# The Mixed Complexes of Mercury(II) with Hydroxide and Iodide

INGRID AHLBERG

*Division of Physical Chemistry I, Chemical Center, University of Lund, P.O.Box 740, S-220 07 Lund 7, Sweden*

The mixed complexes formed between mercury(II), hydroxide and iodide in solutions with 0.5 M sodium perchlorate as supporting electrolyte have been studied at 25°C, by measuring the emf of the cell $-$ GE|S|SE$+$, where GE is a glass electrode and SE a standard reference electrode. S had the general composition: $B$ Hg(II), $H$ H$^+$, $(0.5\ M-2B-H)$ Na$^+$, $X$ I$^-$, $(0.5\ M-X)$ ClO$_4{}^-$ The ratio $X/B$ was 0.5 or 1.0. The experimental data $Z$ (average number of OH$^-$ bound per mercury(II) as a function of log $h$ could be described by assuming one mixed complex, *viz.* HgOHI. The equilibrium constant, $\beta_{1,1,1}$, for the reaction

$$\text{Hg}^{2+} + \text{I}^- + \text{H}_2\text{O} \rightleftharpoons \text{HgOHI} + \text{H}^+$$

was determined as log $\beta_{1,1,1} = 8.9 \pm 0.1$.

The equilibrium between mercury and iodide with 0.5 M NaClO$_4$ as supporting electrolyte has been studied by Sillén *et al.*[1-3] by emf measurements and by Marcus[4] using distribution equilibrium methods. Their results are shown in Table 1. Sillén's values have been used in the calculations. Analogously to the hydrolysis of the mercury bromide,[5] it is $K_{1,2}$, the equilibrium constant for the reaction

$$\text{Hg}^{2+} + \text{HgI}_2 \rightleftharpoons 2\ \text{HgI}^+ \tag{1}$$

that together with $\beta_{1,1,0}$ and $\beta_{2,1,0}$ has to be known when computing the equilibrium constant $K_{1,1}$, for the reaction
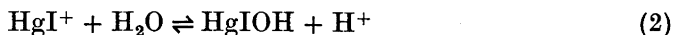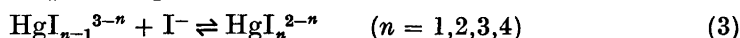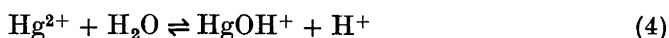
$$\text{HgI}^+ + \text{H}_2\text{O} \rightleftharpoons \text{HgIOH} + \text{H}^+ \tag{2}$$

Table 1 also gives $K_n$, the equilibrium constant for the reaction

$$\text{HgI}_{n-1}{}^{3-n} + \text{I}^- \rightleftharpoons \text{HgI}_n{}^{2-n} \qquad (n = 1,2,3,4) \tag{3}$$

The equilibrium constant for the reactions

$$\text{Hg}^{2+} + \text{H}_2\text{O} \rightleftharpoons \text{HgOH}^+ + \text{H}^+ \tag{4}$$

and

$$\text{Hg}^{2+} + 2\ \text{H}_2\text{O} \rightleftharpoons \text{Hg(OH)}_2 + 2\ \text{H}^+ \tag{5}$$

*Table 1.* Equilibrium constants for the system $Hg^{2+} - I^-$.

| Ref. | Method | $K_{1,2}$ | $\log (K_1/M)$ | $\log (K_2/M)$ | $\log (K_3/M)$ | $\log (K_4/M)$ |
|---|---|---|---|---|---|---|
| Sillén *et al* 1949 [1,2] | red, Hg | 115 | 12.87 | 10.95 | 3.78 | 2.23 |
| Sillén 1949 [3] | | | | | | |
| Marcus [4] | distr. | 81 | | | 3.67 | 2.37 |

have been taken from the work by Hietanen and Sillén,[10] $\log (\beta_{1,1,0}/M) = -3.70 \pm 0.07$, $\log (\beta_{2,1,0}/M^2) = -6.30 \pm 0.05$.

## EXPERIMENTAL

*Chemicals.* Sodium perchlorate, perchloric acid, sodium hydroxide, silver perchlorate, and mercury perchlorate were prepared as described previously.[5,6] Sodium iodide (Mallinckrodt, *p.a.*) was analysed potentiometrically.

*Details of the emf measurements.* In order to produce hydrolysed solutions of $u = 1.0$ the following solutions were carefully mixed into the titration vessel. Since $HgI_2$ is the least soluble species especially the additions of $S_4$ had to be performed very slowly to avoid Tyndall effects.

$S_1$: 0.75 mM Hg(II), 0.08 mM $H^+$, 498.5 mM $Na^+$, 500 mM $ClO_4^-$.
$S_2$: 0.75 mM Hg(II), 0.08 mM $H^+$, 498,5 mM $Na^+$, 496.3 mM $ClO_4^-$, 3.75 mM $I^-$.
$S_3$: 1.50 mM Hg(II), 0.16 mM $H^+$  496.8 mM $Na^+$, 500 mM $ClO_4^-$.
$S_4$: 1.50 mM Hg(II), 0.16 mM $H^+$, 496.8 mM $Na^+$, 492.5 mM $ClO_4^-$. 7.5 mM $I^-$.
$S_5$:13.38 mM NaOH                         500 mM $ClO_4^-$.

The ratio of the volumes of $S_1$ and $S_2$ was 4:1 and of $S_3$, $S_4$ and $S_5$ 4:1:5.

$$S_0 = S_1 + S_2 + S_3 + S_4 + S_5$$

The solutions $S_1$ and $S_3$ were prepared from 100 mM stock solutions of Hg(II) perchlorate. $S_2$ and $S_4$ originated from stock solutions of sodium iodide and mercury(II) perchlorate.

Magnetic stirring was applied and $N_2$ was passed through the solution. This was then immediately titrated with an acid solution which had the same values of $B$ and $X$ as had $S_0$.

## LIST OF SYMBOLS

$B$ = total Hg(II) concentration.
$b$ = concentration of $Hg^{2+}$.
$X$ = total halogen concentration.
$x$ = concentration of free halogenide.
$u$ = $X/B$.
$H$ = analytical hydrogen ion excess concentration.
$h$ = actual concentration of hydrogen ion.
$a$ = $h^{-1}$.
$\beta_{p,q,r}$ = equilibrium constant for the reaction

$$q\,Hg^{2+} + p\,H_2O + r\,X^- \rightleftharpoons Hg_q(OH)_p X_r^{(2q-p-r)+} + p\,H^+ \qquad (6)$$
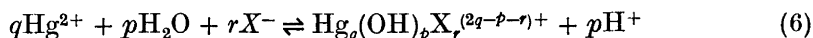
$Z$ average number of hydrogen ions split off per Hg(II)

$$BZ = h - H = p\ \beta_{p,q,r} b^p h^{-p} x^r \tag{7}$$

$Kn$ = equilibrium constant for the reaction

$$HgX_{n-1} + X^- \rightleftharpoons HgX_n; \quad n = (1,2,3,4) \tag{8}$$
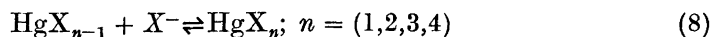
$K_{1,2}$ = equilibrium constant for the reaction

$$Hg^{2+} + HgX_2 \rightleftharpoons 2\ HgX^+ \tag{9}$$

## MEASUREMENTS AND CALCULATIONS

Potentiometric measurements were performed in the cell previously described.[5] The solutions S in the titration vessel had compositions analogous to those described for the bromide systems, *i.e.* $X/B$ was maintained constant in each titration. However, the low solubility of mercury(II) iodide further complicated the study of the mercury–hydroxide–iodide system. When $u = 0.5$, $B$ was 5.00 mM or 2.5 mM. The concentration of free iodide, $x$, increases both with $u$ and $-\log h$.

When $u = 1.0$, it was necessary to lower the total iodide concentration in order to obtain a hydrolysed solution without precipitation of red $HgI_2$. Therefore the value of $B$ was chosen as 0.75 mM.
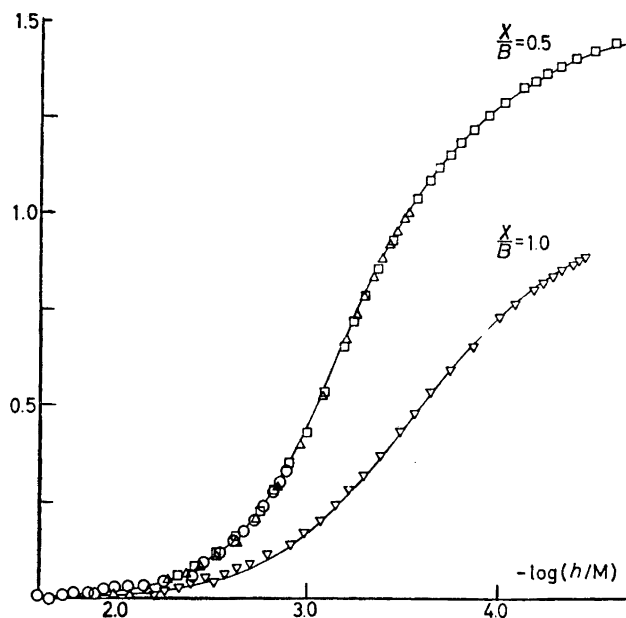


*Fig. 1.* The formation of hydroxo complexes in solutions containing mercury(II) and iodide. The curves have been calculated from the equilibrium constants in Table 3. The experimental points are denoted O, △, □, and △ for $B = 10$, 5, 2.5, and 0.75 mM, respectively.

*Table 2.* Survey of titrations.

---

$u = 0.500$, $B = 5.000$ mM.

$-\log (h/M)$, $Z$; 3.548, 1.001; 3.526, 0.985; 3.485, 0.949; 3.448, 0.915;
3.441, 0.881; 3.364, 0.831; 3.318, 0.782; 3.277, 0.733; 3.219, 0.671;
3.094, 0.522; 2.976, 0.395; 2.861, 0.288; 2.746, 0.204; 2.637, 0.146;
2.541, 0.105; 2.455, 0.083; 2.384, 0.062; 2.271, 0.050; 2.180, 0.023;
2.080, 0.011; 2.002, 0.010.

$u = 0.500$, $B = 2.500$ mM.

$-\log (h/M)$, $Z$; 4.642, 1.444; 4.527, 1.424; 4.432, 1.404; 4.349, 1.384;
4.275, 1.365; 4.215, 1.346; 4.153, 1.327; 4.051, 1.290; 3.967, 1.254;
3.893, 1.218; 3.821, 1.184; 3.762, 1.150; 3.707, 1.117; 3.656, 1.084;
3.590, 1.036; 3.532, 0.989; 3.461, 0.928; 3.385, 0.854; 3.318, 0.783;
3.257, 0.716; 3.204, 0.716; 3.101, 0.532; 3.010, 0.429; 2.919, 0.350;
2.842, 0.277; 2.768, 0.225; 2.640, 0.160; 2.540, 0.115; 2.423, 0.082;
2.337, 0.058.

$u = 1.000$, $B = 0.750$ mM.

$-\log (h/M)$, $Z$; 4.482, 0.888; 4.448, 0.880; 4.414, 0.867; 4.357, 0.853;
4.304, 0.837; 4.255, 0.821; 4.211, 0.805; 4.105, 0.765; 4.025, 0.727;
3.886, 0.655; 3.765, 0.592; 3.663, 0.533; 3.578, 0.479; 3.499, 0.432;
3.397, 0.371; 3.308, 0.317; 3.229, 0.278; 3.161, 0.243; 3.080, 0.202;
2.995, 0.169; 2.925, 0.143; 2.804, 0.116; 2.714, 0.093; 2.640, 0.078;
2.578, 0.064; 2.539, 0.043; 2.478, 0.056; 2.403, 0.046.

---

Values of $Z$, plotted as a function of log $h$, is shown in Fig. 1. The complete data for all the titrations are given in Table 2.

For solutions having a constant $X/B$, the experimental $Z(\log h)$ curves coincide for different $B$-values. They may be described by assuming one mixed complex, HgIOH, corresponding to that of the bromide system.[5] Since the mercury iodide complexes are stronger than the corresponding bromide ones, $x$ has a lower value in the iodide solutions. The same approximations as in Ref. 5 are consequently allowed and we obtain,

$$u = \frac{X}{B} = \frac{\beta_{0,1,1}x + 2\beta_{0,1,2}x^2 + \beta_{1,1,1}ax}{1 + \beta_{1,1,0}a + \beta_{2,1,0}a^2 + \beta_{0,1,1}x + \beta_{0,1,2}x^2 + \beta_{1,1,1}ax} \qquad (10)$$

$$Z = \frac{(\beta_{1,1,0}a + 2\beta_{2,1,0}a^2 + \beta_{1,1,1}ax)(2-u)}{2(1 + \beta_{1,1,0}a + \beta_{2,1,0}a^2) + \beta_{0,1,1}x + \beta_{1,1,1}ax} \qquad (11)$$

$Z$ is a function of the two independent variables $u$ and $a$.

Comparison of the experimental $Z$ curves to those calculated from (14), assuming different values of $\beta_{1,1,1}$ gives the best fit when log $\beta_{1,1,1} = 8.9 \pm 0.1$.

The experimental data were treated by means of the computer program "Letagrop", designed by Sillén et al.[7] The equilibrium constants that minimized the error square sum

$$U = \sum(Z_{exp} - Z_{calc})^2 \qquad (12)$$

was sought.

The values, obtained by the computer are given in Table 3. In the first row all points in Table 2 were used. When the errors in $H_0$, $H_T$ and $E_0$ were treated

*Table 3.* Survey of equilibrium constants in the system Hg(II) − OH − I.

| Constant | Computer | | | Curve-fitting |
| --- | --- | --- | --- | --- |
| | All points | $X/B = 0.5$ | $X/B = 1.0$ | |
| $\beta_{0,1,1}/M^{-1}$ | $7.6 \times 10^{12}$ | $7.4 \times 10^{12}$ | $(1.2 \pm 0.1)10^{13}$ | $7.4 \times 10^{12}$ |
| $\beta_{0,1,2}/M^{-2}$ | $(8 \pm 1)10^{23}$ | $(12.2 \pm 0.5)10^{23}$ | $(8.2 \pm 1.6)10^{23}$ | $6.6 \times 10^{23}$ |
| $\beta_{1,1,0}/M$ | $(2.21 \pm 0.04)10^{-4}$ | $(2.24 \pm 0.09)10^{-4}$ | $2.00 \times 10^{-4}$ | $2.00 \times 10^{-4}$ |
| $\beta_{2,1,0}/M^{2}$ | $(5.35 \pm 0.05)10^{-7}$ | $(5.52 \pm 0.03)10^{-7}$ | $5.01 \times 10^{-7}$ | $5.01 \times 10^{-7}$ |
| $\beta_{1,1,1}$ | $(8.4 \pm 0.5)10^{8}$ | $(6.5 \pm 0.1)10^{8}$ | $(18 \pm 2)10^{8}$ | $(8 \pm 2)10^{8}$ |

as unknown constants, the computer gave high values for $E_0$ in the last titration $(X/B = 1.0)$, where the solutions were supersaturated with respect to $HgI_2$. Therefore the data from this titration were also handled separately. In this way the second and third rows of Table 3 have been obtained.

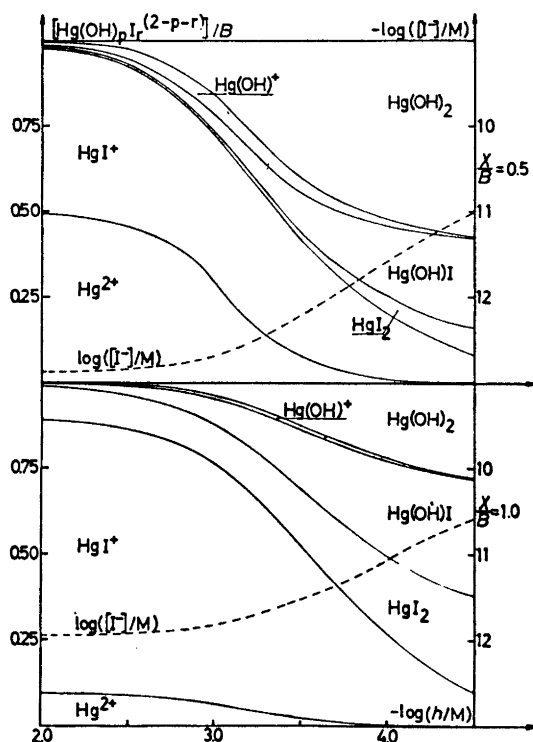Only one mixed complex, Hg(OH)I, was found. Its stability constant $\beta_{1,1,1}$ was $(8 \pm 2) \times 10^8$.



*Fig. 2.* The distribution of the complexes $Hg(OH)_pI_r{}^{2-p-r}$ as a function of $-\log h$.

## RESULTS AND COMMENTS

The distributions of the various species as functions of $-\log h$ at $X/B = 0.5$ and 1.0 is shown in Fig. 2.

The hydrolysed solutions were supersaturated with respect to $HgI_2$, as is seen from the following values which correspond to some of the highest points of the $Z$ curves:

| $u$ | $-\log(h/M)$ | $B/M$ | $[HgI_2]/M$ | $[Hg(OH)_2]/M$ |
|-----|------|------|------|------|
| 0.5 | 4.6 | 0.0025 | $2 \times 10^{-4}$ | $1.4 \times 10^{-3}$ |
| 0.5 | 3.5 | 0.005 | $0.9 \times 10^{-4}$ | $1.6 \times 10^{-3}$ |
| 1.0 | 4.5 | 0.00075 | $2 \times 10^{-4}$ | $0.20 \times 10^{-3}$ |

From Biedermann and Sillén's [8] determination of the solubility of $HgI_2$ it follows that $[HgI_2] = 7 \times 10^{-5}$ M in a saturated solution of mercury(II) iodide. A comparison with the value of $[Hg(OH)_2] = 0.2 \times 10^{-3}$ M in solutions saturated with mercury(II) oxide, which can be deduced from Garett's work,[9] indicates that the two first solutions are also supersaturated with respect to $Hg(OH)_2$.

In a previous publication [5] the acidity of some species $HgX^+$ are given and discussed. For the iodide one gets $K_{1,1} = \beta_{1,1,1}/\beta_{0,1,1} = 1.0 \times 10^{-4}$ M, i.e. $HgI^+$ is a weaker acid than the other mercury monohalide ions studied.

If statistical reasons alone determined the equilibrium constants, $\beta_{1,1,1}$ could be calculated from the relation $\beta_{1,1,1} = 2(\beta_{0,1,2}\beta_{2,1,0})^{\frac{1}{2}}$, which gives $\beta_{1,1,1} = 11 \times 10^8$, close to the experimental value $(8 \pm 2) \times 10^8$.

The value of $\beta_{1,1,1}$ depends on many different constants taken from literature. Systematic errors may also be present because it was rather difficult to prepare a clear $S_0$-solution. Therefore the real error in $\beta_{1,1,1}$ might be much larger than that calculated by the computer.

## REFERENCES

1. Sillén, L. G. and Infeldt, G. Svensk Kem. Tidskr. 58 (1946) 61.
2. Qvarfort, I. and Sillén, L. G. Acta Chem. Scand. 3 (1949) 505.
3. Sillén, L. G. Acta Chem. Scand. 3 (1949) 539.
4. Marcus, Y. Acta Chem. Scand 11 (1957) 599.
5. Ahlberg, I. and Leden, I. Trans. Roy. Inst. Technol. 249 (1972) 17.
6. Ahlberg, I. Acta Chem. Scand. 16 (1962) 887.
7. Ingri, N. and Sillén, L. G. Private communication.
8. Biedermann, G. and Sillén, L. G. Svensk Kem. Tidskr. 61 (1949) 63.
9. Garett, A. B. and Howell, W. W. J. Am. Chem. Soc. 61 (1939) 1730.
10. Hietanen, S. and Sillén, L. G. Acta Chem. Scand. 6 (1952) 747.

# Oxidation of Carbohydrate Derivatives with Silver Carbonate on Celite. VIII. Oxidation of Trioses and Some Related Compounds

SVEIN MORGENLIE

*Agricultural University, Department of Chemistry, N-1432 Ås-NLH, Norway*

Glycolaldehyde and D,L-glyceraldehyde are oxidized by silver carbonate on Celite in methanol to methyl esters of the corresponding acids. Methyl glycolate is also the product obtained on oxidation of dihydroxy acetone. Glyoxal gives methyl glyoxylate with the same oxidant, the second aldehyde group of this compound resisting oxidation. Formaldehyde is oxidized at a somewhat higher temperature than the other compounds.

Methyl esters of oxalic, glyoxylic, glyceric and presumably glycolic acid were found to be secondary products on oxidation of aldopentoses with silver carbonate on Celite in methanol.[1] Glyceraldehyde has been identified as one of the products after oxidation of the pentoses, and small amounts of compounds which were tentatively identified as glycolaldehyde and glyoxal, based on the chromatographic and electrophoretic behaviour, were also detected. To establish whether these compounds might be precursors of the methyl esters mentioned above, it seemed of interest to examine the effect of silver carbonate on Celite on these compounds in methanol. An investigation of the effect of the oxidant on α-hydroxy aldehydes and ketones which are unable to form cyclic hemiacetals was further of general interest, since such compounds would be expected to form hemiacetals with the solvent in methanolic solution, and hence possibly undergo reactions analogous to those occurring with aldoses[1] and ketoses,[2] but in non-cyclic form. Aldoses have been found to give mixtures of aldonolactones and aldoses with a shorter carbon chain,[1] whereas 2-ketoses primarily are cleaved between C-2 and C-3 by this oxidant.[2]

## RESULTS AND DISCUSSIONS

Glycolaldehyde (I) was completely oxidized in methanol by the oxidant within 45 min at 35°C. Methyl glycolate (III) was the only product found after removal of the solvent. Hydrolysis of the ester gave glycolic acid (IV) in
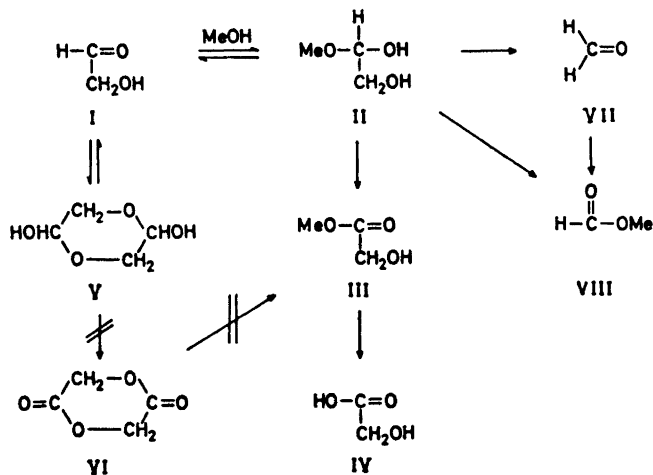
about 55 % yield based on glycolaldehyde. The direct formation of the methyl ester (III) on oxidation of glycolaldehyde indicated that the reaction occurred *via* the hemicaetal (II). Glycolaldehyde crystallizes in the dimeric form (V), and an alternative way to the methyl ester (III) might be an oxidation of this dimer in two steps to the dimeric form (VI) of glycolic acid, and subsequent conversion to the methyl ester in the methanolic solution. This possibility has, however, been excluded by the fact that glycolic acid dimer (VI) is not converted to methyl glycolate (III) under the conditions employed.
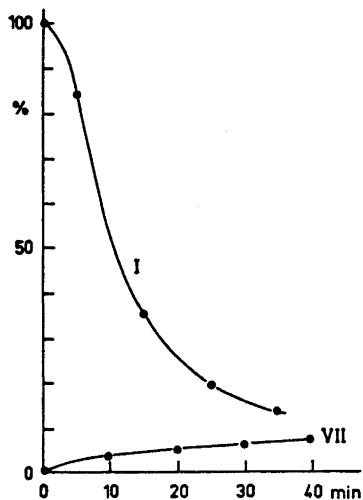


*Fig. 1.* Oxidation of glycolaldehyde. Per cent glycolaldehyde (I) and formaldehyde (VII) present as a function of time.
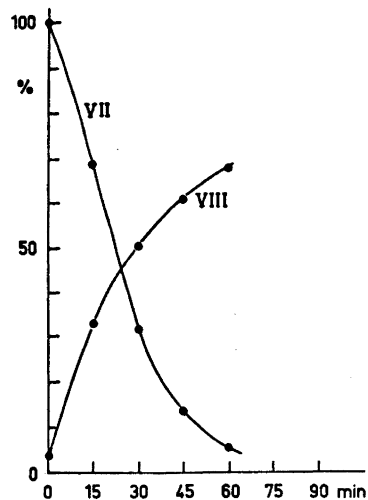
*Fig. 2.* Oxidation of formaldehyde. Per cent formaldehyde (VII) and methyl formate (VIII) present as a function of time.

Since the yield of glycolic acid (IV) from glycolaldehyde is about 55 %, the occurrence of glycol cleavage of the hemiacetal (II) in analogy to the degradation of aldopentoses,[1] is not excluded as a side reaction. The expected products after a glycol cleavage are formaldehyde (VII) and methyl formate (VIII). The presence of formaldehyde is indicated colorimetrically with the acetylacetone-ammonium acetate reagent.[3] Glycolaldehyde interfers slightly in this determination, and thus simultaneous colorimetric determinations of glycolaldehyde with α-naphthol – sulphuric acid [4] and formaldehyde with acetyl acetone – ammonium acetate reagent have been performed. The result is shown in Fig. 1; the formaldehyde curve is corrected for the glycolaldehyde present. It is seen that formaldehyde may be present in about 8 % yield at the end of the reaction.

The question arose whether formaldehyde was further oxidized by the oxidant under the reaction conditions. The effect of silver carbonate on Celite in methanol on formaldehyde (VII) was thus investigated, and it was found that only a slight oxidation occurred at 35°C. At 50°C, however, formaldehyde was almost completely oxidized within 60 min (Fig. 2). Colorimetric determination of ester formed in the solution under the reaction with time, by use of the hydroxylamine – ferric perchlorate reagent [5] (Fig. 2), shows that a possible yield of about 70 % of methyl formate (VIII) is obtained, a slight loss of the low-boiling methyl formate is not excluded. The formation of a formic acid ester in the solution was further indicated by infrared spectroscopy after distillation of the product from the reaction mixture.

DL-Glyceraldehyde (IX) afforded in analogy to glycolaldehyde almost exclusively DL-glyceric acid methyl ester (X) at 35°C. Chromatography indicated the additional formation of traces of methyl glycolate (III), the product expected after degradation of DL-glyceraldehyde to glycolaldehyde (I) followed
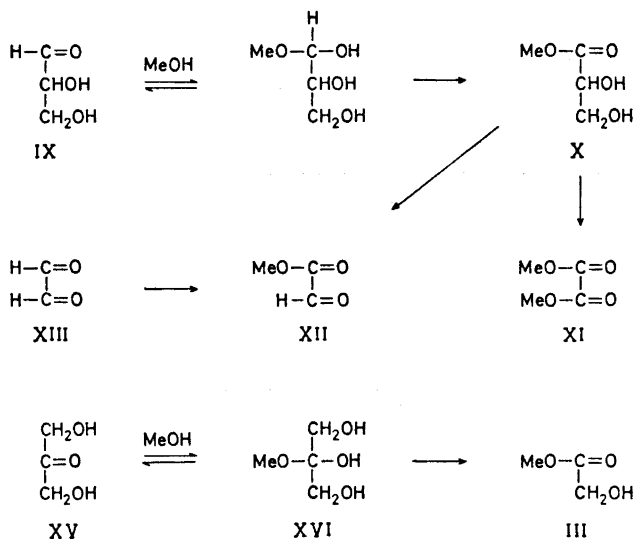
by oxidation of this compound as described above. At 45°C glyceric acid methyl
ester (X) undergoes a slow further oxidation, and the products were found to
be dimethyl oxalate (XI) and methyl glyoxylate (XII) on chromatographic
and spectroscopic evidence.

The presence in addition to methyl glyoxylate of a compound assumed to
be glyoxal (XIII) after oxidation of aldopentoses,[1] suggests a possible rela-
tionship between these compounds in this oxidation. To establish whether
such a relationship may exist, glyoxal (XIII) was also treated with silver
carbonate on Celite in methanol. One of the aldehyde groups of the dialdehyde
was smoothly oxidized to a carbomethoxy group, whereas the remaining
aldehyde group was resistant to oxidation, methyl glyoxylate (XIII) could
not be further oxidized at 45°C. The tendency of methyl glyoxylate (XII) to
hemiacetal formation with methanol must be expected to be greatly reduced
as compared to that of glyoxal (XIII) with an activating second aldehyde
group. Since the hemiacetal form is the form in which all the investigated
compounds obviously are oxidized, the lack of reactivity of methyl glyoxylate
may easily be understood.

The initial attack on 2-ketoses with silver carbonate on Celite in methanol
occurs between C-2 and C-3.[2] One of the reasons for this selectivity may be a
greater reactivity of the secondary hydroxyl group at C-3 than the primary
one. An other explanation could be that in a cyclic form, the hydroxyl groups
at C-2 and C-3 are fixed in a relative orientation particularly suitable for
degradation.

It has been interesting in this connection to find that 1,3-dihydroxy
acetone (XV), with two primary hydroxyl groups next to the ketone func-
tion, needs almost 1 h for a complete oxidation to methyl glycolate (III) at
55°C. This compound is also obviously oxidized by diol cleavage of its hemi-
acetal (XVI). The possibility of two subsequent oxidation steps of the dimeric
form, in which the compound is known to crystallize, to give the glycolic acid
dimer is excluded for the same reasons as in the case of glycolaldehyde (I).

The results presented have shown that the presence of methyl esters of
glycolic, glyoxylic, and glyceric acid after oxidation of aldopentoses may be
due to direct oxidation of the corresponding aldehydes. It is further seen that
dimethyl oxalate may possibly arise from methyl glycerate, in particular
because a temperature of 45°C has been found to be "critical" for this reac-
tion, and dimethyl oxalate was not formed from the aldopentoses at reaction
temperatures lower than this temperature.

The present work has also established that silver carbonate on Celite in
methanol is a convenient oxidant for the conversion of α-hydroxy aldehydes,
and possibly other activated aldehydes, to the corresponding carboxylic acid
methyl esters.

<div align="center">EXPERIMENTAL</div>

Paper chromatography was performed on Whatman No. 1 paper in the solvent system
(v/v) (A) butanone – acetone – formic acid – water 40:2:1:6. Thin-layer chromatography
(TLC) was run on Silica gel G in (B) benzene – ethanol 5:1 and (C) benzene – ethanol 10:1.
As spray reagents were used hydroxylamine – ferric chloride [6] for esters, sulphanilamide –
β-naphthol – sodium nitrite[7] for acids and diphenylamine – aniline – phosphoric acid [8]
for the other compounds.

*Oxidation of glycolaldehyde (I)*. Glycolaldehyde (I) (100 mg) in methanol (50 ml) was stirred with silver carbonate on Celite [9] (6 g) for 35 min at 35°C. The solution was then filtered, and from a part of it, the solvent was evaporated to give chromatographically homogeneous (TLC, solvent C) methyl glycolate (III), indistinguishable from an authentic sample of methyl glycolate. The infrared spectrum was identical with that of authentic methyl glycolate.

To the solution containing methyl glycolate (III) was added sodium hydroxide (200 mg) in water (2 ml). After 2 h, the solution was diluted with water (10 ml), neutralized with Dowex 50 W (H⁺) ion exchange resin and the solvents were evaporated. Glacial acetic acid was evaporated from the residue, which was then kept at $2-3°C$ over night to give crystalline glycolic acid (IV), the yield was 69 mg (54 %), m.p. $75-77°C$, after sublimation *in vacuo* m.p. $77.5-78.5°C$ (lit.[10] 80°).

*Oxidation of glycolaldehyde (I)*. *Colorimetric determination of glycolaldehyde and formaldehyde*. Glycolaldehyde (30 mg) in methanol (20 ml) was stirred with silver carbonate on Celite (2 g) at 35°C. Aliquots (100 $\mu$l) were withdrawn at intervals, diluted with water (to 1 ml) and the amounts of glycolaldehyde and formaldehyde determined colorimetrically with the $\alpha$-naphthol − sulphuric acid reagent [4] and the acetylacetone − ammonium acetate reagent,[3] respectively. The results are shown in Fig. 1.

*Oxidation of formaldehyde (VII)*. Formaldehyde (VII) (6.5 mg) in methanol (10 ml) was stirred with silver carbonate on Celite (1 g) at 50°C. Aliquots (10 $\mu$l and 250 $\mu$l) were withdrawn at intervals, and the amounts of formaldehyde and formate were determined colorimetrically with the acetylacetone − ammonium acetate reagent and the hydroxylamine − ferric perchlorate reagent,[5] respectively. The results are shown in Fig. 2.

After 1 h, the solid material was filtered off. A mixture of the product and methanol was distilled into chloroform by keeping the solution at 60°C for a few min. The infrared spectrum of the resulting chloroform solution showed strong absorption at 1720 cm⁻¹, characteristic of formic esters.[11]

*Oxidation of DL-glyceraldehyde (IX)*. DL-Glyceraldehyde (200 mg) in methanol (100 ml) was oxidized with silver carbonate on Celite (10 g) at 35°C for 45 min. Filtration of the solution and evaporation of the solvent gave syrupy methyl DL-glycerate (X). The compound was chromatographically (TLC, solvent B) indistinguishable from an authentic sample, and the infrared spectra were identical. The product contained traces of a compound with mobility (TLC, solvent C) corresponding to that of methyl glycolate (III).

Hydrolysis of the ester (X) with 0.2 M trifluoroacetic acid at 40°C for 48 h and removal of the acid by repeated distillations with water, afforded syrupy DL-glyceric acid (133 mg). The syrup was chromatographically homogeneous (paper chromatography, solvent A) and the mobility corresponded to that of authentic DL-glyceric acid. M.p. of the derived [12] amide was $86-89°C$ (lit.[12] $91.5-92°C$).

*Oxidation of methyl-DL-glycerate (X)*. Methyl DL-glycerate (190 mg) in methanol (100 ml) was stirred with silver carbonate on Celite (12 g) for 1 h at 45 °C. After filtration of the solution and evaporation of the solvent, the residue was dissolved in chloroform (30 ml). The chloroform layer was extracted with water (6 × 5 ml), dried with sodium sulphate and the solvent evaporated to give dimethyl oxalate (XI) (20 mg) indistinguishable from authentic dimethyl oxalate by TLC (solvent C); the infrared spectrum was identical with that of the authentic sample. The water extracts Nos. 3 to 6 from the extraction mentioned above contained methyl glyoxylate (XII) (14 mg), identical with an authentic sample (TLC, infrared spectrum).

The water extracts Nos. 1 and 2 contained a mixture of starting material and methyl glyoxylate (XII).

*Oxidation of glyoxal (XIII)*. Glyoxal (200 mg) in methanol (100 ml) was oxidized with silver carbonate on Celite (10 g) for 1 h at 45°C. Filtration of the solution and evaporation of the solvent yielded methyl glyoxylate (XII), indistinguishable from an authentic sample (prepared by periodate oxidation of dimethyl tartrate) by TLC (solvent B). The infrared spectrum was identical with that of authentic methyl glyoxylate.

Hydrolysis of the ester (XII) in water (4 ml) containing sodium bicarbonate (0.5 g) for 48 h at room temperature, afforded glyoxylic acid (XIV) (165 mg) as a chromatographically homogeneous syrup (paper chromatography, solvent A). Treatment of this syrup in water (4 ml) with dimedone (300 mg) in ethanol (7.5 ml) and water (7.5 ml) over night yielded the dimedone derivative (133 mg), crystallizing directly from the solution, m.p. 232°C, after sublimation *in vacuo* m.p. $234-238°C$ (lit.[13] $236-238°C$).

*Oxidation of 1,3-dihydroxy-acetone (XV).* 1,3-Dihydroxy-acetone (200 mg) in methanol (100 ml) was treated with silver carbonate on Celite (10 g) at 55°C for 1 h. After filtration, the solvent was evaporated from a part of the solution, yielding methyl glycolate (III), homogeneous by TLC (solvent C). The chromatographic mobility corresponded to that of authentic methyl glycolate, and the infrared spectra (CHCl₃) were identical.

To the solution was added sodium hydroxide (400 mg) in water (4 ml). After 2 h at room temperature, the solution was neutralized with Dowex 50 W ion exchanger (H⁺ form) and the solvent evaporated. From the residue was distilled acetic acid twice, the residue crystallized in refrigerator. The yield was 107 mg (63 %, based on dihydroxy acetone) of glycolic acid (IV), m.p. 72 − 75°C, after sublimation *in vacuo* m.p. 78.5 − 79.5°C (lit.[10] 80°).

## REFERENCES

1. Morgenlie, S. *Acta Chem. Scand.* **27** (1973) 2607.
2. Morgenlie, S. *Acta Chem. Scand.* **27** (1973) 1557.
3. Speck, Jr., J. C. *Methods Carbohyd. Chem.* **2** (1962) 443.
4. Dische, Z. *Mikrochemie* **7** (1929) 33.
5. Goddu, R. F., LeBlanc, N. F. and Wright, C. M. *Anal. Chem.* **27** (1955) 1251.
6. Abdel-Akher, M. and Smith, F. *J. Am. Chem. Soc.* **73** (1951) 5859.
7. Schmidt, G. C., Fischer, C. and McOwen, J. M. *J. Pharm. Sci.* **52** (1963) 468.
8. Scwimmer, S. and Bevenue, A. *Science* **123** (1956) 543.
9. Balogh, V., Fetizon, M. and Golfier, M. *Angew. Chem.* **81** (1969) 423.
10. Rodd, E. H. *Chemistry of Carbon Compounds* **1b** (1952) 784.
11. Thompson, H. W. and Torkington, P. *J. Chem. Soc.* **1945** 640.
12. Frankland, P. F., Wharton, F. M. and Aston, H. *J. Chem. Soc.* **79** (1901) 266.
13. Wolfrom, M. L. and De Lederkremer, R. M. *Carbohyd. Res.* **2** (1966) 426.

# Molecular Structure of Gaseous Tris(methylthio)borane

R. JOHANSEN,[a] E. WISLØFF NILSSEN,[a] H. M. SEIP[a]
and W. SIEBERT[b]

[a] Department of Chemistry, University of Oslo, Oslo 3, Norway and [b] Institut für anorganische Chemie der Universität Würzburg, Würzburg, Germany

Tris(methylthio)borane has been studied by gas electron diffraction. The molecular skeleton was found to be essentially planar with $r_a(B-S) = 1.805(2)$ Å, $r_a(S-C) = 1.825(3)$ Å, and $\angle BSC = 104.5(3)°$. Mean amplitudes of vibration determined from the electron-diffraction data are in fairly good agreement with values computed from spectroscopic data.

The structure determination of tris(methylthio)borane, $B(SMe)_3$, cf. Fig. 1, by gas electron diffraction was carried out as a part of our studies of the nature of the $B-S$ bond, and in particular for comparison with the structure of methylthio-dimethylborane, $Me_2BSMe$, described in the previous paper.[1]

## EXPERIMENTAL

The sample of $B(SMe)_3$ was synthesized by one of us (W.S.). The electron diffraction diagrams were recorded with the Balzer's Eldigraph KDG2 [2,3] in Oslo. The nozzle temperature was about 80°C. Four plates recorded with a nozzle-to-plate distance of 50 cm and wavelength 0.05847 Å and seven plates with a nozzle-to-plate distance of 25.0 cm (the vawelength was 0.05852 Å for five of these plates, 0.05828 Å for two of them) were used. The data were treated as described elsewhere.[4] The levelled intensity curves obtained from each plate were plotted and showed very satisfactory agreement. A composite intensity curve ranging from $s = 2.25$ Å$^{-1}$ to $s = 29.0$ Å$^{-1}$ was computed (see Fig. 2). The $s$ intervals were 0.125 Å$^{-1}$ for $s < 10.0$ Å$^{-1}$ and 0.25 Å for $s > 10.0$ Å$^{-1}$.

The same scattering amplitudes were used as in the previous paper.[1]

## STRUCTURE REFINEMENT

Most of the important interatomic distances may be estimated from the experimental radial distribution (RD) curve [4] shown in Fig. 1. The peaks near 1.81 Å and near 3.12 Å show that the $BS_3$ moiety is planar as expected and give reasonably accurate $B-S$ and $C-S$ bond lengths. The peak around 4.6 Å must correspond to distances of the type $S2\cdots C5$, and shows that the heavy atom skeleton must be nearly planar. The molecular parameters were refined by the least-squares method using a diagonal weight matrix. Very
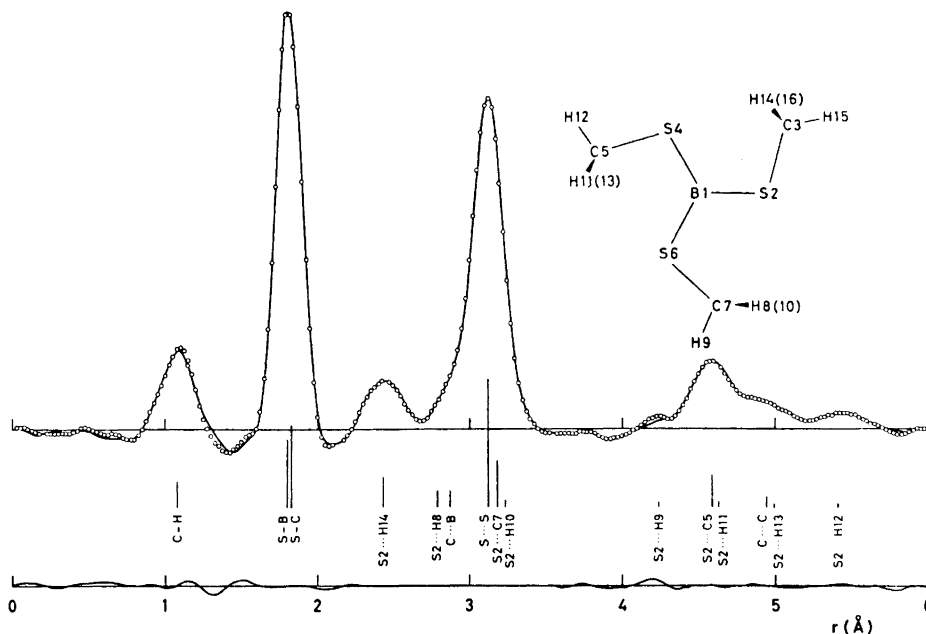
*Fig. 1.* Experimental (circles) and theoretical (full line) radial distribution functions for B(SMe)₃ calculated by Fourier transformation of the curves in Fig. 2 with an artificial damping constant [4] $k = 0.002$ Å². The differences between experimental and theoretical values are also shown. The positions and the approximate areas of the peaks corresponding to the most important interatomic distances are indicated. The figure of the molecule corresponds to $C_{3h}$ symmetry.

satisfactory agreement between experimental and theoretical curves was obtained for a model with $C_3$ symmetry. We assumed further that there was no tilt of the methyl groups. The Bastiansen-Morino shrinkage effect [5] was neg-

*Table 1.* Bond distances, angles, and mean amplitudes of vibration in tris(methylthio)borane. The standard deviations given in parentheses apply to the last decimal place. Mean amplitudes of vibration calculated from spectroscopic data are also given.

| | $r_a$(Å)[3] | $u$(Å) | $u_{calc}$[b](Å) | | angles (degrees) |
|---|---|---|---|---|---|
| (C−H)$_{av}$[a] | 1.089 (4) | 0.085 (5) | 0.078 | ∠SCH | 110.7 (6) |
| S−B[c] | 1.805 (2) | 0.050⎫ (3) | 0.056 | ∠BSC | 104.5 (3) |
| S−C[c] | 1.825 (3) | 0.047⎭ | 0.054 | φ (S4B1S2C3) | 9.9 (30) |
| | | | | φ (B1S2C3H15) | 160.5 (40) |

[a] An asymmetry constant, $\varkappa = 0.000020$ Å,³ was assumed for the C−H bond distances; for all other distances $\varkappa = 0$. [b] At 80°C. [c] If the shrinkage for the S⋯S distance is neglected, 1.804 Å and 1.826 Å are obtained for the S−B and S−C bond lengths.
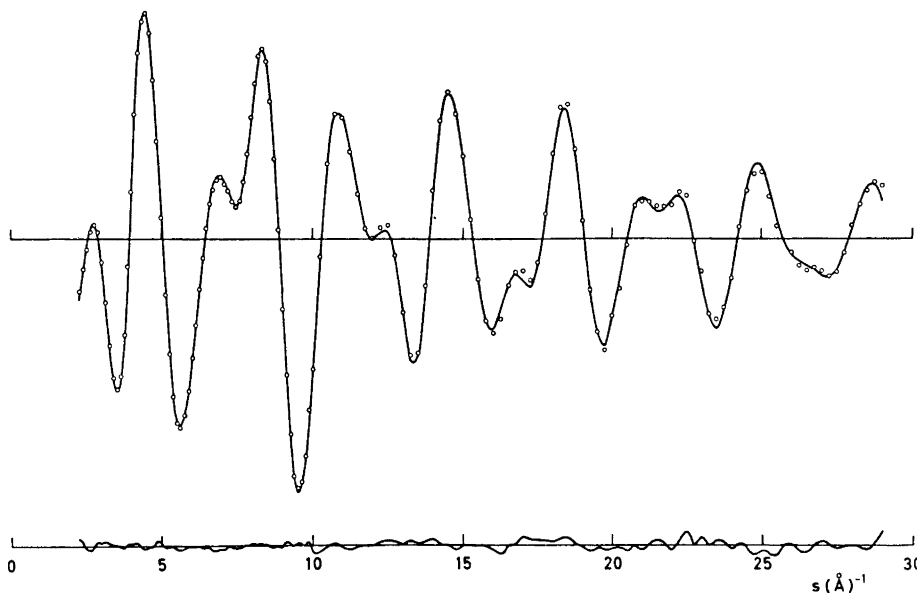
*Fig. 2.* Comparison of the experimental intensity values (circles) and the corresponding theoretical ones (full line) calculated with the parameters in Tables 1 and 2. The differences between experimental and theoretical values are also shown.

lected except for the S $\cdots$ S distance in some refinements where $\delta_a = 0.003$ Å was used. This value was calculated as described in the next section. Some assumptions about the mean amplitudes of vibration $(u)^5$ were also necessary (*cf.* the next section). The bond distances, the corresponding mean amplitudes of vibration, bond angles and torsional angles obtained are given in Table 1. The most important non-bonded distances with the corresponding $u$ values are given in Table 2, and the atomic coordinates in Table 3.

*Table 2.* The most important non-bonded distances and mean amplitudes of vibration.

|  | $r_a$(Å) | $u$ (Å) | | $u_{calc}$(Å) |
|---|---|---|---|---|
| S$\cdots$S | 3.123$^a$ | 0.074 | (2) | 0.075 |
| S2$\cdots$C5 | 4.585 | 0.096 | (5) | 0.095 |
| S2$\cdots$C7 | 3.184 | 0.146 | (8) | 0.145 |
| C$\cdots$B | 2.870 | 0.065 | (8) | 0.096 |
| C$\cdots$C | 4.944 | 0.160 $^b$ | | 0.147 |
| S2$\cdots$H14 | 2.433 | 0.114 | (6) | 0.107 |
| S2$\cdots$H8 | 2.793 | 0.280 | | 0.28 |
| S2$\cdots$H9 | 4.250 | 0.190 | | 0.16 |
| S2$\cdots$H10 | 3.232 | 0.280 | $b$ | 0.28 |
| S2$\cdots$H11 | 4.633 | 0.200 | | 0.18 |
| S2$\cdots$H12 | 5.422 | 0.130 | | 0.12 |
| S2$\cdots$H13 | 4.999 | 0.200 | | 0.18 |

$^a$ A shrinkage of 0.003 Å is included. $^b$ The parameter was not refined.

*Table 3.* Atomic coordinates (Å) for B(SMe)$_3$.

|      | $x$      | $y$      | $z$      |
| ---- | -------- | -------- | -------- |
| B1   | 0.0      | 0.0      | 0.0      |
| S2   | 1.805    | 0.0      | 0.0      |
| C3   | 2.262    | 1.740    | 0.304    |
| S4   | − 0.903  | 1.563    | 0.0      |
| C5   | − 2.638  | 1.089    | 0.304    |
| S6   | − 0.903  | − 1.563  | 0.0      |
| C7   | 0.376    | − 2.829  | 0.304    |
| H8   | 1.088    | − 2.485  | 1.053    |
| H9   | − 0.074  | − 3.754  | 0.662    |
| H10  | 0.925    | − 3.050  | − 0.611  |
| H11  | − 2.697  | 0.300    | 1.053    |
| H12  | − 3.214  | 1.941    | 0.662    |
| H13  | − 3.103  | 0.724    | − 0.611  |
| H14  | 1.608    | 2.185    | 1.052    |
| H15  | 3.288    | 1.812    | 0.662    |
| H16  | 2.179    | 2.326    | − 0.611  |

## VIBRATIONAL FREQUENCIES AND ROOT-MEAN-SQUARE AMPLITUDES OF VIBRATION

The IR and Raman spectra have been studied by Goubeau and Wittmeier [6] and by Vahrenkamp.[7] A calculation of the fundamental frequencies and root-mean-square amplitudes of vibration was carried out by the methods used for Me$_2$BSMe.[1] After some adjustments the force constants given in Table 4 were used. As in the case of Me$_2$BSMe, the torsional and out-of-plane force constants are very uncertain, giving considerable uncertainty in some of the mean ampli-

*Table 4.* Force constants used in the calculation of frequencies and mean amplitudes.

| Stretching force constants (mdyn/Å) | | Bending force constants (mdyn Å/rad²) | | Repulsion force constants (mdyn/Å) | |
| --- | --- | --- | --- | --- | --- |
| B − S | 2.50 | SBS | 0.9  | S···H  | 0.54  |
| S − C | 1.80 | BSC | 0.9  | H···H  | 0.20  |
| C − H | 4.35 | SCH | 0.35 | C3···S4 | 0.007 |
|       |      | HCH | 0.40 |        |       |

| Coupling constants (mdyn/Å) | | Torsional force constants (mdyn Å/rad²) | | | Out-of-plane force constant (mdyn Å/rad²) | |
| --- | --- | --- | --- | --- | --- | --- |
| BS/BS | 0.40 | SBSC | 0.10 | (two for each BS bond) | BS out of SBS plane: | 0.07 (three con- |
|       |      | BSCH | 0.04 | (three for each SC bond) | | tributions) |

*Table 5.* Observed [7] and calculated frequencies (in cm$^{-1}$) for B(SCH$_3$)$_3$ ($C_{3h}$ symmetry).

| | | Symmetry | IR | Raman | Calculated |
|---|---|---|---|---|---|
| $\delta_s$ | (SBS$_2$) | $E'$ | | 162 | 160 |
| $\delta_s$ | (BSC) | $A'$ | | 235 | 219 |
| $\delta_{as}$ | (BSC) | $E'$ | 307 | 305 | 286 |
| $\nu_s$ | (BS$_3$) | $A'$ | 410 | 430 | 429 |
| $\gamma$ | (BS$_3$) | $A''$ | 474 | 481 | 482 |
| $\nu$ | (CS) | $E'$, $A'$ | 709 | 705 | 710, 711 |
| $\nu_{as}$ | (BS$_3$) | $E'$ | 905/930 | 906 | 915/945 |
| $\varrho$ | (CH$_3$) | | 990 | 984 | 977 − 991 |
| $\delta_s$ | (CH$_3$) | | 1320 | 1317 | 1373 |
| $\delta_{as}$ | (CH$_3$) | | 1430 | 1427 | 1406 |
| $\nu_{as}$ | (CH$_3$) | | 2925 | 2925 | 2982 |
| $\nu_{as}$ | (CH$_3$) | | 2995 | 2995 | 2965 |

tudes and in the correction terms necessary to obtain an $r_\alpha$-structure.[8] In Table 5 the computed frequencies are compared to the experimental values using the assignment proposed by Vahrenkamp.[7] The agreement is fairly satisfactory, though improvement in the computed values for the methyl frequencies seems possible.

The computed root-mean-square amplitudes have been included in Tables 1 and 2. The agreement with the electron-diffraction results is acceptable for all parameters except perhaps for $u(\text{C}\cdots\text{B})$.

By approximate methods Vahrenkamp [7] obtained 2.71 mdyn/Å and 2.57 mdyn/Å, respectively, for the B − S stretching force constants in B(SMe)$_3$ and Me$_2$BSH. He concluded that no $\pi$-bonding occurs between boron and sulphur. However, our calculations give a somewhat smaller value for $k(\text{B} - \text{S})$ in B(SMe)$_3$ (2.50 mdyn/Å) compared to 2.85 mdyn/Å in Me$_2$BSMe.[1] Though both values depend to some extent on the values chosen for the other force constants, the results may perhaps be regarded as an indication of a slightly weaker B − S bond in B(SMe)$_3$ than in Me$_2$BSMe.

## DISCUSSION

Tris(methylthio)borane is better suited for electron-diffraction studies than methylthio-dimethylborane. The quality of the observed data was also better, and the uncertainties in the main parameters in Tables 2 and 3 are smaller than in the corresponding parameters given in the previous paper.[1] The standard deviations have been corrected for the effect of correlation between the data.[9] and the uncertainty in the wavelength has been included.

The torsional angle $\phi$ (SBSC) of 9.9° cannot be regarded as significantly different from zero; oscillations about the B − S bonds may lead to an apparent angle of this size. To find if the equilibrium angle is zero, one might compute the $r_\alpha$-structure, but as mentioned in the previous section most of the correction terms were considered to be too inaccurate.

The torsional angle about the $S-C$ bonds ($\phi(\text{B1S2C3H15}) = 160.5°$, *i.e.* about 20° from the staggered position) may possibly also be explained as a result of rather large oscillations. A model with $\phi(\text{B1S2C3H15})$ negative was also tried. The angle refined to $-164°$. The agreement was slightly poorer than for a positive torsional angle, and S2 ⋯ H10 became rather short (about 2.70 Å).

A comparison of the parameters in $B(SMe)_3$ and $Me_2BSMe$ shows that the $B-S$ bond is slightly longer in the former compound. The difference seems to be significant and is consistent with the difference in the force constants discussed in the previous section. It is tempting to ascribe these results to a lower $\pi$-bond order in the BS bonds in $B(SMe)_3$ than in $Me_2BSMe_3$. However, we have also found a bond length of 1.805 (4) Å in $Me_2BSSBMe_2$.[10] The $B-S$ bond length in $B(SMe)_3$ is in good agreement with the average value of 1.807 Å obtained by Hess in $(HSBS)_3$.[11]

The $C-S$ bond lengths in $B(SMe)_3$ and $Me_2BSMe$ are equal as expected. The difference in the BSC angles may be real, but this angle is difficult to determine in $Me_2BSMe$.

## REFERENCES

1. Brendhaugen, K., Wisløff Nilssen, E. and Seip, H. M. *Acta Chem. Scand.* **27** (1973) 2965.
2. Zeil, W., Haase, J. and Wegmann, L. *Z. Instrumentenk.* **74** (1966) 84.
3. Bastiansen, O., Graber, R. and Wegmann, L. *Balzer's High Vacuum Report* **1969** 1.
4. Andersen, B., Seip, H. M., Strand, T. G. and Stølevik, R. *Acta Chem. Scand.* **23** (1969) 3224.
5. Cyvin, S. J. *Molecular Vibrations and Mean Square Amplitudes*, Universitetsforlaget, Oslo and Elsevier, Amsterdam 1968.
6. Goubeau, J. and Wittmeier, H. W. *Z. anorg. allgem. Chem.* **270** (1952) 16.
7. Vahrenkamp, H. *J. Organomet. Chem.* **28** (1971) 181.
8. Kuchitsu, K. and Cyvin, S. J. In Cyvin, S. J., Ed., *Molecular Structures and Vibrations* Elsevier, Amsterdam 1972, Chapter 12.
9. Seip, H. M. and Stølevik, R. In Cyvin, S. J., Ed., *Molecular Structures and Vibrations* Elsevier, Amsterdam 1972, Chapter 11.
10. Johansen, R., Seip, H. M. and Siebert, W. *To be published.*
11. Hess, H. Ninth International Congress of Crystallography, Kyoto, Japan 1972.

# Transfer of Triplet State Energy in Fluid Solution

## V. "Nonclassical" Energy Donor and Acceptor Properties of Benzil and Substituted Benzils

KJELL SANDROS

*Institutionen för fysikalisk kemi, Chalmers Tekniska Högskola, S-402 20 Göteborg 5, Sweden*

Rate constants for triplet energy transfer to and from benzil, *p*-anisil, and *o*-anisil have been determind in cyclohexane solution from measurements of phosphorescence intensity and lifetime. These diketones have different equilibrium conformations in their ground and triplet states. If the energy transfer process is assumed to involve vertical transitions, molecules of this type have less electronic energy available when they act as donors than that which is required when they act as acceptors. Minimum values of the difference between these energies are estimated at 1000, 1000, and 3000 cm$^{-1}$ for benzil, *p*-anisil, and *o*-anisil, respectively.

It is well established that the energy transfer process

$$\text{Donor}_T + \text{Acceptor}_{S0} \rightarrow \text{Donor}_{S0} + \text{Acceptor}_T$$
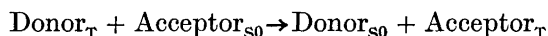
involves an exchange interaction mechanism. The maximum transfer rate is equal to the rate of encounters between excited donors and acceptors. In an earlier investigation [1] comprising a number of molecule pairs (M, N) in benzene solution, rate constants were determined for energy transfer in both directions, that is

$$\text{M}_T + \text{N}_{S0} \rightleftharpoons \text{M}_{S0} + \text{N}_T$$
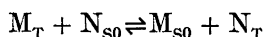
It was found that the rate constants ($k$) obeyed the equation:

$$k = k_D \exp\left(-\Delta E_T/RT\right)/[1 + \exp\left(-\Delta E_T/RT\right)] \tag{I}$$

where $\Delta E_T$ denotes the difference between the electronic excitation energies of the lowest triplet states of acceptor and donor, as obtained from spectroscopic measurements. The equation applies to both positive and negative values of $\Delta E_T$. The value of $k_D$ ($6 \times 10^9$ M$^{-1}$ sec$^{-1}$) is not very far from that calculated for a diffusion-controlled process. The results are compatible with the view that for endothermic energy transfer ($\Delta E_T > 0$) the electronic energy

deficit is made up by Boltzmann distributed vibrational energy of the encounter couples.

An energy transfer behaviour such as that outlined above is denoted as "classical" by Herkstroeter and Hammond.[2] They found that *trans*-stilbene behaved classically as an energy acceptor while the rate constants for endothermic energy transfer with *cis*-stilbene and both isomers of α-methylstilbene as acceptors have much higher values than expected from the spectroscopically obtained triplet state electronic energies of these substances. Hammond and Saltiel[3] had earlier coined the term "nonvertical transition" for the excitation process undergone by acceptors of the latter type. Wagner[4a,b] has shown that biphenyl exhibits a similar acceptor behaviour. Common to all these acceptors is that they have significantly different equilibrium geometries in their ground and excited states. In a comprehensive survey[5] of electronic energy transfer in solution, Lamola presents on p. 67 ff. an attractively simple possibility to explain "nonvertical" excitation behaviour. He points out that activation of a suitable twisting vibrational mode in the ground state of the discussed type of molecules would be especially effective because it reduces the energy required for vertical electronic excitation.

To date there seems to have been only one investigation of the donor properties of substances having different ground and excited state conformations. Wagner[4b] has estimated the rate constant for energy transfer from biphenyl to benzophenone. In the present work energy transfer has been studied in systems where benzil and anisils act both as donors and as acceptors. Convincing arguments[6,7] have been presented for the view that in these molecules the carbonyl groups are coplanar both in the lowest singlet and triplet excited states whereas in the ground state the benzoyl units lie at approximately 90° to each other. These molecules may thus be expected to have potential energy profiles similar to those drawn in Fig. 1. Evidently the energy required for excitation of such a molecule ($E_{TA}$) is higher than the energy available from the excited molecule acting as a donor ($E_{TD}$). "Hot band" transitions of the type proposed by Lamola may be expected to be operative both when the molecule acts as donor and as acceptor.
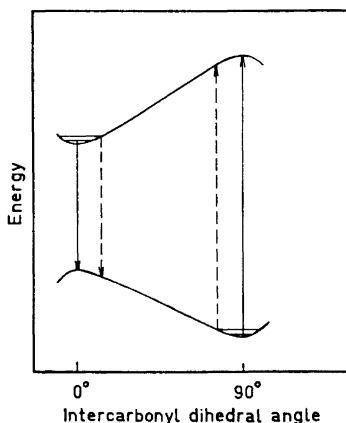


*Fig. 1.* A potential energy model for the ground and lowest triplet states of benzil and anisils, showing a few vertical transitions. The dashed lines represent "hot band" transitions.

## METHODS AND KINETIC ANALYSES

The mixed phosphorescence of a degassed cyclohexane solution of an aromatic diketone (X) and biacetyl (B) upon irradiation by light absorbed mainly by X may be assumed to depend on the following processes:

$$X + h\nu_A \rightarrow X_S' \rightarrow X_T \tag{0}$$

$$X_T + B \rightarrow X + B_T \tag{1}$$

$$B_T + X \rightarrow B + X_T \tag{2}$$

$$X_T \rightarrow X + h\nu_X \tag{3}$$

$$B_T \rightarrow B + h\nu_B \tag{4}$$

$$X_T \rightarrow X \tag{5}$$

$$B_T \rightarrow B \tag{6}$$

The quantum yield of the process (0) is denoted by $\Phi_T$. The rate constants $k_5$ and $k_6$ must be regarded as pseudo first order constants, including bimolecular reactions with solvent and impurities. Introducing $k_X = k_3 + k_5$ and $k_B = k_4 + k_6$ the following equations should apply at a constant light absorption rate of $I_A$:

$$d[X_T]/dt = \Phi_T I_A - [X_T](k_X + k_1[B]) + k_2[X][B_T] = 0 \tag{II}$$

$$d[B_T]/dt = -[B_T](k_B + k_2[X]) + k_1[B][X_T] = 0 \tag{III}$$

These equations give the following steady-state concentrations:

$$[X_T] = \frac{\Phi_T I_A (k_B + k_2[X])}{k_B k_X + k_X k_2[X] + k_B k_1[B]} \tag{IV}$$

$$[B_T] = \frac{\Phi_T I_A k_1[B]}{k_B k_X + k_X k_2[X] + k_B k_1[B]} \tag{V}$$

For systems where $k_1[B]$ and $k_2[X] \gg k_X$ and $k_B$, respectively, the eqns. (IV) and (V) may be approximated to:

$$[X_T] = \frac{\Phi_T I_A k_2[X]}{k_X k_2[X] + k_B k_1[B]} \tag{VI}$$

$$[B_T] = \frac{\Phi_T I_A k_1[B]}{k_X k_2[X] + k_B k_1[B]} \tag{VII}$$

The lifetime $(\tau)$ of the mixed phosphorescence, when the inequalities given above are valid, may be approximated to:

$$\tau = \frac{k_1[B] + k_2[X]}{k_X k_2[X] + k_B k_1[B]} \tag{VIII}$$

as follows from the general expressions given on p. 2357 in Ref. 1. The phosphorescence intensity contributions from $X_T$ and $B_T$, as registered by a spectrofluorimeter, are denoted by $I_X$ and $I_B$, respectively. It follows from eqns. (VI), (VII), and (VIII) that:

$$\tau/I_X = K_1(1 + k_1[B]/k_2[X]) \tag{IX}$$

and

$$\tau/I_B = K_2(1 + k_2[X]/k_1[B]) \tag{X}$$

where $K_1 = (\alpha k_3 \Phi_T I_A)^{-1}$ and $K_2 = (\beta k_4 \Phi_T I_A)^{-1}$, $\alpha$ and $\beta$ being apparatus constants. Measurements of $\tau/I_X$ and of $\tau/I_B$ in a series where $K_1$ and $K_2$ are kept constant thus both permit calculation of the ratio $k_1/k_2$. The value of $k_2$ can be determind from measurements of $I_X/I_B$ in a series where $[X]/[B]$ is kept constant as seen from the following. Eqn. (III) can be written:

$$[X_T]/[B_T] = (k_B + k_2[X])/k_1[B] \tag{XI}$$

Thus:

$$\frac{I_X}{I_B} = \frac{\alpha k_3[X_T]}{\beta k_4[B_T]} = K_3\left(1 + \frac{k_B}{k_2[X]}\right) \tag{XII}$$

where $K_3 = \alpha k_3 k_2[X]/\beta k_4 k_1[B]$.

A plot of $I_X/I_B$ vs. $[X]^{-1}$ should give a straight line with a slope to intercept ratio equal to $k_B/k_2$, and $k_B$ is obtained from the phosphorescence decay in a solution containing biacetyl only.

In the measurements made on the o-anisil — biacetyl system, the inequality $k_2[X] \ll k_B$ was found to be valid. This means that eqn. (V) can be approximated to:

$$[B_T] = \frac{\Phi_T I_A k_1[B]}{k_B k_X + k_B k_1[B]} \tag{XIII}$$

It then follows:

$$\tau_B/I_B = K_2(1 + k_X/k_1[B]) \tag{XIV}$$

where $\tau_B = k_B^{-1}$ is the phosphorescence lifetime as measured upon a flash absorbed by the biacetyl.

The ratio $k_X/k_1$ may thus be determined from a plot of $\tau_B/I_B$ vs. $[B]^{-1}$, and $k_X$ is obtained from the phosphorescence decay in a solution containing only o-anisil.

Some of the energy transfer rate constants have been determined only from phosphorescence lifetime measurements. For the kinetic analyses the reader is referred to appropriate parts of Ref. 1.


### EXPERIMENTAL

For the *phosphorescence intensity* measurements a modified Aminco Bowman spectrophotofluorometer was used. The light from a low pressure mercury "pen-ray" lamp (Ultraviolet Products Inc., Cf. USA, Mod SCTI) passed an interference filter (Thin Film Products, Mass. USA, 253.7 nm, bandwidth 20 nm) and a collimating lens. The excitation beam entered the measuring cell, *via* a quartz rod, in line with the emission entrance path to the monochromator. A UV absorbing filter was placed in front of the emission detector in order to exclude excitation light otherwise appearing in the second order spectrum around 507 nm in the first order.

The equipment for degassing the solutions has been described elsewhere.[8] The measuring procedure was as follows. The emission detector sensitivity was adjusted to give

a constant recorded value of the fluorescence intensity from an acid solution of 3-amino-phthalimide, found to be a suitable reference. The phosphorescence intensity of the degassed cyclohexane solution at 20°C was then measured at the emission maxima of B and X, respectively. The solution was exposed to the exciting light for as short a time as possible to minimize photochemical reactions. The *lifetime* of the mixed phosphorescence was then determined in a flash apparatus described earlier.[9]

From recorded phosphorescence spectra of pure solutions of B and X, respectively, the emission contributions from B and X to the mixed phosphorescence could be separated. The phosphorescence intensities of B and X at their maxima, $I_B$ and $I_X$, were thus calculated. In series where the concentration of X was kept constant, giving an absorbance of about 2 at 253.7 nm, the values of $K_1$ and $K_2$, appearing in eqns. (IX) and (X), were also constant.

*Materials.* 2,2'-Dimethoxybenzil (*o*-anisil) was prepared by the method of Leonard *et al.*[10] and purified by recrystallisation from ethanol. The purification procedures for other chemicals used have been described earlier.[1,8,11,12]

## RESULTS

*Absorptive and emittive properties of the diketones.* For the molar absorptivities ($M^{-1}$ $cm^{-1}$) of the diketones at 253.7 nm in cyclohexane solution the following values were obtained: biacetyl 10, benzil $1.7 \times 10^4$, *p*-anisil $8 \times 10^3$, *o*-anisil $1.7 \times 10^4$. In solutions with comparable concentrations of B and X, 253.7 nm light is thus almost exclusively absorbed by X.

The longest phosphorescence lifetimes (μsec) obtained were: biacetyl 700, benzil 280, *p*-anisil 250, *o*-anisil 45. The corresponding lifetimes in benzene solution[11] are: 1000, 70, 60, 15. The triplet excited aromatic diketones thus seem to react with benzene. This is also indicated by changes in emission spectra on excessive irradiation. The phosphorescence lifetime of *o*-anisil is strongly temperature dependent. The lifetime, in heptane solution, increased from 48 μsec to 143 μsec when the temperature was lowered from 20°C to 0°C.

Phosphorescence spectra of biacetyl, benzil, and *p*-anisil in benzene solution have been reported earlier.[11] In the uncorrected phosphorescence spectra of these substances in cyclohexane solution obtained in this work the emission maxima appeared at: biacetyl 523 nm, benzil 564 nm, *p*-anisil 550 nm. The phosphorescence spectrum of *o*-anisil showed a broad maximum around 560 nm. Since its phosphorescence yield is low, no meaningful values of $I_X$ could be calculated from the mixed phosphorescence of *o*-anisil and biacetyl and only a minor correction had to be applied to the recorded intensity at 523 nm in calculating $I_B$.

*Intensity and lifetime measurements of mixed phosphorescence.* The results of measurements on solutions of *biacetyl* and *benzil* are given in full detail in Table 1 in order to illustrate the calculation procedure. The intensity measurements on the first two solutions are used in calculating $I_B$ and $I_X$ from measured values of $I_{523}$ and $I_{564}$ from the following solutions. The general trend of the $\tau$ values is that expected from eqn. (VIII). In principle, of course, it would be possible to determine the value of $k_1/k_2$ by means of eqn. (VIII). This is a poor method, however, for the biacetyl-benzil system where the values of $k_B$ and $k_X$ are not very different and are small enough to be sensitive to impurities.

*Table 1.* Intensities and lifetimes of the mixed phosphorescence from cyclohexane solutions of biacetyl (B) and benzil (X). For further explanations see text.

| [B] M $\times 10^4$ | [X] M $\times 10^4$ | $I_{523}$ | $I_{564}$ | $I_B$ | $I_X$ | $\tau$ sec $\times 10^6$ | $\tau/I_B$ | $\tau/I_X$ |
|---|---|---|---|---|---|---|---|---|
| 29.0 | — | 56.5 | 14.5 | — | — | 422 | — | — |
| — | 1.28 | 8.5 | 78.5 | — | 78.5 | 277 | — | 3.53 |
| 1.39 | 1.28 | 33.5 | 77.0 | 29.9 | 70.2 | 287 | 11.08 | 4.09 |
| 2.66 | 1.28 | 65.0 | 91.0 | 56.8 | 76.3 | 362 | 6.37 | 4.74 |
| 3.50 | 1.28 | 70.0 | 83.5 | 62.7 | 67.3 | 343 | 5.47 | 5.10 |
| 6.98 | 1.28 | 108.0 | 79.0 | 102.3 | 52.6 | 362 | 3.54 | 6.88 |
| 11.5 | 1.28 | 148.0 | 82.0 | 143.1 | 45.2 | 403 | 2.82 | 8.92 |
| 15.3 | 1.28 | 158.0 | 76.0 | 154.1 | 36.4 | 414 | 2.69 | 11.37 |
| 19.7 | 1.28 | 163.0 | 70.0 | 159.9 | 29.0 | 391 | 2.45 | 13.48 |

Plots of $\tau/I_B$ *vs.* $[B]^{-1}$ and of $\tau/I_X$ *vs.* $[B]$ give straight lines corresponding to:

$$\tau/I_B = 1.75 + 1.28 \times 10^{-3} \, [B]^{-1} \text{ and}$$

$$\tau/I_X = 3.37 + 5.12 \times 10^3 \, [B]$$

Identification with eqns. (X) and (IX) gives $k_1/k_2 = 0.175$ and 0.194, respectively. Determinations of $I_X/I_B$ for a series of solutions with a constant value of $[X]/[B] = 0.27$ and with [X] varying from $2 \times 10^{-5}$ M to $2 \times 10^{-6}$ M were made to determine the value of $k_2$ by means of eqn. (XII). The following relationship was obtained:

$$I_X/I_B = 0.844 + 9.04 \times 10^{-7} \, [X]^{-1}$$

The ratio $k_B/k_2$ may thus be calculated as $1.07 \times 10^{-6}$ M. With $k_B = 1590$ sec$^{-1}$, obtained from the phosphorescence lifetime of a solution containing only biacetyl, this gives $k_2 = 1.49 \times 10^9$ M$^{-1}$ sec$^{-1}$. From the mean value of $k_1/k_2 = 0.184$ it follows that $k_1 = 2.74 \times 10^8$ M$^{-1}$ sec$^{-1}$. It should be noted that the inequalities $k_1[B]$ and $k_2[X] \gg k_X$ and $k_B$ were well fulfilled for the solutions presented in Table 1, justifying the application of eqns. (IX) and (X).

The results of measurements on *biacetyl – p-anisil* solutions may be summarized as follows. Solutions with $[X] = 2.65 \times 10^{-4}$ M and varying biacetyl concentrations gave:

$$\tau/I_B = 1.71 + 3.84 \times 10^{-4} [B]^{-1} \text{ and}$$

$$\tau/I_X = 1.67 + 7.37 \times 10^3 [B]$$

These equations give $k_1/k_2 = 1.18$ and 1.17, respectively.

Measurements on solutions with a constant value of $[X]/[B] = 1.06$ gave:

$$I_X/I_B = 0.90 + 2.17 \times 10^{-6} [X]^{-1}$$

This relationship, the value obtained for $k_B = 1650$ sec$^{-1}$, and the mean value of $k_1/k_2 = 1.175$ give $k_2 = 6.8 \times 10^8$ M$^{-1}$ sec$^{-1}$ and $k_1 = 8.0 \times 10^8$ M$^{-1}$ sec$^{-1}$.

As mentioned earlier, only values of $I_B$ could be accurately determined from intensity measurements on *biacetyl – o-anisil* solutions. Solutions with $[X] = 1.20 \times 10^{-4}$ M gave:

$$\tau_B/I_B = 1.65 + 4.04 \times 10^{-4}[B]^{-1}$$

Almost constant values of $\tau_B$, equal to that in a pure biacetyl solution, were obtained, as expected if $k_2[X] \ll k_B$. Identification of the given relationship with eqn. (XIV) gives $k_X/k_1 = 2.45 \times 10^{-4}$ M. A value of $k_X = 2.22 \times 10^4$ sec$^{-1}$ was obtained from the phosphorescence lifetime in a pure solution of $o$-anisil and thus $k_1 = 9.1 \times 10^7$ M$^{-1}$ sec$^{-1}$.

The low solubility of $o$-anisil in cyclohexane prevented a determination of $k_2$ in this solvent. Some measurements on benzene solutions, presented in Table 2, permit an estimate of the value of $k_2$. The results may be accounted for by assuming that the $o$-anisil sample contains a mol fraction $\gamma$ of an im-

*Table 2.* Phosphorescence decay rate constants ($k$) in benzene solutions of biacetyl (B) and/or $o$-anisil (X).

| Run No. | [B] M $\times 10^5$ | [X] M $\times 10^3$ | $k$ sec$^{-1}$ $\times 10^{-3}$ |
|---|---|---|---|
| 1 | 5.1 | — | 1.11 |
| 2 | 5.1 | 1.27 | 2.06 |
| 3 | 5.1 | 2.57 | 3.05 |
| 4 | 630 | — | 1.12 |
| 5 | 630 | 3.79 | 2.08 |
| 6 | 630 | 6.05 | 2.67 |
| 7 | — | 5.00 | 68 |

purity that quenches biacetyl triplets with a rate constant of $k_q$. If $k_X + k_1[B] \gg k_B + k_2[X]$ the biacetyl phosphorescence decay constant may be approximated to:

$$k = k_{B^o} + \left( \left( k_q\gamma + \frac{k_X}{k_X + k_1[B]} k_2 \right) \right)[X] \qquad \text{(XV)}$$

where $k_{B^o}$ denotes the decay constant in the absence of $o$-anisil. Application of eqn. (XV) to runs $1-3$ and $4-6$, respectively, gives two simultaneous equations from which $k_2$ and $k_q\gamma$ can be evaluated. Insertion of the value of $k_1 = 9.1 \times 10^9$ M$^{-1}$ sec$^{-1}$, valid in cyclohexane solution, and of $k_X = 6.8 \times 10^4$ sec$^{-1}$ from run 7 gives $k_2 = 5.9 \times 10^5$ M$^{-1}$ sec$^{-1}$ and $k_q\gamma = 1.9 \times 10^5$ M$^{-1}$ sec$^{-1}$. If the impurity quenches $o$-anisil triplets with the same rate constant as biacetyl triplets, the neglection of the depencence of $k_X$ on [X] (and thus on the impurity concentration) is justified by the much higher value of $k_X$ than of $k_{B0}$. It should also be noted that, with the biacetyl concentrations chosen, the calculated value of $k_2$ is not strongly dependent on the assumption of equal values of $k_1$ in cyclohexane and benzene solution. Thus values of $k_2$ equal to $6.0 \times 10^5$ M$^{-1}$ sec$^{-1}$ and $6.4 \times 10^5$ M$^{-1}$ sec$^{-1}$ are obtained when the applied value of $k_1$ is doubled and halved, respectively.

Relative triplet quantum yields of the aromatic diketones can be calculated from the values of $K_2$ obtained. The relative yields of benzil, $p$-anisil,

and *o*-anisil are 1:1.02:1.06. Lamola and Hammond [13] have determined the triplet yield of benzil in benzene solution as 0.92. Applying this value triplet yields of 0.94 and 0.98 are obtained for *p*-anisil and *o*-anisil, respectively.

*Energy transfer rate constants from phosphorescence decay measurements.* For systems comprising a diketone and an aromatic noncarbonyl compound energy transfer rate constants were determined from phosphorescence decay measurements only. In Table 3, the results have been summarized together with the rate constants obtained for the systems presented in the preceding section.

*Table 3.* Rate constants for energy transfer from M to N ($k_{M\to N}$) and from N to M ($k_{N\to M}$). The triplet energy of N is denoted by $E_T$.

| M | N | $E_T$ cm$^{-1}$ | $k_{M\to N}$ M$^{-1}$ sec$^{-1}$ | $k_{N\to M}$ M$^{-1}$sec$^{-1}$ |
|---|---|---|---|---|
| Bensil | Biacetyl | 19 600 [1] | 2.7 × 10$^8$ | 1.5 × 10$^9$ |
| *p*-Anisil | Biacetyl | | 8.0 × 10$^8$ | 6.8 × 10$^8$ |
| *o*-Anisil | Biacetyl | | 9.1 × 10$^7$ | 5.9 × 10$^{5a}$ |
| Biacetyl | Pyrene | 16 930 [14] | 8.7 × 10$^9$ | |
| Biacetyl | 1-Chloronaphthalene | 20 645 [15] | 4.0 × 10$^7$ | 4.7 × 10$^9$ |
| Benzil | 1-Chloronaphthalene | | 3.0 × 10$^6$ | 2.8 × 10$^9$ |
| *p*-Anisil | 1-Chloronaphthalene | | 1.4 × 10$^7$ | 2.2 × 10$^9$ |
| *o*-Anisil | 1-Chloronaphthalene | | | 3.5 × 10$^7$ |
| *o*-Anisil | Naphthalene | 21 180 [14] | | 9.1 × 10$^7$ |
| *o*-Anisil | Phenanthrene | 21 600 [14] | | 2.9 × 10$^8$ |
| *o*-Anisil | Triphenylene | 23 250 [16] | | 3.0 × 10$^9$ |
| *o*-Anisil | 2,2′-Dinaphthyl | 19 560 [16] | 9.0 × 10$^7$ | |
| *o*-Anisil | 1,2-Benzpyrene | 18 510 [16] | 2.3 × 10$^9$ | |

*a* In benzene solution.

The experimental conditions and calculation precedures for systems involving 1-chloronaphthalene were similar to those presented for the system biacetyl − 1-chloronaphthalene in benzene solution on p. 2368 in Ref. 1.

In the experiments with *o*-anisil and naphthalene, phenanthrene, or triphenylene, a low flash intensity was used in order to suppress the ratio of delayed fluorescence to phosphorescence from the latter compounds. By adding diphenylamine, which reacts much faster with *o*-anisil triplets than with the noncarbonyl triplets (*cf.* p. 2362 of Ref. 1), the *o*-anisil phosphorescence was quenched. The observed emission was thus almost pure phosphorescence from the noncarbonyl compounds.

The rate constants for energy transfer from *o*-anisil to 2,2′-dinaphthyl and to 1,2-benzpyrene were calculated from "first measurable phosphorescence lifetimes" (*cf.* p. 2361 of Ref. 1).

## DISCUSSION

The rate constant for energy transfer from biacetyl to pyrene, 8.7 × 10$^9$ M$^{-1}$ sec$^{-1}$, may be taken as a representative value for highly exothermic energy transfer in cyclohexane solution at 20°C. This value is somewhat higher than

the corresponding value, $7.6 \times 10^9$, obtained in benzene solution.[1] Similarly, the rate constant values for the system biacetyl $-$ 1-chloronaphthalene, $4.0 \times 10^7$ and $4.7 \times 10^9$, are higher than those measured in benzene solution,[1] $2.9 \times 10^7$ and $3.9 \times 10^9$. On an average, the ratio of the rate constants in cyclohexane and benzene solutions is equal to 1.2 in spite of the higher viscosity of cyclohexane compared to that of benzene, 0.95 and 0.65 cP at 20°C. This is in accordance with the rate constant ratio, 1.3, given by Wagner and Kochewar [17] in their important paper on "How Efficient is Diffusion-Controlled Triplet Energy Transfer?"

For systems behaving "classically", it is expected [see eqn. (I)] that the rate constant for energy transfer in one of the directions should exceed or be equal to $k_D/2$, which is the value corresponding to $\Delta E_T = 0$. In cyclohexane solution this means a value $\geq 4 \times 10^9$ $M^{-1}$ sec$^{-1}$. None of the rate constants for the first three systems presented in Table 3 reach this value, the system $o$-anisil $-$ biacetyl showing the lowest values. This is what may be expected for systems where at least one of the reactants has different ground and excited state geometries. The relative positions of the triplet energy levels of the diketones, as sketched in Fig. 2, should account for the results. No absolute values of the levels for the aromatic diketones can be given since eqn. (I), valid in classical systems, is not applicable. The rate constants obtained for systems involving 1-chloronaphthalene further support Fig. 2.

The logarithms of the rate constant values for systems involving $o$-anisil, the compound showing the most striking nonclassical behaviour, are plotted in Fig. 3 $vs.$ the triplet energy of the other solute of the system. The curve drawn through the points for $o$-anisil acting as an acceptor bears a resemblance to the curve drawn in Fig. 1 of Ref. 2 from a more extensive material for $cis$-stilbene acting as an acceptor. A dashed curve has been drawn from the meagre material available for $o$-anisil acting as a donor. The general features
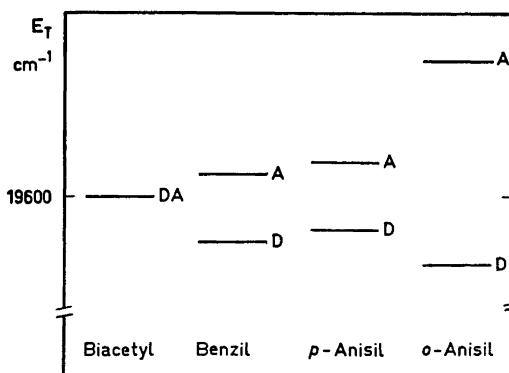


Fig. 2. Relative positions of the triplet electronic energy levels of biacetyl, benzil, $p$-anisil, and $o$-anisil. $D$ represents the energy difference between excited and ground states, both with excited state conformation, which is also the minimum value of available electronic energy from the molecule as a donor. $A$ represents the energy difference between excited and ground states, both with ground state conformation, or the maximum electronic energy required by the molecule as an acceptor.
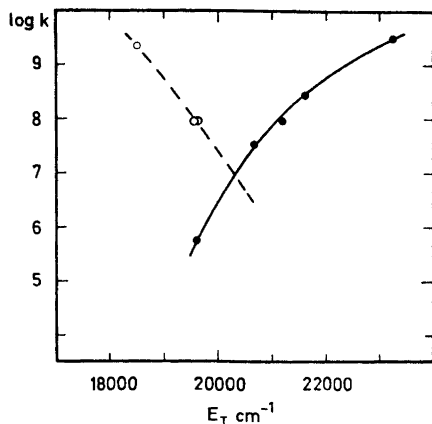
*Fig. 3.* Log $k_{M \to N}$ (O) and log $k_{N \to M}$ (●) *vs.* $E_T$, the triplet energy of N. M denotes *o*-anisil.
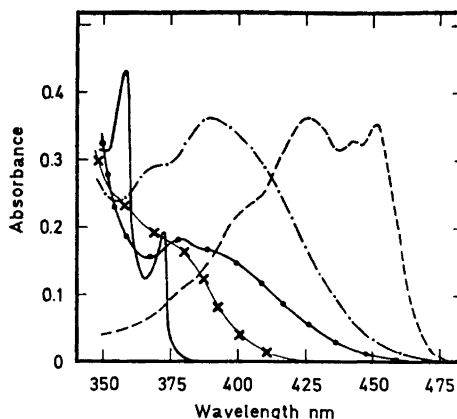


*Fig. 4.* Absorption spectra of $1.7 \times 10^{-2}$ M benzaldehyde ( — ), $1.9 \times 10^{-2}$ M biacetyl ( - - - ), $5.8 \times 10^{-3}$ M benzil ( — . — ), $1.6 \times 10^{-3}$ M *p*-anisil (●), and $1.8 \times 10^{-3}$ M *o*-anisil ( × ) in cyclohexane solution.

of Fig. 3 are quite different from those of Fig. 1 in Ref. 1. The latter figure represents results from systems involving molecules assumed to have equal values of available energy as donor and required energy as acceptor. This evidently does not apply to *o*-anisil. As pointed out above, the results do not permit a determination of the value of $E_{TA} - E_{TD}$. The reason is that the rate constants are certainly higher than those calculated by putting $\Delta E_T$ in eqn. (I) equal to $E_{TA} - E_T$ and to $E_T - E_{TD}$, respectively. However, a minimum value of $E_{TA} - E_{TD}$ may be estimated. The coordinates of the intersection of the curves in Fig. 3 are $E_T = 20300$ cm$^{-1}$ and log $k = 7$. This implies that the rate constant values for energy transfer from *o*-anisil to a molecule with $E_T = 20\,300$ cm$^{-1}$ and for energy transfer from such a molecule to *o*-anisil are both about $10^{-3}$ of the rate constant value for exothermic energy transfer. The activation energy should thus be at least 1500 cm$^{-1}$ for energy transfer in both directions and a minimum value of $E_{TA} - E_{TD} = 3000$ cm$^{-1}$ is obtained. The true value of $E_{TA} - E_{TD}$ is probably much higher. The full drawn curve shows decreasing slope with increasing $E_T$ indicating appreciable effects of favourable activation modes, as discussed in the introduction.

In this connexion, the *o*-anisil emisson studies performed by Almgren [18] are of great interest. In fluid solution at room temperature (solvent CIP: 95 % isopentane, 5 % cyclohexane) he found a phosphorescence maximum at 555 nm and a weak shoulder at 500 nm. The latter emission should probably be regarded as E-type delayed fluorescence.[19] In CIP glass at 80°K, a broad emission spectrum with a maximum at 485 nm was obtained. This was interpreted as phosphorescence from excited molecules for which the conformational relaxation was more or less inhibited by the glassy matrix. The energy difference between the emisson maxima in the two media, 2600 cm$^{-1}$, should

also represent a minimum value of $E_{TA} - E_{TD}$ since total inhibition of conformational changes is not expected. The broad emission spectrum in the glassy matrix may indicate varying degrees of relaxation for the emitting molecules.

For benzil and $p$-anisil the energy transfer results indicate lower values of $E_{TA} - E_{TD}$. Calculations similar to those for $o$-anisil performed on the results from benzil — biacetyl and $p$-anisil — biacetyl indicate a minimum value of $E_{TA} - E_{TD}$ of about 1000 cm$^{-1}$ for both benzil and $p$-anisil. Morantz and Wright [7] have compared the phosphorescence of benzaldehyde and of benzil. The energy difference between the shortest wavelength phosphorescence peaks is about 18 kcal or 6400 cm$^{-1}$. Ignoring interaction between the carbonyl groups and adjoining aromatic groups, Morantz and Wright adopt this energy difference as a measure of the energy difference denoted by $E_{TA} - E_{TD}$ in this work. Such a high value of $E_{TA} - E_{TD}$ for benzil does not seem very probable even though the value 1000 cm$^{-1}$ is certainly much too low.

Absorption spectra of benzaldehyde, biacetyl, benzil, $p$-anisil, and $o$-anisil are given in Fig. 4. The resemblance between the absorption spectra of benzaldehyde and benzil found by Morantz and Wright [7] does not seem very striking. While the long wavelength tail of the benzaldehyde spectrum falls steeply, as does also that of biacetyl, all the aromatic diketones show absorption spectra with long tails. The latter behaviour is to be expected for molecules with different ground and excited state conformations.

It may be noted that Richtol and Belorit [20] have studied the mixed phosphorescence from solutions of benzil and biacetyl excited by 436 nm light. Their interpretation of the results is quite different from that given here. They assume that the energy transfer from benzil to biacetyl is negligible. If this were true no biacetyl phosphorescence should have been observed in the present measurements where the exciting light of wavelength 254 nm was almost exclusively absorbed by benzil. It is then not surprising that the rate constant value obtained for energy transfer from biacetyl to benzil, $5.6 \times 10^5$ M$^{-1}$ sec$^{-1}$, is quite different from the value, $1.5 \times 10^9$ M$^{-1}$ sec$^{-1}$, calculated in the present work.

The reaction scheme proposed by Richtol and Belorit includes the following process:

$$\text{biacetyl}_T + \text{benzil} \rightarrow \text{biacetyl} + \text{benzil}$$
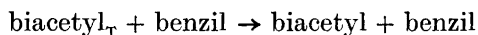
The rate constant for this process is given a value of $7.4 \times 10^5$ M$^{-1}$ sec$^{-1}$. The validity of triplet quantum yield determinations based on measurements of sensitized isomerization reactions,[13] delayed fluorescence,[21] or phosphorescence [8] critically depends on whether the rate of such an energy degradation process is small compared to that of the energy transfer process. The determinations are always performed in systems where the sensitization is an exothermic energy transfer process with close to diffusion-controlled rate. Closely agreeing values of triplet yields for a number of sensitizers have been obtained by the three methods mentioned in which quite different energy acceptors have been involved. This indicates that the energy degradation process cannot compete significantly with the energy transfer process in the systems investigated.

As mentioned in the introduction both the donor and acceptor properties of biphenyl, a substance with different ground and excited state conformations, have been investigated. Making some reasonable assumptions, Wagner [4b] has calculated the rate constants for energy transfer in benzene solution from benzophenone to biphenyl and from biphenyl to benzophenone as $2.5 \times 10^8$ and $3.5 \times 10^7$ $M^{-1}$ $sec^{-1}$, respectively. The $E_T$ value of benzophenone is chosen as 69.5 kcal while the lowest energy $T \leftarrow S$ absorption band and highest energy phosphorescence band of biphenyl correspond to 75.5 and 65.5 kcal, respectively.[4b] Wagner postulates [4a,b] that energy transfer both to and from biphenyl involves a nonvertical transition, the energy difference between the upper and lower states being close to 68.5 kcal. The fact that the energy transfer rate constants both have much lower values than that for a diffusion-controlled process should be a consequence of the greater steric requirements of a process involving nonvertical transitions compared to a process with only vertical ones. Lamola [5] points out that the details of the transfer process are not known and gives preference neither to the model used by Wagner nor to that used in the present work.

## REFERENCES

1. Sandros, K. *Acta Chem. Scand.* **18** (1964) 2355.
2. Herkstroeter, W. G. and Hammond, G. S. *J. Am. Chem. Soc.* **88** (1966) 4769.
3. Hammond, G. S. and Saltiel, J. *J. Am. Chem. Soc.* **85** (1963) 2516.
4. a. Wagner, P. J. *J. Am. Chem. Soc.* **89** (1967) 2820; b. Wagner, P. J. *Mol. Photochemistry* **1** (1969) 71.
5. Lamola, A. A. *Technique of Org. Chemistry*, Interscience, New York 1969, Vol. XIV, p. 17.
6. Evans, T. R. and Leermakers, P. A. *J. Am. Chem. Soc.* **89** (1967) 4380.
7. Morantz, D. J. and Wright, A. J. C. *J. Chem. Phys.* **54** (1971) 692.
8. Sandros, K. *Acta Chem. Scand.* **53** (1969) 2815.
9. Bäckström, H. L. J. and Sandros, K. *Acta Chem. Scand.* **12** (1958) 823.
10. Leonard, N. J., Rapala, R. T., Herzog. H. L. and Blout, E. R. *J. Am. Chem. Soc.* **71** (1949) 2997.
11. Bäckström, H. L. J. and Sandros, K. *Acta Chem. Scand.* **14** (1960) 48.
12. Sandros, K. and Bäckström, H. L. J. *Acta Chem. Scand.* **16** (1962) 958.
13. Lamola, A. A. and Hammond, G. S. *J. Chem. Phys.* **43** (1965) 2129.
14. Evans, D. F. *J. Chem. Soc.* **1957** 1351.
15. Ferguson, J., Iredale, T. and Taylor, J. A. *J. Chem. Soc.* **1954** 3160.
16. Clar, E. and Zander, M. *Chem. Ber.* **89** (1956) 749.
17. Wagner, P. J. and Kochewar, I. *J. Am. Chem. Soc.* **90** (1968) 2232.
18. Almgren, M. *Photochem. and Photobiol.* **9** (1969) 1.
19. Parker, C. A. and Joyce, T. A. *Chem. Commun.* **1968** 1421.
20. Richtol, H. H. and Belorit, A. *J. Chem. Phys.* **45** (1966) 35.
21. Parker, C. A. and Joyce, T. A. *Trans. Faraday Soc.* **62** (1966) 2785.

# Microwave Spectrum, Structural Parameters and Quadrupole Coupling of *trans*-1-Chlorobuten-3-yne

FRED KARLSSON and RAGNAR VESTIN

*Institute of Inorganic and Physical Chemistry, University of Stockholm, Box 6801, S-113 86 Stockholm, Sweden*

The microwave spectra of three isotopic species of *trans*-1-chloro-buten-3-yne: $CH^{35}ClCHCCH$, $CH^{37}ClCHCCH$, and $CH^{35}ClCHCCD$, have been measured in the region 26 500 – 40 000 MHz.

The rotational constants $A$, $B$, and $C$ for the ground state as well as the centrifugal distortion constants, $D_J$ and $D_{JK}$, were determined. From the hyperfine splittings of the rotational lines, the nuclear quadrupole coupling constants $\chi_{aa}$ were calculated for the $CH^{35}ClCHCCH$ and $CH^{37}ClCHCCH$ species, in the principal-axis systems of the molecules. The distance between the chlorine atom and the ethynyl hydrogen atom was determined by isotopic substitution. The molecule length was found to be 6.236 Å.

In order to supply complementary data for electron diffraction measurements the inertial moments corresponding to the average structure were calculated from an estimated force field.

The structure of butenyne has been determined by electron diffraction [1] and microwave spectroscopy [2] in combination. In order to confirm these results on parent molecules we have started to investigate *trans*-1-chloro-buten-3-yne and *cis*-1-chlorobuten-3-yne with microwave spectroscopy. These substances were discovered by Vestin *et al.*[3] They are unstable at room temperature but can be handled at − 70C°.

The original identification of these substances was based on mass spectro-scopical analysis, IR spectroscopy, and their relative retention in gas-liquid chromatography. Microwave spectroscopical analysis confirms the *trans* conformation of *trans*-1-chlorobuten-3-yne.

The *cis*-conformation has a very complicated and yet unassigned spectrum, which was expected from the assumed structure and calculated dipole moment components.

## EXPERIMENTAL

Incomplete dehydrochlorination of 1,4-dichloro-2-butyne by alkali yields small amounts of *cis*- and *trans*-1-chlorobuten-3-yne. These substances can be isolated from the reaction mixture and purified with gas-liquid chromatography. The monodeuteriated

sample of *trans*-1-chlorobuten-3-yne was prepared by reacting the normal species with deuterium oxide $D_2O$ and monodeuteriated ethanol $C_2H_5OD$.

The microwave spectra were recorded on a Hewlett-Packard model 8460 A R-band microwave spectrometer with a phase stabilized source oscillator. The recordings were made at room temperature and a pressure ranging from 10 to 50 mTorr. The frequency region was 26 500 — 40 000 MHz. The precision of the measured transitions was estimated to be 0.05 MHz.

## MICROWAVE SPECTRUM

Most of the lines in the spectrum are grouped in bands at intervals of approximately 2 970 MHz. Each band begins abruptly on the low frequency side and continues for 200 — 300 MHz with decreasing intensity. The very characteristic appearance of a bandhead is shown in Fig. 1.
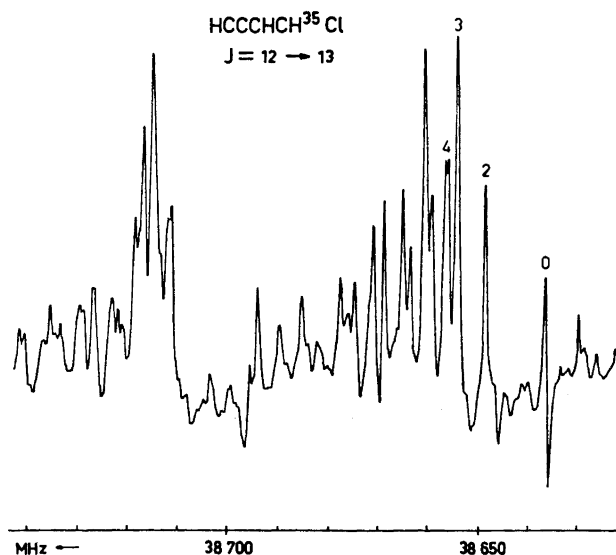


*Fig. 1.* Band of the $J = 12 \rightarrow 13$ transitions of normal *trans*-1-chlorobuten-3-yne near 38 700 MHz. Sweep rate 0.5 MHz/sec.

*trans*-1-Chlorobuten-3-yne is expected to be an almost prolate symmetric rotor; see Fig. 2. Consequently the regions of dense absorption are logically assigned to $\Delta J = +1$, $\Delta K_{-1} = 0$ transitions which are active through the $\mu_a$ dipole moment. CNDO calculation gives the theoretical dipole moment $\mu_a = -1.82$, $\mu_b = -0.64$, and $\mu_c = 0$ debye.

The line abundance of the bands and the repeated structure within the bands indicates the existence of low lying excited vibrational modes, presumably states in which the skeletal bending mode is excited.

The lines from the ground state are easily assigned in high resolution spectra. Outside each group, lines were found which could be identified as $K_{-1} = 0$ and $K_{-1} = 1$ transitions on the basis of their characteristic second-

*Table 1.* Observed rotational transitions and nuclear quadrupole hyperfine splitting in MHz for three isotopic species of *trans*-1-chlorobuten-3-yne.

| J | $K_{-1}$ | $K_{+1}$ | $\leftarrow J$ | $K_{-1}$ | $K_{+1}$ | CH³⁵ClCHCCH $\nu_{obs}$ | $\Delta\nu Q_{obs}$ | CH³⁷ClCHCCH $\nu_{obs}$ | $\Delta\nu Q_{obs}$ | CH³⁵ClCHCCD $\nu_{obs}$ | $\Delta\nu Q_{obs}$ |
|---|---|---|---|---|---|---|---|---|---|---|---|
| 9 | 0 | 9 | 8 | 0 | 8 | 26753.22 | | | | | |
| 9 | 1 | 8 | 8 | 1 | 7 | 26964.30 | | | | | |
| 10 | 1 | 10 | 9 | 1 | 9 | 29498.47 | | 28837.00 | | 28047.45 | |
| 10 | 0 | 10 | 9 | 0 | 9 | 29724.68 | | 29053.30 | | 28255.42 | |
| 10 | 2 | 9 | 9 | 2 | 8 | 29730.68 | | 29058.84 | | | |
| 10 | 3 | 8 | 9 | 3 | 7 | 29733.93 | 0.86 | 29061.19 | 0.61 | | |
| 10 | 1 | 9 | 9 | 1 | 8 | 29960.01 | | 29277.89 | | 28471.31 | |
| 11 | 1 | 11 | 10 | 1 | 10 | 32447.90 | | 31720.30 | | 30851.77 | |
| 11 | 0 | 11 | 10 | 0 | 10 | 32695.75 | | 31957.29 | | 31079.70 | |
| 11 | 2 | 10 | 10 | 2 | 9 | 32703.44 | | 31964.46 | | 31086.62 | |
| 11 | 3 | 9 | 10 | 3 | 8 | 32707.40 | 0.66 | 31968.13 | 0.51 | | |
| 11 | 4 | 8 | 10 | 4 | 7 | 32709.45 | 1.19 | 31970.13 | 0.93 | | |
| 11 | 2 | 9 | 10 | 2 | 8 | 32710.92 | | | | | |
| 11 | 5 | 7 | 10 | 5 | 6 | 32712.43 | 1.85 | 31973.07 | 1.45 | | |
| 11 | 6 | 6 | 10 | 6 | 5 | 32716.30 | 2.63 | | | | |
| 11 | 7 | 5 | 10 | 7 | 4 | 32720.92 | 3.70 | | | | |
| 11 | 8 | 4 | 10 | 8 | 3 | 32726.28 | 4.78 | | | | |
| 11 | 1 | 10 | 10 | 1 | 9 | 32955.53 | | 32205.32 | | 31318.10 | |
| 12 | 1 | 12 | 11 | 1 | 11 | 35397.19 | | 34603.50 | | 33656.09 | |
| 12 | 0 | 12 | 11 | 0 | 11 | 35666.40 | | 34860.95 | | 33903.70 | |
| 12 | 2 | 11 | 11 | 2 | 10 | 35676.08 | | 34869.90 | | 33912.40 | |
| 12 | 3 | 10 | 11 | 3 | 9 | 35680.88 | 0.51 | 34874.38 | 0.36 | 33916.85 | |
| 12 | 4 | 9 | 11 | 4 | 8 | 35683.00 | 0.87 | 34876.48 | 0.71 | 33919.17 | 0.92 |
| 12 | 2 | 10 | 11 | 2 | 9 | 35685.80 | | 34878.94 | | 33920.70 | |
| 12 | 5 | 8 | 11 | 5 | 7 | 35686.28 | 1.33 | | | 33922.67 | 1.28 |
| 12 | 6 | 7 | 11 | 6 | 6 | 35690.41 | 1.94 | | | | |
| 12 | 7 | 6 | 11 | 7 | 5 | 35695.45 | 2.72 | | | | |
| 12 | 1 | 11 | 11 | 1 | 10 | 35951.00 | | 35132.57 | | 34164.75 | |
| 13 | 1 | 13 | 12 | 1 | 12 | 38346.37 | | 37486.59 | | 36460.28 | |
| 13 | 0 | 13 | 12 | 0 | 12 | 38636.59 | | 37764.21 | | 36727.34 | |
| 13 | 2 | 12 | 12 | 2 | 11 | 38648.67 | | 37775.33 | | 36738.00 | |
| 13 | 3 | 11 | 12 | 3 | 10 | 38654.37 | 0.35 | 37780.60 | | 36743.32 | |
| 13 | 4 | 10 | 12 | 4 | 9 | 38656.55 | 0.69 | 37782.84 | 0.55 | 36745.76 | 0.72 |
| 13 | 5 | 9 | 12 | 5 | 8 | 38660.06 | 1.11 | 37786.22 | 0.84 | | |
| 13 | 2 | 11 | 12 | 2 | 10 | 38661.00 | | 37786.64 | | | |
| 13 | 6 | 8 | 12 | 6 | 7 | 38664.50 | 1.52 | 37790.60 | 1.21 | | |
| 13 | 7 | 7 | 12 | 7 | 6 | 38669.93 | 2.09 | 37795.86 | 1.70 | | |
| 13 | 8 | 6 | 12 | 8 | 5 | 38676.22 | 2.84 | 37802.01 | 1.90 | | |
| 13 | 9 | 5 | 12 | 9 | 4 | 38683.55 | 3.48 | | | | |
| 13 | 10 | 4 | 12 | 10 | 3 | 38691.67 | 4.26 | | | | |
| 13 | 1 | 12 | 12 | 1 | 11 | 38946.31 | | 38059.72 | | 37011.37 | |
| 14 | 1 | 14 | 13 | 1 | 13 | | | | | 39264.32 | |
| 14 | 0 | 14 | 13 | 0 | 13 | | | | | 39550.58 | |
| 14 | 2 | 13 | 13 | 2 | 12 | | | | | 39563.57 | |
| 14 | 3 | 12 | 13 | 3 | 11 | | | | | 39569.82 | |
| 14 | 4 | 11 | 13 | 4 | 10 | | | | | 39572.38 | 0.58 |
| 14 | 5 | 10 | 13 | 5 | 9 | | | | | 39576.38 | 0.89 |
| 14 | 2 | 12 | 13 | 2 | 11 | | | | | 39576.82 | |
| 14 | 6 | 9 | 13 | 6 | 8 | | | | | 39581.46 | 1.24 |
| 14 | 7 | 8 | 13 | 7 | 7 | | | | | 39587.55 | 1.68 |
| 14 | 1 | 13 | 13 | 1 | 12 | | | | | 39857.73 | |

order (but unresolved) Stark effects. Within the band the transitions $K_{-1} \geq 2$ were detected by their relative intensities and quadrupole hyperfine splittings which increase with $K_{-1}$; see Table 1.

The rotational constants were fitted to the observed spectrum by the least squares method. It was necessary to include centrifugal distortion terms $D_J$ and $D_{JK}$. The $D_{JK}$ term makes an important contribution and reverses the normal ordering of the $K_{-1}$ values; see Table 2. The vibrational bands

Table 2. Observed rotational constants in MHz for the three isotopic species or *trans*-1-chlorobuten-3-yne.

|         | CH³⁵ClCHCCH          | CH³⁷ClCHCCH          | CH³⁵ClCHCCD          |
|---------|---------------------|---------------------|---------------------|
| $A$     | 48604   ± 41        | 48500   ± 62        | 47730   ± 49        |
| $B$     | 1509.612 ± 0.002    | 1474.986 ± 0.002    | 1434.222 ± 0.002    |
| $C$     | 1463.459 ± 0.002    | 1430.895 ± 0.002    | 1391.832 ± 0.002    |
| $D_J$   | 0.000110 ± 0.000003 | 0.000109 ± 0.000004 | 0.000087 ± 0.000003 |
| $D_{JK}$| − 0.01619 ± 0.00002 | − 0.01572 ± 0.00002 | − 0.01706 ± 0.00002 |

have a very complicated structure in high resolution spectra. All attempts to assign them have been unsuccessful so far.

The CH³⁷ClCHCCH species could be studied at its natural concentration and CH³⁵ClCHCCD was synthesized.

### QUADRUPOLE COUPLING

In good agreement with theory[4] the observable nuclear quadrupole splitting is due to transistions with $\Delta F = +1$. The splitting increases with $K_{-1}$. Thus, for low values of $K_{-1}$, the four quadrupole components merge into one single peak. As $K_{-1}$ increases the peak splits into two, and finally into four, observable peaks.

The nuclear quadrupole energy of a nearly prolate symmetric rotor having one quadrupole nucleus can be written as,[4]

$$E_Q = \frac{\chi_{aa}}{J(J+1)} Y(J,I,F)[3K_{-1}^2 - J(J+1) - 3b_p^2(C_2 + 2C_3 b_p)$$
$$+ \eta(C_1 + 2C_2 b_p + 3C_3 b_p^2 + 4C_4 b_p^3)]$$

where $Y(J,I,F)$ is Casimir's function: $b_p$ is Wang's asymmetry parameter. If $\chi_{gg}$ is the component of the quadrupole coupling tensor along the $g$-principal inertial axis, $\eta$ is defined by $\eta$ $\chi_{aa} = \chi_{bb} - \chi_{cc}$. The constants $C_1$, $C_2$, $C_3$, and $C_4$ could be found in tables.[5]

For *trans*-1-chlorobuten-3-yne the asymmetry parameter $b_p$ is very small: $b_p = -0.0005$. Further, the nuclear quadrupole splitting is only observable for rotational transitions with $K_{-1} \geq 2$ where $C_1 = 0$. Thus the energy expres-

sion above reduces to that of a symmetric rotor, and since only the splitting into doublets is completly resolved, the measurable nuclear hyperfine splitting for $\Delta F = +1$ transitions can be calculated from the formula

$$\Delta\nu_Q = -3K_{-1}{}^2\chi_{aa}/2J(J+1)(J+2)$$

Consequently the quadrupole effect is mainly determined by only one quadrupole coupling constant, $\chi_{aa}$ in this case. For $^{35}Cl$ in $CH^{35}ClCHCCH$ this value was determined to be $\chi_{aa} = -63.6 \pm 0.4$ MHz and for $^{35}Cl$ in $CH^{37}ClCHCCH$ $\chi_{aa} = -51.0 \pm 0.4$ MHz.

## MOLECULAR STRUCTURE

The position of the ethynyl hydrogen atom and the chlorine atom in the main axes system of $CH^{35}ClCHCCH$ was calculated by the method of Costain [6] from the differences in the moments of inertia caused by isotopic substitution of these atoms with deuterium and 37-chlorine. The uncertainty in the $b$-coordinates is expected to be rather great since the atoms concerned are lying very near to the $a$-axis; see Fig. 2. Another ambiguity is introduced by
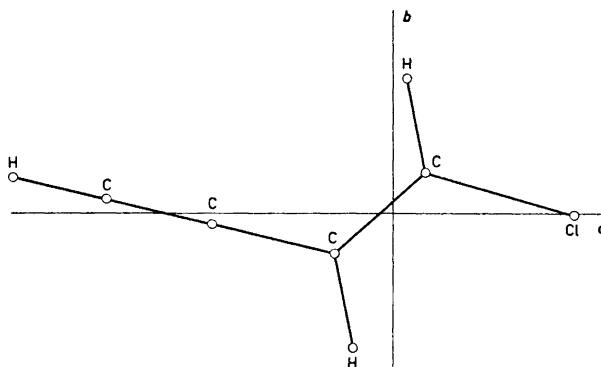


*Fig. 2.* Assumed structure of normal *trans*-1-chlorobuten-3-yne with principal axes of inertia.

the uncertainty in the $I_a$-inertial moment emanating from the fact that we are only observing $a$-type transitions which have a weak dependence on the $A$-rotational constant. The $b$-coordinates however have only a minor effect on the distance between the ethynyl hydrogen atom and the chlorine atom. This length is therefore expected to be accurate and the value is 6.236 Å.

Evidently these substitutions are not sufficient to give the complete $r_s$-structure. The main purpose of this work was therefore to give complementary data for an electron diffraction investigation (in progress) of the molecular structure. The inertial moments however are related to the $r_0$-structure. This is a different vibrational average structure than that observed in electron diffraction.[6] However both of these methods are comparable in the $r_z$-structure

which can be calculated if the harmonic part of the fundamental vibrations are known. In order to see if the $r_z$-structural parameters differ significantly from the corresponding $r_0$-parameters we have calculated the corrections due to harmonic vibrations from a normal coordinate analysis of the molecular vibrations; see Table 3. The force field necessary for this analysis was estimated. The theory for these calculations is given by Herschbach and Laurie [8] and Oka.[9] The computational method used was mainly taken from Oka and Morino.[10]

Actually the moments of inertia also have to be corrected for the centrifugal distortion. Since the molecule is a planar rotor it would seem reasonable to get the centrifugal distortion correction out of a 7 parameter fitting of rotational constants $A$, $B$, $C$, $\tau_{aaaa}$, $\tau_{bbbb}$, $\tau_{abab}$, and $\tau_{aabb}$ to the observed spectra. This was not possible, however, mainly because the near degeneracy to a symmetric rotor spectrum.[11] So we have calculated these centrifugal distortion corrections from the estimated force field.[4] They are actually too small to be significant; see Table 3. The main uncertainty in cal-

Table 3. Vibration-rotation correction for the moments of inertia in the ground vibrational state (in amu Å²). Conversion factor 505 376 amu Å² MHz.

|  | CH³⁵ClCHCCH | | CH³⁷ClCHCCH | | CH³⁵ClCHCCD | |
|---|---|---|---|---|---|---|
|  | $I_b$ | $I_c$ | $I_b$ | $I_c$ | $I_b$ | $I_c$ |
| $r_0$-Parameters | 334.771 | 345.328 | 342.630 | 353.187 | 352.368 | 363.100 |
| Vibration correction | 0.104 | 0.003 | 0.106 | 0.004 | 0.098 | − 0.005 |
| Centrifugal distortion correction | 0.00049 | − 0.00079 | 0.00050 | − 0.00079 | 0.00051 | − 0.00081 |
| $r_z$-Parameters | 334.875 | 345.330 | 342.736 | 353.191 | 352.467 | 353.094 |

culations of the kind mentioned above is the lack of information about the interatomic force field of the molecule. Therefore the calculated $r_z$-parameters must be treated carefully. The $r_z$-length of the molecule derived from these is 6.238 Å. The difference from the $r_s$-length is not significant but for comparison with electron diffraction data we need the absolute values of the inertial moments rather than the differences caused by substitution. For $I_b$ the change from $r_0$ to $r_z$ structure affects the first decimal place; see Table 3. Consequently it cannot be neglected. For $I_c$ on the other hand, the change is minor and presumedly $I_c$ can be used without correction.

REFERENCES

1. Fukuyama, T., Kuchitsu, K. and Morino, Y. Bull. Chem. Soc. Japan 42 (1969) 379.
2. Hirose, C. Bull. Chem. Soc. Japan 43 (1970) 3695.
3. Vestin, R., Borg, A. and Lindblom, T. Acta Chem. Scand. 22 (1968) 687.

4. Gordy, W. and Cook, R. L. *Microwave Molecular Spectra*, Interscience, New York 1970.
5. Townes, C. H. and Schawlow, A. L. *Microwave Spectroscopy*, McGraw, New York 1955.
6. Costain, C. C. *J. Chem. Phys.* **29** (1958) 864.
7. Morino, Y., Kuchitsu, K. and Oka, T. *J. Chem. Phys.* **36** (1962) 1108.
8. Herschbach, D. R. and Laurie, V. W. *J. Chem. Phys.* **37** (1962) 1668.
9. Oka, T. *J. Phys. Soc. Japan* **15** (1960) 2274.
10. Oka, T. and Morino, Y. *J. Mol. Spectry.* **8** (1962) 300.
11. Marstokk, K.-M. and Møllendal, H. *J. Mol. Structure* **8** (1971) 234.

# Bacterial Carotenoids

## XLII* New Keto-carotenoids from *Rhodopseudomonas globiformis* (Rhodospirillaceae**)

KARIN SCHMIDT and SYNNØVE LIAAEN-JENSEN

*Institute of Microbiology, GSF, 34 Göttingen, Germany and Organic Chemistry Laboratories, Norwegian Institute of Technology, University of Trondheim, N 7034 Trondheim, Norway*

Under normal growth conditions the photosynthetic purple non-sulphur bacterium *R. globiformis* produces the four aliphatic, methoxylated keto-carotenoids *1*, *2*, *3*, and *4*; *1*, *2*, and *3* are new compounds.

From cells grown in the presence of diphenylamine the new keto-carotenoids *5*, *6*, and *7* were also isolated.

The keto-carotenoids *1* − *7* all carry the keto groups in the 4(4′)-positions. Their structures were established by means of spectroscopic methods (electronic and mass spectra; for *2*, *3*, and *4* also PMR spectra) and chemical reactions.

Biogenetic considerations suggest that the pathway of carotenoid biosynthesis in *R. globiformis* is common to that of okenone (*25*) synthesis, except that cyclization and aromatization does not occur; no cyclic carotenoids have yet been encountered in photosynthetic purple non-sulphur bacteria.

The carotenoids of the photosynthetic purple nonsulphur bacteria belonging to the family Athiorhodaceae, recently renamed Rhodospirillaceae,[1] have been extensively studied, *e.g.* Refs. 2 − 7. Aliphatic carotenoids with $C_{40}$-skeletons carrying tertiary methoxy or hydroxy groups in the 1,1′-positions are characteristic of this family. Conjugated keto groups in the 2,2′-positions are encountered in many carotenoids of the genus *Rhodopseudomonas*. Cross-conjugated carotenals of the rhodopinal type and glycosidic carotenoids have recently been isolated from some Rhodospirillaceae spp.[6,7]

We now report the carotenoid composition of *Rhodopseudomonas globiformis*, recently isolated by Pfennig.[8] The structures of six new keto-carotenoids, related to the carotenoids previously isolated from other Rhodospirillaceae spp., have been elucidated.

---

* Previous paper. *Acta Chem. Scand.* **27** (1973) 2321.
** Old nomenclature: Athiorhodaceae.

## RESULTS AND DISCUSSION

Under normal, anaerobic growth conditions *R. globiformis* synthesizes four red keto-carotenoids, *1*, *2*, *3*, and *4*.

In the presence of diphenylamine (DPA), a common inhibitor of carotenoid synthesis,[9] three more saturated keto-carotenoids *5*, *6*, and *7* are also produced, see Table 1.

*Table 1.* Carotenoid composition of *Rhodopseudomonas globiformis* grown without or with $10^{-5}$ M DPA in the medium.

| Carotenoid | % of total carotenoid | |
| --- | --- | --- |
| | −DPA | +DPA |
| Unsymmetrical $\xi$-carotene (*23*) | } 2.5 | } 18 |
| Neurosporene (*24*) | | |
| Keto-I   (*1*) | 0.5 | 7 |
| Keto-II  (*2*) | 80 | 18 |
| Keto-III (*3*) | 12 | 7 |
| Keto-IV  (*4*) | 5 | 11 |
| Keto-V   (*5*) | 0 | 12 |
| Keto-VI  (*6*) | 0 | 22 |
| Keto-VII (*7*) | 0 | 5 |

Since no alkali-labile functions are present in *1−7* there is no need of avoiding the saponification step in future isolations.

The experimental evidence for the structures assigned to these compounds referred to as *R.g.* keto-I (*1*, 1-methoxy-1,2-dihydro-$\psi$,$\psi$-caroten-4-one [10]), *R.g.* keto-II (*2*, 1,1'-dimethoxy-1,2,1',2'-tetrahydro-3',4'-didehydro-$\psi$,$\psi$-caroten-4-one), *R.g.* keto-III (*3*, 1,1'-dimethoxy-1,2,1',2'-tetrahydro-$\psi$,$\psi$-caroten-4,4'-dione), *R.g.* keto-IV (*4*, 1-methoxy-1'-hydroxy-1,2,1',2'-tetrahydro-$\psi$,$\psi$-caroten-4-one), *R.g.* keto-V (*5*, 1-methoxy-1,2,7',8',11',12'-hexahydro-$\psi$,$\psi$-caroten-4-one), *R.g.* keto-VI (*6*, 1-methoxy-1,2,7',8'-tetrahydro-$\psi$,$\psi$-caroten-4-one), and *R.g.* keto-VII (*7*, 1-methoxy-1'-hydroxy-1,2,7',8'-tetrahydro-$\psi$,$\psi$-caroten-4-one), will now be discussed.

*R.g.* keto-I (*1*) was available in small quantity. The degree of fine-structure in the electronic spectrum in hexane *contra* ethanol solution (Fig. 1) indicated the presence of a conjugated carbonyl function.[11] The mass spectrum showed diagnostically important fragment ions at $M-31$, $M-101$, and $M-129$ characteristic of the aliphatic okenone and group end $M-69$ and $m/e$ 69 ions typical of the lycopene end group,[11] see Scheme 1. The common $M-92$, $M-106$, and $M-158$ fragment ions caused by elimination from the polyene chain [11] was observed in the mass spectrum of *1* and in all other mass spectra studied here and will be omitted from further discussion. *R.g.* keto-I (*1*) could not be acetylated. Complex metal hydride reduction caused a hypsochromic shift of the electronic spectrum. The reduction product *8* exhibited visible light absorption typical of an aliphatic undecaene (Table 3, Fig. 1) and gave a mono-acetate on acetylation, confirming that *1* is a conjugated mono-ketone.
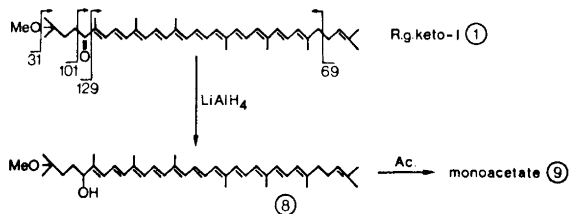
*Scheme 1.*
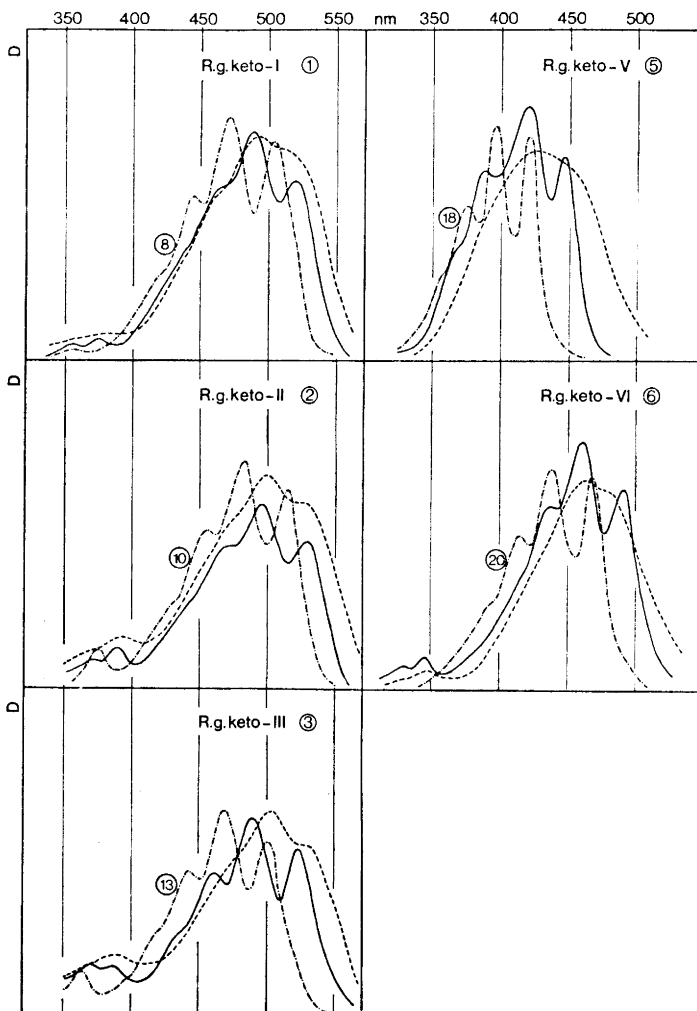


*Fig. 1.* Electronic spectra of *R. globiformis* keto-I (*1*), keto-II (*2*), keto-III (*3*), keto-V (*5*), and keto-VI (*6*) in petroleum ether ———— and ---- ethanol. —.— Hydride reduced derivatives in petroleum ether.

*R.g.* keto-II (*2*) was the major carotenoid of *R. globiformis* grown under normal conditions. The electronic spectrum again showed the solvent effects typical of a conjugated ketone (Fig. 1).

On electron impact the molecular ion was observed at $m/e$ 612 (consistent with $C_{40}H_{54}O(OCH_3)_2$) with diagnostically important fragment ions at $M-31$, $M-87$, and $M-101$ (see Scheme 2). The PMR-spectrum (Fig. 2, including
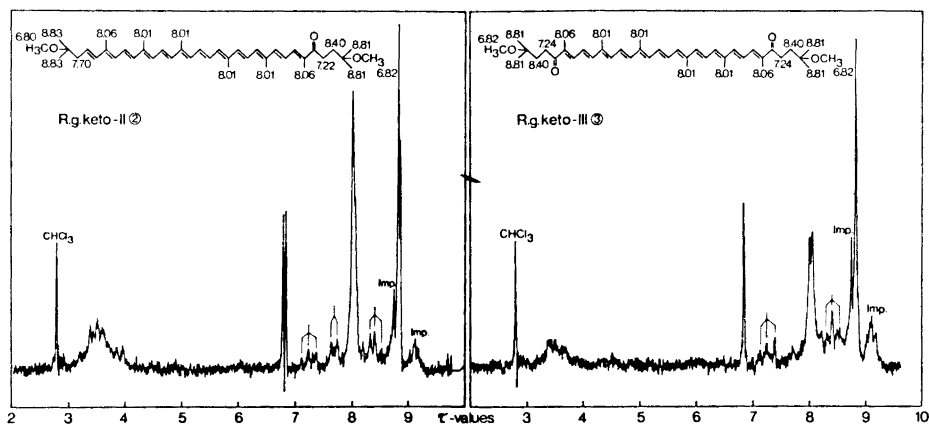


*Fig. 2.* PMR-spectra (CDCl$_3$) of *R. globiformis* keto-II (*2*) and *R. globiformis* keto-III (*3*).

signal assignments) was consistent with structure *2*, demonstrating the presence of two methoxy groups ($\tau$ 6.80 and $\tau$ 6.82) in magnetically non-equivalent environments. Structure *2* was confirmed by hydride reduction to *10* with an aliphatic dodecaene chromophore (Table 3, Fig. 1). Product *10* provided a monoacetate (*11*) on acetylation. On allylic dehydration with acidified chloroform [12] the reduction product *10* gave a product *12* with adsorptive properties, electronic and mass spectra indistinguishable from those of authentic spirilloxanthin (*12*).
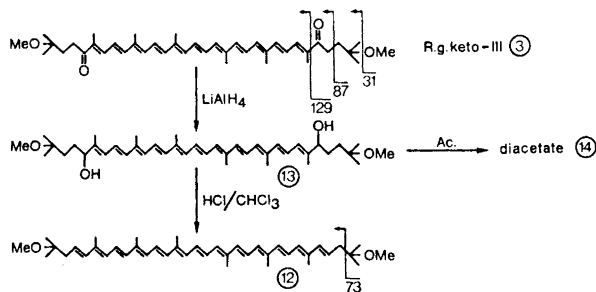


*Scheme 2.*

*Table 2.* Adsorptive properties of the carotenoids from *Rhodopseudomonas globiformis* and their derivatives.

| Carotenoid | $R_F$-values Kieselguhr paper 2%a | 5% | 10% | 20% | Alumina 2%a | 5% | 10% | paper 20% | 30% | Kieselgel G 10%a | Required eluent from Al₂O₃ (activity grade 2) |
|---|---|---|---|---|---|---|---|---|---|---|---|
| Keto-I (1) | 0.45 | | | | | 0.50 | 0.58 | | | 0.24 | 2 %a |
| Keto-II (2) | 0.19 | | 0.50 | | | | 0.50 | | | 0.17 | 5–8 % |
| Keto-III (3) | | | 0.35 | 0.76 | | | 0.38 | | | 0.09 | 10 % |
| Keto-IV (4) | | | 0.33 | 0.74 | | | 0.19 | 0.51 | | 0.04 | 15 % |
| Keto-V (5) | 0.88 | | | | 0.53 | 0.74 | | | | 0.32 | 4–5 % |
| Keto-VI (6) | | | 0.76 | | | 0.60 | 0.78 | | | 0.27 | 5–7 % |
| Keto-VII (7) | | | 0.40 | 0.76 | | | 0.38 | 0.72 | | 0.06 | 15–20 % |
| 8 = reduced 1 | | | | | | | 0.25 | | | | |
| 9 = 1 monoacetate | | | | | | | 0.75 | | | | |
| 10 = reduced 2 | | | | | | | | 0.52 | | | |
| 11 = 10 monoacetate | 0.40 | | | | | | 0.61 | | | | |
| 12 = spirilloxanthin | | | | | | | 0.64 | | | | |
| 13 = reduced 3 | | | | | | | | 0.18 | 0.50 | | |
| 14 = 13 diacetate | | | 0.82 | | | | | | | | |
| 15 = reduced 4 | | | | | | | | | 0.41 | | |
| 16 = 15 monoacetate | | | 0.66 | | | | | | | | |
| 17 = 4 TMS ether | 0.80 | | | | | | | | | | |
| 18 = reduced 5 | 0.59 | | | | | | | | | | |
| 19 = 11,12-dihydro-spheroidene | | | | | | | | | | | |
| 20 = reduced 6 | 0.39 | | | | | 0.73 | | | | | |
| 21 = spheroidene | 0.76 | | | | | | | | | | |
| 22 = reduced 7 | | | | | | | | 0.37 | | | |

*a* Acetone in petroleum ether.

Table 3. Absorption maxima in visible light in hexane solution of the keto-carotenoids from *Rhodopseudomonas globiformis* and their reduction products with lithium aluminium hydride.

| Carotenoid | | Native carotenoid ($\lambda_{max}$ in nm) | | | | | After LiAlH$_4$-reduction | | | | | Polyene chain |
|---|---|---|---|---|---|---|---|---|---|---|---|---|
| Keto-I | (1) | (360) | 375 | (462) | 488 | 520 | (357) | 374 | 448 | 472 | 503 | (8)[a] Undecaene |
| Keto-II | (2) | (368) | 387 | (470) | 494.5 | 527 | (345) | 360 | (456) | 482.5 | 513.5 | (10) Dodecaene |
| Keto-III | (3) | (370) | 387 | 461 | 489 | 522.5 | | | 444 | 469 | 500.5 | (13) Undecaene |
| Keto-IV | (4) | (360) | 377 | (463) | 487 | 519 | | | 446 | 470 | 501 | (15) Undecaene |
| Keto-V | (5) | | | 398.5 | 420 | 446 | | | 374 | 395 | 419 | (18) Heptaene |
| Keto-VI | (6) | (330) | 345 | (436.5) | 460.5 | 490 | | | 414.5 | 438 | 467.5 | (20) Nonaene |
| Keto-VII | (7) | | | (438) | 460 | 491 | | | 416 | 439 | 467 | (22) Nonaene |

[a] Formula number.

*R.g.* keto-III (*3*) was less abundant than *2*, but crystallized in bluish needles of m.p. 179°C, forming aggregates from petroleum ether/ether. As seen from Fig. 1 the electronic spectrum showed the typical solvent effects of conjugated carbonyl compounds. The molecular ion on electron impact occurred at $m/e$ 628 (consistent with $C_{40}H_{54}O_2(OCH_3)_2$). Fragment ions at $M-31$, $M-87$, and $M-129$ (Scheme 3) characterized the end groups. The PMR spectrum (Fig. 2, including signal assignments) revealed a symmetrical molecule with two identical tertiary methoxy groups ($\tau$ 6.80). Structure *3* was confirmed by hydride reduction to *13* with an aliphatic undecaene chromophore (Table 3, Fig. 1), and which could be converted back to keto-III (*3*) by allylic oxidation with *p*-chloranil.[13] The reduction product (*13*) had chromatographic properties (Table 2) indicative of a diol, and acetylation resulted in a diacetate (*14*). Allylic dehydration [12] of *13* gave spirilloxanthin (*12*), identified by co-chromatography tests, electronic and mass spectra.
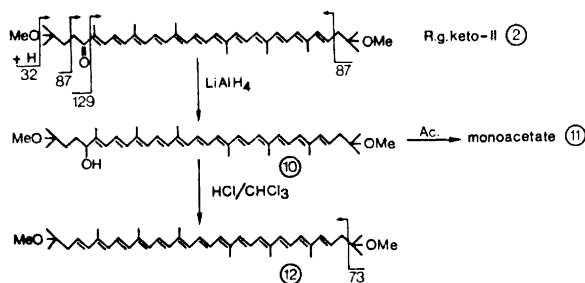


*Scheme 3.*

*R.g.* keto-IV was a minor carotenoid of cells grown under normal conditions. The electronic spectrum (Fig. 1) exhibited the solvent effects characteristic of carotenoid ketones. Hydride reduction gave a product *15* with an aliphatic undecaene chromophore (Table 3, Fig. 1) which provided a monoacetate *16* on acetylation.

Since *R.g.* keto-IV gave a mono(trimethylsilyl)ether (*17*, judged by $R_F$-value and mass spectrum), it may be inferred that keto-IV is a mono-ketone with one tertiary hydroxy group. The mass spectrum of keto-IV exhibited
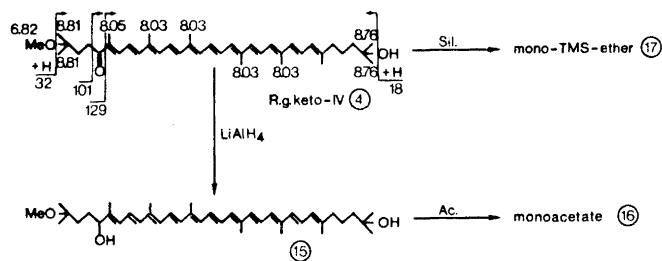


*Scheme 4.*

the molecular ion at $m/e$ 600 (consistent with $C_{40}H_{56}O(OH)OCH_3$) and fragment ions at $M-18$, $M-31$, $M-101$, and $M-129$ defining the end groups (Scheme 4). From these data and the PMR-signals given in Scheme 4, structure 4 is inferred for *R.g.* keto-IV. The same structure has recently been suggested for a minor carotenoid isolated from *Thiothece gelatinosa*, *Thiothece*-OH-484.[14] Co-chromatography tests confirmed their identity.

*R.g.* keto-V (5), isolated from DPA-inhibited cells, is a heptaen-one judged by the electronic spectra of 5 before and after hydride reduction to 18 (Fig. 1, Table 3). The mass-spectrometric fragmentation of *R.g.* keto-V (Scheme 5) was consistent with structure 5: $m/e$ 586 = M (corresponding to $C_{40}H_{59}O(OCH_3)$), $M-69$ and $M-205$ fragment ions defining the hydrocarbon end group and $M-31$, $M-101$, and $M-129$ ions defining the oxygenated end group. On allylic dehydration with acidified chloroform the hydride reduction product 18 gave a conjugated octaene product, tentatively identified as 11,12-dihydrospheroidene (19[5]).
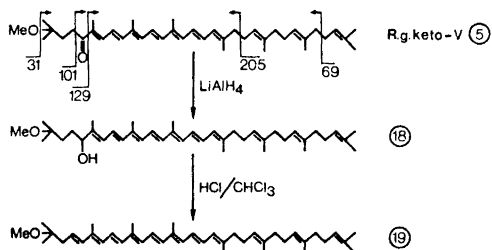


*Scheme 5.*

*R.g.* keto-VI (6) was the major carotenoid in DPA-grown cells. The spectral characteristics in visible light before and after hydride reduction to 20 (Fig. 1, Table 3) and allylic dehydration of 20 to spheroidene (21, identified by co-chromatography tests, electronic and mass spectra) together with the mass spectrum of keto-VI ($m/e$ 584 = M, corresponding to $C_{40}H_{57}O(OCH_3)$; $M-31$, $M-69$, $M-101$, $M-129$, and $M-137$) defined structure 6 for keto-VI, Scheme 6.
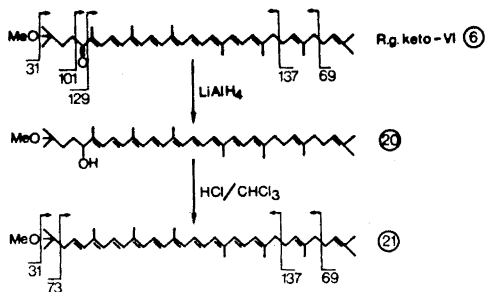


*Scheme 6.*

Finally *R.g.* keto-VII, isolated in minute amounts, was assigned structure 7 on the basis of its electronic spectrum which was identical with that of *R.g.* keto-VI (*6*), mass spectrum (*m/e* 602 = M, corresponding to $C_{40}H_{58}O(OH)OCH_3$; M − 18, M − 31, M − 129, and M − 137 − 18, Scheme 7) and chromatographic properties (Table 2); *R.g.* keto-VII being more polar than *R.g.* keto-VI (*6*).
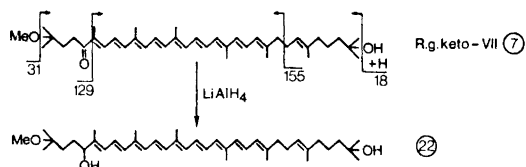


*Scheme 7.*

Hydride reduction of *R.g.* keto-VII (*7*) gave a reduction product (*22*) with the same electronic spectrum as *20* above (Fig. 1), but more polar (Table 2).

## BIOSYNTHETIC CONSIDERATIONS

Since carotenoid biosynthesis normally proceeds towards products of higher dehydrogenation level and DPA is known to inhibit the dehydrogenation steps of the Porter-Lincoln series [15,16] (A, Scheme 8), consideration of the carotenoid composition of cells grown without and in the presence of DPA and the chemical structures of the carotenoids involved permits the postulation of a plausible pathway of carotenoid biosynthesis in *R. globiformis*, Scheme 8.

Starting with unsymmetrical ξ-carotene (*23*) and neurosporene (*24*), present in normal cells (Table 1) and common precursors of carotenoid biosynthesis in photosynthetic bacteria,[16b] the keto-carotenoids typical of normal cells may be formed by the reaction steps A − D (Scheme 8) discussed previously [17,5] and introduction of a carbonyl group. In spheroidenone synthesis the oxygen of the carbonyl groups is derived from molecular oxygen [18] (reaction type E); under anaerobic condition reaction type F *via* alkene, hydrated alkene (secondary alcohol) to ketone may represent a more plausible alternative.

Regarding the position of the more saturated keto-carotenoids *5*, *6*, and *7* isolated only from cells grown in the presence of DPA, these may represent normal precursors of *1*, *2*, *3*, and *4*, or alternatively, abnormal products caused by the enzymatic reactions C, D and B, F when the dehydrogenation reaction A is depressed. Previous work with *Rhodospirillum rubrum* [16] has demonstrated that DPA blocks most efficiently the dehydrogenation step (A*) leading from neurosporene (*24*) to lycopene.

The possible connection between the pathway of carotenoid synthesis in *R. globiformis* and okenone (*25*) synthesis is pointed out. The methoxylated 4-keto-carotenoid okenone (*25*) with one end group in common with *1 − 7* and one aryl end group [19] is synthesized by several purple sulphur bacteria (Thio-
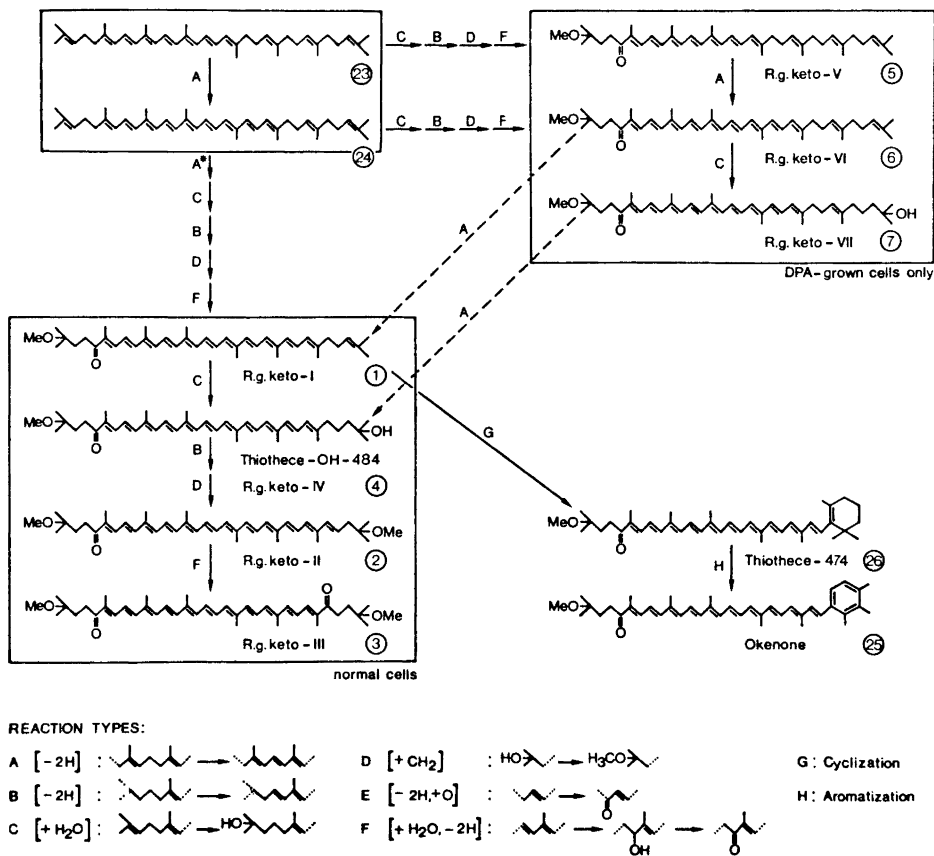
*Scheme 8.*

rhodaceae spp., now Chromatiaceae [1])[20], possibly *via Thiothece*-474 (*26*).[14] However, *R. globiformis*, like all other Rhodospirillaceae hitherto studied, lack the ability to cyclize its carotenoids.


## EXPERIMENTAL PART

*Materials. Rhodopseudomonas globiformis* strain 7950, SMG 161, obtained from Prof. Pfennig's collection (Göttingen institute), was grown anaerobically in the following medium:[21] $KH_2PO_4$ (0.5 g); $MgSO_4.7H_2O$ (0.4 g); NaCl (0.4 g); $NH_4Cl$ (0.4 g); $CaCl_2.2H_2O$ (0.05 g); Difco yeast extract (0.5 g); mannitol (1.5 g); Na-gluconate (0.5 g); trace element solution [22] without $Fe^{2+}$ and EDTA (10 ml); Fe-citrate solution containing 100 mg Fe-citrate/100 ml $H_2O$ (5.0 ml); Biotine solution containing 1 mg biotine/50 ml $H_2O$ (1.0 ml); *p*-aminobenzoic acid solution containing 5 mg *p*-aminobenzoic acid/50 ml $H_2O$ (1.0 ml) in 1000 ml dist. $H_2O$ (pH 4.9). After sterilization 1 ml/100 ml medium of a sterile, filtered 10 % Na-thiosulfate solution was added. For inhibition experiments DPA in a concentration of $10^{-5}$ M was added to the medium. Cells were grown in 500 ml screw cap bottles

at about 2000 Lux at 25 to 28°C. Cells were harvested for extraction by centrifugation after 5–8 days.

Chemicals and solvents were of analytical grade or freshly distilled.

*Methods.* These were as generally used in the Norwegian laboratory.[23] Hydride reduction, acetylation and silylation,[24] allylic oxidation,[25] and allylic elimination[26] were carried out by standard procedures.

*Isolation of the carotenoids.* The centrifuged cell pellet was extracted with acetone and the pigments transferred to ether; yield *ca.* 7 $\mu$g carotenoid/mg protein from normal cells (in total available *ca.* 45 mg carotenoids). From DPA-inhibited cells in total *ca.* 23 mg carotenoids were available.

The pigments mixture was separated by column chromatography on Woelm neutral alumina, activity grade 2. Further purification was obtained by rechromatography on alumina columns or TLC (Kieselgel G). Adsorptive properties of the carotenoids studied are compiled in Table 2. Absorption maxima in visible light are compiled in Table 3. The carotenoid composition of normal and DPA-grown cells is given in Table 1.

*R.g.* keto-I (*1*; 1-methoxy-1,2-dihydro-$\psi,\psi$-caroten-4-one). *Characterization: 1*, available *ca.* 0.2 mg, had: $R_F$-values Table 2; $\lambda_{max}$ Table 3, Fig. 1; *m/e* 582 (M), M−31, M−69, M−92, M−101, M−106, M−129, M−158, M−172, 69. *1* could not be acetylated with acetic anhydride in pyridine. *Reduction product (8). 1*, reduced with KBH$_4$ in ethanol or with LiAlH$_4$ in dry ether, provided *8*: $R_F$-values Table 2; $\lambda_{max}$ Table 3, Fig. 1. *Acetate (9). 8* on standard acetylation gave *9* with unchanged electronic spectrum; $R_F$-value Table 2.

*R.g.* keto-II (*2*, 1,1'-dimethoxy-1,2,1',2'-tetrahydro-3',4'-didehydro-$\psi,\psi$-caroten-4-one). *Characterization: 2* was precipitated together with colourless contaminants from acetone-petroleum ether, yield *ca.* 37 mg; $R_F$-values Table 2; $\lambda_{max}$ Table 3, Fig. 1; $\tau$ (CDCl$_3$) Fig. 2 with signal assignments; *m/e* 612 (M), M−31, M−32, M−73, M−89, M−92, M−101, M−106, M−158. *Reduction product (10). 2*, reduced with KBH$_4$ in ethanol or with LiAlH$_4$ in dry ether, provided *10*; $R_F$-values Table 2; $\lambda_{max}$ Table 3, Fig. 1. *Acetate (11). 10* on standard acetylation gave *11* with unchanged electronic spectrum; $R_F$-value Table 2. *Spirilloxanthin (12). 10* kept in 0.03 N HCl in CHCl$_3$ for 4 min gave *12*. $R_F$-value Table 2, no separation from authentic spirilloxanthin; $\lambda_{max}$ (acetone) 460, 491, 524 nm; *m/e* 596 (M), M−73, M−87, M−92, M−106.

*R.g.* keto-III (*3*; 1,1'-dimethoxy-1,2,1',2'-tetrahydro-$\psi,\psi$-caroten-4,4'-dione). *Characterization: 3* crystallized as bluish, shiny needles forming aggregates from acetone/petroleum ether; yield *ca.* 6 mg; m.p. 179°C; $R_F$-values Table 2; $\lambda_{max}$ Table 3, Fig. 1 (*E* 1 %, 1 cm = 2180 in petroleum ether at 489 nm); $\tau$ (CDCl$_3$) Fig. 2 including signal assignments; *m/e* 628 (M) M−31, M−32, M−92, M−106, M−129, M−158. *Reduction product 13. 3* was reduced with KBH$_4$ in ethanol or with LiAlH$_4$ in dry ether to *13*; $R_F$-values Table 2; $\lambda_{max}$ Table 3, Fig. 1. *13* was oxidized with *p*-chloranil for 3 h, resulting in a 30 % conversion to *3*. *Diacetate 14.* Standard acetylation of *13*, monitored by circular paper chromatography gave an intermediary monoacetate and a final diacetate *14* with unchanged electronic spectrum; $R_F$-value Table 2. *Spirilloxanthin (12). 3*, treated with HCl−CHCl$_3$ like *2* above, gave spirilloxanthin (*12*) identified by the same criteria as after dehydration of *10*.

*R.g.* keto-IV (*4*; 1-methoxy-1'-hydroxy-1,2,1',2'-tetrahydro-$\psi,\psi$-caroten-4-one). *Characterization. 4*, available *ca.* 2 mg, had: $R_F$-values Table 2; $\lambda_{max}$ Table 3, Fig. 1 (as for *1*); $\tau$ (CDCl$_3$) 8.82 (two *gem.* CH$_3$), 8.77 (two *gem.* CH$_3$ at *tert.* OH), 8.18 (one end-of-chain CH$_3$), *ca.* 8.03 (*ca.* four in-chain CH$_3$), 6.82 (one OCH$_3$), see Scheme 4; *m/e* 600 (M), M−18, M−31, M−32, M−32−18, M−92, M−101, M−106, M−129−18, M−158. *Reduction product 15. 4* was reduced in ethanol with KBH$_4$ or in dry ether with LiAlH$_4$ to *15*; $R_F$-values Table 2; $\lambda_{max}$ Table 3, Fig. 1. *Acetate 16. 15* gave on acetylation, monitored by circular paper chromatography, a monoacetate *16* with unchanged electronic spectrum; $R_F$-value Table 2. *Trimethylsilyl ether 17. 15* gave on standard silylation at −35°C a monoether *17* with unchanged electronic spectrum; $R_F$-value Table 2; *m/e* 672 (M), M−15, M−32, M−72, M−90, M−92, M−101, M−106, 131.

*R.g.* keto-V (*5*; 1-methoxy-1,2,7',8',11',12'-hexahydro-$\psi,\psi$-caroten-4-one). *Characterization. 5*, available *ca.* 2.5 mg, had: $R_F$-value Table 2; $\lambda_{max}$ Table 3, Fig. 1; *m/e* 586 (M), M−31, M−69, M−92, M−101, M−106, M−129, M−106−69, M−205, 69. *Reduction product 18. 5* gave on KBH$_4$-reduction in ethanol or on LiAlH$_4$-reduction in dry ether *18*; $R_F$-value Table 2, $\lambda_{max}$ Table 3, Fig. 1. *Dehydration product 19. 18*

was treated with 0.03 N HCl−CHCl$_3$ for 2 min giving *19*; $R_F$-value Table 2; $\lambda_{max}$ 393, 416, and 442 nm in acetone.

*R.g.* keto-VI (*6*; 1-methoxy-1,2,7′,8′-tetrahydro-$\psi,\psi$-caroten-4-one). *Characterization:* *6*, available *ca.* 6.5 mg, had: $R_F$-value Table 2; $\lambda_{max}$ Table 3, Fig. 1; *m/e* 584 (M), M−31, M−32, M−69, M−92, M−101, M−106, M−129, M−137, M−158, M−32−137, 69 (base peak). *Reduction product 20.* *6* was reduced with KBH$_4$ in ethanol or with LiAlH$_4$ in dry ether to *20*, $R_F$-value Table 2; $\lambda_{max}$ Table 3, Fig. 1. *Spheroidene (21)*, *20* was dehydrated in 0.03 N HCl−CHCl$_3$ for 3 min providing *21*, $R_F$-value Table 2; $\lambda_{max}$ (acetone) 432, 454 and 484 nm; *m/e* 568 (M), M−31, M−73, M−92, M−106, M−137, M−158. *21* could not be chromatographically separated from authentic spheroidene (*21*).

*R.g.* keto-VII (*7*; 1-methoxy-1′-hydroxy-1,2,1′,2′,7′,8′-hexahydro-$\psi,\psi$-caroten-4-one). *Characterization:* *7*, available *ca.* 1 mg, had: $R_F$-value Table 2; $\lambda_{max}$ Table 3 and Fig. 1 (as for *6*); *m/e* 602 (M), M−18, M−32, M−50 (M−32−18), M−92, M−106, M−126, M−129, M−155 (M−137−18), M−137−18−32. *Reduction product 22.* *7* gave on reduction with LiAlH$_4$ in dry ether *22*; $R_F$-value Table 2, $\lambda_{max}$ Table 3 and Fig. 1 (as for *20*).

Unsymmetrical $\xi$-carotene (*23*; 7,8,11,12-tetrahydro-$\psi,\psi$-carotene). *Characterization:* *23*, available *ca.* 2 mg, had: $R_F$-value = 0.78 on alumina paper (2 % acetone in petroleum ether); $\lambda_{max}$ (petroleum ether) 374.5, 395, and 419 nm; *m/e* 540 (M), M−69, M−92, M−106, M−137, M−205, 69 (base peak).

Neurosporene (*24*). *Characterization: 24*, available *ca.* 2 mg, had: $R_F$-value = 0.70 on alumina paper (2 % acetone in petroleum ether); $\lambda_{max}$ (petroleum ether) 415.5, 438.5, and 468 nm.

## REFERENCES

1. Pfennig, N. and Trüper, H. G. *Int. J. Syst. Bacteriol.* **21** (1971) 17.
2. Goodwin, T. W. *Arch. Mikrobiol.* **24** (1956) 313.
3. Liaaen Jensen, S. In Gest, H., San Pietro, A. and Vernon, L. P. *Bacterial Photosynthesis*, Antioch, Yellow Springs, Ohio 1963, p. 19.
4. Eimhjellen, K. E. and Liaaen Jensen, S. *Biochim. Biophys. Acta* **82** (1964) 21.
5. Davies, B. H. *Biochem. J.* **116** (1970) 101.
6. Schmidt, K., Francis, G. W. and Liaaen-Jensen, S. *Acta Chem. Scand.* **25** (1971) 2476.
7. Schmidt, K. *Arch. Mikrobiol.* **77** (1971) 231.
8. Pfennig, N. 33. Tagung der Gesellschaft für Hygiene und Mikrobiologie Freiburg, Fischer, Stuttgart 1971.
9. Turian, G. *Helv. Chim. Acta* **33** (1950) 1988.
10. IUPAC Tentative Rules for the Nomenclature of Carotenoids, *Biochemistry. In press.*
11. Vetter, W., Englert, G., Rigassi, N. and Schwieter, U. In Isler, O. *Carotenoids*, Birkhäuser, Basel 1971, Chapter IV.
12. Karrer, P. and Leumann, E. *Helv. Chim. Acta* **34** (1951) 445.
13. Warren, C. K. and Weedon, B. C. L. *J. Chem. Soc.* **1958** 3972.
14. Andrewes, A. G. and Liaaen-Jensen, S. *Acta Chem. Scand.* **26** (1972) 2194.
15. Goodwin, T. W. and Osman, H. G. *Biochem. J.* **56** (1954) 222.
16. Liaaen Jensen, S., Cohen-Bazire, G., Nakayama, T. O. M. and Stanier, R. Y. *Biochim. Biophys. Acta* **29** (1958) 477.
16. b. Davies, B. H. *Biochem. J.* **116** (1970) 93.
17. Liaaen Jensen, S., Cohen-Bazire, G. and Stanier, R. Y. *Nature* **192** (1961) 1168.
18. Shneour, E. A. *Biochim. Biophys. Acta* **65** (1962) 510.
19. Aasen, A. J. and Liaaen Jensen, S. *Acta Chem. Scand.* **21** (1967) 970.
20. Schmidt, K., Pfennig, N. and Liaaen Jensen, S. *Arch. Mikrobiol.* **52** (1965) 132.
21. Pfennig, N. *Personal communication.*

22. Pfennig, N. and Lippert, K. D. *Arch. Mikrobiol.* **55** (1966) 245.
23. Kjøsen, H., Arpin, N. and Liaaen-Jensen, S. *Acta Chem. Scand.* **26** (1972) 3053.
24. Liaaen-Jensen, S. and Jensen, A. *Methods Enzymol.* **23** (1971) 586.
25. Liaaen-Jensen, S. *Acta Chem. Scand.* **19** (1965) 1166.
26. Entschel, R. and Karrer, P. *Helv. Chim. Acta* **41** (1958) 402.

# Kinetics and Mechanism of the Reaction between Vanadium (V) and Hydroxylamine within the Hydrogen Ion Concentration Range 0.005 — 0.2 M

GÖSTA BENGTSSON

*Inorganic Chemistry 1, Chemical Center, University of Lund, P.O.B. 740, S-220 07 Lund 7, Sweden*

The studies of the reaction between vanadium(V) and hydroxylamine within the hydrogen ion concentration range 0.2 – 1.0 M reported previously [1,2] have been continued by a corresponding study within the hydrogen ion concentration range 0.005 – 0.2 M. Within this latter hydrogen ion concentration range the two-stage reaction found in more acid solutions apparently becomes a three-stage reaction. It is shown that this change on decreasing [H$^+$] is due to a side reaction which becomes appreciable only at [H$^+$] < 0.2 M. A mechanism valid within the whole hydrogen ion concentration range studied (0.05 – 1.0 M) is proposed.

A previous investigation [1] of the kinetics of the reduction of vanadium(V) by hydroxylamine within the hydrogen ion concentration range 0.2 – 1.0 M showed that this reaction obeys the rate law

$$-dC_{V(V)}/dt = kC_{V(V)}C_{NH_3OH} + k'C_{V(V)}{}^2 C_{NH_3OH} \tag{1}$$

where $C_{V(V)}$ and $C_{NH_3OH}$ represent the over-all concentrations of vanadium(V) and hydroxylamine, respectively. At sufficiently low values of $C_{V(V)}$ ($\lesssim 5 \times 10^{-4}$ M) the $k'$ term becomes negligible. The following mechanism was proposed for the reaction path corresponding to the $k$ term (*cf.* also Ref. 2)

$$VO_2{}^+ + NH_3OH^+ \overset{\beta_1}{\rightleftharpoons} VO_2NH_3OH^{2+} \quad \text{(rapid)} \tag{I}$$

$$VO_2NH_3OH^{2+} \overset{k''}{\longrightarrow} VO^{2+} + NH_2O\cdot + H_2O \quad \text{(slow)} \tag{II}$$

$$2NH_2O\cdot \longrightarrow N_2 + H_2O \quad \text{(rapid)} \tag{III}$$
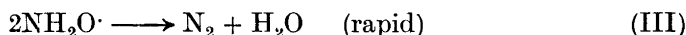
The stability constant $\beta_1 = [VO_2NH_3OH^{2+}]/[VO_2{}^+]$ of the rapid pre-equilibrium (I) has been determined [2] and was found to be independent of [H$^+$] within the hydrogen ion concentration range studied, thus indicating the existence of a protonated complex.

In less strongly acid solutions ($[H^+] < 0.2$ M) the kinetics of the reaction (low $C_{V(V)}$ and a large excess of hydroxylamine) seems to be more complicated. The aim of the present study has been to elucidate the mechanism of this reaction at $[H^+] = 0.005 - 0.2$ M and, if possible, to correlate the results to those obtained in more acid solutions.

## SYMBOLS AND NOTATIONS

$C_M$      over-all concentration of the central ion M $(=VO_2{}^+)$.[3]
$C_L$      over-all concentration of the ligand L $(=NH_3OH^+)$.[4]
$\varepsilon$      molar absorption coefficient (with indices indicating the species).
$A$      absorbance.
$a$      absorption coefficient ($a = A/l$; $l =$ path length).
$\varepsilon$      formal molar absorption coefficient ($\varepsilon = a/C_M$).
$\lambda$      wave length.
$t$      time.

## EXPERIMENTAL

The chemicals used were of the same kind and quality as those described in Ref. 1, as were the methods used for the preparation of the stock solutions and the determination of their concentrations. The temperature was $25.00 \pm 0.05°C$, the ionic strength 1.0 M. Sodium perchlorate and perchloric acid were used to keep the ionic strength constant.

The kinetic and equilibrium measurements were performed spectrophotometrically at $\lambda = 225$ nm by a Zeiss PMQ II Spektralphotometer. Absorption curves were recorded with a Hitachi EPS 3-T spectrophotometer. The reactions were initiated by mixing the proper volumes of the reactant solutions either by pipette or by means of an all glass syringe equipped with a device to allow the delivery of a well-defined volume of the solution in question. By the latter method it was possible to achieve complete mixing (in the absorption cell) within about 2 seconds. The experimental (pseudo-first order) rate constants were calculated from plots of $\ln (A_{max} - A)$ and $\ln (a - a_\infty)$ against $t$ by a least squares program on an electronic computer. The same program was used for the calculation of the intercepts and slopes of the other linear plots in this paper. The error limits represent three standard deviations.

## MEASUREMENTS AND RESULTS

The measurements were carried out at low over-all concentrations of vanadium(V) ($C_M = 0.025 - 0.100$ mM) and generally with a large excess of hydroxylamine ($C_L = 2.50 - 50.0$ mM). At $[H]^+ \geq 0.200$ M the absorbance at 225 nm decreased monotonously with the time after mixing the reactant solutions and the reaction was of the pseudo-first order. At $[H^+] < 0.200$ M, however, three distinct reaction steps could be observed. There was at first an immediate increase of the absorbance leading to an absorbance value which was the same as in more acid solutions under otherwise identical conditions. The absorbance then increased rather slowly with time, passed through a maximum within a few minutes and finally decreased very slowly until it reached a value after a few hours which was approximately equal to that obtained under the same conditions in more acid solutions. Fig. 1 shows a series of absorbance-time curves for $C_M = 0.100$ mM; $C_L = 20.00$ mM at different
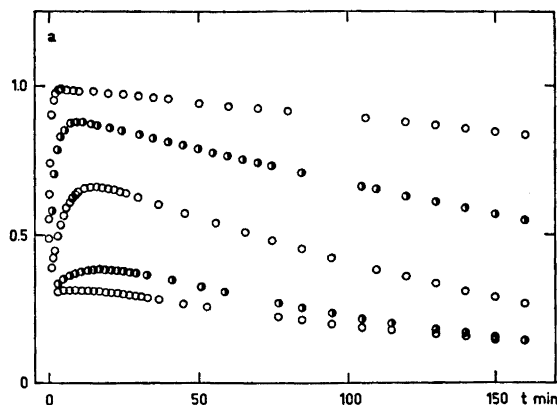
*Fig. 1.* A few absorbance-time curves determined at different $[H^+]$. $C_M = 0.100$ mM; $C_L = 20.00$ mM; $l = 1$ cm; $[H^+]$ from top to bottom: 0.005M, 0.010 M, 0.020 M, 0.050 M, and 0.100 M.

values of $[H^+]$. The three steps of the reaction are as follows: (1) A rapid complex formation equilibrium with the stability constant $\beta_1 = 12.5 \pm 0.4$ M$^{-1}$ (*cf.* Ref. 2). (2) A relatively slow reaction leading to an increase of the absorbance at $\lambda = 225$ nm. (3) A very slow reaction leading to the formation of vanadium(IV) and probably nitrogen gas (*cf.* below).

Step 1 has not been the subject of any kinetic study. The equilibrium has been considered in Ref. 2.

Step 2 is under the prevailing conditions of the pseudo-first order as it can be seen from the fact that $\ln(A_{max} - A)$ *versus* $t$ is linear (Fig. 2) to more than about 60 % of complete reaction (as judged from the height of the maximum). Deviations from the linearity are found at the end of the reaction. These are due to the fact that the succeeding reaction then influences the difference $(A_{max} - A)$ to a noticeable extent. $A_{max}$ is the absorbance at the maximum of the absorbance-time curve. It is proportional to $C_M$ at constant values of $C_L$, $l$, and $[H^+]$. It increases with increasing $C_L$ and decreases with increasing $[H^+]$ (*cf.* Fig. 1), all other factors being kept constant. This indicates that step 2 probably includes an equilibrium reaction in which L is taken up by ML while one or more protons are lost. If it is assumed that steps 1 and 2 constitute the reactions (disregarding the participation of protons)

$$\text{Step 1: M + L} \xrightleftharpoons{\beta_1} \text{ML (rapid)} \qquad \text{(IV)}$$

$$\text{Step 2: ML + L} \xrightleftharpoons[k_2]{k_2} \text{X (slow)} \qquad \text{(V)}$$
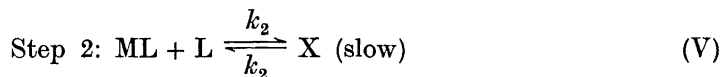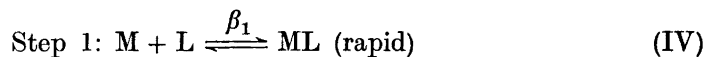
and the equilibrium constant

$$K_2' = [\text{X}]/[\text{ML}][\text{L}] \qquad (2)$$
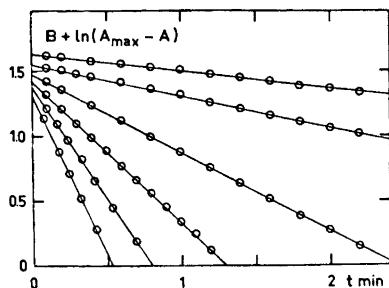
Fig. 2. Step 2. ln $(A_{max} - A)$ versus $t$ for a series of $C_L$-values. $B$ is an arbitrary constant used to make the lines start at roughly the same value. $C_M = 0.100$ mM; $[H^+] = 0.010$ M; $l = 1$ cm; $C_L$ and $B$ from top to bottom: 5 mM, 1.40; 10 mM, 1.05; 20 mM, 0.90; 30 mM, 0.85; 40 mM, 0.85; 50 mM, 0.85.
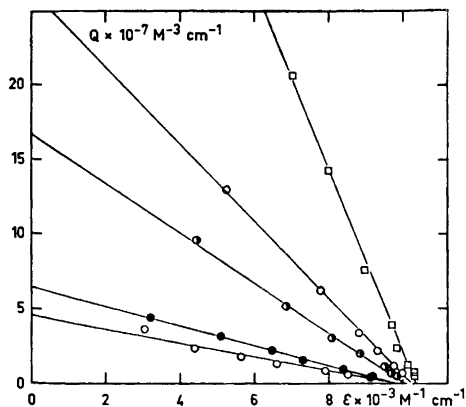
Fig. 3. Step 2. The quantity $Q$ versus $\varepsilon$. $C_M = 0.100$ mM; $[H^+]$ from top to bottom: 5.00 mM; 7.50 mM; 10.00 mM; 15.00 mM; 20.00 mM.

is defined, the following relation can be derived:

$$\varepsilon = \frac{\varepsilon_M + \varepsilon_{ML}\beta_1[L] + \varepsilon_X\beta_1 K'_2[L]^2}{1 + \beta_1[L] + \beta_1 K_2'[L]^2} \tag{3}$$

Since $C_M \ll C_L$ this equation can be transformed to

$$Q = [\varepsilon(1 + \beta_1 C_L) - \varepsilon_M - \varepsilon_{ML}\beta_1 C_L]/C_L^2 = \varepsilon_X\beta_1 K_2' - \varepsilon\beta_1 K_2' \tag{4}$$

All the quantities in the left member of eqn. (4) are known ($\varepsilon = a_{max}/C_M$ is measured as a function of $C_L$; $\beta_1$, $\varepsilon_M$, and $\varepsilon_{ML}$ are obtained from Ref. 2). $Q$ versus $\varepsilon$ yields for a constant value of $[H^+]$ ($[H^+] = 0.005 - 0.020$ M) a straight line with the intercept $\varepsilon_X\beta_1 K_2'$ and the slope $\beta_1 K_2'$ and $\varepsilon_X$ and $K_2'$ can be calculated. The straight lines obtained are shown in Fig. 3, and the values of $\varepsilon_X$ and $K_2'$ are found in Table 1. $K_2'$ is inversely proportional to $[H^+]^2$, so the true equilibrium constant is given by:

$$K_2 = K_2'[H^+]^2 = [X][H^+]^2/[ML][L] \tag{5}$$

The results of the kinetic measurements are also in agreement with this interpretation. The pseudo-first order rate constant, $k_{obs}$, increases strongly with increasing $C_L$ and the order with regard to L is between 1 and 2. From the reactions (IV) and (V) the following expression can be derived

$$k_{obs}(1 + \beta_1 C_L) = k_{-2} + k_{-2}\beta_1 C_L + k_2\beta_1 C_L^2 \tag{6}$$

since $C_L \gg C_M$ and step 2 accordingly can be treated as a reversible first order reaction. $k_{-2}$ can be determined by extrapolating $k_{obs}\,(1 + \beta_1 C_L)$ versus $C_L$ to $C_L = 0$, and then $k_{-2}\beta_1$ and $k_2\beta_1$ can be obtained from the linear relation

$$[k_{obs}(1 + \beta_1 C_L) - k_{-2}]/C_L = k_{-2}\beta_1 + k_2\beta_1 C_L \tag{7}$$

Fig. 4 shows $[k_{obs}\,(1 + \beta_1 C_L) - k_{-2}]/C_L$ versus $C_L$. The values of $k_2$ are shown in Table 1 and are found to be roughly inversely proportional to $[H^+]^2$. The

Table 1. Experimental values of $K_2'$, $K_2$, $\varepsilon_X$, and $k_2$.

| $[H^+]$ mM | $K_2' \times 10^{-3}$ $M^{-1}$ | $K_2$ M | $\varepsilon_X \times 10^{-3}$ $M^{-1}$ $cm^{-1}$ | $k_2$ M $min^{-1}$ |
|---|---|---|---|---|
| 5 | $4.90 \pm 0.32$ | $0.120 \pm 0.008$ | $10.3 \pm 1.3$ | $331 \pm 45$ |
| 7.5 | $2.06 \pm 0.08$ | $0.116 \pm 0.004$ | $10.2 \pm 0.7$ | $231 \pm 41$ |
| 10 | $1.34 \pm 0.10$ | $0.134 \pm 0.010$ | $10.1 \pm 1.3$ | $111 \pm 5$ |
| 15 | $0.535 \pm 0.022$ | $0.120 \pm 0.005$ | $9.7 \pm 0.7$ | $58 \pm 11$ |
| 20 | $0.385 \pm 0.048$ | $0.154 \pm 0.023$ | $9.5 \pm 2.6$ | $36 \pm 14$ |

two sets of values of $k_{-2}$ obtained from graphs corresponding to eqns. (6) and (7) do not agree very well with each other. This can be explained by the fact that $k_{obs}$ at low values of $C_L$ is very unreliable since $A_{max}$ is lower than the true equilibrium value as a consequence of the succeeding reaction. This effect is most pronounced at low $C_L$ (cf. below).

Step 3 is also of pseudo-first order since the lines $\ln (a - a_\infty)$ versus $t$ are straight except within a time interval from $t = 0$ to immediately after the max-
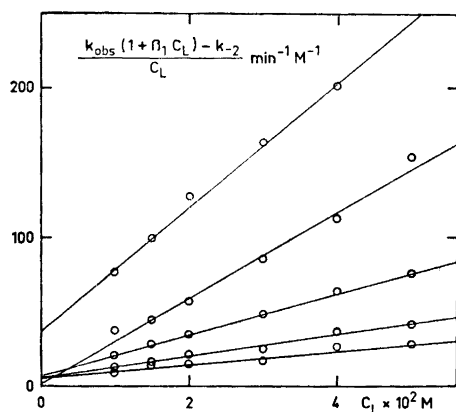


Fig. 4. Step 2. $[k_{obs}\,(1 + \beta_1 C_L) - k_{-2}]/C_L$ versus $C_L$. $C_M = 0.100$ mM; $[H^+]$ from top to bottom: 5.00 mM; 7.50 mM; 10.00 mM; 15.00 mM; 20.00 mM.
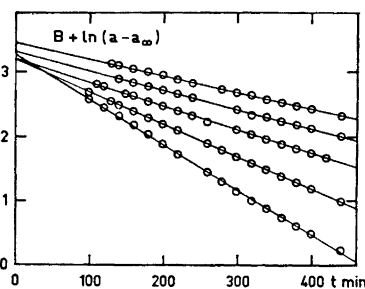


Fig. 5. Step 3. $\ln (a - a_\infty)$ versus $t$ for a series of $C_L$-values. $C_M = 0.100$ mM; $[H^+] = 0.010$ M; $C_L$ from top to bottom. 50.0 mM; 40.0 mM; 30.0 mM; 20.00 mM; 10.00 mM.

imum (Fig. 5). The experimental rate constant $k'_{obs}$ decreases with increasing $C_L$ ([H$^+$] constant) and increases with increasing [H$^+$] ($C_L$ constant). The relation between $k'_{obs}$ and $C_L$ can be roughly represented by the equation

$$k'_{obs} = p + q/C_L \tag{8}$$

where $p$ and $q$ are empirical constants. The fact that the rate law contains two terms indicates the existence of two competing reaction paths, one with X as a reactant and one with ML. The empirical relation can be explained by the reactions:

$$\text{Step 3: } \text{ML} \xrightarrow{k_3} \text{products} \tag{VI}$$

$$\text{X} \xrightarrow{k_4} \text{products} \tag{VII}$$
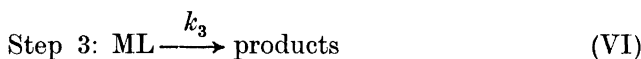
The following relation can be derived from reactions (IV) – (VII), if it is assumed that steps 1 and 2 are much faster than step 3.

$$k'_{obs} = (k_3\beta_1 C_L + k_4\beta_1 K_2' C_L^2)/(1 + \beta_1 C_L + \beta_1 K_2' C_L^2) \tag{9}$$

This equation can be transformed to

$$R = [k'_{obs}(1 + \beta_1 C_L + \beta_1 K_2' C_L^2)]/C_L = k_3\beta_1 + k\beta_1 K_2' C_L \tag{10}$$

Accordingly $R$ is a linear function of $C_L$. Fig. 6 shows this to be the case for [H$^+$] = 0.005 – 0.015 M. At higher [H$^+$] step 3 is too rapid for the assumption made above to be true. If $(1 + \beta_1 C_L) \ll \beta_1 K_2' C_L^2$, then eqn. (9) becomes

Table 2. Experimental values of $k_3$ and $k_4K'_2$.

| [H$^+$] mM | $k_3$ min$^{-1}$ | $k_4K_2'$ M$^{-1}$ min$^{-1}$ |
|---|---|---|
| 5 | 0.144 ± 0.011 | 2.36 ± 0.35 |
| 10 | 0.206 ± 0.014 | 1.27 ± 0.41 |
| 15 | 0.233 ± 0.032 | 1.77 ± 0.99 |

analogous to eqn. (8). Table 2 shows that $k_3$ increases slightly with [H$^+$], whereas $k_4K_2'$ rather decreases. The precision hardly permits the establishment of the exact dependence of these quantities on [H$^+$].

## DISCUSSION

The mechanism proposed above can be summarized in the following reaction-equilibrium scheme:

$$\text{M} \underset{-\text{L}}{\overset{+\text{L}}{\rightleftharpoons}} \text{ML} \underset{-\text{L}}{\overset{+\text{L}}{\rightleftharpoons}} \text{X}$$
$$\downarrow \qquad \downarrow$$
$$\text{products} \quad \text{products}$$
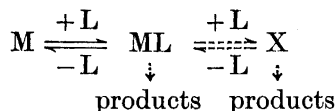
The full drawn arrowds enote rapid reactions (step 1), the dashed arrows relatively slow reactions (step 2), and the pointed arrows very slow reactions (step 3).
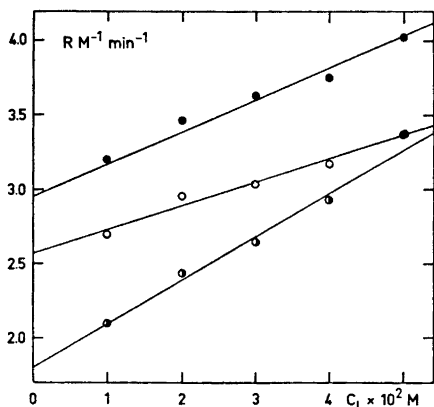


*Fig. 6.* Step 3. The quantity $R$ versus $C_L$. $C_M = 0.100$ mM; ● $[H^+] = 5.00$ mM; ○ $[H^+] = 10.00$ mM; ◑ $[H^+] = 15.00$ mM.
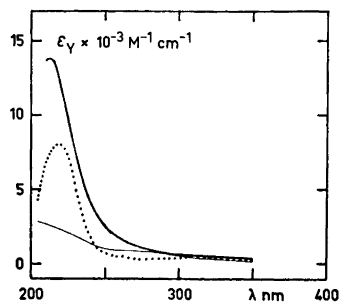
*Fig. 7.* Absorption curves of the species M (——), ML (······), and X (——).

In strongly acid solutions ($[H^+] \geq 0.2$ M) the equilibrium $ML + L \rightleftharpoons X$ is so strongly displaced to the left that the $k_3$ term becomes completely dominating. The formation of X is not noticeable and the over-all reaction is a two-stage reaction. As $[H^+]$ is decreased the equilibrium in question is displaced to the right (the rate of the reaction $ML + L \rightarrow X$ increases) and at sufficiently low $[H^+]$ the formation of X becomes noticeable in the beginning of the third step. At the same time the $k_4$ term becomes appreciable. This indicates that the $k_3$ term is analogous with the first term of the right member of eqn. (1) and that the corresponding reaction is reaction (II). The product emanating from hydroxylamine in this reaction has been established [1] as $N_2$ whereas the product of the reaction corresponding to the $k_4$ term is still uncertain.

The identity of the intermediate X is not known. The complex ML is formed without any loss of protons so this complex should be $VO_2NH_3OH^{2+}$. The addition of a second ligand ($NH_3OH^+$) to this complex is very unfavourable since the resultant complex would acquire a high positive charge. By the formation of X two protons are expelled the origin of which has not been possible to establish. Whatever the structure of X may be, it seems to be a reasonable guess that the final product emanating from hydroxylamine in the reaction corresponding to the $k_4$ term is nitrogen gas. Fig. 7 shows the absorption curves of M, ML, and X within the wave length range $200 - 350$ nm. The curve of ML has been calculated from absorbance values extrapolated to the time $t = 0$ after mixing the reactant solutions using the known values of $\varepsilon_M$ and $\beta_1$. The curve of X has been calculated from the absorbances at maximum of the absorbance-time curve using known values of $\varepsilon_M$, $\varepsilon_{ML}$, $\beta_1$, and $K_2'$ at $[H^+] = 0.005$ M; $C_M = 0.100$ mM; $C_L = 0.020$ M.

## REFERENCES

1. Bengtsson, G. *Acta Chem. Scand.* **26** (1972) 2494.
2. Bengtsson, G. *Acta Chem. Scand. In press.*
3. Rossotti, F. J. C. and Rossotti, H. *Acta Chem. Scand.* **10** (1956) 957.
4. Lumme, P., Lahermo, P. and Tummavuori, J. *Acta Chem. Scand.* **19** (1965) 2175.

Received April 28, 1973.

# Degradation of Cellobiitol and Glucose by Oxygen-Alkali

# Treatment

OLOF SAMUELSON and LENNART STOLPE

*Institutionen för teknisk kemi, Chalmers Tekniska Högskola, Fack, S-402 20 Göteborg 5, Sweden*

An important reaction of cellobiitol during oxygen – alkali treatment at 96° is an oxidation of the glucitol moiety, followed by a liberation of glucose. To a lesser extent, the glucose moiety is oxidized and glucitol liberated in a consecutive reaction. Glucose is decomposed by various reactions. The formation of arabinonic and mannonic acids decreases at high temperature, whereas the reaction paths *via* 3-deoxy-*erythro*-hexosulose become more important. Among the 23 monocarboxylic acids identified after glucose oxidation, formic, acetic, and glycolic acids were the most abundant.

In connection with the recent development of oxygen bleaching of wood pulps, studies of catalysts and inhibitors which affect the degradation of carbo-hydrates by oxygen in alkaline medium have become increasingly important. In these studies it is often advantageous to apply model compounds instead of cellulose. Cellobiitol has been used for this purpose [1] and since the reactions which occur have not been studied previously, an investigation of the reaction products obtained after oxygen-alkali treatment was carried out. The experiments showed that glucose was an important intermediate. Very little is known about the reaction products formed from glucose under comparable conditions and a study of these products was therefore included.

## EXPERIMENTAL

Cellobiitol (6 g), prepared by reduction of cellobiose with sodium borohydride,[2] was dissolved in 300 ml of 0.5 % sodium hydroxide and treated with oxygen under pressure (6 bar) at 96° in the bubbling column described previously.[1] A small amount of hydrogen peroxide (0.67 mmol/l) was added as initiator. The time of reaction was 1.5 h. An aliquot of the solution was used for the determination of peroxide and for alkalimetric determi-nation of organic acids. Another part of the solution was neutralized with acetic acid to pH 8 and separated into an acid fraction and a neutral fraction on an anion exchanger in the acetate form. After the sodium ions were removed on a cation exchanger, both solutions were evaporated and the fractions weighed. The acid fraction amounted to 4.5 % of the added cellobiitol.

The neutral fraction was chromatographed on a preparative scale.[3] The sub-fractions were analyzed automatically by partition chromatography in 85 % ethanol on an anion exchanger in the $SO_4{}^{2-}$ form and on a cation exchanger in the $Li^+$ form[4]. The analyzing system contained two channels, one which recorded all sugars, and one which determined alditols and indicated the presence of ketoses.[5] The presence of glucose and glucitol was confirmed by gas chromatography and gas chromatography-mass spectrometry.[6]

The nonvolatile acids were separated quantitatively on an anion exchange column in 0.08 M sodium acetate (pH adjusted to 5.9 with acetic acid). The chromatogram was recorded automatically by means of a differential refractometer (Waters' Model R-4) and the eluate divided into nine fractions as illustrated in Fig. 1. These were analyzed on anion exchange columns in the acetate form in two media, 0.08 M sodium acetate (pH 5.9) and 0.5 M acetic acid. The chromatograms were recorded with a three-channel analyzer.[7] The volume distribution coefficients and the colour responses were compared to results obtained in previously published papers. This permitted an identification of most compounds. For additional identification, the acids were converted into fully substituted trimethylsilyl esters and identified by gas chromatography and gas chromatography-mass spectrometry.[8] Only one compound recorded on the chromatograms had properties differing from the acids studied in previous work from this laboratory. The mass spectrum revealed that the acid was a 3-deoxyheptonic acid.

A minor amount of organic acids, constituting about 5 % of the total amount of nonvolatile acids, appeared ahead of the first fraction as indicated in Fig. 1. The acids were
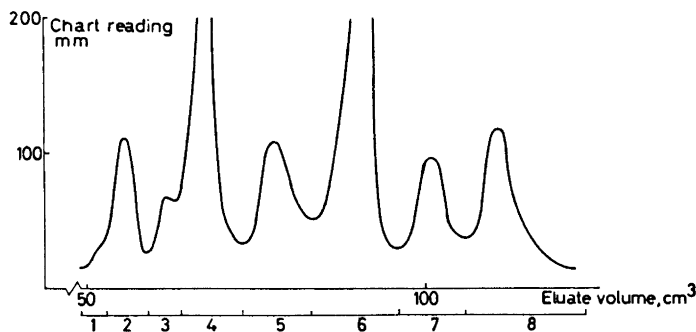


*Fig. 1.* Group separation of monocarboxylic acids obtained by oxygen-alkali treatment of cellobiitol. Column: $10 \times 935$ mm, Dowex 1-X8, $25 - 32\,\mu$. Eluent: 0.08 M sodium acetate, pH $= 5.9$. Detection: Differential refractometer.

rechromatographed on the analysis columns and found to be a complex mixture of aldobionic and similar acids containing one glucose moiety. The amounts were too small for identification.

Formic acid was determined after being extracted with ether from the reaction solution which had been acidified to pH 1. The ether solution was titrated with aqueous 0.1 M NaOH and the aqueous solution chromatographed in 0.3 M sodium acetate on an anion exchange column. The formic acid was recorded automatically by chromic acid oxidation. Acetic acid was obtained as a sodium acetate solution by the same extraction method. The sodium ions were removed by a cation exchange resin and the solution was analyzed by gas chromatography.[9] As a check, the acetic acid was distilled from the reaction solution after acidification with phosphoric acid to pH 2. The distillate was studied by gas chromatography. The values obtained by the two methods differed by less than 10 %.

In the experiment with glucose, the oxygen-alkali treatment was carried out for 15 min. No hydrogen peroxide was added, but in other respects the conditions were the same as those applied with cellobiitol. The pH of the solution was 8.5 at the end of the experiment. The solution was analyzed by the same methods as used in the experiment with cellobiitol.

## RESULTS AND DISCUSSION

*Oxidation of glucose.* The reaction during oxygen-alkali treatment of glucose is very rapid and the treatment was carried out only for 15 min, during which time the sodium hydroxide was consumed completely. In addition to organic acids, a number of neutral sugars were formed by isomerization and fragmentation. Besides glucose (52 %), fructose (37 %) and mannose (7 %) were the most abundant sugars. The presence of psicose, allose, and altrose (1 % of each) showed that not only the substituents at C-1 and C-2, but also those at C-3 were involved in Lobry de Bruyn – Alberda van Ekenstein rearrangements. As expected on the basis of previous results,[10] a small amount of arabinose was formed (0.5 %). It is noteworthy that ribose, the C-2 epimer of arabinose was present in about an equal amount.

A comparison between the organic acids formed by oxygen-alkali treatment at high temperature (96°) in dilute sodium hydroxide (0.5 %) and high

*Table 1.* Organic acids obtained after oxygen-alkali treatment of glucose and cellobiitol. The amounts given as g acid per 100 g of starting material. The nonvolatile compounds are reported as a percentage of the total weight of isolated nonvolatile acids. p = present but not determined.

| Acid | From glucose | | | | From cellobiitol | |
| | 0.5 % NaOH, 96° | | 18 % NaOH, 25° | | 0.5 % NaOH, 96° | |
| | g/100 g | % | g/100 g | % | g/100 g | % |
| | | | | | | |
| Glycolic | 2.67 | 18.6 | 0.67 | 11.0 | 0.52 | 15.0 |
| Glyceric | 2.22 | 15.5 | 0.97 | 15.9 | 0.93 | 26.9 |
| Erythronic | 1.56 | 10.8 | 0.38 | 6.2 | 0.28 | 8.1 |
| 3-Deoxy-*arabino*-hexonic | 1.46 | 10.2 | 0.08 | 1.4 | 0.14 | 4.0 |
| 2-Deoxy-*erythro*-pentonic | 1.38 | 9.6 | 0.11 | 1.7 | 0.05 | 1.4 |
| Arabinonic | 1.15 | 8.0 | 3.03 | 49.7 | 0.08 | 2.3 |
| 2-Hydroxypropionic | 0.65 | 4.5 | 0.21 | 3.4 | 0.31 | 9.0 |
| 3-Deoxytetronic | 0.50 | 3.5 | 0.06[a] | 1.0 | 0.32 | 9.2 |
| 3-Hydroxypropionic | 0.45 | 3.1 | | | | |
| Threonic | 0.42 | 2.9 | | | 0.04 | 1.2 |
| 3-Deoxy-*ribo*-hexonic | 0.33 | 2.3 | 0.08 | 1.4 | 0.05 | 1.4 |
| Ribonic | 0.33 | 2.3 | | | 0.03 | 0.9 |
| 2-Deoxytetronic | 0.23 | 1.6 | 0.06 | 1.0 | 0.11 | 3.2 |
| Gluconic | 0.21 | 1.5 | 0.04 | 0.7 | 0.05 | 1.4 |
| 3-Deoxy-*threo*-pentonic | 0.21 | 1.5 | p | | 0.37 | 10.7 |
| Mannonic | 0.21 | 1.4 | 0.36 | 5.9 | 0.03 | 0.9 |
| 2-Deoxy-*lyxo*-hexonic | 0.15 | 1.1 | | | | |
| 3-Deoxyheptonic | 0.14 | 1.0 | | | | |
| Xylonic | 0.05 | 0.3 | | | | |
| 3-Deoxy-*erythro*-pentonic | 0.05 | 0.3 | 0.04 | 0.7 | 0.11 | 3.2 |
| 2-Deoxy-*threo*-pentonic | 0.01 | 0.1 | | | | |
| 3-Deoxy-*xylo*-hexonic | | | | | 0.03 | 0.9 |
| 2-*C*-Methyl-ribonic | | | | | 0.01 | 0.3 |
| Acetic | 4.1 | | | | 0.04 | |
| Formic | 4.5 | | p | | 0.32 | |
| Carbonic | 1.2 | | | | 0.2 | |

[a] Band 3S1 identified from original chromatograms.

oxygen pressure and those obtained in 18 % solution at room temperature and atmospheric pressure [10] shows that the working conditions exert a great influence. The results obtained in both the present and the previous investigation are given in Table 1. Arabinonic acid was the preponderant acid and mannonic acid was among the major acids obtained at low temperature, whereas the relative amounts produced under the conditions used in the present work were much less. In general, the formation of acids of low molecular weight is favoured under the conditions applied in the present work. A similar influence of an increased temperature was observed by de Wilt [11] and by Malinen and Sjöström.[12]

The formation of arabinonic and mannonic acids, as well as arabinose, can be ascribed to the formation of D-glucosone followed by a benzilic acid rearrangement or a fragmentation between the carbonyl groups.[10,13] These and other reactions of glucosone have recently been studied by Malinen and Sjöström.[12]

The fact that the relative amounts of arabinonic and mannonic acids were lower under the present working conditions than in the earlier experiments indicates that the reaction path via glucosone is less important at high temperature. This is not unexpected since, even in the absence of oxygen, glucose is decomposed very rapidly in hot sodium hydroxide solution and gives rise to 2-hydroxypropionic, 3-deoxy-ribo- and 3-deoxy-arabino-hexonic acids as the preponderant reaction products.[12,14] It is worth mentioning that ribonic acid was more abundant than mannonic acid and that a new reaction path for the formation of ribonic acid from methyl β-glucopyranoside during oxygen-alkali treatment has been suggested recently.[15]

Formic, acetic, and glycolic acids were the three most abundant acids isolated in the present work. Reactions paths which give rise to formic and glycolic acids have been discussed earlier,[10,12,16] whereas acetic acid has escaped observation in previous investigations. Glucosone is one precursor responsible for the formation of formic and glycolic acids, but since this intermediate seems to be less important at high than at low temperature, the reaction path via glucosone cannot explain the large amount of formic acid.

Among the most striking differences between the results obtained by alkali treatment of glucose at high temperature in the absence of oxygen and the results obtained under oxygen pressure is that 2-hydroxypropionic acid is the most abundant acid in the absence of oxygen, whereas the amount formed in the presence of oxygen is fairly small.[12] Instead, very large amounts of acetic acid are formed during oxygen-alkali treatment. It has been reported [17] that pyruvaldehyde, formed after cleavage of glucose between C-3 and C-4, is a precursor of 2-hydroxypropionic acid, i.e. that 2-hydroxypropionic acid is formed by a benzilic acid type rearrangement of this dicarbonyl compound. As pointed out previously, an oxidative cleavage of dicarbonyl compounds between the carbonyl groups is a very important reaction during oxygen-alkali treatment of carbohydrates [18] and it can be concluded therefore that the intermediate pyruvaldehyde is a precursor to acetic acid, which, in this reaction, is formed together with an equimolar amount of formic acid.[19]

No detectable amounts of 2-C-methylpentonic acids were present in the reaction mixture after the oxygen-alkali treatment of glucose. It is possible

that the intermediate, 1-deoxy-2,3-hexodiulose, which is a precursor to these saccharinic acids, [20] is formed, but that it is subjected to an oxidative cleavage of the linkage between the carbonyl groups, which produces equimolar amounts of acetic and erythronic acids. The fact that erythronic acid was among the most abundant acids, but still present in much smaller amounts than acetic acid, can be taken as an indication that this reaction is of importance, but by no means solely responsible for the formation of acetic acid.

Among the nonvolatile acids, 3-deoxyhexonic and 2-deoxy-*erythro*-pentonic acids were much more abundant after the treatment at 96° than at room temperature. The two 3-deoxyhexonic acids mentioned above, which are among the major reaction products after alkaline treatment of glucose and fructose in the absence of oxygen, are formed *via* 3-deoxy-*erythro*-hexosulose by a benzilic acid rearrangement.[21] The results presented in the table indicate that this reaction is of great importance during oxygen-alkali treatment at high temperature. Like other dicarbonyl compounds this intermediate can be subjected to fragmentation between the carbonyl groups. Oxidation will give formic and 2-deoxy-*erythro*-pentonic acid, which were both present in much larger amounts after the high-temperature oxidation than after the reaction at low temperature. The observation by Malinen and Sjöström [12] that the 2-deoxypentonic acid was not formed in the absence of oxygen indicates that the cleavage of the dicarbonyl intermediate by hydrolysis is of little or no importance.

A 3-deoxyheptonic acid was among the minor acids formed in the present work. The formation of acids with a larger number of carbon atoms than the original sugar has previously been observed by Ishizu, Lindberg, and Theander [22] in studies of alkaline treatment of xylose. An aldol condensation is very probably responsible for the formation of a heptose, which then rearranges to a 3-deoxyheptosulose and is converted, by a benzilic acid rearrangement, to 3-deoxyheptonic acids. Like other dicarbonyl sugars, 3-deoxyheptosulose should be subject to fragmentation, which, in this case, should give rise to some 2-deoxyhexonic acid. This reaction path explains the presence of 2-deoxy-*lyxo*-hexonic acid after oxygen-alkali treatment of glucose.

*Oxidation of cellobiitol.* Peroxide is formed during oxygen bleaching of cellulose, and since cellobiitol is very stable towards the attack of oxygen in alkaline medium,[1] a small amount of hydrogen peroxide (0.67 mmol/l) was added to initiate the reaction. It is interesting to note that the final peroxide concentration was the same as that at the beginning of the oxygen treatment. In view of the instability of hydrogen peroxide in hot alkaline solution, it can be concluded that peroxide was formed during the oxygen treatment. It is likely that intermediate carbonyl compounds or enolate anions formed during the degradation of cellobiitol are involved in the reactions which give rise to peroxide.[23]

To simulate the reactions which occur during oxygen-alkali treatment of cellulose, a short time of reaction (1.5 h) was chosen. This means that only a fraction (about 10 %) of the added cellobiitol was attacked. The major portion was recovered in the nonelectrolyte fraction which, in addition, contained glucose and glucitol as major products together with minor amounts of 3-*O*-(α-D-glucopyranosyl)-D-arabinose and 2-*O*-(α-D-glucopyranosyl)-D-erythrose.

The amount of glucose found in the reaction mixture was 3.2 %, calculated as a percentage (by weight) of the organic acids formed during the oxygen-alkali treatment. Since glucose is unstable under the applied working conditions and is rapidly converted into organic acids, it can be concluded that glucose is a very important intermediate.

Glucitol was present in a larger amount (5.3 % calculated on the same basis). Glucitol is much more stable than glucose in the reaction mixture. A separate experiment in which glucitol was treated under the same working conditions as cellobiitol revealed that the rate of formation of acids was roughly the same as that observed with cellobiitol. Evidently, the liberation of glucose from cellobiitol is a much more important reaction than the formation of glucitol.

Separate experiments carried out with cellobiitol in the absence of oxidant showed that neither glucose nor glucitol was formed. The most likely explanation for the formation of glucitol during oxygen-alkali treatment is that an oxidation of the glucose moiety in cellobiitol, resulting in the introduction of a keto group at C-3, occurs and is followed by a $\beta$-elimination at C-1 in the oxidized glucose moiety. Experiments carried out by Theander strongly indicate that oxidation at C-2 or C-3 will give the same reaction pattern since the two carbonyl compounds are rapidly interconverted.[24]

The oxidized glucose unit is unstable in alkali and may also be further oxidized. The consecutive reactions give rise to various fragmentation acids as main end products. Since, as already mentioned, the amount of glucitol was comparatively small, it can be concluded that this reaction path is not very important.

Only a small amount of gluconic acid was present in the reaction mixture (Table 1) indicating that no direct oxidative attack occurs upon the glycosidic bond during oxygen-alkali treatment. Similar observations have been made for aging of alkali cellulose,[25] oxygen bleaching of cellulose,[26] and oxygen alkali treatment of cellobiose.[10,12] In the experiment with glucitol, it was found that gluconic acid was the most abundant acid formed during the oxidation. The working conditions seem to have a great influence upon the products formed from glucitol.[27,28] These results confirm that, in the experiment with cellobiitol, the major part of the liberated glucitol remained unattacked in the reaction mixture.

From the results given above, it can be concluded that a major reaction during the oxygen-alkali treatment results in the liberation of glucose. In analogy with the reactions which seem to be predominant during oxygen-alkali treatment of cellulose [26] and xylan,[29] it can be assumed that the glucose is liberated by $\beta$-elimination after the introduction of a carbonyl group in the glucitol moiety.

The introduction of a keto group at C-2 in the glucitol moiety or an oxidation at C-1 followed by a Lobry de Bruyn – Alberda van Ekenstein transformation, would lead to a $\beta$-elimination with the formation of glucose and 4-deoxy-D-*glycero*-2,3-hexodiulose, according to generally accepted reaction schemes. In the absence of oxygen, this compound rearranges to 3-deoxy-2-*C*-hydroxymethyl-*ribo*- and *arabino*-pentonic acids, whereas oxidation in alkaline medium results in the formation of 2-deoxytetronic

and glycolic acids.[30] Both the rearranged acids and these oxidation products were formed in large amounts when cellobiose was subjected to oxygen-alkali treatment.[10,12] Moreover, these products belonged to the main compounds recovered from the solution when hydrocellulose was subjected to the same treatment.[31] No detectable amounts of isosaccharinic acids were produced from cellobiitol under the applied conditions indicating that this reaction path is of little or no importance as far as the degradation of cellobiitol is concerned.

Another possibility of explaining the formation of glucose would be an oxidation at C-6 in the glucitol moiety followed by a $\beta$-elimination at C-4 with the formation of glucose and 3-deoxy-*threo*-hexosulose. An expected rearrangement product (3-deoxy-*xylo*-hexonic acid) was recorded, but only in trace amounts. Evidently, these reaction schemes cannot explain the main reactions which occur during the oxygen-alkali treatment of cellobiitol.

As shown previously [1] and confirmed in the present work 3-$O$-($\beta$-D-glucopyranosyl)-D-arabinose was formed during the oxygen-alkali treatment of cellobiitol. This intermediate is very unstable in the alkaline medium. A $\beta$-elimination results in the liberation of glucose. A subsequent rearrangement of the intermediate dicarbonyl compound gives rise to the two diastereomeric 3-deoxypentonic acids [10] which were among the major reaction products derived from the glucitol moiety. These results as well as the observation that an appreciable amount of the expected fragmentation acid, 2-deoxytetronic acid, was present permit the conclusion that oxidation of the glucitol moiety to an arabinose moiety is a very important reaction path.

As expected, the relative amounts of the hexonic, pentonic, and tetronic acids were lower in the reaction mixture obtained from cellobiitol than after the treatment of glucose. On the other hand, glyceric and 2-hydroxypropionic acids were much more abundant in the run with cellobiitol. Very probably these acids are formed not only from liberated glucose, but also from the glucitol moiety.

An obvious difference, compared to the reactions which occur with sugars, cellulose and the dicarbonyl compounds referred to above, is that with alditols, straight chain compounds are the primary oxidation products. The results indicate that these are very reactive and give rise to other reaction products than those formed from the corresponding ring-closed compounds.

## REFERENCES

1. Samuelson, O. and Stolpe, L. *Svensk Papperstid.* **72** (1969) 662; **74** (1971) 545.
2. Marchessault, R. H. and Timell, T. E. *J. Polym. Sci. Part C* **2** (1963) 49.
3. Larsson, L.-I. and Samuelson, O. *Acta Chem. Scand.* **19** (1965) 1357.
4. Samuelson, O. and Strömberg, H. *Acta Chem. Scand.* **22** (1968) 1252; *Carbohyd. Res.* **3** (1966) 89.
5. Havlicek, J., Petersson, G. and Samuelson, O. *Acta Chem. Scand.* **26** (1972) 2205.
6. Petersson, G. *Tetrahedron* **25** (1969) 4437.

7. Carlsson, B., Isaksson, T. and Samuelson, O. *Anal. Chim. Acta* **43** (1968) 47.
8. Petersson, G. *Tetrahedron* **26** (1970) 3413.
9. Rexfelt, J. and Samuelson, O. *Svensk Papperstid.* **75** (1972) 299.
10. Samuelson, O. and Thede, L. *Acta Chem. Scand.* **22** (1968) 1913.
11. de Wilt, H. G. J. *Thesis*, University of Technology, Eindhoven 1969.
12. Malinen, R. and Sjöström, E. *Pap. Puu* **54** (1972) 451.
13. Lindberg, B. and Theander, O. *Acta Chem. Scand.* **22** (1968) 1782.
14. Bamford, C. H., Bamford, D. and Collins, J. R. *Proc. Roy. Soc. Ser. A* **204** (1950) 62.
15. Ericsson, B., Lindgren, B. O., Theander, O. and Petersson, G. *Carbohyd. Res.* **23** (1972) 323.
16. Dubourg, J. and Naffa, P. *Bull. Soc. Chim. France* **1959** 1353.
17. Sowden, J. C. *Advan. Carbohyd. Chem.* **12** (1957) 35.
18. Rowell, R. M. *Pulp Pap. Mag. Can.* **72** (1971) T 236.
19. Friedeman, T. E. *J. Biol. Chem.* **73** (1927) 331.
20. Ishizu, A., Lindberg, B. and Theander, O. *Carbohyd. Res.* **5** (1967) 329.
21. Isbell, H. S. *J. Res. Natl. Bur. Std.* **32** (1944) 45.
22. Ishizu, A., Lindberg, B. and Theander, O. *Acta Chem. Scand.* **21** (1967) 424.
23. Entwistle, D., Cole, E. H. and Wooding, N. S. *Text. Res. J.* **19** (1949) 527.
24. Theander, O. *Acta Chem. Scand.* **12** (1958) 1897.
25. Samuelson, O. and Thede, L. *Tappi* **52** (1969) 99.
26. Kolmodin, H. and Samuelson, O. *Svensk Papperstid.* **73** (1970) 93.
27. Minor, J. L. and Sanyer, N. J. *Polym. Sci. Part C* **36** (1971) 73.
28. Malinen, R., Sjöström, E. and Ylijoki, J. *Pap. Puu* **55** (1973) 1.
29. Kolmodin, H. and Samuelson, O. *Svensk Papperstid.* **74** (1971) 301; **76** (1973) 71.
30. Machell, G. and Richards, G. M. *J. Chem. Soc.* **1960** 1932.
31. Kolmodin, H. and Samuelson, O. *Svensk Papperstid.* **75** (1972) 369.

# Molecular Orbital Studies of L-Ascorbic Acid and Some Related Molecules

EVEN FLOOD* and P. N. SKANCKE*

*Department of Chemistry, University of Oslo, Blindern, Oslo 3, Norway*

In this work the structure and UV spectrum of L-ascorbic acid and ascorbate anion are examined through semiempirical calculations. A scheme for $\pi$-electron calculations previously described is extended to include methylene, using 1,3-cyclopentadiene as a reference system. The methylene parameters are used in calculations on $\alpha$-hydroxytetronic acid and $\alpha$-hydroxytetronate, which in the $\pi$-electron system are similar to ascorbic acid and ascorbate. The results for the UV absorption bands are close to the experimental values, the bond lengths are not so well reproduced.

The crystal and molecular structure of L-ascorbic acid (I) and ascorbate anion (II) have been determined by X-ray and neutron diffraction.[1-3] These structures display several interesting features; particularly, in the acid, the carbon-oxygen bond lengths in the two hydroxyl groups are found to be significantly different from each other. One of the purposes of this study is to investigate these structures using semiempirical LCAO–MO–SCF methods.
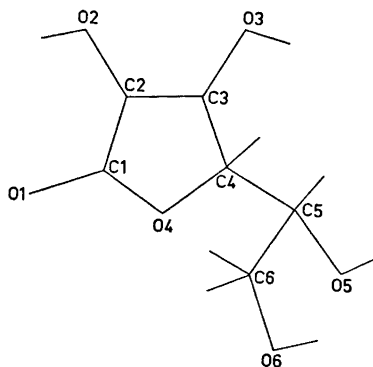


*Fig. 1.* Ascorbic acid with labelling of atoms.

* Present address: University of Tromsø, N-9000 Tromsø, Norway.
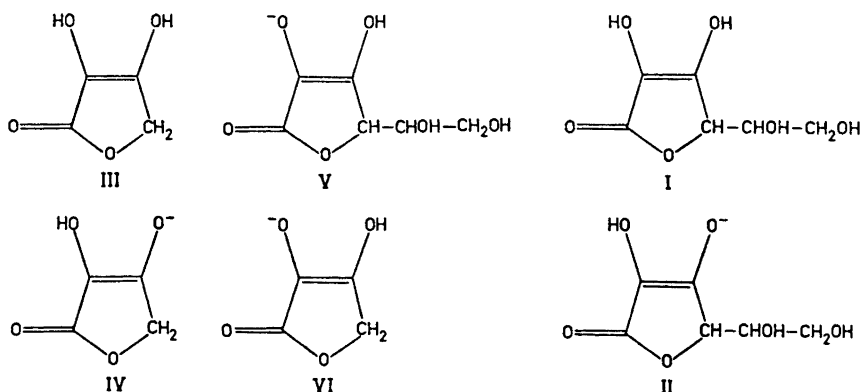
*Fig. 2.* Structure of molecules examined. I L-Ascorbic acid. II Ascorbate anion. III α-Hydroxytetronic acid. IV α-Hydroxytetronate anion.

Most of the calculations were confined to a study of the $\pi$-electrons in the ring, using the ZDO approximation. One problem that arose in this connection was to determine the effect on the electronic structure of the ring when the chain $-\text{CHOH}-\text{CH}_2\text{OH}$ was substituted by a hydrogen atom. This effect was studied using the CNDO/2 method on the molecules with and without chain.[4-6] The latter systems are α-hydroxytetronic acid (III) and α-hydroxytetronate anion (IV). The $\pi$-electron calculations were made on these two molecules.

We also wanted to include the hyperconjugation from the methylene group to the $\pi$-electrons. In order to do that, we had to extend the $\pi$-electron calculations to include parameters for methylene.

When ascorbic acid is protolyzed to ascorbate anion, this can occur in two ways, giving two different ions. Chemical evidence indicates that only one kind is formed. As a part of this work, $\pi$-electron calculations were made to find out if this can be explained from the $\pi$-electron energy differences alone.

For both (I) and (II), experimental UV-data exist. The first transition has been interpreted as a $\pi \rightarrow \pi^*$ transition in both molecules. Another purpose of this work is to calculate these transition energies. The validity of these predictions may give an indication of the extent to which the method can yield quantitatively satisfactory results in cases with several hetero atoms.

## PARAMETERS FOR THE $\pi$-ELECTRON CALCULATIONS

The $\pi$-electron calculations were made using a scheme for the semi-empirical parameters proposed for unsaturated hydrocarbons.[7] The scheme has later been extended to include the carbonyl group,[8] ether oxygen,[9] and other heteroatoms as well as hyperconjugation from the methyl group.[10] For the molecules (III) and (IV) we wanted to include the hyperconjugation from the methylene group. This was done by a method similar to the one used for methyl.[10]

As the parametrization scheme has been described in the papers already referred to, only a brief outline will be given here. The main characteristic is that the one-electron parameter $W_\mu$ is made dependent on the surroundings of the atom $\mu$. This dependence is expressed by

$$W_\mu = W°_\mu + \sum_\nu \Delta W(\nu) \tag{1}$$

where the sum is over nearest neighbours. $\Delta W_\mu(\nu)$ varies with the nature of the neighboring atom $\nu$, and, for some bonds, with the bond length $R_{\mu\nu}$ through the assumed linear relation

$$\Delta W_\mu(\nu) = \Delta W°_\mu(\nu) + \delta W(R_{\mu\nu} - R°_{\mu\nu}) \tag{2}$$

Similarly the two-center parameters $\beta_{\mu\nu}$ and $\gamma_{\mu\nu}$ are made dependent of the bond length through the relations

$$\beta_{\mu\nu} = \beta°_{\mu\nu} + \delta\beta(R_{\mu\nu} - R°_{\mu\nu}) \tag{3}$$

$$\gamma_{\mu\nu} = \gamma°_{\mu\nu} + \delta\gamma(R_{\mu\nu} - R°_{\mu\nu}) \tag{4}$$

The parameters are chosen to fit the UV-spectra and ionisation potentials (using Koopmans' theorem) of several reference molecules.

In addition to the parameters previously determined, we need for this investigation parameters for the methylene group, for the carbon-methylene bond, and for the oxygen-methylene bond. For the methylene group and the carbon-methylene bond, a procedure much similar to the one proposed for methyl [10] is followed.

The methylene group may be described by two $1s$ orbitals from the two hydrogen atoms located symmetrically about the molecular plane chosen as the $xy$-plane, one $2pz$ orbital from carbon, and one $sp^2$ orbital symmetrical about the $xy$-plane. As the group has four electrons, these atomic orbitals (AO's) can be combined to form two doubly occupied quasi AO's:

$$\sigma = c(sp^2) + d(s_1 + s_2) \tag{5}$$

$$\pi = a(pz) + b(s_1 - s_2) \tag{6}$$

where $a$, $b$, $c$, and $d$ are constants. Of these, the first has $\sigma$-symmetry and the second has $\pi$-symmetry. We see that with this description, methylene can be formally treated as a lone pair. In order to calculate $\gamma_{\mu\nu}$ from methylene to a non-neighbouring atom using the ball-approximation,[11] we had to approximate this $\pi$-orbital with two uniformly charged spheres touching each other somewhere on the line from carbon to the line connecting the hydrogen atoms.

The parameters $\gamma_{C\pi}$ and $\beta_{C\pi}$ were assumed independent of $R_{C\pi}$, and $\Delta W_\mu$-(C) was included in $W_\pi$ so the parameter determined was the total $W_\pi$, not $W°_\pi$. Thus, the following five parameters had to be determined: $\beta_{C\pi}$, $\gamma_{C\pi}$, $\nabla W_C(\pi)$, $W_\pi$ and the one-center parameter $\gamma_{\pi\pi}$.

The simplest approach to the problem, is to place the ball center in the middle of the carbon-hydrogen axis, and use the parameters for methyl, following the reasonable chemical argument that the effects from methyl and methylene must be similar. This approach has been tried giving good results [12] (see also Table 2). In the present paper the parameters were obtained from

calculations on 1,3-cyclopentadiene using experimental electronic transition energies and ionisation potentials as reference values.

The electronic transitions of cyclopentadiene have been studied both experimentally [13-15] and theoretically.[16] In the theoretical study referred to, a modified CNDO method with configuration interaction was used. The results obtained indicate that of the four lowest electronic transitions, one band at 7.4 eV represents a $\sigma \to \pi^*$ transition, while the other three bands at 5.34, 6.2, and 7.9 eV correspond to $\pi \to \pi^*$ transitions. Our calculations seem to confirm this, as the value 7.4 eV is very difficult to reproduce as a $\pi \to \pi^*$ transition.

CNDO/2 calculations on cyclopentadiene showed that for the occupied orbitals the coefficients for the $pz$ orbital are larger than for $(s_1 - s_2)$. This led us to place the ball center somewhat closer to the carbon atom than to the hydrogen-hydrogen axis. We chose the distance 0.26 Å from the former, and 0.35 Å from the latter.

The parameter $\gamma_{\pi\pi}$ was difficult to determine using the spectral values as reference. Predicted UV-spectral values and ionisation potential are very insensitive to changes in this parameter. Accordingly, a precise value of this parameter is not important in the present context. To obtain a value we normalized the $\pi$-orbital given by (6), assuming $a/b = 5/4$ for the reason men-

*Table 1.* Parameters for methylene, compared with parameters for methyl.[10] Ball radius in Å and integrals in eV.

| | | | |
|---|---|---|---|
| $\gamma_{CH_3-CH_3}$ | 10.01 | $\gamma_{CH_2-CH_2}$ | 7.42 |
| $W_{CH_3}$ | $-12.0$ | $W_{CH_2}$ | $-13.38$ |
| $\Delta W_C(CH_3)$ | 0.50 | $\Delta W_C(CH_2)$ | 0.636 |
| $\beta_{C-CH_3}$ | $-1.38$ | $\beta_{C-CH_2}$ | $-1.07$ |
| $\gamma_{C-CH_3}$ | 5.70 | $\gamma_{C-CH_2}$ | 5.70 |
| Ball radius | 1.76 | Ball radius | 2.40 |
| | | $\gamma_{O-CH_2}$ | 7.00 |
| | | $\beta_{O-CH_2}$ | $-1.25$ |
| | | $\Delta W_{CH_2}(O)$ | $-0.16$ |
| | | $\Delta W_O(CH_2)$ | 1.51 |

*Table 2.* Semiempirical calculations on 1−3 cyclopentadiene. All values in eV.

| | Exp. values | CNDO | PPP[a] | PPP[b] | PPP[c] |
|---|---|---|---|---|---|
| Ionisation potential | $-8.58^d$ | | $-8.60$ | $-8.60$ | $-8.58$ |
| Transition energies | 5.34 | 4.8 | 5.51 | 5.51 | 5.36 |
| | 6.2 | 6.3 | 6.4 | 6.4 | 6.5 |
| | 7.9 | 7.9 | 7.8 | 7.8 | 7.9 |

[a] Parameters for methyl used for methylene. [b] Same as above, but with $\gamma_{\pi\pi} = 7.42$. [c] Methylene parameters developed in this work. [d] Ref. 17.

tioned above. We then decomposed the integral as a sum of integrals over $2pz$, $s_1$, and $s_2$. Three-center integrals were omitted, and the one- and two-center integrals were estimated from correlation corrected values for $(pzpz|pzpz)$ and $(ss|ss)$. By this method, we arrived at the value 7.42 eV. As seen in Table 2, the change from 10.01 eV for methyl has very little effect. The remaining four parameters were determined so as to give the best fit to the experimental values. The results are given in Tables 1 and 2.

The method used to estimate the parameters $\gamma_{O\pi}$, $\beta_{O\pi}$, $\Delta W_O(\pi)$ and $\Delta W_\pi(O)$ are as follows:

The $\Delta W$ values were assumed to be the same as for the $C-O$ and $C-C$ groups. As the $W_\pi$ determined for methylene is the total value, we estimated an effective $\Delta W_\pi(O)$ from the formula

$$W_\pi(O,C) = W_\pi(C,C) - \Delta W_\pi(C) + \Delta W_\pi(O) = W_\pi(C,C) - \Delta W_C(C) + \Delta W_C(O) \quad (7)$$

where the last two terms give the effective $\Delta W_\pi(O)$ used in the calculation. The value of $\beta_{O\pi}$ was obtained from the relation

$$\beta_{CO}/\beta_{CC} = \beta_{\pi O}/\pi C \quad (8)$$

where all the $\beta$-values were taken at the same bond length, 1.50 Å found through the linear relation (3).

*Table 3.* $\pi$-Electron parameters used in the calculations.

| Carbon-carbon | | Carbon-ether oxygen | | Carbonyl | |
|---|---|---|---|---|---|
| $\gamma_{CC}$ | 11.97 eV | $\gamma_{OO}$ | 18.89 eV | $\gamma_{OO}$ | 18.89 eV |
| $\gamma^\circ_{C-C}$ | 6.91 eV | $\gamma_{CO}$ | 6.20 eV | $\gamma_{CO}$ | 9.33 eV |
| $\delta\gamma_{CC}$ | $-3.99$ eV/Å | | | | |
| $\beta_{CC}$ | $-2.42$ eV | $\beta_{CO}$ | $-1.80$ eV | $\beta_{CO}$ | $-2.46$ eV |
| $\delta\beta_{CC}$ | 3.05 eV/Å | | | | |
| $W_C$ | $-9.84$ eV | $W_O$ | $-11.18$ eV | $W_O$ | $-19.60$ eV |
| $\Delta W_C(C)$ | 0.07 eV | $\Delta W_C(O)$ | $-0.09$ eV | $\Delta W_C(O)$ | $-0.71$ eV |
| $\delta W_{CC}$ | 9.22 eV/Å | $\Delta W_O(C)$ | 1.51 eV | $\Delta W_O(C)$ | 1.30 eV |
| Ball radius | 1.47 Å | | 1.09 Å | | 1.09 Å |
| $R^\circ_{CC}$ | 1.395 Å | $R_{C-O}$ | 1.35 Å | $R_{C-O}$ | 1.22 Å |

The value of $\gamma_{O\pi}$ was interpolated from a curve with the constraints that for $R_{O\pi}=0$, $\gamma_{O\pi}=\frac{1}{2}(\gamma_{OO}+\gamma_{\pi\pi})$ and for $R_{O\pi}=4$ Å, $\gamma_{O\pi}$ was equal to the theoretical value for $\gamma_{OC}$. Interpolation for the value $R_{O\pi}=1.62$ Å gave the value 7.00 eV.

## RESULTS AND DISCUSSION

The structure of L-ascorbic acid and ascorbate anion have been examined by Hvoslef.[1–3] This structure was used as input in the CNDO/2 calculations on the molecules (I) and (II). In (III) and (IV), the ring structures of the first two were used, but the ring was assumed planar and the methylene group was

assumed to be symmetrical about the molecular plane. As the ring is not exactly planar, this assumption introduced some small changes in the oxygen-methylene bond.

The premise for the $\pi$-electron calculations is that the electronic structure of the ring is not much changed when the chain $-\mathrm{CHOH}-\mathrm{CH_2OH}$ is substituted by hydrogen. To test this assumption, CNDO/2 calculations on all four molecules were made, and the charges on the nuclei were compared. The results of this calculation, shown in Table 4, show that the variations are small.

Table 4. CNDO/2 results for charge distributions.

|       | (I)    | (II)   | (III)  | (IV)   |
|-------|--------|--------|--------|--------|
| O(4)  | 6.2414 | 6.3032 | 6.2333 | 6.2774 |
| C(1)  | 3.6213 | 3.6356 | 3.6220 | 3.6356 |
| O(1)  | 6.3224 | 6.4459 | 6.3176 | 6.4193 |
| C(2)  | 3.9961 | 4.1515 | 3.9900 | 4.1561 |
| O(2)  | 6.2453 | 6.2924 | 6.2437 | 6.2322 |
| C(3)  | 3.8446 | 3.7911 | 3.8421 | 3.7949 |
| O(3)  | 6.2341 | 6.4959 | 6.2326 | 6.4999 |
| C(4)  | 3.8848 | 3.9018 | 3.8858 | 3.8951 |
| C(5)  | 3.8476 | 3.8591 |        |        |
| O(5)  | 6.2407 | 6.2882 |        |        |
| C(6)  | 3.8741 | 3.8620 |        |        |
| O(6)  | 6.2577 | 6.2980 |        |        |

This indicates that the calculations made on (III) and (IV) to a good approximation are valid also for (I) and (II). The remaining calculations therefore are concentrated on the first two molecules.

From the structure of ascorbic acid, it is seen that O(2) might be protolyzed as well as O(3), forming the ions (V) and (VI). However, chemical evidence indicates O(3) as the protolytic group for the first protolysis.[3] An attempted explanation for this is that (IV) is stabilized through resonance as shown by the structures



while no similar model can be made for
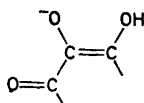
To test this resonance picture, $\pi$-electron calculations were made on (IV) and (VI). For both ions, the structure of (III) was used. From the resonance models, several predictions can be made. In (IV) the charge on O(1) will be larger than in (VI), also (VI) will have larger charge on O(2) than (IV) has on O(3). Further, in (IV) the $\pi$-bond-order for C(2) − C(3) will be smaller and for C(1) − C(2) larger than in (VI).

The result of this calculation is given in Table 7. The charge distribution is not as expected. The predicted effects are present, but they are not large enough to be considered significant. The bond orders are more as expected. The delocalized bonds implied by the resonance model for (IV) are depicted in the almost equal bond order for C(1) − C(2). In (VI) the bond is localized to C(2) − C(3).

Interesting are the high charges on C(2)/C(3) in (IV)/(VI). They indicate that if a resonance picture is used, a more complete one is
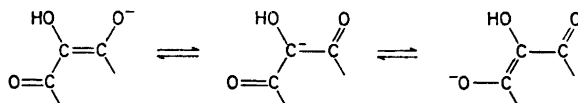


and
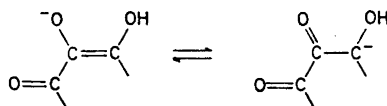


The $\pi$-electron energy for (VI) is 0.02 a.u. higher than for (IV). This corresponds to a Maxwell-Boltzmann distribution, at 300 K,

$$N_{VI}/N_{IV} \approx 10^{-10}$$

so the energy difference alone is satisfactory for explaining why only (II) is observed.

The lowest transition energies of (I) and (II) have been measured in aqueous solutions.[18] The values found are 5.08 eV for the acid and 4.67 eV for the ion. The absorption bands have been assigned to $\pi \rightarrow \pi^*$ transitions of the ring

Table 5. The two lowest calculated transition energies, with oscillator strengths, and the lowest observed bands for (III) and (IV). Energies in eV.

|  | $E$ | $f$ | $E_{obs.}$ |
|---|---|---|---|
| III | 5.20 | 0.321 | 5.08 |
|  | 4.84 | 0.212 |  |
| IV | 6.34 | 0.156 |  |
|  | 4.54 | 0.508 | 4.67 |

electrons.[18] The results of our calculations are shown in Table 5. They show that in (III) we have two transitions at 5.20 eV and 4.84 eV as the lowest values. If we take a weighted mean of these (with respect to the calculated oscillator strength $f$), we obtain 5.06 eV, which is close to the experimental value. For (IV) the calculation gives the lowest transition energy at 4.54 eV with oscillator strength $f = 0.508$. The next transition is at 6.34 eV with $f = 0.158$. It is reasonable to suppose that experimentally these two transitions will come out separately, and that the value measured corresponds to the first predicted transition.

Thus a good agreement with the experimental values is obtained. This shows that the hypothesis that the transition is $\pi \rightarrow \pi^*$ is a reasonable one, and also that the assumptions underlying the calculations used here are valid. The shift in transition energy in going from the acid to the ion is $-0.41$ eV. The calculated shift is $-0.52$ eV, in excellent agreement with the experimental value. It is somewhat surprising that the values for the ion are so well reproduced. The semi-empirical calculations are made on the isolated molecule, which means that solvent effects should be expected to give larger deviations from the theoretical values than we get here.

In the $\pi$-electron approximation, formulas have been made which give an approximate relation between mobile bond order and bond length. These are all of the form

$$R_{\mu\nu} = R^{\circ}{}_{\mu\nu} - cp_{\mu\nu}$$

where $R_{\mu\nu}$ is bond length, $R^{\circ}{}_{\mu\nu}$ is the length for a reference bond, $c$ is a constant and $p_{\mu\nu}$ is the $\pi$-electron bond order. These relations were first used in the Hückel approximation,[19] later it has been shown [20] that they can be used in the ZDO–SCF approximation. In this case the bonds examined are carbon-carbon,[7] carbon-carbonyl oxygen,[8] and carbon-hydroxyl oxygen.[9] The formulas for these bonds are

$$R_{\text{C–C}} = 1.517 - 0.18 \ p_{\text{C–C}} \tag{9}$$

$$R_{\text{C=O}} = 1.365 - 0.18 \ p_{\text{C=O}} \tag{10}$$

$$R_{\text{C–O}} = 1.430 - 0.214 \ p_{\text{C–O}} \tag{11}$$

The bond orders for (III) and (IV) were used to calculate the bond lengths, and the results were compared to the experimental values for (I) and (II). The bond order is not very sensitive to changes in the input structure, so the same input as before was used. The result of these calculations are shown in Table 6.

The deviations from the experimental values are rather large. Especially for the ion, the differences are up to $0.02 - 0.03$ Å. It is interesting, however, that the changes in the bond length in the system $O(1) - C(1) - C(2) - C(3)$ when $O(3)$ is protolyzed, is well reproduced. The most unexpected result is that the calculated bond distances for $O(2) - C(2)$ and $O(3) - C(3)$ in the acid are equal. Also the difference between the calculated and the experimental value for $C(3) - O(3)$ is $0.05$ Å.

This short bond length is connected with the fact that $O(3)$ is the protolytic oxygen. Krogh Andersen [21] has reviewed X-ray structures of several

*Table 6.* Calculated bond lengths compared to experimental values. Values in Å. *a.* (III) compared to (I). *b.* (IV) compared to (II).

| a | Bond order | Bond length calc. | exp. |
|---|---|---|---|
| C(1) − C(2) | 0.308 | 1.441 | 1.452 |
| C(2) − C(3) | 0.882 | 1.359 | 1.338 |
| C(1) − O(1) | 0.710 | 1.237 | 1.216 |
| C(2) − O(2) | 0.249 | 1.377 | 1.361 |
| C(3) − O(3) | 0.252 | 1.376 | 1.326 |
| C(1) − O(4) | 0.468 | 1.330 | 1.355 |

| b | Bond order | Bond length calc. | exp. |
|---|---|---|---|
| C(1) − O(2) | 0.571 | 1.414 | 1.416 |
| C(2) − C(3) | 0.655 | 1.399 | 1.373 |
| C(1) − O(1) | 0.602 | 1.257 | 1.233 |
| C(2) − O(2) | 0.134 | 1.401 | 1.385 |
| C(3) − O(3) | 0.599 | 1.257 | 1.287 |
| C(1) − O(4) | 0.379 | 1.349 | 1.358 |

*Table 6. c.* Changes in bond lengths when O(3) is protolyzed. Values in Å.

| | Calc. | expt. |
|---|---|---|
| C(1) − O(1) | + 0.020 | + 0.017 |
| C(1) − C(2) | − 0.027 | − 0.038 |
| C(2) − C(3) | + 0.040 | + 0.035 |

*Table 7.* Charge distribution for the $\pi$-electrons and $\pi$-bond orders in (IV) and (VI).

| Atom | (IV) | (IV) | Bond | (IV) | (VI) |
|---|---|---|---|---|---|
| C(1) | 0.6796 | 0.5507 | C(1) − C(2) | 0.571 | 0.275 |
| C(2) | 1.2886 | 0.7998 | C(2) − C(3) | 0.655 | 0.763 |
| C(3) | 0.5749 | 1.3884 | C(1) − O(1) | 0.602 | 0.677 |
| CH$_2$ | 1.9846 | 1.9922 | C(2) − O(2) | 0.134 | 0.524 |
| O(1) | 1.7173 | 1.6768 | C(3) − O(3) | 0.599 | 0.127 |
| O(2) | 1.9748 | 1.7597 | | | |
| O(3) | 1.7248 | 1.9733 | | | |
| O(4) | 1.8760 | 1.8588 | | | |

organic acids, among them α-methyltetronic acid and α,γ-dimethyltetronic acid. A linear relation is found between the bond length of the carbon-oxygen bond and the p$K_a$ of the oxygen.

One might argue that the short C−O distance is due to intermolecular forces, in this case hydrogen bonds. In the crystal where all the structure measurements have been made, several hydrogen bonds are present. These might cause perturbations. Against this hypothesis, however, is the fact that semi-empirical calculations made by Lofthus using the Hückel method with overlap give the correct difference in bond order.[22]

## REFERENCES

1. Hvoslef, J. *Acta Cryst.* **B 24** (1968) 23.
2. Hvoslef, J. *Acta Cryst.* **B 24** (1968) 1431.
3. Hvoslef, J. *Acta Cryst.* **B 25** (1969) 2214.
4. Pople, J. A., Santry D. P. and Segal, G. A. *J. Chem. Phys.* **40** (1965) S 129.
5. Pople, J. A. and Segal, G. A. *J. Chem. Phys.* **40** (1965) S136.
6. Pople, J. A. and Segal, G. A. *J. Chem. Phys.* **44** (1966) 3289.
7. Roos, B. and Skancke, P. N. *Acta Chem. Scand.* **21** (1967) 233.
8. Jensen, H. and Skancke, P. N. *Acta Chem. Scand.* **22** (1968) 2899.
9. Höjer, G. *Acta Chem. Scand.* **21** (1969) 2985.
10. Roos, B. *Acta Chem. Scand.* **21** (1967) 2318.
11. Parr, R. G. *J. Chem. Phys.* **20** (1952) 1499.
12. Maggiora, G., Johansen, H. and Ingraham, L. L. *Arch. Biochem. Biophys.* **131** (1969) 352.
13. Price, W. C. and Walsh, A. D. *Proc. Roy. Soc.* **A 179** (1941) 201.
14. Schiebe, G. and Grieneisen, H. *Z. physik. Chem.* **B 25** (1934) 52.
15. Pickett, L. W., Paddock, E. and Sackter, E. *J. Am. Chem. Soc.* **61** (1941) 1073.
16. Del Bene, J. and Jaffe, H. H. *J. Chem. Phys.* **42** (1968) 4050.
17. Streitwieser, A. *J. Am. Chem. Soc.* **82** (1960) 4123.
18. Ogata, Y. and Kosugi, Y. *Tetrahedron* **26** (1970) 4711.
19. Coulson, C. A. *Proc. Roy. Soc.* **A 169** (1939) 413.
20. Skancke, P. N. *Acta Chem. Scand.* **18** (1964) 1671.
21. Krogh Andersen, E. *Experimentelle studier over hydroxyquinoner og deres salte.* Odense Universitets forlag, 1971.
22. Lofthus, A. Physical Institute, University of Oslo. *Unpublished results.*

# Approximate Self-consistent Field Molecular Orbital Calculation on Trithiadiborolane, Dichlorotrithiadiborolane, Dimethyltrithiadiborolane, Trioxadiborolane, Dichlorotrioxadiborolane, and Dimethyltrioxadiborolane

ODD GROPEN* and PER VASSBOTN

Department of Chemistry, University of Oslo, Blindern, Oslo 3, Norway

The electronic structure of trithiadiborolane, dichlorotrithia-diborolane, dimethyltrithiadiborolane, trioxadiborolane, dichlorotrioxadiborolane and dimethyltrioxadiborolane have been investigated using the CNDO/2 method. The calculations indicate a nearly similar degree of multiplicity in the ring bonds for the two types of compounds.

The molecules $H_2S_2$ and $H_2O_2$ have been shown [1-3] to have dihedral angles of 90 and $60-90$ degrees from *trans*, respectively. Later the *cis* barriers for these molecules were calculated by *ab initio* methods [4,5] to 9.33 and 8.35 kcal/mol. The origin of these barriers are widely discussed and it is claimed that the repulsion between the lone pairs in the planar state is mainly responsible for the twisted form.[6]

In ring compounds where $S-S$ and $O-O$ bonds are present one should for the same reason expect a none-planar skeleton, except when conjugation is present in the system. In the case of conjugation one obtains a very favorable delocalization of the $\pi$-electrons, and at the same time the lone pair repulsions are reduced.

In the ring compound trioxadiborolane the boron atom is contributing to the $\pi$-system with a formally vacant $2p_z$-orbital. One should expect this vacant orbital to be especially well suited for conjugation with the $2p_z$ lone pairs on the oxygen atoms. This also seems to be the situation as trioxadiborolane has been established to have planar equilibrium.[7] Semiempirical calculations have suggested considerable $\pi$-bond orders in this ring.[8,9]

---
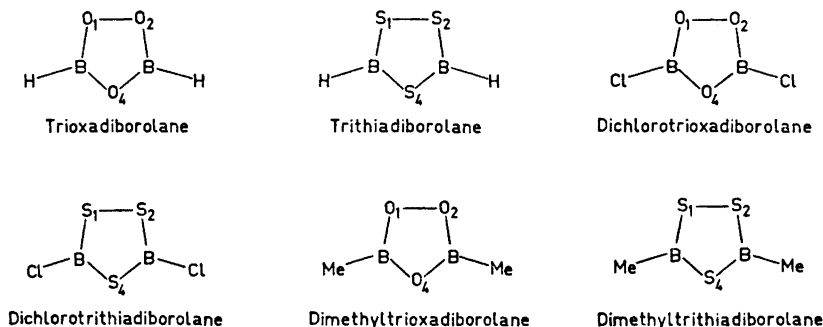
Fig. 1. Labelling of the atoms.

Lately the dichloro-1,2,4-trithia-3,5-diborolane [10] and the dimethyl-1,2,4-trithia-3,5-diborolane [11] were investigated by electron diffraction, and these compounds were also found to have at least nearly planar rings.

To study the electronic structure of these rings, and compare the degree of multiplicity in the ring bonds were either oxygen or sulfur is engaged we have performed semi-empirical calculations on the molecules $(BH)_2O_3$, $(BCl)_2O_3$, $(BCH_3)_2O_3$, $(BH)_2S_3$, $(BCl)_2S_3$ and $(BCH_3)S_3$.

## METHOD AND STRUCTURE PARAMETERS

For only three of the compounds the experimental structure is etablished.[7,10,11] For these compounds the experimental structures are used. For the other three we have made estimates of the necessary geometry parameters. Calculations with different geometries have shown the results not to be sensitive with respect to these variations.

The CNDO-method used here [12,13] is based on a minimal Slater basis for the first and second period, and including $3d$-polarization functions for the third period. Santry and Segal pointed out that calculations including $3d$-orbitals predict experimental results slightly better than without.[14] This is not surprising as several ab initio calculations have shown the importance of including $3d$-orbitals on third period atoms.[15]

Recent calculations with the CNDO-method have, however, shown some difficulties in predicting reasonable charge distribution when $d$-orbitals are included on the third period atoms.[16] We performed calculations both with $3d$-orbitals included and excluded. From these calculations we concluded that the results were not much influenced of the $d$-orbitals except from the charge distribution. Where $d$-orbitals were included a total charge transfer from sulfur to boron was predicted. This result is so unexpected that we decided to concentrate on the results obtained without $d$-orbitals on sulfur and chlorine.

## RESULTS AND DISCUSSION

a. Orbital energies. The calculated orbital energies are presented in Tables 1 and 2. We have given a tentative assignment of the molecular orbitals in terms of $\pi$-orbitals and more or less localized $\sigma$-orbitals. The proposed assignments are presented in the tables.

Disregarding the chlorine lone-pairs we found the highest filled orbital in all the oxygen rings to be a oxygen lone pair, whereas the highest filled orbital

*Table 1.* Orbital energies for the oxygen compounds. All values in a.u.

| Sym. | $(ClB)_2O_3$ Energy | Int.pr. | Sym. | $(HB)_2O_3$ Energy | Int.pr. | Sym. | $(CH_3B)_2O_3$ Energy | Int.pr. |
|------|--------|---------|------|--------|---------|------|--------|---------|
| $1a_1$ | $-1.981$ | $B-O_2$ | $1a_1$ | $-1.951$ | $B-O_2$ | $1a_1$ | $-1.929$ | $B-O_2$ |
| $2a_1$ | $-1.629$ | $B-O_4$ | $2a_1$ | $-1.388$ | $B-O_4$ | $2a_1$ | $-1.569$ | $B-O_4$ |
| $1b_1$ | $-1.374$ | $B-O_2$ | $1b_1$ | $-1.331$ | $B-O_2$ | $1b_1$ | $-1.435$ | $B-C$ |
| $3a_1$ | $-1.173$ | $B-Cl$ | $2b_1$ | $-0.948$ | $B-O_4$ | $3a_1$ | $-1.364$ | $B-C$ |
| $2b_1$ | $-1.160$ | $B-Cl$ | $3a_1$ | $-0.929$ | $O-O$ | $2b_1$ | $-1.249$ | $B-O_2$ |
| $4a_1$ | $-0.957$ | $O-O$ | $4a_1$ | $-0.923$ | $B-H$ | $1b_2$ | $-0.932$ | $\pi$ |
| $1b_2$ | $-0.949$ | $\pi$ | $1b_2$ | $-0.898$ | $\pi$ | $4a_1$ | $-0.907$ | $O-O$ |
| $3b_1$ | $-0.853$ | $B-O_4$ | $3b_1$ | $-0.689$ | $B-H$ | $3b_1$ | $-0.867$ | $B-O_4$ |
| $5a_1$ | $-0.820$ | $1p\ Cl$ | $5a_1$ | $-0.643$ | $1p\ O$ | $5a_1$ | $-0.810$ | $C-H$ |
| $4b_1$ | $-0.707$ | $1p\ Cl$ | $2b_2$ | $-0.633$ | $\pi$ | $1a_2$ | $-0.778$ | $\pi\ C-H$ |
| $2b_2$ | $-0.675$ | $\pi$ | $1a_2$ | $-0.615$ | $\pi$ | $4b_1$ | $-0.741$ | $C-H$ |
| $1a_2$ | $-0.673$ | $\pi$ | $6a_1$ | $-0.614$ | $1p\ O$ | $6a_1$ | $-0.718$ | $C-H$ |
| $6a_1$ | $-0.658$ | $1p\ O$ | $4b_1$ | $-0.597$ | $1p\ O$ | $2b_2$ | $-0.700$ | $\pi\ C-H$ |
| $7a_1$ | $-0.608$ | $1p\ O$ | | | | $5b_1$ | $-0.607$ | $C-H$ |
| $5b_1$ | $-0.581$ | $1p\ O$ | | | | $3b_2$ | $-0.598$ | $\pi$ |
| $2a_2$ | $-0.558$ | $\pi\ Cl$ | | | | $7a_1$ | $-0.584$ | $1p\ O$ |
| $3b_1$ | $-0.557$ | $\pi\ Cl$ | | | | $8a_1$ | $-0.578$ | $1p\ O$ |
| $8a_1$ | $-0.557$ | $1p\ Cl$ | | | | $2a_2$ | $-0.567$ | $\pi$ |
| $6b_1$ | $-0.552$ | $1p\ Cl$ | | | | $6b_1$ | $-0.558$ | $1p\ O$ |

*Table 2.* Orbital energies for the sulfur compounds. All values in a.u.

| Sym. | $(ClB)_2S_3$ Energy | Int.pr. | Sym. | $(HB)_2S_3$ Energy | Int.pr. | Sym. | $(CH_3B)_2S_3$ Energy | Int.pr. |
|------|--------|---------|------|--------|---------|------|--------|---------|
| $1a_1$ | $-1.345$ | $B-S_2$ | $1a_1$ | $-1.309$ | $B-S_2$ | $1a_1$ | $-1.411$ | $B-C$ |
| $1b_1$ | $-1.195$ | $B-Cl$ | $2a_1$ | $-1.034$ | $B-S_4$ | $1b_1$ | $-1.394$ | $B-C$ |
| $2a_1$ | $-1.145$ | $B-Cl$ | $1b_1$ | $-0.988$ | $B-S_2$ | $2a_1$ | $-1.245$ | $B-S_2$ |
| $3a_1$ | $-1.059$ | $B-S_4$ | $3a_1$ | $-0.835$ | $B-H$ | $3a_1$ | $-1.038$ | $B-S_4$ |
| $2b_1$ | $-0.913$ | $B-S_2$ | $2b_1$ | $-0.807$ | $B-S_4$ | $2b_1$ | $-0.924$ | $B-S_2$ |
| $3b_1$ | $-0.752$ | $B-S_4$ | $4a_1$ | $-0.706$ | $S-S$ | $3b_1$ | $-0.811$ | $B-S_4$ |
| $4a_1$ | $-0.747$ | $S-S$ | $1b_2$ | $-0.634$ | $\pi$ | $1b_2$ | $-0.804$ | $\pi_{C-H}$ |
| $1b_2$ | $-0.699$ | $\pi$ | $3b_1$ | $-0.548$ | $B-H$ | $4a_1$ | $-0.781$ | $S-S$ |
| $5a_1$ | $-0.691$ | $1p\ Cl$ | $5a_1$ | $-0.533$ | $1p\ S$ | $1a_2$ | $-0.772$ | $\pi_{C-H}$ |
| $4b_1$ | $-0.614$ | $1p\ Cl$ | $4b_1$ | $-0.482$ | $1p\ S$ | $5a_1$ | $-0.695$ | $C-H$ |
| $1a_2$ | $-0.597$ | $\pi\ Cl$ | $2b_2$ | $-0.476$ | $\pi$ | $4b_1$ | $-0.687$ | $C-H$ |
| $6a_1$ | $-0.595$ | $1p\ Cl$ | $6a_1$ | $-0.460$ | $1p\ S$ | $6a_1$ | $-0.664$ | $C-H$ |
| $2b_2$ | $-0.539$ | $\pi_{Cl}$ | $1a_2$ | $-0.443$ | $\pi$ | $2b_2$ | $-0.569$ | $\pi$ |
| $7a_1$ | $-0.500$ | $1p\ S$ | | | | $5b_1$ | $-0.494$ | $C-H$ |
| $5b_1$ | $-0.495$ | $1p\ Cl$ | | | | $7a_1$ | $-0.491$ | $1p\ S$ |
| $3b_2$ | $-0.489$ | $\pi$ | | | | $3b_2$ | $-0.456$ | $\pi$ |
| $8a_1$ | $-0.474$ | $1p\ S$ | | | | $6b_1$ | $-0.455$ | $1p\ S$ |
| $6b_1$ | $-0.474$ | $1p\ S$ | | | | $8a_1$ | $-0.432$ | $1p\ S$ |
| $2a_2$ | $-0.441$ | $\pi$ | | | | $2a_2$ | $-0.414$ | $\pi$ |

in all the sulfur compounds is a $\pi$-orbital. Also the energy of the totally symmetric $\pi$-orbital we found to be relatively lower in the oxygen compounds than in the sulfur compounds.

This tendency of the $\pi$-orbitals to have a lower energy in the oxygen compounds may indicate a slightly better delocalization in these compounds compared to the sulfur compounds.

*b. Charge distribution.* The gross atomic populations are presented in Table 3. In all rings we found a charge transfer from boron to oxygen or sulfur in the $\sigma$-skeleton, and a smaller backbond effect in the $\pi$-system.

*Table 3.* Gross atomic population.

| Atom | $(ClB)_2O_3$ | | | $(HB)_2O_3$ | | | $(CH_3B)_2O_3$ | | | $(ClB)_2S_3$ | | | $(HB)_2S_3$ | | | $(CH_3B)_2S_3$ | | |
|------|------|------|------|------|------|------|------|------|------|------|------|------|------|------|------|------|------|------|
| | $\sigma$ | $\pi$ | tot. | $\sigma$ | $\pi$ | tot. | $\sigma$ | $\pi$ | tot. | $\sigma$ | $\pi$ | tot. | $\sigma$ | $\pi$ | tot. | $\sigma$ | $\pi$ | tot. |
| O4/S₄ | 4.65 | 1.61 | 6.26 | 4.67 | 1.57 | 6.24 | 4.67 | 1.61 | 6.28 | 4.42 | 1.70 | 6.12 | 4.44 | 1.65 | 6.09 | 4.46 | 1.70 | 6.17 |
| B | 2.07 | 0.47 | 2.54 | 2.23 | 0.43 | 2.65 | 2.19 | 0.46 | 2.66 | 2.30 | 0.44 | 2.74 | 2.46 | 0.38 | 2.83 | 2.40 | 0.42 | 2.82 |
| O2/S₂ | 4.34 | 1.81 | 6.15 | 4.36 | 1.79 | 6.14 | 4.36 | 1.81 | 6.17 | 4.23 | 1.83 | 6.05 | 4.25 | 1.80 | 6.05 | 4.26 | 1.83 | 6.09 |
| Cl/H/CH₃ | 5.26 | 1.91 | 7.17 | 1.08 | | 1.08 | | | 7.05 | 5.27 | 1.88 | 7.15 | 1.07 | | 1.07 | | | 7.00 |

As has been expected the $\pi$-charge transfer into the vacant $2p_z$-orbital on boron is significant. But though the inductive effect in the $\sigma$-skeleton is different in the two types of compounds the back-bonding is almost constant.

CNDO-calculation [17] on aminoborane indicates a $\pi$-charge on boron $(-0.394)$ that is very close to our result. For borazine, however, MWH-technique [18] is predicting a boron $\pi$-charge of $-0.6162$, which should indicate a much stronger conjugation in this compound.

The charge distribution in the rings is almost unaffected by change of substituents.

*c. $\pi$-Bond order.* The bond orders from a CNDO-calculation are usually not invariant under a coordinate transformation. Using only one $2p_z$-orbital for each atom in the $\pi$-representation for a planar molecule, the obtained $\pi$-bond orders may be an indication of the relative conjugation in the systems. The obtained $\pi$-bond orders are presented in Tables 4 and 5. The numbers obtained certainly predict a conjugation in the systems.

*Table 4.* $\pi$-Bond orders for the oxygen compounds.

| Bond | $(ClB)_2O_3$ | $(HB)_2O_3$ | $(CH_3B)_2O_3$ |
|------|------|------|------|
| O – O | 0.020 | 0.033 | 0.028 |
| B – O₄ | 0.514 | 0.548 | 0.516 |
| B – O₂ | 0.537 | 0.577 | 0.536 |

Table 5. $\pi$-Bond orders for the sulfur compounds.

| Bond | $(ClB)_2S_3$ | $(HB)_2S_3$ | $(CH_3B)_2S_3$ |
|------|-------------|-------------|----------------|
| S–S | 0.040 | 0.060 | 0.046 |
| B–S$_4$ | 0.470 | 0.513 | 0.465 |
| B–S$_2$ | 0.510 | 0.569 | 0.510 |

The most striking result is the very small bond orders for the $O-O$ and $S-S$ bonds. This was earlier pointed out by Coulson for the $O-O$ bond.[8] The bond orders are, however, indicating a shortening of these bonds relative to $H_2S_2$ and $H_2O_2$ as far as conjugation is concerned. They also predict a stronger shortening of the $S-S$ bond than the $O-O$ bond relative to $H_2S_2$ and $H_2O_2$, respectively.

The experimental value for the $O-O$ bond length in hydrogen peroxide is not clear as quite different values are presented in the literature (1.475 Å[2] and 1.453 Å[1]). The $O-O$ bond length in trioxa-diborolane is found to be 1.47 Å. For the $S-S$ bond the experimental results are giving a lengthening in the ring (2.067 Å) compared to hydrogen persulfide (2.055 Å).

Coulson [8] has suggested that in $(BH)_2O_3$ the repulsion between the net charges on the oxygen atoms may give just the opposite effect of conjugation. This could be the situation for the sulfur compound too. But probably the variation in the bond lengths are not deducible from our calculations.

Considering the $\pi$-bond order one should expect a shorter $B-O_2$ $(B-S_2)$ bond than $B-O_4$ $(B-S_4)$. This is in agreement with the experimental results for the oxygen compound, but in the two experimentally investigated sulfur compounds the electron diffraction method was not conclusive.

Compared to the CNDO-calculation on the aminoborane we have higher bond orders both for the $B-O$ and the $B-S$ bonds than for the $B-N$ bond (0.305).[17]

## CONCLUSION

The results all predict a high degree of conjugation in the rings. This seems reasonable as they by experimental investigation are concluded to be planar. But what is a little unexpected is the small difference between the rings containing sulfur and oxygen. One should, however, be careful in stressing this point too far as the CNDO/2 method may give wrong conclusions. Especially the lack of $3d$-orbitals may influence the result a great deal.

On the other side, if the conjugation alone is expected to be responsible for the planarity it is not surprising to find the same effects in the sulfur compounds as in the oxygen compounds. This because the calculated barrier to internal rotation about the $S-S$ bond is even higher in hydrogen persulfide [4] than the corresponding barrier in hydrogen peroxide.[5]

We feel that both these questions and the bond length variations may be better understood through *ab initio* calculations. We are therefore now studying the molecules ($H_2B)OH$, $H_2B(SH)$, $(H_2B)O_2(BH_2)$, and $H_2BS_2BH_2$ together with the ring compounds $(BH)_2O_3$ and $(BH)_2S_3$ by *ab initio* calculations.

## REFERENCES

1. Busing, W. R. and Levy, H. A. *J. Chem. Phys.* **42** (1965) 3054.
2. Redington, R. L., Olson, W. B. and Cross, P. C. *J. Chem. Phys.* **36** (1962) 1311.
3. Winnewisser, G., Winnewisser, M. and Gordy, W. *J. Chem. Phys.* **49** (1968) 3465.
4. Veillard, A. and Demuynck, J. *Chem. Phys. Letters* **4** (1970) 476.
5. Dunning, T. H. and Winter, N. W. *Chem. Phys. Letters* **11** (1971) 194.
6. Senning, A. *Sulfur in Organic and Inorganic Chemistry*, Marcel Dekker, New York 1971, Vol. 1.
7. Brooks, W. V. F., Costain, C. C. and Porter, R. F. *J. Chem. Phys.* **47** (1967) 4186.
8. Coulson, C. A. *Acta Cryst.* **B 25** (1969) 807.
9. Leibovici, C. *J. Mol. Struct.* **11** (1972) 141.
10. Almenningen, A., Seip, H. M. and Vassbotn, P. *Acta Chem. Scand.* **27** (1973) 21.
11. Seip, H. M., Seip, R. and Siebert, W. *Acta Chem. Scand.* **27** (1973) 15.
12. Pople, J. A., Santry, D. P. and Segal, G. A. *J. Chem. Phys.* **43** (1965) 129.
13. Pople, J. A. and Segal, G. A. *J. Chem. Phys.* **44** (1966) 3289.
14. Santry, D. P. and Segal, G. A. *J. Chem. Phys.* **47** (1967) 158.
15. Mulliken, R. S. and Bowen, L. *J. Am. Chem. Soc.* **93** (1971) 6738.
16. Gropen, O. and Haaland, A. *Acta Chem. Scand.* **27** (1973) 521.
17. Armstrong, D. R., Duke, B. J. and Perkins, P. G. *J. Chem. Soc.* **1969** 2566.
18. Scherr, V. M. and Haworth, D. T. *Theoret. Chim. Acta* **21** (1971) 143.

# Synthesis of the *N*-Trityl Hexapeptide Hydrazide Corresponding to the Sequence 152—157 of the Coat Protein of Tobacco Mosaic Virus. Comparison of the Homogeneous and the Solid Phase Syntheses

JOHN HALSTRØM, KAROLY KOVÁCS
and KAY BRUNFELDT

*The Danish Institute of Protein Chemistry, Affiliated to the Academy of Technical Sciences,
4 Venlighedsvej, DK-2970 Hørsholm, Denmark*

The pentapeptide derivative benzyloxycarbonyl-threonyl-(benzyl)seryl-glycyl-prolyl-alanine methyl ester was synthesized in solution from alanine methyl ester and on a polymeric support from alanyl-resin (followed by transesterification) by stepwise chain elongation using dicyclohexylcarbodiimide and *tert*-butyloxycarbonyl amino acids. Threonine was introduced as benzyloxycarbonyl-threonine. The over-all yield was 24 % and 28 %, respectively, based on alanine, whereas the efficiency, based on the utilization of amino acids, was 28 % and 9 %, respectively. The products were shown to be identical. Finally, the deprotected pentapeptide methyl ester, obtained by catalytic hydrogenation, was condensed with trityl-tryptophan by the action of dicyclohexylcarbodiimide. The product, trityl-tryptophyl-threonyl-seryl-glycyl-prolyl-alanine methyl ester, was converted to the hydrazide by treatment with hydrazine hydrate in ethanol.

In the present synthesis of a fragment of the C-terminal part of the coat protein of Tobacco Mosaic Virus *(vulgare)* [1] (residues 152 – 157) a pentapeptide derivative, Z-Thr-Ser(Bzl)-Gly-Pro-Ala-OMe,* was used as intermediate. A comparison of its synthesis in solution and on a solid support using the Merrifield method [2] was made. A similar study has been reported for the sequence 81 – 85.[3] Experience with uncontrolled solid-phase synthesis indicates that in general, due to the accumulation of closely related products, only peptides, for which especially favourable isolation procedures are available, can be synthesized in a high state of purity. Cyclic peptides, like antamanid,[4] gramicidin S,[5] and valinomycin,[6] seem especially suited for solid-phase syn-

---

* Abbreviations used in the text: Z= benzyloxycarbonyl; Boc= *tert*-butyloxycarbonyl; Bzl= benzyl; DMF= dimethylformamide; DCC= dicyclohexylcarbodiimide.

thesis, presumably because cyclization and crystallization is an efficient purification. Unfortunately, very few free peptides can be purified by crystallization from organic solvents. However, in the preparation of protected peptides favourable crystallization properties are occasionally encountered.[7] In the rational synthesis of protected peptides for fragment condensation, the fully automated solid-phase synthesis [8] of such intermediates may be competitive with synthesis in solution. In the present case, an over-all yield of 28 % based on the C-terminal residue was obtained, compared with 24 % in solution. However, when comparing the syntheses on an economical basis, the considerable excess of protected amino acids used in the former method should be taken into account. Thus, by calculating the synthesis efficiency according to Rydon,[9] a figure of 9 % is obtained compared with 28 % in solution. Still, it should be emphasized that neither synthesis has been optimized.

## EXPERIMENTAL

Melting points are uncorrected. Ascending thin-layer chromatography was performed on commercial plates (DC-Fertigplatten, Kieselgel F 254, E. Merck AG., Darmstadt). Solvent systems: S1 (chloroform/acetic acid/methanol by volume 90/5/5), S2 (2-butanol/formic acid/water by volume 75/15/10,) S3 (2-butanol/10 % aqueous $NH_3$ by volume 85/15), S4 (1-butanol/pyridine/acetic acid/water by volume 37/25/8/30), S5 (2-methyl-2-propanol/pyridine/heptane by volume 33/13/54), and S7 (1-butanol/acetone/diethylamine/water by volume 37/37/7/19). Chromatograms were visualized by spraying with tert-butyl hypochlorite, followed by p-tolidine/potassium iodide, or by spraying with N hydrogen chloride in acetic acid, followed by ninhydrin. Optical rotation was measured on a Perkin-Elmer model 141 photoelectric polarimeter (tube length 1 dm). The resin (Bio-beads S-X2, 200 – 400 mesh) was obtained from Bio-Rad Laboratories, Richmond, California, and was chloromethylated and esterified with the first amino acid, Boc-alanine, according to the general procedure of Merrifield.[10] Methylene chloride (May and Baker, Ltd. Dagenham, Essex) was stored over potassium carbonate and distilled before use. Acetic acid ("Pronalys" glacial acetic acid, May and Baker Ltd.) was used as such. Ethanol was commercial absolute ethanol. Boc-Gly and Boc-Pro were prepared according to Schnabel [11] whose procedure was also used to prepare Z-Thr at 10°C and pH 8.2. Boc-Ser(Bzl) was purchased from the "Reanal" factory of laboratory chemicals, Budapest. Amino acid analysis was carried out on a Beckman model 120C analyzer after hydrolysis in sealed tubes at 110°C in 6 N hydrochloric acid. Unless otherwise stated, the time of hydrolysis was 24 h. Samples were not dried to constant weight prior to amino acid analysis.

## Synthesis in solution

*Boc-L-Pro-L-Ala-OMe (I).* L-Alanine methyl ester hydrochloride (41.7 g, 300 mmol) was dissolved in DMF (56 ml) and neutralized by addition of triethylamine (40 ml). During the addition, the mixture was diluted with methylene chloride (100 ml) to keep it from solidifying. Excess of volatile base was detected over the liquid surface with the aid of moist indicator paper (Neutralit, Merck). The excess was removed by addition of more L-alanine methyl ester hydrochloride (*ca.* 1 g). After further dilution with methylene chloride (100 ml), a solution of Boc-L-Pro (64.5 g, 300 mmol) in methylene chloride (250 ml) was added, and the mixture cooled to 5°C. After addition of a solution of DCC, Merck, (62.0 g, 300 mmol) in methylene chloride (100 ml), the temperature rose to 20 – 25°C for 5 – 10 min. By immersion in a cooling bath, the temperature was quickly readjusted to about 5°C and the mixture was left to stand at this temperature for 16 h. By filtration the formed dicyclohexylurea (75.0 g), m.p. 196 – 203°C, was isolated, and the filtrate was left to stand at room temperature (22 – 25°C) for 4 h. By concentration *in vacuo* to about

half volume, a further quantity of dicyclohexylurea (9.0 g) could be isolated. The total crude yield of this by-product was 84.0 g (theory: 67.2 g); it was stirred with methylene chloride (200 ml), filtered and dried at 0.1 mmHg. Yield: 68.4 g, mp. 205 – 215°C. The combined filtrates were washed with 5 % aqueous citric acid (200 ml), water (3 × 100 ml), 5 % aqueous sodium bicarbonate solution (200 ml), and water (3 × 100 ml), dried over MgSO₄, filtered and evaporated to dryness at 0.1 mmHg. The yellow syrup (90.0 g, 100 %) was covered with petroleum ether (b.p. 60 – 80°C.) and left to stand for 18 h at room temperature. The crystalline mass was recrystallized from ethyl acetate (80 ml)/petroleum ether (600 ml). Yield: 51.5 g of m.p. 79 – 81°C. Upon evaporation of the mother liquor to dryness and crystallization of the resulting syrup from ethyl acetate (20 ml)/petroleum ether (600 ml) a second crop (15.5 g, m.p. 78 – 80°C.) was obtained. Thus the total yield was 67.0 g (75 %). $[\alpha]_D^{25} = -92.3°$; $[\alpha]_{578}^{25} = -96.6°$ ($c = 1$ in methanol); $R_F S2 = 0.8$; $R_F S5 = 0.6$. (Found: C 56.2; H 8.1; N 9.3. Calc. for $C_{14}H_{24}N_2O_5$ (300.4): C 56.0; H 8.1; N 9.3.) Amino acid content (mol per 300.4 g): Pro 0.98, Ala 0.97.

*Boc-Gly-*L*-Pro-*L*-Ala-OMe (II).* I (60.0 g, 200 mmol) was dissolved in N HCl/glacial acetic acid (500 ml) and left to stand for 90 min at room temperature. Evaporation to dryness at room temperature and 0.2 mmHg left an oil (66 g), which still contained some acetic acid. It was mixed with DMF (10 ml) and kept at 0.2 mmHg and room temperature overnight. Residual acetic acid was removed by adding DMF (15 ml) and precipitating by addition of sodium dried ether (600 ml). The oil was isolated by decantation of the supernatant, and was dried at 0.2 mmHg and room temperature. Yield: 56 g (theory: 47.2 g). It was redissolved in DMF (50 ml) and neutralized by addition of a solution of triethyl amine (27 ml) in methylene chloride (50 ml). The presence of an excess of volatile base was confirmed with the aid of moist indicator paper over the liquid surface. Immediately afterwards Boc-Gly (50.0 g, 286 mmol) was added, dissolved in methylene chloride (200 ml). The mixture was rapidly cooled to − 10°C and a solution of DCC (51.5 g, 250 mmol) in methylene chloride (100 ml) was added. After standing for 1 h at − 10°C the mixture was kept at + 5°C for 4 h, and then at room temperature for 16 h. By filtration, the formed dicyclohexylurea was isolated. It was stirred with methylene chloride (200 ml), filtered and dried at 0.1 mmHg and room temperature. Yield: 51.3 g (92 %), m.p. 215 – 228°C. The combined filtrates were washed with 5 % aqueous citric acid (200 ml), water (3 × 100 ml), 5 % aqueous bicarbonate solution (200 ml), and water (3 × 100 ml), dried over magnesium sulfate, filtered and concentrated to dryness at 1.1 mmHg. The yellow syrup (69 g, 97 %) solidified to a white, compact mass during the evaporation. The product was recrystallized from hot ethyl acetate (270 ml). After standing for 1 h at + 5°C, filtration and drying at 0.1 mmHg the yield of white crystalline product was 51.2 g (72 %), m.p. 152 – 153°C. By dilution of the filtrate with petroleum ether (b.p. 60 – 80°C) (270 ml) and leaving the solution for 16 h at − 18°C a second crop was obtained (2.5 g, 3 %), m.p. 153 – 154°C. $[\alpha]_D^{25} = -110°$; $[\alpha]_{578}^{25} = -116°$ ($c = 1$ in methanol); $R_F S2 = 0.6$. An additional spot ($R_F$ 0.8) revealed the presence of a few percent of dicyclohexylurea. (Found: C 54.7; H 7.8; N 12.2. Calc. for $C_{16}H_{27}N_3O_6$ (357.4): C 53.8, H 7.6; N 11.8.) Amino acid content (mol per 357.4 g): Gly 0.99, Pro 0.99, Ala 0.99.

*HCl.Gly-*L*-Pro-*L*-Ala-OMe (III)* II(36 g, 100 mmol) was dissolved in N HCl/glacial acetic acid (250 ml) and left to stand for 1 h at room temperature. Upon evaporation to dryness *in vacuo*, a crystalline residue was obtained. Recrystallization from methanol-abs. ether afforded a white crystalline product (28 g, 95 %) of m.p. 209°C. $[\alpha]_D^{25} = -110°$; $[\alpha]_{578}^{25} = -118°$ ($c = 1$ in methanol). $R_F S2 = 0.2$ (trace of urea at 0.8). (Found: C 44.7; H 6.9; N 14.2; Cl 12.0. Calc. for $C_{11}H_{20}N_3O_4Cl$ (293.8): C 45.0; H 6.9; N 14.3; Cl 12.1.)

*Boc-*L*-Ser(Bzl)-Gly-*L*-Pro-*L*-Ala-OMe (IV).* III(75 g, 255 mmol) was suspended in a mixture of DMF (43 ml) and methylene chloride (170 ml) and treated with triethylamine (36 ml, 259 mmol) under vigorous stirring. After addition of Boc-L-Ser(Bzl) (95 g, 322 mmol) dissolved in methylene chloride (110 ml) the suspension was stirred for 25 min at room temperature and then cooled to − 15°C. A solution of DCC (66 g, 320 mmol) in methylene chloride (110 ml), precooled to 0°C, was added, and the mixture was stored at − 20°C for 2 h with occasional shaking, and then left overnight at 5°C. After 2 more days at room temperature the mixture was filtered, the filtrate concentrated to dryness, and the resulting oil redissolved in ethyl acetate (800 ml). Undissolved dicyclohexylurea was removed by filtration, and the filtrate was washed with 5 % aqueous citric acid (3 × 100 ml), water (3 × 100 ml), 5 % aqueous sodium bicarbonate solution (2 × 100 ml), and water (3 × 100 ml), and dried over magnesium sulfate. Upon concentrating the

filtrate to dryness, a yellowish oil (140 g, 100 %) was obtained. Attempts at crystalli-
zation from various solvent mixtures (ether/petroleum ether, ethyl acetate/petroleum
ether, and methanol/water) were unsuccessful. Being fairly homogeneous (one major
spot in TLC, $R_F S2 = 0.7$; $R_F S5 = 0.4$) apart from contamination by some dicyclohexyl-
urea, the product was used in the following step without further purification.

*HCl.L-Ser(Bzl)-Gly-L-Pro-L-Ala-OMe (V).* IV (160 g) was dissolved in 1.7 N HCl/
glacial acetic acid (500 ml). After 30 min at room temperature, carbon dioxide evolution
had ceased, and the solution was concentrated to dryness *in vacuo*. The resulting syrup
was triturated three times with hot ethyl acetate. By this process, two impurities, de-
tected by TLC (S5), were removed, leaving a yellowish, crystalline product (120 g, 85 %),
m.p. 80 – 82°C d. (Found: C 53.8; H 7.0; N 11.5; Cl 8.2. Calc. for $C_{21}H_{31}N_4O_6Cl$ (471.0):
C 53.6; H 6.6; N 11.9; Cl 7.5.) $[\alpha]_D^{25} = +10.7$; $[\alpha]_{578}^{25} = +11.0$ $(c = 1$ in methanol).
$R_F S2 = 0.3$ (impurity at 0.4); $R_F S5 = 0.0$.

*Z-L-Thr-L-Ser(Bzl)-Gly-L-Pro-L-Ala-OMe (VI).* V (94.2 g, 200 mmol) was suspended
in a mixture of methylene chloride (100 ml) and ethyl acetate (300 ml) and cooled to
0°C before the addition of triethylamine (30 ml, 216 mmol) under vigorous stirring.
When the mixture had reached room temperature it was filtered (25.9 g triethylammo-
nium chloride, 95 %), and to the filtrate was added Z-L-Thr (75.9 g, 300 mmol). To the
resulting solution, after cooling to 0°C, was added solid DCC (61.8 g, 300 mmol), and the
mixture was left overnight at 5°C. After dilution with ethyl acetate (100 ml), the mixture
was left at room temperature for further 24 h. Upon filtration was obtained a white prod-
uct (160 g), contaminated with dicyclohexylurea. Treatment with boiling methanol
(200 ml) afforded dicyclohexylurea (57 g, 85 %) of m.p. 229 – 223°C and a filtrate, which
upon standing at room temperature overnight deposited a crystalline product (84 g,
63 %) of m.p. 153 – 156°C (with sintering at 85°C). Recrystallization of this product
(100 g) twice from hot methanol (220 ml) gave pure VI (85 g) of m.p. 88 – 90°C, re-solidi-
fication and final m.p. 160 – 161°C. The identity of the substance was proved by a mixed
melting point determination with the purified product from the solid-phase synthesis (X).

Another synthesis of VI was carried out, starting from II, without isolation of III,
IV, and V. The condensation of Z-L-Thr and oily V, was carried out in methylene chloride,
and after filtration of dicyclohexyl urea the filtrate was washed with 5 % aqueous citric
acid, water, 5 % aqueous sodium bicarbonate solution and water, dried over magnesium
sulfate and concentrated to dryness. The resulting yellowish oil was crystallized from
methanol/ethyl acetate/petroleum ether (200/150/600 ml) to yield a white product
(42 % based on II) of m.p. 81 – 83°C. $[\alpha]_D^{25} = -68.0°$; $[\alpha]_{578}^{25} = -71.6°$ $(c = 1$ in methanol).
(Found: C 58.7; H 6.8; N 10.7; O 24.1; $OCH_3$ 4.4. Calc. for $C_{33}H_{43}N_5O_{10}$ (669.7): C 59.2;
H 6.5; N 10.5; O 23,9; $OCH_3$ 4.6.) Amino acid content (mol per 669.7 g): Thr 0.89,
Ser 0.75, Gly 0.92, Pro 0.90, Ala 0.92.

On recrystallization from hot methanol, crystals of m.p. 85 – 89°C, re-solidification
above 90°C and final m.p. 161 – 162°C were obtained. In TLC, complete agreement was
also found between the two products and the purified product from the solid-phase
synthesis (X).

*HCl.L-Thr-L-Ser-Gly-L-Pro-L-Ala-OMe (VII).* VI (6.7 g, 10 mmol) was dissolved in
methanol (70 ml), and 2.8 N methanolic HCl (6.0 ml) was added. Palladium black, ob-
tained by reducing $PdCl_2$ (2.0 g) with formic acid, was added, and hydrogen was passed
through the mixture with vigorous stirring at room temperature and atmospheric pres-
sure. After 4 h the evolution of $CO_2$ had virtually ceased. After further 2 h, the mixture
was filtered, and the filtrate concentrated to dryness. The resulting colourless oil was
dissolved in water (50 ml) and lyophilized. Yield of white, amorphous material: 4.7 g
(92 %). M.p. 103 – 106°C d. $[\alpha]_D^{25} = -92.5$; $[\alpha]_{578}^{25} = -96.6$ $(c = 1$ in methanol); homo-
geneous in TLC $R_F S2 = 0.1$; $R_F S4 = 0.4$; $R_F S7 = 0.5$. (Found: C 42,3; H 6.5; N 13.4;
O 30.3; Cl 9.4; $OCH_3$ 7.1. Calc. for $C_{18}H_{32}N_5O_8$ · $1.3HCl,H_2O$ (510.9): C 42.3; H 6.8; N 13.7;
O 28.2; Cl 9.0; $OCH_3$ 6.1.) Amino acid content (mol per 510.9 g): Thr 0.99, Ser 0.94, Pro
1.00, Gly 1.00, Ala 1.01.

*Trt-L-Trp-L-Thr-L-Ser-Gly-L-Pro-L-Ala-OMe (VIII).* VII [4.2 g, 8.2 mmol (10.7
mmol HCl)] was dissolved in DMF/$H_2O$ (10 ml/1ml) by warming. A solution of N-trityl-
L-tryptophan diethyl ammonium salt (5.7 g, 11.0 mmol) in methylene chloride (35 ml)
was added, and the resulting solution cooled to $-18°C$. DCC (2.3 g, 11.2 mmol) was
added, and the reaction mixture was left to stand, with occasional shaking, at $-18°C$
for 20 h, at $+5°C$ for 48 h, and at room temperature for 4 days. After filtration of the

wine-red mixture, and washing on the filter with methylene chloride, dicyclohexylurea (1.5 g, 60 %) of m.p. 231 – 232°C was isolated.

The combined filtrate and washings were diluted to 100 ml with methylene chloride and washed with water (8 × 25 ml) in a separatory funnel. The organic phase was then concentrated to dryness, and the residue precipitated from methylene chloride by addition of ethyl acetate and petroleum ether, b.p. 60 – 80°C. By filtration and drying to 0.01 mmHg the product was obtained as a yellow solid, (4.0 g, 56 %), m.p. 145 – 155°C. In TLC one large UV-absorbing spot at $R_F S1 = 0.2$ and $R_F S5 = 0.1$ was present. On treatment with chlorine/tolidine, an additional spot was found at $R_F S1 = 0.8$ and $R_F S5 = 0.6$ corresponding to dicyclohexyl urea.

Conditions for preparative silica gel column separation were evaluated using mixtures of chloroform and methanol. By application of the crude product (2.5 g) on a 20 × 4 cm column filled with Kieselgel HF 254 (Merck) (80 g), and elution first with chloroform and then with 5 % methanol in chloroform, a fraction (1.8 g) was obtained, which was almost chromatographically pure (TLC in S1). A previously eluted fraction (0.3 g) contained the impurities with high TLC $R_F$ values. A second portion (1.1 g), applied on the same column, gave 0.9 g of almost pure product. The entire purified quantity (2.7 g) was applied on a fresh column, and eluted in the same way. Yield: 2.5 g (35 % overall yield) of a glass, m.p. 100 – 110°C d. Chromatographically homogeneous, $R_F S1 = 0.2$; $R_F S5 = 0.1$; $[\alpha]_D^{25} = -80.4$; $[\alpha]_{578}^{25} = -84.1$ ($c = 1$ in methanol). On microanalysis, the sum of C, H, N, and O was 89.3 % due to contamination with inorganic material from the silica gel. The values were corrected to give 100 %. (Found C 65.5; H 6.3; N 11.6; O 16.6; OCH$_3$ 3.4. Calc. for $C_{48}H_{55}N_7O_9$ (874.0): C 66.0; H 6.3; N 11.2; O 16.5; OCH$_3$ 3.6.) Amino acid content (mol per 874 g): Trp 0.74, Thr 0.83, Ser 0.80, Gly 0.86, Pro 0.86, Ala 0.86. (8 h hydrolysis).

*Trt*-L-*Trp*-L-*Thr*-L-*Ser*-*Gly*-L-*Pro*-L-*Ala*-$N_2H_3$ *(IX)*. VIII (1.7 g, 1.9 mmol) was dissolved in methanol (15 ml). After addition of hydrazine hydrate (0.6 ml, 12 mmol), the solution was left to stand for 24 h at room temperature. It was then concentrated to half volume on a water-bath at 65 – 70°C, and left for further 24 h. In TLC VIII ($R_F S2 = 0.6$) had disappeared, and only one other spot, visible with UV, acid/ninhydrin, and hypochlorite/tolidine was present at $R_F S2 = 0.3$. By precipitation with water, and reprecipitation from ethanol/water, a suspension (400 ml) was obtained, which could only be filtered with difficulty. On centrifugation for 20 min at 2000 rpm the product was isolated as a yellow glass (1.0 g) of m.p. 160 – 170°C. By concentration of the supernatant to dryness *in vacuo* and precipitating the residue from ethanol/water a further quantity (0.4 g) was obtained. Chromatographically homogeneous; $R_F S2 = 0.3$; $R_F S3 = 0.2$; $R_F S7 = 0.7$. The combined fractions were precipitated from ethanol (5 ml) by addition of ethyl acetate (40 ml) and ether (200 ml). Yield of almost white product: 1.3 g (79 %) and m.p. 160 – 165°C, decomposition above 200°C (evolution of gas, and red colour). $[\alpha]_D^{25} = -76.2$; $[\alpha]_{578}^{25} = -78.2$ ($c = 1$ in methanol). (Found: C 64.5; H 6.0; N 13.9; O 15.5. Calc. for $C_{47}H_{55}N_9O_8 \cdot \frac{1}{2} C_2H_5OH$ (897.1): C 64.3; H 6.5; N 14.1; O 15.2.)

## Synthesis on a solid support

*Z*-L-*Thr*-L-*Ser(Bzl)*-*Gly*-L-*Pro*-L-*Ala*-*OMe* *(X)*. Boc-L-alanyl-resin (45 g, 0.47 mmol Ala/g) was placed in a 1 litre reaction vessel and subjected to four cycles of deblocking, neutralization and coupling. The sequence and quantities of the reagents and solvents employed were the same as previously described.[12] Chloride determination by Volhard titration of the neutralization filtrates gave the following values: 22.3, 23.5, 20.6, and 20.8 mmol Cl⁻. The quantities of amino acid derivatives and coupling reagent employed were: Boc-L-Pro (21.5 g, 100 mmol) and DCC (20.6 g, 100 mmol), Boc-Gly (17.5 g, 100 mmol) and DCC (20.6 g 100 mmol). To reduce waste of the Ser derivative, a smaller excess was used. To ensure a quantitative reaction, two consecutive couplings were carried out, without an intermediate deblocking step. Accordingly: Boc-L-Ser(Bzl) (14.7 g, 50 mmol) and DCC (10.3 g, 50 mmol), having reacted for 90 min were followed, after filtration, by Boc-L-Ser(Bzl) (7.4 g, 25 mmol) and DCC (5.1 g, 25 mmol), which were left to react overnight. In order to reduce the extent of O-acylation Z-L-Thr was also coupled twice, but before each addition of DCC, the derivative solution was filtered

off, and the resin washed three times with methylene chloride. Thus, Z-ʟ-Thr (10.0 g, 40 mmol) and DCC (8.2 g, 40 mmol) was followed by Z-ʟ-Thr (5.0 g, 20 mmol) and DCC (4.1 g, 20 mmol) without an intermediate deblocking step. The combined filtrate and washings following the first salt-formation period were concentrated to dryness at 0.1 mmHg. The recovery of Z-ʟ-Thr was only 1.3 g, m.p. 99 – 101°C. Like Ser, Thr was allowed to react first for 90 min, and then overnight.

After the last coupling the resin was washed once with methylene chloride, six times with ethanol, and once with methanol. Then the entire quantity of peptide resin was transferred to a 3-litre beaker where it was transesterified [13] for 12 h at room temperature in 1.5 litres of 1 N methanolic triethylamine. Concentration of the filtrate to dryness at 0.1 mmHg yielded a colourless oil (13.5 g, 90 % based on the first Volhard titration value). Crystallization from methanol/ethyl acetate/petroleum ether (60 – 80°C) (40 ml/ 40 ml/800 ml) gave a nearly white product (11.2 g, 75 %) of m.p. 150 – 154°C. $[\alpha]_D^{25} = -66.6$; $[\alpha]_{578}^{25} = -70.0°$ ($c = 1$ in methanol). $R_F S2 = 0.6$; $R_F S4 = 0.6$. Inhomogeneous in S5 with $R_F = 0.4$ and 0.7 and in S1 with $R_F = 0.4$ and 0.7, respectively. (Found: C 58.6; H 6.8; N 10.7; O 24.1; $OCH_3$ 5.2. Calc. for $C_{33}H_{43}N_5O_{10}$ (669.7): C 59.2; H 6.5; N 10.5; O 23.9; $OCH_3$ 4.6.) Amino acid content (mol per 669.7 g): Thr 0.87, Ser 0.77, Gly 0.89, Pro 0.95, Ala 0.96.

A second treatment of the resin with 1.5 l of 1 N methanolic triethylamine resulted in the isolation of only 0.5 g of a brown oil. The resin was washed with methanol and dried at 0.1 mmHg. Yield: 40.8 g.

The protected peptide (10.1 g) was dissolved in methanol (25 ml) by warming, and the solution was left to stand at room temperature, in an open flask, for 2 – 3 days. The crystalline product (1.5 g) was collected by filtration, and the yellow filtrate and washings were left to stand for a further period of time. By repeating this procedure for some weeks, a white, crystalline product (4.0 g) of m.p. 161 – 163°C (with sintering at 80 – 90°C) was isolated. A second fraction (1.6 g), m.p. 156 – 160°C, without sintering, was isolated in the same way, leaving a yellow, oily residue.

The combined fractions (5.6 g) could now be recrystallized from hot methanol (20 ml). Yield of white crystals: 4.2 g (28 % over-all). M.p. 86 – 89°C, re-solidification above 90° and final m.p. 162 – 163°C. A mixed melting point with VI was unchanged. In TLC (S1) X was unchanged after being heated to 150°C for 2 min.

## REFERENCES

1. Anderer, F. A., Wittmann-Liebold, B. and Wittmann, H. G. *Z. Naturforsch.* **20b** (1965) 1203.
2. Merrifield, R. B. *Rec. Progr. Hormone Res.* **23** (1967) 451.
3. Pettit, G. R. and Jones, W. R. *J. Org. Chem.* **36** (1971) 870.
4. Wieland, T., Birr, C. and Flor, F. *Ann.* **727** (1969) 130.
5. Halstrøm, J. and Klostermeyer, H. *Ann.* **715** (1968) 208; Klostermeyer, H. *Chem. Ber.* **101** (1968) 2823.
6. Gisin, B. F., Merrifield, R. B. and Tosteson, D. C. *J. Am. Chem. Soc.* **91** (1969) 2691.
7. Meienhofer, J., Trzeciak, A., Havran, R. T. and Walter, R. *J. Am. Chem. Soc.* **92** (1970) 7199.
8. Brunfeldt, K., Halstrøm, J. and Roepstorff, P. *Acta Chem. Scand.* **23** (1969) 2830.
9. Bodanszky, M. In Weinstein, B., Ed., *Peptides, Chemistry and Biochemistry, Proc. 1st. Amer. Peptide Symp. Yale 1968*, Dekker, New York 1970, pp. 1 – 15.
10. Merrifield, R. B. *Biochemistry* **3** (1964) 1385.
11. Schnabel, E. *Ann.* **702** (1967) 188.
12. Brunfeldt, K. and Halstrøm, J. *Acta Chem. Scand.* **24** (1970) 3013.
13. Beyerman, H. C., Hindriks, H. and de Leer, E. W. B. *Chem. Commun.* **1968** 1668.

# The 4-Aminobutyrate Pathway and 2-Oxoglutarate Dehydrogenase in *Escherichia coli*

HEIKKI ROSENQVIST, HEIKKI KASULA
OSMO REUNANEN and VEIKKO NURMIKKO

*Department of Biochemistry, University of Turku, SF-20500 Turku 50, Finland*

The major metabolites of the citric acid cycle and related systems in a wild type *E. coli* grown aerobically on glucose are succinate and lactate. The changes in the levels of the two metabolites were very similar in a batch culture of *E. coli* grown on glucose and on certain other carbon sources. A plot of succinate content against lactate content gave a straight line which may be interpreted as an indication of the energetic function of the system, though during these conditions the role of the citric acid cycle may be mainly biosynthetic.

The specific activities of the enzymes of the 4-aminobutyrate pathway [glutamate decarboxylase (EC 4.1.1.15), 4-aminobutyrate oxoglutarate transaminase (EC 2.6.1.19), succinate semialdehyde dehydrogenase (EC 1.2.1.16)], and of 2-oxoglutarate dehydrogenase (EC 1.2.4.2) are maximal in the lag phase, but decrease in the exponential phase to increase again in the stationary phase. This may be taken as evidence of the repression caused by glucose.

Under a great variety of conditions the rates of synthesis of 4-aminobutyrate oxoglutarate transaminase and succinate semialdehyde dehydrogenase were found to be similar, which may show that the syntheses are regulated coordinately.

In spite of 2-oxoglutarate dehydrogenase and the 4-aminobutyrate pathways being alternatives, only glutamate decarboxylase functions contrary to 2-oxoglutarate dehydrogenase.

Amarasingham and Davis [1] have observed that 2-oxoglutarate dehydrogenase is absent from anaerobic cultures and probably almost absent from cells of *E. coli* grown aerobically on glucose or lactate. They proposed that the citric acid cycle is composed of a biosynthetic branch leading to 2-oxoglutarate, while a reductive branch leads to succinate in *E. coli*. 2-Oxoglutarate dehydrogenase provides an alternative connection between these branches. During anaerobic growth this connection is not necessary, according to Amarasingham and Davis.[1]

Studies with *E. coli* and some other facultative anaerobes have suggested that under anaerobic conditions 2-oxoglutarate causes the end-product inhibition of citrate synthase (EC 4.1.3.7).[2,3] It has been suggested [2] that a similar

inhibition may also exist in cells of *E. coli* grown aerobically. It seems reasonable to suppose that the same mechanism operates also under aerobic conditions or otherwise the supposed end-product inhibition on citrate synthase is not easily explained. On the other hand, it has been found that succinate is accumulated in cells of *E. coli* grown aerobically with glucose as carbon source.[4] These findings may indicate that the citric acid cycle is modified to a branched non-cyclic pathway even under aerobic conditions.

The end-product of the biosynthetic branch of the citric acid cycle, 2-oxoglutarate, does not accumulate.[4] The role of the biosynthetic branch is to synthesize glutamate, because the mutants of *Bacillus subtilis* lacking aconitase
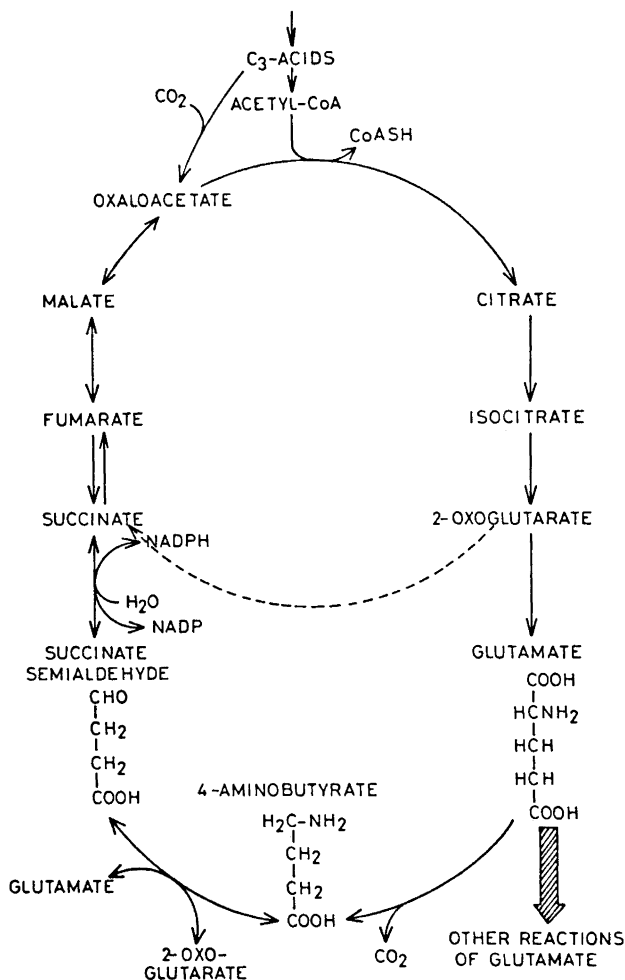


*Fig. 1.* The alternativeness of 4-aminobutyrate bypath and 2-oxoglutarate dehydrogenase (broken line) connecting the reductive and the biosynthetic branch in *E. coli.*

(EC 4.2.1.3)[5,6] and aconitase and isocitrate dehydrogenase (EC 1.1.1.28)[5] or *E. coli* lacking citrate synthase [7] cannot grow on glucose without glutamate, or arginine and proline, which are metabolized to glutamate. Glutamate accumulates during the growth of *E. coli* [8] and some other microorganisms [9,10] when growing on glucose aerobically. When grown on glucose aerobically *E. coli* U5/41 has high levels of glutamate [8] and succinate.[4]

On the other hand, it has been found that *E. coli* demonstrates activity of the enzymes of the 4-aminobutyrate bypass, which metabolizes glutamate *via* its decarboxylation to 4-aminobutyrate, transamination of the 4-aminobutyrate to succinate semialdehyde, and oxidation of the latter to succinate.[11-14] The pathway is catalyzed by glutamate decarboxylase, 4-aminobutyrate oxoglutarate transaminase, and succinate semialdehyde dehydrogenase, respectively (Fig. 1).

When *E. coli* is grown aerobically there are two different pathways connecting the biosynthetic and the reductive branches of the cycle: one through glutamate and the 4-aminobutyrate bypass and the other directly from 2-oxoglutarate to succinate catalyzed by 2-oxoglutarate dehydrogenase (Fig. 1).

This paper presents some results concerning interrelationships of 2-oxoglutarate dehydrogenase and the 4-aminobutyrate bypass of the citric acid cycle in *E. coli* under different growth conditions.

## MATERIALS AND METHODS

*Cultivation of Escherichia coli.* A wild-type *E. coli*, U5/41, was used in the experiments. Its origin and maintenance are reported earlier.[15] The organism was grown in a glucose-mineral salt medium, which was aerated with a mechanical stirrer. The experimental details have been published earlier.[4] When grown anaerobically, $N_2$ was bubbled in the stoppered bottle through the medium, which was shaken in a rotatory shaker (model A from E. Buehler, Tübingen, Germany) at 200 rpm at 37°. The pH was kept at 7.0 with 1.0 M NaOH. The supplements were 25 mM added to the minimal medium. Additional information is given in the legend to the figures.

The turbidity of the medium was measured with a photoelectric Klett-Summerson colorimeter, by using red filter No. 62 (590 – 660 nm).

*Preparation of cell-free extracts.* The samples were removed at different growth phases and centrifuged at 4000 *g* for 10 min and the cells were washed once with cold (+4°C) 0.9 % (w/v) sodium chloride solution. After that the cells were recentrifuged at 6000 *g* for 10 min. The cell pellet was stored at −28°C until ultrasonic treatment (MSE Ultrasonic Disintegrator, 60 W, 20 kHz; Measuring & Scientific Equipments Ltd, Crawley, England) was made for 2 min at 0°C in 2 ml of 20 mM $Na_2HPO_4 - KH_2PO_4$-buffer (pH 7.0) containing 0.01 % (v/v) 2-mercaptoethanol. The suspension was centrifuged (6000 *g*) at 10°C for 10 min and the cell-free extract was used immediately.

The extracts were also dialyzed against the sonication buffer for 12 h at 4°C. We found no significant differences between the dialyzed and non-dialyzed extracts in the assays of 2-oxoglutarate dehydrogenase, succinate dehydrogenase, glutamate decarboxylase, and succinate semialdehyde dehydrogenase. 4-Aminobutyrate oxoglutarate transaminase lost its activity when dialyzed. Therefore, to remove endogenous substrates from the non-dialyzed crude extracts used in the determinations of the activities of succinate semialdehyde dehydrogenase and 4-aminobutyrate oxoglutarate transaminase, the reaction mixtures were allowed to stand in the cuvettes without the substrates for 40 min at room temperature.

*Enzyme, protein, succinate and lactate assays.* All spectrophotometric enzyme assays were performed in 1 ml quartz cuvettes (light path, 1 cm) at 30°C. Enzyme reactions were continuously followed in a Unicam SP. 800B spectrophotometer (Unicam Instruments Ltd, England) fitted to Philips PM 8000 recorder (full scale 10 mV).

2-Oxoglutarate dehydrogenase was assayed, by using a modification of the procedure described by Holms and Bennett, [16] in a reaction mixture containing L-cysteine-HCl (3.3 mM), CoA (0.33 mM), thiamine pyrophosphate (0.33 mM), KCN (5 mM), NAD (1.17 mM), 2-oxoglutarate (adjusted to pH 7.0 with NaOH) and 0.17 M tris buffer, pH 7.5. The reaction was started by the addition of NAD and 2-oxoglutarate and was followed at 340 nm. The KCN solution was prepared at 30 mM and brought to pH 7.5 with HCl. When 2-oxoglutarate dehydrogenase was assayed in preparations from cells grown aerobically on glucose all the mentioned reagents with the exception of 2-oxoglutarate were added to a reaction cuvette; in a blank L-cysteine-HCl, thiamine pyrophosphate, and 2-oxoglutarate were also absent. The reaction was initiated by the addition of 2-oxoglutarate to both cuvettes. The reason for this procedure was the fact that in the cell-free extract of the cells grown aerobically on glucose there was no linear base line activity before the initiation of the reaction, possibly owing to some other reaction, which did not need L-cysteine-HCl and thiamine pyrophosphate. This uneven base line was typical only of cells of E. coli (not, e.g., of Pseudomonas fluorescens UK-1) grown on glucose aerobically (not anaerobically).

4-Aminobutyrate oxoglutarate transaminase, NADP-specific succinate semialdehyde dehydrogenase,[17] and succinate dehydrogenase (EC 1.3.99.1)[18] were measured spectrophotometrically by methods similar to those previously published.

The enzymatic activity of glutamate decarboxylase was monitored by determining the rate of release of $^{14}CO_2$ from DL-glutamic-1-$^{14}C$ acid (New England Nuclear, 575 Albany Street, Boston, Mass. 02118, USA) with a liquid scintillation counter (Decem-NTL,[314] Wallac Oy, Turku, Finland). The procedure was based on a method described elsewhere.[19] The following modifications were made: the reactions were carried out in stoppered scintillation counting vials containing reaction tubes and 0.5 ml ethanolamine-ethylene glycol monomethyl ether (1:2 (v/v)) solution in the bottom of the vial to absorb $^{14}CO_2$. The reaction was initiated by injecting 0.5 ml of cell-free extract through a rubber stopper into the reaction tube; the vials were shaken properly and put into a waterbath of 38°C. Other reagents were prewarmed at 38°C for 1 h. After 10 min the reaction was stopped by injecting 0.4 ml of 2.5 M $H_2SO_4$ into the reaction tube. After being shaken (30 min) at room temperature, the reaction tube was removed and 10 ml of scintillation fluid was added.

The protein content of the extracts was estimated by a modified method of Heepe et al.[20] 4 ml of 0.4 M sulphosalicylic acid was added to a test tube containing 1 ml of enzyme preparation. The content of the tube was mixed and the turbidity of the samples was measured after 10 min in a Klett-Summerson colorimeter by using a filter 42 (390 – 440 nm).

The extractions and the determinations of succinate and lactate were performed as described earlier[4] except that before harvesting, the cultures were cooled with crushed ice.


RESULTS


As has been stated earlier,[4] the major metabolites of the citric acid cycle and related systems in E. coli grown on glucose aerobically are succinate and lactate.

The changes in the levels of succinate and lactate in E. coli are rather similar during batch cultivation in a simple glucose-mineral salt medium. The levels are high in the lag phase, but decrease in the exponential phase to increase again at the end of the exponential and particularly in the stationary phase (Fig. 2a). The decreases in the contents of both succinate and lactate in the late exponential phase compared with the lag phase are about 75 %.

When E. coli is grown aerobically on glucose, the 4-aminobutyrate bypass (glutamate decarboxylase, 4-aminobutyrate oxoglutarate transaminase, and succinate semialdehyde dehydrogenase) is in operation (Fig. 2b). In the lag phase the specific activities of the above mentioned enzymes and 2-oxo-
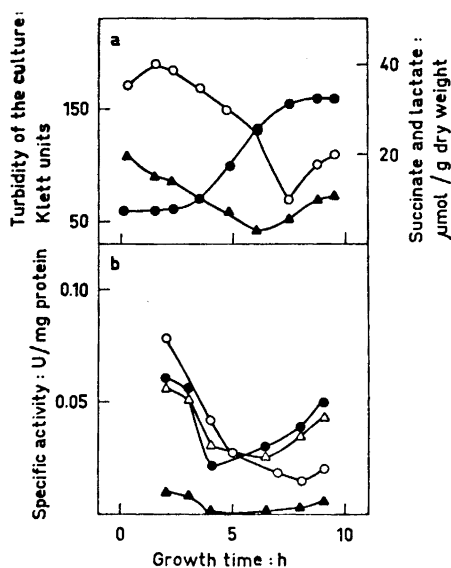
*Fig. 2.* The contents of succinate and lactate and the specific activities of the enzymes of the 4-aminobutyrate bypath and 2-oxoglutarate dehydrogenase during batch cultivation of *E. coli* U5/41 in a simple glucose-mineral salt medium. The cells were harvested to the presented growth from the glucose-mineral salt medium in the stationary phase. a. (●) Turbidity of growth medium; (O) succinate ($\mu$mol/g dry weight); (▲) lactate ($\mu$mol/g dry weight). b. (●) 2-Oxoglutarate dehydrogenase; (O) glutamate decarboxylase; (▲) 4-aminobutyrate oxoglutarate transaminase; (▲) succinate semialdehyde dehydrogenase. The specific activity of glutamate decarboxylase (O) is divided by 2.
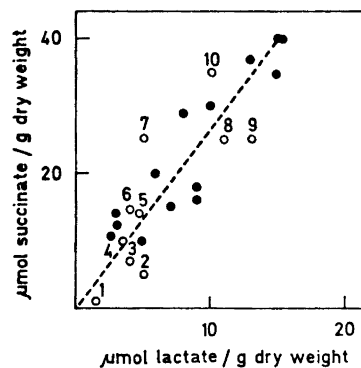
*Fig. 3.* The contents of succinate *versus* the contents of lactate. ●, glucose grown cells, which are harvested in the different points of the growth curve (redrawn from Fig. 2a); O, cells grown on different carbon sources harvested in the late exponential phase. Carbon sources: (1) glutamate, (2) aspartate, (3) 4-aminobutyrate, (4) 2-oxoglutarate, (5) acetate, (6) citrate, (7) pyruvate, (8) lactate, (9) fumarate, and (10) malate.

glutarate dehydrogenase are at their highest. During the lag and the early exponential phases the activities of the enzymes are decreasing until they increase again in the late exponential phase. In order to investigate possible variations of succinate and lactate levels in the energetic or biosynthetic citric acid cycle, *E. coli* U5/41 was grown to the late exponential phase on different carbon sources. The levels of succinate and lactate decreased while grown on glutamate, 4-aminobutyrate or aspartate compared with the levels in *E. coli* grown on glucose in the exponential phase (Fig. 3).

The reason for the decreasing levels of succinate was revealed when *E. coli* was grown on glutamate or 4-aminobutyrate. The specific activities of 2-oxoglutarate dehydrogenase, glutamate decarboxylase, 4-aminobutyrate oxo-

glutarate transaminase, and NADP-specific succinate semialdehyde de-
hydrogenase were estimated during the batch cultivation.

When cultures were grown on glutamate, the specific activity of 2-oxo-
glutarate dehydrogenase increased about 6-fold from the beginning of the
growth period to the end (Fig. 4a). Because the non-cyclic pathway [1] is
evidently not in function in *E. coli* grown on glutamate the high activities of
2-oxoglutarate dehydrogenase (Fig. 4a) and succinate dehydrogenase (un-
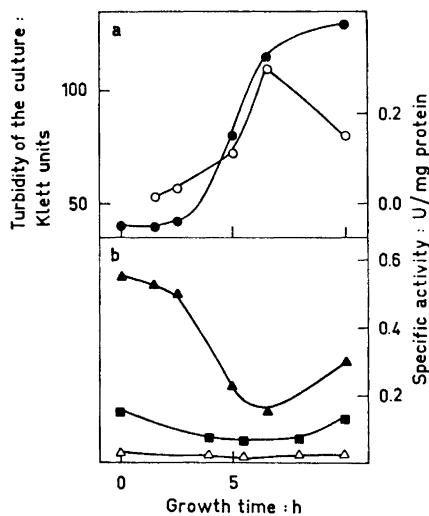


*Fig. 4.* The specific activities of 2-oxo-
glutarate dehydrogenase, glutamate de-
carboxylase, 4-aminobutyrate oxoglutarate
transaminase, and succinate semialdehyde
dehydrogenase during the growth of *E. coli*
U5/41 on glutamate and 4-aminobutyrate.
The cells were precultivated in glucose-
mineral medium to the stationary phase.
Carbon sources: (a) glutamate; (b) 4-
aminobutyrate; ●, 2-Oxoglutarate de-
hydrogenase; O, glutamate decarboxylase;
▲, 4-aminobutyrate oxoglutarate trans-
aminase; △, succinate semialdehyde de-
hydrogenase.
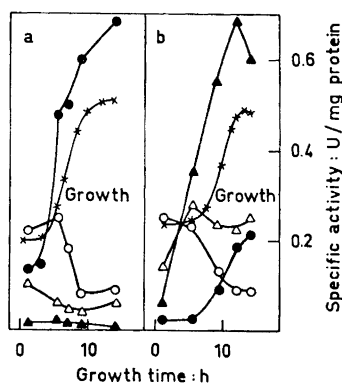
*Fig. 5.* The specific activities of 2-oxo-
glutarate dehydrogenase, glutamate de-
carboxylase, 4-aminobutyrate oxoglutarate
transaminase, and succinate semialdehyde
dehydrogenase during batch cultivation of
*E. coli* U5/41 on succinate as carbon source.
(a) ●, Turbidity of the culture; O, 2-
oxoglutarate dehydrogenase (b) ▲, glu-
tamate decarboxylase; △, 4-aminobutyr-
ate oxoglutarate transaminase; ■, suc-
cinate semialdehyde dehydrogenase.

published data) may cause the low level of succinate. At the same time the
activities of the enzyme of the 4-aminobutyrate bypath decreased (Fig. 4a)
and on the basis of the determinations of the enzyme activities *in vitro* it
seems that during these conditions the carbon flux through 4-aminobutyrate
bypath is decreased.

In *E. coli* grown with 4-aminobutyrate as a carbon source 4-aminobutyrate
oxoglutarate transaminase was induced because the specific activity increased
about 11-fold (Fig. 4b). The level of NADP-specific succinate semialdehyde de-

hydrogenase increased too, but only 1.6-fold (Fig. 4b). The activity of glutamate decarboxylase decreased (Fig. 4b) which is understandable because *E. coli* may not necessarily need it when grown on 4-aminobutyrate. 2-Oxoglutarate dehydrogenase activity increased also at the end of the growth (Fig. 4b). This may explain the low level of succinate in cells grown on 4-aminobutyrate. The situation is comparable with that of *E. coli* grown on succinate (Fig. 5). 4-Aminobutyrate is metabolized through 4-aminobutyrate bypath to succinate, which is rapidly metabolized further.

To test this, *E. coli* was grown on succinate (Fig. 5), and the activity of 2-oxoglutarate dehydrogenase (Fig. 5a) was found to increase until the late exponential phase of growth and after that to decrease. At the same time the activities of glutamate decarboxylase, 4-aminobutyrate oxoglutarate transaminase, and succinate semialdehyde dehydrogenase changed but in opposite directions (Fig. 5b).

This may indicate that when *E. coli* is grown on succinate, the 4-aminobutyrate bypass is used more as 2-oxoglutarate dehydrogenase activity decreases and *vice versa*. The content of succinate is not reported because succinate of the medium might have shown in our gas chromatographic determinations.

It has been stated [1] that 2-oxoglutarate dehydrogenase was absent when *E. coli* was grown anaerobically but that it did appear in an aerobic growth. To reveal possible changes in the enzymes of the 4-aminobutyrate bypass owing to the aeration of the growth medium, the specific activities of 2-oxoglutarate dehydrogenase, glutamate decarboxylase, 4-aminobutyrate oxoglutarate transaminase, and succinate semialdehyde dehydrogenase were estimated in *E. coli* U5/41 grown aerobically and anaerobically.

*Table 1.* The specific activities of the enzymes of the 4-aminobutyrate bypath, 2-oxoglutarate dehydrogenase and succinate dehydrogenase, in the late exponential phase of *E. coli* U5/41 grown aerobically and anaerobically on glucose.

| Enzyme | Specific activity: U/mg protein | |
|---|---|---|
| | aerobic | anaerobic |
| 2-Oxoglutarate dehydrogenase | 0.031 | — |
| Succinate dehydrogenase | 0.130 | 0.070 |
| Glutamate decarboxylase | 0.090 | 0.730 |
| 4-Aminobutyrate oxoglutarate transaminase | 0.019 | 0.005 |
| Succinate semialdehyde dehydrogenase | 0.055 | 0.017 |

The specific activities of 2-oxoglutarate dehydrogenase, succinate dehydrogenase, 4-aminobutyrate oxoglutarate transaminase, and succinate semialdehyde dehydrogenase were higher in aerobiosis than in anaerobiosis, whereas the activity of glutamate decarboxylase was markedly higher in anaerobic growth (Table 1).

### DISCUSSION

The citric acid cycle is a typically aerobic reaction pathway, though part of the citric acid cycle is functional in some anaerobes.[21,22] Facultative anaerobes like *E. coli* have an incomplete citric acid cycle during anaerobic and perhaps sometimes during aerobic conditions.[1,23] According to these reports there was no 2-oxoglutarate dehydrogenase activity during anaerobic growth. It was stated earlier that *Micrococcus lactilyticus* produces succinate dehydrogenase, which catalyzes the reduction of fumarate much faster than the oxidation of succinate.[24,25] Later in *E. coli*[26] and *Streptococcus faecalis*[27] fumarate reductase was isolated, which differs from succinate dehydrogenase in its structure and function. When *E. coli* is grown on glucose aerobically the level of succinate is considerably higher than the levels of the other metabolites of the citric acid cycle.[4] The accumulation of succinate appears to be associated with the lack of activity of 2-oxoglutarate dehydrogenase (Fig. 2b). In a mutant of *Bacillus subtilis* lacking 2-oxoglutarate dehydrogenase it is associated with the activity of fumarate reductase.[5]

It is apparent that the role of the reductive branch of the non-cyclic pathway is also energetic, because it removes excess reductive power, which is seen in the accumulation of succinate. The pool sizes may change during the cooling of the medium with crushed ice and the centrifugation for 10 min before the extraction of succinate and lactate. Therefore the obtained values may not reflect the real steady-state pool sizes. In spite of that, the levels of succinate and lactate change in the same directions during the growth of *E. coli* (Fig. 2a). D-Lactate dehydrogenase (EC 1.1.1.28) and succinate dehydrogenase make use of the same respiratory chain together with NADH dehydrogenases in *E. coli*[28] and the former enzymes have affect partly on the accumulation of lactate and succinate, respectively. The changes in the levels of lactate and succinate are almost similar in the batch culture of *E. coli* grown on glucose and on different carbon sources (Fig. 3). Because D-lactate dehydrogenase and succinate dehydrogenase take part in the respiratory chain the line in the figure may be interpreted as an indication of energetic character of the system, though our opinion is that, during these conditions, the preferred role of the citric acid cycle may be mainly biosynthetic (*e.g.* for the synthesis of glutamate). However, this does not exclude the possibility of energetic control.

During aerobic conditions the specific activities of the enzymes of the 4-aminobutyrate bypath and 2-oxoglutarate dehydrogenase decrease at the beginning of the growth phase and increase in the stationary phase, where the concentration of glucose is apparently small (Fig. 2b). This may be taken as an evidence of the repression by glucose.[13]

When *E. coli* U5/41 was grown on glutamate (Fig. 4a) the synthesis of 2-oxoglutarate dehydrogenase was induced considerably, while the activities of the enzymes of the 4-aminobutyrate bypass were decreasing. The same tendency appeared when *E. coli* U5/41 was grown with succinate as the carbon source (Fig. 5a and b). In these cases it seems obvious that 2-oxoglutarate dehydrogenase and 4-aminobutyrate bypath are the alternative pathways, which are regulated so that when the 4-aminobutyrate bypath is

active the activity of 2-oxoglutarate dehydrogenase is low. This is not, however, always the case. During the preparation of our manuscript Dover and Halpern [12] have reported that a wild type *E. coli* K-12 (CS 101A) cannot grow with 4-aminobutyrate as a carbon source owing to its inability to transport 4-aminobutyrate into the cell. In our studies, wild type *E. coli* U5/41 (and K-12 W 3001) started to grow on 4-aminobutyrate after about a 5 h lag phase during which the activities of 4-aminobutyrate oxoglutarate transaminase, succinate semialdehyde dehydrogenase, and 2-oxoglutarate dehydrogenase increased considerably (Fig. 4b). It seems that glutamate decarboxylase is the only enzyme of the 4-aminobutyrate bypass the function of which is contrary to 2-oxoglutarate dehydrogenase. This is also seen in Table 1.

When *E. coli* U5/41 was grown aerobically and anaerobically on glucose, the activity of glutamate decarboxylase in the latter case was about 70 % higher than in the former, where no activity of 2-oxoglutarate dehydrogenase was found (Table 1). The activities of 4-aminobutyrate oxoglutarate transaminase and succinate semialdehyde dehydrogenase are smaller in anaerobic conditions when the culture is grown on glucose. The two enzymes function like 2-oxoglutarate dehydrogenase in this case. All the enzymes of the 4-aminobutyrate bypass need not necessarily be regulated in the same way.

When 4-aminobutyrate was used as a carbon source, the syntheses of 4-aminobutyrate oxoglutarate transaminase and NADP-specific succinate semialdehyde dehydrogenase were induced (Fig. 4b). The induction of the enzymes of 4-aminobutyrate breakdown may suggest that the catabolism of amines could regulate the above mentioned enzymes (Fig. 4b). This does not, however, mean that the bypass has no meaning when *E. coli* is grown on glucose. In *E. coli*, succinate semialdehyde dehydrogenase has both NAD- and NADP-specific activity (unpublished data). The NADP-specific activity in our studies *in vitro* was found to be higher when grown on glucose.

Glycolysis and the citric acid cycle are the main pathways that provide both energy and many precursors for cell biosynthesis. It has been assumed that with adequate glucose, at least in an organism such as *E. coli* with high aerobic and anaerobic rate of glycolysis, enough energy is produced in the Embden-Meyerhof pathway and that the role of the cycle in producing energy is small.[1,23,29,30] The low activity of 2-oxoglutarate dehydrogenase in the exponential phase may support this view (Fig. 2b). In these conditions NADPH produced by succinate semialdehyde dehydrogenase instead of NADH cannot be used directly in the respiratory chain. Because the preferred role of the citric acid cycle is not perhaps to produce energy under these conditions, the NADP-specific enzyme might be energetically more advantageous.

## REFERENCES

1. Amarasingham, C. R. and Davis, B. D. *J. Biol. Chem.* **240** (1965) 3664.
2. Weitzman, P. D. J. and Dunmore, P. *Fed. Eur. Biochem. Soc. Lett.* **3** (1969) 265.
3. Wright, J. A., Maeba, P. and Sanwal, B. D. *Biochem. Biophys. Res. Commun.* **29** (1967) 34.

4. Rosenqvist, H., Kallio, H. and Nurmikko, V. *Anal. Biochem.* **46** (1972) 224.
5. Fortnagel, P. and Freese, E. *J. Bacteriol.* **95** (1968) 1431.
6. Ramos, F., Wiame, J. M., Wyants, J. and Bechet, J. *Nature* **193** (1962) 704.
7. Ashworth, J. M., Kornberg, H. L. and Nothmann, D. L. *J. Mol. Biol.* **11** (1965) 654.
8. Raunio, R. and Rosenqvist, H. *Acta Chem. Scand.* **24** (1970) 2737.
9. Raunio, R. and Rosenqvist, H. *Suomen Kemistilehti* **B 43** (1970) 8.
10. Tempest, D. W., Meers, J. L. and Brown, C. M. *J. Gen. Microbiol.* **64** (1970) 171.
11. Fonda, M. L. *Biochemistry* **11** (1972) 1304.
12. Dover, S. and Halpern, Y. S. *J. Bacteriol.* **109** (1972) 835.
13. Dover, S. and Halpern, Y. S. *J. Bacteriol.* **110** (1972) 165.
14. Cabaldon, M., Lacomba, T. and Mayor, F. *Rev. Espan. Fisiol.* **26** (1970) 225.
15. Nurmikko, V. and Laaksonen, S. *Suomen Kemistilehti* **B 34** (1961) 7.
16. Holms, W. H. and Bennet, P. M. *J. Gen. Microbiol.* **65** (1971) 57.
17. Jacoby, W. B. (1962) *Methods Enzymol.* **5** (1962) 765.
18. Veeger, C., DerVartanian, D. V. and Zeylemaker, W. P. *Methods Enzymol.* **13** (1969) 81.
19. Hager, L. P. *Methods Enzymol.* **A 17** (1970) 857.
20. Heepe, F., Karte, H. and Lambrecht, E. *Hoppe-Seyler's Z. Physiol. Chem.* **286** (1951) 207.
21. Gottschalk, G. and Barker, H. A. *Biochemistry* **5** (1966) 1125.
22. Stern, J. R., Hegre, C. S. and Bambers, G. *Biochemistry* **5** (1966) 1119.
23. Gray, C. T., Wimpenny, J. W. T. and Mossman, M. R. *Biochim. Biophys. Acta* **117** (1966) 33.
24. Warringa, M. G. P. J. and Guiditta, A. *J. Biol. Chem.* **230** (1958) 111.
25. Warringa, M. G. P. J., Smith, D. H., Guiditta, A. and Singer, T. P. *J. Biol. Chem.* **230** (1958) 97.
26. Hirsch, C. A., Raminsky, M., Davis, B. D. and Lin, E. C. C. *J. Biol. Chem.* **238** (1963) 3770.
27. Aue, B. J. and Deibel, R. H. *J. Bacteriol.* **93** (1967) 1770.
28. Barnes, E. M. and Kaback, H. R. *J. Biol. Chem.* **246** (1971) 5518.
29. Cox, G. B., Newton, N. A., Gibson, F., Snoswell, A. M. and Hamilton, J. A. *Biochem. J.* **117** (1970) 551.
30. Sanwal, B. D. *Bacteriol. Rev.* **34** (1970) 20.

# $^{13}$C-NMR Spectra of Phenyl-substituted Azoles:
# a Conformational Study

MIKAEL BEGTRUP

*Department of Organic Chemistry, Technical University of Denmark, DK-2800 Lyngby, Denmark*

$^{13}$C-NMR Spectra of a number of 1-phenyl-pyrazoles and 1-phenyl-1,2,3-triazoles have been obtained. The effects of substitution with methyl, chlorine, or bromine on $\delta$-values and coupling constants have been measured. The chemical shifts of the benzene carbon atoms depend on the dihedral angle between the rings, a consistency obtaining also in 2-phenyl-1,2,3-triazoles, 1-, 2-, or 4-phenyl-imidazoles, 1-phenyl-pyrrole, and in 1- or 5-phenyl tetrazoles. The parameters most susceptible to changes in the dihedral angle are $\delta_{ortho-C}$ and the difference $\delta_{meta-C} - \delta_{ortho-C}$. Values for these parameters have been determined and their usefulness for conformational studies of phenyl substituted azoles demonstrated.

In unhindered phenyl-substituted azoles, azines, or benzenes the $\pi$-electrons are extensively delocalized over both rings. Steric factors, such as bulky substituents may, however, impede delocalization as a result of augmented torsional energy barriers.[1-10]

The pattern of the phenyl ring protons in the $^1$H-NMR-spectra: multiplet in highly delocalized systems, singlets, or nearly so, in less flexible systems, has been widely used in conformational studies of biphenyls,[1] 2-phenyl-pyridines,[2] 3-phenyl-pyridazines,[3] 2-phenyl-triazines,[2] 3-phenyl-tetrazines,[2] 1-phenyl-pyrazoles,[4-8] 1-phenyl- and 2-phenyl-1,2, 3-triazoles,[7,9] 1-phenyl- and 4-phenyl-1,2,4-triazoles,[7] 1-phenyl-tetrazoles,[7] and 5-phenyl-tetrazoles.[10] However, exceptions to the pattern are known. Thus, in contrast to 2-phenyl-imidazole,[11,12] 1-phenyl-imidazole, an extensively delocalized system,[11,13,14] exhibits a phenyl group singlet at $\delta$ 7.4 (*cf.* Experimental). Conversely, the phenyl group of 1-methyl-2-phenyl-imidazole with an expected higher torsional energy barrier,[12] appears as a multiplet, (see Experimental).

The marked deshielding of the *o*-protons of the phenyl groups in delocalized systems may be caused by several factors the relative weights of which are poorly understood.[1,4,5,7,8,10,15] Presumably, the anisotropy effects induced by the phenyl-substituted ring play a major role. Hence, $^1$H-NMR-spectroscopy

is not an infallible method for conformation analysis of biaromatic systems. The high susceptibility of $^{13}$C-NMR-signals to variation in electron densities of the individual carbon atoms, paired with their relatively small sensitivity to anisotropy factors,[16a,17a] renders $^{13}$C-NMR-spectroscopy a potentially useful tool in studying the extent of delocalization in such systems. We have confirmed experimentally the virtues of $^{13}$C-spectroscopy for this purpose and report the results from studies of a number of phenyl-substituted pyrazoles, imidazoles, 1,2,3-triazoles, and tetrazoles.

## RESULTS

The proton-noise-decoupled $^{13}$C-NMR-data of a series of methyl-, chloro-, and bromo-substituted phenyl-azoles are presented in Table 1.

The signals of 1-phenyl-pyrazole *1a*, 1-phenyl-3-bromo-pyrazole *1c*, 1-phenyl-4-bromo-pyrazole *2c*, and 1-phenyl-5-bromo-pyrazole *3c* were assigned through the proton-undecoupled spectra (Table 2). The signals with the largest splittings were ascribed to the heterocyclic carbon atoms.[17b] The signals which solely exhibited small couplings were assigned to quaternary carbon atoms. Thus, C-3* of *1c* and C-5 of *3c* appeared as broad doublets, and C-4 of *2c* as a triplet. In *1c*, *2c*, and *3c* it was found that $\delta_{C-3} > \delta_{C-5} > \delta_{C-4}$. Consequently, this order is assumed to be valid also in 1-phenyl-pyrazole *1a*. The signal which only exhibited multiplet fine structure due to small couplings was assigned to C-1′. The other benzene carbon atoms showed, besides large $^1J_{CH}$ couplings, smaller coupling constants; the latter were used for the assignments. This fine structure is dominated by coupling to protons in the *m*-positions due to the fact that $J_{CCCH} > J_{CCH}$ and $J_{CCCCH}$ in benzene derivatives.[17c] Thus the signal, exhibiting triplet fine structure in the doublet branches, was attributed to C-4′, the triplet pattern arising from coupling with the two identical *m*-protons. In addition, the C-4′ signal had a lower intensity than signals corresponding to C-2′ and C-3′. The signal with doublet fine structure in its doublet branches, was attributed to C-3′, the small doublets arising from coupling to one *m*-proton. The doublet branches due to C-2′ appeared as frequently blurred triplets or quartets. The fine splitting is caused by coupling to two different *m*-protons. A representative spectrum, illustrating the identification, is shown in Fig. 1.

In the proton-noise-decoupled spectra of *1a*, *1c*, *2c*, and *3c* the intensity of the signals decreased in the order C-3′ > C-2′ > C-4′ > C-3 and C-4 > C-5 > C-1′. Carbon-atoms carrying a substituent appeared with strongly reduced intensity due to loss of Overhauser-enhancement and increase in relaxation time.[16b] The order of intensities was used to identify the signals of the methyl- and chloro-pyrazoles *1d*, *3d*, *1b*, *2b*, and *3b*. The signals of the dihalogeno- and trihalogeno-pyrazoles and of the benzyl-pyrazoles (Table 1) were identified in the same way. If the identity of a signal was considered uncertain, or if

---

* The heterocyclic carbon atoms are numbered according to the IUPAC nomenclature.[18] The phenyl carbon atoms are denoted with a dash. Counting starts with the substituted atom (C-1′).

*Table 1.* 13C-NMR chemical shifts ($\delta$ ppm) of phenyl-substituted azoles.

| Compound[a] | C-2 | C-3 | C-4 | C-5 | C-1' | C-2' | C-3' | C-4' | $CH_2$ or $CH_3$ |
|---|---|---|---|---|---|---|---|---|---|
| 1-Phenyl-pyrrole[b] | 119.0 | 110.1 | | | 140.4 | 120.2 | 129.1 | 125.3 | |
| 1-Benzyl-pyrazole [30] | | 139.2 | 105.7 | 129.0 | 136.3 | 127.4 | 128.5 | 127.7 | 55.7 |
| 1-Benzyl-3-chloro-pyrazole [31] | | 138.9 | 105.1 | 130.9 | 135.3 | 127.7 | 128.6 | 128.0 | 56.3 |
| 1-Benzyl-4-chloro-pyrazole [31] | | 137.5 | 110.1 | 126.8 | 135.4 | 127.5 | 128.6 | 128.0 | 56.7 |
| 1-Benzyl-5-chloro-pyrazole [31] | | 139.5 | 104.9 | 128.2 | 135.8 | 127.2 | 128.6 | 127.7 | 52.5 |
| 1-Phenyl-pyrazole *1a* [32, b] | | 140.7 | 107.3 | 126.2 | 140.7 | 118.8 | 129.1 | 126.0 | |
| 1-Phenyl-3-chloro-pyrazole *1b* [31] | | 141.4 | 106.8 | 128.2 | 139.3 | 118.5 | 129.2 | 126.6 | |
| 1-Phenyl-4-chloro-pyrazole *2b* [33] | | 139.0 | 112.1 | 124.5 | 139.4 | 118.7 | 129.1 | 126.6 | |
| 1-Phenyl-5-chloro-pyrazole *3b* [34] | | 140.3 | 106.3 | 126.9 | 138.3 | 124.7 | 128.6 | 128.0 | |
| 1-Phenyl-3,5-dichloro-pyrazole *5b* [35] | | 140.7 | 105.6 | 128.1 | 137.2 | 124.7 | 128.8 | 128.4 | |
| 1-Phenyl-3-bromo-pyrazole *1c* [31] | | 127.9 | 110.4 | 128.4 | 139.4 | 118.8 | 129.2 | 126.7 | |
| 1-Phenyl-4-bromo-pyrazole *2c* [36] | | 141.3 | 95.5 | 126.8 | 139.4 | 118.8 | 129.4 | 129.9 | |
| 1-Phenyl-5-bromo-pyrazole *3c* [31, a] | | 141.1 | 110.2 | 112.5 | 138.5 | 125.4 | 128.7 | 128.2 | |
| 1-Phenyl-3,4-dibromo-pyrazole *4c* [31] | | 128.5 | 98.9 | 129.4 | 138.9 | 118.6 | 129.4 | 127.3 | |
| 1-Phenyl-3,5-dibromo-pyrazole *5c* [37] | | 128.8 | 112.5 | 114.0 | 138.1 | 125.4 | 128.8 | 128.2 | |
| 1-Phenyl-4,5-dibromo-pyrazole *6c* [31] | | 141.3 | 98.9 | 114.9 | 139.1 | 125.2 | 128.8 | 128.8 | |
| 1-Phenyl-3,4,5-tribromo-pyrazole *7c* [31] | | 128.9 | 101.8 | 116.2 | 138.4 | 125.2 | 129.2 | 129.9 | |
| 1-Phenyl-3-methyl-pyrazole *1d* [38] | | 153.3 | 107.1 | 127.0 | 139.9 | 118.6 | 129.1 | 126.0 | 13.7 |
| 1-Phenyl-5-methyl-pyrazole *3d* [39] | | 139.4 | 106.5 | 138.3 | | 124.5 | 128.5 | 127.3 | 14.6 |
| 1-Phenyl-imidazole *8* [40] | 135.0 | | 129.9 | 117.8 | 136.7 | 121.0 | 129.4 | 128.0 | |
| 2-Phenyl-imidazole *9a* [c, d] | 146.7 | | 122.7 | 122.7 | 130.0 | 125.2 | 128.4 | 128.3 | |
| 1-Methyl-2-phenyl-imidazole *9d* [41] | 147.2 | | 127.8 | 121.9 | 130.1 | 128.0 | 128.0 | 128.0 | 34.4 |
| 4-Phenyl-imidazole *10a* [42, d] | | | | | | 124.7 | 128.5 | 126.7 | |
| 1-Methyl-4-phenyl-imidazole *10a* [43] | 141.7 | 137.4 | 115.5 | 122.2 | 133.6 | 124.3 | 128.1 | 126.2 | |
| 1-Phenyl-1,2,3-triazole *11a* [44] | | | 134.1 | 121.5 | 136.9 | 120.4 | 129.4 | 128.5 | |
| 1-Phenyl-4-chloro-1,2,3-triazole *11b* [33] | | | | 118.9 | | 120.1 | 129.5 | 128.9 | |
| 1-Phenyl-5-chloro-1,2,3-triazole *12b* [45] | | | 131.6 | | 134.6 | 124.5 | 129.1 | 129.1 | |
| 1-Phenyl-4-methyl-1,2,3-triazole *11d* [44] | | | 143.5 | 119.0 | 136.7 | 120.0 | 129.2 | 128.0 | |
| 1-Phenyl-5-methyl-1,2,3-triazole *12d* [46] | | | 132.8 | | 135.9 | 124.4 | 129.0 | 129.9 | |
| 2-Phenyl-1,2,3-triazole *13a* [47] | | | 139.4 | 139.4 | 135.2 | 118.7 | 129.3 | 128.9 | |
| 2-Phenyl-4-methyl-1,2,3-triazole *13d* [47] | | | 144.9 | 134.6 | 139.6 | 118.3 | 128.8 | 126.6 | |
| 1-Phenyl-tetrazole *14* [e] | | | | 140.3 | 133.4 | 120.8 | 129.8 | 129.6 | |
| 1-Methyl-5-phenyl-tetrazole *15* [48] | | | | | | 128.1 | 128.8 | 130.8 | 35.0 |
| 2-Methyl-5-phenyl-tetrazole *16* [48] | | | | | | 126.4 | 128.5 | 129.9 | 39.4 |

[a] The compounds were prepared as described in the references given. [b] The material is commercially available. [c] 13C-NMR data in benzene solution have been published previously.[49] [d] The 13C-NMR spectrum was obtained in a saturated solution accumulating 10 000 scans. [e] The material was kindly supplied by Dr. C. Christoffersen, Department of Chemistry, H. C. Ørsted Institute, University of Copenhagen, Denmark.

Table 2. $^{13}$C-$^1$H NMR-coupling constants of phenyl-substituted azoles.[a]

| Compound | C-2 | C-3 | C-4 $^1J_{CH}$ $^2J_{CCH}$ Hz $^3J_{CXCH}$ | C-5 | C-1' | C-2' | C-3' | C-4' |
|---|---|---|---|---|---|---|---|---|
| 1-Phenyl-pyrrole | 185 | 170 | | | | | 160 | 161 | 165 |
| 1-Phenyl-pyrazole 1a | | 186 | 177 | 185 | | 164 | 161 | 162 |
|  | | 8[b] | 10; 10 | 7[b] | | | | |
|  | | 5 | | 3 | | 5 | 7 | 7 |
| 1-Phenyl-3-bromo-pyrazole 1c | | | 183 | 188 | | 162 | 161 | 162 |
|  | | 11 | 8 | 9 | | | | |
|  | | 1 | | | 9 | 6 | 6 | 7 |
| 1-Phenyl-4-bromo-pyrazole 2c | | 193 | | 194 | | 165 | 161 | 163 |
|  | | 6 | | 5 | | | | |
|  | | | | | | 10 | 5 | 6 |
| 1-Phenyl-5-bromo-pyrazole 3c | | 189 | 182 | | | 162 | 162 | 162 |
|  | | 6 | 11 | 6 | | | | |
|  | | | | | 3 | 6 | | |
| 1-Phenyl-imidazole 8 | 208 | | 190 | 188$_c$ | | 160 | 162 | 160 |
|  | | | 10 | 16 | | | | |
|  | 10; 6 | | 10 | 3 | | 6 | 6 | 6 |
| 1-Methyl-2-phenyl-imidazole 9d | | | 190 | 188 | | 160 | 160 | 160 |
|  | | | 10 | 19 | | | | |
|  | | | | | 7 | | | |
| 1-Phenyl-1,2,3-triazole 11a | | | 195 | 194 | | 160 | | 162 |
|  | | | 11 | 15 | | | | |
| 1-Phenyl-4-chloro-1,2,3-triazole 11b | | | | 202 | | 165 | 161 | 162 |
|  | | | | | | 5 | 7 | 7 |
| 1-Phenyl-5-chloro-1,2,3-triazole 12b | | | 201 | | | 164 | 162 | 164 |
|  | | | | | 5 | 6; 5 | 4 | 3 |
| 2-Phenyl-1,2,3-triazole 13a | | | 194 | 194 | | 165 | 161 | 161 |
|  | | | 14 | 14 | | | | |
|  | | | | | | 6 | 7 | 8 |
| 1-Phenyl-tetrazole 14 | | | | 216 | | 162 | 164 | |
|  | | | | | | 5 | | |

[a] All coupling constants have been obtained by first order analysis. [b] The $^2J_{CCH}$ coupling constants were distinguished from $^3J_{CCCH}$ coupling constants since the former are of the same order of magnitude as $^2J_{CCH}$ of the bromo-substituted pyrazoles 1c, 2c, and 3c. [c] The $^2J_{CCH}$ coupling constants were distinguished from the $^3J_{CXCH}$ coupling constants since the former is of the same order of magnitude as $^2J_{CCH}$ of 1-methyl-2-phenyl-imidazole 9d.

signals coincided, the identity was established by analysis of the proton-undecoupled spectra, as described above.

The $^{13}$C-NMR-signals of 1-phenyl-1,2,3-triazole 11a and of the 4-chloro- and the 5-chloro-derivatives 11b and 12b, respectively (Table 1), were identified analogously through the proton-undecoupled spectra (Table 2).

In the proton-noise-decoupled spectra of 11a, 11b, and 12b the intensity decreased in the order C-3' > C-2' > C-4' > C-4 > C-5 > C-1'. Again, carbon-atoms
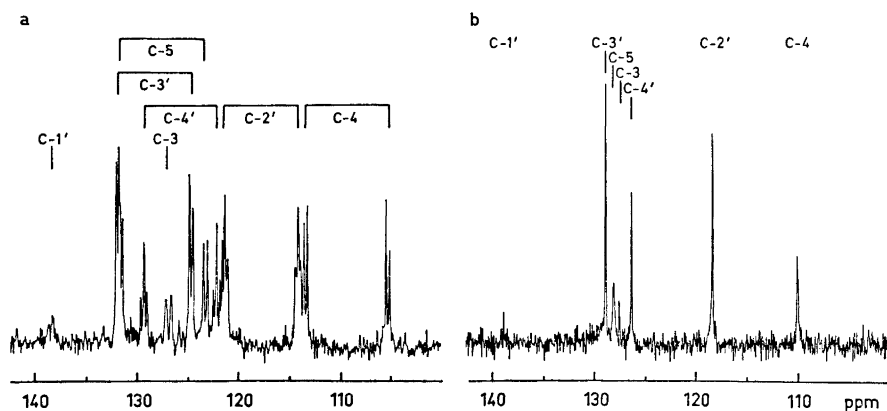
*Fig. 1.* ¹³C-NMR-spectra of 1-phenyl-3-bromo-pyrazole, *1c. a.* Undecoupled. *b.* Proton noise-decoupled.
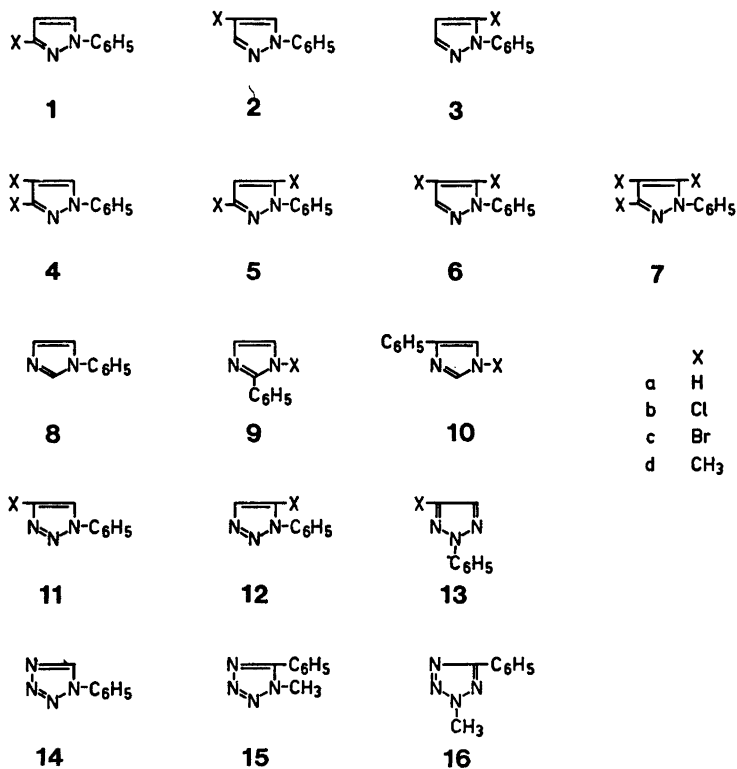
carrying a substituent appeared with strongly reduced intensity. The order of intensities was used to identify the signals of the methyl-1,2,3-triazoles *11c* and *12d*.

The signals of 2-phenyl-1,2,3-triazole *13a*. 1-phenyl-imidazole *8*, 1-methyl-2-phenyl-imidazole *9d*, 1-methyl-4-phenyl-imidazole *10d*, 1-phenyl-tetrazole *14*, 1-methyl-5-phenyl-tetrazole *15*, 2-methyl-5-phenyl-tetrazole *16*, and of 1-phenyl-pyrrole (Table 1) were identified analogously through their proton-undecoupled spectra (Table 2), taking account of the fact that heterocyclic carbon atoms $\beta$ to nitrogen absorb at higher field than those $\alpha$ to nitrogen, while carbon atoms flanked by two nitrogen atoms absorb at the lowest fields.[17e] C-4 and C-5 of *8* and *9d* were assigned assuming the same order as C-3 and C-5 of 1-phenylpyrazole *1a* and 1-methyl-pyrazole,[17e] respectively. The signals of 2-phenyl- and 4-phenyl imidazole, *9a* and *10a*, were identified on the basis of their relative intensity.

A bromine atom shields the bromine-carrying pyrazole ring carbon, C-4 of the pyrazole ring is less shielded than C-3 and C-5. A methyl group deshields the substituent-carrying pyrazole ring carbon. A chlorine atom deshields the substituted carbon, chlorine at C-4 producing larger shifts than chlorine at C-3 or C-5. Carbon atoms adjacent to the substituent are influenced to a minor extent; yet, chlorine at C-3 has a rather large influence on $\delta_{C-5}$. Contributions from more substituent on $\delta_{C-3}$ and $\delta_{C-4}$ are additive inside a maximum range of 0.8 ppm (see Table 1). Contributions from more substituents on $\delta_{C-5}$ are only approximately additive. In this case the maximum difference between $\delta_{C-5}$ observed and $\delta_{C-5}$ calculated by addition of the single contributions from the substituents is 2.2 ppm.

The effects of substituents are different from those found in benzene derivatives,[17d] here obviously depending on the position of substituents, the ring type (compare substituted 1-phenyl-pyrazoles and 1,2,3-triazoles), and finally, the nature of the nitrogen-substituent (compare the chloro-substituted 1-phenyl- and 1-benzyl-pyrazoles).

$^1J_{CH}$ of the heteroaromatic carbons are, as expected,[17b] larger the more electron attracting the surroundings are. Thus $^1J_{HC-5}$ of *14* $>$ $^1J_{HC-2}$ of *8* $>$ $^1J_{HC-4}$ and $^1J_{HC-5}$ of *11a* and $^1J_{HC-4}$ of *13a* $>$ $^1J_{HC-4}$ and $^1J_{HC-5}$ of *8* $>$ $^1J_{HC-3}$ and $^1J_{HC-5}$ of *1a* $>$ $^1J_{HC-4}$ of *1a*. $^1J_{CH}$ for carbon atoms adjacent to an imine-nitrogen atom is larger than $^1J_{CH}$ for carbon atoms adjacent to an amine-nitrogen atom. (Thus, $^1J_{HC-4}$ $>$ $^1J_{HC-5}$ in *8*, $^1J_{HC-3}$ $>$ $^1J_{HC-5}$ in *1a*, and $^1J_{HC-4}$ $>$ $^1J_{HC-5}$ in *11a*).

Bromide and chlorine increase the one bond coupling constant of the adjacent carbon atom with 5.5 − 6.5 Hz and the $\beta$-carbon atom with 3.0 − 3.7 Hz.

$^2J_{CCH}$ of the heteroaromatic carbon atoms is particularly dependent on the surroundings of the hydrogen atom. The value becomes larger the more electron withdrawing the surroundings of the hydrogen atom are. (Thus, $^2J_{HCC-4}$ $>$ $^2J_{HCC-3}$ and $^2J_{HCC-5}$ in *1a*. In addition, $^2J_{HCC-4}$ and $^2J_{HCC-5}$ of *8* and *11a* and $^2J_{HCC-4}$ in *13a* are all larger than $^2J_{HCC-3}$ and $^2J_{HCC-5}$ in *1a*. Finally, $^2J_{HCC-5}$ $>$ $^2J_{HCC-4}$ in *8* and in *11a*).

## DISCUSSION

In 1-benzyl-pyrazole, C-1' resonates at lower field than C-2', C-3', and C-4' due to the electron-attracting amine nitrogen atom. The latter three carbon atoms have similar chemical shifts since they are influenced only by remote inductive effects. A chlorine atom in the heterocyclic ring of 1-benzyl-pyrazole has only a minor influence on the benzene ring carbon atoms, even when chlorine is situated at the 5-position.

In 1-phenyl-pyrazole *1a*, 1-phenyl-3-bromo-pyrazole *1c*, and 1-phenyl-4-bromo-pyrazole *2c* full interannular conjugation prevails.[4–8,11,19,20] C-2' and C-4' resonate at higher field than C-3' because the lone pair of N-1 is delocalized over the *o*- and *p*-positions. C-1' absorbs at lower field than C-3' due to the inductive effect of the adjacent nitrogen atom. The chemical shifts of the different benzene carbon atoms vary less than 1.3 ppm in *1a*, *1c*, and *2c*. Thus bromine in the pyrazole ring shields C-1'. The shielding increases when the bromine is moved from C-4 to C-3. C-2' is not influenced but C-3' and C-4' are deshielded by bromine in the pyrazole ring. The deshielding increases when the bromine is moved from C-4 to C-3.

Whereas bromine in the unhindered 3- and 4-bromo compounds *1c* and *2c* exerts little effect on the phenyl group signals, bromine in 1-phenyl-5-bromo-pyrazole *3c* causes strong low field displacements of C-2' and C-4'. C-1' and C-3' are much less affected. This may be attributable to steric factors interfering with extensive interannular conjugation.[19–21]

Similar results were found for the other compounds studied. Thus, introduction of chlorine at C-3 or C-4 of 1-phenyl-pyrazole *1a* causes small variations in the position of the benzene carbon signals: C-1' is shielded. The shielding increases when the chlorine is moved from C-4 to C-3. C-3' is not influenced, but C-2' is shielded and C-4' is deshielded, the more so when chlorine is moved from C-4 to C-3.

In contrast, chlorine at C-5 causes major displacements similar to those observed when bromine is introduced at C-5.

A methyl group at C-3 of 1-phenyl-pyrazole *1a* does not influence C-3' and C-4' but shields C-2' slightly. In contrast, a methyl group at C-5 again causes displacements similar to those observed with bromine in the 5-position.

The effects of the 5-substituents increase in the order Me, Cl, Br, possibly reflecting an increase in steric hindrance in that order. Inspection of the data reveal $\delta_{C-2}'$ and $\delta_{C-3}' - \delta_{C-2}'$ as the parameters most sensitive to the degree of interannular conjugation. The results indicate that if $\delta_{C-2}' \sim 118.5$ ppm and $\delta_{C-3}' - \delta_{C-2}' \sim 10.5$ ppm in methyl- or chloro-substituted 1-phenyl-pyrazoles the delocalization is extensive. If, however, $\delta_{C-2}' \sim 124.6$ ppm and $\delta_{C-3}' - \delta_{C-2}' \sim 4.0$ ppm delocalization is impeded as a result of higher torsional energy barrier. In bromo-substituted 1-phenylpyrazoles delocalization is extensive if $\delta_{C-2}' \sim 118.8$ ppm and $\delta_{C-3}' - \delta_{C-2}' \sim 10.5$ ppm and strongly diminished if $\delta_{C-2}' \sim 125.4$ ppm and $\delta_{C-3}' - \delta_{C-2}' \sim 3.3$ ppm. The values for 1-phenyl-pyrazole *1a* itself are similar to those of a unhindered bromo-substituted derivative.

*N*-Phenyl substituted 1,2,3-triazoles, -imidazoles, and -tetrazoles behave in the same way as the 1-phenyl-pyrazoles. Thus, introduction of chlorine at

C-4 of 1-phenyl-1,2,3-triazole *11a* causes small displacements of the ^{13}C-NMR-signals of the benzene ring. In contrast, introduction of chlorine at C-5 causes a large low field shift of C-2' and a minor shift of C-3' and C-4'. Similarly, introduction of a methyl group at C-4 of 1-phenyl-1,2,3-triazole *11a* or of 2-phenyl-1,2,3-triazole *13a* produces minor shifts of the benzene carbon signals. However, introduction of a methyl group at C-5 of 1-phenyl-1,2,3-triazole *11a* results in a large low field shift of C-2' and minor shifts of C-3' and C-4'. The effect of chlorine is larger than that of methyl as in the pyrazole series.

This indicates that interannular conjugation is extensive in methyl- or chlorine substituted 1-phenyl-1,2,3-triazoles [22] if $\delta_{C-2'} \sim 120$ ppm and $\delta_{C-3'} - \delta_{C-2'} \sim 9.4$ ppm but reduced if $\delta_{C-2'} \sim 124.5$ ppm and $\delta_{C-3'} - \delta_{C-2'} \sim 4.6$ ppm. In the unhindered 2-phenyl-1,2,3-triazoles *13a* [12,22] and *13d* $\delta_{C-2'} \sim 118.3$ ppm and $\delta_{C-3'} - \delta_{C-2'} \sim 10.6$ ppm. In the unhindered 1-phenyl-imidazole *8* [11,13,14] $\delta_{C-2'} = 121.0$ ppm and $\delta_{C-3'} - \delta_{C-2'} = 9.4$ ppm. In the unhindered 1-phenyl-tetrazole *14* $\delta_{C-2'}$ is 120.8 ppm and $\delta_{C-3'} \sim \delta_{C-2'}$ is 9.0 ppm. In the unhindered 1-phenyl pyrrole [11,23-27] $\delta_{C-2'} = 120.2$ ppm and $\delta_{C-3'} - \delta_{C-2'} = 8.9$ ppm.

The ^{13}C-NMR chemical shifts of C-1' and C-2' of the unhindered *C*-phenyl substituted compounds 2-phenyl-imidazole *9a*,[11,12] 4-phenyl-imidazole *10a*,[11,12] 1-methyl-4-phenyl-imidazole *10d*, and 2-methyl-5-phenyl-tetrazole *16* [10] are different from those of the unhindered *N*-phenyl substituted azoles. Thus, C-1' of *9a*, *10a*, *10d*, and *16* was found to be more shielded than C-1' of the *N*-phenyl azoles in which C-1' is deshielded by the adjacent nitrogen atom. C-2' of *9a*, *10a*, *10d*, and *16* were deshielded compared to C-2' of the unhindered *N*-phenyl azoles. This may be caused by the ability of *C*-phenyl groups to both accept and donate $\pi$-electrons, whereas the latter effect is far less conspicuous in $\pi$-excessive azoles.[28] However, it reduces the electron density at C-2' (and C-4') relative to C-3' and, hence, $\delta_{C-3'} - \delta_{C-2'}$ as compared to the *N*-phenyl substituted azoles, where the phenyl groups act solely as $\pi$-electron acceptors.

Introduction of a methyl group in the 1-position of 2-phenyl-imidazole *9a* caused an appreciable low-field shift of C-2' and minor shifts of C-3' and C-4'. In fact, the signals of C-2', C-3', and C-4' coincided. This clearly demonstrates that interannular conjugation has vanished in the hindered 1-methyl-2-phenyl-imidazole *9d*. Thus, conjugation is present in 2-phenyl-imidazoles if $\delta_{C-2'} \sim 125.2$ ppm and $\delta_{C-3'} - \delta_{C-2'} \sim 3.2$ ppm but absent if $\delta_{C-2'} \sim 128.0$ ppm and $\delta_{C-3'} - \delta_{C-2'} \sim 0$ ppm. Similarly, conjugation prevails in 4-phenyl-imidazoles if $\delta_{C-2'} \sim 124.7$ ppm and $\delta_{C-3'} - \delta_{C-2'} \sim 3.8$ ppm.

Shift of a methyl group from N-2 to N-1 of 5-phenyl-tetrazole causes a low field shift of C-2' and minor shifts of C-3' and C-4'. The ^{13}C-NMR-data of the unhindered [10] 2-methyl-5-phenyl-tetrazole *16* and of the hindered [10] 1-methyl-5-phenyl-tetrazole *15* indicate that interannular conjugation in 5-phenyl-tetrazoles is extensive if $\delta_{C-2'} \sim 126.4$ ppm and $\delta_{C-3'} - \delta_{C-2'} \sim 2.1$ ppm but impeded if $\delta_{C-2'} \sim 128.1$ ppm and $\delta_{C-3'} - \delta_{C-2'} \sim 0.7$ ppm.

## CONCLUSION

The results demonstrate that $^{13}$C-NMR-spectroscopy is a useful tool for the study of the extent of interannular conjugation in $N$- or $C$-phenyl-azoles. The $^{13}$C-NMR-spectra yield unambiguous results in contrast to the $^1$H-NMR-spectra. The combined data indicate that interannular conjugation is extensive in simple $N$-phenyl-azoles if $\delta_{C_{-2}'} \sim 118 - 121$ ppm and $\delta_{C_{-3}'} - \delta_{C_{-2}'} \sim 9.0 - 10.6$ ppm but impeded if $\delta_{C_{-2}'} \sim 124.5 - 125.5$ ppm and $\delta_{C_{-3}'} - \delta_{C_{-2}'} \sim 3.3 - 4.6$ ppm. In simple $C$-phenyl substituted azoles interannular conjugation is extensive if $\delta_{C_{-2}'} \sim 124.5 - 126.4$ ppm and $\delta_{C_{-3}'} - \delta_{C_{-2}'} \sim 3.2 - 3.8$ ppm but impeded if $\delta_{C_{-2}'} \sim 128 - 128.5$ ppm and $\delta_{C_{-3}'} - \delta_{C_{-2}'} \sim 0 - 0.7$ ppm.

So far, only a limited number of compounds have been studied, including very few $C$-phenyl-azoles. Supplementary data will undoubtedly extend the intervals given above. However, when the origin of these differences is taken into account, the differences between the values for unhindered and hindered cases are so large that overlap of the intervals seems unlikely. Thus, application of the $^{13}$C-NMR method for assessing the extent of interannular conjugation in phenyl-azoles may most likely be useful in analogous cases.

Considering the origin of the different intervals observed, it seems likely that the $^{13}$C-NMR method may be put to good use for conformational studies of phenyl-substituted azines and benzenes, as well as of phenyl-substituted, nonaromatic heterocyclic rings.

## EXPERIMENTAL

$^1$H-NMR-spectra were obtained on a Varian A-60 instrument using deuteriochloroform as the solvent. Position of signals are given in ppm ($\delta$-values) relative to tetramethylsilane.

All $^{13}$C-NMR-spectra were obtained in deuteriochloroform solution. The compound (0.695 mmol) was dissolved in 1.20 ml of solvent. Position of signals were measured relative to the center peak of the deuteriochloroform triplet ($\delta$ 76.9 ppm $^{16C}$) and are given in ppm ($\delta$-values) relative to tetramethylsilane. The spectra were obtained on a BRUKER WH-90 instrument using Fast Fourier Transform pulse technique. Unless otherwise stated, 1000 scans were accumulated with 6000 Hz sweep using 8K computer memory. This corresponds to an accuracy of $\pm$ 0.07 ppm in the chemical shifts and of $\pm$ 3 Hz in the coupling constants. The repetition time was 3.0 sec. The decoupled spectra were obtained using proton-noise-decoupling. The undecoupled spectra were measured by the gated decoupling technique [29] in order to maintain part of the Overhauser enhancement of the signals. Thus, the proton-noise-decoupling was interrupted after 1.0 sec. After delay of 0.4 sec, the pulse (4 $\mu$sec) was turned on again. This cycle was repeated every 3.0 sec, 6000 scans being accumulated.

## REFERENCES

1. Murrell, J. N., Gil, V. M. S. and van Duijneveldt, F. B. *Rec. Trav. Chim.* **84** (1965) 1399.
2. Günther, H. and Castellano, S. *Ber. Bunsenges. Physik-Chem.* **70** (1966) 913.
3. Crossland, I. *Acta Chem. Scand.* **20** (1966) 258.
4. Lynch, B. M. and Hung, Y.-Y. *Can J. Chem.* **42** (1964) 1605.
5. Tensmeyer, L. G. and Ainsworth, C. *J. Org. Chem.* **31** (1966) 1878.
6. Elguero, J., Jacquier, R. and Tien Duc, H. C. N. *Bull. Soc. Chim. France* **1966** 3727.
7. Elguero, J., Jacquier, R. and Mondon, S. *Bull. Soc. Chim. France* **1970** 1346.
8. Finar, I. L. and Rackham, D. M. *J. Chem. Soc.* B **1968** 211.

9. Begtrup, M. *Unpublished results.*
10. Fraser, R. R. and Haque, K. E. *Can. J. Chem.* **46** (1968) 2855.
11. Minkin, V. I., Pozharskii, A. F. and Ostroumov, Y. A. *Khim. Geterotsikl. Soedin.* **2** (1966) 413. *Cf. Chem. Abstr.* **66** (1967) 10481t.
12. Hayashi, T. and Midorikawa, H. *Sci. Papers Inst. Phys. Chem. Res.* **58** (1964) 139. *Cf. Chem. Abstr.* **62** (1965) 10317g.
13. Pozharskii, A. F. *Zh. Obshch. Khim.* **1964** 630.
14. Pozharskii, A. F., Sitkina, L. M., Simonov, A. M. and Chegolya, T. N. *Khim. Geterotsikl. Soedin.* **6** (1970) 194. *Cf. Chem. Abstr.* **72** (1970) 111335u.
15. Wilshire, J. F. K. *Austr. J. Chem.* **19** (1966) 1935.
16. Levy, G. and Nelson, G. L. *Carbon-13 Nuclear Magnetic Resonance for Organic Chemists*, Wiley, New York 1972; a p. 22; b p. 29; c p. 23.
17. Stothers, J. B. *Carbon-13 NMR Spectroscopy.* Academic, New York 1972; a p. 102; b p. 332; c p. 348; d p. 196; e p. 253.
18. I. U. P. A. C. Nomenclature of Organic Chemistry Sections A, B, and C. Butterworths, London 1969, p. 53.
19 Tabak, S., Grandberg, I. I. and Kost, A. N. *Tetrahedron* **22** (1966) 2703.
20. Elguero, J., Jacquier, R. and Tien Duc, H. C. N. *Bull. Soc. Chim. France* **1966** 3744.
21. Tabak, S., Grandberg, I. I. and Kost, A. N. *Am. Ass. Brazil. Quim.* **26** (1967) 51. *Cf. Chem. Abstr.* **70** (1969) 36989p.
22. Dal Monte, D., Mangini, A., Passerini, R. and Zauli, C. *Gazz. Chim. Ital.* **88** (1958) 1005.
23. Kofod, H., Sutton, L. E. and Jackson, J. *J. Chem. Soc.* **1952** 1467.
24. Chiang, Y., Hinman, R. L., Theodoropulos, S. and Whipple, E. B. *Tetrahedron* **23** (1967) 745.
25. Jones, R. A., Spotwood, T. McL. and Cheuychit, P. *Tetrahedron* **23** (1967) 4469.
26. Matsuo, T., Shosenji, H. and Miyamoto, R. *Bull. Chem. Soc. Japan* **41** (1968) 2849.
27. Galasso, V. and De Alti, G. *Tetrahedron* **27** (1971) 4947.
28. Albert, A. *Heterocyclic Chemistry*, The Athlone Press, London 1968, p. 52.
29. Feeney, J., Shaw, D. and Pauwels, P. J. S. *Chem. Commun.* **1970** 554.
30. Jones, R. G. *J. Am. Chem. Soc.* **71** (1949) 3994.
31. Begtrup, M. *Acta Chem. Scand.* **27** (1973) 2051.
32. Finar, I. L. and Godfrey, K. E. *J. Chem. Soc.* **1954** 2293.
33. v. Auwers, K. and Kohlhaas, W. *Ann.* **437** (1924) 36.
34. Grandberg, I. I., Gorbachova, L. I. and Kost, A. N. *Zh. Obshch. Khim.* **33** (1963) 511.
35. Michaelis, A. and Röhmer, H. *Ber.* **31** (1898) 3003.
36. Balbiano, L. *Gazz. Chim. Ital.* **19** (1889) 128.
37. Michaelis, A. *Ann.* **385** (1911) 1.
38. v. Auwers, K. and Hollmann, H. *Ber.* **59** (1926) 1282.
39. Claisen, L. and Roosen, P. *Ann.* **278** (1894) 261.
40. Pozharskii, A. F., Martsokha, B. K. and Simonov, A. M. *Zh. Obshch. Khim.* **33** (1963) 1005.
41. Balaban, I. E. and King, H. *J. Chem. Soc.* **127** (1925) 2701.
42. Grant, R. L. and Pyman, F. L. *J. Chem. Soc.* **119** (1921) 1893.
43. Hazeldine, C. E., Pyman, F. L. and Winchester, J. *J. Chem. Soc.* **125** (1924) 1431.
44. Bertho, A. *Ber.* **58** (1925) 861.
45. Dimroth, O. *Ann.* **364** (1908) 183.
46. Dimroth, O. *Ber.* **35** (1902) 1029.
47. Riebsomer, J. L. *J. Org. Chem.* **13** (1948) 815.
48. Rees, R. G. and Green, M. J. *J. Chem. Soc.* **B 1968** 387.
49. Henry, R. A. *J. Am. Chem. Soc.* **73** (1951) 4470.

# Preparation of 2-Deoxy-sugars by Hydrogenolysis of Benzoylated Glycopyranosyl Bromides

STEFFEN JACOBSEN and CHRISTIAN PEDERSEN

*Department of Organic Chemistry, Technical University of Denmark, DK-2800 Lyngby, Denmark*

Hydrogenolysis of tri-*O*-benzoyl-*β*-D-arabinopyranosyl bromide with palladium on carbon as catalyst gives, in addition to the expected 1,5-anhydro-tri-*O*-benzoyl-D-arabinitol, considerable amounts of 1,3,4-tri-*O*-benzoyl-2-deoxy-*β*-D-*erythro*-pentose. A similar treatment of tetra-*O*-benzoyl-*α*-D-glucopyranosyl bromide yields tetra-*O*-benzoyl-2-deoxy-*α*-D-*arabino*-hexopyranose. Hydrogenolysis of tetra-*O*-benzoyl-*α*-D-mannopyranosyl bromide, or of tri-*O*-benzoyl-*β*-D-ribopyranosyl bromide, does not give 2-deoxy-sugars.

The preparation of acetylated or benzoylated 1,5-anhydroalditols by reductive dehalogenation of acylated glycopyranosyl bromides, using palladium on carbon as catalyst in the presence of triethylamine, has been described by Zervas and Zioudrou [1] and by Hedgley and Fletcher.[2] Later Gray and Barker [3] investigated this reaction more closely and found that better yields of 1,5-anhydroalditols were obtained when platinum was used as the catalyst.

In connection with other work we reduced tri-*O*-benzoyl-*β*-D-arabinopyranosyl bromide (*1*) with hydrogen in the presence of palladium on carbon and triethylamine with ethyl acetate as solvent, *i.e.* under conditions which are reported to give an 86 % yield of 1,5-anhydro-tri-*O*-benzoyl-D-arabinitol (*2*).[2] The product was, however, rather impure and examination of it revealed that it contained considerable amounts of 1,3,4-tri-*O*-benzoyl-2-deoxy-*β*-D-*erythro*-pentopyranose (*3*). In view of this rather unexpected result the hydrogenolysis of (*1*), and of other acylated pyranosyl bromides, has been investigated more closely.

In order to optimize the yield of the 2-deoxy-derivative (*3*) a number of exploratory experiments were carried out (Table 1). From these it is seen that only when palladium on carbon, or on barium sulfate, was used as catalyst could significant amounts of (*3*) be obtained. With palladium oxide, platinum oxide, or Raney-nickel (experiments 10, 12, and 13, respectively) only traces of (*3*) were found.
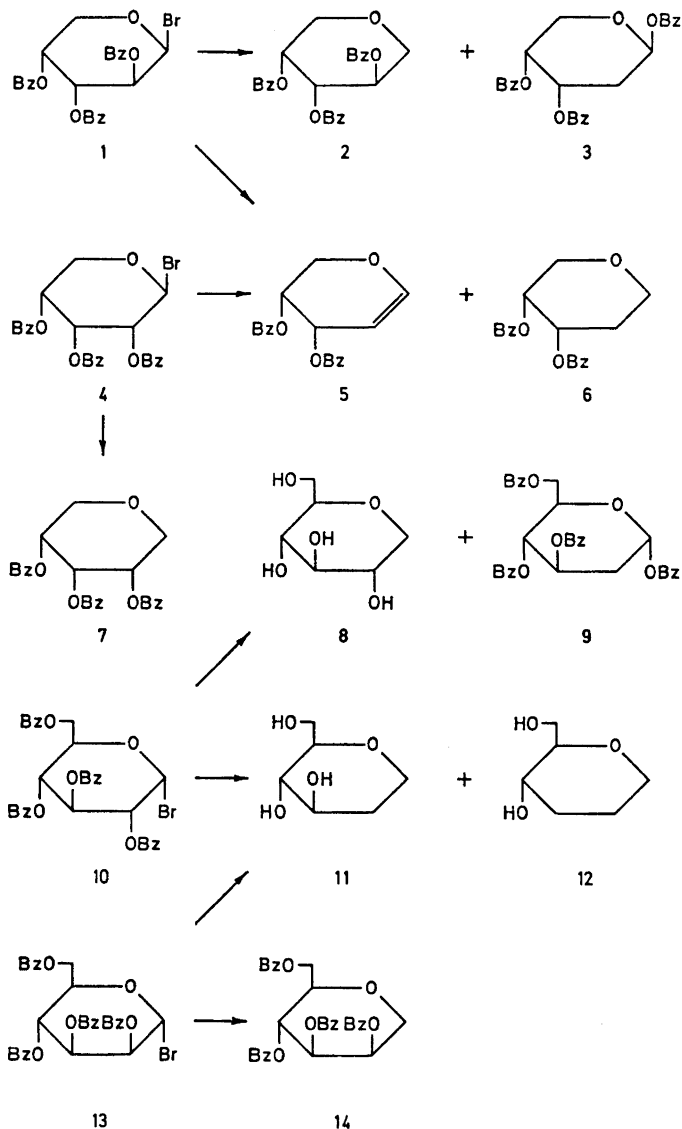
The amount of triethylamine should not be less than 2 molar equivalents (using 200 mg of catalyst) since this resulted in a lower yield of the 2-deoxy-ribose derivative (*3*) (experiment No. 7). A larger amount of triethylamine did, on the other hand, not give more (*3*) (experiments 8 and 9). A larger amount of catalyst gave less (*3*) (experiment 5) unless the amount of triethylamine was increased proportionally (experiment 6). The catalyst is presumably modified by absorption of triethylamine and it is probably this modified catalyst which

*Table 1.* Hydrogenolysis of tri-*O*-benzoyl-β-D-arabinopyranosyl bromide (*1*) (1.0 g was used in each of the experiments). For further details see the experimental section.

| Experiment no. | Ethyl acetate ml | Triethyl-amine ml; molar eqv.'s | | Catalyst | Yield (%) of (*3*) as determined from NMR spectra |
|---|---|---|---|---|---|
| 1 | 7.0 | 0.53; | 2 | 200 mg, 5 % Pd-C | 40 – 50 |
| 2 | 9.5 | 0.53; | 2 | 200 mg, 5 % Pd-C | 40 |
| 3 | 15.0 | 0.53; | 2 | 200 mg, 5 % Pd-C | 24 |
| 4 | 7.0 | 0.53; | 2 | 50 mg, 5 % Pd-C | 45 |
| 5 | 15.0 | 0.53; | 2 | 1.0 g, 5 % Pd-C | 11 |
| 6 | 7.0 | 2.65; | 10 | 1.0 g, 5 % Pd-C | 30 |
| 7 | 7.0 | 0.26; | 1 | 200 mg, 5 % Pd-C | 20 |
| 8 | 5.0 | 5.0; | 19 | 200 mg, 5 % Pd-C | 43 |
| 9 | 0 | 8.0; | 31 | 200 mg, 5 % Pd-C | 34 |
| 10 | 15.0 | 0.53; | 2 | 150 mg, PdO | trace |
| 11 | 7.0 | 0.53; | 2 | 200 mg, 5 % Pd-BaSO₄ | 40 |
| 12 | 9.5 | 0.53; | 2 | 50 mg, PtO₂ | trace |
| 13 | 7.0 | 0.53; | 2 | *ca.* 200 mg, Ra.-Ni | trace |
| 14 | dioxane, 14 ml | 0.53; | 2 | 200 mg, 5 % Pd-C | 24 |

is responsible for the formation of the 2-deoxy-ribose derivative (*3*). Gray and Barker[3] observed that diethylamine has a profound effect on the properties of palladium or platinum when used for the reduction of unsaturated sugars. Addition of more ethyl acetate (experiments 2 and 3) gave less (*3*), probably because the complex formation between the catalyst and the triethylamine was suppressed by dilution. The use of 10 % palladium on carbon gave very nearly the same results as 5 % palladium.

The optimum conditions for the preparation of (*3*) from the bromide (*1*) are those given for experiment No. 1 (Table 1). When the reduction of (*1*) was carried out on a larger scale, using these conditions, (*3*) was readily isolated in 32 % yield. Besides, 1,5-anhydro-tri-*O*-benzoyl-D-arabinitol (*2*) was obtained together with small amounts of 3,4-di-*O*-benzoyl-1,2-dideoxy-D-*erythro*-pent-1-enopyranose (*5*) and its reduction product (*6*).

Hedgley and Fletcher[2] carried out the reduction under almost identical conditions. They, however, used a crude bromide which probably contained some acetic acid and hydrogen bromide. The triethylamine would therefore be partly neutralized and this could affect the reaction. When we carried out the reduction under the conditions of Hedgley and Fletcher the 1,5-anhydride (*2*) was the major product; it did, however, not crystallize well due to the presence of small amounts of other products.

Hydrogenolysis of tetra-*O*-benzoyl-α-D-glucopyranosyl bromide (*10*) under the conditions described above gave a 40 % yield of tetra-*O*-benzoyl-2-deoxy-α-D-*arabino*-hexopyranose (*9*). After debenzoylation of the remaining product 1,5-anhydro-D-glucitol (*8*) and smaller amounts of 1,5-anhydro-2-deoxy-D-*arabino*-hexitol (*11*) and 1,5-anhydro-2,3-dideoxy-D-*erythro*-hexitol (*12*) were

isolated. The latter two products were probably formed *via* unsaturated sugars, analogous to the results described by Gray and Barker.[3]

Both the arabinosyl bromide (*1*) and the glucosyl bromide (*10*) have the bromine atom *cis* to the benzoyloxy-group at C-2, and in both cases the benzoyloxy-group migrated to C-1 without change in configuration. It was therefore of interest to study the hydrogenolysis of compounds in which the bromine is *trans* to the benzoyloxy-group at C-2.

Hydrogenolysis of tetra-*O*-benzoyl-α-D-mannopyranosyl bromide (*13*) gave no detectable amounts of 2-deoxy-derivatives. The main product was 1,5-anhydro-tetra-*O*-benzoyl-D-mannitol (*14*); besides, the 2-deoxy- and the 2,3-dideoxy-1,5-anhydrides (*11*) and (*12*) were isolated as their tri- and dibenzoates, respectively.

Hydrogenolysis of tri-*O*-benzoyl-β-D-ribopyranosyl bromide (*4*) gave 53 % of 1,5-anhydro-tri-*O*-benzoyl-ribitol (*7*) and a trace of the 2-deoxy-1,5-anhydride (*6*). Besides, a very small amount of 1,3,4-tri-*O*-benzoyl-2-deoxy-α-D-*erythro*-pentopyranose was isolated. It seems most likely that this product was formed by hydrogenolysis of tri-*O*-benzoyl-α-D-ribopyranosyl bromide, which could be present as an impurity in the β-bromide (*4*),[4] or it could be formed by anomerization of the latter in the course of the hydrogenolysis.

From the results described above it may be concluded that hydrogenolysis of benzoylated 1,2-*cis*-glycopyranosyl bromides with palladium on carbon in the presence of triethylamine yields substantial amounts of 2-deoxy-sugars in addition to the expected 1,5-anhydro-alditols. Hydrogenolysis of 1,2-*trans*-bromides does not give 2-deoxy-sugars. Similar results have been found for other benzoylated glycosyl bromides; details will be published later.

Hydrogenolysis of tri-*O*-acetyl-β-D-arabinopyranosyl bromide gave a good yield of tri-*O*-acetyl-1,5-anhydro-D-arabinitol and only traces of 2-deoxy-ribose derivatives were formed.

The structure of tetra-*O*-benzoyl-2-deoxy-α-D-*arabino*-hexopyranose (*9*) was confirmed by its reaction with hydrogen bromide, which gave the known tri-*O*-benzoyl-2-deoxy-α-D-*arabino*-hexopyranosyl bromide.[5] The anomeric structure of (*9*) was seen from its NMR spectrum, which showed H-1 at $\delta$ 6.64 as a double doublet, $J_{12e} = 1$ Hz, $J_{12a} = 3$ Hz. Bergmann *et al.*[5] benzoylated 2-deoxy-D-*arabino*-hexose and obtained a tetrabenzoate to which they assigned structure (*9*). However, an NMR spectrum of a product prepared according to Bergmann *et al.* showed H-1 as a double doublet at $\delta$ 6.32, $J_{12e} = 2.5$, $J_{12a} = 9.5$ Hz, clearly indicating that the substance is tetra-*O*-benzoyl-2-deoxy-β-D-*arabino*-hexopyranose. The anomeric structures were further confirmed by the optical rotations, the α-anomer (*9*) being the more dextrorotatory.

## EXPERIMENTAL

Melting points are uncorrected. NMR spectra were obtained on Varian A-60 or HA-100 instruments using deuteriochloroform as solvent. Thin layer chromatography (TLC) was performed on silica gel PF$_{254}$ ("Merck"); for preparative work 1 mm layers were used on 20 × 40 cm plates. Zones were visualized under UV light.

*Catalysts.* Palladium (5 %) on carbon was purchased from "Fluka" (*puriss.*; two different batches were used), or it was prepared according to Ref. 6. No differences were observed between these. 10 % Palladium on carbon was obtained from "Merck". The

palladium oxide was a "Fluka" *puriss.* grade and the platinum oxide was obtained from Johnson Matthey and Co. (England). The Raney nickel was prepared according to Ref. 7.

*Experiments in Table 1.* Tri-O-benzoyl-β-D-arabinopyranosyl bromide [8] (1.0 g) was dissolved in ethyl acetate in a 100 ml roundbottomed flask, the catalyst was added followed by triethylamine. The mixture was then hydrogenated with efficient magnetic stirring at ambient temp. and pressure for 14 − 16 h. The hydrogen uptake was usually completed in *ca.* 6 h.

The mixture was then filtered through a layer of activated carbon and the filter was washed several times with dichloromethane. The filtrate was washed twice with water, dried (MgSO$_4$), and evaporated. The residue (*ca.* 800 mg) was dissolved in tetrachloromethane which was evaporated. This was repeated and an NMR spectrum was then measured in deuteriochloroform solution. The spectra showed H-1 of 1,3,4-tri-O-benzoyl-2-deoxy-β-D-*erythro*-pento-pyranose (*3*) as a broad triplet at $\delta$ 6.7. H-3,4 of (*3*) and H-2,3,4 of the 1,5-anhydride (*2*) gave a broad signal at $\delta$ 5.75. From the integrals of these two signals the yields of (*3*) (Table 1) were calculated. Since products other than (*2*) and (*3*) are present (see below) the values thus obtained are approximations only.

*Hydrogenolysis of tri-O-benzoyl-β-D-arabinopyranosyl bromide (1). A.* To (*1*) (5.0 g) in ethyl acetate (35 ml) was added triethylamine (2.64 ml) and 5 % palladium on carbon (1.0 g). The mixture was then hydrogenated and worked up as described above. The product (4.2 g) was crystallized from ether-pentane to give 1.2 g (28 %) of 1,3,4-tri-O-benzoyl-2-deoxy-β-D-*erythro*-pentopyranose (*3*), m.p. 150 − 152°C. After two additional recrystallizations from ether-pentane the product melted at 156 − 157°C, $[\alpha]_D^{22} = -190°$ (*c* 1.7, CDCl$_3$). (Reported [9] m.p. 159 − 161°C, $[\alpha]_D = -195°$).

A sample (1.50 g) of the material in the mother liquors was separated into 4 fractions by preparative TLC using ethyl acetate-pentane (1:4) as eluent. The fast moving fraction gave 49 mg of 3,4-di-O-benzoyl-1,2-dideoxy-D-*erythro*-pent-1-enopyranose (*5*) as seen from an NMR spectrum, which was identical with that of an authentic sample.[10] The next fraction (114 mg) was crystallized from methanol to give 75 mg of (*3*), m.p. 156 − 157°C. The third fraction (640 mg) was also crystallized from methanol and gave 450 mg (21 %) of 1,5-anhydro-tri-O-benzoyl-D-arabinitol, m.p. 117 − 119°C, $[\alpha]_D^{22} = -214°$ (*c* 1.3, CHCl$_3$). (Reported [2,11] m.p. 120 − 121°C $[\alpha]_D = -220°$). A fourth fraction (120 mg) contained impure (*6*) (see below).

*B.* A suspension of (*1*) (41.0 g) in ethyl acetate (280 ml) and triethylamine (22 ml) was hydrogenated in the presence of 8.0 g of 5 % palladium on carbon. The product was crystallized from ether to give 13.2 g (38 %) of crude (*3*), m.p. 150 − 153°C. One recrystallization from methanol gave 11.2 g (32 %) of (*3*), m.p. 157 − 158°C, $[\alpha]_D^{23} = -195°$ (*c* 1.2, CHCl$_3$).

The mother liquor material was boiled for 3 h with methanol and excess sodium methoxide. The methanol was removed, water was added and the mixture was deionized by passage through columns of Amberlite IR-120 and IR-4 B. The solution was then filtered through activated carbon and evaporated. The residue (3.7 g) was crystallized from ethanol-ethyl acetate to give 800 mg (7.6 %) of 1,5-anhydro-D-arabinitol, m.p. 90 − 93°C.

The remaining material was separated into 4 fractions by chromatography on a column of silica gel (150 g) using butanone-2, saturated with water, as eluent. The first two fractions (91 mg) were not investigated. The third fraction gave 271 mg (3 %) of 1,5-anhydro-2-deoxy-D-*erythro*-pentitol as a syrup. Benzoylation yielded the di-O-benzoate (*6*) which was recrystallized from methanol, yield 200 mg, m.p. 86 − 87°C, $[\alpha]_D^{22} = -64.9°$ (*c* 4.7, CHCl$_3$). (Reported [12] m.p. 89 − 91°C, $[\alpha]_D = -65.1°$). The last fraction (1.119 g) was crystallized from ethanol-ethyl acetate to give 700 mg (6.7 %) of 1,5-anhydro-D-arabinitol, m.p. 93 − 95°C. Recrystallization from ethanol gave a product with m.p. 95 − 97°C, $[\alpha]_D^{22} = -97.5°$ (*c* 3.7, H$_2$O). (Reported [11] m.p. 96 − 97°C, $[\alpha]_D = -98.6°$).

*Tetra-O-benzoyl-α-D-glucopyranosyl bromide* (44.0 g) in ethyl acetate (250 ml) and triethylamine (24 ml) was hydrogenated in the presence of 8.5 g of 5 % palladium on carbon. Work up as described above gave a syrup which was crystallized from ether-pentane. The product (17.5 g), m.p. 149 − 152°C, was recrystallized from ethanol to give 15.6 g (40 %) of tetra-O-benzoyl-2-deoxy-α-D-*arabino*-hexopyranose (*9*), m.p. 152 − 153°C. An additional recrystallization gave the pure product, m.p. 153 − 154°C, $[\alpha]_D^{22} = +68.6°$ (*c* 3.2, CHCl$_3$). (Found: C 70.07; H 4.91. Calc. for C$_{34}$H$_{28}$O$_9$: C 70.36; H 4.86).

The material in the mother liquor was boiled for 3 h with methanolic sodium methoxide, evaporated, dissolved in water, and deionized as described above. The product

was crystallized from ethanol to give 2.55 g (22 %) of 1,5-anhydro-D-glucitol (8), m.p. 135 – 137°C. Additional recrystallization gave a product with m.p. 139 – 141°C, $[\alpha]_D^{23}$ = + 42.0° (c 3.2, H$_2$O). (Reported [13] m.p. 142 – 143°C, $[\alpha]_D$ = + 42.3°).

The material in the mother liquor (1.5 g) was separated into 3 fractions by chromatography on a column of silica gel (150 g) using butanone-2, saturated with water, as eluent. The fastest moving fraction (370 mg, 4.2 %) was pure 1,5-anhydro-2,3-dideoxy-D-*erythro*-hexitol (12) as seen from an NMR spectrum. To confirm its structure it was converted into the 4,6-benzylidene derivative, m.p. 135 – 136°C, $[\alpha]_D^{22}$ = – 3.5° (c 0.2, CDCl$_3$). [Reported [3] m.p. 137.5 – 138.5°C, $[\alpha]_D$ = – 4.1° (tetrachloroethane)].

The next fraction gave 510 mg (5 %) of syrupy 1,5-anhydro-2-deoxy-D-*arabino*-hexitol (11) as seen from an NMR spectrum, which was identical with that of the product described below. Benzoylation and recrystallization from ethanol gave 1,5-anhydro-tri-O-benzoyl-2-deoxy-D-*arabino*-hexitol, m.p. 89 – 90°C, $[\alpha]_D$ = – 8.7° (c 2.5, CHCl$_3$), identical with the product described below.

The last fraction to come off the column gave 1.28 g of rather impure 1,5-anhydro-D-glucitol (8), which was only identified through its NMR spectrum.

*Tetra-O-benzoyl-α-D-mannopyranosyl bromide* [14] (3.8 g) was hydrogenated in ethyl acetate (29 ml) and triethylamine (3.0 ml) with 5 % Pd-C (760 mg) as catalyst. Work up as described above gave 2.9 g of a syrup which crystallized slowly from ether-pentane to give 600 mg (18 %) of crude 1,5-anhydro-tetra-O-benzoyl-D-mannitol (14), m.p. 135 – 138°C.

The material in the mother liquor was separated into 4 fractions by preparative TLC using 2 elutions with ethyl acetate-pentane (1:4). The fastest moving fraction gave 238 mg (12 %) of 1,5-anhydro-di-O-benzoyl-2,3-dideoxy-D-*erythro*-hexitol [the dibenzoate of (12)] as a syrup. The product was identified through its 100 MHz NMR spectrum only, which gave the following $\delta$-values and coupling constants (Hz): H-1e = 4.0; H-1a = 3.46; H-2e, H-2a and H-3a = 1.5 – 2.0; H-3e = 2.3 – 2.5; H-4 = 5.06; H-5 = 3.88; H-6 = 4.4; H-6' = 4.6. $J_{1e1a}$ = 11; $J_{1a2a}$ = 10; $J_{1a2e}$ = ~4; $J_{43e}$ = 4.8; $J_{43a}$ = 10; $J_{45}$ = 10; $J_{56}$ = 5.5; $J_{56'}$ = 2.8.

The next fraction gave 240 mg (9 %) of 1,5-anhydro-tri-O-benzoyl-2-deoxy-D-*arabino*-hexitol which was crystallized from ethanol, m.p. 89 – 90°C. A mixed melting point proved the identity with the product described below. The third fraction (822 mg) was crystallized from ether-pentane to give 633 mg (19 %) of (14), m.p. 140 – 141°C. Further recrystallizations from ethanol gave a product with m.p. 141 – 142°C, $[\alpha]_D^{22}$ = – 145° (c 2.0, CHCl$_3$). (Reported [15] m.p. 145 – 146°C, $[\alpha]_D$ = – 148.4°). The last fraction (237 mg) was not investigated closely. Its NMR spectrum indicated that it was a hydrolysis product of the bromide (13).

*Tri-O-benzoyl-β-D-ribopyranosyl bromide* [4] (2.0 g) in ethyl acetate (14 ml) and triethylamine (1.1 ml) was hydrogenated in the presence of 5 % Pd-C (400 mg). Work up as described above gave 1.6 g of syrup which was separated into several fractions by chromatography on a column of silica gel (150 mg) using ethyl acetate-pentane (1:4) as eluent.

The fastest moving fraction gave 26 mg of a crystalline product which was shown by NMR spectra [16] to be 1,3,4-tri-O-benzoyl-2-deoxy-α-D-*erythro*-pentopyranose, recrystallized from ether-pentane, m.p. 149 – 150°C, $[\alpha]_D^{22}$ = + 42.0° (c 0.4, CHCl$_3$). (Reported [9] m.p. 151 – 152°C, $[\alpha]_D$ = + 41.6°). The next fraction (55 mg) was a mixture. The third fraction (16 mg) was shown by NMR spectroscopy, melting point, and mixed melting point to be identical with (6), described above.

Fraction 4 (1.3 g) was crystallized from ether-pentane to give 900 mg (53 %) of 1,5-anhydro-tri-O-benzoyl-ribitol (7), m.p. 154 – 155°C, $[\alpha]_D$ = 0°. (Reported [17] m.p. 156 – 157°C). The last fraction (150 mg) was not investigated closely. An NMR spectrum indicated that it was a hydrolysis product of the bromide (4).

*Hydrogenolysis with Raney-nickel.* Tri-O-benzoyl-β-D-*arabino*-pyranosyl bromide (5.0 g) in ethyl acetate (40 ml) and triethylamine (2.7 ml) was hydrogenated in the presence of Raney-nickel (ca. 1 g). Work up as described above gave a syrup (4.0 g) which was crystallized from methanol to give 2.2 g (52 %) of (2), m.p. 116 – 118°C, $[\alpha]_D^{22}$ = – 214° (c 3.6, CHCl$_3$). The mother liquor deposited an additional batch of crystals (250 mg) which were recrystallized from ether-pentane to give 120 mg (3 %) of the 2-deoxy-compound (3), m.p. 155 – 157°C.

*Tri-O-benzoyl-2-deoxy-α-D-arabino-hexopyranosyl bromide.* To tetra-O-benzoyl-2-deoxy-α-D-*arabino*-hexopyranose (5.0 g) was added 15 ml of a solution of 32 % hydrogen bromide

in glacial acetic acid and 15 ml of dichloromethane. After 3 h at room temperature more dichloromethane was added and the solution was washed with water and aqueous sodium hydrogen carbonate, dried and evaporated. The residue (4.3 g) was crystallized from ether-pentane to give 2.9 g (62 %) of the α-bromide, m.p. 140−141°C. After an additional recrystallization the melting point was unchanged, $[\alpha]_D^{22} = +115°$ (c 1.5, CHCl$_3$). [Reported [5] m.p. 139°C, $[\alpha]_D^{16} = +121°$ (tetrachloroethane)]. The structure was further confirmed through an NMR-spectrum.

*1,5-Anhydro-tri-O-benzoyl-2-deoxy-*D-arabino-*hexitol.* Tri-O-acetyl-1,2-dideoxy-D-*arabino*-hex-1-enopyranose (5.0 g) in ethyl acetate (25 ml) was hydrogenated in the presence of platinum oxide (200 mg). The product was deacetylated with methanolic sodium methoxide to give 1,5-anhydro-2-deoxy-D-*arabino*-hexitol (*11*) [18] which was purified by distillation, boiling point 170°C (1 mmHg). The product was chromatographically homogeneous, but it could not be induced to crystallize. Benzoylation in the usual manner gave the tribenzoate which crystallized from ether-pentane and was recrystallized from ethanol, m.p. 90−91°C, $[\alpha]_D^{22} = -7.9°$ (c 5.0, CHCl$_3$). (Found: C 70.33; H 5.09. Calc. for $C_{27}H_{24}O_7$: C 70.42; H 5.25).

Microanalyses were performed by Dr. A. Bernhardt.

# REFERENCES

1. Zervas, L. and Zioudrou, C. *J. Chem. Soc.* **1956** 214.
2. Hedgley, E. J. and Fletcher, H. G., Jr. *J. Org. Chem.* **30** (1965) 1282.
3. Gray, G. R. and Barker, R. *J. Org. Chem.* **32** (1967) 2764.
4. Ness, R. K., Fletcher, H. G., Jr. and Hudson, C. S. *J. Am. Chem. Soc.* **73** (1951) 959.
5. Bergmann, M., Schotte, H. and Leschinsky, W. *Ber.* **56** (1923) 1052.
6. *Org. Syn. Coll.Vol.* **3** (1965) 686.
7. *Org. Syn. Coll.Vol.* **3** (1965) 181.
8. Fletcher, H. G., Jr. and Hudson, C. S. *J. Am. Chem. Soc.* **72** (1950) 4173.
9. Pedersen, C., Diehl, H. W. and Fletcher, H. G., Jr. *J. Am. Chem. Soc.* **82** (1960) 3425.
10. Bock, K., Lundt, I. and Pedersen, C. *Acta Chem. Scand.* **23** (1969) 2083.
11. Fletcher, H. G., Jr. and Hudson, C. S. *J. Am. Chem. Soc.* **69** (1947) 1672.
12. Bhattacharya, A. K., Ness, R. K. and Fletcher, H. G., Jr. *J. Org. Chem.* **28** (1963) 428.
13. Fletcher, H. G., Jr. *J. Am. Chem. Soc.* **69** (1947) 706.
14. Ness, R. K., Fletcher, H. G., Jr. and Hudson, C. S. *J. Am. Chem. Soc.* **72** (1950) 2200.
15. Ness, R. K. and Fletcher, H. G., Jr. *J. Am. Chem. Soc.* **75** (1953) 2619.
16. Cushley, R. J., Codington, J. F. and Fox, J. J. *Carbohyd. Res.* **5** (1967) 31.
17. Jeanloz, R., Fletcher, H. G., Jr. and Hudson, C. S. *J. Am. Chem. Soc.* **70** (1948) 4052.
18. Fischer, E. *Ber.* **47** (1914) 196.

# Short Communications

## Asymmetric Induction in a Michael-type Reaction

BENGT LÅNGSTRÖM and
GÖRAN BERGSON

*Department of Organic Chemistry,
University of Uppsala, Box 531, S-751 21
Uppsala, Sweden*



I

II

a) R = H
b) R = CH$_3$–CH–CH$_3$



III

IV

a) R = H
b) R = CH$_3$–CH–CH$_3$

This paper briefly reports some preliminary results which demonstrate asymmetric induction in a base-catalyzed Michael-reaction. Previous studies on asymmetric Michael additions have involved the use of chiral reagents.[1] Walborsky and co-workers,[2] for example, studied the addition of (−)-menthyl chloroacetate to ethyl acrylate using achiral alkoxides as catalysts. Similarly, the addition of Grignard reagents to chiral α,β-unsaturated esters has been extensively studied.[3] Except for some enzymatic reactions, however, the addition of achiral nucleophiles to the carbon-carbon double bond of an achiral substrate under the influence of a chiral catalyst has been little studied.[4] Thus, the present paper is the first report of the use of a chiral catalyst in a Michael addition. Recently, a similar asymmetric induction in an aldol-type reaction [5] was described.

The present investigation deals with the addition of methyl 2-carboxy-1-indanone (I) to acrolein (IIa) or α-isopropylacrolein (IIb) using optically active 2-(hydroxymethyl)-quinuclidine (III) as catalyst in benzene solution at room temperature. The course of the reactions were followed by PMR, with which it was shown that the addition products (IV) are formed quantitatively. The optical rotations of the reaction mixtures were also followed as a function of time and found to change continuously towards a limiting value different from zero, thus indicating the formation of optically active products. The addition products (IVa) and (IVb),
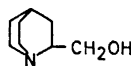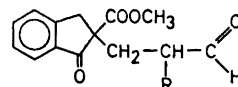
respectively, were isolated and found to be optically active. As an additional test for the optical activity of the products, the semicarbazone derivatives were prepared, purified and tested for optical activity.

The Michael addition reaction involves at least three steps. Firstly, the catalyzing base removes the acidic proton in I with the generation of the nucleophilic stabilized carbanion. Secondly, this nucleophile adds to the activated carbon-carbon double bond in II, and finally the intermediate addition product is protonated at the carbon atom in the α-position to the aldehyde group with the formation of the end product IV. When acrolein (IIa) is used as a reactant, only one asymmetric centre is created in the product IVa. The fact that this product is optically active proves that the catalyzing base, or more precisely its corresponding acid, is present in the second step of the reaction. The most plausible interpretation is that an ion pair between the enolate ion of I and the protonated form of III constitutes the nucleophilic species which adds to the activated double bond in IIa.

When α-isopropylacrolein (IIb) is used as a substrate, the optical activity found

in the product IVb does not prove that the catalyzing base is present in the addition step, since optical activity would also be created in the final protonation step if this is accomplished by the protonated form of III. By analogy with the reaction involving IIa it seems probable, however, that the asymmetric induction also occurs in the addition step for IIb. Product IVb is, of course, a mixture of two diastereomers, as demonstrated by the PMR-spectrum. Preliminary experiments have shown that the initially observed diastereomeric ratio is kinetically controlled.

As yet it is not possible to say anything regarding the degree of asymmetric induction in these reactions.

*Experimental.* The PMR-spectra were recorded with a Varian A60-D instrument at 34°C. Optical rotations were measured with a Perkin-Elmer 141 M apparatus at 546 nm. The microanalyses were performed at the Department of Analytical Chemistry, University of Uppsala.

*Methyl 2-(2-formylethyl)indan-1-on-2-carboxylate (IVa).* In a 100 ml volumetric flask 0.82 g (0.147 mol) of freshly distilled acrolein, 2.76 g (0.146 mol) of 2-carbmethoxy-1-indanone [6] and 0.0058 g (0.00004 mol) of a freshly sublimed and partially resolved (R)-(+)-2-(hydroxymethyl)-quinuclidine (III)[7] ($[\alpha]_{546}^{25.0}$ = +77.0°, 57 % enantiomeric excess[1]) were dissolved in benzene and diluted to 100 ml. The reaction temperature was 22.00 ± 0.02°C. After 20 h, the reaction was complete as determined by PMR and polarimetry. The reaction mixture was washed with 5 × 100 ml of water and 150 ml of a saturated sodium chloride solution. The benzene layer was then dried, evaporated and the residue distilled; b.p. 150 − 152°C/0.1 mmHg. PMR chemical shifts ($\delta$ ppm. relative TMS) methylene 2.00 − 2.75, methylene in the ring 2.85 − 3.85, methyl ester 3.67, aldehyde 9.65, and aromatic protons 7.30 − 7.80. The specific rotation of IVa was $[\alpha]_{546}^{21.0}$ = +8.83° (c 6.53, CCl$_4$). (Found: C 68.70; H 5.75. Calc. for C$_{14}$H$_{14}$O$_4$ (246): C 68.29; H 5.69.)

The semicarbazone derivative[8] of IVa had m.p. 133 − 135°C and a specific rotation $[\alpha]_{546}^{20.0}$ = +3.75° (c 0.96, ethanol). (Found: C 59.44; H 5.66; N 13.82. Calc. for C$_{15}$H$_{12}$N$_3$O$_4$ (303): C 59.40; H 5.61; N 13.86.)

*Methyl 2-(2-formyl-3-methylbutyl)indan-1-on-2-carboxylate (IVb).* As above 2.76 g (0.028

mol) of freshly distilled α-isopropylacrolein[9] and 4.77 g (0.025 mol) 2-carbmethoxy-1-indanone[6] were dissolved in benzene and 0.2376 g (0.0017 mol) of freshly sublimed and partially resolved (R)-(+)-III ($[\alpha]_{546}^{25.0}$ = +77.0°)[7] was added. The mixture was diluted to 100 ml with benzene and kept at 44.00 ± 0.1°C. After 30 days, the reaction was complete according to PMR analysis. The mixture was washed with 5 × 100 ml of water and 150 ml of a saturated sodium chloride solution. The organic layer was dried and evaporated. The residue was not sufficiently stable to be distilled but the raw product of IVb had a specific rotation $[\alpha]_{546}^{44.0}$ = +28.8° (c 5.22, benzene). PMR chemical shifts ($\delta$ ppm. relative TMS) methylene and methine 1.60 − 2.60, methylene in the ring 2.75 − 3.75, methyl 0.80 − 1.10, methyl ester 3.60, aldehyde 9.40 − 9.58 and aromatic protons 7.30 − 7.80.

The semicarbazone derivative of IVb[8] had m.p. 196.0 − 197.5°C and a specific rotation $[\alpha]_{546}^{20.0}$ = − 3.2° (c 0.25, dimethyl sulphoxide). (Found: C 62.34; H 6.69; N 12.10. Calc. for C$_{18}$H$_{23}$N$_3$O$_4$ (345): C 62.60; H 6.66; N 12.17.)

1. Morrison, J. D. and Mosher, H. S. *Asymmetric Organic Reactions*, Prentice-Hall, Englewood Cliffs, New Jersey 1971.
2. a. Inouye, Y., Inamasu, S., Horiike, M., Ohno, M. and Walborsky, H. M. *Tetrahedron* **24** (1968) 2907; b. McCoy, L. L. *J. Org. Chem.* **29** (1964) 240.
3. Inouye, Y. and Walborsky, H. M. *J. Org. Chem.* **27** (1962) 2706.
4. Gavron, O. and Fondy, T. P. *J. Am. Chem. Soc.* **81** (1959) 6333.
5. Obenius, U. and Bergson, G. *Acta Chem. Scand.* **26** (1972) 2546.
6. House, H. O. and Hudson, C. B. *J. Org. Chem.* **35** (1970) 647.
7. Långström, B. *Chem. Scripta. In press.*
8. Shriner, R. L., Fuson, R. C. and Curtin, D. Y. *The Systematic Identification of Organic Compounds*, Wiley, New York 1965, p. 253.
9. Marvel, C. S., Myers, R. L. and Saunders, J. H. *J. Am. Chem. Soc.* **70** (1948) 1694.

# Bourgeanic Acid in the Lichen Stereocaulon tomentosum

TORGER BRUUN

*Institutt for organisk kjemi, Universitetet i Trondheim, Norges tekniske høgskole, N-7034 Trondheim-NTH, Norway*

Stereocaulon tomentosum Fr. (5.8 kg, apparently homogeneous) was collected in August 1955 along the railway line between Agle and Lurudal, some 200 km north of Trondheim. The identity was determined by Dr. I. Mackenzie Lamb. A voucher specimen has been deposited in the collection of the Institutt.

The ground and air dried lichen was extracted for 24 h with ether in a glass Soxhlet apparatus. After the ether extract had been concentrated to a manageable volume and filtered, it was extracted successively with sodium hydrogen carbonate, disodium carbonate, and sodium hydroxide solutions. The disodium carbonate extract weighed 5.9 g. It was treated with 50 ml of boiling petroleum, b.r. $60-70°$, and filtered whilst hot. The filtrate contained 2.0 g, which were chromatographed on 60 g of silica gel with elution successively with benzene, benzene-chloroform 1:1, and chloroform. The volume of each fraction equalled the retention volume, 60 ml. The three fractions eluted with benzene and those eluted with benzene-chloroform 1:1 contained only small amounts of material. The three first fractions eluted with chloroform contained 0.2, 0.9, and 0.5 g of material, respectively. The middle fraction (0.9 g) on crystallisation from petroleum and from acetone afforded crystals (157 mg) of m.p. $121-122°$, $[\alpha]_D$ $+6°$ ($c$ 1.05, chloroform, 1 dm tube).

To the extent that our experiments parallelled those described for bourgeanic acid (*1*) from *Desmaziera evernioides* (Nyl.) Follm. et Hun. and *Ramalina bourgeana* (Mont.),[1] identity with this acid was suggested.

Thanks to the kindness of Dr. B. Bodo a direct comparison of the two acids was possible. They appeared identical by IR and mass spectra and by mixed m.p. determination. Taken at the same time bourgeanic acid melted at $123-124°$, the acid from *S. tomentosum* at $121-122°$, and their mixture at $121-123°$. However, under our conditions (AEI MS 902 instrument, 70 eV) neither bourgeanic acid nor the acid from *S. tomentosum* showed $M^+$ or $[M+1]^+$ as originally reported.[1] The molecular weight of the acid from *S. tomentosum* was arrived at by relying on the $[M-15]^+$ peak of the trimethylsilyl ether of the methyl ester of the acid.

Previous investigations of *S. tomentosum* (compare Ref. 2) have revealed the presence of atranorin, lobaric acid, and stictic acid. The present sample apparently belongs to the Chem. strain 2 of Culberson,[2] since atranorin and lobaric acid were identified.
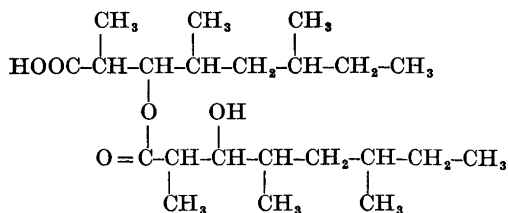
1. Bodo, B., Hebrard, P., Molko, L. and Molko, D. *Tetrahedron Letters* **1973** 1631.
2. Culberson, C. F. *Chemical and Botanical Guide to Lichen Products*, The University of North Carolina Press, Chapel Hill 1969, p. 522.

Received September 28, 1973.



$$\underset{\text{1}}{\begin{array}{c}\overset{\text{CH}_3 \qquad \text{CH}_3 \qquad \text{CH}_3}{\text{HOOC--CH--CH--CH--CH}_2\text{--CH--CH}_2\text{--CH}_3} \\ \text{O} \qquad \text{OH} \\ \text{O=C--CH--CH--CH--CH}_2\text{--CH--CH}_2\text{--CH}_3 \\ \text{CH}_3 \qquad \text{CH}_3 \qquad \text{CH}_3 \end{array}}$$

# Polychlorinated Biphenyls

## VI.* 2,3,7,8-Tetrachlorodibenzofuran, a Critical Byproduct in the Synthesis of 2,2',4,4',5,5'-Hexachlorobiphenyl by the Ullmann Reaction

MARIA MORON, GÖRAN SUNDSTRÖM and CARL AXEL WACHTMEISTER

*Wallenberglaboratoriet, Stockholms Universitet, Lilla Frescati, S-104 05 Stockholm, Sweden*

In connection with structural studies of the components in commercial PCB-mixtures (polychlorinated biphenyls) we have synthesised a number of symmetrically and unsymmetrically substituted chlorinated biphenyls.[2,3] One of these compounds, 2,2',4,4',5,5'-hexachlorobiphenyl, a major component in PCB-mixtures,[4-6] was synthesised in larger amounts by an Ullmann coupling of 2,4,5-trichloroiodobenzene in order to be used in toxicological investigations.

In a study concerning the Ullmann reaction of 2-chloroiodobenzene Nilsson[7] showed that under commonly used conditions dibenzofuran was formed as a byproduct in the coupling reaction. The formation of minor amounts of 2,3,7,8-tetramethoxydibenzofuran in the coupling of 4-bromo-5-iodoveratrole has also been reported.[8] The occurrence of chlorinated dibenzofurans as contaminants in chlorobiphenyl samples prepared for toxicological experiments could be serious in view of the high toxicity of these compounds, recently detected by Vos et al.[9] as contaminants in some commercial PCB-mixtures. We have therefore studied the byproducts in the above coupling reaction with special attention to chlorinated dibenzofurans.

The coupling reaction was performed with commercial 2,4,5-trichloroidobenzene which was thoroughly purified. The copper bronze was of the same quality as the one used by Nilsson[7] and contained a small amount of fatty acids. The use of very pure electrolytic copper did not significantly change the nature or yield of byproducts. No precautions were taken to exclude air from the reaction mixture.

The crude coupling product was fractionated on a silica gel column with hexane

---

\* Part V, see Ref. 1.

as solvent. The fractions eluted after some starting material and the main product were investigated by mass spectrometry for the presence of compounds with the molecular ion 304 m.u. which corresponds to a tetrachlorinated dibenzofuran. Such a compound was also found eluted with some other byproducts, probably chlorinated terphenyls (MS) (cf. Ref. 7). The suspected tetrachlorodibenzofuran could more conveniently be isolated in a pure state by chromatography of the crude coupling product on an alumina column. The compound gave the expected analytical values and mass spectrum. The only peaks exceeding 10 % of the base peak (306 m.u.) in the mass spectrum was found at 241 – 243 m.u. (16 %) which corresponds to loss of ClCO from the molecular ion. This fragmentation was found also by Vos et al.[9] and could be compared with the loss of HCO from the molecular ion of the parent compound, dibenzofuran.[10]

The NMR spectrum showed singlet signals at $\delta$ 7.48 and $\delta$ 7.85, consistent only with a 2,3,7,8-tetrachlorodibenzofuran structure.

Treatment of 2,2',4,4',5,5'-hexachlorobiphenyl with potassium hydroxide at elevated temperatures gave small amounts of the same tetrachlorodibenzofuran (GLC, TLC), probably via a phenolic intermediate.
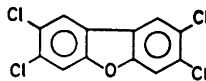


The results presented here show that any preparation of polychlorinated biphenyls synthesised via the Ullmann reaction using iodo-compounds with chlorine atoms in the ortho-positions must be thoroughly analysed for the presence of chlorinated dibenzofurans. A comparison of the toxicity of 2,2',4,4',5,5'-hexachlorobiphenyl, synthesised by the Ullmann method, and a commercial PCB-mixture (Aroclor 1254) was recently published.[11] No details of the purification of the product were given. However, our crude biphenyl contained ca. 3 % tetrachlorodibenzofuran and trace amounts of this compound were detected (GLC) even after repeated crystallisations from hexane, ethanol or acetic acid.

*Experimental.* The melting points were determined on a Kofler micro hot stage. Mass

spectra were recorded on an LKB 9000 spectrometer. The NMR spectrum was obtained on a Varian HA-100D instrument with tetramethylsilane as internal standard.

*Gas chromatography.* The products were characterised by GLC using a Hewlett-Packard 7620A instrument fitted with an EC detector. Glass columns $(0.20 \times 160$ cm) containing 2 % (w/w) Apiezon L on Chromosorb W A/W DMCS (100−120 mesh) at 210° were used. The gas flow (argon-methane, 9:1) was about 25 ml/min.

*Coupling reaction.* 2,4,5-Trichloroiodobenzene (Koch-Light, recrystallised from ethanol or purified on a silica gel column with hexane as solvent, 10 g) was thoroughly mixed with copper-bronze (lithographic bronze, *cf.* Ref. 7; 9.3 g) and the mixture was heated from 180° to 235° during one hour with occasional stirring. Extraction of the reaction mixture in a Soxhlet apparatus with hexane and evaporation of solvent gave 5.7 g of crude product.

*Isolation of 2,2′,4,4′,5,5′-hexachlorobiphenyl.*[5,6,12] 2.5 g of the above product was added to a column $(5.5 \times 62$ cm) of silica gel (Merck, <0.063 mm) which was eluted with hexane. After some starting material 2,2′,4,4′,5,5′-hexachlorobiphenyl was obtained free from byproducts (GLC), 2.05 g, m.p. 103.5−104.5° (EtOH), $\lambda_{max}$ (EtOH) 281 nm ($\varepsilon$ 2040), 290 nm ($\varepsilon$ 1860).

After the major product the tetrachlorodibenzofuran eluted together with some other byproducts, most probably terphenyls (8 Cl) as shown by MS.

*Isolation of 2,3,7,8-tetrachlorodibenzofuran.* When 2.5 g of the crude product was chromatographed on neutral alumina (Merck, activity grade I, $4.2 \times 72$ cm) with hexane as solvent the biphenyl and the suspected terphenyls eluted together. The column was further eluted with hexane-ether (9:1). Finally elution with ether gave a fraction of 2,3,7,8-tetrachlorodibenzofuran (0.08 g) which crystallised from hexane. The compound recrystallised on the hot plate from *ca.* 150° to give needles, m.p. 223−226° (subl. from *ca.* 210°). [Found: C 47.0; H 1.3. M$^+$ 304 m.u. (4 Cl). $C_{12}H_4Cl_4O$ (306.0) requires C 47.1; H 1.3).] (NMR (CDCl$_3$) $\delta$ 7.48 (s) and $\delta$ 7.85 (s). $\lambda_{max}$ (EtOH) 222.5 nm (sh) ($\varepsilon$ 46 500), 228.5 nm

($\varepsilon$ 50 200), 240 nm (sh) ($\varepsilon$ 26 600), 251 nm ($\varepsilon$ 17 400), 259.5 nm ($\varepsilon$ 29 100), 298.5 nm (sh) ($\varepsilon$ 24 500), 304 nm ($\varepsilon$ 28 200), and 314 nm ($\varepsilon$ 23 300).

Retention times on GLC, conditions as described above, for 2,2′,4,4′,5,5′-hexachlorobiphenyl and 2,3,7,8-tetrachlorodibenzofuran were 11.6 and 14.8 min, respectively. Retention times for the terphenyls were several hours under these conditions.

On TLC (silica gel-hexane) the tetrachlorodibenzofuran has an $R_F$ value of 0.30 and the hexachlorobiphenyl 0.41.

1. Sundström, G. *Bull. Environ. Contam. Toxicol. In press.*
2. Sundström, G. *Acta Chem. Scand.* **27** (1973) 600.
3. Sundström, G. *To be published.*
4. Sissons, D. and Welti, D. *J. Chromatogr.* **60** (1971) 15.
5. Webb, R. G. and McCall, A. C. *J. Ass. Off. Anal. Chemists* **55** (1972) 746.
6. Tas, A. C. and deVos, R. H. *Environ. Science Technol.* **5** (1971) 1216.
7. Nilsson, M. *Acta Chem. Scand.* **12** (1958) 537.
8. Baker, W., Barton, J. W., McOmie, J. F. W., Pennek, R. J. and Watts, M. L. *J. Chem. Soc.* **1961** 3986.
9. Vos, J. G., Koeman, J. H., van der Maas, H. L., ten Noever de Brauw, M. C. and deVos, R. H. *Food Cosmetics Toxicol.* **8** (1970) 625.
10. Pring, B. and Stjernström, N. E. *Acta Chem. Scand.* **22** (1968) 549.
11. Vos, J. G. and Notenboom-Ram, E. *Toxicol. Appl. Pharmacol.* **23** (1972) 563.
12. Safe, S. and Hutzinger, O. *J. Chem. Soc. Perkin Trans. 1* **1972** 686.

# Differentiation between α-Glutamyl Peptides, γ-Glutamyl Peptides, and α-Aminoacylglutamic Acids by PMR Spectroscopy

IB KRISTENSEN and
PEDER OLESEN LARSEN

*Department of Organic Chemistry, Royal Veterinary and Agricultural University, DK-1871 Copenhagen, Denmark*

Numerous γ-glutamyl derivatives of amino acids and amines occur naturally,[1] and methods for the unequivocal structure determination of these compounds are therefore of importance. Whereas standard methods can be used to establish the sequence of dipeptides containing glutamic acid the differentiation between α- and γ-glutamyl derivatives poses a specific problem. The only three reliable chemical solutions to this problem are synthesis, quantitative decarboxylation with ninhydrin,[2] and deamination with nitrous acid.[3] The latter two methods are destructive and demand considerable amounts of material. The higher $pK_2$-values for α-glutamyl α-amino acids than for γ-glutamyl α-amino acids determine the elution behaviour on strongly basic ion-exchange resins in the acetate form, γ-glutamyl peptides being eluted last with acetic acid. Differentiation between α- and γ-glutamyl peptides has been made on an amino acid analyser, where γ-glutamyl peptides are eluted before and α-glutamyl peptides after the second amino acid from a strongly acidic ion-exchange resin with citrate buffer.[4] Various methods depending on paper chromatography, electrophoresis, or acid lability for distinction between the two isomer possibilities require both isomers for reliable results.

The δ-value for the α-proton in the glutamic acid moiety is larger for α-glutamyl amino acids than for γ-glutamyl amino acids in aqueous solution, and this difference has been proposed as a means for differentiation between α- and γ-glutamyl derivatives.[4] However, the δ-value for the α-proton in γ-glutamylglutamic acid (3.92 ppm) is higher than the upper limit of 3.90 ppm given for the α-proton in γ-glutamyl derivatives,[4] and similar to the shift for the α-proton in glutamic acid in α-glutamylphenylalanine

(3.93 ppm) and α-glutamyl-β-alanine (3.94 ppm).[4] Again the method will give reliable results only when both isomers are available.

The difference in δ-values for the α-proton is of course due to the different chemical surroundings of the α-protons. The surroundings of the α-protons vary with the ionization state of the dipeptides. Use of the changes in chemical shifts occurring on change in ionization[5] and analysis of the surroundings permits differentiation between the possible isomers in dipeptides containing glutamic acid and a second amino acid. Definite ionization states are obtained (i) in $D_2O$, (ii) in $D_2O$ with excess trifluoroacetic acid, (iii) in $D_2O$ with excess $K_2HPO_4$ (pH 7), and (iv) in $D_2O$ with excess NaOH. In the first case, equal amounts of positively charged amino groups and negatively charged carboxyl groups are obtained, γ-glutamyl amino acids and aminoacylglutamic acids with negative charge on the α-carboxyl group in the glutamic acid moiety, and α-glutamyl α-amino acids with negative charge on the carboxyl group in the second amino acid. In case (ii), all carboxyl groups are free and all amino groups are positively charged, while in case (iii) all carboxyl groups are negatively charged and all amino groups are positively charged. Finally, in case (iv), all carboxyl groups are negatively charged and all amino groups are uncharged.

In Table 1 are listed the δ-values for the α-protons in various glutamic-acid-containing dipeptides and in related compounds. For elucidation the variable surroundings of the α-protons are listed. The changes in δ-values observed are in full agreement with those expected from the substitution patterns. Ionization of a carboxyl group positioned on the same carbon atom as the α-proton results in an upfield shift of from 0.12 to 0.37 ppm. Neutralization of an amino group positioned on the same carbon atom as the α-proton results in an upfield shift of from 0.43 to 0.77 ppm.

Only the signal for the α-proton in the γ-glutamyl peptides exhibits two shifts (between pH < 1 and pH 3 and between pH 7 and pH > 11) characteristic for a proton in a free α-aminocarboxylic acid setting. Therefore when a signal with two shifts is observed, it can be concluded that a γ-glutamyl peptide is present, and assignment of the signals for the two

*Table 1.* $\delta$-Values and chemical surroundings for $\alpha$-protons in glutamic acid containing dipeptides and related compounds.

| | pH < 1[a] | | pH ~ 3[b] | | pH ~ 7[c] | | pH > 11[d] | |
|---|---|---|---|---|---|---|---|---|
| | δ (ppm) | surround-ings | δ (ppm) | surround-ings | δ (ppm) | surround-ings | δ (ppm) | surround-ings |
| **α-Proton in glutamic acid** | | | | | | | | |
| Glutamic acid | 4.17 | | 3.82 | | 3.81 | | 3.23 | |
| Glutamine | 4.20 | | — | | 3.83[b] | | 3.31 | |
| γ-Glutamyl peptides | | | | | | | | |
| γ-Glutamyl-alanine | 4.15 | | 3.82 | | 3.77 | | 3.25 | |
| γ-Glutamyl-glutamic acid | 4.14 | −COOH −NH₃⁺ | 3.92 | −COO⁻ −NH₃⁺ | — | −COO⁻ −NH₃⁺ | — | −COO⁻ −NH₂ |
| γ-Glutamyl-methionine sulfoxide | 4.12 | | 3.89 | | — | | — | |
| γ-Glutamyl-phenylalanine | 4.01 | | 3.70 | | 3.63 | | 3.20[e] | |
| γ-Glutamyl-tyrosine | 4.01 | | 3.72 | | 3.69 | | 3.13 | |
| Glutamic acid α-amide | 4.17 | −CONH₂ −NH₃⁺ | — | — | 4.12[b] | −CONH₂ −NH₃⁺ | 3.35 | −CONH₂ −NH₂ |
| **α-Glutamyl peptides** | | | | | | | | |
| α-Glutamyl-alanine | 4.15 | −CONHR −NH₃⁺ | 4.10 | −CONHR −NH₃⁺ | 4.05 | −CONHR −NH₃⁺ | 3.37 | −CONHR −NH₃ |
| α-Glutamyl-tyrosine | 4.07 | | 4.00 | | 3.97 | | 3.35 | |
| **α-Aminoacyl glutamic acids** | | | | | | | | |
| Alanylglutamic acid | 4.53 | −COOH −NHCOR | 4.27 | −COO⁻ −NHCOR | 4.19 | −COO⁻ −NHCOR | 4.15 | −COO⁻ −NHCOR |
| Tyrosyl-glutamic acid | 4.45[e] | | 4.25[e] | | 4.23[e] | | 4.15 | |
| **α-Proton in second amino acid** | | | | | | | | |
| γ-Glutamyl peptides | | | | | | | | |
| γ-Glutamyl-alanine | 4.29 | | 4.31 | | 4.15 | | 4.15 | |
| γ-Glutamyl-glutamic acid | 4.45 | | 4.42 | | — | | — | |
| γ-Glutamyl-methionine sulfoxide | 4.54 | −COOH −NHCOR | 4.54 | −COOH −NHCOR | — | −COO⁻ −NHCOR | — | −COO⁻ −NHCOR |
| γ-Glutamyl-phenylalanine | 4.72 | | 4.65 | | 4.51 | | 4.50 | |
| γ-Glutamyl-tyrosine | 4.65 | | 4.60 | | 4.48 | | 4.40 | |

*Table 1. Continued.*

α-Glutamyl peptides
α-Glutamyl-

| | | | | | | | | |
|---|---|---|---|---|---|---|---|---|
| alanine | 4.48 ⎫ | − COOH | 4.28 ⎫ | − COO⁻ | 4.22 ⎫ | − COO⁻ | 4.17 ⎫ | − COO⁻ |
| α-Glutamyl-tyrosine | 4.70 ⎭ | − NHCOR | 4.48 ⎭ | − NHCOR | 4.46 ⎭ | − NHCOR | 4.49 ⎭ | − NHCOR |

α-Aminoacyl glutamic acids
Alanyl-

| | | | | | | | | |
|---|---|---|---|---|---|---|---|---|
| glutamic acid | 4.20 ⎫ | − CONHR | 4.15 ⎫ | − CONHR | 4.17 ⎫ | − CONHR | 3.52 ⎫ | − CONHR |
| Tyrosyl-glutamic acid | 4.30$^e$ ⎭ | − NH₃⁺ | 4.20$^e$ ⎭ | − NH₃⁺ | 4.18$^e$ ⎭ | − NH₃⁺ | 3.60 ⎭ | − NH₂ |

$^a$D$_2$O with trifluoroacetic acid. $^b$D$_2$O. $^c$D$_2$O + K$_2$HPO$_4$. $^d$D$_2$O + NaOH. $^e$The exact δ-values are difficult to obtain because of superposition of signals.

α-protons to the two constituent amino acids can be made. The signal for the proton in the second amino acid only shows a shift when pH is raised from 3 to 7. No shift is observed here for the two isomeric possibilities and thus further evidence for a γ-glutamyl structure can be obtained. Both α-glutamyl peptides and α-aminoacylglutamic acids show signals for one proton shifting between pH < 1 and pH 3 and for one proton shifting between pH 7 and pH > 11. Differentiation between these isomers can only be made when the two signals can be assigned to the two constituent amino acids.[6] In the present case this is easily done for the alanine derivatives since the α-proton in alanine gives a signal split into a quartet. For the tyrosine derivatives the coupling of the α-proton in tyrosine with the easily discernible benzylic protons permits assignment.

PMR-spectra of the compounds in different ionization states thus provide an unequivocal and nondestructive method for differentiation between on one side γ-glutamyl peptides and on the other side α-glutamyl peptides and aminoacylglutamic acids. Furthermore differentiation between α-glutamyl peptides and aminoacylglutamic acids can be made provided that the signals for the α-protons can be assigned to glutamic acid and the second amino acid. Not only the changes but also the actual δ-values found may be used for assignment of structure. However, especially when new amino acids are involved such assignments must be made with more caution than those made on the basis of changes in chemical shifts.

*Methods and materials.* PMR-spectra were measured on a JEOL C-6OHL instrument.

δ-Values are in ppm relative to sodium 2,2,3,3-tetradeuterio-3-(trimethylsilyl)propionate. Spectra were measured on solutions containing between 1 and 4 % of peptide in D$_2$O containing excess trifluoroacetic acid (more than 6 %), in D$_2$O, in D$_2$O containing 1.5 mol of K$_2$HPO$_4$ per mol of glutamic acid derivative, and in 0.4 N NaOH in D$_2$O.

γ-L-Glutamyl-L-alanine, α-L-glutamyl-L-alanine, L-alanyl-L-glutamic acid, α-L-glutamyl-L-tyrosine, and L-tyrosyl-L-glutamic acid were obtained from Cyclo Chemical, U.S.A. γ-L-Glutamyl-L-phenylalanine was isolated from seeds of *Fagus silvatica*. L.[5] and unequivocally identified by comparison with previously verified material.[7] γ-L-Glutamyl-L-tyrosine was isolated from *Aubrietia deltoidea* DC.[7] γ-Glutamylglutamic acid and γ-glutamylmethionine sulfoxide were also isolated from seeds of *Fagus silvatica* L. The configurations of these compounds have not been established.[5] L-Glutamic acid α-amide was obtained from Calbiochem, U.S.A.

1. Waley, S. G. *Advan. Protein Chem.* **21** (1966) 1.
2. Sachs, H. and Brand, E. *J. Am. Chem. Soc.* **75** (1953) 4608.
3. Sachs, H. and Brand, E. *J. Am. Chem. Soc.* **76** (1954) 3601.
4. Kasai, T. and Sakamura, S. *Agr. Biol. Chem.* **37** (1973) 685.
5. Kristensen, I. *Free amino acids and γ-glutamyl peptides in* Fagus silvatica L., Diss., Royal Veterinary and Agricultural University, Copenhagen 1973.
6. Sheinblatt, M. *J. Am. Chem. Soc.* **88** (1966) 2845.
7. Larsen, P. O. and Sørensen, H. *Acta Chem. Scand.* **21** (1967) 2908.

# The Effects of Nucleotides on the α-Glucosidase Formation in Baker's Yeast Protoplasts*

SAMPSA HAARASILTA and ERKKI OURA

*Research Laboratories of State Alcohol Monopoly (Alko), SF-00101 Helsinki 10, Finland*

The few papers dealing with yeast and 3',5'-AMP (cAMP) provide some evidence that cyclic cAMP may be involved in the metabolic control of yeast, as has already been well documented for bacteria.[2] It has been reported that the concentration of cAMP in *Schizosaccharomyces pombe, Saccharomyces carlsbergensis* and *Sacch. fragilis* depends on the growth conditions.[3-5] Moreover, it has been demonstrated for *Sacch. cerevisiae* protoplasts that certain nucleotides, including cAMP, can overcome the glucose repression of respiratory adaptation.[6] cAMP has been shown to have a de-repressive effect on the glucose repression of sporulation in intact baker's yeast.[7]

The effects of cAMP and some other nucleotides on the partially repressed α-glucosidase synthesis in baker's yeast protoplasts are reported in this paper.

A commercial baker's yeast strain was used in the experiments. Protoplasts were prepared from an early log-phase culture according to Nurminen *et al.*[8] by using β-mercaptoethanol and *Helix pomatia* snail gut juice. The methods used for the induction and the determination of α-glucosidase were slightly modified from those described by Burger *et al.*[9] The induction medium was 0.7 M in $MgSO_4$ and contained 0.65 % maltose, 1 % Casamino acids and approximately 0.2 % protoplasmic protein (determined according to Lowry *et al.*[10]). In some experiments 0.8 M mannitol was used as the osmotic stabilizer for the protoplasts in place of $MgSO_4$. The pH of the mixture was adjusted to 4.7 with McIlwaine's citrate-

phosphate buffer. Any additions to the induction mixture are indicated. The induction was carried out by incubating 10 ml of the mixture at 30°C in a 50 ml Erlenmeyer flask in a shaker. A preparation for α-glucosidase analysis was made by centrifuging 1 − 2 ml of the induction mixture, suspending the sediment in 1 − 2 ml of distilled water and allowing it to stand with occasional shaking for at least 20 min at 0°C. During this time protoplasts were broken. The supernatant remaining after centrifugation of the broken cell suspension is hereafter referred to as lysate. 50 − 200 μl of lysate were taken for the determination of α-glucosidase activity. It was made by measuring the hydrolysis of *p*-nitrophenyl-α-D-glucoside (PNPG) at 400 nm with a spectrophotometer linked to an automatic recorder. The assay mixture for α-glucosidase was the same as described by Kloet *et al.*[11] One unit was defined as the amount of enzyme which liberated 1 nmol of *p*-nitrophenol in 1 min at 30°C with 1 ml of lysate present in the assay mixture.



*Fig. 1.* Kinetics of α-glucosidase induction in baker's yeast protoplasts. The induction of α-glucosidase, the preparation of a lysate and the assay of α-glucosidase activity were carried out as described in the text. The induction medium (0.7 M $MgSO_4$ as osmotic stabilizer) was supplied with 0.25 % glucose (×), 1 % glucose (□) or 1 % glucose +0.3 mM cAMP (○).

*Table 1.* α-Glucosidase activity. The effect of low $Mg^{2+}$ and $Mn^{2+}$ ion concentrations on the α-glucosidase induction in baker's yeast protoplasts. The effects of cAMP and ATP in the presence of $Mg^{2+}$ and $Mn^{2+}$ ions on the α-glucosidase induction. The induction of α-glucosidase, the preparation of lysate and the assay of α-glucosidase were carried out as described in the text. The supplements to the induction medium (0.8 M mannitol as osmotic stabilizer) are shown in the table. Activities are expressed as nmol of PNPG hydrolyzed/(min ml) lysate. The samples were taken 4 h after the start of induction.

| Supplement | 0.25 % glucose | 1 % glucose | 0.25 % glucose + 1 mM cAMP | 0.25 % glucose + 1 mM ATP |
|---|---|---|---|---|
| — | 134 | 85 | 142 | 157 |
| 5 mM $Mg^{2+}$ | 126 | 57 | 137 | 125 |
| 5 mM $Mn^{2+}$ | 99 | 43 | 157 | 169 |

The kinetics of α-glucosidase formation in the presence of 0.25 % glucose, 1 % glucose and 1 % glucose +0.3 mM cAMP are presented in Fig. 1. No α-glucosidase was synthesized by protoplasts during the first hour. This period was observed to be independent of the glucose concentration and the presence of cAMP. The repressive effect of increased glucose concentration on the α-glucosidase formation was obvious. cAMP does not seem to have any positive effect and, if anything, acts as a weak repressor. The repressive effect, however, could not be observed in all the experiments. The synthesis rate of α-glucosidase began to be accelerated by cAMP about 3.5 h after the beginning of the enzyme induction. The synthesis rate of α-glucosidase in protoplasts induced in the presence of 1 % glucose +0.3 mM cAMP did not quite reach that in protoplasts induced in the presence of 0.25 % glucose.

The effects of cAMP concentration on the α-glucosidase synthesis is shown in Fig. 2. A cAMP concentration of about 0.3 mM gave the maximum de-repressive effect, which decreased slowly at higher concentrations.

The inhibitory effect of $Mg^{2+}$ ions on the α-glucosidase induction in baker's yeast protoplasts was reported by Burger *et al.*[8] It was now observed that, besides $Mg^{2+}$ ions, $Mn^{2+}$ ions have an inhibitory effect on the α-glucosidase induction (Table 1). This effect of $Mn^{2+}$ ions was more intense than that of $Mg^{2+}$ ions, but weaker than that of 1 % glucose. The inhibitory effect of $Mg^{2+}$ ions could no longer be observed when $MgSO_4$ was used as an osmotic stabilizer for the protoplasts (see Ref. 1). This is possibly a consequence of $MgSO_4$
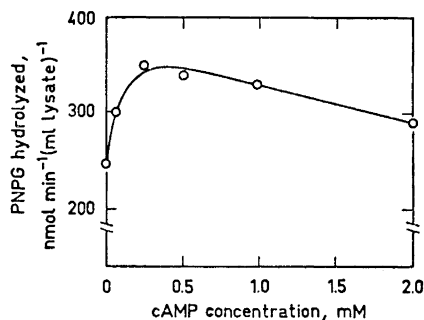


*Fig. 2.* Effect of cAMP concentration on the α-glucosidase induction in baker's yeast protoplasts. The induction of α-glucosidase the preparation of a lysate and the assay of α-glucosidase were carried out as described in the text. The induction medium (0.7 M $MgSO_4$ as osmotic stabilizer) was supplied with 1 % glucose and different cAMP concentrations. The samples were taken 6 h after the start of induction.

being a better osmotic stabilizer than mannitol. The results presented in Table 1 also show that cAMP and ATP nullify the repressive effect of $Mn^{2+}$ ions, and that cAMP can overcome the repressive effect of $Mg^{2+}$ ions as well. The presence of $Mn^{2+}$ ions increase the de-repressive effect of these nucleotides. It is to be noted that the adenyl cyclase in baker's yeast, the only enzyme known to synthesize cAMP is manganese dependent.[12]

The effects of some other nucleotides on α-glucosidase formation were also studied. The results are presented in Table 2. They

*Table 2.* The effect of different nucleotides on the induction of α-glucosidase in baker's yeast protoplasts. The induction of α-glucosidase, the preparation of lysate and the assay of α-glucosidase were performed as described in the text. The induction medium (0.7 M $MgSO_4$ as osmotic stabilizer) was supplied with 1 % glucose and different nucletides to a final concentration of 1 mM. Activities are expressed as nmol of PNPG hydrolyzed/(min ml) lysate. The samples were taken 4.5 h after the start of induction.

| Nucleotide [a] | α-Glucosidase activity |
|---|---|
| None | 155 |
| Cyclic 3′,5′-AMP | 168 |
| ATP | 168 |
| Cyclic 3′,5′-GMP | 163 |
| Cyclic 2′,3′-AMP | 155 |
| Cyclic 3′,5′-UMP | 155 |
| AMP | 150 |
| ADP | 138 |
| O²′-MB cyclic 3′,5′-AMP | 137 |
| N⁶,O²′-DB cyclic 3′,5′-AMP | 137 |
| N⁶-MB cyclic 3′,5′-AMP | 121 |

[a] MB = monobutyryl, DB = dibutyryl.

indicate that the de-repressive effect of cAMP cannot be due to the 3′,5′-ring structure alone; cyclic 3′5′-UMP and butyryl derivatives of cAMP have no de-repressive effects. A definite stimulative effect of ATP was exhibited under these experimental conditions. The de-repressive effect of cyclic 3′5′-GMP was to be expected.

The results obtained support the view that cAMP participated in the catabolite repression of yeast.

1. Haarasilta, S. and Oura, E. *Proceedings of the 3rd International Specialized Symposium on Yeasts, Otaniemi/Helsinki (1973) Part 1, Abstracts*, p. 126.
2. Perlman, R. L. and Pastan, I. In Horecker, B. L. and Stadtman, E. R., Eds., *Current Topics in Cellular Regulation*, Academic, New York and London 1971, Vol. 3, p. 117.
3. Schlanderer, G., Megnet, R. and Dellweg, H. *Jahrb. Vers. Lehranst. Brau. Berlin 1971*, p. 209.
4. Van Wijk, R. and Konijn, T. M. *FEBS Lett.* **13** (1971) 184.
5. Sy, J. and Richter, D. *Biochemistry* **11** (1972) 2788.
6. Fang, M. and Butow, R. A. *Biochem. Biophys. Res. Commun.* **41** (1970) 1579.
7. Tsuboi, M., Kamisaka, S. and Yanagishima, N. *Plant Cell Physiol.* **13** (1972) 585.
8. Nurminen, T., Oura, E. and Suomalainen, H. *Suomen Kemistilehti* **B 38** (1965) 282.
9. Burger, M., Oura, E. and Suomalainen, H. *Suomen Kemistilehti* **B 38** (1965) 285.
10. Lowry, O. H., Rosebrough, N. J., Farr, A. L. and Randall, R. J. *J. Biol. Chem.* **193** (1951) 265.
11. De Kloet, S. R., Van Wermeskerken, R. K. A. and Koningsberger, V. V. *Biochim. Biophys. Acta* **47** (1961) 138.
12. Londesborough, J. C. and Nurminen, T. *Acta Chem. Scand.* **26** (1972) 3396.

Received October 20, 1973.

# Microwave Spectrum of Thiete 1,1-Dioxide

WIKTOR RALOWSKI, STIG LJUNGGREN and JOHAN MJÖBERG

*Division of Physical Chemistry, The Royal Institute of Technology, S-100 44 Stockholm 70, Sweden*

Thiete 1,1-dioxide (*cf.* Fig. 1) was first synthesized by Dittmer and Christy in 1960.[1,2] A complete structural investigation by X-ray diffraction was performed by Lowenstein[3] in 1965. Within the limits of error of the method he found a planar ring structure with the plane of the $O-S-O$ bond perpendicular to the plane of the ring. The refinement of the structure was not carried far enough to reveal the positions of the hydrogen atoms. The results of Lowenstein are tabulated in Table 1.

The effects of some other nucleotides on α-glucosidase formation were also studied. The results are presented in Table 2. They

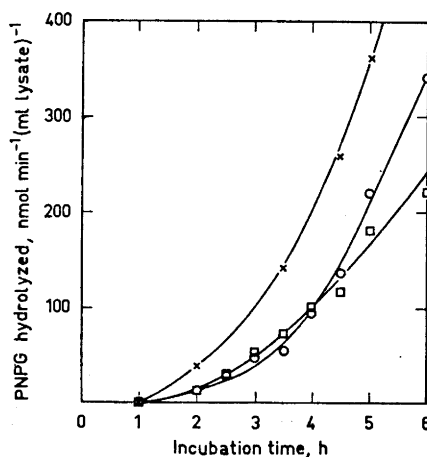Table 2. The effect of different nucleotides on the induction of α-glucosidase in baker's yeast protoplasts. The induction of α-glucosidase, the preparation of lysate and the assay of α-glucosidase were performed as described in the text. The induction medium (0.7 M MgSO$_4$ as osmotic stabilizer) was supplied with 1 % glucose and different nucletides to a final concentration of 1 mM. Activities are expressed as nmol of PNPG hydrolyzed/(min ml) lysate. The samples were taken 4.5 h after the start of induction.

| Nucleotide [a] | α-Glucosidase activity |
|---|---|
| None | 155 |
| Cyclic 3′,5′-AMP | 168 |
| ATP | 168 |
| Cyclic 3′,5′-GMP | 163 |
| Cyclic 2′,3′-AMP | 155 |
| Cyclic 3′,5′-UMP | 155 |
| AMP | 150 |
| ADP | 138 |
| O$^{2'}$-MB cyclic 3′,5′-AMP | 137 |
| N$^{6}$,O$^{2'}$-DB cyclic 3′,5′-AMP | 137 |
| N$^{6}$-MB cyclic 3′,5′-AMP | 121 |

[a] MB = monobutyryl, DB = dibutyryl.

indicate that the de-repressive effect of cAMP cannot be due to the 3′,5′-ring structure alone; cyclic 3′5′-UMP and butyryl derivatives of cAMP have no de-repressive effects. A definite stimulative effect of ATP was exhibited under these experimental conditions. The de-repressive effect of cyclic 3′5′-GMP was to be expected.

The results obtained support the view that cAMP participated in the catabolite repression of yeast.

1. Haarasilta, S. and Oura, E. *Proceedings of the 3rd International Specialized Symposium on Yeasts, Otaniemi/Helsinki (1973) Part 1, Abstracts*, p. 126.
2. Perlman, R. L. and Pastan, I. In Horecker, B. L. and Stadtman, E. R., Eds., *Current Topics in Cellular Regulation*, Academic, New York and London 1971, Vol. 3, p. 117.
3. Schlanderer, G., Megnet, R. and Dellweg, H. *Jahrb. Vers. Lehranst. Brau. Berlin 1971*, p. 209.
4. Van Wijk, R. and Konijn, T. M. *FEBS Lett.* **13** (1971) 184.
5. Sy, J. and Richter, D. *Biochemistry* **11** (1972) 2788.
6. Fang, M. and Butow, R. A. *Biochem. Biophys. Res. Commun.* **41** (1970) 1579.
7. Tsuboi, M., Kamisaka, S. and Yanagishima, N. *Plant Cell Physiol.* **13** (1972) 585.
8. Nurminen, T., Oura, E. and Suomalainen, H. *Suomen Kemistilehti* **B 38** (1965) 282.
9. Burger, M., Oura, E. and Suomalainen, H. *Suomen Kemistilehti* **B 38** (1965) 285.
10. Lowry, O. H., Rosebrough, N. J., Farr, A. L. and Randall, R. J. *J. Biol. Chem.* **193** (1951) 265.
11. De Kloet, S. R., Van Wermeskerken, R. K. A. and Koningsberger, V. V. *Biochim. Biophys. Acta* **47** (1961) 138.
12. Londesborough, J. C. and Nurminen, T. *Acta Chem. Scand.* **26** (1972) 3396.

Received October 20, 1973.

# Microwave Spectrum of Thiete 1,1-Dioxide

WIKTOR RALOWSKI, STIG LJUNGGREN and JOHAN MJÖBERG

*Division of Physical Chemistry, The Royal Institute of Technology, S-100 44 Stockholm 70, Sweden*

Thiete 1,1-dioxide (cf. Fig. 1) was first synthesized by Dittmer and Christy in 1960.[1,2] A complete structural investigation by X-ray diffraction was performed by Lowenstein[3] in 1965. Within the limits of error of the method he found a planar ring structure with the plane of the $O-S-O$ bond perpendicular to the plane of the ring. The refinement of the structure was not carried far enough to reveal the positions of the hydrogen atoms. The results of Lowenstein are tabulated in Table 1.

*Table 1.* Bond lengths and bond angles in thiete 1,1-dioxide as obtained by Lowenstein using X-ray diffraction.

| Bond | Found, Å | Bond angle | Found |
|------|----------|------------|-------|
| C — C | 1.52 ± 0.04 | C — S — C | 80.5° |
| C = C | 1.39 ± 0.03 | S — C — C | 85.1° |
| — C — S | 1.79 ± 0.04 | S — C = C | 90.0° |
| = C — S | 1.77 ± 0.03 | C — C = C | 104.5° |
| S — O | 1.43 ± 0.02 | O — S — O | 115.5° |
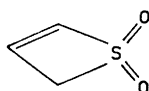


*Fig. 1.* Thiete 1,1-dioxide (thiete sulfone).

In the present investigation microwave spectra of the ground and three vibrationally excited states of thiete 1,1-dioxide and the second excited state of one of these modes were studied in the frequency region 26 500 – 40 000 MHz.

A sample of thiete 1,1-dioxide was kindly supplied by Dr. T. Kempe of the Department of Organic Chemistry, The Royal Institute of Technology, Stockholm.

The spectra were recorded on a Hewlett Packard model 8460 microwave spectrometer with a phase-stabilized source oscillator. All the measurements were carried out at room temperature with sample pressures in the range 15 – 25 mTorr.

Preliminary values of the rotational constants were calculated from an assumed structure based on Lowenstein's results and some reasonable additional assumptions as to the positions of the hydrogen atoms.

Only $a$-type $R$-branch transitions of $C_3H_4{}^{32}SO_2$ were observed. An attempt to identify transitions of the $^{34}S$ species proved fruitless, due to the poor signal-to-noise ratio at the temperature of the experiments. Observed and calculated frequencies of the lines belonging to the ground state are listed in Table 2.

*Table 2.* Ground state rotational spectrum of thiete 1,1-dioxide.

| Transition | Observed [a] frequency (MHz) | Calculated frequency (MHz) | Calc. — obs. frequency (MHz) |
|------------|------------------------------|----------------------------|------------------------------|
| $5_{15} \rightarrow 4_{14}$ | 29 308.78 | 29 308.72 | − 0.06 |
| $5_{05} \rightarrow 4_{04}$ | 29 589.36 | 29 589.30 | − 0.06 |
| $5_{24} \rightarrow 4_{23}$ | 29 718.49 | 29 718.46 | − 0.03 |
| $5_{42} \rightarrow 4_{41}$ | 29 751.91 [b] | 29 751.98 | 0.07 |
| $5_{41} \rightarrow 4_{40}$ | | 29 752.02 | 0.11 |
| $5_{33} \rightarrow 4_{32}$ | 29 759.00 [b] | 29 758.86 | − 0.14 |
| $5_{32} \leftarrow 4_{31}$ | 29 763.34 [b] | 29 763.56 | 0.22 |
| $5_{23} \leftarrow 4_{22}$ | 29 864.38 | 29 864.34 | − 0.04 |
| $5_{14} \leftarrow 4_{13}$ | 30 095.65 | 30 095.59 | − 0.06 |
| $6_{16} \leftarrow 5_{15}$ | 35 152.95 | 35 153.00 | 0.05 |
| $6_{06} \leftarrow 5_{05}$ | 35 435.28 | 35 435.31 | 0.03 |
| $6_{25} \leftarrow 5_{24}$ | 35 648.29 | 35 648.38 | 0.09 |
| $6_{51} \leftarrow 5_{50}$ | 35 700.74 [b] | 35 701.14 | 0.30 |
| $6_{52} \leftarrow 5_{51}$ | | 35 701.14 | 0.30 |
| $6_{43} \leftarrow 5_{42}$ | 35 708.00 [b] | 35 707.84 | − 0.16 |
| $6_{42} \leftarrow 5_{41}$ | | 35 708.04 | 0.04 |
| $6_{34} \leftarrow 5_{33}$ | 35 717.58 [b] | 35 717.71 | 0.13 |
| $6_{33} \leftarrow 5_{32}$ | 35 729.90 [b] | 35 730.17 | 0.27 |
| $6_{24} \leftarrow 5_{23}$ | 35 895.10 | 35 895.13 | 0.03 |
| $6_{15} \leftarrow 5_{14}$ | 36 090.37 | 36 090.42 | 0.05 |

[a] Frequencies are accurate to ± 0.05 MHz.
[b] Not used in calculation of rotational constants. The inaccuracy of these frequencies is caused mainly by overlapping by nearby lines or vibrational satellites.

Tables 3 and 4 present the resulting rotational constants of the ground state and the vibrational satellites. No attempt was made to assign the satellites to any particular vibrational modes. The centrifugal distortion was found to be negligible for the measured transitions. As expected, the $A$ constant of the ground state is less accurately determined than the $B$ and $C$ constants. The rotational constants of the vibrational satellites were calculated from the three best separated and modulated lines observed in the spectrum.

Owing to the low Stark effect we could not determine the dipole moment.

Rough estimates yielded the following values for the intensity ratio of the vibrational satellites to the ground state at 24°C: 0.41 for $v_1 = 1$, 0.23 for $v_2 = 1$ and 0.15 for $v_3 = 1$. From these data the energy differences were calculated to be 184 cm⁻¹, 303 cm⁻¹, and 392 cm⁻¹, respectively. Un-

*Table 3.* Rotational constants and principal moments of inertia[a] of thiete 1,1-dioxide in the ground state.

| Rotational constants | Value MHz | | Principal moment of inertia | Value amu Å² | $\varkappa$ |
|---|---|---|---|---|---|
| A | 5463.98 | $(0.59)^b$ | $I_a$ | 92.492 | |
| B | 3052.679 | (0.006) | $I_b$ | 165.552 | − 0.8768 |
| C | 2894.365 | (0.006) | $I_c$ | 174.607 | |

[a] Conversion factor 505 377 MHz amu Å². [b] Values in parentheses are standard deviations determined by the least squares fitting procedure.

*Table 4.* Rotational constants of thiete 1,1-dioxide in vibrationally excited states.

| Rotational constants | Value MHz | | | |
|---|---|---|---|---|
| | $v_1 = 1$ | $v_1 = 2$ | $v_2 = 1$ | $v_3 = 1$ |
| A | 5465.6 | 5457.7 | 5460.4 | 5465.0 |
| B | 3051.76 | 3050.67 | 3055.42 | 3021.02 |
| C | 2894.24 | 2893.54 | 2891.35 | 2891.98 |

fortunately, there are no reliable far IR data available at present for comparison.

Assuming that the two oxygen and the two out-of-plane hydrogen atoms lie perpendicularly to the plane of the ring, which also contains the two other hydrogen atoms, we attempted to obtain an improved estimate of the distance between the oxygen atoms. Neglecting the vibrational contribution to the effective second moments of inertia [4] we obtain:

$$I_a + I_c - I_b = 2\sum_i m_i b_i{}^2$$

where $b_i$ is the distance of the $i$:th atom from the $ac$ plane and $m_i$ its mass.

If the C−H bond length and the H−C−H angle are assumed to be 1.089 Å and 112.5° the distance, $r_{pO}$, between the plane of the ring and the oxygen atoms calculated by the above formula will be 1.239 Å. The error in $r_{pO}$ caused by neglecting the vibrational contribution and the use of assumed values for the parameters of the hydrogen atoms has been estimated to be less than 0.01 Å.

The value obtained for $r_{pO}$ corresponds either to an increase in the S−O bond length to 1.487 or to an increase in the O−S−O angle to 120.1° as compared to Lowenstein's values (*cf.* Table 1). A lengthening of the S−O bond to 1.49 Å appears unreasonable, whereas a value of 120° for the O−S−O angle can be considered normal.[5]

1. Dittmer, D. C. and Christy, M. E. *J. Org. Chem.* **26** (1961) 1324.
2. Dittmer, D. C., Christy, M. E., Takashina, N., Henion R. S. and Balquist, J. M. *J. Org. Chem.* **36** (1971) 1324.
3. Lowenstein, M. Z. *Diss. Abstr.* **26** (1965) 2500.
4. Herschbach, D. R. and Laurie, V. M. *J. Chem. Phys.* **40** (1964) 3142.
5. Saito, S. and Makino, F. *Bull. Chem. Soc. Japan* **45** (1972) 92.

# Effects of a Europium-shift Reagent Upon the PMR Spectrum of Some Triglycerides

P. E. PFEFFER and H. L. ROTHBART

*Eastern Regional Research Center, Agricultural Research Service, U.S. Department of Agriculture, Philadelphia, Pennsylvania 19118, USA*

In this journal, Almqvist *et al.* recently reported on the PMR spectral analysis (100 MHz) of almond oil dissolved in $CCl_4$, to which various quantities of $Eu(fod)_3$ were added.[1] Shift patterns were reported which they believed differed from those observed in our study (60 MHz) of a number of pure triglycerides in similar solutions.[2] The purpose of this communication is to clarify some of the apparent differences, to draw attention to the effect of some impurities, and to point out a weakness in the use of attenuation factors.

Fig. 1. contains data concerning the apparent shift of protons of *rac*-glycerol 1,2-dipalmitate 3-oleate (PPO). Shifts were measured relative to the internal standard, tetramethylsilane (TMS) proton resonance. The figure indicates that at low values of the $Eu(fod)_3$-to-lipid ratio (X), the curves rise sharply in approximately linear fashion. At higher values
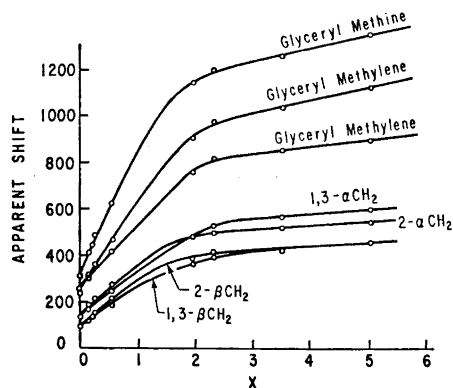


*Fig. 1.* Apparent chemical shifts (Hz) for PPO in $CCl_4$ containing various concentrations of $Eu(fod)_3$. X is the $Eu(fod)_3$/triglyceride molar ratio. Spectrum obtained at 60 MHz using TMS as internal standard.

of X the slopes decrease, and the proton resonances corresponding to the $\beta$- and $\alpha$-methylenes of the fatty acid moieties* exhibit a coalescence in the case of the former and a crossover in the case of the latter.

Although Almqvist *et al.* report the same general shape for the curves in Fig. 1, a number of anomalies were observed. At low values of X, they observed little change in the apparent shift until $X \simeq 0.3$. After this point their curves are similar to ours except for a slight dip reported by Almqvist in the region $X \simeq 2.3$. Thus there is a report of at least one inflection point, although we have seen none in this study. Our data indicate a crossover of the $\alpha$-methylene peaks at $X \simeq 1.8$, but the data of Almqvist *et al.* indicate that this occurs at $X = 2.5$ and do not indicate a coalescence of $\beta$-methylenes even up to $X \simeq 5$.

An important difference in the two studies is reflected in our use of pure model compounds compared to the use of an oil which may have contained traces of free acids. The previous authors have indicated that their assignments of X values might have been slightly high due to this. This is an attractive possibility since

$$(1/X_{true}) = (1/X_{apparent}) + [\text{mmol free acid/mmol } Eu(fod)_3]$$

which would explain the disagreement in X for the phenomena observed. In an attempt to investigate this further, solutions of a triglyceride in which 10 % of the lipid was oleic acid were studied by PMR after successive incremental additions of $Eu(fod)_3$. The shift data from these experiments substantiated the predictions and also helped to explain the relatively flat curve at low X values observed by Almqvist. The resonances associated with the carboxylic acid were imperceptible at these low concentrations. Acid interacts with the shift reagent to a far greater degree than does the triglyceride, resulting in little or no shift of triglyceride resonances until an X value was reached at which virtually all of the acid had been complexed by $Eu(fod)_3$.

It has been our experience that $Eu(fod)_3$ purchased from suppliers is somewhat

---

* We refer to $\alpha$, $\beta$, etc., as the methylene grops along the fatty acid chain, and 1,2,3 as positions on the glyceryl moiety.

variable in properties due probably to contamination by Lewis bases such as water.[3] Some of the materials have been rejected on the basis of depressed transition temperatures [4] determined by differential scanning calorimetry. In other cases, spurious unidentified peaks in the PMR spectra of solutions of the reagents have been observed which led to our rejection of the Eu(fod)$_3$. With samples of Eu(fod)$_3$ which have passed these tests, minor differences in apparent shift at, for example, high values of $X$ have been observed.

In our previous work assignment of α-methylene resonances was made primarily after consideration of the relative peak areas. In order to dispel any doubt concerning these assignments, α-deuteriated oleic acid was prepared and used for the synthesis of selectively deuteriated POP (PO$_{\alpha D_2}$P). Fig. 2a demonstrates the absence of the upfield ($\delta$ 8.2) α-methylene resonance (except for a resonance corresponding to a small amount of proteo isomer). Furthermore, Eu(fod)$_3$-complexed rac-glycerol 1,2-distearate 3-oleate (SSO)

was demonstrated to display spectral characteristics similar to PPO. A sample of SSO$_{\alpha D_2}$ was examined under conditions similar to those employed in the study of PO$_{xD_2}$P, and the absence of the originally observed downfield triplet, of the composite quartet ($\delta$ 9.1) was noted (Fig. 2b).

In view of this evidence, there can be no doubt about our initial assignment of resonances corresponding to the α-methylene protons of the triglycerides. The curve denoted as 1,3-αCH$_2$ in Fig. 1 represents the mean-apparent-shift value of these resonances for the dissymmetric molecular species PPO, and is nearly coincident with the center of gravity of the α-methylene resonances of symmetric species such as POP.

Several authors have used attenuation factors [5] or induced shift rations [1,6] to describe the chemical shift phenomenon. We wish to point out that such attenuation factors should be used with great care, especially in cases where "resonance crossovers" are demonstrated (Fig. 1). Since two protons may appear at an identical chemical shift, separate, and then cross over at higher $X$, attenuation factors may be variable and hence misleading.

In conclusion, we would like to emphasize that Eu(fod)$_3$ can provide important information concerning the structure of triglycerides. However, care should be exercised when relying upon the calculated ratios of Eu(fod)$_3$/lipid and the chemical shift which results from these ratios. It can be particularly misleading to use these values when studying complex mixtures which, as we have shown, can contain spectroscopically undetectable complexible materials.
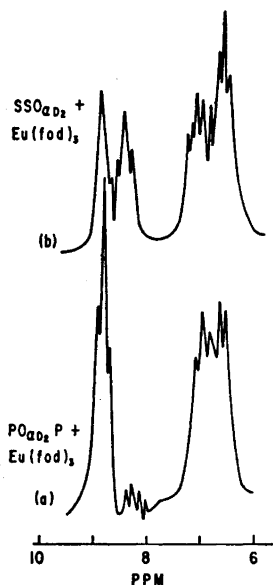


Fig. 2. (a.) PMR spectrum of the α- and β-methylene protons of PO$_{\alpha D_2}$P in CCl$_4$ containing Eu(fod)$_3$ (60 MHz). $X \simeq 2.4$. (b.) PMR spectrum of the è- and β-methylene protons of SSO$_{\alpha D_2}$ in CCl$_4$ containing Eu(fod)$_3$ (60 MHz). $X \simeq 2.4$.

1. Almqvist, S.-O., Andersson, R., Shahab, Y. and Olsson, K. Acta Chem. Scand. 26 (1972) 3378.
2. Pfeffer, P. E. and Rothbart, H. L. Tetrahedron Letters 1972 2533.
3. A recent report notes that water reduces the induced shifts due to Eu(fod)$_3$. Porter, R., Marks, T. J. and Shriver, D. F. J. Am. Chem. Soc. 95 (1973) 3548.
4. Springer, C. S., Jr., Meek, D. W. and Sievers, R. E. Inorg. Chem. 6 (1967) 1105.
5. Sanders, J. K. M. and Williams, D. H. J. Am. Chem. Soc. 93 (1971) 641.
6. Wineburg, J. P. and Swern, D. J. Am. Oil Chemists' Soc. 49 (1972) 267.

# Studies on the Furan Series

## Part V. The Reaction of Furoin and Related Compounds with Vilsmeier Reagents. A Convenient Synthesis of Unsymmetrically 5,5'-Disubstituted Difurylethylene Derivatives

SEPPO PENNANEN

*Department of Chemistry, Helsinki University of Technology, Otaniemi, Finland*

The reaction of furoin (I) with DMF/POCl₃ complex gave both 5-chlorofurfuryl 2'-furyl ketone (II) and 5-formyl-2,2'-furil (III). Under similar conditions thenoin (IV) and benzoin (V) produced α-chloro-2-thenyl 2'-thienyl ketone (VI) and α-chlorobenzyl phenyl ketone (VII), respectively. The diol (IX) obtained by the reduction of furoin gave smoothly (*E*)-1-(5-chloro-2-furyl)-2-(5-formyl-2-furyl)ethene (X) with the DMF/POCl₃ treatment. Analogously 1,2-di(2-thienyl)ethanediol (XI) gave (*E*)-1-(5-chloro-2-thienyl)-2-(2-thienyl)ethene (XII), but 1,2-diphenylethanediol (XIII) gave 1,2-diphenylethanediol diformate (XIV). X was photocyclized to 7-chlorobenzo[1,2-b:4,3-b']-difuran-2-carboxaldehyde (XVIII).

Some unsuccessful attempts to synthesize furohelicenes from the derivatives of X and XVIII are described.

Numerous reactions of DMF complexes have been reported and reviewed.[1] In this work some new pathways in the reactions of Vilsmeier reagents are observed.

When furoin (I), easily obtainable from furfural, was treated with DMF/POCl₃ (1:1) complex in refluxing methylene chloride, the reaction gave no expected products, but 34 % of 5-chlorofurfuryl 2'-furyl ketone (II) and 26 % of 5-formyl-2,2'-furil (III). It seems likely that two competing reactions, leading to II and III, are involved, as the amount of complex used had no noticeable effect on the ratio of yields. On the other hand, other DMF complexes caused a different distribution of products. DMF/COCl₂ and DMF/SOCl₂ gave 47 % of III (traces of II) and 54 % of II (traces of III), respectively (Scheme 1).

Compounds analogous to I, thenoin (IV) and benzoin (V), reacted with DMF/POCl₃ complex giving α-chloro-2-thenyl 2'-thienyl ketone (VI) and α-chlorobenzyl phenyl ketone (VII) (Scheme 1).

I:   X = O
IV:  X = S

V: ⟨☐⟩ = phenyl

II: X = O ; R₁ = H ;
    R₂ = Cl

VI : X = S ; R₁ = Cl ;
     R₂ = H

VII : ⟨☐⟩ = phenyl :

R₁ = Cl ; R₂ = H

III : X = O ; R₃ = CHO

VIII : X = O ; R₃ = H
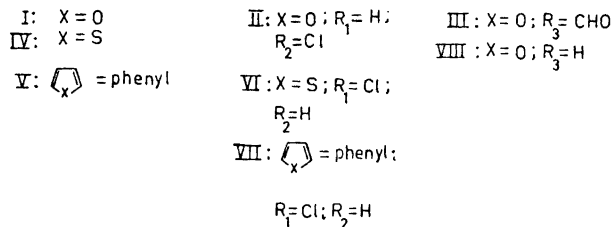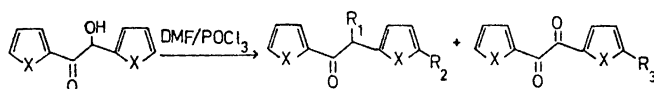
*Scheme 1.*

The formation of II can be considered as a substitution, where the chloride anion of the complex interacts with the hydroxyl group of furoin:
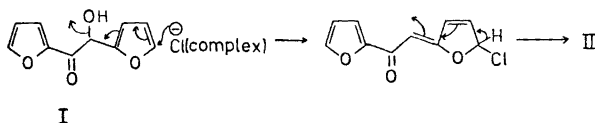


*Scheme 2.*

The compound III cannot be synthesized directly from furil (VIII) with the Vilsmeier reagent. Therefore it seems likely that formylation takes place on the furfuryl alcohol side of I followed by aerial oxidation of the alcohol. This is supported by the fact that under a nitrogen atmosphere no III is formed (only traces of II).

When I was reduced to the vicinal diol (IX) and treated with the Vilsmeier complex, only one yellow compound was produced and identified by spectral data as (*E*)-1-(5-chloro-2-furyl)-2-(5-formyl-2-furyl)ethene (X).



IX : X = O

XI : X = S

X : X = O ; R₁ = Cl ; R₂ = CHO

XII : X = S ; R₁ = Cl ; R₂ = H



XIII                              XIV
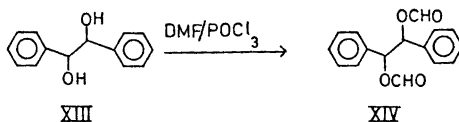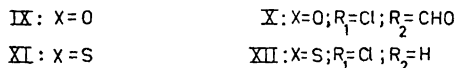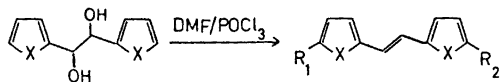
*Scheme 3.*

The reaction presumably starts with substitution, as the chlorinated compound IXa, obtainable from II by reduction, gives X, and continues with the elimination of water; as IXb, obtainable from X by oxidation and decarboxylation, similarly gives X (Scheme 4).
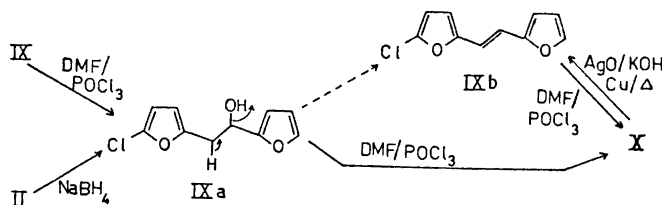


*Scheme 4.*

The reaction of the S-analogue (XI) of IX with DMF/POCl$_3$ stopped after substitution and elimination producing (E)-1-(5-chloro-2-thienyl)-2-(2-thienyl)-ethene (XII). The reaction with the benzenoid analogue, vic.-1,2-diphenyl-ethanediol (XIII), took quite another direction from that taken with IX and XI giving a normal esterification (diformylation) product: 1,2-diphenyl-ethanediol diformate (XIV).



XV: R$_1$ = Ac ; R$_2$ = H          X: R$_2$ = R$_3$ = H

XVI: R$_1$ = H ; R$_2$ = Et or alkyl          XVII : mixture $\begin{cases} R_2=Et(alkyl); R_3=H \\ R_2=H; R_3=Et(alkyl) \end{cases}$
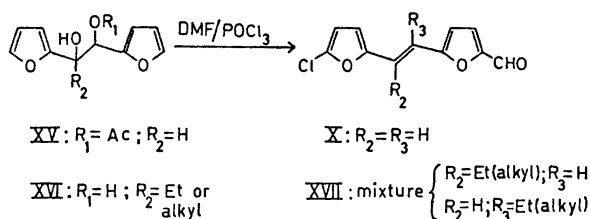
*Scheme 5.*

Some derivatives of IX were prepared (XV and XVI; Scheme 5) in order to see what effect the substituents might have on the reaction (Scheme 3). The compound XV gave X, as expected. XVI gave a mixture of two isomers. The alkyl substituents seem to have no directing effect on the reaction, as the NMR-spectrum of the mixture showed that the ratio of two isomers was about 1:1.

The procedure above constitutes a facile two-step method for the preparation of unsymmetrically 5,5'-disubstituted (E)-difurylethylenes from easily obtainable furoin. The reaction can be run on a large scale without difficulty, and after the first step (reduction of furoin) no special purification of the reaction product is required. Both of the final substituents in the furan rings are quite reactive and make further syntheses possible.

By the method of Kellog et al.[2] X was photocyclized in methanol to a 2,7-disubstituted benzo[1,2-b:4,3-b']difuran (XVIII) in a yield of 30 %.
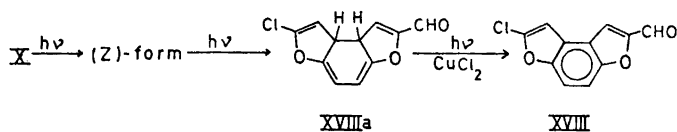
*Scheme 6.*

With a longer reaction time in the photolysis the solvent, methanol, interacted with the formyl group giving the dimethylacetal of XVIII as a byproduct.

The preparation of furohelicenes from the derivatives of X and XVIII was also attempted (Scheme 7).
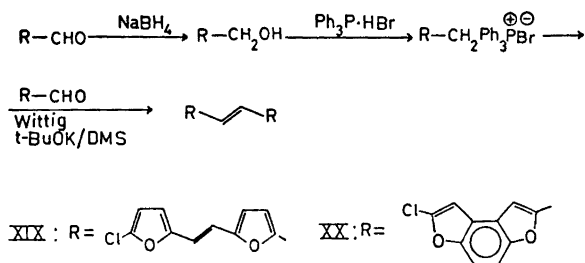


*Scheme 7.*

Both compounds XIX and XX were photolyzed under various conditions,[3] but no furanoid products, such as the thienohelicenes prepared by Groen *et al.*,[3] were formed. The linear tetrafuranoid compound (XIX) is quite labile (it decomposes slowly at room temperature) and therefore probably gave only insoluble (acetone), black resinous material. XX was relatively more stable under the conditions employed, because 75 – 85 % of the starting material was recovered unchanged after photolysis, and no reaction products, except tar, were formed.

## EXPERIMENTAL

*General.* All melting points are uncorrected. The spectra were determined on the instruments described earlier.[4] Furoin (I), thenoin (IV), and benzoin (V) were synthesized from the corresponding aldehydes by the method of Cardon and Lankelma.[5] Vicinal diols IX, XI, and XIII were prepared by $NaBH_4$ reduction from I, IV, and V, respectively, the substituted vicinal diol XV from I *via* acetylation and $NaBH_4$ reduction, and XVI from I *via* the Grignard reaction. All diols were used without further purification.

*Preparation of DMF complexes and reaction conditions.* In the preparation of the DMF complexes in $CH_2Cl_2$ the procedure of Silverstein *et al.*[6] was followed, and purified $POCl_3$, $SOCl_2$ or $COCl_2$ (20 % in toluene) were employed. The equivalent amount or excess of the complexes were used in the reactions. Reaction times were from 15 min

to half an hour in dried, refluxing methylene chloride. Standard work-ups [6] were employed.

## Reaction products of the complexes

*5-Chlorofurfuryl 2'-furyl ketone (II) and 5-formyl-2,2'-furil (III).* 4.20 g of I was used. Elution of the reaction mixture with $CHCl_3$ on a silica gel column gave 1.55 g (34 %) of II and 1.20 g (26 %) of III. Physical properties of II: m.p. 29 – 30°C (recryst. from petroleum ether b.p. 40 – 60°C); $\nu$ 1690, 880 cm⁻¹; $\tau$ 2.42 (1 H d 1.5 Hz), 2.83 (1 H d 3.5 Hz), 3.50 (1 H dd 3.5 and 1.5 Hz), 3.75 (1 H d 3.5 Hz), 3.93 (1 H d 3.5 Hz), 5.91 (2 H s). (Found: C 57.14; H 3.33. Calc. for $C_{10}H_7ClO_3$: C 57.28; H 3.18.) Physical properties of III: m.p. 54 – 55°C (recryst. from petroleum ether b.p. 40 – 60°C); $\nu$ 3120, 1675, 870 cm⁻¹; $\tau$ 0.55 (1 H s), 2.34 (1 H d 1.5 Hz), 3.15 (2 H d 3.5 Hz), 3.42 (1 H dd 3.5 and 1.5 Hz), 3.70 (1 H d 3.5 Hz). (Found: C 61.08; H 2.94. Calc. for $C_{11}H_6O_5$: C 60.55; H 2.75.) The yield of II after $SOCl_2/DMF$ treatment of I was 54 % (traces of III were observed on a TLC plate) and after $COCl_2/DMF$ treatment the yield of III was 47 % (only traces of II).

*α-Chloro-2-thenyl 2'-thienyl ketone (VI).* Yield 0.56 g (54 %), when 1.00 g of IV was used; viscous oil, very soon resinifing after a silica gel column treatment ($CHCl_3$); elemental analysis indicated chlorine; $\nu$ 3100, 2920, 1665, 1510, 1040, 710 cm⁻¹; $\tau$ 2.10 (1 H m), 2.70 (5 H br. m), 3.55 (1 H s).

*α-Chlorobenzyl phenyl ketone (VII).* 1.00 g of V gave 0.95 g (96 %) of VII; m.p. 66 – 67°C (lit.[7] m.p. 66 – 68°C); $\nu$ 3060, 1690 cm⁻¹; $\tau$ 2.00 (2 H m), 2.60 (8 H m), 3.77 (1 H s).

(E)-*1-(5-Chloro-2-furyl)-2-(5-formyl-2-furyl)ethene (X).* 1.90 g of IX gave 1.10 g (52 %) of X; yellow needles from petroleum ether/$CHCl_3$; m.p. 120°C; $\lambda_{max}$ 273 ($\varepsilon$ 8500), 366 ($\varepsilon$ 34 600) nm; $\nu$ 1675, 1620 cm⁻¹; $\tau$ 3.17 (1 H d 15.5 Hz), 2.98 (1 H d 15.5 Hz), 3.47 (1 H d 3.0 Hz), 2.72 (1 H d 3.0 Hz), 3.75 (1 H d 3.5 Hz), 3.53 (1 H d 3.5 Hz), 0.40 (1 H s); $m/e$ 222 (100 %), 193 (12 %), 187 (5 %), 165 (25 %), 159 (71 %), 137 (17 %), 131 (22 %), 102 (34 %). (Found: C 59.71; H 3.27. Calc. for $C_{11}H_7ClO_3$: C 59.45; H 3.14.)

(E)-*1(or 2)-(5-Chloro-2-furyl)-2(or 1)-(5-formyl-2-furyl)-1-butene (XVII).* 1.00 g of XVI gave 0.97 g (47 %) of XVII, viscous pale yellow oil, which according to the NMR-spectrum was a 1:1 mixture of two isomers. $\tau$ 0.52 (1/2 H s), 0.55 (1/2 H s), 2.60 – 3.80 (5 H m), 7.25 (2 H q 7 Hz), 8.78 (3/2 H t 7 Hz), 8.80 (3/2 H t 7 Hz).

(E)-*1-(5-Chloro-2-thienyl)-2-(2-thienyl)ethene (XII).* 1.00 g of XI gave 0.35 g (35 %) of XII; yellow needles from EtOH/$H_2O$; m.p. 69 – 70°C; $\lambda_{max}$ 258 ($\varepsilon$ 7 900), 334 sh ($\varepsilon$ 27 200), 346 ($\varepsilon$ 29 000), 361 sh ($\varepsilon$ 21 900) nm; $\nu$ 3050, 1560, 1520, 1435, 1040, 980, 930, 690 cm⁻¹; $\tau$ 2.98 (1 H d 4 Hz), 3.08 (2 H m), 3.18 (2 H s), 3.30 (2 H s); $m/e$ 226 (100 %), 191 (42 %), 190 (53 %), 181 (15 %), 158 (25 %), 147 (50 %). (Found: C 53.47; H 3.55. Calc. for $C_{10}H_7ClS_2$: C 53.10; H 3.10.)

*1,2-Diphenylethanediol diformate (XIV).* The yield was quantitative from XIII; white prisms from benzene/$CHCl_3$; m.p. 167°C; $\nu$ 2930, 1705, 1150 cm⁻¹; $\tau$ 1.95 (2 H s), 2.72 (10 H s), 3.74 (2 H s); $m/e$ 242 (3 %), 224 (6 %), 197 (5 %), 179 (17 %), 165 (15 %), 152 (8 %), 135 (90 %), 105 (38 %), 77 (100 %). (Found: C 71.38; H 6.01. Calc. for $C_{16}H_{14}O_4$: C 71.11; H 5.81.)

## Preparation of derivatives of X

*7-Chlorobenzo[1,2-b:4,3-b']difuran-2-carboxaldehyde (XVIII).* 0.500 g of X was dissolved in 500 ml of methanol and oxidizing agent [3] (1.25 g of anh. $CuCl_2$ and 0.20 g of $I_2$) was added. The mixture was photolyzed with a Hanau TQ 81 UV-lamp under $N_2$-atmosphere and tap water cooling for 8 h. Methanol was evaporated under reduced pressure, ether added and inorganic salts removed by washing with water. After drying and ether evaporation a yellow viscous oil was obtained, which after elution in a silica gel column with benzene gave 0.15 g (30 %) of white solid; m.p. 159 – 160°C (recryst. from petroleum ether/benzene); $\lambda_{max}$ 265 sh ($\varepsilon$ 5 900), 274 ($\varepsilon$ 20 400), 285 ($\varepsilon$ 28 600), 295 sh ($\varepsilon$ 20 900) nm; $\nu$ 3110, 1680, 1520 cm⁻¹; $\tau$ 0.10 (1 H s), 2.43 (2 H slight br. s), 2.62

(1 H s), 3.17 (1 H s); $m/e$ 220 (100 %), 192 (9 %), 186 (9 %), 185 (6 %), 163 (19 %), 157 (38 %), 129 (34 %). (Found: C 59.85; H 2.18. Calc. for $C_{11}H_5ClO_3$: C 60.00; H 2.27.)

When the reaction time was extended to 24 h and excess of $CuCl_2/I_2$ was employed, the reaction of the solvent and the formyl group of XVIII occurred. 2.00 g of starting material (X) gave 0.25 g (13 %) of XVIII, 0.50 g (23 %) of dimethyl acetal of XVIII (XVIIIb), and 0.22 g of yellow material, which according to the NMR-spectrum was a mixture of $(E)$- and $(Z)$-forms of X. The diluted hydrochloric acid treatment of XVIIIb produced a quantitative yield of XVIII. XVIIIb: viscous pale yellow oil: $\lambda_{max}$ 266 sh ($\varepsilon$ 9000), 273 ($\varepsilon$ 20 100), 284 ($\varepsilon$ 28 000), 294 sh ($\varepsilon$ 6100) nm; $\tau$ 2.56 (2 H s), 2.98 (1 H s), 3.25 (1 H s), 4.32 (1 H s), 6.56 (6 H s).

$(E)$-$1,2$-$Di\{5[(E)$-$2$-$(5$-$chloro$-$2$-$furyl)$-$1$-$ethenyl]$-$2$-$furyl\}$ $ethene$ $(XIX)$. The Wittig compound XXI was prepared from $PhP.HBr$ [8] and $NaBH_4$ reduced X by the procedure of Saikachi $et$ $al.$[9] The Wittig reaction was accomplished in DMS with $t$-BuOK.[10] 1.00 g of XXI and 0.70 g of X gave after column chromatography with benzene and recrystallization from benzene/petroleum ether 0.60 g (46 %) of dark red needles; m.p. 182°C (d); $\lambda_{max}$ 282 sh ($\varepsilon$ 11 700), 286 ($\varepsilon$ 12 400), 330 ($\varepsilon$ 9000), 345 ($\varepsilon$ 13 700), 416 sh ($\varepsilon$ 16 500), 440 ($\varepsilon$ 24 700), 470 ($\varepsilon$ 21 300) nm; $\nu$ 1510, 1460, 970, 955, 940 cm$^{-1}$; $\tau$ 3.15 (6 H m), 3.65 (8 H m); $m/e$ 412 (100 %), 377 (8 %), 349 (21 %), 321 (5 %), 313 (6 %), 285 (6 %), 257 (8 %), 229 (7 %), 207 (22 %), 206 (30 %), 165 (14 %), 143 (20 %). (Found: C 75.66; H 3.89. Calc. for $C_{22}H_{14}Cl_2$: C 75.86; H 4.02.)

$(E)$-$1,2$-$Di(7$-$chloro$-$2$-$benzo[1,2$-$b:4,3$-$b']difuran)ethene$ $(XX)$. The preparation of the phosphorus compound XXI from XVIII and the Wittig reaction with XXI and XVIII were performed as above. After a column chromatography with benzene and recrystallization from cyclohexan/benzene 0.50 g of XXI and 0.20 g of XVIII gave 0.25 g (62 %) orange needles. The compound (XX) had a strong, blue fluorescence in benzene solution. XX: m.p. 264°C; $\lambda_{max}$ 347 sh ($\varepsilon$ 28 500), 363 ($\varepsilon$ 55 200), 383 ($\varepsilon$ 9600), 407 ($\varepsilon$ 97 900) nm; $\nu$ 3120, 1525, 970, 950 cm$^{-1}$; $m/e$ 408 (100 %), 376 (17 %), 374 (52 %), 345 (20 %), 276 (43 %), 204 (20 %).

*Photolysis of XIX and XX.* Both XIX and XX were photolyzed under various conditions [3] and with various oxidazing agents.[2] In every case XIX produced only resinous material. XX gave no reaction products, and 75 − 85 % of the starting material was recovered after photolysis (identification with TLC and UV-spectroscopy).

## REFERENCES

1. Kittilä, R. S. *Dimethylformamide Chemical Uses*, E. I. Du Pont de Nemours & Co., Wilmington, Delaware 1967.
2. Kellog, R. M., Groen, M. B. and Wynberg, H. *J. Org. Chem.* **32** (1967) 3093.
3. Groen, M., Schadenberg, H. and Wynberg, H. *J. Org. Chem.* **36** (1971) 2797.
4. Pennanen, S. I. and Nyman, G. A. *Acta Chem. Scand.* **26** (1972) 1018.
5. Cardon, S. Z. and Lankelma, P. *J. Am. Chem. Soc.* **70** (1948) 4248.
6. Silverstein, R. M., Ryskiewicz, E. E. and Willard, C. *Org. Syn.* **36** (1956) 74.
7. Borowitz, I. J., Rusek, P. E. and Virkhaus, R. *J. Org. Chem.* **34** (1969) 1595.
8. Schwieter, U. S., Planta, C. R., Rüegg, R. and Isler, O. *Helv. Chim. Acta* **45** (1962) 541.
9. Saikachi, H., Ogawa, H., Minami, Y. and Sato, K. *Chem. Pharm. Bull.* **18** (1970) 465.
10. Denney, D. B. and Song, J. *J. Org. Chem.* **29** (1964) 495.

# Determination of the Ethylation Rate of Cellulose

OLLE RAMNÄS

Department of Engineering Chemistry, Chalmers University of Technology,
S-402 20 Göteborg 5, Sweden

The reaction between ethyl chloride and the different hydroxyl groups in cellulose (dissolved and undissolved fibers) was studied. In both cases the substitution was much slower at C-3 than at C-2 and C-6. For the dissolved fibers the rate of reaction was proportional to the hydroxide concentration within the range 0.7 — 3 M sodium hydroxide. For the undissolved fibers the ratio of the rate constants for ethylation at C-2, C-3, and C-6 was found to be 7:1:6.5 and was virtually independent of the sodium hydroxide concentration.

In an earlier paper [1] the distribution of substituents in hydroxyethyl cellulose was determined. In this work the study has been extended to ethyl cellulose. The relative reactivities of the three hydroxyl groups in cellulose during the reaction with ethyl chloride or ethyl sulfate have been studied by several authors, [2-5] who all found that the hydroxyl group at C-3 was the least reactive. Mahoney and Purves [2] and Honeyman [3] found that the primary hydroxyl group at C-6 was the most reactive in contrast to Croon and Flamm [5] whose results indicated that the hydroxyl group at C-2 was the most reactive. The discrepancies may be explained by less satisfactory analytical methods. Considerable progress has been made in developing the analytical technique during the last ten years, and it was therefore of interest to reinvestigate the reaction between cellulose and ethyl chloride. It was also of interest to determine whether the results obtained in hydroxyethylation are valid when other substituents are introduced into cellulose.

## EXPERIMENTAL

In the experiments with dissolved cellulose 3.0 g liquid ethyl chloride was added to a solution of 0.5 g hydrocellulose from rayon [1] in 35 ml aqueous sodium hydroxide (3 — 18 %). The reaction was performed at 20° in a tightly stoppered 100 ml round bottom flask with vigorous shaking so that the ethyl chloride was effectively dispersed in the sodium hydroxide solution. Since ethyl chloride has a low solubility in water and boils at 12°, an excess pressure (about 0.3 bar) was obtained in the flask. Blank experiments were performed without cellulose in order to determine the solubility of ethyl chloride in sodium hydroxide solutions and the decrease in sodium hydroxide concentration because of side reactions.

The ethylation was stopped by neutralization with hydrochloric acid after one and two weeks, respectively. After precipitation in one liter of acetone and filtration, the sodium chloride formed was removed by ultrafiltration (Diaflo Membrane) and washing with water. The derivative was dried in the air.

Purified cotton [6] was used in the experiments with undissolved fibers. The samples (2 g) were treated with aqueous sodium hydroxide (3, 10, and 18 %) at room temperature for 60 min and then pressed to a press-weight ratio of about 3.7. The finely divided cellulose was transferred to a stainless steel autoclave and liquid ethyl chloride (5 ml) was added. The autoclave was rotated in a polyglycol bath at 100° for 300 min and then cooled in ice. The reaction product was suspended in water and neutralized with hydrochloric acid. It was then washed in water and ethanol, sucked off on a Büchner funnel and dried.

The cellulose derivatives were hydrolyzed in sulfuric acid as described previously.[7] After neutralization with barium carbonate and evaporation under reduced pressure, the hydrolyzate was fractionated into four groups by partition chromatography on an anion exchanger in the sulfate form with aqueous ethanol (92.4 % w/w) as eluent.[8] A differential refractometer (Waters R401) was used to detect the chromatographic peaks. The first fraction contained tri- and disubstituted glucoses ($s_{236}$, $s_{23}$, $s_{26}$, and $s_{36}$), the second fraction glucoses monosubstituted at C-2 and C-3 ($s_2$ and $s_3$) and the two last fractions contained 6-O-ethylglucose ($s_6$) and glucose ($s_0$), respectively. The components of the different fractions were converted to their trimethylsilyl (TMS) derivatives [9] and determined quantitatively by gas chromatography on a QF-1 column (3 m; 3 % QF-1 on Gas Chrom Q 100/120 mesh) using a Perkin-Elmer 900 Gas Chromatograph. For $s_{236}$ one peak was recorded and for the other derivatives two peaks were recorded. Xylitol was added as an internal standard to all fractions. The ratio, peak area/weight, of the derivatives relative to that of xylitol, was determined in calibration runs.

Reference substances of all ethylglucoses of interest were isolated from a hydrolyzate of highly substituted ethyl cellulose. After separating into four groups on the sulfate resin, the fractions were evaporated under reduced pressure and rechromatographed on a borate resin with boric acid as eluent.[10] The sugar derivatives were detected according to the orcinol method.[8] By choosing a suitable concentration and pH gradient of the eluent all ethylglucoses, except $s_{236}$, $s_{23}$, $s_{26}$, and $s_2$, could be completely separated. Almost pure substances of these derivatives were obtained by taking the fractions corresponding to the middle part of each elution band. The separation of a mixture of ethylglucoses on an analytical column is shown in Fig. 1. The boric acid in the collected fractions was removed by repeated addition of methanol and evaporation under reduced pressure.
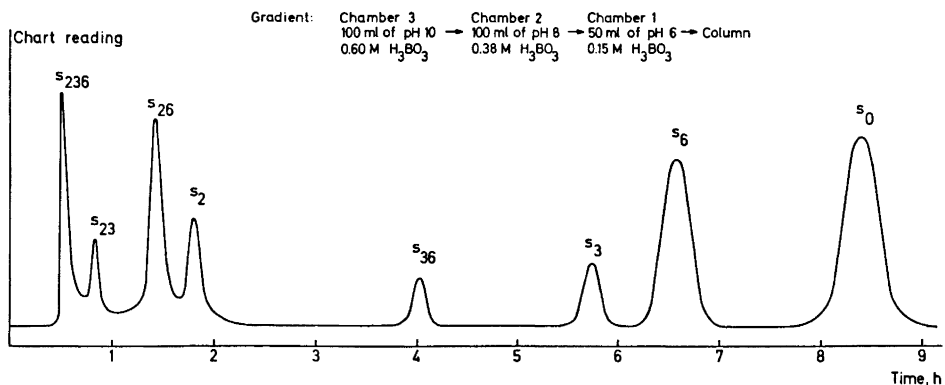


Fig. 1. Separation of a mixture of ethylglucoses as borate complexes by gradient elution at 70°. Resin bed: 2.4 × 1300 mm, Dowex 1-X8, borate form, 20 − 26 μm. Nominal linear flow: 3.9 cm min⁻¹. The Technicon gradient device (Autograd) was used. Chamber 2 was opened after 1 h and chamber 3 after 3.5 h.

The purity of the reference substances was controlled by gas chromatography of their TMS derivatives. A final confirmation of the identity of these derivatives was obtained by mass spectrometry. Since the spectra of the TMS derivatives of 2-O-ethylglucose and some methylglucoses are known,[11] the spectra of the other ethyl substituted glucoses could be predicted. The working conditions for mass spectrometry were the same as previously.[12]

The ethyl chloride concentration in the sodium hydroxide solutions in the blanks was determined after vigorous shaking over night. Without lowering the pressure an aliquot of the aqueous phase was taken and mixed with water containing a small amount of methanol, which was used as an internal standard. The diluted solution was directly analyzed on a Porapak N column using a Perkin-Elmer 990 Gas Chromatograph. It was necessary to clean the glass liner in the injection block often to get reproducible values. On the chromatogram traces of ethanol and diethyl ether could be seen. The solubility of ethyl chloride ($S$) in solutions of different sodium hydroxide concentrations ($0 < c < 5.5$ M) followed Setchenows equation, $\log (S_0/S) = kc$.

With the values $S_0 = 0.158$ and $k = 0.243$ (concentrations given as molarities) the calculated and experimental values agreed within 5 %.

## RESULTS AND DISCUSSION

*Chromatography on ion exchangers.* Most glucose methyl ethers substituted at one or several of the hydroxyl groups at C-2, C-3, and C-6 can be easily separated by partition chromatography on an anion exchanger in the sulfate form with aqueous ethanol as eluent.[8] The corresponding ethyl ethers are not sufficiently polar to be well separated by the same technique. Even at an ethanol concentration of 95 % the two important ethers, $s_2$ and $s_3$, overlapped seriously. The method proved to be very useful for group separations of hydrolyzates of ethyl cellulose, however.

Chromatography of the sugar derivatives on the borate form of an anion exchange resin offers another way for analysis. This method has often been used for separations of unsubstituted sugars.[10] Among common sugars, glucose is held most strongly by the borate resin. This shows that favorable possibilities for complex formation must exist. In the pyranose form the hydroxyl groups of glucose are in a less favorable position for complex formation than in the furanose form.[13] This was in agreement with experiments on 4-O-methyl-glucose, which can only exist in the pyranose form. Its peak elution volume was about half of that for 2-O-methylglucose. The hydroxyl groups at C-1 and C-2 in α-glucofuranose are *cis* to each other and almost in the same plane, which provides excellent possibilities for borate complexes. The great importance of the C-1 – C-2 complex is demonstrated by the fact that all glucoses ethylated at C-2 are eluted much faster than the other derivatives studied. An inspection of a simple stereomodel of glucofuranose shows that borate complexes might also be formed with the following pairs of hydroxyl groups: C-5 and C-6, C-3 and C-5, C-3 and C-6. The complexes involving C-3 seem to exert a larger effect upon the retention than that with C-5 and C-6, since $s_3$ is eluted before $s_6$. These conclusions are supported by the fact that galactose is eluted before xylose.[10] Glucofuranose and galactofuranose have the same structure, except that the side chains containing C-5 and C-6 are located on opposite sides of the ring. This makes the formation of C-3 complexes impossible for galactofuranose. In xylofuranose complexes linked to C-3 and

*Table 1.* Relative intensity of peaks at $m/e = 191 - n44$ ($J_1$ series), $204 - n44$ ($H_1$ series) and $217 - n44$ [$F_1$ ($G_1$) series]. Only peaks greater than 1 % are included. The compounds represent one anomeric form (except for $s_{236}$, which only exhibited one peak on gas chromatography).

| Compound | 191 | 147 | 103 | 204 | 160 | 116 | 217 | 173 | 129 |
|---|---|---|---|---|---|---|---|---|---|
| $s_0$ | 40 | 22 | 6 | 100 | — | — | 18 | — | 6 |
| $s_2$ | 40 | 17 | 9 | 9 | 100 | 2 | 7 | 12 | 6 |
| $s_3$ | 5 | 100 | 12 | 3 | 76 | 3 | 41 | 4 | 12 |
| $s_6$ | 41 | 16 | 6 | 100 | — | 1 | 19 | 4 | 7 |
| $s_{23}$ | 3 | 100 | 15 | 1 | 13 | 93 | 7 | 35 | 11 |
| $s_{26}$ | 32 | 11 | 8 | 8 | 100 | 3 | 2 | 16 | 7 |
| $s_{36}$ | 4 | 93 | 14 | 1 | 100 | 5 | 52 | 6 | 16 |
| $s_{236}$ | 1 | 78 | 16 | — | 12 | 100 | 2 | 42 | 15 |

C-5 can exist, since xylofuranose has the same structure as glucofuranose, except that C-6 is missing.

*Mass spectrometry.* The identification scheme for the determination of the number and position of methoxyl substituents in TMS derivatives of methylated aldohexopyranoses given by Petersson and Samuelson [11] is also valid for the TMS derivatives of glucose ethyl ethers. The relative intensities of the peaks corresponding to the most interesting fragment ions are given in Table 1. Only small differences are observed when the intensities of these ions are compared with the corresponding ions from glucose methyl ethers.

*Side reactions.* During the ethylation of cellulose two side reactions compete with the main reaction:[14]

$$EtCl + OH^- \rightarrow EtOH + Cl^-$$
$$EtCl + EtOH + OH^- \rightarrow EtOEt + Cl^- + H_2O$$
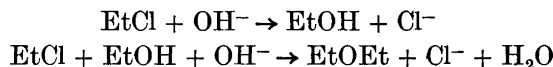
In both reactions hydroxide ions are consumed. The formation of water and ethanol also contributes to a lowered hydroxide concentration. Titration of the blanks with sulfuric acid showed that under the applied conditions the decrease in alkalinity was a linear function of the time. After one week 95.3, 97.4, and 98.3 % of the sodium hydroxide was left in the solutions with the initial concentrations 3, 10, and 18 % sodium hydroxide, respectively. In Figs. 3 and 4 the mean values of the sodium hydroxide concentration during each experiment are used.

Blank experiments were also performed under the same conditions as with the reaction with undissolved fibres. Equal volumes of sodium hydroxide solutions and liquid ethyl chloride (about the same proportions as in the real experiments) were heated in autoclaves at 100° for 1, 2, and 5 h, respectively. The rapid decrease in sodium hydroxide concentration is shown in Fig. 2.

*Reaction with dissolved fibers.* Since ethyl chloride is only slightly soluble in sodium hydroxide solutions, the degree of ethylation was low even though the reaction times were one and two weeks for the reaction with dissolved cellulose. The D.S. values calculated from the composition of the hydrolyzate were $0.02 - 0.10$. The relative rate constants for ethylation at C-2, C-3, and

C-6 ($k_2$:$k_3$:$k_6$) were obtained from the ratio of the amounts of the monosubstituted ethylglucoses in the hydrolyzate. The chromatographic analysis showed that disubstitution could be disregarded. The dependence of the relative reaction rates upon the sodium hydroxide concentration is given in Fig. 3. As can be seen from the figure a straight line relationship seems to exist between the relative rates and the hydroxide concentration. The broken lines represent the corresponding constants for the hydroxyethylation reaction.

The similarity between the two processes is striking. The lines representing the substitution at C-2 are parallel. The lines for the substitution at C-6 are almost parallel and exhibit a more pronounced dependence on the hydroxide concentration than those for the reaction at C-2. The difference between $k_2$ and $k_6$ is smaller for the ethylation than for the hydroxyethylation, except at low hydroxide concentration.

An attempt was made to calculate the rate constants ($k_i'$) for the reaction between ethyl chloride and the different hydroxyl groups in cellulose using a similar method to that applied to the hydroxyethylation reaction.[15] It was assumed that at constant sodium hydroxide concentration the rate of ethylation is proportional to the ethyl chloride concentration [EtCl] and to the concentration of non-substituted hydroxyl groups. Since disubstitution could be disregarded, the rate of ethylation of a hydroxyl group at carbon atom $i$ can be written:

$$d[s_i]/dt = k_i'[\text{EtCl}]([\text{cell}] - [s_i])$$

where [cell] is the molar concentration of glucose units (substituted or unsubstituted) and [$s_i$] the molar concentration of glucose units with an ethyl group at carbon atom $i$. Only a small part of the ethyl chloride was consumed in side reactions and in the reaction with the dissolved cellulose. Most of the ethyl chloride remained undissolved. It was assumed that the ethyl chloride
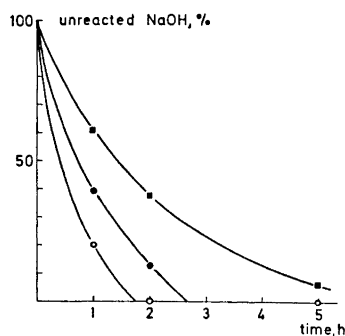


Fig. 2. Reaction between ethyl chloride and sodium hydroxide in autoclaves at 100°. O, initial NaOH-concentration 3 %; ●, initial NaOH-concentration 10 %; ■, initial NaOH-concentration 18 %.
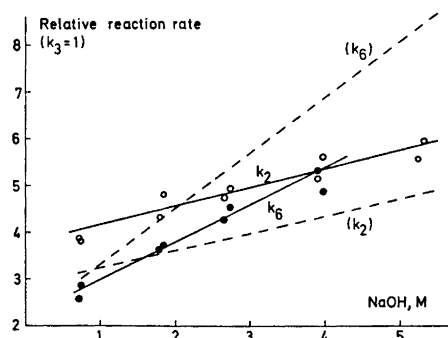
Fig. 3. Relative rate of ethylation of the different hydroxyl groups in cellulose as a function of the sodium hydroxide concentration ($k_3 = 1$). The broken lines and the constants within parenthesis refers to hydroxyethylation (1). ●, ethylation at C-6; O, ethylation at C-2.
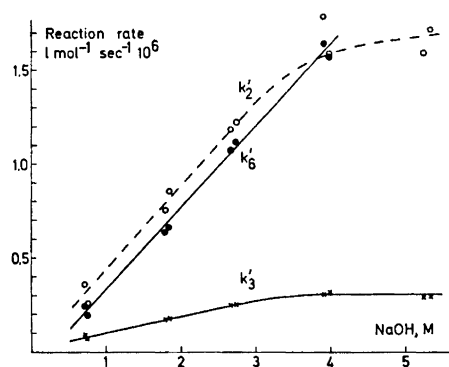
*Fig. 4.* Rate of ethylation of the different hydroxyl groups in cellulose as a function of the sodium hydroxide concentration.

concentration was constant in each experiment and the same as that determined in the corresponding blanks. Since $[s_i]$ is small compared to [cell], $k_i'$ can be calculated from the following equation:

$$k_i' = [s_i]/([EtCl][cell]t)$$

The dependence of $k_i'$ upon the hydroxide concentration is given in Fig. 4. From the figure it is seen that within the range $0.7 - 3$ M sodium hydroxide a straight line relationship exists between the rate constants and the sodium hydroxide concentration. At concentrations greater than 4 M, $k_3'$ is independent of the hydroxide concentration, whereas $k_2'$ exhibits a less pronounced dependence upon the hydroxide concentration. Unfortunately, no reliable determinations of $k_6'$ could be made at the highest concentration. The curves in Fig. 4 are similar to those in Ref. 15 for the reaction between ethylene oxide and cellulose. The hydroxyethylation was about 50 times faster than the ethylation. The similarity between the two reactions was not unexpected, since the ethylation also occurs *via* alkoxide ions. The amount of nucleophilic alkoxide ions seems to be mainly determined by the degree of dissociation, which depends upon the sodium hydroxide concentration. The ethylation is virtually determined by dissociation of the hydroxyl groups up to 3 M sodium hydroxide. The fact that $k_3'$ is almost constant at high hydroxide concentration cannot be explained by a complete dissociation, since the hydroxyl group at C-3 is probably less acidic [16] than those at C-2 and C-6, of which the reactivities increase in this concentration range.

*Reaction with undissolved fibers.* The distribution of substituents after reaction with undissolved cellulose fibers is given in Table 2. Since, the gas chromatographic peaks corresponding to $s_{23}$, $s_{36}$, and $s_{236}$ overlapped and were comparatively small, the amounts of these ethylglucoses were not determined in the hydrolyzate. The sum of the other ethylglucoses and glucose was set to 100 %, which gives rise to a negligible error in their relative amounts.

The distribution of substituents was calculated according to a statistical method suggested by Spurlin.[17] The best agreement between the observed and calculated values was obtained when the relative rate constants $(k_2:k_3:k_6)$ were given the values 7:1:6.5. For the hydroxyethylation the corresponding

Table 2. Observed and calculated distribution of substituents (in mol %) for the reaction with undissolved fibers at different sodium hydroxide concentrations.

| NaOH | 3 % | | 10 % | | 18 % | |
|---|---|---|---|---|---|---|
| | found | calc. | found | calc. | found | calc. |
| $s_0$ | 95.2 | 95.2 | 72.9 | 72.7 | 43.8 | 43.7 |
| $s_2$ | 2.2 | 2.3 | 11.2 | 12.1 | 21.0 | 21.5 |
| $s_3$ | 0.3 | 0.3 | 1.5 | 1.6 | 2.2 | 2.6 |
| $s_6$ | 2.2 | 2.1 | 10.8 | 11.2 | 18.9 | 19.7 |
| $s_{26}$ | 0.1 | — | 3.6 | 1.9 | 14.1 | 9.6 |

relative rate constants were found to be 10:1:10.[1] The experimental and calculated amounts of all ethylglucoses investigated, except $s_{26}$, agreed fairly well as shown in Table 2. One of the assumptions made for the calculations was that the relative rate constants are constant throughout the reaction and that the substitution in one position does not affect the substitution in another position. The bad agreement for $s_{26}$ indicates that this assumption could be invalid.

It was found that the relative rate constants were independent of the hydroxide concentration used in the sodium hydroxide treatment. Similar results were reported by Croon and Flamm [5] in their study of the ethylation of alkali cellulose prepared from cotton linters pulp after steeping in solutions of 16.4 and 32.2 % sodium hydroxide. In the present work experiments were made at such a high sodium hydroxide concentration (18 %) that the cellulose was completely transferred to Na-cellulose I, and at such a low concentration (3 %) that no change occurred. Evidently, the change in the supermolecular structure of cellulose has no influence upon the distribution of substituents.

It is interesting to note that in both the reaction of unbleached cotton treated with sodium hydroxide and in the reaction of the dissolved hydrocellulose with ethyl chloride the substitution was much slower at C-3 than at C-2 and C-6. The low reactivity of the hydroxyl group at C-3 can be explained by hydrogen bonding between this hydroxyl group and the ring oxygen of the adjacent glucose unit.[18]

Large differences in the relative rates during the reaction of ethylene oxide with dissolved rayon and with alkali cellulose were found previously [1] demonstrating that accessibility factors have a great influence upon the distribution of the substituents. The results obtained in the present work on ethylation lend support to this conclusion. It should therefore be expected that the relative rate constants should depend upon the source of cellulose material. This offers an explanation to the fact that the values obtained with cellulose from unbleached cotton in the present work differ more from those reported by Croon and Flamm for the reaction of bleached linters pulp than should be expected with regard to the experimental errors.

## REFERENCES

1. Ramnäs, O. and Samuelson, O. *Svensk Papperstid.* **71** (1968) 829.
2. Mahoney, J. F. and Purves, C. B. *J. Am. Chem. Soc.* **64** (1942) 9.
3. Honeyman, J. *J. Chem. Soc.* **1947** 168.
4. Timell, T. E. *Studies on Cellulose Reactions*, Diss., Stockholm 1950.
5. Croon, I. and Flamm, E. *Svensk Papperstid.* **61** (1958) 963.
6. Dorée, C. *The Methods of Cellulose Chemistry*, Chapman and Hall, London 1950.
7. Ramnäs, O. and Samuelson, O. *Svensk Papperstid.* **71** (1968) 674.
8. Larsson, L.-I., Ramnäs, O. and Samuelson, O. *Anal. Chim. Acta* **34** (1966) 394.
9. Sweeley, C. C., Bentley, R., Makita, M. and Wells, W. W. *J. Am. Chem. Soc.* **85** (1963) 2497.
10. Kesler, R. *Anal. Chem.* **39** (1967) 1416.
11. Petersson, G. and Samuelson, O. *Svensk Papperstid.* **71** (1968) 731.
12. Ramnäs, O. and Samuelson, O. *Carbohyd. Res.* **6** (1968) 355.
13. Khym, J. X., Zill, L. P. and Cohn, W. E. In Calmon, C. and Kressman, T. R. E., Eds., *Ion Exchangers in Organic and Biochemistry*, Interscience, New York 1957.
14. Savage, A. B. *Das Papier* **24** (1970) 916.
15. Ramnäs, O. and Samuelson, O. *Svensk Papperstid.* **76** (1973) 569.
16. Rydholm, S. *Pulping Processes*, Wiley, New York 1965.
17. Ott, E. and Spurlin, H. *Cellulose and Cellulose Derivatives II*, Interscience, New York 1954.
18. Liang, C. Y. and Marchessault, R. H. *J. Polymer Sci.* **37** (1959) 385.

# Studies of the Heterogeneity of *Streptomyces griseus* Protease. Isolation and Characterization of an Alkaline Serine Protease from Commercial Pronase-P Derived from *Streptomyces griseus* K1

CARL-AXEL   BAUER   and   BO   LÖFQVIST

*Biochemistry 1, Chemical Centre, P.O.B. 740, S-220 07 Lund 7, Sweden*

1. A proteolytic enzyme has been mildly isolated from Pronase-P by gel filtration on Sephadex G-75 superfine. The yield was almost optimal and the specific activity of the enzyme was constant throughout the isolation procedure and storage.

2. Analytical polyacrylamide gel electrophoresis at pH 6.8 and 8.5 failed to reveal any impurities in the preparation. When the enzyme was concentrated $5-10$ fold, two minor contaminents could be detected. They were estimated by staining to constitute less than 2 % and by enzymatic activity less than 1 %.

3. The binding of $Ca^{2+}$ to the enzyme has been found to be non-stoikiometric, and leading to a higher electrophoretic mobility with increasing $Ca^{2+}$-content in the buffer. In $Ca^{2+}$-free media the enzyme has an isoelectric point just above 7.

4. Molecular weight was estimated to 18 000. The most striking feature of the amino acid analysis was that no lysine was detected.

5. The enzyme was shown to be most stable in $Ca^{2+}$ containing buffers of neutral pH. In such buffers the enzyme was also stable in the pH-range $5-11$, in this respect being similar to elastase. The pH-optimum of the enzyme towards glutarylphenylalanine *p*-nitroanilide was between pH 10 and 11.

6. The enzyme was inhibited completely by diisopropylfluorophosphate, and partly by inhibitors normally considered to be site-specific for either chymotrypsin or elastase.

7. The enzyme was highly active towards acetyl-L-tyrosine ethyl ester, carbobenzoxy-tyrosine *p*-nitrophenyl ester, and glutaryl-L-phenylalanine *p*-nitroanilide. It was also active towards acetyl-alanyl-alanyl-alanine methyl ester and congo-red elastin as well as towards many other substrates. The activity towards casein at pH 7.5 and pH 10 was approximately identical. Amidase activity of the enzyme was low.

8. The enzyme was classified as an alkaline serine protease, with broad substrate specificity showing similarities with both chymotrypsin and elastase. The results are discussed in relation to earlier investigations on this and similar enzymes.

The heterogeneity of Pronase, the extracellular proteolytic enzyme prep-
aration from *Streptomyces griseus*, has been the subject of several investiga-
tions.[1-3] The most extensive fractionation of Pronase so far has been achieved
by polyacrylamide gel electrophoresis.[3] By this method 14 enzymatically
active protein components were resolved: 8 showing protease activity, 5
showing activity towards LNA,* while one component probably corresponded
to the carboxypeptidase present in Pronase.[1] Only a few of the Pronase com-
ponents, mainly some DFP-sensitive proteases, have been isolated and char-
acterized further.[4-12] At present there is evidence for at least four DFP-
sensitive proteases, three with molecular weights between 15 000 and 20 000,[4-12]
and one with a molecular weight of approximately 28 000.[8,10] One of these
enzymes, the "*Streptomyces griseus* trypsin", with a molecular weight of 20 000,
is well characterized.[4-8] Recently, the other three DFP-sensitive enzymes
were reported to show elastase-like activities.[10]

Although an acceptable fractionation of small amounts of Pronase com-
ponents can be obtained by preparative polyacrylamide gel electrophoresis,
it is not possible to isolate enough quantities for characterization purposes by
this method.[3] In this laboratory, we have therefore developed a method for
fractionating Pronase by gel filtration on Sephadex G-75 superfine, bead size
> 40 $\mu$.[13] Pronase is thereby separated into 7 enzymatically active peaks, de-
signated A–G. Only two of these peaks, E and G, are homogeneous on poly-
acrylamide gel electrophoresis, and correspond to bands 4 and 3, respectively,
of the earlier electrophoretic studies.[3] Since fraction E represents the com-
paratively well characterized "*Streptomyces griseus* trypsin",[3-8] we have chosen
to study fraction G, one of the low molecular weight, DFP-sensitive enzymes.
We have designated this enzyme SGP3, because of its migration in our high
resolution electrophoretic separation system.[3]

Studies by Löfqvist and Sjöberg [3] showed that SGP3 is identical to the
"PNPA hydrolase I" described by Wåhlby,[4,5,9] and to the "alkaline protease
a" described by Narahashi.[1] Wåhlby showed that the amino acid sequence
around the reactive seryl residue of "PNPA hydrolase I" was similar to that
of chymotrypsin. Narahashi describes a purification of "alkaline protease a",
but hardly gives any characterization data. Johnson and Smillie isolated an
enzyme called "SGPA", and partly studied its amino acid sequence.[11,12]
"SGPA" was found to be identical to „PNPA hydrolase I",[14] and should thus
correspond to SGP3. Finally, Gertler and Trop have purified and partly char-
acterized three "elastase-like enzymes from Pronase", of which "Enzyme II"
corresponds to "PNPA hydrolase I",[10] and thus also to SGP3.

---

* *Non-standard abbreviations.* Acetyl, Ac; *N*-acetyl-L-tyrosine ethyl ester, ATEE; *N*-benzoyl-
L-arginine methyl ester, BAME; *N*-benzoyl-D,L-arginine-*p*-nitroanilide, BANA; carbobenzoxy,
CBZ; diisopropylfluorophosphate, DFP; glutaryl-L-phenylalanine-*p*-nitroanilide, GPNA; methyl
ester, ME; *p*-nitrophenyl ester, *p*-NPE; 4-phenyl-azo-benzyloxycarbonyl-L-prolyl-L-leucyl-
glycyl-L-prolyl-D-arginine.2H$_2$O is designated collagenase substrate A; tosyl ... chloromethyl
ketones, T ... CK; L-Leu-$\beta$-naphthylamide, LNA.

Buffer I: 0.03 M borate buffer, pH 7.5, 0.03 M in CaCl$_2$ and containing 0.02 % NaN$_3$. Buffer
II: buffers 0.3 M in H$_3$BO$_3$, 0.15 M in cacodylic acid and 0.1 M in acetic acid, adjusted to a given
pH with NaOH. The enzyme studied throughout this investigation is called *Streptomyces griseus*
protease 3, and is abbreviated SGP3.

Though SGP3 has been subject of some earlier studies, no extensive characterization of the enzyme has been performed by earlier investigators, and further some of their results are highly contradictory. This could partly be due to the fact that hereto used purification procedures have involved conditions, where the enzyme is unstable. Accordingly, figures concerning activity and yield, if presented, often show big losses.

The aim of this work has therefore been to mildly isolate the enzyme, with full control of specific activity and yield. The enzyme has, after this isolation, in many respects been more extensively characterized than earlier, and the results are discussed in relation to earlier investigations on this and similar enzymes.

## EXPERIMENTAL

### Materials

*Enzyme.* Pronase-P was obtained from the Kaken Chemical Company, Tokyo, (lot number 592045).

*Inhibitors.* $^{32}$P-Diisopropylfluorophosphate was obtained from the Radiochemical Centre. Tosyl chloromethyl ketones of L-alanine, L-leucine, L-lysine, L-phenylalanine, and L-valine were purchased from Cyclo. 1-Bromo-4-(2,4 dinitrophenyl)-butan-2-one and acetylprolylalanylprolylalanine chloromethyl ketone * were kindly donated by Professor Elkan Blout, Harvard Medical School, US.

*Enzyme substrates.* (All low-molecular substrates were chromatographically homogeneous.)

*High molecular weight substrates.* Casein of Hammarsten grade was obtained from Merck AG, azocoll from Calbiochem AG, and congo-red elastin from Sigma Chemical Co.

*Methyl and ethyl esters.* N-Acetyl-L-tyrosine ethyl ester, N-benzoyl-L-alanine methyl ester, and N-benzoyl-L-arginine methyl ester.HCl were purchased from Sigma. N-Acetyl-L-alanine methyl ester, N-acetyl-L-alanyl-L-alanine methyl ester, N-acetyl-L-alanyl-L-alanyl-L-alanine methyl ester, and N-benzoyl-glycine methyl ester were all purchased from Cyclo Chemical Co.

p-*Nitrophenyl esters.* N-Carbobenzoxy-L-alanine-p-nitrophenyl ester was obtained from Cyclo, N-carbobenzoxy-glycine-p-nitrophenyl ester, and p-nitrophenyl acetate from Sigma. N-Carbobenzoxy-nitrophenyl esters of L-leucine, L-proline, and L-tyrosine were products of Fluka AG.

*Amides.* N-Acetyl-L-alanine amide, N-carbobenzoxy-glycyl-L-leucine amide, and N-carbobenzoxy-glycyl-L-tyrosine amide were all from Cyclo. N-Carbobenzoxy-glycyl-L-phenylalanine amide was purchased from Sigma.

*Other low-molecular weight substrates.* N-Benzoyl-D,L-arginine-p-nitroanilide.HCl, N-carbobenzoxy-glycyl-L-leucine, and 4-phenylazobenzyloxycarbonyl-L-prolyl-L-leucyl-glycyl-L-prolyl-D-arginine.2H$_2$O were obtained from Fluka AG. Glutaryl-L-phenylalanine-p-nitroanilide was purchased from Merck AG, glutaryl-L-phenylalanine-β-naphthylamide from Mann Research Laboratories, Inc., and L-leucine β-naphthylamide.HCl from Sigma.

Sephadex G-75 superfine (lot number 9070), and G-25 medium were obtained from Pharmacia Fine Chemicals AB. Bio-Rex 70 (200 – 400 mesh) was obtained from Bio-Rad Laboratories. All other chemicals used were of reagent grade or better.

### Preparative methods

*Gel filtration on Sephadex G-75.* Pronase-P, 1.3 g, was dissolved in 16 ml of buffer I and was immediately applied to a Sephadex G-75 column (10 × 90 cm) and eluted at a flow rate of 60 – 70 ml/h according to Klevhag and Löfqvist.[13] A Uvicord (type 4701 A, LKB) set at 280 nm with LKB recorder and collector was used to monitor and collect the eluate. The protein fractions were stored at 4°C. Unless otherwise specified, these or concentrated solutions were used for characterization purposes.

---

* This preparation was not of the highest purity.

*Ultrafiltration* was used for concentration purposes and was carried out in an Amicon diaflo apparatus equipped with UM-05 filter.

*Change of medium on Sephadex G-25.* 7 ml concentrated enzyme solution (absorbance at 280 nm 1.0 – 2.0) was applied to a Sephadex G-25 column (2.5 × 40 cm), and eluted at 40 ml/h with 0.25 M $NH_4HCO_3$ in glass-distilled water, pH 7.7.

*Lyophilization.* The enzyme solution (in 0.25 M $NH_4HCO_3$) was frozen and repeatedly lyophilized to constant weight. Since the lyophilization procedures was found to occasionally cause heterogeneity, each batch was tested for homogeneity by electrophoresis on analytical polyacrylamide gels. Heterogeneous batches were discarded. The use of lyophilized enzyme for characterization was restricted to cases, where it could not be avoided.

*Chromatography on Bio-Rex 70* was carried out essentially as described by Johnson and Smillie.[11] SGP3 (10 mg) or Pronase-P (200 mg) was dissolved in 3 ml of 0.05 M cacodylic-NaOH buffer, pH 6.0, and was applied to a Bio-Rex 70 column (2 × 50 cm). The column was developed with 12 l of cacodylic-NaOH buffer, pH 6.0, followed by 2 l of 0.05 M phosphate buffer, pH 7.5, and 2 l at pH 8.0, which finally released SGP3.

## Assays of purity

*Preparative polyacrylamide gel electrophoresis.* Sample of 100 μl of SGP3 (0.10 – 0.25 mg) or Pronase-P (2 mg), active or $^{32}$P-DFP-inhibited, in sucrose stabilized 0.38 M borate – 0.01 M $Ca^{2+}$-buffer, pH 6.8, were applied to preflushed gels and analyzed according to Löfqvist and Sjöberg.[3]

*Analytical polyacrylamide gel electrophoresis* as described by Löfqvist and Sjöberg[3] was performed on each SGP3 preparation in three different buffer systems. The buffers used were (a) 0.38 M borate – 0.01 M $Ca^{2+}$ pH 6.8, (b) 0.02 M cacodylate – 0.015 M tris buffer, pH 6.8, and (c) 0.005 M tris – 0.04 M glycine buffer, pH 8.5. Samples either of 5 or 20 μl of SGP3 (0.1 – 40 μg) or 5 μl of Pronase-P (100 μg) were applied to the gels, and both anodic and cathodic migrations were performed.

*Determination of $^{32}$P-DFP incorporated into SGP3 in Pronase and in purified SGP3.* The serine enzymes of Pronase were inhibited with $^{32}$P-DFP as described under inhibition assays below. It was specially checked that the GPNA-activity of Pronase was zero. Pentaethylenhexamine was also added (final concentration $10^{-3}$ M) in order to inhibit the $Zn^{2+}$-dependent enzymes, which constitute the rest of the enzymes of Pronase (Löfqvist, B., unpublished). Precautions were thus taken to minimize the digestion. The inhibited Pronase components were separated on a preparative polyacrylamide gel as described above. After electrophoresis, the gel was cut in 1.5 mm thick discs, which were allowed to dry i vials, and 5 ml dioxan containing 0.8 % omnifluor (New England Nuclear) was added. The radioactivity of the $^{32}$P-DFP-labelled components was determined in a Nuclear-Chicago Mark 1 liquid scintillation counter, and the number of SGP3 molecules in Pronase was calculated. No significant leakage of $^{32}$P-DFP-inactivated SGP3 from the gels could be detected. The efficiency was approximately ·82 %. Determination of $^{32}$P-DFP incorporated into purified SGP3 was carried out as described above for SGP3 in Pronase but without pentaethylenhexamine.

*Determination of protein.* The extinction coefficient for the enzyme at 280 nm, $E$ (1 %, 1 cm), was determined by measuring the absorbance of an enzyme solution in 0.25 M $NH_4HCO_3$. A known volume of the solution was then repeatedly lyophilized to constant weight (more than 98 % dry substance). The extinction coefficient was calculated by extrapolation to 1 % protein content.

*Amino acid analyses.* Amino acid analyses were carried out by the analytical division of the Institute of Biochemistry, Uppsala, Sweden, as described by Eaker.[15] Samples (both performic oxidized and unoxidized) were hydrolyzed for 24 h. Tryptophan was estimated by the method of Edelhoch.[16]

## Optimal conditions and stability of the enzyme

*Temperature stability.* The enzyme (0.13 mg) in 500 μl of buffer I was preincubated for 15 min as well as 24 h at 10, 25, 32.5 40, 50, 60, and 70°C. The residual activity was determined at 25°C by adding 2.5 ml GPNA in buffer I (3.3 % methanol) giving a final con-

centration of 1 mM GPNA. Absorbance was measured after 15 min, as described under spectrophotometric assays.

*Temperature optimum.* 2.5 ml of 1.2 mM GPNA in buffer I (3.3 % methanol) were thermostated at 10, 25, 32.5, 40, 50, 60, and 70°C for 15 min. The reactions were started by adding 500 $\mu$l SGP3 (0.065 mg) in buffer I. Absorbance was measured at 410 nm.

*pH-Stability and $Ca^{2+}$-dependence.* 250 $\mu$l of the lyophilized enzyme (0.050 mg) in distilled water, with or without 0.03 M $CaCl_2$, was preincubated in 250 $\mu$l of 15 times diluted buffer II of pH 3.0, 4.0, 5.0, 6.0, 7.0, 7.5, 8.0, 9.0, 10.0, and 11.0 for 15 min as well as 24 h at 25°C, and tested for residual activity by adding 2.5 ml 1.2 mM GPNA in buffer II, pH 7.5 (3.3 % methanol). Absorbance at 410 nm was measured after 15 min at 25°C. The capacity of buffer II was good enough to ensure a pH of $7.5 \pm 0.1$.

*pH-Optimum.* 2.8 ml buffer II of pH 6.0, 7.0, 7.5, 8.0, 9.0, 9.5, 10.0, 10.5, 11.0, 11.5, and 12.0 were thermostated to 25°C and 100 $\mu$l GPNA in methanol added, giving a final concentration of 1 mM. The reaction was started by adding 100 $\mu$l of lyophilized SGP3 (0.050 mg) in 0.01 M $CaCl_2$ solution. Absorbance at 410 nm was measured after 15 min.

*The effect of urea, methanol and acetone.* 0.175 mg lyophilized SGP3 was incubated for 15 min at 25°C in 2.9 ml buffer II, pH 7.5, containing 0, 2, 4, 6 and 8 M urea with or without 0.03 M $CaCl_2$. The residual activity was determined at 25°C by adding 100 $\mu$l GPNA (final concentration 1 mM GPNA, 3.3 % methanol). The effect of various concentrations of acetone and methanol on the enzyme activity was determined towards 5 mM $N$-Ac-Ala$_3$ME as described under titrimetric assays.

## Inhibition assays

*Inhibition with $^{32}$P-DFP* was carried out by adding 25 $\mu$l of 10 mM $^{32}$P-DFP dissolved in propyleneglycol to 250 $\mu$l of SGP3 (0.3 − 0.6 mg) or Pronase-P (2 mg) in buffer I. The degree of inhibition was studied by withdrawing 50 $\mu$l of the solution and testing for activity towards 3 ml of 1 mM GPNA solution as described below.

*Inhibition with tosyl chloromethyl ketones* was carried out according to the method of Shaw et al.[17],[18] 2.9 ml buffer I with 1.67 % methanol, $5 \times 10^{-5}$ M inhibitor and $5 \times 10^{-7}$ M SGP3 was incubated at 25°C. After 20 h, 100 $\mu$l GPNA was added to give a final substrate concentration of 1 mM. The residual enzymatic activity was determined.

*Inhibition with 1-bromo-4-(2,4-dinitrophenyl)-butan-2-one* was carried out essentially as described by Visser et al.[19] $5 \times 10^{-5}$ M inhibitor and $5 \times 10^{-7}$ M SGP3 in 2.9 ml 0.05 M phosphate buffer, pH 6.5, containing $10^{-4}$ M $CaCl_2$ and 5 % $CH_3CN$, was incubated for 10 h at 37°C. Residual enzymatic activity was determined in 1 mM GPNA, 3.3 % in methanol.

*Inhibition with acetylprolylalanylprolylalanine chloromethyl ketone.* $5 \times 10^{-7}$ M enzyme in buffer II, pH 6.5, with a 100 fold molar excess of inhibitor, was incubated for 2 h at 37°C. Residual activity was determined with GPNA.

## Enzyme assays

*Titrimetric assays. Methyl and ethyl esterase activities* were measured titrimetrically with an Autoburette ABU 12 and a Titrator TTT 1 c (Radiometer, Copenhagen). 2.95 ml of 0.1 M KCl-solution containing 2.5 % acetone and the substrate (1 − 20 mM) was added to the thermostated (25°C) reaction vessel. The pH was adjusted to 7.5 and 50 $\mu$l of enzyme in buffer I was added to start the reaction. 4.8 mM NaOH was used to maintain the pH at 7.5 and the measurements were carried out in an atmosphere of nitrogen. No significant adsorption of SGP3 to the electrodes was detected; *cf.* Ref. 10.

*Spectrophotometric assays.* All spectrophotometric determinations were corrected for blanks and were carried out in a Zeiss PMQ II spectrophotometer. *(a) Proteolytic activity* was measured according to the method of Kunitz [20] as described by Löfqvist and Sjö-berg;[3] *(b) collagenolytic activity* was determined according to the method of Wünsch and Heidrich [21] but in buffer I at 25°C; *(c) p-nitrophenyl esterase activity.* The solubility of some of these esters is very low in water. A 0.030 M borate buffer, pH 7.5, containing 10 % acetone was therefore used to make 0.1 − 1 mM *p*-nitrophenyl ester solutions. The reaction was then started by adding 50 $\mu$l of the enzyme (0.115 − 59 $\mu$g) in buffer I to a

cuvette containing 2.95 ml of $p$-nitrophenyl ester solution. In order to minimize autolysis of the substrates, the reaction vessel was thermostated at 10°C. The liberated $p$-nitrophenol was assayed by measuring the optical density at 410 nm; *(d) Peptidase activity* towards BANA and GPNA was determined according to Erlanger *et al.*[22,23] 2.90 ml of 0.25 – 2 mM substrate in buffer I with 3.3 % methanol was incubated with 100 μl of SGP3 (10 μg), and the absorbance was monitored at 410 nm at 25°C. One GPNA-unit of the enzyme was defined as the amount of enzyme hydrolyzing 1 μmol GPNA per minute; *(e) Elastolytic activity* was determined by the congo-red elastin method according to Shotton;[24] *(f) Azocoll activity* was determined according to the method of Moore.[25] 60 mg azocoll was suspended in 16 ml of buffer I and constantly shaken at 25°C. The reaction was started by addition of 4 ml enzyme (0.004 – 0.4 mg) in buffer I. The activity was monitored by measuring the optical density at 520 nm (the absorption maximum of the product formed); *(g) Carboxypeptidase activity*. To 0.9 ml $10^{-4}$ M CBZ-Gly-Leu in buffer I was added 100 μl SGP3. Liberated Leu was assayed by the ninhydrin method;[26] *(h) Amidase activity*. 9.75 ml 1 mM substrate solution in buffer II with 5 % acetone was incubated with 250 μl SGP3 in buffer I. The reaction was carried out at 25°C. 2 ml samples were withdrawn at suitable time intervals and the enzyme was immediately inactivated by addition of $NH_3$-reagent as described by Balis.[27] The colour was fully developed after 2 h, and the absorbance was read at 640 nm; *(i) Activity towards β-naphthylamides* was determined according to the method of Goldbarg and Ruthenburg.[28] 2.90 ml of 0.25 – 2 mM L-Leu-β-naphthylamide in buffer I with 3.3 % methanol at 25°C, was incubated by addition of 100 μl of SGP3 (23 μg) in buffer I. Samples were withdrawn after 1 h and 20 h.

## RESULTS

*Isolation of the enzyme.* Gel filtration of Pronase-P was carried out on a Sephadex G-75 column, and seven peaks (Fig. 1) with enzymatic activity were obtained. Peak G (approximately 300 ml) corresponds to the polyacrylamide
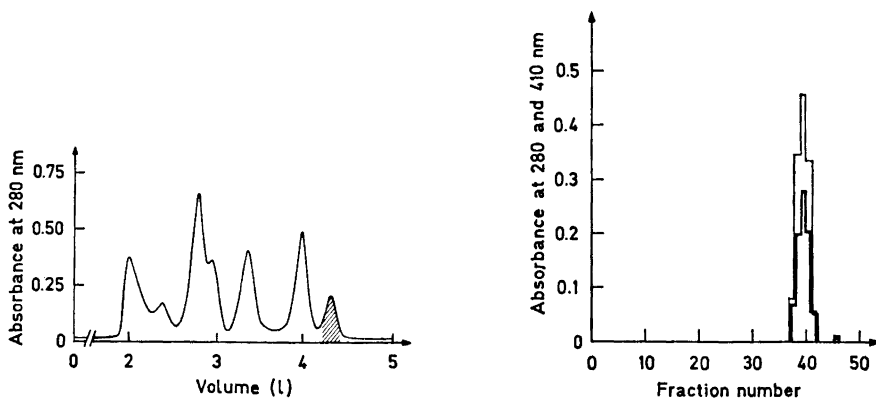




*Fig. 1.* Gelfiltration of Pronase-P on a Sephadex G-75 superfine column (10 × 90 cm). The peaks are designated A, B, C, D, E, F, and G, going from left to right. Fractions from G were pooled as indicated in the figure.

*Fig. 2.* Histogram showing enzymatic activities of peak G found in the different gel fractions of a small preparative polyacrylamide gel after 4 h electrophoresis (cathodic migration) in 0.38 M borate – 0.01 M $Ca^{2+}$ buffer, pH 6.8. The gel fractions (1.5 mm thick) were extracted at pH 7.5 with a 0.03 M borate – 0.03 M $CaCl_2$-buffer, and tested for activity towards casein pH 7.5 (—) and GPNA pH 7.5 ( – ).

gel electrophoresis band 3, as shown by testing each fraction (25 ml) of the peak on analytical gels. At the same time evidence was gathered for homogeneity of the G-fractions. Homogeneous fractions were pooled as indicated in the figure and stored at 4°C.

*Purity of the preparation.* Further tests of purity were carried out with pooled enzyme concentrated 5 − 10 fold by ultrafiltration, in order to detect even very small amounts of impurities. *(a) Preparative polyacrylamide gel electrophoresis.* Proof of homogeneity was gathered by electrophoresis on small preparative gels. The activity of the eluates from the gel slices towards GPNA and casein pH 7.5 was tested. As can be seen from Fig. 2, there is one big peak only with almost coincident GPNA and casein activities from fraction to fraction, a very good criterion of the peak's homogeneity. Fraction 46 corresponds to about 1 % of the total activity towards casein and much less than 1 % of the total activity towards GPNA. *(b) Analytical polyacrylamide gel electrophoresis.* The purity of peak G was further assessed by analytical polyacrylamide gel electrophoresis in three different buffer media (see experimental procedure). Pooled SGP3 proved to be homogeneous in all three buffers. When concentrated enzyme was used it was possible to detect a slower moving impurity, estimated by dilution series to constitute about 1 %. No activity could be assigned to this band. A second contaminating band, similarly estimated to constitute about 1 %, moving faster than SGP3 could sometimes be detected. This faint band probably corresponds to the small impurity detected in fraction 46 of the preparative polyacrylamide gel.

After isolation regarding molecular size, SGP3 has thus been proved by charge-based separation to be about 98 % pure according to protein staining with coomassie blue. Based on catalytic activity the preparations have been found to be about 99 % pure. The 1 % enzymatic impurity detected in fraction 46 of the preparative gel most certainly originated in the F-peak, as it had the same migration position as a component from that peak. This impurity can thus be further minimized by more restrictive pooling. No contamination by aminopeptidases or carboxypeptidases could be detected, as no activity towards L-Leu-β-naphthylamide or CBZ-Gly-Leu could be demonstrated, even upon prolonged incubations.

*Identity.* The results of earlier investigations [1,4−6,9−11,14] lead to the conclusion that there are hardly any media in which Pronase can be dissolved without any change in its identity. A complete control of change in yield and specific activity of the enzyme throughout the separation and storage procedures is therefore a necessary pre-requisite for the characterization. The data in Table 1 give evidence for a high level of stability under the selected conditions. No loss in yield or activity could be indicated during the separation procedure. During storage at 4°C in buffer I, the loss of activity was about 0.3 % a day, as checked both by active site titration and activity towards GPNA. Table 1 also shows that the specific activity towards GPNA is constant throughout the separation procedure and storage, indicating that the loss in activity is followed by a proportional loss of active sites. Thus, no modified DFP-reacting enzyme molecules with altered catalytic activity seem to be generated. Furthermore, electrophoretic analysis of SGP3, which had been stored for six weeks, did not show increased amounts of stainable im-

Table 1. Yield and specific activity of SGP3 at isolation and storage.

| Fraction | Amount of protein mg | Activity nmol GPNA · mg protein⁻¹ min⁻¹ | Total activity towards GPNA μmol GPNA min⁻¹ | Yield (recovered GPNA-activity) % | ³²P-DFP reactive enzyme nmol/mg protein | Specific activity nmol GPNA · nmol ³²P-DFP react. enz⁻¹ min⁻¹ |
|---|---|---|---|---|---|---|
| Pronase-P applied | 1300 | 39.1 | 50.8 | | | |
| Estimated values for SGP 3 in Pronase-P | 52.7ᵃ | 31.3ᵇ | 40.6 | 100 | 2.24ᶜ | 14.0 |
| Peak G | | 782 | 41.2 | 101 | | |
| Pooled fractions (freshly prepared) | 44.6ᵃ | 782 | 34.9 | 86 | 55.5ᶜ | 14.1 |
| Pooled fractions (stored 30 days at 4 °C) | 44.6ᵃ | 717 | 32.0 | 79 | 50.7ᶜ | 14.1 |

ᵃ Calculated from $E$(1 %, 1 cm, 280 nm) = 8.6 and the volume. ᵇ Calculated from our observation that peak G contains about 80 % of the activity of Pronase towards GPNA. ᶜ Calculated from the amount of ³²P-DFP incorporated into SGP3.

purities. This indicates that when autodigestion of an enzyme molecule once has started it seems to be followed by a rapid digestion into rather small fragments.

The charge of the active enzyme molecule also seems unaltered during the separation and storage procedures. Thus the mobility of SGP3 is the same when crude Pronase or freshly prepared or stored SGP3 are studied on analytical polyacrylamide gel electrophoresis.

As far as the identity of the enzyme has been studied during the separation and storage procedures, no change in charge, molecular size, or specific activity towards GPNA could be detected. Yield seems to be optimal, which also shows that digestion during the course of the separation is minimized.

## Extinction coefficient

The extinction coefficient, $E(1 \%, 1$ cm, 280 nm), was determined to 8.6, which is in quite good agreement with Wåhlby's value of 9,[9] while Gertler and Trop on the other hand report $E(0.1 \%, 1$ cm, 280 nm$) = 1.21$.[10] Our absorption determination was made on fresh enzyme in $NH_4HCO_3$ solution, after which the weight was determined upon lyophilization. A 0.1 % solution of those amino acids, which absorb at 280 nm (in the same molar proportions as was found in the protein from amino acid analyses), gave an extinction coefficient of 0.86, which thus must be considered as a maximum value. Lyophilized enzyme was found to give non-reproducible and sometimes too high extinction coefficients. This is probably due to the formation of enzyme aggregates during lyophilization, causing light scattering and consequently too high absorption values and extinction coefficients. We could thus obtain reproducible $E(1 \%, 1$ cm, 280 nm) values only when fresh enzyme, not lyophilized, was used for absorption determinations.

## Calcium effect on electrophoretic mobility

The amount of $Ca^{2+}$ in a lyophilized preparation of SGP3 was determined by atomic absorption on a Perkin-Elmer 303 and found to be less than 0.1 Ca-atoms per enzyme molecule. This preparation was used to demonstrate the relation between electrophoretic mobility and ionic strength of $Ca^{2+}$ in buffers at constant pH (Table 2). The low mobility in $Ca^{2+}$-free solutions

Table 2. The electrophoretic mobility of SGP3 in 6 % polyacrylamide gels, 0.03 M borate buffer of various concentrations of $Ca^{2+}$.

| Concentration of $Ca^{2+}$ in the buffer (M) | Electrophoretic mobility $(cm^2 \ sec^{-1} \ V^{-1}) \times 10^6$ |
|:---:|:---:|
| $10^{-6}$ | 6 |
| $10^{-5}$ | 7 |
| $10^{-4}$ | 15 |
| $10^{-3}$ | 25 |
| $10^{-2}$ | 38 |

([$Ca^{2+}$] $\leq 10^{-5}$ M) indicates that the enzyme is only slightly positively charged at pH 6.8, with an IP just above 7. When more $Ca^{2+}$ is added to the buffer, the mobility increases indicating that $Ca^{2+}$ is bound to the enzyme, thus giving the molecule a more positive net charge. The enzyme does not seem to reach a point of saturation concerning $Ca^{2+}$, even at concentrations as high as 0.01 M.

## Amino acid composition and molecular weight

Amino acid composition has been based on a molecular weight of 18 000 (see below), assuming 10.0 leucine residues. As can be seen from Table 3, there is excellent agreement between our data and the data of Johnson and Smillie.[11]

Table 3. Amino acid analyses of SGP3 and for comparison values from Johnson and Smillie [11] and Gertler and Trop.[10]

| Amino acid residue | Number of amino acid residues per molecule SGP3 (assuming 10.0 Leu) according to: | | | | | |
| | Bauer and Löfqvist | | Johnson and Smillie | | Gertler and Trop | |
| | 24 h hydrolysis | Integral number | [a] | Integral number | 22 h hydrolysis | Integral number |
|---|---|---|---|---|---|---|
| Lys | traces | 0 | 0.15 | 0 | $0.6 \times 2.5 = 1.5$ | 2 |
| His | 2.9 | 3 | 3.00 | 3 | $1.1 \times 2.5 = 2.8$ | 3 |
| Arg | 6.9 | 7 | 6.7 | 7[b] | $2.8 \times 2.5 = 7.0$ | 7 |
| Asp | 16.1 | 16 | 15.9 | 16 | $7.0 \times 2.5 = 17.5$ | 18 |
| Thr | 21.7[c] | 22 | 21.9[c] | 22 | $8.1 \times 2.5 = 20.3$ | 20 |
| Ser | 20.2[c] | 20 | 21.7[c] | 22 | $8.5 \times 2.5 = 21.3$ | 21 |
| Glu | 8.0 | 8 | 8.2 | 8 | $3.6 \times 2.5 = 9.0$ | 9 |
| Pro | 3.9 | 4 | 4.4 | 4 | $2.0 \times 2.5 = 5.0$ | 5 |
| Gly | 31.4 | 31 | 31.7 | 32 | $12.8 \times 2.5 = 32.0$ | 32 |
| Ala | 18.7 | 19 | 18.9 | 19 | $8.1 \times 2.5 = 20.3$ | 20 |
| 1/2 Cys | 3.7[d] | 4 | 4.3[d] | 4 | $1.5 \times 2.5 = 3.8$ | 4 |
| Val | 11.4 | 11 | 11.9[e] | 12 | $5.1^f \times 2.5 = 12.8$ | 13 |
| Met | 1.1[d] | 1 | 1.0[d] | 1 | $0.8 \times 2.5 = 2.0$ | 2 |
| Ile | 7.3 | 7 | 8.2[e] | 8 | $3.1^f \times 2.5 = 7.8$ | 8 |
| Leu | 10.0 | 10 | 10.0 | 10 | $4.0 \times 2.5 = 10.0$ | 10 |
| Tyr | 7.9 | 8 | 8.0 | 8 | $3.0 \times 2.5 = 7.5$ | 8 |
| Phe | 4.8 | 5 | 5.2 | 5 | $2.0 \times 2.5 = 5.0$ | 5 |
| Trp | 1.2[g] | 1 | 0.61[h] | 1 | $0.5^i \times 2.5 = 1.3$ | 1 |

[a] Results are averages of duplicate hydrolyses at 24, 48, 72, and 96 h. [b] Corrected to 8 after partial amino acid sequence determination.[12] [c] Values are extrapolated to zero times of hydrolysis. [d] Values estimated after performic acid oxidation. [e] Average of values after 72 and 96 h. [f] Values after 48 h. [g] Estimated by the method of Edelhoch.[16] [h] Estimated by the method of Harrison and Hofman and calculated relative to the arginine value.[11] [i] Hydrolysed in the presence of 4 % thiodiglycolic acid.[10]

The difference in serine residues is probably due to the use of a wrong correction factor, this amino acid being partly hydrolyzed after 24 h.[29] Our slightly low valine and isoleucine values are certainly due to the short hydrolysis time.[29]

"Enzyme II", one of the "pronase elastases", studied by Gertler and Trop [10] is apparently identical to SGP3, as mentioned in the introduction. The reported number of amino acid residues of "Enzyme II" was, however, very low (Table 3), since it was based on a molecular weight of 7 000 and 4.0 leucine residues. If these values are multiplied by 2.5 (which gives 10.0 leucine residues and a molecular weight around 17 500) it can be seen that there is quite good agreement between the new values for "Enzyme II", our values, and those obtained by Johnson and Smillie.

Wåhlby [9] has shown that one $^{32}$P-DFP-molecule reacts with one molecule of enzyme. The molecular weight can thus also be calculated from the number of $^{32}$P-DFP molecules, which react with a known amount of 100 % active enzyme. As can be seen in Table 1, it has been possible to use this method, and the molecular weight for SGP3 was estimated to 18 000. Molecular weight calculations, based on our amino acid analyses data, give a value around 17 750.
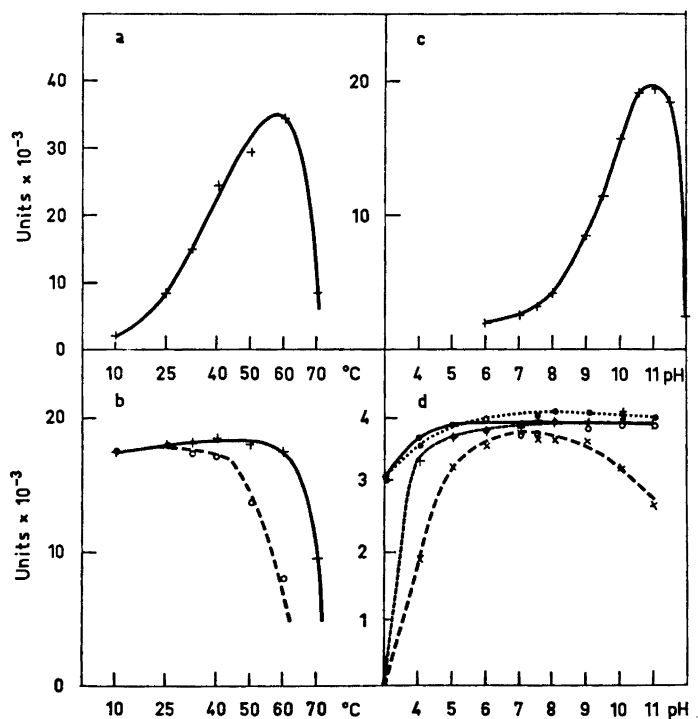


Fig. 3. (a) Temperature optimum after 15 min incubation at pH 7.5, (b) temperature stability after 15 min incubation (+) and 24 h incubation (O) at pH 7.5, (c) pH-optimum after 15 min incubation at 25°C, and (d) pH-stability and Ca$^{2+}$-dependence after 15 min (O) and 24 h (×) without Ca$^{2+}$, and 15 min (O) and 24 h (+) with Ca$^{2+}$ at 25°C. Substrate: 1 mM GPNA.

Optimal  conditions  and  stability  of  the  enzyme

As seen in Fig. 3b, at temperatures over 40°C (pH 7.5) the enzyme is rather unstable even in $Ca^{2+}$-containing buffers when incubated for several hours. Temperature optimum (Fig. 3a) has been estimated to 57°C, for an incubation time of 15 min. The enzyme is stable in the range pH 5.0 − 11.0 (Fig. 3d) when incubated in buffers containing $3 \times 10^{-2}$ M $Ca^{2+}$, but without $Ca^{2+}$ it is stable only in the range around pH 6 − 9. The stability declines abruptly below pH 4, without $Ca^{2+}$ already at pH 5, reaching zero at pH 3, where the enzyme is irreversibly denatured. To minimize the inactivation it is thus recommended to store the enzyme in a buffer 0.03 M in $Ca^{2+}$ even at 4°C.

The pH-optimum of SGP3 (Fig. 3c), when GPNA is used as substrate (15 min assay), is found between pH 10 and 11, where the enzyme is about six times as active as at the commonly used pH 7.5.

The effects of acetone and methanol on the activity of SGP3 towards the watersoluble substrate $N$-Ac-Ala$_3$-ME have briefly been checked. Addition of 2.5 % acetone or methanol caused a decrease of 40 − 50 % in activity and 5 % gave a decrease of 60 − 65 %.

Upon incubation with urea, the activity of the enzyme rapidly decreases (Fig. 4). In 8 M urea the activity is only about 5 % of the original. The residual activities after urea treatment have been measured with GPNA in 3.3 %
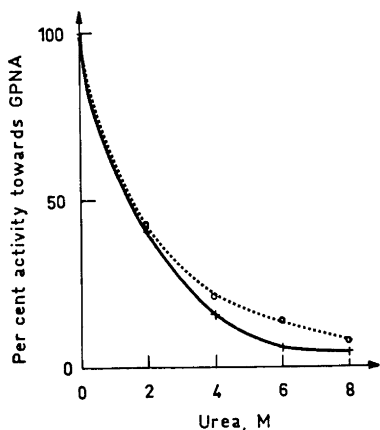


Fig. 4. Influence of urea on the activity of the enzyme as measured with 1 mM GPNA as substrate (3.3 % methanol). (O) with 0.03 M $Ca^{2+}$, ( + ) without $Ca^{2+}$ (lyophilized).

methanol. Since methanol causes decreases in the activity of SGP3, it cannot be outruled that the effect of urea is enhanced by the presence of methanol. Nevertheless the decrease in activity is so rapid, that the enzyme must be considered to be rather susceptible towards urea.

Inhibitor  specificity

Enzyme activity towards GPNA rapidly decreases on incubation with a 20-fold molar excess of DFP, showing that SGP3 is a serine enzyme as earlier pointed out by Wåhlby,[4] and Gertler and Trop.[10] The results of the inhibition

*Table 4.* Inhibition of enzyme activity by tosyl chloromethyl ketones. The results are given in percent inhibition of the activity towards GPNA after 20 h incubation at pH 7.5 and 25°C. The molar ratio of inhibitor to enzyme was 100:1.

| Inhibitor | Inhibition (%) |
|-----------|----------------|
| T Ala CK | 0 |
| T Val CK | 5 |
| T Leu CK | 15 |
| T Phe CK | 20 |
| T Lys CK | 0 |

studies with various tosyl chloromethyl ketones are presented in Table 4. TPheCK, normally considered as a site-specific chymotrypsin inhibitor,[30] is the most potent of these inhibitors, but TLeuCK and, to a lesser extent, T ValCK also inhibit the enzyme.

Two compounds known as powerful elastase inhibitors have also been tested. One of them, 1-bromo-4-(2,4-dinitrophenyl)-butan-2-one, caused, when in 100-fold molar excess over SGP3, only about 5 % inhibition (10 h, 37°C, pH 6.5). Under similar conditions elastase was inhibited to 90 %.[19] The site of inhibition in SGP3 has not been determined, but in elastase the $\gamma$-carboxyl of Glu-6 is alkylated.[19] The other inhibitor, Ac-Pro-Ala-Pro-Ala CK, made as a specific inhibitor for elastase (Professor Blout, personal communication), caused an inhibition of 10 % of SGP3 activity towards GPNA, after 2 h (37°C, pH 6.5) with a 100-fold molar excess of inhibitor.

## Substrate specificity

*1. Specificity towards some natural and some synthetic substrates.* As can be seen in Table 5 the enzyme is about equally active towards casein both at pH 7.5 and pH 10.0. Further, SGP3 is active towards congo-red elastin. Though no unit of activity is defined for congo-red elastin,[24] the activity of SGP3 towards this substrate is found to be 10 – 20 % of that of pure elastase.[24] This is in good agreement with the data of Gertler and Trop.[10]

SGP3 is also active towards the synthetic collagenase A substrate, as well as towards azocoll. GPNA, which is a chymotrypsin substrate,[23] is also a good

*Table 5.* Activity towards some natural and some synthetic substrates at 25°C.

| Substrate | Activity |
|-----------|----------|
| Casein, pH 7.5 | 0.20 $OD_{280}$ units mg enz.$^{-1}$ min$^{-1}$ |
| Casein, pH 10.0 | 0.21 $OD_{280}$ units mg enz.$^{-1}$ min$^{-1}$ |
| Azocoll | 4.0 $OD_{520}$ units mg enz.$^{-1}$ min$^{-1}$ |
| Collagenase A substrate | 6.7 × 10$^{-2}$ $\mu$mol mg enz.$^{-1}$ min$^{-1}$ |

substrate for SGP3 and has been used in many of the assays throughout this investigation, as it is a stable and easily measureable substrate. The kinetic constants for SGP3 using GPNA as substrate are $K_m = 0.91 \times 10^{-3}$ M, $k_{cat} = 0.22$ sec$^{-1}$ and $k_{cat}/K_m = 240$ sec$^{-1}$ M$^{-1}$ (2 % methanol, pH 7.5), whereas the constants for chymotrypsin under similar conditions are $K_m = 2.8 \times 10^{-4}$ M, $k_{cat} = 0.013$ sec$^{-1}$, and $k_{cat}/K_m = 46.4$ sec$^{-1}$ M$^{-1}$.[23] Thus the $K_m$ for chymotrypsin is about 3 times lower, $k_{cat}$ is about 17 times lower and $k_{cat}/K_m$ about 5 times lower than the corresponding constants for SGP3. Thus, SGP3 is more efficient in cleaving GPNA. Methanol (3.3 %) increased $K_m$ 1.5 times, but had little effect on $k_{cat}$ ($K_m = 1.4 \times 10^{-3}$ M, $k_{cat} = 0.24$ sec$^{-1}$ and $k_{cat}/K_m = 170$ sec$^{-1}$ M$^{-1}$).

Interestingly, no activity towards L-Glu-L-Phe-$\beta$-naphthylamide, the $\beta$-naphthylamide analogue of GPNA, could be detected even upon 24 h incubation, indicating that the naphthylamide group is too bulky to permit binding.

2. *Specificity towards methyl and ethyl esters.* ATEE, a chymotrypsin substrate, is the most readily hydrolyzed of these esters, as can be seen in Table 6. SGP3 also shows a little activity towards the trypsin substrate BAME, but even on prolonged incubations it is not at all active towards BANA, another trypsin substrate.[22]

*Table 6.* Activity of SGP3 towards some methyl and ethyl esters, at pH 7.5 in 0.1 M KCl (2.5 % in acetone) at 25°C.

| Substrate | $k_{cat}$ (sec$^{-1}$) | $k_{cat}/K_m$ (sec$^{-1}$ M$^{-1}$) |
|---|---|---|
| ATEE | 360 | 2800 |
| N-Ac-Ala ME | 2 | 15 |
| N-Ac-Ala$_2$ ME | 10 | 450 |
| N-Ac-Ala$_3$ ME | 70 | 4400 |
| N-Benzoyl-Ala ME | 1 | 100 |
| BAME | 0.8 | 250 |

Activity towards the N-benzoyl methylesters of hydrophobic amino acids could not be determined at acceptable acetone concentrations, since the solubilities of some of these compounds are quite low, and the enzyme is most sensitive towards even low concentrations of acetone. It was, however, possible to use the glycine and alanine compounds, but SGP3 was active only towards the latter.

3. *Specificity towards* p-*nitrophenyl esters.* The low solubility and the high rate of self-hydrolysis of these esters makes it difficult to obtain accurate determinations of $K_m$ and $k_{cat}$. Thus our values presented in Table 7 can be regarded as only approximate, though within the right order of magnitude. As can be seen, SGP3 is characterized by very high $k_{cat}/K_m$ values for the Leu and Tyr analogues, like $\alpha$-chymotrypsin, but in contrast to elastase. The figures for the Gly and Ala compounds are, however, similar to those determined for elastase. Interestingly, the $k_{cat}/K_m$ values of SGP3 and

*Table 7.* Comparison of $k_{cat}/K_m$ values for SGP3, alkaline protease C, elastase, and chymotrypsin towards some $p$-NPE compounds. The activity of SGP3 was determined at 10°C in 0.015 M borate buffer, pH 7.5, containing 10 % acetone.

| $p$-NPE compound | SGP3 (Bauer and Löfqvist) | | Alkaline protease C(=SGP1)[a] | Elastase[b,c] | $\alpha$-Chymotrypsin[b] |
|---|---|---|---|---|---|
| | $k_{cat}(\text{s}^{-1})$ | $k_{cat}/K_m(\text{s}^{-1}\text{M}^{-1})$ | $k_{cat}/K_m(\text{s}^{-1}\text{M}^{-1})$ | $k_{cat}/K_m(\text{s}^{-1}\text{M}^{-1})$ | $k_{cat}/K_m(\text{s}^{-1}\text{M}^{-1})$ |
| CBZ-Gly | 5 | $10^4$ | $1.8 \times 10^4$ | $1.5 \times 10^4$ [b] | $1.9 \times 10^5$ |
| CBZ-Ala | 20 | $2 \times 10^5$ | – | $1.85 \times 10^5$ [c] | – |
| CBZ-Leu | 15 | $4 \times 10^6$ | $2.7 \times 10^6$ | $2.9 \times 10^4$ [b] | $3.45 \times 10^6$ |
| CBZ-Tyr | 500 | $5 \times 10^7$ | $1.25 \times 10^7$ | $80$ [b] | $11 \times 10^7$ |
| CBZ-Pro | 0.06 | 200 | – | $20$ [c] | – |
| Ac | 0.04 | 300 | – | $470$ [b] | – |

[a] All assays were conducted at 25°C in phosphate buffer ($I=0.05$, pH 7.5), containing 1.66 % acetonitrile.[31] [b] All assays were conducted at 25°C in 0.1 M phosphate buffer (pH 7.8).[32] [c] All assays were conducted at 25°C in phosphate buffer ($I=0.1$).[33]

*Table 8.* Activity towards amide substrates. Activity is given as % hydrolysis of the amide bond after 72 h at 25°C, pH 7.5 (5 % acetone).

| Substrate | % hydrolysis |
|---|---|
| $N$-Ac-L-Ala·NH$_2$ | 0 |
| $N$-CBZ-Gly-L-Leu·NH$_2$ | 2 |
| $N$-CBZ-Gly-L-Phe·NH$_2$ | 9 |
| $N$-CBZ-Gly-L-Tyr·NH$_2$ | 12 |

Narahashi's "alkaline protease C" ($=$SGP1),[31] reveal very little, if any, difference in specificity as concerns the Gly, Leu, and Tyr analogues.

*4. Specificity towards amide substrates.* As can be seen from Table 8 the amidase activity of the enzyme is very low. Interestingly, the enzyme is more active even towards the phenylalanine than the leucine analogue. Like elastase, this enzyme does not appear to cleave $N$-acetyl-L-Ala amide. Although Thompson and Blout [34] showed this substance to be a competitive inhibitor for elastase, it did not detectably inhibit SGP3.

## DISCUSSION

In this investigation, special attention has been drawn to the stability of enzyme SGP3 during the purification and storage procedures. This is justified by the fact that Pronase-P, the starting material, is a very complex mixture of active proteolytic enzymes, which may cause a number of active and inactive degradation products when subjected to purification. In addition, several of the enzymes in Pronase show amidase activity (Löfqvist, B., unpublished) and may thus cause deamidation reactions. This could *e.g.* be the case in the investigation by Johnson and Smillie.[11] They obtained two proteolytically active peaks on Bio-Rex 70, with identical amino acid compositions but with different specific activities — one (SGPA1) showing only half the specific activity of the other (SGPA2) towards ATEE. Obviously, SGPA1 and SGPA2 differed in charge since they were not equally retarded on the ion exchanger, and Johnson and Smillie also suggested (based on their sequence work) that SGPA1 may be generated from SGPA2 by deamidation of Gln 192 A. If so, this could very well explain the differences both in charge and specific activity, since Gln 192 A ought to be located in the vicinity of the active Ser 195. In this connection it is also interesting to note that elastase has a Gln in position 192 located in the active region of that enzyme.[35]

It is thus evident that care must be taken during the isolation procedure and storage so that no changes of the enzyme identity will occur, and this should thoroughly be checked. As shown in Table 1 it has been possible to accomplish such mild conditions in our separation, as the specific activity is unaltered.

To test the homogeneity of SGP3 we also tried the Bio-Rex 70 separation method of Johnson and Smillie.[11] It was not possible, however, to elute our

SGP3 preparation under the prescribed conditions, but the enzyme was released when a buffer of a higher pH and a higher ionic strength was used. This indicates that our enzyme preparation should have a higher isoelectric point than SGPA2. Both separations were performed in $Ca^{2+}$-free buffers, where we have shown that no $Ca^{2+}$, which could alter the net charge, was bound to the enzyme. Thus, the results suggest that our enzyme preparation should be less deamidated than SGPA2. Analytical polyacrylamide gel electrophoresis of Pronase-P and stored SGP3 also verify that no change in charge and thus no deamidation has occurred at our conditions of isolation and storage.

During storage of SGP3 a loss in total activity, but not in specific activity, is seen (Table 1). As discussed above, deamidation reactions cannot be responsible for this loss in activity, and accordingly the enzyme is exposed to another type of denaturation causing loss of enzyme. Analytical polyacrylamide gel electrophoresis does not reveal any new stainable components, and $K_{av}$ for SGP3 on Sephadex G-75 is not influenced by storage.[13] These facts indicate that the loss in activity is caused by autodigestion of the enzyme into rather small fragments, and that no high molecular intermediates are accumulated during this process. Such a digestion also explains the parallel losses in active sites and amount of enzyme. It is also in good agreement with the findings of Klevhag and Löfqvist,[13] who showed that several of the Pronase-enzymes, including SGP3, were digested into low molecular components in the absence of $Ca^{2+}$ or by prolonged storage at neutral pH. We thus conclude that even if it has not been possible to avoid a certain loss in yield and active sites during our isolation and storage procedures, this has not caused any change in the identity of SGP3.

A third observation concerning the identity of SGP3, which, however, does not overthrow the statements above, may be worth mentioning in this context. Lyophilized preparations of SGP3 sometimes show heterogeneity on polyacrylamide gel electrophoresis. The additional bands are slower migrating than SGP3. They are all active towards casein and GNPA, and the ratio of activity between casein and GPNA for all these components are equal to that of homogeneous SGP3. One possible explanation to the heterogeneity is that lyophilization sometimes may cause the formation of polymeric forms of SGP3.

*Some properties of SGP3 in relation to earlier investigations on this enzyme and chymotrypsin and elastase.* Molecular weight calculations, based on our amino acid analyses data, give a value around 17 750 for SGP3, while Johnson and Smillie [11] similarly derived a molecular weight of 18 276. The latter value is probably the more accurate, since the former is based on results known to be low in some cases. Our determination of molecular weight with ^{32}P-DFP, also gave a value of 18 000. Wåhlby determined, however, a molecular weight of approximately 16 000 by using an ultracentrifugation technique,[9] but a value of 18 000 can possibly be within the limits of error for the technique used. Estimations of molecular weight by gel filtration on Sephadex have given still lower values. Klevhag and Löfqvist [13] estimated a molecular weight of 15 000 on Sephadex G-75, and Awad *et al.*[8] similarly derived 15 500 on Sephadex G-100. These somewhat lower values might possibly indicate a slight interaction between Sephadex and the protein. The extremely low value of

7 000 obtained by Gertler and Trop by gel filtration on Sephadex G-75 must be wrong, and is probably due to an artifact, as they also suggest themselves.[10]

The pH stability curve of SGP3 (in $Ca^{2+}$-buffers) shows that while it is stable between pH 5.0 and 11.0, it is irreversibly denatured at pH 3 (Fig. 3d). This behaviour is in contrast to that of chymotrypsin and trypsin, but similar to that of elastase.[24]

The pH-optimum curve for SGP3 (Figure 3c), with an optimum far on the alkaline side, indicates the dissociation of a functional group around pH 9 and 10.

The effects of urea and methanol and acetone show that SGP3 is most sensitive to the polarity and to the hydrogen bonding capacities of the environment, thus indicating a rather loose tertiary structure.

Earlier inhibition studies with TPheCK have shown both distinctly higher [10] and distinctly lower [11] inhibitions than we have found. These results are not necessarily inconsistent, however, since the excess of the inhibitor and the incubation pH and time have not been the same. The fact that SGP3 is inhibited by certain tosyl chloromethyl ketones (Table 4) might indicate that a histidine residue, necessary for activity, is present in the active site of SGP3, as has been proved for chymotrypsin with TPheCK,[17] and for trypsin with TLysCK.[18] TPheCK, normally considered to be a site-specific inhibitor for chymotrypsin,[30] only partly inhibits SGP3, indicating that the subsites of this enzyme differ from those of chymotrypsin. The low inhibition of SGP3 with inhibitors site-specific for elastase, suggests that the subsites of SGP3 also differ from those of elastase.

From the substrate specificity data (Tables 5 – 8), it can be seen that SGP3 shows a broad substrate specificity, and is highly active towards both typical chymotrypsin substrates (ATEE, CBZ-Tyr-$p$NPE) and typical elastase substrates ($N$-Ac-Ala$_3$ME and congo-red elastin). Like elastase, SGP3 shows high activity towards $N$-Ac-Ala$_3$ME, less towards $N$-Ac-Ala$_2$ME, and low activity towards $N$-Ac-AlaME. This might indicate an extended active center, as postulated for elastase by Thompson and Blout.[34]

The facts that SGP3 has an alkaline pH-optimum, that it is totally inhibited by DFP, and that it is proteolytically active, permit its classification as an alkaline serine protease.

*Relation of SGP3 to some other microbial serine proteases.* The relation of SGP3 to other microbial serine proteases, especially to those in Pronase, is interesting. Though three "elastase-like enzymes" from Pronase have been reported,[10] only two of these, the low molecular weight ones, seem to be closely related, with a sequence around their active seryl residues similar to that of chymotrypsin.[5] The third "elastase-like enzyme", which is of a higher molecular weight, has recently been shown to have an amino acid sequence around its active seryl residue similar to that of subtilisin.[8] What differences could there be between the two low molecular weight enzymes? Table 7 only possibly indicates faint differences in specificity. Preliminary results from our laboratory show, however, that SGP3 has a much higher specific activity towards GPNA than SGP1. Further differences are indicated by Gertler and Trop, who showed that their "Enzyme II" (=SGP3) reacted more rapidly with ATEE than with $N$-Ac-Ala$_3$ME, whereas the reverse was true for "Enzyme

III" (=SGP1).[10] Careful comparative investigations with both SGP1 and SGP3 must evidently be undertaken in order to detect further differences in specificity between these two enzymes.

SGP3 is, as mentioned above, rather susceptible towards urea. This is in marked contrast to the serine enzyme (identical to SGP1) studied by Siegel *et al.*,[36] which was unusually stable in 6 M quanidinium chloride and in 8 M urea. That enzyme also proved to be markedly stabilized by $Ca^{2+}$. As seen from Fig. 4 this is evidently not the case for SGP3. These facts indicate that there could be important structural differences between the two enzymes.

It might be argued that SGP3 is derived from SGP1 by limited digestion, since the latter enzyme seems to have slightly higher molecular weight. Preliminary amino acid analysis of SGP1 from this laboratory, do not verify such a hypothesis, as SGP1 seems to have, for example, fewer Glu/Gln than SGP3.

Interestingly, SGP3 does also appear to have some properties in common with the well-studied α-lytic protease from *Sorangium sp.*[37,38] Thus SGP3, α-lytic protease and elastase are "low-lysine, high-arginine" enzymes,[38] in contrast to chymotrypsin and trypsin. This make the first-mentioned enzymes subject to less losses of net charge, when the pH is increased from 8 to 10. Further, α-lytic protease seems to be quite similar to elastase in specificity, at least towards certain small synthetic substrates. Unlike SGP3, however, it does not hydrolyze ATEE, and is not at all inhibited by tosyl chloromethyl ketones. As stated by Kaplan and Whitaker,[37] "the substrate binding properties of the α-enzyme are appreciably different from those of chymotrypsin". Evidently the α-enzyme also differs from SGP3 in these properties.

REFERENCES

1. Narahashi, Y. *Methods Enzymol.* **19** (1970) 651.
2. Trop, M. and Birk, Y. *Biochem. J.* **116** (1970) 19.
3. Löfqvist, B. and Sjöberg, L.-B. *Acta Chem. Scand.* **25** (1971) 1663.
4. Wåhlby, S. *Biochim. Biophys. Acta* **151** (1968) 394.
5. Wåhlby, S. and Engström, L. *Biochim. Biophys. Acta* **151** (1968) 402.
6. Narahashi, Y. and Fukunaga, J. *J. Biochem. Tokyo* **66** (1969) 743.
7. Jurasek, L., Fackre, D. and Smillie, L. B. *Biochem. Biophys. Res. Commun.* **37** (1969) 99.
8. Awad, W., Soto, A., Siegel, S., Skiba, W., Bernström, G. and Ochoa, M. *J. Biol. Chem.* **247** (1972) 4144.
9. Wåhlby, S. *Biochim. Biophys. Acta* **185** (1969) 178.
10. Gertler, A. and Trop, M. *Eur. J. Biochem.* **19** (1971) 90.
11. Johnson, P. and Smillie, L. *Can. J. Biochem.* **49** (1971) 548.
12. Johnson, P. and Smillie, L. *Can. J. Biochem.* **49** (1971) 1083.
13. Klevhag, J.-E. and Löfqvist, B. *In preparation.*
14. Jurasek, L., Johnson, P., Olafson, R. W. and Smillie, L. B. *Can. J. Biochem.* **49** (1971) 1195.

15. Eaker, D. In *Evaluation of novel protein products*, Pergamon, Oxford and New York 1970, pp. 171–194.
16. Edelhoch, H. *Biochemistry* **6** (1967) 1948.
17. Schoellman, G. and Shaw, E. *Biochemistry* **2** (1963) 252.
18. Shaw, E., Mares-Guia, M. and Cohen, W. *Biochemistry* **4** (1965) 2219.
19. Visser, L., Sigman, D. and Blout, E. *Biochemistry* **10** (1971) 735.
20. Kunitz, M. *J. Gen. Physiol.* **30** (1947) 291.
21. Wünsch, E. and Heidrich, H. G. *Z. physiol. Chem.* **333** (1963) 149.
22. Erlanger, B., Kokowsky, N. and Cohen, W. *Arch. Biochem. Biophys.* **95** (1961) 271.
23. Erlanger, B., Edel, F. and Cooper, A. *Arch. Biochem. Biophys.* **115** (1966) 206.
24. Shotton, D. *Methods Enzymol.* **19** (1970) 113.
25. Moore, G. *Anal. Biochem.* **32** (1969) 122.
26. Yemm, E. and Cocking, E. *Analyst* **80** (1955) 209.
27. Balis, E. *Methods Biochem. Anal.* **20** (1971) 104.
28. Goldbarg, J. A. and Ruthenburg, A. M. *Cancer Philadelphia* **11** (1958) 283.
29. Moore, S. and Stein, W. *Methods Enzymol.* **6** (1963) 819.
30. Shaw, E. *Methods Enzymol.* **25** (1972) 655.
31. Narahashi, Y. *J. Biochem. Tokyo* **71** (1972) 1077.
32. Marshall, T. H., Whitaker, J. R. and Bender, M. L. *Biochemistry* **8** (1969) 4671.
33. Geneste, P. and Bender, M. *Proc. Nat. Acad. Sci. U.S.* **64** (1969) 683.
34. Thompson, R. and Blout, E. *Proc. Nat. Acad. Sci. U.S.* **67** (1970) 1734.
35. Shotton, D. M. and Watson, H. C. *Nature* **225** (1970) 811.
36. Siegel, S., Brady, A. and Awad, W. *J. Biol. Chem.* **247** (1972) 4155.
37. Kaplan, H. and Whitaker, D. R. *Can. J. Biochem.* **47** (1969) 305.
38. Kaplan, H., Symonds, V. B., Dugas, H. and Whitaker, D. R. *Can. J. Biochem.* **48** (1970) 649.

# The Crystal Structure of Perchloro-all-*cis*-tricyclo [5.2.1.0$^{4,10}$]deca-2,5,8-triene

BENGT AURIVILLIUS and GUNNAR MALMROS*

*Division of Inorganic Chemistry 2, Chemical Center, University of Lund, Box 740, S-220 07 Lund 7, Sweden*

The crystal and molecular structure of the chlorocarbon perchloro-all-*cis*-tricyclo[5.2.1.0$^{4,10}$]deca-2,5,8-triene, $C_{10}Cl_{10}$, has been studied with the aid of three-dimensional X-ray diffractometer data. The symmetry is orthorhombic, space group *Pbca*. The unit cell contains eight molecules $C_{10}Cl_{10}$ and has the dimensions $a = 12.666$ Å, $b = 15.630$ Å, and $c = 15.509$ Å.

The structure has been refined to an *R*-value of 0.029 (1837 independent reflections). The molecules $C_{10}Cl_{10}$ deviate slightly from their ideal symmetry $C_{3v}$. Most of the *intra*- and *inter*-molecular distances are normal. A few short non-bonded Cl − Cl distances do, however, occur and are discussed in the text.

A chlorocarbon $C_{10}Cl_{10}$ has been synthesized by chlorination of all-*cis*-tricyclo[5.2.1.0$^{4,10}$]decane by Jacobson.[1] Considering chemical and spectroscopic properties of the compound, Jacobson arrived at the following possible structural formula:



●Cl
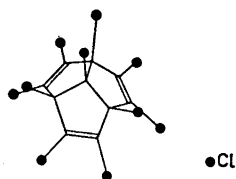
The compound may thus be denoted perchloro-all-*cis*-tricyclo[5.2.1.0$^{4,10}$]-deca-2,5,8-triene. It seemed of interest to get a more direct proof of the molecular structure in question and therefore the present X-ray investigation of

$C_{10}Cl_{10}$ was undertaken. It was hoped that the bonding distances found would further elucidate the proposed formula. In the present paper the chlorocarbon $C_{10}Cl_{10}$ will be denoted PCT.

## UNIT CELL AND SPACE GROUP

A specimen of PCT,[2] where the crystals had been grown in chloroform, was kindly supplied by Dr. Jacobson. From this sample a small crystal, $V \approx 0.003$ mm³, was selected. From Weissenberg and precession photographs the Laue symmetry was found to be *mmm*. The following restrictions limited possible reflections:

$$0kl, \ k = 2n; \ hk0, \ h = 2n; \ h0l, \ l = 2n.$$

This is characteristic of the orthorhombic space group *Pbca* (No. 61). The cell dimensions found from the Weissenberg and precession photographs were used to interpret powder photographs (*cf.* Table 1), taken in a Guinier-Hägg focussing camera. Strictly monochromatized $CuK\alpha_1$ radiation was used and KCl ($a = 6.2909$ Å) added as an internal standard. The following lattice parameters were obtained with the aid of least-squares calculations:

$$a = 12.666(5) \ \text{Å}, \ b = 15.630(5) \ \text{Å}, \ c = 15.509(7) \ \text{Å}.$$

The density of the specimen as determined by the flotation method is 2.08 g cm⁻³, in good agreement with the calculated value of 2.05 g cm⁻³ for eight molecules $C_{10}Cl_{10}$ per unit cell.

## DATA COLLECTION AND DATA REDUCTION

The crystal structure was originally solved using photographic intensity data. Later, data were collected by means of a Pailred linear diffractometer for a refinement of the structure.

*Photographic intensity data.* $CuK\alpha$ radiation was used when collecting the film data. A small crystal was mounted with [011] as rotation axis in an integrating Weissenberg camera. The multiple film technique was used and the intensities of the registered 3002 reflections were estimated visually. After correcting for Lorentz and polarization effects in the usual way, symmetry-related reflections belonging to different layers were put on a common scale by means of least-squares calculations and mean values of $|F_o|$ were calculated. In this way 2297 independent reflections resulted. The film data were regarded as preliminary and no absorption correction was made, though the linear absorption coefficient is 165 cm⁻¹.

*Diffractometer intensity data.* The intensity data were collected using $MoK\alpha$ radiation monochromatized by reflection off the (002) planes of a graphite crystal, the monochromator angle being 6.08°. The single crystal used was a nearly pentagonal plate with the edges 0.15 mm and the thickness 0.075 mm. The plate was mounted along one of its edges which coincides with the direction of the crystallographic *b*-axis. The reflections of the layer lines $h0l - h15l$ were collected for the copper range, $\sin \theta / \lambda \leq 0.65$, using equi-inclination and $\omega$-scan techniques with a scan rate of 1.0°/min. The scan range was 3.0° for all reflections except for those with $\sin \theta < 0.1$ in the layers $6-16$, where the scan range was 4.0°. The stationary background counts were measured for 40 sec at each end of the scan interval. The aperture size of the detector was 2.0°. As a check of the electronic stability during the period of data collection, the intensity of one standard reflection

*Table 1.* X-Ray powder data of perchloro-all-*cis*-tricyclo[5.2.1.0$^{4,10}$]deca-2,5,8-triene. Guinier focusing camera of 80 mm diameter with CuK$\alpha_1$ radiation and KCl as an internal standard.

| h k l | $10^5 \sin^2 \theta_{obs}$ | $10^5 \sin^2 \theta_{calc}$ | $I_{obs}$ |
|-------|------|------|------|
| 1 1 1 | 858 | 859 | vw |
| 0 2 1 | 1214 | 1218 | w |
| 1 0 2 | 1354 | 1356 | w |
| 1 2 1 | 1592 | 1588 | w |
| 1 1 2 | – | 1599 | – |
| 0 2 2 | 1958 | 1958 | w |
| 2 1 1 | – | 1969 | – |
| 1 1 3 | 2823 | 2833 | vvw |
| 2 2 2 | 3435 | 3437 | vw |
| 2 3 0 | 3666 | 3665 | vw |
| 3 1 1 | 3823 | 3818 | vw |
| 2 1 3 | 3932 | 3942 | m |
| 0 0 4 | – | 3947 | – |
| 0 4 1 | 4121 | 4132 | w |
| 3 0 2 | 4318 | 4315 | vw |
| 1 0 4 | – | 4317 | – |
| 1 4 1 | 4503 | 4502 | vw |
| 3 2 1 | – | 4546 | – |
| 3 1 2 | 4560 | 4558 | vvw |
| 1 1 4 | – | 4559 | – |
| 2 2 3 | 4681 | 4671 | vw |
| 1 3 3 | 4784 | 4775 | vvw |
| 0 2 4 | 4919 | 4918 | vvw |
| 3 2 2 | 5282 | 5286 | w |
| 1 2 4 | – | 5288 | – |
| 2 4 0 | 5364 | 5365 | w |
| 2 1 4 | 5676 | 5669 | vw |
| 4 1 0 | 6166 | 6160 | vw |
| 2 2 4 | – | 6397 | – |
| 4 1 1 | 6412 | 6406 | vw |
| 3 3 2 | – | 6500 | – |
| 1 3 4 | 6504 | 6502 | m |
| 3 2 3 | – | 6520 | – |
| 1 5 1 | 6694 | 6687 | vw |
| 4 2 0 | 6886 | 6888 | vw |
| 4 0 2 | – | 6904 | – |
| 4 2 1 | – | 7135 | – |
| 0 2 5 | – | 7138 | – |
| 4 1 2 | 7145 | 7146 | vw |
| 1 2 5 | – | 7508 | – |
| 3 1 4 | 7504 | 7518 | m |
| 2 5 0 | 7560 | 7550 | w |
| 2 4 3 | – | 7585 | – |
| 2 5 1 | 7797 | 7797 | vw |
| 3 4 2 | – | 8200 | – |
| 1 4 4 | 8197 | 8202 | m |
| 3 2 4 | 8235 | 8246 | vw |
| 4 3 1 | 8342 | 8349 | vw |

was measured at regular intervals. The largest difference measured was 1.4 %. Reflections for which the two measured background values differed more than 3.09 times the e.s.d. of their difference were omitted. The integrated peak counts $I$ were calculated from the total integrated peak counts, the background counts, and the counting times in the usual way. If $\sigma(I)/I \geq 0.5$, the reflection was considered unobserved. For each layer line both the reflections $hkl$ and $\bar{h}kl$ were measured, giving a total of 7121 reflections. Of these, 3214 were omitted because of the above-mentioned restrictions. In the final step of refinement mean values of the reflections $hkl$ and $\bar{h}kl$ were taken and only those pairs were considered for which both $hkl$ and $\bar{h}kl$ occurred in the reduced intensity list. In this way 1837 independent reflections finally resulted from the diffractometer measurements. The corrections for Lorentz and polarization effects were performed using the standard procedure. With $MoK\alpha$ radiation the linear absorption coefficient is only 18 cm$^{-1}$. Therefore no absorption correction was made.

*Comparison between the two data sets.* The final $R$-factor, using anisotropic temperature factors for all atoms, was 0.109 for 2297 independent reflections measured with the multiple film technique and 0.029 for 1837 independent reflections using diffractometer data.

The positional parameters obtained from the two data sets agree within 3 e.s.d.'s of the parameters obtained from the film data. The $\sigma$-values of the positional parameters were $1.5 - 2.0$ times larger for film data than for diffractometer data.

## STRUCTURE DETERMINATION

The unit cell contains 80 chlorine and 80 carbon atoms. As the space group is unique and has a centre of symmetry, the best way of attacking the problem seemed to be to use sign relationships.

To perform these calculations the program GAASA [3] was used which one of us (Malmros) had adapted to the computer Univac 1108. According to the method of Wilson, an approximate scale factor and an overall temperature factor was first calculated, followed by a calculation of normalized structure factors. Thereafter, sign relations for 306 reflections with $E > 1.7$ were deduced and sign symbols were introduced for the 10 largest $E$-values. From this basic set new symbols were calculated, using the restriction that those which had a lower probability than 0.975 were discarded. Equations between the remaining symbols were derived and solved if their probabilities were larger than 0.998. After four reiterations 268 phases were described by three symbols, which could, however, be chosen arbitrarily. Thus the phases for the 268 reflections were in fact determined. Starting with the now known 268 phases, all 306 phases but one could be determined.

Using $E$-values a three-dimensional Fourier function was then calculated, which revealed the positions of all chlorine atoms. Based on all observed reflections the parameters of the chlorine atoms were then refined by means of least-squares calculations, giving an $R$-factor of 0.29. The positions of all carbon atoms in the unit cell could be deduced from a three-dimensional difference Fourier function, where the contributions of the chlorine atoms were subtracted. (At this stage it was observed that the carbon atom positions could as well have been obtained from the $E$-map, though other peaks of the same heights occurred there).

*Table 2.* Weight analysis obtained in the final cycle of least-squares refinement. $w$ = weighting factor. $\Delta = ||F_o| - |F_c||$.

| Interval $|F_o|$ | Number of reflections | $w\Delta^2$ | Interval sin $\theta$ | Number of reflections | $w\Delta^2$ |
|---|---|---|---|---|---|
| 0.0 − 18.5 | 182 | 1.777 | 0.000 − 0.274 | 547 | 0.735 |
| 18.5 − 21.3 | 183 | 1.137 | 0.274 − 0.345 | 481 | 0.658 |
| 21.3 − 24.4 | 185 | 1.192 | 0.345 − 0.395 | 351 | 1.036 |
| 24.4 − 28.0 | 182 | 1.106 | 0.395 − 0.435 | 251 | 0.882 |
| 28.0 − 32.4 | 184 | 0.770 | 0.435 − 0.468 | 156 | 1.188 |
| 32.4 − 38.8 | 184 | 0.786 | 0.468 − 0.498 | 44 | 2.012 |
| 38.8 − 47.0 | 183 | 1.159 | 0.498 − 0.524 | 5 | 0.491 |
| 47.0 − 59.5 | 184 | 0.949 | | | |
| 59.5 − 85.8 | 184 | 0.510 | | | |
| 85.8 − 388.2 | 184 | 0.614 | | | |

*Table 3.* Positional and thermal parameters of the atoms of PCT. All numbers are multiplied by $10^5$. Estimated standard deviations are given within brackets. The anisotropic thermal parameters are based on the expression $\exp\ [-(h^2\beta_{11} + k^2\beta_{22} + l^2\beta_{33} + 2hk\beta_{12} + 2hl\beta_{13} + 2kl\beta_{23})]$.

| Atom | $x$ | $y$ | $z$ | $\beta_{11}$ | $\beta_{22}$ | $\beta_{33}$ | $\beta_{12}$ | $\beta_{13}$ | $\beta_{23}$ |
|---|---|---|---|---|---|---|---|---|---|
| Cl(1) | 1444(9) | 25842(7) | 32611(7) | 570(7) | 257(5) | 331(4) | 122(4) | − 60(5) | 24(4) |
| Cl(2) | − 12212(9) | 11033(9) | 43928(8) | 396(6) | 515(6) | 450(6) | 4(5) | 121(5) | − 35(5) |
| Cl(3) | − 7102(11) | − 6101(8) | 32630(11) | 625(9) | 333(6) | 816(9) | − 182(5) | 1(7) | − 97(5) |
| Cl(4) | 10993(11) | − 45(8) | 18240(7) | 819(10) | 453(6) | 283(5) | 59(6) | − 75(5) | − 171(4) |
| Cl(5) | 18552(11) | − 13986(8) | 33085(10) | 834(10) | 198(5) | 681(7) | 39(5) | − 99(7) | − 78(5) |
| Cl(6) | 35994(9) | − 3701(8) | 44744(8) | 521(7) | 380(5) | 484(6) | 128(5) | − 97(6) | 82(4) |
| Cl(7) | 38033(8) | 14764(7) | 34079(8) | 359(6) | 357(5) | 453(5) | 51(4) | 103(5) | 19(4) |
| Cl(8) | 30554(9) | 16094(8) | 54496(7) | 555(7) | 474(6) | 324(4) | 6(5) | − 176(5) | − 64(4) |
| Cl(9) | 6778(9) | 24344(7) | 53232(7) | 645(8) | 432(6) | 267(4) | 115(5) | 30(5) | − 139(4) |
| Cl(10) | 19246(10) | 17782(7) | 22307(6) | 693(8) | 366(5) | 221(4) | 11(5) | 82(5) | 73(3) |
| C(1) | 7116(29) | 16365(23) | 37163(23) | 383(23) | 207(16) | 232(14) | 31(14) | − 51(15) | − 6(11) |
| C(2) | − 1163(29) | 9567(26) | 37836(23) | 349(22) | 352(19) | 219(14) | 35(16) | 17(15) | 0(14) |
| C(3) | 1038(31) | 2576(26) | 33419(27) | 398(24) | 246(19) | 338(18) | − 14(15) | − 73(18) | − 21(13) |
| C(4) | 11727(32) | 2586(26) | 29323(24) | 466(25) | 263(17) | 231(15) | 12(16) | − 11(17) | − 58(12) |
| C(5) | 19532(32) | − 3193(26) | 33928(27) | 506(26) | 193(17) | 348(18) | 23(16) | 50(20) | − 52(13) |
| C(6) | 26558(29) | 1068(25) | 38526(25) | 340(24) | 274(18) | 280(16) | 71(15) | 2(16) | − 3(13) |
| C(7) | 25668(28) | 10548(25) | 37835(24) | 321(21) | 275(17) | 238(14) | − 49(14) | 37(15) | 5(13) |
| C(8) | 22419(28) | 15244(23) | 45833(23) | 403(23) | 227(16) | 226(14) | − 46(15) | − 63(15) | − 8(12) |
| C(9) | 12721(30) | 18461(23) | 45396(24) | 415(24) | 217(16) | 228(14) | − 21(14) | 31(17) | − 48(12) |
| C(10) | 15989(28) | 11855(24) | 31500(22) | 341(21) | 238(16) | 199(14) | 20(13) | 21(14) | 22(11) |

A least-squares refinement of the parameters of all atoms in the unit cell, based on the final diffractometer intensity data set described above, resulted in an $R$-factor of 0.029 (1837 independent reflections), when anisotropic temperature factors were introduced for the atoms. Cruickshank's weighting scheme, with $a = 18.0$, $c = 0.0015$ and $d = 0$, was used in the calculations. The weighting scheme for the last cycle of the refinement is given in Table 2. The final param-

eters of the atoms are presented in Table 3. Lists of observed and calculated structure factors are available on request to the Division of Inorganic Chemistry 2, Chemical Center, Lund.

## DESCRIPTION AND DISCUSSION OF THE STRUCTURE

The labelling of the atoms and the ring planes in the crystal structure of PCT is indicated in a clinographic drawing given in Fig. 1. A stereographic picture of the molecule is presented in Fig. 2. It is immediately seen that the structure of the molecule as obtained from the present investigation confirms the model deduced by Jacobson (*cf*. p. 3172). This model implies a $C_{3v}$ or pseudo-$C_{3v}$ symmetry of the molecule.
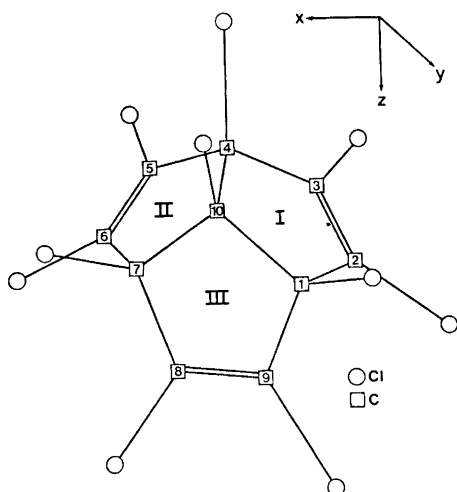


*Fig. 1.* A clinographic view of the molecule of PCT showing the labelling of the carbon atoms (*cf*. Table 3) and the ring planes. Each carbon atom is bonded to a chlorine atom of the same number, C(1) to Cl(1) *etc*. The positions of the three formal double bonds of the molecule are also given.

As seen from Fig. 1, the threefold or pseudo-threefold axis extends along the line $C(10) - Cl(10)$. The present investigation shows a small but significant deviation from $C_{3v}$ symmetry. Neither the threefold axis nor the mirror planes are exactly fulfilled in the molecule.

*Intra-* and *inter-*molecular distances in the structure are given in Table 4 together with the angles within a molecule. The various distances within a molecule are visualized in Fig. 3. As seen from this drawing the deviation from $C_{3v}$ symmetry is quite small. A slight decrease of the distance $C(4) - C(5)$ and a slight increase of the distance $C(4) - Cl(4)$ would remove most of the asymmetry of the distances.

When discussing the bond distances within a molecule on the whole, one may, however, neglect the deviations from $C_{3v}$ and use mean values. With this simplification the molecule may be described with the aid of asymmetric units of composition $C_5Cl_5$ (*cf*. Fig. 4 and Table 4).
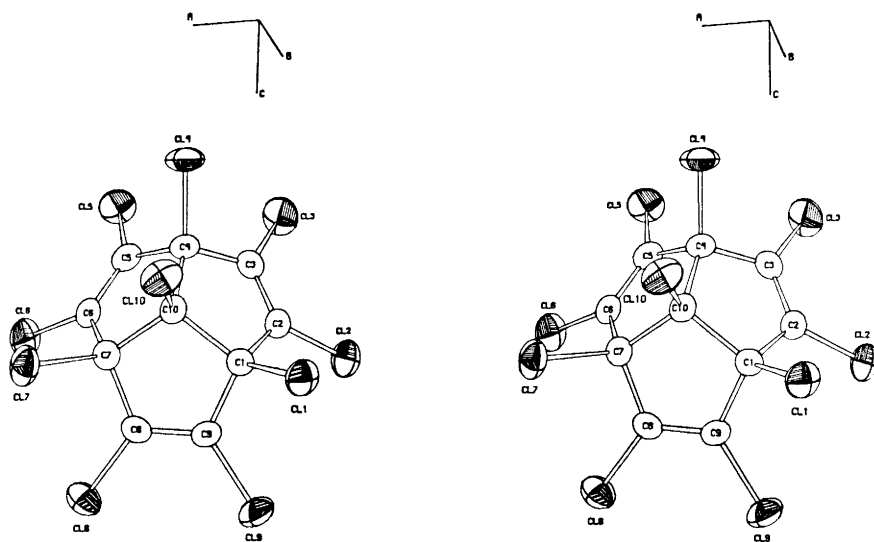
*Fig. 2.* A stereographic view of the molecule of PCT.

*The five-membered rings.* The distance $C(x) - C(x')$ (*cf.* Fig. 4) has a mean length of 1.323(6) Å, in fair agreement with the value 1.337(6) Å given in Ref. 4 for a double carbon-carbon bond. The formal double bond $C(x) - C(x')$ is the shortest one within the ring. The mean value, 1.499(18) Å, of the bonds $C(x) - C(y)$ and $C(x') - C(y')$, which may be considered identical in the simplified model, is not far from the value given for a shortened single bond in the presence
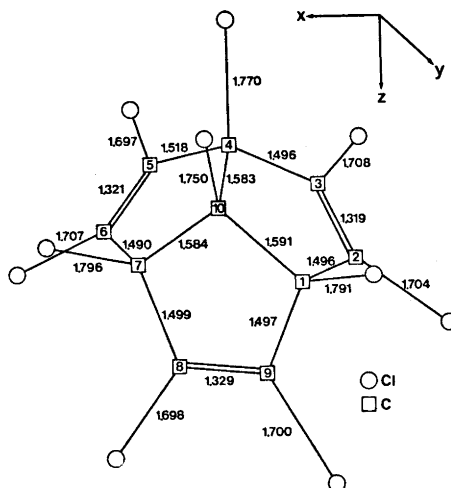


*Fig. 3.* A clinographic view of the molecule of PCT showing the various bonding distances. Notations of the atoms, *cf.* Table 3.
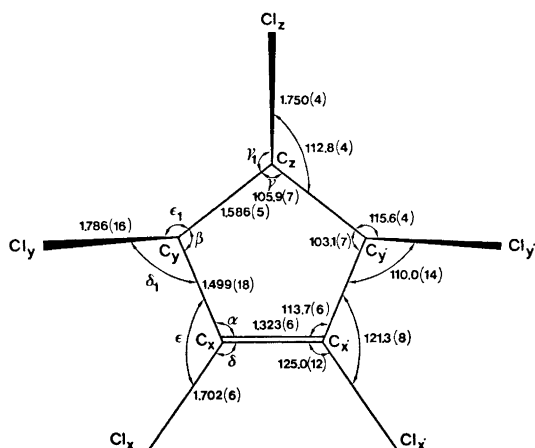
*Fig. 4.* A schematic view of the asymmetric unit $C_5Cl_5$ of PCT. The carbon and the chlorine atoms are marked $x$, $x'$, $y$, $y'$, and $z$. The angles in the five-membered ring are denoted $\alpha$, $\beta$, $\gamma$; remaining angles in the planar part $\delta$ and $\varepsilon$.

of a double bond, 1.53(1) Å.[4] These bonds are the next shortest ones of the ring. The mean value of the bonds $C(y) - C(z)$ and $C(y') - C(z)$ is 1.586(5) Å, definitely longer than a single paraffinic bond, 1.541(3) Å.[4] Lengthened tetrahedral carbon-carbon bonds are not unusual for cage molecules. Thus distances $C - C$ of $1.60 - 1.62$ Å have been observed for photoaldrin.[5]

A structure with more specific bearing on the present one is that of hexacyclo [$10.3.1.0^{2,10}.0^{3,7}.0^{6,15}.0^{9,14}$]hexadecane.[6] In this structure the longest $C - C$ bond is 1.55(2) Å. The reason for the lengthening is assumed to be the interaction of two pairs of eclipsed hydrogen atoms on the respective carbon atoms. Making the same assumption for PCT, the long $C(y) - C(z)$ and $C(y') - C(z)$ distances would be due to the interaction of the eclipsed chlorine atoms $Cl(y) - Cl(z)$ and $Cl(y') - Cl(z)$, which are at short mutual distances. Mean values of the angles are given in Fig. 4 (*cf.* Table 4).

Both the angles and the distances of the five-membered rings show good agreement with the predictions that could be made for the proposed structure.

*The carbon-chlorine distances.* The carbon-chlorine distances fall within three ranges:

(*i*) In the simplified model the distances $C(x) - Cl(x)$ and $C(x') - Cl(x')$ may be considered to be identical. The mean value of the bond length is *1.702(6)* Å, in good agreement with the values given for the non-equivalent $C - Cl$ distances in 1,2,3,4-tetrachlorobutadiene,[7] 1.701(12) and 1.715(11) Å. The bond length $C(x) - Cl(x)$ in PCT is also not far from the value, 1.70 Å, given for an aromatic carbon-chlorine bond.[4]

(*ii*) In the idealized model mean values may be taken for the $C(y) - Cl(y)$ and the $C(y') - Cl(y')$ distances. The mean value is *1.786(16)* Å, in fair agreement with 1.767(2) Å, given for a paraffinic carbon-chlorine bond.[4]

(*iii*) The $C(z)$ and $Cl(z)$ atoms are unique in the molecule of PCT. The bond

*Table 4a.* Selected distances (Å) in the crystal structure of PCT. Estimated standard deviations are given within brackets. Notations, *cf.* Figs. 1 and 4. Mean values of equivalent distances within the five-membered rings are given, in addition to the total mean values between the rings. It is also noted which least-squares plane the atoms belong to (*cf.* Tables 5 and 6).

| Atoms | Bonding distance | Mean value in the rings | Mean value between the rings | Notations *cf.* Figs. 1, 4 | Planes (Tables 5, 6) |
|---|---|---|---|---|---|
| C(2) − C(3) | 1.319(6) | | | | I |
| C(5) − C(6) | 1.321(6) | | 1.323(6) | C(x) − C(x′) | II |
| C(8) − C(9) | 1.329(5) | | | | III |
| C(1) − C(2) | 1.496(5) | 1.496 | | | I |
| C(3) − C(4) | 1.496(6) | | | | I |
| C(4) − C(5) | 1.518(6) | 1.504 | 1.499(5) | {C(x) − C(y) | II |
| C(6) − C(7) | 1.490(6) | | | {C(x′) − C(y′) | II |
| C(7) − C(8) | 1.499(5) | 1.498 | | | III |
| C(1) − C(9) | 1.497(5) | | | | III |
| C(1) − C(10) | 1.591(5) | | | | I, III |
| C(4) − C(10) | 1.583(6) | | 1.586(5) | {C(y) − C(z) | I, II |
| C(7) − C(10) | 1.584(5) | | | {C(y′) − C(z) | II, III |
| C(2) − Cl(2) | 1.704(4) | 1.705 | | | I |
| C(3) − Cl(3) | 1.706(4) | | | | I |
| C(5) − Cl(5) | 1.697(4) | 1.702 | 1.702(5) | {C(x) − Cl(x) | II |
| C(6) − Cl(6) | 1.707(4) | | | {C(x′) − Cl(x′) | II |
| C(8) − Cl(8) | 1.698(4) | 1.699 | | | III |
| C(9) − Cl(9) | 1.700(4) | | | | III |
| C(1) − Cl(1) | 1.791(4) | | | | IV |
| C(4) − Cl(4) | 1.770(4) | | 1.786(10) | {C(y) − Cl(y) | V |
| C(7) − Cl(7) | 1.796(4) | | | {C(y′) − Cl(y′) | VI |
| C(10) − Cl(10) | 1.750(4) | | | C(z) − Cl(z) | IV, V, VI |
| | *Intra*-molecular distances Cl − Cl < 3.6 Å | | | | |
| Cl(1) − Cl(10) | 3.037(1) | | | | IV |
| Cl(4) − Cl(10) | 3.042(2) | | 3.039(3) | Cl(y′) − Cl(z) | V |
| Cl(7) − Cl(10) | 3.036(2) | | | | VI |
| Cl(2) − Cl(3) | 3.265(2) | | | | I |
| Cl(5) − Cl(6) | 3.276(2) | | 3.274(8) | Cl(x) − Cl(x′) | II |
| Cl(8) − Cl(9) | 3.282(2) | | | | III |
| Cl(1) − Cl(2) | 3.381(2) | 3.359 | | | I |
| Cl(3) − Cl(4) | 3.336(2) | | | | I |
| Cl(4) − Cl(5) | 3.311(2) | 3.324 | 3.326(56) | Cl(x) − Cl(y) | II |
| Cl(6) − Cl(7) | 3.336(2) | | | | II |
| Cl(7) − Cl(8) | 3.312(2) | 3.295 | | | III |
| Cl(9) − Cl(1) | 3.277(2) | | | | III |
| | *Inter*-molecular distances Cl − Cl < 3.6 Å | | | | |
| Cl(4) − Cl(8) | 3.461(2) | | | | |
| Cl(5) − Cl(7) | 3.428(2) | | | | |

*Table 4b.* Angles (°) in the approximately planar parts $C_6Cl_5$ of the crystal structure of PCT. Estimated standard deviations are given within brackets. Notations, *cf.* Figs. 1 and 4.

Plane I:   Atoms C(1), C(2), C(3), C(4), C(10), Cl(2), Cl(3)
Plane II:  Atoms C(4), C(5), C(6), C(7), C(10), Cl(5), Cl(6)
Plane III: Atoms C(1), C(7), C(8), C(9), C(10), Cl(8), Cl(9)

| Atoms | Angle | Mean value in the rings | Mean value between the rings | Notations *cf.* Fig. 4 | Planes (Tables 5, 6) |
|---|---|---|---|---|---|
| C(1) – C(2) – C(3) | 113.8(3) | 114.1 | | | I |
| C(2) – C(3) – C(4) | 114.3(4) | | | | I |
| C(4) – C(5) – C(6) | 113.1(4) | 113.7 | 113.7(6) | α | II |
| C(5) – C(6) – C(7) | 114.3(4) | | | | II |
| C(7) – C(8) – C(9) | 113.3(3) | 113.4 | | | III |
| C(8) – C(9) – C(1) | 113.5(3) | | | | III |
| C(3) – C(4) – C(10) | 102.7(3) | 102.7 | | | I |
| C(10) – C(1) – C(2) | 102.6(3) | | | | I |
| C(6) – C(7) – C(10) | 103.4(3) | 103.1 | 103.1(7) | β | II |
| C(10) – C(4) – C(5) | 102.8(3) | | | | II |
| C(9) – C(1) – C(10) | 103.5(3) | 103.6 | | | III |
| C(10) – C(7) – C(8) | 103.8(3) | | | | III |
| C(4) – C(10) – C(1) | 106.4(3) | | | | I |
| C(7) – C(10) – C(4) | 106.2(3) | | 105.9(7) | γ | II |
| C(1) – C(10) – C(7) | 105.2(3) | | | | III |
| C(3) – C(2) – Cl(2) | 124.9(3) | 124.8 | | | I |
| C(2) – C(3) – Cl(3) | 124.6(3) | | | | I |
| C(6) – C(5) – Cl(5) | 126.3(3) | 125.1 | 125.0(12) | δ | II |
| C(5) – C(6) – Cl(6) | 123.8(3) | | | | II |
| C(9) – C(8) – Cl(8) | 124.9(3) | 125.1 | | | III |
| C(8) – C(9) – Cl(9) | 125.3(3) | | | | III |
| C(1) – C(2) – Cl(2) | 121.3(3) | 121.2 | | | I |
| C(4) – C(3) – Cl(3) | 121.1(3) | | | | I |
| C(4) – C(5) – Cl(5) | 120.5(3) | 121.2 | 121.3(8) | ε | II |
| C(7) – C(6) – Cl(6) | 121.9(3) | | | | II |
| C(7) – C(8) – Cl(8) | 121.8(3) | 121.5 | | | III |
| C(1) – C(9) – Cl(9) | 121.2(3) | | | | III |

Angles (°) in the approximately planar parts $C_2Cl_3$ of the crystal structure of PCT. The atoms are situated at the bridge head positions.

Plane IV: Atoms C(1), C(10), Cl(1), Cl(10)
Plane  V: Atoms C(4), C(10), Cl(4), Cl(10)
Plane VI: Atoms C(7), C(10), Cl(7), Cl(10)

| Atoms | Angle | Mean value | Notations | Planes |
|---|---|---|---|---|
| Cl(10) – C(10) – C(1) | 112.4(3) | | | IV |
| Cl(10) – C(10) – C(4) | 113.0(2) | 112.8(4) | $\gamma_1$ | V |
| Cl(10) – C(10) – C(7) | 113.0(2) | | | VI |
| Cl(1) – C(1) – C(10) | 115.6(2) | | | IV |
| Cl(4) – C(1) – C(10) | 116.0(3) | 115.6(4) | $\varepsilon_1$ | V |
| Cl(7) – C(7) – C(10) | 115.2(2) | | | VI |

*Table 4. Continued.*

Angles (°) in the non-planar parts of the molecule of PCT.

| Atoms | Angle | Mean value |
|---|---|---|
| C(2) − C(1) − Cl(1) | 109.5(3) | |
| C(9) − C(1) − Cl(1) | 110.2(3) | 109.9(4) |
| C(5) − C(4) − Cl(4) | 110.7(3) | |
| C(3) − C(4) − Cl(4) | 111.4(3) | 111.1(4) |
| C(8) − C(7) − Cl(7) | 109.2(3) | |
| C(6) − C(7) − Cl(7) | 108.8(3) | 109.2(2) |

Total mean value 110.0 (14), notated $\delta_1$ in Fig. 4.

length C(z) − Cl(z) of *1.750(4)* Å falls in between the values discussed above for paraffinic and olefinic carbon-chlorine bonds.

    Mean values of the various C − C − Cl angles are given in Table 4 but will not be further discussed here.

    *The architecture of the molecule.* Each five-membered ring in the molecule of PCT approximately forms a plane together with the chlorine atoms at each end of the double C − C bond. The least-squares planes (I, II, III) of the actual atoms are given in Table 5 together with the distances of the various atoms to the best plane. The planes each deviate significantly from planarity but no atom has a larger distance from the best plane than 0.08 Å (*cf.* Tables 5 and 3).

    The carbon atoms at the bridge head positions and their attached chlorine atoms, *viz.* the atoms Cl(y), C(y), C(z), Cl(z) and Cl(z), C(z), C(y'), Cl(y') (Fig. 4) each form a plane. The least-squares planes, denoted IV, V, and VI, through these atoms are given in Table 6 together with the distances from the various atoms to the best plane. Considering the e.s.d.'s in the positional parameters (Table 3) of the constituting atoms, not all groups are strictly planar. The deviation from planarity is 0.03 Å or less. A simple interpretation of the structural formula proposed for PCT would predict planarity of the groups.

    *Non-bonded chlorine-chlorine contacts within the molecule.* Within a molecule of PCT there are five different chlorine-chlorine distances shorter than 3.3 Å. The mean value of the Cl(x) − Cl(x') contact is 3.274(8) Å. This distance is, as expected, shorter than the sum of the van der Waals radii, and compares well to the value of 3.292(5) Å found for the corresponding distance in 1,2,3,4-tetrachlorobutadiene.[7]

    The mean value of the Cl(y) − Cl(z) and Cl(y') − Cl(z) distances (Table 4) is 3.039(3) Å. These distances are considerably shorter than those usually found between chlorine atoms bound to adjacent carbon atoms, *e.g.* 3.08 Å, in octachlorocyclobutane.[8,9] The discussed distance is also shorter than contacts of the same type, given by Rudman [10] in his survey over chlorine-chlorine distances in aromatic compounds.

    As indicated above the long C(y) − C(z) and C(y') − C(z) distances may be a consequence of these short Cl − Cl distances.

    *Inter-molecular distances.* There are no short C − C or C − Cl intermolecular contacts (Table 4). The shortest Cl − Cl distances between different molecules

are 3.428(2) and 3.461(2) Å. The values are not abnormally low compared to those given by Rudman.[10]

*Concluding remarks.* The present X-ray investigation has in all main features confirmed the structure of PCT as proposed by Jacobson.[1] As to the details, the X-ray investigation has revealed that the molecule as it appears in the crystalline state shows a small but significant deviation from the expected $C_{3v}$ symmetry, if the standard deviations resulting from the least-squares refinements are reliable and not underestimated. Further work is needed to conclude if the deviation from this symmetry persists also in solution or if it is due to crystal forces.

*Table 5.* Least-squares planes defined by the five-membered carbon ring and the $Cl(x)$ atoms (*cf.* Fig. 4). The normalized equations are given in a Cartesian coordinate system (unit 1 Å) with the axes parallel to the crystallographic ones. All atoms are given unit weight. The distances (Å) of the atoms to the best plane are also presented.

| Plane I[a] | | Plane II[b] | | Plane III[c] | |
|------|----------|------|----------|------|----------|
| Atom | Distance | Atom | Distance | Atom | Distance |
| C(1)  | − 0.05 | C(4)  | 0.05   | C(1)  | − 0.08 |
| C(2)  | − 0.01 | C(5)  | 0.00   | C(7)  | − 0.01 |
| C(3)  | − 0.02 | C(6)  | 0.00   | C(8)  | 0.00   |
| C(4)  | 0.06   | C(7)  | − 0.01 | C(9)  | − 0.01 |
| C(10) | 0.00   | C(10) | − 0.02 | C(10) | 0.07   |
| Cl(2) | 0.05   | Cl(5) | − 0.03 | Cl(8) | − 0.01 |
| Cl(3) | − 0.04 | Cl(6) | 0.02   | Cl(9) | 0.04   |

$^a$ Plane I:      $0.4373\,x - 0.3909\,y + 0.8099\,z - 4.1147 = 0$
$^b$ Plane II:   $-0.6200\,x - 0.0016\,y + 0.7846\,z - 2.5992 = 0$
$^c$ Plane III:   $0.3714\,x + 0.8506\,y - 0.3723\,z - 0.4398 = 0$

*Table 6.* Least-squares planes defined by two carbon and two chlorine atoms at the bridge head positions. The normalized equations and the distances of the atoms are given as in Table 5.

| Plane IV[a] | | Plane V[b] | | Plane VI[c] | |
|-------|----------|-------|----------|-------|----------|
| Atom  | Distance | Atom  | Distance | Atom  | Distance |
| C(1)   | − 0.03 | C(4)   | 0.00 | C(7)   | − 0.02 |
| C(10)  | 0.03   | C(10)  | 0.00 | C(10)  | 0.02   |
| Cl(1)  | 0.02   | Cl(4)  | 0.00 | Cl(7)  | 0.01   |
| Cl(10) | − 0.02 | Cl(10) | 0.00 | Cl(10) | − 0.01 |

$^a$ Plane IV:   $-0.6749\,x - 0.5353\,y - 0.5079\,z - 4.8722 = 0$
$^b$ Plane V:    $-0.9331\,x + 0.3578\,y - 0.0362\,z - 1.4049 = 0$
$^c$ Plane VI:    $0.2037\,x - 0.8563\,y - 0.4747\,z - 3.5144 = 0$

## REFERENCES

1. Jacobson, I. T. *Acta Chem. Scand.* **21** (1967) 2235.
2. Jacobson, I. T. *Acta Chem. Scand.* **26** (1972) 2477.
3. Lindgren, O., Lindqvist, O. and Nyborg, J. *Acta Chem. Scand.* **24** (1970) 732.
4. *International Tables for X-Ray Crystallography*, Kynoch Press, Birmingham 1962, Vol. III.
5. Khan, A. A., Baur, W. H. and Khan, M. A. Q. *Acta Cryst.* **B 28** (1972) 2060.
6. Rao, S. T. and Sundralingam, M. *Acta Cryst.* **B 28** (1972) 694.
7. Otaka, Y. *Acta Cryst.* **B 28** (1972) 342.
8. Owen, T. B. and Hoard, J. L. *Acta Cryst.* **4** (1951) 172.
9. Margulis, T. N. *Acta Cryst.* **19** (1965) 857.
10. Rudman, R. *Acta Cryst.* **B 27** (1971) 262.

# Studies of the Sulfoxidation of Alkanes

## I. The Dependence of the Sulfoxidation Rate on the Conversion and the $SO_2/O_2$ Ratio

BENGT BJELLQVIST*

*Department of Nuclear Chemistry, The Royal Institute of Technology, S-100 44 Stockholm 70, Sweden*

It is shown that in purified dry cyclohexane or n-alkane the sulfoxidation reaction starts spontaneously after an induction period. The reaction rates as a function of time have been determined for different mol ratios $SO_2/O_2$. Initially the reaction rate seems to be growing exponentially. The reaction constant characterizing this behaviour increases with the $SO_2/O_2$ ratio. This result is ascribed to a competition between the reactions

$$R\cdot + SO_2 \rightarrow RSO_2\cdot \qquad (1)$$

and

$$R\cdot + O_2 \rightarrow RO_2\cdot \qquad (2)$$

where the formation of alkylperoxy radicals leads to termination according to

$$RO_2\cdot + radical \rightarrow stable\ product$$
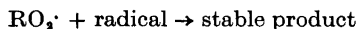
With high gas flows and good mixing the reaction rate reaches a maximum value and then decreases in a manner which indicates inhibition by the products formed. It is shown that addition of sulfuric acid inhibits the reaction. The sulfonic to sulfuric acid molar product ratio is for low conversions $1.3-1.9$. This value increases with reaction time. As a part of this investigation the solubilities of oxygen and sulfur dioxide in cyclohexane, $C_{10}-C_{13}$ and $C_{13}-C_{17}$ n-alkanes were also determined.

The possibility to sulfoxidate cyclohexane and n-alkanes is known since 1940.[1] The reaction is a free-radical chain process and a variety of chain-initiating catalysts, *e.g.* $\gamma$-rays, UV-light, ozone and peroxides[2] have been used. From a study on cyclohexane Graf[3] suggested the following mechanism

---

* Present address: Aminkemi AB, Box 20105, S-161 20 Bromma 20, Sweden.

Propagation
$$C_6H_{11}\cdot + SO_2 \rightarrow C_6H_{11}SO_2\cdot \quad (1)$$
$$C_6H_{11}SO_2\cdot + O_2 \rightarrow C_6H_{11}SO_2O_2\cdot \quad (2)$$
$$C_6H_{11}SO_2O_2\cdot + C_6H_{12} \rightarrow C_6H_{11}SO_2O_2H + C_6H_{11}\cdot \quad (3)$$

Branching and product formation
$$C_6H_{11}SO_2O_2H \rightarrow C_6H_{11}SO_3\cdot + OH\cdot \quad (4)$$
$$C_6H_{11}SO_3\cdot + C_6H_{12} \rightarrow C_6H_{11}SO_3H + C_6H_{11}\cdot \quad (5)$$
$$OH\cdot + C_6H_{12} \rightarrow H_2O + C_6H_{11}\cdot \quad (6)$$
$$H_2O + C_6H_{11}SO_2O_2H + SO_2 \rightarrow C_6H_{11}SO_3H + H_2SO_4 \quad (7)$$

$$C_6H_{11}SO_2O_2H + C_6H_{12} \rightarrow C_6H_{11}SO_3H + C_6H_{10} + H_2O \quad (8)$$

$$C_6H_{11}SO_2O_2H + C_6H_{10} \rightarrow C_6H_{11}SO_3\!\!-\!\!\left\langle\bigcirc\right\rangle\!\!-\!\!OH \quad (9)$$

$$C_6H_{11}SO_3\!\!-\!\!\left\langle\bigcirc\right\rangle\!\!-\!\!OH + H_2SO_4 \rightarrow C_6H_{11}SO_2O\!\!-\!\!\left\langle\bigcirc\right\rangle\!\!-\!\!HSO_4 + H_2O \quad (10)$$

$$C_6H_{11}SO_2O_2\cdot + C_6H_{11}SO_2\cdot \rightarrow 2\,C_6H_{11}SO_3\cdot \quad (11)$$

The steps (1) to (7) have commonly been accepted as correct. If all water produced in reaction (6) were to participate in reaction (7) a 2:1 ratio of $RSO_3H$ to $H_2SO_4$ should result. The reported ratio using anhydrous reactants is appreciably higher and the steps (8) to (11) were proposed to explain this effect as well as the diolester formation. This explanation has been questioned by Black and Baxter [4] who instead suggested two alternative explanations. All the water might not be available for the reduction reaction due to hydrate formation. The rate of reduction is very slow and hence an appreciable concentration of water built up before the rate of reduction of persulfonic acid can approach that of its decomposition. It is also earlier known that, once started, the reaction continues even after the removal of the radical producing agent. Keller [5] has shown that using high pressures and temperatures of $50-60°C$ the sulfoxidation reaction of n-alkanes starts spontaneously if the molar ratio $SO_2$ to hydrocarbon in the liquid phase is bigger than one. In this work it is shown that after an induction period the sulfoxidation of purified, dry cyclohexane as well as higher n-alkanes also starts at room temperature and atmospheric pressure without addition of any catalysts.

Contradictory statements are found in the literature concerning the reaction rate dependence on the $SO_2/O_2$ ratio. Graf [3] studied the UV-initiated sulfoxidation of cyclohexane. $SO_2$ and $O_2$ in different ratios were bubbled through the hydrocarbon and the product was allowed to separate from the reaction mixture and collected at the bottom of the reaction vessel. The highest reaction rates were reported for the molar ratio $SO_2/O_2 = 2$. Graf states that with a higher $SO_2$-content in the gas-phase than 70 % the reaction rate is proportional to the partial pressure of $O_2$. Results similar to Graf's are reported by Black [4] and Dzjagatspanyan.[6] Bertram [7,8] $\gamma$-irradiated closed ampoules containing hexane in which $SO_2$ and $O_2$ were dissolved. In this investigation he found that the chain length was proportional to the square of the $SO_2$ concentration and independent of the oxygen concentration. In several

patents [9],[10] it is claimed that in the technical sulfoxidation of higher n-alkanes the preferred $SO_2/O_2$ ratio is between 6:1 and 15:1.

In the present investigation the reaction rates as function of time have been followed by measuring the gas consumption in the uncatalysed sulfoxidation of cyclohexane and n-alkanes for different $SO_2/O_2$ mol ratios. The effects of adding small amounts of water and sulfuric acid have also been investigated.

## EXPERIMENTAL

*Materials.* The cyclohexane (Merck *p.a.*) and n-alkanes, respectively, (BP CD 331 and CD 364) were shaken with oleum 25 % in $SO_3$ (1 part oleum per 10 parts alkane) until the UV absorption caused by aromatics and olefines completely vanished. The acid breakdown products as well as $SO_2$ and $SO_3$ were extracted with 1 M NaOH. The hydrocarbons were then dried with alkali pellets. The pellets were changed at least twice due to the formation of a white precipitate on the pellets. Finally the hydrocarbons were allowed to stand with the pellets. Immediately before use the alkali pellets were filtered of and the purity once again controlled by UV-spectrometry.[1] 'The gas chromatographically determined composition of the alkane mixtures are given in Table 1.

*Table 1.* Gaschromatographic analysis of the n-paraffin composition.

| Number of C atoms | Per cent of the mixture | |
|:---:|:---:|:---:|
| | $C_{10}-C_{13}$ paraffin | $C_{13}-C_{17}$ paraffin |
| 9 | 0.3 | — |
| 10 | 6.7 | — |
| 11 | 31.3 | 3.6 |
| 12 | 32.7 | 3.5 |
| 13 | 24.4 | 5.4 |
| 14 | 3.1 | 22.8 |
| 15 | 0.1 | 26.7 |
| 16 | — | 22.4 |
| 17 | — | 12.8 |
| 18 | — | 1.2 |
| 19 | — | — |

The gases were dried first with concentrated sulfuric acid and then with $P_2O_5$.

*Measurement of the sulfoxidation reaction rate.* The reaction rates were followed by means of gas consumption measurements. The gas flow before and after the reaction vessel was measured with soap-bubble flow meters. Before and after the flow meters the gases were dried.

With gas flow velocities of 500 ml/min the precision of the measurements is better than $\pm 2$ ml/min. The difference in gas flow was calculated assuming that the gases can be treated as ideal. When cyclohexane was used it was necessary to compensate for the vapour pressure. This was done assuming equilibrium between the liquid and the leaving gas stream. Losses of cyclohexane were eliminated by bubbling the gas stream through cyclohexane at 25°C. The pressure in front of the reaction vessel never increased more than 3 − 4 torr during an experiment. The influence of this effect on the measured gas consumption can be neglected. Due to the finite measuring time, approximately 3 minutes, slightly distorted curves are obtained for experiments in which the increase or decrease in gas consumption is very sharp. Approximately 80 % of the consumed gases are re-

covered as products. This figure is independent of the hydrocarbon conversion in the interval studied. The fact that less than 100 % of the gases are recovered can probably be seen as result of the high solubility of $SO_2$ in the product.

*Experimental conditions.* The reaction vessel, all glass, was filled with 100 ml of a hydrocarbon which first was freed from dissolved $O_2$ by $N_2$-bubbling and then equilibrated with a gas mixture of $SO_2$ and $N_2$ by bubbling. The time necessary for equilibrating the system was 4 h after which the gas stream leaving the system reached a steady-state value. The reaction was started by substituting the $N_2$-stream fully or only partly, with an $O_2$-stream. In some experiments with a long induction period during which the system could reach equilibrium, the hydrocarbon was saturated with $SO_2$ and the reaction started by mixing $O_2$ into the gas stream. The reaction mixture was vigorously stirred and thus the products did not separate. The temperature was $25 \pm 0.2°C$ and the gas flow approximately 500 ml/min.

The reaction was stopped by adding water and due to the heat then evolved it was found necessary to cool the reaction mixture in order to get an uncoloured product.

The water used in the study of the effect of water addition was presaturated with gas of the same composition as used for the reaction. Sulfuric acid added during the reaction was made water-free by mixing with oleum. The liquids were added with a syringe through a septum above the hydrocarbon surface.

*Determination of solubilities.* The hydrocarbons were saturated with oxygen of atmospheric pressure at $25 \pm 0.2°C$ and a sample of $1.00 \pm 0.05$ ml solution was transferred into an evacuated system. The hydrocarbon was frozen out with liquid $N_2$, and $O_2$ was transferred by a Toepler pump to a gas buret. After a number (8 – 10) of freeze-pump-thaw cycles the oxygen was collected and measured.

To determine the $SO_2$-solubility the alkane was first freed from oxygen by $N_2$-bubbling in order to avoid the formation of sulfonic acids. The $N_2$-stream was then mixed with $SO_2$ and from rotameter values the mixing ratio and hence the partial pressure of $SO_2$ was known within 1 %. Four hours $SO_2$-$N_2$-bubbling was used to ensure that equilibrium was reached. The dissolved $SO_2$ was determined iodometrically.[12] The results of the solubility determination are given in Table 2 and Fig. 1. In those cases where these values

*Table 2.* Determined solubilities of $SO_2$ and $O_2$ in the hydrocarbons used, $t = 25°C$, $p = 1$ atm.

| Hydrocarbon | Solubility of $SO_2$ mol/l | Solubility of $O_2$ mol/l | References |
|---|---|---|---|
| Cyclohexane | $0.340 \pm 0.015$ | $0.0112 \pm 0.0010$ | this work |
| Cyclohexane | | 0.0115 | a |
| $C_{10} - C_{13}$ n-Alkanes | $0.284 \pm 0.015$ | $0.0104 \pm 0.0007$ | this work |
| Dodecane | | 0.0083 | a |
| $C_{13} - C_{17}$ n-Alkanes | $0.261 \pm 0.015$ | $0.0087 \pm 0.0007$ | this work |
| $C_{13} - C_{17}$ n-Alkanes | 0.254 (20°C) | 0.0084 (20°C) | 21 |
| Hexadecane | | 0.0077 | a |

[a] from Landolt-Börnstein.

could be compared with those given in the literature, the agreement is good. The $SO_2$- and $O_2$-concentrations given for the sulfoxidation experiments are based on these determinations and it has been assumed that the $O_2$-solubility is proportional to the pressure and independent of the $SO_2$-concentration. The gas consumption in the reaction causes changes in the composition of the gas stream leaving the reaction vessel. In calculations of concentrations, equilibrium has been assumed to exist between leaving gas stream and the reaction mixture.
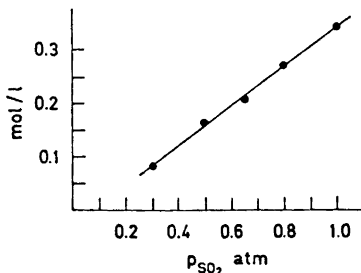
Fig. 1. $SO_2$-concentration in cyclohexane as a function of $p_{SO_2}$ at $t = 25°C$.

Product analysis. The product mixture was freed from dissolved $SO_2$ in a rotating vacuum-evaporator and the analysis of the product phase was made by pH-titration in an acetone – water (9:1) mixture.[13]

## RESULTS AND DISCUSSION

Initial period characterized by increasing reaction rates. The gas consumption as a function of time for the cyclohexane experiments are shown in Figs. 2 – 4. From the mechanism suggested by Graf, which describes the sulf-oxidation as a linearly branched chain reaction, an exponentially increasing
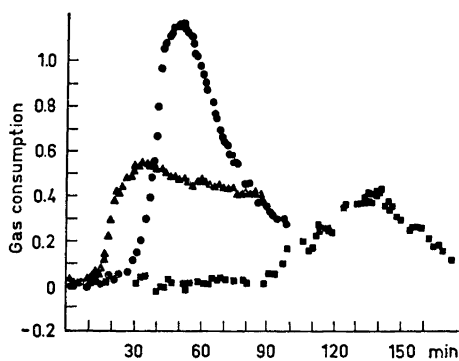




Fig. 2. The gas consumption (l gas (NTP)/l cyclohexane min) as a function of time for different $SO_2/O_2$-ratios at $t = 25°C$. a, ▲ $p_{SO_2} = 0.91$; $p_{O_2} = 0.09$; b, ● $p_{SO_2} = 0.84$; $p_{O_2} = 0.16$; c, ■ $p_{SO_2} = 0.67$; $p_{O_2} = 0.33$.
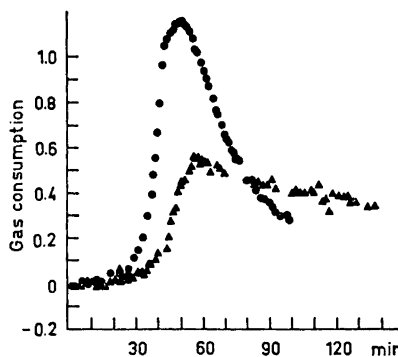
Fig. 3. The gas consumption (cf. text to Fig. 2) as a function of time for the sulfoxidation of cyclohexane at $t = 25°C$. a, ● $p_{SO_2} = 0.84$; $p_{O_2} = 0.16$; b, ▲ $p_{SO_2} = 0.68$; $p_{O_2} = 0.16$.

reaction rate is expected. As can be seen from Fig. 5 the results for the initial period of the sulfoxidation seems to be in agreement with this assumption. The first part of all curves has thus been fitted to the function $Ae^{kt}$ and the resulting constants, $k$, are given in Table 3.

From Fig. 2 can be seen that the reaction constant $k$ increases with increasing $SO_2/O_2$ ratio. In Figs. 3 and 4, respectively, this effect has been

Table 3. Results on the sulfoxidation of cyclohexane.

| Curve No. | $p_{SO_2}$ atm | $p_{O_2}$ atm | $p_{N_2}$ atm | $c_{SO_2}$ M | $c_{O_2}$ M | $\dfrac{c_{SO_2}}{c_{O_2}}$ | Max. reaction rate $\dfrac{l\ gas\ NTP}{l\ min}$ | Integrated gas consumption to the maximum l NTP/l | Time constant $k$ min$^{-1}$ | Induction period min |
|---|---|---|---|---|---|---|---|---|---|---|
| 2a | 0.91 | 0.09 | — | 0.31 | 0.0010 | 300±60 | 0.55 | 7 | 0.258±0.062 | 16 |
| 2b (3a) | 0.84 | 0.16 | — | 0.28 | 0.0018 | 159±33 | 1.16 | 14 | 0.167±0.009 | 29 |
| 2c (4d) | 0.67 | 0.33 | — | 0.22 | 0.0037 | 59±2 | 0.40 | 12 | 0.039±0.023 | 97 |
| 3b (4b) | 0.68 | 0.16 | 0.17 | 0.22 | 0.0017 | 128±8 | 0.71 | 8 | 0.133±0.025 | 38 |
| 4a | 0.68 | 0.08 | 0.25 | 0.22 | 0.0084 | 264±25 | 0.40 | 6 | 0.201±0.043 | 25 |
| 4c | 0.68 | 0.18 | 0.14 | 0.22 | 0.0020 | 111±15 | 0.70 | 13 | 0.086±0.006 | 69 |
| | 0.89 | 0.11 | — | 0.30 | 0.0013 | 239±27 | 0.63 | 8 | 0.33 ±0.13 | 17 |
| | 0.71 | 0.29 | — | 0.23 | 0.0033 | 71±3 | 0.72 | 12 | 0.101±0.028 | 73 |
| | 0.51 | 0.11 | 0.39 | 0.16 | 0.0012 | 134±18 | 0.67 | 13 | 0.117±0.006 | 67 |
| | 0.30 | 0.13 | 0.48 | 0.08 | 0.0014 | ≈60 | | | | >300 |
| | 0.50 | 0.50 | — | 0.16 | 0.0056 | ≈30 | | | | >300 |

Pressures and concentration relates to gas streams leaving the reaction vessel at half the maximum reaction rate. $SO_2/O_2$-consumption-ratio used in calculations=2 corresponding to the assumption that gas not refound as products represents $SO_2$. Concentration ratio limits corresponding to zero reaction rate and maximum reaction rate.
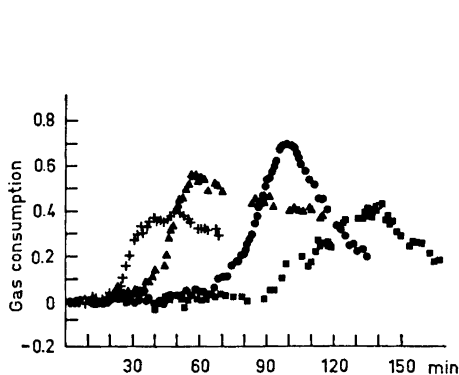
*Fig. 4.* The gas consumption (*cf.* text to Fig. 2) as a function of time for cyclohexane at $t = 25°C$. a, + $p_{SO_2} = 0.68$; $p_{O_2} = 0.075$; b, ▲ $p_{SO_2} = 0.68$; $p_{O_2} = 0.16$; c, ● $p_{SO_2} = 0.68$; $p_{O_2} = 0.18$; d, ■ $p_{SO_2} = 0.67$; $p_{O_2} = 0.33$.
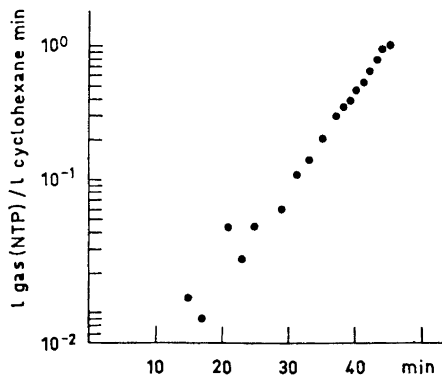


*Fig. 5.* Reaction rate as a function of time for the sulfoxidation of cyclohexane. $p_{SO_2} = 0.84$ atm; $p_{O_2} = 0.16$ atm.

separated into a positive $SO_2$-dependence and a negative $O_2$-dependence, respectively. The most reasonable explanation to the negative $O_2$-dependence is a competition between the reactions

$$R \cdot + SO_2 \rightarrow RSO_2 \cdot \qquad\qquad (1)$$

$$R \cdot + O_2 \rightarrow RO_2 \cdot \qquad\qquad (12)$$

where reaction (12) leads to termination. The rate constant for the reaction between cyclohexylperoxy radical and cyclohexane is very low. *G*-values of resulting products from $\gamma$-irradiation of cyclohexane containing $O_2$ make clear that liquid phase oxidation of alkanes is not a chain reaction at 25°C.[14] As the sulfonylperoxy radical does not seem to react with $SO_2$, this possibility could probably also be disregarded for the cyclohexylperoxy radical.

Applying the mechanism suggested by Graf and assuming reaction (12) to be the dominating radical consuming reaction $k$ is expected to be proportional to the $O_2$-concentration. As can be seen from Fig. 6 a reasonable fit to a linear
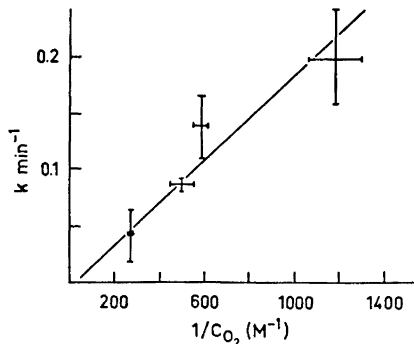


*Fig. 6.* The reaction constant $k$ for the sulfoxidation as a function of 1/oxygen concentration. $p_{SO_2} = 0.68$ atm.

relation results when $k$ is plotted as a function of $1/[O_2]$ for constant $SO_2$-concentration. Competition between reaction (1) and (12) gives a first order dependence of $k$ on the $SO_2$-concentration. Due to the low precision no conclusion can be drawn concerning the $SO_2$-dependence. The conditions for which no reaction is observed (Table 3) indicate that at least for low $SO_2$-concentrations the initial period of the sulfoxidation is not determined solely by the concentration ratio $SO_2/O_2$. This is in agreement with Bertram's [7] finding that the reaction shows a second order dependence on the $SO_2$-concentration. Graf has shown that in $SO_2$-saturated cyclohexane the persulfonic acid forms a complex with $SO_2$. If the branching rather takes place according to

$$RSO_2O_2H \cdot SO_2 \rightarrow RSO_3 \cdot + HSO_3 \cdot \qquad (4a)$$
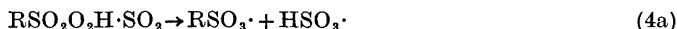
the $SO_2$ dependence might be influenced by the equilibrium

$$RSO_2O_2H + SO_2 \rightleftharpoons RSO_2O_2H \cdot SO_2 \qquad (13)$$
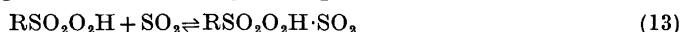
Bertram's results that the chain length is independent of the $O_2$-concentration might be due to trace amounts of impurities consuming radicals. The present experiments are less sensitive towards impurities as these should be consumed in such an early state of the reaction that their influence on $k$-values are negligible. The conditions in works[3-5] leading to the conclusion that the optimal $SO_2/O_2$ ratio is approximately two, differ from those in the present work as the product was allowed to separate continuously from the reaction mixture. The optimum $SO_2/O_2$ ratio of two relates to the steady-state, which as a result of the slow product separation might correspond to a point on the falling part of the rate *versus* time curves presented in Figs. 2 − 4.

Concerning the fate of the cyclohexylperoxy radical the propagation reactions (1) and (2) are addition reactions and probably very fast. Reaction (3) on the other hand is an abstraction reaction where the abstracting entity is a peroxy radical. Normally this type of reaction is very slow at room temperature [15] and thus the sulfonylperoxy radical is assumed to be the dominating radical in the reaction mixture. The probable fate of a cyclohexylperoxy radical will then be to take part in a recombination reaction with a sulfonylperoxy radical. In analogy with the Russel mechanism for recombination of primary and secondary alkylperoxy radicals [16] this reaction might probably involve the decomposition of a cyclic transition state in which one of the α-hydrogen atoms is transferred to give the products ketone and sulfonic acid.



$$(14)$$
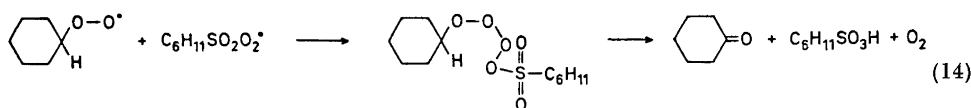
In the presence of sulfuric and sulfonic acids, respectively, the following steps could appear [reactions (15) and (16)].

Assuming inhibition according to reactions (12) and (14) thus gives an alternative possibility to explain the formation of cyclohexandiol-(1,2)-cyclohexylmonosulfonate found in the product as a sulfuric acid ester.[3]
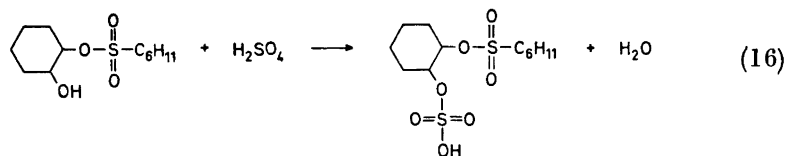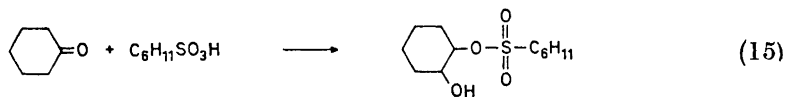
Compared with the mechanism for the diolester production suggested by Graf, the above given mechanism has the advantage of correctly interpreting the variation of diol formation with the $SO_2/O_2$ ratio. For the $SO_2/O_2$ ratio corresponding to the limit of a self-sustained reaction Graf gives the product ratio sulfonic acid/sulfuric acid/acidic diolester as 3:1:1. The limit of a self-sustained reaction corresponds to the point where radical consumption equals radical production, *i.e.* with the above given mechanism, the gas composition for which the rates of reactions (4) and (13) are equal. As the water formed in the reaction (16) should be consumed in reaction (7) this condition gives exactly the product ratios found by Graf. Secondly, for those conditions for which Graf reports a decreased reaction rate with increased oxygen pressure, this decrease of the reaction rate is also connected with an increased ester formation.

The molar ratio sulfonic acid to sulfuric acid in the product for a number of experiments broken off at low conversion falls between 1.3 and 1.9.

The following reaction sequence seems to give a reasonable description of the present knowledge of the initial period of the sulfoxidation in cyclohexane.

$$(R \cdot = C_6H_{11} \cdot)$$

|  |  |  |  |
|---|---|---|---|
| Propagation | $R \cdot + SO_2$ | $\rightarrow RSO_2 \cdot$ | (1) |
| | $RSO_2 \cdot + O_2$ | $\rightarrow RSO_2O_2 \cdot$ | (2) |
| | $RSO_2O_2 \cdot + RH$ | $\rightarrow RSO_2O_2H + R \cdot$ | (3) |
| Branching and product formation | $RSO_2O_2H + SO_2 \rightleftharpoons RSO_2O_2H \cdot SO_2$ | | (13) |
| | $RSO_2O_2H \cdot SO_2$ | $\rightarrow RSO_3 \cdot + HSO_3 \cdot$ | (4a) |
| | $RSO_3 \cdot + RH$ | $\rightarrow RSO_3H + R \cdot$ | (5) |
| | $HSO_3 \cdot + RSO_2O_2H$ | $\rightarrow RSO_3 \cdot + H_2SO_4$ | (6a) |
| Termination | $R \cdot + O_2$ | $\rightarrow RO_2 \cdot$ | (12) |
| | $RO_2 \cdot + RSO_2O_2 \cdot$ | $\rightarrow$ stable product | (14) |
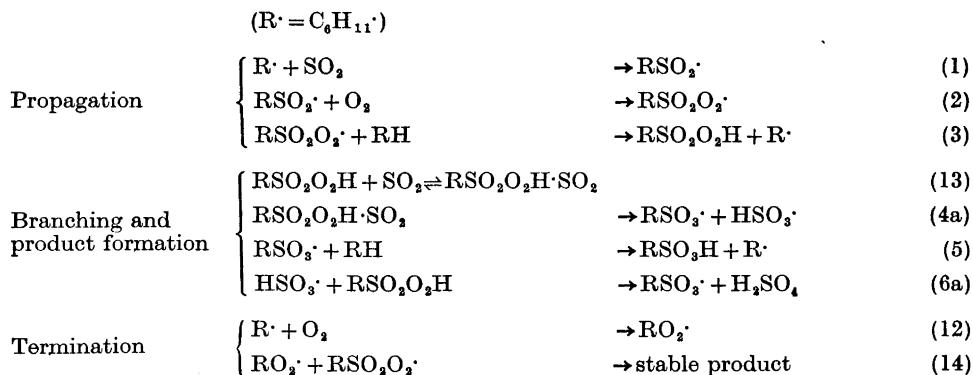
The exponential increase in reaction rate might either be due to an increase of the persulfonic acid concentration or alternatively due to product catalysis of reaction (4a).

*Initiation.* The present investigation gives very little information concerning the nature of the spontaneous initiation. Untreated *p.a.* and *purum* cyclohexane also give a spontaneous reaction but with an increased induction period. Distillation of the purified cyclohexane under argon atmosphere immediately before use did not influence the results. Extrapolating the exponentially increasing gas consumption to $t = 0$ and assuming the resulting gas consumption to be equal to $(2k_1[SO_2]/2k_{12}[O_2]) \times$ (radical production) gives values for the radical production of the order of $10^{-9} - 10^{-10}$ M s$^{-1}$ $(k_1 \approx k_{12})$. For the liquid phase oxidation of n-decane the corresponding value at 150°C has been determined to be $2.6 \times 10^{-9}$ M s$^{-1}$.[14] In this case the radical production is ascribed to the reaction

$$RH + O_2 + RH \rightarrow 2R\cdot + H_2O_2 \qquad (17)$$

For the sulfoxidation the least endothermic radical producing reactions seems to be

$$RH + SO_2 \rightarrow HSO_2\cdot + R\cdot \qquad (18)$$

The strength of the $H - SO_2$ bond has been given as approximately $50 - 60$ kcal/mol.[17] From this value the reaction should be endothermic with an energy of $30 - 40$ kcal/mol. The uncertainties in the initial gas consumptions are very great due to the extrapolations made and from the present investigation no certain conclusion can be drawn concerning the $SO_2$- and $O_2$-dependence, respectively.

*Product inhibition.* In experiments with relatively high oxygen concentrations in the gas phase a maximum in reaction rate appears after a gas consumption of approximately 0.6 mol in cyclohexane and then the reaction rate starts to fall. When the oxygen content in the gas mixture is low, no marked maximum appears and an approximately constant reaction rate is reached at relatively low conversions. The reaction rate reached in these experiments are found to depend on the gas flow velocity and it seems clear that the reaction rate is limited by the diffusion of oxygen. For a mol ratio $SO_2/O_2$ of 9 it has been found that the production of sulfonic acid is approxi-
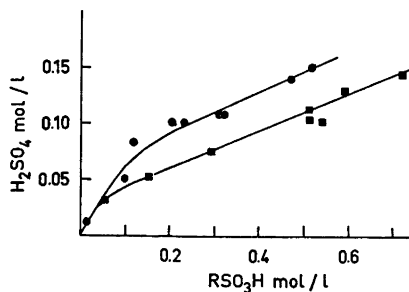


*Fig. 7.* Sulfuric acid yield as a function of the sulfonic acid yield in cyclohexane, at $t = 25$°C.  ● $p_{SO_2} = 0.67$ and $p_{O_2} = 0.33$; ■ $p_{SO_2} = 0.90$ and $p_{O_2} = 0.10$.

mately 6 times the sulfuric acid production at high conversions (Fig. 7). The high molar product ratio resulting when oxygen diffusion limits the reaction rate could be due to competition between reaction (2) and one of the reactions

$$RSO_2\cdot + RSO_2O_2H \rightarrow RSO_3H + RSO_3\cdot \tag{19}$$

$$RSO_2\cdot + RSO_2O_2\cdot \rightarrow RSO_3\cdot + RSO_3\cdot \tag{20}$$
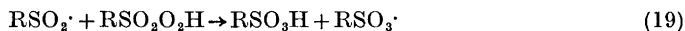
suggested by Bertram and Graf, respectively.

Experiments with higher oxygen content in the gas phase show a similar behaviour. As the maximum reaction rate is approached the sulfonic acid to sulfuric acid ratio starts to increase. The main difference compared with experiments with lower oxygen content in the gas phase is that this increase starts at higher conversion. As pointed out above Graf has found proportionality between oxygen pressure and sulfoxidation rate at conditions which might correspond to high conversions. In the present experiments the decay of the reaction rate is faster the lower the oxygen pressure is. Together these facts indicate that the decay of the reaction rate may be connected with one of the reactions (19) or (20) becoming important.

The experiments with water addition (Figs. 8a – 8c) show that reaction (7) must be fast. Free water in concentrations high enough to explain the deviation in product ratio from 2 should not be possible. The momentary increase in gas consumption, following the water addition, is attributed to the fact that the solubility of $SO_2$ is higher in sulfuric acid than in water.
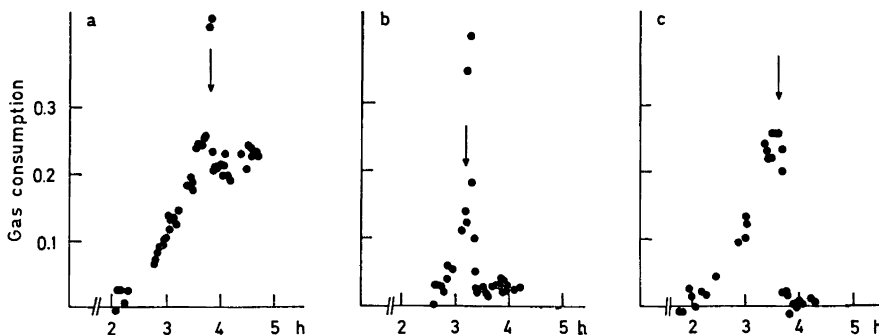


*Fig. 8.* The effect of water addition on the sulfoxidation of $C_{10} - C_{13}$ n-alkanes. The water was presaturated with $SO_2$ and $O_2$. Time for the addition indicated by the arrow. $SO_2/O_2$-ratio = 9:1; $t = 25°C$. *a*, 20 $\mu l$ water added; *b*, 0.2 ml water added; *c*, 1.0 ml water added. Ordinate: 1 gas (NTP)/1 n-paraffin $(C_{10} - C_{13})$ min.

Fig. 9 shows that addition of sulfuric acid inhibits the reaction and thus the decrease in reaction rate is most probably caused by build up of the main products. The position of the maximum seems to be determined solely by the degree of conversion. A visible phase separation could normally be detected 5 – 10 min before the maximum reaction rate was reached indicating that the size of the product drops is increasing.

Asinger and Saus [18] have studied the sulfoxidation of $C_{13} - C_{17}$ n-paraffins and found a very high content of disulfonic acid in the product. This was explained by the assumption that the reaction to an appreciable extent was taking place in the polar product phase. This should be true also for the sulf-

oxidation of cyclohexane, but in this case the disulfonic acid production is suppressed as all the hydrogen atoms in the monosulfonic acid are protected against abstraction by the presence of the sulfonic group in the molecule.[18] In this connection it is interesting to note that Asinger and Saus's data show that the increase in the disulfonic acid to monosulfonic acid ratio is very fast up to $\approx 5$ % conversion and then levels out.[19] The maximum in the reaction rate in our experiments also appears at approximately 5 % conversion.
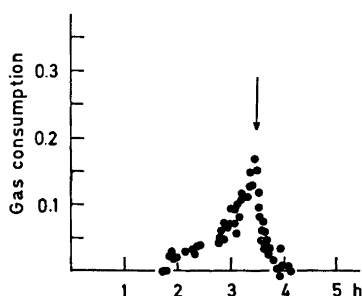


Fig. 9. The effect of sulfuric acid addition on the sulfoxidation of $C_{10} - C_{13}$ n-alkanes. 0.6 ml $H_2SO_4$ added; $SO_2/O_2$-ratio $= 9:1$.
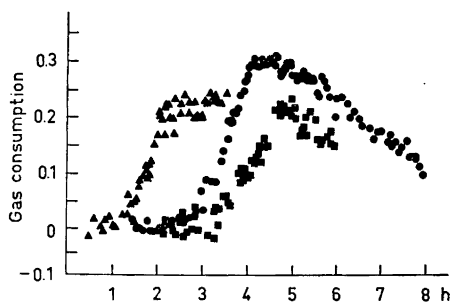


Fig. 10. The gas consumption as a function of time for the sulfoxidation of $C_{10} - C_{13}$ n-alkanes; $t = 25°C$. ▲ $p_{SO_2} = 0.95$ and $p_{O_2} = 0.05$; ● $p_{SO_2} = 0.90$ and $p_{O_2} = 0.10$; ■ $p_{SO_2} = 0.81$ and $p_O = 0.19$.

The solubility of $O_2$ in the product could be expected to be low, analogous with what is known for concentrated sulfuric acid. A marked increase in the size of the product drops connected with the fact that the reaction to an appreciable extent takes place in the product phase could explain that oxygen
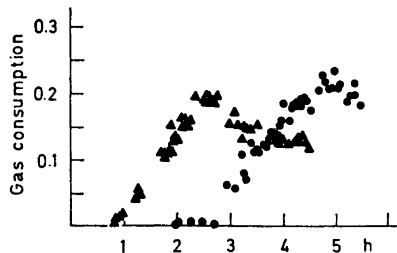


Fig. 11. The gas consumption as a function of time for the sulfoxidation of $C_{13} - C_{17}$ n-alkanes at $t = 25°C$. ▲ $p_{SO_2} = 0.95$ and $p_{O_2} = 0.05$; ● $p_{SO_2} = 0.90$ and $p_{O_2} = 0.10$.
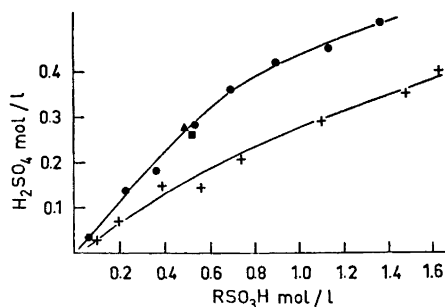


Fig. 12. Sulfuric acid yield as a function of the sulfonic acid yield in n-alkanes at $t = 25°C$. ● $p_{SO_2} = 0.90$ and $p_{O_2} = 0.10$ (with stirring); ▲ $p_{SO_2} = 0.80$ and $p_{O_2} = 0.20$ (with stirring); ■ $p_{SO_2} = 0.95$ and $p_{O_2} = 0.05$ (with stirring); + $p_{SO_2} = 0.90$ and $p_{O_2} = 0.10$ (without stirring).

*Table 4.* Results on the sulfoxidation of n-alkane mixtures.

| Hydrocarbon | $p_{SO_2}$ atm | $p_{O_2}$ atm | Max. reaction rate $\dfrac{\text{l gas NTP}}{\text{l min}}$ | Integrated gas consumption to the maximum l NTP/l | Induction period h | Time-constant $k$ min$^{-1}$ | Relative value of $k$.[a] | Relative length of reaction sequence according to Ref. 19 (cyclohexane=1.00) |
|---|---|---|---|---|---|---|---|---|
| C$_{10}$-C$_{13}$ n-Alkanes | 0.95 | 0.05 | 0.23 | 12 | 1.7 | 0.035±0.023 | 0.089 | |
| » | 0.90 | 0.10 | 0.30 | 17 | 3.3 | 0.023±0.004 | 0.083 | |
| » | 0.81 | 0.19 | 0.22 | 20 | 4 | 0.014±0.006 | | |
| » | 0.67 | 0.33 | | | >6 | | | |
| C$_{13}$-C$_{17}$ n-Alkanes | 0.95 | 0.05 | 0.19 | 10 | 1.7 | | | |
| » | 0.90 | 0.10 | 0.22 | 17 | 3.3 | | | |
| » | 0.80 | 0.20 | | | >6 | | | |
| n-Decane | | | | | | | | 0.21 |
| n-Dodecane | | | | | | | | 0.093 |
| n-Hexadecane | | | | | | | | 0.059 |

[a] In cyclohexane $k=1$, for the pressure used.

diffusion becomes limiting and that thus one of the reactions (19) or (20) starts to compete with reaction (2). This might then explain the product inhibition as well as a proportionality between $O_2$-concentration and reaction rate at high conversions. If the sulfuric acid production is connected with the radical production as suggested by Graf (reactions (4) − (7)), the picture is incomplete and some radical consuming reaction also must contribute to the product yield.

*Sulfoxidation of higher n-alkanes.* As can be seen from Figs. 10 and 11 the $C_{10} - C_{13}$ and $C_{13} - C_{17}$ n-alkanes, respectively, show the same principal behaviour as cyclohexane but increased $SO_2/O_2$ ratios are necessary to achieve a spontaneous reaction. With increased hydrocarbon chain length the induction period increases and at the same time the maximum reaction rate decreases. For $C_{13} - C_{17}$ n-alkanes the time dependence of the reaction rate cannot be described by a simple exponential function. The results are summarized in Table 4. At low conversions the product ratio sulfonic to sulfuric acid for $C_{10} - C_{13}$ n-alkanes is slightly lower than 2 (Fig. 12). A marked increase of this value is not noted before conversions occur appreciably higher than what corresponds to maximum reaction rate. The product ratio in this case seems to be relatively insensitive to changes of the $SO_2/O_2$ ratio from 9/1 to 19/1 resp. 4/1. Performing the experiment without any stirring except what is achieved with the gas bubbling results in a marked increase in the sulfonic acid/sulfuric acid product ratio. The observed behaviour is probably connected with the low reaction rate which makes oxygen diffusion a limiting factor only when the reaction is performed without stirring.

For comparison the kinetic chain length reported by Cerny [20] is given in Table 4. The change in $k$-value going from cyclohexane to $C_{10} - C_{13}$ n-alkanes is in reasonable agreement with the results of Cerny. The very marked decrease in $k$ when going to the n-alkanes cannot be ascribed to different solubilities of $SO_2$ and $O_2$, respectively, in the hydrocarbons as can be seen from Table 2. A condition which could be expected to change appreciably is the distribution of the intermediate radicals and the persulfonic acid between hydrocarbon and product phase. With increased hydrocarbon chain length the intermediates to a greater extent will be found in the hydrocarbon phase. Comparing the concentration ratio $[SO_2]/[O_2]$ in hydrocarbon and product phase, respectively, makes clear that radical recombination according to the reactions (12) and (14) will mainly take place in the hydrocarbon phase and thus an increase in the hydrocarbon chain length will give increased radical recombination rates. Another effect might contribute to the decrease in $k$ if the rate of reaction (4a) is faster in the product phase than in the hydrocarbon phase. The fact that the product inhibition appears at somewhat higher integrated gas consumptions in the sulfoxidation of the n-alkanes might also be due to an increased solubility of the intermediates in the hydrocarbon phase.

REFERENCES

1. Platz, C. and Schimmelschmidt, K. DRP 735.096, 10 Dec. 1940; *Chem. Abstr.* **38** (1944) 1249.
2. Gilbert, E. E. *Sulfonation and Related Reactions*, Wiley, New York 1965, pp. 131 – 134.
3. Graf, B. *Ann.* **578** (1952) 50.
4. Black, J. F. and Baxter, E. F. *2nd United Nations International Conference on the Peaceful Uses of Atomic Energy*, Geneva 1958. *Proceedings* Vol. **20** 162.
5. Keller, K. *Dissertation*, TH, Aachen 1969.
6. Dzjagatspanyan, R. V., Zetkin, V. I. and Zykova, E. N. *2nd Russian Conference on Radiation Chemistry*, Moscow 1960. *Proceedings* pp. 390 – 393.
7. Bertram, D. *Proc. 1962 Tihany Symp. Radiat. Chem.* (1962) 23.
8. Bertram, D. *Dechema-Monographie* **42** (1962) 197.
9. British patent 1.109.415, 10 April 1968.
10. Swiss patent 458.328, 30 August 1968.
11. Nilsson, O. *Acta Chem. Scand.* **21** (1967) 1501.
12. Eriksen, T. E. *Chem. Eng. Sci.* **22** (1967) 729.
13. Carasik, W., Mausner, M. and Spiegelman, G. *Chem. Spec. Mfr. Ass., Proc. Annual Meeting* No. *53* (1966) 97.
14. Emanuel, N. M., Denisov, E. T. and Maizus, Z. K. *Liquid-phase Oxidation of Hydrocarbons*, Plenum Press, New York 1967, pp. 71 – 74 and 182 – 186.
15. Ingold, K. U. *Accounts Chem. Res.* **2** (1968) 1.
16. Russel, G. A. *J. Am. Chem. Soc.* **79** (1957) 3871.
17. Kallend, A. S. *Trans. Faraday Soc.* **63** (1967) 2442.
18. Asinger, E. and Saus, A. *Symposium on the Utilization of Large Radiation Sources and Accelerators in Industrial Processing*, Munich 1969. *Proceedings* pp. 77 – 90.
19. Gubelt, B. *Dissertation*, TH, Aachen 1967.
20. Cerny, O. *Coll. Czech. Chem. Commun.* **33** (1968) 257.
21. Rösinger, S. *Symposium on the Utilization of Large Radiation Sources and Accelerators in Industrial Processing*, Munich 1969, *Proceedings* p. 91.

# On Phase Transitions between the MnP and NiAs Type Structures

KARI SELTE and ARNE KJEKSHUS

*Kjemisk Institutt, Universitetet i Oslo, Blindern, Oslo 3, Norway*

High and low temperature X-ray diffraction studies of TiAs, TiSb, VP, VAs, CrP, CrAs, $Cr_{0.5}Fe_{0.5}As$, $Mn_{0.9}Fe_{0.1}As$, $Mn_{0.15}Fe_{0.85}As$, CoP, CoAs, NiAs, and RhSb show that continuous phase transitions between the MnP and NiAs type structures take place in CrAs $(1173 \pm 20$ K), $Mn_{0.9}Fe_{0.1}As$ $(553 \pm 50$ K), and CoAs $(1248 \pm 20$ K). The results are discussed mainly in terms of a geometrical model for the relationship between the two structure types.

Considering the amount of effort which has been devoted to studies of the physical and chemical properties of the phases with the NiAs and MnP type structures (*cf.*, *e.g.*, surveys in Refs. 1 – 3) surprisingly little attention has been paid to the phase transitions between these structure types (see Refs. 4 – 16). However, for so closely related structure types as NiAs and MnP, fundamental information concerning the factors which lead to preference for one of them in the particular case must be hidden in the transformation characteristics with temperature, pressure, composition, *etc.* as the variables. For this reason, a low and high temperature X-ray study of carefully selected phases with NiAs or MnP type structure was carried out as a part of a protracted research programme on such phases.

## EXPERIMENTAL

Samples of VP, VAs, CrP, CrAs, and CoAs were prepared and characterized by Guinier photographic X-ray data as described previously.[17–20] Samples of TiAs, TiSb, CoP, NiAs, RhSb, $Cr_{0.5}Fe_{0.5}As$, $Mn_{0.9}Fe_{0.1}As$, and $Mn_{0.15}Fe_{0.85}As$ were prepared similarly at 850°C, crushed, subjected to 2 – 3 further annealings at the same temperature (with intermediate crushings), and finally cooled slowly to room temperature. The ternary samples were made from appropriate mixtures of the binary compounds.

The experimental details concerning the low and high temperature X-ray diffraction measurements are described by Furuseth *et al.*[21]
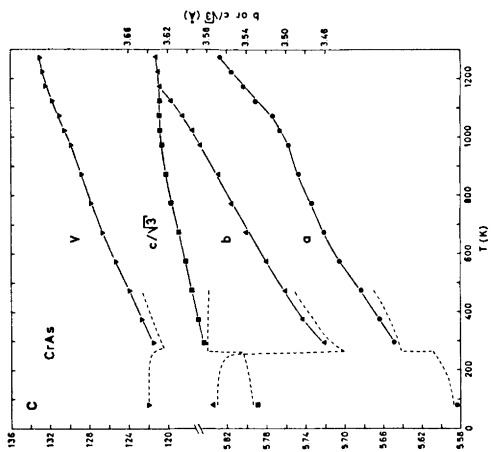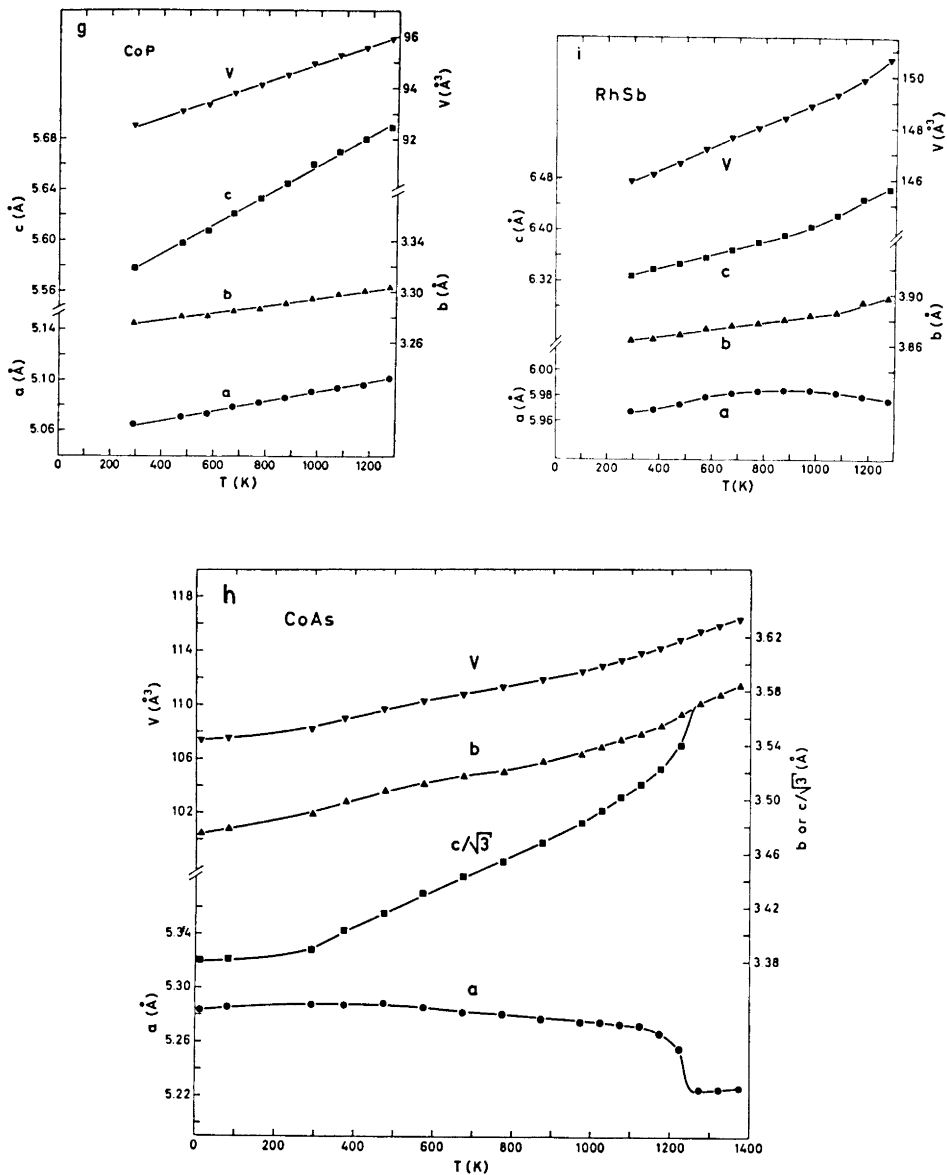
*Fig. 1.* Unit cell dimensions of (a) VAs, (b) CrP, (c) CrAs, (d) $Cr_{0.5}Fe_{0.5}As$, (e) $Mn_{0.9}Fe_{0.1}As$, (f) $Mn_{0.15}Fe_{0.85}As$, (g) CoP, (h) CoAs, and (i) RhSb as functions of temperature. Broken curves in (c) indicate changes in unit cell dimensions induced at the first order magnetic transformation.[15]

## RESULTS

Prior to this work, transformations from the MnP to the NiAs type structure had been detected above room temperature in MnAs,[4,6−8,13] MnAs$_{0.9}$P$_{0.1}$,[9,14] Cr$_{1−t}$Mn$_t$As,[15] and CoAs.[5] These observations together with thermodynamic considerations based on the symmetries of the coordination polyhedra in the two structure types, suggest that other phases with MnP type structure may show the same behaviour. As clearly evinced by data for, e.g., FeAs,[22] phases with MnP type structure do not necessarily transform to NiAs type before the melting point is reached.

A representative selection of binary and a few ternary pnictides (VAs, CrP, CrAs, Cr$_{0.5}$Fe$_{0.5}$As, Mn$_{0.9}$Fe$_{0.1}$As, Mn$_{0.15}$Fe$_{0.85}$As, CoP, CoAs, and RhSb) with the MnP type structure at room temperature have been subjected to a high temperature X-ray study. The temperature dependences of the unit cell dimensions are shown in Fig. 1a − i.

In the same way that phases which possess the MnP type structure at room temperature may transform to the NiAs type at higher temperatures, those with the latter type at room temperature may transform to the MnP type at lower temperatures. Thus, a few potential candidates for such a transformation, viz. TiAs, TiSb, VP, and NiAs, were examined down to liquid helium temperature. However, none of the X-ray diagrams gave indication of transformation. It should be emphasized that the occurrence of additional
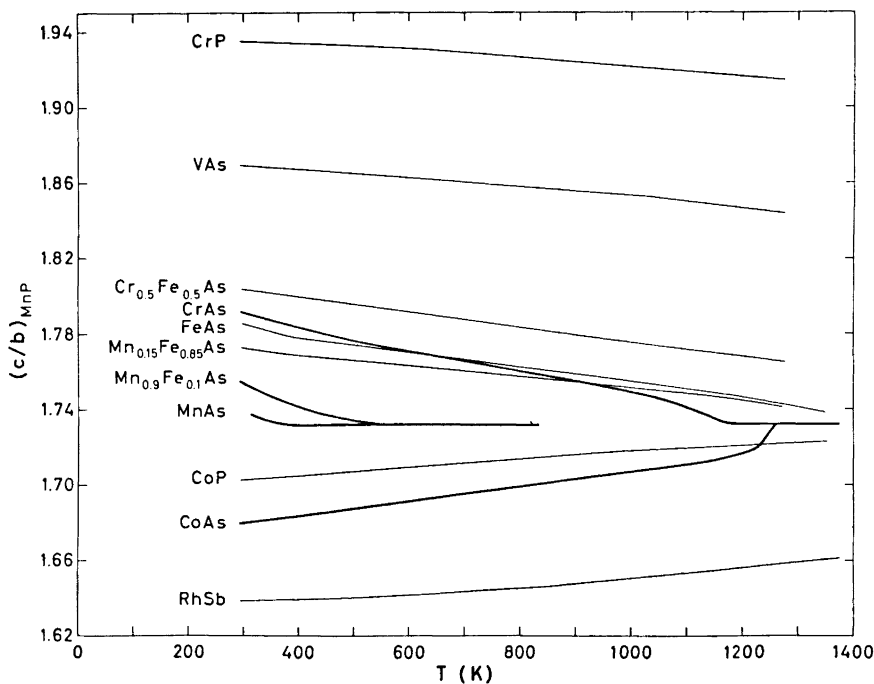


Fig. 2. Temperature dependence of axial ratios $(c/b)_{MnP}$. Heavy lines indicate phases which transform from MnP to NiAs type structure.

reflections and the splitting of those which would be characteristic of the MnP type cell are difficult to detect at the onset of the transformation.

The results of the high temperature study are conveniently divided into three categories:

(1) VAs, CrP, and RhSb show no sign of a beginning transformation up to ∼ 1300 K.

(2) Judging from the close approach of $c/b$ to $\sqrt{3}$, $Mn_{0.15}Fe_{0.85}As$ and FeAs are probably in an intermediate state (see Discussion) near the melting points of $1293 \pm 20$ and $1343 \pm 20$ K, respectively. $Cr_{0.5}Fe_{0.5}As$ and CoP are in a similar situation at the highest temperature of investigation ( ∼ 1300 K).

(3) CrAs, $Mn_{0.9}Fe_{0.1}As$, and CoAs transform, as seen from Fig. 1c, e, and h, at temperatures of $1173 \pm 20$, $553 \pm 50$, and $1248 \pm 20$ K, respectively.

The most important experimental inference of points (1) − (3) is illustrated in Fig. 2, which gives the temperature dependence of the axial ratios $(c/b)_{MnP}$.

In common with the results for MnAs, $MnAs_{0.9}P_{0.1}$, and $Cr_{1-t}Mn_tAs$ quoted above, the data in Figs. 1 and 2 show that the unit cell dimensions vary continuously in the region of transformation, which accordingly must be of second or higher order.

A comparison of the curves in Fig. 1a − i reveals a large degree of individuality in the thermal expansion of the various substances. Due to differences in presentation of the expansion curves the mutual variations are larger than apparent at first sight. In order to elucidate this fact, the relative expansion coefficients $(\alpha_a = (a_T - a_{T'})/a_{300}(T - T')$, and analogously for $\alpha_b$ and $\alpha_c)$ of the various phases have been calculated and listed in Table 1. Apart

*Table 1.* Relative expansion coefficients ($\alpha_a$, $\alpha_b$, and $\alpha_c$) for phases with MnP type crystal structure.

| Phase | $\alpha_a \times 10^6$ (K$^{-1}$) | $\alpha_b \times 10^6$ (K$^{-1}$) | $\alpha_c \times 10^6$ (K$^{-1}$) | Temp. range (K) |
|---|---|---|---|---|
| VAs | 12.2 | 20.8 | 7.7 | 300 − 1200 |
| CrP | 15(av.) | 21(av.) | 12.1 | 300 − 1200 |
| CrAs | 29(av.) | 51(av.) | 18(av.) | 300 − 1000 |
| $Cr_{0.5}Fe_{0.5}As$ | 8(av.) | 37(av.) | 13(av.) | 300 − 1000 |
| $Mn_{0.9}Fe_{0.1}As$ | 80(av.) | 110(av.) | 75(av.) | 300 − 550 |
| $Mn_{0.15}Fe_{0.85}As$ | 11(av.) | 37.4 | 20.8 | 300 − 1200 |
| FeAs [a] | 11(av.) | 44(av.) | 22(av.) | 500 − 1200 |
| CoP | 7.7 | 8.8 | 20.7 | 300 − 1200 |
| CoAs | − 3.5 | 19(av.) | 41.3 | 300 − 1000 |
| RhSb | 5(av.) | 7.0 | 16.9 | 300 − 1000 |

[a] Extracted from Ref. 22.

from the small negative value of $\alpha_a$ for CoAs, the most extreme values in Table 1 are associated with the expansion coefficients for $Mn_{0.9}Fe_{0.1}As$. The generally much larger values for $\alpha_a$, $\alpha_b$, and $\alpha_c$ for Mn-rich samples of the $Mn_{1-t}Fe_tAs$ and other $Mn_{1-t}T$ As phases can almost certainly be associated with variations

in electronic band structure (*viz.* number of "localized" unpaired electrons) as a function of temperature.[23] Among the remainder of the phases in Table 1, the values for $\alpha_a$ of CrAs, $\alpha_b$ of CrAs, $Cr_{0.5}Fe_{0.5}As$, $Mn_{0.15}Fe_{0.85}As$, and FeAs, and $\alpha_c$ for CoAs are notably larger than the other expansion coefficients. Comparison of the data in Fig. 1 and Table 1 shows that a larger expansion coefficient for one or two of the axes is always balanced by a smaller coefficient for the others, giving rise to an approximately constant volume expansion. There is no distinction between the categories (1) − (3) in this respect.

The transformation process between the NiAs and the completely deformed MnP type structure takes place over a temperature interval which varies from ∼50 K in CoAs to ∼300 K in $Mn_{0.9}Fe_{0.1}As$. Since $Mn_{0.9}Fe_{0.1}As$, moreover, has a relatively low transformation temperature, this phase has been selected for a careful examination of both unit cell dimensions and positional parameters as a function of temperature.

<div align="center">DISCUSSION</div>

A schematic presentation of the relationship between the NiAs and MnP type structures is shown in Fig. 3. The illustration is clearly rather simplified and does not, for example, convey the information that the hexagonal NiAs type structure belongs to space group $P6_3/mmc$ and the orthorhombic MnP type to *Pnma*. The setting of the orthohexagonal NiAs unit cell is in accordance with the latter space group. The projection shows the positions of metal and non-metal atoms in the NiAs arrangement, whereas the lengths and directions of the arrows give their main displacements in the MnP type cell.

Important supplementary information for binary $TX$ phases ($T$: $3d$ metal; $X$: P, As, or Sb) with MnP and/or NiAs type structure is given in Table 2. As immediately evident from the table the NiAs type structure has only one structural degree of freedom, $(c/a)_{NiAs} \approx (a/b)_{MnP}$, in addition to the compositional variable $t$ according to the formula $T_{1+t}X$. All carefully examined binary compounds with the MnP type structure exhibit a stoichiometric 1:1 composition, whereas the nominal number of structural variables are increased considerably. The real number of structural variables are smaller. Firstly, only two of the axial ratios are free variables. Secondly, Table 2 shows that the following empirical constraints are obeyed for most compounds with MnP type structure: $(c/a)_{MnP} \approx 1.10$, $x_T \approx 0$, $z_T \approx x_X \approx 0.20$ and $z_X \approx 7/12$. It is perhaps noteworthy that $(a/b)_{MnP}$ varies less than $(c/a)_{NiAs}$ in accordance with the fact that relative sizes of the components are more restricted for the MnP type structure (*vide infra*).

Table 2 comprises representatives with $(c/b)_{MnP}$ both larger and smaller than $\sqrt{3}$, which is the criterion distinguishing between the two sub-classes within the MnP type structure according to Pfisterer and Schubert.[31] As seen from the table, no such distinction is manifested in the positional parameters which satisfy the above approximate constraints equally well regardless of the value of $(c/b)_{MnP}$. Even on a more detailed level such a classification is obscure as may be evidenced by comparisons of the corresponding interatomic distances and angles in FeAs and CoAs,[18,22,29,30] or perhaps even more clearly

*Table 2.* Axial ratios and positional parameters of binary $TX$ phases ($T$: $3d$ metal; $X$: P, As, or Sb) with MnP and/or NiAs type structure. Unless explicitly stated, data refer to room temperature, those for phases with NiAs type structure being converted to an orthohexagonal cell with setting according to space group *Pnma*.

| Phase | $c/a$ | $c/b$ | $a/b$ | $x_T$ | $z_T$ | $x_X$ | $z_X$ | Ref. |
|---|---|---|---|---|---|---|---|---|
| $\beta$-TiAs | 1.02 | $\sqrt{3}$ | 1.69 | 0 | 1/4 | 1/4 | 7/12 | 1 |
| TiSb [a] | 1.118 | $\sqrt{3}$ | 1.549 | 0 | 1/4 | 1/4 | 7/12 | 1 |
| VP | 0.885 | $\sqrt{3}$ | 1.957 | 0 | 1/4 | 1/4 | 7/12 | 20 |
| VAs | 1.076 | 1.872 | 1.740 | 0.0054(10) | 0.1890(4) | 0.1969(6) | 0.5734(3) | 20 |
| VSb [a] | 1.358 | $\sqrt{3}$ | 1.276 | 0 | 1/4 | 1/4 | 7/12 | 1 |
| CrP | 1.122 | 1.933 | 1.722 | 0.0073(3) | 0.1929(3) | 0.1853(5) | 0.5653(3) | 24, 25 |
| CrAs | 1.099 | 1.794 | 1.632 | 0.0065(10) | 0.2001(8) | 0.2012(4) | 0.5770(6) | 17 |
| CrAs, 1173 K | 1.085 | $\sqrt{3}$ | 1.597 | 0 | 1/4 | 1/4 | 7/12 | |
| CrSb [b] | 1.311 | $\sqrt{3}$ | 1.321 | 0 | 1/4 | 1/4 | 7/12 | 26 |
| MnP | 1.126 | 1.866 | 1.658 | 0.0049(3) | 0.1965(2) | 0.1879(5) | 0.5684(4) | 24, 25 |
| MnAs, 328 K | 1.112 | 1.736 | 1.561 | 0.0047(10) | 0.2229(22) | 0.2255(16) | 0.5816(12) | 8 |
| MnAs, 403 K | 1.112 | $\sqrt{3}$ | 1.557 | 0 | 1/4 | 1/4 | 7/12 | 1 |
| MnSb [b] | 1.235 | $\sqrt{3}$ | 1.402 | 0 | 1/4 | 1/4 | 7/12 | 27 |
| FeP | 1.115 | 1.869 | 1.676 | 0.0020(4) | 0.2004(3) | 0.1912(7) | 0.5684(6) | 28 |
| FeAs | 1.108 | 1.787 | 1.614 | 0.0033(1) | 0.1992(1) | 0.1992(1) | 0.5773(1) | 29, 30 |
| FeSb [a] | 1.369 | $\sqrt{3}$ | 1.265 | 0 | 1/4 | 1/4 | 7/12 | 26 |
| CoP | 1.100 | 1.703 | 1.547 | 0.0007(3) | 0.1976(3) | 0.1913(6) | 0.5816(6) | 24, 25 |
| CoAs | 1.110 | 1.682 | 1.515 | 0.0023(10) | 0.2000(5) | 0.1996(7) | 0.5869(3) | 18 |
| CoAs, 1248 K | 1.183 | $\sqrt{3}$ | 1.464 | 0 | 1/4 | 1/4 | 7/12 | |
| CoSb [b] | 1.296 | $\sqrt{3}$ | 1.336 | 0 | 1/4 | 1/4 | 7/12 | 26 |
| NiAs | 1.245 | $\sqrt{3}$ | 1.391 | 0 | 1/4 | 1/4 | 7/12 | 1 |
| NiSb [b] | 1.322 | $\sqrt{3}$ | 1.310 | 0 | 1/4 | 1/4 | 7/12 | 26 |

[a] The phase is reported to deviate from 1:1 composition. [b] The phase is reported to exhibit a range of homogeneity, quoted values refer to 1:1 composition.

seen in CrAs above and below the Néel temperature of $261-272$ K.[17] As pointed out by, e.g., Rundqvist,[24] there is a degree of correlation between $(c/b)_{MnP}$ and the total number of "valence" electrons per formula unit, although this may be a reflection of a consistent trend in the size of the $T$ component rather than the cause of the distinction.

As a reflection of the empirical constraints on the positional parameters, the center of gravity of the six $X$ atoms surrounding each $T$ is shifted in the direction opposite to that of the "central" $T$ atom, and as seen from Fig. 3
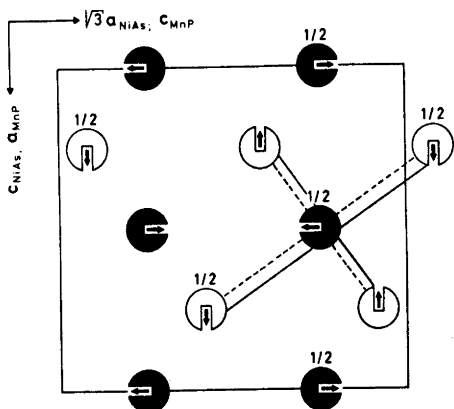


Fig. 3. Relationship between the NiAs and MnP type structures. Filled and open circles represent metal and non-metal atoms, respectively, in the NiAs arrangement. Lengths and directions of arrows give their main displacements in the MnP type cell.

these shifts are of approximately equal magnitude. The most important consequence of this rearrangement is the production of four roughly equal $T-T$ contacts in the MnP type structure as opposed to generally * two in the NiAs type (vide infra). This happens on the expense of the symmetry of the $TX_6$ coordination octahedron, the six equal $T-X$ bonds in the NiAs type structure being splitted into four non-equivalent $(2+2+1+1)$ bond lengths in the MnP type according to Pnma. The immediate implication of this non-equivalence is that no single "radius" can be attributed to $T$ or $X$ in the MnP type structure (vide infra).

On account of the experimental facts for compounds with the MnP and NiAs type structures it is possible to formulate a set of postulates or hypotheses which geometrically governs the occurrence of one or the other of the structure types concerned. Among the most natural and obvious set of such geometrical conditions, some prove to be dependent on others, and the object of the following analysis is to sort them in the two categories. Three unambiguously independent postulates are:

(1) Using the NiAs type structure as the starting point no essential change in the coordination number and symmetry of the $6X$ around $T$, and vice versa, is permitted.

(2) An approximately equal size of $T$ and $X$ is required in the MnP type structure.

---

* In the NiAs type structure of (say) VP there are $2+6$ approximately equal $T-T$ contacts.[20]

(3) The number of $T-T$ contacts are two and four in the NiAs and MnP type structures, respectively.

An additional requirement which is closely associated with (1) can be formulated as:

(4) The average $T-X$ bond length is maintained in the transformation from the NiAs to the MnP type structure, with a minimum scatter in these distances for the latter type.

Symmetry considerations on the basis of (1) and (3) show that the displacements of the $T$ atoms must be perpendicular to $c_{\text{NiAs}}$, and are most efficient, alternately, along $\pm b_{\text{NiAs}}$ $(=\pm\sqrt{3}a_{\text{NiAs}}\approx\pm c_{\text{MnP}})$. The resulting unit cell must consequently be of orthorhombic symmetry. Postulate (2) enters into the considerations as a selection criterion for possible candidates for the MnP type structure. In terms of the unit cell in Fig. 3, the above deduction is summarized as:

(5) The positional parameters of the $T$ atoms in the MnP type structure are restrained by $x_T\approx 0$ (and $y_T\approx 0$, according to $Pn2_1a$, or $y_T=0$, according to $Pnma$) whereas $z_T \neq 1/4$.

As a consequence of these metal displacements, symmetry considerations based on the hypotheses (1)−(4) show that the non-metal atoms must be shifted mainly along $\pm c_{\text{NiAs}}$ $(\approx\pm a_{\text{MnP}})$, viz.:

(6) The positional parameters of the $X$ atoms in the MnP type structures are $x_X \neq 1/4$, with the constraint(s) $z_X\approx 7/12$ (and $y_T\approx 0$ or $y_T=0$, according to $Pn2_1a$ or $Pnma$).

In order to establish semi-theoretical values for $z_T$ and $x_X$ it is convenient first to present some partly incorrect results based only on hypotheses (2) and (3) and simple geometrical considerations. Assuming that $T$ and $X$ are rigid spheres of equal radii which make 6 $T-X$ and 2 $T-T$ contacts in the NiAs type structure, a value of 4/3 is obtained for $(c/a)_{\text{NiAs}}$. Presuming, moreover, that the axial ratios are maintained in the transformation from the NiAs to a MnP type arrangement together with hypothesis (3) it is found that $z_T=0.157$. Provided the unit cell dimensions are kept constant this gives rise to a 15 % increase in $T-T$. This paradoxical conclusion implies that either the first or the latter assumption of this sequence is erroneous. On more careful examination it is seen that already the starting point is incorrect in that the $T$ and $X$ atoms cannot be of spherical shape (and, moreover, $T-T$ in phosphides and arsenides with the MnP type structure appears to be some 10−20 % larger than $T-X$). As one may expect, an extension of the above speculations to the non-metal atoms turns out to be even less realistic.

In order to obtain further progress it is necessary to take experimental facts into account as additional hypotheses:

(7) Compounds with the MnP type structure satisfy the empirical constraint(s) $(c/a)_{\text{MnP}}=1.10$ (and $1.63 < (c/b)_{\text{MnP}} < 1.93$). As a direct consequence potential candidates for a continuous transformation from the NiAs to the MnP type structure must fulfil the requirement, $(c/a)_{\text{NiAs}}\approx 1.6$.

(8) The shortest interatomic $X-X$ distances in the MnP type structure are caused by the geometry of the atomic arrangement, and are consequently non-bonding. This condition acts as the limiting factor for the magnitude of the deformation of the NiAs arrangement.

Equating the two sets of bonding $T-T$ distances in an idealized MnP type arrangement based on hypotheses (1), (3), and (5):

$$\left\{ \left( \frac{a}{2} \right)^2 + [2(\tfrac{1}{4} - z_T)c]^2 \right\}^{\frac{1}{2}} = \left\{ \left( \frac{b}{2} \right)^2 + \left[ \frac{c}{2} - 2(\tfrac{1}{4} - z_T)c \right]^2 \right\}^{\frac{1}{2}}$$

it follows that

$$z_T = \tfrac{1}{4} - \tfrac{1}{8} \left( 1 + \frac{b^2}{c^2} - \frac{a^2}{c^2} \right)$$

Taking advantage of hypothesis (7) one finds that

$$0.181 < z_T < 0.195$$

(Compared with an NiAs type arrangement of the same unit cell dimensions $[(c/a)_{\text{NiAs}} = 1.6]$ this means $< 4 \%$ increase in $T - T$ distance, which is consistent with postulate (3) as well as with the observed data.)

Since the deduced range for $z_T$ is in remarkable accordance with the values listed in Table 2, it is worthwhile to present the results of a similar derivation for $x_X$. This deduction is based on hypotheses (2), (6), and (8), using a 20 % increased average (r.m.s.) $T - X$ bond distance as the limiting value for the shortest permissible $X - X$ distance. (Although the figure of 20 % appears to be somewhat arbitrary at first sight, this criterion is based on experience from a large number of transition metal compounds.) The calculations show that

$$x_X \approx \tfrac{1}{4} - \left( \frac{5}{64} - \frac{c^2}{36a^2} \right) \approx 0.20$$

Thus, the above deductions fully match the experimental facts in Table 2 and this gives rise to a further more precise specification of (5) and (6):

(9) The geometrical constraints on the positional parameters of the MnP type structure are $x_T \approx 0$, $z_T \approx x_X \approx 0.20$, and $z_X \approx 7/12$ (according to $Pnma$).

The fact that the displacements of $T$ and $X$ relative to the idealized NiAs type arrangement must be of the same magnitude, follows in an intuitive manner directly from Fig. 3, bearing in mind that the two kinds of atoms are of approximately equal size.

Towards the end of the geometrical considerations it is tempting to formulate, as a separate point, the conditions governing the volume, although the content of which follows immediately from (1) and (4):

(10) The volume per formula unit is maintained during the continuous MnP⇌NiAs type phase transition, provided the size of $T$ remains virtually constant.

The limitation on (10) applies to the situation in MnAs and ternary Mn-rich phases of the type $Mn_{1-t}T_tAs$, where the size of Mn is sensitive to the number of unpaired electrons. The latter fact provides a natural explanation as to why phase transitions (NiAs→MnP) can be induced in these phases on the application of high pressures.

In summarizing the above discussion the most important geometrical condition which governs the preference of the MnP type structure in relation to the NiAs type is the approximately equal size of $T$ and $X$ which in turn permits an increase from two to four $T - T$ contacts in the former structure type.

NiP breaks the pattern formed by pnictides of the $3d$ series in that it adopts a unique crystal structure, which according to Larsson [32] is closely related to both the NiAs and MnP types. The NiP type atomic arrangement can in a somewhat superficial way be said to be intermediate between the NiAs and MnP types in that each $T$ obtains three close $T-T$ contacts. For this reason it is tempting to apply a geometrical reasoning for the hypothetical transition from NiAs to NiP type structure. Without going into details, the $T$ atoms are shifted (from their positions in the NiAs type cell) perpendicular to $c_{NiAs}$ and mainly, in an alternating manner, along the plus and minus directions of the two hexagonal axes. This corresponds to one of the most efficient ways to produce 3 $T-T$ contacts from an NiAs type arrangement. The resulting unit cell is of orthorhombic symmetry, and in the case of NiP it has a four times larger volume than the NiAs type cell. As a consequence of the displacements of the $T$ atoms, the $X$ atoms in NiP are shifted mainly along $\pm c_{NiAs}$ ($\approx \pm b_{NiP}$), and in a manner which gives rise to five $T-X$ bond distances of approximately equal length, whereas, as a compromise, the sixth necessarily has to be considerably elongated. A characteristic feature of the deformation in the NiP type structure is the rather short $X-X$ distance [2.430(1) Å, $i.e.$ only 10 % larger than the expectation value for the $P-P$ single bond length [33]]. In line with the above geometrical considerations for the relationship between the NiAs and MnP type structures it is suggested that the condition that rules the occurrence of the NiP type structure is the 3 $T-T$ contacts per $T$ atom. The limiting factor is once more the shortest $X-X$ distances, which can be regarded as non-bonding. Contrary to the suggestions of Larsson,[32] we propose therefore that each $T$ is coordinated to 6 $X$ and 3 $T$. The choice between the MnP and NiP type structures cannot be governed by a size factor, since the average $Ni-P$ distance is comparable with the average $Co-P$ distance in CoP with MnP type structure.

The geometrical considerations on the relationship between the NiAs and MnP type structures have necessarily been limited to the initial and final stages of the transition. Since the transitions in all known cases are continuous of second or higher order, more information is at hand. However, the problem is how to utilize this information. Although no experimental evidence concerning the lattice modes of vibration is available, it is probably possible to describe the dynamical mechanism of the NiAs$\rightleftharpoons$MnP type transition in terms of the "soft modes" formalism.[34] The most fundamental question in this connection appears to be how the transition is initiated in the high temperature phase. In order to approach this problem further it is necessary to get some insight into the nature and implications of the $T-T$ contacts. The two $T-T$ contacts in the NiAs type structure and the four in the MnP type unquestionably reflect bonding interaction between the atoms concerned, but the degree of localization and kinds of orbitals involved in these bonds represent a hitherto unsolved problem. Carter [35,36] has, for example, recently advanced a "quasi free electron" model for the $T-T$ interactions in compounds with the NiAs type structure. Provided such a model conveys a reasonable degree of correctness about the nature of these bonds, it is tempting to suggest that the relation between the Fermi surface and the Brillouin zone faces may release the transformation. The increase from two to four $T-T$ contacts is in any case definitely associated with a decrease in the number of "localized" unpaired electrons, and may possibly result from splitting of electronic bands. Without distinguishing between bonding, non-bonding, and possibly anti-bonding bands the experimental evidences show that the MnP type structure occurs at a valence electron concentration of $10-14$ per $TX$ unit. This provides an "explanation" as to why TiSb does not obtain a MnP type arrangement despite the fact that its unit cell proportions should

be favourable. The monochalcogenides of the $3d$ metals appear to prefer the NiAs type structure which permits a larger number of unpaired electrons and variable compositions.

REFERENCES

1. Kjekshus, A. and Pearson, W. B. *Progr. Solid State Chem.* **1** (1964) 83.
2. Pearson, W. B. *A Handbook of Lattice Spacings and Structures of Metals and Alloys*, Pergamon, Oxford-London-Edinburgh-New York-Toronto-Braunschweig 1967, Vol. II.
3. Hulliger, F. *Struct. Bonding (Berlin)* **4** (1968) 83.
4. Willis, B. T. M. and Rooksby, H. P. *Proc. Phys. Soc.* **B 67** (1954) 290.
5. Heyding, R. D. and Calvert, L. D. *Can. J. Chem.* **35** (1957) 449.
6. Kornelsen, R. O. *Can. J. Phys.* **39** (1961) 1728.
7. Kornelsen, R. O. *Thesis*, University of Ottawa 1964.
8. Wilson, R. H. and Kasper, J. S. *Acta Cryst.* **17** (1964) 95.
9. Ido, H. *J. Phys. Soc. Japan* **25** (1968) 1543.
10. Sobczak, R., Boller, H. and Bittner, H. *Monatsh.* **99** (1968) 2227.
11. Sobczak, R., Boller, H. and Nowotny, H. *Third International Conference on Solid Compounds of Transition Elements*, Oslo 1969, p. 154.
12. Menyuk, N., Kafalas, J. A., Dwight, K. and Goodenough, J. B. *Phys. Rev.* **177** (1969) 942.
13. Grønvold, F., Snildal, S. and Westrum, E. F. *Acta Chem. Scand.* **24** (1970) 285.
14. Hall, E. L., Schwartz, L. H., Felcher, G. P. and Ridgley, D. H. *J. Appl. Phys.* **41** (1970) 939.
15. Kazama, N. and Watanabe, H. *J. Phys. Soc. Japan* **30** (1971) 1319.
16. Kjekshus, A. and Jamison, W. E. *Acta Chem. Scand.* **25** (1971) 1715.
17. Selte, K., Kjekshus, A., Jamison, W. E., Andresen, A. F. and Engebretsen, J. E. *Acta Chem. Scand.* **25** (1971) 1703.
18. Selte, K. and Kjekshus, A. *Acta Chem. Scand.* **25** (1971) 3277.
19. Selte, K., Kjekshus, A. and Andresen, A. F. *Acta Chem. Scand.* **26** (1972) 4188.
20. Selte, K., Kjekshus, A. and Andresen, A. F. *Acta Chem. Scand.* **26** (1972) 4057.
21. Furuseth, S., Kjekshus, A. and Andresen, A. F. *Acta Chem. Scand.* **23** (1969) 2325.
22. Selte, K., Kjekshus, A. and Andresen, A. F. *Acta Chem. Scand.* **26** (1972) 3101.
23. Selte, K., Kjekshus, A. and Andresen, A. F. *Acta Chem. Scand.* **27** (1973). *In press.*
24. Rundqvist, S. *Acta Chem. Scand.* **16** (1962) 287.
25. Rundqvist, S. and Nawapong, P. C. *Acta Chem. Scand.* **19** (1965) 1006.
26. Kjekshus, A. and Walseth, K. P. *Acta Chem. Scand.* **23** (1969) 2621.
27. Bouwma, J., van Bruggen, C. F., Haas, C. and van Laar, B. *J. Phys. (Paris)* **C 32** (1971) 78.
28. Selte, K. and Kjekshus, A. *Acta Chem. Scand.* **26** (1972) 1276.
29. Selte, K. and Kjekshus, A. *Acta Chem. Scand.* **23** (1969) 2047.
30. Selte, K. and Kjekshus, A. *Acta Chem. Scand.* **27** (1973) 1448.
31. Pfisterer, H. and Schubert, K. *Z. Metallk.* **41** (1950) 358.
32. Larsson, E. *Arkiv Kemi* **23** (1965) 335.
33. Furuseth, S., Selte, K. and Kjekshus, A. *Acta Chem. Scand.* **19** (1965) 735.
34. Samuelsen, E. J., Andersen, E. and Feder, J. *Structural Phase Transitions and Soft Modes*, Universitetsforlaget, Oslo-Bergen-Tromsø, 1971.
35. Carter, F. L. In Bennett, L. H., Ed., *Electronic Density of States* (NBS Spec. Publ. No. 323) Washington 1971, p. 385.
36. Carter, F. L. *Fourth International Conference on Solid Compounds of Transition Elements*, Geneva 1973, p. 11.

# Reaction of Allenes with Dichlorocarbene

TYGE GREIBROKK*

*Department of Chemistry, University of Oslo, Oslo 3, Norway*

The reactions of allenes with dichlorocarbene, generated by the chloroform/sodium hydroxide method, have been investigated. Alkyl substituted allenes gave spirocyclopentanes in good yields. Phenyl-allene also gave the diadduct which, however, reacted further with the base. The higher substituted phenyl allenes reacted slowly. Triphenylallene gave the monoadduct only, while the allenic double bonds of tetraphenylallene did not react. One product was isolated, however, in which 3 mol of dichlorocarbene had added to one of the benzene rings.

Addition of dihalocarbenes to allenes has been reported on various occasions,[1-6] with the monoadduct as the main product. Some diadducts also have been reported, but usually in poor yields, except for the reaction of allene with phenylbromodichloromethyl mercury, which gave both mono-adduct and diadduct in good yields.[1] In our studies on electrophilic reactions with allenes [7,8] we now also include the reactions of the highly reactive di-chlorocarbene generated by the reaction of chloroform with 50 % aqueous sodium hydroxide, catalyzed by benzyltriethylammonium chloride (BTA), according to Makosza and Wawrzyniewicz.[9] The following compounds have been examined; allene (*1a*), 1,1-dimethylallene (*1b*), tetramethylallene (*1c*), phenylallene (*1d*), triphenylallene (*1e*), and tetraphenylallene (*1f*). When allene (*1a*) was bubbled to a stirred mixture of chloroform, 50 % NaOH and BTA, a mixture of monoadduct (*2a*) and diadduct (*3a*) was isolated and separated by GLPC. With a dry ice condenser connected during the reaction, the spirocyclopentane was isolated in 34 % yield after 2 days reaction. When 1,1-dimethylallene (*1b*) was stirred at 0° for 5 h, the monoadduct (*2b*), from addition to the substituted double bond, was isolated in 88 % yield. After 48 h at room temperature the spirocyclopentane (*3b*) was obtained in 70 % yield. With tetramethylallene (*1c*) the formation of the diadduct (*3c*) was faster; a 90 % yield was achieved after 20 h.

---

* Present address: Institute for Biomedical Research, University of Texas, Austin 78712, U.S.A.

a: $R^1 = R^2 = R^3 = R^4 = H$

b: $R^1 = R^2 = CH_3$, $R^3 = R^4 = H$

c: $R^1 = R^2 = R^3 = R^4 = CH_3$

d: $R^1 = Ph$, $R^2 = R^3 = R^4 = H$

e: $R^1 = H$, $R^2 = R^3 = R^4 = Ph$

f: $R^1 = R^2 = R^3 = R^4 = Ph$

Phenylallene (*1d*) gave a mixture of several products. Small amounts of monoadducts were seen in the NMR spectrum after 8 h. By further reaction these compounds disappeared, leaving a mixture from which one major component was isolated. From the NMR and mass spectra the constitution of this product is expressed by structure *4*. Dehydrohalogenation of the initial diadduct (*3d*) would give *5*, which could add another molecule of dichlorocarbene. Triphenylallene (*1e*) gave mainly the monoadduct (*2e*) which was separated by chromatography on neutral alumina in 40 % yield. Tetraphenylallene (*1f*) reacted slowly, but gave a product which was separated on neutral alumina in 10 % yield. The mass spectrum revealed a triple adduct to a benzene ring by the $M(m/e\ 590)$, $M - Cl$ and $M - nHCl$ ($n = 1 - 6$) fragments. The NMR spectrum was in accordance to addition to only one benzene ring. Three protons at $\delta$ 1.7 and two protons at $\delta$ 1.3 might indicate that one of the cyclopropane rings is *trans* to the others, a less strained configuration than the all-*cis* structure, analogous with the structure of *trans*-benzene trioxide.[10] The presence of a weak allenic absorption at 1940 cm$^{-1}$ in the infrared is also in agreement with structure *6*. The Makosza method, which we have used, evidently is not well suited for addition to allenic double bonds of low reactivity. The addition of dihalocarbenes to phenylallenes is, however, not easily accomplished. Dehmlow [4] reacted phenylallenes with sodium trichloroacetate at 80° and obtained cyclobutanes arising from a cycloaddition with tetrachloroallene (formed in the reaction). A previous attempt to use the haloform/butoxide method resulted in dehydrohalogenation of the product.[11] On the other hand, we have shown that the present method is very efficient in producing tetrachlorospirocyclopentanes from alkyl-substituted allenes.

The same method also furnished the tetrabromo analogs; the yields were, however, low.[12]

## EXPERIMENTAL

The NMR spectra were recorded on a Varian A 60-A spectrometer, the IR spectra on a Perkin Elmer model 457 spectrophotometer and the mass spectral data were obtained on an A.E.I. MS 902 mass spectrometer. The preparative GLC analyses (GLPC) were performed on a Varian Aerograph model 711, equipped with a 20 % SE-30 on Chromosorb column.

*Reaction of allene (1a) with dichlorocarbene.* Allene (1.0 g, 0.025 mol) was slowly bubbled to a stirred mixture of chloroform (100 ml), 50 % NaOH (50 ml), and BTA (100 mg) at 10 − 20° in a bottle equipped with a dry ice condenser. After 2 days, ice-cold water was added, the aqueous phase extracted with chloroform, the organic phase washed with water, dried ($MgSO_4$) and carefully evaporated. The NMR spectrum of the residue (4.0 g) showed a 1:5 ratio of monoadduct and diadduct as the main products. The components were separated by preparative gas chromatography and identified by comparison of the NMR and IR spectra with those previously reported.[1] Distillation of the residue gave 1.7 g (34 %) of the spirocyclopentane (*3a*), b.p. 30° (0.1 mmHg).

*Reaction of 1,1-dimethylallene (1b) with dichlorocarbene.* 1,1-Dimethylallene (1.36 g, 0.02 mol) was stirred in a mixture of chloroform (50 ml), 50 % NaOH (30 ml), and BTA (50 mg) for 5 h at 0°. Work up as above, gave 2.5 g (83 %) of the monoadduct, contaminated by small amounts of diadduct. Distillation gave 1.6 g of the pure *2b*, b.p. 137 − 139°. NMR($CDCl_3$) CH $\delta$ 5.90(s), CH $\delta$ 5.55(s), two $CH_3$ $\delta$ 1,42(s). MS: M (*m/e* 150), M − $CH_3$, M − Cl, M − Cl − HCl. When the reaction mixture was stirred for 2 days, all the monoadduct had reacted. Chromatography on neutral alumina (act. II − III) gave 3.2 g (70 %) of pure *3b*. NMR ($CDCl_3$), CH $\delta$ 1.86(d), CH $\delta$ 1.82(d) (*J* = 7.0 Hz), $CH_3$ $\delta$ 1.57(s), $CH_3$ $\delta$ 1.34(s). MS: M (*m/e* 232), M − Cl, M − 2Cl, M − Cl − HCl, M − Cl − 2HCl.

*Reaction of tetramethylallene (1c) with dichlorocarbene.* Tetramethylallene (1.92 g, 0.02 mol) was reacted as above for 20 h. Washing and evaporation as above gave 4.7 g (90 %) of the solid diadduct (*3c*), m.p. 210 − 212° after recrystallization from chloroform. NMR ($CDCl_3$) $CH_3$ $\delta$ 1.50(s), $CH_3$ $\delta$ 1.37(s). MS: M (*m/e* 260), M − Cl, M − Cl − HCl, M − 2Cl − HCl, M − 3Cl.

*Reaction of phenylallene (1d) with dichlorocarbene.* Phenylallene (2.32 g, 0.02 mol) was reacted as above for 20 h. The same work up as above gave a residue (4.9 g) which was treated with hexane, filtered and the filtrate chromatographed on neutral alumina (act. II − III). Careful elution with hexane gave 1.5 g (23 %) of *4*. NMR ($CDCl_3$) $CH_2$ $\delta$ 2.40(d) (*J* = 2.5 Hz), arom. H $\delta$ 7.1 − 7.6. MS: M (*m/e* 326), M − Cl, M − 2Cl, M − Cl − HCl, M − 3Cl, M − 2Cl − HCl, M − 4Cl, M − 5Cl.

*Reaction of triphenylallene (1e) with dichlorocarbene.* Triphenylallene (1.34 g, 5 mmol) was treated as described above for 2 days, The residue (1.8 g) after the same work up procedure was treated with hexane, filtered and the filtrate chromatographed on neutral alumina (act. II − III). Elution with hexane, evaporation of the eluate and recrystallization from petroleum ether (b.p. 40 − 65°) gave 0.7 g (40 %) of the monoadduct (*2e*), m.p. 138 − 139°. NMR ($CDCl_3$) CH $\delta$ 3.75(s), arom. H $\delta$ 7.0 − 7.5. MS: M (*m/e* 350) − Cl, M − 2Cl, M − 2Cl − Ph.

*Reaction of tetraphenylallene (1f) with dichlorocarbene.* Tetraphenylallene (0.344 g, 1 mmol) was treated as described above for 3 days. The residue (0.7 g) was dissolved in cyclohexane and carefully chromatographed on neutral alumina (act. II − III). Elution with cyclohexane gave 60 mg (10 %) of *6*, contaminated with some starting materials. NMR ($CDCl_3$), three CH $\delta$ 1.7(m), two CH $\delta$ 1.3 (m), arom. H $\delta$ 7.0 − 7.6. MS: M (*m/e* 590), M − Cl, M − *n*HCl (*n* = 1 − 6).

## REFERENCES

1. Seyferth, D., Burlitch, J. M., Minasz, R. J., Yick-Pui Mui, J., Simmonds, H. D., Treiber, A. J. H. and Dowd, S. R. *J. Am. Chem. Soc.* **87** (1965) 4259.
2. Ball, W. J. and Landor, S. R. *Proc. Chem. Soc. (London)* **1961** 246.
3. Peer, H. G. and Schors, A., *Rec. Trav. Chim.* **86** (1967) 161.
4. Dehmlow, E. V. *Chem. Ber.* **100** (1967) 7779.
5. Skattebøl, L. *Tetrahedron Letters* **1965** 2175.
6. Ullman, E. F. and Franshawe, W. J. *J. Am. Chem. Soc.* **83** (1961) 2379.

7. Greibrokk, T. and Skattebøl, L. *Acta Chem. Scand.* **27** (1973) 1421.
8. Greibrokk, T. *To be published*.
9. Makosza, M. and Wawrzyniewicz, M. *Tetrahedron Letters* **1969** 4659.
10. Foster, C. H. and Berchtold, G. A. *J. Am. Chem. Soc.* **94** (1972) 7939.
11. Dehmlow, E. V. *Chem. Ind. (London)* **1966** 1379.
12. Skattebøl, L. and Greibrokk, T. *To be published*.

# Synthesis of Naturally Occurring Quinones

## Alkylation with the Silver Ion-Peroxydisulphate-Carboxylic Acid System

N. JACOBSEN and K. TORSSELL

*Department of Organic Chemistry, University of Aarhus, 8000 Aarhus C, Denmark*

The syntheses of some naturally occurring quinones (primin, lapachol, 2-undecyl-1,4-benzoquinone (intermediate), *etc.*) are reported. The syntheses are performed by alkylation of quinones with radicals obtained from the decarboxylation of carboxylic acids with the silver ion-peroxodisulfate system.

We have previously reported[1] that radicals generated by decarboxylation of carboxylic acids with silver ions and peroxodisulfate (Eqns. 1 and 2) can be used for the alkylation of quinones.

$$Ag^+ + S_2O_8^{2-} \rightarrow Ag^{2+} + SO_4^{\cdot -} + SO_4^{2-} \tag{1}$$

$$Ag^{2+} + RCOOH \rightarrow R^{\cdot} + CO_2 + H^+ + Ag^+ \tag{2}$$
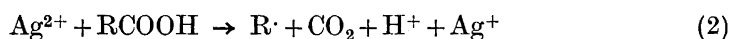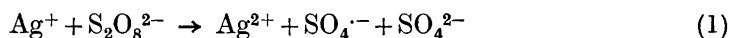
In this paper we demonstrate the utility of this method in the synthesis of some naturally occurring quinones.

## RESULTS

*Primin.* Pentylation of 2-methoxy-1,4-benzoquinone with pentyl radicals from the decarboxylation of hexanoic acid gave the natural product, primin (2-methoxy-6-pentyl-1,4-benzoquinone), together with the two isomeric monopentylated and the three possible dialkylated isomers (Table 1).

It is interesting to note that the methoxy group possesses a stronger directing effect in this type of reaction than does the methyl group.

*Table 1.* Pentylation of 2-methoxy-1,4-benzoquinoue.

| Products (2-Methoxy-1,4-benzoquinones) | No. | Yield % | M.p. °C | M.p. (Ref.). |
|---|---|---|---|---|
| 3-Pentyl | *1* | 2 | Oil | |
| 5-Pentyl | *2* | 34 | 115 – 116 | (114 – 115)[2] |
| 6-Pentyl | *3* | 13 | 62 – 63 | (62 – 63)[3] |
| 3,5-Dipentyl | *4* } | 1[a] | Oil | |
| 3,6-Dipentyl | *5* } | | | |
| 5,5-Dipentyl | *6* | 2 | Oil | |

[a] *4:5 ∼ 2:1*, approximately determined by NMR.



Isopropylation of toluquinone [1]

Isomer ratio
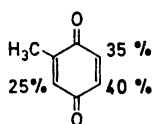
Pentylation of 2-methoxy-1,4-benzoquinone

Isomer ratio
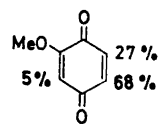
In view of the nucleophilic character of the alkyl radical this distribution pattern is expected.

*γ,γ-Dimethylallylquinones.* The decarboxylation of 4-methyl-3-pentenoic acid *7* was expected to give a delocalized 3,3-dimethylallyl radical *8*.
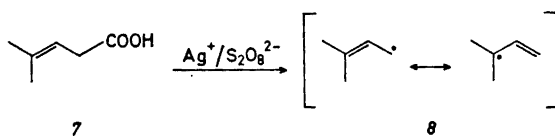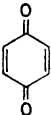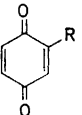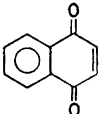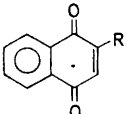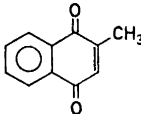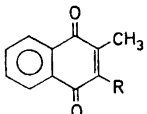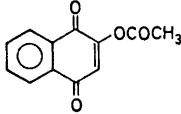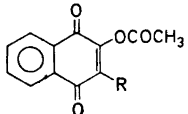


In principle, *8* should be able to attack a quinone molecule with either of the two carbon atoms bearing high spin density, giving rise to either a α,α-dimethylallyl- or a γ,γ-dimethylallylquinone.

Various quinones were alkylated and in all cases only the γ,γ-dimethylallylquinone was isolated.

The same results were obtained when the isomeric 2,2-dimethyl-3-butenoic acid *9* was used instead of *7*, indicating that the same radical is formed in both cases (Table 2).

The 4-methyl-3-pentenoic acid used in these syntheses was contaminated with 15 % of *trans*-4-methyl-2-pentenoic acid *14*, which under the conditions used did not disturb the reaction.

*Table 2.* Products from the alkylation of quinones with radicals from *7* and *9*.

| Quinone | Carboxylic acid | Molar ratio quinone: carboxylic acid: peroxodisulfate | Product R= $-CH_2-CH=C(CH_3)_2$ | | Yield % (based on the quinone) | m.p. °C | m.p. (Ref.) |
|---|---|---|---|---|---|---|---|
|  | 7 | 1:1.5:1.7 |  | *10* | 34 | 25−28 | (30.5)[4] |
|  | 7 | 1:1.3:1.3 |  Deoxylapachol | *11* | 58 | 60−61 | (62)[5] |
|  | 9 | 1:1.3:2 |  Menaquinone - *1* | *12* | 70 | | |
|  | 7 9 | 1:1:1.8 1:1.2:2 |  Lapachol acetate | *13* | 73 79 | 79−80 79−80 | (65−66)[6] (65−66)[6] |

Various α,β-unsaturated carboxylic acids were found to require higher temperatures (10 − 20°) for their decarboxylation than those of their saturated or β,γ-unsaturated analogs; however, when they were decarboxylated in the presence of a quinone, this was recovered unchanged.

Alkaline hydrolysis of lapachol acetate *13* gave lapachol *15*, overall yield calculated on 2-acetoxy-1,4-naphthoquinone or *7*, 61 %.

*2-Undecyl-1,4-benzoquinone 16.* This compound was used as an intermediate in the synthesis of embelin (2-undecyl-3,6-dihydroxy-1,4-benzoquinone) by Asano and Hase.[7]

Decarboxylation of lauric acid in the presence of a fourfold excess of benzoquinone gave *16* in 37 % yield calculated on the lauric acid.

## EXPERIMENTAL

The melting points are uncorrected. NMR spectra were recorded on a Varian A-60, IR spectra on a Perkin-Elmer Infracord, and UV spectra on a Perkin-Elmer 402 spectrometer.

*Alkylation of quinones.* Details of the reaction have been described earlier.[1]

*General procedure.* To a vigorously stirred water-acetonitrile solution or two-phase system of the quinone, the carboxylic acid, and silver nitrate at $60-65°C$ was added an aqueous solution of ammonium peroxodisulfate during 1 h. After further 10 min stirring at $60-65°C$, the mixture was cooled to room temperature and worked up.

*Pentylation of 2-methoxy-1,4-benzoquinone.* The general procedure was followed. To 2-methoxy-1,4-benzoquinone (2.07 g, 0.015 mol), hexanoic acid (2.61 g, 0.0225 mol), silver nitrate (1.5 g) in acetonitrile (60 ml), and water (60 ml) was added ammonium peroxodisulfate (5.13 g, 0.0225 mol) in water (25 ml). The mixture was extracted with methylene chloride, the extract was washed with 10 % sodium bicarbonate until neutral, dried, and concentrated to 10 ml *in vacuo* at room temperature.* Careful chromatography of the solution on silica gel (eluent $CH_2Cl_2$) gave five fractions:

I. 50 mg of a yellow oil *4* and *5*. NMR ($CCl_4$): $\delta$ 0.9 (6 H, distorted t, $J \sim 6$), 1.4 (12 H, m), 2.3 (4 H, distorted t, $\sim J6$), 3.96 and 4.00 (3 H, two singlets assigned to *5* and *4*, resp.), 6.27 and 6.34 (1 H, two triplets, $J = 1.5$ assigned to *4* and *5*, resp.).

II. 75 mg of a yellow oil *1*. Analytical data (after molecular distillation at $120°C/10^{-4}$ mmHg. (Found: C 68.9; H 7.66. Calc.: C 69.2; H 7.74.) UV (EtOH): $\lambda_{max}$ nm (log $\varepsilon$) 254 (4.0), 275 (2.9). IR (film): $cm^{-1}$ 1670(s), 1650(s), 1590(m), 840(m). NMR ($CCl_4$): $\delta$ 0.9 (3 H, distorted t, $J \sim 6$), 1.3 (6 H, m), 2.4 (2 H, t, $J = 7$), 4.0 (3 H, s), 6.5 (2 H, AB-system, $\Delta\nu_{AB} = 3.2$, $J_{AB} = 9.5$).

III. 100 mg of a yellow oil *6*. Analytical data (after molecular distillation at $140°C/10^{-4}$ mmHg. (Found: C 72.9; H 9.48. Calc.: C 73.4; H 9.42.) UV (EtOH): $\lambda_{max}$ nm (log $\varepsilon$) 278 (4.2), 380 (2.8). IR (film): $cm^{-1}$ 1675(s), 1650(s), 1605(s), 850(m). NMR ($CCl_4$): $\delta$ 0.9 (6 H, distorted t, $J \sim 6$), 1.4 (12 H, m), 2.4 (4 H, distorted t, $J \sim 7$), 3.8 (3 H, s), 5.7 (1 H, s).

IV. 1.06 g of yellow crystals *2*. M.p. $115-116°C$ (from $CCl_4$) (lit. $114-115$).[2] UV (EtOH): $\lambda_{max}$ nm (log $\varepsilon$) 266 (4.2), 360 (2.9). IR ($CHCl_3$): $cm^{-1}$ 1680(s), 1650(s), 1610(s), 990(m), 900(m), 860(m). NMR ($CDCl_3$): $\delta$ 0.9 (3 H, distorted t, $J \sim 6$), 1.4 (6 H, m), 2.4 (2 H, distorted t, $J \sim 7$), 3.8 (3 H, s), 5.9 (1 H, s), 6.5 (1 H, t, $J = 1$).

V. 420 mg of yellow crystals *3*. M.p. $62-63°C$ (from light petroleum) (lit. $62-63$).[3] UV (EtOH): $\lambda_{max}$ nm (log $\varepsilon$) 269 (4.1), 366 (2.8). IR ($CCl_4$) $cm^{-1}$ (1680(s), 1655(s), 1605(s), 900(m). NMR ($CCl_4$): $\delta$ 0.9 (3 H, distorted t, $J \sim 6$), 2.4 (6 H, m), 2.4 (2 H, distorted t, $J \sim 7$), 3.8 (3 H, s), 5.8 (1 H, d, $J = 2$), 6.3 (1 H, d, t, $J_1 = 2$, $J_2 = 1$).

*4-Methyl-3-pentenoic acid 7.* 1-Cyano-3-methyl-2-butene, prepared by the method of Ultee,[8] was hydrolyzed according to Reichstein[9] to give *7*, b.p. $101-102°C/10$ mmHg. It contained 15 % of *trans*-4-methyl-2-pentenoic acid (NMR and GC).

*2,2-Dimethyl-3-butenoic acid 9* was prepared according to Engel and Schexsnayder.[10]

*2-Acetoxy-1,4-naphthoquinone* was prepared from 2-hydroxy-1,4-naphthoquinone by the method of Thiele and Winther.[11] M.p. $129-131°C$ (lit.130°).[11]

*2-(γ,γ-Dimethylallyl)-1,4-benzoquinone 10.* The general procedure was followed. To benzoquinone (1.08 g, 0.01 mol), *7* (2.01 g, 85 %, 0.015 mol) and silver nitrate (0.5 g) in water (100 ml) was added ammonium peroxodisulfate (3.88 g, 0.017 mol) in water (20 ml). The reaction mixture was extracted with methylene chloride and the extract washed with 10 % sodium bicarbonate until neutral, dried, and evaporated. The crude oily product, 0.85 g, was crystallized from methanol to give 0.59 g *10*, 34 % based on benzoquinone, m.p. $25-28°C$ (lit. 30.5°).[4] UV (EtOH): $\lambda_{max}$ nm (log $\varepsilon$) 248 (4.2), 320 (2.8). IR (film): $cm^{-1}$ 1660(s), 1605(m), 900(m), 850(m), 815(w), 785(w). NMR ($CCl_4$): $\delta$ 1.66 (3 H, broad s), 1.76 (3 H, d, $J \sim 1$), 3.1 (2 H, broad d, $J = 7.5$), 5.1 (1 H, t, m, $J = 7.5$), 6.5 (1 H, m), 6.7 (2 H, m).

*2-(γ,γ-Dimethylallyl)-1,4-naphthoquinone (deoxylapachol) 11.* The general procedure was followed. To 1,4-naphthoquinone (1.58 g, 0.01 mol), *7* (1.73 g, 85 %, 0.013 mol), silver nitrate (0.5 g) in acetonitrile (17 ml), and water (37 ml) was added ammonium

---

* Evaporation to dryness caused decomposition.

peroxodisulfate (2.96 g, 0.013 mol) in water (15 ml). The reaction mixture was extracted with cyclohexane and the extract washed with 10 % $NaHCO_3$ until neutral, dried, and evaporated. The crude product was chromatographed on silica gel (eluent: methylene chloride) to yield 400 mg of naphthoquinone and 1300 mg of *11* (58 % based on naphthoquinone), m.p. 60 − 61°C (from light petroleum) (lit. 62°).[5] UV (EtOH): $\lambda_{max}$ nm (log $\varepsilon$) 247 (4.2), 252 (4.2), 264 (4.1), 334 (3.4). IR (KBr): cm⁻¹ 1660(s), 1610(m), 1595(m). NMR (CDCl₃): $\delta$ 1.69 (3 H, broad s), 1.79 (3 H, broad s), 3.3 (2 H, broad d, $J = 7.5$), 5.2 (1 H, t, m, $J = 7.5$), 6.8 (1 H, t, $J = 1.5$), 7.5 − 8.3 (4H, m).

*2-Methyl-(γ,γ-dimethylallyl)-1,4-naphthoquinone (menaquinone-1)* *12*. The general procedure was followed. To 2-methyl-1,4-naphthoquinone (0.86 g, 0.005 mol), *9* (0.74 g, 0.005 mol), silver nitrate (0.5 g) in acetonitrile (20 ml), and water (20 ml) was added ammonium peroxydisulphate (2.28 g, 0.1 mol) in water (10 ml). The mixture was neutralized with solid sodium bicarbonate and extracted with ether. The extract was dried and evaporated to give a yellow oil, which after TLC on silica gel (eluent 15 % ether in light petroleum) yielded 845 mg (70 % based on the 2-methyl-1,4-naphthoquinone) of *12* as a yellow oil. UV (EtOH): $\lambda_{max}$ nm (log $\varepsilon$) 245 (4.2), 249 (4.2), 264 (4.1), 272 (4.1), 334 (3.4). IR (film): cm⁻¹ 1665(s), 1630(m), 1610(m). NMR (CCl₄): $\delta$ 1.69 (3 H, broad s), 1.75 (3 H, broad s), 2.1 (3 H, s), 3.3 (2 H, broad d, $J = 7$), 5.0 (1 H, t, m, $J = 7$), 7.5 − 8.2 (4 H, m).

*Lapachol acetate 13.* The general procedure was followed. To 2-acetoxy-1,4-naphthoquinone (1.08 g, 0.005 mol), *7* (0.067 g, 85 %, 0.005 mol), silver nitrate (0.5 g) in acetonitrile (17 ml), and water (20 ml) was added ammonium peroxodisulfate (2.05 g, 0.009 mol) in water (10 ml). The reaction mixture was neutralized with solid sodium bicarbonate and extracted with ether. The extract was dried and evaporated to give 1.2 g of *13* containing about 10 % of 2-acetoxy-1,4-naphthoquinone (NMR). Recrystallization of the crude product from methanol gave 1.04 g *13* (73 %, m.p. 60 − 62°C (lit. 65 − 66°).[6] Recrystallization from light petroleum raised the m.p. to 79 − 80°C. UV (EtOH): $\lambda_{max}$ nm (log $\varepsilon$) 245 (4.2), 251 (4.2), 264 (4.1), 269 (4.1), 336 (3.4). IR (CHCl₃): cm⁻¹ 1780(s), 1675(s), 1640(m), 1600(m). NMR (CCl₄): $\delta$ 1.69 (3 H, broad s), 1.73 (3 H, broad s), 2.3 (3 H, s), 3.2 (2 H, broad d, $J = 7.5$), 5.1 (1 H, t, m, $J \sim 7.5$), 7.5 − 8.2 (4 H, m). By carrying out the same reaction using *9* (0.68 g, 0.006 mol) instead of *7* and ammonium peroxodisulfate (2.28 g, 0.01 mol) 1.12 g (79 %) of almost pure *13* was obtained as crude product.

*Hydrolysis of 13.* 200 mg of crude product from the synthesis of *13* using *7* was heated on a steam bath with 10 ml *1* M sodium carbonate for 30 min. The dark red solution was filtered, cooled in an ice bath, and acidified with concentrated HCl. After 1 h at 0°C, the yellow precipitate of lapachol *15* was filtered and dried *in vacuo* over anhydrous potassium carbonate. The yield was 143 mg, 83 %, m.p. (from CCl₄) 139 − 140°C (lit. 139 − 140°).[12] UV (EtOH): $\lambda_{max}$ nm (log $\varepsilon$) 253 (4.3), 279 (4.1), 333 (3.4). IR (KBr): cm⁻¹ 3320(s), 1660(s), 1640(s), 1590(m). NMR (CDCl₃): $\delta$ 1.68 (3 H, d, $J = 1$), 1.80 (3 H, broad s), 3.3 (2 H, broad d, $J = 7$), 5.2 (1 H, t, m, $J = 7$), 7.5 − 8.3 (4 H, m).

*2-Undecyl-1-4,benzoquinone 16.* The general procedure was followed. To lauric acid (1.00 g, 0.005 mol), benzoquinone (2.16 g, 0.02 mol), and silver nitrate (0.5 g) in acetonitrile (40 ml) was added ammonium peroxodisulfate (2.51 g, 0.011 mol) in water (15 ml). The reaction mixture was cooled to 5° and 20 ml of cold water was added with vigorous stirring. The precipitate (1.12 g) was filtered and dried *in vacuo* over CaCl₂. TLC on silica (eluent 20 % ether in light petroleum) gave 490 mg of *16*, 37 % calculated on the lauric acid, m.p. (CH₃OH) 59 − 60°C (lit. 57 − 59°).[7] UV (EtOH): $\lambda_{max}$ nm (log $\varepsilon$) 249 (3.8). IR (KBr): cm⁻¹ 1660(s), 1600(m), 717(m). NMR (CCl₄): $\delta$ 0.9 (3 H, distorted t, $J \sim 6$), 1.3 (18 H, m), 2.4 (2 H, distorted t, $J \sim 7$), 6.5 (1 H, m), 6.7 (2 H, m).

## REFERENCES

1. Jacobsen, N. and Torssell, K. *Ann.* 763 (1972) 135.
2. Schildknecht, H. and Schmidt, H. *Z. Naturforsch.* **22b** (1967) 287.
3. Schildknecht, H., Bayer, I. and Schmidt, H. *Z. Naturforsch.* **22b** (1967) 36.
4. Bohlman, F. and Kleine, K. M. *Chem. Ber.* **99** (1966) 885.
5. Burnett, A. R. and Thomson, R. H. *J. Chem. Soc.* **C 1967** 2100.
6. Cooke, R. G., Killen Macbeth, A. and Winzor, F. L. *J. Chem. Soc.* **1939** 878.

7. Asano, M. and Hase, Z. *J. Pharm. Soc. Japan* **60** (1940) 650.
8. Ultee Sr., A. J. *Rec. Trav. Chim.* **68** (1949) 495.
9. Reichstein, T. *Chem. Ber.* **63** (1930) 749.
10. Engel, P. S. and Schexsnayder, M. A. *J. Am. Chem. Soc.* **94** (1972) 4357.
11. Thiele, J. and Winther, E. *Ann.* **311** (1900) 341.
12. Burnett, A. R. and Thomson, R. H. *Chem. Ind. (London)* **1968** 1771.

# Crystal Structure of Cyclooctasarcosyl

P. GROTH

*Department of Chemistry, University of Oslo, Oslo 3, Norway*

The crystals belong to the orthorhombic system with space group *Pbca* and cell dimensions $a = 18.34_0$ Å, $b = 18.27_9$ Å, $c = 18.87_5$ Å. There are eight molecules in the unit cell. The phase problem was solved by direct methods. The $R$-value arrived at for 3471 observed reflections was 7.2 %. The ring conformation is surprisingly open with the inner volume filled by a cluster of four water molecules, which participate in a network of inter- and intra-molecular hydrogen bond bridges. Each of the four pairs of diametrically placed amino-acid residues is related by an approximate two-fold axis of symmetry. The conformation is *cis, cis, trans, trans, cis, cis, trans, trans.*

Cyclic oligopeptides of sarcosine of the general formula (I) have been studied by Dale and Titlestad.[1] To account for the relatively high observed

$$\left[ CH_3 - \underset{|}{N} - CH_2 - \overset{\overset{\displaystyle O}{\|}}{C} - \right]_n \qquad n = 2, 3, \cdots, 8 \qquad (1)$$
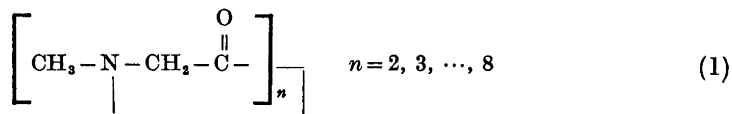
resistance to ring inversion, transannular interactions between N and C (carbonyl) were suggested. Such interactions have been reported to exist in certain cyclic aminoketones.[2] In the 10-ring lactone of 6-keto-9-hydroxy-nonanoic acid[3] there is strong evidence for transannular donor-acceptor attraction between the "ether" oxygen of the ester group and the carbonyl carbon atom.

In order to establish whether transannular N···C (carbonyl) attractions actually are stabilising the oligomers (I), and to obtain detailed information of the ring conformations and the geometries of the amino-acid residues, single crystals of some of these compounds are being examined by X-ray methods. Results for the cases $n = 2$ and $n = 4$ have been reported earlier.[4,5] In cyclo-tetrasarcosyl ($n = 4$) the transannular N···C (carbonyl) distance was $3.08_3$ Å, and no conclusion concerning stabilising transannular donor-acceptor attraction could be drawn. In the present paper the results of the crystal structure determination of cyclooctasarcosyl ($n = 8$) are presented.

The crystals belong to the orthorhombic system and the systematic absences lead to the space group *Pbca*. The cell parameters, measured by means of a four circle diffractometer, and their estimated standard deviations are:

$$a = 18.340(3)\text{Å}, \quad b = 18.279(3)\text{Å}, \quad c = 18.875(2)\text{Å}$$

With eight molecules per unit cell the calculated density is $\varrho_c = 1.20$ g cm$^{-3}$. The observed density, $\varrho_o = 1.34$ g cm$^{-3}$, corresponds to a difference in molecular weight of 72 which is accounted for by assuming the presence of four water molecules per asymmetric unit.

With $2\theta(\max) = 50°$ and MoK$\alpha$-radiation, about 5000 independent reflections were measured on an automatic four-circle diffractometer. Using an observed-unobserved cutoff at $2.5\sigma(I)$, 3471 were recorded as observed. No corrections have been made for absorption or secondary extinction effects.

*Table 1.* Final fractional coordinates and anisotropic thermal vibration parameters with estimated standard deviations (multiplied by $10^5$ for nonhydrogens and $10^4$ for hydrogens). The symbols CC, CM and OV are used for carbonyl carbons, methyl carbons and water oxygens, respectively. Hn1 and Hn2 are bonded to Cn.

| ATOM | x | y | z | θ | B11 | B22 | B33 | B12 | B13 | B23 |
|------|---|---|---|---|-----|-----|-----|-----|-----|-----|
| O1 | 76027(19) | 18723(20) | 35285(20) | | 220( 12) | 353( 15) | 383( 15) | -152( 22) | 136( 24) | -91( 20) |
| O2 | 55212(18) | 28366(17) | 29976(19) | | 256( 13) | 217( 11) | 311( 14) | -19( 19) | -12( 22) | 173( 21) |
| O3 | 43418(20) | 26792(18) | 41380(19) | | 415( 15) | 242( 13) | 263( 13) | 141( 83) | -213( 23) | -126( 21) |
| O4 | 25152(19) | 34898(18) | 39854(20) | | 333( 16) | 177( 11) | 396( 16) | -141( 20) | 62( 24) | 4( 24) |
| O5 | 24755(17) | 57014(19) | 35979(19) | | 200( 12) | 301( 13) | 333( 14) | -83( 20) | -78( 22) | 148( 24) |
| O6 | 44802(17) | 55267(18) | 31185(19) | | 196( 12) | 289( 13) | 307( 13) | 21( 20) | -108( 21) | -179( 22) |
| O7 | 56589(20) | 46143(18) | 41377(19) | | 365( 16) | 278( 13) | 232( 13) | 46( 23) | 118( 23) | 72( 21) |
| O8 | 74555(20) | 40383(19) | 40003(21) | | 295( 14) | 170( 11) | 366( 14) | -60( 19) | -148( 23) | 48( 23) |
| OV1 | 47653(24) | 44883(22) | 20780(22) | | 471( 16) | 412( 16) | 373( 17) | 81( 29) | -131( 29) | -189( 27) |
| OV2 | 52356(29) | 30892(25) | 19460(26) | | 669( 23) | 476( 19) | 627( 22) | 498( 36) | 114( 37) | 382( 34) |
| OV3 | 39965(22) | 42211(23) | 8128(22) | | 392( 16) | 442( 17) | 372( 16) | 8( 27) | -93( 27) | -8( 28) |
| OV4 | 49236(23) | 38748(23) | 3794(24) | | 475( 16) | 455( 17) | 388( 17) | 1( 30) | -87( 29) | -35( 29) |
| N1 | 65806(20) | 12147(20) | 36315(21) | | 168( 13) | 168( 13) | 265( 15) | 28( 21) | 7( 24) | 35( 23) |
| N2 | 45848(20) | 14147(20) | 34810(23) | | 163( 13) | 178( 13) | 389( 17) | 44( 21) | -16( 24) | -40( 24) |
| N3 | 37232(23) | 31473(21) | 31886(22) | | 264( 15) | 228( 14) | 250( 15) | 158( 25) | -78( 26) | -144( 26) |
| N4 | 28332(23) | 45816(20) | 43437(22) | | 293( 16) | 160( 13) | 266( 16) | -43( 24) | 167( 27) | -21( 24) |
| N5 | 34992(21) | 63800(19) | 38955(22) | | 191( 14) | 147( 12) | 317( 16) | 30( 28) | 64( 25) | 29( 24) |
| N6 | 54677(20) | 59628(21) | 36929(22) | | 193( 13) | 185( 13) | 208( 15) | 27( 22) | -25( 26) | -32( 24) |
| N7 | 62824(22) | 42561(21) | 31460(22) | | 244( 15) | 259( 15) | 259( 15) | 114( 23) | -12( 26) | 29( 25) |
| N8 | 71269(21) | 29554(20) | 43841(21) | | 237( 15) | 171( 13) | 278( 15) | 7( 23) | -82( 25) | 35( 24) |
| C1 | 58284(26) | 11303(24) | 38679(22) | | 193( 16) | 127( 14) | 282( 19) | -30( 25) | -7( 29) | 54( 28) |
| C2 | 48744(27) | 19053(27) | 31333(28) | | 181( 17) | 238( 17) | 381( 20) | 68( 29) | 71( 31) | -124( 33) |
| C3 | 36743(27) | 38345(27) | 35561(28) | | 256( 18) | 188( 17) | 292( 19) | 59( 29) | -46( 33) | 18( 31) |
| C4 | 33296(27) | 50974(24) | 43687(27) | | 266( 18) | 139( 14) | 241( 18) | 23( 28) | -42( 31) | -25( 27) |
| C5 | 42516(27) | 62845(24) | 41399(29) | | 200( 17) | 166( 15) | 301( 20) | -18( 27) | -8( 31) | -97( 29) |
| C6 | 59282(25) | 65054(26) | 32387(27) | | 155( 16) | 201( 16) | 263( 19) | 22( 27) | 39( 30) | 108( 30) |
| C7 | 63620(28) | 35600(26) | 34749(29) | | 273( 19) | 163( 16) | 314( 21) | 59( 26) | -77( 34) | 17( 31) |
| C8 | 66769(30) | 23279(28) | 43290(33) | | 200( 19) | 191( 16) | 271( 21) | 3( 30) | 9( 34) | 58( 34) |
| CM1 | 68728(30) | 6696(29) | 31219(31) | | 263( 20) | 246( 20) | 385( 22) | 86( 33) | -11( 35) | -222( 35) |
| CM2 | 42970(31) | 8600(30) | 39737(32) | | 257( 20) | 272( 20) | 367( 23) | -150( 34) | 155( 36) | 50( 37) |
| CM3 | 33320(35) | 38825(32) | 24836(32) | | 303( 26) | 369( 23) | 252( 21) | 202( 40) | -254( 38) | -78( 41) |
| CM4 | 21360(34) | 45611(32) | 47466(35) | | 364( 26) | 296( 23) | 459( 27) | -18( 38) | 905( 44) | 13( 42) |
| CM5 | 32819(31) | 69281(29) | 34494(34) | | 203( 20) | 186( 17) | 413( 26) | 58( 32) | 108( 38) | 235( 36) |
| CM6 | 58018(32) | 62977(32) | 43483(34) | | 315( 23) | 328( 23) | 391( 26) | -58( 36) | -234( 48) | 279( 40) |
| CM7 | 66739(32) | 43997(38) | 24489(38) | | 328( 23) | 326( 22) | 224( 28) | 114( 37) | 163( 35) | 5( 37) |
| CM8 | 77972(32) | 29854(38) | 48336(31) | | 281( 21) | 270( 21) | 344( 23) | -40( 34) | -292( 37) | 120( 37) |
| CC1 | 69905(27) | 17986(26) | 37865(27) | | 189( 17) | 181( 16) | 219( 19) | 55( 28) | -16( 38) | 66( 29) |
| CC2 | 53026(27) | 15588(26) | 34838(29) | | 180( 17) | 148( 15) | 257( 19) | 25( 27) | 19( 30) | -68( 29) |
| CC3 | 40602(26) | 26125(26) | 35389(28) | | 198( 17) | 219( 19) | 237( 19) | 59( 30) | 9( 32) | -86( 32) |
| CC4 | 29560(29) | 38951(26) | 39839(28) | | 253( 19) | 151( 16) | 216( 18) | 67( 29) | -25( 32) | 57( 30) |
| CC5 | 38654(28) | 57222(26) | 39044(27) | | 281( 18) | 186( 16) | 204( 18) | 16( 29) | 56( 30) | -13( 29) |
| CC6 | 47464(26) | 58952(26) | 36073(28) | | 168( 16) | 167( 15) | 232( 18) | 6( 28) | -31( 30) | 1( 29) |
| CC7 | 59450(26) | 47547(27) | 35485(28) | | 171( 17) | 185( 17) | 204( 18) | 13( 28) | -69( 31) | -6( 29) |
| CC8 | 70287(29) | 35365(26) | 39767(28) | | 231( 18) | 156( 16) | 223( 19) | 56( 29) | 14( 31) | -74( 30) |
| H11 | 5748(24) | 1266(23) | 4381(27) | 1,02(1,13) | | | | | | |
| H12 | 5712(25) | 663(25) | 3848(24) | 1,04(1,10) | | | | | | |
| H21 | 3562(26) | 1703(25) | 3170(25) | 1,86(1,10) | | | | | | |
| H22 | 4270(25) | 1981(23) | 2845(27) | 2,93(1,00) | | | | | | |
| H31 | 3686(25) | 4244(25) | 3154(25) | 2,77(1,10) | | | | | | |
| H32 | 4105(27) | 3914(24) | 3877(25) | 4,08(1,11) | | | | | | |
| H41 | 3803(26) | 4946(24) | 4171(24) | 4,08(1,13) | | | | | | |
| H42 | 3354(25) | 5238(24) | 4906(26) | 3,42(1,11) | | | | | | |
| H51 | 4362(25) | 6865(24) | 4595(26) | 1,62(1,10) | | | | | | |
| H52 | 4448(26) | 6725(26) | 4222(24) | 2,30(1,11) | | | | | | |
| H61 | 6429(26) | 5675(24) | 3229(25) | 3,16(1,11) | | | | | | |
| H62 | 5714(25) | 5469(23) | 2653(25) | 4,44(1,12) | | | | | | |
| H71 | 6393(25) | 3196(25) | 3805(25) | 3,35(1,11) | | | | | | |
| H72 | 5874(27) | 3450(25) | 3773(25) | 2,39(1,10) | | | | | | |
| H81 | 6227(27) | 2468(26) | 4244(25) | 3,01(1,15) | | | | | | |
| H82 | 6889(25) | 2119(25) | 4825(27) | 2,79(1,19) | | | | | | |

*Table 2.* Observed and calculated structure factors on 10 times absolute scale.

*Table 2. Continued.*

```
  1  799  743      8  199  195     14  154  157     11  192  176      0  543  557    H= 9,K= 5     H= 6,K= 12      9  266  268
  2   84  100     11  144  136     16  110  117     12  576  581      3  146  149    1 1300 1228     1  138  105    10  248  233
  3  796  689     13  295  275     19  158  129     13  105  104      4  368  365     2  931  933     2  445  468    11  142  176
  4 1143 1042     15  122   78    H= 4,K= 2        14  687  701      7  166  156     4  416  351     3  219  294    13  108   95
  5  982  985     17  163  149     0  591  536     17  167  158      8  134  114     5  853  815     5  473  496    14  111  123
  6  694  689    H= 3,K= 13       1  625  674     18  107   62      9  128  107     6  736  704     7  144  111    15  217  243
  7  110  123     1  164  148     2  618  639     20  138  110     13  176  151     7  343  301     8  335  350    17  123  107
  8  128  202     2  193  202     3 1408 1371    H= 4,K= 9         15  186  188     8  352  319     9  126   54    H= 6,K= 3
  9  806  854     5  199  188     4  158  132      1   93   65    H= 4,K= 18        9  729  756    11  347  388     0  177  241
 10  478  458     6  450  505     5 2050 2010      2  296  282      0  113  124    10  490  533    12  161  155     1  815  782
 11  465  502     7  353  347     7  850  802      3  303  323      1  219  230    11  164  145    13  300  258     2  860  761
 12  240  240     9  109  109     6  173  173      4  432  512      3  115  117    12  132  104    H= 5,K= 13      3  154  110
 14  209  250    10  371  398     9  987 1032      6  342  343     10  161  142    13  265  261     1  127  190     4  204  176
 15  428  420    12  156  150    11 1058 1062      7  154  178     13  129  144    14  254  260     2  609  611     5  540  502
 19  138  120    15  169  155    12  104   76      8  108   83    H= 4,K= 19       15  269  293     3  253  260     6  191  193
 21  122   86    19  109   28    13  381  382      9  495  507      1  350  308    16  146  134     5  165  121     7  343  294
 H= 3,K= 6       H= 3,K= 14      14  137  154     10  190  183      3  131   79    17  120  128     8  115  152     8  237  202
  1  534  479     1  101  109     15  312  303     12  107  110      4  176  166    18  284  270     9  220  229     9  204  197
  2  287  320     2  162  179     17  301  309     14  133  159      5  116  138    H= 5,K= 6      10  378  387    10  210  224
  3  148  148     4  579  531     19  199  207    H= 4,K= 10        6  137   97     1  150  177    12  268  268    11  192  216
  4  673  625     5  149  138    H= 4,K= 3         0  178  190      8  135  126     2  794  840    13  122  112    12  421  398
  5  369  361     7  103  117     2 1194 1158      1  755  755    H= 4,K= 20       3  355  362    H= 5,K= 14     13  271  276
  6  136  152     8  140  170     3 1334 1280      2  216  254      0  568  552     4  153  217     1  139  162    14  161  185
  8  354  336    11  139  142     4  866  725      3  482  484      3  120  121     5   86   49     2  613  623    15  235  242
 11  173  192    14  155  154     5  472  583      4  105   84      4  190  162     6  476  435     3  211  211    16  255  242
 14  354  370    H= 3,K= 15      6  478  515      8  181  155      5  120   99     7  383  403     4  349  339    18  195  177
 15  181  164     1  622  656     8  760  724     10  114  123    H= 4,K= 21       8  517  551     6  479  479    H= 6,K= 4
 18  321  300     2  410  434     9  894  877     15  224  200      0  207  190     9  169  140     8  186  197     0  309  247
 19  105  101     3  235  256    10  179  202     17  284  249      8  128  113    10  556  564    11  122  104     1  145  137
 H= 3,K= 7       5  226  231    11  312  341     19  127  109     10  175  164    11  267  237    16  155  124     2  922  932
  1  607  637     6  186  162    12  373  362    H= 4,K= 11       11  214  192    12  261  261    H= 5,K= 15      3  244  247
  2  294  333     7  103   70    14  380  379      0  921  926    H= 4,K= 22       13  254  260     1  144  178     4  338  346
  3  104  136    10  109  118    15  269  278      1  577  586      6  121  136    15  127  111     4  197  150     5  622  601
  4  222  237    14  156  143    16  109  142      2  279  264      9  203  191    16  189  227     5  204  207     6 1281 1248
  5  746  673    H= 3,K= 16      17  199  196      3  155  179    H= 4,K= 23       17  323  301     6  152  147     7  300  316
  6 1000  969     1   99   28    H= 4,K= 4         4  242  232      0  368  317    18  133  106    11  134  149     8  493  507
  7  462  490     2  309  314     1  345  326      5  170  125      3  123  109    H= 5,K= 7      H= 5,K= 16      9  295  315
  9  429  466     3  413  431     3  824  790      6  372  387    H= 4,K= 24       1  314  316     3  197  209    10  333  346
 10  188  222     4  323  343     4  516  546      7  193  216      1  123   99     2  156  202     4  118  131    14  224  220
 12  577  604     5   99   69     5  388  371      8  204  205    H= 5,K= 0         3  171  145     5  255  251    16  199  179
 13  364  388     7  288  317     6  304  315      9  100  118      4  236  246     5 1172 1150     7  228  216    18  241  232
 14  319  309     8  198  216     8  183  196     10  519  562      6   99  110     6  860  874    16  156  156    19  154  174
 16  215  215     9  140  113    10   88   93     11  372  372      8  211  199     7  107   95    H= 5,K= 7      H= 6,K= 5
 H= 3,K= 8      12  113  138    11  194  194     12  178  177     10  426  414     9  129  148     1  154  169     0  242  223
  1 1812 1867    10  126  109    12  175  200     13  259  278     16  220  251    10  141   98     2  262  272     2   97   61
  2  495  477    16  182  125    16  170  170     14  240  250     18  116   43    11  316  312     3  189  175     3  347  354
  3  655  668    H= 3,K= 17      17  210  218     15  193  185     20  308  287    12  263  241     4  248  244     4  283  307
  4  551  566     1  150  159     19  148  153    H= 4,K= 12      H= 5,K= 1       13  448  453     7  147  134     5  323  289
  5  796  792     2  131  167     21  128   91      0  121  151     2  678  643    15  167  160    10  121  163     6  453  442
  6  197  212     3  169  212    H= 4,K= 5         1  177  189     3  878  974    16  183  150    H= 5,K= 18      7  425  410
  7  203  189     4  263  272     0  741  641      2  137  132     4 1598 1555    18  183  109     3  116  211     8  328  205
  8  346  354     6  218  245     1  148   76      3   92   84     5 2244 2070    19  109   88     4  164  149     9  502  477
  9  288  321     8  198  216     2  218  158      4  892  946     6  338  329    20  181  131     5  157  145    10  176  192
 12  216  176     9  140  113     3  472  431      7  192  200     7  427  412    H= 5,K= 2        6  240  212    11  157  217
 14  375  382    12  113  138     4  646  660      8  774  781     8  822  844     1  679  688     8  178  159    12  116   85
 15  138  148    H= 3,K= 18      5  379  424     13  105   60      9  565  566     2   86  119     11  190  183    13  144  126
 16  202  218     2  341  325     8  501  515     16  171  147    10  427  439     3  434  402    H= 5,K= 19      14   97   99
 17  223  210     5  105  117    10  127  120    H= 4,K= 13      12  285  293     4  133  128     1  255  284    15  219  219
 18  185  197     8  146  169    11  406  402      0  113  137    16  165  167     5  502  517     4  121  136    16  119   69
 H= 3,K= 9      H= 3,K= 0        12  223  234      1  465  456    17  231  214     7  284  280     5  292  287    H= 6,K= 6
  1  215  206     1  182  175    13  207  223      2  164  200    19  283  264     8  182  183     7  180  146     0 1009 1004
  2  511  508     3  106  109    14  136  142      3  249  229    20  197  192    11  166  144    H= 5,K= 20      1  899  912
  3  300  269     7  195  181    17  216  203      5  309  343    H= 5,K= 2      12  354  351     1  112  117     2  481  482
  5  162  140    H= 3,K= 21      H= 4,K= 6         7  262  280     1  186  186    13  148  179     2  233  228     3 1448 1511
  6  437  442     4  139  122     0  441  413      8  190  195     2   75   44    14  373  390     5  190  168     4  456  498
  7  127  169     5  117  111     1  220  288     10  201  251     4 1720 1736    15        ...     H= 6,K= ...    5  584  567
  8  175  230     9  116  111     2  287  233     12  117   67     7  105  113    ...             ...              6  189  218
  9  129  107    H= 3,K= 0        3  476  396     13  197  228    11 1211 1237    ...             ...              7  393  301
 11  112  107     1  156  149     6  697  693     15  219  205     9  142  107    ...             ...              9  443  441
 12  204  242     2  462  490     6   96  120    ...              11  107   96    ...             ...             10  188   66
 13  174  163     5  203  198     7 1340 1397    ...              12  148  168    ...             ...             12  469  453
 14  200  239     6  307  384    H= 3,K= 21      ...              13  215  240    ...             ...             13  443  475
 16  106   77    H= 4,K= 7        9  102   97    ...              14  281  292    ...             ...             14  113  111
 17  162  121     1  156  149    ...             ...              16  116  113    ...             ...             15  140  162
 18  173  148     9  116  111    11  122  136    ...              17  203  272    ...             H= 6,K= ...    H= 6,K= 7
 H= 3,K= 0       H= 3,K= 0       13  134  144    ...              21  190  194    ...             ...              1 1394 1416
  1  469  488     1  156  149    13  215  246    ...             H= 5,K= 3       ...             ...              2  998 1012
  2  906  878     2  462  490    14  112  113    ...              1  416  396    ...             ...              3  804  289
  4  526  481     5  203  198    16  119  108    ...              2  642  601    ...             ...              5  303  202
  5  109  114     6  307  384    H= 4,K= 7       ...              3  636  586    ...             ...              6  437  419
  6  162  120     8  175  182    0  899  929    ...              4  170  158    ...             ...              8  213  219
  7  340  341    H= 3,K= 0       1  384  381    ...              5  590  578    ...             ...              9  138   88
 10  259  242     1  137  184    3  647  640    ...              6  344  281    ...             ...             10  263  219
 11  108  138     3  167  173    6  184  240    H= 5,K= 10       ...             ...             ...             11  261  281
 13  125  115     7  210  181    6  344  353    0  340  384    ...             ...             ...             13  365  369
 14  291  232    H= 4,K= 0       7  274  265    1  294  315    ...             3 1401 1434    ...             14  643  667
 H= 3,K= 11      1  513  422    8  263  252    2  228  247    ...              4  185  196    ...             15  605  608
  1  142  200    2 1376 1293    10   91   65    3  282  282    ...              6  96  131    ...             16  517  508
  2  193  195    6  165   72    12  290  278    4  636  677    ...              7  214  242    ...             18  183  174
  3  432  451    8  701  607    12  238  233    7  172  175    20  138  144    ...              8  234  271    19  144  142
  4  262  252   10  291  330    13  542  540    8  141  155    ...              9  212  219    ...             H= 6,K= ...
  5  425  415   12  730  766    15  436  443    9  209  208   H= 5,K= 11       ...             ...              3  140   45
  6  529  493   16  393  403    15  209  172   10  327  342    1 1198 1143    ...              9  240  240    ...             1  109  110
  7  568  537   20  200  161    17  193  198   12  109  131    3  121  121    ...             10  316  337    ...             2  102  182
  8  231  241   H= 4,K= 1       18  258  268   13  145  129    3 2582 2484    ...             11  106  162    ...             3   83   90
  9  342  349    0 2203 2086   19  153  134    0  772  736    4  536  553    ...             14  122  136    ...             7  756  723
 10  162  161    1  977  930   H= 4,K= 8        1  358  342    6  158  187    ...              5  291  289    ...             13  154  164
 11  275  323    2  954  904    0 1873 1833    3  367  386    8  170   69    ...              8  397  413    ...             16  447  441
 12  196  186    3 3172 1849    1  231  226    4  337  413    9  403  413    ...              3  493  478    ...             17   89  130
 13  155  141    4 1741 1634    2  636  800    5  189  205   12  240  235    ...              8  214  242    ...             19  193  196
 16  132  127    5  723  658    4  920  905    6  101   84   13   98  132    ...              8  234  316    H= 6,K= ...    11  178  196
 19  170  120    6  460  492    5   97   29   10  168  150   16  266  492    ...              9  208  184    ...             14  303  316
 H= 3,K= 12      H= 4,K= 1       7  152  169   11  170  112   16  484  492    ...             11  116  110    ...             18  108  131
  2  153  156    8  156  146    9  248  621   12  230  192   13  383  349    ...             H= 6,K= ...    13  108   98    H= 6,K= 9
  5  266  225   10  418  430   11  225  236   16  111   65   19  100   94   ...              0  980  845
  6  140  157   11  225  236   13  129  147   10  521  512   21  242  237   17  228  220     7  797  773     1  737  710
  7  337  357                                                                                               2  445  453
```

*Table 2. Continued.*

*Table 2. Continued.*

```
H= 10,K= 3        4  479  492     4  281  299    10  109  104    13  119  125     4  112  107     4  214  212    17  179  174
 0  619  617      5  208  257     5  267  273    14  186  150   H= 12,K=  6      6  121   40     5  101   82   H= 14,K=  5
 1  683  698      6  314  332     7  286  296   H= 11,K= 12      0  155  123    H= 13,K=  0      6  357  370     0  527  544
 2  241  261      8  140  133     8  111  128     1  370  357     1  134  102     2  196  193     7  263  304     1  527  533
 3  262  226     11  101   86    10  357  379     2  331  339     4  201  232     4  245  267     8  217  174     2  356  364
 4  259  219     13  108  115    11  193  183     4  101   98     7  632  681     6  144  160    11  122  141     4  247  239
 6  705  706     14  116  118    12  329  322     5  394  368     8  103  122     8  141  126    16  111   80     5  645  673
 7  519  539     16  178  179    13  133  149     7  425  452    11  219  243    10  301  315   H= 13,K= 10      6  475  453
11  243  246    H= 10,K= 12     14  311  291     9  307  312    19  219  186    12  200  180     1  157  200     8  329  301
13  144  140      2  296  298   H= 11,K=  4     11  353  321   H= 12,K=  7      14  220  198     2  126  132    10  220  221
15  185  182      4  145  155     1  811  847   H= 11,K= 13      1  284  300    16  113  113     4  277  292    11  280  243
18  100  122      6  175  173     2  122  100     1  176  187     3  547  550   H= 13,K=  1      5  186  171    13  179  162
19  197  175      8  138  139     3  417  421     2  520  524     4  310  305     1  100   72     6  672  648    17  177  158
H= 10,K=  4     H= 10,K= 13     4   94   83     3  163  172     5  105   86     2  267  246     7  117   89   H= 14,K=  6
 0  830  868      0  212  208     5  594  593     5  160  190     7  511  538     3  126   94     8  182  193     0  107   73
 2  225  217      1  188  165     7  218  224     6  277  268     8  326  302     4  203  226    10  207  175     1  315  309
 3  160  186      3  123  181     8  222  239     7  147  165     9  112   93     5   87   17    14  290  283     3  745  746
 4  743  740      5  112  141     9  150  196     8  188  174    10  250  238     7  350  367   H= 13,K= 11      8  395  394
 5  218  220      7  199  209    10  105  116    12  339  323    11  110  129     8  257  256     1  293  293     7  115  176
 6  715  689      8  184  171    11  130  138   H= 11,K= 14     13  112   59     9  380  387     3  197  210     8  106  124
 7  276  273      9  389  370    12  240  250     1  173  157   H= 12,K=  8     11  103  118     4  281  281     9  322  329
 8  540  546     10  123  111    14  127  134     2  547  588     0  371  375    13  320  293     5  144  146    12  121  145
10  622  623     11  113   89    15  114   62     4  186  157     1  140  146    14  120  108     8  166  175   H= 13,K= 12
12  181  190     17  128   90    17  116  163     5  185  195     2  330  363    17  103  122   H= 14,K=  7
13  155  135    H= 10,K= 14    H= 11,K=  5      8  131  111     5  204  193    H= 13,K=  2      1  489  499     0  918  936
14  201  207      0  220  245     1  251  278    11  182  205     6  280  290     2  444  463     2  362  364     1  447  465
17  251  226      2  147  140     2  235  262    14  114  100     8  543  551     4  406  415     3  626  606     4  463  472
H= 10,K=  5      3  185  204     3  446  429   H= 11,K= 15     10  376  357     6  283  310     4  170  180     5  233  222
 0  167  222      5  131  129     4  536  514     1  103   86    12  218  241     7  126  129     6  259  240     8  153  148
 1  135  180      6  259  268     5   90   46     2  150  181    16  316  297    11  304  302     7  159  172     9  175  201
 2  107  109      9  126  101     7  270  271     3  116   95   H= 12,K=  9     12  236  225     8  211  231    10  217  187
 3  124   92     10  131  142     8  601  629     5  251  274     0  510  508    15  211  199     9  121  109    11  171  196
 4  359  384     11  286  290     9  248  261     9  175  187     1  301  313    17  144  112    10  130  112    12  156  150
 5  231  195    H= 10,K= 15     12  315  318    14  116   33     2   97   82    H= 13,K=  3     11  110  124    13  183  163
 6  348  361      0  602  616    14  184  153   H= 11,K= 16      3  176  184     1   96   77    14  108   81    15  184  179
 7  140  138      1  287  293    15  152  141     1  138  164     4  446  461     2  329  354    H= 13,K= 13    H= 14,K=  8
 8  281  276      2  156  141    16  273  271     4  110   99     5  129  141     3  382  384     2  247  264     0  482  483
 9  251  233      4  479  467    17  102  116    13  115   96     6  222  215     5  139  127     5  180  184     2  266  306
11  419  473      5  259  245    18  159  122   H= 11,K= 17      8  390  388     6  399  406     6  138   92     4  406  397
13  315  309    H= 10,K= 16    H= 11,K=  6      1  109  131    11  160  159     7  161  186     7  142  140     8  184  193
14  116  112      0  110   82     2  418  403     2  141  145    13  105   25    10  432  422     9  129   98    11  122   99
15  155  127      1  211  226     3  163  181     3  131  148    15  161  132    13  145  111   H= 13,K= 14    13  178  188
16  164  119      2  160  132     4  538  582   H= 11,K= 18    H= 12,K= 10     14  139  143     1  301  331    H= 14,K=  9
21  159  156      3  201  224     6  518  515     4  202  187     0  216  204    H= 13,K=  4      5  146  127     0  420  427
H= 10,K=  6      4  133  111     7  316  318     6  110  115     3  591  634     1  592  594   H= 13,K= 15     1  340  340
 1  119  105      6  140  139     9  166  179   H= 11,K= 19      4  496  487     2  128  144     4  103  104     3  325  107
 2   92   42      7  108  128    10  217  216     5  234  201     6  116  123     3  238  236     6  134  120     8  210  206
 5  330  364     10  262  226    11  148  134   H= 12,K=  0      7  516  521     4  128  151   H= 13,K= 16     9  203  198
 7  775  787     14  171  138    13  115  138     0  485  482    11  108   99     5  688  707     3  104  114    12  142  126
 8  228  234    H= 10,K= 17     16  196  174    16  196  174    16  158  129     7  280  286   H= 13,K= 17    15  213  213
11  162  169      3  272  244    18  114   80     4  356  342   H= 12,K= 11      8  127  109     2  238  208    16  120  136
12  264  272      4  154  133    19  164  132     6  820  793     0  276  263     9  223  201     4  110   92    17  196  195
13  373  378      6  194  176    20  222  203     8  398  431     1  338  356    11  551  556   H= 13,K= 18    H= 14,K= 10
15  157  205     10  112  102   H= 11,K=  7     10  363  363     3  535  561    13  468  439     1  140  100     1  140  100
16  127  140    H= 10,K= 18     1  454  459    12  306  326     4  195  165    17  246  223     4  160  141     2  104   88
18  135  125      3  198  181     2  231  235    14  115  125     5  165  165    19  161  152   H= 13,K= 19     5  319  318
H= 10,K=  7      7  122  136     3  240  247   H= 12,K=  1      6  265  300    H= 13,K=  5     1  147  124     6  160  172
 0  522  507     11  114  114     4  174  171     1  287  293     7  299  303     1  297  288   H= 14,K=  0      9  161  152
 1  104   73    H= 10,K= 19     6  382  419     2  347  344    10  232  217     2  835  866     0   96   93   H= 14,K= 11
 4  231  216      0  414  450     9  453  450     4  198  219    14  108  149     3  631  623     2  831  875     0  869  579
 6  153  103      1  240  213    11  164  143     6  121  126   H= 12,K= 12      4  358  369     3  345  325     1  146  183
 7  202  208      4  127  169    15  191  169     7  245  246     1  146  146     5  439  439     6  278  272     2  335  328
 8  256  267    H= 10,K= 20    16  167  163     8  293  293     2  245  267     6  338  321     8  207  225     4  346  328
 9  261  249      9  143  126   H= 11,K=  8      9   94   54     3  148  133     7  324  342    10  372  364     5  132  136
11  113  111    H= 10,K= 22     1  335  366    10  102   94     4  119  122     8  223  201    14  161  172     6  169  197
12  149  134      0  136  122     2  237  254    15  120  122     5  197  209     9  228  218   H= 14,K=  1    H= 14,K= 13
14  110  124      3  125   66     4  198  188   H= 12,K=  2      6  155  173    11  235  247     0  224  265    12  121   83
H= 10,K=  8    H= 11,K=  0      5  201  195     1  378  402     7  175  167    12  116   72     1  103  119    H= 14,K= 12
 0  259  296      2  274  309     6  146  141     3  476  492     8  137  124    13  115   96     2  173  184     0  798  798
 1  179  178      4  217  200     7  130  111     5  198  180    11  121   97    14  151  102     3  384  378     1  78  173
 2  568  578      8  247  277     8  240  257     7  294  334    13  118  113    15  172  135     4  278  272     2  336  352
 3  146  140     10  116  114     9  477  462     9  201  200   H= 12,K= 13    18  111  118     5  130  152     3  112   72
 4  186  169     12  165  184    10  199  214    10   97   33     0  489  479   H= 13,K=  6      6  111  102     4  346  328
 8  106  130     16  138  114    12  189  178   H= 12,K=  3      1  418  440     1  150  145     7  189  199     5  132  136
12  129  133    H= 11,K=  1     13  189  149     0  337  333     2  203  207     2  289  307     8  204  180     6  169  197
13  155  146      1  468  430    14  128  131     1  122   91     3  318  306     3  141  123     9  131  141    H= 14,K= 13
14  121  103      2  712  329    15  233  216     2  126  173     4  116  153     4  594  606    10  168  148     0  393  346
17  115  132      3  479  490    19  176  164     4  140   79     7  164  153     6  239  256    13  201  188     1  323  316
18  164  124      5  148   93   H= 11,K=  9     5  332  339     8  103   78     8  708  718    15  147  161     5  223  213
20  187  162      6  610  400     4  135  118     6  276  261   H= 12,K= 14     10  272  272   H= 14,K=  2      7  363  357
H= 10,K=  9      7  290  264     5  357  378     7  258  260     0  193  220    12  324  320     0  170  178     8  300  277
 0  297  280      8   96   85     6  199  195     8  168  227     1  437  447    16  107  148     1  334  336     9  141  159
 1  375  395     10  452  472     7  253  266     9  492  516     3  536  636   H= 13,K=  7      5  553  553    10  135  149
 3  378  376     11  248  213     8  153  145    10  378  416     4  114  109     1  417  437     7  679  700    11  136  150
 4  126  104     12  112   90     9  199  229    11  424  438     6  453  438     2  430  447     9  418  415    H= 14,K= 14
 5  413  431     13  299  302    10  135  149    12  291  317     6  142  137     3  134  134    11  348  313     0  124   74
 6  457  485     14  148  192    12  152  152    14  161  182   H= 12,K= 15     4  137  136    13  137  181     7  158  158
 7  195  214     15  148  123    13  191  172   H= 12,K=  4     1  245  287     5  118  102    15  208  200   H= 14,K= 15
 8  155  169     18  168  158   H= 11,K= 10     0  228  249     2  144  132     6  334  356   H= 14,K=  3     1  139  117
 9  351  362     19  161  169     2  547  554     2  311  322     4  169  141     7  165  182     0  263  180     8  123  113
10  114  102    H= 11,K=  2     3  212  211     4  195  203     6  138  122     8  245  262     3  148  118    10  171  154
11  283  273      2  171  144     4  546  608     6  484  488    11  131  117    10  280  276     4  307  301    H= 14,K= 16
18  110  114      3  116  132     5  141  131     9  154  166    11  149  123   H= 13,K=  8     5  190  166     1  112  112
H= 10,K= 10     H= 15,K=  0      6  394  416    10  456  458   H= 14,K= 16     1  284  275     7  168  169     4  180  236
 1  488  499      5  102   98     7  122  143    11  164  151     0  295  293     2  235  266     8  771  790     5  167  195
 2  122  100      6  391  392     8  216  275    12  153  148    10  335  316     3  676  614     9  460  445     7  123  100
 3  144  118     10  108  196     9  144  134    14  209  243    H= 14,K= 17     5  352  381    10  384  387     9  194  174
 5  194  195     10  108  132    11  174  163    17   99   87     1  154  118     6  290  298    11  167  150    H= 14,K= 17
 7  113  112     11  324  359    12  333  292   H= 12,K=  5     11  207  214     8  108  126    12  189  153     1  170  150
 8  130  133     12  136  164    15  185  162     0  193  145    11  160  138     9  216  247    13  118  123     8  130  117
11  215  241     14  182  196    18  152  152   H= 11,K= 11     1  411  386    10  206  271    14  219  237    H= 14,K= 18
14  118  105     15  222  202   H= 11,K= 16     2  283  280     1  308  301    11  196  196    H= 14,K=  4     0  180  163
15  281  265     16  105   76     1  299  291     4  179  170     5  203  197    15  196  196     4  112  108    H= 15,K=  0
H= 10,K= 11    H= 11,K=  3     2  142  117     6  237  281   H= 13,K= 20     1  192  203     7  121  129     8  132  160
 0  440  473      1  435  408     3  281  285     8  233  229     0  195  185     2  268  292    11  156  166    12  131  144
 2   99  144      2  327  298     6  337  353     9  324  352     2  138  116     3  118  154   H= 15,K=  1
 3  208  241      3  151  143     7  282  300    11  197  210     3  160  154
```

*Table 2. Continued.*



The structure was solved by direct methods and refined by full-matrix least squares technique. Methylene hydrogen atom positions were calculated assuming C−H bond lenghts of 1.0 Å. Neither the methyl nor the water hydrogens could be localized in the difference Fourier map, and are not included in the calculations. Anisotropic temperature factors were introduced for O, N, and C-atoms, and weights in least squares were calculated from the standard deviations in intensities, $\sigma(I)$, taken as

$$\sigma(I) = [C_T + (0.02 C_N)^2]^{\frac{1}{2}}$$

were $C_T$ is the total number of counts and $C_N$ the net count (peak minus background). The conventional $R$-value arrived at was 7.2 % (weighted value $R_w = 7.7$ %) for 3471 observed reflections. The form factors used were those of Hanson et al.[6] except for hydrogen.[7] Final fractional coordinates and thermal vibration parameters are given in Table 1. The expression for anisotropic vibration is:

$$\exp - (B11h^2 + B22k^2 + B33l^2 + B12hk + B13hl + B23kl)$$

A comparison between observed and calculated structure factors is presented in Table 2.

The principal axes of the thermal vibration ellipsoids for oxygen, nitrogen, and carbon atoms were calculated from the temperature parameters of Table 1. Maximum root mean square amplitudes range from about 0.20 Å for carbonyl carbons to about 0.30 Å for methyl carbon atoms and water oxygens. Due to the size of the molecule, no rigid-body analysis of translational and librational motion has been carried out.

Interatomic distances, bond angles, and dihedral angles are given in Table 3. The standard deviations, given in parentheses, are estimated from the correlation matrix of the last least squares refinement cycle. Fig. 1 shows the molecule viewed along [001].
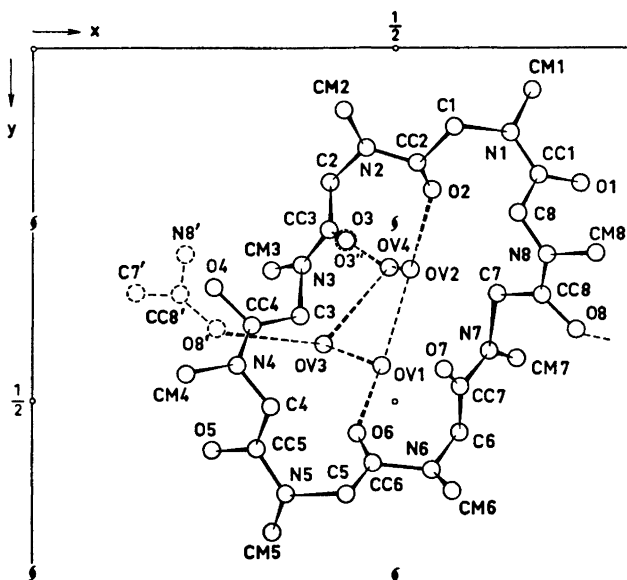


*Fig. 1.* The molecule viewed along [001].

By averaging bond distances of Table 3, and comparing with the results of the corresponding dimeric [4] and tetrameric [5] compounds, no significant differences are observed:

| Distance | Cyclodisarcosyl | Cyclotetrasarcosyl | Cyclooctasarcosyl |
|---|---|---|---|
| CC − CM | 1.506 Å | 1.531 Å | 1.527 Å |
| CC − N | 1.348 Å | 1.358 Å | 1.344 Å |
| CC − O | 1.234 Å | 1.225 Å | 1.228 Å |
| C − N | 1.455 Å | 1.458 Å | 1.456 Å |
| CM − N | 1.475 Å | 1.467 Å | 1.483 Å |

*Table 3.* Interatomic distances, bond angles and dihedral angles with estimated standard deviations.

| DISTANCE | (Å) | DISTANCE | (Å) | DISTANCE | (Å) |
|---|---|---|---|---|---|
| O1 - CC1 | 1.227( 5) | O2 - CC2 | 1.234( 5) | O3 - CC3 | 1.231( 5) |
| O4 - CC4 | 1.222( 5) | O5 - CC5 | 1.219( 5) | O6 - CC6 | 1.233( 5) |
| O7 - CC7 | 1.227( 5) | O8 - CC8 | 1.230( 5) | N1 - CM1 | 1.488( 6) |
| N2 - CM2 | 1.479( 6) | N3 - CM3 | 1.488( 6) | N4 - CM4 | 1.483( 6) |
| N5 - CM5 | 1.481( 6) | N6 - CM6 | 1.487( 6) | N7 - CM7 | 1.487( 6) |
| N8 - CM8 | 1.482( 6) | N1 - C1 | 1.454( 6) | N2 - C2 | 1.462( 6) |
| N3 - C3 | 1.454( 6) | N4 - C4 | 1.440( 6) | N5 - C5 | 1.451( 6) |
| N6 - C6 | 1.466( 6) | N7 - C7 | 1.452( 6) | N8 - C8 | 1.447( 6) |
| N1 - CC1 | 1.352( 6) | N2 - CC2 | 1.352( 6) | N3 - CC3 | 1.339( 6) |
| N4 - CC4 | 1.340( 6) | N5 - CC5 | 1.350( 6) | N6 - CC6 | 1.338( 6) |
| N7 - CC7 | 1.345( 6) | N8 - CC8 | 1.338( 6) | C1 - CC2 | 1.519( 7) |
| C2 - CC3 | 1.520( 7) | C3 - CC4 | 1.536( 7) | C4 - CC5 | 1.531( 7) |
| C5 - CC6 | 1.520( 7) | C6 - CC7 | 1.526( 7) | C7 - CC8 | 1.529( 7) |
| C8 - CC1 | 1.531( 7) | OV1 - OV2 | 2.787( 6) | OV1 - OV3 | 2.743( 6) |
| OV2 - O2 | 2.814( 5) | OV3 - O8' | 2.868( 6) | OV2 - OV4 | 2.928( 7) |
| OV4 - O3' | 2.883( 6) | O6 - OV1 | 2.791( 5) | OV3 - OV4 | 2.864( 6) |

| ANGLE | (°) | ANGLE | (°) |
|---|---|---|---|
| O1 - CC1 - N1 | 121.94(46) | O2 - CC2 - N2 | 121.79(46) |
| O3 - CC3 - N3 | 122.55(47) | O4 - CC4 - N4 | 121.98(48) |
| O5 - CC5 - N5 | 122.93(46) | O6 - CC6 - N6 | 121.99(45) |
| O7 - CC7 - N7 | 121.72(47) | O8 - CC8 - N8 | 121.76(46) |
| O1 - CC1 - C8 | 120.64(46) | O2 - CC2 - C1 | 121.26(43) |
| O3 - CC3 - C2 | 120.92(48) | O4 - CC4 - C3 | 120.86(46) |
| O5 - CC5 - C4 | 120.71(45) | O6 - CC6 - C5 | 120.02(43) |
| O7 - CC7 - C6 | 121.16(47) | O8 - CC8 - C7 | 120.51(45) |
| CM1 - N1 - C1 | 116.87(41) | CM2 - N2 - C2 | 118.99(43) |
| CM3 - N3 - C3 | 116.31(43) | CM4 - N4 - C4 | 116.68(44) |
| CM5 - N5 - C5 | 116.28(41) | CM6 - N6 - C6 | 118.06(41) |
| CM7 - N7 - C7 | 116.89(43) | CM8 - N8 - C8 | 117.33(43) |
| CM1 - N1 - CC1 | 119.15(39) | CM2 - N2 - CC2 | 123.68(43) |
| CM3 - N3 - CC3 | 124.64(43) | CM4 - N4 - CC4 | 118.37(43) |
| CM5 - N5 - CC5 | 119.18(42) | CM6 - N6 - CC6 | 122.83(43) |
| CM7 - N7 - CC7 | 124.27(42) | CM8 - N8 - CC8 | 118.28(42) |
| C8 - CC1 - N1 | 117.36(42) | C1 - CC2 - N2 | 116.88(44) |
| C2 - CC3 - N3 | 116.53(44) | C3 - CC4 - N4 | 117.24(45) |
| C4 - CC5 - N5 | 116.23(43) | C5 - CC6 - N6 | 117.98(44) |
| C6 - CC7 - N7 | 117.11(43) | C7 - CC8 - N8 | 117.73(44) |
| CC1 - N1 - C1 | 123.68(42) | CC2 - N2 - C2 | 116.76(44) |
| CC3 - N3 - C3 | 118.82(43) | CC4 - N4 - C4 | 125.03(45) |
| CC5 - N5 - C5 | 122.72(42) | CC6 - N6 - C6 | 116.57(42) |
| CC7 - N7 - C7 | 116.92(44) | CC8 - N8 - C8 | 123.79(44) |
| N1 - C1 - CC2 | 112.19(42) | N2 - C2 - CC3 | 111.86(43) |
| N3 - C3 - CC4 | 112.61(44) | N4 - C4 - CC5 | 112.44(44) |
| N5 - C5 - CC6 | 112.36(44) | N6 - C6 - CC7 | 118.38(42) |
| N7 - C7 - CC8 | 110.80(44) | N8 - C8 - CC1 | 111.86(44) |
| CC2 - O2 - OV2 | 149.97(33) | O2 - OV2 - OV1 | 132.15(22) |
| OV2 - OV1 - OV3 | 85.23(18) | OV1 - OV3 - O8' | 115.40(19) |
| OV2 - OV4 - O3' | 148.06(22) | OV4 - O3 - CC3 | 144.55(36) |
| OV4 - OV2 - O2 | 134.41(22) | OV4 - OV2 - OV1 | 91.69(17) |
| O6 - OV1 - OV2 | 141.19(20) | O6 - OV1 - OV3 | 127.46(19) |
| OV4 - OV3 - O8' | 121.82(19) | OV3 - OV4 - O3' | 111.78(18) |
| OV1 - OV3 - OV4 | 93.75(17) | OV3 - OV4 - OV2 | 80.68(16) |

| DIHEDRAL ANGLE | (°) | DIHEDRAL ANGLE | (°) |
|---|---|---|---|
| CC1 - N1 - C1 - CC2 | -77.50(60) | N1 - C1 - CC2 - N2 | -167.51(43) |
| C1 - CC2 - N2 - C2 | -169.68(44) | CC2 - N2 - C2 - CC3 | 78.99(61) |
| N2 - C2 - CC3 - N3 | -167.69(44) | C2 - CC3 - N3 - C3 | -178.28(46) |
| CC3 - N3 - C3 - CC4 | 93.10(57) | N3 - C3 - CC4 - N4 | -179.39(43) |
| C3 - CC4 - N4 - C4 | -1.88(75) | CC4 - N4 - C4 - CC5 | -186.89(56) |
| N4 - C4 - CC5 - N5 | 179.76(43) | C4 - CC5 - N5 - C5 | -19.88(69) |
| CC5 - N5 - C5 - CC6 | -72.30(63) | N5 - C5 - CC6 - N6 | -167.04(43) |
| C5 - CC6 - N6 - C6 | -171.72(45) | CC6 - N6 - C6 - CC7 | 77.53(55) |
| N6 - C6 - CC7 - N7 | -173.03(41) | C6 - CC7 - N7 - C7 | -173.94(43) |
| CC7 - N7 - C7 - CC8 | 83.07(57) | N7 - C7 - CC8 - N8 | -172.52(44) |
| C7 - CC8 - N8 - C8 | -5.68(73) | CC8 - N8 - C8 - CC1 | -91.88(58) |
| N8 - C8 - CC1 - N1 | -173.36(42) | C8 - CC1 - N1 - C1 | -9.88(67) |

The geometry of the *cis* and *trans* amide groups, respectively, is roughly the same as for cyclotetrasarcosyl:

| Angle | Cyclotetrasarcosyl | Cyclooctasarcosyl |
|---|---|---|
| (CM−N−CC)*cis* | 119.8° | 118.7° |
| (CM−N−CC)*trans* | 124.3° | 123.9° |
| (C−N−CC)*cis* | 123.9° | 123.8° |
| (C−N−CC)*trans* | 120.1° | 117.2° |

The corresponding angles in cyclodisarcosyl, where the amide group has the *cis* conformation, are 119.7° and 124.6°, respectively.

As may be seen from Fig. 1, the ring has an open conformation with the inner volume filled by a cluster of four water molecules which participate in a network of inter- as well as intra-molecular hydrogen bond bridges. The four water oxygens are situated at the corners of a somewhat distorted square with $OV - OV - OV$ angles of about $81°$, $91°$, $85°$, and $93°$, and $OV \cdots OV$ bondlengths ranging from 2.743 Å to 2.920 Å. The two $OV \cdots O$ bond distances of the intra-molecular hydrogen-bond bridge are 2.791 Å and 2.814 Å, respectively. The $OV \cdots O$ distances of the two inter-molecular bridges, linking different symmetry related molecules, are somewhat longer: $OV3 \cdots O8' = 2.868$ Å, $OV4 \cdots O3'' = 2.883$ Å. The $OV - OV - O$ angles are distributed over a wide range (from $112°$ to $150°$).

There are no direct transannular interactions to be held responsible, as originally thought,[1] for the rigity of this rather large ring. Since, from IR-spectra, it can be stated that the same conformation persists in $CHCl_3$ solution, where no water molecules are present to form transannular bridges, the explanation must be sought in the intrinsic conformation of the peptide chain itself.[8]

Fig. 1 clearly shows that the ring conformation is *cis,cis,trans,trans,cis, cis,trans,trans*. It might also be seen that each of the four pairs of diametrically placed amino-acid residues is related by an approximate two fold axis of symmetry.

Apart from the hydrogen bonds, no short intermolecular distances are observed.

## REFERENCES

1. Dale, J. and Titlestad, K. *Chem. Commun.* **1969** 656.
2. Leonard, N. J., Adamcik, J. A., Djerassi, C. and Halpern, O. *J. Am. Chem. Soc.* **80** (1958) 4858.
3. Fedeli, W. and Dunitz, J. D. *Helv. Chim. Acta* **51** (1968) 445.
4. Groth, P. *Acta Chem. Scand.* **23** (1969) 3155.
5. Groth, P. *Acta Chem. Scand.* **24** (1970) 780.
6. Hanson, H. P., Herman, F., Lea, J. D. and Skillman, S. *Acta Cryst.* **17** (1964) 1040.
7. Stewart, R. F., Davidson, E. R. and Simpson, W. T. *J. Chem. Phys.* **42** (1965) 3175.
8. Titlestad, K., Groth, P., Dale, J. and Ali, M. Y. *Chem. Commun.* **1973** 346.

# Formation of $\mu$-Cyano Species in Reactions between Bis(histidinato)cobalt and Hexacyanoferrate Complexes

SVEN BAGGER and KEITH GIBSON

*Chemistry Department A, Building 207, The Technical University of Denmark, DK-2800 Lyngby, Denmark*

Evidence for the formation of stable, diamagnetic di- and tri-nuclear $\mu$-cyano species in aqueous systems of bis(histidinato)cobalt-(II) plus hexacyanoferrate(III) and of bis(histidinato)cobalt(III) plus hexacyanoferrate(II) is presented.

An intense, red-purple colour is rapidly generated by mixing aqueous solutions of bis(histidinato)cobalt(II) and hexacyanoferrate(III). A similar colour slowly develops when bis(histidinato)cobalt(III) and hexacyanoferrate-(II) are allowed to react in solution. In both cases the colour persists for weeks. The chemistry underlying these phenomena is the subject of this paper.

The reactions studied may be represented by (1), (2), and (3):

$$[\text{Co(his)}_2] + [\text{Fe(CN)}_6]^{3-} \rightarrow \text{products} \xrightarrow{\text{slow}} \text{isolated product} \downarrow \qquad (1)$$
$$\text{I} \qquad\qquad\qquad\qquad\qquad\qquad \text{II}$$

$$trans\text{-imidazole-}[\text{Co(L-his)}_2]^+ + [\text{Fe(CN)}_6]^{4-} \rightarrow \text{products} \qquad (2)$$
$$\text{III}$$

$$rac\text{-all-}cis\text{-}[\text{Co(L-his)(D-his)}]^+ + [\text{Fe(CN)}_6]^{4-} \rightarrow \text{products} \qquad (3)$$
$$\text{IV}$$
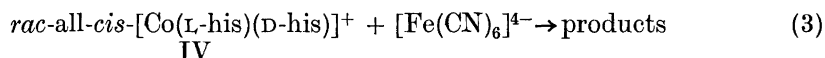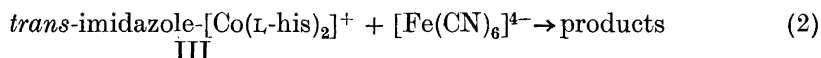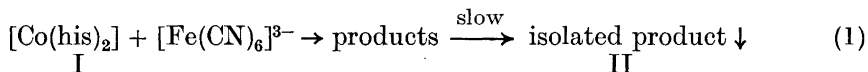
where his stands for histidinate (Fig. 1); I is a mixture of labile cobalt(II) isomers prepared with either L- or $rac$-histidine and III and IV are single isomers of cobalt(III) complexes. The isomerism of bis(histidinato) chelates was treated in a previous paper.[1]

## EXPERIMENTAL RESULTS

The absorption spectra before and immediately after mixing the reactants of (1) are shown in Fig. 2a. The spectral changes were almost identical using either L- or $rac$-histidine. The spectra before and 25 h after mixing the reactants
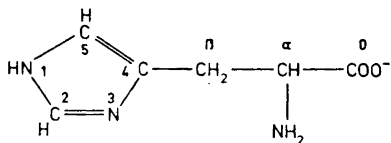
Fig. 1. Histidinate with the numbering system used.

of the slow processes (2) and (3) are shown in Figs. 3a and 3b. The time course was followed at 500 nm (Fig. 4).

To obtain information on the stoichiometry of reactions (1), (2), and (3), Job's method of continuous variation [2] was applied. The results are shown in
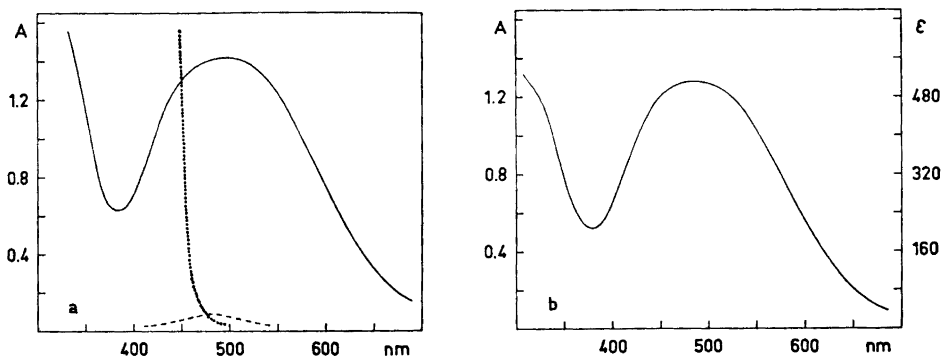


Fig. 2. Absorption spectra of reactants and products of reaction (1). a: – – – 5.0 mM [Co(L-his)$_2$]; ··· 5.0 mM [Fe(CN)$_6$]$^{3-}$; ——— 2.5 mM [Co(L-his)$_2$] + 2.5 mM [Fe(CN)$_6$]$^{3-}$, immediately after mixing. b: 1.25 mM product II, $\varepsilon$ given with respect to the total cobalt concentration (2.5 mM). Path-lengths 1 cm.
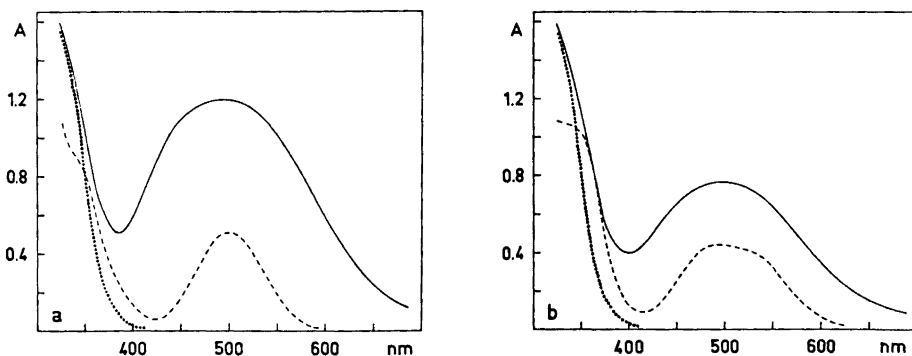


Fig. 3. Absorption spectra of reactants and products of reactions (2) and (3). a: – – – 5.0 mM trans-imidazole-[Co(L-his)$_2$]$^+$; ··· 5.0 mM [Fe(CN)$_6$]$^{4-}$; ——— 2.5 mM[Co(L-his)$_2$]$^+$ + 2.5 mM [Fe(CN)$_6$]$^{4-}$, 25 h after mixing. b: – – – 5.0 mM rac-all-cis-[Co(D-his)(L-his)]$^+$; ··· 5.0 mM [Fe(CN)$_6$]$^{4-}$; ——— 2.5 mM [Co(D-his)(L-his)]$^+$ + 2.5 mM [Fe(CN)$_6$]$^{4-}$, 25 h after mixing. Path-lengths 1 cm.
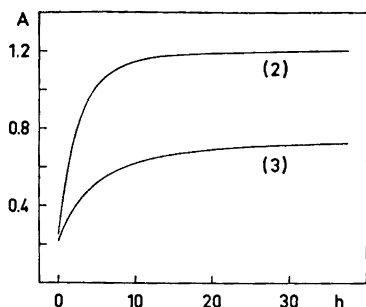
*Fig. 4.* Change of absorbance at 500 nm with time for reactions (2) and (3). (2): 2.5 mM $[Co(L\text{-his})_2]^+$ + 2.5 mM $[Fe(CN)_6]^{4-}$. (3): 2.5 mM $[Co(D\text{-his})(L\text{-his})]^+$ + 2.5 mM $[Fe(CN)_6]^{4-}$. Path-lengths 1 cm.
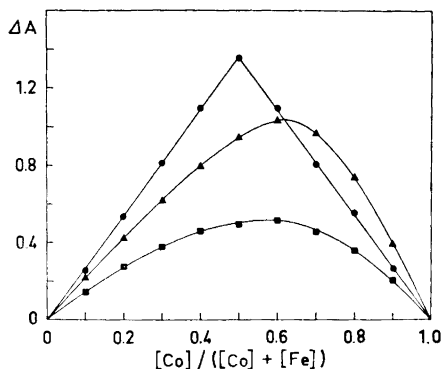
*Fig. 5.* Job plots at 500 nm for reactions (1), (2), and (3). ($\bullet$) $[Co(L\text{-his})_2]$ plus $[Fe(CN)_6]^{3-}$. ($\blacktriangle$) *trans*-imidazole-$[Co(L\text{-his})_2]^+$ plus $[Fe(CN)_6]^{4-}$. ($\blacksquare$) *rac*-all-*cis*-$[Co(D\text{-his})(L\text{-his})]^+$ plus $[Fe(CN)_6]^{4-}$. Path-lengths 1 cm.

Fig. 5, where $\Delta A$, the difference between the measured absorbance and the absorbance calculated assuming no reaction, is plotted against composition. Again the data for reaction (1) were collected immediately after, and those for (2) and (3) 25 h after mixing.

When reaction (1) is performed with concentrated solutions of $[Co(L\text{-his})_2]$ and $[Fe(CN)_6]^{3-}$ in ethanol/water solvent a precipitate is *slowly* formed. (When *rac*-histidinate was used in identical experiments, no precipitate formed.) The isolated material, II, was found to contain Co and Fe in the ratio 2:1, and the analysis was consistent with the formula $K_2\{[Co(L\text{-his})_2]_2Fe(CN)_6\}.2H_2O$. The absorption spectrum of a fresh solution of II is shown in Fig. 2b.

Cationic cobalt complexes in fresh solutions of II or in the immediate products of reaction (1) could not be detected by ion exchange experiments.

Some infrared spectra of aqueous solutions, covering pertinent regions, are given in Fig. 6; the cyanide stretching bands of reaction (1) products and of the isolated complex II are compared to that of $[Fe(CN)_6]^{4-}$, and the carboxylate antisymmetric stretching bands of the same materials are compared to that of $[Co(his)_2]^+$.

Data from proton-decoupled natural abundance $^{13}$C-NMR spectra are summarized in Table 1. Chelated histidine in all cases exhibited sharp lines and the $\delta$-values were approximately the same as in the corresponding spectrum of free histidine; this indicates that all the materials are diamagnetic.

The assignment of the $^{13}$C resonances for free histidine was checked by an off-resonance experiment (two lines are assigned erroneously in Ref. 3).

Circular dichroism spectra of the optically active complexes were measured, and the data are given in Fig. 7.
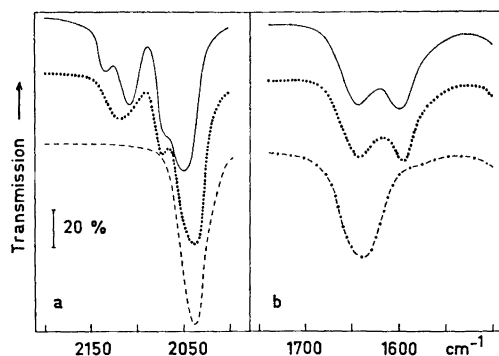
*Fig. 6.* Infrared spectra in aqueous solution. Path-lengths 36 $\mu$m a: —— isolated product II; ··· [Co(L-his)$_2$] + [Fe(CN)$_6$]$^{3-}$; --- [Fe(CN)$_6$]$^{4-}$. [Fe] = 0.1 M in all cases, solvent H$_2$O. b: —— isolated product II: ··· [Co(L-his)$_2$] + [Fe(CN)$_6$]$^{3-}$; — . — . — *trans*-imidazole-[Co(L-his)$_2$]$^+$. [Co] = 0.1 M in all cases, solvent D$_2$O.
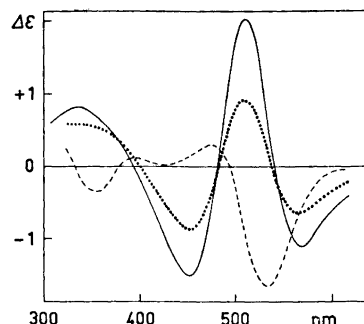
*Fig. 7.* Circular dichroism; $\Delta\varepsilon$ calculated with respect to the total cobalt concentration. —— [Co(L-his)$_2$] + [Fe(CN)$_6$]$^{3-}$ *and* isolated product II (these two curves were the same, within experimental error); ··· *trans*-imidazole-[Co(L-his)$_2$]$^+$ + [Fe(CN)$_6$]$^{4-}$, 25 h after mixing; --- *trans*-imidazole-[Co(L-his)$_2$]$^+$.

*Table 1.* Experimental $^{13}$C chemical shifts.

| | | | | Assignment | | | | |
| | C(0) | C(2) | C(4) | C(5) | C($\alpha$) | C($\beta$) | Terminal CN | Uncertain |
| --- | --- | --- | --- | --- | --- | --- | --- | --- |
| Histidine.HCl | 173.2 | 134.9 | 128.0 | 118.6 | 54.5 | 26.7 | – | – |
| [Co(L-his)$_2$]$^+$ | 184.7 | 137.2 | 132.7 | 117.6 | 56.4 | 27.1 | – | – |
| [Co(L-his)$_2$]$^+$ + [Fe(CN)$_6$]$^{4-}$ | 186.5 | 138.6 | 132.8 | 117.5 | 55.6 | 27.6 | 176.8 | 136.9$^a$ |
| | 175.0 | 140.9 | 135.0 | 116.6 | 53.7 | 26.6 | | |
| Product II | 185.5 | 138.5 | 132.8 | 117.5 | 55.6 | 28.1 | 176.8 | 173.4$^b$ |
| | | 140.4 | 134.9 | 116.5 | 53.7 | 27.3 | | 172.7$^c$ |
| [Fe(CN)$_6$]$^{4-}$ | – | – | – | – | – | – | 176.8 | – |

$^a$ Weak resonance. $^b$ and $^c$ C(0) and possibly bridged CN.

*Apparatus.* Electronic absorption spectra were measured with a Cary 11 spectrophotometer and CD spectra with a Roussel-Jouan Dichrographe II.

Proton-decoupled 22.63 MHz $^{13}$C-NMR spectra were obtained with a Bruker WH 90 spectrometer using the Fourier transform technique; the solvent was D$_2$O and the spectra were run at ambient temperature. $\delta$-Values are reported relative to TMS; dioxane ($\delta$ = 67.40) served as an internal reference.

IR spectra were measured with a Beckman IR 20 spectrometer using solution cells with CaF$_2$ windows.

*Materials.* L-and DL-Histidine (*puriss.*, chromatographic purity) were obtained from Fluka. All other chemicals were analytical grade.

*Cobalt(III) complexes.* rac-all-cis-[Co(L-his)(D-his)]Br was prepared as in Ref. 1.

*trans*-Imidazole-[Co(L-his)$_2$]ClO$_4$ was prepared as follows: CoCl$_2$.6H$_2$O (3.57 g, 15 mmol) and L-histidine (5.13 g, 33 mmol) were dissolved in 50 ml water and 0.5 g activated charcoal was added. Air was bubbled through the solution while the temperature was

maintained at 75°C. After 90 min the solution was cooled, the charcoal filtered off and 60 ml water containing 8 g $NaClO_4$ was added. After standing overnight the pink needle crystals were filtered off and washed with cold water and ethanol. The product was then recrystallized from warm water and air dried. Yield 2.7 g (37 % of total Co). (Found: C 29.18; H 3.72; N 17.08; Cl 6.88. Calc. for $[Co(C_6H_8N_3O_2)_2]ClO_4 \cdot 1.5H_2O$: C 29.19; H 3.87; N 17.10; Cl 7.18.) Samples of this perchlorate salt were washed with water through an anion exchange column (Dowex 1 X-8) in the bromide form; evaporation of the eluent yielded the bromide salt which was used in the NMR experiments. The absorption, CD and PMR spectra of *trans*-imidazole-$[Co(L-his)_2]^+$ prepared in this way were in complete agreement with those reported [1] for the chromatographically purified isomer.

*Job experiments.* Reaction (1): Solutions of $[Co(his)_2]$, pH 9 (5.0 mM, made from $CoCl_2 \cdot 6H_2O$, L- or DL-histidine and NaOH) and of $K_3[Fe(CN)_6]$ (5.0 mM) were mixed in volume ratios $10:0, 9:1, \ldots, 0:10$. The absorption spectra of the resulting solutions were measured immediately. All operations were carried out under strict $O_2$-free conditions at room temperature.

Reactions (2) and (3): Solutions of $[Co(his)_2]^+$ and $K_4[Fe(CN)_6]$ (both 5.0 mM) were mixed in the same way and the spectra were recorded repeatedly until no further change was observed. $O_2$ was excluded and the temperature was maintained at 20°C throughout.

*Isolation and analysis of product* II. A concentrated solution of $[Co(L-his)_2]$ was prepared by adding $CoCl_2.6H_2O$ (1.00 g, 4.20 mmol) to L-histidine (1.38 g, 8.58 mmol) dissolved in 15 ml 0.59 M NaOH. This was cooled in an ice-bath and protected from the atmosphere with a stream of nitrogen. A solution of $K_3[Fe(CN)_6]$ (1.38 g, 4.20 mmol) in 15 ml $H_2O$ was run in with stirring. 14 ml of ethanol was added dropwise and the mixture kept in a refrigerator overnight. The bulky precipitate which formed was filtered off, washed with ice-cold water/ethanol (2:1) and ethanol and air dried. Subsequent drying over $H_2SO_4$ *in vacuo* resulted in a weight loss of *ca.* 15 %. Yield 1.2 g. Red-purple powder, dissolves readily in water to give neutral solutions. (Found: Fe 5.3; Co 11.1; H 3.8; C 32.5; N 23.2. Calc. for $K_2\{[Co(his)_2]_2Fe(CN)_6\}.2H_2O$: Fe 5.3; Co 11.2; H 3.4; C 34.1; N 23.9.)

For the Fe and Co determinations, the complex was destroyed by refluxing with 72 % perchloric acid for 24 h. The resulting clear solution was diluted and Fe determined gravimetrically by the standard cupferron method. The combined filtrates from the Fe determination were reconcentrated to fumes of perchloric acid and Co determined electrolytically after neutralisation with aqueous ammonia. (Test analyses on samples made by combining known amounts of $[Co(L-his)_2]$ and $K_3[Fe(CN)_6]$ gave results within 2 % of the expected.)

C, H, and N analyses were carried out by the Microanalytical Department, Chemistry Laboratory II, University of Copenhagen.

## DISCUSSION

Our interpretation of the experimental results is based upon the following reaction scheme,

$$[Co^{II}(his)_2] + [Fe^{III}(CN)_6]^{3-} \xrightarrow{\text{fast}} [(his)_2Co^{III}(\mu\text{-NC})Fe^{II}(CN)_5]^{3-} \quad (4)$$

$$[(his)_2Co^{III}(\mu\text{-NC})Fe^{II}(CN)_5]^{3-} \xrightleftharpoons{\text{slow}} [Co^{III}(his)_2]^+ + [Fe^{II}(CN)_6]^{4-} \quad (5)$$

$$[(his)_2Co^{III}(\mu\text{-NC})Fe^{II}(CN)_5]^{3-} + [Co^{III}(his)_2]^+ \xrightleftharpoons{\text{slow}}$$
$$[(his)_2Co^{III}(\mu\text{-NC})Fe^{II}(CN)_4(\mu\text{-CN})Co^{III}(his)_2]^{2-} \quad (6)$$
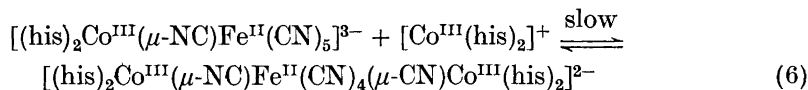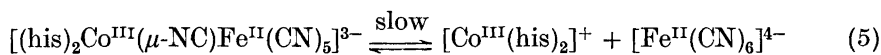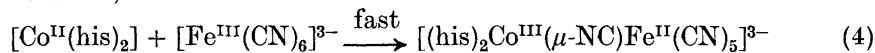
where (4) is orders of magnitude faster than (5) and (6). Thus the observed colour changes result from formation of di- and trinuclear species.

A related, but transient, dinuclear species has been observed [4] as an intermediate in the reaction of $[Co^{II}(edta)]^{2-}$ with $[Fe(CN)_6]^{3-}$.

The proposed reaction scheme predicts that the reaction between $[Co^{II}(his)_2]$ and $[Fe(CN)_6]^{3-}$ would be characterized by a Job plot with a sharp extremum where the concentrations of the two components are equal. This is consistent with Fig. 5. The initial dinuclear products have not been isolated. The substance precipitated from the $[Co(L-his)_2]$ system is a trinuclear complex formed by the subsequent slow, reversible reactions.

The reaction between $[Co^{III}(his)_2]^+$ and $[Fe(CN)_6]^{4-}$ is described by (5) and (6). When equilibrium has been established, then mono-, di-, and also trinuclear species will be present. This will result in a curved Job plot with an extremum where the Co:Fe ratio is $> 1$, in agreement with the experiments (Fig. 5).

The formation of $\mu$-cyano bridges in reactions (5) and (6) must involve bond breaking between low-spin Co(III) and histidinate, and therefore these reactions are expected to be slow.

Bridging cyano groups have previously been shown to exhibit a $25 - 100$ cm$^{-1}$ higher cyanide stretching frequency than terminal cyano groups.[5,6] Accordingly the higher frequency bands in Fig. 6a are taken to prove the occurrence of cyano bridges. The IR spectrum of the solid isolated trinuclear complex in KBr pellets was very similar to the solution spectrum, indicating no change in the cyano groups on dissolution.

It should be noted that the trinuclear species may exist with the bridged cyano groups in either *cis*- or *trans*-positions in the octahedral Fe(II) coordination sphere. Molecular models do not indicate substantial steric crowding in the statistically favoured *cis*-structure.

In both $[Co(his)_2]$ and $[Co(his)_2]^+$ each histidinate is coordinated *via* the imidazole nitrogen number 3, the amino nitrogen, and a carboxylate oxygen. However, in the cyano bridged complexes only five coordination sites on each cobalt are occupied by histidinate. Thus bridge formation must be associated with displacement of one ligating histidinate group, and therefore two types of histidinate, bidentate and tridentate, must result.

If the displaced histidinate group is carboxylate then two IR absorptions, due to the antisymmetric stretching of free and coordinated carboxylate, should be observable, just as in the related case of $[(his)_2Co.O_2.Co(his)_2]$.[7] As is shown in Fig. 6b, two bands are observed both with the products of reaction (1) and with the trinuclear complex II. The higher frequency component is assigned to carboxylate bound to Co(III) and the lower frequency component to uncoordinated carboxylate.

Since two types of histidinate ligands occur, two sets of histidinate resonances arise in the proton-decoupled $^{13}C$ spectra of the complexes containing cyano bridges (Table 1). Unfortunately, the small differences between the $^{13}C$ chemical shifts of CN and COO makes an unambiguous assignment of these difficult in the $\mu$-cyano compounds. The $^{13}C$ resonance of free COO is seen to be shifted *ca.* 11 ppm downfield on coordination to Co(III).

The visible absorption spectrum of a freshly prepared solution of the isolated trinuclear complex II resembles that of the dinuclear product of reaction (4) if the extinction coefficients are calculated with respect to cobalt (see Fig. 2). The high intensities suggest that the visible absorption is dominated by an

Fe(II)→Co(III) charge transfer; apparently this transition is twice as probable in the trinuclear as in the dinuclear complex.

The circular dichroism spectra, when $\Delta\varepsilon$ is calculated with respect to cobalt, are the same for the mono- and dibridged species as is seen in Fig. 7. This is reasonable as the cobalt coordination sphere is supposed to be the same in the two cases.

The CD and absorption spectra of the equilibrated mixtures of $[Co(his)_2]^+$ and $[Fe(CN)_6]^{4-}$ and the corresponding Job plots show that the equilibria (5) and (6) are displaced further in favour of mononuclear complexes with racemic histidinate than with L-histidinate.

In conclusion, $[Co^{II}(his)_2]$ is quantitatively oxidized by $[Fe(CN)_6]^{3-}$ in a one-electron inner-sphere reaction. Both metal ions achieve low-spin $d^6$ electron configuration and a rather stable cyano bridged reaction product results. The same kind of $\mu$-cyano species are formed in simple substitution reactions when isomers of $[Co^{III}(his)_2]^+$ are equilibrated with $[Fe(CN)_6]^{4-}$.

## REFERENCES

1. Bagger, S., Gibson, K. and Sørensen, C. S. *Acta Chem. Scand.* **26** (1972) 2503.
2. Job, P. *Ann. Chim.* [10] **9** (1928) 113.
3. Johnson, L. F. and Jankowski, W. C. *Carbon-13 NMR Spectra*, Wiley-Interscience, New York 1972.
4. Adamson, A. W. and Gonick, E. *Inorg. Chem.* **2** (1963) 129.
5. Dows, D. A., Haim, A. and Wilmarth, W. K. *J. Inorg. Nucl. Chem.* **21** (1961) 33.
6. De Castello, R. A., Mac-Coll, C. P. and Haim, A. *Inorg. Chem.* **10** (1971) 293.
7. Bagger, S. and Gibson, K. *Acta Chem. Scand.* **26** (1972) 3788.

# Activity Coefficients of Alkanoate Ions in Aqueous Three-component Solutions Containing Sodium Alkanoate and Sodium Chloride

SUNE BACKLUND, FOLKE ERIKSSON and RAUNO FRIMAN

*Department of Physical Chemistry, Åbo Akademi, SF-20500 Åbo 50, Finland*

In connection with studies on the self-association of alkali metal alkanoates in the ionic medium 3 M Na(Cl), a method has been developed for the estimation of the alkanoate ion activity coefficients in the three-component system sodium chloride-sodium alkanoate-water at different constant ionic strengths. The activity coefficients are calculated from the activities of the other components in the system using the Gibbs-Duhem equation. The activities have been estimated from potentiometric measurements ($a_{Na^+}$, $a_{Cl^-}$, $a_{Na,Cl}$) and vapour pressures ($a_w$). Results are given for propionate, butyrate, and pentanoate at total ionic strengths of 1.0 mol kg$^{-1}$ and 3.0 mol kg$^{-1}$ Na(Cl) at 25°C.

This paper reports a direct continuation of the attempts to estimate the activity coefficients of alkanoate ions in mixed solutions, which started with a determination of the activity coefficients of acetate ions in sodium chloride solutions.[1] The activity coefficients of propionate, butyrate, and pentanoate ions in sodium chloride solutions are investigated and calculated using the Gibbs-Duhem equation. The experimental part includes potentiometric titrations with a sodium responsive glass electrode, and vapour pressure osmometry determinations of the water activities in the mixtures.

Sodium propionate, butyrate, and pentanoate have previously been investigated by, among others, potentiometric studies of the hydrolytic equilibria in the ionic medium 3 M Na (Cl) (Danielsson;[2] Stenius and Zilliacus[3]). The aim of the present investigation is to clarify to what extent the activity coefficients of the alkanoate ions change in such systems. The object is closely related to the studies of hydrolytic equilibria in that the present investigation also aims at elucidating the association of the anions in the system. A difference, however, is that there are no excess hydrogen ions in the solutions.

Danielsson,[4] using a method developed by McKay and Perring, has calculated mean molar activity coefficients of sodium propionate and butyrate in solutions similar to those discussed here.

*Note.* The symbols and units in this paper follow throughout the recommendations in Ref. 5.

## EXPERIMENTAL

*1. Chemicals.* The sodium chloride (E. Merck AG *p.a.* quality) was dried two days at 200°C and stored in a desiccator. The sodium alkanoates were prepared by neutralizing the corresponding fatty acids (Fluka AG *purissimum* quality) with sodium hydroxide (E. Merck AG "Titrisol") at the boiling point. The salts were dried in an evaporator over diphosphorus pentaoxide for five days at 100°C. The molar masses of the salts were checked by titration with perchloric acid in glacial acetic acid, using crystal violet as indicator. Salts with a molar mass differing more than 0.5 % from the theoretical values were rejected. The water was twice distilled and deionized. Its conductivity was 0.5 $\mu$S cm$^{-1}$ and its pH about 6 at 25°C.

*2. Solutions.* Sodium chloride and sodium alkanoate solutions of equal molality were prepared for each titration at a constant ionic strength. The solutions were saturated with silver chloride and stored in polyethylene bottles in darkness. Extensive precautions were taken to protect the solutions from carbon dioxide. Since all measurements of the water activities of the mixtures were made for solutions whose concentrations were measured in mol dm$^{-3}$ at a constant molar ionic strength,[6] these values have been recalculated as molalities at a constant molal ionic strength.

*3. Potential measurements.* The two following electrode systems were used to measure the sodium and chloride ion activities:

Cell 1: Ag,AgCl/$I_m$ NaCl//$I_m$ (NaCl, NaB)/Na-glass

Cell 2: Ag,AgCl/$I_m$ NaCl//$I_m$ (NaCl, NaB)/AgCl,Ag

where NaB is the sodium alkanoate and $I_m = \frac{1}{2}\sum_i m_i z_i^2$, ($m_i$ = the molality of ionic species i.) The reference electrode vessel, measuring vessel, and the bridge ("Wilhelm" type) were similar to those described by Sillén.[7] The cells were immersed in a water bath kept at $25.00 \pm 0.05$°C, an adequate temperature control for the emf measurements which were made to an accuracy of 0.1 mV. About 6 mol kg$^{-1}$ ammonium nitrate was used in the bridge.

The glass electrode was an Electronic Instruments Ltd Type GNA 33.[8] The potential of the glass electrode was found to vary with the illumination, and so all measurements were made at constant light conditions. The silver-silver chloride electrodes were prepared according to Brown[9] with some minor modifications. The electrode systems were checked by titration in sodium chloride solutions.

The measurements were performed as volumetric titrations with automatic recording of the potentials in the following way. Each titration at a given ionic strength was divided into two parts. In the first part, NaCl of ionic strength $I_m$ was added to 30 cm$^3$ NaB of the same ionic strength. In the second, NaB was added to NaCl.

The emf values were recorded by a digital voltmeter furnished with a printout unit. When cell 1 was used, a preamplifier was connected between the cell and the digital voltmeter. The additions were made with a motor-driven burette controlled by a dial timer. The apparatus has been described previously by, *e.g.*, Danielsson[10] and Backlund.[1]

*4. Vapour pressure osmometry.* The water activities $a_w$ of the mixed electrolytes have been measured by Danielsson *et al.*[6] These measurements have been supplemented by measurements in pure sodium alkanoate solutions. The water activities of pure sodium chloride solutions were taken from Ref. 11. The measurements were performed with a Mechrolab 301 A Vapor Pressure Osmometer.

## RESULTS

### 1. Activity coefficients of sodium and chloride ions. The mean activity coefficients of sodium chloride

The standard state was chosen to give $\lim_{m_\pm \to 0} \gamma_\pm^* = 1$. Moreover, the Guggenheim convention [12] for pure sodium chloride-water systems was used to set the mean activity coefficient $\gamma^*_{\mathrm{Na,Cl}} = \gamma^*_{\mathrm{Na}^+} = \gamma^*_{\mathrm{Cl}^-}$.

The activity coefficients of sodium ion were calculated from emf values measured with cell 1. According to the Nernst equation,

$$E_1 = E^{\ominus\prime}_1 + k \log a_{\mathrm{Na}^+} + E_{\mathrm{diff}\,1} \tag{1}$$

where $E^{\ominus\prime}_1 = E^{\ominus}_{\mathrm{glass}} - E^{\ominus}_{\mathrm{AgCl,Ag}} + k \log a_{\mathrm{Cl}^-}$ and $k = RTF^{-1} \ln 10$. $a_{\mathrm{Cl}^-}$ is the activity of chloride ion at the molality of $I_m$ NaCl. The diffusion potential $E_{\mathrm{diff}\,1}$ is not zero. In measurements in pure sodium chloride solutions, the diffusion potential was shown to be constant with varying $a_{\mathrm{Na,Cl}}$ (i.e. $E_1$ versus $\log a_{\mathrm{Na}^+}$ yielded a straight line of slope $k$).

Ekwall and Stenius [13] found that replacing chloride by formate ions did not change the diffusion potential to any significant extent. If $E^{\ominus\prime}_1$ and $E_{\mathrm{diff}\,1}$ are combined into a single quantity, $E^{\ominus}_1$, the following equation, which may be used to calculate the activity coefficient of the sodium ion, is obtained

$$\log \gamma_{\mathrm{Na}^+} = (E_1 - E^{\ominus}_1 - k \log m_{\mathrm{Na}^+})/k \tag{2}$$

$E^{\ominus}_1$ is calculated from the activity [11] in a pure sodium chloride solution of an ionic strength equal to that of the mixed electrolyte under investigation. Values of $\log \gamma_{\mathrm{Na}^+}$ calculated at $I_m = 1.0$ mol kg$^{-1}$ and $I_m = 3.0$ mol kg$^{-1}$ are given in Tables 1 and 2, respectively.

The activity coefficients of the chloride ion are calculated from the emf values of cell 2. Use of the Nernst equation and application of the same argument to cell 2 as to cell 1, gives the following expression

$$\log \gamma_{\mathrm{Cl}^-} = (E^{\ominus}_2 - E_2 - k \log m_{\mathrm{Cl}^-})/k \tag{3}$$

$E^{\ominus}_2$ consists of the constant terms $E_{\mathrm{diff}\,2}$, $k \log a_{\mathrm{Cl}^-}$, and $E'$, the difference between the standard potentials of the two silver-silver chloride electrodes. $E^{\ominus}_2$ is determined in the same way as $E^{\ominus}_1$. Values of $\log \gamma_{\mathrm{Cl}^-}$ at $I_m = 1.0$ mol kg$^{-1}$ and $I_m = 3.0$ mol kg$^{-1}$ are given in Tables 1 and 2, respectively.

The mean activity coefficients of sodium chloride in the mixed electrolyte solutions were calculated from the defining equation

$$\log \gamma_\pm = \tfrac{1}{2}(\log \gamma_+ + \log \gamma_-) \tag{4}$$

Calculated mean activity coefficients $\gamma_{\mathrm{Na,Cl}}$ at $I_m = 1.0$ mol kg$^{-1}$ and $I_m = 3.0$ mol kg$^{-1}$ are shown in Figs. 1 and 2, respectively.

*Table 1.* Coefficients of the polynomial $\log \gamma_x = \sum_{i=0}^{3} g_i m^i_{NaB}$, where $x = Na^+$, $Cl^-$ and $B^-$, in mixtures of sodium chloride and sodium alkanoate at ionic strength $I_m = 1.0$ mol kg$^{-1}$.

| Alkanoate | $\log \gamma_{Na^+}$ | | | | $\log \gamma_{Cl^-}$ | | | | $\log \gamma_{B^-}$ | | | |
|---|---|---|---|---|---|---|---|---|---|---|---|---|
| | $g_0$ | $g_1$ | $g_2$ | $g_3$ | $g_0$ | $g_1$ | $g_2$ | $g_3$ | $g_0$ | $g_1$ | $g_2$ | $g_3$ |
| Propionate | −0.1831 | −0.0466 | 0.0135 | 0.0000 | −0.1827 | 0.0767 | 0.0290 | 0.0000 | −0.1174 | 0.1560 | 0.0000 | 0.0000 |
| Butyrate | −0.1847 | −0.1210 | 0.1419 | −0.0608 | −0.1815 | 0.1166 | 0.0342 | 0.0000 | −0.0860 | 0.3479 | −0.3275 | 0.1680 |
| Pentanoate | −0.1829 | 0.0106 | −0.0166 | 0.0000 | −0.1836 | 0.0956 | 0.0380 | 0.0000 | −0.1207 | 0.1908 | 0.0000 | 0.0000 |

*Table 2.* Coefficients of the polynomial $\log \gamma_x = \sum_{i=0}^{3} g_i m^i_{NaB}$, where $x = Na^+$, $Cl^-$ and $B^-$, in mixtures of sodium chloride and sodium alkanoate at ionic strength $I_m = 3.0$ mol kg$^{-1}$.

| Alkanoate | $\log \gamma_{Na^+}$ | | | | $\log \gamma_{Cl^-}$ | | | | $\log \gamma_{B^-}$ | | | |
|---|---|---|---|---|---|---|---|---|---|---|---|---|
| | $g_0$ | $g_1$ | $g_2$ | $g_3$ | $g_0$ | $g_1$ | $g_2$ | $g_3$ | $g_0$ | $g_1$ | $g_2$ | $g_3$ |
| Propionate | −0.1469 | −0.0043 | −0.0015 | 0.0000 | −0.1464 | 0.0580 | 0.0030 | 0.0000 | 0.0839 | 0.0727 | 0.0000 | 0.0000 |
| Butyrate | −0.1464 | −0.0091 | −0.0019 | 0.0000 | −0.1466 | 0.0866 | −0.0008 | 0.0000 | 0.2042 | 0.0187 | 0.0277 | −0.0039 |
| Pentanoate | −0.1476 | 0.0417 | −0.0182 | 0.0009 | −0.1485 | 0.0885 | −0.0036 | 0.0000 | 0.3083 | −0.0796 | 0.0145 | 0.0000 |
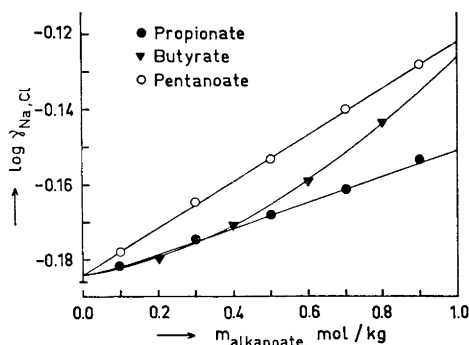
Fig. 1. The logarithm of the mean activity coefficient of the sodium chloride as a function of the alkanoate molality in mixed solutions of sodium chloride and sodium alkanoate at ionic strength $I_m = 1.0$ mol kg$^{-1}$.
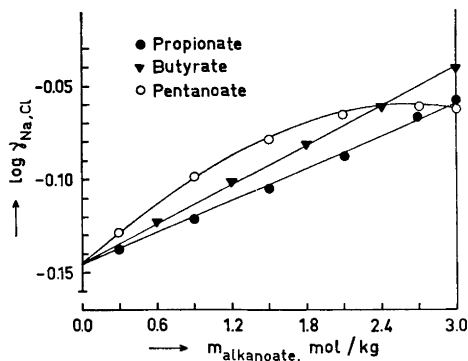
Fig. 2. As Fig. 1, but $I_m = 3.0$ mol kg$^{-1}$.

## 2. The mean activity coefficient of the sodium alkanoate. The activity coefficient of the alkanoate ion

Application of the Gibbs-Duhem equation to the three-component system $NaCl - NaB - H_2O$ gives

$$m_{NaCl}d[\ln(a_{Na}a_{Cl})] + m_{NaB}d[\ln(a_{Na}a_B)] + m_wd(\ln a_w) = 0 \qquad (5)$$

where $m_w$ is the molality of water. All the solutions investigated have the cation in common, and the sodium molality $m_{Na} = m_{Cl} + m_B$ is constant. Therefore, according to Harned,[14]

$$2\, m_{NaCl}d(\log \gamma_{Na,Cl}) + 2\, m_{NaB}d(\log \gamma_{Na,B}) = -\, m_wd(\log a_w) \qquad (6)$$

Integration of (6), from pure NaB to a mixed solution of a given composition, gives

$$\int_{\log \gamma^*_{Na,B}}^{\log \gamma_{Na,B}} m_{NaB}\ d(\log \gamma_{Na,B}) = \frac{m_w}{2}\log\frac{a^*_{wNaB}}{a_w} - \int_{\log \gamma^{tr}_{Na,Cl}}^{\log \gamma_{Na,Cl}} m_{NaCl}\ d(\log \gamma_{Na,Cl}) \qquad (7)$$

where, following Harned and Robinson,[15] $\gamma^{tr}_{Na,Cl} = \lim_{m_{NaCl} \to 0} \gamma_{Na,Cl}$ is called the "trace activity coefficient". $a^*_{wNaB}$ is the water activity of pure sodium alkanoate solution. Eqn. (7) makes it possible to calculate the mean activity coefficients of sodium alkanoate in mixtures of sodium chloride and sodium alkanoate at a *constant* sodium molality.

According to Harned,[11] there are rather simple relationships between the composition and the activity coefficients of solutions of two electrolytes at a constant ionic strength. The right-hand member of eqn. (7) is known for all values of $m_{NaB}$, and it may thus be assumed that it can be expressed as

a polynomial $\sum\limits_{i=0}^{n} b_i \, m_{\mathrm{NaB}}{}^{i+1}$, where $b_i$ are constants which can be determined, e.g. by regression analysis. The units of the $b_i$ are $(\mathrm{kg \, mol^{-1}})^i$, $(i = 0, 1, \ldots, n)$. Eqn. (7) may now be written

$$\int\limits_{\log \gamma^*_{\mathrm{Na,B}}}^{\log \gamma_{\mathrm{Na,B}}} m_{\mathrm{NaB}} \; \mathrm{d}(\log \gamma_{\mathrm{Na,B}}) = \sum_{i=0}^{n} b_i \, m_{\mathrm{NaB}}{}^{i+1} \tag{8}$$

Differentiating with respect to $m_{\mathrm{NaB}}$ and multiplying the result by $m_{\mathrm{NaB}}{}^{-1}$ gives

$$\mathrm{d}(\log \gamma_{\mathrm{Na,B}}) = \sum_{i=0}^{n} b_i(i+1) \, m_{\mathrm{NaB}}{}^{i-1} \; \mathrm{d}(m_{\mathrm{NaB}}) \tag{9}$$

On integration, (9) gives

$$\int\limits_{\log \gamma^*_{\mathrm{Na,B}}}^{\log \gamma_{\mathrm{Na,B}}} \mathrm{d}(\log \gamma_{\mathrm{Na,B}}) = \sum_{i=0}^{n} b_i(i+1) \int\limits_{m_{\mathrm{NaB}} = m_{\mathrm{Na}}}^{m_{\mathrm{NaB}}} m_{\mathrm{NaB}}{}^{(i-1)} \; \mathrm{d}(m_{\mathrm{NaB}})$$

$$\log \gamma_{\mathrm{Na,B}} = \log \gamma^*_{\mathrm{Na,B}} + b_0 \ln 10 \log \frac{m_{\mathrm{NaB}}}{m_{\mathrm{Na}}} + \sum_{i=1}^{n} \frac{b_i(i+1)}{i} (m_{\mathrm{NaB}}{}^{i} - m_{\mathrm{Na}}{}^{i}) \tag{10}$$

According to the definition $\lim\limits_{m_{\mathrm{NaB}} \to 0} \gamma_{\mathrm{N,B}} = \gamma^{\mathrm{tr}}_{\mathrm{Na,B}}$, a finite value of $\gamma_{\mathrm{Na,B}}$ will be obtained on "infinite dilution" of sodium alkanoate in sodium chloride. The values of $\gamma^*_{\mathrm{Na,B}}$ are taken from Robinson and Smith.[16]

Values of mean activity coefficients $\gamma_{\mathrm{Na,B}}$, calculated from (10), are illustrated at $I_m = 1.0$ mol $\mathrm{kg^{-1}}$ and $I_m = 3.0$ mol $\mathrm{kg^{-1}}$ in Figs. 3 and 4, respectively. $\gamma_{\mathrm{B^-}}$ has been calculated from (4) and (2). Values of this quantity are given at the same ionic strengths in Tables 1 and 2, respectively.
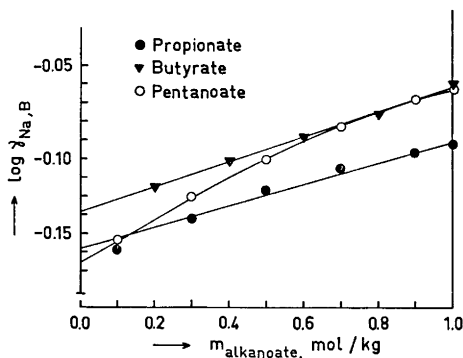


Fig. 3. The logarithm of the mean activity coefficient of the sodium alkanoate as a function of the alkanoate molality in mixed solutions of sodium chloride and sodium alkanoate at ionic strength $I_m = 1.0$ mol $\mathrm{kg^{-1}}$.
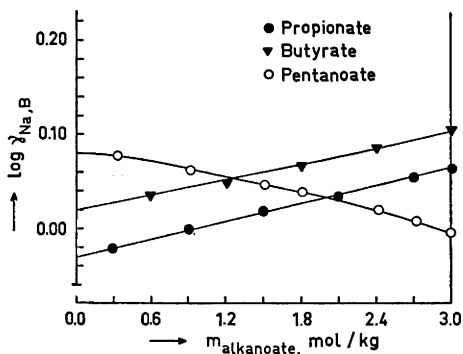
Fig. 4. As Fig. 3, but $I_m = 3.0$ mol $\mathrm{kg^{-1}}$.

## DISCUSSION

A method has been developed to estimate single ion activity coefficients and mean activity coefficients in three-component systems. The method includes experimental determinations as well as theoretical calculations. The advantage of this method compared with those used earlier [1,4] is that it is unnecessary to work over the whole molality range, from zero to a given total molality, in the mixed solution. The mean activity coefficient of one of the components can be calculated from the water activities and the activity coefficients of the other component at a single ionic strength. The method is theoretically correct if it is possible to consider the electrolyte as a $1 - 1$ electrolyte at all the molalities investigated. The weakness of this method, as compared to the method described previously,[1] is that the effects of aggregation on the vapour pressure data for alkanoate solutions without added sodium chloride [16] will influence the activity coefficients and the trace activity coefficients of the same alkanoates in molality regions where there is no association at the same ionic strength.

The largest source of error in experimental determinations is the diffusion potential, which has been assumed to be constant during each titration. However, a comparison with the activity coefficients calculated by Danielsson [4] from vapour pressure data only shows a difference of less than $\pm 1$ %. This indicates that the accuracy of the activity coefficients of the sodium and chloride ions, respectively, are of the same order of magnitude.

The accuracy of the calculation of the mean activity coefficients of the sodium alkanoate is highly dependent on the experimental accuracy of the water activity. In this case too, the differences from Danielsson's [4] values are less than $\pm 1$ %. The activity coefficients of the alkanoate ions studied so far, as well the corresponding activities, are presented for $I_m = 3.0$ mol kg$^{-1}$ in Table 3. The values of the acetate ion are taken from Ref. 1. The ion activities are also given in Fig. 5. The results cannot directly be compared to the values calculated from the combination of gas chromatography and hy-

Table 3. The logarithm of the alkanoate activity coefficient and the alkanoate activity in mixtures of sodium chloride and sodium alkanoate at ionic strength $I_m = 3.0$ mol kg$^{-1}$.

| $m_{NaB}$ | Acetate | | Propionate | | Butyrate | | Pentanoate | |
|---|---|---|---|---|---|---|---|---|
| mol kg$^{-1}$ | log $\gamma_{Ac^-}$ | $a_{Ac^-}$ | log $\gamma_{Pr^-}$ | $a_{Pr^-}$ | log $\gamma_{Bu^-}$ | $a_{Bu^-}$ | log $\gamma_{Va^-}$ | $a_{Va^-}$ |
| 0.00 | 0.000 | 0.000 | 0.083 | 0.000 | 0.204 | 0.000 | 0.308 | 0.000 |
| 0.30 | 0.021 | 0.315 | 0.105 | 0.383 | 0.212 | 0.489 | 0.285 | 0.579 |
| 0.60 | 0.042 | 0.666 | 0.127 | 0.805 | 0.224 | 1.006 | 0.265 | 1.106 |
| 0.90 | 0.063 | 1.040 | 0.149 | 1.269 | 0.240 | 1.566 | 0.248 | 1.595 |
| 1.20 | 0.085 | 1.459 | 0.171 | 1.780 | 0.259 | 2.183 | 0.233 | 2.056 |
| 1.50 | 0.106 | 1.916 | 0.193 | 2.339 | 0.281 | 2.867 | 0.221 | 2.499 |
| 1.80 | 0.127 | 2.413 | 0.214 | 2.950 | 0.304 | 3.631 | 0.212 | 2.934 |
| 2.10 | 0.149 | 2.959 | 0.236 | 3.620 | 0.329 | 4.481 | 0.205 | 3.368 |
| 2.40 | 0.170 | 3.550 | 0.258 | 4.351 | 0.354 | 5.426 | 0.200 | 3.811 |
| 2.70 | 0.191 | 4.139 | 0.280 | 5.146 | 0.379 | 6.464 | 0.199 | 4.271 |
| 3.00 | 0.213 | 4.899 | 0.302 | 6.012 | 0.403 | 7.593 | 0.200 | 4.758 |

*Fig. 5.* The activity of the alkanoate ion as a function of the alkanoate molality in mixed solutions of sodium chloride and sodium alkanoate at ionic strength $I_m = 3.0$ mol kg$^{-1}$.
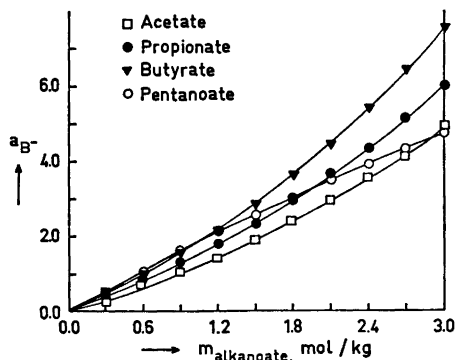
drolytic equilibrium data given by Backlund and Danielsson.[17] Neither the standard state nor the ionic strength is equal in the two cases. Moreover, the experimental uncertainty is larger in the latter case.

If, as a very rough approximation, it is assumed that Harned's rule [11]

$$\log \gamma_{Na,Cl} = \log \gamma^{tr}_{Na,Cl} + \alpha m_{NaCl}$$
$$\log \gamma_{Na,B} = \log \gamma^{tr}_{Na,B} + \beta m_{NaB}$$

is valid for the systems investigated, then

(i)  for propionate and butyrate, $\alpha = -\beta$ and $\gamma^{tr}_{Na,Cl} = \gamma^{tr}_{Na,B}$
(ii) for pentanoate, $\alpha \neq -\beta$ and $\gamma^{tr}_{Na,Cl} \neq \gamma^{tr}_{Na,B}$

The first case has been treated thermodynamically for $1-1$ electrolytes by Guggenheim.[18]

The second is called the "general case"; its thermodynamic treatment is very difficult. The failure of Guggenheim's model to describe the pentanoate can probably be ascribed primarily to the great difference in size between the sodium ion and the pentanoate ion.

The trace activity coefficient of sodium pentanoate seems surprisingly high if it is compared to the trace activity coefficients of sodium propionate and butyrate at $I_m = 3.0$ mol kg$^{-1}$. A possible explanation for this deviation might be the uncertainties in the activity coefficients of sodium pentanoate in chloride-free solutions, as mentioned above.

For this reason, a quantitative estimation of the degree of association of sodium pentanoate from the calculated activity coefficients does not seem to be justified at this stage. However, the results are qualitatively fully compatible with earlier investigations [3] into the structure of sodium pentanoate solutions.

## REFERENCES

1. Backlund, S. *Acta Chem. Scand.* **25** (1971) 2070.
2. Danielsson, I. *Proc. IVth Intern. Congr. Surface Active Substances, Brussels 1964*, Gordon and Breach Science Publishers, New York 1967, Vol. II, p. 555.
3. Stenius, P. and Zilliacus, C.-H. *Acta Chem. Scand.* **25** (1971) 2232.
4. Danielsson, I. *Proc. Vth Intern. Congr. Surface Active Substances, Barcelona 1968*, Ediciones Unidas, S.A., Barcelona 1969, Vol. II, p. 869.
5. McGlashan, M. L. *Manual of Symbols and Terminology for Physicochemical Quantities and Units*, Butterworths, London 1971.
6. Danielsson, I. *Proc. 3rd Scandinavian Symp. Surface Chemistry, Fredensborg 1967*, Nordforsk, pp. 1 — 7.
7. Forsling, W., Hietanen, S. and Sillén, L. G. *Acta Chem. Scand.* **6** (1952) 901.
8. Electronic Instruments Ltd. *TDS-ELECT-9. ISSUE 16th February* (1962) pp. 1 — 6.
9. Brown, A. S. *J. Am. Chem. Soc.* **56** (1934) 646.
10. Danielsson, I. *Kemian Teollisuus* **23** (1966) 1081.
11. Robinson, R. A. and Stokes, R. H. *Electrolyte Solutions*, Butterworths, London 1959.
12. Guggenheim, E. A. *J. Phys. Chem.* **34** (1930) 1758.
13. Ekwall, P. and Stenius, P. *Acta Chem. Scand.* **21** (1967) 1643.
14. Harned, H. S. *J. Am. Chem. Soc.* **57** (1935) 1865.
15. Harned, H. S. and Robinson, R. A. *Multicomponent Electrolyte Solutions*, Pergamon, Glasgow 1968.
16. Smith, E. R. B. and Robinson, R. A. *Trans. Faraday Soc.* **38** (1942) 70.
17. Backlund, S. and Danielsson, I. *Proc. VIth Intern. Congr. Surface Active Substances, Zürich 1972. In press.*
18. Guggenheim, E. A. *Phil. Mag.* [7] **19** (1935) 588.

# An *ab initio* SCF-MO Calculation of Methylenecyclopropene, Cyclopropenimine, and Cyclopropenone

ANNE SKANCKE

*Department of Medical Biology, University of Tromsø, Tromsø, Norway*

An *ab initio* SCF-MO study has been undertaken on the iso-electronic series methylenecyclopropene, cyclopropenimine, and cyclopropenone. A population analysis has been carried out and serves as the basis for a discussion of the chemical properties of the molecules.

The molecular and electronic structure of small, strained ring systems have attracted much interest, and a large amount of theoretical and experimental work has been undertaken in this field. In some previous studies we have investigated the molecular structure and electron distribution in some small ring systems displaying conjugation.[1-3] The methods we used were electron diffraction and semi-empirical molecular orbital calculations, where only the $\pi$-electrons were included explicitly. As a continuation of this research program, we have carried through an *ab initio* all electron calculation on the molecules methylenecyclopropene, cyclopropenimine, and cyclopropenone. The main purpose of the study is to obtain information on the electron distribution in the molecules. Of particular interest in this context is the question whether these molecules have pronounced single-bond double-bond structures or a more uniform distribution of the $\pi$-electrons.

## METHOD OF CALCULATION

The calculations were performed using the computer program REFLECT[4] by which the Roothaan-Hall equations are solved for a Gaussian type basis, making explicit use of the molecular symmetry.

The computations were carried through using (9.5) basis for the carbon, oxygen, and nitrogen atoms. These primitive basis sets were contracted to double zeta basis sets. The orbital exponents and contraction coefficients applied for the heavy atoms were those of Huzinaga.[5] For hydrogen Huzinaga's exponents scaled by the factor 1.25 were used. The assumed geometries used in the calculations are shown in Fig. 1. which also gives the numbering of the
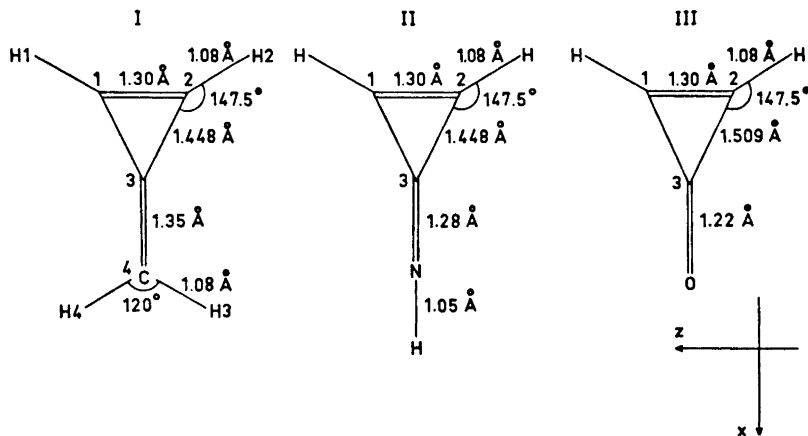
*Fig. 1.* Numbering of atoms. I Methylenecyclopropene, II cyclopropenimine, III cyclo-propenone.

atoms and the coordinate system adopted. For cyclopropenimine, the imino hydrogen atom was assumed to be on the straight line $C=N-H$. This has been done in order to preserve the symmetry plane orthogonal to the ring plane. We assume that this will be an adequate model for the molecule.

## RESULTS AND DISCUSSION

Only the molecular ground states have been considered in this study.

The total molecular energies as well as the orbital energies for all the molecules studied are presented in Table 1, where also the assignments of the molecular orbitals are given.

*Table 1.* Total energy and orbital energies (a.u.) for methylenecyclopropene, cyclopropenimine, and cyclopropenone.

| Methylenecyclopropene | | Cyclopropenimine | | Cyclopropenone | |
|---|---|---|---|---|---|
| $E_{tot}$: | $-153.5916$ | $E_{tot}$: | $-169.5288$ | $E_{tot}$: | $-189.4122$ |
| $1a_1$ | $-11.3105$ | $1a_1$ | $-15.5101$ | $1a_1$ | $-20.5793$ |
| $1b_1$ | $-11.3084$ | $2a_1$ | $-11.3655$ | $2a_1$ | $-11.4262$ |
| $2a_1$ | $-11.3055$ | $3a_1$ | $-11.2990$ | $3a_1$ | $-11.3419$ |
| $3a_1$ | $-11.2098$ | $1b_1$ | $-11.2970$ | $1b_1$ | $-11.3399$ |
| $4a_1$ | $-1.2469$ | $4a_1$ | $-1.2563$ | $4a_1$ | $-1.4156$ |
| $5a_1$ | $-0.9800$ | $5a_1$ | $-1.1163$ | $5a_1$ | $-1.2450$ |
| $2b_1$ | $-0.8026$ | $2b_1$ | $-0.7963$ | $2b_1$ | $-0.8255$ |
| $6a_1$ | $-0.7711$ | $6a_1$ | $-0.7854$ | $6a_1$ | $-0.8063$ |
| $7a_1$ | $-0.6665$ | $7a_1$ | $-0.7286$ | $7a_1$ | $-0.6950$ |
| $3b_1$ | $-0.5904$ | $8a_1$ | $-0.5756$ | $3b_1$ | $-0.6152$ |
| $8a_1$ | $-0.5479$ | $3b_1$ | $-0.5414$ | $8a_1$ | $-0.5944$ |
| $1b_2(\pi_1)$ | $-0.5195$ | $1b_2(\pi_1)$ | $-0.5326$ | $1b_2(\pi_1)$ | $-0.5885$ |
| $4b_1$ | $-0.4477$ | $2b_2(\pi_2)$ | $-0.3483$ | $2b_2(\pi_2)$ | $-0.4362$ |
| $2b_2(\pi_2)$ | $-0.3065$ | $4b_1$ | $-0.3139$ | $4b_1$ | $-0.3931$ |

For computational reasons a decomposing of the total molecular energy providing the necessary data for scaling of the molecular wave function, was not obtained. Hence a reliable estimate of the closeness to the Hartree-Fock limit is rather difficult to make. Huzinaga's calculations on atoms [5] show the need for using eleven $s$ type functions and seven $p$ type functions for carbon, nitrogen, and oxygen, and six $s$ functions for hydrogen. Furthermore, polarization functions would also be needed. The importance of such functions would be enhanced in molecules. For computational reasons we were forced to perform the calculations using smaller basis sets. For one of the molecules, methylenecyclopropene, we have also carried out a calculation using a (7,3) basis for carbon. The total enery in that case was $-153.4285$ a.u. as compared to $-153.5916$ a.u. for the (9,5) calculation. We therefore feel that the total energy given by the latter calculation for this molecule should be at most av few tenths of an atomic unit above the Hartree-Fock limit. Furthermore, a comparative study of molecular properties within this series should be reliable also from a quantitative point of view. Admittedly the relative importance of polarization functions and other extensions of the basis is expected to vary from molecule to molecule in this isoelectronic series. For cyclopropenone, the energy of the present calculation compares favourably with that from a work by Clark et al.[6] In that work a (5,2) basis was employed, giving a total energy of $-187.7254$ a.u.

In Table 2 are given the molecular energies and the sum of the atomic ground state energies calculated by the same basis. The difference between the energies should give a somewhat reliable estimate of the total molecular binding energy in each case. We have here neglected the difference between atomic and molecular correlation energy. The differences, also included in the table, indicate that methylenecyclopropene is the most stable of these systems. Cyclopropenone and cyclopropenimine have rather similar binding energies, the latter being somewhat more stable. A point worth noticing is found in comparing the binding energies of the present calculation with those by Lehn

Table 2. Molecular properties for methylenecyclopropene, cyclopropenimine, and cyclopropenone.

| Properties | Methylene-cyclopropene | Cyclo-propenimine | Cyclo-propenone |
|---|---|---|---|
| Atomic energy (a.u.) | $-152.7376$ | $-168.9488$ | $-188.8543$ |
| Calculated molecular energy (a.u.) | $-153.5916$ | $-169.5288$ | $-189.4122$ |
| Binding energy (a.u.) | 0.8540 | 0.5800 | 0.5579 |
| (kcal/mol) | 536 | 364 | 350 |
| Dipole moment (D) | 2.11 | 1.02 | 4.67 |
| Ionization potentials (eV) | 8.34 | 8.54 | 10.70 |
| | 12.18 | 9.48 | 11.87 |
| | 14.14 | 14.49 | 16.01 |

Table 3. Gross atomic populations for methylenecyclopropene.

| Atomic orbitals | | Molecular orbitals | | | | | | | | | | | | | | Total |
|---|---|---|---|---|---|---|---|---|---|---|---|---|---|---|---|---|
| | | $1a_1$ | $1b_1$ | $2a_1$ | $3a_1$ | $4a_1$ | $5a_1$ | $2b_1$ | $6a_1$ | $7a_1$ | $3b_1$ | $8a_1$ | $1b_2$ | $4b_1$ | $2b_2$ | |
| $C_1C_2$ | $1s+2s$ | 0.984 | 1.000 | 0.067 | 0 | 0.459 | 0.038 | 0.397 | 0.212 | 0.021 | -0.001 | -0.004 | 0 | 0.031 | 0 | 3.153 |
| $C_3$ | $1s+2s$ | 0.0313 | 0 | 1.968 | 0 | 0.272 | 0.316 | 0 | 0.104 | 0.231 | 0 | 0.013 | 0 | 0 | 0 | 2.935 |
| $C_4$ | $1s+2s$ | 0 | 0 | 0 | 2.000 | 0.070 | 0.851 | 0 | 0.053 | 0.178 | 0 | 0.037 | 0 | 0 | 0 | 3.189 |
| $H_1,H_2$ | | 0 | 0 | 0 | 0 | 0.042 | 0.007 | 0.250 | 0.192 | 0.055 | 0.030 | 0.035 | 0 | 0.074 | 0 | 0.685 |
| $H_3,H_4$ | | 0 | 0 | 0 | 0 | 0.001 | 0.098 | 0.001 | 0.033 | 0.169 | 0.265 | 0.055 | 0 | 0.140 | 0 | 0.762 |
| $C_1,C_2$ | $2p_x$ | 0 | 0 | 0 | 0 | 0.046 | 0.026 | 0.002 | 0.335 | 0.004 | 0.082 | 0.197 | 0 | 0.360 | 0 | 1.052 |
| | $2p_y$ | 0 | 0 | 0 | 0 | 0 | 0 | 0 | 0 | 0 | 0 | 0 | 0.620 | 0 | 0.293 | 0.913 |
| | $2p_z$ | 0 | 0 | 0 | 0 | 0.165 | 0.014 | 0.261 | 0.085 | 0.253 | 0.013 | 0.339 | 0 | 0.004 | 0 | 1.134 |
| $C_3$ | $2p_x$ | 0 | 0 | 0 | 0 | 0.193 | 0.424 | 0 | 0.077 | 0.045 | 0 | 0.425 | 0 | 0 | 0 | 1.164 |
| | $2p_y$ | 0 | 0 | 0 | 0 | 0 | 0 | 0 | 0 | 0 | 0 | 0 | 0.614 | 0 | 0.343 | 0.957 |
| | $2p_z$ | 0 | 0 | 0 | 0 | 0 | 0 | 0.173 | 0 | 0 | 0.274 | 0 | 0 | 0.560 | 0 | 1.007 |
| $C_4$ | $2p_x$ | 0 | 0 | 0 | 0 | 0.039 | 0.042 | 0 | 0.054 | 0.541 | 0 | 0.283 | 0 | 0 | 0 | 0.959 |
| | $2p_y$ | 0 | 0 | 0 | 0 | 0 | 0 | 0 | 0 | 0 | 0 | 0 | 0.146 | 0 | 1.070 | 1.216 |
| | $2p_z$ | 0 | 0 | 0 | 0 | 0 | 0 | 0.005 | 0 | 0 | 0.947 | 0 | 0 | 0.222 | 0 | 1.174 |

Table 4. Gross atomic populations for cyclopropenimine.

| Atomic orbitals | | Molecular orbitals | | | | | | | | | | | | | | Total |
|---|---|---|---|---|---|---|---|---|---|---|---|---|---|---|---|---|
| | | $1a_1$ | $2a_1$ | $3a_1$ | $1b_1$ | $4a_1$ | $5a_1$ | $2b_1$ | $6a_1$ | $7a_1$ | $8a_1$ | $3b_1$ | $1b_2$ | $2b_2$ | $4b_1$ | |
| $C_1,C_2$ | $1s+2s$ | 0 | 0 | 1.000 | 1.000 | 0.403 | 0.058 | 0.413 | 0.166 | 0.092 | -0.006 | 0.001 | 0 | 0 | 0.049 | 3.176 |
| $C_3$ | $1s+2s$ | 0 | 2.000 | 0 | 0 | 0.389 | 0.092 | 0 | 0.223 | 0.027 | 0.118 | 0 | 0 | 0 | 0 | 2.849 |
| $N$ | $1s+2s$ | 2.000 | 0 | 0 | 0 | 0.171 | 1.049 | 0 | 0.096 | 0.079 | 0.010 | 0 | 0 | 0 | 0 | 3.405 |
| $H_1,H_2$ | | 0 | 0 | 0 | 0 | 0.036 | 0.009 | 0.248 | 0.116 | 0.109 | 0.061 | 0.080 | 0 | 0 | 0.036 | 0.695 |
| $H_3$ | | 0 | 0 | 0 | 0 | 0.007 | 0.09 | 0 | 0.172 | 0.250 | 0.045 | 0 | 0 | 0 | 0 | 0.564 |
| $C_1,C_2$ | $2p_x$ | 0 | 0 | 0 | 0 | 0.049 | 0.006 | 0.001 | 0.254 | 0.081 | 0.175 | 0.265 | 0 | 0 | 0.237 | 1.068 |
| | $2p_y$ | 0 | 0 | 0 | 0 | 0 | 0 | 0 | 0 | 0 | 0 | 0 | 0.492 | 0.412 | 0 | 0.904 |
| | $2p_z$ | 0 | 0 | 0 | 0 | 0.145 | 0.027 | 0.244 | 0.012 | 0.156 | 0.514 | 0.024 | 0 | 0 | -0.007 | 1.112 |
| $C_3$ | $2p_x$ | 0 | 0 | 0 | 0 | 0.119 | 0.520 | 0 | 0.001 | 0.152 | 0.238 | 0 | 0 | 0 | 0 | 1.030 |
| | $2p_y$ | 0 | 0 | 0 | 0 | 0 | 0 | 0 | 0 | 0 | 0 | 0 | 0.717 | 0.168 | 0 | 0.885 |
| | $2p_z$ | 0 | 0 | 0 | 0 | 0 | 0 | 0.181 | 0 | 0 | 0 | 0.774 | 0 | 0 | 0.041 | 0.996 |
| $N$ | $2p_x$ | 0 | 0 | 0 | 0 | 0.045 | 0.039 | 0 | 0.410 | 0.613 | 0.100 | 0 | 0 | 0 | 0 | 1.207 |
| | $2p_y$ | 0 | 0 | 0 | 0 | 0 | 0 | 0 | 0 | 0 | 0 | 0 | 0.299 | 1.008 | 0 | 1.307 |
| | $2p_z$ | 0 | 0 | 0 | 0 | 0 | 0 | 0.008 | 0 | 0 | 0 | 0.483 | 0 | 0 | 1.33 | 0.821 |

Table 5. Gross atomic populations for cyclopropenone.

| Atomic orbitals | | $1a_1$ | $2a_1$ | $3a_1$ | $1b_1$ | $4a_1$ | $5a_1$ | $2b_1$ | $6a_1$ | $7a_1$ | $3b_1$ | $8a_1$ | $1b_2$ | $2b_2$ | $4b_1$ | Total |
|---|---|---|---|---|---|---|---|---|---|---|---|---|---|---|---|---|
| | | | | | | | | | Molecular orbitals | | | | | | | |
| $C_1,C_2$ | $1s+2s$ | 0 | 0 | 1.000 | 1.000 | 0.038 | 0.441 | 0.416 | 0.218 | 0.034 | 0 | -0.01 | 0 | 0 | 0.064 | 3.201 |
| $C_3$ | $1s+2s$ | 0 | 2.000 | 0 | 0 | 0.222 | 0.169 | 0 | 0.229 | 0.215 | 0 | 0.088 | 0 | 0 | 0 | 2.923 |
| O | $1s+2s$ | 2.000 | 0 | 0 | 0 | 1.347 | 0.076 | 0.241 | 0.055 | 0.297 | 0 | 0.141 | 0 | 0 | 0 | 3.916 |
| $H_1,H_2$ | | 0 | 0 | 0 | 0 | 0.001 | 0.047 | 0.002 | 0.165 | -0.001 | 0.055 | 0.132 | 0 | 0 | 0.055 | 0.674 |
| $C_1,C_2$ | $2p_x$ | 0 | 0 | 0 | 0 | 0.020 | 0.024 | 0.246 | 0.371 | 0 | 0.140 | 0.040 | 0 | 0 | 0.356 | 1.044 |
| | $2p_y$ | 0 | 0 | 0 | 0 | 0 | 0 | 0 | 0 | 0 | 0 | 0 | 0.277 | 0.627 | 0 | 0.904 |
| | $2p_z$ | 0 | 0 | 0 | 0 | 0.007 | 0 | 0 | 0.041 | 0.302 | 0.022 | 0.343 | 0 | 0 | -0.012 | 1.117 |
| $C_3$ | $2p_x$ | 0 | 0 | 0 | 0 | 0 | 0 | 0.171 | 0 | 0 | 0.645 | 0 | 0 | 0 | 0.183 | 0.932 |
| | $2p_y$ | 0 | 0 | 0 | 0 | 0 | 0 | 0 | 0 | 0 | 0 | 0 | 0.740 | 0.008 | 0 | 0.748 |
| | $2p_z$ | 0 | 0 | 0 | 0 | 0.153 | 0.168 | 0 | 0.050 | 0.044 | 0 | 0.288 | 0 | 0 | 0 | 0.999 |
| O | $2p_x$ | 0 | 0 | 0 | 0 | 0 | 0 | 0.018 | 0 | 0 | 0.923 | 0 | 0 | 0 | 0.889 | 1.328 |
| | $2p_y$ | 0 | 0 | 0 | 0 | 0 | 0 | 0 | 0 | 0 | 0 | 0 | 0.707 | 0.737 | 0 | 1.444 |
| | $2p_z$ | 0 | 0 | 0 | 0 | 0.148 | 0.397 | 0 | 0.072 | 0.636 | 0 | 0.472 | 0 | 0 | 0 | 1.830 |

*Table 6.* Total gross atomic charges.

| Atoms | Methylene-cyclopropene | Cyclopropen-imine | Cyclo-propenone |
|---|---|---|---|
| $C_1$, $C_2$ | 6.252 | 6.266 | 6.266 |
| $C_3$ | 6.063 | 5.769 | 5.601 |
| $C_4$ | 6.538 | | |
| O | | | 8.518 |
| N | | 7.740 | |
| $H_1$, $H_2$ | 0.685 | 0.696 | 0.674 |
| $H_3$ | | 0.564 | |
| $H_3$, $H_4$ | 0.762 | | |

and coworkers [7] for cyclopropane, cyclopropene, and diazirine. Diazirine may be thought of as a cyclopropene molecule where two CH groups have been replaced by two N-atoms. The difference in binding energy between these two species was found to be 0.48 a.u., or 0.24 a.u. for each N atom. In cyclopropenimine, one $CH_2$ group in methylenecyclopropene, has been replaced by an NH group. The difference in binding energy in this case is 0.27 a.u. Considering the fact that the systems display some discrepancies, the similarities of these magnitudes are of some interest.

Table 1 gives the orbital energies. In the case of all molecules, the first four orbitals are nearly pure a.o.'s and localized to the heavy atom frame of the systems. For cyclopropenone and cyclopropenimine the orbitals with the highest energy describe the lone pairs in nitrogen and oxygen. The two $\pi$-orbitals are next to highest in energy. For methylenecyclopropene the highest lying $\sigma$-orbital is between the two $\pi$-orbirals.

Table 2 also shows the lowest ionization potentials estimated by means of Koopmans' theorem, and the dipole moments of the molecules. By symmetry, the dipole moment components vanish along the $y$ and $z$ axes and the dipole moments for all three molecules coincide with the positive $x$ direction.

The molecular populations have been calculated from a Mulliken type population analysis. The resulting molecular populations are given in Tables 3 — 5. The total $\sigma$ populations are obtained by adding the $1s$, $2s$, $2px$, and $2pz$ contributions. Table 6 gives the total of these populations. It is seen that all three molecules have practically identical charges on atoms 1 and 2. In cyclopropenimine, the charge on atom $C_3$ is rather low, and compared to the hydrocarbon there is a net flow of electrons to the external heavy atom.

This effect is even more pronounced for the cyclopropenone molecule, where the very high charge of about 8.5 electrons on the oxygen atom is responsible for the unusual high dipole moment of this molecule. A further study of the electronic distribution is made by investigating the overlap populations given in Tables 7 — 9. It is seen from these tables that the C = O bond in cyclopropenone has a smaller overlap population than the external double bond in the two other molecules. This applies to the $\sigma$ part as well as the $\pi$ part of this bond. A remarkable feature is found for the $C_1 - C_2$ bond in cyclopropenimine and cyclopropenone. In these cases the total overlaps are in

Table 7. Overlap populations for methylenecyclopropene.

| Bonds | $1a_1$ | $1b_1$ | $2a_1$ | $3a_1$ | $4a_1$ | $5a_1$ | $2b_1$ | $6a_1$ | $7a_1$ | $3b_1$ | $8a_1$ | $1b_2$ | $4b_1$ | $2b_2$ | Total |
|---|---|---|---|---|---|---|---|---|---|---|---|---|---|---|---|
| $C_1-C_2$ | 0.000 | 0.0 0 | 0.000 | 0.0 0 | 0.192 | 0.017 | 0.026 | 0.062 | 0.024 | −0.040 | 0.181 | 0.131 | −0.376 | 0.120 | 0.388($\pi=$ 0.251) |
| $C_1-C_3$ | 0.000 | 0.000 | 0.000 | 0.000 | 0.125 | 0.018 | 0.043 | −0.005 | −0.008 | 0.012 | −0.121 | 0.105 | 0.124 | −0.106 | 0.183($\pi=$ −0.001) |
| $C_3-C_4$ | 0.000 | 0.000 | 0.000 | 0.000 | 0.019 | 0.273 | 0.002 | 0.022 | 0.020 | 0.090 | −0.014 | 0.052 | −0.113 | 0.206 | 0.540($\pi=$ 0.258) |
| $C_1-H_1$ | 0.000 | 0.000 | 0.000 | 0.000 | 0.010 | 0.002 | 0.132 | 0.115 | 0.035 | 0.016 | 0.015 | 0.000 | 0.016 | 0.000 | 0.341 |
| $C_4-H_4$ | 0.000 | 0.000 | 0.000 | 0.000 | 0.001 | 0.046 | 0.000 | 0.013 | 0.099 | 0.127 | 0.041 | 0.000 | 0.072 | 0.000 | 0.400 |

Table 8. Overlap populations for cyclopropenimine.

| Bonds | $1a_1$ | $2a_1$ | $3a_1$ | $1b_1$ | $4a_1$ | $5a_1$ | $2b_1$ | $6a_1$ | $7a_1$ | $8a_1$ | $3b_1$ | $1b_2$ | $2b_2$ | $4b_1$ | Total |
|---|---|---|---|---|---|---|---|---|---|---|---|---|---|---|---|
| $C_1-C_2$ | 0.000 | 0.000 | 0.000 | 0.000 | 0.166 | 0.019 | 0.008 | 0.080 | −0.002 | 0.221 | −0.162 | 0.098 | 0.145 | −0.578 | −0.003($\pi=$ 0.243) |
| $C_1-C_3$ | 0.000 | 0.000 | 0.000 | 0.000 | 0.124 | 0.027 | 0.044 | −0.019 | −0.005 | −0.155 | 0. 62 | 0.098 | −0.090 | 0.032 | 0.121($\pi=$ 0.008) |
| $C_3-N$ | 0.000 | 0.000 | 0.000 | 0.000 | 0.020 | 0.260 | 0.034 | 0.061 | 0.028 | −0.006 | 0.126 | 0.087 | 0.143 | −0.052 | 0.669($\pi=$ 0.230) |
| $C_1-H$ | 0.000 | 0.000 | 0.000 | 0.000 | 0.000 | 0.000 | 0.131 | 0.067 | 0.070 | 0.032 | 0.038 | 0.000 | 0.000 | −0.031 | 0.316 |
| $N-H_3$ | 0.000 | 0.000 | 0.000 | 0.000 | 0.005 | 0.048 | 0.′00 | 0.096 | 0.151 | 0.026 | 0.000 | 0.000 | 0.000 | 0.000 | 0.326 |

Table 9. Overlap populations for cyclopropenone.

| Bonds | $1a_1$ | $2a_1$ | $3a_1$ | $1b_1$ | $4a_1$ | $5a_1$ | $2b_1$ | $6a_1$ | $7a_1$ | $3b_1$ | $8a_1$ | $1b_2$ | $2b_2$ | $4b_1$ | Total |
|---|---|---|---|---|---|---|---|---|---|---|---|---|---|---|---|
| $C_1-C_2$ | 0.000 | 0.000 | 0.000 | 0.000 | 0.019 | 0.179 | 0.006 | 0.091 | 0.015 | −0.050 | 0.176 | 0.051 | 0.186 | −0.687 | −0.013($\pi=0.237$) |
| $C_1-C_3$ | 0.000 | 0.000 | 0.000 | 0.000 | −0.001 | 0.138 | 0.039 | −0.011 | −0.008 | 0.022 | −0.138 | 0.068 | −0.041 | 0.078 | 0.146($\pi=0.027$) |
| $C_3-O$ | 0.000 | 0.000 | 0.000 | 0.000 | 0.218 | 0.021 | 0.006 | 0.024 | −0.016 | 0.163 | −0.071 | 0.144 | 0.052 | −0.104 | 0.438($\pi=0.196$) |
| $C_1-H_1$ | 0.000 | 0.000 | 0.000 | 0.000 | 0.000 | 0.010 | 0.130 | 0.099 | 0.046 | 0.030 | 0.017 | 0.000 | 0.000 | −0.021 | 0.311 |

fact negative, indicating the instability of these systems. The differences be-
tween the systems are in the $\sigma$ electrons, the $\pi$ electron overlaps are nearly
identical for all three molecules. Indeed, the systems seem unstable; although
the cyclopropenone molecule has been syntesized, it has resisted isolation
from solution.[8]

At this point, one must also question the reliability of the Mulliken type
population analysis for small strained ring systems.

## REFERENCES

1. Skancke, A. and Skancke, P. N. *Acta Chem. Scand.* **22** (1968) 175.
2. Skancke, A. *Acta Chem. Scand.* **22** (1968) 3239.
3. Skancke, A. *Acta Chem. Scand.* **27** (1973) 1735.
4. Siegbahn, P. *Chem. Phys. Lett.* **8** (1971) 245.
5. Huzinaga, S. *J. Chem. Phys.* **42** (1965) 1293.
6. Clark, D. T. and Lilley, D. M. *J. Chem. Commun.* **1970** 148.
7. Kochanski, E. and Lehn, J. M. *Theor. Chim. Acta* **14** (1969) 281.
8. Ryan, G. A. *Diss. Abstr. Int.* **30** (B 1969) 2616.

Received May 15, 1973.

# Organic Hydroxylamine Derivatives

## VIII.* Structural Analogues of GABA of the Isoxazole Enol-Betaine Type. Synthesis of 5,6,7,8-Tetrahydro-4H-isoxazolo[3,4-d]azepin-3-ol Zwitterion and Some Derivatives

POVL KROGSGAARD-LARSEN, HANS HJEDS,
SØREN BRØGGER CHRISTENSEN and LOTTE BREHM

*The Royal Danish School of Pharmacy, Chemical Laboratory C, DK-2100 Copenhagen, Denmark*

The structural analogue of GABA, 5,6,7,8-tetrahydro-4H-isoxazolo[3,4-d]azepin-3-ol zwitterion (V), a new heterocyclic compound, and some derivatives have been synthesized using the reaction of hydroxylamine with enamines of β-ketoesters previously found to give isoxazolin-5-ones.[18] The $pK_A$ values of the isoxazolin-5-ones described have been determined and the enol-betaine character of (V) and of the N-benzyl derivative (VI) has been established.

Some common structural features of GABA, muscimol, and compound (V) are compared.

Structure-activity correlations of conformationally restricted analogues of γ-aminobutyric acid (GABA), an inhibitory transmitter at certain synapses in the mammalian central nervous system,[1,2] are of importance in the investigations of the active conformations of GABA. Recent studies seem to indicate that extended conformations of GABA are important in the initial bindings of GABA to its transport carrier[3] as well as to the active sites of the GABA transaminase enzymes.[4] However, studies of the interactions between GABA analogues and the postsynaptic receptors have provided rather conflicting suggestions as to the active conformations of GABA. On these receptors GABA might be active in extended[5–8] and/or folded conformations.[9,10]

Muscimol (3-hydroxy-5-aminomethylisoxazole) has been demonstrated to be a GABA agonist of restricted conformation[5] and furthermore to be a non-competitive inhibitor of the GABA transport system.[3,11] Further information about the active conformations of GABA might be obtained from structure-activity investigations of pertinent aminoalkyl substituted 3-hydroxyisoxazoles. The zwitterionic character of these 3-hydroxyisoxazole derivatives is

---

* Part VII. *Acta Chem. Scand.* **27** (1973) 2802.

generally accepted and has been confirmed for muscimol and for the homologous compound, 3-hydroxy-5-(2-aminoethyl)isoxazole, by X-ray crystallographic structural analysis.[12,13]

The isoxazolin-5-one nucleus has pronounced acidic properties [14] and amphoteric properties have been shown for 4-(3-aminopropyl)-5-hydroxy-isoxazole,[15*] a very unstable compound which is the hitherto only known 5-hydroxyisoxazole enol-betaine. These protolytic properties indicate that GABA agonists may well be found among 5-hydroxyisoxazole enol-betaines structurally related to muscimol. This paper presents the synthesis of 5,6,7,8-tetrahydro-4H-isoxazolo[3,4-d]azepin-3-ol zwitterion (V), which is a structural analogue of GABA. Two conformers of (V) (A and B in Fig. 1) seem to be almost equally favourable. The approximate intra-molecular distances between the exocyclic oxygen atoms and the azepine nitrogen atoms in A and B are 4.5 and 5.3 Å, respectively (Dreiding stereomodels) (cf. Ref. 12). The structural relationship between GABA, muscimol, and 5,6,7,8-tetrahydro-4H-isoxazolo[3,4-d]azepin-3-ol (V) including their amphoteric properties are shown in Fig. 1.
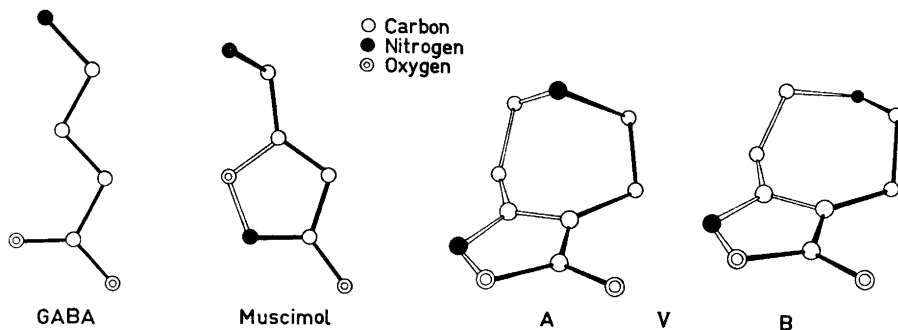


Fig. 1. Similarities of structures (heavy black lines) and amphoteric properties of GABA, muscimol, and two conformers of 5,6,7,8-tetrahydro-4H-isoxazolo[3,4-d]azepin-3-ol zwitterion (VA and VB). $pK_A$-values ($H_2O$): 4.03, 10.6[16] (GABA); 4.78, 8.43[17] (muscimol); 3.3, 9.6 (V).

The synthesis of compound (V) and derivatives as described below are based on the reaction of hydroxylamine with the N-benzylenamines (IIa – c) of the appropriate β-ketoesters (Ia–c) as shown in Scheme 1. This reaction was earlier shown [18] to give isoxazolin-5-ones via the corresponding benzyl-ammonium salts. In Scheme 1 the isoxazolin-5-ones are depicted as the 3-isoxazolin-5-one tautomers, but in fact isoxazolin-5-ones usually are mixtures of at least this tautomer and the 2-isoxazolin-5-one tautomer.[14,19]

---

* In the literature this compound is named 4-(3-aminopropyl)-2-isoxazolin-5-one.
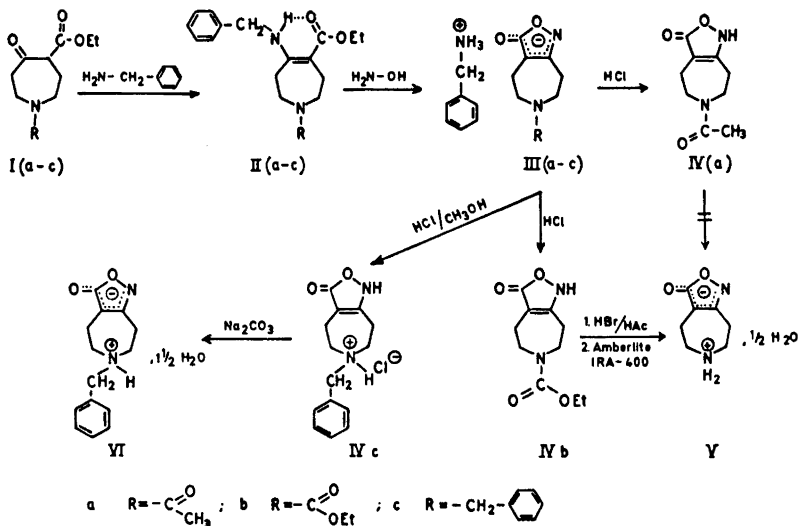
*Scheme 1.*

The $\beta$-ketoesters (Ia–c), prepared by ring expansion of the corresponding 4-piperidone derivatives with ethyl diazoacetate as described by Yamamoto *et al.*[20] and Moriya *et al.*,[21] were treated with benzylamine to give the enamines (IIa–c). The enamine structure of the compounds (IIa–c), each of which form an *intra*molecular hydrogen bond, were established by IR, UV, and ^{1}H NMR spectroscopy, and were in agreement with the previous findings for analogous compounds.[18] The enamines (IIa–c) were treated with hydroxylamine to give the benzylammonium salts (IIIa–c). The structure determinations of (IIIa–c) were based on IR, UV, and ^{1}H NMR spectroscopy and in the case of (IIIb–c) further supported by elemental analyses. Compound (IIIa) could not be obtained in a crystalline state. The spectroscopic data of (IIIa–c) were in accordance with the general findings for analogous products.[18]

Treatment of the benzylammonium salts (IIIa,b) with hydrochloric acid and of (IIIc) with methanolic hydrogen chloride afforded the isoxazolin-5-ones (IVa–c) in good yields. Conclusive evidence of the constitutions of these compounds were provided by elemental analyses and by IR, UV, and ^{1}H NMR spectroscopy. The spectroscopic data were in accordance with the general findings described by Jacquier *et al.*[19]

Attempts to prepare the enol-betaine (V) from the isoxazolin-5-one (IVa) were unsuccessful. Thus, reflux of (IVa) with 6 N hydrochloric acid for 4 h caused extensive decomposition of the molecule and no product was isolated. On the other hand after boiling under reflux of (IVa) with a 43 % solution of hydrogen bromide in glacial acetic acid for 3 h as well as with a 10 % solution of sodium methoxide in methanol for 4 h (IVa) was left almost completely unreacted. In another attempt to prepare (V) the isoxazolin-5-one

(IVb) was refluxed with a 15 % solution of potassium hydroxide in methanol for 24 h after which time the starting material (IVb) could be recovered from the reaction mixture in 90 % yield. Finally (IVb) was cleaved by treatment with a 43 % solution of hydrogen bromide in glacial acetic acid and 5,6,7,8-tetrahydro-4$H$-isoxazolo[3,4-$d$]azepin-3-ol zwitterion (V) was isolated from the reaction mixture in moderate yield using a strongly basic ion exchange resin. The compound was shown to crystallize as a hemihydrate.

The enol-betaine (VI) was isolated from an aqueous solution of the isoxazolin-5-one hydrochloride (IVc) after adjustment of pH of the solution to 6.5. The compound crystallized with 1.5 mol of water.

IR and UV spectroscopic data of the compounds (II)–(VI), which are all new, and p$K_A$ values of the acidic or amphoteric compounds (IV)–(VI) are listed in Table 1. In the IR spectra of the compounds (V) and (VI) carbonyl group signals were absent, and the aromatic character of the isoxazole nucleus of the compounds (V) and (VI) as well as of (IIIa–c) manifests itself as absorp-

*Table 1.* IR and UV data and pertinent p$K_A$ values of the compounds (II) – (VI).

| | IR data [a] (cm⁻¹) | UV data [b] $\lambda_{max}$(nm) | $\varepsilon \times 10^{-3}$ | p$K_A$ values [c] I | II |
|---|---|---|---|---|---|
| IIa | 3250(m), 1650(s), 1630(s), 1595(s) | 304 | 13.3 | | |
| IIb | 3240(m), 1695(s), 1645(s), 1600(s) | 304 | 14.4 | | |
| IIc [d] | 3240(m), 1642(s), 1600(s) | 304 | 13 | | |
| IIIa [d,e] | 3600 − 2300(s), 2150(w), 1680(m), 1640 − 1610(s), 1500 − 1470(s) | 261 | 6.6 | | |
| IIIb [e] | 3200 − 2300(s), 2180(w), 1690(s), 1620(s), 1490 − 1460(s) | 260 | 6.68 | | |
| IIIc [e] | 3300 − 2300(s), 2160(w), 1630 − 1610(s), 1510 − 1460(s) | 261 | 5.95 | | |
| IVa | 3300 − 2600(s), 1720(s), 1640 − 1610(s) | 263 | 8.51 | 4.3 | |
| IVa [f] | 3500 − 2600(m), 1790(m), 1730(s), 1640(s), 1600(m) | | | | |
| IVb | 3300 − 2600(m), 1725(s), 1665(s), 1630(s) | 263 | 8.26 | 4.7 | |
| IVb [f] | 3500 − 2600(m), 1790(m), 1720(s), 1665(s), 1625(s) | | | | |
| IVc | 3200 − 2300(s), 1725(s), 1640(s), 1610(m) | 259 | 7.26 | 3.3 | 8. |
| V | 3600 − 2200(m), 2150(w), 1650 − 1610(s), 1520 − 1470(s) | 255 | 9.00 | 3.3 | 9.6 |
| IV | 3600 − 2000(m), 1650 − 1610(s), 1520 − 1470(s) | 254 | 8.00 | 3.3 | 8.3 |

[a] Unless otherwise stated the IR spectra were recorded in the solid state (KBr). [b] Unless otherwise stated the UV spectra were recorded in ethanol solutions. [c] p$K_A$ values were determined by electrometrical titration in water at 25°C according to the method described by Albert and Serjeant.[23] [d] The IR spectrum was recorded using the film technique. [e] The UV spectra were recorded in tetrahydrofuran solutions. [f] The IR spectra were recorded in chloroform solutions (*cf.* Ref. 19).

tion bands in the 1520 – 1460 and 1650 – 1600 cm⁻¹ regions.[22] Broad absorptions in the IR spectra of (V) and (VI) over the range 3600 – 2000 cm⁻¹ and in the case of compound (V) an absorption band at 2150 cm⁻¹ suggest ammonium salt character of the molecules. These observations compared with the acidic properties of the isoxazolin-5-one nucleus confirm the proposed zwitterionic character of the compounds (V) and (VI). The UV maxima of the enol-betaines (V) and (VI) were observed at wavelengths of 255 and 254 nm, respectively, in agreement with that observed (255 nm) for the zwitterionic compound 4-(3-aminopropyl)-5-hydroxyisoxazole by Quin and Pinion.[15]

## EXPERIMENTAL

Unless otherwise stated the determinations of melting points, the recording of IR, UV, and ¹H NMR spectra, and the performance of microanalyses were accomplished as described in a previous paper.[18] The singlet, doublet, triplet, quartet, and multiplet patterns of the ¹H NMR spectra are designed s, d, t, q, and m, respectively. pH Values were measured on a Radiometer pH meter 26.

*Ethyl 1-acetyl-4-benzylamino-2,3,6,7-tetrahydro-1H-azepine-5-carboxylate (IIa).* A mixture of 8.4 g (37 mmol) of (Ia),[20] 4.4 g (41 mmol) of benzylamine, and 18 g of molecular sieve, Union Carbide 3A, was refluxed in 75 ml of benzene for 5 h. The mixture was filtered and concentrated *in vacuo* to give 8.5 g (73 %) of pale yellow crystals. Recrystallization (cyclohexane) of an analytical sample afforded colourless crystals, m.p. 106.0 – 108.5°C. (Found: C 68.50; H 7.73; N 8.94. Calc. for $C_{18}H_{24}N_2O_3$: C 68.33; H 7.65; N 8.85). ¹H NMR data (CCl₄) δ: 9.7 [broadened t (J = 6 cps), 1 H, $CH_2 - NH - C$]; 7.25 (slightly broadened s, 5 H, $C_6H_5$); 4.36 [d (J = 6 cps), 2 H, $C - CH_2 - NH$]; 4.06 [q (J = 7 cps), 2 H, $O - CH_2 - CH_3$]; 3.7 – 3.1 (m, 4 H, $CH_2 - CH_2 - N - CH_2 - CH_2$); 2.8 – 2.3 (m, 4 H, $CH_2 - CH_2 - C = C - CH_2 - CH_2$); 2.00 [s, 3 H, $CH_3 - C = O$]; 1.21 (t (J = 7 cps), 3 H, $CH_3 - CH_2$].

*Benzylammonium salt of 6-acetyl-5,6,7,8-tetrahydro-4H-isoxazolo[3,4-d]azepin-3-ol (IIIa).* 368 mg (16 mmol) of sodium were allowed to react with methanol (50 ml) and to this solution were added 1.10 g (16 mmol) of hydroxylammonium chloride. After stirring for 5 min 4.5 g (15 mmol) of (IIa) were added and the mixture was refluxed for 2 h. After cooling to room temperature 25 ml of tetrahydrofuran (THF) were added. The mixture was stirred for 5 min, filtered, and evaporated to dryness *in vacuo* to give 4.2 g (97 %) of a glassy compound which on TLC plates [silica gel GF₂₅₄ (Merck), chloroform – methanol – formic acid (66:33:1), ninhydrin] gave two spots corresponding to benzylamine and the isoxazolin-5-one (IVa). ¹H NMR data (DMSO-$d_6$) δ: 7.6 – 7.2 (m, 5 H, $C_6H_5$); 7.1 – 6.4 (broadened signal, 3 H, $CH_2 - NH_3^+$); 3.98 (slightly broadened s, 2 H, $C - CH_2 - NH_3^+$); 3.7 – 3.2 (m, 4 H, $CH_2 - CH_2 - N - CH_2 - CH_2$); 2.7 – 2.0 (m, 4 H, $CH_2 - CH_2 - C = C - CH_2 - CH_2$); 2.03 (s, 3 H, $CH_3 - C = O$).

*6-Acetyl-1,3,4,5,7,8-hexahydro-3-oxo-6H-isoxazolo[3,4-d]azepine (IVa).* 3.4 g (11 mmol) of crude benzylammonium salt (IIIa) were dissolved in 10 ml of water. Upon addition of 5 g of sodium carbonate the mixture was continuously extracted with ether for 1.5 h. The ether phase was discarded, and upon addition of 8 ml of concentrated hydrochloric acid the aqueous phase was continuously extracted with ether – methylene chloride (4:1) for 48 h. The extract was dried, filtered, and evaporated. Recrystallization (methanol) of the residue afforded 1.4 g (64 %) of (IVa) as colourless crystals, m.p. 162.5 – 164.5°C (decomp.). (Found: C 55.10; H 6.28; N 14.35. Calc. for $C_9H_{12}N_2O_3$: C 55.09; H 6.17; N 14.28). ¹H NMR data (DMSO-$d_6$) δ: 3.8 – 3.3 (m, 4 H, $CH_2 - CH_2 - N - CH_2 - CH_2$); 2.8 – 2.1 (m, 4 H, $CH_2 - CH_2 - C = C - CH_2 - CH_2$); 2.06 (s, 3 H, $CH_3 - C = O$). Several ¹H NMR spectra of (IVa) were recorded in DMSO-$d_6$ solution, but in no case could the resonance signal of the acidic proton of (IVa) be detected.

*Diethyl 4-benzylamino-2,3,6,7-tetrahydro-1H-azepine-1,5-dicarboxylate (IIb).* (IIb) was synthesized as described above for (IIa) using 8.6 g (33 mmol) of (Ib)[21] and 3.9 g (36 mmol) of benzylamine to give 11.0 g (95 %) of crude product as a pale yellow oil. An analytical sample was subjected to column chromatography on silica gel (0.05 – 0.20 mm,

Merck), eluent: benzene — ethyl acetate (2:1). The purified enamine (IIb) was crystallized (petroleum ether) to give colourless needles, m.p. 36.5 − 39.0°C. (Found: C 65.75; H 7.64; N 8.07. Calc. for $C_{19}H_{26}N_2O_4$: C 65.87; H 7.57; N 8.09). $^1$H NMR data ($CCl_4$) $\delta$: 9.8 [broadened t ($J = 6$ cps), 1 H, $CH_2 - NH - C$]; 7.20 (slightly broadened s, 5 H, $C_6H_5$); 4.38 [d ($J = 6$ cps), 2 H, $C - CH_2 - NH$]; 4.02 and 3.95 [2 × q ($J = 7$ cps in both cases), 4 H, $2 \times O - CH_2 - CH_3$]; 3.5 − 3.1 (m, 4 H, $CH_2 - CH_2 - N - CH_2 - CH_2$); 2.7 − 2.3 (m, 4 H, $CH_2 - CH_2 - C = C - CH_2 - CH_2$); 1.23 and 1.16 [2 × t ($J = 7$ cps in both cases), 6 H, $2 \times CH_3 - CH_2$].

*Benzylammonium salt of ethyl 5,6,7,8-tetrahydro-4H-isoxazolo[3,4-d]azepin-3-ol-6-carboxylate (IIIb).* (IIIb) was prepared as described above for (IIIa) using 5.0 g (15 mmol) of (IIb) and 1.10 g (16 mmol) of hydroxylammonium chloride to give 5.8 g of a crystalline product. An analytical sample was recrystallized twice (THF) to give (IIIb) as colourless crystals, m.p. 152 − 156°C (decomp.). (Found: C 61.30; H 7.08; N 12.80. Calc. for $C_{17}H_{23}N_3O_4$: C 61.22; H 6.99; N 12.60). $^1$H NMR data (DMSO-$d_6$) $\delta$: 8.3 − 7.5 (broadened signal, 3 H, $CH_2 - NH_3^+$); 7.4 (slightly broadened s, 5 H, $C_6H_5$); 3.94 [q ($J = 7$ cps), 2 H, $O - CH_2 - CH_3$]; 3.94 (slightly broadened s, 2 H, $C - CH_2 - NH_3^+$); 3.6 − 3.1 (m, 4 H, $CH_2 - CH_2 - N - CH_2 - CH_2$); 2.4 − 1.9 (m, 4 H, $CH_2 - CH_2 - C = C - CH_2 - CH_2$); 1.15 [t ($J = 7$ cps), 3 H, $CH_3 - CH_2$].

*Ethyl 1,3,4,5,7,8-hexahydro-3-oxo-6H-isoxazolo[3,4-d]azepine-6-carboxylate (IVb).* (IVb) was synthesized as described above for (IVa) using 5.6 g (17 mmol) of crude (IIIb). Continuous extraction of the acidified aqueous phase with ether-methylene chloride (4:1) for 1.5 h afforded 3.8 g of crude (IVb), which was recrystallized (THF — ether) to give 2.3 g (58 %) of (IVb) as colourless crystals, m.p. 112.0 − 113.0°C (decomp.). (Found: C 53.45; H 6.33; N 12.55. Calc. for $C_{10}H_{14}N_2O_4$: C 53.09; H 6.24; N 12.38). $^1$H NMR data [$CCl_4 - CDCl_3$ (1:1)] $\delta$: 9.8 − 9.4 (broadened signal, 1 H, $NH$); 4.14 [q ($J = 7$ cps), 2 H, $O - CH_2 - CH_3$]; 3.8 − 3.3 (m, 4 H, $CH_2 - CH_2 - N - CH_2 - CH_2$); 3.0 − 2.2 (m, 4 H, $CH_2 - CH_2 - C = C - CH_2 - CH_2$); 1.27 [t ($J = 7$ cps), 3 H, $CH_3 - CH_2$].

*5,6,7,8-Tetrahydro-4H-isoxazolo[3,4-d]azepin-3-ol zwitterion (V).* 3.7 g (17 mmol) of (IVb) were dissolved in 35 ml of glacial acetic acid containing 43 % of hydrogen bromide at 25°C. The solution was heated in an oil bath for 30 min during which time the temperature rose to 90°C. A further amount of 35 ml of glacial acetic acid containing hydrogen bromide (43 %) was carefully added and the solution was refluxed (bath temperature: 90 − 100°C) for 1.5 h. After cooling to 25°C a black oil separated. Upon addition of water (20 ml) the solution was evaporated *in vacuo*. The crystalline residue was dissolved in water (15 ml), refluxed with activated charcoal (2 g) for 2 min, cooled to 25°C, filtered, and evaporated to dryness *in vacuo*. The brown crystalline residue was dissolved in water (10 ml) and passed through a column containing an ion exchange resin [Amberlite IRA 400, (OH), 150 ml] using acetic acid (1 N) as an eluent. Obtained were 2.3 g of crude (V), which crystallized extremely slowly. Extraction twice with 25 ml portions of boiling methanol left 1.6 g (60 %) of (V) as a faint greyish crystalline powder. An analytical sample was recrystallized (ethanol − water) to give (V) as colourless needles, m.p. 215 − 217°C (decomp.). (Found: C 51.50; H 6.79; N 17.10. Calc. for $C_7H_{10}N_2O_2$. 0.5 $H_2O$: C 51.52; H 6.80; N 17.17). [Found after drying of (V) over $P_2O_5$ (60 h; 125°C; 0.1 mmHg): C 54.50; H 6.59; N 18.15. Calc. for $C_7H_{10}N_2O_2$: C 54.53; H 6.54; N 18.17]. $^1$H NMR data [$D_2O$ (acetonitrile was used as an internal standard)] $\delta$: 4.71 (s, 3 H, DO$H$); 3.5 − 3.2 (m, 4 H, $CH_2 - CH_2 - NH_2^+ - CH_2 - CH_2$); 3.1 − 2.5 (m, 4 H, $CH_2 - CH_2 - C = C - CH_2 - CH_2$).

*Ethyl 1-benzyl-4-benzylamino-2,3,6,7-tetrahydro-1H-azepine-5-carboxylate (IIc).* (IIc) was synthesized as described above for (IIa) using 5.5 g (20 mmol) of (Ic) [21] and 2.4 g (22 mmol) of benzylamine to give 6.0 g (82 %) of crude product as a pale yellow oil. An analytical sample was rapidly passed down a short column of silica gel (0.05 − 0.20 mm, Merck) using methylene chloride − ethyl acetate (2:1) as an eluent. The isolated enamine (IIc) was obtained as a yellowish oil. As demonstrated by IR and $^1$H NMR spectroscopy (IIc) contained small amounts of impurities, which could not be removed by repeated chromatographic procedures. $^1$H NMR data ($CCl_4$) $\delta$: 9.8 [broadened t ($J = 6$ cps), 1 H, $CH_2 - NH - C$]; 7.10 and 7.14 (2 × s, 10 H, $2 \times C_6H_5$); 4.32 [d ($J = 6$ cps), 2 H, $C - CH_2 - NH$]; 3.98 [q ($J = 7$ cps), *ca.* 3 H, $O - CH_2 - CH_3$]; 3.36 (s, 2 H, $C - CH_2 - N$); 2.7 − 2.0 (m, 8 H, $CH_2 - CH_2 - N - CH_2 - CH_2$ and $CH_2 - CH_2 - C = C - CH_2 - CH_2$); 1.20 [t ($J = 7$ cps), *ca.* 4 H, $CH_3 - CH_2$].

*Benzylammonium salt of 6-benzyl-5,6,7,8-tetrahydro-4H-isoxazolo[3,4-d]azepin-3-ol (IIIc).* (IIIc) was prepared as described above for (IIIa) using 6.0 g (17 mmol) of crude

(IIc) and 1.24 g (18 mmol) of hydroxylammonium chloride to give 5.4 g (94 %) of crystalline crude product. An analytical sample was recrystallized (THF) to give colourless needles, m.p. 137.5 – 140.0°C (decomp.). (Found: C 71.65; H 7.23; N 11.88. Calc. for $C_{21}H_{25}N_3O_2$: C 71.77; H 7.17; N 11.96). $^1$H NMR data (DMSO-$d_6$) $\delta$: 7.36 and 7.26 (two slightly perturbed s, 10 H, $2 \times C_6H_5$); 5.8 – 5.1 (broad signal, 3 H, $CH_2 - NH_3^+$); 3.91 (s, 2 H, $C - CH_2 - NH_3^+$); 3.65 (s, 2 H, $C - CH_2 - N$); 2.8 – 1.9 (m, 8 H, $CH_2 - CH_2 - N - CH_2 - CH_2$ and $CH_2 - CH_2 - C = C - CH_2 - CH_2$).

*6-Benzyl-1,3,4,5,7,8-hexahydro-3-oxo-6H-isoxazolo[3,4-d]azepine hydrochloride (IVc).* To a solution of 2.9 g (8.3 mmol) of crude (IIIc) in methanol (24 ml) were added with cooling and stirring a methanolic solution of hydrogen chloride, prepared from methanol (20 ml) and acetyl chloride (5 ml). Ether (16 ml) was added and the salt (IVc) was allowed to crystallize at 5°C for 70 h to give 910 mg (39 %) of (IVc) as a white crystalline powder. An analytical sample was recrystallized (methanol) to give colourless crystals, m.p. 186 – 190°C (decomp.). (Found: C 59.90; H 6.21; N 10.12. Calc. for $C_{14}H_{17}ClN_2O_2$: C 59.87; H 6.12; N 9.98). $^1$H NMR data (DMSO-$d_6$) $\delta$: 7.9 – 7.3 (m, 5 H, $C_6H_5$); 4.48 (s, 2 H, $C - CH_2 - NH^+$); 3.6 – 2.4 (m, 8 H, $CH_2 - CH_2 - NH^+ - CH_2 - CH_2$ and $CH_2 - CH_2 - C = C - CH_2 - CH_2$). The acidic protons of (IVc) were not detectable in the spectrum.

*6-Benzyl-5,6,7,8-tetrahydro-4H-isoxazolo[3,4-d]azepin-3-ol zwitterion (VI).* In a solution of 420 mg (1.5 mmol) of (IVc) in water (4.5 ml) the pH was brought to *ca.* 6.5 with 2 N sodium carbonate at 65°C, and the enol-betaine (VI) was allowed to crystallize at 5°C for 18 h to give 350 mg (86 %) as colourless plates, m.p. 138.5 – 141.0°C (decomp.). (Found: C 61.80; H 7.09; N 10.38. Calc. for $C_{14}H_{16}N_2O_2$. 1.5 $H_2O$: C 61.97; H 7.06; N 10.33). [Found after drying of (VI) over $P_2O_5$ (20 h; 60°C; 0.1 mmHg): C 68.90; H 6.93; N 11.57. Calc. for $C_{14}H_{16}N_2O_2$: C 68.83; H 6.60; N 11.47]. $^1$H NMR data (DMSO-$d_6$) $\delta$: 7.36 (slightly broadened s, 5 H, $C_6H_5$); 5.38 (broadened s, 4 H, $NH^+$ and 1.5 $H_2O$); 3.86 (slightly broadened s, 2 H, $C - CH_2 - NH^+$); 3.0 – 2.1 (m, 8 H, $CH_2 - CH_2 - NH^+ - CH_2 - CH_2$ and $CH_2 - CH_2 - C = C - CH_2 - CH_2$).

## REFERENCES

1. Curtis, D. R. and Johnston, G. A. R. *Handbook of Neurochemistry* **4** (1970) 115.
2. Curtis, D. R. and Watkins, J. C. *Pharmacol. Rev.* **17** (1965) 347.
3. Beart, P. M., Johnston, G. A. R. and Uhr, M. L. *J. Neurochem.* **19** (1972) 1855.
4. Beart, P. M., Uhr, M. L. and Johnston, G. A. R. *J. Neurochem.* **19** (1972) 1849.
5. Johnston, G. A. R., Curtis, D. R., DeGroat, W. C. and Duggan, A. W. *Biochem. Pharmacol.* **17** (1968) 2488.
6. Curtis, D. R., Duggan, A. W., Felix, D. and Johnston, G. A. R. *Nature* **226** (1970) 1222.
7. Kier, L. B. and Truitt, E. B. *Experientia* **26** (1970) 988.
8. Beart, P. M., Curtis, D. R. and Johnston, G. A. R. *Nature New Biol.* **234** (1971) 80.
9. Steward, E. G., Player, R., Quilliam, J. P., Brown, D. A. and Pringle, M. J. *Nature New Biol.* **233** (1971) 87.
10. Van Gelder, N. M. *Can. J. Physiol. Pharmacol.* **49** (1971) 513.
11. Johnston, G. A. R. *Phychopharmacologia* **22** (1971) 230.
12. Brehm, L., Hjeds, H. and Krogsgaard-Larsen, P. *Acta Chem. Scand.* **26** (1972) 1298.
13. Brehm, L., Krogsgaard-Larsen, P. and Hjeds, H. *Acta Chem. Scand. To be published.*
14. DeSarlo, F. and Dini, G. *J. Heterocycl. Chem.* **4** (1967) 533.
15. Quin, L. D. and Pinion, D. O. *J. Org. Chem.* **35** (1970) 3130.
16. King, E. J. *J. Am. Chem. Soc.* **76** (1954) 1006.
17. Eugster, C. H. *Fortschr. Chem. Org. Naturst.* **27** (1969) 261.
18. Krogsgaard-Larsen, P., Christensen, S. B. and Hjeds, H. *Acta Chem. Scand.* **27** (1973) 2802.
19. Jacquier, R., Petrus, C., Petrus, F. and Verducci, J. *Bull. Soc. Chim. France* **1970** 2690.

20. Yamamoto, H., Nakata, M., Morosawa, S. and Yokoo, A. *Bull. Chem. Soc. Japan* **44** (1971) 153.
21. Moriya, T., Oki, T., Yamagushi, S., Morosawa, S. and Yokoo, A. *Bull. Chem. Soc. Japan* **41** (1968) 230.
22. Katritzky, A. R. and Boulton, A. J. *Spectrochim. Acta* **17** (1961) 238.
23. Albert, A. and Serjeant, E. P. *Ionization Constants of Acids and Bases*, Methuen, London 1962, p. 16.

# Decyanation of 4-Cyano-2-methyl-1,3,6-triazacycl[3.3.3] azine with Polyphosphoric Acid*

OLOF CEDER and KARIN VERNMARK

*Department of Organic Chemistry, University of Göteborg and Chalmers Institute of Technology, Fack, S-402 20 Göteborg 5, Sweden*

Decyanation of 4-cyano-2-methyl-1,3,6-triazacycl[3.3.3]azine, *1*, with polyphosphoric acid at 200° yields 2-methyl-1,3,6-triazacycl-[3.3.3]azine, *3*. The effect of Eu(fod)₃ on the chemical-shift values of the protons in *3* are reported. The results allow shift assignments to H-7 and H-9.

2-Methyl-4-cyano-1,3,6-triazacycl[3.3.3]azine, *1*, can be easily prepared in quantities [1] and our earlier studies on the chemical and spectral properties of the 1,3,6-triazacycl[3.3.3]azine system have been performed with this derivative. The cyano group in *1* causes an extension of the conjugated system, blocks a position susceptible to substitution, and has a directive and deactivating effect in electrophilic substitution reactions.[2] For these reasons it would be more desirable to carry out such studies on *2* [1] or *3*.[1] Neither of these compounds has been available in amounts sufficient for investigations of this
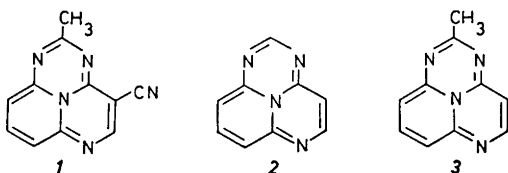


kind. The present communication describes an improved method of synthesis for 2-methyl-1,3,6-triazacycl[3.3.3]azine, *3*, and reports its NMR spectra in CDCl₃ and CF₃COOH solutions. In addition, the chemical shifts of H-7 and H-9 are assigned with the help of the chemical-shift reagent Eu(fod)₃.[3]

We have earlier obtained minute amounts of *2* and *3* when *4* (R = H or CH₃) was ring-closed in diphenylether at 250°.[1] Attempts to increase the yields of *2* or *3* by scaling up or modifying the decarbethoxylation conditions

---

* Presented at "Organikerdagarna", Stockholm, June 12—14, 1972.
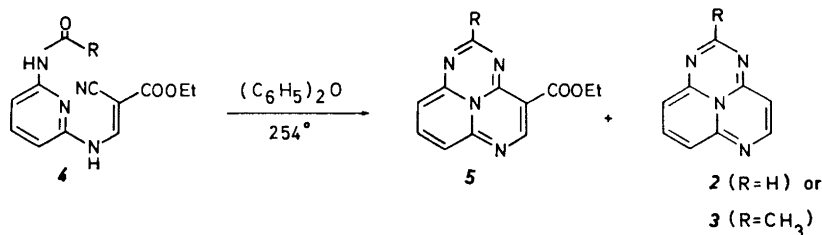
(e.g. by varying the reaction time, temperature, concentration, medium, by the use of p-toluenesulfonic acid as a catalyst, etc.) have not been very successful.

Mosby has reported [4] that 2,3,6,7-tetramethylnaphthalene-1,4-dinitrile lost the two cyano groups and gave a "good yield" of 2,3,6,7-tetramethylnaphthalene when the dinitrile was heated to 200° in polyphosphoric acid. Snyder and Elston [5] observed that aromatic nitriles were converted to amides when they were heated to ca. 100° in polyphosphoric acid for 1 – 2 h. When 1 was kept in polyphosphoric acid [6] at 200° for 30 min, a 25 % yield of 3 and small amounts of the amide 6 were isolated after chromatographic work-up.
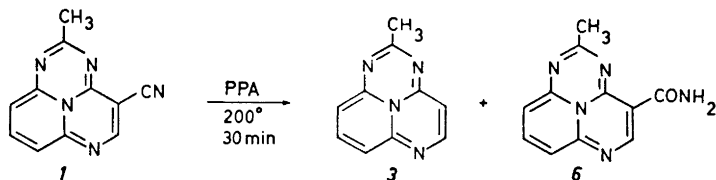


At lower reaction temperatures, (100°; 2h), the major product was the amide 6, which displays physical and spectral properties (cf. Experimental) similar to those of the other members of this system. Attempts to prepare 2 from its 4-cyanoderivative by the same method failed, since 2 decomposes in warm polyphosphoric acid.

The NMR spectra earlier reported were mostly recorded in AsCl₃ and CF₃COOD, where the solubility of the cyclazines is sufficient. These solutions are red, while the solutions in nonacidic, organic solvents are dark-blue. In CF₃COOH and AsCl₃, where the shifts for the corresponding protons are the same, we propose that cyclazinium ions of, e.g., types 7 and 8 are formed. This
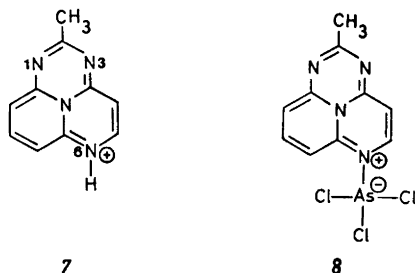
assumption is supported by the observation [7] that a red hydrochloride is formed when dry HCl is passed through a chloroform solution of *1*. The $\delta$-values for the protons in *3* are listed in Table 1. Good correlation is observed between them and the charge-density values [1] at the $sp^2$-hybridized carbon atoms to which the protons are attached. On this basis H-7 and H-9 are assigned the chemical shift values 5.81 and 5.35 ppm, respectively. These assignments agree with the results of lanthanide-shift reagent studies on *3* (*vide*

*Table 1.* Charge densities [a] and chemical-shift values (ppm) for the protons in *3* in $CDCl_3$ and $CF_3COOH$.

| | Charge densities | $CDCl_3$ | $CF_3COOH$ | $\Delta\delta$ |
|---|---|---|---|---|
| H-5 | +0.164 (C-5) | 7.07 | 8.15 | 1.08 |
| H-8 | +0.099 (C-8) | 6.77 | 7.97 | 1.20 |
| H-7 | −0.132 (C-7) | 5.81 | 7.23 | 1.42 |
| H-9 | −0.136 (C-9) | 5.35 | 6.81 | 1.46 |
| H-4 | −0.148 (C-4) | 4.97 | 6.28 | 1.31 |
| $CH_3$ | − | 1.67 | 2.27 | 0.60 |

[a] The charge-density values quoted in Table 1 have been calculated [1] for *2*, but they are assumed to be applicable also to the corresponding atoms in *3*.

*infra*). The displacement of the ring-proton resonances $1.0-1.4$ ppm to lower field (*cf.* Table 1) when the medium is changed from $CDCl_3$ to $CF_3COOH$ indicates that the $12\pi$-electron periphery becomes protonated in the acid medium. The NMR spectrum of *3* in $CF_3COOH$ or in $H_2SO_4$ displays no $CH_2$ signal and the five aromatic proton signals show a 1:1:1:1:1 ratio. The same spectrum of *3* recorded in $D_2SO_4$ displays an identical ratio for the aromatic proton signals, which indicates that none of these protons have been exchanged for deuterium.* Although we cannot localize the $>NH^+$ signal in the NMR spectrum, we conclude that protonation has occurred on nitrogen. Three sites of protonation are possible (N-1, N-3, and N-6; *cf.* structure *7*), but it is not possible to predict from the NMR and electronic spectral data, or from the charge-density values for N-1, N-3, and N-6 ($-0.352$, $-0.354$, and $-0.341$, respectively),[1] if one of these atoms is preferentially protonated. Alkylation of *3*, however, results in three *N*-alkyl derivatives,[9] with one of them predominating. When the NMR spectrum of *3* was recorded in $CF_3COOD$ or $D_2SO_4$, the 2-methylprotons were completely exchanged in *ca.* 20 min. The reactivity of this methyl group will be discussed in a subsequent communication.[9]

It has proved difficult to assign chemical-shift values to H-7 and H-9 in the 1,3,6-triazacycl[3.3.3]azine system.** We have therefore studied the effect of $Eu(fod)_3$-$d_{27}$ [3] on *3*, where the peripheral *N*-atoms represent three possible sites of coordination. The charge-density values for these *N*-atoms are very

---

* *Cf.* the *C*-protonation of cycl[3.2.2]azine.[8]
** The assignment for H-7 and H-9 in Ref. 1, Figs. 3−5, should have the order indicated on those spectra.

close (*cf.* footnote to Table 1), but since N-1 and N-3 are sterically shielded by the 2-methyl group, *N*-6 should be the most likely site of coordination. Consequently, the chemical shifts for H-5 and H-7 should be more affected by the shift reagent than those of H-4 and H-9. When the Eu-ion is placed 5.0 Å from N-6, good, linear correlation between the $\Delta_{Eu}$-values [10] (Table 2) and $(3 \cos^2 \theta_i - 1)/r^3_i$ [11] (*cf.* Fig. 1) is obtained for H-4, H-5, H-7, and H-8 in *3*.
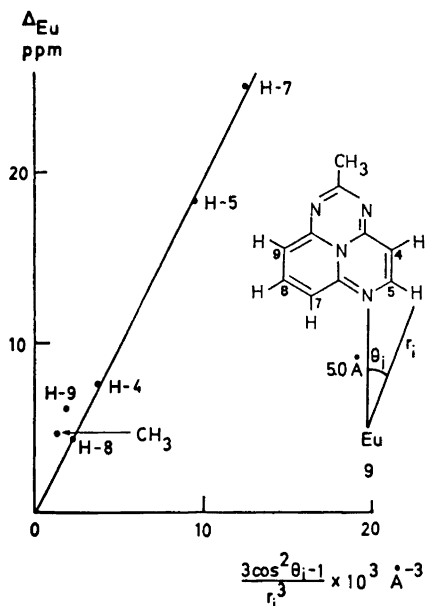


*Fig. 1.* $\Delta_{Eu}$-values for the protons in *9* as a function of $(3 \cos^2 \theta_i - 1)/r_i^3$ for $r = 5.0$ Å.

We therefore assign the signal at 5.81 ppm with the highest $\Delta_{Eu}$-value (Table 2) to H-7 and the signal at 5.35 to H-9. The points for H-9 and the 2-methyl protons deviate and show larger $\Delta_{Eu}$-values than expected. We believe that this deviation is caused by Eu-coordination also at N-1 and N-3.

*Table 2.* $\Delta_{Eu}$-values for the protons in *3*.'

| H-4 | H-5 | H-7 | H-8 | H-9 | 2-CH$_3$ |
|-----|-----|-----|-----|-----|----------|
| 7.5 | 18.3 | 25.0 | 4.3 | 6.1 | 4.6 |

## EXPERIMENTAL

*General.* NMR spectra were recorded with a Varian A-60 spectrometer, using TMS as internal reference. Chemical shifts are given in δ-values. UV and visible spectra were measured in ethanol solution with a Cary Model 15 spectrophotometer. IR spectra were determined in KBr with a Perkin-Elmer 337 spectrophotometer. Mass spectra were

obtained with a GEC–AEI 902 mass spectrometer at the Department of Medical Bio-chemistry, University of Göteborg. Thin-layer chromatography was performed on Silica Gel $GF_{254}$ (Merck) according to Stahl and the colorless spots were visualized with short-wave, ultraviolet light. Elemental analyses were carried out at "Mikroanalytisches Laboratorium, Institut für Physikalische Chemie, Universität Wien".

*Preparation of 2-methyl-1,3,6-triazacycl[3.3.3]azine, 3.* To 7 ml of freshly prepared polyphosphoric acid,[6] kept at 200°, 1 g (5.3 mmol) of *1* was added and the solution was stirred for 35 min. After having been cooled to room temperature, 10 ml of water was added and the deep-red solution was neutralized with 10 % aqueous $NaHCO_3$ and then extracted with chloroform. The extract was dried ($MgSO_4$) and evaporated to dryness, yielding 300 mg (30 %) of *3*, which was purified by column chromatography on 9 g of neutral alumina (Fluka, activity I). Chloroform eluted 207 mg of pure *3* with properties earlier described.[1] NMR data for *3* in $CDCl_3$ and in $CF_3COOH$ are summarized in Table 1.

*Preparation of 4-amido-2-methyl-1,3,6-triazacycl[3.3.3]azine, 6.* To 1.6 ml of freshly prepared polyphosphoric acid,[5] kept at 100°, 200 mg (0.97 mmol) of *1* was added and the solution was stirred for 2 h. The reaction mixture was worked up as described above and 200 mg of a crude mixture of *6* and *1* was obtained. Chromatography on 9 g of silica gel gave ($CHCl_3$-EtOAc; 9:1) 102 mg (51 %) of pure, crystalline *6*, m.p. 294 – 296°C (decomp.). IR: 3310, 3150 (NH), 1690 cm$^{-1}$ (amide C=O), UV: $\lambda_{max}$ at 237 ($\varepsilon = 18\ 011$), 260 ($\varepsilon = 11\ 990$), 332 ($\varepsilon = 14\ 310$), 352 ($\varepsilon = 7650$), 370 ($\varepsilon = 9380$), 388 ($\varepsilon = 7770$), 545 ($\varepsilon = 347$), 586 ($\varepsilon = 400$) and 633 ($\varepsilon = 197$) nm; NMR ($AsCl_3$): singlet at 2.31 (3 H, $CH_3$), doublet ($J = 8$ Hz) at 6.82 (1 H, H-9), doublet ($J = 8$ Hz) at 7.12 (1 H, H-7), triplet ($J = 8$ Hz) at 7.82 (1 H, H-8), doublet ($J = 6$ Hz) at 8.41 (1 H, H-5) ppm, *Anal:* (Found: C 58.30; H 4.09; N 30.53. Calc. for $C_{11}H_9N_5O$: C 58.15; H 3.99; N 30.82), MS: $M^+ = 227$.

*Lanthanide-shift-measurements.* The shifts induced by $Eu(fod)_3$-$d_2$ were measured in a *ca.* 0.3 M solution of *3* in $CDCl_3$, dried over Linde 4A molecular sieve for 1 day. After each addition of shift reagent the solution was left for *ca.* 5 min before the spectrum was determined. The $\Delta_{Eu}$-values for *3* were calculated as the slope of the straight, first part of the curve obtained when the induced shifts (in ppm) were plotted against [Eu-(fod)$_3$]/[*3*]. The curve is linear up to a molar ratio of *ca.* 0.6 for H-5 and H-7 and to *ca.* 1.0 for the remaining protons in *3*. The straight line passing through the origin in Fig. 1 is calculated by the least-squares method excluding the values for H-9 and 2-$CH_3$. The distances $r_i$ and angles $\theta_i$ were estimated from structure *9*. The bond-lenghts and angles quoted in *9* have been obtained from X-ray studies.*

## REFERENCES

1. Ceder, O. and Andersson, J. E. *Acta Chem. Scand.* **26** (1972) 596.
2. Ceder, O., Andersson, J. E. and Johansson, L.-E. *Acta Chem. Scand.* **26** (1972) 624.
3. Rondeau, R. E. and Sievers, R. E. *J. Am. Chem. Soc.* **93** (1971) 1522.
4. Mosby, W. L. *J. Am. Chem. Soc.* **75** (1953) 3600.
5. Snyder, H. R. and Elston, C. T. *J. Am. Chem. Soc.* **76** (1954) 3039.
6. Uhlig, F. and Snyder, H. R. *Advan. Org. Chem.* **1** (1960) 35.
7. Ceder, O. and Samuelsson, M. L. *Acta Chem. Scand.* **27** (1973) 2095.
8. Boekelheide, V., Gerson, F., Heilbronner, E. and Meuche, D. *Helv. Chim. Acta* **46** (1963) 1951.
9. Ceder, O. and Vernmark, K. *To be published.*
10. Demarco, P. V., Elzey, T. K., Lewis, R. B. and Wenkert, E. *J. Am. Chem. Soc.* **92** (1970) 5734.
11. McConnell, H. M. and Robertson, R. E. *J. Chem. Phys.* **29** (1958) 1361.

* An X-ray structure determination, which will be published elsewhere, has been carried out on *1* by Professor Iain C. Paul, University of Illinois, Urbana, Ill.

# Electrophilic Bromination of 1,3,6-Triazacycl[3.3.3]azine

OLOF CEDER and MARIE LOUISE SAMUELSSON

*Department of Organic Chemistry, University of Göteborg and Chalmers Institute of Technology, Fack, S-402 20 Göteborg 5, Sweden*

The electrophilic bromination of 1,3,6-triazacycl[3.3.3]azine, 2, with *N*-bromosuccinimide is described. Under mild conditions, substitution occurs, as predicted by arguments using resonance structures and by HMO-calculations, preferentially (80 %) in position 4. On further bromination, positions 7 and 9 are also attacked.

Electrophilic-substitution studies on the 1,3,6-triazacycl[3.3.3]azine system [1] have earlier been carried out on the 4-cyano-2-methyl derivative *1*, which is available in quantities.[2] As predicted from charge-density values, substitution in this compound occurs in the 7 and 9 positions.[1,2] However, the parent compound *2*[2] is more suitable for such studies than *1* since position 4, which has the lowest charge-density value (*cf.* Table 1), is unsubstituted in *2*.



*1*          *2*
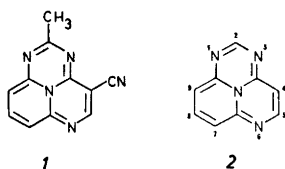
The present communication describes a slight improvement in the preparation of *2* and reports the results of electrophilic-substitution studies on the same compound.

The title compound was prepared as previously described.[2] The last step in this sequence, ring closure of *3* in diphenyl ether at 250°, gave, in low yields, *2* and *4* (0.8 % and 5.4 %, respectively).[2] If instead, a catalytic amount of



*3*          *4*
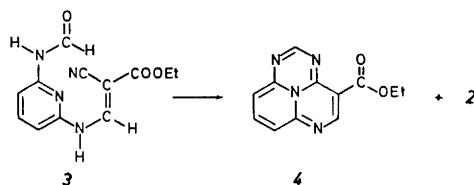
$p$-toluenesulfonic acid was added to the reaction mixture, the yields of 2 and 4 were raised to 5.0 and 7.3 %, respectively. Decarbethoxylation of 4 in the presence of $p$-toluenesulfonic acid gave 16 % of 2, but the over-all yield of 2 (based on 3) was still higher in the modified, one-step method.

1,3,6-Triazacyl[3.3.3]azine is stable both in the solid state and in solution. It is easily soluble in chloroform, acetic and trifluoroacetic acid. The NMR spectra of 2 (in $CDCl_3$ and in $CF_3COOH$) contain an ABX-multiplet (H-7, H-8, and H-9), an AX-quartet (H-4 and H-5), and a one-proton singlet (H-2). The coupling constants and chemical-shift values, which show good correlation with the calculated charge-density values [2] on the adjacent carbon atoms, are listed in Table 1.

Table 1. Charge density values,[2] NMR chemical shifts, and coupling constants (in Hz) for 2.

|  | H-4 | H-9 | H-7 | H-8 | H-5 | H-2 |
|---|---|---|---|---|---|---|
| Charge-density values | −0.148 | −0.136 | −0.132 | +0.099 | +0.164 | +0.231 |
| $\delta_{CDCl_3}$ | 4.86 | 5.29[a] | 5.75[a] | 6.68 | 6.99 | 6.50 |
| $\delta_{CF_3COOH}$ | 6.16 | 6.75 | 7.13 | 7.88 | 8.04 | 7.40 |
| Multiplicity | doublet | multiplet | multiplet | triplet | doublet | singlet |
| Coupling constants ($CDCl_3$) |  | $J_{4-5}=5.2$ | $J_{7-8}=7.6$ | $J_{8-9}=8.5$ | $J_{7-9}=1.3$ |  |

[a] The assignment of chemical-shift values to H-7 and H-9 are based on results of lanthanide-shift-reagent studies on 2-methyl-1,3,6-triazacyl[3.3.3]azine.[3]

The bromination experiments were performed with $N$-bromosuccinimide in chloroform at temperatures between $-7°$ and $+25°$. Bromination of 2 under mild conditions (cf. Experimental) yielded 80 % of 5 and only 7 % of 6 and 7 together (cf. Chart 1). Bromination of 5 under slightly more vigorous conditions (cf. Experimental) yielded one tri- and two dibromo compounds, 10, 8, and 9, respectively. The number of bromine atoms were determined by mass spectrometry from the element profile in the molecular-ion region. The structure of 5 follows from its NMR spectrum (cf. Table 3), which lacks the AX-quartet generated by H-4 and H-5 in the spectrum of 2. The NMR spectra of the dibromo compounds each display two one-proton singlets and, in addition, AB-type signals; they therefore possess structures 8 and 9. Bromination of each one separately led to the same tribromo compound as was isolated previously. The NMR spectrum shows three unsplit, one-proton signals (cf. Table 3) and thus this compound has structure 10. The positions of the substituents in 8 and 9 were derived by comparison of the chemical-shift values for their protons with the values for the corresponding protons in the 4,7- and 4,9-dibromo-2-methyl-1,3,6-triazacyl[3.3.3]azine, 11 and 12.
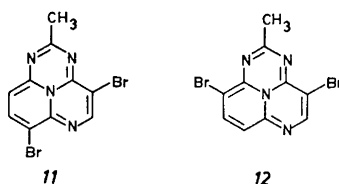
The structure determinations of *11* and *12* are presented in a separate communication.[4] The chemical-shift values for H-5, H-8, and H-9 in *11* and for H-5, H-7, and H-8 in *12* are very close to the observed values for the corresponding protons in *8* and *9* (*cf.* Table 2).

*Table 2.* NMR chemical shifts (solvent: trifluoroacetic acid) of *8, 9, 11,* and *12*.

|        | H-5  | H-7  | H-8  | H-9  |
|--------|------|------|------|------|
| *11*   | 8.45 | –    | 8.07 | 6.58 |
| *8*    | 8.44 | –    | 8.08 | 6.63 |
| *12*   | 8.40 | 7.12 | 7.98 | –    |
| *9*    | 8.37 | 7.11 | 7.96 | –    |

Conversion of *6* and *7* to *8* and *9*, respectively, by bromination with NBS ascertained the structures of the monobromoderivates.

Arguments using resonance structures predict that electrophilic substitution in *2* should occur in positions 4, 7, and 9. In Chart 2, the structures of the intermediates for substitutions at C-4 and C-8 are presented. For 4-substitution, structures *13a – 13d* can be drawn. In *13a*, representing six forms, the positive charge is located on carbon atoms. In the three remaining forms *13b – 13d* the positive charge is located on the central *N*-atom. Here all atoms possess

*Table 3.* NMR spectral data (δ-values and coupling constants) for compounds *5, 8, 9,* and *10* (solvent: trifluoroacetic acid).

| Compound | H-2 | H-5 | H-7 | H-8 | H-9 | $J_{7-8}$ (Hz) | $J_{8-9}$ (Hz) | $J_{7-9}$ (Hz) |
|----------|------|------|------|------|------|------|------|------|
| *5*  | 7.38 | 8.32 | 7.22 | 7.85 | 6.73 | 8.45 | 8.15 | 1.0 |
| *8*  | 7.36 | 8.44 | –    | 8.08 | 6.63 | –    | 9.4  | –   |
| *9*  | 7.39 | 8.37 | 7.11 | 7.96 | –    | 8.5  | –    | –   |
| *10* | 7.38 | 8.48 | –    | 8.26 | –    | –    | –    | –   |

full octets, which is not the case in *13a*. Similar structures can be drawn for electrophilic attack at C-7 and C-9. In *14*, which illustrates the intermediates for substitution on C-8, the charge is located on the peripheral $N$-atoms, and on C-4, C-7, and C-9; no resonance structure exists, where all atoms contain full octets. The predictions are in agreement with the results of the bromination studies.

Compounds *5 – 10* are blue or green and their electronic spectra are similar to those displayed by other brominated derivatives of the 1,3,6-triazacycl[3.3.3]azine system (*cf.* Table 4). The infrared spectra lack characteristic

*Table 4.* Electronic spectral data in the UV-region for *5 – 10*; nm ($\varepsilon \times 10^{-4}$).

| | | | | | | | |
|---|---|---|---|---|---|---|---|
| *5*[a] | 233 (1.49) | 272 (1.16) | 336 (1.22) | 351s(0.85) | 369 (0.85) | 378 (0.67) | 387 (0.79) |
| *6*[a] | 234 (1.69) | 266 (1.77) | 335 (1.69) | 359 (0.84) | 376 (1.15) | 387 (0.97) | 394 (1.01) |
| *7*[a] | 233 (1.72) | 267 (1.50) | 334 (1.61) | 357 (0.78) | 374 (1.00) | 389 (0.86) | |
| *8*[a] | 244 (1.09) | 279 (1.29) | 342 (1.27) | 360 (0.66) | 379 (0.76) | 388s(0.59) | 397 (0.69) |
| *9*[a] | 241 (2.20) | 284 (1.37) | 343 (1.73) | 349s(1.52) | 360s(1.23) | 375 (1.03) | 392 (0.87) |
| *10*[a] | 207 (1.72) | 247 (0.82) | 288 (0.77) | 348 (0.88) | 367s(0.53) | 386 (0.47) | 404 (0.42) |

*Table 4 cont.* Electronic spectral data in the visible region for *5 – 10*; nm ($\varepsilon$).

| | | | |
|---|---|---|---|
| *5*[b] | 560 (125) | 605 (186) | 663 (177) |
| *6*[a] | 555 (145) | 597 (218) | 651 (181) |
| *7*[b] | 550 (167) | 598 (221) | 650 (200) |
| *8*[b] | 566 (83) | 616 (134) | 673 (134) |
| *9*[b] | 575 (82) | 620 (140) | 677 (163) |
| *10*[a] | 580 (86) | 630 (133) | 688 (200) |

[a] Solvent: ethanol; [b] Solvent: acetone.

absorption in the $4000 – 1200$ cm$^{-1}$ region, apart from the C=N band at 1600 cm$^{-1}$. The solubilities seem to depend on the position of the substituent; compounds *2* and *5* are easily soluble, but *8* and *10* only slightly soluble in chloroform.

Attempts to introduce more than three bromine atoms in *2* by using higher temperatures and longer reaction times failed. The presence of ethanol in the reaction medium led to the formation of ethoxy derivatives. One of these was shown (mass and NMR spectra) to contain one ethoxy group and three bromine atoms. Since this compound can be obtained from *10*, the bromine atoms are located in positions 4, 7, and 9. The position of the ethoxy group has not been determined. A compound with one chlorine atom, two bromine atoms, and one ethoxy group was observed as an impurity (MS). It has presumably been formed by a radical-induced exchange of chlorine for bromine. This type of reaction has been discussed in a previous communication.[5]
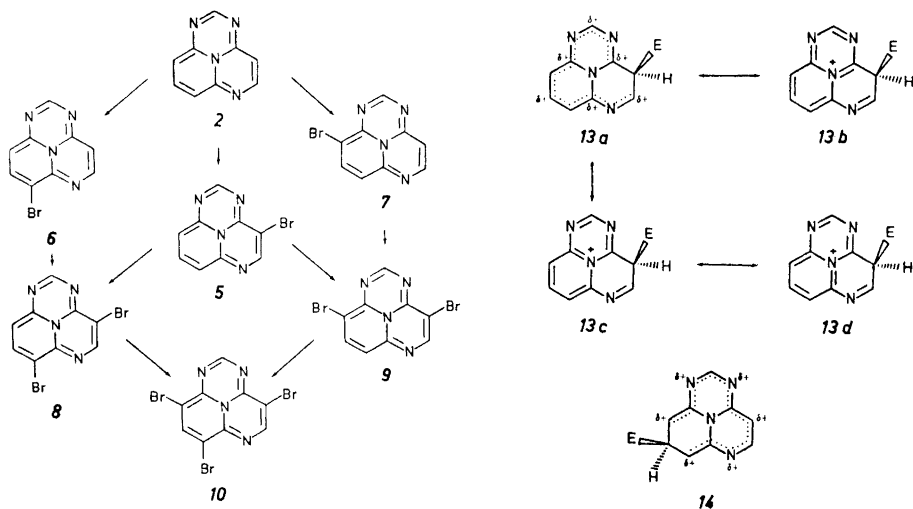
*Chart 1.* Bromination of *2*; products and interrelation of structures.



*Chart 2.* Resonance structures for electrophilic substitution intermediates of *2*.

## EXPERIMENTAL

*General.* The NMR spectra have been measured in $CDCl_3$ or $CF_3CO_2H$ with tetramethylsilane as internal reference using a Varian Model A-60 spectrometer. Mass spectra were recorded with a GEC-AEI 902 mass spectrometer at the Department of Medical Biochemistry, University of Göteborg. The infrared spectra were determined in KBr with a Perkin-Elmer 337 infrared spectrophotometer, and the electronic spectra in ethanol or acetone with a Cary Model 15 spectrophotometer. For column chromatography, neutral aluminium oxide or silica gel ($\phi < 0.08$ mm) was used, and for TLC, Silica Gel $GF_{254}$ (Merck), according to Stahl. *N*-Bromosuccinimide (NBS) was recrystallized from water before use. Compound *3* was prepared by formylation of the condensation product from 2,6-diaminopyridine and ethyl 2-cyano-3-ethoxyacrylate, as earlier described.[a]

*Ring closure of 3 to 2 and 4.* A solution of 5.2 g of *3* in 400 ml of diphenyl ether was heated to 250° and 52 mg of *p*-toluenesulfonic acid was added. The mixture was kept at 250° for 2.5 h, then cooled to *ca.* 30° and passed over a column of 50 g of aluminium oxide (activity I). The column was washed with petroleum ether to remove the diphenyl ether. The coloured compounds were eluted with chloroform, the solvent was evaporated, and the residue separated by preparative TLC (EtOAc − MeOH, 3:1). Yield of *2*: 169 mg (5.0 %); of *4*: 352 mg (7.3 %).

*Decarbethoxylation of 4 to 2.* To 47 mg of *4* in 7 ml of diphenyl ether, kept at 250°, was added 5 mg of *p*-toluenesulfonic acid. The reaction mixture was heated for 4 h and then allowed to cool. The solvent was removed and the blue material eluted as described above. Preparative TLC on the residue after evaporation gave 5.2 mg (15.7 %) of *2*; 11.8 mg (25 %) of *4* was recovered unchanged.

*Bromination of 2.* A solution of 124 mg (0.73 mmol) of *2* and 130 mg (0.73 mmol) of NBS in 35 ml of chloroform was stirred for 30 min at − 7°. The reaction mixture was then filtered to remove succinimide and the solvent evaporated. The following compounds were isolated from the residue by preparative TLC (EtOAc): *5* (145 mg; 80 %) and *6* + *7* (13 mg; 6.7 %). Minute amounts of *8* and *9* were observed (TLC). The mixture of *6* and *7* was separated by preparative TLC ($CH_2Cl_2$; the chromatogram was developed twice). NMR data for *5* are presented in Table 3, UV data for *5 − 7* in Table 4, mass-spectral data, melting points, and chromatographic mobilities in Table 5.

*Table 5.* Mass spectral data, melting points, and chromatographic mobilities of *5 − 10*.

| | M.S. (M$^+$ and intensities) | | M.p., °C | $R_F$ (TLC) |
|---|---|---|---|---|
| 5 | 248, 250 | 1:1 | 189 − 191 | 0.20$^a$ |
| 6 | 248, 250 | 1:1 | 233 − 234 | 0.15$^a$ |
| 7 | 248, 250 | 1:1 | 186 − 188 | 0.15$^a$ |
| 8 | 326, 328, 330 | 1:2:1 | 251 − 253 | 0.36$^b$ |
| 9 | 326, 328, 330 | 1:2:1 | 199 − 200 | 0.42$^b$ |
| 10 | 404, 406, 408, 410 | 1:3:3:1 | 308 − 310 | 0.61$^b$ |

$^a$ Solvent: EtOAc; $^b$ solvent CHCl$_3$− EtOAc, 3:1.

*Bromination of 5.* To a solution of 145 mg (0.58 mmol) of *5* in 20 ml of chloroform was added 100 mg (0.56 mmol) of NBS and the mixture was stirred at − 7°. A sample taken after 20 min still contained starting material (TLC). An additional 30 mg of NBS was added and the temperature was allowed to rise to + 5°. After another 10 min, the mixture was filtered, the solvent evaporated, and the residue analyzed by TLC. Compounds *8, 9,* and *10* had formed with *9* as the main component. The crude product was suspended in 10 ml of chloroform, filtered, and analyzed (TLC). The filtrate contained almost pure *9* and the solid residue mainly *8* and *10*. Further purification was performed by TLC (CHCl$_3$ − EtOAc, 1:3). No yields were determined, since substantial amounts of material were lost during the purification procedure. NMR and UV data for *8 − 10* are presented in Tables 3 and 4; mass-spectral data, melting points, and chromatographic mobilities are summarized in Table 5.

*Bromination of 8 to 10.* Equivalent amounts of *8* (12 mg, 0.037 mmol) and NBS (6.5 mg, 0.037 mmol) were dissolved in 3 ml of chloroform and stirred for 1 h at 25°. TLC showed, that *ca.* 50 % of *8* had reacted to give *10*.

*Bromination of 9 to 10.* Compound *9* was treated as described for *8* above. TLC showed, that *10* had been formed and that no starting material remained.

*Bromination of 6 to 8 and 10.* One crystal each of *6* and of NBS, dissolved in 0.5 ml of chloroform, were shaken for 1 min and the solution was then analyzed by TLC. Two products, *8* and *10*, were observed.

*Bromination of 7 to 9 and 10.* Compound *7* was treated as described for *6* above. According to TLC, *9* and *10* had formed.

*Formation of ethoxyderivatives of* 10. A solution of 30 mg of *10* and 15 mg of NBS in 20 ml of chloroform (stabilized with *ca.* 1 % of ethanol) was stirred for 2 weeks at 25°. After evaporation of the solvent, the residue was separated by preparative TLC (EtOAc). Compound *10* was the main component, but *ca.* 2 mg (6 %) of another blue product was isolated. Since a mass spectrum of the latter compound suggested the presence of an ethoxy group, 30 mg of *2* and 95 mg of NBS (3 equivalents) dissolved in 30 ml of chloroform containing 10 % ethanol was stirred for 3 days at 25°. Preparative TLC (CH$_2$Cl$_2$; the chromatogram was developed twice) yielded the same blue compound as isolated above. M.S.: 448, 450, 452, 454 (intensities 1:3:3:1). NMR (CDCl$_3$): singlets at $\delta$ = 7.60 (1 H) and 7.72 (1 H), quartet at 4.33 (2 H), and triplet at 1.33 (3 H).

## REFERENCES

1. Ceder, O., Andersson, J. E. and Johansson, L.-E. *Acta Chem. Scand.* **26** (1972) 624.
2. Ceder, O. and Andersson, J. E. *Acta Chem. Scand.* **26** (1972) 596.
3. Ceder, O. and Vernmark, K. *Acta Chem. Scand.* **27** (1973) 3259.
4. Ceder, O. and Samuelsson, M. L. *To be published.*
5. Ceder, O. and Samuelsson, M. L. *Acta Chem. Scand.* **27** (1973) 2095.

# The Molecular Structure of Dimethoxymethane, CH₃-O-CH₂-O-CH₃, in the Gas Phase

E. E. ASTRUP

*Department of Chemistry, University of Oslo, Oslo 3, Norway*

The molecular structure of dimethoxymethane (methylal) has been investigated in the gas phase by the electron diffraction method. The molecule has a $C_2$ symmetry and the preferred conformation is found to be *gauche-gauche*. The dihedral angle, $\delta(COCO)$, is 63.3°. The most important parameters are as follows: $r(C-O)_{term.} = 1.432$ (0.004) Å, $r(C-O)_{centr.} = 1.382$ (0.004) Å, $r(C-H) = 1.108$ (0.004) Å, $\angle COC = 114.6$ (0.5)°, $\angle OCO = 114.3$ (0.7)°, $\angle OCH = 110.3$ (0.6)°.

The structure of dimethoxymethane was investigated as part of a study of cyclic [1] and acyclic ethers. A short communication [2] reporting the preliminary results of this work was published in 1971. Dimethoxymethane has previously been investigated, using the electron diffraction technique by Donohue [3] in 1950, by Aoki [4] in 1953, and recently by Andreassen and Bauer. [5] Donohue's work has not been published, but according to the quoted results he apparently assumed a planar all-*anti* conformation. Based on dipole moment
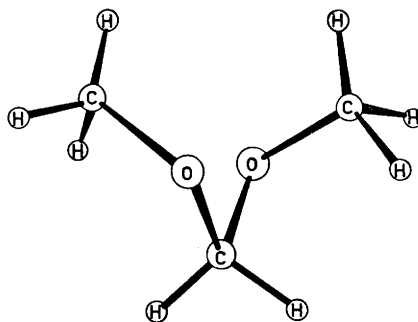


*Fig. 1.* Dimethoxymethane.

measurements [6] Aoki assumed that the most probable conformation should be the one having the two methyl groups located on opposite sides of the OCO plane. Aoki's electron diffraction investigation was based on visually estimated intensity data. The recent work of Andreassen and Bauer is in good agreement with the present work (Table 3).

*Table 1.* Structure parameters for dimethoxymethane obtained by least squares refinement on the intensity data. Distances ($r_a$-values) and mean amplitudes of vibration ($u$-values) are given in Å, angles in degrees. The standard deviations given in parentheses have been corrected to take into account data correlation. The uncertainty arising from error in the electron wavelength is included. (For numbering system of the atoms see Fig. 3.)

| Distances | $r$ | | $u$ | |
|---|---|---|---|---|
| $C_1-O_1$(term.) | 1.432 | (0.004) | 0.052 | |
| $C_2-O_1$(centr.) | 1.382 | (0.004) | | |
| $C-H$ | 1.108 | (0.004) | 0.063 | (0.004) |
| $O_1\cdots O_2$ | 2.320 | (0.017) | 0.072 | |
| $C_1\cdots O_2$ | 2.877 | (0.012) | 0.111 | (0.013) |
| $C_1\cdots C_2$ | 2.366 | (0.012) | 0.066 | (0.012) |
| $C_1\cdots C_3$ | 3.550 | (0.033) | 0.138 | |
| $O_1\cdots H_1$ | 2.023 | (0.007) | 0.085 | |
| $O_1\cdots H_6$ | 2.092 | (0.014) | 0.103 | (0.016) |
| $O_1\cdots H_5$ | 2.477 | (0.026) | 0.112 | |
| $O_1\cdots H_4$ | 3.520 | (0.030) | 0.121 | |
| $O_1\cdots H_3$ | 3.737 | (0.026) | | |
| $C_2\cdots H_5$ | 2.525 | (0.023) | 0.110 | |
| $C_1\cdots H_5$ | 3.175 | (0.048) | 0.130 | |
| $C_1\cdots H_1$ | 3.306 | (0.011) | 0.098 | |
| $C_1\cdots H_3$ | 4.093 | (0.041) | 0.130 | |
| $C_1\cdots H_4$ | 4.451 | (0.027) | | |
| $H_3\cdots H_4$ | 1.799 | (0.014) | | |
| $H_1\cdots H_2$ | 1.810 | (0.006) | | |
| $H_5\cdots H_8$ | 2.596 | (0.043) | | |
| $H_2\cdots H_5$ | 3.585 | (0.018) | | |

| Angles | deg. | |
|---|---|---|
| $\angle$ COC | 114.6 | (0.5) |
| $\angle$ OCO | 114.3 | (0.7) |
| $\alpha$(methoxy)[a] | 116.7 | (0.9) |
| $\angle$ OCH | 110.3 | (0.6) |
| $\tau$(CH$_3$)[b] | 19.8 | (2.0) |
| $\delta$(COCO)[c] | 63.3 | (0.9) |

[a] $\alpha$ is the twist angle of the methoxy groups about the central CO bonds. [b] $\tau$ is the twist angle of the methyl groups about the terminal CO bonds. [c] $\delta$(COCO) is the dihedral angle of the carbon-oxygen chain.

## EXPERIMENTAL

The electron diffraction diagrams of a commercial sample of dimethoxymethane were taken on a Balzer Eldigraph KDG-2. The sample was kept at approximately $-18°C$, and the electron wavelength was 0.05843 Å. The pressure in the apparatus during exposure was about $2 \times 10^{-5}$ torr. Four plates were selected from each nozzle-to-plate distance, 25 cm and 50 cm, respectively. The intensity was recorded on a photometer for each 0.25 mm on the photographic plates. Each plate was oscillated about the centre of the diffraction diagram, and the intensity integrated over the arc. The data were treated the usual

*Table 2.* Correlation matrix ( × 100) for the parameters. (The coefficients having absolute values less than 20 are not given.)

| Parameters | 1 | 2 | 3 | 4 | 5 | 6 | 7 | 8 | 9 | 10 | 11 | 12 | 13 |
|---|---|---|---|---|---|---|---|---|---|---|---|---|---|
| 1 $r(C_1-O_2)$ | 100 | | | | | | | | | | | | |
| 2 $r(C-H)$ | −20 | 100 | | | | | | | | | | | |
| 3 $\angle$ COC | | | 100 | | | | | | | | | | |
| 4 $\angle$ OCO | | | −84 | 100 | | | | | | | | | |
| 5 $\alpha(CH_3O)^a$ | | | −39 | 63 | 100 | | | | | | | | |
| 6 $r(C_2-O_1)$ | −76 | | −22 | | | 100 | | | | | | | |
| 7 $\angle$ OCH | | | −36 | 55 | 38 | | 100 | | | | | | |
| 8 $\tau(CH_3)^b$ | | | −21 | | −21 | | | 100 | | | | | |
| 9 $u_{C-H}$ | −20 | | | | | 32 | | | 100 | | | | |
| 10 $u_{C_1\cdots C_2}$ | | | −77 | 80 | 58 | | 28 | | | 100 | | | |
| 11 $u_{C_2\cdots O_1}$ | | | | | | | | | −38 | | 100 | | |
| 12 $u_{O_1\cdots H_4}$ | | | 20 | | | | | | | | | 100 | |
| 13 scale | 52 | | | | | 51 | | | | | | | 100 |

$^a$ $\alpha$ is the twist angle of the methoxy groups about the central CO bonds. $^b$ $\tau$ is the twist angle of the methyl groups about the terminal CO bonds.

*Table 3.* Comparison of parameters for dimethoxymethane studied by electron diffraction.

| Parameters | This study | | | Andreassen and Bauer [5] | |
|---|---|---|---|---|---|
| $r(C-O)_{term.}$ | 1.432 | (0.004) Å⎫ | | | |
| $r(C-O)_{centr.}$ | 1.382 | (0.004) Å⎭ | | 1.413 | (0.003) Å |
| $r(C-H)$ | 1.108 | (0.004) Å | | 1.119 | (0.013) Å |
| $\angle$ COC | 114.6 | (0.5)° | | 111.9 | (3.6)° |
| $\angle$ OCO | 114.3 | (0.7)° | | 114.0 | (3.5)° |
| $\angle$ OCH | 110.3 | (0.6)° | | 109.6 | (2.2)° |
| $\delta$(COCO) | 63.3 | (0.9)° | | 61.8 | (2.9)° |

way.[7] The average curves from each nozzle-to-plate distance were combined to give one intensity curve covering an $s$-range of $1.75-29.25$ Å$^{-1}$. The intensity curve, modified by $s/|f_c||f_o|$, where $f$ is the complex scattering factor for carbon and oxygen, is presented in Fig. 2.

The distances and vibrational amplitudes estimated from the RD (radial distribution) curve were refined by a least-squares procedure. The calculations have been carried out on a CDC 3300 computer.[8]

## STRUCTURE ANALYSIS AND RESULTS

Approximately values for the parameters used in the least-squares analysis are determined from the experimental RD curve on Fig. 3.

The two first peaks at about 1.1 Å and 1.4 Å on the RD curve represent the $C-H$ and $C-O$ bond distances, respectively. Attempts have been made to
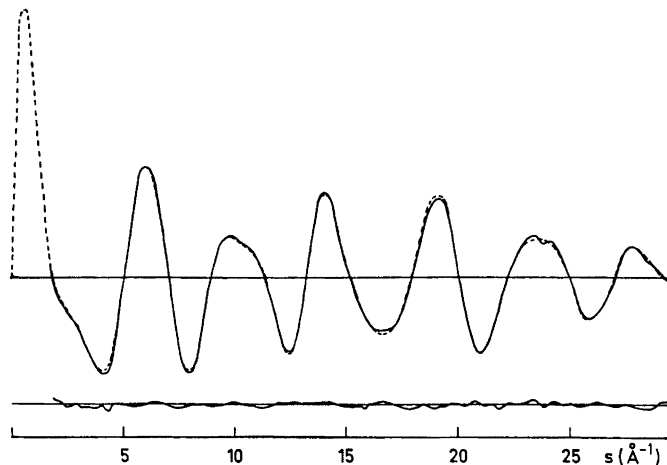
*Fig. 2.* Dimethoxymethane. Experimental (solid line), theoretical (dotted line), and difference molecular intensity curve.
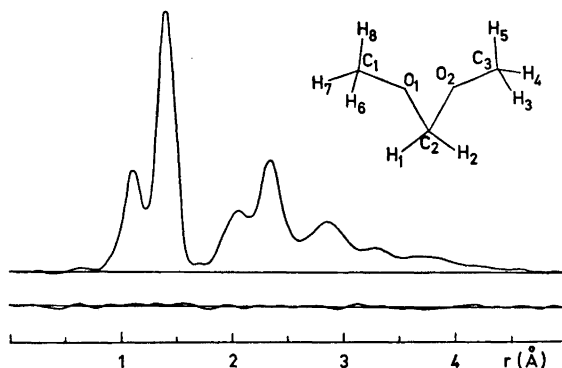


*Fig. 3.* Dimethoxymethane. Experimental radial distribution curve. The lower curve shows the difference between the experimental and the theoretical values. Artificial damping constant $k = 0.002$ Å.

determine whether there is only one $C-O$ bond length (model I) or different lengths of the terminal and central $C-O$ bonds (model II). The least-squares refinement of model I gives a $C-O$ bond distance of 1.405 Å and a corresponding vibrational amplitude ($u$-value) of 0.058 Å. This amplitude is somewhat greater than what has been found for $C-O$ bonds in other electron-diffraction investigations of ethers.[1, 13] However, the peak in question may consist of a sum of contributions from two slightly different bond lengths, which have smaller $u$-values than obtained for one average $C-O$ bond. A least-squares

refinement of two different $C-O$ bond lengths (model II) and their $u$-values do not converge, apparently because of the great correlation between these parameters. If the $u$-values of the two distances are assumed equal, they may be refined simultaneously with the two bond lengths, keeping all other parameters fixed. This gives a $u$-value of the $C-O$ distances of 0.052 Å, which is the same as the one found in 1,2-dimethoxyethane.[12] Subsequent refinements of the structure were performed by keeping this $u$-value fixed and refining the other parameters. The final result for the $C-O$ bonds is $r(C-O)_{terminal} = 1.432$ Å and $r(C-O)_{central} = 1.382$ Å. It should be mentioned that the correlation between the two $C-O$ bonds and their $u$-values makes the bond lengths much dependent of the determined vibrational amplitude. The refinements of the last-mentioned structure model (model II) gives the best fit between the experimental and the theoretical curves obtained in this investigation. One can not conclude unequivocally from these refinements that there are two different carbon-oxygen bond lengths in dimethoxymethane, however, the results indicate that this is the case.

The main contribution to the peak at $2.0-2.1$ Å is from $O \cdots H$ distances between oxygen atoms and hydrogen atoms in $\beta$-positions. The HCH plane of the methylene group is assumed to be perpendicular to the OCO plane and bisecting the angle OCO. The angle HCH in the methylene group is put equal to the tetrahedral angle, 109°28'. The angle OCH in the methoxy groups is determined to be 110.3°.

The best agreement between experimental and theoretical curves is obtained for the $\angle$ OCO equal to 114.3° and the $\angle$ COC equal to 114.6°. These angles do not differ much from what is found in the cyclic ether 1,3,5-trimethyltrioxan,[1] though the OCO angle is found to be the greater in the latter compound. There is, however, a considerable correlation between these valence angles, and the determined difference is not significant.

The next peak in the RD curve at $2.3-2.4$ Å contains contributions from the $O_1 \cdots O_2$ distance and the two $C_1 \cdots C_2$ distances, being 2.320 Å and 2.366 Å, respectively.

The most significant peak for the determination of the conformation is found in the outer part of the RD curve at 2.9 Å. This peak contains contributions from $C_1 \cdots O_2$ and $C_3 \cdots O_1$ distances. The expected unfavourable interaction of lone pair electrons on the oxygen atoms in an all-*anti* conformation should be expected to favour a *gauche-gauche* conformation. This is also consistent with the result of this work. One methyl group is twisted above the OCO plane and the other methyl group below the plane. Convergence of the least-squares analysis could not be obtained in refinements where the two twist angles were refined simultaneously. Assuming equal twist angles for the two methyl groups about the central $C-O$ bonds resulted in a good fit between the experimental and the theoretical curves. The distances $C_1 \cdots O_2$ and $C_3 \cdots O_1$ are then equal, and the obtained $u$-values of 0.111 Å do not deviate from what could be expected for such a distance. Consequently it is reasonable to assume only one twist angle of the methoxy groups. The methoxy groups are found to be twisted 116.7° from an all-*anti* conformation, resulting in a dihedral angle, $\delta(COCO)$, of 63.3°.

The following independent parameters were simultaneously refined: $C-O$(terminal), $C-O$(central), $C-H$, $\angle COC$, $\angle OCO$, the twist angle $\tau(CH_3O)$ of the methyl groups about the central $C-O$ bonds, $\angle OCH(CH_3)$, the twist angle $\tau(CH_3)$ of the methyl groups about the terminal $C-O$ bonds, the mean amplitudes of vibration for the $C-H$ bond distances, the $C_1 \cdots C_2$, the $C_1 \cdots O_2$, and the $O \cdots H$ distances from the oxygen atoms to the methylene hydrogen atoms. The remaining vibrational amplitudes were grouped according to distance types and lengths, and were partly refined in separate cycles, partly assigned reasonable values, so that the sum of square residuals converge to the lowest value.

The vibrational amplitude for the $C-H$ bonds are found to be smaller in this work than usually found. This parameter is only slightly correlated with other parameters and will be of little importance for the over-all result.

The dipole moment of dimethoxymethane in benzene, measured by Krane,[9] is found to be 0.99 D. A simple calculation of the dipole moment is carried out, assuming each oxygen atom to have a dipole moment of 1.2 D. The resultant dipole moment is found to be 1.08 D. Dipole moments of some related ethers referred in the literature [10] are: dimethylether 1.30 D, methoxymethane 1.23 D, diethylether 1.15 D. As can be seen the dipole moment is not much influenced by the increasing chain length. The agreement between the experimental and the calculated value is satisfactory.

The dimethoxymethane may be looked upon as the unit element of the polyoxymethylene chain $(-CH_2-O-)_n$. Polyoxymethylene is reported to have a *gauche-gauche-gauche* conformation and the internal rotation angle is found to be about $77-78°$. In an X-ray investigation by Tadokoro *et al.*[11] the following bond lengths and angles (which are of interest to compare) have been found: $r(C-O) = 1.42$ Å, $\angle OCO = 110.8°$, $\angle COC = 112.4°$, and the internal rotation angle $78.2°$. These values are in satisfactory agreement with the results obtained in this work.

## REFERENCES

1. Astrup, E. E. *Acta Chem. Scand.* **27** (1973) 1345.
2. Astrup, E. E. *Acta Chem. Scand.* **25** (1971) 1494.
3. Allen, P. W. and Sutton, L. E. *Acta Cryst.* **3** (1950) 46. Data provided by J. Donohue.
4. Aoki, K. *J. Chem. Soc. Japan, Pure Chem. Sect.* **74** (1953) 110.
5. Andreassen A. L. and Bauer, S. H. *Unpublished work.*
6. Kubo, V. M. *Sci. Papers Inst. Phys. Chem. Rec. (Tokyo)* **29** (1963) 179.
7. Bastiansen, O. and Skancke, P. N. *Advan. Chem. Phys.* **3** (1960) 323.
8. Andersen, B., Seip, H. M., Strand, T. G. and Stølevik, R. *Acta Chem. Scand.* **23** (1969) 3224.
9. Krane, J. *Private communication.*
10. *Handbook of Chemistry and Physics*, 48th Ed., The Chemical Rubber Co., Cleveland 1967.
11. Tadokoro, H., Yasumoto, T., Murahashi, S. and Nitta, I. *J. Polymer Sci.* **44** (1960) 266.
12. Astrup, E. E. *Unpublished results.*
13. Kimura, K. and Kubo, M. *J. Chem. Phys.* **30** (1959) 151.

# Rotational Isomerism and Nuclear Magnetic Resonance Spectra of Propyl and Butyl Derivatives

DAGFINN W. AKSNES and JAN STØGÅRD

*Chemical Institute, University of Bergen, N-5000 Bergen, Norway*

The 60 MHz NMR spectra of eleven propyl and butyl derivatives have been fully analyzed by means of the computer program UEAITR. A theoretical analysis of the propyl spectrum has also been carried out by the combined use of the composite particle technique, good quantum numbers and symmetry. The spectral parameters of the strongly coupled protons follow from this "direct" analysis. The chemical shifts and coupling constants of the eleven compounds are discussed in terms of substituent and conformational effects.

Rotamer energies of the energetically favoured forms of three butyl halides have been calculated using a semi-empirical method. The calculations indicate that, whereas the *anti* form predominates about the $CH_3CH_2-CH_2CH_2X$ bond by $0.7-1.1$ kcal/mol, the *gauche* form is preferred about the $CH_3CH_2CH_2-CH_2X$ bond by $0.1-0.3$ kcal/mol. It is found that rotamers having an *anti* arrangement of the carbon skeleton contribute as much as 77 % in the gas phase. However, the NMR data suggest an increase of *gauche*-methyl forms by 10 % in the liquid phase owing to dipole interactions.

**R**otational isomerism about single $C-C$ bonds in alkanes and their derivatives has been extensively studied by electron diffraction and various spectroscopy methods.[1] Since the barrier to internal rotation about the $C-C$ bond is low, only time-average NMR parameters are usually measured at room temperature. The spectra of compounds containing three or more strongly coupled methyl or methylene protons are, nevertheless, very complex. Although it might be possible to calculate some of the spectral parameters directly from the spectrum only an "indirect" computer analysis will yield precise parameters.

Experimental and theoretical studies of halogenated ethanes, propanes, and butanes generally agree in indicating that halogen stabilizes *gauche* conformations.[1] However, electron diffraction data on butyl bromide[2] suggest that the distribution of conformers is the same as for pentane[3] in contrast to the situation in butyl chloride.[4] It therefore seemed of interest to investigate the conformations of the butyl halides using NMR and the semi-empirical

method due to Scott and Scheraga.[5] The latter method has been found to reproduce experimental barrier heights and differences in conformational energy satisfactorily for a series of halogenated ethanes and propanes.[6]

The following propyl and butyl derivatives have been studied in this paper: I: propyl chloride; II: propyl bromide; III: propyl iodide; IV: propyl alcohol; V: tripropyl phosphate; VI: tripropyl thiophosphate; VII: butyl chloride; VIII: butyl bromide; IX: butyl iodide; X: butylamine; XI: butyl cyanide.

Twelve years ago Cavanaugh and Dailey [7] studied the NMR spectra of some propyl derivatives on the basis of a perturbation treatment of the $A_3B_2C_2$ spin system. When the present work was initiated, however, no precise NMR data on these compounds were available. During the course of this investigation Schrumpf [8] reported NMR data for several propyl derivatives, including compounds I − III. Schrumpf analyzed the spectra of the propyl halides as $A_3B_2C_2$ systems by iterative fitting of only 30 − 70 lines mainly in the B region.

The present paper also reports a theoretical sub-spectral analysis of the propyl spectrum on the basis of the $A_3BB'XX'$ approximation. This approximation is far better than the one used by Schrumpf in his sub-spectral treatment. This investigation is a continuation of previous work on related compounds.[9−13]

## EXPERIMENTAL

All the compounds were obtained from Fluka AG except V and VI which were provided by one of us (D.W.A.). Compounds V and VI have b.p.$_{10}$ 89 − 90°C and b.p.$_{8}$ 102 − 104°C, respectively. The propyl compounds I − VI were examined as 25 % v/v solutions in methylene chloride whereas compounds VII − XI were studied as neat liquids added 1 % v/v benzene. A trace of trifluoroacetic acid was added to IV to ensure rapid exchange of the hydroxyl proton. A small amount of TMS added to all samples served as internal standard. The samples were thoroughly degassed and sealed under vacuum.

The NMR spectra were run at ambient probe temperature (ca. 27°C) on a JEOL-C-60H spectrometer. The spectra used for the analyses were recorded at 54 Hz sweep width and calibrated, relative to the locking substance, every 5 Hz using a frequency counter. Line positions were obtained by averaging the results of four scans.

Computations were performed on the IBM/50H computer at the University of Bergen. The graphical output was obtained on a Calcomp Plotter.

## ROTAMER ENERGIES OF BUTYL HALIDES

In previous papers the semi-empirical method due to Scott and Scheraga [5] has been used to calculate rotamer energies in halogenated butanes.[6,11,12]

In these calculations the energy ($E$) of a given molecular conformation is broken down into additive non-bonded interactions plus the torsional strain as shown in eqn. (1).

$$E = \tfrac{1}{2}V_0 \,(1 + \cos 3\,\tau) + \sum a_{ij}\exp\,(-b_{ij}r_{ij}) - c_{ij}/r_{ij}{}^6 + d_{ij}/r_{ij} \qquad (1)$$

The significance of the various terms in eqn. (1) and of the parameters has been described previously.[6] $E$ can be calculated once $V_0$, $a_{ij}$, $b_{ij}$, $c_{ij}$, $d_{ij}$ and the molecular geometry are known.

In butyl halides an ethane-like situation exists about two $C-C$ bonds if the orientation of the substituent X is taken into account. It is thus seen that five different staggered rotamers result ($3^2 = 9$ rotamers altogether). With respect to the central $C_2-C_3$ bond two different rotational isomers are found:



anti                    gauche
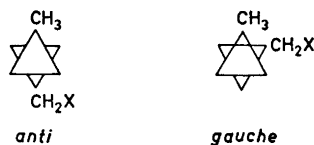
In Table 1 the staggered rotamers are specified by italics $a$ (*anti*) and $g$ (*gauche*) which refer to the relevant dihedral angles. The first italic refers to the dihedral angle ($\tau$) of the $C_1-C_2$ bond relative to the $C_3-C_4$ bond and the second italic refers to the dihedral angle of the $X-C_1$ bond relative to the central $C_2-C_3$ bond.

Average values of bond lengths and angles have been measured for butyl chloride [4] and bromide [5] in the gas phase at room temperature. The corresponding parameters of the butyl halides in the liquid phase have, however, not been reported. For our comparative studies we have therefore found it advantageous to use the same standard values as in previous calculations on similar molecules,[6,11,12] *viz*.: Bond lengths (Å): $C-C = 1.53$, $C-H = 1.09$, $C-Cl = 1.77$, $C-Br = 1.93$, and $C-I = 2.13$. Bond angles (degrees): $C-C-H = H-C-H = 109.47$ and $C-C-X = 111.0$ (X = C, Cl, Br, or I). These standard values do not, in fact, differ significantly from the reported values of gasous

*Table 1.* Calculated rotamer energies (kcal/mol) for the staggered forms of butyl halides.

| Sub-stituent | Rotamer | Dihedral angles (deg.) | | Calculated contributions | | | Total energy |
|---|---|---|---|---|---|---|---|
| | | | | Steric | Polar H···X | Torsional | |
| Cl | | 180, | 180 | 1.31 | −4.37 | 0 | −3.06 |
| Br | (*a,a*) | 180, | 180 | 0.84 | −3.88 | 0 | −3.03 |
| I | | 180, | 180 | 0.79 | −3.05 | 0 | −2.27 |
| Cl | | 68, | 180 | 2.02 | −4.52 | 0.11 | −2.39 |
| Br | (*g,a*) | 68, | 180 | 1.55 | −4.00 | 0.11 | −2.34 |
| I | | 68, | 180 | 1.45 | −3.15 | 0.11 | −1.59 |
| Cl | | 180, | 74 | 1.62 | −4.78 | 0 | −3.16 |
| Br | (*a,g*) | 180, | 74 | 1.06 | −4.26 | 0 | −3.21 |
| I | | 180, | 76 | 1.03 | −3.36 | 0 | −2.33 |
| Cl | | 68, | 74 | 2.77 | −4.95 | 0.11 | −2.06 |
| Br | (*g,g*) | 68, | 70 | 2.24 | −4.56 | 0.11 | −2.20 |
| I | | 68, | 74 | 2.10 | −3.45 | 0.11 | −1.24 |
| Cl | | 70, | 300 | 28.16 | −5.90 | 0.18 | 22.43 |
| Br | (*g,g′*)[a] | 70, | 310 | 21.17 | −5.52 | 0.18 | 15.83 |
| I | | 70, | 310 | 27.46 | −4.42 | 0.18 | 23.22 |

[a] (*g,g′*) represents the form in which the methyl and halogen approach most closely.

butyl chloride and bromide. The calculated energy differences have, never-theless, been found to be fairly insensitive to the choice of bond lengths and bond angles for the range of conformations in which steric interactions are not strong, that is, at the energy minima.[14]

The rotamer energies listed in Table 1 were calculated from eqn. (1) using the previously quoted values of the parameters $V_0$, $a_{ij}$, $b_{ij}$, $c_{ij}$, and $d_{ij}$.[6] The calculated energies are relative and have no absolute significance. The computer program COORD [15] was used for calculating the interatomic distances for a given molecular geometry.

The ratio of the mol fractions of the i'th and j'th rotamers is given by eqn. (2).

$$n_i/n_j = Q_i'(Q_j')^{-1} \exp[-(E_i - E_j)/RT] \tag{2}$$

where $Q_i'$ is the partition function for a particular rotamer i, excluding the steric interaction energy term. It has, however, been shown that the $Q_i''$'s are fairly constant for alkane isomers with the same degree of branching.[16] Errors introduced by assuming that the $Q_i''$'s are independent on conforma-tion in the butyl halides are small compared to the approximations involved in eqn. (1). The distribution of rotamers listed in Table 2 was obtained using eqn. (2) and the rotamer energies in Table 1.

*Table 2.* Distribution of rotamers (%) for butyl halides and pentane at 27°C. The figures take into account the multiplicity.

| Rotamer | Multiplicity | Mol fraction | Cl | Substituent | | |
| | | | | Br | I | $CH_3$[a] |
| --- | --- | --- | --- | --- | --- | --- |
| (a,a) | 1 | $n_0$ | 22.8 | 20.7 | 23.7 | 45.7 |
| (g,a) | 2 | $n_1$ | 14.8 | 13.0 | 15.2 | 24.0 |
| (a,g) | 2 | $n_2$ | 53.9 | 56.0 | 52.4 | 24.0 |
| (g,g) | 2 | $n_3$ | 8.5 | 10.3 | 8.7 | 6.3 |

[a] Based on an assumed difference in energy between *anti* and *gauche* conformations of 0.8 kcal/mol.

## SPECTRAL ANALYSIS

The NMR spectra of the eleven compounds were analyzed by means of the UEANMR II [17] and UEAITR [18] computer programs. These programs make use of magnetic equivalence factoring to reduce the size of the secular matrices. The UEANMR II program was, however, only used in conjunction with the sub-routine KOMBIP [19] to obtain stick- and line-shape plots. The iterative fitting of experimental and calculated transitions was performed by means of the UEAITR program.

(a) *Propyl spectra.* Generally, the protons of a rapidly rotating propyl group constitute an $A_3BB'CC'$ spin system. However, when a strongly electro-negative substituent is attached to the propyl fragment the NMR spectra can be fairly accurately analyzed on the basis of an $A_3BB'XX'$ system. This system

provides a good example of a complex system which can be simplified by the combined use of the composite particle technique, good quantum numbers and symmetry. It follows from the principles of the sub-spectral analysis that the strongly coupled $A_3BB'$ part of the $A_3BB'XX'$ system can be broken down into two $a_3b_2$ and two $a_3bc$ sub-spectra characterized by $m(XX')= \pm 1$ and 0, respectively:[20]

$$A_3BB'(A_3BB'XX') = (a_3b_2)_{+1} + (a_3b_2)_{-1} + (a_3bc)_0(sym.) + (a_3bc)_0(antisym.) \quad (3)$$

These sub-spectra are characterized by the following effective spectral parameters:

$(a_3b_2)_{\pm 1}$ sub-spectra:

$$\nu_a = \nu_A \pm J_{AX}; \; J_{ab} = J_{AB} \quad (4)$$
$$\nu_b = \nu_B \pm N$$

$(a_3bc)_0$ sub-spectra:

$$\nu_a = \nu_A; \; J_{ab} = J_{AB}$$
$$\nu_b = \nu_B + L; \; J_{ac} = J_{AB} \quad (5)$$
$$\nu_c = \nu_B - L; \; J_{bc} = J_{BB'} \pm J_{XX'}$$

where $N = \frac{1}{2}(J_{BX} + J_{BX'})$ and $L = \frac{1}{2}(J_{BX} - J_{BX'})$

These effective spectral parameters are identical with the corresponding transformations of the $ABB'XX'$ system,[21] as expected, since the composite particle method implies identity transformations.

The problem has thus been reduced to solving the general $A_3B_2$ and $A_3BC$ systems. In principle, however, the relevant spectral data of these systems can be obtained from the corresponding $ab_2$ and $abc$ sub-spectra.

In the composite particle notation the following spin states of the $A_3B_2$ system contribute:

$$A_3B_2 = QT + 2DT + QS + 2DS \quad (6)$$

The total relative intensities attributable to these four overall spin states are 46, 22, 10, and 2, respectively. The two latter spin states only contribute 12 intensity units at $\nu_A$.

The transition frequencies of the general $a_3b_2$ system that can be obtained in analytical form are given in Table 3.[22] The relevant spectral lines of a given sub-spectrum can then be found by inserting the appropriate expressions for $\nu_a$, $\nu_b$, and $J_{ab}$ from eqn. (4).

All spectral parameters of the $CH_3-CH_2$-protons, except $L$ and $J_{BB'}$, can be obtained from the $(a_3b_2)_{\pm 1}$ sub-spectra by using, for example, eqns. (7) and (8).

$$\nu_A = \frac{1}{2}(a_6{}^+ + a_6{}^-); \; \nu_B = \frac{1}{4}(b_4{}^+ + b_5{}^+ + b_4{}^- + b_5{}^-) \quad (7)$$

$$J_{AX} = \frac{1}{2}(a_6{}^+ - a_6{}^-); \; N = \frac{1}{4}(b_4{}^+ + b_5{}^+ - b_4{}^- - b_5{}^-)$$

$$J_{AB} = \frac{2}{5}(a_1{}^+ - a_6{}^+ + b_1{}^+ - \frac{1}{2}b_4{}^+ - \frac{1}{2}b_5{}^+) \quad (8)$$

where the superscripts $+$ and $-$ refer to sub-spectra characterized by $m(XX')=1$ and $-1$, respectively.

*Table 3.* Closed-form transition frequencies for the $a_3b_2$ spin system.

| Line | Origin | Frequency [a] |
|---|---|---|
| $a_1$ | $QT$ | $\frac{1}{2}(\nu_a + \nu_b + \frac{5}{2}J_{ab} + R_-)$ |
| $a_2$ | $DT$ | $\frac{1}{2}(\nu_a + \nu_b + \frac{3}{2}J_{ab} + S_+)$ |
| $a_3$ | $QT$ | $\frac{1}{2}(\nu_a + \nu_b - \frac{5}{2}J_{ab} + R_+)$ |
| $a_4$ | $DT$ | $\nu_b + \frac{1}{2}(S_+ + S_-)$ |
| $a_5$ | $DT$ | $\frac{1}{2}(\nu_a + \nu_b - \frac{3}{2}J_{ab} + S_-)$ |
| $a_6$ | $QS + DS$ | $\nu_a$ |
| $b_1$ | $QT$ | $\frac{1}{2}(\nu_a + \nu_b + \frac{5}{2}J_{ab} - R_-)$ |
| $b_2$ | $DT$ | $\frac{1}{2}(\nu_a + \nu_b + \frac{3}{2}J_{ab} - S_+)$ |
| $b_3$ | $QT$ | $\frac{1}{2}(\nu_a + \nu_b - \frac{5}{2}J_{ab} - R_+)$ |
| $b_4$ | $DT$ | $\nu_b + \frac{1}{2}(S_- - S_+)$ |
| $b_5$ | $DT$ | $\nu_b - \frac{1}{2}(S_- - S_+)$ |
| $b_6$ | $DT$ | $\frac{1}{2}(\nu_a + \nu_b - \frac{3}{2}J_{ab} - S_-)$ |

[a] $R_\pm = [(\nu_a - \nu_b \pm \frac{1}{2}J_{ab})^2 + 6J_{ab}^2]^{\frac{1}{2}}$　$S_\pm = [(\nu_a - \nu_b \pm \frac{1}{2}J_{ab})^2 + 2J_{ab}^2]^{\frac{1}{2}}$

The appearance of the $(a_3b_2)_{\pm 1}$ sub-spectra depends only on $T$, where

and
$$T = J_{AB}/(\nu_{AB} \pm (J_{AX} - N)) \qquad (9)$$
$$\nu_{AB} = \nu_A - \nu_B$$

These sub-spectra have similar appearance in the investigated compounds I−IV since $|\nu_{AB}| \gg |J_{AX} - N|$. A fair estimate of $T$ can be obtained directly from the experimental spectra. It was thus possible to identify most of the transitions of the $(a_3b_2)_{\pm 1}$ sub-spectra as shown in Fig. 1 for compound I. Subsequent use of eqns. (7) and (8) then yielded the following NMR data for I:

$\nu_A = 60.0$ Hz, $\nu_B = 106.4$ Hz, $J_{AB} = 7.35$ Hz, $N = 6.70$ Hz, and $J_{AX} = 0$.

The *b*-lines used in this calculation have been indicated with arrows in Fig. 1

Closed-form expressions for the transitions of the ABC system and hence $A_3BC$ system, cannot be obtained, however, since secular matrices of at least third order are involved.

Compounds V and VI can, similarly, be treated as $A_3BB'XX'P$ systems. The phosphorus-proton coupling constants can be obtained directly from the spectra with reasonable accuracy.

The experimental spectra of the terminal $-CH_2R$ protons in compounds I−VI show that these protons are practically magnetically equivalent. The propyl protons thus constitute an $A_3B_2X_2$ system quite closely. It is therefore of interest to look at the features of this system. It follows from eqns. (3)−(5) that the strongly coupled $A_3B_2$ part of the $A_3B_2X_2$ system consists of four $a_3b_2$ sub-spectra with $J_{ab} = J_{AB}$ and the following effective chemical shifts:

$$\nu_a = \nu_A + m(X_2)J_{AX}; \; \nu_b = \nu_B \pm m(X_2)J_{BX} \qquad (10)$$

where $m(X_2) = \pm 1$ and 0. The $a_3b_2$ sub-spectrum corresponding to $m(X_2) = 0$ are doubly degenerate. Closed-form transition frequencies can be obtained
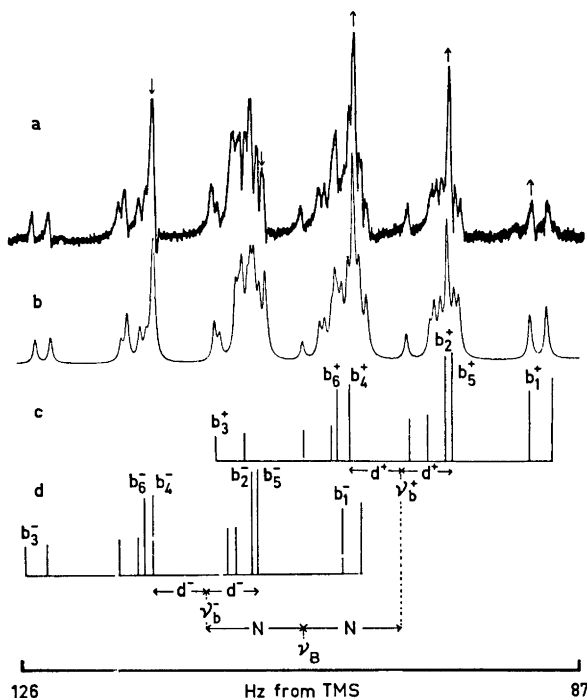
*Fig. 1.* The BB′ region of the 60 MHz spectrum of propyl chloride; a, experimental spectrum; b, computed total spectrum; c, and d, computed stick-plots of the $a_3b_2$ sub-spectra characterized by $m(XX') = 1$ and $-1$, respectively. The numbering of the lines refers to Table 3 and $d = \frac{1}{2}(S_+ - S_-)$.

from Table 3 by inserting the appropriate values of $\nu_a$, $\nu_b$, and $J_{ab}$ from eqn. (10).

The $CH_3 - CH_2$-region of the propyl spectrum can therefore be reproduced reasonably well as a superposition of three similar $a_3b_2$ sub-spectra. These sub-spectra contribute a total of 48 intensity units at $\nu_A$ and account fully for this strong peak.

The final spectral parameters of compounds I−IV obtained from the iterative analyses of the $A_3BB'CC'$ and $A_3BB'CC'P$ spin systems are listed in Table 4. The experimental and calculated B spectra of I and VI are shown in Figs. 1 and 2. It is seen that the doublets at the wings of the spectrum in Fig. 1 are further split into quartets in Fig. 2 due to the $J_{BP}$ coupling.

(b) *Butyl spectra.* Again, rotational averaging simplifies the NMR spectrum to one of the $A_3BB'CC'DD'$ type. All the experimental spectra were, however, satisfactorily reproduced on the basis of an $A_3BB'CC'D_2$ spin system. This implies that the terminal $- CH_2 R$ protons are magnetically equivalent within the accuracy of the experiment.

The secular matrices of this spin system can be considerably reduced by means of a procedure similar to the one used for the propyl spectra. The

*Table 4.* 60 MHz NMR spectral parametres (Hz) of six propyl derivatives in 25 % v/v methylene chloride solution.

| Compound | I | II | III | IV | V[b] | VI[b] |
|---|---|---|---|---|---|---|
| $\nu_A$ [a] | 60.02 | 59.96 | 58.05 | 52.58 | 53.94 | 55.49 |
| $\nu_B$ | 106.55 | 111.10 | 109.12 | 90.76 | 97.99 | 99.44 |
| $\nu_C$ | 209.23 | 202.46 | 190.12 | 209.23 | 237.92 | 237.24 |
| $\nu_{\alpha\beta}$ [c] | 102.68 | 91.36 | 81.00 | 118.47 | 139.93 | 137.70 |
| $J_{AB}$ | 7.34 | 7.30 | 7.31 | 7.39 | 7.36 | 7.38 |
| $J_{AC}$ | −0.04 | −0.04 | −0.04 | −0.05 | −0.03 | −0.07 |
| $J_{BB'} - J_{CC'}$ | −0.95 | −0.90 | −1.02 | −0.92 | −0.99 | −0.94 |
| $J_{BC}$ | 6.60 | 6.64 | 6.73 | 6.59 | 6.39 | 6.67 |
| $J_{BC'}$ | 6.72 | 6.76 | 6.90 | 6.87 | 6.54 | 6.48 |
| $J_{BP}$ | − | − | − | − | −0.20 | −0.71 |
| $J_{CP}$ | − | − | − | − | 8.60 | 8.86 |
| Assigned lines | 130 | 148 | 147 | 130 | 205 | 244 |
| RMS error | 0.06 | 0.06 | 0.07 | 0.09 | 0.09 | 0.10 |
| Max. prob. error | 0.033 | 0.022 | 0.044 | 0.037 | 0.051 | 0.038 |

[a] Chemical shifts downfield from TMS. [b] $J_{AP} = 0$. [c] $\nu_{\alpha\beta} = \nu_C - \nu_B$, *i.e.*, the internal shift difference of protons positioned $\alpha$ and $\beta$ to the substituent.

simplest possible spin state, however, comprises an ABB′CC′ system and is unamenable to calculation by hand. It is thus necessary to use computer analysis in order to obtain the spectral data. The trial values were obtained either from the experimental spectra or else by a tedious trial-and-error procedure. The refined parameters listed in Table 5 were all obtained from the iterative computations. Figs. 3 and 4 show satisfactory agreement between the experimental and calculated spectra of X.



120.2        Hz from TMS        80.1
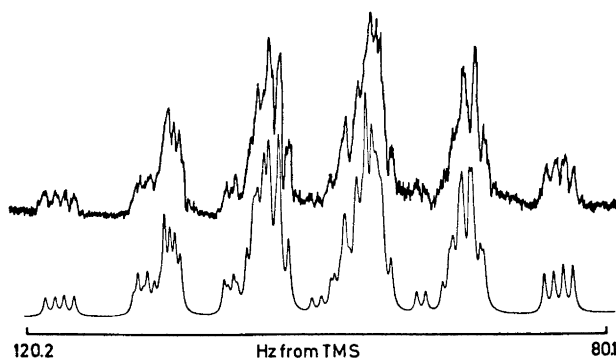
*Fig. 2.* Experimental (upper trace) and calculated (lower trace) 60 MHz spectrum of the BB′ region in tripropyl thiophosphate. Note that the doublets at the wings of the propyl spectrum (Fig. 1) are further split into quartets due to the proton-phosphorus coupling.

*Table 5.* 60 MHz NMR spectral parameters (in Hz) of neat 1-substituted butanes.

| Compound | VII[b] | VIII | IX | X | XI |
|---|---|---|---|---|---|
| $\nu_A$ [a] | 50.98 | 50.20 | 48.34 | 50.58 | 47.57 |
| $\nu_B$ | 82.80 | 81.56 | 77.55 | 76.30 | 77.74 |
| $\nu_C$ | 98.55 | 102.77 | 99.05 | 77.55 | 83.61 |
| $\nu_D$ | 203.17 | 194.82 | 179.73 | 152.31 | 126.94 |
| $\nu_{\alpha\beta}$ [d] | 104.62 | 92.05 | 80.68 | 74.76 | 43.33 |
| $J_{AB}$ | 7.34 | 7.38 | 7.33 | 7.39 | 7.32 |
| $J_{AC}$ [c] | −0.18 | −0.20 | −0.14 | −0.17 | −0.20 |
| $J_{BB'}$ | −12.47 | −12.54 | −12.62 | −12.63 | −12.74 |
| $J_{BC}$ | 5.81 | 5.73 | 5.77 | 5.80 | 5.88 |
| $J_{BC'}$ | 8.83 | 8.94 | 8.93 | 8.95 | 9.05 |
| $J_{BD}$ | −0.22 | −0.23 | −0.07 | −0.20 | −0.11 |
| $J_{CC'}$ | −12.53 | −12.53 | −12.65 | −12.67 | −12.73 |
| $J_{CD}$ | 6.71 | 6.80 | 6.92 | 6.79 | 6.96 |
| Assigned lines | 550 | 446 | 540 | 566 | 399 |
| RMS error | 0.09 | 0.09 | 0.11 | 0.09 | 0.10 |
| Max. prob. error | 0.012 | 0.014 | 0.013 | 0.017 | 0.016 |

[a] Chemical shifts downfield from TMS. [b] Data from Ref. 13 with corrected shift values. $J_{AD} = 0$. [d] $\nu_{\alpha\beta} = \nu_D - \nu_C$.
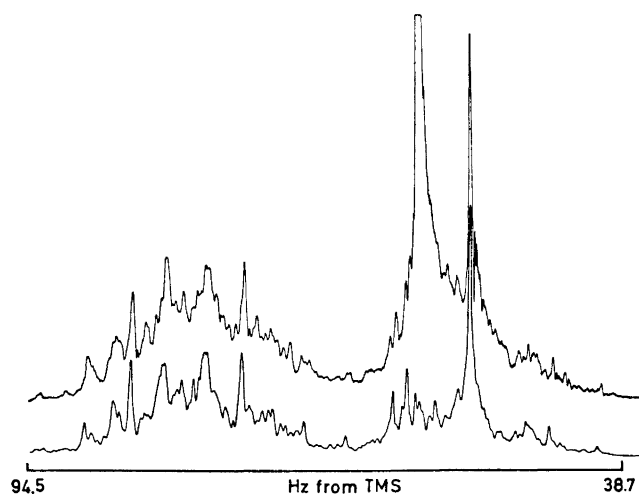


*Fig. 3.* Experimental (upper trace) and calculated (lower trace) 60 MHz spectrum of the $A_3BB'CC'$ region in butylamine. The strong peak adjacent to the methyl signal is due to the $NH_2$ protons.
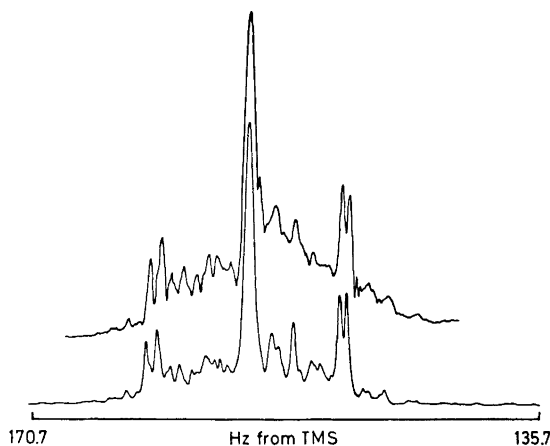
*Fig. 4.* Experimental (upper trace) and calculated (lower trace) 60 MHz spectrum of the $D_2$ region in butylamine.

## DISCUSSION

The calculated rotamer energies of the butyl halides (Table 1) show that, whereas the *anti* form predominates about the $CH_3CH_2 - CH_2CH_2X$ bond by $0.7 - 1.1$ kcal/mol, the *gauche* form is preferred about the $CH_3CH_2CH_2 - CH_2X$ bond by $0.1 - 0.3$ kcal/mol. When the multiplicity is taken into account it is seen from Table 2 that the $(a, g)$ rotamer predominates although the $(a, a)$ conformer has comparable energy for the butyl halides. In contrast, in pentane the all-*anti* conformation abounds. In these molecules the $(a, a)$ and $(a, g)$ rotamers contribute as much as $70 - 77$ % of the staggered forms. This clearly shows that an *anti* or zig-zag conformation of the carbon skeleton is preferred. The calculations indicate, however, that the replacement of one methyl group by a halogen atom in pentane introduces extra stability of the $(a, g)$ conformer at the expence of the $(a, a)$ and $(g, a)$ conformers.

The steric energy for the $(g, g')$ rotamer in Table 1 is, of course, too high since the rigid rotor model used in the present calculations is found to be inadequate when steric interactions are strong.[14] At any rate, however, the contribution of the $(g, g')$ rotamer can be rejected by steric requirements because calculations show that the H-halogen distances would be too short (*ca.* 1.8 Å) to allow the existence of this form without serious distortion of the rest of the molecule.

The present calculations of rotamer distributions deviate, however, considerably from the results obtained from electron diffraction studies of compounds VII [4] and VIII.[2] Surprisingly, in those studies, the $(g, g')$ rotamer was found to contribute as much as 24 % for VII [4] while this rotamer was ruled out by steric requirements for VIII.[2] It is difficult to believe, however, that the present evaluations are so much in error since the same model has been found to reproduce experimental barrier heights and rotamer energy differences

satisfactorily for a series of halogenated ethanes and propanes.[6] At any rate, since the present calculations are strongly dependent upon bond angles it is certain that further improvements in the calculated molecular energies will necessitate more accurate bond angles than yet available. In the analysis of the electron diffraction data for VII a *gauche* angle of 60° was assumed.[4] The authors point out, however, that in the analysis of the radial distribution curve for the longer non-bonded interactions some adjustment of the *gauche* angle may be necessary. In accord with the present work, infrared, electron diffraction, microwave, and theoretical studies of halogenated propanes and butanes generally agree in indicating that fluorine, chlorine, and bromine stabilize *gauche* isomers.[1,4,6,11,12,23] Electron diffraction data for VIII [2] suggest, however, that bromine has a negligible stabilization effect on the *gauche* forms, in contrast to experimental results for propyl bromide.[1,6]

The results of Table 1 show that the steric or van der Waals energy is respulsive whereas the electrostatic energy is attractive for the butyl halides. It is seen that the steric repulsion which is considerable in the rotamers possessing *gauche* methyl, is not balanced by the attractive electrostatic interaction in the $(g, a)$, $(g, g)$ and $(g, g')$ rotamers. The mutual avoidance of the terminal $CH_2X$ and $CH_3$ groups is also implied by the large value of the dihedral angle $\tau$ (68°). The attractive hydrogen-halogen interaction is comparable for VII and VIII but somewhat less for IX. The steric repulsion is, however, about the same for these molecules.

Since the barriers to internal rotation about the $C-C$ single bonds in the propyl and butyl derivatives are low only time-average NMR parameters $P$ defined by eqn. (20) are measured at room temperature.

$$P = \sum_i n_i P_i / \sum_i n_i \qquad (20)$$

where the summation is over all the contributing rotamers.

Let $J_g$ and $J_t$ represent the *gauche* and *trans* coupling constants of the $-CH_2-CH_2-$ fragment in a perfectly staggered conformation. The observed vicinal coupling constants, $J$ and $J'$, can easily be expressed in terms of $J_g$ and $J_t$ by using eqn. (20).[22]

$$J = \tfrac{1}{2}(1 + p)J_g + \tfrac{1}{2}(1 - p)J_t$$
$$J' = (1 - p)J_g + pJ_t \qquad (21)$$

where $p$ is the relative population of all contributing conformers possessing an *anti* arrangement of the $R-C-C-C$ or $C-C-C-C$ bonds, as appropriate. Eqn. (21) is based on the assumption that $J_t$ and $J_g$ are invariant for a particular ethanic fragment of a given compound. This is, of course, an approximation, in particular since the present compounds are not perfectly staggered ($\tau > 60°$).[10,24] It follows from eqn. (21) that

$$2J + J' = 2J_g + J_t \qquad (22)$$

It is possible to calculate $p$ from eqns. (21) and (22) provided that $J$, $J'$ and either $J_g$ or $J_t$ are known.

It follows from eqn. (21) that $J = J'$ when $p = \tfrac{1}{3}$. This is the situation when the energy difference $\Delta E$ between the *anti* form and the two identical *gauche* forms, is zero.

The pair of vicinal coupling constants observed in the $-CH_2-CH_2-R$ fragment of compounds I – XI have identical or nearly identical values for a particular compound. This indicates that the relevant $\Delta E$ values are small in agreement with previous observations for propyl chloride and bromide[1] and 1,4-dihalobutanes.[11,12] Our calculations indicate that $\Delta E = 0.1 - 0.3$ kcal/mol in gaseous butyl halides while the NMR data imply that $\Delta E \simeq 0$ in the liquid phase. The small deviation in $\Delta E$ is reasonable since dipole interactions in the liquid phase would tend to stabilize rotamers having the larger dipole moments, that is, rotamers with a *gauche* substituent.

By inserting $p = n_0 + 2n_2$ in eqn. (21) the $J_{BC}$ and $J_{BC'}$ coupling constants corresponding to $J$ and $J'$, respectively, are obtained. From eqn. (22) and the data of Table 5 it follows that the average value of $2J_g + J_t = 20.44$ Hz for the butyl halides. This value is quite close to the values reported for similar compounds[11,12,22] with the substituents two bonds away from the ethanic fragment. There is considerable experimental evidence for assuming that $J_t \simeq 11$ Hz,[9–12,22] whence $J_g \simeq 4.7$ Hz. By inserting these values together with the average values $J_{BC} = 5.77$ Hz and $J_{BC'} = 8.90$ Hz for the butyl halides (Table 5) it is found that $p = 0.67$ which is about 0.1 less than the theoretical value for the gas phase. This result is consistent with the previous conclusion that *gauche* forms are enriched in the liquid phase. However, in the symmetrically substituted 1,4-dihalobutanes[11,12] the change of phase was found to have little effect on the *anti-gauche* equilibrium about the central $C_2 - C_3$ bond.

The NMR parameters for compounds I – III obtained in this study, deviate considerably from those reported by Cavanaugh and Dailey.[7] Our results are, however, in good agreement with Schrumpfs[8] recent data for the propyl halides. The observed deviations in the chemical shifts can probably be largely ascribed to solvent effects. However, Schrumpf discusses at length certain aspects of the propyl spectrum on basis of the $X_3BB'CC'$ approxiamation. This is a very poor approximation and the $A_3BB'XX'$ system would have been a far better choice. Furthermore, the present work shows that the latter system is easily treated by the sub-spectral method.

The observed chemical shifts for compounds I – XI are generally in keeping with the inductive effect. When the chemical shift differences of the $-CH_2-CH_2R$ protons were plotted against Huggins[25] values of the electronegativities of the first atom in the substituent, a linear relationship was found to exist for the Cl, Br, I, and OH substituents. The electron withdrawing power of the remaining substituents, however, is apparently not adequately described by the electronegativity of the first atom in the bond. Furthermore, on a quantitative basis, other substituent as well as conformational effects have to be taken into account. Specifically, for the CN group the magnetic anisotropy effect contributes significantly to the screening of the adjacent methylene protons. This effect gives rise to shielding along the $C\equiv N$ bond direction.[26] However, since the shielding attenuates rapidly with the distance from the anisotropic center the $\alpha$-protons will experience a larger shielding than the $\beta$-proton resulting in a reduced value of $\nu_{\alpha\beta}$.

The chemical shift difference of the $CH_3 - CH_2-$ protons decreases from propyl to corresponding butyl derivatives in accord with the attenuation of

the inductive effect due to the extra intervening carbon atom.

Although it has not been possible to obtain the individual geminal coupling constants for the propyl compounds the data of Table 4 show that $J_{CC'}$ is more positive than $J_{BB'}$. This observation is in agreement with the following predictions based on MO calculations:[26],[27]

(a) Increasing the HCH angle increases the $s$ character of the orbitals thus resulting in a positive contribution to the coupling.

(b) A substituent which withdraws electrons from the $\sigma$ bond by the inductive effect will give a positive contribution to the coupling and vice-versa.

Strongly electronegative substituents will affect the hybridization of the adjacent carbon atom by preferring to make use of carbon $p$ character. This results in an increase in the $s$ character of the remaining bonds and the geminal coupling constant will get a positive contribution [(a) above]. A similar substituent effect on the geminal coupling constants has also been observed in 1,4-dichlorobutane.[12] In the butyl compounds, however, the measured geminal coupling constants have nearly the same values and are little affected by the substituent due to the extra intervening carbon atom.

The observed decrease in the $-CH_2-CH_2-R$ vicinal coupling constants with increasing electronegativity of the substituent is also in agreement with valence bond calculations which predict that:[27],[28]

(a) electronegative substituents decrease the vicinal coupling and

(b) increase of the HCC bond angles decreases the vicinal coupling.
Electronegative substituents might be expected to increase the HCC bond angle by altering the hybridization as mentioned above.

The vicinal coupling constants of the $CH_3-CH_2$-fragment are virtually identical in the studied compounds. The present results can therefore hardly be taken as support for the idea that strongly electronegative substituents increase vicinal coupling in $H-C-C-H$ fragments separated by an odd number of bonds.[8],[29]

The values of $J_{BC}$ and $J_{BC'}$ in the butyl compounds are determined by conformational rather than substituent effects.

The relatively small magnitude of the long-range coupling constants ($0-0.23$ Hz) is due to rotational averaging. Motionally averaged four-bond coupling constants of comparable magnitude and either sign, have been measured in saturated aliphatic and cyclic compounds.[30] However, no unambiguous substituent trends are discernible from the present data. At any rate, due to conformational effects it would be hazardous to ascribe small changes in the long-range coupling constants to definite substituent effects.

## REFERENCES

1. See, for example, Eliel, E. L., Allinger, N. L., Angyal, S. J. and Morrison, G. A. *Conformational Analysis*, Wiley, New York 1965.
2. Momany, F. A., Bonham, R. A. and McCoy, W. H. *J. Am. Chem. Soc.* **85** (1963) 3077.
3. Bonham, R. A., Bartell, L. S. and Kohl, D. A. *J. Am. Chem. Soc.* **81** (1959) 4765.
4. Ukaji, T. and Bonham, R. A. *J. Am. Chem. Soc.* **84** (1962) 3627, 3631.
5. Scott, R. A. and Scheraga, H. A. *J. Chem. Phys.* **44** (1966) 3054.
6. Abraham, R. J. and Parry, K. *J. Chem. Soc.* B **1970** 539.

 7. Cavanaugh, J. R. and Dailey, B. P. *J. Chem. Phys.* **34** (1961) 1094.
 8. Schrumpf, G. *J. Magn. Resonance* **6** (1972) 243.
 9. Aksnes, D. W. and Albriktsen, P. *Acta Chem. Scand.* **24** (1970) 3764.
10. Aksnes, D. W. and Albriktsen, P. *Acta Chem. Scand.* **26** (1972) 3021.
11. Aksnes, D. W. *Acta Chem. Scand.* **26** (1972)   164.
12. Aksnes, D. W. *Acta Chem. Scand.* **26** (1972) 1883.
13. Aksnes, D. W. and Støgård, J. *Acta Chem. Scand.* **26** (1972) 2552.
14. Radom, L. and Pople, J. A. *J. Am. Chem. Soc.* **92** (1970) 4786.
15. Dewar, M. J. S. and Baird, N. C. *COORD*, Program No. 136, *Quantum Chemistry Program Exchange*, Indiana University, Chemistry Department, Bloomington, Ind.
16. Heatley, F. *J. Chem. Soc. Faraday Trans. II*, **68** (1972) 2097.
17. Woodman, C. M. *Personal communication.*
18. Johannesen, R. B., Ferretti, J. A. and Harris, R. K. *J. Magn. Resonance* **3** (1970) 84.
19. Aksnes, D. W. *KOMBIP*, Program No. 205, *Quantum Chemistry Program Exchange*, Indiana University, Chemistry Department, Bloomington, Ind.
20. Diehl, P., Harris, R. K. and Jones, R. G. *Progr. NMR Spectrosc.* **3** (1967) 1.
21. Diehl, P. *Helv. Chim. Acta* **48** (1965) 567.
22. Emsley, J. W., Feeney, J. and Sutcliffe, L. H. *High Resolution Nuclear Magnetic Resonance Spectroscopy*, Pergamon, New York 1965, Vol. 1.
23. Hirota, E. *J. Chem. Phys.* **37** (1962) 283.
24. Harris, R. K. and Sheppard, N. *Trans. Faraday Soc.* **59** (1963) 606.
25. Huggins, M. L. *J. Am. Chem. Soc.* **75** (1953) 4123.
26. Mathieson, D. W. *Nuclear Magnetic Resonance For Organic Chemists*, Academic, London 1967.
27. Pople, J. A. and Bothner-By, A. A. *J. Chem. Phys.* **42** (1965) 1339.
28. Lynden-Bell, R. M. and Harris, R. K. *Nuclear Magnetic Resonance Spectroscopy*, Nelson, London 1969.
29. Schrumpf, G. and Klein, A.-W. *Chem. Ber.* **106** (1973) 246, 266.
30. Barfield, M. and Chakrabarti, B. *Chem. Rev.* **69** (1969) 757.

# *anti-amphi* and *cis-trans* Isomerisms in Some

# Bis(dioximato)nickel(II) Complexes

SØREN BOLS PEDERSEN and ERIK LARSEN

*Chemistry Department I and II, The H. C. Ørsted Institute, University of Copenhagen, Universitetsparken 5, DK-2100 Copenhagen Ø, Denmark*

Nickel(II) complexes of *vic*-dioximes, particularly camphorquinone dioximes, have been isolated and studied by ^{1}H NMR in $CDCl_3$ solution. Generally the Ni-complexes of *anti* dioximes are more stable than those of *amphi* dioximes, but it is found that for bis(2,3-bornane-dione dioximato)nickel(II) this is not the case. The isomerization of Ni(*anti* dioxime)$_2$ to Ni(*amphi* dioxime)$_2$ is shown to be accelerated by acid. The *cis-trans* isomerism is studied by ^{1}H NMR and for a $BF_2$ derivative of a bis-*anti* complex by ^{19}F NMR. It is concluded that only *trans* isomers are present in measurable quantities.

T he analytically important dioxime complexes of nickel(II) have been investigated to some degree in the past.[1] However, the low solubility of the red compounds like bis(dimethylglyoximato)nickel(II) has made it difficult to study these complexes in solution. In the present paper an investigation is reported on soluble dioxime complexes, which exist in several isomers.

The dioxime of an α-diketone may take the *anti*, *syn*, and *amphi* configurations, and if the diketone is unsymmetric two *amphi* forms may exist. Of these the *syn* form is known to be unable to form metal complexes.[1] The *anti* isomer gives the "usual" red complex, exemplified by the well known bis(dimethylglyoximato)nickel(II). The *amphi* isomers are known to react with nickel(II), but the complexes formed have not been well characterized, and metal:ligand ratios of 1:1 as well as 1:2 have been reported.[1-12] The symbols $\beta$, $\alpha$, and $\delta$ will in the following designate the *anti*, and the two *amphi* forms, respectively.

The possibility of *cis-trans* isomerism exists for nickel(II) complexes of unsymmetric *vic*-dioximes. Both forms may have a twofold axis of symmetry. In the *cis* isomer this axis lies in the coordination plane, and in the *trans* complex the symmetry axis is perpendicular to the coordination plane through the nickel atom.

In the case of unstrained dioximes, the bis($\beta$-dioximato)nickel(II) complex seems to be more stable than the bis(α- or $\delta$-dioximato) complexes. Both more favourable ring size (5 membered *vs.* 6 membered ring) and intramolecular

hydrogen bonding in the complex may stabilize the bis $\beta$-complex, which furthermore is often insoluble. Isomerization of bis($\delta$-dioximato)nickel(II) complexes to the bis $\beta$-complexes have been observed. The conversion can be accomplished by boiling with dilute acetic acid.[1-10]

In bis(4-iminopentane-2,3-dione 3-oximato)nickel(II) one of the oxime groups coordinates *via* nitrogen and the other *via* oxygen giving a five- and a six-membered ring in the same molecule.[13,14] For bis(2,3-bornanedione dioximato)nickel(II) we find evidence for a similar behavior (a $\beta\delta$-complex) and the conditions for isomerization have been studied by PMR. Nuclear magnetic resonance was also used to establish which *cis-trans* isomers of bis(2,3-bornanedione dioximato)nickel(II) were isolated. ^{19}F NMR of the compounds in which the hydroxy hydrogens are replaced by $BF_2$ groups bridging the two ligands was found useful to decide whether a *cis* or a *trans* complex was present.

*cis-trans* Isomerism was suggested by Sugden when two forms of bis-(benzylmethylglyoximato)nickel(II) was isolated.[15,16] Jensen *et al.* held the opinion that the two forms were a crystalline and an amorphous modification of the same *trans* isomer.[17] Thus there has been no unambiguous demonstration of the existence of *cis-trans* isomerism for bis(dioximato)nickel(II) complexes.

The choice of bis(2,3-bornanedione dioximato)nickel(II) for these investigations was decided partly by the possibility that this complex could behave as an optically active model for bis(dioximato)nickel(II) complexes in general with the purpose to get information about the electronic properties by examining the circular dichroism spectrum. However, bis($\beta$-(1$R$,4$S$)-2,3-bornanedione dioximato)nickel(II) only exhibits barely detectably Cotton effects. The chiroptical properties are commented on in the last part of the paper.

The isomer distributions and the abbreviations used in the following are summarized in Table 1.

## EXPERIMENTAL

*Complexes.* The bis(dioximato)Ni(II) complexes were prepared by three methods:
1. Nickel acetate and *vic*-dioxime (1:2 mol) were refluxed in ethanol or dimethyl sulfoxide for about ¼ h. On the addition of water a product precipitated. This product was extracted with chloroform or diethyl ether. The resulting solution was washed with water, dried with sodium sulphate, filtered and evaporated to dryness. The remaining solid was recrystallized from ethanol or hexane.
2. Nickel acetate and *vic*-dioxime (1:2 mol) were mixed in a two-phase system of water-chloroform with stirring at room temperature for about 1 h. The chloroform phase was separated, washed and dried as above.
3. *Vic*-dioxime (2 mol) was suspended in dilute sodium hydroxide containing equivalent amount of base, and nickel nitrate (1 mol) was added. The product was extracted with chloroform and isolated as above.
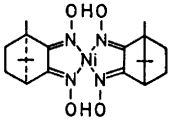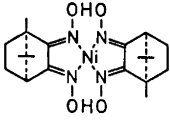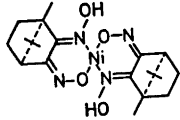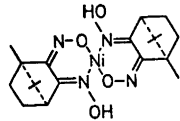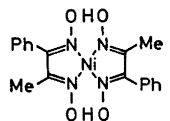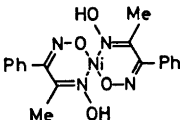
By all three methods Ni($\alpha$-cdo)$_2$ and Ni($\delta$-cdo)$_2$ could be obtained pure. Both compounds are yellowish green. Yields about 50 % after recrystallization from ethanol.

*Ni($\alpha$-cdo)$_2$.* Found: C 53.50; H 6.88; N 12.48; Ni 12.75. Calc. for $NiC_{20}H_{30}N_4O_4$: C 53.47; H 6.73; N 12.47; Ni 13.07.

*Ni($\delta$-cdo)$_2$.* Found C 53.55; H 6.87; N 12.38; Ni 12.85. The compounds showed similar behavior on heating: Around 240°C there was a slow transformation or destruction with colour change to brown without real melting. No melting was observed below 340°C.

## Table 1.

| Formulae | Configuration | Abbreviation |
|---|---|---|
| | cis-anti | $(cis)$Ni$(\beta$-cdo$)_2$ |
| | trans-anti | $(trans)$Ni$(\beta$-cdo$)_2$ |
| | trans-amphi | Ni$(\alpha$-cdo$)_2$ |
| | trans-apmhi | Ni$(\delta$-cdo$)_2$ |
| | trans-anti | Ni$(\beta$-PhMeG$)_2$ |
| | trans-amphi | Ni$(\alpha$-PhMeG$)_2$ |

Ni$(\beta$-cdo$)_2$ was prepared only by methods 2 and 3 in order to avoid contamination with the $\alpha$- and $\delta$-isomers. Attempts to obtain Ni$(\beta$-cdo$)_2$ free from isomers by recrystallization were unsuccessful. It was then purified by column chromatography (2 × 35 cm column, packed with basic silica gel, 0.2 – 0.5 mm particle size) using soda treated chloroform as eluent. The temperature was kept at 5°C. Ni$(\delta$-cdo$)_2$ had a slightly higher mobility than (Ni$(\alpha$-cdo$)_2$, Ni$(\beta$-cdo$)_2$, and Ni$(\beta$-cdo$)(\delta$-cdo) in order. The mobilities were so close that it was necessary to repeat the chromatography on the red fraction. The solvent was distilled off under reduced pressure at 10°C. In this way Ni$(\beta$-cdo$)_2$ was obtained as a red powder, which contained chloroform of crystallization. This was given off by prolonged heating at $\sim$ 80°C *in vacuo*. Yield approx. 25 % (variable) of Ni$(\beta$-cdo$)_2$. (Found: C 53.30; H 6.68; N 12.40; Ni 12.95). When heated it was converted around 165°C with

colour change from red to yellowish brown without melting. There was a further slow transformation or destruction around 230°C, where the compound turned darker brown. It did not melt below 340°.
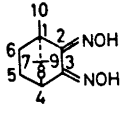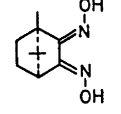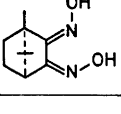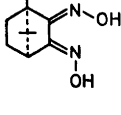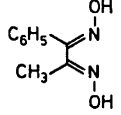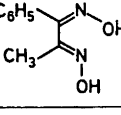
All three isomers are relatively soluble in common organic solvents.

$Ni(\beta\text{-}PhMeG)_2$ could be prepared by all of the three methods. Recrystallization from ethanol gave red crystals, melting point: 248 – 250°C. Yield 60 %. (Found: C 52.50; H 4.45; N 13.62; Ni 14.47. Calc. for $NiC_{18}H_{18}N_4O_4$: C 52.34; H 4.39; N 13.56; Ni 14.21.)

$Ni(\alpha\text{-}PhMeG)_2$ was prepared by methods 2 and 3. Recrystallization from hexane gave yellow crystals, which decompose around 200°C. Yield 45 %. (Found: C 52.60; H 4.41; N 13.38; Ni 14.45).

$Ni(\beta\text{-}PhMeGBF_2)_2$ was prepared by analogy with Schrauzers' method,[18] by the reaction of $Ni(\beta\text{-}PhMeG)_2$ and $BF_3.OEt_2$. The compound was recrystallized from acetone,

*Table 2.* ¹H NMR spectra of isomeric *vic*-dioximes represented as δ-values recorded at 60 MHz with TMS as internal standard.

| | | H-4[c] | CH₃-10[c] | CH₃-7 (or 9) | CH₃-9 (or 7) | OH |
|---|---|---|---|---|---|---|
| (structure) | β-cdoH[a] | 2.99[e] | 1.32[d] | 0.82[d] | 0.82[d] | 10.5[d] |
| (structure) | α-cdoH[a] | 2.38[e] | 1.31[d] | 0.83[d] | 0.83[d] | 11.1, 11.2[d][d] |
| (structure) | δ-cdoH[a] | 3.07[e] | 0.99[d] | 0.88[d] | 0.75[d] | 10.9, 11.1[d][d] |
| | [b] | 3.15[e] | 1.08[d] | 0.94[d] | 0.86[d] | 8.42, 11.3[d][d] |

| $C_6H_5C(NOH)C(NOH)CH_3$ | | CH₃ | C₆H₅ | OH |
|---|---|---|---|---|
| (structure) | β-PhMeGH[a] | 2.05[d] | 7.22[d] | 11.35, 11.37[d][d] |
| (structure) | α-PhMeGH[a] | 2.02[d] | 7.37[f] | 11.1, 11.4[d][d] |

[a] $(CD_3)_2SO$. [b] $CDCl_3$. [c] Ref. 19. [d] Singlet. [e] Average doublet. [f] Multiplet.

giving yellow crystals, which decompose at around 340°C. Yield 50 %. (Found: C 42.42; H 3.40; N 10.87; Ni 11.26. Calc. for $NiC_{18}H_{16}N_4O_4B_2F_4$: C 42.49; H 3.17; N 11.0; Ni 11.54.)

Bis(benzylmethylglyoximato)nickel(II) ($\alpha$ and $\beta$) and other bis(dioximato)Ni(II) complexes were kindly supplied by professor K. A. Jensen. They were identified by melting points and elemental analyses.

NMR spectra were recorded on Varian A-60A and 100A spectrometers. Circular dichroism measurements were performed with Roussel-Jouan Dichrographs (type I and II). The absorption spectra were measured with Cary 14 and Unicam spectrophotometers.

## RESULTS AND DISCUSSION

The preparation and identification of the *vic*-dioxime isomers was achieved by published methods.[1] The ligands and the complexes were isolated and isomeric purity ascertained by chromatography. ^{1}H NMR served to identify the isomers.

In Table 2 are shown the chemical shifts, which are most easily used for the dioximes. The assignments for the camphor derivatives are the same as those proposed by Daniel and Pavia.[19] The H-4 signal occurs as a doublet for these camphor derivatives, as it does [20] in a series of derivatives such as formylcamphor and its enamines. This suggests that ring strain produces a dihedral angle of approximately 90° between H-4 and one of the two H-5 protons, thus giving a very small coupling constant between these two protons. The chemical shift differences between the isomers are quite substantial and make identification easy.

Table 3 contains the ^{1}H NMR signals for the nickel(II) complexes isolated from the dioximes. Chemical shift differences are also big enough in the complexes to ascertain assignments. For the hydroxy protons there is a variation from *ca*. 17 to *ca*. 10 ppm (*vs*. TMS). The former value is characteristic for the bis-$\beta$-complexes, where the OH protons participate in strong and probably nearly symmetric hydrogen bonds. This feature also manifests itself in the

*Table 3.* ^{1}H NMR spectra recorded at 60 MHz in $CDCl_3$ with TMS as internal standard, given as $\delta$-values.

| | H-4 | $CH_3$-10 | $CH_3$-7 (or 9) | $CH_3$-9 (or 7) | OH |
|---|---|---|---|---|---|
| Ni($\beta$-cdo)$_2$ | 2.83[a] | 1.31[b] | 1.00[b] | 0.89[b] | 16.8[b] |
| Ni($\alpha$-cdo)$_2$ | 2.58[a] | 1.37[b] | 0.88[b] | 0.87[b] | 11.0[b] |
| Ni($\delta$-cdo)$_2$ | 3.20[a] | 1.11[b] | 0.94[b] | 0.81[b] | 10.8[b] |
| | $CH_3$ | $C_6H_5$ | OH | | |
| Ni($\beta$-PhMeG)$_2$ | 1.99[b] | 7.35[c] | 17.6[b] | | |
| Ni($\alpha$-PhMeG)$_2$ | 2.06[b] | 7.30[c] | 11.2[b] | | |

[a] App. doublet. [b] Singlet. [c] App. singlet.

infrared spectra of the complexes of *anti-vic*-dioximes by the characteristic band at approximately 2300 cm$^{-1}$.

As already mentioned the H-4 and CH$_3$-10 signals are also in the complexes quite sensitive to the anisotropy of the neighbouring oxime groups. For the two isomers of Ni(PhMeG)$_2$ the differences in chemical shifts of C$_6$H$_5$ and CH$_3$ protons are smaller, but still in accordance with the anisotropy.

$^1$H NMR is thus applicable for the identification of the different isomers of bis(dioximato)nickel(II) complexes that have been isolated. The outlined assignments will later be utilized to identify isomers observed only in solution and not isolated.

*Exchange reactions.* Nickel(II) complexes are known to be rather labile in aqueous solution.[21] Also planar, four-coordinated complexes such as Ni(CN)$_4^{2-}$ exchange ligands very rapidly. In aprotic organic solvents the exchange may become very slow, and this has been shown to be the case for chloroform solutions of bis(dioximato)Ni(II) complexes under certain conditions (acid-free chloroform, *vide infra*). The following reactions have been studied:

$$NiL_2 + L'H \rightleftharpoons NiLL' + LH$$

$$\text{(1)}$$

$$NiLL' + L'H \rightleftharpoons NiL'_2 + LH$$
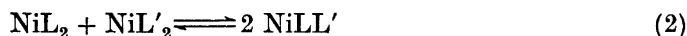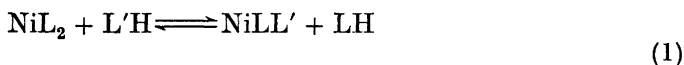
$$NiL_2 + NiL'_2 \rightleftharpoons 2\ NiLL' \qquad \text{(2)}$$

The equilibrium (1) can be established by mixing Ni($\delta$-cdo)$_2$ and $\beta$-PhMeGH (= L'H) in CDCl$_3$. The reaction was followed by $^1$H NMR, and the equilibrium composition of NiL$_2$:NiLL':NiL'$_2$ was found to be 1:2.7:1.9 at 35°C, when the solution was saturated with both LH and L'H. Equilibrium constants of the order of 250 and 70 were found for the two reactions. The time for half conversion is about 80 min at 35°C at usual NMR concentrations. The mixed complex Ni($\delta$-cdo)($\beta$-PhMeG) differ in chemical shifts from the "pure" complexes; see Table 4.

Table 4. $^1$H NMR spectra of mixed complexes recorded at 60 MHz in CDCl$_3$ with TMS as internal standard, given as $\delta$-values.

| | H-4 | CH$_3$-10 | CH$_3$-7 (or 9) | CH$_3$-9 (or 7) | OH | CH$_3$ | C$_6$H$_5$ |
|---|---|---|---|---|---|---|---|
| Ni($\delta$-cdo) ($\beta$-PhMeG) | 3.29 | 1.16 | 0.93[a] | 0.77 | 10.5 17.8 | 2.01 | 7.35[a] |
| Ni($\delta$-cdo) ($\beta$-cdo) | 3.23 2.81[a] | 1.12[a] 1.31[a] | 0.93[a] 0.99[a] | 0.77 0.90[a] | 9.3 18.2 | | |
| Ni($\alpha$-PhMeG) ($\beta$-PhMeG) | | | | | 10.3 18.3 | 2.07[a] 1.92 | 7.28[a] 7.40[a] |

[a] These signals are positioned very near the corresponding signals in the unmixed complexes and have only been visible as shoulders or broadening of the signals; *cf.* Table 3.

A number of systems (including the above mentioned complexes) have been examined to see whether ligand exchange could occur in CDCl$_3$ according to (2) above. However, in all cases it was found that no such reaction takes place within a few days, even in the presence of acid. For this reason the complexes are considered robust in chloroform.

*cis-trans Isomerization.* The earlier reported [15] attempt to isolate *cis-trans* isomers of unsymmetric *vic*-bis(dioximato) complexes was shown by Jensen *et al.*[17] to be inconclusive. However, in view of the above found robust character of these complexes, it might seem likely that both isomers could be present. The two samples of bis(*anti*-benzylmethylglyoximato)nickel(II) used by K. A. Jensen have identical PMR spectra. Therefore, we conclude that only one form is present rather than assuming the *cis* and *trans* forms to have the same chemical shifts for corresponding protons.

For this complex, as for the other *anti*-complexes, we should expect the two bridging protons to be non-equivalent in the *cis* isomer, but equivalent in the *trans* isomer, provided the hydrogen bonds are symmetric. The PMR signal for the two OH protons in Ni($\beta$-cdo)$_2$, Ni($\beta$-PhMeG)$_2$, and bis(*anti*-benzylmethylglyoximato)Ni(II) splits into three components of unequal intensity at low temperature (in the range $-40°C$ to $-20°C$). This is taken as evidence for the presence of different tautomers. For all other protons there is an effective twofold axis in the molecule. Although these results present evidence for the *trans* isomers, it was believed that the complex obtained by introducing BF$_2$ groups instead of H in the O $-$ H $-$ O bridge would give more conclusive results. The configuration of this product is certainly locked, and tautomerization of the molecule is not likely. The $^{19}$F NMR is known to exhibit large chemical shift differences, and since for this complex a *cis* isomer would produce two non-equivalent fluorine nuclei and a *trans* isomer equivalent nuclei, a conclusive result was anticipated. The $^{19}$F NMR of Ni ($\beta$-PhMeGBF$_2$)$_2$ in CH$_3$NO$_2$ at 70°C consisted of a single broad signal at 7058 Hz to higher field from external CF$_3$COOH (recorded at 94.1 MHz).

The $^1$H NMR spectra (see Tables 1 and 3) of the *amphi* complexes also indicate that only the *trans* forms are present in measurable quantities. All the signals are unsplit and the OH signal appears as a sharp singlet over the temperature interval $-40°$ to 30°C.

All our experiments indicate that only *trans* isomers of the complexes with unsymmetric ligands have been isolated. Neither on steric nor on electronic grounds can this finding be rationalized. Instead crystal packing forces may be important in the isolation from solvents in which nickel(II) complexes are labile, and thus all complex is precipitated in the most insoluble form.

*amphi-anti Isomerization* for Ni(cdo)$_2$. As mentioned in the experimental section the preparation of Ni($\beta$-cdo)$_2$ from the corresponding ligand isomer, $\beta$-cdoH, yields products containing different fractions of Ni($\beta$-cdo)$_2$, Ni($\alpha$-cdo)$_2$, Ni($\delta$-cdo)$_2$, and "mixed" complexes. Method of preparation, *i.e.* choice of solvent, pH in the aqueous phase, temperature and length of time for interaction seem to be important for the relative amounts of isomers isolated. No systematic studies were carried out to investigate the conditions. The isomers were isolated by means of column chromatography and identified by PMR. During this work great irreproducibility was noted with respect to both the chro-

matographic separations and the PMR spectra. These circumstances were related to the use of $CHCl_3$ or $CDCl_3$ as solvent and the acid content of the chloroform. The PMR spectra of the $Ni(cdo)_2$ complexes were found to be constant with time only when the $CDCl_3$ used as solvent was carefully treated with $Na_2CO_3$. The following results were obtained with a $CDCl_3$ sample of convenient "natural" acid content. Similar results have been obtained with purified $CDCl_3$ solutions to which were added known amounts of $CF_3COOD$.

The PMR spectra of $Ni(\beta\text{-cdo})_2$, $Ni(\alpha\text{-cdo})_2$, and $Ni(\delta\text{-cdo})_2$, in the above mentioned $CDCl_3$ of suitable acidity, were recorded as a function of time, temperature, and concentration of complex. The change with time is most spectacular for $Ni(\beta\text{-cdo})_2$, where the colour also changes from red to yellow. Fig. 1 shows how $Ni(\beta\text{-cdo})_2$ present at $t = 0$ is isomerized via at least one
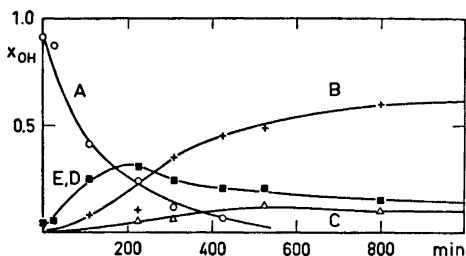


Fig. 1. Isomerization of $Ni(\beta\text{-cdo})_2$. The changes in the mol fractions of the different OH signals as a function of time. Temp. $26.38 \pm 0.02°C$, solvent $CDCl_3$. The chemical shifts are as follows ($\delta$-values with TMS as internal standard) A, ○ 16.8 ppm; B, + 10.9 ppm; C, △ 11.1 ppm; D, ■ 18.2 ppm; E, ■ 9.3 ppm.

intermediate to a mixture of $Ni(\delta\text{-cdo})_2$ and $Ni(\alpha\text{-cdo})_2$. The curve is characteristic for the conversion over the temperature interval $15 - 40°C$. Altogether five different OH proton resonances are observed. More signals may be present, since the detection limit of an isomer was around 5 % of the total. Three of the hydroxyl protons have chemical shifts corresponding to the $\beta_2$, $\alpha_2$, and $\delta_2$ complexes. The remaining two absorb at 18.2 and 9.3 ppm, with a 1:1 intensity relation in all runs. The chemical shifts for the latter two protons and the fact that they have equal concentration indicate that a mixed complex $Ni(\beta\text{-cdo})(\delta\text{-cdo})$ is formed (Table 4). At equilibrium the $CDCl_3$ solution contains $85 - 90$ % of the complex in the form of $Ni(\delta\text{-cdo})_2$, $5 - 10$ % as $Ni(\alpha\text{-cdo})_2$, and about 5 % as $Ni(\beta\text{-cdo})(\delta\text{-cdo})$ over the interval $15°C$ to $40°C$.

$Ni(\alpha\text{-cdo})_2$ isomerizes to the same equilibrium mixture, but the rate is about ten times slower than that of $Ni(\beta\text{-cdo})_2$

The rate of disappearance of the starting isomer was shown to be first order. For $Ni(\beta\text{-cdo})_2$ the halftime for the transformation of complex-bound $\beta$-cdo was estimated from the area under the H-4 signal and the $CH_3$-10 signal as well as from the peak height of $CH_3$-10. The halftime found in this way agrees fairly well with the halftime of transformation of the total anti OH, meaning $x_A$ plus $x_D$ from Fig. 1. The first order kinetics indicate that the reaction closely follows the ideal case where the rate of isomerization of complex-bound $\beta$-cdo is independent of the other ligand. The course of the reaction shown in Fig. 1 further supports this idea, as the time of maximum concentration of the "mixed" complex correspond rather well to two half-

times for conversion of the starting complex, as it would in the ideal case, neglecting the reverse reaction.

In the above mentioned solvent the apparent energy of activation was found to be about 24 kcal mol$^{-1}$ (25°C), and the rate of isomerization corresponds to the rate in a *ca.* $10^{-3}$ M $CF_3COOH$ solution, *vide infra.*

The catalytic effect of acid was demonstrated by following (PMR) solutions of Ni($\beta$-cdo)$_2$ or Ni($\alpha$-cdo)$_2$ in soda-treated CDCl$_3$ after the addition of small amounts of $CF_3COOH$ (up to 5 mol % with respect to nickel complex). The addition of larger amounts of $CF_3COOH$ (*e.g.* equivalent amounts) yields green paramagnetic solutions, which presumably contain ion pairs. No precipitation of free dioxime or nickel trifluoroacetate was noted.

The addition of the weak acid $\beta$-cdoH to Ni($\beta$-cdo)$_2$ in acid-free CDCl$_3$ did not catalyze the isomerization, although ligand exchange occurs under these conditions. Thus we conclude that the isomerization reaction is promoted by the formation of protonated complexes such as Ni($\beta$-cdo)($\beta$-cdoH). This explains the preparative method used earlier.

The Ni($\alpha$-PhMeG)$_2$ complex behaves qualitatively in the same way as the unstable cdo-complexes and isomerizes in acid chloroform to Ni($\beta$-PhMeG)$_2$. Due
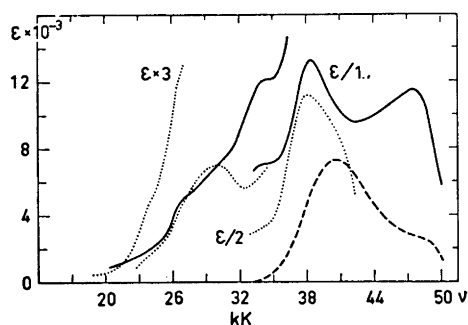


*Fig. 2.* Molar absorption of $\beta$-cdoH (- - -) in methanol, and molar absorption of Ni ($\beta$-cdo)$_2$ in methanol (———), and in chloroform (···).
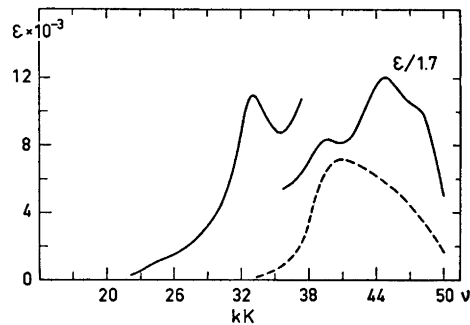
*Fig. 3.* Molar absorption of $\alpha$-cdoH (- - -) and of Ni($\alpha$-cdo)$_2$ (———) in methanol.

to the low solubility of the latter complex the reaction could only be studied at elevated temperatures. In this case also an intermediate, Ni($\alpha$-PhMeG) ($\beta$-PhMeG), was clearly detected (see Table 4). At equilibrium only Ni($\beta$-PhMeG)$_2$ could be detected.

The isomerization has not been studied in detail in other solvents. However, isomerization has been observed to occur in several common organic solvents.

*Electronic spectra* of $\beta$, $\alpha$, and $\delta$-cdoH and their corresponding nickel(II) complexes are shown in Figs. 2, 3, and 4, respectively. The $\alpha$- and $\delta$-compounds exhibit very similar absorption, as expected. The circular dichroism of the two *amphi* complexes, Ni($\alpha$-cdo)$_2$ and Ni($\delta$-cdo)$_2$, are markedly different
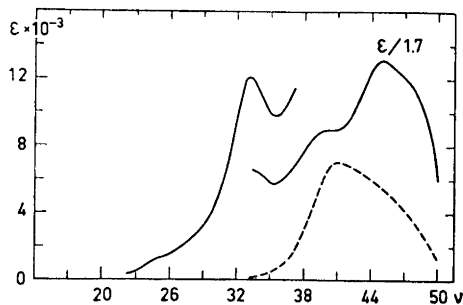
*Fig. 4.* Molar absorption of $\delta$-cdoH (- - -)
and of Ni($\delta$-cdo)$_2$ (——) in methanol.
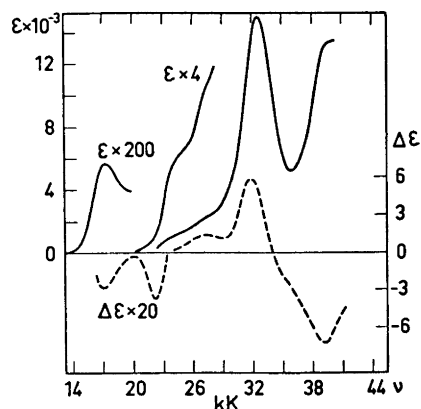


*Fig. 5.* Molar absorption (——) and cir-
cular dichroism (- - -) of Ni($\alpha$-cdo)$_2$ in
chloroform.
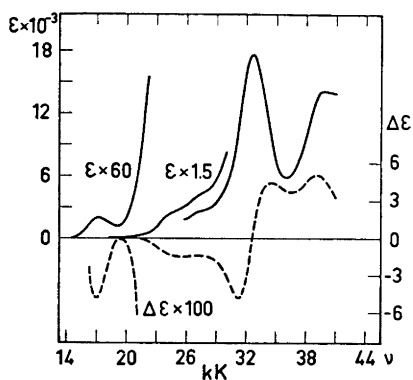


*Fig. 6.* Molar absorption (——) and circular
dichroism (- - -) of Ni($\delta$-cdo)$_2$ in chloro-
form.

(Figs. 5 and 6). The *anti* complex, Ni($\beta$-cdo)$_2$, exhibits only very small Cotton effects. The band at about 24 kK is the only measurable optically active band, with a dissymmetry factor, $\Delta\varepsilon/\varepsilon$, of only $-10^{-4}$. The low activity indicates that the complex (the chromophore) is very nearly planar on a time average.

Ingraham [22] reported a theoretical investigation on bis(dimethyl-glyoximato)nickel(II) and calculated that the energy difference between the lowest unfilled orbital ($2b_{1g}$) and the highest filled orbital ($3b_{3g}$) should be about 1 eV. This suggests that the triplet state might be thermally populated in solution. For Ni($\beta$-cdo)$_2$, which is soluble, this is not the case. The PMR gave sharp signals, without contact shift. Also, the chemical shifts were almost temperature-independent.

## REFERENCES

1. Meisenheimer, J. and Theilacker, W. In Freudenberg, K., Ed., *Stereochemie*, Leipzig 1932, p. 1077.
2. Atack, F. W. *J. Chem. Soc.* **103** (1913) 1317.
3. Ponzio, G. and Avogadro, L. *Gazz. Chim. Ital.* **53** (1923) 25.
4. Avogadro, L. *Gazz. Chim. Ital.* **53** (1923) 698; **54** (1924) 545.
5. Ponzio, G. *Ber.* **61** (1928) 1316.
6. Meisenheimer, J. and Theilacker *Ann.* **469** (1929) 128.
7. Hieber, W. and Leutert, F. *Ber.* **62** (1929) 1839.
8. Brady, O. L. and Muers, M. M. *J. Chem. Soc.* **1930** 1599.
9. Whiteley, M. A. *J. Chem. Soc.* **83** (1903) 24.
10. Forster, M. O. *J. Chem. Soc.* **83** (1903) 514; **103** (1913) 662.
11. Yamasaki, K. and Matsumoto, C. *J. Chem. Soc. Jap.* **76** (1955) 569.
12. Yamasaki, K. Matsumoto, C. and Ryojro, I. *J. Chem. Soc. Jap.* **78** (1957) 126.
13. Lacey, M. J., MacDonald, C. G., Shannon, J. S. and Collin, P. J. *Aust. J. Chem.* **23** (1970) 2279.
14. Lacey, M. J., MacDonald, C. G., Shannon, J. S. and McConnell, J. F. *Chem. Commun.* **1971** 1206.
15. Sugden, S. *J. Chem. Soc.* **1932** 246.
16. Cavell, H. J. and Sugden, S. *J. Chem. Soc.* **1935** 621.
17. Jensen, K. A., Nygaard, B. and Jensen, R. B. *Acta Chem.* Scand. **19** (1965) 770.
18. Schrauzer, G. N. *Chem. Ber.* **95** (1962) 1438.
19. Daniel, A. and Pavia, A. A. *Tetrahedron Letters* **1967** 1145.
20. Jensen, H. P. and Larsen, E. *To be published.*
21. Basolo, F. and Pearsson, R. G. *Mechanisms of Inorganic Reactions*, 2nd. Ed., Wiley, New York 1967.
22. Ingraham, L. L. *Acta Chem. Scand.* **20** (1966) 283.

# Crystal Structure of 2,7-Diphenyl-2,3,5,6-octatetraene

P. GROTH

*Department of Chemistry, University of Oslo, Oslo 3, Norway*

The crystals belong to the monoclinic system with space group $P2_1/c$ and cell dimensions $a = 15.653$ Å, $b = 7.457$ Å, $c = 6.454$ Å, $\beta = 98.20°$. There are two molecules in the unit cell. The phase problem was solved by direct methods, and the $R$-value arrived at by full-matrix least squares refinement was 6.0 % for 1049 observed reflections. The cumulated double bonds are 1.310 Å and 1.306 Å, respectively, and the single bond length 1.470 Å. The torsion angle about the bond to the phenyl ring (of length 1.491 Å) is 20.6°.

W hen properly substituted, a diallene can exist in a *meso*-configuration or as a racemic modification. The synthesis and some thermal reactions of conjugated *meso*-diallenes have been described by Kleveland and Skattebøl.[1] The two-step synthesis consists of the addition of dibromocarbene to the conjugated dienes followed by treatment of the diadducts with methyllithium (R = phenyl and *tert*-butyl):
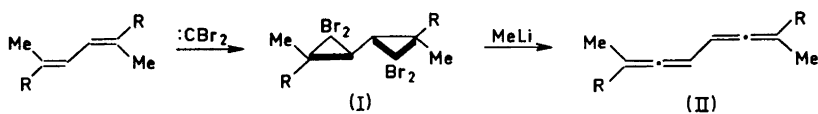


Structural assignments of intermediates (I) and products (II) were based on spectroscopic evidence and crystallographic space group determinations:

| Compound | Space group | Number of molecules in the unit cell |
|---|---|---|
| (I)(R = $C_6H_5$) | *Pbca* | 4 |
| (I)(R = $C(CH_3)_3$) | $P2_1/c$ | 2 |
| (II)(R = $C_6H_5$) | $P2_1/c$ | 2 |
| (II)(R = $C(CH_3)_3$) | $P2_1/c$ | 2 |

*Table 1.* Final fractional coordinates and anisotropic temperature factors with estimated standard deviations (multiplied by $10^5$ for carbon and $10^4$ for hydrogen).

| ATOM | X | Y | Z | B | B11 | B22 | B33 | B12 | B13 | B23 |
|------|---|---|---|---|-----|-----|-----|-----|-----|-----|
| C1 | 24727(16) | 50171(33) | 29575(40) | | 376(12) | 1116(58) | 1982(74) | 150(39) | 59(49) | 247(108) |
| C2 | 31344(19) | 58791(40) | 42239(49) | | 402(14) | 1845(66) | 2233(87) | 133(48) | 53(50) | -824(132) |
| C3 | 39674(18) | 58776(41) | 37485(50) | | 367(14) | 2171(69) | 3066(118) | -71(49) | -16(64) | -117(141) |
| C4 | 41559(20) | 49835(43) | 20154(53) | | 383(14) | 2410(74) | 3131(185) | 173(56) | 561(68) | 686(154) |
| C5 | 35197(20) | 41225(43) | 7361(53) | | 523(16) | 2172(72) | 2508(97) | 78(57) | 653(68) | -275(146) |
| C6 | 26769(18) | 41441(37) | 11948(44) | | 428(14) | 1698(58) | 2208(98) | -34(47) | 188(59) | -194(128) |
| C7 | 15743(16) | 49915(33) | 34765(42) | | 362(12) | 1292(58) | 2878(75) | 135(42) | 33(52) | 84(107) |
| C8 | 9144(16) | 46392(35) | 28454(46) | | 333(11) | 1824(64) | 2375(88) | -56(44) | 334(55) | 138(119) |
| C9 | 2486(16) | 43887(41) | 6355(45) | | 345(13) | 1971(79) | 2658(94) | -72(45) | 198(56) | -411(126) |
| C10 | 14384(24) | 53869(51) | 56922(53) | | 445(16) | 2583(88) | 2788(181) | 217(61) | 421(85) | 744(154) |
| H2 | 3814(15) | 6532(35) | 5228(44) | 3.7(,7) | | | | | | |
| H3 | 4460(17) | 6491(36) | 4896(46) | 5.1(,7) | | | | | | |
| H4 | 4738(17) | 4926(38) | 1655(44) | 5.2(,7) | | | | | | |
| H5 | 3613(17) | 3473(38) | -424(51) | 5.4(,8) | | | | | | |
| H6 | 2220(14) | 3484(31) | 191(40) | 3.5(,6) | | | | | | |
| H9 | 37(16) | 3852(41) | 358(46) | 5.2(,7) | | | | | | |
| H101 | 841(21) | 5229(36) | 5811(49) | 5.3(,8) | | | | | | |
| H102 | 1594(20) | 6553(51) | 6310(57) | 8.4(1,1) | | | | | | |
| H103 | 1838(21) | 4582(44) | 6869(57) | 7.8(,9) | | | | | | |

Under the assumption of an ordered crystal structure, this crystallographic information demands the molecules to be centrosymmetrical, a requirement which is only satisfied by the *meso*-configuration. In order to eliminate the possibility of disorder, a crystal structure determination of (II)(R = $C_6H_5$) has been carried out.

The crystals belong to the monoclinic system and the systematic absences lead to the space group $P2_1/c$. The cell parameters measured by means of a four circle diffractometer, and their estimated standard deviations, are: $a = 15.653(3)$ Å, $b = 7.457(2)$ Å, $c = 6.454(1)$ Å, $\beta = 98.20(2)°$. Since there are two molecules in the unit cell ($\rho_{obs} = 1.15$ g cm⁻³, $\rho_{calc} = 1.14$ g cm⁻³), the molecules themselves must be centrosymmetrical.

With $2\theta(max) = 50°$ and Mo$K\alpha$-radiation, 1445 reflections were measured on an automatic four-circle diffractometer. 1049 were recorded as observed
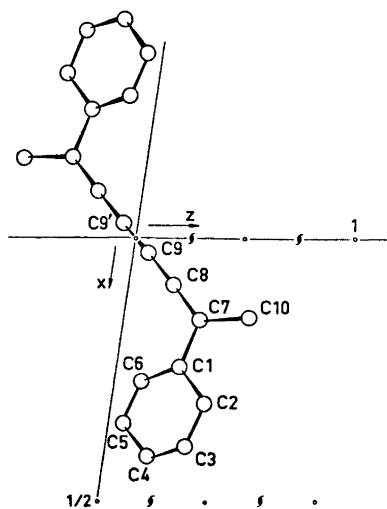


*Fig. 1.* The molecule viewed along [010].

*Table 2.* Observed and calculated structure factors on 10 times absolute scale.

*Table 2. Continued.*

when an observed-unobserved cutoff at 2.5 $\sigma(I)$ was used. No corrections have been made for absorption or secondary extinction effects.

The structure was solved by direct methods and refined by full-matrix least squares technique. Hydrogen atom positions were calculated; for the methyl group with one H in the plane defined by the three nearest carbon atoms. Anisotropic temperature factors were introduced for the carbons, and weights in least squares were calculated from the standard deviations in intensities, $\sigma(I)$, taken as

$$\sigma(I) = (C_T + (0.02\ C_N)^2)^{\frac{1}{2}}$$

were $C_T$ is the total number of counts and $C_N$ is the net count (peak minus background). The conventional $R$-value arrived at was 6.0 % (weighted value $R_w = 6.4$ %) for 1049 observed reflections. The form factors used were those of Hanson *et al.*[2] for C-atoms and those of Stewart *et al.*[3] for hydrogens.

*Table 3.* Interatomic distances and angles with estimated standard deviations.

| DISTANCE | (Å) | DISTANCE | (Å) | DISTANCE | (Å) |
|---|---|---|---|---|---|
| C1 – C2 | 1.385( 4) | C2 – C3 | 1.381( 4) | C3 – C4 | 1.378( 4) |
| C4 – C5 | 1.378( 4) | C5 – C6 | 1.379( 4) | C6 – C1 | 1.385( 4) |
| C1 – C7 | 1.491( 3) | C7 – C10 | 1.505( 4) | C7 – C8 | 1.316( 3) |
| C8 – C9 | 1.386( 3) | C9 – C9 | 1.478( 6) | | |

| ANGLE | (°) | ANGLE | (°) |
|---|---|---|---|
| C1 – C2 – C3 | 121.3( 3) | C2 – C3 – C4 | 120.1( 3) |
| C3 – C4 – C5 | 119.6( 3) | C4 – C5 – C6 | 120.3( 3) |
| C5 – C6 – C1 | 121.1( 3) | C6 – C1 – C2 | 117.6( 3) |
| C2 – C1 – C7 | 121.6( 2) | C6 – C1 – C7 | 120.9( 2) |
| C1 – C7 – C10 | 118.5( 2) | C8 – C7 – C10 | 120.3( 3) |
| C1 – C7 – C8 | 121.2( 2) | C7 – C8 – C9 | 179.9( 3) |
| C8 – C9 – C9 | 124.3( 3) | | |

Final fractional coordinates and thermal vibration parameters are given in Table 1. The expression for anisotropic vibration is:

$$\exp\left[-(B_{11}\,h^2 + B_{22}\,k^2 + B_{33}\,l^2 + B_{12}\,hk + B_{13}\,hl + B_{23}\,kl)\right]$$

The maximum r.m.s. amplitudes obtained by thermal analysis range from 0.22 Å to 0.28 Å. Rigid-body analysis of translational and librational motion [4] gave relatively large r.m.s. discrepancy between atomic vibration tensor components calculated from the thermal parameters of Table 1, and those calculated from the rigid-body parameters. By including all atoms, the value obtained was 0.0040 Å². This number does not support the assumption of regarding the molecule as an oscillating rigid-body, and the coordinates were therefore not corrected for librational motion.

A comparison between observed and calculated structure factors is presented in Table 2. Bond distances and angles are listed in Table 3. The numbering of atoms is shown in Fig. 1 where the molecule is viewed along [010].

The bond distances C7 = C8, C8 = C9, C9 − C9′, and the angle C8 = C9 − C9′ agree closely with the corresponding values obtained by a recent electron diffraction investigation of the free molecule of 1,2,4,5-hexatetraene:[5] 1.316 Å, 1.313 Å, 1.471 Å, 124.0°. The three carbon atoms C7, C8, C9 are, within error limits, situated on a straight line, and the bond lengths C1 − C7(1.491 Å) and C7 − C10(1.505 Å) indicate some degree of conjugation in this part of the molecule.

The phenyl ring is planar to within 0.007 Å, and the torsion angle of 20.6° about C1 − C7 gives contacts between H2 and two methyl hydrogens of 2.42 Å and 2.67 Å, respectively. The ring angles have normal values except for C2 − C1 − C6 which is about 3° smaller. Owing to the electron donating characteristics of the system attached to C1, the effect is what should be expected.[6]

No short inter-molecular contacts are observed.

## REFERENCES

1. Kleveland, K. and Skattebøl, L. *Chem. Commun.* **1973** 432.
2. Hanson, H. P., Herman, F., Lea, J. D. and Skillman, S. *Acta Cryst.* **17** (1964) 1040.
3. Stewart, R. F., Davidson, E. R. and Simpson, W. T. *J. Chem. Phys.* **42** (1965) 3175.
4. Shoemaker, V. and Trueblood, K. N. *Acta Cryst.* **B 24** (1968) 63.
5. Trætteberg, M., Paulen, G. and Hopf, H. *Acta Chem. Scand.* **27** (1973) 2227.
6. Christensen, A. T. and Strømme, K. O. *Acta Cryst.* **B 25** (1969) 657.

Received June 14, 1973.

# Choline Acetylase Inhibitors

## II.* The Preparation of Some 3-Substituted Acetonyltrimethylammonium Salts

BENGT OLOF PERSSON

*Research Institute of National Defence, Dept. 1, S-172 04 Sundbyberg 4, Sweden*

Four 3-halogenoacetonyltrimethylammonium halides have been prepared, one of each of the halogens F, Cl, Br, and I. All except the fluorine derivative showed a strong choline acetyl transferase inhibiting activity. Acetonyl- and 3-diazoacetonyltrimethylammonium salts, which were obtained as intermediates in the synthetic routes, did not possess inhibitor activity.

In the search for a specific choline acetyl transferase inhibitor, we have synthetized some quaternary ammonium salts, structurally related to choline and mainly belonging to the general formula

$$[(CH_3)_3N-(CH_2)_n-CO-X]^+ \ Y^-$$
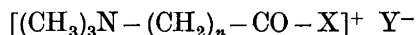
where $n = 1$ or $2$, $X = CH_3$, $CH_2F$, $CH_2Cl$, $CH_2Br$, $CH_2I$, $CHN_2$, $CH_2OH$, $CO-CH_3$, $CH_2N^+(CH_3)_3$ *etc.* and $Y =$ halogen. A previous paper [1] contains a description of one of these, 3-bromoacetonyltrimethylammonium bromide, named BAT by others [2] for convenience. We have now developed an improved method for the preparation of this substance and also found paths to its fluorine, chlorine, and iodine analogues.

The method reported [1] for preparing BAT had the disadvantage of utilizing 1,3-dibromoacetone, which is not commercially available and is obtained *via* careful distillation from a complex mixture of bromination products of acetone. We therefore switched a couple of years ago to the more easily procurable monobromoacetone as starting material in the preparation of BAT. The monobromoacetone is thus reacted with an excess of trimethylamine in, for instance, acetone, and the acetonyltrimethylammonium bromide so obtained is brominated in glacial acetic acid with an equivalent of bromine. The yield exceeds 80 %.

---

* Part I, see Ref. 1.

The iodine analogue, 3-iodoacetonyltrimethylammonium iodide, can be obtained from BAT through a simple Finkelstein exchange, using an equivalent of sodium iodide in acetone. This method, in which initially an iodine-rich, crystalline product formed, which after decomposition in water (to give elemental iodine) and washing with carbon tetrachloride gave 3-iodoacetonyl-trimethylammonium iodide, however, gives a rather low yield. To get a better yield, the 3-iodoacetonyltrimethylammonium iodide could instead be prepared from equimolecular amounts of trimethylamine and 1,3-diiodo-acetone, synthetized from freshly prepared 3-oxoglutaric acid [3] according to Lederer.[4]

The chlorine analogue, 3-chloroacetonyltrimethylammonium chloride, has so far defied all our efforts to isolate it in a pure state from the reaction product of trimethylamine and 1,3-dichloroacetone. The difficulty probably lies in the poor quaternizing ability of the chlorine function, combined with the enhanced probability of condensation and elimination reactions of 1,3-di-chloroacetone under the basic conditions created by the trimethylamine. Tri-methylammonium chloride is a dominant component in the dark-coloured reaction products. This crude reaction product does, however, show a strong choline acetylase inhibiting activity.[5]

The preparation of reasonably pure 3-chloroacetonyltrimethylammonium chloride has been achieved in two ways. In the earlier of these two methods, 3-chlorodiazoacetone, prepared according to Arndt and Amende,[6] was reacted with trimethylamine and the resulting 3-diazoacetonyltrimethylammonium chloride was treated in a second step with hydrogen chloride in anhydrous ethanol. More recently we have obtained 3-chloroacetonyltrimethylammonium chloride in a less elaborate way by converting 3-iodoacetonyltrimethylam-monium iodide with silver chloride in aqueous methanol.

The fluorine analogue, 3-fluoroacetonyltrimethylammonium bromide, fi-nally, has been prepared from 3-bromodiazoacetone, synthetized from bromo-acetyl bromide in strict analogy to the chlorine compound [6] mentioned above. A solution of the diazoketone in benzene or methylene chloride was treated with anhydrous hydrogen fluoride in heterogeneous phase, and the 1-bromo-3-fluoropropan-2-one so obtained reacted with trimethylamine, without in-tervening isolation.

The synthetized trimethylammonium salts have been tested for their in-hibitory action on choline acetylase (acetyl-CoA:choline $O$-acetyl transferase, EC 2.3.1.6) from bovine caudate nucleus. The chloro-, bromo-, and iodo-acetonyltrimethylammonium halides showed a strong inhibitory action, each giving about 90 % inhibition at a concentration of $2 \times 10^{-5}$ M,[7] whereas the acetonyl-, 3-diazoacetonyl-, and 3-fluoroacetonyltrimethylammonium bromides did not inhibit the enzyme to any noticeable extent.[7]


EXPERIMENTAL

*Acetonyltrimethylammonium bromide.* 40.5 g of freshly distilled monobromoacetone was dissolved in 500 ml of dry acetone. Using argon as a carrier gas, 26.1 g (*i.e.* 1.5-fold molar excess) of anhydrous trimethylamine was blown into the solution, stirred and cooled on an ice-salt bath. A cream-coloured precipitate formed during addition of the

amine. The reaction mixture was kept at room temperature overnight and the precipitate was then collected on a filter, washed with dry acetone and recrystallized from anhydrous ethanol. Yield: 51.0 g (88 %) of colourless crystals melting at 187–188°C. (Found: C 36.6; H 7.47; Br 40.5; N 7.40. Calc. for $C_6H_{14}BrNO$: C 36.7; H 7.20; Br 40.8; N 7.14.)

*3-Bromoacetonyltrimethylammonium bromide (BAT), improved method.* 2.00 g of acetonyltrimethylammonium bromide was dissolved in 10 ml of glacial acetic acid. To this solution was added 1.60 g of bromine in 5 ml of glacial acetic acid. During the addition, which was performed at room temperature, dropwise and with stirring, a brick-red, crystalline precipitate was formed. This disappeared when the reaction mixture was kept at room temperature overnight. The yellow solution formed was evaporated to dryness and the cream-coloured residue was crystallized from ethanolic ether to give brilliant, white flakes melting at 129–130°C. Yield: 2.66 g (95 %). (Found: C 25.2; H 4.63; Br⁻ 28.9, Br(total) 58.1; N 4.98. Calc for $C_6H_{13}Br_2NO$: C 26.2; H 4.77; Br⁻ 29.1; Br(total) 58.1; N 5.09.)

*3-Iodoacetonyltrimethylammonium iodide, method A.* A mixture, prepared from a slurry of 0.275 g of BAT in 30 ml of dry acetone and a solution of 0.300 g of sodium iodide in 15 ml of the same solvent, was shaken overnight at room temperature. The reaction mixture was filtered as it still contained a solid phase consisting of unreacted starting material. Evaporation of the filtrate gave some dark amber granules, which on dissolution in water lost iodine. Washing with carbon tetrachloride and evaporation of the water gave a low yield of small, yellow crystals melting at 160–170°C (dec.). (Found: C 19.9; H 3.75; I⁻ 34.1; N 3.92. Calc. for $C_6H_{13}I_2NO$: C 19.5; H 3.55; I⁻ 34.4; N 3.80.)

*Method B, improved method.* A solution was prepared from 375 ml of dry ether and 9.30 g of 1,3-diiodoacetone [4] which had been freshly recrystallized from ether at –78°C. Another solution, made from 1.77 g of anhydrous trimethylamine and 30 ml of dry ether, was added while swirling the flask in a dry ice bath. The reaction mixture was allowed slowly to attain room temperature. After some days the supernatant was decanted and the precipitate was recrystallized from methanol. 4.0 g (36.1 %) of transparent, faintly yellow flakes, melting at about 170°C (dec.), were obtained. The IR spectra of the products from methods A and B were identical. (Found: C 19.6; H 3.55; I⁻ 33.6; I(total) 67.6; N 3.80. Calc. for $C_6H_{13}I_2NO$: C 19.5; H 3.55; I⁻ 34.4; I(total) 68.8; N 3.80.)

*3-Diazoacetonyltrimethylammonium chloride.* To a chilled solution of 0.14 g of 3-chlorodiazoacetone [6] in 5 ml of dry ether was added 0.6 g (8.5-fold molar excess) of anhydrous trimethylamine. The reaction mixture was kept at +5°C for several days, during which time an amorphous, tan to light yellow precipitate formed. Crystallisation from anhydrous ethanolic ether gave clear, faintly yellow crystals, melting at 130–150°C (dec.). Yield: 0.067 g (31.7 %). (Found: Cl 19.6; N 22.7. Calc. for $C_6H_{12}ClN_3O$: Cl 20.0; N 23.7.)

*3-Chloroacetonyltrimethylammonium chloride, method A.* 0.90 g of 3-diazoacetonyltrimethylammonium chloride was dissolved in 100 ml of cold, anhydrous ethanol, which had been saturated shortly before with dry hydrogen chloride. Having been kept at –18°C for three days the reaction mixture was evaporated and the tan, hygroscopic, syrupy residue was immediately transferred to a desiccator, where it was stored *in vacuo.* The yield was quantitative, 0.94 g. Attempts to crystallize the product were not successful. (Found: Cl⁻ 21. Calc. for $C_6H_{13}Cl_2NO$: Cl⁻ 19.)

*Method B, preparation from the iodine analogue.* A slurry of about 0.50 g of silver chloride in 12.5 ml of methanol was prepared by bringing together a hot solution of 0.593 g of silver nitrate in 20 ml of distilled water with a hot solution of 0.204 g of sodium chloride in 20 ml of distilled water under vigorous stirring, and then washing the precipitate several times, at first with water, later with methanol, carefully decanting off the washings so as to minimize the loss of silver chloride. To this slurry, in an ampoule, was added a solution of 0.500 g of 3-iodoacetonyltrimethylammonium iodide in 12.5 ml of distilled water. The ampoule was sealed and shaken for three days at room temperature. The reaction mixture was filtered and the solid phase was thoroughly washed with several portions of (1) ammonia, (2) water, and (3) methanol, dried and weighed. The amount of silver iodide formed was 0.6298 g (98.8 %). The filtrate was evaporated as far as possible and kept for a long time in good vacuum over phosphorus pentoxide. Under these conditions the tan, syrupy residue showed a tendency to develop lightly yellow

crystalline structures. These structures disappeared rapidly, however, when the substance was removed from the desiccator, probably due to hygroscopicity of the substance. Infrared and NMR spectrometry demonstrated the structural identity of the substance with the product prepared from 3-diazoacetonyltrimethylammonium chloride and hydrogen chloride according to method A above. The NMR spectrum from a solution of the substance in deuterium oxide showed the expected three singlets, namely the two-proton singlet from the 1-methylene protons, the two-proton singlet from the 3-methylene protons and the nine-proton singlet from the methyl protons at $\delta$ 4.70, 4.44, and 3.32, respectively, as referred to an external TMS (in chloroform) standard. Despite the vigorous measures for desiccation, it did not seem possible to obtain an anhydrous product. (Found: C 36.9; H 7.53; N 7.08. Calc. for $C_6H_{13}Cl_2NO + 1/2\ H_2O$: C 36.9; H 7.23; N 7.18.)

*3-Bromodiazoacetone.* A dry, pure solution of diazomethane in ether was prepared [8] and standardized [9] by established methods. To 175 ml of the solution (0.35 M with respect to diazomethane), a solution of 4.95 g of bromoacetyl bromide in 50 ml of dry ether was added slowly with efficient stirring. The molar ratio diazomethane:bromo-acetyl bromide 2.5:1 was chosen as a compromise between the desire to suppress the formation of 1,3-dibromoacetone and the wish not to waste diazomethane. After the reaction mixture had been kept at $-20°C$ for three days, the ether, the methyl bromide, and the excess of diazomethane were removed by evaporation, and the residual golden yellow oil, was distilled *in vacuo*, b.p. $52-54°C/0.3$ torr. Further purification was achieved by repeated crystallization from rather concentrated $(15-20\ \%\ v/v)$ solutions in ether at $-78°C$. Yield: 2.3 g (58 %) of faintly yellow crystals, melting at $-1$ to $+1°C$ to form a golden yellow liquid, $n_D^{25}$ 1.5734. The substance was found to be a skin irritant. Its infrared spectrum showed the typical features of an $\alpha$-diazoketone with a diazo stretching frequency of 2100 cm$^{-1}$ and a carbonyl stretching of relatively low frequency, about 1630 cm$^{-1}$. Its NMR spectrum (from a 5 % solution in carbon tetrachloride) showed the expected two singlets, the one-proton singlet at $\delta$ 5.84 and the two-proton singlet at $\delta$ 3.83, as referred to an internal TMS standard. (Found: C 22.3; H 1.89; Br 49.7; N 17.0. Calc. for $C_3H_3BrN_2O$: C 22.1; H 1.86; Br 49.0; N 17.2.)

*3-Fluoroacetonyltrimethylammonium bromide.* In a 25 ml polyethylene bottle, 1.0 g of 3-bromodiazoacetone was dissolved in 10 ml of dry benzene. The solution was cooled until part of the solvent solidified. 0.5 g of anhydrous hydrogen fluoride was added dropwise and the reaction mixture was shaken by hand for a couple of minutes, during which time nitrogen was evolved and the yellow colour of the diazoketone disappeared. The benzene phase was separated from the excessive hydrogen fluoride, treated with freshly fused potassium fluoride and concentrated by evaporation. This benzene solution of the reaction product darkened rather quickly, even at $-20°C$, and attempts to isolate 1-bromo-3-fluoropropan-2-one at room temperature were not successful. However, infrared and NMR spectra, registered on the crude products obtained, indicated that this ketone was the main component. In the NMR spectrum, registered on a carbon tetrachloride solution, the two-proton singlet from the bromomethyl group was found at $\delta$ 4.03, whereas the signal from the fluoromethyl group occurred as a doublet, $J_{HF}$ 47.5 Hz centered at $\delta$ 5.03, as referred to an internal TMS standard.

To a clear, light, freshly-prepared solution of 1-bromo-3-fluoropropan-2-one in benzene was added 6.14 ml of an 1 M solution of trimethylamine in anhydrous ethanol. The reaction mixture was kept at $+5°C$ for several days, during which time the bottom of the reaction vessel became covered with small, colourless crystals; these were collected on a filter and washed with and recrystallized from a mixture of isopropanol and iso-propyl ether. The overall yield, as calculated on the 3-bromodiazoacetone used, was poor and did not exceed 10 %. The colourless to faintly brownish crystals melted at $140-145°C$ (dec.). (Found: C 33.1; H 6.62; Br 36.3; N 6.60. Calc. for $C_6H_{13}BrFNOC$: 33.7; H 6.12; Br 37.3; N 6.54.)

The spectroscopic data reported above have been obtained from the following instruments:

NMR spectra have been recorded on a 60 MHz Varian A 60 a nuclear magnetic resonance spectrometer, using, when possible, carbon tetrachloride solutions with an internal tetramethyl silane (TMS) standard. The salts have been studied in deuterium oxide solutions and compared with an external standard of TMS in chloroform.

Infrared spectra were recorded on a Perkin-Elmer Model 225 grating infrared spectrophotometer, whereby non-ionic substances were studied in carbon tetrachloride solutions

or neat (liquids or smears) or both and salts were studied in solid phase using KBr technique.

Elemental analyses with respect to C, H, and N have been performed on a Hewlett Packard F & M Scientific 185 Carbon Hydrogen Nitrogen Analyzer. Halogen ion has been determined *via* potentiometric titration with silver nitrate using a mercurous sulphate reference electrode. Non-ionic halogen has been transformed, when desired, into ionic form with Schöninger combustion technique.

## REFERENCES

1. Persson, B. O., Larsson, L., Schuberth, J. and Sörbo, B. *Acta Chem. Scand.* **21** (1967) 2883.
2. Steinberg, G. M. and Cramer, J. A. *Biochem. Pharmacol.* **19** (1970) 632.
3. Adams, R., Chiles, H. M. and Rassweiler, C. F. *Org. Syn. Coll. Vol.* **1**, 2nd Ed. (1946) 10.
4. Lederer, L. *Deutsches Reichspatent* Nr. 95440, 1897.
5. Schuberth, J. *Unpublished results*, 1966.
6. Arndt, F. and Amende, J. *Ber.* **61** (1928) 1122.
7. Sollenberg, J. *Private communication*, 1970.
8. de Boer, Th. J. and Backer, H. J. *Org. Syn. Coll. Vol.* **4** (1963) 250.
9. Arndt, F. *Org. Syn. Coll. Vol.* **2** (1943) 166.

# Tetrakis (pyridine) cobalt (III) Complexes

JOHAN SPRINGBORG[a] and CLAUS ERIK SCHÄFFER [b]

[a] Department of General and Inorganic Chemistry, Royal Veterinary and Agricultural University, Thorvaldsensvej 40, DK-1871 Copenhagen V, Denmark and [b] Chemistry Department I (Inorganic Chemistry), University of Copenhagen, H. C. Ørsted Institute, Universitetsparken 5, DK-2100 Copenhagen Ø, Denmark

One of the isomers of carbonatochlorotris(pyridine)cobalt(III) has been prepared for the first time. It gives with pyridine the new carbonatotetrakis(pyridine)cobalt(III) ion, which with acid gives the new *trans*-diaquatetrakis(pyridine)cobalt(III) ion. These two ions have been isolated as their perchlorates. They both have extreme protolytic properties. The carbonato ion in strongly acid water solution protonates in two steps the first of which corresponds to an acidity constant (in 8 M sodium perchlorate) of 0.3 M. The acid decomposition of the carbonato ion to give carbon dioxide is unusually slow and results in the *trans*-diaqua ion whose first acidity constant (in 1 M sodium nitrate) is 0.04 M.

The only tetrakis(pyridine)cobalt(III) complex that has been reported[1] so far is the *trans*-dichloro ion. Among the other metals of the first transition period all the known tetrakis(pyridine) complexes also have the *trans*-structure. In Chemistry Department I several vain attempts have been made to prepare *cis*-complexes within the chromium(III) series.

On the other hand *cis*-complexes are not sterically impossible since they are known among the metals of the second [2,3] and third [4] transition metal series. However, here the greater radii of the ions, and the greater thermodynamic stability and particularly the greater robustness (inertness) of the complexes may be responsible for their apparently greater stereochemical liberalism.

With cobalt(III), as opposed to chromium(III), the carbonato ion is known [5,6] to bind as a bidentate ligand. This property together with the carbonato ion's easy removal with acid, often under stereochemical retention of configuration, has made it widely used for preparing *cis*-complexes of the chromophoric type $CoN_4O_2$ within the amine and ammine series.

Also in the present paper the carbonato ion has been used, and carbonatochlorotris(pyridine)cobalt(III) has been prepared as an initial material for other pyridine-cobalt(III) complexes. Our aim was to prepare the carbonatotetrakis(pyridine)cobalt(III) ion and this aim has been reached. Our further

purpose, however, was to use this compound for preparing other *cis*-tetrakis-(pyridine) complexes, which would be of spectroscopic interest. This purpose has not been achieved. By reaction with acid this carbonato complex gives the *trans*-diaqua ion, or with strong hydrochloric acid the *trans*-dichloro ion, and no evidence has been provided for the existence of *cis*-complexes, except the carbonato complex itself.

## PREPARATIONS

An aqueous solution of the green tris(carbonato)cobalt(III) anion was prepared [7] by addition of a solution of cobalt(II) chloride in dilute hydrogen peroxide to an excess of solid potassium hydrogencarbonate. This solution reacts with a mixture of pyridinium chloride and hydrochloric acid with formation of a blue-violet solution. The blue-violet colour is without doubt due to the replacement of coordinated carbonate ions by pyridine molecules. By evaporation of the reaction mixture at room temperature, carbonatochloro-tris(pyridine)cobalt(III) is formed.

Evaporation at room temperature appeared to be essential. Upon standing at room temperature for two weeks without evaporation no precipitate was formed. Heating of the reaction mixture, on the other hand, caused rapid reduction to cobalt(II).

Some experiments in which nitrate was substituted for chloride were carried out. Nitrate, which generally is a weaker ligator than chloride, was used in an attempt to increase the number of pyridine molecules substituted, in order to obtain the carbonatotetrakis(pyridine)cobalt(III) ion directly from the tris(carbonato)cobalt(III) ion. However, no well-defined products were isolated from these mixtures.

Carbonatochlorotris(pyridine)cobalt(III) dissolves in pyridine with a violet colour. Heating of this solution causes complete reduction to cobalt(II). However, by addition of bis(pyridine)mercury(II) perchlorate to the cold solution and subsequent heating to 50°C, no substantial reduction to cobalt(II) occurs, and the chloride is replaced by pyridine yielding the red carbonato-tetrakis(pyridine)cobalt(III) ion. This was isolated as the red perchlorate salt.

From the reaction of carbonatotetrakis(pyridine)cobalt(III) perchlorate with 12 M perchloric acid at room temperature, the brownish *trans*-diaqua-tetrakis(pyridine)cobalt(III) perchlorate was isolated.

## EXPERIMENTAL

*Materials.* Pyridine, "chem. pure", was purchased from Riedel-de Haën, sodium perchlorate, "*puriss. p.a.*", from Fluka AG, Buchs SG, and sodium nitrate, "zur Analyse", from Merck. [Hgpy$_2$](ClO$_4$)$_2$ was prepared according to the literature.[8] All other chemicals were of reagent grade and were used without further purification.

*Spectra and identification methods.* Absorption spectra in the $300-650$ nm region, recorded using either a Cary Model 14 or a Zeiss DMR 21 spectrophotometer, were used as a check of purity and as characterization of the compounds. Data for maxima, minima, and shoulders have been given below as $(\varepsilon, \lambda)$, the absorbancy $\varepsilon$ in l/mol cm and the wavelength $\lambda$ in nm.

Infrared spectra of the compounds in potassium bromide disks were recorded on a Perkin-Elmer 457 grating infrared spectrophotometer.

Powder X-ray diffraction diagrams were obtained using a Guinier powder camera with Cu-radiation.

*pH-Measurements.* The pH-measurements were made with a G 202 C glass electrode and a K 401 calomel electrode connected to a PHM 52 digital pH-meter, all from Radiometer, Copenhagen.

The pH-meter was adjusted to show $pH = 2.000 \pm 0.002$ in $0.01000$ M $HNO_3$, 1 M $NaNO_3$. It is then assumed that the readings on the meter are equal to $p[H^+]$ in 1 M $NaNO_3$ solutions at 25°C.

# Preparative procedures. Properties of and measurements on the individual compounds

*1. Carbonatochlorotris(pyridine)cobalt(III)*, [Copy₃CO₃Cl]. A solution of $CoCl_2.6H_2O$ (119 g, 0.5 mol) in a mixture of water (2500 ml) and hydrogen peroxide (112 ml, 30 %) was portionwise and with stirring added to solid potassium hydrogencarbonate (750 g, 7.5 mol) in a 4 l beaker. The potassium hydrogencarbonate dissolved with a vigorous evolution of carbon dioxide gas and formation of a green solution of the tris(carbonato)-cobaltate(III) ion. In order to complete the catalytic decomposition of the excess of hydrogen peroxide, the solution was allowed to stand for half an hour at room temperature. It was then cooled in an ice bath to about 5°C. An ice-cold mixture of pyridine (200 ml, 2.48 mol) and 12 M hydrochloric acid (580 ml, 6.96 mol) was then added dropwise to the stirred solution with continued cooling during one hour. Carbon dioxide gas was evolved and the colour of the solution turned from green to red-violet. The mixture was allowed to stand for another 2 h in the ice bath and was then left at room temperature in an open shallow dish. After about a week evaporation had reduced the volume to approximately 1200 ml.* Within two or three days the precipitation of blue-violet crystals of carbonatochlorotris(pyridine)cobalt(III) set in. Brownish by-products and some potassium chloride were also precipitated. The mixture was filtered, washed thoroughly with water and then with methanol (three 100 ml portions). By the washing most of the impurities were removed. Drying in the air yielded 85 g of blue-violet crystals of almost pure carbonatochlorotris(pyridine)cobalt(III) (43 %, based upon cobalt(II) chloride). (Found: Co 15.27; C 48.80; H 3.95; N 10.76; Cl 9.09. Calc. for [Copy₃CO₃Cl]: Co 15.05; C 49.07; H 3.86; N 10.73; Cl, 9.05.) This product was used in the following synthesis. For further purification the almost pure carbonatochlorotris(pyridine)cobalt-(III) (4 g) was dissolved in methanol (300 ml) at 50°C, filtered, and cooled in ice as quickly as possible. Small blue-violet needleshaped crystals separated. After 3 h of cooling the sample was filtered and washed with ice-cold methanol (three 10 ml portions). Drying in air yielded 1.04 g (26 %). A check on the purity was made spectrophotometrically. (Found: Co 15.00; C 48.98; H 3.90; N 10.82; Cl 8.99.) ($\varepsilon$, $\lambda)_{max}$: (50, 577); (60, 409). Medium: 80 % v/v acetonitrile in water.**

*Properties.* Carbonatochlorotris(pyridine)cobalt(III) is sparingly soluble in water and methanol. In aqueous and methanolic solutions it is decomposed so rapidly that measurements of the visible absorption spectrum are difficult. The difficulties also arise from the slow rates at which the compound dissolves in these media. The visible absorption spectrum was therefore measured in 80 % v/v acetonitrile in water, as the compound dissolves readily in this medium. However, also in this medium the decomposition is fast. The colours of the solutions for the three media mentioned above are blue-green in daylight and violet in electric light.

---

* In one experiment with quantities scaled to 1/10 of those given above, the reaction mixture was evaporated at 35°C in a rotating vacuum evaporator within some hours. The yield of carbonatochlorotris(pyridine)cobalt(III) was only 1.05 g (5.3 %).

** The decomposition even in this medium is fast. In the extrapolation of the $\varepsilon$ values at the maxima to the time of dissolution corrections up to 5 % were required, thus increasing the experimental error of the estimated $\varepsilon$ values. A deviation within 2 % was found between the $\varepsilon$ values of this sample and the sample recrystallized four times.

Carbonatochlorotris(pyridine)cobalt(III) reacts within minutes with either 4 M perchloric acid or 4 M hydrochloric acid, in both cases with evolution of carbon dioxide, but yielding different tris(pyridine)cobalt(III) complexes, which will be described in a forthcoming paper.

The infrared spectrum of carbonatochlorotris(pyridine)cobalt(III) was compared with that of trichlorotris(pyridine)cobalt(III) and showed clearly additional bands in the $\nu_1$ (1675 (broad), 1640 (sharp) cm$^{-1}$) and $\nu_5$ (1245 (sharp) cm$^{-1}$) regions [9] of the bidentately coordinated carbonate ion (see also p. 3318).

2. *Carbonatotetrakis(pyridine)cobalt(III) perchlorate*, [Copy$_4$CO$_3$]ClO$_4$.H$_2$O. Bis-(pyridine)mercury(II) perchlorate (7.5 g, 13.4 mmol) was added to cold pyridine (160 ml) in a 250 ml flask. The mercury(II) complex dissolved partly, but yet almost pure carbonatochlorotris(pyridine)cobalt(III) (10 g, 25.5 mmol) was then added. It dissolved partly, giving a violet colour. The flask was equipped with a calcium chloride tube and the mixture stirred under heating in a water bath at 50°C for 45 min. By this treatment all the solids dissolved and the colour changed to red. Cooling for half an hour in ice caused precipitation of red crystals of carbonatotetrakis-(pyridine)cobalt(III) perchlorate. To complete the precipitation 200 ml of dry ether was added. The precipitate was filtered, washed with ether and dried in air. The crude product (13.5 g) was dissolved in water (1500 ml) at room temperature and a saturated water solution of sodium perchlorate (150 ml) was added to the filtered solution with stirring and cooling in ice. The precipitate was filtered and washed with ice-cold water (30 ml) and 96 % ethanol (two 30 ml portions). Drying in air yielded 8.4 g of the almost pure salt (60 % based on carbonatochlorotris(pyridine)cobalt(III)). 2.5 g of this salt was dissolved in water (280 ml) and a saturated water solution of sodium perchlorate (30 ml) was added to the filtered solution. The yield was 2.0 g (80 %). The sample reprecipitated twice was pure. (Found: Co 10.70; C 45.85; N 10.16; H 4.00; Cl 6.46. Calc. for [Copy$_4$CO$_3$]-ClO$_4$.H$_2$O: Co 10.66; C 45.62; N 10.14; H 4.01; Cl 6.41.) Visible spectra in different media are collected together in Table 2.

*Properties.* In contrast to carbonatochlorotris(pyridine)cobalt(III), the carbonato-tetrakis(pyridine)cobalt(III) ion reacts extremely slowly with strong acids. So, the visible absorption spectrum in 1 M hydrochloric acid only changed very slowly at room temperature. Within a period of 2 h the positions of the maxima and minima remained constant and the changes in the $\varepsilon$ values were less than 1 %. Contrary to this the visible absorption spectrum in 1 M HCl, 6 M LiCl changes much more rapidly giving changes in the $\varepsilon$ values up to 30 % within a period of 2 h. These differences are probably due to a faster acid hydrolysis in this medium.

Prolonged treatment with 12 M hydrochloric acid at room temperature yielded within hours the green chloride salt of the *trans*-dichlorotetrakis(pyridine)cobalt(III) ion. The yield was rather poor (20 %), due to reduction to cobalt(II). In a test tube experiment the rate of hydrolysis of [Copy$_4$CO$_3$]$^+$ was compared with that of [Cophen$_2$-CO$_3$]$^+$ (phen = 1,10-phenanthroline) using 12 M hydrochloric acid. The latter compound changed its colour to that of the diaqua complex within a minute, while the pyridine complex had not reacted to any visible extent within 10 min.

In 12 M perchloric acid, the reaction also proceeds slowly, though much faster than in 12 M hydrochloric acid. At room temperature, the reaction is essentially complete within 10 min, yielding the *trans*-diaquatetrakis(pyridine)cobalt(III) ion.

The colours of neutral and dilute acid solutions are purely red, but on addition of large quantities of strong acids an instantaneous colour shift to red-violet is observed, independently of which acid is used.

The visible absorption spectra of the carbonatotetrakis(pyridine)cobalt(III) perchlorate in pure water, in aqueous 7.2 M lithium chloride solution, and in hydrochloric acid solutions (7.2, 9.4, and 12 M) are shown in Fig. 1. The spectrum of the neutral solutions remained constant for 3 h. The extinction values for the acid solutions varied with time, probably owing to the slow acid hydrolysis, and extrapolations back to the time of dissolution were necessary. The extrapolations were performed linearly, based upon absorption curves taken 2 and 7 min, respectively, after the time of dissolution. The corrections of the observed extinction values were only small (0 − 3 %) in 7.2 M and 9.4 M hydrochloric acid, but rather large (5 − 15 %) in 12 M hydrochloric acid.

Carbonatotetrakis(pyridine)cobalt(III) perchlorate is sparingly soluble in water and in 2 M perchloric acid but very soluble in 12 M perchloric acid. Thus it was possible to

dissolve the carbonato complex in 12 M perchloric acid at room temperature and re-
precipitate the salt almost quantitatively by rapid dilution with five volumes of cold
water.

As an attempt at obtaining a quantitative measure of the proton affinity, a de-
termination of the solubilities in neutral and acid aqueous sodium perchlorate media
was performed at $19 \pm 1°C$. The concentrations were determined spectrophotometrically
from the absorbancies at the maxima by comparison with the absorbancies of solutions
of known concentrations. Saturated solutions in 4 M and in 8 M sodium perchlorate were
obtained by treating a large excess of the perchlorate salt with the solvent until no in-
crease in the absorbancy was observed. Saturation was achieved within 2 h. However,
within 8 min a concentration of approximately 90 % of that in the saturated solution was
observed. The preparation of the acid solutions was complicated by the acid hydrolysis.
The solutions were therefore prepared and measured within 10 min, during which time
the absorbancy of a solution at the first absorption band decreased less than 1 % to
decrease much further as the acid hydrolysis took place. So errors due to the hydrolysis
are estimated to be negligible. However, the solutions obtained in this manner were
doubtless not saturated and the values given in Table 1 must therefore represent lower
limits to the solubility in the acid media.

In order to further check that the higher concentrations found in the acid media
were actually due to increased solubility, the following experiment was made. An almost
saturated solution of the carbonato salt in 8 M $NaClO_4$, 0.5 M $HClO_4$ was prepared as
before. Then 38 ml of this solution was partly neutralized immediately after its prepa-
ration by addition of 3 ml of 5 M NaOH producing a solution with 7.8 M $NaClO_4$, 0.1 M
$HClO_4$. Within 3 h red crystals separated. These were identified as $[Copy_4CO_3]ClO_4.H_2O$
by their Guinier powder diffraction pattern and by their infrared spectrum in the region
$4000-250$ cm$^{-1}$. The yield was 60 mg to be compared with the theoretical yield of
$[Copy_4CO_3]ClO_4.H_2O$, 158 mg, calculated from the solubilities above.

The infrared spectrum of carbonatotetrakis(pyridine)cobalt(III) perchlorate was
compared with that of trichlorotris(pyridine)cobalt(III) and showed clearly additional
bands in the $v_1$[1680 (broad), 1640 (sharp) cm$^{-1}$] and $v_5$ [1240 (shoulder) cm$^{-1}$] regions [9]
of the bidentately coordinated carbonate ion.

3. trans-*Diaquatetrakis(pyridine)cobalt(III) perchlorate, trans-*[Copy_4(H_2O)_2](ClO_4)_3.-
4H_2O.* Carbonatotetrakis(pyridine)cobalt(III) perchlorate (4 g, 7.24 mmol) was dissolved
in 70 % perchloric acid (15 ml), and the violet solution allowed to stand at room tempe-
rature for 10 min under carbon dioxide evolution. The colour gradually changed to red-
violet and a brownish precipitate, probably anhydrous *trans*-diaquatetrakis(pyridine)-
cobalt(III) perchlorate, formed. After cooling, ice-cold water (30 ml) was added. Thereby
the precipitate dissolved and after a few seconds brown crystals of *trans*-diaquatetrakis-
(pyridine)cobalt(III) perchlorate with 4 mol of crystal water formed. After cooling for
10 min in ice, the precipitate was filtered, washed with ice-cold 4 M perchloric acid (5 ml)
and sucked as dry as possible. Then the sample was dissolved in ice-cold 0.12 M perchloric
acid (40 ml) and ice-cold 70 % perchloric acid (20 ml) was added to the filtered solution
with stirring and cooling in ice. After some minutes the precipitate was filtered, washed
with ice-cold 4 M perchloric acid (5 ml) and dried with ether.*

Drying in air yielded brown crystals (4.3 g) of pure *trans*-diaquatetrakis(pyridine)-
cobalt(III) perchlorate. (76 %). (Found: Co 7.50; N 7.16; C 30.26; Cl 14.38; H 3.7 Calc. for
$[Copy_4(H_2O)_2]ClO_4)_3.4H_2O$: Co 7.54; N 7.17; C 30.72; Cl 13.60; H 4.1.) $(\varepsilon, \lambda)_{max}$: (43.9,
560); (51.0, 490). $(\varepsilon, \lambda)_{min}$: (43.3, 540); (25.8, 435). Medium: 1 M nitric acid.

## Acid dissociation constant of the *trans*-diaquatetra-kis(pyridine)cobalt(III) ion.

The first acid dissociation constant of the *trans*-diaquatetrakis(pyridine)cobalt(III)
ion was determined at 25°C in 1 M NaNO$_3$. The ion has an acidity comparable to that
of phosphoric acid. Therefore the dissociation constant was calculated directly from pH

---

\* Caution must be taken to avoid leaving the ether with the perchloric acid washings or the
mother liquor.

measurements on solutions of the ion itself, or even better, of the ion itself in 0.01 M $HNO_3$.

As the complex is unstable in water and decomposes rather rapidly, the solutions were made up quickly so as to make the first measurement $30-45$ sec after the dissolution. The measurements were continued over a period of 2 min and the pH data given in Table 3 are the results of a linear extrapolation back to the time of dissolution. The rate of change was in the order of 0.02 pH units per minute for the acid medium, 0.01 M $HNO_3$, 1 M $NaNO_3$, and 0.04 pH units per minute for the neutral medium, 1 M $NaNO_3$. So the rate of decomposition increases with increasing pH and the extrapolated pH-values are more accurate for the more acid solutions. The acid-dissociation constant was calculated [10] by means of the equation:

$$-\log K_{s,1} = -\log [H^+] + \log \left(\frac{1-\bar{\nu}}{\bar{\nu}}\right) + \log \left[1 + \frac{(2-\bar{\nu})K_{s,2}}{(1-\bar{\nu})[H^+]}\right] \qquad (1)$$

where $\bar{\nu}$ equals the average number of protons produced by the diaqua ion and is given by $\bar{\nu} = ([H^+] - [OH^-] - C_{HNO_3})/C_{Co}$ where, for example, $C_{Co} =$ stoichiometric concentration of the complex, and $-\log [H^+] = $ pH (measured). The last term of eqn. (1) was ignored in the calculations of $K_{s,1}$.

As seen from Table 3, the experimental uncertainty is rather large for the data obtained in 1 M $NaNO_3$ as compared with that in 0.01 M $HNO_3$, 1 M $NaNO_3$, although the averages for the two sets of experiments agree well.

Because of the fast decomposition already at $[H^+] = 0.01$ M, we were unable to determine, by this method, the second acid dissociation constant $K_{s,2}$ for the *trans*-diaqua ion. An order of magnitude estimate of $K_{s,2}$ could, however, be obtained from the measurements in the neutral medium using the equation [10]

$$K_{s,2} = \frac{\bar{\nu}[H^+]^2 + (\bar{\nu}-1)[H^+]K_{s,1}}{(2-\bar{\nu})K_{s,1}} \qquad (2)$$

and the value $(1.4 \times 10^{-2}$ M$)$ found for $K_{s,1}$. This estimate of $K_{s,2}$ $(10^{-4}$ M$)$ is as expected for such a diaqua ion and would, according to formula (1), give a correction smaller than 0.02 to $K_{s,1}$. This correction has not been made.

## RESULTS AND DISCUSSION

*Cobalt-carbonato bond breaking.* In the following it is attempted to sum up some features which may be relevant for comparing the present system with other cobalt(III) carbonato systems. The discussion is complicated by the circumstance that it is not known whether the same reaction mechanism applies to the different carbonato systems. So it is probably not justified to discuss the relative rates of reaction on the basis of the following arguments which are essentially of thermodynamic character. Therefore the following discussion should be read with this reservation in mind.

Carbonatochlorotris(pyridine)cobalt(III) hydrolyses much faster with acid than does the carbonatotetrakis(pyridine)cobalt(III) ion. This is probably partly because its lower charge facilitates the attack of the hydrogen ion, but the below-mentioned reasons of sterical or electronic origins are likely to act in the same direction.

In order to try to understand [11] the different rates of hydrolysis of $\alpha$- and $\beta$-[CotrienCO$_3$]$^+$ (trien = triethylenetetramine = 1,4,7,10-tetraazadecane) it was natural to invoke the sterical differences between these two equally charged ions whose electronic situation should not be too different. On the other hand, by the comparison [12],[13] of the fast hydrolysis rates of [Coen$_2$CO$_3$]$^+$

*Acta Chem. Scand.* 27 (1973) No. 9

(en = ethylenediamine) and other analogous amine systems with the slow rates of $[Cobipy_2CO_3]^+$ (bipy = 2,2'-bipyridine) and $[Cophen_2CO_3]^+$ (phen = 1,10-phenanthroline), it was likely that the electronic properties of the N-ligating ligands were causing the main differentiating factor. Here the electron accepting capability of the heterocyclic aromatic ligands was proposed to increase the electron donation to the metal ion from the oxygen ligators of the carbonate ion and thereby strengthen the cobalt to oxygen bonds. This abolition of the charge accumulation on the cobalt by the $\pi$-acid character of the aromatic systems would seem likely to occur also with pyridine as the N-ligator, but in this case to a lower extent than with the larger aromatic ligands. On the other hand, all the aromatic ligands are probably poorer $\sigma$-donors than the amine systems with concomitant smaller charge accumulation on the cobalt, and this probably applies more to pyridine than to the bidentate heteroaromatics. Therefore, the fact that $[Copy_4CO_3]^+$ hydrolyses slowest of all the carbonato complexes mentioned, need not be caused by a steric inhibition of the hydrogen ion attack. However, from the X-ray structure analysis [14] of $[Copy_4CO_3]ClO_4.H_2O$ it can be seen that the $\alpha$-hydrogen atoms of some of the pyridine molecules do shield the ligating oxygen atoms.

The infrared spectra of carbonato-complexes have previously been compared and it has been advocated that the frequency $\nu_1$ ($1600-1650$ cm$^{-1}$), which, according to normal coordinate analysis, essentially is associated with the carbon to oxygen double bond, increases as the cobalt to oxygen bond is strengthened.[9,15] In the region of $\nu_1$ the compound $[Copy_4CO_3]ClO_4.H_2O$ exhibits bands at 1680 (broad) and 1640 (sharp) to be compared with

| | |
|---|---|
| $[Co(NH_3)_4CO_3]Cl$ | 1593;[9] |
| $[Co(ND_3)_4CO_3]Cl$ | 1635, 1607;[9] |
| $[Coen_2CO_3]Br$ | 1628, 1615;[9] 1575;[15] 1613, 1607;[12] |
| $[Coen_2CO_3]ClO_4$ | 1643;[9] |
| $[Coen_2CO_3]Cl$ | 1577;[15] 1613, 1590;[12] |
| $[Cobipy_2CO_3]Cl$ | 1632;[13] |
| $[Cophen_2CO_3]Cl$ | 1650, 1630.[12] |

It is seen that the pyridine complex has the highest $\nu_1$ frequency, which should mean the highest cobalt to oxygen bond order, in agreement with its higher stability toward hydrolysis.

*Protonation of the carbonato group.* A reasonably concentrated solution of $[Copy_4CO_3]ClO_4$ in 12 M perchloric acid reprecipitates the complex perchlorate on addition of water. This would seem to indicate that a protonation had taken place. On the other hand, we have found that $[Cr(NH_3)_6]Cl_3$ dissolves in hydrochloric acid, saturated with HCl at 0°C, and reprecipitates on addition of water. Further, Pfeiffer [16] reports that $[Crpy_3Cl_3]$, which does not dissolve much in concentrated hydrochloric acid, dissolves very well in concentrated nitric acid and reprecipitates on addition of water. We can confirm Pfeiffer's report and add that concentrated perchloric acid does not dissolve $[Crpy_3Cl_3]$ equally well, and it seems unlikely that a well defined protonation takes place, either with $[Cr(NH_3)_6]Cl_3$ or with $[Crpy_3Cl_3]$.

In the following, evidence will be presented that the carbonato group of

$[Copy_4CO_3]^+$ is protonated in at least two steps. The first protonation is demonstrated by solubility measurements, and the further protonation by spectrophotometric measurements.

A quantitative study of the protonation was made by the solubility measurements given in Table 1. The results show unambiguously that a protonation does take place and the variation of solubility with acid concentration shows further that one proton is taken up by the carbonato ion — in this $[H^+]$-region and this medium — and not two at a time.

*Table 1.* Solubilities of $[Copy_4CO_3]ClO_4.H_2O$ in different media (19°C). For the acid media the data are lower limits to the solubilities.

| Medium | Concentration × $10^3$ |
|---|---|
| 8 M NaClO$_4$ | 5.1 M |
| 8 M NaClO$_4$, 0.1 M HClO$_4$ | 6.1 M |
| 8 M NaClO$_4$, 0.5 M HClO$_4$ | 14 M |
| 7.5 M NaClO$_4$, 0.5 M HClO$_4$ | 12 M |
| 4 M NaClO$_4$ | 3.1 M |
| 4 M NaClO$_4$, 0.5 M HClO$_4$ | 5.1 M |

The acid dissociation constant $K$ for $[Copy_4CO_3H]^{2+}$, applicable for the medium 7.5 − 8 M sodium perchlorate, may be estimated as $K = 0.3$ M from the solubilities. For the medium 4 M sodium perchlorate $K$ is estimated as $K = 0.7$ M, or twice the above value. This increase of the basic character of $[Copy_4CO_3]^+$ ion with increasing salt concentration is also reflected in the rate of acid hydrolysis which increases considerably on going from 1 M HCl to 1 M HCl, 6 M LiCl.

It seems to be a general feature of normal salts that their "salting-in" effect on the protonated species (which always has a positive charge which is higher than that of the base by one unit) is the dominating factor to determine the decrease of the acidity constant with increasing salt concentration. This variation has been found before for some cationic chromium(III) complexes,[17] and it is also known for some neutral amines, *e.g.* 4-nitroaniline,[18a] although the salting-out effect on the base may be of importance here. It is noteworthy that with 4-nitroaniline the variation is the opposite when the salt is tetraethylammonium chloride, probably because this organic cation interacts more with the neutral amine than with its cationic corresponding acid.

The protonation of $[Copy_4CO_3]^+$ was further studied by comparing the visible spectra in different media (Table 2, Fig. 1). There are two noteworthy features.

Solutions of $[Copy_4CO_3]ClO_4$ in salt media are more violet than are water solutions of the same concentration. This is associated with a red shift of the first absorption maximum of 4 nm and an increase in the molar absorbancy of 1 − 2 %. This would normally be called a medium effect meaning that we know of no specific chemical interaction that can be made responsible for it. It is nearly independent of the cation, provided this is not a proton. If it is a proton the red-shift of the first absorption band is larger and gradually in-
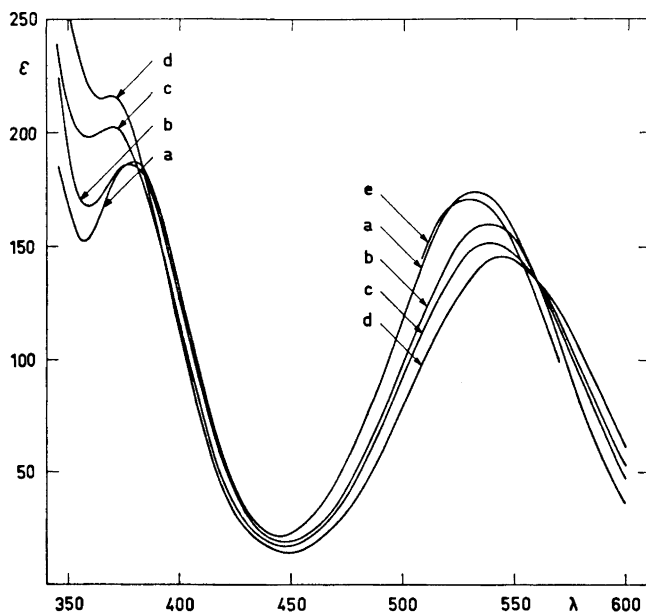
*Fig. 1.* Visible absorption spectra of $[Copy_4CO_3]ClO_4 \cdot H_2O$ at room temperature. 7.2 M LiCl (a), 7.2 M HCl (b), 9.6 M HCl (c), 12 M HCl (d) and water (e).

*Table 2.* Spectral data for $[Copy_4CO_3]ClO_4$ in different media.

| Medium | $(\varepsilon, \lambda_{max})$ | $(\varepsilon, \lambda_{max})$ |
|---|---|---|
| $H_2O$ | (172,530) | (190,379) |
| 6 M LiCl | (174,532) | (187,379) |
| 7.2 M LiCl | (175,532) | (187,378) |
| 12 M LiCl | (174,534) | (188,376) |
| 6 M $CaCl_2$ | (174,534) | (192,376) |
| 4.5 M $MgCl_2$ | (177,534) | (191,376) |
| 0.5 M HCl, 6 M LiCl | (172,532) | (186,378) |
| 1 M HCl, 6 M LiCl | (171,533) | (185,377) |
| 7.2 M HCl | (160,538) | (187,377) |
| 12 M HCl | (146,544) | (215,370)[a] |
| 8 M $NaClO_4$ | (173,532) | (183,379) |
| 0.5 M $HClO_4$, 8 M $NaClO_4$ | (167,533) | (183,378) |
| 4 M $HClO_4$ | (164,535) | (187,379) |
| 7.2 M $HClO_4$ | (145,543) | (213,370)[a] |

[a] The maximum not developed, appears as a shoulder.

creases with the acid concentration to 14 nm and there is a concomitant decrease in the molar absorbancy up to 15 %. This special behaviour of the proton is attributed to protonation of the carbonato complex.

However, the visible absorption spectrum in 0.5 M $HClO_4$, 8 M $NaClO_4$ is almost identical with the spectrum in 8 M $NaClO_4$. As approximately 60 % of the complex is protonated in the acid solution, this means that the absorption spectrum of the carbonato complex is almost unaffected by this first protonation. This observation is in agreement with the fact that the visible absorption spectra in 6 M LiCl and 0.5 M HCl, 6 M LiCl also are nearly identical.

The knowledge that $[Copy_4CO_3]^+$ and $[Copy_4CO_3H]^{2+}$ have similar spectra makes it necessary to attribute the changes of the spectra in strongly acid solutions (Table 2, Fig. 1) to protonation beyond the first proton but it cannot be inferred from the results whether one or more further protons are taken up.

It would be chemically interesting to know where the protons are bound in the carbonato ion. There are three places that one may discuss, the carbonyl oxygen atom and the two ligating oxygen atoms.

The fact that the spectra of $[Copy_4CO_3]^+$ and $[Copy_4CO_3H]^{2+}$ are almost identical would suggest that the first proton is located upon the carbonyl oxygen. It should, however, be noted that the $[H^+]$-independent equilibria between species with differently located protons might invalidate this suggestion to a small extent.

The fact that the second protonation is associated with a colour shift is in agreement with the assumption that this protonation takes place on the ligating oxygen atoms.

Finally, there are two facts that we would like to mention. Firstly, the spectrum of $[Copy_4CO_3]ClO_4$ in 7.2 M perchloric acid resembles that in 12 M hydrochloric acid (Table 2). Secondly, the rate of acid hydrolysis in 12 M perchloric acid as compared with 12 M hydrochloric acid is pronouncedly increased. These results agree qualitatively with the circumstance that perchloric acid in non-aqueous media is a stronger acid than hydrochloric acid and that the same applies to aqueous media for very high acid concentrations.[18b]

*trans-Diaquatetrakis(pyridine)cobalt(III) perchlorate.* The reaction of the carbonatotetrakis(pyridine)cobalt(III) ion with perchloric acid is unusual not only because it is very slow but also because of the fact that the reaction* leads to the *trans*-diaquatetrakis(pyridine)cobalt(III) ion. In contrast to this, the acid hydrolysis of the corresponding carbonato complexes with ammonia and ethylenediamine [5] yields the *cis* isomers.

The assignment of the *trans* structure of the diaquatetrakis(pyridine)-cobalt(III) ion is unambiguous, based on the visible absorption spectrum which exhibits a tetragonal splitting of the first spin-allowed absorption band $^1A_{1g}(O_h) \rightarrow {}^1T_{1g}(O_h)$ into clearly separated components $^1A_{1g}(D_{4h}) \rightarrow {}^1E_g(D_{4h})$ [17 860 $cm^{-1}$] and $^1A_{1g}(D_{4h}) \rightarrow {}^1A_{2g}(D_{4h})$ [20 410 $cm^{-1}$], analogously to the corresponding ethylenediamine complex.[10]

The first acid dissociation constant ($10^{-1.37}$ M in 1 M $NaNO_3$) of the *trans*-diaquatetrakis(pyridine)cobalt(III) ion is pronouncedly higher than that

---

* It may be noted that in the reaction with 12 M hydrochloric acid the first isolable product is the chloride of the *trans*-dichlorotetrakis(pyridine)cobalt(III) ion.

*Table 3.* The first acid-dissociation constant of the *trans*-diaquatetrakis(pyridine)cobalt-(III) ion in 1 M $NaNO_3$ at 25°C.

| | | 0.01000 M $HNO_3$, 1 M $NaNO_3$ | | | |
|---|---|---|---|---|---|
| No. | $C_{co}$ | $-\log[H^+]$ | $[H^+]$ | $\bar{v}$ | $pK_{s,1}$ |
| 1 | 0.01494 | 1.694 | 0.02023 | 0.6847 | 1.358 |
| 2 | 0.02020 | 1.639 | 0.02296 | 0.6416 | 1.386 |
| 3 | 0.02232 | 1.616 | 0.02421 | 0.6366 | 1.373 |
| | | | | Average of $pK_{s,1}$ | 1.37 |

| | | 1 M $NaNO_3$ | | | |
|---|---|---|---|---|---|
| No. | $C_{co}$ | $-\log[H^+]$ | $[H^+]$ | $\bar{v}$ | $pK_{s,1}$ |
| 1 | 0.01703 | 1.876 | 0.01331 | 0.7816 | 1.322 |
| 2 | 0.02095 | 1.831 | 0.01476 | 0.7045 | 1.453 |
| 3 | 0.02698 | 1.732 | 0.01854 | 0.6872 | 1.390 |
| | | | | Average of $pK_{s,1}$ | 1.39 |

($10^{-4.15}$ M in 1 M $NaNO_3$)[10] of the corresponding ethylenediamine complex. These results mean that the hydroxo complexes are more stable relative to the corresponding aqua complexes when the remaining ligands are pyridine molecules than when they are ethylenediamine molecules. This can be rationalized along similar lines to those mentioned on p. 3318.

## REFERENCES

1. Werner, A. *Ber.* **39** (1906) 1538.
2. Cheng, P.-T., Loescher, B. R. and Nyburg, S. C. *Inorg. Chem.* **10** (1971) 1275.
3. Raichart, D. W. and Taube, H. *Inorg. Chem.* **11** (1972) 999.
4. Delépine, M. and Lareze, F. *Compt. Rend.* (a) **256** (1963) 3912; (b) **257** (1963) 3772.
5. Krishnamurty, K. V., Harris, G. M. and Sastri, V. S. *Chem. Revs.* **70** (1970) 171.
6. Piriz Mac-Coll, C. R. *Coord. Chem. Revs.* **4** (1969) 147.
7. Jørgensen, C. K. *Inorganic Complexes*, Academic, London 1963, p. 81.
8. Hofmann, K. A. *Ber.* **38** (1905) 1999.
9. Fujita, J., Martell, A. E. and Nakamoto, K. *J. Chem. Phys.* **36** (1962) 339.
10. Bjerrum, J. and Rasmussen, S. E. *Acta Chem. Scand.* **6** (1952) 1265.
11. Dasgupta, T. P. and Harris, G. M. *J. Am. Chem. Soc.* **93** (1971) 91.
12. Farago, M. E., Keefe, I. M. and Mason, C. F. V. *J. Chem. Soc.* **A 1970** 3194.
13. Francis, D. J. and Jordan, R. B. *Inorg. Chem.* **11** (1972) 461.
14. Kaas, K. and Sørensen, A. M. *Acta Cryst.* **B 29** (1973) 113.
15. Gatehouse, B. M., Livingstone, S. E. and Nyholm, R. S. *J. Chem. Soc.* **1958** 3137.
16. Pfeiffer, P. *Z. Anorg. Chem.* **55** (1907) 97.
17. Josephsen, J. and Schäffer, C. E. *Acta Chem. Scand.* **24** (1970) 2929.
18. Rochester, C. H. *Acidity Functions*, Academic, London 1970, (a) p. 101, (b) p. 39 and p. 43.

# Activities in the Systems $Mg^{2+} - Na^+ - X^- - ClO_4^-$ with

# $X^- = Cl^-$, $Br^-$ and $SCN^-$. The Possible Formation of $MgX^+$

# Ion Pairs

JOSEF HAVEL* and ERIK HÖGFELDT

*Department of Inorganic Chemistry, Royal Institute of Technology (KTH),
S-100 44 Stockholm 70, Sweden*

The changes in the activities of water and some positive and
negative ions in 3 M (Na,Mg)ClO₄ when Na⁺ is replaced with Mg²⁺
have been studied by emf titrations and by vapor phase osmometry
at 25°C. All data are consistent with eqn. (5) below, *i.e.* $z^{-1} \log y_i =
A + B[Mg^{2+}]$, when taking ion pair formation into account, where the
two constants $A$ and $B$ are different for anions and cations and $z$ is
the charge of the ion studied. The following equilibrium constants
are found for the formation of MgCl⁺ (log $K_1 = -0.98 \pm 0.19$), MgBr⁺
(log $K_1 = -1.45$ ($-1.01$)), MgSCN⁺ (log $K_1 = -0.91 \pm 0.19$).

In a study of the equilibria between Mg(II) and phosphate [1] in 3 M (Na)ClO₄
it was sometimes necessary to replace as much as 600 mM of Na⁺ with
Mg(II). Such a substantial change in the ionic medium might cause changes
in the activity coefficients of the species involved and influence the descrip-
tion of the results obtained. In order to elucidate this point further some
measurements have been performed in an attempt to evaluate the variation
of the activity coefficients at about 3 M ionic strength ($\pm$ 10 %) and 25°C in
the systems $Mg^{2+} - Na^+ - X^- - ClO_4^-$ for $X^- = Cl^-$, $Br^-$ and $SCN^-$.

## EXPERIMENTAL

*Chemicals and solutions.* NaCl (Merck, Suprapur) was used directly without further
purification. NaBr (Merck, *p.a.*) was recrystallized twice from water. NaSCN (Mal-
linckrodt, anal.r.) was recrystallized three times from water.
Standard solutions of these salts were prepared from doubly distilled water. The
concentration of NaX was determined by evaporating a known volume and drying in
an oven at 120°C till constant weight, except for NaCl which was ignited at ≈300°C.
The analyses were checked by precipitating the silver salts. The results obtained by the

---

* Present address: Department of Analytical Chemistry, J. E. Purkyně University, Brno,
Czechoslovakia.

two methods agreed to within 0.1 %. A stock solution of $Cd(ClO_4)_2$ was prepared as described by Hietanen et al.[2] and $In(ClO_4)_3$ as described by Biedermann and Wallin.[3] The preparation of the other solutions, used in this paper, has been described elsewhere.[1]

*Apparatus.* The emf titrations were performed in a paraffin oil thermostat at 25°C using the "Wilhelm" type bridge.[4] The Ag,AgCl-electrodes in the reference half-cell were electrolytically prepared according to Brown.[5] Ag,AgBr-electrodes were prepared from Ag,AgCl-electrodes by immersing in 0.1 M NaBr overnight, then carefully washing with distilled water, and equilibrating for a few days in 3 M $NaClO_4$ saturated with AgBr before use. Electrodes, electrolytically prepared according to Brown, gave the same results as those prepared by this method. Ag,AgSCN-electrodes were prepared by a slight modification of the method given by Wanderzee and Smith,[6] *i.e.* by electrolyzing silver-coated Pt-electrodes in a solution containing 0.1 M NaSCN + 0.05 M $HClO_4$ for $\sim 1$ h at $0.2 - 0.5$ mA. Cadmium and indium amalgam electrodes containing 0.01 % metal were prepared coulometrically *in situ*, using either Cd rod (99.99 % purity), In rod (99.99 % purity), or Ag-coated Pt plate as anode and a mercury pool as cathode. The emf of the glass electrodes used, Beckman, type 40498, was measured with a Metrohm compensator, type E388, with an accuracy of $\pm 0.2$ mV. The emf of hydrogen (preparation given in Ref. 1) and Ag,AgX-electrodes was measured with a Cambridge Vernier potentiometer with an accuracy of $\pm 0.02$ mV except for SCN⁻, where the accuracy was $\pm 0.05$ mV. The hydrogen electrode reached a stable potential within 20 min; it was stable to within $\pm 0.1$ mV for 12 h.

The vapor pressure measurements were made with a Hewlett-Packard Vapor Pressure Osmometer, Model 301A using an aqueous probe for 25°C.

*The emf measurements.* The investigation was carried out as a series of potentiometric titrations. The cell employed for studying positive ions can be described by

$$+ \text{ SE} \quad \left| \begin{array}{l} 3 \text{ M } ClO_4^-, \, (3 - 2X - H - z \, B)\text{M Na}^+, \\ X \text{ M Mg}^{2+}, \, H \text{ M H}^+, \, B \text{ M Me}^{z+} \end{array} \right| \begin{array}{l} \text{electrode} \quad - \\ \text{reversible} \\ \text{to Me}^{z+} \end{array} \quad \text{(I)}$$
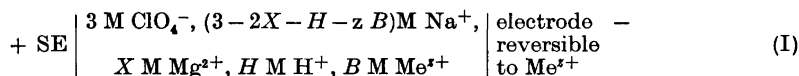
where $Me^{z+} = Ag^+$, $Cd^{2+}$, or $In^{3+}$.
The reference half-cell SE was of the type

$$\text{Ag,AgCl} \mid 0.01 \text{ M Ag}^+, \, 2.99 \text{ M Na}^+, \, 3 \text{ M ClO}_4^- \mid \quad \text{(II)}$$
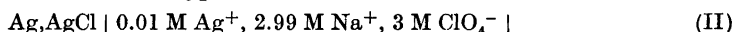
The emf of cell (I) can be expressed by

$$E = E_{0,\text{Me}} + 59.16 \, z^{-1} \log [\text{Me}^{z+}] + 59.16 \, z^{-1} \log y_{\text{Me}} + E_j \quad \text{(1)}$$

where $E_{0,\text{Me}}$ is a constant, different for each kind of electrode; $y_{\text{Me}}$ is the activity coefficient of $Me^{z+}$ on the molarity scale and $E_j$ the diffusion potential.

The cell employed for studying negative ions can be described by

$$\text{SE} \quad \left| \begin{array}{l} (3 - C)\text{M } ClO_4^-, \, C \text{ M X}^-, \, (3 - 2X - H) \text{ M Na}^+, \\ X \text{ M Mg}^{2+}, \, H \text{ M H}^+ \end{array} \right| \begin{array}{l} \text{reversible} \\ \text{electrode} \\ \text{to X}^- \end{array} \quad \text{(III)}$$
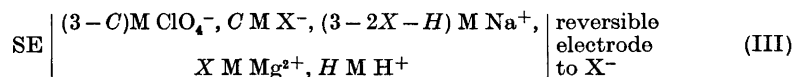
where $X^- = Cl^-$, $Br^-$ or $SCN^-$.
The reference half-cell is that described by (II).

The emf of cell (III) can be expressed by

$$E = E_{0,\text{x}} - 59.16 \, \log[\text{X}^-] - 59.16 \log y_{\text{X}^-} + E_j \quad \text{(2)}$$

where $E_{0,\text{x}}$ and $y_{\text{X}^-}$ are defined analogously to $E_{0,\text{Me}}$ and $y_{\text{Me}}$, and $E_j$ is the diffusion potential.

$E_{0,\text{Me}}$ and $E_{0,\text{x}}$ were determined from the first point of the titration, *i.e.* the point with no $Mg^{2+}$ present, since the solution in the buret (T) always contained $Mg^{2+}$ plus some $H^+$, while the solution in the titrating vessel (S) contained a constant amount of the ion to which the measuring electrode was responding plus ionic media ions; *cf.* (I) and (III). Solution T also contained $X^-$ or $Me^{z+}$ at the same concentration as in S, so that $[X^-]_{\text{tot}}$ and $[Me^{z+}]_{\text{tot}}$ were kept constant during the titration. In this way the variation in $E_j$ represents only the effects arising from the replacement of $Na^+$ with $Mg^{2+}$. All other contributions to $E_j$ are constant during the titration and can be included in $E_0$.

The standard state of the various species can conveniently be defined with reference to 3 M NaClO$_4$, i.e. $y_i = 1$ when $C_i \to 0$ in that medium, where $C_i$ is the concentration of species $i$. In this medium the water activity is 0.88($ = 21/23.74$, cf. below).

*The vapor pressure measurements.* In the Mechrolab Osmometer the resistance difference ($\Delta R$) corresponding to the steady-state temperature difference ($\Delta T$) between two matched thermistors (one containing a drop of the solvent, the other a drop of the solution studied) is measured using a Wheatstone bridge. The quantity $\Delta R$ can be related to the vapor pressure of water, $p_{H_2O}$, by using standard solutions with known vapor pressure. At 25.0°C the standard solutions used were doubly distilled water ($p_{H_2O} = 23.74$ torr), 3 M NaClO$_4$ (21.0 torr)[7] and 3 M HClO$_4$ (19.7 torr).[7]

<div align="center">RESULTS</div>

*The change of water activity.* From the osmometric measurements the change in water activity when replacing Na$^+$ in 3 M (Na)ClO$_4$ with Mg$^{2+}$ can be estimated. In Fig. 1 $p$ is plotted against $\Delta R$ for the solutions studied. A straight
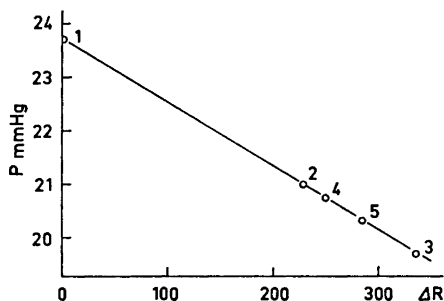


*Fig. 1.* The vapor pressure of water, $p_{H_2O}$ (mmHg), as a function of $\Delta R$. 1, H$_2$O; 2, 3 M NaClO$_4$; 3, 3 M HClO$_4$; 4, a mixture containing 0.60 M Mg(ClO$_4$)$_2$ and 1.80 M NaClO$_4$; 5, 1.5 M Mg(ClO$_4$)$_2$. Points 1, 2, and 3 were used for the definition of the straight line.

line can be fitted to the data and by interpolation it is found that by changing the concentration of Mg$^{2+}$ from 0 to 600 mM the change in water activity is only $= 1.3$ % and to a good approximation negligible.

*The emf measurements for positive ions.* Using cell (I) emf titrations were performed such that the total concentrations of H$^+$ and Me$^{z+}$ were kept constant during each titration except for a slight variation of the In$^{3+}$ concentration, whilst the concentration of Mg$^{2+}$, [Mg$^{2+}$], was varied. In Table 1 the data are collected on the form $V$(ml), [Mg$^{2+}$] (mM), $E_{gl(ass)}$ (mV) $E_{H(hydrogen)}$ (m) or $V$, [Mg$^{2+}$], $E_{Me}$. In Fig. 2 the quantity $E'_j$ defined below, and easily obtained by a rearrangement of eqn. (1)

$$E'_{j,Me} = E_j + 59.16\, z^{-1} \log y_{Me} = E - E_{0,Me} - 59.16\, z^{-1} \log[Me^{z+}] \qquad (3)$$

is plotted against [Mg$^{2+}$] for all the cations studied. Not only do the curves have the same slope, but they all coincide, in the figure they have been shifted 1 mV in order not to crowd the data.

Rather high $H$-values (0.013 $-$ 0.137) were used in order to permit accurate determination of the concentration of free H$^+$, $h$, as well as to prevent hydrolysis of the cations. The $h$-values were determined by separate experiments. Two different $h$-values were used 114.8 mM and 59.0 mM. Measurements with

*Table 1.* The change of activities for some positive ions in 3 M (Na,Mg)ClO$_4$.

Measurements with glass and hydrogen electrodes.

Series 1: S: $H_0 = 114.76$ mM, [Mg$^{2+}$]$_{tot} = 0$.
      T: $H_T = 114.76$ mM, [Mg$^{2+}$]$_{tot} = 1422.6$ mM; $V_0 = 40.04$ ml.
Experimental data [$V$, [Mg$^{2+}$], $E_{gl}$, $E_H$ (corrected for atm. pressure)]:
0.00, 0.0, $-24.6$, $-660.52$; 0.50, 17.79, $-24.3$, $-660.29$; 1.00, 35.15, $-24.05$, $-660.08$;
2.50, 84.78, $-23.4$, $-659.46$; 5.00, 160.16, $-22.4$, $-658.45$; 10.50, 299.73, $-20.45$,
$-656.63$; 20.00, 480.57, $-18.0$, $-654.16$; 40.00, 720.97, $-14.7$, $-650.84$.
Series 2: S: $H_0 = 58.95$ mM, [Mg$^{2+}$]$_{tot} = 0$.
      T: $H_T = 58.95$ mM [Mg$^{2+}$]$_{tot} = 1470.5$ mM; $V_0 = 40.04$ ml.
0.00, 0.0, $-41.0$, $-732.24$; 2.48, 85.77, $-39.85$, $-731.11$; 5.00, 163.25, $-38.9$, $-730.20$;
10.00, 293.88, $-37.1$, $-728.37$; 20.00, 489.86, $-34.2$, $-725.62$; 45.03, 778.44, $-30.00$,
$-721.42$.

Measurements with Ag,AgCl electrode.

$H_{tot} = 114.75$ mM and [Ag$^+$]$_{tot} = 10.06$ mM were kept constant throughout the titration.
S: [Mg$^{2+}$]$_{tot} = 0$; T: [Mg$^{2+}$]$_{tot} = 1437.6$ mM; $V_0 = 40.05$ ml. Experimental data ($V$,
[Mg$^{2+}$], $E$): 0.00, 0.0, $-1.80$; 2.50, 84.56, $-0.77$; 5.00, 159.73, 0.19; 10.00, 287.52, 1.83;
20.00, 479.20, 4.37; 45.04, 761.08, 8.27.

Measurements with Cd amalgam electrode.

$H_{tot} = 13.85$ mM and [Cd$^{2+}$]$_{tot} = 14.67$ mM were kept constant throughout the titration.
$V_0 = 40.05$ ml. Experimental data ($V$,[Mg$^{2+}$],$E$ (0.01 wt.% Cd amalgam used)): 0.00, 0.0,
$-989.85$; 0.50, 18.25, $-989.63$; 1.00, 36.05, $-989.43$; 2.50, 86.94, $-988.78_5$; 5.01, 164.52,
$-987.83$; 7.51, 233.66, $-986.97$; 10.01, 295.88, $-986.175$; 12.52, 335.19, $-985.46$; 15.02,
403.58, $-984.78$; 20.07, 493.98, $-983.58$; 25.07, 569.66, $-982.50$; 30.08, 634.68, $-981.57$;
40.09, 740.23, $-980.07$; 50.10, 822.34, $-978.89$; 60.05, 887.68, $-977.90$.

Measurements with In amalgam electrodes.

$H_{tot} = 136.96$ was kept constant throughout both series of titrations. Series 1: A silver
anode and a Hg pool cathode were used when preparing the In amalgam electrodes.
S: [Mg$^{2+}$]tot $= 0$ mM, [Ag$^+$]tot $= 2.03$ mM, [In$^{3+}$]$_{tot} = 18.42$ mM T: [Mg$^{2+}$]$_{tot} = 1418.8$
mM, [Ag$^+$]$_{tot} = 0$ mM, [In$^{3+}$]$_{tot} = 19.10$ mM. Experimental data ($V$,[Mg$^{2+}$],$E$): 0.0, 0.0,
$-915.8$; 2.50, 109.11, $-914.10$; 5.01, 203.04, $-913.02$; 10.01, 354.89, $-911.32$; 20.02,
567.77, $-909.41$; 32.90, 742.01, $-907.25$.
Series 2: S: [Mg$^{2+}$]$_{tot} = 0.0$ mM, [In$^{3+}$]$^+ = 29.10$ mM.
      T: [Mg$^{2+}$]$_{tot} = 1418.8$ mM, [In$^{3+}$]$_{tot} = 19.10$ mM; $V_0 = 40.04$ ml.
Experimental data ($V$,[Mg$^{2+}$],$E$): 0.00, 0.0, $-934.19$; 0.50, 17.50, $-934.03$; 1.00, 34.57,
$-933.85$; 2.50, 83.38, $-933.31$; 5.01, 157.50, $-932.52$; 10.01, 283.76, $-931.12$; 15.02,
387.04, $-929.90$; 20.02, 472.93, $-928.93$; 40.04, 709.40, $-926.17$; 60.06, 851.27, $-924.25$.

*Table 2.* The change of activities of some negative ions.

1. The change of chloride ion activity during Na$^+$ $-$ Mg$^{2+}$ replacement.

    Series 1: [Cl$^-$]$_{tot} = 1.00$ mM was constant throughout the series, S: [Mg$^{2+}$]$_{tot} = 0.0$
mM; T: [Mg$^{2+}$]$_{tot} = 1499.5$ mM; $V_0 = 50.09$ ml. Experimental data ($V$(ml), [Mg$^{2+}$] (mM),
$E_{Ag,AgCl}$ (mV)): 0.0, 0.0, $-276.34$; 0.25, 7.45, $-276.29$; 0.50, 14.82, $-276.26$; 1.00,
29.35, $-276.12$; 2.51, 71.55, $-275.74$; 5.01, 136.34, $-275.10$; 10.01, 249.74, $-274.07$;
15.02, 345.90, $-273.19$; 20.02, 428.17, $-272.46$; 25.03, 499.62, $-271.81$; 30.03, 562.02,
$-271.23$; 40.04, 666.13, $-270.17$.
    Series 2: [Cl$^-$]$_{tot} = 20.02$ mM, S: [Mg$^{2+}$]$_{tot} = 0.0$ mM; T: [Mg$^{2+}$]$_{tot} = 1490.0$ mM; $V_0 =$
40.05 ml. Experimental data: 0.0, 0.0, $-352.86$; 0.25, 9.24, $-352.79$; 0.50, 18.37, $-352.70$;
1.00, 36.30, $-352.53$; 2.51, 87.87, $-352.04$; 5.01, 165.67, $-351.29$; 7.51, 235.28, $-350.62$;
10.01, 297.94, $-350.07$; 12.51, 354.64, $-349.50$; 15.02, 406.39, $-349.01$; 20.02, 496.58,
$-348.17$; 30.03, 638.48, $-346.86$; 40.04, 744.91, $-345.88$.

*Table 2. Continued.*

Series 3: $[Cl^-]_{tot} = 50.18$ mM, S: $[Mg^{2+}]_{tot} = 0.0$ mM; T: $[Mg^{2+}]_{tot} = 1474.9$ mM; $V_0 = 40.05$ ml. Experimental data: 0.0, 0.0, $-376.47$; 0.25, 9.15, $-376.38$; 0.55, 19.98, $-376.29$; 1.00, 35.93, $-376.12$; 2.51, 86.98, $-375.64$; 5.01, 163.99, $-374.91$; 7.51, 232.90, $-374.22$; 10.01, 294.92, $-373.64$; 15.01, 402.08, $-372.65$; 20.01, 491.39, $-371.82$; 30.00, 631.65, $-370.52$; 39.99, 736.90, $-369.53$.

Series 4: $[Cl^-]_{tot} = 199.85$ mM, S: $[Mg^{2+}]_{tot} = 0.0$ mM; T: $[Mg^{2+}]_{tot} = 1400.1$ mM; $V_0 = 40.05$ ml. Experimental data: 0.0, 0.0, $-411.42$; 0.25, 8.69, $-411.36$; 0.50, 17.26, $-411.27$; 1.00, 34.11, $-411.13$; 2.51, 82.57, $-410.67$; 5.01, 155.67, $-410.01$; 10.01, 279.96, $-408.85$; 15.01, 381.68, $-407.93$; 17.52, 426.08, $-407.52$; 20.02, 466.61, $-407.16$; 30.01, 599.72, $-405.95$; 40.00, 699.60, $-405.05$; 49.99, 777.32, $-404.31$.

## 2. The change of bromide ion activity.

Series 1: $[Br^-]_{tot} = 24.83$ mM, S: $[Mg^{2+}]_{tot} = 0.0$ mM; T: $[Mg^{2+}]_{tot} = 1487.6$ mM; $V_0 = 40.05$ ml. Experimental data ($V$(ml), $[Mg^{2+}]$ (mM), $E_{Ag,AgBr}$(mV)): 0.0, 0.0, $-512.67$; 0.26, 9.59, $-512.60$; 0.50, 18.34, $-512.53$; 1.00, 36.24, $-512.39$; 2.51, 87.73, $-512.02$; 5.02, 165.69, $-511.45$; 7.51, 234.90, $-510.96$; 10.01, 297.46, $-510.51$; 15.01, 405.53, $-509.75$; 20.02, 495.78, $-509.11$; 22.53, 535.56, $-508.84$; 22.05, 572.41, $-508.57$; 30.03, 637.45, $-508.11$; 35.03, 694.06, $-507.68$; 40.06, 743.89, $-507.28$.

Series 2: $[Br^-]_{tot} = 49.66$ mM, S: $[Mg^{2+}]_{tot} = 0.0$ mM; T: $[Mg^{2+}]_{tot} = 1475.2$ mM; $V_0 = 40.05$ ml. Experimental data: 0.0, 0.0, $-530.43$; 0.26, 9.51, $-530.37$; 0.51, 18.55, $-530.29$; 1.00, 35.94, $-530.14$; 2.51, 87.00, $-529.77$; 5.01, 164.02, $-529.21$; 7.51, 232.94, $-528.71$; 10.01, 294.97, $-528.27$; 12.51, 351.11, $-527.86$; 15.02, 402.34, $-527.48$; 20.02, 491.64, $-526.84$; 25.03, 567.36, $-526.29$; 30.03, 632.13, $-525.83$; 32.53, 661.16, $-525.60$; 35.03, 688.27, $-525.40$; 40.06, 737.68, $-525.03$.

Series 3: $[Br^-]_{tot} = 197.60$ mM, S: $[Mg^{2+}]_{tot} = 0.0$ mM; T: $[Mg^{2+}]_{tot} = 1401.2$ mM; $V_0 = 40.05$ ml. Experimental data: 0.0, 0.0, $-565.74$; 0.25, 8.69, $-565.69$; 0.50, 17.28 $-565.65$; 1.00, 34.13, $-565.53$; 2.52, 82.95, $-565.20$; 5.01, 155.79, $-564.69$; 7.51, 221.26,, $-564.22$; 10.01, 280.18, $-563.79$; 15.02, 382.17, $-563.06$; 17.52, 426.42, $-562.74$; 20.02, 466.99, $-562.44$; 25.03, 538.91, $-561.91$; 30.03, 600.43, $-561.49$; 35.03, 653.76, $-561.08$; 40.04, 700.51, $-560.74$.

## 3. The change of thiocyanate ion activity.

Series 1: $[SCN^-]_{tot} = 217.93$ mM, S: $[Mg^{2+}]_{tot} = 0.0$ mM; T: $[Mg^{2+}]_{tot} = 1391.0$ mM; $V_0 = 40.05$ ml. Experimental data ($V$(ml), $[Mg^{2+}]$ (mM), $E_{Ag,AgSCN}$(mV)): 0.0, 0.0, $-547.28$; 0.25, 8.63, $-547.20$; 0.50, 17.15, $-547.15$; 1.00, 33.89, $-546.99$; 2.51, 82.04, $-546.57$; 5.01, 154.66, $-545.93$; 7.51, 219.65, $-545.36$; 10.02, 278.37, $-544.85$; 12.51, 331.08, $-544.39$; 15.02, 379.39, $-543.97$; 20.02, 463.60, $-543.23$; 25.04, 535.13, $-542.64$; 30.03, 596.07, $-542.11$; 35.04, 649.11, $-541.63$; 40.04, 695.43, $-541.22$; 50.04, 772.64, $-540.52$; 60.05, 834.48, $-539.95$.

Series 2: $[SCN^-]_{tot} = 145.08$ mM, S: $[Mg^{2+}]_{tot} = 0.0$ mM; T: $[Mg^{2+}]_{tot} = 1427.5$ mM; $V_0 = 40.05$ ml. Experimental data: 0.0, 0.0, $-537.96$; 0.25, 8.86, $-537.51$; 0.50, 17.60, $-537.41$; 1.00, 34.77, $-537.27$; 2.50, 83.87, $-536.77$; 5.01, 158.71, $-536.08$; 7.51, 225.40, $-535.48$; 10.01, 285.43, $-534.94$; 15.02, 389.33, $-534.05$; 20.02, 475.74, $-533.23$; 25.01, 548.74, $-532.63$; 30.03, 611.68, $-532.11$; 35.04, 666.11, $-531.70$; 40.04, 713.64, $-531.30$; 50.06, 793.02, $-530.62$; 60.06, 856.39, $-530.02$.

Series 3: $[SCN^-]_{tot} = 36.46$ mM, S: $[Mg^{2+}]_{tot} = 0.0$ mM; T: $[Mg^{2+}]_{tot} = 1481.8$ mM; $V_0 = 40.05$ ml. Experimental data: 0.0, 0.0, $-502.85$; 0.25, 9.19, $-502.62$; 0.50, 18.27, $-502.50$; 1.00, 36.10, $-502.31$; 2.50, 87.06, $-501.80$; 5.01, 164.75, $-501.04$; 7.51, 233.98, $-500.39$; 10.01, 296.29, $-499.81$; 12.51, 352.68, $-499.28$; 15.02, 404.14, $-498.76$; 20.02, 493.84, $-497.95$; 25.02, 569.75, $-497.23$; 30.02, 634.83, $-496.64$; 35.54, 696.68, $-496.06$; 40.04, 740.79, $-495.57$; 50.05, 823.11, $-494.86$.

both glass and hydrogen electrodes agreed within the limits of experimental accuracy.

*The emf measurements for negative ions.* Titrations were performed at several rather low $C$-levels for each anion and these were kept constant in each titra-
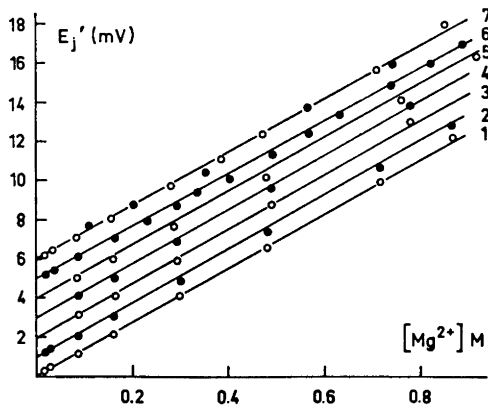
*Fig. 2.* The change of $E'_{j,Me}$, [*cf.* eqn. (3)] with [$Mg^{2+}$] for some positive ions. 1, glass electrode, $H = 114.76$ mM; 2, hydrogen electrode, $H = 114.76$ mM; 3, glass electrode, $H = 58.95$ mM; 4, hydrogen electrode, $H = 58.95$ mM; 5, Ag,AgCl electrode, $H = 114.75$ mM, [$Ag^+$]$_{tot} = 10.06$ mM; 6, Cd amalgam electrode, $H = 13.85$ mM, [$Cd^{2+}$]$_{tot} = 14.67$ mM; 7, In amalgam electrode, $H = 136.96$ mM, open circles [$In^{3+}$] $= 18.42 - 19.10$ mM, dots [$In^{3+}$] $= 19.10 - 29.10$ mM. The full drawn lines correspond to the slope $(13.568 \pm 0.002)$ mV mol$^{-1}$ and they are shifted stepwise by 1.00 mV for the sake of clarity.

tion. The hydrogen ion concentration, $h$, was also kept constant at $\approx 2.5$ mM. For SCN$^-$ the solutions were saturated with AgSCN in order to ensure stable potentials. The results of measurements with cell (III) are collected in Table 2.
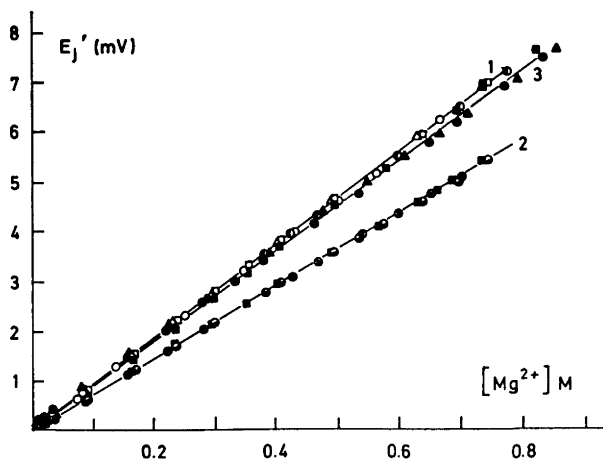


*Fig. 3.* The change of $E'_{j,x}$ [*cf.* eqn. (11)] with [$Mg^{2+}$] in 3 M ($Na^+$, $Mg^{2+}$)ClO$_4$ for some negative ions. 1, Ag,AgCl electrode: 1.00 mM, 20.0 mM, 50.18 mM, 199.85 mM Cl$^-$; 2, Ag,AgBr electrode: 24.83 mM, 49.66 mM, and 197.60 mM Br$^-$; 3, Ag,AgSCN electrode: 36.46 mM, 145.08 mM, and 217.93 mM SCN$^-$. The straight lines through the experimental points are those obtained using LETAGROP, assuming $E'_{j,x}$ to be a linear function of [$Mg^{2+}$] and neglecting any complex formation. The slopes are: $9.29 \pm 0.02$, $7.26 \pm 0.02$, and $9.05 \pm 0.07$ mV mol$^{-1}$ for Cl$^-$(1), Br$^-$(2) and SCN$^-$(3).

In Fig. 3 the quantity $E'_{j,X}$ defined analogously to $E'_{j,Me}$ in eqn. (3) is plotted against $[Mg^{2+}]$ for the anions studied. In this case three separate straight lines are obtained, one for each anion.

## TREATMENT OF DATA

*Positive ions.* The data in Fig. 2, were fitted to a straight line, employing a least squares computer program, giving

$$E_j' = E_j + 59.16\ z^{-1} \log y_{Me} = (13.568 \pm 0.002)[Mg^{2+}] \tag{4}$$

Results [3,8] similar to (4) have been obtained for the replacement of $Na^+$ in 3 M $NaClO_4$ with $In^{3+}$. Biedermann and Wallin [3] found $\log y_{Ag}{}^3/y_{In} = 0.20[In^{3+}]$ while Ferri [8] obtained $\log y_H{}^3/y_{In} = 0.52[In^{3+}]$. The influence of changes in ionic medium has recently been studied by Byé *et al.*[9] They suggest that the activity coefficient for an ion in a system at constant ionic strength ($I$), but varying composition, can be described by

$$\log y_i = F_i(I) + \Sigma a_{ij} C_j \tag{5}$$

where $F_i(I)$ corresponds to the Debye-Hückel term and the second term to a Setchenow salting-out term where $C_j$ is the concentration of species $j$. They report several systems which follow eqn. (5). It is easily seen that expression (4) is of the same type as (5). According to (5) there is one term for each ion, whose concentration varies during the experiment. In the present study $[H^+]$ and $[Me^{z+}]$ were kept constant at rather low values so that only $[Mg^{2+}]$ and $[Na^+]$ varied. To a first approximation, however,

$$2[Mg^{2+}] + [Na^+] \sim 3.0 \pm 0.4 \tag{6}$$

and it is possible to express the variation of $\log y_{Me}$ as a function of $[Mg^{2+}]$ only. If we denote the salting-out terms for $Mg^{2+}$ and $Na^+$ by $a_{Me,Mg}$ and $a_{Me,Na}$ we get

$$\log y_i = F_i(I) + 3a_{Me,Na} + (a_{Me,Mg} - 2a_{Me,Na})[Mg^{2+}] \tag{7}$$

By comparing (4) with (7) we get

$$\frac{-zE_j}{59.16} = F_i(I) + 3a_{Me,Na} \tag{8a,b}$$

and

$$(a_{Me,Mg} - 2a_{Me,Na}) = \frac{13.568}{59.16} z$$

According to eqn. (8a) $-E_j$ must be constant and the difference $a_{Me,Mg} - 2a_{Me,Na}$ must depend only on $z$, which seems somewhat surprising. It is hardly to be expected, however, that $E_j$ is constant during the exchange of $Na^+$ for $Mg^{2+}$. It has recently been shown by Österberg and Sjöberg [10] that changes in sodium ion concentration are reflected in changes in $E_j$.

A correct estimate of $E_j$ is difficult to make. The conditions for which the Henderson [11] and Planck [12,13] equations are derived are practically impossible to fulfil.[14] These equations can therefore only be used as rough guides when

*Table 3.* Treatment of the data for the Ag,AgCl electrode by the program LETAGROP ETITR.

| Run No. | Variable parameters | $k(E_j')$ mV mol$^{-1}$ | $K_1$ | $E_0$ mV | $U$ | $\sigma(E)$ mV |
|---|---|---|---|---|---|---|
| 1 | $k$ | $9.29\pm0.02$ | — | $-453.83$ $-453.35$ $-453.34$ $-452.79$ | 0.163 | 0.06 |
| 2 | $k,E_0$ | $9.29\pm0.02$ | — | $-453.86\pm0.01$ $-453.31\pm0.01$ $-453.29\pm0.01$ $-452.84\pm0.01$ | 0.068 | 0.04 |
| 3 | $k,K_1$ | $8.11\pm0.44$ | $0.048\pm0.018$ | $-452.84\pm0.01$ | 0.059 | 0.04 |
| 4 | $k,K_1,E_0$ | $6.74\pm0.36$ | $0.106\pm0.016$ $\log K_1=$ $-0.98\pm0.19$ | $-453.89\pm0.02$ $-453.33\pm0.01$ $-453.30\pm0.01$ $-452.81\pm0.00_4$ | 0.048 | 0.03 |
| 5 | $k,K_1,E_0,\delta B$ $\delta B=$ $-25.92\pm7.54$ mM $-11.70\pm2.10$ $+18.63\pm2.83$ $+0.48\pm1.73$ | $6.36\pm0.70$ | $0.122\pm0.031$ $\log K_1=$ $-0.914\pm0.056$ | $-453.85\pm0.02$ $-453.35\pm0.01$ $-453.33\pm0.01$ $-452.80\pm0.01$ | 0.019 | 0.02 |

*Table 4.* Treatment of the data for the Ag,AgBr electrode by the program LETAGROP ETITR.

| Run No. | Variable parameters | $k(E_j')$ mV mol$^{-1}$ | $K_1$ | $E_0$ mV | $U$ | $\sigma(E)$ mV |
|---|---|---|---|---|---|---|
| 1 | $k$ | $7.21\pm0.02$ | — | $-607.62$ $-607.57$ $-607.40$ | 0.086 | 0.04 |
| 2 | $k,E_0$ | $7.21\pm0.01$ | — | $-607.62\pm0.01$ $-607.53\pm0.01$ $-607.45\pm0.01$ | 0.022 | 0.02 |
| 3 | $k,K_1,E_0$ | $6.33\pm0.52$ | $0.035\pm0.021$ $\log K_1=$ $-1.45$ (max. $-1.01$) | $-607.62\pm0.01$ $-607.53\pm0.01$ $-607.44\pm0.01$ | 0.021 | 0.02 |

*Table 5.* Treatment of the data for the Ag,AgSCN electrode by the program LETAGROP ETITR.

| Run No. | Variable parameters | $k(E_j')$ mV mol$^{-1}$ | $K_1$ | $E_0$ mV | $U$ | $\sigma(E)$ mV |
|---|---|---|---|---|---|---|
| 1 | $k$ | $9.36\pm0.09$ | — | $-586.42$ $-587.55$ $-587.93$ | 3.65 | 0.28 |
| 2 | $k,E_0$ | $9.05\pm0.07$ | — | $-586.54\pm0.02$ $-587.23\pm0.03$ $-587.58\pm0.04$ | 0.75 | 0.12 |
| 3 | $K_1$ | — | $0.430\pm0.003$ | » | 1.84 | 0.19 |
| 4 | $K_1,E_0$ | — | $0.420\pm0.003$ | $-586.54\pm0.02$ $-587.28\pm0.02$ $-587.75\pm0.03$ | 0.37 | 0.09 |
| 5 | $k,K_1,E_0$ | $6.10\pm1.10$ | $0.123\pm0.045$ $\log K_1=$ $-0.91\pm0.19$ | $-586.50\pm0.03$ $-587.19\pm0.02$ $-587.58\pm0.05$ | 0.32 | 0.07 |

applied to real systems. Nevertheless, Henderson's equation has been used to estimate $E_j$ using some different assumptions.

$$E_j = \frac{\sum u_j/z_j(C_{j,2}-C_{j,1})}{\sum u_j(C_{j,2}-C_{j,1})} + \frac{RT}{F}\ln\frac{\sum u_jC_{j,2}}{\sum u_jC_{j,1}} \tag{9}$$

$C_{j,1}$ and $C_{j,2}$ are ionic concentrations in the two solutions I and II. $z_j$ is the ionic charge and $u_j$ the ionic mobility. Inserting the ionic conductivities $(l_i(=u_iF)$ at infinite dilution $(l_{Na}=50.11$, $l_{ClO_4}=67.32$ and $\frac{1}{2}l_{Mg}=53.06$ ohm$^{-1}$ cm$^2$) [15] we get $E_j=5.07$ mV. On the other hand if we use $\sum u_jC_{j,2}/\sum u_jC_{j,1}=\varkappa_2/\varkappa_1$ where $\varkappa_2$ (54.50) is the conductivity of 3 M NaClO$_4$ and $\varkappa_1$ that of 1.5 M MgClO$_4$ [17] (65.0 as obtained by interpolation) we get $E_j=36.18$ mV. From the slope of eqn. (4) we get 20.35 mV, which is somewhere between the calculated values. It is tempting to assume that the whole variation in $E_j$ is due rather to $E_j$ than to $y_{Me}$, in agreement with the findings of Biedermann and Sillén [7] who found that when replacing Na$^+$ with H$^+$ up to 600 mM in 3 M (Na)ClO$_4$ no change in the activity coefficients of the cations could be observed. However, from the present information it cannot be determined whether both $E_j$ and $y_{Me}$ vary or only $E_j$.

*Negative ions.* (a) *The slope.* The data in Fig. 3 have been treated in the same way as those in Fig. 2 and best straight lines evaluated by a least squares computer method. The results are given in Tables 3 − 5 as run No. 1. In the treatment of these data the program LETAGROP was used and besides the evaluation of the slope $k_j$ in the expression

$$E'_{j,X} = k_j[Mg^{2+}] \tag{10}$$

$E_{0,X}$ in the expression

$$E_{j,X^-} = E_j - 59.16 \log y_X = E - E_{0,X^-} + 59.16 \log[X^-] \tag{11}$$

was evaluated as well. The results of these calculations are given as run No. 2 in Tables 3 − 5. As seen, the $E_{0,X}$-values obtained are within a few hundredths of a millivolt of the directly measured values, except for the less accurate data for SCN$^-$ where the difference in some cases amounts to 0.2 − 0.3 mV. The straight lines in Fig. 3 have been drawn using the results of run No. 2 in Tables 3 − 5.

(b) *The ion pair formation constant.* On considering eqns. (5) and (11) it can be surmised that the different slopes obtained for the three anions can only be due to $y_{X^-}$ varying differently for each anion, since $E_j$ must be the same in all three cases. In their study Biedermann and Sillén [7] found that the activity coefficients of anions varied, but all in the same way. It is thus tempting to try to interpret the differences in the slopes of the three anions studied as being due to ion pair formation. The species MgCl$^+$ [18−22] has been suggested by several investigators and it is thus not unreasonable to attribute the difference in slopes to ion pair formation.

An estimate of the equilibrium constant $K_1$ of the reaction

$$Mg^{2+} + X^- \rightleftharpoons MgX^+ \tag{12}$$

was obtained by neglecting the activity coefficient term in the relation:

$$\log K_1 = \log [MgX^+][Mg^{2+}]^{-1}[X^-]^{-1} + \log \frac{y_{MgX^+}}{y_{Mg^{2+}}y_{X^-}} \qquad (13)$$

In the activity coefficient expression in eqn. (13) the ratio $y_{MgX^+}/y_{Mg^{2+}}$ might be constant if the findings of Biedermann and Sillén [7] can be applied to the systems investigated in this study, while $y_{X^-}$ can be expected to vary. By neglecting the activity coefficient term only a first approroximation to $K_1$ is obtained.

By means of the computer program LETAGROP ETITR developed by Sillén et al.[23] besides $K_1$ the values of $E_{0,X}$ and $k_j$ (cf. eqn. (10)) were varied either one at a time or simultaneously. The results are given in Tables 3 – 5 as runs Nos. 3 – 5. In addition for $Cl^-$ a correction to the $Mg^{2+}$-concentration $\delta B$ in the burette was also varied (run No. 5). From Table 3 we find that run No. 5 gives the best fit to the data as measured by the error squares sum ($U$) defined by

$$U = \sum_{1}^{N} (E_{obs} - E_{calc})^2 \qquad (14)$$

where the summation is taken over all experimental points ($N$). As well as this the standard deviation in the measured emf values $\sigma(E)$ is smallest for run No. 5. However, in this run the correction $\delta B$ obtained is larger (max. 1.85 %) than the experimental uncertainty ($\sim 0.5$ %). For this reason this run has been discarded and the best fit obtained with run No. 4.

For $Br^-$ the best results were obtained with run No. 3 and for $SCN^-$ with run No. 5. In all cases, however, the improvement of the fit to the experimental data on the introduction of $K_1$ is only very slight, the low $K_1$-values found indicate only a very slight ion pair formation. It is interesting to note, however, that the quantity $k_j$ becomes practically the same (6.33, 6.33, and 6.10 for $Cl^-$, $Br^-$, and $SCN^-$) after the correction for ion pair formation. This is what is to be expected when supposing that both $E_j$ and perhaps also $y_{X^-}$ (cf. Ref. 7) might be the same for all anions.

## DISCUSSION

*Activity coefficients.* From the information presently available it is difficult to ascertain whether or how much the activity coefficients of cations and anions change during the exchange of $Na^+$ for $Mg^{2+}$. If they vary, they change linearly with $[Mg^{2+}]$ in agreement with eqn. (5). On the other hand activity coefficient quotients like that in eqn. (13) may stay nearly constant so that the evaluation of stability constants may be quite accurate.

*Ion pair formation.* Table 6 gives the currently known estimates of $K_1$ together with the results of the present study. From Table 6 is evident that the consistency between the various investigations is poor. The estimates obtained by extrapolation from solvent-water mixtures to pure water seem too high, while the values obtained in water show a poor agreement. As recently discussed by Bjerrum [26] equilibrium constants $< 10$ are difficult to estimate with any reasonable certainty as illustrated by, e.g., the case of the formation

*Table 6.* log $K_1$ for reaction (12) and X$^-$ = Cl$^-$, Br$^-$, SCN$^-$.

| Anion | Temp. °C | Medium | log $K_1$ | Ref. |
|-------|----------|--------|-----------|------|
| Cl$^-$ | 35 | 20 % dioxane | 1.3 | 19 |
| | 35 | 30 % dioxane | 1.7 | 19 |
| | 35 | 0 % dioxane | 0.5 | This work/20 |
| | 0 | sat.KClO$_4$ | 0.62 | 20 |
| | 0 | sat.KClO$_3$ | 0.08 | 20 |
| | 0 | →0 | 0.91 | 20 |
| | −40 | C$_2$H$_5$OH,→0 | 3.22 | 24, 25 |
| | −20 | C$_2$H$_5$OH,→0 | 3.40 | 24, 25 |
| | 0 | C$_2$H$_5$OH,→0 | 3.67 | 24, 25 |
| | 20 | C$_2$H$_5$OH,→0 | 3.79 | 24, 25 |
| | 25 | ∼3 M(Na)ClO$_4$ | −0.98 ± 0.19 | This work |
| Br$^-$ | 20 | C$_2$H$_5$OH,→0 | 3.38 | 25 |
| | 25 | ∼3 M(Na)ClO$_4$ | −1.41(−1.01) | This work |
| SCN$^-$ | 25 | ∼3 M(Na)ClO$_4$ | −0.91 ± 0.19 | This work |

of outer-sphere complexes. The low values obtained in the present study indicate weak interactions indeed and it seems highly probable that the MgX$^+$-species discussed can be regarded as Bjerrum's ion pairs rather than complexes in the ordinary sense of the word. The use of Bjerrum's theory and some simplifying assumptions lead to ion pair formation constants about 10 and below. Experimentally, however, it has been found that many 1:2 electrolytes give equilibrium constants of the same order of magnitude as found in this paper.[27] Instead of introducing ion pair formation constants, the results in the present paper can equally well be rationalized in terms of α-coefficients according to Harned's rule [28] and extensions therof.[29] This approach, however, is only a way of representing experimental data and of less interest in the present context, although its applicability emphasizes the difficulty in obtaining unique descriptions, when weak interactions are concerned.

REFERENCES

1. Havel, J. and Högfeldt, E. *Chemica Scripta. In press.*
2. Hietanen, S., Sillén, L. G. and Högfeldt, E. *Chemica Scripta* **3** (1973) 65.
3. Biedermann, G. and Wallin, T. *Acta Chem. Scand.* **14** (1960) 594.
4. Forsling, W., Hietanen, S. and Sillén, L. G. *Acta Chem. Scand.* **6** (1952) 901.
5. Brown, A. S. *J. Am. Chem. Soc.* **57** (1934) 646.
6. Wanderzee, C. E. and Smith, W. E. *J. Am. Chem. Soc.* **78** (1956) 721.

 7. Biedermann, G. and Sillén, L. G. *Arkiv Kemi* **5** (1953) 425.
 8. Ferri, D. *Personal communication.*
 9. Byé, J, Fischer, R., Krumenacher, L., Lagrange, J. and Vierling, F. *Trans. Royal Inst. Technol.* No. 255 (1972).
10. Österberg, R. and Sjöberg, B. *Trans. Royal Inst. Technol.* No. 275 (1972).
11. Hendersen, P. *Z. physik. Chem. (Leipzig)* **59** (1907) 118.
12. Planck, M. *Ann. Phys. (Leipzig)* **39** (1890) 161.
13. Planck, M. *Ann. Phys. (Leipzig)* **40** (1890) 561.
14. Vetter, K. J. *Electrochemical Kinetics,* Academic, New York 1967, p. 50.
15. Conway, B. E. *Electrochemical Data,* Elsevier, Amsterdam 1952, p. 145.
16. Janz, G. J., Oliver, B. G., Lahshminarayanan, G. R. and Mayer, G. *J. Phys. Chem.* **74** (1970) 1285.
17. van Rysselberghe, P. and McGee, J. M. *J. Am. Chem. Soc.* **65** (1943) 737.
18. Ohtaki, H. and Yamasaki, K. *Bull. Chem. Soc. Japan* **31** (1958) 445.
19. Das, P. B., Das, P. K. and Patnaik, D. *J. Indian Chem. Soc.* **36** (1959) 761.
20. Kenttämaa, J. *Suomen Kemistilehti* **32** (1959) 68.
21. Griffin, R. G., Amis, E. S. and Wear, J. O. *J. Inorg. Nucl. Chem.* **28** (1966) 543.
22. Grinberg, A. A. and Kiseleva, N. V., *Zh. Neorg. Khim.* **3** (1959) 1804.
23. Brauner, P., Sillén, L. G. and Whiteker, R. *Arkiv Kemi* **31** (1969) 365.
24. Golben, M. and Dawson, L. R. *J. Phys. Chem.* **64** (1960) 37.
25. Golben, M. *Thesis* 1949, Univ. Kentucky, Univ. Microfilms Co., 1223.
26. Bjerrum, J. *Trans. Royal Inst. Technol.* No. 253 (1972).
27. Denney, T. O. and Monk, C. B. *Trans. Faraday Soc.* **47** (1951) 992.
28. Harned, H. S. and Owen, B. B. *The Physical Chemistry of Electrolytic Solutions,* 3rd Ed., Reinhold, New York 1958, Chapter 14, p. 585.
29. Ginstrup, O. *Acta Chem. Scand.* **24** (1970) 875.

# Multicomponent Polyanions

## VI. The Molecular and Crystal Structure of $Na_4H_2Mo_5P_2O_{23}(H_2O)_{10}$, a Compound Containing Sodium-coordinated Dihydrogenpentamolybdodiphosphate Anions

### BRITT HEDMAN

*Department of Inorganic Chemistry, University of Umeå, S-901 87 Umeå, Sweden*

The crystal structure of $Na_4H_2Mo_5P_2O_{23}(H_2O)_{10}$ has been determined from three-dimensional X-ray diffraction data collected with a PAILRED diffractometer using $MoK\alpha$-radiation. The cell dimensions of the monoclinic $(P2_1/n)$ unit cell are $a = 26.388(2)$ Å, $b = 13.661(1)$ Å, $c = 8.041(1)$ Å, and $\beta = 91.37(1)°$, and it contains four formula units. The structure consists of $H_2Mo_5P_2O_{23}{}^{4-}$-groups linked together by direct sodium bridges $(O-Na-O)$ in the $y$- and $z$-directions forming infinite layers parallel to the $yz$-plane. The layers are held together by $O-Na-H_2O-Na-O$ linkages. Each sodium ion is surrounded by six oxygen atoms (water oxygens and group oxygens), which form an octahedron. The structure has been refined by least squares methods using anisotropic vibrational parameters and the final $R$-value is 0.053, based on 3897 independent reflexions.

In emf-investigations of aqueous equilibria involving $H^+$, $MoO_4{}^{2-}$ and $HPO_4{}^{2-}$, the complexes $(H^+)_8(MoO_4{}^{2-})_5(HPO_4{}^{2-})_2{}^{6-}$, $(H^+)_9(MoO_4{}^{2-})_5(HPO_4{}^{2-})_2{}^{5-}$, and $(H^+)_{10}(MoO_4{}^{2-})_5(HPO_4{}^{2-})_2{}^{4-}$ have been reported.[1] In connection with these studies different crystalline phases have been obtained. X-Ray diffraction investigations have been carried out with some of these.[2] The crystal structure of $Na_6Mo_5P_2O_{23}(H_2O)_{13}$, corresponding to the complex $(H^+)_8(MoO_4{}^{2-})_5(HPO_4{}^{2-})_2{}^{6-}$, has been completely determined.[2]

The present work presents the crystal data and structure of $Na_4H_2Mo_5P_2O_{23}(H_2O)_{10}$, the phase which corresponds to the complex $(H^+)_{10}(MoO_4{}^{2-})_5(HPO_4{}^{2-})_2{}^{4-}$. For brevity, $Na_6Mo_5P_2O_{23}(H_2O)_{13}$ and $Na_4H_2Mo_5P_2O_{23}(H_2O)_{10}$ will be referred to in the text as (8,5,2) and (10, 5,2), respectively.

### EXPERIMENTAL

*Crystal preparation and analyses.* In a typical preparation of the crystals, $Na_2MoO_4.2H_2O$ and $NaH_2PO_4.2H_2O$ were dissolved in concentrated $HClO_4$. The concentrations were $[MoO_4{}^{2-}]_{tot} = 1.60$ M, $[HPO_4{}^{2-}]_{tot} = 0.64$ M, and $[HClO_4]_{tot} = 2.57$ M.

After a few days (sometimes weeks) of evaporation at room temperature colourless acicular crystals were formed. The crystals were not stable in air, and during the X-ray exposures they were sealed together with part of the mother liquid in a capillary of Lindeman glass. The contents of Na, Mo, and P were determined by elemental analyses (carried out at the Department of Analytical Chemistry, University of Umeå). (Found: Na 7.9; Mo 41.0; P 5.2. Calc.: Na 7.8; Mo 40.5; P 5.2.) The water content of the crystal was investigated by Karl Fischer titration and a value of 16.2 % (calc. 15.2 %) was found. Thermobalance analysis confirmed the amount of water.

*Crystal data and space group.* Rotation photographs around [100], [010] and [001] and the corresponding Weissenberg photographs (zero, first and second layer lines) taken with $CuK\alpha$-radiation ($\lambda = 1.5418$ Å) revealed that the crystals were monoclinic. This was confirmed from precession photographs.

Accurate unit cell dimensions were determined with a Hägg-Guinier camera with Si as internal standard. The parameters and their corresponding standard deviations are: $a = 26.388 \pm 0.002$ Å, $b = 13.661 \pm 0.001$ Å, $c = 8.041 \pm 0.001$ Å, $\beta = 91.37° \pm 0.01°$, $V = 2897.8$ Å³.

The calculated density with $Z = 4$ is 2.71 g cm⁻³, which is in agreement with the observed density of $2.71 \pm 0.01$ g cm⁻³ determined by flotation in a bromoform-carbon tetrachloride solution. Systematic extinctions were found for $h0l$, $h + l = 2n + 1$ and $0k0$, $k = 2n + 1$ and the space group was uniquely determined as $P2_1/n$ ($P2_1/c$, No. 14 in Ref. 3, in a different orientation).

*Collection and reduction of intensity data.* Three-dimensional intensity data were at 25°C collected with a Philips PAILRED linear diffractometer using $MoK\alpha$-radiation reflected off the (200) plane of a LiF-monochromator crystal ($\lambda = 0.7107$ Å). A crystal of approximate dimensions $0.07 \times 0.20 \times 0.26$ mm was mounted and rotated along the $c$-axis (parallel to the 0.26 mm-edge of the crystal). A total of 6834 reflexions of the type $hkl$ and $\bar{h}kl$ from the layers $hk0 - hk7$ were scanned up to a limit of $\sin \theta \approx 0.55$. The integrated reflexions were corrected for background in the usual way,[4] and since the zero level reflexions $hk0$ and $\bar{h}k0$ were equivalent within experimental error, the $hk0$ reflexions were used. Reflexions with a relative statistical error of $\Delta I_0/I_0$ greater than 0.3 were omitted leaving a remaining data set of 4538 unique observed reflexions.

During the refinement it became obvious that some reflexions of high $\sin \theta$-values showed noticeable differences between the observed and calculated structure factor values. A thorough investigation including comparison with films and analyses of the reflexion profiles on the charts showed that extra peaks had occurred. Since the $a$-axis is 26.388 Å, these were possibly caused by strong reflexions of about the same $\sin \theta$. 104 reflexions showing this effect were deleted from the material. In addition the 537 reflexions from the $hk7$ layer were omitted since no film for comparison was available. The refinements were then based on the remaining 3897 reflexions. The intensities were corrected for Lorentz and polarization effects and absorption correction was applied with a $4 \times 10 \times 12$ grid ($\mu = 23.65$ cm⁻¹).

*Computer programs used.* The computer programs for Lorentz, polarization and absorption corrections were originally written by P. Coppens, L. Leiserowitz and D. Rabinovich. Fourier summations and calculation of distances and angles were performed with programs originally written by A. Zalkin. A modified version of a program written by Gantzel, Sparks and Trueblood was used in the least squares refinements of the structural parameters (full-matrix) and for block-diagonal refinements the program BLOCK written by Ove Lindgren, University of Gothenburg, was used. The stereoscopic figures were produced by the program ORTEP.[5] The computations were carried out with a CDC 3200 computer in Umeå and an IBM 360/65 computer in Gothenburg.

Crystal data:
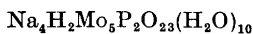
$Na_4H_2Mo_5P_2O_{23}(H_2O)_{10}$                         F. W. = 1183.8
Monoclinic $P2_1/n$, all atoms in 4(e): $\pm (x, y, z; \frac{1}{2} + x, \frac{1}{2} - y, \frac{1}{2} + z)$

$a = 26.388(2)$ Å
$b = 13.661(1)$ Å
$c = 8.041(1)$ Å                                         $Z = 4$
$\beta = 91.37(1)°$                                       $D_x = 2.71$ g cm⁻³
$V = 2897.8$ Å³                                           $D_m = 2.71 \pm 0.01$ g cm⁻³
                                                          $\mu = 23.63$ cm⁻¹

## STRUCTURE DETERMINATION AND REFINEMENT

The space group implies that symmetry vectors on a Harker line $(\frac{1}{2}, 2y + \frac{1}{2}, \frac{1}{2})$ and in a Harker plane $(2x + \frac{1}{2}, \frac{1}{2}, 2z + \frac{1}{2})$ should be found in a Patterson synthesis. The computed three-dimensional synthesis [normalized to $P(0,0,0) = 999$] contained three peaks on the line and eleven in the plane, all of them of height $130 - 160$. In addition a peak of height $\approx 300$ was found at $(0.5, 0, 0.3)$. Two of the Harker line vectors could be shown to be doublets, and in combination with $(2x, 2y, 2z)$ vectors four molybdenum atoms were located. The coordinates of the fifth atom were obtained from cross vectors. The $(0.5, 0, 0.3)$ vector was explained as a multiple cross vector between different formula units.

A Fourier synthesis based on the molybdenum atoms gave a conventional $R$-value of 0.338. It confirmed the positions of the molybdenum atoms and also gave the positions of phosphorus and oxygen atoms belonging to the $H_2Mo_5P_2O_{23}{}^{4-}$-group. In a second Fourier synthesis four sodium atoms and ten water oxygen atoms could be located, while the $R$-value decreased to 0.243. The positional parameters and isotropic temperature factors for the 44 non-hydrogen atoms in the asymmetric unit were refined by full-matrix least squares methods. The function minimized was $\sum \omega(|F_o| - |F_c|)^2$ and the residual $R = \sum ||F_o| - |F_c|| / \sum |F_o|$ was reduced from 0.243 to 0.073 in five iterations. The refinements were then continued with anisotropic vibrational parameters using a block-diagonal matrix approximation which resulted in a final $R$-value of 0.053.

The atomic scattering factors used for $Mo^{3+}$ were those given by Cromer and Waber,[6] for P those given by Hanson, Herman, Lea and Skillman,[7] and for $Na^+$, $O^-$, and O the values in International Tables.[8] To obtain electroneutrality $f(O)$ was used for water oxygen atoms and $f(O^-)$ for the remainder. Account was taken of the real part of the dispersion correction.[8]

A weighting scheme according to Cruickshank[9] was applied:
$\omega = 1/(a + |F_o| + c|F_o|^2 + d|F_o|^3)$ where the values of the constants were $a = 60$, $c = 0.008$, and $d = 0$.

A difference Fourier synthesis based on 2809 reflexions with a maximum of $\sin \theta \approx 0.45$ was searched for possible hydrogen atom peaks around the $H_2Mo_5P_2O_{23}{}^{4-}$-group. Two peaks at acceptable oxygen-hydrogen distances were found and the positional parameters were included in a block-diagonal least squares refinement (scattering factors for H from Stewart et al.[10]). The decrease in $R$-value was significant on the 10 %-level according to the Hamilton test as approximated by Pawley.[11] However, since there were higher peaks in the difference Fourier for which no explanations were found, no values of hydrogen atom parameters are given. The sites for the tested peaks are identical with the hydrogen atom positions as discussed later in the text.

Final atomic coordinates and vibrational parameters and corresponding standard deviations are given in Tables 1 and 2, and a comparison of the observed and calculated structure factors is given in Table 3.

## DESCRIPTION AND DISCUSSION OF THE STRUCTURE

The structure is built up from $H_2Mo_5P_2O_{23}{}^{4-}$-anions, $Na^+$-ions and $H_2O$ molecules. The Mo atoms in the $H_2Mo_5P_2O_{23}{}^{4-}$-groups form pentagons the

*Table 1.* The fractional atomic coordinates and in parentheses their estimated standard deviations (referring to the last decimal place given).
For the oxygen atoms $O(ij)$ or $OP(ij)$ the index means that the atom is bonded to the molybdenum atoms $i$ and $j$. $Aq(ij)$ is a water oxygen bonded to the sodium ions $i$ and $j$.

|           | $x$          | $y$          | $z$           |
|-----------|-------------|-------------|---------------|
| Mo1       | 0.23748(3)  | 0.25607(7)  | 0.2772 (1)    |
| Mo2       | 0.16157(3)  | 0.44947(6)  | 0.3501 (1)    |
| Mo3       | 0.03942(3)  | 0.37272(6)  | 0.3485 (1)    |
| Mo4       | 0.04162(3)  | 0.12885(6)  | 0.1540 (1)    |
| Mo5       | 0.16453(3)  | 0.05712(6)  | 0.1832 (1)    |
| P1        | 0.1257(1)   | 0.2143(2)   | 0.4824 (4)    |
| P2        | 0.1269(1)   | 0.2913(2)   | 0.0398 (4)    |
| O1(1)     | 0.2765(3)   | 0.2726(6)   | 0.4481(11)    |
| O2(1)     | 0.2792(3)   | 0.2421(6)   | 0.1211(11)    |
| O(12)     | 0.2148(3)   | 0.3869(5)   | 0.2307(11)    |
| O(15)     | 0.2161(3)   | 0.1229(5)   | 0.3119(10)    |
| OP(12)    | 0.1696(3)   | 0.2849(5)   | 0.4470 (9)    |
| OP(15)    | 0.1713(2)   | 0.2230(5)   | 0.0825(10)    |
| O1(2)     | 0.1916(3)   | 0.4860(6)   | 0.5294(11)    |
| O2(2)     | 0.1577(3)   | 0.5514(5)   | 0.2298(11)    |
| O(23)     | 0.0933(2)   | 0.4515(5)   | 0.4382(10)    |
| OP(23)    | 0.1127(3)   | 0.3556(5)   | 0.1897 (9)    |
| O1(3)     | −0.0041(3)  | 0.3836(6)   | 0.5002(10)    |
| O2(3)     | 0.0154(3)   | 0.4493(5)   | 0.1934(10)    |
| OP(3)     | 0.0783(3)   | 0.2677(5)   | 0.5301(10)    |
| O(34)     | 0.2172(3)   | 0.2509(5)   | 0.2497(10)    |
| O1(4)     | 0.1719(3)   | 0.0525(6)   | 0.3013(12)    |
| O2(4)     | −0.0006(3)  | 0.1176(6)   | −0.0082(12)   |
| OP(4)     | 0.0800(2)   | 0.2369(5)   | −0.0170(10)   |
| O(45)     | 0.0964(3)   | 0.0522(5)   | 0.0783(10)    |
| OP(45)    | 0.1134(3)   | 0.1488(5)   | 0.3279(10)    |
| O1(5)     | 0.1601(3)   | −0.0441(6)  | 0.3053(13)    |
| O2(5)     | 0.1955(3)   | 0.0190(7)   | 0.0104(12)    |
| OP1       | 0.1464(3)   | 0.1466(6)   | 0.6255(10)    |
| OP2       | 0.1468(3)   | 0.3600(5)   | −0.0999(10)   |
| Na1       | 0.5239(2)   | 0.2485(4)   | 0.2542 (7)    |
| Na2       | 0.3678(3)   | 0.1989(5)   | 0.3726 (9)    |
| Na3       | 0.3225(2)   | 0.2003(5)   | −0.1183 (8)   |
| Na4       | 0.2599(2)   | 0.4092(5)   | 0.6927 (8)    |
| Aq(1)     | 0.4715(4)   | 0.3517(6)   | 0.0862(13)    |
| Aq(12)    | 0.4640(4)   | 0.1493(7)   | 0.4056(13)    |
| Aq(2)     | 0.3946(5)   | 0.3365(9)   | 0.4890(23)    |
| Aq1(23)   | 0.3966(3)   | 0.1998(8)   | 0.0651(13)    |
| Aq2(23)   | 0.3468(4)   | 0.1202(7)   | 0.6404(13)    |
| Aq1(34)   | 0.2391(4)   | 0.2381(10)  | 0.7848(13)    |
| Aq2(34)   | 0.3386(4)   | 0.3754(9)   | 0.8427(20)    |
| Aq(4)     | 0.2391(3)   | 0.4996(6)   | 0.9402(12)    |
| Aq1       | 0.0847(3)   | 0.0166(7)   | 0.7479(11)    |
| Aq2       | 0.0811(3)   | 0.4796(7)   | −0.2383(12)   |

*Table 2.* The final anisotropic thermal parameters ($\times 10^4$) and their estimated standard deviations ($\times 10^4$) in parentheses. The parameters are calculated according to the formula

$$\exp\ [-(h^2\beta_{11}+k^2\beta_{22}+l^2\beta_{33}+hk\beta_{12}+hl\beta_{13}+kl\beta_{23})]$$

|        | $\beta_{11}$ | $\beta_{22}$ | $\beta_{33}$ | $\beta_{12}$ | $\beta_{13}$ | $\beta_{23}$ |
|--------|--------|--------|---------|---------|---------|---------|
| Mo1    | 6(0)   | 28(0)  | 70(2)   | 4(0)    | 10(1)   | 10(1)   |
| Mo2    | 6(0)   | 21(0)  | 70(2)   | −2(0)   | 8(1)    | −6(1)   |
| Mo3    | 6(0)   | 20(0)  | 75(2)   | 1(0)    | 10(1)   | −11(1)  |
| Mo4    | 6(0)   | 20(0)  | 79(2)   | −2(0)   | 5(1)    | −9(1)   |
| Mo5    | 7(0)   | 25(0)  | 87(2)   | 8(0)    | 3(1)    | −9(1)   |
| P1     | 6(0)   | 22(1)  | 55(6)   | 0(1)    | 7(2)    | 6(3)    |
| P2     | 6(0)   | 21(1)  | 57(6)   | 0(1)    | 5(2)    | 4(3)    |
| O1(1)  | 8(1)   | 40(5)  | 119(19) | 1(4)    | −1(6)   | 30(13)  |
| O2(1)  | 9(1)   | 44(5)  | 73(17)  | 8(4)    | 19(6)   | 6(13)   |
| O(12)  | 6(1)   | 22(3)  | 92(17)  | 1(3)    | 17(5)   | 12(11)  |
| O(15)  | 7(1)   | 27(4)  | 59(16)  | 8(3)    | 0(5)    | 21(11)  |
| OP(12) | 9(1)   | 25(3)  | 29(15)  | −3(3)   | 14(5)   | −7(10)  |
| OP(15) | 6(1)   | 24(3)  | 67(16)  | 10(3)   | 4(5)    | −4(10)  |
| O1(2)  | 7(1)   | 46(5)  | 78(17)  | −8(4)   | 0(6)    | −53(13) |
| O2(2)  | 12(1)  | 25(4)  | 88(18)  | 4(3)    | 22(6)   | 24(12)  |
| O(23)  | 5(1)   | 19(3)  | 94(16)  | 0(3)    | 6(5)    | −27(10) |
| OP(23) | 7(1)   | 19(3)  | 50(15)  | 3(3)    | 17(5)   | −9(9)   |
| O1(3)  | 7(1)   | 35(4)  | 61(16)  | 0(3)    | 24(6)   | −45(11) |
| O2(3)  | 8(1)   | 25(4)  | 81(17)  | 6(3)    | 7(6)    | −14(11) |
| OP(3)  | 7(1)   | 22(3)  | 82(17)  | −1(3)   | 21(5)   | −4(10)  |
| O(34)  | 8(1)   | 24(3)  | 74(16)  | 6(3)    | 16(5)   | −33(11) |
| O1(4)  | 11(1)  | 30(4)  | 114(19) | −8(4)   | 6(7)    | 2(13)   |
| O2(4)  | 9(1)   | 28(4)  | 135(20) | −3(3)   | 5(6)    | −39(13) |
| OP(4)  | 6(1)   | 22(3)  | 74(16)  | −1(3)   | −8(5)   | −3(10)  |
| O(45)  | 8(1)   | 23(3)  | 71(17)  | 6(3)    | 5(5)    | −16(11) |
| OP(45) | 8(1)   | 27(4)  | 65(16)  | 4(3)    | 7(5)    | −26(11) |
| O1(5)  | 11(1)  | 31(4)  | 153(21) | 4(4)    | −6(7)   | 22(14)  |
| O2(5)  | 10(1)  | 49(5)  | 124(20) | 18(4)   | 10(7)   | −42(15) |
| OP1    | 9(1)   | 34(4)  | 49(16)  | 3(3)    | −1(5)   | 25(11)  |
| OP2    | 9(1)   | 32(4)  | 58(16)  | 0(3)    | 7(6)    | 32(11)  |
| Na1    | 9(1)   | 73(4)  | 91(11)  | −3(3)   | 4(4)    | 5(9)    |
| Na2    | 20(1)  | 60(3)  | 215(15) | −24(3)  | 35(6)   | −101(12) |
| Na3    | 11(1)  | 78(4)  | 129(12) | 10(3)   | 5(4)    | −41(11) |
| Na4    | 19(1)  | 85(4)  | 128(14) | 28(4)   | −5(5)   | 18(12)  |
| Aq(1)  | 15(1)  | 33(4)  | 146(22) | 2(4)    | 17(8)   | 19(14)  |
| Aq(12) | 15(1)  | 49(5)  | 134(22) | 2(5)    | 7(8)    | 13(16)  |
| Aq(2)  | 16(2)  | 49(7)  | 519(49) | 5(6)    | −18(15) | −82(28) |
| Aq1(23)| 10(1)  | 60(6)  | 204(24) | 3(5)    | 14(8)   | 39(19)  |
| Aq2(23)| 15(1)  | 44(5)  | 140(21) | 4(5)    | 9(8)    | −1(15)  |
| Aq1(34)| 10(1)  | 120(10)| 111(24) | 2(6)    | −7(8)   | −36(22) |
| Aq2(34)| 15(2)  | 76(8)  | 301(34) | 3(6)    | 6(12)   | 125(28) |
| Aq(4)  | 12(1)  | 44(5)  | 111(20) | 10(4)   | 6(7)    | −5(14)  |
| Aq1    | 13(1)  | 54(5)  | 106(20) | 21(5)   | 15(7)   | 16(15)  |
| Aq2    | 12(1)  | 50(5)  | 86(19)  | −20(4)  | 5(7)    | −7(14)  |

planes of which are approximately parallel to the $xy$-plane. Three of the Na$^+$-ions act as links in O−Na−O-bridges between adjacent groups and two symmetry-related zigzag chains parallel to the $y$-axis are formed this way (Fig. 1). The difference in $z$ between the chains is about 4 Å. The fourth Na$^+$-ion

*Table 3.* Observed and calculated structure factors. The columns are $h$, $|F_o|$, and $F_c$, respectively.

```
  H 17  0        H  9  0       2  243 -232      8  120  113      20   64  -63     -17   89   86
10  58  -65    28   30  -31    1   51  -53     10  372 -372      19   73   76     -19   31  -31
 6 104 -105    26   40  -39                    12  138  133      17   37  -34     -23   63  -60
 4  75  -77    24   83   81       H  4  0      14  276 -277      15  100 -103     -24  110 -104
               22   31  -27    0   63   59     16  277 -268      14   27   33     -27   75  -67
  H 16  0       20  130  133    1   50   48     18   97   96      13   49  -49
 0 143  151    19   32   36    2  421 -410     20   42  -36      10   41   45       H 10  1
 1  33  -37    18   60   52    4   55  -58     24  238  225       9  130 -134     -27   87  -64
 4  79   83    16  107  108    5   25  -27     26  140  128       8   30  -36     -23   51   48
 8  38  -40    15   35   37    6  163 -157     28   80  -74       7   35   39     -21   40  -40
10  86  -95    14   58  -57    8   87   58     30  109   99       6   25  -20     -20   80  -62
14  70  -75    10  100 -101    9   20   20     34   84  -78       5   46   44     -19   46  -45
                8   54  -52   10   98  101                        3   27  -18     -18   72  -72
  H 15  0        6  176 -178   12  328  338      H 17  1          2   74  -70     -17  104  102
18  54  -56     4  109 -107   14   82   93      7   35   36       1  148  145     -16   58  -58
16  76  -79     2  169 -165   16  106  115      6   32   35       0   44  -47     -14   40  -38
14 103  112     1   24  -26   18   43  -45      3   74  -76      -1  148  144     -13  113 -110
12  27  -30                   20  148 -150      1   48  -53      -2   31  -27     -12   60   58
 8  74   77       H  8  0     22  102 -100      0   80   92      -6   38  -41     -11   87   85
 6 100  105     0  223  206   24  102  -99     -3   44  -46      -7   65   60     -10   50  -47
 2  50   53     2  145  143   26   89  -85     -4   32  -34      -8   34   31      -9   82  -83
                3   64   69   28  174 -167     -5   38  -39      -9  141 -140      -8   98   93
  H 14  0        4  382  377   30   30   26     -7   45   48     -12   42   39      -7   52  -47
 0  26   29     5   97  -99                   -10   49  -48     -13   63  -61      -6  130  126
 1  28   28     6  226 -228     H  3  0                        -15   64  -64      -4   96   95
 2  49   47     7   40   40   32  131 -122       H 16  1       -16   30   33      -1  211 -202
 3  28  -27     8   28   25   29   42   36    -10   47   55     -17   43  -44       0   62   64
 4  78  -81    10   83  -86   28   83  -76     -9   60   60     -19   79   80       1  215  210
 5  37   34    12  221 -227   24   56  -54     -7   87   88     -21   55  -61       2   76  -75
 6  40   42    13   27   26   23   24   20     -6   54   61     -22   42  -41       3   46  -45
 7  29  -25    14   87  -88   22  135  131     -5   44   55     -23   70   69       4   68  -64
12  70  -74    18  128 -133   20  115 -114     -1   86   89                        6  116 -118
14  38  -38    19   27   24   19   38  -38      0   42  -40       H 12  1          7   81   83
               20   55   52   18  308  310      1   71  -73    -23   70   72       8   29  -36
  H 13  0       22  150  150   16   88   50      2   72   79    -22   40   40       9   86   97
20  45   44    26  125  124   14   22   15      4   42  -45    -19   63   61      11  146 -159
18 106 -108    28  110  109   13   40  -41      5   70  -74    -18   54   57      13  173  185
16  95  -95    30   29  -25   12   75  -77      6   46  -47    -17  122  121      14   26  -28
 9  30  -27                   10  105  110      7   62  -63    -15   35  -33      16   36   38
 8 185  190      H  7  0      8  190 -213      9   73  -75    -14   67  -64      17   99 -103
 7  37   42    30  116  112    7   26   28     12   34  -37    -10   64   65      18   77   77
 3  39  -42    26   25  -21    6  149 -130     13   27  -26     -9   86  -67      20   58   53
 2 175  174    24   28  -23    3   38  -31     14   37   38     -8  105  -99      21   31   31
 1  45   43    20  191 -193    2  220 -212                      -7  165 -163      23   73  -73
               18   28   27                     H 15  1        -4   32  -37      24   42   40
  H 12  0       16   91  -91     H  2  0      14   80  -83     -3  152 -151      25   30   25
 0 245 -238    14   73  -75    0  121 -124     13   35   37     -2   31  -30
 2 123 -125    10  205  212    2   33   30      9   66  -69     -1   45  -45       H  9  1
 4  96   98     8   25  -33    3   44  -49      8   47  -50      1   79   79     29   45  -42
 6 165 -171     6  195  200    4  161 -161      5   65   67      2   64   62     28   36   38
 7  37   40     5   29  -29    5   58   65      4   54   56      3  112  115     26   48   51
 8  72   71     4  184  185    6  284  296      3   26  -27      6   82   83     25   98  -97
10 109  114     2   37  -32    7   50  -55      2   29   27      7  172  175     22   53   53
12  84   88     1   35   36    8  261 -265      1   75   77      9   43   45     21   74  -75
14  55   52                   9   36   32     -1   94   98     10   48  -48     17   32  -34
16 103  102      H  6  0     12  210  214     -2   61   62     11   35   36     15  105  111
18  64  -61     0  224 -213   13   33   32     -3   29  -33     14   59   62     13   78   81
20  26  -29     2  171  169   14   43   46     -5   58   59     15   35  -31     12   39  -43
24 146 -145     3   33  -29   15   29   27     -6   56   54     16   65  -65     11  127  132
25  29   26     4  158 -157   16  157 -164     -8   42  -43     17  121 -128     10   36   39
                5   42   45   18   96   59     -9   45  -46     19   35  -35      6   62  -67
  H 11  0       8   76  -75   19   23  -22    -10   38  -40     21   41  -41      7   33   31
25  31   30    10  104  110   20  131  129    -11   52  -54     23   67  -70      5   51  -51
24  39  -41    11   52  -55   22  105 -103    -12   48  -47     25   54   48      4  154  155
23  42  -40    12  185 -194   23   34  -34    -13   63   61                       3   61  -58
22  85   81    13   27  -28   24   64   59    -15   88  -91      H 11  1          2  104  109
20  62   58    15   35   32   25   35  -35    -16   70  -72     24   37  -31      1   87  -86
18  79   77    16   42   38   28   48  -43                     23   78  -78     -1  138 -133
16  34  -34    18   57  -61   32   49   42      H 14  1        22   32  -32     -2   99   87
15  38  -34    20   59   61   34   80  -74    -18   87   88     21   28  -26     -3   58  -54
14 168  174    22   43   40                  -16   83   82     18   43  -44     -4  178  167
13  42   43    27   47   47     H  1  0     -15   45  -53     17   70   73     -5   35  -24
12  26  -34    28   72   70   34   49  -44    -14   35  -36     16   90   95     -6   45  -43
10  72  -74    30   48  -48   33   28  -20    -11   27   27     15   36  -36     -7   36   34
 6  59  -59                   32   30  -27     -9   19  -23     13  107  115     -8   53  -35
 4 115 -119      H  5  0     30   71  -57     -8   73  -73     11   55   61    -11  162  153
               30   98   90   27   26  -23     -7   45   46     10   65   65    -12   51  -49
  H 10  0       28  146  143   26  158 -148     -6   55  -55      9   29   30    -13   32   31
 0 294 -284    27   30   37   24  113  106     -3   51   53      8   64   67    -14   40  -39
 1  47   47    26  150 -146   22   73   70     -2   86  -86      7   40   39    -15  134  129
 2  29   27    24   89   87   20  117  120     -1   30  -25      3   97  -93    -16   48   45
 6  89  -88    22   45  -44   18   24  -22      0   28   22      2   35  -32    -18   70  -65
10 143  146    20  118 -116   17   37   36      1   39   39      1   30  -27    -20   66   64
11  31  -34    19   32   34   16  156  153      2   39   39      0  131 -126    -21   65  -68
12 151 -150    18  183 -185   14   79  -77      3   79  -81     -3   97  -95    -22   75   72
13  53   49    17   64  -68   12   65   65      4   26   30     -4   51  -47    -25   91  -87
14  69   74    15   26   33   11   26   26      5   26   31     -8   75   74    -26   34   32
16 173  173    14  348 -357   10  172 -173      7   43  -48     -9   32   33    -28  110  104
18  66  -69    12   20  -12    8  153 -164      8   95   98    -10   85   84
22  91   87    10  173  175    7   30  -34     11   49  -48    -11   64   61      H  8  1
23  33  -32     8   36  -30    6  183 -172     16   57  -58    -12   53  -52    -29   87   77
26  49  -48     6   59   76    4  116 -126     18   72  -74    -13  128  125    -26   40   37
28  60   59     4  186  196                                   -14   89   85    -25   57  -47
                3   74   79     H  0  0        H 13  1        -15   56  -56    -23   40   40
                             6  237  255     21   61  -58     -16   75   75    -22   54  -52
```

## Table 3. Continued.

**Column 1**

```
-21 122 -117
-19 101  -99
-17  25  -21
-16  44  -40
-15 167 -163
-13  90  -86
-12  30   24
-11 183  176
-10  68   64
 -9  60   56
 -8  32   31
 -7  29  -32
 -6  53   48
 -5 394  379
 -4  63  -62
 -3  63  -61
 -2  86   84
 -1  26  -21
  1  32   30
  2  57  -59
  3  33   36
  5 359 -375
  6  22   23
  7  40   39
  8  33  -34
  9 124 -131
 10  59  -61
 11 117 -124
 13 116  124
 14  34   37
 15 133  139
 19 152  154
 21 125  127
 23  53  -54
 25  51   50
 26  47  -44
 29 115 -109
 30  56   49

     H  7  1
 29  56   55
 27  53   52
 25  65   63
 24  62   62
 22  25   24
 21 145  146
 20  38   38
 19  78  -79
 18  73  -77
 16  88   89
 13  52  -54
 12 151 -159
 11 173 -190
 10  52  -59
  9  66   55
  8  84   88
  7 120 -127
  5  20  -23
  4  40   38
  3 132  132
  2 150  147
  1  58   55
  0  53  -50
 -1  60   56
 -2 157  149
 -3  64   64
 -4  75   68
 -5  61   58
 -7 171 -164
 -9  73   71
-10  82   78
-11 171 -170
-12 292 -280
-13  58  -54
-15  65  -62
-16 101   97
-17  34   40
-18  62  -54
-19 103 -102
-21 120  116
-22 132  124
-24  32   29
-25  45   44
-26  59   58
-27  27   28
-29  64   59
-31  58  -51

     H  6  1
-31  29  -28
-30  51  -48
-29  54   54
-28  79  -72
-27  44  -41
-22  66   62
-20 145  141
-17  40   38
-16  64   62
-15  52  -48
-14 155  155
-13  75  -74
-11 115  107
```

**Column 2**

```
-10 262 -252
 -8  57  -52
 -6 143 -132
 -4 170 -152
 -3 111  110
 -1 195 -176
  1 212  200
  2  99  -90
  3 106 -110
  4 234  240
  5  39  -44
  6  81   83
  8  50   55
  9  47   50
 10 160  170
 11 174 -183
 12  61   66
 13  80   84
 14 164 -176
 15  45   42
 16  27  -27
 17  21  -21
 19  37   38
 20  91  -93
 21  23   21
 22  58  -60
 24  26   26
 25  39   39
 29  54  -49
 31  27   27

     H  5  1
 32  24  -21
 31  39  -38
 30  28  -23
 27 190  189
 25  32  -31
 24  82  -83
 23 115  113
 22  39  -32
 21  57   55
 17 101 -111
 16  46  -48
 15 105  113
 13 244 -264
 12  86   96
 11 139 -150
 10  97  106
  9  57   56
  8 120 -125
  7 126 -137
  6  41  -47
  5 101 -102
  4  43  -35
  3 191  199
  2 125 -120
  1  54   47
  0  64  -68
 -1  25   14
 -2 199 -181
 -3 267  245
 -4  61  -54
 -5 118 -103
 -6  52   50
 -7 171 -156
 -8 150 -143
-10  80   76
-11  62  -62
-12 152  149
-13 276 -279
-15  94   94
-16  46  -44
-17 117 -114
-21  32   30
-22  61  -61
-23 120  118
-24 101  -98
-25  38  -32
-26  53  -49
-27 138  136

     H  4  1
-33  60  -54
-32  58   53
-30  80  -74
-29 113 -109
-26  72   70
-25  27  -29
-23  66   64
-22  38  -31
-21 107  105
-20  91   90
-19 100   95
-18  31  -31
-17  89   82
-16  83  -84
-15  98  100
-14  87   90
-13  73   79
-12  51  -51
-11 241 -241
-10  22  -21
```

**Column 3**

```
 -9  59   50
 -7 214 -206
 -6 146 -134
 -5 257 -225
 -4 191 -176
 -3 277 -244
 -2 352  312
 -1  89   87
  0  56  -55
  1 145 -137
  2 184 -174
  3 316  320
  4  76   81
  5 268  271
  6 135  142
  7 167  184
 10  55   60
 11 202  224
 12  58  -64
 13  73  -92
 15  68  -72
 16  37   37
 17 121 -125
 18  23   21
 19 131 -133
 20  40  -40
 21 127 -128
 22  25   21
 23  46  -44
 26  36  -34
 29 132  122
 30  48   44
 31  38   32
 33  59   53

     H  3  1
 33  89   80
 32  39   36
 31  76  -70
 28  60  -54
 27  34  -31
 26  33  -33
 25  65  -62
 23 120 -116
 22  65  -66
 21 106  106
 19 173 -176
 18  44  -41
 17  70   73
 16  25   26
 15 141  151
 14  80   83
 13  78   85
 11  30   30
  9 134  150
  8  60   67
  7  60  -57
  6 109  109
  5 127 -133
  4 211 -232
  3  55   43
  2 152 -158
  1 261 -274
  0  44   44
 -1 307 -298
 -2 115 -116
 -3  28   17
 -4 240 -236
 -5 113 -101
 -6  98   87
 -7  98  -99
 -8  38   34
 -9 181  190
-10  48   51
-11  47   46
-13  44   44
-14  82   86
-15 125  129
-17 120  128
-19 152 -151
-20  54  -55
-21 103  107
-22  85  -81
-23  92  -91
-24  35  -36
-25  47  -47
-26  33  -31
-27  30  -23
-28 102 -104
-29  25   19
-31  56  -52
-32  52   49
-33  57   52

     H  2  1
-33  67   65
-32  95   86
-31  46  -45
-30  27   28
-28  26   27
-26  74   73
-25  45   44
```

**Column 4**

```
-24  63  -60
-23  95  -96
-22  89  -85
-21 103  105
-20  58  -58
-19  37   37
-18 176 -179
-17  86  -88
-16 131 -133
-15  87   83
-14  68   66
-13  88   90
-12  18  -15
-11  72  -74
-10  38  -37
 -9  26   19
 -8 265  256
 -7 275  275
 -6 249  243
 -5 302 -289
 -4 100   97
 -3 111  119
 -2 146  130
 -1  21  -19
  0  39  -40
  2  93  -89
  3  85 -103
  4  76  -84
  5 306  332
  6 196 -200
  7 344 -371
  8 234 -239
  9  46   55
 10  84   84
 11  84   89
 13  93  -98
 14  34  -34
 15 125 -125
 16  95   94
 17 161  163
 18 123  120
 19  85  -87
 20  55   52
 21  75  -73
 22  70   64
 23  71   67
 24  28   28
 25  47  -47
 26  36  -30
 29  56  -52
 30  26  -24
 32  47  -41
 33  57  -48

     H  1  1
 34  27  -19
 30  39   37
 29  69  -63
 27  40   39
 26  51   46
 25 156 -160
 24  50   52
 23  37  -41
 22  32   35
 21  56  -55
 20  48   44
 18  50   49
 17 102 -105
 16  70  -68
 15 231  233
 14  86  -89
 12  50   43
 11 111  120
 10  60   55
  9 128  130
  8 164 -168
  6  69   75
  5 128 -131
  4  18   29
 -5 167 -169
 -6 107  116
 -7  93  107
 -8 147 -144
-10  40  -49
-11 129  138
-12 103   98
-13  57   56
-14 121 -128
-15 211  225
-16  95  -97
-17 103 -107
-18  81   82
-19  22   19
-20  73   75
-21  52  -51
-24 118  115
-25 128 -125
-26  48   47
-28  24  -18
-29  48  -45
-30  64   61
-34  78  -74
```

**Column 5**

```
     H  0  1
-33  67   62
-31 102   93
-29  36  -35
-27 108  106
-23 121 -120
-17 298 -310
-13  95   97
-11  48  -61
 -9 350  371
 -7 275  279
 -5  44   39
  5 125 -130
  7 308 -310
  9 253 -258
 11  65  -52
 13 120 -113
 15 106  106
 17 318  316
 19  22  -24
 21  56   57
 23 151  146
 25  68  -65
 27 119 -113
 29  41   40
 31 136 -124
 33  96  -69

     H 17  2
  7  53  -56
  4  46   44
  1  64  -66
 -1  65   65
 -3  30   31
 -6  42  -41
 -7  38   38
 -9  62   62

     H 16  2
-13  39   43
-11  42   40
-10  35   31
 -9  42  -37
 -7  42   42
 -6  28  -24
 -5  33  -28
 -3  59  -59
  0 107 -106
  3  44  -93
 10  74   76
 13  48   50
 14  44   46

     H 15  2
 13  28  -27
  9  43  -46
  8  44  -47
  7  93  -94
  6  42  -41
  5  67  -66
  4  33  -39
  2  48  -48
  1  46  -45
  0  36  -38
 -2  73   74
 -3  86   88
 -4  36  -42
 -5  35   35
 -7 108  107
 -8  34   40
 -9  43   46
-10  64   67
-12  42  -39
-14  33   36
-17  94  -96

     H 14  2
-15 126 -127
-11  79  -81
-10  42  -45
 -9 106 -109
 -8  75   71
 -5  37   37
 -3  39  -36
 -1 169  169
  0  72   71
  1  90   90
  2  85  -86
  4  36   39
  5  34   34
  8  33   33
  9 143 -150
 13  47  -46
 15  97 -100
 16  45   44
 17  29  -27
 19  54   55
 20  34  -31

     H 13  2
 20  44  -43
 19  58  -57
```

**Column 6**

```
 18  80   79
 17  50  -51
 16  39   35
 12  29  -30
 10  57   60
  9  57   56
  8  62  -67
  7  61   59
  6  72  -74
  3  71   70
  2  79  -79
 -3  37  -37
 -5  37  -37
 -6  40   26
 -7  69  -71
 -8  90   88
-10  63  -65
-17  89   88
-18  78  -75
-20  41   44
-23  31   27

     H 11  2
 24  49   50
 23  39  -39
 21  47  -44
 18  79  -80
 17 160 -166
 16  26   29
 14  40  -41
 13  25   31
 11  51  -53
 10  37  -44
  9  41   49
  8  40  -49
  7 162  165
  6  71   73
  4  65   66
  3  69   68
  2  59  -58
  1 133  129
 -1 143 -137
 -2  74   73
 -3  59  -60
 -4  96  -93
 -7 158 -149
 -9 141 -134
-10  59   58
-11 107  105
-13  51  -47
-14  36   45
-15  27   29
-16  68  -68
-17 135  130
-18 102  102
-19  94   92
-23  94   86
-24  39  -27
-25  46  -36
-26  54   39
-27  58  -44

     H 10  2
-27  72  -54
-26  66   42
-25  66  -58
-23  82  -79
-21  78  -76
-18  64   62
-17  46  -47
```

*Table 3. Continued.*

```
-15  71   64      -6 180  166      1 123  113      -8 128 -125     -18  76  -78      -8  36   34
-14  30  -22      -5  38  -35      2 176 -168      -7  89  -88     -17 102  101      -6  76  -69
-13 152  150      -4  83  -76      3 379  392      -6  36  -31     -16  47   47      -4 216 -228
-11 102   99      -3  55   49      4 180  177      -5 103   92     -15 225  232       4 228 -242
-10  77  -78      -2  30  -34      5  31  -35      -4 179 -154     -14  84  -84       8  68  -67
 -9 106  109      -1 127 -120      7  83  -87      -3 219  197     -13  91   92      10 369  367
 -8 117  101       0  85  -77      8  97  102      -2  23  -14     -12  36  -23      12 176 -188
 -6  76   75       1  54  -54      9  48   51      -1  97  -87     -11 194  195      14 245  249
 -5  44  -40       3  32   29     10 133 -144       1  56  -53     -10  50   52      16 156  151
 -4  35  -33       4 121 -124     11 231 -244       3 229  229      -9 337  347      18  67  -67
 -3 148 -142       5  21   25     12  84   92       4 153 -154      -7 100  -99      22 121  114
 -1  74  -72       6 199  198     13 222 -237       8 162 -175      -6 102 -105      24 104 -100
  0 217  209       7  74  -76     14  81  -90       9  69   76      -5  82  -79
  1 151 -146       8  95  -97     15  52   54      10  33   31      -4 393  381          H 17 3
  2 114 -110       9  89   93     17  92  -52      11  83  -90      -3  87  -76       8  60   56
  3 128 -128      10  82   85     19  65  -70      12 228 -241      -2 199 -172       7  39   38
  4  61   60      11  42   42     20  35   35      13  76  -78      -1 372 -341       6  38  -37
  5  23  -22      12 110  116     21 124  126      14  21   23       0 129 -123       0  63  -65
  6  93   92      14  92   97     22  61  -61      15 112  114       1 329 -319      -6  31  -34
  7  29   31      15  26   27     23  69   67      16  58  -57       2  44  -28      -7  31  -23
  8  63   64      17  62   63     25  40   35      17  43  -42       4 286  307
  9  66   71      18 103  105     27 111  107      19  97  -98       5 180 -195          H 16 3
 10  90  -95      19  55  -53     28  41  -46      21  86   84       6 186 -204     -14  54   55
 11 117  120      20  34  -33     30  41   38      22  69   70       8 193  195     -12  32  -34
 12  74   80      22  69  -67     31  29  -37      24  55   58       9 302  313     -10  47  -48
 13  77   82      25  41  -40                      25  64  -60      10  38  -41      -8  46   44
 14  69  -74      28  37  -39         H 5 2         26  55   50      11 144  143      -6  54  -54
 15  81   85                      28  89 -104      27  63   64      12  66  -62      -4  45  -50
 17  36   42          H 7 2       26  67   71      28  35   37      13  88   91      -3  43   48
 18  29   29      30  39  -44     25  31   32                       14  92  -91      -1  40  -40
 20  37  -34      29  66  -72     24  57  -62          H 3 2        15 236  240       1  28   36
 21  81  -81      27  24  -27     23  41  -41      32  75   98      16  76   75       2  41  -40
 22  39  -40      24  30   31     22  48   50      31  33   45      17  40   37       4  96  102
 23  29  -28      22  64  -64     21  72  -74      29  62   79      18 107 -107       7  39  -35
 24  40   41      21  58   59     20  60   60      26  41   47      19  27  -26       9  35   42
 25  69  -69      20  97   98     19  71  -72      25  28  -32      20  91   92      10  50   49
 27  63  -56      19 156  156     18  98   95      24  60   65      21  55  -56      11  40  -40
 28  53  -56      17  34  -37     17  32  -36      23  35   40      23 111 -101
                  16  37   42     16  45  -50      22 190 -194      24 118 -107          H 15 3
     H 9 2        15  53   55     15  81  -81      21  60  -56      25 129 -120      12  32   36
 26  55   54      13 101  108     14 197  204      20 106  105      27  28  -29      10  64   68
 25  51   52      12  38   43     13  20  -17      19 130 -126      28  25   30       8  51   51
 24  32  -33      11  35  -38     12  46  -48      18  62  -60      29  53  -55       6  27  -26
 23  40  -36      10 165 -176     10  52  -58      17  68  -68      33  30   42       2  52  -53
 21  48   47       9 153 -161      9  94  105      14  56  -57                        1  38   35
 20  65  -61       8  21   16      8  83   88      13  75  -78          H 1 2         0  98  -99
 19  66   69       7  32  -31      7 153  168      12  18   16      33  41  -56      -2  86  -82
 18  50   53       6  79  -82      6  39   41      11  42   49      31  47  -67      -6  34  -37
 16  86  -91       5 169 -172      4 118 -120      10  75  -77      30  52   72      -8  54   58
 15  42   44       4  53  -51      3 169  162       9  64   69      27  37  -46      -9  59  -57
 13  72   72       3 120 -114      2  77  -71       8 168  114      26  23   27     -10  43   47
 11 124 -129       1  58   53      1  56   55       7 149  155      25 337  -46     -11  30   31
 10 114  118      -1  23  -23     -1  61  -57       6  19  -18      24  62  -66     -12  61   60
  9  63  -67      -2  36  -22     -2  30   23       5 157  177      23  84   89     -14  47   48
  8  42   44      -3  87   80     -3 192 -171       3  75   78      22  93   86     -16  56   60
  6  40   41      -4  77  -65     -4 161  147       2 235  232      20  58  -58
  5 176 -180      -5 175  161     -6  70  -67       1  84  -84      19  72   73          H 14 3
  4  66   63      -6 191  178     -7 176 -180       0  54  -55      17 215  213     -18 111 -107
  3  56  -56      -7  88   81     -8  31  -22      -1  68   64      16 134 -130     -16  71  -76
  2  30   35      -8  76  -72     -9 110 -110      -2 101  -93      15  46   44     -14  37   41
  1  93   87      -9 106  100    -10  83  -80      -3  62  -54      14 133  131     -12  55  -52
  0  34   34     -10 157  151    -11  47  -45      -4 106  -92      13 107 -114      -9  55   56
 -1  62  -58     -12 138  138    -12 132  132      -5 199 -197      12  19   18      -6 159  163
 -2 102  -97     -13 136 -126    -13  58   59      -6 100  103      11 178  176      -6  29   36
 -4  27  -26     -14  23   21    -14 193 -159      -7 133 -136      10 158  152      -2 172  172
 -5 256  238     -15  89  -85    -15  59   56      -8 195 -197       9  63  -65       0  54  -56
 -6  90  -89     -16  70  -65    -16  34   41      -9 128 -128       7 251 -265       1  70  -71
 -7  25   24     -17  35   32    -17  76   78     -10 159  157       6 257  264       2 107 -108
 -9  58   60     -18  49   56    -18 103 -104     -11  50  -56       4  65   59       3  45   48
-10 178 -171     -19 118 -124    -19  61   62     -12  85  -87      -5 111 -105       5  45  -48
-11 110  102     -20 103  -94    -21  87   84     -13  64   63      -6 245 -247       6  76  -77
-12  76   74     -21 138 -134    -22  90  -90     -14 132  135      -7 241  250       8 147 -154
-13  38  -35     -22  42   42    -23  32   31     -15  74   81      -8  32   25      10  57   57
-14  66  -66     -23  47   44    -24  53   51     -16  98 -100      -9 154  157      15  40   48
-15 112 -107     -29 106  100    -26  40  -37     -17  39   42     -10 244 -247      16  83   86
-16  53   53     -31  41   42    -27  48  -53     -18  87   86     -11 204 -205      18  61   81
-17  39   36                     -28  35   32     -19 160  160     -13  51   55
-18  45  -45          H 6 2      -29  35  -31     -20 105 -104     -14 185 -191          H 13 3
-19  98  -98     -31  50  -49    -31  51  -47     -21  71   67     -15  45   52      20  30   25
-20  58   58     -30  49   44    -33  50  -41     -22 152  152     -16 144  151      19  36  -35
-21  84  -81     -29  37   36                     -23  29  -27     -17 273 -289      17  35   31
-22  32  -23     -28  47  -42         H 4 2       -24  37  -37     -19  69  -72      14  60  -65
-23  62   56     -27 136  127    -33  36   34     -28  53  -49     -20  25   24      13  24  -23
-24  60   56     -24  58  -58    -32  40   35     -29 102  -99     -22  84  -83      10  63  -67
-26  39  -34     -23 109  102    -31  83  -79     -31  57  -57     -23 123 -122       8  49  -46
-29 103   96     -21 155  150    -30  37  -33     -32  32  -29     -24  69   71       6  65   62
                 -19 116 -118    -29  45   43                     -25  27   29       4  71   77
     H 8 2       -17  56  -60    -28  60   55          H 2 2       -27 102  101      -2  77   77
-29  27   23     -16  80  -79    -27  68   65     -34  63   58     -28  27   25      -3  36  -36
-25  45  -45     -13 275 -280    -26  39  -32     -33  64   54     -30  44  -41      -4  36  -36
-24  29   18     -11 219 -217    -25  97  -93     -32  57  -52     -31  70   66      -5  32   30
-22  52  -45     -10  58  -58    -24  88   88     -31  32  -33     -33  92   86      -7  27  -23
-20  44   46      -9  69   64    -23  35   30     -30  41   38                       -8  58  -56
-19  31  -31      -8  73   66    -21  86   85     -29  42  -39          H 0 2       -10  44  -43
-17  53   55      -7 168 -166    -19 131 -129     -27  33  -34     -34  36  -28     -11  75  -73
-15  62   64      -6  58   49    -16  53   53     -25 156 -154     -32  63   60     -12  48  -49
-14  75   67      -5  38   35    -15 135  138     -24 133 -129     -26  52  -53     -15  74  -79
-13  52  -55      -4 151  149    -14  67  -61     -23 106 -105     -24  76   76     -16  72  -74
-12 146  138      -3 431  404    -13 163 -167     -22  65   70     -22  42   42
-11  48   46      -2 152 -138    -12 148 -148     -21  46  -47     -16 197  210          H 12 3
 -9  40   37      -1  80   72    -10  28   27     -20  50   53     -12  31  -35     -21  57   64
 -8  61  -60       0 195  184     -9  81   80     -19  51  -52     -10 212  212     -18  50  -48
```

*Table 3. Continued.*

```
-17   31   31      23   24  -23       3   37   36      -2   74   67       5   52   51      13  116  119
-16   33  -39      22   88  -87       2  276 -273      -3   51   42       4  128  131      12   21  -22
-15   58   55      19   55  -54       1   21   24      -4   31   29       2  177  175      11   65  -63
-14   31   34      18   85   87       0   94   88      -5  135  125       1   45  -42      10  247  252
-10   32  -36      17   59   60      -1   35  -33      -6   45   43      -1   25  -23       9   88   78
 -8  107  108      16   28  -28      -2  183 -169      -7  142 -137      -2  167  151       8  192  197
 -5   67  -68      14   24   23      -3  127  117      -8  149 -142      -3   25  -20       6  119 -125
 -4   45  -44      12  225  233      -4  219 -202      -9   82   76      -4  240  217       5   18  -19
 -2   67   66      10   30   27      -5   68  -69     -10  133 -133      -5   41   39      -5   76   80
 -1   62  -62       9   45   51      -6   73   70     -11  133 -133      -6   97  -99      -6   51  -59
  1   63   62       8   88  -88      -7  125  120     -12   55  -58      -7  154  145      -7  164 -167
  2   73  -70       6  125  127      -8  127  117     -13   36   36      -8  115 -114      -8   52   50
  4  101  101       5   42   42      -9   90  -89     -14   90  -92      -9   36  -34      -9  230  249
  6   79  -80       4   33  -33     -10   23   25     -15   63  -65     -11   89   96     -10  338  359
  7   52  -53       2  174 -171     -12  170  165     -16  122 -124     -12  214 -217     -11  108 -110
  8   61  -62       1   49  -50     -13  157 -162     -17   77   78     -13  110 -111     -13  120  127
  9   83   84      -1   33   33     -14   57   58     -19   87  -89     -14  164 -176     -14  136  149
 10   30   29      -2   87  -83     -15   64   62     -21   97   99     -15  124  131     -15   24  -19
 11   34  -33      -3   91  -87     -16   61   60     -22   48   46     -16   55   58     -16  154  165
 14   53  -55      -4  153 -147     -17   61  -62     -24   27   24     -17   24  -23     -17   57   61
 15   36  -33      -5   35   35     -18   80   81     -25   34   31     -18  118 -123     -18   61  -61
 16   87   96      -6  182  175     -19   53   54     -26   58   60     -19   27   22     -19   82  -86
 19   36  -34      -8   63  -62     -22  127 -123     -27   29   27     -20   30  -29     -20   32  -35
 22   48   48      -9   73   74     -26   38  -35     -28   36   34     -21   85  -89     -21   64   68
                  -11   70  -70     -27   47   42     -32   50  -45     -22  129  132     -22   48   54
   H 11  3        -12  187  180     -28   93  -95                      -24   56   54     -23   88  -91
 24  103   97     -13   93   53                        H  4  3        -25   79  -81     -24  148 -153
 22   28   25     -14  135  138       H  6  3         -32   51  -46     -26   40   35     -25   29  -23
 19   44   46     -16  104 -103     -31   36   38     -31   79  -78     -28   40   43     -26   83  -80
 18   58   60     -17   44   49     -30  125  121     -30   47   45     -33   39   38     -28   41   41
 16   71  -71     -18  105  110     -28   69   64     -27   69  -72                      -30   53  -55
 15   36   31     -19   49  -46     -27   30   28     -26   33  -34       H  2  3        -31   21  -20
 14  108 -109     -22  102  -94     -26   60  -61     -25   60   58     -34   60  -59     -32   27  -28
 12   41  -44     -23   65  -66     -24   67   65     -24   74   79     -33   50  -46     -34   80   78
 11   30   29     -27   35  -26     -21   48  -49     -23   29  -28     -32  113 -110
 10  109 -111     -28   68  -66     -20  213 -213     -21   60   57     -31   51   48       H  0  3
  8   86  -89                      -18   53  -48     -20  125 -127     -29   29  -31     -33   85   87
  6   75   78       H  8  3        -16   44  -44     -19   52   52     -28   52  -49     -25   70   80
  1   50  -55     -29   82   81     -14  103 -101     -18  116  118     -27   39   38     -23   82  -86
  0  175  162     -25   30   26     -12  132  135     -17   43   45     -26  105 -107     -21   70  -71
 -1   62  -58     -24   31   28     -10   57   59     -16   53   60     -24   66   69     -19   39  -45
 -2   47   40     -20   27  -30      -6  396  374     -15   51   49     -23   31   29     -17   63  -70
 -3   35   40     -19   56  -51      -5   87   78     -14  181 -188     -22  105  106     -15   84  -86
 -5   52  -47     -18   86   87      -4  272  250     -12  113  114     -21   30  -32     -13   41   35
 -6   88   86     -15   53  -52      -3   33  -31     -10  177  177     -20   40   37     -11   82   91
 -7   44   40     -14   95  -97      -2  147 -132      -9  103 -100     -18  175  182      -5  116  107
 -8   35  -26     -13   26   26      -1   58   56      -8  174 -172     -17   39  -28       7   82  -82
-10  183 -180     -12   66   61       0   42   40      -7   61  -61     -16  150  157       9   65   62
-11   58   64     -10   83   86       1   28  -30      -6   45   44     -15   55   53      11  151 -156
-12   34  -34      -8   75  -75       2   82   80      -5  161 -150     -14   33  -32      13   71   71
-14   86  -90      -7  120  119       3   28  -26      -4  176  160     -13   20   24      15   27  -32
-15   60   58      -6   70  -67       4  343 -349      -3   62   49     -12   90   93      17   47   42
-16   79  -79      -5   37   35       5   93  -94      -2  182 -160     -11   86  -93      19   26   24
-17   63  -61      -4   30   26       6  200 -205       0   99   86     -10   51  -55      21   84   78
-19   64   62      -3   53   49       7   66   71       2  110  104      -9  124 -116
-20   48   46      -2   32  -28       8   82  -86       3   89  -92      -8  371 -383       H 17  4
-24  107  108      -1   81  -74       9   62  -63       4  217 -223      -7   47  -41       7   52   54
-26   70   66       0   35   34      10   99 -109       5  211  227      -6   66  -65       4   39   34
                    1   95   91      11   60   64       7   34  -32      -5   82   78       1   54   49
   H 10  3          3   86  -86      12   70  -75       8  184  201      -4   83  -83      -1   37  -30
-27   39   36       4   21  -21      13   44  -47       9  100  109      -2  272 -247      -4   73  -80
-26   42  -32       5   26   29      14  116  123      10  269 -292       0   52   48      -7   29  -25
-23   39   38       6   56   60      18  134  134      11   75  -77       2  197  209      -8   50  -47
-20  108  106       7  168 -174      19   31   30      13  111  116       4   65   68
-18   65   65       8   95   86      20  160  160      14  151  155       5  146 -155       H 16  4
-17   33   34       9   56   59      23   25   26      15  128 -132       6  195  208     -14   37   35
-16   70   69      10  119 -126      26   51   49      16  123 -125       7  183  195     -13   51  -59
-14   79   79      11   61  -59      28  107 -100      17   52   50       8  321  326     -12   52   57
-13   45  -41      13   32   34      30  118 -106      18   54  -54      10   35  -28     -10   63   71
-10  116 -118      14   85   87                       19   59  -58      11   93   96      -7   46  -50
 -9   33   36      15   40  -42       H  5  3         20  150  146      13   83  -89      -2   68  -65
 -8  116 -116      16   62  -63      31   35  -29      21   24   25      15   42   39       0   48  -51
 -7   70  -69      17   63   60      29   37   35      22   77  -75      16  192 -192       3   63   70
 -6   93  -87      18   67  -69      28   41   39      23   25  -26      17   67  -64       5   51  -53
 -4  152 -145      19   30  -31      27   45  -42      24   31  -29      18  142 -140       8   50   58
 -1   47   49      20   41   39      26   49   44      26   54   52      19  101   98       9   28   38
  0   45  -33      22   40  -39      25   61   57      28   33  -33      20   67  -63      12   58   61
  1   76  -75      23   23   21      24   49   46      32   41   34      21   38  -34      13   42  -45
  2   87   86      24   27  -21      23   34  -30                       22  125 -127
  3   65   65                       22   26   27       H  3  3         25   26   30       H 15  4
  4  113  111       H  7  3         21   24   27      33   39  -33      26   95  102       9   27   34
  6   97  100      30   49   43      20   59   57      31   38   34      28   23   15       8   43  -46
  7   57   62      28   85  -79      19   30  -28      28   40   33      30   31   37       7   70   73
  8  104  108      26   61  -58      18   42  -42      26   52   48      32  133  114       3   35   38
  9   74  -75      23   34   35      17   70   72      25   39  -37      33   33   31       2   68  -71
 10  136  144      22   91  -88      16   54  -55      24   38   35                       -2   35   38
 11   65   66      21   40  -42      15   23  -23      23   54   52       H  1  3        -3   44  -43
 12   43  -43      20   84  -80      14  133 -139      22  112  106      31   44  -42      -4   35   33
 13   44  -48      18  106  106      12   57  -63      21   89  -90      30   84  -77      -6   30  -32
 14   46  -47      17   25  -18      11   39  -41      20   36   34      29   29   27      -7   69  -76
 15   34   33      16   42   41      10   59  -61      18  118 -116      28   26   22      -8   82   81
 16   80  -82      15   27   25       9   19   20      16   22   20      26   29  -26     -10   40  -37
 17   44  -47      14   53   52       8  135 -140      15   52   53      25   37   33     -17   44   53
 18   67  -64      13   63  -67       7   47  -49      14   65  -67      24  168 -156     -18   46  -43
 20  106 -105      12  135  139       6   73  -75      13   58  -58      23   88  -77
 23   34   30      10   41   45       5   39   43      12  223 -231      22   26  -28       H 14  4
 26   42   34       9   49  -49       4   88   88      11   25   25      21   46   46     -17   30   34
                    8   43   45       3   99   91      10   89  -94      20   40   41     -16   58   59
   H  9  3          7   48   49       2  103  103       9   43  -46      18  101 -104     -15   59   59
 27   27  -26       6  145  150       1   71  -67       8   39  -41      16  125  121     -11   68   71
 26   52  -48       5   55   57       0   98   92       7   86   88      15   43  -47     -10   31   30
 24   35   31       4  156 -158      -1   41  -37       6   55  -59      14  186  190      -9   91   85
```

*Table 3. Continued.*

Column 1:

```
-7    73  -75
-5    28  -23
-4    46  -44
-3    38   37
-2    32  -34
-1   117 -116
 0    47  -49
 1    40  -40
 4    89  -89
 5    37  -40
 6    36   27
 7    32  -34
 9   122  131
13    65   55
14    51   52
15    77   75
19    40  -43

H 13  4
20    38   32
18    40   36
17    33   35
16    68   69
15    51   51
14    35  -40
 8    53  -56
 7    64  -64
 6   108 -107
 4    32  -30
 2    37  -38
 1    37  -35
 0    44  -43
-2    96   96
-3    55   55
-5    31  -29
-6   102  102
-8    81   79
-9    53   58
-10   39   35
-12   58  -59
-14   92   87
-16   71  -71
-17   48  -53
-18   81  -80
-20   32  -37

H 12  4
-22   52   51
-19   30  -32
-16  109 -105
-14   76  -78
-13   48  -48
-11   27   24
-10  104 -102
-9    63   62
-8    69  -64
-7    40  -36
-4    62   61
-3    41   43
-2    32   28
 0   146  140
 2    28   23
 3    80   74
 4    55   56
 5    87  -83
 8    24  -23
 9    58   57
10   109 -111
13    51  -52
14    98 -102
15    61   62
16    47  -47
20    51   49
21    30   29
23    34  -31
24    32   33

H 11  4
24    46  -42
23    60   61
22    32   31
21    48   44
20    38  -42
18    26  -18
17    82   78
16    30  -30
15    43   42
13    33  -32
11    54   55
10    44   47
 9    42  -44
 8    26   32
 7   111 -113
 6    55   58
 5    40  -38
 4   129  126
 2    65  -59
 1    88  -83
-1    57   51
-2    28   31
-3    71   56
-6   165 -159
```

Column 2:

```
-7    50   48
-9   116  110
-10   79  -78
-11   66  -68
-14   30  -30
-16   61   64
-17   48  -49
-19   67  -64
-20   83   80
-23   80  -80
-27   47   48

H 10  4
-27   48   43
-25   57   56
-24   92   87
-22   48  -47
-21   66   55
-20   60   40
-19   39  -37
-13   79  -77
-11   65  -65
-10   43  -45
-7    24  -22
-6    67   66
-5    26  -27
-4    81  -78
-3   129  119
-2    46   42
-1    66   61
 0    55   54
 1   100   96
 3    59   59
 4    77  -74
 6    98   96
 7    33  -33
 8    72  -73
11   112 -114
12    46  -48
13    66  -68
14    36   34
16    61  -61
18    52   53
19    28  -25
21    69   63
22    26   26
23    39   39
25    57   53
27    38   33

H 9  4
27    42   36
24    26   28
23    60   58
22    50  -47
21    27  -29
19   102 -100
18    89  -89
17    44   46
16    32  -34
14    64  -63
13    89  -90
12    30  -32
11    97  100
10    43   44
 9    68   68
 8   113  115
 7    66  -68
 5    99   92
 3   132  123
 2   141  131
 1    72  -70
 0    57  -53
-1    54   51
-3    51  -49
-4   111 -105
-5   174 -166
-7    60   58
-8   147 -140
-11  132 -128
-12   67  -68
-14  119  116
-15   96   92
-16   35   41
-17   81  -80
-18   96  100
-19   51   53
-20   40   31
-21   65   66
-22   75   74
-24   30  -26
-28   39  -38
-29   58  -51

H 8  4
-28  107 -104
-24   73  -69
-22   72  -68
-20   47  -50
-19   73   76
-18   44   47
-17   48  -47
```

Column 3:

```
-14  120  121
-13   74   71
-12  189  183
-10   56   56
-9   113 -109
-8    55   50
-7    62   59
-6    37   37
-5    42   42
-4    48  -44
-3    83  -75
-2   122 -113
-1    38   37
 0    40   38
 1    83  -80
 2   172 -167
 4    47   45
 5    83   85
 6    35  -35
 8    65   68
 9   122 -127
1C    64   65
11    81   85
12   183  190
15    51  -54
16    78   78
19    46   50
20    27  -25
21    27  -32
22    63  -61
26    50  -46
28    29  -33

H 7  4
29    82   75
28    52  -50
26    27   26
25    32  -27
24    48  -45
23    35   33
22    44   42
20    34   36
19   112 -111
18    44   48
17    35  -35
15    23  -21
14   117  119
12    30  -31
11    73   77
10    39  -39
 9    39   36
 8    21  -19
 7    54   53
 6    50  -50
 5   161  158
 4    72  -72
 3    97   92
 1   103  -96
 0    48   45
-1    49   43
-2    92  -81
-4   169  159
-5   184 -169
-7   121 -115
-8    59   54
-10   27  -26
-11   81  -73
-12  116  114
-14  185 -182
-18   50  -54
-19   81   79
-20   66  -76
-21   75   76
-22   42  -41
-23   63  -62
-24   58   56
-26   52   48
-29   40  -31
-30   67   62
-31   36  -34

H 6  4
-30   34  -32
-29   58  -61
-27   36  -32
-26   33  -32
-25   40   37
-24   55   54
-23   95  -93
-22   78  -69
-21   67  -67
-20   68   73
-19   61   57
-15   36   36
-14   25  -22
-13  136  136
-12   68   68
-8    31  -34
-7   130  123
-5    80  -80
-4   130 -117
-3   277 -255
```

Column 4:

```
 0   122 -113
 1    47  -41
 2    30  -26
 3   284 -279
 4    89  -92
 5    46   45
 6    80   82
 7    62   63
 8   140 -143
10   124  133
11    68   70
12    44  -46
13   145  149
14    68   67
16    46  -48
17    94   95
18    73   77
19    27   26
20    33  -34
21   151 -148
22    37   38
27   104  -95
31    62   54

H 5  4
31    49  -43
30    77  -67
29    37  -33
26    32  -31
24    48   46
23    35   32
22    31  -29
20   120  117
19    49   40
17   107  108
15    41   40
14    44   44
13    54  -54
11    19   19
10   135 -139
 8    18  -18
 7   122 -126
 6    64  -69
 5    37  -46
 4   212 -207
 3    83  -83
 2    30  -27
 0    45  -36
-2    87   77
-4   135  119
-5    36   39
-6   246  233
-7   136  137
-8    97  -91
-9    50   49
-10  222  219
-13   26   31
-14   30  -29
-16   67  -69
-17   91  -93
-18   70   75
-19   40  -31
-20  196 -201
-21   34  -31
-28   37   37
-30   91   88
-31   50   49

H 4  4
-32   61  -58
-31   45   40
-30   33   27
-26  120  124
-25   76   70
-24   27   20
-23   43  -46
-22   87   89
-21   64  -65
-20   37  -34
-19  112  113
-18   72  -73
-16   86  -85
-15  113 -113
-14  114 -112
-13  131  135
-12  148 -151
-11   36  -28
-10  157 -158
-9   170 -171
-7   161  156
-6    52  -47
-4    68   63
-3   194 -173
-2   160  137
-1   151  139
 0   359  324
 1    88  -82
 2    57   59
 3   184 -182
 4   116  119
 5   175  183
 6   100 -104
```

Column 5:

```
 9   213 -225
10   174 -181
11   101  102
12    63  -63
13    46   48
14   151 -152
15   127 -129
17    70   72
18   136 -137
19    66   65
20    30   27
21    97  -94
22    22   17
24    66   61
25    53   52
26    48   49
27    44  -42

H 3  4
30    46   45
29    30  -36
28    27  -32
27    36  -36
26    70   74
24    45  -43
23    29  -26
22    26  -26
21    62   62
20    62  -64
19   130  126
17    29  -28
16    83  -84
15    24   27
14    31   33
13    72   75
12    21   22
11    71  -74
10    22   23
 9   119 -126
 8   173  184
 7    36  -38
 6    41   45
 5   143 -148
 4    51   56
 3    94  -92
 2   131  128
 1    39   37
 0   158  146
-1    55  -46
-2   341 -302
-3    72   65
-5   213  205
-6   126 -131
-7    44   48
-8    72  -70
-9    81   79
-10  182 -186
-11   87   89
-12  135  139
-14  137 -142
-15   80  -77
-16  144  154
-17   31   31
-19   53  -54
-20   62   64
-21   98 -101
-22   32   32
-24   83   83
-25   28   29
-26   94  -99
-31   27   22
-32   71  -74

H 2  4
-31   49   49
-30   65  -65
-28  113  115
-27   28   24
-26   57  -57
-25  110  114
-23   31   30
-22   49   50
-21   31   32
-20   72   78
-19   36   29
-18   82  -93
-16   69   77
-15   77  -87
-14   31  -29
-11  126 -125
-10   60   55
-9   152 -152
-8    88  -88
-7    67   71
-5    31   30
-2    20   18
-1    96   91
 0   141 -129
 1   140  134
 2    62   65
 4    70  -69
 5    77   82
```

Column 6:

```
 6    66   68
 8   136 -141
 9   177 -182
10   137  143
11    66  -66
12   122 -124
13    54  -57
14    96   98
15   134 -137
16    49  -53
17    19   23
18    53   50
22    56   54
23    91   94
24    35  -38
25   102  111
26    26   28
28    28   30
29    43   41
31    29   31
33    44  -56

H 1  4
32    44   59
31    53   72
28    60   70
27    36   41
26    26  -30
25    53   58
24    26   30
23    95 -103
21    56  -60
20    26   27
18   155 -153
17   133 -128
16    68  -67
15    75  -75
14    44  -40
13    44   46
12    19  -23
11    91  -52
10    67  -64
 8    76   72
 7   285  293
 6    99  108
 5    47  -51
 4    27   28
-7   181 -192
-8   216 -224
-9   126 -132
-10   93  100
-11  101  108
-12   41  -42
-14   86   89
-17  120  120
-18  227  241
-19   37   36
-22   29   29
-23   93  102
-27   71  -73
-28   60  -59
-30   58  -63
-32   62  -62
-33   63  -63
-34   30  -24

H 0  4
-34  112  110
-28   71  -73
-26   37  -37
-24  133 -139
-20  143 -156
-18   22  -18
-16  161  176
-14  137  145
-12   54   53
-10  299  322
-8    91   97
-6   139 -149
 4   138  134
 6   262 -266
 8   264  274
10   109  109
12   159  156
14    92   90
16   184  185
18   134 -135
22    59  -60
24    31  -31
26    39  -48
28    42  -49

H 17  5
 1    58   60
 0    43   44
-1    34   38
-3    77   78

H 16  5
-7    57  -64
-6    41   43
-3    77  -79
```

*Table 3. Continued.*

```
0   29   25        1   25   20       -8   43   31       15   47  -45            H   3   5        12   56   57
1   46   48       -1   27   27       -7   74  -70       16   73   71       29   54   53        11   23  -23
2   31   29       -3   57   53       -6   73  -72       17   39   41       28   29  -20        10   57  -58
3   36   39       -5   94   87       -5  247 -228       18   26  -27       27   42  -52         9  119 -118
4   40  -38       -7  126 -121       -4   57  -55       19   61  -61       25   88  110         8   68  -65
7  107  108       -9   25   21       -3   87  -78       20   69  -64       23   45   55         7   91  -54
                 -10   66   64       -2   90   81       21   23   20       22   25  -26         6   63   63
    H 15  5      -11   44  -46       -1   33   28       22   33   32       20   49  -49         5  105  107
9   80   83      -12   43  -38        0   69  -66                         19   20  -20         4   49   49
6   40   34      -13   36  -35        1   72  -67            H   5   5     18   41   39        -6   76   78
5   65  -61      -15   50  -48        2   23   22       31   34   42       17   79   80        -7   51   56
3   61   62      -19   38  -45        3  229  219       29   27  -39       16   48   48        -8   33   25
1   55  -55      -20   51  -46        4   74   73       25   37  -46       15  129 -122        -9  187 -193
-1   70  -68     -21   72   91        5  113  109       24   30  -37       14   22  -26       -10   82  -83
-6   43   41                          7   52   49       21  131 -137       13   50  -52       -12   41   41
-7   90  -94         H 10  5          8   53  -56       19   37   39       11   60  -62       -13  105 -117
-9   84   89      -26   28  -17        9   52   58       17   24   22       10   47   40       -14   19   19
-11  34   32      -25   30   27       10   45   44       16   23  -25        9  162 -164       -15   72  -73
                 -24   36  -34       11  133  134       14   23   22        8   39  -40       -17  108 -117
    H 14  5      -23  108 -110       13  125 -123       13  131  132        7   47   45       -19   71   80
-17  39   42      -22   65   50       17   71  -70       11  165  168        5  120  123       -20   28   26
-5   46  -47      -21   66   64       19  108 -104       10   20   20        3   52  -54       -23   35   37
-4   27   22      -17   53  -51       20   23  -18        9   38  -40        2  136 -130       -25   67   73
-2   46  -39      -12   26  -25       21   94  -90        6   69  -74        1   66   65       -26   55   38
0   29   28      -11   50  -50       22   30   32        5  106  104       -1  348  310       -27   82   91
5   78   74       -9   76   66       25   31  -27        4   47   47       -2   46  -40       -29   24   21
8   61   60       -7   51   49       27   36   38        3  216 -209       -3  148 -129       -32   29   26
10   57  -57       -5   97  -96       29   51   59        2   37  -29       -4  111 -104       -33   32  -27
12   32   31       -4   48   42                          1   61  -58       -5   63   62
15   44  -44       -3  100   89           H   7   5      0   67  -59       -6   33   29            H   0   5
16   59  -55       -2   37  -33       27   64  -74       -1   56  -86       -7  115  110       -33  109 -117
19   37  -30       -1   34   30       23   49  -52       -2   34  -28       -8   33  -33       -31   40  -43
                   1   91  -63       22   25   28       -3  140 -125       -9  106 -103       -29   73  -79
    H 13  5        3   28  -28       21   46  -47       -5  106  -93      -11  201 -206       -27   60  -67
19   33  -32        5   97   93       20   33   30       -6   31  -23      -17   25  -23       -23  145  156
18   25  -22        6   55  -54       18   59  -61       -7  210  195      -13   54   58       -21   36  -37
17   26  -23        7  140 -139       17   64   67       -8   36  -37      -14   27  -22       -19  150  164
16   26  -24        8   26   33       16   28   25       -9  138 -130      -15  171 -183       -17  146  155
15  111  108        9   25   27       15   23  -25      -11  132  132      -18   54   55       -15   22  -22
14   29   20       17   84   82       13  100  103      -12   39  -39      -19   72   73       -13   34  -32
13   35   34       19   80  -77       12   77  -77      -13  187  188      -25  167  172       -11  105  112
11   24   16       20   46   43       11  111  114      -15   82   83      -26   26   23        -9  153 -165
9  110  108       21   47   43        9   39  -38      -17   54  -56      -31   63   68        -7  241 -200
8   26   25       22   26  -22        7   51   47      -19   96  100      -33   39  -18        -5   55  -58
6   26  -25       23   51   48        6   31   34      -20   38   35                            5  114  117
5   78  -78       25   28  -30        5   30   26      -21  113 -113           H   2   5         7  102  231
3   44  -42                           3   85  -77      -23   92  -91      -29   90   93         9   28  -25
1   42  -38           H  9  5         2   52   51      -24   27  -26      -27  106 -114        11   49   44
-1  140 -131       27   40   44        1  153 -135      -27   66  -63      -25   40   40        13   34   33
-2   41  -37       26   40   44        0   21   18      -29   64  -68      -23   29   28        15   38  -40
-4   29   27       25   47   52       -1   40   42      -31   34   35      -22   30   26        17  190 -188
-5   89  -86       24   36  -39       -2   63   62                        -20   23  -20        21   83  -82
-6   26  -27       23   79   79       -3  221 -202           H   4   5    -19   89  -93        23   75  -80
-8   34  -35       22   29   25       -4   17  -17      -31   93  105      -17   93   99        27   44   66
-9   66   64       20   64   62       -5   55   52      -28   29   24      -14   48   45        29   32   37
-11  115  112      19   27   29       -6   44   40      -27   73   76      -12   74  -75        31   49   69
-13   33  -34      18   53  -51       -8   27   23      -25   34  -27      -11   76   73        33   27   32
-14   38  -25      17   45  -45       -9   55   57      -24   50  -45      -10   60  -73
-15  130  133      15   25  -24      -10   25   24      -22   33  -31       -9   77  -73            H 17  6
-17   30   32      14   23   22      -12   37  -36      -21  135 -141       -8   89   94         8   39  -45
-19   59  -59      13   92  -90      -13  171  173      -18   21  -38       -6   51  -53         4   33  -36
                  11   89  -82      -15   37  -38      -17  146 -154       -5  120  113        -4   49   55
    H 12  5        9   53  -50      -17   47   49      -15  110 -115       -4   33  -32        -6   35   44
-19   60  -58       8   51   50      -19   32   27      -14   22  -25       -3   24  -26        -7   32  -38
-17  125 -124       6   71  -67      -21   35  -49      -13   36  -37       -1  176 -156
12   59   58        5   22   22      -22   33   32      -11  122  126        1  227  224            H 16  6
-9  104   98        4   48   46      -23   97 -100      -10   30   32        2   17  -20        -8   36   37
-7  128  125        2   70   68      -27   52  -52       -9  109  107        3  119 -123        -2   60   60
-5   72   70        1  178  167      -29   43  -47       -8   70   68        4   90   96         3   56   54
-3   33   34       -1  119  111      -31   40   33       -7   99   98        5   47  -50         2   27   26
-1   47   46       -2   24   17                          -6  115 -103        6   45  -49         6   38   48
1   50  -54       -3  106  100           H   6   5       -5  188  177        7   38   41         8   85  -88
4   63  -64       -4  117  106      -30   36   23       -4   35  -29        8   62  -64        11   25  -22
5  112 -108       -5   32  -31      -28   26   19       -3   77   66        9   55   52
7  102 -102       -6   41  -41      -24   50  -45       -2  131  113       10  116  121            H 15  6
9   83  -81       -7   61   55      -23   68  -63       -1   47   47       11  151 -146        10   54  -56
10   27  -32       -9  120 -110      -22   43   43        0   80  -76       13  121  122         9   27   18
11   36   39      -10   40   40      -21   75   75        1   58  -51       14   26  -29         6   73   73
12   41  -41      -11   52  -45      -18   65  -69        2   56  -54       15   69  -71         8   48   48
13   40  -39      -12   36   36      -15   33   34        3   52  -52       16   60   58         5   45   44
14   68   65      -13  118 -114      -14   65   64        4   93   94       18   47   44         4   50  -48
15   60   58      -14   28  -27      -12   57  -61        5  170 -176       19   40   38         2   37   43
16   35  -24      -15   30  -26      -11   45  -40        7   53  -56       22   27   28        -2   32  -30
17   74   72      -16   34   39      -10   56  -56        8   95  -98       23   61  -62        -5   28  -29
19   70   63      -17   59  -61       -8   54   48        9  174 -173       25   69   76        -6   32   31
23   60   53      -23   74   73       -7   53   45       10   71   74       26   29  -33        -8  103 -106
                 -25   79   75       -5  103  -99       11   30  -32       29   33  -40        -9   66  -68
    H 11  5      -27   57   55       -4   63  -58       15  173  173                           -12   31   35
23   28  -31      -28   25   30       -3   65   63       16   54   57            H   1   5
21   83   77                          -2   42   38       16   54   57       33   33  -54            H 14  6
17   40  -37          H  8  5         -1   51  -47       17   24   25       30   35   45       -15   29   30
16   26   26      -29  122 -121        0   39  -35       19  119  117       27   60   73       -13   30   34
15   36  -35      -25   47  -42        1   38   29       20   53  -51       25   24   32       -12   28  -33
14   29   25      -21  105  104        3   26  -20       21   51   52       24   53   67       -11   41   45
12   39  -38      -20   27   25        4   96   92       22   82   83       23   56   68        -1   28  -28
11   59  -58      -19  129  133        5   81   82       23   32   37       19   78   82         0   37   40
10   25   27      -16   25   29        6   81  -82       25   36  -36       18   29   23         1   48  -46
8   54   52      -15  163  158        7  102 -102       26   45  -50       17   57  -58         3   28  -24
5   32  -35      -14   28  -35        8   37   41       28   32   41       15  131 -130         5   25  -22
4   38  -32      -12   56  -53        9   77   75       29   49  -56       14   54  -53         8   32   32
3  123  118      -11  142 -138       10   62   63       31   43  -52       13   62  -65        10   26  -23
2   34   38      -10   33   26       14   63  -62       32   29  -42                           11   50   49
```

*Table 3. Continued.*

Column 1:

```
14   38   -33
16   25    24
18   32   -26

        H 13   6
17   28    23
16   84   -82
12   25    22
 9   39   -37
 8   98   100
 6   66    65
 5   24   -21
 2   53    50
 1   26   -14
 0   70    69
-1   37    41
-2  124  -122
-3   27   -28
-6   37   -41
-7   37    36
-8   72   -71
-10  76   -74
-12  40    50
-14  50   -54
-16  54    59
-18  51    53

        H 12   6
-16  80    82
-12  68    75
-10  77    76
-6   43   -43
-4   25   -25
-3   28   -28
-2   71   -72
-1   49   -46
 0  150  -148
 4   69   -66
 6   26   -34
 9   26    23
10  107   106
14   98    93
17   30    22

        H 11   6
22   41   -34
20   72    66
19   31    23
18   30    34
14   48    46
13   28    28
12   26    19
10   69   -72
 9   43   -44
 8   33   -33
 7   41   -38
 4   99   -96
 3   69   -67
 2   36    35
 1   25   -26
 0   31   -29
-3   58    60
-4   27    21
-6  104   106
-7   65    63
-8   48   -46
-9   36    31
-10  88    92
-11  40    39
-14  40   -38
-16  46   -48
-17  38   -35
-18  35    28
-21  33   -32

        H 10   6
-25  31    30
-24  57   -53
-23  74    71
-22  86    90
-20  72   -77
-16  63    66
-14  23   -15
-13  80   -85
-12  56   -57
-11  28   -28
-10  99   101
```

Column 2:

```
-7   33   -33
-6   51   -51
-5   29    25
-4  108   108
-2   34   -33
-1   86    82
 0   44   -40
 1   56    54
 2   57    56
 4   23    25
 6   96   -93
 7   32    25
 8  113   115
 9   29   -26
10   28   -23
11   53   -56
12   27   -30
14   36    35
16   44    43
17   26   -30
18   95   -93
20   65    60
23   35    32
24   44   -42

        H 9   6
25   31    26
22   63    58
21   35   -32
18   74    70
16   58    54
14   35    38
13   22   -26
10   44   -46
 9   23    21
 6  108  -110
 4   24   -22
 3   51    45
 2   83   -79
 0   60    59
-2   24   -23
-3   60   -54
-4   97    95
-5   26   -22
-8  123   119
-9   26    27
-11  65   -61
-12  34    33
-13  45    48
-14  53   -56
-15  33    29
-18  94   -96
-21  42    47
-28  36    35
-29  29   -27

        H 8   6
-29  31    33
-28 121   123
-24  73    77
-22  75    77
-20  32    45
-18  70   -68
-16  60    65
-15  55   -57
-14 123  -126
-12  92   -92
-10  23    22
-9   50   -42
-8   76   -71
-6   60   -53
-5   68    66
-4  104    98
-2  112   103
-1   23   -23
 2  185   178
 3   28    23
 6   46   -46
12  195  -190
14   30    30
15   34   -36
16   47   -47
19   28    27
20   57    54
21   27    26
22   98    90
23   47   -41
```

Column 3:

```
25   24    16
26  119    97
27   26    19
28   45    39

        H 7   6
28   83    76
26   39   -39
24   24    26
22   23   -19
20   65   -60
18   84   -82
17   78   -75
16   20    18
15   20   -17
14   81   -79
13   25    20
12   25   -26
11   21   -19
10   70    71
 8   57   -56
 7   44    49
 6   22    22
 5   39    40
 4  124   118
 2   51    50
 1   25   -23
 0  126  -119
-1   39   -37
-2  135   121
-4  163  -151
-5   41   -37
-6   57   -56
-7   83   -79
-9   24   -22
-10  36    35
-12  86   -84
-14 122   122
-15  37    38
-17  57    56
-19  53    75
-20  85    88
-21  33    33
-22  54    59
-24  45   -46
-27  27    24
-29  54   -49
-30  69   -70
-31  46   -47

        H 6   6
-31  27    31
-29  51   -52
-28  25   -16
-27  47   -51
-26  33    25
-25  33   -32
-24  74   -80
-22  65    67
-21  90   -85
-20  78   -58
-19  50   -40
-18  23    29
-17  64    66
-15  49    46
-13  27    21
-12  64   -65
-11  62    63
-10  62    63
-9   52    57
-8   20   -17
-7   36    29
-6   26   -25
-5   21   -25
-4   70    71
-3   67   -58
-2   34   -31
-1   44   -45
 1   20   -18
 3   54   -51
 4   51    53
 5   53   -51
 6   64   -67
 7   73    73
 8   77    83
 9   38    43
10   31   -36
```

Column 4:

```
11   18    19
12   27   -29
13   24    20
14   32   -34
15   98    96
16   32    35
18   66   -66
19   32   -34
20   57    58
22   37   -33
25   31   -23
27   30   -24

        H 5   6
30   55    56
29   27   -26
28   32    33
24   36   -33
22   54    51
20  141  -137
18   60   -56
17   46    49
14   80   -80
13   40   -40
10  146   155
 8   34    33
 7   30   -29
 5   89   -88
 4  272   275
 3   36    33
 2   49   -46
 1   32   -29
-1   55    52
-4   82   -72
-5   54    44
-6  291  -267
-7   60    58
-8  113   113
-9   50    49
-10 133  -139
-11  33   -28
-12  85   -92
-14  41    41
-16  87    94
-17  46   -49
-18  42   -39
-19  40   -64
-20 133   143
-22  33    36
-24  36   -40
-26  46    48
-29  37    39
-30  74   -76
-31  40    38

        H 4   6
-32  60    60
-30  60   -60
-27  27   -25
-26  86   -85
-23  27   -27
-22  99  -109
-20  31    30
-19  30    30
-18  43   -44
-16  95   101
-15  28   -24
-14  65    74
-13  34    37
-12  84    81
-11  33    33
-10  26    29
-9   46   -50
-6   33    32
-5   60    58
-4  165  -151
-3   51    46
-2  107   -98
-1   87   -76
 0  194  -178
 1   36   -35
 2   95   -92
 3   68    68
 4  120  -125
 5   33    37
 6   56    60
 7   37   -39
```

Column 5:

```
 8   34   -34
 9   23    29
10  110   108
11   21    17
12   39    37
14  147   145
18   49    47
20   76   -71
22   33   -31
23   32   -37
24   80   -70
26   27   -25
28   76   -63

        H 3   6
30   67   -55
28   54    47
26   86   -74
24   30    33
22   64    58
21   37    33
16  160   149
15   25    21
14   44   -33
13   46    49
12   75   -76
10   71    68
 9   52   -55
 6  106  -114
 5   24   -26
 4   35   -36
 3   45   -39
 1   64   -55
 0  162  -150
-2  252   228
-3  103    91
-4  101   -96
-5   64    62
-6  132   129
-8  159   159
-9   46    45
-10 113   109
-11  45    51
-12  87   -93
-13  44   -48
-14 134   140
-15  20   -27
-16  81   -91
-17  32   -30
-18 102  -104
-19  52   -57
-21  40   -43
-23  29   -29
-24  80   -68
-26  36    39
-27  29    25
-28  25    26
-29  37    45
-32  63    62

        H 2   6
-30  55    53
-28  78   -88
-27  37    41
-26  57    66
-25  52    59
-24  52   -61
-23  57    63
-22  24   -28
-18  79    90
-16 125  -142
-14  34    37
-13 104  -113
-12  58    61
-11  69   -74
-10 106  -112
-8   48    51
-7   21    15
-6  142   148
-4   40   -40
-3   41    31
-1  148   133
 0  142   129
 1   98   100
 2  154  -164
 3   33    31
```

Column 6:

```
 4  134   146
 5   18    15
 6   99   105
 8   59   -63
10   54   -49
11   91   -89
12  118   114
13   44   -46
14  129  -124
16   24    21
17   24   -25
18   33    28
22   89   -78
23   34    34
24   49    50
26   46   -49
27   30    32
30   23    25

        H 1   6
32   74   -66
28   45   -54
24   23   -25
22   83    97
18   80    72
16   52    51
14   76    70
13   21   -20
10   36   -38
 9   73    70
 8   38   -35
 7   38    39
 6  116  -119
 5   31    31
 4   35    32
-6   55   -54
-7   82   -84
-8  145   146
-9   72   -74
-11  26   -35
-12  50    51
-14  70   -76
-16  47   -51
-17  57    57
-18  99   -99
-22  76   -78
-23  36    35
-24  36   -44
-26  27    34
-27  41   -43
-28  38    41
-32  35    38
-33  36   -35

        H 0   6
-34  84   -95
-32  66    79
-28  31    39
-26  83    89
-24 153   160
-22  84   -86
-20 144   149
-16  27   -26
-14  78   -74
-12  37   -32
-10 185  -193
-8   23    24
-6  129   129
 4   15   -13
 6  188   184
 8  173  -169
10   48   -45
12   82   -80
14   61   -52
16   92   -83
18  170   152
20   69   -63
22   67    58
24  152   125
26   86    71
30   90    70
32   48   -38
```

connects equivalent chains in different unit cells by forming $O-Na-O$-bridges in the z-direction. The layers parallel to the yz-plane that are formed this way are connected by $O-Na-H_2O-Na-O$ linkages (Fig. 2).

The $H_2Mo_5P_2O_{23}^{4-}$-*group*. The group differs only slightly in bond lengths and angles from the $Mo_5P_2O_{23}^{6-}$-group in (8, 5, 2).[2] It consists of five $MoO_6$-

*Fig. 1.* A view in the $-z$-direction of the zig-zag arrangement of $H_2Mo_5P_2O_{23}^{4-}$-groups linked by three types of $Na^+$-bridges. The chain on $z \approx 0.75$ is drawn with thick lines.
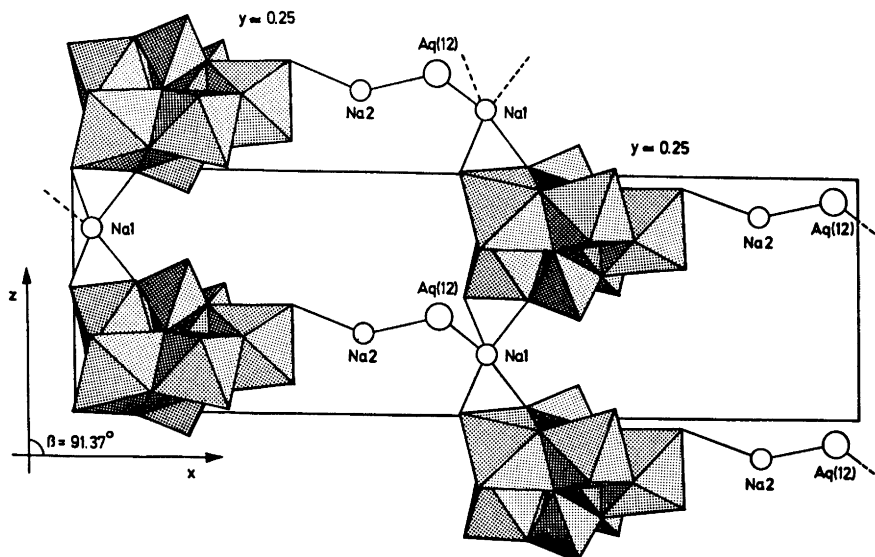


*Fig. 2.* A view in the $y$-direction of the $Na^+$-connections between $H_2Mo_5P_2O_{23}^{4-}$-groups in the $z$-direction, and the $O-Na-H_2O-Na-O$ links between layers in the $x$-direction.

octahedra which form a ring. The octahedra are joined together through common edges, except in one contact where they share a corner. Two $PO_4$-tetrahedra are attached to the ring, one above and the other below it. Each tetrahedron has three of its four oxygen atoms in common with Mo. Two of these are coordinated to two Mo atoms, the third oxygen to one Mo only. There are in all twelve unshared oxygens in the group. A stereoscopic figure of the group, including the designations of the atoms, is shown in Fig. 3. The two-fold rotation axis through Mo1 and O(34) in (8, 5, 2) is not included in this space group, but the deviations from this molecular symmetry are rather small in (10, 5, 2).
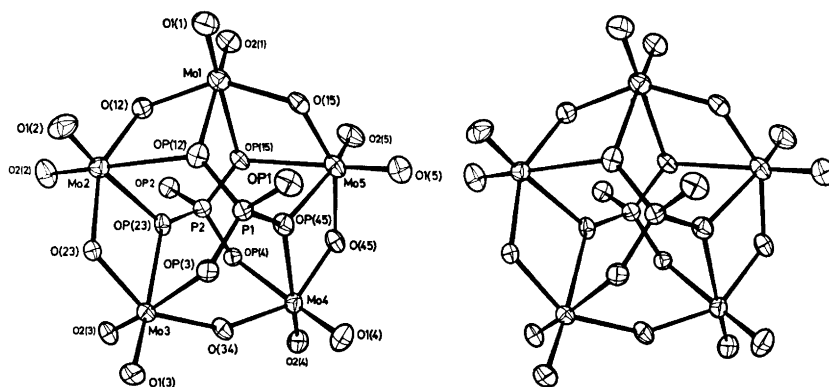


*Fig. 3.* Stereoscopic view of the $H_2Mo_5P_2O_{23}{}^{4-}$-group with thermal ellipsoids scaled to include 50 % probability.

The distances between two Mo atoms in octahedra sharing edges vary between 3.38 and 3.41 Å and increase to 3.681(1) Å when only a corner is shared (Mo3 − Mo4). The cross distances within the ring lie in the range $5.51 − 5.61$ Å. The Mo − P distances vary between 3.30 and 3.61 Å while the P − P distance is 3.712(4) Å. Distances and angles between the Mo and P atoms in the group and the corresponding values for (8, 5, 2) are listed in Table 4.

A comparison shows that all the Mo − Mo distances are $0.02 − 0.06$ Å longer in (10, 5, 2) than in (8, 5, 2). The P − P distance is 0.11 Å shorter in (10, 5, 2) and the P atoms seem to be pressed together. No tendency towards ring-fracture can be noted. The Mo − Mo distances between $MoO_6$-octahedra sharing edges can also be compared with $3.309 − 3.351$ Å reported for $Na_3(CrMo_6O_{24}H_6).8\ H_2O$ [12] and $3.20 − 3.44$ Å for $(NH_4)_6Mo_7O_{24}.4H_2O$ [13].

*The coordination of Na$^+$-ions around the* $H_2Mo_5P_2O_{23}{}^{4-}$*-groups.* In the structure there are four kinds of crystallographically different Na$^+$-ions and they are all coordinated to two $H_2Mo_5P_2O_{23}{}^{4-}$-groups at the same time. Na1, which is the atom that connects groups in the z-direction, coordinates O1(3) and OP(3) from one group and O2(4) and OP(4) from the other. Na2 and Na3 are both attached to two oxygen atoms, one in each group. For Na2 the oxygen

*Table 4.* Distances (Å) and angles (degrees) within the $H_2Mo_5P_2O_{23}{}^{4-}$-group (and for the Mo and P atoms in the $Mo_5P_2O_{23}{}^{6-}$-group in (8,5,2)).
The designation of the atoms is explained in Table 1. The estimated standard deviations are given in parentheses and refer to the last decimal place given. The values are based on parameters from block-diagonal least squares refinements.

| | (10,5,2) | (8,5,2) | | (10,5,2) | (8,5,2) |
|---|---|---|---|---|---|
| Mo1–Mo2 | 3.375(1) | 3.364(1) | P1-Mo1 | 3.461(3) | 3.439(3) |
| Mo1–Mo3 | 5.507(1) | 5.459(2) | P1-Mo2 | 3.521(3) | 3.505(3) |
| Mo1–Mo4 | 5.520(1) | 5.459(2) | P1-Mo3 | 3.303(3) | 3.335(3) |
| Mo1–Mo5 | 3.405(1) | 3.364(1) | P1-Mo4 | 3.602(3) | 3.644(3) |
| Mo2–Mo3 | 3.389(1) | 3.356(1) | P1-Mo5 | 3.401(3) | 3.432(3) |
| Mo2–Mo4 | 5.608(1) | 5.566(1) | P2-Mo1 | 3.482(3) | 3.439(3) |
| Mo2–Mo5 | 5.526(1) | 5.493(2) | P2-Mo2 | 3.409(3) | 3.432(3) |
| Mo3–Mo4 | 3.681(1) | 3.647(2) | P2-Mo3 | 3.606(3) | 3.644(3) |
| Mo3–Mo5 | 5.609(1) | 5.566(1) | P2-Mo4 | 3.306(3) | 3.335(3) |
| Mo4–Mo5 | 3.391(1) | 3.356(1) | P2-Mo5 | 3.534(3) | 3.505(3) |
| | | | P1-P2 | 3.712(4) | 3.822(6) |

| | (10,5,2) | (8,5,2) |
|---|---|---|
| Mo2–Mo1–Mo5 | 109.19(3) | 109.44(5) |
| Mo3–Mo2–Mo1 | 109.00(3) | 108.63(4) |
| Mo4–Mo3–Mo2 | 104.89(3) | 105.18(3) |
| Mo5–Mo4–Mo3 | 104.89(3) | 105.18(3) |
| Mo1–Mo5–Mo4 | 108.63(3) | 108.63(4) |

| | O1(1) | O2(1) | O(12) | O(15) | OP(12) | OP(15) |
|---|---|---|---|---|---|---|
| Mo1 | 1.713(9) | 1.701(8) | 1.919(7) | 1.928(7) | 2.313(7) | 2.361(7) |
| O1(1) | | 2.665(13) | 2.830(11) | 2.801(11) | 2.828(10) | |
| OP(15) | | 2.869(10) | 2.773(10) | 2.562(11) | 3.052(11) | |
| O(12) | | 2.767(11) | | | 2.549(10) | |
| O(15) | | 2.812(11) | | | 2.766(10) | |
| O1(1)–Mo1– | | 102.7(4) | 102.3(4) | 100.4(4) | 87.9(4) | |
| OP(15)–Mo1– | | 88.3(4) | 80.0(3) | 72.6(3) | 81.5(3) | |
| O(12)–Mo1– | | 99.5(4) | | | 73.4(3) | |
| O(15)–Mo1– | | 101.4(4) | | | 80.9(3) | |

| | O1(2) | O2(2) | O(12) | O(23) | OP(12) | OP(23) |
|---|---|---|---|---|---|---|
| Mo2 | 1.703(8) | 1.697(8) | 1.921(7) | 1.951(7) | 2.388(7) | 2.212(7) |
| O1(2) | | 2.701(12) | 2.837(12) | 2.718(10) | 2.882(11) | |
| OP(23) | | 2.941(10) | 2.741(9) | 2.453(11) | 2.705(10) | |
| O(12) | | 2.704(10) | | | 2.549(10) | |
| O(23) | | 2.774(11) | | | 3.037(10) | |
| O1(2)–Mo2– | | 105.2(4) | 102.9(4) | 95.9(3) | 87.9(4) | |
| OP(23)–Mo2– | | 96.7(4) | 82.8(3) | 71.9(3) | 71.9(3) | |
| O(12)–Mo2– | | 96.6(4) | | | 71.6(3) | |
| O(23)–Mo2– | | 98.8(4) | | | 88.3(3) | |

| | O1(3) | O2(3) | O(23) | O(34) | OP(3) | OP(23) |
|---|---|---|---|---|---|---|
| Mo3 | 1.702(8) | 1.735(8) | 1.911(7) | 1.898(7) | 2.275(7) | 2.354(7) |
| O1(3) | | 2.687(11) | 2.790(10) | 2.806(11) | 2.696(10) | |
| OP(23) | | 2.868(10) | 2.453(11) | 2.845(10) | 3.143(11) | |
| O(23) | | 2.811(11) | | | 2.650(10) | |
| O(34) | | 2.752(10) | | | 2.684(11) | |

*Table 4. Continued.*

|  |  |  |  |  |
|---|---|---|---|---|
| O1(3)–Mo3– | 102.8(4) | 100.9(4) | 102.3(3) | 84.1(3) |
| OP(23)–Mo3– | 87.7(3) | 69.3(3) | 83.3(3) | 85.5(3) |
| O(23)–Mo3– | 100.8(3) |  |  | 78.1(3) |
| O(34)–Mo3– | 98.4(3) |  |  | 79.5(3) |

|  | O1(4) | O2(4) | O(34) | O(45) | OP(4) | OP(45) |
|---|---|---|---|---|---|---|
| Mo4 | 1.715(9) | 1.702(9) | 1.915(7) | 1.898(7) | 2.273(7) | 2.343(7) |
| O1(4) |  | 2.674(13) | 2.745(11) | 2.787(11) |  | 2.863(11) |
| OP(4) |  | 2.682(10) | 2.676(11) | 2.670(10) |  | 3.130(11) |
| O(34) |  | 2.811(12) |  |  |  | 2.850(10) |
| O(45) |  | 2.784(11) |  |  |  | 2.434(11) |
| O1(4)–Mo4– |  | 103.0(4) | 98.1(4) | 100.8(4) |  | 88.3(4) |
| OP(4)–Mo4– |  | 83.6(3) | 78.9(3) | 79.0(3) |  | 85.4(3) |
| O(34)–Mo4– |  | 101.9(4) |  |  |  | 83.4(3) |
| O(45)–Mo4– |  | 101.2(4) |  |  |  | 69.2(3) |

|  | O1(5) | O2(5) | O(15) | O(45) | OP(15) | OP(45) |
|---|---|---|---|---|---|---|
| Mo5 | 1.701(9) | 1.709(10) | 1.914(7) | 1.968(7) | 2.414(7) | 2.195(7) |
| O1(5) |  | 2.710(14) | 2.718(11) | 2.781(12) |  | 2.916(11) |
| OP(15) |  | 2.920(12) | 2.562(11) | 3.057(10) |  | 2.720(11) |
| O(15) |  | 2.850(12) |  |  |  | 2.739(10) |
| O(45) |  | 2.721(11) |  |  |  | 2.434(11) |
| O1(5)–Mo5– |  | 105.2(5) | 97.3(4) | 98.3(4) |  | 96.1(4) |
| OP(15)–Mo5– |  | 88.5(4) | 71.5(3) | 87.9(3) |  | 72.2(3) |
| O(15)–Mo5– |  | 103.6(4) |  |  |  | 83.3(3) |
| O(45)–Mo5– |  | 95.2(4) |  |  |  | 71.3(3) |

|  | OP1 | OP(3) | OP(12) | OP(45) |
|---|---|---|---|---|
| P1 | 1.564(8) | 1.506(7) | 1.538(7) | 1.559(8) |
| OP1 |  | 2.546(10) | 2.458(11) | 2.527(11) |
| OP(3) |  |  | 2.525(10) | 2.493(11) |
| OP(12) |  |  |  | 2.550(10) |
| OP1–P1– |  | 112.1(4) | 104.8(4) | 108.1(4) |
| OP(3)–P1– |  |  | 112.1(4) | 108.9(4) |
| OP(12)–P1– |  |  |  | 110.8(4) |

|  | OP2 | OP(4) | OP(15) | OP(23) |
|---|---|---|---|---|
| P2 | 1.565(8) | 1.504(7) | 1.530(7) | 1.545(8) |
| OP2 |  | 2.537(10) | 2.456(11) | 2.518(11) |
| OP(4) |  |  | 2.527(9) | 2.463(10) |
| OP(15) |  |  |  | 2.546(10) |
| OP2–P2– |  | 111.5(4) | 105.0(4) | 108.1(4) |
| OP(4)–P2– |  |  | 112.8(4) | 107.7(4) |
| OP(15)–P2– |  |  |  | 111.7(5) |

atoms are O1(1) and O2(2) and for Na3 O2(1) and O1(2) in group one and two, respectively. Na4 is in contact with O1(1) and O1(2) in one group and with O2(5) in another. (Na2–4 are the bridge ions in the previously mentioned zig-zag chains.) Consequently there are eight sodium ions coordinated to seven of the twelve unshared oxygen atoms and to two of the shared oxygen atoms in a $H_2Mo_5P_2O_{23}^{4-}$-group. Since every ion is shared between two groups the average number of $Na^+$-ions around a group is four, which implies that the
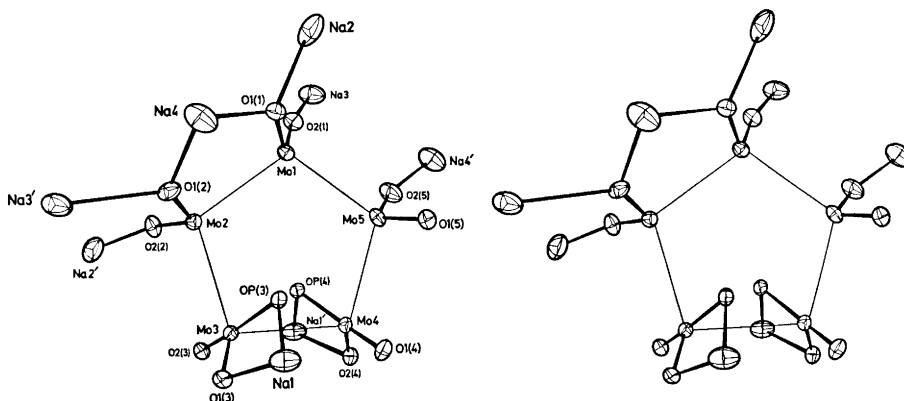
*Fig. 4.* Stereoscopic view of the sodium coordination to the $H_2Mo_5P_2O_{23}{}^{4-}$-group (for clarity all shared oxygen atoms except two have been omitted). The thermal ellipsoids are scaled to include 50 % probability.

charge of the group has been neutralized. The configuration of $Na^+$-ions around a group is shown in Fig. 4.

*The sodium-oxygen arrangement.* Every sodium ion is surrounded by six group- or water-oxygen atoms forming an octahedron, which can be written schematically as $NaO_x(H_2O)_{6-x}$. For Na1 $x = 4$, for Na2 and Na3 $x = 2$, and for Na4 $x = 3$. The octahedra are coupled together to form an $Na_4O_9(H_2O)_8$-unit by sharing oxygen atoms as shown in Fig. 5.

The Na1 octahedron has a corner [Aq(12)] in common with the Na2 octahedron, while the latter also shares Aq2(23) with the Na3 octahedron and O1(1) with the Na4 octahedron. The Na3 and Na4 octahedra share an edge through Aq1(34) and Aq2(34). The $Na_4O_9(H_2O)_8$-unit is the smallest unit
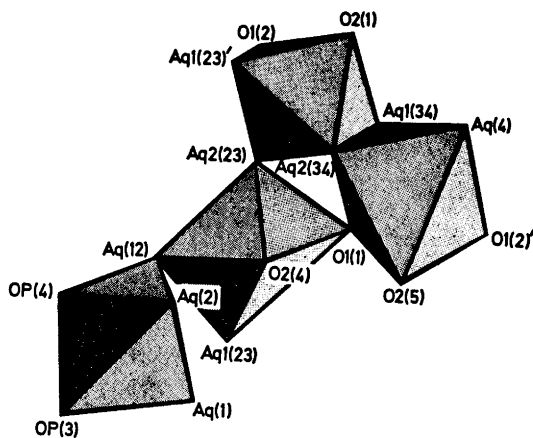


*Fig. 5.* The $Na_4O_9(H_2O)_8$-unit schematically drawn with octahedra.

necessary to describe the network that is formed since Aq1(23) and O1(2) are also shared with other units. The Na−Na distances are in the range 3.61−4.83 Å.

*The two "free" water molecules.* There are two water molecules, Aq1 and Aq2, which are not coordinated to any $Na^+$-ion. They are situated one on each side of the $H_2Mo_5P_2O_{23}^{4-}$-group, Aq1 2.617(12) Å from OP1 and Aq2 2.613(12) Å from OP2. They also seem to be related by the near two-fold rotation axis mentioned.

*The $MoO_6$-octahedra.* The $MoO_6$-octahedra are somewhat distorted from an ideal octahedron and the Mo−O distances can be divided into three groups according to the number of atoms that the oxygen atom is coordinated to: (1) coordinated to one Mo atom, the distance varies between 1.70 and 1.74 Å (2) coordinated to two Mo atoms, the distance varies between 1.90 and 1.97 Å (3) coordinated to P and to one or two Mo atoms, the distance varies between 2.20 and 2.41 Å.

This increasing distance with increasing coordination is found in (8, 5, 2) as well as in other structures referred to in an earlier paper.[2]

It is apparent that the O−O distance is shorter (2.43−2.56 Å) when the oxygen atoms form a shared edge between two octahedra than the distance in unshared edges (2.65−3.14 Å). Distances and angles in the $MoO_6$-octahedra are listed in Table 4.

*The $PO_4$-tetrahedra.* It can be seen from the distances and angles in Table 4 that the $PO_4$-tetrahedra are not far from regular. The P−O distances are in the range 1.50−1.57 Å and the different O−P−O angles vary between 105 and 112°. These values and the values of the O−O distances (2.46−2.55 Å) agree well with distances found in other compounds containing phosphate groups.[14,15]

In (8, 5, 2) the shortest P−O distance (1.495(9) Å) is to the unshared oxygen, while in (10, 5, 2) this distance is the longest one [1.564(8) and 1.565(8) Å]. In the crystal structure of $H_3PO_4$ a significantly longer P−O distance is found when a hydrogen atom is bonded to an oxygen atom and also takes part in a hydrogen bond than when no hydrogen atom is present.[14] The difference found between (8, 5, 2) and (10, 5, 2) can probably be explained in the same way. The hydrogen atoms in the $H_2Mo_5P_2O_{23}^{4-}$-group could, if situated on one unshared P-oxygen each, cause the elongation in the P−O distance especially if a suitable hydrogen bond to some other atom occurred. The two non-coordinated water molecules are situated at reasonable hydrogen bond distances from these oxygen atoms. However, no definite positions of the hydrogen atoms are available to prove this assumption.

*The sodium-oxygen octahedra.* The octahedra are quite distorted from an ideal octahedron with Na−O distances in the range 2.21−2.63 Å, with five exceptions (Table 5). Three of these occur when the same group oxygen is shared between different sodium ions [2.694(10), 2.753(11) and 3.038(11) Å]. The other two [2.733(10) and 2.811(10) Å] are in the octahedron around Na1, which is the most distorted one since four of its oxygens are $H_2Mo_5P_2O_{23}^{4-}$-oxygens and dominated by the coordination to Mo-atoms.

*Table 5.* Distances (Å) within the sodium—oxygen octahedra. The designation of the atoms is explained in Table 1. The estimated standard deviations are given in parentheses and refer to the last decimal place given. The values are based on parameters from block-diagonal least squares refinements.

| | O1(3) | O2(4) | OP(3) | OP(4) | Aq(1) | Aq(12) |
|---|---|---|---|---|---|---|
| Na1 | 2.811(10) | 2.733(10) | 2.341(9) | 2.343(9) | 2.374(11) | 2.431(11) |
| O1(3) | | | 2.696(10) | 4.858(11) | 3.353(12) | 3.415(13) |
| O2(4) | | | 4.763(12) | 2.683(10) | 3.353(14) | 3.385(13) |
| OP(3) | | | | 3.665(11) | 3.297(12) | |
| Aq(12) | | | | 3.477(12) | 3.782(14) | |

| | O1(1) | O2(2) | Aq(2) | Aq(12) | Aq1(23) | Aq2(23) |
|---|---|---|---|---|---|---|
| Na2 | 2.694(10) | 2.274(10) | 2.208(15) | 2.633(12) | 2.604(14) | 2.482(13) |
| O1(1) | | 3.783(11) | 3.244(15) | | 4.581(14) | 3.167(13) |
| Aq(12) | | 3.623(13) | 3.225(16) | | 3.301(15) | 3.682(14) |
| O2(2) | | | | | 3.000(13) | 3.122(14) |
| Aq(2) | | | | | 3.888(21) | 3.446(16) |

| | O2(1) | O1(2) | Aq1(23) | Aq2(23) | Aq1(34) | Aq2(34) |
|---|---|---|---|---|---|---|
| Na3 | 2.331(10) | 3.038(11) | 2.423(12) | 2.331(12) | 2.374(11) | 2.452(14) |
| O2(1) | | 3.787(12) | 3.194(12) | | 2.881(14) | 3.310(16) |
| Aq2(23) | | 3.401(13) | 3.789(15) | | 3.491(15) | 3.856(16) |
| O1(2) | | | 3.800(13) | | 4.161(15) | |
| Aq2(34) | | | 3.342(17) | | 3.253(16) | |

| | O1(1) | O1(2) | O2(5) | Aq(4) | Aq1(34) | Aq2(34) |
|---|---|---|---|---|---|---|
| Na4 | 2.753(11) | 2.442(10) | 2.528(12) | 2.417(12) | 2.517(15) | 2.421(14) |
| O1(1) | | 3.744(11) | 3.460(13) | | 2.942(14) | 3.805(17) |
| Aq(4) | | 3.510(13) | 4.059(14) | | 3.785(16) | 3.238(15) |
| O1(2) | | | 3.039(11) | | 4.139(15) | |
| Aq2(34) | | | 3.549(18) | | 3.253(16) | |

There is no significant difference between the Na−O distances arising from water oxygen atoms or group oxygen atoms and no systematic effects on the distortion of the octahedra apart from those mentioned are evident.

## REFERENCES

1. Pettersson, L. *Acta Chem. Scand.* **25** (1971) 1959.
2. Strandberg, R. *Acta Chem. Scand.* **27** (1973) 1004.
3  *International Tables for X-Ray Crystallography*, Kynoch Press, Birmingham 1965, Vol I.
4. Ivarsson, G., Lundberg, B. K. S. and Ingri, N. *Acta Chem. Scand.* **26** (1972) 3005.
5. Johnson, C. K. ORTEP. Report ORNL-3794, Oak Ridge National Laboratory, Oak Ridge, Tennessee.

6. Cromer, D. T. and Waber, J. T. *Acta Cryst.* **18** (1965) 104.
7. Hanson, H. P., Herman, F., Lea, J. D. and Skillman, S. *Acta Cryst.* **17** (1964) 1040.
8. *International Tables for X-Ray Crystallography*, Kynoch Press, Birmingham 1962, Vol III.
9. Cruickshank, D. W. J. *Computing Methods in Crystallography*, Pergamon, London 1965, p. 114.
10. Stewart, R. F., Davidson, E. R. and Simpson, W. T. *J. Chem. Phys.* **42** (1965) 3175.
11. Pawley, G. S. *Acta Cryst.* **A 26** (1970) 691.
12. Perloff, A. *Inorg. Chem.* **9** (1970) 2228.
13. Evans, H. T., Jr. *J. Am. Chem. Soc.* **90** (1968) 3275.
14. Furberg, S. *Acta Chem. Scand.* **9** (1955) 1557.
15. Jönsson, P.-G. *Acta Chem. Scand.* **26** (1972) 1599.

# The Crystal and Molecular Structure of

# Diethylthioselenophosphinatothallium (I)

STEINAR ESPERÅS and STEINAR HUSEBYE

Chemical Institute, University of Bergen, N-5000 Bergen, Norway

The crystal and molecular structure of diethylthioselenophos-phinatothallium(I), [Tl(Et$_2$PSeS)], has been determined and refined by three-dimensional X-ray methods. The crystals are monoclinic and belong to the space group $C_{2h}^3 - C2/m$. There are four formula units in the cell with $a = 10.342(3)$ Å, $b = 9.116(3)$ Å, $c = 10.154(2)$ Å, and $\beta = 101.98(2)°$. Calculated density is 2.88 g/cm$^3$. For the structure analysis 997 reflection intensities above background were collected on a Siemens AED-1 single-crystal diffractometer. Full-matrix least squares refinement resulted in a conventional $R$-value of 0.088.

The structure can be considered as built up of dimeric units, [Tl(Et$_2$PSeS)]$_2$, linked together in two-dimensional polymeric layers parallel to the $ab$-plane. Each thallium atom is coordinated to two sulphur and two selenium atoms in the dimer and to two more distant selenium atoms belonging to different neighbour dimers. The Tl$-$S and Tl$-$Se bond lengths in the dimer are 3.237(5) Å and 3.424(4) Å, respectively, while the intermolecular Tl$-$Se contacts are 3.594(3) Å.

Monovalent thallium has the $(n-1)d^{10}ns^2$ configuration found also in tetravalent tellurium and selenium, trivalent arsenic, antimony, and bismuth and in divalent lead and tin. Studies of complexes of these elements have shown that the $ns^2$ lone pair in some compounds is stereochemically inert.[1] In other compounds it occupies either a position in the coordination polyhedron,[2-9] or it has some $p$-character, pointing in between some weak central atom to ligand bonds.[10] The latter type of stereochemical activity has been found in monovalent thallium compounds.[10]

In many respects the thallium(I) compounds bear a certain resemblance to the alkali and the coinage metals. Structural studies of dithiocarbamates of monovalent gold,[11] copper,[12] silver,[13] cesium[14], and thallium[15,16] have shown a tendency for these metal complexes to occur as polymers. While the complexes of the first three metals are arranged as isolated low polymers, the others can be considered as interconnected dimers having very interesting structures. Dipropyldithiocarbamatothallium(I),[15] [Tl{(n-pr)$_2$NCS$_2$}], is built as a chain arrangement of dimeric units, while in diisopropyldithiocarbamatothallium(I),[16]

[Tl{(iso-pr)$_2$NCS$_2$}], and in dibutyldithiocarbamatocesium(I),[14] [Cs{(bu)$_2$NCS$_2$}], the dimers are linked together into layers.

The present structure determination was undertaken to further investigate the polymeric nature of Tl(I) compounds and also the role of the lone pair of electrons in such compounds as mentioned above.

## EXPERIMENTAL

For the present study, the thioselenophosphinate complex of monovalent thallium was prepared by Kuchen *et al.* by reaction between trivalent thallium and diethylthio-selenophosphinate ions.[17]

$$Tl^{3+} + 3Et_2PSeS^- = Tl(Et_2PSeS) + (Et_2PSeS)_2$$
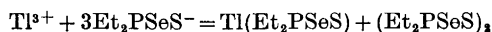
The crystals were recrystallized from chloroform solution as small colorless prisms elongated along the *c* axis.

Preliminary cell dimensions and the space group were determined by film methods.

For recording of data, a Siemens automatic, off-line single-crystal diffractometer (AED-1) was used. The diffractometer was operated as a three-circle instrument using Nb-filtered Mo$K\alpha$ radiation. A crystal with dimensions $0.22 \times 0.13 \times 0.09$ mm$^3$ was mounted with the *c* axis along the $\phi$-axis of the instrument.

During exposure to X-rays, the crystal surface became slowly covered by a yellow powder. This decomposition caused the intensities of the standard reflections to decrease nearly 20 % during the data collection. The crystal orientation and unit cell dimensions were determined by measuring $\theta$, $\chi$, and $\phi$ angles for 15 reciprocal vectors. The setting angles for all reflections could then be calculated.

For determination of accurate unit cell parameters by means of least squares methods, the $\theta$ angles of 18 reflections with high $\theta$ were measured. The cell data are $a = 10.342(3)$ Å, $b = 9.116(3)$ Å, $c = 10.154(2)$ Å, and $\beta = 101.98(2)°$. There are four formula units in the cell with calculated density 2.88 g/cm$^3$. The systematic absences are $hkl$ for $h + k = 2n + 1$, in the monoclinic crystal system. Thus the space group is either $C2$, $Cm$, or $C2/m$.

The intensity data were collected using the five-value measuring procedure and $\theta - 2\theta$ scan technique.[18] The scan speed was 2.5°/min, with automatic setting of higher speed for strong reflections. To avoid counting losses for high intensity reflections, the diffractometer inserts a proper attenuation filter into the primary beam. Each reflection was scanned between $\theta_1 = \theta - 0.5°$ and $\theta_2 = \theta + 0.5°$, where $\theta$ is the Bragg angle for the $\alpha_1$-peak. The scanning was performed by going from $\theta$ to $\theta_1$, then from $\theta_1$ to $\theta_2$ and finally from $\theta_2$ to $\theta$. The intensities for all three scans and their sum, $I_t$, were recorded. Likewise the background was measured for one half of the total scan time at each side of the reflection, and the respective intensities and their sum $I_b$ were also recorded. The net count for a reflection, $I_N$, was put equal to $I_t - I_b$.

In order to bring the net intensities to a common scale and to check the crystal orientation, two reference reflections were measured at intervals of 50 reflections. Out of 1193 reflections attainable with $\theta \leq 28°$, 997 were found to have intensities stronger than twice the standard deviation. The remaining reflections were labelled as unobserved and each assigned an intensity equal to twice its standard deviation. This standard deviation was defined as the square root of the sum of the total intensity and the intensity of the background.

The data were corrected for Lorentz and polarization effects. During the refinement an absorption correction was applied ($\mu = 219$ cm$^{-1}$) using the Gaussian integration method as described by Coppens *et al.*[19] However, as both the standard deviations of the parameters and the $R$-factor increased afterwards, this data correction was omitted. The reason for this negative result may be the decomposition of the crystal as mentioned above. No extinction correction was found necessary.

The calculated structure factors were based on the atomic scattering curves given in *International Tables for X-ray Crystallography*,[20] Table 3.3.1 A. The curves for thallium were corrected for anomalous dispersion using the $\Delta f'$ and $\Delta f''$ values given by Cromer,[21] and taking the amplitude of $f$ as the corrected value.

## STRUCTURE DETERMINATION AND REFINEMENT

A three-dimensional Patterson map, calculated on the basis of the 997 observed reflections, could only be interpreted in terms of a dimeric complex. In the centric space group $C2/m$, which was the first choice, the dimers had to occupy special twofold positions with the thallium atoms on a twofold axis parallel with $b$ and the selenium, sulphur, and phosphorus atoms lying in a mirror plane halfway between the two thallium atoms and at right angles to $b$. The center of the dimer, $i.e.$ the intersection between the twofold axis and the mirror plane, is thus a center of symmetry.

The thallium position was taken from the Patterson map. A Fourier map with signs based on the thallium contribution then allowed the location of the selenium, sulphur, and phosphorus atoms. From the next electron density map, the positions of the carbon atoms were found.

Full-matrix least squares refinement was then carried out using a program (BDLS) which minimizes the expression $r = \sum w(|F_o| - K|F_c|)^2$. Here $K$ is a variable scale factor and $w$, the relative weight assigned to a reflection, is equal to $1/\sigma^2$ $(F_o)$. The variance of $F_o$ is evaluated as $F_o^2\{(I_t + I_b + k^2(I_t - I_b)^2\}/4(I_t - I_b)^2$, where $k$ may be interpreted as the relative standard deviation in the scaling curve based on the reference reflections. Non-observed reflections with $K|F_c|$ larger than the observable limit are included in the refinement with $F_o$ put equal to the limit.

After a few cycles of refinement of coordinates and isotropic temperature factors for all atoms except hydrogen, the reliability index, $R = \sum||F_o| - |F_c||/\sum|F_o|$, reached a value of 0.109.

After introducing anisotropic temperature factors for all atoms (except hydrogen) the $R$-factor converged to a value of 0.088. The shifts were less than one tenth of the estimated standard deviations.

In the light of the high temperature factors of selenium related to those of sulphur ($U = 0.093$ for Se, and 0.042 for S), disorder in the positions of these atoms could be possible. Subsequent refinement based on two different configurations of the dimers, such that the selenium and sulphur atoms exchanged positions resulted in the original single configuration.

Attempts to refine the structure in the non-centric alternative space groups were not successful.

A final difference electron density map showed a maximum peak of 2.8 e/Å³ near the thallium position. Possible explanations could be the omission of an absorption correction, termination of series errors, and the somewhat poor quality of the data due to the decomposition of the crystal. Similar peaks have also been found in difference maps for other Tl(I) compounds.[22,23]

Observed and calculated structure factors following the last refinement cycle can be obtained from the authors, upon request.

## RESULTS AND DISCUSSION OF THE STRUCTURE

The final positional and thermal parameters are listed in Tables 1 and 2. Interatomic distances and angles are listed in Tables 3 and 4.

*Table 1.* Final atomic coordinates in fraction of cell edges with standard deviations in brackets.

|         | $x$         | $y$        | $z$       |
|---------|-------------|------------|-----------|
| Tl      | 0.0         | 0.2117(2)  | 0.0       |
| Se      | −0.2578(4)  | 0.0        | 0.0533(5) |
| S       | 0.0551(6)   | 0.0        | 0.2616(7) |
| P       | −0.1441(8)  | 0.0        | 0.2521(9) |
| $C_1$   | −0.188(3)   | 0.157(4)   | 0.351(3)  |
| $C_2$   | −0.135(4)   | 0.298(4)   | 0.317(4)  |

*Table 2.* Components of atomic vibration tensors, $U \times 10^3$, in $Å^2$ with standard deviations, referred to crystallographic axes. For all atoms the expression is
$$\exp\{-2\pi^2[h^2a^{-2}U_{11} + k^2b^{-2}U_{22} + l^2c^{-2}U_{33} + 2hka^{-1}c^{-1}U_{12} + 2klb^{-1}c^{-1}U_{23} + 2hla^{-1}c^{-1}U_{13}]\}.$$

| Tl    | 63.2(0.8)   | 63.6(0.9)    | 62.9(0.8)   | $(U_{11}, U_{22}, U_{33})$ |
|-------|-------------|--------------|-------------|---------------------------|
|       | 0.0         | 0.0          | 19.1(0.6)   | $(U_{12}, U_{23}, U_{13})$ |
| Se    | 68.4(2.6)   | 118.0(3.8)   | 95.2(3.1)   |                           |
|       | 0.0         | 0.0          | 11.7(2.3)   |                           |
| S     | 20.8(2.9)   | 68.6(4.8)    | 44.3(3.7)   |                           |
|       | 0.0         | 0.0          | 8.6(2.6)    |                           |
| P     | 39.4(4.2)   | 93.3(7.0)    | 61.9(5.2)   |                           |
|       | 0.0         | 0.0          | 18.5(3.7)   |                           |
| $C_1$ | 78.1(17.9)  | 123.2(27.6)  | 113.3(22.7) |                           |
|       | 22.0(18.4)  | −41.1(21.0)  | 38.0(16.5)  |                           |
| $C_2$ | 152.4(32.0) | 78.5(23.5)   | 178.1(38.0) |                           |
|       | 44.1(23.8)  | 22.4(24.1)   | 64.3(27.9)  |                           |

*Table 3.* Interatomic distances (Å) and angles (°) within the dimeric $[Tl(Et_2PSeS)]_2$ unit. Standard deviations in brackets. For atomic labels, see Fig. 2.

| Bond lengths |           | Bond angles       |           |
|--------------|-----------|-------------------|-----------|
| Tl−Se        | 3.424(4)  | Se−Tl−S           | 62.9(1)   |
| Tl−S         | 3.237(5)  | Tl−Se−P           | 81.6(2)   |
| P−Se         | 2.115(9)  | Tl−S−P            | 87.5(3)   |
| P−S          | 2.042(10) | Se−P−S            | 113.6(4)  |
| P−$C_1$      | 1.86(4)   | Se−P−$C_1$        | 111.5(9)  |
| $C_1$−$C_2$  | 1.46(5)   | S−P−$C_1$         | 109.3(8)  |
|              |           | P−$C_1$−$C_2$     | 113.7(25) |
|              |           | $C_1$−P−$C_1$     | 100.7(15) |
| Interatomic contacts |   | S−Tl−S′           | 106.8(1)  |
|              |           | S−Tl−Se′          | 77.5(1)   |
| Tl···Tl′     | 3.859(2)  | Se−Tl−Se′         | 111.4(1)  |
| Se···S       | 3.479(7)  | Tl−Se−Tl′         | 68.6(1)   |
| Tl···P       | 3.753(8)  | Tl−S−Tl′          | 73.2(1)   |

*Table 4.* Some interatomic distances (Å) and angles (°) involving dimer-dimer interactions. Standard deviations in brackets. For atomic labels, see Fig. 2.

| Tl···Se = 3.594(3) | | |
|---|---|---|
| | Se(I)···Tl···Se(II) | 86.0(1) |
| | Se(I)···Tl···Se | 158.4(1) |
| | Se(I)···Tl···Se' | 84.0(1) |
| | Se(I)···Tl···S | 108.3(1) |
| | Se(I)···Tl···S' | 123.9(1) |
| | Tl(I)···Se···Tl(II) | 94.0(1) |
| | Tl(I)···Se···Tl | 158.4(1) |
| | Tl(I)···Se···Tl' | 96.0(1) |

Some bond lengths and angles in a diethylthioselenophosphinatothallium(I) dimer are shown in Fig. 1. Views of the unit cell contents seen along the *c* and the *a* axis are shown in Fig. 2 and Fig. 3, respectively. A stereoscopic drawing showing the packing of molecules is given in Fig. 4.

The crystal structure can be regarded as built up of dimeric units, [Tl(Et₂PSeS)]₂, linked together in two-dimensional polymeric layers parallel to the *ab*-plane. Each thallium atom is bonded to two sulphur and two selenium atoms in the dimer, thallium being at the top of an approximately square pyramid with the latter atoms forming its base. However, each thallium atom also has two more distant selenium neighbours in the opposite direction, belonging to different adjacent dimers. The metal atom is thus coordinated by six atoms situated at the corners of a distorted trigonal prism. In each layer the metal atoms form a central sheet surrounded on both sides by the ligands. The only interactions between adjacent layers are of van der Waals type between the alkyl groups.

The crystal structure resembles those found for dipropyldithiocarbamato-thallium(I) [15] and diisopropyldithiocarbamatothallium(I),[16] where the same type of dimers and ligand bridges are observed. In the dipropyl complex the dimers are linked into chains, while in its diisopropyl analogue the dimers are connected into layers. The similarities are even greater in dibutyldithiocarba-matocesium(I),[14] where the layer structure is essentially the same as in the
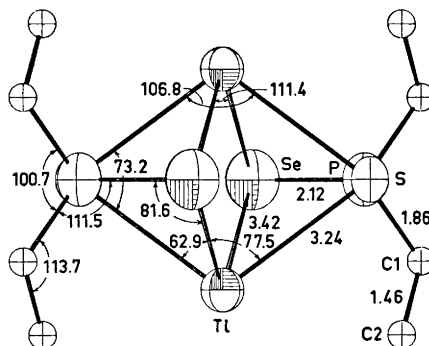


*Fig. 1.* The [Tl(Et₂PSeS)]₂ dimer as seen along the *c* axis with some bond lengths and bond angles indicated. The thermal ellipsoids of Tl, Se, S and P correspond to 50 % probability.
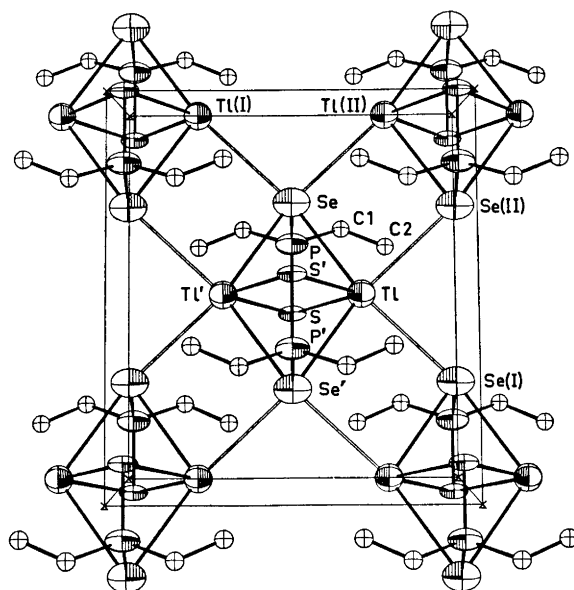
*Fig. 2.* A view of the unit cell as seen along the *c* axis. Unfilled bonds represent dimer-dimer contacts.
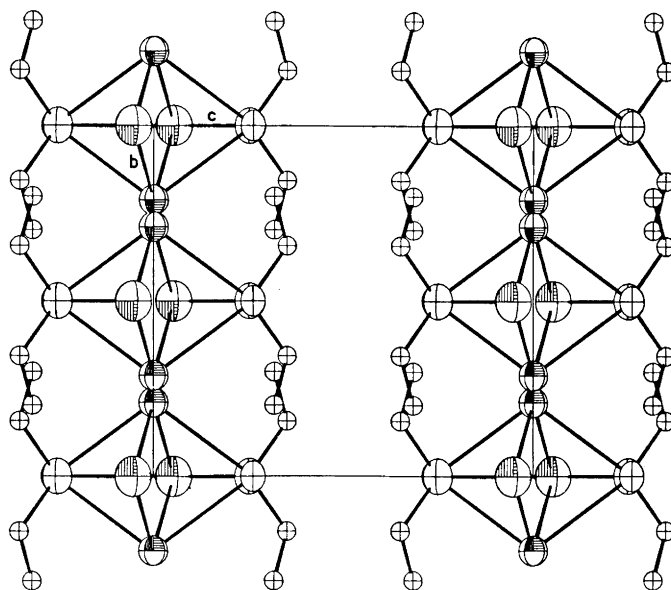


*Fig. 3.* A view of the unit cell as seen along the *a* axis.

present complex. A recently terminated structure investigation of diethyldithio-phosphinatothallium(I),[23] [Tl(Et$_2$PS$_2$)], shows this structure to consist of monomeric units, linked together in two-dimensional polymeric layers.

The thallium-sulphur and thallium-selenium bond lengths within the dimeric unit are found to be 3.237(5) Å and 3.424(4) Å, respectively. The dimers are linked together in two-dimensional polymeric layers by thallium-selenium contacts of 3.594(3) Å. The view that the structure is built up of dimeric units is justified by the shorter thallium-selenium coordination distances within the dimer and the shorter Tl...Tl separation. In the dimer the intermetallic distance is found to be 3.859(2) Å, while the corresponding distance between adjacent dimers is 5.2 Å. Similar metal-metal distances are observed in thallium(I) methoxide,[24] TlOCH$_3$, where the intermetallic separation within the tetrameric molecules are on the average 3.84 Å. In [Tl{n-pr)$_2$NCS$_2$}][15] the alternating interatomic distances are 3.98 Å and 4.00 Å, while in the cyclopentadienyl compound, C$_5$H$_5$Tl,[25] the metal-metal separations are all equal to 3.99 Å. In [Tl{(iso-pr)$_2$NCS$_2$}],[16] the distance between the two metal atoms in the same dimeric unit is found to be 3.584(5) Å, and this is significantly shorter than the corresponding distance in the former compounds. Whether bonding interactions between the metal atoms in all these structures occur is not clear, but according to Frasson et al.[25] the metal-metal distances are such as to allow the possibility of metal-metal interactions. For comparison, the shortest intermetal distances in the α-form of thallium are 3.41 Å and 3.46 Å.[26]

Similar metal-coordination as in the present investigation of diethylthio-selenophosphinatothallium(I), or more correctly of bis(diethylthioseleno-phosphinatothallium(I)), is found in some lead salts of dithioacids. Both in diethyldithiophosphatolead(II),[27] [Pb{(EtO)$_2$PS$_2$}$_2$], and in diethyldithiocarb-amatolead (II),[28] [Pb(Et$_2$NCS$_2$)$_2$], the coordination around the lead atom is a distorted tetragonal pyramid, with two distant sulphur neighbours in the opposite direction. The latter two lead-sulphur distances are, however, too large for any
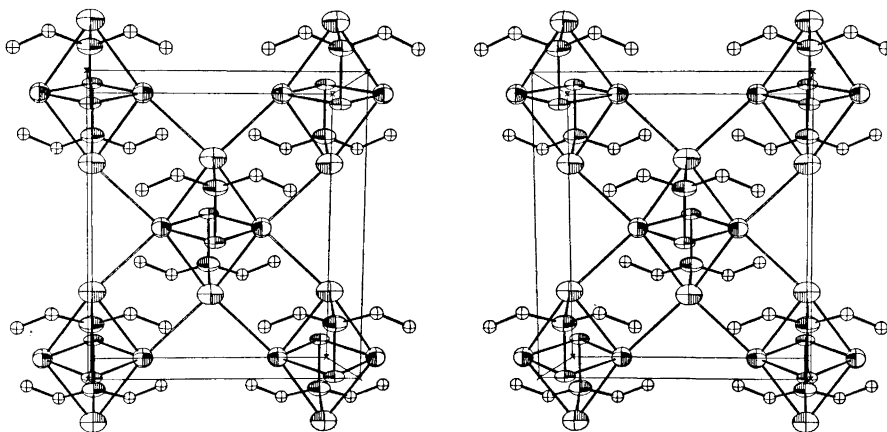


*Fig. 4.* A stereoscopic drawing showing the packing of molecules as seen along the *c* axis.

bonding interaction.[27,28] A somewhat similar configuration is also found in red PbO,[29,30] except that there Pb(II) has four distant neighbours as compared to the two found here for Tl(I). It is believed that in PbO the $6s$ electron pair in Pb(II) occupies a $sp$ hybridized orbital pointing away from the four near neighbours and that the repulsion between this lone pair of electrons and the ligands explains the deviation from cubic symmetry.[10,29] Exactly the same structure is found for SnO.[10,29] In TlI[31] there are five near neighbours and two distant ones, with the lone pair localized between the two weaker bonds. In the present case, the $sp$-hybridized lone pair then correspondingly points away from the four near sulphur and selenium neighbours and is located in between the two weak intermolecular Tl...Se bonds.

The thallium-sulphur bond lengths of 3.237(5) Å found in the present investigation may seem large. Bond distances of the same order of magnitude are, however, found in other thallium(I) compounds. In dipropyldithiocarbamatothallium(I)[15] the Tl−S coordination distances within the dimer range from 2.88 Å to 3.29 Å, while in the diisopropyl analogue[16] the corresponding lengths show smaller variations and vary between 2.98 Å and 3.05 Å. In diethyldithiophosphinatothallium(I)[23] the intramolecular Tl−S bonds are found to be 3.056(7) Å, while the intermolecular Tl−S distances are 3.429(10) Å and 3.453(7) Å. In $Tl_2S.Tl_2S_3$, studied by Hahn and Klingler[32] where the monovalent thallium atoms are eight-coordinated the Tl(I)−S distance is determined to be 3.32 Å, a bond length in accordance with the sum of the Pauling ionic radii of $Tl^+$ and $S^{2-}$ of 3.28 Å.[33] The authors also interpreted the interaction to be mainly ionic. A similar interpretation is given by Verhoef, Boeyens and Herbstein to the Tl−S coordination distances ranging from 3.38 Å to 3.45 Å found in some thiourea complexes of thallous salts.[34-36] As a larger bond distance than the sum of the ionic radii was found, the interaction was proposed to be of ion-dipole type. There does not seem to be any definite covalent radius for thallium available in the literature; however, a covalent Tl−S distance varying between 2.5 Å and 2.8 Å seems to be probable.[32,34] According to Slater the sum of the atomic radii of thallium and sulphur is 2.90 Å.[37]

The intramolecular thallium-selenium bond of 3.424(4) Å is relatively weaker than the thallium-sulphur bond, as the difference in bond lengths is larger than the difference in the selenium and sulphur covalent radii. This is, however, not surprising as only the selenium atoms are engaged in dimer-dimer interactions. This difference between sulphur and selenium is further reflected in the corresponding Se−P and S−P bond lengths of 2.115(9) Å and 2.042(10) Å, respectively. The former is just significantly larger (0.04 Å) than 2.07 Å, the sum of the P and Se double bond radii, while the latter is 0.10 Å larger than a P=S double bond.[33] For comparison the P−Se and P−S single bond lengths corrected for bond polarity are 2.24 Å and 2.10 Å, respectively. The relatively strong P−S and P−Se bonds found are not unexpected in view of the large Tl−S and Tl−Se coordination distances. The double-bond character of these bonds is also indicated from IR spectra recorded by Kuchen and Hertel.[38]

The large Tl−S and Tl−Se bond lengths in the present structure investigation are probably partly due to a high degree of ionic character and partly to the bridging nature of the sulphur and selenium atoms.

*Table 5.* Selected interatomic distances in some Tl(I) compounds in Å. Standard deviations in brackets.

| $a$ | Tl−S | Tl−Se | Tl−Tl |
|---|---|---|---|
| [Tl(Et₂PSSe)] | 3.237(5) | 3.424(4) | 3.859(2) |
| [Tl{(n-pr)₂NCS₂}] [15] | 2.88 − 3.29(0.015) | | 3.977(4) |
| [Tl{(iso-pr)₂NCS}] [16] | 2.977 − 3.050(0.103) | | 3.584(5) |
| Tl₂S.Tl₂S₃ [32] | 3.32 | | |
| [Tl(tu)₄]NO₃ [34] | 3.43(0.015) | | |
| [Tl(tu)₄]ClO₄ [34] | 3.43 | | |
| | 3.46 | | |
| [Tl(tu)₄]H₂PO₄ [35] | 3.446(8) | | |
| | 3.410(8) | | |
| [Tl(tu)₄]C₆H₅COO [36] | 3.45(1) | | |
| | 3.38(1) | | |
| Sum of Slater atomic radii [37] | 2.90 | 3.05 | 3.80 |
| Sum of Pauling ionic radii [33] | 3.28 | 3.42 | 2.88 |

$a$ tu = thiourea, n-pr = propyl and iso-pr = isopropyl.

The intermolecular thallium-selenium distance of 3.594(3) Å is significantly larger than the sum of the Pauling ionic radii of Tl⁺ and Se²⁻ of 3.42 Å.[33] However, there is no doubt that a dimer-dimer interaction exists.

For comparison, selected interatomic distances in some Tl(I) compounds are given in Table 5.

The phosphorus-carbon and carbon-carbon bonds correspond to normal values within the error limits, and the bond angles on the phosphorus atom are in good agreement with $sp^3$-hybridization on this atom.

The shortest interlayer contact is found to be 3.91(5) Å, and this is the only distance shorter than 4 Å. This is between the methylene carbons in the ethyl groups. The weak interlayer contacts may perhaps be the cause of the relatively high temperature factors found for the structure.

## REFERENCES

1. Gillespie, R. J. *J. Chem. Educ.* **47** (1970) 18.
2. Hazell, A. C. *Acta Chem. Scand.* **26** (1972) 1510.
3. Krebs, B., Buss, B. and Altena, D. *Z. anorg. allgem. Chem.* **386** (1971) 257.
4. Maslin, S. H., Ryan, P. R. and Asprey, L. B. *Inorg. Chem.* **9** (1970) 2100.
5. Maslin, S. H. and Ryan, P. R. *Inorg. Chem.* **10** (1971) 1757.
6. Poore, M. C. and Russel, D. R. *Chem. Commun.* **1** (1971) 18.
7. Curry, J. D. and Jondace, R. J. *J. Chem. Soc. Dalton* **1972** 1120.
8. Mumme, W. G. and Winter, G. *Inorg. Nucl. Chem. Letters* **7** (1971) 505.
9. Lawton, S. L. and Kokotailo, G. *Nature* **221** (1969) 550.
10. Dunitz, J. D. and Orgel, L.E. *Advan. Inorg. Chem. Radiochem.* **2** (1960) 1.
11. Hesse, R. In *Advances in the Chemistry of the Coordination Compounds*, New York 1961, p. 314.

12. Hesse, R. *Arkiv Kemi* **20** (1963) 481.
13. Hesse, R. and Nilson, L. *Acta Chem. Scand.* **23** (1969) 825.
14. Aava, U. and Hesse, R. *Arkiv Kemi* **30** (1969) 149.
15. Nilson, L. and Hesse, R. *Acta Chem. Scand.* **23** (1969) 1951.
16. Jennische, P., Olin, Å. and Hesse, R. *Acta Chem. Scand.* **26** (1972) 2799.
17. Knop, B. *Dissertation*, Technische Hochschule, Aachen, 1965.
18. Troughton, P. G. H. *Siemens Review* XXXVII (1970), Fourth Special Issue, "X-Ray and Electron Microscopy News", p. 22.
19. Coppens, P., Leiserowitz, L. and Rabinovich, D. *Acta Cryst.* **18** (1965) 1035.
20. *International Tables for X-Ray Crystallography*, Kynoch Press, Birmingham 1962, Vol. III.
21. Cromer, O. T. *Acta Cryst.* **18** (1965) 17.
22. Olofsson, O. and Gullman, J. *Acta Chem. Scand.* **25** (1971) 1327.
23. Esperås, S. and Husebye, S. *To be published.*
24. Dahl, L. F., Davis, G. L., Wampler, D. L. and West, R. *J. Inorg. Nucl. Chem.* **24** (1962) 357.
25. Frasson, E., Monegus, F. and Panattoni, C. *Nature* **199** (1963) 1087.
26. *Tables of Interatomic Distances and Configuration in Molecules and Ions*, The Chemical Society, Burlington House, W. 1., London 1958.
27. Ito, T. *Acta Cryst.* **B 28** (1972) 1034.
28. Iwasaki, H. and Hagihara, H. *Acta Cryst.* **B 28** (1972) 3070.
29. Moore, W. J. and Pauling, L. *J. Am. Chem. Soc.* **63** (1941) 1392.
30. Byström, A. *Arkiv Kemi, Mineral. Geol.* **A 20** (1945) No. 11.
31. Helmholz, L. *Z. Krist.* **95** (1936) 129.
32. Hahn, H. and Klingler, W. *Z. anorg. Chem.* **260** (1949) 10.
33. Pauling, W. *The Nature of the Chemical Bond*, 3rd. Ed., Cornell University Press, Ithaca, New York 1960.
34. Boeyens, J. C. A. and Herbstein, F. H. *Inorg. Chem.* **6** (1967) 1408.
35. Verhoef, L. H. W. and Boeyens, J. C. S. *Acta Cryst.* **B 24** (1968) 1262.
36. Verhoef, L. H. W. and Boeyens, J. C. A. *Acta Cryst.* **B 25** (1969) 607.
37. Slater, J. C. *J. Chem. Phys.* **41** (1964) 3199.
38. Kuchen, W. and Hertel, H. *Angew. Chem.* **4** (1969) 127.

# Oxidation of α-Hydroxy Ketones with *m*-Chloroperbenzoic Acid

TYGE GREIBROKK*

*Department of Chemistry, University of Oslo, Oslo 3, Norway*

A series of α-hydroxy ketones have been oxidized by *m*-chloroperbenzoic acid at 0°. The products were mixtures of aldehydes and carboxylic acids. The reactions did not follow a Baeyer-Villiger mechanism, but have been suggested to go through an enediol intermediate. Second order rate constants have been measured.

We recently found that the oxidation of phenylallene with *m*-chloroperbenzoic acid (MCPBA) gave benzaldehyde as the main product.[1] It was suggested that this compound resulted from a further oxidation of an intermediate α-hydroxy ketone. Such compounds have previously been obtained as products from oxidation of allenes with peracids.[2,3] Some of these non-enolizable compounds reacted further with more peracid at room temperature, while others were resistant.[2] Hence we wanted to study the behaviour of α-hydroxy ketones to peracids. Peracetic acid oxidation of benzoin and phenyl substituted derivatives of benzoin at room temperature already has been reported. The products, however, were exclusively benzoic acids.[4] In analogy with the oxidation of ketones a Baeyer-Villiger mechanism for the reaction was suggested.[4]

We have been interested in performing the oxidations in the cold with a moderately strong peracid. Therefore a dilute solution of the respective compounds was stirred at 0° with equivalent amounts of MCPBA. The consumption of peracid was followed by iodometric titration. The oxidation rates were high compared with those of simple ketones; acetophenone did not react even after one week at 0°, while benzoin (I) was completely oxidized after a few hours. The oxidized benzoin solution was washed with sodium carbonate in water, from which a mixture of *m*-chlorobenzoic acid and benzoic acid could be isolated. From the organic phase benzaldehyde was isolated in 90 % yield.

---

*Present address: Institute for Biomedical Research, University of Texas, Austin, Texas 78712, U.S.A.

The oxidation of acetoin (II) gave only acetic acid in addition to some un-reacted acetoin. The reaction rate obviously was too low to prevent further oxidation of acetaldehyde. 2-Hydroxy-1-phenyl-propan-1-one (III)[5] also reacted slowly. The isolated products were benzoic acid and about 40 % un-reacted starting material. On the other hand the isomeric 1-hydroxy-1-phenyl-propan-2-one (IV)[1] reacted very fast, though slower than benzoin, to give benzaldehyde in 81 % yield.

Introduction of an ether group in place of the hydroxy group, as in the methyl ether of benzoin (V),[6] provided a mixture of benzaldehyde and methyl-benzoate. The oxidation rate was decreased compared to that of benzoin (Table 1).

*Table 1.*

$$R^1 - \overset{\overset{\text{O}}{\|}}{C} - \overset{\overset{\text{OR}^4}{|}}{\underset{\underset{R^2}{|}}{C}} - R^3$$
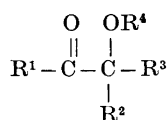
| Comp. | $R^1$ | $R^2$ | $R^3$ | $R^4$ | $K_2$ |
|-------|-------|-------|-------|-------|-------|
| I | phenyl | phenyl | H | H | $10.5 \times 10^{-3}$ |
| II | $CH_3$ | $CH_3$ | H | H | $0.7 \times 10^{-3}$ |
| III | phenyl | $CH_3$ | H | H | $0.8 \times 10^{-3}$ |
| IV | $CH_3$ | phenyl | H | H | $2.3 \times 10^{-3}$ |
| V | phenyl | phenyl | H | $CH_3$ | $1.3 \times 10^{-3}$ |
| VIII | phenyl | phenyl | $CH_3$ | H | No reaction |

$$R-\overset{\overset{\text{O}}{\|}}{C}-\overset{\overset{\text{OH}}{|}}{C}H-R \; \rightleftharpoons \; R-\overset{\overset{\text{OH}}{|}}{C}=\overset{\overset{\text{OH}}{|}}{C}-R \; \longrightarrow \; R-\overset{\overset{\text{OH}}{|}}{\underset{\diagdown}{C}}\overset{}{\underset{O}{}}\overset{\overset{\text{OH}}{|}}{\underset{\diagup}{C}}-R \; \longrightarrow \; RCHO + RCOOH$$

$$\text{VI} \qquad\qquad \text{VII}$$

$$Ph-\overset{\overset{\text{O}}{\|}}{C}-\overset{\overset{\text{OMe}}{|}}{C}H-Ph \; \longrightarrow \; Ph-\overset{\overset{\text{OH}}{|}}{\underset{\diagdown}{C}}\overset{}{\underset{O}{}}\overset{\overset{\text{OMe}}{|}}{\underset{\diagup}{C}}-Ph \; \longrightarrow \; PhCHO + PhCOOMe$$

$$\text{V}$$
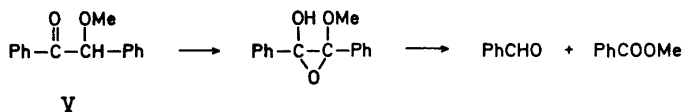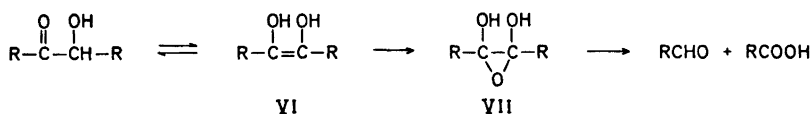
From the higher migratory aptitude of a phenyl group compared to a methyl group,[7] a Baeyer-Villiger oxidation of IV would be expected to be slow compared to the oxidation of III. The contrary, however, was found. We suggest that the peracid oxidation of α-hydroxy ketones at 0° go through an enediol intermediate (VI). Epoxidation of VI gives a 2,3-dihydroxy epoxide (VII) which rearranges[7] to a mixture of an aldehyde and a carboxylic acid. A strong indication for the enediol intermediate in these reactions was found in the oxidation of methylbenzoin (VIII); in this case no reaction occurred even

after several days at 0°. If a Bayer-Villiger mechanism were operating, this compound should have reacted very fast.

The oxidations approximately followed second order kinetics. The rate constants were comparable to those observed in the allene oxidations.[1] Our results indicate that the rate-determining step involves the α-hydroxy ketone-enediol equilibrium, as seen in the difference in reaction rates between IV and V.

The reaction was not catalyzed by acid, as the Baeyer-Villiger oxidation is known to be.[8] Indeed, when two drops of sulphuric acid were added to a solution of benzoin and MCPBA, the reaction was greatly retarded.

## EXPERIMENTAL

*Kinetics.* 0.01 mol of the α-hydroxy ketone was added to a solution of 70 % MCPBA (0.01 mol) in dichloromethane (100 ml) at 0°. The solution was stirred at 0° and the amount of peracid titrated iodometrically. The first 50 % of the oxidations was found to follow a second order plot. Rate constants were calculated from these plots.

*Oxidation of benzoin (I).* Benzoin (4.24 g, 0.02 mol) was added to the solution of MCPBA (0.02 mol) in 200 ml $CH_2Cl_2$ at 0°. After 15 h at 0° the solution was washed with a sodium carbonate solution, dried ($Na_2CO_3$) and evaporated. The residue consisted of fairly pure benzaldehyde, 1.92 g (90 %). From the aqueous phase addition of acid precipitated a mixture of benzoic acid and *m*-chlorobenzoic acid.

*Oxidation of acetoin (II).* The equivalent amounts of acetoin and MCPBA were reacted as previously shown. Careful evaporation of the solvent after one week at 0° and distilation of the residue gave a mixture of acetic acid and unreacted starting material.

*Oxidation of 2-hydroxy-1-phenyl-propan-1-one (III).* Amounts and conditions were similar to those in the oxidation of benzoin. After 4 days at 0° anhydrous $Na_2CO_3$ (10 g) was added to the reaction mixture, stirred for one hour, filtered and the filtrate evaporated. The residue consisted mainly of unreacted material, 1.2 g (40 %). From the alkaline precipitate a mixture of benzoic acid and *m*-chlorobenzoic acid was isolated.

*Oxidation of 1-hydroxy-1-phenyl-propan-2-one (IV).* Amounts, reaction conditions and work up procedure were analogous to the former, except that the reaction was finished over night. The residue consisted of fairly pure benzaldehyde, 1.6 g (81 %).

*Oxidation of the methyl ether of benzoin (V).* Amounts, reaction conditions (three days at 0°) and work up procedure followed the former reaction. From the filtrate a mixture of starting material, benzaldehyde (30 % yield) and methylbenzoate (50 % yield) was isolated. Chromatography on neutral alumina (act. II−III) gave the pure methyl-benzoate with benzene.

## REFERENCES

1. Greibrokk, T. and Skattebøl, L. *Acta Chem. Scand.* **27** (1973) 1421.
2. Crandall, J. K., and Machleder, W. H. *J. Am. Chem. Soc.* **90** (1968) 7292.
3. Crandall, J. K., Machleder, W. H. and Thomas, M. J. *J. Am. Chem. Soc.* **90** (1968) 7346.
4. Franzen, V. *Chem. Ber.* **88** (1955) 717.
5. Klemmensen, P., Schroll, G. and Lawesson, S. O. *Arkiv Kemi* **28** (1968) 405.
6. Quelet, R. and Frainnet, E. *Compt. Rend.* **235** (1953) 492.
7. Lewis, S. V. *Oxidation* **1** (1969) 213.
8. Hamthorne, F. and Emmous, W. D. *J. Am. Chem. Soc.* **80** (1958) 6398.

# Addition of Iodine Isocyanate to Allenes

TYGE GREIBROKK*

*Department of Chemistry, University of Oslo, Oslo 3, Norway*

Reactions of iodine isocyanate with allenes have been investigated. Absorption of one mol of the reagent at −78° gave addition preferentially to the substituted double bond of alkyl allenes. Addition at 0° gave a 1:1 mixture of isomers from addition to either double bond, except in the case of 1,1-dimethylallene, which gave preferentially addition to the unsubstituted double bond. Phenylallene in both cases furnished a 1:1 mixture of isomers.

Addition of the pseudohalogen iodine isocyanate (INCO) to olefins and acetylenes has been reported.[1-5]

Reactions with cumulated double bonds have not been examined, although Grimwood and Swern [2] observed, without isolating the product that methylallene absorbed one mol of INCO. As a part of our studies on electrophilic reactions with allenes,[6,7] we have investigated the reactions with iodine isocyanate.

Allene (*1a*), methylallene (*1b*), 1,1-dimethylallene (*1c*), tetramethylallene (*1d*), and phenylallene (*1e*) were treated with 2 mol of INCO in ether at −78° to 0°. Since INCO is a highly reactive electrophilic agent,[4] addition to both the double bonds of reactive allenes could not be excluded. We were, however, in no case able to observe any diadducts. In order to minimize the amounts of diiodo adducts,[1] further preparations were conducted with equimolar amounts of INCO and allenes. Because of low stability the isocyanates *2, 3* were transformed to the corresponding carbamates *4, 5* with methanol.

Allene (*1a*) gave a complex mixture of diiodo compounds, carbamates and polymeric material from which no major component could be separated. The symmetric allene *1d* gave only one product (*4d*), while the allenes *1b* and *1e* gave the isomeric carbamates (*4b, 5b* and *4e, 5e*) in a ratio of about 1:1, after reaction at 0°. 1,1-Dimethylallene (*1c*) under the same conditions furnished a 1:9 mixture of the isomers *4c* and *5c*. The combined yields in each case were 60 − 70 %. Separation of isomers were effected by chromatography on neutral alumina.

---

* Present address: Institute for Biomedical Research, University of Texas, Austin, Texas 78712, U.S.A.

When the methylallenes *1b* and *1c* were reacted at $-78°$, addition to the substituted double bond was preferred in a ratio of 2:1. Phenylallene (*1e*) still gave the 1:1 ratio at $-78°$. The NMR spectra showed that without exception iodine had substituted the central carbon atom of the allenic linkage. Together with the mass spectra these spectroscopic data were analogous to those previously observed for iodo carbamates.[5]



*a*: $R^1 = R^2 = R^3 = R^4 = H$
*b*: $R^1 = CH_3$, $R^2 = R^3 = R^4 = H$
*c*: $R^1 = R^2 = CH_3$, $R^3 = R^4 = H$
*d*: $R^1 = R^2 = R^3 = R^4 = CH_3$
*e*: $R^1 = Ph$, $R^2 = R^3 = R^4 = H$
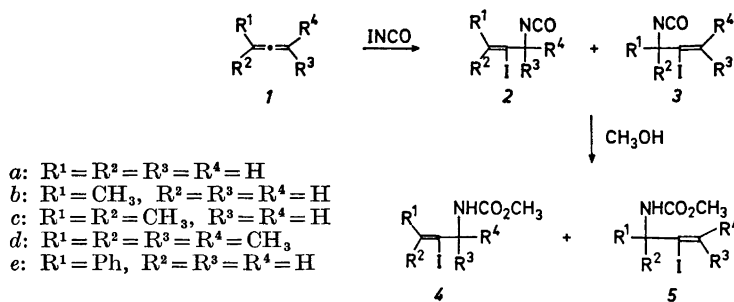
Mechanistically the methylallenes are expected to add INCO preferentially at the substituted double bond.[8] This was mainly true when the reaction was performed at low temperature, but not at $0°$. In order to examine if the latter was a result of a thermodynamically controlled reaction, as in the addition of bromine to allenes,[9] the isocyanate isomer mixtures *2, 3c* and *2, 3e*, synthesized at $-78°$, were kept at $0°$ for 2 h. No change in the isomer ratio was observed. Thus, the product composition must be the result of a kineticly controlled reaction.

### EXPERIMENTAL

The NMR spectra were recorded on a Varian A 60-A spectrometer and the mass spectral data were obtained on a A.E.I. MS 902 mass spectrometer.

*General procedure.* To a preformed solution of INCO [1] (0.03 mol) in dry ether (200 ml) the allene (0.03 mol) in ether (50 ml) was added under nitrogen with stirring at $-78°$ (or $0°$, respectively) during 10 min. After 4 h stirring at the same temperature, the suspension was filtered. To the filtrate methanol (150 ml) and 3 drops of a 0.1 M MeOLi solution (in methanol) was added. After 15 h at $20°$ in the dark, the solution was concentrated to a small volume, dissolved in ether (100 ml), washed with water containing a trace of sodium bisulfite, then with water, dried ($MgSO_4$) and evaporated. The carbamate isomers were separated by chromatography on neutral alumina (activity II), whereby the isomers *4*, together with minor amounts of diiodo adducts, were carefully eluted with hexane/cyclohexane. The other isomers (*5*) were then eluted with ether. A second identical chromatography procedure, combined with recrystallization from cyclohexane, was necessary to achieve analytically pure compounds.

*Addition to methylallene (1b).* The reaction at $-78°$ gave 4,8 g of a crude product whose NMR spectrum showed a 2:1 mixture of the isomers *4b* and *5b*, together with some diiodo adducts.

Reaction at $0°$ gave 6.5 g of carbamates *4b* and *5b* in a ratio of 1:1.

Elution with cyclohexane on neutral alumina gave 2.6 g (34 %) of *4b*, contaminated with small amounts of the other isomer. Further purification on neutral alumina and recrystallisation from cyclohexane gave analytical pure *4b*, m.p. $81-83°$. NMR($CDCl_3$) $CH_3$ $\delta$ 1.25 (d, $J = 7.0$ Hz), CH $\delta$ 4.0 (q), $CH_2$ $\delta$ 6.3 (d, $J = 2.0$ Hz) and $\delta$ 5.8 (d) NH $\delta$ 5.1 (b), $OCH_3$ $\delta$ 3.7 (s). MS: M(*m/e* 255) $- CH_3OH$, $M - NHCO_2CH_3$, $M - I$ (base peak).

Elution with ether twice from neutral alumina gave 2.5 g (32 %) of the pure, not crystalline *5b*. NMR(CDCl$_3$) CH$_3$ $\delta$ 1.8 (d, $J$ = 6.5 Hz), CH $\delta$ 5.8 (q), NCH$_2$ $\delta$ 4.1 (q), NH $\delta$ 5.3 (b), OCH$_3$ $\delta$ 3.7 (s). MS: M(*m/e* 255) − CH$_3$OH, M − NHCO$_2$CH$_3$, M − I (base peak).

*Addition to 1,1-dimethylallene (1c)*. The reaction at − 78° gave 4.9 g of the crude 2:1 mixture of isomers *4c* and *5c* (together with diiodo adducts).

Reaction at 0° gave 5.5 g of 1:9 mixture of isomers *4c* and *5c*. Elution with ether as above gave 4.4 g (55 %) of pure, not crystalline *5c*. NMR(CDCl$_3$) CH$_3$ $\delta$ 1.95(s), NCH$_2$ $\delta$ 4.14 (d), NH $\delta$ 5.3 (b), OCH$_3$ $\delta$ 3.65 (s). MS: M(*m/e* 269) − H, M − CH$_3$OH, M − CO$_2$CH$_3$, M − NHCO$_2$CH$_3$, M − I (base peak).

From the low temperature reaction crude *4c* was isolated. An analytically pure product was, however, not obtained because of the presence of small amounts of *5c*. NMR(CDCl$_3$) CH$_3$ $\delta$ 1.5 (s), CH$_2$ $\delta$ 6.25 (d, $J$ = 2.5 Hz) and $\delta$ 5.85 (d), NH $\delta$ 5.3 (b), OCH$_3$ $\delta$ 3.6 (s).

*Addition to tetramethylallene (1d)*. Reaction at 0° gave 6.0 g (67 %) of crude *4d*. Recrystallization from petroleum ether (b.p. 40 − 65°) gave pure *4d*, m.p. 68 − 69° NMR(CDCl$_3$) CH$_3$ $\delta$ 2.02 (s), CH$_3$ $\delta$ 2.08 (s), two CH$_3$ $\delta$ 165 (s), NH $\delta$ 5.1 (b), OCH$_3$ $\delta$ 3.6 (s). MS: M(*m/e* 297) − CH$_3$OH, M − CH$_3$OH − CH$_3$, M − NHCO$_2$CH$_3$, M − I, M − NHCO$_2$CH$_3$ (base peak).

*Addition to phenylallene (1e)*. The reaction at − 78° gave 7.2 g of the 1:1 mixture isomers *4e* and *5e*.

Reaction at 0° gave 8.0 g of the same 1:1 mixture. Elution with cyclohexane gave 3.0 g (31 %) of the crude isomer *4e*. A second elution gave pure *4e*, m.p. 88 − 91°. NMR(CDCl$_3$) CH$_2$ $\delta$ 6.40 (d, $J$ = 2.0 Hz) and $\delta$ 5.95 (d), CH and NH $\delta$ 5.3 (b), OCH$_3$ $\delta$ 3.7 (s), Ph $\delta$ 7.3 (s). MS: M(*m/e* 317) − I (base peak), M − I − CH$_3$OH, M − I − CO$_2$CH$_3$, M − I − NHCO$_2$CH$_3$. Elution with ether gave 2.9 g (30 %) of crude *5e*. Further purification from neutral alumina gave pure *5e*, m.p. 110 − 115°. NMR(CDCl$_3$) CH $\delta$ 6.95 (s), NCH$_2$ $\delta$ 4.2 (q), NH $\delta$ 5.2 (b), OCH$_3$ $\delta$ 3.7 (s), Ph $\delta$ 7.3 (m). MS: M(*m/e* 317) − CH$_3$OH, M − I (base peak), M − I − CH$_3$OH, M − I − CO$_2$CH$_3$, M − I − NHCO$_2$CH$_3$.

# REFERENCES

1. Hassner, A., Lorber, M. E. and Heathcock, C. J. *J. Org. Chem.* **32** (1967) 540.
2. Grimwood, B. E. and Swern, D. *J. Org. Chem.* **32** (1967) 3665.
3. Drefahl, G., Ponsold, K. and Köllner, J. *J. prakt. Chem.* **23** (1964) 136.
4. Gebelein, C. G. and Swern, D. *Chem. Ind. (London)* **1965** 1462.
5. Greibrokk, T. *Acta Chem. Scand.* **26** (1972) 3305.
6. Greibrokk, T. *To be published*.
7. Greibrokk, T. and Skattebøl, L. *Acta Chem. Scand.* **27** (1973) 1421.
8. Waters, W. L., Linn, W. S. and Caserio, M. C. *J. Am. Chem. Soc.* **90** (1968) 6741, and references therein.
9. Federova, A. V. *J. Gen. Chem. USSR* **33** (1963) 3508.

# The Primary Structure of Soybean Leghemoglobin

## II. Amino Acid Sequence of Seventeen Peptides Isolated from the Tryptic Hydrolysate of the Slow Component

NILS ELLFOLK and GUNNEL SIEVERS

Department of Biochemistry, University of Helsinki, SF-00170 Helsinki 17, Finland

The amino acid sequences of seventeen peptides which had been isolated from the tryptic hydrolysate of the apoprotein of the slow component (Lba) of soybean leghemoglobin have been determined. The amino terminal peptide has been identified as *Val-Ala-Phe-Thr-Glu-Lys*.

In the preceding paper[1] the purifications and amino acid composition of seventeen peptides from the tryptic digest of the slow components of soybean leghemoglobin (Lba) have been described. All these peptides were obtained in a homogeneous state and in sufficient quantity to allow the structural studies to be performed. The determination of the sequence of these peptides is described in this communication.

## MATERIALS AND METHODS

*Leghemoglobin.* The slow component of soybean leghemoglobin (Lba) and its apoprotein were prepared as previously described.[2,3]

*Peptides.* As described in the preceding paper,[1] each peptide isolated was finally dissolved in 2 ml of deionized water and stored at $-16°C$. Aliquots were removed and taken to dryness just before use for the structural studies.

*Enzymes.* Carboxypeptidase A was a crystallized, DFP-treated preparation and subtilopeptidase A a crystallized preparation, both from Sigma Chemical Company (St. Louis, U.S.A.). Three times crystallized chymotrypsin and leucine aminopeptidase were preparations from Worthington Biochemical Corporation (Freehold, New Jersey, U.S.A.). Thermolysin was a crystalline preparation from Merck AG (Germany).

*Digestion of the peptides with enzymes.* Hydrolysis with chymotrypsin was carried out on 0.2 to 0.5 $\mu$mol of peptides in $0.2-0.5$ ml of 1 % ammonium bicarbonate solution of pH 8.1 at 37°C for the appropriate time by addition of chymotrypsin at an enzyme-substrate ratio 1:100 (w/w). After digestion the solution was taken to dryness *in vacuo.*

---

*Abbreviations.* 1-Dimethyl-amino-5-naphthalenesulfonyl-, dansyl-, DNS-; 3-phenyl-2-thiohydantoin-, PTH-.

The digest with subtilopeptidase A was performed on 0.2 – 0.5 μmol of peptide in 0.2 M N-ethylmorpholine-acetic acid buffer, pH 8.0, containing 0.5 μmol peptide/ml with a 1:100 molar ratio, at 37°C for the appropriate time. The reaction was terminated by holding the hydrolysate at 100°C for 3 min after which it was lyophilized.

Hydrolysis with thermolysin was performed in a 0.2 % ammonium carbonate solution, pH 8.3, containing 1 μmol of peptide in 1 ml of solution at 37°C with a 1:100 molar ratio for 20 h, after which the digest was lyophilized.

*Partial hydrolysis with dilute hydrochloric acid.* 0.2 – 0.5 μmol of peptide was hydrolyzed in 0.5 ml of 0.03 N HCl in sealed tubes for 15 h at 105°C. After hydrolysis the solution was taken to dryness *in vacuo* over pellets of sodium hydroxide.

*Partial hydrolysis with concentrated hydrochloric acid.* A sample of peptide solution containing 0.1 μmol of peptide was evaporated to dryness, dissolved in 0.2 ml of 12 N hydrochloric acid and incubated at 37°C for 15 – 42 h. After hydrolysis the solution was taken to dryness *in vacuo* over pellets of sodium hydroxide.

*Chromatography of peptides.* The column chromatography and paper chromatography employed for the isolation and purification of the peptides were carried out as described in the preceding paper.[1] The chromatographic mobility was determined relative to leucine and denoted by $R_{Leu}$.

*High voltage paper electrophoresis.* Purification of peptides by electrophoresis was carried out on Whatman No. 3MM paper in cooled tanks[4] at 60 V/cm. The electrophoresis buffers were pyridine-acetic acid at pH 6.5 and 3.5, 8 % acetic acid – 2 % formic acid at pH 1.9, and ammonium carbonate (1 %) at pH 8.9.[5] The electrophoretic mobilities at pH 6.5 were determined relative to lysine and aspartic acid and are denoted by $E_{Lys}$ and $E_{Asp}$, respectively.

*Amino acid analyses.* The amino acid content of the peptides was determined after hydrolysis at 108°C for 18 h on an automatic amino acid analyzer (Beckman/Spinco 120 B).[6] The general method of Spackman *et al.*[6] was used for determining the glutamine or asparagine content of peptides hydrolyzed with leucine aminopeptidase or carboxypeptidase A. The elution program used did not separate glutamine, asparagine, and serine. Tryptophan was quantitatively determined according to Spies and Chambers' method K.[7]

*Amino acid sequence analyses.* The phenylisothiocyanate method of Sjöquist *et al.*[8] and Blombäck *et al.*[9] was used. The thiohydantoins obtained were identified by thin layer chromatography in the solvent systems of Jeppsson and Sjöquist.[10] Subtractive Edman degradation was performed according to Königsberg and Hill.[11,12] Edman-dansyl-degradation was performed according to Gray and Hartley,[13,14] and the DNS-amino acids were identified by electrophoresis at pH 4.38 at 4800 V for 2.5 h on a high voltage cold plate (Shandon Southern, Great Britain).[13,14] The DNS derivatives of serine, alanine, and glycine were further separated at pH 2.0 as described by Milstein.[15] The DNS derivatives were also identified by thin layer chromatography according to Woods and Wang.[16]

*Amide residues.* Amide residues were assigned on the basis of electrophoretic mobilities of the peptides at pH 6.5 according to Offord[17] and by digestion with leucine aminopeptidase.

*Hydrazinolysis.* For hydrazinolysis the peptide sample was dried thoroughly over $P_2O_5$ and traces of moisture were removed by addition of 0.15 ml of benzene and repeating the drying procedure. The dry sample was sealed in an evacuated tube together with 0.1 ml of anhydrous hydrazine and heated for 16 h at 80°C. The sample was taken to dryness *in vacuo* over $P_2O_5$ and $H_2SO_4$, and the liberated amino acid was determined with the amino acid analyzer.

*Digestion with carboxypeptidase A.* The incubation of 0.05 – 0.1 μmol of peptide was performed in 0.2 ml of 0.2 M sodium bicarbonate buffer, pH 8.3, as previously described.[18] The liberated amino acids were determined with the automatic amino acid analyzer.

*Digestion with leucine aminopeptidase.* The incubation of 0.05 – 0.1 μmol of peptide was performed as previously described in 0.1 ml of 0.1 M Tris-HCl buffer of pH 8.5.[18] Liberated amino acids were determined using the automatic amino acid analyzer.

*Nomenclature of leghemoglobin.* Leghemoglobin was abbreviated Lb and the different components of leghemoglobin as previously described.[2]

*Nomenclature of peptides.* The principles employed for numbering the peptides are identical with those used previously.[1] The letter before the peptide number indicates

the hydrolysis procedure used: "T" refers to trypsin, "Th" to thermolysin, "C" to chymotrypsin, "S" to subtilopeptidase A, "A" to hydrolysis with dilute and "H" with 12 N hydrochloric acid.

## RESULTS

*The amino-terminal sequence of Lba.* Amino-terminal valine was estimated in high yield as its PTH-derivative, as was the second amino acid alanine. The third, phenylalanine, was also conclusively identified, and the fourth amino acid seemed to be threonine. However, the fifth amino acid residue from the amino-terminus could not be clearly identified. The amino terminal of Lba is therefore *Val-Ala-Phe-Thr-*.

*The sequence of the individual peptides.* The sequences shown in Table 1 were obtained from enzymatic digestions and Edman degradations of the

*Table 1.* Amino acid sequence of the tryptic peptides from the slow component (Lba) of soybean leghemoglobin.

| Peptide number | Amino acid sequence |
|---|---|
| aT1[a] | Lys |
| aT2 | Ala-Pro-Ala-Ala-Lys |
| aT3 | Leu-Phe-Ala-Leu-Val-Arg |
| aT4 | Ala-Lys |
| aT5 | Thr-Ile-Lys |
| aT6 | Ala-Ser-Gly-Thr-Val-Val-Ala-Asp-Ala-Ala-Leu-Gly-Ser-Val-His-Ala-Gln-Lys |
| aT7 | Ala-Val-Thr-Asn-Pro-Glu-Phe-Val-Val-Lys |
| aT8 | Ala-Ala-Val-Gly-Asp-Lys |
| aT9 | Asp-Ser-Ala-Gly-Glu-Leu-Lys |
| aT10 | Glu-Ala-Leu-Leu-Lys |
| aT11 | Leu-Thr-Gly-His-Ala-Glu-Lys |
| aT12 | Val-Ala-Phe-Thr-Glu-Lys |
| aT13[b] | Glp-Asp-Ala-Leu-Val-Ser-Ser-Ser-Phe-Glu-Ala-Phe-Lys |
| aT14 | Asp-Leu-Phe-Ser-Phe-Leu-Ala-Asn-Pro-Thr-Asp-Gly-Val-Asn-Pro-Lys |
| aT15 | [Glu-Asn-Ala-Leu] - [Val-Ser-Ser] - [Ser, Tyr] - [Glu-Ala-Tyr] - Lys |
| aT16 | Trp-Ser-Asp-Glu-Leu-Ser-Arg |
| aT17 | Ala-Trp-Glu-Val-Ala-Tyr-Asp-Glu-Leu-Ala-Ala-Ala-Ile-Lys |
| aT18 | Ala-Asn-Ile-Pro-Gln-Tyr-Ser-Val-Val-Phe-Tyr-Thr-Ser-Ile-Leu-Glu-Lys |

[a] Assumed to be formed by secondary splitting of the peptides or free lysine contaminating the apoprotein. [b] Glp, abbreviation used for pyrrolidone-carboxylic acid.

tryptic peptides of component *a* of soybean leghemoglobin (Lba). The sequence of the histidine containing heptapeptide, *a*T11, published earlier,[18] is also included in the table. The peptides are discussed in the order in which they were originally isolated. The exact amino acid composition has been reported previously.[1] The amino acid composition of the peptides before and after each stage of the Edman degradation is expressed as mol ratios. Im-

purities generally amounted to 0.1 or less residues per mol and were not reported. Peptides which contain a lysine or arginine residue are assumed to be COOH-terminal.

*Peptide aT1.* This was identified as free *lysine* by paper electrophoresis, paper chromatography and by its position on the amino acid analyzer.

*Peptide aT2.* The amino acid sequence of this peptide was deduced from two steps of the Edman degradation presented in Table 2.

*Peptide aT3.* This peptide was degraded by the Edman technique through four steps, giving the sequence shown in Table 2.

*Table 2.* Amino acid sequences of peptides *a*T2, *a*T3, and *a*T5.

| Sequence *a*T2 | Ala - Pro - Ala - Ala - Lys | | | | | |
|---|---|---|---|---|---|---|
| Edman degradation | | | | | | |
| Step 1 | *0.00* | 1.00 | 2.14 | | | *a* |
| Step 2 | 0.00 | *0.00* | 2.0 | | | *a* |
| | | | | | | |
| Sequence *a*T3 | Leu - Phe - Ala - Leu - Val - Arg | | | | | |
| Edman degradation | | | | | | |
| Step 1 | *0.00* | 1.00 | 1.06 | 0.97 | 0.82 | *a* |
| Step 2 | 0.00 | *0.07* | 0.78 | 1.23 | 0.93 | *a* |
| Step 3 | — | 0.00 | *0.34* | 1.03 | 0.93 | *a* |
| Step 4 | — | — | 0.00 | *0.39* | 1.00 | *a* |
| | | | | | | |
| Sequence *a*T5 | Thr - Ile - Lys | | | | | |
| Edman degradation | | | | | | |
| Step 1 | *0.00* | 1.00 | *a* | | | |

*a* Not determined.

*Peptide aT4.* From the specificity of trypsin, the dipeptide had to be *Ala-Lys.* In confirmation, the amino terminal endgroup was found to be alanine identified as PTH-alanine.

*Peptide aT5.* One step of Edman degradation (Table 2) showed threonine to be the $NH_2$-terminal amino acid of this tripeptide.

*Peptide aT6.* The sequence of this peptide has earlier been reported.[18] The amino acids of positions 5 − 7 of this peptide were re-investigated. A thermolysin digestion of the peptide yielded four peptides, Th1, Th2, Th3, and Th4, which were isolated by electrophoresis at pH 6.5 and 1.9. Peptide Th2 was a pentapeptide containing two valine, one alanine, and one aspartic acid. It was subjected to three steps of Edman degradation, which formulated the sequence as *Val-Val-Ala-Asp,* (Table 3), a sequence identical to that reported by Aggarwal and Riggs.[19]

*Peptide aT7.* Five steps of Edman degradation and digestion with leucine aminopeptidase yielded the $NH_2$-terminal sequence *Ala-Val-Thr-Asn-Pro-* for this peptide (Table 4). When *a*T7 was subjected to hydrolysis with subtilopeptidase A, four principal peptides were formed, S1, S2, S3, and S4.

*Table 3.* Amino acid sequence of peptide $a$T6.

| Sequence | Ala-Ser-Gly-Thr-Val-Val-Ala-Asp-Ala-Ala-Leu-Gly-Ser-Val-His-Ala-Gln-Lys |
|---|---|
| | \|—— Th1 ——\|———— Th2 ————\|— Th3 —\|———— Th4 ————\| |
| Thermolytic peptides | |
| Th1 (neutral) | Ala, 1.05; Ser, 1.01; Gly, 1.07; Thr, 0.87 |
| Th2 ($E_{Asp}$, 0.39) | Val, 1.38; Ala, 3.20; Asp, 1.42 |
| Edman degradation | |
| Step 1 | *Val, 0.93*; Ala, 2.93; Asp, 1.13 |
| Step 2 | *Val, 0.00*; Ala, 2.85; Asp, 1.15 |
| Step 3 | —          *Ala, 1.90*; Asp, 1.10 |
| Step 4 | —          Ala, 2.00; *Asp. 0.68* |
| Th3 (neutral) | Leu, 0.90; Gly, 1.09; Ser, 1.01 |
| Th4 ($E_{Lys}$, 0.74) | Val, 0.75; His, 0.40; Ala, 1.13; Glu, 1.04; Lys, 1.07 |

*Table 4.* Amino acid sequence of peptide $a$T7.

| Sequence | Ala-Val-Thr-Asn-Pro-Glu-Phe-Val-Val-Lys |
|---|---|
| | \|———— S1 ————\| S2 \|— S3 —\| |
| | \|– S4 –\| |
| | \|———— Th1 ————\|—Th2 ——\| |
| | \|———— Th3 ——\| |
| Edman degradation | |
| Step 1 | *Ala, 0.00*; Val, 2.73; Thr, 0.99; Asp, 1.08; Pro, 1.25; Glu, 1.11; Phe, 0.84; Lys, [a] |
| Step 2 | Ala, 0.00; *Val, 1.88*; Thr, 1.04; Asp, 1.07; Pro, 1.10; Glu, 1.06; Phe, 0.85; Lys [a] |
| Step 3 | Ala, 0.00; Val, 1.93; *Thr, 0.25*; Asp, 1.06; Pro, 0.89; Glu, 1.12; Phe, 1.00; Lys, [a] |
| Step 4 | Ala, 0.00; Val, 1.86; Thr, 0.00; *Asp, 0.47*; Pro, 1.12; Glu, 1.13; Phe, 0.90; Lys, [a] |
| Step 5 | Ala, 0.00; Val, 2.02; Thr, 0.00; Asp, 0.00; *Pro, 0.37*; Glu, 1.29; Phe, 0.69; Lys, [a] |
| Leucine amino peptidase A 30 min. | Ala, 1.00; Val, 0.98; Thr, 0.48; Asn, 0.42 |
| Subtilopeptidase peptides | |
| S1 ($E_{Asp}$, 0.35) | Ala, 0.82; Val, 0.96; Thr, 0.98; Asp, 1.10; Pro, 1.10; Glu, 1.03 |
| Edman degradation | |
| Step 1 | *Ala, 0.00*; Val, 0.82; Thr, 0.89; Asp, 1.06; Pro, 1.29; Glu, 0.95 |
| Step 2 | Ala, 0.00; *Val, 0.00*; Thr, 0.87; Asp, 1.09; Pro, 0.98; Glu, 1.06 |
| Step 3 | —          Val, 0.00; *Thr, 0.00*; Asp, 0.93; Pro, 1.11; Glu, 0.97 |
| Step 4 | —          —          Thr, 0.00; *Asp, 0.60*; Pro, 0.98; Glu, 1.02 |
| Step 5 | —          —          —          Asp, 0.00; *Pro, 0.50*; Glu, 1.00 |
| S2 (neutral) | Phe, 1.00 |
| S3 (neutral) | Val, (2) |
| S4 ($E_{Lys}$, 0.51) | Val, 1.03; Lys, 0.97 |
| Thermolytic peptides | |
| Th1 ($E_{Asp}$, 0.32) | Ala, 0.96; Val, 1.04; Thr, 1.00; Asp, 0.99; Pro, 1.10; Glu, 1.03; Phe, 0.88 |
| Th2 ($E_{Lys}$, 0.47) | Val, 2.18; Lys, 1.00 |
| Th3 ($E_{Lys}$, 0.40) | Phe, 0.93; Val, 2.07; Lys, 1.00 |

[a] Not determined.

These were separated by electrophoresis at pH 6.5 and 1.9 and finally by paper chromatography with the butanol-acetic acid-water system. The amino acid sequence of S1 was derived from five steps of Edman degradation. The acidic electrophoretic mobility at pH 6.5 suggests that glutamic acid must be in the acid form. Since the $NH_2$-terminal sequence of $a$T7 was confirmed by the Edman degradation on S1, this is placed in the $NH_2$-terminus of $a$T7. Since lysine is placed at the COOH-terminus of $a$T7 and considering the specificity of trypsin, the structure of S4 can only be *Val-Lys*. S2 is found to be free phenylalanine and S3 a dipeptide *Val-Val*. For confirmation and completion of the sequence, $a$T7 was digested with thermolysin. Three main subpeptides were formed, Th1, Th2, and Th3, which were isolated by electrophoresis at pH 6.5. Th1 gives the necessary overlap for S1 and S2, Th2 overlaps S3 and S4 and Th3 overlaps S2 and S3.

*Table 5.* Amino acid sequences of peptides $a$T8, $a$T9, $a$T10, and $a$T12.

| Sequence $a$T8 | Ala - Ala - Val - Gly - Asp - Lys | | | | | |
|---|---|---|---|---|---|---|
| Edman degradation | | | | | | |
| Step 1 | *0.00* | 1.15 | 0.91 | 0.96 | 0.98 | [a] |
| Step 2 | 0.00 | *0.35* | 0.90 | 1.04 | 1.06 | [a] |
| Step 3 | — | 0.00 | *0.00* | 0.99 | 1.01 | [a] |
| Step 4 | — | — | 0.00 | *0.64* | 1.00 | [a] |
| | | | | | | |
| Sequence $a$T9 | Asp - Ser - Ala - Gly - Gln - Leu - Lys | | | | | |
| | \|——— Th1 ———\|— Th2 —\| | | | | | |
| Edman degradation | | | | | | |
| Step 1 | *0.00* | 0.99 | 1.03 | 1.00 | 1.00 | 0.96 | [a] |
| Step 2 | 0.00 | *0.00* | 1.03 | 1.03 | 1.05 | 0.89 | [a] |
| Step 3 | — | 0.00 | *0.30* | 1.09 | 1.03 | 0.88 | [a] |
| Step 4 | — | — | 0.00 | *0.70* | 1.02 | 0.98 | [a] |
| | | | | | | |
| Thermolytic peptides | | | | | | |
| Th1 ($E_{Asp}$, 0.48) | Asp, 0.99; Ser, 0.90; Ala, 1.10; Gly, 1.02; Gln, 1.01 | | | | | |
| Th2 | Leu, 0.96; Lys, 1.04 | | | | | |
| | | | | | | |
| Sequence $a$T10 | Glu - Ala - Leu - Leu - Lys | | | | | |
| Edman degradation | | | | | | |
| Step 1 | *0.00* | 0.98 | 2.01 | [a] | | |
| Step 2 | 0.00 | *0.00* | 2.00 | [a] | | |
| | | | | | | |
| Sequence $a$T12 | Val - Ala - Phe - Thr - Glu - Lys | | | | | |
| Edman degradation | | | | | | |
| Step 1 | *0.00* | 0.96 | 1.01 | 0.97 | 1.07 | [a] |
| Step 2 | 0.00 | *0.00* | 0.88 | 1.06 | 1.06 | [a] |
| Step 3 | — | 0.00 | *0.00* | 0.93 | 1.07 | [a] |
| Step 4 | — | — | 0.00 | *0.00* | 1.00 | [a] |

[a] Not determined.

*Peptide aT8.* The results of the Edman degradation presented in Table 5 permit the determination of the amino acid sequence of this peptide. The aspartic acid residue in the peptide must be in the acid form because of the neutral mobility of the peptide on electrophoresis at pH 6.5.

*Peptide aT9.* The Edman degradation of this peptide was carried out through four steps which yielded the $NH_2$-terminal sequence *Asp-Ser-Ala-Gly-* (Table 5). Digestion of aT9 with thermolysin yielded two peptides, Th1 and Th2, which were purified by paper electrophoresis at pH 6.5. Th1 was an acidic pentapeptide which, after removal of aspartic acid by the Edman technique, yielded an electrophoretically neutral peptide indicating the presence of glutamine. Th2 was a basic peptide containing leucine and lysine. Since lysine is the COOH-terminus of aT9, the sequence of Th2 is *Leu-Lys.*

*Peptide aT10.* Two steps of Edman degradation (Table 5) established the complete sequence of this peptide. The glutamic acid residue in the peptide was shown to be in the acid form by its neutral behaviour on paper electrophoresis at pH 6.5.

*Peptide aT11.* No sequence studies were performed as the structure of this histidine peptide has been reported earlier.[18]

*Peptide aT12.* Four steps of Edman degradation established the sequence of this peptide (Table 5). The glutamic acid residue must be in the acid form because of the neutral electrophoretic mobility of the whole peptide at pH 6.5. The sequence of the first four amino acids of this peptide is identical to that obtained for the $NH_2$-terminal end of the intact peptide chain of Lba, which indicates that aT12 represents the $NH_2$-terminal sequence of Lba.

*Peptide aT13.* One step of Edman degradation gave no change in the amino acid composition of the peptide compared to the untreated sample. It was assumed that a pyrrolidone carboxylic acid occupied the $NH_2$-terminal position and that the transformation of a glutamine residue may have occurred during isolation of the peptide. When the peptide was subjected to thermolytic hydrolysis five principal peptides were formed, Th1, Th2, Th3, Th4, and Th5. These were separated electrophoretically at pH 6.5 and further at pH 1.9. Table 6 shows their amino acid composition. Since Th1, like aT13 itself, shows no $NH_2$-terminal amino acid by Edman degradation, Th1 had to represent the $NH_2$-terminal position of aT13. The amino acid sequence of Th1 was derived after partial hydrolysis of the peptide with 12 N HCl at 37°C. The hydrolysate was resolved by electrophoresis at pH 6.5, and free glutamic acid, aspartic acid, and alanine were isolated in addition to a dipeptide Th1-H1 the sequence of which was *Asp-Ala* as shown by one step of Edman degradation (Table 6). The aspartic acid residue of Th1 is present in the acid form. When precautions were taken to avoid degradation of the assumed labile $NH_2$-terminal glutamine, a thermolytic peptide Th1A was isolated containing aspartic and glutamic acid and alanine. Its electrophoretic mobility shows only one acidic group to be free, which indicates that glutamic acid is amidated. Two steps of dansyl-Edman degradation yielded the sequence *Gln-Asp-Ala.* The composition of Th2 suggests its structure to be identical with that of Th1 elongated by one amino acid, leucine. This conclusion is supported by carboxypeptidase A, establishing Leu as the COOH-terminus of the peptide. Its electrophoretic mobility showed two

*Table 6.* Amino acid sequence of peptide aT13.

| | |
|---|---|
| Sequence [b] | Glp-Asp-Ala-Leu-Val-Ser-Ser-Ser-Phe-Glu-Ala-Phe-Lys |
| | \|— Th1 —\|——— Th4 ———\|—— Th3 —\|—Th6—\| |
| | \|——— Th2 ——\|— Th5 ——\| |
| | \|——— S1 ——\|——S4 —\|      \|— S3 ——\| |
| | \|— S2 ———\| |
| | |
| Edman degradation | |
| Step 1 | Glu, 1.95; Asp, 1.09; Ala, 2.09; Leu, 1.06; Val, 1.03; |
| | Ser, 2.86; Phe, 1.77; Lys [a] |
| | |
| Thermolytic peptides | |
| Th 1 ($E_{Asp}$, 1.07) | Asp, 1.03; Glu, 0.96; Ala, 1.00 |
| | |
| Hydrolysis in 12 N HCl | |
| Th1-H1 | Asp, 1.00; Ala, 1.00 |
| Edman degradation | |
| Step 1 | *Asp, 0.00*; Ala, 1.00 |
| Th1A ($E_{Asp}$, 0.59) | Asp, 1.04; Glu, 0.99; Ala, 0.98 |
| Edman degradation | Direct examination of dansyl derivatives |
| Step 1 | DNS-Glu |
| Step 2 | DNS-Asp |
| | |
| Th2 ($E_{Asp}$, 0.92) | Asp, 0.99; Glu, 0.85; Ala, 0.99; Leu, 1.16 |
| Carboxypeptidase A 100 min | Leu, 0.52 |
| Th2A ($E_{Asp}$, 0.50) | Amino acid composition identical with that of Th2 |
| | |
| Th3 ($E_{Asp}$, 0.52) | Phe, 0.75; Glu, 1.00; Ala, 1.00 |
| Edman degradation | |
| Step 1 | *Phe, 0.00*; Glu, 1.00; Ala, 1.00 |
| Step 2 | —   *Glu, 0.00*; Ala, 1.00 |
| | |
| Th4 (neutral) | Leu, 0.91; Val, 1.01; Ser, 3.13 |
| Edman degradation | |
| Step 1 | *Leu, 0.00*; Val, 0.94; Ser, 3.05 |
| Step 2 | —   *Val, 0.00*; Ser, 3.00 |
| | |
| Th5 (neutral) | Val, 1.13; Ser, 2.86 |
| | |
| Th6 ($E_{Lys}$, 0.63) | Phe, 1.00; Lys, 1.00 |
| | |
| Subtilopeptidase peptides | |
| S1 ($E_{Asp}$, 0.92) | Glu, 0.95; Asp, 0.98; Ala, 1.00; Leu, 1.07 |
| | |
| S2 ($E_{Asp}$, 0.52) | Glu, 1.00; Ala, 1.05; Phe, 0.95 |
| Edman degradation | |
| Step 1 | *Glu, 0.00*; Ala, 1.01; Phe, 0.99 |
| Step 2 | —   *Ala, 0.00*; Phe, 1.00 |
| | |
| S3 ($E_{Asp}$, 0.43) | Ser, 1.10; Phe, 1.02; Glu, 1.02; Ala, 0.86 |
| | |
| S4 | Val, 0.86; Ser, 2.15 |
| Edman degradation | |
| Step 1 | *Val, 0.00*; Ser, 2.00 |

[a] Not determined. [b] Glp, abbreviation used for pyrrolidone carboxylic acid.

acidic groups to be free. The composition of Th2A is identical to that of Th2 except that it has only one free acidic group, a relationship identical to that of Th1 and Th1A. Th6 contains the lysine residue of $a$T13, and therefore occupies the COOH-terminal portion of the peptide. Its sequence, *Phe-Lys*, is deduced by considering the specificity of trypsin. Th3 was determined as *Phe-Glu-Ala* by two steps of Edman degradation. The glutamic acid residue of this peptide must be in the acid form because of the acidic electrophoretic mobility of the peptide at pH 6.5. Th4 was deduced to be *Leu-Val-Ser-Ser-Ser* by two steps of Edman degradation. Th5 was assumed to be *Val-Ser-Ser-Ser* by referring to the sequence of Th4. Th3 and Th4 both represent the middle portion of the peptide $a$T13, Th2 giving the overlap between Th1 and Th4. The order of these components was further established and confirmed by the overlapping peptides obtained from a subtilopeptidase A digest of $a$T13. Four peptides, S1, S2, S3, and S4, were isolated by electrophoresis at pH 6.5 and 1.9. The amino acid composition of these subpeptides is given in Table 6. S1 contained the $NH_2$-terminal four residues and electrophoresis at pH 6.5 showed it to have two free acidic groups. Two steps of Edman degradation and acidic mobility at pH 6.5 showed the sequence of S2 to be *Glu-Ala-Phe*. The sequence of S4 was deduced to be *Val-Ser-Ser* from one step of Edman degradation. S1 gives the overlap of Th1 and Th4, S2 that of Th4 and Th3, and S3 that of Th3 and Th6.

*Peptide $a$T14.* The $NH_2$-terminal sequence of the peptide was found to be *Asp-Leu-Phe-Ser-Phe-Leu-* as revealed by six steps of subtractive and dansyl Edman procedures (Table 7). Hydrolysis in 0.03 N HCl produced free aspartic acid and four peptide fragments, A1, A2, A3, and A4 which were isolated by paper electrophoresis at pH 6.5 and further at pH 1.9. A1 represents the $NH_2$-terminal part of the peptide containing five of the $NH_2$-terminal amino acid residues. Its sequence is therefore concluded to be *Leu-Phe-Ser-Phe-Leu-Ala*. A4 represents the COOH-terminal portion of the peptide. Its sequence had to be *Pro-Lys* from the specificity of trypsin; the sequence was also confirmed by dansylation (Table 7). A2 and A3 are derived from the middle portion of the original peptide and the sequences were found to be *Pro-Thr* and *Gly-Val*, respectively (Table 7). The liberation of *Pro-Thr*, *Gly-Val*, and *Pro-Lys* indicates the sequences *Asx-Pro-Thr-Asx*, *Asx-Gly-Val-Asx*, and *Asx-Pro-Lys* considering the specificity of the mild acid hydrolysis. For completion of the sequence, $a$T14 was subjected to hydrolysis with subtilopeptidase A. In addition to free serine, leucine, and lysine, six peptide fragments were formed, S1, S2, S3, S4, S7, and S8, which were isolated by electrophoresis at pH 6.5 and 1.9. Table 7 shows their amino acid composition. S1 and S2 both represent the $NH_2$-terminal portion of the original peptide, $a$T14. The electrophoretic mobility of these two peptides at pH 6.5 indicated the presence of nonamidated aspartic acid. The sequence for S1 was found to be *Asp-Leu* and for S2 *Asp-Leu-Phe* by dansyl-Edman degradation. S7 and S8 both contained lysine and therefore represent the COOH terminus of the original peptide. S8 is a basic peptide on electrophoresis at pH 6.5, indicating the fourth aspartic acid residue of the original peptide to be amidated. Three steps of dansyl-Edman showed its sequence to be *Gly-Val-Asn-Pro-Lys*. S7, which contains the third and fourth aspartic

*Table 7.* Amino acid sequence of peptide *a*T14.

| Sequence | Asp-Leu-Phe-Ser-Phe-Leu-Ala-Asn-Pro-Thr-Asp-Gly-Val-Asn-Pro-Lys |
|---|---|

```
Asp-Leu-Phe-Ser-Phe-Leu-Ala-Asn-Pro-Thr-Asp-Gly-Val-Asn-Pro-Lys
|─────── A1 ───────|  |─ A2 ─|   |─ A3 ─|   |─ A4 ─|
|──── S2 ────|─S5─|  |──── S4 ────|  |─────── S7 ───────|
                                          |──── S8 ────|
|─ S1 ─|              |──────── S3 ────────|
```

**Edman degradation**

Step 1 — *Asp, 2.97*; Leu, 1.87; Phe, 1.67; Ser, 1.00; Ala, 1.04; Pro, 2.23; Thr, 1.02; Gly, 1.06; Val, 0.93; Lys [a]

Step 2 — Asp, 3.07; *Leu, 0.98*; Phe, 1.62; Ser, 1.22; Ala, 1.02; Pro, 2.08; Thr, 1.01; Gly, 1.11; Val, 0.90; Lys [a]

Step 3 — Asp, 2.93; Leu, 0.95; *Phe, 0.87*; Ser, 1.20; Ala, 1.03; Pro, 2.27; Thr, 0.90; Gly, 1.05; Val, 0.83; Lys [a]

Direct examination of dansyl derivatives

Step 4 — DNS-Ser
Step 5 — DNS-Phe
Step 6 — DNS-Leu

**Hydrolysis with 0.03 N HCl**

A1 — Leu, 2.04; Phe, 1.84; Ser, 1.15; Ala, 0.98

A2 — Pro, 1.15; Thr, 0.85
Dansylation — DNS-Pro

A3 — Gly, 1.01; Val, 0.99
Dansylation — DNS-Gly

A4 — Pro, 0.98; Lys, 1.02
Dansylation — DNS-Pro

**Subtilopeptidase peptides**

S1 ($E_{Asp}$, 0.67) — Asp, 1.03; Leu, 0.97
Dansylation — DNS-Asp

S2 ($E_{Asp}$, 0.51) — Asp, 1.05; Leu, 0.98; Phe, 0.98
Edman degradation
 Step 1 — *Asp, 0.25*; Leu, 1.0; Phe, 0.85
 Step 2 — — *Leu, 0.61*; Phe, 1.00

S3 ($E_{Asp}$, 0.31) — Leu, 0.87; Ala, 1.11; Asp, 1.93; Pro, 1.05; Thr, 0.89; Gly, 1.14
Dansylation — DNS-Leu

S4 (neutral) — Leu, 0.93; Ala, 0.93; Asp, 1.13
Edman degradation
 Step 1 — *Leu, 0.00*; Ala, 0.96; Asp, 1.04
 Step 2 — — *Ala, 0.00*; Asp, 1.00

S5 — Ser

S6 — Leu

S7 (neutral) — Thr, 1.01; Asp, 2.00; Gly, 1.20; Val, 0.88; Pro, 1.20; Lys, 0.98
Direct examination of dansyl derivatives
Edman degradation
 Step 1 — DNS-Thr
 Step 2 — DNS-Asp
 Step 3 — DNS-Gly

S8 ($E_{Lys}$, 0.51) — Gly, 1.03; Val, 1.00; Asp, 1.33; Pro, 0.60; Lys, 0.97
Direct examination of dansyl derivatives
Edman degradation
 Step 1 — DNS-Gly
 Step 2 — DNS-Val
 Step 3 — DNS-Asp

S9 — Lys

[a] Not determined.

acid residue of aT14, was found to be neutral on electrophoresis at pH 6.5, so indicating the third aspartic acid residue to be in the acid form. After three steps of dansyl-Edman degradation and by referring to the sequence of S8, the sequence of S7 is concluded to be *Thr-Asp-Gly-Val-Asn-Pro-Lys*. S3 and S4 represent the middle portion of the original peptide. The neutral electrophoretic mobility of S4 at pH 6.5 showed the second aspartic acid residue of aT14 to be amidated, the sequence of the peptide being *Leu-Ala-Asn* as shown by two steps of Edman degradation. S3 is an acidic peptide which contains the second and the third aspartic acid residue of aT14 and confirms that third aspartic acid residue is in the acid form. The sequence of S3 is concluded to be *Leu-Ala-Asn-Pro-Thr-Asp-Gly* referring to the sequences of A2, S4, and S7.

*Peptide aT15.* The amino acid composition of this peptide shows it to be identical to that of aT13 except for two phenylalanyl residues which are assumed to be exchanged into two tyrosyl residues. Subpeptides of a subtilopeptidase digest were studied to confirm this assumption. Six peptides could be isolated electrophoretically at pH 6.5 and 1.9: S1, S2, S3, S4, S5, and S6 (Table 8). Two steps of Edman degradation and an acidic mobility on electrophoresis at pH 6.5 showed the sequence of S1 to be *Glu-Ala-Tyr*.

*Table 8.* Amino acid sequence of peptide aT15.

| Sequence | [Glu-Asn-Ala-Leu]-[Val-Ser-Ser]-[Ser, Tyr]-[Glu-Ala-Tyr]-Lys |
|---|---|
|  | \|———— S2 ————\| \|—— S4 ——\|          \|—— S1 ——\|-S6-\| |
| Subtilisin peptides | |
| S1 ($E_{Asp}$, 0.45) | Glu, 1.05; Ala, 1.04; Tyr, 0.91 |
| Edman degradation | |
| Step 1 | *Glu, 0.00*; Ala, 1.13; Tyr, 0.87 |
| Step 2 | —    *Ala, 0.65*; Tyr, 1.00 |
| S2 ($E_{Asp}$, 0.42) | Glu, 1.01; Asp, 1.04; Ala, 1.05; Leu, 0.90 |
| Edman degradation | |
| Step 1 | *Glu, 0.00*; Asp, 1.07; Ala, 1.05; Leu, 0.88 |
| Step 2 | —    *Asp, 0.48*; Ala, 1.17; Leu, 0.83 |
| Step 3 | —      —    *Ala, 0.37*; Leu, 0.83 |
| Carboxypeptidase A | |
| 30 min | Leu, 1.00; Ala, 0.39; Asn (Ser) 0.10 |
| S3 | Ser, 1.00 (2) |
| S4 | Val, 1.03; Ser, 1.97 |
| Edman degradation | |
| Step 1 | *Val, 0.00*; Ser, 2.00 |
| S5 | Val, 0.92; Ser, 1.13 |
| Edman degradation | |
| Step 1 | *Val, 0.00*; Ser, 1.00 |
| S6 ($E_{Lys}$, 1.00) | Lys, 1.00 |

Three steps of Edman degradation and carboxypeptidase A digestion indicated the sequence of S2 to be *Glu-Asn-Ala-Leu*. On the basis of electrophoresis at pH 1.9, S3 seems to be *Ser-Ser*. S4 was shown to be *Val-Ser-Ser* and S5 *Val-Ser*, both by one step of Edman degradation. S6 was found to be free lysine. The sequences of the subpeptides confirm our assumption of a homology between $a$T13 and $a$T15 and are put in order according to the sequence of $a$T13.

*Peptide* a*T16*. Five steps of Edman degradation established the sequence of this peptide (Table 9). The aspartic and glutamic acid residues must be

*Table 9.* Amino acid sequence of peptide $a$T16.

| Sequence | Trp-Ser-Asp-Glu-Leu-Ser-Arg |
|---|---|
| | \|———— Th1 ————\|—— Th2 ——\| |
| Edman degradation | |
| Step 1 | *Trp, 0.00*; Ser, 1.77; Asp, 1.13; Glu, 1.15; Leu, 0.95; Arg [a] |
| Step 2 | — *Ser, 1.07*; Asp, 1.03; Glu, 1.06; Leu, 0.88; Arg [a] |
| Step 3 | — Ser, 1.01; *Asp, 0.49*; Glu, 1.06; Leu, 0.93; Arg [a] |
| Step 4 | — Ser, 1.06; Asp, 0.00; *Glu, 0.68*; Leu, 0.94; Arg [a] |
| Step 5 | — Ser, 1.00; Asp, 0.00; Glu, 0.56; *Leu, 0.41*; Arg [a] |
| Thermolysin peptides | |
| Th1 ($E_{Asp}$, 0.64) | Trp, +; Ser, 0.92; Asp, 1.02; Glu, 1.06 |
| Th2 ($E_{Lys}$, 0.53) Edman degradation | Leu, 0.96; Ser, 1.09; Arg, 0.95 |
| Step 1 | *Leu, 0.00*; Ser, 1.00; Arg,[a] |

[a] Not determined.

in the acid form because of the electrophoretic mobility of the whole peptide at pH 6.5. The sequence was further confirmed by thermolytic fragments, Th1 and Th2, which were isolated by paper electrophoresis at pH 6.5. Th1 contained the four $NH_2$-terminal residues and Th2 represented the COOH-terminal position of the whole peptide. One step of Edman degradation on Th2 confirmed the sequence *Leu-Ser-Arg*.

*Peptide* a*T17*. The Edman degradation revealed the $NH_2$-terminal alanine of this peptide (Table 10). Digestion by chymotrypsin yielded two principal components, C1 and C2, which were separated by electrophoresis at pH 6.5. C1 represents the $NH_2$-terminal portion of the whole peptide because it contains the $NH_2$-terminal alanine. C2 represents the COOH-terminal portion of the whole peptide because it contains lysine. Three steps of Edman degradation yielded the COOH-terminal sequence *Ala-Ala-Ala-Ile-Lys*. On hydrolysis with thermolysin, five peptides were formed, Th1, Th2, Th3, Th4, and Th5, which were separated on electrophoresis at pH 6.5 and 1.9. Th3 represented the $NH_2$-terminal portion of the whole peptide. Two steps of Edman degradation established the sequence *Ala-Trp-Glu*. Th5 contains the lysine residue of peptide $a$T17 and therefore represents the COOH-terminal

*Table 10.* Amino acid sequence of peptide *a*T17.

| Sequence | Ala-Trp-Glu-Val-Ala-Tyr-Asp-Glu-Leu-Ala-Ala-Ala-Ile-Lys |
| --- | --- |
| | |————————— C1 —————————————|————— C2 ———| |
| | |— Th3 —|—————— Th1 ———|—— Th4 ———|—Th5-| |
| | |—————————— Th2 ———————————| |
| Edman degradation | |
| Step 1 | *Ala, 4.02*; Trp, 1.00; Glu, 2.04; Val, 0.88; Tyr, 0.92; Asp, 1.25; Leu, 1.25; Ile, 0.80; Lys [a] |
| | |
| Chymotryptic peptides | |
| C1 ($E_{Asp}$, 0.47) | Ala, 1.92; Trp, 1.00; Glu, 1.99; Val, 0.97; Tyr, 0.43; Asp, 1.12; Leu, 1.00 |
| Dansylation | DNS-Ala |
| | |
| C2 ($E_{Lys}$, 0.48) | Ala, 3.09; Ile, 0.92; Lys, 0.99 |
| Edman degradation | |
| Step 1 | *Ala, 2.16*; Ile, 0.84; Lys [a] |
| Step 2 | *Ala, 1.17*; Ile, 0.83; Lys [a] |
| Step 3 | *Ala, 0.49*; Ile, 0.84; Lys [a] |
| | |
| Thermolytic peptides | |
| Th1 ($E_{Asp}$, 0.65) | Val, 0.98; Ala, 1.03; Tyr, 0.90; Asp, 1.13; Glu, 0.99 |
| Edman degradation | |
| Step 1 | *Val, 0.00*; Ala, 0.93; Tyr, 1.03; Asp, 1.03; Glu, 1.01 |
| Step 2 | Val, 0.00; *Ala, 0.28*; Tyr, 0.46; Asp, 1.14; Glu, 1.00 |
| Step 3 | — Ala, 0.00; *Tyr, 0.29*; Asp, 1.06; Glu, 1.00 |
| Step 4 | — — Tyr, 0.00; *Asp, 0.76*; Glu, 1.00 |
| | |
| Th2 ($E_{Asp}$, 0.59) | Val, 0.91; Ala, 3.19; Tyr, 0.53; Asp, 1.00; Glu, 0.92; Leu, 0.96 |
| | |
| Th3 ($E_{Asp}$, 0.41) | Ala, 0.98; Trp, +; Glu, 1.02 |
| Edman degradation | |
| Step 1 | *Ala, 0.26*; Trp, +; Glu, 1.00 |
| Step 2 | Ala, 0.00; *Trp*, —; Glu, 1.00 |
| | |
| Th4 (neutral) | Leu, 0.87; Ala, 3.13 |
| Edman degradation | |
| Step 1 | *Leu, 0.30*; Ala, 3.00 |
| | |
| Th5 ($E_{Lys}$, 0.72) | Ile, 0.99; Lys, 1.01 |

[a] Not determined.

portion of the peptide. Its sequence had to be *Ile-Lys*. Th1 is a component derived from the middle portion of the whole peptide and was determined to be *Val-Ala-Tyr-Asp-Glu* by four steps of Edman degradation. The electrophoretic mobility of the peptide at pH 6.5 shows aspartic and glutamic acid to be in the acid form. Th4 is another component from the inner portion of the whole peptide. One step of Edman degradation yielded the sequence *Leu-Ala-Ala-Ala*. Th2 gives the overlap between Th1 and Th4.

*Peptide aT18.* Alanine was identified as the $NH_2$-terminal residue by dansylation. Thermolytic digestion of the peptide yielded eight peptide frag-

*Table 11.* Amino acid sequence of peptide *a*T18.

Sequence

Ala-Asn-Ile-Pro-Gln-Tyr-Ser-Val-Val-Phe-Tyr-Thr-Ser-Ile-Leu-Glu-Lys

```
|————————— Th1 ——————————|————————— Th4 —————————|——— Th8 ———|
|————————— Th2 ———|—Th6 —|————————— Th3 —|————————— Th7 ————————|
                                          |— Th5 ———|
|————————— S1 ————————|— S4 —|                                |— S6 —|
|————————————— S2 ———————————————————————————|—S3—|——— S5 ———|
```

| | |
|---|---|
| Dansylation | DNS-Ala |
| **Thermolysin peptides** | |
| Th1 (neutral) | Ala, 0.98; Asp, 1.00; Ile, 1.15; Pro, 1.25; Glu, 1.09; Tyr, 0.87; Ser, 0.91 |
| Hydrazinolysis | Ser, 0.80 |
| | |
| Th2 (neutral) | Ala, 0.86; Asp, 1.03; Ile, 1.04; Pro, 1.44; Glu, 1.07 |
| Edman degradation | |
|     Step 1 | *Ala, 0.00*; Asp, 0.98; Ile, 1.04; Pro, 0.84; Glu, 1.13 |
|     Step 2 | —      *Asp, 0.12*; Ile, 1.01; Pro, 0.88; Glu, 1.12 |
|     Step 3 | —      —      *Ile, 0.11*; Pro, 0.91; Glu, 1.09 |
|     Step 4 | —      —      —      *Pro, 0.00*; Glu, 1.00 |
| | |
| Th3 (neutral) | Val, 1.90; Phe, 1.09; Tyr, 0.60 |
| (70 h hydrolysis) | |
| Edman degradation | Direct examination of dansyl derivatives |
|     Step 1 | DNS-Val; DNS-Val-Val |
|     Step 2 | DNS-Val |
|     Step 3 | DNS-Phe |
| | |
| Th4 (neutral) | Val, 1.86; Phe, 1.23; Tyr, 0.60; Thr, 0.80; Ser, 0.92 |
| (70 h hydrolysis) | |
| Dansylation | DNS-Val; DNS-Val-Val |
| Hydrazinolysis | Ser, 0.92 |
| Hydrolysis in 12 N HCl | |
| Th4-H1 (70 h hydrolysis) | Val, 2.02; Phe, 0.98 |
|    Th4-H2 | Tyr, 0.55; Thr, 1.04; Ser, 0.96 |
| | |
| Th5 (neutral) | Tyr, 0.86; Thr, 1.09; Ser, 1.09 |
| Edman degradation | Direct examination of dansyl derivatives |
|     Step 1 | DNS-Tyr |
|     Step 2 | DNS-Thr |
| | |
| Th6 | Tyr, 0.90; Ser, 1.00 |
| Edman degradation | |
|     Step 1 | *Tyr, 0.00*; Ser, 1.00 |
| | |
| Th7 (neutral) | Thr, 0.87; Ser, 0.98; Ile, 0.89; Leu, 0.99; Glu, 1.11; Lys, 1.05 |
| Edman degradation | Direct examination of dansyl derivatives |
|     Step 1 | DNS-Thr |
|     Step 2 | DNS-Ser |
|     Step 3 | DNS-Ile |
|     Step 4 | DNS-Leu |
| | |
| Th8 (neutral) | Ile, 0.91; Leu, 0.98; Glu, 1.12; Lys, 0.99 |
| Edman degradation | |
|     Step 1 | *Ile, 0.00*; Leu, 0.87; Glu, 1.17; Lys [a] |
|     Step 2 | —      *Leu, 0.00*; Glu, 1.00; Lys [a] |

*Table 11. Continued.*

| Subtilopeptidase peptides | |
|---|---|
| S1 (neutral) | Ala, 0.80; Asp, 0.95; Ile, 1.12; Pro, 0.90; Glu, 1.16; Tyr, 1.07 |
| S2 (neutral) | Ala, 0.97; Asp, 1.12; Ile, 1.10; Pro, 1.02; Glu, 1.03; Tyr, 1.22 (2); Ser, 1.05; Val, 0.68 (2) [b]; Phe, 0.89; Thr, 0.81 |
| S3 | Ser |
| S4 | Ser, 1.03; Val, 0.97 |
| Dansylation | DNS-Ser |
| S5 (neutral) | Ile, 1.00; Leu, 1.00; Glu, 1.30; Lys, 1.17 |
| S6 (neutral) | Glu, 0.92; Lys, 1.08 |

[a] Not determined. [b] Incomplete hydrolysis of the Val-Val bond in 18 h hydrolysis.

ments, Th1, Th2, Th3, Th4, Th5, Th6, Th7, and Th8, which were electro-phoretically separated at pH 6.5 and 1.9. Th1 and Th2 are the only peptides containing the $NH_2$-terminal alanine. Four steps of Edman degradation of Th2 established the sequence *Ala-Asn-Ile-Pro-Gln*. Since Th1 and Th2 were neutral on electrophoresis at pH 6.5, the glutamic and aspartic acid residues must be in amide form. Th6 was found to be *Tyr-Ser* after one step of Ed-man degradation. The COOH-terminal amino acid residue in Th1 was found to be serine by hydrazinolysis and the sequence of the peptide was concluded to be *Ala-Asn-Ile-Pro-Gln-Tyr-Ser* referring to the sequence of Th2 and Th6. Th8 represents the COOH-terminal portion of the peptide containing lysine. Two steps of Edman degradation established its sequence as *Ile-Leu-Glu-Lys*. Since the peptide was neutral on electrophoresis at pH 6.5, the glutamic acid residue is in the acid form. Th3, Th4, and Th5 represent the middle portion of peptide $aT18$. The presence of two valine residues in Th3 was confirmed by a 70 h acid hydrolysis of the peptide, which also indicated the sequence *Val-Val*, known to be highly resistant to acid hydrolysis. The dansyl-Edman procedure established the sequence *Val-Val-Phe-Tyr* for Th3. Two steps of dansyl-Edman degradation showed the sequence of Th5 to be *Tyr-Thr-Ser*. Dansylation of Th4 revealed *Val-Val* as the $NH_2$-terminal sequence and hydrazinolysis identified serine as the COOH-terminal residue. Hydrol-ysis with 12 N HCl results in two main peptide fragments which were con-cluded to be *Val-Val-Phe* and *Tyr-Thr-Ser*. The sequence of Th4 is accordingly *Val-Val-Phe-Tyr-Thr-Ser*. The order of the thermolytic subpeptides was fur-ther established and their sequences were confirmed by overlapping peptides obtained from a subtilopeptidase A hydrolysis of $aT18$. In addition to free serine, five peptide fragments, S1, S2, S4, S5, and S6, were isolated by electro-phoresis at pH 1.9. Their amino acid compositions are given in Table 11. The sequence of S4 was found to be *Ser-Val* by dansylation. S1 confirms the sequence of Th1 and S5 and S6 that of Th8. S4 gives the overlap between Th1 and Th4 as well as between Th6 and Th3. The overlap is further estab-lished by S2.

## DISCUSSION

The amino acid sequences of seventeen peptides isolated from the tryptic hydrolysates of the slow component of soybean leghemoglobin have been determined. With the exception of peptide $a$T15, all other peptides were obtained in sufficient amount to establish the sequence unequivocally. The proposed sequences depend on evidence obtained by enzymatic digestion of the tryptic peptides with chymotrypsin, subtilopeptidase A, thermolysin, and by Edman sequential degradation. The presence of amides in aspartyl or glutamyl residues was determined from the behaviour of peptides on electrophoresis or by quantitative determination of free amino acids released by the action of leucine aminopeptidase or carboxypeptidase on the peptide containing the amino acids in question.

The nature of peptide bonds that are cleaved by trypsin conform to known specificity requirements of the enzyme. However, the rate of hydrolysis of various bonds differs. The presence of aspartic acid in a position $NH_2$-terminal to lysine *(-Asp-Lys-)* decreases the rate of hydrolysis. This sequence occurs in peptide $a$T8. The isolation of the ditryptic peptide, $a$T8, $a$T16, in good yield clearly indicates the resistance of this bond in contrast to peptides having glutamic acid in the same position *(-Glu-Lys-)*, e.g. $a$T11, $a$T12, and $a$T18.

As was expected from the known specificity of chymotrypsin, cleavage occurred at peptide bonds involving the carboxyl groups of the tyrosine, phenylalanine, and leucine residues. The only exception was the tyrosylaspartyl bond in peptide $a$T17. In addition, it was observed that chymotrypsin hydrolyzed a particular peptide linkage at a much faster rate than other potentially sensitive ones. Hirs et al.[20] have suggested that a longer sequence may determine the ability of a particular bond to be cleaved. To what extent the conformation of the peptide might be decisive remained to be clarified.

Thermolysin was found to be highly specific in hydrolyzing bonds involving the amino groups of tyrosine, phenylalanine, leucine, valine, and isoleucine. However, an exceptional splitting at the carboxyl group of tyrosine was observed with one of the thermolytic subpeptides of $a$T18. A preference of some bonds was also observed with thermolysin. In peptide $a$T16 the *-Gly-Val-* sequence was not attacked by the enzyme. In the case of thermolysin too it is evident that something more than the presence of a specific amino acid residue is required for the enzyme specificity.

The proposed amino acid sequence of the tryptic peptides is primarily based on the data of subtractive- and dansyl-Edman sequential techniques. The cyclization of the $NH_2$-terminal glutamine residue to pyrrolidone carboxylic acid, one of the sources of difficulty with the Edman procedure, was encountered only with peptide $a$T13. By separating the tryptic peptides electrophoretically, we were able to determine the $NH_2$-terminal glutamine residue before cyclization.

The peptide $a$T15 is a minor component isolated from one leghemoglobin preparation only. Because the preparation of leghemoglobin requires the use of a pool of nodules from hundreds of plants the noted heterogeneity can be due to an intraspecies variation. Further sequence studies on the other soybean leghemoglobin components may shed some light on the origin of this leghemoglobin form.

## REFERENCES

1. Ellfolk, N. and Sievers, G. *Acta Chem. Scand.* **26** (1972) 1155.
2. Ellfolk, N. *Acta Chem. Scand.* **14** (1960) 609.
3. Ellfolk, N. *Acta Chem. Scand.* **16** (1962) 831.
4. Ryle, A. P., Sanger, F., Smith, L. F. and Kitai, R. *Biochem. J.* **60** (1955) 541.
5. Ambler, R. P. *Biochem. J.* **89** (1963) 349.
6. Spackman, D. H., Stein, W. H. and Moore, S. *Anal. Chem.* **30** (1958) 1190.
7. Spies, J. R. and Chambers, D. C. *Anal. Chem.* **21** (1949) 1249.
8. Sjöquist, J., Blombäck, B. and Wallén, P. *Arkiv Kemi* **16** (1960) 425.
9. Blombäck, B., Blombäck, M., Edman, P. and Hessel, B. *Biochim. Biophys. Acta* **115** (1966) 371.
10. Jeppsson, J. D. and Sjöquist, J. *Anal. Biochem.* **18** (1967) 264.
11. Konigsberg, W. and Hill, R. J. *J. Biol. Chem.* **237** (1962) 2547.
12. Konigsberg, W. *J. Biol. Chem.* **241** (1966) 4534.
13. Gray, W. R. and Hartley, B. S. *Biochem. J.* **89** (1963) 59P.
14. Gray, W. R. and Hartley, B. S. *Biochem. J.* **89** (1963) 379.
15. Milstein, C. *Biochem. J.* **101** (1966) 338.
16. Woods, K. R. and Wang, K.-T. *Biochim. Biophys. Acta* **133** (1967) 369.
17. Offord, R. E. *Nature* **211** (1966) 591.
18. Ellfolk, N. and Sievers, G. *Acta Chem. Scand.* **23** (1969) 2994.
19. Aggarwal, S. J. and Riggs, A. *Acta Chem. Scand.* **24** (1970) 2234.
20. Hirs, C. H. W., Moore, S. and Stein, W. H. *J. Biol. Chem.* **235** (1960) 633.

# Initial Thermoelectric Powers of the Silver-Silver Ion
# Electrode in Acetonitrile-Water and Ethanol-Water Mixtures

SVEIN ELIASSEN and HANS HOLTAN

The University of Trondheim, Norwegian Institute of Technology, Department of Industrial Electrochemistry, N-7034 Trondheim-NTH, Norway

Initial thermoelectric powers of the silver-silver nitrate couple were measured in solvent mixtures of acetonitrile-water and ethanol-water at different concentrations of silver nitrate. It was found that the solvent composition has a great influence on the initial thermoelectric power. In the acetonitrile-water system the sign is changed from negative in water to positive in acetonitrile. Small additions of acetonitrile to water increases the initial thermoelectric power markedly before the curve is flattening out towards acetonitrile, indicating the strong interactions between the silver ion and acetonitrile.

In the ethanol-water system the initial thermoelectric power reaches its minimum at about 20 wt. % of ethanol. This confirms the fact that the solvent system reaches its maximum structure ordering at this composition.

In a previous paper[1] results from measurements of initial thermoelectric powers ($\varepsilon_0$) in ethanol-water and acetonitrile-water mixtures were presented using the quinhydrone ($Q - QH_2$) electrode. The electrolytes were HCl and $HClO_4$ and it was found that $\varepsilon_0$ got more positive in the solutions rich in acetonitrile. At about 65 wt. % of acetonitrile it even changed its sign from negative to positive. The quinhydrone electrode, however, is not quite satisfactory in the solutions with high contents of acetonitrile. We now report the results of some work done with the silver-silver nitrate electrode in acetonitrile-water and ethanol-water mixtures.

$\varepsilon_0$ measurements may reveal interesting information concerning the structure of the solution and the transport properties of solvated ions in a temperature gradient. Work on initial thermoelectric powers in nonaqueous solutions have only been carried out in a few systems.[1–4]

Measurements of $\varepsilon_0$ requires a stable and reversible electrode. In nonaqueous solvents many of the usual reference electrodes in water are not satisfactory. Butler[5] has recently reviewed works reported on reference electrodes in aprotic solvents, but still much work has to be done in finding suitable electrodes in

nonaqueous solvents. The silver-silver ion couple is stable and reversible in acetonitrile. This has been confirmed by potentiometric technique by several authors.[6-9] Measurements of $\varepsilon_0$ with this electrode are not reported in non-aqueous solvents, but in aqueous solutions the method has been applied by several authors.[10-15]

The general equation for the initial thermoelectric power of an electrolytic thermocell is developed by Holtan [16] on the basis of the thermodynamics of irreversible processes by applying Onsagers reciprocal relations.

For the thermocell

$$Ag|AgNO_3 \text{ (solution)} \underset{T_1 T_2}{\parallel} AgNO_3 \text{ (solution)} \mid Ag$$
$$T_1 \qquad\qquad T_1 T_2 \qquad\qquad T_2$$

the solvent being a mixture of acetonitrile-water or ethanol-water, $\varepsilon_0$ is given as

$$F\varepsilon_0 = t_{NO_3^-}S^*_{NO_3^-} - t_{Ag^+}S^*_{Ag^+} - S^*_{el} + S_{Ag} \tag{1}$$
$$- t_{NO_3^-}S_{AgNO_3^-} + \Delta N_{H_2O}S_{H_2O} + \Delta N_2 S_2$$

where

$F$ = the Faraday;
$\varepsilon_0$ = the initial thermoelectric power;
$t$ = the true ionic transport number;
$S^*$ = the transported entropies of the solvated ions and the electrons, respectively;
$S$ = the partial molar entropy;
$\Delta N$ = the number of moles of solvent transported from the anode to the cathode compartment, when on Faraday of electricity has passed through the solution

The number 2 is referring to the nonaqueous solvent.

Expressions similar to the general equation of Holtan are given by Haase,[17] Agar,[18] and Tyrell.[19] The advantage of Holtan's equation is that the thermo-static part (the part that does not contain any transported entropies) of the equations will not contain any ionic entropies, but only partial molar entropies of the neutral components. These can in principle be measured separately. Holtan has also taken into account the solvent transport due to the fact that the solvation shell round the ions will be transported in an electric field. By using the Hittorf reference system the terms containing transport of solvent fall out, according to Haase.[17] Some questions can, however, be put forward using the Hittorf reference system in a system with a temperature gradient. These questions will be discussed in a later paper.

## EXPERIMENTAL

The cell used for measuring the initial thermoelectric power in this work is the same as in the previous paper.[1] It is earlier described by Tyrell and Hollis [13] and Haase and Schönert.[20]

The reagents were of Merck preparations of *p.a.* quality and distilled and deionised water. Acetonitrile and ethanol were redistilled.

The silver electrodes were prepared by heating freshly prepared silver oxide on a silver plate in an electric furnace at about 400°C for 30 min. The silver oxide was precipitated from a solution of silver nitrate and sodium hydroxide and washed several times by deionised water. The silver oxide decomposes at this temperature yielding a silver surface of high reactivity. Silver electrodes prepared in this way are extremely reproducible, and isothermal emf's above 20 $\mu V$ were a scarceness in both water and the nonaqueous solvents.

Measurements of emf were made using a digital voltmeter of type Solartron LM 1604.2. The isothermal emf was measured before and after the experiment. The thermopotential was measured at a mean temperature of 298 K and the temperature difference between the electrodes was 10 K. The halfcells were kept at the desired temperature by circulating water from the two thermostats for one hour to obtain thermal equilibrium before the measurement. The emf was then measured and the process was repeated, but now the electrode being the warm in the first case was the cold one. The mean value of the two thermopotentials is divided by the temperature difference giving the initial thermoelectric power, assuming that $\varepsilon_0$ is temperature-independent or a linear function of the temperature in the interval.

## RESULTS AND DISCUSSION

The cell emf is considered positive when the hot electrode is positive.

*Acetonitrile-water mixtures.* The initial thermoelectric powers were measured as a function of the concentration of silver nitrate and the solvent composition. The results are presented in Table 1.

*Table 1.* Initial thermoelectric powers in mV/deg. as function of the concentration of $AgNO_3$ and the solvent composition in acetonitrile-water mixtures.

| Mol % CH₃CN | 1.0 N | 0.5 N | 0.1 N | 0.05 N | 0.01 N | 0.001 N |
|---|---|---|---|---|---|---|
| 0 | − 0.271 | − 0.323 | − 0.445 | − 0.500 | − 0.622 | − 0.798 |
| 1.8 | − 0.225 | − 0.170 | − 0.045 | − 0.082 | − 0.147 | − 0.318 |
| 3.7 | − 0.121 | + 0.024 | + 0.124 | + 0.090 | − 0.001 | − 0.167 |
| 5.7 | + 0.016 | + 0.179 | + 0.209 | + 0.160 | + 0.078 | − 0.090 |
| 7.9 | + 0.142 | + 0.268 | + 0.248 | + 0.202 | + 0.124 | − 0.040 |
| 10.3 | + 0.246 | + 0.324 | + 0.272 | + 0.224 | + 0.149 | − 0.009 |
| 12.9 | + 0.301 | + 0.366 | + 0.298 | + 0.245 | + 0.166 | + 0.011 |
| 18.7 | + 0.358 | + 0.393 | + 0.323 | + 0.271 | + 0.194 | + 0.038 |
| 25.6 | + 0.385 | + 0.412 | + 0.361 | + 0.293 | + 0.214 | + 0.058 |
| 34.0 | + 0.419 | + 0.430 | + 0.384 | + 0.310 | + 0.229 | + 0.074 |
| 44.6 | + 0.458 | + 0.471 | + 0.414 | + 0.343 | + 0.258 | + 0.098 |
| 58.0 | + 0.500 | + 0.501 | + 0.460 | + 0.391 | + 0.325 | + 0.172 |
| 75.6 | + 0.558 | + 0.542 | + 0.520 | + 0.468 | + 0.394 | + 0.266 |
| 99.0 | + 0.591 | + 0.578 | + 0.559 | + 0.508 | + 0.450 | + 0.358 |

$\varepsilon_0$ is much more positive in acetonitrile than in water. $\varepsilon_0$ is directly related to the entropy of electrochemical transport involved in the reduction of silver ion to silver metal. The solvent ordering in acetonitrile solutions is therefore greater than in aqueous solutions. Several factors may cause this difference. One is that there are strong interactions between the silver ion and acetonitrile

as indicated by the fact that the standard reduction potential is 0.57 V lower in acetonitrile than in water [21] and as is shown by the formation of silver-acetonitrile complexes.[22] Another factor is that solvation of small ions decreases the high degree of structure normally present. The solvent ordering would be opposed by initial structure breaking effects, making the overall entropy change smaller. Liquid acetonitrile is relatively nonstructured compared to water.[23] Thus the structure breaking effects of ions would be smaller in acetonitrile than in water. The stronger interactions and the smaller structure breaking effects should predict a more positive entropy change in acetonitrile and therefore a more positive $\varepsilon_0$.

Small additions of acetonitrile have a great influence on $\varepsilon_0$. At a concentration of 0.1 N AgNO$_3$ $\varepsilon_0$ increases 0.653 mV/deg. with an addition of 5.7 mol % of acetonitrile to pure water. An addition of 23.4 mol % of water to 99 % acetonitrile, however, only decreases $\varepsilon_0$ by 0.039 mV/deg.

For the thermocell

$$Pt|Q-QH_2|HCL \ \text{(solution)} \ || \ HCl \ \text{(solution)} \ | \ Q-QH_2|Pt$$
$$T_1 \qquad\qquad T_1T_2 \qquad\qquad T_2$$
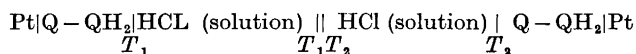
where $Q-QH_2$ is the quinhydrone electrode and the solvent is a mixture of acetonitrile and water, the opposite effect was found.[1] A small addition of acetonitrile to water did not increase the thermoelectric power. $\varepsilon_0$ on the contrary slightly decreased in the solutions rich in water to about 10 mol % of acetonitrile where it reached its minimum. In the solutions rich in acetonitrile addition of water markedly decreased $\varepsilon_0$. This is due to the strong interactions between water and the hydrogen ion, which is dominating in the solutions rich in water. The smaller structure breaking effects in acetonitrile compared to water are only coming into account in the solutions rich in acetonitrile making $\varepsilon_0$ increase.

Strehlow and Koepp [24] have measured the selective solvation in the system $AgNO_3 - H_2O - CH_3CN$ by a transference method. They found that the silver ion is selective solvated by acetonitrile and the nitrate ion by water. IR, NMR and Raman spectra [25,26] of this solution have shown similar results. The curvature of $\varepsilon_0$ as function of mol % of acetonitrile is indicating the same. Oliver and Janz [26] have found that the silver ion is solvated by acetonitrile in a solution with an acetonitrile content as low as 4.7 mol %. This is the point where the curve of $\varepsilon_0$ as function of the solvent composition is flattening out. $\varepsilon_0$ measurements may therefore give information of the solvation of ions in solvent mixtures.

The thermostatic part ($\varepsilon_0'$) of eqn. 1 reads in pure acetonitrile,

$$F\varepsilon_0' = S_{Ag} - t_{NO_3}-(S^\circ_{AgNO_3} - 2R \ln C - 2R \ln \gamma_\pm \qquad (2)$$
$$- 2RT \ d \ln \gamma_\pm/dT) + \Delta N_{CH_3CN}S_{CH_3CN}$$

where

| | |
|---|---|
| $S^\circ_{AgNO_3}$ | = the hypothetical standard partial molar entropy of AgNO$_3$; |
| $C$ | = the concentration; |
| $\gamma_\pm$ | = the mean ionic activity coefficient of AgNO$_3$. |
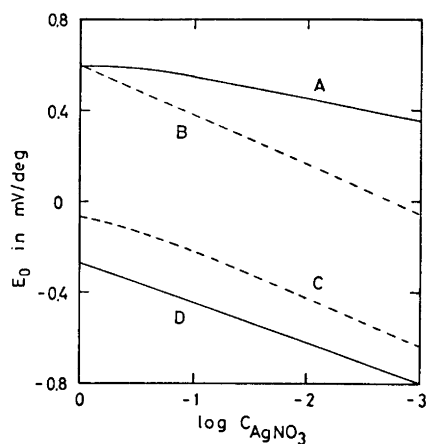
*Fig. 1.* $\varepsilon_0$ as function of the concentration of $AgNO_3$ in: A, $CH_3CN$ and D, $H_2O$. The stippled lines are: C the term $t_{NO_3}- \times 2RF^{-1} \ln C\gamma_\pm$ in $H_2O$, and B the term $\varepsilon_0(1) + t_{NO_3}-2RF^{-1}\ln C$ in $CH_3CN$.

In Fig. 1 $\varepsilon_0$ is presented as function of the concentration of $AgNO_3$ in pure acetonitrile and water. In Fig. 1 is also presented the term (stippled line C)

$$t_{NO_3}-2RF^{-1} \ln C\gamma_\pm$$

in pure water. The transport numbers are taken from McInnes and Longs-worth [27] and the activity coefficients are taken from McInnes and Brown [28] and Robinson and Tait.[29] The stippled line B is the term

$$\varepsilon_0(1\ N) + t_{NO_3}-2RF^{-1} \ln C$$

in pure acetonitrile. The transport numbers are taken from Strehlow and Koepp.[24]

In the water solutions $\varepsilon_0$ are close to the ideal slope when corrected for the activity coefficients, indicating that the other terms of eqn. 1 are not influenced by concentration changes or have the same concentration depen-dence. In pure acetonitrile $\varepsilon_0$ as function of the concentration is far from the ideal slope. The activity coefficients of $AgNO_3$ in acetonitrile are therefore markedly lower than one, which is earlier noticed by Pleskov.[7] This may be due to partial association of $AgNO_3$ in acetonitrile. This is earlier demon-strated by conductance [30] and potentiometric [9] measurements even in dilute solutions.

*Ethanol-water mixtures.* The $\varepsilon_0$ measurements in ethanol-water solutions are presented in Table 2. In the solutions rich in ethanol measurements of $\varepsilon_0$ could not be carried out in concentrated solutions of $AgNO_3$ because of the smaller solubility of $AgNO_3$.

The results are not so striking as those of the acetonitrile-water solutions. $AgNO_3$ has stronger interactions with water than with ethanol. When ethanol is added to water $\varepsilon_0$ decreases slightly until the composition reaches a value

*Table 2.* Initial thermoelectric powers in mV/deg. as function of the concentration of AgNO$_3$ and the solvent composition in ethanol-water mixtures.

| Mol % EtOH | 1.0 N | 0.1 N | 0.01 N | 0.001 N |
|---|---|---|---|---|
| 0 | − 0.270 | − 0.445 | − 0.622 | − 0.799 |
| 3.2 | − 0.302 | − 0.478 | − 0.653 | − 0.830 |
| 6.8 | − 0.320 | − 0.503 | − 0.680 | − 0.858 |
| 11.1 | − 0.329 | − 0.514 | − 0.687 | − 0.867 |
| 16.2 | − 0.314 | − 0.490 | − 0.662 | − 0.835 |
| 22.2 | − 0.299 | − 0.470 | − 0.639 | − 0.809 |
| 29.5 | − | − 0.594 | − 0.759 | − 0.759 |
| 38.8 | − | − 0.393 | − 0.558 | − 0.718 |
| 50.8 | − | − 0.363 | − 0.526 | − 0.687 |
| 66.3 | − | − 0.307 | − 0.438 | − 0.592 |
| 76.2 | − | − | − 0.296 | − 0.428 |
| 99.4 | − | − | − 0.062 | − 0.157 |
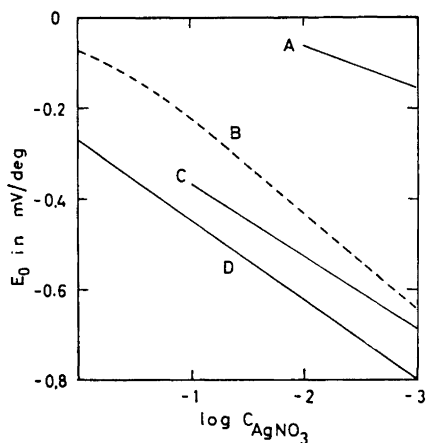


*Fig. 2.* $\varepsilon_0$ as function of the concentration of AgNO$_3$ in: A, EtOH, C, 50.8 mol % EtOH, and D, H$_2$O. The stippled line B is the term $t_{NO_3^-} \ 2RF^{-1} \ln \ C\gamma_\pm$ in H$_2$O.
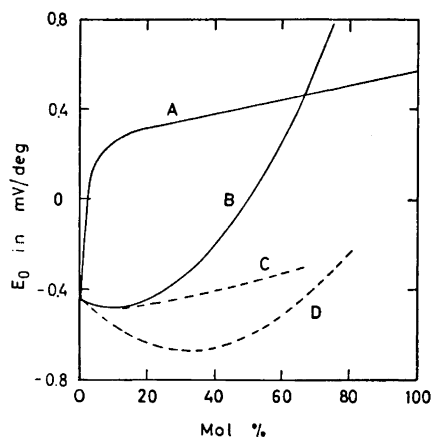
*Fig. 3.* $\varepsilon_0$ as function of the solvent composition. The mol % is mol % nonaqeuous solvent. Electrolyte concentration is 0.1 N. A, Ag|AgNO$_3$ in CH$_3$CN; B, Q-QH$_2$|HCl in CH$_3$CN; C, Ag|AgNO$_3$ in EtOH; and D, Q-QH$_2$|HCl in EtOH. B and D from Ref. 1.

of about 20 wt. % of ethanol. $\varepsilon_0$ is then increasing when the composition changes towards pure ethanol, but $\varepsilon_0$ is negative at all concentrations. Other measurements [31] have indicated that small additions of ethanol to water increase the order in the structure of the solvent. The maximum structural order is found to be at about 20 wt. % of ethanol. The structure breaking of the solvation of ions are therefore greatest at this solvent composition, explaining that $\varepsilon_0$ reaches its minimum at this point. For the HCl solutions using the quinhydrone electrode the minimum of $\varepsilon_0$ was found to be at about

40 wt. % of ethanol. Other effects than the structure of the solvent must influence $\varepsilon_0$ in this case.

The measurements are also showing that the activity coefficients of $AgNO_3$ are smaller in ethanol than in water. In Fig. 2, $\varepsilon_0$ is presented as function of the concentration of $AgNO_3$ in pure water, 50.8 mol % ethanol, and absolute ethanol. The slopes are indicating more non-ideality going from pure water to pure ethanol.

In Fig. 3, $\varepsilon_0$ measurements in 0.1 N electrolytes as function of the solvent composition are presented together. This figure shows the interesting influence of different solvents on $\varepsilon_0$. Because of the lack of thermodynamic data, the explanation can not be given.

## REFERENCES

1. Holtan, H. and Eliassen, S. *Acta Chem. Scand.* **27** (1973) 429.
2. Haase, R. and Jansen, H. J. *Z. physik. Chem. (Frankfurt)* **61** (1968) 310.
3. Lin, J. and de Haven, J. J. *J. Electrochem. Soc.* **116** (1969) 805.
4. Lin, J. *J. Electrochem. Soc.* **116** (1969) 1708.
5. Butler, J. M. *Advan. Electrochem. Electrochem. Eng.* **7** (1970) 77.
6. Koch, F. K. V. *J. Chem. Soc.* **1928** 524.
7. Pleskov, V. A. *Zh. Fiz. Khim.* **22** (1948) 351.
8. Koepp, H. M., Wendt, H. and Strehlow, H. *Z. Electrochem.* **64** (1960) 483.
9. Kratochvil, B., Lorah, E. and Garber, C. *Anal. Chem.* **41** (1969) 1793.
10. Burian, R. *Z. Electrochem.* **37** (1931) 238.
11. Lange, K. and Hesse, T. *Z. Electrochem.* **38** (1932) 428.
12. Khoroshin, A. B. and Temkin, M. N. *Zh. Fiz. Khim.* **26** (1952) 773.
13. Tyrell, H. J. V. and Hollis, G. L. *Trans Faraday Soc.* **48** (1952) 893.
14. Haase, R. and Behrend, G. *Z. physik. Chem. (Frankfurt)* **31** (1962) 375.
15. Haase, R. and Koch, K. *Z. physik. Chem. (Frankfurt)* **46** (1965) 63.
16. Holtan, H. *Electric Potentials in Thermocouples and Thermocells*, Thesis, Utrech 1953, p. 42.
17. Haase, R. *Thermodynamics of Irreversible Processes*, Addison-Wesley, Reading 1969, p. 385.
18. Agar, J. N. *Advan. Electrochem. Electrochem. Eng.* **3** (1963) 31.
19. Tyrell, H. J. V. *Diffussion and Heat Flow in Liquids*, Butterworth, London 1961.
20. Haase, R. and Schönert, H. *Z. physik. Chem. (Frankfurt)* **25** (1960) 372.
21. Strehlow, H. *Chem. Non-aqueous Solvents* **1** (1966) 129.
22. Janz, G. J. and Taniguchi, H. *Chem. Rev.* **53** (1953) 397.
23. Janz, G. J., Marchinkowsky, A. E. and Ahmad, I. *J. Electrochem. Soc.* **112** (1965) 104.
24. Strehlow, H. and Koepp, H. M. *Z. Electrochem.* **62** (1958) 372.
25. Baddiel, C. B., Tait, M. C. and Janz, G. J. *J. Phys. Chem.* **69** (1965) 3634.
26. Oliver, B. G. and Janz, G. J. *J. Phys. Chem.* **74** (1970) 3819.
27. McInnes, D. A. and Longsworth, G. L. *Chem. Rev.* **11** (1932) 171.
28. McInnes, D. A. and Brown, A. S. *Chem. Rev.* **18** (1936) 335.
29. Robinson, R. A. and Tait, D. A. *Trans Faraday Soc.* **37** (1941) 569.
30. Yeager, H. and Kratochvil, *J. Phys. Chem.* **73** (1969) 1963.
31. Franks, F. and Ives, D. J. G. *Quart. Rev. Chem. Soc.* **20** (1966) 1.

# The Conformation of 1,4,7,10-Tetraoxacyclododecane

## and its 1:1 Lithium Salt Complexes

F. A. L. ANET,[a] J. KRANE,[a] JOHANNES DALE,[b]
KARI DAASVATN[b] and PER OLAV KRISTIANSEN[b*]

[a] Department of Chemistry, University of California, Los Angeles, California 90024, and
[b] Kjemisk Institutt, Universitetet i Oslo, Oslo 3, Norway

Infrared spectroscopy and low-temperature ¹H and ¹³C NMR spectroscopy show that both in the free and complexed form this cyclic tetra-ether adopts a "square" conformation with ether oxygen on "side" positions. Dynamic NMR spectroscopy reveals two site exchange processes, the nature of which is discussed in detail.

The medium-ring hydrocarbon cyclododecane is unable to adopt a conformation of diamond-lattice type because of the strong transannular hydrogen interactions that would result. The conformation actually chosen both in the solid [1] and in solution [2] has been established to be of the "square" type with $D_4$ symmetry shown in Fig. 1. Strain-energy calculations [3] also give as a result that this is the lowest-energy conformation for cyclododecane.
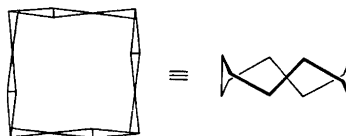


*Fig. 1.* Two representations of the cyclo-dodecane conformation.

In order to study the conformational effect of replacing in a symmetrical fashion four methylene groups by ether oxygen, we have now studied another 12-membered ring, 1,4,7,10-tetraoxacyclododecane, the tetramer of ethylene oxide.[4] Since we observed that this tetra-ether forms stable 1:1 cation complexes with lithium salts such as LiSCN, LiBr, LiCl, and LiF, it also became of interest to establish whether the ring-conformation in this complex is the same as, or different from, that of the free ring. Analogous 2:1 complexes are formed with sodium salts; with potassium salts they are much less stable. A

---

* Present address: Dyno Industrier, N-2001 Lilleström, Norway.

series of transition metal halides, like $CuCl_2$, $CoCl_2$, $NiCl_2$, and $FeCl_2$, also form crystalline 1:1 complexes.

## INFRARED SPECTRA

The crystalline lithium bromide complex has a particularly simple infrared spectrum with sharp bands (Fig. 2). The spectrum of the lithium isothiocyanate complex is practically identical except for the additional bands due to the anion. The sodium salt complexes also have very similar spectra. A comparison with the infrared spectra of the ethylene oxide polymer and the potassium bromide complex of the cyclic hexamer, which both have conformationally equivalent monomer units,[5] strongly suggests a similar situation here. In particular, the presence of only two bands in the $800-1000$ cm$^{-1}$ region can be taken as an indication of just one type of $-CH_2-CH_2-$units, and since all experimental data for the polymer point to a strong *gauche*-preference for the
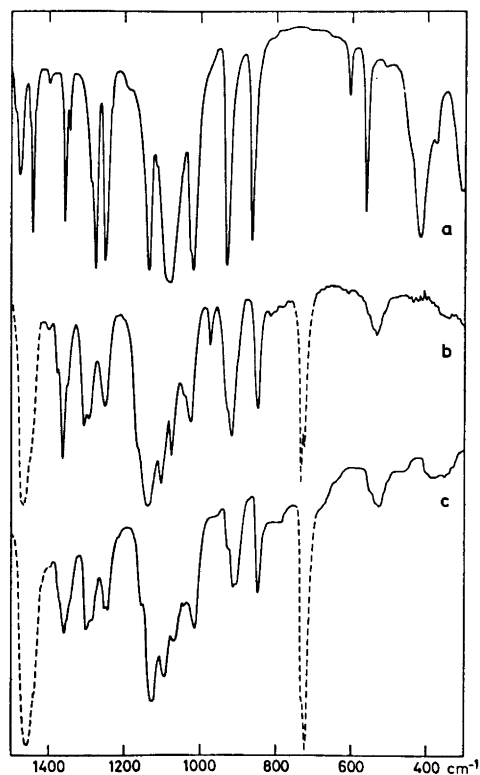


*Fig. 2.* Infrared spectra of 1,4,7,10-tetraoxacyclododecane as a 1:1 complex with LiBr pressed in KBr (a), alone as liquid at 30° (b) and alone as solid at $-60°$ (c). Absorption bands of the protecting polyethylene film are indicated by dashed curves.
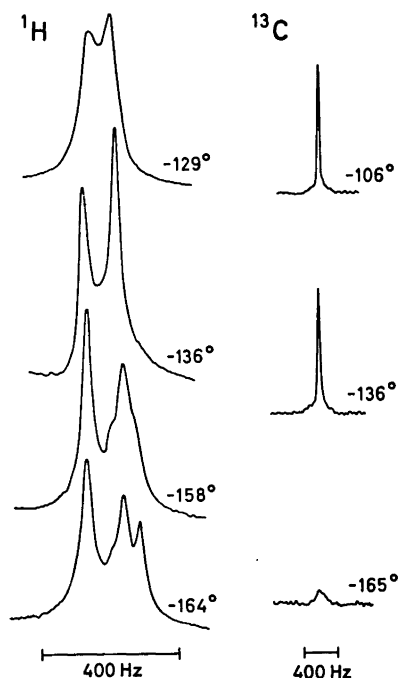
Fig. 3. 251 MHz $^1$H and 63.1 MHz $^{13}$C
NMR spectra of 1,4,7,10-tetraoxacyclo-
dodecane in $CHCl_2F/CHClF_2$ (1:2) solution.

CC-bonds and *anti*-preference for the CO-bonds,[6] there can be little doubt
that the tetra-ether ring has the "square" conformation of Fig. 1 with all
ether oxygens in "side" positions and not at the "corners". This is obviously
also the only way in which all four oxygens can coordinate equally to one
and the same Li-cation.*

The uncomplexed tetra-ether melts at 17° and shows sufficient similarity
between its infrared spectra in the melt (and solution) and in the crystal (Fig.
2) to suggest that the compound is conformationally homogeneous. It may
be more difficult, however, to draw a final conclusion about the identity of this
conformation. The infrared spectrum differs somewhat from that of the
complex as regards band positions, but not in general character, as the strong
band present only in lithium and not in sodium complexes at 420 cm$^{-1}$ can
be assigned to LiO stretching. The conformation may therefore be essentially
the same in the free ring as in the complex, but less rigid.

## MOLECULAR DIPOLE MOMENT

Dipole moment measurements in benzene and in carbon tetrachloride solu-
tion gave values of 2.50 and 2.40 D, respectively. This is so far from the value
of about 5 D expected for the complexing conformation with all oxygens on

* The crystal structure of the complexes is being determined by Dr. Frank, UCLA.

"side" positions with their dipoles pointing in the same direction, and also so far from the zero value expected if all oxygens are on corner positions, that a variety of alternative "quadrangular" ring conformations were examined as candidates. Those which reproduced the observed molecular dipole moment had, however, a very high calculated energy as the corresponding hydro-carbon,[7] and too low symmetry to be compatible with the simplicity of the observed infrared spectrum, and had therefore to be rejected.

The use of a measured molecular dipole moment in conformational analysis when several dipoles are present in the molecule may often be hazardous, except when they add up to the maximum possible value or when there is com-plete cancellation. Intermediate dipole moments may be simulated by vector addition in too many different ways. Also, if the molecule is flexible, a large atomic polarization may increase the apparent value of an intrinsically small molecular moment, while large amplitudes of thermal vibrations may decrease the apparent value of an intrinsically large molecular moment.

In the present tetra-ether, the experimentally determined value is the same as expected if the four ether dipoles were present in separate molecules. Also for the higher cyclic oligomers of ethylene oxide the observed molecular dipole moments [5] are close to the values expected for free relative orientation of the dipoles. That thermal vibrations have indeed large amplitudes in these polyoxyethylene rings is seen from their broad infrared bands [5] (Fig. 2) as compared with those of the stiffened complexing molecules. This may be related to the *gauche* preference about the CC-bond; the apparent lack of repulsion between two ether oxygen atoms in 1,4-*gauche* relationship [6] would be expected to reduce also the energy of adjoining rotational barriers and so create a rather shallow torsional potential.

## DYNAMIC NMR SPECTROSCOPY

[1]H resonance spectroscopy at 251 MHz shows two processes becoming slow for the uncomplexed tetra-ether (Fig. 3). The single room-temperature line at $\delta$ 3.65 has split into two bands at $-133°$ ($T_c \sim -126°$, $\Delta G^{\ddagger} = 6.8 \pm 0.3$ kcal/mol). At still lower temperature, about $-160°$, a further splitting takes place; the high-field band gives two new bands, while the low-field band only broadens ($\Delta G^{\ddagger} = 5.5 \pm 0.3$ kcal/mol). In ^{13}C resonance at 63.1 MHz the single room-temperature line at 70.0 ppm (downfield from TMS) on cooling remains a single line after the first process, and only broadens after the second without giving resolved lines. This broadening is not caused by magnetic inhomogeneity because the TMS-signal remains quite sharp. Broadening due to dipole-dipole relaxation can also be ruled out since no further broadening is observed at still lower temperature ($-172°$). It seems therefore to be due to near coin-cidence of chemical shifts for different carbon atoms; a similar situation has been encountered for the $-O-CH_2CH_2-O-$unit in 1,3,6-trioxacyclooctane.[8]

Of the lithium cation complexes, only the one having isothiocyanate as a counter ion was studied by low-temperature spectroscopy. Here also two dynamic processes are revealed by ^{1}H resonance (Fig. 4). The single-room-temperature line at $\delta$ 3.55 is split into two partially overlapping broad bands
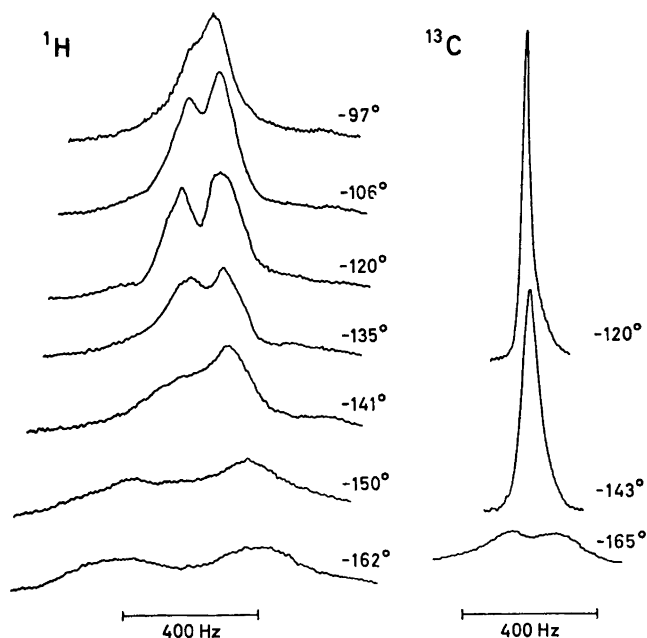
*Fig. 4.* 251 MHz ¹H and 63.1 MHz ¹³C NMR spectra of the 1:1 LiNCS complex of 1,4,7,10-tetraoxacyclododecane in $CHCl_2F/CHClF_2$ (1:2) solution.

at $-106°$ ($T_c \sim -96°$, $\Delta G^{\ddagger} = 8.2 \pm 0.3$ kcal/mol). At $-135°$ a second process starts to become slow, and at $-160°$ two very broad bands are seen, separated by a larger chemical shift than observed for the free ring. In ¹³C resonance the single room-temperature line at 71.2 ppm on cooling remains single after the first process. After the second process has become slow, two broad bands are now seen ($\Delta G^{\ddagger} = 5.6 \pm 0.3$ kcal/mol). The tendency for broader signals and larger chemical shift differences in lithium complexes has been observed earlier.[9]

The NMR-spectra obtained at the lowest temperature when both processes are slow are clearly in agreement with the "square" conformation with the oxygen atoms at "side" positions both for the free and the complexed ring. If the oxygen atoms were at corner positions, only a single ¹³C line and two ¹H bands should have been observed. The presence of two distinct site-exchange processes is also consistent with oxygen atoms at "side" positions as will be shown below.

## SITE EXCHANGE PROCESSES

For cyclododecane a ring atom and substituent exchange mechanism has been proposed [7] which involves the stepwise movement of each corner by one
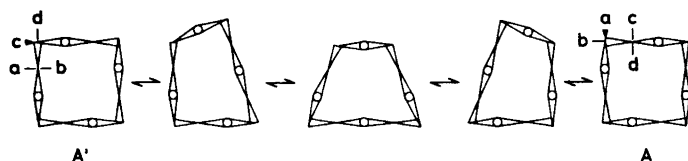
*Fig. 5.* Proposed one-cycle conformational interconversion path for the low-barrier site-exchange process.

position and passes through higher-energy quadrangular conformations. A complete cycle comprises the passage of four barriers and leads to the enantiomeric "square" conformation with all atoms moved by one step around the ring.

Applying this conformational interconversion mechanism to 1,4,7,10-tetraoxacyclododecane, the stable conformation A can either be transformed in one direction (Fig. 5) through one cycle to its mirror image A′, or in the other direction (Fig. 6) through two cycles to an identical conformation A″. In both cases the two types of carbon atoms exchange sites. In the former case (Fig. 5) also the *cis*-related protons of each unit exchange sites ($H_a = H_c$; $H_b = H_d$), while in the latter case (Fig. 6) the *trans*-related protons are exchanged ($H_a = H_d$; $H_b = H_c$). Thus, either of the two paths could in principle represent the low-barrier process since half of the protons would remain different from the other half. The other path would then lead to full exchange and represent the high-barrier process.

A decision can be reached by considering the relative barrier heights. The one-cycle path (Fig. 5) involves passage over four barriers, identical in pairs. Both have been estimated [7] to be < 14 kcal/mol for cyclododecane, and the kinetically decisive of these determined experimentally to be 7.3 kcal/mol.[2] If the barrier is defined [7] as the moment the bond between the old and new corner atom becomes *syn*-eclipsed, all these barriers are seen to involve eclipsing of the CC-bond, so that the critical interaction must be between the adjoining oxygen atoms (Fig. 7a); hence all four barriers must be lower than in the hydrocarbon.
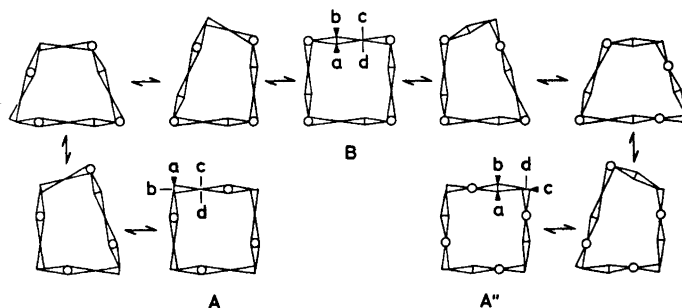


*Fig. 6.* Proposed two-cycle conformational interconversion path for the high-barrier site-exchange process.
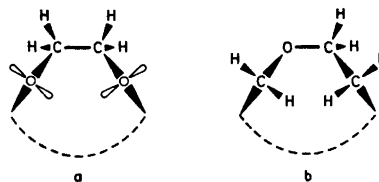
*Fig. 7.* Critical eclipsed interaction in all barriers on the one-cycle path (a) and on the two-cycle path (b).

On the other hand, the two-cycle path (Fig. 6) involves passage over eight barriers, pairs of which are identical, but these are all seen to involve eclipsing of a CO-bond. The critical interaction is therefore between two methylene groups (Fig. 7b); hence all eight barriers are expected to remain high.

A support for the assignment of path A⇌A′ to the low-barrier process and path A⇌B⇌A″ to the high-barrier process comes from the observed increase of the higher barrier on complexation with lithium isothiocyanate and the lack of an observed effect on the lower barrier. All along path A⇌A′ (Fig. 5) the four ether oxygen atoms point to the same side of the ring, and no real dissociation of the complex is necessary. On the other hand, it is seen that half-way through path A⇌A″ (Fig. 6) the intermediate "square" conformation B has got all oxygen atoms at corner positions so that the complex must become completely dissociated and then can only form again if the lithium cation reenters the A″ ring from the opposite side. The activation energy must therefore be increased by an amount corresponding to the stabilization obtained by complexing.

## EXPERIMENTAL

*1,4,7,10-Tetraoxacyclododecane.* This compound was prepared from ethylene oxide in diethyl ether solution using triethylaluminium as a catalyst.[4] The distilled crude product had to be crystallized from pentane at $-20°$ to remove acyclic material, then dried over $P_2O_5$. M.p. 17°.

*Lithium salt complexes.* The lithium bromide complex was prepared by dissolving equimolar quantities of dry lithium bromide and 1,4,7,10-tetraoxacyclododecane in methanol, evaporating the solution, and drying the solid in vacuum at 100°. (Found: C 36.02; H 6.09; Br 30.37. Calc. for $C_8H_{16}O_4LiBr$: C 36.54; H 6.12; Br 30.38.)

The lithium isothiocyanate complex was also prepared from a solution of equimolar quantities of salt and cyclic tetra-ether in methanol; the complex started to crystallize during concentration in a rotating evaporator and was filtered off. M.p. $240-243°$. (Found: C 45.25; H 6.60. Calc. for $C_8H_{16}O_4LiSCN$: C 45.00; H 6.65).

The sodium isothiocyanate complex crystallized from a concentrated methanol solution of the components and was filtered off. M.p. $159-163°$. It had a 2:1 stoichiometry and contained methanol as evidenced by OH absorption in the infrared and by analysis (Found: C 45.80; H 7.22. Calc. for $C_{16}H_{32}O_8.NaSCN.2CH_3OH$: C 45.82; H 8.06.)

*Infrared spectroscopy.* The spectra were recorded in a Perkin-Elmer Grating Infrared Spectrophotometer 457. Liquid films between pressed KBr disks protected by thin polyethylene films were cooled in a RIIC low-temperature cell to obtain the spectrum of crystalline tetra-ether. The lithium and sodium salt complexes could be ground with KBr and pressed into a pellet without any cation exchange taking place.

*Dipole moments.* Dielectric constants were measured at 25°C in a Weilheim Dipolmeter DM 01 on four different solutions in benzene. Refractive indices were measured on the same solutions in a Brice-Phoenix Differential Refractometer. Calculation of dipole moments was performed according to Hedestrand,[10] using no correction for atomic polarization.

*NMR spectroscopy.* The spectra of $CHCl_2F/CHClF_2$ (1:2) solutions were obtained on a superconducting solenoid NMR spectrometer [11] operating at 251 MHz for protons and at 63.1 MHz for $^{13}C$. Acquisition and Fourier transform of free induction spectra were carried out with a Data General Nova computer having 12 K 16-bit words, of which 8 K were used for data.[12]

REFERENCES

1. Dunitz, J. D. and Shearer, H. M. M. *Helv. Chim. Acta* **43** (1960) 18.
2. Anet, F. A. L., Cheng, A. K. and Wagner, J. J. *J. Am. Chem. Soc.* **94** (1972) 9250.
3. Wiberg, K. B. *J. Am. Chem. Soc.* **87** (1965) 1070; Bixon, M. and Lifson, S. *Tetrahedron* **23** (1967) 769.
4. Stewart, D. G., Waddan, D. Y. and Borrows, E. T. *Brit. Pat*, 2,293,868. (1957).
5. Dale, J. and Kristiansen, P. O. *Chem. Commun.* **1971** 670; *Acta Chem. Scand.* **26** (1972) 1471.
6. Flory, P. J. *Statistical Mechanics of Chain Molecules*, Interscience, New York 1969, p. 165.
7. Dale, J. *Acta Chem. Scand.* **27** (1973) 1130.
8. Degen, P. J., *Ph.D. Thesis*, University of California, Los Angeles 1972.
9. Dale, J. and Krane, J. *Chem. Commun.* **1972** 1012.
10. Hedestrand, G. *Z. physik. Chem.* **B 2** (1929) 428.
11. Anet, F. A. L., Buchanan, G. W. and Bradley, C. H. Paper presented at the 11th Experimental NMR Conference, Pittsburgh, Pa., April 1970.
12. Anet, F. A. L., Basus, V. J., Bradley, C. H. and Cheng, A. K. Paper presented at the 12th Experimental NMR Conference, Gainesville, Fla., Feb. 1971.

# Crystal Structures of Synthetic Analgetics

## I. Dextropropoxyphene Hydrochloride

### ERIK BYE

*Department of Chemistry, University of Oslo, Oslo 3, Norway*

The molecular and crystal structure of dextropropoxyphene hydrochloride has been determined by X-ray methods. The crystals are orthorhombic, space group $P2_12_12_1$; with unit cell dimensions $a = 11.997$ Å; $b = 12.835$ Å; $c = 13.830$ Å. The phase problem was solved by the heavy atom method and the model refined to an $R$-value of 0.032 for 1643 observed reflections. The absolute configuration has been established; estimated standard deviations are $0.003 - 0.004$ Å in interatomic distances and $0.2 - 0.3°$ in angles.

The crystal packing is dominated by a very strong $N^+ - H \cdots Cl^-$ hydrogen bond of 3.03 Å. There is no evidence of any interaction between the protonated nitrogen atom and the ester group. The latter is planar and the two phenyl rings form an angle of 86.6°.

Propoxyphene, first synthesized by Pohland *et al.* in 1953,[1] is a synthetic analgetic with morphine-like action. It belongs to a group of ester-compounds with the general formula

$$
\begin{array}{c}
\mathrm{Ph} \\
| \\
\mathrm{CH_2} \qquad \mathrm{R^3} \\
| \qquad\quad | \\
\mathrm{R^1 - C - O - C - CH - CH - R^4} \\
\;\;\; \| \qquad | \quad\; | \\
\;\;\; \mathrm{O} \qquad \mathrm{Ph} \;\; \mathrm{R^2}
\end{array}
$$
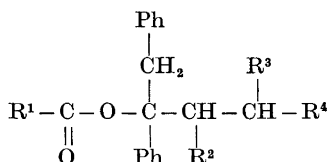
where $R^1 = Et$; $R^2 = Me$; $R^3 = H$; $R^4 = N(CH_3)_2$. The morphine-like action is believed to be dependent on a particular molecular conformation, resulting from an interaction between the basic nitrogen atom and the ester group. This particular conformation for synthetic analgetics was first proposed by Casy from a study of methadone .[2] The present structure determination was carried out to obtain information about the structure, and correlate this to the activity of analgetics. This is the first of several compounds related to methadone to be examined by X-ray methods in this laboratory.

Fig. 1 shows the propoxyphene molecule with the numbering scheme of the atoms (Cl and H excluded).
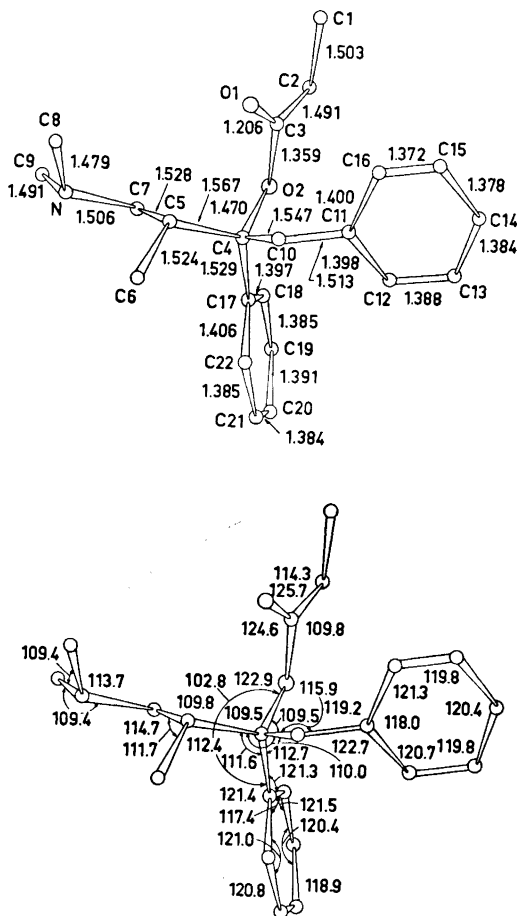


*Fig. 1.* Bond lengths (Å) and angles (°) in dextropropoxyphene hydrochloride.

## EXPERIMENTAL

Commercially available propoxyphene hydrochloride was recrystallized from a solution of acetone/ether. The compound crystallizes as colourless, transparent parallel-epipeds. Oscillation and Weissenberg photographs indicated orthorhombic symmetry, systematically absent reflections were $h00,0k0,00l$ for odd indices, and the space group is $P2_12_12_1$. Unit cell dimensions were determined from measurements on a manual Picker four-circle diffractometer with $CuK\alpha$-radiation. The density was measured by flotation.

A crystal of dimensions 0.4 mm × 0.4 mm × 0.3 mm was used for the collection of three-dimensional intensity data on a Syntex P1 diffractometer using graphite crystal monochromated MoKα-radiation. The $2\theta - \theta$ autocollection program was applied with variable scan rate and a cut-off at $2\sigma_I$. The scan range was from 0.6° below $2\theta(\alpha_1)$ to 0.7° above $2\theta(\alpha_2)$, and the backgrounds were counted 0.7 times the intensity measuring time. The intensities of three standard reflections were measured periodically during the data collection. They showed an average decrease of 4 % and the intensities were corrected for this effect. Estimated standard deviations in the intensities were assigned as the square root of the total counts with a 2 % addition for instrumental instability.

A total of 1795 independent reflections were recorded within the limit of sin $\theta/\lambda$ 0.76, 1647 having a net count larger than $2\sigma_I$.

The data were corrected for Lorentz and polarization effects but not for absorption ($\mu = 2.01$ cm⁻¹ MoKα) or secondary extinction.

All calculations were performed on a CDC 3300 computer using the programs described in Ref. 3. Atomic form factors were those of Hanson et al.[4] for C, O, N, and C, and of Stewart et al.[5] for H.

## CRYSTAL DATA

Dextropropoxyphene hydrochloride, $C_{22}H_{29}NO_2$ HCl, orthorhombic.
$a = 11.997$ (1) Å, $b = 12.835$ (1) Å, $c = 13.830$ (1) Å.
$V = 2129.6$ Å³, $M = 375.94$, $Z = 4$.
Melting point: 166.5 − 167.5°C.
$D_{obs} = 1.18$ g cm⁻³, $D_{calc} = 1.19$ g cm⁻³.
Systematic absences: $h00$ when $h$ is odd, $0k0$ when $k$ is odd, $00l$ when $l$ is odd; space group $P2_12_12_1$.

## STRUCTURE DETERMINATION

The coordinates of the chlorine ions were determined from a three-dimensional Patterson synthesis. A Fourier map revealed 18 of the 26 heavy atom positions. Two successive Fourier refinement served to establish a trial structure of all the non-hydrogen atoms. Successive cycles of full matrix least squares refinement, first with isotropic then with anisotropic thermal parameters yielded an $R$-value of 0.07. None of the hydrogen atoms could be localized in a difference Fourier map, and approximate positions were calculated from stereochemical considerations. A distance of 3.01 Å between Cl and N was supposed to correspond to a hydrogen bond from a protonated nitrogen atom. Giving the atoms individual isotropic thermal parameters, the block-diagonal least squares refinement converged at $R = 0.034$.

To establish the absolute configuration, the structure factors were calculated including anomalous dispersion effects for the chlorine ion. The two $R$-values calculated, with $\Delta f''$ positive and negative were 0.034 and 0.033, respectively. The diastereomer corresponding to the lower $R$-value could be assigned the configuration $4S{:}5R$, following the numbering in the present paper. This corresponds to the absolute configuration assigned to the (+)-isomer by Sullivan et al.[6] from chemical evidence. The $R$-ratio 0.034/0.033 may be accepted at a significance level better than 0.005 with Hamilton's test.[7]

The reflections 012, 023, 031, 102, and 113 were the strongest ones and had to be measured with reduced intensity of the primary beam. They showed

*Table 1.* Observed and calculated structure factors. The columns are $h$, $k$, $l$, $10|F_o|$ and $10|F_c|$.

*Table 1. Continued.*

Table 1. Continued.



*Fig. 2.* The crystal structure of dextropropoxyphene hydrochloride as seen along the c-axis.

great differences $(F_o - F_c)$ and were excluded from the further refinement.

Final block-diagonal least squares refinement, including anomalous dispersion effects gave an $R$-value of 0.032 ($R_w = 0.032$). In the last cycle the average shift in the parameters were $0.1\sigma$ for the 1643 observed reflections.

A total difference Fourier map showed electron densities in the range $\pm 0.2$ eÅ$^{-3}$.

Observed and calculated structure factors are listed in Table 1, and the atomic parameters in Tables 2 and 3. The anisotropic temperature factor is given by

*Table 2.* Fractional atomic coordinates and thermal parameters with standard deviations $(10^5)$ for non-hydrogen atoms.

| Atom | $x$ | $y$ | $z$ | $B_{11}$ | $B_{22}$ | $B_{33}$ | $B_{12}$ | $B_{13}$ | $B_{23}$ |
|---|---|---|---|---|---|---|---|---|---|
| Cl | 44808 | − 37286 | 6017 | 872 | 674 | 959 | 371 | 133 | 210 |
|  | 7 | 7 | 7 | 7 | 5 | 7 | 11 | 13 | 11 |
| N | 22449 | − 26439 | 7777 | 647 | 410 | 515 | − 56 | − 125 | 11 |
|  | 18 | 15 | 16 | 17 | 14 | 14 | 27 | 30 | 25 |
| O1 | 4785 | 2717 | 18542 | 627 | 833 | 559 | − 292 | − 82 | − 311 |
|  | 15 | 16 | 14 | 15 | 16 | 12 | 28 | 25 | 24 |
| O2 | 19313 | 6478 | 8602 | 492 | 452 | 443 | 19 | 15 | − 45 |
|  | 13 | 13 | 12 | 13 | 10 | 10 | 21 | 21 | 20 |
| C1 | − 10477 | 13028 | 6017 | 671 | 1419 | 824 | 553 | − 28 | − 365 |
|  | 27 | 34 | 26 | 26 | 37 | 25 | 56 | 46 | 55 |
| C2 | 1644 | 11802 | 3593 | 651 | 661 | 567 | 49 | 31 | − 139 |
|  | 23 | 24 | 21 | 23 | 21 | 19 | 39 | 36 | 36 |
| C3 | 8386 | 6512 | 11201 | 535 | 425 | 484 | − 141 | 88 | 164 |
|  | 21 | 20 | 18 | 20 | 16 | 16 | 33 | 31 | 31 |
| C4 | 28210 | 2555 | 14942 | 524 | 415 | 387 | 6 | 29 | 5 |
|  | 21 | 19 | 18 | 21 | 17 | 15 | 32 | 23 | 27 |
| C5 | 26550 | − 9410 | 16661 | 682 | 411 | 402 | − 40 | − 113 | − 32 |
|  | 22 | 20 | 19 | 22 | 17 | 15 | 34 | 33 | 28 |
| C6 | 36101 | − 14228 | 22381 | 1214 | 507 | 678 | 202 | 590 | − 23 |
|  | 29 | 24 | 23 | 32 | 20 | 21 | 47 | 47 | 37 |
| C7 | 24782 | − 14938 | 6994 | 730 | 373 | 455 | − 116 | − 58 | − 17 |
|  | 22 | 20 | 19 | 24 | 16 | 16 | 33 | 35 | 29 |
| C8 | 13405 | − 29022 | 14640 | 1135 | 604 | 930 | − 408 | − 771 | − 147 |
|  | 30 | 26 | 26 | 32 | 22 | 26 | 48 | 54 | 43 |
| C9 | 19621 | − 30635 | − 1969 | 1280 | 566 | 629 | − 286 | 171 | 257 |
|  | 29 | 24 | 23 | 35 | 21 | 21 | 48 | 48 | 37 |
| C10 | 27871 | 8435 | 24706 | 502 | 502 | 401 | − 42 | − 106 | 97 |
|  | 21 | 20 | 18 | 20 | 17 | 15 | 33 | 33 | 29 |
| C11 | 25933 | 20030 | 24103 | 594 | 476 | 372 | 45 | 130 | 172 |
|  | 21 | 21 | 18 | 21 | 17 | 15 | 33 | 32 | 29 |
| C12 | 34187 | 26995 | 21334 | 788 | 514 | 633 | 7 | 16 | 301 |
|  | 24 | 23 | 23 | 25 | 19 | 20 | 39 | 39 | 35 |
| C13 | 32227 | 37612 | 21427 | 1175 | 526 | 642 | − 217 | 237 | 29 |
|  | 28 | 24 | 23 | 33 | 20 | 21 | 47 | 44 | 37 |
| C14 | 22051 | 41337 | 24349 | 1508 | 547 | 644 | 740 | 761 | 261 |
|  | 32 | 24 | 22 | 38 | 21 | 21 | 51 | 53 | 38 |
| C15 | 13794 | 34577 | 27151 | 890 | 767 | 795 | 705 | 402 | 466 |
|  | 27 | 26 | 24 | 28 | 25 | 24 | 47 | 46 | 43 |
| C16 | 15710 | 24064 | 26963 | 631 | 700 | 623 | 299 | 57 | 403 |
|  | 23 | 23 | 22 | 23 | 22 | 20 | 39 | 38 | 38 |
| C17 | 38751 | 4836 | 9145 | 543 | 358 | 476 | 76 | − 86 | 104 |
|  | 21 | 18 | 19 | 20 | 16 | 16 | 31 | 35 | 30 |
| C18 | 38502 | 5533 | − 871 | 637 | 673 | 428 | − 200 | − 106 | 67 |
|  | 23 | 23 | 19 | 23 | 21 | 16 | 39 | 36 | 34 |
| C19 | 48077 | 7323 | − 6169 | 917 | 830 | 489 | − 96 | − 352 | − 53 |
|  | 26 | 26 | 21 | 29 | 25 | 18 | 47 | 39 | 38 |
| C20 | 58223 | 8554 | − 1573 | 623 | 804 | 687 | − 77 | − 473 | 12 |
|  | 23 | 25 | 22 | 24 | 24 | 21 | 42 | 39 | 40 |
| C21 | 58658 | 7818 | 8357 | 506 | 856 | 711 | 226 | − 86 | 136 |
|  | 23 | 25 | 23 | 21 | 24 | 20 | 40 | 39 | 43 |
| C22 | 49114 | 5937 | 13679 | 564 | 618 | 531 | 154 | − 96 | 60 |
|  | 23 | 23 | 20 | 21 | 22 | 17 | 38 | 34 | 35 |

*Table 3.* Fractional coordinates (10⁴) and isotropic thermal parameters (Å²) with standard deviations for hydrogen atoms.

| Atom | $x$ | $y$ | $z$ | $B$ |
|------|------|------|------|------|
| H1C1 | − 1378 | 1681 | 86 | 8.0 |
|  | 2: | 27 | 23 | .9 |
| H2C1 | − 1100 | 1728 | 1222 | 9.7 |
|  | 34 | 30 | 24 | 1.1 |
| H3C1 | − 1379 | 683 | 847 | 11.0 |
|  | 33 | 33 | 27 | 1.2 |
| H1C2 | 294 | 752 | − 254 | 5.7 |
|  | 21 | 22 | 18 | .7 |
| H2C2 | 506 | 1802 | 260 | 4.5 |
|  | 20 | 20 | 18 | .6 |
| HC5 | 1998 | − 992 | 2055 | 3.5 |
|  | 20 | 20 | 18 | .6 |
| H1C6 | 3723 | − 1044 | 2817 | 8.5 |
|  | 29 | 28 | 23 | 1.0 |
| H2C6 | 3424 | − 2145 | 2410 | 6.5 |
|  | 25 | 26 | 21 | .8 |
| H3C6 | 4334 | − 1405 | 1820 | 7.1 |
|  | 24 | 26 | 21 | .8 |
| H1C7 | 3202 | − 1446 | 242 | 5.0 |
|  | 20 | 22 | 19 | .7 |
| H2C7 | 1875 | − 1195 | 332 | 3.6 |
|  | 19 | 19 | 17 | .6 |
| HN | 2964 | − 2948 | 931 | 5.9 |
|  | 22 | 22 | 20 | .7 |
| H1C8 | 1209 | − 3618 | 1509 | 6.4 |
|  | 24 | 24 | 19 | .7 |
| H2C8 | 678 | − 2489 | 1227 | 8.5 |
|  | 28 | 28 | 23 | 1.0 |
| H3C8 | 1604 | − 2726 | 2197 | 5.9 |
|  | 23 | 24 | 21 | .8 |
| H1C9 | 1819 | − 3804 | − 169 | 4.0 |
|  | 18 | 19 | 17 | .6 |
| H2C9 | 2624 | − 2996 | − 572 | 6.0 |
|  | 22 | 23 | 21 | .7 |
| H3C9 | 1604 | − 2722 | − 506 | 8.7 |
|  | 31 | 30 | 24 | 1.0 |
| H1C10 | 3559 | 744 | 2835 | 3.6 |
|  | 19 | 19 | 16 | .6 |
| H2C10 | 2193 | 525 | 2860 | 2.1 |
|  | 17 | 16 | 15 | .5 |
| HC12 | 4151 | 2384 | 1962 | 4.8 |
|  | 21 | 21 | 18 | .6 |
| HC13 | 3828 | 4248 | 3935 | 5.6 |
|  | 22 | 22 | 19 | .7 |
| HC14 | 2065 | 4868 | 2444 | 7.1 |
|  | 24 | 25 | 21 | .8 |
| HC15 | 693 | 3767 | 2919 | 6.2 |
|  | 23 | 24 | 20 | .7 |
| HC16 | 939 | 1921 | 2887 | 5.1 |
|  | 23 | 22 | 19 | .7 |
| HC18 | 3148 | 547 | − 389 | 3.2 |
|  | 18 | 18 | 16 | .5 |
| HC19 | 4800 | 760 | − 1303 | 4.9 |
|  | 21 | 21 | 18 | .6 |
| HC20 | 6552 | 971 | − 524 | 4.4 |
|  | 19 | 19 | 17 | .6 |
| HC21 | 6583 | 863 | 1208 | 4.7 |
|  | 20 | 20 | 16 | .6 |
| HC22 | 4930 | 575 | 2059 | 4.5 |
|  | 23 | 22 | 18 | .7 |

*Table 4.* Bond lengths (Å) and bond angles (°) for the nonhydrogen atoms, with standard deviations.

| | Bond length Uncorrected | Corrected | Angles | |
|---|---|---|---|---|
| C1 − C2 | 1.503 (4) | | C1 − C2 − C3 | 114.3 (.3) |
| C2 − C3 | 1.491 (4) | | C2 − C3 − O1 | 125.7 (.2) |
| C3 − O1 | 1.206 (3) | | C2 − C3 − O2 | 109.8 (.2) |
| C3 − O2 | 1.359 (3) | | O1 − C3 − O2 | 124.6 (.2) |
| O2 − C4 | 1.470 (3) | | C3 − O2 − C4 | 122.9 (.2) |
| C4 − C5 | 1.567 (4) | | O2 − C4 − C5 | 109.5 (.2) |
| C5 − C6 | 1.524 (4) | | O2 − C4 − C10 | 109.5 (.2) |
| C5 − C7 | 1.528 (4) | | O2 − C4 − C17 | 102.8 (.2) |
| C7 − N | 1.506 (3) | | C4 − C5 − C6 | 112.4 (.2) |
| C8 − N | 1.479 (4) | | C4 − C5 − C7 | 109.8 (.2) |
| C9 − N | 1.491 (4) | | C6 − C5 − C7 | 111.7 (.2) |
| C4 − C10 | 1.547 (3) | | C5 − C7 − N | 114.7 (.2) |
| C10−C11 | 1.509 (4) | 1.513 | C7 − N − C8 | 113.7 (.2) |
| C11−C12 | 1.388 (4) | 1.398 | C7 − N − C9 | 109.4 (.2) |
| C12−C13 | 1.383 (4) | 1.388 | C8 − N − C9 | 109.4 (.2) |
| C13−C14 | 1.372 (5) | 1.384 | C5 − C4 − C10 | 110.0 (.2) |
| C14−C15 | 1.373 (5) | 1.378 | C5 − C4 − C17 | 111.6 (.2) |
| C15−C16 | 1.369 (4) | 1.372 | C4 − C10−C11 | 115.9 (.2) |
| C16−C11 | 1.389 (4) | 1.400 | C10−C11−C12 | 122.7 (.2) |
| C4 − C17 | 1.527 (4) | 1.529 | C11−C12−C13 | 120.7 (.3) |
| C17−C18 | 1.389 (4) | 1.397 | C12−C13−C14 | 119.8 (.3) |
| C18−C19 | 1.382 (4) | 1.385 | C13−C14−C15 | 120.4 (.3) |
| C19−C20 | 1.382 (4) | 1.391 | C14−C15−C16 | 119.8 (.3) |
| C20−C21 | 1.378 (4) | 1.384 | C15−C16−C11 | 121.3 (.3) |
| C21−C22 | 1.382 (4) | 1.385 | C16−C11−C12 | 118.0 (.3) |
| C22−C17 | 1.400 (4) | 1.406 | C16−C11−C10 | 119.2 (.2) |
| | | | C5 − C4 − C17 | 111.6 (.2) |
| | | | C10−C4 − C17 | 112.7 (.2) |
| Hydrogen bond length | | | C4 − C17−C18 | 121.3 (.2) |
| N − H···Cl⁻ | 3.031 (2) | | C17−C18−C19 | 121.5 (.3) |
| | | | C18−C19−C20 | 120.4 (.3) |
| | | | C19−C20−C21 | 118.9 (.3) |
| | | | C20−C21−C22 | 120.8 (.3) |
| | | | C21−C22−C17 | 121.0 (.3) |
| | | | C22−C17−C18 | 117.4 (.2) |
| | | | C22−C17−C4 | 121.4 (.2) |

*Table 5.* Bond lengths (Å) involving hydrogen atoms.

| | | | | |
|---|---|---|---|---|
| C1−H1C1 | 0.96 | | C9 − H1C9 | 0.97 |
| C1−H2C1 | 1.01 | | C9 − H2C9 | 0.95 |
| C1−H3C1 | 0.95 | | C9 − H3C9 | 1.02 |
| C2−H1C2 | 1.02 | | C10−H1C10 | 1.06 |
| C2−H2C2 | 0.94 | | C10−H2C10 | 0.98 |
| C5−HC5 | 0.96 | | C12−HC12 | 1.00 |
| C6−H1C6 | 0.95 | | C13−HC13 | 1.00 |
| C6−H2C6 | 0.98 | | C14−HC14 | 0.96 |
| C6−H3C6 | 1.04 | | C15−HC15 | 0.96 |
| C7−H1C7 | 1.08 | | C16−HC16 | 1.02 |
| C7−H2C7 | 0.96 | | C18−HC18 | 0.94 |
| N − HN | 0.97 | | C19−HC19 | 0.95 |
| C8−H1C8 | 0.93 | | C20−HC20 | 1.02 |
| C8−H2C8 | 1.01 | | C21−HC21 | 1.00 |
| C8−H3C8 | 1.09 | | C22−HC22 | 0.96 |

Standard deviations are in the range 0.02−0.03 Å.

$$\exp - (B_{11}h^2 + B_{22}k^2 + B_{33}l^2 + B_{12}hk + B_{13}hl + B_{23}kl)$$

The e.s.d. in bond lengths and angles were calculated to be $0.003 - 0.004$ Å and $0.3°$, respectively.

## DISCUSSION

Interatomic distances and bond angles are given in Tables 4 and 5, and are shown in Fig. 1. The analysis of the thermal parameters showed that the two benzyl parts of propoxyphene could be regarded as rigid bodies, and the positional parameters of these atoms were corrected for librational effects. The corrected bond lengths are also listed in Table 4.

Fig. 2 illustrates the crystal structure which is dominated by a very strong hydrogen bond (3.03 Å) between the protonated nitrogen atom and the chlorine ion; the distance between the hydrogen atom (HN) and the chlorine ion being 2.08 Å.

There are no other particularly short intermolecular distances in the structure.

The distance $C1 - C2$ (1.503 Å) is found to be shorter than the normal, 1.537 Å.[8] This is probably due to the considerable thermal motion of the methyl carbon atom.

The mean $C - N$ bond length is 1.492 Å, in agreement with the value reported by Marsh et al. (1.487 Å).[9] The mean aromatic $C - C$ distance is 1.383 Å (1.389 Å corrected).

Owing to the two large aromatic groups at C4, the angle $O2 - C4 - C17$ is as small as $102.8°$. To compensate the strain around C4, the angle $C4 - C10 - C11$ is $115.9°$. Both values are significantly different from the normal tetrahedral angle.

The phenyl rings A and B are planar. C4 is co-planar with plane B, whereas C10 is 0.09 Å out of plane A. This deviation from planarity may be caused by the repulsions around C4 mentioned above. The two planes A and B form an angle of $86.6°$. The dihedral angles $C12 - C11 - C10 - C4$ and $C18 - C17 - C4 - O2$ are $76.2°$ and $-28.3°$, respectively.

The ester group (C2,C3,O1,O2) is planar to within 0.004 Å, the planes through C1,C2,C3 and C3,O2,C4 form angles of $5.4°$ and $5.6°$ with this plane, respectively, C1 and C4 being on the same side.

The butylamine part of the molecule is nearly fully extended, the torsional angles around the bonds $C10 - C4$, $C4 - C5$ and $C5 - C7$ being $-162.6°$, $169.8°$ and $-176.7°$. Owing to the strong hydrogen bond between the nitrogen atom and the chlorine ion there is no interaction between the $NH^+(CH_3)_2$ and the ester groups. The bond $N - H$ is pointing away from the ester group, and the suggested morphine-like conformation is not found in this hydrochloride of dextropropoxyphene. In the present structure the distance $H1C7 - O1$ is 3.27 Å, and a rotation about the bonds $C5 - C7$ and $C7 - N$ may thus bring the nitrogen atom in close contact with the carbonyl group. This rotation may take place in the free molecule or related compounds; the crystal structure of methadone now being under investigation in this laboratory may give an answer to this.

## REFERENCES

1. Pohland, A. and Sullivan, H. R. *J. Am. Chem. Soc.* **75** (1953) 4458.
2. Casy, A. F. *J. Chem. Soc.* **B 1966** 1157.
3. Dahl, T., Gram, F., Groth, P., Klewe, B. and Rømming, C. *Acta Chem. Scand.* **24** (1970) 2232.
4. Hanson, H. P., Herman, F., Lea, J. D. and Skillman, S. *Acta Cryst.* **17** (1964) 1040.
5. Stewart, R. F., Davidson, E. R. and Simpson, W. T. *J. Chem. Phys.* **42** (1965) 3175.
6. Sullivan, H. R., Beck, J. R. and Pohland, A. *J. Org. Chem.* **28** (1963) 2381.
7. Hamilton, W. C. *Acta Cryst.* **18** (1965) 502.
8. *Interatomic Distances, Suppl.* The Chemical Society, London 1965.
9. Marsh, R. E. and Donohue, J. *Advan. Protein Chem.* **22** (1967) 235.

# The Molecular Structure of

# Hexachloro-3,4-dimethylenecyclobutene

ANNE SKANCKE

*Department of Chemistry, University of Oslo, Blindern, Oslo 3, Norway\**

The molecular structure of gaseous hexachloro-3,4-dimethylene-cyclobutene has been investigated by electron diffraction. The molecule is found to be planar. The average value of the C—Cl distances is 1.695(6) Å. The carbon skeleton is almost unchanged from that of the unsubstituted hydrocarbon.

The main conclusions from the experimental study have been satisfactorily confirmed by an SCF-MO calculation including the $\pi$-electrons only.

The molecular structure of 3,4-dimethylenecyclobutene has previously been elucidated by an electron diffraction investigation.[1] The experimental results obtained were found to be in accordance with properties calculated by the ZDO approximation in the SCF theory.[2]

The aim of the present work is to study the geometric stability of the carbon skeleton of the perchlorinated derivative of the molecule. The main results from the electron diffraction study have been confirmed by semi-empirical calculations of the same kind as those used for the unsubstituted hydrocarbon. A sample of the compound was kindly given to me by Drs. E. D. Bergmann and I. Agranat of the Hebrew University of Jerusalem.

## ELECTRON DIFFRACTION STUDIES

The electron scattering patterns were recorded on the Oslo electron diffraction unit[3] with a nozzle temperature of 140° and a nozzle-to-photographic plate distance of about 48 cm. Due to thermal instability of the compound, attempts at recordings at shorter distances were not successful, and the structure calculations were based on intensity data from one nozzle-to-plate distance only. The optical densities of four plates in the region $s = 1.375$ Å$^{-1}$ to 19.75 Å$^{-1}$ were measured at $\Delta s = 0.125$ Å$^{-1}$ intervals, and the data were processed in the usual manner.[4]

---

\* Present address: Institute of Medical Biology, University of Tromsø, Tromsø, Norway.

Theoretical intensity curves were calculated from the approximation

$$I^{ClCl}(s) = \sum \frac{|f_i(s)|\ |f_j(s)|}{|f_{Cl}(s)|^2} \cos\left[\eta_i(s) - \eta_j(s)\right] \frac{\sin\,(R_{ij}s)}{R_{ij}} \exp\left(-\tfrac{1}{2}u_{ij}^2 s^2\right) \qquad (1)$$

The sum extends over all atomic pairs i, j in the molecule.

As usual, $R_{ij}$ denotes the internuclear distance, $u_{ij}$ the root mean square amplitude of vibration, and $f_i(s) = |f_i(s)| \exp\left[i\eta_i(s)\right]$ is the atomic scattering factor for atom i. For the carbon and chlorine atoms values from nonrelativistic Hartree-Fock calculations have been used.[5,6]

Radial distribution curves were calculated by Fourier inversions of experimental and theoretical intensity curves.

Because of the short intensity range in the data the constant k in the general formula for the radial distribution curve

$$RD = (2\pi)^{-\frac{1}{2}} \sum_{s\,=\,S_{min}}^{S_{max}} Im(s) \exp\left(-ks^2\right) \sin\,(rs)\varDelta s \qquad (2)$$

was put equal to 0.020.

The best agreement between experimental and theoretical curves was obtained by assuming the molecule to be planar. The carbon − carbon distances 1 − 2 and 2 − 3 were assumed to be 1.45 Å and the carbon − carbon distances 2 − 5 and 1 − 4 were assumed equal to 1.37 Å. The C − Cl bonds were assumed to be 1.69 Å, and a least squares refinement was carried out. For labelling of atoms, see Fig. 1.

Because of lack of intensity data at s-values above 20 Å⁻¹ and strong scattering contribution from the six C − Cl distances, it was not possible to refine the C − C distances and the corresponding u-values. The external angles and the average C − Cl bond distance and corresponding u-value were refined.
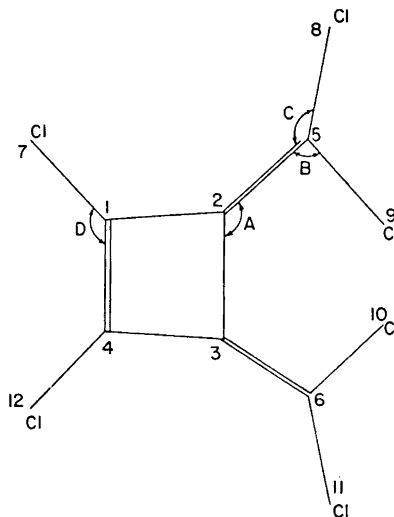


*Fig. 1.* Notation of atoms.

*Table 1.* Experimental and calculated distances in hexachloro-3,4-dimethylenecyclo-butene. Calculated values for the unsubstituted hydrocarbon included for comparison.

| Dist. | $R(Å)$ exp | Stand. dev. | $R$ calc. | $R$ calc. for hydroc. |
|-------|-----------|-------------|-----------|------------------------|
| $C_1-C_2$ | 1.45 | | 1.469 | 1.468 |
| $C_2-C_3$ | | | 1.477 | 1.476 |
| $C_2-C_5$ | 1.37 | | 1.351 | 1.350 |
| $C_1-C_4$ | | | 1.356 | 1.354 |
| $(C-Cl)_{av.}$ | 1.695 | 0.006 | 1.721 | |

*Table 2.* Interbond angles from least squares refinement. For labelling of angles see Fig. 1.

| Angle | Degrees | Stand. dev. (degr.) |
|-------|---------|----------------------|
| A | 134.4 | 0.9 |
| B | 127.4 | 1.9 |
| C | 118.7 | 1.5 |
| D | 134.9 | 0.9 |

The results are given in Tables 1 and 2. Other $u$-values were refined with the constraint that the $u$-values for all distances of one type and belonging to the same peak in the radial distribution curve are identical. The final results were used to calculate theoretical radial distribution curves, shown in Fig. 2. The final results for the experimental structure parameters are given in Table 1.

## MOLECULAR ORBITAL CALCULATIONS

The procedure applied in these calculations has been presented in detail previously.[7-9] The parameters appropriate to the carbon-carbon bond have
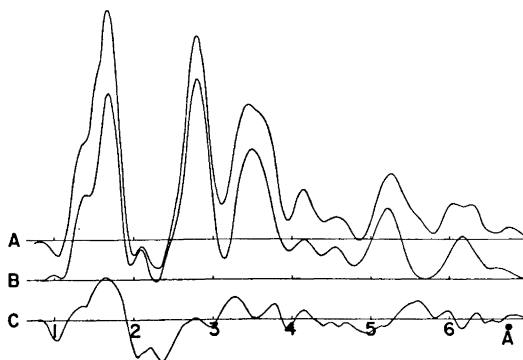


*Fig. 2.* Radial distribution curves. A, experimental; B, theoretical; C, A−B.

been taken from a paper by Roos and Skancke,[7] and for the chlorine-carbon bond parameters evaluated by Grabe [9] have been used. Her paper, however, does not give a relation between bond order and bond length for the $C-Cl$ bond. All the molecules chosen for the parameterization have bond lengths very close to 1.718 Å, and also her calculated bond orders varied very little, between 0.14 and 0.18.

For the carbon-carbon bond, the relation $R_{\mu\nu} = 1.517 - 0.18\ p_{\mu\nu}$ has been successfully used in previous papers. $p_{\mu\nu}$ is here the bond order between neighboring atoms $\mu$ and $\nu$ as calculated by this parameterization scheme. The constant 0.18, the slope of the bond distance to bond order graph, seems to change little when one atom is a hetero atom. If we assume the value 0.18 also for the chlorine-carbon bond, and use the experimental bond distance for $o$-dichlorobenzene and 1,2,4,5-tetrachlorobenzene which are both determined to 1.717 Å ± 0.005 Å,[10] and the calculated bond order 0.150, we obtain the relation

$$R_{\mu\nu} = 1.744 - 0.18\ p_{\mu\nu} \tag{3}$$

By using the experimental bond distance [11] and calculated bond order for $cis$-1,2-dichloroethylene, however, one arrives at a relation

$$R_{\mu\nu} = 1.755 - 0.18\ p_{\mu\nu} \tag{4}$$

The CCCl bond angles of the benzene derivatives are 120°, and the corresponding angle for $cis$-1,2-dichloroethylene is 121°33′, so the difference can hardly be explained as due to hybridization. Eqn. (3) based upon benzene derivative data are used in the present work to calculate C–Cl bond distances from bond orders, but the uncertainty at this point should be kept in mind.

## RESULTS AND DISCUSSION

Table 1 gives the bond distances of the molecule. In spite of the rather poor resolution of the radial distribution function the experimental results show a planar molecule with a strongly alternating ring system similar to the one in the unsubstituted hydrocarbon. This conclusion is confirmed by the molecular orbital calculations.

The difference between the experimental and the theoretical value for the C–Cl bond is hard to explain. Partly it may be ascribed to the uncertainty in the bond order to bond distance relationship for the $C-Cl$ bond. The bond orders for the C–Cl bonds in this molecule were all equal to 0.132 as compared to about 0.15 for the molecules chosen for the parameterization. This should indicate a C–Cl distance larger than 1.718 Å for the molecule investigated here. Because of the strong contribution from this distance in the radial distribution curve (see Fig. 1) its experimental value should be quite reliable.

In Table 3 the calculated $\pi$-electron charges are compared with those in the hydrocarbons.[2] It is seen that the chlorine atoms increase the electron density in the ring, while atoms 5 and 6 have reduced atomic net charges as compared to the hydrocarbon.

The experimental UV spectrum of the molecule recorded in $n$-heptane solution [12,13] is given in Table 4. This shows two pronounced absorption maxima,

Table 3. Calculated $\pi$-electron atomic charges in hexachloro-3,4-dimethylenecyclobutene (I), and in the substituted hydrocarbon (II). For labelling of atoms see Fig 1.

| Atom No. | I | II |
|---|---|---|
| 1 | 1.017 | 0.988 |
| 2 | 0.994 | 0.878 |
| 5 | 1.045 | 1.132 |
| 7 | 1.982 | |
| 8 | 1.981 | |
| 9 | 1.981 | |

Table 4. Calculated and observed electronic transitions in hexachloro-3,4-dimethylenecyclobutene. Frequencies in $cm^{-1}$.

| $\nu_{calc.}$ | $\nu_{obs.}$ | $f_{calc.}$ | $\log E_{obs.}$ |
|---|---|---|---|
| 37 000 | 34 700 | 0.15 | |
| 38 300 | 35 700 | 0.0 | |
| 47 000 | 39 700 | 0.82 | 4.5 |
| 48 000 | 41 700 | 0.84 | 4.56 |

one at about 35 000 $cm^{-1}$ and one at about 40 000 $cm^{-1}$. Both peaks exhibit fine structure. By a comparison to the calculated counterparts, the experimental transition at 41 700 $cm^{-1}$ ($\log E = 4.56$) has to be assigned to the calculated strong transition at 48 000 $cm^{-1}$. The close-lying transition of 39 700 ($\log E = 4.5$) must correspond to the calculated value of 47 000 $cm^{-1}$. As a shoulder on this dominating double peak are two transitions at 34 700 $cm^{-1}$ and 35 700 $cm^{-1}$, respectively. These are most likely related to the calculated values of 37 000 $cm^{-1}$ and 38 300 $cm^{-1}$. The experimental intensities of these weak transitions are very uncertain.

The discrepancies between experimental and calculated values for the strong transitions may partly be due to solvent shifts.

REFERENCES

1. Skancke, A. *Acta Chem. Scand.* **22** (1968) 3239.
2. Skancke, A. and Skancke, P. N. *Acta Chem. Scand.* **22** (1968) 175.
3. Bastiansen, O., Hassel, O. and Risberg, F. *Acta Chem. Scand.* **9** (1955) 232.
4. Andersen, B., Seip, H. M., Strand, T. G. and Stølevik, R. *Acta Chem. Scand.* **23** (1969) 3224.
5. Watson, R. E. and Freeman, A. J. *Phys. Rev.* **123** (1961) 521.
6. Strand, T. G. and Bonham, R. A. *J. Chem. Phys.* **40** (1964) 1686.
7. Roos, B. and Skancke, P. N. *Acta Chem. Scand.* **21** (1967) 233.
8. Roos, B. *Acta Chem. Scand.* **21** (1967) 2318.
9. Grabe, B. *Acta Chem. Scand.* **22** (1968) 2237.
10. Strand, T. G. and Cox, H. L., Jr. *J. Chem. Phys.* **44** (1966) 2426.
11. Shimizu, T. and Takuma, H. *J. Phys. Soc. Japan* **15** (1960) 646.
12. Roedig, A., Bischoff, F., Burkhard, H. and Märkl, G. *Ann.* **670** (1963) 8.
13. Ziegler, E. and Brandmüller, J. *Z. anal. Chem.* **210** (1965) 193.

# Crystal Structure of Cyclopentasarcosyl Dihydrate

## P.  G R O T H

*Department of Chemistry, University of Oslo, Oslo 3, Norway*

The crystals belong to the monoclinic system with space group $P2_1/c$ and cell dimensions $a = 9.31_6$ Å, $b = 30.15_4$ Å, $c = 7.81_8$ Å, $\beta = 113.7_1°$. There are four molecules in the unit cell. The phase problem was solved by direct methods, and the $R$-value arrived at for 2298 observed reflections was 7.6 %. The conformation is *cis, cis, cis, trans, trans*. The water molecules participate in a network of intermolecular hydrogen-bond bridges. Bond distances and angles are compared with those of cyclotetrasarcosyl and cyclooctasarcosyl.

$\mathbb{C}$yclic oligopeptides of sarcosine of the general formula are studied by Dale and Titlestad, mainly by spectroscopic methods.[1,2] For the pentameric

$$
\left[ -\text{N} - \text{CH}_2 - \overset{\displaystyle \text{O}}{\underset{\displaystyle \|}{\text{C}}} - \right]_n \qquad n = 2, \cdots, 12
$$

$$\begin{array}{c}\text{CH}_3 \\ | \end{array}$$
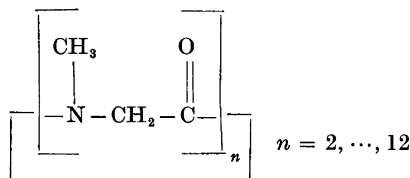
compound there is strong NMR-evidence for one preferred conformation in solution.[1] From symmetry arguments it could be concluded that the conformation is a mixture of *cis* and *trans* amino acid residues. Whether or not this conformation persists in the solid could not be decided by IR-spectroscopy. However, by dissolving the crystals in chloroform at low temperature ($-50°$C), and slowly heating the solution, no essential changes in the NMR-spectra recorded at different temperatures were observed.[2] In order to obtain detailed information of the molecular geometry, an X-ray crystallographic investigation of cyclopentasarcosyl has been carried out.

The crystals belong to the monoclinic system and the systematic absences lead to the space group $P2_1/c$. The cell parameters measured by means of a four circle diffractometer, and their estimated standard deviations are:

$$a = 9.316(2) \text{ Å}, \quad b = 30.154(8) \text{ Å}, \quad c = 7.818(1) \text{ Å}, \quad \beta = 113.71(1)°$$

With four molecules per unit cell the calculated density is $\varrho_c = 1.17$ g cm$^{-3}$.

19

The observed density, $\varrho_o = 1.28$ g cm$^{-3}$, corresponds to a difference in molecular weight of 36, which is accounted for by assuming the presence of two water molecules per asymmetric unit.

Whith $2\theta(\text{max}) = 50°$ and MoK$\alpha$-radiation, about 3800 independent reflections were measured on an automatic four-circle diffractometer. Using an observed-unobserved cutoff at $2.5\sigma(I)$, 2298 were recorded as observed. No corrections have been made for absorption or secondary extinction effects.

The structure was solved by direct methods and refined by full-matrix least squares technique. Methylene hydrogen atom position were calculated. Neither the methyl nor the water hydrogens could be localized in the difference Fourier map, and are not included in the calculations. Anisotropic temperature factors were introduced for O, N, and C-atoms, and weights in least squares were calculated from the standard deviations in intensities, $\sigma(I)$, taken as

$$\sigma(I) = [C_T + (0.02\ C_N)^2]^{\frac{1}{2}}$$

where $C_T$ is the total number of counts and $C_N$ the net count (peak minus background). The conventional $R$-value arrived at was 7.6 % (weighted value $R_W = 7.9$ %) for 2298 observed reflections. The form factors used were those of Hanson et al.[3] except for hydrogen.[4] The final fractional coordinates and thermal vibration parameters are given in Table 1. The expression for anisotropic vibration is:

$$\exp\left[-(B_{11}h^2 + B_{22}k^2 + B_{33}l^2 + B_{12}hk + B_{13}hl + B_{23}kl)\right]$$

Table 1. Final fractional coordinates and anisotropic thermal vibration parameters with estimated standard deviations (multiplied by $10^5$ for non-hydrogens and $10^4$ for hydrogens). The symbols CC, CM, and OV are used for carbonyl carbons, methyl carbons, and water oxygens, respectively. Hn1 and Hn2 are bonded to Cn.

| ·ATOM | X | Y | Z | B | B11 | B22 | B33 | B12 | B13 | B23 |
|---|---|---|---|---|---|---|---|---|---|---|
| O1 | 50660(43) | 21235(12) | 38273(53) | | 1798(69) | 182(6) | 2326(97) | -93(32) | 1361(139) | -419(38) |
| O2 | 130430(41) | 19168(12) | 54720(49) | | 1132(57) | 169(6) | 2629(92) | -86(30) | -327(127) | 26(37) |
| O3 | 109303(46) | 5189(13) | 51840(53) | | 1986(72) | 176(6) | 3841(102) | 576(36) | 1364(140) | 396(40) |
| O4 | 73795(42) | 13112(12) | -6463(46) | | 1965(69) | 117(6) | 2306(98) | 1(32) | 1192(127) | 155(34) |
| O5 | 45592(43) | 11314(11) | 8056(49) | | 1963(70) | 122(5) | 2850(85) | 25(30) | 716(126) | 206(34) |
| N1 | 77820(45) | 21664(13) | 32392(54) | | 1137(65) | 184(5) | 2134(102) | -84(32) | 128(138) | 13(37) |
| N2 | 92079(48) | 18394(14) | 49216(56) | | 1380(72) | 111(6) | 2158(102) | 206(34) | 668(147) | 30(39) |
| N3 | 88357(54) | 6512(13) | 8449(56) | | 1848(85) | 121(6) | 2846(184) | 156(37) | 1296(161) | 88(48) |
| N4 | 43094(52) | 11318(14) | -21666(59) | | 1814(83) | 124(6) | 1696(99) | -4(36) | 1411(150) | -113(41) |
| N5 | 35051(48) | 19509(13) | 8079(59) | | 1198(72) | 131(6) | 2175(110) | 102(34) | 55(147) | -87(42) |
| CC1 | 49181(60) | 20529(15) | 22189(70) | | 1280(89) | 84(6) | 2325(137) | 107(38) | 536(195) | -8(47) |
| CC2 | 87292(56) | 18488(16) | 42763(67) | | 978(79) | 122(7) | 1921(114) | -19(41) | 697(157) | -46(47) |
| CC3 | 99383(63) | 7810(18) | 41560(74) | | 1308(89) | 116(7) | 2287(137) | 122(44) | 794(197) | 172(52) |
| CC4 | 70372(66) | 9280(19) | -4598(69) | | 1944(187) | 115(7) | 1853(124) | 81(50) | 1871(196) | -85(51) |
| CC5 | 41179(55) | 13153(16) | -7323(70) | | 1118(82) | 107(7) | 1878(125) | -148(39) | -174(172) | 23(52) |
| C1 | 63016(58) | 20856(18) | 16591(71) | | 1219(86) | 95(7) | 1786(120) | -36(39) | 257(107) | 24(49) |
| C2 | 88572(67) | 13746(17) | 39860(91) | | 1437(96) | 97(7) | 2145(149) | 175(42) | 378(213) | -48(49) |
| C3 | 95861(71) | 8138(22) | 28653(81) | | 1781(112) | 152(9) | 2633(153) | 142(53) | 1413(213) | 269(61) |
| C4 | 63914(78) | 7571(20) | -17262(91) | | 2312(128) | 114(8) | 2232(150) | -93(54) | 663(238) | -176(58) |
| C5 | 34220(70) | 17843(18) | -9447(74) | | 1221(93) | 129(8) | 1778(131) | 19(46) | -323(183) | 122(53) |
| CM1 | 82944(67) | 26407(16) | 36136(74) | | 2121(111) | 93(7) | 2763(143) | -351(45) | 767(289) | -119(48) |
| CM2 | 95820(69) | 9854(18) | 69566(68) | | 2427(124) | 158(8) | 1661(124) | 23(52) | 12321(207) | 93(52) |
| CM3 | 77119(88) | 1788(17) | 18415(82) | | 3285(149) | 86(7) | 3254(169) | 116(54) | 1929(244) | 204(54) |
| CM4 | 39808(79) | 13655(21) | -39755(78) | | 2881(138) | 222(10) | 1435(124) | 181(63) | 786(214) | 144(57) |
| CM5 | 21624(68) | 18815(26) | 13183(93) | | 1816(92) | 346(15) | 3961(198) | -40(61) | 1779(231) | -326(86) |
| OV1 | 26896(46) | -2653(13) | 38564(59) | | 2249(88) | 194(6) | 3907(125) | 69(37) | 2635(166) | -42(43) |
| OV2 | 49560(59) | 4579(16) | 33197(71) | | 3054(106) | 254(8) | 5903(171) | 299(49) | 3731(229) | 1364(61) |
| H11 | 6073(58) | 2335(17) | 692(69) | 5,2(1,3) | | | | | | |
| H12 | 6355(43) | 1813(13) | 922(51) | 2,6(,9) | | | | | | |
| H21 | 7641(59) | 1358(16) | 2688(74) | 4,5(1,3) | | | | | | |
| H22 | 7269(67) | 1378(18) | 4585(73) | 6,4(1,6) | | | | | | |
| H31 | 10614(72) | 553(18) | 1748(77) | 8,4(1,6) | | | | | | |
| H32 | 9655(56) | 1125(17) | 1728(63) | 4,8(1,3) | | | | | | |
| H41 | 5919(67) | 529(19) | -1867(77) | 6,4(1,7) | | | | | | |
| H42 | 5318(51) | 648(14) | -3847(67) | 4,1(1,1) | | | | | | |
| H51 | 2242(70) | 1837(17) | -1784(73) | 6,3(1,3) | | | | | | |
| H52 | 4854(49) | 1968(13) | -1413(54) | 2,9(1,0) | | | | | | |

A comparison between observed and calculated structure factors is presented in Table 2.

*Table 2.* Observed and calculated structure factors on 10 times absolute scale.

*Table 2. Continued.*

*Table 2. Continued.*

The principal axes of the thermal vibration ellipsoids for oxygen, nitrogen, and carbon atoms were calculated from the temperature parameters of Table 1. Maximum root mean squares amplitudes range from about 0.28 Å for carbonyl carbons to about 0.40 Å for methyl carbon atoms and water oxygens. Due to the size of the molecule, no rigid-body analysis of translational, librational, and screw motion has been carried out.

Interatomic distances, bond angles and dihedral angles are given in Table 3. The standard deviations, given in parantheses, are estimated from the correlation matrix of the last least squares refinement cycle. Fig. 1 shows the molecule viewed along [0 0 1].
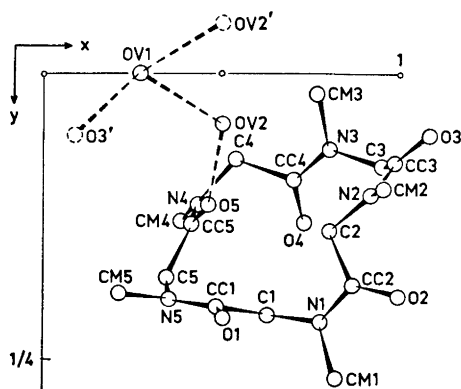


Fig. 1. The molecule viewed along [001].

By averaging bond distances of Table 3, and comparing with the results of the corresponding tetrameric [5] and octameric [6] compounds, no significant differences are observed:

| Distance | cycotetrasarcosyl | cyclooctasarcosyl | cyclopentasarcosyl |
|---|---|---|---|
| CC–C | 1.531 Å | 1.527 Å | 1.530 Å |
| CC–N | 1.358 | 1.344 | 1.345 |
| CC–O | 1.225 | 1.228 | 1.232 |
| C–N | 1.458 | 1.456 | 1.453 |
| CM–N | 1.467 | 1.483 | 1.487 |

The somewhat longer CM–N distances of cycloocta- and cyclopentasarcosyl are possibly connected with the fact that methyl hydrogens were localized for the tetrameric compound, but not for the other two.

The geometry of the *cis* and *trans* amide groups, respectively, is also roughly the same:

| Angle | cyclotetrasarcosyl | cyclooctasarcosyl | cyclopentasarcosyl |
|---|---|---|---|
| (CM–N–CC)*cis* | 119.8° | 118.7° | 118.6° |
| (CM–N–CC)*trans* | 124.3 | 123.9 | 123.5 |
| (C–N–CC)*cis* | 123.9 | 123.8 | 122.8 |
| (C-N-CC)*trans* | 120.1 | 117.2 | 117.5 |

*Table 3.* Interatomic distances, bond angles and dihedral angles with estimated standard deviations.

| DISTANCE | (Å) | DISTANCE | (Å) | DISTANCE | (Å) |
|---|---|---|---|---|---|
| O1 – CC1 | 1.236( 6) | O2 – CC2 | 1.227( 5) | O3 – CC3 | 1.236( 6) |
| O4 – CC4 | 1.223( 6) | O5 – CC5 | 1.236( 6) | N1 – CM1 | 1.499( 6) |
| N2 – CM2 | 1.495( 6) | N3 – CM3 | 1.479( 6) | N4 – CM4 | 1.487( 6) |
| N5 – CM5 | 1.473( 7) | CC1 – N6 | 1.367( 6) | CC2 – N1 | 1.352( 6) |
| CC3 – N2 | 1.325( 6) | CC4 – N3 | 1.357( 6) | CC5 – N4 | 1.326( 6) |
| CC1 – C1 | 1.518( 7) | CC2 – C2 | 1.517( 7) | CC3 – C3 | 1.537( 7) |
| CC4 – C4 | 1.541( 8) | CC5 – C5 | 1.537( 7) | N1 – C1 | 1.486( 6) |
| N2 – C2 | 1.455( 6) | N3 – C3 | 1.459( 7) | N4 – C4 | 1.468( 7) |
| N5 – C5 | 1.433( 6) | O3 – OV1 | 2.748( 6) | O5 – OV2 | 2.747( 5) |
| OV1 – OV2 | 2.735( 6) | OV1 – OV2 | 2.736( 6) | | |

| ANGLE | (°) | ANGLE | (°) |
|---|---|---|---|
| N5 – CC1 – O1 | 122.2( 5) | O1 – CC1 – C1 | 121.7( 5) |
| N1 – CC2 – O2 | 122.8( 4) | O2 – CC2 – C2 | 121.9( 4) |
| N2 – CC3 – O3 | 121.1( 5) | O3 – CC3 – C3 | 117.9( 5) |
| N3 – CC4 – O4 | 122.6( 5) | O4 – CC4 – C4 | 118.6( 5) |
| N4 – CC5 – O5 | 122.1( 5) | O5 – CC5 – C5 | 116.6( 5) |
| C1 – N1 – CM1 | 116.4( 4) | CM1 – N1 – CC2 | 119.9( 4) |
| C2 – N2 – CM2 | 117.5( 5) | CM2 – N2 – CC3 | 118.4( 4) |
| C3 – N3 – CM3 | 116.5( 5) | CM3 – N3 – CC4 | 124.4( 5) |
| C4 – N4 – CM4 | 118.7( 5) | CM4 – N4 – CC5 | 122.5( 5) |
| C5 – N5 – CM5 | 119.8( 5) | CM5 – N5 – CC1 | 117.5( 5) |
| N5 – CC1 – C1 | 116.1( 5) | N1 – CC2 – C2 | 116.1( 4) |
| N2 – CC3 – C3 | 121.8( 5) | N3 – CC4 – C4 | 118.8( 5) |
| N4 – CC5 – C5 | 119.1( 5) | CC1 – C1 – N1 | 113.1( 4) |
| CC2 – C2 – N2 | 112.5( 4) | CC3 – C3 – N3 | 114.8( 5) |
| CC4 – C4 – N4 | 107.9( 4) | CC5 – C5 – N5 | 111.2( 4) |
| C1 – N1 – CC2 | 123.6( 4) | C2 – N2 – CC3 | 124.1( 5) |
| C3 – N3 – CC4 | 119.8( 5) | C4 – N4 – CC5 | 116.8( 5) |
| C5 – N5 – CC1 | 120.8( 5) | OV1 – OV2 – O5 | 128.8( 2) |
| OV2 – O5 – CC5 | 157.7( 3) | O3 – OV1 – OV2 | 118.2( 2) |
| CC3 – O3 – OV1 | 126.1( 4) | O3 – OV1 – OV2 | 113.1( 2) |
| OV2 – OV1 – OV2 | 87.7( 2) | OV1 – OV2 – O5 | 139.7( 2) |

| DIHEDRAL ANGLE | (°) | DIHEDRAL ANGLE | (°) |
|---|---|---|---|
| N5 – CC1 – C1 – N1 | -176.2( 4) | CC1 – C1 – N1 – CC2 | 89.1( 6) |
| C1 – N1 – CC2 – C2 | -9.1( 7) | N1 – CC2 – C2 – N2 | 173.4( 5) |
| CC2 – C2 – N2 – CC3 | -192.8( 6) | C2 – N2 – CC3 – C3 | -1.1( 8) |
| N2 – CC3 – C3 – N3 | -78.0( 7) | CC3 – C3 – N3 – CC4 | 122.7( 5) |
| C3 – N3 – CC4 – C4 | -179.1( 5) | N3 – CC4 – C4 – N4 | 147.7( 5) |
| CC4 – C4 – N4 – CC5 | -63.6( 7) | C4 – N4 – CC5 – C5 | 161.7( 5) |
| N4 – CC5 – C5 – N5 | -171.9( 5) | CC5 – C5 – N5 – CC1 | 68.6( 6) |
| C5 – N5 – CC1 – C1 | 14.1( 7) | | |

Fig. 1 shows that the ring conformation is *cis, cis, cis, trans, trans*. The two water molecules participate in a network of *inter*-molecular hydrogen-bond bridges only. The four OV–O– and OV–OV distances are all about 2.74 Å. The angle OV2–OV1–OV2′ is 87.7°, while other angles of the hydrogen-bond bridges range from 110° to 158°.

Since the shortest CC···N distance across the ring is longer than 3.5 Å, no direct transannular contact can be held responsible for the rigidity of this 15-membered ring. As in the case of cyclooctasarcosyl, the explanation must be sought in the intrinsic conformation of the peptide chain itself.[2]

Apart from the hydrogen bonds, there are no short inter-molecular contacts.

FERERENCES

1. Dale, J. and Titlestad, K. *Chem. Commun.* **1969** 656.
2. Titlestad, K., Groth, P. and Dale, J. *Chem. Commun.* **1973** 646.
3. Hanson, H. P., Herman, F., Lea, J. D. and Skillman, S. *Acta Cryst.* **17** (1964) 1040.
4. Stewart, R. F., Davidson, E. R. and Simpson, W. T. *J. Chem. Phys.* **42** (1965) 3175.
5. Groth, P. *Acta Chem. Scand.* **24** (1970) 780.
6. Groth, P. *Acta Chem. Scand.* **27** (1973) 3302.

# On the Mass Spectral Fragmentation of 2,5-Diphenyl-*p*-benzoquinones

MAURI LOUNASMAA* and ARTO KARJALAINEN**

*Department of Chemistry, University of Oulu, Oulu, Finland*

The mass spectra of 14 2,5-diphenyl-*p*-benzoquinones are measured.
The characteristics of the fragmentation patterns are discussed.

Several studies concerning the mass spectral fragmentation of benzoquinones are available.[1–9] Most of these, however, concern either relatively simple benzoquinone derivatives, or isoprenoid benzoquinones where the main interest in the fragmentation pattern is due to the side chain. In connection with an investigation of some fungal benzoquinones the mass spectra of several 2,5-diphenyl-*p*-benzoquinones were measured. Because there is, as far as we know, no systematic mass spectral investigation of this type of benzoquinones
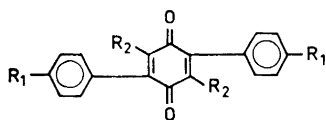


(I)   $R_1 = R_2 = H$
(II)   $R_1 = OH$; $R_2 = H$
(III)   $R_1 = OCH_3$; $R_2 = H$
(IV)   $R_1 = H$; $R_2 = OH$
(V)   $R_1 = R_2 = OH$
(VI)   $R_1 = OCH_3$; $R_2 = OH$
(VII)   $R_1 = OH$; $R_2 = OCH_3$
(VIII)   $R_1 = R_2 = OCH_3$
(IX)   $R_1 = H$; $R_2 = Br$
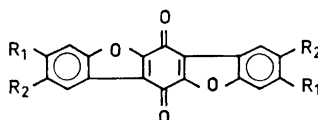
(X)   $R_1 = R_2 = OCOCH_3$
(XI)   $R_1 = R_2 = OCH_3$
(XII)   $R_1 = R_2 = OSi(CH_3)_3$
(XIII)   $R_1 = OCOCH_3$; $R_2 = H$
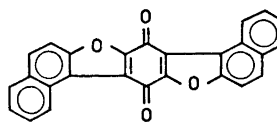
(XIV)

* Present address: Technical Research Centre of Finland, Chemical Laboratory, SF-02150 Otaniemi, Finland.
** Present address: Pharmaceutical Factory Leiras, SF-20100 Turku, Finland.

available (however, *cf*. Ref. 10), it seemed to us worthwhile to report the results obtained. In this paper we present the results concerning 2,5-diphenyl-*p*-benzoquinone (I), as well as 13 of its derivatives (II – XIV).

By analogy with the general fragmentation pattern of benzoquinones,[1] three initial fragmentation paths may be suggested.

*Route A*. Cleavage of the 1 – 2 and 3 – 4 bonds.

*Route B*. Elimination of carbon monoxide (eventually elimination of CHO).

*Route C*. Fission of the molecule into two halves due to the cleavage of the 1 – 2 and 4 – 5 bonds.

These three initial fragmentations, as well as some further cleavages, applied to the case of 2,5-diphenyl-*p*-benzoquinone (I), are presented in Scheme 1.



*Scheme 1.*
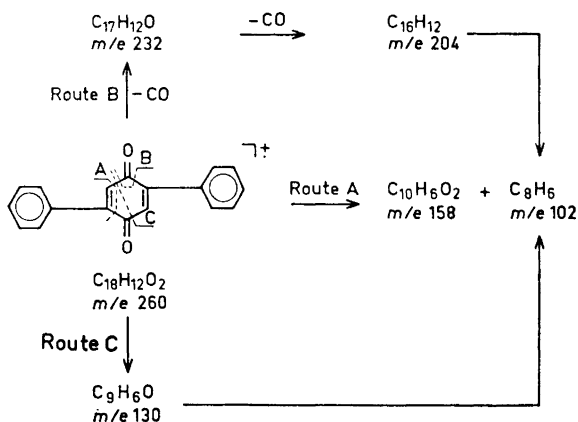
In the mass spectrum of 2,5-diphenyl-*p*-benzoquinone (I) (Fig. 1) Routes B and C are well represented. The absence of the peak corresponding to $m/e$ 158 seems to indicate that very little fragmentation occurs according to Route A. However, the spectrum taken at low electron voltage suggests that
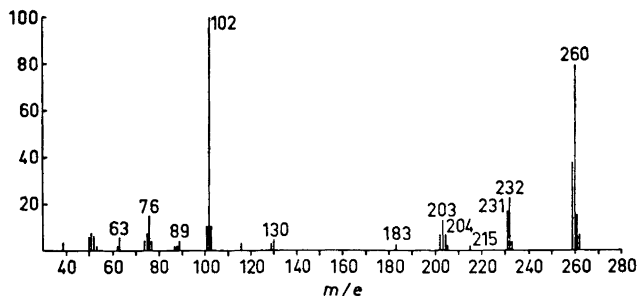


*Fig. 1.* Mass spectrum (70 eV) of 2,5-diphenyl-*p*-benzoquinone (I).

*Table 1.* Mass spectra (70 eV) of compounds (II), (III), (IV), (VI), (VIII), (X), (XI), (XII), (XIII) and (XIV). Only the ions of integral mass values having an abundance of 2 % of the base peak or greater are recorded. The relative abundance is given in parenthesis.

---

Compound (II): $m/e$ (%) 39(10), 40(3), 41(4), 42(3), 44(5), 46(2), 50(3), 51(7), 53(6), 55(6), 57(4), 58(12), 62(5), 63(15), 64(6), 65(5), 69(4), 73(3), 74(4), 75(4), 76(4), 77(4), 89(22), 90(5), 91(5), 109(4), 117(7), 118(100), 119(12), 121(6), 132(3), 145(4), 146(5), 147(8), 149(6), 181(3), 189(4), 199(4), 207(3), 219(4), 223(3), 235(6), 236(12), 237(4), 247(9), 248(3), 263(12), 264(13), 265(4), 275(14), 276(4), 291(14), 292(58), 293(14), 294(22), 295(7).

Compound (III): $m/e$ (%) 39(4), 43(5), 45(6), 51(4), 60(5), 62(4), 63(12), 74(2), 75(4), 76(3), 77(2), 88(3), 89(37), 90(3), 94(2), 101(3), 102(5), 103(2), 116(3), 117(27), 118(3), 132(100), 133(9), 135(3), 138(2), 146(3), 160(5), 161(2), 178(3), 188(2), 189(4), 205(2), 206(2), 213(2), 218(3) ,221(4), 233(2), 224(2), 249(11), 250(2), 258(2), 261(14), 262(4), 263(2), 264(7), 277(17), 278(4), 289(41), 290(9), 291(9), 292(12), 293(2), 305(8), 320(96), 321(22), 322(16), 323(3).

Compound (IV): $m/e$ (%) 39(5), 51(4), 62(2), 63(6), 64(2), 65(4), 75(2), 76(3), 77(6), 78(2), 89(17), 90(7), 91(6), 102(3), 105(4), 117(2), 118(11), 119(4), 129(10), 130(2), 137(2), 145(2), 146(2), 147(3), 164(2), 173(4), 178(6), 179(3), 189(6), 207(6), 208(2), 218(3), 236(2), 245(2), 246(3), 247(2), 263(2), 264(5), 292(100), 293(19), 294(6).

Compound (VI): $m/e$ (%) 39(10), 41(6), 43(7), 44(10), 50(8), 51(20), 53(6), 55(7), 62(7), 63(10), 65(12), 69(5), 75(5), 76(18), 77(20), 78(12), 79(8), 88(6), 89(13), 90(6), 91(7), 105(17), 108(12), 119(30), 120(18), 121(31), 122(2), 132(6), 133(22), 134(8), 135(11), 139(5), 147(14), 148(33), 149(15), 150(2), 152(6), 153(6), 159(22), 160(6), 165(8), 175(6), 176(10), 177(7), 181(5), 188(5), 203(18), 204(2), 237(5), 244(4), 251(4), 253(4), 267(5), 281(4), 309(4), 321(3), 323(3), 324(30), 325(8), 326(3), 337(5), 352(100), 353(24), 354(7).

Compound (VIII): $m/e$ (%) 39(11), 41(11), 43(20), 44(13), 45(4), 50(11), 51(9), 53(6), 56(9), 57(6), 58(7), 62(8), 63(9), 65(19), 74(6), 75(13), 76(40), 77(17), 78(8), 79(8), 87(7), 88(16), 89(11), 90(4), 91(6), 92(5), 104(10), 105(6), 116(8), 117(6), 118(6), 119(100), 120(13), 121(12), 131(6), 132(9), 133(11), 134(5), 135(14), 144(6), 145(7), 146(5), 147(35), 148(8), 149(10), 150(5), 151(4), 152(8), 159(17), 160(5), 161(11), 163(6), 164(7), 165(7), 175(10), 176(13), 189(6), 190(8), 191(5), 195(10), 223(21), 224(6), 235(7), 238(15), 239(4), 250(6), 251(7), 263(2), 266(6), 281(78), 282(17), 283(3), 291(4), 309(40), 310(9), 311(6), 318(5), 319(6), 320(4), 321(4), 332(2), 333(3), 334(4), 335(9), 336(5), 337(28), 338(6), 339(4), 347(11), 348(5), 349(5), 352(21), 353(6), 365(5), 380(100), 381(27), 382(16), 383(4).

Compound (X): $m/e$ (%) 39(7), 40(5), 41(22), 42(57), 43(100), 44(25), 45(5), 58(16), 63(4), 64(22), 65(5), 66(12), 68(9), 69(7), 77(6), 79(5), 91(13), 92(3), 149(7), 172(9), 252(2), 253(6), 254(2), 255(2), 294(4), 295(2), 296(2), 336(7), 337(2), 338(2), 351(12), 352(78), 353(22), 354(11), 355(3), 378(2), 394(17), 395(6), 396(6), 397(2), 436(10), 437(4), 438(6), 439(3), 478(6),479(3), 480(5), 481(2), 520(4), 521(2), 522(4), 523(2).

Compound (XI): $m/e$ (%) 43(2), 44(3), 47(3), 49(2), 62(2), 69(3), 77(2), 83(17), 85(11), 87(2), 90(2), 133(2), 147(3), 149(3), 152(2), 161(7), 204(9), 205(2), 279(3), 294(2), 307(2), 309(2), 321(2), 322(3), 337(8), 347(3), 348(2), 349(2), 350(2), 365(10), 366(2), 392(2), 393(4), 394(2), 395(2), 408(100), 409(26), 410(7).

Compound (XII): $m/e$ (%) 43(6), 44(8), 45(45), 46(4), 47(3), 57(2), 58(3), 59(5), 66(3), 73(440[a]), 74(45), 75(28), 76(3), 91(3), 131(4), 133(3), 147(18), 148(3), 149(6), 229(5), 455(3), 464(7), 465(4), 537(6), 538(3), 539(2), 552(12), 553(6), 554(5), 555(2), 568(9), 569(4), 570(3), 610(2), 611(3), 612(2), 625(17), 626(9), 627(6), 628(3), 640(100), 641(58), 642(35), 643(14), 644(4).

*Table 1. Continued.*

Compound (XIII): $m/e$ (%) 41(6), 42(24), 43(55), 44(6), 45(15), 50(2), 51(2), 52(2), 53(2), 55(2), 57(2), 58(2), 60(12), 74(2), 75(6), 76(2), 77(3), 79(3), 87(2), 104(3), 131(2), 149(4), 150(4), 151(3), 152(3), 179(3), 207(2), 208(2), 236(3), 263(3), 291(3), 320(100), 321(19), 322(16), 323(4), 334(38), 335(9), 336(6), 348(6), 362(11), 363(3), 364(5), 376(6), 404(4), 406(3).

Compound (XIV): $m/e$ (%) 112(2), 124(3), 125(4), 137(14), 138(23), 166(2), 180(8), 194(10), 274(9), 275(4), 276(9), 277(2), 303(3), 304(2), 332(2), 360(2), 388(100), 389(29), 390(6).

 *a* $m/e$ 640 used as base peak.

the peak at $m/e$ 102, which in the normal spectrum represents the base peak, arises partly from the molecular ion. This indicates that the cleavage of the 1 − 2 and 3 − 4 bonds (Route A) takes place, but in this case the charge remains mainly in the acetylenic moiety. This phenomenon is a general feature in the mass spectral fragmentation of 2,5-diphenyl-$p$-benzoquinones and is especially pronounced in the cases where positions 3 and 6 are unsubstituted [compounds (I), (II) and (III)].
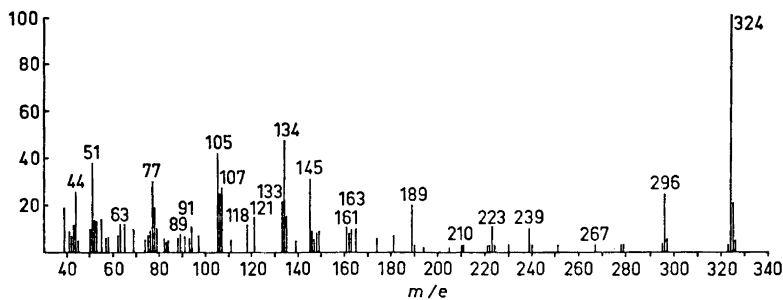


*Fig. 2.* Mass spectrum (70 eV) of 2,5-bis-($p$-hydroxyphenyl)-3,6-dihydroxy-$p$-benzo-quinone (V).

The mass spectra of the hydroxy-$p$-benzoquinone derivatives investigated (IV), (V), and (VI) (Fig. 2 and Table 1) show a fragmentation pattern basically analogous to that of 2,5-diphenyl-$p$-benzoquinone (I) (Fig. 1). The base peak in these spectra corresponds to the molecular ion. This is in agreement with earlier observations of Williams et al.,[1] concerning the mass spectral behaviour of hydroxybenzoquinones.

According to Williams et al.[1] the cleavage of the 1 − 2 and 4 − 5 bonds (Route C) of hydroxybenzoquinones occurs mainly with hydrogen rearrangement from the hydroxyl group. This process is also seen from the mass spectra of compounds (IV), (V), and (VI) (Fig. 2 and Table 1), by the presence of peaks at $m/e$ 147 ($C_9H_7O_2^+$), $m/e$ 163 ($C_9H_7O_3^+$), and $m/e$ 177 ($C_{10}H_9O_3^+$), respectively. These hydroxybenzoquinone compounds also show peaks at $m/e$ 173 ($C_{10}H_5O_3^+$), $m/e$ 189 ($C_{10}H_5O_4^+$), and $m/e$ 203 ($C_{11}H_7O_4^+$). A plausible
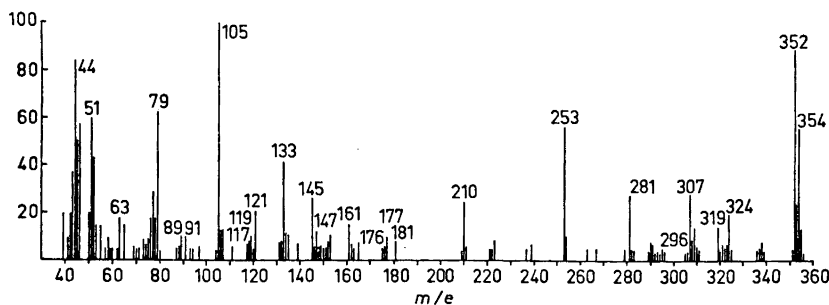
*Fig. 3.* Mass spectrum (70 eV) of 2,5-bis-(*p*-hydroxyphenyl)-3,6-dimethoxy-*p*-benzoquinone (VII).

explanation for these peaks is the cleavage of the $1-2$ and $3-4$ bonds (Route A) with hydrogen rearrangement.

The mass spectra of the methoxy-*p*-benzoquinone derivatives investigated (VII) and (VIII) (Fig. 3 and Table 1) show fragmentation patterns, where Routes A, B and C are involved. However, because the positions 3 and 6 of the quinone ring are substituted, the cleavage of the $1-2$ and $3-4$ bonds (Route A) (combined with the remaining of the charge in the acetylenic moiety), is much less pronounced than in the above mentioned case of 2,5-diphenyl-*p*-benzoquinone (I).

In the case of 2,5-bis-(*p*-hydroxyphenyl)-3,6-dimethoxy-*p*-benzoquinone (VII) the peaks at $m/e$ 324 and 296 (weak) are obviously due to successive losses of carbon monoxide from the molecular ion (Route B). The initial fragmentation according to Route C is responsible for the formation of the ion $C_{10}H_8O_3{}^+$ ($m/e$ 176).

Williams *et al.*[1] have pointed out that the most general feature of the spectra of methoxybenzoquinones is associated with the appearance of an ion, which, in the case of 2,5-bis-(*p*-hydroxyphenyl)-3,6-dimethoxy-*p*-benzoquinone (VII) would be (XVI)($C_9H_5O_3{}^+$; $m/e$ 161).



(XVI)
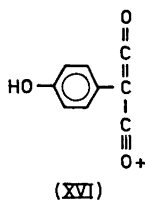
Williams *et al.*[1] have also found that another common process leads to pronounced $M-71$ peaks. This process arises from the formal loss of two molecules of carbon monoxide and a methyl group from the molecular ion. This process and some further fragmentations applied to the case of 2,5-bis-(*p*-hydroxyphenyl)-3,6-dimethoxy-*p*-benzoquinone (VII) are shown in Scheme 2.

A plausible representation for the ion of $C_7H_5O^+$ corresponding to the base peak at $m/e$ 105 is the cation (XVII). As indicated by the spectra (Fig. 3 and Table 1) both these processes take place in the fragmentation of compounds (VII) and (VIII).



$C_{20}H_{16}O_6$
$m/e$ 352

$C_{17}H_{13}O_4$
$m/e$ 281

$C_{16}H_{13}O_3$,
$m/e$ 253

$C_7H_5O$
$m/e$ 105

$-CO$

$C_8H_5O_2$
$m/e$ 133

$C_{14}H_{10}O_2$
$m/e$ 210

(XVII)
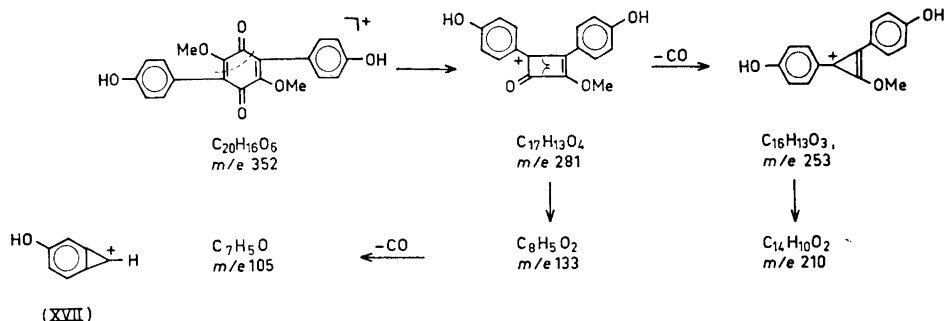
*Scheme 2.*

The mass spectrum of 2,5-diphenyl-3,6-dibromo-$p$-benzoquinone (IX) (Fig. 4) shows three molecular peaks at $m/e$ 420, 418, and 416, the intensities of which correspond to the relative abundance of the bromine isotopes. The fragmentation of this compound is very much dominated by the presence of the two bromine atoms. The cleavage of the first bromine atom leads to the ions of $m/e$ 339 and 337, which can then lose the second one giving rise to the ion of $m/e$ 258. A bromine atom may also be eliminated under form of hydrogen bromide (peaks at $m/e$ 338 and 336). The formal loss of two molecules of hydrogen bromide and two molecules of carbon monoxide from the molecular ions leads to the ion of $m/e$ 200.

Due to the low volatility, the fungal 2,5-diphenyl-$p$-benzoquinone derivative (XVIII), known as thelephoric acid, does not give a readable mass spectrum. However, the conversion of the compound into more volatile derivatives permits its mass spectral investigation. Thus the corresponding tetra-acetate
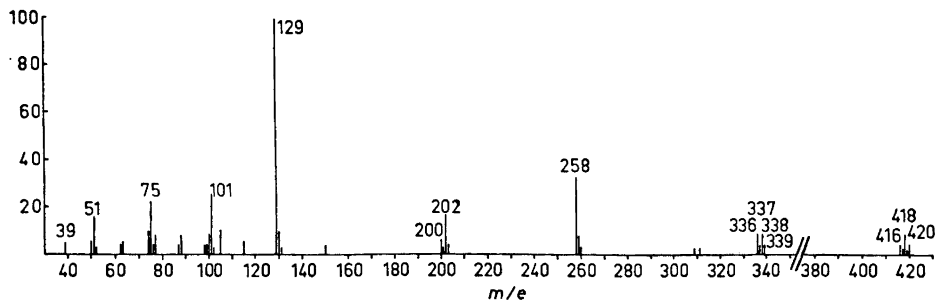


*Fig. 4.* Mass spectrum (70 eV) of 2,5-diphenyl-3,6-dibromo-$p$-benzoquinone (IX).

shows the molecular peak at $m/e$ 520 (Table 1) in accordance with the proposed structure (X). The fragmentation is very much dominated by successive losses of acetoxyl groups in the form of ketene, as indicated by appreciable peaks at $m/e$ 478, 436, 394, and 352. The existence of these peaks may be used for quantitative determination of hydroxyl groups in thelephoric acid (XVIII). In the mass spectrum of the corresponding tetramethyl ether (XI) (Table 1) the base peak at $m/e$ 408 corresponds to the molecular ion. Fragmentation is very poor except for the cleavage of the $CH_3 \cdot$ radical from one of the methoxyl groups followed by losses of two CO units. There is also some fission of the molecule into two halves according to Route C.



(XVIII)
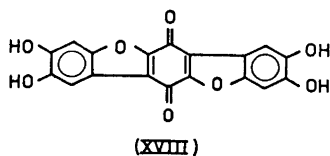
The tetra-trimethylsilyl ether derivative of thelephoric acid (XII) shows a strong molecular peak at $m/e$ 640 (Table 1). The mass spectrum exhibits only a few other peaks in the higher mass region except for the peaks at $m/e$ 625 ($M^+ - CH_3 \cdot$) and 568 ($M^+ - C_3H_8Si$). The peaks at $m/e$ 75 and 73 (base peak), which are always observed in the mass spectra of trimethylsilyl ethers,[11] are caused by $(CH_3)_2Si = \overset{+}{O}H$ and $(CH_3)_3Si^+$, respectively. The peaks at $m/e$ 147 and 59 are artifacts. The first one is due to an ion formed by expulsion of a methyl group from hexamethyldisiloxane and the second one to a small amount of acetamide present, which is formed during the preparation of trimethylsilyl ether derivative (XII) using trimethylsilylacetamide.[12]

The compound (XIII) (Table 1) shows a fragmentation pattern analogous to that of compound (X), as may be expected. Thus the main fragmentation, as indicated by the peaks at $m/e$ 362 and 320 (base peak), consists of losses of the acetoxyl group in the form of ketene from the molecular ion ($C_{22}H_{12}O_8^+ \cdot$; $m/e$ 404).

In the mass spectrum of compound (XIV) (Table 1) the base peak at $m/e$ 388 corresponds to the molecular ion. Although the fragmentation is very poor Routes B and C can be recognized in the spectrum.

Several mass spectra examined exhibit peaks at $M + 2$ due to the corresponding hydroquinones formed by dismutation reactions in the ionization chamber.[5,9,13,14,15]

Moreover, in several cases doubly charged molecular and other ions are formed, as indicated by the presence of small peaks, due to doubly charged ^{13}C isotopic ions (not presented in the figures or in Table 1), at 1/2 mass unit higher than the corresponding fragment.[16] This means that, e.g., the peaks assigned above to the fission of the molecules into two halves (cf. Route C) are partly due to doubly charged molecular ions.

Mass spectra were recorded on a Hitachi Perkin-Elmer RMU-6E double-focusing mass spectrometer using direct sample insertion into the ion source which was at a tem-

perature between 120° and 150°. In several cases relatively high probe temperatures (about 300°) were necessary for sufficient vaporization of samples.

## REFERENCES

1. Bowie, J. H., Cameron, D. W., Giles, R. G. F. and Williams, D. H. *J. Chem. Soc.* **B** **1966** 335.
2. Elwood, T. A. and Bursey, M. M. *Org. Mass Spectrosc.* **1** (1968) 537.
3. Heiss, J., Zeller, K.-P. and Rieker, A. *Org. Mass Spectrosc.* **2** (1969) 1325.
4. Misiti, D., Moore, H. W. and Folkers, K. *J. Am. Chem. Soc.* **87** (1965) 1402.
5. Das, B. C., Lounasmaa, M., Tendille, C. and Lederer, E. *Biochem. Biophys. Res. Commun.* **21** (1965) 318.
6. Griffiths, W. T. *Biochem. Biophys. Res. Commun.* **25** (1966) 596.
7. Das, B. C., Lounasmaa, M., Tendille, C. and Lederer, E. *Biochem. Biophys. Res. Commun.* **26** (1967) 211.
8. Muraca, R. F., Whittick, J. S., Doyle Daves, Jr., G., Friis, P. and Folkers, K. *J. Am. Chem. Soc.* **89** (1967) 1505.
9. Morimoto, H., Shima, T., Imada, I., Sasaki, M. and Ouchida, A. *Ann.* **702** (1967) 137.
10. Gaylord, M. C. and Brady, L. R. *J. Pharm. Sci.* **60** (1971) 1503.
11. Budzikiewicz, H., Djerassi, C. and Williams, D. H. *Mass Spectrometry of Organic Compounds*, Holden-Day, San Francisco, 1967, p. 472.
12. Ref. 11, p. 476.
13. Spiteller, G. *Massenspektrometrische Strukturanalyse organischer Verbindungen*, Verlag Chemie, Weinheim 1966, p. 270.
14. Aplin, R. T. and Pike, W. T. *Chem. Ind. London* **1966** 2009.
15. Ukai, S. Hirose, K., Tatematsu, A. and Goto, T. *Tetrahedron Letters* **1967** 4999.
16. Biemann, K. *Mass Spectrometry*, McGraw, New York 1962, p. 157.

# Association Equilibria and Micelle Formation of Fatty Acid Sodium Salts. II. An Investigation of Straight-chain Salts by Vapour Pressure Osmometry

PER STENIUS

*Department of Physical Chemistry, Åbo Akademi, Porthansgatan 3—5, SF-20500 Åbo 50, Finland*

The vapour pressures of mixed aqueous solutions of sodium chloride and sodium acetate, propionate, butyrate, and hexanoate, respectively, have been measured. From these, using a method suggested by McKay and Perring [1] the mean activity coefficients of the sodium chloride and the sodium carboxylates have been calculated. The regularities shown by the changes in activity in solutions where there is no association (in these, the activity coefficients generally follow Harned's rule) make it possible to estimate the mean aggregation number of the butyrate and hexanoate anions. These agree with previously reported potentiometric determinations of association equilibria [2] and show that the aggregation occurs in alkaline solutions, too. The method cannot be applied to solutions containing aggregates of micellar size, due to their high vapour pressure.

It is generally accepted [3] that small aggregates are formed in measurable amounts by surfactants in aqueous solutions below the critical micelle concentration, c.m.c. However, the structure and size of these aggregates is not very well established. Different suggestions have been made,[2-8] most of them indicating that the submicellar aggregates, similarly to micelles, are held together mainly by forces of attraction between hydrocarbon chains in conjunction with a reduction in the water structure on association (hydrophobic bonding). The possibility that the binding of counter ions plays a role cannot, however, be ruled out. It may be expected that more could be learned about the structural changes in the solutions from a detailed examination of the association equilibria in solutions of compounds with a very high c.m.c. These give rise to the formation of appreciable amounts of smaller aggregates and, at higher concentrations, to micelles.[1,8]

Such investigations, at least if thermodynamic properties are studied, are rendered difficult by the fact that effects caused by changes in the concentrations of different species cannot be distinguished from changes in their activity coefficients.[9,10] In this investigation it has been found possible to make some

reasonable predictions concerning the variation in activity coefficients by utilizing the regularities shown by the activity coefficients of the different components in mixed electrolyte solutions.

Investigations of the activity of water in aqueous solutions of short-chain alkanoates were made very early in the history of surfactant science.[11],[12] Smith and Robinson [13] made extensive isopiestic investigations of pure sodium carboxylate solutions. From their data, it is clearly seen that carboxylates with five or more carbon atoms in the chain do associate, but it is not possible to draw definite conclusions regarding the size of the aggregates formed. A few [14–18] investigations of the activities in mixtures of short-chain carboxylates with simple electrolytes have been reported. Some of the data used for the calculations below have been published before,[19] but complete tables are given here to give a comprehensive picture of the calculations and results.

## LIST OF SYMBOLS

$a_i$ = activity of substance i
$n_i$ = amount of substance i
$m_i$ = molality of substance i
$m$ = total molality of NaCl and NaR in mixed solutions
$\bar{q}$ = mean number of anions per carboxylate aggregate
$u_1$ = $m_{1r}/m$, $u_2 = m_{2r}/m$
$x_{12}$ = $m_1/m_2$, $x_1 = m_1/m$, $x_2 = m_2/m$
$y$ = $\ln a_w$, $z_1 = m_{1r}\phi_{1r}$, $z_2 = \nu_{2r}m_{2r}\phi_{2r}$
$\nu_i$ = mean number of ions formed by substance i
$\gamma_i$ = mean activity coefficient of substance i (molality basis)
$\nu$ = mean amount of ions per unit amount of mixed electrolyte

Subscripts: $_w$ = water, $_1$ = NaCl (in mixed solutions), $_{1r}$ = NaCl (in reference solutions), $_2$ = Na-carboxylate (NaR, in mixed solutions), $_{2r}$ = NaR (in reference solutions).

## METHOD OF CALCULATION

*Mean activity coefficient of sodium chloride.* Consider a system of sodium chloride (1) and sodium carboxylate, (2) dissolved in water (w). Application of the Gibbs-Duhem equation to this system gives, at constant temperature and pressure,

$$n_1 \, \mathrm{d} \ln a_1 + n_2 \, \mathrm{d} \ln a_2 + n_w \, \mathrm{d} \ln a_w = 0 \qquad (1)$$

where $n_i$ is the amount of substance i and $a_i$ its activity.

Several methods to utilize eqn. (1) to calculate the activities of different components in ternary systems have been discussed recently.[20–24] For our purposes, it has been found convenient to modify the method outlined by McKay and Perring [1] in the following way, which makes it possible to estimate the relative influence of association and intermolecular interactions as the concentration of electrolyte increases.

The experimentally determined quantities in vapour pressure osmometry are the water activities $a_w$ at different molalities of NaCl, $m_1$, and NaR, $m_2$.

As suggested by McKay and Perring,[1] it is convenient to transform (1) to an expression where $\ln a_w \equiv y$ and $m_1/m_2 \equiv x_{12}$ are used as independent variables. On changing to molalities, (1) can be written

$$-d \ln a_2 = x_{12} \, d \ln a_1 + m_w/m_2 \, dy \qquad (2)$$

where $m_w$ is the molality of water ($=55.508 \text{ mol kg}^{-1}$).
Differentiating $\ln a_1 = f(x_{12}, y)$ gives

$$d \ln a_1 = \left( \frac{\partial \ln a_1}{\partial x_{12}} \right)_y dx_{12} + \left( \frac{\partial \ln a_1}{\partial y} \right)_{x_{12}} dy \qquad (3)$$

Introduction of (3) into (2) yields the following equation:

$$-d \ln a_2 = \left[ x_{12} \left( \frac{\partial \ln a_1}{\partial y} \right)_{x_{12}} + \frac{m_w}{m_2} \right] dy + x_{12} \left( \frac{\partial \ln a_1}{\partial x_{12}} \right)_y dx_{12} \qquad (4)$$

(4) is of the general form $dF(y, x_{12}) = G(y, x_{12})dy + H(y, x_{12})dx_{12}$, where $dF$ is a total differential. Then $(\partial G/\partial x_{12})_y = (\partial H/\partial y)_{x_{12}}$ or from (4):

$$\left( \frac{\partial \ln a_1}{\partial y} \right)_{x_{12}} = -m_w \left[ \frac{\partial(1/m_2)}{\partial x_{12}} \right]_y \qquad (5)$$

From an experimental point of view, it is convenient to use the quantity

$$x_2 = \frac{m_2}{m_1 + m_2} = \frac{m_2}{m} = \frac{1}{1 + x_{12}} \qquad (6)$$

instead of $x_{12}$. Introducing this variable into the right hand member of (5) gives

$$\left[ \frac{\partial(1/m_2)}{\partial x_{12}} \right]_y = \frac{x_2}{m^2} \left( \frac{\partial m}{\partial x_2} \right)_y + \frac{1}{m} \qquad (7)$$

The molality of $Na^+$ ions is $m_1 + m_2 = m$ and the molality of $Cl^-$ ions is $m_1$. The NaCl activity hence is given by $a_1 = \gamma_1^2 m_1 m$ where $\gamma_1$ is the mean activity coefficient of NaCl. But $m_1/m = 1 - x_2$ and thus

$$a_1 = \gamma_1^2 m^2 (1 - x_2) \, ; \, (\partial \ln a_1)_{x_2} = 2(\partial \ln \gamma_1 m)_{x_2} \qquad (8)$$

Introduction of (7) and (8) into (5) yields

$$\frac{2}{m_w} \left( \frac{\partial \ln \gamma_1 m}{\partial y} \right)_{x_2} = -\frac{x_2}{m_2} \left( \frac{\partial m}{\partial x_2} \right)_y - \frac{1}{m} \qquad (9)$$

This equation might be used to calculate $\gamma_1$ from $y$ and $x_2$. The integrand in the right hand member of (9), however, becomes uncertain as $m \to 0$. This difficulty can be circumvented by utilizing the known activity coefficients $\gamma_{1r}$ in an isopiestic pure sodium chloride solution of molality $m_{1r}$. The Gibbs-Duhem equation for this solution gives [25]

$$\frac{2}{m_w} \frac{d \ln \gamma_{1r} m_{1r}}{dy} = -\frac{1}{m_{1r}} \qquad (10)$$

Since $a_w$ is the same in this reference solution and the mixed electrolyte solution, subtraction of (10) from (9) gives

$$\frac{2}{m_w}\left[\frac{\partial \ln (\gamma_1 m/\gamma_{1r}m_{1r})}{\partial y}\right]_{x_2} = -\frac{x_2}{m^2}\left(\frac{\partial m}{\partial x_2}\right)_y - \frac{1}{m} + \frac{1}{m_{1r}} \qquad (11)$$

This equation now is integrated at constant $x_2$, yielding values for $\gamma_1$ at a given ratio $m_1/m$. In the limit, $m \to 0$, $\gamma_1 m \to \gamma_{1r} m_{1r}$ and $a_w \to 1$; (11) then can be written

$$\frac{2}{m_w}\ln\frac{\gamma_1 m}{\gamma_{1r}m_{1r}} = -\int_0^y\left[\frac{x_2}{m^2}\left(\frac{\partial m}{\partial x_2}\right)_y + \frac{1}{m} - \frac{1}{m_{1r}}\right]_{x_2} dy \qquad (12)$$

(12) is McKay's and Perring's equation (6) in our notation.
The osmotic coefficient of the reference solution, $\phi_{1r}$, is defined by

$$y \equiv \ln a_w = -\frac{2}{m_w}m_{1r}\phi_{1r} \qquad (13)$$

For convenient calculations, (12) is further modified by introducing (13) and the symbols

$$m_{1r}\phi_{1r} = z_1 \; ; \; m_{1r}/m = u_1 \qquad (14)$$

giving the final equation for $\gamma_1$:

$$\ln \gamma_1 = \ln (\gamma_{1r}u_1) - \int_0^{z_1}\frac{1}{m_{1r}}\left[x_2\left(\frac{\partial u_1}{\partial x_2}\right)_{m_{1r}} - u_1 + 1\right]_{x_2} dz_1 \qquad (15)$$

This equation contains no approximation except the assumption that the free Na+-ion molality is $m_1 + m_2$, i.e. that no sodium ions are bound to the carboxylate aggregates. This is probably a good approximation except in solutions containing aggregates of micellar size.

*Mean aggregation number of the carboxylates.* If it is assumed that the carboxylate dissociates completely into two ions, i.e. the association to polynuclear aggregates is disregarded, an equation exactly analogous to (15) is valid for the activity coefficient of NaR, $\gamma_2'$:

$$\ln \gamma_2' = \ln (\gamma_{2r}'u_2) - \int_0^{z_2}\frac{1}{m_{2r}}\left[x_1\left(\frac{\partial u_2}{\partial x_1}\right)_{m_{2r}} - u_2 + 1\right]_{x_1} dz_2 \qquad (16)$$

where $\gamma_{2r}'$ and $m_{2r}$ are the activity coefficient (disregarding association) and molality, respectively, of an isopiestic reference solution of NaR, and

$$u_2 = \frac{m_{2r}}{m} \; ; \; x_1 = \frac{m_1}{m} \; ; \; z_2 = m_{2r}\phi_{2r} \qquad (17)$$

However, it is possible to estimate the effects of association upon $\gamma_2'$. It is experimentally found that in solutions where there is no association, $m_{1r}$ and $m_{2r}$ are linear functions of $x_2$ and $x_1$ at constant m:

$$m_{1r}/m = 1 + a'x_2 \tag{18}$$

$$m_{2r}/m = 1 + a''x_1 \tag{19}$$

where $a'$ and $a''$ are constants which are different for different values of m. These relationships are illustrated for sodium acetate in Figs. 1 and 2, which
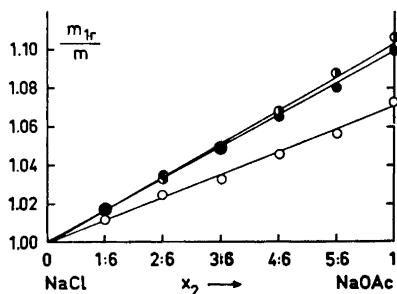


*Fig. 1.* The molality of an isopiestic solution of NaCl, $m_{1r}$, as a function of the fraction of sodium acetate $x_2$ in a mixed aqueous solution of NaCl and NaOAc for different total molalities m. ○ 1.0, ● 2.0 and ◖ 3.0 mol kg$^{-1}$.
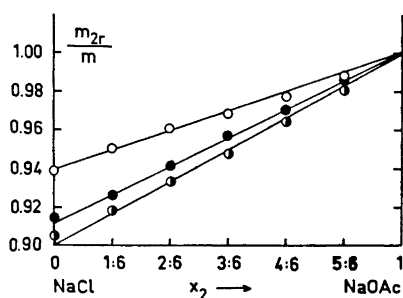
*Fig. 2.* The molality of an isopiestic solution of NaOAc, $m_{2r}$, as a function of the fraction of sodium acetate, $x_2$, in a mixed aqueous solution of NaCl and NaOAc for different total molalities m. Symbols as in Fig. 1.

show that straight lines are obtained within experimental error. If (18) is introduced into (15), the integrand becomes zero.

The condition of vapour pressure equilibrium between the reference solution and the mixed solution demands that [26]

$$\phi_{1r}m_{1r}\nu_{1r} = \phi m \nu \tag{20}$$

where $\nu_{1r}$ is the mean amount of ions formed per unit amount of reference electrolyte, $\nu$ the corresponding quantity for the mixed electrolyte and $\phi$ the osmotic coefficient of the mixed electrolyte solution. Then

$$\phi\nu/\phi_{1r}\nu_{1r} = u_1 \tag{21}$$

If the integral in (15) is denoted by $A_1$, (15) may be transformed to

$$\gamma_1/\gamma_{1r} = u_1 e^{-A_1} \tag{22}$$

and thus

$$\phi\nu/\phi_{1r}\nu_{1r} = (\gamma_1/\gamma_{1r})e^{A_1} \tag{23}$$

If there is no association $\nu = \nu_{1r} = 2$. If this is combined with the experimental fact that $A_1 = 0$ under these circumstances, (23) becomes

$$\phi/\phi_{1r} = \gamma_1/\gamma_{1r} \quad \text{(no association)} \tag{24}$$

It seems resonable to assume that (24) will hold for the non-associating component, *i.e.* for the NaCl, even in solutions where the other component does form aggregates. This implies that the term $e^{A_1}$ just reflects the effect

of the association of the other component upon the ratio $\phi \nu/\phi_{1r}\nu_{1r}$, *i.e.* the fact that $\nu$ is less than 2. Introducing (24) into (23) gives

$$\nu = 2\,e^{A_1} \tag{25}$$

since it can be assumed that $\nu_{1r} = 2$ for all $m_{1r}$.

The mean aggregation number of the carboxylate anions is defined by

$$\bar{q} = m_2/m_{aggr} \tag{26}$$

where $m_{aggr}$ is the molality of the aggregates, including monomers. Assuming that no sodium ions are bound to the aggregates, $\nu m = m_{Na} + m_{Cl} + m_{aggr}$; $m_{Na} = m$ and $m_{Cl} = (1 - x_2)m$, giving

$$\bar{q} = x_2/(\nu + x_2 - 2) \tag{27}$$

*Mean activity coefficient of the carboxylate.* It is, as can be seen from Fig. 3, which shows $\nu$ for sodium hexanoate, possible to extrapolate the values for
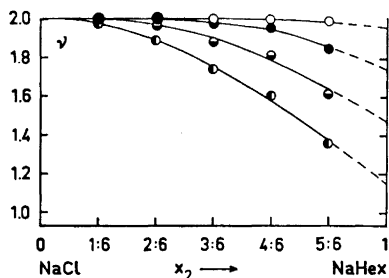


*Fig. 3.* The mean amount of ions $\nu$ formed per unit amount of mixed electrolyte in aqueous $NaCl - Na$ hexanoate mixtures at different total molalities m as a function of the fraction of Na hexanoate. ○ 0.5, ● 1.0, ◓ 2.0, and ◐ 3.0 mol $kg^{-1}$.

$\nu$ calculated from (25) to $x_2 = 1$, *i.e.* to pure carboxylate solutions. These extrapolated values, $\nu_{2r}$, may then be utilized to calculate the activity coefficient of the carboxylates in pure solutions *with the association taken into account* in the following way:

From the Gibbs-Duhem equation,

$$m_{2r}\,d \ln a_{2r} = -m_w\,d \ln a_w = -m_w dy \tag{28}$$

If the carboxylate dissociation is written

$$NaR \rightarrow Na^+ + \frac{1}{q}\,R_q^{\bar{q}-} = Na^+ + (\nu_{2r} - 1)R_q^{\bar{q}-} \tag{29}$$
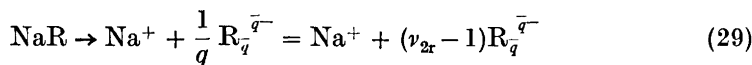
the mean carboxylate activity is defined by

$$a_{2r} = (\nu_{2r} - 1)^{\nu_{2r}-1}(\gamma_{2r}m_{2r})^{\nu_{2r}} \tag{30}$$

and the mean activity coefficient is given by

$$\gamma_{2r} = (\gamma_R^{\nu_{2r}-1}\gamma_{Na})^{1/\nu_{2r}} \tag{31}$$

where $\gamma_R$ and $\gamma_{Na}$ are the single ionic activity coefficients of the $R_q^{\bar{q}-}$ and $Na^+$ ions, respectively. Introducing (30) and the osmotic coefficient

$$\phi_{2r} = -\frac{m_w y}{\nu_{2r} m_{2r}} \tag{32}$$

into (28) gives, after slight rearrangement

$$d \ln [(\nu_{2r} - 1)^{\nu_{2r}-1}(\gamma_{2r} m_{2r})^{\nu_{2r}}] = \frac{1}{m_{2r}} dz_{2r} \tag{33}$$

where $z_{2r} = \nu_{2r} m_{2r} \phi_{2r}$. As $m_{2r} \to 0$, the integration of (33) becomes uncertain. This difficulty may be circumvented by using a value of $\gamma_{2r}$ at a concentration which is low enough to make the assumption $\nu_{2r} = 2$ certain, as an integration constant. This integration constant, $\gamma_{2r}^{\circ}$ at $m_{2r} = m_{2r}^{\circ}$ may be calculated in the conventional way from osmotic coefficients.[26] Introducing $\gamma_{2r}^{\circ}$ and $m_{2r}^{\circ}$, the integrated form of (33) is

$$\ln \gamma_{2r} = -\ln m_{2r} + \frac{2}{\nu_{2r}} \ln m_{2r}^{\circ} \gamma_{2r}^{\circ} - \frac{1}{\nu_{2r}} \ln (\nu_{2r} - 1)^{\nu_{2r}-1} + \frac{1}{\nu_{2r}} \int_{z_{2r}^{\circ}}^{z_{2r}} \frac{dz_{2r}}{m_{2r}} \tag{34}$$

where $z_{2r}^{\circ} = 2 m_{2r}^{\circ} \phi_{2r}^{\circ}$. If $\nu_{2r} = 2$ throughout, (34) reduces to

$$\ln \gamma_{2r}' = -\ln m_{2r} + \ln m_{2r}^{\circ} \gamma_{2r}^{\circ} + \int_{\phi_{2r}^{\circ} m_{2r}^{\circ}}^{\phi_{2r} m_{2r}} \frac{d(\phi_{2r} m_{2r})}{m_{2r}} \tag{35}$$

In the mixed solutions, the association may be taken into account in a similar way. The sodium ion activity is $a_{Na} = \gamma_{Na} m$ and the carboxylate ion activity is $a_R = \gamma_R \nu_R m_2 = \gamma_R (\nu_2 - 1) x_2 m$, giving the mean carboxylate ion activity

$$a_2 = \gamma_{Na} m [\gamma_R m x_2 (\nu_2 - 1)]^{\nu_2-1} = [x_2 (\nu_2 - 1)]^{\nu_2-1} (\gamma_2 m)^{\nu_2} \tag{36}$$

where

$$\gamma_2 = (\gamma_{Na} \gamma_R^{\nu_2-1})^{1/\nu_2} \tag{37}$$

is the mean activity coefficient of the carboxylate with the association taken into account. Using this activity, an equation for the calculation of $\gamma_2$ from $a_w$ may now be derived in a way exactly analogous to the derivation of (15). In analogy with (7),

$$\left[\frac{\partial(1/m_1)}{\partial x_{21}}\right]_y = \frac{x_1}{m^2}\left(\frac{\partial m}{\partial x_1}\right)_y + \frac{1}{m} \tag{38}$$

where $x_1 = 1 - x_2$ and $x_{21} = m_2/m_1$. Differentiation of (36) after taking logarithms and introducing $x_1 = 1 - x_2$ yields

$$(\partial \ln a_2)_{x_1} = [\ln(\nu_2 - 1)^{\nu_2-1}(\gamma_2 m)^{\nu_2}]_{x_1} \tag{39}$$

and the equation analogous to (9) is

$$\frac{1}{m_w}\left(\frac{\partial \ln[(\nu_2 - 1)^{\nu_2-1}(\gamma_2 m)^{\nu_2}]}{\partial y}\right)_{x_1} = -\frac{x_1}{m^2}\left(\frac{\partial m}{\partial x_1}\right) - \frac{1}{m} \tag{40}$$

To avoid uncertainty in the integration of (40), activity coefficients calculated from (34) may be utilized.

Introducing $m_w(\partial y)_{x_1} = -\partial(v_2 m_2 \phi_2)_{x_1} = -\partial z_2$ and subtracting (33) from (40) gives

$$d \ln \frac{(v_2-1)^{v_2-1}(\gamma_2 m)^{v_2}}{(v_2-1)^{v_{2r}-1}(\gamma_{2r} m_{2r})^{v_{2r}}} = \left[\frac{x_1}{m^2}\left(\frac{\partial m}{\partial x_1}\right)_{z_2} + \frac{1}{m} - \frac{1}{m_{2r}}\right]_{x_1} dz_2 \qquad (41)$$

As $m \to 0$, the logarithm also becomes 0. The final expression for $\ln \gamma_2$ then is

$$\ln \gamma_2 = \ln m + \frac{1}{v_2}\left\{\ln \frac{(v_{2r}-1)^{v_{2r}-1}(m_{2r}\gamma_{2r})^{v_{2r}}}{(v_2-1)^{v_2-1}} - \int_0^{z_1} \frac{1}{m_{2r}}\left[\left(\frac{\partial u_2}{\partial x_1}\right)_{m_{1r}} x_1 - u_2 + 1\right]_{x_1} dz_2\right\} \qquad (42)$$

where $u_2 = m_{2r}/m$.

The calculation of $\gamma_2$ is limited to solutions which have a vapour pressure which is equal to the pressure of a reference solution of the pure carboxylate. This limits the possibilities to calculate $\gamma_2$ to cases where there is not very extensive association. It is thus, unfortunately, not possible to calculate $\gamma_2$ in micellar solutions. However, in such solutions the assumption that no sodium ions are bound is probably not correct, *i.e.* the calculation of $v$ from (25) becomes very questionable and the whole method breaks down for this reason, too.

The calculation of $\gamma_1$ from (15), $\bar{q}$ and $v$ from (26) and (25), and $\gamma_2$ from (42) were performed by numerical integration and differentiation using a program written in Algol for a Univac 1108 computer.

The calculation of the derivatives in (15), (16), (42) was performed by fitting a cubic polynomial to the functions $u_1(x_2)$ and $u_2(x_1)$ at constant $m_{2r}$ and $m_{1r}$, respectively. The values for $u_1$ and $u_2$ used for this fitting were obtained by quadratic interpolation from the experimental values of $u_1$ and $u_2$ which may be calculated from the points given in Tables 2 − 5.

*Table 1.* Densities of sodium carboxylates in aqueous solution at 25°C.

| $c_{NaR}$ mol dm$^{-3}$ | $\varrho_{NaR}$, g cm$^{-3}$ | | | |
| --- | --- | --- | --- | --- |
| | Sodium acetate | Sodium propionate | Sodium butyrate | Sodium hexanoate |
| 0.250 | 1.0072 | 1.0094 | 1.0083 | 1.0064 |
| 0.400 | 1.0134 | 1.0149 | 1.0137 | 1.0120 |
| 0.500 | 1.0176 | 1.0187 | 1.0174 | 1.0155 |
| 0.700 | 1.0257 | 1.0263 | 1.0248 | 1.0226 |
| 1.000 | 1.0377 | 1.0376 | 1.0361 | 1.0327 |
| 1.300 | 1.0496 | 1.0490 | 1.0476 | 1.0419 |
| 1.500 | 1.0573 | 1.0566 | 1.0557 | 1.0475 |
| 1.800 | 1.0688 | 1.0679 | 1.0661 | 1.0554 |
| 2.100 | 1.0842 | 1.0793 | 1.0770 | 1.0627 |
| 2.400 | 1.0927 | 1.0906 | 1.0872 | 1.0695 |
| 2.700 | 1.1030 | 1.1020 | 1.0961 | 1.0760 |
| 3.000 | 1.1140 | 1.1133 | 1.1053 | 1.0822 |

*Table 2.* Experimental results for sodium acetate/sodium chloride solutions.
$x_2 =$ (carboxylate molality): (total molality); m = total molality of the sample solution;
$m_{1r} =$ molality of a NaCl solution with the same water activity as the sample solution.

$x_2 = 0.1667$: (m, $m_{1r}$); 0.252, 0.254; 0.405, 0.408; 0.507, 0.511; 0.713, 0.720; 1.020, 1.040;
1.237, 1.251; 1.558, 1.576; 1.884, 1.916; 2.215, 2.250; 2.552, 2.590; 2.894, 2.940; 3.243, 3.289.
$x_2 = 0.3333$: (m, $m_{1r}$); 0.252, 0.255; 0.405, 0.411; 0.508, 0.515; 0.715, 0.729; 1.030, 1.055;
1.243, 1.270; 1.567, 1.607; 1.898, 1.958; 2.234, 2.306; 2.577, 2.655; 2.926, 3.021; 3.283, 3.377.
$x_2 = 0.5000$: (m, $m_{1r}$); 0.253, 0.256; 0.406, 0.414; 0.509, 0.520; 0.717, 0.737; 1.034, 1.069;
1.249, 1.292; 1.577, 1.639; 1.911, 2.004; 2.253, 2.363; 2.603, 2.723; 2.959, 3.107; 3.325, 3.474.
$x_2 = 0.6667$: (m, $m_{1r}$); 0.253, 0.257; 0.407, 0.417; 0.510, 0.524; 0.719, 0.745; 1.038, 1.087;
1.255, 1.316; 1.586, 1.659; 1.925, 2.048; 2.273, 2.422; 2.628, 2.798; 2.993, 3.197; 3.368, 3.580.
$x_2 = 0.8333$: (m, $m_{1r}$); 0.253, 0.258; 0.407, 0.420; 0.511, 0.529; 0.721, 0.752; 1.042, 1.104;
1.261, 1.340; 1.596, 1.713; 1.939, 2.097; 2.292, 2.485; 2.655, 2.877; 3.028, 3.292; 3.412, 3.693.
$x_2 = 1.000$: (m, $m_{1r}$); 0.253, 0.259; 0.408, 0.423; 0.512, 0.534; 0.723, 0.760; 1.046, 1.122;
1.267, 1.368; 1.606, 1.750; 1.954, 2.148; 2.313, 2.550; 2.683, 2.958; 3.064, 3.390; 3.457, 3.819.

*Table 3.* Experimental values for sodium propionate/sodium chloride solutions. Symbols:
as in Table 2.

$x_2 = 0.1667$: (m, $m_{1r}$); 0.400, 0.408; 0.508, 0.512; 0.714, 0.727; 1.241, 1.263; 1.564, 1.595;
1.892, 1.935; 2.227, 2.283; 2.567, 2.636; 2.914, 2.994; 3.268, 3.368.
$x_2 = 0.3333$: (m, $m_{1r}$); 0.400, 0.413; 0.509, 0.519; 0.718, 0.736; 1.250, 1.299; 1.579, 1.650;
1.915, 2.010; 2.258, 2.376; 2.621, 2.757; 2.968, 3.123; 3.336, 3.526.
$x_2 = 0.5000$: (m, $m_{1r}$); 0.400, 0.418; 0.511, 0.527; 0.721, 0.749; 1.260, 1.334; 1.594, 1.703;
1.938, 2.075; 2.290, 2.470; 2.660, 2.870; 3.024, 3.251; 3.407, 3.675.
$x_2 = 0.6667$: (m, $m_{1r}$); 0.400, 0.422; 0.513, 0.534; 0.724, 0.763; 1.270, 1.370; 1.610, 1.757;
1.961, 2.153; 2.323, 2.565; 2.696, 2.982; 3.082, 3.389; 3.418, 3.835.
$x_2 = 0.8333$: (m, $m_{1r}$); 0.400, 0.428; 0.514, 0.542; 0.727, 0.777; 1.280, 1.410; 1.626, 1.814;
1.985, 2.234; 2.357, 2.670; 2.742, 3.110; 3.143, 3.527; 3.558, 3.995.
$x_2 = 1.000$: (m, $m_{1r}$): 0.410, 0.433; 0.516, 0.550; 0.730, 0.792; 1.290, 1.447; 1.625, 1.875;
2.010, 2.316; 2.392, 2.774; 2.790, 3.249; 3.205, 3.668; 3.639, 4.177.

*Table 4.* Experimental values for sodium butyrate/sodium chloride solutions. Symbols:
as in Table 2.

$x_2 = 0.1667$: (m, $m_{1r}$); 0.405, 0.410; 0.716, 0.728; 1.030, 1.066; 1.352, 1.391; 1.570, 1.617;
1.902, 1.991; 2.239, 2.322; 2.585, 2.680; 2.938, 3.062; 3.298, 3.446.
$x_2 = 0.3333$: (m, $m_{1r}$); 0.407, 0.418; 0.721, 0.747; 1.040, 1.093; 1.368, 1.445; 1.592, 1.694;
1.934, 2.104; 2.284, 2.449; 2.645, 2.840; 3.016, 3.257; 3.398, 3.675.
$x_2 = 0.5000$: (m, $m_{1r}$); 0.408, 0.425; 0.725, 0.761; 1.050, 1.127; 1.385, 1.503; 1.614, 1.774;
1.967, 2.219; 2.330, 2.569; 2.708, 3.000; 3.097, 3.446; 3.505, 3.915.
$x_2 = 0.6667$: (m, $m_{1r}$); 0.410, 0.431; 0.730, 0.778; 1.060, 1.164; 1.402, 1.557; 1.637, 1.850;
2.002, 2.329; 2.379, 2.690; 2.774, 3.147; 3.188, 3.628; 3.619, 4.130.
$x_2 = 0.8333$: (m, $m_{1r}$); 0.411, 0.438; 0.734, 0.797; 1.070, 1.120; 1.419, 1.615; 1.660, 1.916;
2.037, 2.440; 2.430, 2.809; 2.843, 3.294; 3.281, 3.800; 3.741, 4.325.
$x_2 = 1.000$: (m, $m_{1r}$); 0.412, 0.441; 0.739, 0.822; 1.080, 1.244; 1.437, 1.683; 1.684, 2.011;
2.074, 2.495; 2.483, 2.935; 2.916, 3.490; 3.380, 3.937; 3.870, 4.640.

## EXPERIMENTAL

*I. Chemicals.* The sodium acetate was *p.a.* grade from E. Merck. Other fatty acid
salts were synthesized by neutralization of the acids (*purissimum* grade from Fluka)
with sodium ethylate in dry ethanol. The salts were dried in vacuum at 110°C and their
molecular weights then checked by titration with $HClO_4$ in glacial acetic acid. Only salts
with a molecular weight differing less than 0.25 % from the theoretical weight were
accepted.

The sodium chloride was *p.a.* grade from E. Merck. It was dried before use in vacuum at 110°C.

The water was doubly distilled and passed through an ion exchanger (Dowex) immediately before use. Its conductivity was about 0.5 $\mu$S cm$^{-1}$.

*II. Preparation of solutions.* Mixed electrolyte solutions were prepared by mixing appropriate volume proportions of stock sodium chloride and sodium carboxylate solutions of the same concentration. The molalities were calculated from the densities given for NaCl solutions in Ref. 27 and the pycnometrically determined carboxylate densities given in Table 1; the densities of mixed electrolyte solutions were assumed to change linearly with the amount of carboxylate in a solution of constant concentration. By checking the densities of some solutions this was shown to hold to an accuracy which was better than the difference in molality that could be detected with the vapour pressure osmometer. To all solutions were added 10$^{-4}$ mol/l NaOH to suppress effects of hydrolysis. This amount is too small to affect the water activities to a measurable extent.

*III. Measurement of water activities.* Water activities were measured with a Mechrolab model 301 Vapour Pressure Osmometer, using sodium chloride solutions of suitable concentration as standards. The resistance difference $\Delta R$ between the two thermistors was calibrated as a function of the difference in water activity between the solutions surrounding the drops by using NaCl solutions of known water activity (taken from Ref. 28). At least six $\Delta R$ values were taken for each point. The standard deviation in $\Delta R$ is $\pm 0.2$ ohm corresponding to a difference in water activity of about $\pm 0.001$. Fig. 4
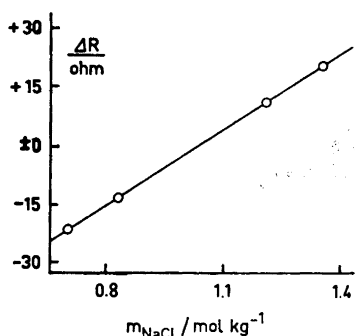


*Fig. 4.* A sample calibration curve showing the resistance difference $\Delta R$ between the VPO thermistors as a function of the NaCl molality using 1.0 mol kg$^{-1}$ NaCl as a reference solution.

exemplifies a calibration curve. Measurements of the vapour pressures of the sample solutions were made in the same way and the molality of the isopiestic NaCl solution was read directly from the $\Delta R$ *versus* m$_{NaCl}$ curve.

All measurements were performed at $(25 \pm 0.01)$°C.

*Table 5.* Experimental values for sodium hexanoate/sodium chloride solutions. Symbols: as in Table 2.

$x_2 = 0.1667$: (m, m$_{1r}$); 0.253, 0.256; 0.406, 0.414; 0.510, 0.520; 0.718, 0.737; 1.037, 1.070; 1.362, 1.413; 1.583, 1.645; 1.920, 2.001; 2.266, 2.370; 2.619, 2.753; 2.982, 3.120; 3.360, 3.549.
$x_2 = 0.3333$: (m, m$_{1r}$); 0.254, 0.263; 0.409, 0.422; 0.513, 0.533; 0.726, 0.762; 1.052, 1.115; 1.388, 1.482; 1.619, 1.730; 1.974, 2.115; 2.341, 2.500; 2.721, 2.876; 3.116, 3.190; 3.527, 3.557.
$x_2 = 0.5000$: (m, m$_{1r}$); 0.255, 0.267; 0.411, 0.430; 0.517, 0.544; 0.733, 0.784; 1.068, 1.157; 1.416, 1.540; 1.656, 1.789; 2.030, 2.168; 2.422, 2.603; 2.834, 2.810; 3.267, 3.107; 3.724, 3.456.
$x_2 = 0.6667$: (m, m$_{1r}$); 0.255, 0.271; 0.413, 0.436; 0.521, 0.555; 0.740, 0.804; 1.084, 1.190; 1.443, 1.574; 1.696, 1.822; 2.092, 2.129; 2.512, 2.402; 2.959, 2.663; 3.435, 2.955; 3.946, 3.327.
$x_2 = 0.8333$: (m, m$_{1r}$); 0.256, 0.273; 0.416, 0.442; 0.525, 0.565; 0.748, 0.823; 1.100, 1.220; 1.475, 1.577; 1.739, 1.775; 2.159, 2.008; 2.610, 2.244; 3.096, 2.476; 3.624, 2.772; 4.198, 3.140.
$x_2 = 1.000$: (m, m$_{1r}$); 0.257, 0.267; 0.418, 0.432; 0.528, 0.560; 0.756, 0.872; 1.118, 1.240; 1.508, 1.600; 1.785, 1.793; 2.231, 2.003; 2.718, 2.180; 3.253, 2.450; 3.841, 2.790; 4.493, 3.250.

*Table 6.* Activity coefficients of sodium chloride (1) and sodium acetate (2) in mixed aqueous solutions at different ionic strengths.

| m mol kg⁻¹ | $x_2=0$ | | $x_2=1:6$ | | $x_2=1:3$ | | $x_2=1:2$ | | $x_2=2:3$ | | $x_2=5:6$ | | $x_2=1$ | | |
|---|---|---|---|---|---|---|---|---|---|---|---|---|---|---|---|
| | $\gamma_1{}^a$ | $\gamma_2$ | $\gamma_1$ | $\gamma_2$ | $\gamma_1$ | $\gamma_2$ | $\gamma_1$ | $\gamma_2$ | $\gamma_1$ | $\gamma_2$ | $\gamma_1$ | $\gamma_2$ | $\gamma_1$ | $\gamma_2$ | $\gamma_2{}^a$ |
| 0.500 | 0.681 | 0.713 | 0.686 | 0.718 | 0.692 | 0.719 | 0.697 | 0.723 | 0.700 | 0.727 | 0.704 | 0.731 | 0.707 | 0.736 | 0.735 |
| 1.000 | 0.657 | 0.718 | 0.665 | 0.720 | 0.673 | 0.729 | 0.681 | 0.733 | 0.689 | 0.742 | 0.696 | 0.750 | 0.699 | 0.759 | 0.757 |
| 1.500 | 0.660 | 0.748 | 0.667 | 0.726 | 0.678 | 0.755 | 0.690 | 0.764 | 0.700 | 0.775 | 0.708 | 0.787 | 0.712 | 0.800 | 0.799 |
| 2.000 | 0.668 | 0.789 | 0.681 | 0.782 | 0.695 | 0.792 | 0.707 | 0.806 | 0.720 | 0.820 | 0.730 | 0.835 | 0.736 | 0.851 | 0.851 |
| 2.500 | 0.688 | 0.840 | 0.702 | 0.827 | 0.719 | 0.840 | 0.732 | 0.856 | 0.746 | 0.872 | 0.758 | 0.892 | 0.767 | 0.914 | 0.914 |
| 3.000 | 0.714 | 0.896 | 0.728 | 0.896 | 0.745 | 0.889 | 0.760 | 0.910 | 0.777 | 0.933 | 0.791 | 0.958 | 0.803 | 0.982 | 0.982 |
| 3.500 | 0.746 | 0.953 | 0.757 | 0.926 | 0.772 | 0.940 | 0.789 | 0.963 | 0.807 | 1.004 | 0.824 | 1.025 | 0.843 | 1.063 | 1.057 |

*a* From Ref. 29.

*Table 7.* Activity coefficients of sodium chloride (1) and sodium propionate (2) in mixed aqueous soutlions at different ionic strengths.

| m mol kg⁻¹ | $x_2=0$ | | $x_2=1:6$ | | $x_2=1:3$ | | $x_2=1:2$ | | $x_2=2:3$ | | $x_2=5:6$ | | $x_2=1$ | | |
|---|---|---|---|---|---|---|---|---|---|---|---|---|---|---|---|
| | $\gamma_1{}^a$ | $\gamma_2$ | $\gamma_1$ | $\gamma_2$ | $\gamma_1$ | $\gamma_2$ | $\gamma_1$ | $\gamma_2$ | $\gamma_1$ | $\gamma_2$ | $\gamma_1$ | $\gamma_2$ | $\gamma_1$ | $\gamma_2$ | $\gamma_2{}^a$ |
| 0.500 | 0.681 | 0.721 | 0.687 | 0.740 | 0.696 | 0.748 | 0.703 | 0.756 | 0.710 | 0.758 | 0.720 | 0.764 | 0.745 | 0.771 | 0.764 |
| 1.000 | 0.657 | 0.731 | 0.667 | 0.754 | 0.678 | 0.768 | 0.690 | 0.781 | 0.705 | 0.788 | 0.723 | 0.800 | 0.740 | 0.812 | 0.808 |
| 1.500 | 0.660 | 0.759 | 0.671 | 0.792 | 0.685 | 0.816 | 0.702 | 0.833 | 0.721 | 0.848 | 0.740 | 0.864 | 0.765 | 0.882 | 0.876 |
| 2.000 | 0.668 | 0.804 | 0.686 | 0.843 | 0.705 | 0.877 | 0.724 | 0.899 | 0.747 | 0.920 | 0.770 | 0.942 | 0.797 | 0.969 | 0.966 |
| 2.500 | 0.688 | 0.861 | 0.709 | 0.909 | 0.731 | 0.944 | 0.753 | 0.973 | 0.779 | 1.002 | 0.804 | 1.029 | 0.832 | 1.064 | 1.061 |
| 3.000 | 0.714 | 0.927 | 0.739 | 0.982 | 0.764 | 1.023 | 0.788 | 1.056 | 0.813 | 1.081 | 0.847 | 1.113 | 0.866 | 1.151 | 1.160 |
| 3.500 | 0.746 | 1.005 | 0.789 | 1.069 | 0.808 | 1.114 | 0.835 | 1.142 | 0.857 | 1.170 | 0.883 | 1.196 | 0.902 | 1.232 | – |

*a* From Ref. 29.

*Table 8.* Mean aggregation number ($\bar{q}$) of the butyrate anions and activity coefficients of the sodium chloride ($\gamma_1$) and the sodium butyrate ($\gamma_2$) in mixed aqueous solution at different total molalities. $\gamma_2' =$ activity coefficient of sodium butyrate without association taken into account.

| $x_2$ | | m, mol kg$^{-1}$ | | | | | | |
| --- | --- | --- | --- | --- | --- | --- | --- | --- |
| | | 0.500 | 1.000 | 1.500 | 2.000 | 2.500 | 3.000 | 3.500 |
| 0 | $\gamma_1{}^a$ | 0.681 | 0.657 | 0.656 | 0.668 | 0.688 | 0.714 | 0.746 |
| | $\gamma_2$ | 0.731 | 0.755 | 0.807 | 0.897 | 0.999 | 1.119 | 1.235 |
| 1:6 | $\gamma_1$ | 0.690 | 0.673 | 0.680 | 0.696 | 0.721 | 0.755 | 0.796 |
| | $\gamma_2$ | 0.736 | 0.772 | 0.843 | 0.933 | 1.035 | 1.155 | 1.283 |
| | $\nu$ | 2.00 | 1.99 | 1.97 | 1.96 | 1.96 | 1.96 | 1.95 |
| | $\bar{q}$ | 1.00 | 1.03 | 1.04 | 1.04 | 1.04 | 1.05 | 1.05 |
| 1:3 | $\gamma_1$ | 0.694 | 0.689 | 0.704 | 0.726 | 0.754 | 0.794 | 0.841 |
| | $\gamma_2$ | 0.750 | 0.792 | 0.868 | 0.958 | 1.061 | 1.189 | 1.329 |
| | $\nu$ | 2.00 | 1.97 | 1.96 | 1.94 | 1.95 | 1.93 | 1.90 |
| | $q$ | 1.00 | 1.02 | 1.04 | 1.04 | 1.04 | 1.05 | 1.06 |
| 1:2 | $\gamma_1$ | 0.699 | 0.706 | 0.716 | 0.752 | 0.786 | 0.833 | 0.890 |
| | $\gamma_2$ | 0.758 | 0.808 | 0.900 | 0.987 | 1.092 | 1.223 | 1.385 |
| | $\nu$ | 2.00 | 1.98 | 1.96 | 1.93 | 1.93 | 1.91 | 1.88 |
| | $\bar{q}$ | 1.00 | 1.02 | 1.04 | 1.05 | 1.07 | 1.11 | 1.13 |
| 2:3 | $\gamma_1$ | 0.708 | 0.719 | 0.744 | 0.777 | 0.817 | 0.869 | 0.933 |
| | $\gamma_2$ | 0.761 | 0.825 | 0.919 | 1.024 | 1.131 | 1.263 | 1.425 |
| | $\nu$ | 2.00 | 1.99 | 1.98 | 1.94 | 1.94 | 1.91 | 1.89 |
| | $\bar{q}$ | 1.00 | 1.02 | 1.04 | 1.05 | 1.08 | 1.12 | 1.15 |
| 5:6 | $\gamma_1$ | 0.718 | 0.729 | 0.757 | 0.794 | 0.841 | 0.895 | 0.963 |
| | $\gamma_2$ | 0.766 | 0.847 | 0.954 | 1.060 | 1.171 | 1.302 | 1.450 |
| | $\nu$ | 2.00 | 1.99 | 1.97 | 1.97 | 1.96 | 1.91 | 1.88 |
| | $\bar{q}$ | 1.00 | 1.01 | 1.04 | 1.05 | 1.07 | 1.11 | 1.16 |
| 1 | $\gamma_1$ | 0.740 | 0.751 | 0.756 | 0.824 | 0.853 | 0.918 | 0.979 |
| | $\gamma_2$ | 0.784 | 0.849 | 0.927 | 1.106 | 1.206 | 1.332 | 1.577 |
| | $\gamma_2'$ | 0.786 | 0.869 | 0.962 | 1.095 | 1.185 | 1.307 | 1.380 |
| | $\nu$ | 2.00 | 1.98 | 1.97 | 1.96 | 1.93 | 1.90 | 1.87 |
| | $\bar{q}$ | 1.00 | 1.01 | 1.04 | 1.04 | 1.05 | 1.08 | 1.16 |
| | $\gamma_2'{}^a$ | 0.782 | 0.868 | 0.982 | 1.083 | 1.182 | 1.278 | 1.368 |

$^a$ From Ref. 29.

## RESULTS AND DISCUSSION

The experimental results (total molalities, and molalities of isopiestic NaCl solutions for different $m_{\text{NaR}}/m_{\text{NaCl}}$ ratios) are given in Tables 2 – 5.

From these data values of $\gamma_1$, $\gamma_2$, $\gamma_2'$, $\nu$, and $\bar{q}$ have been calculated; these are given in Tables 6 – 9. The logarithms of $\gamma_1$ and $\gamma_2$ at a few constant molalities are given in Figs. 5 – 12.

The results are in good agreement with previously determined activity coefficients,[18] as can be seen from the figures. This gives strong support to the applicability of the method to systems of this type. The values obtained

*Table 9.* Mean aggregation number ($\bar{q}$) of the hexanoate anions and activity coefficients of the sodium chloride ($\gamma_1$) and sodium hexanoate ($\gamma_2$) in mixed aqueous solutions at different total molalities. $\gamma_2'$ = activity coefficient of sodium hexanoate without association taken into account.

| $x_2$ | | m, mol kg⁻¹ | | | | | | |
|---|---|---|---|---|---|---|---|---|
| | | 0.500 | 1.000 | 1.500 | 2.000 | 2.500 | 3.000 | 3.500 |
| 0 | $\gamma_1{}^a$ | 0.681 | 0.657 | 0.656 | 0.668 | 0.688 | 0.714 | 0.746 |
| | $\gamma_2$ | 0.787 | | | | | | |
| 1:6 | $\gamma_1$ | 0.694 | 0.677 | 0.684 | 0.702 | 0.739 | 0.771 | 0.811 |
| | $\gamma_2$ | 0.805 | 0.895 | 1.021 | | | | |
| | $\nu$ | 2.00 | 2.00 | 2.00 | 2.00 | 1.99 | 1.97 | 1.95 |
| | $\bar{q}$ | 1.00 | 1.00 | 1.01 | 1.02 | 1.07 | 1.20 | 1.40 |
| 1:3 | $\gamma_1$ | 0.708 | 0.698 | 0.711 | 0.734 | 0.765 | 0.787 | 0.825 |
| | $\gamma_2$ | 0.854 | 1.043 | | | | | |
| | $\nu$ | 2.00 | 1.99 | 1.98 | 1.96 | 1.93 | 1.89 | 1.84 |
| | $\bar{q}$ | 1.00 | 1.02 | 1.06 | 1.12 | 1.26 | 1.57 | 2.00 |
| 1:2 | $\gamma_1$ | 0.718 | 0.720 | 0.739 | 0.765 | 0.780 | 0.783 | 0.808 |
| | $\gamma_2$ | 0.866 | 1.089 | | | | | |
| | $\nu$ | 1.99 | 1.97 | 1.96 | 1.88 | 1.81 | 1.74 | 1.64 |
| | $\bar{q}$ | 1.01 | 1.07 | 1.15 | 1.26 | 1.59 | 2.03 | 2.67 |
| 2:3 | $\gamma_1$ | 0.735 | 0.746 | 0.763 | 0.784 | 0.798 | 0.806 | 0.821 |
| | $\gamma_2$ | 0.867 | 1.053 | | | | | |
| | $\nu$ | 1.99 | 1.95 | 1.92 | 1.80 | 1.76 | 1.60 | 1.55 |
| | $\bar{q}$ | 1.07 | 1.14 | 1.27 | 1.50 | 2.10 | 2.96 | 4.25 |
| 5:6 | $\gamma_1$ | 0.757 | 0.775 | 0.782 | 0.782 | 0.784 | 0.804 | 0.844 |
| | $\gamma_2$ | 0.851 | 0.993 | | | | | |
| | $\nu$ | 1.98 | 1.84 | 1.75 | 1.61 | 1.48 | 1.36 | 1.26 |
| | $\bar{q}$ | 1.11 | 1.24 | 1.47 | 1.74 | 2.68 | 4.81 | 10.13 |
| 1 | $\gamma_1$ | 0.769 | 0.801 | 0.826 | | | | |
| | $\gamma_2$ | 0.799 | 0.869 | 0.916 | 0.898 | 0.854 | 0.857 | |
| | $\nu$ | 1.92 | 1.73 | 1.60 | 1.47 | 1.30 | 1.16 | |
| | $\bar{q}$ | 1.20 | 1.38 | 1.64 | 2.00 | 3.38 | 11.28 | |
| | $\gamma_2'$ | 0.801 | 0.858 | 0.847 | 0.769 | 0.678 | 0.617 | 0.583 |
| | $\gamma_2'^a$ | 0.794 | 0.858 | 0.850 | 0.763 | 0.673 | 0.612 | 0.576 |

*a* From Ref. 29.

for the activity coefficients of pure carboxylates in aqueous solution, as calculated without taking the association into account, are in close agreement with those reported by Smith and Robinson,[13,29] as can be seen from Tables 6 – 9.

According to the well-known empirical equation called Harned's rule,[30]

$$\log \gamma_1 = \log \gamma_1{}^{tr} + \alpha\, m_1$$

where $\gamma_1$ is the activity coefficient of electrolyte 1 in a mixture of electrolytes 1 and 2 at constant molality, $m_1$ is the molality of 1 in this mixture and

$\gamma_1^{tr}$ is the activity coefficient of 1 in infinite dilution at this ionic strength. As can be seen from Figs. 5, 7, 9 and 11, Harned's rule is valid for the NaCl in all solutions except those at high ionic strengths and high hexanoate concentrations.

In these regions, aggregation is quite extensive (Table 9) and the assumptions made are probably too crude, especially as regards the binding of sodium ions to the aggregates.

Harned's rule is also valid for the carboxylates except for butyrate at very high concentrations and for hexanoate. This is to be expected since the assumptions made are not valid in these solutions. Moreover, it can be seen
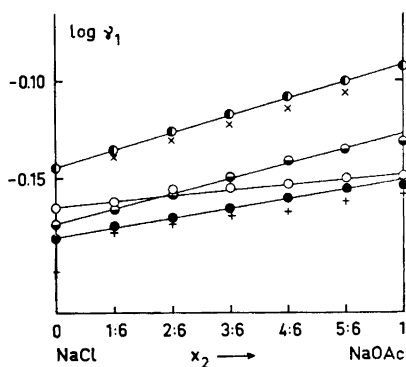


*Fig. 5.* The logarithm of the activity coefficient of sodium chloride in aqueous NaCl – Na acetate mixtures as a function of $x_2 = m_{NaOAc}/m$ at different total concentrations m. O 0.5, ● 1.0, ◒ 2.0, ◐ 3.0, × 3.0 (Ref. 18), and + 1.0 mol kg⁻¹. (Ref. 18).
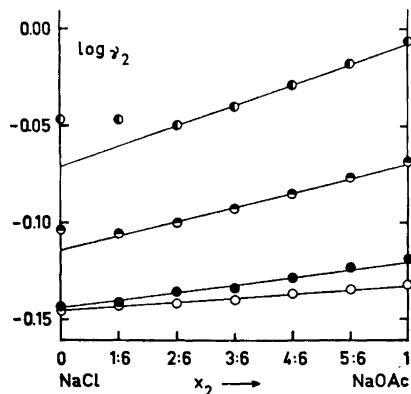
*Fig. 6.* The logarithm of the activity coefficient of sodium acetate in aqueous NaCl – Na acetate mixtures as a function of $x_2 = m_{NaOAc}/m$ at different total concentrations m. O 0.5, ● 1.0, ◒ 2.0, and ◐ 3.0 mol kg⁻¹.

that $\gamma^{tr}$ and $|\alpha|$ are equal for the sodium chloride and sodium acetate in NaCl/NaOAc mixtures, for the sodium chloride and sodium propionate in NaCl/NaPr mixtures and for the sodium chloride and sodium butyrate in NaCl/NaBu mixtures. Some theoretical justification for this phenomenon has been given by Guggenheim;[31] since one of the main assumptions of his theory is that the ionic radii are equal, it seems very resonable that the hexanoate deviates quite drastically from the rule.

The aggregation numbers are in good agreement with those found previously.[2,32] It should be remembered, that the numbers given here include monomers. It is clearly seen that aggregation becomes noticeable in butyrate solutions at total molalities above 1.5 m; this agrees quite well with previous potentiometric results which indicate aggregation at concentrations higher than 1.0 mol/l at the ionic strength 3 mol/l. Considerable aggregation is indicated at high hexanoate concentrations; however, the actual mean aggregation numbers obtained should be regarded as indicative only because of the uncertainty of the extrapolations.

Fig. 7. The logarithm of the activity coefficient of sodium chloride in aqueous NaCl − Na propionate mixtures as a function of $x_2 = m_{NaPr}/m$ at different total molalities m. Symbols as in Fig. 5.
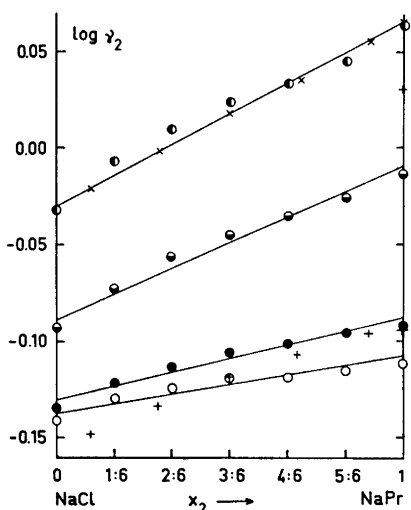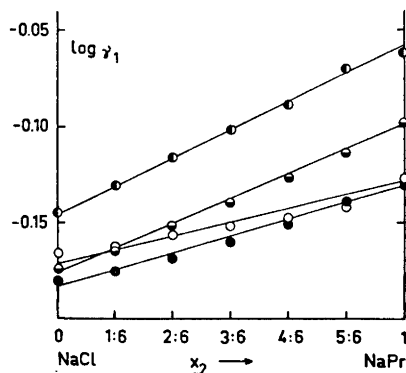


Fig. 8. The logarithm of the activity coefficient of sodium propionate in aqueous NaCl − Na propionate mixtures as a function of $x_2 = m_{NaPr}/m$ at different total molalities m. ○ 0.5, ● 1.0, ◐ 2.0, ◑ 3.0, × 3.0 (Ref. 24), and + 1.0 (Ref. 24).
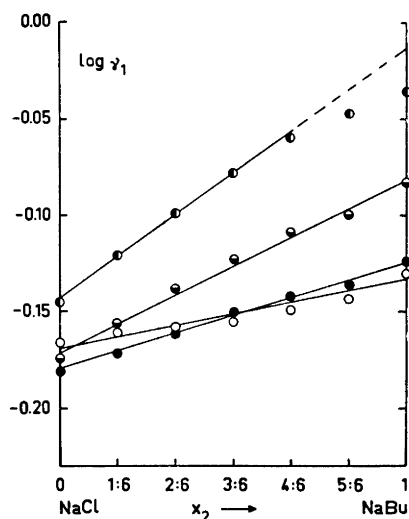


Fig. 9. The logarithm of the activity coefficient of sodium chloride in aqueous NaCl − Na butyrate mixtures as a function $x_2 = m_{NaBu}/m$ at different total molalities m. Symbols as in Fig. 8.

The results given in part I [2] of this series indicate that all complexes formed by carboxylates bind hydrogen ions. It was asserted that this was probably a result of using hydrogen ion activity measurements for the investigation of the aggregation. The vapour pressure measurements have been made at a pH of about 9, which is well above the highest pH at which any binding of hydrogen ions is indicated by potentiometric measurements. One may conclude, that

(a) small aggregates are formed by butyrate and hexanoate anions; the hexanoate forms quite large aggregates (micelles) at high concentration;

(b) hydrogen ions are not necessary to stabilize these aggregates, *i.e.*, they are probably not held together by hydrogen bonding. This conclusion is supported by recent NMR investigations;[33]

(c) this does not exclude the possibility that the sodium ions play an important part in forming ion pairs with the aggregates; some indication of this is given by independent sodium ion activity measurements [8] which show a decrease in activity as aggregates are formed. This is also supported by the results of this work, which indicate that the assumption that sodium ions are not bound to the aggregates leads to strongly decreasing sodium chloride activity coefficients when the hexanoate association becomes extensive;
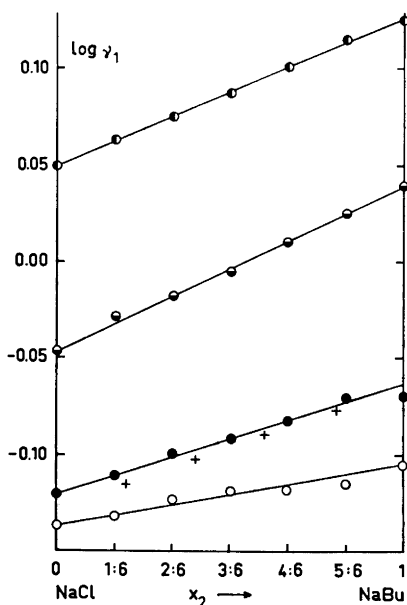


*Fig. 10.* The logarithm of the activity coefficient of sodium butyrate in aqueous NaCl — Na butyrate mixtures as a function of $x_2 = m_{\text{NaBu}}/m$ at different total molalities m. Symbols as in Fig. 8.
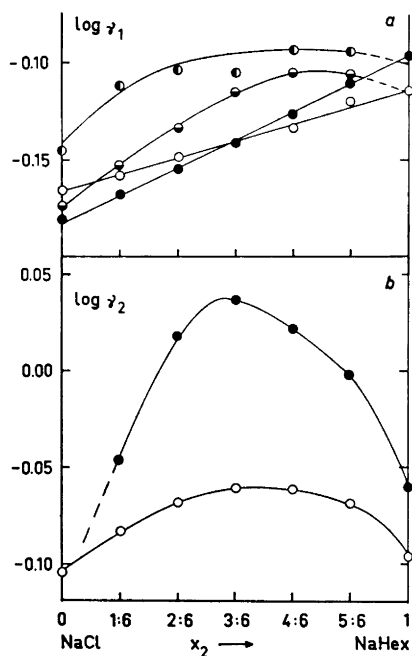
*Fig. 11.* The logarithms of the activity coefficient of (a) sodium chloride and (b) hexanoate in aqueous NaCl — Na hexanoate mixtures as a function of $x_2 = m_{\text{NaHex}}/m$ at different total molalities m. Symbols as in Fig. 8.

(d) the very slow rise in mean aggregation number as the concentration increases indicates quite low formation constants. This lends some support to the view that the hydrocarbon chains in the small aggregates are held together by hydrophobic bonding; there does not seem to be any strong and specific attraction between the carboxylate anions.

## REFERENCES

1. McKay, H. A. C. and Perring, J. K. *Trans. Faraday Soc.* **49** (1953) 163.
2. Stenius, P. and Zilliacus, C. H. *Acta Chem. Scand.* **25** (1971) 2232.
3. Mukerjee, P. *Advan. Colloid Interface Sci.* **1** (1967) 241.
4. Franks, F. and Smith, H. T. *J. Phys. Chem.* **68** (1964) 3581.
5. Franks, F., Quickenden, M. J., Ravenhill, J. R. and Smith, H. T. *J. Phys. Chem.* **72** (1968) 2668.
6. Stead, J. A. and Taylor, H. *Australasian J. Pharm.* **51** (1970) 51.
7. Proust, J. and Ter-Miniassan-Saraga, L. *Compt. Rend.* **270** (1970) 1354.
8. Danielsson, I. and Stenius, P. *J. Colloid Interface Sci.* **37** (1971) 264.
9. van Voorst Vader, F. *Trans. Faraday Soc.* **57** (1961) 110.
10. Birch, B. J. and Hall, D. G. *J. Chem. Soc. Faraday Trans.* **1 1972** 2350.
11. Krafft, F. and Strutz, A. *Ber.* **29** (1896) 1329.
12. McBain, J. W. and Salmon, C. S. *J. Am. Chem. Soc.* **43** (1920) 426.
13. Smith, E. R. B. and Robinson, R. A. *Trans. Faraday Soc.* **38** (1942) 70.
14. Ekwall, P. and Harva, O. *Finska Kemistsamfundets Medd.* **52** (1943) 257.
15. Kolthoff, I. M. and Johnson, W. F. *J. Phys. Chem.* **52** (1948) 22.
16. Lanier, R. D. *J. Phys. Chem.* **69** (1965) 3993.
17. Persson, H. *Acta Chem. Scand.* **25** (1971) 1775.
18. Backlund, S. *Acta Chem. Scand.* **25** (1971) 2070.
19. Danielsson, I. *Chim. Phys. Appl. Prat. Ag. Ag. Surface, C. R. Congr. Int. Deterg., 5th,* **2** (1968) 1041.
20. Robinson, R. A., Wood, R. H. and Reilly, P. J. *J. Chem. Thermodyn.* **3** (1971) 461.
21. Rush, R. M. and Johnson, J. S. *J. Chem. Thermodyn.* **3** (1971) 779.
22. Pepela, C. N. and Dunlop, P. *J. Chem. Thermodyn.* **4** (1972) 115.
23. Downes, C. J. *J. Chem. Soc. Faraday Trans.* **1 1972** 1964.
24. Backlund, S., Eriksson, F. and Friman, R., *Acta Chem. Scand.* **27** (1973) 3234.
25. Robinson, R. A. and Stokes, R. H. *Electrolyte Solutions*, Revised Ed., Butterworths, London 1965, p. 34.
26. *Ibid.* p. 179.
27. Landolt-Börnstein, *Physikalisch-Chemische Tabellen, III Erg. Bd.* Springer, Berlin 1935.
28. Ref. 25, p. 476.
29. Ref. 25, pp. 492 – 933.
30. Ref. 25, p. 438.
31. Guggenheim, E. A. *Phil. Mag.* **19** (1935) 588.
32. Danielsson, I. and Koivula, T. In Ekwall, P. and Runnström-Reio, V., Eds., *Surface Chemistry*, Munksgaard, Copenhagen 1965, p. 137.
33. Ödberg, L., Svens, B. and Danielsson, I. *J. Colloid Interface Sci.* **41** (1972) 298.

# Association Equilibria and Micelle Formation of Fatty Acid Sodium Salts. III. The Association of Sodium Butyrate at 40° in 3 M Na(Cl)

PER STENIUS

*Department of Physical Chemistry, Åbo Akademi, Porthansgatan 3—5, SF-20500 Åbo 50, Finland*

A potentiometric investigation has been made of the self-association of sodium butyrate (NaB) at 40°C in the ionic medium 3 M Na(Cl). The following complexes and stability constants ($\beta$) have been found:

$$B^- + H_2O \rightarrow HB + OH^- \qquad -\log \beta_{1,1} = 8.630 \pm 0.021$$
$$5\,B^- + 2\,H_2O \rightarrow H_2B_5^{3-} + 2\,OH^- \qquad -\log \beta_{2,5} = 17.170 \pm 0.029$$

The results indicate (i) that the aggregates formed are slightly larger than those formed at 25°C; (ii) that the association is endothermic, the standard enthalpy of association being about 20 kJ/mol butyrate; (iii) that the increase in entropy of the system on association is very large (about 65 J mol$^{-1}$ K$^{-1}$), and (iv) that these aggregates probably are formed by hydrophobic bonding.

$\mathbf{P}$arts I and II [1,2] in this series show quite conclusively that small aggregates are formed by sodium alkanoates with more than 3 carbon atoms in the hydrocarbon chain. The aim of the present investigation is to obtain a better understanding of the forces holding the molecules together in these aggregates by investigating the dependence of the aggregation processes in sodium butyrate solutions on temperature. Previous investigations [1-8] indicate that the nature of these forces is similar to those causing micelle formation; the hydrocarbon chains are held together by hydrophobic bonding and the repulsion between the carboxylate end groups is decreased by ion pair formation.

## LIST OF SYMBOLS

$[B^-]$ = concentration of free butyrate ions
$C_B$ = total concentration of sodium butyrate
$C_H$ = analytical excess of hydrogen ions; $C_H^\circ$ = initial excess of hydrogen ions

| | | |
|---|---|---|
| $E$ | = | experimental electromotive force; $E_{OH}°$, $E_{H}°$ = constants (standard cell potentials), $E_j$ = liquid junction potential |
| $K_w$ | = | ionic product of water |
| $k$ | = | $RTF^{-1} \ln 10$ |
| $p, q$ | = | number of hydrogen and butyrate ions in complex $H_pB_q$ |
| $U$ | = | error square sum |
| $V$ | = | volume of solution |
| $Z_{exp}$ | = | $(C_H - [H^+])/C_B$; $Z_{calc}$ = defined by eqn. (8) |
| $\beta_{p,q}$ | = | stability constant of complex $H_pB_q$ (defined by eqn. 15) |
| $\sigma(y)$ | = | standard deviation in $Z$ |
| $\ominus$ | = | standard state |

## EXPERIMENTAL

*I. Potentiometric titrations.* The self-association of butyrate anions was studied by investigating the hydrolysis of butyric acid as a function of the total butyrate concentration $C_B$ in a series of potentiometric titrations. These were all performed in solutions made 3 M in Na$^+$ by addition of NaCl, in order to make it possible to use concentrations instead of activities.[9],[10] $C_B$ was kept constant in each titration, the analytical excess of hydrogen ions, $C_H$, being varied by coulometric addition of OH$^-$-ions. The concentration of free hydrogen ions was measured with a hydrogen electrode in combination with the reference electrode

$$Ag|AgCl|3 \text{ M NaCl (satd. with AgCl)}|(3M - C_B)\text{NaCl}, \; C_B \text{ NaB}|$$
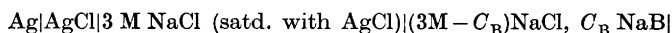
where NaB denotes sodium butyrate. The bridge solution thus was a neutral solution of similar composition to the solution titrated. The complete cell may be written

$$Pt|H_2|H^+ \quad (\text{in}(3M - C_B)\text{NaCl}, \; C_B \text{ NaB})|\text{ref.electr.}$$
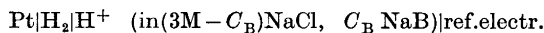
and its emf is given by

$$\begin{aligned} E &= E_H° - k \log[H^+] + E_j \\ &= E_{OH}° + k \log[OH^-] + E_j \\ &= E_{OH}° + k \log K_w - k \log[H^+] + E_j \end{aligned} \qquad (1)$$

where $E_H°$ and $E_{OH}°$ are constant potentials, $k = RTF^{-1} \ln 10 = 62.132$ mV at 40°C and $E_j$ is the liquid junction potential.

The titration vessel and the system used to record the emf have been described in detail elsewhere.[11],[12] The titrations were performed automatically. A digital voltmeter with a printout unit was used to measure the emf of the cell for 30 min after each addition of OH$^-$. The voltmeter was then turned off and the coulometer started, electrolytic addition of OH$^-$ being performed for 30 min, followed by a new 30 min recording period. The emf values recorded, except for a few points in the immediate vicinity of the equivalence point, were stable within ± 0.1 mV for 15 − 20 min; the zero-point drift of the system was less than 0.2 mV/24 h. The highest currents used in the electrolysis was 2 mA. The titration vessel was thermostated at 40.0 ± 0.1°C.

*II. Cell calibration and calculation of* $[H^+]$. In each titration, $E_{OH}°$ was determined according to the method developed by Biedermann and Sillén.[9] Known excess concentrations of OH$^-$ were added and the experimental quantity $E - k \log [OH^-] = E_{OH}° + E_j$ then was plotted against OH$^-$ and extrapolated to $[OH^-] = 0$. This procedure invariably yielded straight lines and the intercept was taken as $E_{OH}°$. The equivalence point was determined using Gran plots[13] from the $E$-values measured on the alkaline side of the equivalence point.

To calculate $[H^+]$ in the acid solutions, $K_w$ was determined in 3 M NaCl at 40°C using the method described by Ingri *et al.*[14] A solution 0.05 M in HCl, was titrated in the same way as the butyrate solutions. Since $[H^+] = C_H°$ in this solution, $E_H°$ may be determined
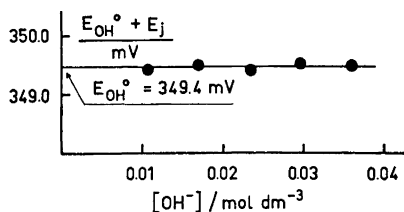
*Fig. 1.* The potential $E_{OH}° + E_j$ as a function of $[OH^-]$ in the titration of 0.5 M sodium butyrate.

in the same way as $E_{OH}°$ by plotting $E + k \log[H] = E_H + E_j$ against $[H^+]$ and extrapolating to $[H^+] = 0$. Then $K_w$ may be calculated from [eqn. (1)]:

$$\log K_w = (E_H° - E_{OH}°)/k \tag{2}$$

The value obtained for $K_w$ in this way was used to calculate $[H^+]$ in all solutions at all $C_B$. $E_j$ was found to be negligibly small for all concentrations of $[H^+]$ or $[OH^-]$ used in our titrations; the slopes of the plots of $E_H° + E_j$ and $E_{OH}° + E_j$ were found to be zero (see Fig. 1). pOH thus was calculated from the simplified equation

$$pOH = -\log[OH^-] = (E - E°)/k \tag{3}$$

*III. Electrodes.* The Ag/AgCl electrode was prepared by a method slightly modified from that of Brown.[15]

The hydrogen electrode was prepared according to Bates.[16] Commercially avaiable hydrogen was purified by passing it through (i) a platinum catalyst to remove traces of oxygen, (ii) a 10 % $H_2SO_4$ solution, (iii) a 10 % NaOH solution, (iv) two wash bottles containing 3 M NaCl, and (v) a glass spiral of 1 m length. Vessels (ii) − (v) were all thermostated at 40°C. In this way it was found possible to ensure that (a) the hydrogen gas did not cause temperature changes in the titration vessel, (b) there were no changes in concentration due to evaporation of solvent with the hydrogen gas.

New Ag/AgCl and hydrogen electrodes were prepared for each titration. The stabilizing time for a fresh electrode system was 2 − 3 h.

The discharge electrode was made of platinum. It had an area of *ca* 4 cm² and was covered with platinum black by electrolysis in aqueous $K_4PtCl_6$. The anode was a silver plate heavily coated with AgCl and immersed in 3 M NaCl.

*IV. Chemicals. Sodium butyrate* was prepared by neutralization of hot butyric acid (Fluka *puriss.* grade) with 1 M NaOH (Merck p.a. grade). The salt was dried in a vacuum oven at 110°C for about a week. The molecular weight was checked by titration with perchloric acid in glacial acetic acid and was found to differ less than 0.25 % from the theoretical value. *Sodium chloride,* Merck *p.a.* was dried in a vacuum oven at 110°C for a week before use. The *water* was distilled, passed through an ion exchange column and then redistilled. Its conductivity was about 0.5 $\mu$S cm⁻¹. The *solutions* were prepared in volumetric flasks previously calibrated at 40°C.

## TREATMENT OF EXPERIMENTAL DATA

Since the electrode system is calibrated with a known excess of $OH^-$ ions, one may calculate $E_{OH}°$, $[OH^-]$, and $C_H$ directly from the experimental emf values and hydroxide ion additions. To calculate $[H^+]$, the value of $K_w$ should be known. This cannot be determined in each solution, since the limited solubility of butyric acid does not allow a determination of $E_H°$. For this reason, it is preferred to write the equilibria studied in the following way

$$qB^- + pH_2O \rightleftharpoons H_pB_q^{(p-q)-} + pOH^- \tag{4}$$
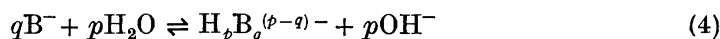
The stability constant for this reaction is given by

$$\beta_{pq}{}' = \frac{[H_pB_q][OH^-]^p}{[B^-]^q[H_2O]^p} = \frac{\beta_{pq}}{[H_2O]^p} = \frac{\beta_{pq}{}''K_w{}^p}{[H_2O]^p} \tag{5}$$

where $\beta_{pq}{}''$ is the stability constant if the reaction is written

$$pH_3O^+ + qB^- \rightleftharpoons H_pB_q{}^{(p-q)-} + H_2O \tag{6}$$
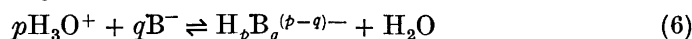
Following Sillén,[17] the quantity

$$Z_{exp} = (C_H - [H^+])/C_B \tag{7}$$

i.e. the number of hydrogen ions bound per carboxylate anion, is calculated. $[H^+]$ can be calculated from (1) if $K_w$ is known; since $C_H \gg [H^+]$ in all experiments a small error in $K_w$ in this case is of no consequence. Theoretically, $Z$ may also be calculated from, using the law of mass action,

$$Z_{calc} = (\sum p[OH^-]^{-p}[B^-]^q\beta_{pq})/C_B \tag{8}$$

the sum being taken over the $p,q$-values giving all the complexes occurring in the solution. $[B^-]$ may be calculated by solving the equation

$$C_B = [B^-] + \sum q[OH^-]^{-p}[B^-]^q\beta_{pq} \tag{9}$$

The error square sum minimization procedure LETAGROPVRID [18],[19] developed by Sillén and co-workers, has been used in the present work to find values of $p$, $q$, and $\beta_{pq}$ which give values for $Z_{calc}$ that agree within experimental error with $Z_{exp}$. In this procedure, guesses are made for possible values of $p$ and $q$, i.e. possible complexes, and the $\beta_{pq}$-values are then adjusted to give a minimum in the sum of the squares of the errors

$$U = \sum_{i=1}^{n} (Z_{calc,i} - Z_{exp,i} + \delta Z)^2 \tag{10}$$

where $n$ is number of experimental points and $\delta Z$ is a possible systematic error which may be different for each titration (for example, an error in $C_B$ or $C_H$). As an indication of the agreement between experiments and the suggested complex formation in the solutions, one may also use the standard deviation

$$\sigma(y) = \sqrt{U_0/(n-1)} \tag{11}$$

which is conveniently compared with the experimental error in $Z_{exp}$. However, the quantity $U_0$ used in this equation is not the $U$ value in (10), but the minimum in $U$ for the second-degree surface which is used to approximate the true $U$-function in the search for a minimum. If the found minimum is a good one, the difference between $U$ and $U_0$ will be small.

## RESULTS AND CALCULATIONS

*The ionic product of water at 40°C.* $K_w$ at 40°C was determined in two titrations of 0.05 M HCl in 3 M NaCl. The values of $\log K_w$ calculated from (2) were $-13.58$ and $-13.54$, respectively. The value $\log K_w = -13.56$ was used in subsequent calculations of $Z_{exp}$.
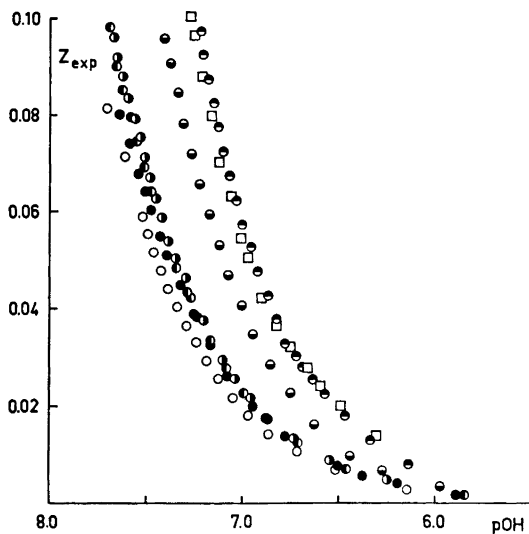
*Fig. 2.* The hydrolysis of sodium butyrate at different concentrations. The quantity $Z_{exp} = (C_H - [H^+])/C_B$ is plotted against $-\log [OH^-]$. Temperature $= 40°C$. Some points in Tables 1−7 have been left out. Concentrations of $C_B$: ○ 0.5 M; ● 1.0 M; ◐ 1.2 M; ◑ 1.5 M; ◔ 2.0 M; ◕ 2.5 M; □ 3.0 M.

*Table 1.* Titration of 0.500 M sodium butyrate at 40°C.

$C_B = 0.500$ M $\qquad\qquad\qquad$ $\delta Z = 0.0036 \pm 0.0004$
$C_H{}° = 0.04025$ M $\qquad\qquad$ $E_{OH}{}° = 349.4$ mV
$V = 30.00$ ml

| Amount of OH⁻ added mmol | $E$ mV | $p$OH | $Z_{exp}$ | $1000(Z_{calc} - Z_{exp})$ |
|---|---|---|---|---|
| 0 | − 128.7 | 7.695 | 0.0837 | − 2.3 |
| 0.1865 | − 123.7 | 7.614 | 0.0712 | − 2.2 |
| 0.3731 | − 118.1 | 7.524 | 0.0588 | − 1.5 |
| 0.4290 | − 116.1 | 7.492 | 0.0551 | − 1.4 |
| 0.4850 | − 113.9 | 7.457 | 0.0513 | − 1.4 |
| 0.5410 | − 111.6 | 7.420 | 0.0476 | − 1.3 |
| 0.5969 | − 109.2 | 7.381 | 0.0439 | − 1.2 |
| 0.6529 | − 106.5 | 7.338 | 0.0402 | − 1.1 |
| 0.7088 | − 103.7 | 7.293 | 0.0364 | − 0.7 |
| 0.7648 | − 100.5 | 7.241 | 0.0327 | − 0.5 |
| 0.8208 | − 97.0 | 7.185 | 0.0290 | − 0.2 |
| 0.8767 | − 93.0 | 7.120 | 0.0252 | 0.2 |
| 0.9327 | − 88.5 | 7.048 | 0.0215 | 0.5 |
| 0.9887 | − 83.1 | 6.961 | 0.0178 | 0.9 |
| 1.044 | − 76.5 | 6.855 | 0.0140 | 1.5 |
| 1.100 | − 67.8 | 6.715 | 0.0103 | 1.9 |
| 1.156 | − 55.4 | 6.515 | 0.0066 | 2.5 |
| 1.212 | − 32.2 | 6.142 | 0.0028 | 3.1 |
| 1.231 | − 16.1 | 5.883 | 0.0016 | 3.3 |

*Potentiometric titrations of sodium butyrate.* Seven different concentrations of sodium butyrate were titrated, starting from solutions to which were added HCl to give $Z_{exp}$ ca. 0.1. For each concentration, two titrations were performed. These generally gave values for $Z_{exp}$ which agreed within $\pm 0.005$ units in $Z$. As discussed in part I, this is the accuracy that may be expected considering the errors inherent in the experimental method. To decrease calculation time, one titration only for each concentration was used in LETA-GROPVRID. The additions, emf values, $Z_{exp}$, and $p$OH for these titratons are given in Tables $1-7$ and in Fig. 2. The constant $E_{OH}°$ for each titration is also given in the tables, and as a function of $C_{OH}°$ in Fig. 3. The slope of the straight line defined by these values is 13 mV/mol; at 25°C it is 10 mV/mol.[20]

*Calculations with LETAGROPVRID.* The version of LETAGROPVRID described in Ref. 19, adapted to an UNIVAC 1108 computer, was used to find the values of $p,q$, $\delta Z$, and $\beta_{pq}$ that were able to explain the experimental results within experimental error. The calculations are summarized in Table 8. The final result, giving a standard deviation in $Z$ of 0.0067, is that only butyric, acid and the complex $H_2B_5$ are formed. It should be emphasized, however that this does not rule out the existence of, for example, the complexes $H_1B_5$

*Table 2.* Titration of 1.000 M sodium butyrate at 40°C.

$C_B = 1.000$ M

$C_H° = 0.08013$ M

$V = 30.00$ ml

$\delta Z = 0.0046 \pm 0.0005$

$E_{OH}° = 354.9$ mV

| Amount of OH⁻ added mmol | $E$ mV | $p$OH | $Z_{exp}$ | $1000(Z_{calc} - Z_{exp})$ |
|---|---|---|---|---|
| 0 | $-119.2$ | 7.631 | 0.0801 | 3.4 |
| 0.1865 | $-116.2$ | 7.582 | 0.0739 | 1.4 |
| 0.3731 | $-113.4$ | 7.537 | 0.0677 | 0.7 |
| 0.4290 | $-112.0$ | 7.519 | 0.0658 | $-0.0$ |
| 0.4850 | $-111.3$ | 7.503 | 0.0639 | $-0.3$ |
| 0.5410 | $-110.2$ | 7.486 | 0.0621 | $-1.0$ |
| 0.5969 | $-109.1$ | 7.468 | 0.0602 | $-1.4$ |
| 0.6529 | $-108.0$ | 7.450 | 0.0583 | $-1.7$ |
| 0.7088 | $-106.9$ | 7.433 | 0.0565 | $-2.0$ |
| 0.7648 | $-105.8$ | 7.415 | 0.0546 | $-2.2$ |
| 0.8208 | $-104.6$ | 7.396 | 0.0527 | $-2.4$ |
| 0.8767 | $-103.4$ | 7.376 | 0.0509 | $-2.7$ |
| 1.063 | $-99.6$ | 7.315 | 0.0447 | $-2.4$ |
| 1.249 | $-95.2$ | 7.244 | 0.0384 | $-2.1$ |
| 1.436 | $-90.2$ | 7.164 | 0.0322 | $-1.5$ |
| 1.623 | $-84.1$ | 7.066 | 0.0260 | $-0.8$ |
| 1.809 | $-76.5$ | 6.943 | 0.0198 | 0.2 |
| 1.996 | $-66.1$ | 6.776 | 0.0136 | 1.3 |
| 2.182 | $-49.3$ | 6.506 | 0.0073 | 2.7 |
| 2.238 | $-41.3$ | 6.377 | 0.0055 | 3.1 |
| 2.294 | $-29.9$ | 6.193 | 0.0036 | 3.6 |
| 2.350 | $-10.4$ | 5.879 | 0.0018 | 4.0 |
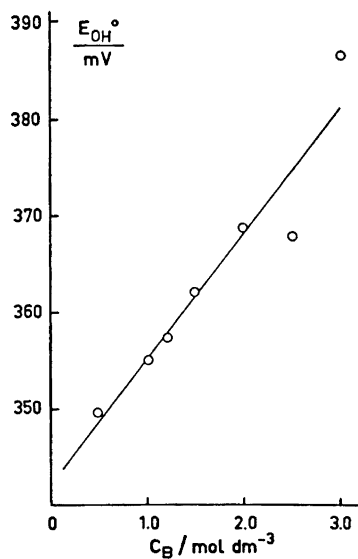
*Fig. 3.* The change in $E_{OH}°$ with $C_B$ for sodium butyrate at 40°C.

*Table 3.* Titration of 1.2 M sodium butyrate at 40°C.

$C_B = 1.200$ M          $\delta Z = 0.0022 \pm 0.0006$
$C_H° = 0.1141$ M        $E_{OH}° = 357.2$ mV
$V = 30.00$ ml

| Amount of OH⁻ added mmol | $E$ mV | $p$OH | $Z_{exp}$ | $1000(Z_{calc} - Z_{exp})$ |
|---|---|---|---|---|
| 0 | − 120.3 | 7.685 | 0.0950 | 6.9 |
| 0.1865 | − 118.1 | 7.650 | 0.0898 | 4.8 |
| 0.3731 | − 116.0 | 7.616 | 0.0847 | 3.2 |
| 0.5596 | − 113.9 | 7.582 | 0.0795 | 2.1 |
| 0.7462 | − 111.7 | 7.547 | 0.0743 | 1.1 |
| 0.9327 | − 109.4 | 7.510 | 0.0691 | 0.2 |
| 1.119 | − 107.0 | 7.471 | 0.0639 | − 0.5 |
| 1.305 | − 104.3 | 7.428 | 0.0587 | − 1.4 |
| 1.492 | − 101.6 | 7.384 | 0.0536 | − 1.8 |
| 1.678 | − 98.6 | 7.336 | 0.0484 | − 2.2 |
| 1.865 | − 95.3 | 7.283 | 0.0432 | − 2.5 |
| 2.052 | − 91.6 | 7.223 | 0.0380 | − 2.6 |
| 2.238 | − 87.5 | 7.157 | 0.0328 | − 2.5 |
| 2.425 | − 82.6 | 7. 78 | 0.0277 | − 2.5 |
| 2.611 | − 76.8 | 6.985 | 0.0225 | − 2.1 |
| 2.798 | − 69.5 | 6.868 | 0.0173 | − 1.5 |
| 2.984 | − 59.6 | 6.708 | 0.0122 | − 0.7 |
| 3.171 | − 44.1 | 6.459 | 0.0069 | 0.3 |
| 3.357 | − 6.2 | 5.849 | 0.0017 | 1.7 |

*Table 4.* Titration of 1.5 M sodium butyrate at 40°C.

$C_B = 1.500$ M  
$C_H{}^\circ = 0.1439$ M  
$V = 30.00$ ml

$\delta Z = -0.006 \pm 0.002$  
$E_{OH}{}^\circ = 361.8$ mV

| Amount of OH⁻ added mmol | $E$ mV | $p$OH | $Z_{exp}$ | $1000(Z_{calc} - Z_{exp})$ |
|---|---|---|---|---|
| 0 | −115.3 | 7.680 | 0.0959 | 15.7 |
| 0.1865 | −113.1 | 7.645 | 0.0917 | 11.9 |
| 0.3731 | −111.4 | 7.618 | 0.0876 | 10.1 |
| 0.5596 | −109.7 | 7.590 | 0.0834 | 8.5 |
| 0.7462 | −108.0 | 7.563 | 0.0793 | 7.1 |
| 0.9327 | −106.2 | 7.534 | 0.0752 | 5.5 |
| 1.119 | −104.5 | 7.506 | 0.0710 | 4.5 |
| 1.305 | −102.7 | 7.478 | 0.0669 | 3.4 |
| 1.492 | −100.8 | 7.447 | 0.0627 | 2.3 |
| 1.678 | −98.8 | 7.415 | 0.0586 | 1.2 |
| 1.865 | −96.6 | 7.379 | 0.0544 | −0.1 |
| 2.052 | −94.3 | 7.342 | 0.0503 | −1.3 |
| 2.238 | −91.1 | 7.291 | 0.0461 | −3.8 |
| 2.425 | −89.2 | 7.260 | 0.0420 | −3.4 |
| 2.611 | −86.3 | 7.214 | 0.0378 | −4.3 |
| 2.798 | −83.0 | 7.161 | 0.0337 | −5.4 |
| 2.984 | −79.4 | 7.103 | 0.0296 | −6.3 |
| 3.171 | −75.2 | 7.035 | 0.0254 | −7.0 |
| 3.357 | −70.4 | 6.958 | 0.0213 | −7.5 |
| 3.544 | −64.6 | 6.864 | 0.0171 | −7.6 |
| 3.731 | −56.2 | 6.729 | 0.0130 | −8.2 |
| 3.917 | −44.8 | 6.546 | 0.0088 | −8.0 |
| 4.104 | −26.7 | 6.254 | 0.0047 | −7.4 |

*Table 5.* Titration of 2.0 M sodium butyrate at 40°C.

$C_B = 2.000$ M  
$C_H{}^\circ = 0.2681$ M  
$V = 30.00$ ml

$\delta Z = 0.0068 \pm 0.0004$  
$E_{OH}{}^\circ = 368{,}5$ mV

| Amount of OH⁻ added mmol | $E$ mV | $p$OH | $Z_{exp}$ | $1000(Z_{calc} - Z_{calc})$ |
|---|---|---|---|---|
| 0 | −102.8 | 7.585 | 0.1340 | 0.5 |
| 0.3731 | −100.7 | 7.552 | 0.1278 | −0.8 |
| 0.7462 | −98.8 | 7.521 | 0.1216 | −1.2 |
| 1.119 | −96.9 | 7.491 | 0.1154 | −1.4 |
| 1.492 | −95.1 | 7.462 | 0.1091 | −1.0 |
| 1.865 | −93.2 | 7.431 | 0.1029 | −0.9 |
| 2.238 | −91.2 | 7.399 | 0.0957 | −0.9 |
| 2.611 | −89.2 | 7.367 | 0.0905 | −0.7 |
| 2.984 | −87.1 | 7.333 | 0.0843 | −0.6 |
| 3.357 | −84.9 | 7.297 | 0.0780 | −0.4 |

*Table 5. Continued.*

| | | | | |
|---|---|---|---|---|
| 3.731 | − 82.5 | 7.259 | 0.0718 | − 0.5 |
| 4.104 | − 79.9 | 7.217 | 0.0656 | − 0.6 |
| 4.477 | − 77.1 | 7.172 | 0.0594 | − 0.8 |
| 4.850 | − 74.0 | 7.122 | 0.0532 | − 1.1 |
| 5.223 | − 70.6 | 7.067 | 0.0470 | − 1.2 |
| 5.596 | − 66.8 | 7.006 | 0.0407 | − 1.1 |
| 5.969 | − 62.4 | 6.935 | 0.0345 | − 1.0 |
| 6.342 | − 57.3 | 6.853 | 0.0283 | − 0.6 |
| 6.715 | − 51.0 | 6.752 | 0.0221 | 0.1 |
| 7.088 | − 43.0 | 6.623 | 0.0159 | 1.4 |
| 7.462 | − 31.7 | 6.441 | 0.0096 | 3.4 |
| 7.648 | − 20.8 | 6.266 | 0.0065 | 4.2 |
| 7.835 | − 2.5 | 5.971 | 0.0034 | 5.2 |

*Table 6.* Titration of 2.5 M sodium butyrate at 40°C.

$C_B = 2.500$ M $\qquad\qquad\qquad \delta Z = 0.019 \pm 0.002$
$C_H° = 0.4047$ M $\qquad\qquad\quad E_{OH}° = 367.7$ mV
$V = 30.00$ ml

| Amount of OH⁻ added mmol | $E$ mV | $p$OH | $Z_{exp}$ | $1000(Z_{calc} - Z_{exp})$ |
|---|---|---|---|---|
| 0 | − 92.2 | 7.402 | 0.1619 | − 26.9 |
| 0.3731 | − 91.0 | 7.383 | 0.1569 | − 25.8 |
| 0.7462 | − 90.5 | 7.375 | 0.1519 | − 22.5 |
| 1.119 | − 89.6 | 7.360 | 0.1469 | − 20.4 |
| 1.492 | − 88.8 | 7.347 | 0.1420 | − 18.0 |
| 1.865 | − 88.0 | 7.334 | 0.1370 | − 15.6 |
| 2.238 | − 87.3 | 7.323 | 0.1320 | − 12.8 |
| 2.611 | − 86.5 | 7.310 | 0.1270 | − 10.3 |
| 2.984 | − 85.6 | 7.296 | 0.1221 | − 8.2 |
| 3.357 | − 84.7 | 7.281 | 0.1171 | − 5.9 |
| 3.731 | − 83.7 | 7.265 | 0.1121 | − 3.9 |
| 4.104 | − 82.8 | 7.251 | 0.1071 | − 1.6 |
| 4.477 | − 81.8 | 7.235 | 0.1022 | 0.4 |
| 4.850 | − 80.7 | 7.217 | 0.0972 | 2.2 |
| 5.223 | − 79.5 | 7.198 | 0.0922 | 3.8 |
| 5.596 | − 78.1 | 7.175 | 0.0872 | 5.0 |
| 5.969 | − 76.7 | 7.153 | 0.0823 | 6.1 |
| 6.342 | − 75.0 | 7.125 | 0.0773 | 6.7 |
| 6.715 | − 73.3 | 7.098 | 0.0723 | 7.4 |
| 7.088 | − 71.3 | 7.066 | 0.0674 | 7.6 |
| 7.462 | − 69.3 | 7.033 | 0.0624 | 8.0 |
| 7.835 | − 67.0 | 6.996 | 0.0574 | 8.1 |
| 8.208 | − 64.7 | 6.959 | 0.0524 | 8.5 |
| 8.581 | − 62.2 | 6.919 | 0.0475 | 8.8 |
| 8.954 | − 59.4 | 6.874 | 0.0425 | 9.1 |
| 9.327 | − 56.2 | 6.823 | 0.0375 | 9.3 |
| 9.700 | − 52.7 | 6.766 | 0.0325 | 9.8 |
| 9.887 | − 50.1 | 6.724 | 0.0300 | 9.3 |
| 10.07 | − 47.2 | 6.678 | 0.0276 | 8.8 |
| 10.26 | − 44.1 | 6.628 | 0.0251 | 8.7 |
| 10.44 | − 40.6 | 6.571 | 0.0226 | 8.6 |
| 10.82 | − 34.1 | 6.467 | 0.0176 | 10.0 |
| 11.19 | − 25.8 | 6.333 | 0.0126 | 11.8 |
| 11.56 | − 13.8 | 6.140 | 0.0077 | 14.1 |

*Table 7.* Titration of 3.0 M sodium butyrate at 40 °C.

$C_B$ = 3.000 M  
$C_H{}^\circ$ = 0.4877 M  
$V$ = 30.00 ml

$\delta Z = -0.0060 \pm 0.0009$  
$E_{OH}{}^\circ = 386.4$ mV

| Amount of OH⁻ added mmol | $E$ mV | $p$OH | $Z_{exp}$ | $1000(Z_{calc} - Z_{exp})$ |
|---|---|---|---|---|
| 0 | − 81.4 | 7.529 | 0.1626 | − 1.2 |
| 0.3731 | − 79.8 | 7.503 | 0.1584 | − 2.5 |
| 0.7462 | − 78.5 | 7.482 | 0.1543 | − 2.7 |
| 1.119 | − 77.3 | 7.463 | 0.1501 | − 2.6 |
| 1.492 | − 76.3 | 7.447 | 0.1460 | − 1.8 |
| 1.865 | − 75.2 | 7.429 | 0.1418 | − 1.3 |
| 2.238 | − 74.2 | 7.413 | 0.1377 | − 0.5 |
| 2.611 | − 73.2 | 7.397 | 0.1335 | 0.4 |
| 2.984 | − 72.3 | 7.383 | 0.1294 | 1.5 |
| 3.357 | − 71.3 | 7.367 | 0.1252 | 2.4 |
| 3.731 | − 70.2 | 7.349 | 0.1211 | 2.9 |
| 4.104 | − 69.3 | 7.334 | 0.1170 | 4.1 |
| 4.477 | − 68.2 | 7.317 | 0.1128 | 4.7 |
| 4.850 | − 66.9 | 7.296 | 0.1087 | 4.6 |
| 5.223 | − 65.8 | 7.278 | 0.1045 | 5.3 |
| 5.596 | − 64.6 | 7.259 | 0.1004 | 5.6 |
| 5.969 | − 63.5 | 7.241 | 0.0962 | 6.4 |
| 6.342 | − 62.3 | 7.222 | 0.0921 | 6.7 |
| 6.715 | − 60.9 | 7.199 | 0.0879 | 6.6 |
| 7.088 | − 59.5 | 7.177 | 0.0838 | 6.5 |
| 7.462 | − 58.1 | 7.154 | 0.0796 | 6.5 |
| 7.835 | − 56.8 | 7.133 | 0.0755 | 6.8 |
| 8.208 | − 55.2 | 7.107 | 0.0714 | 6.3 |
| 8.581 | − 53.6 | 7.082 | 0.0672 | 6.0 |
| 8.954 | − 51.9 | 7.054 | 0.0631 | 5.4 |
| 9.327 | − 50.0 | 7.024 | 0.0589 | 4.6 |
| 9.700 | − 48.1 | 6.993 | 0.0548 | 3.8 |
| 10.07 | − 46.0 | 6.959 | 0.0506 | 2.8 |
| 10.44 | − 43.9 | 6.926 | 0.0465 | 2.0 |
| 10.82 | − 41.5 | 6.887 | 0.0423 | 0.9 |
| 11.19 | − 38.9 | 6.845 | 0.0382 | − 0.4 |
| 11.37 | − 37.1 | 6.816 | 0.0361 | − 1.8 |
| 11.56 | − 35.1 | 6.784 | 0.0340 | − 3.3 |
| 11.75 | − 33.1 | 6.752 | 0.0320 | − 4.7 |
| 11.93 | − 30.8 | 6.715 | 0.0299 | − 6.2 |
| 12.12 | − 28.4 | 6.676 | 0.0278 | − 7.5 |
| 12.31 | − 25.7 | 6.633 | 0.0257 | − 8.8 |
| 12.49 | − 22.9 | 6.588 | 0.0237 | − 10.0 |
| 12.68 | − 19.8 | 6.538 | 0.0216 | − 10.9 |
| 12.87 | − 16.2 | 6.480 | 0.0195 | − 11.8 |
| 13.05 | − 12.1 | 6.414 | 0.0175 | − 12.6 |
| 13.43 | − 4.7 | 6.295 | 0.0133 | − 12.1 |

*Table 8.* Calculations with LETAGROPVRID on the hydrolysis of sodium butyrate at 40°C.

| p,q | Stability constants $(-\log \beta_{pq})$ of tried complexes $(p,q)$ | | | | | | |
|---|---|---|---|---|---|---|---|
| | I | II | III | IV | V[a] | VI[b] | VII[b] |
| 1,1 | 8.84 ± 0.07 | 8.84 ± 0.07 | 8.725 ± 0.002 | 8.725 ± 0.002 | 8.725 ± 0.002 | 8.749 ± 0.058 | 8.630 ± 0.021 |
| 1,2 | rej[c] | | | | rej. | rej. | rej. |
| 1,3 | | rej. | rej. | | | | |
| 2,3 | | rej. | rej. | rej. | | | |
| 3,3 | | | | rej. | | | |
| 1,4 | 9.68 ± 0.25 | 9.68 ± 0.25 | rej. rej. | | rej. | rej. | |
| 2,4 | 16.95 ± 0.06 | 16.95 ± 0.06 | | | rej. | 17.020 ± 0.082 | |
| 3,4 | rej. | | | | rej. | rej. | |
| 1,5 | | rej. | rej. | rej. | rej. | | rej. |
| 2,5 | | | 17.257 ± 0.036 | 17.257 ± 0.036 | 17.257 ± 0.036 | | 17.170 ± 0.029 |
| 3,5 | | | | rej. | rej. | | rej. |
| 4,5 | | | | rej. | | | |
| 1,6 | | rej. | rej. | | | | |
| 2,6 | | | | | rej. | | |
| 1,7 | | | rej. | | | | |
| 2,7 | | | rej. | | | | |
| U | 0.023444 | 0.023444 | 0.010936 | 0.010936 | 0.010936 | 0.009113 | 0.007763 |
| σ(y) | 0.0114 | 0.0114 | 0.00777 | 0.00777 | 0.00777 | 0.00726 | 0.00670 |

[a] A systematic error $Z = 0.021 \pm 0.002$ was introduced for the Z-values in titration 6. [b] Systematic errors for all titrations were introduced; values for run VII are given in Tables 1—7. [c] rej. = rejected. The complex was tried together with the complexes for which stability constants are given in the same column, but the standard deviation came out more than twice as large as the stability constant.

or $H_3B_5$. Indeed, introduction of $H_1B_5$ together with HB and $H_2B_5$ gives a slightly lower value of $U$, but the uncertainty in the stability constant for $H_1B_5$ is too large to merit a value for this constant bo be given in Table 2. Introduction of $H_3B_5$ also yields a slightly lower value of $U$ but values for the stability constants have not been given for the same reason as above.

The standard deviation is of the same order of magnitude as the estimated experimental error in $Z_{exp}$. The difference $Z_{calc} - Z_{exp}$ is given for each point in Tables 1 — 7. It is seen that most of the large differences fall in $p$OH ranges where $Z_{exp}$ is very low, *i.e.*, close to the equivalence point. Hence, the value of $\sigma(y) = 0.0067$ should be considered quite satisfactory. The systematic errors in $Z$ for each titration are of the same magnitude as the estimated experimental uncertainties with the exception of titration 6 at $C_B = 2.5$ M, where $\delta Z = 0.019$. It is seen from Fig. 2 that this curve seems to be slightly higher than all the others.

*The variation in* $E_{OH}^{\circ}$ *with* $C_B$. In the previous investigations of carboxylates it was found that the constant $E_{OH}^{\circ}$ varies linearly with $C_B$. This is so also in the present case, as is seen from Fig. 3. The reasons for this variation

have been discussed in Refs. 21 and 22. It is only noted here that the un-certainties in the calculations due to the shift in the energy of $OH^-$ ions in the standard state which seems to be reflected in the variation in $E_{OH}^{\circ}$ apply to these calculations in the same way as those reported before.

## DISCUSSION

The final result is compared to results at 25°C in Table 9. The following differences are noted

(i) no improvement in the fit of theoretical data to the experiments can be obtained by introducing dimers at 40°C;

(ii) The complex found at 40°C is larger than any of those found at 25°C.

Both results indicate an increased association at 40°C. There does not seem to be any specific chemical bonds (or hydrogen bonds) holding the aggregates together, since the aggregation numbers are not very definitive and probably should be considered as mean aggregation numbers. This conclusion is supported by the following attempt to estimate the enthalpy of aggregate formation.

It was assumed that only HB and $H_2B_4$ or HB and $H_2B_5$ are formed at 25°C and the resulting stability constants were calculated with LETAGROP-VRID. These results are compared to the results from similar calculations for the data at 40°C in Table 9 (rows B and C). It is seen, that these assumptions decrease the agreement between the values predicted by the assumed asso-ciation equilibria and the experiments at 25°C. However, the standard deviation $\sigma(y)$ is still smaller than at 40°C and close to the experimental error.

For this reason, it seems feasible to estimate the enthalpy of formation of HB and $H_2B_5$ using van't Hoff's equation

$$\ln(\beta'/\beta'') = (\Delta H^{\ominus}/R)(1/T'' - 1/T') \qquad (12)$$

and the values of $\beta_{1,1}$ and $\beta_{2,5}$ found at 25°C and 40°C, respectively. The stand-ard Gibbs' energy of formation is calculated from

*Table 9.* A comparison of the complex formation of sodium butyrate at 25°C and 40°C.

| Temp. °C | $-\log \beta_{1,1}$ | $-\log \beta_{1,2}$ | $-\log \beta_{1,4}$ | $-\log \beta_{2,4}$ | $-\log \beta_{1,5}$ | $-\log \beta_{2,5}$ | $U$ | $\sigma(y)$ |
|---|---|---|---|---|---|---|---|---|
| 40 | 8.630 ± 0.021 | | | | | 17.170 ± 0.029 | 0.0078 | 0.0067 |
| 25 A | 9.216 ± 0.005 | 9.89 ± 0.06 | 11.03 max[a] 10.76 | 19.17 ± 0.25 | 27.89 ± 0.17 | | 0.0013 | 0.0025 |
| 25 B | 9.200 ± 0.005 | | | 18.619 0.035 | | | 0.0031 | 0.0038 |
| 25 C | 9.187 ± 0.005 | | | | | −18.843 ± 0.048 | 0.0046 | 0.0047 |

[a] max.; The standard deviation is larger than about 30 % of the stability constant, and a maximum value for the stability constant is given instead of a standard deviation.

$$\Delta G^{\ominus} = -RT \ln \beta \qquad (13)$$

and the following results then are obtained:

|  | $\Delta G^{\ominus}{}_{298}$ kJ/mol | $\Delta H^{\ominus}{}_{298}$ kJ/mol |  |
|---|---|---|---|
| $B^-(aq) + H_2O \rightarrow OH^-(aq) + HB(aq)$ | 52.51 | 56.61 | (14) |
| $5\ B^-(aq) + 2\ H_2O \rightarrow H_2B_5{}^{3-}(aq) + 2OH^-(aq)$ | 107.5 | 189.0 | (15) |
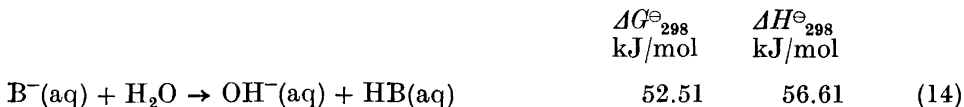
The standard Gibbs' energy and enthalpy of formation with hydrogen ions was obtained by adding the energies for the association [23]

|  | $\Delta G^{\ominus}{}_{298}$ kJ/mol | $\Delta H^{\ominus}{}_{298}$ kJ/mol |
|---|---|---|
| $H^+(aq) + OH^-(aq) \rightarrow H_2O$ | $-79.78$ | $-58.41$ |

once to (14) and twice to (15). This gives

|  | $\Delta G^{\ominus}$ kJ/mol | $\Delta H^{\ominus}$ kJ/mol |  |
|---|---|---|---|
| $B^-(aq) + H^+(aq) \rightarrow HB(aq)$ | $-27.27$ | $-1.79$ | (14a) |
| $5B^-(aq) + 2H^+(aq) \rightarrow H_2B_5{}^{3-}(aq)$ | $-52.08$ | 95.14 | (15a) |

It is seen that the process of aggregation is endothermic and that the aggregation of the anions probably causes the large change in enthalpy, since the enthalpy for (14a) is very small. Subtracting (14a) twice from (15a) gives

|  | $\Delta G^{\ominus}$ kJ mol$^{-1}$ | $\Delta H^{\ominus}$ kJ mol$^{-1}$ | $\Delta S^{\ominus}$ kJ mol$^{-1}$K$^{-1}$ |  |
|---|---|---|---|---|
| $3B^-(aq) + 2HB^-(aq) \rightarrow H_2B_5{}^{3-}(aq)$ | 2.46 | 98.72 | 322.8 | (16) |
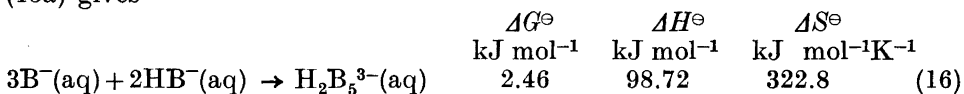
The standard Gibbs energy of formation now becomes positive, $i.e.$ the strong tendency of the carboxylate groups to bind hydrogen ions in the cause of the negative $\Delta G^{\ominus}$ in eqn. 15a. This is a strong case for assuming that hydrogen bonding cannot be an important part of the forces that hold the aggregates together. They are formed only at very high concentrations even in acid solutions. Moreover, there is evidence that they do exist also in weakly alkaline solutions (pH > 9).[2,24]

A very rough estimate of the different contributions to $\Delta G^{\ominus}$ may be made in the following way:

$\Delta G^{\ominus}$ is divided into three parts:

$$\Delta G^{\ominus} = \Delta G^{\ominus}{}_{el.stat} + \Delta G^{\ominus}{}_{aggr.entr.} + \Delta G^{\ominus}{}_{sol}$$

(a) $\Delta G^{\ominus}{}_{el.stat}$ is the contribution to $\Delta G^{\ominus}$ from the energy required to bring the three charges close together in $H_2B_5{}^{3-}$. Assuming that the aggregate is spherical with a diameter $r$ equal to the length of the butyrate chain $+0.2$ nm and that this sphere bears the charge $q = 3\ e^-$ (that is, ion pair formation is neglected), the work of charging the sphere may be calculated from

$$W_{\text{charging}} = \int_0^{3\,e^-} \frac{q}{\varepsilon_r r} \; dq; \; \Delta G^{\ominus}{}_{\text{el.stat.}} = N_A W_{\text{charging}} \qquad (17)$$

where $\varepsilon_r$ is the dielectric constant of water at $25°$ ($= 78.30$).[25] This gives

$$\Delta G^{\ominus}{}_{\text{el.stat}} = 35.73 \text{ kJ mol}^{-1} \qquad (18)$$

(b) $\Delta G_{\text{aggr.entr.}}$ is the contribution' to $\Delta G^{\ominus}$ from the decrease in entropy due to the aggregation of five molecules into one. This may be calculated from

$$\Delta G^{\ominus}{}_{\text{aggr.entr.}} = -T\Delta S_{\text{aggr.entr.}} = -RT \ln \frac{x_{2,5}}{x_m} =$$
$$= -RT \ln 0.2 = 2.89 \text{ kJ mol}^{-1}$$

since the mol fraction of aggregates, $x_{2,5}$ is $1/5$ of the mol fraction of the monomers forming the aggregate.

(c) If it is assumed that no other forces bind the hydrophilic parts of the molecule together, the residual change in Gibbs' energy is due to attraction forces between the hydrocarbon chains and/or rearrangements in the solute-solvent interaction and is given by

$$\Delta G^{\ominus}{}_{\text{sol}} = \Delta G^{\ominus} - \Delta G^{\ominus}{}_{\text{el.stat}} - \Delta G^{\ominus}{}_{\text{aggr.entr.}}$$
$$= -36.57 \text{ kJ/mol}$$

This negative contribution thus according to the admittedly very crude calculation given above is the cause of the formation of aggregates. The enthalpy change is too large to be explained by the energy required to force the charges together only. It seems that one may at least draw the conclusion, that there is a large increase in entropy due to an increased mobility of the hydrocarbon chains and/or rearrangements in the water structure on association which is the ultimate cause of aggregation. This is in agreement with other investigations,[3-8] of which particular importance should be given to the non-thermodynamic confirmation given by recent NMR investigations.[24] However, it is not possible to assert whether the entropy change is due to a rearrangement of solvent molecules around the changed end-groups or due to hydrophobic hydration. There is some evidence that the first few $CH_2$ groups close to the polar group in a surfactant are strongly affected by the solvation water of surrounding the polar end group.[26,27] Very recently, Birch and Hall [28] have pointed out that it is not possible to assert with certainty whether the enthalpies of dilution of surfactants below the c.m.c. can be explained by the Debye-Hückel theory for monomeric $1-1$ electrolytes or by the formation of dimers. The main difficulty according to these authors is insufficient knowledge of activity coefficients. It seems that the investigation reported here shows that it is possible to circumvent these difficulties by working at high constant ionic strengths.

REFERENCES

1. Stenius, P. and Zilliacus, C.-H. *Acta Chem. Scand.* **25** (1971) 2232 (Part I).
2. Stenius, P. *Acta Chem. Scand.* **27** (1973) 3435.
3. Mukerjee, P. *Advan. Colloid Interface Sci.* **1** (1967) 241.
4. Franks, F. and Smith, H. T. *J. Phys. Chem.* **68** (1964) 3581.
5. Franks, F., Quickenden, M. J., Ravenhill, J. R. and Smith, H. T. *J. Phys. Chem.* **72** (1968). 2268.
6. Stead, J. A. and Taylor, H. *Australas. J. Pharm.* **51** (1970) 51.
7. Proust, J. and Ter-Miniassan-Saraga, L. *Compt. Rend.* **270** (1970) 1354.
8. Danielsson, I. and Stenius, P. *J. Colloid Interface Sci.* **37** (1971) 264.
9. Biedermann, G. and Sillén, L. G. *Arkiv Kemi* **5** (1952) 425.
10. Hietanen, S. and Sillén, L. G. *Acta Chem. Scand.* **13** (1959) 533.
11. Forsling, W., Hietanen, S. and Sillén, L. G. *Acta Chem. Scand.* **6** (1952) 901.
12. Danielsson, I. *Kemian Teollisuus* **23** (1966) 1081.
13. Gran, G. *Analyst* **77** (1952) 61.
14. Ingri, N., Lagerström, G., Frydman, M. and Sillén, L. G. *Acta Chem. Scand.* **11** (1957) 1034.
15. Brown, R. *J. Am. Chem. Soc.* **56** (1934) 646.
16. Bates, R. *Determination of pH*, Wiley, New York 1965, p. 241.
17. Sillén, L. G. *Acta Chem. Scand.* **10** (1956) 186.
18. Sillén, L. G. *Acta Chem. Scand.* **18** (1964) 1085.
19. Sillén, L. G. and Warnqvist, B. *Arkiv Kemi* **31** (1969) 315, 341.
20. Danielsson, I. *Chem. Phys. Appl. Surface Active Subst., Proc. Int. Congr., 4th 1964*, Gordon and Breach, New York 1967, Vol. 2, p. 555.
21. Ginstrup, O. *Acta Chem. Scand.* **24** (1970) 875.
22. Danielsson, I. and Stenius, P. *Trans. Roy. Inst. Technol. Stockholm; Pure Appl. Chem*,. **34** (1972) 81.
23. Arnek, R. *Arkiv Kemi* **32** (1970) 66.
24. Ödberg, L., Svens, B. and Danielsson, I. *J. Colloid Interface Sci.* **41** (1972) 298.
25. Malmberg, C. G. and Maryott, A. A. *J. Res. Natl. Bur. Std.* **56** (1956) 1.
26. Corkill, J. M., Goodman, J. F., Robson, P. and Tate, J. R. *Trans. Faraday Soc.* **62** (1966) 987.
27. Corkill, J. M., Goodman, J. F. and Tate, J. R. *Trans. Faraday Soc.* **60** (1964) 996.
28. Birch, B. J. and Hall, D. G. *J. Chem. Soc. Faraday Trans. 1* **1972** 2350.

# The Crystal Structure of a Basic Hafnium Chromate

MARGARETA HANSSON and WANDA MARK

*Department of Inorganic Chemistry, Chalmers University of Technology and The University of Göteborg, P.O. Box, S-402 20 Göteborg 5, Sweden*

Hafnium chromate of approximate formula $Hf_4(OH)_8(CrO_4)_4.H_2O$ crystallizes in space group *Pnnm* with $a = 11.543$, $b = 13.587$, $c = 6.847$ Å and $Z = 2$. It is isotypic with a corresponding zirconium compound with the formula $Zr_4(OH)_6(CrO_4)_5.H_2O$.

The crystal structure of the hafnium compound has been determined from X-ray single crystal data by means of three dimensional Fourier syntheses. Least squares refinement of the structural parameters based on 818 independent reflexions yielded a final $R$ value of 0.061.

The hafnium atoms are joined by double oxygen bridges to form planar infinite chains with the composition $[Hf(OH)_2]_n{}^{2n+}$. The chains are connected by chromate groups to form a three-dimensional structure. Seven oxygen atoms are coordinated to each hafnium atom in a pentagonal bipyramidal arrangement. The Hf—O distances range from 2.01 to 2.25 Å.

$S$ome investigations have been performed in order to elucidate the differences between zirconium and hafnium with respect to their chemical behaviour and atomic sizes. The hydrolysis systems $ZrO_2 - SO_3 - H_2O$ and $HfO_2 - SO_3 - H_2O$ have been investigated by McWhan, Lundgren and Hansson [1,2] and the two systems show discrepancies as regards the conditions under which the different phases are formed.

In the hydrolysis system $ZrO_2 - CrO_3 - H_2O$, three principally different crystalline phases are obtained.[3] In attempts to prepare the corresponding phases in the $HfO_2 - CrO_3 - H_2O$ system, only one crystalline phase was found, namely $4HfO_2.4.3CrO_3.5.4H_2O$, the corresponding phase in the zirconium system having the composition $4ZrO_2.4.9CrO_3.3.7H_2O$.[3] Apart from the different compositions of the products, crystallization is more readily brought about in the zirconium system. The crystalline hafnium chromate is formed in very low yield and the crystals are small.

## EXPERIMENTAL

The hafnium chromate investigated was prepared by hydrothermal hydrolysis of an amorphous hafnium chromate in a 10 M chromium trioxide solution at 165°C.

Due to the small amount obtained, the hafnium and chromium contents were determined by electron probe microanalysis. The results indicate an approximate formula of $Hf_4(OH)_8(CrO_4)_4.H_2O$, which can also be written $4HfO_2.4CrO_3.5H_2O$. By refining the structure with three-dimensional X-ray data, it was possible to establish the composition $4HfO_2.4.3CrO_3.5.4H_2O$. The experimental and calculated hafnium and chromium contents are:

|  | % Hf | % Cr |
|---|---|---|
| Experimental | 53.9 | 16.2 |
| Calculated for: |  |  |
| $4HfO_2.4CrO_3.5H_2O$ | 53.6 | 15.6 |
| $4HfO_2.4CrO_3.6H_2O$ | 52.9 | 15.4 |
| $4HfO_2.4.3CrO_3.5.4H_2O$ | 52.2 | 16.3 |

## PROCESSING OF DATA

From Guinier and Weissenberg photographs it was evident that the hafnium chromate structure is very nearly isomorphous with that of the corresponding zirconium chromate.

The crystals are red truncated double pyramids, that used for the structure determination having a basal plane of $0.03 \times 0.05$ mm$^2$ ($y$ and $z$ directions) and a height of 0.05 mm.

Due to the positions of the hafnium atoms in the structure, reflexions with $k = 2n$ are very strong while those with $k = 2n + 1$ are very weak. The crystal was therefore mounted along the $y$ axis in a single crystal diffractometer (Philips PAILRED) and reflexions from the reciprocal layers $h0l - h14l$ and $\bar{h}0l - \bar{h}14l$ with $k$ even were registered with Mo$K\alpha$ radiation. The $\omega$ scanning speed was 1°/min, and the total time for registration of one reflexion was 3 min for the lower levels and 6 min for the higher levels. A total of 1196 reflexions were collected with $k$ even. The intensities of the reflexions with $k$ odd are on an average one tenth of those with $k$ even. In order to be able to estimate these weak reflexions with a better accuracy, they were registered with multiple film Weissenberg techniques and Cu$K\alpha$ radiation. Each layer ($h1l - h9l$, $k = 2n + 1$) was exposed for $2 - 3$ weeks and the intensities of the 311 independent reflexions thus obtained were estimated visually by comparison with an intensity scale.

## UNIT CELL DIMENSIONS

The crystals have orthorhombic symmetry and the conditions for reflexion are:

$h0l$ with $h + l = 2n$
$0kl$ with $k + l = 2n$

The conditions are in accordance with space groups No. 34, $Pnn2$, and No. 58, $Pnnm$.

Accurate cell dimensions were obtained by least squares refinement of the cell parameters using the program POWDER.[4] For this purpose 41 lines were indexed on a Guinier powder photograph taken with Cu$K\alpha_1$ radiation, using lead nitrate as an internal standard ($a_{Pb(NO_3)_2} = 7.8566$ Å at 21°C).[5] The cell dimensions and their standard deviations were found to be (for com-

*Table 1.* Guinier powder data. $\lambda_{CuK\alpha_1} = 1.54050$ Å.

| $h\,k\,l$ | $10^5 \sin^2 \theta$ obs | $10^5 \sin^2 \theta$ calc | $d$ Å calc | $I$ obs |
|---|---|---|---|---|
| 1 0 1 | 1715 | 1711 | 5.8892 | st |
| 1 2 0 | 1734 | 1731 | 5.8549 | st |
| 2 0 0 | 1785 | 1781 | 5.7715 | st |
| 1 3 0 | 3346 | 3338 | 4.2162 | vvw |
| 3 1 0 | 4341 | 4329 | 3.7021 | w |
| 2 2 1 | | 4332 | 3.7008 | |
| 2 3 0 | 4683 | 4673 | 3.5630 | vw |
| 0 0 2 | 5069 | 5062 | 3.4237 | vst |
| 0 4 0 | 5146 | 5142 | 3.3968 | vst |
| 3 0 1 | 5274 | 5273 | 3.3544 | vst |
| 3 2 0 | 5299 | 5293 | 3.3480 | vst |
| 1 2 2 | 6801 | 6792 | 2.9555 | vvw |
| 2 0 2 | 6851 | 6843 | 2.9446 | m |
| 1 4 1 | | 6852 | 2.9425 | |
| 2 4 0 | 6934 | 6923 | 2.9275 | st |
| 4 2 1 | 9682 | 9675 | 2.4763 | st |
| 0 4 2 | 10195 | 10203 | 2.4114 | vw |
| 3 2 2 | 10359 | 10354 | 2.3937 | vw |
| 3 4 1 | 10412 | 10415 | 2.3868 | vw |
| 1 0 3 | 11840 | 11834 | 2.2391 | w |
| 2 4 2 | 11990 | 11984 | 2.2250 | vw |
| 1 6 0 | 12035 | 12014 | 2.2222 | w |
| 4 4 0 | 12276 | 12266 | 2.1993 | vw |
| 5 2 0 | 12433 | 12417 | 2.1859 | m |
| 2 6 1 | 14619 | 14615 | 2.0148 | w |
| 3 0 3 | 15420 | 15396 | 1.9631 | w |
| 3 6 0 | 15587 | 15576 | 1.9516 | m |
| 1 4 3 | 16969 | 16975 | 1.8695 | w |
| 1 6 2 | 17077 | 17076 | 1.8640 | vvw |
| 5 2 2 | 17484 | 17479 | 1.8424 | w |
| 6 2 1 | 18581 | 18580 | 1.7869 | m |
| 4 2 3 | 19784 | 19798 | 1.7311 | w |
| 4 6 1 | 19944 | 19959 | 1.7241 | w |
| 0 0 4 | 20250 | 20246 | 1.7118 | vw |
| 0 8 0 | 20593 | 20567 | 1.6984 | w |
| 3 6 2 | | 20638 | 1.6955 | |
| 1 2 4 | 22013 | 21977 | 1.6431 | vw |
| 2 0 4 | | 22027 | 1.6412 | |
| 1 8 1 | 22273 | 22278 | 1.6319 | vvw |
| 2 8 0 | 22351 | 22348 | 1.6293 | w |
| 5 6 0 | 22727 | 22701 | 1.6166 | w |
| 7 0 1 | 23090 | 23083 | 1.6032 | m |
| 7 2 0 | | 23103 | 1.6025 | |
| 2 6 3 | 24740 | 24738 | 1.5486 | vvw |
| 3 2 4 | 25571 | 25539 | 1.5242 | vw |
| 0 8 2 | | 25629 | 1.5215 | |
| 2 4 4 | 27176 | 27169 | 1.4777 | vvw |
| 5 6 2 | 27741 | 27762 | 1.4619 | vvw |
| 6 2 3 | 28716 | 28703 | 1.4377 | vw |
| 6 6 1 | 28880 | 28864 | 1.4337 | vw |

parison those of the corresponding zirconium compound are given within brackets):

$$a = 11.543 \pm 0.002 \text{ Å} \quad (11.629)$$

$$b = 13.587 \pm 0.002 \text{ Å} \quad (13.653)$$

$$c = \phantom{0}6.847 \pm 0.001 \text{ Å} \quad (6.882)$$

$$V = 1073.9 \pm 0.3 \quad \text{Å}^3 \quad (1092.7)$$

The observed and calculated values of $\sin^2\theta$ less than 0.30 are listed in Table 1, together with the calculated inter-planar spacings. As the experimental density could not be determined, the number of formula units per unit cell was assumed to be $Z = 2$ as in the corresponding zirconium chromate structure. On the basis of this assumption, the calculated density is 4.18 g/cm$^3$, which seems reasonable.

## STRUCTURE DETERMINATION AND REFINEMENT

The two sets of data were corrected for Lorentz, polarization and absorption effects with the programs DATAP1 and DATAP2,[6] respectively. To bring the different data sets on to the same scale, a structure factor calculation was performed, which was based on the hafnium atoms, assuming that the positional parameters were the same as in $4ZrO_2.4.9CrO_3.3.7H_2O$. Successive three dimensional Fourier syntheses were calculated (program DRF [6]) to obtain the positions of the chromium and oxygen atoms. In the calculations, the space group $Pnnm$ was used and the positions of the atoms labelled $Cr_1$, $Cr_2$, $O_1 - O_{10}$, and $O_{12}$ could be determined without any ambiguity. All atoms occupy the special position $4(g)$ except $O_1$ and $O_2$ which are situated in the general position $8(h)$. This implies the composition $Hf_4(OH)_8(CrO_4)_4.2H_2O$ or $4HfO_2.4CrO_3$. $6H_2O$. The $O_{12}$ atoms correspond to the two water molecules of crystallization per formula unit. A Fourier synthesis, based on the refined atomic parameters, showed small excesses of electron density at very nearly the same positions as the $Cr_3$ atoms in the zirconium chromate structure. It was therefore considered likely that the hafnium compound contained a small additional amount of chromate ($Cr_3$). These chromate groups must be statistically distributed between four equivalent positions, as will be seen later. As the additional chromate oxygen atoms ($O_{11}$) could not be located from the Fourier syntheses, they were assumed to occupy the same positions as in the zirconium structure. Refinement of the parameters was performed with the program BLOCK,[6] different occupation numbers being assigned to $Cr_3$. In the different refinements, the occupation number of $O_{11}$ was assigned the same value, $q$, as that of $Cr_3$. The occupation number for $O_{12}$, $(1 - q)$, (cf. later) was deduced from the positional relationship between $Cr_3$ and $O_{12}$. The best fit with the experimental data was obtained for an occupation number of 0.14 for $Cr_3$ and thus of 0.86 for $O_{12}$.

A few cycles of refinement with the least squares full matrix program LINUS [6] showed that secondary extinction effects were of little importance. The final cycles of refinement were performed with the program LALS.[6]

*Table 2.* Observed and calculated structure factors for $\sim Hf_4(OH)_8(CrO_4)_4 \cdot H_2O$.

```
H  0  0        H  0  11       9 125 -125      H  4  8        H  6  8        H  8  9
 2 513  457     1 105  111    13  84   89      0 237 -228     3 155  152     1 154  162
 6 150 -131     3 105  100                     2 141 -149     5 175  173     9  96 -101
 8 211 -187     9  95  -87     H  2  9         10 154  157     7 119  129
10 350 -335                    4 160 -165      12 129  136     9  94   88     H  8  10
12 289 -266     H  0  12       6 192 -196                                    0 132  152
14 104  -93     0 126  144     8  99  -99      H  4  9         H  6  9       2 122  115
20  87   82    10  95  -84                     1 148 -153     2  94   92    10 126 -101
22  78   90    12  80  -75     H  2 10         3 125 -129     4 153  160
                                3 146 -136     7  97   87     6 156  158     H  8  11
 H  0  1        H  0  13       5 118 -137      9 127  125     8 101   88     1 105  112
 1 448  432     1  94   84     7 111 -110     11 113  113
 3 478  455                                   13  86   80     H  6  10      H  10  0
 5  70   65     H  0  14       H  2 11                        3 118  126     3 214 -216
 7 359 -314     0  96   99     4 109 -113      H  4  10       5 133  143     5 405 -394
 9 270 -258                    6 131 -137      0 189 -187     7 110  103     7 285 -283
11 187 -184     H  2  0                        2 119 -122     9  94   63     9 105 -108
13 181 -169     1 291 -296     H  2 12        10 118  126                   13  93   97
15 134 -116     3 501 -493     3  85  -83                     H  6  11      15 151  141
                5 490 -453                     H  4  11       4 104  109    17 121  122
 H  0  2        7 314 -314     H  4  0         1 110 -104     6 118  111
 0 803  816     9 271 -255     2 377 -383      3  98  -90                    H  10  1
 2 294  300    13 204  188     4 215 -208                     H  8  0        1  33  -25
 8 110 -113    15 184  177     6  86   74      H  4  12       2 334  333     2 204 -213
10 294 -282    17 106  110     8 228  223      0 133 -119     4 179  180     4 253 -245
12 256 -245                   10 343  331      2  95  -76     6  98  -89     6 254 -252
14 103 -100     H  2  1       12 273  260                     8 250 -231    10 107  -91
                2 108 -112    14  94   54      H  6  0       10 261 -252    12 113   92
 H  0  3        4 372 -380                     1 206  249    12 204 -191    14 154  137
 1 453  454     6 524 -509     H  4  1         3 476  454    14 114 -105    16 111  116
 3 399  405     8 236 -223     1 315 -345      5 442  426    20  99   80
 5  65   51    14 123  120     3 329 -337      7 270  269                    H  10  2
 7 317 -310    16 194  183     5 161 -144      9 169  164     H  8  1        1  68  -26
 9 267 -265    18 120  118     7 192  187     13 133 -129     1 350  378     3 155 -153
11 177 -186                    9 295  282     15 159 -153     3 222  220     5 325 -327
13 148 -153     H  2  2       11 253  243     17 148 -125     7 144 -130     7 240 -248
15 125 -100     1 205 -212    13 156  159                     9 219 -209     9 105 -107
19  88   93     3 298 -311    15  84   81      H  6  1       11 235 -232    13  97   79
21  82   80     5 319 -316    19  93  -84      2 232  233    13 158 -151    15 141  128
                7 249 -255                     4 396  393                   17 128  119
 H  0  4        9 268 -248     H  4  2         6 377  374     H  8  2
 0 631  661    13 166  158     0 457 -461      8 165  170     0 374  369     H  10  3
 2 256  304    15 157  159     2 250 -264     16 178 -157     2 248  258     2 208 -213
 6  85  -72    17 105  108     4 161 -171     18 109 -106     4 148  159     4 241 -259
 8 135 -132    19  88   77     8 158  153                     8 193 -179     6 244 -249
10 251 -263                   10 287  282      H  6  2       12 185 -176     8 211 -205
12 212 -221     H  2  3       12 257  240      1 192  189    14 127 -109    10  87  -75
14  95  -85     2 173 -161    14 117  101      3 313  321                   12 110   95
                4 412 -415                     5 320  326     H  8  3       14 147  135
 H  0  5        6 478 -480     H  4  3         7 215  225     1 383  383    16 115  111
 1 250  266     8 209 -211     1 382 -384      9 177  163     3 206  214
 3 255  269    12  89   78     3 309 -320     15 146 -130     7 137 -144     H  10  4
 5  80   61    14 122  122     5 111 -108     17 141 -122     9 205 -212     3 149 -163
 7 195 -193    16 176  172     7 201  207                    11 220 -224     5 301 -303
 9 182 -189    18 104  107     9 277  280      H  6  3       13 151 -139     7 225 -227
11 136 -144                   11 236  234      2 242  241    17  89   33     9  85  -93
13 134 -135     H  2  4       13 133  145      4 384  399                   15 116  119
15 100  -96     1 188 -189                     6 344  362     H  8  4       17 104  108
19  80   79     3 321 -317     H  4  4         8 166  167     0 346  347
                5 304 -310     0 440 -443     14 132 -120     2 247  250     H  10  5
 H  0  6        7 233 -240     2 275 -272     16 173 -149     4 149  139     2 145 -148
 0 430  466     9 207 -205     4 139 -139                     8 179 -175     4 178 -181
 2 230  239    13 163  150     8 155  160      H  6  4       10 202 -204     6 178 -187
 8  96 -113    15 146  148    10 261  262      1 164  161    12 168 -160     8 166 -165
10 200 -216    17  99   96    12 214  215      3 303  302                   14 114  108
12 182 -183                   14  87   86      5 304  312     H  8  5
                H  2  5                        7 218  214     1 249  261     H  10  6
 H  0  7        2  80  -80     H  4  5         9 136  138     3 154  155     3 130 -139
 1 233  245     4 254 -260     1 227 -237     13  94 -104     7  97  -89     5 235 -246
 3 198  213     6 337 -338     3 213 -229     15 126 -129     9 157 -156     7 191 -187
 7 169 -169     8 163 -165     5  91  -93     17 114 -110    11 189 -179    15 109  101
 9 171 -173    14  99   91     7 128  129                    13 120 -122
11 124 -128    16 149  147     9 199  201      H  6  5                       H  10  7
13 105 -106                   11 175  182      2 142  148     H  8  6        2 116 -132
15  87  -70     H  2  6       13 124  129      4 249  261     0 258  275     4 158 -170
                1 146 -140    15  88   69      6 258  261     2 199  202     6 162 -165
 H  0  8        3 249 -250                     8 132  136     4 106  111     8 131 -134
 0 263  295     5 226 -246     H  4  6        14 102  -92     8 154 -145
 2 142  160     7 190 -195     0 343 -346     16 133 -127    10 166 -170     H  10  8
 8  79  -70     9 146 -162     2 220 -219     18  96  -88    12 153 -134     5 164 -174
10 149 -156    13 109  125     4  94 -104                                   7 131 -137
12 133 -140    15 124  125     8 133  132      H  6  6        H  8  7
                               10 215  216     1 112  118     1 227  232     H  10  9
 H  0  9        H  2  7       12 181  177      3 240  235     3 105  133     4 122 -121
 1 151  165     2  88  -96    14  82   71      5 241  251     9 148 -142     6 101 -118
 3 140  146     4 244 -242                     7 169  177    11 157 -153     8 101 -100
 7 114 -114     6 277 -280     H  4  7         9 109  111
 9 136 -122     8 137 -135     1 221 -224     15  94 -110     H  8  8        H  10  10
               16 129  123     3 182 -185                     0 177  184     3  85  -84
 H  0  10                     7 148  126      H  6  7        2 134  141     5 140 -141
 0 226  229     H  2  8       9 182  178      2 134  137     4  81   82
 2 130  134     1  87  -94   11 134  154      4 229  233     8  90  -99     H  10  11
10 121 -126     3 151 -161   13  91  102      6 228  224    10 112 -124     2  79  -65
12 108 -107     5 145 -164                    8 125  116    12  98 -103     6  98  -84
                7 139 -139                   16 101 -106
```

*Table 2. Continued.*

```
H 12 C              H 14 4           7   -  -16*       7   33   28      13   16  -17        6   62  -51
2  256 -265     3  141  145      8   26   30       8    -    8*                          7   80  -65
4  180 -169     5  228  239      9   39  -36       9   76   75       H 5 3           8    -    4*
6   89   83     7  169  171     10   50   59      10    -    6*     0   23   28        9   34  -30
8  218  215                     11    -   -4*     11   56   62      1   24   26       10    -    C*
10 182  181         H 14 5      12   33   45      12    -  -14*     2    -   18*      11   43   44
12 110  132     2  153  146     13   21   42      13   12   15      3   57   57       12   62  -66
                4  157  160                                        4   20  -28
F 12 1          6  121  128       H 1 5             H 3 4           5   43  -36        F 7 3
1  316 -332     8  125  119     0    -   -9*       1   34   41      6   68   57       0   54   54
3  133 -131                     1    -  -12*       2   53  -62      7   74  -63       1   40  -41
7   75   74         H 14 6      2    -   -6*       3    -  -15*     8   72   66       2   34  -25
9  168  160     3  125  122     3   25  -25       4    -   -2*      9   25  -25       3    -  -25*
11 218  208     5  204  200     4    -    5*       5   21   15     10    -   -3*      4  105 -106
13 122  126     7  146  144     5    -   15*       6   30   35     11   42  -50       5   84   72
                                6   38  -44       7   59   60     12   33  -42       6    -  -13*
H 12 2              H 14 7      7   29   33       8    -    6*     13   35  -57       7    -   -8*
0  257 -241     2  133  128     8   27  -34       9   34   40                        8    -   12*
2  218 -222     4  130  145     9    -   1C*      10  34   34       F 5 4           9   67  -66
4  141 -155     6  107  115    10    -    0*      11  29  -34      1   40  -37       10  25  -14
8  183  180     8  106  100·   11   19   30       12  54   69      2   39  -43       11  52  -59
10 147  157                                                       3   47   50
12 111  122         H 14 8       H 1 6             H 3 5           4    -   13*      H 7 4
                5  152  148     1    -    8*       0   33  -38      5   52   53       1   54  -58
H 12 3          7   98  109     2    -   10*       1   26   31      6   20   20       2   78   79
1  330 -326                     3    -  -29*       2   18   16      7    -   -1*      3   19   23
3  132 -131         F 14 9      4    -   -7*       3    -    6*      8   39  -38       4    -    5*
7   83   85     2   90   93     5    -  -29*       4   43   52      9    -  -13*      5    -   -8*
9  177  161     4  105  105     6    -    1*       5   39  -52     10   75  -85       6   45  -47
11 207  201     6   88   84     7    -  -16*       6   24   20     11   25   29       7   60  -62
13 115  117                     8    -   26*       7    -    9*     12  25  -36       8    -   -5*
                H 1 0          9   20  -28       8    -    0*                        9   26  -26
F 12 4          2   30   30    1C   3C   45       9   42   48       H 5 5          10    -   -5*
C  233 -232     3  100  -71                      10    -   11*     0    -   18*      11  34   46
2  2C7 -2C9     4    -  -12*     H 1 7             11  31   45      1    -   15*
4  135 -138     5   99  -70     0    -   -7*                       2    -    6*      H 7 5
6   79   61     6    -   -1*    1    -  -12*       H 3 6           3   34   35       0   33   36
8  171  172     7   27  -16     2    -   -7*       1   19   28      4   24  -31       1   27  -29
10 149  150     8   61   53     3   18  -19       2   32  -42      5   25  -32       2   20  -23
                9   64  -48     4    -   -7*       3    -   -3*      6   40   41       3    -  -14*
H 12 5          10  94   81     5    -    9*       4    -    3*      7   34  -38       4   63  -69
1  248 -241     11   -    2*    6   27  -40       5    -   14*      8   46   53       5   54   60
3  110  -98     12  56   57     7   22   33       6   22   26      9    -   -4*      6    -    1*
9  126  122     13  62   58     8   17  -27       7   36   46     10    -    4*      7    -    3*
11 169  164     14  16   18                      8    -    8*     11  21  -31       8    -   16*
13 111  103                     H 3 C             9   24   32                       9   42  -46
                F 1 1          1   70   68       10  17   28       H 5 6
H 12 6          0   21  -25     2  117 -104                        1   24  -28       H 7 6
0  179 -192     1   19  -23     3   41  -34       F 3 7           2   27  -31       1   35  -42
2  186 -172     2   10  -11     4    -    7*      0   18  -24      3   29   39       2   47   57
4  112 -113     3   72  -56     5   61   39       1    -   16*      4    -   10*      3    -   14*
8  135  143     4   17   21     6   68   52       2    -   12*      5   30   40       4    -    5*
10 119  127     5   38   33     7  108   84       3    -    4*      6    -   15*      5    -  -10*
12 104   95     6   99  -74     8   21   17       4   33   46      7    -    0*      6   30  -36
                7   70   55     9   57   53       5   24  -34      8   23  -34       7   39  -49
F 12 7          8   66  -53    10   64   47       6   21   26      9    -   11*      8    -   -7*
1  210 -210     9   31   12    11   51   -5C      7   14   16
3   84  -88     10   -    7*   12   93   85                        H 5 7           H 7 7
9  128  111     11  4C   44    13   69  -60       F 5 0          0    -   19*      0   21   26
11 159  141     12  23   20    14  29   31       1   33  -42      1    -   18*      1    -  -19*
                13  45   47                      2   36  -46      2    -    7*      2    -  -16*
H 12 8          14  18   21     F 3 1            3   70   67      3    -   28*      3    -  -12*
0  131 -132                     0   78  -88       4    -   17*      4    -  -16*      4   39  -58
2  115 -124         H 1 2      1   62   70       5  108   82      5   18  -24       5   28   40
8   85  1C3      1   24   29     2   31   28       6   31   27      6   24   37
                2   32   40     3    -   13*       7    -   -3*      7   23  -37       H 9 C
H 12 9          3   51  -47     4  114   93       8   74  -58                       1   51   60
1  145 -151     4    -  -11*    5  102  -5C       9    -   13*      H 7 0          2   61   59
3   71  -63     5   39  -34     6   44   29       10 132 -114     1   67  -80       3   65  -67
                6    -  -10*    7   28   18       11  40   28      2  111  115       4   27  -26
F 12 10         7    -   -8*    8    -    2*       12  48  -47      3   38   36       5   77  -62
0  100 -111     8   29   20     9   89   71       13  32  -30      4    -   -4*      6    -  -12*
2   97 -1C1     9   51  -45    10    -   12*                       5   34  -23       7    -    5*
                10  66   58    11  68   62       F 5 1          6   80  -67       8   79   71
H 14 0          11   -  -14*   12    -   -1*      0    -   16*      7  103  -83       9   29  -15
1   31   47     12  44   46    13  21   15       1   11   12      8    -  -12*      10  82   88
3  188  186     13  43   39    14  36  -43       2   32   22      9   36  -35       11  40  -34
5  296  294     14  17   23                      3   74   65      10  24   -7       12   -   23*
7  201  206                     F 3 2            4   39  -46      11  70   62
15 106 -1C8         H 1 3      1   56   59       5   43  -42      12  83  -71       H 9 1
                0   18  -22     2   83  -83       6   77   56      13  34   41       0   33  -40
H 14 1          1   28  -29     3   35  -31       7   83  -59                       1   29  -33
2  193  196     2    -  -10*    4    -   -2*       8   91   74       H 7 1          2    -    0*
4  225  214     3   42  -44     5    -    3*       9    -  -11*     0   54   66       3   55  -51
6  168  168     4    -   -5*    6   46   36       10   -    3*      1   46  -55       4   75   67
8  136  149     5   22   25     7   80   64       11  50  -44      2   41  -33       5   89   72
10  97   77     6   75  -73     8    -   -7*       12  38  -36      3   16  -26       6   75  -60
14 110 -113     7   63   60     9   53   48       13  55  -60      4  132 -110       7   52   43
16 108  -9C     8   46  -48    10  45   30                        5  111   91       8   96  -83
                9   31   29    11  29  -30       F 5 2          6    -    1*       9    -    2*
F 14 2          10   -   10*   12  76   76       1   48  -52      7    -    0*      10    -   -8*
3  142  149     11  37   48    13  43  -39       2   50  -61      8   26   20       11  50   44
5  258  256     12  21   30    14  24   36       3   55   50      9   80  -65       12  35   40
7  184  184     13  30   44                      4    -   11*     10    -  -21*
15 102  -98                     H 3 3            5   71   58      11  70  -61       F 9 2
                H 1 4          0   51  -61       6   34   31                       1   71   67
H 14 3          1    -   15*    1   38   44       7    -   -5*      H 7 2          2   70   66
2  191  192     2    -   20*    2   23   20       8   33  -29      1   76  -77       3   58  -53
4  224  215     3   40  -41     3    -   11*       9    -   17*     2  104  105       4   25  -18
6  177  167     4    -  -10*    4   91   92       10  98  -88      3   38   38       5   62  -51
8  138  143     5   33  -37     5   67  -69       11  42   41      4    -    8*      6    -  -14*
14 128 -111     6    -   -1*    6   44   41       12  37  -35      5    -    4*      7    -    2*
```

*Table 2. Continued.*

```
  8  53  46      3  44  -46      H  9  4        5  -  -14*      5  42  49      4  22  -11
  9  23  -20     4  53   50     1  48   48     10  43   67      6  36  -43      5  31  -36
 10  64  67      5  65   60     2  49   47                      7  23   30      6  -   -5*
 11  41  -41     6  59  -55     3  46  -47      H  9  5         8  49  -61
                 7  48   48     5  48  -45      0  -  -22*                      H  9  6
  H  9  3        8  73  -72     6  -   -8*      1  -  -19*      H  9  6         1  31   35
  0  36  -41     9  -   16*     7  -    0*      2  -    3*      1  31   35      2  28   33
  1  34  -35    10  -   -3*     8  44   50      3  30  -28      2  28   33      3  25  -36
  2  -   -4*    11  35   48                     4  33   43      3  25  -36
```

These were based on a data set consisting of 509 strong structure factors with $k = 2n$ and 313 weak structure factors with $k = 2n + 1$. Mean values of $F_{hkl}$ and $F_{\bar{h}kl}$ for $k = 2n$ were used, those reflexions that did not occur twice being eliminated. Positional parameters, including isotropic temperature factors, and layer scale factors were refined, only one of the four oxygen atoms $O_7 - O_{10}$ being refined at a time. These four oxygen atoms were refined alternately until the shifts were negligible. This method of refinement was necessary owing to coupling between the $x$ and $y$ parameters of $O_7 - O_{10}$. Cruickshank's weighting scheme was used, and the refinement yielded a final $R$ value of 0.061. The final $R$ factor based on the strong structure factors was 0.046, while that based on the weak structure factors was 0.158.

No correction was made for anomalous dispersion since the data set consisted partly of reflexions obtained with copper and partly of reflexions obtained with molybdenum radiation.

The positional parameters were also refined with all atoms occupying the general position 4(c) in space group $Pnn2$. After several cycles of refinement, the parameter shifts had still not converged. The space group $Pnnm$ was therefore considered to be the correct one.

*Table 3.* Atomic coordinates, expressed as fractions of the cell edges, and isotropic thermal parameters in Å². Standard deviations are given within brackets.

| Atom | Occ. number | $x$ | $y$ | $z$ | $B$ |
|---|---|---|---|---|---|
| $Hf_1$ | 1 | 0.0505(1) | 0.1246(3) | 0 | 0.95(2) |
| $Hf_2$ | 1 | 0.0421(1) | 0.6269(3) | 0 | 0.88(2) |
| $Cr_1$ | 1 | 0.3716(5) | 0.1608(6) | 0 | 1.1(1) |
| $Cr_2$ | 1 | 0.3622(5) | 0.5910(6) | 0 | 1.1(1) |
| $Cr_3$ | 0.14 | 0.191(3) | 0.872(5) | 0 | 1.2(6) |
| $O_1$ | 1 | 0.068(1) | 0.134(2) | 0.304(2) | 1.3(3) |
| $O_2$ | 1 | 0.049(1) | 0.628(3) | 0.303(3) | 1.7(3) |
| $O_3$ | 1 | 0.243(2) | 0.110(2) | 0 | 0.6(3) |
| $O_4$ | 1 | 0.227(2) | 0.637(3) | 0 | 1.5(4) |
| $O_5$ | 1 | 0.354(3) | 0.276(3) | 0 | 2.8(7) |
| $O_6$ | 1 | 0.351(4) | 0.476(4) | 0 | 4.4(11) |
| $O_7$ | 1 | 0.107(2) | 0.271(2) | 0 | 1.6(4) |
| $O_8$ | 1 | 0.089(2) | 0.775(2) | 0 | 1.7(5) |
| $O_9$ | 1 | 0.092(3) | 0.963(2) | 0 | 1.9(5) |
| $O_{10}$ | 1 | 0.093(3) | 0.467(2) | 0 | 1.9(5) |
| $O_{11}$ | 0.14 | 0.282(12) | 0.868(16) | 0.184(22) | 2.2(23) |
| $O_{12}$ | 0.86 | $-0.305(5)$ | 0.122(5) | 0 | 5.6(13) |

*Table 4.* Distances (Å) and angles (°) in $\sim Hf_4(OH)_8(CrO_4)_4 \cdot H_2O$. Standard deviations are given within parentheses.

Within the $HfO_7$ pentagonal bipyramids:
axial oxygen
atoms:

| | | | |
|---|---|---|---|
| $Hf_1 - 2O_1$ | 2.10(2) | $Hf_2 - 2O_2$ | 2.08(2) |

equatorial
oxygen atoms:

| | | | |
|---|---|---|---|
| $Hf_1 - O_3$ | 2.24(2) | $Hf_2 - O_4$ | 2.13(3) |
| $Hf_1 - O_7$ | 2.09(3) | $Hf_2 - O_7$ | 2.21(3) |
| $Hf_1 - O_8$ | 2.12(3) | $Hf_2 - O_8$ | 2.08(3) |
| $Hf_1 - O_9$ | 2.25(3) | $Hf_2 - O_{10}$ | 2.25(3) |
| $Hf_1 - O_9'$ | 2.03(3) | $Hf_2 - O_{10}'$ | 2.01(3) |
| | | | |
| $O_1 - Hf_1 - O_1$ | 167(1) | $O_2 - Hf_2 - O_2$ | 176(1) |
| $O_3 - Hf_1 - O_7$ | 77(1) | $O_4 - Hf_2 - O_8$ | 71(1) |
| $O_7 - Hf_1 - O_8$ | 68(1) | $O_8 - Hf_2 - O_7$ | 66(1) |
| $O_8 - Hf_1 - O_9'$ | 76(1) | $O_7 - Hf_2 - O_{10}$ | 78(1) |
| $O_9' - Hf_1 - O_9$ | 66(1) | $O_{10} - Hf_2 - O_{10}'$ | 66(1) |
| $O_9 - Hf_1 - O_3$ | 73(1) | $O_{10}' - Hf_2 - O_4$ | 78(1) |

ax. – eq.:

| | | | |
|---|---|---|---|
| $O_1 - O_3$ | 2.92(2) | $O_2 - O_4$ | 2.92(3) |
| $O_1 - O_7$ | 2.82(3) | $O_2 - O_7$ | 3.07(3) |
| $O_1 - O_8$ | 3.03(3) | $O_2 - O_8$ | 2.92(4) |
| $O_1 - O_9$ | 3.13(4) | $O_2 - O_{10}$ | 3.06(4) |
| $O_1 - O_9'$ | 3.08(3) | $O_2 - O_{10}'$ | 2.94(3) |

eq. – eq.:

| | | | |
|---|---|---|---|
| $O_3 - O_7$ | 2.70(4) | $O_4 - O_8$ | 2.46(5) |
| $O_7 - O_8$ | 2.34(4) | $O_8 - O_7$ | 2.34(4) |
| $O_8 - O_9'$ | 2.56(5) | $O_7 - O_{10}'$ | 2.67(5) |
| $O_9' - O_9$ | 2.34(6) | $O_{10}' - O_{10}$ | 2.33(6) |
| $O_9 - O_3$ | 2.65(4) | $O_{10} - O_4$ | 2.78(5) |

Within the $CrO_4$ tetrahedra sharing vertices with $HfO_7$:

| | | | |
|---|---|---|---|
| $Cr_1 - 2O_2$ | 1.69(2) | $Cr_2 - 2O_1$ | 1.67(2) |
| $Cr_1 - O_3$ | 1.63(2) | $Cr_2 - O_4$ | 1.68(3) |
| $Cr_1 - O_5$ | 1.57(4) | $Cr_2 - O_6$ | 1.56(5) |
| | | | |
| $O_2 - Cr_1 - O_2$ | 106(1) | $O_1 - Cr_2 - O_1$ | 107(1) |
| $O_2 - Cr_1 - O_3$ | 112(1) | $O_1 - Cr_2 - O_4$ | 108(1) |
| $O_3 - Cr_1 - O_5$ | 108(2) | $O_4 - Cr_2 - O_6$ | 107(2) |
| $O_5 - Cr_1 - O_2$ | 109(1) | $O_6 - Cr_2 - O_1$ | 113(1) |

Within the $CrO_4$ tetrahedra sharing an edge with $HfO_7$:

| | | | |
|---|---|---|---|
| $Cr_3 - O_8$ | 1.78(6) | $O_8 - Cr_3 - O_9$ | 95(2) |
| $Cr_3 - O_9$ | 1.69(6) | $O_9 - Cr_3 - O_{11}$ | 118(7) |
| $Cr_3 - 2O_{11}$ | 1.64(15) | $O_{11} - Cr_3 - O_8$ | 113(7) |
| | | $O_{11} - Cr_3 - O_{11}$ | 101(10) |

Other distances:

| | | | |
|---|---|---|---|
| $O_{12}(H_2O) - O_8$ | 2.86(7) | $Hf_1 - Hf_1$ | 3.581(9) |
| $O_{12}(H_2O) - O_9'$ | 2.71(7) | $Hf_1 - Hf_2$ | 3.542(6) |
| | | $Hf_2 - Hf_2$ | 3.583(9) |

The observed and calculated structure factors together with those corresponding to the unobserved $k = 2n + 1$ reflexions are listed in Table 2. The atomic positions and their standard deviations are given in Table 3.

## DESCRIPTION OF THE STRUCTURE

$4HfO_2.4.3CrO_3.5.4H_2O$ is isomorphous with $4ZrO_2.4.9CrO_3.3.7H_2O$ apart from the different $Cr_3$ chromate and water contents. The most important distances and angles are given in Table 4. To facilitate a comparison between the structures of the zirconium and hafnium chromates the labelling of the atoms and the lay-out of the table are the same as for $4ZrO_2.4.9CrO_3.3.7H_2O$.

The hafnium atoms are joined by double hydroxide bridges involving the oxygen atoms $O_7 - O_{10}$. Planar infinite chains of composition $[Hf(OH)_2]_n^{2n+}$, running parallel to the $y$ axis, are thus formed. In addition, there are three oxygen atoms from three different chromate groups coordinated to each hafnium atom. All the hafnium atoms are thus seven coordinated the oxygen atoms being situated at the vertices of distorted pentagonal bipyramids. The chromate groups $Cr_1$ and $Cr_2$ each share three vertices with three $HfO_7$ polyhedra belonging to different chains. The chains are thus connected in the $x$ and $z$ directions to form a three-dimensional network. The structure described has the composition $4HfO_2.4CrO_3.6H_2O$ if the two water molecules of crystallization are taken into account. The additional chromate groups, corresponding to the $Cr_3$ atoms, are situated in the same holes in the structure as the water molecules, though not simultaneously. Each $CrO_4^{2-}$ entering such a hole expels $2OH^-$ in the $[Hf(OH)_2]_n^{2n+}$ chain and thus shares one tetrahedron edge with a pentagonal bipyramid. The occupation number of $O_{12}$, as deduced from the Fourier synthesis, is very nearly 1 and the compound can therefore be formulated as $4HfO_2.(4+x)CrO_3.(6-2x)H_2O$. The $x$ value may vary between 0 and 2 without changing the structure, since $Z = 2$. For this crystal $x$ was found to be 0.28.

In Fig. 1, approximately one formula unit of the structure is depicted in perspective with distances given in Å. The Hf $-$ Hf distances are on an average $3.56_2$ Å and are significantly shorter than the average Zr $-$ Zr distance
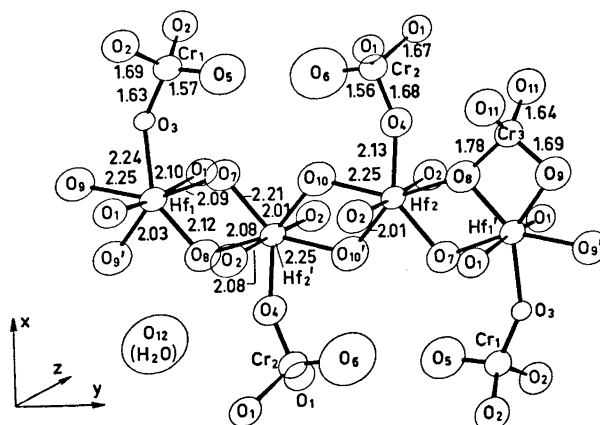


*Fig. 1.* One approximate formula unit of $4HfO_2.4.3CrO_3.5.4H_2O$ shown in perspective. The thermal motions are outlined as spheres and the distances are given in Å.

(3.597 Å) in zirconium chromate. Assuming that the $O-Me-O$ angles in the $Me-(OH)_2$ bridges are not altered, the short $Hf-Hf$ distance results in a displacement of the bridging oxygen atoms in opposite directions in order to avoid too close an oxygen-oxygen contact. The $Hf-O$ distances are hence alternately short and long, as can be seen from Table 4 and Fig. 1.

Since the structure is held together by chromate groups, there may be structural constraints on the chains due, for example, to the close contact (2.73 Å) between the chromate oxygen atoms $O_5$ and $O_6$. However, due to experimental difficulties, the results obtained do not permit a more detailed comparison between this hafnium chromate and the structures of other similar zirconium and hafnium compounds.

## REFERENCES

1. McWhan, D. B. and Lundgren, G. *Inorg. Chem.* **5** (1966) 284.
2. Hansson, M. *Acta Chem. Scand. To be published.*
3. Mark, W. *Acta Chem. Scand.* **27** (1973) 177.
4. Lindqvist, O. and Wengelin, F. *Arkiv Kemi* **28** (1967) 179.
5. *International Tables for X-Ray Crystallography*, Kynoch Press, Birmingham 1962, Vol. III, p. 122.
6. The program library of the Dept. of Inorg. Chem. Göteborg. DATAP1 and BLOCK have been written locally by O. Lindgren, DATAP2 was originally written by Coppens, Leiserowitz and Rabinowich (1965), DRF by A. Zalkin, Berkeley, California, and LALS by P. Gantzel, R. Sparks and K. Trueblood.

Received June 19, 1973.

# Preparation and PMR Analysis of *cis* and *trans* Isomers of 2-Chloro-5-methyl-1,3,2-oxathiaphospholane and 2-Phenyl-5-methyl-1,3,2-oxathiaphospholane

KNUT BERGESEN and MALVIN BJORØY

*Chemical Institute, University of Bergen, N-5000 Bergen, Norway*

The high resolution magnetic resonance spectra of the *cis* and *trans* isomers of 2-chloro- and 2-phenyl-5-methyl-1,3,2-oxathiaphospholane have been completely analysed. The geminal *cis, trans* and the proton phosphorus coupling constants and the shift values are reported. The *trans* isomer is found mainly to exist in an equilibrium between two envelope conformations, while only one conformation predominates in the *cis* isomer. In both isomers the carbon atom 5 is found to be out of the ring plane.

Five membered ring compounds, such as 1,3,2-oxathiaphospholanes,[1-3] are suitable for conformational investigation. The PMR spectra are simplified because of the large chemical shift difference of the ring protons caused by the more deshielding effect of the ring oxygen atom as compared to the sulfur atom. From the PMR analysis of phosphorus substituted 1,3,2-oxathiaphospholanes [1-2] the ring was found to exist mainly in an equilibrium between two envelope conformations, where the carbon atom in position 5 is out of the ring plane. However, in 2-methylthio-1,3,2-oxathiaphospholane [3] the ring was found to exist in a fixed conformation, in agreement with the large difference in the *cis* and *trans* coupling constants and the large difference of the phosphorus proton coupling constants observed for the protons in the oxygen part of the ring.

In order to obtain useful information about the 1,3,2-oxathiaphospholane ring when substituted in the 5 position, the *cis* and *trans* isomers of 2-chloro- (I) and 2-phenyl-5-methyl-1,3,2-oxathiaphospholane (II) were prepared and their PMR spectra analysed in detail with respect to both coupling constants and chemical shifts. The PMR spectra of I and II indicate the presence of two isomers in the ratio 1:2, which complicated the analysis to some extent. The total spectra of the ring protons were extremely complex due to the overlapping of the protons of the isomers. However, the signals

I : R = Cl
II : R = Ph
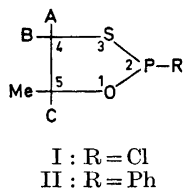
of the ring protons from the major *trans* isomer can be separated from the rest of the spectrum as it appears to be an $ABMX_3P$ spin system.

The 60 MHz spectrum of the ring protons of I consists of four main regions ($\delta = 2.5 - 3.0$, $3.0 - 3.5$, $4.0 - 4.6$, and $4.6 - 5.3$). The two low field bands are assigned to the methine proton at carbon 5 because of the deshielding effect of the group attached to the phosphorus atom. The methine proton of the *trans* isomer is found to resonance at lower field as compared to the methine proton of the *cis* isomer.

The complex band at high field of the spectrum is due to the protons at carbon 4 of the two isomers. The B proton of the *cis* and *trans* isomers is observed to give resonance at higher field as compared to the A protons. The two doublets at high field in the total spectrum is assigned to the methyl group.

The 60 MHz spectrum of the ring protons of II consists of two main regions ($\delta = 1.8 - 3.0$ and $3.7 - 4.7$). The low field band is assigned to the methine proton of the two isomers, while the high field band is due to the protons at carbon 4.
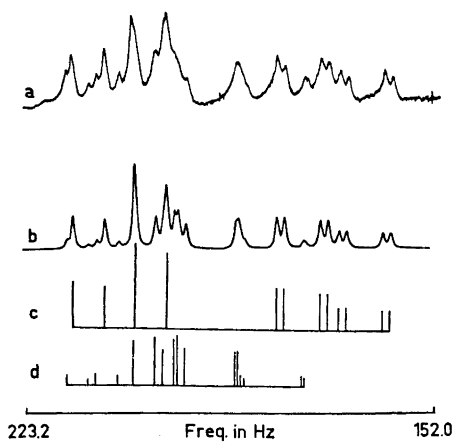


*Fig. 1.* The AB part of the 60 MHz spectrum of the *cis* and *trans* isomers of I: (a) experimental spectrum; (b) computed total lineshape spectrum; (c) computed stickplot of the AB protons in the *trans* isomer; (d) computed stick-plot of the AB protons in the *cis* isomer.
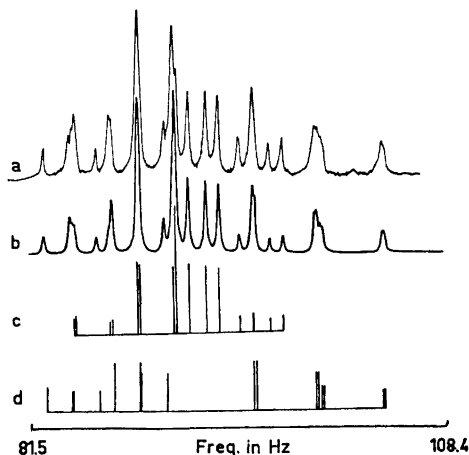
*Fig. 2.* The AB part of the 60 MHz spectrum of the *cis* and *trans* isomers of II: (a) experimental spectrum; (b) computed total line-shape spectrum; (c) computed stick-plot of the AB protons in the *trans* isomer; (d) computed stick-plot of the AB protons in the *cis* isomer.
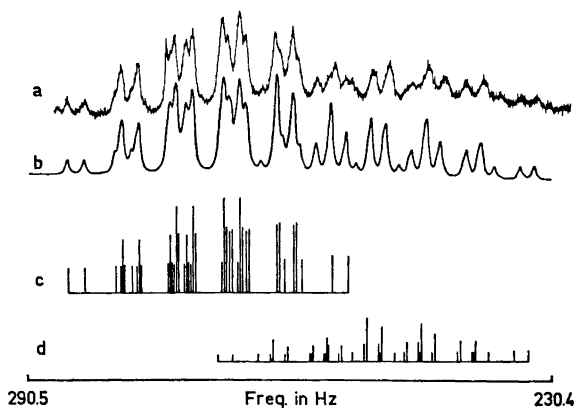
*Fig. 3.* The C part of the 60 MHz spectrum of the *cis* and *trans* isomers of II: (a) experimental spectrum; (b) computed total line-shape spectrum; (c) computed stick-plot of the C proton in the *trans* isomer; (d) computed stick-plot of the C proton of the *cis* isomer.

The PMR spectra of I and II were analysed as an $ABMX_3P$ spin system by means of the computer program UEAITR [4] and KOMBIP.[5] The fully computer analysed 60 MHz and 100 MHz spectra resulted in a good correlation between calculated and experimental spectra, Figs. 1, 2, and 3. The final RMS error observed was 0.06 or less when all parameters were allowed to vary. The probable errors of the coupling constants are 0.02 to 0.03 Hz. The spectral parameters are listed in Table 1.

Recent articles on geminal coupling constants in 1,3,2-dithiaphospholanes [1,6-9] and 1,3,2-dithiarsolanes [10] indicate the range $-11.0$ to $-12.5$ Hz in the $C-CH_2-S$-moiety. The observed values for I and II are in the expected range. These coupling constants are smaller (more negative) than those found in the 1,3,2-dioxaphospholanes and 1,3,2-dioxaarsolanes, which probably is due to a combination of a reduced $H-C-H$ angle and a smaller electron withdrawal effect of sulfur as compared to oxygen.
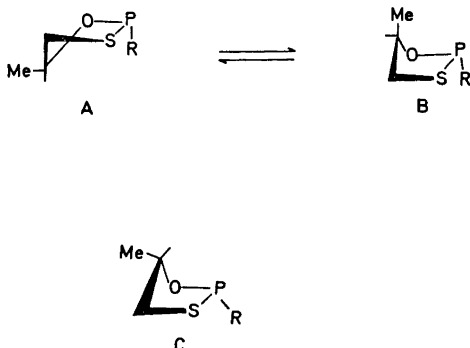
*Table 1.* Chemical shifts and coupling constants for the *cis* and *trans* isomers of I and II.

| Compound | Isomer | CH$_3$ | A | B | C |
|---|---|---|---|---|---|
| I | *cis* | 1.60 | 3.38 | 3.12 | 4.59 |
| | *trans*[a] | 2.23 | 3.09 | 2.48 | 4.80 |
| II | *cis* | 1.40 | 2.79 | 2.19 | 4.17 |
| | *trans* | 1.19 | 2.71 | 2.47 | 4.49 |

| Compound | Isomer | Coupling constants, Hz | | | | | | | |
|---|---|---|---|---|---|---|---|---|---|
| | | $J_{AB}$ | $J_{AC}$ | $J_{AP}$ | $J_{BC}$ | $J_{BP}$ | $J_{CP}$ | $J_{CH_3-C-H}$ | $J_{P-O-C-CH_3}$ |
| I | *cis* | −11.79 | 4.82 | 4.24 | 11.13 | 0.13 | 4.53 | 6.10 | −0.01 |
| | *trans*[a] | −10.90 | 5.53 | −0.01 | 7.65 | 1.36 | 3.22 | 6.20 | 0.03 |
| II | *cis* | −11.97 | 4.66 | 4.69 | 11.11 | 0.31 | 1.73 | 6.36 | 0.34 |
| | *trans* | −11.31 | 6.60 | 0.17 | 5.14 | 2.57 | 1.89 | 6.10 | 0.04 |

[a]Values obtained from 100 MHz spectra.

The vicinal coupling constants for 1,3,2-oxathiaphospholanes [1-3] are in the range $J_{cis} = 4.3 - 7.4$ Hz and $J_{trans} = 5.9 - 6.9$ Hz for most of the comdounds studied, except for 2-methylthio-1,3,2-oxathiaphospholane,[3] where the *cis* and *trans* coupling constants are quite different in magnitude. The *cis* and *trans* coupling constants in the *trans* isomer of I and II are very similar in magnitude to those found for most of the 1,3,2-oxathiaphospholanes,[1-2] which probably indicates that this five-membered oxathiaphospholane mainly exists in an equilibrium between two envelope conformation A and B with carbon atom 5 out of the ring plane.

This is also in agreement with the small difference between the phosphorus proton coupling constant observed for the AB protons in the sulfur part of the ring.

The *cis* and *trans* coupling constants observed in the *cis* isomer of I and II are quite different (Table 1), which probably indicates that only one conformer predominates, C.

This assumption is in agreement with that found from the Dreiding stereo-models where the carbon in position 5 is out of the ring plane and with an equatorial position of both the methyl group and the substituent attached to the phosphorus atom. The difference in the phosphorus proton coupling constant for the AB protons in the *cis* isomer is also in agreement with conformation C. The same relation has been found for the *cis* isomers of 2-chloro- and 2-phenyl-4-methyl-1,3,2-dithiaphospholane [9] and 2-chloro- and 2-phenyl-4-methyl-1,3,2-dithiarsolane.[11] Further analyses of other ringsubstituted 1,3,2-oxathiaphospholanes are in progress in this laboratory.

## EXPERIMENTAL

*2-Chloro-5-methyl-1,3,2-oxathiaphospholane (I)* was prepared from 3-mercaptopropan-2-ol and phosphorus trichloride in ether solution using triethylamine as base, b.p.$_{10}$ 68°C.

*2-Phenyl-5-methyl-1,3,2-oxathiaphospholane (II)* was prepared from 3-mercapto-propan-2-ol and dichlorophenylphosphine in ether solution using triethylamin as base, b.p.$_{0.5}$ 93°C.

The PMR spectra of I and II were measured as 50 % solution in CDCl$_3$. The spectra were recorded on a 60 MHz JEOL, C-60 H and a 100 MHz Varian HA-100 spectrometer. In the PMR sample tubes, small amounts of TMS were added to serve as reference and locking substance. The tubes were degassed and sealed under vacuum. The spectra were recorded in internal lock mode with frequency sweep at approx. 50 Hz sweep width and calibrated every 5 Hz using a frequency counter. The counter is accurate to 0.1 Hz to a 10 sec count. Line positions were taken by averaging the data from four spectra, and are assumed to be correct to about 0.05 Hz. The computation was carried out using a UNIVAC 1110 computer and graphical output was obtained using a Calcomp Plotter.

## REFERENCES

1. Bergesen, K., Bjorøy, M. and Gramstad, T. *Acta Chem. Scand.* 26 (1972) 3037.
2. Bergesen, K., Bjorøy, M. and Gramstad, T. *Acta Chem. Scand.* 26 (1972) 2156.
3. Bergesen, K. and Bjorøy, M. *Acta Chem. Scand.* 27 (1973) 357.
4. Johannessen, R. B., Fenetti, I. A. and Harris, R. K. *J. Magn. Resonance* 3 (1970) 84.
5. Aksnes, D. W. KOMBIP, Quantum Chemistry Program Exchange, Indiana University, Chemistry Department, Indiana, U.S.A.
6. Albrand, J. P., Cogne, A., Gagnaire, D., Martin, J., Robert, J. B. and Verrier, J. *Org. Magn. Resonance* 3 (1971) 75.
7. Peake, S. C., Fild, M., Schmutzler, R., Harris, R. K., Nichols, J. M. and Rees, R. G. *J. Chem. Soc. Perkin Trans.* 2 1971 380.
8. Albrand, J. P., Gagnaire, D., Martin, J. and Robert, J. B. *Org. Magn. Resonance* 5 (1973) 33.
9. Bergesen, K. and Bjorøy, M. *Acta Chem. Scand.* 27 (1973) 1103.
10. Aksnes, D. W. and Vikane, O. *Acta Chem. Scand.* 27 (1973) 1337.
11. Aksnes, D. W. and Vikane, O. *Acta Chem. Scand.* 27 (1973) 2135.

# The Crystal Structure of Potassium Oxopentacyanovanadate(IV), $K_3[VO(CN)_5]$

SUSAN JAGNER and NILS-GÖSTA VANNERBERG

*Department of Inorganic Chemistry, University of Göteborg and Chalmers University of Technology, P.O. Box, S-402 20 Göteborg 5, Sweden*

The crystal structure of potassium oxopentacyanovanadate(IV), $K_3[VO(CN)_5]$, has been determined by single crystal X-ray methods. $K_3[VO(CN)_5]$ crystallizes with a so-called OD structure and the crystal structure of $K_3[VO(CN)_5]$ can be characterised in terms of the family of structures represented by the OD groupoid symbol:

$$\begin{matrix} P & m & 2_1 & (n) \\ \{c_2 & 2_1 & (n\bar{\tfrac{1}{2}},_1)\} \end{matrix}$$

Following an approximate determination of the superposition structure, the structure of the ordered orthorhombic form ($MDO_1$) has been determined from Weissenberg data and refined with least squares methods to an $R$ value of 0.083, based on a total of 527 reflections. The superposition structure belongs to space group No. 36, $Cmc2_1$ with $A = 4.2646 \pm 0.0003$ Å, $b = 13.4700 \pm 0.0012$ Å, $c = 9.7818 \pm 0.0015$ Å and $Z = 2$, whereas the $MDO_1$ structure belongs to space group No. 33, $Pna2_1$ with $a = 13.4700 \pm 0.0012$ Å, $b = 8.5292 \pm 0.0006$ Å, $c = 9.7818 \pm 0.0015$ Å and $Z = 4$.

Potassium oxopentacyanovanadate(IV) contains discrete $[VO(CN)_5]^{3-}$ ions in which the $V = O$ bond distance is 1.64 Å, the mean $V - C(eq)$ bond distance is 2.14 Å and the $V - C(ax)$ bond distance is 2.31 Å. The $[VO(CN)_5]^{3-}$ ion would thus appear to exhibit the distortion characteristic of many vanadyl(IV) complex ions, namely a long vanadium-ligand bond *trans* to the $V = O^{2+}$ entity.

Although vanadium forms a wide range of complex cyanides,[1] few of these are well-characterised. In connection with an investigation on transition metal hexacyanides and cyanide complexes in progress at this department, the crystal structures of $K_2[V(CN)_6]$, $K_3[V(CN)_6]$ and $K_4[V(CN)_6]$ were of considerable interest. The crystal structure of $K_3[V(CN)_5NO].2H_2O$,[2] previously thought to be $K_5[V(CN)_5NO].H_2O$,[3] had already been determined in connection with a series of investigations on transition metal pentacyanonitrosyl ions.[4–6]

In their investigation on complex cyanides of vanadium, Bennett and Nicholls [7] were unable to confirm the reported preparation [8] of $K_2[V(CN)_6]$,

and instead obtained $K_3[VO(CN)_5]$. Similarly, they found the vanadium(III) cyanide to be more consistent with the formula $K_4[V(CN)_7].H_2O$ than $K_3[V(CN)_6]$.[9] This was in accordance with the findings of Chadwick and Sharpe [1] who had formulated the scarlet compound as $K_4[V(CN)_7].2H_2O$. The complex cyanide of vanadium(III) has now unequivocally been shown to be $K_4[V(CN)_7].2H_2O$ in a recent crystal structure determination by Towns and Levenson.[10] The crystal structure of $K_4[V(CN)_6]$, which is, like that of $K_3[VO(CN)_5]$, an OD structure, is now under investigation by the authors.

Although Bennett and Nicholls [7] were the first to characterise the potassium salt of $[VO(CN)_5]^{3-}$, other oxopentacyanovanadates, namely those of caesium, tetramethylammonium, and tetraethylammonium, had been prepared previously.[11] For the purposes of comparison with $K_3[V(CN)_5NO].2H_2O$, to which $K_3[VO(CN)_5]$ was expected to show structural similarities, and in order to obtain more information concerning $V-C$ coordination distances in cyanovanadates, it was decided to investigate the crystal structure of $K_3[VO(CN)_5]$. The oxopentacyanovanadate(IV) ion has additional interest in that it contains the $VO^{2+}$ entity which has been the subject of much attention in recent years.[12,13]

## PREPARATION AND ANALYSIS

Single crystals of potassium oxopentacyanovanadate(IV) were prepared from $VOSO_4.5H_2O$, according to a slightly modified version of the original method due to Bennett and Nicholls.[7] $VOSO_4.5H_2O(s)$ was added to saturated aqueous potassium cyanide at room temperature, the resulting green solution was filtered from undissolved solid and methanol was slowly added. After re-filtration, the solution was allowed to crystallize in an argon-filled desiccator, green needle-shaped crystals of suitable size for single crystal X-ray work being deposited after a few weeks.

The *potassium* and *vanadium* contents were determined by means of atomic absorption spectroscopy using a Perkin Elmer 403 spectrometer. [Found: K 36.3; V 16.2. Calc. for $K_3[VO(CN)_5]$: K 37.4; V 16.2]. No attempt was made to determine the oxygen and cyanide contents. The infra-red spectrum, registered with a Beckman IR9 spectrophotometer, showed complete agreement with that given by Bennett and Nicholls.[7] This, together with the experimental density and the results of the potassium and vanadium analyses and of the crystal structure determination, can leave little doubt that the compound investigated was indeed $K_3[VO(CN)_5]$.

## OD STRUCTURE

Crystals of $K_3[VO(CN)_5]$ were mounted along the needle-axis in glass capillaries, and rotation photographs were recorded about this axis, which will in the following be assumed to coincide with the crystallographic $c$ axis. The rotation photographs showed continuous streaks perpendicular to the layer lines, indicating a lack of periodicity in the $c$ direction. It was thus apparent that potassium oxopentacyanovanadate(IV) crystallizes with a so-called OD structure,[14] that is, a structure which can be described in terms of ordered layers stacked in a disordered manner in the $c$ direction. Weissenberg photographs recorded for layer lines corresponding to a $c$ axis of approximately 13.5 Å showed, apart from discrete reflections, truncated horizontal streaks (constant $Y$). The discrete or "family" reflections had orthorhombic symmetry

as did those parts of the streaks corresponding to a unit cell with the ap-
proximate dimensions: $a = 8.5$ Å, $b = 9.7$ Å, and $c = 13.5$ Å.

The following conditions of reflection were noted:

(i)   discrete reflections, $hkl$, for $h = 2H$
     diffuse streaks, $hk\zeta$, for $h = 2H + 1$, where $\zeta$ can assume any value
(ii)  $Hkl$: $H + l = 2n$
(iii) $hk0$: $h + k = 2n$
(iv)  $0kl$: $l = 2n$

According to (i) and (ii), the superposition structure,[14] corresponding to the
family reflections, $Hkl$, has an $a$ axis of one-half 8.5 Å and is $B$ face-centred
with $Bmmb$ and $Bm2_1b$ as possible space groups [$cf$. (ii) and (iii)]. Reflection
condition (iii) indicates the presence of an $n$ glide perpendicular to the $c$ di-
rection. This is independent of the mode of stacking of the layers and must
therefore be a layer symmetry operation. Reflection condition (iv) is a special
case of (ii) but also indicates the presence of a $c$ glide perpendicular to the $a$
axis in the larger orthorhombic cell, $i.e.$ that with the approximate dimensions
$a = 8.5$ Å, $b = 9.7$ Å, and $c = 13.5$ Å.

The information which could be obtained from the reflection conditions
was thus that the space group of the superposition structure was $Bmmb$ or
$Bm2_1b$, that one of the ordered extreme structures, $i.e.$ so-called "structure of
maximum degree of order," MDO,[14] was orthorhombic, belonging to space
group $Pc2_1n$, and that the unit cell of the former structure was related to that
of the latter by a halving of the $a$ axis. From this information it was then
possible to determine the OD groupoid.[14]

The derivation of the OD groupoid may be illustrated by means of symbols
as, for example, in Fig. 1a. This figure shows the packing of the layers $L_0$,
$L_1$, and $L_2$ in the orthorhombic structure of maximum degree of order, MDO$_1$.
According to reflection condition (iii), the minimum symmetry of a single
layer is $P11(n)$. The $B$ face-centring of the superposition structure implies, as
will be seen later, that $L_1$ is related to $L_0$ by a translation of $\vec{a}/4$. In the ordered
orthorhombic structure, MDO$_1$, there is a $c$ glide plane perpendicular to the
$a$ axis [$cf$. reflection condition (iv)]. This means that the third layer, $L_2$, must
come directly under the first in the $c$ direction and, moreover, that the minimum
layer symmetry $P11(n)$ is insufficient, the true layer symmetry being $Pm2_1(n)$.
The symmetry operations which convert $L_0$ into $L_1$ are then seen to be
$_{0,1}[c_2 2_1 n_{\bar{\frac{1}{4}},1}^-]$, while $L_1$ is converted into $L_2$ by the operations $_{1,2}[c_2 2_1 n_{\frac{1}{4},1}]$.

Potassium oxopentacyanovanadate(IV) can thus be said to crystallize
as a family of structures whose symmetry is characterised by the OD groupoid
symbol [14]

$$P \quad m \quad 2_1 \quad (n)$$
$$\{c_2 \quad 2_1 \quad (n_{\bar{\frac{1}{4}},1}^-)\}$$

This symbol gives the total symmetry of any pair of consecutive layers,
$L_p$ and $L_{p+1}$.

Whereas the $c_2$ glide is a total symmetry operation in the ordered
orthorhombic structure, it can be just a partial operation, as illustrated in
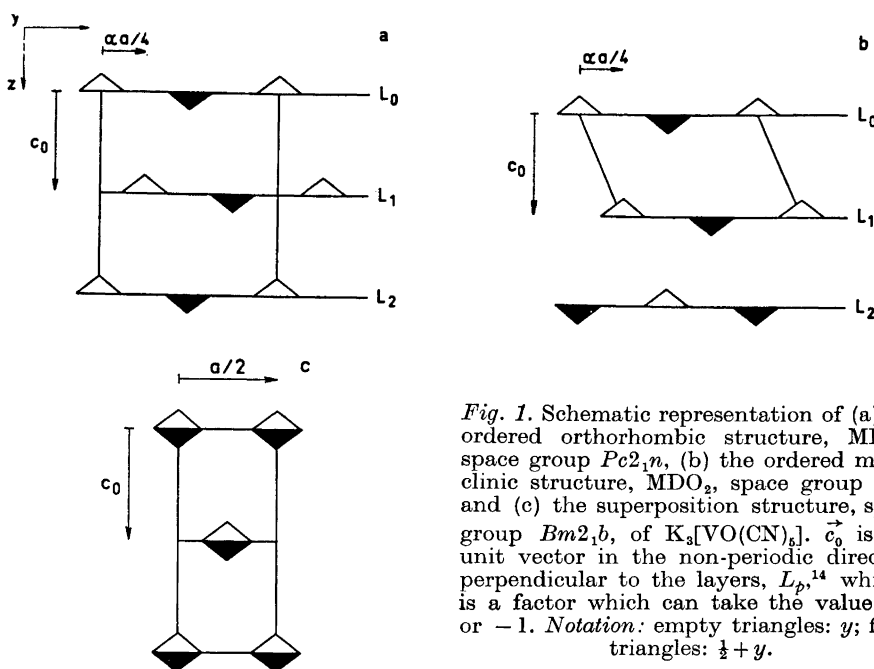
*Fig. 1.* Schematic representation of (a) the ordered orthorhombic structure, $MDO_1$, space group $Pc2_1n$, (b) the ordered monoclinic structure, $MDO_2$, space group $P2_1$, and (c) the superposition structure, space group $Bm2_1b$, of $K_3[VO(CN)_5]$. $\vec{c_0}$ is the unit vector in the non-periodic direction perpendicular to the layers, $L_p$,[14] while $\alpha$ is a factor which can take the value $+1$ or $-1$. *Notation:* empty triangles: $y$; filled triangles: $\frac{1}{2} + y$.

Fig. 1b. This gives rise to a monoclinic structure which is the other ordered extreme structure ($MDO_2$).

In other words, successive layers may be regarded as being related to one another by the translation $\alpha \vec{a}/4$, where $\alpha$ can take the value $+1$ or $-1$. If $\alpha$ is alternately $= \pm 1$, an ordered orthorhombic structure ($MDO_1$) with the approximate unit cell dimensions $a = 8.5$ Å, $b = 9.7$ Å, and $c = 2c_0 = 13.5$ Å is obtained. As is apparent from Fig. 1a, the space group of this structure is $Pc2_1n$ (conventional setting:[15] No. 33, $Pna2_1$). An oblique stacking of the layers, *i.e.* $\alpha = +1$ (or $\alpha = -1$) only, as illustrated in Fig. 1b, results in a monoclinic structure ($MDO_2$), belonging to space group $P2_1$, whose unit cell is given by $\vec{a}_{mon} = \vec{a}$, $\vec{b}_{mon} = \vec{b}$, $\vec{c}_{mon} = \frac{1}{4}\vec{a} + \vec{c_0}$ and $\beta \approx 107°$. In principle, each crystal can exhibit a different sequence of $\alpha$ values so that the structure of a given crystal is most appropriately described in terms of contributions from the two ordered extreme structures.

The superposition structure is obtained by taking any given arrangement, translating through $\vec{a}/2$ and superimposing on the original arrangement (*cf.* Fig. 1c), *i.e.*

$$\hat{\varrho}(x,y,z) = \frac{1}{2}[\varrho(x,y,z) + \varrho(x + \tfrac{1}{2},y,z)]$$

where $\varrho(x,y,z)$ represents the superposition structure and $\varrho(x,y,z)$ the real structure. This structure is a fictitious structure which is the same for all members of the OD family. As is apparent from Fig. 1c, the space group of

this structure can unequivocally be derived to be $Bm2_1b$ (conventional setting:[15] No. 36, $Cmc2_1$).

There is another OD groupoid which is consistent with the reflection conditions, namely

$$P \quad m \quad m \quad (n)$$
$$\{c_2 \quad n_{2,\frac{1}{2}} \quad (n_{\frac{1}{2},1}^-)\}$$

The possibility that $K_3[VO(CN)_5]$ crystallized as a family of structures characterised by this OD groupoid could, however, be ruled out since the groupoid implies the centrosymmetric $Pcmn$ (conventional setting:[15] No. 62, $Pnma$) as space group for the orthorhombic structure of maximum degree of order. As will be apparent from the atomic coordinates obtained in $Pna2_1$, this would necessitate statistical occupation for vanadium, which would be most unlikely to occur in an ordered extreme structure.


ACCURATE UNIT CELL PARAMETERS

Crystals of $K_3[VO(CN)_5]$ were picked out of their mother-liquor under a microscope, dried between filter papers and pulverised. Powder photographs

Table 1. X-Ray powder diffraction data for $K_3[VO(CN)_5]$ .Guinier camera, $CuK\alpha_1$ radiation ($\lambda = 1.54050$ Å).

| H k l | $10^5 \sin^2 \theta_{obs}$ | $10^5 \sin^2 \theta_{calc}$ | $I_{calc}$ (relative scale) | $I_{obs}$ |
|---|---|---|---|---|
| 0 2 0 | 1311 | 1308 | 63 | m |
| 0 0 2 | 2479 | 2480 | 68 | m |
| 1 1 0 | 3588 | 3589 | 208 | s |
| 0 2 2 | 3785 | 3788 | 714 | vs |
| 1 1 1 | 4211 | 4209 | 74 | m |
| 0 4 0 | 5231 | 5232 | 68 | m |
| 1 3 0 | 6202 | 6205 | 638 | vs |
| 1 3 1 | 6826 | 6825 | 666 | vs |
| 0 4 2 | 7714 | 7712 | 21 | vw |
| 1 3 2 | 8674 | 8685 | 153 | m − s |
| 1 1 3 | 9170 | 9170 | 335 | s |
| 0 0 4 | 9914 | 9921 | 60 | w |
| 0 6 1 | 12394 | 12391 | 47 | w |
| 2 0 0 | 13044 | 13049 | 160 | m − s |
| 1 5 2 | 13906 | 13917 | 169 | m − s |
| 0 6 2 | 14256 | 14252 | 115 | m |
| 0 4 4 | 15152 | 15153 | 46 | w |
| 2 2 2 | 16837 | 16837 | 109 | m |
| 2 4 0 | 18284 | 18281 | 47 | w |
| 2 4 1 | 18900 | 18901 | 8 | vvw |
| 1 7 1 | 19901 | 19904 | 36 | w |
| 0 8 0 | 20922 | 20927 | 10 | vvw |
| 2 6 1 | 25438 | 25440 | 22 | vw |
| 2 6 2 | 27302 | 27300 | 73 | m |
| 2 4 4 | 28206 | 28202 | 32 | vw |
| 3 3 1 | 32918 | 32923 | 21 | vw |

were taken in a Guinier focusing camera with $CuK\alpha_1$ radiation, using KCl as an internal standard ($a_{KCl} = 6.2919_4$ at $20°C$ [16]). Twenty-six family reflections, $Hkl$, were indexed and used to refine the unit cell dimensions of the superposition structure with the program POWDER.[17] The following values were obtained:

$$A = \phantom{0}4.2646 \pm 0.0003 \text{ Å}$$
$$b = 13.4700 \pm 0.0012 \text{ Å}$$
$$c = \phantom{0}9.7818 \pm 0.0015 \text{ Å}$$
$$V = 562 \text{ Å}^3$$

the axes being labelled in accordance with the conventional setting [15] of $Bm2_1b$, i.e. $Cmc2_1$. Observed and calculated $\sin^2 \theta$ values are listed in Table 1.

The calculated density based on two formula units of $K_3[VO(CN)_5]$ in the unit cell of the superposition structure is $1.86$ g $cm^{-3}$. The experimental density as determined by the method of flotation using bromoform and carbon tetrachloride is $1.88$ g $cm^{-3}$.

The unit cell dimensions of the ordered orthorhombic structure, $MDO_1$, are thus $a = 13.4700 \pm 0.0012$ Å, $b = 8.5292 \pm 0.0006$ Å, $c = 9.7818 \pm 0.0015$ Å, and $V = 1124$ Å$^3$, the axes being labelled in accordance with space group No. 33, $Pna2_1$. Each unit cell contains four formula units of $K_3[VO(CN)_5]$.

## DETERMINATION OF THE SUPERPOSITION STRUCTURE

A crystal was mounted along the $b$ axis (direction of non-periodicity when axes labelled in accordance with space groups No. 63,[15] $Cmcm$ and No. 36,[15] $Cmc2_1$, i.e. $A = 4.2646$ Å, $b = 13.4700$ Å, $c = 9.7818$ Å) and Weissenberg photographs of the layers $h0l - h7l$ were registered with $CuK\alpha$ radiation, using multiple film equi-inclination techniques. The intensities of the 121 discrete, or "family", reflections, $Hkl$, were estimated visually by comparison with a logarithmic intensity scale and the reflections from the different layers were scaled together approximately according to the times of exposure. Since the linear absorption coefficient for $K_3[VO(CN)_5]$ in $CuK\alpha$ radiation is 177 $cm^{-1}$, there were appreciable absorption errors in the data.

After correction of the $H0l - H7l$ data for Lorentz and polarisation effects with the program DATAP2,[17] a three-dimensional Patterson calculation (program DRF [17]) revealed the position of the vanadium atom and of one of the potassium atoms (K1). The approximate positions of the remaining atoms were obtained from successive electron density calculations (DRF [17]). Owing to the poor quality of the films, it was not at this stage possible to ascertain the symmetry of the diffuse streaks and thus unequivocally determine the OD groupoid. The superposition structure was therefore, for the time being, assumed to belong to the centrosymmetric space group No. 63,[15] $Cmcm$, this space group occurring far more often than $Cmc2_1$ as space group for superposition structures.[14] As mentioned above, once the OD groupoid had been determined, it was, however, possible to show that $Cmc2_1$ was the correct space group for the superposition structure.

After a few cycles of refinement of the positional and isotropic thermal parameters for all atoms, using the block diagonal least squares program BLOCK,[17] an $R$ value of 0.154 was obtained. Owing to the paucity of data and the overlap of atoms, this refinement was conducted in a series of small steps, only a few parameters being varied at a time, individual layer scale factors being refined alternately with an overall scale factor. The atomic scattering factors of Cromer and Waber [18] were used for all atoms and each $F_o$ value was weighted according to Cruickshank's weighting scheme,[19] $w = (a + F_o + cF_o{}^2 + dF_o{}^3)^{-1}$, with $a = 10.0$, $c = 0.05$ and $d = 0$. The positional and thermal parameters thus obtained are listed in Table 2.

Table 2. Approximate positional and thermal parameters in the superposition structure of $K_3[VO(CN)_5]$ according to space group No. 63, *Cmcm*.

| Atom | Occupation No. | $x$ | $y$ | $z$ | $B$ (Å²) |
|------|------|------|------|------|------|
| V | 4a | 0.50 | 0.000 | 0.000 | 0.000 | 5.0 |
| K(1) | 8f | 0.50 | 0.000 | 0.264 | 0.219 | 4.1 |
| K(2) | 8f | 0.25 | 0.500 | 0.470 | 0.079 | 4.6 |
| N(1) | 8f | 1.00 | 0.500 | 0.157 | 0.090 | 8.3 |
| N(2) | 8f | 0.25 | 0.500 | 0.420 | 0.267 | 8.7 |
| C(1) | 16h | 0.50 | 0.339 | 0.091 | 0.057 | 8.9 |
| C(2) | 8f | 0.25 | 0.500 | 0.445 | 0.268 | 4.6 |
| O(1) | 8f | 0.25 | 0.500 | 0.446 | 0.148 | 7.9 |

As will be apparent after the description of the ordered orthorhombic structure, there is considerable overlap of atoms in the superposition structure. It was not therefore considered worthwhile to refine the structure further or to attempt to locate the positions of the individual atoms more accurately by trial and error. The nitrogen position, N(1), for example, arises from the superposition of four different nitrogen equipoints [N(1) – N(4)] in the ordered orthorhombic structure. Similarly, the position C(1) is a crude approximation of the superposition of C(1) – C(4) in the ordered orthorhombic structure, the positions of these atoms when superimposed by no means eclipsing one another completely. For the same reason, the separation of C(2), N(2), and O(1) in the superposition structure is essentially arbitrary. Nor was it considered worthwhile, once the ordered orthorhombic structure had been determined, to redetermine the superposition structure in the correct space group, $Cmc2_1$. The superposition structure is, after all, essentially fictitious and has value only as a means to determining the true structure, approximate to one, or both, of the ordered extremes, since bond distances and angles derived from such a superposition structure must inevitably be mean values.

DETERMINATION AND REFINEMENT OF THE MDO₁ STRUCTURE

A new crystal was mounted along the $a$ axis (direction of non-periodicity when axes labelled in accordance with space group No. 33,[15] $Pna2_1$, *i.e.* $a =$

13.4700 Å, $b = 8.5292$ Å, and $c = 9.7818$ Å) and Weissenberg photographs of the layers $0kl - 12kl$ were recorded with $MoK\alpha$ radiation, using multiple film equi-inclination techniques. The intensities of the 292 family reflections, $hKl$, and of the streaks at the orthorhombic lattice points (*i.e.* corresponding to a unit cell of the dimensions $a = 13.4700$ Å, $b = 8.5292$ Å, and $c = 9.7818$ Å) were estimated visually by comparison with a logarithmic intensity scale. Owing to the way in which the data were collected, *i.e.* for an $a$ axis of 13.4700 Å, it was not possible to estimate the intensities of the streaks at the monoclinic lattice points and thus also determine the $MDO_2$ structure.

For each of the layers $0kl - 12kl$, the reflections were divided into two groups, one comprising the family reflections, $hkl$, with $k = 2K$ and one the non-family reflections, $hkl$, with $k = 2K + 1$. Each group was assigned a separate scale factor, provision thus being made for twenty-six "layers", rather than thirteen. Approximate layer scale factors were calculated from exposure times and the data were corrected for Lorentz and polarisation effects with the program DATAP2.[17] No correction was applied for absorption (linear absorption cofficient for $K_3[VO(CN)_5]$ in $MoK\alpha$ radiation $= 20.2$ cm$^{-1}$).

A Patterson synthesis of the non-family data ($0kl - 12kl$, with $k = 2K + 1$, 235 reflections in all) was calculated with the program DRF.[17] From such a calculation [14] it is possible to obtain vectors between atoms within a single layer. The most dominant peaks, together with their relative heights and interpretation are listed in Table 3. It was thus possible to obtain the positions of the K(1) and K(2) potassium atoms relative to vanadium, these being a single position, K(1), in the superposition structure. Unfortunately no constructive information concerning the relative positions of K(3) and V could be obtained from the Patterson synthesis.

*Table 3.* Analysis of the most dominant vectors in the Patterson synthesis of the $0kl$-$12kl$, $k = 2K + 1$ data for $K_3[VO(CN)_5]$. Height of origin peak $= 999$.

| Peak No. | $u$ | $v$ | $w$ | Peak height | Interpretation |
|----------|--------|--------|--------|------|------------|
| 1 | 0.0000 | 0.5000 | 0.0891 | 374 | V − K(3) |
| 2 | 0.2998 | 0.0002 | 0.2170 | 160 | V − K(1) |
| 3 | 0.2637 | 0.5001 | 0.2875 | 151 | V − K(2) |
| 4 | 0.0000 | 0.0000 | 0.4160 | 318 | V − K(3) |
| 5 | 0.0000 | 0.5000 | 0.5000 | 459 | V − V |

In the superposition structure the vanadium atom was found to occupy the position $Cmcm$: $4a$. Initially, therefore, V was placed in $Pna2_1$: $4a$ with $x = \frac{1}{4}$, $y = \frac{1}{8}$, $z = 0$, which corresponds to the origin in the superposition structure. Successive electron density calculations (DRF [17]) using the signs obtained with the potassium and vanadium atoms in the following approximate positions:

| | | $x$ | $y$ | $z$ |
|---|---|---|---|---|
| V | $4a$ | 0.250 | 0.125 | 0.000 |
| K(1) | $4a$ | 0.050 | 0.375 | 0.217 |
| K(2) | $4a$ | 0.486 | 0.375 | 0.788 |
| K(3) | $4a$ | 0.220 | 0.125 | 0.411 |

revealed the positions of the ligand atoms. The other possible positions of K(3) relative to V according to the superposition structure could be discarded since the above set yielded the lowest $R$ value ($R = 0.28$). Once the ligand atoms had been determined it became, however, apparent that K(3) and V had been wrongly labelled. This was supported by the results of a few cycles of block diagonal least squares refinement, a much lower isotropic temperature coefficient being obtained for K(3) (1.2 Å²) than for V (4.4 Å²), both K(1) and K(2) having $B \approx 3.5$ Å².

When the positions of all the atoms had been determined the structure was refined using the block diagonal least squares program, BLOCK.[17] The atomic scattering factors of Cromer and Waber [18] were used for all atoms and Cruickshank's weighting scheme [19] was employed with $a = 25.0$, $c = 0.02$ and $d = 0$. At first all twenty-six scale factors were allowed to vary independently and, after a few cycles of refinement, the mean ratio between the scale factors for the non-family reflections and the family reflections for each layer was seen to be approximately 1.9. An attempt was then made to determine an approximate value for the percentage contribution from the $MDO_1$ structure in order to be able to hold this parameter constant in the subsequent refinement. The structure was therefore refined with the non-family data only. This refinement had to be carried out in small steps, a few parameters being varied at a time, owing to the paucity of the data (235 reflections). The layer scale factors thus obtained were then used to scale the data into two "layers", one comprising all the family reflections and the other all the non-family reflections. Refinement based on this data set then yielded a scale factor between the $F_o$ values of the non-family and the family reflections and thus an estimate of the percentage of $MDO_1$ structure in the actual crystal studied. This procedure was repeated, a scale factor of 1.89 being finally adopted. This would appear to correspond to a $MDO_1$ contribution of just over 50 %. (Attempts were made to find a crystal which had a structure better approximating that of either the $MDO_1$ or the $MDO_2$ structure. Those crystals investigated all yielded, however, approximately the same intensity distribution as the crystal described in this paper, i.e. they all contained roughly equal contributions from the two MDO structures.)

The data were then re-stored in the thirteen layers $0kl - 12kl$, the $F_o$ values of all the non-family reflections being multiplied by 1.89. Individual layer scale factors, atomic parameters and isotropic temperature coefficients were refined with the program BLOCK.[17] For the final cycles of refinement the full matrix least squares program LALS [17] was used with an overall scale factor and anisotropic temperature coefficients for K(1), K(2), K(3) and V. The refinement was terminated when the parametral shifts for the majority of the atoms were less than 10 % of the standard deviations, those for $z_{N(3)}$ and $z_{C(3)}$ being approximately 20 % of the corresponding e.s.d.'s. A final $R$

Table 4. Atomic coordinates, expressed as fractions of the cell edges, and thermal parameters for $K_3[VO(CN)_5]$. The estimated standard deviations of the parameters ($\times 10^4$; $\times 10^2$ for $B$) are given within parentheses. Anisotropic temperature coefficients are of the form exp $\{-(h^2\beta_{11}+k^2\beta_{22}+l^2\beta_{33}+hk\beta_{12}+hl\beta_{13}+kl\beta_{23})\}$ and isotropic temperature coefficients of the form exp $\{-B(\sin^2\theta/\lambda^2)\}$.

| Atom | $x$ | $y$ | $z$ | $B$ (Å²) | $\beta_{11}$ | $\beta_{22}$ | $\beta_{33}$ | $\beta_{12}$ | $\beta_{13}$ | $\beta_{23}$ |
|---|---|---|---|---|---|---|---|---|---|---|
| V | 0.2251(3) | 0.1279(6) | 0.4226(6) | | 0.0038(2) | 0.0076(4) | 0.0072(3) | 0.0000(7) | 0.0021(5) | 0.0017(22) |
| K(1) | 0.0197(4) | 0.3672(24) | 0.2171(9) | | 0.0044(4) | 0.0087(12) | 0.0119(6) | 0.0012(12) | −0.0050(7) | −0.0073(24) |
| K(2) | 0.4899(5) | 0.3608(21) | 0.7411(8) | | 0.0047(4) | 0.0057(17) | 0.0130(7) | 0.0010(9) | −0.0003(6) | 0.0015(17) |
| K(3) | 0.2534(4) | 0.1256(9) | 0.0000 | | 0.0047(3) | 0.0101(6) | 0.0094(5) | −0.0003(12) | 0.0007(6) | 0.0034(25) |
| N(1) | 0.3986(21) | 0.4013(31) | 0.3868(25) | 4.95(57) | | | | | | |
| N(2) | 0.4139(19) | 0.3542(50) | 0.0624(22) | 3.83(55) | | | | | | |
| N(3) | 0.0864(18) | 0.3933(51) | 0.5565(22) | 3.84(53) | | | | | | |
| N(4) | 0.1004(20) | 0.3535(44) | 0.8989(28) | 5.00(53) | | | | | | |
| N(5) | 0.3332(31) | 0.1306(46) | 0.7303(58) | 4.41(38) | | | | | | |
| C(1) | 0.3360(21) | 0.2983(27) | 0.3951(25) | 3.34(48) | | | | | | |
| C(2) | 0.3678(21) | 0.4478(30) | 0.0042(30) | 2.75(43) | | | | | | |
| C(3) | 0.1332(22) | 0.3027(30) | 0.5207(28) | 3.08(50) | | | | | | |
| C(4) | 0.1610(26) | 0.4523(34) | 0.9091(41) | 3.90(53) | | | | | | |
| C(5) | 0.2979(31) | 0.1315(44) | 0.6359(42) | 3.83(40) | | | | | | |
| O(1) | 0.1739(13) | 0.1325(29) | 0.2703(15) | 3.54(29) | | | | | | |

*Table 5.* Observed and calculated structure factors for K₃[VO(CN)₅]. The columns are *l*, $F_o$, $F_c$ and the phase in radians, respectively. Unobserved reflections are denoted with an asterisk. For each layer the family reflections are listed before the non-family reflections. The reflections 242 and 642 were too strong to be measured accurately and were therefore omitted from the data set.

```
   0  0  L            3  69  56 -1.06        8   -  16 -0.48*       7   -  21  1.59*       4  20  20 -2.54
 4 154 135 -0.74      4   -  14 -1.60*       9   -  10 -2.12*       8  22  20  2.84         5  37  42  1.80
 6 108  98  2.50      5  45  51 -0.92       10   -   1  3.02*       9  25  22  0.68         6  25  26 -2.79
 8  31  33  0.70      6  29  29  0.54       11   -  14 -2.87*      10   -   9  0.12*        7  18  15  1.60
10  32  36  1.09      7  50  47 -1.56       12   -   1  2.33*      11   -   7  0.17*        8   -  15  1.68*
12  19  19 -0.30      8   -  10 -1.94*       2  5  L              12   -   1  2.92*        9  26  25  0.52
   0  4  L            9   -  18 -2.16*       0  17  16  0.00        3  5  L               10   -   2  0.55*
 2  25  24  0.56     10   -  11  0.61*       1  29  31 -2.37       0  17  15 -0.00        11   -   5 -0.82*
 4  93  89  2.42       1  5  L               2  17  19 -1.30       1  20  18 -2.78        12   -   6  0.23*
 6  61  59 -0.44      0   -   1  0.00*       3  34  36  2.16       2   -   8 -0.53*          4  5  L
 8  11  10 -2.99      1  21  16  0.72        4   -  10 -1.11*      3  23  25  2.34         0   -   9 -3.14*
10  21  23 -1.78      2  21  20  1.81        5  34  39  2.41       4   -  11 -1.40*        1   -   5 -0.59*
12  13  13  2.86      3  34  34 -0.73        6   -   1 -1.55*      5  39  41  1.73         2  20  19  2.18
   0  8  L            4   -   7 -1.93*       7  38  41  1.23       6   -   5  1.45*        3  31  34 -0.48
 0  83  83 -0.00      5  28  30 -1.05        8   -   5  1.49*      7  26  24  1.34         4   -   7 -2.14*
 2  12  14 -2.81      6   -  12  1.07*       9   -   7  0.99*      8   -  11  2.92*        5  40  45 -1.46
 4  37  41 -0.82      7  30  28 -1.92       10   -   6  0.29*      9   -  16  0.81*        6   -  18  0.63*
 6  20  24  2.86      8   -  13 -2.41*      11   -  12  0.32*     10   -   8  0.67*        7  25  22 -1.27
 8   -   3 -1.15*     9   -  15 -2.83*       2  7  L              11   -   3  0.96*        8   -  11 -1.03*
   0 12  L            1  7  L               0   -   7 -0.00*       3  7  L               9  25  23 -2.19
 0  31  34  3.14      0   -   8  0.00*       1   -   4 -2.49*      0   -   0 -3.14*       10   -   4  0.25*
 2   -   5  1.85*     1  24  20 -2.21        2   -   3  0.62*      1   -  11 -0.39*       11   -   2 -0.84*
 4  14  17  2.23      2   -   3 -2.79*       3  23  27  2.24       2   -  11  2.60*         4  7  L
   0  1  L            3  30  28  2.41        4   -   3  0.04*      3  23  20 -0.47        0   -   1 -3.14*
 5  59  60  1.80      4   -  16  0.81*       5  17  18  2.38       4   -  10  0.98*        1   -  12 -0.89*
 7  33  32  1.53      5  26  29  2.07        6   -   3  2.99*      5  28  28 -0.90        2  20  18  1.78
 9  34  33  0.40      6   -  14 -2.55*       7  27  24  1.22       6   -   1 -0.69*        3   -  10 -0.58*
11   -   5  1.07*     7  30  27  1.35        8   -   5  2.96*      7   -  14 -1.24*        4   -   7  0.67*
   0  3  L            8   -   7  1.21*       9   -   6  0.69*      8   -  14 -0.12*        5  22  24 -1.37
 1  21  20  2.33      1  9  L              10   -   1 -0.53*       9   -  14 -2.32*       6   -  10  0.58*
 3  42  43  2.10      0   -   6 -3.14*       2  9  L             10   -   6 -2.39*        7   -   9 -1.40*
 5  59  58  1.74      1   -   6  1.99*       0   -   5 -3.14*      3  9  L               8   -   6 -1.76*
 7  36  34  1.75      2   -  11 -1.47*       1   -  13  0.58*      0   -   9  3.14*        9   -  15 -2.44*
 9  31  27  0.81      3   -  14  2.17*       2   -  13  1.38*      1   -   9  0.74*         4  9  L
11   -   8  1.61*     4   -   6  3.00*       3   -  13 -1.12*      2   -   6  1.03*        0   -   9 -0.00*
   0  5  L            5   -  14  2.07*       4   -  12  0.96*      3   -   6 -0.56*        1   -   5 -1.70*
 1  14  15  0.79        2  0  L               5   -  19 -0.58*      4   -  12  1.06*        2   -  13 -1.10*
 3  40  41 -0.29      0  13  14 -0.00        6   -   7  0.07*      5   -  16 -1.52*        3   -  18  3.06*
 5  34  37 -1.03      1  45  38  0.38        7   -  21 -1.89*        4  0  L               4   -   2 -2.71*
 7  19  22 -1.20      2   - 126 -0.43*       2 11  L              4 115 109 -0.79         5   -  19  1.57*
 9  22  25 -2.76      3  47  38  2.60        0   -   5  3.14*      5  28  28  0.50          6   -  12 -2.76*
11   -   3  2.98*     4  27  28 -2.60        1   -   2  2.10*      6  20  22 -2.86          4 11  L
   0  7  L            5  18  18 -0.80        2   -   3 -2.41*      7  23  22 -1.90        0   -   1 -3.14*
 1  21  18  0.64      6  54  47 -1.16        3   -  13 -0.79*      8  14  20 -1.23         1   -   8  2.34*
 3  16  15 -0.43      7  14  17 -2.15        4   -   3 -2.90*      9   -  12  2.06*        2   -   6 -1.13*
 5  32  32 -1.46      8  35  32  1.70        5   -   5 -1.03*     10  25  25  1.46         3   -   4  2.17*
 7  19  16 -1.73      9   -  10 -1.74*        3  2  L             11  13  13  2.73         4   -   2 -2.46*
 9   -  17 -2.64*    10  12  13  0.45        3  62  56  2.73       12   -  12  0.04*        5   -  12  1.88*
   0  9  L           11   -   2  1.85*       4  44  47 -1.05        4  4  L                5  2  L
 1   -   6  1.57*    12  15  18  0.60        5 105  94 -0.72       1  35  37 -2.42         3  56  54 -2.91
 3  19  19  2.72       2  8  L               6  28  31  2.42       2   -  10  1.42*        4  23  27  1.10
 5   -  20  2.09*     0   -   8  3.14*       7  36  38  3.09       3  60  54  2.90         5  37  35 -0.61
 7   -  16  2.31*     1  18  18 -2.92        8  17  19  1.54       4  82  82  2.37         6  25  28  2.36
   0 11  L            2  69  57  2.71        9  12  14 -1.47       5  16  17  2.91         7  47  48  1.68
 1   -  10 -2.55*     3   -   1 -0.22*      10  19  21  0.87       6  16  16 -0.48         8  26  25 -1.80
 3   -   3 -3.02*     4  12  14  0.43       11  14  14  1.80       7  22  24  1.11         9  16  17 -0.33
   1  2  L            5  16  15  2.08       12   -  13  0.01*      8  12  13  2.75        10  17  18 -2.55
 4  69  65  2.24      6  22  22  1.92        3  6  L              9  11  12 -0.96        11   -   6  0.12*
 5  23  24 -0.59      7   -   9  1.06*       0  95  86  3.14       10  25  25 -1.95       12  15  16 -2.77
 6  29  39  1.37      8  20  17 -1.41        1  71  69 -3.01      11   -  10 -0.66*       13  15  11 -1.66
 7  34  32  1.91      9   -   4  1.20*       2  31  35  2.60       12  13  13 -3.06         5  6  L
 8  15  15 -1.88     10   -   7 -2.61*       3  48  50 -0.62        4  8  L               0   -   3  3.14*
 9  24  27 -1.24       2 12  L               4  23  29  1.89       0  72  67 -0.00        1  33  33  2.51
10  16  19 -1.96      0   -   6 -0.00*       5  31  36  2.75       1  14  15  1.10         2  54  52 -0.40
11   -   4  1.36*     1   -   5  0.64*       6  14  15 -0.25       2   -  10 -0.97*        3  37  37 -0.13
   1  6  L            2  26  23 -0.49        7  19  20 -0.56       3  24  23 -0.23         4  11  11 -2.22
 0  99  87 -0.00        2  1  L               8   -   8 -1.09*      4  36  38 -0.77         5  15  14  2.67
 1  43  42  2.86      4  12  13  2.73        9   -  10  1.55*      5   -   7 -0.47*        6  20  21 -1.16
 2  55  56 -0.66      5  51  54 -0.78       10   -  12 -2.19*      6  13  11  2.32         7  34  32 -1.36
 3  54  49 -0.29      6  15   7  0.41       11  14  11 -0.98       7  14  14 -1.98         8   -   7  1.91*
 4  27  35 -1.10      7  57  55 -1.92       12   -   8 -3.13*      8   -   7  0.03*        9   -   8  2.89*
 5  27  31  2.18      8   -  14 -0.84*       3 10  L              9   -   6  2.34*        10   -   5  0.95*
 6   -  12 -2.17*     9  16  10 -2.33        0  32  31 -0.00       10  16  16  1.07         5 10  L
 7  15  16 -1.01     10   -   6 -1.94*       1  26  27  0.16        4 12  L               0   -   8  3.14*
 8  18  21  1.18     11  17  14 -2.83        2  14  14 -0.54       0  20  20  3.14         1  14  14 -0.92
 9  15  16  1.92     12   -   6 -1.78*       3   -  14  2.46*      1   -   5 -1.56*        2  26  25  2.68
10   -  19  0.88*      2  3  L               4   -  15 -1.14*      2   -   3  1.23*        3  21  20  3.00
   1 10  L            2  23  19  1.30        5  18  18 -0.69       3   -   5  3.09*        4   -   5  1.19*
 0  28  28  3.14      3  53  51 -1.12        3  1  L              4  14  12  2.17         5   -   4 -0.29*
 1  16  17 -0.28      4  19  18  0.69        4  14  13  1.47        4  1  L               6   -   6  1.77*
 2  18  21  2.53      5  33  38 -0.65        5  59  60 -1.30       3  46  45  2.69         7  15  13  1.62
 3  20  19  2.78      6  19  22  0.07        6   -   4 -2.10*      4   -   7  1.07*        5  1  L
 4   -  12  1.95*     7  37  43 -1.83        7  26  31 -1.72       5  64  62  1.84         3  43  43  2.17
 5   -  11 -0.84*                            8   -  13 -0.17*      6  30  27 -2.48         4   -   6 -0.88*
   1  1  L                                   9  27  25 -2.32       7  28  28  1.98         5  34  36  1.94
 4  19  21  1.05                            10   -  10 -3.03*      8  18  16  2.09         6  34  34 -2.78
 5  54  56  2.26                            11   -   7 -2.38*      9  30  28  0.90         7  34  31  1.39
 6  21  19 -2.13                            12   -   4 -1.37*      10   -   4  2.91*        8   -  17  1.97*
 7  48  47  1.40                             3  3  L             11   -   1 -1.51*        9   -  16  1.38*
 8   -  16  0.59*                           1  17  20 -3.12       12   -   9  0.65*       10   -   7  2.63*
 9   -  20  0.42*                           2  36  35 -1.41        4  3  L               11   -   9  0.39*
10   -   7 -2.41*                           3  24  31  2.65       0  14  16 -0.00        12   -   8  0.44*
11   -  10  0.08*                           4  38  35 -2.40       1  15  16 -2.70        13   -   2  1.95*
   1  3  L                                   5  43  43  2.13       2  59  51 -1.38         5  3  L
 2  26  23  1.06                            6  19  16  3.00       3  26  30  3.11         0  39  43  3.14
```

**Table 5. Continued.**

```
 1  29   24  1.16        9   -    9 -2.03*       7   -    8  2.30*       1   -    7  0.93*       8   -    1 -2.85*
 2  57   50  1.74       10   -   11 -2.35*       8   -   10  2.96*       2   -   14 -1.11*       9  14   15 -2.47
 3  31   37 -0.47       11   -    7 -3.09*       9   -   15  0.96*       3   -   12  2.71*      10   -    8 -0.47*
 4  19   16  1.82          6 5 L                    7 7 L                  4   -    7 -1.91*      11  13   11  2.10
 5  32   32 -1.21        0   -   15 -0.00*        0   -    8  3.14*       5   -   10  1.38*         10 8 L
 6  24   29  0.26        1  21   21  2.10         1   -    7 -0.53*       6   -   10 -2.55*       0  11    8 -C.00
 7  30   29 -2.00        2  18   15 -1.63         2  21   20  2.48          8 11 L               1  17   18 -2.83
 8  21   19 -1.62        3  15   15  2.02         3   -    9 -0.05*       0   -    2  0.00*       2  15   16  3.08
 9   -   11 -2.29*       4  26   24 -1.88         4   -   17  0.92*       1   -    3  2.34*       3   9    8 -2.21
10   -    4 -1.48*       5  23   23  2.42         5  23   22 -1.51        2   -    7 -0.87*       4   -    2 -2.40*
11   -    9  3.01*       6  17   18  2.95         6   -    8 -0.19*       3   -    0  1.65*       5  21   20  2.26
12   -   10 -2.69*       7  17   15  1.49         7   -    7 -1.13*       4   -    4 -2.96*       6  12   14  2.75
   5 5 L                 8   -   17  3.11*           7 9 L                   9 2 L               7   -    2  1.09*
 0   -    6  3.14*       9   -   11  1.73*        0   -    8  3.14*       3  79   77  3.12          10 1 L
 1  17   13 -1.59       10   -    8  1.21*        1   -   10 -0.85*       4  19   20 -1.19        4  34   31  1.21
 2  18   14  2.00          6 7 L                  2   -    6  1.92*       5  17   16  0.69        5  11   11 -1.43
 3  28   29 -0.52        0  16   17 -0.00         3   -    4 -0.81*       6  15   16  2.50        6  17   18 -0.66
 4   -    2 -2.52*       1   -    3 -2.31*        4   -    9  1.47*       7  28   27  1.98        7  15   12 -1.83
 5  25   23 -0.99        2  17   10 -1.60         5   -   13 -1.38*       8  10    9 -1.23        8  14   14 -0.09
 6  22   22  0.47        3   -   13  2.02*           8 0 L               9  21   21 -0.20        9   -    6 -1.23*
 7  23   22 -1.63        4  18   15 -1.96         4  72   65 -0.41       10   -    8  1.76*      10  16   14 -1.97
 8   -   11 -0.94*       5   -   13  1.59*        5  16   16 -2.75       11   -    5 -0.50*         10 3 L
 9   -   11 -1.74*       6   -   11  2.62*        6  15   15  1.29          9 6 L               1  22   25 -1.49
10   -    6 -0.32*       7  20   17  1.08         7  44   46 -1.59        0   9    6 -0.00       2  10    8  1.01
11   -    7 -3.01*       8   -    9  2.67*        8  24   22 -0.40        1  30   33  1.89       3  15   12 -2.06
   5 7 L                 9   -    6  1.39*        9  16   15 -3.13        2  52   50 -0.21       4  26   28  1.17
 0  21   19  0.00          6 9 L                 10  17   16  1.10        3  52   50  0.02       5   -    7 -0.96*
 1   -    3 -2.39*       0   -   12 -3.14*       11  10    8  2.63        4  11   12  1.26       6   -   13 -0.22*
 2  31   24 -1.67        1   -   10 -0.14*       12   -   10  0.10*       5  13   12 -2.23       7   -   12 -1.28*
 3   -   18  2.49*       2   -    8  2.35*          8 4 L               6  15   15 -0.36        8  18   15  0.21
 4   -   11 -1.34*       3   -    8 -0.81*        0  62   54  2.14       7  16   17 -1.47        9   -    8 -1.15*
 5   -   17  2.22*       4   -   11  1.63*        1  46   50 -0.82       8  11   10  1.20       10   -    9 -1.83*
 6   -   19 -2.74*       5   -   15 -0.70*        2  10   11  1.70       9  19   18  2.80          10 5 L
 7   -   19  1.53*       6   -    6 -0.56*        3  50   44 -3.06          9 10 L              0  27   25  0.00
 8   -    9  1.46*       7   -   10 -1.99*        4  39   41  2.53       0   -    1  0.00*       1   -   12  2.68*
 9   -    8  1.47*          6 11 L               5  14   12 -0.51        1  11   12 -1.10       2  17   15 -C.61
   5 9 L                 0   -    6  3.14*        6  13   11 -0.97        2  18   18  2.98       3   -    6  1.30*
 0   -    6 -0.00*       1   -    2 -2.98*        7  31   31  1.64       3  19   19 -3.10       4  25   23 -1.83
 1   -    3 -1.93*       2   -    4  0.94*        8  15   15  2.52          9 1 L               5  15   10  1.87
 2   -   11 -0.70*       3   -    6 -1.11*        9  11   11  0.06       4  24   26 -1.84       6  16   12  2.51
 3   -   13  2.51*       4   -    8  1.12*       10  10   10 -1.98       5   -    3  1.55*       7   -    9  1.23*
 4   -    2  2.13*       5   -    3 -1.63*       11   -    9 -0.29*       6  23   23  3.11       8   -   12 -3.12*
 5   -    8  1.99*          7 2 L                   8 8 L               7  17   18  1.32          10 7 L
 6   -    8 -2.79*       3  22   29  1.21         0  26   25 -0.00       8   -   10  2.36*      0   -   11 -0.00*
   6 C L                 4  55   57 -0.88         1  18   23  2.17       9   -    6  2.35*       1   -   10  1.69*
 4  45   44 -0.38        5  57   51 -0.50         2   -    5 -2.09*      10   -    9  1.54*      2   -    6 -1.64*
 5  71   67  2.14        6  11    9  0.65         3  22   24  0.04       11   -    6  0.53*      3   -    6  1.53*
 6  38   35  2.70        7  16   20  3.01         4  17   20 -0.67          9 3 L               4  20   16 -1.81
 7  17   23  0.83        8   -   11 -1.40*        5   -    5  2.28*       0  12   16 -3.14       5   -    4  2.26*
 8  30   28 -0.75        9   -   11 -2.47*        6   -    7  2.56*       1  23   25 -1.72       6   -    6  2.78*
 9  13   15  0.74       10  18   18  0.86         7  15   15 -1.60       2  12   10  1.45          11 2 L
10  10   10  2.69       11  23   21  2.24         8   -    7 -0.85*      3  24   26 -1.13       3   8   11  1.43
11  11   11 -1.36          7 6 L                    8 12 L              4  21   18  1.60        4  47   47 -0.26
   6 4 L                 0  36   34  3.14         0  12   12  3.14       5   -    8 -0.80*       5  27   27 -0.73
 0  17   14  0.00        1  52   48 -2.89         1   -    8 -1.38*      6  22   19  0.19        6  15   14  1.25
 1  75   67  0.49        2  12   12 -2.84         2   -    2  2.94*      7  18   20 -1.48        7  15   16 -2.22
 2   -  123 -0.28*       3  11   12 -2.74         3  13   12  2.98       8   -   10 -0.04*       8  22   20 -0.85
 3  23   26  1.05        4  37   36  2.55         4  13    9  2.76       9   -   10 -0.76*       9  12   14 -1.85
 4  33   33  3.08        5  43   41  2.37            8 1 L              10   -    9 -1.08*      10   -    6  C.67*
 5  36   37 -0.91        6  10   11 -2.69         4  25   25 -2.21          9 5 L              11  11   11  2.42
 6  21   21 -0.40        7  12   15  0.46         5  19   22  1.27       0  20   22  3.14          11 6 L
 7  11   15 -2.76        8   -    8  1.86*        6  29   28 -2.90       1   -    5  3.10*      0  37   34  3.14
 8  25   25  2.07        9   -    9  0.95*        7  15   13  1.94       2  19   21  1.88        1  28   29 -2.07
 9  10   14 -2.74       10  14   14 -2.23         8   -   14  1.98*      3   -   11 -1.20*      2  11   11 -0.04
10  12   12 -0.13       11  13   12 -1.09         9  17   16  1.15       4  18   17  1.03        3  10   12 -1.84
11  12   12  1.99          7 10 L                10   -    7  1.82*      5   -    5 -2.62*      4  25   25  2.69
   6 8 L                 0  20   20 -0.00        11   -    2  0.86*      6  16   16 -0.14        5  15   15  2.56
 0   -    6  3.14*       1  19   19  0.41            8 3 L              7  16   15 -2.07        6  12   10 -1.47
 1  29   30 -2.53        2   -    5 -0.36*        0   -    6  0.00*      8   -    9 -1.23*      7  10   12  0.38
 2  54   54  2.82        3   -    6  1.30*        1  21   21  1.68       9   -    4 -1.32*      8  13   11  2.34
 3  12   16 -1.84        4  13   14 -0.86         2  19   23 -0.63          9 7 L              9   -    8  0.72*
 4  14   13  0.11        5  16   16 -0.71         3  25   26  2.39       0   -   18 -0.00*     10   -    5 -2.72*
 5  13   16  2.29        6   -    4  1.25*        4   -    4 -1.52*      1   -   10  1.44*     11  12   10 -C.80
 6  11   12  2.58          7 1 L                  5  27   29  1.56       2   -   10 -1.50*        11 10 L
 7   -    7  0.17*       4  40   37  0.97         6  18   17 -2.68       3   -   12  2.07*     0  12   12 -0.00
 8  13   13 -1.24        5  32   35 -1.44         7  16   14  1.84       4   -   13 -1.58*     1  11   12  0.89
 9   -    9  0.26*       6  19   22 -C.21         8   -   10  2.27*      5   -    3  3.02*     2   -    5  2.45*
10  11    7 -3.08        7   -   10 -0.87*        9   -   14  1.25*      6   -   15 -3.13*     3   -    5  0.79*
   6 12 L                8  19   20 -0.26        10   -    9  2.15*      7   -   11  1.50*     4  13   12 -0.29
 0   -    1 -3.14*       9  20   19 -2.07            8 5 L                 9 9 L              5  11    9 -0.62
 1   -    9  0.40*      10   -   11 -1.99*        0  15   14 -3.14       0   -    4 -0.00*        11 1 L
 2  15   16 -0.28       11   -    1  1.63*        1  13   10 -2.43       1   -    6  0.73*     4  18   19  0.97
   6 1 L                   7 3 L                  2  36   34  1.92       2   -    7 -1.35*     5  14   15 -1.76
 3  23   22 -1.02        0  22   19 -0.00         3   -   14 -0.10*      3   -    9  1.79*     6   -   10  0.29*
 4  39   35  1.32        1  20   20  2.72         4  26   22  0.97          10 0 L            7   -    6 -0.87*
 5  29   32 -0.91        2  29   31 -0.43         5  18   13 -1.96       4  11   12  3.11     8   -   1C -C.52*
 6  24   21 -0.21        3  19   24  2.84         6  23   23  0.31       5  41   40  2.33     9   -    9 -1.84*
 7  21   23 -1.71        4  19   17 -1.78         7   -    9 -0.89*      6  30   34  2.85    10   -    9 -1.76*
 8  17   17 -0.02        5  44   46  1.66         8   -   13 -1.18*      7  11   13 -0.49        11 3 L
 9  18   16 -1.57        6   -    9  2.63*        9   -   10 -1.96*      8   -    4 -1.91*    1  21   21  1.57
10   -    9 -2.35*       7  17   13  1.69            8 7 L              9  18   19  0.26     2  20   21 -1.00
11   -   10 -2.87*       8  18   16  2.94         0   -    6 -3.14*     10  12   13  2.95     3   -    9  0.09*
   6 3 L                 9  19   19  1.07         1   -    8 -1.24*     11  21   17 -1.09     4  27   26 -2.37
 0  43   41  3.14       10   -   12  1.17*        2   -   15  2.39*         10 4 L            5   -    7  0.95*
 1  22   21  0.63          7 5 L                  3   -    8 -0.66*      0  16   18 -3.14     6  17   14 -2.67
 2  23   23  2.11        0   -    9 -0.00*        4   -    5  0.42*      1  31   35  0.37     7   -    8  2.98*
 3  23   28 -0.73        1  19   19  1.90         5   -   12 -1.54*      2  29   30 -0.05     8   -   12  2.87*
 4  24   24  1.61        2  22   21 -1.50         6   -   13  0.26*      3  16   20  0.90     9   -   10  1.60*
 5  30   32 -1.35        3   -    2 -2.63*        7   -    4 -1.26*      4   9    8  0.30        11 5 L
 6   -   14 -0.78*       4  28   29 -2.14         8   -    8 -0.95*      5  35   35 -0.81     0   -   11  0.00*
 7  29   28 -2.16        5  18   19  1.80            8 9 L              6  24   28 -0.38     1  15   14  2.10
 8   -   11 -0.54*       6   -   14  3.00*        0   -    6 -0.00*      7   -    3  2.87*    2  15   15 -0.50
```

*Table 5. Continued.*

```
3   -   5  1.56*    3   -   4 -3.02*    7  17  18  1.64    6  15  15 -2.53    2  13  13  2.34
4   -  10 -2.24*      12   0  L         8  13  14  2.67    7   -   9  1.88*   3  14  14 -1.16
5  15  13  1.39     4  31  29  0.21     9  12  11 -0.46    8   -  10  2.03*   4   -   6  0.93*
6   -   8  2.94*    5   -   5  2.54*   10   -   3  0.30*   9   -   5  2.73*   5   -   3 -2.85*
7   -   3  2.31*    6  13  12  2.53      12   8  L        10   -   7  2.33*   6   -  12  0.77*
8   -   9  2.50*    7  17  17 -1.50    0  13  13 -0.00      12   3  L         7   -   9 -1.17*
   11   7  L        8  13  13 -0.45    1  14  15  2.11    1  15  14  0.86    8   -   7 -1.11*
0   -   3  3.14*    9  14  15  2.62    2   -   5  1.53*   2  18  19 -1.17      12   7  L
1   -  10 -1.42*   10   -   4 -2.36*   3  23  22 -0.19    3   -   7  0.77*   0   -   3  3.14*
2  17  17  2.33    11   -   8  2.90*   4  20  20  0.26    4  18  15 -2.59    1   -   7 -2.13*
3   -   2 -2.46*      12   4  L        5   -   1 -1.15*   5   -   9 -0.66*   2  13  11  2.10
4  19  16  0.77     0  28  28  3.14    6   -   4  0.44*   6  15  16 -2.67    3   -   6 -1.99*
5   -   7 -1.91*    1  25  29 -1.06    7  11  11 -1.52    7   -   5  2.02*   4   -   7  0.51*
6   -   7  0.41*    2   6   8 -1.36    8   9   9 -0.44    8   -   9  2.03*   5   -   4 -2.60*
   11   9  L        3  43  41  2.98      12   1  L        9   -   5  2.12*   6   -   8  0.55*
0   -   3 -3.14*    4  35  34 -2.86    3  14  16  1.88      12   5  L        7   -   5 -1.64*
1   -   8 -1.22*    5   -   2  0.89*   4  11  11 -2.46    0   -   8  3.14*
2   -   4  2.12*    6   -   4 -1.78*   5   -   5  0.20*   1  14  16 -1.96
```

*Table 6.* Bond distances (Å) and angles (°) within the $[VO(CN)_5]^{3-}$ complex ion. Standard deviations of the distances ($\times 10^3$) and the angles are given within parentheses.

Distances

| | | | |
|---|---|---|---|
| $V-C(1)$ | 2.102(26) | $C(1)-N(1)$ | 1.220(37) |
| $V-C(2)$ | 2.136(28) | $C(2)-N(2)$ | 1.160(44) |
| $V-C(3)$ | 2.161(28) | $C(3)-N(3)$ | 1.057(45) |
| $V-C(4)$ | 2.148(32) | $C(4)-N(4)$ | 1.178(46) |
| $V-C(5)$ | 2.306(41) | $C(5)-N(5)$ | 1.039(68) |
| $V-O(1)$ | 1.642(16) | | |

Angles

| | | | |
|---|---|---|---|
| $C(1)-V-C(2)$ | 164.1(1.1) | $C(3)-V-C(5)$ | 80.4(1.2) |
| $C(1)-V-C(3)$ | 89.3(1.0) | $C(3)-V-O(1)$ | 98.4(1.1) |
| $C(1)-V-C(4)$ | 88.1(1.1) | $C(4)-V-C(5)$ | 76.2(1.4) |
| $C(1)-V-C(5)$ | 78.7(1.2) | $C(4)-V-O(1)$ | 105.1(1.3) |
| $C(1)-V-O(1)$ | 99.6(1.0) | $C(5)-V-O(1)$ | 177.9(1.3) |
| $C(2)-V-C(3)$ | 89.7(1.0) | $V-C(1)-N(1)$ | 176.0(2.2) |
| $C(2)-V-C(4)$ | 86.6(1.2) | $V-C(2)-N(2)$ | 172.5(2.5) |
| $C(2)-V-C(5)$ | 85.5(1.3) | $V-C(3)-N(3)$ | 173.0(2.6) |
| $C(2)-V-O(1)$ | 96.3(1.1) | $V-C(4)-N(4)$ | 178.0(3.1) |
| $C(3)-V-C(4)$ | 156.5(1.3) | $V-C(5)-N(5)$ | 177.6(4.1) |

value of 0.083 was obtained for the complete data set ($R = 0.080$ for the family reflections and 0.086 for the non-family reflections). The corresponding atomic parameters are given in Table 4 and observed and calculated structure factors in Table 5. The high $F_c$ values corresponding to some of the unobserved non-family reflections are acceptable, bearing in mind the size of the scale factor by which the $F_o$ values of all the non-family reflections have been multiplied. Bond distances and angles within the $[VO(CN)_5]^{3-}$ ion, calculated with the program DISTAN,[17] are given in Table 6.

The proposed structure was tested by means of a three-dimensional $F_o - F_c$ Fourier synthesis (DRF[17]) which showed a maximum electron density of 1.4 e/Å³.

## DESCRIPTION AND DISCUSSION OF THE STRUCTURE

The ordered orthorhombic structure of $K_3[VO(CN)_5]$ is composed of potassium ions and distorted octahedral $[VO(CN)_5]^{3-}$ ions packed as illustrated in Fig. 2. If the axes are labelled in accordance with $Pna2_1$, the direction of non-
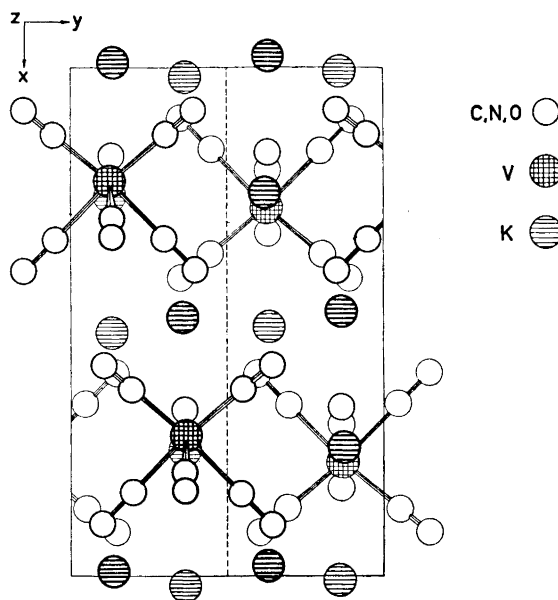
*Fig. 2.* Projection of the unit cell of the $MDO_1$ structure of $K_3[VO(CN)_5]$ along [001].

periodicity in the actual crystals coincides with the $x$ direction and the ordered layers are thus perpendicular to this direction. The first such layer, $L_0$, (*cf.* Fig. 1a) in the unit cell of the ordered orthorhombic structure, may be visualized as comprising the two $[VO(CN)_5]^{3-}$ ions and the two K(3) potassium ions in the upper half of the unit cell shown in Fig. 2, together with the K(1) and K(2) potassium ions, four in all, directly above and below these complex ions in the $x$ direction. The second layer, which is identical with the first, is related to the latter by a translation of $\vec{b}/4$, while the third layer is related to the second by a translation of $-\vec{b}/4$ and lies directly under the first layer in the $x$ direction (*cf.* Fig. 1a). Two of the four K(1) and K(2) potassium ions belonging to the third layer are visible at the lower edge of the unit cell illustrated in Fig. 2.

The superposition structure can be visualized by taking the left-hand half of the unit cell depicted in Fig. 2, translating through $\vec{b}/2$ and superimposing it on the right-hand half of the unit cell. The above-mentioned overlap of atoms in the superposition structure then becomes apparent.

As may be seen from Table 6, the $[VO(CN)_5]^{3-}$ ion has approximately $C_{4v}$ symmetry and shows the distortion characteristic of many vanadyl(IV) complex ions,[12,13] namely a long vanadium-ligand bond *trans* to the $V = O^{2+}$ entity. The $V - C(eq)$ bonds range from 2.10 to 2.16 Å with a mean distance of 2.14 Å while the $V - C(ax)$ bond is 2.31 Å. The $C - N$ distances within the equatorial cyanide groups range from 1.06 to 1.22 Å with a mean distance of 1.15 Å

and the axial C−N distance is 1.04 Å. All the V−C−N linkages are linear within the limits of the standard deviations (3 $\sigma$).

The spread in the V−C(ax) and C−N bond lengths is rather large, as are the standard deviations of all the bond distances and angles. This ought not to be interpreted in terms of severe distortions from the ideal $C_{4v}$ symmetry, but instead as indicative of a slightly lower accuracy and precision in the determination than is usual, as a consequence of the disorder. That this is necessarily the case is apparent on consideration of Fig. 2 and of the super-position structure derived from this figure. The family reflections, $hKl$, which yield the superposition structure, are obviously very insensitive to the posi-tions of the individual ligand atoms. The intensities of the non-family reflec-tions, on the other hand, are difficult to determine accurately owing to asym-metric intensity fluctuations along the streaks and to the fact that most of these reflections are very weak, since the contribution from the ordered orthorhombic structure to the structure of the crystal is not more than ap-proximately 50 %. The mean V−C(eq) bond length of 2.14 Å, is, however, in good agreement with the V−C bond lengths found in $K_4[V(CN)_7] \cdot 2H_2O$,[10] i.e. mean V−C(eq) = 2.149 Å and mean V−C(ax) = 2.144 Å, and is slightly, though not significantly, shorter than the mean V−C distance (2.17 Å) ob-tained in $K_3[V(CN)_5NO] \cdot 2H_2O$.

The V=O bond length is $1.64 \pm 0.02$ Å, which agrees well with correspond-ing distances in other vanadyl(IV) compounds, e.g. $[VOSO_4(H_2O)_4] \cdot H_2O$ ($1.591 \pm 0.005$ Å),[20] $VOSO_4$ ($1.594 \pm 0.017$ Å),[21] and $(NH_4)_2[VO(NCS)_4(H_2O)] \cdot 4H_2O$ ($1.62 \pm 0.06$ Å).[22] The slight, though not significant, increase in the V=O bond length in the compounds $[VOSO_4(H_2O)_4] \cdot H_2O$, $(NH_4)_2[VO(NCS)_4(H_2O)] \cdot 4H_2O$, and $K_3[VO(CN)_5]$ is in accordance with a decrease in $\nu(V=O)$, as is seen from Table 7. Several attempts have been made [12,12,23,24] to correlate the

*Table 7.* V=O bond lengths and infra-red stretching frequencies for some vanadyl(IV) compounds.

| Compound | Ligand atoms other than vanadyl oxygen | $\nu(V=O)$ cm$^{-1}$ | $d(V=O)$ Å | Ref. |
|---|---|---|---|---|
| $[VOSO_4(H_2O)_4] \cdot H_2O$ | $O(H_2O, SO_4^{2-})$ | 1003, 975 | $1.591 \pm 0.005$ | 20,23 |
| $(NH_4)_2[VO(NCS)_4(H_2O)] \cdot 4H_2O$ | $N(NCS^-), O(H_2O)$ | 982, 963 | $1.62 \pm 0.06$ | 22 |
| $K_3[VO(CN)_5]$ | $C(CN^-)$ | 929 | $1.64 \pm 0.02$ | 7, present work |

V=O stretching frequency with the environment of the $VO^{2+}$ entity, but, although there would seem to be an obvious correlation for the three com-pounds cited in Table 7, the general validity of such a correlation would appear to be doubtful.[12]

In order to ascertain whether or not the vanadium atom lies in the equa-torial ligand plane, the least squares plane through the four equatorial carbon atoms, C(1), C(2), C(3), and C(4), coordinated to the vanadium atom in $x=$

0.2251, $y = 0.1279$, $z = 0.4226$, was calculated with the program PLANEFIT.[17] The distances of the defining atoms and the vanadium atom from this plane, whose equation (Cartesian coordinates, Å) is

$$- 0.3648\ X - 0.0011\ Y - 0.9311\ Z + 5.3256 = 0$$

are $d_{C(1)} = 0.07$ Å, $d_{C(2)} = 0.08$ Å, $d_{C(3)} = -0.07$ Å, $d_{C(4)} = -0.07$ Å, and $d_V = 0.37$ Å. The vanadium atom would thus appear to be displaced slightly, more towards the vanadyl oxygen atom in $[VO(CN)_5]^{3-}$ than in $[VOSO_4(H_2O)_4]$, where the corresponding displacement was found to be 0.28 Å.[20]

Several theoretical models have been suggested for vanadyl complexes and, in particular, for the $[VO(H_2O)_5{}^{2+}]$ ion, that due to Ballhausen and Gray [25] being most often quoted. Since teh molecular orbital description of $[VO(H_2O)_5{}^{2+}]$ closely resembles that of $[Me(CN)_5NO]^{n-}$, where $Me = V$, Cr, Mn, Fe,[26-28] it is perhaps profitable to compare the geometries of $[VO(CN)_5]^{3-}$ and $[V(CN)_5NO]^{3-}$ in the light of these models. For $[V(CN)_5NO]^{3-}$, molecular orbital calculations [27,28] indicate a strong axial $V \rightarrow \pi^* NO$ transfer, which is supported by the extremely short $V-N$ distance (1.66 Å) and long $N-O$ distance (1.29 Å) obtained for $K_3[V(CN_5)NO]2.H_2O$.[2] In $[VO(CN)_5]^{3-}$, by analogy with $[VO(H_2O)_5]^{2+}$, there is also a strong axial metal-ligand $\pi$ bond, but this is essentially an oxygen to vanadium transfer. $[VO(CN)_5]^{3-}$ would thus be expected to have the ground state configuration $...(e_\pi)^4(2b_2)^1$, whereas in $[V(CN)_5NO]^{3-}$ the $2b_2$ orbital is empty, the ion presumably having the ground state configuration $...(6e)^4$. It is interesting, in the light of these ground state configurations, to note that, whereas $VO^{2+}$ ions are generally regarded as V(IV) or $d^1$ species, $[V(CN)_5NO]^{3-}$ is normally regarded as a $d^4$ or V(I) ion. This clearly illustrates that the assignment of an oxidation state to the central metal atom in complex ions in which there is appreciable metal-ligand double bonding must essentially be purely formal.

Another feature of the $[Me(CN)_5NO]^{n-}$ ions is that the central metal atom is displaced approximately 0.2 Å (0.16 Å in $K_3[Mn(CN)_5NO].2H_2O$ [5] and 0.2 Å in $Na_2[Fe(CN)_5NO].2H_2O$ [29]) from the equatorial ligand plane towards the nitrosyl group. This has been interpreted [5] in terms of the weak antibonding rather than nonbonding nature of the $2b_2$ ($d_{xy}$) orbital as a result of the equatorial $M-\pi(CN)$ and $M-\pi^*(CN)$ interactions. Since the $2b_2$ orbital is empty in $[V(CN)_5NO]^{3-}$, a smaller displacement was expected in this case, but, owing to the disorder, it was not, however, possible to draw any conclusions concerning this feature from the crystal structure of $K_3[V(CN)_5NO].2H_2O$.[2] In $K_3[VO(CN)_5]$ the displacement of the vanadium atom from the equatorial ligand plane would appear to be slightly larger than in $[VO(SO_4)(H_2O)_4].H_2O$. This could be interpreted in terms of a slightly more antibonding $2b_2$ ($d_{xy}$) orbital in $[VO(CN)_5]^{3-}$ as compared with the approximately nonbonding $b_2$ orbital in $[VO(H_2O)_5]^{2+}$,[25] and presumably also in $[VO(SO_4)(H_2O)_4]$.[26]

The K(3) potassium ion is octahedrally coordinated by five nitrogen atoms and an oxygen atom at distances of $2.85 - 3.01$ Å. There are five carbon atoms only slightly more remote so that the K(3) potassium ion can be regarded as having eleven nearest neighbours, $i.e.$ as being octahedrally coordinated by five cyanide groups and an oxygen atom. The K(1) and K(2) potassium ions are, on the other hand, each surrounded by six cyanide groups in the form

of a somewhat distorted trigonal prism, two of the prism faces being capped by a seventh cyanide group and an oxygen atom, respectively. A similar potassium-ligand coordination polyhedron was found in $K_3[Mn(CN)_5NO]$.$2H_2O$,[5] while in $K_3[V(CN)_5NO].2H_2O$ [2] the potassium ions were octahedrally and square antiprismatically coordinated.

## REFERENCES

1. Chadwick, B. M. and Sharpe, A. G. *Advan. Inorg. Chem. Radiochem.* **8** (1966) 83.
2. Jagner, S. and Vannerberg, N.-G. *Acta Chem. Scand.* **24** (1970) 1988.
3. Griffith, W., Lewis, J. and Wilkinson, G. *J. Chem. Soc.* **1959** 1632.
4. Vannerberg, N.-G. *Acta Chem. Scand.* **20** (1966) 1571.
5. Tullberg, A. and Vannerberg, N.-G. *Acta Chem. Scand.* **21** (1967) 1462.
6. Svedung, D. H. and Vannerberg, N.-G. *Acta Chem. Scand.* **22** (1968) 1551.
7. Bennett, B. G. and Nicholls, D. *J. Chem.Soc.* **A 1971** 1204.
8. Yakimach, A. *Compt. Rend.* **191** (1930) 789.
9. Locke, J. and Edwards, G. H. *Amer. Chem. J.* **20** (1898) 594.
10. Towns, R. L. R. and Levenson, R. A. *J. Am. Chem. Soc.* **94** (1972) 4345.
11. Selbin, J. and Holmes, L. H. *J. Inorg. Nucl. Chem.* **24** (1962) 1111.
12. Selbin, J. *Coord. Chem. Rev.* **1** (1966) 293.
13. Selbin, J. *Chem. Rev.* **65** (1965) 153.
14. Dornberger-Schiff, K. *Lehrgang über OD-Strukturen*, Akademie-Verlag, Berlin 1966.
15. *International Tables for X-Ray Crystallography*, Kynoch Press, Birmingham 1959.
16. Hambling, P. *Acta Cryst.* **6** (1953) 98.
17. Modified and in use at this Department, *DATAP2* was originally written by Coppens, P., Leiserowitz, L. and Rabinowich, D., *LALS* by Gantzel, R., Sparks, K. and Trueblood, K., *DRF* and *DISTAN* by Zalkin, A., *POWDER* by Lindqvist, O. and Wengelin, F., *BLOCK* by Lindgren, O. and *PLANEFIT* by Wengelin, F.
18. Cromer, D. T. and Waber, J. T. *Acta Cryst.* **18** (1965) 104.
19. Cruickshank, D. W. J. *The Equations of Structure Refinements*, Glasgow 1964.
20. Ballhausen, C. J., Djurinskij, B. F. and Watson, K. J. *J. Am. Chem. Soc.* **90** (1968) 3305.
21. Kierkegaard, P. and Longo, J. M. *Acta Chem. Scand.* **19** (1965) 1906.
22. Hazell, A. C. *J. Chem. Soc.* **1963** 5745.
23. Selbin, J., Holmes, L. H. and McGlynn, S. P. *J. Inorg. Nucl. Chem.* **25** (1963) 1359.
24. Garvey, R. G. and Ragsdale, R. O. *J. Inorg. Nucl. Chem.* **29** (1967) 745.
25. Ballhausen, C. J. and Gray, H. B. *Inorg. Chem.* **1** (1962) 111.
26. Manoharan, P. T. and Gray, H. B. *J. Am. Chem. Soc.* **87** (1965) 3340.
27. Manoharan, P. T. and Gray, H. B. *Inorg. Chem.* **5** (1966) 823.
28. Fenske, R. F. and DeKock, R. L. *Inorg. Chem.* **11** (1972) 437.
29. Manoharan, P. T. and Hamilton, W. C. *Inorg. Chem.* **2** (1963) 1043.

# The Stability Constants for Complexes between Nickel(II) and Squaric Acid

DAGMAR ALEXANDERSSON and NILS-GÖSTA VANNERBERG

*Department of Inorganic Chemistry, Chalmers University of Technology and the University of Göteborg, P.O. Box, S-402 20 Göteborg 5, Sweden*

The formation of complexes between nickel(II) and squaric acid has been studied at 25°C with spectrophotometric methods in solutions in which the total molarity was held constant at 3 M by the addition of $NaClO_4$. The total concentrations of nickel perchlorate and sodium squarate ranged from 0 to 600 mM and 0.1 to 3 mM, respectively. The pH range was 1.3 — 5.0. Preliminary constants were obtained graphically and were then refined with the generalized least squares program Letagrop. The experimental data could best be explained in terms of the following equilibria and corresponding stability constants in the $Ni^{2+} - H^+ - C_4O_4^{2-}$ system:
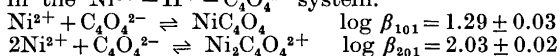
$Ni^{2+} + C_4O_4^{2-} \rightleftharpoons NiC_4O_4$     $\log \beta_{101} = 1.29 \pm 0.03$
$2Ni^{2+} + C_4O_4^{2-} \rightleftharpoons Ni_2C_4O_4^{2+}$     $\log \beta_{201} = 2.03 \pm 0.02$

The errors given correspond to an error of $3\sigma$ in $\beta$, where $\sigma$ is the standard deviation in $\beta$.

Squaric acid (3,4-dihydroxy-3-cyclobutene-1,2-dione, $H_2C_4O_4$) was not known until 1959, when it was first synthetized by Cohan *et al.*[1] The aromatic character of the anion, $A^{2-}$, its stability and its solubility in water have, since then, stimulated a number of investigations on the acid and its metal complexes. A survey of reported values for the acidity constants at varying ionic strength has been given previously.[2] Recently acidity constants have been reported by Gelb[3] ($pK_{a1} = 0.51$) and by Schwartz and Howard[4,5] ($pK_{a1} = 0.5$ and $pK_{a2} = 3.48$).

Schwartz and Howard carried out conductance measurements as well as potentiometric titrations, while Gelb measured conductometrically. They all worked with varying ionic strength and used calculated activity coefficients to determine the thermodynamic acidity constants.

The formation of squarate complexes with metal ions has been studied by Tedesco and Walton,[6] who determined formation constants for iron(III), uranium(VI), aluminium(III), copper(II), manganase(II), cobalt(II), and nickel(II), and by Cilindro *et al.*[7] who studied complex formation with some

actinides. In their investigation of nickel(II) squarate complexes, Tedesco and Walton used a paper chromatographic method with 0.5 M $NaClO_4$ as supporting electrolyte. The pH range was $3.5-4$ and the temperature $25°C$. Only a preliminary constant was thus obtained. In connection with our work on squaric acid and its complex formation with transition metal ions a more exhaustive investigation was desirable.

## EXPERIMENTAL

*Chemicals and analyses. Nickel(II) perchlorate* was prepared from nickel carbonate (BDH) and perchloric acid (Merck *p.a.*). The nickel perchlorate was recrystallized several times by dissolving in hot water, cooling and filtering off the precipitated crystals. The nickel perchlorate solution was standardized against a standard EDTA solution, using murexide as indicator according to Vogel.[8] The EDTA solution was prepared from Titriplex III (Merck *p.a.*) by dissolving a weighed amount of the salt. The EDTA concentration was checked with a zinc chloride solution, prepared from zinc sticks (Merck *p.a.*) and hydrochloric acid (Merck *p.a.*), as described by Vogel.[9]

The *free hydrogen ion* concentration in the nickel perchlorate solution was determined by Gran methods.[10]

*Perchloric acid, sodium perchlorate,* and *sodium squarate* were prepared and analyzed as described elsewhere.[2]

*Apparatus.* The *ultra-violet absorption measurements* were performed on a Gilford 240 spectrophotometer. Matched quartz cells of path lengths 0.01, 0.05, 0.1, 0.2, 0.5, and 1 cm were employed, these being calibrated before use. During the measurements, the sample compartment was thermostated to $25.0 \pm 0.1°C$.

The solutions to be investigated were prepared by mixing solutions of nickel(II) perchlorate, sodium squarate and perchloric acid, the total molarity being held constant at 3 M by addition of sodium perchlorate. The total concentrations of sodium squarate, $A$, and nickel perchlorate, $B$, varied within the ranges $0.1-3$ mM and $0-600$ mM, respectively. The concentration of the free squarate ion, $a$, ranged, however, from 0.004 to 1 mM, owing to the varying hydrogen ion and nickel ion concentrations. The variation is limited by the slight solubility of squarates and by their high molar absorptivities. The free hydrogen ion concentration, $h$, was measured in each solution by emf methods as is described previously.[2] The sodium perchlorate concentration was then 3.000 M $-2A-2B-h$.

No nickel hydroxide complexes were formed, according to calculations using the formation constants for nickel(II) hydroxide complexes, determined by Burkov *et al.*[11]

The absorbance was measured at 26 wavelengths ranging from 220 to 290 nm. Sixteen of these absorbances corresponding to wavelengths ranging from 240 to 270 nm were used in the calculations. The stability of the sodium squarate solutions as well as of the nickel squarate solutions is good. For some solutions the absorbances were measured again after $6-9$ months and found to have changed only by $1-2 \%$.

## LIST OF SYMBOLS

| | |
|---|---|
| $A$ | total concentration of squaric acid, $H_2A$ |
| $a$ | free concentration of squarate ions, $A^{2-}$ |
| $B$ | total concentration of nickel ions, $Ni^{2+}$ |
| $b$ | free concentration of nickel ions, $Ni^{2+}$ |
| $H$ | total concentration of hydrogen ions, $H^+$ |
| $h$ | free concentration of hydrogen ions, $H^+$ |
| $c_{pqr}$ | free concentration of $Ni_pH_qA_r^{(2p+q-2r)+}$ |
| $A_s$ | absorbance |
| $l$ | optical pathlength |

$\varepsilon$      apparent molar absorptivity

$\beta_{qpr}$    equilibrium constant for the reaction

$$p\text{Ni}^{2+} + q\text{H}^+ + r\text{A}^{2-} \rightleftharpoons \text{Ni}_q\text{H}_p\text{A}_r^{(2p+q-2r)+}$$
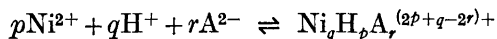
defined so that

$$c_{pqr} = \beta_{pqr}\, b^p h^q a^r$$

$\varepsilon_{pqr}$    molar absorptivity for the complex $\text{Ni}_p\text{H}_q\text{A}_r^{(2p+q-2r)+}$

$v_0, A_0, H_0$ volume and total concentrations in the starting solution in the emf measurements

$v_t, A_t, B_t, H_t$ volume and total concentrations in the solution added in the emf measurements

$E$      potential

## SPECTROPHOTOMETRIC MEASUREMENTS

Squaric acid and its anions show strong absorption of radiation in the ultraviolet but not in the visible range. Nickel squarates also absorb in the ultraviolet region but the absorbance of nickel perchlorate is very weak. In this work the variation of the absorbance with changes in the concentrations of
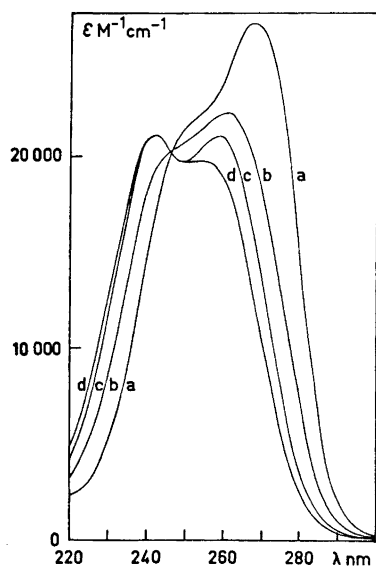


*Fig. 1.* $\varepsilon$ data as a function of $\gamma$ for sodium squarate solutions with different hydrogen ion concentrations. The measurements were made every 2nd nm, all points falling on the curves. The following values for $-\log h$ were used: a. 6.21; b. 3.31; c. 2.06; d. 1.08.
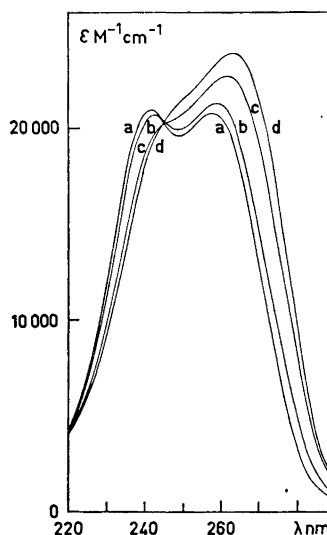
*Fig. 2.* $\varepsilon$ data as a function of $\lambda$ for solutions with $A = 0.1201$ mM and different nickel perchlorate concentrations. The following values for $B$ and $-\log h$ were used: a. 0 mM and 2.03; b. 85.18 mM and 2.00; c. 352.4 mM and 1.93; d. 598.6 mM and 1.86.

the components has been used to determine the stability constants of the complexes. Spectra were registered for solutions of sodium squarate with varying $h$ values (cf. Fig. 1) and for solutions containing both sodium squarate and nickel perchlorate. The absorbances of series of solutions with pH 2 and pH 5, respectively, are shown in Figs. 2. and 3. According to determinations made previously [2] the HA⁻ anion dominates the squaric acid system at pH 2 while the A²⁻ anion dominates at pH 5 (cf. Fig. 4).

When the nickel perchlorate concentration is varied from 0 to 100 mM at pH 5 and the sodium squarate concentration is kept constant, the absorbances change only slightly (cf. Fig. 3). This may either be due to the fact that the complexes formed have about the same molar absorptivities as the squarate ion, A²⁻, or that complex formation is negligible.
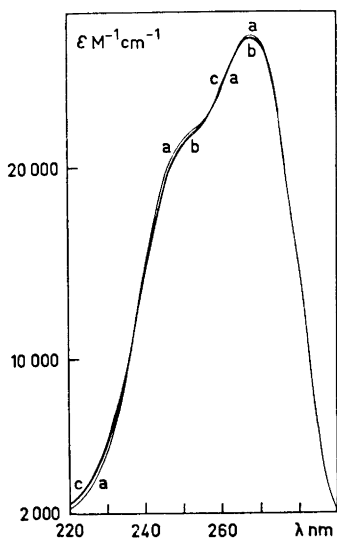


Fig. 3. $\varepsilon$ data as a function of $\lambda$ for solutions with $A = 1.000$ mM and different nickel perchlorate concentrations. The following values for $B$ and $-\log h$ were used: a. 0 mM and 4.96; b. 60.00 mM and 5.01; c. 100.0 mM and 4.95.
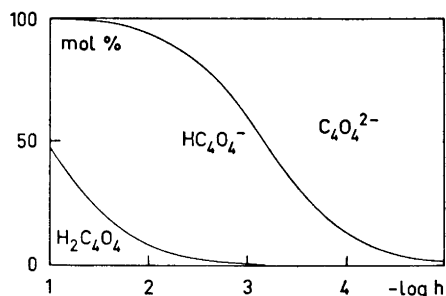
Fig. 4. The distribution of complexes as a function of $-\log h$ for squaric acid.

The change in absorbance is more pronounced in solutions with pH 2 (cf. Fig. 2). Nickel complexes would therefore appear to be formed at this pH.

## TREATMENT OF THE DATA

The absorbance, $A_s$, may be expressed:

$$A_s = \varepsilon l A = l \sum_p \sum_q \sum_r \varepsilon_{pqr} c_{pqr} \tag{1}$$

Inserting the expression

$$c_{pqr} = \beta_{pqr} b^p h^q a^r$$

in eqn. (1) gives

$$\varepsilon = \frac{\sum_p \sum_q \sum_r \varepsilon_{pqr} \beta_{pqr} b^p h^q a^r}{\sum_p \sum_q \sum_r r \beta_{pqr} b^p h^q a^r} \qquad (2)$$

I. $p = 0$. In solutions where no nickel is present

$$\varepsilon = \frac{\varepsilon_{001} + \varepsilon_{011}\beta_{011}h + \varepsilon_{021}\beta_{021}h^2}{1 + \beta_{011}h + \beta_{021}h^2} \qquad (3)$$

The constants $\beta_{011}$ and $\beta_{021}$ have been determined earlier by means of emf methods at the same ionic strength,[2] *i.e.* log $\beta_{011} = 3.19 \pm 0.001$ and log $\beta_{021} = 4.15 \pm 0.02$, the errors given corresponding to an error of $3\sigma$ in $\beta$. Using these values of the constants, the experimental data from solutions not containing nickel were processed with the spectrophotometric version of the "Letagrop" program.[12] When $\beta_{011}$ was varied together with $\varepsilon_{001}$, $\varepsilon_{011}$, and $\varepsilon_{021}$ for the 16 wavelengths, log $\beta_{011} = 3.13 \pm 0.05$ was obtained as "the best value". The $\beta$ values calculated from the emf measurements were used in the following, since these are the most accurate values. The $\varepsilon$ values calculated holding these $\beta$ values constant are given in Table 1 and used in the following.

*Table 1.* Molar absorptivities, $\varepsilon_{pqr}$, in $M^{-1}$ $cm^{-1}$ calculated with the Letagroup program. The errors are given as $3\sigma$ where $\sigma$ is the standard deviation in $\varepsilon$.

| $\lambda$nm | $\varepsilon_{021}$ | $\varepsilon_{011}$ | $\varepsilon_{001}$ | $\varepsilon_{101}$ | $\varepsilon_{201}$ | $\varepsilon_{100}$ |
|---|---|---|---|---|---|---|
| 240 | $20\,800 \pm 470$ | $21\,100 \pm 120$ | $14\,800 \pm 140$ | $13\,100 \pm 560$ | $16\,300 \pm 310$ | 0.011 |
| 242 | $21\,100 \pm 440$ | $21\,400 \pm 120$ | $16\,900 \pm 120$ | $15\,000 \pm 510$ | $18\,000 \pm 260$ | 0.011 |
| 244 | $21\,000 \pm 460$ | $20\,900 \pm 120$ | $18\,600 \pm 130$ | $17\,100 \pm 330$ | $19\,400 \pm 180$ | 0.011 |
| 246 | $20\,800 \pm 470$ | $20\,200 \pm 120$ | $20\,000 \pm 140$ | $18\,600 \pm 310$ | $20\,600 \pm 160$ | 0.010 |
| 248 | $20\,500 \pm 450$ | $19\,700 \pm 120$ | $20\,900 \pm 130$ | $19\,900 \pm 360$ | $21\,500 \pm 200$ | 0.010 |
| 250 | $20\,200 \pm 440$ | $19\,600 \pm 110$ | $21\,500 \pm 130$ | $20\,600 \pm 310$ | $22\,200 \pm 210$ | 0.010 |
| 252 | $19\,900 \pm 380$ | $19\,800 \pm 100$ | $21\,900 \pm 110$ | $21\,100 \pm 320$ | $22\,700 \pm 210$ | 0.009 |
| 254 | $19\,300 \pm 380$ | $20\,300 \pm 100$ | $22\,200 \pm 110$ | $21\,400 \pm 300$ | $23\,100 \pm 210$ | 0.009 |
| 256 | $18\,600 \pm 390$ | $20\,800 \pm 100$ | $22\,600 \pm 110$ | $21\,900 \pm 350$ | $23\,600 \pm 230$ | 0.009 |
| 258 | $17\,500 \pm 420$ | $21\,100 \pm 110$ | $23\,200 \pm 120$ | $22\,600 \pm 370$ | $24\,300 \pm 240$ | 0.009 |
| 260 | $16\,100 \pm 450$ | $21\,000 \pm 120$ | $24\,100 \pm 130$ | $23\,600 \pm 400$ | $25\,000 \pm 260$ | 0.009 |
| 262 | $14\,600 \pm 540$ | $20\,400 \pm 140$ | $25\,100 \pm 160$ | $24\,700 \pm 470$ | $25\,600 \pm 300$ | 0.009 |
| 264 | $12\,800 \pm 650$ | $19\,300 \pm 170$ | $26\,100 \pm 190$ | $25\,700 \pm 500$ | $26\,100 \pm 370$ | 0.009 |
| 266 | $10\,900 \pm 760$ | $17\,700 \pm 200$ | $26\,800 \pm 220$ | $26\,400 \pm 490$ | $26\,300 \pm 370$ | 0.008 |
| 268 | $9\,000 \pm 940$ | $15\,600 \pm 250$ | $27\,200 \pm 270$ | $26\,700 \pm 510$ | $26\,000 \pm 360$ | 0.008 |
| 270 | $7\,000 \pm 1080$ | $13\,400 \pm 280$ | $26\,900 \pm 320$ | $26\,500 \pm 450$ | $25\,300 \pm 400$ | 0.007 |

II. $q = 1$. In eqn. (1) $Ni_p H_q A_r^{(2p+q-2r)+}$ represents the general form for a nickel complex. In the pH range $1.3 - 5$ it is, however, probable that not more than one hydrogen ion is bound per complex. The total concentration of squaric

acid is rather low, $A \leq 3$ mM so that $r = 1$ seems to be most likely. Neglecting the weak absorbance of the nickel ions (cf. Table 1) eqn. (2) is reduced to the form

$$\varepsilon = \frac{\varepsilon_{001} + \varepsilon_{011}\beta_{011}h + \varepsilon_{021}\beta_{021}h^2 + \sum_p \varepsilon_{p11}\beta_{p11}b^p h + \sum_p \varepsilon_{p01}\beta_{p01}b^p}{1 + \beta_{011}h + \beta_{021}h^2 + \sum_p \beta_{p11}b^p h + \sum_p \beta_{p01}b^p} \tag{4}$$

or

$$[\varepsilon(1 + \beta_{011}h + \beta_{021}h^2) - (\varepsilon_{001} + \varepsilon_{011}\beta_{011}h + \varepsilon_{021}\beta_{021}h^2)]/\varepsilon b =$$
$$= -\sum_p b^{p-1}(\beta_{p11}h + \beta_{p01}) + \sum_p b^{p-1}(\varepsilon_{p11}\beta_{p11}h + \varepsilon_{p01}\beta_{p01})\varepsilon^{-1} \tag{5}$$

In order to investigate whether the complexes $Ni_pHA^{(2p-1)+}$ were present, all other nickel complexes were neglected and all terms in eqn. (5) divided by a factor $h$. Data from solutions with $A = 1.157$ mM, $B = 500.0$ mM and pH varying from 1.3 to 3.7 were then inserted. Since $B \gg A$, $b$ can be replaced by $B$. All quantities on the left-hand side of the equation are then known and the coefficient for the term $\varepsilon^{-1}$, $\sum_p B^{p-1} \varepsilon_{p11}\beta_{p11}$, is constant. The left-hand side of the equation was plotted against $\varepsilon^{-1}$, (cf. Fig. 5) to test whether or not there was a linear correlation. It was obvious that there was no linear correlation $Ni_pHA^{(2p-1)+}$ thus not being the main complexes formed.
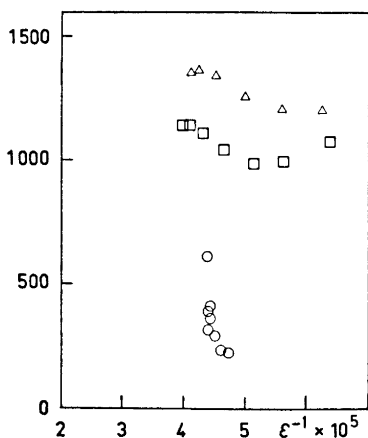


Fig. 5. The left-hand side of eqn. (5) divided by $h$, as a function of $\varepsilon^{-1}$ for different wavelengths. $A = 1.157$ mM, $B = 500.0$ mM and the values for $\lambda$ are ○ 254 nm, □ 268 nm and △ 270 nm.
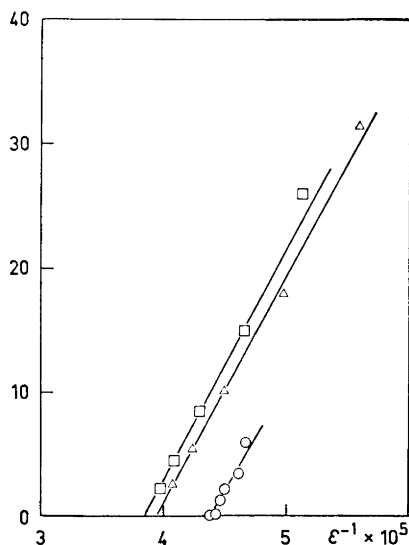
Fig. 6. The left-hand side of eqn. (5) as a function of $\varepsilon^{-1}$ for different wavelengths. $A = 1.157$ mM, $B = 500.0$ mM and $1.3 \leq -\log h \leq 3.7$. The $\lambda$ values are ○ 254 nm, □ 268 nm and △ 270 nm. From the slope and intercept for $\lambda = 270$ nm $\sum_p \beta_{p01}b^{p-1} = 72$ M$^{-1}$ and $\varepsilon_{101} = 25\ 300$ M$^{-1}$ cm$^{-1}$ are obtained.

III. $q = 0$. The complexes $Ni_p HA^{(2p-1)+}$ were then neglected and the complexes $Ni_p A^{(2p-2)+}$ tested by inserting the same data in eqn. (5) (cf. Fig. 6). This time a linear correlation was obtained. The complexes $Ni_p A^{(2p-2)+}$ must therefore be present both in solutions with pH 2 and in those with pH 5. From Fig. 3 it is seen that these complexes have molar absorptivities which differ little from that of the squarate ion, $\varepsilon_{001}$. Supposing all $\varepsilon_{p01} \approx \varepsilon_{101}$, the slope and intercept of the line give

$$\sum_p \beta_{p01} B^{p-1} = 72; \quad \varepsilon_{101} = 25\ 300$$

for $\lambda = 270$ nm.

Data from solutions with pH 2 and varying $A$ and $B$ values were then used for the wavelength $\lambda = 270$ nm. In Fig. 7 the left-hand side of eqn. (5) has been plotted against $\varepsilon^{-1}$. If NiA is supposed to be the only nickel complex present, the slope and intercept of the line give
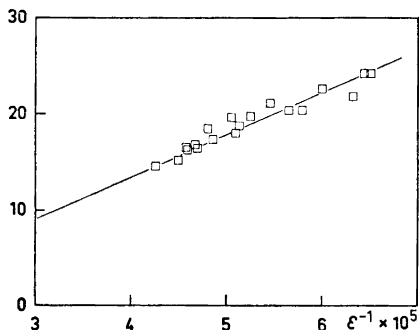


Fig. 7. The left-hand side of eqn. (5) as a function of $\varepsilon^{-1}$ for $\lambda = 270$ nm, different $A$ and $B$ values and pH $\sim$ 2. From the slope and intercept $\beta_{101} = 4$ M$^{-1}$ and $\varepsilon_{101} = 108\ 000$ M$^{-1}$ cm$^{-1}$ are obtained.
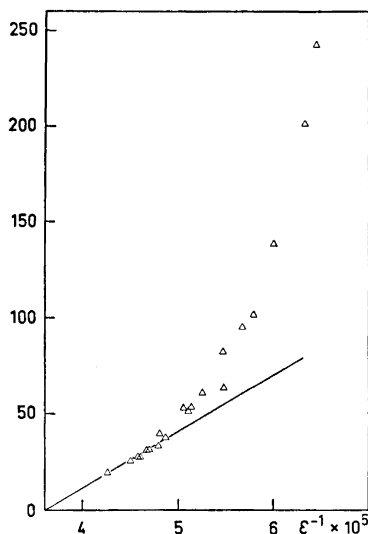
Fig. 8. The left-hand side of eqn. (5) divided by a factor $B$, as a function of $\varepsilon^{-1}$ for $\lambda = 270$ nm, different $A$ and $B$ values and pH $\sim$ 2. From the slope and intercept $\beta_{201} = 107$ M$^{-2}$ and $\varepsilon_{201} = 27\ 600$ M$^{-1}$ cm$^{-1}$ are obtained.

$$\beta_{101} = 4; \quad \varepsilon_{101} = 108\ 000$$

The $\varepsilon_{101}$ value obtained seemed to be too high compared to $\varepsilon_{001} = 26\ 900$. To test whether or not the complex $Ni_2 A^{2+}$ was formed, all terms in eqn. (5) were divided by a factor $B$ and the left-hand side of the new equation was plotted against $\varepsilon^{-1}$ (cf. Fig. 8). If all nickel complexes except $Ni_2 A^{2+}$ were neglected and data from solutions with the highest $B$ values (and thus the highest $\varepsilon$ values) were used, then

*Table 2.* Spectrophotometric data for 14 solutions. The values given are log *h*, *A* and *B* for each solution, followed by $\varepsilon$, $\varepsilon_{calc}$, and $\varepsilon_{calc} - \varepsilon$ for the 16 wavelengths. The concentrations are expressed in M and the molar absorptivities in $M^{-1}\ cm^{-1}$, all absorptivities are multiplied by a factor $10^{-1}$.

| | | | | | | | | |
|---|---|---|---|---|---|---|---|---|
| -2.006399 | 0.000120 | 0.085180 | | | | | | |
| 2010.000 | 2001.513 | -8.487 | 2064.000 | 2055.626 | -8.373 | 2061.000 | 2053.878 | -7.121 |
| 2023.000 | 2018.762 | -4.237 | 1995.000 | 1995.149 | 0.149 | 1993.000 | 1997.508 | 4.508 |
| 2018.000 | 2022.696 | 4.696 | 2057.000 | 2061.246 | 4.246 | 2096.000 | 2101.508 | 5.508 |
| 2125.000 | 2128.220 | 3.220 | 2127.000 | 2127.914 | 0.914 | 2091.000 | 2087.901 | -3.099 |
| 2009.000 | 2002.890 | -6.110 | 1886.000 | 1876.455 | -9.545 | 1724.000 | 1709.944 | -14.056 |
| 1534.000 | 1518.044 | -15.955 | | | | | | |
| -1.577699 | 0.000120 | 0.200400 | | | | | | |
| 1927.000 | 1914.278 | -12.722 | 2004.000 | 1992.687 | -11.313 | 2027.000 | 2024.615 | -2.385 |
| 2019.000 | 2023.357 | 4.357 | 2012.000 | 2024.872 | 12.872 | 2022.000 | 2041.216 | 19.216 |
| 2052.000 | 2069.748 | 17.748 | 2090.000 | 2108.779 | 18.779 | 2131.000 | 2150.328 | 19.328 |
| 2167.000 | 2184.606 | 17.606 | 2184.000 | 2200.076 | 16.077 | 2172.000 | 2184.211 | 12.211 |
| 2120.000 | 2130.231 | 10.231 | 2025.000 | 2036.253 | 11.253 | 1892.000 | 1901.754 | 9.754 |
| 1727.000 | 1736.506 | 9.506 | | | | | | |
| -1.937099 | 0.000120 | 0.352400 | | | | | | |
| 1846.000 | 1838.382 | -7.618 | 1946.000 | 1941.315 | -4.685 | 2002.000 | 2005.917 | 3.917 |
| 2029.000 | 2038.667 | 9.667 | 2047.000 | 2065.158 | 18.158 | 2072.000 | 2095.802 | 23.802 |
| 2106.000 | 2127.829 | 21.829 | 2146.000 | 2167.909 | 21.909 | 2189.000 | 2211.139 | 22.139 |
| 2230.000 | 2253.098 | 23.098 | 2259.000 | 2283.868 | 24.869 | 2271.000 | 2291.619 | 20.619 |
| 2251.000 | 2268.308 | 17.308 | 2195.000 | 2206.470 | 11.470 | 2090.000 | 2103.388 | 13.388 |
| 1548.000 | 1563.847 | 15.847 | | | | | | |
| -1.908400 | 0.000120 | 0.462100 | | | | | | |
| 1818.000 | 1806.648 | -11.352 | 1927.000 | 1921.815 | -5.184 | 1998.000 | 2002.263 | 4.263 |
| 2042.000 | 2051.729 | 9.729 | 2075.000 | 2090.542 | 15.542 | 2109.000 | 2128.380 | 19.380 |
| 2146.000 | 2162.013 | 16.013 | 2186.000 | 2202.814 | 16.814 | 2228.000 | 2247.021 | 19.021 |
| 2273.000 | 2292.837 | 19.837 | 2310.000 | 2331.036 | 21.036 | 2329.000 | 2350.318 | 21.318 |
| 2320.000 | 2342.089 | 22.089 | 2276.000 | 2295.893 | 19.893 | 2192.000 | 2208.179 | 16.179 |
| 2056.000 | 2080.873 | 24.873 | | | | | | |
| -1.888100 | 0.000120 | 0.541400 | | | | | | |
| 1786.000 | 1791.965 | 5.965 | 1904.000 | 1913.836 | 9.837 | 1987.000 | 2002.824 | 15.825 |
| 2045.000 | 2061.301 | 16.301 | 2086.000 | 2106.822 | 20.822 | 2126.000 | 2148.621 | 22.621 |
| 2165.000 | 2183.019 | 18.019 | 2207.000 | 2224.275 | 17.275 | 2246.000 | 2269.059 | 23.059 |
| 2291.000 | 2316.995 | 25.995 | 2334.000 | 2359.200 | 25.200 | 2360.000 | 2384.720 | 24.720 |
| 2360.000 | 2384.687 | 24.687 | 2325.000 | 2346.867 | 21.868 | 2251.000 | 2267.480 | 16.480 |
| 2130.000 | 2146.621 | 16.621 | | | | | | |
| -1.871200 | 0.000120 | 0.598600 | | | | | | |
| 1773.000 | 1785.295 | 12.296 | 1897.000 | 1910.945 | 13.945 | 1987.000 | 2004.688 | 17.688 |
| 2052.000 | 2068.163 | 16.163 | 2100.000 | 2117.454 | 17.454 | 2143.000 | 2161.494 | 18.494 |
| 2182.000 | 2196.228 | 14.228 | 2220.000 | 2237.750 | 17.750 | 2262.000 | 2282.850 | 20.850 |
| 2310.000 | 2331.951 | 21.951 | 2355.000 | 2376.353 | 21.353 | 2385.000 | 2405.326 | 20.327 |
| 2390.000 | 2405.865 | 19.865 | 2360.000 | 2376.638 | 16.638 | 2292.000 | 2301.898 | 9.898 |
| 2175.000 | 2184.529 | 5.529 | | | | | | |
| -4.973000 | 0.001000 | 0.0 | | | | | | |
| 1477.000 | 1490.305 | 13.305 | 1688.000 | 1698.283 | 10.284 | 1862.000 | 1866.789 | 4.789 |
| 1590.000 | 2000.327 | 10.327 | 2082.000 | 2090.958 | 8.959 | 2143.000 | 2150.799 | 7.799 |
| 2180.000 | 2189.603 | 9.603 | 2211.000 | 2220.864 | 9.864 | 2250.000 | 2261.027 | 11.027 |
| 2310.000 | 2320.537 | 10.537 | 2392.000 | 2401.067 | 9.067 | 2491.000 | 2501.405 | 10.405 |
| 2585.000 | 2598.861 | 13.861 | 2653.000 | 2669.023 | 16.023 | 2679.000 | 2698.136 | 19.136 |
| 2657.000 | 2672.805 | 15.805 | | | | | | |
| -4.948999 | 0.001000 | 0.075000 | | | | | | |
| 1428.000 | 1433.390 | 5.391 | 1591.000 | 1625.018 | 34.018 | 1802.000 | 1805.594 | 3.594 |
| 1933.000 | 1948.490 | 15.490 | 2037.000 | 2053.266 | 16.266 | 2111.000 | 2123.266 | 12.266 |
| 2155.000 | 2167.078 | 12.078 | 2190.000 | 2203.135 | 13.135 | 2231.000 | 2247.674 | 16.674 |
| 2298.000 | 2313.771 | 15.771 | 2386.000 | 2401.393 | 15.393 | 2485.000 | 2499.301 | 14.301 |
| 2578.000 | 2589.467 | 11.467 | 2641.000 | 2649.609 | 8.609 | 2661.000 | 2666.507 | 5.508 |
| 2630.000 | 2632.617 | 2.817 | | | | | | |
| -4.757999 | 0.001000 | 0.100000 | | | | | | |
| 1435.000 | 1443.375 | 8.375 | 1627.000 | 1631.480 | 4.480 | 1801.000 | 1809.844 | 8.844 |
| 1944.000 | 1951.833 | 7.833 | 2048.000 | 2056.284 | 8.285 | 2120.000 | 2126.832 | 6.832 |
| 2165.000 | 2171.412 | 6.412 | 2202.000 | 2208.619 | 6.619 | 2245.000 | 2253.965 | 8.965 |
| 2314.000 | 2320.336 | 6.336 | 2401.000 | 2406.990 | 5.990 | 2506.000 | 2502.103 | -3.896 |
| 2595.000 | 2588.605 | -6.395 | 2656.000 | 2644.988 | -11.012 | 2674.000 | 2657.325 | -16.675 |
| 2641.000 | 2615.813 | -21.187 | | | | | | |
| -2.711300 | 0.001157 | 0.500000 | | | | | | |
| 1563.000 | 1592.073 | 29.073 | 1732.000 | 1753.831 | 21.831 | 1884.000 | 1896.000 | 12.001 |
| 2007.000 | 2013.313 | 6.313 | 2102.000 | 2098.282 | -3.717 | 2166.000 | 2162.509 | -3.491 |
| 2212.000 | 2208.750 | -3.250 | 2253.000 | 2252.319 | -0.681 | 2302.000 | 2301.344 | -0.656 |
| 2363.000 | 2363.726 | 0.726 | 2431.000 | 2433.394 | 2.394 | 2493.000 | 2499.833 | 6.833 |
| -1.000 | -1.000 | 0.0 | -1.000 | -1.000 | 0.0 | 2518.000 | 2545.053 | 27.054 |
| 2453.000 | 2472.620 | 19.620 | | | | | | |
| -2.400299 | 0.001157 | 0.500000 | | | | | | |
| 1628.000 | 1632.189 | 4.189 | 1783.000 | 1783.525 | 0.526 | 1913.000 | 1911.684 | -1.316 |
| 2017.000 | 2014.389 | -2.611 | 2095.000 | 2088.930 | -6.070 | 2152.000 | 2147.378 | -4.622 |
| 2158.000 | 2191.875 | -6.125 | 2240.000 | 2235.325 | -4.675 | 2288.000 | 2283.915 | -4.085 |
| 2345.000 | 2343.264 | -1.736 | 2404.000 | 2406.472 | 2.472 | 2455.000 | 2462.808 | 7.808 |
| 2484.000 | 2501.152 | 17.152 | 2481.000 | 2508.197 | 27.197 | 2444.000 | 2467.195 | 23.195 |
| 2365.000 | 2383.060 | 18.060 | | | | | | |
| -2.117999 | 0.001157 | 0.500000 | | | | | | |
| 1724.000 | 1692.787 | -31.213 | 1861.000 | 1828.344 | -32.656 | 1957.000 | 1935.475 | -21.525 |
| 2034.000 | 2016.330 | -17.670 | 2092.000 | 2075.207 | -16.793 | 2141.000 | 2124.790 | -16.210 |
| 2180.000 | 2166.314 | -13.686 | 2223.000 | 2209.037 | -13.963 | 2269.000 | 2256.242 | -12.757 |
| 2319.000 | 2310.222 | -8.777 | 2367.000 | 2362.944 | -4.056 | 2401.000 | 2403.422 | 2.422 |
| 2411.000 | 2421.616 | 10.617 | 2390.000 | 2407.035 | 17.035 | 2330.000 | 2345.527 | 15.527 |
| 2225.000 | 2243.851 | 18.851 | | | | | | |
| -1.845199 | 0.001157 | 0.500000 | | | | | | |
| 1807.000 | 1775.016 | -31.984 | 1911.000 | 1889.073 | -21.927 | 1977.000 | 1968.004 | -8.996 |
| 2021.000 | 2019.746 | -1.254 | 2056.000 | 2057.583 | 1.583 | 2091.000 | 2094.801 | 3.801 |
| 2128.000 | 2131.456 | 3.456 | 2169.000 | 2171.847 | 2.847 | 2214.000 | 2215.382 | 1.382 |
| 2251.000 | 2260.134 | 3.134 | 2290.000 | 2296.830 | 6.830 | 2302.000 | 2314.320 | 12.320 |
| 2285.000 | 2304.240 | 15.240 | 2239.000 | 2259.716 | 20.716 | 2144.000 | 2170.429 | 26.429 |
| 2007.000 | 2045.278 | 38.278 | | | | | | |
| -1.584200 | 0.001157 | 0.500000 | | | | | | |
| 1514.000 | 1671.577 | -42.423 | 1989.000 | 1960.196 | -28.804 | 2024.000 | 2006.737 | -17.262 |
| 2036.000 | 2025.455 | -10.545 | 2047.000 | 2039.055 | -7.945 | 2069.000 | 2061.030 | -7.970 |
| 2093.000 | 2090.156 | -2.844 | 2140.000 | 2124.890 | -15.110 | 2180.000 | 2160.227 | -19.773 |
| 2212.000 | 2189.930 | -22.070 | 2226.000 | 2203.915 | -22.085 | 2214.000 | 2191.219 | -22.781 |
| 2168.000 | 2145.918 | -22.082 | 2080.000 | 2064.940 | -15.060 | 1948.000 | 1943.136 | -4.863 |
| 1750.000 | 1791.134 | 1.134 | | | | | | |

*Table 3.* Survey of the results from the calculation of the $\beta$ constants, I by graphical methods, II, III, and IV using the Letagrop program.

| | | Number of experimental $\varepsilon$ values | $\beta_{pqr}$ varied $(pqr)$ | $\beta_{pqr}$ constant $(pqr)$ 021, 011 and | $\varepsilon_{pqr}$ varied $(pqr)$ | $\log(\beta_{pqr} \pm 3\sigma)$ | $U \times 10^7$ | $\sigma(\varepsilon)$ |
|---|---|---|---|---|---|---|---|---|
| I. | Fig. 9 | | 101 | | | 1.28 | | |
| | Fig. 8 | | 201 | | | 2.03 | | |
| II. | Different | 138 | 101 | | 101 | $1.89 \pm 0.05$ | 0.71 | 240 |
| | $h$ values | 138 | 201 | | 201 | $2.20 \pm 0.05$ | 0.71 | 240 |
| | $A$ and $B$ | 138 | 111 | | 111 | $2.80 \pm 0.14$ | 6.0 | 700 |
| | constant | 138 | 122 | | 122 | $8.83 \pm 0.23$ | 7.1 | 770 |
| III. | Different | 656 | 101 | | 101 | $1.61 \pm 0.02$ | 9.7 | 420 |
| | $A$ and $B$ | 656 | 201 | | 201 | $2.23 \pm 0.02$ | 5.2 | 290 |
| | values | 656 | 301 | | 301 | $2.78 \pm 0.04$ | 12 | 450 |
| | | 656 | 102 | | 102 | $5.70 \pm 0.05$ | 95 | 1280 |
| IV. | II+III | 772 | $\begin{cases}101\\201\end{cases}$ | | $\begin{matrix}101\\201\end{matrix}$ | $\left.\begin{matrix}1.27 \pm 0.07\\2.05 \pm 0.05\end{matrix}\right\}$ | 2.53 | 185 |
| | | 182 | 101 | 201 | 101 | $1.32 \pm 0.05$ | 0.44 | 163 |
| | | 404 | 201 | 101 | 201 | $2.01 \pm 0.03$ | 1.29 | 183 |
| | | 772 | $\begin{cases}101\\201\end{cases}$ | | $\begin{matrix}-\\-\end{matrix}$ | $\left.\begin{matrix}1.29 \pm 0.03\\2.03 \pm 0.02\end{matrix}\right\}$ | 2.57 | 183 |

$$\beta_{201} = 107; \quad \varepsilon_{201} = 27\ 600$$

were obtained.

Since it seemed probable that both complexes were present in the solutions, eqn. (5) was re-written:

$$[\varepsilon(1 + \beta_{011}h + \beta_{021}h^2) - (\varepsilon_{001} + \varepsilon_{011}\beta_{011}h + \varepsilon_{021}\beta_{021}h^2)]/\varepsilon B - [(\varepsilon_{201} - \varepsilon)\beta_{201}B]/\varepsilon =$$
$$- \beta_{101} + \varepsilon_{101}\beta_{101}\varepsilon^{-1} \qquad (6)$$

and

$$\beta_{201} = 107; \quad \varepsilon_{201} = 25\ 300$$

were inserted. The $\varepsilon_{201}$ value obtained when only one complex was supposed to be present is probably too large. A new plotting (*cf.* Fig. 9) gave

$$\beta_{101} = 19; \quad \varepsilon_{101} = 28\ 100$$

Compared to the result above $\sum_p \beta_{p01}b^{p-1} = 72$, these $\beta$ values give

$$\beta_{101} + B\beta_{201} = 19 + 0.500 \times 107 = 73$$

IV. *"Letagrop" calculations.* The experimental data were also processed with the spectrophotometric version of the "Letagrop" program.[12] In Table 2 some experimental and calculated data are presented and in Table 3 a survey of the results of the calculations is given. $U$ is the error squares sum, defined as $U = \sum(\varepsilon_{\mathrm{calc}} - \varepsilon)^2$ and $\sigma(\varepsilon)$ the standard deviation in $\varepsilon$ as defined in the program. The $\varepsilon_{100}$ values (*cf.* Table 1), determined in nickel(II) perchlorate

solutions, were used in the "Letagrop" calculations.

In group II and III, Table 3, one complex at a time was included in the calculations. Since the best fit was obtained for the complexes with $(pqr) =$ (101) and (201), these were included together. Efforts were made to determine $\beta_{111}$, $\beta_{102}$ or $\beta_{301}$, together with $\beta_{101}$ and $\beta_{201}$, by processing three complexes simultaneously. During the calculations, however, the third $\beta$ value either became negative, or attained a small positive value with standard deviations of the same magnitude. It did not therefore seem likely that the three former complexes were present.
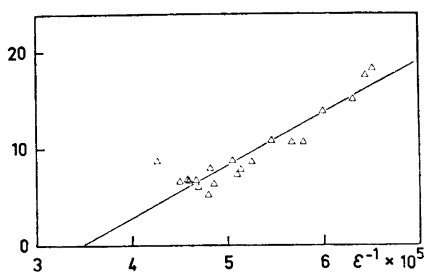


Fig. 9. The left-hand side of eqn. (6) as a function of $\varepsilon^{-1}$ for $\lambda = 270$ nm, different $A$ $B$ values and pH $\sim 2$. $\beta_{201} = 107$ and $\varepsilon_{201} =$ 25 300 are inserted. From the slope and intercept of the line $\beta_{101} = 19$ M$^{-1}$ and $\varepsilon_{101} =$ 28 100 M$^{-1}$ cm$^{-1}$ are obtained.
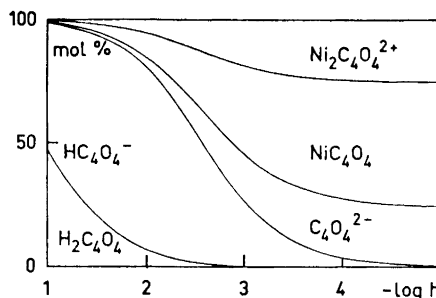


Fig. 10. The distribution of squaric acid as a function of $-\log h$ for the nickel squarate system when $B = 100.0$ mM.

As no complexes other than (101) and (201) could be detected, final calculations were performed. Solutions containing the highest percentage of the (101) complex were chosen and the $\beta_{101}$ and $\varepsilon_{101}$ values varied in the calculations while the $\beta_{201}$ and $\varepsilon_{201}$ values were kept constant. In this way the $\varepsilon_{101}$ values could be determined with the highest possible accuracy. The $\varepsilon_{201}$ values were determined in a similar manner. These $\varepsilon_{101}$ and $\varepsilon_{201}$ values (cf. Table 1) were then inserted in a final calculation, using data from all the solutions, the following values being obtained for the stability constants:

$$\beta_{101} = (19.5 \pm 1.2)\text{M}^{-1}; \quad \log \beta_{101} = 1.29 \pm 0.03$$

$$\beta_{201} = (106 \pm 4)\text{M}^{-2}; \quad \log \beta_{201} = 2.03 \pm 0.02$$

EMF MEASUREMENTS

In order to confirm the results obtained by spectrophotometric methods, some potentiometric titrations were carried out. The distribution of complexes can be seen in Figs. 4, 10, 11, and 12. If a nickel solution is added to a sodium squarate solution, both solutions having pH 3, and if $A$ is kept constant, the free hydrogen ion concentration increases. Owing to the slight solubility

of squarate complexes $A$ is rather low and only small amounts of hydrogen ions will be liberated and thus only small changes in $h$ can be detected if no precipitates are allowed to form.
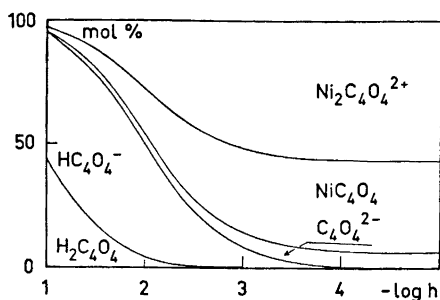


*Fig. 11.* The distribution of squaric acid as a function of $-\log h$ for $B = 300.0$ mM.
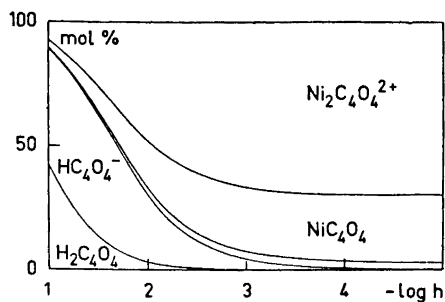
*Fig. 12.* The distribution of squaric acid as a function of $-\log h$ for $B = 500.0$ mM.

In order to avoid the formation of precipitates without starting with too small an $A$ value, sodium squarate solutions were diluted with nickel perchlorate solutions, *i.e.* $A$ decreased with increasing $B$ during the titrations (*cf.* Table 4). The hydrogen ion concentrations were measured by means of the cell described earlier.[2]

*Table 4.* Emf data. The concentrations of NiA and $Ni_2A^{2+}$ have been calculated by means of the formulae $\beta_{101}$ $a$ $b$ and $\beta_{201}$ $a$ $b^2$, respectively. $\Delta_1 E$ is the "error" when the complexes with $(pqr)$ (011), (021), (101) and (201) are included in the calculations and $\Delta_2 E$ the error based on (011) and (021) only. The $\beta_{101}$ and $\beta_{201}$ values obtained by spectrophotometric methods have been used.

| $A$ mM | $B$ mM | NiA mM | $Ni_2A^{2+}$mM | $-\log h_{calc}$ | $\dfrac{H - h_{calc}}{A}$ | $\Delta_1 E$ mV | $\Delta_2 E$ mV |
|--------|--------|--------|----------------|------------------|---------------------------|-----------------|-----------------|
| 2.150 | 0 | 0 | 0 | 3.234 | 0.480 | 0.2 | 0.2 |
| 1.843 | 71.44 | 0.59 | 0.22 | 3.054 | 0.327 | −0.2 | −10.5 |
| 1.613 | 125.0 | 0.59 | 0.40 | 3.001 | 0.240 | 0.3 | −13.0 |
| 1.433 | 166.7 | 0.53 | 0.48 | 2.985 | 0.188 | 0.1 | −13.8 |
| 1.290 | 200.0 | 0.50 | 0.54 | 2.983 | 0.155 | 0.1 | −13.8 |
| 1.075 | 250.0 | 0.37 | 0.51 | 2.992 | 0.116 | 0.2 | −13.0 |
| 0.921 | 285.8 | 0.30 | 0.47 | 3.006 | 0.094 | −0.1 | −12.2 |
| 0.806 | 312.6 | 0.26 | 0.44 | 3.004 | 0.083 | −0.1 | −11.2 |
| 0.717 | 333.4 | 0.22 | 0.40 | 3.015 | 0.074 | −0.1 | −10.3 |

## TREATMENT OF THE DATA

Data from the titrations are given in Table 4. Using the symbols $v_0$, $H_0$ and $A_0$ for the volume and total concentrations of the original sodium squarate solution and $v_t$, $H_t$, and $B_t$ for those of the nickel perchlorate solution added, then

$$H = \frac{v_0 H_0 + v_t H_t}{v_0 + v_t} \ ; \ A = \frac{v_0 A_0}{v_0 + v_t} \ ; \ B = \frac{v_t B_t}{v_0 + v_t}$$

The "Letagrop" program for potentiometric titrations [13] was used to calculate $-\log h_{calc}$, $H$, $(H - h_{calc})/A$, and $\Delta E$, where $\Delta E = E_{calc} - E$ was the "error" in the potential. The $\beta$ values determined spectrophotometrically were inserted and not varied during the calculations.
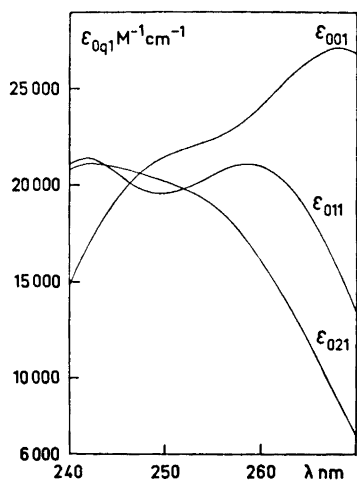


Fig. 13. $\varepsilon_{0q1}$ as a function of $\lambda$. The $\varepsilon_{0q1}$ values are calculated by the Letagrop program.
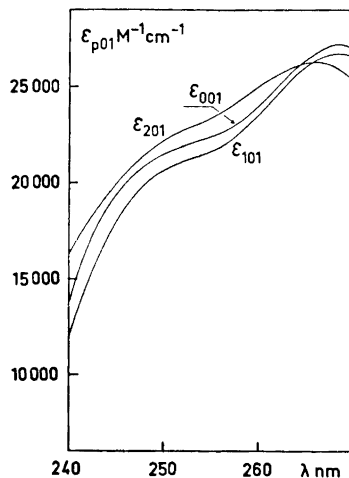
Fig. 14. $\varepsilon_{p01}$ as a function of $\lambda$. The $\varepsilon_{p01}$ values are calculated by the Letagrop program.

The $(-\log h)$ values decreased when the nickel perchlorate solution with $-\log h = 3.19$ was added, as long as the concentrations of the nickel squarate complexes increased. The "errors" $\Delta_1 E$ obtained when the two nickel complexes were included in the calculations, were small, whereas $\Delta_2 E$, obtained when these complexes were excluded, were significant. The emf measurements thus confirm the $\beta$ values determined by spectrophotometric methods.

## RESULTS AND DISCUSSION

The "best values" obtained from the spectrophotometric data are

$$\log \ \beta_{101} = 1.29 \pm 0.03$$
$$\log \ \beta_{201} = 2.03 \pm 0.02$$

where the errors given correspond to an error of $3\sigma$ in $\beta$. The corresponding $\varepsilon$ values are shown in Table 1.

These $\beta$ values have been used together with the previously determined

$$\log \ \beta_{011} = 3.19$$

$$\log \quad \beta_{021} = 4.15$$

to calculate the distribution of the squarate ion, $A^{2-}$, between the different complexes at some nickel concentrations (cf. Figs. 10, 11, and 12). From the diagrams it would seem most favourable to study the complex formation at pH $4-5$. At this pH, however, most of the squaric acid, not bound to nickel, is present as the squarate ion, $A^{2-}$, with molar absorptivities very similar to those for NiA and $Ni_2A^{2+}$ (cf. Table 1). Hence if spectrophotometric methods are used it is necessary to work at other pH values. At pH 2, for instance, $A^{2-}$, NiA, and $Ni_2A^{2+}$ together represent 68 % of the total squaric acid concentration when $B = 0.5$ M and $A^{2-}$ 6 % when $B = 0$.

The absence of complexes containing more than one squarate ion is not surprising considering the low total concentration of squarate ions, $A \leq 3$ mM compared to the total nickel ion concentration, $B \leq 600$ mM. The similarity of the absorptivities for the squarate ion and its metal complexes was also noticed by Tedesco and Walton.[6] They found that the association of the squarate ion with copper(II) or iron(III) did not affect the ultra-violet absorption of the ion for $\lambda > 225$ nm. In their spectrophotometric measurements they used the absorption of the copper(II) and iron(III) complexes in the visible range of the spectrum. No such absorption occurs, however, for the nickel complexes. In their work on nickel(II) squarate complexes they used a paper chromatographic method and, assuming that only one complex, $NiC_4O_4$, was formed they obtained the formation constant $\log \beta = 1.48$. This value agrees well with those determined in this work, i.e. $\log \beta_{101} = 1.29$ and $\log \beta_{201} = 2.03$, considering the differences in assumptions and ionic strength.

In more concentrated nickel squarate solutions precipitates are formed after some time. The formation of precipitates can be related to the concentration of the complex $Ni_2A^{2+}$ and not to that of the complex NiA. Some solutions were prepared with constant $A = 5.07$ mM and $B = 300$ mM and varying perchlorate ion concentrations ranging from 600 to 1800 mM. These solutions thus had varying total molarity. Precipitates were only formed in the solutions with the highest perchlorate concentrations. It therefore seems probable that the precipitate contains the ions $Ni_2A^{2+}$ and $ClO_4^-$. Analysis of the precipitate gave the following results: Found: C 8.8; H 2.7; Cl 12.6. Calc. for $Ni_2C_4O_4(ClO_4)_2$ $7H_2O$: C 8.7; H 2.5; Cl 12.8.

The complex formation between nickel(II) and squarate ions is weaker than was expected, when the investigation was started. The rather small stability constants and the fact that the electronic spectrum of the squarate ion is only slightly affected by the complex formation show that the bonds between the central ion and the ligand involve rather weak $\sigma$- or electrostatic interactions. $\pi$-Bonding between the nickel $d$-orbitals and the empty antibonding orbitals of the aromatic system can be disregarded.

## REFERENCES

1. Cohan, S., Lacher, J. R. and Park, J. D. *J. Am. Chem. Soc.* **81** (1959) 3480.
2. Alexandersson, D. and Vannerberg, N. G. *Acta Chem. Scand.* **26** (1972) 1909.
3. Gelb, R. I. *Anal. Chem.* **43** (1971) 1110.
4. Schwartz, L. M. and Howard, L. O. *J. Phys. Chem.* **74** (1970) 4374.
5. Schwartz, L. M. and Howard, L. O. *J. Phys. Chem.* **75** (1971) 1798.
6. Tedesco, P. H. and Walton, H. F. *Inorg. Chem.* **8** (1969) 932.
7. Cilindro, L. G., Stadlbauer, E. and Keller, C. *J. Inorg. Nucl. Chem.* **34** (1972) 2577.
8. Vogel, A. I. *Quantitative Inorganic Analysis*, Longmans 1961, p. 435.
9. Vogel, A. I. *Quantitative Inorganic Analysis*, Longmans 1961, p. 432.
10. Gran, G. *Analyst* **77** (1952) 661.
11. Burkov, K. A., Lilic, L. S. and Sillén, L. G. *Acta Chem. Scand.* **19** (1965) 14.
12. Sillén L. G. and Warnqvist, B. *Arkiv Kemi* **31** (1969) 377.
13. Brauner, P., Sillén, L. G. and Whiteker, R. *Arkiv Kemi* **31** (1969) 365.

# The Crystal and Molecular Structure of *cis*-Dichloro-bis(1,2-ethanediol)manganese(II) [MnCl₂(C₂H₆O₂)₂]

BRITT-MARIE ANTTI

*Department of Inorganic Chemistry, University of Umeå, S-901 87 Umeå, Sweden*

The crystal structure of [MnCl₂(C₂H₆O₂)₂] has been determined and refined from three-dimensional X-ray diffraction data. The crystals are monoclinic, space group $P2_1/c$, with the following cell dimensions and their estimated standard deviations; $a = 9.491 \pm 0.001$ Å, $b = 7.223 \pm 0.001$ Å, $c = 14.213 \pm 0.001$ Å and $\beta = 92.229 \pm 0.007°$. There are four formula units per unit cell and each atom occupies a general fourfold position. The intensity material was collected with the Weissenberg equi-inclination technique from the $b$-axis using a linear diffractometer and Mo$K\alpha$-radiation. With anisotropic temperature factors for all the non-hydrogen atoms the refinement terminated at a final conventional $R$-value of 0.053. The Mn²⁺ ion is octahedrally surrounded by the four glycol * oxygens and the two chlorine atoms. In this way neutral molecules [MnCl₂(C₂H₆O₂)₂] are formed and these are held together through hydrogen bonds of the type O−H···Cl. A tentative proposal for the positions of the hydrogen atoms is given.

A n investigation of complexes between polyols and divalent transition metal ions is currently in progress in this department. The first work in this series, a crystal structure determination of [Cu(C₂H₆O₂)₃]SO₄, was recently published by the author.[1] The crystal structure determination [MnCl₂(C₂H₆O₂)₂] which is presented below forms the second paper in the series.

## EXPERIMENTAL

*Crystal preparation and analyses.* The crystals were prepared by dissolving 7.5 g MnCl₂.4H₂O in 7 g glycol by heating on a water bath. The solution obtained was placed over sulphuric acid *in vacuo*. Pink crystals, in the form of somewhat irregular hexagonal plates, separated after a short time. The chlorine content of the crystals was determined gravimetrically to be 27.14 %. (Calculated for [MnCl₂(C₂H₆O₂)₂], 28.36 %.) No other analyses were made.

*Crystal data and space group.* From rotation photographs around the *a*- and *b*-axes and the corresponding Weissenberg photographs (zero- and first layers) it was concluded

---

\* Throughout this paper 1,2-ethanediol will be referred to as glycol.

that the crystals are monoclinic. The cell dimensions were refined from a powder photograph taken in a camera of Guinier-Hägg type and with Si as internal standard. (To avoid fluorescence the $CuK\alpha$-radiation was filtered through copper foil before being diffracted in the crystal powder.) The following parameters and their corresponding standard deviations were obtained $a = 9.491 \pm 0.001$ Å, $b = 7.223 \pm 0.001$ Å, $c = 14.213 \pm 0.001$ Å and $\beta = 92.229 \pm 0.007°$. The density of the crystals was determined by the flotation method using bromoform and xylene. The experimental value was 1.68 $g/cm^3$ and the value calculated for four formula units in the unit cell was 1.70 $g/cm^3$. Systematic extinctions were found for $h0l$ when $l$ is odd and for $0k0$ when $k$ is odd. This is characteristic for the space group $P2_1/c$ (No. 14).[2]

*Intensity data.* The intensities from the crystal $[MnCl_2(C_3H_6O_2)_2]$ were collected and measured with an automatic linear diffractometer, PAILRED, and $MoK\alpha$-radiation. The crystal used was hygroscopic and therefore it was enclosed in a capillary of Lindeman glass during the measurements. It was rotated around the $b$-axis and intensities for $h0l - h8l$ were measured. Reflexions with a total number of counts less than 4000 during one scan interval were measured twice. The half-scan interval for reflexions with $\theta \geq 22°$ ($\Omega_1$) varied between $0.9° - 1.2°$ and for those with $\theta \leq 22°$ ($\Omega_2$) between $1.8°$ and $2.1°$ for $h0l - h3l$. From $h3l$ to $h8l$, $\Omega_1$ was $1.2°$ and $\Omega_2$ was $2.1°$. The scan speed used was $1°/min$. Background intensities, $B_1$ and $B_2$, were measured during 40 sec ($t_B$) before and after each scan. The intensity for a reflexion, $TI$, was calculated from the measured total intensity, $T$, (peak + background) by subtracting the background counts $B_1$ and $B_2$ according to the relation

$$TI = T/TN - [t_T/(t_B/60)](B_1 + B_2)$$

where $t_T$ stands for the total scanning time $[\Omega_{1\ or\ 2}/(\text{scan speed/min})]$ and $TN$ is the number of times the reflexion is measured. The relative counting statististical error of each reflexion $\Delta T/TI$, was calculated using the formula

$$\frac{\Delta T}{TI} = \frac{[T/TN^2 + t^2(B_1 + B_2) + T^2/TN^2 \times 0.0001]^{1/2}}{T/TN - t(B_1 + B_2)}$$

where $t = t_T/(t_B/60)$ and $T^2/TN^2 \times 0.0001$ is a term that corrects for the linear error in the diffractometer. Out of a total of 3291 measured intensities those with $\Delta T/TI > 0.5$ were omitted leaving 1969 independent reflexions for the refinement.

Besides the normal correction for Lorentz and polarization factors absorption correction was also made. The linear absorption coefficient was 19.1 $cm^{-1}$ and the greatest difference in transmission was 18 %. When the refinement was terminated, structure factors for all the omitted reflexions within the copper sphere were calculated. These were all weak reflexions, weaker or equal to the threshold value of the intensity material.

The diffractometer data correction program used was the modified version of a program originally written by Ivarsson and Lundberg.[3] The computer programs used were the same as described by Antti and Lundberg.[4]

## STRUCTURE DETERMINATION AND REFINEMENT

The manganese and chlorine atoms were located from a three-dimensional Patterson synthesis, and all the other atoms were found by standard Fourier methods.

The atomic parameters and the atomic temperature factors were refined by full matrix least-squares techniques. The reflexion material was weighted according to the method proposed by Cruickshank,[5] with $a = 50$, $c = -0.015$ and $d = 0.0001$. The atomic scattering factors for $Mn^{2+}$, $Cl^-$, O, and C were used and taken from the International Tables[6] and account was taken of the real parts of the dispersion corrections for the manganese and the chlorine atoms. With isotropic temperature factors for all atoms the refinement converged to a conventional $R$-value of 0.083. A final refinement including

anisotropic temperature factors for all atoms resulted in a final $R$-value of 0.053. All parameter shifts in the last refinement were less than 10 % of the estimated standard deviations.

Finally a difference Fourier synthesis was calculated. From the twenty highest peaks which appeared in this map twelve corresponded to reasonable positions for the twelve independent hydrogen atoms in general positions. Four of the hydrogen atoms, those bound to oxygen atoms, were suitably located for hydrogen bonding to chlorine atoms.

After two cycles of least-squares refinement of the positional parameters for all the hydrogen atoms the $R$-value decreased to 0.046. During this refinement the isotropic thermal parameters of the hydrogen atoms and the positional and anisotropic thermal parameters of all the other atoms were kept constant. The scattering factors for the hydrogen atoms used were those proposed by Stewart, Davidson and Simpson.[7] When the non-hydrogen atoms were refined in two further cycles, while the hydrogen atom positions were kept constant, there was a further decrease in the $R$-value to 0.044.

The significance of this decrease in $R$-value from 0.053 to 0.044 was tested by a method proposed by Hamilton (1965)[8] and somewhat simplyfied by Pawley (1970).[9] The decrease proved to be significant with more than 99 % certainty. The present material gave an $R$-ratio of 1.205 which should be compared with the calculated ratio $\mathscr{R}_{48,1821,0.01} = 1.017$. The indices 48, 1821, and 0.01 refer to the dimension of the hypothesis, the degrees of freedom, and the significance level, respectively. Although the determination of the hydrogen atom positions cannot be considered especially accurate, the introduction of them made the values of the estimated standard deviations for all the non-hydrogen atoms 16 to 23 % lower.

Under these circumstances it seems to be justified to include the hydrogen atom positions. A last difference Fourier map was then calculated in which no abnormalities could be detected. A list of the final positional parameters and the thermal parameters is given in Tables 1 $a$ and 1 $b$. The observed and calculated structure factors are listed in Table 2.


## DESCRIPTION AND DISCUSSION OF THE STRUCTURE

The structure is built up from discrete molecules [MnCl$_2$(C$_2$H$_6$O$_2$)$_2$], which are held together through weak hydrogen bonds and van der Waals contacts. The hydrogen bonds are of the type Cl$\cdots$O$-$H. A drawing illustrating the packing and the hydrogen bond contacts is shown in Fig. 1.

In the molecule [MnCl$_2$(C$_2$H$_6$O$_2$)$_2$] manganese(II) coordinates to four oxygen atoms and two chlorine atoms in a somewhat distorted octahedral arrangement as can be seen in Fig. 2. The chlorine atoms, which are in *cis*-positions, are at nearly equal distances, 2.463 Å and 2.464 Å, respectively, from the manganese atom. The distances between the oxygen and manganese atoms are very similar and lie between 2.184 Å and 2.247 Å. The angles within the octahedron show a rather wide variation around the ideal value. For example, the angles that should be 90° in a regular octahedron, *i.e.* the angles $L-M-L$ where the $L$:s stand for ligands in adjacent corners and $M$ is the

*Table 1a.* The atomic positional fractional coordinates and the anisotropic thermal parameters. All values have been multiplied by $10^4$. (Standard deviations for the last significant figure are given in parentheses). Anisotropic temperature factors have been calculated according to the formula $\exp[-(h^2\beta_{11}+k^2\beta_{22}+l^2\beta_{33}+hk\beta_{12}+hl\beta_{13}+kl\beta_{23})]$.

|       | $x$      | $y$     | $z$       | $\beta_{11}$ | $\beta_{22}$ | $\beta_{33}$ | $\beta_{12}$ | $\beta_{13}$ | $\beta_{23}$ |
|-------|----------|---------|-----------|----------|----------|----------|----------|----------|----------|
| Mn    | 2510(1)  | 1621(1) | 4293(0.4) | 62(1)    | 108(1)   | 30(0.3)  | $-10(1)$ | $-4(1)$  | 3(1)     |
| Cl(1) | 2062(1)  | 1399(2) | 5984(1)   | 101(1)   | 197(2)   | 29(0.4)  | $-44(3)$ | 5(1)     | 1(2)     |
| Cl(2) | 2981(1)  | 6680(1) | 9004(1)   | 100(1)   | 107(2)   | 50(1)    | $-7(2)$  | $-6(1)$  | 1(2)     |
| O(11) | 4586(3)  | 2841(5) | 4587(2)   | 74(3)    | 210(8)   | 38(2)    | $-44(8)$ | $-13(3)$ | 14(5)    |
| O(12) | 3430(3)  | 2324(5) | 2904(2)   | 104(4)   | 188(7)   | 29(1)    | $-44(8)$ | $-4(3)$  | 34(5)    |
| O(21) | 1583(3)  | 4463(4) | 4231(2)   | 87(3)    | 126(6)   | 57(2)    | 8(7)     | $-7(4)$  | 10(5)    |
| O(22) | 371(3)   | 1362(5) | 3657(2)   | 70(3)    | 164(7)   | 54(2)    | $-29(7)$ | $-21(4)$ | 4(5)     |
| C(11) | 4536(5)  | 8155(8) | 1203(4)   | 72(5)    | 229(12)  | 57(3)    | 42(12)   | 24(5)    | $-12(9)$ |
| C(12) | 4513(5)  | 3715(7) | 2987(3)   | 103(5)   | 165(10)  | 48(2)    | $-15(11)$| 42(6)    | 35(7)    |
| C(21) | 448(6)   | 4623(8) | 3550(4)   | 119(7)   | 182(12)  | 63(3)    | 97(14)   | $-23(7)$ | 16(9)    |
| C(22) | 494(5)   | 8005(8) | 1326(4)   | 74(5)    | 234(14)  | 78(4)    | $-61(12)$| $-19(7)$ | 23(10)   |

*Table 1 b.* Atomic positional fractional coordinates for the hydrogen atoms. All values have been multiplied by $10^3$. (Standard deviations for the last significant figure are given in parentheses). The thermal parameters have not been refined.

|          | $x$      | $y$     | $z$     | $B$  |
|----------|----------|---------|---------|------|
| H(O11)   | 506(5)   | 258(8)  | 12(4)   | 4.0  |
| H(O12)   | 298(5)   | 238(8)  | 236(3)  | 4.0  |
| H(O21)   | 207(5)   | 574(8)  | 423(3)  | 4.0  |
| H(O22)   | 12(5)    | 537(8)  | 110(3)  | 4.0  |
| H(C11)1  | 409(6)   | 683(9)  | 138(4)  | 5.0  |
| H(C11)2  | 381(6)   | 914(9)  | 108(4)  | 5.0  |
| H(C12)1  | 406(6)   | 497(9)  | 310(4)  | 5.0  |
| H(C12)2  | 501(6)   | 381(8)  | 243(4)  | 5.0  |
| H(C21)1  | 89(6)    | 467(9)  | 281(4)  | 5.0  |
| H(C21)2  | $-11(6)$ | 589(9)  | 363(4)  | 5.0  |
| H(C22)1  | 94(6)    | 807(9)  | 70(4)   | 5.0  |
| H(C22)2  | 126(6)   | 806(9)  | 180(4)  | 5.0  |

central atom, vary between 72.4° and 104.7°. For a complete list of distances and angles within the octahedron, see Table 3.

A comparison can be made between $[MnCl_2(C_2H_6O_2)_2]$, the subject of this report, and the structure of $MnCl_2.4H_2O$.[10] It is interesting to observe that the manganese atom has retained its configuration although water has been substituted by glycol. In $MnCl_2.4H_2O$ there are also discrete molecules or octahedra where the manganese atom coordinates two chlorine atoms at an average distance of 2.488 Å and four oxygen atoms at an average distance of 2.206 Å. These distances should be compared with those obtained from the structure $[MnCl_2(C_2H_6O_2)_2]$, which are 2.464 Å and 2.215 Å respectively. The average $Mn-Cl$ distance of 2.464 Å in the glycol compound is significantly shorter

Table 2. Observed and calculated structure factors ($\times 10$). Values marked with an asterisk were not included in the refinements.

*Table 2. Continued.*

(Structure factor table — columns of H, L, F$_o$, F$_c$ values)

```
                          H  L
                          7  1  128  136
K= 3                      7  2  161  170
                          7  3  110  120
2 -6  242  227            7  4  140  156
2 -7  439  439            7  5   98   84
2 -8  151  155            7  6   58   80
2 -9  181  172            7  7  185  196
2-10   73   76            7  9  102  110
2-11  161  152            7 10   85   91
2-17   77   71            7 13   72   51
2-18   70   50            6 14  173  176
1-19  126  118            6 13   67   54
1-17  189  175            6 12  157  154
1-13  131  126            6 11   84   91
1-12   66   48            6  9   67   45
1-11  253  244            6  8  397  405
1-10  116  109            6  6  194  202
1 -9  297  296            6  4  106  102
1 -8   77   75            6  3  166  165
1 -7  114  109            6  2  264  273
1 -6  137  130            6  1  308  316
1 -5  468  454            6  0  222  223
1 -4  234  229            6 -1  126  134
1 -3  876  869            6 -2   96   96
1  3  681  669            6 -3  333  335
1  4  401  382            6 -5  303  304
1  5  381  387            6 -6   98   96
1  6  279  271            6 -9  232  225
1  8   58   63.           6-11  179  170
1  9  323  316            6-12  101   91
1 11  381  375            6-15   79   89
1 12  178  175            6-17   90   92
1 13  194  189            5-16  162  147
1 15   86   90            5-15  112  112
1 17  143  144            5-13  127  125
1 19  114  111            5-12  113  110
1 18   84   81            5-10  165  159
1 16   83   61            5 -9  135  130
0 13  257  244            5 -8  165  150
0 12  118  109            5 -7  168  153
0 11  331  318            5 -6  167  161
0 10  114  120            5 -5  216  220
0  8   62   74            5 -4  124  131
0  7  654  630            5 -3   95   91
0  6  113   47            5 -2  230  235
0  5 1038 1004            5 -1  340  345
0  3  168  161            5  0  117  123
0  2   42   39            5  1  143  145
                          5  2  270  262
K= 4                      5  3  197  201
                          5  5  202  203
12  5  119  108           5  6   79   79
12  3  176  182           5  8   94   88
12 -1  124  115           5  9   80   76
12 -3  160  149           5 10   63   62
12 -5   69   58           5 12  116  115
11-10   66   51           5 13   81   85
11 -8   64   61           5 14   73   67
11 -7  115  128           5 15  121  122
11 -5   92   93           5 17  120  104
11 -4  110  122           4 13  120  163
11 -2   72   57           4 13  120  114
11 -1  165  160           4 12  184  180
11  1  129  141           4 10   78   71
11  2   99   90           4  8  270  265
11  4   66   91
11  5  124  106           K= 5
11  7  126  140
10 11   95   91           12  4  164  157
10 10   90   92           12  2   90   84
10  9  136  146           12 -2  124  127
10  8  127  125           12 -4  116  105
10  5   95  117           11 -2   89   95
10  3  192  196           11 -5   65   37.
10  1  112  124           11  0   81   95
10 -1   99  106           11  2   90   95
10 -3  210  218           11  5   78   79
10 -5  124  110           11  4   80   95
10 -7   81   81           11  0   63   86
10 -9  146  152           10 -8  153  139
10-13   63   17.          10-10   87   91
 9-13   89   82           10 -6  207  201
 9-10  123  123           10 -2  180  184
 9 -9   63   48           10  0  232  227
 9 -8   83   68           10  4  154  146
 9 -7  157  147           10  7   82   81
 9 -5  191  180           10  8  108  104
 9 -4  153  142           10 10   69   77
 9 -3   66   59            9 11  103   81
 9 -2  122  120            9  8   98  101
 9  1  209  211            9  6  125  115
 9  1  226  231            9  5   66   52
 9  2  122  123            9  4   77   88
 9  6   62   65            9  2   77   88
 9  5  137  131            9  0  154  155
 9  6   68  114            9 -2  100   42
 9  7   99  107            9 -4  155  147
 9 10   83   50            9 -5  115  115
 9 13   87   73            9 -6  205  201
 8 12   84   71            9 -8  104   94
 8  9   76   68            9-10   69   77
 8  8  199  197            9-11   90   88
 8  7  110  114            9-14   97   76
 8  9   94   91            8 13   60   42
 8  5   86   94            8 11   72   81
 8  4  121  119            8 10  123  110
 8  3  291  296            8  9   60   60
 8  2  251  255            8  7  128  123
 8  1  177  187            7 11  128  123
 8 -1  164  182            7  8  191  191
 8 -2   95  101            7  7   65   59
 8 -3  360  362            7  5  180  189
 8 -4   66   47            7  5  205  201
 8 -5  205  199            7  3  103  108
 8 -7   67   70            7  2   86   83
 8 -9  228  220            7  1  129  127
 8-10  130  133            7  0  290  285
 8-11  109  107            7  1   90   88
 8-14   82   62            7  0  291  280
 7-14   75   64            6 14   97   81
 7-13   71   64            6 13   60   42
 7-12  104  114            6 11   98   84
 7-11  107   88            6  9  154   96
 7-10  135  138            6  6  117   88
 7 -9  116  120            6  4  436  435
 7 -8   82   82            6  2  222  228
 7 -7  268  262            6  1  237  238
 7 -6  179  176            6 -2  271  276
 7 -5   91   94            6 -3  437  430
 7 -4  264  259            6 -3  271  276
 7 -3  155  160            6 -1  214  220
 7 -1  225  232            5  3  194  201
                          5  3  100   96
                          5  3  324  321
                          5  1   91   87
                          4  8  188  156
                          4  7  215  212
                          3  6   53  29.
                          3  9  142  135
                          3 11   64   36.
                          3 12  153  155
                          3 13   91   72
                          3 10  104  104
                          2 17  115  115
                          2 14   57   56.
                          2 12  197  197
                          2 11  165  171
                          2  9   54   53
                          2  8  283  282
                          2  7  155  150
                          2  5  558  563
                          2  5   91  114
                          2  4   96   94
                          2  3  186  191
                          2  2  579  582
                          2  1  437  436
                          2  0  530  542
                          2 -1  262  259
                          2 -2  322  329
                          2 -3  269  284
```

```
 H  L
 2 -4  416  408        6-10  325  304
 2 -5  626  631         6 -9   76   53
 2 -6  328  333         6 -8  256  242
 2 -7  281  271         6 -6  339  328
 2 -9  119  117         6 -4  516  507
 2-10  153  149         6 -2  174  167
 2-11  325  328         6  0  276  261
 2-12   75   80         6  1   81   88
 2-13  200  202         6  2  428  429
 2-14   95   84         6  3  102   89
 2-15   91   81         6  5   92   88
 2-17  164  160         6  6   57   57
 2-19   91   81         6  7  143  138
 1-19   79   57         6  8   82   79
 1-18  114  120         6  9  105  103
 1-16  110   96         6 14   91   85
 1-15  171  158         5 16   81   64
 1-13  197  194         5 14  105  179
 1-12  144  139         5 12   76   85
 1-10  144  141         5 11  110  118
 1 -9  218  204         5  9  164  171
 1 -7  363  363         5  8  254  247
 1 -6   77   74         5  6  274  266
 1 -5   87   97         5  5  148  149
 1 -3  266  267         5  4   57   51
 1 -3  286  286         5  3  180  180
 1  2  183  187         5  2  126  131
 1  3  145  135         5  0  429  433
 1  4  223  231         5 -1  161  160
 1  5  179  189         5 -2  166  164
 1  6   89   81         5 -3   92   96
 1  7  340  346         5 -4   85   95
 1  8   68   63         5 -5   97   92
 1  9  261  259         5 -6  286  277
 1 10  193  194         5 -7  101   93
 1 12  206  209         5 -8  231  218
 1 13  193  190         5-10   55   53
 1 14   69   57         5-12   58   63
 1 15  177  180         5-14  144  143
 1 18  126  126         5-16   73   60
 1 19   74  40.         4-16  240  210
 0 19  111  103         4-15   69   46
 0 17  182  177         4-12  245  226
 0 15  102   97         4-10  429  411
 0 13  234  226         4 -9   81   79
 0 12  182  180         4 -8   99  101
 0 11  387  376         4 -7  104   98
 0 10  199  192         4 -6  350  350
 0  9  161  161         4 -5  135  131
 0  8   67   60         4 -4  373  369
 0  7  249  237         4 -2  249  252
 0  5  315  317         4 -1   55   57
 0  4  502  491         4  0  270  266
 0  2  295  292         4  1   90   89
                       4  2  208  201
K= 5                    4  3  107  102
                       4  4   62   67
12  4  164  157         4  7  108  108
12  2   90   84         4  9   89   75
12 -2  124  127         4 10  163  160
12 -4  116  105         4 13   89   72
11 -2   89   95         4 14  131  125
11  0   81   95         3 15   74   74
11  2   90   95         3 14  149  150
11  5   78   79         3 13   93   84
                       3 12  109  109
                       3 11  102  109
                       3 10  125  113
                       3  9  157  157
                       3  6  308  201
                       3  5  216  220
                       3  4   86   82
                       3  0  277  275
                       3  0  387  386
                       3 -1  236  231
                       3 -2  237  237
                       3 -3  283  284
                       3 -4  212  222
                       3 -6  262  257
                       3 -7  127  117
                       3 -8  283  277
                       3-10   50  14.
                       3-12  146  142
                       3-14  117   89
                       2-18  148  133
                       2-16  174  158
                       2-12  294  281
                       2-11   79   80
                       2-10  368  362
                       2 -8   93   94
                       2 -6  416  405
                       2 -5  145  140
                       2 -4  346  344
                       2 -2  108  101
                       2 -1  376  375
                       2  0  210  208
                       2  1  393  397
                       2  4   58   54
                       2  5   78   80
                       2  6  197  207
                       2  7  131  137
                       2  9  258  254
                       2 10   81   85
                       2 11  140  137
                       2 14  140  137
                       2 15   61   55
                       2 18  176  161
                       1 16   81   73
                       1 14  135  135
                       1 12  136  132
                       1  9  247  243
                       1  8  250  252
                       1  7  247  240
                       1  6  155  146
                       1  4   67   61
                       1  3  459  459
                       1  2  255  262
                       1  0  158  154
                       1 -2  136  137
                       1 -5  205  205
                       1 -6  247  245
                       1 -7  153  143
                       1 -8  194  116
                       1 -9  118  125
                       1-12  125  120
```

```
 H                           H  L
 1-13   56   43              4 -2   80   74
 1-14   98   90              4 -3   70   62
 1-15   70   52              4 -4  304  316
 1-16   66   54              4 -5   79   84
 0  2  135  131              4 -6  120  131
 0  4   52   59              4 -7  106  118
 0  6  238  232              4-11   74   71
 0  7  253  255              4-16   80   84
 0  8  200  202              3-16   74   61
 0 10  179  167              3-12   78   64
 0 11   99   98              3-11   58   53
 0 12  329  315              3-10  165  176
 0 13   88   76              3 -9   74   72
 0 14  130  126              3 -8  119  117
 0 16  141  133              3 -4  236  236
 0 18  196  188              3 -3  100   98
                            3 -2  408  407
K= 6                         3  1  136  147
                            3  5  105  101
12 -2   75   66              3  2  229  227
11 -7   71   60              3  3  434  431
11 -4   95   88              3  5  193  197
11  4   76   84              3  6  153  161
11  6   65   60              3  7  178  182
10 10   66   89              3  8  160  159
10  8  109  101              3  9   58   66
10  3   85   81              3 10  190  193
10  2   64   57              3 11  110  107
10 -3  123  134              3 12  138  128
10 -7   61   56              3 16   79   63
10 -8   85   72              3 18   68   73
10-10   81   73              2 14  107  107
 9-12   71   79              2 12  218  216
 9-10   78   84              2  8  309  305
 9 -6   63   67              2  3  210  206
 9  0   70  33.              2  2  441  444
 9  1   95   96              2  0  475  487
 9  2   76   65              2 -1  200  203
 9  3   79   71              2 -2  171  171
 9  4  111  121              2 -3  130  328
 9  6   81   79              2 -5  151  146
 9  8   74  19.              2 -6  308  307
 9  9   69   75              2 -7  125  142
 9 10  109  109              2 -8   92   86
 9 12   90   81              2 -9  123  140
 8 14  116  115              2-10   98  102
 8 10   85   75              2-11   93  100
 8  8  218  217              2-12   89   87
 8  6   94   97              2-17   72   75
 8  5   58  17.              1-18   89   87
 8  4  104  100              1-16   61   53
 8  2  180  176              1-12   74   77
 8  0   57   53              1-11   85   79
 8 -5   67   67              1-10  161  163
 8 -8   83   78              1 -8  120  128
 8 -9   58   60              1 -7   82   89
 8-11   60  32.              1 -5  301  307
 8-14   85   99              1 -4  329  336
 7-12   96  102              1 -2  359  362
 7-10   78   84              1  2  307  307
 7 -9   66   44              1  4  421  412
 7 -8   60   44              1  7  122  122
 7 -7   58  25.              1  6  104   90
 7 -4  147  141              1  7   81   82
 7 -3  107  106              1  8  144  147
 7 -2  155  159              1 10  234  223
 7 -1   90   88              1 11  109   99
 7  0   85   76              1 12  120  121
 7  2  137  141              1 13   68   84
 7  3   90   96              1 15   80   66
 7  4  207  208              1 16   63   66
 7  5   83   78              1 18   98   76
 7  6  140  149              1 17   61   64
 7  7  112   99              0 13  151  142
 7 10  182  170              0 11  101  112
 7 12   92   91              0 10   88   72
 6 14  183  176              0  9  113  117
 6 12  127  134              0  7   73   72
 6 11   68   74              0  4  436  424
 6  9  209  212              0  4  363  354
 6  5   74   62              0  3  163  163
 6  3   91   98              0  2  298  305
 6  2  257  263
 6  1   73   73              K= 7
 6  0  232  231
 6 -3  102  101              10 10  107   64
 6 -4   87   85              10  8   62   47
 6 -5   70   79              10  4  105  117
 6 -6   81   87              10  3   65   55
 6 -9   61   47              10 -8  111  108
 6 -8   58   70              10 -1   66   41
 5-17   95   79              10 -2  122  117
 5-16   95   79              10 -8   66  109
 5-13   72  38.              10 -8   66   50
 5-12  103   93              9 -16  135  142
 5-11   54   54              9 -3   98   97
 5-10  117  117              9 +3   93   97
 5 -8  102   97              9 -2   89   95
 5 -7   66   61              9 13  137  132
 5 -6  137  140              1 -1   94   97
 5 -4  171  179              3 137  132
 5 -3  266  262              5 10   79   79
 5  2  194  191              5 11   70  119
 5  1  155  159              8  7  120  132
 5  0   92   84              8 12  131  138
 5 -1   89   89              8 11  118  131
 4 299  298              8 10  110   97
 4 194  192              8  9   97   97
 4   64   62              8 -1   93   61
 4  0  127  126              8 -2  199  113
 5 10  147  138              8 -8   92  101
 5 12  147  138              8-10   61   54
 5 13   75   63              7-14   70   67
 5 16  108   92              7-12   78   68
 4 14  170  163              7-11   71   70
 4 13  188  178              7 -9  102  120
 4 12  194  191              7 -8  107  120
 4  9   98   90              7 -5   89   84
 4  8  322  313              7  3   74   68
 4  4  424  427              7  1  133  133
 4  3  174   69              7 -1   63   49
 4  2  442              7  0  171  179
 4  1  111  118              7  4   71   84
 4  0  426  423              7  6   68   62
 4 -1   73   62
```

```
 H  L
 7  9   62   65
 7 15   61  5.
 6 13  103  105
 6  9  112  114
 6  7  150  166
 6  3  163  166
 6  2  141  151
 6  1  132  136
 6  0  102  106
 6 -2  112  116
 6 -3  106  108
 6 -4  185  194
 6 -5   67   77
 6 -6   91   95
 6 -8   73   81
 6-10  108  122
 5-14   79  101
 5-12   87   87
 5-11   76   96
 5-10   70   50
 5 -9   73   59
 5 -8  186  194
 5 -6  131  127
 5 -5  119  130
 5 -3  130  137
 5 -2  183  195
 5  0   94   95
 5  1   83   79
 5  2   48   63
 5  3   92   81
 5  5   56   70
 5 10   56   42
 4 13  103  109
 4 12   82   67
 4  9   98   90
 4  8   52   29
 4  7  227  233
 4  5  148  162
 4  4   48   39
 4  3  103  105
 4  2  138  153
 4  1  289  290
 4  0   93   98
 4 -1  102  123
 4 -2   60   61
 4 -3  121  116
 4 -4  163  180
 4 -5   74   87
 4 -6  157  164
 4-10  126  148
 4-12   82  103
 3-14  105  120
 3-12   65   66
 3-10   58   81
 3 -9   96   98
 3 -8  240  250
 3 -7   61   78
 3 -6  100  109
 3 -5  120  112
 3 -4  120  112
 3 -2  190  202
 3  0   98  104
 3  1  102  101
 3  3  137  134
 3  5   84   70
 3  7   56   53
 3  8   68   57
 3 10   68   50
 3 13   58   58
 3 16   62   55
 3 14  125  129
 2 12  145  155
 2 10   75   77
 2  5  280  281
 2  2   84   89
 2  1  225  236
 2  0  157  160
 1-14  213  223
 2 -3   61   80
 2 -4  193  204
 2 -5  210  210
 2 -7  161  166
 2-10  196  205
 2-11  102  115
 1-18   66  26.
 1-17   78   89
 1-16   91   89
 1-14  105  128
 1-11  127  139
 1-10  157  161
 1 -8  204  206
 1 -6   71   51
 1 -4  281  278
 1 -3  291  291
 1  1  201  204
 1  3  100   97
 1  5  117  121
 1  6   69   70
 1  8  131  138
 1 11   52   31
 1 14  110  120
 1 13  131  131
 1 12  110  120
 1 16   65   69
 1 17   69   62
 1  5   76   55
 0 12  160  163
 0 11  115  124
 0 10   89   88
 0  7   52   48
 0  6  139  146
 0  5  153  354
 0  2   68   76
```

*Table 2. Continued.*

| H | L | | | H | L | | | H | L | | | H | L | | | H | L | | | H | L | | | H | L | | |
|---|---|---|---|---|---|---|---|---|---|---|---|---|---|---|---|---|---|---|---|---|---|---|---|---|---|---|---|
| | | | | 8 | 8 | 59 | 45 | 6 | 3 | 129 | 129 | 4 | -9 | 144 | 141 | 3 | -2 | 159 | 168 | 2 | 6 | 88 | 93 | 1 | -9 | 131 | 136 |
| K= | 8 | | | 8 | 9 | 77 | 75 | 6 | 9 | 57 | 37 | 4 | -7 | 71 | 67 | 3 | -6 | 64 | 64 | 2 | 7 | 52 | 60 | 1 | -10 | 60 | 61 |
| | | | | 7 | 13 | 67 | 54 | 5 | 14 | 63 | 41 | 4 | -5 | 225 | 235 | 3 | -7 | 131 | 143 | 2 | 11 | 113 | 116 | 1 | -13 | 76 | 76 |
| 9 | 7 | 77 | 77 | 7 | 7 | 95 | 87 | 5 | 13 | 65 | 53 | 4 | -3 | 158 | 167 | 3 | -8 | 56 | 56 | 2 | 13 | 105 | 104 | 1 | -15 | 72 | 78 |
| 9 | 6 | 73 | 64 | 7 | 6 | 89 | 73 | 5 | 10 | 91 | 92 | 4 | -1 | 48 | 58 | 3 | -9 | 89 | 90 | 2 | 17 | 74 | 75 | 0 | 2 | 91 | 97 |
| 9 | 5 | 67 | 76 | 7 | 5 | 91 | 80 | 5 | 9 | 76 | 67 | 4 | 1 | 170 | 181 | 3 | -12 | 66 | 30* | 1 | 15 | 65 | 68 | 0 | 3 | 48 | 51 |
| 9 | 4 | 58 | 29* | 7 | 1 | 119 | 116 | 5 | 7 | 110 | 116 | 4 | 3 | 70 | 75 | 3 | -13 | 100 | 95 | 1 | 13 | 85 | 66 | 0 | 4 | 61 | 55 |
| 9 | 1 | 101 | 109 | 7 | 0 | 92 | 91 | 5 | 6 | 103 | 97 | 4 | 11 | 85 | 67 | 2 | -17 | 80 | 98 | 1 | 10 | 78 | 67 | 0 | 5 | 135 | 134 |
| 9 | 0 | 59 | 41 | 7 | -1 | 121 | 122 | 5 | 5 | 63 | 60 | 4 | 13 | 96 | 93 | 2 | -15 | 56 | 58 | 1 | 9 | 104 | 111 | 0 | 6 | 89 | 87 |
| 9 | -1 | 111 | 111 | 7 | -2 | 61 | 62 | 5 | 4 | 117 | 117 | 3 | 15 | 72 | 79 | 2 | -13 | 86 | 81 | 1 | 8 | 160 | 156 | 0 | 7 | 142 | 139 |
| 9 | -5 | 71 | 75 | 7 | -4 | 56 | 67 | 5 | 1 | 124 | 131 | 3 | 13 | 91 | 88 | 2 | -11 | 191 | 192 | 1 | 7 | 82 | 89 | 0 | 11 | 157 | 162 |
| 9 | -7 | 89 | 68 | 7 | -5 | 91 | 82 | 5 | 0 | 60 | 80 | 3 | 10 | 89 | 69 | 2 | -9 | 121 | 125 | 1 | 4 | 215 | 218 | 0 | 13 | 94 | 104 |
| 9 | -13 | 62 | 44 | 7 | -7 | 136 | 133 | 5 | -1 | 169 | 186 | 3 | 9 | 88 | 87 | 2 | -8 | 83 | 81 | 1 | 3 | 86 | 89 | 0 | 17 | 104 | 95 |
| 8 | -11 | 76 | 75 | 7 | -13 | 71 | 76 | 5 | -3 | 82 | 77 | 3 | 8 | 105 | 101 | 2 | -7 | 115 | 125 | 1 | 2 | 124 | 137 | | | | |
| 8 | -9 | 100 | 102 | 7 | -14 | 70 | 45 | 5 | -5 | 77 | 90 | 3 | 7 | 123 | 126 | 2 | -5 | 170 | 170 | 1 | -2 | 179 | 193 | | | | |
| 8 | -8 | 67 | 24* | 6 | -14 | 60 | 18* | 5 | -7 | 175 | 183 | 3 | 5 | 69 | 75 | 2 | -3 | 73 | 74 | 1 | -3 | 68 | 67 | | | | |
| 8 | -7 | 61 | 41 | 6 | -11 | 118 | 127 | 5 | -9 | 70 | 80 | 3 | 4 | 117 | 122 | 2 | -2 | 55 | 54 | 1 | -4 | 120 | 123 | | | | |
| 8 | -5 | 128 | 127 | 6 | -9 | 155 | 163 | 4 | -17 | 74 | 74 | 3 | 2 | 143 | 146 | 2 | -1 | 59 | 58 | 1 | -5 | 79 | 80 | | | | |
| 8 | -3 | 155 | 158 | 6 | -5 | 195 | 206 | 4 | -11 | 149 | 153 | 3 | 1 | 106 | 101 | 2 | 0 | 82 | 85 | 1 | -6 | 57 | 54 | | | | |
| 8 | 1 | 132 | 132 | 6 | -3 | 189 | 192 | 4 | -10 | 55 | 23* | 3 | 0 | 54 | 43 | 2 | 1 | 39 | 40 | 1 | -7 | 147 | 162 | | | | |
| 8 | 3 | 138 | 156 | 6 | 1 | 143 | 152 | | | | | 3 | -1 | 160 | 161 | 2 | 5 | 76 | 54 | 1 | -8 | 66 | 60 | | | | |

than the 2.488 Å separation in the tetrahydrate, while the Mn – O distances in both the compounds are of about the same order of magnitude. It seems that the exchange from water to glycol has had some effect on the Mn – Cl bond. In both structures the chlorine atoms are adjacent to each other and participate in hydrogen bonds to oxygen atoms in neighbouring octahedra. Evidently the exchange from water to glycol increases the distortion of the octahedral arrangement around the manganese atom. In $MnCl_2.4H_2O$ the angles between opposite corners *via* the central atom are very near 180°. One angle differs from this value by 11° and the other two by 6° and 3°, respectively. In [MnCl₂(C₂H₆O₂)₂] none of these angles differs by less than 16° and by more than 22°.

Comparisons can also be made with the dihydrate of $MnCl_2$.[11] This compound consists of polymeric chains of metal and chlorine ions arranged in a near square planar configuration with each chlorine ion shared by two metal ions. The water molecules which fill the remaining octahedral positions around the metal ion also link adjacent chains through hydrogen bonding. In this compound the Mn – Cl distances of 2.515 Å and 2.592 Å are significantly longer than in the glycol compound while the Mn – O distance of 2.150 Å is significantly shorter than the Mn – O distances in the glycol compound. There seems to be a tendency for the Mn – Cl distance to decrease in the series $MnCl_2.2H_2O \rightarrow MnCl_2.4H_2O \rightarrow$ [MnCl₂(C₂H₆O₂)₂] and at the same time the Mn – O distances increase. In the same series the Cl – Cl distances within the coordination octahedra vary from 3.530 Å and 3.691 Å for $MnCl_2.2H_2O$ to 3.708 Å for the tetrahydrate and 3.717 Å for [MnCl₂(C₂H₆O₂)₂]. The angles Cl – Mn – Cl show the same trend; they are 87°, 96°, and 98° respectively.



*Fig. 1.* A stereoscopic illustration of the molecular packing and the hydrogen bond contacts in a unit cell of [MnCl₂(C₂H₆O₂)₂].

*Fig. 2.* A stereoscopic view of the atoms in the asymmetric unit, showing the coordination around manganese. Thermal ellipsoids are scaled to enclose 50 % probability.

The greatest differences in angles and distances occur between $MnCl_2.2H_2O$ on the one hand and $MnCl_2.4H_2O$ and $[MnCl_2(C_2H_6O_2)_2]$ on the other. It is also between the two $MnCl_2$-hydrates that a structural change occurs from polymeric chains to discrete octahedra, the latter being retained in $[MnCl_2(C_2H_6O_2)_2]$.

The glycol molecules act as bidentate ligands coordinating to the manganese atom through the two *vicinal* hydroxyl groups. As can be seen from Fig. 2 the glycol molecules do not expand in the same plane but are twisted in relation to each other. This is a natural consequence of the *cis*-configuration of the molecule. The angles between connected planes [1] in the two glycol ligands are nearly the same, 52.3° and 52.1° for Glycol I and II, respectively. The equations for these planes are given in Table 4. In the structure $[Cu(C_2H_6O_2)_3]SO_4$ these angles varied between 45.9° to 55.3° for the three glycol ligands.[1] When the glycol molecule is unstrained the carbon-carbon bond is twisted in such a way

*Table 3.* Dimensions of the octahedron around manganese in $[MnCl_2(C_2H_6O_2)_2]$. (Standard deviations for the last significant figure are given in parentheses.)

| Atoms | Distance, Å. | Atoms | Angle(°) | Atoms | Angle(°) |
|---|---|---|---|---|---|
| Mn — Cl(1) | 2.463(1) | Cl(1) — Mn — Cl(2) | 98.0(0.4) | O(11) — Mn — O(21) | 89.3(1) |
| Mn — Cl(2) | 2.464(1) | Cl(1) — Mn — O(11) | 91.6(1) | O(11) — Mn — O(22) | 157.7(1) |
| Mn — O(11) | 2.184(3) | Cl(1) — Mn — O(21) | 90.9(1) | O(11) — Mn — O(12) | 72.4(1) |
| Mn — O(12) | 2.247(3) | Cl(1) — Mn — O(22) | 101.8(1) | O(21) — Mn — O(22) | 72.9(1) |
| Mn — O(21) | 2.233(3) | Cl(1) — Mn — O(12) | 163.7(1) | O(21) — Mn — O(12) | 85.6(1) |
| Mn — O(22) | 2.197(3) | Cl(2) — Mn — O(11) | 104.7(1) | O(22) — Mn — O(12) | 92.4(1) |
| | | Cl(2) — Mn — O(21) | 163.1(1) | | |
| | | Cl(2) — Mn — O(22) | 91.1(1) | | |
| | | Cl(2) — Mn — O(12) | 89.6(1) | | |

*Table 4.* The equations for the planes $1-4$ in the glycol ligands. The numbering of the planes is the same as in Table 5.

$$1:\quad 0.584587x - 0.523141y - 0.620146z - 1.627167 = 0$$
$$2:\quad -0.093764x - 0.959094y - 0.267110z - 4.092643 = 0$$
$$3:\quad 0.549048x - 0.521635y - 0.653027z - 4.908709 = 0$$
$$4:\quad -0.116435x - 0.060177y - 0.991374z - 5.225780 = 0$$

*Table 5.* Dimensions of the two glycol ligands I and II. (Standard deviations of the last significant figure are given in parentheses.)

| Atoms | Distance, Å | Plane | Atoms | Angle(°) |
|---|---|---|---|---|
| | | I | | |
| O(11) − C(11) | 1.442(6) | 1 | O(11) − C(11) − C(12) | 107.0(3) |
| O(12) − C(12) | 1.439(6) | 2 | O(12) − C(12) − C(11) | 106.5(4) |
| C(11) − C(12) | 1.490(7) | 1 − 2 | | 52.3 |
| | | II | | |
| O(21) − C(21) | 1.425(6) | 3 | O(21) − C(21) − C(22) | 107.3(4) |
| O(22) − C(22) | 1.444(6) | 4 | O(22) − C(22) − C(21) | 107.4(4) |
| C(21) − C(22) | 1.486(8) | 3 − 4 | | 52.1 |

*Table 6.* Hydrogen bond distances and their estimated standard deviations. (All distances represent hydrogen bonding between atoms in different octahedra).

| Bond | Distance, Å |
|---|---|
| O(11) − H···Cl(2) | 3.112(3) |
| O(12) − H···Cl(1) | 3.116(3) |
| O(21) − H···Cl(2) | 3.108(3) |
| O(22) − H···Cl(1) | 3.109(3) |

as to achieve a *staggered* conformation and this angle is approximately 55°. In [MnCl₂(C₂H₆O₂)₂] the glycol molecules are evidently somewhat strained in order to achieve a molecular packing with lowest possible energy. This fact is also reflected in the O − C − C angles in the glycol ligands, which deviate significantly from the tetrahedral angle of 109.5°. The mean values of the O − C − C angles for Glycol I is 106.8° and for Glycol II 107.4°. With regard to the interatomic distances within the glycol ligands, there are no significant deviations from earlier reported values.[1] A complete list of bond distances and angles in the two glycol ligands is presented in Table 5.

As mentioned earlier the whole structure is held together by weak hydrogen bonds and van der Waals contacts. Each oxygen atom in the two glycol ligands is involved in a hydrogen bond to a chlorine atom in a neighbouring molecule. The hydrogen bond distances are listed in Table 6.

The O − H distances calculated from the parameters listed in Tables 1a and 1b are 0.92 Å, 0.87 Å, 1.04 Å, and 0.93 Å for O(11), O(12), O(21), and O(22), respectively. The C − H distances are 1.08 Å and 1.00 Å for C(11); 1.02 Å and 0.94 Å for C(12), 1.15 Å and 1.07 Å for C(21), and 1.00 Å and 0.97 Å for C(22). No detailed list of distances and angles concerning the hydrogen atoms is represented because of the limited accuracy of the hydrogen parameters.

In octahedral complexes of the type $MeA_4B_2$ there are two possible ways of arranging the atoms, which lead to the *cis-* and *trans*-form, respectively.[12]

This also holds true when $A_4$ represents the four coordinating atoms from two bidentate chelating agents as in $[MnCl_2(C_2H_6O_2)_2]$ the subject of this report. Thus it would appear possible that the *trans*-form of this compound may also be found.

$MnCl_2.4H_2O$ appears in two monoclinic crystal modifications.[13,14] One of them, the $\alpha$-form, is stable at room temperature and the other, the $\beta$-form, is metastable at room temperature. When preparing the $[MnCl_2(C_2H_6O_2)_2]$ crystals the $\alpha$-form was used. In $\alpha$-$MnCl_2.4H_2O$ the chlorine atoms are in the *cis*-position as mentioned earlier and the derived compound $[MnCl_2(C_2H_6O_2)_2]$ has retained this *cis*-configuration. $\beta$-$MnCl_2.4H_2O$ is isomorphous with $FeCl_2.4H_2O$,[14] the structure of which has been determined by Penfold and Grigor.[15] In this structure the chlorine atoms are in the *trans*-position, an thus should also be so in the isomorphous compound $\beta$-$MnCl_2.4H_2O$. It therefore seems possible that the *trans*-form of $[MnCl_2(C_2H_6O_2)_2]$ should arise if the crystals are prepared from $\beta$-$MnCl_2.4H_2O$ and glycol. The metastability of $\beta$-$MnCl_2.4H_2O$ would serve as an explanation for the failure of the *trans*-compound to form at room temperature.

REFERENCES

1. Antti, B.-M., Lundberg, B. K. S. and Ingri, N. *Acta Chem. Scand.* **26** (1972) 3984.
2. *International Tables for X-Ray Crystallography*, Kynoch Press, Birmingham 1965, Vol. I.
3. Ivarsson, G., Lundberg, B. K. S. and Ingri, N. *Acta Chem. Scand.* **26** (1972) 3005.
4. Antti, C.-J. and Lundberg, B. K. S. *Acta Chem. Scand.* **25** (1971) 1758.
5. Cruickshank, D. W. J. *Computing Methods in Crystallography*, Pergamon, London 1965, p. 114.
6. *International Tables for X-Ray Crystallography*, Kynoch Press, Birmingham 1962, Vol. III.
7. Stewart, R. F., Davidson, E. R. and Simpson, W. T. *J. Chem. Phys.* **42** (1965) 3175.
8. Hamilton, W. C. *Acta Cryst.* **18** (1965) 502.
9. Pawley, G. S. *Acta Cryst.* A **26** (1970) 691.
10. Zalkin, A., Forrester, J. D. and Templeton, D. H. *Inorg. Chem.* **3** (1964) 529.
11. Morosin, B. and Graeber, E. J. *J. Chem. Phys.* **42** (1965) 898.
12. Werner, A. *Ber.* **45** (1911) 121.
13. Groth, P. *Chemische Krystallographie*, Wilhelm Engelmann, Leipzig 1908, Vol. I.
14. Dawson, H. M. and Williams, P. *Z. physik. Chem. (Leipzig)* **31** (1899) 59.
15. Penfold, B. R. and Grigor, J. A. *Acta Cryst.* **12** (1959) 850.

# Metal Complexes with Mixed Ligands

## 8. The Crystal Structure of Diperchlorato-tetraimidazolo-copper(II); Cu(C₃H₄N₂)₄(ClO₄)₂

GUN IVARSSON

*Department of Inorganic Chemistry, University of Umeå, S-901 87 Umeå, Sweden*

The crystal structure of diperchlorato-tetraimidazolo-copper(II) has been determined using three-dimensional X-ray diffraction data. The crystals are monoclinic, space group $P2_1/n$, with two formula units in the unit cell. The cell dimensions with corresponding standard deviations are $a = 8.198 \pm 0.001$ Å, $b = 16.293 \pm 0.002$ Å, $c = 9.353 \pm 0.002$ Å and $\beta = 125.81 \pm 0.01°$. The intensities were collected and measured with a linear diffractometer and MoKα-radiation. The structure was solved by routine heavy-atom methods and refined by a full-matrix least squares method with anisotropic temperature factors for all nonhydrogen atoms to a final $R$-value of 0.060. The structure is built up of uncharged octahedral complexes $Cu(C_3H_4N_2)_4$-$(ClO_4)_2$. The complexes are held together through hydrogen and van der Waals bonds. The distances between copper and imidazole nitrogens are 1.997 Å and 2.007 Å and the two distances between copper and perchlorate oxygens are 2.625 Å. The hydrogen atoms were located from a difference Fourier map.

The present investigation forms part of an X-ray crystal structure study of crystalline phases obtained from hydrolyzed aqueous $Cu^{2+} - C_3H_4N_2 - ClO_4^-$-solutions. Hitherto the phases $Cu_3(C_3H_3N_2)_2(C_3H_4N_2)_8(ClO_4)_4$[1] and $Cu(C_3H_4N_2)_4(ClO_4)_2$ have been prepared and ivestigated by X-ray methods. The crystal structure of the former was presented in part 2 of this series and the crystal structure of the latter will be presented and discussed in the present paper. The equilibrium investigations by Sjöberg[2] provide the solution chemistry background to the present crystal structure study.

## EXPERIMENTAL

*Crystal preparation and analyses.* The crystals used were prepared by adding 5.8 ml of a solution with the composition: $[Na^+] = 3.495$ M; $[ClO_4^-] = 3.000$ M; $[OH^-] = 0.495$ M to 5.6 ml of a solution with the composition $[Na^+] = 2.430$ M; $[ClO_4^-] = 3.000$ M; $[Cu^{2+}] =$

0.034 M; $[H^+] = 0.357$ M and $[C_3H_5N_2^+] = 0.179$ M. After mixing welldefined blue-violet prismatic crystals were formed within a few days.

The copper content of the crystals was determined electrolytically and the nitrogen content was determined using the Kjeldahl method. (Found: Cu, 11.47; N, 20.7. Calc. for $Cu(C_3H_4N_2)_4(ClO_4)_2$: Cu, 11.88; N, 21.0.)

*Crystal data and space group.* From rotation photographs around the *c*- and *b*-axis and the corresponding Weissenberg photographs (zero, first, and second layer lines) taken with $CuK\alpha$-radiation it was concluded that the crystals were monoclinic. The cell dimensions were refined from a Guinier photograph giving 67 lines. The following parameters and their corresponding standard deviations were obtained: $a = 8.198 \pm 0.001$ Å, $b = 16.293 \pm 0.002$ Å, $c = 9.353 \pm 0.002$ Å, $\beta = 125.81 \pm 0.01°$, $V = 1011.79$ Å³.

By the flotation method (using bromoform and acetone) the density was determined to be 1.75 g/cm³. With two of the above mentioned formula units in the cell the calculated density is 1.755 g/cm³. Systematic extinctions were found for $h0l$, $h + l = 2n + 1$ and $0k0$, $k = 2n + 1$. This is characteristic for the space group $P2_1/n$ (a transformation of $P2_1/c$, No. 14 in International Tables).[3]

*Collection and reduction of intensity data.* Single-crystal intensity data were collected and measured with an automatic linear diffractometer (PAILRED). The radiation was $MoK\alpha$ with a LiF monochromator. The crystal was rotated along the *c*-axis and intensities for $hk0 - hk8$ were measured ($\sin \theta_{MoK\alpha} \leq 0.54$). The half scan intervals were for $hk0 - hk3$ equal to 0.6° for $\theta > 20°$ and equal to 1.2° for $\theta < 20°$. Corresponding values for $hk4 - hk8$ were 1.0° and 2.0°. The scan speed used was 0.5°/min. Weak reflexions (counts less than 1000) were measured up to three times. Background radiation was measured during 20 sec intervals on each side of the reflexion.

The intensities of approixmately 3400 reflexions were measured. Reflexions with a relative counting statistical error of $\Delta I/I > 1.0$ were omitted, which left 1612 observed intensities. The intensities were corrected for Lorentz and polarization factors and absorption. The linear absorption coefficient was calculated to be 14.45 cm⁻¹. The absorption correction gave differences in the transmission between $0.81 - 0.93$.

The computer programs used were the same as in a paper previously published by Ivarsson *et al.*[1]

## STRUCTURE DETERMINATION AND REFINEMENT

The copper, chlorine, and oxygen atoms were located from a three dimensional Patterson synthesis and the other nonhydrogen atoms were found by standard Fourier methods.

The structure was refined by full-matrix least squares techniques. The weighting scheme of Cruickshank[4] was applied to the observed reflexions. The atomic scattering factors for $Cu^{2+}$, $Cl^-$, O, N, C, and H were used.[5] With individual isotropic temperature factors the refinement converged to a conventional *R*-value of 0.146; the hydrogen atoms were not included. Anisotropic temperature factors were then applied to all nonhydrogen atoms and the *R*-value dropped to 0.065. At this stage of the refinement a difference Fourier map was made in order to try to find the hydrogen positions. The maxima that were found could be explained by hydrogen atoms. Subsequent least squares cycles with these hydrogen atom positions included also reduced the *R*-value and a final *R*-value of 0.060 was obtained. The decreace in *R*-value was significant on the 0.1 %-level according to the Hamilton test as approximated by Pawley.[6] All parameter shifts in the final cycle were less than 10 % of the estimated standard deviation. A final difference Fourier synthesis was calculated in which no abnormalities could be detected. The final atomic coordinates and vibrational parameters are given in Tables 1 and 2. A comparison between the observed and calculated structure factors is given in Table 3.

*Table 1.* The final atomic positional fractional coordinates and vibrational parameters and their estimated standard deviations ($\sigma$ in parenthesis). All values multiplied by $10^4$. Anisotropic temperature factors have been calculated according to the formula $\exp[-(h^2B_{11}+k^2B_{22}+l^2B_{33}+hkB_{12}+hlB_{13}+klB_{23})]$.

| | $x$ | $y$ | $z$ | $B_{11}$ | $B_{22}$ | $B_{33}$ | $B_{12}$ | $B_{13}$ | $B_{23}$ |
|---|---|---|---|---|---|---|---|---|---|
| Cu | 0 | 0 | 0 | 145 (2) | 19(0) | 131 (2) | − 16 (1) | 168 (3) | 13 (1) |
| Cl | 1186 (2) | 1176(1) | − 2843 (2) | 221 (3) | 31(0) | 197 (4) | 37 (2) | 312 (6) | 31 (2) |
| O1 | − 50 (7) | 659(3) | − 2587 (6) | 249(11) | 33(2) | 225(11) | 11 (7) | 314(19) | − 41 (7) |
| O2 | 872(11) | 987(4) | − 4458 (8) | 595(26) | 78(4) | 243(15) | 76(16) | 586(33) | 43(11) |
| O3 | 3217(10) | 1022(7) | − 1481(11) | 236(17) | 189(9) | 398(22) | 88(19) | 331(32) | 18(22) |
| O4 | 673(16) | 1988(3) | − 2833(16) | 1266(50) | 25(2) | 1225(49) | 35(17) | 2334(95) | 21(16) |
| N1 | 2790 (6) | 410(3) | 1850 (6) | 158(10) | 25(1) | 133 (9) | − 25 (6) | 172(16) | − 5 (6) |
| N2 | 6037 (8) | 426(3) | 3861 (8) | 171(12) | 42(2) | 224(13) | 7 (9) | 167(21) | 13 (9) |
| N3 | − 1170 (7) | 1022(2) | 238 (6) | 175(10) | 23(2) | 152(10) | − 5 (6) | 210(17) | 13 (6) |
| N4 | − 2540 (9) | 1870(3) | 1037 (9) | 325(17) | 33(2) | 265(15) | − 52 (9) | 453(28) | 19 (8) |
| C1 | 4441(10) | − 37(4) | 2748(11) | 231(16) | 34(2) | 268(17) | − 13(11) | 313(27) | − 12(11) |
| C2 | 5431(10) | 1212(5) | 3684(10) | 207(16) | 45(3) | 216(17) | 38(12) | 144(26) | 35(11) |
| C3 | 3417(11) | 1191(4) | 2433(11) | 249(17) | 26(2) | 255(17) | − 5(10) | 166(28) | 37(10) |
| C4 | − 1806(11) | 1122(4) | 1228 (9) | 304(18) | 33(2) | 188(15) | − 38(11) | 355(28) | − 6 (9) |
| C5 | − 2353(11) | 2282(4) | − 115(11) | 340(20) | 29(2) | 267(18) | − 76(11) | 445(34) | − 30(10) |
| C6 | − 1523(11) | 1756(4) | − 617(10) | 344(20) | 28(2) | 229(16) | − 55(11) | 435(32) | − 32 (9) |

*Table 2.* The final fractional coordinates and their estimated standard deviation for the hydrogen atoms. (All values multiplied by $10^3$). The hydrogen atoms were given an isotropic thermal parameter of 5.0 which was not refined.

| | $x$ | $y$ | $z$ |
|---|---|---|---|
| H$_1$ | 448(10) | − 61(4) | 268 (9) |
| H$_2$ | 735(10) | 25(4) | 477(10) |
| H$_3$ | 652(10) | 160(4) | 448 (9) |
| H$_4$ | 258(10) | 159(4) | 202 (9) |
| H$_5$ | − 192(10) | 57(4) | 201 (9) |
| H$_6$ | − 302(10) | 209(4) | 165 (9) |
| H$_7$ | − 300(10) | 285(4) | − 46 (9) |
| H$_8$ | − 128(10) | 181(4) | − 134 (9) |

## DESCRIPTION AND DISCUSSION OF THE STRUCTURE

The structure is built up of uncharged octahedral complexes $Cu(C_3H_4N_2)_4(ClO_4)_2$. The complexes are held together through hydrogen and van der Waals bonds. A drawing of the complex is shown in Fig. 1 and in Fig. 2 the packing of the complexes is illustrated.

*The $Cu(C_3H_4N_2)_4(ClO_4)_2$ complex.* In the complex the four imidazole nitrogens and the $Cu^{2+}$-ion are on the basis of symmetry, placed in the same plane and form a slightly distorted plane quadratic nitrogen coordination around $Cu^{2+}$. The $Cu-N$ distances (2.010 Å and 1.998 Å) are quite normal

*Table 3.* Observed and calculated structure factors ( × 10). Values marked with an asterisk were not included in the final refinement.

*Table 3. Continued.*

[Table of structure factors with columns H, K and associated values — dense numerical crystallographic data]

and the N–Cu–N angles are very near to 90°. Above and below this plane two oxygen atoms from the perchlorate groups are symmetrically placed and complete the octahedral coordination. The Cu–O distances are 2.625 Å and the angles O–Cu–O, O–Cu–N₁, and O–Cu–N₃ are 180°, 93°, and 94°, respectively. These angles and distances strongly indicate a nearly regular octahedral coordination around the copper atom.

*The ligands imidazole and perchlorate.* The dimensions of the imidazole

*Fig. 1.* Stereoscopic diagrams of the Cu-coordination with thermal ellipsoids of the non-hydrogen atoms scaled to enclose 50 % probability.
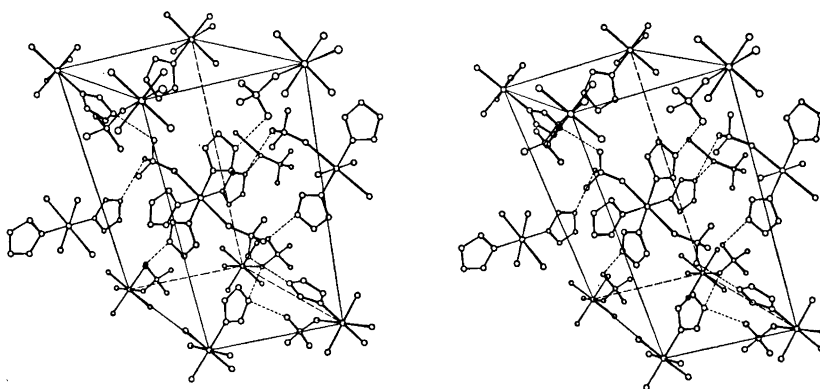


*Fig. 2.* Stereoscopic illustration of the molecular packing of $Cu(C_3H_4N_2)_4(ClO_4)_2$ in the unit cell. The cell is tilted to avoid overlaping. The broken lines mark hydrogen bonds.

rings are of the same size as found in other studies.[1,7-9] The planarity of the imidazole rings is shown in Table 5, where the planes of best fit are given.

No abnormalities could be found in the perchlorate group. The Cl $-$ O distances range from 1.391 Å to 1.442 Å, the longest distance being to the copperbonded oxygen.

*The hydrogen positions and hydrogen bonds.* The positions of the hydrogen atoms are shown in Fig. 1 and the coordinates are given in Table 2.

The hydrogen atoms which are bonded to the carbon atoms in the imidazole rings are placed in the expected positions. The hydrogen atoms on the pyrrole nitrogens ($N_2$ and $N_4$) take part in hydrogen bonds of which there are two

*Table 4.* Bond lengths and bond angles and their estimated standard deviations.

| Bond | $l(\sigma(l) \times 10^3)$,Å | Angle | $\theta(10\sigma(\theta))°$ | Bond | $l(\sigma(l) \times 10^3)$,Å |
|---|---|---|---|---|---|
| $Cu-O_1$ | 2.625(5) | $N_1-Cu-N_3$ | 90.3(2) | | |
| $Cu-N_1$ | 2.010(4) | $O_1-Cu-N_1$ | 86.9(2) | | |
| $Cu-N_3$ | 1.998(4) | $O_1-Cu-N_3$ | 90.7(2) | | |
| $N_1-C_1$ | 1.319(8) | $N_1-C_1-N_2$ | 110.9(6) | $C_1-H_1$ | 0.938(70) |
| $C_1-N_2$ | 1.331(9) | $C_1-N_2-C_2$ | 108.6(6) | $N_2-H_2$ | 0.947(69) |
| $N_2-C_2$ | 1.348(9) | $N_2-C_2-C_3$ | 104.9(6) | $C_2-H_3$ | 0.988(70) |
| $C_2-C_3$ | 1.355(10) | $C_2-C_3-N_1$ | 110.7(6) | $C_3-H_4$ | 0.852(70) |
| $C_3-N_1$ | 1.361(8) | $C_3-N_1-C_1$ | 104.8(5) | | |
| $N_3-C_4$ | 1.311(9) | $N_3-C_4-N_4$ | 110.9(6) | $C_4-H_5$ | 1.200(70) |
| $C_4-N_4$ | 1.325(8) | $C_4-N_4-C_5$ | 108.0(6) | $N_4-H_6$ | 0.937(70) |
| $N_4-C_5$ | 1.353(10) | $N_4-C_5-C_6$ | 106.2(6) | $C_5-H_7$ | 1.019(68) |
| $C_5-C_6$ | 1.339(10) | $C_5-C_6-N_3$ | 109.4(6) | $C_6-H_8$ | 0.834(71) |
| $C_6-N_3$ | 1.372(8) | $C_6-N_3-C_4$ | 105.5(5) | | |
| $Cl-O_1$ | 1.442(5) | $O_1-Cl-O_2$ | 110.2(4) | $O_1\cdots H_2$ | 2.217(71) |
| $Cl-O_2$ | 1.409(7) | $O_1-Cl-O_3$ | 108.7(5) | $O_2\cdots H_2$ | 2.403(70) |
| $Cl-O_3$ | 1.406(7) | $O_1-Cl-O_4$ | 108.1(5) | $O_4\cdots H_6$ | 2.056(69) |
| $Cl-O_4$ | 1.391(6) | $O_2-Cl-O_3$ | 108.0(5) | | |
| | | $O_2-Cl-O_4$ | 110.4(6) | | |
| | | $O_3-Cl-O_4$ | 111.4(7) | | |

*Table 5.* (a) Planes of best fit (least squares).

Imidazole ring $(N_1C_1N_2C_2C_3)$
$0.6902x - 0.1445y - 0.7090z - 2.9100 = 0$

Imidazole ring $(N_3C_4N_4C_5C_6)$
$-0.5774x + 0.3185y - 0.7517z - 1.0066 = 0$

(b) Deviation (Å) from planes (max standard deviation of the atomic positional fractional coordinates $xyz \times 10^4$ in parentheses).

| | | | | | | | |
|---|---|---|---|---|---|---|---|
| $N_1(6)$ | 0.003 | Cu(0) | −0.016 | $N_3(7)$ | 0.000 | Cu(0) | −0.037 |
| $C_1(10)$ | −0.004 | $H_1(100)$ | 0.047 | $C_4(11)$ | 0.003 | $H_5(100)$ | −0.139 |
| $N_2(8)$ | 0.003 | $H_2(100)$ | 0.134 | $N_4(9)$ | −0.005 | $H_6(100)$ | 0.041 |
| $C_2(10)$ | −0.001 | $H_3(100)$ | 0.024 | $C_5(11)$ | 0.005 | $H_7(100)$ | −0.094 |
| $C_3(11)$ | −0.002 | $H_4(100)$ | −0.003 | $C_6(11)$ | −0.003 | $H_8(100)$ | −0.053 |

kinds in the structure. A schematic drawing illustrating these hydrogen bonds is shown in Fig. 2. The two broken lines from an imidazole nitrogen to two different perchlorate groups show a suggested bifurcated hydrogen bond. Distances are given in Table 4. By comparing the distances there seems to be a stronger interaction to the copperbonded oxygen $O_1(O_1\cdots N_2 = 3.000$ Å) than to $O_2(O_2\cdots N_2 = 3.221$ Å). An interaction to $O_2$ cannot be excluded. The

distances between $N_4$ and $O_4$, where a single hydrogen bond is proposed, is 2.921 Å.

As can be seen from Fig. 2, hydrogen bonds connect the complexes forming coupled sheets within the structure.

## REFERENCES

1. Ivarsson, G., Lundberg, B. K. S. and Ingri, N. *Acta Chem. Scand.* **26** (1972) 3005.
2. Sjöberg, S. *Acta Chem. Scand.* **25** (1971) 2149.
3. *International Tables for X-Ray Crystallography*, Kynoch Press, Birmingham 1962, Vol. I.
4. Cruickshank, D. W. J. *Computing Methods in Crystallography*, Pergamon, London 1965, p. 114.
5. *International Tables for X-Ray Crystallography*, Kynoch Press, Birmingham 1962, Vol. III.
6. Pawley, G. S. *Acta Cryst.* **A 26** (1970) 691.
7. Lundberg, B. K. S. *Acta Chem. Scand.* **26** (1972) 3902.
8. Fransson, G. and Lundberg, B. K. S. *Acta Chem. Scand.* **26** (1972) 3969.
9. Lundberg, B. K. S. *Acta Chem. Scand.* **26** (1972) 3977.

# The Crystal Structure of Thallium(I)

# Dimethyldithiocarbamate

PER JENNISCHE and ROLF HESSE

*Institute of Chemistry, University of Uppsala, Box 531, S-751 21, Uppsala, Sweden*

The crystal structure of thallium(I) dimethyldithiocarbamate, $TlS_2CN(CH_3)_2$, has been determined from 3-dimensional X-ray data. The crystals are monoclinic, space group $P2_1/a$, with unit cell dimensions: $a = 9.101$, $b = 6.673$, $c = 11.379$ Å, $\beta = 98.90°$. There are four formula units in the elementary cell.

The structure is composed of dimers, $[TlS_2CN(CH_3)_2]_2$, which are joined by thallium-sulphur coordination to form layers parallel to the $(a,b)$-plane. The thallium atoms are situated close to the layer plane, whereas the ligands protrude from both sides of the plane. Only van der Waals forces exist between successive layers, which are stacked in the $c$-direction. The thallium atoms achieve 7-coordination by using sulphur atoms from five ligands in the layer. The coordination distances are in the range 3.0 to 3.7 Å. The four closest sulphur atoms belong to the same dimer as the thallium atom. The thallium atoms within a layer form a 3-connected net with the interatomic distances 3.64 and 3.85 Å.

The dimers are related to those found in the structures of the corresponding propyl and isopropyl compounds, but in the latter the dimers are linked to form chains. The importance of packing effects and the particular coordination requirements of thallium(I) in determining the structures of these compounds are discussed.

The crystal structures of thallium(I) dipropyldithiocarbamate[1] and thallium(I) di-isopropyldithiocarbamate[2] were determined at this Institute as part of a systematic investigation of the coordination chemistry of compounds having the composition AX. The same type of dimeric molecules are found in both structures but the dimers are arranged quite differently in the two cases. In the isopropyl compound the dimers are nicely packed in layers determined by van der Waals forces. The layers are stacked in such a way that chains of dimers are formed, but only weak thallium-sulphur forces act between adjacent dimers in the chains. Similar chains are also found in the structure of the propyl compound, but the packing is quite different. No layers are formed and the dimers along the chains are connected by strong thallium-sulphur bonds. In the structure of the isopropyl compound, which appears to be de-

termined mainly by packing requirements, the symmetry of the dimer is the same as that expected for an isolated dimer. In the structure of the propyl compound, however, the dimer is considerably distorted.

The observed structural effects of changes in the ligands are related to those found in the dithiocarbamates and monothiocarbamates of copper(I) and silver(I).[3]

## EXPERIMENTS

A sample of thallium(I) dimethyldithiocarbamate was kindly prepared by Dr. S. Åkerström according to his published method.[4] It consisted of pale yellow four-sided platelets. Most of the crystals were too thin for X-ray investigation, but suitable crystals could be cut from the corners of larger crystals. Their density was measured by the flotation method using an aqueous solution of $K_2HgI_4$. The unit cell dimensions were found from a powder photograph taken on an IRDAB XDC 700 camera using $CuK\alpha_1$ radiation with silicon as an internal standard. Equi-inclination Weissenberg photographs were taken using $CuK\alpha$ radiation and Ilford Industrial G film. The multiple-film technique (using four films) was used. The exposure times were approximately 50 h. For the lowest layers the strong reflexions were collected separately at exposure times of roughly 5 h. The decomposition of the crystal was comparatively slow. It was thus possible to collect the layers $0kl$ to $6kl$ using one crystal of dimensions $0.04 \times 0.13 \times 0.19$ mm³, with the rotation axis in the plane of the crystal and bisecting one of the corners. A second crystal of dimensions $0.04 \times 0.11 \times 0.15$ mm³ was used for the layers $7kl$ and $8kl$. This crystal was then remounted and rotated about an axis approximately normal to the plate to collect the layers $hk3$ and $hk6$. These were used for interlayer scaling.

The intensities were measured using an automatic SAAB film scanner [5] connected on-line to an IBM 1800 processor controller. Process and integration programs written by Werner were used.[6] The parameters for the integration procedure (IVRUT = IRRUT = 10, BAK = 0.85, SBAK = 0.90, MYT = 0, FK = 0.5) were chosen so that the minimum transmission point for each reflexion was at the centre of a rectangle $1.89 \times 1.26$ mm² corresponding to 441 measuring spots of the size $0.09 \times 0.06$ mm². The rectangle was large enough to include both the $\alpha_1$ and $\alpha_2$ reflexion. The average of the transmission values along the edges of the rectangle was taken as the background transmission $T_b$. All $n$ spots within the rectangle with transmission value, $T_i$, less than $0.85T_b$ were used in the calculation of $I_{obs} = 10 \ln 10 \sum_{i=1}^{n} D_i$. The corrected optical density, $D_i$, was cal-culated as $D_i = D'(1 + 0.5D')$, where $D' = \log T_b/T_i$. The factor 0.5, which corrects for the negative errors in the intensities of the strong reflexions, has been suggested by Werner.[7] In this way intensities in the range 50 to 1000 were obtained corresponding to peak optical densities in the range 0.1 to 1.5. Despite the correction factor the high intensities were found to be unreliable, and only measurements in the range 50 to 450 were actually used.

During the integration procedure a number of streaks present on the films were interpreted as reflexions. In order to facilitate their elimination a program was written to produce a plot of each film on an IBM 1627 plotter. The plot showed the position in the reciprocal layer of each reported reflexion together with the position corresponding to the indices calculated for that reflexion by the integration program. From these plots it was possible to detect reflexions displaced from the crystallographic positions. Systematic mistakes in the indexing caused by errors in the alignment of the film in the film scanner were sometimes observed for the high-angle reflexions on a film. These were easily detected on the plots. After a simulated movement of the film by the program to produce a new set of indices for the reflexions, a new plot could be drawn with no such mistakes occurring.

The 786 independent reflexions were corrected for Lorentz and polarization effects, as well as for absorption ($\mu = 520$ cm⁻¹) but not for extinction. Interlayer scale factors for the layers $0kl$ to $8kl$ were obtained by comparison of the intensities of the reflexions in this data-set with the intensities of the corresponding reflexions in the two layers

$hk3$ and $hk6$. The scale factors were themselves included in the final refinement, and found to differ on average by 5 % (max. 11 %) from the experimental values.

## DETERMINATION OF THE ATOMIC POSITIONS

A layer structure was suggested at an early stage by the plate-like crystal habit and by the very high intensity of the 001 line on the powder photograph; the $c^*$-axis was normal to the plate. The approximate position of the thallium atom was found from a 3-dimensional Patterson synthesis. The positions of the two independent sulphur atoms were then determined from a difference Fourier synthesis. After a least-squares refinement of the coordinates and isotropic temperature factors of the thallium and sulphur atoms, the positions of the remaining nitrogen and carbon atoms were found from a new difference synthesis. No attempt was made to determine the positions of the hydrogen atoms. At this point anisotropic temperature factors were introduced for the thallium and sulphur atoms and the refinement converged to an $R$-value of 0.130. Certain large $\Delta F$'s remained for the strong reflexions, and the errors were traced to the film factors, which had initially been calculated using conventional methods for visually estimated data. They appeared to be generally too small for the low layers and too large for the high layers. New film factors were then applied which were calculated from the reported film factor value of 2.93 for Ilford Industrial G film [8] at perpendicular incidence. A simple Lambert-Beer expression was assumed to account for the increased film thickness at higher angles of incidence. With this modification the refinement was continued and the $R$-value decreased to 0.105.

The scattering factors for thallium were taken from the tables provided by Cromer and Waber,[9] and for the remaining elements from Hanson et al.[10] Anomalous dispersion corrections were applied for thallium and sulphur.[11]

The final atomic coordinates and temperature factor coefficients are given in Table 1. A difference synthesis calculated with these parameters revealed no significant features. The observed and calculated structure amplitudes are shown in Table 2.

Table 1. Atomic coordinates and thermal parameters, listed as isotropic $B$ or anisotropic $b_{ij}$. The anisotropic temperature factor is defined as $\exp(-b_{11}h^2 - 2b_{12}hk...)$. The standard deviation corresponding to the last digit is shown in parentheses.

| Atom | $x$ | $y$ | $z$ | $B(\text{Å}^2)$ |
|---|---|---|---|---|
| Tl | 0.2087(3) | −0.0489(2) | 0.0494(1) | |
| S1 | −0.0323(8) | −0.2729(13) | −0.1530(7) | |
| S2 | 0.0149(11) | 0.1571(16) | −0.2057(9) | |
| N | 0.100(3) | −0.141(6) | −0.333(3) | 4.5(6) |
| C | 0.033(3) | −0.095(4) | −0.237(2) | 2.8(5) |
| C1 | 0.121(4) | −0.345(7) | −0.370(3) | 4.8(7) |
| C2 | 0.172(5) | 0.006(8) | −0.397(5) | 6.2(9) |

| Atom | $b_{11}$ | $b_{22}$ | $b_{33}$ | $b_{12}$ | $b_{13}$ | $b_{23}$ |
|---|---|---|---|---|---|---|
| Tl | 0.0147(19) | 0.0218(5) | 0.0083(2) | 0.0011(2) | 0.0014(1) | −0.0026(2) |
| S1 | 0.0153(21) | 0.0161(20) | 0.0085(6) | 0.0013(10) | 0.0029(6) | 0.0012(9) |
| S2 | 0.0202(24) | 0.0168(24) | 0.0120(9) | 0.0031(13) | 0.0045(8) | −0.0017(2) |

*Table 2.* Observed and calculated structure factors. Reflexions marked with an asterisk were not included in the refinement.

[Table of observed and calculated structure factors, organized in column groups headed 0,K,L; 1,K,L; 2,K,L; 3,K,L; 4,K,L; 5,K,L; 6,K,L; 7,K,L; 8,K,L — each listing index, observed and calculated values.]

## UNIT CELL AND SYMMETRY

Formula unit: $TlS_2CN(CH_3)_2$
Crystal system: monoclinic
Unit cell parameters: $a = 9.101(2)$ Å; $b = 6.673(2)$ Å; $c = 11.379(3)$ Å;
$\qquad\qquad \beta = 98.90(2)°$
Volume of unit cell: 683 Å$^3$
Density (measured): 3.16 g cm$^{-3}$
Number of formula units per unit cell: 4
Density (calculated): 3.158 g cm$^{-3}$
Diffraction symmetry: $2/m$
Systematic absences: $h0l$ for $h = 2n + 1$; $0k0$ for $k = 2n + 1$
Space group: $P2_1/a$
Coordinates of equivalent positions: $\pm (x,y,z); \pm (\frac{1}{2}+x, \frac{1}{2}-y, z)$

## DESCRIPTION AND DISCUSSION OF THE STRUCTURE

*General features.* The structure of thallium(I) dimethyldithiocarbamate is made up of dimers having the composition $[TlS_2CN(CH_3)_2]_2$. There are two such dimers in the unit cell with their centres at 0,0,0 and $\frac{1}{2},\frac{1}{2},0$. The dimer is illustrated in Fig. 1 which also shows the atom notation used. The dimers are linked by thallium-sulphur coordination in layers parallel to the $(a,b)$-plane in such a way that the thallium atoms are all situated very close to the plane; Fig. 2. The ligands project from both sides of this plane as seen in the figure. The layers are stacked upon one another in the direction of **c**, so that only carbon-carbon and carbon-nitrogen contacts are formed. The layer is shown in Fig. 3. Within the layer the metal atoms form a distorted hexagonal net
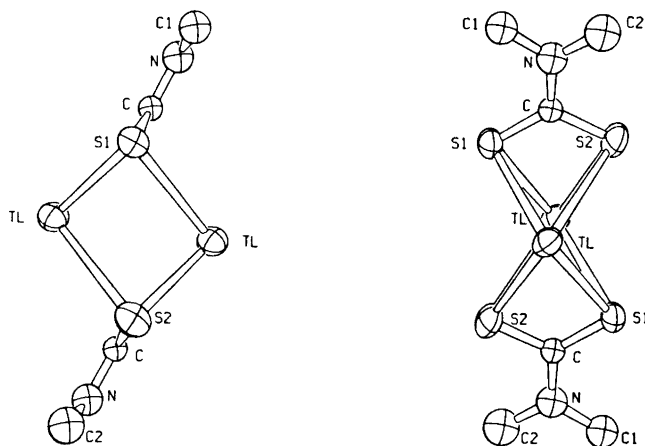


*Fig. 1.* The dimeric thallium(I) dimethyldithiocarbamate molecule in two orientations; left: sulphur plane normal to the plane of the paper (superimposed carbon and sulphur atoms omitted); right: sulphur plane in the plane of the paper.
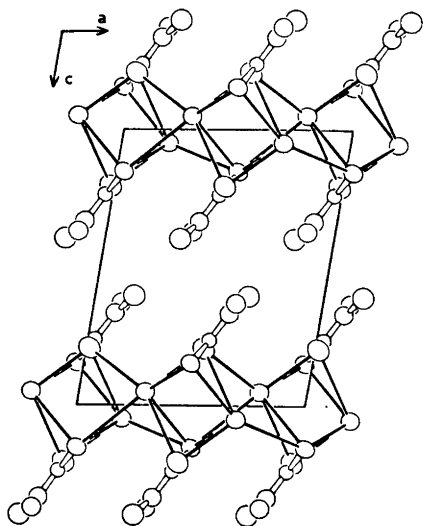
*Fig. 2.* Projection of the structure with
the layers normal to the plane of the paper.
The dimers shown have their centres at
0,0,0; $\frac{1}{2},\frac{1}{2}$,0; 1,0,0; 0,0,1; $\frac{1}{2},\frac{1}{2}$,1; 1,0,1. The
thallium-sulphur coordination in the layer
is indicated by thin black lines.
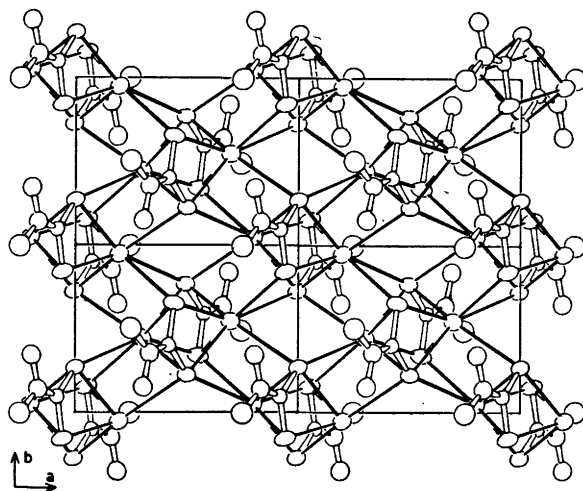


*Fig. 3.* View of the layer. All the dimers have their centres in the plane $z = 0$. The thallium-
sulphur coordination is indicated by thin black lines. The sevenfold coordination of the
thallium atoms is clearly seen although one of the bonds is almost hidden.


as shown in Fig. 4. The figure also shows how the sulphur atoms within the
layer are confined to almost planar strips. The distances shorter than 4 Å
between atoms in different dimeric units are listed in Table 3.

*Table 3.* Distances shorter than 4 Å between atoms in different dimers. If the two atoms are situated in different layers the distance is set in italics. The relationship between the coordinates of the second atom and those of Table 1 $(x,y,z)$ is indicated.

| Atoms | | | Distance (Å) | Atoms | | | Distance (Å) |
|---|---|---|---|---|---|---|---|
| Tl | S2 | $\frac{1}{2}-x,-\frac{1}{2}+y,-z$ | 3.46(1) | N | C2 | $-x,-y,-1-z$ | *3.75(6)* |
| Tl | S1 | $\frac{1}{2}-x,\frac{1}{2}+y,-z$ | 3.52(1) | S1 | C1 | $-\frac{1}{2}+x,-\frac{1}{2}-y,z$ | 3.78(3) |
| C2 | C2 | $-x,-y,-1-z$ | *3.61(10)* | C | C1 | $-\frac{1}{2}+x,-\frac{1}{2}-y,z$ | 3.84(4) |
| C1 | C2 | $\frac{1}{2}-x,-\frac{1}{2}+y,-1-z$ | *3.62(6)* | S1 | C2 | $-\frac{1}{2}+x,-\frac{1}{2}-y,z$ | 3.88(5) |
| Tl | Tl | $\frac{1}{2}-x,\frac{1}{2}+y,-z$ | 3.637(2) | S1 | S2 | $x,-1+y,z$ | 3.89(1) |
| Tl | Tl | $\frac{1}{2}-x,-\frac{1}{2}+y,-z$ | 3.637(2) | Tl | C1 | $\frac{1}{2}-x,\frac{1}{2}+y,-z$ | 3.98(4) |
| S1 | N | $-\frac{1}{2}+x,-\frac{1}{2}-y,z$ | 3.69(3) | Cl | Cl | $-x,-1-y,-1-z$ | *3.98(8)* |
| Tl | S1 | $\frac{1}{2}+x,-\frac{1}{2}-y,z$ | 3.74(1) | | | | |

*The dimer.* The centrosymmetric dimeric unit is shown in Fig. 1. From consideration of the bonds within the molecule the expected point symmetry is *mmm*; but the molecule is in fact found to be somewhat distorted. The four sulphur atoms form a parallelogram which is almost rectangular, the acute angle being 88°. The edges are 2.98 Å and 4.13 Å. Ths short edges connect sulphur atoms in the same ligand. The two thallium atoms are located on each side of the sulphur plane to form a double pyramid. The thallium-thallium vector makes a small angle, 10°, to the normal of the sulphur plane. Each thallium atom is thus closer to the sulphur atoms of one ligand, 2.99 and 3.03 Å, than to those of the other, 3.28 and 3.44 Å. The double pyramid is shown in Fig. 5.
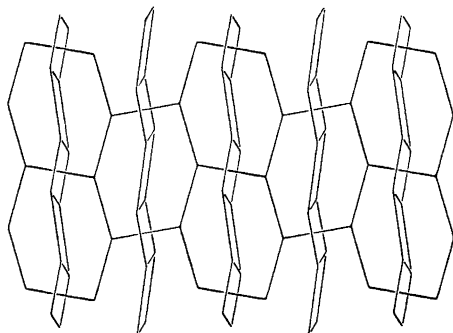


*Fig. 4.* Simplified drawing showing the 3-connected metal atom net and the intersecting sulphur strips. The figure has the same orientation as Fig. 3. The short thallium-thallium distances, 3.64 Å, run in the direction of **b**, the longer ones, 3.85 Å, in the direction of **a**.
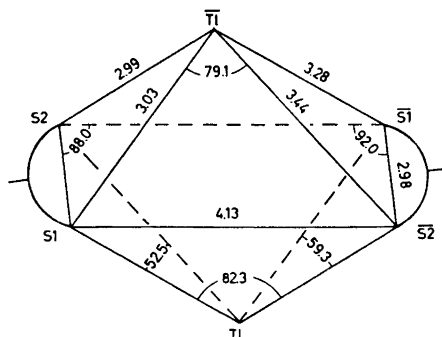
*Fig. 5.* Angles and distances in the central double pyramid in the dimer. Centrosymmetrically related atoms are denoted by a bar.

*Table 4.* Distances and angles in the dimethyldithiocarbamate ligand. The notation used is shown in Fig. 1.

| Atoms | Distance(Å) | Atoms | Angle(°) |
|-------|-------------|-------|----------|
| S1 − C | 1.69(3) | S1 − C − S2 | 121(2) |
| S2 − C | 1.74(3) | S1 − C − N | 123(2) |
| C − N | 1.36(3) | S2 − C − N | 117(2) |
| N − C1 | 1.44(5) | C − N − C1 | 123(3) |
| N − C2 | 1.44(6) | C − N − C2 | 123(4) |
| S1 ... S2 | 2.98(1) | C1 − N − C2 | 114(3) |

The angles and distances in the dithiocarbamate ligand are given in Table 4. They agree well with those found in other dithiocarbamates. The ligands are almost planar, except for the hydrogen atoms. The maximum deviation from the least-squares plane is 0.07 Å. The planes of the two ligands, required by symmetry to be parallel, make dihedral angles of 30° with the sulphur plane. The molecule thus acquires the shape of a paddle-wheel as seen in Fig. 1.

Although the molecule is distorted, the distances between each of the thallium atoms and the two inner carbon atoms remain the same, 3.42 and 3.43 Å, as do those between the thallium atoms and the nitrogen atoms, 4.36 and 4.37 Å. This may follow from a tendency of the thallium-sulphur-carbon angles to take up equal values. Repulsion between the thallium atoms and the carbon and nitrogen atoms may also be responsible, since there appears to be some positive charge on these atoms associated with the conjugated $\pi$-system. According to a recent calculation,[12] these charges are 0.41 and 0.34, respectively. Neither of these explanations is entirely satisfying, however. In general, it is not feasible to isolate such interactions from the other forces in the crystal which influence the geometry of the dimer. Some of these forces will be discussed later.

As mentioned above, the thallium atom is closer to the sulphur atoms of one ligand than to those of the other. The thallium atom is thus 0.74 Å from the plane of the closest ligand, see Fig. 1. Although this could suggest that the dimer may be considered as made up of two planar monomers which are slightly deformed, the compound is nonetheless known [4] to form dimers in solution. The monomeric picture would not appear then to be particularly useful in discussing the crystal structure.

*Table 5.* Distances of coordination. The relationship between the coordinates of the sulphur atoms to those given in Table 1 $(x,y,z)$ is shown.

| Atoms | | | Distance (Å) |
|-------|--|--|--------------|
| Tl | S2 | $-x, -y, -z$ | 2.991(10) |
| Tl | S1 | $-x, -y, -z$ | 3.027(8) |
| Tl | S1 | $x, y, z$ | 3.284(8) |
| Tl | S2 | $x, y, z$ | 3.442(10) |
| Tl | S2 | $\frac{1}{2} - x, -\frac{1}{2} + y, -z$ | 3.458(10) |
| Tl | S1 | $\frac{1}{2} - x, \frac{1}{2} + y, -z$ | 3.519(8) |
| Tl | S1 | $\frac{1}{2} + x, -\frac{1}{2} - y, z$ | 3.736(8) |

Similar dimers have been found in thallium(I) dipropyldithiocarbamate[1] and in thallium(I) di-isopropyldithiocarbamate.[2] In the isopropyl compound the dimer is quite regular, the thallium-thallium vector being normal to the sulphur parallelogram and the least-squares plane through the $S_2CNC_2$ part of the ligand being coplanar with the sulphur plane. In the propyl compound, the dimer is considerably distorted. The sulphur atoms do not form a plane, and the molecule is not centrosymmetric.

*The coordination.* As shown in Table 5, there are seven atoms at distances ranging from 3.0 to 3.8 Å from the thallium atom. There are no other sulphur atoms closer to the thallium atom than 5 Å. The four closest sulphur atoms all belong to the same dimer as the thallium atom itself, whereas the remaining three belong to three different ligands in two other dimers; see Fig. 3. The dimeric unit is thus clearly distinguishable in the structure. The coordination polyhedron is illustrated in Fig. 6. It is most conveniently described as a tri-
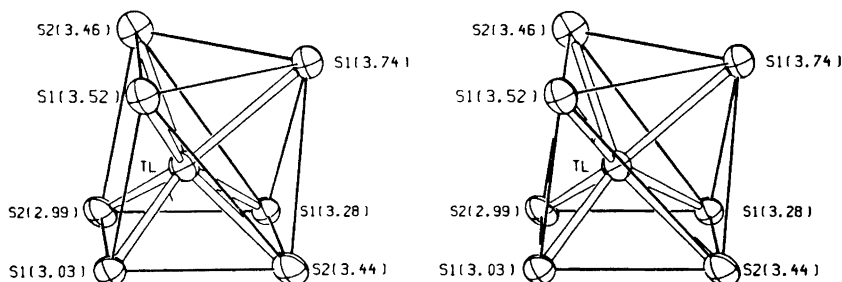


*Fig. 6.* Stereoscopic illustration of the coordination polyhedron. The distances of coordination are shown. See also Table 5.

gonal prism of six sulphur atoms with the seventh atom outside one of the faces of the prism. The four sulphur atoms in the dimer make up one of the faces of the prism. This face is planar and is directed downwards in the figure. The two remaining quadrangular faces are not exactly planar, but the two calculated least-squares each show a maximum deviation of 0.06 Å from the four defining points. All three faces are thus effectively planar. Furthermore, since the sum of the dihedral angles between them is 180.0° they are all parallel to a common line. The seventh atom is situated outside the largest of these three faces. The two triangular faces of the prism are not parallel.

The observed polyhedron is well known for 7-coordination; examples are found [13] in the complex ions $NdF_7^{2-}$ and $TaF_7^{2-}$. 8-Coordination rather than 7-coordination appears to be the preferred arrangement for thallium(I) with respect to sulphur. In thallium sulphide,[14] TlS, one half of the thallium atoms is univalent and one half trivalent. The univalent ions are surrounded by eight sulphur atoms at the corners of a square antiprism at a distance of 3.33 Å. In this compound the sulphur atoms can easily be accomodated around the thallium atom, and can form bonds to thallium atoms in several directions. 8-Coordination also occurs in the thiourea complexes of ionic thallium(I) salts. For these compounds an idealized structure has been proposed [15] which in-

volves square antiprismatic coordination. Here the sulphur atoms belong to thiourea molecules which are uncharged so that the most favourable stoichiometry with respect to coordination may be adopted.

In the dithiocarbamates the conditions for a high coordination number and a regular coordination geometry are less favourable. Packing restrictions are imposed because the ligands are quite large and unsymmetrical. They are also charged so that the stoichiometry is determined. A lower coordination number than eight would thus be anticipated. It is interesting to note that the highest coordination number observed so far is found in the structure of the methyl compound which has the smallest ligand. In fact, the connection with the square antiprismatic coordination may be observed in the structure of this compound. The coordination polyhedron, Fig. 6, may be seen as consisting of a base parallelogram and a top triangle. The centrosymmetrically related coordination polyhedra are joined in the $a$-direction by sharing of either the base parallelograms or one edge of the top triangles. When the two triangles share an edge they form, by symmetry, a parallelogram, which is almost parallel to the base parallelogram, dihedral angle 3°. The thallium atoms are thus sandwiched between parallelograms of sulphur atoms, as may be seen in Fig. 4. They are closer to the parallelogram comprising the sulphur atoms in the dimer than to the other parallelogram, 1.90 $vs.$ 2.62 Å. In the idealized structure of the thiourea complexes of the ionic thallium salts [15] a similar arrangement is found, but the parallelograms are squares and the thallium atoms are at equal distances from the two surrounding squares. As a particularly¦ interesting aspect of this comparison it should be mentioned that this idealized structure was proposed mainly from considerations of electrostatic forces.

Deformed coordination polyhedra with various coordination numbers and ranges of bonding distances are common in thallium(I) systems. Interesting examples are given by Ohmasa and Nowacki in reports of the structures of various thallium containing minerals.[16] These are sulfosalts with the donating sulphur atoms occurring in rigid groups where all the atoms are bound by covalent bonds. It is therefore not possible for the thallium atoms to achieve a regular coordination environment. A similar case has been found in $TlP_5$ [17] where the donating phosphorus atoms are members of a rigid phosphorus network. In these cases the conditions for a regular coordination would appear extremely unfavourable.

The same type of dimeric unit is found in the three thallium(I) dialkyl-dithiocarbamates which have been discussed here (propyl, isopropyl, and methyl) but the coordination numbers differ. Thus, 7-coordination is found in the methyl compound but only 5-coordination in the isopropyl compound. In the propyl compound there are two independent thallium atoms which exhibit 5- and 6-coordination. A comparison of the geometry of the dimers in the structures suggests a connection between a high coordination number and a strong deformation of the internal geometry of the dimer. Consequently, very little distorsion is observed in the iso-propyl compound. All four independent thallium-sulphur distances in the dimer are very close to 3.0 Å. The higher coordination numbers in the two other compounds are associated with considerable deformation of the geometry of the dimer. In each case a range

of distances is observed: 2.99 to 3.44 Å in the methyl and 2.88 to 4.37 Å in the propyl compound. If the thallium atom employs sulphur atoms from other dimers to increase its coordination number, the sulphur atoms must coordinate to thallium atoms outside their own dimers. These double engagements evidently disturb the bonding forces within the dimer.

Interesting features of the bonding between thallium(I) and sulphur are the variations of the bond distances, the coordination numbers and the geometries observed in different compounds, as discussed above. The structural behaviour of thallium(I) with respect to sulphur may then be summarized in the statement that *thallium(I) has weak coordination requirements*. Gold(I) may serve as an example of a species with considerably stronger coordination requirements. It is known to exhibit twofold linear coordination not only in the dithiocarbamates (propyl [18] and butyl [19]) but also in a number of other compounds.

*The metal atom arrangement.* The distance between the two thallium atoms in a dimer is $3.847 \pm 0.006$ Å, but even shorter distances, $3.637 \pm 0.002$ Å, exist between thallium atoms in different dimers. A thallium atom in a given dimer thus has two neighbours at 3.64 Å in different dimers as well as the neighbour at 3.85 Å in its own dimer. In this way a 3-connected net of metal atoms is formed. The net is somewhat puckered, the thallium atoms alternating between $z = \pm 0.05$, *i.e.* $\pm 0.57$ Å. The net is illustrated in Fig. 4 together with a schematic illustration of the coordinated sulphur atoms.

The metal atom net found in the structure of thallium(I) dimethyldithiocarbamate may be compared with the metal atom chains observed in the propyl and isopropyl homologues. In these two structures the metal atoms form equidistant nonlinear chains with steps 3.6 Å in the isopropyl and 4.0 Å in the propyl compound. In the chains every second step connects metal atoms situated within one dimer. The shortest metal-metal distance between two chains is about 9 Å in both the propyl and the isopropyl compound. If the chains were to approach one another more closely, so that these distances become similar in magnitude to those within the chains, a 2-dimensional net would result. The appearance of chains in the two latter compounds is associated with the greater size of their ligands, and this evidently prevents the closer approach of the dimers.

It is interesting to note the structure of caesium(I) dibutyldithiocarbamate [20] which strongly resembles that of the present compound. It is made up of dimers arranged in layers with no caesium-sulphur interaction between the layers. However, the metal-metal distances within the dimer, 4.29 Å, are considerably shorter than those appearing between metal atoms in different dimers (minimum distance 5.03 Å). The metal atom arrangement is thus most naturally described as being made up of pairs, and the chain or net models are not particularly useful.

*The linkage.* It was mentioned above that thallium(I) exhibits a tendency to assume 8-coordination with respect to sulphur. Since the thallium atom in the dimethyldithiocarbamate is coordinated to only four sulphur atoms within the dimer, the higher coordination number must be associated with the linkage of the dimeric units. In the structure, each dimer is linked by thallium-sulphur coordination to four other dimers to form a layer arrange-

ment, as shown in Fig. 3. An idealized form of this linkage is illustrated in
Fig. 7. Here the bonds within the dimers are heavily drawn and the sulphur
parallelograms are shaded. The dimers are arranged very simply so that the
sulphur atoms form planar "ladders". The metal atoms are situated between
these in positions of 8-coordination. It is easily seen that each dimer is linked
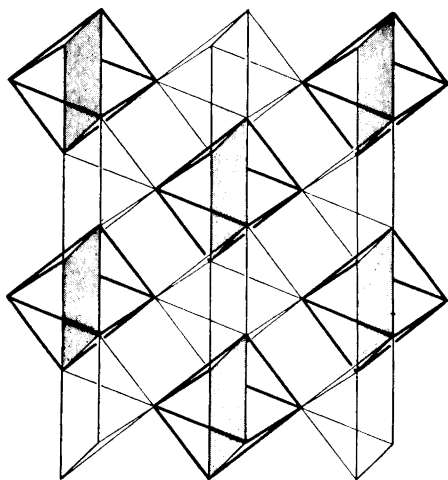


*Fig. 7.* Layer arrangement of the dimeric
molecules giving eightfold coordination.
The sulphur parallelograms of the dimers
are shaded. The thallium-sulphur bonds
within the dimers are heavily drawn. The
outer parts of the ligands, which project
upwards and downwards from the layer,
    have been omitted from the figure.
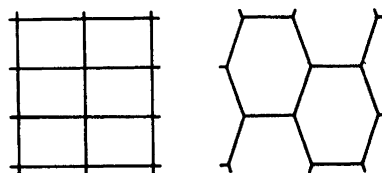
*Fig. 8.* The 4-connected metal atom net in
the model structure (left) and the ob-
served 3-connected hexagonal net (right).

to four others. The metal atoms form a simple 4-connected rectangular net.
This "ideal" arrangement is somewhat distorted in the real structure but
the nature of the distortions can be easily understood. The steps of the ladders
cannot be equal since every second step of sulphur atoms along the ladders
are interconnected by sulphur-carbon-sulphur bonds. The intermediate pairs
have no such connections. The former sulphur-sulphur distances are thus
shorter than the latter, 2.97 *vs.* 3.89 Å. However, as the latter are very little
longer than the sum of two ionic radii for $S^{2-}$, 3.68 Å, they also represent
quite a close sulphur atom approach. The thallium atom is then stituated be-
tween two parallelograms, one small and one large. The small one belongs to
the same dimer as the thallium atom; it is thus closer than the large one. In
this way pairs of metal atoms are distinguishable so that the metal atom
net is distorted to form the 3-connected "hexagonal" net as shown in Fig. 8.
Further complications result from the necessity to pack the ligands in a
favourable way both within and between the layers. The nature of the packing
can be appreciated in Fig. 2. Although the structural effects of the packing

requirements are generally very difficult to analyze, it is here reasonable to assume that the ligands are responsible for the folding of the sulphur ladders to form strips. These strips are somewhat inclined, so that the metal atom net is puckered and not planar. After this distorsion the metal atom retains bonds to all four sulphur atoms in the dimer, but the bond to one of the four other atoms is lost, the corresponding distance being larger than 5 Å. The coordination number is therefore only seven.

It is to be expected that the idealized arrangement would be even further destroyed if the ligands were larger. The increased packing difficulties caused by the presence of larger alkyl groups would restrict the number of dimers to which a given dimer could be linked. In the propyl and isopropyl compounds each dimer is linked to only two other dimers, so that chains of dimers are formed instead of the layers found in the methyl compound. The coordination numbers are lower; five and six for the two non-equivalent thallium atoms in the propyl compound and five in the isopropyl compound.

On the other hand, it is expected that the destruction of the idealized arrangement would be less pronounced if the metal-sulphur distances were larger. The alkyl groups would then possess more space, so that the effects of the packing requirements would be less severe. The ligands of caesium di-butyldithiocarbamate [20] are, of course, much larger than those in thallium(I) dimethyldithiocarbamate. The similarities between the two structures can be seen as resulting from the large metal-sulphur distances in the dimer of the caesium compound, average 3.58 Å, compared to the average value of 3.18 Å in the dimer of the thallium compound. In the caesium compound each dimer is linked to four others, as in thallium(I) dimethyldithiocarbamate, but only one of the sulphur atoms in each ligand is involved in the linkage. The coordination number is then only six. The possibility of obtaining higher coordination numbers in the lower homologues of the caesium series is interesting and will be investigated further.

## REFERENCES

1. Nilson, L. and Hesse, R. *Acta Chem. Scand.* **23** (1969) 1951.
2. Jennische, P., Olin, Å. and Hesse, R. *Acta Chem. Scand.* **26** (1972) 2799.
3. Jennische, P. and Hesse, R. *Acta Chem. Scand.* **25** (1971) 423.
4. Åkerström, S. *Arkiv Kemi* **24** (1965) 495.
5. Abrahamson, S. *J. Sci. Instr.* **43** (1966) 931.
6. Werner, P.-E. *Arkiv Kemi* **31** (1969) 505.
7. Werner, P.-E. *Acta Chem. Scand.* **25** (1971) 1297.
8. Morimoto, H. and Uyeda, R. *Acta Cryst.* **11** (1963) 1107.
9. Cromer, D. T. and Waber, J. T. *Acta Cryst.* **18** (1965) 104.
10. Hanson, H. P., Herman, F., Lea, J. D. and Skillman, S. *Acta Cryst.* **17** (1964) 1040.
11. Cromer, D. T. *Acta Cryst.* **18** (1965) 17.
12. Nikolov, G. St. and Tyutyulkov, N. *Inorg. Nucl. Chem. Letters* **7** (1971) 1209.
13. Wells, A. F. *Structural Inorganic Chemistry,* Oxford University Press, Oxford 1962, p. 685.

14. Scatturin, V. and Frasson, E. *Ric. Sci.* **26** (1956) 3382; *Structure Reports* **20** 192.
15. Boeyens, J. C. A. *Acta Cryst.* **B 26** (1970) 1251.
16. Ohmasa, M. and Nowacki, W. *Z. Krist.* **134** (1971) 360.
17. Olofsson, O. and Gullman, J. *Acta Chem. Scand.* **25** (1971) 1327.
18. Hesse, R. and Jennische, P. *Acta Chem. Scand.* **26** (1972) 3855.
19. Jennische, P. and Hesse, R. *To be published.*
20. Aava, U. and Hesse, R. *Arkiv Kemi* **30** (1968) 149.

# Isolation and Characterization of Egg Lecithin

BO LUNDBERG

*Department of Biochemistry and Pharmacy, Åbo Akademi, SF-20500 Åbo, Finland*

A modified method for the isolation of chromatographically and spectroscopically pure egg lecithin is described and the final product is characterized. Instead of the customary ethanol or chloroform-methanol, diethyl ether is used for extraction in this method. The chromatography is carried out on a silicic acid-silicate column with 6:1 and 3:1 (v/v) mixtures of chloroform and methanol, pure methanol, and pure chloroform as eluting solvents.

The special precautions taken to avoid degradation and oxidation of the product were deoxygenation of the solvents and addition of 4-methyl-2,6-*tert*-butylphenol (BHT) as antioxidant. Moreover, the chromatography was carried out at +4°C under nitrogen.

The values obtained in the characterization of the product are compared with those reported earlier by other authors. Similar values were obtained for the percentages of nitrogen, phosphorus, glycerol, and total fatty acids, but the fatty acid composition differs considerably. This stresses the importance of a well-defined method for the isolation of egg lecithin.

No satisfactory method for the isolation of egg lecithin was found in the literature when the author first undertook the study of its physical-chemical properties. The major features required of such a method are that it is fast and cheap and gives a homogeneous and undegraded product.

The classical method for the isolation of egg lecithin is the cadmium chloride procedure.[1] Isolation with solvents and column chromatographic methods are nowadays used. Before the extraction of the phospholipids, egg yolks are usually treated with acetone, whereupon dehydration takes place at the same time as the neutral lipids are dissolved and the phospholipids are precipitated.[2-5] Lyophilization before extraction with acetone has also been used.[3] Ethanol [2,4,5] and chloroform-methanol mixtures [3] have been used to extract the crude phospholipids.

Silicic acid [4] and alumina,[2,5] alone and in combination, have been used in the column chromatographic separation of the phospholipids isolated by solvent extraction. It has been reported that the silicic acid-silicate column is the only one that separates lecithin and sphingomyelin quantitatively.[6] Ethanol [2] and various methanol-chloroform mixtures have been used as

eluents.[3-5] Degradation of lecithin in alumina columns has been reported by Renkonen.[7] In contrast, no degradation has been detected in silicic acid columns.[8]

The results of earlier characterizations of egg lecithin differ considerably.[2,5,9] This shows that different methods may give products of variable composition. Because the physical-chemical properties of lecithins vary with the fatty acid composition, it is of great importance that the isolated product is homogeneous and well-defined. IR spectra of egg lecithin have apparently not been reported earlier, but density values for egg lecithin have been presented by Elworthy.[10]

## EXPERIMENTAL

*Materials and methods.* The yolks used in the work were taken from fresh eggs and the treatment was begun immediately after the whites had been separated.

All solvents were guaranteed reagents from E. Merck AG. They were deoxygenated and 0.005 % 4-methyl-2,6-tert-butylphenol (BHT) was added as an antioxidant.

Silica Gel G, according to Stahl, E. Merck AG, was used in the TLC analyses. The silicic acid used in column chromatography was an analytical reagent (100 mesh) from Mallinckrodt that had been treated according to Rouser and co-workers.[6]

The column used was a Pharmacia column of type SR 25/45 which was connected to a pressure vessel containing the solvent.

The lecithin standard was chromatographically homogeneous L-α-lecithin from the California Biochemical Corporation.

In the chemical characterization of the lecithin, glycerol was estimated according to Renkonen,[11] nitrogen with a Coleman Model 29 Nitrogen Analyzer and phosphorus by the perchloric acid procedure.[12] The fatty acid composition was estimated by GLC of their methyl esters on a Perkin-Elmer F 11 Gas Chromatograph equipped with a column of Chromosorb W coated with EGGS-X. The temperature was programmed from 150 to 180°C at a rate of 4°C/min. Nitrogen was used as carrier gas. Total fatty acids were determined by the method of Tattrie.[9]

The IR spectrum was recorded with a Perkin-Elmer Model 700 Infrared Spectrophotometer equipped with a sodium chloride cell. The solvent was carbon tetrachloride. The UV spectrum was measured with a Perkin-Elmer Model 402 UV-visible Spectrophotometer using petroleum ether as solvent.

The thin-layer plates were developed as described by Skipsky and co-workers.[13]

The density was measured by the displacement method.[10]

The lyophilization was carried out in a Christ Model L 2 Freeze Dryer.

*Extraction of crude phospholipids.* The yolks (about 60 g) of twelve eggs were lyophilized overnight. The resulting cake was homogenized by mixing with 150 ml of diethyl ether in a Waring blendor. The mixture was filtered and the filtrate evaporated almost to dryness in a rotary evaporator. The crude phospholipids were precipitated by adding 150 ml of cold acetone. The precipitation was repeated by dissolving the phospholipids in 10 ml of cold diethyl ether, filtering to remove any undissolved matter and adding 100 ml of cold acetone. The solvent was then removed and the crude phospholipids were stored under nitrogen at −20°C until further treated. The average yield of crude phospholipids was 4 % based on the weight of the fresh yolks.

*Column chromatographic separation.* The Pharmacia type SR 25/45 column that was used was filled with 100 g of activated silicic acid − silicate. The crude phospholipids were applied in 5 ml of chloroform. The load was 1 mg P/g SiO$_2$. The flow rate was held at 2 ml/min with compressed nitrogen, and 10 ml fractions were collected on a fraction collector. The chromatography was carried out at +4°C in a thermostated room. The eluting solvents were (1) 200 ml of 6:1 chloroform:methanol, (2) 150 ml of 3:1 chloroform: methanol, (3) 150 ml of pure methanol, and (4) 200 ml of pure chloroform. After such an elution sequence, the column was ready to be used again. The cephalin was eluted by solvent (1), the lecithin by solvent (2), and sphingomyelin and lysolecithin by solvent (3).

After the elution (6 h), the contents of the tubes were analysed by TLC. The tubes containing pure lecithin were evaporated to dryness under nitrogen in a rotary evaporator. The product was stored in acetone at $-20°C$ or, if it was used at once, was lyophilized and dried to constant weight over phosphorus pentoxide under nitrogen in a vacuum desiccator. The average yield of pure lecithin from 60 g of fresh yolks was 1.6 g.

*Characterization of the product.* The purity of the final product was tested by TLC. Only one spot was detected on charring with sulphuric acid. Because this method is sensitive to 0.1 $\mu$g of lipids, the product was regarded as chromatographically pure (see Fig. 1).
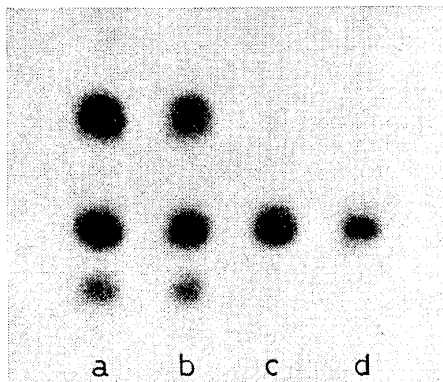


*Fig. 1.* Thin-layer chromatograms of (a) total phospholipids in egg yolk, (b) phospholipids applied to the column, (c) final product, (d) synthetic L-α-lecithin.

As further evidence of the purity of the product, the IR and UV spectra were recorded. The spectra showed that the product was spectroscopically pure and undegraded (see Figs. 2 and 3).

The results of the chemical analyses of the pure product can be compared with those of Hanahan et al.,[2] Singleton et al.,[5] and Tattrie [9] in Table 1.

The fatty acid composition, expressed as percentages of the total fatty acids in the homogeneous egg lecithin, determined by GLC analysis in this work and those reported by Hanahan et al.,[2] Singleton et al.,[5] and Tattrie,[9] is as shown in Table 2.
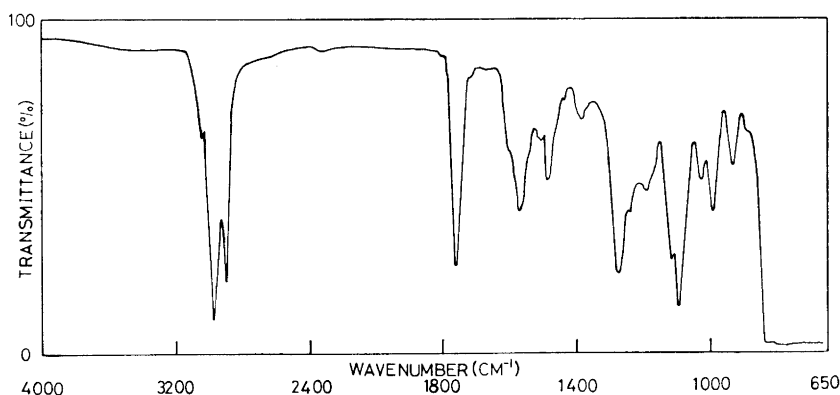


*Fig. 2.* IR spectrum of pure egg lecithin in carbon tetrachloride. The absence of the sphingomyelin absorption band at 1640 cm$^{-1}$ is to be noted.

*Table 1.* Analytical data of the isolated egg lecithin compared with those found by other authors.

|  | This work | Ref. 2. | Ref. 5. | Ref. 9. |
|---|---|---|---|---|
| N, % | 1.82 | 1.79 | — | 1.82 |
| P, % | 4.02 | 3.90 | 3.97 | 3.94 |
| Glycerol, % | 12.00 | — | — | — |
| Fatty acids, % | 71.2 | 70.0 | 69.5 | 70.3 |
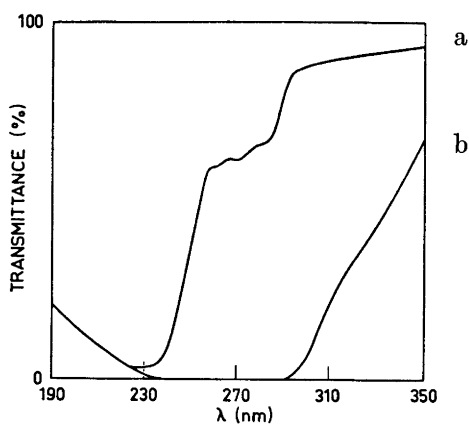


*Fig. 3.* UV spectra of pure egg lecithin in petroleum ether. Curve (a) is the spectrum of lecithin stored one week in acetone at − 20°C and curve (b) that of lecithin stored one week in air at + 4°C.

*Table 2.* Fatty acid composition of the isolated egg lecithin compared with that found by other authors.

| Fatty acid | This work | Ref. 2. | Ref. 5. | Ref. 9. |
|---|---|---|---|---|
| Palmitic | 35.9 | 32.0 | 37.7 | 35.7 |
| Palmitoleic | 0.9 | 1.0 | 3.1 | Trace |
| Stearic | 18.4 | 16.0 | 9.2 | 14.9 |
| Oleic | 28.7 | 30.0 | 32.9 | 37.0 |
| Linoleic | 13.9 | 17.0 | 17.0 | 12.4 |
| Arachidonic | 2.2 | — | — | — |

The average molecular weight of the fatty acids calculated from these values is 273.4. According to this average value the molecular weight of the egg lecithin was 768. The measured density of the lecithin was 1.018 g/cm³.

## DISCUSSION

Much time is saved in evaporating the solvent by using diethyl ether instead of ethanol or a chloroform:methanol mixture for the extraction. At the same time most of the sphingomyelin, which is insoluble in diethyl ether,

is separated. Most of the cephalin could have been separated by extraction with ethanol, but this is of lesser importance because it is much easier to separate cephalin than sphingomyelin from lecithin by chromatography. Because the evaporation of ethanol is very lengthy, this solvent was not used. One important condition that must be fulfilled when diethyl ether is used for extraction, however, is that the yolk has been completely dried. Besides lyophilization, dehydration with acetone was tried; but this proved less effective.

The chromatography was performed at about $+4°C$ in order to avoid oxidation and degradation during column chromatography as far as possible. This required the testing of a particular elution sequence in chromatography at this temperature. Water was avoided so that the column would remain active. With the elution schemes described the column retained its activity for up to one year.

The data obtained in the analysis of the pure egg lecithin agree fairly well with those reported in earlier investigations. However, divergent fatty acid compositions are obtained when different isolation methods are used. This shows the importance of a well-defined method for the separation of egg lecithin because its molecular weight and physical-chemical qualities vary with the fatty acid composition.

## REFERENCES

1. Levene, P. A. and Rolf, I. P. *J. Biol. Chem.* **72** (1937) 587.
2. Hanahan, D. J., Turner, M. B. and Jayko, M. E. *J. Biol. Chem.* **192** (1951) 623.
3. Rhodes, D. N. and Lea, C. H. *Biochem. J.* **65** (1957) 526.
4. Saunders, L. *J. Pharm. Pharmacol.* **9** (1957) 834.
5. Singleton, W. S., Gray, M. S., Brown, M. L. and White, J. L. *J. Am. Oil Chemists' Soc.* **38** (1961) 565.
6. Rouser, G., O'Brien, J. and Heller, D. *J. Am. Oil Chemists' Soc.* **38** (1961) 14.
7. Renkonen, O. *J. Lipid Res.* **3** (1962) 181.
8. Newman, H. A. I., Ching-Tong Liu and Silversmit, D. B. *J. Lipid Res.* **2** (1961) 403.
9. Tattrie, N. H. *J. Lipid Res.* **1** (1959) 60.
10. Elworthy, P. H. *J. Chem. Soc.* **1959** 1951.
11. Renkonen, O. *Biochim. Biophys. Acta* **56** (1962) 367.
12. Rouser, G., Siakotos, A. N. and Fleischer, S. *Lipids* **1** (1966) 85.
13. Skipsky, V. P., Peterson, R. F. and Barclay, M. *Biochem. J.* **90** (1964) 374.

Received May 17, 1973.

# Complex Formation between Silver and Iodide Ions in Fused Potassium-Sodium Nitrate. II. Phase Transformation at High Iodide Concentrations

BERTIL HOLMBERG

*Division of Physical Chemistry, Lund University, Chemical Center, P.O.B. 740, S-220 07 Lund 7, Sweden*

The transition from a solid to a liquid silver iodide phase in equilibrium with iodide-containing melts of equimolar $(K,Na)NO_3$ at 280°C has been studied. At a total iodide concentration of 0.93 mol $kg^{-1}$ in the nitrate phase a solid solution $(K,Ag)I(s)$ transforms into a liquid solution $(K,Ag)I(l)$, in which the mol ratio I:Ag increases from 1.30 to 1.50 when the iodide concentration in the nitrate melt increases from 0.93 to 1.58 mol $kg^{-1}$. These findings are considered in relation to the phase diagram of the system $AgI - KI$ and the structure of $\alpha$-AgI.

The solubility of equimolar $(K,Na)I(s)$ in the nitrate melt has been determined at various amounts of $AgNO_3$ added to this melt. The results indicate the presence of $AgI_4^{3-}$ as well as polynuclear species.

In a previous paper[1] potentiometric data on the complex formation between silver and iodide ions in fused equimolar $(K,Na)NO_3$ at 280°C have been reported. The stabilities of the complex ions $AgI_2^-$, $AgI_3^{2-}$, and $Ag_2I_6^{4-}$ were determined. Evidence was also found for the presence of $AgI_4^{3-}$, but the value of the corresponding stability constant could be given only as a rough estimate. Thus, the nature of the complex species richest in iodide is still somewhat unclear. The need for additional studies employing other experimental methods, such as solubility measurements, is obvious. The conventional solubility method, however, cannot be applied to this system at high iodide concentrations. In their study of silver iodide complexes in equimolar melts of $KNO_3$ and $NaNO_3$ at 280°C, Elding and Leden[2] did not perform solubility measurements at iodide concentrations above 0.8 mol $kg^{-1}$ [*i.e.* mol per kg solvent, $(K,Na)NO_3$]. They found, that a further increase in the iodide concentration made the solid AgI transform into a deeply coloured melt with a density considerably higher than that of the nitrate melt with which it is in equilibrium. Miscibility gaps of this kind have been reported

for similar systems before. Such systems are Na,Ag/NO$_3$,I[3] and K,Ag/NO$_3$,I.[4] Different factors that seem to be of importance in determining the extent of immiscibility in this kind of fused salt systems have been thoroughly discussed by Ricci,[5] Marcus,[6,7] and Belyaev.[8] Generally the different character of the chemical bonding in the components of the system contributes to the tendency of liquid immiscibility. Differences in the anion or cation radii and in ion polarizabilities between the constituent ions in the two phases also seem to be of importance for the phase separation. Hence the two liquid phases are expected to exhibit rather different properties.

The present investigation has been undertaken in order to (a) elucidate the phase transition that made an unambiguous interpretation of Elding's and Leden's solubility data difficult; (b) provide additional qualitative information on the complex formation at high ligand concentrations. Such information may be gained from a careful study of the solubility of the ligand (i.e. (K,Na)I(s)) in the nitrate melt when various amounts of AgNO$_3$ are added to this melt.

## EXPERIMENTAL

*Chemicals used.* Potassium nitrate and sodium nitrate (Merck, *p.a.*) were powdered, ground together and dried at 120°C for at least ten days. Potassium iodide (Merck, *p.a.*) and sodium iodide (Mallinckrodt, *p.a.*) were dried at 140°C. These chemicals were used without further purification.

Silver iodide was prepared by precipitation from hot dilute solutions of potassium iodide and silver nitrate (Engelhard, *p.a.*). The precipitate was washed with 1 % nitric acid and large amounts of water. After drying for one day at 110°C the silver iodide was stored protected from light.

*Apparatus.* Large Pyrex test tubes were used as reaction vessels in a high-temperature thermostat bath similar to the one used by Cigén and Mannerstrand.[9] The temperature was maintained at (280 ± 1)°C.

*Procedure.* For the phase transition investigation, weighed amounts of (K,Na)I (equimolar mixture) and AgI were added to 50.00 g of liquid (K,Na)NO$_3$ (equimolar mixture), and the system was agitated by vigorous stirring with a Pyrex propeller. Equilibrium was attained within less than 40 h. After equilibration the system was allowed to stand without stirring for at least 1 h in order to effect properly separated phases.

Samples from the nitrate phase were taken with a pre-heated pipette. Samples from the heavy, liquid AgI phase were isolated from the system in the following way.

One end of a Pyrex glass tube (inner diameter 5 mm) was drawn to a fine capillary, which was introduced into the liquid AgI phase, while the other end of the tube was closed. Then the liquid was sucked up into the tube through the capillary. The sample was poured out into a small beaker, thermostated at 280°C, where the procedure could be repeated. It appeared that one separation of this kind is enough to eliminate all observable traces of the nitrate phase. The distribution of Ag and I between the two phases was determined in systems containing 4.50 g AgI. The total concentrations of silver and iodide in the nitrate melt were determined. Samples from the liquid AgI phase were isolated and analyzed for silver and iodide and in some cases for sodium and potassium. Occasional qualitative tests for nitrate were also made.

The solubility of (K,Na)I was measured in systems containing 50.00 g (K,Na)NO$_3$, 21.00 g (K,Na)I and various amounts of AgNO$_3$.

Some melts with high iodide concentrations were analyzed for iodide after 10 days at 280°C. No oxidation of iodide could be detected.

*Analyses.* The silver content was determined by electroanalytical precipitation on a rotating platinum cathode from hot cyanide solutions.

For the iodide analyses the solidified samples were suspended in an aqueous dex-

trin solution (in order to prevent coagulation of AgI). The amount of iodide not present
as solid AgI was determined by titration with a standard $AgNO_3$ solution using eosine
as indicator. The total amount of iodide was calculated from these titration data and
the known value of the silver content. The iodide analyses were reproduced to $\pm 0.5 \%$
or better.

The content of alkali metal ions was determined from atomic absorption measure-
ments on samples dissolved in 50 mM cyanide solutions.

*X-Ray powder photographs* of samples from the liquid AgI phase were recorded
in a Hägg-Guinier camera within a few hours after the sample had been quenched.
Another powder photograph of each specimen was recorded after three days. No change
in the diffraction pattern could be detected.

## RESULTS AND DISCUSSION

The following symbols are used:

$n_A$ = amount of species A.
$y$ = mol ratio $n_I/n_{Ag}$ in the iodide phase.
$q_{Na}$ = $n_{Na}/(n_{Na}+n_K+n_{Ag})$, calculated for the iodide phase.
$x_K$ = $n_K/(n_K+n_{Na})$, calculated for the system as a whole.
$C_{Ag}$ = total concentration of silver(I) in the nitrate melt.
$C_I$ = total concentration of iodide in the nitrate melt.
$\bar{n}$ = $(C_I-[I^-])/C_{Ag}$, the average ligand number.

*The phase transition.* The only components of importance in the liquid
AgI phase are AgI and KI. No nitrate could be detected, and from the fig-
ures of Table 1 it follows that sodium accounts for less than 0.3 % of the
total cation amount. Therefore, the sodium content has been ignored in the
calculation of the composition of the AgI phase. The traces of sodium might
possibly result from contamination by the nitrate melt, but this view is to
some degree contradicted by the monotonous variation in $q_{Na}$ with $y$.

*Table 1.* The sodium ratio $q_{Na}$ at different values of $y$ in the liquid AgI phase.

| $y$, $q_{Na} \times 10^3$; | | | | |
|---|---|---|---|---|
| 1.304, 1.0; | 1.360, 1.4; | 1.423, 2.1; | 1.469, 2.7; | 1.503, 2.8 |

The composition of the liquid AgI phase has been directly determined
from the silver and iodide analyses. For the solid phase, which is difficult
to separate quantitatively from the nitrate melt, the composition is cal-
culated from the difference between the added and found amounts of iodide
in the nitrate melt. Fig. 1 shows $y$ as a function of $C_I$.

The phase transition occurs at $C_I = (0.930 \pm 0.006)$ mol $kg^{-1}$ (*vide* Table 2).
The point in Fig. 1 marked with a half-filled circle refers to a three-phase
system where the liquid nitrate and AgI phases are in equilibrium with solid
(K,Na)I. Hence, the range of existence for the liquid AgI phase at 280°C
is $1.30 \leq y \leq 1.50$. For the solid AgI phase $y$ deviates markedly from 1 in
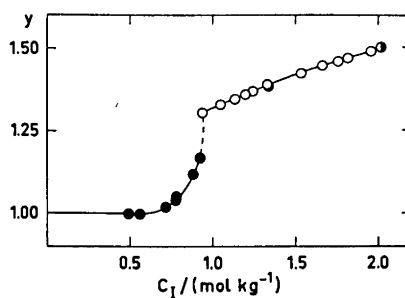
*Fig. 1.* Variation of $y$ with $C_I$. Symbols: (K,Ag)I(s) (●), (K,Ag)I(l) (○), three-phase system (K,Ag)I(l) — (K,Na)I(s) — nitrate melt (◑).

*Table 2.* The equilibrium compositions of the nitrate and iodide phases. Data of the left hand side of the table refer to systems (K,Ag)I(s)-nitrate melt; those of the right hand side refer to (K,Ag)I(l)-nitrate melt.

| $\dfrac{C_I}{\text{mol kg}^{-1}}$ | $\dfrac{C_{Ag}}{\text{mol kg}^{-1}}$ | $y$ | $\dfrac{C_I}{\text{mol kg}^{-1}}$ | $\dfrac{C_{Ag}}{\text{mol kg}^{-1}}$ | $y$ |
|---|---|---|---|---|---|
| 0.492 | 0.00789 | 1.00 | 0.936 | 0.0300 | 1.304 |
| 0.561 | 0.00937 | 1.00 | 1.048 | 0.0374 | 1.330 |
| 0.715 | 0.01672 | 1.02 | 1.132 | 0.0456 | 1.347 |
| 0.773 | 0.01994 | 1.04 | 1.198 | 0.0479 | 1.360 |
| 0.779 | 0.02065 | 1.05 | 1.241 | 0.0528 | 1.370 |
| 0.881 | 0.02690 | 1.12 | 1.329 | 0.0603 | 1.389 |
| 0.923 | 0.02969 | 1.17 | 1.333 | 0.0596 | 1.386 |
|  |  |  | 1.533 | 0.0810 | 1.423 |
|  |  |  | 1.661 | 0.0927 | 1.446 |
|  |  |  | 1.755 | 0.1039 | 1.459 |
|  |  |  | 1.817 | 0.1110 | 1.469 |
|  |  |  | 1.954 | 0.1293 | 1.489 |
|  |  |  | 2.013 | 0.1330 | 1.503[a] |

[a] In equilibrium with solid (K,Na)I.

a narrow concentration range preceding the solid-liquid transition. This obviously means that KI migrates into the high-temperature modification of silver iodide, $\alpha$-AgI, forming a solid solution. At $C_I = 0.93$ mol kg$^{-1}$ the concentration of potassium iodide in the solid phase is high enough to make the iodide lattice of the $\alpha$-AgI collapse — the solid melts. (From the measurements reported here it is of course impossible to distinguish between KI and NaI in the *solid* solution. The reluctance of AgI to accept NaI in liquid solution at this temperature suggests, however, that KI is the solute in the solid as well.)

Extensive investigations of systems of the type AgI — MI have been made recently by Burley and Kissinger [10] and by Bradley and Greene.[11],[12] Burley and Kissinger claim that the AgI — KI system contains one compound, KAg$_3$I$_4$, stable up to 268°C, where it melts congruently. No solid solution was indicated.

According to Bradley and Greene,[11] the AgI−KI system contains two intermediate compounds, $K_2AgI_3$ and $KAg_4I_5$. $K_2AgI_3$ disproportionates to solid $KAg_4I_5$ and KI at 130°C. The compound $KAg_4I_5$ is stable between 38°C and 253°C. Below 38°C it disproportionates to the hexagonal $\beta$-AgI and $K_2AgI_3$. At 253°C $KAg_4I_5$ melts incongruently. No solid solutions have been reported. Topol and Owens [13] later verified the diagram published by Bradley and Greene in all essentials.

Thus, AgI and KI do not form any solid intermediate compound at 280°C. According to Bradley and Greene, the system is liquid in a range between 23 and 34 mol % KI at this temperature. The limits $1.30 \leq y \leq 1.50$ for the liquid AgI phase in the systems studied in this work are in perfect agreement with these figures.

The consistency with the findings of Bradley and Greene has been further confirmed by X-ray diffraction measurements on powder of quenched samples of the liquid AgI phase. All samples gave identical powder photographs where no traces of KI could be detected. The diffraction pattern showed that the samples consisted of $\beta$-AgI and $K_2AgI_3$. The structure of the latter compound has been determined by Brink and Kroese.[14] For comparison powder photographs from a model powder were recorded. This powder was made by melting together KI and AgI in the mole proportions 1:3 at 280°C followed by a rapid cooling to room temperature. The model powder and the samples from the liquid AgI phase gave identical diffraction patterns.

Thus, there is good agreement with the phase diagram of Bradley and Greene except for the rather narrow range where a solid solution of KI in $\alpha$-AgI has been observed in this work.

In the solid $\alpha$-AgI, which is stable above 146°C, the iodide ions are arranged in a body-centered cubic lattice [15,16] while the silver ions are thought to be randomly distributed over a large number of sites. A formation of solid solution with, for instance, those alkali metal iodides where no sterical obstacles arise, should obviously be facilitated by this type of structure. This fact has also been stressed by Krogh-Moe [17] in his discussion of different factors of importance for formation of solid solutions with compounds of B 23 structure.

The crystal ionic radii of $K^+$ and $Ag^+$ are not very different: 1.33 Å and 1.26 Å, respectively. The potassium ions might possibly be accommodated in the 12d positions, which are the largest cation sites in $\alpha$-AgI. Such an arrangement can not be realized, however, without a considerable distortion of the iodide lattice. This might be the cause of the final breakdown of the crystal structure at a critical concentration of potassium ion, which is reached at the point of phase transition.

*The ligand solubility.* The solubility of (K,Na)I(s) at various $C_{Ag}$ has been determined for $0 \leq C_{Ag} \leq 0.13$ mol kg$^{-1}$ and the results are given in Table 3.

It is well known that KI and NaI form a continuous range of solid solutions at high temperatures.[18-20] No solid solution or intermediate compound with $KNO_3$ or $NaNO_3$ is found at 280°C.[20] Furthermore, it appeared from the analyses for silver in the nitrate melt that no detectable amounts of $AgNO_3$ are present in the solid (K,Na)I at equilibrium. Separate experiments have shown that the solubility of (K,Na)I in fused (K,Na)$NO_3$ is independent of

*Table 3.* The solubility of (K,Na)I at different $C_{Ag}$ and the corresponding ligand numbers, $\bar{n}_{exp}$. For comparison the ligand numbers, calculated from the set of stability constants of Ref. 1 ($\bar{n}_{calc}$) are included.

| $\dfrac{C_{Ag}}{\text{mol kg}^{-1}}$ | $\dfrac{C_I}{\text{mol kg}^{-1}}$ | $\bar{n}_{exp}$ | $\bar{n}_{calc}$ |
|---|---|---|---|
| 0 | 1.577 | | |
| 0.01121 | 1.611 | $3 \pm 1$ | 3.07 |
| 0.02470 | 1.659 | $3.3 \pm 0.4$ | 3.06 |
| 0.03984 | 1.707 | $3.3 \pm 0.2$ | 3.05 |
| 0.04919 | 1.735 | $3.2 \pm 0.1$ | 3.05 |
| 0.0619 | 1.773 | $3.19 \pm 0.08$ | 3.04 |
| 0.0761 | 1.816 | $3.14 \pm 0.08$ | 3.04 |
| 0.0913 | 1.858 | $3.08 \pm 0.07$ | 3.04 |
| 0.0955 | 1.868 | $3.05 \pm 0.06$ | 3.04 |
| 0.1087 | 1.906 | $3.02 \pm 0.05$ | 3.03 |
| 0.1199 | 1.936 | $3.00 \pm 0.05$ | 3.03 |
| 0.1300 | 1.965 | $2.98 \pm 0.04$ | 3.03 |
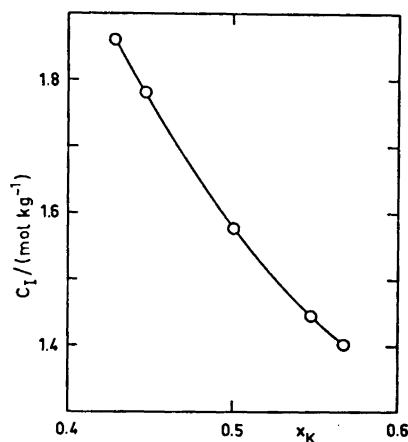


*Fig. 2.* The solubility of (K,Na)I(s) at various $x_K$. $C_{Ag} = 0$.

the mass ratio of solid (K,Na)I to liquid (K,Na)NO$_3$, indicating that the ratio $n_K : n_{Na}$ is the same (*i.e.* 1:1) in the solid and in the nitrate melt. On the other hand, there is a strong dependence on the K − Na balance in the entire system. This is illustrated in Fig. 2 where the solubility, $C_I$, is given for $C_{Ag} = 0$ as a function of $x_K$ around $x_K = 0.5$.

At $x_K = 0.500$ the solubility in pure (K,Na)NO$_3$ is $1.577 \pm 0.004$ mol kg$^{-1}$. In systems containing silver(I) there is an appreciable increase of the solubility for increasing $C_{Ag}$. Since $x_K$ has been kept constant at 0.500 in all systems investigated, it is very reasonable to assume the free iodide concentration, [I$^-$], to be 1.58 mol kg$^{-1}$ in melts containing silver(I) as well. Hence, the mean ligand number $\bar{n}$ may be directly calculated from the corresponding values of $C_{Ag}$ and $C_I$. In Table 3 the ligand numbers evaluated

in this direct way are compared with values calculated from the set of stability constants given in Ref. 1.

Two important pieces of information about the higher complexes can be derived from the experimental $\bar{n}$-data: (a) The monotonous variation of $\bar{n}$ with $C_{Ag}$ at $[I^-] = 1.58$ mol kg$^{-1}$ indicates that polynuclear species are present since $\bar{n}$ is a function solely of the free ligand concentration in a mononuclear complex system;[21] (b) Despite the poor accuracy in the $\bar{n}$-values at the smallest $C_{Ag}$ (due to small differences $C_I - [I^-]$), it is evident that $\bar{n}$ exceeds 3 at low $C_{Ag}$, indicating the presence of $AgI_4^{3-}$.

The $\bar{n}_{exp}$-values of Table 3 show a more pronounced decrease with increasing $C_{Ag}$ than do the $\bar{n}_{calc}$-values. At high $C_{Ag}$ the two sets of $\bar{n}$-values coincide. The reason for this trend might be a too low value of the stability constant $\beta_{41}$ of $AgI_4^{3-}$ calculated from the emf measurements in unsaturated melts. This possibility has been discussed in a previous paper.[1]

A more thorough discussion of the complex formation at high $C_I$ will appear in a subsequent paper,[22] treating the distribution equilibria between $(K,Ag)I(s)$ or $(K,Ag)I(l)$ and the nitrate melt.

## REFERENCES

1. Holmberg, B. *Acta Chem. Scand.* **27** (1973) 875.
2. Elding, I. and Leden, I. *Acta Chem. Scand.* **23** (1969) 2430.
3. Zakharchenko, M. A. and Bergman, A. G. *J. Gen. Chem. USSR* **25** (1955) 833.
4. Dombrovskaya, N. S. and Koloskova, Z. A. *Izv. Sektora Fiz. Khim. Anal., Inst. Akad. Nauk SSSR* **22** (1953) 178.
5. Ricci, J. E. In Blander, M., Ed., *Molten Salt Chemistry*, Interscience, New York 1964, p. 239.
6. Marcus, Y. In Dyrssen, D., Liljenzin, J. O. and Rydberg, J., Eds., *Solvent Extraction Chemistry*, North-Holland, Amsterdam 1967, p. 555.
7. Marcus, Y. In Braunstein, J., Mamantov, G. and Smith, G. P., Eds., *Advances in Molten Salt Chemistry*, Plenum Press, New York 1971, Vol 1, p. 76.
8. Belyaev, N. *Russian Chem. Rev.* **29** (1960) 428.
9. Cigén, R. and Mannerstrand, N. *Acta Chem. Scand.* **18** (1964) 1755.
10. Burley, G. and Kissinger, H. E. *J. Res. Natl. Bur. Std.* A **64** (1960) 403.
11. Bradley, J. N. and Greene, P. D. *Trans Faraday Soc.* **62** (1966) 2069.
12. Bradley, J. N. and Greene, P. D. *Trans. Faraday Soc.* **63** (1967) 424.
13. Topol, L. E. and Owens, B. B. *J. Phys. Chem.* **72** (1968) 2106.
14. Brink, C. and Kroese, H. A. S. *Acta Cryst.* **5** (1952) 433.
15. Strock, L. W. *Z. physik. Chem. Leipzig* **25** (1934) 441.
16. Hoshino, S. *J. Phys. Soc. Japan* **12** (1957) 315.
17. Krogh-Moe, J. In Førland, T., Grjotheim, K., Motzfeldt, K. and Urnes, S., Eds., *Selected Topics in High Temperature Chemistry*, Univ. forl., Oslo 1966, p. 79.
18. Kurnakow, N. S. and Zemczuźny, S. F. *Z. anorg. Chem.* **52** (1907) 186.
19. Bergman, A. G. and Platonov, F. P. *Izv. Sektora Fiz. Khim. Anal., Inst. Akad. Nauk SSSR* **10** (1937) 253.
20. Vasenin, F. I. and Bergman, A. G. *Izv. Sektora Fiz. Khim. Anal., Inst. Akad. Nauk SSSR* **11** (1938) 169.
21. *E.g.* Rossotti, F. J. C. and Rossotti, H. *The Determination of Stability Constants*, McGraw, New York 1961.
22. Holmberg, B. *Acta Chem. Scand.* **27** (1973) 3657.

# Analysis of Acetylated Methyl Glycosides as Their Trimethylsilyl Derivatives by Gas-Liquid Chromatography and Mass Spectrometry

HANS B. BORÉN, PER J. GAREGG, LENNART KENNE,
ÅKE PILOTTI, SIGFRID SVENSSON and CARL-GUNNAR SWAHN

Department of Organic Chemistry, Arrhenius Laboratory, University of Stockholm,
S-104 05 Stockholm, Sweden

The separation, by gas liquid chromatography, of the trimethylsilyl ether derivatives of thirty-one methyl D-hexopyranoside acetates with the O-acetyl groups in the 2-, 3-, 4-, 6-, 2,3-, 3,6-, and 4,6-positions is described. The number and position(s) of the O-acetyl groups are unequivocally determined by mass spectrometry.

Partially O-acetylated glycosides are of interest in carbohydrate chemistry from several points of view. They are useful intermediates in synthesis, in particular for the protection of specific hydroxyl groups.[1] Advantage can be taken of their nucleophilic properties in operations involving neighbouring group participation.[2] Their tendency to undergo acyl migration[3] can be troublesome, although this very property has on occasion been put to advantage.[4] Many naturally-occurring polysaccharides are partially O-acetylated, Some of these O-acetylated polysaccharides are of biological importance and the O-acetyl group itself can contribute to the biological activity. Partially O-acetylated glycosides are therefore useful in model studies on  biological interactions, such as the determination of enzyme specificities and investigations of biological systems. For these reasons, the assignment of the number and positions of O-acetyl groups in a glycoside is a problem of general interest. A prerequisite for any method used is that conditions which promote acyl migration must be avoided. Migration of O-acetyl groups is catalyzed by acid and base [1,3] and is also promoted by elevated temperature.[5] The number and position(s) of the O-acetyl groups can be determined by NMR since the O-acetyl function exerts a deshielding effect and the assignments may be facilitated by using lanthanide shift reagents.[6,7] Recently, a method was introduced by de Belder and Norrman in which the free hydroxyl groups are converted into acetal functions. The acetalized compound is then treated with base and methylated and, after hydrolysis, the resulting partially methylated sugars

can be analyzed as their alditol acetates, by gas-liquid chromatography (GLC) and mass spectrometry (MS).[8]

In the present paper we describe the separation and analysis of several O-acetylated glycosides, as their trimethylsilyl ethers, by GLC. The number and position(s) of the O-acetyl groups were determined by MS.

The various acetates used in this study were all available from previous work [9,10] and their synthesis will therefore not be repeated here. The relative retention times of the methyl hexopyranosides acetates on GLC are given in Table 1. The column used (OV 225) generally gives adequate separations for analytical purposes.

*Table 1.* Relative GLC retention times of acetylated methyl glycosides as their trimethylsilyl derivatives.

| Position of O-acetylation | GLC retention time[a] | | | | | | |
|---|---|---|---|---|---|---|---|
| | 2 | 3 | 4 | 6 | 2,3 | 3,6 | 4,6 |
| Methyl glycopyranoside of: | | | | | | | |
| α-D-Galactose | 2.09 | 2.77 | — | 2.42 | 5.23 | 8.35 | 3.59 |
| β-D-Galactose | 4.25 | 2.42 | 1.60 | 2.43 | 6.84 | — | 4.31 |
| α-D-Glucose | 2.07 | 1.64 | 2.75 | 4.10 | 5.25 | — | 7.77 |
| β-D-Glucose | 3.48 | 2.32 | 2.73 | 3.45 | — | — | 7.46 |
| α-D-Mannose | 1.11 | 1.67 | 1.54 | 1.89 | — | — | 4.45 |
| β-D-Mannose | 2.23 | 1.32 | — | — | 4.86 | — | — |

[a] on an OV-225 (S.C.O.T.) column at 165° relative to methyl tetra-O-(trimethylsilyl)-α-D-glucopyranoside.

The ions obtained, by electron impact mass spectrometry, from methyl D-hexopyranosides acetylated in the 2-, 3-, 4-, 6-, 2,3-, 3,6-, and 4,6-positions are given in Table 2. Since variations in the configurations of the molecules only gave rise to minor variations in the relative abundance of the ions obtained, only the MS for the methyl β-galactopyranosides (α-anomer of the 3,6-diacetate) are given in Table 2. The fragmentation patterns observed are analogous to those observed by DeJongh and co-workers for methyl glycoside trimethylsilyl ethers.[11] Mass differences are observed, however, owing to the replacement of O-trimethylsilyl groups by O-acetyl groups and also by the elimination of acetic acid and ketene during the fragmentation of the O-acetylated glycosides. In the following discussion, the nomenclature proposed by Kochetkov and Chizhov [12] is used.

For the monoacetates, ions are produced from the parent ion ($M^{\cdot+}$) corresponding to ($M^{\cdot+} - CH_3^{\cdot}$), ($M^{\cdot+} - CH_3^{\cdot} - CH_3OH$), ($M^{\cdot+} - CH_3^{\cdot} - CH_3COOH$), ($M^{\cdot+} - CH_3^{\cdot} - CH_3OH - CH_3COOH$) and [$M^{\cdot+} - CH_3^{\cdot} - CH_3COOH - (CH)_3-SiOH$]. The parent ions ($M^{\cdot+}$] were not observed.

The A-series type of fragmentation produces a fragment $m/e$ 331 ($A_2$) for the 2-, 3-, and 6-acetates.

$$M^{\cdot+} \xrightarrow{\ -\cdot OCH_3\ } A_1 \xrightarrow{\ -TMSOH\ } A_2^1\ m/e\ 331$$
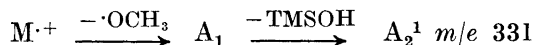
*Table 2.* Fragments obtained on MS of acetylated methyl glycosides as their trimethylsilyl derivatives.

| m/e | Relative peak intensities [a] | | | | m/e | Relative peak intensities [a] | | | |
| | 2-acetate | 3-acetate | 4-acetate | 6-acetate | | 2-acetate | 3-acetate | 4-acetate | 6-acetate |
| --- | --- | --- | --- | --- | --- | --- | --- | --- | --- |
| 437 | 0.2 | 0.2 | 0.2 | 0.1 | 203 | 4 | 2 | — | — |
| 405 | 0.2 | 0.1 | 0.3 | 0.2 | 199 | — | 1 | — | — |
| 378 | 0.4 | — | — | 0.2 | 193 | — | 2 | — | — |
| 377 | 0.5 | 1.5 | 0.3 | 0.4 | 192 | — | 4 | — | — |
| 363 | 0.2 | 0.8 | — | — | 191 | 10 | 21 | 4 | 3 |
| 362 | — | — | — | 0.2 | 189 | 5 | 3 | 3 | 3 |
| 361 | — | 0.3 | — | 0.4 | 187 | 3 | — | — | — |
| 349 | 0.6 | — | — | — | 185 | — | 2 | — | 2 |
| 347 | 1.1 | — | 0.2 | 0.3 | 175 | 5 | 5 | — | 4 |
| 346 | — | — | 0.2 | — | 174 | 12 | 28 | — | — |
| 345 | 0.7 | 0.9 | 0.8 | 0.4 | 173 | — | 2 | — | — |
| 335 | 0.8 | 0.9 | — | 0.4 | 171 | 3 | 2 | — | — |
| 334 | 1.5 | 2.9 | — | — | 169 | — | 3 | 2 | — |
| 333 | 5.0 | 7.9 | 0.5 | — | 163 | — | 2 | — | — |
| 332 | 0.6 | 3.2 | 0.3 | 0.3 | 161 | 3 | 2 | 3 | — |
| 331 | 0.6 | 1.3 | — | 0.6 | 159 | 6 | 4 | 2 | 3 |
| 319 | — | — | — | 1.2 | 157 | — | 3 | 2 | 2 |
| 318 | 0.6 | — | 0.2 | 1.6 | 155 | — | 3 | 3 | 1 |
| 317 | 1.4 | 0.8 | 0.9 | 5.3 | 149 | 4 | 4 | 3 | 3 |
| 306 | 0.8 | — | — | 0.7 | 148 | 5 | 3 | 2 | 3 |
| 305 | 3.1 | 0.6 | 0.2 | 2.6 | 147 | 32 | 27 | 16 | 23 |
| 304 | 1.4 | — | — | — | 146 | — | 4 | 2 | 4 |
| 303 | 5.3 | — | 0.5 | — | 145 | 9 | 4 | 5 | 5 |
| 291 | 0.5 | — | 0.7 | 0.6 | 143 | 4 | 5 | 4 | 3 |
| 290 | — | — | — | 0.5 | 142 | — | 13 | 9 | — |
| 289 | 1.3 | 2.0 | 0.6 | 0.3 | 135 | — | — | — | 1 |
| 288 | — | 0.9 | 0.7 | 0.3 | 134 | 3 | 4 | 2 | 2 |
| 287 | 1.2 | 2.7 | 2.3 | 1.1 | 133 | 19 | 18 | 22 | 23 |
| 276 | — | 0.7 | — | — | 132 | 43 | 69 | 6 | — |
| 275 | 1.0 | 2.4 | — | — | 131 | 5 | 6 | 5 | 4 |
| 274 | 0.5 | 1.8 | — | — | 130 | — | 4 | — | 1 |
| 273 | 1.8 | 2.4 | 1.0 | 0.5 | 129 | 11 | 34 | 8 | 8 |
| 272 | — | — | — | 0.4 | 119 | 2 | 4 | 6 | — |
| 271 | — | 1.5 | — | 1.2 | 118 | 2 | 2 | 2 | — |
| 265 | 0.7 | — | — | — | 117 | 16 | 26 | 28 | 5 |
| 261 | 1.3 | 1.4 | 2 | — | 116 | 4 | 7 | 3 | 2 |
| 260 | 3.7 | 1.2 | 8 | 1.2 | 115 | — | — | — | 1 |
| 259 | 1.1 | 1.0 | — | 0.5 | 113 | — | 2 | — | 2 |
| 257 | — | 0.8 | — | — | 103 | 14 | 11 | 8 | 3 |
| 248 | — | — | — | — | 101 | 3 | 3 | 3 | 2 |
| 247 | 4 | 2 | — | 1 | 95 | 2 | 2 | 3 | 11 |
| 246 | 1 | — | — | — | 93 | 5 | 6 | 8 | 5 |
| 245 | 5 | 3 | 2 | — | 89 | 6 | 11 | 9 | 5 |
| 244 | 2 | 5 | 3 | — | 85 | — | — | — | 2 |
| 243 | 4 | 11 | 5 | 2 | 81 | 3 | 2 | 3 | 3 |
| 233 | 1 | — | 1 | — | 75 | 18 | 24 | 28 | 15 |
| 232 | — | 2 | 2 | — | 74 | 9 | 6 | 7 | 5 |
| 231 | 4 | 3 | 8 | — | 73 | 100 | 100 | 100 | 73 |
| 230 | 2 | 3 | — | — | 72 | — | 2 | 2 | — |
| 229 | — | — | — | — | 71 | — | 1 | — | — |
| 220 | — | 2 | — | — | 69 | — | 2 | 3 | — |
| 219 | 9 | 8 | — | 3 | 61 | — | — | — | 1 |
| 218 | 31 | 24 | — | 8 | 59 | 5 | 6 | 5 | 4 |
| 217 | 39 | 61 | 3 | 43 | 55 | — | 2 | — | 2 |
| 207 | — | — | — | 3 | 45 | 8 | 7 | 8 | 6 |
| 206 | — | — | 8 | 8 | 44 | 7 | 6 | 5 | 4 |
| 205 | 6 | 3 | 26 | 22 | 43 | 16 | 15 | 21 | 16 |
| 204 | 7 | 2 | 99 | 100 | | | | | |

*Table 2. Continued*

| $m/e$ | Relative peak intensities [a] 2,3-acetate | 3,6-acetate | 4,6-acetate | $m/e$ | Relative peak intensities [a] 2,3-acetate | 3,6-acetate | 4,6-acetate |
|---|---|---|---|---|---|---|---|
| 407 | 0.2 | — | 0.4 | 187 | 14 | — | 2 |
| 375 | 0.1 | 1.0 | 0.1 | 185 | 3 | 4 | — |
| 348 | 0.2 | — | — | 183 | 3 | 5 | 2 |
| 347 | 0.2 | 0.5 | 0.4 | 175 | 4 | 8 | 5 |
| 333 | 0.3 | 1.0 | — | 174 | — | 25 | — |
| 322 | — | 2.1 | — | 173 | 4 | — | — |
| 319 | 0.6 | — | — | 172 | 3 | — | — |
| 317 | 0.6 | — | — | 171 | 16 | — | — |
| 314 | — | — | 0.7 | 170 | 7 | — | — |
| 306 | 0.8 | — | — | 169 | 3 | — | — |
| 305 | 3.5 | — | — | 161 | 4 | — | 3 |
| 304 | 1.4 | — | — | 159 | 4 | 5 | — |
| 303 | 3.9 | 2.1 | — | 158 | 6 | — | — |
| 302 | 0.6 | 2.1 | — | 157 | 7 | — | — |
| 301 | 0.6 | — | — | 155 | 5 | 7 | 6 |
| 291 | 1.3 | — | — | 149 | 5 | — | — |
| 289 | 0.8 | 2.1 | — | 148 | 3 | — | — |
| 288 | 0.5 | — | 0.5 | 147 | 23 | 7 | 8 |
| 287 | 2.5 | 5 | 2.8 | 146 | 3 | 13 | 3 |
| 275 | 0.8 | — | — | 145 | 27 | 22 | 5 |
| 274 | 1.4 | — | — | 143 | 6 | 7 | 4 |
| 273 | 5.2 | 4 | 0.4 | 142 | — | 13 | 11 |
| 272 | — | — | 0.4 | 134 | — | 6 | 3 |
| 271 | — | 3 | 0.4 | 133 | 13 | 25 | 21 |
| 262 | 1.3 | — | 0.9 | 132 | 9 | 89 | 4 |
| 261 | 5.0 | — | 3.1 | 131 | 4 | 8 | 3 |
| 260 | — | — | 9.5 | 130 | 3 | — | — |
| 259 | 2.6 | — | — | 129 | 23 | 23 | 3 |
| 257 | 1.3 | — | 1.1 | 119 | 9 | 6 | 6 |
| 246 | 1 | — | — | 118 | 3 | 7 | — |
| 245 | 4 | 5 | 1 | 117 | 41 | 48 | 17 |
| 244 | 1 | 7 | — | 116 | 7 | 11 | 4 |
| 243 | 5 | 33 | 2 | 115 | 3 | — | 2 |
| 242 | 2 | — | — | 113 | 3 | — | — |
| 241 | — | 3 | — | 112 | 4 | — | — |
| 233 | — | — | 1 | 109 | — | — | 2 |
| 231 | 3 | — | — | 103 | 19 | 4 | 3 |
| 230 | 2 | — | — | 101 | 5 | 5 | 2 |
| 221 | — | — | 1 | 95 | 4 | 5 | 2 |
| 220 | 3 | — | — | 93 | 8 | 14 | 5 |
| 219 | 8 | 6 | — | 89 | 8 | 13 | 5 |
| 218 | 29 | 11 | — | 87 | 8 | — | — |
| 217 | 29 | 51 | 2 | 85 | 4 | 4 | 2 |
| 215 | 4 | — | — | 81 | 6 | 8 | 4 |
| 213 | 4 | — | — | 75 | 29 | 43 | 19 |
| 206 | — | — | 7 | 74 | 10 | 9 | 7 |
| 205 | 6 | 6 | 16 | 73 | 100 | 100 | 67 |
| 204 | — | 6 | 100 | 69 | — | — | 3 |
| 203 | 4 | — | — | 61 | 3 | 4 | — |
| 201 | — | — | 3 | 59 | 7 | 9 | 4 |
| 199 | 3 | — | — | 55 | 3 | 4 | — |
| 191 | 8 | 7 | — | 45 | 13 | 16 | 7 |
| 189 | 5 | — | 3 | 44 | 14 | 36 | 10 |
| 188 | 3 | 5 | — | 43 | 84 | 73 | 44 |

[a] Peaks of relative intensity $<1$ were omitted below $m/e$ 250.

Other types of $A_2$-fragments, at $m/e$ 361, are also given by the 3- and 6-acetates, by the elimination of acetic acid from the $A_1$-fragment.
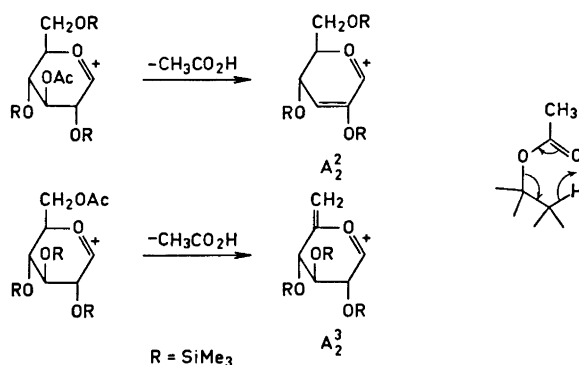


In the ensuing fragmentation, $A_2{}^2$ and $A_3{}^2$ can lose a molecule of trimethyl silanol [TMSOH (90)] yielding $A_3$-fragments at $m/e$ 271.

Fragments corresponding to the B-, C-, D- and E-series are weak. Strong fragments derived from the H- and K-series type of fragmentation are observed (Tables 2 and 3).

In order to distinguish between the monoacetates, reference may be made to the spectra in Table 2. Alternatively, the substitution pattern of a fully trimethylsilylated methyl hexopyranoside monoacetate may be unequivocally determined from some of the most abundant fragments (Table 3).

Table 3. Abundant fragments obtained from monoacetylated methyl glycosides as their trimethylsilyl derivatives.

| Frag-ment ($m/e$) | Probable major structure (TMS = $(CH_3)_3Si$-) | Relative peak intensities | | | |
|---|---|---|---|---|---|
| | | 2-acetate | 3-acetate | 4-acetate | 6-acetate |
| 219 | [TMSO − ·CHCH$_2$CH$_2$OTMS]$^+$ | 9 | 8 | — | 3 |
| 218 | [TMSO − CH = CHCH$_2$OTMS]$^+$ | 31 | 24 | — | 8 |
| 217 | [TMSO − CH = CH − CH = OTMS]$^+$ | 39 | 61 | 3 | 43 |
| 205 | [TMSO − ·CH − CH$_2$OTMS]$^+$ | 6 | 3 | 26 | 22 |
| 204 | [TMSO − CH = CH − OTMS]$^+$ | 7 | 2 | 99 | 100 |
| 174 | [TMSO − CH = CH − OAc]$^+$ | 12 | 28 | — | — |
| 142 | Probably $C_3 - C_4$ fragm. | — | 13 | 9 | — |
| 132 | [TMSO − CH$_2$CHO]$^+$ | 43 | 69 | 6 | — |

The molecular ions of the diacetates are not seen, but fragments are obtained corresponding to $(M^{·+} - CH_3{}^· - CH_3COOH)$. The $A_1$-, B-, C-, D-, and E-series of fragments are only found in low abundance. The position of the

*O*-acetyl groups can readily be determined by inspection of the H- and K-type fragments (Table 4) or from a comparison with the reference spectra.

*Table 4.* Abundant fragments obtained from diacetylated methyl glycosides as their trimethylsilyl derivatives.

| Fragment (m/e) | Probable major structure (TMS = (CH₃)₃Si-) | Relative peak intensities 2,3-acetate | 3,6-acetate | 4,6-acetate |
|---|---|---|---|---|
| 243 | possibly $M^{.+}$ – TMSO$^{.}$ – TMSOH | 5 | 33 | 2.5 |
| 218 | [TMSO – CH = CH – CH₂OTMS]⁺ | 29 | 11 | – |
| 217 | [TMSO – CH = CH – CH = OTMS]⁺ | 29 | 51 | 2 |
| 204 | [TMSO – CH = CH – OTMS]⁺ | – | 6 | 100 |
| 174 | [AcO – CH = CH – OTMS]⁺ | – | 25 | – |
| 171 | – | 16 | – | – |
| 147 | [(CH₃)₃SiOSi(CH₃)₂]⁺ | 23 | 7 | 8 |
| 145 | – | 27 | 22 | 5 |
| 142 | Probably $C_3 - C_4$ fragm. | – | 13 | 11 |
| 132 | [TMSO – CH₂CHO]⁺ | 9 | 89 | 4 |
| 129 | [TMSO – ·CH – CH = CH₂]⁺ | 23 | 23 | 3 |

## EXPERIMENTAL

The various glycoside acetates were available from previous studies.[9],[10] They were converted into the fully trimethylsilylated derivatives as described by Sweeley.[13] GLC was performed on a Perkin-Elmer 900 instrument fitted with an OV-225 S.C.O.T. column at 165°. The mass spectra, using a Perkin-Elmer 270 gas chromatograph mass spectrometer, were recorded at a manifold temperature of 200°, an ionization potential of 70 eV, an ionization current of 80 μA and an ion source temperature of 120°.

## REFERENCES

1. Wolfrom, M. L. and Szarek, W. A. In Pigman, W. and Horton, D., Eds., *The Carbohydrates. Chemistry and Biochemistry.* Academic, New York and London 1972, Vol. 1A, p. 217.
2. Paulsen, H., Behre, H. and Herold, C.-P. *Fortsch. Chem. Forsch.* **14** (1970) 472.
3. Sugihara, J. M. *Advan. Carbohyd. Chem.* **8** (1953) 1.
4. Bouveng, H. O., Lindberg, B. and Theander, O. *Acta Chem. Scand.* **11** (1957) 1788.
5. Garegg, P. J. *Arkiv Kemi* **23** (1964) 255.
6. Butterworth, R. F., Pernet, A. G. and Hanessian, S. *Can. J. Chem.* **49** (1971) 981.
7. Borén, H. B., Garegg, P. J., Pilotti, Å. and Swahn, C.-G. *Acta Chem. Scand.* **26** (1972) 3261.
8. de Belder, A. N. and Norrman, B. *Carbohyd. Res.* **8** (1968) 1.
9. Borén, H. B., Garegg, P. J., Kenne, L., Maron, L. and Svensson, S. *Acta Chem. Scand.* **26** (1972) 644.
10. Borén, H. B., Garegg, P. J., Kenne, L., Pilotti, Å., Svensson, S. and Swahn, C.-G. *Acta Chem. Scand.* **27** (1973) 2740.
11. De Jongh, D. C., Radford, T., Hritar, J. D., Hanessian, S., Preber, M., Dawson, S. and Sweeley, C. C. *J. Am. Chem. Soc.* **91** (1969) 1728.
12. Kochetkov, N. K. and Chizhov, O. S. *Advan. Carbohyd. Chem.* **21** (1966) 39.
13. Sweeley, C. C., Bentley, R., Makita, M. and Wells, W. W. *J. Am. Chem. Soc.* **85** (1963) 2487.

# Cadmium-Imidazole Complex Formation in Aqueous Solutions. Preparation and Characterization of Compounds with Five and Six Ligands

JØRGEN BIRGER JENSEN

*Fysisk-Kemisk Institut, DTH 206, DK-2800 Lyngby, Denmark*

The fifth and sixth complex compound between cadmium and imidazole have been isolated and characterized. The counterions were perchlorate and nitrate, respectively. With chloride as counterion in the corresponding complex compound the Cd-ion probably enters the crystal lattice in an oxidation state lower than 2.

The formulas of the fifth and sixth complex compound were found to be Cd $im_5aq(ClO_4)_2$ and Cd $im_6(NO_3)_2$, respectively (im = imidazole). Concerning the complex compound with chloride as counterion the formula $Cd_4^{II}(Cd_2^{I})im_{28}Cl_{10}$ is suggested.

Reactions in which divalent Cd-ions may undergo reductions to a lower oxidation state than 2 are discussed.

From analysis of the polarographic results from the cadmium-imidazole system and estimation of activity coefficients of imidazole it was shown in a previous paper [1] that the maximum coordination number of the Cd-ion against imidazole was 6.

In order to support the results from the polarographic studies our efforts have been directed towards the preparation of complex compounds with five and six imidazole ligands per cadmium ion by suitable synthetical methods. To our knowledge none of these compounds have previously been isolated.

Earlier it was reported [2] that $Cd^{2+}$-ethylenediamine complexes form slightly soluble perchlorates and nitrates. Therefore our experiments have been concentrated mainly on these two ions. In addition, some experiments have been carried out with chloride.

## EXPERIMENTAL

*Preparations.* According to Leden [3] Cd(ClO$_4$)$_2$ was prepared by dissolving CdCO$_3$ in HClO$_4$. The crude product was recrystallized by dissolving in hot water and cooling in an ice bath. The Cd-content was controlled by potentiometric titrations. All other chemicals mentioned below were of reagent grade and were used without further purification. The temperature was kept constant at $25 \pm 0.1°C$ by means of a thermostated water-bath.

1. The perchlorate precipitate was prepared by dissolving 0.5 mol imidazole into 1 liter well-stirred 1.0 M NaClO$_4$. pH was adjusted to 9.5 by addition of HClO$_4$ using a glass electrode. To this solution, 1 ml 1.0 M Cd(ClO$_4$)$_2$ was added. Immediately a white, voluminous precipitate was formed. This precipitate was isolated by filtration, quickly washed with cooled ethanol and dried in vacuum. (Found: Cd $17.0 \pm 0.2$; im $51.5 \pm 0.5$; ClO$_4$ $29.4 \pm 1$. Calc. for Cd im$_5$aq (ClO$_4$)$_2$: Cd 16.8; im 50.8; ClO$_4$ 29.7). The term im is used as an abbreviation for the unprotonated imidazole molecule.

2. The nitrate precipitate was prepared by dissolving 0.5 mol imidazole into 1 liter well-stirred 1.0 M NaNO$_3$ and adjusting the pH to 9.5 by adding HNO$_3$. 10 ml 1.0 M Cd(NO$_3$)$_2$ was added. After stirring for about $10-15$ min, a crystalline precipitate appeared. The precipitate was isolated by filtration, washed with ethanol and dried in vacuum. (Found: Cd $17.2 \pm 0.2$; im $64.0 \pm 0.5$; NO$_3$ $19.4 \pm 0.5$. Calc. for Cd im$_6$(NO$_3$)$_2$: Cd 17.4; im 63.3; NO$_3$ 19.2).

3. In a stirred solution of 1 liter 0.5 M imidazole at an ionic strength 1.0 established with KCl, the pH was adjusted to 9.5 by addition of HCl. Finally, 10 ml 1.0 M CdCl$_2$ was added. The solution was left unstirred and undisturbed, and after 1 or 2 d the crystallization was gradually initiated yielding pale white, almost colourless crystals. The crystallization continued for several days. The crystals were isolated, washed with ethanol and dried in vacuum. (Found: Cd $23.0 \pm 0.2$; im $65.5 \pm 0.5$; Cl $12.0 \pm 0.1$. Calc. for Cd$_4^{II}$(Cd$_2^{I}$)im$_{28}$Cl$_{10}$: Cd 23.0; im 65.0; Cl 12.0).

*Analysis and measurements.* The imidazole analyses were performed on an automatic titration equipment (SBR2, PHM26, TTT11, ABU1, TTA3, Radiometer, Copenhagen, Denmark). The pH was initially adjusted to 3.00 using HClO$_4$, HNO$_3$, and HCl, respectively, and the imidazole content was determined from difference titration curves, *i.e.* the difference between titration curves for complex compounds and acids. To avoid precipitation of Cd(OH)$_2$ the titrations were terminated at approximately pH 9.5. In addition some titrations were carried out on solutions from which the Cd$^{2+}$-ions had beforehand been removed with Na$_2$S.
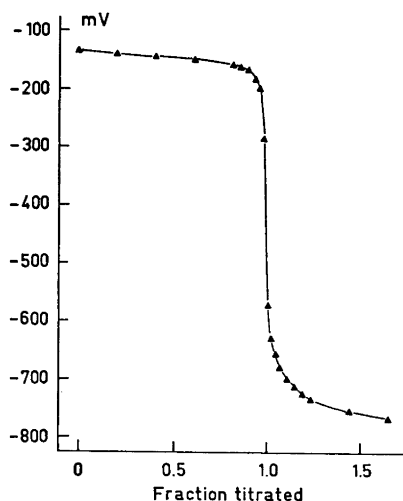


*Fig. 1.* Na$_2$S titrations of CdSO$_4$, $^8/_3$ H$_2$O using Ag/Ag$_2$S as indicator electrode and Hg/Hg$_2$SO$_4$, Na$_2$SO$_4$(s) as reference electrode. The mV-values are converted to values relative to a saturated calomel electrode.

The chloride analyses were carried out by potentiometric titration using Ag/AgCl and $Hg/Hg_2SO_4$, $Na_2SO_4(s)$ electrodes. Likewise, the cadmium analyses were carried out potentiometrically, using the method described by Hiltner and Grundmann.[4] The Ag/$Ag_2S$ electrode was prepared from a silver pellet electrode (Radiometer P4011) on which $Ag_2S$ was deposited by electrolysis. By means of this electrode the cadmium ions could be determined very precisely by potentiometric titrations [4] using a $Hg/Hg_2SO_4$, $Na_2SO_4(s)$ electrode as reference electrode. Duplicate experiments showed that it was possible to determine the cadmium content with a reproducibility of about 0.5 %. A titration curve is shown in Fig. 1. The potentials are converted to values relative to a saturated calomel electrode. Regarding the $Ag/Ag_2S$ electrode as a second order electrode, the electrode potential can be calculated from the Nernst-equation:

$$(\pi - \psi) = \pi^0 - 29.56 \log a_{S^{2-}} \quad (25°C)$$

where $(\pi - \psi)$ indicated the electrode potential, expressed in mV, $\pi^0$ the oxidation potential at $a_{S^{2-}} = 1$, and $a_{S^{2-}}$ the activity of sulphide ion. According to Latimer [5] $\pi^0$ has the value $-690$ mV $vs.$ normal hydrogen electrode at ionic strength $= 0$. At the equivalence point $a_{S^{2-}} = a_{Cd^{2+}} = (L_{CdS})^{\frac{1}{2}}$ where $L_{CdS}$ is the solubility product of CdS. Using this information the potential at the equivalence point of the titration curve was calculated to approx. $-475$ mV $vs.$ saturated calomel electrode in good agreement with the experimental results shown in Fig. 1. The freezing point measurements were carried out on a Fiske osmometer (Fiske Associates, Inc., Uxbridge, Mass. USA), and vapour pressure measurements on a Knauer osmometer (H. Knauer & Co., GmbH, Berlin, BRD). The DTA measurements were carried out on a DTA-equipment from Bureau de Liaison, Paris. The absorbance spectra were obtained on a Beckmann DB spectrophotometer. Nitrate and perchlorate analyses were performed using nitron as described by Busch.[6]

## RESULTS AND DISCUSSION

*The complex compound from the perchlorate solution,* here abbreviated as Cd-im-ClO$_4$, crystallizes easily in white very voluminous threads almost like cotton. In all probability the crystals can be classed within the monoclinic crystal group. The solubility of Cd-im-ClO$_4$ is strongly dependent on temperature. This gave us a convenient way to determine its solubility product. A solution containing $5 \times 10^{-4}$ M $Cd(ClO_4)_2$, 1.0 M $NaClO_4$, and 0.5 M imidazole at pH $= 9.5$ and 25°C is just saturated and without precipitate. When lowering the temperature to 23°C white crystals of Cd-im-ClO$_4$ are formed. However, they redissolve when the temperature is raised to 25°C. Earlier [1] it was shown that in a solution of the above mentioned composition only about 24 % of the cadmium ions are in the $Cd im_5 aq^{2+}$ form. Since the experiments were carried out in a 1.0 M $NaClO_4$ solution it may be assumed that the activity coefficients of all the ions present in the solution are determined by the $NaClO_4$. Assuming that $\log \gamma_{Cd\,im_5aq(ClO_4)_2} = 3 \log \gamma_{NaClO_4}$ is valid in the present solution we are able to calculate the solubility product by means of tabulated values for $\gamma_{NaClO_4}$ from Robinson and Stokes [7]

$$L_{sp} = c_{Cd\,im_5aq^{2+}} c_{ClO_4^-}{}^2 \gamma_{NaClO_4}{}^3 = \text{approx. } 2 \times 10^{-5} \text{ mol}^3/\text{l}^3$$

This is in good agreement with the results shown in Table 1 where the solubility of the Cd-im-ClO$_4$ in 0.1 M HClO$_4$ is tabulated together with the solubilities of the NO$_3^-$ and Cl$^-$ complex compounds in 0.1 M of their corresponding acids, *i.e.* 0.1 M HNO$_3$ and 0.1 M HCl, respectively, to prevent precipitation of Cd(OH)$_2$.

*Table 1.* The solubilities of the investigated cadmium imidazole complex compounds in 0.1 M of their corresponding acids. $t = 25°C$. +indicates formation of precipitates, −indicates no precipitate.

| Concentration of complex compounds mol/l | Counterion (in brackets the corresponding acid) | | |
|---|---|---|---|
| | $ClO_4^-$ $(HClO_4)$ | $Cl^-$ $(HCl)$ | $NO_3^-$ $(HNO_3)$ |
| 0.05 | − | − | − |
| 0.1 | + | (+) very little precipitate formed | − |
| 0.2 | + + | + + | + |

In Fig. 2 is shown the mol percentage of individual cadmium-imidazole complexes as a function of log of imidazole activity at ionic strength 1.0 with sodium perchlorate. From this figure it appears that the fifth complex compound has its maximum value at $C_{im} \cong 4.0 \times 10^{-1}$ M ($a_{im} \cong 3.5 \times 10^{-1}$ M). In
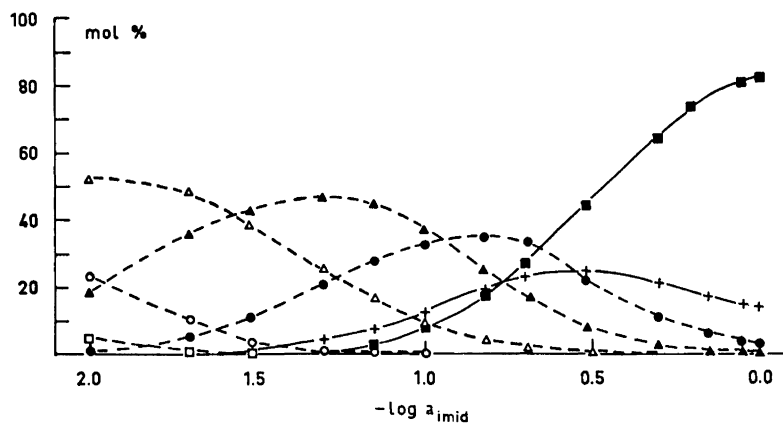


*Fig. 2.* Percentage of individual cadmium-imidazole complexes as a function of log of imidazole activity. Ionic strength = 1.0 with sodium perchlorate. Total Cd-contents = $5 \times 10^{-4}$ M, pH = 9.5, $t = 25°C$. Only the last two curves are fully drawn up. For details: see text. Explanation of symbols: □ Cd $aq_6^{2+}$, ○ Cd $imaq_5^{2+}$, △ Cd $im_2aq_4^{2+}$, ▲ Cd $im_3aq_3^{2+}$, ● Cd $im_4aq_2^{2+}$, + Cd $im_5aq^{2+}$, ■ Cd $im_6^{2+}$.

other words when more imidazole is added to a solution of 0.4 M imidazole with a small precipitate of Cd $im_5aq(ClO_4)_2$ it must be expected that precipitate would redissolve due to the reaction Cd $im_5aq^{2+} + im \rightarrow$ Cd $im_6^{2+} + aq$, *i.e.* the solubility product of Cd $im_5aq(ClO_4)_2$ is no longer exceeded. This is actually what happens: In a solution of 0.1 M imidazole, $1.0 \times 10^{-3}$ M Cd$(ClO_4)_2$, and 1.0 M NaClO$_4$ at 25°C and pH = 9.5 no precipitate is found. When more imidazole is added stepwise, the precipitation starts at 0.2 M, the maximum value

being reached at 0.4 M. At a concentration of imidazole of 1.0 M the precipitate has dissolved again. The fact that the formation curve in Fig. 2 may be reconstructed in this way supports the result from the analyses and makes it very likely that the precipitate has the postulated composition, Cd im$_5$aq(ClO$_4$)$_2$ a postulate which is further supported by freezing point and vapour pressure measurements.

Fig. 3 shows the results from the freezing point measurements. Curve B represents the points measured directly, and in curve A the points are cor-
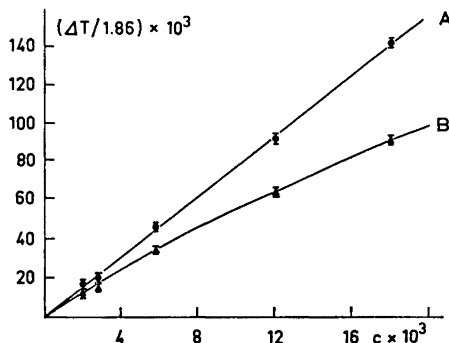


Fig. 3. Dependence of the freezing point depression of the perchlorate complex on the concentration of this complex. Curve B: measured values. Curve A: The measured values corrected for complex formation by which a straight line is formed. The slope of this line has the value 7.85 indicating the formula Cd im$_5$aq(ClO$_4$)$_2$ for the complex compound.

rected for complex formation by means of which a straight line is formed. The slope of this line has the value 7.85 indicating that the most likely number of dissociated particles from the investigated compound is 8 in agreement with the previously mentioned composition. The results from vapour pressure



Fig. 4. Vapour pressure measurements on the perchlorate complex. The dotted line with open circles represents values from measurements on sodium chloride solutions. The horizontal dotted line represents the same values corrected for osmotic coefficients. The condition that all the curves must coincide at infinite dilution is seen to be fulfilled only when $v$ is given the value 8, corresponding to the formula Cd im$_5$aq (ClO$_4$)$_2$ for the perchlorate complex. The letter R on the ordinate axis indicates the measured value in arbitrary units.
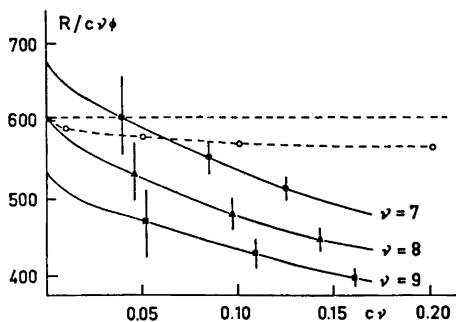
measurements are represented in Fig. 4. The calibration curve based on measurements on NaCl is shown as dotted lines. When extrapolated to infinite dilution the curves must coincide at a point on the ordinate axis determined by the NaCl curve. This condition can only be fulfilled when $v$ is given the value 8.

Care must be taken when $Cd\,im_5aq(ClO_4)_2$ is prepared to avoid precipitation of complex compound coordinated with six im-molecules, i.e. $Cd\,im_6(ClO_4)_2$. From Fig. 2 it appears that in a solution of 1.0 M imidazole, 1.0 M $NaClO_4$, and $5 \times 10^{-4}$ M $Cd(ClO_4)_2$ at pH = 9.5 the larger part of the cadmium ions is coordinated with six im, whereas only a small amount has five im. In this solution, no precipitation was observed at 25°C. When adding more $Cd(ClO_4)_2$ to a well-stirred solution of this composition white crystals are formed at once. When analyzed in the normal way the precipitate turns out to be an inhomogeneous mixture of the fifth and sixth complex compound. In other words by this procedure the solubility product is exceeded for the perchlorates of both of the two complexes.

Results from solubility experiments in organic solvents showed that $Cd\,im_5aq(ClO_4)_2$ is very soluble in both ethanol and acetone but almost insoluble in ether. The heat stability has been examined by DTA measurements. The temperature was increased from 25°C to 130°C. According to the results from these experiments $Cd\,im_5aq(ClO_4)_2$ is stable up to 110°C. At 120°C a weak exothermic reaction occurs, probably caused by decomposition. Analyses (of $Cd^{2+}$, im, and $ClO_4^-$) on crystals, which were kept at 100°C for 24 h, and on vacuum dried crystals, gave identical results.

*The complex compound from the nitrate solution* forms trigonal, optically active, almost colourless crystals built as parallelepipedons. According to the results from analyses the crystals were identified as the six-coordinated complex compounds, i.e. $Cd\,im_6(NO_3)_2$, and only this compound was found in the precipitate from the nitrate solutions. This indicates greater solubility of $Cd\,im_5aq(NO_3)_2$ compared with $Cd\,im_6(NO_3)_2$ contrary to what was the case in perchlorate solutions. Consequently, in nitrate solutions, more crystals are formed when more imidazole is added, contrary to what happened in perchlorate solutions where the almost insoluble $Cd\,im_5aq(ClO_4)_2$ in this way was converted to the more soluble $Cd\,im_6(ClO_4)_2$ and the crystals disappeared.

The solubility of $Cd\,im_6(NO_3)_2$ is strongly temperature dependent, just as that of the perchlorate complex, and the solubility product could therefore be determined by the same method. The solubility product was calculated to

$$L_{sp} = c_{Cd\,im_6^{2+}}\ c_{NO_3}^{-2}\ \gamma_{NaNO_3}^{3} \cong 4 \times 10^{-4}\ mol^3/l^3$$

Table 1 summarizes the solubilities of $Cd\,im_6(NO_3)_2$ in 0.1 M $HNO_3$. Results from solubility experiments in organic solvents showed that $Cd\,im_6(NO_3)_2$ is very soluble in ethanol but almost insoluble in acetone and ether.

The DTA measurements showed that $Cd\,im_6(NO_3)_2$ was stable up to a temperature of 80°C where a weak endothermic reaction occurred and the compound got an amorphous plastic-like consistency. At approximately 100°C the colour changed from white to yellow. All the crystals were lost and a yellow liquid was formed. When cooled no crystals were reformed whereas the result was an amorphous glass-like solid.

*The complex compound from the chloride solutions* form crystals which most probably can be classed within the hexagonal crystal group. According to results from analyses the only way to explain the electroneutrality for the crystals is to assume that cadmium is present in the crystal partly as ions in a lower oxidation state than 2.

The existence of the monovalent cadmium ion is established in the literature.[5] Grantham [8] demonstrated that the cadmium dimer ion $Cd_2^{2+}$ is extremely stable in $Cd\text{-}CdCl_2$ melts at temperatures near the freezing point of the salt. Very recently [9,10] it has been suggested that when cadmium and zinc are electrolytically dissolved in alkaline solutions, monovalent ions are found in both cases. In accordance with this, the composition of the precipitate formed in the system containing 0.01 M $CdCl_2$, 0.5 M imidazole, and 1.0 M KCl at pH = 9.5 is assumed to have the formula $Cd_4^{II}(Cd_2^{I})im_{28}Cl_{10}$. This assumption is based partly on the results from experiments carried out in this laboratory, partly on the above mentioned investigations.

1. Before the cadmium ion is able to enter the crystal lattice as monovalent ion it must undergo a reduction and, of course, simultaneously another component must be oxidized. Imidazole is known [11] to be very stable to oxidizing agents, and so it is only possible to create monovalent cadmium ions in solutions where the anions can be oxidized. With $Cl^-$ as anion the redox process is supposed to be:

$$2\ Cd^{2+} + 2\ Cl^- \rightleftharpoons Cd_2^{2+} + Cl_2 \tag{1}$$
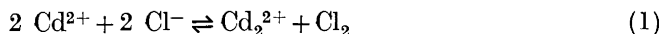
Neither $NO_3^-$ nor $ClO_4^-$ are able to take part in a redox process similar to (1) and consequently $Cd_2^{2+}$ cannot be found in these solutions. The chlorine formed according to reaction (1) will not be identified as free $Cl_2$. According to Albert [11] halogenation of imidazole in alkaline solutions is very brisk, i.e. if the reaction (1) takes place we would expect to find the chlorine bound to imidazole.

Since it might be expected that the absorbance spectrum from this chlorinated imidazole molecule is different from that of the free imidazole, an attempt was made to identify this compound by means of spectrophotometric measurements. In Fig. 5 is shown the UV absorbance spectra from these experiments. No difference in the absorbance spectra was observed in the visible region. Curve A shows the absorbance spectrum of 0.5 M chlorinated imidazole, prepared in this institute, in 1.0 M KCl, pH = 9.5. Curve B shows the absorbance spectrum of 0.5 M pure imidazole in 1.0 M KCl, pH = 9.5. In both
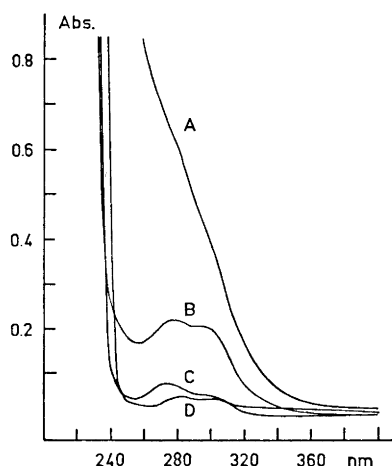


Fig. 5. Absorbance spectra of curve A: 0.5 M chlorinated imidazole in 1.0 M KCl, curve B: 0.5 M imidazole in 1.0 M KCl. Reference solution for A and B: 1.0 M KCl. Curve C: Filtrate from the KCl solution in which the complex compound was precipitated, curve D: 0.5 M imidazole in 1.0 M KCl. Reference solution for C and D: 0.495 M imidazole in 1.0 M KCl. In all solutions pH was 9.5.

curve A and B the reference solution was 1.0 M KCl, pH$\cong$9.5. The solution containing the complex compound as precipitate was filtered through a glass filter, and the filtrate was used in the spectrophotometric measurements. The result appears in curve C. Curve D belongs to pure 0.5 M imidazole in 1.0 M KCl, pH = 9.5. Reference solution in case C and D was solution D diluted with 1% KCl in order to obtain the same concentration of imidazole in solution C and D. Since the difference between the curves C and D is greatest at approx. 270 nm, where also the difference between the curves A and B is very great, the assumption can be made that the solution in which the complex precipitate is formed most likely also contains the chlorinated imidazole compound and consequently Cd-ions in a lower oxidation state than 2 according to eqn. (1).

2. When the crystals formed from complex formation were dissolved in hydrochloric acid, a gas evolution was observed. As suggested by Latimer [8] the gas evolution can be explained by the following reaction:

$$Cd_2^{2+} + 2 \ H^+ \rightleftharpoons 2 \ Cd^{2+} + H_2 \tag{2}$$

This reaction — or a reaction similar to it — also explains why the cadmium ions, when titrated with sodium sulphide, always react as divalent Cd-ions. This appears from titration curves, which indicate only one point of equivalence together with the fact that the total amount of $Cd^{2+}$, imidazole, and $Cl^-$ determined as earlier mentioned yields within the experimental error 100 %. If the Cd-ions should exist in the crystals solely as divalent ions, then the mol ratio between Cl and Cd-ions should be 2:1 in order to fulfill the condition of electroneutrality. Experimentally, we found the ratio 1.67:1, indicating that the cadmium ions are present in the crystal in lower valency than two, possibly as the dimer $Cd_2^{2+}$ as suggested by Grantham.[8] Reaction (2) can also be observed titrimetrically. A difference in base consumption when two specific amounts of hydrochloric acid with and without complex compound are titrated with sodium hydroxide, indicates that some cadmium ions are oxidized and free hydrogen is formed. The results from four such experiments showed that 40 ± 5 % of the Cd-ions were oxidized according to (2).

These experiments involved some uncertainty mainly due to trouble in connection with exclusion of air, but the effect was very clear: less base consumption for titration of hydrochloric acid in the case where the complex compound was dissolved in the acid, in full agreement with reaction (2). At the present time more experiments are prepared in this institute to support the assumption of monovalent Cd-ions. The results from these experiments will be discussed elsewhere but on the basis of the present experiments it seems possible to assume that the Cd-ions exist in the crystal probably in the dimer form $Cd^+ - Cd^+$ similar to the mercuro ions, and so we here propose the formula: $Cd_4^{II}(Cd_2^{I})im_{28}Cl_{10}$. In the DTA measurements the temperature was increased continuously from 25°C to 100°C. From these experiments it appeared that no heat involving reactions occurred within these limits of temperature. The results from the solubility experiments in 0.1 M HCl are summarized in Table 1. Results from solubility experiments in organic solvents showed that $Cd_4^{II}(Cd_2^{I})im_{28}Cl_{10}$ is almost insoluble in ethanol, acetone, and ether. Just like in the case of Cd $im_5aq(ClO_4)_2$ and Cd $im_6(NO_3)_2$ the solubility

of the complex compound with $Cl^-$ as counterion was found to be strongly temperature dependent. Using this information we found the solubility at 25°C to be approximately $5 \times 10^{-2}$ mol $Cd_4^{II}(Cd_2^{I})im_{28}Cl_{10}$ per litre.

## REFERENCES

1. Jensen, J. B. *Acta Chem. Scand.* **26** (1972) 4031.
2. Glöckner, W. *Die Komplexverbindungen*, Aulis Verlag Deubner & Co., KG., Köln, BRD, 1962.
3. Leden, I. *Potentiometrisk undersökning af några kadmiumsalters komplexitet*, Glerupska Univ. Bokhandeln, Lund 1943.
4. Hiltner, W. and Grundmann, W. *Z. physik. Chem.* **168** (1933) 291.
5. Latimer, W. M. *The oxidation states of the elements and their potentials in aqueous solutions*, 2nd Ed., Prentice-Hall, Englewood Cliffs, New Jersey 1952.
6. Busch, M. *Ber.* **38** (1905) 861.
7. Robinson, R. A. and Stokes, R. H. *Electrolyte Solutions*, Butterworths, London 1955.
8. Grantham, L. F. *J. Chem. Phys.* **44** (1966) 1509.
9. Bockris, J. O. M., Nagy, Z. and Damjanovic, A. *J. Electrochem. Soc.* **119** (1972) 285.
10. Azin, A. A. A. and El-Sobki, K. M. *Electrochim. Acta* **17** (1972) 601.
11. Albert, A. *Hetereocyclic Chemistry*, 2nd Ed., The Athlone Press, London 1968.

# Nucleophilic Reactivity

## Part VIII. Kinetics of Reactions of Acetic Anhydride with Nucleophiles in Water

SIRKKA LEPPÄNEN, LIISA STRANDMAN, STINA TAKALA PETRI PAJUNEN and JOUKO KOSKIKALLIO

Department of Physical Chemistry, University of Helsinki, Meritullinkatu 1 C, Helsinki 17, Finland

Rate constants of the reactions of acetic anhydride with the nucleophiles $OH^-$, $PhO^-$, 4-$MePhO^-$, 4-$ClPhO^-$, 4-$NO_2PhO^-$, $PO_4^{3-}$, $CO_3^{2-}$, $HPO_4^{2-}$, $H_2PO_4^-$, and $H_2O$ were measured in aqueous solutions at different temperatures. A linear free energy relationship between the logarithm of the rate constant and the $pK_a$ values of the conjugate acid of the nucleophile was found for a restricted group of reactions. When the leaving group of the substrate was weakly basic (e.g. acetic anhydride and 2,4-dinitrophenyl acetate) the values of the slope of the linear free energy relationship of the reactions of phenyl acetate and nitrosubstituted phenyl acetates with similar nucleophiles were found to be constant, about 0.44, whereas a slope of about 0.56 was obtained when the substrate involved a relatively more strongly basic leaving group (phenyl and 4-nitrophenyl acetates). The experimental second-order rate constant was found to be equal to the rate constant of the formation of the addition intermediate for reactions connected with relatively low values of the slope (0.44). For the steeper slope values (0.56), the experimental rate constant is equal to the product of the rate constant of the formation of the addition intermediate and the ratio of the rate constants of decomposition of the intermediate to products or to starting materials.

## EXPERIMENTAL

*Reaction of acetic anhydride with hydrogen phosphate ion.* Reaction rates were measured with a recording spectrophotometer Beckman DK-2 at 240 nm. Acetic anhydride was added to a 1 cm cell containing a 1:1 molar ratio mixture of potassium dihydrogen phosphate and disodium hydrogen phosphate at constant temperature. The concentration of acetic anhydride was initially about 0.05 M and the total phosphate salt concentrations were varied between 0.01 M and 0.1 M. First-order rate constants were calculated using the Guggenheim method.[1] The second-order rate constants of the reaction between acetic anhydride and hydrogen phosphate ion were obtained from the slope of the plot of the first-order rate constants against the hydrogen phosphate ion concentration. These values are shown in the Table 1. Alkaline hydrolysis and the reaction with dihydrogen phosphate ion are negligible.

This reaction was also studied with a Radiometer TTT1e pH-stat. Acetic anhydride was added at constant temperature to a reaction mixture containing an approximately 10:1 molar ratio mixture of disodium hydrogen phosphate and potassium dihydrogen phosphate. The concentration of anhydride was initially about 0.01 M and the total phosphate salt concentrations were varied from zero to about 0.2 M. The reaction mixture was automatically titrated at constant pH with 0.1 M potassium phosphate solution.

The pH-meter was calibrated at each temperature with three standard buffer solutions,[2] 0.05 M potassium hydrogen phthalate, 0.025 M potassium hydrogen phosphate and disodium hydrogen phosphate, and 0.01 M borax solutions.

The second-order rate constant $k_{HPO_4}$ is equal to the slope of the straight line obtained by plotting the first-order rate constants against the hydrogen phosphate ion concentrations. The values of the rate constants are shown in Tables 1 and 2, as are the rate constants $k_{OH}$ of the alkaline hydrolysis of acetic anhydride obtained by extrapolating the rate constants to zero phosphate concentration. The rate constants $k_{HPO_4}$ obtained by the two different methods differ somewhat because of experimental errors. Kirsch and Jencks[3] have reported a value of $k_{HPO_4} = 148 \times 10^{-3}$ M$^{-1}$ s$^{-1}$ at 25°C.

*Reaction of acetic anhydride with dihydrogen phosphate ion.* The sum of the first-order rate constants of the hydrolysis of acetic anhydride and its reaction with dihydrogen phosphate ion were obtained by the photometric method in solutions containing a large excess of potassium dihydrogen phosphate which was varied between 0.1 M and 1 M. The ratio of the two rate constants was calculated from the analysis of the reaction products of acetic anhydride with water and dihydrogen phosphate ion by hydrolysing the acetyl phosphate produced in the reaction. Values of both rate constants $k_{H_2PO_4}$ and $k_{H_2O}$ could be obtained separately and are shown in Table 1. The value of $k_{H_2PO_4}$ is rather inaccurate because a maximum of about one percent of anhydride reacted with dihydrogen phosphate ion. The increase in the total rate observed when increasing the hydrogen phosphate ion concentration is mainly due to a positive salt effect of the hydrolysis reaction of acetic anhydride.

*Table 1.* Second-order rate constants $k_2$ of reactions of acetic anhydride with nucleophiles N in water at different temperatures.

| N | 5°C | 10°C | 15°C | 25°C | Method |
|---|---|---|---|---|---|
| | | $10^3 k_2$/M$^{-1}$s$^{-1}$ | | | |
| OH$^-$ | 270 000 | | 505 000 | 895 000 | pH-stat, phosphate |
| OH$^-$ | 360 000 | | | 1 110 000 | pH-stat, carbonate |
| PhO$^-$ | | 432 000 | | | pH-stat |
| 4-MePhO$^-$ | | 862 000 | | | pH-stat |
| 4-ClPhO$^-$ | | 419 000 | | | pH-stat |
| 4-NO$_2$PHO$^-$ | | 14 300 | | | pH-stat |
| PO$_4^{3-}$ | 370 | | 1 780 | | product analysis |
| PO$_4^{3-}$ | 580 | | 1 190 | 2 810 | pH-stat |
| CO$_3^{2-}$ | 640 | | 1 550 | 2 500 | pH-stat |
| HPO$_4^{2-}$ | 25 | | 52 | 99 | photom. |
| HPO$_4^{2-}$ | 24.3 | | 57.3 | 144 | pH-stat |
| H$_2$PO$_4^-$ | | | 0.16 | | product analysis |
| H$_2$O | 0.0126 | | 0.0260 | 0.472 | photom. |

*Reaction of acetic anhydride with phosphate and hydroxide ions.* The first-order rate constants of acetic anhydride in reaction mixtures containing potassium phosphate and disodium hydrogen phosphate at constant pH were obtained by the pH-stat method. Four simultaneous reactions should be considered:

$$k = k_{H_2O} + k_{OH}\, c_{OH} + k_{HPO_4}\, c_{HPO_4} + k_{PO_4}\, c_{PO_4} \tag{1}$$

This equation can be rearranged to:

$$(k - k_{H_2O} - k_{HPO_4}\, c_{HPO_4})\, f_{OH} = k_{OH}\, K_w/a_H + k_{PO_4}\, c_{PO_4}\, f_{OH} \tag{2}$$

when $c_{OH}$ is replaced by $K_w/a_H\, f_{OH}$. $a_H$ is constant at constant pH. The activity coefficient $f_{OH}$ was calculated using the following equation:

$$\log f = -A\; z_1^2 \left( \frac{I^{\frac{1}{2}}}{1+I^{\frac{1}{2}}} - bI \right) \tag{3}$$

A value of $b = 0.25$ was used.[4,5] Values of $k_{H_2O}$, $k_{HPO_4}$, $c_{HPO_4}$, and $c_{PO_4}$ are known individually. The rate constant $k_{PO_4}$ was obtained from the slope of a plot of the left side of eqn. 2 against values of $c_{PO_4}\, f_{OH}$. Values of $k_{OH}$ were calculated using the reported [6] values of $K_w$. The results are shown in Tables 1 and 2. The values of $k_{PO_4}$ are inaccurate because of the experimental difficulties in measuring fast reactions by the pH-stat method and in calculating activity coefficients at high ionic strength.

*Table 2.* First-order rate constants $k_1$ and second-order rate constants $k_{HPO_4}$ obtained as intercept and slope, respectively, when plotting the observed first-order rate constants against the disodium hydrogen phosphate concentrations. Values of $k_{PO_4}$ were obtained from slopes when plotting $(k_{obs} - k_{H_2O} - k_{HPO_4}\, c_{HPO_4})\, f_{OH}$ against $c_{PO_4}\, f_{OH}$.

| $T°C$ | pH | $10^3 k_1/s^{-1}$ | $10^3 k_{PO_4}/s^{-1}M^{-1}$ | $10^3 k_{HPO_4}/s^{-1}M^{-1}$ | $k_{OH}/s^{-1}M^{-1}$ |
|---|---|---|---|---|---|
| 5 | 7.81 | 0.74 | | 24.3 | |
| 5 | 9.99 | 6.54[a] | 710 | | 258 |
| 5 | 10.53 | 20.5[a] | 450 | | 285 |
| 15 | 7.62 | 1.50 | | 57.5 | |
| 15 | 9.68 | 11.0[a] | 580 | | 508 |
| 15 | 10.20 | 35.8[a] | 1800 | | 498 |
| 25 | 7.47 | 2.80 | | 144 | |
| 25 | 9.45 | 25.6[a] | 2810 | | 895 |

[a] $k_1 = k_{OH}\, K_w/a_H$

Values of $k_{PO_4}$ were also obtained by measuring the ratio of the amounts of products formed in a simultaneous hydrolysis reaction and the reaction of phosphate ion with acetic anhydride. An aqueous solution of acetic anhydride was rapidly mixed with a solution containing disodium hydrogen phosphate and potassium phosphate of about 20:1 molar ratio and the consumption of phosphate at the end of the reaction was analysed by titrating with a hydrochloric acid solution. The hydroxide ion and phosphate ion concentrations in the reaction mixture were calculated using the values [6] of the base constant of phosphate ion $K_b = 0.0053$ and 0.0110 mol $dm^{-3}$ at 5°C and 15°C, respectively, and the values of activity coefficients obtained using eqn. 3. Because phosphate ions were present in excess compared to anhydride, the ratio $c_{OH}/c_{PO_4}$ remains approximately constant during the reaction and $k_{PO_4}$ can be calculated.

$$k_{PO_4} = k_{OH}\, \frac{c_{OH}}{c_{PO_4}}\, \frac{n_{OH}}{n_{PO_4}} - k_{HPO_4}\, \frac{c_{HPO_4}}{c_{PO_4}} \tag{4}$$

The values of $k_{PO_4}$ were calculated from the amount of anhydride which reacted with hydroxide ions $n_{OH}$ and with phosphate ions $n_{PO_4}$ and the known values of the rate constants $k_{HPO_4}$. These values shown in Table 1 are rather inaccurate due to experimental difficulties and errors in calculating activity coefficients in solutions of high ionic

strength. The error limits are expected to be about 50 %.

*Reaction of acetic anhydride with carbonate ion.* The first-order rate constant $k$ of acetic anhydride when reacting in reaction mixtures containing sodium carbonate and sodium hydrogen carbonate was determined by pH-stat method. The reaction mixture initially contained about 0.01 M acetic anhydride. The concentration of sodium hydrogen carbonate was varied from zero to about 0.5 M and the concentration of sodium carbonate from zero to about 0.005 M. The reaction mixture was titrated with 0.1 M sodium carbonate solution. The second-order rate constants $k_{CO_3}$ and $k_{OH}$ were calculated according to the equation:

$$\left(k - k_{H_2O}\right) f_{OH} = k_{OH}\frac{K_w}{a_H} + \left(k_{CO_3} + k_{HCO_3}\frac{c_{HCO_3}}{c_{CO_3}}\right) c_{CO_3} f_{OH} \qquad (5)$$

The values of the slope of the linear plot of the left side of eqn. 5 against $c_{CO_3} f_{OH}$ are equal to $k_{CO_3} + k_{HCO_3}(c_{HCO_3}/c_{CO_3})$. Values of $k_{HCO_3}(c_{HCO_3}/c_{CO_3})$ were found to be negligible in our experiments. Values of $k_{CO_3}$ and $k_{OH}$ are shown in Tables 1 and 3. Measurements at low pH are necessary in order to obtain values of $k_{HCO_3}$, but complications due to the slow reaction $CO_2 + H_2O = H_2CO_3$ and the volatility of carbon dioxide make it difficult to obtain reliable data.

*Table 3.* First-order rate constants $k_1 = k_{OH}K_w/a_H$ and second-order rate constants $k_{CO_3}$ obtained as intercept and slope, respectively, by plotting $(k_{obs} - k_{H_2O}) f_{OH}$ against $c_{CO_3} f_{OH}$.

| $T°C$ | pH | $10^3 k_1/s^{-1}$ | $10^3 k_{CO_3}/M^{-1}s^{-1}$ | $k_{OH}/M^{-1}s^{-1}$ |
|---|---|---|---|---|
| 5 | 9.13 | 1.00 | 660 | 316 |
| 5 | 9.67 | 4.20 | 530 | 386 |
| 5 | 10.21 | 14.4 | 730 | 380 |
| 25 | 8.48 | 3.80 | 2880 | 1250 |
| 25 | 8.98 | 13.6 | 2180 | 1075 |
| 25 | 9.48 | 32.8 | 2370 | 1150 |

The values of $k_{OH}$ obtained from experiments in, respectively, phosphate and carbonate buffer solutions differ somewhat. The results obtained in carbonate buffer solutions are possibly less reliable because of the simultaneous reactions of carbon dioxide. Kirsch and Jencks[3] have reported a value of $k_{OH} = 967$ M$^{-1}$ s$^{-1}$ at 25°C and Bunton and Fendler[7] a value of $k_{OH} = 158$ M$^{-1}$ s$^{-1}$ at 0°C. Previously reported[6] values of $k_{OH}$ obtained by a flow method are about 20 times larger than the present values and must be considered to be in error. The previously reported[9] value of $k_{OH}/k_{PhO} = 1.36$ at 25°C obtained from product analysis can be combined with the value of $k_{PhO} = 432$ M$^{-1}$ s$^{-1}$ at 10°C from Table 1. A value of $k_{OH} = 588$ M$^{-1}$ s$^{-1}$ at 10°C is obtained which is within the range of $k_{OH}$ values obtained by the other methods.

*Reactions of acetic anhydride with phenoxide ions.* The first-order rate constants were calculated by the Guggenheim method[1] from measurements by the pH-stat method in reaction mixtures containing initially about $10^{-4}$ M anhydride and about 0.01 M phenol by titrating with 0.002 M sodium carbonate solution at constant pH and temperature, 10°C. The respective concentrations of phenoxide ion and substituted phenoxide ions in the reaction mixtures were calculated using values of $pK_a = 10.12$, 10.48, 9.63, and 7.33 at 10°C which in turn were calculated using values[10] of $pK_a = 9.90$, 10.26, 9.40, and 7.15 at 25°C and values[11] of the enthalpies of ionization of $\Delta H = 5.65$, 5.65, 5.80, and 4.70 kcal mol$^{-1}$ for phenol, $p$-cresol, $p$-chlorophenol, and $p$-nitrophenol, respectively. Mean values of the second-order rate constants $k_{PhO}$ obtained from kinetic measurements at different initial phenol concentrations and different pH values are collected in Table 1.

DISCUSSION

A linear free energy relationship is obtained for the reactions of acetic anhydride with basic oxygen-containing nucleophiles when the logarithms of the rate constants $k$ are plotted against the $pK_a$ values, Table 4, of the conjugate acids of the nucleophiles; Fig. 1.

$$\log \ k = (0.45 \pm 0.01) \ pK_a - 4.95 \pm 0.01 \tag{6}$$

Table 4. Parameters of the Arrhenius equation for the reactions of acetic anhydride with nucleophiles in water.

| N | $\log A$ | $E/\mathrm{kJ \ mol^{-1}}$ | $3 + \log k$ 5°C | $pK_a$ 5°C |
|---|---|---|---|---|
| $OH^-$ | 12.01 | 40.5 | 5.431 | 16.475 |
| 4-MePhO$^-$ | | | 5.936[a] | 10.48[a] |
| PhO$^-$ | | | 5.636[a] | 10.12[a] |
| 4-ClPhO$^-$ | | | 5.622[a] | 9.63[a] |
| 4-NO$_2$PhO$^-$ | | | 4.156[a] | 7.53[a] |
| PO$_4^{3-}$ | 10.21 | 54.5 | 2.76 | 12.46 |
| CO$_3^{2-}$ | 8.56 | 46.7 | 2.806 | 10.553 |
| HPO$_4^{2-}$ | 8.77 | 55.3 | 1.393 | 7.281 |
| H$_2$PO$_4^-$ | | | −1.1 | 2.073 |
| H$_2$O | | | −1.900 | −1.745 |

[a] at 10°C.

The rate constants of the hydrolysis reaction and the reactions of phosphate and phenoxide ions with anhydride deviate from this linear free energy relationship. The rate constants of various hydrolysis reactions commonly deviate from linear free energy relationships when water is used as solvent. The deviation of the rate constant of the phosphate ion reaction from eqn. 6 is unexpected but could at least partly be due to the relatively large experimental error anticipated for this reaction. Positive deviations of eqn. 6 are observed for the reactions of different phenoxide ions with anhydride, Fig. 1. The value of the ratio $k_{OH}/k_{PhO} = 1.0$ at 5°C, however, is not very different from the values 1.04, 1.28, and 1.26 obtained previously [12] for the ratio of the rate constants of the reactions of methyl benzenesulphonate at 25°C, methyl nitrate at 90°C, and methyl perchlorate at 0°C, respectively. Linear free energy relationships similar to eqn. 6 were also obtained [12] for these three reactions. The slope of the linear free energy relationship is 0.24 for all three. The rate constants of the reactions with hydroxide ion deviate from the straight line [12] but those of reactions with phenoxide ion do not.[12] Hydroxide and phenoxide ions involving a $\sigma$-type bond between oxygen and carbon show a different kind of reactivity compared with the reactions of nucleophiles containing oxygen bonded to carbon, nitrogen, phosphorus, etc. by $\pi$-type bonds with carbon atoms involving only $\sigma$-type bonds (e.g. the methyl group) or with carbon atoms involving also $\pi$-type bonds (e.g. the carbonyl group of acetic anhydride).
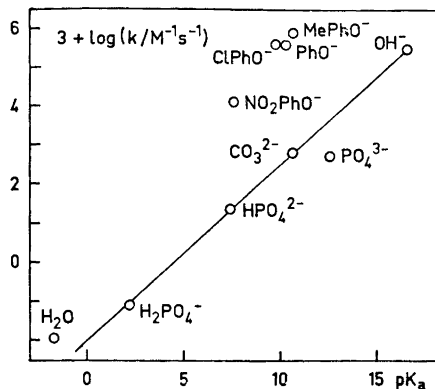
*Fig. 1.* Logarithms of the second-order rate constants of the reactions of acetic anhydride with nucleophiles in water at 5°C plotted against the $pK_a$ values of the conjugate acids of the nucleophiles in water at 25°C.
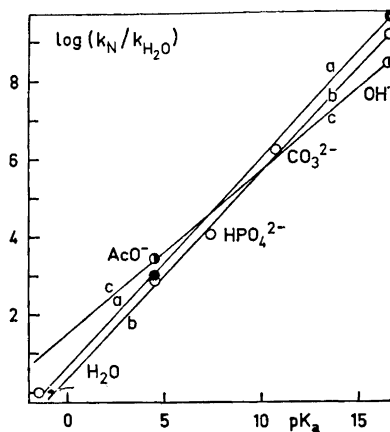


*Fig. 2.* Logarithms of the ratios of the second-order rate constants of the reactions of phenyl acetate (a), 4-nitrophenyl acetate (b), and 2,4-dinitrophenyl acetate (c) with nucleophiles and water, respectively, in water at 25°C plotted against the $pK_a$ values of the conjugate acids of the nucleophiles in water at 25°C.

A linear free energy relationship similar to eqn. 6 is also obtained [13],[14] for reactions of 4-nitrophenyl acetate with basic oxygen-containing nucleophiles, Fig. 2. The slope is, however, different, about $0.54 \pm 0.02$. It is useful to compare the rates of reactions of 4-nitrophenyl acetate with acetate ions and the rates of reactions of acetic anhydride with 4-nitrophenoxide ions because in both cases the same addition intermediate is expected:

$$
\begin{array}{ccc}
\overset{O}{\overset{||}{CH_3-C}}-O-\overset{O}{\overset{||}{C}}-CH_3 & \underset{k_{-1}}{\overset{k_1}{\rightleftharpoons}} \text{ intermediate } \underset{k_{-2}}{\overset{k_2}{\rightleftharpoons}} & \overset{O}{\overset{||}{CH_3-C}}+{}^-O-\overset{O}{\overset{||}{C}}-CH_3 \\
+ & & | \\
{}^-OPhNO_2 & & OPhNO_2
\end{array} \qquad (7)
$$
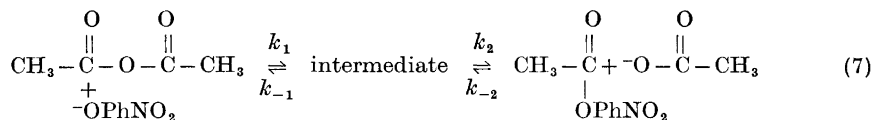
By steady state treatment eqn. 8 is obtained for the experimental rate constants for the overall reactions from left to right, $k_{PhO}$, and from right to left, $k_{AcO}$.

$$k_{PhO} = k_1/(1 + k_{-1}/k_2) \text{ and } k_{AcO} = k_{-2}/(1 + k_2/k_{-1}) \qquad (8)$$

If it is assumed that $k_2 \ll k_{-1}$ then [13] $k_{AcO} = k_{-2} = 5.0 \times 10^{-4}$ M$^{-1}$ s$^{-1}$ at 25°C and $(k_{-1}/k_2)k_{PhO} = (k_{-1}/k_2)50 \gg 50$ M$^{-1}$ s$^{-1}$ at 25°C. $k_{PhO}$ is estimated from the value obtained at 10°C. It is, however, unlikely that the addition of 4-nitrophenoxide ion to the carbonyl group of acetic anhydride would be more than $10^5$ times faster than the addition of acetate ion to the carbonyl group of 4-nitrophenyl acetate because the basicities of acetate ion ($pK_a = 4.76$) and 4-nitrophenoxide ion ($pK_a = 7.15$) are not very different. It is therefore more likely that $k_2 \gg k_{-1}$, as one would expect because acetate ion is a better leaving

group than 4-nitrophenoxide ion. In this case $k_{PhO} = k_1 = 50$ $M^{-1}$ $s^{-1}$ and $k_2 \gg 5.0$ $10^{-4}$ $M^{-1}$ $s^{-1}$.

The value of the slope 0.45, obtained for reactions of acetic anhydride with nucleophiles, is a measure of the sensitivity of $k_1$ of the addition reaction to changes in the basicity of the nucleophile when attacking the carbonyl carbon of acetic anhydride. On the other hand the value of the slope 0.54 is a measure of the sensitivity of $k_{-2} k_{-1}/k_2$ to changes in the basicity of the nucleophile in reactions with 4-nitrophenyl acetate. If the sensitivities of addition reactions of nucleophiles to the carbonyl group of acetic anhydride and 4-nitrophenyl acetate are about equal, then the difference in the values of the slopes $0.54 - 0.45 = 0.09$ would approximately represent the sensitivity of the ratio $k_{-1}/k_2$ to changes in basicity of the nucleophile when it adds to 4-nitrophenyl acetate. As expected, the value is positive, because an increase in the basicity of the nucleophile would decrease the reverse reaction of the intermediate to the starting materials.

A value of 0.43 is obtained for the slope of the linear free energy relationship for the reactions of 2,4-dinitrophenyl acetate with the nucleophiles [15] $OH^-$, $AcO^-$ at 25°C. This is close to the value of the slope (0.45) obtained for acetic anhydride, as would be expected for substrates with a good leaving group ($AcO^-$, $pK_a = 4.74$ and 2,4-dinitrophenoxide ion, $pK_a = 4.08$). For the reactions [15] of phenyl acetate with the nucleophiles $OH^-$ and $AcO^-$, a value of 0.54 is obtained for the slope, which is close to the value (0.54) obtained for the reactions of 4-nitrophenyl acetate with the nucleophiles. In these cases the substrate does not have a good leaving group (phenoxide ion, $pK_a = 9.90$ and 4-nitrophenoxide ion, $pK_a = 7.15$). Values of the slope $A$ of eqn. 6 could perhaps serve as a guide when studying the mechanism of nucleophilic reactions at carbonyl carbon for choosing between the two possibilities $k_{-1} \gg k_2$ or $k_{-1} \ll k_2$.

## REFERENCES

1. Guggenheim, E. A. *Phil. Mag.* **2** (1926) 538; Frost, A. A. and Pearson, R. G. *Kinetics and Mechanism*, Wiley, New York 1961, p. 49.
2. Bates, R. G. *Determination of pH*, Wiley, New York 1964, p. 76.
3. Kirsch, J. F. and Jencks, W. P., *J. Am. Chem. Soc.* **84** (1964) 837.
4. Davies, C. W. *Ion Association*, Butterworths, London 1962, pp. 39, 41.
5. Bates, R. G. *Determination of pH*, Wiley, New York 1964, p. 406.
6. *Stability Constants of Metal-Ion Complexes*, Special Publ. Nos. 17 and 25, The Chemical Society, London 1964 and 1971.
7. Bunton, C. A. and Fendler, J. H. *J. Org. Chem.* **32** (1967) 1547.
8. Koskikallio, J. *Ann. Acad. Sci. Fennicae* **A II 57** (1957).
9. Koskikallio, J. *Suomen Kemistilehti* **B 32** (1959) 161.
10. Kortum, G., Vogel, V. and Andrussow, K. *Dissociation Constants of Organic Acids in Aqueous Solution*, Butterworths, London 1961.
11. Fernandez, L. P. and Hepler, L. G. *J. Am. Chem. Soc.* **81** (1959) 1783.
12. Koskikallio, J. *Acta Chem. Scand.* **26** (1972) 1201.
13. Jencks, W. P. and Carriulo, J. *J. Am. Chem. Soc.* **82** (1960) 1778.
14. Bruice, T. C. and Lapinski, R. *J. Am. Chem. Soc.* **80** (1958) 2265.
15. Jencks, W. P. and Gilchrist, M. *J. Am. Chem. Soc.* **90** (1968) 2622.

# Peroxide-induced Rearrangement of Carbohydrate Acetals

LISSI M. JEPPESEN, INGE LUNDT and
CHRISTIAN PEDERSEN

*Department of Organic Chemistry, Technical University of Denmark,
DK-2800 Lyngby, Denmark*

When acetylated methyl 4,6-*O*-benzylidene-α-D-glucopyranoside is treated with di-*tert*-butyl peroxide a rearrangement takes place to a methyl 6-deoxy-α-D-glucopyranoside. A similar treatment of methyl 4,6-*O*-benzylidene-α-D-galactopyranoside yields a mixture of 6-deoxy-galactoside and 4-deoxy-D-*xylo*-hexopyranoside. 3-*O*-Benzoyl-5,6-*O*-benzylidene-1,2-*O*-isopropylidene-α-D-glucofuranose and 6-*O*-benzoyl-3,5-*O*-benzylidene-1,2-*O*-isopropylidene-α-D-glucofuranose both give a 5-deoxy-D-*xylo*-hexofuranose as the main product. Methyl 5-*O*-benzoyl-2,3-*O*-benzylidene-β-D-ribofuranoside forms a mixture of 2- and 3-deoxy-D-*erythro*-pentofuranosides when heated with peroxide.

It has been reported that cyclic acetals, when heated with di-*tert*-butyl peroxide, will undergo a radical—induced rearrangement to give carboxylic esters. Thus Huyser and Garcia [1] found that 2-phenyl-1,3-dioxolane could be rearranged into ethyl benzoate. This type of rearrangement has also been achieved by an acetone sensitized photochemical reaction.[2–4] If such reactions could be applied to cyclic acetals derived from carbohydrates they would provide a convenient route for the preparation of deoxy-sugars since many carbohydrate acetals are readily available.

The photochemically induced rearrangement has actually been attempted in the sugar series by Matsuura *et al.*[5] who subjected methyl 2,3-*O*-benzylidene-β-D-ribofuranoside to photolysis. They, however, did not isolate any deoxy-ribose derivatives, but found that methyl 2- or 3-*O*-benzoyl-β-D-ribofuranoside had been formed. We have found that cyclic acetals of carbohydrates will undergo peroxide induced rearrangement to give deoxy-sugars in moderate yields.

Thus, when methyl 2,3-di-*O*-acetyl-4,6-*O*-benzylidene-α-D-glucopyranoside (Ia) was heated with di-*tert*-butyl peroxide at 140°C for 7 h methyl 2,3-di-*O*-acetyl-4-*O*-benzoyl-6-deoxy-α-D-glucopyranoside (IIa) was obtained in 41 % yield. The isomeric 4-deoxy-D-*xylo*-pyranoside (V) was not found. The corresponding dibenzoate (Ib) under similar conditions gave methyl tri-*O*-benzoyl-α-D-quinonopyranoside (IIb) in 27 % yield.

a : R = R' = CH₃ , R² = C₆H₅
b : R = CH₃, R' = R² = C₆H₅
c : R = CH₃CO, R' = R² = CH₃
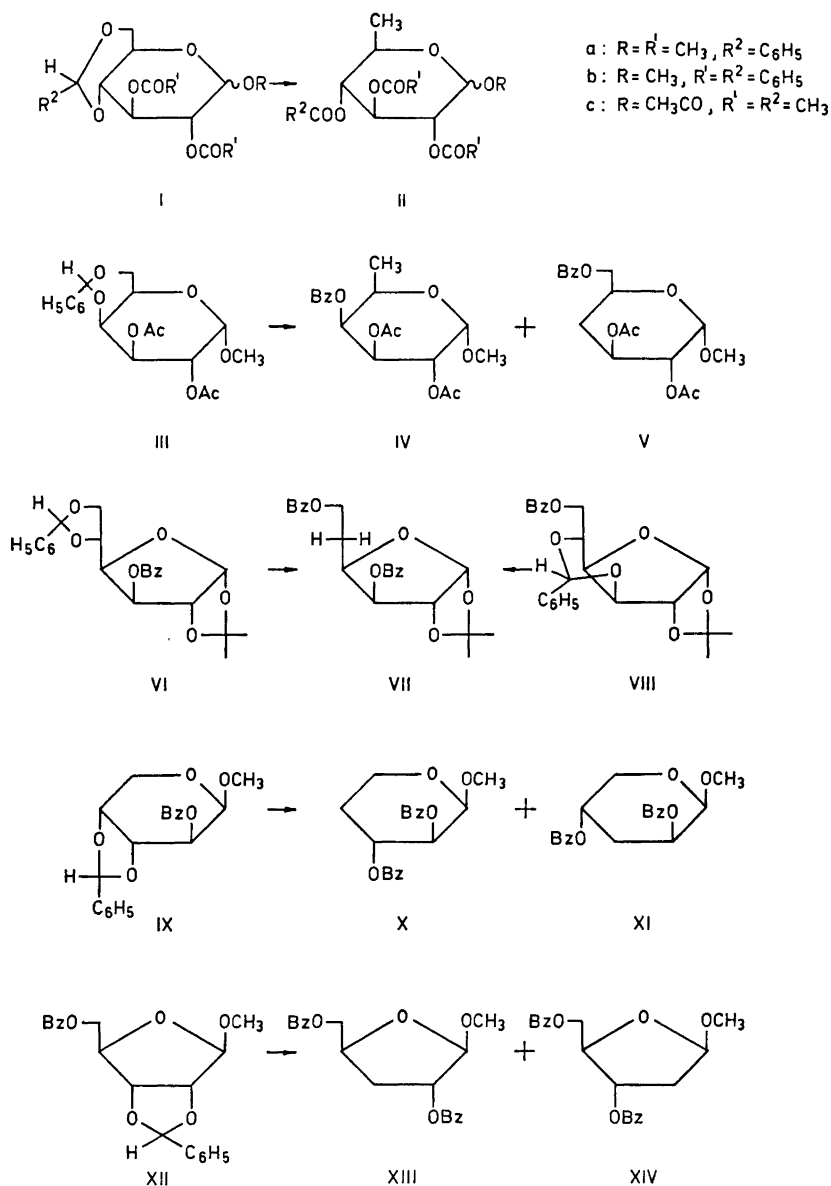
In these experiments di-*tert*-butyl peroxide was used in excess, thus serving as a solvent. The yields were rather low due to radical or thermally induced decomposition of the products. Since the benzoate (Ib) was rather insoluble in di-*tert*-butyl peroxide it was attempted to dilute the reaction mixture with

chlorobenzene, which has a boiling point (132°C) at which the peroxide decomposes to radicals at a reasonable rate.[6] This did, however, not improve the yield of (IIb). Attempts to rearrange unacylated compounds, such as methyl 4,6-O-benzylidene-α-D-glucopyranoside, were not successful because of the low solubility of such compounds in di-*tert*-butyl peroxide and in chlorobenzene.

In analogy with the results described above treatment of 4,6-O-ethylidene-tri-O-acetyl-β-D-glucopyranose (Ic) with di-*tert*-butyl peroxide gave tetra-O-acetyl-6-deoxy-β-D-glucopyranose (IIc).

Whereas the glucose derivatives (I) gave only 6-deoxy-compounds treatment of methyl di-O-acetyl-4,6-O-benzylidene-α-D-galactopyranoside (III) with di-*tert*-butyl peroxide yielded a mixture of methyl 2,3-di-O-acetyl-4-O-benzoyl-6-deoxy-α-D-galactopyranoside (IV) and methyl 2,3-di-O-acetyl-6-O-benzoyl-4-deoxy-α-D-*xylo*-hexopyranoside (V) with the latter predominating.

The two benzylidene derivatives (VI) and (VIII), both derived from 1,2-O-isopropylidene-α-D-glucofuranose, were found to react more readily with peroxide than the pyranose derivatives described above. Thus (VI) and (VIII) had disappeared completely after treatment with peroxide for 3 − 6 h at 120°C whereas most of the pyranose derivatives required *ca.* 20 h. Both (VI) and (VIII) gave 3,6-di-O-benzoyl-5-deoxy-1,2-O-isopropylidene-α-D-*xylo*-hexofuranose (VII) as the main product, and only traces of the isomeric 6-deoxy-D-glucofuranose and 3-deoxy-D-*ribo*-hexofuranose derivatives, which could arise from (VI) and (VIII), respectively, were found.

Methyl-2-O-benzoyl-3,4-O-benzylidene-β-D-arabinopyranoside (IX) required 20 h heating with di-*tert*-butyl peroxide for complete conversion and gave a mixture of the 4- and the 3-deoxy-pentosides (X) and (XI). These could not be separated; but chromatography of the debenzoylated product gave methyl 4-deoxy-β-D-*threo*-pentopyranoside and methyl 3-deoxy-β-D-*threo*-pentopyranoside, identical with those described by Hanessian *et al.*[7,8]

The reaction of methyl 5-O-benzoyl-2,3-O-benzylidene-β-D-ribofuranoside (XII) with di-*tert*-butyl peroxide was completed within 3 h at 120°C and gave a 55 % yield of a product which consisted mainly of methyl 2,5-di-O-benzoyl-3-deoxy-β-D-*erythro*-pentofuranoside (XIII) mixed with a small amount of the 2-deoxy-ribose derivative (XIV). The two compounds could not be separated; but chromatography of the debenzoylated product gave 8 % methyl 2-deoxy-β-D-*erythro*-pentofuranoside, identified as its di-*p*-nitrobenzoate,[9] and 33 % methyl 3-deoxy-β-D-*erythro*-pentofuranoside. The latter was converted into the pure dibenzoate (XIII).[10]

The rearrangements described above probably follow the pathway suggested for 2-substituted 1,3-dioxolanes.[1] The initial step is an abstraction of the acetalic hydrogen atom followed by rearrangement of the cyclic radical thus formed. Recombination with a hydrogen atom finally yields the deoxy-sugar.

Attempts to carry out the rearrangement with dibenzoyl peroxide, in boiling benzene or chlorobenzene, were unsuccessful; only unreacted starting material was found. We also tried to carry out a photochemically induced rearrangement [2-4] by irradiation of the benzylidene derivative (Ia), or the ethylidene derivative (Ic), in acetone solution with a medium pressure mercury lamp. However, no reaction took place in the course of 24 h.

## EXPERIMENTAL

Thin layer chromatography (TLC) was performed on silica gel $PF_{254}$ (Merck); for preparative work 1 mm layers were used on $20 \times 40$ cm plates. NMR spectra were obtained on Varian A-60 or HA-100 instruments.

*Di-tert-butyl peroxide* was a commercial product. It was kept for 24 h over potassium hydroxide and distilled *in vacuo* before use.

*Methyl-2,3-di-O-acetyl-4-O-benzoyl-6-deoxy-α-D-glucopyranoside (IIa).* A mixture of methyl 2,3-di-O-acetyl-4,6-O-benzylidene-α-D-glucopyranoside [11] (450 mg) and di-*tert*-butyl peroxide (1.0 ml) was stirred magnetically while heated to 140°C in an oil bath for 7 h. Evaporation *in vacuo* gave a residue which was purified by preparative TLC, using ether − pentane (1:2) as eluent, to give 185 mg (41 %) of (IIa) as a colourless syrup, $[\alpha]_D^{23} = +59.4°$ (c 6, CHCl$_3$). (Found: C 59.16; H 6.12. Calc. for $C_{18}H_{22}O_8$: C 59.00; H 6.05). An NMR spectrum (Table 1) was in agreement with the proposed structure.

*Methyl tri-O-benzoyl-6-deoxy-α-D-glucopyranoside (IIb).* Methyl 2,3-di-O-benzoyl-4,6-O-benzylidene-α-D-glucopyranoside (Ib) [11] (327 mg) and di-*tert*-butyl peroxide (1.0 ml) were heated to 160°C for 20 h. Evaporation *in vacuo* gave a dark syrup which was separated into two components by preparative TLC (ether − pentane 1:2). The fast moving compound was the 6-deoxy-compound (IIb) 88 mg (27 %), which was recrystallized from methanol, m.p. 142 − 143°C, $[\alpha]_D^{23} = +52.0°$ (c 2.3, CHCl$_3$) (reported [12] m.p. 146 − 147°C, $[\alpha]_D = +57°$). NMR spectral data are given in Table 1.

In a separate experiment (Ib) (336 mg) was dissolved in chlorobenzene (8 ml); *ca.* 4 ml was then distilled off and peroxide (1.0 ml) was added. The solution was heated at a bath temperature of 135°C and monitored by TLC (ether − pentane 1:2). After 7 h starting material was still present; more peroxide (0.5 ml) was added and the heating was continued over night (23 h total). Work up as described above gave 110 mg (32 %) of (IIb), m.p. 140 − 141°C.

*Tetra-O-acetyl-6-deoxy-β-D-glucopyranose (IIc).* Tri-O-acetyl-4,6-O-ethylidene-β-D-glucopyranose (Ic) [13] (403 mg) was heated to 125°C for 20 h with peroxide (2.0 ml). The solvent was evaporated and the residue was purified by preparative TLC (benzene − ethyl acetate 4:1). The main fraction gave 93 mg (23 %) of (IIc) which was recrystallized from ether − pentane, m.p. 144 − 145°C, $[\alpha]_D = +20.0°$ (c 2.2, CHCl$_3$) [reported [14] m.p. 145°C, $[\alpha]_D^{24} = +22°$ (c 4, CHCl$_3$)].

In a separate experiment 2.16 g of (Ic) was heated with peroxide (6.0 ml) to 125°C for 24 h. Evaporation of the peroxide gave a syrup which contained a trace of the starting material (Ic) as seen from an NMR spectrum. The product was dissolved in ether and treated with activated carbon, the ether was evaporated and the residue was crystallized from methanol to give 225 mg (10 %) of (IIc), m.p. 134 − 138°C. The material in the mother liquor was purified by preparative TLC, using two elutions with ethyl acetate-pentane (1:4), to give an additional 526 mg (24 %) of (IIc), m.p. 128 − 135°C.

*Rearrangement of methyl di-O-acetyl-4,6-O-benzylidene-α-D-galactopyranoside (III).* A mixture of (III) [15] (362 mg) and peroxide (1.0 ml) was heated to 120°C for 8 h. The product was separated into two fractions by preparative TLC (ether − pentane 1:1). The fast moving fraction gave 58 mg (16 %) of methyl 2,3-di-O-acetyl-4-O-benzoyl-6-deoxy-α-D-galactopyranoside (IV), crystallized from methanol, m.p. 76 − 77°C, $[\alpha]_D = +187°$ (c 3, CHCl$_3$); (Found: C 59.17; H 5.96. Calc. for $C_{18}H_{22}O_8$: C 59.00; H 6.05).

The slow moving fraction gave 91 mg (25 %) of methyl 2,3-di-O-acetyl-6-O-benzoyl-4-deoxy-α-D-*xylo*-hexopyranoside (V) as a syrup, $[\alpha]_D^{21} = +111°$ (c 4.6, CHCl$_3$). (Found: C 59.43; H 6.44). NMR spectral data of (IV) and (V) are given in Table 1.

*Rearrangement of 3 -O-benzoyl-5,6-O-benzylidene-1,2-O-isopropylidene-α-D-glucofuranose (VI).* The peroxide (2.0 ml) and (VI) [16] (418 mg) was heated to 120°C for 3 h. Preparative TLC with ether − pentane (1:4) as eluent gave two fractions. The fast moving fraction gave 32 mg (8 %) of a compound which, as seen from an NMR spectrum, was 3,5-di-O-benzoyl-6-deoxy-1,2-O-isopropylidene-α-D-glucofuranose. It was not investigated further.

The next fraction gave 3,6-di-O-benzoyl-5-deoxy-1,2-O-isopropylidene-α-D-*xylo*-hexofuranose (VII) as a syrup, 189 mg (45 %), $[\alpha]_D^{23} = -27.0°$ (c 7.8, CHCl$_3$). (Found: C 66.85; H 5.98; Calc. for $C_{23}H_{24}O_7$: C 66.99; H 5.87). Its NMR spectrum (Table 1) was identical with that of a compound prepared by benzoylation of 5-deoxy-1,2-O-isopropylidene-α-D-*xylo*-hexofuranose. [17]

*Table 1.* NMR spectra of deoxy-sugars in deuteriochloroform. Chemical shifts ($\delta$-values) and coupling constants (Hz).

| Compound | H 1 | H 2 | H 3 | H 4 | H 5 | H 6 | −OCH$_3$ | −OAc |
|---|---|---|---|---|---|---|---|---|
| αIIa | ~4.9<br>$J_{12}=4$ | ~4.95<br>$J_{23}=9.5$ | 5.08<br>$J_{34}=9.5$ | 5.66<br>$J_{45}=9.8$ | 4.03<br>$J_{56}=6.5$ | 1.25 | 3.44 | 1.68 |
| αIIb | 5.18 | 5.28<br>$J_{23}=9.5$ | 6.14<br>$J_{34}=9.5$ | 5.36<br>$J_{45}=9.5$ | 4.2<br>$J_{56}=6.3$ | 1.35 | 3.47 | 2.08 |
| βIIc | $J_{12}=3.8$<br>5.74 | 4.87<br>$J_{23}=9$ | 5.26<br>$J_{34}=9.5$ | 5.12<br>$J_{45}=9.5$ | 3.75<br>$J_{56}=6.5$ | 1.25 | 3.48 | 2.04, 2.08 |
| IV | $J_{12}=8$<br>5.1 | 5.3 | 5.58<br>$J_{34}=3$ | 5.6<br>$J_{45}=0.6$ | 4.3<br>$J_{56}=6.6$ | 1.28 | | 2.15 |
| V | $J_{12}=3.4$<br>4.94<br>$J_{12}=3.8$ | $J_{23}=10$<br>4.80<br>$J_{23}=10$ | 5.31<br>$J_{34e}=5.5$<br>$J_{34a}=11.5$ | $J_{45}=0.6$<br>4a=1.67<br>4e=2.24<br>$J_{4a4e}=12$ | 4.2<br>$J_{4e5}=2.5$<br>$J_{4a5}=12$ | 4.3−4.45<br>$J_{56}\cong 3$<br>$J_{56}\cong 4$ | 3.68 | 1.98<br>2.1<br>1.97<br>2.0 |
| VII | 5.98<br>$J_{12}=3.7$ | 4.68<br>$J_{23}=0$ | 5.45<br>$J_{34}=2.8$ | ~4.6<br>$J_{45}=J_{45'}=6.6$ | H5=H5′=2.2<br>$J_{56}=6.6$ | 4.3−4.6<br>$J_{66'}=13.6$ | H$_3$C−C−CH$_3$<br>1.55, 1.34<br>3.43 | |
| X | 5.1<br>$J_{12}=3.5$ | 5.28<br>$J_{23}=10.0$ | 5.73<br>$J_{34a}=10.6$<br>$J_{34e}=5.4$ | 4a=2.4<br>4e=2.63<br>$J_{4e5a}=2.2$ | 5a=3.95<br>5e=3.75 | $J_{4e4a}=12.3$<br>$J_{5a5e}=12.3$ | | |
| XI | 5.05<br>$J_{12}=3.6$ | 5.5<br>$J_{23}=5.8$<br>$J_{23'}=10.8$ | 2.3−2.6<br>$J_{35e}=1.6$<br>$J_{45e}=1.6$ | ~5.6<br>$J_{45a}=1.7$<br>$J_{5a5e}=12.8$ | 5a=2.8<br>5a=4.0<br>5e=3.8 | | | |
| XIII | 5.08<br>$J_{12}=0$<br>$J_{23}=4.6^{[b]}$ | 5.43<br>$J_{23'}=1.4^{[b]}$<br>$J_{33'}=14.5^{[b]}$ | 3=2.05$^{[b]}$, 3′=1.83$^{[b]}$<br>$J_{34}=8.5^{[b]}$<br>$J_{3,4}=7.0^{[b]}$ | ~4.75<br>$J_{45}=4.1$<br>$J_{45}=6.2$ | H5=4.5<br>H5′=4.6<br>$J_{55'}=11.8$ | | | |
| a | 5.27<br>$J_{12}=2.4$<br>$J_{12'}=5.0$ | H2=2.63<br>H2′=2.44 | 5.69<br>$J_{22}=14$<br>$J_{23}=7.0$ | 4.8−4.4<br>$J_{2'3}=5.0$ | $J_{34}=2.4$ | | 3.4 | |

$^{a}$ Methyl 2-deoxy-3,5-di-*O*-*p*-nitrobenzoyl-β-D-*erythro*-pentofuranoside. $^{b}$ in benzene solution.

*Rearrangement of 6-O-benzoyl-3,5-O-benzylidene-1,2-O-isopropylidene-α-D-glucofuranose (VIII)*. A mixture of (VIII)[18] (502 mg) and peroxide (2.0 ml) was heated at 125°C for 6 h. The product was separated into 3 fractions by preparative TLC using 2 elutions with ethyl acetate-pentane (1:4). The fast moving zone gave the 5-deoxy-compound (VII) (152 mg, 32 %), identical with the product described above as seen from an NMR spectrum. The next fraction contained unchanged (VIII) (47 mg, 9 %). The slow moving fraction yielded 47 mg (9 %) of a product which was not investigated closely. An NMR spectrum indicated that it was 5,6-di-O-benzoyl-3-deoxy-1,2-O-isopropylidene-α-D-*ribo*-hexofuranose.

*Rearrangement of methyl 2-O-benzoyl-3,4-O-benzylidene-β-D-arabinopyranoside (IX)*. A mixture of (IX)[19] (293 mg) and peroxide (1.0 ml) was heated to 125°C for 20 h. Preparative TLC (ether − pentane 1:2) gave 104 mg (36 %) of a product which was a mixture of two deoxy-compounds as seen from NMR spectra. They could not be separated completely. The NMR spectra (Table 1) were measured on almost pure products, obtained after several chromatographic separations.

In a separate experiment (IX) (1.0 g) and peroxide (6.0 ml) were kept at 120°C for 20 h. The peroxide was then evaporated and the residue was debenzoylated with sodium methoxide in methanol. After neutralisation with Amberlite IR-120 and evaporation a brown syrup was obtained. This was separated into 2 fractions by preparative TLC (chloroform − methanol 9:1). The fast moving fraction (109 mg) was rechromatographed to give 54 mg (19 %) of methyl 4-deoxy-β-D-*threo*-pentopyranoside as a syrup, $[\alpha]_D^{23} = -157°$ (c 2, MeOH) (reported[7] $[\alpha]_D = -151°$).

The slow moving fraction gave 135 mg which was also rechromatographed. This gave 90 mg (22 %) of methyl 3-deoxy-β-D-*erythro*-pentopyranoside as a syrup, $[\alpha]_D^{23} = -176°$ (c 4, MeOH) (reported[7] $[\alpha]_D = -176°$). NMR spectra of the two products in $D_2O$ confirmed their structures. Their mass spectra were identical with those reported by Hanessian.[7,8]

*Rearrangement of methyl 5-O-benzoyl-2,3-O-benzylidene-β-D-ribofuranoside (XII)*. (XII)[20] (234 mg) was heated with peroxide (1 ml) at 120°C for 4 h. The product was purified by preparative TLC (ether − pentane 1:2) to give 135 mg (56 %) of a product which was shown from NMR spectra to consist mainly of methyl 2,5-di-O-benzoyl-3-deoxy-β-D-*erythro*-pentofuranoside (XIII) and a small amount of the 2-deoxy-compound (XIV). These two could not be separated.

In a separate experiment 1.5 g of (XII) was heated with peroxide (5.0 ml) to 120°C for 4 h. The product was debenzoylated as described above and the debenzoylated material was chromatographed on a column of silica gel (75 g) using chloroform-methanol (9:1) as eluent.

The first fraction (54 mg, 8 %) gave an NMR spectrum in $D_2O$ which showed that it was methyl 2-deoxy-β-D-*erythro*-pentofuranoside. It was treated with p-nitrobenzoyl chloride (250 mg) in pyridine (5 ml) and worked up in the usual way to give 157 mg (8 %) of methyl 2-deoxy-3,5-di-O-p-nitrobenzoyl-β-D-*erythro*-pentofuranoside. The product was purified by preparative TLC (ether − pentane 1:2) and crystallized from benzene-pentane, m.p. 142 − 143°C, $[\alpha]_D^{23} = -5.9°$ (c 5, CHCl₃) (reported[9] m.p. 143 − 144°C, $[\alpha]_D = -5.4$).

The next fraction (52 mg, 8 %) was a mixture of 2- and 3-deoxy-compounds. The third fraction (204 mg, 33 %) was shown by NMR spectra in $D_2O$ to be methyl 3-deoxy-β-D-*erythro*-pentofuranoside. Benzoylation with benzoyl chloride (0.5 ml) in pyridine (5 ml) gave 408 mg (27 %) of (XIII) which was recrystallized from ether − pentane, m.p. 80 − 81°C, $[\alpha]_D = -33°$ (c 2.2, CHCl₃) [reported[10] m.p. 80 − 81, $[\alpha]_D = -32°$ (c 1.7, CHCl₃)]

Microanalyses were performed by Dr. A. Bernhardt.

## REFERENCES

1. Huyser, E. S. and Garcia, Z. J. *Org. Chem.* 27 (1962) 2716.
2. Elad, D. and Youssefyeh, R. D. *Tetrahedron Letters* 1963 2189.
3. Seyfarth, H. E., Hesse, A. and Pastohr, H. *Z. Chem.* 9 (1969) 150.
4. Hartgerink, J. W., van Der Laan, L. C. J., Engberts, J. B. F. N. and De Boer, Th. J. *Tetrahedron* 27 (1971) 4323.

5. Matsuura, K., Maeda, S., Arahi, Y. and Ishido, Y. *Bull. Chem. Soc. Japan* **44** (1971) 292.
6. Walling, C. *Free Radicals in Solution* Wiley, New York 1957.
7. Hanessian, S. and Plessas, N. R. *J. Org. Chem.* **34** (1969) 1053.
8. De Jongh, D. C., Hribar, J. D. and Hanessian, S. *Advan. Chem. Ser.* No. 74, American Chemical Society, 1968, p. 202.
9. Ness, R. K., McDonald, D. L. and Fletcher, H. G., Jr. *J. Org. Chem.* **26** (1961) 2895.
10. Walton, E., Holly F. W., Boxer, G. E., Nutt, R. F. and Jenkins, S. R. *J. Med. Chem.* **8** (1965) 659.
11. Ansell, E. G. and Honeyman, J. *J. Chem. Soc.* **1952** 2778.
12. *Methods Carbohyd. Chem.* **6** (1972) 178.
13. Hall, D. M. and Stamm, O. A. *Carbohyd. Res.* **12** (1970) 421.
14. Bonner, W. A. *J. Am. Chem. Soc.* **81** (1959) 5171.
15. Bell, D. J. and Greville, G. D. *J. Chem. Soc.* **1955** 1136.
16. Levene, P. A. and Raymond, A. L. *Ber.* **66** (1933) 384.
17. Hedley, E. J., Mérész, O. and Overend, W. G. *J. Chem. Soc.* **C 1967** 888.
18. Brigl, P. and Grüner, H. *Ber.* **65** (1932) 1428.
19. Baggett, N., Buck, K. W., Foster, A. B. and Webber, J. M. *J. Chem. Soc.* **1965** 3401.
20. *To be published.*

# Reaction of Sugar Esters with Hydrogen Fluoride

## XII. Derivatives of D-Galactofuranose and D-Talofuranose

KLAUS BOCK, CHRISTIAN PEDERSEN and LARS WIEBE

*Department of Organic Chemistry, Technical University of Denmark,
DK-2800 Lyngby, Denmark*

Tetra-*O*-acetyl- and tetra-*O*-benzoyl-β-D-galactofuranosyl fluoride
were prepared by brief treatment of the corresponding ethyl glyco-
sides with anhydrous hydrogen fluoride. Prolonged treatment of
tetra-*O*-benzoyl-β-D-galactofuranosyl fluoride with hydrogen fluoride
led to rearrangement and tetra-*O*-benzoyl-α-D-talofuranosyl fluoride
could be isolated in good yield.

In a previous paper it was shown that acetylated or benzoylated glucofuranose
derivatives could be rearranged to mannofuranose derivatives by treatment
with anhydrous hydrogen fluoride.[1] In the present paper a corresponding
rearrangement of D-galactofuranoses to derivatives of D-talofuranose is
described.

Brief treatment of ethyl tetra-*O*-benzoyl-β-D-galactofuranoside (*1b*) with
anhydrous hydrogen fluoride gave a good yield of tetra-*O*-benzoyl-β-D-
galactofuranosyl fluoride (*β-3b*) as the only detectable product. A similar
treatment of the tetraacetate (*1a*) gave the β-fluoride (*β-3a*) together with
small amounts of tetra-*O*-acetyl-α-D-galactofuranosyl fluoride and 2,3,5,6-
tetra-*O*-acetyl-α-D-galactofuranose, the latter isolated as the pentaacetate
after acetylation.

The further reaction of the fluorides (*3a* and *b*) and of the glycosides (*1a*
and *b*) with hydrogen fluoride was first studied by NMR spectroscopy. The
acetylated fluoride (*β-3a*) was dissolved in anhydrous hydrogen fluoride at
0°C and an NMR spectrum was obtained after *ca.* 5 min. This spectrum showed
that the 1,2-acetoxonium ion (*2a*) was present as the main product, as seen
from an acetoxonium ion signal at 2.98 ppm; H-1 gave a doublet at 7.36 ppm,
$J_{12} = 5.3$ Hz. Thus the fluoride (*β-3a*) is immediately converted into the
acetoxonium ion (*2a*) in hydrogen fluoride, in agreement with previous results.[1,2]
When the solution was kept at room temperature further reaction took place
and after 24 h spectra showed that (*2a*) was no longer present. After 12 days
the diacetoxium ion (*5a*) was the only product as seen from NMR spectra

a : R = CH₃

b : R = C₆H₅

c : R = p-NO₂C₆H₄
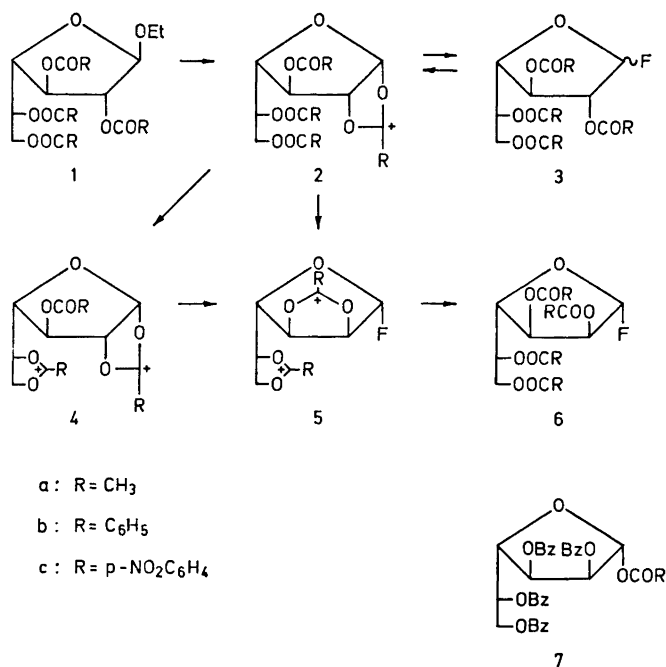
which gave acetoxonium ion signals at 2.86 and 2.97 ppm; a signal integrating to 6 H corresponding to 2 equivalents of acetic acid was found at 2.52 ppm. The anomeric proton was a doublet centered at 6.51 ppm with a spacing of 61.5 Hz ($J_{1F}$). Since $J_{12}$ was less than 0.5 Hz the product must be the α-fluoride (*5a*).[3] In analogy with the corresponding reaction in the glucofuranose series [1] the diacetoxonium ion (*4a*) might be expected to be an intermediate in the conversion of (*2a*) into (*5a*), this ion could, however, not be detected with certainty in the NMR spectra. Reaction of the ethyl furanoside (*1a*) with hydrogen fluoride gave the same result. The 1,2-acetoxonium ion was formed at once, and hydrolysis of the solution which contained this ion gave the β-fluoride (*β-3a*) as described above. On further reaction the diacetoxonium ion (*5a*) was formed. The ethanol which was cleaved off from (*1a*) in hydrogen fluoride was quantitatively converted into ethyl acetate by reaction with acetic acid. This is analogous to the reaction of methanol with acetic acid in hydrogen fluoride solution.[2,4]

Work up of the hydrogen fluoride solution which contained the diacetoxonium ion (*5a*) gave only small amounts of products, probably because the diacetates formed by hydrolysis of (*5a*) are water soluble and therefore are lost.

Reaction of the benzoates (*1b*) or (*β-3b*) with hydrogen fluoride proceeded analogously to the reaction of the acetates. Both (*1b*) and (*β-3b*) gave the 1,2-benzoxonium ion (*2b*) at once when dissolved in hydrogen fluoride. The

signal of the anomeric proton was hidden by the aromatic protons; H2 was found at 6.66 ppm, H3 at 6.27, H4 at 5.57, H5 at 6.45, and H6 and H6' at 5.0 – 5.2 ppm; $J_{12} = 5.3$ Hz; $J_{23} = 0.5$; $J_{34} = 2.5$; $J_{45} = 2.5$. The ion (2b) had disappeared completely after 24 h at room temperature. The further reaction was rather slow, but after ca. 25 days at room temperature the dibenzoxonium ion (5b) was formed as the only detectable product. Its spectrum was quite similar to that of (5a); H1 gave a doublet centered at 6.70 ppm, $J_{12} = 0$, $J_{1F} = 60.0$ Hz.

When the hydrogen fluoride solution, which contained (5b), was hydrolyzed a mixture of partially benzoylated products was obtained. After benzoylation tetra-O-benzoyl-α-D-talofuranosyl fluoride (6b) could be isolated in ca. 60 % yield. Besides, a smaller amount of penta-O-benzoyl-α-D-talofuranose (7b) was obtained. The latter product must arise via a partial hydrolysis of the fluoride during the work up of the hydrogen fluoride solution. In order to increase the yield of the fluoride (6b) the benzoylated product was treated briefly with hydrogen fluoride to convert the pentabenzoate to the fluoride. After this treatment 76 % of (6b) was obtained from the galactose derivative (3b).

Treatment of (6b) with hydrogen bromide in acetic acid gave crude tetra-O-benzoyl-D-talofuranosyl bromide. Hydrolysis and p-nitrobenzoylation of this gave the known [5] 2,3,5,6-tetra-O-benzoyl-1-O-p-nitrobenzoyl-α-D-talofuranose (7c).

## EXPERIMENTAL

NMR spectra were obtained on Varian A-60 and HA-100 instruments. Spectra in anhydrous hydrogen fluoride were measured in Teflon sample tubes. Positions of signals in hydrogen fluoride are given in ppm relative to $(CH_3)_3SiCH_2CH_2CH_2SO_3Na$. [19]F spectra were measured at 94.1 MHz. Positions of signals ($\phi$F) are given in ppm relative to internal methyl trifluoroacetate. Thin layer chromatography (TLC) was performed on silica gel $PF_{254}$ (Merck); for preparative work 1 mm layers were used on 20 × 40 cm plates.

*Ethyl tetra-O-benzoyl-β-D-galactofuranoside (1b).* Ethyl β-D-galactofuranoside [6] (1.51 g) was benzoylated in the usual manner with benzoyl chloride in pyridine. The product crystallized from ether – pentane to give 4.30 g (94 %) of (1b) with m.p. 100 – 101°C. An additional recrystallization did not change the melting point, $[\alpha]_D^{24} = -7.1°$ (c 1.4, $CHCl_3$). (Found: C 69.44; H 5.11. Calc. for $C_{36}H_{32}O_{10}$: C 69.23; H 5.16).

*Tetra-O-acetyl-β-D-galactofuranosyl fluoride (β-3a).* Ethyl tetra-O-acetyl-β-D-galactofuranoside [7] (2.86 g) was dissolved in anhydrous hydrogen fluoride (8 ml) and the solution was kept at 0°C for 15 min. It was then diluted with dichloromethane and poured on ice. The organic phase was washed with aqueous sodium hydrogen carbonate, dried and evaporated. The residue (2.17 g) was crystallized from ether-pentane (seed crystals were obtained in a separate experiment in which the product was purified by preparative. TLC using ether – benzene (1:1) as eluent) to give 1.01 g (36 %) of (β-3a), m.p. 71 – 73°C Recrystallization from ether – pentane gave the pure product, m.p. 76 – 77°C, $[\alpha]_D^{24} = -15.2°$ (c 1.5, $CHCl_3$). (Found: C 48.20; H 5.53. Calc. for $C_{14}H_{19}FO_9$: C 48.02; H 5.47.)

The material in the mother liquors was separated into 2 fractions by preparative TLC (benzene – ether 1:1). The fast moving fraction (500 mg, 17 %) consisted of the β-fluoride (β-3a) mixed with a small amount of tetra-O-acetyl-α-D-galactofuranosyl fluoride (α-3a) as seen from an NMR spectrum (Table 1).

The slow moving fraction was acetylated to give 200 mg (7 %) of penta-O-acetyl-β-D-galactofuranose, which crystallized from ethanol, m.p. 91 – 95°C, $[\alpha]_D^{24} = -33.3°$ (c 1.2, $CHCl_3$) (recorded [8] m.p. 96 – 97°C, $[\alpha]_D = -41.5°$). An NMR spectrum confirmed

*Table 1.* NMR spectra of D-galactofuranose and D-talofuranose derivatives in deuteriochloroform.

| Com-pound | Chemical shifts ($\delta$-values) | | | | | | | | Observed 1st. order coupling constants (Hz) | | | | | | | | | |
|---|---|---|---|---|---|---|---|---|---|---|---|---|---|---|---|---|---|---|
| | H 1 | H 2 | H 3 | H 4 | H 5 | H 6 | H 6' | $\phi_F$ | $J_{1F}$ | $J_{12}$ | $J_{2F}$ | $J_{23}$ | $J_{34}$ | $J_{4F}$ | $J_{45}$ | $J_{56}$ | $J_{56}'$ | $J_{66}'$ |
| $\beta$-3a | 5.74 | 5.23 | 5.08 | 4.49 | 5.42 | 4.35 | 4.20 | −52.2 | 58.0 | ∼0 | 7.3 | 1.4 | 4.5 | 1.9 | 4.5 | 4.6 | 6.8 | 12.0 |
| $\alpha$-3a | 5.6 | | | | | | | −48.4 | 65.0 | 3.3 | 19.0 | | | 6.5 | | | | |
| $\beta$-3b | 6.04 | 5.67 | 5.75 | 4.96 | 6.14 | 4.70− | 4.85 | −49.3 | 59.0 | | 6.5 | | ≃4 | 1.5 | ≃5 | 4.5 | 7.0 | |
| 6b | 6.00 | 5.70 | | 4.99 | 6.00 | 4.83 | 4.73 | −40.5 | 61.0 | ∼0 | 2.3 | | 3.6 | 7.5 | 6.0 | 4.0 | 6.0 | 12.0 $J_{3F}=4.5$ |
| 7b | 6.69 | 5.8−6.1 | | 5.02 | 5.87 | 4.7 | 4.8 | | ∼0 | | | | | | | | | |
| 7c | 6.70 | 5.9 | 6.0 | 5.01 | 5.86 | 4.6 | 4.8 | | ∼0 | | | | | | | | | |

the structure and showed that the product contained small amounts of the corresponding α-anomer.

*Tetra-O-benzoyl-β-D-galactofuranosyl fluoride (β-3b).* Ethyl tetra-O-benzoyl-β-D-galactofuranoside (*1b*) (4.12 g) was dissolved in hydrogen fluoride (12 ml) and the solution was kept at 0°C for 45 min. Work up as described above gave a crystalline product (3.76 g) which was recrystallized from ether − pentane to give 2.84 g (72 %) of (β-3b), m.p. 110 − 111°C, $[\alpha]_D^{24}= +14.9°$ (c 1.6, CHCl₃). (Found: C 68.07; H 4.69. Calc. for C₃₄H₂₇FO₉: C 68.21; H 4.55).

*Tetra-O-benzoyl-α-D-talofuranosyl fluoride (6b).* A solution of tetra-O-benzoyl-β-D-galactofuranosyl fluoride (2.04 g) in anhydrous hydrogen fluoride (8 ml) was kept for 21 d at room temperature. The mixture was then worked up as described above and the crude product was benzoylated with benzoyl chloride (7.0 ml) in pyridine (15 ml). Work up in the usual way gave 2.36 g of product.

A sample of this (800 mg) was separated into two fractions by preparative TLC with ether − pentane (1:1) as eluent. The fast moving fraction gave 400 mg of pure (6b) as seen from NMR spectra. The slower moving fraction gave 135 mg of penta-O-benzoyl-α-D-talofuranose (*7b*) as a syrup, $[\alpha]_D^{24} = −30.3°$ (c 1.5, CHCl₃). (Found: C 70.09; H 4.63. Calc. for C₄₁H₃₂O₁₁: C 70.30; H 4.59.).

The remaining product (1.56 g) was treated with anhydrous hydrogen fluoride (6 ml) at 0°C for 5 min. Work up gave a syrup (1.5 g) which was purified by preparative TLC with ether − pentane (1:1) to give 1.22 g of (6b) as seen from an NMR spectrum.

In a separate experiment tetra-O-benzoyl-β-D-galactofuranosyl fluoride (1.66 g) was kept in hydrogen fluoride (8 ml) for 29 d at room temp. The product was benzoylated and the benzoylated product was treated with hydrogen fluoride for 5 min at 0°C. Work up and chromatography of the product gave 1.26 g (76 %) of tetra-O-benzoyl-α-D-talofuranosyl fluoride. A sample was rechromatographed using ether − pentane (1:1) as eluent, $[\alpha]_D^{24} = −90.3°$ (c 3.9, CHCl₃). (Found: C 68.06; H 4.73. Calc. for C₃₄H₂₇FO₉: C 68.21; H 4.55.).

*2,3,5,6-Tetra-O-benzoyl-1-O-p-nitrobenzoyl-α-D-talofuranose (7c).* The fluoride (*6b*) (700 mg) was kept in a solution of 30 % HBr in glacial acetic acid (10 ml) over night at +5°C. Dichloromethane was then added and the mixture was washed with water and aqueous sodium hydrogen carbonate, dried and evaporated. The crude tetra-O-benzoyl-D-talofuranosyl bromide (740 mg) was dissolved in 10 ml of a mixture of acetone and water (9:1) and stirred with silver carbonate (1.0 g) for 3 h. Filtration and evaporation gave 550 mg of crude 2,3,5,6-tetra-O-benzoyl-D-talofuranose. This was nitrobenzoylated in the usual manner with p-nitrobenzoyl chloride (190 mg) in pyridine (5 ml). The product was crystallized from ethanol to give 543 mg (62 %) of (*7c*), m.p. 175 − 185°C. Two additional recrystallizations from dichloromethane-methanol gave 250 mg of pure

product, m.p. $189-190°C$, $[\alpha]_D^{20} = -27.0°$ ($c$ 2.8, $CHCl_3$) (reported [5] m.p. $189-189.5°C$, $[\alpha]_D = -25.0°$). NMR data are shown in Table 1.

  Microanalyses were performed by Dr. A. Bernhardt.

## REFERENCES

1. Bock, K. and Pedersen, C. *Acta Chem. Scand.* **26** (1972) 2360.
2. Bock, K. and Pedersen, C. *Acta Chem. Scand.* **27** (1973) 2701.
3. Hall, L. D., Steiner, P. R. and Pedersen, C. *Can. J. Chem.* **48** (1970) 1155.
4. Lundt, I. and Pedersen, C. *Acta Chem. Scand.* **26** (1972) 1938.
5. Kohn, P., Samaritano, R. H. and Lerner, L. M. *J. Am. Chem. Soc.* **87** (1965) 5475.
6. Green, J. W. and Pacsu, E. *J. Am. Chem. Soc.* **59** (1937) 1208.
7. Janson, J. and Lindberg, B. *Acta Chem. Scand.* **14** (1960) 877.
8. Chittenden, G. J. F. *Carbohyd. Res.* **25** (1972) 35.

# Short Communications

## Normalized Projection Maps Calculated and Plotted by Computer

DIEGO FERRI,[a] OLOF WAHLBERG[a,b] and ERIK HÖGFELDT[a]

[a]Department of Inorganic Chemistry, The Royal Institute of Technology (KTH), S-100 44 Stockholm 70 and [b]Departments of Inorganic and Structural Chemistry, The Arrhenius Laboratory, P.O.B., S-104 05 Stockholm 50, Sweden

The theory of normalized projection maps was outlined in the 1950's by Sillén,[1-3,5] Biedermann,[3] and the Rossottis'.[4-6] The information about the average composition of complexes obtained by the MESAK method [7] combined with that from normal-

* Present address: Università di Napoli, Instituto Chimico, 80134 Napoli, Italy.

ized projection maps often gives the main species present in a given system. Further calculations with LETAGROP [8-10] gives an improved set of equilibrium constants and makes it possible to test the uniqueness of the model as well as the possible presence of minor constituents and systematic errors. An instructive example of what can be achieved by combining the MESAK method with projection maps can be found in a paper by Ingri.[11]

In order to simplify the use of normalized projection maps Ferri and Wahlberg [12] prepared an Algol program NORMEX for calculating such maps. The maps can be plotted using a line printer.

Photograpic plots can also be obtained by using a program recently designed by Warnqvist.[13] NORMEX is constructed in a way that allows a high degree of freedom in the choice of normalizing conditions. At present the program is written for one, two, or three components, but an extension to four or more can easily be



Fig. 1. $-\log b$ plotted against $-\log (B-b)b$ for the system In(III)—Cl$^-$ studies by Ferri.[14] The points are experimental and the curves computed with NORMEX and log $\beta_1$ = 2.57, log $\beta_2$ = 3.84, and log $\beta_3$ = 4.2.

made if the need arises. The use of NORMEX is illustrated in Fig. 1, where $-\log b$ is plotted against $-\log (B-b)b$ for the system $In^{3+} - Cl^-$ in 3 M $NaClO_4$ studied by one of us.[14] $B$ is the total concentration of indium and $b$ the concentration of free $In^{3+}$ as measured by an indium amalgam electrode. The points are experimental and the curves have been computed with NORMEX using a model including the formation of $InCl^{2+}$, $InCl_2^+$, and $InCl_3$ with $\log \beta_1 = 2.57 \pm 0.02$, $\log \beta_2 = 3.84 \pm 0.02$, and $\log \beta_3 = 4.2 \pm 0.1$, which compares well with the values obtained by LETAGROP:

$\log \beta_1 = 2.58 \pm 0.01$, $\log \beta_2 = 3.84 \pm 0.01$, $\log \beta_3 = 4.25 \pm 0.02$

A detailed description of NORMEX and examples of how to use it are given in the paper by Ferri and Wahlberg,[12] and anyone interested can write to Dr. Wahlberg at the University of Stockholm for reprints and further information.

1. Sillén, L. G. *Acta Chem. Scand.* **10** (1956) 186.
2. Sillén, L. G. *Acta Chem. Scand.* **10** (1956) 803.
3. Biedermann, G. and Sillén, L. G. *Acta Chem. Scand.* **10** (1956) 203.
4. Rossotti, F. J. C. and Rossotti, H. S. *Acta Chem. Scand.* **9** (1955) 1166.
5. Rossotti, F. J. C., Rossotti, H. S. and Sillén, L. G. *Acta Chem. Scand.* **10** (1956) 203.
6. Rossotti, F. J. C. and Rossotti, H. S. *The Determination of Stability Constants,* McGraw, New York 1961.
7. Sillén, L. G. *Acta Chem. Scand.* **15** (1961) 1981.
8. Ingri, N. and Sillén, L. G. *Arkiv Kemi* **23** (1965) 97.
9. Sillén, L. G. and Warnqvist, B. *Arkiv Kemi* **31** (1969) 341.
10. Brauner, P., Sillén, L. G. and Whiteker, R. *Arkiv Kemi* **31** (1969) 377.
11. Ingri, N. *Acta Chem. Scand.* **17** (1963) 597.
12. Ferri, D. and Wahlberg, O. *Chem. Commun.,* Univ. Stockholm 1973, No. XII.
13. Warnqvist, B. *Personal communication* 1971.
14. Ferri, D. *Acta Chem. Scand.* **26** (1972) 733.

Received November 2, 1973.

# Polymannuronic Acid 5-Epimerase from the Marine Alga *Pelvetia canaliculata* (L.) Dcne. et Thur.

JOHN MADGWICK, ARNE HAUG and BJØRN LARSEN

*Institutt for marin biokjemi, N-7034 Trondheim-NTH, Norway*

Polymannuronic acid 5-epimerase was first demonstrated as an extracellular product of the bacterium *Azotobacter vinelandii* (Lipmann).[1] Subsequent work dealt with characterisation of the enzymic epimerisation,[2] the nature of the alginate from *A. vinelandii*,[3] and the mechanism of the enzymatic reaction.[4,5] However, although it seemed likely that brown algae must contain a similar epimerase, it was hard to prove because these plants' enzymes are so difficult to extract due to the presence of large amounts of sulphated polysaccharides and phenolic compounds.[6] This communication presents evidence for an algal alginate epimerase and describes the preparation of a soluble enzyme system from the brown alga *P. canaliculata*. An ammonium sulphate fraction was obtained which catalysed the conversion of polymannuronic acid to a mixed polymer containing guluronic acid residues. The epimerisation reaction was revealed by changes in carbazole reactives[7] and with incorporation of tritium into the polyuronide fraction.[4]

*Materials and methods: P. canaliculata* was harvested from Lade and Flakk, Trondheimsfjord, on 18.5.1973 and 19.8.1973, respectively, and deep-frozen at $-15°C$. A brei of *P. canaliculata* was made in water at $0°C$, (800 ml/100 g wet wt.), using an Ultra-Turrax® blendor. The material remaining after filtration with gauze (*ca.* 0.5 mm, 4 layers) was discarded. Centrifugation, $(7000\,g, 10\,min, 4°C)$, gave a pellet which was resuspended in iced water and resedimented. An acetone powder, (500 mg/100 g wet algae), was prepared from the washed pellet,[8] and subsequently extracted, (4 h, $20°C$), with a solution containing phosphate buffer, (pH 7.8, 0.05 M), NaCl, (0.2 M), and dithiothreitol $(10^{-4}\,M)$. Solubles were separated by centrifugation, treated with ammonium sulphate at $0°C$, and the precipitates between 40 % and 90 % saturation combined and dialysed against tris(hydroxymethyl)ami-

made if the need arises. The use of NORMEX is illustrated in Fig. 1, where $-\log b$ is plotted against $-\log (B-b)b$ for the system $In^{3+} - Cl^-$ in 3 M $NaClO_4$ studied by one of us.[14] $B$ is the total concentration of indium and $b$ the concentration of free $In^{3+}$ as measured by an indium amalgam electrode. The points are experimental and the curves have been computed with NORMEX using a model including the formation of $InCl^{2+}$, $InCl_2^+$, and $InCl_3$ with $\log \beta_1 = 2.57 \pm 0.02$, $\log \beta_2 = 3.84 \pm 0.02$, and $\log \beta_3 = 4.2 \pm 0.1$, which compares well with the values obtained by LETAGROP:

$\log \beta_1 = 2.58 \pm 0.01$,     $\log \beta_2 = 3.84 \pm 0.01$, $\log \beta_3 = 4.25 \pm 0.02$

A detailed description of NORMEX and examples of how to use it are given in the paper by Ferri and Wahlberg,[12] and anyone interested can write to Dr. Wahlberg at the University of Stockholm for reprints and further information.

1. Sillén, L. G. *Acta Chem. Scand.* **10** (1956) 186.
2. Sillén, L. G. *Acta Chem. Scand.* **10** (1956) 803.
3. Biedermann, G. and Sillén, L. G. *Acta Chem. Scand.* **10** (1956) 203.
4. Rossotti, F. J. C. and Rossotti, H. S. *Acta Chem. Scand.* **9** (1955) 1166.
5. Rossotti, F. J. C., Rossotti, H. S. and Sillén, L. G. *Acta Chem. Scand.* **10** (1956) 203.
6. Rossotti, F. J. C. and Rossotti, H. S. *The Determination of Stability Constants,* McGraw, New York 1961.
7. Sillén, L. G. *Acta Chem. Scand.* **15** (1961) 1981.
8. Ingri, N. and Sillén, L. G. *Arkiv Kemi* **23** (1965) 97.
9. Sillén, L. G. and Warnqvist, B. *Arkiv Kemi* **31** (1969) 341.
10. Brauner, P., Sillén, L. G. and Whiteker, R. *Arkiv Kemi* **31** (1969) 377.
11. Ingri, N. *Acta Chem. Scand.* **17** (1963) 597.
12. Ferri, D. and Wahlberg, O. *Chem. Commun.,* Univ. Stockholm 1973, No. XII.
13. Warnqvist, B. *Personal communication* 1971.
14. Ferri, D. *Acta Chem. Scand.* **26** (1972) 733.

Received November 2, 1973.

# Polymannuronic Acid 5-Epimerase from the Marine Alga *Pelvetia canaliculata* (L.) Dcne. et Thur.

JOHN MADGWICK, ARNE HAUG and BJØRN LARSEN

*Institutt for marin biokjemi, N-7034 Trondheim-NTH, Norway*

Polymannuronic acid 5-epimerase was first demonstrated as an extracellular product of the bacterium *Azotobacter vinelandii* (Lipmann).[1] Subsequent work dealt with characterisation of the enzymic epimerisation,[2] the nature of the alginate from *A. vinelandii*,[3] and the mechanism of the enzymatic reaction.[4,5] However, although it seemed likely that brown algae must contain a similar epimerase, it was hard to prove because these plants' enzymes are so difficult to extract due to the presence of large amounts of sulphated polysaccharides and phenolic compounds.[6] This communication presents evidence for an algal alginate epimerase and describes the preparation of a soluble enzyme system from the brown alga *P. canaliculata*. An ammonium sulphate fraction was obtained which catalysed the conversion of polymannuronic acid to a mixed polymer containing guluronic acid residues. The epimerisation reaction was revealed by changes in carbazole reactives[7] and with incorporation of tritium into the polyuronide fraction.[4]

*Materials and methods:* *P. canaliculata* was harvested from Lade and Flakk, Trondheimsfjord, on 18.5.1973 and 19.8.1973, respectively, and deep-frozen at $-15°C$. A brei of *P. canaliculata* was made in water at $0°C$, (800 ml/100 g wet wt.), using an Ultra-Turrax® blendor. The material remaining after filtration with gauze (*ca.* 0.5 mm, 4 layers) was discarded. Centrifugation, (7000 $g$, 10 min, 4°C), gave a pellet which was resuspended in iced water and resedimented. An acetone powder, (500 mg/100 g wet algae), was prepared from the washed pellet,[8] and subsequently extracted, (4 h, 20°C), with a solution containing phosphate buffer, (pH 7.8, 0.05 M), NaCl, (0.2 M), and dithiothreitol ($10^{-4}$ M). Solubles were separated by centrifugation, treated with ammonium sulphate at 0°C, and the precipitates between 40 % and 90 % saturation combined and dialysed against tris(hydroxymethyl)ami-

nomethane/HCl buffer (pH 8.3, 0.012 M, at 0°C, 1 h). Enzymatic activity was detected using a carbazole assay,[7] and by the incorporation of tritium.[4] The amount of tritium incorporation was estimated by liquid scintillation counting as described previously.[4] Protein was determined according to Lowry et al.[9]

Results. Table 1 shows the changes in carbazole colour of polymannuronic acid after treatment over an extended reaction time. In the absence of borate, mannuronic acid gives a low extinction in the carbazole

Table 1. Assay of epimerase activity in P. canaliculata using the carbazole reaction.

| Incubation time (h) | Carbazole reactives (extinction at 530 nm) | | Ratio With borate/ without borate |
|---|---|---|---|
| | Without borate | With borate | |
| 0 | 0.58 | 0.72 | 1.24 |
| 0.5 | 0.64 | 0.80 | 1.25 |
| 1.5 | 0.72 | 0.74 | 1.03 |
| 4.5 | 0.96 | 0.70 | 0.73 |
| 18.0 | 1.36 | 0.61 | 0.45 |

Incubation mixture: Enzyme solution, 1.5 mg/ml protein (albumin equivalents); TRIS-HCl, pH 8.3, 12 mM; $CaCl_2$, 2.6 mM; Polymannuronic acid 7 mM; NaCl 150 mM; Dithiothreitol, 1.24 mM; 20°C. (P. canaliculata harvested 18.5.73).

reaction, and the increases observed must be due to the transformation of mannuronic acid residues into guluronic acid residues, having a much higher extinction in the absence of borate.[2,7] In the presence of borate, the two monomers have approximately the same extinctions. The ratio of these extinctions, which gives the changing proportion of mannuronic to guluronic acid, decreased significantly within 90 min. The exact amount of conversion to guluronic acid is unknown because the enzyme extract contained considerable polysaccharide, including alginic acid of undetermined uronic acid composition. The epimerisation of polymannuronic to a mixed, guluronic acid containing polymer was also checked independently on these samples using electrophoretic separation on paper,[10] of the hydrolysed polymer. Visual examination of the paper strips

showed the appearance of guluronic acid after 5 h incubation.

In a separate experiment, the P. canaliculata enzyme system, (harvested 19.8.73), was assayed in tritiated water (total activity approximately 20 mCi).[4] The reaction was terminated with acid, (0.1 N, HCl), and the whole reaction mixture dialysed against distilled water. Total counts were measured on redissolved precipitates, and also on the individual uronic acids after hydrolysis and ion-exchange chromatography. Table 2 shows that of the

Table 2. Incorporation of tritium by uronic acids during enzymic epimerisation of polymannuronic acid.

| Time (h) | Activity, (counts per minute) | | |
|---|---|---|---|
| | Total | Guluronic acid | Mannuronic acid |
| 0 | 14840 | 5 | 33 |
| 5 | 49630 | 2539 | 672 |

Incubation mixture: Enzyme solution, 1.2 mg/ml protein (albumin equivalents); Collidine, pH 7.0, 25 mM; $CaCl_2$, 2.6 mM; Polymannuronic acid, 0.7 mM; Tritium, 2 mCi/ml; 20°C. (P. canaliculata harvested 19.8.73).

activity found in the incubation mixture at the start of the experiment, only an insignificant amount was present in the uronic acids. After 5 h incubation a significant proportion of the activity was recovered in the uronic acid fraction with about four times more in the guluronic as in the mannuronic acid fraction. Compared with the results obtained for the Azotobacter epimerase, as discussed in some detail in a previous publication,[4] the present work indicates the presence of polymannuronic acid epimerase in Pelvetia canaliculata. The fact that relatively more activity was found in the mannuronic acid, than was found in Azotobacter experiments, might mean that there was a higher degree of reversibility for the algal enzyme.

1. Haug, A. and Larsen, B. Biochim. Biophys. Acta 192 (1969) 557.
2. Haug, A. and Larsen, B. Carbohyd. Res. 17 (1971) 297.

3. Larsen, B. and Haug, A. *Carbohyd. Res.* **17** (1971) 287.
4. Larsen, B. and Haug, A. *Carbohyd. Res.* **20** (1971) 225.
5. Larsen, B. and Haug, A. Paper read at Seventh International Seaweed Symposium, Sapporo, Japan, August 8th, (1971) 491.
6. Johnston, C. S. and Davies, J. M. Paper read at Sixth International Seaweed Symposium, Santiago, Spain, September 9th, (1968) 501.
7. Knutson, C. A. and Jeanes, A. *Anal. Biochem.* **24** (1968) 470.
8. Madgwick, J., Haug, A. and Larsen, B. *Acta Chem. Scand.* **27** (1973) 711.
9. Lowry, O. H., Rosebrough, N. J., Farr, A. L. and Randall, R. J. *J. Biol. Chem.* **193** (1951) 265.
10. Haug, A. and Larsen, B. *Acta Chem. Scand.* **15** (1961) 1395.

Received October 8, 1973.

# Alkylation Reactions of the Tellurocyanate Ion

TOR AUSTAD, STEINAR ESPERÅS and JON SONGSTAD

*Chemical Institute, University of Bergen, N-5000 Bergen, Norway*

This paper reports a study on the reaction between a primary alkyl halide and the tellurocyanate ion in acetonitrile. Methyl iodide and methyl tosylate were first used as substrates, but because of the obnoxious odour of the product(s) from these reactions a primary alkyl halide of higher molecular weight was chosen. Benzyl bromide was found to be ideal for several reasons. The product obtained was a crystalline compound, sufficiently stable for elemental analysis and only slightly malodourous. Furthermore, the reaction was rapid and the experimental difficulties due to the reaction between the tellurocyanate ion and traces of oxygen and moisture [1] were thus negligible. Although the rate of the reaction is high at room temperature, a kinetic study was possible and the rate of the reaction was determined. As the rates of the reactions between benzyl bromide and the selenocyanate ion and between benzyl bromide and the thiocyanate ion could be determined as well, a picture of the relative nucleophilicity of the tellurocyanate ion could be obtained.

Benzyl halides have been known for a long time to form exclusively benzyl thiocyanate [2] and benzyl selenocyanate [3] when they react with ionic thiocyanate and selenocyanate, respectively. From the reaction between equivalent amounts of benzyl bromide and tetraphenylarsonium tellurocyanate in acetonitrile, a slightly yellowish crystalline compound was obtained in high yield. This compound was insoluble in diethyl ether while readily soluble in acetonitrile and acetone. An IR spectrum of the product did not show a peak due to the tellurocyanate ion at 2081 cm⁻¹.[1] As the characteristic peaks of the tetraphenylarsonium ion were present, the product from the reaction necessarily had to be a salt.

The product decomposed slowly in water and protic solvents with the formation of elemental tellurium. The usual qualitative tests for nitrogen and bromine were positive. Elemental analysis suggested the product to be considered as an adduct between tetraphenylarsonium bromide and benzyl tellurocyanate, tetraphenylarsonium bromocyanobenzyltellurate(II).

$$\text{Ph}_4\text{As}^+ \qquad \underset{\underset{\underset{N}{\overset{|||}{C}}}{\overset{|}{\text{PhCH}_2\text{Te}^-}}}{\overset{\text{Br}}{\overset{|}{\phantom{x}}}}$$

The compound, crystallized from acetonitrile, is nearly colourless. The prism-shaped crystals are extended along the $a$ axis. Unit cell parameters were calculated from 89 high-order reflections read from Weissenberg $0kl$ and $h0l$ films, employing Ni-filtered $\text{Cu}K\alpha$ radiation. Refinement by a least squares program gave final values of $a = 9.471(4)$ Å, $b = 26.345(9)$ Å, $c = 12.899(5)$ Å and $\beta = 114.63(4)°$. There are four formula units per unit cell. (Density, found by flotation 1.60; calc. 1.61 g/cm³.) From systematic absences, $h0l$ for $l = 2n + 1$ and $0k0$ for $k = 2n + 1$, the space group is $C_{2h} - P2_1/c$.

3. Larsen, B. and Haug, A. *Carbohyd. Res.* **17** (1971) 287.
4. Larsen, B. and Haug, A. *Carbohyd. Res.* **20** (1971) 225.
5. Larsen, B. and Haug, A. Paper read at Seventh International Seaweed Symposium, Sapporo, Japan, August 8th, (1971) 491.
6. Johnston, C. S. and Davies, J. M. Paper read at Sixth International Seaweed Symposium, Santiago, Spain, September 9th, (1968) 501.
7. Knutson, C. A. and Jeanes, A. *Anal. Biochem.* **24** (1968) 470.
8. Madgwick, J., Haug, A. and Larsen, B. *Acta Chem. Scand.* **27** (1973) 711.
9. Lowry, O. H., Rosebrough, N. J., Farr, A. L. and Randall, R. J. *J. Biol. Chem.* **193** (1951) 265.
10. Haug, A. and Larsen, B. *Acta Chem. Scand.* **15** (1961) 1395.

Received October 8, 1973.

# Alkylation Reactions of the Tellurocyanate Ion

TOR AUSTAD, STEINAR ESPERÅS and JON SONGSTAD

*Chemical Institute, University of Bergen, N-5000 Bergen, Norway*

This paper reports a study on the reaction between a primary alkyl halide and the tellurocyanate ion in acetonitrile. Methyl iodide and methyl tosylate were first used as substrates, but because of the obnoxious odour of the product(s) from these reactions a primary alkyl halide of higher molecular weight was chosen. Benzyl bromide was found to be ideal for several reasons. The product obtained was a crystalline compound, sufficiently stable for elemental analysis and only slightly malodourous. Furthermore, the reaction was rapid and the experimental difficulties due to the reaction between the tellurocyanate ion and traces of oxygen and moisture [1] were thus negligible. Although the rate of the reaction is high at room temperature, a kinetic study was possible and the rate of the reaction was determined. As the rates of the reactions between benzyl bromide and the selenocyanate ion and between benzyl bromide and the thiocyanate ion could be determined as well, a picture of the relative nucleophilicity of the tellurocyanate ion could be obtained.

Benzyl halides have been known for a long time to form exclusively benzyl thiocyanate [2] and benzyl selenocyanate [3] when they react with ionic thiocyanate and selenocyanate, respectively. From the reaction between equivalent amounts of benzyl bromide and tetraphenylarsonium tellurocyanate in acetonitrile, a slightly yellowish crystalline compound was obtained in high yield. This compound was insoluble in diethyl ether while readily soluble in acetonitrile and acetone. An IR spectrum of the product did not show a peak due to the tellurocyanate ion at 2081 cm$^{-1}$.[1] As the characteristic peaks of the tetraphenylarsonium ion were present, the product from the reaction necessarily had to be a salt.

The product decomposed slowly in water and protic solvents with the formation of elemental tellurium. The usual qualitative tests for nitrogen and bromine were positive. Elemental analysis suggested the product to be considered as an adduct between tetraphenylarsonium bromide and benzyl tellurocyanate, tetraphenylarsonium bromocyanobenzyltellurate(II).

$$\text{Ph}_4\text{As}^+ \qquad \underset{\overset{|}{\underset{\overset{|}{\underset{N}{\overset{|||}{C}}}}{\text{Te}^-}}}{\overset{\overset{\text{Br}}{|}}{\text{PhCH}_2}}$$

The compound, crystallized from acetonitrile, is nearly colourless. The prism-shaped crystals are extended along the $a$ axis. Unit cell parameters were calculated from 89 high-order reflections read from Weissenberg $0kl$ and $h0l$ films, employing Ni-filtered Cu$K\alpha$ radiation. Refinement by a least squares program gave final values of $a = 9.471(4)$ Å, $b = 26.345(9)$ Å, $c = 12.899(5)$ Å and $\beta = 114.63(4)°$. There are four formula units per unit cell. (Density, found by flotation 1.60; calc. 1.61 g/cm$^3$.) From systematic absences, $h0l$ for $l = 2n + 1$ and $0k0$ for $k = 2n + 1$, the space group is $C_{2h} - P2_1/c$.

The compound is probably an example of a four-electron three-center tellurium compound with a close to linear (N)C−Te−Br bond. The exceptional ability of the tellurium atom to be the central atom in four-electron three-center systems is well documented.[4,5] Recently, several salts of anions of the general type $PhTeX_2^-$ have been isolated.[6]

Freshly prepared samples of the compound have no odour, but on storage at room temperature an unpleasant odour is produced though no significant decomposition was observed. On recrystallization of pure samples, tetraphenylarsonium bromide crystallized as a minor recrystallization product. It is therefore probable that the following equilibrium exists,

$$PhCH_2\overset{\overset{\displaystyle Br}{|}}{\underset{\underset{\displaystyle N}{\overset{\displaystyle |||}{\underset{\displaystyle C}{|}}}}{Te^-}} \rightleftharpoons PhCH_2TeCN + Br^-$$
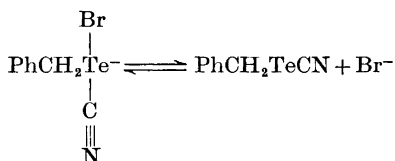
and that the unpleasant odour is due to traces of benzyl tellurocyanate or subsequent products. No yield of dibenzyl telluride or dibenzyl ditelluride could be detected.

The reaction between tetraphenylarsonium tellurocyanate and benzyl bromide in acetonitrile was found to be strictly second order, first order in each reactant, and one equivalent of benzyl bromide consumed one equivalent of the tellurocyanate ion. As the rate of the reaction is high, $t_{\frac{1}{2}} \approx 2$ min for concentrations of reactants of 0.01 M, the accuracy of the rate measurements was limited. Benzyl chloride was found to react at least three orders of magnitude slower than benzyl bromide, but as severe decomposition of the tellurocyanate ion was observed for such long reaction times, the rate of this reaction could not be accurately determined. A $k_{Br}/k_{Cl}$ ratio of $> 10^3$, however, for a non-transition metal nucleophile, is unusual. The results of the kinetic studies are listed in Table 1.

The observed reactivity sequence is thus $NCTe^- > NCSe^- > NCS^-$. This reactivity sequence appears to be the same as when the ions act as electrophiles toward polarizable nucleophiles.[5,7]

Further studies on alkylation reactions of the tellurocyanate ion are in progress in this laboratory.

*Table 1.* Second order rate constants at 21.0°C for nucleophiles reacting with benzyl bromide in acetonitrile. Concentrations of reactants, $6.0 \times 10^{-3}$ M.

| | $k_2$ M$^{-1}$ sec$^{-1}$ |
|---|---|
| NCTe$^-$ | 1.20 |
| NCSe$^-$ | $1.95 \times 10^{-1}$ |
| NCS$^-$ | $3.24 \times 10^{-2}$ |

*Experimental.* Acetonitrile was purified as previously reported [1] and carefully flushed with nitrogen prior to use. Tetraphenylarsonium tellurocyanate, thiocyanate, and selenocyanate were synthesized and purified as reported.[1] Benzyl bromide, Fluka *puriss.*, was distilled in vacuum and stored in a dark bottle in the refrigerator.

*Tetraphenylarsonium bromocyanobenzyltellurate(II).* To 1.343 g tetraphenylarsonium tellurocyanate, $2.5 \times 10^{-3}$ mol, in 30 ml acetonitrile, was slowly added a solution of an equivalent amount of benzyl bromide, 0.428 g, in 20 ml acetonitrile. A slight increase of the yellow colour of the solution could be observed. The reaction mixture was stirred for 15 min at room temperature and traces of tellurium dioxide was removed by filtration. Due to the high solubility of the product in acetonitrile, the volume had to be reduced in vacuum to 15 ml. On addition of a small amount of diethyl ether, the product, slightly yellowish, crystallized. Yield of crude product, 1.624 g, 92 %. IR of the product showed no peak at 2081 cm$^{-1}$ due to ionic tellurocyanate while a very weak peak at 2162 cm$^{-1}$ could be observed. The mother liquor from the crystallization was evaporated to dryness and a minute amount of residue was obtained. No known compounds, however, could be isolated from the residue, which, on standing, deposited traces of elemental tellurium.

The product was dissolved in a minimum of luke-warm acetonitrile, filtered, and the solution allowed to cool in the refrigerator. The first crystals which deposited, less than 0.1 g, mainly consisting of tetraphenylarsonium bromide, were discarded. After 12 h in the refrigerator, 1.28 g, 73 %, of pure product, slightly yellowish, was obtained. M.p. 118°C. The compound decomposed in the melting point capillary at $\approx 160$°C. (Found: C 54.63; H 3.62; N 2.06. Calc. for $C_{32}H_{27}AsBrNTe$: C 54.28; H 3.84; N 1.98). The compound, dissolved in acetonitrile, appeared stable in the

presence of lithium perchlorate, while water slowly deposited elemental tellurium.

*Kinetic study.* The rate constants were determined by measuring the disappearance of the peaks at 2081 $cm^{-1}$ (TeCN$^-$), 2068 $cm^{-1}$ (SeCN$^-$), and 2059 $cm^{-1}$ (SCN$^-$) at varying concentration of the pseudohalide ions and benzyl bromide in the $4-10 \times 10^{-3}$ M concentration range. The rate constants in Table 1 refer to measurements with initial concentrations of reactants of $6 \times 10^{-3}$ M. When the thiocyanate ion and the selenocyanate were the nucleophiles, 0.1 cm liquid cells were used. Due to the considerably lower extinction coefficient of the tellurocyanate ion at 2081 $cm^{-1}$,[1] 0.15 cm liquid cells were used in these reactions. The rate constants for the selenocyanate ion and the thiocyanate ion are probably good to $\pm$ 3 % while the rate constant for the reaction between the tellurocyanate ion and benzyl bromide is probably of considerably lower accuracy, $\approx \pm 5$ %, due to the high rate of this reaction. A very weak peak at $\sim 2162$ $cm^{-1}$ could be observed in completed reaction mixtures. For all examined reactions, the rate plots were linear up to two or three half-lives. Due to traces of oxygen in the applied solvent, the rate constant for the very slow reaction between tetraphenylarsonium tellurocyanate and benzyl chloride could not be accurately determined.

The stoichiometry of the reaction between tetraphenylarsonium tellurocyanate and benzyl bromide was determined in more concentrated solutions by measuring the reduction of the peak due to the tellurocyanate ion as a function of added benzyl bromide. All measurements confirmed the reaction to be a 1:1 reaction.

*Acknowledgement.* The authors are indebted to Dr. O. Foss for valuable discussions.

1. Austad, T., Songstad, J. and Åse, K. *Acta Chem. Scand.* **25** (1971) 331.
2. Henry, L. *Ber.* **2** (1869) 636.
3. Jackson, C. L. *Ann.* **179** (1875) 1.
4. Foss, O. *Selected Topics in Structure Chemistry,* Universitetsforlaget, Oslo 1967, p. 145.
5. Austad, T., Rød, T., Åse, K., Songstad, J. and Norbury, A. H. *Acta Chem. Scand.* **27** (1973) 1939.
6. Vikane, O. *Personal communication.*
7. Stangeland, L. J., Austad, T. and Songstad, J. *Acta Chem. Scand.* **27** (1973). *In press.*

Received October 25, 1973.

# Reactions of Diphenylditelluride with Halogens in Presence of Ligands Containing Sulphur or Selenium as Donor Atoms

SVERRE HAUGE and OLAV VIKANE

*Chemical Institute, University of Bergen, N-5000 Bergen, Norway*

Phenyltellurium trichloride dissolved in methanol reacts with aqueous thiourea (tu) to give thiourea complexes of divalent tellurium, $C_6H_5Te(tu)Cl$ and $C_6H_5Te(tu)_2Cl$.[1]

It has now been found that diphenylditelluride dissolved in methanol reacts with halogen (chlorine or bromine) and ligands containing sulphur or selenium to form complexes of divalent tellurium:

$$C_6H_5TeTeC_6H_5 + X_2 + 2\ L = 2C_6H_5TeLX \quad (1)$$

or

$$C_6H_5TeTeC_6H_5 + Br_2 + 4\ L^- =$$
$$2\ C_6H_5TeL_2^- + 2\ Br^- \quad (2)$$

In the first case L is thiourea, selenourea, triphenylphosphineselenide, or trimorpholylphosphineselenide. In the second case $L^-$ is thiocyanate or selenocyanate. The anionic complexes formed have been isolated as tetramethylammonium salts.

By use of 4 mol of selenourea (su) and 1 mol chlorine the complex $C_6H_5Te(su)_2Cl$ was formed:

$$C_6H_5TeTeC_6H_5 + Cl_2 + 4\ su =$$
$$2\ C_6H_5Te(su)_2^+ + 2\ Cl^-$$

The analogous complex with thiourea is known.[1]

When potassium selenocyanate instead of tetramethylammonium selenocyanate was used in reaction (2) a blue-violet compound separated from the solution. The compound was shown to be bis(benzenetellurenyl) selenide, $C_6H_5TeSeTeC_6H_5$. A possible mechanism may be that benzenetellurenyl selenocyanate is formed first, and then (Ar $= C_6H_5$):

$$ArTeSeCN + SeCN^- = Se(CN)_2 + ArTeSe^-$$
$$ArTeSeCN + ArTeSe^- = ArTeSeTeAr +$$
$$SeCN^-$$

The same compound, bis(benzenetellurenyl) selenide, was isolated from a reaction between selenourea-benzenetellurenyl chloride, $C_6H_5Te(su)Cl$, and potassium selenocyanate. The reaction is probably

presence of lithium perchlorate, while water slowly deposited elemental tellurium.

*Kinetic study.* The rate constants were determined by measuring the disappearance of the peaks at 2081 cm$^{-1}$ (TeCN$^-$), 2068 cm$^{-1}$ (SeCN$^-$), and 2059 cm$^{-1}$ (SCN$^-$) at varying concentration of the pseudohalide ions and benzyl bromide in the $4-10 \times 10^{-3}$ M concentration range. The rate constants in Table 1 refer to measurements with initial concentrations of reactants of $6 \times 10^{-3}$ M. When the thiocyanate ion and the selenocyanate were the nucleophiles, 0.1 cm liquid cells were used. Due to the considerably lower extinction coefficient of the tellurocyanate ion at 2081 cm$^{-1}$,[1] 0.15 cm liquid cells were used in these reactions. The rate constants for the selenocyanate ion and the thiocyanate ion are probably good to $\pm 3$ % while the rate constant for the reaction between the tellurocyanate ion and benzyl bromide is probably of considerably lower accuracy, $\approx \pm 5$ %, due to the high rate of this reaction. A very weak peak at $\sim 2162$ cm$^{-1}$ could be observed in completed reaction mixtures. For all examined reactions, the rate plots were linear up to two or three half-lives. Due to traces of oxygen in the applied solvent, the rate constant for the very slow reaction between tetraphenylarsonium tellurocyanate and benzyl chloride could not be accurately determined.

The stoichiometry of the reaction between tetraphenylarsonium tellurocyanate and benzyl bromide was determined in more concentrated solutions by measuring the reduction of the peak due to the tellurocyanate ion as a function of added benzyl bromide. All measurements confirmed the reaction to be a 1:1 reaction.

*Acknowledgement.* The authors are indebted to Dr. O. Foss for valuable discussions.

1. Austad, T., Songstad, J. and Åse, K. *Acta Chem. Scand.* **25** (1971) 331.
2. Henry, L. *Ber.* **2** (1869) 636.
3. Jackson, C. L. *Ann.* **179** (1875) 1.
4. Foss, O. *Selected Topics in Structure Chemistry*, Universitetsforlaget, Oslo 1967, p. 145.
5. Austad, T., Rød, T., Åse, K., Songstad, J. and Norbury, A. H. *Acta Chem. Scand.* **27** (1973) 1939.
6. Vikane, O. *Personal communication.*
7. Stangeland, L. J., Austad, T. and Songstad, J. *Acta Chem. Scand.* **27** (1973). *In press.*

Received October 25, 1973.

# Reactions of Diphenylditelluride with Halogens in Presence of Ligands Containing Sulphur or Selenium as Donor Atoms

SVERRE HAUGE and OLAV VIKANE

*Chemical Institute, University of Bergen, N-5000 Bergen, Norway*

Phenyltellurium trichloride dissolved in methanol reacts with aqueous thiourea (tu) to give thiourea complexes of divalent tellurium, $C_6H_5Te(tu)Cl$ and $C_6H_5Te(tu)_2Cl$.[1]

It has now been found that diphenylditelluride dissolved in methanol reacts with halogen (chlorine or bromine) and ligands containing sulphur or selenium to form complexes of divalent tellurium:

$$C_6H_5TeTeC_6H_5 + X_2 + 2\ L = 2C_6H_5TeLX \quad (1)$$

or

$$C_6H_5TeTeC_6H_5 + Br_2 + 4\ L^- =$$
$$2\ C_6H_5TeL_2^- + 2\ Br^- \quad (2)$$

In the first case L is thiourea, selenourea, triphenylphosphineselenide, or trimorpholylphosphineselenide. In the second case L$^-$ is thiocyanate or selenocyanate. The anionic complexes formed have been isolated as tetramethylammonium salts.

By use of 4 mol of selenourea (su) and 1 mol chlorine the complex $C_6H_5Te(su)_2Cl$ was formed:

$$C_6H_5TeTeC_6H_5 + Cl_2 + 4\ su =$$
$$2\ C_6H_5Te(su)_2^+ + 2\ Cl^-$$

The analogous complex with thiourea is known.[1]

When potassium selenocyanate instead of tetramethylammonium selenocyanate was used in reaction (2) a blue-violet compound separated from the solution. The compound was shown to be bis(benzenetellurenyl) selenide, $C_6H_5TeSeTeC_6H_5$. A possible mechanism may be that benzenetellurenyl selenocyanate is formed first, and then (Ar $= C_6H_5$):

$$ArTeSeCN + SeCN^- = Se(CN)_2 + ArTeSe^-$$
$$ArTeSeCN + ArTeSe^- = ArTeSeTeAr + SeCN^-$$

The same compound, bis(benzenetellurenyl) selenide, was isolated from a reaction between selenourea-benzenetellurenyl chloride, $C_6H_5Te(su)Cl$, and potassium selenocyanate. The reaction is probably

similar to the conversion of the adduct of thiourea with $o$-nitrobenzeneselenenyl ion, $ArSeSC(NH_2)_2^+$, to bis($o$-nitrobenzeneselenenyl)sulphide, $ArSeSSeAr$.[2]

In an attempt to prepare a phenyldibromotellurate(II) complex a compound which was shown to be tetramethylammonium phenyltetrabromotellurate(IV) crystallized from the solution:

$$C_6H_5TeTeC_6H_5 + 2 Br_2 + 2 Br^- =$$
$$2 C_6H_5TeBr_4^-$$
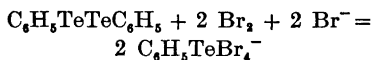
There is probably, in the solution, an equilibrium between tellurate(II) and tellurate(IV). The solubility and the stability of the complexes under the conditions employed, favour the tellurate(IV).

Space groups and unit cell dimensions were determined from single-crystal oscillation and Weissenberg photographs using CuKα radiation. The unit cell dimensions are believed to be accurate to within 0.5 %. Densities were determined by flotation. Melting points are corrected.

Diphenylditelluride was prepared according to the method of Haller and Irgolic.[3] Potassium selenocyanate was prepared as described in *Inorganic Syntheses*.[4] Tetramethylammonium selenocyanate was prepared as described elsewhere.[5] Triphenylphosphineselenide and trimorpholylphosphineselenide were gifts from J. Songstad of this Institute.

*Thiourea-benzenetellurenyl bromide*, $C_6H_5Te$-(tu)Br. 2.5 mmol (1.025 g) of diphenylditelluride and 5 mmol (0.38 g) of thiourea were dissolved in 20 ml of warm methanol, and 2.5 mmol of bromine dissolved in 2.5 ml methanol was added under rapid stirring. After filtering, a clear orange red solution resulted, from which the compound crystallized on standing. Yield, 1.62 g (90 %). The product was recrystallized from methanol, and identified by its melting point and by X-ray photographs. The thiourea-benzenetellurenyl bromide has earlier been prepared from phenyltellurium trichloride, thiourea, and potassium bromide.[1]

*Selenourea-benzenetellurenyl chloride*, $C_6H_5Te$-(su)Cl, was prepared in the same way as the thiourea compound, using 2.5 mmol (1.025 g) of diphenylditelluride and 5 mmol (0.62 g) of selenourea, dissolved in 20 ml of warm methanol, and 2.5 mmol of chlorine dissolved in 5 ml methanol. Yield, 1.63 g (89 %). It could be recrystallized from methanol (1 g dissolved in about 30 ml at boiling temperature). M.p. 165° (dec.). (Found: C 23.11; H 3.55; N 7.79. Calc. for $C_7H_9ClN_2SeTe$: C 23.14; H 3.42; N 7.71).

The crystals are orange-red, monoclinic prisms extended along the $a$ axis, with $a = 6.28$ Å, $b = 10.70$ Å, $c = 15.34$ Å, $\beta = 90.6°$. There are four molecules per unit cell; density, calc. 2.34, found 2.35 g/cm³. The space group, from systematic absences, is $P2_1/n$ (No. 14). The crystals are isomorphous with the corresponding thiourea complex.[1]

*Selenourea-benzenetellurenyl bromide*, $C_6H_5Te$-(su)Br, was prepared and recrystallized as described above for the chloride, using 2.5 mmol (1.025 g) of diphenylditelluride and 5 mmol (0.62 g) of selenourea dissolved in 20 ml of warm methanol, and 2.5 mmol of bromine dissolved in 2.5 ml methanol. Yield, 1.46 g (72 %). M.p. 195° (dec.). (Found: C 20.76; H 2.31; N 7.02. Calc. for $C_7H_9BrN_2SeTe$: C 20.62; H 2.21; N 6.87).

The crystals are isomorphous with those of the chloride, and have the same colour and morphology. The unit cell dimensions are, $a = 6.50$ Å, $b = 10.73$ Å, $c = 15.41$ Å, $\beta = 91.2°$, density, calc. 2.52, found 2.51 g/cm³.

*Trimorpholylphosphineselenide-benzenetellurenyl chloride*, $C_6H_5TeSeP(NC_4H_8O)_3Cl$, was prepared as described above for the selenourea compounds, using 1.25 mmol (0.50 g) of diphenylditelluride and 2.5 mmol (0.92 g) of trimorpholylphosphineselenide dissolved in 40 ml warm methanol, and 1.25 mmol of chlorine dissolved in 3.6 ml methanol. The compound was not recrystallized. Yield, 1.10 g (72 %). M.p., 137° (dec.). (Found: C 35.47; H 4.72; N 6.87; O 7.89; P 5.02. Calc. for $C_{18}H_{29}N_3O_3PClSeTe$: C 35.53; H 4.77; N 6.91; O 7.89; P 5.09).

The crystals form orange-red, monoclinic prisms extended along the $a$ axis, with $a = 9.13$ Å, $b = 18.70$ Å, $c = 14.76$ Å, $\beta = 116.4°$. There are four molecules per unit cell; density, calc. 1.78, found 1.77 g/cm³. The space group, from systematic absences, is $P2_1/c$ (No. 14).

*Trimorpholylphosphineselenide-benzenetellurenyl bromide*, $C_6H_5TeSeP(NC_4H_8O)_3Br$, was prepared as described above for the chloride, using 1.25 mmol bromine dissolved in 2.4 ml methanol instead of the chlorine solution. Yield, 1.30 g (79 %). M.p., 138° (dec.). (Found: C 33.03; H 4.35; N 6.35; O 7.32; P 4.87. Calc. for $C_{18}H_{29}N_3O_3PBrSeTe$: C 33.11; H 4.44; N 6.44; O 7.36; P 4.75).

The crystals are isomorphous with those of the chloride, and show the same colour and morphology. The unit cell dimensions are, $a = 9.23$ Å, $b = 18.84$ Å, $c = 14.86$ Å, $\beta = 117.2$. Density, calc. 1.88, found 1.87 g/cm³.

*Triphenylphosphineselenide-benzenetellurenyl bromide*, $C_6H_5TeSeP(C_6H_5)_3Br$, was prepared in the same way as trimorpholylphosphineselenide-benzenetellurenyl bromide, using 1.25

mmol (0.50 g) of diphenylditelluride and 2.5 mmol (0.86 g) of triphenylphosphineselenide dissolved in 40 ml of methanol, and 1.25 mmol of bromine dissolved in 2.5 ml methanol. Yield, 1.1 g (70 %). M.p., 127° (dec.). (Found: C 46.14; H 3.30; P 4.96. Calc. for $C_{24}H_{20}PBrSeTe$: C 46.05; H 3.20; P 4.95).

The crystals are orange-red, monoclinic prisms extended along the long $ac$ diagonal, with $a = 12.79$ Å, $b = 9.93$ Å, $c = 18.60$ Å, $\beta = 104.8°$. There are four formula units per unit cell; density, calc. 1.82, found 1.80 g/cm³. The space group, from systematic absences, is $P2_1/n$ (No. 14).

*Diselenourea-benzenetellurenyl     chloride*, $C_6H_5Te(su)_2Cl$. To a solution of 2.5 mmol (1.025 g) of diphenylditelluride and 10 mmol (1.23 g) of selenourea in 30 ml of warm methanol was added slowly under vigorous stirring, 2.5 mmol of chlorine dissolved in 2.5 ml methanol. After filtering, a bright yellow solution resulted, from which the complex crystallized on standing in a refrigerator. Yield, 1.72 g (70 % based on $C_6H_5TeTeC_6H_5$). It may be recrystallized from a warm solution of selenourea in methanol. M.p., 169° (dec.). (Found: C 19.86; H 2.65; N 11.56. Calc. for $C_8H_{13}N_4ClSe_2Te$: C 19.75; H 2.67; N 11.52).

The crystals form yellow, triclinic prisms with $a = 11.22$ Å, $b = 12.06$ Å, $c = 5.91$ Å, $\alpha = 98.95°$, $\beta = 93.86°$, $\gamma = 62.17°$. With two formula units in unit cell, the calculated density is 2.30, found 2.28 g/cm³.

The complex was also prepared from $C_6H_5Te(su)Cl$ and selenourea. About 0.2 g of selenourea was dissolved in a mixture of 5 ml water, 5 ml methanol, and 0.5 ml conc. hydrochloric acid. About 0.2 g of selenourea-benzenetellurenyl chloride was added and the mixture was heated until all had dissolved. A mixture of triselenourea dichloride hydrate[6] and diselenourea-benzenetellurenyl chloride crystallized on standing. When prepared in this way, the crystals of diselenourea-benzenetellurenyl chloride were orthorhombic long needles extended along the $c$ axis, with $a = 11.99$ Å, $b = 21.24$ Å, $c = 5.89$ Å. There are four formula units per unit cell; density, calc. 2.15, found 2.14 g/cm³. The space group, from systematic absences, is $P2_12_12_1$ (No. 19). In this form, the crystals are isomorphous with those of the corresponding thiourea complex.[1]

*Tetramethylammonium    phenyldiselenocyanatotellurate(II)*, $(CH_3)_4NC_6H_5Te(SeCN)_2$. To a solution of 1.25 mmol (0.50 g) of diphenylditelluride and 10 mmol (1.79 g) of tetramethylammonium selenocyanate in 30 ml of warm methanol, was added, under vigorous stirring, 1.25 mmol of bromine dissolved in 2 ml of

methanol. After filtering, a clear orange-red solution resulted, from which the tellurate(II) crystallized on standing. Yield, 0.95 g (78 %). The compound can be recrystallized from a solution of tetramethylammonium selenocyanate in methanol. M.p., 134° (dec.). (Found: C 29.79; H 3.47; N 8.72; Se 30.06. Calc. for $C_{12}H_{17}N_3Se_2Te$: C 29.48; H 3.48; N 8.60; Se 32.33).

The crystals form orange-red prisms and plates. The prisms are extended along the $b$ axis, with $a = 15.84$ Å, $b = 9.34$ Å, $c = 23.38$ Å, $\beta = 100.7°$. There are eight formula units in the unit cell; density, calc. 1.87, found 1.86 g/cm³. The space group, from systematic absences, is $Cc$ (No. 9) or $C2/c$ (No. 15).

*Tetramethylammonium    phenyldithiocyanatotellurate(II)*, $(CH_3)_4NC_6H_5Te(SCN)_2$, was prepared in the same way as the analogous selenocyanate complex, using 10 mmol (1.32 g) of tetramethylammonium    thiocyanate. The crystals were washed with minute amounts of cold water, cold ethanol, and finally with ether, whereby co-precipitated $(CH_3)_4NSCN$ was removed. Yield, 0.64 g (65 %). M.p., 108° (dec.). (Found: C 36.34; H 4.34; N 10.43; S 16.18. Calc. for $C_{12}H_{17}N_3S_2Te$: C 36.49; H 4.31; N 10.64; S 16.22).

The crystals are isomorphous with those of the selenocyanato complex, and show the same colour and morphology. The unit cell dimensions are, $a = 15.78$ Å, $b = 9.18$ Å, $c = 23.15$ Å, $\beta = 100.6°$, and density, calc. 1.59, found 1.58 g/cm³.

*Tetramethylammonium    phenyltetrabromotellurate(IV)*, $(CH_3)_4NC_6H_5TeBr_4$. In an attempt to prepare tetramethylammonium phenyldibromotellurate(II), 2.5 mmol (1.025 g) of diphenylditelluride was dissolved in 15 ml methanol, and 6.9 mmol (1.05 g) of tetramethylammonium bromide was dissolved in 10 ml of water and a small amount of hydrobromic acid, and the two solutions were mixed. 2.5 mmol of bromine dissolved in 2.5 ml methanol was added with stirring. The orange-red solution was stored in a refrigerator for 12 h. Bright yellow crystals had formed which later were shown to be tetramethylammonium phenyltetrabromotellurate(IV). Yield, 0.41 g, or 83 % based on the amount of bromine employed. M.p., 290° (dec.). (Found: C 20.19; H 2.92; N 2.47; Br 53.55. Calc. for $C_{10}H_{17}NBr_4Te$: C 20.06; H 2.84; N 2.34; Br 53.43).

Some diphenylditelluride was isolated from the mother liquor after evaporation.

The crystals of the phenyltetrabromotellurate(IV) are triclinic plates with $a = 13.08$ Å, $b = 15.85$ Å, $c = 9.33$ Å, $\alpha = 91.3°$, $\beta = 104.4°$, $\gamma = 104.8°$. The density, calc. for four formula

units in the unit cell, is 2.30, found 2.29 g/cm³.

*Bis(benzenetellurenyl) selenide*, $(C_6H_5Te)_2Se$. To a solution of 2.5 mmol (1.025 g) diphenyl-ditelluride and 10 mmol (1.44 g) of potassium selenocyanate dissolved in 30 ml of warm methanol was added, under vigorous stirring, 2.5 mmol of bromine dissolved in 2 ml methanol. The solution was stored in a refrigerator for 24 h. The blue-violet crystals of $(C_6H_5Te)_2Se$ were then filtered off. Yield, 1.18 g, or 97 % based on the amount of diphenylditelluride employed. M.p., 64°. (Found: C 30.45; H 2.32; Se 16.42. Calc. for $C_{12}H_{10}SeTe_2$: C 29.50; H. 2.03; Se 16.18).

The crystals are monoclinic, and form long thin needles.

1. Foss, O. and Hauge, S. *Acta Chem. Scand.* **13** (1959) 2155.
2. Eriksen, R. *Acta Chem. Scand.* **26** (1972) 1274.
3. Haller, W. S. and Irgolic, K. J. *J. Organometal. Chem.* **38** (1972) 97.
4. Waitkins, G. R. and Shutt, R. *Inorg. Syn.* **2** (1946) 186.
5. Hauge, S. *Acta Chem. Scand.* **25** (1971) 3081.
6. Hauge, S., Opedal, D. and Aarskog, J. *Acta Chem. Scand.* **24** (1969) 1107.

# Loroxanthin from Chlamydomonas reinhardti

GEORGE W. FRANCIS,[a]
GJERT KNUTSEN[b] and TORLEIV LIEN[b]

[a] *Department of Chemistry and* [b] *Botanical Laboratory, University of Bergen, N-5000 Bergen, Norway*

Previous workers [1-3] have identified the main carotenoid pigments of the green alga *Chlamydomonas reinhardti* as β-carotene, lutein, violaxanthin, trollein and neoxanthin. We have now reinvestigated the carotenoids of *Chl. reinhardti*, strain No. 11−32 (90) from the algal collection of the Institute of Plant

Physiology, University of Göttingen, Germany.

Pigments were extracted from the damp-dried algal mass with acetone/methanol (2/1) mixtures, the total extract taken to dryness under reduced pressure and after saponification with methanolic KOH, the carotenoids were separated by thin layer chromatography on Kieselgel G layers with acetone/petrol solvent mixtures. The pigments described by previous workers were readily recognised from their visible light absorption spectra and chromatographic properties. The total pigment content (*ca.* 1.4 mg/g wet weight) and the distribution among the individual pigments were close to those previously reported.

Mass spectrometry showed the expected molecular weights for all polyenes as judged by the observation of molecular ions (M) and ions at M − 92 (P), M − 106 (Q) and M − 158 (T) mass units.[4,5] These ions are formed by the extrusion of 6 or 10 consecutive C-atoms of the conjugated chain with the methyl groups carried by these atoms according to the mechanism of Fig. 1.[6] Treatment with acidified ethanol [7] produced the expected shifts to lower wavelength in the visible light absorption spectra of the epoxides, violaxanthin and neoxanthin. However, while acetylation, with acetic anhydride in pyridine, of lutein, violaxanthin and neoxanthin yielded the required diacetates, the triol previously described as trollein provided a triacetate. Since trollein (*1*) contains only two acetylable hydroxy groups,[8] the identity of the triol with this compound is disproved.

The triol had visible light absorption maxima at 473, 446, (423) nm in acetone and thus had a nonaene chromophore of the type found in lutein (*2*). Mass spectrometry of the triol, in addition to M (584), P (492 = M − 92), Q (478 = M − 106) and T (426 = M − 158) ions, provided an ion at $m/e$ 462 (M − 122). The mass spectrum of the triacetate (M = 710) showed an analogous ion at $m/e$ 546 (M − 164). The possibility that these latter ions were Q' ions formed by species in which one of the extruded C-atoms of the chain bore a hydroxymethyl or an acetoxymethyl group, respectively, rather than a methyl group was apparent.[9,10] The partial mass shift of the Q ion, but not of the P ion, was indicative that the substituent was at C − 19 rather than at C − 20.[10,11]

Further information about the position of the hydroxy groups of the triol was

units in the unit cell, is 2.30, found 2.29 g/cm³.

*Bis(benzenetellurenyl) selenide*, $(C_6H_5Te)_2Se$. To a solution of 2.5 mmol (1.025 g) diphenyl-ditelluride and 10 mmol (1.44 g) of potassium selenocyanate dissolved in 30 ml of warm methanol was added, under vigorous stirring, 2.5 mmol of bromine dissolved in 2 ml methanol. The solution was stored in a refrigerator for 24 h. The blue-violet crystals of $(C_6H_5Te)_2Se$ were then filtered off. Yield, 1.18 g, or 97 % based on the amount of diphenylditelluride employed. M.p., 64°. (Found: C 30.45; H 2.32; Se 16.42. Calc. for $C_{12}H_{10}SeTe_2$: C 29.50; H. 2.03; Se 16.18).

The crystals are monoclinic, and form long thin needles.

1. Foss, O. and Hauge, S. *Acta Chem. Scand.* **13** (1959) 2155.
2. Eriksen, R. *Acta Chem. Scand.* **26** (1972) 1274.
3. Haller, W. S. and Irgolic, K. J. *J. Organometal. Chem.* **38** (1972) 97.
4. Waitkins, G. R. and Shutt, R. *Inorg. Syn.* **2** (1946) 186.
5. Hauge, S. *Acta Chem. Scand.* **25** (1971) 3081.
6. Hauge, S., Opedal, D. and Aarskog, J. *Acta Chem. Scand.* **24** (1969) 1107.

# Loroxanthin from *Chlamydomonas reinhardti*

GEORGE W. FRANCIS,[a]
GJERT KNUTSEN[b] and TORLEIV LIEN[b]

[a]*Department of Chemistry and* [b]*Botanical Laboratory, University of Bergen, N-5000 Bergen, Norway*

**P**revious workers [1-3] have identified the main carotenoid pigments of the green alga *Chlamydomonas reinhardti* as β-carotene, lutein, violaxanthin, trollein and neoxanthin. We have now reinvestigated the carotenoids of *Chl. reinhardti*, strain No. 11−32 (90) from the algal collection of the Institute of Plant

Physiology, University of Göttingen, Germany.

Pigments were extracted from the damp-dried algal mass with acetone/methanol (2/1) mixtures, the total extract taken to dryness under reduced pressure and after saponification with methanolic KOH, the carotenoids were separated by thin layer chromatography on Kieselgel G layers with acetone/petrol solvent mixtures. The pigments described by previous workers were readily recognised from their visible light absorption spectra and chromatographic properties. The total pigment content (*ca.* 1.4 mg/g wet weight) and the distribution among the individual pigments were close to those previously reported.

Mass spectrometry showed the expected molecular weights for all polyenes as judged by the observation of molecular ions (M) and ions at M − 92 (P), M − 106 (Q) and M − 158 (T) mass units.[4,5] These ions are formed by the extrusion of 6 or 10 consecutive C-atoms of the conjugated chain with the methyl groups carried by these atoms according to the mechanism of Fig. 1.[6] Treatment with acidified ethanol [7] produced the expected shifts to lower wavelength in the visible light absorption spectra of the epoxides, violaxanthin and neoxanthin. However, while acetylation, with acetic anhydride in pyridine, of lutein, violaxanthin and neoxanthin yielded the required diacetates, the triol previously described as trollein provided a triacetate. Since trollein (*1*) contains only two acetylable hydroxy groups,[8] the identity of the triol with this compound is disproved.

The triol had visible light absorption maxima at 473, 446, (423) nm in acetone and thus had a nonaene chromophore of the type found in lutein (*2*). Mass spectrometry of the triol, in addition to M (584), P (492 = M − 92), Q (478 = M − 106) and T (426 = M − 158) ions, provided an ion at *m/e* 462 (M − 122). The mass spectrum of the triacetate (M = 710) showed an analogous ion at *m/e* 546 (M − 164). The possibility that these latter ions were Q′ ions formed by species in which one of the extruded C-atoms of the chain bore a hydroxymethyl or an acetoxymethyl group, respectively, rather than a methyl group was apparent.[9,10] The partial mass shift of the Q ion, but not of the P ion, was indicative that the substituent was at C − 19 rather than at C − 20.[10,11]

Further information about the position of the hydroxy groups of the triol was

*Fig. 1.* Mechanism for the formation, by either electron bombardment or prior thermal decomposition, of P (M−92), Q (M−106), and T (M−158) ions observed in the mass spectra of carotenoids.[6]

sought by subjecting it to *p*-chloranil oxidation for 6 h under standard conditions.[12] This reagent is known to effect oxidation of hydroxy groups allylic to the main chromophore, but to leave hydroxy groups allylic to isolated double bonds unaffected. This treatment yielded a single product, somewhat less polar than the starting material, (TLC on Kieselgel G, with 30 % acetone in petrol as eluent, gave the following $R_F$-values: triol, 0.30; oxidised triol, 0.37; lutein, 0.51) having one absorption maximum only in the visible light region, at 476 nm in acetone and 480 nm in ethanol. Mass spectrometry showed this product to have a molecular weight of 582 and a prominent peak due to loss of 120 mass units at *m/e* 462 was explicable as a Q′ ion. A diacetate of molecular weight 666 could be obtained from this product.



The above evidence shows that only a single oxidisable hydroxy group is allylic to the main chromophore in the triol. Further, the observation of a large shift in the position of the main visible light absorption maximum, 30 nm, on oxidation is believed to be characteristic for carotenoids where one of the normal in-chain methyl groups has been replaced by a hydroxymethyl group.[10,13] Having thus located the oxidised methyl group at C−19 or C−19′, the two remaining hydroxy groups must be placed in the end groups in a way that explains their non-oxidation. The co-occurrence of the triol with lutein in this organism suggests that these hydroxy groups are similarly placed in each case and such an arrangement satisfies the above condition.

Loroxanthin (3) is known [10] to occur in a few species of green algae and the data reported for that compound and its *p*-chloranil oxidation product, loroxanthal (4), accord with those here reported for the triol and its oxidation product. We thus conclude that the triol, present in *Chlamydomonas reinhardti* and previously identified as trollein (1), is in fact loroxanthin (3).

When the other xanthophylls present in *Chlamydomonas reinhardti* were subjected to *p*-chloranil oxidation under the same conditions as the triol, no less polar products were formed. However, in the case of the epoxides, prolonged treatment yielded unidentified more polar products,

and since the effects of the epoxy functions in this reaction are unknown the possibility that these compounds contain hydroxy-methyl groups cannot be completely ruled out. The weight of available evidence, however, suggests that $\beta$-carotene, lutein, violaxanthin, and neoxanthin have been correctly identified by the previous workers.[1-3]

Culturing conditions[14] and chemical methods[15] have been described elsewhere.

1. Krinsky, N. I. and Levine, R. P. *Plant Physiol.* **39** (1964) 680.
2. Stolbova, A. V. *Genetika* **7** (1971) 90.
3. Sirevåg, R. and Levine, R. P. *Planta* **111** (1973) 73.
4. Schwieter, U., Bolliger, H. R., Chopard-dit-Jean, L. H., Englert, G., Kofler, M., König, A., v. Planta, C., Rüegg, R., Vetter, W. and Isler, O. *Chimia* **19** (1965) 294.
5. Enzell, C. R., Francis, G. W. and Liaaen-Jensen, S. *Acta Chem. Scand.* **23** (1969) 727.
6. Francis, G. W. *Acta Chem. Scand.* **26** (1972) 1443.
7. Karrer, P. and Jucker, E. *Carotenoids*, Elsevier, Amsterdam 1950.
8. Straub, O. In Isler, O. *Carotenoids*, Birkhäuser, Basel 1971.
9. Francis, G. W. and Liaaen-Jensen, S. *Acta Chem. Scand.* **24** (1970) 2705.
10. Aitzetmüller, K., Strain, H. H., Svec, W. A., Grandolfo, M. and Katz, J. J. *Phytochemistry* **8** (1969) 1761.
11. Enzell, C. R. and Liaaen-Jensen, S. *Acta Chem. Scand.* **25** (1971) 271.
12. Liaaen-Jensen, S. *Acta Chem. Scand.* **19** (1965) 1166.
13. Aasen, A. J. and Liaaen-Jensen, S. *Acta Chem. Scand.* **21** (1967) 2185.
14. Lien, T. and Knutsen, G. *Exptl. Cell Res.* **78** (1973) 79.
15. Halfen, L. N. and Francis, G. W. *Arch. Mikrobiol.* **81** (1972) 25.

Received September 24, 1973.

# Crystalline Leghemoglobin

## XIV. Transfer of Hematin from Lba and Lbc to Horse-radish Peroxidase Apoprotein

NILS ELLFOLK, ULLA PERTILÄ and GUNNEL SIEVERS

*Department of Biochemistry, University of Helsinki, SF-00170 Helsinki 17, Finland*

In 1960 Rossi-Fanelli and Antonini noted the transfer of hematin from *Aplysia* methemoglobin to horse apomyoglobin.[1] Until then the bond between heme and globin had been considered very stable under physiological conditions. A similar migration of hematin has also been shown to take place between some other hemo-proteins, *e.g.* myoglobin and horse-radish apoperoxidase (apoHRP).[2] In the present investigation the transfer of hematin from the fast and slow components of soybean leghemoglobin, Lba and Lbc, to apoHRP has been studied. The appearance of the peroxidase activity is taken as evidence for the correct binding of hematin to apoHRP. For comparison, the transfer of the hematin of horse myoglobin (Mb I) to apoHRP was also studied.

*Materials and methods.* Lba, Lbc and yeast cytochrome $c$ peroxidase (YCCP) were prepared as described previously.[3,4] Horse heart cytochrome $c$ was a commercial preparation (Type III) from Sigma Chemical Company (St. Louis, U.S.A.). Horse myoglobin (Mb I) was isolated according to Åkeson and Theorell.[5] Horse radish peroxidase, component C (HRP C) was prepared according to Paul,[6] and its apoprotein according to Theorell and Maehly.[7] The heme-binding capacity of apoHRP was determined by titration with hematin. The peroxidase activity was assayed by the guaiacol method.[8] The concentration of hydrogen peroxide was determined enzymatically according to Yonetani.[9] ApoHRP and leghemo-globin or myoglobin, respectively, were incubated in 0.02 M sodium phosphate buffer, pH 7.0, for 18 h at 25°C. The peroxidatic activity of the solution was measured and the amount of HRP formed calculated.

*Results and discussion.* Fig. 1 portrays the transfer of hematin from Lba, Lbc and Mb I to apoHRP at pH 7.0. The values obtained were corrected for the inherent

and since the effects of the epoxy functions in this reaction are unknown the possibility that these compounds contain hydroxymethyl groups cannot be completely ruled out. The weight of available evidence, however, suggests that $\beta$-carotene, lutein, violaxanthin, and neoxanthin have been correctly identified by the previous workers.[1-3]

Culturing conditions [14] and chemical methods [15] have been described elsewhere.

1. Krinsky, N. I. and Levine, R. P. *Plant Physiol.* **39** (1964) 680.
2. Stolbova, A. V. *Genetika* **7** (1971) 90.
3. Sirevåg, R. and Levine, R. P. *Planta* **111** (1973) 73.
4. Schwieter, U., Bolliger, H. R., Chopard-dit-Jean, L. H., Englert, G., Kofler, M., König, A., v. Planta, C., Rüegg, R., Vetter, W. and Isler, O. *Chimia* **19** (1965) 294.
5. Enzell, C. R., Francis, G. W. and Liaaen-Jensen, S. *Acta Chem. Scand.* **23** (1969) 727.
6. Francis, G. W. *Acta Chem. Scand.* **26** (1972) 1443.
7. Karrer, P. and Jucker, E. *Carotenoids*, Elsevier, Amsterdam 1950.
8. Straub, O. In Isler, O. *Carotenoids*, Birkhäuser, Basel 1971.
9. Francis, G. W. and Liaaen-Jensen, S. *Acta Chem. Scand.* **24** (1970) 2705.
10. Aitzetmüller, K., Strain, H. H., Svec, W. A., Grandolfo, M. and Katz, J. J. *Phytochemistry* **8** (1969) 1761.
11. Enzell, C. R. and Liaaen-Jensen, S. *Acta Chem. Scand.* **25** (1971) 271.
12. Liaaen-Jensen, S. *Acta Chem. Scand.* **19** (1965) 1166.
13. Aasen, A. J. and Liaaen-Jensen, S. *Acta Chem. Scand.* **21** (1967) 2185.
14. Lien, T. and Knutsen, G. *Exptl. Cell Res.* **78** (1973) 79.
15. Halfen, L. N. and Francis, G. W. *Arch. Mikrobiol.* **81** (1972) 25.

Received September 24, 1973.

# Crystalline Leghemoglobin

## XIV. Transfer of Hematin from Lba and Lbc to Horse-radish Peroxidase Apoprotein

NILS ELLFOLK, ULLA PERTILÄ and GUNNEL SIEVERS

*Department of Biochemistry, University of Helsinki, SF-00170 Helsinki 17, Finland*

In 1960 Rossi-Fanelli and Antonini noted the transfer of hematin from *Aplysia* methemoglobin to horse apomyoglobin.[1] Until then the bond between heme and globin had been considered very stable under physiological conditions. A similar migration of hematin has also been shown to take place between some other hemoproteins, *e.g.* myoglobin and horse-radish apoperoxidase (apoHRP).[2] In the present investigation the transfer of hematin from the fast and slow components of soybean leghemoglobin, Lba and Lbc, to apoHRP has been studied. The appearance of the peroxidase activity is taken as evidence for the correct binding of hematin to apoHRP. For comparison, the transfer of the hematin of horse myoglobin (Mb I) to apoHRP was also studied.

*Materials and methods.* Lba, Lbc and yeast cytochrome *c* peroxidase (YCCP) were prepared as described previously.[3,4] Horse heart cytochrome *c* was a commercial preparation (Type III) from Sigma Chemical Company (St. Louis, U.S.A.). Horse myoglobin (Mb I) was isolated according to Åkeson and Theorell.[5] Horse radish peroxidase, component C (HRP C) was prepared according to Paul,[6] and its apoprotein according to Theorell and Maehly.[7] The heme-binding capacity of apoHRP was determined by titration with hematin. The peroxidase activity was assayed by the guaiacol method.[8] The concentration of hydrogen peroxide was determined enzymatically according to Yonetani.[9] ApoHRP and leghemoglobin or myoglobin, respectively, were incubated in 0.02 M sodium phosphate buffer, pH 7.0, for 18 h at 25°C. The peroxidatic activity of the solution was measured and the amount of HRP formed calculated.

*Results and discussion.* Fig. 1 portrays the transfer of hematin from Lba, Lbc and Mb I to apoHRP at pH 7.0. The values obtained were corrected for the inherent

*Fig. 1.* The formation of HRP from apoHRP and Lb*a* (○), Lb*c* ( ● ) and MbI ( ▲ ) in 0.02 M sodium phosphate buffer, pH 7.0. Ordinate: HRP formed as calculated from the activity measurements; abscissa: concentration of hemoglobin in incubation solution.

peroxidatic activity of Lb*a*, Lb*c*, Mb I, and apoHRP. The activity obtained is therefore a consequence of the formation of holoHRP.

Banerjee [10] has defined the equilibrium constant for the dissociation of a hemoprotein to yield dimeric hematin and protein and derived the value log $K = 15.24$ at 25°C for metmyoglobin at pH 7.0. A comparison of the affinities of the apoproteins of Lb*a*, Lb*c*, and Mb I allows a relative value of 12.81 for Lb*a* and 12.91 for Lb*c* to be estimated for the hematin-protein association constant, assuming the constant for Mb I to be equal to the above-mentioned 15.24.

These findings present a new case of hematin transfer between proteins. Under the conditions studied (pH 7.0) heme is about 370 times more firmly bound to the apoprotein in horse Mb I than in Lb*a*, and 250 times more firmly than in Lb*c*. A comparative study on urea denaturation of Lb*a*, Lb*c* and sperm whale myoglobin indicates that sperm whale myoglobin is more stable to urea denaturation than the

two leghemoglobin components.[11] It appears therefore, as through the "heme pocket" of Lb*a* and Lb*c* is more open than that of myoglobin, and allows an easier migration of the heme.

1. Rossi-Fanelli, A. and Antonini, E. *J. Biol Chem.* **235** (1960) PC 4.
2. Rosenquist, U. and Paul, K.-G. *Acta Chem. Scand.* **18** (1964) 1802.
3. Ellfolk, N. *Acta Chem. Scand.* **14** (1960) 609.
4. Ellfolk, N. *Acta Chem. Scand.* **20** (1966) 1427.
5. Åkeson, Å. and Theorell, H. *Arch. Biochem. Biophys.* **91** (1960) 319.
6. Paul, K.-G. *Acta Chem. Scand.* **12** (1958) 1312.
7. Theorell, H. and Maehly, A. C. *Acta Chem. Scand.* **4** (1950) 422.
8. Chance, B. and Maehly, A. C. *Methods Enzymol.* **2** (1955) 764.
9. Yonetani, T. *J. Biol. Chem.* **240** (1965) 4509.
10. Banerjee, R. *Biochem. Biophys. Acta* **64** (1962) 368, 385.
11. Sievers, G., Harmoinen, A. and Ellfolk, N. *Abstr. 9th Intern. Congr. Biochem., Stockholm*, (1973) Commun. No. 2j41.

# On the Nonsymmetry of Reaction Parameter ( $\varrho$ ) and the Substituent Parameter ( $\sigma$ ) in the Hammett Equation and Similar Extrathermodynamic Relationships

SVANTE WOLD*

*Research Group for Chemometrics, Institute of Chemistry, Umeå University, S-901 87 Umeå, Sweden*

The Hammett equation (1) has empirically been found to well describe aromatic

* 1973–74 on leave to Department of Statistics, University of Wisconsin, 53706 Wisconsin, USA.

*Fig. 1.* The formation of HRP from apoHRP and Lba (O), Lbc (●) and MbI (▲) in 0.02 M sodium phosphate buffer, pH 7.0. Ordinate: HRP formed as calculated from the activity measurements; abscissa: concentration of hemoglobin in incubation solution.

peroxidatic activity of Lba, Lbc, Mb I, and apoHRP. The activity obtained is therefore a consequence of the formation of holoHRP.

Banerjee [10] has defined the equilibrium constant for the dissociation of a hemoprotein to yield dimeric hematin and protein and derived the value $\log K = 15.24$ at 25°C for metmyoglobin at pH 7.0. A comparison of the affinities of the apoproteins of Lba, Lbc, and Mb I allows a relative value of 12.81 for Lba and 12.91 for Lbc to be estimated for the hematin-protein association constant, assuming the constant for Mb I to be equal to the above-mentioned 15.24.

These findings present a new case of hematin transfer between proteins. Under the conditions studied (pH 7.0) heme is about 370 times more firmly bound to the apoprotein in horse Mb I than in Lba, and 250 times more firmly than in Lbc. A comparative study on urea denaturation of Lba, Lbc and sperm whale myoglobin indicates that sperm whale myoglobin is more stable to urea denaturation than the

two leghemoglobin components.[11] It appears therefore, as through the "heme pocket" of Lba and Lbc is more open than that of myoglobin, and allows an easier migration of the heme.

1. Rossi-Fanelli, A. and Antonini, E. *J. Biol Chem.* **235** (1960) PC 4.
2. Rosenquist, U. and Paul, K.-G. *Acta Chem. Scand.* **18** (1964) 1802.
3. Ellfolk, N. *Acta Chem. Scand.* **14** (1960) 609.
4. Ellfolk, N. *Acta Chem. Scand.* **20** (1966) 1427.
5. Åkeson, Å. and Theorell, H. *Arch. Biochem. Biophys.* **91** (1960) 319.
6. Paul, K.-G. *Acta Chem. Scand.* **12** (1958) 1312.
7. Theorell, H. and Maehly, A. C. *Acta Chem. Scand.* **4** (1950) 422.
8. Chance, B. and Maehly, A. C. *Methods Enzymol.* **2** (1955) 764.
9. Yonetani, T. *J. Biol. Chem.* **240** (1965) 4509.
10. Banerjee, R. *Biochem. Biophys. Acta* **64** (1962) 368, 385.
11. Sievers, G., Harmoinen, A. and Ellfolk, N. *Abstr. 9th Intern. Congr. Biochem., Stockholm,* (1973) Commun. No. 2j41.

Received October 25, 1973.

# On the Nonsymmetry of Reaction Parameter ( $\varrho$ ) and the Substituent Parameter ( $\sigma$ ) in the Hammett Equation and Similar Extrathermodynamic Relationships

SVANTE WOLD*

*Research Group for Chemometrics, Institute of Chemistry, Umeå University, S-901 87 Umeå, Sweden*

The Hammett equation (1) has empirically been found to well describe aromatic

* 1973—74 on leave to Department of Statistics, University of Wisconsin, 53706 Wisconsin, USA.

reactivity data ($m$ and $p$ substitution) of reaction series of type I (for recent reviews, see Refs. 1 and 2):
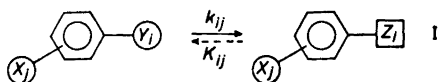


Often, the Hammett equation is written in the reduced form as

$$\log k_{ij} - \log k_{i0} = \varrho_i \sigma_j \qquad (1a)$$

However, as will be argued below, for mathematical and statistical reasons, the following, full formulation, should be preferred

$$\log k_{ij} = \alpha_i + \varrho_i \sigma + e_{ij} \qquad (1b)$$

In eqn. 1b, the parameters $\alpha_i$ and $\varrho_i$ are specific for the $i$:th reaction (defined by the reaction center $Y_i$ in scheme I). The former ($\alpha_i$) is closely, but not exactly, corresponding to $\log k_{i0}$ in eqn. 1a. The substituent parameter $\sigma_j$ is specific for the $j$:th substituent ($X_j$ in scheme I). The residuals ($e_{ij}$) denote the part of the observed data ($\log k_{ij}$) which is not described by the systematic part in eqn. 1b. They contain contributions of two, principally different, types, namely (a) errors of measurement and (b) model errors, due to simplifications inherent in eqn. 1.*

Hine,[3] making a theoretical interpretation of the Hammett equation in terms of free energy differences between reactant and products (or transition states) in scheme I in conjunction with a complementary scheme describing the change of the substituent $X_j$ to the substituent $W_j$, arrived at the following formulation of the Hammett equation, which is formally symmetrical in the reaction and substituent variable

$$\log k_{ij} - \log k_{i0} = \tau_{ij}(\sigma Y_i - \sigma z_i)\sigma x_i \qquad (2)$$

Wepster[4] recently extended this formalism also to the extended Hammett equation of Yukawa and Tsuno,[5] obtaining the following equation

$$\log k_{ij} - \log k_{i0} = \tau_{ij}[(\sigma Y_i - \sigma z_i)\sigma x_j + (\sigma Y_i{}^R - \sigma z_i{}^R)\sigma x_j{}^R] \qquad (3)$$

---

* Eqn. 1 is empirically valid both for rate ($k$) and equilibrium ($K$) constants. For brevity, however, the notation is restricted to the former.

Though the derivations of Hine and Wepster are formally correct, and consequently also eqns. (2) and (3), these formulations imply, incorrectly, a symmetry between the reaction variable(s) and substituent variable(s) in the Hammett and Yukawa-Tsuno equations. However, in their full formulations (eqn. 1b and analogously for the Yukawa-Tsuno equation), these equations are not symmetrical. In the Hammett equation, the variation of the reaction center is described by *two* parameters ($\alpha_i$ and $\varrho_i$), while the variation of the substituent can be described by a single parameter ($\sigma_j$). The nature of this assymmetry can, moreover, be formulated in stringent mathematical terms as follows (a full account of this treatment is given in Ref. 6):

Consider the variation in reaction center in scheme I as being described (formally) by the macroscopic variable $t$, varying among the states $t_i$ with each state corresponding to a particular reaction $Y_i \rightarrow Z_i$. Similarly, the variation of the substituent ($X_j$ in scheme I) is described by the variable $r$ with the states $r_j$. In addition, the influence of these macroscopic variables ($t$ and $r$) on the observed variable ($\log k_{ij}$) is symbolized to occur *via* the microscopic (hypothetical) vector variables $z$ and $x$, respectively.
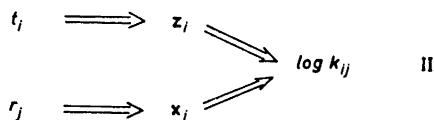


Hence, $\log k_{ij}$ is a function of two vector variables, say $F(z,x)$. The behaviour of this function can be studied by means of Taylor expansions; different cases can be seen:

1. The vector variables $z$ and $x$ contain only one independent variable each, denoted by $z$ and $x$, respectively. The Taylor expansion is, in the usual symbols:

$$\log k_{ij} = F(z,x) = F(z_0,x_0) + F_z{}'(z-z_0) + F_x{}'(x-x_0) + \tfrac{1}{2}F_{zz}{}''(z-z_0)^2 + F_{zx}{}''(z-z_0)(x-x_0) + \tfrac{1}{2}F_{xx}{}''(x-x_0)^2 + R(3) = F(z_0,x_0) - F_z{}'F_x{}'/F_{zx}{}'' + (F_x{}' + F_{zx}{}''(z-z_0) + F_{zz}{}''F_{zx}{}''(z-z_0)^2/2F_z{}')(F_x{}'/F_{zx}{}'' + (x-x_0) + F_{xx}{}''/2F_x{}'(x-x_0)^2) + R_2(3)$$
$$= C + h(z)g(x) + R_2(3) \qquad (4)$$

Here $F_z{}'$ denotes the value of $\delta F/\delta x$ at the point $(z_0,x_0)$ and so on. The remainders, $R(3)$ and $R_2(3)$, which are different, contain terms of third and higher orders, such as $F_{xxx}{}'''(z-z_0)(x-x_0)^2$.

Since now the macroscopic variables $t$ and $r$ vary discretely, so do the microscopic variables $z$ and $x$. Rewriting $h(z_i)$ as $\beta_i$ and $g(x_j)$ as $\theta_j$, we see that, provided that the variation of the microscopic variables $z$ and $x$ over the experimental range of $t$ and $r$ is sufficiently small to make the remainder $R_2(3)$ small compared to the errors of measurement of $\log k_{ij}$, the data will in this first case conform well to the simple one-component model:

$$\log k_{ij} = c + \beta_i\,\theta_j + e_{ij} \qquad (5)$$

2. Analogously, it can be shown that for the case that the vector variable $z$ contains *several* independent variables while the vector variable $x$ still contains only one, a second order approximation is [6]

$$F(z,x) = f(z) + h(z)g(x) + R(3) \qquad (6)$$

which, translated to the discrete case in the same way as above, gives:

$$\log k_{ij} = \alpha_i + \beta_i\theta_j + e_{ij} \qquad (7)$$

3. Finally, higher order approximations of functions in both single variables and vector variables ($z$ and/or $x$) all give the same discrete model:

$$\log k_{ij} = \alpha_i + \sum_{a=1}^{M} \beta_{ia}\theta_{aj} + e_{ij} \qquad (8)$$

We are now in the position to make a rigorous interpretation of the simple Hammett equation (1b) which is seen to be equivalent to eqn. (7). This implies that *several* microscopic variables (denoted by the vector $z$) vary with the variation of the reaction center (the macroscopic variable $t$), while only one microscopic variable ($x$) varies with the variation of the substituent (the macroscopic variable $r$). In addition, the variation of these microscopic variables over the experimental range where the Hammett equation is valid, is so small that the second order approximation holds good ($R(3)$ is small).

The formalism of Hine and Wepster is relevant only for cases when data are well fitted by the simpler model (5), indicating that both the reaction variable and the substituent variable influence the reaction rate (or equilibrium constant) *via* one single microscopic variable each.

From the present derivation it also follows that it is of less importance which transformation of the observed data which is used in the models. The function $F(z,x)$ can as well correspond to $\sqrt{k_{ij}}$ or $\log \log k_{ij}$ as to $\log k_{ij}$. The parameter scales will naturally be different, but there is presently no indication that $\log k_{ij}$ will always be the best transformation for the use in an empirical model of the ETR type.

Finally, the present treatment shows that, since the influence of any number of macroscopic variables can be incorporated in the variable $z$, it is indeed possible to formulate the Hammett equation and other similar ETR's with a single substituent scale which is independent of temperature, pressure, solvent, and so on. The influence of the latter variables can in principle be incorporated in the vector variable $z$ and hence be described by the two parameters $\alpha_i$ and $\varrho_i$ in eqn. (1b). Whether this is possible for a particular class of chemical phenomena, however, is a question that only can be settled by the analysis of corresponding emprical data. The present derivation only shows the possible existence of such a single substituent scale, not the experimental domain where it is applicable.

1. Hammett, L. P. *Physical Organic Chemistry,* 2nd Ed., McGraw, New York 1971.
2. Exner, O. In Chapman, N. B. and Shorter, J., Eds., *Advances in Linear Free Energy Relationships,* Plenum, London 1972.
3. a. Hine, J. *Physical Organic Chemistry,* McGraw, New York 1962, p. 84; b. Hine, J. *J. Am. Chem. Soc.* **81** (1959) 1126.
4. Wepster, B. M. *J. Am. Chem. Soc.* **95** (1973) 102.
5. a. Tsuno, Y., Ibata, T. and Yukawa, Y. *Bull. Chem. Soc. Japan* **32** (1959) 960; b. Yukawa, Y. and Tsuno, Y. *Ibid.* **32** (1959) 965, 971.
6. Wold, S. *Chem. Scripta* **3** (1973). *In press.*

# Organic Selenium Compounds

## XII.* Coordination Compounds of Carbon Diselenide

K. A. JENSEN and E. HUGE-JENSEN

*Department of General and Organic Chemistry, University of Copenhagen, The H. C. Ørsted Institute, DK-2100 Copenhagen, Denmark*

The interesting investigations by Wilkinson *et al.*[1] have demonstrated that carbon disulfide is able to function as a ligand in coordination compounds. Within the compass of our investigations of the chemical reactions of carbon diselenide we have tried to prepare the corresponding compounds of carbon diselenide. This has, however, a pronounced tendency to polymerize, and in most experiments we were only able to isolate poly(carbon diselenide)[2] or compounds that probably contain a tetraselenooxalate ion (see below).

Only in one case did we isolate a substance containing monomeric carbon diselenide, namely the compound $[Pt(Ph_3P)_2(CSe_2)]$, which was obtained as a light green solid by the interaction of tris(triphenylphosphine)platinum(0) at room temperature with exactly the calculated amount of carbon diselenide. As soon as an excess of carbon diselenide was added the green compound was transformed into a brown solid.

The above mentioned complex has a strong band in the infrared spectrum at 995 cm$^{-1}$, which is attributed to the stretching frequency of the carbon-selenium double bond. Free carbon diselenide has the corresponding band at 1270 cm$^{-1}$ (in $CCl_4$). The shift is similar to that found for coordinated carbon disulfide (1157 cm$^{-1}$) *versus* free carbon disulfide (1522 cm$^{-1}$). Otherwise the infrared spectrum differs from that of triphenylphosphine practically only in the intensities of the bands. The 1090 cm$^{-1}$ band of triphenylphosphine (the "X-sensitive" phenyl band, *cf*. Ref. 3) appears at 1100 cm$^{-1}$ with increased intensity in the spectrum of the platinum compound.

From $[Ni(Ph_3P)_2(CO)_2]$ or $[Rh(Ph_3P)_3Cl]$ and carbon diselenide we have only been able to isolate compounds which analytically contain 2 mol of carbon diselenide. The reaction of $[Ni(Ph_3P)_2(CO)_2]$ with carbon diselenide shows convincingly that no compound containing 1 mol of carbon diselenide can be formed. When carbon diselenide is added to a benzene solution of the nickel compound, CO is evolved and the solution first becomes dark red and later almost black, and a blackred solid precipitates. When only 1 mol of carbon diselenide had been added, the filtered solution still contained half of the $[Ni(Ph_3P)_2(CO)_2]$ unchanged; when 2 mol of carbon diselenide was added a practically insoluble compound with the composition $[Ni(Ph_3P)_2(CSe_2)_2]$ was obtained in almost quantitative yield. Similarly, the rhodium compound obtained from $[Rh(Ph_3P)_3Cl]$ analytically corresponds to the formula $[Rh(Ph_3P)_2Cl(CSe_2)_2]$.

The infrared spectra of these two compounds do not exhibit the absorption band near 1000 cm$^{-1}$, found in the spectrum of the platinum compound. The main difference between the infrared spectra of the starting materials and those of the $CSe_2$ compounds is the appearance of a strong band at 870 cm$^{-1}$. Since the asymmetric stretching vibration of a diselenocarboxylate group occurs near 900 cm$^{-1}$,[4] we conclude that these compounds probably contain a coordinated tetraselenooxalate ion. The reduction of 2 $CSe_2$ to $(CSeSe^-)_2$ would correspond to an oxidation of Ni(0) to Ni(II) and of Rh(I) to Rh(III). The properties of the nickel compound (colour, diamagnetism) also indicate that it is a square-planar complex. Poly(carbon diselenide) exhibits an absorption in the same range[2] but the stoichiometric composition of the compounds isolated makes it improbable that they contain polymeric carbon diselenide.

Our efforts to obtain a definite proof of the presence of a tetraselenooxalate group in these compounds have not been successful. It has not been possible to get crystals suited for an X-ray structural analysis, and it has not been possible to prepare complexes with aliphatic phosphines which might be more soluble. Various attempts have been made to prove the presence of tetraselenooxalate in a purely chemical way. So far these have been unsuccessful, but they will be pursued further.

*Experimental.* *Tris(triphenylphosphine)-platinum(0)*, $[Pt(Ph_3P)_3]$, was prepared es-

* Part XI: *Acta Chem. Scand.* 24 (1970) 1092. Parts XIV – XVII have been published: *Acta Chem. Scand.* 24 (1970) 2055, 2061, 2065, 3213.

sentially according to the directions given by Malatesta and Cariello,[5] but the starting material, [PtI$_2$(Ph$_3$P)$_2$], was prepared in a simpler way.

[PtI$_2$(Ph$_3$P)$_2$]. A solution of 2 g of K$_2$PtCl$_4$ in 20 ml of water was mixed with a solution of 4 g of KI in 20 ml of water. After 15 min a solution of 5.2 g of triphenylphosphine in 50 ml of abs. ethanol was added to the mixture with stirring. The yellow precipitate was filtered off, washed with water and ethanol, collected, dried and crystallized from chloroform. This product is [Pt(Ph$_3$P)$_4$][PtI$_4$], m.p. ca. 290°C (decomp.). On boiling with water for 1 h it was transformed into [PtI$_2$(Ph$_3$P)$_2$], m.p. 258°C.

[Pt(Ph$_3$P)$_3$]. Anhydrous hydrazine (1 ml) was added to a suspension of [PtI$_2$(Ph$_3$P)$_2$] in 10 ml of abs. ethanol and the mixture was refluxed for 10 min. The hot solution was decanted from a little precipitate and yielded on cooling and standing a yellow precipitate which was isolated by centrifugation, washed with warm ethanol, water and again with warm ethanol and dried in vacuum. Yield almost quantitative. M.p. 125−130°C in accordance with lit.[5] (Found: C 66.2; H 4.69. Calc. for C$_{54}$H$_{45}$P$_3$Pt: C 66.2; H 4.58).

[Pt(Ph$_3$P)$_2$(CSe$_2$)]. Carbon diselenide (43 mg) was added with stirring to a suspension of [Pt(Ph$_3$P)$_3$] (250 mg) in dry ether (10 ml). The yellow solid soon became green. The green product was isolated by centrifugation, washed three times with ether and dried in vacuum. M.p. 158−163°C (decomp.). (Found: C 50.15; H 3.39; Se 17.77. Calc. for C$_{37}$H$_{30}$P$_2$PtSe$_2$: C 50.00; H 3.38; Se 17.75). Infrared spectrum: CSe$_2$-band at 995 cm$^{-1}$ (s).

The compound was insoluble in ether or ethanol. It dissolved in benzene or dichloromethane but was thereby transformed into a brown product. A similar product was also obtained when excess carbon diselenide was added to a solution of [Pt(Ph$_3$P)$_3$] in ether. The selenium content of the brown products was higher than that of the green compound but lower than calculated for a compound containing 2 mol of CSe$_2$. In the infrared spectrum of the brown products the intensity of the 995 cm$^{-1}$ band had decreased considerably and a rather weak and broad band had appeared in the 850−870 cm$^{-1}$ region. According to these results it is doubtful whether a compound analogous to the nickel and rhodium compounds, described below, was formed or whether the product only contained polymeric carbon diselenide.

[Ni(Ph$_3$P)$_2$(CSe$_2$)$_2$]. Carbon diselenide (220 mg) was added to a solution of 400 mg of [Ni(Ph$_2$P)$_2$(CO)$_2$][6] in 10 ml of benzene. The solution instantly turned red and CO was evolved; after 1 h the mixture was opaque and a reddish-black precipitate had formed. The precipitate was isolated by centrifugation,

washed with ether and dried in vacuum. Yield 470 mg (83 %). M.p. 167°C (decomp.). (Found: C 49.00; H 3.31; Se 34.16. Calc. for C$_{38}$H$_{30}$NiP$_2$-Se$_4$: C 49.43; H 3.25; Se 34.24).

The complex is slightly soluble in chloroform with a red colour. Absorption maxima of a CHCl$_3$ solution (0.1 mg/ml): 454 nm (log $\varepsilon$ 3.61) and 550 nm (log $\varepsilon$ 3.45). Infrared spectrum: CSe$_2$-band at 870 cm$^{-1}$ (s).

[Rh(Ph$_3$P)$_2$(CSe$_2$)$_2$Cl]. Carbon diselenide (85 mg) was added to a suspension of [Rh(Ph$_3$P)$_3$Cl][7] (231 mg) in benzene (10 ml). The colour changed from red to dark brown. After 1 h the precipitate was isolated by filtration, washed with ether and dried in vacuum. Yield 150 mg (60 %). (Found: C 45.51; H 3.31; Cl 3.54; Se 31.10. Calc. for C$_{38}$H$_{30}$ClP$_2$RhSe$_4$: C 45.49; H 2.99; Cl 3.54; Se 31.52). Infrared spectrum: CSe$_2$-band at 865 cm$^{-1}$ (s).

From a solution of [Rh(Ph$_3$P)$_2$(CO)Cl] in benzene and carbon diselenide a brown-black product was obtained which still contained CO ($\nu$CO 1970 cm$^{-1}$) and approximately had the composition of the starting material with 1 mol CSe$_2$ added. It was, however, unstable and was transformed into the above-mentioned compound.

Infrared spectra of KBr discs were recorded on a Perkin Elmer model 337 grating spectrophotometer and visible spectra on a Unicam SP. 800 A instrument.

1. Baird, M. C. and Wilkinson, G. Chem. Commun. 1966 514; Baird, M. C., Hartwell, G., Mason, R., Rae, A. I. M. and Wilkinson, G. Chem. Commun. 1967 92; Baird, M. C. and Wilkinson, G. J. Chem. Soc. A 1967 865; Baird, M. C., Hartwell, G. and Wilkinson, G. J. Chem. Soc. A 1967 2037; Yagupsky, M. P. and Wilkinson, G. J. Chem. Soc. A 1968 2813; Mason, R. and Rae, A. I. M. J. Chem. Soc. A 1970 1767; Commereuc, D., Douek, I. and Wilkinson, G. J. Chem. Soc. A 1970 1771.
2. Brown, A. J. and Whalley, E. Inorg. Chem. 7 (1968) 1254.
3. Jensen, K. A. and Nielsen, P. H. Acta Chem. Scand. 17 (1963) 1875.
4. Jensen, K. A., Henriksen, L. and Nielsen, P. H. In Klayman, D. L. and Günther, W. H. H., Eds., Organic Selenium Compounds, Wiley-Interscience, New York 1973, pp. 846−848.
5. Malatesta, L. and Cariello, C. J. Chem. Soc. 1958 2323.
6. Rose, J. D. and Statham, F. S. J. Chem. Soc. 1959 69.
7. Osborn, J. A., Jardin, F. H., Young, J. F. and Wilkinson, G. J. Chem. Soc. A 1966 1730; Osborn, J. A. and Wilkinson, G. Inorg. Syn. 10 (1967) 68.

# On the Crystallographic Phase Transformation in $Mn_{0.9}Fe_{0.1}As$

KARI SELTE,[a] ARNE KJEKSHUS[a] and ARNE F. ANDRESEN[b]

[a] Kjemisk Institutt, Universitetet i Oslo, Blindern, Oslo 3, Norway and [b]Institutt for Atomenergi, Kjeller, Norway

Some phases which have the orthorhombic MnP type crystal structure at room temperature transform continuously to the hexagonal NiAs type at higher temperatures.[1] The former type may be regarded as a distorted variant of the latter, the distortion of the atomic arrangement being completed when the positional parameters $z_T$ (T: metal) and $x_X$ (X: non-metal) both have reached a value of $\sim 0.20$, as compared with 1/4 in the orthohexagonal NiAs cell, with setting according to $Pnma$. The positional parameters $x_T$ and $z_X$ take values of $\sim 0$ and $\sim 7/12$, respectively, in both structure types.

The purpose of the present communication is to report the *simultaneous* variations in positional parameters and unit cell dimensions over a complete transformation interval between the MnP and NiAs type structures. Previous studies have either concerned the temperature dependence of the unit cell dimensions or the positional parameters. An idea of the behaviour of the structural variables during transformation can be obtained by comparing the data for the unit cell proportions of $MnAs_{0.9}P_{0.1}$ by Ido [2] with the positional parameters $z_T$ and $x_X$ of $MnAs_{0.92}P_{0.08}$ by Hall et al.[3]

Several factors are of importance in the selection of suitable candidates for such a study. When the sample is in a polycrystalline state, the neutron diffraction technique is best fitted for the purpose in view of the convenient profile refinement procedure,[4] which evaluates all structural variables simultaneously. $Mn_{0.9}Fe_{0.1}As$ was chosen due to its relatively low transformation temperature. This phase has previously been subjected to a detailed neutron diffraction study of its cooperative magnetic properties at low temperatures ($T_N = 206 \pm 1$ K).[5] There is, however, one complicating factor associated with our choice in that the crystallographic transformation in $Mn_{0.9}Fe_{0.1}As$ is accompanied by a change of Mn from a "high spin" state in the region where the NiAs type structure prevails, to a "low spin" state in the MnP type region.[5] (A similar behaviour is found for other Mn-rich $Mn_{1-t}T_tAs$ phases.) This change in electronic state of the Mn atoms results in a distinct volume change of the MnP type unit cell during the transformation, as opposed to the situation in, e.g., CrAs and CoAs.[1]

The variation above room temperature of the relative intensity (background subtracted) of the characteristic reflection 101 of the MnP type cell of $Mn_{0.9}Fe_{0.1}As$ is shown in the upper part of Fig. 1. According to these data, the transformation (MnP$\rightleftharpoons$NiAs) temperature is determined as $673 \pm 20$ K, which is considerably higher than that $(553 \pm 50$ K) obtained [1] more qualitatively by X-ray diffraction.

The profile refinement technique was found to be quite suitable up to 560 K. Above this temperature the deviations from the orthohexagonal NiAs symmetry have become too small for a simultaneous refinement of so many coupled parameters.

The refined structural parameters of $Mn_{0.9}Fe_{0.1}As$ are presented in Fig. 1 as $(a/b)_{MnP}$, $(c/a)_{MnP}$, $(c/b)_{MnP}$, $x_T$, $(1/4 - z_T)$, $(1/4 - x_X)$, and $(7/12 - z_X)$ *versus* temperature. In the range $558 - 673$ K the most probable temperature variations of the parameters are indicated by broken lines. As is clearly evident from the diagram all these variables show a continuous variation through the region of transformation, thus confirming that the transition is of second or higher order. The virtually parallel behaviour of $z_T$ and $x_X$ presents additional confirmation of the geometrical model outlined in Ref. 1. The transformation interval is seen to extend over some 500 K which is appreciably larger than in $MnAs_{0.9}P_{0.1}$ ($\sim 200$ K [2,3]). When expressing the data in terms of a reduced temperature variable, $T/T_{trans.}$, it is also found that the transformation characteristics are no universal function. The latter inference is furthermore supported by the more qualitative data for CrAs and CoAs.[1]

Unfortunately, the relatively sparse neutron diffraction data at each temperature do not permit an evaluation of anisotropic temperature factors. The latter type of data would be of considerable interest in relation to the question of whether the "soft modes" formalism can describe the kinetics of this transformation.
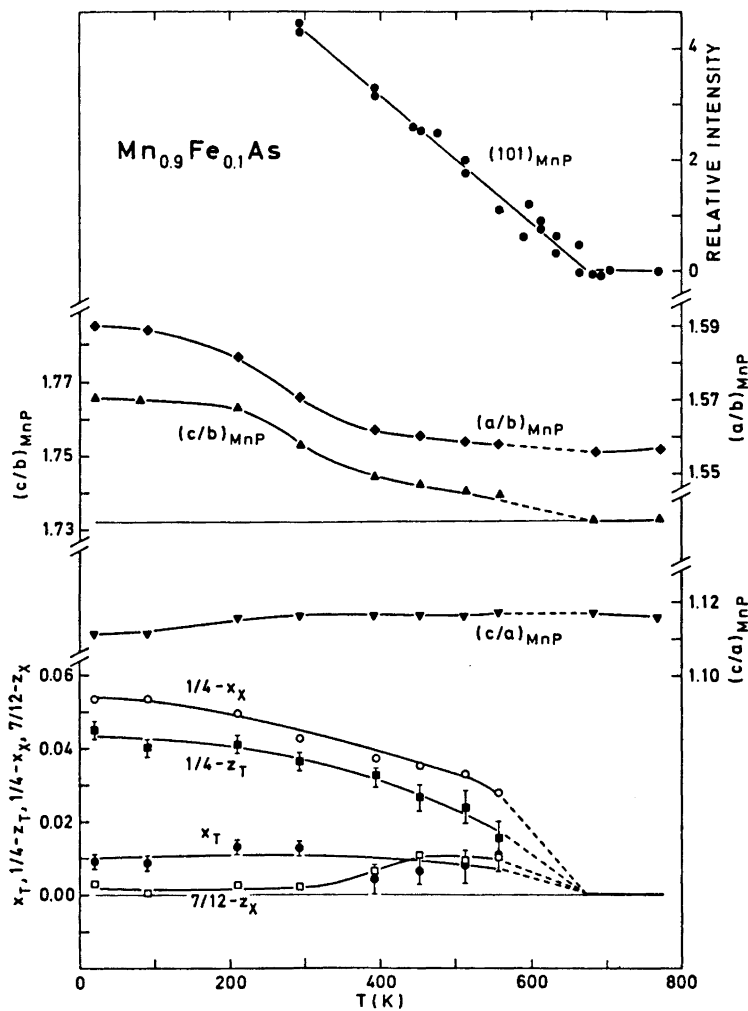
*Fig. 1.* Relative intensity of $(101)_{MnP}$, $(a/b)_{MnP}$, $(c/a)_{MnP}$, $(c/b)_{MnP}$, $x_T$, $(1/4 - z_T)$, $(1/4 - x_X)$. and $(7/12 - z_X)$ for $Mn_{0.9}Fe_{0.1}As$ as functions of temperature. Error bar gives estimated standard deviation when this exceeds size of symbol.

1. Selte, K. and Kjekshus, A. *Acta Chem. Scand.* **27** (1973) 3195.
2. Ido, H. *J. Phys. Soc. Japan* **25** (1968) 1543.
3. Hall, E. L., Schwartz, L. H., Felcher, G. P. and Ridgley, D. H. *J. Appl. Phys.* **41** (1970) 939.
4. Rietveld, H. M. *J. Appl. Crystallogr.* **2** (1969) 65.
5. Selte, K., Kjekshus, A. and Andresen, A. F. *Acta Chem. Scand.* **A 28** (1974). *In press.*

# Isopropylidene Derivatives of α-D-Galactofuranose

## SVEIN MORGENLIE

*Department of Chemistry, Agricultural University, N-1432 Ås-NLH, Norway*

1,2:5,6-Di-*O*-isopropylidene-α-D-galactofuranose (I) has found only limited use in synthetic carbohydrate chemistry, being less accessible than the corresponding D-glucose derivative. This di-*O*-isopropylidene-galactofuranose has been synthesized by two different routes from the corresponding D-glucose derivative in three [1] and six [2] steps, respectively. Formation of the compound in low yield directly from D-galactose by treatment with acetone — cupric sulphate at 100°C has, however, been reported.[3] Isolation of this compound from the main product, 1,2:3,4-di-*O*-isopropylidene-α-D-galactopyranose (II), was achieved by gas-liquid chromatography, and the method is not suitable on a synthetic scale. 1,2:5,6-Di-*O*-isopropylidene-α-D-galactofuranose (I) was required as precursor in the synthesis of the 1,2-*O*-isopropylidene derivative, and it was hoped that a modification of the direct acetonation method might offer a simple way to the di-*O*-isopropylidene-galactofuranose (I) also on a larger scale.

Treatment of D-galactose with cupric sulphate in refluxing acetone after prior
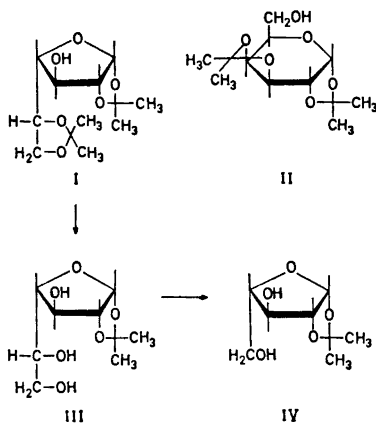


dissolution of the sugar in hot dimethylformamide was found to enhance the proportion of 1,2:5,6-di-*O*-isopropylidene-α-D-galactofuranose (I) relative to the pyranose derivative (II). The total yield of di-*O*-isopropylidene derivatives was, however, reduced to 50 – 60 %. The furanose and pyranose diacetals were formed in about equal amounts, and it was possible to isolate much of the furanose isomer by crystallization from the product mixture. The furanose diacetal (I) was obtained in this way in 20 – 22 % yield in one step from D-galactose without chromatographic separation, and despite the low yield, the method should offer a useful alternative to the previously reported three- and six-step syntheses.[1,2]

Partial acid hydrolysis of the 5,6-*O*-isopropylidene group of the diacetal (I) yielded 1,2-*O*-isopropylidene-α-D-galactofuranose (III). This compound could be obtained in 24 % yield from D-galactose by taking advantage of the stability of 1,2:3,4-di-*O*-isopropylidene-α-D-galactopyranose (II) at conditions sufficient to remove the 5,6-*O*-isopropylidene group of the furanose isomer (I). Weak acid hydrolysis of the di-*O*-isopropylidene-galactose mixture thus gave 1,2-*O*-isopropylidene-α-D-galactofuranose (III) as the only monoisopropylidene derivative, easily separable from the unhydrolyzed 1,2:3,4-di-*O*-isopropylidene-α-D-galactopyranose (II).

The identity of the monoisopropylidene-galactose (III) was established by periodate oxidation followed by borohydride reduction to 1,2-*O*-isopropylidene-β-L-arabinofuranose (IV), and by re-acetonation of the monoisopropylidene-galactose (III) with cupric sulphate-acetone, which gave the di-isopropylidene-galactofuranose (I) exclusively.

High temperature [4,5] and dimethylformamide as a solvent [6,7] are factors known to favor furanose formation in solutions of reducing sugars, and a furanose content higher than 50 % was indicated for D-galactose under conditions similar to those employed in the synthesis of the di-*O*-isopropylidene-galactofuranose (I) by trimethylsilylation and subsequent GLC in this laboratory. This high furanose content is possibly the explanation of the relatively high yield of di-*O*-isopropylidene-galactofuranose obtained.

*Experimental.* Thin layer chromatography (TLC) was performed on silica gel G in benzene — ethanol 3:1 (v/v) and benzene — ethanol 4:1; the spots were detected with diphenylamine — aniline — phosphoric acid.[8] Paper chromatography was run on Whatman No. 1 paper

in butanol—pyridine—water 5:3:2, and electrophoresis on Whatman No. 1 paper in borate buffer, pH 10; the spots were detected with aniline hydrogenphthalate. Gas-liquid chromatography (GLC) was effected with a Perkin Elmer F-11 gas chromatograph, equipped with a flame ionization detector and a stainless steel column (2 m × 3 mm) containing 3 % XE-60 on Gas Chrom Q (100/120 mesh); the nitrogen flow rate was 20 ml/min. The operating temperature was 175°C.

*1,2:5,6-Di-O-isopropylidene-α-D-galactofuranose (I).* A solution of D-galactose (3 g) in hot dimethylformamide (30 ml) was added to rapidly stirred anhydrous cupric sulphate (15 g) in acetone (90 ml), and stirring under reflux was continued for 24 h. After addition of more cupric sulphate (5 g) and acetone (100 ml), the mixture was stirred under reflux for additional 24 h. Solid material was then filtered off, and the solution concentrated to a thin syrup. The syrup was dissolved in water (50 ml) and the water solution extracted with chloroform (5 × 10 ml). The combined chloroform extracts were dried over sodium sulphate, and the solvent was evaporated. The residue (2.3 g) contained two compounds, indistinguishable from authentic 1,2:3,4-di-O-isopropylidene-α-D-galactopyranose (II) and 1,2:5,6-di-O-isopropylidene-α-D-galactofuranose (I) by TLC and GLC, the latter having the lowest mobility by both methods. Quantitative GLC showed that the ratio of the amounts of the furanose (I) to pyranose (II) derivative was 6:5. The mixture of di-isopropylidene derivatives was extracted with light petroleum (b.p. 40—56°C) (3 × 10 ml) at 35°C to remove some of the di-isopropylidenegalactopyranose derivative (II). The residue was dissolved in light petroleum-diethyl ether, from which 1,2:5,6-di-O-isopropylidene-α-D-galactofuranose (I) crystallized, (0.95 g, 22 %), m.p. after recrystallization from the same solvent mixture 97—98°C (lit.[1] 97.5—98°C), [α]$_D$ −34° (c 1, methanol) (lit.[1] −35.3°).

*1,2-O-Isopropylidene-α-D-galactofuranose (III).* A mixture of di-O-isopropylidenegalactose derivatives (I and II) prepared from D-galactose (3 g) as described above, was dissolved in 40 % aqueous acetic acid (30 ml), and the solvents were evaporated in a stream of air over night. The residue was dissolved in chloroform (25 ml), and the chloroform solution was extracted with water (2 × 15 ml). The combined water extracts were re-extracted with chloroform (2 × 10 ml), and the water evaporated under reduced pressure. Crystallization of the residue from ethyl acetate gave 1,2-O-isopropylidene-α-D-galactofuranose (III) (870 mg, 24 % based on galactose), m.p. 102—103°C, [α]$_D$ −27° (c 2, water). (Found: C 48.83; H 7.24. Calc. for C$_9$H$_{16}$O$_6$: C 49.08; H 7.34.)

*1,2-O-Isopropylidene-β-L-arabinofuranose (IV).* To 1,2-O-isopropylidene-α-D-galactofuranose (III) (40 mg) in water (2.5 ml) was added sodium periodate (60 mg) in water (3 ml). After 20 min 0.5 M barium acetate solution was added until complete precipitation, and the solution was filtered and treated with Dowex 50 W (H$^+$) ion exchanger. Sodium borohydride (50 mg) in water (3 ml) was then added, the solution kept at room temperature for 2 h and then treated with Dowex 50 W (H$^+$) ion exchanger once more. The solvent was evaporated, and the boric acid removed by repeated codistillation with methanol. The residue gave a single spot when subjected to TLC. Preparative TLC and crystallization from ethyl acetate gave 1,2-O-isopropylidene-β-L-arabinofuranose (IV) (9 mg), m.p. 113—115°C (lit.[9] 117—118°C). Hydrolysis of the product at 100°C for 4 h in 30 % aqueous acetic acid and subsequent removal of the solvents under reduced pressure, gave a syrup which was indistinguishable from authentic arabinose by paper chromatography and electrophoresis.

*1,2:5,6-Di-O-isopropylidene-α-D-galactofuranose (I) from 1,2-O-isopropylidene-α-D-galactofuranose (III).* 1,2-O-Isopropylidene-α-D-galactofuranose (III) (20 mg) in acetone (5 ml) was stirred with anhydrous cupric sulphate (0.5 g) for 2 h. TLC and GLC showed the presence of a single component, indistinguishable from authentic 1,2:5,6-di-O-isopropylidene-α-D-galactofuranose (I). Filtration of the solution and evaporation of the solvent gave a crystalline residue (22 mg, 93 %) m.p. 94—97°C, mixed m.p. 95—97°C.

1. Paulsen, H. and Behre, H. *Carbohyd. Res.* **2** (1966) 80.
2. Brimacombe, J. S., Gent, P. A. and Stacey, M. *J. Chem. Soc.* **C 1968** 567.
3. DeJongh, D. C. and Biemann, K. *J. Am. Chem. Soc.* **86** (1964) 67.
4. Acree, T. E., Shallenberger, R. S., Lee, C. Y. and Einset, J. W. *Carbohyd. Res.* **10** (1969) 355.
5. Acree, T. E., Shallenberger, R. S. and Mattick, L. R. *Carbohyd. Res.* **6** (1968) 498.
6. Hveding, J. A., Kjølberg, O. and Reine, A. *Acta Chem. Scand.* **27** (1973) 1427.
7. Kuhn, R. and Grassner, H. *Ann.* **610** (1957) 122.
8. Schwimmer, S. and Bevenue, A. *Science* **123** (1956) 543.
9. Levene, P. A. and Compton, J. *J. Biol. Chem.* **116** (1936) 189.

# Further Studies on the Degradation of Folic Acid in a

# Growing Culture of *Pseudomonas fluorescens* UK-1

JUHANI SOINI and KARIN MAJASAARI

*Department of Biochemistry, University of Turku, SF-20500 Turku 50, Finland*

*Pseudomonas fluorescens* UK-1 has been cultivated aerobically in a mineral medium with folic acid as a sole source of carbon and nitrogen. The accumulation of the degradation products of folic acid in the culture medium has been followed during the growth of the organism. Folic acid begins to split to pterine-6-carboxylic acid and PABGA * at the beginning of cultivation and the folic acid, as such, is exhausted before the middle of the logarithmic growth phase. The consumption of PABGA becomes very significant in the early logarithmic phase at the same time as PABA begins to accumulate in the medium. The utilization of PABA is a slow process, for traces of it can be found even after the organism has been growing for 100 hours, *i.e.* at the end of the growth cycle. Pterine-6-carboxylic acid is first consumed after the logarithmic phase of growth. Carboxypeptidase activity has been estimated during the early logarithmic phase and compared with the results obtained for other pseudomonads.

Pseudomonads are able to utilize numerous organic compounds as sole source of carbon and nitrogen. Several studies have been made on the splitting of folic acid and related molecules, but these concentrated on the isolation and characterization of the enzymes catalyzing the breakdown of $N$-acetyl-glutamate linkages.[1-4] The aim of this investigation was to follow the degradation of folic acid during the growth cycle of *Pseudomonas fluorescens* UK-1, the initiation of which has been described in an earlier paper.[5] Chromatographic separation has been used for the detection and identification of the degradation products.

## METHODS

*Reagents.* All chemicals were guaranteed reagents from Sigma Chemical Co. or AnalaR reagents from The British Drug Houses Ltd.

*Culture conditions and preparation of cell extract. Ps. fluorescens* UK-1 was preserved and cultivated in 5 mM pantothenate medium as described earlier.[5] The main cultivation

---

* In this publication PABGA=*p*-aminobenzoyl-L-glutamic acid, PABA=*p*-aminobenzoic acid.

was carried out in a medium which was 2.25 mM in folic acid, this providing the only source of carbon and nitrogen. The cells were separated from 100 ml specimens taken during the growth of the organism and treated as before.[5]

*Determination of degradation products.* Samples were centrifuged and the clear supernatant reduced to 1 ml at 40° in a rotating vacuum evaporator in order to study the compounds accumulating in the medium during bacterial growth. 100 $\mu$l of this solution was pipetted onto Whatman No. 3 paper and chromatographed using a 1:2 1 % $NH_3$-propanol mixture as solvent.[6] After drying, the chromatograms were photographed in ultraviolet light with a Desaga MinUVIS lamp at a wavelength of 254 nm. Parallel chromatograms were diazo-stained.[7] Spots from these chromatograms in which PABA and PABGA became visible were cut off and eluted with 3 ml of $H_2O$. The colour intensity was measured with a Beckman DB spectrophotometer at a wavelenght of 520 nm. Authentic PABA and PABGA were used as standards. Known amounts of these compounds were chromatographed, eluted and measured for preparing the standard curves.

## RESULTS AND DISCUSSION

Figs. 1 and 2 show that, in a growing culture of *Ps. fluorescens* UK-1, the degradation of folic acid begins almost immediately after the cells have been transferred into the main culture medium. The first degradation products, PABA and PABGA (Fig. 1), and the pterine moiety (Fig. 2), appear in the medium, indicating that the enzymes catalyzing the degradation are situated in the periplasmic space of the cell. PABGA is detectable in the medium



| 1 | 2 | 3 | 4 | 5 | 6 | 7 | 8 | 9 | 10 |
|---|---|---|---|---|---|---|---|---|---|
Specimen No.

| 2 | 8 | 23 | 35 | 46 | 48 | 50 | 52 | 76 | 96 |
Growth time, h
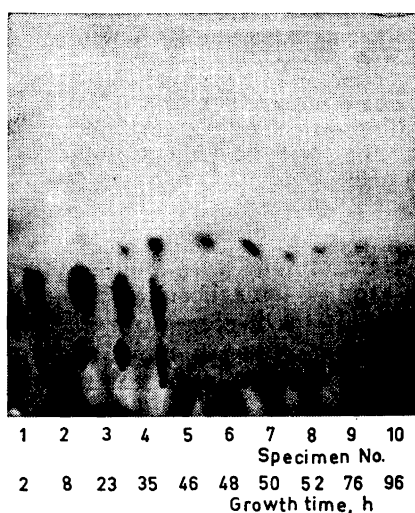
*Fig. 1.* A diazo-stained chromatogram made from specimens taken from the culture medium during growth of *Ps. fluorescens* UK-1. Top row, PABA; middle row, PABGA; bottom row, folic acid remaining in the medium.



| 1 | 2 | 3 | 4 | 5 | 6 | 7 | 8 | 9 | 10 |
|---|---|---|---|---|---|---|---|---|---|
Specimen No.

| 2 | 8 | 23 | 35 | 46 | 48 | 50 | 52 | 76 | 96 |
Growth time, h
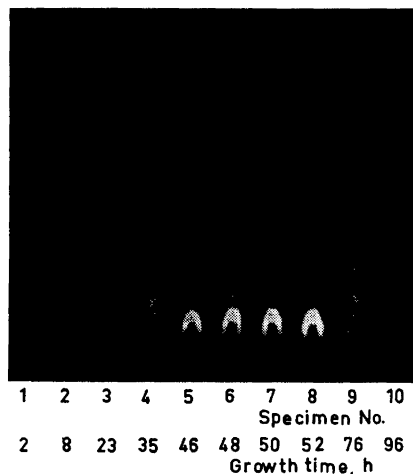
*Fig. 2.* Same chromatogram as in Fig. 1, but photographed in UV-light before diazo-staining. Dark spots at an $R_F$-value of 0.13 in specimens 1 – 4 are pterine-6-carboxylic acid almost completely covered by folic acid remaining in the medium. Bright spots at $R_F$-value 0.18 in specimens 5 – 8 are pterine-6-carboxylic acid, which disappears in specimens 9 and 10.

during the 35 h after the transfer, and thereafter disappears. PABA starts to accumulate before the PABGA has been exhausted. This is a consequence of the bacterium utilizing the glutamyl residue of PABGA, for traces of PABA remain until the end of the growth period.

The colour intensities of the spots of PABA and PABGA were measured to determine the concentration of these compounds in the culture medium. The results are presented in Fig. 3. After the bond between PABGA and the pterine splits at the beginning of bacterial growth, the utilization of the glutamyl residue of PABGA begins. Thus the amount of PABGA decreases by 15 $\mu$mol/100 ml of growth medium during the first 35 h while the concentration
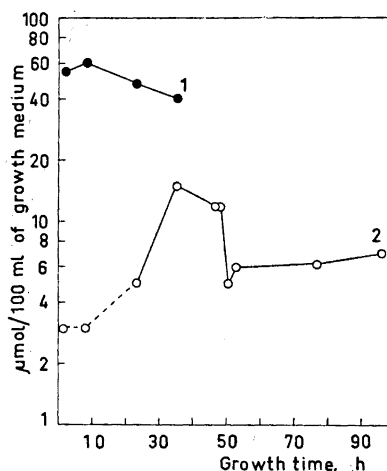


*Fig. 3.* Concentrations of PABGA (curve 1) and PABA (curve 2) in culture medium during the growth of *Ps. fluorescens* UK-1. Concentrations have been estimated from the spots in the diazo-stained chromatogram (Fig. 1) and calculated as $\mu$mol/100 ml of growth medium.

of PABA increases by 12 $\mu$mol. The concentrations of the first two PABA spots have been marked with a dotted line because accurate determination of these faint spots was difficult. After 35 h. *Ps. fluorescens* UK-1 obviously begins to utilize PABA for its concentration in the growth medium diminishes significantly.

The pterine formed from the degradation of folic acid was identified in our earlier paper as pterine-6-carboxylic acid.[5] This compound is present in the growth medium from the beginning of the experiment, but it is mostly covered with intact folic acid in the first four spots of the UV-photograph (Fig. 2). It becomes clearly visible in specimens taken after 35 h, and can be seen in samples over the next 10 h. At the end of the growth period it disappears, clearly indicating that *Ps. fluorescens* UK-1 can utilize pterine-6-carboxylic acid as well as PABGA and PABA. We intend to investigate the utilization of this acid in future studies.

Specimens from the growing culture of *Ps. fluorescens* UK-1 were collected between 20 and 30 h in order to study the velocities with which folic acid is split under *in vitro* conditions. The chosen time interval was such that PABGA was continuing to decrease and the formation of PABA had clearly started in
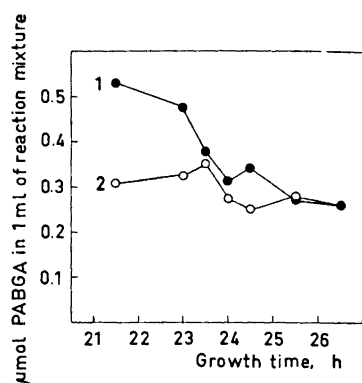
Fig. 4. Formation of PABGA from folic acid after 15 sec (curve 1) and 1 h (curve 2). Enzyme preparations were made from cell specimens taken at intervals during the early logarithmic phase of *Ps. fluorescens* UK-1 growth. The reaction mixture contained folic acid at 2.3 $\mu$mol/ml of 0.05 M TRIS-HCl buffer, pH 7.3. Temperature was 30° and protein concentration 0.1 mg/ml. The reaction was started by addition of enzyme and stopped by immersing the tube in an ice bath. 200 $\mu$l of the reaction mixture was pipetted onto Whatman No. 3 paper. After the chromatographic run and diazo-staining, the spots were eluted and the concentrations of PABGA calculated.
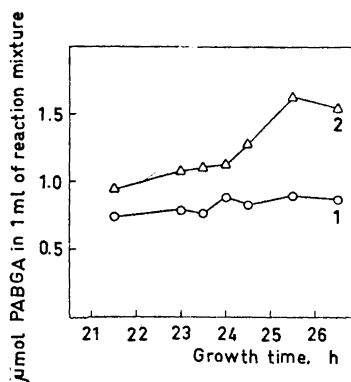
Fig. 5. Formation of PABA from PABGA after 1 h (curve 1) and 3 h (curve 2). The experimental conditions were the same as in Fig. 4 except that the substrate (PABGA) concentration was 3.8 $\mu$mol/ml.

the growth medium (Fig. 3). Cells treated with ultrasonic waves and strepto-mycin were used as enzyme preparation, and folic acid and PABGA as sub-strates. The results are shown in Figs. 4 and 5. In Fig. 4, curve 1 shows that PABGA is split off from folic acid within 15 seconds after adding the enzyme. The rate of formation of PABGA is probably constant in enzyme preparations made from specimens taken between 21 and 27 h, but the in-crease of PABA (Fig. 3) during this period leads to an apparent decrease in PABGA concentration. Curve 2 in Fig. 4 shows the PABGA concentration in reaction mixtures after 1 h, and establishes the constant consumption of PABGA.

The splitting of PABGA in cell specimens is presented in Fig. 5 as a func-tion of time. After 3 h incubation time, the rate of formation of PABA accel-erates continually. The maximum value for PABA formation is 1.6 $\mu$mol/ml of reaction mixture, indicating that 42 % of PABGA has been converted to PABA. The low value is obviously due to the PABA formed being further me-tabolized (*cf.* Fig. 3).

Because of the yellow precipitate produced during the growth of *Ps. fluorescens* UK-1, it is difficult to draw any growth curve as a function of time.

McCullough *et al.*,[4] however, report a 24 h generation time for *Ps. stutzeri* when grown on leucovorin, and, according to Goldman and Levy,[2] a pseudomonad isolated from mud is in the late logarithmic phase after 36 h when grown on methotrexate. From these it can be estimated that *Ps. fluorescens* UK-1 is in an early logarithmic phase between 20 and 30 h. It can be calculated from Fig. 5 that during this period the activity of the enzyme that releases PABA from PABGA increases from a value of 17 milli-units/mg to 30 milli-units/mg when ultrasonic and streptomycin treated cells are used. These values are in good agreement with those obtained earlier with a similar enzyme preparation: after protamine treatment, 38 milli-units/mg in the logarithmic phase[1] and 22 milli-units/mg at the end of the logarithmic phase.[2] In *Ps. stutzeri* the value is very high: after 24 h the activity of carboxypeptidase $G_1$ is 1.8 units/mg after protamine treatment.[4]

## REFERENCES

1. Levy, C. and Goldman, P. *J. Biol. Chem.* **242** (1967) 2933.
2. Goldman, P. and Levy, C. *Proc. Nat. Acad. Sci. U. S.* **58** (1967) 1299.
3. Levy, C. and Goldman, P. *J. Biol. Chem.* **243** (1968) 3507.
4. McCullough, J., Chabner, B. and Bertino, J. *J. Biol. Chem.* **246** (1971) 7207.
5. Soini, J. and Majasaari, K. *Acta Chem. Scand.* **27** (1973) 2115.
6. Goto, M., Forrest, H., Dickerman, L. and Urushibara, T. *Arch. Biochem. Biophys.* **111** (1965) 8.
7. Lawson, R., Elliot, W., Elliot, D. and Jones, K., Eds., *Data for Biochemical Research*, 2nd Ed., Clarendon Press, Oxford 1969, pp. 521 – 522.

Received July 20, 1973.

# The Mutarotation of D-Glucose and Its Dependence on Solvent*

## I. Studies of Reaction and Equilibrium in the Mutarotation Catalyzed by Water

FREDERICK GRAM, JOHAN A. HVEDING and ANDREAS REINE

*Department of Chemistry, University of Oslo, Oslo 3, Norway*

The rate of anomerization and the equilibrium of D-glucose at 20, 30, and 40°C were determined in water and in water-DMF mixtures of high water content. Only in such mixtures was the mutarotation found to be simple. The specific rotations of the pyranoses were determined also for mixtures with lower concentration of water. GLC technique was used to correct for anomeric impurity. For the temperature interval 20 – 30°C $\Delta H$ for the $\alpha \rightarrow \beta$ conversion in water was found to be about $-280$ cal mol$^{-1}$. This value agrees better with earlier thermochemical results than with $\Delta H$ values earlier determined polarimetrically.

Equations for a two-step reversible path give an expression for the "mutarotation constant" $k$ as a function of the elementary rate constants $k_{12}$ and $k_{32}$. The experimental data found for the change in $k$ with water concentration in the water/DMF system, and also those found by other authors in the water/dioxane and water/methanol systems, seem to indicate that the ring opening reaction steps are second order in water. The results give some support to the Lowry idea of a concerted acid-base mechanism for the special case of catalytic action of water.

Quantitative investigations of the reactions[1] involved in the mutarotation** of free aldoses have usually been carried out with aqueous solutions. The intention of the present investigation has been primarily to study the influence of the water concentration upon the anomerization reaction of D-glucose. To this end we have employed the classical method of varying the concentration of the catalytic solvent by dilution with another liquid. The diluent we have chosen, $N,N$-dimethylformamide (DMF), was assumed

---

\* Presented in part at the 11th National Meeting of the Norwegian Chemical Society, June 1970, and a short abstract was printed in *Tidsskr. Kjemi, Bergvesen Met.* **30** No. 6 (1970) 8.

\*\* The term mutarotation is here throughout used in its original meaning to denote a change in the optical rotation of a solution.

to have, in both the pure state and in mixtures, very little catalytic influence on the anomerization.

The mechanism of the acid-base catalysis in mutarotation reactions and in other proton transfer reactions has been a subject of great interest. The idea of a concerted push-pull mechanism was first proposed by Lowry [2] to explain the result on tetramethylglucose in nonaqueous solvents.[3] According to this mechanism the reaction should be trimolecular with the substrate, an acid, and a base, giving for the total rate of reaction

$$v = \{S\} \sum_i \sum_j k_{ij} \{A_i\} \{B_j\}$$

and resulting in second order catalyst terms. According to Pedersen [4] the reactions showing acid-base catalysis proceed in two bimolecular steps. The rate expression in this case should give first order catalyst terms:

$$v = \{S\} \sum (k_A \{A\} + k_B \{B\})$$

Dawson and Spivey,[5] examining the enolization of acetone in acetic acid/acetate ion buffered aqueous solutions, found a small catalytic product term containing $\{AcOH\}\{AcO^-\}$. Pedersen, however, has held this term to be much smaller than could be predicted on the basis of a concerted mechanism. In 1950 it was shown by Swain [6] that Pedersen's argument is not valid since it ignores the experimental equivalence of some kinetic terms. Some more recent experiments by different workers have brought Swain and his collaborators [7] to doubt the general validity of Lowry's concept, especially the catalysis of the anomerization of tetramethylglucose by pyridine and pyridinium ion in aqueous acetone. No second order catalyst term was detected in this reaction. Another example mentioned in which such terms are said to be conspicuously missing is the anomerization of D-glucose in buffered aqueous solutions of varying methanol content, studied by Hill and Thumm.[8] We believe, however, that the way in which these authors tested the kinetic order of water is somewhat unsatisfactory. The amphiprotic properties of methanol ought not to have been neglected in testing the *third* order kinetics as combined action of water and methanol may well be of importance (see Discussion).

The conversion of $\alpha$-D-glucopyranose ($\alpha$-gl$p$) to the $\beta$-pyranose form ($\beta$-gl$p$) and *vice versa* is now generally accepted to pass through the aldehyde form ($\mu$), the ring openings being the slow, rate-determining reaction steps. The reaction scheme may thus be written

$$\alpha\text{-gl}p \underset{k_{21}}{\overset{k_{12}}{\rightleftharpoons}} \mu \underset{k_{32}}{\overset{k_{23}}{\rightleftharpoons}} \beta\text{-gl}p$$
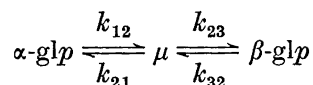
The solution [9] of the differential equations for this scheme leads, when $k_{21}, k_{23} \gg k_{12}, k_{32}$,[10] to the following expression for the rotation at the time $t$: $\gamma_t = \gamma_\infty + (\gamma_0 - \gamma_\infty) \exp(-kt)$, where

$$k = (k_{12}k_{23} + k_{32}k_{21})/(k_{21} + k_{23}) \tag{1}$$

The $\beta/\alpha$ equilibrium constant $(K)$ is given by

$$K = k_{12}k_{23}/k_{32}k_{21} \tag{2}$$

Using the numerical values obtained by polarography,[10] the maximum concentration of $\mu$ [11] is found to be less than 0.01 % of the total sugar concentration. Under such conditions $K$ can be determined experimentally from the well known formula

$$K = ([\gamma_\alpha]_\lambda^T - [\gamma_\infty]_\lambda^T)/([\gamma_\infty]_\lambda^T - [\gamma_\beta]_\lambda^T) \tag{3}$$

Combining eqns. (1) and (2), we arrive at

$$k = [(K+1)/K]/(1/Kk_{32} + 1/k_{12}) \tag{4}$$

Eqn. (4) relates the rate constants $k_{12}$ and $k_{32}$ of the ring opening reaction steps to the "mutarotation constant" ($k$) and equilibrium constant ($K$) found experimentally (see Discussion).

## EXPERIMENTAL

*Materials.* α-D-Glucose (Eastman Kodak Co., *anhydrous*) and β-D-glucose (Koch-Light, *pure*) showed both $[\gamma_\infty]_D^{19.99} = + 52.67 \pm 0.04°$ (*c* 2.998, water), in accordance with literature values. The anomeric purity was tested by GLC. We used a method of trimethylsilylation similar to that described by Sweeley *et al.*[12] To be quite sure that no anomerization takes place before the silylation the reagents, hexamethyldisilazane and trimethylchlorosilane, were added to the solvent, DMF, previous to the addition of the sugar. The "α-D-glucose" was found to contain as a mean 4.3 % (4.2, 4.4, 4.2, 4.4) of β-D-glucose and the "β-D-glucose" as a mean 1.26 % (1.21, 1.27, 1.31) of α-D-glucose. However, instead of using purification procedures, which according to literature are assumed to leave some uncertainty as to the anomeric purity, we preferred to use the commercial glucose products and correct for the contents of the opposite anomer.

*N,N*-Dimethylformamide (E. Merck AG, *Uvasol*) was found by GLC to contain *ca.* 0.05 wt. % water. The liquid was stored in a dark, tightly stoppered bottle in a refrigerator. Distilled water was used in the mutarotation experiments.

*Instruments.* A Perkin-Elmer 141 digital polarimeter, with a glass standard cell of 5 ml volume and 1 dm length, was used for the measurements of optical rotation. All measurements were made at 589 nm and the $\gamma$ values for the equilibrium solutions were estimated to be correct to $\pm 0.001°$.

Two Colora ultrathermostats were used for temperature control: (a) A Colora TS of water volume 22 l and pumping speed 16 l/min was used to supply the water jacket of the polarimeter cell through an isolated rubber tube. The tolerance quoted for this instrument was $\pm 0.005°C$. (b) A Colora KT 10 was used as a fore-thermostat to circulate water through the cooling spiral of the precision thermostat.

The thermometer (Thermo-Schneider, 0.1°C division) was compared with a calibrated platinum resistance thermometer and from several readings was found to show a one hundredth of a degree higher temperature. We judge the temperature data given in this paper to be the true temperatures to within $\pm 0.01°C$.

For the analysis of anomeric purity we used a Varian Aerograph 1200, equipped with a flame ionization detector. The column was stainless steel, 150 cm × 3 mm, containing 5 % SE-30 on Chromosorb W, and kept at 160°C.

*Procedures.* A careful experimental technique, especially in order to find correct initial rotations, was required. The calculated weight quantities of water and DMF to give a certain composition were mixed in a glass-stoppered flask and brought, in the thermostat, to the desired temperature. A quantity of sugar to give a concentration of 3 g per 100 ml solution was then added. With agitation of the flask in the thermostat the dissolution took only about 15 sec in the case of water and some longer time in the case of mixed solvents. The preheated polarimeter cell was quickly filled with the solution and readings began. Time was measured with a stop watch. The initial rota-

tions, $y_0$, found by extrapolation to zero time of course have some limit to their accuracy caused by the time required for dissolution. To enable an accurate calculation of the concentrations in weight/volume units the densities of the various sugar solutions at the experimental temperatures were determined separately.

Measurements of mutarotation were carried out at three temperatures, 19.99, 29.99, and 39.99°C, with water, DMF, and 12 water-DMF mixtures as solvents. The "mutarotation constant" ($k$) was calculated from $\ln(y_t - y_\infty) = -kt + \ln(y_0 - y_\infty)$ by a least squares method. The values of the variable $\ln(y_t - y_\infty)$ were given weight according to $(y_t - y_\infty)$.[13] Calculations of the $k$ values and their standard deviations were performed on a CDC 3300 computer.

## RESULTS

The calculations showed that the mutarotation follows the simple logarithmic law only when the mol fraction ($x_w$) of water in the solvent was higher than about 0.7. Mixtures with lower water content showed an important deviation from simple linearity. The mutarotation in DMF-rich solvents has been subject to further investigations.[14]

*Specific rotations.* Knowledge of the anomeric composition of both species used in our experiments made it possible to calculate the specific rotations, $[\gamma_\alpha]_D{}^T$ and $[\gamma_\beta]_D{}^T$, of pure $\alpha$-D-glucose and pure $\beta$-D-glucose from polarimetrically determined initial specific rotations $S_\alpha$ and $S_\beta$. Assuming the measured rotations to be linear functions of the composition, the equations $0.957 [\gamma_\alpha]_D{}^T + 0.043[\gamma_\beta]_D{}^T = S_\alpha$ and $0.0126 [\gamma_\alpha]_D{}^T + 0.9874[\gamma_\beta]_D{}^T = S_\beta$ are valid. The $S$ values are obtained ($S = y_0/\varepsilon d$) from the initial rotations $y_0$ determined polarimetrically, the weight fraction $\varepsilon$ of the sugar, and the solution density $d$. Table 1 contains $[\gamma_\alpha]_D{}^T$ (columns 2, 3, and 4) and $[\gamma_\beta]_D{}^T$ (columns 5, 6, and 7) at the different mol fractions and temperatures. $[\gamma_\infty]_D{}^T$ for the solutions showing simple mutarotation are given in Table 2.

*Table 1.* Specific rotations of $\alpha$- and $\beta$-D-glucose in water-DMF mixtures.

| $x_w$ | $[\gamma_\alpha]_D{}^{19.99}$ | $[\gamma_\alpha]_D{}^{29.99}$ | $[\gamma_\alpha]_D{}^{39.99}$ | $[\gamma_\beta]_D{}^{19.99}$ | $[\gamma_\beta]_D{}^{29.99}$ | $[\gamma_\beta]_D{}^{39.99}$ |
|---|---|---|---|---|---|---|
| 1 | 112.9 | 112.8 | 112.7 | 17.37 | 17.25 | 17.11 |
| 0.976 | 113.7 | 113.4 | 113.2 | 17.06 | 16.98 | 16.69 |
| 0.950 | 114.4 | 114.1 | 113.8 | 16.89 | 16.65 | 16.17 |
| 0.897 | 116.0 | 115.6 | 115.1 | 16.46 | 16.37 | 16.06 |
| 0.849 | 117.1 | 116.6 | 116.1 | 16.22 | 16.19 | 15.85 |
| 0.750 | 120.0 | 118.8 | 118.6 | 15.84 | 15.69 | 15.43 |
| 0.650 | 122.8 | 121.9 | 121.2 | 15.79 | 15.66 | 15.53 |
| 0.500 | 126.3 | 125.5 | 124.9 | 16.08 | 15.94 | 15.74 |
| 0.350 | 130.0 | 129.2 | 128.3 | 16.80 | 16.60 | 16.35 |
| 0.256 | 132.3 | 131.6 | 130.4 | 17.49 | 17.23 | 16.89 |
| 0.156 | 134.6 | 133.9 | 132.6 | 18.38 | 17.97 | 17.55 |
| 0.100 | 135.6 | 134.9 | 134.0 | 18.90 | 18.46 | 17.95 |
| 0.0504 | 136.8 | 136.0 | 135.1 | 19.39 | 18.92 | 18.38 |
| 0 | 137.8 | 137.0 | 136.1 | 20.00 | 19.45 | 18.87 |

*Table 2.* Equilibrium specific rotations of D-glucose in water-DMF mixtures.

| $x_w$ | $[\gamma\infty]_D^{19.99}$ | $[\gamma\infty]_D^{29.99}$ | $[\gamma\infty]_D^{39.99}$ |
|---|---|---|---|
| 1 | 52.67 | 52.89 | 53.17 |
| 0.976 | 53.37 | 53.52 | 53.71 |
| 0.950 | 53.87 | 54.00 | 54.17 |
| 0.897 | 54.69 | 54.88 | 55.05 |
| 0.849 | 55.31 | 55.51 | 55.72 |
| 0.750 | 56.36 | 56.59 | 56.85 |

Without correction for anomeric impurity our specific rotation data for $\alpha$-D-glucose would have been from 3.6 to 3.7 % lower, *e.g.* for water at 19.99°C, 108.8° instead of 112.9°. The highest value quoted in the literature seems to be 113.4° at 20°C, found by Hudson and Yanovsky.[15] For the $\beta$ form the lowest value given in the literature (for water at 20°C) seems to be 17.5°, found by Nelson and Beegle.[16] This agrees fairly well with our corrected value, 17.37°. We believe that the variety of specific rotations of the D-glucose anomers quoted in the literature may be partly due to the presence of varying amounts of the opposite anomer.

*Table 3.* $\beta/\alpha$ ratio ($K$) in equilibrium solutions. The molar enthalpies ($\Delta H$) calculated from the $K$ values.

| $x_w$ | $K(19.99°C)$ | $K(29.99°C)$ | $K(39.99°C)$ | $\Delta H(20-30°C)$ cal mol$^{-1}$ | $\Delta H(30-40°C)$ cal mol$^{-1}$ |
|---|---|---|---|---|---|
| 1 | 1.708 | 1.681 | 1.652 | $-280$ | $-330$ |
| 0.976 | 1.662 | 1.640 | 1.607 | $-230$ | $-390$ |
| 0.950 | 1.636 | 1.608 | 1.569 | $-310$ | $-460$ |
| 0.897 | 1.603 | 1.576 | 1.539 | $-300$ | $-440$ |
| 0.849 | 1.579 | 1.553 | 1.516 | $-290$ | $-460$ |
| 0.750 | 1.571 | 1.522 | 1.491 | $-560$ | $-390$ |

*The equilibrium constant.* Table 3 contains the $K$ values, calculated by eqn. (3), for the solutions showing simple mutarotation. It is interesting to note that the excess of $\beta$- over $\alpha$-D-glucose in the equilibrium is diminished with increasing fraction of the organic solvent. The temperature coefficient is clearly negative. In this table are also included the molar enthalpies of the $\alpha \rightarrow \beta$ transformation calculated using the van't Hoff equation. From repeated experiments at $x_w = 1$ the uncertainty in $K$ is calculated to be 0.15, 0.35, and 0.85 % at 20, 30, and 40°C, respectively. Calculations based on $K$ values of so nearly the same magnitude give, of course, very large relative errors in $\Delta H$ (*e.g.* 25 % or 70 cal for the interval 20−30°C). The very good agreement of our value of $-280$ cal mol$^{-1}$ in water with $\Delta H$ determined calorimetrically by Sturtevant[17] and by Kabayama *et al.*[18] may therefore be casual.

*Table 4.* The "mutarotation constant" ($k$) at different solvent compositions and temperatures.

| $x_w$ | $k \times 10^2(19.99°C)$ min$^{-1}$ | $k \times 10^2(29.99°C)$ min$^{-1}$ | $k \times 10^2(39.99°C)$ min$^{-1}$ |
|---|---|---|---|
| 1 | 1.48 | 3.88 | 9.34 |
| 0.976 | 1.24 | 3.19 | 7.67 |
| 0.950 | 0.978 | 2.52 | 6.38 |
| 0.897 | 0.632 | 1.72 | 4.11 |
| 0.849 | 0.418 | 1.13 | 2.88 |
| 0.750 | 0.182 | 0.492 | 1.28 |

*Kinetic results.* Table 4 contains the "mutarotation constant" ($k$) at the different mol fractions and temperatures. The standard deviation in $k$ in single runs were never greater than 0.11 %. Duplicate runs were made in a number of cases, *e.g.* four runs in water at 39.99°C gave $k \times 10^2 = 9.398$, 9.285 starting with "α-D-glucose" and $k \times 10^2 = 9.346$, 9.312 starting with "β-D-glucose". The reproducibility in $k$ was good enough to make the uncertainty in all cases less than 1 %.

*Table 5.* $k/c_w{}^n$ data, calculated from the $k$ values in Table 4, with $n = 1$, 2, and 3. Sugar concentration: About 3 g in 100 ml solution. $k' = k/c_w$, $k'' = k/c_w{}^2$, and $k''' = k/c_w{}^3$.

| $x_w$ | $c_w$ mol l$^{-1}$ | $k' \times 10^4$ l mol$^{-1}$ min$^{-1}$ | $k'' \times 10^6$ l$^2$ mol$^{-2}$ min$^{-1}$ | $k''' \times 10^8$ l$^3$ mol$^{-3}$ min$^{-1}$ |
|---|---|---|---|---|
| | | 19.99°C | | |
| 1 | 54.30 | 2.73 | 5.02 | 9.24 |
| 0.976 | 49.34 | 2.51 | 5.09 | 10.3 |
| 0.950 | 44.71 | 2.19 | 4.89 | 10.9 |
| 0.897 | 37.12 | 1.70 | 4.59 | 12.4 |
| 0.849 | 31.54 | 1.33 | 4.20 | 13.3 |
| 0.750 | 23.05 | 0.790 | 3.43 | 14.9 |
| | | 29.99°C | | |
| 1 | 54.18 | 7.16 | 13.2 | 24.4 |
| 0.976 | 49.21 | 6.48 | 12.2 | 26.8 |
| 0.950 | 44.57 | 5.65 | 12.7 | 28.5 |
| 0.897 | 36.96 | 4.65 | 12.6 | 34.1 |
| 0.849 | 31.35 | 3.60 | 11.5 | 36.7 |
| 0.750 | 22.87 | 2.15 | 9.40 | 41.1 |
| | | 39.99°C | | |
| 1 | 53.99 | 17.3 | 32.0 | 59.4 |
| 0.976 | 49.00 | 15.7 | 32.0 | 65.2 |
| 0.950 | 44.35 | 14.4 | 32.4 | 73.2 |
| 0.897 | 36.70 | 11.2 | 30.5 | 83.1 |
| 0.849 | 31.12 | 9.25 | 29.7 | 95.5 |
| 0.750 | 22.68 | 5.64 | 24.9 | 109.8 |

*Table 6.* $k/c_w{}^n$ data for mutarotation of D-glucose in water/dioxane solvents at 25°C. Sugar concentration: About 4 g in 100 ml solution. $k'$, $k''$ and $k'''$, see Table 5.

| $x_w$ | $c_w$ mol l$^{-1}$ | $k \times 10^2$ min$^{-1}$ | $k' \times 10^4$ l mol$^{-1}$ min$^{-1}$ | $k'' \times 10^6$ l$^2$ mol$^{-2}$ min$^{-1}$ | $k''' \times 10^8$ l$^3$ mol$^{-3}$ min$^{-1}$ |
|---|---|---|---|---|---|
| 1 | 54.0 | 2.42 | 4.48 | 8.29 | 15.3 |
| 0.950 | 43.6 | 1.47 | 3.36 | 7.72 | 17.7 |
| 0.876 | 32.9 | 0.838 | 2.55 | 7.74 | 23.5 |
| 0.826 | 27.5 | 0.596 | 2.17 | 7.87 | 28.6 |
| 0.759 | 22.0 | 0.387 | 1.76 | 8.01 | 36.4 |

*Table 7.* $k/c_w{}^n$ data for mutarotation of D-glucose in water/methanol solvents at 20°C. $k'$, $k''$ and $k'''$, see Table 5.

| $x_w$ | Sugar conc. % | $c_w$ mol l$^{-1}$ | $k \times 10^2$ min$^{-1}$ | $k' \times 10^4$ l mol$^{-1}$ min$^{-1}$ | $k'' \times 10^6$ l$^2$ mol$^{-2}$ min$^{-1}$ | $k''' \times 10^8$ l$^3$ mol$^{-3}$ min$^{-1}$ |
|---|---|---|---|---|---|---|
| 1 | 5 | 53.7 | 1.46 | 2.72 | 5.07 | 9.45 |
| 0.941 | 3 | 48.1 | 1.18 | 2.45 | 5.10 | 10.6 |
| 0.910 | 3 | 45.1 | 1.05 | 2.33 | 5.16 | 11.4 |
| 0.807 | 3 | 36.4 | 0.77 | 2.11 | 5.81 | 16.0 |
| 0.727 | 5 | 30.2 | 0.625 | 2.07 | 6.86 | 22.7 |
| 0.633 | 3 | 24.5 | 0.48 | 1.96 | 7.99 | 32.6 |

*Dependence of* k *on water concentration.* In order to examine how $k$ depends on the molar concentration of water, $c_w$, when DMF is the diluent, we have listed in Table 5 the "water constants" found by division of the $k$ values by different powers of $c_w$. The effect of two other diluents, dioxane and methanol, is represented in the same way in Tables 6 and 7. The $k$ data for the dioxane and methanol systems are taken from Rowley and Hubbard [19] and Richards, Faulkner, and Lowry,[20] respectively. To find the water concentrations it was necessary to determine the densities of the sugar solutions used by these authors. From the tables can be seen that the second power relation clearly is preferred when dioxane is the diluent. This is, at first sight, less obvious for the two other solvent systems. Evidently the three systems differ in catalytic properties.

DISCUSSION

The reduction of the surplus of $\beta$ form in aqueous equilibrium solutions by the addition of DMF may have a connection with the anomeric effect and its dependence on the dielectric properties and solvation.

The question of whether acid-base catalyses generally are concerted or not will be a matter of dispute so long no conclusive experimental proof or disproof can be delivered. In the case of highly aqueous solutions without stronger ionic catalysts there seems, however, to be some evidence that water molecules obtain their relatively high catalytic power from a con-

certed mechanism. A support to this view is the relatively high isotope effect, $k_{H_2O}/k_{D_2O}$ being from 3.5 to 4.0 (cf. Ref. 1b, p. 34).

A concerted mechanism should give second or higher order in water for the ring opening reaction steps (e.g. $k_{12} = k_{12}''c_w^2$). Assuming that the ring opening reaction steps are both nth order in water, it can be derived from eqn. (4) that $k$ must be nearly proportional to $c_w^n$. The known variations in $K$ and the approximate magnitude expected for the $k_{12}/k_{32}$ ratio [10] implies that the water/DMF and water/methanol systems in none of the mixtures examined should deviate more than a few per cent from this proportionality. In the case of water/dioxane it has been difficult to find enough rotation [19] or $K$ data to calculate the deviation from proportionality, but the error factor for the lowest water concentration may be estimated to be greater than 0.9.

In view of the above considerations the "water constant" data for the water/dioxane system indicate that the ring opening reaction steps are essentially second order in water. In the water/DMF system these reaction steps also seem to be preferentially of this order, but a downward drift of the $k''$ values is apparent, especially at the lowest water concentrations. The drift in this case may be understood when considering the thermodynamic excess properties of water-DMF mixtures. Dimethylformamide is known extensively to form hydrogen-bonded complexes $HCON(CH_3)_2.nH_2O$, where $n = 2 - 4$.[21] Determination of partial vapour pressures has given that the activity coefficients of water in water-DMF mixtures at our solvent compositions are below unity.[22] This ought to reduce $k$ more than by an ideal dilution. Table 5 shows that the decrease in $k''$ is less at higher temperature, and this may be expected if the decrease results from water-DMF complexing. It is of interest in this connection to note that in the water-dioxane and water-methanol mixtures the activity coefficients of water are found to be above unity.[23,24] We believe that in the water/methanol system the amphiprotic properties of methanol should give a substantial increase in $k''$ caused by a combined action of water and methanol in a concerted mechanism. The effect on the rate constants $k_{12}$ and $k_{32}$ by $c_{MeOH}c_w$ terms, and consequently an increase in $k''$, should be most visible at the lowest water concentrations here examined (see $k''$ column in Table 7).

The polarimetric rate data we have considered here, even if indicating the existence of second order catalyst terms, cannot of course be regarded as a conclusive proof of a concerted bimolecular water catalysis. For a further approach more experimental material, not least from polarographic studies on the elementary rate constants in mixed solvents, is desirable.

## REFERENCES

1. a. Pigman, W. and Isbell, H. S. *Advan. Carbohydrate Chem.* **23** (1968) 11; b. Isbell, H. S. and Pigman, W. *Advan. Carbohydrate Chem. Biochem.* **24** (1969) 14.
2. Lowry, T. M. *J. Chem. Soc.* **129** (1927) 2554.
3. Lowry, T. M. and Faulkner, I. J. *J. Chem. Soc.* **127** (1925) 2883.
4. Pedersen, K. J. *J. Phys. Chem.* **38** (1934) 581.
5. Dawson, H. M. and Spivey, E. *J. Chem. Soc.* **1930** 2180.
6. Swain, C. G. *J. Am. Chem. Soc.* **72** (1950) 4578.

7. Swain, C. G., Di Milo, A. J. and Cordner, J. P. *J. Am. Chem. Soc.* **80** (1958) 5983.
8. Hill, D. G. and Thumm, B. A. *J. Am. Chem. Soc.* **74** (1952) 1380.
9. Rakowski, A. *Z. physik. Chem.* **57** (1906) 321.
10. a. Los, J. M. and Wiesner, K. *J. Am. Chem. Soc.* **75** (1953) 6346; b. Los, J. M., Simpson, L. B. and Wiesner, K. *J. Am. Chem. Soc.* **78** (1956) 1564.
11. Lowry, T. M. and John, W. T. *J. Chem. Soc.* **97** (1910) 2634, p. 2637.
12. Sweeley, C. C., Bentley, R., Makita, M. and Wells, W. W. *J. Am. Chem. Soc.* **85** (1963) 2497.
13. Schmid, H. and Bauer, G. *Z. Naturforsch.* **21b** (1966) 1009.
14. Hveding, J. A., Kjølberg, O. and Reine, A. *To be published.*
15. Hudson, C. S. and Yanovsky, E. *J. Am. Chem. Soc.* **39** (1917) 1013.
16. Nelson, J. M. and Beegle, F. M. *J. Am. Chem. Soc.* **41** (1919) 559.
17. Sturtevant, J. M. *J. Phys. Chem.* **45** (1941) 127.
18. Kabayama, M. A., Patterson, D. and Piche, L. *Can. J. Chem.* **36** (1958) 557.
19. Rowley, H. H. and Hubbard, W. R. *J. Am. Chem. Soc.* **64** (1942) 1010.
20. Richards, E. M., Faulkner, I. J. and Lowry, T. M. *J. Chem. Soc.* **129** (1927) 1733.
21. Geller, B. E. *Russ. J. Phys. Chem.* **35** (1961) 542.
22. Jones, J. *M. S. Thesis*, University of Oklahoma, Norman, Oklahoma 1969.
23. Goates, J. R. and Sullivan, R. J. *J. Phys. Chem.* **62** (1958) 188.
24. Gölles, F. *Monatsh. Chem.* **92** (1961) 981.

# On the Question of Tautomerism of
# Solid Dinitrophenylazo-alkylphenols

PAUL JUVVIK and BJØRN SUNDBY*

*Chemical Institute, University of Bergen, N-5000 Bergen, Norway*

Infrared spectra indicate that many solid 4-(2',4'-dinitrophenyl-azo)-alkylphenols exist as tautomeric mixtures with alkyl-1,4-benzo-quinone 2',4'-dinitrophenylhydrazones. There is also some indication that both tautomers are packed into a common crystal lattice. 2,5-Diisopropylquinone 2',4'-dinitrophenylhydrazone was isolated in two interconvertible, solid modifications of seemingly different tautomeric composition.

Arylazonaphthols are known to exhibit tautomerism in solution (*cf.* Refs. in a previous paper[1]). Infrared studies of 1-phenylazo-2-naphthol,[2] 2-phenylazo-1-naphthol,[2] and 4-phenylazo-1-naphthols[3] as potassium bromide discs seem to indicate the existence of tautomeric mixtures (*cf.* Formula II) also in the solid state, contrary to the rule of thumb that one type of molecule only may be packed into a crystal lattice.[2] Application of X-ray methods has led to a similar conclusion:[4] one of the two crystalline modifications of 4-phenylazo-1-naphthol is mainly hydrazonic, the other azophenolic.

Arylazophenols have been much less thoroughly studied, and to the best of the authors' knowledge, nothing is known of their structure in the solid state. In the present paper the infrared spectra of solid dinitrophenylazo-alkylphenols [II, R = alkyl(s); R' = 2',4'-$(NO_2)_2$] are discussed from the tau-tomerism point of view; this work is closely related to a study of the tau-tomerism in tetrachloroethylene solution.[1]

## EXPERIMENTAL

Preparation and purification of the mono- and dinitrophenylazoalkylphenols II have been mentioned elsewhere.[1]

Compound 16 (Table 1) was isolated from the preparative-layer chromatogram in the form of a dark, red-brown oil which solidified on standing. M.p. about 165° (dec.); solid

---

* Present address: Division of Chemical Oceanography, Bedford Institute of Oceanography, Dartmouth, Nova Scotia, Canada.

IR-spectrum, Fig. 1a. On rubbing in the presence of a little solvent (petroleum ether 40 − 60° and dichloromethane were tested) the solid rapidly and quantitatively passed into a yellow modification: m.p. 165° (dec.) after turning brown at about 150°; solid IR-

*Table 1.* Infrared spectral data and probable tautomer composition of solid 4-(mono- and dinitrophenyl)-azophenols.

| No. | R in II[a] | cm⁻¹ stretch (KBr discs)[b] | | | Tautomer composition[c] |
| | | C=O | NH | OH | |
|---|---|---|---|---|---|
| | *R′ = 1′,4′-dinitro* | | | | |
| 1 | H | | 0 | 3475s,b | A |
| 2 | 2-Et | 1613 | 3292w | 3510w 3420m 3180m,b | M |
| 3 | 2-Pr | | 0 | 3445s,b | A |
| 4 | 2-Bu | | 0 | 3474s,b | A |
| 5 | 3-Me | | 3290w | 3180s,b | M |
| 6 | 3-Et | 1615 | 3288m | 3120s,b | M |
| 7 | 3-Bu | | 3274m | 3090s,b | M |
| 8 | 3,5-Me₂ | | 0 | 3458s,b | A |
| 9 | 3-Me-5-Et | 1616sh | 3311m | 3110m,b | M |
| 10 | 3-Me-5-Pr | | 0 | 3335m,b 3557w,b | A |
| 11 | 2,3-Me₂ | | 3295w | 3360m,b | M |
| 12 | 2,5-Me₂ | | 3280m | 3110s,b | M |
| 13 | 2-Me-5-Pr | | 3292w | 3090s,b | M |
| 14 | 2-Pr-5-Me | | 3315w | 3280m,b | M |
| 15 | 2-Bu-5-Me | | 3272 | 3120s,b | M |
| 16a | 2,5-Pr₂ brown mod. | 1616s | 3295w | 3410w,b 3110m,b | M |
| 16b | 2,5-Pr₂ yel. mod. | 1617s | 3295m | 3405b | M |
| 17 | 2,5-Bu₂ | 1618s | 3301w | 3160s,b | M |
| 18 | 2,3,5-Me₃ | | 3307m | 3080s,b | M |
| 19 | 2,6-Me₂ | 1615s | 3290m | | H |
| 20 | 2-Me-6-Bu | 1614s | 3296s | 3520m,b | M |
| 21 | 2,6-Pr₂ | 1613s | 3285s | | H |
| 22 | 2,6-Bu₂ | 1616s | 3290s | | H |
| 23 | 2,3,6-Me₃ | 1617s | 3300s | | H |
| 24 | 2,3,5,6-Me₄ | 1614sh | 3332s | | H |
| | *R′ = 2′-nitro* | | | | |
| 25 | 3-Et | | 0 | 3415s,b | A |
| 26 | 2-Pr-5-Me | 1612[d] | 3293w | 3130s,b | M |
| 27 | 2,6-Pr₂ | 1612[d] | 3295w | 3395s,b | M |
| 28 | 2,6-Bu₂ | 1612s | 3301s | | H |
| | *R′ = 4′-nitro* | | | | |
| 29 | 3-Et | | 0 | 3415s,b | A |
| 30 | 2-Pr-5-Me | | 0 | 3455s,b | A |
| 31 | 2,6-Pr₂ | | 0 | 3235w,b 3520s,b | A |
| 32 | 2,6-Bu₂ | | 3296w | 3420w,b 3596w | M |

[a] Me=methyl; Et=ethyl; Pr=isopropyl; Bu=*tert*-butyl. [b] w=weak; m=medium; s=strong; b=broad; sh=shoulder. [c] A=azo; H=hydrazone; M=tautomeric mixture. [d] C=O+C=C (see text).
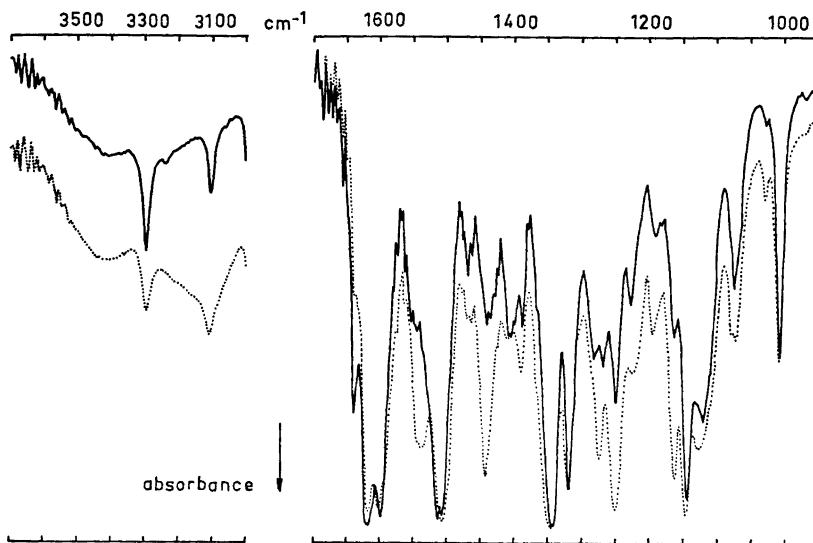
*Fig. 1.* Infrared solid spectra as KBr pellets. (*a*): Brown (···; No. 16*a*) and (*b*): yellow (——; No. 16*b*) modifications of 2,5-diisopropylquinone 2′,4′-dinitrophenylhydrazone. The broad bands at about 3420 cm⁻¹ are partially due to moisture. In the 3700 − 3000 cm⁻¹ region the spectra are vertically displaced for clarity; in the 1700 − 950 cm⁻¹ region they have a common base line.

spectrum, Fig. 1*b*. Both solids are stable in a dry condition. The reverse transformation could be brought about by dissolving the yellow form in, *e.g.*, dichloromethane and rapidly evaporating to dryness; on rubbing or standing, the solvent-free, brown oil solidified to a brown solid as before. Several of the other compounds were tested in a similar way, but could not be induced to undergo such transformations.

Infrared spectra were recorded with Unicam SP 100 and SP 200G instruments on potassium bromide pellets containing 0.5 − 1 % w/w of the solid compounds. Some spectra (*cf.* Fig. 2) were recorded at elevated temperatures up to 190°, using a specially constructed pellet holder fitting into a Beckman-RIIC variable temperature unit.

Electronic spectra (Fig. 3) were recorded with a Beckman DB instrument on well-ground, glass-clear potassium bromide pellets pressed from 30 − 50 μg of substance in 200 mg of salt.

## RESULTS

*Infrared spectra.* Some of the dinitrophenylazo-alkylphenols show a strong OH band but no NH band (Fig. 4*a*), and hence are probably pure azo in the solid state (Nos. 1, 3, 4, 8, 10, 25, 29 − 31). Others apparently lack any OH band, whereas the NH band is as sharp and strong as in aliphatic dinitro-phenylhydrazones (Fig. 4*b*); these are pure hydrazones (Nos. 19, 21 − 24, 28). Nos. 11, 16*b*, 20, 27 show a more or less well-defined NH-band at the ordinary frequency 3300 cm⁻¹,[5] together with a broad band at higher frequencies clearly due to bonded OH (Fig. 4*c*); these compounds apparently are tautomeric mixtures. In some instances (Nos. 2, 5 − 7, 9, 12 − 15, 16*a*, 17, 18, 26, 32)
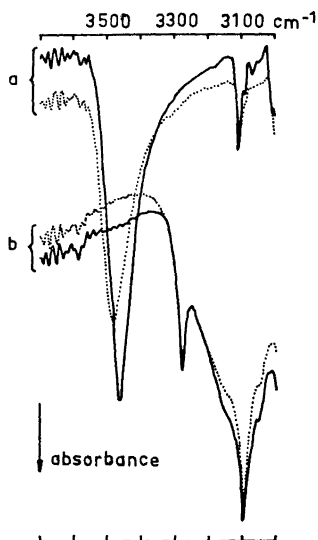
Fig. 2. Infrared solid spectra as KBr pellets. (a): 2-tert-butylquinone 4-(2',4'-dinitrophenylhydrazone) (No. 4) at 25° (——) and at 180° (···). (b): 2,5-dimethyl-quinone 2',4'-dinitrophenylhydrazone (No. 12) at 25° (——) and at 150° (···). Spectra (b) are vertically displaced for clarity.
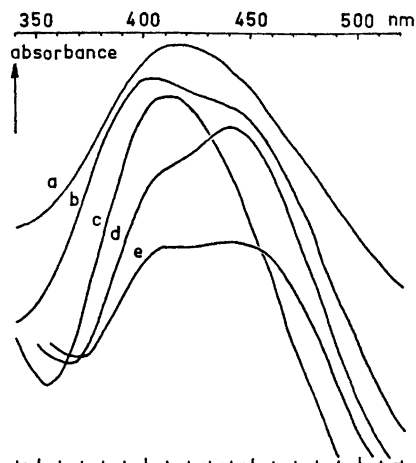
Fig. 3. Ultraviolet-visible solid spectra as KBr pellets (a): 4-(2',4'-Dinitrophenyl-azo)-3-methylphenol (No. 5). (b): 2,3,5,6-Tetramethylquinone 2',4'-dinitrophenyl-hydrazone (No. 24). (c): 4-(2',4'-Dinitro-phenylazo)-3-methyl-5-isopropylphenol (No. 10). (d): 2,6-Diisopropylquinone 4-(2',4'-dinitrophenylhydrazone) (No. 21). (e): 2,5-Di-tert-butylquinone 2',4'-dinitro-phenylhydrazone (No. 17). The spectra are vertically displaced for clarity.

the broad maximum comes below the NH position, and its nature (bonded OH, bonded NH, or both) then is more indeterminable (Fig. 4d). The width of the band ($\Delta\nu\frac{1}{2}$ several hundred cm$^{-1}$) indicates, however, that much bonded OH is present, and hence also these compounds are tautomeric mixtures.

In the carbonyl region the dinitro compounds show a complex band centred at about 1610 cm$^{-1}$. One of the main peaks in this band, at 1612 – 1620 cm$^{-1}$, is missing in just the five compounds which also lack the NH band (Nos. 1, 3, 4, 8, 10), and hence this particular peak may be assigned to the C = O stretching vibration. Regrettably the partial overlap with the other bands restricts the diagnostic value of the C = O band of dinitrophenylazophenols to a mere qualitative confirmation of what may be deduced from the NH bands and only to cases where much hydrazone is present. The C = O band positions, in the solid DNPAP's are essentially the same as in tetrachloroethylene solution.[1]

In the 2'-nitro compounds the C = O band apparently overlaps completely with the higher one (1612 – 1614 cm$^{-1}$) of two bands representing the double bond vibrations, and in the 4'-nitro series the nearly systematic lack of
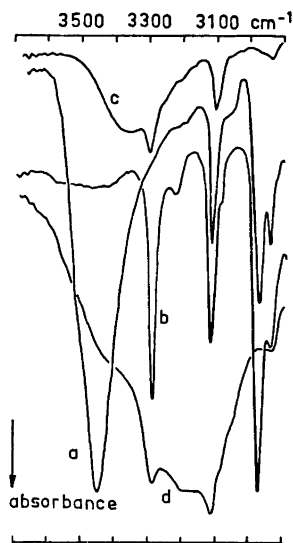
*Fig. 4.* Infrared solid spectra as KBr pellets. (*a*): 2-Isopropylquinone 4-(2',4'-dinitrophenylhydrazone) (No. 3). (*b*): 2,6-Diisopropylquinone 4-(2',4'-dinitrophenyl-hydrazone) (No. 21). (*c*): 2,3-Dimethyl-quinone 2',4'-dinitrophenylhydrazone (No. 11). (*d*): 4-(2',4'-Dinitrophenylazo)-3-methylphenol (No. 5). The spectra are vertically displaced for clarity.

hydrazone [1] makes the assignment of a C=O band fortuitous.

*Electronic spectra.* Ultraviolet-visible (UV) spectra of the solids in the form of potassium bromide pellets have been used in the phenylazonaphthol series for confirming the presence of the azo form;[2] the positions of the UV azo and hydrazone maxima were found to fall at about the same wavelengths as in relatively polar solution. When this technique was applied to selected compounds of the present series (Fig. 3) no correspondence with the infrared spectra could be found: there is a single maximum in the azo region whether IR indicates absence (No. 10) or presence (No. 9) of NH; two UV bands appear, with the azo band the larger one (Nos. 22 and 24) or the smaller one (No. 21), even when IR shows no OH bands at all; or the azo and hydrazone bands are of about the same intensity (No. 17), whereas IR indicates only small amounts of NH. This behaviour is explained by the observations that the hydrazone tautomer of some 2'-nitro- and 2',4'-dinitro-phenylazo-alkyl-phenols,[6] quinone *N*-methyl 2,4-dinitrophenylhydrazones,[6] and strongly conjugated, aliphatic DNPH's [7-9] shows two UV bands in the "azo" and "hydrazone" regions in low-polar as well as high-polar solution. It must be concluded, therefore, that unless interpreted with extreme care, UV spectra are useless for detecting or confirming tautomerism in solid nitrophenyl-azophenols.

## DISCUSSION

There are two possible explanations of the presence of both tautomers in the solid state: two kinds of crystals may be present in admixture, or the molecules of both tautomers may be packed into the same crystal lattice. In the case of 1,2-naphthoquinone hydrazones Hadži[2] found no evidence of two

types of crystals. This is perhaps more obvious with 1,2- (I) than with 1,4-
(II) derivatives, since in the former a dynamic tautomerism may take place
by an intramolecular hydrogen-transfer mechanism without
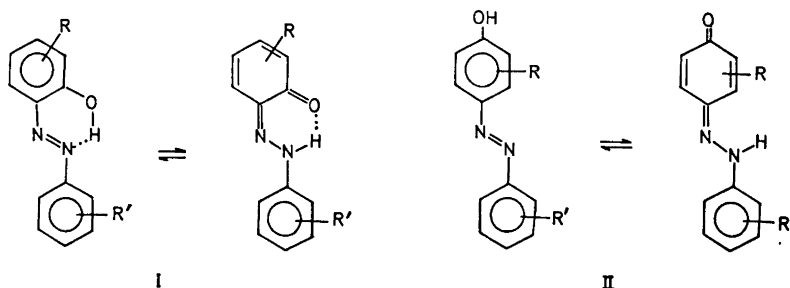


significant variation of molecular dimensions or orientation. However, the
1,4-tautomers differ mainly in the position of the small, active hydrogen, and
also these should be sufficiently similar to allow for packing into a common
lattice. 2,4-Dinitrophenylhydrazones are notorious of exhibiting polymorphism
and forming solid solutions.[10,11]

The assumption of mixed crystal lattices is supported by the IR data
discussed above, and by the observation that No. 16 occurs in two inter-
convertible modifications. The properties of the two forms in the dissolved
state (chromatography, IR-, and UV-spectra) are identical, as expected,
whereas the IR solid spectra are clearly different (Fig. 1). The spectra indicate
that the yellow modification (16b) contains much hydrazone, and the brown
one (16a), considerably less. Thus both modifications probably are tautomeric
mixtures, differing only in composition and stability. At room temperature
the yellow, more hydrazonic form is the thermodynamically more stable one;
at about 150° the azo form appears to be formed spontaneously. This is con-
sistent with the relative stabilities found in similar tautomeric systems.[12]

The lack of relationship between the tautomeric compositions in tetra-
chloroethylene solution and in the solid state is notable. Nos. 2, 11, 13, 14,
17, 26, and 27 are predominantly azophenolic in the solid state, whereas in
solution they are $64-97$ % hydrazonic.[1] Even more striking are Nos. 3, 4, 8,
25, 29, and 30. These solids have practically identical spectra in the $3800-$
$3000$ cm$^{-1}$ region (cf. Fig. 4a) which indicate complete absence of hydrazone.
In solution, however, Nos. 3 and 4 contain 68 and 84 % of hydrazone, against
10, 0, and 0 % in Nos. 25, 29, and 30.[1] Moreover, the spectra of Nos. 3, 4, and
8 are radically different from those of the other 2- and 3,5-alkylated dinitro
compounds (Nos. 2, 9, 10; cf. Fig. 4c and d), which in solution contain 68,
15, and 14 % of hydrazone,[1] respectively. These lacks of relationship may be
explained by different possibilities of intermolecular hydrogen bonding in
the compounds. The various types of bonding ($> N-H\cdots O=$; $\geqslant N\cdots H-O-$;
$> N-H\cdots$nitro; $-O-H\cdots$nitro; $\geqslant N-H\cdots O-H$; etc.) and their relative
amounts in a given compound probably depend on, among other things, the
steric conditions imposed by the alkyl substituents in one molecule on the

various donating and accepting centres in the neighbouring molecules. This also influences the tautomeric composition.

If this assumption of a mixed, tautomeric crystal lattice is correct, the question arises whether the tautomeric equilibrium is static or dynamic on a molecular scale. The stability of the yellow form of No. 16 up to 150° and the lack of significant changes in the solid spectra of other sample compounds up to some 190° (cf. Fig. 2) seem to give preference to the static version. The high conversion temperature indicates a high energy of activation of the hydrogen transfer reaction, hydrazone → azo. Consequently the tautomerically active bonds $> N - H \cdots O =$ and $\geqslant N \cdots H - O -$ are probably inactive at lower temperatures. The other types of bonding ($- O - H \cdots$nitro, etc.) are tautomerically fixed and require complete rearrangement of the crystal lattice, or melting, to allow for transition of the hydrogen.

Infrared spectroscopy certainly is not the ideal method for an exhaustive study of tautomerism in solid azophenols. It appears from the results above, however, that Hadži's doubt [2] that an X-ray examination would yield nothing else than the average structure is too pessimistic, and that X-ray work in this field should be encouraged.

## REFERENCES

1. Juvvik, P. and Sundby, B. *Acta Chem. Scand.* **27** (1973) 1645.
2. Hadži, D. *J. Chem. Soc.* **1956** 2143.
3. Morgan, K. J. *J. Chem. Soc.* **1961** 2151.
4. Kishimoto, S., Hirashima, T., Manabe, O. and Hiyama, H. *Kogyo Kagaku Zasshi* **70** (1967) 1379; *Chem. Abstr.* **68** (1968) 48769p.
5. Jones, L. A., Holmes, J. C. and Seligman, R. B. *Anal. Chem.* **28** (1956) 191.
6. Juvvik, P. and Sundby, B. *Acta Chem. Scand.* **27** (1973) 3632.
7. Heggelund, A. and Juvvik, P. *Unpublished work.*
8. Juvvik, P. and Solheim, E. *Unpublished work.*
9. Juvvik, P. and Sire, J. *Unpublished work.*
10. Buckingham, J. *Quart. Rev. Chem. Soc.* **23** (1969) 37.
11. Kitaev, Yu. P., Buzykin, B. I. and Troepol'skaya, T. V. *Russ. Chem. Rev.* **39** (1970) 441.
12. Fischer, E. and Frei, G. *J. Chem. Soc.* **1959** 3159.

# Ultraviolet — Visible Spectra of Azophenols:

# Absorption of the Hydrazone Form in the "Azo Region"

PAUL JUVVIK and BJØRN SUNDBY*

*Chemical Institute, University of Bergen, N-5000 Bergen, Norway*

The ultraviolet — visible spectra of the hydrazone tautomer of 4-(2′,4′-dinitrophenylazo)-alkylphenols show two distinct absorption maxima, at about 383 − 402 and 417 − 440 nm, in tetrachloroethylene solution. The shorter-wavelength band occurs in the same region as the main band of the azo tautomer, and thus interferes with the detection of that form. Similar spectra are given by quinone 2′-nitrophenylhydrazones, and by the $N$-methyl derivatives of quinone 2′- and 4′-nitro- and 2′,4′-dinitrophenylhydrazones. The longer-wavelength maximum is tentatively assigned to the degenerate transitions of the NH nitrogen lone pair to the nitro groups and the quinone oxygen, and the shorter-wavelength band is proposed to be the displaced, next-lower band among the four commonly found in dinitrophenylhydrazones.

Ever since the work of Kuhn and Bär[1] it has been generally assumed[2,3] that the hydrazone species (I) of the arylazophenol — quinone arylhydrazone tautomeric system absorbs at a longer ultraviolet — visible (UV) wavelength than the azophenol (II). *Vice versa*, it has been assumed that substances of this type are actually present as equilibrium mixtures of the two forms whenever the UV spectra of their solutions [4-7] or of the solids [6,7] show two bands at the appropriate positions. The assignment of the bands originally was deduced [1,4] from the spectra of the $O$- and $N$-methylated species, which represent unambiguous azo and hydrazone structures; later, it has been confirmed by relation to the infrared [7] and nuclear magnetic resonance [8,9] spectra. It will appear from the results reported below, however, that UV spectroscopy is less generally useful for detecting and studying tautomerism than was formerly believed: several quinone 2′,4′-dinitrophenylhydrazones (DNPHs) and 2′-nitrophenylhydrazones (2′-NPHs), which are 100 % hydrazones according to infrared,[10] show two distinct UV maxima, the lower of which coincides with

---

* Present address: Division of Chemical Oceanography, Bedford Institute of Oceanography, Dartmouth, Nova Scotia, Canada.
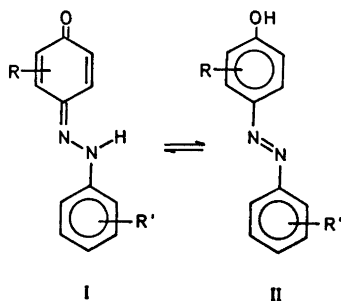
the maximum of the azo tautomer. This would induce the erroneous conclusion that a considerable proportion of the azo form were present.

## EXPERIMENTAL

The preparation and purification of compounds Nos. *1 — 30, 36 — 39,* and *42 — 45* (Table 1) are described elsewhere.[10] The *N*-methyl hydrazones were prepared by treating the quinone with the appropriate 1-methyl-1-arylhydrazine [11] in hot, 2 N ethanolic hydrochloric acid (Nos. *32, 33, 36, 40, 46, 56*), or in anhydrous formic acid at room temperature (No. *31*), and purified by preparative-layer chromatography (PLC) [10] on silica gel. Oxidation of the hydrazine to *N*-methyl-mono- or -dinitroaniline, and demethylation of the hydrazone, were troublesome side reactions. The *O*-methyl azo compounds Nos. *34, 35, 41,* and *47* were made from the dinitrophenylazophenol with diazomethane in ether solution, followed by PLC.

*Table 1.* Ultraviolet — visible spectra of dinitrophenylazophenols and related compounds in tetrachloroethylene solution.

| No. R in I or II [a,b] | Lower band [c,d,e] | | Higher band [d,e,f] | | Int. ratio [g] | % NH [h] | $\Delta\lambda$ nm [f] |
|---|---|---|---|---|---|---|---|
| | $\lambda$ nm [f] | $\varepsilon \times 10^{-4}$ | $\lambda$ nm [f] | $\varepsilon \times 10^{-4}$ | | | |
| **R' = 2',4'-(NO$_2$)$_2$** | | | | | | | |
| 1 H | 383 | | — | | | 8 | |
| 2 2-Me | 393 | 2.61 | 429 | 2.59 | 0.99 | 60 | 36 |
| 3 2-Et | 393 | | 430 | | 1.04 | 64 | 37 |
| 4 2-Pr | 394 | | 433 | | 1.09 | 68 | 39 |
| 5 2-Bu | 394 | | 435 | | 1.19 | 84 | 41 |
| 6 2-Ph | 394 | 1.87 | — | | | 4 | |
| 7 3-Me | 392 | 2.08 | (430) | (0.84) | 0.40 | 25 | (38) |
| 8 3-Et | 391 | 2.07 | (427) | (0.59) | 0.29 | 27 | (36) |
| 9 3-Pr | 396 | 2.74 | (432) | (0.67) | 0.24 | 19 | (36) |
| 0 3-Bu | 392 | | (428) | | 0.35 | 20 | (36) |
| 1 3-Ph | 396 | 2.06 | — | | | 7 | |
| 2 3,5-Me$_2$ | 399 | | — | | | 22 | |
| 3 3-Me-5-Et | 402 | | — | | | 15 | |
| 4 3-Me-5-Pr | 395 | | — | | | 14 | |
| 5 3-Me-5-Bu | 402 | 2.40 | — | | | 14 | |

(*Table 1, continued*)

| | | | | | | | | |
|---|---|---|---|---|---|---|---|---|
| 16 | 2,3-Me$_2$ | 398 | | 434 | | 1.18 | 80 | 36 |
| 17 | 2,5-Me$_2$ | 391 | | 428 | | 1.16 | 90 | 37 |
| 18 | 2-Me-5-Pr | 392 | | 427 | | 1.12 | 89 | 35 |
| 19 | 2-Pr-5-Me | 393 | 3.49 | 430 | 3.96 | 1.14 | 94 | 37 |
| 20 | 2-Bu-5-Me | 393 | | 430 | | 1.14 | 91 | 37 |
| 21 | 2,5-Pr$_2$ | 396 | 2.06 | 432 | 2.34 | 1.14 | 93 | 36 |
| 22 | 2,5-Bu$_2$ | 395 | | 431 | | 1.09 | 97 | 36 |
| 23 | 2,3,5-Me$_3$ | 389 | | 417 | | 0.98 | 81 | 28 |
| | | | | | | | | |
| 24 | 2,6-Me$_2$ | 397 | | 437 | | 1.25 | 95 | 40 |
| 25 | 2,6-Pr$_2$ | 400 | | 440 | | 1.24 | 98 | 40 |
| 26 | 2-Me-6-Bu | 398 | | 437 | | 1.24 | 98 | 39 |
| 27 | 3-Cl-2,6-Pr$_2$ | 395 | 2.66 | 440 | 4.00 | 1.49 | 100 | 45 |
| 28 | 2,6-Bu$_2$ | 401 | 2.86 | 440 | 3.31 | 1.14 | 100 | 39 |
| 29 | 2,3,6-Me$_3$ | 399 | 4.02 | 435 | 4.56 | 1.16 | 100 | 36 |
| 30 | 2,3,5,6-Me$_4$ | 391 | 3.08 | 421 | 2.94 | 0.90 | 100 | 30 |
| | | | | | | | | |
| 31 | H N-Me-(I) | (345) | | 426 | | 3.84 | | (79) |
| 32 | 2-Pr-5-Me N-Me-(I) | 346 | 0.79 | 448 | 1.20 | 1.72 | | 102 |
| 33 | 2,6-Bu$_2$ N-Me-(I) | 351 | | 446 | | 2.32 | | 95 |
| 34 | H O-Me-(II) | 390 | | — | | | | |
| 35 | 2-Pr-5-Me O-Me-(II) | 414 | | — | | | | |
| | R′= 2′-NO$_2$ | | | | | | | |
| 36 | 3-Et | 364 | 2.12 | 444 | 0.36 | 0.17 | 10 | 70 |
| 37 | 2-Pr-5-Me | 399 | 2.35 | 449 | 1.82 | 1.28 | 82 | 50 |
| 38 | 2,6-Pr$_2$ | 395 | 1.96 | 457 | 3.22 | 1.64 | 93 | 62 |
| 39 | 2,6-Bu$_2$ | 395 | 1.69 | 457 | 2.56 | 1.49 | 100 | 62 |
| | | | | | | | | |
| 40 | 2-Pr-5-Me N-Me-(I) | (368) | | 435 | | 1.68 | | (67) |
| 41 | 2-Pr-5-Me O-Me-(II) | 375 | | | | | | |
| | R′= 4′-NO$_2$ | | | | | | | |
| 42 | 3-Et | 378 | 3.94 | — | | | 0 | |
| 43 | 2-Pr-5-Me | 387 | 1.99 | — | | | 0 | |
| 44 | 2,6-Pr$_2$ | 386 | 2.80 | — | | | 0 | |
| 45 | 2,6-Bu$_2$ | 386 | | (449) | | 0.21 | 4 | (54) |
| | | | | | | | | |
| 46 | 2-Pr-5-Me N-Me-(I) | 346 | | 453 | | 2.35 | | 107 |
| 47 | 2-Pr-5-Me O-Me-(II) | 391 | | — | | | | |

[a] Or in derivatives of I or II, as remarked. [b] Me= methyl; Et= ethyl; Pr= isopropyl; Bu= *tert*-butyl; Ph= phenyl. [c] Lower band of hydrazone form, or main band of azo form, or both. [d] Main band of hydrazone form. [e] $\varepsilon$ is in l mol$^{-1}$ cm$^{-1}$. [f] Values in parenthesis are geometrically resolved, submerged bands. [g] Intensity ratio higher/lower band. [h] Percentage of hydrazone form, according to infrared spectra (Ref. 10).

Compounds Nos. *48—55* were made in the usual way.[12] Of Nos. *52—55*, the main isomer (*trans*, or *E*[13]) was isolated by PLC, and its identity checked by infrared spectra in tetrachloroethylene solution. Compounds Nos. *48, 49,* and *51* probably are *E* isomers as obtained.[14,15] Compounds Nos. *57,*[16,17] *58,*[18,19] and *59*[20] were made according to published methods, and Nos. *60—62* by coupling of 2,4-pentanedione with the appropriate diazonium tetrafluoroborate[21] in acetic acid solution.

UV spectra were recorded of $2-5 \times 10^{-5}$ M solutions in Merck Uvasol tetrachloroethylene, or in Fluka *p.a.* acetonitrile, using a Beckman DB instrument and 10 mm quartz cells, usually at 25°.

*Table 2.* Ultraviolet — visible spectra of 2,4-dinitrophenylhydrazones in tetrachloro-ethylene solution.[a]

| No. | Carbonyl comp. and hydrazone[b] | | *para*[c] band $\lambda$ nm | *ortho*[c] band $\lambda$ nm[d] | $\Delta\lambda$ nm[e] | Int. ratio[f] |
|---|---|---|---|---|---|---|
| *48* | 2-Butanone | DNPH | 351 | (425) | 74 | 0.16 |
| *49* | 3-Methyl-2-butenal | DNPH | 371 | (440) | 69 | 0.21 |
| *50* | Phorone | DNPH | 382 | (453) | 71 | 0.21 |
| *51* | Benzaldehyde | DNPH | 366 | (433) | 67 | 0.22 |
| *52* | 2-Furaldehyde | DNPH | 374 | (440) | 66 | 0.21 |
| *53* | Ethyl pyruvate | DNPH | 347 | (393) | 46 | 0.33 |
| *54* | Methylglyoxal 1-mono-DNPH | | 338 | (381) | 43 | 0.42 |
| *55* | Methylglyoxal 2-mono-DNPH | | 341 | (390) | 49 | 0.33 |

[a] Molar absorptivities were not determined. [b] Isomerism: *cf.* Experimental section. [c] Assignment: *cf.* text. [d] Values in parenthesis are for geometrically resolved, submerged bands. [e] $\lambda_{ortho} - \lambda_{para}$. [f] Intensity ratio *ortho/para* band, by graphical analysis.

## RESULTS

The "azo" and "hydrazone" absorption regions (about 400 and 450 nm, respectively) of the series of dinitro compounds (Nos. *1 — 30*) are defined [1,4] approximately by the spectra of the *N*- and *O*-methyl compounds Nos. *31 — 35* (*cf.* Fig. 1: *31, 32,* and *34*). Two bands are found in these regions in most of the compounds. The maxima are particularly well developed (*cf.* Fig. 1: *2*
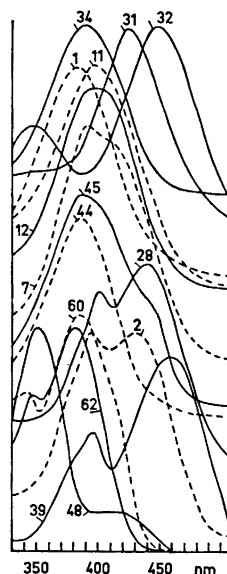


*Fig. 1.* Ultraviolet — visible spectra of quinone hydrazones and azophenols in tetrachloroethylene solution. Numbers refer to the tables. The spectra are vertically displaced for clarity. The absorbances are arbitrary.

and *28*) in compounds Nos. *2 – 5*, and *16 – 30*, which all contain much of the hydrazone tautomer (60 – 100 % [10]). In these compounds, the lower band (389 – 401 nm) is always the minor one (40 – 65 % relative intensity, by graphical analysis), and it coincides fairly exactly with the band given by the azo tautomer (394 – 402 nm). When less hydrazone is present, the higher band is reduced in the same measure (Fig. 1: *7*, *12*, *11*, *1*). When the molecule is locked in the hydrazone structure by *N*-methylation (Nos. *31 – 33*), two bands are still present, but the lower band is shifted towards the blue.

Two bands are found also in the compounds of the 2′-nitro series (Fig. 1: *39*); here, the two regions are farther apart, and the lower band of the hydrazone occurs some 20 nm higher than the azo band. With *N*-methyl (No. *40*), there are still two similar bands.

In the 4′-nitro series, which are usually pure azo compounds,[10] there is a single, practically symmetrical band in the azo region (Fig. 1: *44*). Only No. *45* gives two additional shoulders (*cf.* Fig. 1), of which that at the higher wavelength perhaps is due to the 4 % of hydrazone tautomer present,[10] as deduced from the *N*-methyl derivative No. *46*. The latter, which has the hydrazone structure, again shows two bands.

Two bands, very similar to those found in the quinone DNPHs and 2′-NPHs, are also shown by di-heteroconjugated DNPHs and 2-NPHs,[22] as exemplified by Nos. *60* and *62* (Table 3, and Fig. 1). The corresponding 4-nitro compounds (No. *61*) show a single band, however.[22]

*Table 3.* Ultraviolet – visible spectra of hydrazones and azo compounds in acetonitrile solution.

| No. | Compound [a] | $\lambda$ nm[b]; $\varepsilon \times 10^{-4}$ [b,c] | | | | |
|---|---|---|---|---|---|---|
| *33* | 2,6-Bu$_2$-benzoquinone *N*-Me DNPH | (222) $d$ | 284 $d$ | (348) $d$ | 446 $d$ | |
| *46* | 2-Pr-5-Me-benzoquinone *N*-Me 4′-NPH | (258) (0.86) | (296) (0.76) | (355) (0.76) | 461 2.77 | |
| *56* | Benzoquinone *N*-Me 4′-NPH | (236) (0.32) | (260) (0.48) | (295) (0.42) | (342) (0.32) | 443 3.13 |
| *57* | 2-Nitroazobenzene | 229 1.12 | (269) (0.70) | 316 1.76 | 435[e] 0.060 | |
| *58* | 2,4-Dinitroazobenzene | 231 1.14 | (260) (0.86) | 331 2.19 | 444[e] 0.078 | |
| *59* | 1-(2′,4′-Dinitrobenzeneazo)-2,3-Me$_2$-butadiene | 231 1.17 | 270 0.43 | 405 1.71 | | |
| *60* | 2,3,4-Pentanetrione 3-(2′-NPH) | (228) (1.67) | (244) (1.90) | (278) (1.70) | (330) (2.24) | 390 2.99 |
| *61* | 2,3,4-Pentanetrione 3-(4′-NPH) | 237 0.93 | (297) (0.26) | 375 3.07 | | |
| *62* | 2,3,4-Pentanetrione 3-(DNPH) | 243 1.01 | (275) (0.74) | (337) (1.01) | 383 2.41 | |

[a] Abbreviations: *cf.* footnote *b* to Table 1, and text. [b] Values in parenthesis are for graphically resolved bands. [c] $\varepsilon$ is in l mol$^{-1}$cm$^{-1}$. [d] Not determined. [e] $n \rightarrow \pi^*$ band.

## DISCUSSION

*Hydrazone spectra.* Since DNPHs are derivatives of benzene, their spectra may generally be regarded as modified benzene spectra, where the bands are displaced and their intensity altered under the influence of the substituents.[23,24] More specifically, of the two bands found at long wavelengths in aliphatic and aromatic DNPHs (*cf.* Fig. 1: *48*), the main one has been considered to represent the charge-transfer transition from nitrogen 2 to the *para* nitro group (III), and the shoulder, the analogous transition to the *ortho* group (IV).[14]
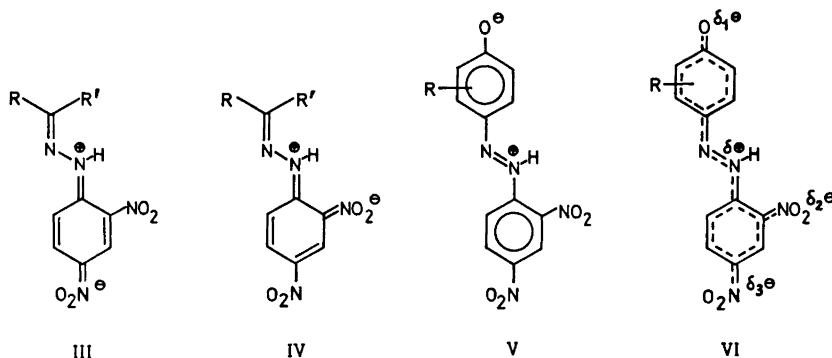


This assignment was based on the observation that 2-NPHs absorb at longer wavelengths, and with less intensity, than the corresponding 4-NPHs.[14] The similar spectra found in 2,4-dinitroaniline and its *N*-monoalkyl derivatives were interpreted in the same way.[25]

This assignment apparently cannot be applied uncritically to the spectra of quinone DNPHs, or di-heteroconjugated DNPHs of the type of No. *62*, since the minor band now occurs to the other side of the main band (*cf.* Fig. 1: *28*), and is sharper and stronger ($\Delta\lambda_{\frac{1}{2}} \approx 25$ nm; $40-65$ % rel. intensity) than that of ordinary DNPHs ($\Delta\lambda_{\frac{1}{2}} \approx 60$ nm; $20-25$ %). Moreover, according to the same interpretation[14] quinone 2'-NPHs and di-heteroconjugated 2-NPHs should give a single band only, whereas two bands are actually present (*cf.* Fig. 1: *39* and *60*).

Therefore, the main band of the quinone DNPHs is now proposed to arise from the degenerate transitions to the nitro groups and the quinone oxygen (III≡IV≡V), while the minor band probably is identical to the displaced, next-lower band among the four bands commonly occurring in DNPHs.[23]

As regards the main band, the assumption of overlap between III and IV finds support in the observation that the distance between the III and IV bands is noticeably shorter in mono-heteroconjugated (*cf.* Nos. *53-55*) than in ordinary saturated, unsaturated, or aromatic DNPHs (Ref. 23, and Table 2); hence, it may be expected to be still shorter in the quinone and di-hetero-conjugated DNPHs, in which the degree of conjugation is still higher. Further, since this overlap is obviously induced by the presence of the cross-conjugated quinone ring, the strongly electron-withdrawing quinone oxygen probably

takes part to some extent in the partial delocalisation; this leads to VI as a tentative structure of the ground state. The extension of the absorbing electron system beyond the $C=N$ bond is indicated by the higher molar absorptivity and longer wavelength maxima of quinone DNPHs ($3-4 \times 10^4$; $420-440$ nm; *cf.* Nos. *24−27*), compared to those of saturated DNPHs ($2-3 \times 10^4$, $350-370$ nm [23],[26]). Similarly, electron-attracting groups in *para*-position of aromatic DNPHs also lead to a slight increase in absorptivity.[14],[26],[27] An even more obvious example of degeneracy analogous to the excitation of VI is found in the single-band spectra of the probably completely delocalised anions of quinone [28] and mono-[22],[29] and di-heteroconjugated [22] DNPHs; this is contrasted by the anions of ordinary, nonheteroconjugated DNPHs, which give two bands.[23],[29],[30] The latter bands have been assigned to the separate transfers of charge to the two nitro groups.[30] The spectra of quinone DNPH anions are further discussed elsewhere.[28]

Structures similar to VI are proposed for the ground state of quinone 2′-NPHs, and for the *N*-methyl derivatives of quinone DNPHs, 2′-NPHs, and 4′-NPHs, to account for the main band in their two-band spectra. Similarly, excitation of VII explains the main band of the di-heteroconjugated DNPHs, and analogous structures are adopted for the ground states of di-heteroconjugated 2-NPHs and 4-NPHs, *e.g.*, Nos. *60* and *61*.

As to the minor band, the next-lower band of ordinary DNPHs is proposed to be displaced to the close vicinity of the main band in the quinone DNPHs,



VII                                    VIII
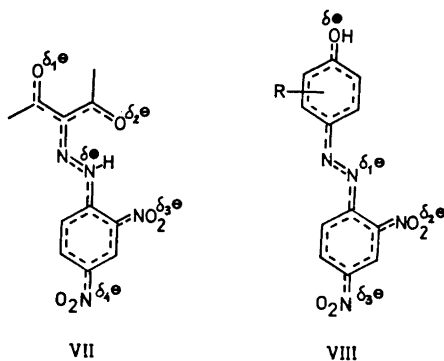
as a result of the presence of the cross-conjugated quinone oxygen. Similar shifts towards the red on introduction of unsaturation are observed for all the four bands usually given by DNPHs,[23] and the shift may be expected to be greater with heteroconjugation, as was found for the band distance discussed above. Since the minor band thus is probably due to a local transition in the substituted benzene ring, it should occur in 2-NPHs and 4-NPHs as well. The apparent lack of it in the di-heteroconjugated 4-NPHs (*cf.* No. *61*) may be due to overlap with the main band, since the latter occurs at lower wavelengths than in the corresponding 2-NPHs and DNPHs (*cf.* Nos. *60−62*), and introduction of a 4-nitro group in a 2-NPH (to give a DNPH) results in a red shift of the minor band (No. *60 vs.* No. *62*).

*Azo spectra.* The existence of a "single" band in the spectra of the azo tautomer (Nos. *1, 6, 11 – 15; cf.* Fig. 1: *1, 11*) seems to be characteristic of the azo structure, since the same is found in the *O*-methyl compounds (Nos. *34* and *35; cf.* Fig. 1: *34*) and in simple azo compounds (Nos. *57 – 59*). The absence of $sp^3$ electrons on nitrogen 2 excludes transitions of the types III and IV, whereas excitation of the $sp^2$ electrons $(n \rightarrow \pi^*)$ is forbidden.[31] A very weak band at about 440 nm due to the latter transition is found in the simple azo compounds Nos. *57* and *58*, but not in the other azo compounds examined, probably because it is masked by the main band.

The main band hence is probably the usual "conjugation" (K) band [24] of azo compounds, shifted to long wavelengths by the combination of electron-donating and -withdrawing substituents on the rings: the ground state may be represented by VIII, and on excitation, degeneracy between the transitions to the nitro groups and the strongly electron-attracting nitrogen 2 is postulated. The absence of the cross-conjugated oxygen atom characteristic of the hydrazone structure may explain the "absence" of a minor band close to the main band: the distance between the main band and the next-lower band is noticeably longer in the azo compounds (*cf.* Table 3).

It is noted that whereas 2-NPHs seem to absorb generally at longer wavelengths than 4-NPHs or DNPHs,[14] (*cf.* also Nos. *60 – 62*), this sequence is reversed in the case of azo compounds (*cf.* Nos. *35, 41, 47*, and Nos. *58, 59*). This perhaps is another indication that the main bands of the hydrazone and azo tautomers are of different origin.

## REFERENCES

1. Kuhn, R. and Bär, F. *Ann.* **516** (1935) 143.
2. Zollinger, H. *Azo and Diazo Chemistry. Aliphatic and Aromatic Compounds*, Interscience, New York 1961, pp. 322 – 327.
3. Bershtein, I. Ya. and Ginzburg, O. F. *Russ. Chem. Rev.* **41** (1972) 97.
4. Ospenson, J. N. *Acta Chem. Scand.* **4** (1950) 1351; **5** (1951) 491.
5. Burawoy, A. and Thompson, A. R. *J. Chem. Soc.* **1953** 1443.
6. Hadži, D. *J. Chem. Soc.* **1956** 2143.
7. Morgan, K. J. *J. Chem. Soc.* **1961** 2151.
8. Kaul, B. L., Nair, M., Rao, A. V. R. and Venkataraman, K. *Tetrahedron Letters* **1966** 3897.
9. Hofer, E. and Uffmann, H. *Tetrahedron Letters* **1971** 3241.
10. Juvvik, P. and Sundby, B. *Acta Chem. Scand.* **27** (1973) 1645.
11. Blanksma, J. J. and Wackers, M. L. *Rec. Trav. Chim. Pays-Bas* **55** (1936) 655; *Chem. Abstr.* **30** (1936) 7104.
12. Vogel, A. I. *A Textbook of Practical Organic Chemistry*, 3rd Ed., Longmans, London 1967, p. 1061 (Method 2).
13. IUPAC Tentative Rules for the Nomenclature of Organic Chemistry. Section E. Fundamental Stereochemistry, *J. Org. Chem.* **35** (1970) 2849.
14. Rappoport, Z. and Sheradsky, T. *J. Chem. Soc.* **B 1968** 277.
15. Karabatsos, G. J., Shapiro, B. L., Vane, F. M., Fleming, J. S. and Ratka, J. S. *J. Am. Chem. Soc.* **85** (1963) 2784.
16. Meisenheimer, J. *Ber.* **36** (1903) 4174.
17. Bamberger, E. and Hübner, R. *Ber.* **36** (1903) 3803.
18. Willgerodt, C. and Hermann, B. *J. prakt. Chem.* [2] **40** (1889) 252.
19. Willgerodt, C. and Ferko, M. *J. prakt. Chem.* [2] **37** (1888) 351.
20. Meyer, K. H. *Ber.* **52** (1919) 1468.

21. Messmer, A. and Krasznay, I. *Acta Chim. Acad. Sci. Hung.* **28** (1961) 399; *Chem. Zentr.* **1964** 1 – 0824.
22. Juvvik, P., Sire, J. and Solheim, E. *Unpublished results.*
23. Timmons, C. J. *J. Chem. Soc.* **1957** 2613.
24. Stern, E. S. and Timmons, C. J. *Gillam and Stern's Introduction to Electronic Absorption Spectroscopy in Organic Chemistry*, Edward Arnold, London 1970, pp. 113 – 133.
25. Kaplan, M. J., Adolph, H. G. and Hoffsommer, J. C. *J. Am. Chem. Soc.* **86** (1964) 4018.
26. Jones, L. A. and Hancock, C. K. *J. Org. Chem.* **25** (1960) 226.
27. Jones, L. A. and Mueller, N. *J. Org. Chem.* **27** (1962) 2356.
28. Juvvik, P. and Sundby, B. *Acta Chem. Scand.* **27** (1973) 3641.
29. Haldorsen, K. M., Heggelund, A., Juvvik, P. and Schønfelder, T. *Unpublished results.*
30. Wells, C. F. *Tetrahedron* **22** (1966) 2685.
31. Rau, H. *Angew. Chem.* **85** (1973) 248.

# Acid Strengths of Some Dinitrophenylazo-
# alkylphenols

PAUL JUVVIK and BJØRN SUNDBY*

Chemical Institute, University of Bergen, N-5000 Bergen, Norway

The acid strengths of thirty 4-(2',4'-dinitrophenylazo)-alkylphe-
nols, tautomeric with alkylquinone 2',4'-dinitrophenylhydrazones,
have been measured in 50 % aqueous dimethyl sulfoxide solution.
For 29 of the compounds, $pK_a$ was between 7.33 and 8.69. 3-Chloro-
2,6-diisopropyl-1,4-benzoquinone 4-(2',4'-dinitrophenylhydrazone)
probably is the most strongly acidic hydrazone recorded ($pK_a$ 5.91).

The change of colour which occurs when 2,4-dinitrophenylhydrazones (DNPH's) are treated with bases [1] forms the basis of much work on the analysis of carbonyl compounds.[2,3] The colour produced, and the NH acid strength of the hydrazones, are both influenced by the structure of the substituents on the carbonyl carbon atom.[4] *Vice versa*, knowledge of the acid strength is of interest in identification work. The literature records $pK_a$ values of some saturated [4,5] and unsaturated [4] aliphatic, unsubstituted aromatic,[4-6] and some other [4] DNPH's, and of a series of DNPH's of substituted benzaldehydes and acetophenones.[6] Since different solvents were used in these works, the values can be compared only *via* compounds which are common to the series, *e.g.*, benzaldehyde DNPH. On this basis, the $pK_a$ values of the various DNPH's lie between about 9.4 and 12.4, referred to 50 % aqueous dioxane as solvent,[6] and with benzaldehyde DNPH at 10.90.[6]

2-Methylnaphthoquinone 4-DNPH has been measured at $pK'$ 4.1 in ethanol containing 10 % of chloroform:[4] this corresponds to $pK_a$ 10.2 in 50 % dioxane. The 4-(2',4'-dinitro-6'-chlorophenylhydrazone) of thymoquinone seems to be somewhat more acidic, as indicated by its $pK_a$ of 8.33 in aqueous ethanol.[7] It has also been observed that some chloroquinone DNPH's dissolve in neutral ethanol with blue or green colours,[8] and that some alkylquinone DNPHs move as greenish spots on neutral silica gel thin-layer chromatograms;[9] this indicates partial dissociation, and a higher acidity than of the DNPH's mentioned above.

---

* Present address: Division of Chemical Oceanography, Bedford Institute of Oceanography, Dartmouth, Nova Scotia, Canada.

The acid strengths of a series of alkylquinone DNPH's have now been determined in 50 % aqueous dimethyl sulfoxide (DMSO) solution. The chromatographical properties [9] of the compounds and their tautomerism with dinitrophenylazo-alkylphenols [10,11] have been discussed elsewhere. For brevity, the compounds are referred to below as DNPAP's (dinitrophenylazophenols), without regard to their actual structure in the solvent used.

## EXPERIMENTAL

The preparation and purification of the compounds have been described before.[10] The method used for determining the $pK_a$ values is a simplification of a standard spectrophotometric method.[6,12] The simplification involves omitting the buffer solutions and instead adjusting the sample pH by adding small amounts of base or acid, and measuring the pH directly in the cuvette with a combination electrode. The advantages of the method include more rapid measurements, extremely low ionic strength, and reduced consumption of solvent, without sacrifice in accuracy.

*Measurements.* Stock solutions were prepared containing about 0.4 mg of compound in 2 ml of pure DMSO (Fluka). The alkaline spectrum was recorded (Beckman DB or DB-GT instruments at 25°) of a sample made by diluting $50-100$ $\mu$l of stock solution to 2 ml with 50 % (v/v) DMSO in a 1 cm cuvette, and injecting 5 $\mu$l of $10^{-2}$ N potassium hydroxide in 50 % DMSO. The amount of sample was adjusted to give an absorbance of about 0.8 at the maximum absorbance wavelength. The acid spectrum was recorded using a fresh sample of the same concentration and containing 5 $\mu$l of $10^{-2}$ N hydrochloric acid in 50 % DMSO.

To obtain readings in the intermediate pH range, microliter amounts of $10^{-3}$ N potassium hydroxide in 50 % DMSO was injected into a fresh sample to give an absorbance of about 0.2 at the alkaline maximum wavelength. The pH then was measured in the cuvette (Radiometer pH-meter Type 28, with glass/calomel electrode GK 2321 C), and immediately afterwards, the exact absorbance was read. More base then was injected to increase the absorbance slightly, *etc.* Between readings, the electrode was blotted with tissue paper. Four to eight readings were taken in the $0.2-0.7$ absorbance range. After each series, the electrode was rinsed with water, wiped dry, and immersed in an aqueous buffer (Beckman pH 7.00; Radiometer pH 4.65 and 9.22) until the correct reading was obtained, usually after 5 sec. Rinsing with water and drying was repeated when returning to a new sample; the response time now was $\frac{1}{2}-2$ min. The sample was stirred magnetically during the pH-measurements (Bel-Art Spectrophotometric Cell Stirrer), and the stirrer was left in the cuvette during the spectral readings.

The slightly soluble Nos. *28* and *31* could not be measured accurately owing to precipitation at low or intermediate pH values. No. *31* was measured at a greater dilution in a 4 cm cuvette. By starting from the alkaline side, it was possible to obtain an approximate $pK_a$ value for No. *28*. Owing to the precipitation, the full spectrum of No. *28* could not be obtained in acid solution.

*Calculations.* The apparent $pK_a$ values (Table 1) were calculated from the usual buffer equation,[6,12] assuming all activity coefficients equal to unity. The deviation within each series of readings, and between duplicate series, was $\pm 0.08$ to 0.02 $pK_a$ unit.

## RESULTS AND DISCUSSION

*Spectra.* Depending on the alkylation pattern, the DNPAP's show one or two absorption bands in acid solution. No. *1* and the mono- and 3,5-dialkyl compounds (Nos. *2 – 15*) give a single band below 406 nm. A single band, but now at $412-427$ nm, is also given by the 2,3- and 2,5-substituted compounds (Nos. *16 – 23*), whereas the 2,6-alkylated compounds (Nos. *24 – 30*) show two bands, at $383-400$ and $443-456$ nm. The latter two bands may indicate the presence of a tautomeric mixture of azo and hydrazone forms, or the com-

*Table 1.* Apparent $pK_a$ values and spectral data of 4-(2′,4′-dinitrophenylazo)alkyl-phenols, or alkyl-1,4-benzoquinone 4-(2′,4′-dinitrophenylhydrazones), in 50 % aqueous dimethyl sulfoxide.

| No. | Alkyl,[a] or full name | $\lambda_{HA}$ nm[b] | | $\varepsilon_{HA}{}^{c}$ $\times 10^{-4}$ | $\lambda_{A}$-nm | $\varepsilon_{A}-$ $\times 10^{-4}$ | $\varepsilon_{A}-/\varepsilon_{HA}$ | $pK_a$ |
|---|---|---|---|---|---|---|---|---|
| 1 | H | 387 | | 2.12 | 553 | 3.85 | 1.82 | 8.05 |
| 2 | 2-Me | 400 | | 2.01 | 580 | 4.94 | 2.46 | 8.04 |
| 3 | 2-Et | 402 | | 2.12 | 590 | 5.07 | 2.39 | 8.04 |
| 4 | 2-Pr | 403 | | 2.06 | 595 | 5.21 | 2.53 | 8.00 |
| 5 | 2-Bu | 405 | | 2.07 | 604 | 6.11 | 2.95 | 8.27 |
| 6 | 2-Ph | 402 | | 1.70 | 586 | 4.24 | 2.49 | 7.92 |
| 7 | 3-Me | 402 | | 1.97 | 575 | 4.15 | 2.11 | 7.95 |
| 8 | 3-Et | 402 | | 2.06 | 577 | 4.92 | 2.39 | 8.11 |
| 9 | 3-Pr | 404 | | 2.15 | 575 | 4.63 | 2.15 | 7.66 |
| 10 | 3-Bu | 405 | | 1.94 | 592 | 4.62 | 2.38 | 8.27 |
| 11 | 3-Ph | 398 | | 1.59 | 564 | 3.31 | 2.08 | 7.63 |
| 12 | 3,5-Me$_2$ | 402 | | 2.18 | 566 | 4.02 | 1.85 | 8.01 |
| 13 | 3-Me-5-Et | 403 | | 2.27 | 564 | 4.47 | 1.97 | 8.28 |
| 14 | 3-Me-5-Pr | 402 | | 1.78 | 564 | 3.68 | 2.07 | 8.37 |
| 15 | 3-Me-5-Bu | 406 | | 1.60 | 576 | 4.00 | 2.50 | 8.27 |
| 16 | 2,3-Me$_2$ | 412 | | 2.03 | 603 | 5.50 | 2.71 | 8.13 |
| 17 | 2,5-Me$_2$ | 417 | | 2.03 | 599 | 5.50 | 2.71 | 7.86 |
| 18 | 2-Me-5-Pr | 414 | | 2.00 | 593 | 5.10 | 2.55 | 8.06 |
| 19 | 2-Pr-5-Me | 417 | | 2.19 | 596 | 6.26 | 2.86 | 8.10 |
| 20 | 2-Bu-5-Me | 421 | | 1.67 | 601 | 5.06 | 3.03 | 8.31 |
| 21 | 2,5-Pr$_2$ | 417 | | 2.20 | 598 | 6.28 | 2.86 | 7.99 |
| 22 | 2,5-Bu$_2$ | 427 | | 1.75 | 614 | 6.72 | 3.84 | 8.69 |
| 23 | 2,3,5-Me$_3$ | 412 | | 1.85 | 596 | 4.63 | 2.50 | 8.53 |
| 24 | 2,6-Me$_2$ | (383) | 443 | 1.37 | 604 | 4.22 | 3.08 | 7.46 |
| 25 | 2-Bu-6-Me | (400) | 455 | 2.57 | 612 | 5.78 | 2.28 | 7.68 |
| 26 | 2,6-Pr$_2$ | (399) | 454 | 2.80 | 612 | 7.50 | 2.68 | 7.33 |
| 27 | 3-Cl-2,6-Pr$_2$ | (394) | 452 | 3.33 | 606 | 6.10 | 1.83 | 5.91 |
| 28 | 2,6-Bu$_2$ | [d] | 456 | 2.78 | 613 | 8.04 | 2.89 | 8.4[g] |
| 29 | 2,3,6-Me$_3$ | (397) | 453 | 2.81 | 610 | 6.08 | 2.19 | 7.95 |
| 30 | 2,3,5,6-Me$_4$ | (392) | 445 | 2.02 | 608 | 4.59 | 2.27 | 8.59 |
| | *DNPH's of:* | | | | | | | |
| 31 | Benzaldehyde | 402 | | 2.83 | 472[e] | 3.25[e] | 1.15 | 11.48 |
| 32 | Phorone | 400 | | 2.63 | 475[f] | 2.27[f] | 0.87 | 13.36 |

[a] Me = methyl; Et = ethyl; Pr = isopropyl; Bu = *tert*-butyl; Ph = phenyl. [b] Values in parentheses are graphically resolved, submerged bands. [c] Main band only. [d] Unresolved, submerged band present (*cf.*, Experimental). [e] Submerged band at 550 nm ($\varepsilon \approx 1.44 \times 10^4$). [f] Submerged band at 568 nm ($\varepsilon \approx 1.37 \times 10^4$). [g] Approximate value (*cf.*, Experimental).

pound may exist entirely in the hydrazone form, which is known [13] to give two bands. The intermediate position of the single band of Nos. *16 – 23* suggests it to be composed of two overlapping, closely spaced bands. By comparison with determinations of the tautomeric composition of similar com-

pounds in other solvents,[10],[14] Nos. *1* and *6 — 15* probably are pure azo in 50 % DMSO; Nos. *2 — 5* and *16 — 26* tautomeric mixtures; and No. *28*, perhaps also Nos. *27, 29*, and *30*, pure hydrazones. The tentative assignments of the two bands of the hydrazone and the single band of the azo form in tetrachloroethylene solution have been discussed before.[13] The same assignments apply also to the present spectra in acid, 50 % DMSO.

In basic solution, ordinary DNPH's give two bands (*cf.* Fig. 1: A), which have been assigned to the separate transfers of charge to the two nitro groups
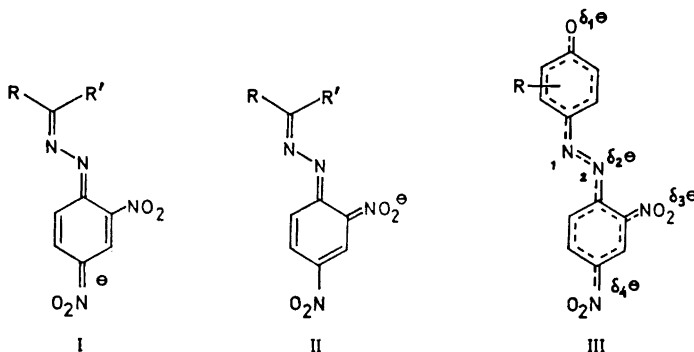


(I — II).[2] This assignment does not fit the single band given by the DNPAP anions, except if one assumes degeneracy between the transitions corresponding to I and II. The consistent occurrence of a single band, independent of the probable tautomeric composition (Fig. 1: *1, 14, 19, 28*), thus indicates structure III for the mesomeric, common anion in the ground state. This structure is supported by the long wavelengths of absorption in basic solution relative to saturated DNPH's (about 440 nm [2],[4]), and by the ratio between the absorptivities in basic and acid solution, which is about 2 — 4 for the DNPAP's *vs.* about 1 or less for saturated DNPH's.[4],[6]

Alkylation in 2- and 2,6-position leads to a red-shift of the absorption maximum in basic solution, relative to 3- and 3,5-alkylation. This resembles the effect of alkyl on the tautomeric composition in tetrachloroethylene solution,[10] where 2- and 2,6-alkyl lead to much higher contents of hydrazone than do 3- and 3,5-alkyl. Probably the redshift is caused by the larger partial charge on nitrogen 2 with 2- and 2,6-alkyl, as was assumed for the contents of hydrazone.[10] If so, the basic absorption wavelength of a given DNPAP, relative to a definitely non-hydrazonic DNPAP (*e.g.*, No. *1* in 50 % DMSO), may be taken as a measure of the tautomeric composition.

*Acidities.* Recalculation of the acidity values given by Timmons,[4] which are in fact $-pK_b{'}$ values, using phorone DNPH (No. *32*) as a reference compound, gives $10.5 - 13.5$ as the probable range of $pK_a$ of his series of aliphatic and aromatic DNPH's when transferred to 50 % DMSO. Similar calculations on the values given by Jones and Mueller [6] indicate $11.0 - 12.2$ as the probable range for their aromatic DNPH's in 50 % DMSO. In this relation the DNPAP's are more acidic by 1.8 $pK_a$ units or more.
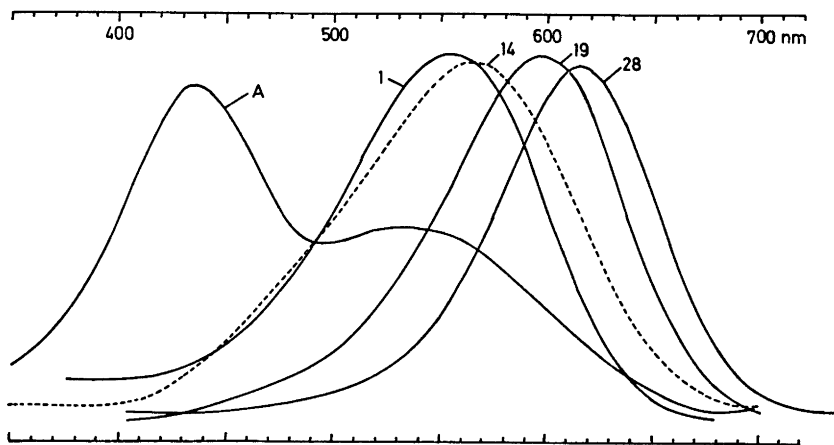
*Fig. 1.* Ultraviolet-visible spectra of dinitrophenyl-hydrazones and dinitrophenylazo-phenols in alkaline, 50 % aqueous dimethyl sulfoxide solution. Numbers refer to Table 1.
A = 2-Butanone 2,4-dinitrophenylhydrazone.

Owing to the limited solubility of the DNPAP's in 50 % DMSO, it was not possible to determine the tautomeric composition and, hence, the acid strengths of the individual tautomers [15] with any certainty. A detailed discussion of substituent and positional effects of the alkyl groups therefore is not worth-while. However, chlorine (No. *27*) exerts the ordinary inductive effect, which seems to be effectively transmitted across the C=N−N bridge: No. *27* prob-ably is the most strongly acidic DNPH recorded, being at least 4.6 p$K_a$ units more acidic than ordinary DNPH's, and 1.4 units more than No. *26*.

Similarly, the mesomeric effect of the C=O group of the hydrazonic Nos. *24−26* and *28−30* is transmitted to the NH group, as judged from their higher acidities relative to ordinary DNPH's. On the other hand, No. *32* is about 2 units less acidic than saturated DNPH's: in the absence of C=O conjugation, C=C conjugation decreases, rather than increases, the acidity. Thus, the conclusions of Jones and Mueller,[6] that mainly the dinitrophenyl group is responsible for the acidity of DNPH's, and that transmission across the hydrazone bridge does not occur with any great facility, seem to be valid only for hydrazones without inductive or mesomeric groups.

## REFERENCES

1. Bohlmann, F. *Chem. Ber.* **84** (1951) 490.
2. Wells, C. F. *Tetrahedron* **22** (1966) 2685.
3. Jart, A. and Bigler, A. J. *J. Chromatogr.* **23** (1966) 261.
4. Timmons, C. J. *J. Chem. Soc.* **1957** 2613.
5. Schaal, R. and Gadet, C. *Bull. Soc. Chim. Fr.* **1961** 2154.
6. Jones, L. A. and Mueller, N. *J. Org. Chem.* **27** (1962) 2356.
7. Mukerji, S. K. and Sharma, H. L. *Talanta* **14** (1967) 1123.
8. Schildknecht, H. *Angew. Chem.* **75** (1963) 762.

 9. Juvvik, P. and Sundby, B. *J. Chromatogr.* **76** (1973) 487.
10. Juvvik, P. and Sundby, B. *Acta Chem. Scand.* **27** (1973) 1645.
11. Juvvik, P. and Sundby, B. *Acta Chem. Scand.* **27** (1973) 3625.
12. Jaffé, H. H. and Orchin, M. *Theory and Applications of Ultraviolet Spectroscopy*, Wiley, New York 1962, pp. 560 – 572.
13. Juvvik, P. and Sundby, B. *Acta Chem. Scand.* **27** (1973) 3632.
14. Hofer, E. and Uffmann, H. *Tetrahedron Letters* **1971** 3241.
15. Zollinger, H. *Azo and Diazo Chemistry. Aliphatic and Aromatic Compounds*, Interscience, New York 1961, pp. 330 – 331.

# Mass Spectrometric Studies of 1-Acylaminoisoquinolines

# and of Some *N*-(2-Isoquinolinio)amidates

J. MØLLER,[a] J. BECHER,[b] C. LOHSE,[b] K. LEMPERT[c] and B. ÁGAI[c]

[a] *Physical Laboratory II, The H. C. Ørsted Institute, University of Copenhagen, DK-2100 Copenhagen.* [b] *Department of Chemistry, University of Odense, DK-5000 Odense, Denmark.* [c] *Department of Organic Chemistry, Technical University, Budapest, Hungary*

A possible correlation between the initial electron-impact promoted processes and those induced by photochemical means of *N*-(2-iso-quinolinio)amidates has been studied. No similarity between the two types of processes was found. The mass spectra of twelve *N*-(2-iso-quinolinio)amidates and of ten of their 1-acylaminoisoquinoline photoisomers have been recorded and compared. The main fragmentation modes are inferred from the results of high resolution mass measurements, deuterium labelling and the metastable defocusing technique and are reported in details for the 1-acylaminoisoquinolines.

The mass spectral fragmentation behaviour of *N*-(1-pyridinio)amidates and a few *N*-(2-isoquinolinio)amidates has been investigated by Ikeda *et al.*[1] Completely analogous behaviour was reported for the two types of compounds. Furthermore Ikeda *et al.* have compared the electron-impact induced fragmentation of *N*-(1-pyridinio)benzamidates with that caused by thermolysis.

The *N*-(2-isoquinolinio)amidates are known to be photo reactive and their photochemical rearrangement* to 1-acylaminoisoquinolines (*A* to *B*) has recently been described.[2]
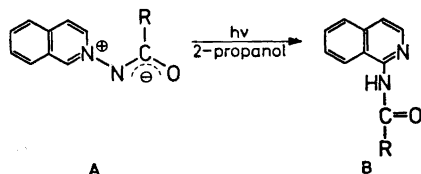


Striking similarities between the initial electron-impact induced processes and those induced by photochemical means have been reported [3] for quinoline

---

* The photochemical rearrangements were carried out in one of the following solvents: 2-propanol, methylene chloride, water, methanol or ethanol; *cf.* Ref. 2.

$N$-oxide and isoquinoline $N$-oxide. They appeared to follow the same fragmentation routes as their photo isomers, carbostyril and isocarbostyril. As the ground state charge distribution of $A$ and the isoelectronic isoquinoline $N$-oxide may be considered to be similar it is of interest to ascertain whether a similar relationship exists for the $N$-(2-isoquinolinio)amidate series. We have, therefore, measured and interpreted mass spectra of compounds of the general structures $A$ and $B$.

## TYPE B COMPOUNDS

The present investigation includes the compounds $1-10$ of type $B$.

Compound, R
1: $C_6H_5$
2: $C_6D_5$
3: $o$-$CH_3OC_6H_4$
4: $m$-$CH_3OC_6H_4$
5: $p$-$CH_3OC_6H_4$

Compound, R
6: $CH_3$
7: $(CH_3)_3C$
8: $(CH_3)_3CCH_2$
9: $C_2H_5O$
10: $NH_2$

Results from IR and NMR spectroscopy suggest [2b,c] that compounds $6-10$ exist largely in the amide form $(Ba)$ whereas compounds $1$, $4$, and $5$ are best described by the tautomeric structure $(Bb)$. Compound $3$ displayed IR-absorptions indicative of the presence of both OH-groups and of NH-groups. These findings, also supported by NMR results, indicate that $3$ is best described as a mixture of the tautomers $(Ba)$ and $(Bb)$.



Ba                    Bb
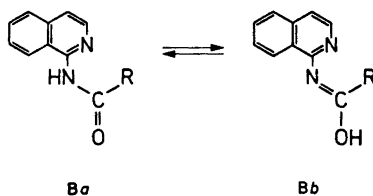
The structures of the molecular ions formed upon electron impact, may, however, differ considerably from the "ground state", due to the large amount of excess energy ($\sim 5$ eV [4]).

## DISCUSSION

The mass spectra of $1$, $4$, and $5$ (Fig. 1) exhibit similar fragmentation patterns, which may best be rationalized if structures for the molecular ions other than $(Bb)$ are considered.

Abstraction of one hydrogen atom from the molecular ion gives rise to abundant $[M-1]$ ions. The mass spectrum of $2$ indicates that the hydrogen lost in this process originates from the phenyl group, suggesting the following structures for this species $c$ or $d$:
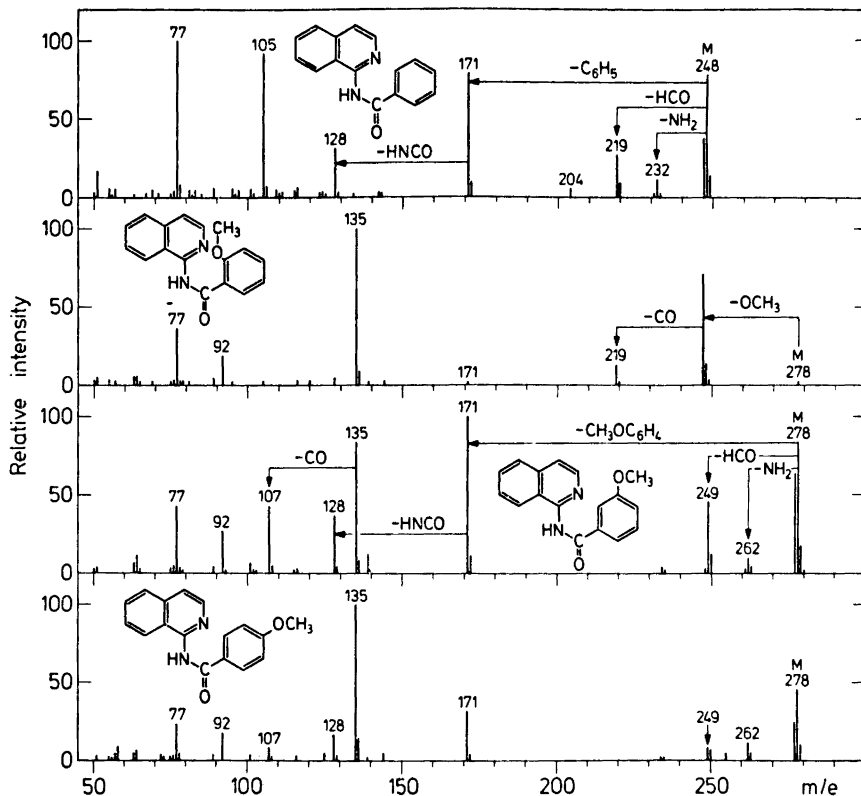
*Fig. 1.*
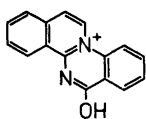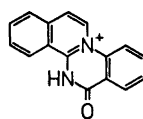


In addition, elimination of $NH_2$, CO, and CHO from the molecular ion is observed.

From the mass spectrum of *2* it is inferred that the hydrogen atom involved in the CHO loss originates from the phenyl group, as does one of the hydrogens in the $NH_2$ loss. Labelling by exchange of *2* with $D_2O$ and subsequent measurement of the mass spectrum, proves that the last labelled hydrogen is also eliminated quantitatively in the $NH_2$ loss.

This collective evidence suggests that the molecular ions of *1*, *4*, and *5*

may also exist in the amide form. Hydrogen transfer from an *ortho*-position to either NH or O followed by bond formation from the ring nitrogen to the *ortho*-postition and subsequent ejection of NH$_2$ or CHO may lead to the following [M − NH$_2$] and [M − CHO] ions:
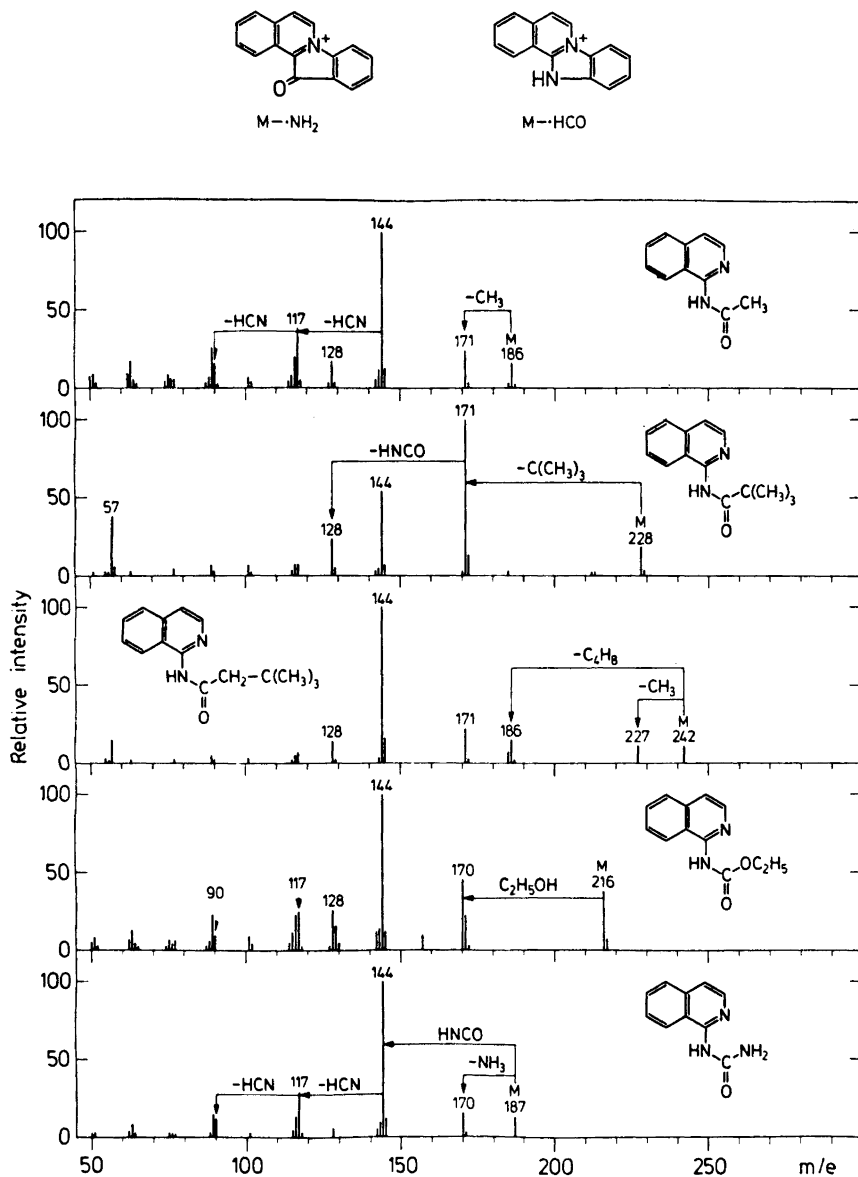




Fig. 2.

Metastable peaks also indicate the fragmentation sequence $M - CO - H$ suggesting that the above mentioned CHO· loss may as well be a concerted loss of CO and H·.

The amide structure of the molecular ions of these compounds is consistent with the dominating α-cleavage (with respect to the carbonyl group) which gives rise to the very abundant [RCO] ions (base peak in the case of *5*). A similar ion is also found to be responsible for the base peak in the spectrum of *3* (Fig. 1). In the rest of the compounds, where R = alkyl, no such ion is seen (Fig. 2).

In the case of the *o*- and *p*-methoxy compounds (*3* and *5*) the RCO ions are assumed to have, respectively, *o*- and *p*-quinoid structures:



For the corresponding ion in the spectrum of *4* no quinoid form can be written:
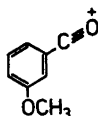


The difference in the structure of these ions is clearly demonstrated by their further fragmentation. The loss of CO from the [RCO] ion in the spectrum of *4* gives rise to an abundant ion. This is not the case for *3* and *5*.

The α-cleavage with elimination of R gives rise to important ions at $m/e$ 171 in all spectra (Figs. 1 and 2) but two: *3* and *10*. The ion formed in this process may be depicted in the following way:
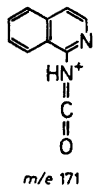


*m/e* 171

Subsequent loss af HNCO then leads to the ion at $m/e$ 128.

In the spectrum of *10* the ion of $m/e$ 171 is formed in very low relative abundance. In this case α-cleavage is followed by hydrogen transfer leading to elimination of $NH_3$. Deuterium labelling, performed in the ion source by simultaneous introduction of $D_2O$ through the gas inlet system, revealed that the three labelled hydrogens were lost in the $NH_3$ elimination which may be explained by the following process:

**9**                          m/e 170
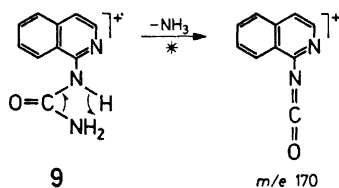
A similar rearrangement may be responsible for the elimination of $C_2H_5OH$ recorded in the spectrum of *9*.

A rearrangement process with hydrogen transfer to the NH group is responsible for the formation of the base peaks (m/e 144) in all the aliphatic substituted compounds but one, *7*. The m/e 144 ion may be depicted as:



*m/e* 144
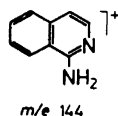
and shows the same fragmentation as observed for authentic 1-aminoisoquinoline:* *i.e.* the successive loss of two molecules of HCN which probably involves ring expansion in one of the steps.

From the above mentioned fragmentations compounds *1–10* may be divided into two main groups where R = aryl and R = alkyl, respectively. The molecular ion of compound *3*, however, exhibits a completely different fragmentation pattern owing to the predominant elimination of the *o*-methoxy group.

This process is analogous to the loss of the phenyl hydrogen in the other aromatic substituted compounds but the characteristic fragmentations of the rest of the group are almost completely suppressed and the relative abundance of the molecular ion is diminished to only 2.5 %.

TYPE A COMPOUNDS

The present investigation concerns the following compounds of type *A*:



**A**
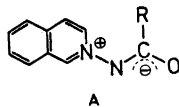
Compound, R
*11*: $C_6H_5$
*12*: $C_6D_5$
*13*: $o$-$CH_3OC_6H_4$
*14*: $m$-$CH_3OC_6H_4$
*15*: $p$-$CH_3OC_6H_4$
*16*: $o$-$NO_2C_6H_4$

Compound, R
*17*: $m$-$NO_2C_6H_4$
*18*: $p$-$NO_2C_6H_4$
*19*: $(CH_3)_3C$
*20*: $(CH_3)_3CCH_2$
*21*: $C_2H_5O$
*22*: $NH_2$

* measured in our laboratory

The mass spectra of two of these compounds $(R = C_6H_5)$ *11* and $(R = NH_2)$ *22* have already been published [1] and shown to be analogous to those of the corresponding pyridinium compounds.

The predominant fragmentation process is $\alpha$-cleavage with elimination of R· and formation of the $m/e$ 171 ion:



*m/e* 171
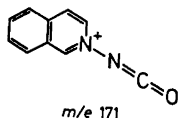
This ion then loses NCO· to furnish the isoquinoline ion at $m/e$ 129.

The ion of $m/e$ 129 may also be formed in a one step process from the molecular ion as shown by the presence of the appropriate metastable peak, detectable by the application of the metastable defocusing technique (shown for *11* and *20*). Furthermore it should be noted that a thermal degradation of these compounds prior to ionization is possible, as the relative abundances of the various ions depend on the ion source temperature and other instrumental parameters. This may explain the rather big differences of the relative ion abundances when spectra from the present investigation are compared with those reported by Ikeda *et al.* as shown in Table 1.

*Table 1.* Principal mass spectral peaks of $N$-(2-isoquinolinio)benzamidate *(11)* and $N$-(2-isoquinolinio)carbamidate *(22)*. a: Ikeda *et al.*,[1] b: present study.

| Compound *11* | | | | | | | | | | |
|---|---|---|---|---|---|---|---|---|---|---|
| $R = C_6H_5$, $m/e$: | 248 | 247 | 171 | 129 | 102 | 110 | 105 | 103 | 91 | 77 |
| (% rel. int.) a: | (75) | (100) | (63) | (53) | (29) | (21) | (18) | (18) | (14) | (35) |
| (% rel. int.) b: | (64) | (100) | (49) | (55) | (13) | (−) | (9) | (5) | (4) | (28) |

| Compound *22* | | | | | | | | |
|---|---|---|---|---|---|---|---|---|
| $R = NH_2$, $m/e$: | 187 | 186 | 171 | 129 | 102 | 144 | 117 | 90 |
| (% rel. int.) a: | (10) | (5) | (14) | (100) | (30) | (15) | (10) | (7) |
| (% rel. int.) b: | (75) | (21) | (92) | (100) | (21) | (16) | (10) | (9) |

The relative intensities of the most important peaks in the mass spectra of type *A* compounds are given in Table 2. These values should, for the reasons given, be regarded with caution (*cf.* Table 1).

In the cases where R is aromatic the molecular ions are comparatively abundant and the [M − 1] ions give rise to the base peaks except for the two *ortho*-substituted phenyl derivatives (*cf.* Table 2).

The mass spectrometric behaviour of the *ortho*-nitro substituted compound *(16)* is clearly different from that of the *meta*- and *para*-isomers (*17* and *18*). Only the mass spectrum of *16* exhibits a fragment ion at $m/e$ 134 (100 % rel. abundance), which is found to have the molecular ion as precursor.

*Table 2.* Principal mass spectral peaks of *N*-(2-isoquinolinio) amidates (% Rel. Int.).

| Compound | R | [M] | [M−H] | [M−R] | [C$_9$H$_7$N] | [RCON] | [RCO] | Other peaks | | | |
|---|---|---|---|---|---|---|---|---|---|---|---|
| 11 | C$_6$H$_5$ | 248 (64) | 247 (100) | 171 (49) | 129 (55) | 119 (5) | 105 (9) | 102 (13) | | | |
| 13 | o-CH$_3$OC$_6$H$_5$ | 278 (15) | 277 (12) | 171 (12) | 129 (100) | 149 (6) | 135 (8) | 102 (14) | 134 (6) | | |
| 14 | m-CH$_3$OC$_6$H$_5$ | 278 (66) | 277 (100) | 171 (58) | 129 (78) | 149 (7) | 135 (15) | 102 (17) | 134 — | | |
| 15 | p-CH$_3$OC$_6$H$_4$ | 278 (64) | 277 (100) | 171 (31) | 129 (53) | 149 (7) | 135 (24) | 102 (14) | 134 (15) | | |
| 16 | o-NO$_2$C$_6$H$_4$ | 293 (30) | 292 (22) | 171 (53) | 129 (96) | 164 — | 150 (3,5) | 102 (19) | 159 (5) | 134 (100) | 104 (25) |
| 17 | m-NO$_2$C$_6$H$_4$ | 293 (64) | 292 (100) | 171 (74) | 129 (93) | 164 (3,0) | 150 (7) | 102 (20) | 246 (16) | | |
| 18 | p-NO$_2$C$_6$H$_4$ | 293 (54) | 292 (100) | 171 (43) | 129 (80) | 164 — | 150 (4,5) | 102 (19) | 246 (25) | | |
| 19 | (CH$_3$)$_3$C | 228 (12) | | 171 (100) | 129 (46) | | | 102 (9) | 57 (11) | | |
| 20 | (CH$_3$)$_3$CCH$_2$ | 242 (32) | 241 (3) | 171 (93) | 129 (100) | | | 102 (25) | 57 (7) | 186 (90) | 185 (71) | 144 (72) |
| 21 | C$_2$H$_5$O | 216 (18) | | 171 (22) | 129 (100) | | | 102 (17) | 144 (13) | | |
| 22 | NH$_2$ | 187 (75) | 186 (21) | 171 (92) | 129 (100) | | | 102 (21) | 144 (16) | | |
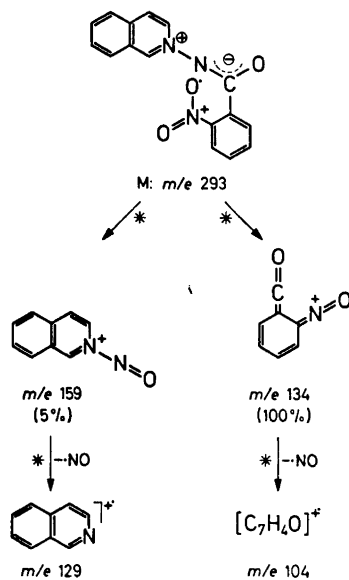


Scheme 1.

A reasonable mechanism for the formation of the $m/e$ 134 ion is shown in Scheme 1.

The *meta-* and *para*-nitro substituted compounds (*17* and *18*) have similar mass spectra. This is also the case for the *meta-* and *para*-methoxy substituted compounds (*14* and *15*), except for one difference. The [RCON] ion (*m/e* 149) exhibits in the case of the *para*-methoxy isomer (*15*) a loss of methyl group to give an ion (*m/e* 134) of similar abundance as that of *m/e* 149. This process is also observed for the *ortho*-isomer (*13*), but not for the *meta*-substituted compound (*14*).

In the case of the neopentyl substituted compound (*20*) the abundant ion at $m/e$ 186 ($C_{11}H_{10}N_2O$) is probably formed by a McLafferty rearrangement of the molecular ion with elimination of $(CH_3)_2C=CH_2$. The ion at $m/e$ 185 ($C_{11}H_9N_2O$) may be due to $C-C$ bond cleavage at the tertiary carbon atom, and the ion of $m/e$ 144 is, according to accurate mass measurement, $C_9H_8N_2$.

## CONCLUSION

Comparison of the mass spectra of type *A* compounds with those of type *B* shows several differences, and although the predominant fragmentation mode in both cases is initiated by $\alpha$-cleavage with elimination of R the further decompositions of the [M − R] ions are different (loss of NCO· *versus* loss of HNCO). It can therefore be concluded that there is no similarity between the initial electron-impact promoted processes and those induced by photochemical means of *N*-(2-isoquinolinio)amidates.

This result is consistent with the conclusion of a recent review [5] of attempts to correlate these two types of processes for aromatic amine *N*-oxides. A similarity was concluded to exist for some of the *N*-oxides examined but no general correlation could be found.

## EXPERIMENTAL

Mass spectra were obtained on a MS902 mass spectrometer using the direct sample insertion system (ion source temperature: $100-180°C$), and an electron energy of 70 eV. All transitions given are verified by the presence of metastable peaks or by the application of the metastable defocusing technique and the elemental compositions are substantiated by high resolution mass measurements ($\pm 5$ ppm). Peaks corresponding to double charged ions appearing at half masses and peaks of lower abundance than 2 % are omitted.

Microanalyses were carried out in the Microanalytical Department of the University of Copenhagen by Mr. Preben Hansen. Melting points (uncorrected) were determined on a Büchi melting point apparatus. Infrared spectra were recorded on a Perkin Elmer Model 137 infrared spectrophotometer. Ultraviolet spectra were determined on a Beckman ACTA III ultraviolet spectrophotometer by Mrs. Bodil Kroneder. Proton magnetic resonance spectra were recorded on a Jeol C-60H1 NMR spectrometer.

Labelling with deuterium of the NH group in some of the 1-acylaminoisoquinolines was carried out by recrystallization twice from $D_2O/CD_3OD$ mixtures containing a trace of $D_2SO_4$, the incorporation was checked by NMR.

The *N*-(2-isoquinolinio)amidates were all prepared as described in Ref. 2c, the data for four new *N*-(2-isoquinolinio) amidates are given here. Compounds *6*, *9* and *10* were prepared as described in the literature.[6,2b]

*N-(2-Isoquinolinio)-o-nitrobenzamidate* (16). Yield 27 %, yellow crystals, m.p. 140 − 142° (benzene). (Found: C 65.35; H 3.83; N 14.23. Calc. for $C_{16}H_{11}N_3O_3$: C 65.52; H 3.78; N 14.33). IR, $\nu_{max}$ (KBr) 1640, 1590, 1575 cm$^{-1}$. UV, $\lambda_{max}$ (log $\varepsilon$), (2-propanol) 323 (3.99),

276 (3.92) nm. NMR, (DMSO-$d_6$), $\tau$ 1.45 $-$ 2.45 (m, aryl H, 10 H), $\tau$ 0.14 (s, H$_1$, 1 H) ppm.

N-*(2-Isoquinolinio)*-m-*nitrobenzamidate* (17). Yield 24 %, yellow crystals, m.p. 228 $-$ 230° (dioxane, cyclohexane). (Found: C 65.65; H 3.86; N 14.18). IR, $\nu_{max}$ (KBr) 1650, 1600, 1565 cm$^{-1}$. UV, $\lambda_{max}$ (log $\varepsilon$), (2-propanol) 331 (4.02), 268 Sh (4.21) nm. NMR (trifluoroacetic acid) $\tau$ 2.20 $-$ 1.25 (m, aryl H, 9 H), $\tau$ 0.95 (s, aryl H, 1 H), $\tau$ 0.14 (s, H$_1$, 1 H) ppm.

N-*(2-Isoquinolinio)*-p-*nitrobenzamidate* (18). Yield 27 % yellow crystals, m.p. 220 $-$ 221° (dioxane). (Found: C 65.70; H 3.83; N 14.18. IR, $\nu_{max}$ (KBr) 1640, 1610, 1570 cm$^{-1}$. UV, $\lambda_{max}$ (log $\varepsilon$), (2-propanol) 331 (4.08), 278 (4.16) nm. NMR (DMSO-$d_6$) $\tau$ 1.34 $-$ 2.77 (m, aryl H, 10 H), $\tau$ 0.00 (s, H$_1$, 1 H) ppm.

N-*(2-Isoquinolinio)pentadeuteriobenzamidate* (12). Yield 42 %, golden needles, m.p. 181 $-$ 183° (benzene). (Found: C 75.90; D+H 4.96; N 10.92. Calc. for C$_{16}$H$_7$D$_5$N$_2$O: C 75.88; D+H 4.78; N 11.07). IR, $\nu_{max}$ (KBr) 1532, 1570 cm$^{-1}$. UV, $\lambda_{max}$ (log $\varepsilon$), (abs. ethanol) 332 (4.03), 274 Sh (3.97) nm. NMR (DMSO-$d_6$) $\tau$ 2.66 (s), $\tau$ 1.43 $-$ 2.30 (m, H$_{3-8}$, s+m, 6 H), $\tau$ 0.05 (s, H$_1$, 1 H) ppm.

*1-(Pentadeuteriobenzoyl)amino isoquinoline* (2). Irradiation was carried out according to Ref. 2c. Thus 0.5 g of *12* dissolved in 600 ml of 2-propanol was irradiated for 8 h yielding yellow crystals (0.5 g). Recrystallization from ethanol, water (7/3) yielded 0.29 g colourless crystals, m.p. 101 $-$ 103°. (Found: C 75.80; D+H 4.92; N 11.07). IR, $\nu_{max}$ (KBr) 1610 broad, 1530 cm$^{-1}$. UV, $\lambda_{max}$ (log $\varepsilon$), (abs. ethanol) 375 (3.90), 357 (3.94), 321 (3.70), 282 (4.04) nm. NMR (DMSO-$d_6$) $\tau$ 3.10 $-$ 2.30 (m, H$_{3-8}$, 6 H), $\tau$ 1.15 (s, broad, NH, 1 H) ppm.

## REFERENCES

1. Ikeda, M., Tsujimoto, N. and Tamura, Y. *Org. Mass Spectrom.* 5 (1971) 61.
2. a. Tamura, Y., Tsujimoto, N., Ishibashi, H. and Ikeda, M. *Chem. Pharm. Bull.* 19 (1971) 1285; b. Agai, B. and Lempert, K. *Tetrahedron* 28 (1972) 2069; c. Becher, J. and Lohse, C. *Acta Chem. Scand.* 26 (1972) 4041.
3. Buchardt, O., Duffield, A. M. and Shapiro, R. H. *Tetrahedron* 24 (1968) 3139.
4. Cooks, R. G. *Org. Mass Spectrom.* 2 (1969) 481.
5. Spence, G. G., Taylor, E. C. and Buchardt, O. *Chem. Rev.* 70 (1970) 231.
6. Craig, J. J. and Cass, W. E. *J. Am. Chem. Soc.* 64 (1942) 783.

# Complex Formation between Silver and Iodide Ions in Fused Potassium-Sodium Nitrate. III. Heterogeneous Equilibria Involving Solid and Liquid AgI Solutions

BERTIL HOLMBERG

*Division of Physical Chemistry, Lund University, Chemical Center, P.O.B. 740, S-220 07 Lund 7, Sweden*

A thermodynamic calculation method of treating data pertinent to the distribution of AgI between solid or liquid (K,Ag)I and a nitrate melt is described. The heterogeneous equilibrium constants are estimated and the stability constants $\beta_{nm}$ for the proposed complexes in the nitrate phase are computed and compared to results from previous studies. From this comparison it is concluded that the species $Ag^+$, $AgI$, $AgI_2^-$, $AgI_3^{2-}$ and $Ag_2I_6^{4-}$ are present in the nitrate melt, whereas clearcut evidence for $AgI_4^{3-}$ cannot be established.

The complex formation between $Ag^+$ and $I^-$ in liquid equimolar $(K,Na)NO_3$ has recently been studied at this laboratory with different experimental methods.[1-3] One aim of these investigations is to compare the results concerning the iodide-rich complexes obtained with different experimental techniques in order to see whether or not the various kinds of experimental data can be satisfactorily described by one single model of the system.

Unfortunately, the conventional solubility method cannot be utilized in the whole concentration range of interest, since the solid silver iodide phase undergoes a phase transition to a reddish liquid at high iodide concentrations in the nitrate melt.[1] This phase transition has been treated in detail in a previous paper.[3] The liquid iodide phase can be formulated as $(K,Ag)I(l)$ and the solid phase as $(K,Ag)I(s)$. As pointed out earlier,[3] the solute in the solid solution cannot be proved to be exclusively either KI or NaI. It is obvious, however, that the same results would be obtained if NaI were dissolved to some extent in the solid, and there would be no difference in the numerical calculations (*vide infra*).

In this paper a simple thermodynamic calculation routine will be described and applied to the distribution equilibria between $(K,Ag)I(s)$ or $(K,Ag)I(l)$ and the nitrate melt in order to yield information on the nature and stability

4

of the complex species in the nitrate phase. The method may be regarded as an extension of the well established solubility method [4] to heterogeneous equilibria involving non-ideal solid and liquid solutions, with both solute and solvent taking part in the complex formation equilibria under study.

<div align="center">EXPERIMENTAL</div>

*Chemicals, apparatus and analyses* have been described elsewhere.[3]

*Procedure.* Weighed amounts of equimolar (K,Na)I and AgI were added to 50.00 g of equimolar (K,Na)NO$_3$. The distribution of silver and iodide between the two phases was determined in three series of measurements with different amounts of AgI in the systems, namely: 0.700 g AgI (series A), 2.200 g AgI (series B), and 4.50 g AgI (series C). For all three series the total concentrations of silver and iodide in the nitrate melt were determined. The composition of the iodide phase was determined for systems in series C only. The experimental technique was the same as described previously.[3]

<div align="center">CALCULATIONS</div>

The following symbols are used:

$C_{Ag}$ = total concentration of Ag$^+$-ion in the nitrate melt.

$C_I$ = total concentration of I$^-$-ion in the nitrate melt.

[A] = denotes the concentration in the nitrate phase of species "A".

$\bar{n}$ = $(C_I - [I^-])C_{Ag}^{-1}$, the ligand number.

$\beta_{nm}$ = $[Ag_m I_n^{(n-m)-}][Ag^+]^{-m}[I^-]^{-n}$

$K_n$ = $[AgI_n^{(n-1)-}][AgI_{(n-1)}^{(n-2)-}]^{-1}[I^-]^{-1}$

$x_i$ = mol fraction of component "$i$" in the iodide phase.

$a_i$ = activity of component "$i$" in the iodide phase.

$f_i$ = $a_i x_i^{-1}$

$x_i', a_i', f_i'$ etc. denote quantities valid for the solid iodide phase.

$x_i'', a_i'', f_i''$ etc. denote quantities valid for the liquid iodide phase.

The indices 1 and 2 are used for AgI and KI, respectively.

$R$ = $([K^+][I^-])^{-1}$

$R_0$ = value of $R$ in a system where $x_2' = 0$

$R^*, []^*, ()^*$ etc. denote the values of the quantities in question at the point of phase transition.

Sternberg and coworkers [5] have performed emf measurements in liquid AgI $-$ KI mixtures in the temperature range $400 - 680°C$ [6] and have found considerable deviations from ideality in such systems. Nevertheless, the concentration product $[Ag^+][I^-]$ in a nitrate melt in equilibrium with a liquid AgI-KI phase may be calculated for each $C_I$. The evaluation of the stability constants for the complex species in the nitrate melt may then be extended to the concentration range $C_I \geq 0.5$ mol kg$^{-1}$. The calculation routine outlined below requires the following conditions to be met:

*i.* The true equilibrium state must be reached. For the distribution of a solute between a liquid and a solid solution it is often difficult to ascertain that this condition has been fulfilled. In the present case, however, there is no doubt that the figures of Table 1 refer to a true equilibrium state. Obviously the high temperature and the structure of $\alpha$-AgI strongly promote the equilibration.

*ii.* The total composition of each phase must be known in the entire concentration range under study, since the calculations involve an integration of functions of the composition variables.

*iii.* The activity coefficients for $K^+$ and the solute species in the nitrate melt should be constant in the pertinent concentration range. This condition, originating from the definitions of the equilibrium constants (*vide infra*), has been discussed in a recent paper.[2]

Consider the following heterogeneous equilibria, where the species of the right hand members are present in the nitrate melt:

AgI(solid iodide solution, $a_1'$) $\rightleftharpoons Ag^+ + I^-$
KI(solid iodide solution, $a_2'$) $\rightleftharpoons K^+ + I^-$
AgI(liquid iodide solution, $a_1''$) $\rightleftharpoons Ag^+ + I^-$
KI(liquid iodide solution, $a_2''$) $\rightleftharpoons K^+ + I^-$
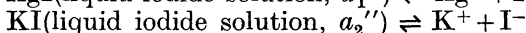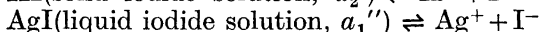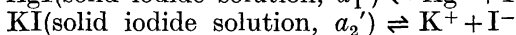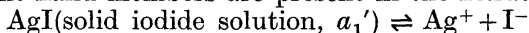
with the equilibrium constants

$$K_1' = [Ag^+][I^-]/a_1' \tag{1}$$

$$K_2' = [K^+][I^-]/a_2' \tag{2}$$

$$K_1'' = [Ag^+][I^-]/a_1'' \tag{3}$$

$$K_2'' = [K^+][I^-]/a_2'' \tag{4}$$

In eqn. (1) $K_1'$ is identical with the conventional solubility product, $K_{s,0}$, determined by Elding and Leden,[1] since $a_1' = 1$ in pure $\alpha$-AgI, which is taken as the standard state for AgI in the solid solution. From the Gibbs-Duhem equation we have

$$d \ln a_1' = -(x_2'/x_1') \, d \ln a_2' \tag{5}$$

Eqn. (2) yields

$$d \ln a_2' = d \ln [K^+][I^-])$$

and hence

$$\ln a_{1j}' = \int_{\ln R_0}^{\ln R_j} (x_2'/x_1') \, d \ln R \tag{6}$$

The index $j$ is used to denote corresponding values of different quantities referring to the same actual system. From eqns. (1) and (6) we obtain

$$([Ag^+][I^-])_j = K_1' \exp \left[ \int_{\ln R_0}^{\ln R_j} (x_2'/x_1') \, d \ln R \right] \tag{7}$$

Eqn. (7) may be used to evaluate $([Ag^+][I^-])$ in the region $C_I \leq C_I^*$. For systems with $C_I \geq C_I^*$ the following expression, analogous to eqn. (6), is valid

$$\ln (a_1'')_j - \ln (a_1'')^* = \int_{\ln R^*}^{\ln R_j} (x_2''/x_1'') \, d \ln R \tag{8}$$

Taking the hypothetical pure liquid AgI at 280°C as the standard state where $a_1'' = 1$, we define an activity scale for the liquid iodide phase in accordance

with normal conventions. The choice of standard state for the liquid iodide solution is, however, of no importance for the determination of the product $[Ag^+][I^-]$. From eqns. (3) and (8) we have

$$([Ag^+][I^-])_j = K_1''(a_1'')^* \exp\left[\int_{\ln R^*}^{\ln R_j}(x_2''/x_1'')\ \mathrm{d}\ln R\right] \tag{9}$$

At the point of phase transition, $([Ag^+][I^-])^*$ can be expressed by means of both eqns. (1) and (3), and hence

$$K_1''(a_1'')^* = K_1'(a_1')^* \tag{10}$$

Eqn. (6) yields

$$(a_1')^* = \exp\left[\int_{\ln R_0}^{\ln R^*}(x_2'/x_1')\ \mathrm{d}\ln R\right] \tag{11}$$

By combination of eqns. (9), (10), and (11) we obtain

$$([Ag^+][I^-])_j = K_1'\exp\left[\int_{\ln R_0}^{\ln R^*}(x_2'/x_1')\ \mathrm{d}\ln R + \int_{\ln R^*}^{\ln R_j}(x_2''/x_1'')\ \mathrm{d}\ln R\right]$$

which finally can be rewritten in the more general form

$$([Ag^+][I^-])_j = K_1'\exp\left[\int_{\ln R_0}^{\ln R_j}(x_2/x_1)\ \mathrm{d}\ln R\right] \tag{12}$$

This expression is identical with eqn. (7). Consequently, the integration may be performed continuously, irrespective of the phase transition, even if a graph of $x_2/x_1$ vs. $\ln R$ displays a discontinuity at the transition point (cf. Fig. 1). Furthermore, the derivation of eqn. (12) is rather general and will apply to any phase transition. Hence, regarding the solid-liquid equilibria, the calculation method is not restricted to cases when a so called "continuous range of solid solution" is formed, but any phase transformation in the solid
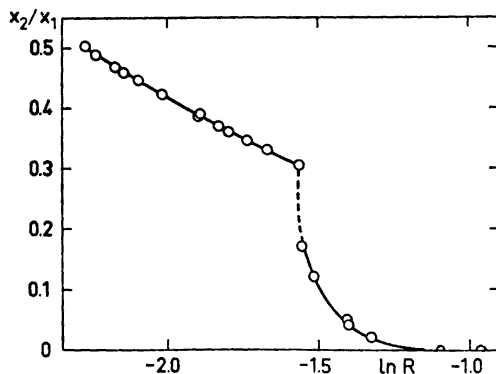


*Fig. 1.* A plot of $x_2/x_1$ vs. $\ln R$, calculated according to alt. I. The integration is performed along the smooth curve.

may occur as long as there is no change in the components of the solid solution and the proper values of $x_2$ and $R$ are known.

For $R_j \leq R^*$ the exponential factor in the right hand member of eqn. (12) is proportional to $a_1''$ and may be written $\lambda_1 a_1''$. This quantity is directly obtained from the integration process and is tabulated in Table 1. A simple calculation gives $\lambda_1 = K_1''/K_1'$.

Table 1. Experimental data and calculated quantities (alternative I). Interpolated values are denoted i. Data above the line refer to systems (K,Ag)I(s)-nitrate melt; those below the line refer to (K,Ag)I(l)-nitrate melt.

| Series | $C_I$ / mol kg$^{-1}$ | $C_{Ag} \times 10^2$ / mol kg$^{-1}$ | $x_1$ | $a_1'$ or $\lambda_1 a_1''$ | $a_1''$ | $f_1$ | $a_2$ | $f_2$ | $[Ag^+][I^-] \times 10^{10}$ / (mol kg$^{-1})^2$ | $\bar{n}$ | $[I^-]$ / mol kg$^{-1}$ |
|---|---|---|---|---|---|---|---|---|---|---|---|
| C | 0.492 | 0.789 | 1.00 | 1 | | 1 | 0 | | 6.20 | 3.20 | 0.467 |
| C | 0.561 | 0.937 | 1.00 | 1 | | 1 | 0 | | 6.20 | 3.25 | 0.531 |
| C | 0.715 | 1.672 | 0.98 | 0.9984 | | 1.02 | 0.0067 | 0.3 | 6.19 | 3.32 | 0.659 |
| C | 0.773 | 1.994 | 0.96 | 0.9962 | | 1.04 | 0.0072 | 0.18 | 6.18 | 3.34 | 0.706 |
| C | 0.779 | 2.065 | 0.95 | 0.9960 | | 1.05 | 0.0073 | 0.14 | 6.18 | 3.35 | 0.710 |
| C | 0.881 | 2.690 | 0.89 | 0.9879 | | 1.11 | 0.0081 | 0.07 | 6.12 | 3.37 | 0.790 |
| A | 0.908 | 2.819 | | | | | | | 6.10 i | 3.38 | 0.813 |
| C | 0.923 | 2.969 | 0.85 | 0.9822 | | 1.15 | 0.0085 | 0.06 | 6.09 | 3.38 | 0.823 |
| C | 0.936 | 3.00 | 0.767 | 0.9806 | 0.49 | 0.63 | 0.39 | 1.68 | 6.08 | 3.39 | 0.834 |
| A | 0.942 | 3.01 | | | | | | | 6.07 i | 3.39 | 0.840 |
| B | 0.961 | 3.23 | | | | | | | 6.04 i | 3.39 | 0.851 |
| B | 0.998 | 3.43 | | | | | | | 5.97 i | 3.40 | 0.881 |
| A | 1.046 | 3.78 | | | | | | | 5.88 i | 3.41 | 0.917 |
| C | 1.048 | 3.74 | 0.752 | 0.9477 | 0.47 | 0.62 | 0.44 | 1.76 | 5.87 | 3.41 | 0.920 |
| B | 1.099 | 4.19 | | | | | | | 5.79 i | 3.42 | 0.956 |
| C | 1.132 | 4.56 | 0.742 | 0.9271 | 0.46 | 0.62 | 0.46 | 1.80 | 5.75 | 3.42 | 0.976 |
| A | 1.139 | 4.47 | | | | | | | 5.73 i | 3.43 | 0.986 |
| C | 1.198 | 4.79 | 0.735 | 0.9070 | 0.45 | 0.61 | 0.49 | 1.87 | 5.62 | 3.44 | 1.033 |
| B | 1 212 | 4.96 | | | | | | | 5.60 i | 3.44 | 1.041 |
| C | 1.241 | 5.28 | 0.730 | 0.8974 | 0.44 | 0.61 | 0.51 | 1.89 | 5.56 | 3.44 | 1.059 |
| A | 1.255 | 5.42 | | | | | | | 5.55 i | 3.44 | 1.068 |
| B | 1.310 | 5.94 | | | | | | | 5.47 i | 3.45 | 1.105 |
| C | 1.329 | 6.03 | 0.720 | 0.8763 | 0.43 | 0.60 | 0.54 | 1.94 | 5.43 | 3.45 | 1.121 |
| C | 1.333 | 5.96 | 0.722 | 0.8742 | 0.43 | 0.60 | 0.55 | 1.96 | 5.42 | 3.45 | 1.127 |
| B | 1.404 | 6.72 | | | | | | | 5.33 i | 3.46 | 1.171 |
| C | 1.533 | 8.10 | 0.703 | 0.8321 | 0.41 | 0.59 | 0.62 | 2.08 | 5.16 | 3.46 | 1.253 |
| B | 1.572 | 8.32 | | | | | | | 5.10 i | 3.46 | 1.284 |
| C | 1.661 | 9.27 | 0.691 | 0.8047 | 0.40 | 0.58 | 0.67 | 2.16 | 4.99 | 3.47 | 1.339 |
| B | 1.715 | 10.01 | | | | | | | 4.93 i | 3.47 | 1.368 |
| C | 1.755 | 10.39 | 0.685 | 0.7874 | 0.39 | 0.57 | 0.70 | 2.22 | 4.88 | 3.47 | 1.394 |
| C | 1.817 | 11.10 | 0.681 | 0.7761 | 0.38 | 0.56 | 0.72 | 2.26 | 4.81 | 3.48 | 1.431 |
| B | 1.856 | 11.77 | | | | | | | 4.78 i | 3.48 | 1.446 |
| C | 1.954 | 12.93 | 0.672 | 0.7534 | 0.37 | 0.56 | 0.77 | 2.34 | 4.67 | 3.48 | 1.504 |
| B$^a$ | 1.995 | 13.36 | | | | | | | 4.62 i | 3.48 | 1.530 |
| C$^a$ | 2.013 | 13.30 | 0.665 | 0.7408 | 0.37 | 0.55 | 0.79 | 2.37 | 4.59 | 3.48 | 1.550 |

[a] Three-phase system (K,Ag)I(l)−(K,Na)I(s)-nitrate melt.

The activity of KI in the solid iodide solution might in principle be obtained by integrating some function based on the Gibbs – Duhem relation. Since no such function can be extrapolated to $x_2' = 0$ with an acceptable accuracy, another method has been tried. From the limiting value $\lim_{x_1' \to 0} f_2' = 1$ we obtain

$$\lim_{x_2' \to 0} [x_2'/([K^+][I^-])] = K_2'^{-1} \tag{13}$$

Hence, $K_2'$ may be estimated from a graphical extrapolation according to eqn. (13) and the activities $a_2'$ can then be calculated from eqn. (2).

Similar methods may be utilized to obtain estimates of $K_1''$ and $K_2''$, although the extrapolation range is considerably larger in these cases. The working equations are

$$\lim_{x_1'' \to 1} [x_1''/([Ag^+][I^-])] = K_1''^{-1} \tag{14}$$

$$\lim_{x_2'' \to 0} [x_2''/([K^+][I^-])] = K_2''^{-1} \tag{15}$$

The activities $a_1''$ and $a_2''$ are computed from eqns. (3) and (4).

## RESULTS

In Table 1 the results from all three series of measurements have been collected. An inspection of the experimental data reveals that series with different amounts of AgI phase give the same corresponding values of $C_I$ and $C_{Ag}$ within the limits of error. This means, that deviations from the original K – Na balance (1:1) in the nitrate melt, originating from the potassium iodide migration into the AgI phase, are so small that they do not cause any observable changes in the relations between $C_I$ and $C_{Ag}$.

The product $[Ag^+][I^-]$ was calculated from the data of series C by means of graphical integration according to eqn. (12). The value of $K_1'$ was taken from Ref. 1. Recalling that systems of series C contain 0.2686 mol $KNO_3$, 0.01917 mol AgI and 50.00 g $(K,Na)NO_3$, we obtain

$$R^{-1} = \left[ \frac{0.2686}{0.0500} \text{ mol kg}^{-1} + \frac{C_I}{2} - \frac{x_2}{x_1} \left( \frac{0.01917}{0.0500} \text{ mol kg}^{-1} - C_{Ag} \right) \right] (C_I - \bar{n} C_{Ag})$$

With $\bar{n} = 3$ as a starting value, a first set of products $([Ag^+][I^-])_j$ was calculated and used to evaluate a set of stability constants yielding better values of $\bar{n}$ and $[I^-]$. The calculations were iterated until the variables remained unaltered. Fig. 1 gives the graph of $x_2/x_1$, versus the final values of $\ln R$.

For the determination of the stability constants the $(C_I; C_{Ag})$ data from series A and B were incorporated into the experimental material utilized. The corresponding values of $[Ag^+][I^-]$ were obtained by graphical interpolation between the values from series C.

From previous studies [1-3] it may be concluded that the concentrations of the species $AgI_3^{2-}$, $AgI_4^{3-}$, and $Ag_2I_6^{4-}$ or a combination of two of them give the

main contributions to $C_{Ag}$ in the pertinent range of $C_I$. Since $AgI_2^-$ is not quite negligible at the smallest $C_I$, a small correction has been applied, *viz.* $C_{corr} = C_{Ag} - [AgI_2^-]$. The correction term was calculated from the value of $\beta_{21}$ of Ref. 1. Hence

$$C_{corr}[Ag^+]^{-1} = \beta_{31}[I^-]^3 + \beta_{41}[I^-]^4 + 2\beta_{62}[Ag^+][I^-]^6 \tag{16}$$

The stability constants were evaluated from eqn. (16) with standard graphical and least-squares methods.

It appeared that the experimental results could not be satisfactorily described by a model with only four mononuclear complexes. Hence, the last term of the right hand member of eqn. (16) cannot be omitted. Since the terms are all of a rather high order in $[I^-]$, it is, on the other hand, difficult to judge whether the $AgI_4^{3-}$ term should be discarded or not. The calculations were performed both on the assumption that $AgI_3^{2-}$, $AgI_4^{3-}$ and $Ag_2I_6^{4-}$ are present in significant amounts (alternative I) and on the assumption that $AgI_3^{2-}$ and $Ag_2I_6^{4-}$ are the only prevailing species (alternative II). The calculated stability constants are found in Table 3. In Table 1 the ligand numbers *etc.* for all the experimental material (according to alternative I) are given. The thermodynamic quantities pertaining to the iodide phase and the distribution equilibria (*vide* Table 1) also refer to alternative I, but the changes in the numerical values of these quantities would be very small if they were derived according to alternative II instead.

When the concentrations $[Ag^+]$, $[K^+]$, and $[I^-]$ had been determined, the constants $K_2'$, $K_1''$, and $K_2''$ were estimated by extrapolations according to
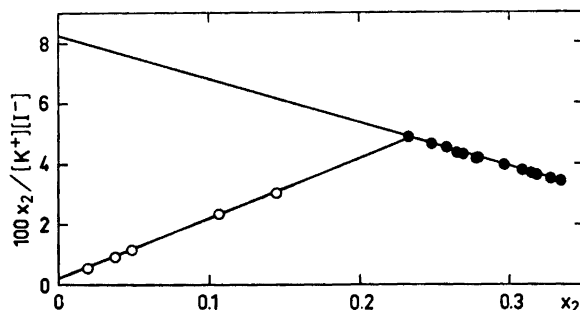


*Fig. 2.* Estimation of $K_2'$ and $K_2''$ by extrapolation according to eqns. (13) and (15). Notations: (K,Ag)I(s) (○); (K,Ag)I(l) (●).

eqns. (13), (14), and (15). Fig. 2 gives an example of this extrapolation procedure. The results are collected in Table 2, where the cation exchange equilibrium constants $K_{12}' = K_1'/K_2'$ and $K_{12}'' = K_1''/K_2''$ have also been included. The standard free energy changes for the corresponding exchange reactions are calculated according to $\Delta G^\circ = -RT \ln K_{12}$ and the results are included in Table 2.

*Table 2.* The estimated heterogeneous equilibrium constants and free energy changes. $K_1'$ from Ref. 1. The equilibrium constants for reactions I − IV are expressed in $(\text{mol kg}^{-1})^2$.

| Equilibrium reaction | Equilibrium constant | | $\Delta G°$ |
|---|---|---|---|
| | Symbol | Value | $(\text{kJ mol}^{-1})$ |
| I.   AgI(solid iodide solution)$\rightleftharpoons$Ag$^+$+I$^-$ | $K_1'$ | $(6.2 \pm 0.1) \times 10^{-10}$ | |
| II.  AgI(liquid iodide solution)$\rightleftharpoons$Ag$^+$+I$^-$ | $K_1''$ | $(1.25 \pm 0.08) \times 10^{-9}$ | |
| III. KI(solid iodide solution)$\rightleftharpoons$K$^+$+I$^-$ | $K_2'$ | $(5.6 \pm 0.6) \times 10^2$ | |
| IV   KI(liquid iodide solution)$\rightleftharpoons$K$^+$+I$^-$ | $K_2''$ | $12.2 \pm 0.4$ | |
| V.   AgI(solid iodide solution + K$^+$$\rightleftharpoons$ KI(solid iodide solution) + Ag$^+$ | $K_{12}'$ | $1.1 \times 10^{-12}$ | 127 |
| VI.  AgI(liquid iodide solution + K$^+$$\rightleftharpoons$ KI(liquid iodide solution) + Ag$^+$ | $K_{12}''$ | $1.0 \times 10^{-10}$ | 106 |

## DISCUSSION

*Heterogeneous equilibria.* The equilibrium constants of Tables 2 and 3 give a good description of the two-phase systems in the composition range investigated. The estimates of $K_1''$ and $K_2''$, and hence $a_1''$ and $a_2''$, may of course be subject to considerably larger errors than those quoted in Table 2, which are three standard deviations, estimated from the linear regression. No theoretical argument can justify a linear extrapolation to $x_2 = 0$ according to eqns.

*Table 3.* Sets of stability constants in nitrate melts at 280°C.

| | $\dfrac{\beta_{11} \times 10^{-3}}{(\text{mol kg}^{-1})^{-1}}$ | $\dfrac{\beta_{21} \times 10^{-6}}{(\text{mol kg}^{-1})^{-2}}$ | $\dfrac{\beta_{31} \times 10^{-7}}{(\text{mol kg}^{-1})^{-3}}$ | $\dfrac{\beta_{41} \times 10^{-7}}{(\text{mol kg}^{-1})^{-4}}$ | $\dfrac{\beta_{62} \times 10^{-16}}{(\text{mol kg}^{-1})^{-7}}$ |
|---|---|---|---|---|---|
| Solubility data, Ref. 1 | $4.2 \pm 0.3$ | $3.6 \pm 0.2$ | $2.9 \pm 0.3$ | — | — |
| This work, alt. I | — | — | $2.4 \pm 0.3$ | $3.6 \pm 0.7$ | $1.6 \pm 0.7$ |
| This work, alt. II | — | — | $3.8 \pm 0.6$ | — | $3.1 \pm 0.6$ |
| Emf data, Ref. 2: | | | | | |
| unsaturated melts | — | $3.1 \pm 0.3$ | $2.27 \pm 0.06$ | $0.28 \pm 0.06$ | $1.9 \pm 0.7$ |
| melts  saturated | | | | | |
| with (K,Na)I, A[a] | — | *3.1* | *2.27* | *1.6* | *1.9* |
| B[a] | — | *3.1* | *2.27* | *0.28* | 0.64 |
| Probable values | 4.2 | 3.1 | 2.3 | $\approx 1$ | 1.9 |

[a] Set of constants that describes the experimental data. The values in italics are taken from the emf data in unsaturated melts; the fourth is calculated from the data on saturated melts.

(13), (14), and (15), although the points fall on a straight line within the range of the experiments. A comparison with thermodynamic literature data can be made, however, in the following way.

The proportionality factor $\lambda_1 = K_1''/K_1'$ is related to the standard free energy change, $\Delta G°$, for the process

$$\alpha\text{-AgI(s)} \rightarrow \text{AgI(l)}$$
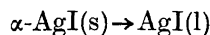
at 280°C by the equation $\varDelta G° = RT \ln \lambda_1$. Hence an estimate of $\lambda_1$ may be obtained from an approximate value of $\varDelta G°$. Recently Hamer, Malmberg and Rubin [7] published a set of calculated emf's for formation cells based on a critical compilation of thermodynamic data up to 1500°C. From their results the value $\varDelta G° = (3 \pm 1) \times 10^3$ J mol$^{-1}$, valid at 280°C, may be estimated, yielding $\lambda_1 = 2.0 \pm 0.4$. From the constants in Table 2 we obtain $\lambda_1 = 2.0 \pm 0.2$ This agreement indicates that the linear extrapolations give estimates of the constants that may be better than just to the correct order of magnitude. Hence, we can regard the $\varDelta G°$ values of Table 2 with some confidence, and it may be of interest to note that the liquid-liquid cation exchange reaction is associated with quite a large $\varDelta G°$-value, only 20 % smaller than that for the solid-liquid reaction.

In the solid (K,Ag)I solution the activity factor $f_2'$ decreases very rapidly from the limiting value 1 to rather small values near the phase transition point (*vide* Table 1). These large deviations from ideality are in good agreement with the picture of the possible structure of the solid solution outlined in a previous paper.[3] This pronounced non-ideal behaviour should be expected if the K$^+$ ions preferentially occupy the largest cation sites and simultaneously cause a considerable distortion of the iodide lattice.

*The complex formation equilibria in the nitrate melt.* Table 3 contains sets of over-all stability constants, obtained from different experimental methods. From a comparison of the results of this work with previous findings, it is evident that alternative II must be discarded, since the values of $\beta_{31}$ and $\beta_{62}$ both markedly disagree with results from conventional solubility [1] and emf [2] measurements.

In the set of constants according to alternative I, $\beta_{31}$ is in good agreement with the values from both solubility and emf data, and $\beta_{62}$ agrees well with the value obtained from emf measurements in unsaturated melts. The discrepancy with previous results is large for $\beta_{41}$. It has been pointed out before,[2] however, that the rather small value of $\beta_{41}$ from emf measurements in unsaturated melts might emerge from systematic errors which might be caused by liquid junction potentials. This assumption was to some degree qualitatively supported by the ligand solubility data.[3] Assuming reasonable values of $\beta_{31}$ and $\beta_{62}$, the emf measurements in melts saturated with (K,Na)I also favour a model that includes a fourth mononuclear complex with $\beta_{41}$ in the order of magnitude of $10^7$ (mol kg$^{-1}$)$^{-4}$ (*vide* Table 3).

On the other hand, variations in activity coefficients of the solute species may be of importance at large $C_I$ and $C_{Ag}$. Remembering that $\beta_{41}$ is obtained more or less as a correction term in the calculations, we must conclude that the variations of the $\beta_{41}$ values in Table 3 are too large to permit us to decide for certain whether or not a fourth mononuclear complex is really formed.

To sum up, the presence of three mononuclear species and the dinuclear complex $Ag_2I_6{}^{4-}$ has been proved by different experimental methods. The most probable values of the corresponding stability constants are given in Table 3. In addition, effects that might emerge from the presence of $AgI_4{}^{3-}$ have been observed, but it follows from the magnitude of the equilibrium constants that the concentration of $AgI_4{}^{3-}$ will never become large enough

*Table 4.* The stepwise stability constants and quotients.

| Medium | Quantity | $n=1$ | $n=2$ | $n=3$ | $n=4$ |
|---|---|---|---|---|---|
| $H_2O$, 18°C, $I=0$ [11] | $K_n/M^{-1}$ | $3.8 \times 10^6$ | $1.4 \times 10^5$ | 87 | 0.27 |
| $H_2O$, 25°C, $I=4$ M($NaClO_4$) [9] | $K_n/M^{-1}$ | $(10^8)$ | $(10^3)$ | 600 | 4 |
| (K,Na)$NO_3$(l), 280°C | $K_n/(\text{mol kg}^{-1})^{-1}$ | 4200 | 740 | 7 | $\approx 0.5$ |
| $H_2O$, 18°C, $I=0$ [11] | $K_n/K_{(n+1)}$ | 27 | 1600 | 320 | |
| $H_2O$, 25°C, $I=4$ M($NaClO_4$) [9] | $K_n/K_{(n+1)}$ | $(10^5)$ | (1.7) | 150 | |
| (K,Na)$NO_3$(l), 280°C | $K_n/K_{(n+1)}$ | 5.7 | 100 | $\approx 10$ | |

to be measured with any accuracy. A reasonable estimate of $\beta_{41}$ would be $10^7$ (mol kg$^{-1}$)$^{-4}$.

The relative stability of the different complexes may be judged from the quotients $K_n/K_{(n+1)}$, *i.e.* the equilibrium constants for the reactions

$$AgI_{(n-1)}^{(n-2)-} + AgI_{(n+1)}^{n-} \rightleftharpoons 2AgI_n^{(n-1)-}$$
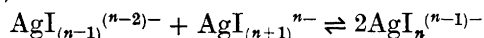
Since $K_n/K_{(n+1)}$ is a dimensionless quantity, a direct comparison may be made between, *e.g.*, aqueous solutions and molten salt media. The stepwise stability constants $K_n$ and the quotients are given in Table 4. The second complex is evidently the most stable one in the nitrate melt. In aqueous solution, this behaviour is in fact a rather general feature of Ag(I)-halide complex formation.

The abnormally high stability of AgI reported by Leden [8,9] is evidently erroneous. His much too high value of $\beta_{11}$ was caused by too primitive experimental facilities.[10] Lieser [11] later found a sequence of stabilities in aqueous solution which is in good agreement with the general pattern (*cf.* Table 4). The values of $K_3$ and $K_4$, and hence $K_3/K_4$, obtained by Lieser, must be looked upon with some scepticism, however, since Lieser did not use a constant ionic medium but tried to estimate the activity coefficients for the solute species. The stability constants for the complexes richest in iodide may therefore be subject to considerable errors. A far more reliable value of $K_3/K_4$ can be calculated from the data of Leden [8,9] (*cf.* Table 4).

From the discussion above it is evident that no definite support can be found for the view [12] that only three halide ions may be coordinated to silver(I) in nitrate melts. In fact, $K_3/K_4 \approx 10$ is a rather normal value for complexes formed stepwise.

## REFERENCES

1. Elding, I. and Leden, I. *Acta Chem. Scand.* **23** (1969) 2430.
2. Holmberg, B. *Acta Chem. Scand.* **27** (1973) 875.
3. Holmberg, B. *Acta Chem. Scand.* **27** (1973) 3550.
4. Johansson, L. *Coord. Chem. Rev.* **3** (1968) 293, and papers cited therein.

5. Sternberg, S., Adorian, I. and Galasiu, I. *Electrochim. Acta* **11** (1966) 385.
6. Sternberg, S. *Private communication.*
7. Hamer, W. J., Malmberg, M. S. and Rubin, B. *J. Electrochem. Soc.* **112** (1965) 750.
8. Leden, I. *Acta Chem. Scand.* **10** (1956) 540.
9. Leden, I. *Acta Chem. Scand.* **10** (1956) 812.
10. Leden, I. *Private communication.*
11. Lieser, K. H. *Z. anorg. allgem. Chem.* **292** (1957) 97.
12. Cigén, R. and Mannerstrand, N. *Acta Chem. Scand.* **18** (1964) 1755; **18** (1964) 2203.

# Studies on Orchidaceae Alkaloids

## XXXVIII.* Asymmetric Synthesis of 2-Isobutylmalic Acid and 2-(Cyclohexylmethyl)malic Acid

SVANTE BRANDÄNGE, STAFFAN JOSEPHSON and
STAFFAN VALLÉN

Department of Organic Chemistry, Arrhenius Laboratory, University of Stockholm,
S-104 05 Stockholm, Sweden

In order to determine the absolute configurations of 2-isobutyl-malic acid (I) and 2-benzylmalic acid (II), the (+)-dimethylesters of the former acid and of 2-(cyclohexylmethyl)malic acid (IX) were prepared by asymmetric syntheses. Results from studies of these synthetic materials and from CD studies of the molybdate complexes of the natural and synthetic acids and of (S)-(+)-citramalic acid (III), indicate that the natural acids I and II both have the R-configuration.

The Orchidaceae alkaloids cornucervine [1] and phalaenopsine La [2] are esters of 2-isobutylmalic acid (I) and 2-benzylmalic acid (II), respectively. Several 2-alkylmalic acids occur naturally, but for only one of these, 2-methylmalic acid (citramalic acid), does the absolute configuration seem to be known. Thus, (+)-citramalic acid (III) possesses the S-configuration.[3,4]

$$R-\underset{\underset{\displaystyle OH}{|}}{\overset{\overset{\displaystyle COOH}{|}}{C}}-CH_2-COOH$$
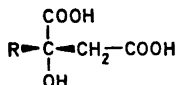
III : R = CH₃

X : R = H

We recently reported an asymmetric synthesis of (+)-diethyl citramalate.[5] Ethyl pyruvate was added to a solution of the lithium enolate formed from (−)-menthyl acetate and lithium diisopropylamide at −70°, and the resulting mixed ester was transferred into the diethyl ester. (S)-(+)-Diethyl citramalate was obtained in 26 % optical yield.

* For No. XXXVII in this series, see Ref. 10.

Repetition of this synthesis using ethyl 4-methyl-2-oxo-pentanoate (IV), gave (+)-dimethyl 2-isobutylmalate (V). From the optical rotation, assuming that the natural (−)-ester is the pure enantiomer, the optical yield was found to be approximately 20 %. A corresponding synthesis of dimethyl 2-(cyclohexylmethyl)malate (VII) was carried out, starting from VIII, and the (+)-form was obtained in excess. This synthesis was considered more favourable than that of dimethyl 2-benzylmalate (VI) as ethyl cyclohexylpyruvate (VIII) should give less enolisation than ethyl phenylpyruvate on reaction with the lithium enolate of (−)-menthyl acetate. The dimethyl ester VII was also prepared by catalytic hydrogenation of VI having a natural origin. Due to the small amount available, the optical rotation of the sample of VII thus formed was not determined.

R—CH₂—C(=O)COOEt  →  R—CH₂—C(COOEt)(OH)—CH₂—COO—[menthyl]  →  R—CH₂—C(COOR')(OH)—CH₂—COOR'

IV : R = i-Pr
VIII : R = c-hexyl

V : R = i-Pr, R' = Me
VI : R = phenyl, R' = Me
VII : R = c-hexyl, R' = Me
I : R = i-Pr, R' = H
II : R = phenyl, R' = H
IX : R = c-hexyl, R' = H
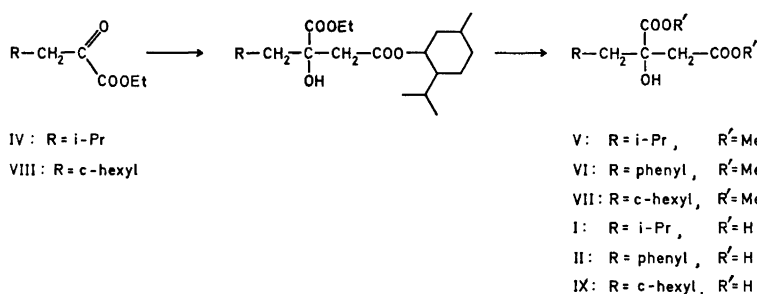
It is reasonable to assume that the asymmetric syntheses of the esters of 2-methyl-, 2-isobutyl-, and 2-(cyclohexylmethyl)malic acid (IX) all follow the same steric course, and that these esters should consequently all have the $S$-configuration. The dimethyl ester of the natural 2-isobutylmalic acid has the opposite optical rotation and should therefore have the $R$-configuration.

CD spectra of α-hydroxyacids, as their molybdate complexes, give valuable information for the determination of their absolute configurations.[6] The molybdate complexes of $(S)$-(+)-malic acid [6] (X) and $(S)$-(+)-citramalic

Table 1. Molecular ellipticities obtained in the CD spectra of molybdate complexes of some 2-alkylmalic acids (nm, $[\theta] \times 10^{-4}$).

| Acid | pH | Lowest wave-length measured | Third extremum | | Second extremum | | | | First extremum | |
|---|---|---|---|---|---|---|---|---|---|---|
| Natural I | 3.5 | 225, +20 | 237, −20 | 243, 0 | 251, +29 | 259, 0 | | | 272, −25 | |
| Natural II | 3,4 | 220, +27 | 236, −27 | 247, 0 | 250, +3.2 | 253, 0 | | | 267, −27 | |
| IX (derived from natural II) | 3.6 | 224, +17 | 239, −8.5 | 247, 0 | 250, +1.3 | 253, 0 | | | 268, −11 | |
| II | 4.2 | 210, −28 | 237, +13 | 250, 0 | 250, 0 | 250, 0 | | | 270, +11 | |
| Synthetic I | 3.8 | 225, −8.0 | 237, +3.6 | 243, 0 | 250, −7.2 | 259, 0 | | | 272, +5.6 | |
| Synthetic II | 3.5 | 233, +1.0 | 237, +2.9 | 242, 0 | 251, −7.9 | 259, 0 | | | 272, +6.2 | |

acid (III) show similar CD spectra. The spectra of the acids themselves, however, show bands at 212 nm with $[\theta]$ $+0.26 \times 10^4$ and $[\theta]$ $-1.6 \times 10^4$ degree $mol^{-1}$ $cm^2$, respectively.

The above synthetic esters were transformed into the acids, and the CD spectra of their molybdate complexes were recorded. The results are summarised in Table 1. The acids III, I, and IX all gave similar CD spectra, indicating that they have the same absolute configuration, for III known to be $S$. The molybdate complexes of the natural acids I and II, and of IX, the latter prepared from VI with natural origin, show the opposite Cotton effects and should consequently have the $R$-configuration. From the magnitudes of the Cotton effects the optical yields of I and IX could be estimated as 22 and 63 %, respectively, provided that the natural acids and IX, prepared from one of them, are optically pure.

The CD spectra of the molybdate complexes are considerably influenced by the pH value,[6] as exemplified in Fig. 1 for 2-benzylmalic acid. Small variations in the pH value were found when determining the other spectra, and this explains minor differences in shape between spectra given by enantiomers.
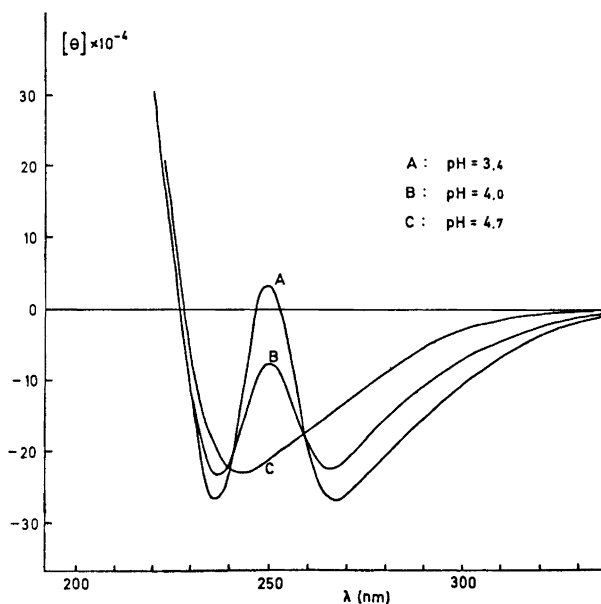


*Fig. 1.* Molybdate complex of natural II at different pH values.

## EXPERIMENTAL

GLC was performed as described previously.[5] Optical rotations were measured on a Perkin-Elmer 141 polarimeter. A Nester-Faust NFT-51 spinning band column was used in the distillations. A Cary 60 spectropolarimeter was used for the measurements of CD spectra (cell length 0.1 cm) and a Beckman pH meter (accuracy 0.1 units) was used for the pH determinations. The CD spectra were measured in dilute hydrochloric acid solu-

tions, containing 2.3 − 2.5 mol of sodium molybdate per mol hydroxyacid. Molecular ellipticities are given in degree mol$^{-1}$ cm$^2$.

(S)-(+)-Citramalic acid [7] in hydrochloric acid (pH 0.8) gave the following CD spectrum (0.043 M solution): $[\theta]_{240}$ − 0.07 × 10$^4$, $[\theta]_{230}$ − 0.42 × 10$^4$, $[\theta]_{220}$ − 1.18 × 10$^4$, $[\theta]_{212}$ − 1.56 × 10$^4$ (min), $[\theta]_{203}$ − 1.30 × 10$^4$ (!).

Ethyl 4-methyl-2-oxo-pentanoate (IV) was obtained from isobutylmagnesium bromide, diethyl oxalate and water according to Akimova.[8] The product was distilled (b.p. 70 − 72°, 10 mm) giving an 80/20 mixture of keto and enol forms (NMR). The enol content increased on storage.

2-Isobutylmalic acid (I). Ethyl (−)menthyl 2-isobutylmalate was synthesised (the yield according to GLC was approximately 70 %) as described previously for ethyl (−)menthyl citramalate,[5] using lithium diisopropylamide as base. The crude reaction product was stirred under vacuum (1 mm, 100°) to remove volatile impurities, and was then hydrolysed with 2 M potassium hydroxide in ethanol (reflux overnight). Part of the ethanol was evaporated, water was added, and the aqueous layer was washed several times with ether. After acidification and concentration of the aqueous layer, methanol was added, and the mixture was refluxed for three days. Part of the methanol was evaporated and the residue was partitioned between water and chloroform. The chloroform layer was dried (Na$_2$SO$_4$) and concentrated and pure dimethyl ester V was obtained by preparative GLC, $[\alpha]_{578}$ + 0.17°, $[\alpha]_{436}$ − 0.05°, $[\alpha]_{365}$ − 0.68° (c 9.8, ethanol). The same compound obtained by methanolysis of cornucervine showed $[\alpha]_{578}$ − 0.64°, $[\alpha]_{436}$ + 0.16°, $[\alpha]_{365}$ + 3.9° (c1,9, ethanol).[1] The acid I was obtained by hydrolysis of the dimethyl ester with 4 M hydrochloric acid (115°, 2 days) followed by evaporation (15 mm, 40°). The molybdate solution was prepared using the acid thus formed.

Synthesis of ketoester VIII. A solution of sodium dihydro-bis(2-methoxyethoxy)-aluminate (333 g, 1.3 mol) in benzene and tetrahydrofuran (300 ml) was added in portions to a stirred solution of cyclohexylmethanoic acid (78 g, 0.61 mol) in tetrahydrofuran (700 ml) during 1 h, and the mixture was then stirred overnight. Dilute hydrochloric acid and ether were added, and the organic layer was dried (Na$_2$SO$_4$) and concentrated. The residue was distilled giving cyclohexylmethanol (57 g, 82 %). The corresponding bromide was obtained in 60 % yield by reaction with phosphorus tribromide.[9] The keto-ester VIII was synthesised analogously to IV. After distillation somewhat impure VIII (6.6 g, b.p. 94 − 98°, 7 mm) was obtained from 24 g of the bromide. The enol content was less than 3 % (NMR). Preparative GLC gave an analytical sample. (Found: C 65.8; H 9.05. Calc. for C$_{11}$H$_{18}$O$_3$: C 66.6; H 9.15.) MS (m/e, relative intensity): M$^+$ = 198(3), 125(96), 97(100). Impure VIII was used in the reaction with (−)-menthyl acetate.

2-(Cyclohexylmethyl)malic acid (IX). Ethyl (−)-menthyl 2-(cyclohexylmethyl)malate was synthesised (the yield according to GLC was approximately 80 %) analogously to ethyl (−)-menthyl 2-isobutylmalate, and was converted into the dimethyl ester VII which was purified by preparative GLC, $[\alpha]_{578}^{23}$ + 3.3° (c 2,5, ethanol). MS: M$^+$ = 258 lacking, 199(75), 125(100), 97(56). Hydrolysis of this purified dimethyl ester with 4 M hydrochloric acid (115°, 3 days) and evaporation (15 mm, 40°) yielded the acid IX.

Acid IX, derived from phalaenopsine La. The dimethyl ester VI,[2] obtained by methanolysis of the alkaloid, was hydrogenated (5 atm, 3 h) in acetic acid using PtO$_2$. Ether was added and the mixture was extracted repeatedly with sodium hydrogen carbonate solution, and finally with water. The ether layer was dried (Na$_2$SO$_4$). The solution gave a single peak on GLC (3 % JXR) with the same retention time as the starting material VI. The intensity of the mass spectra peaks, e.g. those at m/e 91 and 97, clearly showed, however, that very little of the starting material was left. The ester VII was hydrolysed to IX as described above.

2-Benzylmalic acid (II) was prepared by hydrolysis as above. No dehydrated material could be detected in the product (NMR).

## REFERENCES

1. Brandänge, S., Lüning, B., Moberg, C. and Sjöstrand, E. *Acta Chem. Scand.* **25** (1971) 349.
2. Brandänge, S. and Lüning, B. *Acta Chem. Scand.* **23** (1969) 1151.
3. vonder Mühll, P. A., Settimj, G., Weber, H. and Arigoni, D. *Chimia* **19** (1965) 595.
4. Weber, H. *Dissertation*, Eidgenössische Technische Hochschule, Zürich 1965.
5. Brandänge, S., Josephson, S. and Vallén, S. *Acta Chem. Scand.* **27** (1973) 1084.
6. Voelter, W., Bayer, E., Barth, G., Bunnenberg, E. and Djerassi, C. *Chem. Ber.* **102** (1969) 2003.
7. Barker, H. A. *Biochem. Prep.* **9** (1962) 25.
8. Akimova, L. N. *Vestn. Mosk. Univ. Khim.* **24** (1969) 124; *Chem. Abstr.* **72** (1970) 21255.
9. Hiers, G. S. and Adams, R. *J. Am. Chem. Soc.* **48** (1926) 2385.
10. Blomqvist, L., Brandänge, S., Gawell, L., Leander, K. and Lüning, B. *Acta Chem. Scand.* **27** (1973) 1439.

# Multicomponent Polyanions

## VII. The Molecular and Crystal Structure of $Na_6Mo_7O_{24}(H_2O)_{14}$, a Compound Containing Sodium-coordinated Heptamolybdate Anions

KERSTIN SJÖBOM and BRITT HEDMAN

*Department of Inorganic Chemistry, University of Umeå, S-901 87 Umeå, Sweden*

The crystal structure of $Na_6Mo_7O_{24}(H_2O)_{14}$ has been determined from three-dimensional X-ray diffraction data collected with a Philips PAILRED diffractometer, using $MoK\alpha$-radiation. $Na_6Mo_7O_{24}$-$(H_2O)_{14}$ crystallizes in the orthorhombic space group $P2_1ab$ with unit cell dimensions $a = 15.626(1)$ Å, $b = 21.130(1)$ Å, and $c = 10.377(1)$ Å. There are four formula units in the cell. The structure has been refined by full-matrix least squares methods, with isotropic temperature factors using 2372 independent reflexions, and the final $R$-value is 0.056.

The structure consists of $Mo_7O_{24}{}^{6-}$-anions embedded in a sodium-water oxygen double-chain arrangement along the $y$-axis, with the sodium ions directly coordinated to the anions. The configuration of the $Mo_7O_{24}{}^{6-}$-anion is the same as in $(NH_4)_6Mo_7O_{24}.4H_2O$ [1–3] and $K_6Mo_7O_{24}.4H_2O$,[4] *i.e.* seven $MoO_6$-octahedra are joined together by common edges. Each sodium ion is octahedrally surrounded by six water and group oxygen atoms. These octahedra form chains by sharing edges and corners.

The short $Mo-Mo$ distances are in the range $3.19-3.45$ Å, and the $Mo-O$ distances fall in three ranges, $1.67-1.76$ Å, $1.88-2.01$ Å, and $2.11-2.33$ Å, depending on coordination number.

The first determination of a heptamolybdate structure was made by Lindqvist [1] in 1950. He investigated the paramolybdate salt $(NH_4)_6Mo_7O_{24}.4H_2O$, and concluded from a determination of the molybdenum atom positions that the compound was built up of isolated $Mo_7O_{24}{}^{6-}$-groups, consisting of shared $MoO_6$-octahedra as shown in Fig. 1. Through recent complete structure determinations of this compound, Lindqvist's structure proposal has been fully confirmed (Shimao,[2] Evans [3]). The corresponding potassium compound, $K_6Mo_7O_{24}.4H_2O$, investigated by Gatehouse,[4] has also been found to contain isolated heptamolybdate ions. An interesting question in connection with these structures is whether the cations are coordinated to the polyanions or not. From the data hitherto published no answer to the question can be given

since in the short communications presented by Evans and Gatehouse no cation positions have been listed.

In recent polyanion structure determinations it has been found that the cations are often directly coordinated to the polyanion group, thus forming a sort of cation-coordinated polyanion complex. This seems to be the case particularly when small cations like $Na^+$ or $Li^+$ are used. In the structures of $Na_6Mo_5P_2O_{23}(H_2O)_{13}$ [5] and $Na_4H_2Mo_5P_2O_{23}(H_2O)_{10}$ [6] it has been found that all $Na^+$-ions are directly bonded to the polyanions present in the structure ($Mo_5P_2O_{23}{}^{6-}$ and $H_2Mo_5P_2O_{23}{}^{4-}$, respectively). In order to see whether hepta-molybdate anions may be directly coordinated by $Na^+$-ions in a similar way, we have undertaken some crystal structure investigations particularly of sodium salts crystallized from aqueous solutions.

So far the crystalline phases $Na_6Mo_7O_{24}(H_2O)_x$ with $x \approx 21-23$ and $Na_6Mo_7O_{24}(H_2O)_{14}$ have been prepared. The space group of the former compound is $P2/c$ or $Pc$, and the unit cell dimensions are $a = 12.91$ Å, $b = 10.07$ Å, $c = 20.14$ Å and $\beta = 126.8°$ with $Z = 2$ and $D_m \approx 2.52$ g cm$^{-3}$. Data collection for this compound is in progress. In the present paper the crystal structure of $Na_6Mo_7O_{24}(H_2O)_{14}$ will be described and discussed.

An additional aim of these crystal structure determinations is to obtain accurate model data for use in the large angle X-ray scattering studies of aqueous sodium heptamolybdate solutions being performed with Doc. Georg Johansson, KTH, Stockholm.[7] Preliminary results seem to indicate that the structure of heptamolybdates in solution is very similar to that of a hepta-molybdate in a crystal.

## EXPERIMENTAL

*Crystal preparation and analyses.* In a typical preparation solutions of the composition $[MoO_4{}^{2-}]_{tot} = 2.04$ M and $[HClO_4]_{tot} = 2.33$ M were placed for slow evaporation at room temperature and two colourless crystalline phases were obtained within a few days. The orthorhombic crystals showed a long prismatic habit while the monoclinic crystals were short prismatic. Both of them were unstable in air, and during the X-ray exposures the crystal was sealed, together with part of the mother liquid, in a glass capillary.

The content of Mo and Na was determined by elemental analyses (Department of Analytical Chemistry, University of Umeå). (Found: Mo 45.3; Na 9.6. Calc.: Mo 46.5; Na 9.5.) The content of crystal water was found to be 17.3 % (calc 17.4 %) by thermo-balance analysis.

*Crystal data and space group.* From rotation photographs around [100] and [001], and from the corresponding Weissenberg photographs (zero, first, and second layer lines) taken with Cu$K\alpha$-radiation, the crystals were determined to be orthorhombic.

The cell dimensions were refined with a Hägg-Guinier camera with Si as internal standard (25°C). The parameters and their corresponding standard deviations are $a = 15.626 \pm 0.001$ Å, $b = 21.130 \pm 0.001$ Å, $c = 10.377 \pm 0.001$ Å and $V = 3426.3$ Å$^3$.

Systematic extinctions $hk0$, $k = 2n+1$ and $h0l$, $h = 2n+1$ gave two possible space groups $P2_1ab$ and $Pmab$ of which $P2_1ab$ was shown later to be the correct one (No. 29, Ref. 8). The observed density, 2.75 g cm$^{-3}$, was determined by flotation in a bromoform-carbon tetrachloride solution. With $Z = 4$ the calculated density is 2.80 g cm$^{-3}$.

*Collection and reduction of intensity data.* Three-dimensional intensity data were collected with a PAILRED diffractometer (equi-inclination geometry). Mo$K\alpha$-radiation monochromated with a LiF-crystal was used ($\lambda = 0.7107$ Å, 25°C). A crystal of approximate dimensions $0.21 \times 0.15 \times 0.13$ mm was mounted and rotated along the $a$-axis (parallel to the 0.21 mm-edge). Intensities for $0kl - 9kl$ were measured with half-scan intervals $0.6 - 1.2°$ and at a scan-speed of 0.5° min$^{-1}$. In all 3399 reflexions of the type $hkl$ were

scanned up to a limit of $\sin \theta \approx 0.54$. Reflexions with a relative statistical error $\Delta I_o/I_o$ greater than 0.5 were omitted which reduced the number of unique observed reflexions to 2372. The intensities were corrected for background as described in an earlier paper,[9] and for Lorentz, polarization and absorption effects ($\mu = 26.38$ cm$^{-1}$).

*Computer programs used.* The computer programs for Lorentz, polarization and absorption corrections were originally written by P. Coppens, L. Leiserowitz and D. Rabinovich. In direct methods the program GAASA[10] was used. Fourier summations and calculations of distances and angles were performed with programs originally written by A. Zalkin. Modified versions of LALS, written by Gantzel, Sparks and Trueblood, and LINUS, written by Hamilton and Ibers were used in the least squares refinements of the structural parameters (full-matrix) and for block-diagonal refinements the program BLOCK, written by Ove Lindgren, University of Gothenburg, was used. The stereoscopic figures were produced by the program ORTEP.[11] The computations were carried out with a CDC 3200/3300 computer in Umeå and an IBM 360/65 computer in Gothenburg.

Crystal data:

$Na_6Mo_7O_{24}(H_2O)_{14}$        F.W. $= 1445.7$

Orthorhombic $P2_1ab$

$a = 15.626(1)$ Å        $Z = 4$
$b = 21.130(1)$ Å        $D_x = 2.80$ g cm$^{-3}$
$c = 10.377(1)$ Å        $D_m = 2.75$ g cm$^{-3}$
$V = 3426.3$ Å$^3$        $\mu = 26.38$ cm$^{-1}$

## STRUCTURE DETERMINATION AND REFINEMENT

The determination of the Mo atom positions was carried out with both Patterson synthesis and direct methods. The three-dimensional Patterson synthesis showed extremely strong overlapping of symmetry and cross vectors, and attempts to solve it failed at first. Direct methods were then applied, and these gave useful information of the arrangement of adjacent Mo atoms, but no descrete anions appeared. By applying the information from the direct methods to the Patterson synthesis, seven four-fold positions could be obtained. All high peaks were explained in this way. A least squares refinement at this stage gave a conventional $R$-value of 0.256. With standard Fourier and least squares techniques, the group oxygen, sodium and water oxygen atoms could be located. The positions of the water oxygen atoms were also confirmed in a series of difference Fourier computations.

To save computer time the refinements of the structural parameters were performed with block-diagonal least squares methods in an intermediate stage. In the final cycles, full-matrix refinements were made and a weighting scheme $w = (a + |F_o| + c|F_o|^2 + d|F_o|^3)^{-1}$ with $a = 250$, $c = -0.11$, and $d = 0.00002$ was applied. In these refinements an isotropic secondary extinction parameter was also included, as described by Coppens and Hamilton.[12] In the final cycle the resulting $R$-value, $R = \sum ||F_o| - |F_c||/\sum |F_o|$, was 0.056, and the last shifts were less than 10 % of the estimated standard deviations for all parameters except for five isotropic temperature factors. No refinements with anisotropic thermal parameters were made, since it would have meant only five reflexions per parameter refined and extreme computer times. The atomic scattering factors used were for Mo$^{3+}$ those given by Cromer and Waber[13] and for Na$^+$, O$^-$, and O the values in Ref. 8. Account was taken of the real part of the dispersion correction.[14] To obtain electroneutrality $f(O)$ was used

*Table 1.* The fractional atomic coordinates and isotropic thermal parameters. The estimated standard deviations in parentheses refer to the last decimal place given. For the oxygen atoms $O(ij..)$ the index means that the atom is bonded to the molybdenum atoms $i, j,....$ $Aq(ij)$ is a water oxygen atom bonded to the sodium ions $i$ and $j$.

| | x | y | z | B |
|---|---|---|---|---|
| Mo1 | 0.1281 (3) | 0.47122(7) | 0.9476 (1) | 1.043(28) |
| Mo2 | 0.1315 (3) | 0.62569(8) | 0.9712 (2) | 1.181(29) |
| Mo3 | 0.3199 (3) | 0.48018(8) | 0.6701 (2) | 1.146(31) |
| Mo4 | 0.3194 (3) | 0.63503(8) | 0.6859 (2) | 1.114(30) |
| Mo5 | 0.1500ᵃ | 0.39637(8) | 0.6803 (2) | 1.214(30) |
| Mo6 | 0.1276 (3) | 0.55849(7) | 0.6708 (1) | 0.890(28) |
| Mo7 | 0.1493 (3) | 0.71738(8) | 0.7256 (2) | 1.202(29) |
| O1(1) | 0.1959(15) | 0.4174 (7) | 0.0156(14) | 1.10(25) |
| O2(1) | 0.0365(16) | 0.4722 (8) | 0.0450(16) | 1.64(29) |
| O(12) | 0.1849(15) | 0.5468 (7) | 0.0090(14) | 1.19(27) |
| O(15) | 0.0714(16) | 0.4168 (8) | 0.8169(15) | 1.61(28) |
| O(126) | 0.0713(14) | 0.5521 (6) | 0.8304(13) | 0.77(23) |
| O(1356) | 0.2024(15) | 0.4800 (7) | 0.7700(13) | 0.97(24) |
| O1(2) | 0.2003(18) | 0.6742 (8) | 0.0499(17) | 2.05(32) |
| O2(2) | 0.0411(16) | 0.6216 (8) | 0.0695(16) | 1.75(31) |
| O(27) | 0.0742(15) | 0.6882 (7) | 0.8573(15) | 1.46(28) |
| O(2467) | 0.2009(15) | 0.6286 (7) | 0.7894(14) | 1.19(26) |
| O1(3) | 0.3684(15) | 0.4274 (8) | 0.7656(16) | 1.66(30) |
| O2(3) | 0.3884(15) | 0.4870 (7) | 0.5390(14) | 1.19(26) |
| O(34) | 0.3512(15) | 0.5546 (8) | 0.7625(16) | 1.84(32) |
| O(35) | 0.2406(14) | 0.4236 (7) | 0.5710(14) | 0.87(24) |
| O(346) | 0.2364(16) | 0.5611 (8) | 0.5890(15) | 1.45(28) |
| O1(4) | 0.3621(14) | 0.6836 (7) | 0.8028(15) | 1.26(28) |
| O2(4) | 0.3893(18) | 0.6361 (9) | 0.5604(18) | 2.39(36) |
| O(47) | 0.2410(15) | 0.6953 (7) | 0.6092(15) | 1.51(29) |
| O1(5) | 0.2006(17) | 0.3312 (8) | 0.7500(16) | 1.80(31) |
| O2(5) | 0.0797(16) | 0.3650 (7) | 0.5699(15) | 1.59(29) |
| O(56) | 0.0816(15) | 0.4943 (7) | 0.5885(14) | 1.16(26) |
| O(67) | 0.0784(16) | 0.6242 (8) | 0.6007(15) | 1.50(29) |
| O1(7) | 0.2003(18) | 0.7746 (9) | 0.8084(19) | 2.82(40) |
| O2(7) | 0.0771(16) | 0.7558 (7) | 0.6288(13) | 1.06(24) |
| Na1 | 0.4852(12) | 0.3876 (6) | 0.5880(12) | 3.41(25) |
| Na2 | 0.5105(10) | 0.5590 (5) | 0.5767(10) | 2.19(18) |
| Na3 | 0.4773(10) | 0.7214 (5) | 0.4488 (9) | 2.09(18) |
| Na4 | 0.2960 (9) | 0.3569 (4) | 0.1322 (9) | 1.75(16) |
| Na5 | 0.2946 (9) | 0.5180 (4) | 0.1636 (9) | 1.73(16) |
| Na6 | 0.3681(10) | 0.6963 (5) | 0.0429(10) | 2.25(19) |
| Aq(12) | 0.5535(17) | 0.4692 (9) | 0.6983(17) | 2.11(33) |
| Aq1(13) | 0.5437(19) | 0.2973 (9) | 0.6959(18) | 2.61(38) |
| Aq2(13) | 0.3824(18) | 0.3185 (9) | 0.5001(20) | 2.71(39) |
| Aq(2) | 0.5673(19) | 0.6151(10) | 0.7406(20) | 3.12(43) |
| Aq(36) | 0.3888(19) | 0.6788 (9) | 0.2768(19) | 2.79(40) |
| Aq(4) | 0.4072(16) | 0.3080 (9) | 0.2437(17) | 2.04(34) |
| Aq1(45) | 0.3909(17) | 0.4381 (9) | 0.0685(17) | 2.23(34) |
| Aq2(45) | 0.2417(19) | 0.4291(10) | 0.2960(21) | 3.27(45) |
| Aq(46) | 0.3435(20) | 0.8066(10) | 0.0747(21) | 3.36(46) |
| Aq1(5) | 0.4132(19) | 0.5437(10) | 0.2963(22) | 3.27(46) |
| Aq2(5) | 0.2207(16) | 0.5788 (8) | 0.3218(19) | 2.23(34) |
| Aq(56) | 0.3767(15) | 0.5854 (7) | 0.0242(14) | 1.14(26) |
| Aq(6) | 0.5219(26) | 0.7097(15) | 0.0384(30) | 6.01(74) |
| Aq | 0.2232(17) | 0.7159 (9) | 0.3529(18) | 2.26(35) |

ᵃ Arbitrarily fixed.

*Table 2.* Observed and calculated structure factors. The columns are $k$, $|F_o|$, $|F_c|$ and phase angle $\alpha$ (radians), respectively.

```
     0 K 14            12  43  55 -3.14      8  69  79 -0.00     12  51  43  2.18        1 K 5
 0 149 139  3.14       11 227 232 -0.00     10  36  31  3.14     13  61  71 -0.69     25  55  55  2.91
 2  92  88 -3.14       10  38  18 -0.00     11 178 175  3.14     14  41  34  1.98     24  64  58 -0.29
 3  48  43 -3.14        9  66  57 -3.14     13 216 211  3.14     15  51  55  2.70     23  86  95  2.57
 4  55  67  0.00        8  48  47  0.00     14 104 103  3.14     17 110  99  2.29     22  60  57 -2.79
 5  48  40 -0.00        7  82  82 -0.00     15  50  63  3.14     18  47  30 -2.32     21 126 130 -0.74
                        6  76  63 -3.14     16  71  67 -0.00     19  55  49  0.52     20  51  57 -2.09
     0 K 13             5 195 189 -0.00     17  50  60 -0.00     20  53  51 -0.27     19 127 130 -1.16
 9  58  40  3.14        4 111 111  3.14     18 115 118  3.14                          17 112 122 -1.03
 4  53  60 -3.14        3  63  75  3.14     20  61  68  3.14         1 K 9            16  81  71 -0.85
 3  61  55 -3.14        2 107  99 -3.14     23  40  12 -3.14     20  72  68  0.02     14  58  60 -1.91
 0  60  46  3.14        1  40  43  0.00     24 108 112 -0.00     19  63  71 -1.46     12 218 217  2.90
                        0  98  99  0.0      25  41  24 -0.00     17  45  34 -2.84     11 142 140 -0.59
     0 K 12                                 26 108 116 -0.00     16  41  47  0.77     10  75  70  1.85
 0  59  67  0.0             0 K 6           27  44  41  3.14     15  58  57  1.24      9 169 168  2.13
 1  58  50 -3.14        0 225 220  0.0                           14 113 110  0.21      8  41  41  3.13
 2 104 112 -0.00        1  38  40  0.00         0 K 1            12 121 119  0.41      7  70  69  2.07
 6  49  40  3.14        2 198 192 -0.00     26  78  79 -0.00     11  59  58 -1.39      6 279 277 -1.38
 8  69  55 -3.14        3  49  52  3.14     25 101  94 -3.14     10  56  63 -0.22      5 206 207  1.99
11 143 132  3.14        4  88  88  3.14     24  94  99 -0.00      8 157 162  2.13      4  61  58  2.99
12  46  42  0.00        5  65  56 -0.00     23  82  77 -3.14      7  42  45  1.33      3  66  62 -1.16
13  68  81  3.14        7 134 136 -0.00     21  81  72  0.00      6 122 108  1.38      2  63  60  2.44
                        8  78  78  0.00     20 107 109  3.14      4 145 136  2.15
     0 K 11            10  41  21 -3.14     18 146 148  3.14      3 101 102 -2.05         1 K 4
18  85  81 -0.00       13  70  69  3.14     16  40  36  3.14      2  49  28 -1.10      1 279 284  2.64
17  73  80  3.14       15 139 137 -0.00     15 127 137  0.00      1  82  81  0.45      2  72  68 -2.77
16  45  63  3.14       16  63  55 -0.00     14 130 126 -3.14                           3  46  42  2.73
15  65  64  3.14       17  38  20  3.14     13 554 551 -0.00         1 K 8             4 102 106 -0.91
14  63  71 -0.00       19  45  38  3.14     12  97  99 -3.14      1 117 113  0.70      5  93  87 -1.81
13  50  50 -3.14       21  40  46  3.14     11 256 254 -0.00      2 104 103  1.28      6  88  89 -0.58
12  43  53  0.00       24  83  84  3.14      8  29  18 -3.14      3 135 129 -0.32      7 215 216 -2.37
11 137 133  3.14       26 109 111  3.14      7  90  81 -0.00      4  95  89 -2.67      8  85  83 -1.06
 9  98 113  3.14                             6 122 117 -0.00      5  82  89  1.65      9 207 197 -2.94
 8  48  63  3.14            0 K 5             5  87  77  0.00      6 110 105 -2.87     10 166 163  2.80
 7  40  34 -0.00       26 106 108 -0.00      4  30  29 -3.14      7  66  71  1.04     11 184 181 -0.17
 5  71  69 -0.00       24 109 118 -0.00      3 122 119 -0.00      8  51  59 -0.26     12  46  47 -0.96
 4  93 106  0.00       19  89  92  3.14                           9 138 134  2.32     13 116 117 -0.74
 2 192 198 -3.14       17  46  43 -0.00         0 K 0            10 126 120  2.35     15  55  61 -0.72
 1  86  83 -3.14       16 108 101 -0.00      4  71  68 -3.14     11  99 101 -0.31     17  85  77  0.95
 0 258 249  3.14       15  77  70  3.14     10  56  58  0.00     12 170 167  2.89     18  40  12  0.68
                       12  64  60  0.00     12 404 404  3.14     14 120 122  2.97     19  92  87  1.26
     0 K 10            11 154 162  3.14     14  72  76 -0.00     16  52  37  0.59     21  64  59 -0.42
 0  69  82  3.14        7 211 207 -0.00     16  67  67 -0.00     18  62  61 -0.56     22  74  63 -0.81
 2  74  63 -3.14        5  46  39 -0.00     20 184 190  3.14     19  73  73 -1.56     23  66  63 -0.74
 3 116 111 -3.14        1  35  28  0.00     22  38  35  3.14     20  80  82 -2.31     24  49  47  2.64
 4 118 130  3.14        0 167 175  3.14     24 124 112  3.14     21  71  73 -0.87     25 153 152 -0.25
 5 102 105 -0.00                            26 193 200  3.14     22  48  40 -1.31     27  66  70  0.10
 6  54  55 -3.14            0 K 4                               23 100 109  2.64
 9  90  86  3.14        0 193 180  0.0          1 K 14          24  65  54  0.03         1 K 3
11 110 113 -0.00        1  37  19 -0.00      1  69  63 -0.55                          26  76  71  2.50
13 179 175 -0.00        2 114 110 -3.14      3  91  85 -0.20         1 K 7            25  77  79  2.75
15 138 132 -0.00        5  99 104 -0.00      5  86  77 -0.36     23  65  64 -0.60     24  88 125  2.77
16  56  55 -0.00        7 213 216 -0.00                          22  67  70 -0.83     23  41  49 -0.10
17 113 111  3.14        9  35  40 -3.14         1 K 13          19  80  81  0.63     22  74  81 -0.34
20  54  60 -0.00       10  59  59 -0.00     10  47  45 -1.64     18  40  40 -1.89     20 110 111  1.12
                       11 230 229 -0.00      8  83  93  2.13     17  63  67  1.74     19 124 129 -0.84
     0 K 9             12 108 101 -3.14      6  52  44  1.11     16  50  34 -3.05     18  93  94  1.98
20  71  64 -0.00       13 365 371 -0.00      5  96  91 -1.02     14  58  52  2.49     17  48  40 -1.57
16 100  94 -0.00       16  48  52  3.14      1  87  93  2.96     13 134 127 -0.60     16  38  32  2.47
13  61  67  3.14       17  71  81 -3.14                          12  65  67  2.37     14 268 270 -0.23
12  53  50  0.00       19  89  96  3.14         1 K 12          11 102 102 -0.33     13 104 102 -0.34
11 107 103  3.14       20 116 117  3.14      1  81  88 -0.10     10 175 173  2.64     12 367 372 -0.34
10  39  45  3.14       21  73  65 -0.00      2  46  29  0.32      9  63  63 -2.86     11  59  60 -2.35
 7 109 108 -0.00       22  46  39 -0.00      3  87  75 -1.07      8  45  46 -2.85     10  56  46  1.05
 6  57  60  3.14       24  99  97  0.00      4  87  78  2.44      7 215 212 -2.66      9  48  41  0.04
 5  41  37  0.00       25 131 134  3.14      6 113 110  1.99      6 132 126  2.72      8  51  53 -0.06
 4 120 116  3.14                             7  42  39  0.32      5 197 199 -0.87      7 124 122  2.27
 2 132 138  0.00           0 K 3             8  65  64  2.20      4  38  49 -1.26      6  99 104  0.98
 0  57  62  0.0        27  52  51  3.14      9  42  45  1.78      3  37  17  2.58      5 167 162  0.25
                       26 152 149  3.14     11  49  52 -1.42      2  55  55 -2.74      4 130 130  2.76
     0 K 8             24  59  54  3.14     12  90  81  0.01      1 280 279  2.67      3 221 204  3.09
 0 376 365  3.14       22  59  59  3.14     15  54  58  1.96                           1  97  84  1.96
 1 123 119 -3.14       21  76  69  3.14                             1 K 6
 2 224 227 -3.14       20  64  66  3.14         1 K 11           1 116 106  1.94         1 K 2
 7 109 109  0.00       17  49  58  3.14     18  77  87 -0.76      2  89  84  3.07      1 343 339  0.29
 8  56  61 -3.14       15 125 127 -0.00     15  54  47  2.82      3 109 104  2.65      2  83  77  1.56
11 140 146  3.14       13  45  53  3.14     14 140 139  2.86      4 130 121  2.07      3  46  50  1.97
12  77  86 -0.00       12 240 240  3.14     12 134 126  2.87      5  37  38 -1.07      4  40  33 -2.42
13  38  32 -0.00       11 180 179 -0.00     10 105 113  2.46      6 160 155  1.48      5  83  84  2.13
14  43  30  0.00        8 104 112 -0.00      9  93  88  2.41      7 180 177  2.20      6 476 469 -1.09
15  76  87  3.14        6 120 114 -3.14      8  41  27 -0.33      8 214 210  2.14      7 137 136  0.96
18  40  55 -0.00        5  78  82 -0.00      7  74  67  2.38      9  73  76  0.01      8  40  40  0.12
19  71  87 -3.14        4  93  94 -3.14      6  97 102  2.99     10  61  45 -0.01      9  72  68  0.06
21  46  31 -0.00        3 158 150  3.14      3 115 115 -0.34     12 148 148 -0.27     10  56  52 -0.78
24 101 103 -0.00        2 263 253 -0.00      1  59  66 -0.14     13 106 111 -0.71     11  63  53 -2.50
                        1 180 173 -0.00                          14 172 162 -0.29     12 172 171  2.76
     0 K 7             0 749 803  0.0           1 K 10          15  54  57  1.47     13  63  61 -0.72
22  70  80 -0.00                             1 205 196  2.99     17  45  41 -1.63     14  94  92 -1.81
21  75  69 -0.00           0 K 2             3  55  47 -2.21     18  88  91  2.31     15  69  75  0.18
19  39  33  3.14        0 239 216  3.14      4  50  23  2.91     19 136 138 -0.88     16 108 105 -0.97
18  66  54 -0.00        2  72  71 -0.00      5 144 145 -0.76     20  78  70  0.54     17  83  93 -1.40
17 100 100 -3.14        4  49  58  3.14      6  58  55  1.84     22  48  41  0.82     18  69  75  2.12
15 162 169 -0.00        5  85  88 -0.00      7 107 116  3.01     25  84  82  2.59     19 145 141 -1.28
14 127 131 -0.00        6  92  89 -0.00      8 114 113  2.85     26  49  46  2.66     21  49  44 -0.84
13 286 287 -0.00        7 122 117 -0.00     10  89  85  2.52                          22  51  53  2.90
```

*Table 2. Continued*

```
23    50    60 -2.98     15    73    68  2.16     11   119   126 -0.55     11    59    53  2.67      4    51    57  1.83
24    54    59  0.23     17   103   109 -1.38     10    99   103 -1.63     10    76    74 -1.01      3    38    34  0.80
25   143   136  2.95     19    72    71 -2.08      9   147   143  1.50      8   237   229  1.76      2   152   148 -1.82
26    88    94  2.36                               8   207   209  1.07      7   173   174 -2.17      1   143   137 -1.88
27    68    66 -2.73        2  K   9               7   331   340  1.67      6   236   224  1.64
                        21    62    54  1.06        6   178   181  1.61      5   332   339 -1.91        3  K   7
   1  K   1             20   140   140  1.48        5   275   276  1.21      3   142   143  1.83      1   167   164 -2.76
27    60    70  0.25     18   106   115  1.21       4   109   107 -2.41                               2    83    81  3.05
26    74    91  2.54     16   122   126  1.63       3    93    92  2.05        2  K   0               3    50    56 -1.86
25   153   164 -0.31     14    46    36 -0.96       2    47    51  1.03      4    64    56 -0.78       5   175   175  1.29
24    51    56  1.81     13    52    44  0.81       1   144   144 -1.25      6   344   344 -1.78       6   108   107 -2.24
22    36    13 -3.13     12    70    71  1.56       0   131   131  0.43      8    98    87  1.96       7    95    90  1.06
21    53    47  0.02     11    83    80 -1.81                             12   224   224 -1.69        8    52    43  1.13
19   112   110  1.59      9    55    51 -2.53         2  K   4           14   123   125 -2.45        9    64    58  0.72
18    73    85  2.65      8   131   129 -2.00       0    70    75  1.64    16    95    85 -1.01       10    94    91 -1.88
16    62    62 -0.97      7   140   139  1.63       1    44    42 -1.65    18   229   221  1.21       11    42    40 -1.25
15    50    50 -2.57      6   108   113 -1.66       3   100    95  1.24    20    65    77 -0.45       12    48    43  1.66
14   127   132 -1.61      5   121   111  1.28       4    40    37  0.15    22    68    57 -1.61       13   135   134  1.16
13    48    57 -0.16      4   138   143 -1.33       5    77    81 -2.20    24    59    53  0.57       14    38    21 -2.74
12   219   211 -2.36      3    89    94 -1.53       6    83    86  0.87    26    87    87 -0.32       15    50    42  1.56
11   127   123 -0.12      2    89    92  3.07       7   113    99 -1.52                               16    40    32  2.17
 9   112   112 -3.11      1   142   143 -1.92       8   209   199  1.53        3  K  13              17    94    93 -2.26
 8    71    79 -1.11      0   132   137 -2.26       9    97    95  1.35     1    45    32  2.47       18    48    48  1.34
 7   198   191 -1.78                              10    34    34  0.64     2   109   106  1.24       19    77    76 -1.60
 6   326   320 -1.05        2  K   8             11   116   113  2.25     3    74    58  1.51       22    99    91  0.74
 5    32    23  0.95      0    71    73 -0.98     12   138   139 -1.64     5   127   120  0.99       23    75    70  1.12
 4    90    96 -1.27      1   147   150 -1.27     13   206   201  2.36     7    74    64  1.06       25    49    41 -1.23
 3    61    63 -0.79      2   133   137 -1.36     14    54    49  1.29    10    88    87  1.49
                         4    44    45  2.95     16    98   104 -1.81    11    49    30 -1.16          3  K   6
   1  K   0              5   132   130  1.36     17    88    86 -0.99                               25    49    47 -2.06
 4   261   258 -0.22      6    99    97  1.41     19   117   124 -1.83        3  K  12              24    42    40  1.34
 6    83    68  0.99      7   147   159  1.57     20   127   127 -1.51    15    94   105 -2.02       22    48    49 -2.91
 8    89    93 -0.31      8   107   114  0.96     21    56    60 -2.37    13    50    38 -1.65       21    48    58  0.44
10    39    42 -3.06      9    61    62  1.67     24    69    61  2.26    11    87    93  1.06       20    58    54 -1.98
12   389   388 -0.25     11    96    98 -1.01     25    92    88 -1.17     9    54    52 -2.39       19   192   183  1.20
14   431   427 -0.41     13    92    89  1.38     26    43    22 -1.87     8   109    98 -2.09       18   106   109 -1.99
18   109   109  2.03     14   106   106  1.68     27    77    77 -1.57     6   141   144 -2.01       15    61    69 -1.11
20   122   130  1.48     15    49    59  0.40                             4    98    96 -2.23       14    78    82 -0.01
22    90    91 -0.14     16    50    52  1.08        2  K   3            3   106   101  0.97       13   101   101  0.93
24   168   172  2.86     18    78    70 -2.30     27    73    77 -1.27                              12    62    53 -1.05
26    94   103  2.49     20    57    55 -1.95     26    62    60 -0.34        3  K  11              11   101   100  0.99
28    55    45  1.79     21    70    79  1.36     25    44    42 -1.95     2    73    80 -1.74        8   225   222 -1.94
                        22    43    49  1.56     24    41    34 -0.72     3    45    47  0.59        7   233   225 -1.82
   2  K  14             23    47    30  1.62     22    54    48 -2.01     4    60    52  1.36        6   154   151 -2.29
 0    66    51 -0.68     24    52    63  2.01     21    55    51 -0.79     7    69    59 -2.19        5    48    42  1.55
 4    79    75  1.86                             19    39    40  1.39     8    68    81  1.53        4   174   169 -2.25
 6    57    65  1.23        2  K   7             18   170   166  1.46     9    90    85 -2.09        3    59    52 -2.08
                        21   102    96 -2.33     17    89    94 -1.69    10   115   113 -1.84        2    70    72  2.46
   2  K  13             20    40     8 -1.91     15   142   136  1.67    14    45    40 -2.63        1   128   120 -2.10
12    70    79  1.56     19   108   112 -1.80     14    87    86 -2.06    15    46    13 -2.46
11    47    38 -2.82     18    69    67  1.31     13    61    57 -0.42    18    88    87  1.23          3  K   5
10    44    40  1.23     17   101   112 -1.35     12   107   111 -1.37                               1   158   158 -1.42
 9    93    86 -1.81     15    61    57  2.05     11    54    55  0.39        3  K  10               2   129   119 -1.68
 8    62    43 -2.06     14    70    68  2.12      9    71    72  1.52    19    69    74 -1.89        3    36    38 -2.87
 7    93    99 -1.73     13   129   122  2.52      8    44    35 -1.45    17   127   128 -2.21        4    36    36 -0.65
 5    81    81 -1.79     11    93    90  2.32      7   113   110  2.05    15    41    38 -3.02        5   159   158 -1.65
 3    89    91 -1.69     10   102   105  1.30      6   177   179 -1.38    14    45    52 -2.70        6   334   338  1.04
 0    95    98 -1.69      8    36    39 -1.74      5   191   190  2.04    13    79    75  1.13        7   209   210 -2.48
                         7   140   137 -2.04      4    97    92 -0.79    12    70    58 -2.42        8    40    34 -0.40
   2  K  12              6    50    45 -0.58      3    34    36 -1.40    11    47    48 -1.06        9   156   163 -2.23
 1   110   123 -1.61      5   111   114 -2.35      2    91    89  2.33    10    53    48  2.64       10    57    60 -1.99
 2    53    40 -3.12      4    49    49  0.35      0   443   441  2.13     9    57    52  1.10       11   121   122  1.03
 3    65    56 -1.86      3    52    49 -2.29                             8    62    60 -2.16       12    48    42 -3.01
 4    60    73 -2.27      2   111   104 -1.51        2  K   2            6    81    86 -2.27       13    70    73  1.14
 6    82    81 -1.74      1    47    59  0.94      0   279   279  0.15     5   189   190  1.09       14   122   114  1.58
 7    61    64  1.57      0    42    51  1.16      1    63    54 -2.03     3    54    52  0.63       15    55    37  0.10
 8    89    90 -1.68                              2   226   230  1.56     2    65    75  1.30       16    38    32  1.32
 9    57    69 -1.98        2  K   6             3    39    40  0.06     1    60    46 -2.59       17   129   123  1.01
11   106   108 -1.35      0   192   198  3.01      4    77    83 -1.33                              19   181   184  1.03
13    63    58  0.45      1    96    91 -2.43      5   352   345  1.44        3  K   9              20   112   106  1.13
16    53    58  1.11      2   109   106  2.82      6   253   248  1.43     1    52    51 -2.41       21   152   149  1.20
                         3   136   137 -1.29      7   293   288  1.89     3    97    92  1.34       23    54    55 -2.20
   2  K  11              4   170   169 -1.28      8   246   247  0.89     4   178   174 -2.15
18    48    49 -2.56      5   249   249  1.59      9    82    80  1.54     6   172   171 -2.18          3  K   4
17    42    36 -0.11      6   234   245 -1.66     10   156   159 -1.49     7   134   136 -1.88       27    61    55 -1.62
16    41    28 -0.93      7   254   255  1.72     11    69    69 -1.65     8   201   204 -2.05       26    46    25 -3.01
15    43    36  0.26      8   231   232 -2.25     12    98   105 -2.21    11   112   114  0.89       25    46    25  0.31
14   107   121  1.56      9    85    85 -2.76     13    82    72  0.39    12    56    53 -2.00       22   104    97  1.06
11    56    60 -1.05     13    91    97  0.97     14   114   113 -0.85    14    43    34 -2.50       21    68    67  0.42
 8    50    51  0.32     14    51    49 -1.71     15    64    67  0.78    15    94    90 -2.07       20    42    22 -2.05
 7    80    81  1.08     15   113   110  2.00     16   104    98  1.91    18    83    83 -1.98       19   133   131 -1.83
 5    64    68  1.24     16   118   126  1.63     18   225   220 -1.51    19   135   126  1.26       17    46    58 -2.04
 4    62    59  2.51     17   100   100 -1.54     19   100    95  1.34    21    43    39  0.54       16    52    42  1.79
 3    44    35 -0.23     18   135   141  1.38     20   153   161 -1.92    22    55    44 -2.14       15   114   117  1.30
 2   132   135 -1.28     20   142   141  1.38     21    58    59  1.07                               14    61    59  1.87
 1    63    63 -0.70     24    49    44 -0.59     24    72    72  2.19        3  K   8              13    99    94  1.41
 0    92    84 -0.53     26    56    51 -1.86     26    62    68  2.91    22    59    54  0.71       11    61    55  0.56
                                                28    71    57 -1.47    21   125   118  1.18       10   137   138 -1.90
   2  K  10                2  K   5                                     20    88    87  1.15        9    72    74 -1.05
 0    65    66 -1.86     26    48    49 -3.08        2  K   1           19   109   103  0.89        8   174   176  1.05
 1    42    59  1.55     25    53    58 -1.39     28    46    40 -1.58    18    75    60  1.30        7   285   287  1.04
 2    40    34 -0.81     24    82    79  1.93     27    52    32 -1.85    17    77    68  1.27        6    96    94  1.56
 3   104   109 -1.58     22    59    46  1.30     25    61    54 -1.12    14    65    60  2.72        5    82    81  0.47
 4    45    38 -0.03     21    79    78  1.23     24    54    59  1.91    13    44    33  0.54        4   125   121  1.21
 5    91    97 -2.45     20    96    93 -1.63     21   103    98 -2.57    12    64    61 -2.48        3    54    48  2.20
 6    47    49 -0.98     19    56    56  0.08     20   198   199 -1.64    11    91    85  1.02        2    68    64 -2.08
 7    85    92 -1.92     18   158   148 -1.64     19   185   184 -1.83    10   152   149 -2.00        1   117   118 -1.86
 9    58    52 -0.78     17    56    57  1.96     18   154   148 -1.84     9   179   175 -2.03
10    81    70  1.33     16   109   112  1.60     15    58    44 -1.81     8    43    51  2.41          3  K   3
11    59    62  2.35     15    60    56 -0.24     14    86    86 -1.39     7   119   116 -2.81       1   208   205 -2.25
12    48    62  1.19     14    52    54  0.76     13   267   257  2.62     6   153   149  1.10        2   108   103  2.28
13    73    66  2.97     13   111   122  1.31     12   148   147 -1.58     5   136   137 -'.72        3   150   138 -1.27
```

*Table 2. Continued.*

```
4   124  120 -2.64      1   114  119  0.75      7    85   85  1.60      9    37   37  2.12           5 K 11
5   193  189  1.94      3    47   44  1.35      6    70   66  1.70      8   218  220  2.04     18   51   57  2.87
6   327  309 -1.65      4    55   51  1.34      5    92   96  2.14      7   261  260 -3.09     15   54   34 -0.31
7   320  317 -2.66      5    52   53 -1.40      4    91   83 -0.99      6   219  214  1.04     14  139  145 -0.73
8   105   98 -1.70      6    75   67  0.85      3    49   46 -0.26      5   216  212 -2.63     12  138  136 -0.68
9   125  124  2.05      7    69   64 -2.05      2   149  154  0.07      4   129  125  0.84     10   57   67 -0.49
10   51   52 -1.12      8    76   71  0.63      1    62   62 -1.24      3   172  170  0.95      9   65   47 -0.82
11   63   64  1.00      9    49   41  0.71      0    52   62 -0.11      2   167  160  3.08      8   66   65 -2.76
12   59   57  1.05     11   107  113  0.21                             1    60   60 -2.33      7   48   47 -0.59
13  135  140  0.68     12    48   30 -2.52           4 K 6             0   403  418  3.10      6   91   91 -0.76
14   59   64  0.21     14    43   28  2.32      0   211  219  2.41                              5   65   69  2.19
15   63   60 -1.25                              1    61   60  1.95           4 K 2             3  106  104  2.40
17   38   26  0.00           4 K 11             2   121  122  2.89      0   105  104 -0.91      2   51   55  1.07
18  148  153 -2.16     17    43   53 -1.14      3   138  143  0.88      1   138  132  2.05      1   58   56  2.36
19  140  147  1.01     14   108  115 -2.21      4   189  198  0.60      2   215  204 -2.15
20  156  165 -1.97     12    60   73  2.08      5   207  209 -2.50      3    83   78  1.24           5 K 10
24   43   43 -2.24     11    92   89 -0.33      6   191  188  0.98      4    75   73  0.68      1  202  200 -0.75
25   54   42 -1.78     10    42   31  2.06      7   164  165 -2.59      5   163  174 -2.54      5  135  138  3.05
26   75   82 -2.37      9    99   98 -0.67      8    40   50  1.15      6   209  212 -2.83      7   86   87 -0.53
27   48   42  1.09      8    50   49 -1.29      9    38   17  1.03      7   285  281 -1.87      8   82   76 -0.61
28   50   37 -1.67      7    47   42 -2.34     11    49   41 -2.72      8   204  197 -2.88      9   43   28 -2.39
                       6    68   70 -1.74     12    36   29 -1.23      9    61   57 -2.48     10   64   80 -0.90
      3 K 2            5    69   59 -3.06     13    53   52 -1.56     10    97   95  1.34     11   54   42  1.80
27   48   51  1.59      4    42   52 -2.38     14    55   74  0.92     11    43   51 -0.49     13   70   68  2.94
26   67   86 -2.45      2   118  113  0.16     15   135  131 -2.91     13   135  131 -0.64     14   44   53 -0.47
24   47   40 -1.27      0   153  151 -0.67     16   122  129 -2.95     14    74   79 -0.17     15   72   69 -1.08
22   60   54 -0.90                             17    64   62  0.98     15    93   93 -2.28     16   51   55 -0.80
21   67   73  1.43           4 K 10            18   127  124 -2.28     16    81   74 -2.18     17   62   64 -0.40
20   92   89  0.94      0    95   85  0.10     19    43   50 -0.79     18   217  220  0.53     20   59   47  2.23
19  260  262  1.10      1    76   76 -1.69     20   111  103 -2.16     19    53   33 -1.53
18   51   55 -2.16      2    85   93 -0.48     23    46   47  0.92     20   108  110  0.37           5 K 9
17  174  173  1.09      3    81   83 -0.16     24    69   69 -0.60     21    53   54 -0.91     21   69   67  2.76
16   93   90  2.01      4    61   54 -0.62     25    60   53  0.11     23    38   26 -0.17     20   55   61  2.85
15   61   68 -0.79      5    65   58  1.94     26    97   91 -0.98     24    87   84  3.12     17   41   24  0.03
14  147  147  1.14      7    92   86  1.03                            27    42   43 -0.32     14  107  114  2.72
13   47   45 -0.33      9    67   65  0.51           4 K 5            28    79   73  0.66     13   60   48  1.22
11  110  113  1.53     10    40   39 -2.67     26    55   72  2.62                             12   76   74  2.43
9   102   98 -1.23     11    45   53 -3.11     25    56   52  0.34           4 K 1            11   63   69 -2.50
8   210  204 -0.28     12    57   50 -2.79     24    90   97  3.09     28    45   41  0.84     10   65   74  2.65
7   380  377 -1.67     13   109  106  2.39     20    94   82  0.85     27    47   37  1.63      8  148  154  0.03
6   464  466  0.57     14    56   44  2.03     19    72   81 -0.97     26    55   59  2.51      7   49   45  1.17
5   200  198 -2.39     15    97   90 -3.09     18   164  160  0.88     25    78   77 -0.11      4   96   99 -0.28
4   112  103  1.10     17   113  106  0.50     17    59   61 -2.63     24    62   65 -2.77      1   49   60  1.85
3   102   97 -1.59     18    54   49 -2.88     16    63   67 -2.44     23    46   49 -0.99
2   187  176 -1.81                             15    53   54 -1.45     22    44   38 -0.23           5 K 8
1   110  106 -2.00           4 K 9             13   172  178 -1.88     20   138  134  0.38      1   46   62 -2.67
                      20   107  116 -2.60     12    82   80  1.98     19   136  138  0.76      3   92   93  2.28
      3 K 1           18    78   71 -2.63     11    84   88 -0.42     18   112  118  0.51      4   56   49  0.09
3    84   79  2.06     16   118  121 -2.91     10    75   76  1.21     16    44   43 -1.71      5   48   54  0.95
4   214  204  0.69     15    48   42 -2.78      9    66   72 -1.96     15   155  154  1.58      6   73   70 -0.92
5   112  100  0.59     14    42   53  1.49      8   139  134 -2.34     14    39   37 -0.37      7   45   50 -0.65
6   454  458  1.10     13    62   55 -2.12      7   303  306 -2.57     13   251  251  2.90      8   46   46 -2.20
7   256  259  0.99     12    49   57 -2.64      6   149  147 -2.11     12   130  132  0.01      9  103  101 -0.37
8   138  135  0.49     11    58   63  0.19      5   235  245 -2.62     11   128  128  2.04     10  126  126 -0.07
9    84   82 -1.58     10    38   34 -0.52      4    89   85  0.66     10    81   78  1.68     11   96   97  3.07
10   40   35 -1.43      8    41   38  0.86      3    93   88 -2.86      9    41   34 -1.99     12  211  219 -0.85
11   44   42  0.27      7   103  108 -2.39      2    46   46 -0.77      8   108  101 -1.34     13   49   46  1.80
13   89   90  2.33      6   100   98  0.94      1   161  162  0.96      7   144  144  1.25     14  131  137 -0.73
14  172  178  1.04      5    68   75 -2.10      0   228  220 -0.42      6    81   74 -1.04     16   48   52 -2.82
15  101   98  1.77      4   124  122  0.47                             5   245  232  1.21     17   42   42 -2.87
16   60   56  1.68      3    65   62  1.18           4 K 4             4    21   20 -0.17     18   65   61 -2.95
17   69   70 -2.10      2    76   85 -3.00      0   368  369 -2.32      3   216  207 -2.14     19   56   56  2.36
19  213  211 -1.91      1    66   68  0.34      1    65   65 -1.05                             20   46   39 -0.01
20   57   56  1.18      0    40   42  1.22      2    82   83  0.02           4 K 0            21   77   74  3.13
24   40   45 -2.53                              3   125  122 -1.71      4    55   55  0.19     22   58   43  1.74
25   68   62  0.61           4 K 8             4    80   79 -1.14      6   255  254  1.65     23   94   99 -0.58
26   69   84 -2.47      0   175  175 -0.68      5   185  178  1.54      8   218  214  1.72     24   83   72  2.11
                       1    68   69  0.63      6    90   91 -1.79     10   104  102 -1.71
      3 K 0            2   133  133 -0.31      7   161  163  1.86     12   204  206 -0.21           5 K 7
28   74   69 -2.03      3    60   69 -2.25      8    55   51 -2.05     14    79   88  0.59     23   75   62  3.01
26   58   73 -2.37      5   136  130  3.11      9    48   43 -2.07     16   120  119  1.93     22   87  102  2.71
24  101   98 -2.18      6   109  109 -1.33     10    58   62  3.05     18   214  212 -1.65     21   57   44  2.14
22   54   44  1.26      7   177  173 -2.73     11   191  195  2.82     20    55   60 -0.57     19  104  101  2.09
20  187  193 -1.85      9    63   69 -0.93     12   110  113  0.13     24    60   65 -0.64     18   46   30 -1.35
18  117  118 -1.98     11   119  120  0.02     13   315  322  3.00     26   109  113 -0.55     16   75   71 -0.60
16   58   51 -1.06     12    70   71  2.18     14    48   53 -2.48     28    53   64 -1.35     15   45   44 -1.53
14  134  140  0.43     13    63   52 -1.83     15    82   78  2.49                             13  113  116  2.93
12  276  282  0.98     14   107  104 -2.41     17    56   45  0.00           5 K 14           12   53   48 -1.72
10   49   50 -0.95     15    55   44  0.85     19   146  145  0.63      2    68   60  1.77     11  112  119  2.02
8    46   48  0.90     17    53   50 -1.70     20   101   99  0.52      3    94   95  2.17     10  147  153 -0.54
6   345  341 -1.63     18    81   83  1.80     21    57   63  1.19      5    89   95  2.40      9   67   72  0.52
4    41   39  0.92     19    48   48  0.05     23    56   56 -0.72      6    59   50 -1.07      7  128  132 -0.37
                      20    67   72  1.08     24    53   50  3.14                              6   42   40 -0.77
      4 K 14          21    55   52 -2.84     25   124  123 -0.12           5 K 13            5   83   94  2.85
0   113  114 -0.41     22    51   37 -2.46     26    52   34  1.77      8    69   88 -0.37      2   93   98 -0.24
1    48   34 -1.81     23    44   34 -3.02     27    53   60  0.85      5    88   88  2.72      1  372  379 -0.69
2    74   67 -0.29     24    79   78 -2.98                             2    70   73 -2.66
4    69   67 -2.70                                   4 K 3            1    87   95 -0.90           5 K 6
6    49   48 -2.47           4 K 7             28    54   57 -0.94                              1   74   71 -1.76
                      24    50   60 -3.03     27    59   55  0.17           5 K 12            2  106  104 -1.51
      4 K 13          20    46   18  0.91     26   104  104 -0.63      1    86   88  2.70      3   93   89 -0.23
12   68   72 -2.39     19    87   91  0.70     24    69   58 -0.39      2    42   42 -2.22      4   41   41  0.03
10   48   26 -1.42     18    55   58 -2.51     22    41   38 -0.55      3    59   63  3.04      6   92   99  1.92
9    72   76  0.29     17   113  114  0.56     20    89   90 -1.34      4    69   61 -0.58      7  136  139 -0.03
7    97   93  0.74     16    51   55  0.99     18   142  144 -2.00      8    55   42 -0.31      8  108  112 -0.14
5    78   59  1.00     15   108  116  2.75     17    53   57  1.06      9    48   45 -0.31      9   86   89 -2.59
3    72   74 -0.23     14    60   60  2.92     16    49   42  2.11     10    67   66  2.24     10   57   67 -2.71
2    49   60 -2.02     13   230  234  2.69     15   114  111 -2.58     12    73   69  2.40     12  147  157  2.64
0    79   72  0.63     11   143  150  2.97     14    53   55  1.18     14    53   49  2.10     13   80   78  2.85
                      10    77   76 -2.68     12   173  172 -0.32     15    46   39  0.21     14  193  190  2.45
      4 K 12          9    39   42  1.43     11    82   82 -2.88                              15   47   53  1.95
0    55   53  1.55     8   116  110  2.88     10    60   67 -0.98                              17   39   35  0.97
```

*Table 2. Continued.*

```
18   66    78  -0.26
19  122   115   3.00
20   75    72   2.65
25   65    69  -0.37

      5  K  5
25   77    87  -0.93
24   77    76   2.49
23   84    81  -0.15
21   92    89  -3.12
19   76    81   2.57
17   51    49   2.49
15   39    49   2.13
14  106   105  -1.01
13   82    92   2.14
12  227   234  -0.38
11  115   115  -3.02
10   55    48  -0.95
 9   74    69   0.04
 7   38    43  -1.31
 6  111   114  -2.52
 5  105   102   0.18
 4   73    73  -0.29
 3   56    51   2.37
 2   94    99   0.60

      5  K  4
 1  599   619  -0.65
 2  181   172  -0.36
 3   58    53  -1.38
 4  127   123   2.53
 5  114   118  -2.43
 6   49    51   0.99
 7  118   111  -1.47
 8  100   104   3.03
 9  126   133   0.01
10  139   151  -0.46
11  170   176   2.42
12   37    35  -0.89
13  115   111   2.78
14   53    64  -2.22
15   51    57  -1.70
16   64    61  -1.27
17   52    54   2.02
19  137   132   1.73
21   90   101   2.42
22   64    63   2.82
25  145   138   2.42
27   83    91   2.09
28   50    29  -0.30

      5  K  3
26   77    76  -0.34
25   52    54  -0.39
24  103   100  -0.56
22   62    50   2.91
21   66    68   1.80
20   54    51   1.62
19  103   101   2.89
18   86    91  -0.12
15   65    73   2.69
14  302   308   2.35
13  104   104   2.28
12  358   371   2.44
10   44    45   1.70
 9   56    47  -3.08
 8   56    52   1.51
 7  198   200  -0.22
 6  321   317   1.58
 5   34    33   1.81
 4   85    79   3.04
 3  142   135  -0.44
 2  140   141  -1.00
 1  178   172  -2.02

      5  K  2
 1  253   250   2.23
 2   46    51   1.10
 3   29    35   1.32
 4   94    94   0.60
 5   46    42  -0.66
 6  229   234   2.93
 7  193   191   0.70
 8   91    94   1.67
 9   39    43   2.84
11   74    77  -1.23
12  162   157  -0.22
13   53    58   2.50
14   44    23  -2.04
15   98   103   1.55
18   45    48  -1.01
19  105   103   3.09
20   41    44  -2.00
22   62    53   0.55
24   47    53   3.04
25  146   148  -0.67
26   80    85  -0.49
27   63    68  -1.02
28   58    51  -1.46

      5  K  1
27   52    58   1.90

26   81    72  -0.73
25  174   169   2.69
21   74    69   3.07
20   46    41  -1.12
19   75    68   0.71
15   89    80  -1.80
13   56    53   2.20
12   95    93  -0.49
11  171   176   2.58
10   71    77  -0.87
 9  162   163   0.17
 8  124   134   2.56
 7  121   122   2.78
 6  140   143   2.33
 5   32    30  -0.69
 4   91    89   2.97
 3   53    54  -2.75

      5  K  0
 4  114   113  -3.11
 6   93    98   2.70
 8  123   126   2.41
10   64    66   1.77
12  425   431   2.60
14  289   290   2.47
16   43    43   0.53
18  107   115  -0.73
20   48    27  -1.31
22   93    88  -2.91
24  155   153  -0.59
26   75    86  -0.48
28   46    32   0.64

      6  K  14
 0  125   126   2.18
 2   58    60   2.18
 3   50    63   2.42
 4   58    67  -0.88
 5   49    30  -0.46

      6  K  13
12   50    40  -1.32
11   63    63  -0.42
 8   47    30   0.27
 4   79    78   2.72
 3   80    71   1.30
 0   46    45   1.50

      6  K  12
 0   57    49  -0.52
 1   66    68   2.46
 2   73    65  -0.63
 4   50    28  -0.90
 5   49    53   2.62
 8   47    44   1.02
 9   61    63   0.28
11  104   108   2.13
15   44    26   2.56
16   46    37  -1.90

      6  K  11
18   55    54  -0.51
17   59    45   2.14
14   73    63  -0.76
11  112   114   2.08
10   52    48  -1.35
 9   98   101   2.04
 8  103    95   2.57
 4   92    96  -0.57
 2  137   143   2.19
 0  160   164   2.18

      6  K  10
 0   76    71   1.41
 2   69    82   1.97
 3  107   109   1.87
 4  100    98   2.35
 5   63    65  -0.11
 9   66    67   2.16
11  118   126  -0.58
12   42    38  -2.03
13  143   143  -0.86
15   98   100  -0.81
16   54    33  -1.08
17  116   112   2.33
18   49    36  -1.77
20   66    49  -1.17
21   58    46  -0.29

      6  K  9
20   73    80  -1.31
19   45    55   2.23
18   77    73  -1.98
17   58    65  -0.11
16  104   115  -1.24
14   59    55  -3.10
13   45    45  -3.06
11   69    70   2.33
 9   44    38   0.02
 8   61    67   0.88
 7   68    71  -1.03
 5   46    57  -2.07

 4   86    87   1.98
 2  118   116  -0.09
 1   62    74   1.34
 0  119   115  -0.31

      6  K  8
 0  214   215   2.33
 1   99   107   2.12
 2  131   135   1.58
 3   53    61  -1.34
 4   58    60   0.44
 5  128   133  -1.90
 6   42    38  -3.04
 7  108   105  -1.51
 8   87    95   3.06
10   43    49  -2.65
11  114   113   2.29
12   58    44  -0.64
14   81    77  -0.86
15   90    83   3.04
18   43    42  -0.33
19   51    46   2.81
20   41    10  -2.29
21   62    62  -1.54
23   48    22  -1.73
24   85    89  -0.79

      6  K  7
21   82    81   0.01
18   54    65  -0.73
17  128   130   2.43
16   44    41  -2.75
15  149   152  -1.15
14   76    86  -0.95
13  246   248  -1.07
11  134   143  -0.91
10   47    50  -1.57
 9   39    45  -2.24
 8   70    74  -1.29
 7   69    73  -1.02
 6   62    66   3.12
 5  141   148  -0.57
 4   67    60   1.63
 3   80    80   1.71
 2  178   185   2.15
 1   61    55   1.93
 0   54    51  -1.14

      6  K  6
 0  276   270  -0.91
 1   78    78  -0.17
 2  190   197  -0.87
 3   49    51   2.87
 4  150   149  -2.23
 5  113   114  -1.45
 6   61    64  -0.02
 7  144   150  -1.29
 8  144   149  -0.26
 9   98    99  -1.03
10   68    72   1.14
13   83    87  -3.02
15   80    87  -1.17
16  133   146  -1.33
18   72    80  -2.58
19   48    37   1.84
24   94    91   2.24
25   56    50   1.02
26  108    97   2.09

      6  K  5
26   99    99  -0.77
25   63    60   1.72
24   89    85  -1.06
22   41    21   2.23
21   44    44  -3.07
19   78    79   2.28
16   58    51  -0.80
15   49    41   2.94
14   72    80   2.31
13   95   100   2.32
12   48    47  -0.34
11  129   134   2.21
10   64    68  -2.64
 9   69    65  -1.96
 8  127   131  -2.77
 7  105   111  -1.59
 6   72    76  -1.74
 5  166   171  -2.13
 4   41    37   0.58
 3   90    90  -1.92
 2   52    55   1.18
 1   77    77   2.12
 0  297   302   2.36

      6  K  4
 0  152   144   0.75
 1  259   258   1.80
 2  164   167   2.30
 3  107   103  -0.21
 4   52    51  -0.02
 5  148   139  -0.71
 6   68    69   2.48

 7   59    63  -0.92
 8  104   104  -1.85
 9   78    87  -2.34
11  101   106  -1.07
12  109   124   2.04
13  372   392  -0.96
14   71    76  -0.40
15  112   116  -1.38
17   41    46   1.64
18   51    40  -0.43
19   82    79   1.37
20   60    62   1.85
21  106   110  -0.22
23   58    59   1.43
24   87    84  -0.93
25  126   127   2.04
26   48    16  -1.61
27   53    36   1.57

      6  K  3
27   75    82   1.91
26  139   135   2.29
24   88    92   2.32
21   53    49   2.56
20   53    61   2.01
18   65    57  -2.27
17   62    57   2.22
16   87    96  -1.86
15  103   104  -1.38
13   93    93  -2.87
12  163   168   2.08
11   64    59  -0.50
10   94    93   0.75
 9   48    58  -1.44
 8  157   163  -0.66
 7  140   146  -1.45
 6   54    47   0.37
 5  207   198  -1.42
 4  133   132   2.34
 3  108   109   3.10
 2  187   192  -0.96
 1  158   156  -0.22
 0  462   479  -0.78

      6  K  2
 0  162   162   2.89
 2   19    18  -1.23
 3   63    58  -2.77
 4   38    33   1.34
 5  208   207  -1.72
 6   76    80  -1.91
 7  213   209  -1.10
 8  172   168  -2.50
 9   35    33  -1.88
10   61    54   2.40
11  113   115   2.61
12   63    64   1.10
13  196   203   2.70
14  119   129   2.25
16   57    56  -0.19
18   78    81   1.76
20  113   114   1.39
21   83    77   2.92
24   88    87  -0.93
26   99   106  -0.65
28   45    39   2.58

      6  K  1
26   50    50  -0.51
25  109   100   2.38
24   85    83  -0.69
21  129   135  -0.20
20   96   107   1.67
19   41    38   1.44
18  105   105   1.92
16   55    52   0.12
15   60    66   2.93
13  341   353  -0.76
12   84    82   1.51
11  172   170  -0.94
10   58    53   1.91
 9   65    66  -2.13
 8  169   173  -1.73
 7   39    39   1.22
 6  147   146  -1.30
 5   48    46  -0.06
 4   23    19   0.54
 3   92    93  -0.14

      6  K  0
 4   36    39   2.48
 6   35    23   0.48
 8  337   339  -1.02
10  103   111   0.89
16  272   277   2.18
18  125   123   2.72
20   80    88   2.29
24  110   112   2.34
26  163   165   2.38

      7  K  14
 3   46    44  -1.60

 4   53    47  -2.91
 5   63    69  -1.23

      7  K  13
12   45    34   0.59
10   52    52  -2.36
 8   76    71   2.03
 7   65    70   3.12
 5  118   110  -1.93
 4   43    14   1.91
 3   60    45  -2.11
 2   79    74  -2.34
 1   63    58   2.46

      7  K  12
 3   80    82  -2.25
 4   62    71   0.33
 5   64    79   2.49
 6  104   100   0.68
 7   56    68  -0.29
 8   68    71   0.99
 9   57    61   1.11
10   44    40  -0.64
11   65    62  -2.06
14   44    43   0.05
15   82    72   0.89

      7  K  11
18   66    58  -1.66
16   50    25  -0.11
14   62    75   1.85
12   72    72   1.88
10   62    64   1.57
 9   67    56   0.70
 8   65    65  -1.02
 6   69    75   2.62
 3   52    44  -1.45
 2   52    58   1.59
 1   37     5   1.32

      7  K  10
 1   99    98   1.92
 5  133   138  -1.81
 6   83    84   0.98
 7  110   115   2.94
 8   46    41   2.13
 9   69    76  -2.90
10   44    33   2.09
11   52    47   2.39
12   44    44   0.43
13   64    69  -1.29
14   53    50   0.72
17   87    91   0.69

      7  K  9
20   76    75  -0.43
19   77    77  -2.38
18   51    52   1.15
15   54    61   1.08
14   78    86  -0.65
12   68    62  -0.12
11   68    79  -2.37
10   62    74  -0.79
 8  144   159   1.19
 7   98   106   0.17
 6  115   125   0.43
 5   46    58   2.99
 4  133   141   0.74
 3   41    53  -2.48
 2   46    42  -0.38
 1   71    79   0.36

      7  K  8
 1   92    93  -0.03
 2   80    84   0.88
 3   96    93  -1.05
 4   52    51   2.85
 5   57    60   1.15
 6   84    88   3.03
 7  108   111   0.18
 9  107   103   1.08
10   88    95   0.92
11   46    53  -1.59
12  119   123   1.93
13   53    54  -2.67
14   74    73   1.87
16   71    69  -0.56
17   64    67  -2.29
18   50    33  -1.24
19   96   107  -2.40
20   60    82   3.09
21   72    85  -2.06
22   73    79  -2.75
23   71    73   1.89

      7  K  7
23   64    49  -1.35
22   88    97  -1.74
21   50    34  -2.76
17   80    74   0.62
16   40    50   2.47
```

*Table 2. Continued.*

```
13   97   96 -1.83        7 K 2         13   42   25 -1.41        0  176  184 -1.21        9 K 13
10  120  134  1.82     1  162  158 -0.56  15   62   59  0.33                            11   46   33 -1.62
 9   62   62  2.87     2   81   80  0.45  17  106  102 -1.92        8 K 4             10   60   57  0.45
 7   94   96  3.04     3   46   48  1.53  18   60   57  0.59     0  183  183  0.72      5   91   91  0.23
 6   53   65  2.59     4  113  116 -3.13  19   69   80 -3.02     2   97   96 -1.84      3   63   42 -0.02
 5  109  115 -1.31     5   33   27  0.93                        3  122  124  1.72      2   75   85  0.35
 4   41   50 -1.25     6  366  377 -2.09        8 K 9          4   72   80  1.47
 3   51   40 -0.74     7  257  265  0.56  20  125  128  0.74     5  134  139 -2.55        9 K 12
 2   43   45  1.34     8  110  109 -3.00  18  129  129  0.10     6   72   72  0.02      3   71   73 -0.06
 1  237  246  1.62     9  134  142 -0.04  16  100  111  0.51     7  128  130 -1.66      4   71   70  2.88
                      10   48   44 -0.84  14   79   81 -1.16     8  114  116  0.08      5   50   64 -1.86
      7 K 6          11   41   39 -2.69  13   74   73  0.35     9   41   37 -0.05      6   88   84  2.90
 1  115  117  0.39    12  144  148  2.44  12   79   72  0.77    10   69   69 -0.95      8   76   86 -2.77
 2   42   45 -0.43    13   56   64 -2.39  11   71   73 -2.23    11   52   46  0.26     11   96   94  0.85
 3   44   35  2.30    14  146  155 -2.53  10   50   41  3.04    12   86   85 -2.09     12   49   30 -1.90
 4  159  163  0.63    15   55   73  2.99   9   85   81 -2.98    13   81   80  0.57     15   65   73 -2.78
 5   35   24  2.94    16   66   81 -0.50   8   98   96 -3.04    15   67   65 -0.79
 6  135  140  0.37    17   95   99 -2.90   7  112  111  0.43    18   64   69  2.91        9 K 11
 7  139  147  1.01    18   41   44  1.54   6  134  133 -2.89    19  170  170 -2.71     14   75   81  2.18
 8  130  138  1.63    19  144  154 -2.43   5  147  139  0.35    20   94   93 -2.65     12   87   78  1.88
 9   49   55 -1.02    20   91   92 -2.50   4  124  125 -2.20    21   96   93  2.95     10   79   68  3.05
11   71   75 -2.58    21   70   68 -2.44   3   54   46 -2.45    25   54   57 -2.56      9   70   55  2.77
12  109  101 -0.97    22   68   71  2.51   1   93   92 -2.08    27   57   66 -2.68      8   88   87  0.73
13   74   84 -2.33    25   97  102  2.04   0  103  107 -2.39                            7   46   47  2.89
14  115  117 -0.90    26   76   79  1.01                            8 K 3              6   59   58  1.25
17   42   31 -2.40                              8 K 8          25   47   56  3.05      4   49   42  0.34
18   86   95  1.22        7 K 1           0   45   37 -2.80    23   54   49 -2.57      3   82   80 -1.08
19  133  132 -2.15    26   70   70  0.84   1   71   69 -2.03    20   53   44  0.90      2  104  108 -2.19
20   91   92 -0.19    25  112  109 -0.95   2   97   94 -2.40    18  152  147  0.74
25   56   60  1.86    21   52   58 -1.32   3   48   51  0.29    17   59   57 -2.56        9 K 10
26   70   50  1.97    20   61   70  2.71   4   56   58  2.69    16   67   66 -0.67      1   84   89  2.03
                      19  132  128  1.00   5  120  120  0.29    15  117  117  0.62      2   69   67  0.58
      7 K 5          17   58   67 -0.03   6   94   88  0.67    14   62   69 -1.74      5  172  175  0.26
24   49   56 -1.18    16   50   53 -0.30   7  147  151  0.54    13  113  113 -0.02      6   75   78 -3.02
23   76   67  1.66    15   73   73 -1.49   8  116  109 -0.03    12  103  103 -2.43      8   59   57  0.09
22   68   70  3.03    14   39   51 -2.19  10   41   42 -0.86    11   69   76  0.35     11   81   87 -1.72
21   94  106 -2.27    12   64   68 -2.98  13   96   88  0.55    10   72   75  1.83     12   63   64  2.50
20   83   79 -2.68    11   85   91 -1.56  14  117  112  0.90     8  120  118 -2.97     13   48   50  0.51
19  154  160 -2.44    10   33   35  1.74  17   43   49  1.36     7  122  124  0.15     14   53   59  2.78
17  111  117 -2.26     9  200  211  2.18  18   53   64 -2.49     6  192  195 -2.47     15   75   66  1.87
16   41   51  0.05     8  176  174 -2.29  20   76   63 -2.19     5  171  171  0.37     17   95   90 -3.11
15   40   50 -2.65     7  223  227 -2.22  21   52   58  0.31     4   80   81 -2.37     18   45   15  0.60
14  104  108  2.38     6  219  230 -2.17                        3  137  138 -2.00     19   61   60 -2.67
13   69   63 -2.20     5   42   38 -2.31        8 K 7          2   47   46 -0.75
12  146  153  2.05     4  168  168 -3.14  21   78   69  2.83     0  169  167  0.72        9 K 9
11   91   89 -2.13     3   96   99 -0.62  19  101  112 -2.94                           19   75   79  0.18
10   78   82  0.75                        18   44   49  0.63        8 K 2             18   64   66 -2.62
 9  145  154  0.74        7 K 0          17   78   84 -2.20     0  295  305 -0.17     15   89   97 -2.68
 8   46   39 -2.68     4  101  106 -0.24  16   45   52 -1.51     2  174  175  0.99     14   55   49 -2.17
 7  176  181  0.38     6   55   52 -0.60  15   62   67  0.26     3   92   96 -0.95     12   54   59 -2.33
 6  206  217 -2.05     8   69   74 -1.81  14   42   47  0.92     4   58   64 -2.28     11  103  109  0.33
 5  128  133  1.51    10   81   84  2.31  11   58   66  1.12     5  281  283  0.36      8  166  167 -2.95
 4  108  111  2.63    12  239  241 -1.13  10   68   57  0.48     6  177  179  0.46      7  103   99 -3.08
 3   82   92 -0.66    14   67   67 -1.37   8   45   48 -0.02     7  281  285  0.29      6  125  118  2.89
 2  114  114  0.45    16   58   61  2.32   7   60   55 -1.76     8  224  224  0.22      5   50   56 -1.16
 1  170  168  0.15    18  118  126  1.25   6   42   42  3.12    10  122  125 -1.53      4  122  120  2.99
                      20  146  145  0.67   5   51   48 -2.70    12  127  132  2.99      3   51   45 -0.07
      7 K 4          22  133  123 -0.66   4   45   62  1.80    15   80   88  1.07      2   79   81  1.53
 1  462  476  1.81    24   74   84  1.66   3   78   78  2.82    16   93   96  1.50      1   63   61  2.99
 2  141  137  1.88    26   74   87  1.21   2   77   88 -2.29    17   37   12  1.47
 3   81   83 -0.32                         1   61   68  1.43    18  192  194 -2.64        9 K 8
 4   84   91 -1.86        8 K 13          0   79   97  1.95    19   79   79  1.13      1   69   62 -2.96
 5   74   74 -2.11     9   67   73 -2.80                       20  137  145 -2.78      2  133  120 -2.66
 6  134  145 -2.75     7  103   97 -2.70        8 K 6         21   89   89 -0.27      3   50   39 -0.76
 7   84   85 -2.30     5   83   85 -3.05   0  119  112  2.94    25   64   49  2.79      5   71   75 -2.57
 8   85   93 -1.82     3   58   59  3.05   1   58   54  2.49    27   45   33  2.60      6  112  113  0.92
 9  118  129  2.55     2   45   35  1.51   2   84   87  2.34    28   82   78 -2.27      7   95   86  2.60
10   90  104  1.82     0  108  101 -2.91   3  105  108 -1.95                            8   64   64  1.63
11   61   62 -1.67                         4   94   90 -2.80        8 K 1              9  130  127  2.99
12   40   39 -1.67        8 K 12          5  200  208  0.26    24   49   50  0.54     10   90   90  2.72
13  118  130 -2.32     0   68   62 -2.76   6   94   90 -2.80    23   50   40  2.24     11   74   82  0.37
15   59   63  2.98     1  110  114 -2.23   7  115  113  0.04    21  111  109  2.81     12   78   78  2.14
17   50   54  0.38     2   48   39 -2.59   8   51   67  2.65    20  144  144 -2.65     14   62   53  2.03
19   50   47  0.14     3   50   48 -2.84  12   41   35  1.10    19  138  144 -2.59     15   50   26 -0.85
20   42   52  2.45     4   48   51 -2.58  13  101   97 -0.69    18  152  161 -2.89     17   52   58 -0.36
21   55   60 -1.96     5   74   67  0.07  14   76   86 -1.84    16   38   33  2.57     18   46   41  0.39
22   87   90 -2.03     6   91   92 -2.80  15   93   93  0.72    15  145  143 -1.78     19   81   81 -0.40
25  118  112 -0.84     7   56   65  1.02  16  102   98  0.30    14   67   72  2.44     20   58   48 -0.05
                       8   96   87 -2.99  17   71   66 -2.67    13   79   87  1.77     21  106  100  0.08
      7 K 3           9   78   85 -3.12  18  143  138  0.29    12  129  132 -2.71     22   44   44 -0.69
26   53   64  1.23    11   95   92 -2.35  20   91   94  0.75    10   41   50 -1.19
25   60   59  2.09    12   48   30  0.49  23   61   47 -2.95     9   47   49  0.59        9 K 7
24   59   66  1.59    13   72   62  0.79                        8  245  250  0.45     22   95   82  0.09
22   60   67 -0.32    14   57   40 -0.72        8 K 5          7  214  211 -2.75     21   53   58 -1.32
20  124  125  0.17                        25   72   74 -3.09     6  136  136  0.18     19   84   87 -2.05
19  132  136 -2.12        8 K 11         20   74   77 -2.65     5  243  244 -2.82     17   83   87 -2.88
18  106  111  0.92    14   97  100  0.88  18  146  145 -2.51     3  152  157  1.72     15   70   76  0.90
15   42   41 -1.22     8   94   84 -0.03  17   53   47  1.00                           13   81   79 -0.20
14  189  200 -1.29     6   83   93  0.47  16   71   66  0.94        8 K 0             12   74   70  1.40
13   62   75 -1.88     4   57   56  1.72  15   82   84  0.04     4   22   22 -2.07     11  120  120 -1.67
12  255  264 -1.10     2   78   76 -2.79  13  140  141  0.19     6  218  216 -2.86     10   94   94  2.54
11   84   85  2.92     0   41   36  2.82  12   69   74  2.80     8  238  239  3.02      8   74   81  1.13
 9   92   99 -1.21                        11   89   84 -0.86    10   79   78  1.50      7   54   55 -1.66
 8   39   49  2.08        8 K 10         10   75   79 -1.56    12  134  136 -2.35      6   83   83 -1.71
 7  115  113  0.86     0   98  100 -3.02   8  133  134  0.06    14   43   49 -2.12      5  120  123  0.52
 6  124  127 -0.02     1   47   52  1.47   7  207  209  0.29    16  113  110 -1.06      4   61   66  0.31
 5   55   48  0.50     3   81   74 -2.76   6  136  134  0.66    18  164  156  0.63      3   54   54  2.20
 4  134  133 -0.32     5   89   93  3.14   5  251  249  0.06    22   60   62 -2.87      1  155  152  2.18
 3   87   88  1.97     7  108  107 -2.49   4  100  103  3.10    28   54   49  1.39
 2   72   70  0.62     9  108  103 -2.44   3   77   72  0.31                               9 K 6
 1  216  215  0.11    10   65   52  0.38   2   50   41  1.86        9 K 14            1   95   97  2.41
                      12   78   77  0.14   1  152  155 -1.96     3   51   61 -1.65
```

*Table 2. Continued.*

```
 2 129 128  1.48    11  80  78  0.58    24  51  36 -2.58     3  53  56 -2.05    15 107 100  0.93
 3  36  27  1.28    10  43  53  1.68    26  50  39  1.98     4 101 108 -1.59    14 104 107  0.01
 4 120 126 -3.08     9  69  69  2.91    27  72  80 -1.68     5 133 131 -2.78    13  46  48 -1.09
 6  89  85 -2.56     7  73  65 -2.70                         6 350 360  0.20    12  58  60 -0.97
 7  97  98 -2.83     6 183 183  0.45         9 K  3          7 239 236 -3.08    11  79  74 -1.22
 8 107 105 -2.50     5  92  89 -2.57                         8  75  78  0.09    10  36  27  0.12
 9  63  58  1.14     4  66  70 -1.21    27  51  51  0.53     9 101 108  2.10     9  95  99 -1.79
10  41  33  0.20     3  39  41 -1.68    25  58  34  3.09    10  47  46  1.63     8 137 138  0.00
11  61  55  0.05     2 117 116 -2.53    24  59  54  1.96    11  75  74  0.37     7 278 282  0.57
12  89  85 -1.46     1  83  82  3.13    22  46  42  1.53    12  43  42  1.02     6 323 331 -0.18
13  69  71 -0.61                        21  51  50 -1.15    13  54  34 -1.90     5  75  73  1.24
14  68  71 -1.51         9 K  4         20 105 100  3.13    14 117 119  0.45     4  46  50 -0.62
15  48  49 -2.20                        19 114 115 -0.04    15  74  70 -1.90     3  83  86  1.12
16  53  46 -2.44     1 267 263  2.13    18 109 112  3.11    17  97  91 -0.27
18  89  85 -2.90     2  86  92 -2.84    17  67  55 -0.90    18  49  57  2.42         9 K  0
19 124 127  0.00     3  74  72  1.63    16  73  76 -2.19    19 172 162  0.23
24  61  60  0.72     4  91  96  0.19    14 154 152 -1.13    20 106  95  0.66     4 135 139  0.34
26  50  42 -2.23     5  80  80  0.64    13  52  54 -0.03    21  49  58 -0.36     6 310 313 -2.05
                     6  80  85 -0.90    12 118 123 -1.19    22  48  37 -1.71     8 128 130 -0.71
     9 K  5          7 159 159  0.77     9  79  77  0.60    26  79  78  2.86    10  96  89 -1.94
                     8 134 137  0.49     8  70  74 -1.68    27  55  59  1.23    12 185 184 -0.71
25  61  60  1.78     9  56  72 -1.94     7 167 172 -2.64                        14 179 171 -1.28
23  61  52  3.00    10  68  67  3.06     6 195 196 -2.28         9 K  1         16  86  80 -2.27
22  60  57 -1.58    11 136 135 -1.02     5  62  64  0.52                        18  92  92  2.93
21 101  98 -0.05    12  60  62  1.74     4  52  51  2.36    28  48  38  2.52    20 115 114 -3.03
20  97  97  0.27    13  84  86 -0.75     3  46  44  2.79    27 105 100 -2.11    22  78  68  1.41
19 124 120 -0.16    14  38  33 -0.37     2 130 126  1.60    26  53  71  2.70    24  80  87  2.54
17  71  75 -0.24    15 103 105  0.91     1  66  69  2.66    25  54  54 -0.59    26  72  73  2.83
15  62  65 -1.52    17  61  60 -3.02                        23  56  52 -1.06    28  58  61 -2.52
14  61  50  1.07    18  51  62  1.65         9 K  2         19 187 175 -2.47
14  94  94 -1.00    19 149 147 -2.26                        18  43  47  2.33
13  94  94 -1.00    22  76  73  0.15     1  56  56  3.12    17  62  56 -3.12
12  76  81  2.39                         2 109 111 -2.33
```

for water oxygen atoms and $f(O^-)$ for the remainder. A difference Fourier synthesis based on the listed parameters showed no abnormalities. No attempts to locate hydrogen atoms were made.

Final atomic coordinates and isotropic thermal parameters and corresponding standard deviations are given in Table 1, and a comparison of observed and calculated structure factors is made in Table 2.

## DESCRIPTION AND DISCUSSION OF THE STRUCTURE

The structure is built up from $Mo_7O_{24}^{6-}$-ions, $Na^+$-ions and $H_2O$ molecules. The $Mo_7O_{24}^{6-}$-ion consists of seven $MoO_6$-octahedra joined together by sharing edges as shown in Fig. 1.

A characteristic feature of the structure is that all $Na^+$-ions are directly coordinated to $Mo_7O_{24}^{6-}$-groups, and most of them act as links in $O-Na-O$
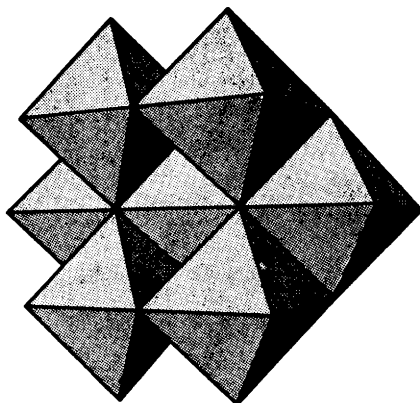


*Fig. 1.* The $Mo_7O_{24}^{6-}$-anion schematically drawn as a regular polyhedron.
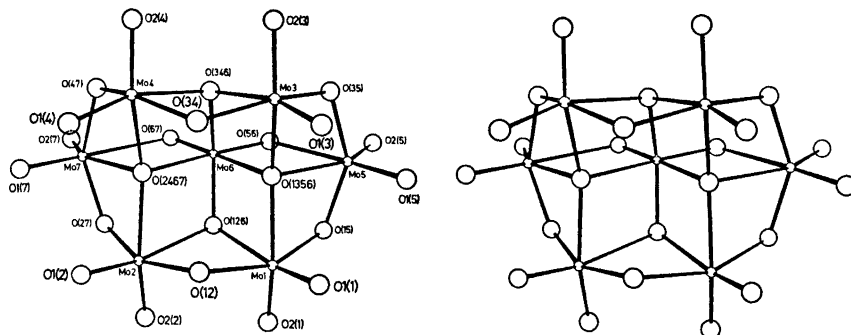
*Fig. 2.* A stereoscopic view of the $Mo_7O_{24}^{6-}$-anion.

bridges in the $x$-, $y$-, and $z$-directions. In Fig. 3 these connections are illustrated schematically.

Each $Na^+$-ion is octahedrally surrounded by oxygen atoms donated by both $H_2O$ molecules and $Mo_7O_{24}^{6-}$-groups. The octahedra are all coupled together through common edges and corners forming a double-chain arrangement in which the $Mo_7O_{24}^{6-}$-groups are embedded. The double-chains are approximately parallel with the $yz$-plane and stretch along the $y$-axis. The arrangement is shown in Fig. 4.

In the structure there are also $O-Na-H_2O-Na-O$ linkages as well as numerous hydrogen bonds indicated by short $Aq-O$ and $Aq-Aq$ distances.
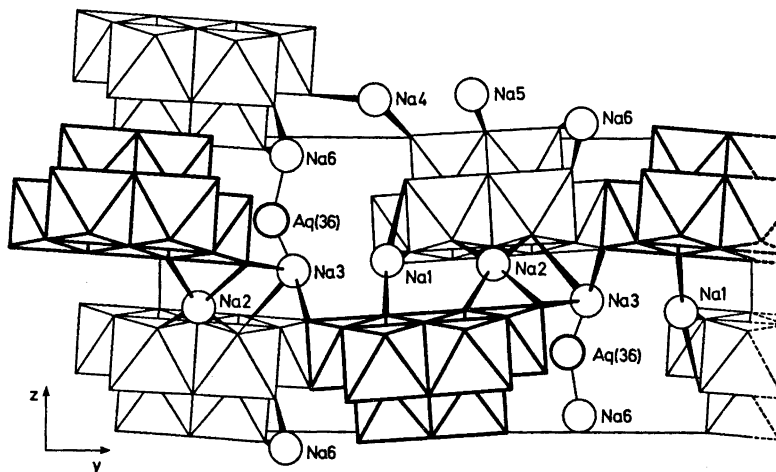


*Fig. 3.* A schematic drawing of all the $O-Na-O$ connections between $Mo_7O_{24}^{6-}$-anions in the structure. The $Mo_7O_{24}^{6-}$-anions are idealized and anions on $x \approx 0.7$ are drawn with thick lines, anions on $x \approx 0.2$ with thin lines.
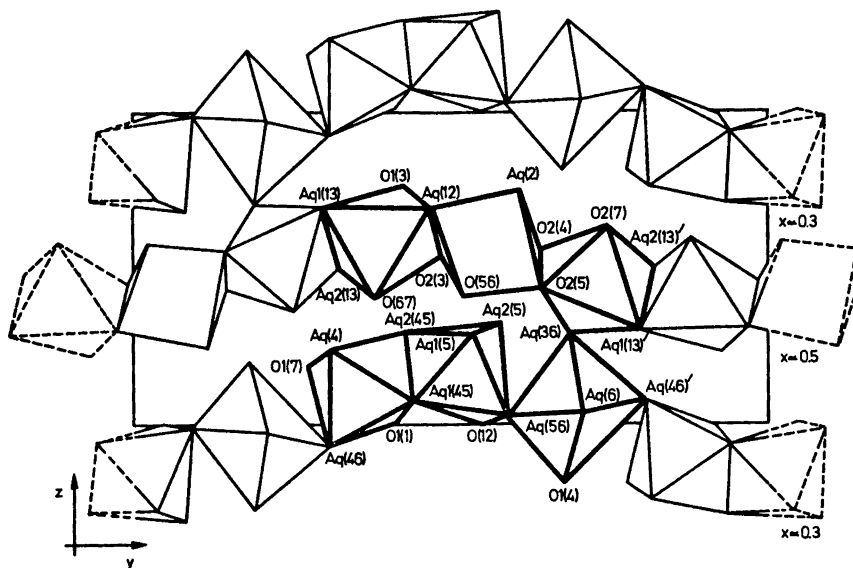
*Fig. 4.* A schematic drawing of the double-chain arrangement of $NaO_x(H_2O)_{6-x}$-octahedra, with repetition units in both strings marked with thick lines.

*Table 3.* Least squares planes through the $Mo_7O_{24}^{6-}$-group, the distances (Å) for plane-defining atoms and for some selected atoms to the planes. The selected atoms show pairs with the smallest and largest differences in distance from both planes, and an intermediate pair. The angle between the planes is 89.96°.

Plane I: $0.7062x + 0.0501y - 0.7062z - 2.9091 = 0$

| Defined by | | | | Samples | | |
|---|---|---|---|---|---|---|
| Mo5 | 0.002 | O(56) | 0.021 | O(126) | −1.805 | O1(1) | −1.930 |
| Mo6 | −0.008 | O(67) | 0.034 | O(346) | 1.795 | O1(3) | 1.816 |
| Mo7 | −0.002 | O1(5) | −0.023 | O(27) | −1.824 | O1(2) | −1.861 |
| O(1356) | 0.007 | O1(7) | 0.015 | O(47) | 1.840 | O1(4) | 1.746 |
| O(2467) | 0.007 | O2(5) | −0.001 | O2(2) | −3.818 | | |
| | | O2(7) | −0.048 | O2(4) | 3.772 | | |

Plane II: $-0.0004x - 0.9975y - 0.0701z - 12.2533 = 0$

| Defined by | | | | Samples | | |
|---|---|---|---|---|---|---|
| Mo6 | −0.007 | O(12) | 0.006 | O(1356) | 1.574 | O(56) | 1.406 |
| O(126) | 0.012 | O(34) | 0.012 | O(2467) | −1.572 | O(67) | −1.342 |
| O(346) | −0.003 | | | O(15) | 2.874 | O2(1) | 1.540 |
| | | | | O(27) | −2.877 | O2(2) | −1.627 |
| | | | | O2(3) | 1.594 | | |
| | | | | O2(4) | −1.564 | | |

*Table 4.* Distances (Å) and angles (degrees) within the $Mo_7O_{24}{}^{6-}$-group. The designation of the atoms is explained in Table 1. The estimated standard deviations are given in parentheses and refer to the last decimal place given.

| | | | | |
|---|---|---|---|---|
| Mo1 – Mo2 | 3.274(2) | | Mo1 – Mo6 – Mo2 | 57.20 (5) |
| Mo3 – Mo4 | 3.276(2) | | Mo1 – Mo6 – Mo3 | 74.90 (9) |
| Mo1 – Mo5 | 3.211(2) | | Mo1 – Mo6 – Mo4 | 102.46(11) |
| Mo2 – Mo7 | 3.214(2) | | Mo1 – Mo6 – Mo5 | 55.84 (5) |
| Mo3 – Mo5 | 3.193(4) | | Mo1 – Mo6 – Mo7 | 112.96 (6) |
| Mo4 – Mo7 | 3.204(6) | | Mo2 – Mo6 – Mo3 | 100.75(11) |
| Mo1 – Mo3 | 4.161(5) | | Mo2 – Mo6 – Mo4 | 75.29 (9) |
| Mo2 – Mo4 | 4.175(5) | | Mo2 – Mo6 – Mo5 | 112.61 (6) |
| Mo6 – Mo1 | 3.413(2) | | Mo2 – Mo6 – Mo7 | 55.97 (5) |
| Mo6 – Mo2 | 3.426(2) | | Mo3 – Mo6 – Mo4 | 57.23 (9) |
| Mo6 – Mo3 | 3.431(5) | | Mo3 – Mo6 – Mo5 | 55.35 (6) |
| Mo6 – Mo4 | 3.409(6) | | Mo3 – Mo6 – Mo7 | 112.76(14) |
| Mo6 – Mo5 | 3.445(2) | | Mo4 – Mo6 – Mo5 | 112.40(11) |
| Mo6 – Mo7 | 3.422(2) | | Mo4 – Mo6 – Mo7 | 55.94(10) |
| | | | Mo5 – Mo6 – Mo7 | 163.91(12) |

| | O1(1) | O2(1) | O(12) | O(15) | O(126) | O(1356) |
|---|---|---|---|---|---|---|
| Mo1 | 1.71(2) | 1.75(2) | 1.94(2) | 1.99(2) | 2.28(2) | 2.19(2) |
| O1(1) | | 2.76(3) | 2.74(2) | 2.84(3) | | 2.87(2) |
| O(126) | | 2.85(2) | 2.57(3) | 2.86(2) | | 2.63(3) |
| O2(1) | | | 2.83(3) | 2.70(2) | | |
| O(1356) | | | 2.87(2) | 2.49(3) | | |
| O1(1)    – Mo1 – | | 106.0 (9) | 97.4 (8) | 100.0 (8) | | 94.3 (8) |
| O(126)  – Mo1 – | | 88.9 (8) | 74.7 (7) | 84.1 (6) | | 72.1 (6) |
| O2(1)    – Mo1 – | | | 100.1 (8) | 92.1 (9) | | |
| O(1356) – Mo1 – | | | 87.9 (7) | 73.2 (8) | | |

| | O1(2) | O2(2) | O(12) | O(27) | O(126) | O(2467) |
|---|---|---|---|---|---|---|
| Mo2 | 1.70(2) | 1.75(2) | 1.91(2) | 1.99(2) | 2.33(2) | 2.18(2) |
| O1(2) | | 2.73(4) | 2.74(2) | 2.82(3) | | 2.87(2) |
| O(126) | | 2.92(2) | 2.57(3) | 2.89(2) | | 2.63(3) |
| O2(2) | | | 2.82(3) | 2.66(2) | | |
| O(2467) | | | 2.87(2) | 2.45(3) | | |
| O1(2)    – Mo2 – | | 105.2(10) | 98.8 (9) | 99.8 (8) | | 94.9 (9) |
| O(126)  – Mo2 – | | 90.4 (8) | 73.9 (7) | 83.6 (6) | | 71.1 (6) |
| O2(2)    – Mo2 – | | | 101.0 (8) | 90.9 (9) | | |
| O(2467) – Mo2 – | | | 89.1 (7) | 72.0 (8) | | |

| | O1(3) | O2(3) | O(34) | O(35) | O(346) | O(1356) |
|---|---|---|---|---|---|---|
| Mo3 | 1.67(2) | 1.74(2) | 1.91(2) | 2.01(2) | 2.31(2) | 2.11(2) |
| O1(3) | | 2.69(2) | 2.70(2) | 2.84(3) | | 2.82(3) |
| O(346) | | 2.89(3) | 2.55(3) | 2.91(2) | | 2.60(2) |
| O2(3) | | | 2.79(2) | 2.69(3) | | |
| O(1356) | | | 2.81(3) | 2.46(2) | | |
| O1(3)    – Mo3 – | | 103.9(10) | 97.8 (8) | 100.7 (8) | | 95.9 (9) |
| O(346)  – Mo3 – | | 90.1 (8) | 73.6 (8) | 84.5 (7) | | 71.8 (7) |
| O2(3)    – Mo3 – | | | 99.7 (8) | 91.7 (8) | | |
| O(1356) – Mo3 – | | | 88.7 (8) | 73.3 (7) | | |

*Table 4. Continued.*

| | O1(4) | O2(4) | O(34) | O(47) | O(346) | O(2467) |
|---|---|---|---|---|---|---|
| Mo4 | 1.72(2) | 1.70(2) | 1.94(2) | 1.94(2) | 2.27(2) | 2.15(2) |
| O1(4) | | 2.74(3) | 2.76(2) | 2.77(3) | | 2.78(3) |
| O(346) | | 2.88(3) | 2.55(3) | 2.85(2) | | 2.58(2) |
| O2(4) | | | 2.78(3) | 2.68(4) | | |
| O(2467) | | | 2.84(3) | 2.43(2) | | |
| O1(4)    −Mo4− | | 106.4(10) | 97.7 (8) | 98.2 (8) | | 91.1 (8) |
| O(346)   −Mo4− | | 92.1 (9) | 74.0 (8) | 84.8 (7) | | 71.6 (7) |
| O2(4)    −Mo4− | | | 99.3 (9) | 94.8(10) | | |
| O(2467) −Mo4− | | | 87.7 (8) | 72.6 (8) | | |

| | O1(5) | O2(5) | O(15) | O(35) | O(56) | O(1356) |
|---|---|---|---|---|---|---|
| Mo5 | 1.75(2) | 1.72(2) | 1.93(2) | 1.90(2) | 2.52(2) | 2.16(2) |
| O1(5) | | 2.75(3) | 2.80(3) | 2.77(2) | | 3.15(2) |
| O(56) | | 2.74(2) | 2.89(2) | 2.90(3) | | 2.68(3) |
| O2(5) | | | 2.79(2) | 2.80(3) | | |
| O(1356) | | | 2.49(3) | 2.46(2) | | |
| O1(5)    −Mo5− | | 105.1 (9) | 99.3 (8) | 98.6 (9) | | 107.2 (8) |
| O(56)    −Mo5− | | 78.1 (7) | 79.8 (7) | 80.9 (7) | | 69.6 (6) |
| O2(5)    −Mo5− | | | 99.8(10) | 101.2 (8) | | |
| O(1356) −Mo5− | | | 75.0 (8) | 74.2 (6) | | |

| | O(56) | O(67) | O(126) | O(346) | O(1356) | O(2467) |
|---|---|---|---|---|---|---|
| Mo6 | 1.76(2) | 1.75(2) | 1.88(2) | 1.90(2) | 2.27(2) | 2.24(2) |
| O(56) | | 2.75(2) | 2.80(2) | 2.80(3) | 2.68(3) | |
| O(2467) | | 2.74(3) | 2.63(3) | 2.58(2) | 3.15(2) | |
| O(67) | | | 2.83(2) | 2.81(3) | | |
| O(1356) | | | 2.63(3) | 2.60(2) | | |
| O(56)    −Mo6− | | 103.4 (9) | 100.5 (8) | 99.8 (9) | 82.4 (7) | |
| O(2467) −Mo6− | | 85.9 (8) | 78.7 (7) | 76.7 (8) | 88.3 (6) | |
| O(67)    −Mo6− | | | 102.6 (8) | 100.6 (9) | | |
| O(1356) −Mo6− | | | 77.8 (7) | 76.3 (7) | | |

| | O1(7) | O2(7) | O(27) | O(47) | O(67) | O(2467) |
|---|---|---|---|---|---|---|
| Mo7 | 1.69(2) | 1.71(2) | 1.90(2) | 1.93(2) | 2.60(2) | 2.15(2) |
| O1(7) | | 2.71(3) | 2.73(3) | 2.74(3) | | 3.09(3) |
| O(67) | | 2.80(2) | 2.99(2) | 2.95(3) | | 2.74(3) |
| O2(7) | | | 2.77(2) | 2.87(3) | | |
| O(2467) | | | 2.45(3) | 2.43(2) | | |
| O1(7)    −Mo7− | | 105.7 (9) | 99.1 (9) | 98.1(11) | | 107.0 (9) |
| O(67)    −Mo7− | | 77.7 (7) | 81.4 (7) | 79.7 (7) | | 69.7 (6) |
| O2(7)    −Mo7− | | | 99.7(10) | 103.6 (8) | | |
| O(2467) −Mo7− | | | 74.2 (8) | 72.7 (7) | | |

Table 5. A comparison between corresponding distances (Å) in Na$_6$Mo$_7$O$_{24}$(H$_2$O)$_{14}$ and in other structures containing Mo$_7$O$_{24}^{6-}$-anions.

| Defining atoms | Na$_6$Mo$_7$O$_{24}$(H$_2$O)$_{14}$ | (NH$_4$)$_6$Mo$_7$O$_{24}$·4H$_2$O [1] | (NH$_4$)$_6$Mo$_7$O$_{24}$·4H$_2$O [2] | (NH$_4$)$_6$Mo$_7$O$_{24}$·4H$_2$O [3] (average distances) | K$_6$Mo$_7$O$_{24}$·4H$_2$O [4] |
|---|---|---|---|---|---|
| Mo1–Mo2<br>Mo3–Mo4 | 3.274(2)<br>3.276(2) | 3.27<br>3.28 | 3.179<br>3.250 | 3.257 | 3.240<br>3.253 |
| Mo5–Mo1, Mo3<br>Mo7–Mo2, Mo4 | 3.19–3.21 | 3.21–3.31 | 3.08–3.30 | 3.206 | 3.16–3.26 |
| Mo6–all Mo atoms | 3.41–3.45 | 3.29–3.48 | 3.18–3.50 | 3.405, 3.434 | 3.38–3.45 |
| Mo1–Mo3<br>Mo2–Mo4 | 4.161(5)<br>4.175(5) | 4.30<br>4.27 | 4.176<br>4.225 | – | 4.272<br>4.244 |
| Mo–O | 1.67–2.33<br>[2.52(2), 2.60(2)] | – | 1.65–2.51 | 1.71–2.42 | 1.61–2.45<br>(1.51, 2.62) |

There is also a "free" water molecule, since one of the fourteen water molecules is not coordinated to any $Na^+$-ion (binds to other atoms through hydrogen bonds).

*The $Mo_7O_{24}^{6-}$-group.* The group is shown as a polyhedron with idealized octahedra in Fig. 1, and in more detail with the designation of the atoms included, in Fig. 2.

The molybdenum atoms Mo1 − 4 are situated at the corners of an approximate rectangle, with Mo6 lying above the centre of the rectangle, and with an Mo5 − Mo6 − Mo7 angle of 163.91(12)°. The $Mo_7O_{24}^{6-}$-group has no symmetry required by the crystal symmetry, but is very close to 2mm $(C_{2v})$. In Table 3 are given the equations of two least squares planes corresponding to approximate mm-symmetry, the atoms defining these planes, and the distances from the planes to these atoms and to some other atoms. It can be noted that the differences between corresponding distances are less than 0.12 Å. The angle between the planes is 89.96°.

As can be seen from Table 4 the Mo − Mo distances between atoms in edgesharing octahedra can be divided into three significantly different intervals, 3.19 − 3.21 Å (Mo5 − Mo1 and Mo3, Mo7 − Mo2 and Mo4), 3.27 − 3.28 Å (Mo1 − Mo2, Mo3 − Mo4) and 3.41 − 3.45 Å (Mo6 − all other Mo atoms). When sharing corners the distances are 4.161(5) and 4.175(5) Å. In Table 5 a comparison of distances between atoms in this structure and in other heptamolybdate structures is made, and the values are in agreement with those found in $K_6Mo_7O_{24}.4H_2O$ [4] and $(NH_4)_6Mo_7O_{24}.4H_2O$ according to Evans.[3] With regard to the distances given by Shimao,[2] there seems to be some discrepancy between values given and values computed from the parameters listed, thus making a relevant comparison difficult.

The $MoO_6$-octahedra are somewhat distorted from an ideal octahedron with Mo − O distances in three ranges depending on coordination number: 1.67 − 1.76 Å, 1.88 − 2.01 Å, and 2.11 − 2.33 Å for oxygen atoms coordinated to one, to two, and to three or four Mo atoms, respectively. In each octahedron there are two short, two intermediate, and two long Mo − O distances. Such regularities have been found previously in the structure determinations of the ammonium[3] and potassium[4] analogues, as well as in $MoO_3$[15] and $Na_6Mo_5P_2O_{23}(H_2O)_{13}$.[5] The $MoO_6(6)$ octahedron is an exception in that the three kinds of distances fall in the ranges mentioned, but the coordination is to two, three, and four Mo-atoms, respectively. The Mo − O distances Mo5 − O(56) and Mo7 − O(67) [2.52(2) and 2.60(2) Å] fall outside the ranges mentioned, and these oxygen atoms seem to be more strongly bonded to Mo6 than to Mo5 and Mo7 [distances to Mo6 1.76(2) and 1.75(2) Å]. Distances and angles in the $Mo_7O_{24}^{6-}$-group are collected in Table 4.

*The sodium arrangement around and between the $Mo_7O_{24}^{6-}$-groups.* The $Mo_7O_{24}^{6-}$-group has twelve unshared oxygen atoms. $Na^+$-ions are coordinated to nine of these and to three of the shared ones. A stereoscopic view of this coordination is shown in Fig. 5. The total number of $Na^+$-ions in the figure is eleven, since of the six crystallographically different $Na^+$-ions in the structure, Na3 is coordinated to three groups at the same time, Na1, Na2, and Na4 to two groups, and Na5 and Na6 to one group only. In this way the $Na^+$-ions act as links in O − Na − O bridges, connecting $Mo_7O_{24}^{6-}$-groups in the
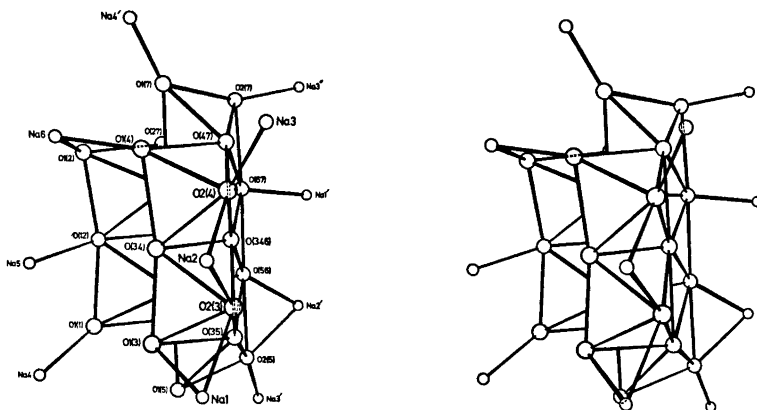
*Fig. 5.* A stereoscopic view of the $Na^+$-coordination around an $Mo_7O_{24}{}^{6-}$-anion. The anion is visualized as a polyhedron with spheres representing oxygen atoms.

$x$-, $y$-, and $z$-directions and forming a three-dimensional network. They also take part in $O-Na-H_2O-Na-O$ linkages. In Fig. 3 a schematic drawing of all the $O-Na-O$ bridges between $Mo_7O_{24}{}^{6-}$-groups is shown.

*The sodium-oxygen arrangement.* Each $Na^+$-ion is octahedrally surrounded by water and group oxygen atoms. The types of octahedra thus obtained may be written $NaO_x(H_2O)_{6-x}$, and there are four kinds of such arrangements in the structure, one with $x=1$, two with $x=2$, two with $x=3$, and one with $x=4$. The sodium-oxygen octahedra are all coupled together to form a double-chain arrangement by sharing edges and corners. This double-chain lies along the $y$-axis as shown in Fig. 4.

The repetition units in the two strings of the double-chain have the compositions $Na_3O_7(H_2O)_{4.5}$ and $Na_3O_5(H_2O)_{8.5}$. In Fig. 4 these repetition units are marked with thick lines. As can be seen from the figure, all three octahedra in the first unit are coupled together by sharing edges, and the connection between units is also achieved in this way. The octahedra in this unit are of the types $x=3$, 4, and 3 and with the sodium ions denoted Na1, Na2, and Na3, respectively.

In the second unit two octahedra are coupled together by sharing an edge, and the third one is connected through a shared corner. Coupling between the units is achieved by shared corners. The sodium ions in this unit are denoted Na4, Na5, and Na6, with octahedra of types $x=2$, 1, and 2, respectively.

Above and below the double-chain shown in Fig. 4 there are symmetry related chains on half a unit cell distance in $x$, and with hydrogen bonds as the only contacts. Between two different repetition units a shared water oxygen atom [Aq (36)] forms the only connection, apart from hydrogen bonds.

The sodium-oxygen octahedra are quite distorted in an irregular way, with the most distorted one, that around Na2, being close to trigonal prism. This occurs since four of its oxygen atoms are donated by two $Mo_7O_{24}{}^{6-}$-groups, which dominate the coordination figure. The $Na-O$ distances are in

*Table 6.* Distances (Å) within the sodium-oxygen octahedra. The designation of the atoms is explained in Table 1. The estimated standard deviations are given in parentheses and refer to the last decimal place given.

| | O1(3) | O2(3) | O(67) | Aq(12) | Aq1(13) | Aq2(13) |
|---|---|---|---|---|---|---|
| Na1 | 2.73(3) | 2.64(2) | 2.45(2) | 2.33(3) | 2.39(3) | 2.35(3) |
| O1(3) | | 2.69(2) | | 3.10(3) | 3.95(3) | 3.60(3) |
| O(67) | | 4.05(3) | | 3.70(2) | 3.54(3) | 3.46(4) |
| O2(3) | | | | 3.09(3) | | 3.58(2) |
| Aq1(13) | | | | 3.64(3) | | 3.27(4) |

| | O2(3) | O2(4) | O2(5) | O(56) | Aq(12) | Aq(2) |
|---|---|---|---|---|---|---|
| Na2 | 2.47(3) | 2.50(3) | 2.46(2) | 2.33(2) | 2.38(2) | 2.26(3) |
| O2(3) | | 3.16(2) | | 3.32(3) | 3.09(3) | |
| O2(4) | | | 3.27(4) | | | 3.38(4) |
| O2(5) | | | | 2.74(2) | | 3.26(3) |
| Aq(12) | | | | 3.11(2) | | 3.12(3) |

| | O2(4) | O2(5) | O2(7) | Aq1(13) | Aq2(13) | Aq(36) |
|---|---|---|---|---|---|---|
| Na3 | 2.55(3) | 2.44(2) | 2.48(2) | 2.43(2) | 2.59(3) | 2.43(3) |
| O2(4) | | 3.27(4) | 3.79(3) | | 3.91(3) | 3.08(3) |
| Aq1(13) | | 3.71(3) | 3.59(2) | | 3.27(4) | 3.49(4) |
| O2(5) | | | 3.10(2) | | | 3.51(4) |
| Aq2(13) | | | 3.68(4) | | | 3.75(3) |

| | O1(1) | O1(7) | Aq(4) | Aq1(45) | Aq2(45) | Aq(46) |
|---|---|---|---|---|---|---|
| Na4 | 2.35(2) | 2.38(3) | 2.33(3) | 2.36(2) | 2.44(2) | 2.51(3) |
| O1(1) | | 3.53(3) | 3.13(3) | 3.01(2) | 3.42(3) | |
| Aq(4) | | 3.35(4) | 3.31(3) | 3.68(3) | 3.45(3) | |
| O1(7) | | | | 3.50(3) | 3.62(4) | |
| Aq1(45) | | | | 3.32(3) | 3.24(3) | |

| | O(12) | Aq1(5) | Aq2(5) | Aq1(45) | Aq2(45) | Aq(56) |
|---|---|---|---|---|---|---|
| Na5 | 2.43(2) | 2.37(3) | 2.38(2) | 2.47(2) | 2.47(2) | 2.40(2) |
| O(12) | | 3.36(3) | | 4.00(3) | 3.98(2) | 3.11(3) |
| Aq1(5) | | | 3.11(4) | 3.27(3) | 3.61(4) | 3.01(3) |
| Aq2(5) | | | | | 3.19(3) | 3.94(3) |
| Aq1(45) | | | | | 3.32(3) | 3.16(2) |

| | O1(2) | O1(4) | Aq(36) | Aq(46) | Aq(56) | Aq(6) |
|---|---|---|---|---|---|---|
| Na6 | 2.67(3) | 2.51(2) | 2.48(2) | 2.39(3) | 2.35(2) | 2.42(4) |
| O1(2) | | 3.61(3) | 3.77(4) | 3.59(3) | 3.35(3) | |
| Aq(6) | | 3.54(4) | 3.30(4) | 3.48(5) | 3.47(4) | |
| O1(4) | | | | 3.85(3) | 3.10(2) | |
| Aq(36) | | | | 3.49(3) | 3.29(3) | |

the range $2.29-2.71$ Å and there is no significant difference in distances from Na to water oxygen or group oxygen atoms. These distances are comparable to the distances found in $Na_6Mo_5P_2O_{23}(H_2O)_{13}$ [5] and $Na_4H_2Mo_5P_2O_{23}(H_2O)_{10}$.[6] Distances within the sodium-oxygen octahedra are listed in Table 6.

*The "free" water molecule.* The structure also includes a water molecule which is not coordinated to any $Na^+$-ion, but which is probably bonded by hydrogen bonds. It is situated at about the same distance from three $Mo_7O_{24}{}^{6-}$-groups and has five nearest neighbour oxygen atoms at distances of $2.68-2.91$ Å. Of these, three are water oxygen atoms [Aq1(13), Aq(36) and Aq2(5)] and two group oxygen atoms [O(47) and O1(5)]. The distances to other atoms are longer than 3.29 Å.

## REFERENCES

1. Lindqvist, I. *Arkiv Kemi* **2** (1950) 325.
2. Shimao, E. *Bull. Chem. Soc. Japan* **40** (1967) 1609.
3. Evans, H. T., Jr. *J. Am. Chem. Soc.* **90** (1968) 3275.
4. Gatehouse, B. M. and Leverett, P. *Chem. Commun.* **15** (1968) 901.
5. Strandberg, R. *Acta Chem. Scand.* **27** (1973) 1004.
6. Hedman, B. *Acta Chem. Scand.* **27** (1973) 3335.
7. Johansson, G., Pettersson, L. and Ingri, N. *To be published.*
8. *International Tables for X-Ray Crystallography*, Kynoch Press, Birmingham 1965, Vol I.
9. Ivarsson, G., Lundberg, B. K. S. and Ingri, N. *Acta Chem. Scand.* **26** (1972) 3005.
10. Lindgren, O., Lindqvist, O. and Nyborg, J. *Acta Chem. Scand.* **24** (1970) 732.
11. Johnson, C. K. ORTEP. Report ORNL-3794, Oak Ridge National Laboratory, Oak Ridge, Tennessee.
12. Coppens, P. and Hamilton, W. C. *Acta Cryst.* **A 26** (1970) 71.
13. Cromer, D. T. and Waber, J. T. *Acta Cryst.* **18** (1965) 104.
14. *International Tables for X-Ray Crystallography*, Kynoch Press, Birmingham 1962, Vol. III.
15. Kihlborg, L. *Arkiv Kemi* **21** (1963) 357.

# A New Method for Specific Degradation of Polysaccharides

LENNART KENNE, JÖRGEN LÖNNGREN and
SIGFRID SVENSSON

*Department of Organic Chemistry, Arrhenius Laboratory, University of Stockholm,
S-104 05 Stockholm, Sweden*

A new method for the specific degradation of polysaccharides
is presented. It involves the preparation of a methylated poly-
saccharide containing a limited number of free hydroxyl groups, at
defined positions, oxidation of these to carbonyl groups by ruthenium
tetraoxide and subsequent β-elimination by treatment with base.
Analysis of the degraded product provides evidence concerning the
sequence of sugar residues in the original polysaccharide. The utility
of the method is demonstrated with two polysaccharides of known
structures, the lipopolysaccharide from *Salmonella typhimurium* LT2
and the capsular polysaccharide from *Klebsiella* type 47.

It is possible to prepare methylated polysaccharides with a limited number of free hydroxyl groups, by using suitable selective procedures. Suitable methods are the acid hydrolysis of furanosidic or other acid labile linkages, sulphone degradation[1] or base-catalysed elimination of pyranosidouronate residues.[2,3] Oxidation with ruthenium tetraoxide[4] would then give carbonyl groups, and methoxyl or glycosyl residues in β-positions to these would be eliminated on treatment with base. A carbonyl group at the 3-position would lead to cleavage of the glycosidic linkage. Analysis of the degraded product should give information on the sequence of sugar residues in the original polysaccharide. We have recently studied the β-elimination with model substances of low-molecular weight[5-7] and demonstrated that the elimination goes to completion. We now report the application of this degradation method to two bacterial polysaccharides of known structure.

## RESULTS AND DISCUSSION

The O-specific side chains in the lipopolysaccharide (LPS) from *Salmonella typhimurium* LT2 are composed of repeating units with the structure I. The D-glucose connected with a dotted arrow is only present in some of the repeating units. Some of the abequose residues are acetylated at C-2. This structure has been demonstrated by chemical[8,9] and biosynthetic[10] studies. The LPS was fully methylated by the Hakomori procedure.[11] Part of the product was

hydrolysed and the mixture of partially methylated sugars was analysed by GLC – MS [12] (Table 1, column A). This analysis was in accordance with that of previous investigations.[8] The methylated LPS was subjected to mild acid hydrolysis and the polysaccharide, free from lipid and components of low-molecular weight, was recovered by gel filtration. Part of this product was methylated using trideuteriomethyl iodide, hydrolysed and analysed (Table 1, column B). Most of the 4,6-di-$O$-methyl-D-mannose now appeared as 3,4,6-tri-$O$-methyl-D-mannose, with a trideuteriomethyl group at the 3-position, demonstrating that most of the abequose residues had been hydrolysed off. The only free hydroxyl groups in the recovered polysaccharide are consequently those at the 3-position of the mannose residue. The product was oxidised with ruthenium tetraoxide, thus transforming the secondary alcohol groups into keto groups.

The oxidised polysaccharide was treated with sodium ethoxide in ethanol-dichloromethane and part of the product was hydrolysed and analysed (Table 1, column C). This analysis indicated that the oxidation was virtually complete, as the percentage of 4,6-di-$O$-methyl-D-mannose was approximately the same as after trideuteriomethylation of the mild acid degraded polysaccharide (Table 1, column B). Another portion of the degraded material was trideuterio-methylated and hydrolysed. Analysis of this material (Table 1, column D) showed that most of the 2,3-di-$O$-methyl-L-rhamnose now appeared as 4-$O$-trideuteriomethyl-2,3-di-$O$-methyl-L-rhamnose. This demonstrates that, in

Table 1. Methylation analyses of the original and modified *S. typhimurium* LT2 poly-saccharides.

| Methylated sugar[a] | $T^b$ | Mol %[c] | | | |
|---|---|---|---|---|---|
| | | A | B | C | D |
| 2,4-Abe[d] | 0.32 | 8 | 1 | 1 | < 1 |
| 2,3,4 CD$_3$-Rha[d] | 0.46 | – | – | – | 32 |
| 2,3-Rha[e] | 0.98 | 20 | 22 | 34 | 2 |
| 2,3,4,6-G[e] | 1.00 | 14 | 17 | 20 | 33 |
| 2,3,4,6-Gal | 1.25 | 2 | 3 | 2 | 3 |
| 3 CD$_3$, 4,6-Man | 1.95 | – | 23 | – | – |
| 2,4,6-Man | 2.09 | 2 | – | – | – |
| 2,4,6-Gal | 2.28 | 12 | 14 | 15 | 10 |
| 3,4,6-Gal | 2.50 | 2 | 1 | 2 | 1 |
| 4,6-Man | 3.29 | 22 | 2 | 3 | < 1 |
| 2,6-Gal | 3.62 | 15 | 15 | 21 | 17 |
| 3,6-G | 4.30 | 1 | 1 | 1 | 1 |
| 2,4-G | 5.10 | 3 | 1 | 2 | 1 |

[a] 2,4-Abe = 2,4-di-$O$-methyl-abequose, 2,3,4 CD$_3$-Rha = 2,3-di-$O$-methyl-4-mono-$O$-trideuterio-methyl-L-rhamnose, *etc.* [b] Retention time of the corresponding alditol acetate relative to 1,5-di-$O$-acetyl-2,3,4,6-tetra-$O$-methyl-D-glucitol on an ECNSS-M column at 170°. [c] A: original poly-saccharide; B: methylated, acid degraded and trideuteriomethylated polysaccharide (see text); C: methylated, acid degraded, oxidised and alkali treated polysaccharide (see text); D: methyl-ated, acid degraded, oxidised, alkali treated and trideuteriomethylated polysaccharide (see text). [d] Part of this volatile ether and its corresponding alditol acetate was probably lost during the work up procedure. [e] These components were separated on an OV-225 SCOT column, on which they showed $T$ 0.92 and 1.00, respectively.

the original polysaccharide, the D-mannose residue was linked to the L-rhamnose at position 4. The stoichiometry of the latter analysis (Table 1, column D) is not very good. This may be due to non-sugar components and to losses of volatile L-rhamnose derivatives. This, however, does not affect the interpretation of the results, which are in agreement with previous results,[10] obtained by other methods. The different steps in the degradation are depicted in Scheme 1. It is assumed, in this scheme, that all positions in the sugar residues are methylated unless otherwise indicated.
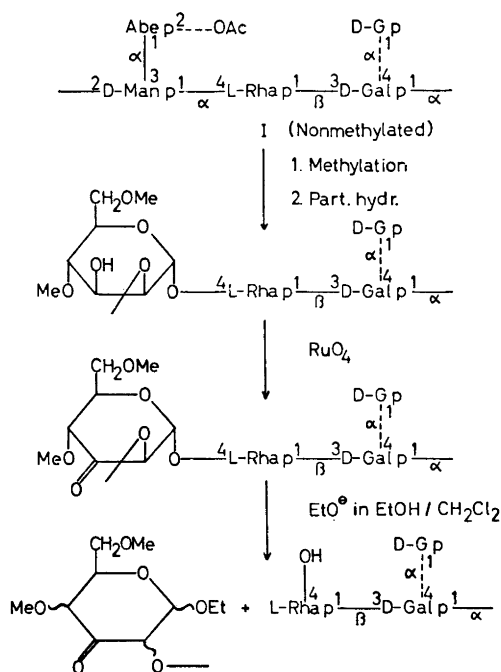


*Scheme 1.*

The capsular polysaccharide elaborated by *Klebsiella* type 47 is composed of tetrasaccharide repeating units, the structure of which (II) has recently been determined.[13] On treatment of the fully methylated polysaccharide with base followed by mild acid hydrolysis, the side chains are eliminated and a linear, methylated polysaccharide with free hydroxyls at position 3 in the L-rhamnose residues can be recovered.[2] Methylation analysis of the original and degraded polysaccharide (Table 2, column A and B) demonstrated that the degradation was essentially complete. The degraded polysaccharide was oxidised with ruthenium tetraoxide and treated with sodium ethoxide in ethanol-dichloromethane. Part of the product was hydrolysed and analysed (Table 2, column C). The presence of some 2-O-methyl-L-rhamnose in the hydrolysate of this material indicates that some 20 % of the L-rhamnose

*Table 2.* Methylation analyses of the original and modified *Klebsiella* type 47 polysaccharides.

| Methylated sugar[a] | $T^b$ | Mol %[c] | | | |
|---|---|---|---|---|---|
| | | A | B | C | D |
| 2,3,4-Rha[d] | 0.46 | 19 | 3 | 4 | 1 |
| 2,3 CD₃-Rha | 0.98 | — | 51 | — | — |
| 2,3 Et-Rha | 0.92 | — | — | — | 11 |
| 2,3 Et, 4,6-Gal | 1.23 | — | — | — | 77 |
| 2-Rha | 1.52 | 32 | 2 | 17 | — |
| 2,4,6-Gal | 2.28 | 27 | 44 | 80 | 11 |
| 2,3-G | 5.39 | 22 | — | — | — |

[a] See Table 1, note *a*. [b] See Table 1, note *b*. [c] A: original polysaccharide, carboxyl-reduced after methylation; B: methylated polysaccharide, degraded at the uronic acid residue and trideuteriomethylated (see text and Ref. 2); C: methylated, degraded, oxidised and alkali treated polysaccharide (see text); D: methylated, degraded, oxidised, alkali treated and ethylated polysaccharide (see text). [d] See Table 1, note *d*.

residues were not oxidised. On prolonged oxidation, some methoxyls were converted into formate ester groups. Another portion of the product was ethylated, hydrolysed and analysed (Table 2, column D). The presence of 3-*O*-ethyl-2-*O*-methyl-L-rhamnose, and a comparable amount of 2,4,6-tri-*O*-methyl-D-galactose, supports the assumption that some L-rhamnose residues had not been oxidised. The main product, however, was 3-*O*-ethyl-2,4,6-tri-*O*-methyl-D-galactose, demonstrating that the branching L-rhamnose residues are linked to the 3-position of the D-galactose residues in the original polysaccharide. The consecutive degradations depicted in Scheme 2, leaving essentially only the D-galactose residue intact, afford chemical evidence for the presence of a repeating unit in this polysaccharide. It is assumed, in this scheme, that all positions in the sugar residues are methylated unless otherwise indicated. Similar evidence for other capsular polysaccharides has previously been obtained by biosynthetic studies [14] and by hydrolysis with phage-induced enzymes.[15,16]

In the examples discussed above, a free hydroxyl was generated at C-3 in a sugar residue of a polysaccharide. The glycosidic linkage of that residue was then cleaved by oxidation, followed by base-catalysed elimination. Secondary alcoholic hydroxyls may, however, also be liberated in 2- or 4-positions in glycopyranosides. By the same sequence of reactions, the substituent at C-4 or C-2, respectively, would be eliminated. If a methylated sugar residue is eliminated, the reducing sugar thus formed can be subjected to a second elimination,[17] thus providing further structural evidence. Additional information may be obtained by degradation of unsaturated carbonyl sugar by mild acid hydrolysis with concomitant release of substituents other than those in the β-position to the carbonyl group.[18]

The oxidation with ruthenium tetraoxide was performed in a two-phase system, with the methylated polysaccharide in dichloromethane and ruthenium dioxide-periodate in water.[4] The latter system generates ruthenium tetra-

*Scheme 2.*

oxide, which dissolved in the organic phase. During the oxidation, black ruthenium dioxide is formed. When the rate of oxidation decreases, both phases turn yellow, as almost all ruthenium is present as ruthenium tetraoxide. Prolonged oxidation should be avoided as methoxyl groups may be oxidised into formate esters groups.[18] We have also found that acetylated $\beta$-glucopyranosides may be oxidised into 5-hexosulosonates,[19] as has been observed with chromic trioxide in acetic acid [20] and with ozone.[21]

The two-phase oxidation has another advantage as it prevents the formation of ruthenium dioxide on to which the polysaccharide may be adsorbed, thereby preventing complete oxidation.

The presented degradation method permits the step-wise elimination of sugar residues in a methylated polysaccharide, thus providing a method which, in combination with methylation analysis, should be valuable for sequencing large structural entities.

## EXPERIMENTAL

*General methods.* Concentrations were performed under diminished pressure, at bath temperatures not exceeding 40°. For GLC, a Perkin-Elmer 900 instrument, fitted with flame-ionisation detectors, was used. Separations were performed on (a) glass-columns (190 × 0.15 cm) containing 3 % ECNSS-M on Gas Chrom Q (100 − 120 mesh) at 170°, (b) OV-225 SCOT columns (15 m × 0.5 mm) at 190°. For quantitative evaluations of the GLC, a Hewlett Packard 3370 B integrator was used. For GLC − MS a Perkin-Elmer 270 instrument and the same columns as above were used.

# Sequential degradation of the LPS from *S. typhimurium* LT 2

*Methylation.* LPS [8] (60 mg) in dimethyl sulphoxide (20 ml) was treated with 2 M methylsulphinyl anion (20 ml) under nitrogen. The resulting solution was agitated ultrasonically for 30 min and then kept for 4 h at room temperature. Methyl iodide (10 ml) was then added dropwise with external cooling. The turbid solution was agitated ultrasonically for 30 min, giving a clear solution. Methyl iodide was then distilled off and the solution was dialysed against running tap water overnight and then against distilled water overnight. The resulting suspension was freeze-dried giving methylated LPS (73 mg). A sample (3 mg) was hydrolysed, transformed into alditol acetates and analysed by GLC − MS [12] (Table 1, column A).

*Partial acid hydrolysis.* Methylated LPS (70 mg) was treated with 50 % aqueous acetic acid (90 ml) for 14 h on a boiling water bath. The solution was evaporated to dryness and the product was fractionated on a Sephadex LH 20 column (28 × 3 cm) using chloroform-acetone (3:1) as irrigant. The separation was monitored polarimetrically. The modified polysaccharide (30 mg) was eluted with the void volume. Part of the product was trideuteriomethylated and analysed as described earlier (Table 1, column B). The partially methylated alditol acetate with a trideuteriomethoxyl group gave a mass spectrum in which fragments containing this group were shifted by three mass units.

*Oxidation.* Methylated partially hydrolysed polysaccharide (10 mg) in dichloromethane (3 ml) was treated with 0.08 M ruthenium tetraoxide in dichloromethane (8 ml). After addition of a saturated aqueous solution of sodium metaperiodate the reaction mixture was shaken vigorously until the solution became yellow ($\simeq$ 15 min). The aqueous layer was separated and the organic phase was washed with water (4 × 5 ml) and evaporated to dryness.

*Alkaline degradation.* The oxidised material from above was dissolved in dichloromethane (4 ml) and ethanolic 1 M sodium ethoxide (2 ml) was added. The reaction mixture was kept at room temperature for 30 min and then evaporated. The material was divided into two portions. One was hydrolysed and the sugars were analysed as before (Table 1, column C). The other portion was reetherified using trideuteriomethyl iodide, hydrolysed and analysed as before (Table 1, column D).

# Sequential degradation of the capsular polysaccharide from *Klebsiella* type 47

*Methylation and elimination of the uronosylic residue and isolation of the degraded polysaccharide* was performed as earlier described [2] (Table 2, column A and B).

*Oxidation* of a 10 mg sample of methylated, degraded polysaccharide was performed as described above.

*Alkaline degradation.* The oxidised material was dissolved in dichloromethane (4 ml) and ethanolic 1 M sodium ethoxide (2 ml) for 30 min, neutralised with acetic acid and evaporated. The material was divided into two portions. One was hydrolysed and the sugars analysed as before (Table 2, column C). The other portion was reetherified using ethyl iodide, hydrolysed and analysed as before (Table 2, column D). The partially methylated and ethylated alditol acetate gave a mass spectrum in which fragments containing an ethoxy group were shifted fourteen mass units.

# REFERENCES

1. Lindberg, B. and Lundström, H. *Acta Chem. Scand.* **20** (1966) 2423.
2. Lindberg, B., Lönngren, J. and Thompson, J. L. *Carbohyd. Res.* **28** (1973) 351.
3. Aspinall, G. O. and Barron, P. E. *Can. J. Chem.* **50** (1972) 2203.
4. Beynon, P. J., Collins, P. M., Doganges, P. T. and Overend, W. G. *J. Chem. Soc.* **C** **1966** 1131.
5. Kenne, L. and Svensson, S. *Acta Chem. Scand.* **26** (1972) 2144.
6. Kenne, L., Larm, O. and Svensson, S. *Acta Chem. Scand.* **26** (1972) 2473.
7. Kenne, L., Larm, O. and Svensson, S. *Acta Chem. Scand.* **27** (1973) 2797.
8. Hellerqvist, C. G., Lindberg, B., Svensson, S., Holme, T. and Lindberg, A. A. *Carbohyd. Res.* **9** (1969) 237.
9. Hellerqvist, C. G., Larm, O., Lindberg, B. and Lindberg, A. A. *Acta Chem. Scand.* **25** (1971) 744.
10. Robbins, P. W. and Wright, A. *Microbial toxins*, Academic, New York 1971, Vol. 4, p. 351.
11. Hakomori, S. *J. Biochem. (Tokyo)* **55** (1964) 205.
12. Björndal, H., Hellerqvist, C. G., Lindberg, B. and Svensson, S. *Angew. Chem. Int. Ed.* **9** (1970) 610.
13. Björndal, H., Lindberg, B., Lönngren, J. Rosell, K.-G. and Nimmich, W. *Carbohyd. Res.* **27** (1973) 373.
14. Troy, F. A., Frerman, F. E. and Heath, E. C. *J. Biol. Chem.* **246** (1971) 118.
15. Sutherland, I. W. and Wilkinson, J. F. *Biochem. J.* **110** (1968) 749.
16. Yurewicz, E. C., Ghalambor, M. A. and Heath, E. C. *J. Biol. Chem.* **246** (1971) 5596.
17. Anet, E. F. L. J. *Chem. Ind. (London)* **1963** 1035.
18. Kenne, L., Rosell, K.-G. and Svensson, S. *Unpublished results.*
19. Hoffman, J., Kenne, L. and Svensson, S. *Unpublished results.*
20. Angyal, S. J. and James, K. *Aust. J. Chem.* **23** (1970) 1209.
21. Deslongchamps, P. and Moreau, C. *Can. J. Chem.* **49** (1971) 2465.

# Deamination of Methyl 2-Amino-2-deoxy-α- and -β-D-glucopyranosides

CHRISTINA ERBING, BENGT LINDBERG and
SIGFRID SVENSSON

*Department of Organic Chemistry, Arrhenius Laboratory, University of Stockholm*
*S-104 05 Stockholm, Sweden*

Deamination of methyl 2-amino-2-deoxy-α-D-glucopyranoside yields a mixture (3:1) of 2,5-anhydro-D-mannose and methyl 2-deoxy-2-C-formyl-D-*arabino*-pentofuraroside. The latter substance is readily epimerized to the D-*ribo*-isomer. Analogous results are obtained in the β-series.

The deamination of 2-amino-2-deoxy-D-glucose was first investigated by Ledderhose in 1880,[1] although it was not until later that the product was identified as 2,5-anhydro-D-mannose. This reaction and the deamination of 2-amino-2-deoxy-D-glucopyranosides have subsequently been studied by several groups, and have recently been reviewed by Defaye.[2] The deamination reaction has also been used for the controlled degradation of polysaccharides (*e.g.* Ref. 3) and glycoproteins [4] containing 2-amino-2-deoxy-D-glucopyranose residues. With the aim of using this reaction for the same purpose, we have reinvestigated the deamination of methyl 2-amino-2-deoxy-α- and -β-D-glucopyranoside.

## RESULTS AND DISCUSSION

The deamination was performed with sodium nitrite at pH 3.5 and the product was reduced with sodium borohydride or sodium borodeuteride. The reduced product was acetylated before the analysis by GLC-MS. The results are shown in Table 1. The 2,5-anhydro-D-mannitol tetra-acetate (1) gave the expected MS and NMR-spectrum. The origins of the major fragments in the MS are indicated in Scheme 1. (Figures in brackets refer to the compound monodeuteriated at C-1.)

On deamination, followed by reduction and acetylation, the α- and β-glycoside each yielded two components which were faster, on GLC, than *1*. The MS of these four components were almost identical. The fragmentation

Table 1. Products formed by deamination and reduction of methyl 2-amino-2-deoxy-α-
and -β-D-glucopyranosides.

| Products | T-value[a] | | Yield (mol %) | |
| --- | --- | --- | --- | --- |
| | OV-225 | ECNSS-M | Me-α-GNH$_2$[b] | Me-β-GNH$_2$ |
| 2,5-Anhydro-D-mannitol | 1.51 | 1.95 | 73 | 84 |
| Methyl 2-deoxy-2-$C$-hydroxymethyl-α-D-*ribo*-pentofuranoside | 0.69 | 0.79 | | |
| Methyl 2-deoxy-2-$C$-hydroxymethyl-α-D-*arabino*-pentofuranoside | 0.69 | 0.85 | 27 | |
| Methyl 2-deoxy-2-$C$-hydroxymethyl-β-D-*ribo*-pentofuranoside | 0.74 | 0.90 | | |
| Methyl 2-deoxy-2-$C$-hydroxymethyl-β-D-*arabino*-pentofuranoside | 0.76 | 0.99 | | 16 |

[a] T-values for the corresponding sodium borohydride-reduced acetates relative to L-fucitol pentaacetate. [b] Me-α-GNH$_2$ = Methyl 2-amino-2-deoxy-α-D-glucopyranoside.
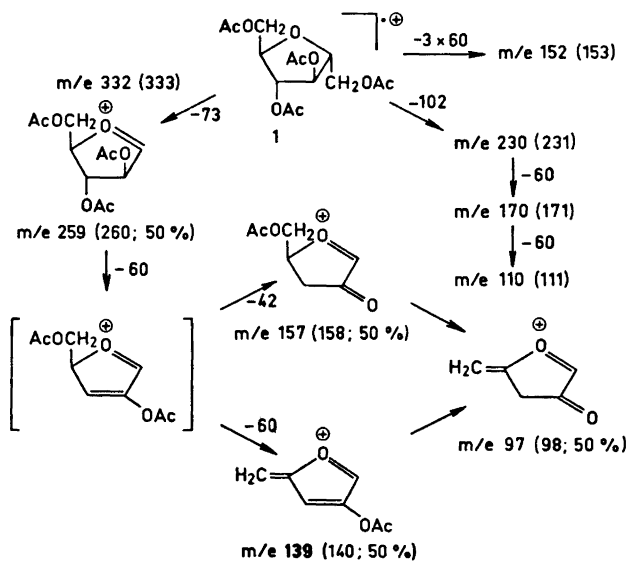


Scheme 1.

pattern is identical with that expected for an acetylated methyl 2-deoxy-2-$C$-hydroxymethyl-pentofuranoside (Scheme 2). (Figures in brackets refer to the compound monodeuteriated at the 2-$C$-acetoxymethylgroup.)

The mixture of the two isomeric methyl α-2-deoxy-2-$C$-hydroxymethyl-pentofuranoside acetates was isolated by chromatography on silicic acid. The
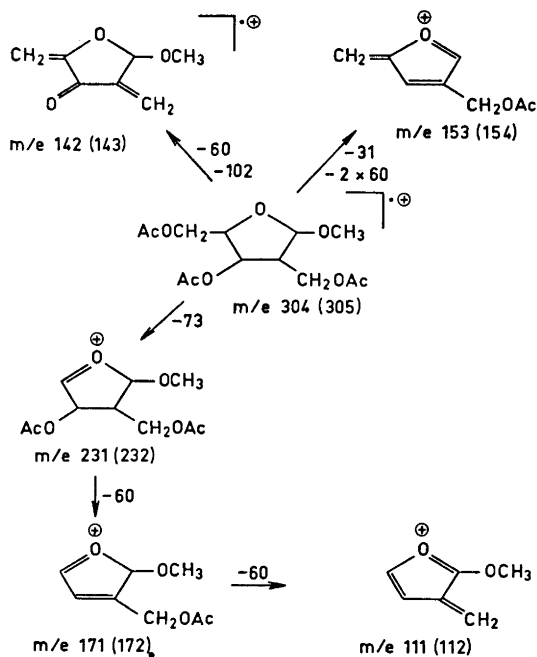
*Scheme 2.*

NMR spectrum of this mixture showed the presence of acetoxyl protons, methoxyl protons, and other protons in the relative proportions 9:3:8 in agreement with the postulated structures. Part of the isolated mixture was hydrolysed, reduced with sodium borohydride or sodium borodeuteride and acetylated. GLC revealed only one alditol-acetate (ECNSS-M or OV 225). The MS demonstrated that it was a fully acetylated 2-deoxy-2-*C*-hydroxy-methyl-pentitol *(2)*. The primary fragmentation of the compound is indicated in formula *2*.
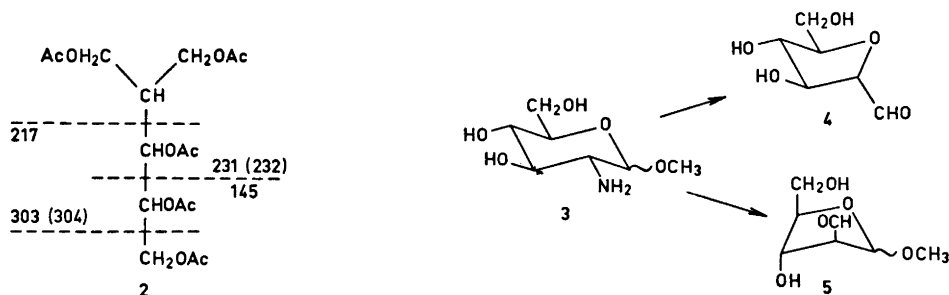
The formation of these products in analogous to the deamination of amino-cyclohexane derivatives, wherein a stereospecific rearrangement resulting from the attack on the diazonium ion by the group *trans* and antiparallel to this is observed.[5] For the methyl 2-amino-2-deoxy-D-glucopyranosides (3), attack by the ring oxygen gives 2,5-anhydro-D-mannose *(4)*, whereas attack by the carbon atom, C-4, with retention of the configuration, gives methyl 2-deoxy-2-C-formyl-D-*arabino*-furanoside *(5)*.

The latter reaction is similar to the deamination of methyl 3-amino-3-deoxy-α-D-glucopyranoside *(6)* yielding methyl 3-deoxy-3-C-formyl-α-D-*xylo*-furanoside which cyclises to the cyclic hemiacetal *7*.[6]
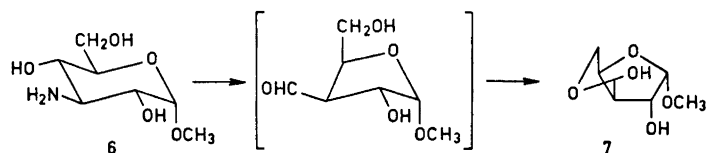


When methyl 3-acetamido-3,6-dideoxy-2-O-methanesulphonyl-α-L-gluco-pyranoside *(8)* was heated with methoxide, a similar ring contraction, yielding compounds *9* and *10*, was observed.[7]
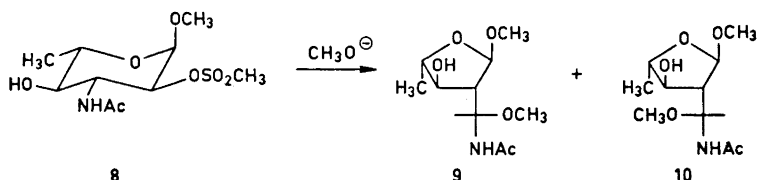


For both the α- and the β-anomer of *3* the component *5* after reduction consisted of 2 isomers. When the deamination and the reduction of either the α- or β-isomer were performed in $D_2O$ using sodium borodeuteride as reducing agent, MS showed that the minor slower moving isomer contained two deuterium atoms. It therefore seems probable that the slower moving isomer is formed by epimerization of the D-*arabino*-isomer into the D-*ribo*-isomer *(5→11)*. This epimerization probably occurs during the borodeuteride reduction alkaline conditions, but does not reach equilibrium, as only small amounts of deuterium are incorporated in *5*. The total amount of the two isomers was virtually constant but their relative proportions varied in different experiments. The minor component accounted for between 10 and 40 % of the total amount.
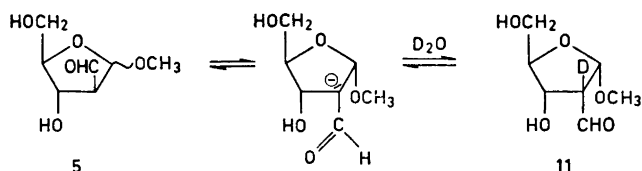
The formation of *1* (73 %) and *3* (27 %) (including epimerized component) by deamination of methyl 2-amino-2-deoxy-α-D-glucopyranoside accounted for all the starting material. The corresponding figures for the β-series were 84 % of *1* and 16 % of *3* (including epimerized component).

When the deamination reaction is applied to the controlled degradation of a polysaccharide containing 2-amino-2-deoxy-D-gluco-pyranose residues, the reaction will presumably follow the same two routes as observed for the low-molecular weight glycosides. The 2-amino-2-deoxy-D-glucopyranosidic linkages will, however, only be cleaved by the major pathway. This should not diminish the value of the method as the linkages of the 2-deoxy-2-*C*-formyl-furanose residues, or the corresponding reduced residues, are labile to acid hydrolysis and will be cleaved under conditions which leave ordinary glycosidic linkages virtually unaffected.

## EXPERIMENTAL

*General methods.* Concentrations were performed under diminished pressure, at bath temperatures not exceeding 40°. For GLC, a Perkin-Elmer 900 instrument, equipped with flame-ionisation detectors, was used. The separations were performed on glass columns (180 × 0.15 cm) packed with (a) 3 % OV 225 on Gas Chrom Q (100 − 200 mesh), (b) 3 % ECNSS-M on Gas Chrom Q (100 − 200 mesh) or (c) 3 % UC W-98 on Chromosorb Q (80 − 100 mesh) at 190°C. For quantitative evaluations of the GLC, a Hewlett Packard 3370 B integrator was used. For GLC-MS, a Perkin-Elmer 270 combined GLC-MS instrument fitted with the appropriate column was used. Mass spectra were recorded at an ionisation potential of 70 eV, an ionisation current of 80 $\mu$A and an ion source temperature of 80°C. NMR was recorded on a Varian A 60 A using tetramethyl-silane as reference.

*Deacetylation of methyl 2-acetamido-2-deoxy-α-D-glucopyranoside.* Methyl 2-acetamido-2-deoxy-α-D-glucopyranoside (78.0 mg) and L-fucitol (75.0 mg, internal standard) were added to a solution of $Ba(OH)_2.6H_2O$ (1.0 g) in deaerated water (10 ml). The resulting mixture was heated in a sealed steel ampoule for 4 h at 135°C under nitrogen. The reaction mixture was then cooled and neutralised with carbon dioxide. After filtration, the water solution was concentrated to dryness. Part of the product ($\simeq$ 5 mg) was dissolved in water (5 ml) and passed through a column of Dowex 50 ($H^+$). The eluate was concentrated to dryness, acetylated and analysed by GLC (column C). This analysis showed only fucitol pentaacetate. Another part of the deacetylated product was reacetylated and analysed by GLC (column C). This analysis demonstrated that all methyl 2-acetamido-2-deoxy-D-glucopyranoside appeared on reacetylation.

*Treatment of methyl 2-amino-2-deoxy-α and -β-D-glucopyranoside with nitrous acid.* Methyl 2-acetamido-2-deoxy-α- or -β-D-glucopyranoside ($\simeq$ 10 mg, accurately weighed) and L-fucitol ($\simeq$ 10 mg, accurately weighed) was deacetylated as above. The deacetylated product was dissolved in a sodium acetate buffer (1 ml, 8 M; pH 3.5) and mixed with an equal volume of sodium nitrite in water (2 % w/v). The solution was kept at room temperature overnight. To the reaction mixture was then added an excess of sodium borohydride or borodeuteride and after 18 h the solution was adjusted to pH 3.0 by the addition of acetic acid. The mixture was then concentrated to dryness and boric acid was removed by codistillations with methanol. The reaction product was acetylated and analysed by GLC-MS (columns A and B). In a separate experiment, the deamination and reduction were carried out in $D_2O$. The results of the GLC analyses are given in Table 1. The mass spectra of the two fastest components (Table 1) were virtually identical and displayed peaks at $m/e$ 43(100), 54(10) [55(11)], 69(6) [69(5)], 71(11) [72(6)], 82(5), 87(9) [87(5)], 98(5), 99(12) [100(6)], 100(13) [101(6)], 111(35) [111(9), 112(38)], 142(12) [143(5)], 153(16) [153(4), 154(11)], 171(4) [172(5)], 231(4) [232(4)]. The values for the components which had been reduced with sodium borodeuteride are given in angular brackets. The mass spectra for the two fastest components obtained when the deamination and reduction were carried out in $D_2O$ were identical except for a shift of the peak at $m/e$ 232(233) by

one mass unit. The mass spectrum for the slowest components (Table 1) had peaks at $m/e$ 43(100), 44(3), 69(4) [69(3), 70(2)], 85(2) [85(2), 86(2)], 97(23) [97(10), 98(11)], 110(22) [111(18)], 115(3) [115(2), 116(1)], 139(23) [139(7), 140(8)], 152(8), 153(3) [153(6), 154(2)], 157(3) [157(1), 158(1)], 170(1) [171(1)], 259(3) [259(1), 260(1)].

*Isolation of the reaction products.* Methyl 2-acetamido-2-deoxy-α-D-glucopyranoside (1.6 g) was *N*-deacetylated and treated with nitrous acid as described above. The crude acetylated product was fractionated on a Silica Gel column (50 × 5 cm) using light petroleum — ethyl acetate (2:1 w/v) as irrigant. The separation was monitored by TLC. Two fractions were obtained; I, $R_F = 0.37$ (330 mg) and II, $R_F = 0.31$ (700 mg). GLC-MS analysis showed that fraction I was a mixture of two peracetylated methyl 2-deoxy-2-*C*-hydroxymethyl-pentofuranosides and that II was peracetylated 2,5-anhydrohexitol. The NMR spectrum of fraction I showed peaks at τ 7.90, 6 H, singlet, *O*-acetyl; τ 6.58, 3 H, singlet, *O*-methyl; τ 5.1 — 5.9, 5 H, multiplet, 2 H-1, H-2, H-3 and H-4; a 4.67 — 5.16, 2 H, multiplet, 2 H-6. The NMR spectrum of fraction II had protons at τ 7.88, 12 H, singlet, *O*-acetyl; τ 5.70, 6 H, broad singlet, 2 H-1, H-2, H-3, H-4 and H-5; τ 4.77, 2 H, broad singlet, 2 H-6.

Part of fraction I (5 mg) was hydrolysed with aqueous sulphuric acid (3 ml) at 100° for 1 h. The hydrolysate was neutralised with barium carbonate, filtered and reduced with sodium borohydride or sodium borodeuteride. The reduced product was acetylated and analysed by GLC-MS. The GLC analysis showed only one component with the *T*-value 4.75 on column A and 6.1 on column B. The mass spectrum had peaks at $m/e$ 43(100), 103(7), 129(16) [130(16)], 145(7), 154(2) [155(2)], 171(3) [172(3)], 189(2) [190(2)], 201(4) [202(4)], 215(1), 217(0.5), 231(5) [232(5)]. Values for peaks after reduction of the products with sodium borodeuteride are given in angular brackets, after corresponding figures for the non-deuterated analogue.

*Added in proof.* Dmitriev, B.A., Knirel, Yu.A. and Kochetkov, N.K. [*Carbohyd. Res.* **29** (1973) 451, **30** (1973) 45] have investigated the deamination of two disaccharide glycosides containing 2-amino-2-deoxy-D-glucose residues. In addition to the 2,5-anhydromannose derivatives, they also, for each disaccharide, obtain smaller amounts of an unidentified component. This, in the light of the present study, should most probably be the 2-deoxy-2-*C*-formyl-D-*arabino*-pentofuranose derivative.

# REFERENCES

1. Ledderhose, G. *Z. Physiol. Chem.* **4** (1880) 139.
2. Defaye, J. *Advan. Carbohyd. Chem. Biochem.* **25** (1970) 181.
3. Foster, A. B., Harrison, R., Inch, T. D., Stacey, M. and Webber, J. M. *J. Chem. Soc.* **1963** 2279.
4. Isemura, M. and Schmid, K. *Biochem. J.* **124** (1971) 591.
5. Chérest, M., Felkin, H., Sicher, J., Šipoš, F. and Tichy, M. *J. Chem. Soc.* **1965** 2513.
6. Inoue, S. and Ogawa, H. *Chem. Pharm. Bull.* **8** (1960) 79.
7. Čapek, K., Jåry, J. and Samek, Z. *Chem. Commun.* **1969** 1162.

# Refinement of the Crystal Structure of the Non-stoichiometric Boride IrB~1.35

TORSTEN LUNDSTRÖM and LARS-ERIK TERGENIUS

*Institute of Chemistry, University of Uppsala, Box 531, S-751 21 Uppsala 1, Sweden*

The structure of IrB~1.35 has been refined using a single-crystal diffractometer technique. Variations in the cell dimensions have been observed, indicating a small homogeneity range.

The structure is described in terms of puckered boron layers and puckered metal double layers, which also contain boron atoms in trigonal prismatic interstices. The structure does not contain a three-dimensional boron network.

The microhardness of IrB~1.35 was found to be $(1380 \pm 80) \times 10^7$ N/m².

Two of the phases in the iridium-boron system were characterized crystallo-graphically in the early sixties by Aronsson and co-workers [1-3] using powder as well as single-crystal techniques. The phases were denoted IrB~1.1 and IrB~1.35. Recently two further phases were discovered by Rogl, Nowotny and Benesovsky,[4] who claimed the composition to be close to IrB~0.9 for both phases. One of these phases is stable at high temperatures, crystallizing in the WC-type structure. The other phase is a low-temperature modification, which crystallizes in a new, unique structure. Iridium-boron alloys were also studied by Reinacher,[5] using high-temperature microscopical techniques, and by Samsonov *et al.*,[6] who studied the sintering reaction between boron and iridium.

The purpose of the present investigation was to study the boron network of IrB~1.35 using single-crystal diffractometry.

## EXPERIMENTAL DETAILS

The samples were prepared from iridium powder (Johnson, Matthey and Co., London, claimed purity min. 99.8 %) and crushed crystalline boron (H. C. Starck, Werk Goslar, claimed purity min. 99.8 %) by arc-melting under an inert atmosphere of purified argon. Many crystal fragments were examined in a Weissenberg camera until a crystal suitable for X-ray intensity measurement was found. The crystal fragment selected was taken from an alloy of nominal composition IrB~1.4, which in addition contained β-rhombo-hedral boron crystals. The *h0l* Weissenberg layer of the crystal selected displayed weak

streaks surrounding the reflexions and extending in directions perpendicular to the vector $\vec{R}(hkl)$ in the reciprocal lattice. Weak streaks were also found in the $b*$ direction.

The X-ray intensities were measured with an automatic single-crystal diffractometer (PHILIPS-STOE) using $\theta - 2\theta$ integration and monochromatized molybdenum radiation (graphite monochromator). A total of 1729 independent reflexions with $2\theta < 120°$ were recorded. All observed intensities less than $2\sigma$ were excluded from the refinement procedure. Three standard reflexions (400, $\bar{1}11$, and 312) were measured 53 times each during the data collection period but no significant changes in their intensities were detected. Corrections were applied for Lorentz, polarization (correction factor $p = (1 + \cos^2 2\theta_M \cos^2 2\theta)/(1 + \cos^2 2\theta_M)$ with $\theta_M = 6.1°$) and absorption effects using the program DATAPH, originally written by Coppens et al.[7] The calculated value of the linear absorption coefficient was 1504 cm$^{-1}$. The shape of the crystal was approximated by ten boundary planes. The size of the crystal was roughly $41 \times 42 \times 27$ $\mu$m in the directions $a$, $b$, and $c$, respectively. The agreement factor

$$\Sigma |F_o - F_{o,av}|/\Sigma F_o$$

decreased through the application of the absorption correction from 5.2 % to 4.0 % for 109 pairs of equivalent reflexions (those related by the two-fold axis).

## CELL DIMENSIONS AND MICROHARDNESS

X-Ray powder photographs were taken with a Guinier-Hägg focusing camera using $CuK\alpha_1$ radiation and zone-refined silicon ($a = 5.43054$ Å) as internal calibration standard for the determination of the cell dimensions.

The cell dimensions were refined using a least-squares computer program (CELNE) written by J. Tegenfeldt and N.-O. Ersson of the Institute of Chemistry, Uppsala, Sweden.

The microhardness measurements were performed with the DURIMET Micro hardness tester (LEITZ, Wetzlar). The indentations were made with a pyramidal Vickers diamond, using a load of $49.03 \times 10^{-2}$ N (50 p).* The load was applied for ten seconds for all measurements. An oil immersion objective in combination with a green-filter was used in measuring the indentations. The hardness determination was based on the measurements of both diagonals for 17 ($= n$) crack-free indentations, at different parts of the specimen. A hardness value was calculated for each indentation, based on the arithmetic mean of the two diagonals. The calculated standard deviation was obtained using the following expression:

$$\sigma = [\sum_{i=1}^{n} (H_{vi} - \bar{H}_v)^2/(n-1)]^{1/2}$$

The surface was prepared for the hardness measurements by sawing, wet grinding on carborundum disks and polishing with diamond paste. No etching procedure was performed on the polished surface.

Cell dimensions and microhardness were measured at room temperature and are collected in Table 1.

---

* 1 N (Newton) = 101.972 p.

*Table 1.* Cell dimensions and microhardness [$49.03 \times 10^{-2}$ N (50 p) load] for the monoclinic IrB~1.35. Standard deviations are given in parentheses.

| Compound | Cell dimensions (Å) | Monoclinic angle (°) | Cell volume (Å³) | Microhardness (N/m² × 10⁻⁷) |
|---|---|---|---|---|
| IrB~1.35 B-rich | $a = 10.5300(9)$ $b = 2.9038(3)$ $c = 6.1013(5)$ | $\beta = 91.119(9)$ | 186.52(6) | $1380 \pm 80^a$ |
| IrB~1.35 B-poor | $a = 10.5421(10)$ $b = 2.8905(3)$ $c = 6.1003(4)$ | $\beta = 91.143(6)$ | 185.85(6) | |

$^a$ 1 N/m² $= 1.01972 \times 10^{-7}$ kp/mm².

## STRUCTURE REFINEMENT AND RESULTS

The crystal structure of IrB~1.35 was refined using alternatively a least-squares procedure and Fourier difference technique. The programs used were the full-matrix program UPALS [8] and the Fourier summation program DRF.[9] The atomic scattering factors were taken from Refs. 10 and 11 and were corrected for dispersion effects.[12] The least-squares refinements were based on statistical weights modified according to $w = 1/\{(C_1\sigma)^2 + (C_2F_o)^2\}$. The best weighting analysis was obtained using $C_1 = 1.0$ and $C_2 = 0.08$. The discrepancy indices, $R$ and $R_w$, are based on $F_o$ using unity weights and the weights described above, respectively.

An analysis of the corrected intensity data corroborated the choice of space groups proposed by Aronsson,[3] namely $C2/m$, $Cm$, or $C2$. The atomic coordinates given in Ref. 3 were used in the first refinement cycles, using space group $C2/m$. A very high temperature factor was obtained for the B(5) atom (notation according to Ref. 3), which indicated non-occupancy of the proposed atomic position. A Fourier difference synthesis, based solely on the iridium contributions to $F_c$, supported this conclusion. The refinement further yielded approximately 50 % occupation of the atomic position of B(6) as obtained with a fixed value for the temperature factor for this atom. The composition of the crystal investigated is thus IrB~1.25, which is of a slightly but not necessarily significantly lower boron content than that proposed by Aronsson.[3] The Fourier difference map also displayed electron density peaks approximately 0.1 Å outside the mirror plane, which indicated that the metal atoms might partially occupy a general atomic position close to the mirror plane. Refinement of this model yielded $y$ coordinates for the iridium atoms that were significantly different from those of the mirror plane ($\sim 60\sigma$). The metal atoms thus occupy positions on one side or the other of the mirror plane in a more or less disordered way.

It is possible, however, that the observed disorder of the metal atoms in the $b$ direction may be described as anisotropic thermal vibrations of the atoms. The structure was accordingly refined using anisotropic temperature factors for the atoms. This refinement yielded 10 % lower estimated standard

deviations for the atomic coordinates and $R_w = 9.3$ %. The thermal vibrations of the metal atoms were significantly anisotropic, the r.m.s. vibrations in the $b$ direction being $18\sigma$ larger than those in the $ac$ plane. However, the difference synthesis based on the anisotropic refinement displayed peaks extending in the $b$ direction from the mirror plane, which supports the model described above with the iridium atoms in general positions. Furthermore, there are no evident physical grounds for markedly anisotropic thermal vibrations of the metal atoms in the structure. These circumstances infer that the most likely structure model involves the iridium atoms in general positions outside the mirror plane.

The structure was also refined in the lower space groups $C2$ and $Cm$, in order to investigate possible disorder in the $ac$ plane, for which some indications were found in the Fourier difference synthesis. These refinements did not improve the agreement between observed and calculated structure factors. Consequently the space group $C2/m$ was chosen for the description of the structure.

*Table 2.* Final structure data for IrB$_{\sim 1.35}$. Standard deviations are given in parentheses. Space group $C2/m$ (No. 12). Cell dimensions: $a = 10.5300(9)$ Å, $b = 2.9038(3)$ Å, $c = 6.1013(5)$ Å and $\beta = 91.119(9)°$.

| Atom | Position | $x$ | $y$ | $z$ | $B$ | Occupancy |
|------|----------|-----|-----|-----|-----|-----------|
| Ir(1) | 8($j$) | 0.09933(9) | 0.0310(5) | 0.13856(13) | 0.56(2) | 1/2 |
| Ir(2) | 8($j$) | 0.35745(9) | 0.0292(5) | 0.28858(13) | 0.59(2) | 1/2 |
| B(3) | 4($i$) | 0.5545(37) | 0 | 0.3808(56) | 1.3(3) | 1 |
| B(4) | 4($i$) | 0.1804(22) | 0 | 0.4689(35) | 0.6(2) | 1 |
| B(6) | 4($i$) | 0.745(10) | 0 | 0.056(16) | 1.9(9) | 0.51(15)[a] |

[a] Refined with fixed temperature factor.

The final structure data are collected in Table 2. The final $R_w$ was 0.100, based on all observed reflexions (1006), while R was 0.082 based on 632 reflexions with $0.5 < \sin\theta/\lambda < 1.04$. The interatomic distances are presented in Table 3.

## DISCUSSION

Since diffractometer data were used, the agreement between observed and calculated structure factors as obtained in the refinement was not so good as might have been anticipated. There are at least two factors that might be responsible for the less satisfactory agreement. One factor is the imprecise nature of the absorption correction originating in the large absorption coefficient and the irregular shape of the crystal. Secondly, there is a possibility that for different reflexions different proportions of the X-ray intensity within the streaks have escaped measurement. It is estimated that for this reason some of the reflexions may have up to 15 % too low observed intensity.

*Table 3.* Interatomic distances for IrB$_{\sim 1.35}$ (in Å units). Distances listed are 0.2 Å < Ir — Ir < 3.8 Å, Ir — B < 3.5 Å, and B — B < 2.6 Å. The estimated standard deviations are given in parentheses.

| Ir(1) — | | | Ir(2) — | | |
|---|---|---|---|---|---|
| | B(6) | 2.04(11) | | B(4) | 2.059(16) |
| — | B(3) | 2.07(3) | — | B(3) | 2.14(4) |
| — | B(6) | 2.12(8) | — | B(4) | 2.175(15) |
| — | B(4) | 2.18(2) | — | B(4) | 2.19(2) |
| — | B(3) | 2.19(3) | — | B(3) | 2.21(4) |
| — | B(6) | 2.24(8) | — | B(6) | 2.28(8) |
| — | Ir(1) | 2.664(2) | — | B(6) | 2.35(10) |
| — | Ir(1) | 2.670(2) | — | B(6) | 2.39(8) |
| — | Ir(1) | 2.723(3) | — | Ir(2) | 2.734(3) |
| — | Ir(2) | 2.851(1) | — | Ir(1) | 2.851(1) |
| — | Ir(2) | 2.856(1) | — | Ir(1) | 2.856(1) |
| — 2Ir(1) | | 2.904(0) | — 2Ir(2) | | 2.904(0) |
| — | Ir(2) | 2.946(1) | — | Ir(1) | 2.946(1) |
| — | Ir(2) | 3.008(2) | — | Ir(1) | 3.008(2) |
| — | Ir(2) | 3.023(1) | — | Ir(1) | 3.023(1) |
| — | Ir(2) | 3.028(1) | — | Ir(1) | 3.028(1) |
| — | Ir(2) | 3.084(2) | — | Ir(1) | 3.084(2) |
| — | Ir(2) | 3.089(2) | — | Ir(1) | 3.089(2) |
| — | Ir(2) | 3.113(1) | — | Ir(1) | 3.113(1) |
| — | Ir(2) | 3.172(2) | — | Ir(1) | 3.172(2) |

| B(3) — | | | B(4) — | | |
|---|---|---|---|---|---|
| | B(3) | 1.87(7) | | 2B(3) | 2.03(3) |
| — 2B(4) | | 2.03(3) | — 2Ir(2) | | 2.059(16) |
| — 2Ir(1) | | 2.07(3) | — 2B(4) | | 2.09(3) |
| — 2Ir(2) | | 2.14(4) | — 2Ir(2) | | 2.175(15) |
| — 2Ir(1) | | 2.19(3) | — 2Ir(1) | | 2.18(2) |
| — 2Ir(2) | | 2.21(4) | — 2Ir(2) | | 2.19(2) |

| B(6) — 2B(6) | | | B(6) — 2Ir(2) | | |
|---|---|---|---|---|---|
| | | 1.61(9) | | | 2.28(8) |
| — 2Ir(1) | | 2.04(11) | — 2Ir(2) | | 2.35(10) |
| — 2Ir(1) | | 2.12(8) | — 2Ir(2) | | 2.39(8) |
| — 2Ir(1) | | 2.24(8) | | | |

However, the results as regards the boron network were unambiguous, although the standard deviation of the occupational parameter of the B(6) atom is large.

The structure can be described most concisely as a stacking in the c direction of puckered boron layers (B) and puckered double layers of metal atoms (A). The stacking is simple without displacements, *i.e.* the stacking sequence is ABAB... . Projections of these layers in the c direction are shown in Fig. 1. The B(3) and B(4) atoms form the boron layer, having three and four close boron neighbours, respectively, within the layer. The iridium atoms have five close iridium neighbours within a layer and another two or three adjacent iridium atoms in the other half of the double layer. Boron atoms are also found in the trigonal prismatic interstices of the metal double layer. A full occupation of these interstices would imply the formation of boron chains with a B — B distance of 1.61 Å. However, the B(6) atoms occupy the position only to approximately 50 %. If these atoms occupy the interstices in an ordered way, there are no B — B contacts between B(6) atoms. If on the other hand the occupation is disordered, boron pairs or short boron chains might occasionally

| B(3) | B(4) | B(4) | B(3) |
|------|------|------|------|
| B | O | ◉ | ● | ● |
| z | 0.38 | 0.47 | 0.53 | 0.62 |

| Ir(1) | Ir(2) | Ir(1) | Ir(2) | |
|-------|-------|-------|-------|--|
| Ir | O | ◑ | ⬭ | ⬮ | B(6) O |
| z | 0.14 | 0.29 | -0.14 | -0.29 | z ±0.06 |

0 _____ 5 Å

a                                                b
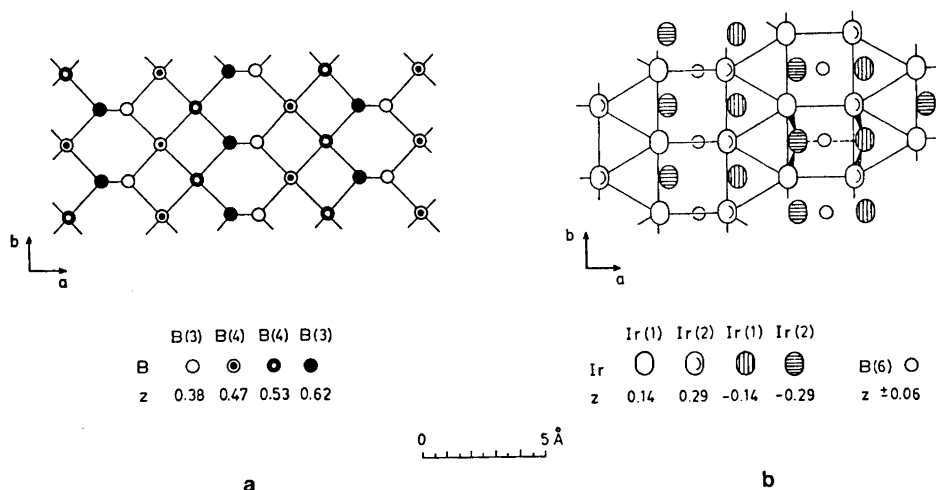
*Fig. 1.* The crystal structure of IrB$_{\sim1.35}$ may be described as a simple stacking of puckered boron layers (B) and double layers of metal atoms (A). (*a*) A puckered boron layer. (*b*) A puckered double layer of metal atoms containing isolated boron atoms. These boron atoms have a trigonal prismatic environment of metal atoms as indicated in (*b*). The metal atoms of the upper half of the double layer are connected with unbroken lines.

occur. The accuracy of the present investigation does not permit a choice between these two possibilities.

The structure differs in some respect from that earlier proposed by Aronsson,[3] based on photographic data. The iridium atoms occupy partially a general position close to the mirror plane while they were earlier believed to be situated exactly on the mirror plane. One proposed boron position, B(5), does not occur at all in the present refinement, which precludes the possibility of a three-dimensional boron network. Similar non-occurrence of boron atoms was recently demonstrated in the crystal structures of Ru$_2$B$_3$,[13] WB$_{2.0}$,[13] and Mo$_{1-x}$B$_3$.[14]

In general the interatomic distances obtained in this investigation do not differ appreciably from those obtained by Aronsson,[3] disregarding distances associated with the non-existent B(5) position.

From Table 1 it is apparent that IrB$_{\sim1.35}$ displays a range of homogeneity. The unit cell volume of boron-rich IrB$_{\sim1.35}$ is larger than that of boron-poor composition. Furthermore, an increase of the boron content of the phase involves a decrease of the *a* axis and an increase of the *b* axis while the *c* axis is not influenced. It appears as if the B(6) atoms may explain this behaviour to some extent. If it is assumed that the boron-poor composition corresponds to a half occupation of the B(6) position, the introduction of further boron atoms into the structure would involve the formation of more and more boron chains in the *b* direction. Since the B—B contacts formed are shorter than the remaining B—B distances in the structure (see Table 3), an expansion in the *b* direction is expected. The rigidity of the boron layer causes a minor contrac-

tion in the $a$ direction. The $c$ axis is not very much affected, since the bonding in the $c$ direction mainly consists of metal-metal bonds between the two halves of the double layer and metal-boron bonds between the two types of layers.

## REFERENCES

1. Aronsson, B., Stenberg, E. and Åselius, J. *Acta Chem. Scand.* **14** (1960) 733.
2. Aronsson, B., Stenberg, E. and Åselius, J. *Nature* **195** (1962) 377.
3. Aronsson, B. *Acta Chem. Scand.* **17** (1963) 2036.
4. Rogl, P., Nowotny, H. and Benesovsky, F. *Monatsh. Chem.* **102** (1971) 678.
5. Reinacher, G. *Metall* **19** (1965) 707.
6. Samsonov, G. V., Kosenko, V. A., Rud', B. M. and Sidorova, V. G. *Izv. Akad. Nauk. SSSR, Neorgan. Materialy* **8** (1972) 771.
7. Coppens, P., Leiserowitz, L. and Rabinovich, D. *Acta Cryst.* **18** (1965) 1035.
8. Lundgren, J.-O. Institute of Chemistry, Uppsala, Sweden 1972. *Unpublished.*
9. Zalkin, A., Berkeley, Calif., USA, Liminga, R. and Lundgren, J.-O., Institute of Chemistry, Uppsala, Sweden.
10. Cromer, D. T. and Waber, J. T. *Acta Cryst.* **18** (1965) 104.
11. Hanson, H. P., Herman, F., Lea, J. D. and Skillman, S. *Acta Cryst.* **17** (1964) 1040.
12. Cromer, D. T. *Acta Cryst.* **18** (1965) 17.
13. Lundström, T. *Arkiv Kemi* **30** (1968) 115.
14. Lundström, T. and Rosenberg, I. *J. Solid State Chem.* **6** (1973) 299.

# On the Electrical Properties of AgNO₃, TlNO₃, and NH₄NO₃

J H. FERMOR and A. KJEKSHUS

*Kjemisk Institutt, Universitetet i Oslo, Blindern, Oslo 3, Norway*

Values of the dielectric constant and resistivity measured at 1 kHz
are presented for polycrystalline AgNO₃, TlNO₃, and NH₄NO₃ below
room temperature. Results are also given for AgNO₃ and TlNO₃ in
hitherto unexplored regions above room temperature. The data show
dielectric transitions in AgNO₃, TlNO₃, and NH₄NO₃, with the critical
temperatures − 35, − 35, and − 32°C, respectively. Previously pub-
lished values of the heat capacity of TlNO₃ are examined, and shown
to contain an anomaly at ∼ − 35°C which appears to be associated
with the dielectric transition there. Consideration of the present and
other results for NH₄NO₃ leads to the conclusion that a previously
detected transition in the dielectric constant at − 32°C on cooling is
of the same character as those found at comparable temperatures in
other univalent nitrates, rather than a consequence of the IV→V
structural transition. A maximum in the dielectric constant of AgNO₃
is found at 110°C.

Two structural phases have been identified hitherto in solid AgNO₃ at
atmospheric pressure. On heating samples from room temperature, the
calorimetrically determined phase II→I transition temperature is reported as
158.9 to 160.6°C,[1] in good agreement with that given by Bridgman,[2,3] who
identified four structural modifications at pressures of up to 50 kbar. The phase
diagram for AgNO₃ is of quite a different form from that for TlNO₃, whose
properties closely resemble those of RbNO₃ and CsNO₃, however. Measure-
ments of specific heat from 15 to 300 K [4] do not show any anomalies which
could indicate additional phase transformations at atmospheric pressure.

The melting point of carefully dried AgNO₃ is reported to be 209.6°C.[5] Appreciable
decomposition of the melt has been reported for temperatures in the range 305 to 450°C,[6,7]
although the density and electrical conductivity were found to be reversible for tem-
perature cycles with a maximum temperature of 320°C.[8] X-Ray measurements on the
solid were, however, affected by decomposition of phase I crystals.[9]
   Phase I AgNO₃ has trigonal symmetry,[9] whereas phase II is orthorhombic.[10,11] This
phase is weakly birefringent, and has rather high values of refractive indices [12] compared,
for example, with those for KNO₃ in the orthorhombic phase II.[13]

The large refractive indices of AgNO₃ are mainly due to the large electronic
polarizability of Ag⁺ compared with that for K⁺, the values of this parameter
having been given as 2.4 and 1.33 Å³, respectively.[14] This, together with the

distinctive phase diagram, suggests that the lattice bonding and hence also the electrical properties of $AgNO_3$ might differ considerably from those of the alkali metal nitrates. In order to test this point, it is of interest to compare the frequencies of a lattice mode of vibration for the various compounds. The frequencies of strong absorption peaks of this part of the IR spectrum are shown as a function of the cation radius for $LiNO_3$, $NaNO_3$, $AgNO_3$, $KNO_3$, $TlNO_3$, and $NH_4NO_3$ in Fig. 1. It is seen that the frequency varies regularly
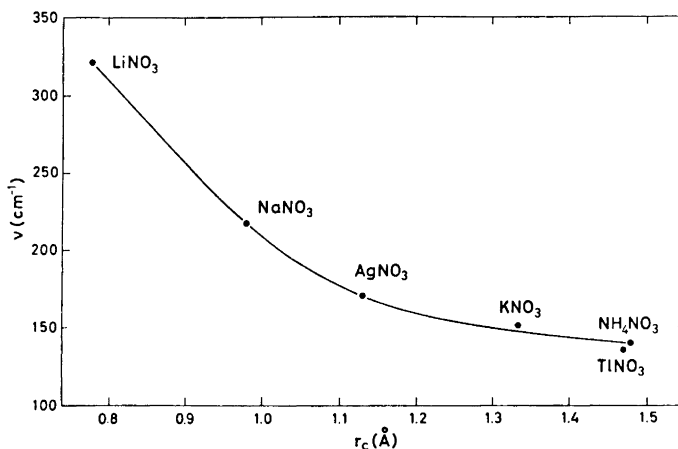


Fig. 1. A lattice mode frequency $\nu$ for univalent nitrates at room temperature *versus* cation radius $r_c$. The value of $\nu$ for $NH_4NO_3$ is from Landolt-Börnstein [15] and Newman and Halford;[16] for $TlNO_3$, Newman and Halford;[16] the remaining data are taken from Ferraro and Walker.[17]

with cation radius, and therefore with the anion-cation separation. Thus it seems from this dynamic property of the lattice that the interionic bonding is of a uniform nature in the compounds, and it is to be expected that the electrical among other ionic properties of $AgNO_3$ will conform with those of the alkali metal nitrates.

According to dilatometric measurements, the volume expansion coefficient of $AgNO_3$ drops sharply at the II→I transition or a few degrees above.[18] Sparse d.c. two-terminal resistivity data for $t > 140°C$ indicate a sharp minimum at the I→II transition.[18] Measurements of a.c. conductivity have been obtained in the vicinity of the melting point.[19] The dielectric constant $\epsilon$ has been given as 9.0 at 20°C for a measuring frequency of 3 MHz.[20]

By means of optical microscopy, it was shown that $TlNO_3$ adopts three modifications between room temperature and the melting point, the structural symmetries in order of increasing temperature being orthorhombic, rhombohedral, and cubic.[21] The cubic phase I was confirmed to be optically isotropic, the melting point being 210.4°C.[22-24]

Differential thermal analysis has showed the III→II transition temperature to be 79°C, and II→I at 144°C, the II→III transition being diffuse.[22] A calorimetric investigation gave the I→II transition temperature range as 142.5 to 143.8°C, compared with the value 144.6°C given by Bridgman.[2] The latter author found the II→III transition to occur at 75°C and recorded no additional phases at pressures of up to 12 kbar.

The orthorhombic, room temperature phase III has been studied by several authors using X-ray diffraction.[22,25-27] From measurements of the anisotropic IR absorption spectra for this phase, the directions of the two-fold axes of the nitrate groups, which lie in planes equidistant from those through the metal atoms, were deduced to bisect the angle between the $a$ and $b$ axes; the molecular planes being tilted about these directions.[16]

A large polarizability of $Tl^+$ [28] is reflected in both the refractive index [29] and the dielectric constant at room temperature (16.5),[20] but as in the case of $AgNO_3$, this does not appear to influence the IR response, as may be seen in Fig. 1.

A determination of the electrical conductivity at 900 Hz and 30 kHz did not show the III→II transition, but the II→I transition produced an overall increase of ∼1.5 orders of magnitude in $\sigma$.[30] Later measurements showed a decrease in $\sigma$ by a factor of 200 at III→II,[22] probably due to a partial disintegration of the sample, which may have included water. An increase in $\sigma$ of two orders of magnitude was noted at II→I.

The values of the specific heat $C_p$ for $TlNO_3$ according to two calorimetric investigations are shown in Fig. 2, where there is seen to be a small change in slope at $238 \pm 5$ K. Apparently undetected hitherto, this effect seems to exceed the experimental error; the two sets of data agreeing well in the region
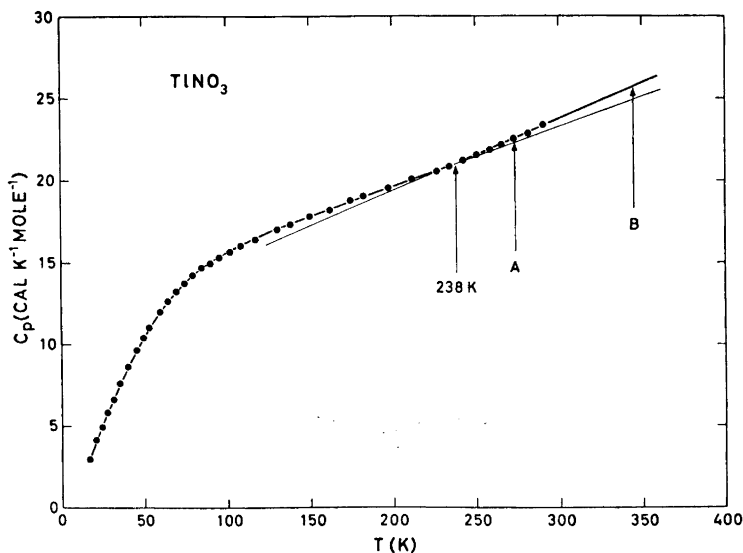


Fig. 2. The specific heat $c_p$ of $TlNO_3$ as a function of the absolute temperature $T$, showing a discontinuity of slope at $238 \pm 5$ K. The experimental points are from Latimer and Ahlberg,[31] and the section A−B of the curve is drawn according to the equation given by Satoh.[32]

of overlap. The anomaly may indicate a threshold in the bonding or disorder properties of the ions, and will be shown to coincide with a dielectric transition.

By means of optical spectroscopic and dilatometric observations, it was found that orthorhombic, room temperature phase IV crystals of $NH_4NO_3$ transform at $\sim -16°C$ into a tetragonal low temperature phase V, of lesser birefringence.[21] Samples were also found to be optically uniaxial at $-50°C$. By using a dilatometer, the same author found that on increasing the temperature, the expansion coefficient diminished at $-16°C$, and was followed by a region of contraction over the range $-14$ to $-8°C$, above which the crystals expanded normally. Later dilatometric experiments yielded the V→IV transition temperature of $-18°C$.[33] In common with several other univalent nitrate phases, the anions lie in parallel planes, in the present case parallel to (010). [34-38]

Although X-ray diffraction measurements indicated the symmetry of phase V to be hexagonal or pseudohexagonal, with only expansion differences between the unit cell dimensions at $-78$, $-33$, and $-18°C$,[36] the earlier suggestion of tetragonal symmetry,[21] has been confirmed at $-50°C$.[37,38]

Specific heat measurements showed a sharp peak in value at $-60.4°C$,[39] and this anomaly was later noted in addition to others at $-160$ and $-18°C$.[40] The transformations at $-160$ and $-60.4°C$ were absent from other calorimetric investigations, however,[41,42] the temperatures reported for the V→IV and IV→III transitions being $-16.9$ and $32.2°C$.

Measurements of dielectric constant at 100 kHz for a powdered sample showed an increase in value at $-33°C$ on cooling, and hysteresis to $-6°C$ on heating.[43] A two-terminal conductivity measurement for $t > -25°C$, at a sample voltage of 200 V, showed an anomaly at $\sim -6°C$ on heating.[37]

Observations of the electron paramagnetic resonance (EPR) of $VO^{2+}$ included in the $NH_4NO_3$ lattice have shown that a rapid readjustment of the ion which is present at 25°C is totally absent at $-70°C$. The gradual onset of the motion appears to occur over the range $-30$ to $-20°C$.[44]

An ideal study of the low frequency (or non-optical) properties of a compound would probably consist of measurements of the temperature dependence of the four-terminal conductivity and dielectric constant, virtually from d.c. to a practical upper limit in the radio frequency range. The investigation would also provide data on polarization barrier formation and the influence of substitutional impurities in single crystals; together with the detection of any non-linearity of displacement current. The effect of pressure upon the electrical parameters would also be determined. Actual investigations usually only fulfil part of these requirements, but nevertheless provide a useful addition to the information gained using other, and often more sophisticated techniques.

The present work was aimed primarily at discovering whether electrical anomalies of the type found in the alkali metal nitrates [45-49] occur also in $AgNO_3$, $TINO_3$, and $NH_4NO_3$. Satisfactory techniques for the measurement of four-terminal resistivity and dielectric constant below room temperature in these compounds are still to be fully developed, and the series of measurements is therefore restricted to a.c. two-terminal parameters for polycrystalline samples. The measurements were extended above room temperature for $AgNO_3$ and $TINO_3$.

Of the three compounds measured, $NH_4NO_3$ has been most thoroughly studied below room temperature, and it is the only univalent nitrate known

to have a structural phase transition in this region. It is not possible to reconcile all of the reported physical properties of the compound, however; and some extra complexity is to be expected when both ions are non-spherical.

## EXPERIMENTAL

The *p.a.* grade compounds were finely divided by crushing, and dried under vacuum; $AgNO_3$ (E. Merck A.G.) and $TlNO_3$ (Fluka A.G.) at $\sim 120°C$ for 24 h, $NH_4NO_3$ (E. Merck A.G.) at 70°C for 1 h. Laminar polycrystalline samples were then formed by cooling the melt between silver electrode plates of $\sim 10$ cm² area, spacers of quartz or Pyrex being used to obtain separations of $\sim 0.3$ mm.

The apparatus used to control the sample temperature and measure dielectric constant and dissipation at 1 kHz were as described previously.[45,46]
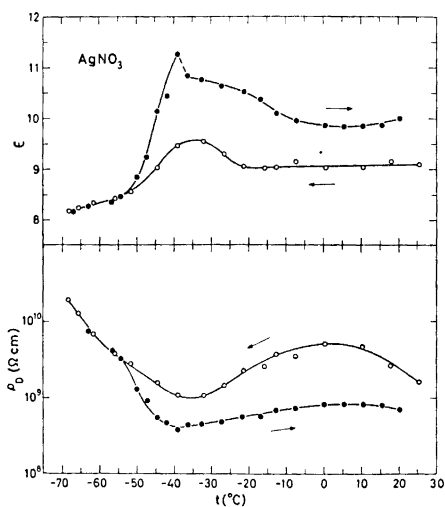


*Fig. 3.* Dielectric constant $\epsilon$ and resistivity $\varrho_D$ for $AgNO_3$ as functions of temperature. In this and the following diagrams open circles denote values obtained with decreasing temperature; filled circles with increasing temperature.
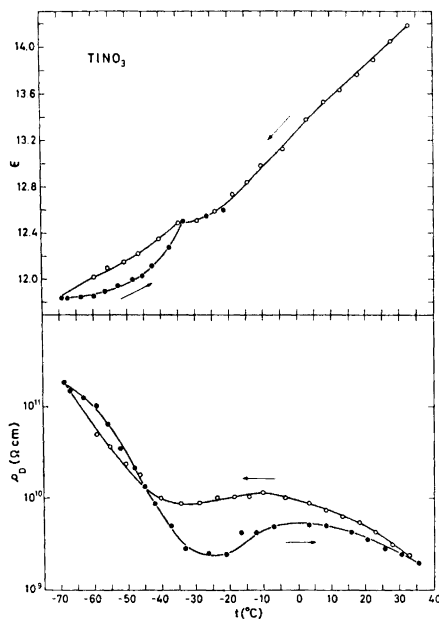
*Fig. 4.* Dielectric constant $\epsilon$ and resistivity $\varrho_D$ for $TlNO_3$ *versus* temperature.

## RESULTS AND DISCUSSION

Values of the dielectric constant $\epsilon$ and resistivity $\varrho_D$ at 1 kHz for $AgNO_3$, $TlNO_3$, and $NH_4NO_3$ below room temperature are shown in Figs. 3 to 5, and results obtained above room temperature for $AgNO_3$ and $TlNO_3$ in Figs. 6 and 7.
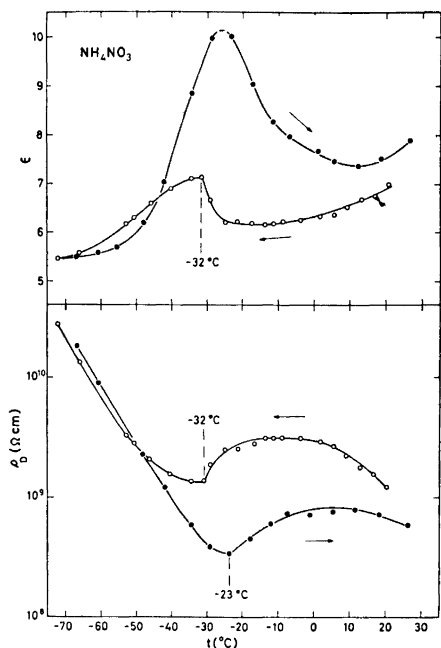
Fig. 5. Dielectric constant $\epsilon$ and resistivity $\varrho_D$ for $NH_4NO_3$ as functions of temperature.
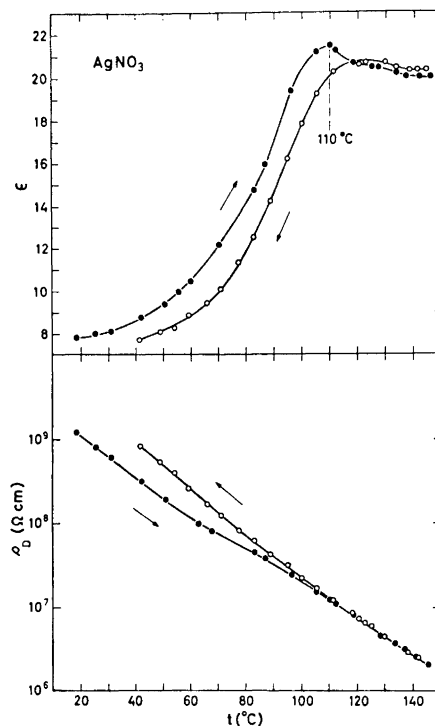
Fig. 6. Dielectric constant $\epsilon$ and resistivity $\varrho_D$ for $AgNO_3$ versus temperature.

The form of the samples yielding these data is both convenient and suitable when the temperature variation of parameters rather than their absolute values are of primary interest. It is clear, however, that when a compound is allowed to freeze in contact with metal electrode plates, there is little control over the growth of the crystallites, which is governed by such factors as rate of cooling, degree of purity of the sample, condition of the electrode surface, etc. With anisotropic compounds the samples may include preferred directions of crystal growth, which are not easily ascertained. It may also be difficult to measure the sample geometry with high precision. Variations in absolute value from sample to sample have been found, and the results are therefore not necessarily those for a bulk sample of small, randomly oriented grains. The temperature dependent forms of the anomalies seen in the results are reproducible, however.

Below room temperature, the curves for $AgNO_3$, $TlNO_3$, and $NH_4NO_3$ show dielectric transitions which are similar in form to those found in the alkali metal nitrates.[45-49] The temperatures marked on the curves are taken as being characteristic of the anomalies for the purpose of comparison. The forms of the anomalies suggest the presence of structural or order-disorder
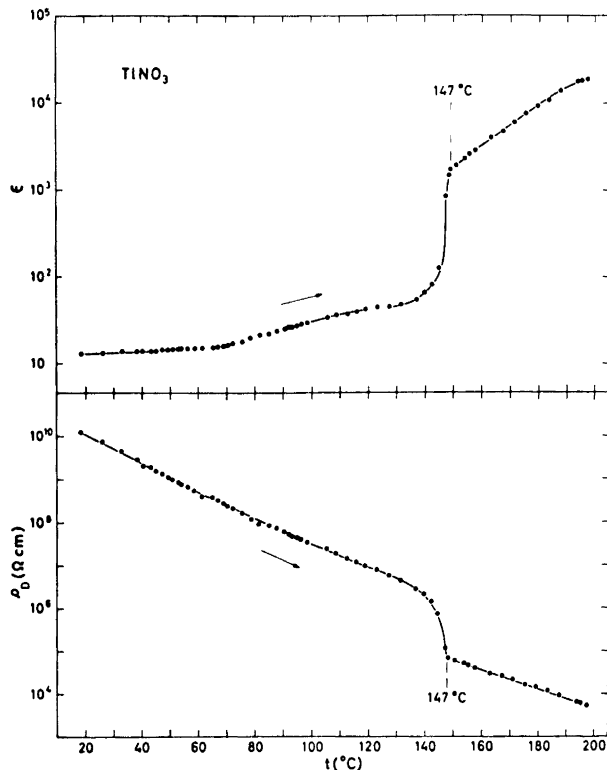
*Fig. 7.* Dielectric constant $\epsilon$ and resistivity $\varrho_D$ for $TlNO_3$ as functions of temperature.

transformations in the compounds, and in the case of $TlNO_3$ the dielectric transition temperature of $-35°C$ (Fig. 4) agrees well with that of the discontinuity in slope of the specific heat curve of Fig. 2.

The maximum at $-32°C$ in the values of $\epsilon$ obtained on cooling for $NH_4NO_3$ (Fig. 5) is very similar to the effect found by Kamiyoshi and Yamakami [43] at the same temperature. The latter authors employed a frequency of 100 kHz, and a powdered sample, and the differences between the two sets of data are no greater than may be expected from the techniques used. On heating, the present results show less hysteresis than those of Kamiyoshi and Yamakami.

The resistivity $\varrho_D$ of $NH_4NO_3$ (Fig. 4) reflects the course of $\epsilon$, showing that the increased polarizability is accompanied by relaxation. In addition, the $\varrho_D$ curves show slight, but important minima at $\sim -20°C$ on cooling and $\sim -3°C$ on heating. The latter effect corresponds to the d.c. conductance anomaly found by Brown and McLaren at $\sim -6°C$ on heating, and identified as being due to the $V \rightarrow IV$ transformation.[37] From a comparison of these results, it appears that the dielectric transitions do not coincide with the $IV \rightleftharpoons V$ transformations, and that negligible changes in $\epsilon$ are associated with the structural

transitions, although variations in a.c. and d.c. resistivity do occur. This interpretation is supported by the large discrepancy between the dielectric transition temperature ($-32°C$) and that detected by other means ($\sim -18°C$)* on cooling.

On the other hand, the anomalous variations of $\epsilon$ and $\varrho_D$ for $NH_4NO_3$ below room temperature are clearly of the same nature as those found in the other univalent nitrates, implying that the effect is not a disorder property of the $NH_4^+$ ion, although the latter could be involved in the $V \rightarrow IV$ transformation. It may be significant that the EPR measurements [44] on $NH_4NO_3$ containing $VO^{2+}$ showed the onset of rapid reorientation of the ion to occur over the hysteresis interval of the dielectric transition. This is not the case for $NaNO_3$, $KNO_3$, and $CsNO_3$, however.[44]

The results for $AgNO_3$ above room temperature (Fig. 6) show a maximum in $\epsilon$ at 110°C, succeeded by a plateau region at higher temperatures. The increase in $\epsilon$ of $\sim 2.5$ times the room temperature value is not associated with an increase in dissipation, the values of $\varrho_D$ being substantially linear, especially on cooling. Thus the increased polarizibility involves purely elastic displacements or rotations. It is not known whether the anomaly is reflected in the d.c. resistivity, the measurements of Davis et al.[18] commencing above 110°C. The dielectric anomaly does not appear to be directly connected with the $II \rightarrow I$ transformation at $\sim 160°C$.

The data obtained for $TlNO_3$ above room temperature (Fig. 7) show a gradual increase in $\epsilon$ above $\sim 70°C$, i.e. in the phase II region. The onset of the $II \rightarrow I$ transition is gradual, and the change completed at 147°C. The rather steeply increasing value of $\epsilon$ in phase I resembles those of the isostructural phase III of $RbNO_3$.[49] No appreciable change in $\varrho_D$ occurs at $III \rightarrow II$, in accordance with the use of a dry sample (cf. Ref. 22). Apart from the effects of the $II \rightarrow I$ transition, which has a gradual onset, the variation in resistivity is substantially linear. Of all of the known structural transformations in univalent nitrates, the $III \rightarrow II$ transition in $TlNO_3$ has the least effect upon the electrical parameters.

REFERENCES

1. Arell, A. *Ann. Acad. Sci. Fennicæ Ser. A VI* **1962** No. 100.
2. Bridgman, P. W. *Proc. Am. Acad. Arts Sci.* **51**( 1916) 579.
3. Bridgman, P. W. *Proc. Am. Acad. Arts Sci.* **72** (1937) 44.
4. Smith, W. V., Brown, O. L. I. and Pitzer, K. S. *J. Am. Chem. Soc.* **59** (1937) 1213.
5. Janz, G. J., James, D. W. and Goodrin, J. *J. Phys. Chem.* **64** (1960) 937.
6. Gordon, S. and Campbell, C. *Anal. Chem.* **27** (1955) 1102.
7. Patil, K. C., Gosavi, R. K. and Rao, C. N. R. *Inorg. Chim. Acta* 1 (1967) 155.
8. Murphy, J. W. and Wetmore, F. E. W. *Can. J. Chem.* **37** (1959) 1397.
9. Fischmeister, H. F. *J. Inorg. Nucl. Chem.* **3** (1956) 182.
10. Levin, E. M. *J. Am. Ceram. Soc.* **52** (1969) 53.
11. Zachariasen, W. H. *Skrifter Norske Videnskaps-Akad. Oslo I. Mat. Naturv. Kl.* **1928** No. 4.

* See introductory section.

12. Swanson, H. E., Gilfrich, N. T. and Ugrinic, G. M. *Natl. Bur. Std. (U.S.) Circ.* No. **539**, V (1955) p. 59.
13. Washbuen, E. W. (Ed.) *International Critical Tables* Vol. VII, McGraw, New York 1930.
14. Tessman, J. R. and Kahn, A. H. *Phys. Rev.* **92** (1953) 890.
15. *Landolt-Börnstein* 6th Ed., Vol. I, Part 4, Springer, Berlin-Göttingen-Heidelberg 1955.
16. Newman, R. and Halford, R. S. *J. Chem. Phys.* **18** (1950) 1276.
17. Ferraro, J. R. and Walker, A. *J. Chem. Phys.* **42** (1965) 1273.
18. Davis, W. J., Rogers, S. E. and Ubbelohde, A. R. *Proc. Roy. Soc. (London) Ser. A* **220** (1953) 14.
19. Cerisier, P. and Bizouard, M. *Compt. Rend.* **261** (1965) 5100.
20. Eucken, A. and Büchner, A. *Z. physik. Chem.* **B 27** (1934) 321.
21. Wallerant, F. *Bull. Soc. Franc. Mineral.* **28** (1905) 311.
22. Brown, R. N. and McLaren, A. C. *Acta Cryst.* **15** (1962) 977.
23. Rolla, M., Franzosini, P. and Riccardi, R. *Discussions Faraday Soc.* **32** (1961) 84.
24. Finbak, C. and Hassel, O. *Z. physik. Chem.* **B 35** (1937) 25.
25. Rivoir, L. and Abbad, M. *Anales Fis. Quim. (Madrid)* **39** (1943) 306.
26. Ferrari, A. and Cavalca, L. *Gazz. Chim. Ital.* **80** (1950) 199.
27. Hinde, R. M. and Kellett, E. A. *Acta Cryst.* **10** (1957) 383.
28. Roberts, S. *Phys. Rev.* **76** (1949) 1215.
29. Miller, W. H. *Proc. Roy. Soc. (London)* **14** (1865) 555.
30. Komatsu, H. *Rept. Inst. Sci. Technol. Univ. Tokyo* **5** (1951) 15.
31. Latimer, W. M. and Ahlberg, J. E. *J. Am. Chem. Soc.* **54** (1932) 1900.
32. Satoh, S. *Bull. Inst. Phys. Chem. Res. (Tokyo)* **21** (1942) 127.
33. Behn, U. *Proc. Roy. Soc. (London) Ser. A* **80** (1908) 444.
34. Bragg, W. H. *Trans. Faraday Soc.* **20** (1924) 59.
35. West, C. D. *J. Am. Chem. Soc.* **54** (1932) 2256.
36. Hendricks, S. B., Posnjak, E. and Kracek, F. C. *J. Am. Chem. Soc.* **54** (1932) 2766.
37. Brown, R. N. and McLaren, A. C. *Proc. Roy. Soc. (London) Ser. A* **266** (1962) 329.
38. Hendricks, S. B., Deming, W. E. and Jefferson, M. E. *Z. Krist.* **85** (1933) 143.
39. Crenshaw, J. L. and Ritter, I. *Z. physik. Chem.* **B 16** (1932) 143.
40. Jaffray, J. *Compt. Rend.* **224** (1947) 1346.
41. Stephenson, C. C., Bentz, D. R. and Stevenson, D. A. *J. Am. Chem. Soc.* **77** (1955) 2161.
42. Nagatani, M., Seiyama, T., Sabiyama, M., Suga, H. and Syuzo, S. *Bull. Chem. Soc. Japan* **40** (1967) 1833.
43. Kamiyoshi, K. and Yamakami, T. *Sci. Rep. Tohoku Univ.* **A 11** (1959) 418.
44. Rao, K. V. S., Sastry, M. D. and Venkateswarlu, P. *J. Chem. Phys.* **52** (1970) 4035.
45. Fermor, J. H. and Kjekshus, A. *Acta Chem. Scand.* **22** (1968)  836.
46. Fermor, J. H. and Kjekshus, A. *Acta Chem. Scand.* **22** (1968) 1628.
47. Fermor, J. H. and Kjekshus, A. *Acta Chem. Scand.* **22** (1968) 2054.
48. Fermor, J. H. and Kjekshus, A. *Acta Chem. Scand.* **23** (1969) 1581.
49. Fermor, J. H. and Kjekshus, A. *Acta Chem. Scand.* **26** (1972) 2645.

# Metal Complexes with Mixed Ligands

## 7. An Emf-Investigation of the Complex Formation between Binuclear Dihydroxo-bridged Copper(II) Cations and Imidazole Ligands

STAFFAN SJÖBERG

Department of Inorganic Chemistry, University of Umeå, S-901 87, Umeå, Sweden

Equilibria between copper(II), imidazole $(C_3H_4N_2)$ and $OH^-$ have been studied in the three media 3.0 M $(Na)ClO_4$, 3.0 M $(Na)Cl$, and 5.0 M $(Na)Cl$. The measurements have been performed as potentiometric (glass electrode) titrations at 25°C. Besides pure binary hydrolytic species $CuOH^+$ and $Cu_2(OH)_2{}^{2+}$ and unhydrolyzed copper-imidazole complexes $Cu(C_3H_4N_2)_n{}^{2+}$, $n = 1, 2, 3, 4$, all data could be explained with the ternary complexes $Cu(OH)C_3H_4N_2{}^+$ and $Cu_2(OH)_2(C_3H_4N_2)_4{}^{2+}$. In 3.0 M $(Na)ClO_4$ medium $Cu_2(OH)_2(C_3H_4N_2)_2{}^{2+}$ also seems to be formed. The equilibrium constants determined are given in Tables 4 and 6.

Data have been analyzed with the least squares computer program LETAGROPVRID.

In part 1 [1] of this series equilibria in the system $Cu^{2+} - OH^- -$ imidazole were studied at 25°C in 3.0 M $(Na)ClO_4$. It was found that for ratios $C/B \geq 8$ ($C =$ total imidazole concentration and $B =$ total copper concentration) all data could be explained by a series of stepwise binary complexes $Cu(C_3H_4N_2)_n{}^{2+}$ with $n = 1, 2, 3, 4$, and 6 (possibly also small amounts of a complex with $n = 5$). For $C/B < 8$ the data also indicated formation of ternary complexes and the effects found were tentatively explained by a single complex $Cu_2(OH)_2-(C_3H_4N_2)_3{}^{2+}$.

Using solely the data available from the part 1 investigation it was impossible to decide whether the composition $Cu_2(OH)_2(C_3H_4N_2)_3{}^{2+}$ really corresponded to a single complex or if it instead was a mean composition of a number of complexes. To clarify the situation it is necessary to collect data where the steps between different $C/B$ ratios lie much closer together than in the earlier investigation. Supplementary data were therefore collected and a new detailed mathematical analysis was performed. Special attention was paid to the possibility of formation of stepwise binuclear copper-complexes of the type $Cu_2(OH)_2(C_3H_4N_2)_n{}^{2+}$. The results of this analysis will be reported below.

## PREVIOUS STUDIES ON BINARY AND TERNARY HYDROLYZED COPPER(II)-SPECIES

*Binary hydrolytic $Cu_q(OH)_p$-species.* The main complex in hydrolyzed $Cu^{2+}$-solutions, $Cu_2(OH)_2{}^{2+}$ was first reported by Hagisawa[2] in 1939. Since then this complex has been confirmed and more accurately determined especially through the investigations of Pedersen,[3] Berecki-Biedermann[4] (3.0 M (Na)ClO$_4$, 25°C) and Ohtaki[5] (dioxane-water mixture, 3.0 M (Li)ClO$_4$, 25°C).

Perrin[6] claimed that the hydrolysis of $Cu^{2+}$ proceeds by a "core- and links"[7] mechanism to form di-, tri-, and polynuclear complexes of the type $Cu_n$-$(OH)_{2n-2}{}^{2+}$. However, neither Berecki-Biedermann nor Ohtaki found any evidence for the formation of trinuclear or higher complexes. The existence of a mononuclear, $CuOH^+$, complex has also been reported and is formed in appreciable amounts only at low concentrations of copper.

*Ternary hydrolytic $Cu_q(OH)_pL_n$-species.* Both mononuclear $(q=1)$ and polynuclear $(q>1)$ complexes have been described. In the systems studied the ligands used have been predominantly bidentate in character. Hitherto only two systems with monodentate nitrogen containing ligands appear to have been investigated. In the system $Cu^{2+} - OH^- - NH_3$, it has been proposed that a series of complexes $Cu(OH)_n(NH_3)_{4-n}$ with $n=1$, 2, and 3 is formed.[8,29] Other species such as $Cu(OH)NH_3{}^+$ have also been reported.[29] The other system studied, was the system $Cu^{2+} - OH^- -$ pyridine. It was proposed[9] that the main complex is $Cu_2(OH)_2(pyridine)_4{}^{2+}$ with $\log K(2\ Cu^{2+} + 2OH^- + 4L \rightleftharpoons Cu_2(OH)_2L_4{}^{2+}) = 24.71$. However, mononuclear ternary complexes of the type $Cu(OH)L_n{}^+$, with $n=1$, 2, 3 have also been reported.[10] Information concerning complexes with bidentate ligands may be found in the editions of Stability Constants.[11] The most frequently reported complexes are $Cu(OH)L$ and $Cu_2(OH)_2L_2$ [the complex $Cu_2(OH)_2L_2$ is supposed to be formed by dimerization of $Cu(OH)L$]. Other types of complexes have also been described; *e.g.* Vacca[12] in an investigation of the system $Cu^{2+} - OH^- - N,N,N',N'$-tetramethylethylenediamine found evidence for the formation of trinuclear complexes. The complete set of ternary complexes necessary for explaining his data were: $Cu(OH)L^+$, $Cu_2(OH)_2L^{2+}$, $Cu_2(OH)_2L_2{}^{2+}$, $Cu_3(OH)_4L_2{}^{2+}$, and $Cu(OH)_2L$. The choice of this chemical model was, however, a matter of personal judgement. Vacca's computer calculations indicated that four other models were also possible.

*Crystal structures.* Numerous crystal structures of $Cu_2(OH)_2L_n$-complexes are described in the literature. In all of these the central unit of the complex consists of two copper atoms bonded together through two OH-bridges with the ligands occupying the available coordination sites around the copper atoms. Structures with both monodentate and bidentate ligands have been reported. The following structures with bidentate ligands have been described: $Cu_2(OH)_2(2,2'$-bipyridyl)$_2(NO_3)_2$,[13] $Cu_2(OH)_2(2,2'$-bipyridyl)$_2SO_4.5H_2O$,[14] $Cu_2$-$(OH)_2(N,N,N',N'$-tetramethylethylenediamine)$_2Br_2$,[15] and $Cu_2(OH)_2(2$-(2-ethylaminoethyl)pyridine)$_2(ClO_4)_2$[30] and for monodentate ligands, $Cu_2(OH)_2(methylamine)$_4SO_4.H_2O$.[16] No crystal structure determinations of any $Cu(OH)_pL_n$ complexes have yet been made. This is probably due to the difficulties involved in preparing crystals.

## EXPERIMENTAL

*Chemicals and analysis.* The perchlorate solutions used were prepared and analyzed as described earlier.[1] Stock solutions of $CuCl_2$ were prepared by dissolving recrystallized $CuCl_2 \cdot (H_2O)_2$ (Merck *p.a.*) in water and analyzed for copper as earlier described.[1] Hydrochloric acid (Merck *p.a.*) was used without further purification.

*Apparatus.* The thermostat, cell arrangement, and electrodes used were the same as described earlier. The potentiometric titrations were performed with an automatic system for precise emf-titrations, a system constructed and built at this institute by O. Gintstrup.[17]

*Method.* The measurements were carried out as a series of potentiometric titrations. In general the total copper(II) concentration, $B$, and the total imidazole concentration, $C$, were kept constant in each of the titrations. The free hydrogen ion concentration, $h$, was varied by adding hydroxide ions and measured with a glass electrode. Calibrations and assumptions in connection with the use of the glass electrode were the same as described earlier.[1] The liquid junction potentials used were $E_j = -16.3\ h$, $-17.0\ h$, $-3.8\ h$ mV in 3.0 M(Na)$ClO_4$, 3.0 M (Na)Cl, and 5.0 M (Na)Cl, respectively. The reversibility of the equilibria was tested by making back titrations (addition of $H^+$) to hydrolyzed solutions. However, for the $C/B$ ratios $< 2.5$ this was impossible due to the precipitation of $Cu(OH)_{1.6}(ClO_4)_{0.4}$, which occurred on the $H^+$ additions. For testing equilibria at these ratios dilution experiments were carried out. (Solutions of different $Z$-values were diluted with pure medium.) It was found that the equilibria were reversible at all the ratios studied. The precipitate obtained for $C/B < 2.5$ was always of the type $Cu(OH)_{1.6}X_{0.4}(X = Cl, ClO_4)$ whereas at higher ratios copper-imidazole complexes were precipitated. In perchlorate solutions this precipitate was either the trinuclear imidazole-imidazolate complex $Cu_3(C_3H_4N_2)_8(C_3H_3N_2)_2(ClO_4)_4$ or $Cu(C_3H_4N_2)_4(ClO_4)_2$ or a mixture of both. In both cases precipitation causes an increase in acidity and limits the available $-\log h$ range approximately to $-\log h < 8$.

*Data treatment.* The mathematical analysis of data was made with the least squares program LETAGROPVRID[18] (version ETITR[19]). On treating the emf data the error squares sum $U = \sum(Z_{calc} - Z_{exp})^2$ was minimized. The standard deviations were defined and calculated according to Sillén.[20] The computation was performed on a CD 3200 computer.

In the least squares calculations use was made of the quantity $Z$, which is defined as the average number of $OH^-$ bound or reacted per $Cu^{2+}$-ion. This quantity can be determined from the analytical excess of $OH^-$ over the zero level of $Cu^{2+}$, $C_3H_5N_2^+$, $H_2O$ and from the measured $h$ with the relationship

$$Z = (h - H - K_w h^{-1})/B \tag{1}$$

where $K_w$ is the ionic product of water. In the present study the term $K_w h^{-1}$ can be neglected. Another quantity that will be used in the present paper is $\bar{n}$, which in the part 1[1] investigation was denoted as $Z_n$. $\bar{n}$ is given by the relationship

$$\bar{n} = (h - H - [C_3H_4N_2])/B \tag{2}$$

For the case when only complexes of the type $Cu_q(C_3H_4N_2)_r^{2q+}$ are formed, $[C_3H_4N_2]$ can be calculated from the relationship

$$[C_3H_4N_2] = K_a h^{-1} [C_3H_5N_2]^+ = K_a h^{-1}(C + H - h) \tag{3}$$

where $K_a$ is the acidity constant of $C_3H_5N_2^+$. In this particular case $\bar{n}$ is the average number of imidazole molecules bound per copper atom. In all other cases $[C_3H_4N_2]$ must be considered as a calculated quantity, which is used only for testing how well or how poorly a set of experimental data fits a series of complexes $Cu_q(C_3H_4N_2)_r^{2+}$.

## DATA, CALCULATIONS AND RESULTS

*Binary data.* The mononuclear complexes of the series $Cu(C_3H_4N_2)_n^{2+}$ were accurately determined by making separate calculations with data for $C/B \geq 8$ only. The results of these calculations with complexes and best equilibrium

*Table 1.* The acidity constant of $C_3H_5N_2^+$ and equilibrium constant for the mononuclear complexes $Cu(C_3H_4N_2)_n^{2+}$ with $n = 1,2,3,4$. The constants have been determined in separate investigations with $C/B \geq 8$ and are defined according to:

$$pH^+ + qCu^{2+} + rC_3H_5N_2^+ \rightleftharpoons (H^+)_p(Cu^{2+})_q (C_3H_5N_2^+)_r; \ \beta_{pqr}.$$

The errors given are 3 $\sigma(\log \beta_{pqr})$.
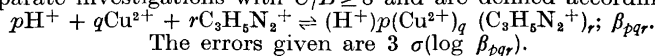
| $\log \beta_{pqr}$ | 3.0 M $(Na)ClO_4$[a] | 3.0 M $(Na)Cl$ | 5.0 M $(Na)Cl$ |
|---|---|---|---|
| $\log \beta_{-1\,01}$ | $-7.913 \pm 0.002$ | $-7.637 \pm 0.001$ | $-8.118 \pm 0.002$ |
| $\log \beta_{-1\,11}$ | $-3.27 \pm 0.03$ | $-3.238 \pm 0.015$ | $-3.610 \pm 0.019$ |
| $\log \beta_{-2\,12}$ | $-7.23 \pm 0.03$ | $-7.209 \pm 0.014$ | $-7.920 \pm 0.016$ |
| $\log \beta_{-3\,13}$ | $-11.82 \pm 0.04$ | $-11.85 \pm 0.02$ | $-12.98 \pm 0.03$ |
| $\log \beta_{-4\,14}$ | $-17.04 \pm 0.04$ | $-17.17 \pm 0.02$ | $-18.43 \pm 0.03$ |

[a] From the part 1[1] investigation with $C/B \geq 8$.

constants are collected in Table 1. For the binary hydrolytic complexes $Cu_q(OH)_p$ we have used the results of Berecki-Biedermann's emf-investigation[4] (3.0 M $(Na)ClO_4$, 25°C) and it has been assumed that the main complexes are $Cu(OH)^+$ and $Cu_2(OH)_2^{2+}$ with the equilibrium constants $\beta_{-110} = 1.0 \times 10^{-8}$ M and $\beta_{-220} = 2.5 \times 10^{-11}$ M.

In the search for ternary complexes it was assumed that the binary equilibria in the three-component system were completely explained with the above mentioned complexes and no attempts were made to adjust their equilibrium constants or to introduce new binary species. Only in the very last steps of the refinements was a covariation of the binary constants together with the ternary constants made. The purpose of this variation was to determine whether this covariation affected the ternary complexes found (by changing their equilibrium constants or in the worst case by rejecting one or more of them).

*Ternary data.* Experimental data were collected covering the following concentration ranges: 5 mM $\leq B \leq$ 160 mM, 5 mM $\leq C \leq$ 166 mM and $1 < -\log h < 8$. All experimental data from the 3.0 M$(Na)ClO_4$ medium are collected in Table 2. In order to separate and accurately determine for instance setwise polynuclear complexes of the type $Cu_2(OH)_2(C_3H_4N_2)_n^{2+}$, it was found necessary to keep the $C/B$ ratios studied rather close to each other, thus in 3.0 M $(Na)ClO_4$ we have used the ratios: 0.5, 0.8, 1, 1.7, 2.5, 3.3, in 3.0 M $(Na)Cl$ 0.5, 1, 1.5, 2, 2.5, 3, 4, and in 5.0 M $(Na)Cl$ 0.125, 0.25, 0.5, 1, 2, 4, respectively. In order to visualize the magnitudes of the effects which must be explained and also to illustrate how poorly (or well) the present data conform with solely $Cu(C_3H_4N_2)_n^{2+}$-complexes, we have constructed Bjerrum-plots, $\bar{n}(\log[C_3H_4N_2])$ for the 3.0 M $(Na)ClO_4$ medium. The plots are shown in Fig. 1. It can be seen that for $C/B < 8$ there are pronounced effects which must be due to complexes other than $Cu(C_3H_4N_2)_n^{2+}$. It was also found that the data available for the 3.0 M perchlorate medium were considerably greater than for the chloride media. This arises from the fact that the precipitated $Cu(OH)_{1.6}(ClO_4)_{0.4}$ is more soluble than the corresponding chloride compound.

*Table 2.* Experimental data $Z(\log h)$ at different $C/B$ ratios (3.0 M (Na)ClO$_4$ medium). For each point the quantities, $H$(in mM), $\log h$, $Z$, $\Delta Z_0$ and $\Delta Z_1$ are given. $\Delta Z$ is the residual $(Z_{\mathrm{exp}} - Z_{\mathrm{calc}}) \times 1000$ and the indices 0 and 1 refer to the assumptions: 0. Binary complexes $Cu(C_3H_4N_2)_n{}^{2+}$ only with constants given in Table 1 together with hydrolysis species $CuOH^+$ and $Cu_2(OH)_2{}^{2+}$ with constants proposed by Berecki-Biedermann.[4] 1. Binary complexes and proposed ternary complexes with equilibrium constants given in Table 4.

**SATS 1   C/B=0.4897**

| H | logh | Z | $\Delta Z_0$ | $\Delta Z_1$ |
|---|---|---|---|---|
| -0.27 | -4.148 | 0.033 | -1.99 | -2.05 |
| -0.44 | -4.301 | 0.048 | -0.59 | -0.70 |
| -0.61 | -4.429 | 0.063 | 0.60 | 0.40 |
| -0.77 | -4.539 | 0.078 | 0.91 | 0.61 |
| -1.09 | -4.723 | 0.108 | -0.22 | -0.83 |
| -1.38 | -4.863 | 0.137 | -0.17 | -1.18 |
| -1.67 | -4.970 | 0.164 | 2.37 | 0.92 |
| -1.94 | -5.068 | 0.190 | 3.82 | 1.81 |
| -2.19 | -5.153 | 0.215 | 5.70 | 3.06 |
| -2.68 | -5.310 | 0.262 | 6.77 | 2.51 |
| -3.12 | -5.425 | 0.305 | 13.55 | 7.58 |
| -3.53 | -5.535 | 0.345 | 16.53 | 8.39 |

**SATS 2   C/B=0.4895**

| H | logh | Z | $\Delta Z_0$ | $\Delta Z_1$ |
|---|---|---|---|---|
| 1.06 | -2.960 | 0.003 | -0.59 | -0.59 |
| -0.20 | -3.869 | 0.025 | -0.97 | -0.96 |
| -0.37 | -4.017 | 0.035 | -0.35 | -0.40 |
| -0.54 | -4.150 | 0.045 | -0.46 | -0.54 |
| -0.71 | -4.265 | 0.057 | -0.66 | -0.78 |
| -0.87 | -4.360 | 0.068 | -0.11 | -0.29 |
| -1.03 | -4.451 | 0.080 | -0.64 | -0.90 |
| -1.19 | -4.530 | 0.093 | -0.72 | -1.07 |
| -1.35 | -4.598 | 0.105 | 0.17 | -0.27 |
| -1.51 | -4.667 | 0.117 | -0.20 | -0.78 |
| -1.66 | -4.730 | 0.130 | -0.10 | -0.81 |
| -1.81 | -4.789 | 0.142 | 0.00 | -0.87 |
| -1.96 | -4.845 | 0.154 | 0.23 | -0.83 |
| -2.11 | -4.897 | 0.167 | 0.72 | -0.54 |
| -2.26 | -4.946 | 0.179 | 1.60 | 0.12 |
| -2.40 | -4.995 | 0.192 | 2.07 | 0.34 |
| -2.54 | -5.043 | 0.204 | 2.61 | 0.60 |
| -2.82 | -5.137 | 0.229 | 2.70 | 0.01 |
| -3.09 | -5.229 | 0.254 | 2.55 | -0.29 |
| -3.36 | -5.313 | 0.279 | 3.37 | -1.15 |
| -3.62 | -5.391 | 0.304 | 5.34 | -0.29 |
| -3.88 | -5.448 | 0.330 | 13.14 | 6.51 |

**SATS 3   C/B=0.8287**

| H | logh | Z | $\Delta Z_0$ | $\Delta Z_1$ |
|---|---|---|---|---|
| 2.99 | -2.481 | 0.006 | -0.60 | -0.60 |
| -0.53 | -3.125 | 0.027 | -0.56 | -0.57 |
| -3.63 | -3.701 | 0.086 | -1.12 | -1.17 |
| -6.40 | -4.031 | 0.153 | 0.09 | -0.08 |
| -8.88 | -4.282 | 0.223 | 0.11 | -0.30 |
| -11.06 | -4.494 | 0.291 | -1.45 | -2.25 |
| -13.09 | -4.685 | 0.361 | -0.95 | -2.40 |
| -14.93 | -4.868 | 0.431 | -0.07 | -2.48 |
| -16.62 | -5.048 | 0.501 | 1.64 | -2.43 |
| -18.17 | -5.228 | 0.571 | 4.60 | -2.21 |
| -19.59 | -5.406 | 0.641 | 10.62 | -0.72 |

**SATS 4   C/B=0.8302**

| H | logh | Z | $\Delta Z_0$ | $\Delta Z_1$ |
|---|---|---|---|---|
| -1.10 | -3.463 | 0.042 | -0.23 | -0.25 |
| -2.82 | -3.825 | 0.087 | -1.06 | -1.12 |
| -4.49 | -4.068 | 0.136 | -2.00 | -2.27 |
| -6.14 | -4.256 | 0.186 | -3.04 | -3.41 |
| -7.74 | -4.412 | 0.236 | -3.40 | -3.98 |
| -9.31 | -4.552 | 0.286 | -3.37 | -4.30 |
| -10.85 | -4.681 | 0.337 | -2.89 | -4.26 |
| -12.36 | -4.806 | 0.387 | -2.54 | -4.52 |
| -13.83 | -4.927 | 0.438 | -2.07 | -4.91 |
| -15.28 | -5.047 | 0.488 | -0.50 | -4.50 |
| -16.69 | -5.168 | 0.539 | 1.02 | -4.66 |
| -18.08 | -5.290 | 0.590 | 3.36 | -4.73 |
| -19.44 | -5.404 | 0.640 | 10.29 | -1.00 |

**SATS 5   C/B=0.8302**

| H | logh | Z | $\Delta Z_0$ | $\Delta Z_1$ |
|---|---|---|---|---|
| -17.66 | -5.430 | 0.639 | 13.59 | 1.79 |
| -16.20 | -5.463 | 0.639 | 13.99 | 1.37 |
| -14.97 | -5.492 | 0.639 | 14.47 | 1.07 |
| -13.91 | -5.519 | 0.639 | 15.02 | 0.86 |
| -12.99 | -5.544 | 0.639 | 15.66 | 0.75 |
| -12.18 | -5.568 | 0.639 | 16.07 | 0.46 |
| -11.47 | -5.590 | 0.639 | 16.42 | 0.09 |
| -10.84 | -5.611 | 0.639 | 16.83 | -0.19 |
| -10.27 | -5.629 | 0.639 | 17.44 | -0.22 |
| -9.76 | -5.648 | 0.639 | 17.95 | -0.36 |
| -9.30 | -5.665 | 0.639 | 18.47 | -0.47 |

**SATS 6   C/B=0.8302**

| H | logh | Z | $\Delta Z_0$ | $\Delta Z_1$ |
|---|---|---|---|---|
| -9.30 | -5.665 | 0.639 | 18.70 | -0.24 |
| -8.53 | -5.696 | 0.639 | 19.11 | -1.05 |
| -7.88 | -5.724 | 0.639 | 19.89 | -1.39 |
| -7.32 | -5.749 | 0.639 | 21.01 | -1.31 |
| -6.83 | -5.772 | 0.639 | 21.93 | -1.41 |
| -6.41 | -5.794 | 0.639 | 22.84 | -1.49 |
| -6.03 | -5.814 | 0.639 | 23.92 | -1.32 |
| -5.70 | -5.832 | 0.639 | 24.94 | -1.19 |
| -5.40 | -5.849 | 0.639 | 26.13 | -0.84 |
| -5.13 | -5.865 | 0.639 | 27.64 | -0.08 |

**SATS 7   C/B=0.8302**

| H | logh | Z | $\Delta Z_0$ | $\Delta Z_1$ |
|---|---|---|---|---|
| -5.12 | -5.865 | 0.638 | 27.02 | -0.69 |
| -4.27 | -5.923 | 0.638 | 30.17 | -0.71 |
| -3.67 | -5.972 | 0.638 | 33.16 | -0.58 |

**SATS 8   C/B=1.000**

| H | logh | Z | $\Delta Z_0$ | $\Delta Z_1$ |
|---|---|---|---|---|
| 0.26 | -3.512 | 0.009 | -0.28 | -0.28 |
| -0.12 | -4.163 | 0.038 | 0.63 | 0.56 |
| -0.30 | -4.427 | 0.068 | 1.28 | 1.07 |
| -0.47 | -4.612 | 0.099 | 2.36 | 1.91 |
| -0.63 | -4.766 | 0.130 | -0.48 | -1.32 |
| -0.79 | -4.873 | 0.160 | 0.99 | -0.26 |
| -0.93 | -4.971 | 0.189 | -0.11 | -1.89 |
| -1.07 | -5.049 | 0.216 | 1.14 | -1.20 |
| -1.21 | -5.120 | 0.243 | 1.33 | -1.67 |
| -1.46 | -5.238 | 0.293 | 3.37 | -1.96 |
| -1.79 | -5.383 | 0.360 | 5.08 | -1.92 |
| -2.09 | -5.503 | 0.419 | 6.40 | -3.62 |
| -2.44 | -5.634 | 0.489 | 9.52 | -5.04 |
| -2.75 | -5.738 | 0.551 | 15.10 | -4.36 |
| -3.02 | -5.826 | 0.604 | 21.14 | -3.52 |
| -3.25 | -5.901 | 0.651 | 27.73 | -2.29 |

**SATS 9   C/B=1.000**

| H | logh | Z | $\Delta Z_0$ | $\Delta Z_1$ |
|---|---|---|---|---|
| 0.00 | -3.555 | 0.023 | -0.57 | -0.58 |
| -0.31 | -3.798 | 0.039 | -0.41 | -0.44 |
| -0.61 | -4.005 | 0.060 | -0.51 | -0.58 |
| -0.91 | -4.164 | 0.083 | 0.34 | 0.22 |
| -1.20 | -4.294 | 0.107 | 1.34 | 1.12 |
| -1.75 | -4.502 | 0.157 | 3.50 | 2.98 |
| -2.29 | -4.676 | 0.208 | 3.26 | 2.29 |
| -2.80 | -4.820 | 0.259 | 5.07 | 3.50 |
| -3.29 | -4.951 | 0.310 | 5.67 | 3.27 |
| -4.42 | -5.242 | 0.438 | 8.28 | 2.54 |
| -5.05 | -5.401 | 0.515 | 11.45 | 2.45 |
| -5.64 | -5.553 | 0.592 | 16.42 | 2.74 |
| -6.20 | -5.704 | 0.669 | 21.96 | 1.42 |

**SATS 10   C/B=1.000**

| H | logh | Z | $\Delta Z_0$ | $\Delta Z_1$ |
|---|---|---|---|---|
| 0.96 | -3.006 | 0.003 | -2.61 | -2.61 |
| 0.14 | -3.524 | 0.016 | -2.27 | -2.27 |
| -0.25 | -3.869 | 0.038 | 0.09 | -0.03 |
| -0.63 | -4.161 | 0.070 | -1.15 | -1.27 |
| -1.00 | -4.350 | 0.104 | 0.35 | 0.09 |
| -1.35 | -4.501 | 0.139 | -0.01 | -0.49 |
| -1.70 | -4.619 | 0.172 | 0.73 | -0.01 |
| -2.03 | -4.724 | 0.205 | -0.61 | -1.69 |
| -2.67 | -4.893 | 0.269 | 0.11 | -1.82 |
| -3.29 | -5.035 | 0.330 | 0.84 | -2.21 |
| -3.87 | -5.153 | 0.388 | 3.76 | -0.63 |
| -4.43 | -5.262 | 0.443 | 6.28 | 0.22 |
| -4.95 | -5.360 | 0.496 | 9.15 | 1.11 |
| -5.93 | -5.542 | 0.594 | 13.26 | -0.17 |
| -6.83 | -5.701 | 0.683 | 21.76 | 0.97 |

**SATS 11   C/B=1.035**

| H | logh | Z | $\Delta Z_0$ | $\Delta Z_1$ |
|---|---|---|---|---|
| -10.81 | -3.583 | 0.138 | -0.14 | -0.19 |
| -14.88 | -3.747 | 0.188 | 2.44 | 2.33 |
| -22.36 | -4.007 | 0.281 | -1.34 | -1.60 |
| -28.95 | -4.186 | 0.362 | 1.03 | 0.57 |
| -34.90 | -4.342 | 0.437 | 0.02 | -0.73 |
| -40.26 | -4.472 | 0.503 | 1.53 | 0.64 |
| -45.11 | -4.594 | 0.564 | 0.59 | -0.97 |
| -51.57 | -4.753 | 0.645 | 2.91 | 0.46 |
| -59.03 | -4.935 | 0.738 | 11.20 | 6.99 |

**SATS 12   C/B=1.035**

| H | logh | Z | $\Delta Z_0$ | $\Delta Z_1$ |
|---|---|---|---|---|
| -4.43 | -2.854 | -0.047 |  | -0.51 |
| -7.57 | -3.042 | -0.009 |  | -0.11 |
| -9.13 | -3.117 | -0.081 | 1.27 | 1.26 |
| -10.64 | -3.193 | -0.093 | 0.75 | 0.73 |
| -12.13 | -3.260 | -0.105 | 0.54 | 0.52 |
| -13.60 | -3.318 | -0.118 | 1.41 | 1.39 |
| -15.04 | -3.375 | -0.131 | 1.31 | 1.28 |
| -16.47 | -3.418 | -0.143 | 4.26 | 4.22 |
| -19.22 | -3.511 | -0.168 | 5.72 | 5.67 |
| -21.96 | -3.602 | -0.194 | 5.48 | 5.40 |
| -24.56 | -3.683 | -0.220 | 5.56 | 5.46 |
| -27.12 | -3.754 | -0.246 | 7.68 | 7.55 |
| -29.61 | -3.829 | -0.271 | 6.87 | 6.70 |
| -32.03 | -3.893 | -0.297 | 8.75 | 8.55 |

**SATS 13   C/B=1.667**

| H | logh | Z | $\Delta Z_0$ | $\Delta Z_1$ |
|---|---|---|---|---|
| -3.78 | -3.475 | 0.101 | 1.73 | 1.69 |
| -7.67 | -3.887 | 0.207 | 1.89 | 1.73 |
| -11.04 | -4.175 | 0.318 | 0.85 | 0.42 |
| -13.27 | -4.353 | 0.402 | 0.51 | -0.23 |
| -16.21 | -4.587 | 0.528 | 1.50 | 0.04 |
| -17.94 | -4.731 | 0.612 | 1.62 | -0.54 |
| -19.77 | -4.885 | 0.710 | 6.54 | 3.35 |
| -21.43 | -5.041 | 0.809 | 8.09 | 3.33 |
| -22.91 | -5.194 | 0.906 | 8.93 | 2.00 |
| -24.47 | -5.370 | 1.018 | 12.32 | 1.67 |
| -25.71 | -5.526 | 1.117 | 16.94 | 1.30 |
| -26.21 | -5.594 | 1.159 | 19.49 | 0.96 |
| -26.85 | -5.686 | 1.215 | 24.07 | 0.78 |
| -27.31 | -5.757 | 1.257 | 27.91 | 0.11 |
| -27.61 | -5.804 | 1.286 | 30.94 | -0.40 |
| -27.76 | -5.827 | 1.300 | 32.93 | -0.31 |
| -27.90 | -5.831 | 1.314 | 35.07 | -0.18 |
| -28.05 | -5.874 | 1.328 | 37.29 | -0.12 |
| -28.47 | -5.943 | 1.370 | 45.89 | 1.43 |
| -28.88 | -6.013 | 1.412 | 55.09 | 2.01 |
| -29.27 | -6.080 | 1.454 | 67.21 | 4.75 |

**SATS 14   C/B=1.66**

*Table 2. Continued.*

| H | logh | z | $\Delta z_0$ | $\Delta z_1$ |
|---|---|---|---|---|
| -3.12 | -3.567 | 0.101 | 0.35 | 0.31 |
| -5.97 | -3.885 | 0.184 | 0.16 | 0.01 |
| -8.71 | -4.107 | 0.270 | 0.74 | 0.41 |
| -11.37 | -4.288 | 0.357 | 1.30 | 0.70 |
| -13.94 | -4.446 | 0.444 | 1.19 | 0.20 |
| -16.42 | -4.590 | 0.531 | 0.92 | -0.56 |
| -18.83 | -4.725 | 0.618 | 1.49 | -0.65 |
| -21.16 | -4.854 | 0.706 | 2.57 | -0.42 |
| -23.43 | -4.980 | 0.793 | 3.35 | -0.74 |
| -27.75 | -5.232 | 0.968 | 6.80 | -0.91 |
| -26.79 | -5.296 | 1.012 | 8.10 | -0.91 |
| -29.81 | -5.360 | 1.055 | 9.91 | -0.65 |
| -30.82 | -5.425 | 1.099 | 11.93 | -0.51 |
| -31.82 | -5.490 | 1.143 | 15.10 | 0.45 |
| -32.80 | -5.558 | 1.187 | 17.43 | -0.00 |
| -33.76 | -5.626 | 1.230 | 20.94 | 0.17 |
| -34.72 | -5.695 | 1.274 | 25.80 | 0.96 |
| -35.66 | -5.763 | 1.318 | 32.56 | 2.86 |
| -36.58 | -5.830 | 1.362 | 41.69 | 6.27 |

SATS 15   C/B=1.664

| H | logh | z | $\Delta z_0$ | $\Delta z_1$ |
|---|---|---|---|---|
| -5.48 | -3.855 | 0.171 | -1.72 | -1.86 |
| -8.00 | -4.072 | 0.250 | -1.64 | -1.93 |
| -10.43 | -4.244 | 0.330 | 0.00 | -0.52 |
| -12.79 | -4.394 | 0.411 | 1.08 | 0.25 |
| -15.07 | -4.529 | 0.491 | 3.22 | 1.94 |
| -17.27 | -4.656 | 0.572 | 4.79 | 3.03 |
| -19.42 | -4.779 | 0.653 | 4.99 | 2.53 |
| -21.49 | -4.896 | 0.733 | 6.93 | 3.61 |
| -23.50 | -5.014 | 0.814 | 6.88 | 2.39 |
| -25.46 | -5.130 | 0.895 | 8.86 | 2.88 |
| -27.35 | -5.244 | 0.976 | 9.08 | 1.06 |
| -29.19 | -5.369 | 1.057 | 11.16 | 0.37 |
| -30.98 | -5.561 | 1.137 | 14.41 | 0.26 |
| -32.72 | -5.616 | 1.218 | 20.16 | -0.01 |
| -33.58 | -5.674 | 1.259 | 27.55 | 4.12 |
| -35.24 | -5.804 | 1.339 | 38.30 | 5.46 |

SATS 16   C/B=1.664

| H | logh | z | $\Delta z_0$ | $\Delta z_1$ |
|---|---|---|---|---|
| -35.24 | -5.804 | 1.338 | 37.73 | 4.86 |
| -31.00 | -5.856 | 1.338 | 38.71 | 2.16 |
| -27.67 | -5.901 | 1.338 | 40.33 | 0.37 |
| -24.99 | -5.946 | 1.338 | 42.29 | -0.87 |
| -22.78 | -5.976 | 1.338 | 44.06 | -2.17 |
| -20.93 | -6.007 | 1.338 | 46.51 | -2.51 |
| -19.36 | -6.031 | 1.338 | 50.91 | -0.34 |
| -16.01 | -6.054 | 1.338 | 54.93 | 1.52 |
| -16.83 | -6.074 | 1.338 | 59.83 | 4.59 |

SATS 17   C/B=1.664

| H | logh | z | $\Delta z_0$ | $\Delta z_1$ |
|---|---|---|---|---|
| -5.63 | -4.839 | 0.448 | 6.61 | 4.21 |
| -6.64 | -4.982 | 0.537 | 8.65 | 5.03 |
| -8.56 | -5.248 | 0.715 | 11.72 | 4.36 |
| -9.96 | -5.439 | 0.849 | 14.67 | 2.83 |
| -10.84 | -5.561 | 0.938 | 19.58 | 3.63 |
| -12.53 | -5.816 | 1.117 | 29.14 | -0.14 |
| -12.74 | -5.847 | 1.139 | 31.74 | 0.25 |
| -12.94 | -5.879 | 1.161 | 33.83 | -0.17 |
| -13.14 | -5.911 | 1.184 | 35.84 | -0.90 |
| -13.34 | -5.944 | 1.206 | 38.35 | -1.31 |
| -13.54 | -5.975 | 1.228 | 41.57 | -1.17 |
| -13.74 | -6.010 | 1.251 | 43.10 | -3.18 |
| -13.93 | -6.043 | 1.273 | 46.20 | -3.90 |
| -14.13 | -6.074 | 1.295 | 50.65 | -3.23 |
| -14.32 | -6.107 | 1.318 | 54.03 | -4.24 |

SATS 18   C/B=2.489

| H | logh | z | $\Delta z_0$ | $\Delta z_1$ |
|---|---|---|---|---|
| 0.20 | -2.872 | 0.034 | 0.73 | 0.73 |
| -1.26 | -3.133 | 0.060 | 1.39 | 1.38 |
| -2.70 | -3.362 | 0.095 | 0.19 | 0.08 |
| -4.11 | -3.538 | 0.134 | -0.42 | -0.54 |
| -5.50 | -3.678 | 0.175 | -1.09 | -1.17 |
| -8.21 | -3.899 | 0.261 | -2.03 | -2.22 |
| -10.83 | -4.075 | 0.347 | -3.94 | -4.33 |
| -13.37 | -4.222 | 0.434 | -4.39 | -4.97 |
| -15.82 | -4.353 | 0.521 | -4.34 | -5.20 |
| -20.51 | -4.587 | 0.695 | -3.53 | -5.11 |
| -24.91 | -4.799 | 0.870 | -2.24 | -4.82 |
| -29.07 | -5.002 | 1.045 | -1.75 | -5.63 |
| -34.86 | -5.300 | 1.307 | -0.06 | -6.66 |
| -40.20 | -5.607 | 1.570 | 2.21 | -8.55 |
| -45.12 | -5.931 | 1.832 | 12.67 | -5.66 |
| -46.08 | -6.049 | 1.920 | 16.49 | -6.21 |
| -48.20 | -6.172 | 2.007 | 22.65 | -6.16 |
| -49.68 | -6.301 | 2.095 | 31.93 | -5.59 |
| -51.13 | -6.437 | 2.182 | 44.79 | -5.46 |
| -52.54 | -6.578 | 2.270 | 64.38 | -3.87 |
| -53.92 | -6.726 | 2.357 | 90.57 | -3.01 |
| -55.26 | -6.880 | 2.445 | 124.91 | -2.54 |
| -56.58 | -7.036 | 2.532 | 167.80 | -2.01 |

SATS 19   C/B=2.489

| H | logh | z | $\Delta z_0$ | $\Delta z_1$ |
|---|---|---|---|---|
| -53.15 | -6.853 | 2.425 | 117.75 | -1.96 |
| -47.70 | -6.887 | 2.425 | 121.50 | -2.41 |
| -43.26 | -6.918 | 2.425 | 124.92 | -2.87 |
| -39.58 | -6.944 | 2.425 | 128.60 | -2.76 |
| -36.48 | -6.968 | 2.425 | 132.10 | -1.72 |
| -33.82 | -6.990 | 2.425 | 135.40 | -1.33 |
| -31.53 | -7.010 | 2.425 | 138.62 | -0.63 |
| -29.53 | -7.029 | 2.425 | 141.72 | 0.12 |
| -27.76 | -7.046 | 2.425 | 144.71 | 0.92 |
| -26.20 | -7.062 | 2.425 | 147.55 | 1.65 |
| -24.80 | -7.078 | 2.425 | 150.29 | 2.39 |

SATS 20   C/B=2.489

| H | logh | z | $\Delta z_0$ | $\Delta z_1$ |
|---|---|---|---|---|
| -6.02 | -4.692 | 0.491 | 5.29 | 3.48 |
| -11.72 | -5.384 | 1.048 | 12.72 | 3.38 |
| -16.47 | -6.018 | 1.606 | 23.13 | -3.19 |
| -19.74 | -6.574 | 2.053 | 59.75 | -2.10 |
| -21.22 | -6.886 | 2.277 | 106.88 | 1.85 |
| -21.58 | -6.966 | 2.333 | 124.64 | 4.26 |
| -21.76 | -7.006 | 2.360 | 135.04 | 6.45 |
| -21.93 | -7.045 | 2.388 | 146.15 | 8.89 |

SATS 21   C/B=3.322

| H | logh | z | $\Delta z_0$ | $\Delta z_1$ |
|---|---|---|---|---|
| 0.52 | -2.830 | 0.034 | -0.22 | -0.22 |
| -2.26 | -3.340 | 0.099 | -0.65 | -0.69 |
| -4.84 | -3.678 | 0.191 | -1.29 | -1.39 |
| -7.25 | -3.912 | 0.288 | -1.49 | -1.62 |
| -9.51 | -4.097 | 0.388 | -1.09 | -1.45 |
| -11.62 | -4.256 | 0.487 | -1.70 | -2.37 |
| -15.48 | -4.525 | 0.688 | -0.15 | -1.51 |
| -16.91 | -4.762 | 0.888 | 0.93 | -1.37 |
| -21.98 | -4.982 | 1.089 | 1.80 | -1.51 |
| -26.02 | -5.296 | 1.391 | 3.59 | -1.54 |
| -28.41 | -5.502 | 1.592 | 4.04 | -2.06 |
| -30.58 | -5.709 | 1.793 | 4.30 | -2.49 |
| -31.59 | -5.814 | 1.894 | 4.09 | -3.04 |
| -35.27 | -6.397 | 2.422 | 3.99 | -5.71 |
| -37.05 | -6.520 | 2.523 | 3.39 | -8.05 |
| -38.53 | -6.781 | 2.724 | 8.67 | -9.66 |
| -39.91 | -7.056 | 2.925 | 34.79 | 1.89 |

SATS 22   C/B=3.329

| H | logh | z | $\Delta z_0$ | $\Delta z_1$ |
|---|---|---|---|---|
| -2.07 | -3.934 | 0.171 | -0.50 | -0.75 |
| -3.87 | -4.269 | 0.315 | 1.47 | 0.87 |
| -5.57 | -4.511 | 0.463 | 2.81 | 1.63 |
| -7.19 | -4.710 | 0.611 | 5.24 | 3.22 |
| -8.73 | -4.887 | 0.760 | 6.75 | 3.61 |
| -10.19 | -5.052 | 0.909 | 7.60 | 3.26 |
| -11.58 | -5.207 | 1.058 | 9.47 | 3.62 |
| -12.91 | -5.358 | 1.207 | 10.33 | 3.00 |
| -14.18 | -5.505 | 1.356 | 11.95 | 3.23 |
| -15.39 | -5.650 | 1.505 | 13.35 | 3.39 |
| -16.55 | -5.796 | 1.654 | 14.04 | 3.11 |
| -17.66 | -5.943 | 1.804 | 14.49 | 3.29 |
| -18.73 | -6.092 | 1.953 | 15.14 | 3.10 |
| -19.75 | -6.244 | 2.102 | 15.42 | 2.98 |
| -20.73 | -6.400 | 2.251 | 16.63 | 3.42 |
| -21.67 | -6.564 | 2.400 | 16.89 | 2.01 |
| -22.57 | -6.736 | 2.550 | 19.03 | 0.68 |
| -23.44 | -6.918 | 2.699 | 24.63 | -0.25 |
| -23.87 | -7.014 | 2.774 | 28.90 | -0.94 |
| -24.28 | -7.113 | 2.848 | 35.17 | -1.44 |
| -24.69 | -7.216 | 2.923 | 43.66 | -1.80 |
| -25.09 | -7.325 | 2.997 | 54.41 | -2.54 |
| -25.48 | -7.439 | 3.072 | 68.81 | -3.07 |
| -25.87 | -7.542 | 3.147 | 94.50 | 6.20 |
| -26.25 | -7.686 | 3.221 | 109.99 | -5.52 |
| -26.62 | -7.817 | 3.296 | 139.30 | -5.17 |
| -26.99 | -7.950 | 3.371 | 175.92 | -3.22 |

SATS 23   C/B=3.329

| H | logh | z | $\Delta z_0$ | $\Delta z_1$ |
|---|---|---|---|---|
| -2.07 | -3.936 | 0.171 | -1.57 | -1.73 |
| -7.19 | -4.710 | 0.611 | 5.17 | 3.08 |
| -17.11 | -5.867 | 1.729 | 16.92 | 5.63 |
| -22.12 | -6.643 | 2.475 | 23.19 | 6.99 |
| -25.87 | -7.542 | 3.147 | 94.50 | 6.20 |

SATS 24   C/B=3.319

| H | logh | z | $\Delta z_0$ | $\Delta z_1$ |
|---|---|---|---|---|
| -1.09 | -4.183 | 0.165 | -1.80 | -2.08 |
| -3.46 | -4.837 | 0.515 | 1.59 | -1.02 |
| -5.67 | -5.249 | 0.870 | 7.49 | 0.45 |
| -7.73 | -5.603 | 1.226 | 12.41 | -0.20 |
| -9.67 | -5.939 | 1.583 | 18.66 | 1.43 |
| -11.48 | -6.278 | 1.940 | 22.29 | 2.83 |
| -13.19 | -6.633 | 2.296 | 26.37 | 4.90 |
| -14.80 | -7.023 | 2.653 | 38.25 | 4.72 |
| -15.57 | -7.238 | 2.831 | 52.79 | 3.06 |
| -15.94 | -7.352 | 2.920 | 64.96 | 2.75 |
| -16.31 | -7.470 | 3.010 | 81.32 | 2.64 |
| -16.64 | -7.595 | 3.099 | 102.29 | 2.08 |
| -17.04 | -7.725 | 3.188 | 129.29 | 1.49 |
| -17.40 | -7.860 | 3.277 | 163.61 | 2.10 |

SATS 25   C/B=3.319

| H | logh | z | $\Delta z_0$ | $\Delta z_1$ |
|---|---|---|---|---|
| -0.48 | -3.868 | 0.087 | -1.18 | -1.25 |
| -1.09 | -4.181 | 0.166 | -0.20 | -0.48 |
| -2.30 | -4.571 | 0.339 | -0.36 | -1.50 |
| -5.13 | -5.155 | 0.782 | 5.01 | -0.78 |
| -8.72 | -5.776 | 1.405 | 10.78 | -4.46 |
| -11.48 | -6.281 | 1.939 | 18.60 | -0.77 |
| -12.35 | -6.454 | 2.117 | 21.71 | 1.70 |
| -13.19 | -6.638 | 2.296 | 21.32 | -0.20 |
| -14.00 | -6.826 | 2.474 | 26.82 | 1.48 |
| -14.79 | -7.024 | 2.652 | 36.40 | 2.89 |
| -15.18 | -7.129 | 2.741 | 43.40 | 3.02 |
| -15.56 | -7.243 | 2.830 | 48.35 | -1.84 |
| -15.94 | -7.353 | 2.920 | 63.03 | 0.63 |
| -16.31 | -7.473 | 3.009 | 78.43 | -0.75 |
| -16.68 | -7.598 | 3.098 | 99.68 | -1.11 |

*Analysis of 3.0 M $(Na)ClO_4$-data.* The search for the ternary complexes was started by assuming the formation of a series of complexes $Cu_2(OH)_2L_n^{2+}$ with $n = 1$, 2, 3, and 4. We found that this series could satisfactorily explain

*Fig. 1.* Experimental data (3.0 M (Na)ClO$_4$) plotted as curves $\bar{n}$ (log [C$_3$H$_4$N$_2$]) for $C/B$ ratios 0.5, 0.8, 1.0, 1.7, 2.5, and 3.3. Half-filled symbols mark titrations where $B$ and $C$ have been kept constant. All other symbols represent starting concentrations. The full curve has been calculated with the set of mononuclear complexes Cu(C$_3$H$_4$N$_2$)$_n^{2+}$ given in Table 1. The symbols stand for the following $B$ and $C$ (in mM): (a) ■ 10-5, ▲ 20-10, ◯ 38-32, ● 30-25, ▽ 5-5, ◑ 20-20, ◐ 80-80, (b) ⬡ 15-25, ■ 26-44, □ 38-64, ◯ 38-95, ▲ 22-55, △ 15-38, ▲ 7-25, ◖ 15-51, ■ 38-127.

the data. For the two regions Data 1 ($0.5 \leq C/B \leq 1.7$) and Data 2 ($1.7 \leq C/B \leq 3.3$), $\sigma(Z)$ values were 0.0035 and 0.0058, respectively. (See Table 3.)

Even though this model explained the data rather well, further tests were carried out. The mononuclear complexes Cu(OH)L$^+$, Cu(OH)L$_2^+$, and Cu(OH)L$^+_3$ were systematically tested. Table 3 shows that the addition of the complex Cu(OH)L$^+$ causes a replacement of the two complexes Cu$_2$(OH)$_2$L$^{2+}$ and Cu$_2$(OH)$_2$L$_3^{2+}$. The calculations also show that the ternary complex

*Table 3.* Results of LETAGROP calculations for some different assumptions concerning the ternary complexes formed in 3.0 M $(Na)ClO_4$ medium. In the calculations, the binary constants given in Table 1 together with the hydrolysis constants given by Berecki-Biedermann,[4] have not been varied. The constants $p_{qr}$ are defined as in Table 1 and the errors 3 $\sigma(\log p_{qr})$ are given when the corresponding equilibrium constant has been varied. Ranges 1 and 2 refer to data with $0.5 \le C/B \le 1.7$ and $1.7 \le C/B \le 3.3$, respectively. R denotes a rejected complex.

| Range | $\sigma(z) \times 1000$ | Cu(OH)L $\log(\beta_{-211} \pm 3\sigma)$ | $Cu_2(OH)_2L$ $\log(\beta_{-321} \pm 3\sigma)$ | $Cu_2(OH)_2L_2$ $\log(\beta_{-422} \pm 3\sigma)$ | $Cu_2(OH)_2L_3$ $\log(\beta_{-523} \pm 3\sigma)$ | $Cu_2(OH)_2L_4$ $\log(\beta_{-624} \pm 3\sigma)$ | $\log(\beta_{pqr} \pm 3\sigma)$ | $p,q,r$ |
|---|---|---|---|---|---|---|---|---|
| 1 (215 points) | 3.48 | $-10.42 \pm 0.11$ | $-14.10 \pm 0.07$ | $-17.72 \pm 0.06$ | | | | |
| | 2.69 | $-10.42 \pm 0.05$ | $-15.15 \pm 0.60$ | $-17.88 \pm 0.08$ | | | | |
| | 2.69 | $-10.42 \pm 0.05$ | | $-17.87 \pm 0.07$ | | | R | $-3,1,1$ |
| | 2.69 | $-10.47 \pm 0.08$ | | $-17.87 \pm 0.07$ | | | $-8.95 \pm 0.30$ | $-2,2,1$ |
| | 2.47 | $-10.44 \pm 0.05$ | | $-17.83 \pm 0.08$ | | | $-12.35 \pm 0.25$ | $-3,2,2$ |
| | 2.60 | $-10.41 \pm 0.05$ | | $-17.92 \pm 0.08$ | | | $-16.22 \pm 0.31$ | $-4,2,3$ |
| | 2.66 | $-10.40 \pm 0.05$ | | $-18.02 \pm 0.19$ | | | R | $-6,3,2$ |
| | 2.69 | $-10.43 \pm 0.06$ | | $-17.89 \pm 0.07$ | | | $-16.04 \pm 0.26$ | $-4,3,2$ |
| | 2.62 | $-10.42$ | | $-17.91 \pm 0.08$ | | | | |
| | 5.75 | $-10.42$ | | $-17.87$ | | | | |
| 2 (177 points) | 3.51 | $-10.42$ | | $-17.89 \pm 0.04$ | $-22.71 \pm 0.15$ | $-27.28 \pm 0.07$ | | |
| | 3.51 | $-10.42$ | | $-17.89 \pm 0.04$ | R | $-27.20 \pm 0.02$ | | |
| | 3.23 | $-10.42$ | | $-17.91 \pm 0.04$ | | $-27.30 \pm 0.06$ | $-15.70 \pm 0.22$ | $-3,1,2$ |
| | 3.48 | $-10.42$ | | $-17.88 \pm 0.05$ | | $-27.23 \pm 0.09$ | $-21.34 \pm 0.52$ | $-4,1,3$ |
| | 3.51 | $-10.42$ | | $-17.89 \pm 0.04$ | | $-27.19 \pm 0.02$ | R | $-12,3,10$ |
| | 3.50 | $-10.42$ | | $-17.90 \pm 0.04$ | | $-27.19 \pm 0.02$ | R | $-5,2,4$ |
| | 3.50 | $-10.42$ | | $-17.90 \pm 0.04$ | | $-27.19 \pm 0.02$ | $-26.37 \pm 1.32$ | $-6,2,5$ |
| | 3.51 | $-10.42$ | | $-17.90 \pm 0.05$ | | $-27.20 \pm 0.03$ | R | $-8,3,6$ |

*Table 4.* Results of final covariations of binary and ternary constants in the three media investigated. When no $3\,\sigma(\log{}_{pqr})$ is given the formation constant has not been varied. R denotes a rejected complex.

| Medium | Range | $\sigma(Z)$ $\times 1000$ | CuL²⁺ $\log(\beta_{-111})$ $\pm 3\,\sigma$ | CuL₂²⁺ $\log(\beta_{-212})$ $\pm 3\,\sigma$ | CuL₃²⁺ $\log(\beta_{-313})$ $\pm 3\,\sigma$ | CuL₄²⁺ $\log(\beta_{-414})$ $\pm 3\,\sigma$ | Cu₂(OH)₂²⁺ $\log(\beta_{-220})$ $\pm 3\,\sigma$ | Cu(OH)L⁺ $\log(\beta_{-211})$ $\pm 3\,\sigma$ | Cu₂(OH)₂L₂²⁺ $\log(\beta_{-422})$ $\pm 3\,\sigma$ | Cu₂(OH)₂L₄²⁺ $\log(\beta_{-624})$ $\pm 3\,\sigma$ |
|---|---|---|---|---|---|---|---|---|---|---|
| 3.0 M(Na)ClO₄ | $1/2 \leq C/B \leq 7/2$ (350 points) | 2.91 | $-3.261$ $\pm 0.003$ | $-7.219$ $\pm 0.003$ | $-11.816$ $\pm 0.006$ | $-17.035$ $\pm 0.013$ | $-10.59$ $\pm 0.04$ | $-10.44$ $\pm 0.06$ | $-17.90$ $\pm 0.07$ | $-27.18$ $\pm 0.02$ |
| 3.0 M(Na)Cl | $1/2 \leq C/B \leq 4$ (204 points) | 3.21 | $-3.218$ $\pm 0.003$ | $-7.187$ $\pm 0.005$ | $-11.827$ $\pm 0.008$ | $-17.17$ | R | $-10.37$ $\pm 0.04$ | R | $-28.01$ $\pm 0.03$ |
| 5.0 M(Na)Cl | $1/8 \leq C/B \leq 4$ (229 points) | 3.68 | $-3.588$ $\pm 0.003$ | $-7.917$ $\pm 0.009$ | $-12.96$ $\pm 0.02$ | $-18.43$ | R | $-10.23$ $\pm 0.04$ | R | $-27.80$ $\pm 0.07$ |

$Cu(CH)L_2^+$ may be present in small amounts. However, calculations which included this complex gave a rather high value of $3\sigma(\log \beta_{-311}) = 0.22$. Similar calculations were made assuming complexes of the type $Cu(OH)_2L_n$, $Cu_2$-$(OH)L_n^{3+}$, $Cu_3(OH)_2L_n^{4+}$, and $Cu_3(OH)_4L_n^{2+}$. Table 3 indicates that none of these complexes give any appreciable improvement.

Thus it may be concluded that the main ternary complexes are $Cu(OH)L^+$, $Cu_2(OH)_2L_2^{2+}$, and $Cu_2(OH)_2L_4^{2+}$. In a covariation of binary constants against ternary constants it was found that none of the complexes was rejected and that the standard deviations $3\ \sigma(\log \beta_{pqr})$ for the ternary complexes were less than 0.07. The values of the binary equilibrium constants did not change significantly; see Table 4.

*Analysis of (Na)Cl data.* Because of the restricted data range available for these two media no separate mathematical analysis of the data was made as for the 3.0 M $(Na)ClO_4$ medium. Instead the "best" model found for the 3.0 M $(Na)ClO_4$ medium was tested. The results of this test are given in Table 4. It is seen that in both media the data can be explained well with the complexes $Cu(OH)L^+$ and $Cu_2(OH)_2L_4^{2+}$ only. (The equilibrium constants for $Cu_2(OH)_2^{2+}$ and $Cu_2(OH)_2L_2^{2+}$ were always zero).

A final covariation of binary constants and ternary constants gave satisfactory results. The standard deviations $3\ \sigma(\log \beta_{pqr})$ for the ternary complexes also in these media were less than 0.07; see Table 4.

<div style="text-align:center">DISCUSSION</div>

The present investigation has given the intermediate hydrolytic species formed when imidazole is added successively to hydrolyzed Cu(II)-solutions. The main species in hydrolyzed pure Cu(II)-perchlorate solutions are $Cu_2(OH)_2^{2+}$ and $CuOH^+$. Our results seem to indicate that these hydroxo ions and imidazole molecules form complexes in the solution and in 3.0 M $(Na)ClO_4$ medium the following equilibria could be established

$$CuOH^+ + C_3H_4N_2 \rightleftharpoons CuOH(C_3H_4N_2)^+ \tag{4}$$

$$Cu_2(OH)_2^{2+} + 2C_3H_4N_2 \rightleftharpoons Cu_2(OH)_2(C_3H_4N_2)_2^{2+} \tag{5}$$

$$Cu_2(OH)_2^{2+} + 4C_3H_4N_2 \rightleftharpoons Cu_2(OH)_2(C_3H_4N_2)_4^{2+} \tag{6}$$
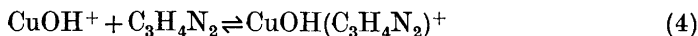
with $\log K = 5.47$, 8.53, and 16.06 for reactions (4), (5), and (6), respectively.

In the chloride media equilibrium (5) could not be detected. Alternatively the results may be interpreted as a series of hydrolysis reactions of Cu(II)-imidazoles where the equilibria present may be written

$$Cu(C_3H_4N_2)^{2+} + H_2O = CuOH(C_3H_4N_2)^+ + H^+ \tag{7}$$

$$2Cu(C_3H_4N_2)^{2+} + 2H_2O = Cu_2(OH)_2(C_3H_4N_2)_2^{2+} + 2H^+ \tag{8}$$

$$2Cu(C_3H_4N_2)_2^{2+} + 2H_2O = Cu_2(OH)_2(C_3H_4N_2)_4^{2+} + 2H^+ \tag{9}$$
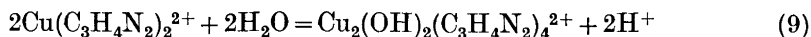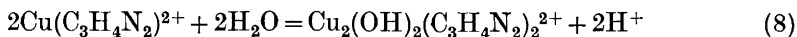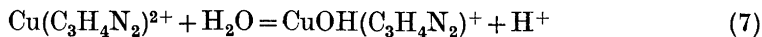
with equilibrium constants given in Table 5.

It is perhaps necessary to point out that we have assumed that we really have $OH^-$ in the complexes. However, an $OH^-$-group together with a $C_3H_4N_2$-

*Table 5.* Acidity and dimerization constants of some hydrolyzed copper(II)-complexes. The constants are defined according to the equilibria given. For brevity the charges of the complexes have been omitted.

| Equilibria | $H_2O$ ($n=0$) | Imidazole ($n=1$) | Imidazole ($n=2$) | Histamine ($n=1$) | Histidine ($n=1$) |
|---|---|---|---|---|---|
| $CuL_n + H_2O \rightleftharpoons Cu(OH)L_n + H^+$ | $-8^a$ | $-7.18^b$ $-7.15^c$ $-6.64^d$ | $-8.5^b$ | $-7.0^e$ $-7.1^f$ | $-7.39^g$ $-7.18^h$ $-6.63^i$ $-8.00^j$ |
| $2CuL_n + 2H_2O \rightleftharpoons Cu_2(OH)_2L_{2n} + 2H^+$ | $-10.6^a$ | $-11.37^b$ | $-11.75^b$ $-13.63^c$ $-11.97^d$ | $-11.8^e$ $-11.99^k$ | $-12.15^g$ $-12.44^j$ |
| $2Cu(OH)L_n \rightleftharpoons Cu_2(OH)_2L_{2n}$ | $5.4^a$ | $3.0^b$ | $4.2^b$ | $2.2^e$ | $2.63^j$ $3.76^g$ |

Temperature and medium: [a] 25°C, 3 M(Na)ClO$_4$, [b] 25°C, 3 M(Na)ClO$_4$, [c] 25°C, 3 M(Na)Cl, [d] 25°C, 5 M(Na)Cl, [e] 25°C, 0.1 (KNO$_3$),[22] [f] 36°C, 1.5(K$_2$SO$_4$),[23] [g] 37°C, 0.15(KNO$_3$),[24] [h] 25°C, 0.01,[25] [i] 25°C, 3 M(Na)ClO$_4$,[26] [j] 25°C, 0.1(KNO$_3$),[27] [k] 20°C, 0.1(KNO$_3$).[28]

molecule may equally well be interpreted as an imidazolate group $C_3H_3N_2^-$; thus the complexes proposed could also be $Cu(C_3H_3N_2)^+$, $Cu_2(C_3H_3N_2)_2^{2+}$, and $Cu_2(C_3H_3N_2)_2(C_3H_4N_2)_2^{2+}$. However, for structural reasons the presence of hydroxide groups in the complexes is more probable. With regard to the aqueous structure of the complexes formed, we may tentatively propose that copper is surrounded by ligands including also one or two perchlorate groups in the coordination sphere. It has been found that in the X-ray investigated compound, $Cu(C_3H_4N_2)_4(ClO_4)_2$,[31] the structure is built up of isolated Cu-$(C_3H_4N_2)_4(ClO_4)_2$ molecules held together solely by hydrogen and van der Waals bonds.

As can be seen from Table 4 the standard deviations of the proposed complexes are rather low and the complexes may thus be considered as well determined. The strengths of the complexes are illustrated by the distribution diagrams given in Fig. 2. It may be noted that in 3.0 M (Na)ClO$_4$ for instance the maximum amounts of $Cu_2(OH)_2^{2+}$, $Cu(OH)L^+$, $Cu_2(OH)_2L_2^{2+}$, and $Cu_2(OH)_2L_4^{2+}$ as percentages of total copper are estimated to be 3, 10, 10, and 15 respectively.

In Table 5 acidity and dimerization constants are given for some copper(II)-complexes with the ligands $H_2O$, imidazole, histamine, and histidine. It can be seen that $K_a(Cu(C_3H_4N_2)^{2+})$ is greater than $K_a(Cu^{2+})$. Thus the introducing of a ligand increases the acidity of the copper ion. Furthermore if we compare complexes Cu(OH)L with ligands imidazole, histamine, and histidine we see that the log $K_a$(CuL)-values reported usually fall within the ranges $7.2 \pm 0.2$. The dimerization constants indicate that there is more extensive dimerization when the ligands are $H_2O$-molecules than when they are mixed $H_2O$ and imidazole, histidine or histamine species. Thus the enolization reac-
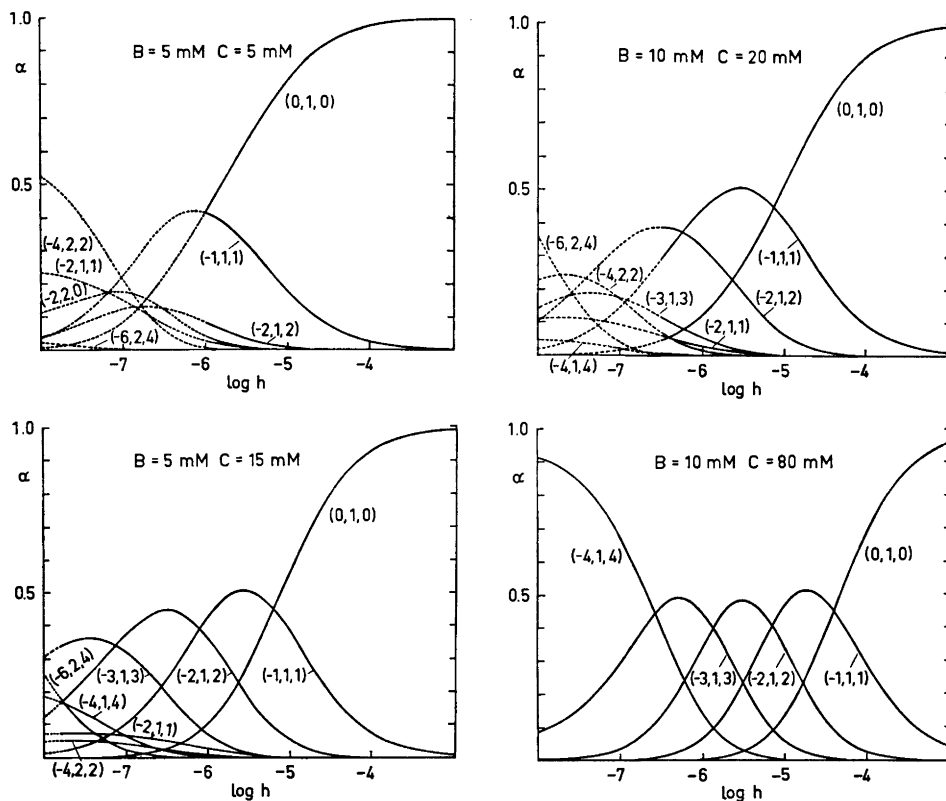
*Fig. 2.* Distribution diagrams $\alpha$ (log $h$)$_{B,C}$. $\alpha$ is defined as the ratio between copper(II) in a species and total copper(II). The computer program HALTAFALL [21] was used for the calculations with the constants given in Table 4 [3.0 M (Na)ClO$_4$]. Broken lines denote ranges where no measurements have been performed due to precipitation (extrapolated range).

tion seems to be hindered when the ligands imidazole, histamine, or histidine are introduced around the copper ion.

For complex formation in the two chloride media, the formation of chloro complexes must be taken into consideration. Many workers [11] have reported that copper(II) ions form weak complexes with chloride ions. Bjerrum,[32] in a spectrophotometric investigation, has shown that the species $CuCl^+$, $CuCl_2$, $CuCl_3^-$, and $CuCl_4^{2-}$ are formed with $K_1 < 1$, $K_2 \approx 0.1 - 0.4$, $K_3 \approx 0.02 - 0.06$, and $K_4 \approx 0.003 - 0.001$ M$^{-1}$, respectively.

The stability constants given in Tables 1 and 4, calculated from the experimental data in the two chloride media, are not true stability constants but rather "conditional" constants. This is because it is assumed that no complex formation has taken place between copper and chloride ions. However, by assuming the equilibria

$$Cu^{2+} + nCl^- \rightleftharpoons CuCl_n^{2-n}, \quad n = 1, 2, 3, 4 \tag{10}$$
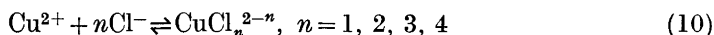
to be known (with equilibrium constants given by Bjerrum) it is possible to calculate new conditional constants $\beta_{pqr}'$ which are corrected for the equilibria (10) through the relation

$$\beta_{pqr}' = \beta_{pqr}(1 + \beta_{010})^q \tag{11}$$

where $\beta_{010} = K_1.[Cl^-] + K_1K_2[Cl^-]^2 + K_1K_2K_3[Cl^-]^3 + K_1K_2K_3K_4[Cl^-]^4$ (12)

$\beta_{010}$ is a constant provided [Cl$^-$] remains constant during the titrations.

The values of $\beta_{pqr}'$ from the two chloride media are given in Table 6. As is seen from this table the values of the $\beta_{pqr}'$ constants are usually greater than those in the perchlorate medium, thus indicating that $(H^+)_p(Cu^{2+})_q$ $(C_3H_5N_2^+)_r(Cl^-)_s$ complexes are also formed. However, in order to determine the formation constants of these mixed complexes, it is necessary to perform measurements in perchlorate media containing varying amounts of chloride, e.g. [ClO$_4^-$] + [Cl$^-$] = 3.0 M. Further studies in this direction are planned.

Table 6. "Conditional stability constants" $\beta_{pqr}'$ defined according to $pH^+ + qCu^{2+} + rC_3H_4N_2 \rightleftharpoons (H^+)_p(Cu^{2+})_q(C_3H_4N_2)_r^{(2q+p)}$ and calculated from the relation $\beta_{pqr}' = \beta_{pqr}$ $(1 + \beta_{010})^q$. The values of $\beta_{pqr}$ are calculated from constants given in Table 4. Approximate values of $\beta_{010}$ have been calculated (see eqn. 12) by assuming $K(CuCl^+) = 1$, $K(CuCl_2) = 0.2$, $K(CuCl_3^-) = 0.004$, $K(CuCl_4^{2-}) = 0.006$ and [Cl$^-$] = 3 and 5 M in each chloride media, respectively.

| Medium | CuL$^{2+}$ log $\beta_{011}'$ | CuL$_2^{2+}$ log $\beta_{012}'$ | CuL$_3^{2+}$ log $\beta_{013}'$ | CuL$_4^{2+}$ log $\beta_{014}'$ | Cu(OH)L$^+$ log $\beta_{-111}'$ | Cu$_2$(OH)$_2$L$_4^{2+}$ log $\beta_{-224}'$ |
|---|---|---|---|---|---|---|
| 3.0 M (Na)ClO$_4$ | 4.652 | 8.607 | 11.92 | 14.62 | −2.53 | 4.47 |
| 3.0 M (Na)Cl | 5.197 | 8.865 | 11.86 | 14.16 | −1.95 | 4.10 |
| 5.0 M (Na)Cl | 5.610 | 9.399 | 12.48 | 15.13 | −1.04 | 6.83 |

## REFERENCES

1. Sjöberg, S. Acta Chem. Scand. 25 (1971) 2149.
2. Hagisawa, H. Bull. Inst. Phys. Res. (Tokyo) 18 (1939) 275.
3. Pedersen, K. J. Kgl. Danske Videnskab. Selskab, Mat.-Fys. Medd. 20 (1943) No. 7.
4. Berecki-Biedermann, C. Arkiv Kemi 9 (1956) 175.
5. Ohtaki, H. Inorg. Chem. 7 (1968) 1205.
6. Perrin, D. D. J. Chem. Soc. 1960 3189.
7. Sillén, L. G. Acta Chem. Scand. 8 (1954) 299.
8. Fisher, J. F. and Hall, J. L. Anal. Chem. 39 (1967) 1550.
9. Leussing, D. L. and Hansen, R. C. J. Am. Chem. Soc. 79 (1957) 4270.

10. Strel'tsova, E. M. and Petreshan, V. I. *Izv. Vyss. Ucheb. Zavod. Khim. i Khim. Tekhnol.* **8** (1965) 373.
11. Sillén, L. G. and Martell, A. E. (compilers) *Stability Constants*, Chem. Soc. London, Spec. Publ. No. 17 (1964) and No. 25 (1971).
12. Vacca, A., Sabatini and Gristina, M. A. *Coord. Chem. Rev.* **8** (1972) 45.
13. Majeste, R. J. and Meyers, E. A. *J. Phys. Chem.* **74** (1970) 3497.
14. Casey, A. T., Hoskins, B. F. and Whillans, F. D. *Chem. Commun.* **1970** 904.
15. Mitchell, T. P., Bernard, W. H. and Wasson, J. R. *Acta Cryst.* **B 26** (1970) 2096.
16. Iitaka, Y., Shimizu, K. and Kwan, T. *Acta Cryst.* **20** (1966) 803.
17. Ginstrup, O. *Chem. Instrum.* **4** (3) (1973) 141.
18. Ingri, N. and Sillén, L. G. *Arkiv Kemi* **23** (1964) 97.
19. Arnek, R., Sillén, L. G. and Wahlberg, O. *Arkiv Kemi* **31** (1969) 353; Brauner, P., Sillén, L. G. and Whiteker, R. *Arkiv Kemi* **31** (1969) 365.
20. Sillén, L. G. *Acta Chem. Scand.* **16** (1962) 159; Sillén, L. G. and Warnqvist, B. *Arkiv Kemi* **31** (1969) 341.
21. Ingri, N., Kakolowicz, W., Sillén, L. G. and Warnqvist, B. *Talanta* **14** (1967) 1261.
22. Doran, M. A., Chaberec, S. and Martell, A. E. *J. Am. Chem. Soc.* **86** (1964) 2129.
23. Zarembowitch, J. *J. Chim. Phys.* **63** (1966) 420.
24. Perrin, D. D. and Sharma, V. S. *J. Chem. Soc.* **A 1967** 724.
25. Leberman, R. and Rabin, B. R. *Trans. Faraday Soc.* **55** (1959) 1660.
26. Williams, D. R. *J. Chem. Soc.* **7** (1972) 790.
27. Freeman, H. C. and Martin, R.-P. *J. Biol. Chem.* **244** (1969) 4823.
28. Perrin, D. D. and Sharma, V. S. *J. Inorg. Nucl. Chem.* **28** (1966) 1271.
29. Gübeli, A. O., Hébert, J., Côte, P. A. and Taillon, R. *Helv. Chim. Acta* **53** (1970) 186.
30. Lewis, D. L., Hatfield, W. E. and Hodgson, D. J. *Inorg. Chem.* **11** (1972) 2216.
31. Ivarsson, G. *To be published.*
32. Bjerrum, J. *Kgl. Danske Videnskab. Selskab, Mat.-Fys. Medd.* **22** (1946) No. 18.

# On the Molecular Structure of Monomeric Dimethyl-(cyclopentadienyl)aluminium, $(CH_3)_2Al(C_5H_5)$

D. A. DREW and ARNE HAALAND

*Department of Chemistry, University of Oslo, Blindern, Oslo 3, Norway*

The electron scattering pattern from gaseous monomeric $(CH_3)_2$-$Al(C_5H_5)$ has been recorded from $s = 1.50$ Å$^{-1}$ to $s = 30.00$ Å$^{-1}$. The data rule out models containing *monohapto* ($\sigma$-bonded) or *pentahapto* (symmetrically $\pi$-bonded) $C_5H_5$ rings.

The four possible models of $C_s$ symmetry containing *polyhapto* (asymmetrically $\pi$-bonded) rings were refined by least squares calculations on the intensity data, and satisfactory agreement was obtained for all four. The values obtained for the perpendicular distances from the Al atom to the plane of the $C_5H_5$ ring and to the (approximate) fivefold symmetry axis of the ring ranged from 2.05 to 2.20 Å and from 0.9 to 1.4 Å, respectively.

CNDO/2 calculations indicate that the equilibrium conformation of monomeric $(CH_3)_2Al(C_5H_5)$ is as model (I) in Fig. 5, that the barrier to internal rotation of the $C_5H_5$ ring is of the order of 5 kcal mol$^{-1}$ or less, and that the barrier to exchange of the methyl groups is between 10 and 20 kcal mol$^{-1}$.

The most important structure parameters obtained by refinement of model (I) are: Perpendicular distance from the Al atom to the ring: 2.10 (2) Å, perpendicular distance from the Al atom to the symmetry axis of the ring: 0.99(10) Å. $C-C = 1.422(2)$ Å, $Al-C(Me) = 1.952$ (3) Å.

The nature of the bonding is discussed.

$\mathbf{T}$he first cyclopentadienyl-aluminium compound, $Et_2AlCp$ ($Et = C_2H_5$, $Cp = C_5H_5$), was synthesized by Giannini and Cesca in 1961.[1] Since the compound is partly associated in freezing benzene and since it forms a 1:1 complex with diethylether, Giannini and Cesca suggested that it contains *monohapto*, or $\sigma$-bonded, cyclopentadienyl rings and that dimerization occurs through ethyl bridges.

Several years later, Kroll and Naegele reported the $^1$H NMR spectra of $Me_2AlCp$ ($Me = CH_3$), $Et_2AlCp$ and $Bu^i_2AlCp$ ($Bu^i = iso\text{-}C_4H_9$).[2] In each compound the five ring protons gave rise to only one line in the $^1$H NMR spectrum, and this line remained unsplit when $Et_2AlCp$ in cyclopentane was cooled to $-60°$ or when $Bu^i_2AlCp$ in cyclopentane was cooled to $-91°$. It was there-

fore suggested that the Cp rings undergo rapid $1-2$ or $1-3$ shifts which render the ring protons equivalent on the NMR time scale.

Kroll and coworkers subsequently synthesized and investigated the analogous dialkyl(methylcyclopentadienyl) derivatives.[3] The ^{1}H NMR spectrum of $Me_2Al(C_5H_4Me)$ in cyclopentane at $+10°$ consisted of two singlets arising from the four ring protons, one singlet arising from the ring Me group and one singlet from the Me groups bonded to the metal. Cooling to $-40°$ produced no change except broadening. The spectrum therefore seemed to be in agreement with a model in which the Al atom and the Me group are bonded to the same atom in the Cp ring. Furthermore it was pointed out that this compound too is associated. That the Me group bonded to Al gives only a singlet in the ^{1}H NMR spectrum at $-40°$ would therefore seem to imply that either bridge-terminal exchange is more rapid than in $Me_6Al_2$ or that the Cp rings occupy the bridging position.

More recently Haaland and Weidlein have recorded the IR and Raman spectra of solid $Me_2AlCp$.[4] The spectra provided strong evidence against the presence of bridging Me groups and $\sigma$-bonded Cp groups. Haaland and Weidlein therefore proposed that solid $Me_2AlCp$ contains $\pi$-bonded Cp rings of approximate $D_{5h}$ symmetry. In view of the low solubility and volatility and the high melting point of the compound they further proposed a polymeric structure with bridging *pentahapto* Cp rings as shown schematically in Fig. 1 A. Such
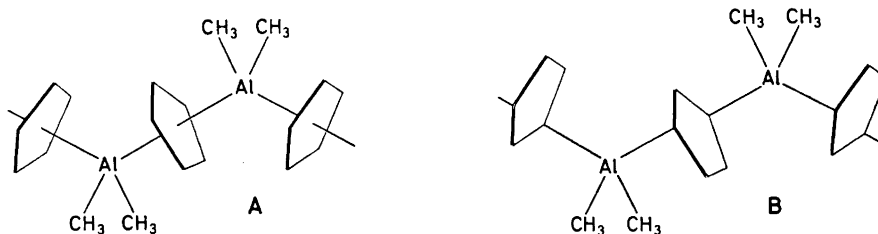


*Fig. 1.* A. Structure model of solid $Me_2AlCp$ proposed by Haaland and Weidlein.[4] B. Revised model of solid $Me_2AlCp$.

bridging Cp groups have been found in crystalline InCp [5] and $PbCp_2$.[6] Finally it was suggested that the polymer is broken down to a mixture of monomeric and oligomeric species in solution and in the gas phase, and that the Cp rings remain $\pi$-bonded in the monomer.

We now report the result or a gas phase electron diffraction investigation of monomeric $Me_2AlCp$. A preliminary account has appeared elsewhere.[7]

## EXPERIMENTAL AND CALCULATION PROCEDURE

$Me_2AlCp$ was prepared from NaCp and $Me_2AlCl$ as described by Kroll and Naegele.[2] The electron scattering pattern was recorded on the Oslo electron diffraction unit [8] with the sample reservoir at $105°$ and nozzle temperatures of $110°$ and $130°$. $Me_2AlCp$ is thermally stable up to $145°$.[4] There were no significant differences between the data collected at the two temperatures. The structure refinement was carried out on the data

collected at 130°. Exposures had been made with nozzle to photographic plate distances of 48 cm and 20 cm. The optical densities of five plates from the first set were recorded at $\Delta s = 0.125$ Å$^{-1}$ intervals, the optical densities of five plates from the last were recorded at $\Delta s = 0.250$ Å$^{-1}$ intervals. (The scattering parameter $s = (4\pi/\lambda) \sin (\theta/2)$ where $\lambda$ is the electron wavelength and $\theta$ the diffraction angle). The optical densities were converted into intensities and the data prosessed in the usual way.[9]

Every second of the modified molecular intensity points obtained from the 48 cm plates is shown in Fig. 2 A and the modified intensity points obtained from the 20 cm plates are shown in Fig. 3 A.
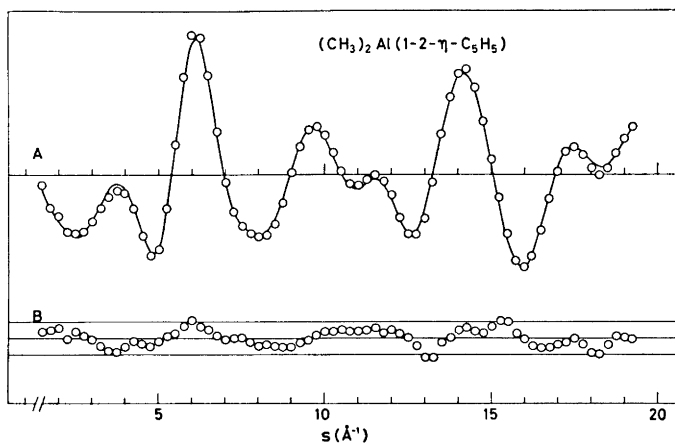


*Fig. 2.* A. ○; Experimental modified molecular intensity points from $s = 1.50$ to $19.25$ Å$^{-1}$. Full line; theoretical modified molecular intensity curve calculated for model (I) and parameter set P.A. B. ○; Difference points. The two full lines indicate the estimated uncertainty (three standard deviations) of the experimental intensity points. *Note:* The scale of B is twice that of A.
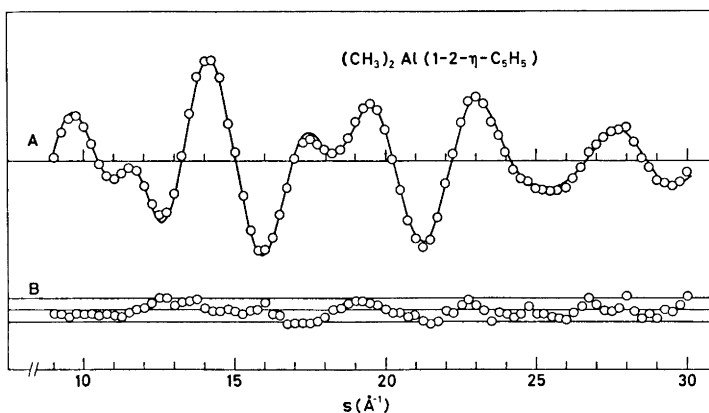


*Fig. 3.* A. ○; Experimental modified molecular intensity points from $s = 9.00$ Å$^{-1}$ to $30.00$ Å$^{-1}$. Full line; theoretical modified molecular intensity curve calculated for model (I) and parameter set PA. B. ○; Difference points. The two full lines indicate the estimated uncertainty (three standard deviations) of the experimental intensity points. *Note:* The scale of B is twice that of A.

Theoretical intensity curves were calculated from:

$$I^{\text{AlC}}(s) = \sum_{i \neq j} \frac{|f_i(s)||f_j(s)|}{|f_{\text{Al}}(s)||f_{\text{C}}(s)|} \cos\left[\eta_i(s) - \eta_j(s)\right] \frac{\sin(R_{ij}s)}{R_{ij}} \exp\left(-\tfrac{1}{2}l^2_{ij}s^2\right)$$

The sum extends over all atom pairs i,j in the molecule. $R_{ij}$ is the internuclear distance, $l_{ij}$ the root mean square amplitude of vibration. $f_j(s) = |f_j(s)| \exp[i\eta_j(s)]$ is the complex atomic scattering factor of atom j. It has been calculated for Al, C, and H by the partial wave approximation with a program written by Peacher.[10] The scattering potentials of Al and C have been found by non-relativistic Hartree-Fock calculations.[11,12]

Radial distribution functions were calculated by Fourier inversion of experimental and theoretical intensity curves after multiplication with the artificial damping function $\exp(-ks^2)$. The experimental intensity functions obtained with different nozzle-to-plate distances were then first spliced to each other and to the theoretical curve calculated for the best model below $s = 1.50$ Å$^{-1}$.

The molecular structure was refined by least-squares calculations on the intensity data with a non-diagonal weight matrix and a separately refined scale factor for the intensity data obtained for each nozzle to plate distance.[13]
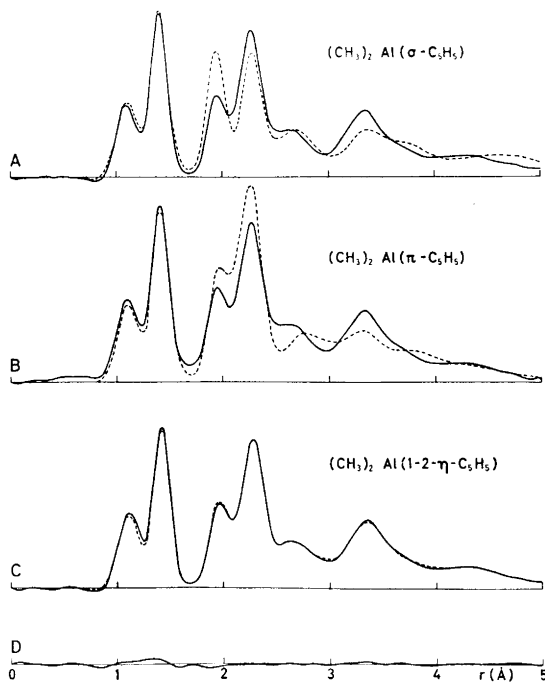


*Fig. 4.* A, B and C. Full line; experimental RD curves. A. Stipled line; theoretical RD curve calculated for model containing σ-bonded Cp ring. B. Stiplet line; theoretical RD curve calculated for model containing symmetrically π-bonded Cp ring. C. Stipled line: theoretical RD curve calculated for model containing asymmetrically π-bonded [model (I), parameter set PA] Cp ring. D. Difference between the two RD curves in C. Artificial damping constant $k = 0.002$ Å$^2$.

STRUCTURE ANALYSIS

In Fig. 4 A and B the experimental RD-curve for $Me_2AlCp$ (full line) is compared to theoretical RD-curves (stipled lines) calculated for models containing *monohapto*, or $\sigma$-bonded, and *pentahapto*, or symmetrically $\pi$-bonded, cyclopentadienyl rings. Both models lead to serious disagreement between experimental and calculated curves in the region around $r = 2.0$ Å, *i.e.* in the region containing the $Al - C$ bond distances, and may confidently be ruled out.

The four possible models of $Me_2AlCp$ with $C_s$ symmetry and the numbering of the C atoms in each model are shown in Fig. 5. The H atoms were given the same number as the C atoms to which they are bonded. For all models the following assumptions were made:

(i) The Cp rings have $D_{5h}$ symmetry. The point at which the fivefold axis intersects the ring plane is denoted by $o$.

(ii) The $Me_2Al$ fragment has $C_{2v}$ symmetry. The projection of the Al atom onto the ring plane is denoted by $p$. The distance $o - p$ is therefore equal to the perpendicular distance from the Al atom to the fivefold symmetry axis.

(iii) The Me groups have $C_{3v}$ symmetry with the threefold axes coinciding with the $Al - C$ bonds, and are oriented in such a way that one $C_6 - H_6$ bond is *anti* to the $Al - C_7$ bond.

The four models shown in Fig. 5 are closely related and may be regarded as rotational isomers: Model (II) may be obtained from model (I) by rotating the Cp ring 36° about its fivefold symmetry axis. Model (III) can be obtained
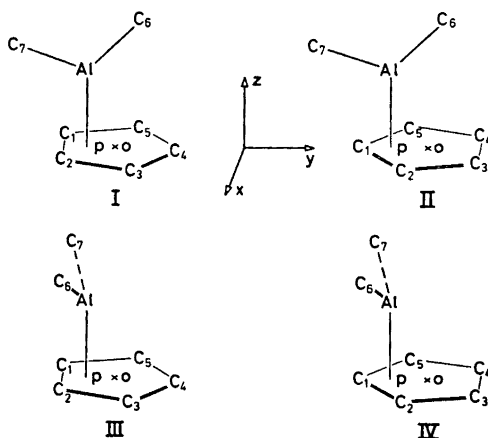


*Fig. 5.* Molecular models of $Me_2AlCp$.

from model (I) by rotating the $Me_2Al$ fragment 90° about its twofold symmetry axis. Model (IV) can be obtained from model (III) by a 36° rotation of the Cp ring or from model (II) by a 90° rotation of the $Me_2Al$ fragment.

Specifically the models differ in the values assigned to the angle between the $AlC_6C_7$ plane and the $y - z$ plane [0° for models (I) and (II), 90° for (III)

and (IV)] and the value assigned to the angle between $o\text{-}C_4$ and the $y$-axis [0° for models (I) and (III), 36° for (II) and (IV)].

After the assumptions (i) to (iii) regarding the local symmetry have been made, the structure of each of the four models is completely determined by the same nine parameters, $i.e.$ by the $C_1 - H_1$, $C_1 - C_2$, $Al - C_6$, and $C_6 - H_6$ bond distances, the $\angle\, C_6 - Al - C_7$ and $\angle\, Al - C_6 - H_6$ valence angles, the perpendicular distance from Al to the ring, $Al - p$, the distance from Al to the fivefold axis of the ring, $o - p$, and finally the angle between the fivefold axis of the ring and the twofold symmetry axis of the $Me_2Al$ fragment. The latter angle was denoted as $\alpha$ and was defined as positive when $C_6$ and $C_7$ are moved towards the negative part of the $y$-axis; hence all models as shown in Fig. 5 have $\alpha$ greater than zero.

It should be emphasized that models containing $\sigma$-bonded or symmetrically $\pi$-bonded Cp rings only are special cases of the four models in Fig. 5: Values of $o - p$ and $\alpha$ close to or equal to zero would correspond to a symmetrically $\pi$-bonded ring, while a value of $o - p$ equal to about 2.20 Å, of $Al - p$ equal to about 1.65 Å (which together would give $Al - C_1 = 1.95$ Å) and of $\alpha$ equal to about 30° for models (II) and (IV) would correspond to a $\sigma$-bonded ring.

For each model the nine structure parameters were refined by least-squares calculations on the intensity data along with the root-mean-square vibrational amplitudes of all bond distances as well as all non-bonded $Al\cdots C$ and $C\cdots C$ distances except $C_6\cdots C_7$. The amplitude of the latter distance was fixed at $l = 0.133$ Å, the value found in monomeric $(CH_3)_3Al$.[14]

It was found that all models could be brought into satisfactory agreement with the electron diffraction data. The generalized $R$-factors [13]

$$R_3 = 100 \left[ \sum_k \sum_l P_{kl} V_k V_l / \sum \sum P_{kl} I_k I_l \right]$$

obtained were 15.6, 15.8, 16.3, and 14.9, respectively. Since we have made assumptions about local symmetry, since not all vibrational amplitudes have been refined, and since shrinkage has been neglected, we do not feel that these numbers are significantly different.

The most important parameter values obtained for each model are shown in Table 1 along with their estimated standard deviations. The four sets of structure parameters have been denoted as PA, PB, PC, and PD. The amplitudes of the $C(Me)\cdots C(Cp)$ distances are not listed. For each model they ranged from 0.1 to 0.4 Å with estimated standard deviations ranging from 0.02 to 0.2 Å. Theoretical intensity curves calculated for model (I) with parameter set PA are compared to the experimental intensity data in Fig. 2 and Fig. 3. The corresponding RD curve is compared to the experimental RD-curve in Fig. 4 C and D. The agreement is seen to be satisfactory. The theoretical curves calculated for the best models (II), (III), and (IV) do not differ significantly from those shown.

At the first glance it is surprising that four models that should differ so much in the non-bonded $C(Me)\cdots C(Cp)$ distances all can be brought into agreement with the electron diffraction data. Inspection of Table 1 shows that this has been possible only with very different values for some structure parameters, particularly $Al - p$, $o - p$, $\alpha$, and $\angle\, C_6 - Al - C_7$.

*Table 1.* Structure parameters for $Me_2AlCp$ obtained by least-squares refinement on the four models shown in Fig. 5. Estimated standard deviations are given in parantheses in the units of the last digit.

| Model Parameter set | I PA R (Å) | II PB R (Å) | III PC R (Å) | IV PD R (Å) |
|---|---|---|---|---|
| $C_1-C_2$ | 1.422(2) | 1.422(2) | 1.421(2) | 1.421(2) |
| $C_1 \cdots C_3$ | 2.300(2) | 2.300(3) | 2.300(3) | 2.300(3) |
| $C_1-H_1$ | 1.06(2) | 1.08(3) | 1.12(2) | 1.13(2) |
| $Al-C_1$ | 2.21(2) | 2.20(3) | 2.19(2) | 2.16(1) |
| $Al-C_2$ | $-$ [b] | 2.55(4) | $-$ [b] | 2.63(8) |
| $Al \cdots C_3$ | 2.75(5) | 3.03(7) | 2.84(4) | 3.24(17) |
| $Al \cdots C_4$ | 3.04(7) | $-$ [c] | 3.18(6) | $-$ [c] |
| $Al \cdots p$ | 2.10(2) | 2.19(3) | 2.06(2) | 2.16(2) |
| $o \cdots p$ | 0.99(10) | 0.99(9) | 1.21(6) | 1.33(22) |
| $Al-C_6$ | 1.952(3) | 1.957(4) | 1.953(3) | 1.957(3) |
| $C_6-H_6$ | 1.14(2) | 1.14(3) | 1.09(2) | 1.10(2) |
| $\angle C_6-Al-C_7$ | 124(3)° | 117(4)° | 109(3)° | 109(6)° |
| $\angle Al-C_6-H_6$ | 113(2)° | 118(2)° | 116(3)° | 116(3)° |
| $\alpha$ [a] | 13(2)° | 1(2)° | $-9(4)°$ | $-19(9)°$ |
| | $l$ (Å) | $l$ (Å) | $l$ (Å) | $l$ (Å) |
| $C_1-C_2$ | 0.049(2) | 0.051(2) | 0.049(2) | 0.051(2) |
| $C_1 \cdots C_3$ | 0.060(2) | 0.060(3) | 0.062(2) | 0.053(3) |
| $C_1 \cdots H_1$ | 0.06(2) [d] | 0.07(2) [d] | 0.07(1) [d] | 0.08(1) [d] |
| $Al-C_1$ | 0.130(8) | 0.092(10) | 0.120(17) | 0.060(8) |
| $Al-C_2$ | $-$ | 0.35(7) | $-$ | 0.28(4) |
| $Al \cdots C_3$ | 0.29(6) | 0.31(6) | 0.26(4) | 0.31(12) |
| $Al \cdots C_4$ | 0.28(12) | $-$ | 0.30(24) | $-$ |
| $Al-C_6$ | 0.064(3) | 0.067(3) | 0.065(3) | 0.063(3) |
| $C_6-H_6$ | 0.06(2) [d] | 0.07(2) [d] | 0.07(1) [d] | 0.08(1) [d] |

[a] $\alpha$ is the angle between the line bisecting the $\angle C_6-Al-C_7$ angle and the $Al-p$ vector. For definition of sign see text. [b] By symmetry equal to $Al-C_1$. [c] By symmetry equal to $Al \cdots C_3$. [d] $l(C_1-H_1)$ and $l(C_6-H_6)$ were assumed equal.

*Table 2.* Binding energies (in atomic units) and energies in excess of model (I) (in kcal $mol^{-1}$) obtained by CNDO/2 calculations on the four models in Fig. 5 with various parameter sets (see Table 1). (1 atomic unit = 627.13 kcal $mol^{-1}$).

| Parameter set | Basis | I | II | III | IV |
|---|---|---|---|---|---|
| PA | $(sp)$ | BE = $-7.4483$ $\Delta E = 0$ | BE = $-7.4417$ $\Delta E =$ 4.1 | BE = $-7.4212$ $\Delta E =$ 17.0 | BE = $-7.4200$ $\Delta E =$ 17.7 |
| PB | $(sp)$ | BE = $-7.4874$ $\Delta E = 0$ | BE = $-7.4835$ $\Delta E =$ 2.5 | | |
| PC | $(sp)$ | BE = $-7.4464$ $\Delta E = 0$ | | BE = $-7.4242$ $\Delta E =$ 13.9 | |
| PD | $(sp)$ | BE = $-7.4515$ $\Delta E = 0$ | | | BE = $-7.4449$ $\Delta E =$ 4.2 |
| PA | $(spd)$ | BE = $-8.2913$ $\Delta E = 0$ | BE = $-8.2813$ $\Delta E =$ 6.2 | BE = $-8.2747$ $\Delta E =$ 10.4 | BE = $-8.2758$ $\Delta E =$ 9.7 |

## MOLECULAR ORBITAL CALCULATIONS

A series of CNDO/2 molecular orbital calculations [15,16] were carried out on the four models with various sets of structure parameters. Calculations were carried out with both $(sp)$ and $(spd)$ bases. The binding energies obtained are listed in Table 2.

It is seen that for parameter set PA model (I) gives lower energy than the three other models, and that for each of the three parameter sets PB, PC, and PD model (I) gives lower energy than the model for which the parameter set was obtained. The calculations therefore suggest that the equilibrium conformation of $Me_2AlCp$ is (I) but that the barrier to rotation of the Cp ring via (II) is of the order of 5 kcal mol$^{-1}$ or less, and that the barrier to exchange of the two Me groups via (III) or (IV) is between 10 and 20 kcal mol$^{-1}$.

The atomic charges on Al and C atoms obtained by calculations on model (I) with parameter set PA and the $(sp)$ basis are listed in Table 3. Very similar charges were obtained in the other calculations.

*Table 3.* Atomic charges (in 0.01 electron units) obtained by CNDO/2 calculations on model (I) with parameter set PA and $(sp)$ basis. $\mu = 2.23$ Debye.

|       | $q$  |      | $q$  |
|-------|------|------|------|
| $C_1$ | $-7$ | $C_5$ | $-3$ |
| $C_2$ | $-7$ | Al    | $+75$ |
| $C_3$ | $-3$ | $C_6$ | $-23$ |
| $C_4$ | $-9$ | $C_7$ | $-24$ |

## DISCUSSION

The close agreement obtained between experimental and calculated RD curves (Fig. 4 C and D) shows that $Me_2AlCp$ indeed is monomeric under the experimental conditions: In associated species the ratio of nonbonded to bonded distances would be greater than for the monomeric unit. Hence if the gas jet had contained significant amounts of associated species, the integrated area under the outer part of the experimental RD-curve would have been greater than the area under the theoretical curve calculated for any model of the monomeric unit.

The electron diffraction data rule out models for the monomeric unit containing $\sigma$-bonded or symmetrically $\pi$-bonded Cp rings. Unfortunately, however, the data do not allow a distinction to be made between the four models of $C_s$ symmetry shown in Fig. 5.

The $Al-C$ bridge bond in dimeric $Me_3Al$ determined by electron diffraction is 2.140(4) Å.[14] In $B_9C_2H_{11}AlEt$ where the Al atom occupies a corner of a distorted icosahedron and is bonded to three B atoms and two C atoms within the icosahedral unit, the two $Al-C(B_9H_2H_{11})$ distances are 2.173(7) Å.[17] Inspection of Table 1 therefore suggests that there is appreciable bonding between Al and $C_1$ and $C_2$ in models (I) and (III). These models may therefore be described as containing *dihapto* Cp rings. The $Al-C(Cp)$ distances obtained by refinement of models (II) and (IV) suggest appreciable bonding only be-

tween Al and $C_1$, though there probably is some additional bonding between Al and $C_2$ and $C_5$. These models may perhaps best be described as containing *trihapto* rings.

Since the distance from $o$ to the center of the $C_1 - C_2$ bond is 0.98 Å, the Al atom in model (I) is actually situated directly above the center of this bond, while in model (III) the metal atom is situated 0.2 Å *outside* the edge of the ring. Since the distance $o - C_1$ is 1.21 Å the Al atom is situated 0.2 Å inside the ring in model (II), 0.1 Å outside in model (IV).

In $(CH_3)Be(C_5H_5)$ the Be atom is situated at the fivefold symmetry axis of the ring.[18] It has been suggested that the Be atom is $(sp)$ hybridized, bonding with hybrid orbitals to the methyl C atom and to the $a_1$ $\pi$-orbital of the ring. The two unhybridized $2p$ orbitals on Be overlap with the $e_1$ $\pi$-orbitals of the ring forming two degenerate bonding molecular orbitals. The Cp ring serves as a five-electron ligand and the Be atom is surrounded by an octet of electrons. The assymetric structure of $Me_2AlCp$ is probably due to the fact that in this compound the Cp ring only need function as a three-electron ligand for the Al atom to be surrounded by an octet of electrons: After the two $Al - C(Me)$ bonds have been formed, the Al atom is left with one electron and two atomic orbitals to effect bonding to the ring. One of these orbitals is $2p_x$, the other an $(sp)$ type hybrid pointing towards a point near $p$.

The molecular orbital calculations show that the $a_1$ and the two $e_1$ $\pi$-orbitals of the ring interact with the atomic orbitals on Al. For model (I) and parameter set PA the resulting molecular orbitals are approximately:

$$\psi_1 = 0.43z_1 + 0.43z_2 + 0.39z_3 + 0.38z_4 + 0.39z_5 + 0.18s_{Al} - 0.17z_{Al}$$
$$\psi_2 = -0.38z_1 + 0.38z_2 + 0.54z_3 - 0.54z_5 + 0.31x_{Al}$$
$$\psi_3 = 0.41z_1 + 0.41z_2 - 0.23z_3 - 0.60z_4 - 0.23z_5 - 0.17z_{Al} + 0.14y_{Al}$$

where $s_{Al}$, $x_{Al}$, $y_{Al}$, and $z_{Al}$ are the $3s$, $3p_x$, $3p_y$, and $3p_z$ orbitals on Al and $z_1$ to $z_5$ the $2p_z$ orbitals of the five carbon atoms in the ring.

It is therefore clear that the four models are best described as $\pi$-complexes, albeit asymmetric. Furthermore it should be noted that allthough the metal atom is bonded to the ring *via* two or three C atoms, the bonding molecular orbitals are not restricted to Al and the C atoms in question, but are delocalized over the entire ring.

Since model (I) has two $Al - C(Cp)$ bond distances near 2.20 Å while model (II) has only one, it might be thought that the bonding between Al and Cp is stronger in (I) than in (II). The molecular orbital calculations indicate that the effect is small: The energy of the three Al to Cp bonding orbitals change only slightly, and the total binding energy for (II) calculated with parameter set PA is only 4.1 kcal mol$^{-1}$ higher than the binding energy of (I).

It might further be thought that model (I) is more favorable than models (III) or (IV) since it allows for effective overlap between the $3p_x$ orbital on Al and the appropriate $e_1$ $\pi$-orbital on the ring. This hypothesis receives support from the molecular orbital calculations: When calculations are carried out on models (III) or (IV) with parameter set PA, the energy of $\psi_2$ rises significantly and the total binding energies obtained are 17 kcal mol$^{-1}$ higher than for model (I).

The molecular orbital calculations therefore indicate that the equilibrium

structure of $Me_2AlCp$ is (I). This model is moreover, when the two Me groups are replaced by *pentahapto* Cp rings, entirely analogous to the structure of $(C_5H_5)_3Ti$ as recently determined by X-ray diffraction.[19]

The CNDO calculations also indicate that the barrier to internal rotation of the Cp ring *via* (II) is only a few kcal $mol^{-1}$. This is in agreement with the large vibrational amplitudes obtained for the $Al - C(Cp)$ distances (see Table 1). Neither, of course, is this low barrier or the moderate barrier obtained for exchange of the Me groups in disagreement with the $^1H$ NMR spectrum of $Me_2AlCp$ in benzene solution at ambient temperature which concists of one singlet corresponding to the six Me protons and another singlet corresponding to the five Cp protons.[2] It must be kept in mind, however, that $Me_2AlCp$ is partly associated in benzene and that there therefore may be other mechanisms of exchange.

The atomic charges on Al and C atoms obtained by CNDO calculations on model (I) are listed in Table 3. All H atoms were found to carry small (less than 0.02 e.u.) charges. Very similar charges were obtained by calculations on the other models. The Me group C atoms carry the same charge as in monomeric $Me_3Al$,[20] $- 0.23$ e.u. The Al atom carries a larger positive charge than in $Me_3Al$, $+ 0.63$ e.u. The negative charge on the ring is fairly uniformly distributed.

The $Al - C(Me)$ bond distances in $Me_2AlCp$ are not significantly different from the terminal $Al - C$ bonds in dimeric $Me_3Al$ or dimeric $Me_2AlH$, 1.957(3) Å [14] and 1.949(3) [21] Å, respectively, as determined by gas phase electron diffraction.

The $C_1 - C_2$ bond distance is very similar to the $C - C$ bond distance in MeBeCp, 1.420(1) Å.[18] The values obtained for the vibrational amplitude of the $C - C$ bond in the two molecules, 0.051(1) Å in MeBeCp and 0.049(2) in $Me_2AlCp$ are also very similar. This indicates that the five $C - C$ bonds in $Me_2AlCp$ must be very nearly equal.

After Haaland and Weidlein published their spectroscopic evidence against $\sigma$-bonded Cp rings in solid $Me_2AlCp$, Einstein, Gilbert and Tuck have determined the crystal structure of $InCp_3$.[22] This compound is polymeric in the solid phase. Each In atom is $\sigma$-bonded to two terminal Cp rings and is linked to two bridging Cp rings. The latter show small, though definite, deviations from fivefold symmetry. Each bridging Cp group is bonded to two In atoms that are lying on opposite sides of the ring. Only two contacts, $In - C_1$ and $C_3 - In'$ are short enough to indicate appreciable bonding. We believe that the model for solid $Me_2AlCp$ should be modified to contain similar bridging groups as shown schematically in Fig. 1 B.

Conversely we would propose that monomeric $InCp_3$ has a structure analogous to that of monomeric $Me_2AlCp$, *i.e.* that the bridging Cp rings become assymetrically $\pi$-bonded in the monomer. The $^1H$ NMR spectrum or the degree of association of $InCp_3$ in inert solvents have not been reported. The $^1H$ NMR spectra of $InCp_3$ in $CDCl_3$ down to $- 70°$ or in $CH_2Cl_2$ down to $- 90°$ consists of one narrow line only.[23] If the compound is monomeric in these solvents and if the structure of the monomer is not influenced, the $^1H$ NMR spectra would indicate rapid exchange of the $\sigma$- and asymmetrically $\pi$-bonded rings.

## REFERENCES

1. Giannini, N. and Cesca, S. *Gazz. Chim. Ital.* **91** (1961) 597.
2. Kroll, W. R. and Naegele, W. *Chem. Commun.* **1969** 246.
3. Kroll, W. R., McDivitt, J. R. and Naegele, W. *Inorg. Nucl. Chem. Letters* **5** (1969) 973.
4. Haaland, A. and Weidlein, J. *J. Organometal. Chem.* **40** (1972) 29.
5. Frasson, E., Menegus, F. and Panattoni, C. *Nature* **199** (1963) 1087.
6. Panattoni, C., Bambieri, G. and Croatto, U. *Acta Cryst.* **21** (1966) 823.
7. Drew, D. A. and Haaland, A. *Chem. Commun.* **1972** 1300.
8. Bastiansen, O., Hassel, O. and Risberg, E. *Acta Chem. Scand.* **9** (1955) 232.
9. Andersen, B., Seip, H. M., Strand, T. G. and Stølevik, R. *Acta Chem. Scand.* **23** (1969) 3224.
10. Peacher, J. L. and Wills, J. C. *J. Chem. Phys.* **46** (1967) 4807.
11. Watson, R. E. and Freeman, A. J. *Phys. Rev.* **123** (1961) 521.
12. Clementi, E., Roothaan, C. C. J. and Yoshimine, M. *Phys. Rev.* **127** (1962) 1618.
13. Seip, H. M., Strand, T. G. and Stølevik, R. *Chem. Phys. Letters* **3** (1969) 617.
14. Almenningen, A., Halvorsen, S. and Haaland, A. *Acta Chem. Scand.* **25** (1971) 1937.
15. Santry, D. P. and Segal, G. A. *J. Chem. Phys.* **47** (1967) 158.
16. Pople, J. A. and Beveridge, D. L. *Approximate Molecular Orbital Theory*, McGraw, New York 1970.
17. Churchill, M. R. and Reis, A. H. *J. Chem. Soc. Dalton Trans.* **1972** 1317.
18. Drew, D. A. and Haaland, A. *Acta Chem. Scand.* **26** (1972) 3079.
19. Lucas, C. R., Green, M., Forder, R. A. and Prout, K. *Chem. Commun.* **1973** 97.
20. Gropen, O. and Haaland, A. *Acta Chem. Scand.* **27** (1973) 521.
21. Almenningen, A., Andersen, G. A., Forgaard, F. R. and Haaland, A. *Acta Chem. Scand.* **26** (1972) 2315.
22. Einstein, F. W. B., Gilbert, M. M. and Tuck, D. G. *Inorg. Chem.* **11** (1972) 2832.
23. Poland, J. S. and Tuck, D. G. *J. Organometal. Chem.* **42** (1972) 307.

# Infrared Studies on the Thiocyanate Ion and its Complexes

# with Palladium (II)

ATIS MIEZIS

*Inorganic Chemistry 1, Chemical Center, University of Lund, Box 740, S-220 07 Lund 7,
Sweden*

The frequencies and the integrated absorption intensities for the
stretching vibrations of the thiocyanate group in NaSCN and various
mixed thiocyanato complexes of palladium(II) have been measured.
A normal coordinate analysis of these vibrations has been carried
out for the thiocyanate ion in order to relate the measured intensities
to dipole moment changes with a stretching of an individual bond.
The high values of $\partial\mu/\partial r$ indicate a large contribution from the
"delocalization moment".

The spectral data have been used to distinguish between the bond
types Pd — SCN and Pd — NCS. The dependence of the bonding on
the nature of the other ligands in the mixed complexes is discussed.

It has been known for many years that infrared spectroscopy presents a
good method for determination of the mode of bonding between a metal
ion and the thiocyanate ion. The linear triatomic ion SCN⁻ has four normal
vibrations, of which two are degenerated. They are all infrared active. On
coordination, all these shift frequencies and the shifts are characteristic of
the mode of bonding. The vibrations may be described approximately as a
C—N stretch ($\nu_{CN}$), a C—S stretch ($\nu_{CS}$), and a S—C—N bend ($\delta_{SCN}$).
Their frequencies are found in the following ranges: $\nu_{CN}$ 1950—2120 cm⁻¹
(generally above the value of the "free" thiocyanate ion, 2060—2070 cm⁻¹,
but below 2100 cm⁻¹), $\nu_{CS}$ 760—880 cm⁻¹, $\delta_{SCN}$ 450—490 cm⁻¹ for the N-
bonded group and $\nu_{CN}$ 2080—2130 cm⁻¹, $\nu_{CS}$ 690—720 cm⁻¹, $\delta_{SCN}$ 400—440
cm⁻¹ for the S-bonded group. As may be seen there is often an overlap of the
$\nu_{CN}$ for the two types of bonding.

The behaviour of all but one of the frequencies can easily be explained by
regarding how the contributions of the three resonance structures[1]

$$N \equiv C - S^- \ (a) \qquad {}^-N = C = S \ (b) \qquad {}^{2-}N - C \equiv S^+ \ (c) \qquad (1)$$
$$71 \ \% \qquad\qquad 12 \ \% \qquad\qquad 17 \ \%$$
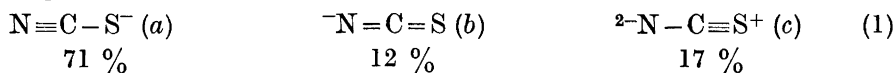
would be changed upon coordination.[2,3] The only unexpected frequency shift
is towards higher frequencies usually shown by the C—N stretch in N-bonded

complexes. This fact is commented upon elsewhere [3] with reference to the work of Porai-Koshits et al.[4] However, $\nu_{CN}$ values also well below that of the "free" thiocyanate ion have been reported, namely 1963 – 1980 cm$^{-1}$ for HNCS [5,6] and around 1990 – 1980 cm$^{-1}$ for the N-bonded hexathiocyanates of Zr(IV), Hf(IV) [7] and Nb(V), Ta(V).[8] In these cases it is probable that the electron redistribution effect, caused by a high covalency, is great enough to cancel out the positive frequency shift predicted from the model of Porai-Koshits et al.[4] i.e. one with little or no change in the force constants of the C – N and C – S bonds for the N-coordinated thiocyanate ion relative to that for the "free" ion.

Besides the frequency shifts, the intensity of the C – N stretching vibration has been developed as a criterion of the bonding type.[2,9-11] The intensity criterion says, roughly, that the integrated absorptions for the N-bonded complexes are larger and for the S-bonded ones smaller than the same quantity for the "free" thiocyanate ion. The technique was first limited to compounds which can be dissolved in a suitable solvent without dissociation or formation of mixed complexes. Later, the procedure was extended to solid samples [3] and it was found that the solid state technique (KBr-disks), in spite of some loss of accuracy, could also be used to distinguish between N- and S-bonded thiocyanato complexes. Bailey et al.[12] have recently reported successful measurements on the solid state intensities with a somewhat modified method.

It was found [13] that metals of class a (as classified by Ahrland, Chatt and Davis [14]) generally are bonded to the thiocyanate ion via the nitrogen atom, whereas class b metals are bonded via the sulphur atom. However, Turco and Pecile [15] found that in mixed complexes of such typical b-metals as palladium(II) and platinum(II) the mode of bonding depends upon the nature of the other ligands present. They suggested that the M – SCN bond usually is the most stable with these metals because of the $\pi$-bonding contribution caused by a back donation of electrons from the filled nonbonding d-orbitals of the metal to vacant orbitals located on the sulphur atom of the thiocyanate ion. But when strong $\pi$-acceptors, as for example tri-substituted phosphines, are introduced into the complex, the $\pi$-bonding contribution to the M – SCN bond is reduced and in such a case a M – NCS bond may become energetically more favourable. As a consequence of this one would expect a critical value in the $\pi$-acceptor strength for which the energy difference between the S- and N-bonded isomers is small enough to permit isolation of both isomers by an adjustment of the conditions of preparation. Subsequently, Burmeister and Basolo [16,17] could prepare the first thiocyanate linkage isomers Pd[As(C$_6$H$_5$)$_3$]$_2$-(NCS)$_2$ – Pd[As(C$_6$H$_5$)$_3$]$_2$(SCN)$_2$ and Pd(bipy)(NCS)$_2$ – Pd(bipy)(SCN)$_2$.

Because of the frequent overlap of $\nu_{CN}$ for the N- and S-bonded thiocyanate groups in these complexes, the type of bonding is usually determined on the basis of the position of $\nu_{CS}$ and $\delta_{SCN}$ [7-19] but also some examples of the application of the intensity criterion are available.[3,11,20]

In a previous paper [3] was discussed how the increase and decrease of the intensity of the C – N stretching vibration for the N- and S-bonded species, respectively, as compared with the "free" ligand, could be rationalized from a simple valence bond picture, using a fixed charge model. Attention was also drawn to a breakdown of the simple model when there is a large redistribu-

tion of the electron cloud upon coordination (strongly covalent bonding). In this work, the intensity measurements have been extended to the $C-S$ stretching region as this vibration seems to be more readily influenced by the degree of interaction between metal and the thiocyanate ion than the $C-N$ stretching vibration.

<div align="center">EXPERIMENTAL</div>

*Preparation of the complexes.* Palladium(II) complexes of the general formula $PdL_2X_2$ and $PdLX_2$, where X is NCS or SCN and L various mono- or bidentate organic ligands, have been prepared. The following ligands are used: Triphenylphosphine ($Ph_3P$), triisopropylphosphine [$(i-Pr)_3P$], tributylphosphine [$(n-Bu)_3P$], triphenylarsine ($Ph_3As$), triphenylstibine ($Ph_3Sb$), pyridine (py), 4-nitropyridine, 4-cyanopyridine, 4-benzoylpyridine, methyl isonicotinate (i-nicotin), 4-acetylpyridine (4-Acpy), isonicotinaldehyde or pyridine-4-aldehyde (4-CHOpy), 4-benzylpyridine, $\gamma$-picoline or 4-methylpyridine (4-Mepy), 4-aminopyridine, 2,2'-bipyridine (bipy), 4,4'-dimethyl-2,2'-bipyridine (4,4'-dimethylbipy), 1,10-phenanthroline (phen), 5-nitro-1,10-phenanthroline (5-nitrophen), 5,6-dimethyl-1,10-phenanthroline (5,6-dimethylphen), thiourea (tu), and ethylenethiourea (etu). All these ligands except 4-nitropyridine are commercially available. 4-nitropyridine was prepared from 4-nitropyridine-1-oxide according to the procedure described by Ochiai.[21]

The complexes were prepared by mixing alcoholic solutions of 1 mmol of $Na_2Pd(SCN)_4$ and the stoichiometric quantity of ligand. Mostly, the complexes precipitated immediately but in some cases stirring for a period of time was necessary. Then they were filtered, washed with alcohol and ether and dried *in vacuo* over phosphorus pentoxide. All chemicals used were of analytical grade. The preparation of the linkage isomers $Pd(AsPh_3)_2(NCS)_2$ and $Pd(AsPh_3)_2(SCN)_2$ has been described before.[3] Carbon, hydrogen, and nitrogen analyses were performed on the samples by the Division of Analytical Chemistry, Chemical Center, Lund, and some examples are given in Table 1.

*Table 1.* The analytical data (%) for some of the palladium(II) complexes.

| Compound | Calculated | | | Found | | |
|---|---|---|---|---|---|---|
| | C | H | N | C | H | N |
| $Pd(PPh_3)_2(NCS)_2$ | 61.1 | 4.05 | 3.75 | 60.9 | 4.06 | 3.7 |
| $Pd(AsPh_3)_2(NCS)_2$ | 54.7 | 3.62 | 3.36 | 54.3 | 3.68 | 2.7 |
| $Pd(bipy)(NCS)_2$ | 38.0 | 2.13 | 14.79 | 37.5 | 2.22 | 14.4 |
| $Pd(4,4'$-dimethylbipy)(NCS)(SCN) | 41.3 | 2.97 | 13.78 | 41.6 | 2.95 | 13.9 |
| $Pd(phen)(SCN)_2$ | 41.8 | 2.00 | 13.91 | 42.9 | 2.45 | 13.4 |
| $Pd(4$-cyanopy$)_2(SCN)_2$ | 39.0 | 1.87 | 19.50 | 38.2 | 2.04 | 19.9 |
| $Pd(\gamma$-pic$)_2(SCN)_2$ | 41.2 | 3.45 | 13.71 | 40.8 | 3.51 | 13.8 |
| $Pd(tu)_2(SCN)_2$ | 12.8 | 2.15 | 22.43 | 13.3 | 2.29 | 22.5 |

*Recording of spectra.* The infrared spectra of the samples in KBr disks were recorded on Perkin-Elmer Models 521 and 180 grating spectrophotometers. The accuracy of the frequency readings is $\pm 0.5$ and $\pm 0.25$ $cm^{-1}$ and of the transmittance $\pm 0.5$ and $\pm 0.4$ %, respectively, according to the performance specifications of the instruments. The scale on the wavenumber axis was expanded 10 times, that is 10 and 5 $cm^{-1}$ per 1 cm of chart paper in the $\nu_{CN}$ and $\nu_{CS}$ range, respectively. From the spectra both frequencies ($\nu$) and the integrated absorptions ($A$) of the bands could be determined.

$A$ is defined as

$$A = \frac{1}{cd}\int \ln\left(\frac{I_0}{I}\right)_\nu \, d\nu$$

where $c =$ concentration, $d =$ thickness of sample, $\nu =$ frequency, $I_0(I) =$ the true intensity of the incident (transmitted) radiation of frequency $\nu$. Ramsay [22] has shown that if the bands could be described by Lorentz functions $A = (K/cd) \ln (T_0/T)\nu_{\max}{}^a \times \Delta\nu_{1/2}{}^a$. Here $T_0$ and $T$ are the apparent intensities of the incident and transmitted light at finite slit widths, respectively, and $\Delta\nu_{1/2}{}^a$ is the apparent half-band width. $K$ is a correction factor related to the ratio of the slit width to the apparent hald-banf width. By using Ramsay's tables of $K$-values and the spectral slit width of the spectrophotometer, one can easily determine the integrated absorption (Ramsay's method of direct integration). Normally for small ratios slit width/half-band width, $K$ is approximately $\pi/2$ and $A = (\pi/2)$ (ln $10)\varepsilon_{\max} \times \Delta\nu_{1/2}$ where $\varepsilon_{\max}$ is the molar absorptivity as defined by $\varepsilon_{\max} = (1/cd)$ log $(T_0/T)\nu_{\max}$. Unfortunately, the shapes of the $\nu_{CN}$ and $\nu_{CS}$ bands in the solid thiocyanato complexes were in most cases not true Lorentzian. In addition to the fact that the method of Ramsay is derived for liquids and solutions, this made us determine the integrated absorption by direct graphical integration. The spectra were run with linear absorbance and the areas under the curves were measured with a planimeter. The spectral slit width (resolution) of the spectrophotometer was about 1.5 cm⁻¹. The values of the integrated absorption determined by graphical integration were generally smaller than those obtained from Ramsay's method.

The assignment of bands due to the thiocyanate group was made by comparing the spectra of the thiocyanates with the spectra of the corresponding chloro compounds. The concentration of the solid sample in a KBr disk was obtained by accurate weighing of the sample before it was mixed with potassium bromide and by determination of the volume of the disk when it had been pressed. Every compound was examined in about ten disks with varying compositions and from the recorded spectra the accuracy of the integrated absorption (given in Table 2) was estimated to be within 10 %.

In addition to frequencies from infrared spectra also some Raman values are included in Table 2. These were obtained with the new commercial Laser-Raman spectrophotometers Cary Model 82 and Spex Ramalog.

## CALCULATIONS ON THE SCN⁻ ION

*The method of normal coordinate analysis.* The intensities of bands arising from the fundamental vibrations are proportional to the square of the dipole derivative with respect to the $Q_i$ normal coordinate. If $A_i$ is the integrated absorption in M⁻¹ cm⁻² the proportionality is given by [23]

$$A_i = \frac{N\pi}{3c^2 \times 10^3} \times \left(\frac{\partial\mu}{\partial Q_i}\right)^2 \tag{2}$$

Here $N$ is Avogadro's number, $c$ the velocity of light in cm/s and $\mu$ the total dipole moment of the molecule in esu cm.* Hence, the absolute value of $\partial\mu/\partial Q_i$ could be obtained from experimental determinations of the integrated absorption:

$$\left|\frac{\partial\mu}{\partial Q_i}\right| = \left(\frac{3c^2 \times 10^3 A_i}{N\pi}\right)^{\frac{1}{2}} (\text{esu g}^{-\frac{1}{2}}) \tag{3}$$

Eqn. (2) is derived for isolated molecules in the gas phase and when handling solid samples one must consider changes in the vibrational intensities caused

* For the sake of convenient comparison with existing data the CGS system has been used in the derivations and the integrated absorption is expressed in M⁻¹ cm⁻². The SI unit for the integrated absorption would be m mol⁻¹, for the velocity of light m s⁻¹ and for the dipole moment C m. In this case eqn. (2) becomes $A_i = 8.988 \times 10^9 \dfrac{N\pi}{3c^2}\left(\dfrac{\partial\mu}{\partial Q_i}\right)^2$.

Table 2. Spectral data of the investigated complexes. The values of $\epsilon$, $\epsilon \times \Delta\nu_{1/2}$, and $A$ are calculated per SCN group.

| | Compound | $\nu_{CN}$ (cm⁻¹) | $\epsilon$ (M⁻¹cm⁻¹) | $\Delta\nu_{1/2}$ (cm⁻¹) | $\epsilon \times \Delta\nu_{1/2} \times 10^{-4}$ (M⁻¹cm⁻²) | $A_{CN} \times 10^{-4}$ (M⁻¹cm⁻²) | $\nu_{CS}$ (cm⁻¹) | $\epsilon$ (M⁻¹cm⁻¹) | $\Delta\nu_{1/2}$ (cm⁻¹) | $\epsilon \times \Delta\nu_{1/2}$ (M⁻¹cm⁻²) | $A_{CS}$ (M⁻¹cm⁻²) | $\delta_{SCN}$ (cm⁻¹) |
|---|---|---|---|---|---|---|---|---|---|---|---|---|
| A | NaSCN | 2070 | 310 | 39 | 1.22 | 3.25 | 755 | 6 | 10 | 60 | 150 | {484 / 470} |
| B | Pd(PPh₃)₂(NCS)₂ | 2092 | 720 | 24.5 | 1.76 | 5.76 | {851 / 846sh} | (70) | (13) | (900) | 2200 | 448 |
| C | Pd[P(i-Pr)₃]₂(NCS)₂ | 2106 | 900 | 23 | 2.07 | 6.05 | 848 | 130 | 6 | 780 | 2600 | |
| D | Pd[P(n-Bu)₃]₂(NCS)₂ | 2105 | 990 | 23 | 2.28 | 6.70 | 847 | 120 | 9 | 1080 | 3100 | |
| E | Pd(AsPh₃)₂(NCS)₂ | 2088 | 720 | 27 | 1.94 | 6.03 | 853 | 100 | 10 | 1000 | 2250 | 448 |
| F | Pd(4-nitropy)₂(NCS)₂ | 2109 | 700 | 29 | 2.03 | 5.96 | a | a | a | a | a | 455ᵇ |
| G | Pd(bipy)(NCS)₂ | 2099 | 700 | 32 | 2.24 | 5.62 | {843 / 849sh} | (38) | (9) | (340) | 990 | 458 |
| H | Pd(5-nitrophen)(NCS)(SCN) | 2090 | 340 | 46 | 1.58 | 4.13 | | a | | | a | {457 / 424 / 419} |
| | | 2120 | 290 | 15 | 0.44 | 1.09 | 692 | 4 | 7 | 28 | 64 | |
| I | Pd(4,4'-dimethylbipy)(NCS)(SCN) | 2099 | 610 | 36 | 2.18 | 6.17 | 839ᵇ | 58ᵇ | 9ᵇ | 522ᵇ | 1014ᵇ | 455 |
| | | 2121 | 310 | 11 | 0.34 | 0.84 | 702 | 4.5 | 9 | 41 | 121 | |
| J | Pd(AsPh₃)₂(SCN)₂ | 2119 | 350 | 8 | 0.28 | 0.87 | a | a | a | a | a | a |
| K | Pd(SbPh₃)₂(SCN)₂ | 2093 | 720 | 11 | 0.79 | 2.80 | a | a | a | a | a | 417 |
| L | Pd(phen)(SCN)₂ | 2116 | 400 | 9 | 0.36 | 1.12 | 695 | 3.5 | 7 | 25 | 60 | 418 |
| M | Pd(5,6-dimethylphen)(SCN)₂ | {2112 / 2106} | 490 / 490 | 7 / 7 | {0.34 / 0.34} | 2.11 | 698 | 3.5 | 7 | 25 | 70 | 420 |

*Table 2. Continued.*

| | | | | | | | | | | | |
|---|---|---|---|---|---|---|---|---|---|---|---|
| N | Pd(4-cyanopy)$_2$(SCN)$_2$ | 2113 | 470 | 10 | 0.47 | 1.35 | {701, 696} | 10, 11 | 3, 4 | {30, 44} | 265 | 419 |
| | Raman | 2119 | | | | | | | | | | |
| O | Pd(4-benzoylpy)$_2$(SCN)$_2$ | 2119 | 370 | 7 | 0.26 | 0.95 | {702, 699} | a | a | a | a | |
| P | Pd(i-nicotin)$_2$(SCN)$_2$ | 2117 | 350 | 9 | 0.31 | 1.04 | a | a | a | a | a | |
| Q | Pd(4-Acpy)$_2$(SCN)$_2$ | 2120 | 350 | 12 | 0.42 | 1.30 | 706 | 6 | 10 | 60 | 134 | 424 |
| R | Pd(4-CHOpy)$_2$(SCN)$_2$ | 2117 | 250 | 24 | 0.60 | 1.41 | 697 | 3 | 9 | 27 | 62 | |
| S | Pd(py)$_2$(SCN)$_2$ | {2114, 2102sh} | (300) | (9) | (0.27) | 1.67 | a | a | a | a | a | 426 |
| T | Pd(4-benzoylpy)$_2$(SCN)$_2$ | 2117 | 320 | 7 | 0.22 | 0.83 | 702 | 9 | 3 | 27 | 71 | |
| U | Pd(4-Mepy)$_2$(SCN)$_2$ | 2110 | 280 | 10 | 0.28 | 0.91 | 698 | 3 | 6 | 18 | 50 | |
| V | Pd(4-aminopy)$_2$(SCN)$_2$ | 2116 | 580 | 14 | 0.81 | 2.40 | 716 | 4 | 8 | 32 | 106 | |
| W | Pd(tu)$_2$(SCN)$_2$ | 2110 | 740 | 12 | 0.89 | 2.90 | {714, 704, 716} | 7, 11 | 50, 41 | {350, 450} | 2370 | |
| | Raman | 2110 | | | | | | | | | | |
| X | Pd(etu)$_2$(SCN)$_2$ | 2103 | 310 | 13 | 0.40 | 1.61 | 703 | 4 | 7 | 28 | 90 | |
| Y | K$_2$Pd(SCN)$_4$ | {2094, 2124} | {140, 190} | {12, 8} | {0.17, 0.15} | 0.97 | {704, 698sh} | (5) | (7) | (35) | 120 | |

[a] Band masked by the absorption of the organic ligand. [b] The values are uncertain because of a large absorption of the organic ligand in that region. Abbreviations: For the abbreviations in the formulae of the compounds see text below "EXPERIMENTAL"; sh means shoulder.

by intermolecular interactions and also the dependency of the intensity on the refractive index of the phase.[24] Ratajczak and Orville-Thomas [25] have derived a general formula which applies to molecules in any phase. However, the results of Yamada and Person [26] in their studies of the infrared intensities in the solid phase of linear triatomic molecules indicate that the intensities of the stretching vibrations of, *e.g.*, a thiocyanate group in the solid phase probably would not differ drastically from those in the gas phase and therefore eqn. (2) would be a good approximation in this case.

Since all atoms in the molecule move in phase for each fundamental vibration the normal coordinates are complicated functions of changes in bond lengths and bond angles. It is desirable from a chemical point of view to relate the change of dipole moment to the individual bonds. This could be done by carrying out a normal coordinate analysis which is based on accurate knowledge of the potential and kinetic energy of the system. Reviews of the method of normal coordinate calculations and the nomenclature used can be found in Refs. 27 and 28. In the following a calculation of the change of dipole moment with the bond lengths in the "free" thiocyanate group will be made in a manner similar to the procedure of Robinson [29] and Orville-Thomas *et al.*[30,31]

The normal coordinates $Q_i$ (in terms of a column matrix Q) are related to the symmetry coordinates $S_i$ (S) by a transformation

$$S = LQ \text{ or } Q = L^{-1}S \tag{4}$$

where $L^{-1}$ is the inverse of matrix L. The linear NCS group belongs to the point group $C_{\infty v}$. That means that the two stretching vibrations and the doubly degenerate bending vibration are in different symmetry classes ($\Sigma^+$ and $\Pi$, respectively) and therefore they can be treated separately. For the two stretching vibrations (4) can be written

$$Q_i = L_{i1}^{-1}S_1 + L_{i2}^{-1}S_2 \quad (i = 1,2)$$

As the stretching vibrations imply changes only in the interatomic distances, a relevant connection between the symmetry and the internal coordinates is $S_1 = \Delta r_1 = \Delta r_{NC}$ and $S_2 = \Delta r_2 = \Delta r_{CS}$. Thus

$$Q_i = L_{i1}^{-1} \Delta r_1 + L_{i2}^{-1} \Delta r_2 \quad (i = 1, 2) \tag{5}$$

Using the GF matrix technique of Wilson [27,32] the vibrational problem leads to a secular equation which symbolically can be written as $|GF - E\lambda| = 0$. Here both F and G are symmetrical matrices. The components of F are the force constants $F = \begin{pmatrix} f_1 & f_{12} \\ f_{12} & f_2 \end{pmatrix}$ where $f_1$ and $f_2$ are the force constants of the N$-$C and C$-$S bonds, respectively, and $f_{12}$ is the bond-bond interaction constant. The elements of the G matrix can easily be shown to be (see Ref. 27 SEC. 4$-$2)

$$G = \begin{pmatrix} \mu_N + \mu_C & -\mu_C \\ -\mu_N & \mu_C + \mu_S \end{pmatrix}$$

where $\mu$ is the reciprocal mass. The homogeneous equations for the amplitudes ($L^{-1}$) for this form of the secular equation are (eqn. 42 in Ref. 32)

$$[(GF)_{11} - \delta_{1l}\lambda_m]L_{m1}^{-1} + [(GF)_{21} - \delta_{2l}\lambda_m]L_{m2}^{-1} = 0$$

where $l$, $m = 1$ or $2$ and $\delta_{kl}$, the Kronecker delta symbol, is unity if $k = l$ and is zero otherwise. $\lambda$ is determined from the observed wave numbers of the two stretching vibrations by $\lambda = 4\pi^2 c^2 \bar{\nu}^2$.

These homogeneous equations give only the ratios of the components of $L^{-1}$. Thus for $l = 1$

$$\frac{L_{m2}^{-1}}{L_{m1}^{-1}} = -\frac{(GF)_{11} - \lambda_m}{(GF)_{21}} \qquad (6)$$

$(GF)_{11}$ and $(GF)_{21}$ are elements of a matrix GF. That is, in this case,

$$(GF)_{11} = (\mu_N + \mu_C)f_1 - \mu_C f_{12} \qquad (7a)$$

$$(GF)_{21} = -\mu_C f_1 + (\mu_C + \mu_S)f_{12} \qquad (7b)$$

The separate values of the elements of $L^{-1}$ can be obtained by the normalization condition. This may be written [32] as $L^{-1}G(L')^{-1} = E$ where $L'$ is the transpose of $L$ and $E$ is the unit matrix. If $(L_0^{-1})_{mk}$ is the unnormalized value of $(L^{-1})_{mk}$ and $K_m$ the normalizing constant then

$$K_m = [\sum_{k,l=1}^{2} (L_0^{-1})_{mk}(L_0^{-1})_{ml} \, G_{kl}]^{-\frac{1}{2}}$$

If for example $(L_0^{-1})_{ml}$ taken equal to unity then

$$K_m = [G_{11} + 2(L_0^{-1})_{m2} \, G_{12} + (L_0^{-1})_{m2}^2 \, G_{22}]^{-\frac{1}{2}} \qquad (8)$$

The knowledge of the ratio $L_{m2}^{-1}/L_{m1}^{-1}$ now directly gives the separate normalized values of $L^{-1}$.

The dipole derivative with respect to the changes in bond legths $\partial\mu/\partial r_k$ can be written as

$$\frac{\partial\mu}{\partial r_k} = \left(\frac{\partial\mu}{\partial Q_1}\right)\left(\frac{\partial Q_1}{\partial r_k}\right) + \left(\frac{\partial\mu}{\partial Q_2}\right)\left(\frac{\partial Q_2}{\partial r_k}\right) \qquad (9)$$

From eqn. (5) is obtained

$$\frac{\partial Q_i}{\partial r_k} = L_{ik}^{-1}$$

which on substitution in eqn. (8) gives

$$\frac{\partial\mu}{\partial r_1} = L_{11}^{-1}\frac{\partial\mu}{\partial Q_1} + L_{21}^{-1}\frac{\partial\mu}{\partial Q_2} \qquad (10a)$$

$$\frac{\partial\mu}{\partial r_2} = L_{12}^{-1}\frac{\partial\mu}{\partial Q_1} + L_{22}^{-1}\frac{\partial\mu}{\partial Q_2} \qquad (10b)$$

*Results.* The wave numbers and the integrated absorptions of the two stretching vibrations of the "free" thiocyanate ion (NaSCN) used in the calcultions can be found in Table 2. The force constants have previously been determined by Jones [1] ($f_1 = 15.95 \times 10^5$, $f_2 = 5.18 \times 10^5$ and $f_{12} = 0.9 \times 10^5$ dyn/cm.

This leads to the following $L^{-1}$ matrix elements

$L_{11}^{-1} = \pm 3.088 \times 10^{-12}$     $L_{12}^{-1} = \mp 0.335 \times 10^{-12}$     $(g^{\frac{1}{2}})$

$L_{21}^{-1} = \pm 2.898 \times 10^{-12}$     $L_{22}^{-1} = \pm 4.866 \times 10^{-12}$     $(g^{\frac{1}{2}})$

With these values inserted in eqns. 10 a and b together with the $\partial\mu/\partial Q_i$'s from eqn. 3 the absolute values of the dipole derivative can be derived. Since the sign of the $\partial\mu/\partial Q_i$ is not known, the values of $\partial\mu/\partial r_i$ will be dependent on the sign combination chosen.

$$\left|\frac{\partial\mu}{\partial r_1}\right| = \begin{array}{l} 1.30 \quad \text{a.u. (different signs for } \partial\mu/\partial Q_i) \text{ or} \\ 1.48 \quad \text{a.u. (similar signs for } \partial\mu/\partial Q_i) \end{array}$$

$$\left|\frac{\partial\mu}{\partial r_2}\right| = \begin{array}{l} 0.30 \quad \text{a.u. (different signs for } \partial\mu/\partial Q_i) \text{ or} \\ 0.002 \quad \text{a.u. (similar signs for } \partial\mu/\partial Q_i) \end{array}$$

As will be discussed later, the values obtained for similar signs for $\partial\mu/\partial Q_i$ can definitely be excluded.

The dipole moment of a molecule, symbolized $\mu$, is defined as the distance between the centres of positive and negative charge, multiplied by the size of one of them. For an ion, e.g. $NCS^-$, with a total negative charge, this charge would not contribute to the dipole moment or the change of dipole moment in a vibration as it all the time is situated in the centre of negative charge. The total dipole moment could be written as a sum of the bond moments

$$\mu = \mu_1 + \mu_2$$

and if the charge distribution is (when leaving the negative unit charge out of account)

$$\overset{-q_1}{N}\overset{r_1}{-\!\!-}\overset{+q_2}{C}\overset{r_2}{-\!\!-}\overset{-q_3}{S}$$
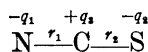
the dipole moment is $\mu = q_2 r_2 - q_1 r_1$ $(q_1 + q_2 = q_3)$. When this relation is derived (a) with respect to $r_1$ keeping $r_2$ constant, (b) with respect to $r_2$ keeping $r_1$ constant one gets

$$\frac{\partial\mu}{\partial r_1} = r_2\frac{\partial q_2}{\partial r_1} - q_1 - r_1\frac{\partial q_1}{\partial r_1} = -q_1 - M_1 \tag{11a}$$

$$\frac{\partial\mu}{\partial r_2} = q_2 + r_2\frac{\partial q_2}{\partial r_2} - r_1\frac{\partial q_1}{\partial r_2} = q_2 + M_2 \tag{11b}$$

$M_1$ and $M_2$ would correspond to the "delocalization moment" of Person and Hall[33] and is a measure of the contribution to the dipole moment change from the movements of delocalized electrons of the vibrating thiocyanate ion.

The charge distribution in the thiocyanate ion has been calculated by Di Sipio et al.[34] Their charges on the sulphur and nitrogen atoms are $q_S = -0.48$ and $q_N = -0.51$, which are in good agreement with the values expected from the resonance structures (1). However, other calculations[35] indicate more negative values, at least for sulphur, and so does an estimation made by Folkesson.[36] Using the ESCA technique, he measured the $N1s$ and $S2p$ electron binding energies of NaSCN. Then, from a correlation of binding energies of

other N and S containing substances and corresponding MO SCF calculated charges (cf., e.g., Ref. 37), he could obtain the values $q_S = -0.72$ and $q_N = -0.70$ a.u. As has been mentioned above, the negative unit charge of the thiocyanate ion does not effect the dipole moment and could be placed in the negative charge centre. Jones [1] has determined the bond distances to be $r_{CN} = 1.17$ Å and $r_{CS} = 1.61$ Å and therefore the negative charge centre is situated somewhere between the carbon and the sulphur. If the values of Folkesson are used, the effective charges would be $q_1$, $q_2 \approx 0.21$ a.u. When the values of $q_1$ and $q_2$ are inserted in eqns. 11a and b together with the $\partial\mu/\partial r_i$'s two different cases appear: Ratio $\partial\mu/\partial Q_i$ negative: $M_1 = 1.09$ a.u., $M_2 = 0.09$ a.u.; positive: $M_1 = 1.27$ a.u., $M_2 = -0.21$ a.u.

In the valence bond description the "delocalization moment" is connected with the changes in the relative weights of the resonance hybrids (1) of the thiocyanate ion during the vibration. A stretching of a bond tends to favour the structure in which that bond is single and it is obvious that this effect works in the same direction upon the change of the dipole moment as the stretching of a bond in a fixed charge model would do. Therefore, a negative value of M is unacceptable and makes it possible to exclude the $\partial\mu/\partial r_i$ values for similar signs for $\partial\mu/\partial Q_i$.

The contribution from the "delocalization moment" is very large, especially for the C−N stretching vibration. The value of $\partial\mu/\partial r_{CN}$ expected from a fixed charge model would be 0.21 a.u., that is only one sixth of the value calculated from the integrated absorption experimentally determined. Therefore, it seems obvious that such a model is insufficient when treating molecules of this kind and that the possibility of delocalized charges must be considered in understanding infrared intensities.


### RESULTS OF THE MEASUREMENTS ON THE Pd-COMPLEXES

In Table 2 all the spectral data of the bands assigned to the C−N and C−S stretching vibrations of the thiocyanate group are listed for the complexes investigated. In some special cases the frequency of the bending vibration is included. The type of bonding is determined mostly on the basis of the integrated absorption of the C−N vibration ($A_{CN}$) and the C−S frequency ($\nu_{CS}$). When the latter is questionable or when the band is masked by the absorption of the other ligand present, also the NCS bending frequency is used as a supporting criterion. Thus the compounds B−G are believed to be fully N-bonded and compounds J−Y S-bonded.

All compounds listed in Table 2 are probably square-planar with *trans* configuration [17] except, of course, those containing a bidentate ligand, such as compounds G, H, I, L, and M, in which the two thiocyanate groups necessarily must be *cis* to each other. In such *cis* compounds both the in-phase and out-of-phase vibrational modes associated with the C−N (C−S) stretching of the two thiocyanate groups are infrared active, whereas in the *trans* compounds only the out-of-phase one is infrared active. Thus, one should expect a splitting of the absorption bands in the *cis* compounds. As seen in Table 2 there is a splitting of the C−N frequency for compounds H, I and M (see
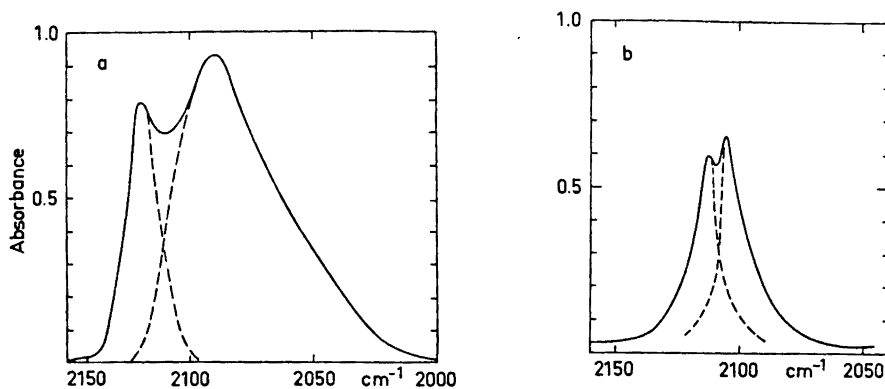
*Fig. 1.* Spectra of (a) Pd(5-nitrophen)(NCS)(SCN), (b) Pd(5,6-dimethylphen)(SCN)$_2$.

also Fig. 1), but for **G** and **L** only a single band is observed, possibly owing to accidental degeneracy. Contrary to the case in compound **M** (Fig. 1b), the two absorption bands in the C − N stretching range of the compounds **H** (Fig. 1a) and **I** showed very different shapes, one having integrated absorption as a N-bonded thiocyanate group, the other as a S-bonded group. Moreover, the existence of bands both in the N- and the S-bonded ranges of the C − S stretching and SCN bending vibrations, makes it plausible that in these compounds one thiocyanate group is linked *via* nitrogen and one *via* sulphur. Of course it could just as well be a mixture of PdL(NCS)$_2$ and PdL(SCN)$_2$ but, as Bertini and Sabatini [19] have pointed out, one would not expect the same spectrum of a mixture when it was prepared at two widely different temperatures. We have prepared the compounds **G** and **H** at − 20°C and + 25°C, warmed them to 130°C and used varying pressures when pressing the KBr disks, but found no difference in the spectrum. Palladium(II) complexes with mixed thiocyanate bonding in the same molecule, as compounds **H** and **I** are believed to be, are not too numerous but recently Meek *et al.*[20] have reported several examples of this kind when bidentate ligands are present.

Splitting is also observed for some of the complexes with *trans*-configuration. Causes of these splittings may be distortions from the regular $D_{4h}$ symmetry brought about by, *e.g.*, non-linearity, but also, as the samples are solid, owing to site symmetry and other solid-state effects.

## DISCUSSION

As mentioned in the introduction above, the transformation from the normally more stable Pd − SCN bonding to Pd − NCS bonding could be ascribed to a high π-bonding ability of the other ligands present. Thus, the π-bonding hypothesis has been used [18] to explain the change from S-bonded thiocyanates for triphenylstibine to both S- and N-bonded for triphenylarsine and to N-bonded for triphenylphosphine by the order of increasing π-

capacity of the ligands. However, this order is somewhat ambiguous [38,39] and also steric factors can promote a change of the bonding type in these systems. From theoretical considerations [13] one would expect a $M-SCN$ complex to be bent whilst a $M-NCS$ complex could be either linear or bent. Not very many structural studies on N-bonded thiocyanato complexes of palladium(II) have been carried out but in $Pd[(C_6H_5)_2PCH_2CH_2CH_2N(CH_3)_2](SCN)(NCS)$ [40] the angle between Pd and the NCS group is 177.6° whilst that between Pd and the SCN group is 107.3°. If the bond angles are similar in the mixed complexes mentioned above, the change from $M-SCN$ to $M-NCS$ bonding could as well be explained by the smaller size of phosphorus as compared with arsenic and antimony which places the phenyl groups nearer to the metal, thus producing a greater steric hindrance to an angular $M-SCN$ arrangement than to a linear $M-NCS$.

Among the ligands with nitrogen as donor atom shown in Table 2, only the bidentate 2,2'-bipyridine, 4,4'-dimethyl-2,2'-bipyridine, and 5-nitro-1,10-phenanthroline and the monodentate 4-nitropyridine are able to promote N-bonded thiocyanates. 1,10-Phenanthroline itself gives S-bonded thiocyanates, but when a strongly electron-withdrawing group such as $-NO_2$ is substituted onto it, one of the thiocyanate groups will change its bonding mode. On the other hand, alkyl substitution (in 5,6-dimethyl-1,10-phenanthroline) would enhance the S-bonding, as it decreases the ability of the ligand to withdraw charge from the central metal atom. This electronic effect could be treated more quantitatively for the *para*-substituted pyridines.

The ability of a substituent to either withdraw electrons from an aromatic ring or donate them into it can be expressed by its Hammett constant, $\sigma$.[41,42] Thus, a positive value of $\sigma$ means that a substitution decreases the electron density of the ring and *vice versa*. Table 3 shows the effective substituent constant $\bar{\sigma}$ derived by Fischer *et al.*[43] for *para*-substituted pyridine systems. The $\bar{\sigma}$ values are related to the basic strength of the substituted compound (*cf.* the $pK_a$ values of the corresponding pyridinium ions, also included in Table 3). In a series of such analogous compounds, increasing $\bar{\sigma}$ (decreasing basicity) would be related to lower electronic density on the pyridine nitrogen and, at coordination, a pronounced electron withdrawal from the central metal atom either by an inductive or $\pi$-electron accepting mechanism. Therefore, one expects that a change of substituents with increasing $\bar{\sigma}$ would cause a continuous decrease of the $\pi$-bonding contribution to the $Pd-SCN$ bond in

*Table 3.* The effective Hammett substituent constants $\bar{\sigma}$ and the $pK_a$ values of the *para*-substituted pyridines. Values are taken from Ref. 43.

| Substituent | $\bar{\sigma}$ | $pK_a$ | Substituent | $\bar{\sigma}$ | $pK_a$ |
|---|---|---|---|---|---|
| 4-NH$_2$ | $-0.65$ | 9.12 | 4-COCH$_3$ | 0.28 | 3.51 |
| 4-CH$_3$ | $-0.14$ | 6.03 | 4-COOCH$_3$ | 0.28 | 3.49 |
| 4-CH$_2$.C$_6$H$_5$ | $-0.07$ | 5.59 | 4-COC$_6$H$_5$ | 0.31 | 3.35 |
| H | 0 | 5.21 | 4-CN | 0.55 | 1.86 |
| 4-CHO | 0.11 | 4.52 | 4-NO$_2$ | 0.63 | 1.39 |

$PdL_2(SCN)_2$ ($L = para$-substituted pyridine) and that at some point a change to $PdL_2(NCS)_2$ may occur. As can be seen in Table 2, this happens when the nitro group with the largest $\bar{\sigma}$ is substituted. The effect of increasing $\bar{\sigma}$ on the complexes which remain S-bonded is illustrated in Fig. 2 with respect to their integrated absorption $A_{CN}$. Even if a certain amount of $\pi$-bonding is accepted
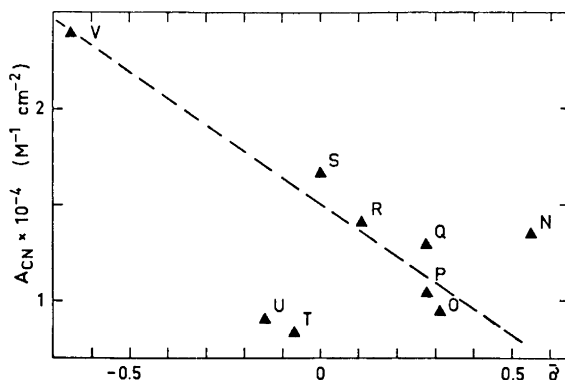


*Fig. 2.* The dependence of the integrated absorption $A_{CN}$ of $PdL_2(SCN)_2$ ($L = para$ substituted pyridine) on the effective Hammett substituent constants $\bar{\sigma}$.

in a $Pd-SCN$ bond, it must be remembered that it for the main part is a $\sigma$ bond resulting from a lone-pair donation from the sulphur atom. Such a donation would be facilitated if a strong electron-withdrawing group is introduced into the complex. From the simple valence bond picture [2,3] using the canonical structures of Jones (1), a decrease of $A_{CN}$ is expected when $\bar{\sigma}$ is increased. Such a decrease may also be found in Fig. 2 although it is not continuous if all the values are regarded.

Also the other complexes in Table 2 are approximately ordered in a series of falling electron-accepting ability of the organic ligand. As no definite correlation between this ability, the frequencies and the integrated absorptions within the groups of N- or S-bonded thiocyanate complexes could be found, there must be other factors than the electronic, which are important. Thus, steric requirements may cause deviations in the metal-thiocyanate bond angles from one complex to another and would change the frequencies and perhaps also the intensities of the thiocyanate group vibrations.

The change in $A_{CN}$ upon coordination can qualitatively be explained by the aid of the resonance structures (1) of the thiocyanate ion,[2,3] if an increase of dipole moment over the $C-N$ bond also implies an increased value of the dipole derivate. For $A_{CS}$, the same procedure would predict a decrease of the "free ion" value upon coordination *via* N and an increase upon coordination *via* S. But the report of Tramer [9] that for $Hg(SCN)_4{}^{2-}$ in acetone solution the ratio $A_{CS}(Hg(SCN)_4{}^{2-})/A_{CS}(SCN^-) < 1$ indicated that the prediction above would be wrong and this is confirmed by the results given in Table 2. However, the suggestion that a larger dipole moment means a larger dipole derivate

and thus integrated absorption cannot be fully true if there is a "delocalization moment" contributing to the static one. An N-coordination for example would favour the resonance structures $b$ and $c$ in (1), that is there would be an increase in bond order and probably a decrease of the $C-S$ bond moment. But when the $C-S$ bond is stretched the structure $a$ where this bond is single would be promoted, and this structure has the largest $C-S$ bond moment of all. Therefore, during the vibration (stretching) an N-coordinated thiocyanate ion would have a greater change of dipole moment over the $C-S$ bond than the uncoordinated ion. The situation would be the reverse when there is S-coordination.

As can be seen in Table 2, $A_{CN}(M-SCN)$ and $A_{CS}(M-SCN)$ are generally about one half of the corresponding values of NaSCN. $A_{CN}(M-NCS)$ is twice the $A_{CN}(SCN^-)$ but $A_{CS}(M-NCS)$ is about twenty times as large as $A_{CS}$-$(SCN^-)$. The same relationships are shown by $Hg(SCN)_4{}^{2-}$ in acetone solution [9] and gaseous HNCS as could be estimated from the spectra reported by Reid.[5] The large value of the $A_{CS}(M-NCS)$, which means 4.5 times larger $\partial\mu/\partial Q_i$ than for the "free" thiocyanate ion, is very interesting, but difficult to explain quantitatively at this point. But it may certainly be connected with a much more pronounced "delocalization moment" at the $C-S$ stretching vibration for the S-bonded thiocyanate ion than for the other forms.

Generally, the differences in absorption frequencies and integrated absorption within the groups of N- and S-bonded thiocyanates are not very great but some examples of abnormal values are found, $viz.$ the $C-S$ stretching intensity of the thiourea compound $\mathbf{W}$ and that of the 4-cyanopyridine compound $\mathbf{N}$. (The frequencies of these compounds are not remarkable and are nearly the same when determined with Raman.) This large intensity, at least for the thiourea compound, is likely to be caused by Fermi resonance. Two bands are observed in the $C-S$ stretching region of the S-bonded thiocyanate ion but probably one of them corresponds to a $C=S$ and $N-C-N$ stretching of the $thiourea$. This band usually is found at about 730 cm$^{-1}$, but it should be lowered at coordination because of the reduced double bond character of the $C=S$ bond. This vibration is of $A_1$ symmetry type [44] and so is the $C-S$ stretching vibration of the thiocyanate group ($\Sigma^+ \equiv A_1$). Furthermore, these two vibrations probably would be of nearly the same energy. Under these conditions, Fermi resonance often produces vibrational perturbations [45] between the two vibrations which involve, besides frequency shifts, an enlargement of the absorption bands.

REFERENCES

1. Jones, L. H. *J. Chem. Phys.* **25** (1956) 1069.
2. Fronæus, S. and Larsson, R. *Acta Chem. Scand.* **16** (1962) 1447.
3. Larsson, R. and Miezis, A. *Acta Chem. Scand.* **23** (1969) 37.

4. Kharitonov, Yu. Ya., Tsintsadze, G. V. and Porai-Koshits, M. A. *Russ. J. Inorg. Chem.* **10** (1965) 427.
5. Reid, C. *J. Chem. Phys.* **18** (1950) 1512.
6. Barakat, T. M., Legge, N. and Pullin, A. D. E. *Trans. Faraday Soc.* **59** (1963) 1764.
7. Bailey, R. A., Michelsen, T. W. and Nobile, A. A. *J. Inorg. Nucl. Chem.* **32** (1970) 2427.
8. Knox, G. F. and Brown, T. M. *Inorg. Chem.* **8** (1969) 1401.
9. Tramer, A. *J. Chim. Phys.* **59** (1962) 232.
10. Larsson, R. and Miezis, A. *Acta Chem. Scand.* **19** (1965) 47.
11. Pecile, C. *Inorg. Chem.* **5** (1966) 210.
12. Bailey, R. A., Michelsen, T. W. and Mills, W. N. *J. Inorg. Nucl. Chem.* **33** (1971) 3206.
13. Lewis, J., Nyholm, R. S. and Smith, P. W. *J. Chem. Soc.* **1961** 4590.
14. Ahrland, S., Chatt, J. and Davies, N. R. *Quart. Rev. Chem. Soc.* **12** (1958) 265.
15. Turco, A. and Pecile, C. *Nature* **191** (1961) 66.
16. Basolo, F., Burmeister, J. L. and Poe, A. J. *J. Am. Chem. Soc.* **85** (1963) 1700.
17. Burmeister, J. L. and Basolo, F. *Inorg. Chem.* **3** (1964) 1587.
18. Sabatini, A. and Bertini, I. *Inorg. Chem.* **4** (1965) 1665.
19. Bertini, I. and Sabatini, A. *Inorg. Chem.* **5** (1966) 1025.
20. Meek, D. W., Nicpon, P. E. and Meek, V. I. *J. Am. Chem. Soc.* **92** (1970) 5351.
21. Ochiai, E. *J. Org. Chem.* **18** (1953) 534.
22. Ramsay, D. A. *J. Am. Chem. Soc.* **74** (1952) 72.
23. Thorndike, A. M., Wells, A. J. and Wilson, E. B. *J. Chem. Phys.* **15** (1947) 157.
24. Steele, D. *Quart. Rev. Chem. Soc.* **18** (1964) 21.
25. Ratajczak, H. and Orville-Thomas, W. J. *Trans. Faraday Soc.* **61** (1965) 2603.
26. Yamada, H. and Person, W. B. *J. Chem. Phys.* **43** (1965) 2519.
27. Wilson, E. B., Decius, J. G. and Cross, P. C. *Molecular Vibrations*, McGraw, New York 1955.
28. Nakamoto, K. *Infrared Spectra of Inorganic and Coordination Compounds*, Wiley, New York and London 1963.
29. Robinson, D. Z. *J. Chem. Phys.* **19** (1951) 881.
30. Rowland Davies, P. and Orville-Thomas, W. J. *J. Mol. Structure* **4** (1969) 163.
31. Thomas, G. A., Ladd, J. A. and Orville-Thomas, W. J. *J. Mol. Structure* **4** (1969) 179.
32. Wilson, E. B. *J. Chem. Phys.* **9** (1941) 76.
33. Person, W. B. and Hall, L. C. *Spectrochim. Acta* **20** (1964) 771.
34. DiSipio, L., Oleari, L. and deMichelis, G. *Coord. Chem. Rev.* **1** (1966) 7.
35. Karlsson, G. and Manne, R. *Phys. Scripta* **4** (1971) 119.
36. Folkesson, B. *Private communication.*
37. Folkesson, B. *Acta Chem. Scand.* **27** (1973) 287.
38. Chatt, J., Duncanson, L. A. and Venanzi, L. M. *J. Chem. Soc.* **1955** 4461.
39. Horrocks, Jr., W. D. and Craig Taylor, R. *Inorg. Chem.* **2** (1963) 723.
40. Clark, G. R. and Palenic, G. J. *Inorg. Chem.* **9** (1970) 2754.
41. Hammett, L. P. *Physical Organic Chemistry*, McGraw, New-York 1940.
42. Jaffé, H. H. *Chem. Rev.* **53** (1953) 191.
43. Fischer, A., Galloway, W. J. and Vaughan, J. *J. Chem. Soc.* **1964** 3591.
44. Yamaguchi, A., Penland, R. B., Mizushima, S., Lane, T. J., Curran, C. and Quagliano, J. V. *J. Am. Chem. Soc.* **80** (1958) 527.
45. Szymanski, H. A. *Theory and Practice of Infrared Spectroscopy*, Plenum Press, New York 1964, p. 149.

# On the Standard Potential of the $Eu^{3+}$ — $Eu^{2+}$ Couple

# in 1 M $LiClO_4$ Medium

GEORG BIEDERMANN and HERBERT B. SILBER*

Department of Inorganic Chemistry, The Royal Institute of Technology,
S-100 44 Stockholm 70, Sweden

On the basis of emf measurements with cells involving mercury redox electrodes the standard potential for $Eu^{3+} + e^- \rightleftharpoons Eu^{2+}$ has been determined at 25°C and in the medium 1 M $LiClO_4$ to have the value of $-379 \pm 1$ mV. The main results are summarized in Table 2.

The coulometric approach employed for the determination of the standard potential has been found to be easily adaptable for equilibrium analysis.

In a previous report [1] of this laboratory a coulometric method was described for the study of redox couples of high reducing power, and the method was applied for the determination of the standard potential of the $Eu^{3+}-Eu^{2+}$ half-cell in the ionic medium 1 M $(CH_3)_4NCl$. This solvent salt was chosen because of its inertness in redox reactions including cathodic reduction with a mercury electrode.

To work with tetramethylammonium chloride solutions entails, however, some disadvantages.

We have been unable to develop a practical method for the preparation of substantial amounts of $(CH_3)_4NCl$ of sufficiently high purity. As a consequence of the presence of traces of unidentified contaminants the life-time of europium(II) ions proved to be quite short. The rate of oxidation of $Eu^{2+}$ by $H^+$ was found to be increased with the ratio $[Eu^{2+}][Eu^{3+}]^{-1}$ and this reaction hindered the study of tetramethylammonium solutions containing a high portion of europium ions in the oxidation state two. Moreover, the $(CH_3)_4N^+$ ion forms slightly soluble compounds with many ligands, and thus our main intention to introduce the $Eu^{3+}-Eu^{2+}$ half-cell into equilibrium analysis may be realized to a limited extent only.

Finally, attention is called to the great need for creating a consistent set of standard potentials. This should replace the present data which have been

---

* Present address: Department of Chemistry, University of Maryland, Baltimore County, Baltimore, Md. 21228, USA.

evaluated partly from measurements with dilute solutions and partly on the basis of investigations carried out in various media of high ionic strengths. For many experimental and theoretical reasons lithium perchlorate seems to be particularly well suited to serve as the solvent salt when redox equilibria have to be studied, and to establish a reliable scale of standard potentials one would be inclined to choose a $LiClO_4$ concentration level, e.g. 1 M, as the ionic medium.

With these ideas in mind a series of preliminary coulometric experiments were made to test the reactivity of the $Li^+$ and $ClO_4^-$ ions in the presence of $Eu^{2+}$. As we could not detect any evidence for the reduction of $ClO_4^-$ and for the participation of $Li^+$ in the cathode reaction, we decided to undertake a precise determination of the $Eu^{3+} - Eu^{2+}$ standard potential in 1 M $LiClO_4$ medium. This forms the subject of the present publication.

*The method of investigation.* In this work the europium redox couple was studied by starting with deoxygenated test solutions of precisely determined initial acidity and generating $Eu^{2+}$ ions *in situ* by constant current coulometry. After each step of electrolytic reduction a local excess of $Eu^{2+}$ is built up in the vicinity of the mercury cathode, and a certain period — 10 to 30 min — is needed until the solution attains a uniform $[Eu^{2+}]$. By placing several mercury redox electrodes into the test solution, and by measuring the emf among them and the cathode the disappearance of concentration differences could be readily followed.

Whatever precautions we have taken, as soon as an appreciable europium(II) concentration was produced a slow but steady decrease in the $[Eu^{2+}]$ occurred due to the reaction

$$Eu^{2+} + H^+ \rightarrow Eu^{3+} + \tfrac{1}{2}H_2 \qquad (1)$$
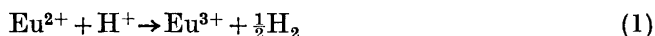
which was recognized by measuring the potential change of the mercury redox electrodes as well as that of a glass electrode. The simultaneous determination of the instantaneous values of the prevailing hydrogen ion concentration and of the redox potential enabled us in combination with the stoichiometric and the electrolysis data to calculate the standard potential for each pair of emf measurements.

In detail, for each series of measurements a test solution of the initial composition

$$B \text{ M } Eu^{3+}, H_0 \text{ M } H^+, (1.00 - 3B - H_0) \text{ M } Li^+, 1.00 \text{ M } ClO_4^-$$
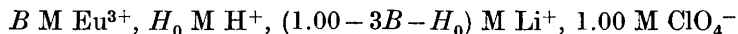
was taken which in the following discussion will be denoted by $S_0$, while the solution arising from $S_0$ by electrolysis and reaction (1) will be represented by S.

$B$ values ranging from 0.5 to 10 mM were studied; in more dilute solutions difficulties were encountered with the redox electrodes, higher europium concentrations would require current strengths not attainable with our equipment.

Since all our subsequent conclusions are based on the value of the *initial hydrogen ion concentration*, $H_0$, prior to the redox potential measurements a coulometric titration was carried out with $S_0$ to obtain this master variable as accurately as possible. For this purpose a platinum foil was immersed into

$S_0$ and it served as the anode in the electrolysis circuit (constant current supply)

$$-Ag \quad \begin{array}{|c|} 100 \text{ m M Ag}^+ \\ 900 \text{ m M Li}^+ \\ 1000 \text{ m M ClO}_4^- \end{array} \quad \Big| \; 1 \text{ M LiClO}_4 \; \Big| \; \text{solution S} \; \Big| \; \text{Pt} +$$
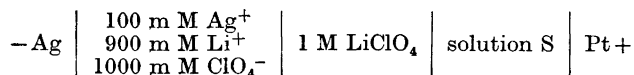
which was employed to generate exact amounts of hydrogen ions in S by the oxidation of water.

After each step of electrolysis the emf of the cell

$$-\text{glass electrode} \mid S \mid RE+ \tag{G}$$
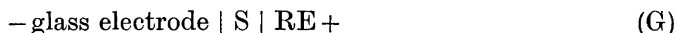
where RE denotes the reference half-cell

$$\Big| \; 1 \text{ M LiClO}_4 \; \Big| \; \begin{array}{c} 100 \text{ mM Ag}^+ \\ 900 \text{ mM Li}^+ \\ 1000 \text{ mM ClO}_4^- \end{array} \; \Big| \; Ag$$
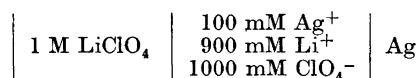
was determined. The emf of cell (G) can be written at 25°C

$$E_G = E_{G,0} - 59.16 \log h \tag{2}$$

In eqn. (2) $E_{G,0}$ represents a constant, which includes the potential of the reference half-cell, and $h$ is the symbol for the hydrogen ion concentration. As the sum of $B$ and $h$ was chosen never to exceed 2 % of the $[ClO_4^-]$, the activity factor of hydrogen ions [as well as those of the europium(III) and europium(II) ions] could be regarded as constants. The standard state is chosen so that the activity factors of all the reacting species tend to unity as their concentrations in the solvent 1 M $LiClO_4$ approach zero. Moreover we ascribe the value of zero to the standard potential of the hydrogen half-cell in the solvent 1 M $LiClO_4$, thus for the potential of a half-cell consisting of hydrogen of $p$ atmosphere and a 1 M $ClO_4^-$ solution containing $h$ M $H^+$ and $(1.00 - h)$ M $Li^+$ with $h \ll 1$ we may write $e = 59.16 \log (hp^{-\frac{1}{2}})$.

On the basis of the corresponding data pairs $(E_G, \mu_A)$ where $\mu_A$ is employed to represent the number of faradays passed through solution S for acidification, a Gran-type plot was constructed which served for the evaluation of the initial hydrogen ion concentration, $H_0$, and of the constant $E_{G,0}$. The $H_0$ value so obtained differed sometimes as much as 2 % from the value calculated from the hydrogen ion concentrations of the stock solutions.

We first attempted to find $H_0$ and $E_{G,0}$ by alkalification which would be expected to yield more accurate results and which could be performed in chloride solutions.[1] In the presence of $ClO_4^-$, however, alkalification resulted inevitably, even at such a low current level as 0.1 mA, in the formation of some europium hydroxide which redissolved but slowly in our slightly acidic solutions.

After having completed the titration for $H_0$ the platinum foil anode was immersed in a mercury pool, and the polarity of the constant current supply was reversed. Next oxygen was expelled by passing through S nitrogen overnight and then the *main experiment*, the reduction of the europium(III) ions, was started.

In each series of measurements a glass electrode and three mercury pools were employed, one having a great surface served as the cathode and the two

others for the measurements of the redox potential. No redox potential value was accepted as significant unless all the pools, including that one which was used as the cathode but after electrolysis was disconnected from the current supply, were found to agree to within $0.2 - 0.3$ mV.

To obtain the standard potential for the europium couple the instantaneous value of the emf of the cell

$$- Hg \mid S \mid RE + \tag{R}$$

was determined. By recalling the arguments brought out in connection with cell (G) the emf of cell (R) may be expressed by the equation

$$E_R = e_{ref} - e_R^\circ - 59.16 \log[Eu^{3+}]/[Eu^{2+}] \tag{3}$$

where $e_{ref}$ denotes the potential of the reference half-cell and $e_R^\circ$ is the symbol for the standard potential of the europium couple. In every experiment a set of corresponding data triplets $(E_R, E_G, \mu)$ was obtained where the symbol $\mu$ is introduced for the number of faradays employed for reduction.

On the basis of each data triplet a value could be obtained for $(e_{ref} - e_R^\circ)$ by combining equations (3) and (2) with the stoichiometric relationships

$\mu = $ number of faradays employed for the reduction of $Eu^{3+} =$

$$= V([Eu^{2+}] + \Delta h) \tag{4}$$

$$\Delta h = h_0 - h \tag{5}$$

$$[Eu^{3+}] = B - [Eu^{2+}] \tag{6}$$

where $V$ denotes the volume of the test solution, $h_0$ is the hydrogen ion concentration attained at the end of the preliminary acidification and $h$ is the instantaneous value of the hydrogen ion concentration. A part of a typical series is shown for illustration in Table 1.

*Table 1.* Some data selected from series 7.

$B = 10.86$ mM     $E_{G,0} = 12.7$ mV     $e_{ref} = 676.0$ mV
$h_0 = 1.846$ mM     $V = 50.00$ ml

| $\mu$ $\mu F$ | Time | $E_G$ mV | $E_{R,1}$ mV | $E_{R,2}$ mV | $E_{cathode}$ mV | $h$ mM | $[Eu^{2+}]$ mM | $-e_R^\circ$ mV |
|---|---|---|---|---|---|---|---|---|
| 167.84 | 12:40 | 177.3 | 1030.5 | 1030.5 | 1030.9 | $1.65_1$ | $3.16_2$ | 377.5 |
|  | 12:58 | 177.7 | 1030.8 | 1030.7 | 1030.7 | $1.62_5$ | $3.13_7$ | 378.0 |
|  | 13:07 | 177.8 | 1031.0 | 1030.7 | 1031.1 | $1.62_0$ | $3.13_1$ | 378.1 |
| 195.81 | 14:22 | 178.5 | 1034.5 | 1034.3 | 1034.9 | $1.57_6$ | $3.64_7$ | 376.1 |
|  | 14:40 | 178.6 | 1034.6 | 1034.4 | 1034.8 | $1.57_0$ | $3.64_1$ | 376.2 |
| 251.75 | 17:20 | 181.8 | 1045.3 | 1045.1 | 1045.6 | $1.38_6$ | $4.57_6$ | 377.4 |
|  | 17:40 | 182.1 | 1045.8 | 1045.6 | 1045.8 | $1.37_0$ | $4.55_9$ | 378.0 |
| 336.59 | 21:50 | 187.2 | 1059.7 | 1059.7 | 1060.3 | $1.12_3$ | $6.00_9$ | 378.4 |
|  | 21:55 | 187.2 | 1059.4 | 1059.4 | 1059.9 | $1.12_3$ | $6.00_9$ | 378.1 |
|  | 22:10 | 187.4 | 1058.9 | 1058.8 | 1059.2 | $1.11_4$ | $6.00_1$ | 377.6 |
|  | 22:15 | 187.9 | 1058.8 | 1058.7 | 1059.0 | $1.09_3$ | $5.97_9$ | 377.6 |

In order to calculate the standard potential itself, $e_R°$, the value of the reference half-cell potential, $e_{ref}$, is required. This has shown a slow trend in the course of this work which comprised several months. The drift can be ascribed to the contamination of the solutions kept in the half-cell vessel with stopcock grease and with substances dissolved from glass, and to the disappearance of lattice imperfections in the silver electrode.

The actual value of $e_{ref}$ was determined by measuring immediately after the completion of a reduction experiment the emf of the cell

$$-\text{Pt, quinhydrone}(s)|11.0 \text{ mM H}^+, 989 \text{ mM Li}^+, 1 \text{ M ClO}_4^-|\text{RE}+ \qquad (Q)$$
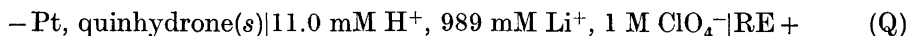
By taking into account the liquid junction potential which was calculated on the basis of an unpublished work in this laboratory to amount to $0.066 \times 11.0 = 0.73$ mV, the emf of cell (Q) provided the value $e_Q° - e_{ref}$ where $e_Q°$ denotes the standard potential of the quinhydrone half-cell. This in turn was obtained by the emf of the cell

$$-\text{H}_2 \ (p \text{ atm}) \ |\text{S}_1|\text{S}_1|\text{S}_1|\text{quinhydrone} \ (s), \text{Pt}+ \qquad (H)$$
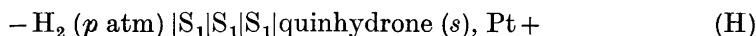
where $S_1$ denotes the test solution of cell (Q) and $p = p_{atm} - p_{H_2O}$. The vapor pressure of a 1 M $\text{LiClO}_4$ solution was estimated from the data of Rush and Johnson [2] to amount to 22.8 torr, and thus we could calculate from the average value of several $E_H$ determinations that in 1 M $\text{LiClO}_4$ medium $e_Q° = 686.1 \pm 0.1$ mV.

Substitution of the quinhydrone for the hydrogen half-cell in the daily routine saved us much time and effort, and it influenced the precision of the standard potential values but little if at all.

## EXPERIMENTAL

### Reagents and analyses

The life-time of the $\text{Eu}^{2+}$ ions was found to depend primarily on the purity of the *water* employed to make up the test solutions. To keep this source of contamination at a minimum some potassium permanganate and sodium hydroxide were first added to water purified by ion exchanger treatment (which was available from a large scale central unit), and the resulting alkaline solution was then slowly distilled while nitrogen was passed through it. The distillate was next acidified with some sulfuric acid and was redistilled in a nitrogen atmosphere. Care was taken to protect the distillates from atmospheric contamination, especially dust, by maintaining above them a slight over-pressure of nitrogen throughout these and the subsequent manipulations.

*Europium(III) perchlorate* stock solutions were prepared from a europium oxide preparation of 99.99 % purity supplied by Typpi Oy, Oulu, Finland. After overnight ignition at 900°C which was needed to transform the small amounts of carbonate ions always present to oxide ions, the sample was dissolved in a slight excess of a standardized perchloric acid solution. The $[\text{Eu}^{3+}]$ of this stock solution was checked gravimetrically by precipitating europium(III) oxalate; this was transformed after washing and drying by ignition to $\text{Eu}_2\text{O}_3$.

*Lithium perchlorate* solutions were prepared as usual in this laboratory.[3] In an attempt to remove dust and other suspended material, such as filter paper fibre, the final product was twice recrystallized from purified water. The perchlorate concentration of the stock solution was determined by passing a sample through a column of a cation exchanger in the hydrogen form and titrating the eluate with a standardized NaOH solution. The hydrogen ion concentration of the stock was determined potentiometrically by coulometric alkalification.

The *silver perchlorate* solutions used in the reference half-cells were prepared from silver carbonate. This was made by adding portionwise 0.1 M $Na_2CO_3$ to a 0.2 M $AgNO_3$ solution. The coarse $Ag_2CO_3$ so formed was washed free by decantation from $Na^+$ and $NO_3^-$ ions, and then it was dissolved in dilute $HClO_4$. The silver content of the stock solution was determined by potentiometric titration with a solution of sodium chloride prepared from a sample of NaCl which serves as a primary standard in this laboratory.

Impurities which gather at the surface must be absent from *mercury* to be employed as a redox electrodes. We started from Hg of commercial quality, this was then distilled twice in vacuum. For each series freshly purified mercury was used which was in addition let to pass through a sintered glass filter immediately before its introduction into the cell.

# Apparatus

All the emf measurements were carried out in a thermostated room kept at 25.0 ± 0.5°C.

The *cell arrangement* was similar to that described in the previous communication dealing with europium.[1] The vessel for the test solution was somewhat modified for greater convenience. It is provided with eight ground glass inlets so that a reagent can be added and a sample can be withdrawn without admitting air. The nitrogen inlet and outlet are made to form parts of the vessel itself, the inlet tube terminates close to the central receptacle which is designed to contain the cathode pool. This is kept in a constant motion by the nitrogen current, and thereby the local excess of $Eu^{2+}$ in the vicinity of the cathode can be prevented to attain a high value.

The *nitrogen* employed for deoxygenation and for the maintenance of an indifferent atmosphere was taken from a cylinder and it was led first through a column containing finely divided copper and then in succession 1 M LiOH, 1 M $HClO_4$, water, and 1 M $LiClO_4$. A sintered glass filter was inserted between the last solution and the inlet tube to remove dust and droplets carried by the gas stream.

The emfs of the glass and redox cells were measured with valve potentiometers of the type E 388 of the Metrohm AG, Herizau, Switzerland. The uncertainty of the emf measurements never exceeded 0.2 mV.

A Metrohm type E 211 coulometer was applied as the constant current source. The current levels were calibrated by inserting into the circuit standard resistances, supplied by the Leeds and Northrup Co., and measuring the average value of the resulting potential drop with a recently certified digital voltmeter.

Beckman general purpose glass electrodes of the types 40498 and 41263 were employed throughout this work. They were calibrated by measuring the emf of the cell

$H_2(p_{atm} - pH_2O)$, Pt | $h$ M $H^+$, $(1.000 - h)$ M $Li^+$, 1.00 M $ClO_4^-$ | glass electrode
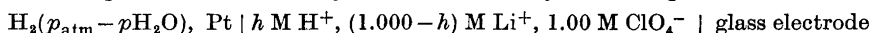
as a function of $h$ in the range 0.1 to 1 mM. In each experiment the emf was found to remain constant to within ± 0.1 mV. The other electrodes were prepared and treated as usual in this laboratory.

# RESULTS

The standard potential values obtained in the seven final series of measurements as well as the main experimental conditions are concisely summarized in Table 2.

As the most important result we may infer on the basis of the data of this table, which cover the log $B$ range $-3.4$ to $-2$ and the log $h$ range $-5$ to $-3$, that the $e_R^\circ$ values do not show any appreciable trend either with the europium or with the hydrogen ion concentration. Thus our two fundamental assumptions expressed by eqns. (3) and (4) may be regarded as close approximations.

This conclusion is further corroborated by the examination of the in-

*Table 2.* Summary of the results.

| Series | $B$ mM | $h_0$ mM | $e_{ref}$ mV | Range of $[Eu^{3+}][Eu^{2+}]^{-1}$ | Range of $h$ mM | Number of reduction steps | Average $-e_R^\circ$ value of the series, mV |
|---|---|---|---|---|---|---|---|
| 1 | 0.424 | 0.500 | 678.0 | 1.00 − 0.594 | 0.220 − 0.114 | 8 | $378._9 \pm 0.9$ |
| 2 | 0.511 | 0.344 | 677.8 | 2.66 − 2.11 | 0.0566 − 0.0051 | 4 | $378._6 \pm 0.8$ |
| 3 | 0.996 | 0.820 | 677.1 | 4.59 − 0.20 | 0.733 − 0.338 | 35 | $380._0 \pm 1.2$ |
| 4 | 1.55 | 0.507 | 677.8 | 1.96 − 0.80 | 0.208 − 0.0130 | 14 | $379._3 \pm 0.9$ |
| 5 | 1.97 | 0.686 | 677.4 | 1.02 − 0.24 | 0.571 − 0.371 | 21 | $379._7 \pm 0.8$ |
| 6 | 10.24 | 1.605 | 676.2 | 3.84 − 0.46 | 1.474 − 1.062 | 17 | $377._7 \pm 1.1$ |
| 7 | 10.86 | 1.846 | 676.0 | 2.47 − 0.81 | 1.65 − 1.09 | 14 | $377._9 \pm 0.7$ |

fluence of the $[Eu^{3+}][Eu^{2+}]^{-1}$ ratio on the $e_R^\circ$ values of the individual series; in no case could any systematic variation be detected. Fig. 1, which shows data pertaining to the $B$ level 1.97 mM, illustrates a typical random spread in $e_R^\circ$. We would therefore propose as the most probable value the mean of the individual averages

$$e_R^\circ = -379 \pm 1 \text{ mV}$$

Thus the magnitude of the europium standard potential in 1 M $LiClO_4$ medium differs by 2 mV only from that valid in 1 M $(CH_3)_4NCl$ where $e_R^\circ$ was found to equal $-381$ mV.[1] The proximity of the two results is somewhat unexpected since both the cations and the anions of the solvent salts were chosen different. The little effect of the replacement of the large $(CH_3)_4N^+$ ion by the small and strongly hydrated $Li^+$ ion is especially remarkable.

Before turning to a discussion of some additional experiments the question should be raised how could the precision of the redox potential measurements, which in the present work was about 1 mV, be improved. As the hydrolysis of the $Eu^{3+}$ ions is certainly negligible for $\log h > -5$, we could always choose a $h B^{-1}$ ratio less than unity in our experiments. As a consequence the rate of oxidation of $Eu^{2+}$ by $H^+$ could be kept low, and therefore − as a straightforward error calculation applied to eqn. (3) shows − the effect of the uncertainty of the instantaneous hydrogen ion concentration determination on the evaluation of $e_R^\circ$ is less than that of the difference usually found among simultaneously employed redox electrodes.
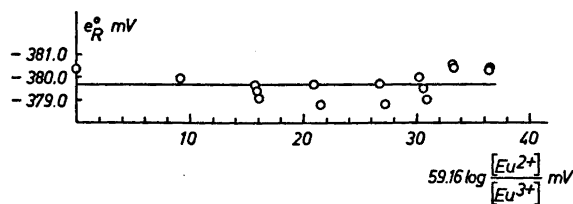


*Fig. 1.* The standard potential $e_R^\circ$ as a function of $59.16 \log[Eu^{2+}]/[Eu^{3+}]$. The data were taken from series 5 pertaining to the $B$ level 1.97 mM, *cf.* Table 2. The horizontal line represents the average value of the standard potential, $-379.7$ mV.

The main source of the uncertainty is probably the presence of traces of impurities in our test solutions. The contaminants which may react at the mercury cathode and (or) protolyze at the low acidities studied, arise from the lithium perchlorate and the nitrogen employed. A cell design recently developed in this laboratory which makes it possible to work under a slight overpressure would eliminate the contamination from the protecting gas; however, we have not been able to find a method for the removal of the remaining, mainly organic, impurities from our lithium perchlorate preparations, which for safety reasons cannot be brought to a high temperature.

*Additional experiments.* At the conclusion of the experiments serving for the evaluation of the standard potential some pioneering work was made to determine the solubility products of europium(III) hydroxide and europium(II) sulfate.

To precipitate europium(III) hydroxide such a high $[Eu^{2+}][Eu^{3+}]^{-1}$ ratio was achieved by cathodic reduction of a test solution S that the $Eu^{2+}$ ions became rapidly oxidized by hydrogen ions. Thereby $h$ diminished so far that colloidal europium(III) hydroxide started to form. The continuous rapid decrease of the $[Eu^{3+}]$ and the increase of $h$ was followed for several days but, as no evidence was found for the approachment of a steady state, the experiment was discontinued.

We were somewhat more successful with europium(II) sulfate. Its solubility product was studied by adding an oxygen-free lithium sulfate solution of $[Li^+] = 1$ M to an S solution made by cathodic reduction to contain 8 mM $Eu^{2+}$, 3.1 mM $Eu^{3+}$ and 0.1 mM $H^+$. In the first three days the redox electrode has shown the $[Eu^{2+}]$ to decrease with a diminishing rate while the glass electrode indicated $h$ to remain constant to within a few percent.

After about 96 h the europium(II) concentration seemed to attain a steady level as no further systematic change in $E_R$ could be detected for additional 24 h. On the basis of this final $E_R$ value $pK_s$ for $EuSO_4(s) \rightleftharpoons Eu^{2+} + SO_4^{2-}$ was calculated to equal 6.3. This result, which we cannot claim to correspond to equilibrium, is not far from the value of Koz'min *et al.*[4] who reported $pK_s = 6.6$ in 1 M KCl medium.

By employing a cell technique not requiring a steady stream of protecting gas and which allows contact between the test and the bridge solutions to be made only when it is needed, we hope to find reliable data for these important heterogeneous equilibria attainable but slowly.

REFERENCES

1. Biedermann, G. and Terjošin, G. S. *Acta Chem. Scand.* **23** (1969) 1896.
2. Rush, R. M. and Johnson, J. S. *J. Phys. Chem.* **72** (1968) 767.
3. Biedermann, G. and Ciavatta, L. *Arkiv Kemi* **22** (1964) 253.
4. Koz'min, Yu. A., Shulgin, L. P. and Ponomarev, V. D. *Zh. Neorg. Khim.* **9** (1964) 2532.

# Chemical Modification in the Active Site of δ-Chymotrypsin

## BENT H. HAVSTEEN

*Institute of Medical Biochemistry, University of Aarhus, Aarhus, Denmark*

The properties of the active site of δ-chymotrypsin were studied by specific modification of two side chains with dimethyl diimidates of aliphatic dicarboxylic acids. The sites of modification were identified as His-57 and Met-192 using ^{14}C-labelled reagent and amino acid sequence analysis of the NH-terminal portion of modified peptides. The latter were liberated from the modified enzyme by limited proteolysis and isolated. The active site titer remained unity after the modification, but the substrate specificity had changed in favour of specific esters. In contrast, the specific amidase activity was diminished. Treatment of derivatives of His and Met with the reagent confirmed the feasibility of the modification reaction proposed. The optical characteristics of the modified enzyme (MCT) support the chemical evidence for the nature of the modification.

Chemical modification in the active site of an enzyme is one of the most direct approaches to study the catalytic mechanism. Covalent derivatives of functional groups which in the native state of the enzyme participate in the conversion of the substrate are almost invariably inactive, or nearly so, but a few exceptions exist.[1,2] One example is reported here. The retention of the catalytic power by the derivative was probably due to enhancement by the modification of the very property, *e.g.* nucleophilicity or basicity, which represented the normal action of the functional group. The specificity, however, was, in the case of chymotrypsin (CT),* sharpened and shifted in the direction from amidase toward esterase activity.[3]

Initially, the project was designed to anchor a group, the NH-terminus of the B-chain, which was expected to participate in the stabilization of the active site by electrostatic clamping of the Asp-194 carboxylate group. The latter side chain would otherwise rotate into the polar environment of the active site and more or less directly impede the productive binding of the substrate. An amidination of Ile-16 would, if it had been successful, have

---

* *Abbreviations:* ATEE, *N*-acetyl-L-tyrosine ethyl ester; CT, Chymotrypsin; DNS, 1-Dimethylamino-naphthalene-5-sulfonamide; MCT, CT modified by dimethyl malondiimidate; NMR, Nuclear magnetic resonance; ORD, Optical rotatory dispersion; PTH, Phenyl-thiohydantoin; RNase, Ribonuclease; Tris, Tris(hydroxymethyl)aminomethane.

shifted the $pK$-value of the $\alpha$-amino group sufficiently in alkaline direction to keep the group almost fully charged under physiological conditions and hence fulfil the intended mission. However, this NH-terminus proved to be much less reactive (only 22 % of the value to be expected from the Brønsted-plot)[4] than normally. This has recently been independently confirmed.[44] Instead of NH-modification, a derivative of high, specific esterase activity and low, specific amidase activity appeared. Its characterization is described below.

Since selectivity of the modification reaction is essential if the observations are intended for mechanistic interpretation, the derivativation was commenced by reversible or irreversible masking of potentially competing groups, such as the $\varepsilon$-amino groups. The latter are in the case of CT known to be unimportant to the catalysis of the native enzyme and should, therefore, be prevented from interfering with the intended, specific modification of the active site.[3] The $\varepsilon$-amino groups were maleylated or carbamylated in the zymogen where the active site is protected (see Fig. 1). Full activity appeared upon activation of the masked zymogen by the conventional procedure.
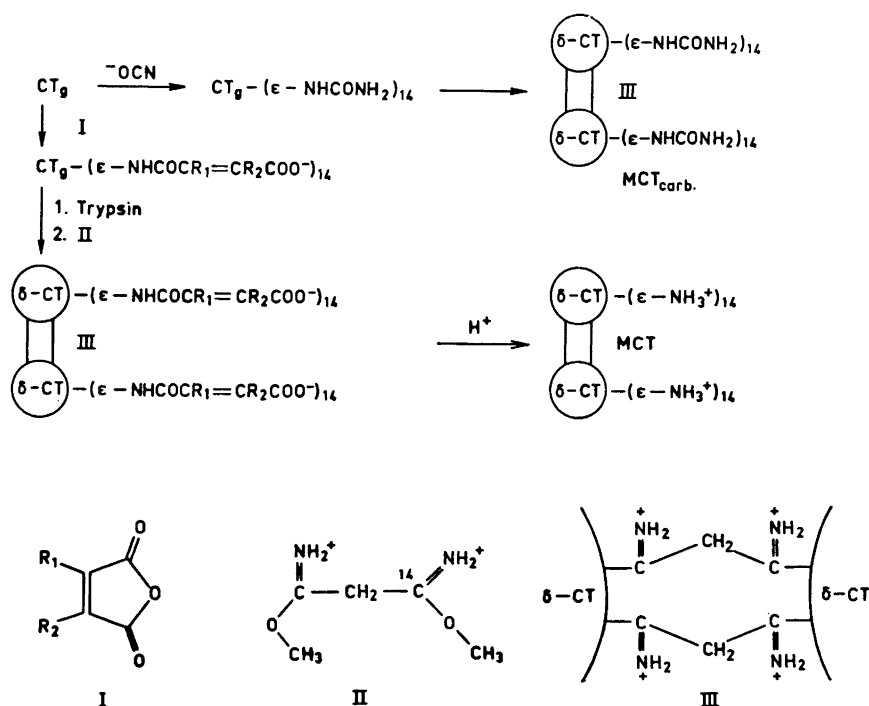


Fig. 1. Summary of the procedure for preparation of MCT. Two alternative pathways are shown. Native chymotrypsinogen is used in both. The two methods of protective masking of competing groups are used for different purposes: Carbamylated MCT is used for quantitative isotope studies whereas transient maleylation is used for crystallization of MCT, for X-ray diffraction work, sequenation, kinetics, and optical measurements. (See also text).

A bifunctional, rather than a monofunctional, reagent was initially chosen because the aim of the project then was to anchor a group ($\alpha$-NH$_2$ of Ile-16) by a short bridge. Besides, exploratory experiments had indicated that monofunctional imidates had no effect on the activity of CT.[6] Dimethyl diimidates of short chain, aliphatic dicarboxylic acids, however, had a marked effect on the catalytic efficiency and specificity.

Imidates are useful reagents because they normally are specific for amino groups and react under mild conditions but they are difficult to prepare in pure state. However, the impurities, which normally consist of small amounts of carboxylic acids, nitriles and ammonium salts, do not interfere with the intended reaction.

Most modification reactions designed to elucidate enzyme mechanisms employ reagents which per molecule attack a single site, but in a few instances, bifunctional reagents have been used.[7-11] In this case, a short chain was preferred to favour a rigid fixation of the reacting groups. This resulted in a stabilization of the active site and in a rate enhancement which increased with decreasing bridge length.[3]

*Table 1.* NMR-Resonance of histidine and malonic acid derivatives. Comparison between the NMR spectra of compounds closely related to dimethyl malondiimidate and the reaction product of this compound with *N*-acetyl-L-His. Operating frequency: 60 MHz. Sweep times: 50 and 500 sec. R. F. field: 0.02 and 0.04 mG. Temp. 23°. Solvent = D$_2$O.

| Compound | $\delta^a$ ppm | $\Delta\delta^f$ | Multiplicity | H$^b$ | Assignment | Area ratio |
|---|---|---|---|---|---|---|
| Imidazol | 7.22 | | Douplet $J=1^c$ | 3 | $\geq$ C−H | 10 |
| | 7.85 | | Singlet $^d$ | | | 7 |
| L-His | 7.08 | | Douplet $J=1$ | 2 | $\geq$ C−H | 1 |
| | 7.79 | | Douplet $J=1$ | | | 1 |
| *N*-Ac-L-His | 7.49 | | 2 Douplets $J=1.5$ and 5 | 2 | $\geq$ C−H | 1 |
| | 8.49 | | 2 Douplets $J=1.5$ and 8 | | | 1 |
| His-der.$^g$ | 7.37 | 0.12 | Douplet $J=1.5$ | 2 | $\geq$ C−H | 1 |
| | 8.20 | 0.29 | Douplet $J=2.5$ | | | 1 |
| Dimethyl malon- | 3.82 | | Singlet$^d$ | 6 | − OCH$_3$ and | |
| diimidate | 3.82 | | Multiplet | 2 | − CH$_2$− | |
| Malonoditril $^h$ | 7.58 | | Triplet | 2 | − CH$_2$− | 1 : 2 : 1 |
| Malonic acid | 3.54$^e$ | | Singlet $^d$ | 2 | − CH$_2$− | |
| L-His | 3.18 | | Multiplet | 2 | − CH$_2$− | 2.0 |
| | 4.00 | | Triplet | 1 | $\alpha$-H | 1.0(1 : 2 : 1) |
| *N*-Ac-L-His | 2.07 | | Singlet $^d$ | 3 | − COCH$_3$ | 9 |
| | 2.13 | | Singlet | 2 | − CH$_2$− | 6 |
| | 3.40 | | Triplet | 1 | $\alpha$-H | *Ca.* 1 : 2 : 1 |
| His-der.$^g$ | 1.92 | 0.15 | Singlet $^d$ | 6 | − COCH$_3$− | 1 |
| | 1.95 | 0.18 | Douplet $J=5$ | 6 | − CH$_2$− | 1 |
| | 3.00 | 0.40 | Multiplet | 2 | $\alpha$-H | |

$^a$ Chemical shift. Standard: Tetramethylsilan. $^b$ Number of hydrogen atoms involved. $^c$ Two overlapping doublets + 1 singlet. $J$ = coupling factor in cps. $^d$ Sharp peak. $^e$ The peak vanishes due to D − H exchange. Half time = 1 min. $^f$ ($\delta N$-$Ac$-L-$His$ − $\delta His$-$der$). $^g$ His-der.: Product of the reaction of *N*-acetyl-L-His with dimethyl malondiimidate. $^h$ Solvent: DMS.

## METHODS

*Preparation of the reagent.* Dimethyl malonic- and succindiimidates were prepared by the method of Hunter and Ludwig [12] with the following modification: The corresponding dinitrile was dissolved in methanol instead of ether or chloroform. The reaction product was identified by determination of the melting point (about 98°), by measurement of IR, NMR, and mass spectra and by elemental analysis. The IR-spectrum displayed the ester absorption band and the UV-spectrum the imidoester chromophore. The NMR-spectrum showed the expected resonances (see Table 1) and the fragmentation pattern obtained by mass spectrometry was compatible with the assumed structure.

A radioactive label ($^{14}$C) was introduced in the carboxyl groups.[13,14] The specific radioactivity of the compound was determined by scintillation counting using Bray's solution and calibration with standard $^{14}$C-toluene.

*Treatment of N-acetyl-L-Met by dimethyl malondiimidate.* The purpose of this experiment was to prove that the Met side-chain could react with the diimidate. The procedure which was employed followed the one for MCT (see below) as closely as possible. Example of an experiment:

Three mg of *N*-acetyl-L-Met were dissolved in 20 ml of an 0.1 M Tris—HCl buffer at pH 8.0. An 0.2 ml aliquot of this stock solution was diluted to 2.00 ml with the buffer in the cuvette at 25° and the reaction was started by addition of 1.0 mg of dimethyl malondiimidate and mixing. Full UV-spectra were recorded immediately and repeated every 10 min. The reaction product was characterized by spectrophotometry since it was so labile that it was difficult to isolate.

*Treatment of N-acetyl-L-His by dimethyl malondiimidate.* This experiment is analogous to the one above. In a typical experiment 5 mg of *N*-acetyl-L-His were dissolved in 10 ml of an 0.1 M Tris buffer at pH 8.1. An aliquot of 3.00 ml was placed in a cuvette and the reaction was initiated by addition of 2.5 mg of dimethyl malondiimidate. Complete UV-spectra were recorded until near completion of the reaction. Since Beer's law was not obeyed, the concentration dependence of the extinction coefficient was determined by serial dilution. Extrapolation to infinite dilution and to saturation yielded limiting values which were used for the determination of the prototropic dissociation constants after repetition of the experiment at a number of pH-values.

The amidine chromophores at 1580 cm$^{-1}$ and at about 240 nm were observed by IR- and UV-spectrophotometry.[15] The content of C, H, and N was determined by microanalysis and the molecular weight was calculated from the colligative properties. The structure was also studied by mass spectrometry.

*Masking of ε-amino groups in chymotrypsinogen. (a) Reversible masking.* The procedure was essentially that described earlier by Harris, Perham et al.[16,17] In a typical experiment 50 mg of the zymogen was dissolved in 10 ml of an 0.05 M phosphate buffer at pH 7.5 and 4°. Dimethyl maleic anhydride was then added in a 50-fold molar excess. The progress of the reaction was followed in a pH-stat. After near completion of the hydrolysis of excess reagent, the by-products were removed by dialysis at pH 5.0.

*(b) Irreversible masking.* The cyanate method of Stark [18] was used for this step. Fifty mg of the zymogen was dissolved in 10 ml of an 0.02 M borate buffer at pH 8.0. The buffer contained 0.2 M KOCN and 8 M urea. The reaction was allowed to proceed at room temperature for 1 h. Then, the solution was dialyzed.

*Activation of chymotrypsinogen with masked ε-amino groups.* The modified zymogen was activated by a brief exposure to trypsin according to the procedure of Jacobsen.[5] The activity gain and the detection by the DNS-method (see below) of Ile (but not of Ala) as NH-terminus proved that the reaction had taken the desired course.

*The modification reaction.* The modification was performed at pH 9.7 and 7° in the presence of a large excess (400-fold) of specific substrate (ATEE) to ensure that the enzyme would become locked in an active and not in an inactive conformation. The reagent, dimethyl malondiimidate was added to the zymogen (in which the ε-NH groups had been masked) in 2000-fold excess in two equal batches, the second 10 min after the first. The progress of the reaction was followed with a pH-stat. The reaction was complete in 30 — 60 min. Excess reagent was hydrolyzed and all by-products were removed by exhaustive dialysis at pH 3 and 4 for 25 h with 4 changes (each 4 l) of HCl solution. Usually, 50 — 100 mg of chymotrypsinogen was used for preparation of a batch of modified enzyme The dialyzed solution of this enzyme (MCT) was distributed in small plastic vials and

frozen. In the frozen state the compound was stable for several months since the UV-spectrum and the specific esterolytic activity (toward ATEE) remained unchanged. The entire procedure for preparation of MCT is summarized in Fig. 1.

*Measurement of the incorporation of $^{14}C$-reagent into the enzyme.* The concentration of MCT on a monomer basis was determined from the absorption at 280 nm using the extinction coefficient which was obtained by correlation of the Kjeldahl analysis with the UV-spectrum.[3] The specific $^{14}C$-activity of MCT was measured on a low-level counter (background: $2-4$ cpm). Measured samples of MCT were pipetted into shallow trays (15 cm $\phi$, Al) and dried under infrared light before counting. From this information, the number of equivalents of $^{14}C$-labelled reagent incorporated in each CT-monomer could be calculated with a relative error of a few percent.[19]

*Determination of the operational active site titer of MCT and CT.* The spectrophotometric cinnamoyl imidazole titration method of Schonbaum *et al.*[20] was used. The relative error involved was a few percent. The cinnamoyl imidazole reagent was prepared by the method of Schonbaum *et al.*[20] and recrystallized. Its melting point and UV-visible spectrum were checked.

*Identification of the modified sites. (a) Amino acid sequence analysis.* A sample of MCT was treated with an excess of dithiothreitol by the method of Cleland[21] to cleave the disulfide linkages reductively. Subsequently, the sulfhydryl groups were completely masked by alkylation with an excess of iodoacetate in 4 M urea.[21] The A-chain was removed by exhaustive dialysis at pH 3.[25] The remaining chains were subjected to sequential, limited proteolysis at 25° in the pH-stat by trypsin[22] at pH 8 (for 20 h) and thermolysin (for 6 h at 40° and pH 7.5).[23,24] The resulting peptides were fractionated by three, consecutive column chromatographic steps:[25]

Gel filtration: Sephadex G-25 in 0.05 M phosphate at pH 7.5 and 4° (72 × 2.7 cm).

Ion exchange: Dowex 50 at 4° and pH $3.1-5.6$ (gradient) in pyridine−acetate (72 × 2.7 cm).

Gel filtration: Sephadex G-10 at 4° and pH 7.5 in 0.05 M phosphate, 8 M urea (48 × 2.7 cm).

The last step was repeated until the fractionation appeared to be complete. The elution profile for $^{14}C$ was in each step used to locate the labelled peptides. Four radioactive peptides ($D_1$, $D_2$, $E_{1a}$, and $E_{1b}$) representing 90 % of the radioactivity were sequenced. All the four peptides displayed the amidine chromophore at about 250 nm. Their homogeneity was tested after rechromatography on Sephadex G-10 or Dowex 50 by high voltage paper electrophoresis at pH 6.5 and 10° for 30 min. Since it was found to be satisfactory, amino acid sequence analysis was performed on the four peptides by the subtractive method of Hartley and Grey.[26]

Polyamide sheets were used to separate the DNS-amino acids.[27] The phenylthiohydantoins were collected at each stage and their radioactivity was measured. Samples of each peptide were subjected to hydrolysis for 20 h at 110° in 6 N HCl and the amino acid composition was determined by the ninhydrin method after ion exchange chromatography.

The following solvents were used for the chromatography of DNS-amino acids on polyamide sheets.

In the first direction: Formic acid in water (1.5 % v/v). In the second direction: Benzene−acetic acid (9:1, v/v).

After drying, again in the 2nd direction: Ethyl acetate−methanol−acetic acid (20:1:1, v/v).

Standards: DNS-Gly, DNS-Glu, DNS-Ile, DNS-Phe, DNS-Pro, DNS-Ser, and DNS-Arg.

The standards were applied on one side of the sheet, the sample on the opposite. A small portion of the sample was also applied to the reference side. In this way, the conditions for chromatography of the unknown sample and the reference became identical. The sample spots on the reference side of the sheet could be distinguished from the reference spots by the difference in the intensity of the fluorescence.

*(b) Selective performic acid oxidation of Met-192 prior to the reaction with diimidate.* The method of Weiner *et al.*[28] was used to destroy a suspected site of modification. In the subsequent attempt to modify the enzyme by the diimidate reaction according to the procedure described above, the process failed to take the usual course.

*Estimation of the molecular weight of MCT.* Two different methods, gel filtration at

4° on calibrated columns and analytical ultracentrifugation, were employed for this purpose. In the former, Sephadex G-100 (medium) was used in an 0.05 M phosphate buffer at pH 7.5 with and without 8 M urea. The low temperature was chosen to reduce autolysis and uncontrolled denaturation. The columns were calibrated with chymotrypsinogen, pepsin, $\beta$-lactoglobulin, pepsinogen, hemoglobin, fibrinogen, and blue dextran.

Since the gel filtration method requires that the proteins have a spherical shape, the experiment was repeated in a denaturing solvent (8 M urea), which is believed to favour this shape since it weakens the intramolecular, non-covalent interactions.[29] In addition, this solvent served to cleave possible non-covalent aggregates of MCT. The compounds were identified by their individual UV- or visible spectra and the elution volumes were used to compute the parameter, $K_{av}$, which resembles the partition coefficient. This parameter served to define the calibration curve for estimation of the molecular weight.[30]

Analytical ultracentrifugation was applied to check the estimate of the molecular weight of MCT. This was performed in buffer solution at 25° by the Archibald approach to equilibrium method and by combination of sedimentation velocity and boundary spreading data. The molecular weight of $\alpha$-CT was also determined to check the methods. The agreement with known data was good.

*Other physical measurements.* The protein concentration was determined by measurement of the extinction at 280 nm.[3] Infrared spectra were recorded on a Beckman instrument. The NMR-spectra were measured on a Varian instrument (60 MHz). Elemental analysis and determination of the molecular weight of the reaction product of $N$-acetyl-L-His with dimethyl malondiimidate were performed by Beller Micro-analytical Laboratory, Göttingen. Optical rotatory dispersion was recorded on a Spectropol 1 spectropolarimeter from FICA. The active site titrations of the operational normality of the enzyme [19] were performed on a Cary-14 spectrophotometer.

*Materials.* The chymotrypsinogen was a 6-times crystallized product from British Drug Houses, $\alpha$-chymotrypsin a crystalline preparation (activity: 1100 NG/mg) from NOVO Industries, Copenhagen, and the marker proteins, crystalline products from Miles-Seravac, Worthington and Boehringer. Chymotrypsin was purified from a contaminating peptide by gel filtration according to the method of Yapel *et al.*[32] The organic compounds used for the syntheses were analytical grade reagents from Fluka, British Drug Houses, and Koch & Light. The solvents were dried and distilled. The polyamide sheets were purchased from Cheng Chin Trading Co., Hankow St., Taipei, Taiwan. Radioactive NaCN ($^{14}$C) was purchased from the Radiochemical Center, Amersham, England. Its specific activity was 52.8 mC/mmol. Standard $^{14}$C-toluene was acquired from the same source.

## RESULTS

*The reactivity of methionyl and histidyl side chains toward dimethyl malondiimidate.* The rate constants for the modification of $N$-acetyl-L-Met were determined by recording the absorbance as a time function at a band, 266.7 nm, which is characteristic of the modified Met side chain. The spectrum of the Met derivative is shown in Fig. 3. The kinetics of its formation were analyzed as described in the legend of Fig. 4. The corresponding plot is shown in Fig. 4. The maximal absorbance change under the conditions of this experiment was 0.360 which corresponds to a difference extinction coefficient of 1432 l mol$^{-1}$ cm$^{-1}$. The rate constant for the modification of Met is compared with that of similar reactions in Table 3. Table 3 shows that both $N$-Ac-L-Met and $N$-Ac-L-His can react with dimethyl diimidate and that the 2nd order rate constants are of the same magnitude as those found for similar imidates when they react with amino groups.

The stability of the Met derivative was studied at 255.8 nm (39.1 kc). At pH 7.0 and 25°, the reaction follows pseudo first order kinetics.
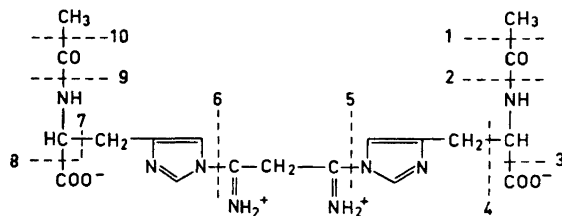
*Fig. 2.* The suggested structure of the reaction product of the treatment of $N$-acetyl-L-His with dimethyl malondiimidate. The numbers indicate the fragmentation points by mass spectrometry which are expected from comparison with the decomposition of similar compounds.
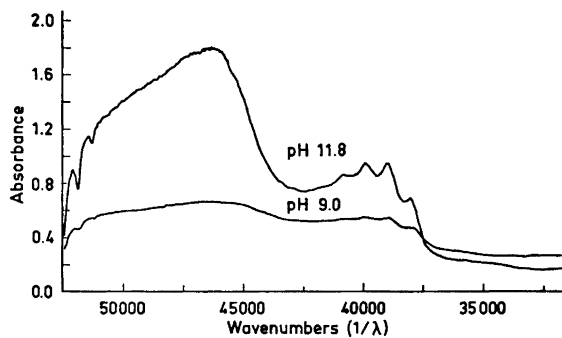


*Fig. 3.* The UV-spectrum of the product of the reaction of $N$-acetyl-L-Met with dimethyl malondiimidate $(2.5 \times 10^{-4}$ M in $H_2O$ at $25°)$. Reference: $H_2O$. Light path: 1 cm.

*Fig. 4.* The kinetics of the reaction of $N$-acetyl-L-Met with dimethyl malondiimidate at pH 8.0 and $25°$ in 0.1 M Tris $-$ HCl measured at 266.7 nm. None of the reactants have an absorption band in that range. Assuming the reaction

$$2A + B \xrightarrow{k_1} AB + A \xrightarrow{k_2} ABA,$$
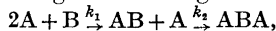
additivity of the absorption contributions from the two chromophores: $\varepsilon_{AB} = 1/2$ $\varepsilon_{ABA}$ and that AB is in the steady state, the parameter $k_1 k_2/(k_2 - k_1) =$ $= (2.30 \pm 0.02) \times 10^{-2}$ l mol$^{-1}$ sec$^{-1}$ may be evaluated from the slope

$[ = \{(2\ b_0 - a_0) k_1 k_2/(k_2 - k_1)\} \times 0.868]$.

Symbols: $a_0 =$ initial conc. of $N$-Ac-L-Met $=$ $= 7.85 \times 10^{-4}$ M; $b_0 =$ initial conc. of dimethyl malondiimidate $= 2.48 \times 10^{-4}$ M.
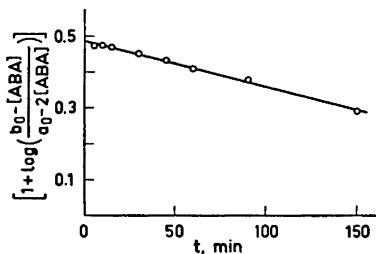
The modified Met displayed in the alkaline range a characteristic 5-member absorption band resembling that of benzene. This spectrum could be directly observed in the modified enzyme under the same conditions (see Fig. 5). The spectrophotometric titration curve for one of these bands (the one at 250.2 nm) was determined because the p$K$-value of the corresponding function had to be taken into account by the interpretation of changes in the pH-dependence of the kinetic parameters upon conversion of $\delta$-CT to MCT and for studies of the ionization properties of the Tyr side chains in the modified enzyme.

The His derivative was subjected to a similar analysis. Its formation was too fast to be followed with the equipment available. However, the compound was stable enough to be isolated by crystallization and was subsequently studied by mass spectrometry, UV-spectrophotometry (see Fig. 6), elemental analysis (Found: C 47.1; H 6.4; N 6.1. Calc. for His der.: C 46.7; H 5.6; N 12.1.
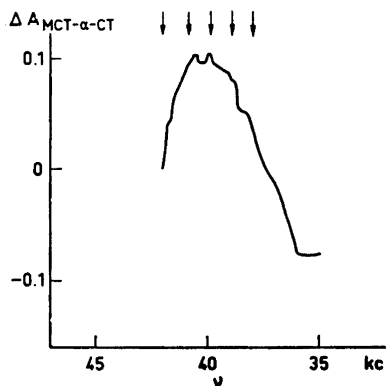


*Fig. 5.* Difference spectrum between MCT and $\alpha$-CT at pH 9.8 and 23°. The chromophore of the modified Met is seen superimposed upon the band of the modified His (see Fig. 6) and those of the perturbed Trp and Tyr residues. The arrows show the position of the bands in the model compound (see Fig. 3). Conc.: MCT = $\alpha$-CT = $10^{-5}$ M; $\nu = 1/\lambda$ (wavenumber).
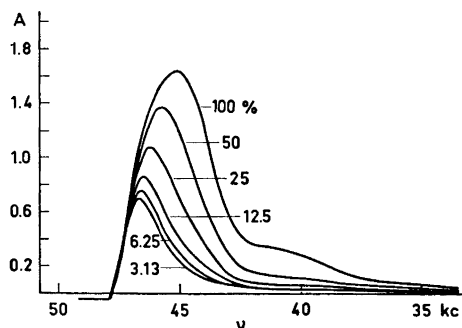
*Fig. 6.* Spectra of the product of the reaction of $N$-Ac-L-His with dimethyl malondiimidate (2.54 and 12.4 mM, respectively) at pH 9.7 in 0.1 M Tris. The spectra were recorded at pH 10.1 *vs.* 0.1 M Tris (1 cm light path, 23°) after completion of the reaction and the following serial dilution: 100, 50, 25, 12.5, 6.25, and 3.13 % of original conc. Ordinate: Absorption. Abscissa: Wavenumber (1/$\lambda$).

Calc. for N-Ac-His: C 48.5; H 6.1; N 21.2) and molecular weight determination (Found: 440; Calc. for His der.: 462. Calc. for N-Ac-His: 198). The fragmentation pattern was analyzed on the basis of the hypothetical structure [33],[34] which is shown in Fig. 2. The results are presented in Table 2.

The first order rate constant for hydrolysis at pH 9.7 and 4° of dimethyl malondiimidate ($k = 0.136$ min$^{-1}$) was taken as a measure of the reactivity of the compound. This value may be compared with 0.018 min$^{-1}$ at pH 9.0 and 25° and 0.024 min$^{-1}$ at pH 10.6 and 25° for methyl acetimidate [12] and 0.00033

*Table 2.* Fragmentation pattern of the His derivative. Mass spectrum of the product of reaction of $N$-acetyl-L-His with dimethyl malondiimidate. Conditions: 300°, 1600 V, 100 $\mu$A. Symbols: M, The assumed structure (intact) as shown in Fig. 2; i, M cleaved at point 5 and/or 6 ($C_8H_9N_3O_3$); B: C——$CH_2$——C (bridge); I:

$$\begin{array}{ccc} & C{-}{-}CH_2{-}{-}C & \\ & \| \qquad\quad \| & \\ & NH_2{}^+ \qquad NH_2{}^+ & \end{array}$$



$(C_4H_4N_2)$
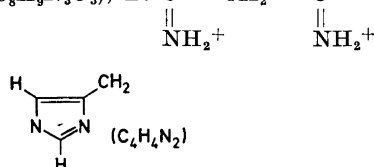
| $m/e$ | | Composition | Cleavage | Fragments | Components |
|---|---|---|---|---|---|
| Obs. | Calc. | | points | | |
| 501 | 501 | $C_{17}H_{18}N_8O_6Cl_2$ | 1, 10 | $MCl_2 - 2CH_3$ | |
| 372 | 372 | $C_{17}H_{24}N_8O_2$ | 3, 8 | $M - 2\ CO_2$ | |
| 266 | 266 | $C_{11}H_{14}N_6Cl$ | 4, 7 | $M - 2CHNH(CO)CH_3$ $\quad\quad\quad\;\; \mid$ $\quad\quad\quad\;\; CO_2{}^-$ | |
| 256 | 256 | $C_{13}H_{16}N_6$ | 3, 8 | | $B + 2\ I + 2\ CH$ |
| 237 | 237 | $C_{10}H_{13}N_4O_3$ | | | $i + CH_2 - C = NH_2{}^+$ |
| 180 | 180 | $C_7H_6N_3O_3$ | 1, 5, 6, 10 | $i - CH_3$ | |
| 151 | 151 | $C_7H_9N_3O$ | 3, 5 | $i - CO_2$ | |

*Table 3.* Rate constants of product formation. Comparison between the reactivities ($k$) of various groups in amino acids towards imidates.

| Amino acid or peptide | Imidate | Temp. °C | pH | $k$ l mol$^{-1}$ min$^{-1}$ | Product |
|---|---|---|---|---|---|
| $\varepsilon$-NH$_2$-caproic acid | Methyl benzimidate | 25 | 8 | $2.2^a$ | Amidine |
| Gly — Gly | Methyl benzimidate | 25 | 8 | $4.2^a$ | Amidine |
| None | Methyl benzimidate | 39 | 8.5 | $< 0.0001$ | Benzoic acid |
| $N$-Ac-L-Met | Dimethyl malondiimidate | 25 | 9.7 | 1.4 | Di-thioimidate[b] |
| $N$-Ac-L-His | Dimethyl malondiimidate | 25 | 9.7 | $>15$ | Amidine [b] |
| $N$-Ac-L-His | Methyl acetimidate | 25 | 7.4 | 0 | Amidine [b] |
| None | Methyl acetimidate | 25 | 7.4 | 0.0003 | Acetic acid. |

[a] Ref. 12. [b] Suggested on the basis of spectral and titrimetric evidence (see text).

min$^{-1}$ for methyl benzimidate [12] at pH 9.6 and 39°. The malondiimidate is clearly much more reactive than the previously used monofunctional imidates.

The spectrophotometric titration curve for modified $N$-acetyl-L-His was difficult to obtain because this compound undergoes reversible oligomerization. Therefore, the spectrum of the monomer had to be constructed from the spectra of the substance at $5-6$ different concentrations (serial dilution) at each

pH-value (see Fig. 6). The data listed in Table 4 are based on the Linderstrøm-Lang theory [35] and on the reported $pK'$-values, $pK_{intr}$-values, electrostatic parameters, and difference extinction coefficients per prototropic group.[31]

*Table 4.* Protolytic and spectroscopic parameters of enzymes, derivatives and model compounds. The data in this table were collected at room temperature (*ca.* 23°) unless otherwise stated. They serve to aid the identification of sites of chemical modification or changed environment and the characterization of the nature of such alterations (*e.g.* electrostatic field, polarity of environment or conformational changes).

| Compound | $pK'$ | $pK'_{intr}$ | $h$ | $w$ | $\Delta\varepsilon^{294}$ 1 mol$^{-1}$ cm$^{-1}$ | Tentative assignment |
|---|---|---|---|---|---|---|
| His-der [a] | 9.43 | 7.48 | 1.85 | 0.90 | | ring 1 |
| | 10.10 | | | | | ring 2 |
| | 10.40 | | | | | amidine 1 |
| | 10.76 | | | | | amidine 2 |
| | 11.55 | 8.94 | | 1.21 | | amidine 3 |
| Met-der [b] | 9.29 ± 0.09 | 8.87 ± 0.08 | 1.26 ± 0.01 | 0.42 | | imido 1 |
| | 12.2 | | | | | imido 2 |
| MCT [c] | 6.32 | | 4.97 | | 160 000 | His 1 |
| 8 M urea | 7.41 | | 3.08 | | 16 000 | His 2 |
| 24° | 8.56 | | 8.56 | | 14 000 | His 3 |
| | 9.82 ± 0.03 | | | | | |
| | 10.25 | | | | | |
| | 11.00 ± 0.02 | 9.92 ± 0.03 | 0.60 ± 0.04 | 0.17 ± 0.01 | | |
| α-CT [c] | 7.02 | 5.29 | 2.20 | 0.67 | | 2 His |
| 25° | 8.15 | | | | | 2 −NH₂ |
| 0.15 M KCl | 6.20 | | | | | 1 COO⁻ |
| | 5.75 | | | | | 1 COO⁻ |

[a] The product of the reaction of *N*-acetyl-L-His with dimethyl malondiimidate. [b] The product of the reaction of *N*-acetyl-L-Met with dimethyl malondiimidate. [c] Protolytic titration. Ref. 42. *h* Slope of log A/HA *vs.* pH-function. *w* Electrostatic factor (see text). $\Delta\varepsilon^{294}$ Difference extinction coefficient at 294 nm.

NMR-spectra of derivatives of His and malonic acid were recorded. The resonance frequencies, multiplicities, and area ratios are listed in Table 1. These data are in agreement with the values reported in the literature for similar compounds. The treatment of *N*-acetyl-L-His with dimethyl malondiimidate gives rise to a shielding effect of the resonances of the protons at the ring, the α-C, the β-C, and the acetyl group. This diamagnetic shift is more pronounced for the His side chain than for the acetyl group.

*Characterization of the modified enzyme.* The elution profile, gel electrophoresis at pH 6.5 and determination of the number of NH-termini were used as criteria for the purity of the preparation. The curves for the determination of the molecular weight by gel filtration were illustrated in Fig. 1 of a preliminary communication.[3] In the same article, the data for the extinction coefficients at 280 nm and the number of amide and free amino groups in α-CT, dimethyl maleylated δ-CT, and carbamylated δ-CT were given in Table 1.

In addition, the extinction coefficient at 280 nm for $\delta$-CT modified by dimethyl succindiimidate was listed. The latter was prepared by a method analogous to the one described in this article for dimethyl malondiimidate.

The results of the cinnamoyl imidazole titration of the operational titer of active sites in $\alpha$-CT and MCT are shown in Table 5 which also contains the value for the incorporation ratio of carboxyl-^{14}C-labelled dimethyl malondiimidate into MCT.

Table 5. Comparison between the covalent dimer and the monomer. Evidence for the molecularity of the modification reaction and the accessibility of the active site in MCT for a specific substrate. The molecular weight was estimated by gel filtration on calibrated columns with and without denaturing agents (8 M urea) and checked by hydrodynamic measurements. The active site titer (= operational normality of the enzyme) was determined with *trans*-cinnamoylimidazole. The number of reagent molecules introduced per monomer was assayed with ^{14}C-dimethyl malondiimidate (carboxyl-labelled). The absence of sulfhydryl groups after the reaction was confirmed with Ellman's reagent.

| Enzyme | M | Active sites/monomer eq./mol | [14]C/mon. g-atom/mol | SH/monomer eq./mol |
|---|---|---|---|---|
| CT-monomer | 25000 | $1.00 \pm 0.03^a$ | | $0.00 \pm 0.02$ |
| M-$\delta$-CT | $47000 \pm 3000$ | $1.03 \pm 0.03$ | $1.030 \pm 0.03$ | $0.10 \pm 0.02$ |

$^a$ This value was $0.91 \pm 0.03$ before gel filtration.

*Investigation of the possibility of disulfide cleavage in MCT during the modification reaction.* Native chymotrypsin does not contain any sulfhydryl groups, but it was conceivable that imidates were sufficiently nucleophilic to break disulfide linkages, *e.g.* followed by the formation of a thioimidate with the reagent (dimethyl malondiimidate). The most reactive of these sites is the one involving Cys-191, the nearest neighbour to one of the expected sites of reaction.[35] An Ellman titration showed that this did not occur to any appreciable extent (see Table 5).[37]

*Fractionation of peptides from MCT after disulfide cleavage and limited proteolysis by trypsin and thermolysin.* The elution profile of two of the three chromatographic steps are shown in Figs. 7 − 8. The fractions which were taken for further purification are shown on the figures. Each fraction was pooled and concentrated by ultrafiltration before application to the next column. The gradient was chosen empirically. It was generated by a gradient former with two cylindrical vessels containing pyridine-glacial acetic acid buffers: 1. pH 3.1 and 5.0; 2. pH 5.0 and 5.6; 3. pH 5.6.[38] The fractions A − F were separately evaporated to dryness on Al-plates (15 cm $\varnothing$), weighed and counted. The radioactivity was related to the number of peptide linkages. The latter, which was taken as a measure of the length of the peptide, was estimated from the extinction at 230 nm which largely is due to this chromophore since the peptides are in the random coil conformation and since the content of aromatic side chains is low.
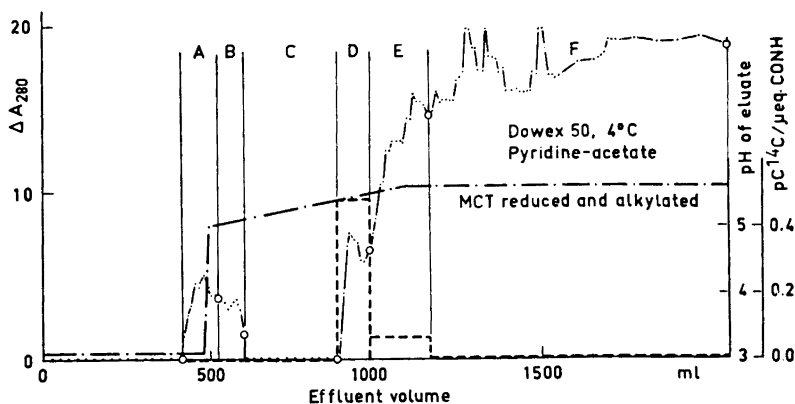
*Fig. 7.* Elution profile at 4° of peptides from limited proteolysis of carbamylated, reduced, alkylated M-δ-CT by trypsin and thermolysin. The column consisted of Dowex 50 × 2 ion exchange resin in equilibrium with pyridine-glacial acetic acid at pH 3.1. The buffer was a mixture of pyridine and glacial acetic acid (see text). Elution rate: 10 ml/h. Symbols: ————, absorption at 280 nm; — · —, pH of the buffer gradient; — — —, the specific ^{14}C-activity in cpm per equiv. of peptide linkage. The fractions A-E were separately collected. Fractions D and E, which contained all of the ^{14}C-label, were further fractionated on Sephadex G-10.
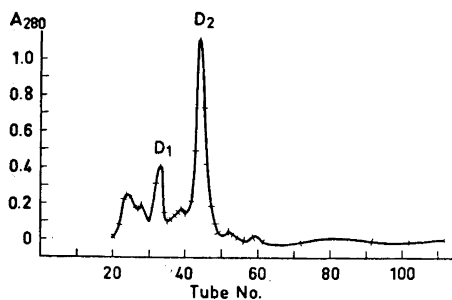


*Fig. 8.* Elution diagram showing the fractionation of fraction D (see Fig. 7). on Sephadex G-10 in 0.05 M phosphate, 8 M urea at 5° and pH 7.5. Flow rate: 10 ml/h. Column 57 × 2.7 cm. Ordinate: Absorption at 280 nm. Abscissa: Glass number (*ca.* 6.5 ml/glass). The fractions $D_1$ (glass 30 − 36 incl.) and $D_2$ (glass 40 − 50 incl.) were after urea removal and further homogeneity tests (see text) sequenced. The bridge chromophore at about 250 nm was visible in the fractions $D_1$ and $D_2$ (as well as in $E_{1a}$ and $E_{1b}$).

*Determination of the* N-*terminal sequence of the* [14]-*C-labelled peptides.* The peptides $D_1$, $D_2$, $E_{1a}$, and $E_{1b}$, which represent *ca.* 90 % of the radioactivity, were sufficiently pure for sequence analysis by the criteria mentioned above (see section on methods). In each cycle of the Edman procedure, two DNS-amino acids appeared which shows the presence of two different, but non-separable, chains. On completion of each cycle, the phenyl-thiohydantoins were collected and counted on the low level apparatus. In Table 6, the ratio of the disintegration rate to the standard deviation of the counting technique is related to the amino acids found in each cycle. These results are compared with the known amino acid sequence of CT. The relevant segments of the B- and C-chains are shown in Fig. 9. In this way, the sites of modification could

*Table 6.* Identification of amino acid side chain carrying $^{14}$C-labelled covalent bridge which connects two $\delta$-CT monomers. The exclusive location of $^{14}$C in His-57 and Met-192 was proven by isolation of $^{14}$C-PTH which sequentially was released from the four peptides. The residual peptide did not contain significant amounts of the tracer in any of the four sequencing experiments The loss of $^{14}$C occurred primarily during the preparation of the reagent and the modification of CT. The purity of the peptides was tested by examination of the elution profile, by electrophoresis and by observation of the number of amino acids which appeared after each cycle of the sequencing procedure. A trace of Tyr was ascribed to the adsorption of a small amount of this amino acid. Tryptic release of Tyr-146 (C-terminal after slight autolysis of $\delta$-CT) was anticipated since the next neighbour is Arg. The peptides sequenced account for 90 % of the labelled protein.

| Peptide[a] | Amino acid No.[b] | cpm./$s_d$[c] | Significance [d] | DNS-Edman [e] |
|---|---|---|---|---|
| D$_1$ | 1 | 5.5 | 1:1.7 × 10$^6$ | His*, Met* |
| | 2 | 0.9 | 1:1.7 | CM-Cys, Gly |
| | 3 | 0.6 | — | Gly, Asp |
| | 4 | 0.2 | — | Val, Ser |
| | 5 | 0.2 | — | Thr, Gly |
| | 6 | 0.8 | 1:1.4 | Thr, Gly |
| | Residual | 1.5 | 1:6.5 | — |
| D$_2$ | 1 | 3.2 | 1:727 | His*, Met* |
| | 2 | 0.2 | — | CM-Cys, Gly |
| | 3 | 0.2 | — | Gly, Asp |
| | 4 | 0.2 | — | Val, Ser |
| | 5 | 0.2 | — | Thr, Gly |
| | 6 | 0.8 | — | Thr, Gly |
| | Residual | 0.4 | 1:1.4 | — |
| E$_{1a}$ | 1 | 1.4 | 1:5.2 | Ala, Met* |
| | 2 | 1.7 | 1:10.2 | His*, Gly |
| | 3 | 0.6 | — | CM-Cys, Asp |
| | 4 | 0.8 | 1:1.4 | Gly, Ser |
| | 5 | 0.1 | — | Val, Gly |
| | 6 | 0.1 | — | Thr, Gly |
| | Residual | 0.6 | — | — |
| E$_{1b}$ | 1 | 4.4 | 1:8 × 10$^5$ | His,* Cys |
| | 2 | 2.0 | 1:21 | CM-Cys, Met* |
| | 3 | — | — | Gly, Gly |
| | 4 | — | — | Val, Asp |
| | 5 | — | — | Thr, Ser |
| | 6 | — | — | Thr, Gly |
| | Residual | — | — | — |

[a] The peptides are electrophoretically homogeneous at pH 6.5 (30 min). [b] From NH-terminal (1). [c] Measured on isolated PTH, $s_d$ = Standard deviation of mean. [d] Significance of decay rate data in previous column, *i.e.* of presence of $^{14}$C in the aminoacid. [e] Subtractive Dansyl-Edman method.[26] [f] Acid hydrolysis apparently cleaves the cross-bridge without affecting the mobility of the amino acids. The amino acids which are expected to be labelled are marked with an asterisk. The chromatographic mobilities of the labelled amino acids indicate that $\varepsilon$-DNS-His and $\varepsilon$-DNS-Met were obtained and that the presumed cross-bridge either was cleaved without affecting the thioether function or the imidazole ring or failed to change the mobilities significantly.

Covalent sidechain linkage between 2 molecules of $\delta$-chymotrypsin.

```
       57   58    59     60     61     62
   ... His . Cys . Gly . Val . Thr . Thr ... B-chain
         |     |
         |    CM
         |
   ... Met . Gly . Asp . Ser . Gly . Gly ... C'-chain
       192' 193'  194'   195'   196'   197'
```
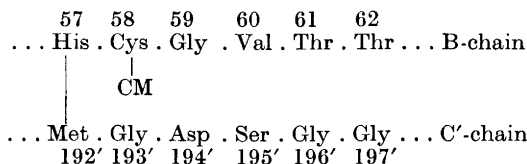
*Fig. 9.* Summary of the amino acid sequence results and the ^{14}C-PTH-amino acid data showing the unique sequences which contain the bridge(s). The prime refers to the neighbouring molecule.

uniquely be assigned to His-57 and Met-192 (see Fig. 10). The amino acid composition analyses of the peptides are consistent with this finding.
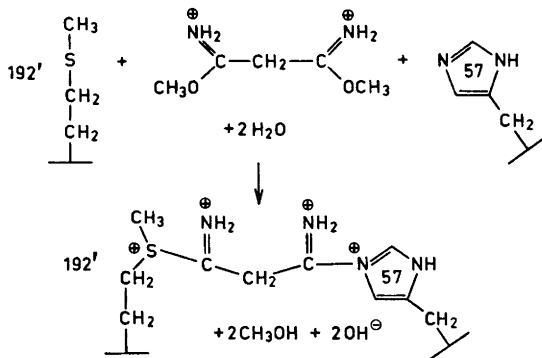


*Fig. 10.* Reaction scheme favoured by the accumulated evidence. It requires the presence of two analogous bridges which connect the two molecules of $\delta$-CT.

*Optical rotatory dispersion of MCT and CT.* The difference ORD-curve between the modified enzyme and CT displayed small anomalies in the region of the aromatic side chains (260 − 270 nm). This range also corresponds to the absorption bands of the new chromophore in MCT and may be due to small Cotton effects. These, however, were so small that it was difficult to extract further information from them. The corresponding difference spectrum in the UV range between MCT and CT displayed, in addition to the chromophore already mentioned, also a band at 290 nm resembling the one reported by Wootton and Hess [39] as characteristic of the acyl enzyme. The origin of the effect was identified as a single Trp residue.

*Stabilizing effect of the modification of the enzyme on the active conformation.* MCT and $\alpha$-CT were reduced and alkylated as described above. The A-chain and the by-products of the reaction were removed by dialysis and the kinetic parameters for the catalyzed hydrolysis of a specific substrate, *N*-acetyl-L-Tyr, were then determined. The results are listed in Table 7. Although the specificity coefficient, $k_{cat}/K_m^{app}$, is much diminished after the cleavage

of the disulfide linkages, a much greater fraction of the active sites remain intact in MCT than in α-CT.

*Table 7.* Stabilizing effect of cross-bridge in MCT. The disulfide bridges in δ-CT and MCT were reduced by Cleland's reagent and alkylated (see text). The three experiments with the reduced and alkylated MCT were carried out at different times after the dialysis. The experimental error listed is the standard deviation. All parameters were evaluated by linear regression using about 8 observations at different substrate concentrations. The UV-spectrum of the preparation used in exp. 2 showed that the protein still was native $(A_{280}/A_{260} = 1.76)$.

| Enzyme | $\dfrac{k_{cat}}{K_m{}^{app}}$ $sec^{-1}$ $mM^{-1}$ | $k_{cat}$ $sec^{-1}$ | $K_m{}^{app}$ mM | Relative efficiency |
|---|---|---|---|---|
| α-CT[a] | 215 | 236 | $1.1 \pm 0.3$ | 1 |
| δ-CT[b] | 211 | 201 | 0.95 | 1.0 |
| MCT[a] | 740 | 519 | $0.7 \pm 0.2$ | 3.4 |
| δ-CT, reduced and alkylated [a] | 0.2 | $0.22 \pm 0.02$ | $1.0 \pm 0.4$ | 1 |
| MCT, reduced and alkylated exp. 1[a] | 0.78 | 0.86 | 1.1 | 4 |
| MCT, reduced and alkylated exp. 2[c] | $97 \pm 7$ | $448 \pm 18$ | $4.6 \pm 0.3$ | $490 \pm 38$ |
| MCT, reduced and alkylated exp. 3[a] | 34 | 17 | 0.5 | 68 |

[a] 25°C, pH 8.0, N-Ac-L-tyr-OEt, 0.1 M KCl. [b] pH 8.5, 0.45 M KCl. [c] pH 8.0, 0.04 M Tris, 20°C.

## DISCUSSION

The evidence for the structure of the product of the reaction of dimethyl malondiimidate with N-acetyl-L-Met is the following:

1. The only function in N-Ac-L-Met which can react with an imidate is the thioether since the masking of the amino group was effective. This was checked by IR-measurement and by dansylation.

2. The kinetics supports the proposed molecularity.

3. The rate constant for formation of the derivative has the magnitude which could be expected from a reaction of the type suggested.

4. A small amount of homoserine was detected in the hydrolysate of MCT but not of CT. This indicates that Met has been attacked.

5. The spectral changes following the addition of the imidate to the N-Ac-Met or the enzyme could not be due to hydrolysis of dimethyl malondiimidate since the small spectral contribution of the latter at the wavelength of observation was subtracted.

6. Sulfonium compounds are known to exhibit multiple bands in the range where the Met derivative and MCT display such bands.[40]

7. Construction of the molecular model of the suggested Met derivative shows that the formation of this compound is feasible and plausible.

8. The alternative hypothesis: The existence of a strong ionic linkage between sulfonium and the imidate is excluded by the observation of the persistence of the characteristic band in MCT after thorough purification of the latter in the presence of a high concentration of salt and urea.

The conclusion must be that both MCT and the model compound contain the thioimidate group.

In the case of the His derivative, the evidence is:

1. The only group in $N$-Ac-L-His which can react with an imidate is the imidazole ring, since the masking of the amino group was effective. This was checked by IR- and NMR-measurement and by dansylation.

2. The expected molecular weight and decomposition pattern were found for the His derivative by mass spectrometry[33,34] (see Table 3). Fragments larger than the reactants were found.

3. The changes in spectrum and p$K$-values (see Figs. 3 and 8) show that a reaction has occurred and that the ring is involved. The spectrum resembles that of an amidine.

4. The elemental analysis and molecular weight determination from the colligative properties exclude other possible structures.

5. ^{14}C-labelled His was found in a partial hydrolysate of the modified enzyme.

The reported failure of previous attempts of modifying imidazole with an imidate may be explained by the difference in pH of the solution and in the reactivity of the reagents.[12] Amidination reactions are known to possess sharp pH-optima.[43] Since imidates require a nucleophile, only the nitrogen atoms of the ring need to be considered as reaction sites. The NMR-data are compatible with thus suggestion. The shielding effect on the imidazole ring of the His derivative (see Table 1) may be due to its participation in the mesomerism of the amidine. The diamagnetic shift of the protons on the $\alpha$- and $\beta$-carbon atoms may be due to either an inductive effect or to the high electric field at the bridge. The latter is the more likely explanation since the $\alpha$-C, which displays the larger deshielding effect can approach the bridge closer than the $\beta$-C can. The NMR-data are compatible with the hypothesis of the formation of the bridge and no plausible alternative seems apparent.

The incorporation ratio (see Table 5) shows that each CT-monomer carries one molecule of the modifying reagent. The sites of modification were identified as Met-192 and His-57 by amino acid sequence analysis of peptides which had been carefully purified and satisfied the homogeneity criteria. Since the disulfides were exhaustively reduced and carboxymethylated prior to the limited proteolysis and the fractionation and since the two modified amino acids are located in two different peptide chains (B and C), their presence in the same molecule shows that the two chains have become connected by a covalent bridge. No other amino acids than the two mentioned carried the ^{14}C-label in the four peptides which were sequenced and which represent 90 % of the label in the protein. Since all ether amino acids remained intact, the covalent bridge must connect Met-192 and His-57 directly. No homologous bridges (His-His or Met-Met) were found in the four peptides which were sequenced and an examination of the total model of the enzyme revealed that the formation of two such bridges as required by the measured incorporation ratio, was highly unlikely.[36]

An intramolecular His-57-Met-192 bridge is feasible in $\delta$-CT but it is likely to impede the binding of specific substrates. Since both $N$-acetyl-L-Trp and $N$-acetyl-L-Tyr were good substrates of MCT and since the molecular weight

determinations indicated the existence of the covalent dimer, this structure was favoured. An examination of the model shows that the formation of a dimer stabilized by two covalent malono-bridges is feasible and plausible. The suggested bond types in the bridge are shown in Fig. 10.

In the dimer model, there is free access for a specific substrate molecule to either of the two active sites and they can be charged simultaneously and act in mutual independence. This is in keeping with the finding of 1.0 active site per molecule of monomer (see Table 5) by the cinnamoyl-imidazole titration.

The reactivity of $N$-acetyl-L-His and of $N$-acetyl-L-Met toward dimethyl malondiimidate shows that the suggested type of modification of CT should occur unless there are special difficulties, such as local steric hindrance or unfavourable electronic conditions. The CT-model does not exhibit any obvious features of that nature. On the contrary, both side-chains are located on the surface and in a position suitable for a bridge formation. Such a bridge would be expected to stabilize the active site, and it was actually possible to cleave the disulfide bridges and carboxymethylate them without loss of catalytic activity toward ATEE under standard assay conditions (see Table 7).

The direct observation of the characteristic thioimidate band in the spectrum of MCT at alkaline pH supports the involvement of Met in the modification reaction. The failure of the usual reaction with dimethyl malondiimidate after selective destruction of the Met-192 side chain by oxidation with performic acid suggests that this residue is involved. Amino acid analysis of MCT shows that one of the two methionines remain intact after the diimidate reaction and the location of the tracer identifies Met-181 as the noninvolved.

Direct evidence of the involvement of His-57-imidazole ring, other than the sequencing and amino acid composition analysis, is more difficult to obtain. A comparison between the p$K$-values of His in the model compound, in CT and in MCT is not easy because the correct assignment of these values to specific groups in the absence of high resolution NMR-data is uncertain. However, since the imidazole ring by amidination should become more basic and since base catalysis undoubtedly is an important part of the mechanism of chymotryptic catalysis,[41] the existence of a His-57-ring amidine in MCT offers a reasonable, partial explanation of the observed enhancement of the catalytic efficiency. The position of the side chain of His-57 in the molecule, which is influenced by hydrogen bonds between Asp-102-carboxylate and $N_1$ and between Ser-195-OH and $N_3$, suggests that the latter, rather than $N_1$, forms the amidine. The ratios of the shielding effects are consistent with the hypothesis that also in the model compound it is $N_3$, and not $N_1$ which reacts.

## REFERENCES

1. Kang, E. P., Storm, C. B. and Carson, F. W. *Biochem. Biophys. Res. Commun.* **49** (1972) 621.
2. Coleman, J. E. and Vallee, B. L. *J. Biol. Chem.* **235** (1960) 390.
3. Havsteen, B. H. *Acta Chem. Scand.* **24** (1970) 2675.
4. Kaplan, H. *J. Mol. Biol.* **72** (1972) 153.
5. Jacobsen, C. F. *Compt. Rend. Trav. Lab. Carlsberg, Ser. Chim.* **25** (1947) 325.
6. Labouesse, B., Oppenheimer, H. and Hess, G. P. In *Symposium on Structure and Activity of Enzymes*, Academic, London 1964, p. 134.
7. Lawson, W. B. and Schramm, H. J. *J. Am. Chem. Soc.* **84** (1962) 2017.
8. Sigman, D. S. and Blout, E. R. *J. Am. Chem. Soc.* **89** (1967) 1747.
9. Fasold, H. *Biochem. Z.* **342** (1965) 288, 295.
10. Quiocho, F. A. and Richards, F. M. *Proc. Natl. Acad. Sci. U. S.* **52** (1964) 833.
11. Hartman, F. C. and Wold, F. *J. Am. Chem. Soc.* **88** (1966) 3890.
12. Hunter, M. J. and Ludwig, M. L. *J. Am. Chem. Soc.* **84** (1962) 3491.
13. Inglis, J. K. H. *Org. Syn. Coll. Vol.* 1 2nd Ed. (1967) 254.
14. Corson, B. B., Scott, R. W. and Vose, C. E. *Ibid.* p. 179.
15. Spackman, D. H., Stein, W. H. and Moore, S. *Anal. Chem.* **30** (1958) 1190.
16. Butler, P. J. G., Harris, J. I., Hartley, B. S. and Leberman, R. *Biochem. J.* **103** (1967) 78 p.
17. Dixon, H. B. F. and Perham, R. N. *Biochem. J.* **109** (1968) 312.
18. Stark, G. R. *Biochemistry* **4** (1965) 1030.
19. Havsteen, B. H. *Chimica* **25** (1971) 28.
20. Schonbaum, G. R., Zerner, B. and Bender, M. L. *J. Biol. Chem.* **236** (1961) 2930.
21. Cleland, W. W. *Biochemistry* **3** (1964) 480.
22. Vithayathil, P. J. and Richards, F. M. *J. Biol. Chem.* **235** (1960) 2343.
23. Huszar, G. and Elzinga, M. *Biochemistry* **10** (1971) 229.
24. Morihara, K. and Ebata, M. *J. Biochem. (Tokyo)* **16** (1967) 149.
25. Hartley, B. S. *Brookhaven Symp. Biol. No. 15* (1962) 85.
26. Hartley, B. S. *Biochem. J.* **119** (1970) 805; Gray, W. R. *Methods Enzymol.* **11** (1967) 469.
27. Woods, K. R. and Wang, K.-T. *Biochim. Biophys. Acta* **133** (1967) 369.
28. Weiner, H., Batt, C. W. and Koshland, D. E., Jr. *J. Biol. Chem.* **241** (1966) 2687.
29. Gutfreund, H. In *An introduction to the study of enzymes*, Blackwell Scientific Publ., Oxford 1965, p. 191.
30. Flodin, P. *Dissertation*, Uppsala 1962.
31. Bates, R. G. *Electrometric pH Determinations*, Wiley, New York 1954.
32. Yapel, A., Han, M., Lumry, R., Rosenberg, A. and Shiao, D. F. *J. Am. Chem. Soc.* **88** (1966) 2573.
33. Fairweather, R. B., Tanzer, M. L. and Gallop, P. M. *Biochem. Biophys. Res. Commun.* **48** (1972) 1311.
34. Biemann, K. and Mc Closkey, J. A. *J. Am. Chem. Soc.* **84** (1962) 2005.
35. Linderstrøm-Lang, K. *Compt. Rend. Trav. Lab. Carlsberg, Ser. Chim.* **25** (1924) 325.
36. Birktoft, J. J., Matthews, B. W. and Blow, D. M. *Biochem. Biophys. Res. Commun.* **36** (1969) 131.
37. Ellman, G. L. *Arch. Biochem. Biophys.* **82** (1959) 70.
38. Schroeder, W. A. *Methods Enzymol.* **11** (1967) 351.
39. Wootton, J. F. and Hess, G. P. *J. Am. Chem. Soc.* **84** (1962) 440.
40. Jaffé, H. H. and Orchin, M. In *Theory and Applications of UV Spectroscopy*, Wiley, New York 1966, p. 497.
41. Bender, M. L., Kézdy, F. J. and Gunter, C. R. *J. Am. Chem. Soc.* **86** (1964) 3714.
42. Havsteen, B. H. and Hess, G. P. *Biochem. Biophys. Res. Commun.* **14** (1964) 313.
43. Hand, E. S. and Jencks, W. P. *J. Am. Chem. Soc.* **84** (1962) 3505.
44. Fersht, A. R. *FEBS Letters* **29** (1973) 283.

# Structural Studies on the *Klebsiella* O Group

# 7 Lipopolysaccharide

BENGT LINDBERG,[a] JÖRGEN LÖNNGREN,[a] WOLFGANG NIMMICH[b] and ULLA RUDÉN[a]

[a] *Department of Organic Chemistry, Arrhenius Laboratory, University of Stockholm, S-104 05 Stockholm, Sweden and*
[b] *Institut für Medizinische Mikrobiologie und Epidemiologie der Universität Rostock, DDR-25 Rostock, German Democratic Republic*

The structure of the O-specific side chains in the *Klebsiella* O group 7 lipopolysaccharide has been investigated, using methylation analysis, partial hydrolysis and Smith degradation studies. In the modification of the Smith degradation used here, the polyalcohol obtained after periodate oxidation-borohydride reduction was methylated before and ethylated after the mild acid hydrolysis. The product obtained was then hydrolysed and analysed, as alditol acetates, by GLC-MS. From these studies, it is concluded that the side chains are composed of tetrasaccharide repeating units, and a structure for these units is proposed.

The twelve different *Klebsiella* O group lipopolysaccharides (LPS) studied by Nimmich and Korten [1] all contain glucose, galactose, a heptose, N-acetyl-glucosamine and a 3-deoxyoctulosonic acid (KDO), which most probably are components of the basal core. In two of them, O7 and O10, the O-specific side chains contained rhamnose and ribose. The O group 10 LPS also contained a low percentage of 3-O-methyl-L-rhamnose, not observed in the O7 LPS. We recently reported structural studies on the O10 LPS [2] and now report similar studies on the O7 LPS.

The LPS was isolated as previously described [1] and showed $[\alpha]_{578}$ $-26°$. Analysis of a hydrolysate by GLC [3]-MS [4] showed that the LPS contained rhamnose, ribose, galactose, glucose, and a heptose in the relative proportions 71:20:2:4:3. D-Arabinose was used as internal standard and the analysis showed that the LPS contained 45 % of "anhydro-sugar" residues.

The main components of the hydrolysate, rhamnose and ribose, were isolated and proved to have the L- and D-configurations, respectively. The LPS showed only a weak absorption around 1735 cm$^{-1}$ in the IR, indicating the absence of O-acetyl or other O-acyl groups in the O-specific side chains. This was confirmed by subjecting the LPS to an O-acyl determination by the

method devised by de Belder and Norrman [5] whereby no methylated sugars were produced.

The LPS was methylated by the method of Hakomori,[6] hydrolysed and the mixture of methylated sugars analysed, as the alditol acetates, by GLC-MS.[7] The results are given in Table 1, column A. The O-specific side chains in LPS from Gram-negative bacteria are generally composed of oligosaccharide repeating units. There are, however, no simple stoichiometric proportions be-

Table 1. Methylation analyses of the original and modified *Klebsiella* O group 7 LPS.

| Methylated sugar | $T^b$ | Mol % $^c$ | | | |
|---|---|---|---|---|---|
| | | A | B | C | D |
| 2-Et-3,5-Rib $^{a,d,e}$ | 0.38 | — | — | — | 20 |
| 2,3,4-Rha $^{a,d}$ | 0.46 | — | 18 | — | — |
| 3-Et-2,4-Rha $^{d,e}$ | 0.44 | — | — | — | 4 |
| 3,5-Rib | 0.77 | 19 | 12 | 26 | 9 |
| 3,4-Rha | 0.92 | 22 | 24 | < 1 | < 1 |
| 2,4-Rha $^e$ | 0.98 | 50 | 33 | 68 | 58 |
| 2,3,4,6-G $^e$ | 1.00 | 2 | 5 | 2 | < 1 |
| Others $^f$ | — | 8 | 9 | 4 | 9 |

$^a$ 2-Et-3,5-Rib = 2-O-ethyl-3,5-di-O-methyl-D-ribose,  2,3,4-Rha = 2,3,4-tri-O-methyl-L-rhamnose, *etc.*

$^b$ Retention time of the corresponding alditol acetate relative to 1,5-di-O-acetyl-2,3,4,6-tetra-O-methyl-D-glucitol on an ECNSS-M column.

$^c$ A, original lipopolysaccharide; B, lipopolysaccharide, partially degraded with acid; C, periodate oxidized and reduced lipopolysaccharide; D, Smith degraded lipopolysaccharide (see text).

$^d$ Part of these volatile derivatives was probably lost during working up.

$^e$ These compounds were separated on an OV-225 SCOT-column.

$^f$ Some of these are probably non-sugar components.

tween either L-rhamnose (71 %) and D-ribose (20 %) in the sugar analysis or between 3,5-di-O-methyl-D-ribose (19 %), 3,4-di-O-methyl-L-rhamnose (22 %), and 2,4-di-O-methyl-L-rhamnose (50 %) in the methylation analysis. D-Ribose is more labile than L-rhamnose during acid hydrolysis but this was compensated for in the sugar analysis. The most reasonable assumption seems to be that the O-specific side chains are composed of linear tetrasaccharide repeating units, containing one D-ribofuranose and three L-rhamnopyranose residues. Although a nonasaccharide repeating unit would give better agreement with the experimental results, repeating units of this size have not been demonstrated in LPS. The D-ribofuranose residue and one of the L-rhamnopyranose residues should be linked at the 2-positions, the two other L-rhamnopyranose residues should be linked at the 3-position. Assuming that the main contribution to the optical rotation of the LPS is due to the O-specific side chains, all or, less probably, three of the four sugar residues should give negative contributions to the optical rotation (*cf.* β-D-ribofuranosides and α-L-rhamnopyranosides).

The D-ribofuranosidic linkages in the LPS were cleaved by mild acid hydrolysis and the product was then reduced with sodium borohydride and

subjected to methylation analysis. The results are given in Table 1, column B. The 1,3,4,5-tetra-*O*-methyl-D-ribitol, from the D-ribosidic end-groups, is volatile and was not accounted for. Although the stoichiometry in the analysis is not very good, the formation of 2,3,4-tri-*O*-methyl-L-rhamnose and the decrease in the 2,4-di-*O*-methyl-L-rhamnose demonstrate unambiguously that the D-ribofuranose residues are linked to the 3-position of L-rhamnose in the original polysaccharide.

In order to determine the complete sequence, the LPS was subjected to a Smith degradation.[8] The procedure was somewhat modified in that the poly-alcohol obtained after periodate oxidation-borohydride reduction was meth-ylated before and ethylated after the mild acid hydrolysis. Part of the methylated polyalcohol was hydrolysed and the methylated sugars analysed, as the alditol acetates, by GLC-MS. The results given in Table 1, column C, demonstrate that all the 2-linked L-rhamnose residues have been oxidised. A sugar analysis using an internal standard showed that the other sugar residues remained essentially intact. The analysis of the hydrolysed and ethyl-ated product is given in Table 1, column D. The presence of 3,5-di-*O*-methyl-D-ribose and 3-*O*-ethyl-2,4-di-*O*-methyl-L-rhamnose reveals that not all the acyclic acetals on the modified L-rhamnose residues have been hydrolysed and that some of the acid-labile D-ribofuranosidic linkages have been hydro-lysed. A comparable amount of 3-*O*-ethyl-2,4-di-*O*-methyl-L-rhamnose was also formed when a sample of fully methylated original LPS was hydrolysed under the same conditions as in the Smith degradation experiment and sub-jected to ethylation analysis. The high percentage of 2-*O*-ethyl-3,5-di-*O*-methyl-D-ribose, however, demonstrates that the 2-linked L-rhamnose is linked to the 2-position of the D-ribofuranose residue in the original LPS.

As a result of these studies, structure I is proposed for the tetrasaccharide repeating unit in the O-specific side chains of the *Klebsiella* O group 7 LPS. It cannot be decided whether the "biological" repeating unit has this structure or a cyclic permutation of this, as no methylated sugar deriving from the non-reducing terminal was observed in the methylation analysis. This negative evidence would suggest that the O-specific side chains are long. We cannot exclude the possibility that the anomeric nature of one of the four sugar residues in this structure should be reversed.

$$\rightarrow 2)\text{-}\alpha\text{-L-Rha}p\text{-}(1\rightarrow 2)\text{-}\beta\text{-D-Rib}f\text{-}(1\rightarrow 3)\text{-}\alpha\text{-L-Rha}p\text{-}(1\rightarrow 3)\text{-}\alpha\text{-L-Rha}p\text{-}(1\rightarrow$$
$$\text{I}$$
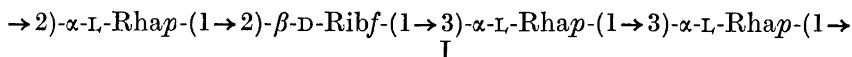
The modified procedure for the Smith degradation described above has some advantages. Acetal migration during the hydrolysis of the polyalcohol, which may complicate the results, is eliminated. It is possible to perform a degradation with only small amounts of material. With the methylation-ethylation technique, structural information may be obtained which is lost in a conventional Smith degradation.

## EXPERIMENTAL

(c 0.3, water). In the IR spectra (KBr) no significant absorption around 1735 cm$^{-1}$ was observed. Preparation of acetalated LPS by reaction with methyl vinyl ether and methylation analysis of the product were performed as previously described.[5,9] The content of phosphorus in the LPS was 0.9 %.

*Sugar analysis.* The LPS (3 mg) and D-arabinose were treated with 0.12 M sulphuric acid at 100° for 14 h. In separate experiments it was demonstrated that complete hydrolysis was obtained under these conditions but that 7 % of the D-ribose was decomposed. The sugars in the hydrolysate were analysed, as alditol acetates, as previously described.[3,4,9] L-Rhamnose, [α]$_{578}^{20}$ + 7° (c 0.3, water) and D-ribose, [α]$_{578}^{20}$ − 19° (c 0.1, water), were isolated from a hydrolysate of the LPS (20 mg) by paper chromatography.

*Methylation analyses* of original and partially degraded LPS were performed as previously described.[6,10,11] Ethylation was performed by procedures similar to those used for methylation. The location of ethyl groups in partially etherified alditol acetates by MS was unambiguous and will not be discussed.

*Analysis of partially hydrolysed LPS.* The LPS (8 mg) in 0.01 M sulphuric acid (4 ml) was kept at 100° for 45 min. After neutralization with Dowex 3 (free base), sodium borohydride (30 mg) was added and the solution was kept at room temperature for 4 h. The solution was then treated with Dowex 50 (H$^+$), concentrated and boric acid removed by repeated distillations with methanol. The product was dissolved in water, lyophilized and subjected to methylation analysis (column B in the Table).

*Smith degradation of the LPS.* The LPS (28 mg) was dissolved in 0.1 M acetate buffer of pH 3.9, 0.2 M sodium metaperiodate (5 ml) was added and the solution was kept in the dark at 4° for 120 h. Excess periodate was destroyed with ethylene glycol (1 ml), the solution was dialysed against tap water overnight and concentrated to 50 ml. Sodium borohydride (300 mg) was added and the solution kept at room temperature for 8 h. Excess borohydride was decomposed by addition of 50 % aqueous acetic acid and the solution was dialysed overnight. Part of this material (6 %) was used for sugar analysis, with D-arabinose (0.5 mg) added as internal standard. The main part was lyophilized and methylated. Part of this product (30 %) was hydrolysed and analysed as alditol acetates (column C in Table 1). The other part was treated with 50 % aqueous acetic acid for 1 h at 100°, concentrated to dryness, dissolved in dioxane-ethanol (3:1, 10 ml), reduced with sodium borohydride (50 mg) at room temperature overnight, worked up using Dowex 50 (H$^+$) followed by distillations with methanol and ethylated. The analysis of this material is given in Table 1, column D.

## REFERENCES

1. Nimmich, W. and Korten, G. *Pathol. Microbiol.* **36** (1970) 179.
2. Björndal, H., Lindberg, B. and Nimmich, W. *Acta Chem. Scand.* **24** (1970) 3414.
3. Sawardeker, J. S., Sloneker, J. H. and Jeanes, A. R. *Anal. Chem.* **37** (1965) 1602.
4. Chizhov, O. S., Golovkina, L. S. and Wulfson, N. S. *Izv. Akad. Nauk SSSR Ser. Khim.* **1966** 1915.
5. de Belder, A. N. and Norrman, B. *Carbohyd. Res.* **8** (1968) 1.
6. Hakomori, S. *J. Biochem. (Tokyo)* **55** (1964) 205.
7. Björndal, H., Hellerqvist, C. G., Lindberg, B. and Svensson, S. *Angew. Chem.* **82** (1970) 643.
8. Goldstein, I. J., Hay, G. W., Lewis, B. A. and Smith, F. *Methods Carbohyd. Chem.* **5** (1965) 361.
9. Lindberg, B., Lönngren, J. and Nimmich, W. *Carbohyd. Res.* **23** (1972) 47.
10. Lindberg, B., Lönngren, J. and Nimmich, W. *Acta Chem. Scand.* **26** (1972) 2231.
11. Hellerqvist, C. G., Lindberg, B., Svensson, S., Holme, T. and Lindberg, A. A. *Carbohyd. Res.* **8** (1968) 43.

# Investigation of the Protease Forming Ability

# of *Serratia marcescens* and One of its Mutant Strains

CURT OVENFORS, MONICA MARKLUND,
ELISABETH JOHNSSON and GUNNAR LUNDBLAD

*Chemistry Department, Statens Bakteriologiska Laboratorium,
S-105 21, Stockholm, Sweden*

The ability of eleven different strains of bacteria to form pro-
teolytic enzymes was investigated. *Serratia marcescens*, SBL-strain
was found to be amongst the best producers of these enzymes. The
strain was cultivated in 10 litre batches and it was demonstrated that
only extracellular enzymes were formed. By means of UV-radiation
a good protease forming, unpigmented mutant strain was obtained.
The enzyme from the mutant strain was purified and concentrated
in the same way as that from the natural strain. The mutant strain
produced a proteolytic enzyme with a pH-optimum of 5.4 on milk-
agar-plates and had an abnormal high tolerance against merthiolate.
Studies were also made of the pH-dependence and temperature sta-
bility of the enzyme formed by the mutant strain.

In the last few years considerable importance has been placed upon proteo-
lytic enzymes as tools for studies on the structure of proteins and for in-
vestigation of split products of biological or biochemical interest. Since the
specificity of proteolytic activity towards different proteins can vary con-
siderably among different enzymes the main purpose of this investigation has
been to look for an enzyme system with as unspecific an activity as possible,
which might be useful in tissue culture technique.

## I. INVESTIGATION OF THE ABILITY OF SOME DIFFERENT
MICROORGANISMS TO PRODUCE PROTEOLYTIC ENZYMES

The formation of proteolytic enzymes in the following strains was in-
vestigated: 1, *Serratia marcescens*, SBL-strain;* 2, *Serratia marcescens*, U 18;
3, *Serratia marcescens*, strain from Karolinska Institutet, Stockholm; 4, *Ser-
ratia rubidae*, SBL-strain; 5, *Streptococcus faecalis*, 16908, SBL-strain; 6,
*Streptococcus faecalis*, M 19, SBL-strain; 7, *Streptococcus faecium*, $A_2$1, SBL-

---

* The strain stored at our laboratory for reference use.

strain; 8, *Streptococcus mitis*, SBL-strain; 9, *Proteus vulgaris*, U 26, SBL-strain; 10, *Lactobacillus casei*, SBL-strain; 11, *Proteus mirabilis*, SBL-strain.

# Materials and methods

*Media.* 1, Medium 59, v. Hofsten and Tjeder.[1] 2, Tryptone-medium, 0.2 % with addition of 40 mg/l $CaCl_2$, Mac Donald *et al.*[2] 3, Medium 63 with addition of gelatin and peptone.[3] 4, Nutrient Agar (slant tubes) SBL 541493. 5, Nutrient Agar (Deep agar tubes) SBL 541494. 6, Nutrient Broth, Difco B 3. 7, Trypticase-Soy (TS), BBL 11768. 8, AC-medium, Bleiweiss and Zimmerman, Difco B 3 A.[4] 9, NZ-case, synthetic medium, Bleiweis and Zimmerman.[4] 10, Murakami's medium, Murakami *et al.*[5] 11, Tomato Juice Agar, Difco B 31. 12, Micro Assay Culture Agar, Difco B 319. 13, Glucose-Yeast Extract-Milk-medium, Brandsaeter and Nelson.[6] 14, Skim milk, Brandsaeter and Nelson.[6] 15, Peptonized milk, Difco B 35. 16, Micro Inoculum Broth, Difco B 320. 17, Modified Briggs Medium, Brandsaeter and Nelson.[6] 18, Mills' Medium, Mills *et al.*[7]

*Culture methods. Serratia*-strains cultivated on agar slants were used to inoculate 5 ml nutrient broth tubes which were incubated at 30°C. After 24 h 1.25 ml of each culture was transferred to flasks containing 25 ml medium. The outgrowth of each strain was tested in the media 1 – 3 and 10 at 25°C with agitation. Tests for growth and enzyme production were made. For the cultivation of *Serratia rubidae* nutrient broth was used as the enzyme-forming medium. Murakami's medium with bovine albumin as enzyme-inducing component was tested on the four *Serratia*-strains but cultivation was done in nutrient broth. Growth at 25°C with agitation as well as growth at 30°C without agitation were tested. Tests for determination of proteolytic activity, growth and pH were taken after 24 and 48 hours.

*Streptococcus*-strains. From agar slants and deep agar tubes cells were transferred to tubes containing 5 ml nutrient broth and to tubes containing 5 ml Trypticase-Soy-medium. After 24 h 0.25 ml of the culture was transferred to 5 ml AC-medium and after another 24 h the culture was transferred to NZ-case. The inoculum was 1 % of the total volume of medium. The growth temperature was 37°C and each strain was grown with or without agitation. According to the method of Bleiweis and Zimmerman,[4] 50 % of the culture volume was changed with fresh medium after 24 h and the growth continued. By this means the cells were maintained in log-phase to reach maximum enzyme formation. Tests were taken when the medium was changed. The cultivations were run at pH 7, 6.0, and 5.5. In the last two pH's the medium was not exchanged. The most active enzyme producer *Streptococcus faecalis* 16908 and *Streptococcus faecalis* M 19 were also tested at pH 7 without changing the medium.

*Proteus vulgaris.* Tests for enzyme formation were negative and therefore this bacterium was not used further.

*Proteus mirabilis.* From agar slants and deep agar tubes, cells were transferred to 5 ml Trypticase-Soy-medium. After 24 h 1.25 ml was inoculated into 25 ml Mills' medium and medium 63 supplemented with gelatin and peptone. Incubation at 37°C was made with and without agitation. Tests for enzyme formation, pH, and bacterial density were taken after 24 and 48 h.

*Lactobacillus casei.* Streak plates were made on Tomato Juice Agar and Micro Assay Culture Agar. After 48 h at 30°C and 37°C, respectively, the cells were transferred to 3 ml each of the media glucose-yeast extract-milk, skim milk, peptonized milk and micro inoculum broth. They were incubated at 30°C and 37°C for 48 h, then 1.25 ml from each tube was transferred to 25 ml of Briggs medium. Different incubation times were tried before enzyme tests were taken.

*Enzyme tests.* For determination of proteolytic activity the following three methods were used: viscosimetry, Kunitz' method modified by Rydén and von Hofsten and the agar plate method.[8-11] Agar- or agaroseplates, diameter 14 cm, containing hemoglobin, milk or albumin were prepared as follows:

*Hemoglobin plates.* 1 g agar or agarose was dissolved in 50 ml boiling buffer-solution (see buffer-solution). 25 ml 4 % bovine hemoglobin was mixed with 25 ml buffer solution (see buffer solution). The two solutions were carefully mixed with each other.

*Milk plates.* 1 g agar or agarose was dissolved under boiling in 50 ml buffer-solution. 50 ml 3 % fat-free dry milk (Semper) in distilled water was added.

*Albumin plates.* 1 g agar or agarose was dissolved under boiling in 50 ml buffer-solution after which the mixture was cooled to 80°C. A solution containing 5 ml 10 % bovine albumin in 50 ml buffer solution was added to the agar solution. The resulting solution was heated instantly to 87°C. 3 mm holes were made in the agar plates into which the test materials were placed. The enzyme activity was demonstrated by clear zones formed around the holes. The logarithm of the diameter of the zones is directly proportional to the actual enzyme activity. The tests were carried out at pH 5, 6, 7, and 8. Each plate contained 35 ml agar or agarose and 14 holes per plate were made and filled with 20 $\mu$l test solution.

The bacterial cultures were centrifuged. To the supernatants merthiolate was added to a final concentration of 0.01 %. Then the supernatants were put into the holes. The plates were incubated at 30°C for the *Serratia*-strains and at 37°C for the other organisms. After a defined time the plates were read. At the same time corresponding tests were carried out with NBC Trypsin (1:300), crystallized trypsin, and subtilisin.

*Buffer solutions.* 0.1 M phosphate buffer was made up to the various pH's used except for pH 5, where 0.1 M citrate-phosphate-buffer was employed. The buffer solutions were prepared according to Augustinsson.[12] To all plates merthiolate was added to a final concentration of 0.01 %.

# Results and discussion

The *Serratia*-strains with the exception of *Serratia rubidae* were easy to cultivate and formed large quantities of the red pigment prodigiosin. The proteolytic activity seemed to be proportional to pigment formation and growth. Medium 63 with peptone and gelatin yielded the best cultures after 48 h incubation at 25°C. Strains of *Serratia marcescens* gave the best proteolytic activity. Optimum activity was obtained at pH 8 on milk agar plates after 48 h incubation (Table 1).

*Table 1.* Proteolytic activity of tested organisms. Enzyme tests carried out at pH 8.0.

| Organism | Enzyme activity, zone diam. in mm | | | Culture conditions | Media number |
| --- | --- | --- | --- | --- | --- |
| | Hemo-globin | Milk | Albumin | | |
| *Serratia marcescens,* SBL | 12 | 14 | 6 | a | 3 |
| *Serratia marcescens,* U18 | 11 | 13 | 0 | a | 3 |
| *Serratia marcescens,* KI | 11 | 12 | 0 | a | 3 |
| *Serratia rubidae* d | 0 | — | 0 | a | 3 |
| *Proteus mirabilis* | 0 | 15 | 8 (pH 7.0) | b | 16 |
| *Streptococcus faecium,* A$_2$I | 0 | 0 | — | c | 7 |
| *Streptococcus faecalis* 16908 | 10 | 15 | 9 | c | 7 |
| *Streptococcus faecalis,* M 19 | 8 | 8 | 0 | c | 7 |
| *Streptococcus mitis* | 0 | 0 | — | c | 7 |
| *Lactobacillus casei* d | 0 | 0 | 0 | | — |

[a] Agitation, 25°C. [b] Agitation, 37°C. [c] Without agitation at pH 7.0 with media exchange 37°C. [d] *Serratia rubidae* and *Lactobacillus casei* do not form protease and showed a weak growth.

The best cultivation of *Streptococcus*-strains was obtained after a change of medium and cultivation without agitation at 37°C. The best enzyme activity was obtained from *Streptococcus faecalis* 16908 on milk agar plates at pH 8 (Table 1).

Of the *Proteus*-strains studied, *Proteus mirabilis* was found to yield growth after 24 h in Mills' medium with agitation at 37°C. The best enzyme activity was obtained at pH 8 on milk agar plates (Table 1).

*Lactobacillus casei* gave bad growth in several media. No proteolytic activity could be detected.

## II. CULTIVATION OF *SERRATIA MARCESCENS* (SBL-STRAIN) AND PURIFICATION OF ITS PROTEOLYTIC ENZYME

### Materials and methods

*Serratia marcescens* (SBL-strain) was cultivated in 10 litres scale using medium 63 supplemented with gelatin and occasionally peptone. The medium was sterilized in an autoclave at 120°C for 60 min. It was inoculated with 195 ml bacteria suspension and the culture incubated for 60 h at 25°C with an agitation speed of 400 rpm by daytime and 250 rpm by night. The air flow was 1.2 − 1.5 l/min. Antifoam Emulsion FG was added. Tests for determination of enzymatic activity were taken at equal time intervals. pH and growth were measured at the same time. For determination of the number of bacteria at the end of the cultivation, 10-fold dilutions were made in a buffer containing 8 g/l NaCl, 1.89 g/l $Na_2HPO_4.12H_2O$, 0.2 g/l KCl and 0.2 g/l $KH_2PO_4$, pH 7.3 − 7.4 (dilution buffer). A volume of 0.1 ml culture was spread on Trypticase Soy agar plates. They were read after 24 h incubation at 37°C. Determination of dry weight of cells was made at the same time by desiccation at 105°C for 24 h. The bacterial suspension obtained was centrifuged at 2000 $g$ for 1 h and washed two times in the dilution buffer mentioned. After the last washing the supernatant was stored at 4°C and the pellet resuspended in the dilution buffer mentinoed above and also stored at 4°C.

An investigation was made to determine the amount of cell-bound proteolytic enzymes. An aliquot of the washed centrifugate was agitated and treated with ultrasonic waves at an energy of 20 kc/s for 3 × 1 min and also for 10 × 1 min both at +4°C. Then the samples were centrifuged at 10 000 $g$ for 30 min. The purification of the proteolytic enzyme was carried out according to von Hofsten *et al.*[13] To 1 litre of the supernatant 10 g Whatman cellulose powder was added after which 700 g ammonium sulphate was dissolved under agitation. The solution was stored for 24 h at +4°C, then it was filtered through a sintered glass filter. The cellulose powder was washed with 50 ml 50 % ammonium sulphate solution. The pale pink coloured cellulose powder was agitated in 250 ml 50 % ammonium sulphate solution and stored at +4°C. Then the cellulose suspension was packed in a column. A clear eluate was obtained. The cellulose was sucked to dryness, then suspended in 25 ml 0.1 M Tris-HCl, pH 8.0, packed in another column and the enzyme was eluted with the buffer. The eluent was recirculated until it was clear. More Tris-HCl was added and eluted. The total volume of the eluate was measured and solid ammonium sulphate was added to a final concentration of 0.4 g/ml. The solution was stored for 24 h at +4°C. The resulting precipitate was sedimented by centrifugation at 10 000 $g$ for 30 min. The centrifugate was suspended in 25 ml distilled water, then dialyzed first against distilled water and after that against 0.05 M Tris-HCl, pH 8.0. The dialysate contained a dark red precipitate which was separated by centrifugation at 10 000 $g$ for 30 min. The supernatant received was concentrated by sequestering the water from the dialysis bags. Part of the concentrate was gel filtered on Sephadex G 75 in 0.1 M phosphate buffer, pH 7.2.

### Results

The changes in growth, protease activity, and pH during the cultivation appears in Fig. 1. The number of bacteria at the end of the cultivation was

*Fig. 1.* Growth, protease activity and pH of *Serratia marcescens* culture in 10 litre culture. (O), Protease (CTU = Comparative Trypsin Units); — — — pH; (↑) Addition of 1 ml antifoam.
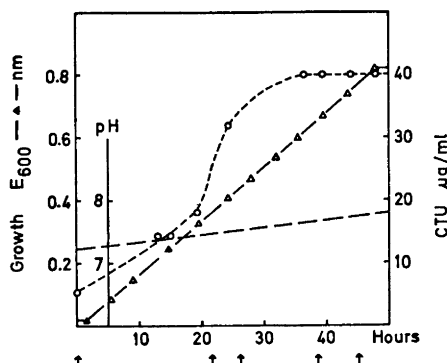
$3.0 \times 10^9$/ml and the cell density was 1.25 g/l. Microscopic investigation showed that the cells which had been treated with ultrasonic waves were destroyed but no proteolytic activity was obtained. This result indicates that only extracellular enzymes have been formed. The result from the purification appears in Fig. 2. Two extinction peaks were obtained and the proteolytic activity was present in only one of them.
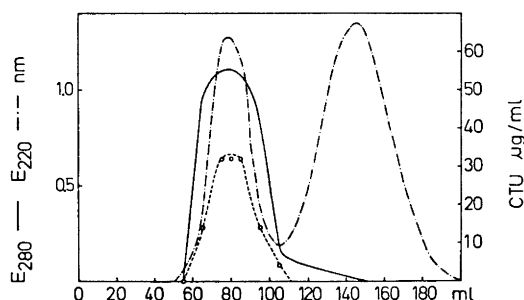


*Fig. 2.* Extinction diagram and protease activity obtained by gel filtering on Sephadex G75 of enzyme solution from *Serratia marcescens*. (O) Protease (CTU = Comparative Trypsin Units).

## III. CULTIVATION OF *SERRATIA MARCESCENS* MUTANT STRAIN AND PURIFICATION OF ITS PROTEOLYTIC ENZYME

### Materials and methods

Attempts were made with UV-radiation to obtain a mutant capable of producing higher proteolytic activity. A 24 h nutrient broth culture was centrifuged and the cells suspended in the dilution buffer and six 10-fold dilutions were made. The three last dilutions were irradiated with a UV-lamp (Westinghouse sterillamp 782 L-20, 14 W) at a distance of 50 cm for 10, 20, 45, and 60 sec, in Petri dishes with 10 ml in each dish. They were slowly rotated during the test. Photoreactivation was avoided by covering the dishes with aluminum foil after the UV-treatment. UV-irradiation for 60 sec yielded about 2 % survivors, for 45 sec about 50 %, and for 20 sec about 80 %. Irradiation for a shorter time than 10 sec had no effect. Many white colonies were found when after irradiation

*Table 2.* Protein- and pH-effect on growth and protease activity of *Serratia marcescens*, natural and mutant strains. Protease activity measured after incubation during 24 h at 30°C.

| Organ-ism | Medium [a] | Growth $(E_{600\ nm})$ [b] | pH [c] | Protease activity, milk-agar (diam. mm) | |
|---|---|---|---|---|---|
| | | | | pH 8 | pH 6 |
| | | 48 h culture | 48 h culture | 48 h culture | 48 h culture |
| Natural | I | 0.57 | 7.8 | 16 | 15 |
| strain | II | 0.92 | 8.4 | 11 | 7 |
| | III | 0.66 | 7.4 | 14 | 13 |
| | IV | 1.02 | 6.5 | 12 | 12 |
| Mutant | I | 0.27 | 7.4 | precipitation | 6 |
| strain | II | 0.89 | 8.4 | precipitation | 0 |
| | III | 0.21 | 7.2 | precipitation | precipitation |
| | IV | 0.29 | 6.2 | precipitation | precipitation |

[a] See Materials and methods. [b] Tests and blanks diluted 1:5 in dist. water. [c] Original pH = 7.2 (except medium IV with pH 6.0).

0.1 ml suspension was spread on nutrient milk agar plates (3 plates per dilution). At the same time unirradiated cells were spread for control. The plates were incubated for 120 h at 30°C. A mutant was isolated and the optimum culture and enzyme-inducing conditions were investigated. The effect of different proteins and the influence of pH were investigated. Medium 63 supplemented with peptone and one of the following protein sources was used (Table 2). I, Gelatin, Difco, pH 7.2; II, Casein hydrolysate (Casamino Acids, Difco) pH 7.2; III, Casein according to Hammarsten (Merck) pH 7.2; IV, Casein according to Hammarsten (Merck) pH 6.0.

On nutrient-milk agar plates the irradiated colonies were surrounded by a clear zone with a diameter of only 3 mm. The corresponding diameter for the natural strain was 9 mm, although the size of the colonies was similar.

# Results

*Effect of mercury-compounds.* It was found that addition of merthiolate in ordinary concentrations to the mutant strain culture did not inhibit the growth. The tolerance of the mutant strain against merthiolate was compared with the natural strain of *Serratia marcescens* and some other bacteria (Table 3). To Medium 63 supplemented with peptone and gelatin, pH 7.2, different amounts of merthiolate were added. The cultures were incubated for 22 h at 25°C with agitation. A 24 h old Trypticase-Soy-culture was used as inoculum. Measurement of bacterial density was made in a Beckman DB-G spectrophotometer at 600 and 660 nm in a 10 mm cuvette. The medium was used as blank.

The mutant strain was cultured in 10 litres-scale in the same way as described for the natural strain. Medium 63 supplemented with peptone and gelatin pH 7.2 was used as before. The cultivation was run at 25°C with an agitation speed of 300 rpm by day and 200 rpm by night. The air flow was 1.2 − 1.5 l/min by day and 0.5 − 0.6 l/min by night. When necessary Antifoam Emulsion FG was added. The medium was inoculated with 200 ml of a 48 h

Table 3. Effect of mercury-compounds on growth of some bacteria.

| Organism | Conc. Hg$^{2+}$ | | | Inhibition % | Reference |
|---|---|---|---|---|---|
| | mM | g/l | Hg-compound | tion % | |
| *Serratia marcescens* | | | | | |
| Natural strain | 0.246 | 0.05 | (merthiolate) | 97 | SBL-strain, natural strain used in the investigation |
| Mutant strain | 8.85 | 1.79 | (merthiolate) | 100 | SBL-strain mutant used in the investigation |
| Mutant strain | 4.425 | 0.90 | (merthiolate) | 83 | SBL-strain mutant used in the investigation |
| Mutant strain | 2.2 | 0.45 | (merthiolate) | 29 | SBL-strain mutant used in the investigation |
| Mutant strain | 1.106 | 0.225 | (merthiolate) | 19 | SBL-strain mutant used in the investigation |
| *E. coli* | 0.246 | 0.05 | (merthiolate) | 97 | SBL-strain, natural strain used in the investigation. |
| *E. coli* | 0.008 | 0.0016 | | 100 | Cooper and Mason [14] |
| *E. coli* | 0.06 | 0.0119 | | 100 | Cook and Steel [15] |
| *B. subtilis* | 1 | 0.201 | *p*-mercuri-benzoate | 97 | Falcone *et al.*[16] |

culture. Tests were taken at equal time intervals for determination of enzyme activity, growth, and pH. The number of bacteria and the cell mass were determined at the end of the cultivation. The culture was stopped by adding 0.01 % merthiolate. The bacteria were centrifuged and washed. The supernatant was sterilized by filtration to avoid further growth. The centrifugate was diluted in the dilution buffer. Both supernatant and centrifugate were stored at +4°C.

*Preliminary purification of protease from the mutant strain.* The protease produced by the mutant strain was purified and concentrated in the same manner as described for the natural strain except that the enzymes produced by the mutant strain were precipitated with ammonium sulphate only. 1000 ml culture supernatant was precipitated with 700 g $(NH_4)_2SO_4$. The precipitate was sedimented by centrifugation and dissolved in $10^{-3}$ M phosphate buffer, pH 7.5. The proteolytic activity was found in this solution. The dissolved centrifugate was dialyzed first against distilled water and then against $10^{-3}$ phosphate buffer, pH 7.5. All the activity was recovered in the dialysate, which was concentrated by ultrafiltration. One ml concentrate from the natural and mutant strain was applied to a Sephadex G 100 column (Fig. 3). The pH- and temperature-dependence of the protease from the natural and mutant strain was tested with the supernatants from the respective 10 litre scale cultures. As substrate milk agar pH 4 – 9 was used and the proteolytic assay was carried out as described in part I. The pH-dependence can be seen in Fig. 5. The temperature dependence of the enzyme activity was tested after exposure to 0°, 20°, 30°, 37°, 60°, and 100°C for 5, 10, 15, 30, 60 min, and 24 h. After the treatment the solutions were rapidly cooled and placed in
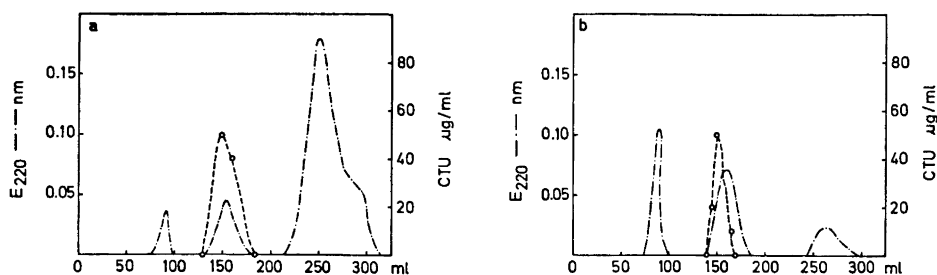
*Fig. 3.* Extinction and proteolytic activity obtained by gel filtering on Sephadex G100 of a concentrated enzyme solution from *Serratia marcescens.* (O) Protease (CTU = Comparative Trypsin Units). (a) Mutant strain; (b) natural strain.

holes in the agar plates. The plates were incubated for 24 h at 30°C before reading. As an alternative test cooled enzyme solutions (0°C) were placed on the substrate plates after which they were incubated at the various temperatures given above for 24 h before reading. The temperature 100°C could not be tested in this case.

The mutant protease showed an acid pH-optimum on milk agar. At pH 6 a clear zone of 13 mm and 11 mm diameter was formed after 24 h incubation at 30°C with the mutant and natural strain, respectively. Merthiolate added to the milk agar inhibited the growth of the natural strain but had no effect on the mutant strain. The investigation of optimum growth and enzyme formation is shown in Table 2. Medium 63 supplemented with peptone and gelatin, pH 7.2, gave the largest protease activity for both the natural and mutant strain. In other experiments it was found that casein hydrolysate yielded better growth than gelatin in this medium. A pH close to neutral gave optimal enzyme production from both organisms in spite of the fact that the protease of the mutant strain had an acid pH-optimum and that good growth occurred on milk agar, pH 5.

Table 3 shows the influence of mercury-compounds. 100 % inhibition of the mutant strain required 8.85 mM merthiolate whereas the natural strain
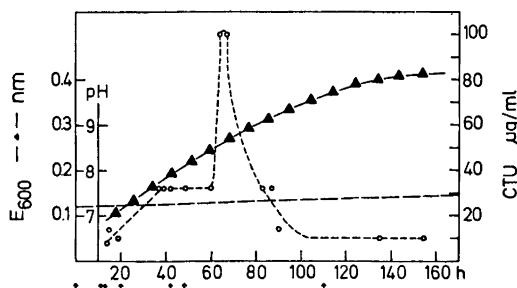


*Fig. 4.* Growth, protease activity and pH of *Serratia marcescens,* mutant strain in 10 litre culture. (▲), Growth, $E_{600}$ nm (blank and test diluted 1:5 in dist. water); (O), Protease (CTU = Comparative Trypsin Units); — — — pH; (↑) Addition of 1 ml antifoam.
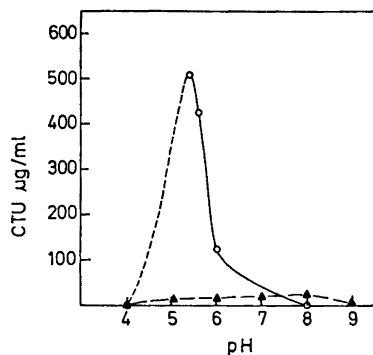
Fig. 5. Protease activity from *Serratia marcescens*, natural and mutant strain as a function of pH on milk agar plates after 24 h at 30°C. (▲) Protease activity, natural strain (CTU = Comparative Trypsin Units); (○) Protease activity, mutant strain.
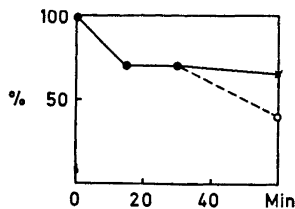
Fig. 6. Remaining activity in % of original activity after heating at 60°C for different periods. (×) Natural strain at pH 8.0. (○) Mutant strain at pH 6.0.

was fully inhibited at 0.246 mM. In comparison with other organisms the mutant strain also showed a much larger tolerance against merthiolate. Fig. 4 shows that the mutant strain grew slower than the natural strain in 10 litre cultures. The protease activity reached its maximum after about 60 h. $(NH_4)_2$-$SO_4$ precipitation was the most suitable method for separating the proteolytic activity from the medium for both the mutant and natural strain. The yield in this case was 30 % and 40 %, respectively. With gel filter three peaks were obtained at about 90, 150, and 250 ml. All proteolytic activity was found in peak number 2 (about 150 ml), see Fig. 3. The protease from the natural and mutant strains had an optimal activity around pH 8 and pH 5.4, respectively (Fig. 5). Temperature stability studies (Fig. 6) showed that after 15 min at 60°C the activity was reduced by 30 %. After 60 min at 60°, 65 % and 40 % of the proteolytic activity from the natural and mutant strain, respectively, remained. All activity was lost after 5 min boiling. The optimum temperature was 30°C. Attempts to demonstrate intracellular enzymes were negative; only extracellular proteases were found.

*Conclusions.* The very marked resistance of the mutant strain to merthiolate (Table 3), and perhaps other mercury compounds is being investigated further to detect what mechanism is responsible for this resistance. More extensive work on the purification and characterization of these proteolytic enzymes is in progress.

## REFERENCES

1. v. Hofsten, B. and Tjeder, C. *Biochim. Biophys. Acta* **110** (1965) 576.
2. Mac Donald, I. J. and Chambers, A. K. *Can. J. Microbiol.* **9** (1963) 871.
3. Rydén, A.-C. and v. Hofsten, B. *Acta Chem. Scand.* **22** (1968) 2803.
4. Bleiweis, A. S. and Zimmerman, L. N. *J. Bacteriol.* **88** (1964) 653.
5. Murakami, M., Fukunaga, K., Matsuhashi, M. and Ono, M. *Biochim. Biophys. Acta* **192** (1969) 378.
6. Brandsaeter, E. and Nelson, F. E. *J. Bacteriol.* **72** (1956) 68.
7. Mills, G. L. and Wilkins, J. M. *Biochim. Biophys. Acta* **30** (1958) 63.
8. Hultin, E. *Svensk Kem. Tidskr.* **58** (1946) 281.
9. Lundblad, G. and Johansson, B. *Enzymologia* **35** (1968) 345.
10. Rydén, A.-C. and v. Hofsten, B. *Acta Chem. Scand.* **22** (1968) 2803.
11. Rutqvist, L. and Lundblad, G. *Acta Vet. Scand.* **10** (1969) 1.
12. Augustinsson, K.-B. *Experimentell Biokemi*, Fr. Bagges Kgl. Hofbogtrykkeri, Copenhagen 1966, pp. 494−95.
13. v. Hofsten, B., Vankley, J. and Eaker, D. *Biochim. Biophys. Acta* **110** (1965) 585.
14. Cooper, E. A. and Mason, J. *J. Hyg.* **26** (1927) 118.
15. Cook, A. M. and Steel, K. J. *J. Pharm. Pharmacol.* **11** (1959) 666.
16. Falcone, G., Salvatore, G. and Covelli, I. *Biochim. Biophys. Acta* **36** (1959) 390.

# An Infrared Spectroscopic Study on some Thiocyanato Complexes of Cobalt (II) in Non-aqueous Solutions

ATIS MIEZIS

*Inorganic Chemistry 1, Chemical Center, University of Lund, Box 740, S-220 07 Lund 7, Sweden*

The frequency and intensity of the C — N stretching vibration have been measured for the thiocyanate ion and the thiocyanato complexes of cobalt(II) in five different non-aqueous solvents (acetonitrile, propane-1,2-diolcarbonate, trimethylphosphate, dimethylacetamide, and dimethyl sulfoxide). It has been concluded that the thiocyanate groups are N-bonded and that the first complex has an octahedral configuration $[Co(NCS)D_5]^+$ (D is the solvent).

The stability constants of the first complex have also been determined and the results are discussed with regard to the donor properties of the solvents.

The majority of useful solvents in coordination chemistry appears to have donor properties. Therefore, the ligands to be coordinated to a metal ion in such solvents would have to compete with the solvent molecules for the coordination sites. The stability of a metal-ligand complex system would then be dependent on the donor strength of the solvent. Gutmann *et al.*[1] have made calorimetric measurements on the interactions of a large number of solvent molecules (D) with antimony(V) chloride as reference acceptor in an inert solvent (dichloroethane), and determined the heats of reaction for

$$D + SbCl_5 \rightleftharpoons DSbCl_5; \quad -\Delta H_{DSbCl_5}$$

For the reactions investigated this quantity is proportional to the logarithm of the formation constant of $DSbCl_5$ obtained from spectrophotometric [1] and NMR-measurements.[2]

Gutmann[3] suggests that the $-\Delta H_{DSbCl_5}$ values can be used as representative expressions for the degree of interaction between donor and acceptor and defines the donor number (DN) as the numerical quantity of $-\Delta H_{DSbCl_5}$

$$DN_{SbCl_5} \equiv -\Delta H_{DSbCl_5}$$

The donor numbers of many solvents together with their dielectric constants can be found, *e.g.* in Ref. 3, p. 69. These values for the solvents studied in this paper are also given in Table 1.

*Table 1.* The donor numbers $DN_{SbCl_5}$ and the dielectric constants $\varepsilon$ of the solvents used.[3]

| Solvent | $DN_{SbCl_5}$ | $\varepsilon$ |
|---------|---------------|---------------|
| Acetonitrile (AN) | 14.1 | 38.0 |
| Propane-1,2-diolcarbonate (PDC) | 15.1 | 69.0 |
| Water | 18.0 | 81.0 |
| Trimethylphosphate (TMP) | 23.0 | 20.6 |
| N,N-Dimethylacetamide (DMA) | 27.8 | 38.9 |
| Dimethyl sulfoxide (DMSO) | 29.8 | 45.0 |

Of course, the numerical values of the donor numbers are only valid for $SbCl_5$ as acceptor, but one could expect that their relative order is maintained with other acceptors if the bonding character is not changed too much. Gutmann[3] has demonstrated this by studies on the stability of halido and pseudo-halido complexes of Co(II) in various donor solvents. Thus, the molar ratios $X^-/Co^{2+}$ required to obtain the tetrahedral $CoX_4^{2-}$ for various solvents usually increase with increasing donor number of the solvent but the correlation is not perfect.

The general study of complex formation in non-aqueous solvents has been neglected up to the present time. The best way to describe a complex system is to determine the stability constants by equilibrium analysis. One of the ligands used by Gutmann in his studies of the influence of solvent donor properties on the stability of a complex system is the thiocyanate ion, $SCN^-$. The thiocyanato complexes can with advantage be studied by infrared spectroscopy[4] owing to the distinct absorption band of the $C-N$ stretching vibration.

Usually there is no detectable difference in the frequency of this vibration between consecutively formed complexes. But when this frequency of the complexes is compared with that of the "free" ligand there would often be a frequency shift. If the frequency shift is large it is possible to obtain the stability constants from "free" ligand concentration measurements using the "free" ligand band.[5] For the $Co^{2+}-NCS^-$ systems in this study, however, the consecutively formed complexes do not have the same frequency of the $C-N$ stretching vibration. Furthermore, only the first complex shows a large frequency shift upon coordination whereas the frequencies of the other complexes lie close to that of the "free" ligand. This makes it impossible to use the "free" ligand band for the determination of the stability constants. In its place the first complex band can be used and the method is described below. Of course, only the stability constant of the first complex may be determined in this way but nevertheless any constants would be of value when discussing donor properties of solvents.

The solvents investigated were: acetonitrile ($CH_3CN$), propane-1,2-diolcarbonate ($C_4H_6O_3$), trimethylphosphate [($CH_3O)_3PO$], N,N-dimethylacetamide [$CH_3CON(CH_3)_2$] and dimethyl sulfoxide [($CH_3)_2SO$].

## PRINCIPLE OF INVESTIGATION

The method is thoroughly described in Ref. 5, and therefore only a short presentation will be made here of the actual conditions and the equations used in the calculations.

*Notations*

$C_M$ = total concentration of metal
$C_L$ = total concentration of ligand
$[M]$ = free concentration of metal
$[L]$ = free concentration of ligand
$[ML]$ = concentration of the first complex
$\beta_1$ = $[ML]/[M][L]$ = stability constant of the first complex
$A_\nu$ = absorbance at the band maximum of the first complex (at the wave number $\nu$)
$A_\nu{}^\circ$ = absorbance when $C_M \to \infty$
$\varepsilon_1$ = molar absorption coefficient of the first complex at the band maximum
$\varepsilon_{L\nu}$ = molar absorption coefficient of the "free" ligand at the wave number $\nu$
$d$ = the cell thickness

For all experimental series, $C_L$ was kept constant while $C_M$ was varied. If $C_M > C_L$ it may be assumed that ML was the only mononuclear complex of importance. The existence of polynuclear complexes was excluded as it probably would imply an absorption band at somewhat higher frequencies and no such band was found for the actual systems. Then

$$C_M = [M] + [ML] \tag{1}$$

$$C_L = [L] + [ML] \tag{2}$$

$$\text{and } A_\nu = \varepsilon_1[ML]d + \varepsilon_{L\nu}[L] \tag{3}$$

In the systems investigated there was always a large difference in frequency between the absorption band maxima of the ligand and the first complex. Therefore, $\varepsilon_{L\nu}$ would be very small and the last term in eqn. (3) may be neglected. Then, by combining eqns. (1)−(3) (*cf.* Ref. 5, p. 1437) one can obtain the following relation:

$$A_\nu = A_\nu{}^\circ - A_\nu/[\beta_1(C_M - C_L A_\nu/A_\nu{}^\circ)]$$

Thus, $A_\nu$ plotted against $A_\nu/(C_M - C_L A_\nu/A_\nu{}^\circ)$ should give a straight line with the slope $-1/\beta_1$. $A_\nu{}^\circ$ was not known at first but may as a first approximation be set to $A_\nu{}^\circ \approx A_\nu$. That means that first $A_\nu$ was plotted against $A_\nu/(C_M - C_L)$ and a new value of $A_\nu{}^\circ$ was obtained as the intercept on the ordinate axis. With this value of $A_\nu{}^\circ$ inserted a renewed plotting could be done and so on until no perceivable change in the parameters was found.

## EXPERIMENTAL CONDITIONS

*Chemicals used.* All the chemicals used were of analytical grade. The solutions to be investigated were made from anhydrous stock solutions of cobalt(II) perchlorate and sodium thiocyanate in five different solvents. They were: *Acetonitrile*, purified by repeated distillations over $P_2O_5$, until this no longer became brown-coloured, and then once over $CaCO_3$.[6] *Propane-1,2-diolcarbonate*, distilled before use.[1] *Trimethylphosphate*, boiled over CaO and then distilled over dried $Na_2CO_3$.[7] N,N-*Dimethylacetamide*, purified according to Gutmann *et al.*[8] *Dimethyl sulfoxide*, purified as described by Schläfer and Schaffernicht.[9]

Anhydrous cobalt(II) perchlorate was prepared by resolution of the hexahydrated salt.[10] This was dissolved in the respective solvent (except acetonitrile) and the solution was evaporated to near dryness. Then the residue was redissolved and the procedure repeated twice. After that a stock solution could readily be made by filling up solvent to the required volume. The solutions of cobalt(II) perchlorate in acetonitrile were prepared in another way. The hexahydrated salt dissolved in acetonitrile was stirred several times with $P_2O_5$ and then refluxed for 2 h with an additional portion of $P_2O_5$. When the mixture was filtered into anhydrous ethyl ether there was a precipitation of a compound which analysis showed to be $Co(CH_3CN)_6(ClO_4)_2$ (*cf.* Ref. 11). From this the stock solutions could be prepared.

No special examinations of the purity of the solutions have been made. A water content would be observable in the infrared spectra of the solutions [12] but no such absorptions have been noticed.

Unfortunately, the measurements had to be performed in solutions with uncontrolled ionic strengths because the solubilities of possible supporting electrolytes were low. Thus, the formal ionic strength is that originating from the concentrations of the ionic species in solution. For aqueous solutions, however, the stability constants obtained in this way seem to be rather independent of the total salt concentration [5] and it is reasonable to presume that this could be valid also for the solutions used here.

*Recording of the spectra.* The measurements were made using a Perkin-Elmer 521 grating spectrophotometer. Matched cells with windows of $CaF_2$ were used in both the sample and reference beam. The content of the reference cell was pure solvent. The cells were of the semi-permanent type which can be completely dismantled for path-length alterations. The maximum thicknesses of the spacers that could be used were about 0.5 mm for acetonitrile and 0.2 for the other solutions because of solvent absorption in the spectral region. The exact thicknesses of the cells were determined using the usual interference fringe technique. The spectra were run with an expanded wave number scale and the spectral slit width of the instrument was about 1.5 cm⁻¹. The wave number readings in the spectral region under investigation were checked periodically by measuring the spectra of carbon monoxide in a 10 cm gas cell.

## RESULTS

*Measurements on NaSCN.* In order to verify Lambert-Beer's law and to obtain spectral data of the "free" thiocyanate ion, measurements on the $C-N$ stretching vibration of NaSCN were made. When the absorbance at the band maximum were plotted against the concentration good straight lines were obtained. Examples of these are given in Fig. 1. From the slopes of the lines the molar absorption coefficients could be calculated. They are summarized in Table 2 together with the wave numbers, band half-widths ($\Delta\nu_{1/2}$) and integrated absorptions ($\varepsilon \times \Delta\nu_{1/2}$).[13]

*Measurements on the cobalt(II) thiocyanate systems.* All the systems show the same essential features and as representative examples of the spectra those of the system $Co^{2+}-NCS-TMP$ have been chosen (Fig. 2). When the ratio $C_{SCN}-/C_{Co^{2+}}$ is small there is a shift of the $C-N$ stretching band to a frequency $25-35$ cm⁻¹ higher than that of the "free" thiocyanate ion (see
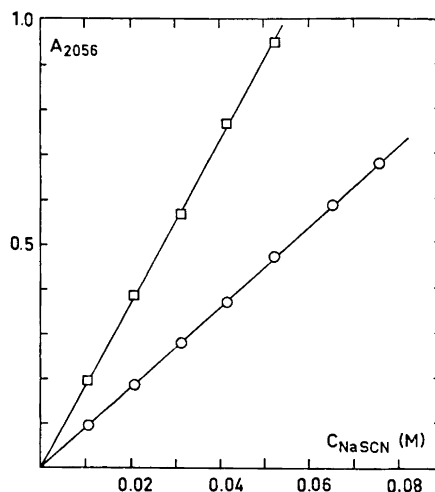
*Fig. 1.* The Beer-law plots of NaSCN in DMSO. $d = 0.105$ (O) and 0.214 mm (□).

*Table 2.* Infrared spectral data for NaSCN and the thiocyanato complexes of Co(II) in various solvents together with the stability constants of the first complex.

| Solvent, D | $\nu$ (cm$^{-1}$) | NaSCN $\varepsilon_{SCN^-}$ (M$^{-1}$cm$^{-1}$) | $\Delta\nu_{1/2}$ (cm$^{-1}$) | $\varepsilon_{SCN^-}\Delta\nu_{1/2}$ ×10$^{-4}$ (M$^{-1}$cm$^{-2}$) | $\nu$ (cm$^{-1}$) | [Co(NCS)D$_5$]$^+$ $\varepsilon_1$ (M$^{-1}$cm$^{-1}$) | $\Delta\nu_{1/2}$ (cm$^{-1}$) | $\varepsilon_1\Delta\nu_{1/2}$ ×10$^{-4}$ (M$^{-1}$cm$^{-1}$) | $\beta_1$ (M$^{-1}$) | Co(NCS)$_4$$^{2-}$ $\nu$ (cm$^{-1}$) | $\varepsilon\Delta\nu_{1/2}$ ×10$^{-4}$ $^b$ (M$^{-1}$cm$^{-2}$) |
|---|---|---|---|---|---|---|---|---|---|---|---|
| AN | 2062 | 701 | 18.5 | 1.3 | 2090 | 1050 | 22 | 2.3 | 730 ± 150 | 2070 | 3.9 |
| PDC | 2057 | 571 | 22 | 1.3 | 2092 | 650 | 26 | 1.7 | — | 2068 | 2.7 |
| TMP | 2059 | 525 | 15 | 0.8 | 2093 | 1110 | 18 | 2.0 | 500 ± 100 | 2072 | 3.6 |
| DMA | 2058 | 913 | 12 | 1.1 | 2082 | 1030 | 25 | 2.4 | 490 ± 100 | 2070 | 4.1 |
| DMSO | 2056 | 850 | 13 | 1.1 | 2083 | 840 | 25 | 2.1 | 150 ± 30 | — | — |
| H$_2$O$^a$ | 2066 | 537 | 37 | 2.0 | 2112 | 700 | 29 | 2.0 | 8.9 | 2075 | 4.9 |

$^a$ Values taken from Refs. 5 and 15. $^b$ Calculated per SCN group.

Fig. 2a; the frequency of the "free" ligand is indicated by an arrow). However, when the ratio is increased the main absorption band is moved to around 2070 (Fig. 2b) and for a large ratio also the band of the "free" ion can be distinguished (Fig. 2c). Usually consecutively formed complexes M(NCS)$_n$ or M(SCN)$_n$ show no detectable difference between the C − N stretching frequencies of the thiocyanate groups,[5,14] so the explanation in this case must be that some of the species have either different types of bonding or different configurations. By experience one would expect all these complexes to be N-bonded and this is also supported by the measured integrated absorptions in this work. The possibility of different configurations is more plausible, especially as there is a distinct change in colour of the solutions from reddish to bright blue when the ratio $C_{SCN^-}/C_{Co^{2+}}$ is increased. Fronæus and Larsson[15] have proposed

Fig. 2. Spectra of the $Co^{2+} - NCS^-$ system in TMP. The cell thickness is 0.214 mm.
a. $C_{Co^{2+}} = 0.0819$ M and $C_{SCN^-} = 0.0204$ M.
b. $C_{Co^{2+}} = 0.0051$ M and $C_{SCN^-} = 0.0153$ M.
c. $C_{Co^{2+}} = 0.0020$ M and $C_{SCN^-} = 0.0204$ M.

that there would be a much stronger electron exchange between ligand and metal for tetrahedral than for octahedral complexes. Such an electron exchange would decrease the bond order of the $C-N$ bond of the thiocyanate group and thus probably the frequency of the $C-N$ stretching vibration. The effect on the integrated absorption would be an increase when going from octahedral to tetrahedral complexes and such an increase is also found (see Table 2). As a matter of fact also Gutmann and Bohunowsky [16] have suggested that the first thiocyanato complex would be a somewhat distorted octahedral $[Co(NCS)D_5]^+$ where D is the donor solvent, while the higher ones would be tetrahedral, e.g. $Co(NCS)_4^{2-}$.

Neither the low-frequency absorption band of the coordinated thiocyanate ion nor that of the "free" ion may be used for a quantitative equilibrium analysis because they are too close together and difficult to resolve. It is possible to obtain the stability constant of the first complex, however, from the high-frequency band found for small ratios $C_{SCN^-}/C_{Co^{2+}}$ according to the method described above. The experimental data are collected in Tables 3 − 6. After

*Table 3.* The $Co^{2+} - NCS^-$ system in AN. Constant $C_L = 0.0051$ M. Cell thickness 0.564 mm. $A_{2090}° = 0.303$.

| $C_M$ (M) | $A_{2090}$ | $\dfrac{A_{2090}}{C_M - C_L}$ (M$^{-1}$) | $\dfrac{A_{2090}}{C_M - C_L A_{2090}/A_{2090}°}$ (M$^{-1}$) |
|---|---|---|---|
| 0.1212 | 0.3005 | 2.588 | 2.588 |
| 0.1010 | 0.2988 | 3.116 | 3.113 |
| 0.0808 | 0.2967 | 3.919 | 3.914 |
| 0.0606 | 0.2993 | 5.393 | 5.387 |
| 0.0505 | 0.2923 | 6.438 | 6.413 |
| 0.0404 | 0.2919 | 8.269 | 8.225 |
| 0.0303 | 0.2876 | 11.41 | 11.30 |
| 0.0253 | 0.2796 | 13.84 | 13.58 |

*Table 4.* The $Co^{2+} - NCS^-$ system in TMP. Constant $C_L = 0.0302$ M. Cell thickness 0.0150 mm. $A_{2093}° = 0.353$.

| $C_M$ (M) | $A_{2093}$ | $\dfrac{A_{2093}}{C_M - C_L}$ (M$^{-1}$) | $\dfrac{A_{2093}}{C_M - C_L A_{2093}/A_{2093}°}$ (M$^{-1}$) |
|---|---|---|---|
| 0.2406 | 0.3495 | 1.661 | 1.660 |
| 0.1805 | 0.3476 | 2.314 | 2.307 |
| 0.1504 | 0.3474 | 2.891 | 2.881 |
| 0.1203 | 0.3494 | 3.879 | 3.865 |
| 0.0995 | 0.3430 | 4.950 | 4.893 |
| 0.0902 | 0.3368 | 5.613 | 5.494 |
| 0.0753 | 0.3396 | 7.530 | 7.351 |
| 0.0666 | 0.3348 | 9.221 | 8.834 |
| 0.0602 | 0.3321 | 11.10 | 10.48 |

*Table 5.* The $Co^{2+} - NCS^-$ system in DMA. Constant $C_L = 0.0153$ M. Cell thickness 0.2165 mm.

| $C_M$ (M) | $A_{2082}$ | $\dfrac{A_{2082}}{C_M - C_L}$ (M$^{-1}$) [a] | $\dfrac{A_{2082}}{C_M - C_L A_{2082}/A_{2082}°}$ (M$^{-1}$) [b] |
|---|---|---|---|
| 0.2006 | 0.3349 | 1.807 | 1.805 |
| 0.1605 | 0.3351 | 2.308 | 2.305 |
| 0.1204 | 0.3346 | 3.184 | 3.178 |
| 0.1003 | 0.3314 | 3.899 | 3.885 |
| 0.0802 | 0.3284 | 5.060 | 5.021 |
| 0.0702 | 0.3288 | 5.989 | 5.935 |
| 0.0602 | 0.3257 | 7.254 | 7.158 |
| 0.0502 | 0.3185 | 9.126 | 8.897 |

[a] $A_{2082}° = 0.339$.  [b] $A_{2082}° = 0.340$.

*Table 6.* The $Co^{2+} - NCS^-$ system in DMSO. Constant $C_L = 0.0301$ M. Cell thickness 0.1050 mm.

| $C_M$ (M) | $A_{2083}$ | $\dfrac{A_{2083}}{C_M - C_L}$ $(M^{-1})$ [a] | $\dfrac{A_{2083}}{C_M - C_L A_{2083}/A_{2082}{}^\circ}$ $(M^{-1})$ [b] |
|---|---|---|---|
| 0.2500 | 0.2595 | 1.180 | 1.176 |
| 0.2000 | 0.2552 | 1.502 | 1.492 |
| 0.1750 | 0.2544 | 1.756 | 1.740 |
| 0.1500 | 0.2510 | 2.093 | 2.066 |
| 0.1250 | 0.2483 | 2.616 | 2.565 |
| 0.1000 | 0.2435 | 3.484 | 3.363 |

[a] $A_{2083}{}^\circ = 0.265$. [b] $A_{2083}{}^\circ = 0.266$.

the second plotting $(A_\nu$ against $A_\nu/C_M - C_L A_\nu/A_\nu{}^\circ)$ no further changes in $A_\nu{}^\circ$ and $\beta_1$ could be observed and the values so obtained are those in Table 2. $\varepsilon_1$ is calculated from $A_\nu{}^\circ$ using the relation $A_\nu{}^\circ = \varepsilon_1 d C_L$.

The method described is not applicable to very stable systems, because the slope of the straight lines $(-1/\beta)$ would be then very small. For the $Co^{2+} - NCS^-$ system in PDC the slope was approximately zero when the plotting of $A_\nu$ against $A_\nu/C_M - C_L$ was made. This would imply a larger $\beta_1$ value for the system in PDC than in the other solvents, that is $\beta_1(PDC) > 730$ $M^{-1}$.

In Table 2 also some values of the frequencies and integrated absorptions of $Co(NCS)_4{}^{2-}$ are given. These values should be considered as rough estimates. They are obtained from spectra similar to that in Fig. 2c by resolving the two bands. The ratios $C_{SCN^-} > C_{Co^{2+}}$ of the solutions used for this are large enough [16] to make it probable that $Co(NCS)_4{}^{2-}$ is the only complex present. Nevertheless, as could be seen in Fig. 2c, there are traces of shoulders on the high frequency side of the main absorption band. If this is a remainder of the band of an octahedral complex or some other effect cannot be accounted for at present. No values of frequency and integrated absorption are given in Table 2 for $Co(NCS)_4{}^{2-}$ in DMSO since complete formation of this complex would require such a large excess of ligand $(C_{SCN^-}/C_{Co^{2+}} > 200)$ [16] that it is not possible to resolve the complex band from the "free" ligand band.

## DISCUSSION

All the solvents used in this investigation could be classed as dipolar aprotic.[17] They are highly polar but have no hydrogen atoms which could be involved in hydrogen bonding. They are all capable of donating a free electron pair situated on the oxygen (nitrogen in acetonitrile) into empty orbitals of a metal ion. The binding effect originating from such an electron donation as well as possible dipole-ion attractions would be expressed by the donor numbers of Gutmann [3] (Table 1). It is reasonable to assume that cobalt(II) ion is fully solvated in such solvents and that the formation of thiocyanato complexes could be represented as ligand exchange reactions, *e.g.*

$$CoD_6{}^{2+} + NCS^- \rightleftharpoons [Co(NCS)D_5]^+ + D$$
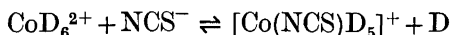
The stability of this complex in the various solvents is expressed by the $\beta_1$ values, and as the ligand exchange will be dependent on the relative donor properties of the solvent molecules as compared to that of the thiocyanate ion, one would expect a relation between the $\beta_1$ values and the donor numbers. As a matter of fact, such a relation is found between the $\beta_1$ values determined in this work (Table 2) and the $DN_{SbCl_5}$ values of Gutmann (Table 1). However, $\beta_1$ in PDC, which could not be determined, is probably larger than in AN and $\beta_1$ in aqueous solution is much smaller than would be expected from the donor number of water. Thus, it is quite evident that in this case the coordination can not be described in the simple terms of donor numbers. Water is a protic solvent and in such solvents anions are solvated not only by ion-dipole interactions but also by strong hydrogen bonding.[17] This anion solvation together with the high dielectric constant of water could be responsible for the weak coordinating ability of the thiocyanate ion in aqueous solvents. Gutmann[3] has also called attention to the steric factors, because the water molecule is much smaller than the other solvent molecules and would be of a more "suitable" shape for solvent coordination. Steric requirements could also be responsible for a greater stability of the thiocyanato complexes in PDC than in AN although PDC has a larger donor number than AN.

It has been mentioned above that all the thiocyanato complexes of cobalt-(II) would be N-bonded in the non-aqueous solvents used. This is concluded from the large values of the integrated absorption for the C–N vibration of the coordinated thiocyanate group, as compared to that of "free" ligand.[13,15] Furthermore, these values indicate that the $M-NCS$ bond, even in the octahedral complexes, would have a distinct covalent character in these solvents. In water, however, the integrated absorption of the first thiocyanato complex is the same as that of the "free" ion. This invariance tells us that there would be very little electron exchange between ligand and metal, and the bond must be regarded as essentially electrostatic in water. When discussing this electron exchange, it seems that bulk physical properties of the solvent such as the dielectric constant would be more useful than the donor number. Thus, a rather good correlation is found between the relative integrated absorption
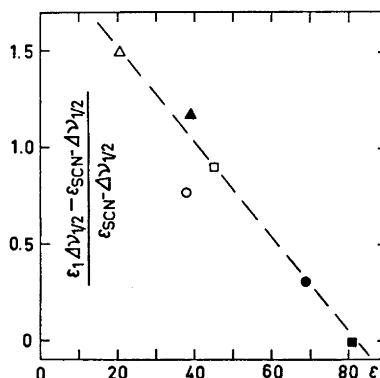


*Fig. 3.* The dependence of the relative integrated absorption $(\varepsilon_1 \Delta \nu_{1/2} - \varepsilon_{SCN^-} \Delta \nu_{1/2})/(\varepsilon_{SCN^-} \Delta \nu_{1/2})$ on the dielectric constant $\varepsilon$. The line is drawn only to emphasize the trend. ○ AN, ● PDC, △ TMP, ▲ DMA, □ DMSO and ■ $H_2O$.

in each solvent, $(\varepsilon_1 \Delta \nu_{1/2} - \varepsilon_{SCN}\text{-}\Delta \nu_{1/2})/\varepsilon_{SCN}\text{-}\Delta \nu_{1/2}$, and the dielectric constant (Fig. 3).

It must be fully understood that a distinction between the effects of the donor strength and the polarity of a solvent on the complex formation is usually difficult to make. Nevertheless, this investigation shows that the donor numbers of Gutmann may be of use when the relative stabilities of complexes in different solvents are discussed.

REFERENCES

1. Gutmann, V., Steininger, A. and Wychera, E. *Monatsh. Chem.* **97** (1966) 460.
2. Gutmann, V., Wychera, E. and Mairinger, F. *Monatsh. Chem.* **97** (1966) 1265.
3. Gutmann, V. In Ebsworth, E. A. V., Maddock, A. G. and Sharpe, A. G., Eds., *New Pathways in Inorganic Chemistry*, Cambridge University Press, London 1968, Chapter 4.
4. Larsson, R. *Rec. Chem. Progr.* **31** (1970) 171.
5. Fronæus, S. and Larsson, R. *Acta Chem. Scand.* **16** (1962) 1433.
6. Walden, P. and Birr, E. *Z. physik. Chem. Leipzig* **144** (1929) 269.
7. Gutmann, V. and Hampel, G. *Monatsh. Chem.* **94** (1963) 830.
8. Gutmann, V., Peychal-Heiling, G. and Michlmayr, M. *Anal. Chem.* **40** (1968) 619.
9. Schläfer, H. and Schaffernicht, W. *Angew. Chem.* **72** (1960) 618.
10. Gutmann, V. and Fenkart, K. *Monatsh. Chem.* **98** (1967) 1.
11. Wickendeu, A. E. and Krause, R. A. *Inorg. Chem.* **4** (1965) 404.
12. Greinacher, E., Lüttke, W. and Mecke, R. *Z. Elektrochem.* **59** (1955) 23.
13. Larsson, R. and Miezis, A. *Acta Chem. Scand.* **23** (1969) 37.
14. Larsson, R. and Miezis, A. *Acta Chem. Scand.* **22** (1968) 3261.
15. Fronæus, S. and Larsson, R. *Acta Chem. Scand.* **16** (1962) 1447.
16. Gutmann, V. and Bohunovsky, O. *Monatsh. Chem.* **99** (1968) 751.
17. Parker, A. J. *Quart. Rev.* **16** (1962) 163.

# Conformational Analysis of Coordination Compounds

## II. Dimethyl-substituted Five- and Six-membered Metal Chelate Rings

S. R. NIKETIĆ* and F. WOLDBYE

*Chemistry Department A, The Technical University of Denmark,
DTH 207, DK-2800 Lyngby, Denmark*

Steepest descent energy minimization technique has been applied to the conformational analysis of tris(chelate)metal complexes containing dimethyl substituted metal-diamine rings. Eight conformers of tris(2,3-diaminobutane) and five conformers of tris(2,4-diaminopentane) complexes were submitted to energy minimization, including complexes containing the ligands in their chiral as well as their *meso* forms.

Conformational energies are presented and partly interpreted in terms of energy differences between *lel* and *ob* rings, and between equatorial and axial methyl substituents.

The general problem of "local minima" inherent in the method is clearly exemplified.

As in our previous paper[1] the basic goal of this research was to explore the capabilities of a steepest descent energy minimization program for the conformational analysis of the tris-diamine metal complexes.

Here we report our analysis of the conformations of various forms of $M(2,3\text{-bn})_3$ and $M(2,4\text{-ptn})_3$** and compare their strain energies and geometries. The computational model was that of full relaxation of internal coordinates. Minimization was performed over the sum of energy terms due to bond stretching, angle bending, torsional and non-bonded contributions. Energy functions and parameters were the same as those used previously[1] for the analysis of the $Co\ tn_3$ system and labeled FF-1.

As illustrated in the following, conformational analysis of 2,3-bn and 2,4-ptn complexes is considerably more complicated than that of unsubstituted complexes (of, *e.g.*, en and tn) due to the presence of methyl groups

---

* On leave of absence from Department of Chemistry, University of Beograd, P.O. BOX 550, 11001 Beograd, Yugoslavia.
** Abbreviations: M = central metal ion. M — N bond lengths are chosen to correspond to M = Co(III); 2,3-bn = 2,3-diaminobutane; 2,4-ptn = 2,4-diaminopentane; tn = 1,3-diaminopropane; en = ethylenediamine. Ionic charges are omitted for simplicity.

whose internal rotation makes the potential energy surface particularly intricate.

## The metal-2,3-bn chelate ring

First we have analyzed the conformations of a single isolated M-2,3-bn ring. This system may correspond to a square planar $M(2,3\text{-bn})X_2$ complex in which the interactions between ligands X and chelate ring as well as non-bonded interactions involving M are neglected.*

The ring assumes the puckered form in which methyl groups could be equatorial (eq) or axial (ax). The resulting stereochemistry of the single M-2,3-bn chelate ring is indicated in Fig. 1.
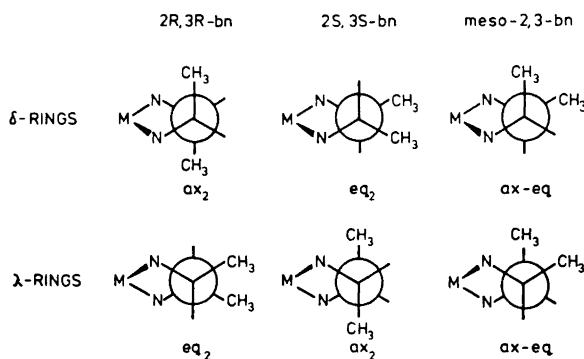


Fig. 1. The stereochemistry of a single metal-2,3-bn chelate ring.

As starting conformations for minimization we constructed two planar M-2,3-bn chelate rings having *meso* and optically active configurations of 2,3-bn. During the minimization, the ring containing the ligand in its chiral form converged rapidly towards the puckered $eq_2$ form characterised by endocyclic and exocyclic torsional angles about the $C-C$ bond of $41.2°$ and $77.7°$, respectively.

In contrast, the M-*meso*-2,3-bn ring remained planar on minimization retaining an unrealistically high strain energy in comparison to the ring with the chiral ligand. Even when the ring atoms of the initial conformation were slightly off-set alternately up and down with respect to the plane of the ring, the structure remained essentially planar on minimization. This may be due to the intrinsic property of the steepest descent minimization technique to tend to retain the initial symmetry ($C_2$ of chiral and $C_s$ of *meso*-2,3-bn) of the chelate rings.

In order to approach the minimum of the puckered form of the M-*meso*-2,3-bn ring we have inverted the position of one of the methyl groups of

---

* The latter type of interaction is not considered quantitatively negligible; it was omitted for the lack of adequate potential functions.
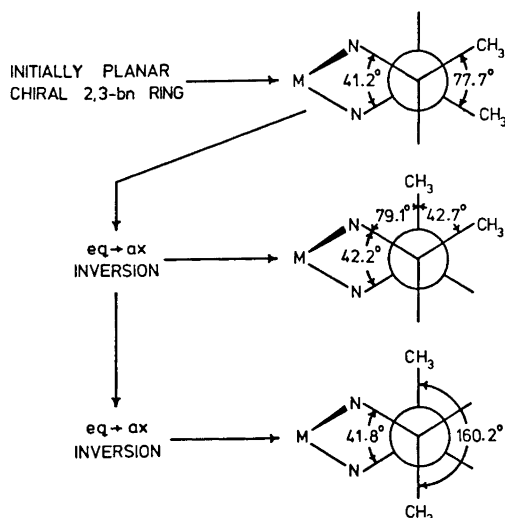
*Fig. 2.* Summary of the minimization of a single metal-2,3-bn chelate ring.

the minimized $eq_2$ ring into the ax position. This new starting conformation proved to be very close to the minimum both in energy and in conformational space, and upon minimization indeed converged rapidly. For comparison, we have constructed an $ax_2$ conformer by inverting both of the methyl groups of the minimized $eq_2$ ring containing chiral ligand. Minimization of this conformer did not lead back to the $eq_2$ conformation; the structure remained in its own local minimum indicating the existence of a barrier to ring inversion.

Results of the minimization of a single M-2,3-bn ring are summarized in Fig. 2.

## Tris(2,3-bn) chelate complexes

With either one of the optically active forms of the ligand $M(2,3\text{-bn})_3$ may exist as 2 stereoisomers ($\varDelta$ and $\varLambda$) each of which may adopt 4 conformations (combinations of $\delta$ and $\lambda$) yielding a total of 8 energetically unique structures. The complex containing the ligand in its *meso* form may be expected to exist in a total of 24 pairwise enantiomeric forms yielding 12 energetically unique structures, namely 2 stereoisomers (*fac* and *mer*), in 4 and 8 conformations, respectively.

In order to see if conformational energy differences between such structures could be interpreted in terms of energy differences between *lel* and *ob* chelate rings, between equatorial and axial methyl groups, and between *fac* and *mer* configurations, we have selected 8 of the above mentioned 20 energetically unique structures for minimization (Fig. 3).

Initial conformations were constructed by placing methyl groups on the

appropriate positions of the frameworks of three conformations of M en₃:
*lel₃*, *lel₂ob*, and *ob₂lel*, for which the coordinates of chain atoms were taken
from the X-ray diffraction data [2] on Cr(III) complexes.

Geometry parameters of the final minimized conformations* show that
the variations in bond lengths are not very important in the discussion of
the resulting structures. Slight irregularities in bond angles and steady con-
traction of chelate angles in all cases is a result of the interannular non-bonded
interactions which are most easily alleviated *via* the angle deformations.[1]
The order of conformational energies of the final minimized forms with chiral
2,3-bn is presented in Fig. 3. Differences in strain energies among the iso-
mers of $M(2,3\text{-bn})_3$ arise primarily from non-bonded interactions. Other
energy terms (particularly bond-stretching and $N-M-N$ angle bending
contributions) follow the increase in non-bonded terms in an approximately
regular way.

The energy differences between the conformations containing the chiral
form of the ligand (Fig. 3) may, in fact, be interpreted by assigning $\approx 2.2$
kcal/mol $CH_3$ to the equatorial preference of methyl groups and $\approx 0.8$ kcal/mol
ring to the preference of *lel* ring conformation. In addition, eq/ax differences
appeared to be slightly greater in *ob* than in *lel* rings.

The *mer* and *fac* isomers with *meso*-2,3-bn ($eq_3ax_3$ conformations), al-
though constructed from the same M en₃ framework, remained on minimi-
zation at higher energies than $ax_6$ conformation of optically active 2,3-bn.
This was considered to be a physically unrealistic situation so we sought
other starting points which might lead to lower points on the energy surface
of $M(meso\text{-}2,3\text{-bn})_3$. Indeed, when we restarted the minimization from the
points artificially generated by eq→ax inversion of the appropriate three
methyl groups in the $eq_6$ conformer, or by a similar ax→eq inversion in the
$ax_6$ conformer (both of which have previously been minimized) we obtained
structures that were lower in energy than the $ax_6$ conformer containing
chiral ligands. An estimate of the energy could be made by applying the
energy values for the eq/ax preference of the methyl groups in the complex
containing the *chiral* form of the ligand to the complex containing its *meso*
form. This estimate (6.8 kcal/mol, *i.e.*, the average value of the $lel_3eq_6$ and
$lel_3ax_6$ conformations), however, is about 4 kcal/mol lower than the values
found by minimization (*vide* Fig. 3). The difficulties in the minimization
of *mer* and *fac* isomers probably originate in the particularly intricate form
of the energy surface of these systems.

It is interesting to note that the energy contributions corresponding to
the interannular non-bonded interactions were approximately the same in
*mer* and *fac* isomers of $M(meso\text{-}2,3\text{-bn})_3$.

## T r i s ( 2 , 4 - p t n )   c h e l a t e   c o m p l e x e s

In the $M(2,4\text{-ptn})_3$ system conformations with axial methyl groups are
sterically too strained to be appreciably populated. Therefore, the discussion
of the stereochemistry of this system reduces itself to the following three

---

* Which may be obtained from the authors upon request.

E
(kcal/mol)

19.4 —— $ob_2lel$ $ax_4eq_2$

13.5 —— $lel_3$ $ax_6$

11.4 —— meridional $lel_3$ $eq_3ax_3$
10.9 —— $lel_2ob$ $ax_4eq_2$
10.7 —— facial $lel_3$ $eq_3ax_3$

7.2 —— $lel_2ob$ $eq_4ax_2$
6.8 —— $ob_2lel$ $eq_4ax_2$

0.0 —— $lel_3$ $eq_6$
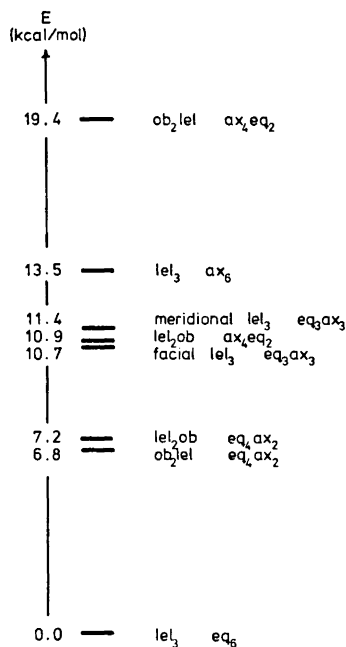
*Fig. 3.* Comparison of minimized energies of M(2,3-bn)$_3$ conformations.

E
(kcal/mol)

5.3 —— $ob_3$ (X-ray minimized)
4.5 —— $ob_3$ (calc.)

3.5 —— $(C_3)$-chair$_3$ $(\alpha < 90°)$

0.2 —— $lel_3$
0.0 —— $(C_3)$-chair$_3$ $(\alpha > 90°)$
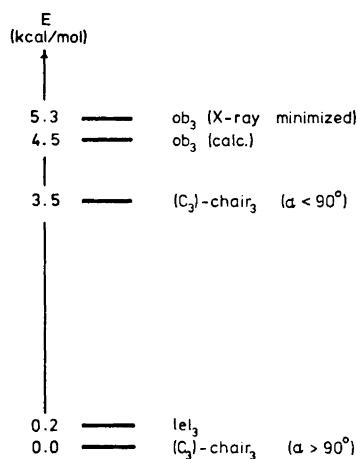
*Fig. 4.* Comparison of minimized energies of M(2,4-ptn)$_3$ conformations.

energetically unique structures all being eq$_6$: $(C_3)$-chair$_3$, $\delta_3$, and $\lambda_3$ formed on coordination of 2R,4S-ptn (*meso* form), 2S,4S- and 2R,4R-ptn, respectively. The latter two forms containing optically active 2,4-ptn appear, for example, as $lel_3$ and $ob_3$ conformations in the complexes of $\Lambda$ absolute configuration.

Four starting conformations for energy minimization were obtained by substitution of methyl groups on eq(2) and eq(4) positions on the frameworks of four of the conformations of Co tn$_3$ described in Ref. 1, namely on $(C_3)$-chair$_3$ (with N−Co−N angle > 90° and < 90°), $lel_3$, and $ob_3$.

The two chair forms with acute and obtuse chelate angles which were shown[1] to represent two points belonging to the same overall minimum on the energy surface of the Co tn$_3$ led to two quite different local-minimum conformations of M(*meso*-2,4-ptn)$_3$ system. The conformer with obtuse chelate angles proved to be stabilized over the other by ≈ 3.5 kcal/mol. The $lel_3$ conformation containing chiral 2,4-ptn rings was found to be very close to the $(C_3)$-chair$_3$ in conformational energy. The other structure containing chiral 2,4-ptn, $ob_3$ conformation, was about 4.5 kcal/mol above the $lel_3$ form indicating the conformational preference for *lel* rings of ≈ 1.5 kcal/mol ring in M(2,4-ptn)$_3$ system (Fig. 4).

For comparison we have also minimized the $ob_3$ conformation corresponding to the structure of $\Lambda$-[Co(2R,4R-ptn)$_3$] ion as known from the X-ray diffrac-
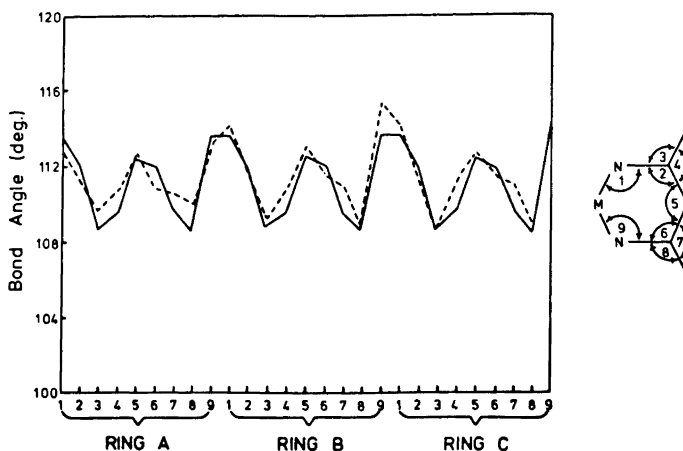
*Fig. 5.* Comparison of bond angles in minimized generated $ob_3$ (——), and in minimized X-ray $ob_3$ (- - -) conformations of Co(2,4-ptn)$_3$. The values of chelate angles (not shown in figure) are 88.1°, 87.9°, and 88.0° for the minimized generated $ob_3$, and 87.8°, 86.9°, and 87.3° for the minimized X-ray $ob_3$ conformation.

tion study.[3] The final minimized conformation obtained in this way was very close to the minimized $ob_3$ conformation described above. Bond lengths and torsional angles were almost identical in both of the structures; differences between the structures — although marginal — were found only in the bond angles (*vide* Fig. 5).

As already concluded in our previous paper[1] the conformational analyses of systems of the type studied here have not yet shown a reliability or general validity comparable to those obtained by applying similar methods to certain classes of hydrocarbons. The capricious behaviour of the M(*meso*-2,3-bn)$_3$ system, for example, may appear somewhat discouraging. Nevertheless, we find these results and their agreement with experimental energy values in the admittedly few cases (*e.g.* the eq/ax preferences) where comparisons could be ventured, promising enough to warrant the efforts involved in improving our approach by developing more versatile, refined and powerful computational methods. The development of such methods based on the original work by Lifson and Warshel[4] is currently in progress in our laboratory.

## REFERENCES

1. Niketić, S. R. and Woldbye, F. *Acta Chem. Scand.* **27** (1973) 621, and *Corrigenda and Addenda. Ibid. A* **28** (1974). *In press.*
2. Raymond, K. N., Corfield, P. W. R. and Ibers, J. A. *Inorg. Chem.* **7** (1968) 1362; Duesler, E. N. and Raymond, K. N. *Ibid.* **10** (1971) 1486.
3. Kobayashi, A., Marumo, F. and Saito, Y. *Acta Cryst.* **B 28** (1972) 3591.
4. Lifson, S. and Warshel, A. *J. Chem. Phys.* **49** (1968) 5116; Warshel, A. and Lifson, S. *Ibid.* **53** (1970) 582.

# The Primary Structure of Soybean Leghemoglobin

## III. Fractionation and Sequence of Chymotryptic Peptides of the Apoprotein of the Slow Component

NILS ELLFOLK and GUNNEL SIEVERS

Department of Biochemistry, University of Helsinki, SF-00170 Helsinki 17, Finland

The peptides from the chymotryptic digest of the apoprotein of the slow component of soybean leghemoglobin were fractionated by chromatography on Dowex 1 and high voltage paper electrophoresis. A suitable combination of these methods enables the isolation of 23 peptides, the amino acid compositions of which have been determined. The amino acid sequence of the peptides forming bridges between tryptic peptides was determined. The present results allow the combination of the tryptic peptides into four fragments.

The isolation of seventeen tryptic peptides from the slow component (Lba) of soybean leghemoglobin and their sequences have recently been reported.[1,2] A digestion of Lba was performed with chymotrypsin in order to elucidate the complete primary structure of Lba by combining the different tryptic peptides. This communication reports the fractionation, purification, and amino acid compositions of the chymotryptic peptides obtained. The determination of the amino acid sequence has been performed mainly for the bridge peptides. Non-bridge peptides provided valuable confirmatory data on the amino acid sequence of the tryptic peptides already worked out.

## EXPERIMENTAL

*Materials.* The slow component (Lba) of soybean leghemoglobin and its apoprotein were prepared as described previously.[3,4] Carboxypeptidase A was a crystallized, DFP-treated preparation, and subtilopeptidase A a crystallized preparation, both from Sigma Chemical Company (St. Louis, U.S.A). Three times crystallized chymotrypsin and leucine aminopeptidase were preparations from Worthington Biochemical Corporation (Freehold, New Jersey, U.S.A.) Trypsin was a crystalline, chymotrypsin-free preparation from Serva AG (Heidelberg, West-Germany).

---

* *Abbreviation.* 1-Dimethyl-amino-5-naphthalenesulfonyl-, dansyl, DNS-.

14

*Chymotryptic digestion.* The apoprotein of Lb*a* (192 mg) was denatured by incubation at pH 9.7 for 4 min at 95°C. Digestion was performed in 20 ml of solution at pH 8.00 and 25°C. 3.55 mg of chymotrypsin in 1 ml of 0.001 N HCl were added initially. Hydrolysis was performed in a Radiometer pH-stat by continuous titration to pH 8.00 with 1 N NaOH. After hydrolysis (3 h) the pH of the solution was reduced to 5.8. The precipitate formed was removed by centrifugation and the supernatant was lyophilized.

*Column chromatography of chymotryptic peptides.* The lyophilized digest was dissolved in 5 ml of water, adjusted to pH 8.8 with 1 N NaOH and added to a column (1.5 × 80 cm) of Dowex 1 × 2 (200-400 mesh) equilibrated to pH 8.4 at 35°C in a buffer composed of 1 % 2,4,6-collidine and 1 % pyridine adjusted to pH 8.4 with glacial acetic acid. Elution was initiated with pH 8.4 buffer at a flow rate of 25 ml/h, and 2.5 ml fractions were collected. After fraction No. 24 a gradient was set up with 300 ml of pH 8.4 buffer in a closed mixing chamber and a buffer of 1 % 2,4,6-collidine and 1 % pyridine adjusted to pH 6.5 with glacial acetic acid. The pH 6.5 buffer was changed to 0.5 N acetic acid at fraction 144 and this to 1 N acetic acid at fraction 176 and, finally, at fraction No. 256 to glacial acetic acid. A 0.1 ml aliquot of each tube was hydrolyzed with alkali and analyzed by the ninhydrin method previously described.[1] The contents of the tubes representing each peak were combined, dried *in vacuo*, dissolved in 2 ml of water and examined for purity as described previously.[1]

*Further purification of peptides.* Heterogeneous peptide fractions were further fractionated into their components either by the paper chromatography or the high voltage paper electrophoresis that had revealed the heterogeneity. The paper chromatography was performed in the butanol − acetic acid − water system as previously described.[1] The electrophoresis was performed at buffers of pH 1.9, 3.5, 6.4, and 8.9, the compositions of which have been reported earlier.[1,2].

*Amino acid composition of peptides.* A measured aliquot of peptide solution was hydrolyzed in 2 ml of 6 N HCl in evacuated sealed tubes for 18 h and the amino acid
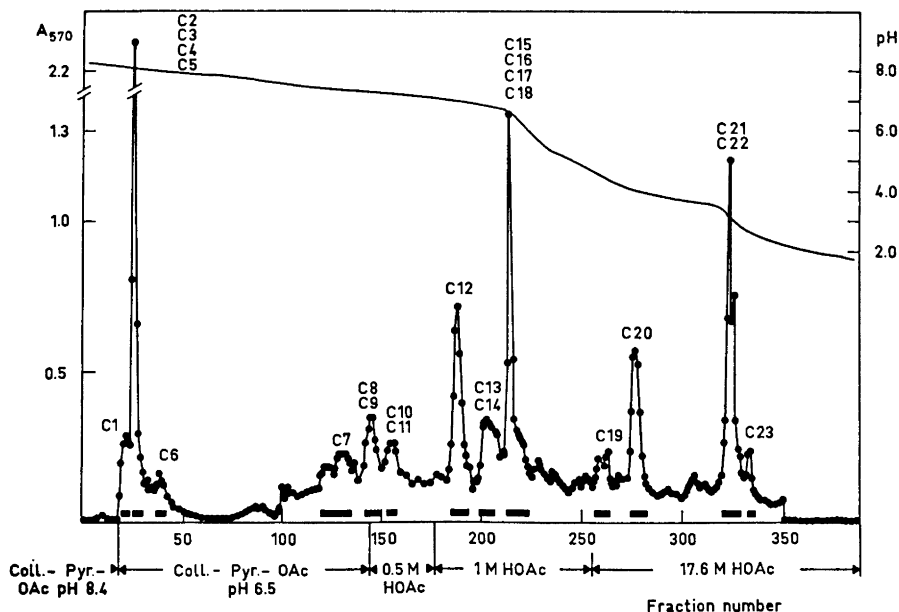


*Fig. 1.* Fractionation of peptides from a chymotryptic digest of 12.6 μmol of the slow component (Lb*a*) of soybean leghemoglobin on a Dowex 1 × 2 column (1.5 × 80 cm) at 35°C. The flow rate was 25 ml/h and 2.5 ml fractions were collected. Experimental details are given in the text. The pooled fractions are indicated by black bars.

*Table 1.* Amino acid compositions of the chymotryptic peptides of the slow component (Lb$a$) of soybean leghemoglobin. The values given in the table are mol ratios and are not corrected for losses of amino acids during hydrolysis.

| Amino acid | $a$C1 | $a$C2 | $a$C3 | $a$C4 | $a$C5 | $a$C6 | $a$C7 | $a$C8 |
|---|---|---|---|---|---|---|---|---|
| Aspartic acid | | | 1.03 | | | | | 1.76 |
| Threonine | | | 0.89 | | | | | 1.34 |
| Serine | | | | | | | 0.98 | |
| Glutamic acid | | | | | | | | 1.98(3) |
| Proline | | | | | | | | 1.02 |
| Glycine | | | 0.95 | | | | | |
| Alanine | 3.82 | 2.82 | 2.03 | 2.98 | 0.80 | 1.07 | 1.60 | 3.49 |
| Valine | | | 0.95 | | | | | 2.02 |
| Isoleucine | 0.94 | 1.03 | 0.98 | 0.76 | 1.04 | | | |
| Leucine | | | | | | | | 2.20 |
| Tyrosine | | | | | | | | |
| Phenylalanine | | | | | | | | 0.75 |
| Tryptophan | | | +[a] | | | | +[a] | |
| Lysine | 2.24 | 1.15 | 3.19 | 2.27 | 2.15 | 0.93 | | 2.17 |
| Histidine | | | | | | | | |
| Arginine | | | | | | | 1.03 | |
| No. of residues | 7 | 5 | 11 | 6 | 4 | 2 | 4 | 17 |
| $E_{Lys}$ / $E_{Asp}$ | 0.69 | 0.50 | 0.50 | 0.76 | 0.89 | 0.78 | 0.50 | neutr. |
| $R_{Leu}$ | 0.10 | 0.40 | 0.11 | 0.41 | 0.29 | 0.19 | 0.45 | 0.22 |

[a] Positive Ehrlich reaction on paper.

| Amino acid | $a$C9 | $a$C10 | $a$C11 | $a$C12 | $a$C13 | $a$C14 | $a$C15 |
|---|---|---|---|---|---|---|---|
| Aspartic acid | 1.15 | 1.06 | 1.03 | 1.03 | 1.13 | 0.91 | 0.91 |
| Threonine | 0.98 | | 0.91 | | | 0.94 | |
| Serine | 2.01 | 0.89 | | 1.00 | | 0.90 | |
| Glutamic acid | | 1.14 | 2.05 | 1.08 | 1.03 | 1.08 | 1.05 |
| Proline | | | 1.03 | | 1.24 | 1.07 | 0.87 |
| Glycine | 2.06 | 1.01 | | 1.06 | | | |
| Alanine | 3.93 | 2.01 | 2.14 | 1.18 | 2.82 | 3.03 | 1.11 |
| Valine | 2.16 | 0.99 | 2.89 | 0.91 | | | |
| Isoleucine | | | | | | 0.96 | 0.93 |
| Leucine | 1.06 | 1.92 | 1.93 | 1.11 | 1.01 | 2.00 | |
| Tyrosine | | | | | | | 0.67 |
| Phenylalanine | | | 0.93 | | 0.79 | 0.91 | |
| Tryptophan | | | | | | | |
| Lysine | 0.92 | | 2.10 | | 1.99 | 2.09 | |
| Histidine | 0.71 | | | | | | |
| Arginine | | 0.86 | | 0.73 | | | |
| No of residues | 16 | 10 | 15 | 8 | 10 | 14 | 6 |
| $E_{Lys}$ / $E_{Asp}$ | 0.19 | neutr. | neutr. | neutr. | neutr. | neutr. | neutr. |
| $R_{Leu}$ | 0.38 | 0.62 | 0.68 | 0.37 | 0.24 | 0.12 | 0.39 |

*Table 1. Continued.*

| Amino acid | aC16 | aC17 | aC18 | aC19 | aC20 | aC21 | aC22 | aC23 |
|---|---|---|---|---|---|---|---|---|
| Aspartic acid | | | 2.95 | 1.05 | 1.05 | | 1.06 | 1.12 |
| Threonine | | | 1.72 | 0.87 | 0.86 | | | |
| Serine | 2.97 | | | | 2.42 | | 1.78 | |
| Glutamic acid | | | 1.30 | 2.04 | 1.89 | 0.98 | 1.00 | 2.42 |
| Proline | | | 1.78 | | | | | |
| Glycine | | | 2.03 | | | | | |
| Alanine | | 1.06 | 2.37 | 1.06 | 1.11 | 1.09 | 1.10 | 1.10 |
| Valine | 1.00 | 0.97 | 1.10 | | 0.91 | | | 0.74 |
| Isoleucine | | | | | | | | |
| Leucine | | | 2.83 | 0.97 | 0.95 | | 0.98 | 0.88 |
| Tyrosine | | | | | | | | 0.74 |
| Phenylalanine | 1.03 | 0.96 | 1.02 | | 0.82 | 0.93 | | |
| Tryptophan | | | | | | | $+^a$ | |
| Lysine | | | 1.95 | 1.02 | 1.00 | | | |
| Histidine | | | 0.75 | | | | | |
| Arginine | | | | | | | 0.87 | |
| No. of residues | 5 | 3 | 20 | 7 | 11 | 3 | 8 | 7 |
| $E_{Lys}$ | | | | | | | | |
| $E_{Asp}$ | neutr. | neutr. | neutr. | 0.26 | 0.22 | 0.50 | 0.22 | 0.78 |
| $R_{Leu}$ | 0.67 | 1.09 | 0.13 | 0.28 | 0.60 | 0.95 | 0.44 | 0.99 |

$^a$ Positive Ehrlich reaction on paper.

composition determined on the amino acid analyzer (Beckman/Spinco 120B). The Ehrlich reaction was employed to detect peptides containing tryptophan.[1] Amide residues were assigned on the basis of electrophoretic mobilities of the peptides at pH 6.5, according to Offord.[5]

*Sequence studies.* The chymotryptic peptides containing lysine or arginine residues were hydrolyzed with trypsin. A solution of the peptide, 1 $\mu$mol in 1 ml of 1 % ammonium bicarbonate buffer of pH 8.1 was treated with trypsin, 10 $\mu$l of a 1 % solution in 0.001 N HCl, and incubated at 37°C for 24 h. The resulting tryptic peptides were designated by the prefix T −. Digestion with subtilopeptidase A was carried out under the same experimental conditions as previously described.[2] The resulting peptides were designated by the prefix S−. Hydrolysis with leucine aminopeptidase and carboxypeptidase A was performed under the same conditions as reported earlier.[2] Subtractive- and dansyl-Edman degradation procedures were performed as described in the preceding paper.[2]

*Nomenclature of peptides.* The peptides isolated from the different fractions were numbered according to the same principles as described previously.[1] The prefix C is placed before peptide number to indicate that the peptide was obtained from a chymotryptic digest. "*a*" before C indicates Lb*a*, the slow component of soybean leghemoglobin.

## RESULTS

*Amino acid composition of chymotryptic peptides.* Fig. 1 shows the elution pattern of the chymotryptic peptides from a Dowex 1 column. The fractions were combined, checked for homogeneity and, if necessary, further purified by high voltage paper electrophoresis. Homogeneous peptides were subjected to amino acid analysis yielding the results shown in Table 1.

*Amino acid sequence of chymotryptic peptides.* The deduced sequences of the chymotryptic peptides isolated are given in Table 2. Because the sequences of the tryptic peptides of Lba have already been established,[2] those of most chymotryptic peptides could be evaluated from their amino acid compositions and their $NH_2$-terminal analyses. Structural studies were performed mainly on bridge-peptides containing lysine and arginine. In the succeeding section the peptides are considered individually and the evidence for their amino acid sequence is presented.

*Table 2.* Deduced amino acid sequences of the chymotryptic peptides from the slow component (Lba) of soybean leghemoglobin.

| Peptide number | Amino acid sequence |
|---|---|
| aC1 | Ala-[Ala,Ala,Ile]-Lys-Ala-Lys |
| aC2 | Ala-Ala-Ala-[Ile,Lys] |
| aC3 | Lys-Thr-Ile-Lys-Ala-[Ala,Val,Gly,Asp]Lys-Trp |
| aC4 | Ala-[Ala,Ile,Lys,Ala,Lys] |
| aC5 | Ile-Lys-Ala-Lys |
| aC6 | Ala-Lys |
| aC7 | Ser-Arg-Ala-Trp |
| aC8 | Ala-Gln-Lys-Ala-[Val,Thr,Asn,Pro,Glu,Phe,Val,Val]-Lys-Glu-Ala-Leu-Leu |
| aC9 | Lys-Ala-[Ser,Gly,Thr,Val,Val,Ala,Asp,Ala,Ala,Leu,Gly,Ser,Val,His] |
| aC10 | Ala-Leu-Val-Arg-Asp-Ser-[Ala,Gly,Gln]-Leu |
| aC11 | Lys-Ala-Val-[Thr,Asn,Pro,Glu,Phe,Val,Val,Lys,Glu,Ala,Leu,Leu] |
| aC12 | Val-Arg-Asp-Ser-Ala-[Gly,Gln]-Leu |
| aC13 | Glu-Lys-Ala-[Pro,Ala,Ala]-Lys-Asp-[Leu,Phe] |
| aC14 | Thr-Ser-Ile-Leu-Glu-Lys-Ala-Pro-Ala-Ala-Lys-Asp-Leu-Phe |
| aC15 | Ala-[Asn,Ile,Pro,Gln,Tyr] |
| aC16 | Val-Ser-Ser-Ser-Phe |
| aC17 | Val-Ala-Phe |
| aC18 | Leu-Ala-[Asn,Pro,Thr,Asp,Gly,Val,Asn,Pro]-Lys-Leu-[Thr,Gly,His,Ala, Glu]-Lys-Leu-Phe |
| aC19 | Thr-[Glu,Lys,Gln,Asp,Ala]-Leu |
| aC20 | Thr-Glu-Lys-Gln-[Asp,Ala,Leu,Val,Ser,Ser]-Ser-Phe |
| aC21 | Glu-Ala-Phe |
| aC22 | Ser-Asp-Glu-[Leu,Ser]-Arg-Ala-Trp |
| aC23 | Glu-Val-[Ala,Tyr,Asp,Glu]-Leu |

*Peptide aC1.* Alanine was established as the $NH_2$-terminal residue by dansylation. Tryptic digestion of aC1 produced two fragments, T1 and T2, which were isolated by electrophoresis at pH 6.5. The amino acid composition (Table 3) of T1 corresponds uniquely to the COOH-terminal portion of aT17 and that of T2 to aT4. Dansylation confirmed the sequence of T2 as *Ala-Lys*. Therefore, aC1 provides overlap joining aT17 to aT4.

*Peptide aC2.* Three steps of Edman degradation established the $NH_2$-terminal sequence *Ala-Ala-Ala-* (Table 3). aC2 represents the COOH-terminal portion of tryptic peptide aT17.

*Peptide aC3.* Three stages of Edman degradation indicated that the $NH_2$-terminal sequence is *Lys-Thr-Ile-*. Tryptic digestion of aC3 yielded four

*Table 3.* Amino acid sequences of peptides aC1, aC2, and aC3.

| | |
|---|---|
| Sequence aC1 | Ala-[Ala,Ala,Ile]-Lys-Ala-Lys |
| | \|————T1————\|–T2—\| |
| Dansylation | DNS-Ala |
| Tryptic peptides | |
| T1 | Ala,2.90; Ile,0.92; Lys,1.08 |
| ($E_{Lys}$,0.50) | |
| Dansylation | DNS-Ala |
| T2 | Ala,1.03; Lys,0.97 |
| ($E_{Lys}$,0.79) | |
| Dansylation | DNS-Ala |
| | |
| Sequence aC2 | Ala-Ala-Ala-[Ile,Lys] |
| Edman degradation | Direct examination of dansyl derivatives |
| Step 1 | DNS-Ala |
| Step 2 | DNS-Ala |
| Step 3 | DNS-Ala |
| | |
| Sequence aC3 | Lys-Thr-Ile-Lys-Ala-[Ala,Val,Gly,Asp]-Lys-Trp |
| | \|·T4·\|——T3——\|————————T2————————\|·T1·\| |
| Edman degradation | Direct examination of dansyl derivatives |
| Step 1 | DNS-Lys |
| Step 2 | DNS-Thr |
| Step 3 | DNS-Ile |
| Tryptic peptides | |
| T1 | Trp +[a]) |
| Dansylation | DNS-Trp |
| T2 | Ala,1.77; Val,1.02; Gly,1.00; Asp,1.15; Lys,1.03 |
| (neutral) | |
| Dansylation | DNS-Ala |
| T3 | Thr,0.73; Ile,1.00; Lys,1.03 |
| ($E_{Lys}$,0.58) | |
| Dansylation | DNS-Thr |
| T4 | Lys,1.00 |
| ($E_{Lys}$,1.00) | |

[a] Positive Ehrlich reaction on paper.

fragments, T1, T2, T3, ãnd T4, which were purified by electrophoresis at pH 6.5 and 1.9 (Table 3). T1 represented free tryptophan as identified by paper electrophoresis and paper chromatography. The amino acid compositions of T2 and T3 were compatible with those of aT8 and aT5, respectively. T4 was found to be free lysine. Three tryptic peptides have COOH-terminal sequences, which should yield free lysine on chymotryptic hydrolysis, aT9, aT10, and aT13. Because tryptophan is the unique $NH_2$-terminal amino acid residue of aT16, aC3 provides the overlap establishing the tryptic peptide order aT5-aT8-aT16.

*Peptide aC4 and aC5.* Both these peptides confirm the tryptic peptide linkage aT17 to aT4. Three steps of Edman degradation established the sequence *Ile-Lys-Ala-Lys.*

*Peptide aC6.* One step of Edman degradation established the sequence *Ala-Lys.*

*Peptide aC7.* Dansylation established the NH$_2$-terminal serine residue. A COOH-terminal tryptophan residue is consistent with the specificity of chymotrypsin. Tryptic digestion of *a*C7 yielded two fragments, T1 and T2, which were isolated by electrophoresis at pH 6.5. Their amino acid composition is given in Table 4. The sequence of T1 was found to be *Ala-Trp* and that of T2 *Ser-Arg.* Peptide *a*C7, therefore, represents the overlap between *a*T16 and *a*T17.

*Table 4.* Amino acid sequences of peptides *a*C4, *a*C5, *a*C6, and *a*C7.

| | |
|---|---|
| Sequence *a*C4 | Ala-[Ala,Ile,Lys,Ala,Lys] |
| Dansylation | DNS-Ala |
| | |
| Sequence *a*C5 | Ile-Lys-Ala-Lys |
| Edman degradation | Direct examination of dansyl derivatives |
| Step 1 | DNS-Ile |
| Step 2 | DNS-Lys |
| Step 3 | DNS-Ala |
| | |
| Sequence *a*C6 | Ala-Lys |
| Edman degradation | |
| Step 1 | Ala, 0; Lys, 1.0 |
| | |
| Sequence *a*C7 | Ser-Arg-Ala-Trp |
| | \|—T2—\|—T1—\| |
| Dansylation | DNS-Ser |
| Tryptic peptides | |
| T1 | Ala, 1.00; Trp, +$^a$ |
| (neutral) | |
| Dansylation | DNS-Ala |
| T2 | Ser, 1.02; Arg, 0.98 |
| ($E_{\text{Lys}}$, 0.78) | |
| Dansylation | DNS-Ser |

$^a$ Positive Ehrlich reaction on paper.

*Peptide aC8.* Alanine was the NH$_2$-terminal amino acid residue as found by dansylation. Digestion of *a*C8 with trypsin produced three fragments, T1, T2, and T3, which were isolated by electrophoresis at pH 6.5 and their amino acid composition is given in Table 5. Two steps of Edman degradation showed T1 to have the sequence *Glu-Ala-Leu-Leu* corresponding to residues 1 − 4 of the tryptic peptide *a*T10. The amino acid composition and analysis of the NH$_2$-terminal amino acid shows T2 to be identical with *a*T7. The sequence of T3 was *Ala-Gln-Lys,* which is compatible with the COOH-terminal sequence of *a*T6. Thus, peptide *a*C8 unambiguosly indicates the tryptic peptide order *a*T6-*a*T7-*a*T10.

*Peptide aC9.* Dansylation showed lysine as the NH$_2$-terminal amino acid residue. Tryptic digestion produced two fragments, T1 and T2, which were separated on electrophoresis at pH 6.5. Their amino acid contents are given in Table 5. T1 represents the NH$_2$-terminal portion of *a*T6 as decided from its

amino acid composition and determination of the $NH_2$-terminal amino acid residue. T2 was found to be free lysine. Three tryptic peptides, $a$T9, $a$T10, and $a$T13, have COOH-terminal sequences which allow liberation of free lysine on hydrolysis with chymotrypsin. Of these, $a$T10 is excluded because of its position COOH-terminal to $a$T7.

*Table 5.* Amino acid sequences of peptides $a$C8 and $a$C9.

| | |
|---|---|
| Sequence $a$C8 | Ala-Gln-Lys-Ala-[Val,Thr,Asn,Pro,Glu,Phe,Val,Val]-Lys- |
| | \|——T3——\| \|————————————————————T2————————————\| |
| | Glu-Ala-Leu-Leu |
| | \|——T1——\| |
| Dansylation | DNS-Ala |
| Tryptic peptides | |
| T1 | Glu, 1.07; Ala, 1.17; Leu, 1.76 |
| ($E_{Asp}$, 0.48) | |
| Edman degradation | |
| Step 1 | *Glu, 0.57*; Ala, 1.18; Leu, 1.82 |
| Step 2 | *Ala, 0.68*; Leu, 2.00 |
| T2 | Ala, 1.08; Val, 2.56; Thr, 1.00; Asp, 1.17; Pro, 0.70; Glu, 1.11 |
| (neutral) | Phe, 0.71; Lys, 0.98 |
| Dansylation | DNS-Ala |
| T3 | Ala, 1.10; Glu, 1.00; Lys, 0.90 |
| ($E_{Lys}$, 0.58) | |
| Dansylation | DNS-Ala |
| | |
| Sequence $a$C9 | Lys-Ala-[Ser,Gly,Thr,Val,Val,Ala,Asp,Ala,Ala,Leu,Gly, |
| | \|-T2-\|————————————————————T1———————————— |
| | Ser,Val,His] |
| | ————————\| |
| Dansylation | DNS-Lys |
| Tryptic peptides | |
| T1 | Ala, 3.81; Ser, 2.25; Gly, 1.94; Thr, 0.75; Val, 2.00(3); |
| ($E_{Asp}$,0.24) | Asp, 1.10; Leu, 1.09; His, 0.95 |
| Dansylation | DNS-Ala |
| T2 | Lys, 1.00 |
| ($E_{Lys}$, 1.00) | |
| Dansylation | DNS-Lys |

*Peptide aC10.* Alanine was established as the $NH_2$-terminal amino acid residue. A COOH-terminal leucine residue was assigned on the basis of the specificity of chymotrypsin. Two fragments, T1 and T2, were obtained on hydrolysis with trypsin and isolated by electrophoresis at pH 6.5. Their amino acid contents are given in Table 6. Two steps of Edman degradation on T1 showed the sequence *Asp-Ser-(Ala, Gly, Gln)-Leu*, which is compatible with the $NH_2$-terminal sequence of $a$T9. Two steps of Edman degradation on T2 established the sequence *Ala-Leu-Val-Arg*, representing the COOH-terminal sequence of $a$T3. $a$C10, therefore, provides the overlap joining $a$T3 to $a$T9.

*Peptide aC11.* This peptide (Table 6) provided further evidence of the linkage between the tryptic peptides $a$T7 and $a$T10.

*Peptide aC12.* Dansylation revealed valine as the $NH_2$-terminal amino acid residue. A COOH-terminal leucine residue was assigned on the basis of

*Table 6.* Amino acid sequences of peptides aC10 and aC11.

| | |
|---|---|
| Sequence aC10 | Ala-Leu-Val-Arg-Asp-Ser-[Ala,Gly,Gln]Leu |
| | \|————T2————\|————————T1————————\| |
| Dansylation | DNS-Ala |
| Tryptic peptides | |
| T1 | Asp, 0.99; Ser, 0.86; Ala, 1.02; Gly, 1.01; Glu, 1.11; Leu, 1.03 |
| $(E_{Asp},0.43)$ | |
| Edman degradation | Direct examination of dansyl derivatives |
| Step 1 | DNS-Asp |
| Step 2 | DNS-Ser |
| T2 | Ala, 1.16; Leu, 0.99; Val, 1.01; Arg, 0.90 |
| $(E_{Lys},0.52)$ | |
| Edman degradation | Direct examination of dansyl derivatives |
| Step 1 | DNS-Ala |
| Step 2 | DNS-Leu |
| | |
| Sequence aC11 | Lys-Ala-Val-[Thr,Asn,Pro,Glu,Phe,Val,Val,Lys,Glu,Ala, Leu,Leu] |
| Edman degradation | Direct examination of dansyl derivatives |
| Step 1 | DNS-Lys |
| Step 2 | DNS-Ala |
| Step 3 | DNS-Val |

*Table 7.* Amino acid sequences of peptides aC12 and aC13.

| | |
|---|---|
| Sequence aC12 | Val-Arg-Asp-Ser-Ala-[Gly,Gln,Leu] |
| | \|—T2—\|————————T1————————\| |
| Dansylation | DNS-Val |
| Tryptic peptides | |
| T1 | Asp, 0.84; Ser, 0.87; Ala, 1.03; Gly, 0.97; Glu, 1.01; Leu, 1.12 |
| $(E_{Asp},0.43)$ | |
| Edman degradation | Direct examination of dansyl derivatives |
| Step 1 | DNS-Asp |
| Step 2 | DNS-Ser |
| Step 3 | DNS-Ala |
| T2 | Val, 1.03; Arg, 0.97 |
| $(E_{Lys},0.80)$ | |
| Dansylation | DNS-Val |
| | |
| Sequence aC13 | Glu-Lys-Ala-[Pro,Ala,Ala]-Lys-Asp-[Leu,Phe] |
| | \|————————T2————————\|————T1————\| |
| | \|————T3————————\| |
| Dansylation | DNS-Glu |
| Tryptic peptides | |
| T1 | Asp, 1.12; Leu, 1.05; Phe, 0.82 |
| $(E_{Asp},0.51)$ | |
| Dansylation | DNS-Asp |
| T2 | Glu, 0.96; Lys, 1.97; Ala, 3.04; Pro, 1.02 |
| $(E_{Lys},0.38)$ | |
| Dansylation | DNS-Glu |
| T3 | Ala, 2.95; Pro, 1.07; Lys, 0.98 |
| $(E_{Lys},0.55)$ | |
| Dansylation | DNS-Ala |

the specificity of chymotrypsin. Hydrolysis with trypsin yielded two fragments, T1 and T2, which were isolated by electrophoresis at pH 6.5 and had the amino acid contents given in Table 7. Peptide *aC12* provided further support for the linkage of the tryptic peptides *aT3* and *aT9*.

*Peptide aC13.* Glutamic acid was the $NH_2$-terminal amino acid residue as found by dansylation. Tryptic hydrolysis produced three fragments, T1, T2, and T3, which were isolated by electrophoresis at pH 6.5 and had the amino acid compositions given in Table 7. T1 represents the unique NH-₂terminal portion of the tryptic peptide *aT14*, and T3 that of the tryptic peptide *aT2*. This indicates the tryptic peptide order *aT18-aT2-aT14*, which was further confirmed by the chymotryptic peptide *aC14*.

*Peptide aC14.* Edman degradation and leucine amino peptidase digestion gave the $NH_2$-terminal sequence *Thr-Ser-Ile-Leu-Glu-* (Table 8). Carboxypeptidase A digestion revealed the COOH-terminal sequence *-Leu-Phe*. Tryptic digestion yielded three fragments, T1, T2, and T3, which were isolated on electrophoresis at pH 6.5 and 1.9 and found to have the amino acid compositions given in Table 8. By Edman degradation the sequence of T1 was found to be *Asp-Leu-Phe-*, the unique $NH_2$-terminal sequence of tryptic peptide *aT14*, and that of T2 *Thr-Ser-Ile-Leu-Glu-Lys* the COOH-terminal

*Table 8* Amino acid sequences of peptides *aC14* and *aC15*.

| Sequence *aC14* | Thr-Ser-Ile-Leu-Glu-Lys-Ala-Pro-Ala-Ala-Lys-Asp-Leu-Phe |
| --- | --- |
| | \|————T2————\|————T3————\|——T1——\| |
| Edman degradation | Direct examination of dansyl derivatives |
| Step 1 | DNS-Thr |
| Step 2 | DNS-Ser |
| Step 3 | DNS-Ile |
| Leucine amino- | |
| peptidase, 30 min | Thr, 1.00; Ser, 1.00; Ile, 0.48; Leu, 0.45; Glu, 0.28 |
| Carboxypeptidase A | |
| 20 min. | Leu, 0.60; Phe, 1.00 |
| Tryptic peptides | |
| T1 | Asp, 1.04; Leu, 1.02; Phe, 0.95 |
| ($E_{Asp}$,0.51) | |
| Edman degradation | Direct analysis of dansyl derivatives |
| Step 1 | DNS-Asp |
| Step 2 | DNS-Leu |
| T2 | Thr, 0.92; Ser, 1.10; Ile, 0.90; Leu, 0.91; Glu, 1.02; Lys, 1.16 |
| (neutral) | |
| Edman degradation | Direct examination of dansyl derivatives |
| Step 1 | DNS-Thr |
| Step 2 | DNS-Ser |
| Step 3 | DNS-Ile |
| T3 | Ala, 2.95; Pro, 1.07; Lys, 0.98 |
| ($E_{Lys}$,0.52) | |
| Edman degradation | Direct examination of dansyl derivatives |
| Step 1 | DNS-Ala |
| Step 2 | DNS-Pro |
| Sequence *aC15* | Ala-[Asn,Ile,Pro,Gln,Tyr] |
| Dansylation | DNS-Ala |

portion of the tryptic peptide $a$T18. T3 was found to be the tryptic peptide $a$T2. These results indicate the tryptic peptide order $a$T18-$a$T2-$a$T14.

*Peptide aC15.* Dansylation showed alanine to be the $NH_2$-terminal residue (Table 8). Peptide $a$C15 represents the $NH_2$-terminal sequence of the tryptic peptide $a$T18.

*Peptide aC16.* Three steps of Edman degradation revealed the $NH_2$-terminal sequence *Val-Ser-Ser-* (Table 9). A COOH-terminal phenylalanine residue was assigned on the basis of chymotryptic specificity. The sequence of $a$C16 was concluded to be *Val-Ser-Ser-Ser-Phe*, representing the middle portion of the tryptic peptide $a$T13.

*Peptide aC17.* Two steps of Edman degradation established the sequence *Val-Ala-Phe* (Table 9), which is the $NH_2$-terminal portion of the tryptic peptide $a$T12 and the Lb$a$ chain.

*Table 9.* Amino acid sequences of peptides $a$C16, $a$C17, and $a$C18.

| | |
|---|---|
| Sequence $a$C16 | Val-Ser-Ser-[Ser,Phe] |
| Edman degradation | Direct examination of dansyl derivatives |
| Step 1 | DNS-Val |
| Step 2 | DNS-Ser |
| Step 3 | DNS-Ser |
| | |
| Sequence $a$C17 | Val-Ala-Phe |
| Edman degradation | Direct examination of dansyl derivatives |
| Step 1 | DNS-Val |
| Step 2 | DNS-Ala |
| | |
| Sequence $a$C18 | Leu-Ala-[Asn,Pro,Thr,Asp,Gly,Val,Asn,Pro]-Lys- |
| | \|————————————————T1————————————————\| |
| | Leu-[Thr, Gly, His, Ala, Glu]-Lys-Leu-Phe |
| | \|————————————T3————————————\|——T2—\| |
| Dansylation | DNS-Leu |
| Tryptic peptides | |
| T1 | Leu, 0.78; Ala, 1.07; Asp, 2.98; Pro, 2.04; Thr, 1.00; Gly, 1.11; |
| ($E_{Asp}$,0.28) | Val, 0.97; Lys, 1.03 |
| Edman degradation | Direct examination of dansyl derivatives |
| Step 1 | DNS-Leu |
| Step 2 | DNS-Ala |
| T2 | Leu, 1.06; Phe, 0.94 |
| (neutral) | |
| Edman degradation | Direct examination of dansyl derivatives |
| Step 1 | DNS-Leu |
| Step 2 | DNS-Phe |
| T3 | Leu, 0.96; Thr, 0.97; Gly, 1.04; His, 0.93; Ala, 1.03; Glu, 1.02; |
| | Lys, 0.99 |
| Dansylation | DNS-Leu |

*Peptide aC18.* Dansylation showed leucine as the $NH_2$-terminal residue. Hydrolysis with trypsin yielded three fragments, T1, T2, and T3, which were electrophoretically isolated at pH 6.5 and 1.9. The amino acid content of these fractions is given in Table 9. Two steps of Edman degradation on T1 indicated the sequence *Leu-Ala-* which, in addition to the amino acid content,

shows Tl to represent the COOH-terminal portion of the tryptic peptide
aT14. The sequence of T2 was found to be *Leu-Phe* by dansylation, and
represents the unique $NH_2$-terminal sequence of the tryptic peptide aT3.
The amino acid composition of T3 was compatible with that of the tryptic
peptide aT11. Therefore, peptide aC18 provides evidence of the tryptic peptide
order aT14-aT11-aT3.

*Peptide aC19.* Threonine was established as the $NH_2$-terminal residue
and leucine as the COOH-terminal residue using carboxypeptidase A (Table
10). aC19 indicates the tryptic peptide sequence aT12–aT13, which was fur-
ther confirmed by peptide aT20.

*Peptide aC20.* Leucine amino peptidase digestion established the $NH_2$-
terminal sequence as *Thr-Glu-.* The phenylalanine residue was positioned at
the COOH terminus from chymotryptic specificity, and the action of carboxy-

*Table 10.* Amino acid sequences of peptides aC19, aC20, and aC21.

| | |
|---|---|
| Sequence aC19 | Thr-[Glu,Lys,Gln,Asp,Ala]-Leu |
| Dansylation | DNS-Thr |
| Carboxypeptidase A | |
| 20 min | Leu, 1.0 |
| | |
| Sequence aC20 | Thr-Glu-Lys-Gln-[Asp,Ala,Leu,Val,Ser,Ser]-Ser-Phe |
| | \|———T2———\|—————————————T1—————————————\| |
| Dansylation | DNS-Thr |
| Leucine amino- | |
| peptidase, 30 min | Thr, 1.00; Glu, 0.48 |
| Carboxypeptidase A | |
| 30 min | Phe, 1.00; Ser, 0.47 |
| Tryptic peptides | |
| T1 | Glu, 1.03; Asp, 0.95; Ala, 1.33; Leu, 1.07; Val, 1.08; |
| $(E_{Asp},0.31)$ | Leu, 1.07; Phe, 0.86 |
| Dansylation | DNS-Glu |
| T2 | Thr, 0.91; Glu, 1.04; Lys, 1.05 |
| (neutral) | |
| Dansylation | DNS-Thr |
| Subtilopeptidase A | |
| peptides | |
| S1 | Asp, 0.98; Ala, 1.03; Leu, 0.98 |
| $(E_{Asp},0.55)$ | |
| Edman degradation | |
| Step 1 | *Asp, 0.00*; Ala,0.98; Leu, 1.02 |
| Step 2 | *Ala, 0.00* Leu, 1.00 |
| S2 | Thr, 0.94; Glu, 2.06; Lys, 1.00 |
| (neutral) | |
| S3 | Val, 1.14; Ser, 2.80 |
| (neutral) | |
| Edman degradation | |
| Step 1 | *Val, 0.00* Ser, 3.00 |
| | |
| Sequence aC21 | Glu-Ala-Phe |
| Edman degradation | Direct examination of dansyl derivatives |
| Step 1 | DNS-Glu |
| Step 2 | DNS-Ala |
| Step 3 | DNS-Phe |

peptidase A on aC20 confirmed the COOH-terminal sequence as -Ser-Phe. aC20 was redigested with trypsin and two fragments were obtained, T1 and T2, which were isolated on electrophoresis at pH 6.5. The amino acid composition of T1 and T2 is given in Table 10. Dansylation on T2 established the sequence *Thr-Glu-Lys* for the neutral peptide. To confirm the sequence and the position of the amide, aC20 was subjected to hydrolysis with subtilopeptidase A, whereupon three major fragments, S1, S2, and S3, were isolated by electrophoresis at pH 6.5 and 1.9. Two steps of Edman degradation on S1 gave the sequence *Asp-Ala-Leu*. S2 was found to be neutral at pH 6.5 indicating that the second glutamic acid was amidated, and the sequence was concluded to be *Thr-Glu-Lys-Gln*. One step of Edman degradation for S3 gave the sequence *Val-Ser-Ser-Ser*. Thus the tryptic peptide sequence of aT12–aT13 is indicated.

*Peptide aC21.* Three steps of Edman degradation established the sequence *Glu-Ala-Phe* (Table 10), which represents residues $10-12$ of the COOH-terminal portion of the tryptic peptide aT13.

*Peptide aC22.* Three steps of Edman degradation established the NH$_2$-terminal sequence as *Ser-Asp-Glu-*. A COOH-terminal tryptophan was assigned on the basis of the specificity of chymotrypsin. Hydrolysis with trypsin yielded two fragments, T1 and T2, which were isolated on electrophoresis at pH 6.5 and 1.9. Their amino acid contents are given in Table 11.

*Table 11.* Amino acid sequences of peptides aC22 and aC23.

| Sequence aC22 | Ser-Asp-Glu-[Leu,Ser]-Arg-Ala-Trp |
|---|---|
| | \|————————T1————————\|—T2—\| |
| Edman degradation | |
| Step 1 | *Ser, 1.08* Asp, 1.00; Glu, 0.97; Leu, 0.98; Arg, +; Ala, 0.97 |
| Step 2 | Ser, 1.05; *Asp, 0.25* Glu, 0.95; Leu, 1.02; Arg, +; Ala, 0.98 |
| Step 3 | Ser, 1.09; Asp, 0.00; *Glu, 0.39* Leu, 0.89; Arg +; Ala, 1.03 |
| Tryptic peptides | |
| T1 | Ser, 1.79; Asp, 1.05; Glu, 1.02; Leu, 1.07; Arg, 1.06 |
| ($E_{Asp}$,0.34) | |
| Edman degradation | Direct examination of dansyl derivatives |
| Step 1 | DNS-Ser |
| Step 2 | DNS-Asp |
| T2 | Ala, 1.00; Trp, +[a]) |
| (neutral) | |
| Edman degradation | Direct examination of dansyl derivatives |
| Step 1 | DNS-Ala |
| Step 2 | DNS-Trp |
| | |
| Sequence aC23 | Glu-Val-[Ala,Tyr,Asp,Glu]-Leu |
| Edman degradation | |
| Step 1 | DNS-Glu |
| Step 2 | DNS-Val |
| Carboxypeptidase A | |
| 30 min | Leu, 1.0 |

[a] Positive Ehrlich reaction on paper.

Two steps of Edman degradation showed the sequence of T2 to be *Ala-Trp*. Peptide *a*C22 provides further support for the linkage of *a*T16 to *a*T17.

*Peptide aC23.* This peptide is assumed to represent the $NH_2$-terminal portion of the tryptic peptide *a*T17, corresponding to residues 2 − 8 on the basis of the amino acid composition and $NH_2$-terminal analysis (Table 11).

## DISCUSSION

The amino acid sequence of all the peptides obtained from the chymotryptic digest of Lb*a* could be evaluated from the direct evidence obtained in the present study and the known sequences of tryptic peptides.

With exception of some peptides ending in lysine, the COOH-terminal residues of the chymotryptic peptides studied seemed to be compatible with the known specificity of chymotrypsin. Peptides *a*C1, *a*C3, and *a*C4 all end in *Ala-Lys*, thus indicating a linkage between *a*T17 and *a*T4. Therefore *a*T17-*a*T4 is assumed to represent the COOH-terminus of Lb*a*. Peptide *a*C2 represents the COOH-terminus of *a*T17 with isoleucine next to lysine. Peptide *a*C15 also indicates a hydrolysis at the Lys-Ala bond, in which lysine is evidently preceded by a phenylalanine residue. Chymotryptic hydrolysis of a bond involving the carboxyl group of lysine is unusual, but it has been observed in a Lys-Ala bond in the γ-chain of human hemoglobin,[6] where the sequence *Val-Lys-Ala-His* was hydrolyzed.

The present study on the chymotryptic peptides permits the arrangement of the tryptic peptides into four fragments: *a*T12-*a*T13, *a*T18-*a*T2-*a*T14-*a*T11-*a*T3-*a*T9, *a*T6-*a*T7-*a*T10, and *a*T5-*a*T8-*a*T16-*a*T17-*a*T4. *a*T12-*a*T13 and *a*T5-*a*T8-*a*T16-*a*T17-*a*T4 represent, respectively, the $NH_2$- and COOH-terminal portions of Lb*a*. The two additional fragments both represent the middle portion of the peptide chain of Lb*a*. However, their internal order cannot be decided simply on the basis of the chymotryptic peptides isolated. If *a*T13 is assumed to be linked to *a*T18, then the distance between the two hemin binding histidines includes 30 amino acid residues, and if *a*T13 were bound to *a*T15 this separation would be 56 amino acid residues. In vertebrate hemoglobin chains the distance is 28 residues. Therefore *a*T13 is assumed to be linked to *a*T18. The lack of direct evidence for the attachment of *a*T13 to *a*T18, *a*T9 to *a*T6, and *a*T10 to *a*T5 is a result of the liberation of lysine as the $NH_2$-terminal residue on chymotryptic attack on these peptides because of their COOH-terminal portions *-Phe-Lys* for *a*T13, and *Leu-Lys* for *a*T9 and *a*T10, respectively. Complementary information is provided by isolating the overlapping peptides from a thermolytic digest of Lb*a*, the description of which is given in the next paper of this series.

The position of many of the chymotryptic peptides that did not contain lysine or arginine was deduced on the basis of their amino acid composition. Thus we were able to account for all the residues in the Lb*a* chain in terms of pure chymotryptic peptides, with the exception of a portion of *a*T18 and *a*T14. These results have led to the tentative formulation of the Lb*a* chain sequence shown in Fig. 2.

```
|----------T12-----------|----------------T13---------------|-------
NH₂-Val-Ala-Phe-Thr-Glu-Lys-Gln-Asp-Ala-Leu-Val-Ser-Ser-Ser-Phe-Glu-Ala-Phe-Lys-Ala-Asn-
|-------C17---|------------------C20---------------------|---C21---|  |----
          |----------C19----------|-----C16------|


|----------------------T18-------------------|---------T2--------|-------
Ile-Pro-Gln-Tyr-Ser-Val-Val-Phe-Tyr-Thr-Ser-Ile-Leu-Glu-Lys-Ala-Pro-Ala-Ala-Lys-Asp-Leu-
----C15-------|                   |----------------------C14----------------
                                          |-------------------C13-------


|-------------------------T14-----------------|---------------T11------------|--
Phe-Ser-Phe-Leu-Ala-Asn-Pro-Thr-Asp-Gly-Val-Asn-Pro-Lys-Leu-Thr-Gly-His-Ala-Glu-Lys-Leu-
---|        |----------------------------C18----------------------|
   |


-----------T3-----------|------------T9----------|----------------------------T6----
Phe-Ala-Leu-Val-Arg-Asp-Ser-Ala-Gly-Gln-Leu-Lys-Ala-Ser-Gly-Thr-Val-Val-Ala-Asp-Ala-Ala-
---|--------C10---------|                        |----------------------C9------------
       |----------C12---------|


----------------------------|----------------T7--------------------|--------T10----
Leu-Gly-Ser-Val-His-Ala-Gln-Lys-Ala-Val-Thr-Asn-Pro-Glu-Phe-Val-Val-Lys-Glu-Ala-Leu-Leu-
               |----------------------------C8-------------------------|
                   |--------------------------C11----------------------------|


---|-----T5----|--------T8---------|--------------T16----------|-----------
Lys-Thr-Ile-Lys-Ala-Ala-Val-Gly-Asp-Lys-Trp-Ser-Asp-Glu-Leu-Ser-Arg-Ala-Trp-Glu-Val-Ala-
|-----------------C3----------------|---------------C22---------|----------
                                               |---C7-------|


-----T17---------------------|----T4------|
Tyr-Asp-Glu-Leu-Ala-Ala-Ala-Ile-Lys-Ala-Lys-COOH
----C23---------|----------------C1----------------|
           |---------C2---------|-----C6------|
                   |------C4------|
                       |----------C5------------|
```

*Fig. 2.* The proposed amino acid sequence of soybean leghemoglobin *a*. The tryptic peptides (T) are shown above the sequence and the chymotryptic peptides (C) are shown below it.

### REFERENCES

1. Ellfolk, N. and Sievers, G. *Acta Chem. Scand.* **26** (1972) 1155.
2. Ellfolk, N. and Sievers, G. *Acta Chem. Scand.* **27** (1973) 3371.
3. Ellfolk, N. *Acta Chem. Scand.* **14** (1960) 609.
4. Ellfolk, N. *Acta Chem. Scand.* **16** (1962) 831.
5. Offord, R. E. *Nature* **211** (1966) 591.
6. Schroeder, W. A., Shelton, J. R., Shelton, J. B., Cormick, J. and Jones, R. T. *Biochemistry* **2** (1963) 992.

Received May 31, 1973.

# Kinetics, Medium, and Deuterium Isotope Effects in the Alkaline Decomposition of Quaternary Phosphonium Salts I. Tetraphenylphosphonium Chloride in Dioxane-Water Mixtures

FAYEZ Y. KHALIL* and GUNNAR AKSNES

*Chemical Institute, University of Bergen, N-5000 Bergen, Norway*

The alkaline decomposition of tetraphenylphosphonium chloride in $0-80$ % dioxane-water mixtures was studied kinetically at $20-55°C$. The reaction rate, which is first-order in phosphonium cation and second-order in hydroxide anion, is strongly accelerated by addition of dioxane, being $5 \times 10^7$ times as large in 80 % dioxane-water as in water at 35°C. The rate constant is expressed by $k' = 19.6\ e^{-33500RT}\ l^2\ mol^{-2}\ sec^{-1}$ in water, and $k' = 10.7\ e^{-10630RT}\ l^2\ mol^{-2}\ sec^{-1}$ in 80 % dioxane-water. The solvent deuterium isotope effect in 30 % $D_2O$-dioxane confirmed the current mechanistic views of the reaction. The termodynamic data are discussed as functions of solvent composition and solvation properties of the reaction medium.

The alkaline decomposition of quaternary phosphonium salts is known to yield phosphine oxide and hydrocarbon. It has long been assumed that the decomposition proceeds through a pentacovalent phosphorus intermediate whose formation is rate determining.[1-3] Although such reactions have been investigated from different points of view, systematic studies of solvent effects are lacking. The alkaline phosphonium decomposition is an example of an ion-ion interaction and is therefore expected to exhibit considerable medium effects. In the present rate study various dioxane-water mixtures are chosen as solvents, in which the dielectric constant can be varied over a wide range. The reaction is also studied in 70 % dioxane-$D_2O$ mixture in order to provide additional mechanistic information.

---

* On leave of absence from Alexandria University. Permanent address: Chemistry Department, Faculty of Science, Alexandria University, Alexandria, Egypt.

## EXPERIMENTAL

*Materials.* Tetraphenylphosphonium chloride (Fluka, Analytical Grade) was of sufficient purity to allow of its use without further purification. Fresh, UV spectroscopic grade, dioxane (Fluka) was used. The heavy water employed (Norsk Hydro) contained 99.8 % $D_2O$.

*Kinetic Procedure.* The reaction was followed by determining the decrease in concentration of the hydroxide or deuteroxide ion. The solvent composition covered the range 0 to 80 % (v/v) of dioxane. Experiments with NaOD were made in 70 % dioxane $-$ 30 % $D_2O$. In a typical run an accurately measured volume of 0.02 M solution of NaOD or NaOH in the appropriate solvent mixture was placed in a thermostat adjusted to within $\pm$ 0.05°C of the required temperature. After thermal equilibrium, the solution was poured into an accurately weighed amount of the phosphonium salt to give a 0.02 M solution after mixing. The mixture was shaken vigorously and replaced in the thermostat. At various intervals, aliquots were withdrawn, poured into an excess of standard HCl solution and back titrated with standard NaOH. The reaction was investigated in the temperature range 20 $-$ 55°C. The results were found to be reproducible within 2 %.

## RESULTS

The third-order rate constants of the reaction were obtained from the slopes of the linear plots represented in Fig. 1. It was found, however, that in solvents containing less than 40 % dioxane, precipitation of phosphine oxide took place causing marked enhancement in rate due to surface adsorption of the phosphonium salt.[4,5] In such cases the reaction was followed only up to 30 % conversion. The rate constants and activation energies are tabulated in Table 1. The dielectric constants were interpolated from the findings of Åkerlöf and Short.[6] The data for the kinetic deuterium isotope effect are also reported in Table 1 (9th entry). Attempts to measure the rate in pure $D_2O$ suffered from rapid precipitation of phosphine oxide due to its lower solubility in $D_2O$ compared to $H_2O$, causing a very high catalytic effect after a short time of reaction. Tetraphenylphosphonium chloride undergoes no deuterium exchange when treated with deuteroxide anion in $D_2O$. The incorporation of deuterium necessitates the presence of $\alpha$-hydrogen in the phosphonium salt.[7,8]
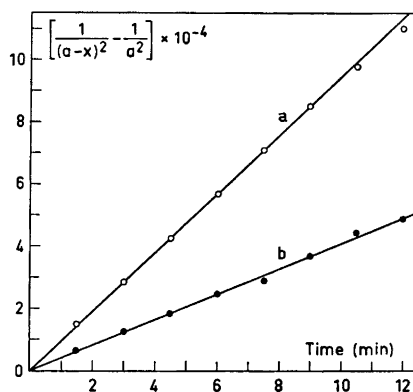


*Fig. 1.* Typical third-order plots for the alkaline decomposition of tetraphenylphosphonium chloride in dioxane-$H_2O$ and dioxane-$D_2O$ mixtures at 25°C. (a) 70 % dioxane-$D_2O$; (b) 70 % dioxane-$H_2O$.

*Table 1.* Third-order rate constants $k'$ and activation energies $E$ for the alkaline decomposition of tetraphenyl-phosphonium chroride in dioxane-water and dioxane-$D_2O$ mixtures.[a,b]

| Dioxane, vol % | $k'$, $l^2$ $mol^{-2}$ $min^{-1}$ | | | | | | | | $E$, kcal/mol |
|---|---|---|---|---|---|---|---|---|---|
| | 20° | 25° | 30° | 35° | 40° | 45° | 50° | 55° | |
| 0 | | 0.00053[c] | | 0.0033 | 0.0079 | 0.018 | 0.043 | 0.096 | 33.50 |
| 10 | | 0.00234[c] | | 0.013 | 0.030 | 0.066 | 0.149 | 0.303 | 32.24 |
| 20 | | 0.00708[c] | | 0.037 | 0.081 | 0.175 | 0.379 | 0.741 | 30.71 |
| 30 | | 0.02818[c] | | 0.141 | 0.309 | 0.660 | 1.318 | 2.639 | 29.61 |
| 40 | | 0.2042[c] | | 0.933 | 1.950 | 3.981 | 7.943 | 15.49 | 28.34 |
| 50 | | 3.516[c] | | 10.96 | 19.05 | 32.55 | 52.08 | 91.20 | 21.26 |
| 60 | 33.88 | 57.54 | 107.2 | 173.8 | 288.4 | 478.6[c] | | | 17.54 |
| 70 | 1 324 | 2 046 | 3 333 | 4 786 | 7 188 | 10 230[c] | | | 15.35 |
| 70−30 $D_2O$ | 3 125 | 4 737 | 6 313 | 8 636 | 11 100 | 15 850[c] | | | 11.52 |
| 80 | 66 070 | 89 130 | 120 200 | 158 500 | 208 000 | 272 300[c] | | | 10.63 |
| $k'_{DO^-}/k'_{HO^-}$ | 2.36 | 2.32 | 1.90 | 1.81 | 1.55 | | | | |
| Ratio: $k'$ 80 % dioxane/$k'$ water | | | | $4.8 \times 10^7$ | $2.6 \times 10^7$ | | | | |

[a] Equivalent concentrations of phosphonium and hydroxide or deuteroxide ions (0.02 M) were used throughout. [b] Total ionic strength amounts to 0.04. No corrections for zero ionic strength or thermal expansions were made. [c] Extrapolated.

## DISCUSSION

### Isotope effect and mechanism

The value of the kinetic isotope ratio $k'_{DO^-}/k'_{HO^-}$, given in Table 1, is the inverse of that expected for a primary isotope effect where an $O-H$ or $O-D$ bond is broken in the rate-determining step. This finding agrees with McEwen's elaboration [9] of Ingold's scheme.[2] The accepted mechanism may thus be illustrated as in Scheme 1.
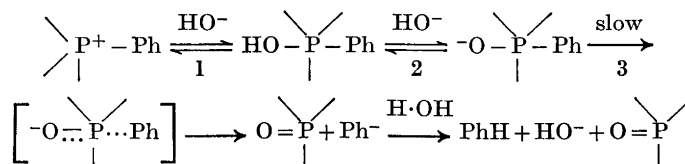
*Scheme 1.*

Hence, the higher rate in dioxane$-D_2O$ than in dioxane$-H_2O$ mixture is to be ascribed to a secondary isotope effect. The greater base strength of $DO^-$ compared to $HO^-$ anions [10] may be the main explanation for this effect. Calculations by Bunton and Shiner [11] on the relative nucleophilicities of $HO^-$ and $DO^-$, taking into account the differences in vibration forces of H-bonded or D-bonded ions, gave a 1.9 times rate increase in $D_2O$ if covalent bond is

formed with the oxyanion. Swain and Bader,[12] using a somewhat different approach, reported 3.2 times stronger basicity of $DO^-$ than $HO^-$. Dahlgram and Long [13] came to a similar result based on kinetic data for proton removal. This leads one to conclude that the present secondary isotope effect is due to stronger solvation of $HO^-$ in $H_2O$ than $DO^-$ in $D_2O$. The value obtained for $k'_{DO^-}/k'_{HO^-}$ is of the magnitude expected for such an effect. Since two $HO^-$ (or $DO^-$) ions are involved prior to the rate-determining step, the observed rates comprise the product of the rate constants of these two steps. In the second step, where a base of comparable basicity to $HO^-$ is formed, the difference in the amount of solvation between reactants and products ought to be small, resulting in a minor solvent isotope effect. In the first step, however, where a covalent neutral intermediate is formed from two ions, the secondary isotope effect due to solvation differences will be strong. In the rate-determining step, where breaking of the $P-C$ bond takes place, it is the difference in solvation of the transition state and the reacting anion which will contribute to the secondary isotope effect. Studies of the isotope content of the hydrocarbon in 50 % $H_2O - D_2O$ mixture showed very little discrimination between hydrogen and deuterium uptake.[7] In line with the general view, Corfield and Trippett [7] concluded, therefore, that the $P-C$ bond in the transition state suffers only very slight breaking. Applying this conclusion to the secondary isotope effect of the same step, the reactant-like transition state suggests also minor solvation effects and a correspondingly small secondary isotope effect in this step.

The temperature effect on the kinetic ratio $k'_{DO^-}/k'_{HO^-}$ is rather high compared to those hitherto reported in secondary isotope rate studies. Thus, in the alkaline hydrolysis of alkyl halogenides [14] the ratio changes only by 5 % from 35 to 80°C. In the present reaction, however, the change is about 40 % in the range 20 to 40°C. As seen from Tables 1 and 2, the differences in $E$ and $\Delta S^*$ in dioxane $- D_2O$ and dioxane $- H_2O$ are: $\Delta E = -3.8$ kcal/mol and $\Delta \Delta S^* = -11.2$ e.u. Such pronounced differences can only be understood if a considerable number of $D_2O$ or $H_2O$ solvent molecules, respectively, are involved, since the reactants, being charged species, have to get rid of their solvation shells prior to reaction.

## Rate, activation energy, and solvent composition

The drastic influence of solvent composition is depicted in Table 1, where the rate at 35°C in 80 % dioxane-$H_2O$ is $4.8 \times 10^7$ times faster than in water. The rate increase is caused mainly by a tremendous decrease in $E$ (33.5 kcal/mol in $H_2O$ and 10.6 kcal/mol in 80 % dioxane $- H_2O$). To a considerable extent, the decrease in $E$ is, however, counteracted by a corresponding decrease in $\Delta S^*$ (Table 2), and confirms the involvement of many water molecules in the solvation shells of reactants. The main contribution to the decrease in $E$ is, as already mentioned, believed to be due to the first step of reaction, involving the formation of a neutral pentacovalent phosphorane from the two ionic species $Ph_4P^+$ and $HO^-$. The increase in solvation of the phosphorane as well as the decrease in solvation of $Ph_4P^+$ and $HO^-$ with increasing dioxane content of the medium will both decrease the activation energy.

*Table 2.* Thermodynamic parameters of activation and frequency factors at 25°C.

| Dioxane, vol % | $\Delta F^*$, kcal/mol | $\Delta H^*$, kcal/mol | $\Delta S^*$, cal/mol deg | log (A, l² mol⁻²) sec⁻¹) |
|---|---|---|---|---|
| 0 | $24.3^a$ | $32.9^a$ | $+29.1^a$ | $19.6^a$ |
| 10 | $23.4^a$ | $31.7^a$ | $+27.8^a$ | $19.3^a$ |
| 20 | $22.7^a$ | $30.1^a$ | $+25.1^a$ | $18.7^a$ |
| 30 | $21.9^a$ | $29.0^a$ | $+23.9^a$ | $18.5^a$ |
| 40 | $20.7^a$ | $27.8^a$ | $+23.6^a$ | $18.4^a$ |
| 50 | $19.1^a$ | $20.7^a$ | $+5.4^a$ | $14.4^a$ |
| 60 | 17.4 | 17.0 | $-1.5$ | 12.9 |
| 70 | 15.3 | 14.8 | $-1.8$ | 12.9 |
| 70 – 30 D₂O | 14.8 | 10.9 | $-13.0$ | 10.4 |
| 80 | 13.1 | 10.0 | $-10.2$ | 10.7 |

[a] Based on extrapolated rate constants.

## Effect of the dielectric constant

As a first approximation, the solvent effect can be expressed on the basis of Born's solvent model using the macroscopic dielectric constant,[15] $D$, as follows:

$$\ln k' = \ln k_0' - NZ_A Z_B e^2/DRTr^*$$

where $\ln k_0'$ is the rate at infinite dielectric constant, $N$ is the Avogadro number, $Z_A$ and $Z_B$ the charges of reacting ions, $e$ the electronic charge, $R$ the gas constant, and $r^*$ the average distance between the centers of reacting ions in the activated complex (closest distance of approach). The plot of $\ln k'$ against $1/D$ should be linear with a slope of $N\, e^2/RTr^*$ for a uni-univalent ionic reaction. In Fig. 2, deviations from linearity at low dielectric constants may be attributed to selective solvation or solvent sorting.[15] The average $r^*$ value obtained from the linear portions of the plots in Fig. 2 is 1.3 Å which is much smaller than the value expected from the sum of radii of the unsolvated reacting ions $Ph_4P^+$ and $OH^-$ (about $5-6$ Å).[16] This reveals the inadequacy of the idealized Born model using the macroscopic dielectric constant in explaining the microscopic events of the present reaction.

Since $E$ is proportional to $RT \ln k'$, it follows from the Born approximation that $E$ ought to change linearly with $1/D$. Fig. 3 shows, however, a non-linear behaviour and a rapid change through an inflection point around $40-50$ % dioxane. This clearly illustrates the important role played by specific solvent effects which may suggest two underlying main types of mixtures: (a) "water-like", *i.e.*, water successively diluted with dioxane and (b) "dioxane-like", *i.e.*, dioxane successively diluted with water. Presumably water can be diluted with certain amounts of dioxane before its characteristic structure breaks down and, *vice versa*, that dioxane can be diluted with water, still keeping its "dioxane structure" up to a certain limit. Consequently, there will exist a transition region where the solvent mixture is neither water nor
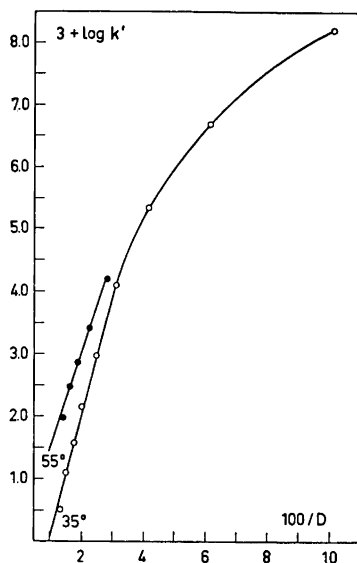
Fig. 2. Variation of log $k'$ of reaction with $1/D$ of solvent mixture.
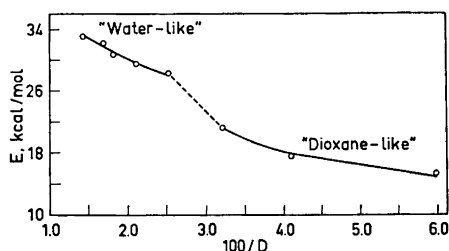
Fig. 3. Dependence of the activation energy of the reaction on $1/D$.

dioxane-like. It is a plausible assumption, therefore, that the characteristic features of Fig. 3 are caused by such structural changes of the solvent mixture, which appear as changes of $E$.

## Thermodynamic parameters of activation

The activation parameters $\Delta F^*$, $\Delta H^*$, and $\Delta S^*$ and frequency factor log $A$ (Table 2) show strong dependence on solvent composition. Thus, $\Delta F^*$ decreases at 25°C from 24.3 to 13.1 kcal/mol with increase of dioxane content from 0 to 80 %. The contributions to $\Delta S^*$ from relative changes in solvation sheaths of the reactants and transition states as the reaction proceeds are quite considerable. Progressive addition of water to dioxane will increase hydrogen bonding with reactants, which will add to $\Delta H^*$ the enthalpy associated with breaking such bonds, and hence $\Delta H^*$ increases. This increase is sharp first, until a sufficient amount of $H_2O$ has been added to cause considerable solvation of all reactants, then further addition will have little effect on hydrogen bonding and hence on $\Delta H^*$. The rate increase is due entirely to the decreased enthalpy since entropy changes oppose rate increase. The large changes in log $A$ are also brought about mainly by changes in solvation of reactants and activated complexes. Nevertheless, the changes in $E$ are much more pronounced since, according to the Arrhenius' equation, they outweigh the changes in $A$, causing rate changes. The relation between log $A$ and $E$ takes the form

$$\log A \ (l^2 \ mol^{-2} \ sec^{-1}) = 5.1 + 0.44 \ E \ (kcal \ mol^{-1})$$

The present thermodynamic parameters are, however, complicated by being resultants of components involving two fast preequilibria and a slow rate-determining step.

## REFERENCES

1. Hey, L. and Ingold, C. K. *J. Chem. Soc.* **1933** 531.
2. Fenton, G. W. and Ingold, C. K. *J. Chem. Soc.* **1929** 2342.
3. Berlin, K. D. and Butler, J. B. *Chem. Rev.* **60** (1960) 243.
4. Aksnes, G. and Songstad, J. *Acta Chem. Scand.* **16** (1962) 1426.
5. Hoffman, H. *Ann.* **634** (1960) 1.
6. Åkerlöf, G. and Short, O. A. *J. Am. Chem. Soc.* **58** (1936) 1241.
7. Corfield, J. R. and Trippett, S. *Chem. Commun.* **1970** 1267.
8. Cremer, E. S. and Chorvat, R. J. *Tetrahedron Letters* **1966** 419.
9. McEwen, W. E., Kumli, K. F., Blade-Font, A., Zanger, M. and Vander Werf, C. A. *J. Am. Chem. Soc.* **86** (1964) 2378.
10. Wiberg, K. *Chem. Rev.* **55** (1955) 713.
11. Bunton, C. A. and Shiner, V. J., Jr. *J. Am. Chem. Soc.* **83** (1961) 42, 3207.
12. Swain, C. G. and Bader, R. F. W. *Tetrahedron* **10** (1960) 182.
13. Dahlgram, G. and Long, F. A. *J. Am. Chem. Soc.* **82** (1960) 1303.
14. Heppolette, R. L. and Robertson, R. E. *J. Am. Chem. Soc.* **83** (1961) 1834.
15. Amis, E. S. *Solvent Effects on Reaction Rates and Mechanism*, Academic, New York and London 1966.
16. Grunwald, E., Baughman, G. and Kohnstam, G. *J. Am. Chem. Soc.* **82** (1960) 5801.

# Influence of Cosolutes upon the Conformation of Carbohydrates in Aqueous Solutions. II. Demonstration of the Anomeric Effect in Cellobiose and Maltose, and Proposal of a Mechanism for the Influence of Inorganic Ions upon its Magnitude

TERENCE PAINTER

*Institute of Marine Biochemistry, N-7034 Trondheim-NTH, Norway*

In sulphuric acid at 70° and 40°, the ratio $(K_\beta/K_\alpha)$ of the rates of hydrolysis of cellobiose and maltose changed very little as the concentration of acid was increased up to 10 N, but then it increased by a factor of 2 as the acid-concentration was further increased to 16 N.

In hydrobromic acid at 40°, 50°, and 60°, increasing concentration of acid caused $K_\beta/K_\alpha$ first to decrease to about half its value in dilute acid, and then slightly to increase again. For a given concentration of hydrobromic acid, $K_\beta/K_\alpha$ first decreased, and then increased again, as the temperature was raised from 40° to 70°.

Zucker-Hammett and Arrhenius plots of the data, together with the results of experiments on the salting-in and salting-out of methyl cellulose, indicated that the changes in $K_\beta/K_\alpha$ were associated with changes in the degree of hydration of the disaccharides, dehydration causing it to increase, and enhanced hydration causing it to decrease.

The behaviour throughout was qualitatively similar to that of the methyl D-glucopyranosides. From this and earlier evidence, it is concluded that the changes in $K_\beta/K_\alpha$ represent changes in the magnitude of the anomeric effect, resulting from changes in the extent to which the dipole interaction between the ring- and glycosidic-oxygen atoms is quenched by hydrogen-bonding to water molecules. A lack of strict parallelism with the behaviour of the methyl glucopyranosides suggests, however, that at least in cellobiose, it is partly quenched also by intramolecular hydrogen bonding.

An attempt is made to interpret the phenomena in terms of the zonal model of Frank and Wen for the structure of water around an ion. It is suggested that anions, generally, orientate water molecules so that they are unable to form hydrogen bonds with the ring- and glycosidic-oxygen atoms, while cations, including the hydrogen ion, orientate them in such a way as to enhance such hydrogen-bonding. It would then follow that the behaviour in sulphuric acid is dominated by the anion throughout, while in hydrobromic acid, the net effect of the two ions is a sensitive function in concentration and temperature.

In Part I of this series,[1] it was shown that the ratio $(K_\beta/K_\alpha)$ of the rates of hydrolysis of $\beta$- and $\alpha$-methyl D-glucopyranoside in sulphuric, phosphoric, hydrochloric, and hydrobromic acids at 70° depended upon both the concentration of acid and the identity of the anion. In all four acids at this temperature, it increased with increasing concentration of acid, but, for a given value of the Hammett acidity function $(H_0)$, the magnitude of the effect decreased in the order in which the acids are named.

Chromatography of the glucosides on silica gel, with the acids as mobile phases, showed that there was no significant salting-in or salting-out of one anomer relatively to the other, so that the phenomenon could not be attributed to primary salt effects. Similarly, studies of the dependence of the rates of hydrolysis upon the Hammett acidity function $(H_0)$ showed that the anions were not participating directly in the reaction as nucleophiles. From this, and studies of the dependence of the activation parameters upon the concentration of acid, it was concluded that the phenomenon was caused by the anomeric effect, which would be expected to increase as the activity of water in the system decreased, leading to desolvation of the glycosides.[1]

The activity of water is a macroscopic quantity, and, for a given value of $H_0$, it is the same for all acids.[2] The magnitude of $K_\beta/K_\alpha$, and, hence, the anomeric effect cannot therefore be a simple function in the activity of water alone. The present extension of the earlier work was undertaken in an attempt to understand, at the molecular level, why different anions differ in their capacity to desolvate the glycosides. Any such attempt must necessarily make use of existing knowledge about the influence of ions upon the structure of water, which is very incomplete. The conclusions will therefore have the status of a working hypothesis, which may require modification in the light of new evidence.

In the earlier paper,[1] brief mention was made of some unusual effects which had been noted in working with hydrobromic acid. This therefore seemed to provide a good starting-point for further work, especially since more is known about the effect of halide ions upon water than about other anions.

A second objective in the present work was to make the systems a little more closely analogous to the biological situation. To this end, temperatures lower than 70° have been investigated, and two new substrates, cellobiose and maltose, have been introduced, since these are better models for polysaccharides than the methyl glucosides.

## THEORY

This section gives a documented summary of the principal theoretical concepts that will be used in discussing the results.

*The anomeric effect as a measure of solvation.* The chair form of an *O*-pyranoside in which O(1) is axial is more stable, and the one in which it is equatorial is less stable, than in the corresponding cyclohexane analogues.[3-5] This phenomenon is described as *the anomeric effect.* It arises because of a repulsive, dipole interaction between the ring- and glycosidic oxygen atoms

in the pyranoid compounds, which is stronger in the equatorial anomer than in the axial one.[3-5]

The *magnitude* of the anomeric effect has been defined [6-9] as the measured difference in free energy, $\Delta G^{\circ}_{\alpha,\beta}$, between an anomeric pair of glycosides, minus that, $\Delta G^{\circ}_{s}$, expected for the corresponding derivatives of cyclohexane, due attention being paid to the sign of the free-energy change in each case.

It has previously been determined mainly by measurement of the position of the equilibrium in anomerisation reactions.[3,4,6,9] For certain sugar derivatives and simpler derivatives of tetrahydropyran, whose free energies in the $C$-1 and 1-$C$ conformations are not widely different, it has also been determined by using NMR spectroscopy to observe directly the relative amounts of the two conformers present at equilibrium.[7,8,10-14] In Part I of this series, it was measured by a kinetic method.[1]

It has long been known that the magnitude of the anomeric effect is dependent upon the solvent, and that any polar solvent has a capacity to diminish it.[3,9] Recently, however, Lemieux and his co-workers [12-14] have shown that the capacity of a solvent to quench the anomeric effect is not a simple function in its dielectric constant. Protic solvents, which are able to solvate the ring- and glycosidic-oxygen atoms, specifically by forming hydrogen bonds with them, have a much greater capacity to quench the anomeric effect than aprotic solvents with a similar dielectric constant. Water is an extreme example of such a solvent.[12-14]

It is obvious that water can solvate the hydroxyl groups of a glycoside in the same way, that is to say, by contributing a proton to form a hydrogen bond with the oxygen atom. These hydroxyl groups can, however, also form hydrogen bonds with water by themselves contributing their proton to the bond. The anomeric effect, as it has been defined,[6-9] does not measure this kind of solvation. This provides a possible basis for understanding why the magnitude of the anomeric effect need not necessarily be a simple function in the activity of water alone.

*The ratio $(K_{\beta}/K_{\alpha})$ as a measure of the magnitude of the anomeric effect.* The proposition that the ratio of the rates of acid-hydrolysis of an anomeric pair of glycopyranosides under the same conditions is a simple function in the magnitude of the anomeric effect rests upon the validity of Edward's hypothesis.[15] It assumes that the transition state is common to both anomers, and that the difference in their rates of hydrolysis is therefore due solely to the difference in their free energies, $\Delta G^{\circ}_{\alpha,\beta}$, in the ground state. This idea has been discussed in detail, and justified in Part I.[1]

This difference in free energy will be a function in the magnitude of the anomeric effect, together with a steric contribution, $\Delta G^{\circ}_{s}$. If it can be assumed that $\Delta G^{\circ}_{s}$ is independent of the medium, then $K_{\beta}/K_{\alpha}$ will be a *unique* function in the magnitude of the anomeric effect, insofar as this will be the only solvent-dependent variable.

This assumption must, however, be examined very critically. So far as carbon atoms and methine hydrogen atoms are concerned, tabulated values [16] for the conformational energies of alkyl groups do provide reasonable assurance that their van der Waals radii are virtually independent of the solvent. For hydroxyl groups, however, values ranging from 0.29 to 1.25 kcal mol$^{-1}$ are

reported.[16] These seem to be more dependent upon the method of measurement than the solvent, but nevertheless, there is no overt reason for believing that the conformational size of an oxygen atom should be independent of whether or not it is hydrogen-bonded to the solvent.

In considering the possible solvent-dependence of $\Delta G°_s$, it is convenient to divide it into two parts, (A) and (B). Part (A) represents the contribution from non-bonded interactions between O(1) and the rest of the glycose ring, which are present in the axial anomer but absent in the equatorial one, while part (B) results from interactions between the glycose ring and the aglycone.

For the glucopyranose ring, the significant interactions of type (A) are, importantly, all between O(1) and C(3), C(5), H(3), and H(5), since the *gauche* interaction with O(2) is common to both anomers. This means that any dependence of this part of the steric factor upon the medium will still be a unique function in the solvation of the glycosidic oxygen atom, and will be operationally indistinguishable from the anomeric effect itself.

With regard to interactions of type (B), consideration of models of α- and β-methyl D-glucopyranoside shows that the only interactions between the methyl group and the glycose ring that are not common to both anomers occur in the $A$-3 rotameric form [5] of the α-anomer, and again, these are with C(3), C(5), H(3), and H(5). No oxygen atom is involved which is not common to both anomers.

These arguments indicate that, whereas the measurement of $K_\beta/K_x$ may possibly not give correct values for the absolute magnitude of the anomeric effect, it does, at least for the methyl glucopyranosides, provide a valid method for studying its dependence upon the concentration and identity of different anions.

*The anomeric effect in disaccharides.* The value of $K_\beta/K_\alpha$ for the glucopyranosides of all primary alcohols is, for hydrolysis in dilute acid, consistently between about 1.6 and 2.4, indicating that only the alcoholic methylene group interacts significantly with the glycose ring.[17,18] For glucopyranosides of secondary aliphatic alcohols, it is slightly lower,[17] while for α- and β-phenyl D-glucopyranoside, the familiar ratio is more than reversed,[15,19] the α-anomer being hydrolysed, in 2 N hydrochloric acid at 60°, about 4 times faster than the β-anomer.[19] Edward attributed this to a particularly strong steric interaction between the phenyl group and positions 3 and 5 in the α-anomer, pointing out that the $-O-Ph$ system would tend to be planar because of the partial, double-bond character of the O(1)$-$Ph bond.[15] Overend et al.[19] subsequently found that the entropy of activation was higher for the α-anomer than for the β-anomer, so that highly restricted rotation about the C(1)$-$O(1) bond is more likely to account for its higher free energy in the ground state.

For disaccharides, the only evidence obtained so far for the existence of the anomeric effect has been with the 1,6'-linked anomeric pair, gentiobiose and isomaltose, which exhibit the usual ratio characteristic for the glucopyranosides of primary alcohols.[20] For the other anomeric pairs of glucobioses, namely, cellobiose and maltose, laminaribiose and nigerose, and sophorose and kojibiose, $K_\beta/K_\alpha$ in dilute acid is in the range 0.3$-$0.7, and the reason is unknown.[20] BeMiller[18] suggests that, as in the case of the phenyl

glucopyranosides, the steric factor for the $\alpha$-anomer is simply larger than it is for the glucopyranosides of primary aliphatic alcohols.

There is, however, a serious reason for questioning whether the anomeric effect exists in these disaccharides at all. This is because of the possibility of intramolecular hydrogen-bonding between the ring- and glycosidic-oxygen atoms in the glycose moiety, and hydroxyl groups in the aglycone. Thus, the disaccharides may contain their own "solvent", which could partly replace the hydration which can be brought about by water.*

For example, the hydroxyl group at C(6) of the reducing unit could form a hydrogen bond with the glycosidic oxygen atom. This can be seen, not only from models, but also from the known fact that *pseudo*-cellobiouronic acid and polyuronides are hydrolysed, between pH 2 and pH 4, partly by intramolecular, general-acid catalysis.[21],[22] In this reaction, the unionised carboxyl group at C(6) of the aglycone donates a proton directly to the glycosidic oxygen atom attached to it at C(4). It is obvious that an intramolecular hydrogen bond must be formed as an intermediate in this step.

The ring-oxygen atoms in the non-reducing glucose residues could also form intramolecular hydrogen bonds in these disaccharides. In cellobiose, the hydroxyl group at C(3) of the reducing unit would be ideally situated to act as the hydrogen-donor, and indeed, such a hydrogen bond is already postulated to exist in the Hermans "bent-chain" model for crystalline cellulose.[23] In the case of maltose, a model shows that the primary hydroxyl group in the reducing unit could form a hydrogen bond with the ring-oxygen atom of the non-reducing unit without any serious steric clashes.

The possible occurrence of such intramolecular hydrogen bonding in polysaccharides in aqueous solution has been much debated in recent years, and is clearly of key importance. Since it is now known that the magnitude of the anomeric effect can be varied at will, by carrying out hydrolysis in different acids of different concentrations,[1] it is possible to introduce a new kind of evidence into this area. Thus, if the higher rate of hydrolysis of maltose is due simply to a larger steric factor, then, even though the absolute values of $K_\beta/K_\alpha$ are lower for cellobiose and maltose than they are for $\beta$- and $\alpha$-methyl D-glucopyranoside, a close parallelism in the response of these values to changes in the medium should still be observed for the two pairs of glucosides. If, however, there is any significant, intramolecular hydrogen-bonding of the type just discussed, it might be expected that the anomeric effect would be suppressed in the disaccharides, and that there would be no significant parallelism between the two sets of values of $K_\beta/K_\alpha$.

*The effect of ions upon the structure of water.* There is much controversy about the detailed structure of liquid water, but it is undisputed that the molecules are associated by hydrogen-bonding, and that it is therefore a partial polymer.[24-27] The average degree of polymerisation decreases with increasing temperature. It is also undisputed that inorganic ions are, in general, hydrated in solution, and that, for closed-shell ions like the halides, the alkali-metal ions, and tetra-alkylammonium ions, the mechanism is simply dipole-attraction.[24],[27],[28]

---

* Since each oxygen atom can form 0,1 or 2 hydrogen bonds, nine different possible states of hydration can be formally recognised.

This mechanism is universally accepted to imply that, around an anion, the water molecules are orientated with their hydrogen atoms pointing, at least on an average, towards the anion, while around a cation, it is the oxygen atoms that are pointing inwards. The extent of this orientation, or "electrostriction", depends upon the electrostatic field at the surface of the ion, and is therefore inversely related to the ionic radius (distance from the nucleus). Thus, ions like $F^-$ and $Li^+$ are powerful electrostrictors, while $I^-$ and $Cs^+$, and especially tetra-alkylammonium ions, are weak ones.[24,27,28] Consistently with this, the proton is a strong electrostrictor,[24] and the hydronium ion, $H_3O^+$, is thought to be associated with at least four other water molecules in dilute solution.[2] The hydroxyl ion is also considered to be a strong electrostrictor.[24,27]

Attempts to develop this simple, electrostatic model through *a priori* calculations are complicated by the need to make simplifying assumptions about the distribution of charge in the water molecule. With one such model, Bernal and Fowler[24] concluded that a monovalent ion would be an electrostrictor only if its ionic radius were less than 1.6 Å. This implies that, among the halides, only $F^-$ would be a significant electrostrictor, whereas, among the alkali-metal ions, only $Cs^+$ would not be. Later models,[28] by assuming a different charge-distribution, predict that anions, generally, should be stronger electrostrictors than cations of the same charge and radius. This comes about essentially because its smaller radius allows a hydrogen atom to get closer to an anion than an oxygen atom can get to a cation.[28]

Little has been stated about the sulphate ion, but from its double charge, its tendency to form hydrated salts, and its high position in the Hofmeister lyotropic series, it is reasonable to infer that it is a powerful electrostrictor. For metal ions with vacant orbitals, there is, of course, the possibility of co-ordination, but here again, the generalisation that the oxygen atoms of water point towards cations and away from anions holds true. For anions like $HSO_4^-$ and $H_2PO_4^-$, the situation is clearly more doubtful.

Frank and Wen[29] have described the electrostricted layer of water molecules as "zone A". Nothing is known about its thickness, and there is no agreement as to how it should be defined, because different methods for measuring "hydration numbers" give widely different results.[27] It is only certain that, for a series like the halides at a given concentration and temperature, its thickness decreases with increasing ionic radius. It has been claimed that, for the iodide ion, it does not exist at all.[30]

Except for very dilute solutions, it follows as a direct consequence of the electrostatic model that the thickness of zone A will depend upon both the identity of the counterion, and the overall concentration of salt. This is because, as the concentration of salt increases, and the anions and cations approach one another more closely, each will start to neutralise the electrostatic field of the other, leading to a breaking-down of the respective A-zones.[31]

For certain ions, notably the larger halide and alkali-metal ions, there is evidence that, outside zone A, there exists a second zone, B, in which the molecules have a higher entropy, and a lower average degree of polymerisation, than they have in pure water at the same temperature.[29] Since the thickness of zone B seems to increase with increasing ionic radius, and hence to be

inversely related to the thickness of zone A, relevant ions like $K^+$, $Rb^+$, $Cs^+$, $Br^-$, and $I^-$ are described [29] as "net structure breakers".* For dilute solutions, it is formally necessary to recognise that, outside zone B, there exists a third zone, C, which is the same as pure water.[29]

It seems to be possible to make the following inferences:

(a) For a given salt or acid at a given temperature, one ion will, in general, be a stronger electrostrictor than the other. As the salt is added to water, zone C will gradually disappear, and electrostricted water will be generated in the two A-zones, in proportion to their relative thicknesses. As the concentration increases still further, and the anions and cations approach one another, the A-zones will start to break down, that of the weaker electrostrictor disappearing first. Since this may be the origin of the B-zones, it cannot be inferred that the B-zones will disappear before the A-zones start to break down.

(b) For a given concentration of salt or acid, an increase in temperature will lead to an increase in the volume of the B-zones at the expense of the A-zones, and also at the expense of zone C, when it is present. Otherwise expressed, the A-zones, and the C-zone if any, will "melt". The A-zone of the weaker electrostrictor will melt first. The higher the concentration of salt, the lower should these "melting points" be, because, with the diminished net electrostatic field, the amount of energy required to break down the zones will be smaller.

*A working hypothesis.* Against this theoretical background, and on the basis of the results described in Part I,[1] the following two postulates are made:

(1) Anions generally, in water, increase the magnitude of the anomeric effect, and their capacity to do so is directly correlated with their electrostrictive power.[1] The magnitude of the anomeric effect is a direct measure of the extent to which the ring- and glycosidic oxygen atoms are solvated by water molecules, through hydrogen-bond formation with their hydrogen atoms.[12-14] At the periphery of a hydrated anion, the hydrogen atoms of the water molecules are pointing inwards, so that, in order to solvate these oxygen atoms, they would have to be re-orientated against the electrostatic field of the anion. This is why such solvation is diminished by anions. The glycosides are not excluded from the domain of the anions, that is to say, they are not significantly salted-out. Chromatographic evidence shows this.[1] This is because their hydroxyl groups are still able to form hydrogen bonds with the electrostricted water molecules, by themselves contributing the proton. Such hydrogen-bond formation should, in fact be promoted, because the density of electrons on the oxygen atoms of the electrostricted water molecules should be enhanced by the electrostatic field of the anion.

(2) Cations, generally, decrease the magnitude of the anomeric effect by orientating the water molecules so as to favour hydrogen-bond formation with the ring- and glycosidic oxygen atoms. They should also enhance the capacity of these molecules to act as hydrogen donors, by virtue of their electrostatic fields. These electrostricted water molecules are also able to form hydrogen bonds with the hydroxyl groups of the glycosides, the oxygen atoms of these groups acting as the proton acceptors.

---

* It is not apparent to this author that such a generalisation can be made without specifying the identity of the counterion, the total concentration of salt, and the temperature.

It is evident that it is not possible for postulate (1) to be correct without postulate (2) also being correct. A way to substantiate the truth of postulate (1) is therefore to seek evidence for the truth of postulate (2). This introduces the main purpose of the present work. To obtain the required evidence, it was clear that an acid should be chosen whose anion is a sufficiently weak electrostrictor to "allow" the hydronium cation, $H_3O^+$, to be the dominant electrostrictor. Ideally, hydrogen iodide should have been chosen, but it could not be used because the liberation of elementary iodine by dissociation and oxidation made the solutions too dark to be measured in the polarimeter.

*The Zucker-Hammett plot* [32] *as a measure of solvation.* This has been discussed in detail in Part I.[1] If the mechanism of hydrolysis is A-1, and if the activity coefficient of the substrate does not change relatively to that of the Hammett base as the concentration of acid increases, then a plot of the logarithms of the *pseudo*-first order rate-coefficients against the Hammett acidity function ($-H_0$) will have unit slope when the free energy of activation ($\Delta G^{\neq}$) is independent of acid-concentration. When $\Delta G^{\neq}$ increases with increasing acidity, the plot is sigmoid, and the slope at the point of inflexion is less than unity, and when $\Delta G^{\neq}$ decreases with increasing acidity, the plot is also sigmoid, but the slope at the point of inflexion is greater than unity.

Such a medium-dependence of $\Delta G^{\neq}$ has been identified with changes in the degree of hydration of the substrate in the ground state, *relative* to that in the transition state, by simultaneous studies of the medium-dependence of the activation parameters.[1] Thus, if the entropy of activation ($\Delta S^{\neq}$) decreases with increasing acidity, then the *difference* between the degree of hydration in the ground and transition states is decreasing, but if it increases, the opposite is true.

In the earlier study of the hydrolysis of the methyl glucopyranosides in sulphuric acid,[1] it was found that $\Delta S^{\neq}$ decreased sharply with increasing concentration of acid. Since this was accompanied by an increase in the magnitude of the anomeric effect, it was concluded that dehydration was taking place in the ground state. In order to understand why a parallel dehydration of the transition state was not taking place, it was necessary to assume that, in acid of any strength, the transition state is always less hydrated than the ground state. Specifically, it was suggested that the hydrate always decomposes when the molecule passes through the transition state, and that this is probably connected with the conformational change, from chair to half-chair, that is entailed in the formation of the transition state.

Insofar as this last assumption can be held to be generally true, it is seen that a decrease in $\Delta S^{\neq}$ will always mean that the ground state is being dehydrated, and that an increase in $\Delta S^{\neq}$ will always mean that it is being hydrated.

*Theoretical aspects of the temperature of precipitation of methyl cellulose.* By measuring the *ratio* ($K_\beta/K_\alpha$) of the rates of hydrolysis of an anomeric pair of glucopyranosides, all medium effects on the rest of the molecule should be compensated for, and a specific measure obtained of hydrogen-bonding to the ring- and glycosidic-oxygen atoms. Because of the unusual results obtained in the present work with hydrobromic acid, it was desirable to seek con-

firmatory evidence of a more conventional kind, even though it would lack this compensatory feature.

Any suitable experimentation would necessarily entail some kind of measurement of solubility, and it was important that this should be carried out in the same temperature-range, namely, $40-70°$. The idea of using the temperature at which methyl cellulose precipitates from aqueous solution [33] met this requirement, and possessed the additional feature that the methoxyl groups would resemble the ring- and glycosidic-oxygen atoms insofar as they could only be hydrated in the capacity of proton acceptors. This kind of approach to the study of solvation phenomena is well precedented, for example, in the experiments of Klotz [34] on the effect of salts on the temperature of precipitation ("cloud point") of polyvinylmethyloxazolidinone, and in the similar experiments of Ciferri and Orofino [35] on poly-L-proline. There are, however, theoretical difficulties in interpretation.

When a polymer dissolves in a solvent, there may be a net decrease in entropy because of an ordering effect upon the solvent molecules. In such a case, an increase in temperature will lead to a decrease in solubility. The phenomenon is a general one, and has been discussed in detail by Patterson.[36] The difficulty is that the solvent molecules may be ordered either because of a direct association with polar groups in the polymer, or because non-polar groups in the polymer give rise to "ice-like" structures in the solvent of the type discussed by Frank and Evans.[37] The ability of a cosolute to affect the temperature of precipitation is, therefore, not necessarily a measure of its ability to modify the extent to which the polar groups are solvated. The mechanism could consist simply in a modification of the free-energy change associated with the exposure of the non-polar groups to the solvent. This could come about, for example, through a change in the surface tension of the solvent.

Another difficulty in the present case is that fully methylated cellulose is insoluble in water, and the well-known temperature effect is observable only for partially methylated cellulose, with a degree of substitution in the range of $1.6-2.0$ (Ref. 33). The possible effect of solvent upon the remaining hydroxyl groups must, therefore, also be considered.

In an attempt to distinguish between these three possibilities, auxiliary experimentation was carried out as described in the section on results. An interesting review of similar problems in the field of protein chemistry is given by Von Hippel and Schleich.[38]

<div style="text-align:center">

EXPERIMENTAL

</div>

*Kinetics of acid-hydrolysis.* Apart from the following, additional details, the procedure and materials were exactly as described in Part I.[1]

$\beta$-Cellobiose was obtained from Theodor Schuchardt, München, and $\beta$-maltose monohydrate from Merck, A/G, Darmstadt. Both products were chromatographically homogeneous, had the correct specific rotations, and were used without further purification. This was also the case for methyl 2,3,4,6-tetra-O-methyl $\alpha$-D-glucopyranoside, which was obtained from Koch-Light Laboratories, Ltd., Colnbrook, Buckinghamshire, England.

The initial concentration of the disaccharides in the reaction mixtures was 2 % w/v, calculated as anhydrous glucose. In each separate concentration of acid, and at each temperature, the "infinity" readings were obtained with freshly-prepared solutions of glucose, also at a concentration of 2 % w/v.

With the reducing disaccharides, the initial optical rotations were more sensitive to changes in acid-concentration than in the case of the methyl glucopyranosides, doubtless because of the anomeric effect. The earlier procedure of extrapolating the readings to zero time was therefore discarded in favour of taking the "initial" reading as the first reading to be taken after the establishment of thermal equilibrium. This is valid, because the rate-coefficient is independent of the concentration of substrate (cf. Overend et al.[19]).

*Measurements of the temperature of precipitation of methyl cellulose.* Methylated cellulose ("Methocel MC", U.S.P., 4000 cps.) was obtained from Fluka A/G, Buchs, Switzerland. An aqueous solution (1 % w/v) was centrifuged for 30 min at 40 000 g, and at 30°, before use. The other reagents were of Merck analytical grade.

For experiments with acids up to a concentration of 1 M, and with other reagents, the stock, 1 % w/v solution of methyl cellulose was mixed with an equal volume of reagent solution at room temperature, and placed in a test-tube in a large, insulated, well-stirred water-bath, which was heated at a rate of about 0.5° per min. With practice the temperature at which turbidity first appeared could be measured reproducibly to within 0.5°. The "cloud-point" was independent of thermal history, provided that the methyl cellulose was completely dissolved beforehand. Because of the difficulty in providing uniform conditions of agitation, no attempt was made to determine the temperature at which the precipitate redissolved upon cooling.

In experiments with acids at a concentration higher than 1 M, the foregoing procedure gave spuriously high results for the cloud-point, because of hydrolysis of the methyl cellulose during the period of heating. In these cases, more-approximate readings were obtained by varying the procedure as follows. When there was salting-in, the solutions of methyl cellulose and acid were heated separately to just below the cloud-point in water (about 52°), mixed, and then heated rapidly, at a rate of about 5° per min, until precipitation occurred. When there was salting-out, the temperature of precipitation was determined roughly by heating the solutions separately to a series of pre-determined temperatures, and observing the presence or absence of a precipitate immediately after mixing.

## RESULTS

*Cellobiose and maltose in sulphuric acid.* In the first series of experiments, $K_\beta/K_\alpha$ for the disaccharides was studied as a function in the concentration of sulphuric acid at 70°, in order to compare the results directly with those obtained earlier[1] for the methyl glucopyranosides at the same temperature. It was, however, only possible to do this up to a concentration of 10 N acid, because the absolute rates of hydrolysis then became too high to be measured accurately. The results are shown in Fig. 1 (Curve A). Another series of experiments was then carried out at 40°, and in this case it was possible to work with concentrations of acid up to 16 N, before acid-catalysed dehydration-reactions started to cause serious departure from first order kinetics (cf. Part I).[1] The results are shown in Fig. 1 (Curve B).

In Fig. 2, the rate-coefficients obtained for cellobiose and maltose at 70° are shown separately, in the form of Zucker-Hammett plots. Unit slope is indicated by a broken line. Similar plots of the results obtained at 40° are shown in Fig. 3. All the values of $-H_0$ in these plots are taken from published tables,[2] and corrected for temperature with published values[2] of the temperature coefficient of $-H_0$.

Thin-layer chromatography of the disaccharides and of a Hammet base (p-nitroaniline) in various concentrations of sulphuric acid was carried out as described earlier,[1] and the results (Table 1) indicated that there was no tendency for the disaccharides to be salted-in or salted-out relatively to one another or to the Hammett base.
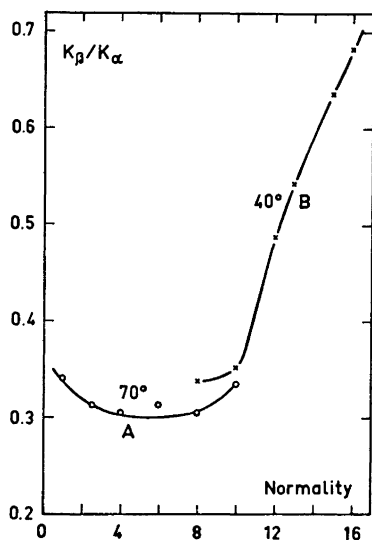
*Fig. 1.* Dependence upon acid-concentration of the ratio $(K_\beta/K_\alpha)$ of the rates of hydrolysis of cellobiose and maltose in sulphuric acid at 68.7° (O) and 39.6° ( × ).
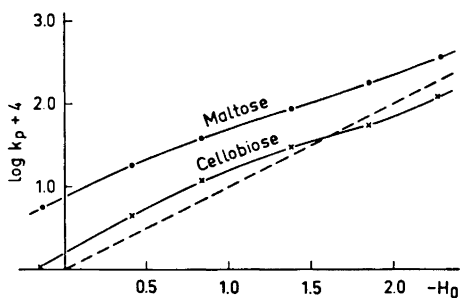
*Fig. 2.* Zucker-Hammett plots for hydrolysis of maltose (●) and cellobiose ( × ) in sulphuric acid at 68.7°. The rate-coefficients $(k_p)$ were calculated by using logarithms to the base 10. The broken line indicates unit slope.

*Table 1.* Chromatographic mobilities ($R_F$ values) of maltose, cellobiose and $p$-nitroaniline (PNA) on thin (0.75 mm) layers of silica gel, with various acids as the mobile phase.

| Acid | $R_F$ values of | | |
| | Maltose | Cellobiose | PNA |
| --- | --- | --- | --- |
| 4 N $H_2SO_4$ | 0.94 | 0.95 | 0.83 |
| 5 N $H_2SO_4$ | 0.95 | 0.96 | 0.79 |
| 8 N $H_2SO_4$ | 0.95 | 0.95 | 0.76 |
| 10 N $H_2SO_4$ | 0.94 | 0.95 | 0.80 |
| 12 N $H_2SO_4$ | 0.95 | 0.95 | 0.80 |
| 16 N $H_2SO_4$ | 0.96 | 0.96 | 0.78 |
| 1 N HBr | 0.99 | 0.99 | 0.76 |
| 3 N HBr | 0.99 | 0.99 | 0.84 |
| 5 N HBr | 0.99 | 0.99 | 0.81 |

*Cellobiose and maltose in hydrobromic acid.* There were no problems due to dehydration in this acid, but the range of acid-concentrations studied at each temperature was limited by the requirement that the absolute rates of hydrolysis should not be too high to be measured accurately, nor too low to be measured conveniently. The results obtained for $K_\beta/K_\alpha$ at 40°, 50°, 60°, and 70° are shown in Fig. 4.
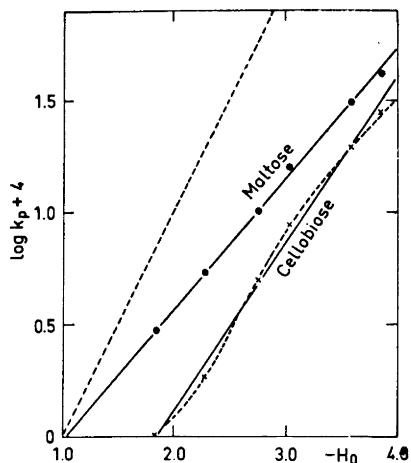
*Fig. 3.* Zucker-Hammett plots for hydrolysis of maltose (●) and cellobiose (×) in sulphuric acid at 39.6°.
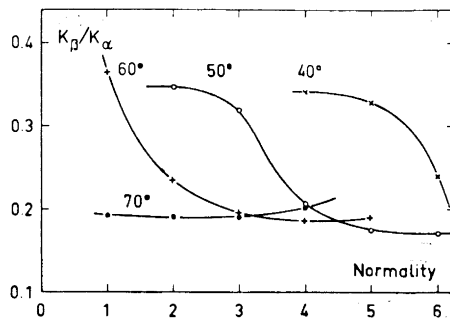


*Fig. 4.* Dependence upon acid-concentration of the ratio $(K_\beta/K_\alpha)$ of the rates of hydrolysis of cellobiose and maltose in hydrobromic acid at 39.5° (×), 49.4° (O), 58.5° (+) and 68.5° (●).
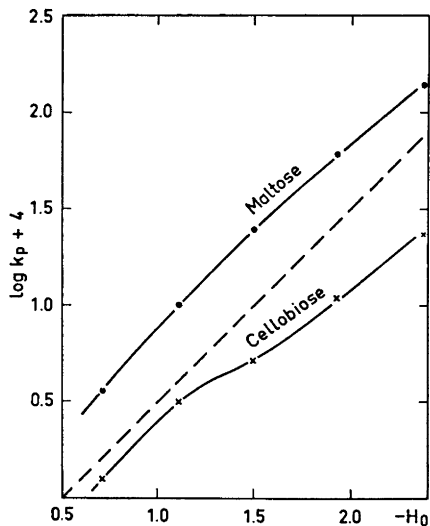


*Fig. 5.* Zucker-Hammett plots for hydrolysis of maltose (●) and cellobiose (×) in hydrobromic acid at 49.4°.
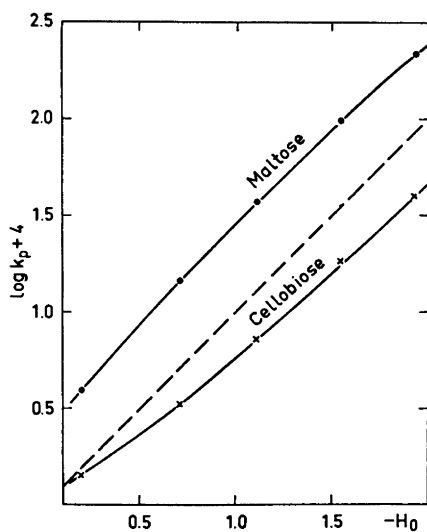


*Fig. 6.* Zucker-Hammett plots for hydrolysis of maltose (●) and cellobiose (×) in hydrobromic acid at 58.5°.

Since it was possible to study five different concentrations of acid at both 50° and 60°, Zucker-Hammett plots for these temperatures are shown in Figs. 5 and 6, respectively. The values of $-H_0$, taken from tables,[2] are valid at 25°, and are not corrected for temperature, because the temperature-coefficient of $-H_0$ is not reported for this acid. A preliminary study in this laboratory indicated that the temperature coefficient is negative (with respect to $-H_0$), and becomes more so with increasing acid-concentration, so that the slopes of the curves are a little too low. The matter was not pursued further, however, because the main purpose of Figs. 5 and 6 is to compare the behaviour of cellobiose with that of maltose.

Thin-layer chromatography of the disaccharides and of $p$-nitroaniline was also carried out in various concentrations of hydrobromic acid, and the results are included in Table 1. The $R_F$ values of the disaccharides are so high in this acid, that it might reasonably be questioned whether the evidence is satisfactory. There was no flattening of the spots, however, which is usually indicative of complete exclusion from the stationary phase, and a proportionate salting-in was also observed for the Hammett base. Because of this, and of the similar results obtained for the methyl glucopyranosides, whose $R_F$ values are lower,[1] it is very unlikely that the different behaviour of the two disaccharides is due to primary salt effects.

The kinetic data also allowed the temperature-dependence of $K_\beta/K_\alpha$ in 2 N, 3 N, 4 N, and 5 N hydrobromic acid to be illustrated, as shown in Fig. 7. There is an evident paucity of experimental points in the individual curves,
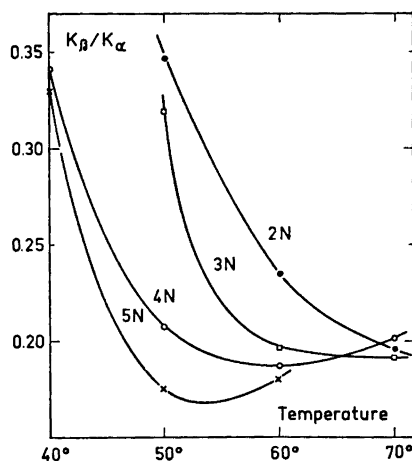


*Fig. 7.* Dependence upon temperature of the ratio $(K_\beta/K_\alpha)$ of the rates of hydrolysis of cellobiose and maltose in hydrobromic acid at concentrations of 5 N ( × ), 4 N (O), 3 N (□), and 2 N (●).
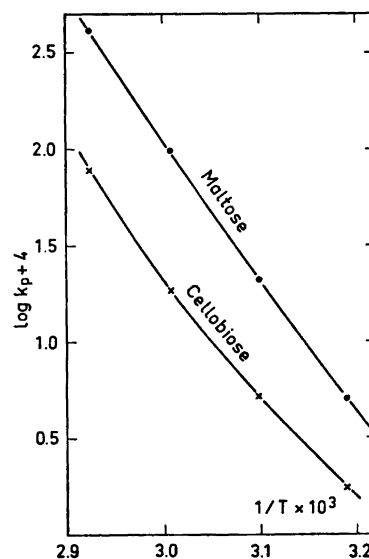
*Fig. 8.* Arrhenius plots for the hydrolysis of maltose (●) and cellobiose ( × ) in 4 N hydrobromic acid.

*Table 2.* Energies $(E_A)$ and entropies $(\Delta S^{\ddagger})$ of activation for hydrolysis of maltose and cellobiose in 4 N hydrobromic acid at 40° and 70°.

|  | $(E_A)$ 70° | $(E_A)$ 40° | $(\Delta S^{\ddagger})$ 70° | $(\Delta S^{\ddagger})$ 40° |
|---|---|---|---|---|
| Maltose | 34.4 | 30.0 | + 20.1 | + 6.8 |
| Cellobiose | 35.8 | 23.3 | + 20.9 | − 16.7 |

but qualitatively, the existence of a series of troughs is clear, even though their exact positions are not precisely known. With such a temperature-dependence, it is not surprising that the kinetics were non-Arrhenian. This is shown in Fig. 8, where the separate data for cellobiose and maltose in 4 N hydrobromic acid are plotted. Both plots are curved, and show that the energy of activation increases with increasing temperature for both disaccharides. The numerical values for the activation parameters were not very accurate, because they had to be measured from the slopes of tangents, but very approximate values are given in Table 2.

*Methyl* α- *and* β-D-*glucopyranoside in hydrobromic acid.* An almost identical series of experiments was carried out on the methyl glucopyranosides, and plots of $K_\beta/K_\alpha$ against normality of hydrobromic acid at the four different temperatures are shown in Fig. 9. They may be compared directly with the results for the disaccharides in Fig. 4. All the other plots of the data were sufficiently similar, in the qualitative sense, to those already shown for the disaccharides in this acid, that it is not necessary to show them. The relevant differences can be most clearly seen from Figs. 4 and 9.
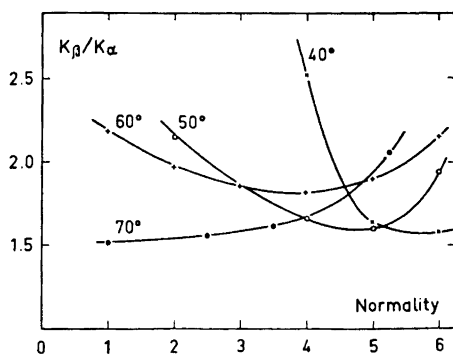


*Fig. 9.* Dependence upon acid-concentration of the ratio $(K_\beta/K_\alpha)$ of the rates of hydrolysis of the anomeric methyl D-glucopyranosides in hydrobromic acid at 39.5° ( × ), 49.5° (O), 58.5° ( + ) and 68.5° ( ● ).
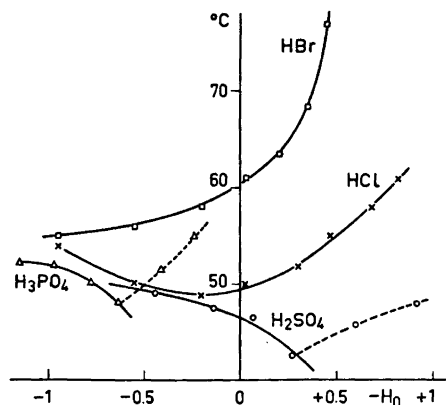


*Fig. 10.* Dependence upon acid-concentration of the cloud-point of methyl cellulose in hydrobromic acid (☐), hydrochloric acid ( × ), phosphoric acid (△), and sulphuric acid (O). The points adjoined by broken curves are assumed to be spurious because of acid-degradation.
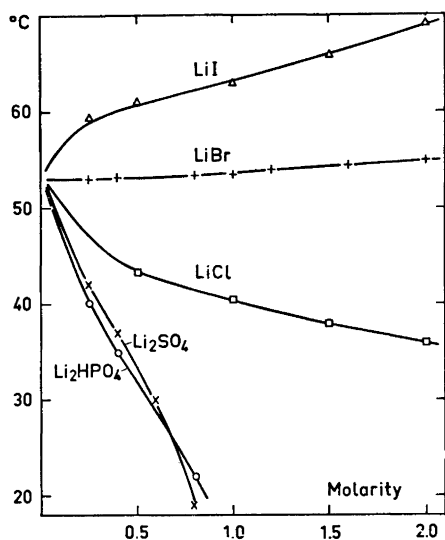
Fig. 11. Dependence upon salt-concentration of the cloud-point of methyl cellulose in lithium iodide ($\triangle$), bromide ($+$), chloride ($\square$), sulphate ($\times$), and monohydrogen phosphate ($\bigcirc$).
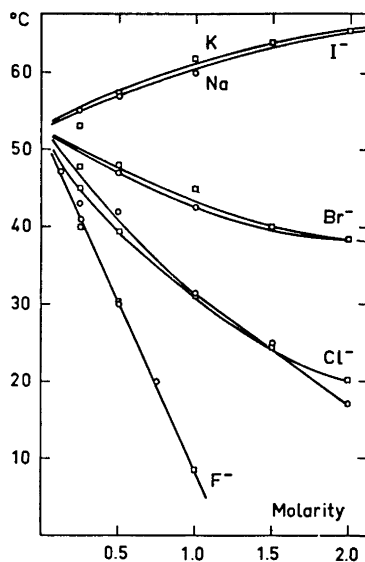
Fig. 12. Dependence upon salt-concentration of the cloud-point of methyl cellulose in the iodides, bromides, chlorides, and fluorides of sodium ($\bigcirc$) and potassium($\square$).

*Effect of the acids and of model cosolutes upon the temperature of precipitation of methyl cellulose.* The results obtained for sulphuric, phosphoric, hydrochloric, and hydrobromic acids are shown in Fig. 10. The Hammett acidity function ($-H_0$) is chosen as the measure of acid-concentration, because this assures that, at a given value of $-H_0$, the samples of methyl cellulose are protonated to the same extent in the four different acids, so that their different solubilities cannot be due to differences in charge. In agreement with theory,[36] even mild acid-hydrolysis brought about a marked increase in the cloud-point, so that all the results are probably too high.

Because of this difficulty, it was of interest to replace the hydrogen ion by $Li^+$, which might be expected to behave similarly, because it is also a strong electrostrictor. Fig. 11 shows the results obtained with $Li_2SO_4$, $LiH_2PO_4$, $LiCl$, $LiBr$, and $LiI$, up to a concentration of 2 M. When a weaker electrostrictor than $Li^+$ was chosen as the cation, the bromide ion was no longer associated with salting-in, although the iodide ion still was. This and several other points of interest are shown in Fig. 12.

Experiments were then carried out to determine to what extent these effects could be due to changes in the hydration of the unmethylated hydroxyl groups. Since alkalis are good solvents for unmethylated polysaccharides, the behaviour in LiOH, NaOH, and KOH was determined. The results (Fig. 13) are shown with the $H^-$ acidity function [2] as the measure of alkali-concentra-
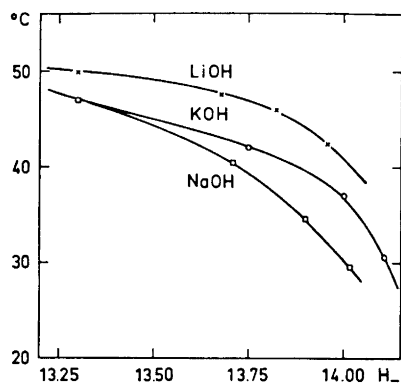
Fig. 13. Dependence upon alkali-concentration of the cloud-point of methyl cellulose in the hydroxides of lithium ($\times$), sodium ($\square$), and potassium (O).
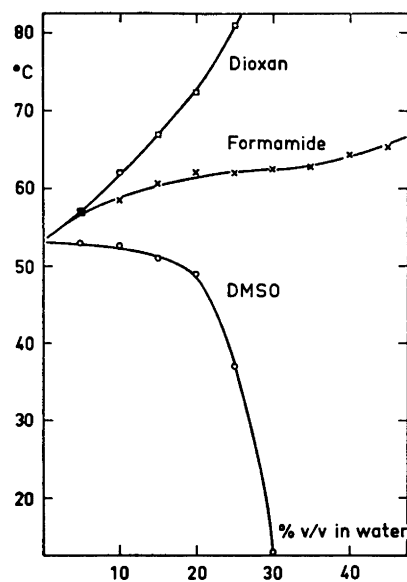
Fig. 14. Dependence of the cloud-point of methyl cellulose upon the concentration in water of dioxan ($\square$), formamide ($\times$) and dimethyl sulphoxide (O).

tion, since this assures that the hydroxyl groups are, for a given value of $H^-$, ionised to the same extent in the three alkalis.

Three organic solvents were next investigated: dioxan, because it is a good solvent for non-polar compounds; dimethyl sulphoxide, because it is a powerful proton-acceptor, and hence a good solvent for unmethylated polysaccharides; and formamide, because it is a good proton-donor. The results are shown in Fig. 14.

Table 3. Pseudo-first order rate-coefficients ($k_p$) and energies ($E_A$) and entropies ($\Delta S^{\ddagger}$) of activation for hydrolysis of methyl 2,3,4,6-tetra-O-methyl-$\alpha$-D-glucopyranoside in 1 N and 12 N sulphuric acid. The rate-coefficients ($k_p$) were calculated by using logarithms to the base 10.

| Temp. (°C) | Normality of acid | $10^4 k_p$ (min$^{-1}$) | $E_A$ (kcal mol$^{-1}$) | $\Delta S^{\ddagger}$ (e.u.) |
|---|---|---|---|---|
| 87.4 | 1.0 | 5.04 | | + 58.4 |
| 82.7 | 1.0 | 1.96 | 51.0 | + 58.4 |
| 78.1 | 1.0 | 0.75 | | + 58.4 |
| 68.5 | 12.0 | 68.8 | | − 0.8 |
| 57.9 | 12.0 | 14.4 | 30.7 | − 0.3 |
| 49.4 | 12.0 | 4.79 | | + 0.1 |
| 39.6 | 12.0 | 1.04 | | + 0.1 |

Finally, direct support was sought for the assumption that the methoxyl groups in methyl cellulose are hydrated in aqueous solution, with their oxygen atoms acting as proton-acceptors. This was done by taking methyl 2,3,4,6-tetra-$O$-methyl-$\alpha$-D-glucopyranoside as a model, and measuring the activation parameters for hydrolysis in both 1.0 N and 12 N sulphuric acid. The results (Table 3) show that the decrease in both the energy and entropy of activation that occurs upon increasing the concentration of acid is even larger than in the corresponding unmethylated compound.[1]

## DISCUSSION

*The anomeric effect in cellobiose and maltose.* The overall impression given by the results in sulphuric acid (Fig. 1) is that, whereas the molecules as a whole are, like the methyl glucopyranosides,[1] smoothly dehydrated by increasing concentrations of acid (Figs. 2 and 10), this is not associated with very much change in the magnitude of the anomeric effect until a transition, occurring only in cellobiose (Fig. 3), suddenly allows it to increase in that sugar. Whether a similar transition in maltose, or a second transition in cellobiose, would occur at a still-higher acid-concentration, cannot be determined with sulphuric acid because of decomposition of the sugars, but the use of a neutral salt as the dehydrating agent might possibly provide an answer to this question.

The effect of hydrobromic acid (Fig. 4) is more uniformly manifested in both disaccharides. This acid clearly enhances hydration (Table 2 and Fig. 10), and this is seen in Figs. 5 and 6 to lead to simultaneous stabilisation of cellobiose and destabilisation of maltose. Even here, however, the changes that occur are sharper and are displaced towards higher acid-concentrations compared to the corresponding changes in the methyl glucopyranosides (Fig. 9).

Decomposition of the disaccharides prevented the measurement of $K_\beta/K_\alpha$ in concentrations of sulphuric acid higher than 16 N, so that its upper limit is still not known. However, the total, measured range of variation in $K_\beta/K_\alpha$, from the minimum of 0.17 in hydrobromic acid (Fig. 4) to the maximum of 0.68 in sulphuric acid (Fig. 1), corresponds to a variation in the magnitude of the anomeric effect, at 40°, of 860 cal mol$^{-1}$. This was calculated from eqn. (4) in Part I,[1] with the ratios of the activity coefficients set equal to unity, in accordance with the chromatographic evidence (Table 1).

This result may be compared with the corresponding figure of about 700 cal mol$^{-1}$, obtained earlier [1] for the methyl glucopyranosides at 70°. It is therefore reasonable to infer that the anomeric effect is just as strong in di- and poly-saccharides generally, as it is in simple glycosides.

*Intramolecular hydrogen-bonding in cellobiose and maltose.* The transition that occurs in cellobiose as the concentration of sulphuric acid increases from 10 N to 16 N at 40° (Fig. 3) is unlikely to be due to a sudden change in the steric factor, because the molecules have already been extensively dehydrated before it occurs (Fig. 2), and no similar change occurs in maltose, even though the steric factor should be larger for this disaccharide.

It is evident that further work on other disaccharides, and on derivatives in which specific hydroxyl groups are removed by substitution or reduction,

is needed to settle this question. However, it may be significant that a concentration of 16 N is not very much lower than that at which sulphuric acid becomes a good solvent for cellulose.[39]

*The mechanism whereby inorganic ions influence the magnitude of the anomeric effect.* One may begin by considering whether it could be the A-zone of the bromide ion that diminishes the magnitude of the anomeric effect. To do this, of course, it would have to be fundamentally different from the A-zones of the other anions that have been investigated,[1] and there is no theoretical or experimental basis for introducing such an assumption. It is therefore necessary first to enquire whether the facts can be accounted for within the framework of existing theories.

The second possibility is that it is the B-zone of the bromide ion that decreases $K_\beta/K_\alpha$. The difficulty with this is that it does not explain the temperature-dependence (Figs. 7 and 8, and Table 2). Evidence was obtained in Part I that the water molecules that solvate the ring- and glycosidic-oxygen atoms, and the other oxygen atoms in the same manner, have a lower entropy than they have in the bulk of the solution, at least in dilute sulphuric acid.[1] Extrapolation to infinite dilution implies that this is also true for solutions in pure water. If, therefore, the water molecules in a B-zone have a higher entropy than they have in pure water at the same temperature, then an increase in temperature can only result in the dehydration of the ring- and glycosidic oxygen atoms of any glycoside molecule that is present in the zone.

The third possibility is that it is the A-zone of the hydrogen ions that diminishes the magnitude of the anomeric effect. If this is accepted, the other facts fall into place in a reasonably straightforward manner. Thus, if the A-zone of the hydrogen ions is larger than that of the bromide ions, as the electrostatic theory would predict, increasing concentration of hydrobromic acid should lead to a net increase in the hydration of the two glycosides, stabilising the $\beta$-anomer, and de-stabilising the $\alpha$-anomer (Figs. 5 and 6). As the concentration of acid increases still further, the A-zones should start to break up. That of the bromide ion should break up first, which would diminish $K_\beta/K_\alpha$ still further, but that of the hydrogen ion should finally start to break up also, leading to an increase in $K_\beta/K_\alpha$ (Figs. 4 and 9).

The temperature-dependence of $K_\beta/K_\alpha$ (Fig. 7) can be interpreted by assuming that the troughs represent "melting points" of the A-zone of the bromide ion. Consistently with this, the melting point is lowest when the concentration of acid is highest. The melting points are not sharp, but this would not be expected if there are two or more layers of electrostricted water molecules surrounding the bromide ions. The final increase in $K_\beta/K_\alpha$ could be explained by assuming either that the A-zone of the hydrogen ion has started to melt, or that the B-zone has now become so large that the entropically favourable dehydration of glycoside molecules in this zone has become the dominant process.

Systems exhibiting non-Arrhenian kinetics are, of course, well known. The examples most commonly cited are reactions for which the energy of activation is very small,[40] or in which quantum-mechanical tunneling is possible.[41,42] Reactions which are heterogeneous, in the macroscopic sense, are also cited,[40] and of course there must exist a range of temperatures for which every enzymic

reaction is non-Arrhenian. It might be a useful generalisation to state that non-Arrhenian kinetics can always be expected, whenever one of the components of the system is undergoing a change of state. One can imagine, for example, the likely temperature-dependence of a reaction carried out in a solution containing ice. Another relevant example is the hydrolysis of sucrose in dilute acid, for which the activation energy decreases sharply as the temperature increases from $0°$ to $40°$ (Ref. 43). In this case, it may be supposed that the solvent sheath around the sucrose molecules is melting.

Independent evidence for the idea that the A-zone of the bromide ion is able to melt under the conditions of these experiments can be seen in the negative temperature-dependence of $-H_0$ for hydrobromic acid. The standard entropy-change that is associated with the proton-transfer reaction is positive,[44] so that, if the bromide ion were playing no part, the temperature coefficient of $-H_0$ would be expected to be positive. The fact that it is negative can be readily explained by assuming that the A-zone of the bromide ion melts, leading to an increase in the activity of water, and, hence, to a decrease in the activity of the hydrogen ions.[2]

In a series of experiments to be reported in detail elsewhere, the effect of hydrobromic and sulphuric acids upon the optical rotation of 2,3,4,6-tetra-$O$-methyl-D-glucose has been studied. This derivative was chosen because it cannot form furanoid or septanoid rings. Its optical rotation might therefore be expected to give an approximate measure of the relative amounts of $\alpha$- and $\beta$-pyranoid forms present at equilibrium, and, hence, of the magnitude of the anomeric effect. Possible objections to this assumption will be discussed, but it is an empirical fact that a close parallelism was observed between the results of this static method, and the kinetic one described here.

A final possibility that must be considered is that anions are able to change the magnitude of the anomeric effect by associating directly with the glycoside molecules. This idea implies an equilibrium-controlled association between glycoside molecules and the anions, taking place competitively with water molecules.

In considering the likelihood of this, it must be remembered that, even in 16 N sulphuric acid, the ratio of water molecules to disaccharide molecules (at the used concentration of 2 % w/v) is still about 500:1, and the ratio of water molecules to anions is still more than 5:1. In 6 N hydrobromic acid, the molar ratio of water to disaccharide is 790:1, and the ratio of water molecules to anions is 7.5:1.

It must also be remembered that, for the methyl glucopyranosides, $K_\beta/K_\alpha$ reaches a maximum in 20 N sulphuric acid,[1] so that, for such a mechanism to be operative, it would be necessary to assume that all the glucoside molecules are fully complexed with anions in acid of that concentration. The chromatographic evidence[1] provides no support for this idea, and it is very unlikely that the association constant could be so large, when the mechanism of the association would necessarily be very similar to that whereby water molecules are themselves attracted to the anions.

Finally, it is, of course, impossible to explain both the initial decrease, and also the final increase, in $K_\beta/K_\alpha$ that takes place with increasing concentration of hydrobromic acid, on a basis of direct anion-substrate associa-

tion alone. Considered together, these facts leave little doubt that the observed effects are, at least primarily, hydration phenomena.

*Relationship to solubility phenomena.* As early as 1926, Kruyt and Robinson [45] suggested that, when a polar non-electrolyte orientates water molecules in the same sense as a particular ion, it will be salted-out by that ion, but salted-in by an ion of opposite charge.

In 1931, Meyer and Dunkel [46] classified the alkali-metal halides into "aquo-bases" or "aquo-acids", according to whether the smaller ion was an anion or a cation, respectively. They then sought to explain the solubilities of organic compounds in solutions of these salts by proposing that proton-acceptors, such as pyridine, dioxan and ethyl acetate, should be selectively bound to the solvation shells of cations, while compounds like phenol and carboxylic acids, which were expected to act primarily as proton-donors, should be bound to the solvent shells of anions. Conversely, it was expected that bases would be exluded from the solvent shells of anions, and acids from those of cations. The net effect of any salt was expected to be determined by the smaller ion.

The validity of these early ideas appears to have been challenged, only in the sense that, as an explanation for the solubility of organic compounds in aqueous salt solutions, they are incomplete. Mainly through the work of Mc-Devit and Long,[47] it is now known that a well-defined salting-out order exists even for non-polar compounds like benzene, that it is connected with the changes in volume that occur when a salt is added to water, and that the mechanism consists in a physical "squeezing-out" of the organic solute, as the water molecules become selectively compressed in the domains of the anions and cations. Non-polar compounds can also be salted-in, most notably by large, organic ions, the mechanism being, almost certainly, direct ion-solute interaction.[48]

For polar non-electrolytes, very different salting-out orders have been noted, and salting-in is commonly brought about by simple, inorganic salts.[48] In a comprehensive review,[48] Long and McDevit have discussed these phenomena, with the fairly clear conclusion that, at least for weak organic acids and bases of low dielectric constant, the reversals in the salting-out order for non-polar compounds that are observed can best be explained by the water-orientation hypothesis of Kruyt and Robinson [45] and Meyer and Dunkel.[46]

The present study of the anomeric effect is not concerned with solubility as such, and it will be recognised that the working hypothesis advanced here consists essentially in the re-application of the ideas of Meyer and Dunkel to a system which is uncomplicated by other considerations. In seeking to confirm that hydrobromic acid enhances direct hydration of a glycoside, by having recourse to measurements of solubility, these complications are re-introduced.

The interpretation of the data obtained for the cloud-point of methyl cellulose (Figs. 10 – 14) is fortunately simplified by the evidence [47,48] that $H^+$, $Li^+$, $Na^+$, $K^+$, $Br^-$, and $I^-$ do not normally salt-in non-polar compounds. The salting-in of methyl cellulose that is brought about by HBr (Fig. 10), by LiBr and LiI (Fig. 11), and by NaI and KI (Fig. 12) is therefore difficult to explain, unless it is assumed that direct hydration is being enhanced. Moreover, the data in Figs. 13 and 14, and in Table 3, indicate that it is mainly the methoxyl groups that are being hydrated. This is consistent with the idea

that the hydration is being brought about by the cations, and that the bromide ion is sufficiently large to "allow" both $H^+$ and $Li^+$ to be the dominant electrostrictor, while the iodide ion is large enough to allow even $Na^+$ and $K^+$ to be the dominant species.

It is tempting to interpret the instances of salting-out in Figs. 10 – 13, also in terms of the water-orientation hypothesis, but a useful warning is provided by the data in Fig. 13. Here it is seen that NaOH salts-out more effectively than KOH. This is contrary to the water-orientation hypothesis, but consistent with the solvent-compression hypothesis of McDevit and Long.[47] This makes it clear that, even for a highly oxygenated molecule like methyl cellulose, the effects described by McDevit and Long are still operative, and that all the data in Figs. 10 – 13 must be regarded as a manifestation of the two effects operating simultaneously.

## REFERENCES

1. Painter, T. *Acta Chem. Scand.* **27** (1973) 2463.
2. Rochester, C. H. *Acidity Functions*, Academic, London and New York 1970, p. 58.
3. Angyal, S. J. In *Conformational Analysis*, Interscience, New York, London and Sydney 1965, p. 375.
4. Lemieux, R. U. In De Mayo, P., Ed., *Molecular Rearrangements*, Interscience, New York, London and Sydney 1964, Vol. 2, p. 735.
5. Stoddart, J. F. In *Stereochemistry of Carbohydrates*, Wiley-Interscience, New York, London, Sydney and Toronto 1971, p. 72.
6. Bishop, C. T. and Cooper, F. P. *Can. J. Chem.* **41** (1963) 2742.
7. Anderson, C. B. and Sepp, D. T. *Chem. Ind. (London)* **1964** 2054.
8. Anderson, C. B. and Sepp, D. T. *Tetrahedron* **24** (1968) 1707.
9. Eliel, E. L. and Giza, C. A. *J. Org. Chem.* **33** (1968) 3754.
10. Anderson, C. B. and Sepp, D. T. *J. Org. Chem.* **32** (1967) 607.
11. Durette, P. L. and Horton, D. *Chem. Commun.* **1970** 1608.
12. Lemieux, R. U. and Pavia, A. A. *Can. J. Chem.* **46** (1968) 1453.
13. Lemieux, R. U., Pavia, A. A., Martin, J. C. and Watanabe, K. A. *Can. J. Chem.* **47** (1969) 4427.
14. Lemieux, R. U. and Pavia, A. A. *Can. J. Chem.* **47** (1969) 4441.
15. Edward, J. T. *Chem. Ind. (London)* **1955** 1102.
16. Eliel, E. L., Allinger, N. L., Angyal, S. J. and Morrison, G. A. *Conformational Analysis*, Interscience, New York, London and Sydney 1965, p. 436.
17. BeMiller, J. N. and Doyle, E. R. *Carbohyd. Res.* **20** (1971) 23.
18. BeMiller, J. N. *Advan. Carbohyd. Chem.* **22** (1967) 25.
19. Overend, W. G., Rees, C. W. and Sequeira, J. S. *J. Chem. Soc.* **1962** 3429.
20. Wolfrom, M. L., Thompson, A. and Timberlake, C. E. *Cereal Chem.* **40** (1963) 82.
21. Smidsrød, O., Haug, A. and Larsen, B. *Acta Chem. Scand.* **20** (1966) 1026.
22. Smidsrød, O., Larsen, B., Painter, T. and Haug, A. *Acta Chem. Scand.* **23** (1969) 1573.
23. Hermans, P. H. *Physics and Chemistry of Cellulose Fibers*, Elsevier, New York 1949.
24. Bernal, J. D. and Fowler, R. H. *J. Chem. Phys.* **1** (1933) 515.
25. Eisenberg, D. and Kauzmann, W. *The Structure and Properties of Water*, Oxford University Press, Oxford 1969.
26. Frank, H. S. *Science* **169** (1970) 633.
27. Blandamer, M. J. *Quart. Rev. Chem. Soc.* **24** (1970) 169.
28. Conway, B. E. and Bockris, J. O. In Bockris, J. O., Ed., *Modern Aspects of Electrochemistry*, Butterworths, London 1954, p. 47.

29. Frank, H. S. and Wen, W.-Y. *Discussions Faraday Soc.* **24** (1957) 133.
30. Hertz, H. G. and Zeidler, M. D. *Ber. Bunsengesellschaft Phys. Chem.* **67** (1963) 774.
31. Friedman, H. L. *J. Chem. Phys.* **32** (1960) 1351.
32. Zucker, L. and Hammett, L. P. *J. Am. Chem. Soc.* **61** (1939) 2791.
33. Croon, I. and Manley, R. St. J. *Methods Carbohyd. Chem.* **3** (1963) 287.
34. Klotz, I. M. *Federation Proc.* **24** (1965) S24.
35. Ciferri, A. and Orofino, T. A. *J. Phys. Chem.* **70** (1966) 3277.
36. Patterson, D. *Macromolecules* **2** (1969) 672.
37. Frank, H. S. and Evans, M. W. *J. Chem. Phys.* **13** (1945) 507.
38. Von Hippel, P. H. and Schleich, T. In Timasheff, S. N. and Fasman, G. D., Eds., *Structure and Stability of Biological Macromolecules*, Biological Macromolecules Series, Marcel Dekker, Inc., New York 1969, Vol. 2, p. 417.
39. Jayme, G. and Lang, F. See Ref. 33, p. 75.
40. Frost, A. A. and Pearson, R. G. *Kinetics and Mechanism*, Wiley, New York 1953.
41. Wayne, R. P. In Bamford, C. H. and Tipper, C. F. H., Eds., *Comprehensive Chemical Kinetics*, Elsevier, Amsterdam, London and New York 1969, Vol. 2, pp. 208, 249.
42. Laidler, K. J. *Theories of Chemical Reaction Rates*, McGraw, New York, St. Louis, San Francisco, London, Sydney, Toronto, Mexico and Panama 1969, p. 59.
43. Moelwyn-Hughes, E. A. *The Kinetics of Reactions in Solution*, Oxford University Press, London 1947, p. 57.
44. Conway, B. E. In Bockris, J. O. and Conway, B. E., Eds., *Modern Aspects of Electrochemistry*, Butterworths, London 1964, Vol. 3, p. 43.
45. Kruyt, H. R. and Robinson, C. *Proc. Acad. Sci. Amsterdam* **29** (1926) 1244.
46. Meyer, K. H. and Dunkel, M. *Z. physik. Chem.* (Bodenstein Festband) (1931) 553.
47. McDevit, W. F. and Long, F. A. *J. Am. Chem. Soc.* **74** (1952) 1773.
48. Long, F. A. and McDevit, W. F. *Chem. Rev.* **51** (1952) 119.

# Canaline

## Characterization of Enzyme-Pyridoxal Phosphate Complex

E.-L. RAHIALA

*Finnish Red Cross Blood Transfusion Service, Helsinki, Finland*

A method of preparation of canaline is described. Canavanine, isolated from Jack bean meal, is enzymatically hydrolyzed with commercial arginase, chromatographed on an cation exchange resin and prepared saltfree. The yield from canavanine obtained suggests losses during the preparation not in excess of approximately 10 % of that expected.

The mode of canaline inhibition of the ornithine ketoacid aminotransferase reaction was studied (a) by analyzing spectrophotometrically the complex formed between canaline and pyridoxal phosphate, the coenzyme of this transamination, and (b) by characterization of the inhibition under various conditions. The results suggest the formation of a covalent bond between canaline and pyridoxal phosphate, stable within a wide range of ionic strenght and temperature, but unstable at high pH. Competitive inhibition of the transamination was demonstrated when the ornithine concentration of the assay medium was the variable factor and uncompetitive when $\alpha$-ketoglutarate concentration was varied. This finding is in accord with the concept that the formation of an oxime-type compund with pyridoxal phosphate is the mechanism of canaline-induced inhibition of transamination.

Canaline, $\alpha$-amino-$\gamma$-aminooxybutyrate, an analogue of ornithine inhibits ornithine-$\alpha$-ketoglutarate transamination. In addition, a chemical homologue of canaline canavanine ($\alpha$-amino-$\gamma$-guanidinooxybutyrate) has been shown to competitively inhibit a number of reactions of arginine, a homologue of ornithine. Ornithine is involved in a number of enzymic reactions, some of which are inhibited by canaline;[1,2] and of these which are inhibited all require pyridoxal phosphate as coenzyme.[2] Other reactions catalyzed by pyridoxal enzymes are also inhibited by canaline.[2] In addition it has been demonstrated that canaline alters the specific adsorption maximum of pyridoxal phosphate in a manner suggestive of a chemical reaction between the two molecules.[2] Thus we suggested that the effect of canaline in the reactions involving ornithine may be due to a monovalent non-catalyzed reaction between canaline

and pyridoxal phosphate, possibly *via* the formation of an oxime, rather than to the structural similarity of ornithine and canaline.

This study describes the purification of canaline, characterizes the canaline-pyridoxal phosphate complex and the kinetics of the canaline-induced inhibition of transaimination. Due to the strong and irreversible inhibition of ornithine-α-ketoglutarate transamination by canaline,[2] and to the detailed knowledge of its kinetic proporties,[3-5] this enzyme, ornithine ketoacid aminotransferase (OKT) (EC 2.6.1.13), was chosen as a model for the inhibition studies.

## MATERIALS AND METHODS

*Ornithine ketoacid aminotransferase (OKT)*. OKT was partially purified from rat liver according to Peraino *et al.*[5] Comparison of the specific enzymic activity of the final preparation with that of the crude homogenate indicated a 600-fold purification.

*Enzyme assay.* OKT-activity was measured with *o*-aminobenzaldehyde as described by Matsuzawa *et al.*[6]

*Preparation of canaline from Jack bean seeds.* A 200 g portion of finely ground Jack bean seeds was defatted with petroleum ether and extracted with 50 % ethanol.[7] Canavanine was precipitated from the extract with absolute ethanol at 4°C and the precipitate was redissolved in water. The resulting solution was deproteinized by the addition of a saturated solution of lead acetate in water. Excess lead ions in the supernatant fluid were precipitated as the sulphate by the addition of 5 M $H_2SO_4$ to a final pH of 3.0.

The supernatant fluid, rich in canavanine but containing amino acid impurities, was purified from the neutral amino acids by a cation exchange resin (Dowex 50 × 8, $NH_4^+$-form) according to Thompson *et al.*[8] Preliminary experiments indicated that canavanine, like the other dibasic amino acids, was eluted quantitatively from the column with 4 M $NH_4OH$.[8] The eluate containing approximately 4 g of canavanine, was evaporated *in vacuo* at ambient temperature. The yellow residue was dissolved in a 0.1 M phosphate buffer pH 7.8, the solution heated to 100°C, and covered with a layer of liquid paraffin. Fifty mg of arginase (Sigma Chemical Corporation, St. Louis, Mo., USA) was added and hydrolysis of canavanine to canaline and urea was carried out at 42°C. The reaction was followed by serial determinations of urea concentration[9] in aliquots of the incubation system at 6 h intervals. The incubation was discontinued after the urea concentration had reached a maximum.[10] Dissolved canaline was dialyzed from the incubation mixture, concentrated *in vacuo*, and chromatographed on Dowex 50 × 8 ($Na^+$-form).[11] All of the canaline-containing fractions, identified with high voltage electrophoresis and ninhydrin staining, were then purified from acid and neutral impurities with cation exchange resin (Dowex 50 × 8, $NH_4^+$-form),[8] reprecipitated with ethanol, dried *in vacuo* and weighed. The purity of the preparate was tested using a small lot of canaline purchased from Sigma as a reference standard.

*Characterization of the pyridoxal phosphate-canaline complex.* The absorption spectrum of an equimolar solution of canaline and pyridoxal phosphate was analyzed between 700 nm and 300 nm with a Coleman 124 spectrophotometer. The effect of varying pH on the complex was tested in 0.1 M phosphate buffer in the pH range of 6.0 to 7.5 and in 0.1 M tris-HCl buffer in the pH range of 7.5 to 9.0. The stability of the complex was also examinated in tris-HCl buffer at pH 8.0 with a concentration from $1 \times 10^{-3}$ M to 2 M. The effect of temperature on the complex was studied at pH 8.0 using 0.1 M tris-HCl buffer and temperatures from 20 to 60°C.

*Analysis of the inhibition of OKT by canaline.* The inhibition of canaline in transamination of ornithine was estimated according to the graphic method of Lineweaver and Burk by varying the concentration of canaline in the reaction mixture from 0 to $2.5 \times 10^{-6}$ M. In these experiments, the concentrations of ornithine and α-ketoglutarate were $1 \times 10^{-4}$ M. When examining the type of canaline inhibition, the concentration of ornithine and α-ketoglutarate was varied from 0 to $5 \times 10^{-3}$ M.

*Characterization of the OKT-pyridoxal phosphate-canaline complex.* The stability of the enzyme-inhibitor complex was tested under similar conditions to those used for the

pyridoxal phosphate-canaline complex. In these studies the concentration of canaline selected was that which resulted in a 50 % inhibition of OKT in optimal enzyme assay conditions (at pH 8.0, in 0.1 M tris-HCl buffer concentration and at 37°C).

## RESULTS

*The yield and characteristics of the purified canaline.* Based on the amount of urea produced by the arginase reaction, the content of canavanine in Jack bean meal was 1.8 % (w/w). This agrees well with earlier findings.[12],[13] The final canaline yield was 2.5 g, which indicates that about 10 % of canaline produced by the arginase reaction was lost during the purification procedures.

The final purity of the product was studied with ascending paper chromatography using three different solvent systems and with high voltage electrophoresis at two different pH's. When butanol − glacial acetic acid − water (120:30:50) was used as the solvent, the $R_F$ value of canaline was 0.11; using butanol − glacial acetic acid − pyridine − water (120:30:30:60) the $R_F$ value was 0.20; and using propanol − NH$_4$OH − water (70:10:20) the $R_F$ value was 0.53. With high voltage electrophoresis (50 V/cm) at pH 3.4 the $R_F$ value was 11.8 (the $R_F$ value of glutamine is chosen as 1.0) and at pH 2.1 the $R_F$ value was 2.2. All of these systems contained only one ninhydrin positive spot which had a mobility identical to that of the Sigma canaline standard.

*Stability of the pyridoxal phosphate-canaline complex.* In agreement with earlier studies,[5] pyridoxal phosphate exhibited an absorption maximum at 420 nm at pH ≥ 7.0. At lower pH's the maximum shifted to 390 nm. Interaction with canaline obliterates both of the maxima. When the pH was raised up to 9.0 an absorption peak reappeared at 420 nm (Fig. 1). Neither the ionic strength nor the temperature of the buffer affected the absorption spectrum of the complex within the limits tested (Fig. 1). Canaline alone did not have any absorption maxima between 300 nm and 700 nm.
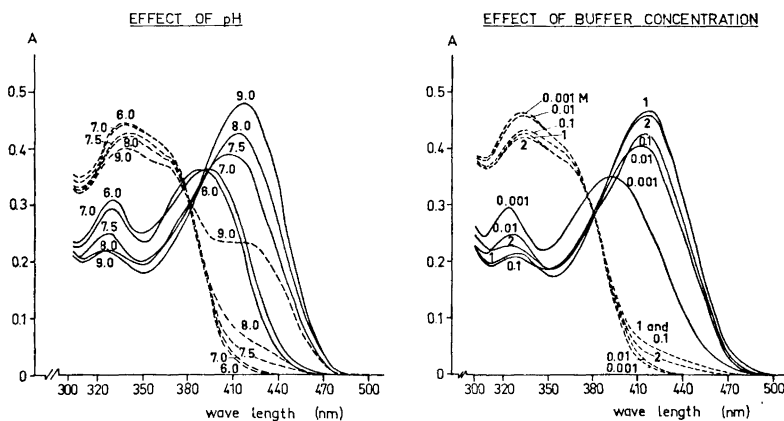


*Fig. 1.* The absorption spectra of pyridoxal phosphate and pyridoxal phosphate-canaline complex: left, at different pH's; right, at different buffer concentrations. ———— pyridoxal phosphate. − − − pyridoxal phosphate-canaline complex.
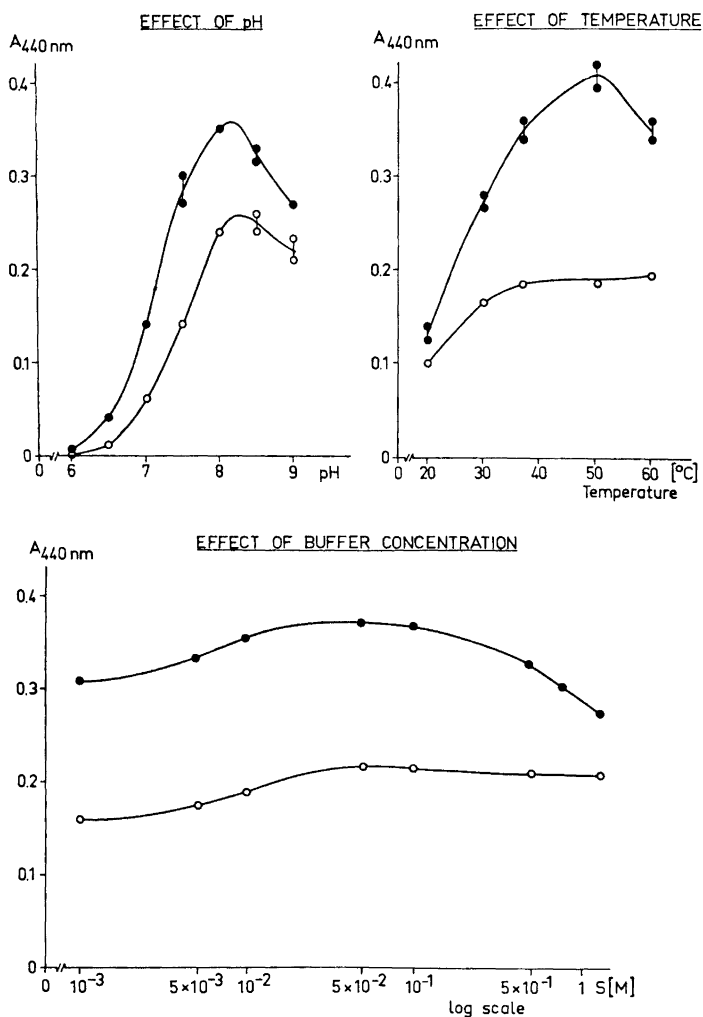
*Fig. 2.* The effect of pH, temperature, and buffer concentration on the stability of the OKT-canaline complex. The concentration of canaline used was $1.9 \times 10^{-7}$ M.

*Stability of the OKT-pyridoxal phosphate-canaline complex.* The addition of canaline did not change the pH-, temperature- or buffer concentration optima of OKT (Fig. 2). The canaline inhibition was strongest at optimal OKT-assay conditions.

*Inhibition of OKT by canaline.* The inhibition constant $(K_i)$ for canaline is between $1 - 2 \times 10^{-7}$ M (Fig. 3). The inhibition of ornithine $\alpha$-ketoglutarate transamination was competitive when the concentration of ornithine was varied and uncompetitive when varying $\alpha$-ketoglutarate (Fig. 4).
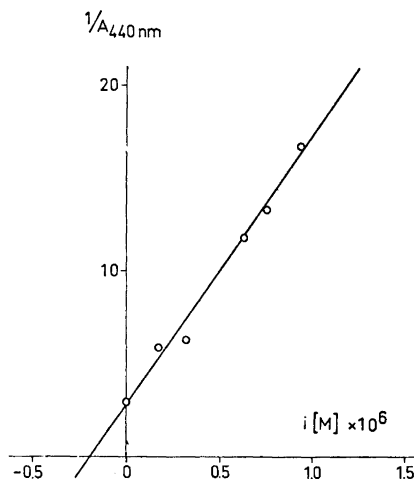
*Fig. 3.* The inhibition with canaline (i) under optimal ornithine ketoacid aminotransferase assay conditions (see text for details).

## DISCUSSION

The results of this study suggest that the canaline induced inhibition of OKT may result from covalent binding of canaline to the pyridoxal phosphate cofactor. The addition of canaline obliterates the typical absorption maximum of pyridoxal phosphate at 390 nm (pH $\leq$ 7.0) or at 420 nm (pH $\geq$ 7.0) between pH 6.0 and 8.5. The complex is not stable at pH 9.0, which reflects dissociation of the pyridoxal phosphate-canaline complex in alkaline medium. Altering the concentration of the buffer between $1 \times 10^{-3}$ M and 2 M or the incubation temperature between 20 and 60°C provided no evidence for any dissociation of the complex. The OKT-canaline complex was also stable at pH $\leq$ 8.5, and the per cent OKT inhibition due to canaline did not change between pH 6.0 and 8.5, but at pH > 8.5 the per cent inhibition was less, perhaps a result of the dissociation of the enzyme-inhibitor complex. In 1 M buffer the per cent inhibition was also less than at concentrations between $1 \times 10^{-3}$ M and 1 M. The incubation temperature had no effect on the per cent inhibition. According to earlier studies [2] the activity of OKT could not be restored by additional pyridoxal phosphate. This was interpreted as evidence for both the stability of the pyridoxal phosphate-canaline complex, and the irreversibility of the binding between OKT and pyridoxal phosphate, in clear contrast to that of pyridoxal phosphate and other apoenzymes. These results are consistent with our earlier findings.

OKT was inhibited irreversibly by canaline with an inhibition constant ($K_i$) between $1 - 2 \times 10^{-7}$ M.* Complete inhibition of this transamination was found in the presence of $1 \times 10^{-6}$ M canaline, using a highly purified enzyme preparation.[3] With crude liver homogenate $3 \times 10^{-6}$ M canaline resulted in a 50 % inhibition,[2] indicating canaline binding by the homogenate in addition to

---

* Because of a very complicated inhibition kinetics in this enzyme system, only an approximate value of the inhibition constant can be given.
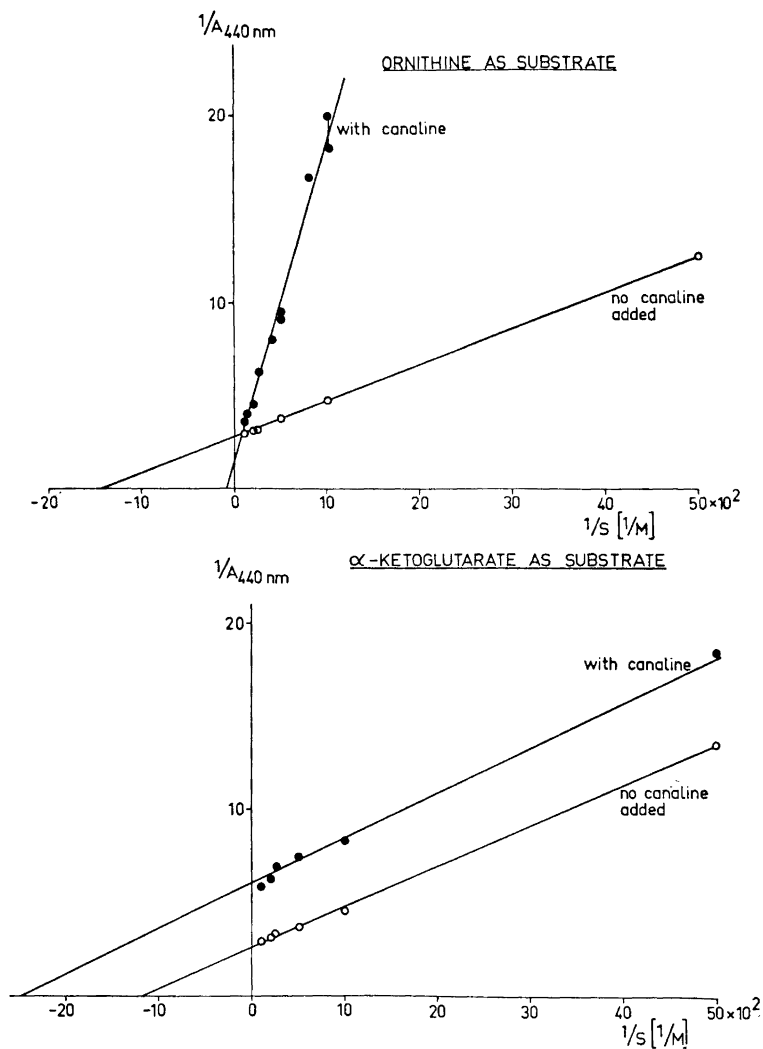
*Fig. 4.* Estimation of the type of canaline inhibition: upper, the concentration of ornithine was varied; and lower, the concentration of α-ketoglutarate was varied. The concentration of canaline in the assay system was $1.9 \times 10^{-7}$ M.

OKT. The graphic analysis of the kinetic of canaline-induced inhibition of OKT, using varying concentrations of either ornithine or α-ketoglutarate, demonstrates different patterns of inhibition (Fig. 4). When the concentration of ornithine was varied the inhibition was competitive, whereas it was uncompetitive when varying the concentration of α-ketoglutarate. This result is consistent with the earlier hypothesis that the inhibitory action of canaline is based on the formation of an oxime with the aldehyde group of pyridoxal

phosphate.[2] Similar to the action of other aminooxy compounds [2,14,15] canaline combines with the same enzyme form as ornithine during transamination, thus acting as a dead-end inhibitor for OKT. In contrast, $\alpha$-ketoglutarate reacts with the enzyme when the prosthetic group, pyridoxal phosphate, is in the aminoform $(-C-NH_2)$. Therefore $\alpha$-ketoglutarate does not compete with canaline, and the resulting inhibition is uncompetitive in type.[16] These results can be interpreted to indicate the formation of an oxime in the reaction between canaline and pyridoxal phosphate, the chemical basis of inhibition of the pyridoxal phosphate dependent enzymes by canaline.

## REFERENCES

1. Kekomäki, M., Rahiala, E.-L. and Räihä, N. C. R. *Ann. Med. Exp. Biol. Fenn.* **47** (1969) 33.
2. Rahiala, E.-L., Kekomäki, M., Jänne, J., Raina, A. and Räihä, N. C. R. *Biochim. Biophys. Acta* **227** (1971) 337.
3. Katunuma, N., Okada, M., Matsuzawa, T. and Otsuka, Y. *J. Biochem. (Tokyo)* **57** (1965) 445.
4. Katunuma, N., Matsuda, Y. and Tomino, I. *J. Biochem. (Tokyo)* **56** (1964) 449.
5. Peraino, C., Bunville, L. G. and Tahmisian, N. *J. Biol. Chem.* **244** (1969) 2241.
6. Matsuzawa, T., Katsunuma, T. and Katunuma, N. *Biochem. Biophys. Res. Commun.* **32** (1968) 161.
7. Damodaran, M. and Narayana, K. G. A. *Biochem. J.* **33** (1939) 1740.
8. Thompson, J. P., Morris, C. J. and Gering, R. K. *Anal. Chem.* **131** (1959) 1028.
9. Searcy, R. L., Gough, G. S., Korotzer, J. L. and Bergquist, L. M. *Amer. J. Med. Technol.* **27** (1961) 255.
10. Greenberg, D. M. In Boyer, P. D., Lardy, H. and Myrbäck, K., Eds., *The Enzymes* Academic, New York 1960. Vol. 4, p. 257.
11. Moore, S. and Stein, W. H. *J. Biol. Chem.* **192** (1951) 663.
12. Miersch, J. *Naturwiss.* **54** (1967) 169.
13. Rindeknecht, H. *Nature* **186** (1960) 1047.
14. DaVanzo, J. P., Matthews, R. J., Young, G. A. and Wingerson, F. *Toxicol. Appl. Pharmacol.* **6** (1964) 396.
15. Persinkin, E. N. and DaVanzo, J. P. *Biochem. Pharmacol.* **17** (1968) 2498.
16. Plowman, K. M. *Enzyme Kinetics*, McGraw, New York 1972, p. 56.

# Tris(hydroxymethyl)aminomethane Buffer and
# Amino Acid Analysis

GREGORY C. GIBBONS, STEFFEN STRØBÆK and
ERLING AA. GEERTSEN

*Institute of Biochemical Genetics and Institute of Genetics, The University of Copenhagen,
Øster Farimagsgade 2 A, DK-1353 Copenhagen K, Denmark*

Amino acid analysis of 14 commercially obtained lots of tris(hydroxymethyl)aminomethane buffer (TRIS) has revealed the presence of either one or two ninhydrin-positive components which chromatograph in the region of the basic amino acids.

The major TRIS component, found in all grades of the buffer tested here, is stable to acid hydrolysis and obeys Beer's Law in the concentration range of 1 to 100 mM.

Tris(hydroxymethyl)aminomethane (2-amino-2-hydroxymethyl-1,3-propane-diol; $(HOCH_2)_3CNH_2$; commonly designated as TRIS) is a widely used buffer for *in vitro* biochemical and biological investigations. TRIS has the disadvantage however, that by virtue of its primary amino group, it interferes with the most commonly used protein assays:[1-2] the Folin-Lowry,[3] the Biuret,[4-6] and the Kjeldahl.[4] In practice this interference can be minimised by choice of suitable blanks and standards,[4-5] by removal of TRIS by dialysis[3] or, by precipitation of the protein, washing to remove TRIS, and analysis of the separated precipitate.[7]

In the course of recent experiments we observed that with proteins dissolved in TRIS buffer, amino acid analysis was complicated by the appearance of either one or two ninhydrin-positive peaks which eluted in the region of the basic amino acids. It was possible to eliminate these TRIS peaks by either dialysis of the protein solution against a non-TRIS containing buffer, or by precipitation of the protein and washing prior to acid hydrolysis. We chose however, to retain the buffer, and investigate more closely the chromatographic properties of TRIS.

## MATERIALS

Tris (hydroxymethyl) aminomethane was obtained from the following sources:
1. Sigma Chemical Co., Missouri, U.S.A. "Sigma 7 – 9" lot 68B – 5220; lot 70B – 5630; lot 96B – 5280; lot 127B – 5110; lot 31C – 5230; lot 71C – 5220; lot 121C – 5140. "Trizma" lot 90C – 5400; lot 121C – 5430.

2. Merck, Darmstadt, Germany. Tris(hydroxymethyl)aminomethane Art. 8382 lot 2481999; Art. 8365 lot 2612546.

3. British Drug Houses, Poole, England, Tris(hydroxymethyl)methylamine Lab. Reagent 27119 lot 1205080; Analar 10315 lot 1261560; Aristar 45205 lot 1402350.

Standard amino acid mixture was obtained from Bio-Cal Instruments, Gräfelfing, Germany.

## METHODS

### Acid hydrolysis

Acid hydrolysis was carried out under a vacuum of 0.1 mmHg in 6 N redistilled hydrochloric acid at 110°C for 20, 24, 48, or 72 h.

### Amino acid analysis

*1. Bio-Cal single column system.* A model BC-201 Bio-Cal amino acid analyser was used under the following conditions: Bio-Rad Aminex A-6 resin (15.5 − 19.5 μm); column 0.9 × 54 cm; flow-rate 80 ml/h buffer, 20 ml/h ninhydrin; buffers: A 0.2 N Na citrate, pH 3.25; B 0.2 N Na citrate, pH 4.25; C 0.2 N Na citrate, 1.0 N NaCl, pH 6.50; buffer changes A to B 59 min, B to C 99 min, C to NaOH 207 min; temperature 58°C.

*2. Durrum system.* A Durrum model D-500 amino acid analyser was used under the following conditions: Durrum resin (8 ± 2 μm, 8 % crosslinkage); column 0.175 × 50 cm; flow-rate 10 ml/h buffer, 5 ml/h ninhydrin; buffers: A 0.2 N Na citrate, pH 3.25; B 0.2 N Na citrate, pH 4.25; C 0.4 N Na citrate, 0.7 N NaCl, pH 7.9; buffer changes A to B 25 min 30 sec, B to C 44 min 30 sec, C to NaOH 76 min; temperature 0 to 35 min 36 sec 52°C, 35 min 36 sec to 76 min 75°C.

*3. Bio-Cal short basic column system.* A model BC-201 Bio-Cal amino acid analyser was used as follows: Bio-Rad Aminex A-5 resin (11.5 − 15.5 μm); column 0.9 × 15 cm; flow-rate 80 ml/h buffer, 20 ml/h ninhydrin; buffer D 0.35 N Na citrate, pH 5.28; temperature 58°C.

### Ninhydrin reaction

*1. Manual reaction.* The manual ninhydrin method was similar to that of Moore and Stein [8] with some minor modifications. The ninhydrin solution was identical to that used in the Bio-Cal BC-201 analyser and contained per liter: Recrystallized ninhydrin 20 g, SnCl$_2$ anhydrous 0.336 g, methyl cellosolve 750 ml, 4 N K/Na acetate buffer (3 N K acetate, 1 N Na acetate, 3H$_2$O, 12 mM K citrate, pH 5.13) 250 ml.

All samples were adjusted to pH 6 and 2 ml aliquots containing 2 μmol of amino acid or 1000 μmol of TRIS were added to 1 ml of ninhydrin solution. The samples were mixed for 30 sec on a Whirlmixer and after sealing with aluminium foil, heated in a boiling water bath for 10 min. After cooling for 10 min the samples were diluted 15 times in 1:1 ethanol/water and spectra measured within 30 min in a Cary model 17 spectrophotometer. Blank samples contained water in the place of amino acids and were otherwise treated as above.

When the reaction was carried out under nitrogen both the samples and ninhydrin solution were extensively washed in dry nitrogen and the heating carried out in sealed ampoules under nitrogen.

*2. Bio-Cal BC-201.* The ninhydrin solution was that described above for the manual method. The sample/ninhydrin ratio used in the BC-201 was 2:1 and the absorbance was measured at 570 and 440 nm after 8 min heating at 100°C in a closed system.

*3. Durrum D-500.* The ninhydrin solution used was Nin-Sol obtained commercially from Pierce Chemical Company, (Rockford, Illinois) and contained per liter: 20 g ninhydrin, 0.625 g hydrindantin, 2H$_2$O, 250 ml 4 M Li acetate buffer, pH 5.2, and 750 ml dimethyl sulphoxide. Reaction conditions in the Durrum were 2:1 sample/ninhydrin ratio, heating for 1.5 min at 125°C, absorbance measured at 590 nm.

## RESULTS

TRIS buffer from all of the sources here tested showed a major peak which chromatographically behaved as a basic amino acid (Fig. 1). On the one column system of the Bio-Cal BC-201 the major TRIS peak appeared between phenyl-
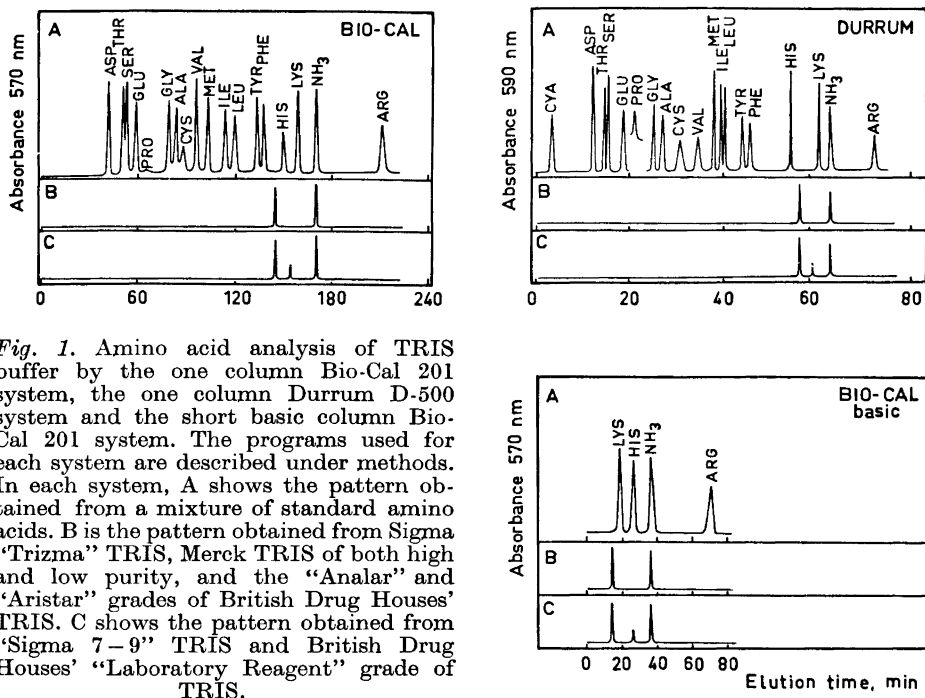


Fig. 1. Amino acid analysis of TRIS buffer by the one column Bio-Cal 201 system, the one column Durrum D-500 system and the short basic column Bio-Cal 201 system. The programs used for each system are described under methods. In each system, A shows the pattern obtained from a mixture of standard amino acids. B is the pattern obtained from Sigma "Trizma" TRIS, Merck TRIS of both high and low purity, and the "Analar" and "Aristar" grades of British Drug Houses' TRIS. C shows the pattern obtained from "Sigma 7 − 9" TRIS and British Drug Houses' "Laboratory Reagent" grade of TRIS.

alanine and histidine. In the one column high-speed Durrum D-500 system the major TRIS peak appeared between histidine and lysine. On the short basic column of the Bio-Cal BC-201 a system similar to the second column of the Beckman 120 C system, the major TRIS peak ran off slightly before lysine.

In samples of TRIS of lower purity ("Sigma 7 − 9" and BDH laboratory reagent) a minor peak was seen which occurred between histidine and lysine on the one column Bio-Cal system, between the major TRIS peak and lysine on the Durrum D-500, and together with histidine on the basic Bio-Cal column (Fig. 1). The magnitude of this minor peak varied from 10 % to 32 % of the area under the major peak. It was noted, however, that the absolute area under the major peak was constant in all cases where the minor peak was observed. The major TRIS peak is characterized by its high 440 nm absorbance in relation to the absorbance at 570 nm (Fig. 2). The spectrum of the major TRIS ninhydrin product, as determined after a manual ninhydrin reaction is qualitatively and quantitatively different from that of leucine, valine, or proline. The magnitude of the TRIS/ninhydrin absorbance at 570 nm is greatly affected
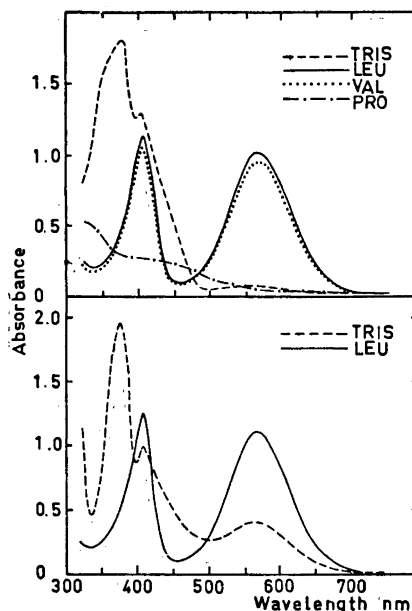
Fig. 2. Visible spectra of the manual ninhydrin reaction products of TRIS (500 mM), leucine (1 mM), valine (1 mM) and proline (1 mM). The manual ninhydrin reaction was carried out as described under methods. Upper half — heating carried out in air; Lower half — heating carried out under oxygen-free nitrogen.

by the presence of oxygen in the system. The bottom half of Fig. 2 shows the increase in absorbance at 570 nm as a result of carrying out the manual nin-hydrin reaction in sealed ampoules under nitrogen. The colour yield of the major TRIS peak in the red region of the spectrum is therefore variable depending upon the exact reaction conditions used while remaining constant for any one set of conditions (Table 1).

The area under the major TRIS peak is linearly dependent on the con-centration of TRIS in the range of 1 to 100 $\mu$mol/ml. Varying amounts of pro-

Table 1. Colour yield of TRIS.

| Method | Colour yield Leucine equiv. | |
|---|---|---|
| Manual ninhydrin | 0.0001 | $\pm 3 \%$ |
| Manual ninhydrin under N$_2$ | 0.0007 | $\pm 3 \%$ |
| Bio-Cal 201 | 0.0013 | $\pm 2 \%$ |
| Durrum D-500 | 0.0039 | $\pm 3 \%$ |

The colour yield of Sigma "Trizma" lot 90C—5400 was measured after manual ninhydrin determination as described in Fig. 2. The colour yield on the Bio-Cal BC-201 of the same lot of "Trizma" TRIS was determined after amino acid analysis of a mixture containing 25 nmol of leucine and 50 $\mu$mol of TRIS. On the Durrum D-500 the colour yield was determined with a mixture containing 2.5 nmol of leucine and 200 nmol of the same lot of TRIS as above.

tein do not influence this relationship. TRIS is not significantly affected by acid hydrolysis for times up to 72 h, the differences observed over 72 h being within the limits of error of the amino acid analyser.

## DISCUSSION

TRIS buffer and ninhydrin react in a manner which bears some similarities to the reaction between α-amino acids and ninhydrin. The TRIS/ninhydrin reaction mechanism appears, however, different, as evidenced by the low colour yield and the visible spectrum of the reaction product(s). The colour yield of the reaction at 570 nm is constant for one set of reaction conditions but variable between different reaction conditions. The absorbance of the TRIS/ninhydrin product(s) at 570 nm obeys Beer's Law in the concentration range of 1 to 100 $\mu$mol/ml (1 − 100 mM) under any one set of conditions.

TRIS yields either one or two ninhydrin-positive peaks on amino acid analysis. The major peak is present in all the grades of TRIS examined in the course of this work, whilst a minor peak was observed in TRIS grades of lower purity. Both the major and the minor TRIS peaks chromatographed together with the basic amino acids on the three column systems tested here. In both the higher and lower purity TRIS grades the elution position and magnitude of the major TRIS peak was not significantly affected by hydrolysis in 6 N hydrochloric acid for periods up to 72 h.

It can thus be noted that if TRIS is suspected as a contaminant during amino acid analysis the major TRIS peak can be immediately identified by its position and in the case of analysers equipped with 440 nm optics, by the high relative absorbance of the TRIS peak at this wavelength. If it is not possible or desired to remove TRIS from samples before acid hydrolysis, it is therefore suggested that grades of TRIS which are free from the minor component are used to simplify the interpretation of resulting chromatograms.

## REFERENCES

1. Layne, E. *Methods Enzymol.* **3** (1957) 447.
2. Jacobs, S. *Methods Biochem. Anal.* **13** (1965) 241.
3. Gellert, M. F., von Hippel, P. H., Schachman, H. K. and Morales, M. F. *J. Am. Chem. Soc.* **81** (1959) 1384.
4. Robson, R. M., Goll, D. E. and Temple, M. J. *Anal. Biochem.* **24** (1968) 339.
5. Stewart, L. E., Thomas, J. W. and Hull, G. E. *Anal. Chim. Acta* **44** (1969) 453.
6. Munro, H. N. and Fleck, A. In Munro, H. N., Ed., *Mammalian Protein Metabolism*, Academic, New York 1969, Vol. III, p. 542.
7. Robinson, H. W. and Hogden, C. G. *J. Biol. Chem.* **135** (1940) 707.
8. Moore, S. and Stein, W. H. *J. Biol. Chem.* **176** (1948) 367.

# Complex Dibenzofurans

## XIV.* An Investigation of the Acid-catalysed Demethylation and Dehydration of Some Tetramethoxyterphenyls

BRIAN G. PRING

*Research and Development Laboratories, Astra Läkemedel AB, S-151 85 Södertälje, Sweden*

The reactions of 2,4′,6′,2″-tetramethoxy-*m*-terphenyl (I), 2,2′,5′,2″-tetramethoxy-*p*-terphenyl (II), and 2,2′,3′,2″-tetramethoxy-*p*-terphenyl (III) with refluxing hydrobromic acid have been investigated. All three compounds were rapidly demethylated to the corresponding tetrahydroxyterphenyls, but only the polyphenol from compound II underwent facile dehydration to give first a dibenzofuran then a benzobisbenzofuran as the final product. Dehydration of the tetrahydroxy-*m*-terphenyl was sluggish, only a little of the benzobisbenzofuran being formed after prolonged reaction. No ring-closure product was formed from compound III. These observations are discussed in the light of the resonance structures of the reaction intermediates.

In previous papers in this series, the acid-catalysed demethylation and subsequent dehydration of substituted 2,2′-dimethoxybiphenyls has been investigated.[1-3] It was found that the dehydration step only proceeds readily in hydrobromic acid under reflux if resorcinol or hydroquinone groupings are present in at least one of the rings, whereas monophenolic and catechol groupings do not facilitate ring-closure.[1,3] Furthermore, it was established that the hydroxyl group of the hydroquinone or resorcinol grouping, not that of the monohydroxy-substituted ring, is eliminated in the acid-catalysed dehydrations of 2,5,2′-trihydroxybiphenyl and 2,4,2′-trihydroxybiphenyl, respectively.[2]

In accordance with the observations on 2,2′-dimethoxybiphenyls, the reactions of suitably substituted polymethoxyterphenyls with refluxing hydrobromic acid afford benzobisbenzofurans or polyhydroxyterphenyls, depending on the substitution of the methoxyl groups in the rings.[4-6] For example, hexamethoxy-*p*-terphenyls containing a hydroquinone grouping in the central ring and hydroquinone or suitable resorcinol groupings in the outer rings afford dihydroxybenzo[1,2-b:4,5-b′]bisbenzofurans with refluxing hydro-

---

* Part XIII. *Acta Chem. Scand.* **22** (1968) 681.

bromic acid, whereas 2,3,2',5',2'',3''-hexamethoxy-$p$-terphenyl and 2,3,4,2',-5',2'',3'',4''-octamethoxy-$p$-terphenyl, containing catechol and pyrogallol groupings, respectively, in the outer rings, afford the corresponding poly-hydroxy-$p$-terphenyls.[4,5] As expected, 2,4,4',6',2'',4''-hexamethoxy-$m$-ter-phenyl, containing resorcinol groupings in all three rings, affords 3,9-dihydroxy-benzo[1,2-b:5,4-b']bisbenzofuran under the reaction conditions.[6]

It was considered it to be of interest to study the acid-catalysed demethyla-tion and dehydration of some tetramethoxyterphenyls, in which the outer rings were monosubstituted and the central ring disubstituted. Three com-pounds were chosen, 2,4',6',2''-tetramethoxy-$m$-terphenyl (I), 2,2',5',2''-tetramethoxy-$p$-terphenyl (II), and 2,2',3',2''-tetramethoxy-$p$-terphenyl (III), in which the central ring contains resorcinol, hydroquinone, and catechol groupings, respectively.



II   R = R'' = OCH$_3$ ,   R' = H

III  R = R' = OCH$_3$ ,   R'' = H

IV   R = R'' = OH ,   R' = H

V   R = R' = OH ,   R'' = H

I   R = OCH$_3$

VI  R = OH
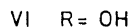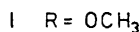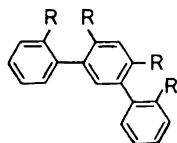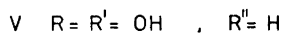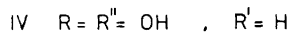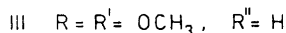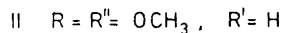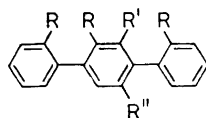
The compounds were prepared by mixed Ullmann couplings between excess 2-iodoanisole and a suitable diiododimethoxybenzene. In order to prepare compound III, the previously unknown 3,6-diiodoveratrole was required. This compound could be obtained in 60 % yield from 3,6-diaminoveratrole, prepared in a several step synthesis essentially according to the method of Oxford,[7] by bis-diazotizing and treating the diazonium solution with potassium iodide. However, a more direct method was to metallate veratrole with excess butyl-lithium in the presence of $N,N,N',N'$-tetramethylethylenediamine [8] (TMEDA) and to iodinate the product. Although the required compound was formed in only 2 % yield, it was easily isolated by chromatography on silica.

The course of the reactions of the compounds I − III with refluxing 48 % hydrobromic acid was followed by means of thin layer chromatography. In the reaction of 2,4',6',2''-tetramethoxy-$m$-terphenyl (I), demethylation was complete within 1 h and only one phenol was detected after this time. On working up the reaction mixture after 1 h, 2,4',6',2''-tetrahydroxy-$m$-terphenyl (VI) was obtained. If the reaction was allowed to continue, another phenol was detectable within 2 h. This gradually increased in amount as the reaction proceeded, and a non-phenolic compound could be detected after 3 days. On working up the reaction mixture after 4 days, the main products were the

tetrahydroxy-$m$-terphenyl (VI) and 2-(2'-hydroxyphenyl)-3-hydroxydibenzo-furan (VII). A small amount of benzo[1,2-b:5,4-b']bisbenzofuran (VIII) was also obtained. Demethylation of 2,2',5',2''-tetramethoxy-$p$-terphenyl (II) was also complete within 1 h. After this time, TLC showed the presence of two phenols, one giving rise to an intense spot and the other to a faint spot. On working up the reaction mixture, 2,2',5',2''-tetrahydroxy-$p$-terphenyl (IV) having the same $R_F$ value as the intense spot could be isolated and identified as the tetraacetate. On allowing the reaction to proceed, a non-phenolic compound was detected after 2 h. The amount of compound IV in the reaction mixture appeared to decrease, while that of the other two compounds increased for some time, but then the other phenol also decreased in amount and after 70 h, only the non-phenolic compound was detected. On working up the reaction mixture after this time, benzo[1,2-b:4,5-b']bisbenzofuran (X) was obtained. The phenol giving rise to the faint spot could be isolated by preparative TLC following work up of the reaction mixture after 48 h. It proved to be 3-(2'-hydroxyphenyl)-2-hydroxydibenzofuran (IX). The reaction with 2,2',3',2''-tetramethoxy-$p$-terphenyl (III) gave 2,2',3',2''-tetrahydroxy-$p$-terphenyl (V) as the final product, and was complete within 1 h.

In the reaction of compound II, double ring-closure to the benzobisbenzofuran occurs readily, the dibenzofuran being an intermediate. This reaction may be expected to take place *via* protonation of the ring containing the hydroquinone grouping in analogy with previous results.[2] The proposed reaction mechanism is outlined in Fig. 1.

The ring-closure reaction of compound I is apparently sluggish, double ring-closure to the benzobisbenzofuran being particularly retarded. According to the expected reaction mechanism (Fig. 2), protonation at the 5'-position
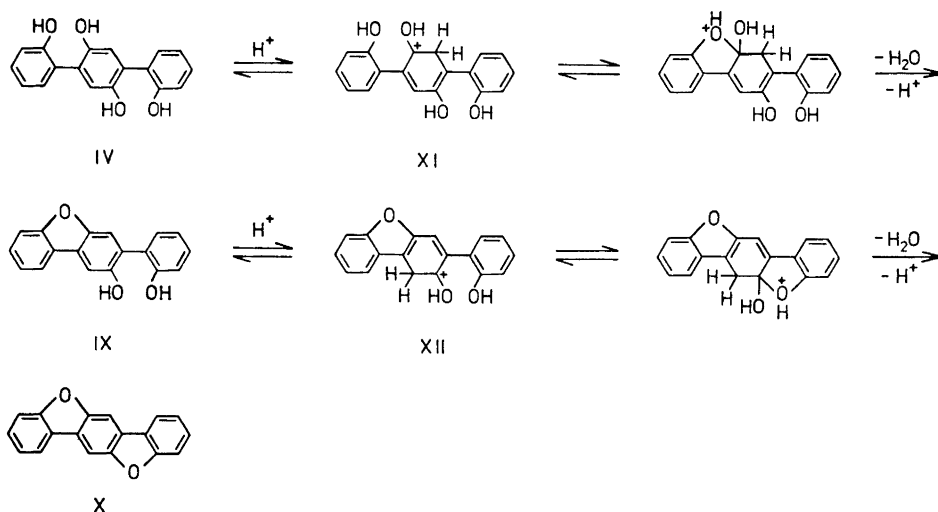


*Fig. 1.* Proposed mechanism for the acid-catalysed dehydration of 2,2',5',2''-tetrahydroxy-$p$-terphenyl, (IV) to 3-(2'-hydroxyphenyl)-2-hydroxydibenzofuran (IX) and benzo-[1,2-b:4,5-b']bisbenzofuran (X).

of the central ring is necessary to lead to ring closure. Comparison of the protonated intermediates XI and XII (Fig. 1) on the one hand and XIII and XIV (Fig. 2) on the other reveals that only XI and XII can have additional resonance forms due to conjugation with a 2-hydroxyphenyl group. Thus intermediates XI and XII should be more stable than XIII and XIV, respectively, and their formation should be more favoured. Consequently, the activation energies of the two ring-closure steps in the reaction of 2,2',5',2''-tetrahydroxy-$p$-terphenyl (IV) with refluxing hydrobromic acid should be lower than those of the corresponding ring closure steps in the reaction of 2,4',6',2''-tetrahydroxy-$m$-terphenyl (VI). Thus the former tetrahydroxy-terphenyl should react more rapidly, this being in agreement with the experimental findings.
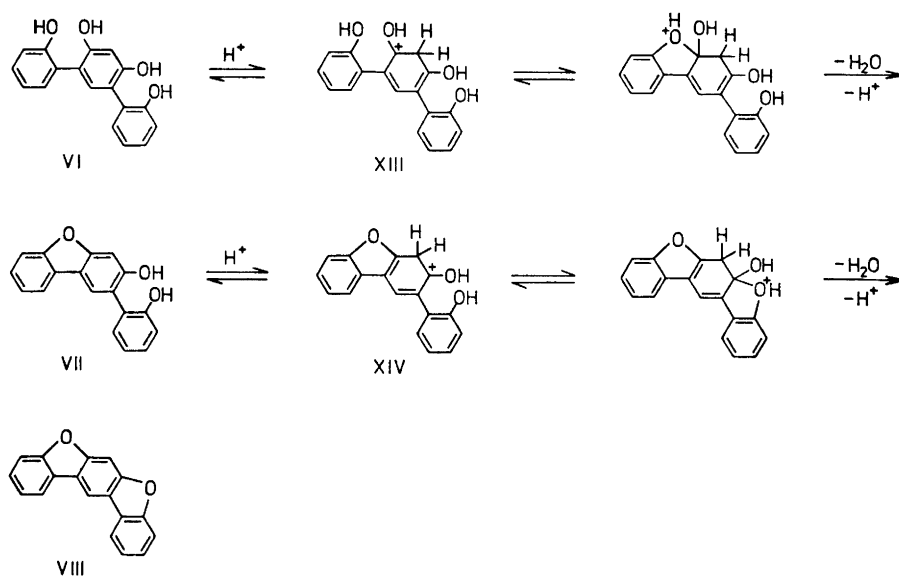


Fig. 2. Proposed mechanism for the acid-catalysed dehydration of 2,4',6',2''-tetrahydroxy-$m$-terphenyl (VI) to 2-(2'-hydroxyphenyl)-3-hydroxydibenzofuran (VII) and benzo-[1,2-b:5,4-b']bisbenzofuran (VIII).

That no ring-closure product is obtained with compound III may be expected in accordance with previous observations on polyhydroxybiphenyls and polyhydroxyterphenyls containing catechol groupings.[1,3,5] However, it is interesting to note that there is a possibility of stabilization of the intermediate arising by protonation of compound V in the 5'-position, in the same way as intermediate XI is stabilized by the 2-hydroxyphenyl group in the 4'-position. In spite of this extra possibility of stabilization, no ring-closure occurs indicating the reason that catechol groupings do not facilitate the reaction is not due to instability of the requisite protonated intermediate. Recent evidence suggests that a stabilizing interaction between the ortho-hydroxyl groups best explains this lack of reactivity.

## EXPERIMENTAL

All melting points are uncorrected. NMR spectra were measured on a Varian T-60 Spectrometer operating at 60 Mc/s with TMS as internal standard. Low resolution mass spectra were recorded on an LKB 9000 mass spectrometer operating at 70 eV and the high resolution mass spectrum on a Varian SM 1 instrument. IR spectra were recorded on a Perkin-Elmer Model 457 Infrared Spectrophotometer. Microanalyses were carried out at the Department of Analytical Chemistry, University of Lund or at the Microanalysis Laboratory, Lantbrukshögskolan, Uppsala.

*2,4′,6′,2″-Tetramethoxy-*m-*terphenyl (I).* A mixture of 2-iodoanisole (20.0 g) and 4,6-diiodoresorcinol dimethyl ether (3.9 g) with copper bronze (35 g) was heated to 220° whereupon an exothermic reaction occurred and the temperature rose to 270°. After cooling, the mixture was extracted in a soxhlet with chloroform. After removal of the solvent under reduced pressure, most of the 2,2′-dimethoxybiphenyl present was removed by distillation (b.p. 166−8°/10 mm) and the remaining material chromatographed on 160 g standardized aluminium oxide (Merck) deactivated by addition of 5 % water, the column being constructed in cyclohexane. Elution was carried out using a cyclohexane-benzene gradient. The fractions giving a spot $R_F$ 0.39 on TLC (Merck Aluminiumoxid $F_{254}$) with benzene as moving phase were combined and the solvent removed. After two recrystallizations of the solid residue from cyclohexane-benzene, 1.01 g of crystalline product, m.p. 181.5−183° remained. Yield 29 %. NMR (CDCl₃): τ 2.5−3.2 (m, 9 H), 3.36 (s, 1 H), 6.19 (s, 6 H), 6.23 (s, 6 H). [Found: C 75.4; H 6.30; mol. wt. 350 (mass spectrometry). Calc. for $C_{22}H_{22}O_4$: C 75.4; H 6.33; mol. wt. 350.4.]

*2,4′,6′,2″-Tetrahydroxy-*m-*terphenyl (VI).* Compound I (100 mg) was heated under reflux for 1 h with a mixture of 10 ml 48 % hydrobromic acid and 10 ml glacial acetic acid under argon. After cooling, the reaction mixture was poured into water and extracted with ether. The ether phase was washed with saturated sodium bicarbonate solution and water, then dried over sodium sulphate. After removal of solvent, the residue was recrystallized twice from chlorobenzene giving 60 mg product, m.p. 185−186° (after sublimation *in vacuo*). [Found: C 73.2; H 4.76; mol. wt. 294 (mass spectrometry). Calc. for $C_{18}H_{14}O_4$: C 73.4; H 4.79; mol. wt. 294.3.]

*2-(2′-Hydroxyphenyl)-3-hydroxydibenzofuran (VII).* Compound I (250 mg) was heated under reflux for 96 h with a mixture of 15 ml 48 % hydrobromic acid and 15 ml glacial acetic acid under argon. The reaction mixture was poured into water (100 ml) and extracted with ether (3 × 30 ml). After washing the ether phase with saturated sodium bicarbonate solution and water and drying over sodium sulphate, the solvent was removed and the residue chromatographed on 25 g silica (Mallinckrodt SilicAR CC 4 100−200 mesh), the column being constructed in benzene and elution being performed with a benzene-ethyl acetate gradient. Three compounds were isolated, the first being benzo-[1,2-b:5,4-b′]bisbenzofuran (VIII) (13 mg, 7 %), m.p. 229−231° after two recrystallizations from glacial acetic acid (lit.[6] m.p. 229−231°). The second compound eluted (65 mg, 33 %) was recrystallized once from cyclohexane and twice from aqueous acetic acid giving the required product m.p. 150−151°. [Found: C 77.9; H 4.41; mol. wt. 276 (mass spectrometry). Calc. for $C_{18}H_{12}O_3$: C 78.2; H 4.38; mol. wt. 276.3.] The third compound eluted (92 mg, 44 %), m.p. 184−185° after recrystallization from chlorobenzene, was identical with compound VI (no depression of m.p. on admixture).

*2,2′,5′,2″-Tetramethoxy-*p-*terphenyl (II).* A mixture of 2-iodoanisole (20.0 g) and 2,5-diiodohydroquinone dimethyl ether (3.9 g) with copper bronze (35 g) was heated to 215°. An exothermic reaction occurred, the temperature rising to 280°. After cooling, the residue was extracted with chloroform in a soxhlet. After removal of the solvent, the residue was distilled *in vacuo*. A fraction, b.p. 200−210°/0.02 mm (1.3 g) was collected and recrystallized twice from acetic acid giving 1.1 g, 31 %, m.p. 184.5−186°. An analytical sample was prepared by chromatographing 220 mg of this material on 20 g standardized aluminium oxide (Merck) deactivated with 5 % water, benzene being used as eluent. Fractions giving a spot $R_F$ 0.42 on TLC (Merck Aluminiumoxid $F_{254}$) with benzene as moving phase were combined and the solvent removed giving a residue which was recrystallized from benzene-cyclohexane, m.p. 184.5−186°. NMR (CDCl₃): τ 2.4−3.1 (m, 8 H), 3.08 (s, 2 H), 6.19 (s, 6 H), 6.28 (s, 6 H). [Found: C 75.8; H 6.31; mol. wt. 350 (mass spectrometry). Calc. for $C_{22}H_{22}O_4$: C 75.4; H 6.33; mol. wt. 350.4.]

*2,2′,5′,2‴-Tetrahydroxy-p-terphenyl (IV)*. Compound II (100 mg) was heated under reflux for 1 h with a mixture of 10 ml 48 % hydrobromic acid and 10 ml glacial acetic acid under argon. After cooling, the reaction mixture was poured into water and extracted with ether. The ether phase was washed with saturated sodium bicarbonate solution and water, then dried over sodium sulphate. After removal of the solvent, the residue was recrystallized from chlorobenzene giving 65 mg product, m.p. 231 − 233° (after sublimation *in vacuo*). [Found: mol. wt. 294 (mass spectrometry). Calc. mol. wt. 294.3.] The crystals became bluish-coloured on exposure to air due to superficial oxidation and the compound was therefore converted to *2,2′,5′,2‴-tetraacetoxy-p-terphenyl* by acetylation with acetic anhydride in pyridine. The crude acetate was chromatographed on Merck Kieselgel 60 deactivated with 15 % water, the column being constructed in benzene and a benzene-isopropyl ether gradient being used as eluent. Fractions giving a spot $R_F$ 0.29 on TLC (Merck Kieselgel $F_{254}$) with isopropyl ether as moving phase were combined and solvent removed giving the required compound, which was recrystallized twice from cyclohexane and once from ethanol giving a product m.p. 126.5 − 127.5°. NMR (CCl$_4$): τ 2.4 − 3.0 (m, 8 H), 2.99 (s, 2 H), 7.98 (s, 6 H), 8.03 (s, 6 H). IR (KBr): $\nu_{C=O}$ 1762 cm$^{-1}$. [Found: C 66.9; H 4.90; mol. wt. 462 (mass spectrometry). Calc. for C$_{26}$H$_{22}$O$_8$: C 67.5; H 4.80; mol. wt. 462.5.] The mass spectrum showed the presence of an impurity corresponding to the tetraacetate substituted with one bromine atom M$^+$, *m/e* 540 (rel. int. to *m/e* 462, 1.3 %) and *m/e* 542 (rel. int. to *m/e* 462, 1.3 %). This impurity was not removed by recrystallization.

*Benzo[1,2-b:4,5-b′]bisbenzofuran (X)*. Compound II (200 mg) was heated under reflux for 72 h with 20 ml 48 % hydrobromic acid and 20 ml glacial acetic acid under argon. After cooling the reaction mixture, the solid product was removed by filtration, washed with water and triturated with ethyl acetate. After washing the ethyl acetate solution with 2 N sodium hydroxide solution and water, it was dried over sodium sulphate. Removal of the solvent afforded 33 mg product (m.p. 263 − 265° after sublimation *in vacuo*) (lit.[4] m.p. 265.5 − 266.5°). Yield 22 %. The alkaline washings afforded no residue on acidification, extracting with ether and removal of the solvent. However, there was a considerable trituration residue of black, presumably polymeric, material.

*3-(2′-Hydroxyphenyl)-2-hydroxydibenzofuran (IX)*. Compound II (100 mg) was heated under reflux for 48 h with a mixture of 10 ml 48 % hydrobromic acid and 10 ml glacial acetic acid under argon. After cooling, the reaction mixture was poured into water and extracted with ether. The ether solution was washed with saturated sodium bicarbonate solution and water, then dried over sodium sulphate. The solution gave 4 spots on a TLC plate (Merck Kieselgel $F_{254}$) with acetic acid-ethyl acetate-petroleum ether (1:2:7) as moving phase. These had $R_F$ values 0.0, 0.30 (corresponding to compound IV), 0.55, and 0.80 (corresponding to compound X). The first three spots gave a positive phenolic reaction with bis-diazotized benzidine while the fourth was observable in short wave UV light. On removal of the solvent from the ether solution, 70 mg residue remained. This was chromatographed on two 20 × 20 cm preparative TLC plates (Merck PSC Fertigplatten, Kieselgel $F_{254}$) using the same moving phase as with analytical TLC. The material corresponding to the spot $R_F$ 0.55 was extracted from the silica with chloroform. On removal of the solvent, *ca.* 4 mg crystalline residue remained which was sublimed *in vacuo*, m.p. 137 − 141°. (High resolution mass spectrometry: M$^+$, *m/e* 276.0784. Calc. for C$_{18}$H$_{12}$O$_3$: *m/e* 276.0786.)

*3,6-Diiodoveratrole. Method 1*. 3,6-Diaminoveratrole dihydrochloride [7] (0.60 g, 2.5 mmol) was bis-diazotized according to the method of Schoutissen [10] by dissolving in 8.75 ml 85 % orthophosphoric acid and stirring at − 5° while adding dropwise a solution of sodium nitrite (0.38 g, 5.5 mmol) in 3.8 ml 98 % sulphuric acid at − 5° for 30 min, 0.26 g urea was added to destroy excess nitrous acid. The solution was then added to a solution of potassium iodide (1.30 g, 6.0 mmol) in a minimum volume of ice-cold water. After 4 h, the mixture was diluted with water, extracted with chloroform and the organic phase washed with saturated sodium bisulphite solution and water, then dried over magnesium sulphate. After removal of the solvent, the residue (0.81 g) was chromatographed on a column of 25 g silica (Merck 0.05 − 0.20 mm) packed in cyclohexane. Elution was carried out using a cyclohexane-benzene gradient. The fractions giving a spot $R_F$ 0.55 on TLC (Merck Kieselgel $F_{254}$) with isopropyl ether as moving phase were combined and the solvent removed giving a colourless oil, which was crystallized from ethanol giving 0.58 g product. Yield 59 %, m.p. 45.5 − 47° (after recrystalliza-

tion from aqueous ethanol). NMR (CDCl₃): τ 2.77 (s, 2 H), 6.13 (s, 6 H). (Found: C 25.0; H 1.94; I 64.4. Calc. for $C_8H_8I_2O_2$: C 24.6; H 2.07; I 65.1.)

*Method 2.* A solution of TMEDA (14.52 g, 0.125 mol) in 25 ml dry heptane was added to 66 ml of 1.9 M butyllithium (0.125 mol) in hexane under argon. A pale yellow precipitate formed and to the stirred suspension, a solution of veratrole (6.91 g, 0.050 mol) in 25 ml dry heptane was added. After stirring at room temperature for 20 h, the suspension was added during 1 h to a stirred mixture of iodine (38.1 g, 0.150 mol) and 100 ml dry heptane at − 70° under argon. The mixture was stirred for 22 h during which time the temperature was allowed to rise to 10°. After addition of 50 ml water, the organic phase was separated and the aqueous phase extracted with ethyl acetate. The combined organic phases were washed with sodium bisulphite solution and water, then dried over magnesium sulphate. On removal of the solvent, 10.3 g residue remained which was chromatographed on a column of 200 g silica (Merck 0.05 − 0.20 mm) packed in cyclohexane. Elution was carried out as in method 1. Evaporation of the fractions containing the required product afforded a colourless oil which gave 0.35 g crystals on crystallization from aqueous ethanol, m.p. 45 − 46.5° after recrystallization. Yield 2.0 %. There was no depression of m.p. on admixture with the product of method 1.

*2,2′,3′,2″-Tetramethoxy-p-terphenyl (III).* A mixture of 3,6-diiodoveratrole (0.39 g) and 2-iodoanisole (2.34 g) with copper bronze (3.5 g) was heated to 220° whereupon an exothermic reaction occurred and the temperature rose to 280°. After allowing to cool, the residue was extracted in a soxhlet with chloroform. After removal of the solvent, the residue was distilled *in vacuo* and the fraction b.p. 170 − 200°/0.015 mm (0.33 g) collected and chromatographed on a column of 20 g aluminium oxide (Merck, standardized) deactivated with 5 % water. The column was constructed in cyclohexane and elution carried out with a cyclohexane-benzene gradient. Fractions giving a spot $R_F$ 0.50 on TLC (Merck Aluminium oxide $F_{254}$) with benzene as moving phase were combined and the solvent removed giving an oil which was crystallized from ethanol giving 0.11 g, m.p. 98 − 100° (after recrystallization from ethanol). Yield 31 %. NMR (CDCl₃): τ 2.6 − 3.3 (m, 10 H), 6.24 (s, 6 H), 6.40 (s, 6 H). [Found: C 75.1; H 6.41; mol. wt. 350 (mass spectrometry). Calc. for $C_{22}H_{22}O_4$: C 75.4; H 6.33; mol. wt. 350.4.]

*2,2′,3′,2″-Tetrahydroxy-p-terphenyl (V).* Compound III (10 mg) was heated under reflux for 2 h with 1 ml glacial acetic acid and 1 ml 48 % hydrobromic acid under argon. After cooling, the mixture was diluted with 10 ml water, extracted with ether and the ether phase washed with saturated sodium bicarbonate solution and water, then dried over sodium sulphate. After removal of solvent, 8 mg residue remained, m.p. 166 − 168° (after recrystallization from toluene). On subliming *in vacuo*, crystals, m.p. 225 − 226°, were obtained. Both samples gave one spot, $R_F$ 0.17 (red-brown colouration with bis-diazotized benzidine), on TLC (Merck Kieselgel $F_{254}$) with acetic acid − ethyl acetate − petroleum ether (1:2:7) as moving phase. On melting the material with the lower m.p., seeding with material with the higher m.p., allowing to solidify and remelting, the m.p. rose to 225 − 226° indicating the two samples to be dimorphic crystalline forms of the same compound. [Found: C 73.1; H 4.80; mol. wt. 294 (mass spectrometry). Calc. for $C_{18}H_{14}O_4$: C 73.4; H 4.79; mol. wt. 294.3.]


# Demethylation and dehydration experiments followed by thin layer chromatography

*General procedure.* The tetramethoxyterphenyl (10 mg) was heated under reflux with a mixture of 1 ml 48 % hydrobromic acid and 1 ml glacial acetic acid under argon, the bath temperature being 140°. Samples (0.1 ml) were withdrawn from the reaction mixture at certain intervals (0, 1, 2, 5, 10, 15, 30 min, 1, 1.5, 2, 3, 5, 8, 24, 48, 72, 96 h with some variations), diluted to 1 ml with water and extracted with 0.2 ml ether. An aliquot (20 μl) of each ether solution was applied to a TLC plate (Merck Kieselgel $F_{254}$, 20 × 20 cm) and the plate developed with acetic acid − ethyl acetate − petroleum ether (1:2:7) as moving phase. The chromatograms were investigated in UV light before spraying with bis-diazotized benzidine.

*Reaction of 2,4′,6′,2″-tetramethoxy-m-terphenyl (I).* After only 2 min, five spots coloured by bis-diazotized benzidine could be detected. Only one of these remained after

1 h, and corresponded to 2,4′,6′,2″-tetrahydroxy-m-terphenyl (VI) ($R_F$ 0.21). Another phenolic compound, $R_F$ 0.50 (corresponding to compound VII), was detected after 1.5 h. After 72 h, a third spot ($R_F$ 0.73) visible in UV, but not giving a positive phenolic reaction appeared. This corresponds to benzo[1,2-b:5,4-b′]bisbenzofuran (VIII). After 96 h, the main spots were those due to compounds VI and VII.

*Reaction of 2,2′,5′,2″-tetramethoxy-p-terphenyl (II)*. After 1 min, four spots giving a positive phenolic reaction were observable. One of these remained after 1 h and corresponded to 2,2′,5′,2″-tetrahydroxy-p-terphenyl (IV) ($R_F$ 0.30). A faint spot $R_F$ 0.55, corresponding to compound IX, had appeared after 30 min. After 2 h, a spot not giving a positive phenolic reaction was detected ($R_F$ 0.80). This corresponded to benzo[1,2-b:4,5-b′]bisbenzofuran (X). As the reaction proceeded, the spot $R_F$ 0.30 decreased in intensity while that with $R_F$ 0.80 increased in intensity. The spot $R_F$ 0.55 increased in intensity at first, but appeared to remain constant after ca 5 h, then became weaker again after 48 h until only the spot at $R_F$ 0.80, together with a spot $R_F$ 0.0, remained after 72 h.

*Reaction of 2,2′,3′,2″-tetramethoxy-p-terphenyl (III)*. After 5 min, five spots coloured by bis-diazotized benzidine were detected. After 1 h, only one spot remained, $R_F$ 0.21, corresponding to 2,2′,3′,2″-tetrahydroxy-p-terphenyl (V). No other spots had been formed after 43 h.

## REFERENCES

1. Stjernström, N. E. *Svensk Kem. Tidskr.* **75** (1963) 184.
2. Pring, B. G. and Stjernström, N. E. *Acta Chem. Scand.* **22** (1968) 538.
3. Pring, B. G. and Stjernström, N. E. *Acta Chem. Scand.* **22** (1968) 681.
4. Erdtman, H. and Stjernström, N. E. *Acta Chem. Scand.* **13** (1959) 653.
5. Stjernström, N. E. *Acta Chem. Scand.* **14** (1960) 1274.
6. Stjernström, N. E. *Acta Chem. Scand.* **16** (1962) 553.
7. Oxford, A. E. *J. Chem. Soc.* **1926** 2004.
8. Mallan, J. M. and Bebb, R. L. *Chem. Rev.* **69** (1969) 693.
9. Pring, B. G. *Chem. Commun. Univ. Stockholm* **1973** No. 14.
10. Schoutissen, H. A. J. *J. Am. Chem. Soc.* **55** (1933) 4535.

# Structures of Linear Multisulphur Systems

## V. The Crystal and Molecular Structure of α-[7-(5-t-Butyl-1,2--dithiole-3-ylidene)-4,5,6,7-tetrahydro-1,2-benzodithiole-3-ylidene]-acetophenone

JORUNN SLETTEN and MAGNAR VELSVIK

*Chemical Institute, University of Bergen, 5000 Bergen, Norway*

The structure of α-[7-(5-t-butyl-1,2-dithiole-3-ylidene)-4,5,6,7-tetrahydro-1,2-benzodithiole-3-ylidene]-acetophenone has been determined by X-ray crystallographic methods. 4759 independent reflections were measured on a diffractometer using the $\theta - 2\theta$ scan technique and MoK$\alpha$ radiation. The structure was solved by direct methods and refined by full-matrix least-squares to $R = 0.050$. The four sulphur atoms and the oxygen atom are arranged on an approximately linear row, with interatomic distances: $S(1) - S(2) = 2.064(1)$ Å, $S(2) - S(3) = 2.856(1)$ Å, $S(3) - S(4) = 2.110(1)$ Å, and $S(4) - O = 2.327(2)$ Å. The two short bond lengths are close to a normal $S(II) - S(II)$ single bond of 2.10 Å. The $S - O$ and the long $S - S$ bond are both in the region between single bond and van der Waals distance.

Poirier and Lozac'h have described the synthesis of a dithiafurophthene, II, by the reaction of diazoacetophenone and 1,2-dithiole-3-thione.[1] By the action of $P_4S_{10}$ on II the oxygen is substituted by sulphur, giving a thiathiophthene, III.

R, S ... S—S ... (I) + N₂CH R' ... O ... (II) → R ... R' ... S—S O ... P₄S₁₀ → R ... R' ... S—S S ... (III)

Stavaux and Lozac'h have used an analogous method to synthesize compound V, and the corresponding five-sulphur compound, VI.[2]

A large number of both experimental and theoretical investigations have been undertaken to determine the structures and electronic properties of compounds analogous to I, II, and III. (See references 3 – 5 for recent review articles.) The structures of compounds IV and VI and five other linear four- and five-sulphur compounds have been determined.[6-12] The sulphur-sulphur

$R_1$ = *t*-butyl
$R_2$ = phenyl

bonding scheme in IV seems to be adequately described in terms of two isolated dithiole systems,[6] while in compound VI delocalized $\sigma$-bonding extending across all sulphur atoms apparently exists.[7] A comparison of the UV and visible spectra of II and III shows that the replacement of oxygen by sulphur causes a bathochromic shift in the visible region and introduces a stronger absorption in the UV region.[13] A corresponding change in the spectrum is observed by going from V to VI.[14]

The present structure investigation, of compound V, was undertaken to determine whether this type of molecule may be regarded as an extended thiafurophthene system.

## EXPERIMENTAL

The compound was supplied as a micro-crystalline sample. Several attempts to grow crystals suitable for X-ray work failed. Crystallization problems have been encountered with a number of the compounds studied in this series. In the present case the most satisfying results were obtained by evaporation at room temperature from a carbon disulphide solution.

The crystals grew elongated along the *a*-axis direction. As the crystals fracture easily, a solvent saw [15] was used to cut the crystal chosen for data collection to a suitable length. The dimension of the crystal was 0.76 mm × 0.25 mm × 0.15 mm. Some of the reflections showed splitting, indicating that the crystal was slightly fractured. Determination of space group and preliminary cell dimensions were carried out using Weissenberg and precession photographs. More accurate cell dimensions were determined by measuring setting angles for 16 reflections on an off-line diffractometer using Mo$K\alpha$ radiation. The density were measured by flotation. The crystal data are as follows:

$C_{23}H_{22}OS_4$                         $M.W. = 430.67$

Crystal system orthorhombic; space group *Pbca* (No. 61); cell dimensions:

$a$     $= 10.979(2)$ Å,  $b = 17.549(4)$ Å,  $c = 21.832(4)$ Å
$V$     $= 4206(2)$ Å$^3$
$D_m$  $= 1.359$ g cm$^{-3}$, $D_x = 1.360$ g cm$^{-3}$, $Z = 8$, $\mu_{MoK\alpha} = 4.52$ cm$^{-1}$

4759 unique reflections with $2\theta \leqslant 55°$ were measured by the $\theta - 2\theta$ scan technique on an off-line four-circle diffractometer using niobium-filtered Mo$K\alpha$ radiation ($\lambda = 0.71069$ Å). The "five value" measurement procedure was employed, and scan ranges for low and high $2\theta$ sides were calculated according to the tangent relationship given by Alexander and Smith.[16]

The intensities of two reference reflections were recorded for every 50 reflections. These measurements were used to bring the data to a common scale. The uncertainty in scale factors were estimated at 2 %. The standard deviations in intensities were taken as $\sigma_I = [\sigma_c^2 + (0.02\sigma_c^2)^2]^{1/2}$, where $\sigma_c$ is the error due to counting statistics. $\sigma_F$ was calculated as $\sigma_I/2(I\ Lp)^{1/2}$. 1264 reflections were measured to be less than $2\sigma_c$. These reflections were given a threshold value of $2\sigma_c$ and included in the refinement only when $|F_{calc}| > |F_{threshold}|$. Data were corrected for Lorentz and polarization effects. An absorption correction according to the method described by Coppens *et al.*[17] was applied.

## SOLUTION AND REFINEMENT

The structure was solved by a symbolic addition procedure programmed by Long.[18] Signs for 259 reflections with $|E| \geqslant 1.70$ were derived by reiterative application of Sayre's equation. An $E$-map[19] calculated from the most probable set of phases clearly revealed the sulphur atoms, the oxygen and 13 out of the 22 carbon atoms. Smaller peaks were also observed in reasonable positions for the remaining atoms. Carbon atom C(15) was represented by a double peak in the $E$-map, and was later shown to be disordered. Structure factors were calculated based on four sulphur atoms, one oxygen and thirteen carbon atoms, and in the subsequent Fourier map the remaining carbon atoms were located. The structure was refined by full-matrix least-squares. At an $R$ of 0.17 $(R = \sum ||F_o| - |F_c||/\sum|F_o|)$, anisotropic temperature factors were introduced. The thermal parameters of C(15) were abnormally high $(U \approx 0.2 \text{ Å}^2)$, indicating disorder. A difference map confirmed the presence of disorder, and two atoms, C(151) and C(152), each with multiplicity 0.5 and isotropic temperature factor, were introduced in positions as found from the difference map. These positions are in good agreement with those observed in the $E$-map. The fractional atoms refined satisfactorily. C(16) is also apparently disordered; however, judging from the thermal parameters the separation between the fractional sites are less than for C(15). An attempt to refine two fractional atoms in this case was not successful.

From a difference map all the hydrogen atoms were found, except those on C(14), C(151), C(152), and C(16), which due to the disorder could not be unambiguously located. Hydrogen atoms were refined isotropically; however, the $t$-butyl hydrogen atoms refined to unreasonable positions, and were therefore kept fixed at the positions obtained from the difference map and with $U$ values comparable to the carbon atoms to which they are attached. At the end of the refinement a secondary extinction correction was carried out.[20] The extinction coefficient was found to be $0.12 \times 10^{-6}$, the maximum correction in $F_{obs}$ being 14 %. The final agreement factor is 0.050. The function minimized in the refinement was $\sum w(|F_o| - |F_c|)^2$, where $w = 1/\sigma_F^2$. Scattering factors used were for sulphur, oxygen, and carbon atoms those of Hanson et al.[21] and for hydrogen those of Stewart et al.[22]

At the end of the refinement a residual difference map was calculated. In the disordered region electron densities up to 0.50 e.Å$^{-3}$ are found.

## RESULTS AND DISCUSSION

Atomic coordinates and thermal parameters are listed in Tables 1 and 2. The molecular dimensions are shown in Fig. 1 and in Tables 3 and 4. The four sulphur atoms and the oxygen atom constitute an approximately linear row, the pertinent angles being $\angle S(1) - S(2) - S(3) = 179.57°$, $\angle S(2) - S(3) - S(4) = 175.26°$, and $\angle S(3) - S(4) - O = 174.25°$.

A least-squares plane through the atoms of rings A, B, C, and D (Fig. 1) shows that there is a small but significant deviation from planarity in this part of the molecule. The molecule is slightly twisted at C(4), so as to leave S(2) slightly above and S(3) slightly below the least-squares plane. In addition the

*Table 1.* Fractional atomic coordinates with the corresponding standard deviations, referring to the last decimal places, listed in parentheses. The standard deviations are derived from the inverse least-squares matrix, except those for H(111) through H(133), which are estimated from the difference Fourier map.

| Atom | $X/a$ | $Y/b$ | $Z/c$ |
|---|---|---|---|
| S(1) | 0.36393(7) | 0.13110(6) | 0.41865(5) |
| S(2) | 0.51640(7) | 0.09645(5) | 0.46647(4) |
| S(3) | 0.72702(6) | 0.04740(4) | 0.53233(3) |
| S(4) | 0.87622(6) | 0.01532(4) | 0.58749(3) |
| O | 1.05219(17) | −0.01093(11) | 0.64380(9) |
| C(1) | 0.44138(24) | 0.19513(15) | 0.37182(12) |
| C(2) | 0.56056(25) | 0.20036(18) | 0.38128(13) |
| C(3) | 0.62155(24) | 0.15549(15) | 0.42776(12) |
| C(4) | 0.74281(24) | 0.15841(15) | 0.44162(12) |
| C(5) | 0.80433(23) | 0.11425(14) | 0.48786(12) |
| C(6) | 0.92669(23) | 0.12168(14) | 0.50169(12) |
| C(7) | 0.97708(23) | 0.07687(15) | 0.54986(12) |
| C(8) | 1.09644(25) | 0.07882(17) | 0.56984(13) |
| C(9) | 1.13102(25) | 0.03197(15) | 0.61942(12) |
| C(10) | 0.36503(25) | 0.23717(18) | 0.32371(14) |
| C(11) | 0.44505(36) | 0.29401(28) | 0.28870(19) |
| C(12) | 0.31060(44) | 0.17953(26) | 0.27913(19) |
| C(13) | 0.26315(34) | 0.28073(23) | 0.35547(18) |
| C(14) | 0.82339(29) | 0.21363(25) | 0.40548(17) |
| C(151) | 0.93275(55) | 0.23539(37) | 0.43470(29) |
| C(152) | 0.94837(53) | 0.19873(35) | 0.40322(27) |
| C(16) | 1.00657(27) | 0.17673(19) | 0.46731(17) |
| C(17) | 1.25662(25) | 0.03187(16) | 0.64441(12) |
| C(18) | 1.35125(27) | 0.07215(19) | 0.61802(15) |
| C(19) | 1.46632(30) | 0.07157(21) | 0.64353(17) |
| C(20) | 1.48836(34) | 0.02995(22) | 0.69621(17) |
| C(21) | 1.39537(39) | −0.01044(26) | 0.72198(18) |
| C(22) | 1.28275(35) | −0.00950(22) | 0.69665(17) |
| H(2) | 0.6098(23) | 0.2385(16) | 0.3633(12) |
| H(8) | 1.1490(22) | 0.1138(15) | 0.5533(12) |
| H(111) | 0.4670(60) | 0.3350(35) | 0.3170(30) |
| H(112) | 0.4000(60) | 0.3180(35) | 0.2670(30) |
| H(113) | 0.5000(60) | 0.2600(35) | 0.2670(30) |
| H(121) | 0.4000(60) | 0.1550(35) | 0.2670(30) |
| H(122) | 0.2330(60) | 0.1980(35) | 0.2500(30) |
| H(123) | 0.2670(60) | 0.1290(35) | 0.3000(30) |
| H(131) | 0.2190(60) | 0.3100(35) | 0.3260(30) |
| H(132) | 0.3180(60) | 0.3170(35) | 0.3850(30) |
| H(133) | 0.2110(60) | 0.2360(35) | 0.3750(30) |
| H(18) | 1.3328(26) | 0.1060(18) | 0.5818(14) |
| H(19) | 1.5245(30) | 0.1031(20) | 0.6238(16) |
| H(20) | 1.5700(32) | 0.0284(19) | 0.7195(15) |
| H(21) | 1.4077(30) | −0.0405(19) | 0.7533(16) |
| H(22) | 1.2273(27) | −0.0310(18) | 0.7095(14) |

*Table 2.* Thermal parameters with the corresponding standard deviations in parentheses. Anisotropic temperature factors are given by:

$$T_i = \exp[-2\pi^2(U_{11}h^2a^{*2} + U_{22}k^2b^{*2} + U_{33}l^2c^{*2} + 2U_{12}hka^*b^* + 2U_{23}klb^*c^* + 2U_{13}hla^*c^*)],$$

and isotropic temperature factors by: $T_i = \exp(-8\pi^2 U \sin^2 \theta/\lambda^2)$. For non-hydrogen atoms the values are multiplied by $10^4$, for hydrogen atoms by $10^3$.

| Atom | $U_{11}$ | $U_{22}$ | $U_{33}$ | $U_{12}$ | $U_{23}$ | $U_{13}$ |
|---|---|---|---|---|---|---|
| S(1) | 375(4) | 744(6) | 1016(7) | −98(4) | 331(5) | −70(5) |
| S(2) | 372(4) | 558(5) | 841(6) | −59(3) | 266(4) | −2(4) |
| S(3) | 373(4) | 482(4) | 538(4) | −76(3) | 124(4) | 27(3) |
| S(4) | 416(4) | 440(4) | 475(4) | −27(3) | 98(3) | 52(3) |
| O | 509(11) | 622(13) | 573(13) | −51(10) | 115(11) | 78(10) |
| C(1) | 461(16) | 439(16) | 491(16) | −25(13) | −42(13) | −18(14) |
| C(2) | 431(16) | 551(18) | 481(17) | −88(15) | 60(15) | −20(14) |
| C(3) | 423(15) | 376(14) | 460(16) | −42(12) | −6(12) | 49(13) |
| C(4) | 409(14) | 440(16) | 440(15) | −45(13) | 45(13) | 12(13) |
| C(5) | 394(14) | 379(14) | 401(15) | −46(12) | −1(11) | 58(11) |
| C(6) | 382(14) | 368(14) | 402(15) | −30(12) | −2(12) | 55(12) |
| C(7) | 397(14) | 374(14) | 429(15) | −18(12) | −20(12) | 81(12) |
| C(8) | 396(15) | 447(16) | 485(17) | −29(13) | 46(14) | 42(13) |
| C(9) | 461(16) | 434(16) | 430(16) | 27(13) | −13(13) | 78(13) |
| C(10) | 505(17) | 597(20) | 545(19) | 4(15) | −11(15) | −102(15) |
| C(11) | 931(28) | 1406(40) | 1021(34) | 72(29) | 713(31) | −152(26) |
| C(12) | 1553(42) | 1002(33) | 1036(32) | 111(32) | −301(26) | −719(32) |
| C(13) | 785(25) | 920(28) | 962(28) | 367(22) | 51(24) | −117(23) |
| C(14) | 473(18) | 1261(34) | 935(28) | −352(21) | 641(26) | −127(19) |
| C(16) | 410(16) | 479(18) | 610(21) | −72(14) | 86(17) | 12(16) |
| C(17) | 459(16) | 429(16) | 396(15) | 35(14) | −5(13) | 25(13) |
| C(18) | 477(18) | 592(19) | 541(20) | 43(15) | 88(16) | −15(15) |
| C(19) | 476(19) | 724(23) | 734(24) | −32(17) | 58(20) | −41(18) |
| C(20) | 596(21) | 792(25) | 708(24) | 101(19) | −32(21) | −21(20) |
| C(21) | 827(29) | 933(30) | 632(24) | 42(24) | 23(23) | −19(22) |
| C(22) | 609(23) | 773(26) | 593(22) | −51(20) | 220(19) | −30(19) |

| | $U$ | | | $U$ | | $U$ |
|---|---|---|---|---|---|---|
| C(151) | 553(15) | | H(113) | 120 | H(133) | 120 |
| C(152) | 490(14) | | H(121) | 120 | H(18) | 65(10) |
| H(2) | 46(8) | | H(122) | 120 | H(19) | 79(12) |
| H(8) | 38(7) | | H(123) | 120 | H(20) | 82(11) |
| H(111) | 120 | | H(131) | 120 | H(21) | 73(11) |
| H(112) | 120 | | H(132) | 120 | H(22) | 56(11) |
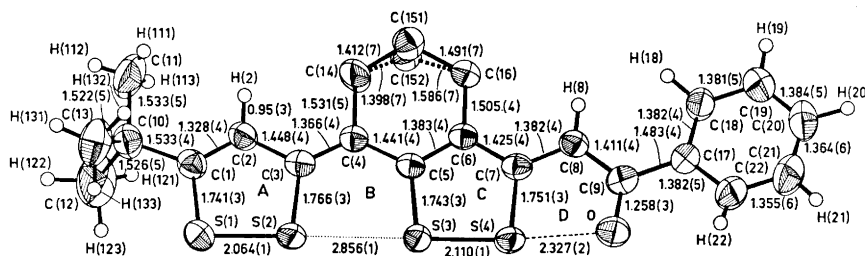


*Fig. 1.* ORTEP-plot [23] of the molecule showing thermal ellipsoids at the 50 % probability level. Hydrogen atoms are drawn with fixed radius. Bond distances are given with the corresponding standard deviations in parentheses.

*Table 3.* C−H bond distances in Å units with the corresponding standard deviations in parentheses.

| | | | | | |
|---|---|---|---|---|---|
| C(2)−H(2) | 0.95(3) | C(12)−H(122) | 1.11(7) | C(18)−H(18) | 1.01(3) |
| C(8)−H(8) | 0.92(3) | C(12)−H(123) | 1.11(7) | C(19)−H(19) | 0.95(3) |
| C(11)−H(111) | 0.98(7) | C(13)−H(131) | 0.96(7) | C(20)−H(20) | 1.03(3) |
| C(11)−H(112) | 0.80(7) | C(13)−H(132) | 1.08(7) | C(21)−H(21) | 0.87(3) |
| C(11)−H(113) | 0.97(7) | C(13)−H(133) | 1.07(7) | C(22)−H(22) | 0.77(3) |
| C(12)−H(121) | 1.10(7) | | | | |

*Table 4.* Intramolecular angles (in degrees) with the corresponding standard deviations in parentheses.

| | | | |
|---|---|---|---|
| S(2)−S(1)−C(1) | 95.2(1) | C(12)−C(10)−C(13) | 109.6(3) |
| S(1)−S(2)−S(3) | 179.57(4) | C(10)−C(11)−H(111) | 108(4) |
| S(1)−S(2)−C(3) | 96.6(1) | C(10)−C(11)−H(112) | 106(4) |
| S(3)−S(2)−C(3) | 83.6(1) | C(10)−C(11)−H(113) | 102(4) |
| S(2)−S(3)−S(4) | 175.26(4) | H(111)−C(11)−H(112) | 98(5) |
| S(2)−S(3)−C(5) | 84.9(1) | H(111)−C(11)−H(113) | 127(5) |
| S(4)−S(3)−C(5) | 96.9(1) | H(112)−C(11)−H(113) | 115(5) |
| S(3)−S(4)−O | 174.25(6) | C(10)−C(12)−H(121) | 94(4) |
| S(3)−S(4)−C(7) | 93.4(1) | C(10)−C(12)−H(122) | 118(4) |
| O−S(4)−C(7) | 80.9(1) | C(10)−C(12)−H(123) | 116(4) |
| S(4)−O−C(9) | 103.8(2) | H(121)−C(12)−H(122) | 131(5) |
| S(1)−C(1)−C(2) | 115.8(2) | H(121)−C(12)−H(123) | 100(5) |
| S(1)−C(1)−C(10) | 116.5(2) | H(122)−C(12)−H(123) | 98(5) |
| C(2)−C(1)−C(10) | 127.8(2) | C(10)−C(13)−H(131) | 109(4) |
| C(1)−C(2)−C(3) | 121.8(2) | C(10)−C(13)−H(132) | 99(4) |
| C(1)−C(2)−H(2) | 123(2) | C(10)−C(13)−H(133) | 102(4) |
| C(3)−C(2)−H(3) | 114(2) | H(131)−C(13)−H(132) | 111(5) |
| S(2)−C(3)−C(2) | 110.6(2) | H(131)−C(13)−H(133) | 113(5) |
| S(2)−C(3)−C(4) | 123.6(2) | H(132)−C(13)−H(133) | 120(5) |
| C(2)−C(3)−C(4) | 125.8(2) | C(4)−C(14)−C(151) | 115.5(4) |
| C(3)−C(4)−C(5) | 126.3(2) | C(4)−C(14)−C(152) | 117.8(3) |
| C(3)−C(4)−C(14) | 118.2(2) | C(14)−C(151)−C(16) | 119.4(4) |
| C(5)−C(4)−C(14) | 115.5(2) | C(14)−C(152)−C(16) | 114.2(4) |
| S(3)−C(5)−C(4) | 121.6(2) | C(6)−C(16)−C(151) | 111.4(3) |
| S(3)−C(5)−C(6) | 114.5(2) | C(6)−C(16)−C(152) | 111.2(3) |
| C(4)−C(5)−C(6) | 123.9(2) | C(9)−C(17)−C(18) | 123.0(2) |
| C(5)−C(6)−C(7) | 119.9(2) | C(9)−C(17)−C(22) | 119.8(2) |
| C(5)−C(6)−C(16) | 121.2(2) | C(18)−C(17)−C(22) | 117.2(3) |
| C(7)−C(6)−C(16) | 119.7(2) | C(17)−C(18)−C(19) | 121.1(3) |
| S(4)−C(7)−C(6) | 116.2(2) | C(17)−C(18)−H(18) | 118(2) |
| S(4)−C(7)−C(8) | 117.8(2) | C(19)−C(18)−H(18) | 120(2) |
| C(6)−C(7)−C(8) | 126.0(2) | C(18)−C(19)−C(20) | 119.9(3) |
| C(7)−C(8)−C(9) | 118.9(2) | C(18)−C(19)−H(19) | 115(2) |
| C(7)−C(8)−H(8) | 119(2) | C(20)−C(19)−H(19) | 125(2) |
| C(9)−C(8)−H(8) | 122(2) | C(19)−C(20)−C(21) | 119.1(3) |
| O−C(9)−C(8) | 118.6(2) | C(19)−C(20)−H(20) | 125(2) |
| O−C(9)−C(17) | 119.2(2) | C(21)−C(20)−H(20) | 116(2) |
| C(8)−C(9)−C(17) | 122.2(2) | C(20)−C(21)−C(22) | 120.6(3) |
| C(1)−C(10)−C(11) | 110.2(2) | C(20)−C(21)−H(21) | 121(2) |
| C(1)−C(10)−C(12) | 109.4(3) | C(22)−C(21)−H(21) | 118(2) |
| C(1)−C(10)−C(13) | 109.4(2) | C(17)−C(22)−C(21) | 122.2(3) |
| C(11)−C(10)−C(12) | 109.8(3) | C(17)−C(22)−H(22) | 125(2) |
| C(11)−C(10)−C(13) | 108.8(3) | C(21)−C(22)−H(22) | 113(2) |

molecule is slightly bent around bond S(3) – C(5), the dihedral angle between the planes of A and C + D is 4.4°. A similar and somewhat more pronounced puckering has been observed in molecule IV.[6] The phenyl group is twisted 6.0° relative to the plane of ring D.

The bond C(10) – C(11) in the *t*-butyl group and bond C(2) – H(2) are eclipsed. The fractional atoms C(151) and C(152) are situated 0.4 and – 0.5 Å, respectively, out of the plane through C(4), C(5), C(6), C(14), C(16). Since the disorder of atom C(16) could not be resolved, the bond distances between C(16) and the adjacent atoms are not realistic. In a case like this, the standard deviations obtained from the inverse least-squares matrix are underestimated.
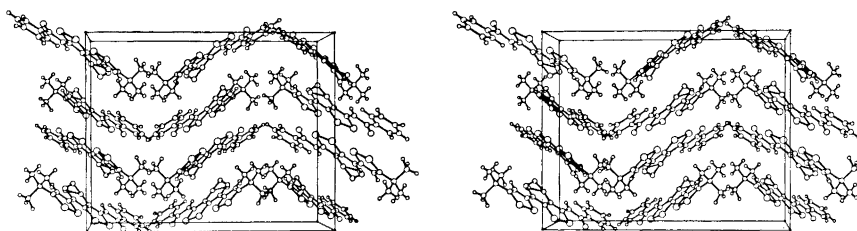


*Fig. 2.* Stereoscopic drawing showing the molecular packing as viewed down the *a*-axis.

The packing of molecules in the crystal is shown in a stereoplot (Fig. 2). Centrosymmetrically related molecules, *e.g.* the reference molecule and its inversion through $1,0,\frac{1}{2}$, partially overlap, the distance between the least-squares planes being 3.4 Å. The shortest intermolecular sulphur-sulphur distances occur between the reference molecule and its inversion through $\frac{1}{2},0,\frac{1}{2}$, the short contacts being: S(1) – S(3)′ = 3.458 Å, S(1) – S(4)′ = 3.684 Å, S(2) – S(3)′ = 3.676 Å, and S(2) – S(2)′ = 3.706 Å.

In compound IV,[6] which is closely related to the present structure, the two terminal S – S bonds are of the same lengths as those found in isolated 1,2-dithiolium rings,[3] while the central S···S distance is slightly shorter than Huggins' constant energy distance of 2.92 Å.[24] When considering the possibility of partial bonding between atoms held in a covalent framework, it is probably more relevant to compare an experimentally determined distance with Huggins' constant energy distance than with the usually quoted sum of van der Waals radii. The effect of extending the linear row by introducing an oxygen atom is clearly demonstrated in the present structure. There is a pronounced lengthening of the bond S(3) – S(4) adjacent to the oxygen atom from 2.062 Å to 2.110 Å, the latter being significantly longer than the single bond distance of 2.10 Å.[25] The S(4)···O distance of 2.327 Å is appreciably shorter than the sum of the constant energy radii of 2.58 Å,[24] indicating a significant interaction between S(4) and O. Rings C + D constitute a system analogous to the dithiafurophthenes, II. For these compounds S – S and S – O distances in the regions 2.101 – 2.137 Å and 2.184 – 2.443 Å, respectively, have been found.[26–30] The S(3) – S(4) and S(4)···O distances observed in the

present compound fit nicely into this pattern. The influence of the oxygen atom on the bonding between the sulphur atoms can also be detected in the slight change in the $S(2)\cdots S(3)$ distance. However, the effect is, as might be expected, minor and within the experimental error. The terminal $S(1)-S(2)$ bonds in the two compounds are identical. This indicates that a delocalized $\sigma$-system in the present compound does not include all the atoms in the linear row.

In compound VI, on the other hand, where the oxygen has been replaced by a sulphur atom the extention of the chain profoundly affects the bonding between all the atoms in the row. Thus compound VI, in contrast to the present compound, V, possesses an extended delocalized $\sigma$-system including all five atoms in the linear row.

Lists of observed and calculated structure factors may be obtained from the authors.

## REFERENCES

1. Poirier, Y. and Lozac'h, N. *Bull. Soc. Chim. France* **1967** 2090.
2. Stavaux, M. and Lozac'h, N. *Bull. Soc. Chim. France* **1968** 4273; **1969** 4184.
3. Hordvik, A. *Quart. Rep. Sulphur Chem.* **5** (1970) 21.
4. Hordvik, A. and Sæthre, L. J. *Israel J. Chem.* **10** (1972) 239.
5. Lozac'h, N. *Advan. Hetrocycl. Chem.* **13** (1971) 162.
6. Sletten, J. *Acta Chem. Scand.* **26** (1972) 873.
7. Sletten, J. *Acta Chem. Scand.* **24** (1970) 1464.
8. Hordvik, A. *Acta Chem. Scand.* **19** (1965) 1253; Hordvik, A., Sletten, E. and Sletten, J. Paper given at the *6th Nordic Structure Chemistry Meeting in Århus*, Denmark, Jan. 1967.
9. Sletten, J. *Chem. Commun.* **1969** 688; *Acta Chem. Scand.* **25** (1971) 3577.
10. Sletten, J. *Acta Chem. Scand.* **27** (1973) 229.
11. Oliver, J. E., Flippen, J. L. and Karle, J. *Chem. Commun.* **1972** 1153.
12. Kristensen, R. and Sletten, J. *Acta Chem. Scand.* **25** (1971) 2366; **27** (1973) 2517.
13. Behringer, H. and Weber, D. *Chem. Ber.* **97** (1964) 2567.
14. Stavaux, M. *Bull. Soc. Chim. France* **1971** 4429.
15. Peterson, J., Steinrauf, L. K. and Jensen, L. H. *Acta Cryst.* **13** (1960) 104.
16. Alexander, L. E. and Smith, G. S. *Acta Cryst.* **17** (1964) 1195.
17. Coppens, P., Leiserowitz, L. and Rabinovich, D. *Acta Cryst.* **18** (1965) 1035.
18. Long, R. E. *Ph. D. Dissertation*, University of California at Los Angeles 1965.
19. Karle, I. L., Hauptman, H., Karle, J. and Wing, A. B. *Acta Cryst.* **11** (1958) 257.
20. Zachariassen, W. H. *Acta Cryst.* **16** (1963) 1139.
21. Hanson, H. P., Hermann, F., Lea, J. D. and Skillmann, S. *Acta Cryst.* **17** (1964) 1040.
22. Stewart, R. F., Davidson, E. R. and Simpson, W. T. *J. Chem. Phys.* **42** (1965) 3175.
23. Johnson, C. K. *ORTEP* Report ORNL-3794, Oak Ridge National Laboratory, Oak Ridge, Tenn.
24. Huggins, M. L. *J. Am. Chem. Soc.* **75** (1953) 4126.
25. Hordvik, A. *Acta Chem. Scand.* **20** (1966) 1885.
26. Mammi, M., Bardi, R., Traverso, G. and Bezzi, S. *Nature* **192** (1961) 1282.
27. Hordvik, A., Sletten, E. and Sletten, J. *Acta Chem. Scand.* **23** (1969) 1377.
28. Pinel, R., Mollier, Y., Llaguno, E. C. and Paul, I. C. *Chem. Commun.* **1971** 1352.
29. Llaguno, E. C., Paul, I. C., Pinel, R. and Mollier, Y. *Tetrahedron Letters* **46** (1972) 4687.
30. Hordvik, A. and Sæthre, L. J. *Acta Chem. Scand.* **26** (1972) 849.

# NMR Experiments on Cyclic Sulfites

## V* High Resolution $^{13}$C Spectra of Trimethylene Sulfites by Fourier Transform NMR

PER ALBRIKTSEN

*Chemical Institute, University of Bergen, N-5000 Bergen, Norway*

The high resolution $^{13}$C NMR spectra of trimethylene sulfite, 5-methyl-, 5-*tert*-butyl-, 5-phenyl-, 5,5-dimethyl-, and 4-methyl trimethylene sulfite obtained without proton noise decoupling, have been analysed. The spectra are consistent with a rigid or anancomeric ring system. The $^{1}J_{CH}$ is found to be larger when the proton has a *cis* lone-electron pair vicinal or remote as compared to the geminal equatorial proton. The $^{2}J_{CH}$ and $^{3}J_{CH}$ are shown to have different values for couplings to an axial as compared to an equatorial proton. The vicinal carbon-proton coupling constant, $^{3}J_{CH}$, is found to be dependent on the dihedral angle of the $^{13}C-C-C-H$ moiety.

The cyclic trimethylene sulfites (TM-sulfites) have been studied in detail by proton NMR.[1-4] It is well known that the TM-sulfites exist mainly in a chair conformation with the $S=O$ group preferentially in the axial position. It has been an increasing interest in the measurement of coupling constants between carbon atoms and protons to which they may or may not be directly bonded. Apart from the inherent interest in such coupling constants, they are expected to give valuable information about molecular structures and conformations.

The recent developed method of pulsed-Fourier transform NMR spectroscopy[5] is shown to be particularly suited for $^{13}$C NMR studies of organic compounds containing natural abundance of $^{13}$C. This work was undertaken in an attempt to obtain experimental data for an angular dependence of the vicinal coupling, $J_{^{13}CCCH}$. One problem of high resolution $^{13}$C NMR arises from the fact that the carbon-hydrogen couplings over more than two bonds, are not always attenuated by interposition of an additional bond.[6] The complexity of the spectrum is increased by the number of coupled protons. One simplification is, however, obtained due to the large chemical shift between carbon and proton. The $^{13}$C spectra can be analysed according to first order rules and hence the signs are not easily obtained.

---

\* Part IV is Ref. 4.

## EXPERIMENTAL

The compounds studied were synthesized as reported previously.[1,3] The spectra were obtained of samples containing the TM-sulfites diluted to *ca.* 30 % v/v in $CDCl_3$. The spectra were obtained at ambient temperature on either a JEOL PFT-100 or a Varian associates XL-100-15 spectrometer, both equipped for continuous wave, CW, and Fourier transform, FT, operation.

The spectrometers were only operated in FT mode at 25.2 MHz. The XL-100-15 spectrometer was connected to a Varian 620i Computer with 4K memory available for data acumulation. The JEOL PFT-100 spectrometer was connected to a JEC-6 computer with 8K available data storage capacity. The spectra were obtained using 12 mm (Varian) or 8 mm (JEOL) O.D. sample tubes with internal $^2H$ lock to $CDCl_3$. All undecoupled spectra which were used in the detailed analyses were obtained using 8K data points. In the FT mode 8 to 9 μsec pulses were applied to either a 2 kHz region or separately to two 1 kHz regions.

The resolution was limited by the computer and is *ca.* 0.5 Hz for a 2 kHz and *ca.* 0.25 Hz for a 1 kHz spectral window, corresponding to 4096 output datapoints in the absorption spectrum. The proton undecoupled $^{13}C$ spectra were recorded after performing 10 000 to 20 000 spectral accumulations, and no line broadening was observed. The spectral windows were carefully chosen to avoid any folding to obscure the spectral regions of interest.

## SPECTRAL ANALYSIS

The $^{13}C$ spectra were analysed using the iterative programs [7] LAOCN3, LACX, and UEAITR. The TM-sulfite were analysed as an AA'BB'CDX (X = $^{13}C$) spin system with the observed spectrum consisting of two separate seven-spin systems (Fig. 1). Iterativ calculations were performed only for the spectral part involving the carbon in position 5.
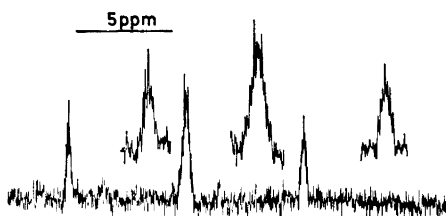


*Fig. 1.* The $^{13}C$ spectrum of carbon 5 of TM-sulfite at 25.2 MHz. The inserts are expanded twice. The spectrum is obtained using 4K data points on a 500 Hz spectral window.

The 5-*tert*-butyl- (Fig. 2) and 5-phenyl-TM sulfite were analysed as an AA'BB'CX spin system with respect to the nuclei in the TM-sulfite ring. Iterative computations were, however, carried out only for the cases with $^{13}C$ in positions 4 or 6. The $^{13}C$ signals due to $C_5$ were in both cases broadened by long range couplings to protons of the substituent. These couplings resulted in non-resolvable fine structure of the signals due to $^{13}C_5$.

The 5-*e*-methyl-TM-sulfite (Fig. 3) was analysed as an AA'BB'CD₃X spin system only for the $^{13}C$ in positions 4 and 6. Treating the $^{13}C$ spectrum of $C_{4(6)}$ as an AA'BB'CX spin-system gave the same results as the complete AA'BB'CD₃X spin-system. The spectrum due to $^{13}C$ in position 5 was not analysed because the long range C−H couplings (a doublet) have no resolvable fine structure.

Trial $^{13}C$ parameters for all compounds studied were obtained by inspection of the undecoupled $^{13}C$ spectra. The proton-proton couplings and proton
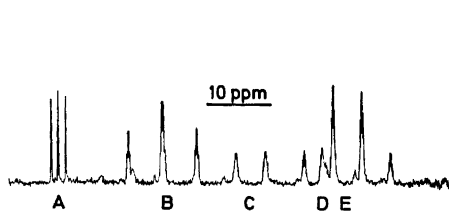
*Fig. 2.* The total $^{13}$C NMR spectrum of 5-*e-tert*-butyl-TM sulfite at 25.2 MHz; A, CDCl$_3$ solvent signals; B, the carbons 4 and 6; C, the carbon 5; D, the tertiary carbon of the *tert*-butyl group. (The signal is saturated due to experimental conditions); E, the carbons of the methyl groups. The spectral window is 2 kHz and the spectrum is recorded with 8K data points.
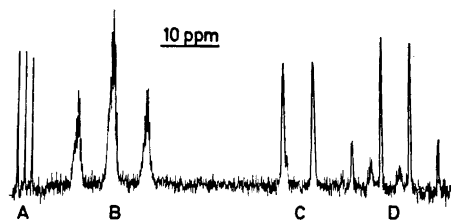
*Fig. 3.* The $^{13}$C NMR spectrum at 25.2 MHz of the 5-*e*-methyl-TM sulfite; A, signals due to the solvent, CDCl$_3$; B, the carbons 4 and 6; C, the carbon 5; D, the carbon of the methyl group. The spectrum is recorded with 8K data points on a 2 kHz spectral window.

chemical shifts are published previously.[1,3,4] Only $^{13}$C spectral parameters were allowed to vary during the iterative calculations. The RMS values were better than 0.3 Hz for all cases when fitting all theoretical transitions to observed lines. Visual comparisons of observed spectra with theoretical Lorentz-shape spectra indicated that the computed intensities were satisfactory in each case. The calculations were performed using an IBM 360/50 computer and the theoretical spectra were plotted using a Calcomp Plotter.

## DISCUSSION

The $^{13}$C NMR data (Tables 1 and 2) are consistent with earlier observations that the unsubstituted and 5-substituted TM-sulfites are in a rigid chair conformation. The direct carbon proton coupling, $^1J_{CH}$, is different for the two geminal protons in the 4 (or 6) position as well as in the 5 position in the ring (Table 1). Laszlo [8] postulated that the direct $^{13}$C$-$H coupling in a methylene group is dependent on two terms, one inversely proportional to the angle defined by the bonds between $^{13}$C and the substituents and secondly, effects of a ionic perturbation caused by a hetero atom attached to the methylene carbon. The angular dependence of $^{13}$C couplings cannot account for a difference in the direct coupling between $^{13}$C and H$_a$ as compared to the coupling to H$_e$. The ionic perturbations are not assumed to perturb the couplings differently.

The $^1J_{CH}$ couplings to the carbon atoms in positions 4 and 6 in the sulfite ring are about 147 Hz and 155 Hz for the spin-spin interaction involving the axial and equatorial protons, respectively. The larger coupling is assigned to the direct $J_{CH}$ to the equatorial proton situated *cis* to the equatorial lone pair electrons on the oxygen, based on the observations for the 4-*e*-methyl TM-sulfite (see Table 1).

Rattet *et al.*[9] reported different direct C$-$H couplings, 141.0 Hz and 139.6 Hz, to the two non-equivalent methylene protons in acetaldehyde

*Table 1.* $^{13}$C $-$ H coupling constants in Hz.
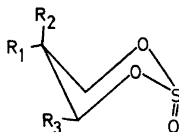


| R$_1$,R$_2$,R$_3$ | $^{13}$C$_{4(6)}$ | | | $^{13}$C$_5$ | | $-$CH$_3$ |
|---|---|---|---|---|---|---|
| | $^1J_{CH}$ | $^2J_{CH}$ | $^3J_{CH}$ | $^1J_{CH}$ | $^2J_{CH}$ | |
| I H,H,H | 153.9<br>147.8 | 7.5<br>1.3 | 7.5<br>3.2 | 127.5<br>131.9 | 2.6<br>1.4 | |
| II CH$_3$,H,H | 153.3<br>146.9 | 7.3 | 7.3<br>2.9 | 132.0 | a | $^1J_{CH}=127.4$<br>$^2J_{CH}=\phantom{0}3.9$ |
| III t-Bu,H,H | 153.6<br>146.6 | 6.2 | 6.3<br>2.4 | 132.1 | a | $^1J_{CH}=125.4$<br>$^3J_{CH}=\phantom{0}3.0$ |
| IV Ph,H,H | 156.5<br>148.4 | 5.7 | 5.9<br>2.3 | 132.6 | a | |
| V H,H,CH$_3$ | 147.5$^b$<br>155.0$^b$<br>148.9$^c$ | 5.6$^b$<br>1.3$^b$<br>5.9$^c$ | a<br>a | 127.0<br>131.0 | a<br>a | $^1J_{CH}=127.0$<br>$^2J_{CH}=\phantom{0}2.9$ |

$^a$ Not calculated, because bands did not show any resolved fine structure. $^b$ Coupling to carbon 6. $^c$ Coupling to carbon 4.

*Table 2.* Chemical shift in ppm from TMS.

| | C$_4$ | C$_5$ | C$_6$ | CH$_3$ | |
|---|---|---|---|---|---|
| I | 56.92 | 25.23 | 56.92 | — | |
| II | 60.30 | 28.01 | 60.30 | 10.63 | |
| $^a$ | 61.05 | 27.62 | 61.05 | 12.88 | |
| III | 58.64 | 44.33 | 58.64 | 26.46 | $^{13}$C$_{tert}$ 30,22 |
| IV | 60.01 | 40.41 | 60.01 | — | |
| $^b$ | 65.79 | 30.84 | 65.79 | 21.71 | |
| V | 63.61 | 32.63 | 56.85 | 20.52 | |

$^a$ 5-$a$-Methyl TM-sulfite. $^b$ 5,5-Dimethyl TM-sulfite.

diethylacetal. The direct $^{13}$C $-$ H coupling value, apparently, reflect decisively a non-equivalence of methylene protons. The occurrence of two distinct $^{13}$C $-$ H couplings in methylene groups means that non-equivalence can be localized in the two corresponding C $-$ H bonds. The presence of an S $=$ O group in the proximity of a C $-$ H bond could create field effects which would lower the average triplet exitation energy. Such lowering might produce

changes in $^1J_{CH}$ without rehybridization occurring at the carbon atom. The effect of the $S=O$ group is expected to be small because polar substituents at remote positions affect the direct $C-H$ coupling to a minor extent (vide infra). The lone pair electrons on a nitrogen or an oxygen atom affects the geminal proton-proton coupling in an adjacent $CH_2$ group.[10,11] The directly bonded $^{13}C-H$ coupling constant is shown to depend upon the orientation of a nitrogen lone pair electrons,[12,13] with the direct coupling of a $C-H$ group cis to lone pair electrons larger as compared to $^1J_{CH}$ of the trans $C-H$ group. The difference between $^1J_{CH}(cis)$ and $^1J_{CH}(trans)$ is ca. 10 Hz for $N$-methyl aziridine[12] and ca. 14 Hz for the methyl proton of acetaldoxime.[12] The difference in $^1J_{CH}$, of the sulfites, involving $C_4$ or $C_6$, of ca. 8 Hz between values for axial and equatorial oriented CH groups is mainly due to the effect of the equatorial lone pair electrons on the oxygens. The smaller difference as compared to for example aziridine[12] may be attributed to the field effect of a syn axial $S=O$ group which would oppose the effect of the equatorial lone pair electrons of the ring oxygen. The observed difference between the two direct couplings for the sulfite is substantial with a magnitude of about 50 % of the total effect produced by an oxygen atom substituted into methane.[14] It has, however, in some cases been reported that $^{13}C-H$ couplings are affected by the medium.[15,16]

Moreover, the difference in $^1J_{CH}$ of carbon 5, about 4 Hz, is significant and is parallelled by the observation that the axial proton at carbon 5 in TM-sulfites resonates at higher frequency as compared to the equatorial proton.[1] This is the reversed sequence with respect to cyclohexane. It has been pointed out that the reason for this, as regards dioxanes,[19] might be an interaction between $H_{5e}$ and the $p$-orbitals of the ring oxygens. Such an effect could account for the observed difference in $^1J_{CH}$ between the axial and equatorial $C_5-H$ groups of the TM-sulfites. The observed direct couplings to carbon 5 are of the magnitude 127.5 Hz and 132.5 Hz for TM-sulfite and ca. 127 Hz and 131 Hz for 4-$e$-methyl TM-sulfite. The larger value is the coupling to the axial proton which has two remote syn axial lone pair electrons. This assignment is consistent with values obtained for $C-H_{5a}$ (ca. 132 Hz) in 5-$e$-methyl, 5-$e$-phenyl and 5-$e$-tert-butyl TM-sulfite (see Table 1).

The magnitude of two and three bond coupling constants involving carbon atoms in positions 4 and 6 of 5-equatorial substituted TM-sulfites are in the range 7.5 Hz to 1.3 Hz. The values of the pertinent coupling constants to carbon 6 obtained for 4-$e$-methyl TM-sulfite are 5.6 and 1.3 Hz. The observed values in TM-sulfite involving carbons 4 or 6 are 7.5 Hz, 7.5 Hz, 3.2 Hz, and 1.3 Hz. The observed values $7.5-6.0$ Hz and $2.0-1.3$ Hz may be assigned to the $^2J_{CH}$ involving the carbons 4 or 6. The larger value is assigned to the coupling to $H_{5a}$, which is consistent with the values obtained for 5-$e$-substituted TM-sulfites. Accordingly, the other pair of values, $7.5-5.9$ Hz and $3.2-2.3$ Hz, may be assigned to $^3J_{CH}$. The larger value is attributed to the spin-spin interaction involving $C_6$ and $H_{4e}$. This is consistent with the observation of only one large vicinal coupling, 5.6 Hz, to carbon 6 in the 4-$e$-methyl TM-sulfite. Moreover, it is apparent that both the $^2J_{CH}$ and $^3J_{CH}$ (Table 1) have pairs of different coupling values, ca. 6.0 Hz and 2.0 Hz, indicating conformational dependence of these two coupling constants.

The two bond $C-H$ couplings involving carbon 5 in TM-sulfite, also, have two distinct values, 2.6 Hz and 1.4 Hz. The difference in values obtained for $^2J_{CH}$ involving carbon 5 as compared to carbons 4 (or 6) indicates substantial effects due to electronegativity of the substituent attached to the carbon. Moreover, the difference between the two $^2J_{CH}$ indicates that this coupling is dependent on the orientation of the coupling path relative to the substituent on the coupled carbon atom. The observed two bond $^{15}N-H$ coupling in aliphatic nitrogen compounds is found to be stereospecific and dependent on orientation of the nitrogen lone-pair.[18] Similar observations have been made for $^2J_{PH}$ in tervalent phosphorus. Theoretical INDO MO calculations [19] verify the effect of the nitrogen lone-pair for aliphatic amines. As regards the sulfites, the observed values of $^2J_{CH}$ are different whether an *axial* or an *equatorial* proton is involved in the spin-spin interaction. It is apparent that there exists a correlation of the sign and magnitude of $^2J_{CH}$ with molecular structure.[29] The $^2J_{CH}$ has been reported to hold either signs,[20-23] but INDO MO calculations [29] suggest that the sign of this coupling constant is negative as regards propane and butane.

The proton-carbon coupling constants through three bonds, $^3J_{^{13}CCCH}$, are in the range 2.3 Hz to 7.5 Hz for the TM-sulfites (Table 1). Karabatsos and Orzech [24] reported coupling constants in the range 3.59 Hz to 5.99 Hz for $sp^3$ hybridized $^{13}C$. The variation of $^3J_{CH}$ indicates that in addition to the $s$-character of the $^{13}C$ hybrid atomic orbital, other factors must affect this coupling. Long range coupling between protons is generally believed to be dominated by the Fermi contact interaction. These terms may also give rise to the most significant contribution to the coupling between other nuclei such as carbon and proton. Substituents bonded to $^{13}C$ should affect the $^3J_{CH}$ due to its electronegativity.

Increasing electronegativity of the substituent should increase $^3J_{CH}$ by virtue of increasing the $s$-character [25] of the $^{13}C$ atomic orbital used in the carbon-carbon bond. It is reasonable to assume that a relationship similar to the Karplus [25] relation also relating the $^3J_{CH}$ with the dihedral angle in a $^{13}C-C-C-H$ fragment. Wasylishen and Schaefer [27] recently proposed an angle dependence of the vicinal $^{13}C-H$ coupling constant in propane from INDO MO calculations. Their calculations predicted a dihedral angle dependence similar to that observed for $^3J_{CH}$ in the TM-sulfites. The observation that the vicinal $C-H$ coupling in TM-sulfites to the equatorial and the axial proton is different, 7.5 Hz and 3.2 Hz, respectively, supports the theoretical calculations of Schaefer *et al.*[27] and adds evidence to the assumption that the TM-sulfite exists in a rigid or anancomeric system.

One of the problems in the interpretation of chemical shifts in $^{13}C$ magnetic resonance is adequate to take into account effects produced by the anisotropy of neighbouring atoms or groups. It has been assumed that in contrast to the $^{13}C$ coupling constants the $^{13}C$ chemical shifts should be sensitive to anisotropy, medium effects and factors which do not complicate the interpretation of the coupling constants. Moreover, it appears that $^{13}C-H$ coupling constants provide a direct and resonably reliable measure of the $s$-character in the carbon bonding orbital. It might be expected that in the absence of medium effects *etc.* a close relation should exist between $^{13}C$ shifts and $^1J_{CH}$. Such a correlation

is not easily obtained from the available data on TM-sulfites, so it might be relevant to compare shift data for TM-sulfites with those for cyclohexanes [22],[23] (Fig. 4) and 1,3-dioxanes [28] (Fig. 5). Plotting the chemical shifts of carbons 4 (or 6) and carbon 5 in 5-substituted TM-sulfites *versus* the pertinent shift values for either 5-substituted 1,3-dioxanes [28] or monosubstituted cyclohexanes [22],[23] indicates a linear relationship (Figs. 4 and 5). It is apparent that an alkyl substituent affects the chemical shift of the α- or β-carbon in TM-
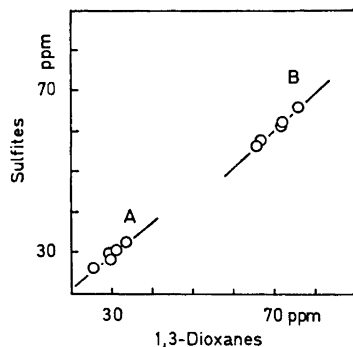


*Fig. 4.* The plot of ^{13}C shifts of the TM-sulfites *versus* the pertinent carbon shifts of 1,3-dioxanes;[28] A, the carbon holding the substituent; B, the β-carbon relative to the substituent. The shifts is measured relative to the TMS ^{13}C signal.
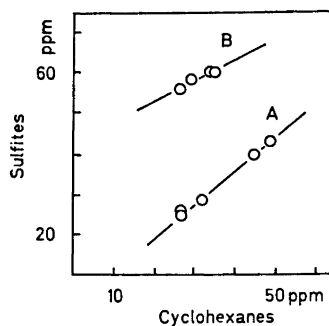
*Fig. 5.* The plot of ^{13}C shifts (ppm from TMS ^{13}C) of the 5-substituted-TM sulfites *versus* the pertinent ^{13}C shift of the related mono-substituted cyclohexanes;[22],[23] A, α-carbon *i.e.* the carbon holding the substituent; B, β-carbon relative to the substituent.

sulfites (Table 3) to the same extent as in cyclohexane.[22],[23] The shift of carbon 5 is hardly affected by the $S = O$ group. Comparison of the geminal (H,H) coupling constants for sulfites and dioxanes suggests that electronegativity differences between the $O - C - O$ and $O - S(O) - O$ moieties are responsible for the difference in carbon chemical shifts in the two types of compounds. Any substituent into a ring appears to have little effect on the chemical shift of a remote ring-carbon. The effect on the chemical shifts (Table 3) of introducing a phenyl group into the TM-sulfite ring gives rise to similar effects as

*Table 3.* Substituent effects on ^{13}C chemical shifts (ppm) in TM-sulfites.

| Substituent | $C_4$ | $C_5$ | $C_6$ |
|---|---|---|---|
| 5-*e*-Me | + 3.4 | + 2.8 | + 3.4 |
| 5-*a*-Me | + 4.1 | + 2.4 | + 4.1 |
| 5,5-Me$_2$ | + 8.9 | + 5.5 | + 8.9 |
| 5-*e*-*t*-Bu | + 1.7 | + 19.1 | + 1.7 |
| 5-*e*-Ph | + 3.1 | + 15.2 | + 3.1 |
| 4-*e*-Me | + 6.7 | + 7.4 | − 0.1 |

observed for cyclohexanes.[22,23] The introduction of geminal methyl groups does not change the carbon chemical shift an amount equal to the sum of the changes on introducing the equatorial and axial methyl groups separately.

## REFERENCES

1. Albriktsen, P. *Acta Chem. Scand.* **25** (1971) 478.
2. Green, C. H. and Hellier, D. G. *J. Chem. Soc. Perkin Trans. 2* **1972** 458.
3. Albriktsen, P. *Acta Chem. Scand.* **26** (1972) 1783.
4. Albriktsen, P. *Acta Chem. Scand.* **26** (1972) 3678.
5. Farrar, T. C. and Becker, E. D. *Pulse and Fourier Transform NMR*, Academic, New York 1971.
6. Mooney, E. F. and Wenson, P. H. *Ann. Rev. NMR Spectroscopy* **2** (1969) 204.
7. Harris, R. K. and Stokes. J. *A Library of Computer Programs for NMR Spectroscopy*, Science Research Council, (Atlas Computer Laboratory) 1971, and references therein.
8. Laszlo, S. *Bull. Soc. Chim. France* **1966** 558.
9. Rattet, L. S., Mandell, L. and Goldstein, J. H. *J. Am. Chem. Soc.* **89** (1967) 2253.
10. Chang, C. F., Fairless, B. J. and Willcott, M. R. *J. Mol. Spectry.* **22** (1967) 112.
11. Pople, J. A. and Bothner-By, A. A. *J. Chem. Phys.* **42** (1965) 1339.
12. Yonezawa, T. and Morishima, I. *J. Mol. Spectry.* **27** (1968) 210.
13. Yonezawa, T., Morishima, I., Fukuta, K. and Ohmori, Y. *J. Mol. Spectry.* **31** (1969) 341.
14. Mullier, N. and Pritchard, D. E. *J. Chem. Phys.* **31** (1959) 1471.
15. Evans, D. T. *J. Chem. Soc.* **1963** 5575.
16. Watts, V. S. and Goldstein, J. H. *J. Phys. Chem.* **70** (1966) 3887.
17. Anteunis, M., Tavernier, D. and Borremans, F. *Bull. Soc. Chim. Belges* **75** (1966) 396.
18. Randell, E. W. and Gillies, D. G. *Progress in NMR*, Vol. 6, p. 119.
19. Wasylishen, E. and Schaefer, T. *Can. J. Chem.* **50** (1972) 2989.
20. Freeman, R. and Anderson, W. A. *J. Chem. Phys.* **39** (1963) 806.
21. Dreeskamp, H. and Sackmann, E. *Z. physik. Chem. Frankfurt am Main.* **34** (1962) 273.
22. Pehk, T. and Lippman, E. *Org. Magn. Resonance* **3** (1971) 679.
23. Dalling, D. K. and Grant, D. M. *J. Am. Chem. Soc.* **89** (1967) 6612.
24. Karabatsos, G. J. and Orzech, C. E., Jr. *J. Am. Chem. Soc.* **87** (1965) 560.
25. Bent, H. A. *Chem. Rev.* **61** (1961) 275.
26. Karplus, M. *J. Am. Chem. Soc.* **85** (1965) 2870.
27. Wasylishen, R. and Schaefer, T. *Can. J. Chem.* **50** (1972) 2710.
28. Kelhie, G. M. and Riddell, F. G. *J. Chem. Soc.* **B 1971** 1030.
29. Albriktsen, P. and Fægri, K. *Unpublished work.*

# Association Equilibria and Micelle Formation of Fatty Acid Sodium Salts. IV. A Comparison between the Association of Sodium Pentanoate, Sodium 3-Methylbutyrate and Sodium Trimethylacetate

PER STENIUS

*Department of Physical Chemistry, Åbo Akademi, Porthansgatan 3—5, SF-20500 Åbo 50, Finland*

A potentiometric investigation of the self-association of sodium 3-methylbutyrate and sodium trimethylacetate has been made in the ionic medium 3 M Na(Cl) at 25°C. The following complexes and stability constants have been found:

Sodium 3-methylbutyrate: ($B^- =$ the 3-methylbutyrate anion)

| | |
|---|---|
| $B^- + H_2O \rightarrow HB + OH^-$ | $-\log \beta_{1,1} = 9.232 \pm 0.016$ |
| $4B^- + H_2O \rightarrow HB_4{}^{3-} + OH^-$ | $-\log \beta_{1,4} = 9.169 \pm 0.052$ |
| $15B^- \rightarrow B_{15}{}^{15-}$ | $-\log \beta_{0,15} = 6.35$ (max. 6.06) |

Sodium trimethyl acetate: ($B^- =$ the trimethylacetate anion)

| | |
|---|---|
| $B^- + H_2O \rightarrow HB + OH^-$ | $-\log \beta_{1,1} = 8.8593 \pm 0.0022$ |
| $4B^- + H_2O \rightarrow HB_4{}^{3-} + OH^-$ | $-\log \beta_{1,4} = 9.848 \pm 0.067$ |
| $4B^- + 2 H_2O \rightarrow H_2B_4{}^{2-} + OH^-$ | $-\log \beta_{2,4} = 17.481 \pm 0.073$ |
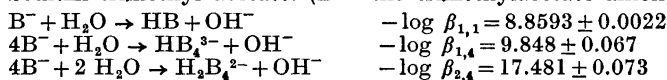
3-Methylbutyrate anions form micelles of about the same size as those of the pentanoate [1] but their stability constant is lower. The compact shape of the trimethyl acetate ions obviously prevents micelle formation, (the increase in mobility of the hydrocarbon part necessary to form stable micelles is not possible), but the small aggregates formed probably are stabilized by hydrophobic bonding.

In a number of investigations,[1-5] it has been shown that straight-chain sodium carboxylates with more than three carbon atoms in the hydrocarbon chain form small aggregates with $4-5$ anions, and that the smallest carboxylate molecule forming micelles is the pentanoate anion. Thermodynamic [4] as well as spectroscopic [5] results indicate that the attractive forces leading to formation of these aggregates probably are hydrophobic bonding, possibly in conjunction with ion-pair formation, since the sodium ion activity decreases when the association becomes appreciable.[4] This picture is consistent with several previous investigations of the pre-micellar aggregation of surfac-

Table 1. Titration of 0.1 M sodium 3-methylbutyrate at 25°C.

$C_B = 0.1000$ M          $E_{OH}° = 342.95$ mV
$C_H° = 0.009678$ M       $V = 40.00$ ml

| Amount of OH⁻ added mmol | $E$ mV | pOH | $Z_{exp}$ | $1000(Z_{exp} - Z_{calc})$ |
|---|---|---|---|---|
| 0 | − 146.7 | 8.277 | 0.0967 | − 0.9 |
| 0.01865 | − 145.1 | 8.250 | 0.0920 | − 1.5 |
| 0.03731 | − 143.6 | 8.225 | 0.0874 | − 1.6 |
| 0.05596 | − 142.0 | 8.198 | 0.0827 | − 1.6 |
| 0.07462 | − 140.2 | 8.167 | 0.0781 | − 2.1 |
| 0.09327 | − 138.4 | 8.137 | 0.0734 | − 2.2 |
| 0.1119 | − 136.5 | 8.105 | 0.0687 | − 2.2 |
| 0.1305 | − 134.5 | 8.071 | 0.0641 | − 2.3 |
| 0.1492 | − 132.3 | 8.034 | 0.0594 | − 2.4 |
| 0.1678 | − 129.9 | 7.993 | 0.0547 | − 2.5 |
| 0.1865 | − 127.3 | 7.949 | 0.0501 | − 2.7 |
| 0.2052 | − 124.6 | 7.904 | 0.0454 | − 2.5 |
| 0.2238 | − 121.5 | 7.851 | 0.0408 | − 2.6 |
| 0.2425 | − 118.0 | 7.792 | 0.0361 | − 2.6 |
| 0.2611 | − 114.1 | 7.726 | 0.0314 | − 2.5 |
| 0.2798 | − 109.4 | 7.647 | 0.0268 | − 2.6 |
| 0.2984 | − 103.9 | 7.554 | 0.0221 | − 2.5 |
| 0.3171 | − 97.3 | 7.442 | 0.0174 | − 2.1 |
| 0.3357 | − 88.0 | 7.285 | 0.0128 | − 2.1 |
| 0.3544 | − 74.4 | 7.055 | 0.0081 | − 1.8 |
| 0.3731 | − 44.5 | 6.550 | 0.0034 | − 1.4 |

Table 2. Titration of 0.5 M sodium 3-methylbutyrate at 25°C.

$C_B = 0.500$ M          $E_{OH}° = 348.4$ mV
$C_H° = 0.05530$ M       $V = 40.00$ ml

| Amount of OH⁻ added mmol | $E$ mV | pOH | $Z_{exp}$ | $1000(Z_{exp} - Z_{calc})$ |
|---|---|---|---|---|
| 0.1865 | − 147.3 | 8.380 | 0.1013 | 22.3 |
| 0.3731 | − 140.6 | 8.266 | 0.0919 | 7.4 |
| 0.5596 | − 135.7 | 8.183 | 0.0826 | 1.6 |
| 0.7462 | − 131.3 | 8.109 | 0.0733 | − 0.9 |
| 0.9327 | − 126.9 | 8.035 | 0.0640 | − 1.8 |
| 1.119 | − 122.1 | 7.954 | 0.0546 | − 2.1 |
| 1.305 | − 116.8 | 7.864 | 0.0453 | − 1.9 |
| 1.492 | − 110.4 | 7.766 | 0.0360 | − 1.6 |
| 1.548 | − 108.3 | 7.720 | 0.0332 | − 1.4 |
| 1.604 | − 105.9 | 7.680 | 0.0304 | − 1.3 |
| 1.660 | − 103.2 | 7.634 | 0.0276 | − 1.2 |
| 1.716 | − 100.3 | 7.585 | 0.0248 | − 1.1 |
| 1.772 | − 97.2 | 7.533 | 0.0220 | − 0.9 |
| 1.828 | − 93.6 | 7.472 | 0.0192 | − 0.8 |
| 1.884 | − 89.3 | 7.399 | 0.0164 | − 0.7 |
| 1.940 | − 84.3 | 7.315 | 0.0136 | − 0.6 |
| 1.996 | − 77.9 | 7.206 | 0.0108 | − 0.6 |
| 2.052 | − 69.8 | 7.069 | 0.0080 | − 0.6 |
| 2.108 | − 58.0 | 6.870 | 0.0052 | − 0.5 |

*Table 3.* Titration of 0.75 M sodium 3-methylbutyrate at 25°C.

$C_B = 0.750$ M $\quad\quad E_{OH}° = 351.8$ mV
$C_H° = 0.07353$ M $\quad\quad V = 40.00$ ml

| Amount of OH⁻ added mmol | $E$ mV | pOH | $Z_{exp}$ | $1000(Z_{exp} - Z_{calc})$ |
|---|---|---|---|---|
| 0 | − 132.2 | 8.182 | 0.0980 | − 4.7 |
| 0.1865 | − 130.4 | 8.151 | 0.0918 | − 3.5 |
| 0.3731 | − 128.2 | 8.114 | 0.0856 | − 3.1 |
| 0.5596 | − 126.0 | 8.077 | 0.0794 | − 2.4 |
| 0.7462 | − 123.6 | 8.036 | 0.0731 | − 1.8 |
| 0.9327 | − 121.0 | 7.992 | 0.0669 | − 1.3 |
| 1.119 | − 118.1 | 7.943 | 0.0607 | − 0.9 |
| 1.305 | − 115.0 | 7.891 | 0.0545 | − 0.5 |
| 1.492 | − 111.5 | 7.832 | 0.0483 | − 0.3 |
| 1.678 | − 107.6 | 7.766 | 0.0421 | 0 |
| 1.734 | − 106.3 | 7.744 | 0.0402 | 0.1 |
| 1.790 | − 105.0 | 7.722 | 0.0383 | 0.3 |
| 1.846 | − 103.5 | 7.697 | 0.0365 | 0.1 |
| 1.902 | − 102.0 | 7.671 | 0.0346 | 0.2 |
| 1.958 | − 100.4 | 7.644 | 0.0327 | 0.2 |
| 2.014 | − 98.8 | 7.617 | 0.0309 | 0.2 |
| 2.070 | − 97.0 | 7.587 | 0.0290 | 0.2 |
| 2.126 | − 95.0 | 7.553 | 0.0271 | 0.1 |
| 2.182 | − 92.9 | 7.517 | 0.0253 | − 0.1 |
| 2.238 | − 90.6 | 7.479 | 0.0234 | − 0.1 |
| 2.294 | − 88.2 | 7.438 | 0.0215 | − 0.2 |
| 2.350 | − 85.4 | 7.391 | 0.0197 | − 0.4 |
| 2.405 | − 82.4 | 7.340 | 0.0178 | − 0.5 |
| 2.461 | − 79.0 | 7.282 | 0.0159 | − 0.6 |
| 2.517 | − 75.0 | 7.215 | 0.0141 | − 0.9 |
| 2.573 | − 70.4 | 7.137 | 0.0122 | − 1.1 |
| 2.629 | − 64.8 | 7.042 | 0.0103 | − 1.3 |
| 2.685 | − 57.7 | 6.922 | 0.0085 | − 1.6 |
| 2.741 | − 47.9 | 6.757 | 0.0066 | − 1.9 |
| 2.797 | − 32.3 | 6.493 | 0.0048 | − 2.2 |
| 2.853 | 3.7 | 5.884 | 0.0029 | − 2.3 |
| 2.909 | 75.2 | 4.676 | 0.0010 | − 1.0 |

tants with larger hydrophobic moieties.[6-8] Similar considerations [9-10] are generally offered to explain micelle formation in general. A very important contribution to the decrease in Gibbs' energy of the surfactant molecules on micelle formation is the increased mobility of the hydrocarbon chains in the interior of the micelle, as compared to the mobility in water.[6,11] This contribution can hardly be conceived to play any important part in the formation of small aggregates with 2 − 4 ions. It also follows that micelles should not be formed by substances in which the structure of the hydrocarbon portion is such that it cannot increase its mobility on association with other similar molecules.

A method to test this model experimentally is to investigate substances in which the hydrocarbon portions are increasingly branched isomers of the

same compound. This has been done in the present investigation, where the aggregation processes in aqueous solutions of the sodium salts of 3-methylbutyric acid and trimethylacetic acid are compared to the association taking place in aqueous solutions of sodium pentanoate.

## LIST OF SYMBOLS

$[B^-]$ = concentration of free carboxylate ions
$C_B$  = total concentration of sodium carboxylate
$C_H$  = analytical excess of hydrogen ions; $C_H{}^\circ$ = initial excess of hydrogen ions
$E$  = experimental electromotive force; $E_{OH}$ = constant (standard cell potential), $E_j$ = liquid junction potential
$K_w$ = ionic product of water
$k$  = $RTF^{-1}\ln 10$
$\mathbf{k}$  = Boltzmann constant
$p, q$ = number of hydrogen and carboxylate ions
$U$  = error square sum
$V$  = volume of solution
$Z_{exp}$ = $(C_B - [H^+])/C_B$; $Z_{calc}$ = defined by eqn. (6)
$\beta_{p,q}$ = stability constant of complex $H_pB_q{}^{(q-p)-}$ [defined by eqn. (4)].
$\sigma(y)$ = standard deviation in $Z$

Table 4. Titration of 1.0 M sodium 3-methylbutyrate at 25°C.

$C_B$  = 1.000 M           $E_{OH}{}^\circ$ = 355.2 mV
$C_H{}^\circ$ = 0.09205 M           $V$  = 40.00 ml

| Amount of OH⁻ added mmol | $E$ mV | pOH | $Z_{exp}$ | $1000(Z_{exp} - Z_{calc})$ |
|---|---|---|---|---|
| 0 | − 123.1 | 8.085 | 0.0920 | − 2.3 |
| 0.1865 | − 120.7 | 8.045 | 0.0874 | − 3.5 |
| 0.3731 | − 118.8 | 8.013 | 0.0827 | − 3.1 |
| 0.5596 | − 117.0 | 7.982 | 0.0780 | − 2.3 |
| 0.7462 | − 115.1 | 7.950 | 0.0734 | − 1.7 |
| 0.9327 | − 113.2 | 7.918 | 0.0687 | − 0.8 |
| 1.119 | − 111.3 | 7.886 | 0.0640 | 0.3 |
| 1.305 | − 109.3 | 7.852 | 0.0594 | 1.2 |
| 1.492 | − 106.8 | 7.810 | 0.0547 | 1.6 |
| 1.678 | − 104.5 | 7.771 | 0.0500 | 2.6 |
| 1.865 | − 101.7 | 7.724 | 0.0454 | 2.9 |
| 2.052 | − 98.8 | 7.675 | 0.0407 | 3.5 |
| 2.238 | − 95.4 | 7.617 | 0.0361 | 3.6 |
| 2.425 | − 91.7 | 7.555 | 0.0314 | 3.9 |
| 2.611 | − 87.2 | 7.478 | 0.0267 | 3.8 |
| 2.798 | − 81.8 | 7.387 | 0.0221 | 3.4 |
| 2.984 | − 75.1 | 7.274 | 0.0174 | 2.9 |
| 3.171 | − 66.3 | 7.125 | 0.0127 | 2.2 |
| 3.357 | − 53.1 | 6.902 | 0.0081 | 1.2 |
| 3.544 | − 24.5 | 6.419 | 0.0034 | − 0.2 |

Table 5. Titration of 1.2 M sodium 3-methylbutyrate at 25°C.

$C_B = 1.200$ M  $E_{OH}° = 355.9$ mV
$C_H° = 0.1136$ M  $V = 40.00$ ml

| Amount of OH⁻ added mmol | $E$ mV | pOH | $Z_{exp}$ | $1000(Z_{exp} - Z_{calc})$ |
|---|---|---|---|---|
| 0.1865 | − 117.0 | 7.994 | 0.0907 | − 4.0 |
| 0.3731 | − 115.0 | 7.960 | 0.0868 | − 4.4 |
| 0.5596 | − 113.6 | 7.937 | 0.0829 | − 3.4 |
| 0.7462 | − 112.3 | 7.915 | 0.0791 | − 2.1 |
| 0.9327 | − 111.1 | 7.894 | 0.0752 | − 0.6 |
| 1.119 | − 109.8 | 7.872 | 0.0713 | 0.8 |
| 1.305 | − 108.5 | 7.850 | 0.0674 | 2.3 |
| 1.492 | − 107.1 | 7.827 | 0.0635 | 3.7 |
| 1.678 | − 105.6 | 7.801 | 0.0596 | 5.0 |
| 1.865 | − 103.9 | 7.773 | 0.0557 | 6.0 |
| 2.052 | − 102.1 | 7.742 | 0.0519 | 6.7 |
| 2.238 | − 100.1 | 7.708 | 0.0480 | 7.7 |
| 2.425 | − 97.9 | 7.671 | 0.0441 | 8.3 |
| 2.611 | − 95.5 | 7.631 | 0.0402 | 8.7 |
| 2.798 | − 92.8 | 7.585 | 0.0363 | 9.0 |
| 2.984 | − 89.7 | 7.533 | 0.0324 | 9.0 |
| 3.171 | − 86.2 | 7.474 | 0.0285 | 8.8 |
| 3.357 | − 82.1 | 7.404 | 0.0246 | 8.4 |
| 3.544 | − 77.3 | 7.323 | 0.0208 | 7.6 |
| 3.731 | − 71.3 | 7.222 | 0.0169 | 6.6 |
| 3.787 | − 69.4 | 7.190 | 0.0157 | 6.4 |
| 3.842 | − 67.2 | 7.152 | 0.0145 | 6.0 |
| 3.898 | − 64.8 | 7.112 | 0.0134 | 5.5 |
| 3.954 | − 62.1 | 7.066 | 0.0122 | 5.1 |
| 4.010 | − 59.2 | 7.017 | 0.0110 | 4.7 |
| 4.066 | − 55.8 | 6.960 | 0.0099 | 4.0 |
| 4.122 | − 52.0 | 6.895 | 0.0087 | 3.5 |
| 4.178 | − 47.5 | 6.819 | 0.0075 | 2.9 |
| 4.234 | − 41.9 | 6.725 | 0.0064 | 2.1 |
| 4.290 | − 35.1 | 6.610 | 0.0052 | 1.4 |
| 4.346 | − 25.8 | 6.452 | 0.0041 | 0.6 |
| 4.402 | − 11.0 | 6.202 | 0.0029 | − 0.2 |
| 4.458 | 21.3 | 5.656 | 0.0017 | − 0.9 |
| 4.514 | 90.5 | 4.486 | 0.0006 | − 0.6 |

## EXPERIMENTAL

*I. Potentiometric titrations.* The association of sodium trimethylacetate and sodium 3-methylbutyrate was studied in a series of potentiometric titrations in solutions made 3 M in Na⁺ by addition of NaCl. The procedure followed was essentially the same as that described in parts I and III.[1,3] In the titrations, the hydrolysis of trimethylacetic acid and 3-methylbutyric acid, respectively, was studied as a function of the total concentration $C_B$ of the sodium salts. The analytical excess of hydrogen ions, $C_B$, was varied by coulometric addition of OH⁻ ions. The concentration of free hydrogen ions was measured with a hydrogen electrode in combination with the reference electrode

Ag|AgCl|3 M NaCl (satd. with AgCl)
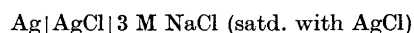
*Table 6.* Titration of 1.5 M sodium 3-methylbutyrate at 25°C.

$C_B = 1.500$ M $\qquad\qquad E_{OH}° = 362.1$ mV
$C_H° = 0.1594$ M $\qquad\qquad V = 40.00$ ml

| Amount of OH⁻ added mmol | $E$ mV | pOH | $Z_{exp}$ | $1000(Z_{exp} - Z_{calc})$ |
|---|---|---|---|---|
| 0.3731 | − 103.1 | 7.864 | 0.1000 | − 15.2 |
| 0.7462 | − 101.2 | 7.832 | 0.0938 | − 12.5 |
| 1.119 | − 99.4 | 7.801 | 0.0876 | − 9.5 |
| 1.492 | − 97.7 | 7.773 | 0.0814 | − 6.2 |
| 1.865 | − 95.9 | 7.742 | 0.0751 | − 3.0 |
| 2.238 | − 94.1 | 7.712 | 0.0689 | 0.3 |
| 2.611 | − 92.1 | 7.678 | 0.0627 | 3.3 |
| 2.984 | − 89.8 | 7.639 | 0.0565 | 6.0 |
| 3.357 | − 87.2 | 7.595 | 0.0503 | 8.4 |
| 3.731 | − 84.2 | 7.544 | 0.0440 | 10.5 |
| 4.104 | − 80.6 | 7.484 | 0.0378 | 12.0 |
| 4.477 | − 76.1 | 7.408 | 0.0316 | 12.7 |
| 4.850 | − 70.8 | 7.318 | 0.0254 | 13.0 |
| 5.223 | − 63.5 | 7.195 | 0.0192 | 12.0 |
| 5.596 | − 52.9 | 7.015 | 0.0130 | 9.7 |
| 5.969 | − 35.2 | 6.716 | 0.0067 | 6.1 |
| 6.342 | 62.4 | 5.066 | 0.0005 | − 0.2 |

and the bridge solution $|(3\ M - C_B)\ NaCl,\ C_B\ NaB|$, where B denotes the carboxylate anion. The complete cell may be written

$$Pt\,|\,H_2\,|\,H^+\ (in\ (3\ M - C_B)\ NaCl,\ C_B\ NaB)\,|\,bridge\,|\,ref.electr.$$
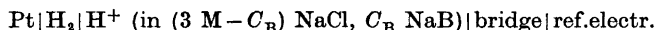
and its emf is given by

$$E = E_H° - k\ \log\ [H^+] + E_j = E_{OH}° + k\ \log\ [OH^-] + E_j \qquad (1)$$

where $E_j$ is the liquid junction potential and $k = RTF^{-1}\ln 10$. The constant ionic strength makes it possible to assume that the activity coefficient of $[OH^-]$ and $[H^+]$ may be included in the constants $E_{OH}°$ and $E_H°$, respectively.[12,13] $E_{OH}°$ was determined by addition of a known excess of $OH^-$ ions and by plotting the quantity $E - k\ \log\ [OH^-] = E_{OH}° + E_j$ against this excess. Since $E_j$ is a linear function of $[OH^-]$, $E_{OH}°$ may be determined by extrapolation to zero $[OH^-]$.[12,13] To calculate $[OH^-]$, the equivalence point was determined using a Gran plot.[14] The titrations were performed automatically with a stabilization period of 30 min after each addition of reagent before the final emf value was registered. The emf then generally was stable within ± 0.1 mV. The apparatus used has been described in detail in Ref. 15.

The silver/silver chloride electrode was prepared in a procedure slightly modified from that of Brown [16] and conditioned for several days in 3 M NaCl saturated with AgCl before use. The hydrogen electrode was prepared according to Bates.[17] The hydrogen gas used was passed through 10 % KOH, 10 % H₂SO₄, and two solutions of 3 M NaCl and then into the solution, to avoid evaporation of water from the solution.

*II. Chemicals. Sodium trimethylacetate* and *sodium 3-methylbutyrate* were prepared by neutralization of the corresponding acids (Fluka *purissimum* grade) with 1 M NaOH (Merck "Titrisol"). The salts were dried in a vacuum oven at 110°C. Their molecular weight was checked by titration with perchloric acid in glacial acetic acid and was found to differ less than 0.25 % from the theoretical value. *Sodium chloride.* (Merck *p.a.*) was dried in a vacuum oven at 110°C for a week before use. *Water* was distilled, passed through an ion exchange column, and then redistilled. Its conductivity was about 0.5 $\mu$S cm⁻¹. The *solutions* were prepared in volumetric flasks previously calibrated at 25°C.

## TREATMENT OF EXPERIMENTAL DATA

From the values of $E_{OH}°$ determined in the experiments one may calculate $E_H°$; using (1), and the relationship

$$E_H° = E_{OH}° + k \log K_w \qquad (2)$$

If $E_H°$ and $E_j$ are known, [H$^+$] and pH in the solutions can be calculated. In our titrations, $E_j$ was never larger than about 0.2 mV at pOH $ca.$ 11. In acid solutions, $E_j$ increases about 20 mV/mol H$^+$.[18] Since the pH in the solutions in this experiment is never lower than 5, it may safely be assumed that $E_j \approx 0$. However, it is possible that $K_w$ varies somewhat with $C_B$,[19] and this makes the calculation of pH in the solutions somewhat uncertain. For this reason, the association equilibria are written

$$q B^- + p H_2O \rightleftharpoons H_p B_q^{(q-p)-} + p OH^- \qquad (3)$$
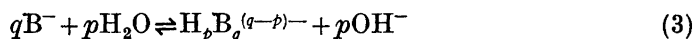
and the stability constants are defined by

*Table 7.* Titration of 2.0 M sodium 3-methylbutyrate at 25°C.

$C_B = 2.000$ M  
$C_H° = 0.3120$ M  
$\delta Z = 0.015 \pm 0.002$

$E_{OH}° = 234.2$ mV (369.5 mV) [a]  
$V = 40.00$ ml

| Amount of OH$^-$ added mmol | $E$ mV | pOH | $Z_{exp}$ | $1000(Z_{exp} - Z_{theor})$ |
|---|---|---|---|---|
| 3.731 | −209.1 | 7.470 | 0.1093 | −21.8 |
| 4.104 | −207.7 | 7.445 | 0.1046 | −19.3 |
| 4.477 | −206.2 | 7.419 | 0.1000 | −16.6 |
| 4.850 | −204.7 | 7.394 | 0.0953 | −14.0 |
| 5.223 | −203.2 | 7.367 | 0.0907 | −11.4 |
| 5.596 | −201.6 | 7.338 | 0.0860 | −8.9 |
| 5.969 | −199.9 | 7.308 | 0.0813 | −6.5 |
| 6.342 | −198.1 | 7.276 | 0.0767 | −4.1 |
| 6.715 | −196.2 | 7.244 | 0.0720 | −1.7 |
| 7.088 | −194.3 | 7.210 | 0.0673 | 0.3 |
| 7.462 | −192.3 | 7.171 | 0.0627 | 2.6 |
| 7.835 | −190.0 | 7.129 | 0.0580 | 4.6 |
| 8.208 | −187.5 | 7.083 | 0.0487 | 6.3 |
| 8.581 | −184.8 | 7.032 | 0.0440 | 8.0 |
| 8.954 | −181.8 | 6.975 | 0.0394 | 9.3 |
| 9.327 | −178.4 | 6.912 | 0.0347 | 11.3 |
| 9.700 | −174.7 | 6.835 | 0.0300 | 12.4 |
| 10.07 | −170.4 | 6.752 | 0.0254 | 12.8 |
| 10.44 | −165.2 | 6.640 | 0.0207 | 12.9 |
| 10.82 | −158.6 | 6.496 | 0.0160 | 12.9 |
| 11.19 | −150.1 | 6.277 | 0.0114 | 12.4 |
| 11.56 | −137.1 | 5.839 | 0.0067 | 11.8 |

[a] Since the range of the digital voltmeter was $\pm 230.0$ mV, a compensating potential of 135.3 mV was connected in series with the cell in this titration; the $E_{OH}°$ value 369.5 mV is the value without compensating potential.

*Table 8.* Titration of 3.0 M sodium 3-methylbutyrate at 25°C.

$C_B = 3.000$ M
$C_H° = 0.320$ M
$\delta Z = 0.0049 \pm 0.0006$

$E_{OH}° = 247.6$ mV   (382.9) [a]
$V = 40.00$ ml

| Amount of OH⁻ added mmol | $E$ mV | pOH | $Z_{exp}$ | $1000(Z_{ber} - Z_{exp})$ |
|---|---|---|---|---|
| 0 | − 193.6 | 7.458 | 0.1066 | − 9.0 |
| 0.3731 | − 192.3 | 7.436 | 0.1035 | − 8.2 |
| 0.7462 | − 191.0 | 7.414 | 0.1004 | − 7.4 |
| 1.119 | − 190.0 | 7.397 | 0.0973 | − 6.0 |
| 1.492 | − 188.8 | 7.377 | 0.0942 | − 5.1 |
| 1.865 | − 187.6 | 7.357 | 0.0911 | − 4.1 |
| 2.238 | − 186.2 | 7.333 | 0.0860 | − 3.5 |
| 2.611 | − 184.8 | 7.309 | 0.0849 | − 3.0 |
| 2.984 | − 183.3 | 7.284 | 0.0817 | − 2.4 |
| 3.357 | − 181.8 | 7.259 | 0.0786 | − 2.0 |
| 3.731 | − 180.4 | 7.235 | 0.0755 | − 1.4 |
| 4.104 | − 178.9 | 7.210 | 0.0724 | − 1.0 |
| 4.477 | − 177.2 | 7.181 | 0.0693 | − 0.8 |
| 4.850 | − 175.6 | 7.154 | 0.0662 | − 0.5 |
| 5.223 | − 173.9 | 7.125 | 0.0631 | − 0.2 |
| 5.596 | − 172.3 | 7.098 | 0.0600 | 0.3 |
| 5.969 | − 170.7 | 7.071 | 0.0569 | 0.8 |
| 6.342 | − 169.0 | 7.042 | 0.0538 | 1.3 |
| 6.715 | − 167.3 | 7.014 | 0.0507 | 1.8 |
| 7.088 | − 165.5 | 6.983 | 0.0475 | 2.4 |
| 7.462 | − 163.4 | 6.948 | 0.0444 | 2.6 |
| 7.835 | − 161.1 | 6.909 | 0.0413 | 2.6 |
| 8.208 | − 158.6 | 6.867 | 0.0382 | 2.6 |
| 8.581 | − 156.0 | 6.823 | 0.0351 | 2.7 |
| 8.954 | − 153.3 | 6.777 | 0.0320 | 2.9 |
| 9.327 | − 150.3 | 6.726 | 0.0289 | 3.0 |
| 9.700 | − 147.1 | 6.672 | 0.0258 | 3.2 |
| 10.07 | − 143.4 | 6.610 | 0.0227 | 3.3 |
| 10.44 | − 139.3 | 6.540 | 0.0196 | 3.5 |
| 10.82 | − 134.2 | 6.454 | 0.0164 | 3.6 |
| 11.19 | − 127.8 | 6.346 | 0.0133 | 3.5 |
| 11.56 | − 119.8 | 6.211 | 0.0102 | 3.5 |
| 11.93 | − 107.8 | 6.008 | 0.0071 | 3.4 |
| 12.31 | − 86.0 | 5.639 | 0.0040 | 3.3 |

[a] See note to Table 7.

$$\beta_{p,q} = ([H_p B_q][OH^-]^p)/[B^-]^q \tag{4}$$

The experimental values for $C_B$, $C_H$, and $[OH^-]$ are used to calculate the quantity

$$Z_{exp} = (C_H - [H^+])/C_B \tag{5}$$

which is the mean number of protons bound per carboxylate anion. In this equation $[H^+]$ may safely be calculated using $K_w$ for 3 M NaCl, since $C_H \gg [H^+]$ in all titrations and a small error in $[H^+]$ is of no consequence.
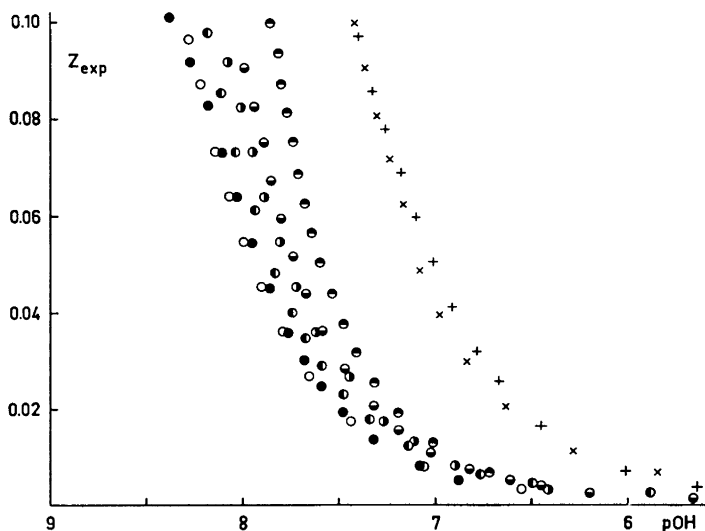
*Fig. 1.* The hydrolysis of sodium 3-methylbutyrate. $Z_{exp} = (C_H - [H^+])C_B$ plotted against pOH for different total concentrations $C_B$. Some of the points in Tables 1 − 8 have been left out. Concentrations of $C_B$ (M): 0.1 O; 0.5 ●; 0.75 ◖; 1.0 ◑; 1.2 ◒; 1.5 ◓; 2.0 ×; 3.0 +.

If the complexes formed in the solutions and their stability constants are known, a theoretical value for $Z$ can be calculated from [20],[21]

$$Z_{calc} = \frac{\sum p[OH^-]^{-p}[B^-]^q \beta_{pq}}{C_B} \qquad (6)$$

using experimental values for $[OH^-]$ and values of the free carboxylate ion concentration, $[B^-]$ calculated by solving the equation

$$C_B = [B^-] + \sum q[OH^-]^{-p}[B^-]^q \beta_{pq} \qquad (7)$$

the summation being taken over all combinations of $p$, $q$ defining existing complexes in the solution. The computer program LETAGROPVRID [22] developed by Sillén and co-workers, which has been used in the present work, uses guessed values for $p$, $q$, and $\beta_{pq}$ and experimental values for $C_B$ and $OH^-$ to calculate $Z_{calc}$ for each of the $n$ experimental points and then minimizes the sum of the squares of the errors

$$U = \sum_{i=1}^{n} (Z_{calc,i} - Z_{exp,i} + \delta Z)^2 \qquad (8)$$

by adjusting the $\beta_{pq}$ in (6). Here, $\delta Z$ is a systematic error in $Z_{exp}$, which may be different for each titration. As measures of the agreement between $Z_{exp}$ and $Z_{calc}$, $U$ and the quantity

*Table 9.* Calculations with LETAGROPVRID on the hydrolysis of sodium 3-methylbutyrate.

| p,q | Stability constants ($-\log \beta_{p,q}$) of tried complexes $H_pB_q$ | | | | | | | | | | | |
|---|---|---|---|---|---|---|---|---|---|---|---|---|
| | I | II | III | IV | V | VI | VII | VIII | IX | X | XI | XII |
| | Titr. 1−6 | Titr. 1−6 | Titr. 1−6 | Titr. 1−6 | All titr. | All titr. | All titr. | All titr. | All titr. | All titr. | All titr. | All titr. |
| 1,1 | 9.256± 0.017 | 9.268± 0.020 | 9.241± 0.015 | 9.2545± 0.0089 | 9.255± 0.040 | 9.270± 0.043 | 9.290± 0.098 | 9.290± 0.098 | 9.290± 0.098 | 9.290± 0.098 | 9.290± 0.098 | 9.252± 0.016 |
| 1,2 | | rej.[b] | | | | | | | | | | |
| 1,3 | | 9.264± 0.045 | | 9.63± 0.16 | | | 9.22± 0.015 | | | | | |
| 2,3 | | rej. | | | | | | | | | | |
| 1,4 | 9.50± 0.14 | rej. | rej. | 9.177± 0.054 | 9.267± 0.094 | | 9.071± 0.049 | 9.066± 0.050 | 9.071± 0.049 | 9.066± 0.052 | 9.166± 0.055 | 9.168± 0.052 |
| 2,4 | 17.73± 0.15 | rej. | rej. | | rej. | 17.85 max 17.60 | | | rej. | rej. | | |
| 3,4 | | rej. | rej. | | | | | | | | | |
| 1,5 | | | rej. | | | | | | | | | |
| 2,5 | | | 17.491± 0.046 | 17.71± 0.12 | | | 17.79 max 17.56 | | | | | |
| 1,8 | | | | | rej. | | | | | | | |
| 0,10 | | | | | | | | | 4.64± 0.23 | | | |
| 1,10 | | | | | | | | | | rej. | | |
| 0,12 | | | | | | | | 5.57± 0.30 | | rej. | | |
| 0,13 | | | | | | | | | rej. | rej. | | |
| 1,13 | | | | | | | rej. | rej. | rej. | 5.88[a] max. 5.62 | | |
| 0,14 | | | | | | | | | | | | |
| 0,15 | | | | | | | | | | | rej. | 6.35[a] max. 6.06 |
| 1,15 | | | | | | | | | | | rej. | |
| 1,16 | | | | | | | | rej. | | | rej. | |
| 1,20 | | | | | | | | | | | | |
| U | 0.00199 | 0.00263 | 0.00214 | 0.00152 | 0.01689 | 0.01573 | 0.01679 | 0.01149 | 0.01212 | 0.01149 | 0.01723 | 0.00748 |
| $\sigma(y)$ | 0.00377 | 0.00432 | 0.00389 | 0.00328 | 0.00917 | 0.00889 | 0.00919 | 0.00762 | 0.00780 | 0.00758 | 0.00926 | 0.00377 |

[a] max.: the standard deviation is larger than about 20 % of the stability constant and only a maximum value for the constant is given.
[b] rej.=rejected. The complex was tried together with other complexes in the same column, but the standard deviation was larger than 50 % of the stability constant.

Table 10. Titration of 1.00 M sodium trimethylacetate at 25°C.

$C_B = 1.000$ M
$C_H° = 0.05570$ M

$E_{OH}° = 216.3_5$ mV
$V = 40.00$ ml

| Amount of OH⁻ added mmol | $E$ mV | pOH | $Z_{exp}$ | $1000(Z_{calc} - Z_{exp})$ |
|---|---|---|---|---|
| 0 | − 253.3 | 7.635 | 0.0557 | 11.4 |
| 0.1865 | − 232.6 | 7.589 | 0.0510 | 9.5 |
| 0.3731 | − 230.0 | 7.545 | 0.0463 | 8.5 |
| 0.5596 | − 227.2 | 7.498 | 0.0417 | 7.5 |
| 0.7462 | − 224.0 | 7.444 | 0.0370 | 6.4 |
| 0.9327 | − 220.4 | 7.383 | 0.0324 | 5.3 |
| 1.119 | − 216.2 | 7.312 | 0.0277 | 4.3 |
| 1.305 | − 211.2 | 7.227 | 0.0230 | 3.3 |
| 1.492 | − 205.2 | 7.126 | 0.0184 | 2.4 |
| 1.678 | − 197.3 | 6.993 | 0.0137 | 1.5 |
| 1.734 | − 194.7 | 6.949 | 0.0123 | 1.4 |
| 1.790 | − 191.5 | 6.894 | 0.0109 | 1.2 |
| 1.846 | − 188.0 | 6.835 | 0.0095 | 1.0 |
| 1.902 | − 183.9 | 6.766 | 0.0081 | 0.9 |
| 1.958 | − 178.9 | 6.681 | 0.0067 | 0.7 |
| 2.014 | − 172.9 | 6.580 | 0.0053 | 0.5 |
| 2.070 | − 165.0 | 6.447 | 0.0039 | 0.4 |
| 2.126 | − 153.6 | 6.254 | 0.0025 | 0.2 |
| 2.182 | − 132.8 | 5.902 | 0.0011 | 0.1 |

Table 11. Titration of 1.2 M sodium trimethylacetate at 25°C.

$C_B = 1.200$ M
$C_H° = 0.08425$ M

$E_{OH}° = 219.1$ mV
$V = 40.00$ ml

| Amount of OH⁻ added mmol | $E$ mV | pOH | $Z_{exp}$ | $1000(Z_{calc} - Z_{exp})$ |
|---|---|---|---|---|
| 0 | − 232.4 | 7.632 | 0.0702 | 2.8 |
| 0.1865 | − 231.6 | 7.619 | 0.0663 | 4.6 |
| 0.3731 | − 230.3 | 7.597 | 0.0624 | 5.1 |
| 0.5596 | − 228.5 | 7.566 | 0.0585 | 4.4 |
| 0.7462 | − 226.8 | 7.538 | 0.0546 | 4.4 |
| 0.9327 | − 224.9 | 7.506 | 0.0507 | 4.0 |
| 1.119 | − 222.7 | 7.468 | 0.0469 | 3.3 |
| 1.305 | − 220.4 | 7.430 | 0.0430 | 2.9 |
| 1.492 | − 217.8 | 7.386 | 0.0391 | 2.3 |
| 1.678 | − 214.9 | 7.337 | 0.0352 | 1.7 |
| 1.865 | − 211.5 | 7.279 | 0.0313 | 1.0 |
| 2.052 | − 207.8 | 7.217 | 0.0274 | 0.5 |
| 2.238 | − 203.4 | 7.142 | 0.0235 | − 0.1 |
| 2.425 | − 198.4 | 7.058 | 0.0197 | − 0.5 |
| 2.611 | − 192.3 | 6.954 | 0.0158 | − 0.8 |
| 2.798 | − 184.0 | 6.814 | 0.0119 | − 1.1 |
| 2.984 | − 171.6 | 6.605 | 0.0080 | − 1.4 |
| 3.078 | − 162.0 | 6.442 | 0.0061 | − 1.6 |
| 3.096 | − 159.5 | 6.400 | 0.0057 | − 1.6 |
| 3.283 | − 86.7 | 5.196 | 0.0018 | − 1.6 |
| 3.301 | − 68.9 | 4.868 | 0.0014 | − 1.3 |
| 3.320 | − 50.7 | 4.561 | 0.0010 | − 0.9 |
| 3.339 | − 33.1 | 4.263 | 0.0006 | − 0.6 |

*Table 12.* Titration of 1.50 M sodium trimethylacetate at 25°C.

$C_B$ = 1.500 M  $E_{OH}°$ = 223.3 mV
$C_H°$ = 0.1108 M  $V$ = 40.00 ml

| Amount of OH⁻ added mmol | $E$ mV | pOH | $Z_{exp}$ | $1000(Z_{calc} - Z_{exp})$ |
|---|---|---|---|---|
| 0 | − 221.3 | 7.516 | 0.0738 | − 6.1 |
| 0.1865 | − 220.5 | 7.502 | 0.0707 | − 5.0 |
| 0.3731 | − 219.9 | 7.492 | 0.0676 | − 3.3 |
| 0.5596 | − 219.3 | 7.482 | 0.0645 | − 1.6 |
| 0.7462 | − 218.2 | 7.463 | 0.0614 | − 1.1 |
| 0.9327 | − 217.0 | 7.443 | 0.0583 | − 0.6 |
| 1.119 | − 215.8 | 7.423 | 0.0551 | 0.1 |
| 1.305 | − 214.3 | 7.397 | 0.0520 | 0.1 |
| 1.492 | − 212.8 | 7.372 | 0.0489 | 0.4 |
| 1.678 | − 211.1 | 7.343 | 0.0458 | 0.5 |
| 1.865 | − 209.4 | 7.315 | 0.0427 | 0.8 |
| 2.052 | − 207.5 | 7.282 | 0.0396 | 0.8 |
| 2.238 | − 205.4 | 7.247 | 0.0365 | 0.9 |
| 2.425 | − 203.0 | 7.206 | 0.0334 | 0.8 |
| 2.611 | − 200.5 | 7.164 | 0.0303 | 0.9 |
| 2.798 | − 197.5 | 7.113 | 0.0272 | 0.7 |
| 2.984 | − 194.2 | 7.058 | 0.0241 | 0.7 |
| 3.171 | − 190.3 | 6.992 | 0.0209 | 0.6 |
| 3.357 | − 185.7 | 6.914 | 0.0178 | 0.5 |
| 3.544 | − 180.0 | 6.818 | 0.0147 | 0.4 |
| 3.731 | − 172.6 | 6.692 | 0.0116 | 0.2 |
| 3.197 | − 162.2 | 6.517 | 0.0085 | 0.2 |
| 4.104 | − 144.9 | 6.224 | 0.0054 | 0.2 |
| 4.122 | − 142.4 | 6.182 | 0.0051 | 0.2 |
| 4.141 | − 139.7 | 6.136 | 0.0048 | 0.2 |
| 4.160 | − 136.7 | 6.086 | 0.0045 | 0.2 |
| 4.178 | − 133.4 | 6.030 | 0.0042 | 0.2 |
| 4.197 | − 129.5 | 5.964 | 0.0038 | 0.3 |
| 4.216 | − 125.0 | 5.888 | 0.0035 | 0.4 |
| 4.234 | − 119.7 | 5.798 | 0.0032 | 0.4 |
| 4.253 | − 113.1 | 5.687 | 0.0029 | 0.4 |
| 4.272 | − 105.0 | 5.550 | 0.0026 | 0.5 |
| 4.290 | − 94.8 | 5.377 | 0.0023 | 0.6 |
| 4.309 | − 82.3 | 5.166 | 0.0020 | 0.7 |
| 4.327 | − 68.2 | 4.928 | 0.0017 | 0.9 |
| 4.346 | − 53.4 | 4.677 | 0.0014 | 1.1 |
| 4.365 | − 37.6 | 4.410 | 0.0010 | 1.5 |
| 4.383 | − 20.5 | 4.121 | 0.0007 | 1.7 |

$$\sigma(y) = \sqrt{U_0/(n-1)} \tag{9}$$

may be used. Here, $U_0$ is the value of the minimum in the second-degree surface used to approximate the real $U$-function by LETAGROPVRID which is defined by the $\beta_{pq}$-values that are used to calculate the real $U$. If the real $U$ in fact is a minimum, the difference between $U$ and $U_0$ is small, and $\sigma(y)$ defines a standard deviation in $Z$.

*Table 13.* Titration of 1.8 M sodium trimethylacetate at 25°C.

$C_B = 1.800$ M          $E_{OH}° = 228.8$ mV
$C_H° = 0.1067$ M        $V = 40.00$ ml

| Amount of OH⁻ added mmol | $E$ mV | pOH | $Z_{exp}$ | $1000(Z_{exp} - Z_{theor})$ |
|---|---|---|---|---|
| 0 | − 208.5 | 7.392 | 0.0592 | − 1.4 |
| 0.1865 | − 207.4 | 7.374 | 0.0596 | − 1.2 |
| 0.3731 | − 206.2 | 7.353 | 0.0540 | − 1.1 |
| 0.5596 | − 205.0 | 7.333 | 0.0514 | − 0.9 |
| 0.7462 | − 203.8 | 7.313 | 0.0488 | − 0.6 |
| 0.9327 | − 202.5 | 7.291 | 0.0463 | − 0.4 |
| 1.119 | − 201.1 | 7.267 | 0.0437 | − 0.3 |
| 1.305 | − 199.6 | 7.242 | 0.0411 | − 0.2 |
| 1.492 | − 198.0 | 7.215 | 0.0385 | − 0.1 |
| 1.678 | − 196.2 | 7.184 | 0.0359 | − 0.1 |
| 1.865 | − 194.3 | 7.152 | 0.0333 | − 0.1 |
| 2.052 | − 192.4 | 7.120 | 0.0307 | 0.1 |
| 2.238 | − 190.2 | 7.083 | 0.0281 | 0.1 |
| 2.611 | − 185.0 | 6.995 | 0.0229 | 0.0 |
| 2.984 | − 178.5 | 6.885 | 0.0178 | − 0.1 |
| 3.357 | − 169.8 | 6.738 | 0.0126 | − 0.1 |
| 3.544 | − 163.8 | 6.637 | 0.0100 | − 0.2 |
| 3.600 | − 161.9 | 6.605 | 0.0092 | − 0.1 |
| 3.656 | − 159.7 | 6.567 | 0.0084 | − 0.1 |
| 3.712 | − 157.3 | 6.527 | 0.0077 | − 0.1 |
| 3.768 | − 154.6 | 6.481 | 0.0069 | − 0.1 |
| 3.824 | − 151.6 | 6.430 | 0.0061 | − 0.1 |
| 3.880 | − 148.1 | 6.371 | 0.0053 | 0.0 |
| 3.936 | − 144.0 | 6.302 | 0.0045 | 0.0 |
| 3.992 | − 139.3 | 6.223 | 0.0038 | 0.0 |
| 4.048 | − 133.4 | 6.123 | 0.0030 | − 0.1 |
| 4.104 | − 125.9 | 5.996 | 0.0022 | 0.0 |
| 4.160 | − 114.7 | 5.807 | 0.0014 | 0.0 |
| 4.216 | − 95.4 | 5.480 | 0.0007 | 0.0 |

## RESULTS AND CALCULATIONS

*I. Sodium 3-methylbutyrate.* The experimental values for sodium 3-methyl-butyrate are listed in Tables 1 − 8, and are summarized in Fig. 1. The titrations were carried out either in duplicate or in triplicate. For each of the concentrations, the titrations agreed within 0.005 units in $Z$. As discussed in Ref. 1, this is the best agreement that can be expected on the basis of an estimation of experimental errors. One of the titrations only was chosen for the calculations with LETAGROPVRID, to save calculation time. The reported values are those used in the calculations.

The calculations performed with LETAGROPVRID are summarized in Table 9.

(i) In four calculations, the titrations up to 1.5 M 3-methylbutyrate only were used. The reason for this is, that the titrations of $C_B = 2.0$ M and 3.0 M

almost coincide, indicating the dominance of large complexes. It was thus possible to rule out a large number of small complexes in a minimum of computing time. The results indicated the possible complexes $H_1B_3$, $H_1B_4$, $H_2B_4$, and $H_2B_5$.

(ii) In subsequent titrations, a value for the stability constant of 3-methylbutyric acid was first calculated using only the titration at $C_B = 0.1$ M. The $Z$ curve for this titration very closely coincides with the theoretical curve for a titration in which only a monobasic acid exists in the solution. This value for $\beta_{1,1}$ then was used in subsequent calculations without variation. It was then found, that the small complex giving the "best" values of $Z_{calc}$ was $H_1B_4$.

(iii) Addition of a larger complex with $10-16$ anions always decreased $U$ considerably. However, it was very difficult to distinguish between complexes of different size. The LETAGROPVRID procedure selects the complexes that are accepted on the basis of the magnitude of the standard deviations of the stability constants of the tried complexes. Introduction of two large complexes, say, $HB_{13}$ and $HB_{14}$, invariably resulted in the rejection of both, since the standard deviations were of the same magnitude as the constants themselves. Different complexes then were tried one by one. The uncertainties in the stability constants of the tried complexes then were $20-40$ %, but the error

Table 14. Titration of 2.0 M sodium trimethylacetate at 25°C.

$C_B = 2.000$ M    $E_{OH}° = 232.5$ mV
$C_H° = 0.1198$ M    $V = 40.00$ ml

| Amount of OH⁻ added mmol | $E$ mV | pOH | $Z_{exp}$ | $1000(Z_{calc} - Z_{exp})$ |
|---|---|---|---|---|
| 0 | − 200.5 | 7.319 | 0.0593 | − 4.7 |
| 0.3731 | − 198.4 | 7.284 | 0.0547 | − 4.3 |
| 0.7462 | − 196.1 | 7.245 | 0.0500 | − 3.9 |
| 1.119 | − 193.7 | 7.205 | 0.0453 | − 3.2 |
| 1.492 | − 191.0 | 7.159 | 0.0407 | − 2.8 |
| 1.865 | − 188.0 | 7.108 | 0.0360 | − 2.3 |
| 2.052 | − 186.3 | 7.080 | 0.0337 | − 2.2 |
| 2.238 | − 184.7 | 7.053 | 0.0313 | − 1.7 |
| 2.425 | − 182.8 | 7.020 | 0.0290 | − 1.6 |
| 2.611 | − 180.7 | 6.985 | 0.0267 | − 1.4 |
| 2.798 | − 178.5 | 6.948 | 0.0243 | − 1.1 |
| 2.984 | − 175.9 | 6.904 | 0.0220 | − 1.1 |
| 3.171 | − 173.1 | 6.856 | 0.0197 | − 1.0 |
| 3.357 | − 169.9 | 6.802 | 0.0174 | − 0.9 |
| 3.544 | − 166.2 | 6.740 | 0.0150 | − 0.8 |
| 3.731 | − 162.0 | 6.669 | 0.0127 | − 0.7 |
| 3.917 | − 156.8 | 6.581 | 0.0104 | − 0.6 |
| 4.104 | − 150.3 | 6.471 | 0.0080 | − 0.4 |
| 4.153 | − 148.3 | 6.437 | 0.0074 | − 0.4 |
| 4.340 | − 138.9 | 6.278 | 0.0051 | − 0.3 |
| 4.526 | − 122.9 | 6.008 | 0.0027 | − 0.1 |
| 4.582 | − 115.4 | 5.881 | 0.0020 | − 0.1 |
| 4.638 | − 104.7 | 5.700 | 0.0013 | 0.0 |
| 4.694 | − 86.1 | 5.386 | 0.0006 | 0.0 |

*Table 15.* Titration of 2.5 M sodium trimethylacetate at 25°C.

$C_B = 2.500$ M          $E_{OH}° = 239.6$ mV
$C_H° = 0.1474$ M        $V = 40.00$ ml

| Amount of OH⁻ added mmol | $E$ mV | pOH | $Z_{exp}$ | $1000(Z_{exp} - Z_{calc})$ |
|---|---|---|---|---|
| 0 | − 185.3 | 7.183 | 0.0589 | − 6.7 |
| 0.1865 | − 184.4 | 7.167 | 0.0571 | − 6.6 |
| 0.3731 | − 183.6 | 7.154 | 0.0552 | − 6.1 |
| 0.5596 | − 182.6 | 7.137 | 0.0533 | − 5.0 |
| 0.7962 | − 181.7 | 7.122 | 0.0515 | − 5.7 |
| 0.9372 | − 180.7 | 7.105 | 0.0496 | − 5.5 |
| 1.119 | − 179.8 | 7.090 | 0.0477 | − 5.0 |
| 1.305 | − 178.8 | 7.073 | 0.0459 | − 4.7 |
| 1.492 | − 177.8 | 7.056 | 0.0440 | − 4.3 |
| 1.678 | − 176.7 | 7.037 | 0.0421 | − 4.1 |
| 1.865 | − 175.6 | 7.019 | 0.0403 | − 3.7 |
| 2.052 | − 174.5 | 7.000 | 0.0384 | − 3.3 |
| 2.238 | − 173.2 | 6.978 | 0.0365 | − 3.1 |
| 2.425 | − 171.9 | 6.956 | 0.0347 | − 2.9 |
| 2.611 | − 170.6 | 6.934 | 0.0328 | − 2.5 |
| 2.798 | − 169.1 | 6.909 | 0.0309 | − 2.3 |
| 2.984 | − 167.5 | 6.882 | 0.0291 | − 2.1 |
| 3.171 | − 165.7 | 6.851 | 0.0272 | − 2.0 |
| 3.357 | − 163.9 | 6.821 | 0.0253 | − 1.8 |
| 3.544 | − 162.0 | 6.789 | 0.0235 | − 1.6 |
| 3.731 | − 159.9 | 6.753 | 0.0216 | − 1.4 |
| 3.917 | − 157.7 | 6.716 | 0.0197 | − 1.2 |
| 4.104 | − 155.1 | 6.672 | 0.0179 | − 1.1 |
| 4.290 | − 152.4 | 6.627 | 0.0160 | − 0.9 |
| 4.477 | − 149.3 | 6.574 | 0.0141 | − 0.7 |
| 4.850 | − 141.6 | 6.444 | 0.0104 | − 0.4 |
| 5.223 | − 130.5 | 6.256 | 0.0067 | − 0.2 |
| 5.596 | − 110.3 | 5.915 | 0.0030 | − 0.0 |
| 5.783 | − 86.9 | 5.519 | 0.0011 | 0.1 |
| 5.839 | − 72.6 | 5.278 | 0.0005 | 0.2 |

square sum decreased significantly (*cf.* for example, columns VI and IX in Table 9). The lowest $U$-value was attained with the complex $B_{15}$, but it should be emphasized that the difference in $U$ between different complexes was quite small (*cf.* for example, columns VIII and X in Table 9).

(iv) Finally, a systematic error $\delta Z$ was introduced in titrations 7 and 8 to check whether the occurrence of a large complex could not be explained just as well as the result of systematic errors. It was found that this improved the value for $\beta_{0,15}$ and decreased $U$; the systematic error in titration 7 is 0.015 $Z$-units (which seems very resonable on inspection of Fig. 1) and the error in titration 8 is insignificant. There is little doubt that on the basis of these potentiometric experiments, micelle-like aggregates are formed by sodium 3-methylbutyrate. The last columns in Tables 1 − 8 show that there is agreement between experimental and theoretical $Z$ values within experimental error ( ± 0.004 $Z$ units).

*Table 16.* Titration of 3.0 M sodium trimethylacetate at 25°C.

$C_B = 3.000$ M       $E_{OH}° = 250.0$ mV

$C_H° = 0.2383$ M      $V = 40.00$ ml

| Amount of $OH^-$ added mmol | $E$ mV | pOH | $Z_{exp}$ | $1000(Z_{exp} - Z_{calc})$ |
|---|---|---|---|---|
| 0 | −180.4 | 7.276 | 0.0794 | −1.5 |
| 0.1865 | −180.0 | 7.269 | 0.0778 | −0.9 |
| 0.3731 | −179.2 | 7.255 | 0.0763 | −1.4 |
| 0.5596 | −178.7 | 7.247 | 0.0747 | −0.9 |
| 0.7462 | −178.0 | 7.235 | 0.0731 | −1.0 |
| 0.9327 | −177.5 | 7.227 | 0.0716 | −0.6 |
| 1.119 | −176.9 | 7.217 | 0.0700 | −0.4 |
| 1.305 | −176.3 | 7.206 | 0.0685 | −0.3 |
| 1.492 | −175.7 | 7.196 | 0.0669 | 0.0 |
| 1.678 | −175.3 | 7.189 | 0.0654 | 0.6 |
| 1.865 | −174.8 | 7.181 | 0.0638 | 1.2 |
| 2.052 | −174.3 | 7.173 | 0.0623 | 1.6 |
| 2.238 | −173.6 | 7.161 | 0.0607 | 1.8 |
| 2.425 | −173.0 | 7.155 | 0.0592 | 2.1 |
| 2.611 | −172.2 | 7.137 | 0.0576 | 2.0 |
| 2.798 | −171.6 | 7.127 | 0.0560 | 2.4 |
| 2.984 | −170.9 | 7.115 | 0.0545 | 2.5 |
| 3.171 | −170.2 | 7.103 | 0.0529 | 2.8 |
| 3.357 | −169.4 | 7.090 | 0.0514 | 2.9 |
| 3.544 | −168.6 | 7.076 | 0.0498 | 3.0 |
| 3.731 | −167.8 | 7.063 | 0.0483 | 3.1 |
| 3.917 | −167.0 | 7.049 | 0.0467 | 3.3 |
| 4.104 | −166.1 | 7.034 | 0.0452 | 3.3 |
| 4.290 | −165.2 | 7.019 | 0.0436 | 3.4 |
| 4.477 | −164.3 | 7.004 | 0.0421 | 3.5 |
| 4.663 | −163.4 | 6.988 | 0.0405 | 3.7 |
| 4.850 | −162.3 | 6.970 | 0.0389 | 3.7 |
| 5.036 | −161.2 | 6.951 | 0.0374 | 3.5 |
| 5.223 | −160.0 | 6.931 | 0.0358 | 3.5 |
| 5.410 | −158.7 | 6.909 | 0.0343 | 3.2 |
| 5.596 | −157.1 | 6.882 | 0.0327 | 2.8 |
| 5.783 | −155.7 | 6.858 | 0.0312 | 2.5 |
| 5.969 | −154.3 | 6.834 | 0.0296 | 2.5 |
| 6.156 | −152.8 | 6.809 | 0.0281 | 2.3 |
| 6.342 | −151.2 | 6.782 | 0.0265 | 2.2 |
| 6.529 | −149.4 | 6.752 | 0.0250 | 2.0 |
| 6.715 | −147.7 | 6.723 | 0.0234 | 1.9 |
| 6.902 | −145.9 | 6.692 | 0.0218 | 1.9 |
| 7.088 | −143.7 | 6.655 | 0.0203 | 1.6 |
| 7.275 | −141.6 | 6.620 | 0.0187 | 1.6 |
| 7.462 | −139.2 | 6.579 | 0.0172 | 1.4 |
| 7.648 | −136.9 | 6.540 | 0.0156 | 1.5 |
| 7.835 | −134.1 | 6.493 | 0.0141 | 1.3 |
| 8.021 | −131.0 | 6.441 | 0.0125 | 1.2 |
| 8.208 | −127.7 | 6.385 | 0.0110 | 1.1 |
| 8.394 | −123.6 | 6.316 | 0.0094 | 1.0 |
| 8.581 | −118.9 | 6.236 | 0.0079 | 0.8 |
| 8.767 | −113.0 | 6.136 | 0.0063 | 0.7 |
| 8.954 | −105.5 | 6.010 | 0.0047 | 0.5 |
| 9.141 | −95.0 | 5.832 | 0.0032 | 0.3 |
| 9.327 | −77.3 | 5.533 | 0.0016 | 0.2 |
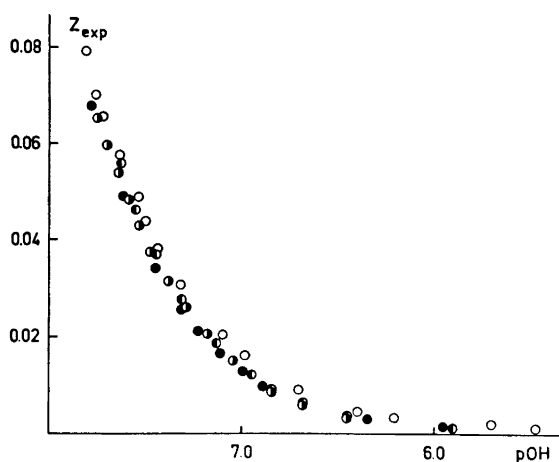
*Fig. 2.* The hydrolysis of sodium trimethylacetate at low concentrations. Concentrations of $C_B$ (M): 0.1 ○; 0.5 ●; 0.75 ◖; 1.0 ◖.
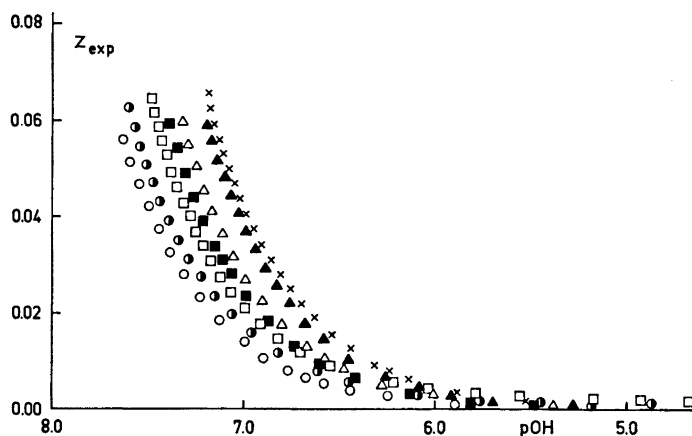


*Fig. 3.* The hydrolysis of sodium trimethylacetate at higher concentrations. Some of the points in Tables $10-16$ have been left out. Concentrations of $C_B$ (M): 1.0 ○; 1.2 ◖; 1.5 □; 1.8 ■; 2.0 △; 2.5 ▲; 3.0 ×.

*II. Sodium trimethylacetate.* The experimental values for titrations of seven different concentrations of sodium trimethyl acetate are given in Tables $10-16$. The experimental results are summarized in Figs. 2 and 3.

The $Z$ curves for all concentrations up to 1.0 M trimethylacetate coincide within experimental error (Fig. 2). Their shape is that of a theoretical normalized curve for a monobasic acid. Obviously, unassociated trimethylacetic

acid only occurs at these concentrations. A value for $\beta_{1,1}$ was calculated with LETAGROPVRID using the four titrations shown in Fig. 2. This value then was used without variation in subsequent calculations. In these, titrations at concentrations above 0.75 M only were utilized.

As Fig. 3 shows, there is a shift of the $Z$ curves indicating complex formation as the concentration exceeds 1 M. Two or three titrations were performed for each concentration and one of these was chosen for use in calculations with LETAGROPVRID on the same grounds as those discussed for sodium 2-methylbutyrate.

The calculations with LETAGROPVRID were fairly straight forward and are summarized in Table 17. The complexes that give the "best" fit to experimental values contain 4 anions. It is seen from the last columns in Tables 10 − 16 that the agreement between theoretical and experimental values is excellent.

*III. Changes in* $E_{OH}^{\circ}$ *with* $C_B$. Fig. 4 shows the shift in $E_{OH}^{\circ}$ with $C_B$ for both salts. This linear change is similar to and of the same magnitude (15 − 16 mV/mol B) as the change found in earlier investigations of straight-chain carboxylates.[1,3,23,24] The reasons for this shift have been discussed elsewhere.[19,25] It is suggested that it is caused by a shift in the standard state energy of OH⁻ ions as $C_B$ increases. This may cause errors in the complex

*Table 17.* Calculations with LETAGROPVRID on the hydrolysis of sodium trimethylacetate.

| $p,q$ | Stability constants ($-\log \beta_{p,q}$) of tried complexes $H_pB_q$ | | | |
|---|---|---|---|---|
|  | I | II | III | IV |
| 1,1 | 8.8593 ± 0.0022 | 8.8593 ± 0.0022 | 8.8593 ± 0.0022 | 8.8593 ± 0.0022 |
| 1,2 | rej.[a] | rej. | | |
| 1,3 | rej. | 9.488 ± 0.029 | | |
| 2,3 | rej. | | | |
| 1,4 | 9.855 ± 0.036 | | | 9.848 ± 0.067 |
| 2,4 | 17.460 ± 0.074 | 17.60 ± 0.14 | | 17.481 ± 0.073 |
| 3,4 | rej. | | | |
| 1,5 | rej. | | 10.331 ± 0.0088 | |
| 2,5 | rej. | | 17.600 ± 0.057 | |
| 1,6 | | | | rej. |
| 1,8 | | | | rej. |
| 1,10 | rej. | | | |
| 1,12 | | | | rej. |
| $U$ | 0.001635 | 0.002064 | 0.002661 | 0.001426 |
| $\sigma(y)$ | 0.00278 | 0.00312 | 0.00354 | 0.00260 |

[a] See note [b] to Table 16.
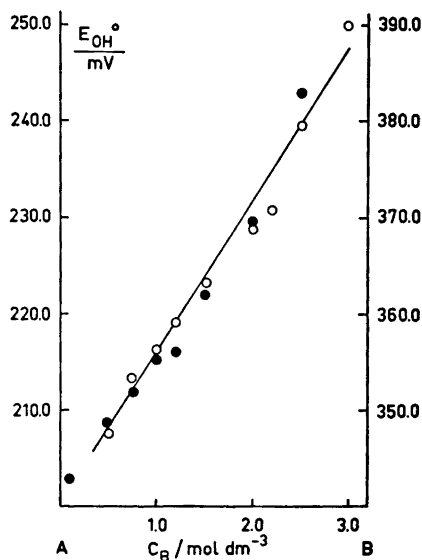
*Fig. 4.* The variation in standard potential $E_{OH}°$ of the cell used in the study of the hydrolysis of sodium 3-methylbutyrate (B; ●) and trimethylacetate (A; ○) as a function of the total carboxylate concentration $C_B$.

formation found with LETAGROPVRID. It might be conceived that the shift in $Z$ curves is caused by a shift in the pOH scale which is dependent on $E_{OH}°$. However, the facts that no shift in the $Z$ curves is found for the short-chain salts that do not associate (acetate, propionate [1]) and that there is independent spectroscopic indication that at least butyrate anions do associate [5] seem to make the results given above fairly reliable.

*Table 18.* A comparison between the complexes formed by different isomers of sodium pentanoate. The stability constants ($-\log \beta_{p,q}$) for the different complexes $H_pB_q$ are given. The values for the pentanoate are taken from Ref. 1.

|  | $-\log \beta_{1,1}$ | $-\log \beta_{1,4}$ | $-\log \beta_{2,4}$ | $-\log \beta_{1,11}$ | $-\log \beta_{0,15}$ |
|---|---|---|---|---|---|
| Pentanoate $CH_3(CH_2)_3COO^-$ | 9.199 ± 0.022 |  | 17.077 ± 0.077 | 12.22 max. 12.01[a] |  |
| 3-Methylbutyrate $\frac{CH_3}{CH_3}$> CH−CH$_2$−COO$^-$ | 9.232 ± 0.016 | 9.168 ± 0.052 |  |  | 6.35 max. 6.06[a] |
| Trimethylacetate $H_3C-\overset{\overset{CH_3}{\mid}}{\underset{\underset{CH_3}{\mid}}{C}}-COO^-$ | 8.8593 ± 0.0022 | 9.848 ± 0.067 | 17.481 ± 0.073 |  |  |

[a] See note to Table 16.

## DISCUSSION

The stability constants of the complexes found for the three pentanoate isomers investigated are compared in Table 18. The following conclusions may be drawn:

(i) All three salts form aggregates with four anions; the difference in stability between these is remarkably small.

(ii) Micellar aggregates are formed by sodium pentanoate and sodium 3-methylbutyrate, with 11 and 15 anions, respectively. As discussed above, not too much significance should be attached to the actual aggregation numbers found, since they represent the best alternative of several almost equal possibilities. Only a crude estimation of the relative stability of the micelles can be made. The stability constant for the proton-free pentanoate micelle, $-\log \beta_{0,11}$, can be roughly estimated by subtracting $\log \beta_{1,1}$ from $\log \beta_{1,11}$; this gives $\log \beta_{11} - \log \beta_{0,11} = 3.0$. This is a considerably larger value than the stability constant found for the 3-methylbutyrate micelles, i.e. the micelles of pentanoate are more stable and their concentration becomes appreciable at lower concentrations than the micelles of 3-methylbutyrate.

(iii) Sodium trimethylacetate does not form micelles, but the smaller aggregates formed by this compound are similar to those found for the other isomers, for sodium butyrate and for sodium hexanoate.[1]

These conclusions are remarkably consistent with current concepts of micelle formation and hydrophobic hydration,[10] as discussed in the introduction. On addition of hydrocarbon to an aqueous solution there is "increased structuring" of the water ("cage formation", "iceberg formation", "hydrophobic hydration")[26] which decreases the reorientation time of the water molecules [27] and causes a large entropy decrease. For this reason, hydrocarbon chains are very sparingly soluble in water; if other parts of the molecule are strongly solvated the hydrocarbon chains tend to associate, since this causes a large increase in the entropy of water (hydrophobic bonding).[28] This explains the formation of smaller aggregates of amphiphilic molecules, e.g. the compounds in Table 18.

Micelle formation proper takes place if a further increase in entropy can be attained by increasing the mobility of the hydrocarbon chains when they are transferred to a hydrocarbon solvent.[10] In the present case, it is very reasonable to assume that it is possible for the n-pentanoate and 3-methylbutyrate chains to increase their mobility, while the very compact trimethylacetate anion cannot form a sufficiently liquid micellar core. The role of hydrophobic factors in the process of formation of micelles from monomers thus can be divided into two steps:

(i) the formation of smaller aggregates, which decreases the hydrophobic hydration of the hydrocarbon chains,

(ii) the formation of micelles from these aggregates, which increases the mobility of the hydrocarbon chains.

A quantitative indication of the feasibility of this model is given in a recent paper by Lin and Somasundaran,[11] where it is found that the total free energy change per $CH_2$ group is $-1.39 \, kT$ to $-1.41 \, kT$ for the transfer from aqueous solution to hydrocarbon solution, $-1.10 \, kT$ to $-1.22 \, kT$ for the transfer

from aqueous solution to micelles and $-0.61$ k$T$ to $-0.69$ k$T$ for the transfer from an aqueous solution of ionic surfactants to micelles. The authors suggest that the difference between the two last processes partly might be explained by the fact that the transfer from a solution of ionic surfactants probably takes place from smaller aggregates. The model is also supported by the investigation of the temperature dependence of the stability of sodium butyrate complexes reported in part III,[3] which shows that the formation of small aggregates is accompanied by a large increase in entropy.

In part I,[1] it is reported that the decrease in free energy per $CH_2$ group on transfer from monomers to aggregates with four anions is about $-0.8$ k$T$. This would imply an energy of transfer of $-0.30$ to $-0.42$ k$T$ from small aggregates to micelles, if the values for transfer from aqueous solution to micelle cited above are used. Considering the fact that these are valid for pure aqueous solution, the agreement between these experiments and the values of Lin and Somasundaran is acceptable. This gives some further support to the two-step model of the hydrocarbon chain aggregation suggested above. If it can be assumed that very extensive rearrangement of the solvatation water around the polar end groups does not take place in the transfer from small aggregates to micelles, the increase in internal mobility of the hydrocarbon chain thus causes a decrease in free energy of about $0.3-0.4$ k$T$.

## REFERENCES

1. Stenius, P. and Zilliacus, C. H. *Acta Chem. Scand.* **25** (1971) 2232 (part I).
2. Stenius, P. *Acta Chem. Scand.* **27** (1973) 3435 (part II).
3. Stenius, P. *Acta Chem. Scand.* **27** (1973) 3452 (part III).
4. Danielsson, I. and Stenius, P. *J. Colloid Interface Sci.* **37** (1971) 264.
5. Ödberg, L., Svens, B. and Danielsson, I. *J. Colloid Interface Sci.* **41** (1972) 298.
6. Mukerjee, P. *Advan. Colloid Interface Sci.* **1** (1967) 241.
7. Stead, J. A. and Taylor, H. *Australas. J. Pharm.* **51** (1970) 51.
8. Proust, J. and Ter-Miniassan-Saraga, L. *Compt. Rend.* **270** (1970) 1354.
9. Anacker, E. W. In Jungermann, E., Ed., *Surfactant Science Series IV. Cationic Surfactants*, Marcel Dekker, New York 1970, p. 203.
10. Ekwall, P., Danielsson, I. and Stenius, P. In Kerker, M., Ed., *Surface Chemistry and Colloids*, *MTP Int. Rev. Science, Phys. Chem. Ser. 1*, vol. 7, Butterworths, London 1972, p. 97.
11. Lin, I. J. and Somasundaran, P. *J. Colloid Interface Sci.* **37** (1971) 731.
12. Biedermann, G. and Sillén, L. G. *Arkiv Kemi* **5** (1952) 425.
13. Hietanen, S. and Sillén, L. G. *Acta Chem. Scand.* **13** (1959) 533.
14. Gran. G. *Analyst* **77** (1952) 61.
15. Danielsson, I. *Kemian Teollisuus* **23** (1966) 1081.
16. Brown, R. *J. Am. Chem. Soc.* **56** (1934) 646.
17. Bates, R. *Determination of pH*, Wiley, New York 1965, p. 241.
18. Ingri, N., Lagerström, G., Frydman, M. and Sillén, L. G. *Acta Chem. Scand.* **11** (1957) 1034.
19. Danielsson, I. and Stenius, P. *Trans. Royal. Inst. Technol., Stockholm; Pure Appl. Chem.* **34** (1972) 81.
20. Sillén, L. G. *Acta Chem. Scand.* **10** (1956) 186.

21. Sillén, L. G. *Acta Chem. Scand.* **18** (1964) 1085.
22. Sillén, L. G. and Warnqvist, B. *Arkiv Kemi* **31** (1969) 315, 341.
23. Danielsson, I. and Suominen, T. *Acta Chem. Scand.* **17** (1963) 979.
24. Danielsson, I., Mäntylä, A., Kreutzman, E. and Ritola, P. *Acta Acad. Aboensis Math. Phys.* **24** (1964) 4.
25. Ginstrup, O. *Acta Chem. Scand.* **24** (1970) 875.
26. Franks, F. In Covington, A. K. and Jones, P., Eds., *Hydrogen Bonded Solvent Systems*, Taylor and Francis, London 1968, p. 31.
27. Franks, F., Ravenhill, J., Egelstaff, P. and Page, D. I. *Proc. Roy. Soc. (London)* **A 319** (1970) 189.
28. Poland, D. C. and Sheraga, H. A. *J. Phys. Chem.* **69** (1965) 2431.

# The Reaction between Triphenylmethyl Isoselenocyanate and Tervalent Phosphorus Compounds. A Kinetic Study

LEIV J. STANGELAND, TOR AUSTAD and JON SONGSTAD

*Chemical Institute, University of Bergen, N-5000 Bergen, Norway*

Triphenylmethyl isoselenocyanate has been found to be deselenated rapidly and cleanly by various tervalent phosphorus compounds. Triphenylmethyl isonitrile and the corresponding selenophosphorus compounds are formed in close to quantitative yields.

A kinetic study has been performed with cyclohexane and aceto-nitrile as solvents and the reactions were found to follow second-order kinetics. The rates of deselenization are enhanced in the solvent of highest polarity, but the rate enhancement is very dependent upon the nature of the applied tervalent phosphorus compound.

From observed reactivity sequences in the two solvents, solvent influence on reaction rates, and activation parameters in cyclohexane, various possible reaction mechanisms are discussed.

O rganic and inorganic selenium compounds appear to be considerably less studied than the corresponding sulfur compounds.[1–4] Apart from the ob-vious difference in biological importance of the two classes of compounds, studies of the chemistry of the selenium compounds appear to have been seriously hindered due to their generally lower stability, their toxicity and, in the case of most organic selenium compounds, their most unpleasant odour.[2]

When focusing on the reactivity of selenium compounds and the various allotropic forms of selenium, no accurate kinetic studies appear to have been performed apart from studies where the selenocyanate ion is involved. In many respects, the chemistry of the selenium compounds appears to be far more dif-ficult to examine than the chemistry of the corresponding sulfur compounds. Due to the lower electronegativity and the greater polarizability of selenium compared with sulfur, selenium compounds are generally better electrophiles than the corresponding sulfur compounds. Furthermore, the greater polariz-ability of the selenium atom causes selenium compounds having a lone pair or a negative charge to be generally better nucleophiles than the corresponding sulfur compounds toward soft substrates.[5] The selenocyanate ion is thus able to react as a biphile towards certain substrates, in contrast to what has been found for the thiocyanate ion.[6] Due to the large difference in size between selenium and first-row elements like carbon and oxygen, the bonds between

these elements are considerably weaker than the corresponding $S-O$ and $S-C$ bonds.[7,8] When linear three-center systems, however, are possible, the selenium compounds are considerably more stable than the corresponding sulfur compounds.[9]

The combination of weaker bonds to most elements and the ability of the selenium atom in the various compounds to act as both acceptor and donor as required, causes the majority of the reactions where selenium is involved to be extremely rapid and not readily accessible to kinetic studies.[2]

With regard to the various modifications of elemental selenium, several reactions indicate the anticipated close similarity with the corresponding reactions of elemental sulfur.[10] Very polarizable nucleophiles like tervalent phosphorus compounds react most readily with both elements.[11,12] The reactions of sulfur and selenium with organic isonitriles are usually very slow reactions, but provide important routes to organic isothiocyanates and isoselenocyanates which are not readily obtainable by other means.[13-20] Interestingly, triethylamine is able to catalyze reactions of both elemental sulfur[21] and selenium,[22,23] probably by polarization of the $S-S$ and the $Se-Se$ bonds. This extreme dependence of reaction rates upon polarizing agents, present as for example impurities in solvents and reactants, combined with the limited solubility of these two elements in most solvents, make kinetic studies of this type of reaction most difficult.[11,24]

For kinetic studies toward selenium one thus has to find compounds which readily, but not too rapidly, expel the selenium atom, make stable selenated products, and most important, make deselenated products of very low selenium basicity to ensure complete reaction.

Nicpon and Meek[25] found that triaryl phosphines deselenated potassium selenocyanate rapidly in acetonitrile, a reaction which has proved to be a simple route to selenophosphorus compounds[25,26] (Eqn. 1).

$$R_3P + SeCN^- \xrightarrow{\text{MeCN}} R_3P = Se + CN^- \tag{1}$$
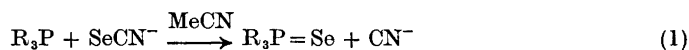
This reaction, however, is not suitable for detailed kinetic studies as the rates of the reactions are highly dependent upon the cation, the solvent, and the purity of the solvent.[27] In a very pure aprotic solvent and by applying an onium cyanide, the reverse of the reaction in eqn. 1 takes place.[28]

Hofmann[29] noted more than a century ago that at elevated temperatures trialkyl phosphines desulfurized isothiocyanates while triphenylphosphine was inactive. We have found that several tervalent phosphorus compounds react readily with triphenyl isoselenocyanate at room temperature in the usual organic solvents in clean and non-malodorous reactions, forming the corresponding selenophosphorus compounds and triphenylmethyl isonitrile in close to quantitative yield, eqn. 2,

$$Ph_3CNCSe + P \diagup \longrightarrow Ph_3CNC + Se = P \diagup \tag{2}$$
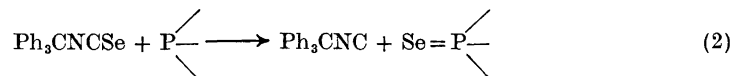
taking advantage of the low nucleophilicity of the isonitrile toward selenium as mentioned above.

As the rates of the reactions were in most cases found to be within an acceptable range for the determination of rate constants, a kinetic study of the reaction depicted in eqn. 2 using a variety of tervalent phosphorus compounds was performed. The reactions were most conveniently followed by UV spectroscopy at appropriate wavelength in the 250 – 270 nm range measuring the decrease in optical density.

Both in acetonitrile and in cyclohexane, the reactions followed second-order kinetics and it was in most cases possible to follow the reactions up to 4 or 5 half-lives. The only exception was the reaction of ethyl diphenylphosphinite in acetonitrile where no simple kinetic laws were found to be obeyed. As this reaction mixture rapidly started to yield malodorous by-products, it was not further examined.

Triphenylmethyl isoselenocyanate decomposes slowly in acetonitrile.[30] For this reason and as the reactions usually were too fast for accurate rate determinations, it was not possible to obtain thermodynamic parameters for the reactions in this solvent. The rate of reaction of tris(morpholino)phosphine was too rapid even in cyclohexane to allow the determination of sufficiently accurate rate constants for the calculation of thermodynamic parameters.

Due to extensive ring-opening in the reaction between the cyclic phosphite, 2-methoxy-1,3-dioxaphospholane, and the isoselenocyanate, the UV method was not applicable in this reaction. The rate of this reaction was therefore determined from the disappearance of the peak at 2100 cm$^{-1}$ in IR. Due to the broadness of this peak, the rate constants for this reaction were considerably less accurate than the rates determined by the UV method. As the rate of the reaction in acetonitrile between the cyclic phosphite and the isoselenocyanate was rather low, the rate of reaction could not be determined due to the instability of triphenyl isoselenocyanate in this solvent at room temperature.

The reaction between ionic cyanide and triphenyl isoselenocyanate in acetonitrile appeared extremely rapid and the rate could thus not be determined. Solutions of triphenyl arsine and triphenylmethyl isoselenocyanate were found to be completely stable in cyclohexane and no reaction could be detected. The rate of decomposition of the isoselenocyanate in acetonitrile was found to be unaffected by the presence of triphenyl arsine. Triphenylmethyl isonitrile is probably a better selenium base in cyclohexane than is triphenyl arsine. The very unstable nature of triphenyl arsine selenide has been noted.[31]

The observed rate constants with calculated activation parameters are listed in Tables 1 and 2.

Tris(morpholino)phosphine was chosen as an example of a tris(dialkylamino)phosphine due to its facile synthesis and, as it is a crystalline compound with high melting point, its purification was rather simple. Furthermore, its stability and crystalline state facilitated the kinetic experiments.

Generally, tris(dialkylamino)phosphines exhibit a very small tendency to act as electrophiles forming pentacovalent phosphoranes. When reacting with biacetyl,[33] ketenes,[34] dialkyl peroxides,[35] and related compounds, with which phosphites and most phosphines readily form pentacovalent species, the aminophosphines react via an ionic mechanism. Only with α,α-diketones with strongly electronegative substituents are the aminophosphines capable of forming isolable phosphoranes.[33]

*Table 1.* Rate constants for the reaction in cyclohexane between triphenylmethyl iso-selenocyanate (Ph$_3$CNCSe) and various tervalent phosphorus compounds (R$_3$P), together with calculated activation parameters.

| R$_3$P | $k_2 \times 10^2$ M$^{-1}$ sec$^{-1}$ 25°C | $k_2 \times 10^2$ M$^{-1}$ sec$^{-1}$ 40.0°C | $\Delta H^*$kcal M$^{-1}$ $\pm 0.4$ | $\Delta S^*$ e.u. $\pm 4$ |
|---|---|---|---|---|
| (Morph)$_3$P | 810 | | | |
| (n-but)$_3$P | 190 | 430 | 9.5 | $-21$ |
| Ph$_2$POEth | 113 | 263 | 9.4 | $-22$ |
| Ph$_2$POMe | 99 | 230 | 9.7 | $-21$ |
| Ph$_3$P | 19.3 | 30.8(35.0°C)$^a$ | 8.6 | $-28$ |
| (MeO)$_3$P | 2.4 | 6.0 | 10.7 | $-25$ |
| PhP(OMe)$_2$ | 1.6 | 3.9 | 10.6 | $-27$ |
| $\begin{array}{l}\text{CH}_2\text{—O}\\\text{CH}_2\text{—O}\end{array}\!\!\!\big> \text{P—OMe}$ | 0.042 | 0.073(35°C)$^b$ | $9.8 \pm 0.8$ | $-40 \pm 8$ |

$^a$ $k_2$ at 45°C = 0.51 M$^{-1}$sec$^{-1}$. $^b$ $k_2$ at 20°C = 3.2 × 10$^{-4}$ M$^{-1}$sec$^{-1}$.

*Table 2.* Rate constants in acetonitrile, $k_2$ (MeCN) and cyclohexane, $k_2$ (chex), with calculated rate ratios at 25.0°C.

| R$_3$P | $k_2$(MeCN) × 10$^2$M$^{-1}$sec$^{-1}$ | $k_2$(chex) × 10$^2$M$^{-1}$sec$^{-1}$ | $\dfrac{k_2(\text{MeCN})}{k_2(\text{chex})}$ |
|---|---|---|---|
| Ph$_3$P | 450 | 19.3 | 23 |
| Ph$_2$POMe | 410 | 99 | 4.1 |
| PhP(OMe)$_2$ | 475 | 1.6 | 300 |
| (MeO)$_3$P | 45 | 2.4 | 19 |

Toward certain substrates, which are known to react *via* transition states with large charge separation, the aminophosphines are by far the most reactive tervalent phosphorus compounds,[36] probably as a result of their being able to act as α-nucleophiles.[37] The finding in this work that tris(morpholino)phosphine is the most reactive of the tervalent phosphorus compounds studied, clearly suggests that the tervalent phosphorus compounds act as nucleophiles in the present reaction. This conclusion is supported by the fact that triphenylphosphine, being a far better nucleophile than is trimethylphosphite, is more reactive than the latter compound and that the acyclic phosphite is considerably more reactive than is the cyclic homolog [38] (Table 1).

Fundamentally, compounds like triphenylmethyl isoselenocyanate and related compounds may react in a number of ways, and, neglecting the very improbable S$_N$Ar reactions when tervalent phosphorus compounds are the nucleophiles, these compounds could possibly provide four different electrophilic centres and thus react in four different ways (1, 2, 3 and 4).

$$\text{Ph}_3\text{C} - \text{N} = \text{C} = \text{Se}$$

1    2    3    4
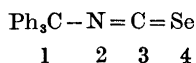
On chemical grounds, paths 1 and 2 can be readily dismissed although Leffler and co-workers [39] have shown that triphenyl phosphine attacks the α-nitrogen atom in triphenylmethyl azide. One is thus left with the following mechanisms where the transition states are depicted in the following scheme:

A $\quad$ $Ph_3C-N=C\overset{\delta-}{=\!=\!=}Se\overset{\delta+}{-\!-\!-}P\!\!\diagup$ $\quad$ Attack on selenium (atom 4)

B $\quad$ $Ph_3C-N=\overset{\delta+}{C}---P\diagdown\!\!\diagup$

$\qquad\qquad\qquad \parallel \quad \diagdown$

$\qquad\qquad\quad Se$

$\qquad\qquad\qquad \overset{\delta-}{} \quad |$

C $\quad$ $Ph_3C-N=C---P\!\!-\!\!$ $\quad$ Insertion reaction (atoms 3 and 4)

$\qquad\qquad\qquad \parallel\!\!\diagup\diagdown$

$\qquad\qquad\quad Se$
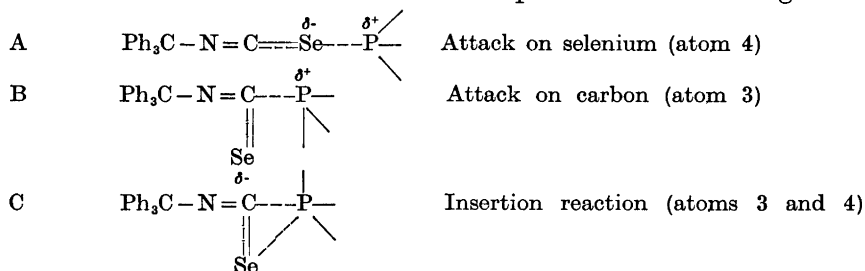
The simple deselenating mechanism depicted in A appears to be the most likely one as this transition state will have some charge separation and a rate increase from cyclohexane to acetonitrile is to be anticipated (Table 2). The rate increases observed, however, are considerably less than those observed for reactions between triaryl phosphines and elemental sulfur,[11] but this may be due to the greater polarizability of the selenium atom.

When neglecting the rate of reaction of the cyclic phosphite, the rate differences between the various tervalent phosphorus compounds is very small. This is further evidence for mechanism A as it is well known that increasing polarizability of the electrophilic center levels the reactivity of tervalent phosphorus compounds.[40]

The mechanism as depicted by B, being rather similar to the one for the Perkow reaction, is in principle far more complicated than suggested. A better picture of this mechanism may be the following one; eqn. 3:[41,42]

$$Ph_3CNCSe + P\!\!\diagup_{\diagdown} \underset{k_{-1}}{\overset{k_1}{\rightleftharpoons}} Ph_3C-N=C-\overset{\delta+}{P}\diagup \overset{k_2}{\longrightarrow} Ph_3CNC + SeP\!\!\diagup \qquad (3)$$
$$\overset{\parallel\ \diagdown}{\underset{\underset{\delta-}{Se}}{}}$$
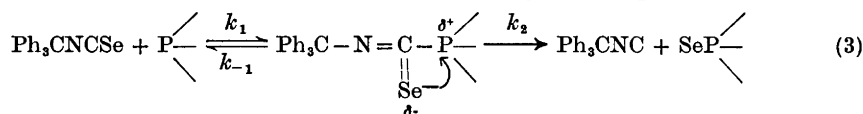
Thus, all rate constants, $k_1$, $k_{-1}$, and $k_2$ have in fact to be considered and it is impossible to predict the effect upon reaction rates of solvent and the groups linked to the phosphorus atom. From Borowitz' extensive studies on the Perkow reaction [41,42] and from similar studies,[43] the effect of solvent is very small, suggesting a very small charge separation in the transition state. The mere fact that the aminophosphine is by far the more reactive one does not accord with this mechanism. Although nitrogen bases are known to attack exclusively the carbon atom in organic isoselenocyanates forming selenoureas and selenocarbamates,[23] it is hard to imagine how very polarizable nucleophiles such as tervalent phosphorus compounds can bypass a very soft electrophilic atom like the selenium atom and attack a hard sterically hindered carbon atom alpha to it. The mechanism as depicted by B thus appears to be rather unlikely.

However, a simple mechanism as depicted by A does not provide a satisfactory explanation for the exceptional reactivity of the alkyl diphenyl-

phosphinites in cyclohexane and the very small observed rate dependence upon solvent (Tables 1 and 2). Numerous reactions between tervalent phosphorus compounds and various substrates are known where no solvent dependence is observed. The most notable examples are the reaction of episulfides,[44] β-peroxylactones,[45] peroxydicarbonates,[46] benzils,[47] various aromatic nitro compounds,[48] etc. with tervalent phosphorus compounds. As there appears to be limited evidence for radical mechanisms in these reactions, the only possible explanation seems to be the formation of non-charged pentacovalent species in the rate determining step. This may indicate that phosphinites in a non-polar solvent as cyclohexane react by mechanism C. There is considerable evidence for the more facile formation of phosphoranes from tervalent phosphorus compounds containing one and only one substituent of exceptional apicophilicity as for the case of phosphinites.[34,37]

In a more polar solvent like acetonitrile, the pentacovalent phosphorane mechanism, mechanism C, is probably unable to compete with the ionic mechanism, mechanism A.[49]

The thermodynamic parameters listed in Table 1 appear to be of little use in discussing the various possible mechanism. Only very accurate kinetic data, beyond the scope of the present study, may provide additional information. The rather similar values for $\Delta H^*$ and $\Delta S^*$ for the various reactions in cyclohexane accord with the small dependence of reaction rates upon substituents bonded to the reacting phosphorus atom. The fact that the cyclic phosphite reacts with an activation enthalpy which is not significantly larger than that of the acyclic phosphite is in accord with results obtained on alkylation reactions of acyclic and cyclic phosphites.[37] Hudson and co-workers [38] have recently discussed the various factors for the significantly more negative entropies of activation for reactions of cyclic phosphites than of acyclic phosphites.

The results obtained in this study do not shed much light upon the electrophilic nature of the selenium atom in selenium compounds. The very polarizable nature of this atom makes transition states of high charge separation less necessary than for the corresponding sulfur compounds and thus levels the reactivity of the tervalent phosphorus compounds.

The exceptional reactivity of the phosphinites in cyclohexane suggests that a special mechanism is available for these compounds in this solvent. Provided the pentacovalent species are sufficiently stable to undergo pseudo rotation [50] prior to the formation of the isonitrile and the selenophosphorus compounds, such a mechanism may be proved possible by stereochemical studies as has been shown by Bodkin and Simpson [50] for alkylation reaction of cyclic six-membered phosphites. The presence of penta-covalent species in the reaction between tervalent amine oxides and tervalent phosphorus compounds has not been confirmed in stereochemical studies.[51]

## EXPERIMENTAL

Acetonitrile and cyclohexane were purified as previously reported.[52] Mid-fractions from the final distillations, carefully flushed with nitrogen, were used in crystallization and for the kinetic studies. Benzene, toluene, diethyl ether, and various petroleum ethers were dried with sodium prior to use.

Methyl diphenylphosphinite, b.p. 102°C (0.75 mm), ethyldiphenylphosphinite, b.p. 157°C (10 mm), and dimethylphenylphosphonite, b.p. 86 − 87°C (10 mm) were made, according to standard procedures, from the corresponding chloro compounds and distilled under nitrogen until their UV spectra in cyclohexane were constant. Trimethyl phosphite, b.p. 110°C (760 mm), and 2-methyl-1,3-dioxaphospholane, $(CH_2O)_2P−OMe$, b.p. 38°C (8 mm) were treated several times with sodium, a large volume petroleum ether (40 − 60°C) was added, and the solutions were stored at − 20°C for 24 h prior to filtration and final distillation. Tris(morpholino)phosphine, m.p. 156°C, was made according to Michaelis[53] or Burgada,[54] crystallized from toluene and finally from acetonitrile. Great care was exercized to exclude moisture from these compounds and their solutions. Triphenyl phosphine, triphenyl arsine, and tributyl phosphine were commercial products and purified by standard methods.

Trityl isoselenocyanate was prepared according to Pedersen [55] from trityl chloride and potassium selenocyanate in acetone. As traces of trityl carbinol could not be removed from the isoselenocyanate by crystallization, the trityl chloride and the ionic selenocyanate were carefully purified and dried prior to the synthesis. The compound was finally crystallized from low-boiling petroleum ether and cyclohexane, dried in vacuum and stored in a dark bottle in the refrigerator. M.p. 129 − 130°C, $\lambda_{max}(CCl_4) = 2100$ cm$^{-1}$, $\Delta\lambda_{\frac{1}{2}} = 110$ cm$^{-1}$, $A = 17 \times 10^4 M^{-1}cm^{-2}$.

Trityl isonitrile, m.p. 136°C, was prepared from trityl chloride and tetramethyl-ammonium dicyanoargentate.[56] Tetraphenylarsonium cyanide was made as reported.[52]

*Reaction between triphenyl phosphine and trityl isoselenocyanate.* To 17.4 g trityl isoselenocyanate, 0.050 mol, in 100 ml diethyl ether, was added 13.1 g triphenyl phosphine, 0.050 mol, in 25 ml diethyl ether. After stirring for a few min, a white crystalline compound started to separate. The reaction mixture was stirred for 2 h at room temperature and then set aside overnight. Yield of crystalline product, triphenyl phosphine selenide, 17.5 g; calculated 17.0 g. After one crystallization from ethanol with close to quantitative yield, the phosphine selenide was obtained pure, m.p. 188 − 189°C (187 − 188°C [25]).

The mother liquor from the reaction was evaporated to dryness and the residue, 12.5 g, was crystallized from cyclohexane yielding 8.9 g trityl isonitrile, 67 %, in the first crop. The melting point and the IR spectrum was the same as that of the isonitrile formed from trityl chloride and tetramethyl dicyanoargentate.[56] However, even after repeated purification, this sample of trityl isonitrile attained a pink colour when exposed to daylight, suggesting it to be contaminated by traces of triphenyl phosphine selenide or trityl isoleselenocyanate and preventing it being used as a UV standard.

As the synthesis of the various selenophosphorus compounds from trityl isoselenocyanate and the corresponding tervalent phosphorus compounds was rather tedious, these compounds were generally made using grey selenium as selenating agent in toluene. After the exothermic reactions were over, the reaction mixtures were refluxed until all the selenium had reacted. Methyl and ethyl diphenyl selenophosphinate were alternatively easily obtained by alcoholysis of chloro diphenyl phosphine selenide, b.p. 215°C (8 mm).

In those reactions where metallic selenium was applied as reagent and the products, the selenophosphorus compounds, had to be purified by distillation, it was necessary to use a small excess of the tervalent phosphorus compounds to obtain pure products. If selenium was used in excess, the products were slightly yellow-greenish and deposited selenium on standing, even after repeated distillations. Unreacted tervalent phosphorus compounds, on the other hand, were easily separated from the products due to the large differences in boiling points. The products were usually obtained in from 80 to 90 % yield. The selenophosphorus compounds from 2-methoxy-1,3-dioxophospholane decomposed on attempted distillation, but as the rate of the reaction between this cyclic phosphite and trityl isoselenocyanate was determined by the IR technique, the rates of reaction could be obtained in this case without the use of a pure product.

The following selenophosphorus compounds were synthesized.

Triphenylphosphine selenide. M.p. 188 − 189°C (187 − 188°C [25]).

Tri-butylphosphine selenide. B.p. 131°C (0.5 mm) [150 − 151°C (0.80 mm) [57]].

Tris(morpholino)phosphine selenide. M.p. 154 − 155°C.

(Found: C 38.96; H 6.72; N 11.29. Calc. for $C_{12}H_{24}N_3O_3PSe$: C 39.12; H 6.57; N 11.41).

*O*-Methyldiphenyl selenophosphinate. M.p. 88 − 89°C (89°C [58]).

(Found: C 53.34; H 4.21; Calc. for $C_{13}H_{13}POSe$: C 52.90; H 4.44).

*O*-Ethyl diphenyl selenophosphinate. M.p. 61 − 62°C.

(Found: C 54.68; H 4.65; P 10.09. Calc. for $C_{14}H_{15}POSe$: C 54.38; H 4.89; P 10.00).
$O,O$-Dimethyl phenyl selenophosphonate. B.p. $100-101°$ (0.8 mm).
(Found: C 40.04; H 4.30: Calc. for $C_8H_{11}PO_2Se$: C 38.57; H 4.45).
$O,O,O$-Trimethyl selenophosphate. B.p. $75-76°C$ (12 mm). The melting points are corrected.

*Kinetic studies.* The rates of the reactions, with the exception of the reaction between the cyclic phosphite and triphenylmethyl isoselenocyanate, were determined from the decrease of absorptions at appropriate wavelengths in the $250-270$ nm range. The principle cause of the decrease was the disappearance of the tervalent phosphorus compounds, but the absorptions due to the other species present could not be neglected. As an example the extinction coefficients are given at 260 nm in cyclohexane for the reactants and the products for the reaction between triphenyl phosphine and triphenyl isoselenocyanate, trNCSe (in $M^{-1}$ $cm^{-1}$): $Ph_3P$ 10 720; trNCSe 2470; $Ph_3PSe$ 3740; trNC 680.

The reactions in acetonitrile were considerably more rapid than the isomerization of trityl isonitrile to trityl cyanide in this solvent.[59] Furthermore, as the UV spectra of these two compounds were rather similar in the measured region, the effect due to the isomerization of trityl isonitrile could be neglected.

The following reaction takes place; eqn. 2:

$$\text{trNCSe} + \text{P}{<} \longrightarrow \text{trNC} + \text{SeP}{<} \tag{2}$$
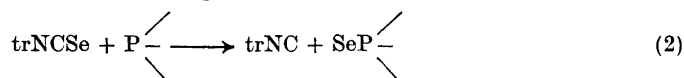
or simplified for the further calculations:

$$\text{A} + \text{B} \longrightarrow \text{C} + \text{D} \tag{4}$$
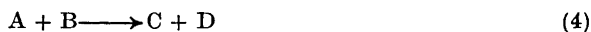
For a second-order reaction, first order in each of the reactants, the following rate equation is obtained:

$$(a-b)^{-1}\ln[b(a-x)/a(b-x)] = k_2t \tag{5}$$

where $a$ and $b$ are the concentrations of species A and B, respectively, at $t=0$.

When $\varepsilon_A$, $\varepsilon_B$, $\varepsilon_C$, and $\varepsilon_D$ are the extinction coefficients of the respective species at a given wavelength, and $x$ is the amount of A reacted at time $t$, the absorption at this wavelength is given by

$$A_t = \varepsilon_A(a-x) + \varepsilon_B(b-x) + \varepsilon_C x + \varepsilon_D x \tag{6}$$

The following general rate equation is thus readily obtained:

$$(a-b)^{-1}\ln \frac{b}{a} \times \frac{A_t - a(\varepsilon_C + \varepsilon_D - \varepsilon_B) - b\varepsilon_B}{A_t - b(\varepsilon_C + \varepsilon_D - \varepsilon_A) - a\varepsilon_A} = k_2t \tag{7}$$

When it was experimentally possible to use identical concentrations of triphenylmethyl isoselenocyanate and the phosphorus compounds, $a$, eqn. 7 reduces to:

$$\frac{A_t - a\varepsilon_A - a\varepsilon_B}{a(a\varepsilon_C + a\varepsilon_D - A_t)} = k_2t \tag{8}$$

The rates of reactions were determined from runs with concentrations of reactants in the $5 \times 10^{-4}$ M $- 4 \times 10^{-3}$ M region, depending upon the rates of reaction and, to some extent, upon extinction coefficients of the reactants used. For various concentrations of the reactants, rate plots were found to be linear up to four or five half-lives when the usual second order rate equation was applied, confirming the clean second-order kinetics, first order in each reactant. The rates of reaction were usually reproducible to within 3 to 4 % in cyclohexane, while the accuracy was considerably less for the reactions in acetonitrile due to the high rates of reactions.

The rate studies were performed on a Beckman DB spectrophotometer, using 0.1 and 1.0 cm cells. The thermostated compartments were kept at the given temperatures $\pm 0.05°C$.

As the calculations according to eqns. 7 and 8 were quite time-consuming, a Fortran N program for Watfor compiler [60] was applied for the evaluation of the rate constants.

The rate of reaction between the cyclic phosphite and triphenylmethyl isoselenocyanate was determined by measuring the disappearance of the peak at 2100 $cm^{-1}$

using a Unicam SP 200G Infrared Spectrophotometer. The rates of reaction in cyclohexane were in this case generally reproducible to within 5 %. The integrated extinction coefficients of triphenylmethyl isoselenocyanate in carbon tetrachloride was calculated from measurements performed with a Perkin Elmer 225 Grating Infrared Spectrophotometer.

## REFERENCES

1. Foss, O. *Organic Sulfur Compounds*, Pergamon, London 1961, Vol. 1, Chapter 9.
2. Fava, A. *Organic Sulfur Compounds*, Pergamon, London 1961, Vol. 2, Chapter 2.
3. Ciuffarin, E. and Fava, A. *Progr. Phys. Org. Chem.* **6** (1968) 81.
4. Bagnall, K. W. *The Chemistry of Selenium, Tellurium and Polonium*, Elsevier, Amsterdam 1966.
5. Pearson, R. G., Sobel, H. and Songstad, J. *J. Am. Chem. Soc.* **90** (1968) 319.
6. Cattalini, L. *Progr. Inorg. Chem.* **13** (1970) 263.
7. Bürger, H. and Schmid, W. *Z. anorg. allgem. Chem.* **388** (1972) 67.
8. Norbury, A. H., Austad, T. and Songstad, J. *To be published.*
9. Foss, O. *Selected Topics in Structure Chemistry*, Universitetsforlaget, Oslo 1967, p. 145.
10. Davis, R. E. *Proc. Indiana Acad. Sci.* **70** (1961) 100.
11. Bartlett, P. D. and Meguerian, G. *J. Am. Chem. Soc.* **78** (1956) 3710.
12. Zingaro, R. A. *Ann. N. Y. Acad. Sci.* **192** (1972) 72.
13. Weith, W. *Ber.* **6** (1873) 210.
14. Nef, J. U. *Ann.* **280** (1894) 291.
15. Jensen, K. A. and Fredriksen, E. *Z. anorg. allgem. Chem.* **230** (1935) 31.
16. Franklin, W. J. and Werner, R. L. *Tetrahedron Letters* **1965** 3003.
17. Collard-Charon, C. and Renson, M. *Bull. Soc. Chim. Belges* **72** (1963) 315.
18. Bulka, E., Ahlers, K. D. and Tucek, E. *Chem. Ber.* **100** (1967) 1367.
19. Boyer, J. H. and Ramakrishnan, J. H. *J. Org. Chem.* **37** (1972) 1360.
20. Kristian, P. and Suchar, G. *Collect. Czech. Chem. Commun.* **37** (1972) 3066.
21. Davis, R. E. and Nakshbendi, H. F. *J. Am. Chem. Soc.* **84** (1962) 2085.
22. Sonoda, N., Yasuhara, T., Ikeda, T., Kondo, K. and Tsutsumi, S. *J. Am. Chem. Soc.* **93** (1971) 6344.
23. Sonoda, N., Yamamoto, G. and Tsutsumi, S. *Bull. Chem. Soc. Japan* **45** (1972) 2937.
24. Bartlett, P. D., Cox, E. F. and Davis, R. E. *J. Am. Chem. Soc.* **83** (1961) 103.
25. Nicpon, P. and Meek, D. W. *Inorg. Chem.* **5** (1966) 1297.
26. Ellermann, J. and Schirmacher, D. *Chem. Ber.* **100** (1967) 2220.
27. Songstad, J. and Stangeland, L. J. *Acta Chem. Scand.* **24** (1970) 804.
28. Austad, T. *To be published.*
29. Hofmann, A. W. *Ber.* **3** (1870) 766.
30. Tarantelli, T. and Pecile, C. *Ann. Chim. (Roma)* **52** (1962) 75.
31. Jensen, K. A. and Nielsen, P. A. *Acta Chem. Scand.* **17** (1963) 1963.
32. Amonoo-Neizer, E. H., Ray, S. K., Shaw, R. A. and Smith, B. C. *J. Chem. Soc.* **1965** 4296.
33. Harpp, D. N. and Mathiaparanam, P. *J. Org. Chem.* **37** (1972) 1367.
34. Bentrude, W. G., Johnson, W. D. and Khan, W. A. *J. Am. Chem. Soc.* **94** (1972) 3058.
35. Denney, D. B., Denney, D. Z., Chang, B. C. and Marsi, K. L. *J. Am. Chem. Soc.* **91** (1969) 5243.
36. Harpp, D. N. and Gleason, J. G. *J. Am. Chem. Soc.* **93** (1971) 2437.
37. Stangeland, L. J., Austad, T. and Songstad, J. *To be published.*
38. Hudson, R. F. and Brown, C. *Accounts Chem. Res.* **5** (1972) 204.
39. Leffler, J. E., Honsberg, U., Tsuno, Y. and Forsblad, I. *J. Org. Chem.* **26** (1961) 4810.
40. Pearson, R. G., Sobel, H. and Songstad, J. *J. Am. Chem. Soc.* **90** (1968) 319.
41. Borowitz, I. J., Fürstenberg, S., Borowitz, G. B. and Schuessler, D. *J. Am. Chem. Soc.* **94** (1972) 1623.
42. Borowitz, I. J. and Crouch, R. K. *Phosphorus* **2** (1973) 209.
43. Konecny, J., Dousse, R. and Rosales, J. *Helv. Chim. Acta* **55** (1972) 3048.
44. Denney, D. B. and Boskin, M. J. *J. Am. Chem. Soc.* **82** (1960) 4736.
45. Adam, W., Ramirez, R. J. and Tsai, S.-C. *J. Am. Chem. Soc.* **91** (1969) 1254.

46. Adam, W. and Rios, A. *J. Org. Chem.* **36** (1971) 407.
47. Ogata, Y. and Yamashita, M. *Tetrahedron* **27** (1971) 2725.
48. Cadogan, J. I. G. *Quart. Rev. Chem. Soc.* **22** (1968) 222.
49. Denney, D. B., Denney, D. Z., Hall, C. D. and Marsi, K. L. *J. Am. Chem. Soc.* **94** (1972) 245.
50. Bodkin, C. L. and Simpson, W. J. *Chem. Commun.* **1970** 1579.
51. Stec, W. J. *Personal communication.*
52. Austad, T., Songstad, J. and Åse, K. *Acta Chem. Scand.* **25** (1971) 331.
53. Michaelis, A. and Luxembourg, C. *Ber.* **28** (1895) 2205.
54. Burgada, R. *Ann. Chim. (Paris)* **8** (1963) 347.
55. Pedersen, C. T. *Acta Chem. Scand.* **17** (1963) 1459.
56. Austad, T., Songstad, J. and Stangeland, L. J. *Acta Chem. Scand.* **25** (1971) 2327.
57. Zingaro, R. A. and McGlothlin, R. E. *J. Chem. Eng. Data* **8** (1963) 226.
58. Lepicard, G., de Saint-Giniez-Liebig, D., Laurent, A. and Rerat, C. *Acta Cryst.* **B 25** (1969) 617.
59. Austad, T. and Songstad, J. *Acta Chem. Scand.* **26** (1972) 3141.
60. Cress, P., Dirksen, P. and Graham, J. W. *Fortran IV with Watfor*, Prentice-Hall Inc., New Jersey 1968.

# A Theory of Surface Nucleation, its Relation to Erofeyev's Equation, and its Application to the Thermal Decomposition of Cobalt(II) Carbonate and Nickel Oxalate

ARNE ENGBERG

*The Technical University of Denmark, Chemistry Department A, Building 207, DK-2800 Lyngby, Denmark*

A theory of surface nucleation has been developed for the thermal decomposition of solids. The nuclei were presumed to be randomly distributed on a certain number of lines, which again were randomly distributed over the surface of prismatic crystals. Hereby, were explained the non-integral and varying values for the apparent reaction order, which occurs in Erofeyev's equation. Thus, the decomposition of cobalt(II) carbonate could be described satisfactorily by a model of instantaneous nucleation of only a single pair of (opposite) crystal faces, while the decomposition of nickel oxalate, which is accompanied by a considerable induction period, first at the later stages followed the same kinetics as for the cobalt(II) carbonate.

Though dehydration of salt hydrates or calcination of carbonates may seem to be simple processes, the kinetics for those and other thermal decompositions have been shown to be far from simple. Depending on the experimental conditions (*e.g.* atmosphere, vapour pressure, and prehistory of the solid) the recorded reaction curve (degree of reaction *versus* time) may or may not exhibit a sigmoid shape. In the latter case the initial straight line and the succeeding decay period have been explained by the growth of a uniform product layer from the outside of the particles leaving a kernel of unreacted material. Consequently, the kinetics could be derived from the outer geometry of the particles as has been done for spheres [1] and parallelepipeds,[2] though it was found later that the size distribution of the particles should also be taken into consideration.[3-5] In case of a sigmoid curve the acceleratory period has been explained by the activation and growth of a limited number of growth nuclei located either on the surface [6,7] or in the volume.[10-17] The decay period can also be described in many cases − if not in all by reversible reactions − by the topochemical kinetics mentioned above.[1-5] Thus surface nucleation tends to be favoured. However, the expressions derived by Mampel,[7] extended by Delmon,[8] and reviewed by Young [9] have not been much used, probably be-

cause of their rather complicated nature. So far they have been overshadowed by the theories based on volume nucleation, including those of Avrami,[10-11] Erofeyev,[12] Prout-Tompkins,[13] and the versions of Garner's theory of linear branching chains.[14-17] While the Avrami-Erofeyev equation may be expected to describe satisfactorily such physical processes as recrystallizations and phase transitions, the assumption of volume nucleation appears unrealistic for chemical processes where gases are involved. Due to larger lattice vibrations caused by the partial potential, the probability of a chemical dissociation and, hence, of a nucleation should be larger at the surface. This may be the reason why deviations have been observed even in the allotropic transformation of tin [18] for the ultimate part of the reaction curve.

In the Avrami-Erofeyev equation, which reads

$$\alpha = 1 - e^{-Kt^m} \tag{1}$$

the exponent, $m = n + i$, is assumed to be the sum of the dimensionality, $n$, and the number of nucleation steps, $i$. Thus, an integral number should be expected for the slope, $m$, when $\ln[-\ln(1-\alpha)]$ is plotted against $\ln(t)$. In practice, however, broken or extremely low or high values may be found together with deviations from the straight line in the decay period. From the literature the initial and final values of $m$ for following decompositions can be extracted: $2.5 - 3.1$, $2.9 - 5.1$ ($KMnO_4$),[19] $5.0$, $3.2$ ($NiC_2O_4$), [20] $0.7 - 1.9$, $0.7 - 1.0$ ($MgC_2O_4$),[21] and $1.48$, $1.67$ ($CoCO_3$).[22]

In the following it will be shown how $m$ may be rationalized into meaningful values by allowance of a certain induction period, $t_0$, (the observed times, $t_{obs}$, being reduced by $t_0$; that is, $t = t_{obs} - t_0$) and how the decay period can be explained by surface nucleation.

While Avrami [10] supposed nucleation to be a first order process (to be derived, if all germs are nucleated with the same probability), Mampel [7] considered the extreme case of a constant nucleation rate. Here, the other extreme case, that of instantaneous nucleation, will be considered. The latter case not only leads to especially simple equations, but is presumed to represent the decomposition of solids in a dynamic vacuum more realistically than does a constant nucleation rate.

Instead of a random nucleation, as supposed by Avrami, Mampel, and Delmon, a distribution of the germs on certain lines will be assumed in harmony with the inference given by Young [23] for the decomposition of nickel oxalate and the observations made on calcite [24] and nickel sulphate hexahydrate.[25]

The basis of the growth nuclei on the surface has formerly been considered as circular in harmony with the observations on tin [18] and chrome alum [26] (with the nuclei growing inwards as hemispheres). However, a square basis will be assumed here in harmony with that observed on nickel sulphate hexahydrate.[25] In order to further facilitate the calculations the growth nuclei will be considered as hemicubes instead of the hemioctahedra that are observed.[25]

## THE SURFACE REACTION

Consider a rectangular planar surface with sides $b$ and $c$ and containing a number of lines, $l_0$, running parallel to $c$, but randomly distributed over the surface. Furthermore let the basis of the growth nuclei be squares of sides $2k_g t$, orientated parallel to $b$ and $c$, and with their centers located on the lines so that each line contains $m_0$ randomly distributed centers (see Fig. 1).
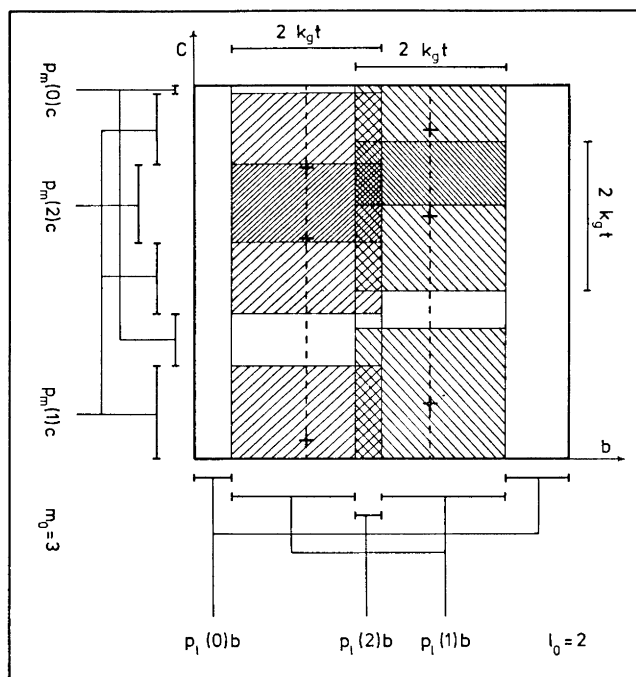


*Fig. 1.* Model for coverage of a crystal surface with growth nuclei. The centers of the growth nuclei (+) are located on two lines (- - -) running parallel to the side $c$.

Now, according to Mampel,[7] the probability that a given point on a growth line has been covered by $i$ overlapping growth nuclei originating from the same line should be given by the Poisson formula

$$p_m(i) = (\mu^i/i!)e^{-\mu} = [(2k_g tm_0/c)^i/i!]e^{-(2k_g tm_0/c)} \tag{2}$$

where the average, $\mu$, for the present case will equal the total length of the nuclei, $2k_g tm_0$, divided by the length of the line, $c$. The probability that a point on the surface has been covered by $j$ overlapping growth lines is expressed in a similar way by

$$p_l(j) = [(2k_g tl_0/b)^j/j!]e^{-(2k_g tl_0/b)} \tag{3}$$

It will appear from Fig. 1 that the total area of the uncovered surface can be estimated by the sum of the areas for the rectangles of breadths $p_1(j)b$ and hereto corresponding lengths $[p_m(0)]^j c$. Thus, the degree of covered surface, $\theta$, should amount to

$$\theta(t) = 1 - \sum_{j=0}^{l_0} p_1(j)[p_m(0)]^j \tag{4}$$

which on insertion of (2) and (3) gives

$$\theta(t) = 1 - \sum_{j=0}^{l_0} \frac{(2k_g t l_0/b)^j}{j!} \, \mathrm{e}^{-(2k_g t l_0/b)} \, \mathrm{e}^{-j(2k_g t m_0/c)} \tag{5}$$

By introduction of a reduced time, $u$,

$$u = 2k_g t/a \tag{6}$$

where $a$ is the thickness of the crystal (normal to the surface under consideration), and the reduced number of germs, $M$, and lines, $L$,

$$M = m_0 a/c \tag{7}$$

$$L = l_0 a/b \tag{8}$$

eqn. (5) simplifies to

$$\theta(u) = 1 - \sum_{j=0}^{L} \frac{(Lu)^j}{j!} \, \mathrm{e}^{-Lu} \, \mathrm{e}^{-jMu} \tag{9}$$

The upper summation limit should not have been changed into $L$ (unless $l_0 = L$ for $a = b$) but the error thus produced will be of minor importance.

For description of the acceleratory phase of the reaction the exponential terms in (9) can be expanded in a power series, yielding

$$\theta(u) = LMu^2[1 - \tfrac{1}{2}Mu - \tfrac{1}{2}M(L - \tfrac{1}{3}M)u^2 + \tfrac{1}{2}M^2(L - \tfrac{1}{12}M)u^3 + \cdots] \tag{9a}$$

Thus, $\theta(u)$ tends to approach $LMu^2$ at the very beginning, which is to be expected, when $LM = N$ represents the reduced number of growth nuclei in total and $u^2$ stands for the reduced area for a single growth nucleus.

If $Mu$ is very small compared to unity, then eqn. (9) reduces to

$$\theta(u) = 1 - \mathrm{e}^{-LMu^2} = 1 - \mathrm{e}^{-Nu^2} \tag{9b}$$

to be expected for a completely random distribution of the germs. If on the other hand $Mu$ is very large compared to unity, then eqn. (9) reduces to

$$\theta(u) = 1 - \mathrm{e}^{-Lu} \tag{9c}$$

to be expected for the growth from randomly distributed lines. Thus, the ratio $M/L$ will be determining for the tendency of the germs to array themselves on a line.

## THE VOLUME REACTION

Consider a rectangular parallelepiped as shown in Fig. 2, where the faces normal to the sides $a$, $b$, and $c$ have reacted to the respective degrees of surface coverage, $\theta_a$, $\theta_b$, and $\theta_c$. Provided that nucleation is instantaneous and that the growth nuclei are hemicubes (or just cylindrical with the axis normal to the surface), the degree of coverage for a plane parallel to the surface and at a certain distance below it will be independent of the depth when this is smaller than $k_g t$. Otherwise the degree of coverage will be zero. Hereby, the evalua-



Fig. 2. Penetration of the growth layers from the various faces of the model crystal shown by dotted lines. Ingestion of the growth layers from either two or three faces are shown by the hatched areas, respectively.
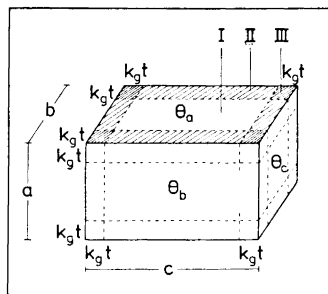
tion of the reacted volume has been greatly simplified. It will appear from Fig. 2 that there are three growth domains in the model crystal: I with growth from a single face, and II and III with interfering growth from two and three faces, respectively. For the first domain the reacted volume, $v_I$, is found as a sum of the areas, e.g. $(b - 2k_g t)(c - 2k_g t)$, multiplied by their respective degrees of coverage, $\theta_a$, and the depth $k_g t$,

$$v_I = 2k_g t \sum_a^c (b - 2k_g t)(c - 2k_g t)\theta_a \tag{10}$$

When the overlapping growth nuclei originate from more than one face, the resultant probability for an uncovered surface element should be the product of the individual probabilities for uncovering for the faces in question. Hence, for that part of domain II, where growth layers normal to $a$ and $b$ are overlapping, the total degree of covering, $\theta_{ab}$, becomes

$$\theta_{ab} = 1 - (1 - \theta_a)(1 - \theta_b) \tag{11}$$

In a similar way the degree of coverage, $\theta_{abc}$, is obtained for domain III,

$$\theta_{abc} = 1 - (1 - \theta_a)(1 - \theta_b)(1 - \theta_c) \tag{12}$$

Consequently, the reacted volumes of domains II and III become

$$v_{II} = 4(k_g t)^2 \sum_a^c (a - 2k_g t)[1 - (1 - \theta_b)(1 - \theta_c)] \tag{13}$$

$$v_{III} = 8(k_g t)^3 [1 - (1 - \theta_a)(1 - \theta_b)(1 - \theta_c)] \tag{14}$$

By introduction of (6) and the elongations $l_1$ and $l_2$,

$$l_1 = b/a; \; l_2 = c/a \tag{15}$$

the degree of reacted volume, $\alpha$, can be expressed by

$$\alpha = (v_{\mathrm{I}} + v_{\mathrm{II}} + v_{\mathrm{III}})/abc = (\theta_a + \theta_b/l_1 + \theta_c/l_2)u - (\theta_b\theta_c/l_1l_2 + \theta_a\theta_c/l_2 + \theta_a\theta_b/l_1)u^2 + (\theta_a\theta_b\theta_c/l_1l_2)u^3 \tag{16}$$

where $\theta_a$, $\theta_b$, and $\theta_c$ depend on $u$ according to (9).

The universality of the expression given above will be shown in the following by the extremes that can be derived from it. The first one to be considered is that derived when the ratios $\theta_b/l_1$ and $\theta_c/l_2$ are either vanishing or identical with $\theta_a$ $(=\theta)$,

$$\alpha(u) = 1 - (1 - \theta u)^n \qquad (n = 1, 2, \text{ or } 3) \tag{16a}$$

which further simplifies for $\theta = 1$ to the well known expression for a $n$-dimensional phase boundary reaction. Thus, a low dimensionality of a reaction can be produced either by a preferential nucleation of some of the faces ($\theta_b$ or $\theta_c$ vanishing) or by a preferential growth of the dimensions ($l_1$ or $l_2$ large).

At this stage it must be emphasized that (16) should apply equally well for anisotropic reactions, provided that the geometric elongations defined in (15) have been replaced by the corresponding kinetic quantities

$$l_1 = (k_a/k_b)(b/a); \; l_2 = (k_a/k_c)(c/a) \tag{15a}$$

obtained by multiplication of the geometric elongations by the proper ratios of the anisotropic rate constants $k_a$, $k_b$, and $k_c$ (for reactions along $a$, $b$, and $c$, respectively).

The second extreme to be mentioned is that occurring when the faces have been covered totally by the growth nuclei. By a reasonable large number of germs this may be realized even in an early stage of the process, whereafter the general topochemical expression [5] should be followed,

$$\alpha(u) = \frac{l_1 + l_2 + l_1l_2}{l_1l_2} u - \frac{1 + l_1 + l_2}{l_1l_2} u^2 + \frac{1}{l_1l_2} u^3 \tag{16b}$$

At the end of the reaction, when $2k_g t$ has grown larger than one of the dimensions corresponding to $u$ larger than unity (when $a$ is smallest dimension), at least one pair of the growth layers which originate from opposite faces, would have grown into each others. As the phenomenon has not been considered by the derivations, (16) should apply strictly for the previous period only ($u$ less than unity). In practice, however, the equation may reproduce also the following period satisfactorily, especially for an apparent three-dimensional reaction. Thus, the transition ($u = 1$) should occur at a degree of reaction of at least $\alpha_{\mathrm{trans}} = 1 - e^{-3} = 0.95$ (corresponding to $ML = 1$) and usually at much higher values (e.g. $\alpha_{\mathrm{trans}} = 0.9998$ for $ML = 3$).

Greatest deviations should be expected for an apparent unidimensional reaction, where the transition may occur at a degree of reaction as low as 0.63. Therefore, the correct treatment shall be given for this type of reaction. Putting $\theta_b/l_1$ and $\theta_c/l_2$ equal to zero in (16) or $n$ equal to unity in (16a) results in the description of the first period ($u \leq 1$; $k_g t \leq a/2$),

$$\alpha(u) = \theta u = \left[ 1 - \sum_{j=0}^{L} \frac{(Lu)^j}{j!} e^{-Lu} e^{-jMu} \right] u \tag{17a}$$

In the following period $(1 \le u \le 2)$ the two growth layers have grown into each other within a layer of reduced thickness $u-1$ in the middle of the particle. Then, according to (11), the degree of covering within the overlap layer should amount to $2\theta - \theta^2$, provided that the surface coverages, $\theta$, are identical for the two nucleation faces in question. As $2-u$ will represent the thickness of the other layers (the bread of the sandwich), the degree of reacted volume should be given by

$$\alpha(u) = \theta(2-u) + (2\theta - \theta^2)(u-1) = \theta u - \theta^2(u-1) \tag{17b}$$

When the growth layers have reached the opposite faces $(2 \le u)$, no further growth in thickness is possible, the growth being limited to the two other dimensions for completion of the reaction. The ultimate period is thus described by

$$\alpha(u) = 2\theta - \theta^2 \tag{17c}$$

By introduction of a cutting-off function $\mathrm{F}(x)$, defined as

$$\mathrm{F}(x) = \begin{cases} 0 & (x \le 0) \\ x & (0 \le x \le 1) \\ l & (l \le x) \end{cases} \tag{18}$$

the kinetics for the three periods given above can be combined into the following expression,

$$\alpha(u) = 2\theta\, \mathrm{F}(u/2) - \theta^2\, \mathrm{F}(u-1)$$

$$= 2 \left[ 1 - \sum_{j=0}^{L} \frac{(Lu)^j}{j!} e^{-Lu} e^{-jMu} \right] \mathrm{F}(u/2) -$$

$$\left[ 1 - \sum_{j=0}^{L} \frac{(Lu)^j}{j!} e^{-Lu} e^{-jMu} \right]^2 \mathrm{F}(u-1) \tag{19}$$

## REACTION OF HETEROSIZED PARTICLES

Besides overlap and ingestion of the growth nuclei described above the decay period of the reaction curve may be influenced by the diffusion of gaseous products and, when particulate samples are used, by the particle size distribution. As long as reactions of small particles in dynamic vacuum are discussed, the diffusion may be of minor importance. Therefore, the discussion will concentrate on the effect from the particle size distribution.

Let the sample consist of crystals with a pair of invariant nucleation faces, $bc$, and with the thickness, $a$, being distributed over a certain number of classes, such that the $i$-th class contains a number, $n_i$, of crystals of dimension $a_i$. Instead of (19) it can then be shown that

$$\alpha(u) = 2\theta \sum \frac{n_i a_i}{\sum n_i a_i} \mathrm{F}\left( \frac{u \sum n_i a_i}{2 a_i \sum n_i} \right) - \theta^2 \sum \frac{n_i a_i}{\sum n_i a_i} \mathrm{F}\left( \frac{u \sum n_i a_i - 1}{a_i \sum n_i} \right) \tag{20}$$

provided that the reduced time $u$ is on basis of the mean dimension $\bar{a}$,

$$\bar{a} = \sum(n_i a_i / \sum n_i) \tag{21}$$

to be inserted in (6).

The expression can be simplified somewhat by introduction of the normalized frequencies, $f_i$, and the reduced dimensions, $q_i$,

$$f_i = n_i / \sum n_i \tag{22}$$

$$q_i = a_i / \bar{a} \tag{23}$$

whereby (20) reduces to

$$\alpha(u) = 2\theta \sum f_i q_i \, \mathrm{F}\left(\frac{u}{2q_i}\right) - \theta^2 \sum f_i q_i \, \mathrm{F}\left(\frac{u}{q_i} - 1\right) \tag{24}$$

## RESULTS AND DISCUSSION

Some calculations have been made on a Wang model 700 desk computer using a program written for the purpose and based on (9) and (20) (or (24)). The program was designed to operate mainly with the number distributions determined by microscopy of a relatively low number of particles. For this reason and because of the low storage capacity of the computer (120 registers), the particle size distribution was assumed to be present as a ten-class histogram. In the calculations to be reported here approximations to the log-normal weight distribution were used. This is the distribution which to a greater extent was found obeyed for precipitates such as AgCl in photographic emulsions,[27] $BaSO_4$,[28] and $CuSO_4 \cdot 5H_2O$.[29] Consequently, the corresponding number distribution should be given by

$$f_i = (\text{constant}) \, q_i a^3 \exp\left[-(\ln q_i - \ln q_{\text{mode}})^2 / 2\sigma^2\right] \tag{25}$$

with the constant $= \exp\left[-2\sigma^2\right]/[\sigma(2\pi)^{\frac{1}{2}}]$

*Table 1.* Approximated number distributions for log-normal weight distributions with the frequency given in percentage.

| $\sigma$ | 0.4 | 0.5 | 0.6 | 0.7 | 0.8 | 0.9 | 1.1 | 1.3 | 1.5 | 1.7 | $1/q_{\text{mode}}$ |
|---|---|---|---|---|---|---|---|---|---|---|---|
| | | | | | $q/q_{\text{mode}}$ | | | | | | |
| 0.1 | | | | 0.54 | 9.03 | 56.70 | 32.30 | 1.42 | 0.01 | | 0.9602 |
| 0.2 | 0.04 | 0.89 | 5.39 | 14.17 | 21.24 | 32.70 | 19.52 | 5.01 | 0.89 | 0.15 | 0.8961 |
| 0.3 | 4.30 | 10.09 | 15.85 | 17.80 | 16.00 | 18.49 | 11.22 | 4.19 | 1.40 | 0.66 | 0.7919 |

| $\sigma$ | 0.2 | 0.3 | 0.4 | 0.5 | 0.7 | 0.9 | 1.1 | 1.5 | 1.9 | 2.5 | $1/q_{\text{mode}}$ |
|---|---|---|---|---|---|---|---|---|---|---|---|
| | | | | | $q/q_{\text{mode}}$ | | | | | | |
| 0.2 | | | 0.04 | 3.38 | 29.64 | 40.37 | 24.37 | 2.15 | 0.05 | | 0.8891 |
| 0.3 | 0.02 | 0.53 | 4.90 | 19.66 | 33.74 | 23.40 | 14.58 | 2.84 | 0.31 | 0.02 | 0.7757 |
| 0.4 | 1.72 | 6.96 | 13.25 | 28.56 | 25.07 | 13.30 | 8.41 | 2.22 | 0.45 | 0.06 | 0.6546 |
| 0.5 | 10.82 | 17.28 | 17.96 | 24.32 | 15.69 | 7.30 | 4.74 | 1.42 | 0.39 | 0.08 | 0.5253 |

For the precipitates mentioned above $\sigma$ was observed in the range of 0.2 – 0.5. In Table 1 the histograms are given which have been used to reproduce (25). It will appear that two sets of class interval have been chosen in order to obtain reasonable approximations over the whole range of the dispersion.

The results in Fig. 3 are shown for the case in which the reaction is under the influence of particle size distribution alone ($M = L = \infty$). Apart from the mean size, whose influence has been eliminated by introduction of the reduced time $u$, the further influence — namely that from the dispersion — is seen to result in a retardation of the later stages of the reaction. In fact, for all
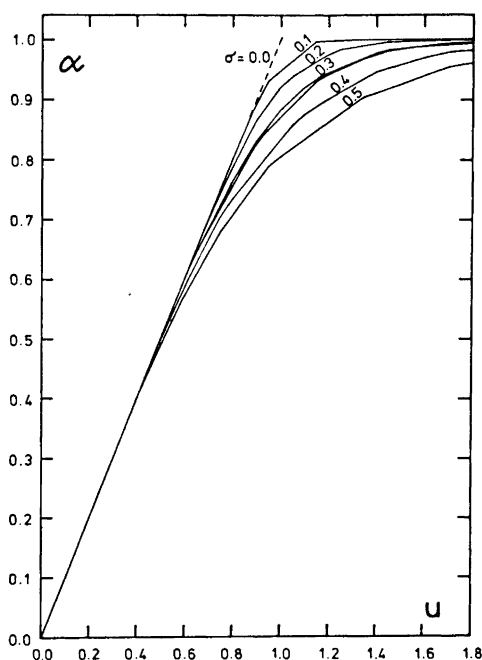


*Fig. 3.* Reaction curves for an apparent unidimensional reaction in the topochemical limit ($\theta = 1$) for particles with approximated log-normal weight distributions (Table 1).
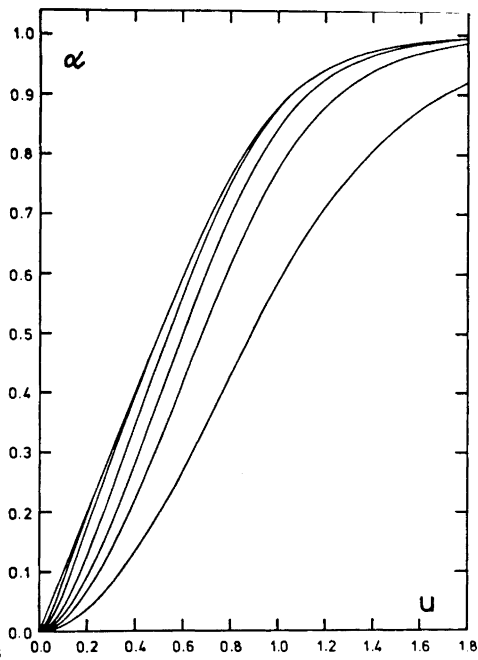
*Fig. 4.* Reaction curves for an apparent unidimensional reaction for particles with an approximated log-normal weight distribution ($\sigma = 0.3$) and with solid ($M = \infty$) growth lines of following numbers: $L = \infty$, 20, 10, 5, 3, 2, 1 (for the curves from top to bottom).

relevant magnitudes of the dispersion only the upper halfs of the reaction curves will be affected by the particle size distribution, which is in agreement with earlier findings.[5] Although the curves may appear somewhat edged because of the coarseness in the histograms used, the duplicates (for $\sigma = 0.2$ and 0.3) run close together, which indicate that the deviations from the master curves (those for the true log-normal distribution) are relatively small.

When the reaction initiates from a limited number of growth lines, a more or less pronounced acceleratory period is found even if an infinite number of growth nuclei are present as shown in Fig. 4. The reaction curves begin as parabolas which can be realized by the approximation of (17a),

$$\alpha(u) = [1 - e^{-Lu}]u + \cdots = Lu^2 + \cdots \tag{26}$$

but because of the growth overlap they soon approach the corresponding topochemical curve (*cf.* Fig. 3) until practical coincidence, the occurrence of which is determined by $L$. For many lines ($L > 20$) the coincidence occurs already in the first stages of the reaction ($\alpha \leq 0.2$), while few lines ($L < 4$) can remove the coincidence. It must also be emphasized that the infinite number of lines assumed in topochemical kinetics, in practice is satisfied, when $L$ is in the order of 100. When $L$ is larger than 10, the coincidence will occur within the first half of the reaction, which means that the two phenomena, growth from nucleation lines and particle size distribution, can be discussed independently of each other. All of the curves are remarkably close to straight lines when $0.2 < \alpha < 0.6$ but their slopes deviate somewhat from that of the interfacial reaction ($L = \infty$) within the limits of 10 % above ($L = 10$) and 20 % below ($L = 1$). Consequently, the rapid estimate of $k_g/a$ obtained from the slope may be inaccurate, while a more reliable estimate must be gained from the ultimate part of the reaction where the influence from the growth lines has been reduced to a minimum.

According to (26) an estimate of $L$ may be obtained from the initial slope of $[\alpha(u)]^{\frac{1}{2}}$, but an examination of Fig. 5 reveals that the predicted straight line is followed over a very narrow range ($0 < \alpha < 0.006$) when $M$ is large. When $M$ is small, however, $d[\alpha(u)]^{\frac{1}{2}}/du$ is constant over a considerably larger part of
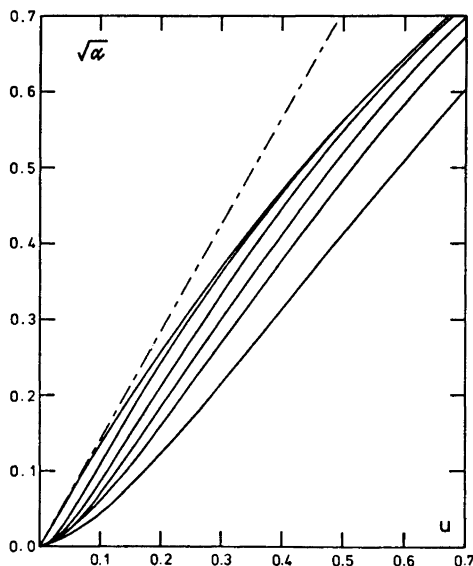


*Fig. 5.* The acceleratory period ($\alpha^{\frac{1}{2}}$ *versus* $u$) for one of the reaction curves in Fig. 4 ($L = 2$, $M = \infty$) together with curves for a decreasing number of nuclei, $M = \infty, 10, 5, 3, 2, 1$ (for the curves from top to bottom).

the curves, but the slope is somewhat dependent on $M$: 1.414 $(M = \infty)$, 1.377 $(M = 10)$, 1.249 $(M = 5)$, 1.160 $(M = 3)$, 1.096 $(M = 2)$, 1.000 $(M = 1)$.

When the reaction curves are transformed into Erofeyev plots, nearly straight lines are produced and in such a way that each curve may be approximated by two lines bisecting each other at about 0.4. In Fig. 6 such curves have been drawn for the same material as presented in Fig. 4. The apparent reaction order given by the slope is dependent on $L$, but the variations are largely concentrated to the lower half of the reaction as can be realized from the following figures: 1.06, $1.63(L = \infty)$; 1.32, $1.63(L = 20)$; 1.57, $1.63(L = 10)$; 1.68, $1.74(L = 5)$; 1.84, $1.91(L = 3)$; 1.96, $2.00(L = 2)$; 1.94, 1.89 $(L = 1)$. The first of these figures are valid for the region $0.05 < \alpha < 0.2$ while
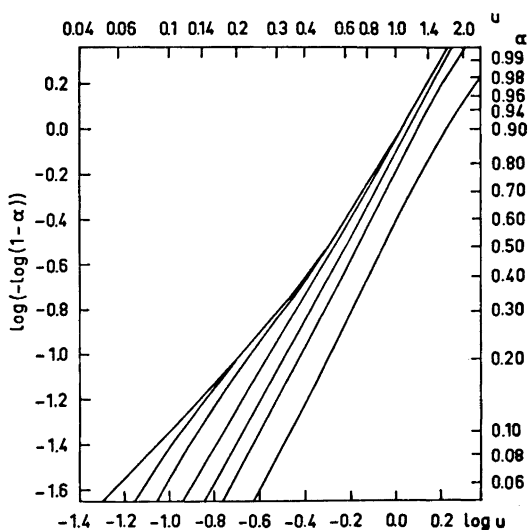


*Fig. 6.* Erofeyev plot $(\log[-\log(1-\alpha)]$ *versus* $\log u)$ for the same reaction curves as in Fig. 4.

the second ones are valid for the region $0.5 < \alpha < 0.9$. This is just in accordance with the theory since the first reaction order should be affected by the number and distribution of the growth nuclei and thus vary between the topochemical limit (1) and the limit of a two dimensional growth of nuclei (2), while the final reaction order should be determined by the topochemical properties of the sample material.

Although the above discussion has been limited to the apparent unidimensional reactions, it is also true that for other types of reactions a non-integral or varying reaction order may in general be explained by a surface nucleation.

Finally, some experimental results will be taken from the literature and related to the theory. For the thermal decomposition of commercial cobalt(II) carbonate Avramov and Janatchkova [22] found the Erofeyev equation to be obeyed with reaction orders ranging from 1.37 (at 220°C) to 2.54 (at 270°C) in

dependence of temperature. The kinetics could have been described better by the Erofeyev equation if an induction period had been included. Thus, for the lowest temperature the initial reaction order (taken for the region $0.05 \leq \alpha \leq 0.20$) could be moved from 1.48 ($t_0 = 0$) to 1.67 ($t_0 = 5$) and 2.00 ($t_0 = 10$ min), whereas the final reaction order of 1.67 (for the region $0.5 \leq \alpha \leq 0.9$) is scarcely changed. By the first movement the reaction is described by a constant reaction order, and by the second movement the initial reaction order assumes a meaningful value. The discrepancy between the slopes reported here (1.48) and those reported earlier (1.37) originates from the fact that Avramov and Janatchkova did not normalize $\alpha$ to unity for the maximum degree of reaction as done here. Their values for $\alpha$ were based on the reaction scheme

$$CoCO_3 + \tfrac{1}{6}O_2 \rightarrow \tfrac{1}{3}Co_3O_4 + CO_2 \tag{27}$$
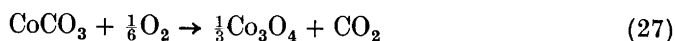
Their final values amounting to $75 - 77 \%$ indicate, however, that the sample material after drying at $130°C$ must have been a basic carbonate
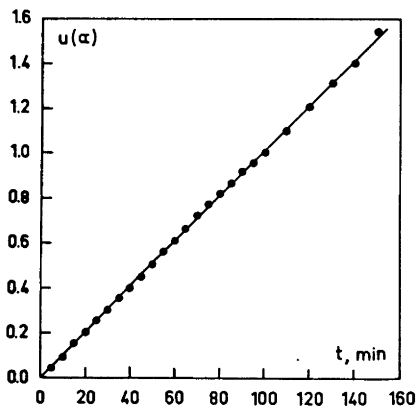


*Fig. 7.* The inverse reaction curve ($u(\alpha)$ *versus t*) for the decomposition of cobalt(II) carbonate at 220°C.
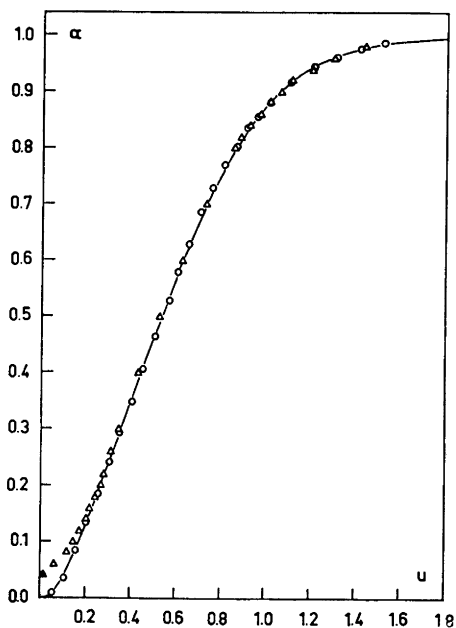
*Fig. 8.* Reduced reaction curves for the thermal decomposition of cobalt(II) carbonate at 220°C (O) and nickel oxalate at 240°C ($\triangle$). $u = 2k_g(t_{obs} - t_0)/a$ with $t_0 = 0$ for cobalt(II) carbonate and $t_0 = 98$ min for nickel oxalate. The solid line represents an unidimensional reaction of log-normal weight distributed particles ($\sigma = 0.3$) with $L = 5$ and $M = 20$.

instead of the neutral one assumed. For instance, $2CoCO_3.Co(OH)_2.H_2O$ yields a weight loss of 77.60 % of the reaction scheme mentioned above.

In contrast to the theories of Avrami and Erofeyev the apparent two-dimensional growth in the acceleratory period and a smaller dimensionality in the later stages of the reaction can be explained easily by the present theory. The magnitudes of $L$, $M$, and $k = k_g/a$ were estimated in the following way. $L$ was estimated by a comparison of the Erofeyev plot for the observed $\alpha$ with the corresponding theoretical curves in Fig. 6. A translation of the observed curve over the theoretical ones with respect to the time axis gave a practical coincidence of the curves when $L = 5$ ($M = \infty$). A somewhat better fit was obtained when $\alpha$ was corrected by an amount $\alpha_0 = 0.02$ so that $\alpha_{corr} = (\alpha - \alpha_0)/(1 - \alpha_0)$, the quantity $\alpha_0$ being determined as the intercept of the smoothed curve from a $\alpha, t^2$ plot. A still better fit was also obtained when $M$ was finite, say $M = 20$ ($15 < M < 100$). Furthermore the constant could have been obtained from the comparison mentioned above, as the translation will amount to $\log k$. More accurately, however, $k$ is found as the slope of the straight line obtained, when $u(\alpha)$ has been plotted against $t$, as shown in Fig. 7. In the present case the linear regression analysis yields $k = (1.013 \pm 0.012) \times 10^{-2}$ min$^{-1}$ with a negligible induction period $t_0 = -0.16 \pm 0.15$ min, and a standard deviation on $t$ of $\pm 0.68$ min (corresponding to 0.3 mm on the published curve). The goodness of the fit for the final results can also be realized from Fig. 8. The above mentioned correction by $\alpha_0$ may be justified if excess water is present and given off rapidly. The observed increase of the reaction order for increasing temperatures may be explained by a lower activation energy for the nucleation than for the growth. Then growth will be more enhanced than nucleation by an increase in temperature with a resulting decrease in number of effective growth nuclei and, consequently (cf. Fig. 6), an increase of the reaction order.

When the experimental curves for higher temperatures were treated as above, $N = LM$ was found to decrease gradually from about 100 (220°C) down to 1 (270°C). The apparent activation enthalpy for $k$ of 22.8 kcal/mol then became much closer to the thermodynamic value of 21.8 kcal/mol for bond breaking (removal of carbon dioxide without oxidation of the metal) than did Avramov and Janatchkova's value of 27.85 kcal/mol. If in addition the metal is allowed to oxidize, the latter deviates even more from the thermodynamic value, which amounts to only 9 kcal/mol.

Nearly the same kinetics as given above have been found for nickel oxalate, although without a considerable induction period. So, the thermal decomposition of the oxalate can not occur by just a bond breaking as in case of the carbonate but must pass through several steps before the ordinary growth nuclei can be formed, namely: (1) charge transfer (of an electron) from the surface anion to an anion vacant site, (2) dissociation of the anion radical into gaseous carbon dioxide, (3) diffusion of the vacant anion sites into the body of the crystal, and (4) migration of the trapped electrons to the cation sites under production of free metal. This scheme was already mentioned by Allen and Scaife [30] and later adopted by Jacobs and Kureishy [31] and others.[23,32-34] As the rather large anion will possess a low mobility, the third step should be the rate determining one until so many vacant sites are formed that the

structure in the outer layer collapses under formation of metallic nuclei, after which the nuclei are expected to grow at normal rate.

When the induction period was eliminated by subtraction of an appropriate value for $t_0$ (98 min), the resulting reduced data for the reaction (240°C) in hydrogen [20] may be shown to fall on the same curve in Fig. 8 as that given for the cobalt carbonate. Following the curve for $L = 5$ and $M = 20$ the data indicate a pronounced tendency for the nuclei to align themselves on lines, a result which has already been observed by electron microscopy.[34] In the acceleratory period the experimental data for nickel oxalate appear somewhat high, however, which suggests that the growth nuclei first acquire their final number at a later stage. A more satisfactory description could be obtained by allowance of a certain $\alpha_0$ (0.02). Together with a diminished induction period ($t_0 = 65.8$ min) this gave the best fit to (24) but not, however, without changes of $L$ (2) and $M$ (2). Even the deviations were reduced but they were not removed, indicating the aforementioned nucleation period.

## CONCLUSION

From the kinetic model of surface nucleation followed by three-dimensional growth it turns out that Erofeyev's equation and the equation for the contracting rectangle (or sphere, envelope and line) are two of the extremes from a more general description. Thus, the apparent reaction order in Erofeyev's equation is affected by the number of nuclei and their possible alignment for the acceleratory phase and to a lesser extent by the particle geometry and size distribution for the decay period. Furthermore, if the number of nuclei depend on temperature and Erofeyev's method is used, the activation energy will not correspond to the interfacial reaction, as exemplified by the reaction of the cobalt carbonate. If only a few nuclei are present, several solutions for the constants $k$, $L$, and $M$ may apply to the experimental data (*cf.* nickel oxalate) whereby the magnitudes of the constants can only be assigned within wide limits rather than with definite values. Then the correct solution must be obtained from, *e.g.*, microscopical examinations of the reaction. The aim of the present work, however, has been concentrated on obtaining a family of reasonable solutions to the observed kinetics, of which only one, of course, will be correct.

## REFERENCES

1. Roginsky, S. and Schulz, E. *Z. phys. Chem.* **A 138** (1928) 21.
2. Hume, J. and Colvin, J. *Proc. Roy. Soc. (London)* **A 132** (1932) 548; **A 125** (1929) 635.
3. Trambouze, M. T. and Imelik, B. *J. Chim. Phys.* **57** (1960) 656.
4. Delmon, B. *Rev. Inst. Franc. Petrole* **16** (1961) 1477.
5. Engberg, A. *Acta Chem. Scand.* **24** (1970) 931; **25** (1971) 3743.
6. Fischbeck, K. and Spingler, H. *Z. anorg. allgem. Chem.* **241** (1939) 209.
7. Mampel, K. *Z. phys. Chem.* **A 187** (1940) 43, 235.
8. Delmon, B. *Rev. Inst. Franc. Petrole* **18** (1963) 760.
9. Young, D. A. *Decompositions of Solids*, Pergamon, New York 1966.
10. Avrami, M. *J. Chem. Phys.* **7** (1939) 1103; **8** (1940) 212; **9** (1941) 177.
11. Jacobs, P. W. M. *Proc. 6th Int. Symp. Reactivity of Solids*, Schnenectady 1968, (1969) 207; *Mater. Sci. Res.* (Plenum) **4** (1969) 37.

12. Erofeyev, B. V. *C. R. Acad. Sci. USSR* **52** (1946) 511.
13. Prout, E. G. and Tompkins, F. C. *Trans. Faraday Soc.* **42** (1946) 468.
14. Garner, W. E. and Hailes, H. R. *Proc. Roy. Soc. (London)* **A 139** (1933) 576.
15. Hailes, H. R. *Trans. Faraday Soc.* **29** (1933) 544.
16. Hill, R. A. W. *Trans. Faraday Soc.* **54** (1958) 685.
17. Delmon, B. and Roman, A. *Rev. Inst. Franc. Petrole* **23** (1968) 1073; *Proc. 6th Int. Symp. Reactivity of Solids*, Amsterdam 1968.
18. Burgers, W. G. and Groen, L. J. *Discussions Faraday Soc.* **23** (1957) 183.
19. Erofeyev, B. V. *Proc. 4th Int. Symp. Reactivity of Solids, Amsterdam 1960*, Elsevier 1961, p. 273.
20. Doremieux, J.-L. and Brissaud, P. *C. R. Acad. Sci. Paris* **C 269** (1969) 1465.
21. Yankwich, P. E. and Zavitsanos, P. D. *J. Phys. Chem.* **69** (1965) 442.
22. Avramo, L. K. and Janatchkova, J. M. *Z. phys. Chem. (Leipzig)* **241** (1969) 244.
23. Dominey, D. A., Morley, H. and Young, D. A. *Trans. Faraday Soc.* **61** (1965) 1246.
24. Renshaw, G. D. and Thomas, J. M. *Nature* **209** (1966) 196; *J. Chem. Soc.* **A 1967** 2058.
25. Thomas, J. M. and Renshaw, G. D. *J. Chem. Soc.* **A 1969** 2753.
26. Cooper, J. A. and Garner, W. E. *Trans. Faraday Soc.* **32** (1936) 1739; *Proc. Roy. Soc. (London)* **A 174** (1940) 487.
27. Loveland, R. P. and Trivelli, A. P. H. *J. Franklin Inst.* (1927) 193, table I.
28. Liteanu, C. and Lingner, H. *Talanta* **17** (1970) 1045, table I.
29. Engberg, A. *To be published*.
30. Allen, J. A. and Scaife, D. E. *J. Am. Chem. Soc.* **58** (1954) 666.
31. Jacobs, P. W. M. and Kureishy, A. R. T. *Proc. 4th Int. Symp. Reactivity of Solids, Amsterdam 1960*, Elsevier 1961, p. 352; *Trans. Faraday Soc.* **58** (1962) 551.
32. Kadlec, O. and Danes, V. *Collection Czech. Chem. Commun.* **32** (1967) 1871.
33. Charcosset, H., Tournayan, L. and Trambouze, Y. *Bull. Soc. Chim. France* **1968** 925.
34. Tournayan, L., Charcosset, H., Wheeler, B. R., McGinn, J. M. and Galwey, A. K. *J. Chem. Soc.* **A 1971** 868.

# The Friedel-Crafts Reactions of 2-Substituted Oxetanes*

P. O. I. VIRTANEN, S. PELTONEN and J. HYYPPÄ

*Department of Chemistry, University of Oulu, SF-901 00 Oulu 10, Finland*

The aluminium chloride-catalyzed Friedel-Crafts reactions of 2-phenyloxetane and 2-methyloxetane with solvent benzene, toluene, and mesitylene have been studied and found to give 3-aryl-3-phenyl-propan-1-ols and 3-aryl-3-methylpropan-1-ols, respectively, as the main condensation products.

3-Phenylpropan-1-ol and diarylmethanes were formed as side products in the reactions of 2-phenyloxetane, while 3-chlorobutan-1-ol and 4-chlorobutan-2-ol were minor components from the reactions of 2-methyloxetane.

The relative rate constants for the main hydroxyalkylation reactions have been determined by the competitive method. The reactions are subject to a relatively low intermolecular selectivity.

It has been suggested for these reactions that the rate is determined by a slow formation of a π-complex, but in the transition state of 2-phenyloxetane the new carbon-carbon bond has been partially formed.

In contrast to oxirans, oxetanes are relatively stable toward nucleophiles in neutral solution but, like oxirans, smoothly undergo a wide variety of nucleophilic substitution reactions in acidic conditions.[1,2] It is also well established that oxirans can be used in the Friedel-Crafts hydroxyalkylation of aromatic hydrocarbons.[3]

Searles [4] has found that oxetane reacts with benzene and mesitylene in the presence of aluminium chloride to yield 50 − 70 % of the corresponding 3-hydroxypropyl derivative. Later, Japanese workers [5] studied the reactions of oxetane and 2-methyloxetane with benzene. However, detailed knowledge of the effect of Lewis acid-type catalysts on the reactions of oxetanes is still limited. We report here the results of our studies concerning the aluminium chloride-catalyzed reactions of 2-phenyloxetane and 2-methyloxetane with benzene, toluene, mesitylene, and other compounds.

---

* Presented in part at the Symposium on Synthetic Chemistry at Kemian Päivät, Helsinki, Finland, November 1973.

## RESULTS AND DISCUSSION

Experiments for examining the products of the reactions were performed by adding oxetane dissolved in hydrocarbon to a suspension of aluminium chloride in hydrocarbon, under conditions similar to those usually employed for the Friedel-Crafts reactions of oxirans.

3-Phenylbutan-1-ol and 3-chlorobutan-1-ol were isolated from the products of the reaction between 2-methyloxetane and benzene. Determined by gas-chromatography from the reaction mixture, they amounted to 75 % and 4 %, respectively. About 1 % of 4-chlorobutan-2-ol was also detected.

The reaction of 2-phenyloxetane with benzene gave 3,3-diphenylpropan-1-ol (rel. amount 83 %), diphenylmethane (10 %), and 3-phenylpropan-1-ol (7 %). The yield of the main product was 28 % calculated on equimolar starting quantities of 2-phenyloxetane and aluminium chloride. This implies that polymerization and other side reactions play a considerable role in these reactions.

The aluminium chloride-catalyzed reactions of propylene oxide with benzene has been reported to give a 64 % yield of 2-phenylpropan-1-ol and no 1-phenylpropan-2-ol.[6] When benzene was alkylated by 1,2-dimethyl-,[7] 1,1-dimethyl-,[7] or 1-methyl-2-phenyloxirane,[8] only minor quantities of the expected alcohols were isolated from the reaction mixtures.

It is now generally accepted that the acid-catalyzed reactions of oxirane and oxetane occur by a borderline $S_N2$-mechanism, and the same seems to be reliable for the 2-methyl- and 2-phenyl-substituted compounds as well. Thus Berti et al.[9] have found that the extent of inversion in the reaction of styrene oxide with hydrogen chloride greatly depends on the solvent, varying from 24 % in dioxane to 83 % in chloroform. Chapman and co-workers [10] have recently reported that 89 % inversion of configuration occurs in the acid-catalyzed methanolysis of styrene oxide. They interpreted this observation in terms of a borderline $S_N2$-mechanism. The same conclusion has been drawn from the values of the entropy of activation and the Hammett $\varrho$-values for the acid-catalyzed alcoholysis of substituted styrene oxides.[11]

Although the hydrogen ion-catalyzed reactions of oxetanes take place by a bimolecular nucleophilic substitution reaction, this is no proof that the aluminium chloride-catalyzed reactions must also do so. The bond-polarizing effect of the latter catalyst seems to be stronger, as we will show later in this discussion.

A collection of the available information [12] suggests the following course for the formation of the main product. A donor-acceptor complex or an intimate ion-pair (I) is first formed from oxetane and aluminium chloride. Thereafter an intermediate benzenium ion (III), i.e. a $\sigma$-complex, is formed in a two-step process which involves a $\pi$-complex (II) as the first intermediate. The benzenium ion is then converted into the products by hydrogen transfers.

Ring fission in the reactions of 2-phenyloxetane studied in this work took place solely between the oxygen atom and substituted carbon atom. The same is evident in the reaction of 2-phenyloxetane with hydrogen chloride in benzene,[13] aqueous solvents,[13] and dioxane,[14] and in the reaction of 2-phenyl-oxetane with acetyl chloride,[13] but not in the reductive cleavage of 2-phenyl-

oxetane with lithium aluminium hydride or lithium borohydride,[15] nor in the reaction of 2-phenyloxetane with methyl magnesium bromide.[1] Clearly the former reaction group includes reactions where powerful catalysts function.
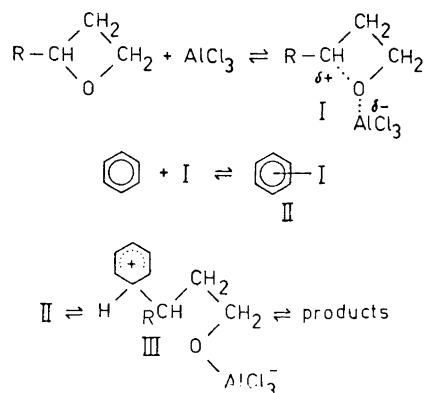
In the acid-catalyzed reaction between 2-methyloxetane and hydrogen chloride in ten solvents or solvent mixtures, and in the concurrent acid-catalyzed methanolysis in four solvents, the main product has been found to result from the ring fission between oxygen and the unsubstituted carbon atom.[16] In these reactions the product ratios vary with changes in the nucleophilicity of the attacking reagent and in the polarity of the reaction medium.

A higher positive charge exists on the carbon atom of the reaction centre in the transition state when the catalyst is aluminium chloride than when it is hydrogen ion, and this can explain the product ratios observed in this work. This charge is located more favourable on the secondary carbon atom than on the primary, and is higher in the case of 2-phenyloxetane than that of 2-methyloxetane.

Consequently, in the reaction of 2-methyloxetane with chloride ion, more secondary chloride is formed when aluminium chloride functions as catalyst than in the hydrogen ion-catalyzed reaction. In the aluminium chloride-catalyzed reaction of 2-methyloxetane with the less nucleophilic aromatic hydrocarbons, and in the catalyzed reactions of 2-phenyloxetane, the bond stretching is so important that it dominates all other forces controlling the course of the reaction.

Diphenylmethane was one of the products from the reaction of 2-phenyloxetane with benzene. This compound has probably been formed from formaldehyde and benzene through the influence of aluminium chloride, for the corresponding product in the reaction of toluene was a mixture of 4,4'-, 2,4'-, and 2,2'-dimethyldiphenylmethanes. This composition was confirmed by gas-chromatographic comparison with authentic samples of all three isomers prepared individually by Grignard reactions.

A mixture of 4,4'- and 2,4'-dimethyldiphenylmethanes was obtained when hydrogen chloride gas was passed into a mixture of toluene, paraformaldehyde, and hydrochloric acid at $60-70°C$.

2-Phenyloxetane has been found to fragment by electron impact partly to formaldehyde.[17] Raising the temperature has been reported to lead to an increasing removal of formaldehyde from 2-phenyloxetane. Thus, at least partly, this is a thermal reaction.

3-Phenylpropan-1-ol was formed in the reactions of 2-phenyloxetane with benzene, toluene, and mesitylene. The product is evidently a result of hydride-ion transfer. The source of hydride-ions may well be diarylmethane, by analogy with the cycloalkylations reported by Ipatieff et al.[18]

The main Friedel-Crafts hydroxyalkylation products were isolated from the reactions of 2-methyloxetane and 2-phenyloxetane with benzene, toluene, and mesitylene.

Chlorobenzene reacted more slowly and gave more side products. The main product in the reaction of 2-phenyloxetane amounted to about 40 % of the volatile components, but at least fifteen others were observed. The corresponding reaction of 2-methyloxetane gave about 70 % of two products with closely similar retention times. We have abandoned further study of these reactions because of their complexity.

The kinetic Friedel-Crafts hydroxyalkylation experiments were performed by the competitive method. To minimize the contribution of disturbing side reactions, the oxetane solution was added gradually to the stirred aluminium chloride suspension in hydrocarbon mixtures or in ethylene dichloride solution at 0°C. After the aluminium chloride had dissolved, samples were withdrawn from the reaction mixture, quenched and analyzed by gas-chromatography.

The kinetic results are collected in Tables 1 − 3. Owing to the decomposition and polymerization reactions, and to the partly heterogeneous conditions, the accuracy of the rate constants is not high. Nevertheless, we consider them sufficiently reliable to draw the following brief conclusions which we believe are useful as a guide.

As may been seen from the tables, the reactions investigated imply a decreasing intermolecular selectivity in the sequence: 2-phenyloxetane in hydrocarbons, 2-methyloxetane in hydrocarbons, 2-methyloxetane in ethylene dichloride. The selectivities are lower than those observed in acylation reactions, but resemble those reported for the various alkylation reactions.[19]

For comparison, the relative rate constants obtained are collected in Table 4 together with those for aluminium chloride-catalyzed acylation with benzoyl chloride in ethylene dichloride [20] and for aluminium chloride-catalyzed alkylation with benzyl chloride in nitromethane.[21] The relative stabilities of the $\pi$-complexes of the aromatic compounds with iodine and iodine monochloride in carbon tetrachloride [22] are also included in the table.

The relative rate constants of 2-methyloxetane closely resemble the relative stabilities of the $\pi$-complexes formed by iodine and iodine monochloride. The selectivity of the reactions of 2-phenyloxetane is lower than that of benzoyl chloride but higher than that of benzyl chloride.

The values 2.4 and 1.64 have been obtained for the kinetic isotope effect $(k_H/k_D)$ in the aluminium chloride-catalyzed benzoylation of, respectively, $p$-deuteriotoluene and hexadeuteriobenzene in benzoyl chloride.[24] Isotope effects of considerable magnitude have also been reported for other acylation reactions.[25] These values reveal that proton elimination is part of the rate-

*Table 1.* The relative rates of the aluminium chloride-catalyzed reactions of 2-methyl-oxetane in ethylene dichloride.

| Hydrocarbons | Molarity mol/1 | Ratio of rate constants | Relative rate | Yield % |
|---|---|---|---|---|
| Toluene | 0.512 | $\dfrac{k_T}{k_B} = 1.7$ | 1.7 | 16 |
| Benzene | 0.537 | | 1.0 | |
| *m*-Xylene | 0.456 | $\dfrac{k_{m\text{-}X}}{k_T} = 1.3$ | 2.2 | 21 |
| Toluene | 0.435 | | | |
| *o*-Xylene | 0.434 | $\dfrac{k_{o\text{-}X}}{k_T} = 1.4$ | 2.4 | 24 |
| Toluene | 0.565 | | | |
| *p*-Xylene | 0.473 | $\dfrac{k_{p\text{-}X}}{k_T} = 1.6$ | 2.7 | 22 |
| Toluene | 0.462 | | | |
| Mesitylene | 0.535 | $\dfrac{k_M}{k_{m\text{-}X}} = 1.9$ | 4.2 | 35 |
| *m*-Xylene | 0.522 | | | |

*Table 2.* The relative rates of the aluminium chloride-catalyzed reactions of 2-methyl-oxetane in mixtures of hydrocarbons.

| Hydrocarbons | mmol | Ratio of rate constants | Relative rate | Yield % |
|---|---|---|---|---|
| Toluene | 6.1 | $\dfrac{k_T}{k_B} = 2.7$ | 2.7 | 34 |
| Benzene | 19.3 | | 1.0 | |
| Mesitylene | 6.0 | $\dfrac{k_M}{k_B} = 8.2$ | 8.2 | 56 |
| Benzene | 19.3 | | | |
| Mesitylene | 6.6 | $\dfrac{k_M}{k_T} = 4.5$ | (12) | 62 |
| Toluene | 15.3 | | | |

*Table 3.* The relative rates of the aluminium chloride-catalyzed reactions of 2-phenyl-oxetane in mixtures of hydrocarbons.

| Hydrocarbons | mmol | Ratio of rate constants | Relative rate | Yield % |
|---|---|---|---|---|
| Toluene | 31.1 | $\dfrac{k_T}{k_B} = 35$ | 35 | 44 |
| Benzene | 37.5 | | 1.0 | |
| Mesitylene | 22.4 | $\dfrac{k_M}{k_T} = 1.9$ | 67 | 84 |
| Toluene | 29.2 | | | |
| Mesitylene | 3.4 | $\dfrac{k_M}{k_B} = 36$ | | |
| Toluene | 3.7 | | | 93 |
| Benzene | 52.1 | $\dfrac{k_T}{k_B} = 27$ | | |

*Table 4.* The relative rates of the aluminium chloride-catalyzed reactions of methyl-substituted benzenes with 2-phenyloxetane, 2-methyloxetane, benzoyl chloride, and benzyl chloride, and the relative stabilities of iodine and iodine monochloride complexes.

| Aromatic compound | Relative rate constants | | | | | Relative stabilities | |
|---|---|---|---|---|---|---|---|
| | 2-Phenyl-oxetane [a] | 2-Methyl-oxetane [a] | 2-Methyl-oxetane [b] | Benzoyl chloride [c] | Benzyl chloride [d] | Iodine [e] | Iodine mono-chloride [e] |
| Benzene | 1.0 | 1.0 | 1.0 | 1.00 | 1.00 | 1.0 | 1.0 |
| Toluene | 35 | 2.7 | 1.7 | 117 | 3.20 | 1.1 | 1.6 |
| m-Xylene | | | 2.2 | 698 | 4.64 | 2.1 | 2.6 |
| o-Xylene | | | 2.4 | 1076 | 4.25 | 1.8 | 2.3 |
| p-Xylene | | | 2.7 | 106 | 4.35 | 2.1 | 2.8 |
| Mesitylene | 67 | 8.2 | 4.2 | 125 000 [f] | 5.20 | 5.5 | 8.5 |

[a] This work, in aromatic hydrocarbons. [b] This work, in ethylene dichloride. [c] Ref. 20, in ethylene dichloride. [d] Ref. 21, in nitromethane. [e] Ref. 22, in carbon tetrachloride. [f] Ref. 23, in nitromethane.

determining step. Accordingly, a σ-complex transition state must be accepted for these reactions.

From the observed relative rate constants and other results for aluminium chloride-catalyzed alkylation with benzyl chloride, Olah and co-workers [21] have suggested that the transition state in the displacement step could best be represented as an oriented π-complex containing a partially formed carbon-carbon bond and a partially broken carbon-chloride bond.

To account for the data, we consider that the rate for the aluminium chloride-catalyzed Friedel-Crafts reactions of 2-methyloxetane and 2-phenyloxetane is most probably determined by the slow formation of a π-complex. This step is followed by a faster isomerization of the complex to the benzenium ion. In the transition state of 2-phenyloxetane the new carbon-carbon bond from oxetane to the aromatic compound has been partially formed. This is reflected in the increased intermolecular selectivity.

## EXPERIMENTAL

*Chemicals.* 2-Methyloxetane and 2-phenyloxetane were synthesized by the methods described previously.[14,16]

Benzene and the alkylbenzenes were purified and used at purities comparable to those used in an earlier investigation.[12] Chlorobenzene was distilled from phosphorus pentoxide. Ethylene dichloride, a *purum* product from Fluka AG, was shaken with sodium hydroxide pellets, allowed to stand over phosphorus pentoxide and fractionally distilled from fresh $P_2O_5$. A middle fraction, b.p. 83.5°, was used in the kinetic experiments.

Aluminium chloride, a *zur Synthese* product from Merck AG, was sublimed several times *in vacuo*.

*Reaction of 2-methyloxetane with benzene.* 2-Methyloxetane, 5.22 g (0.0725 mol) in 20 ml of benzene was added over 90 min to a magnetically stirred mixture of 9.70 g (0.0727 mol) of aluminium chloride in 31.5 ml of benzene under nitrogen. The temperature was held at $5-10°$ with the aid of the ice-water bath. After the aluminium chloride had dissolved, the reaction mixture was allowed to attain room temperature and was left over night. The mixture was then poured gradually into a mixture of 170 g of ice and

50 ml of concentrated hydrochloric acid and mixed until the precipitated aluminium hydroxide had dissolved. The benzene layer was separated and the aqueous layer extracted twice with benzene. The combined benzene solutions were washed with water, 5 % sodium bicarbonate and again water. After drying with magnesium sulphate, the solution was analyzed by gas-chromatography. It contained 75 % of a main product and 5 % of side products calculated on the equimolar quantities of 2-methyloxetane and aluminium chloride. The products were isolated by distillation.

The side products, b.p. 65°/11 torr, $n_D^{25}$ 1.4399, were shown to be composed of 3-chlorobutan-1-ol and 4-chlorobutan-2-ol in the ratio of 4:1 by comparison with known compounds using gas-chromatography.

4-Chlorobutan-2-ol was prepared from 2-methyloxetane and hydrogen chloride in dioxane.[16] 3-Chlorobutan-1-ol was synthesized by allowing the neutral sulphate of 1,3-butanediol to react with hydrochloric acid, as described by Lichtenberger and Lichtenberger.[26]

The identity of the main product, b.p. 120−121°/11 torr, $n_D^{25}$ 1.5178 (lit.:[27] b.p. 132.5−135°/18−19 torr, $n_D^{25}$ 1.5184), was confirmed by its PMR and mass spectra as 3-phenylbutan-1-ol. PMR spectrum: $\delta$ 1.22 (3 H) (doublet, methyl protons), 1.72 (2 H) (multiplet, C-2 methylene protons), 2.83 (1 H) (multiplet, benzylic proton), 3.40 (2 H) (triplet, C-1 methylene protons), 7.16 (5 H) (singlet, aromatic protons). Mass spectrum: $m/e$ M$^+$ 150 (36 %), 132 (41 %), 117 (100 %), 106 (64 %), 105 (75 %), 91 (72 %), 79 (39 %), 77 (45 %).

*Reaction of 2-methyloxetane with toluene.* This was run as in the preceding experiment, except that the mixing time at room temperature was 4 h. 2-Methyloxetane, 5.07 g (0.0704 mol), 9.66 g (0.0724 mol) of aluminium chloride, and 45 ml of toluene gave, by GLC, 73 % of 3-(4′-methylphenyl)-butan-1-ol, b.p. 150−152°/24 torr, $n_D^{25}$ 1.5186. PMR spectrum: $\delta$ 1.18 (3 H) (doublet, methyl protons), 1.69 (2 H) (multiplet, C-2 methylene protons), 2.28 (3 H) (singlet, methyl protons), 2.82 (1 H) (multiplet, benzylic proton), 3.32 (2 H) (multiplet, C-1 methylene protons), 6.97 (4 H) (multiplet, aromatic protons).

*Reaction of 2-methyloxetane with mesitylene.* Using a procedure similar to that of the preceding experiment, 2-methyloxetane, 4.19 g (0.0582 mol), 8.00 g (0.0600 mol) of aluminium chloride, and 40 ml of mesitylene gave, by GLC, 88 % of 3-(2′,4′,6′-trimethylphenyl)-butan-1-ol, b.p. 156−158°/15 torr, $n_D^{25}$ 1.5265. PMR spectrum: $\delta$ 1.23 (3 H) (doublet, methyl protons), 1.88 (2 H) (multiplet, C-2 methylene protons), 2.27 (9 H) (singlet, methyl protons), 2.90−3.55 (3 H) (multiplet, C-1 methylene and benzylic protons), 6.67 (2 H) (singlet, aromatic protons).

*Reaction of 2-phenyloxetane with benzene.* With the same procedure as for 2-methyloxetane, 2-phenyloxetane, 10.02 g (0.0746 mol), 10.00 g (0.0750 mol) of aluminium chloride, and 80 ml of benzene gave a mixture of 82 % (rel. amount by GLC) of 3,3-diphenylpropan-1-ol, 10 % of diphenylmethane, and 9 % of 3-phenylpropan-1-ol. On distillation, 4.48 g (28 % of theory) of 3,3-diphenylpropan-1-ol were collected, b.p. 133−137°/0.1 torr, $n_D^{22}$ 1.5827 (lit.[28] :b.p. 164−166°/2.5 torr, $n_D^{25}$ 1.5814). PMR spectrum: $\delta$ 2.15 (2 H) (multiplet, C-2 methylene protons), 4.05 (1 H) (triplet, benzylic proton), 7.10 (10 H) (singlet, aromatic protons). Mass spectrum: $m/e$ M$^+$ 212, 168 (45 %), 167 (100 %), 165 (35 %), 118 (33 %), 105 (30 %), 92 (30 %), 91 (57 %), 77 (37 %).

*Reaction of 2-phenyloxetane with toluene.* 2-Phenyloxetane, 10.15 g (0.0757 mol), 10.23 g (0.0767 mol) of aluminium chloride, and 84 ml of toluene gave a mixture of 91 % (rel. amount by GLC) of 3-(4′-methylphenyl)-3-phenylpropan-1-ol, 7 % of a mixture of 2,2′-, 2,4′-, and 4,4′-dimethyldiphenylmethanes, and 2 % of 3-phenylpropan-1-ol. 8.52 g (50 % of theory) of the main product were isolated by distillation, b.p. 131−132°/0.1 torr, $n_D^{22}$ 1.5771. PMR spectrum: $\delta$ 2.15 (2 H) (multiplet, C-2 methylene protons), 2.24 (3 H) (singlet, methyl protons), 3.41 (2 H) (triplet, C-1 methylene protons), 4.00 (1 H) (triplet, benzylic proton), 6.96 (4 H) (singlet, aromatic protons), 7.10 (5 H) (singlet, aromatic protons).

*Preparation of 2,2′-, 2,4′-, and 4,4′-dimethyldiphenylmethanes.* These compounds were prepared by known Grignard syntheses from methylphenyl bromides and methylbenzyl chlorides or bromides. The GLC retention times were 14.8, 14.4, and 14.2 min for the 4,4′-, 2,4′-, and 2,2′-substituted compounds, respectively. A 2 m column of 10 % Silicone Gum Rubber SE-30 on Chromosorb W, NAW, was used at 160°.

*Reaction of toluene with formaldehyde.* Hydrogen chloride gas was passed into a mixture of 100.0 g (1.09 mol) of toluene, 20.0 g (0.667 mol) of paraformaldehyde, and 220 ml of

concentrated hydrochloric acid at $60-70°$. The reaction time was 2.5 h. The organic layer was separated, washed with ice-water, 5 % sodium bicarbonate and water, and dried with magnesium sulphate. 1.86 g of a fraction boiling at $157-166°/14$ torr were collected and shown by GLC, PMR, and MS to be composed of 49 % 4,4'- and 51 % 2,4'-dimethyldiphenylmethanes.

*Reaction of 2-phenyloxetane with mesitylene.* 2-Phenyloxetane, 10.0 g (0.0747 mol), 10.0 g (0.0752 mol) of aluminium chloride, and 85 ml of mesitylene reacted to give a mixture of 90 % (rel. amount by GLC) of the main product, about 0.5 % of 3-phenyl-propan-1-ol, and traces of other products. When distilled, 4.05 g of a solid fraction boiling at $130-132°/0.08$ torr were collected. After recrystallization from light petroleum (b.p. $40-65°$), 3.75 g (20 % of theory) of 3-(2',4',6'-trimethylphenyl)-3-phenylpropan-1-ol, m.p. $85.5-88°$ were obtained. PMR spectrum: $\delta$ 2.14 (6 H) (singlet, methyl protons), 2.22 (3 H) (singlet, methyl protons), 2.42 (2 H) (multiplet, C-2 methylene protons), 3.55 (2 H) (triplet, C-1 methylene protons), 4.64 (1 H) (triplet, benzylic proton), 6.74 (2 H) (singlet, aromatic protons), 7.12 (5 H) (singlet, aromatic protons).

*Competitive experiments.* Oxetane solution was added to a suspension of aluminium chloride in either a mixture of two or three hydrocarbons or their solution in ethylene dichloride at 0°C. The reaction mixture was then allowed to attain room temperature. After the aluminium chloride had dissolved (about 10 min in the case of 2-methyloxetane, about 20 min for 2-phenyloxetane), 0.5 ml samples were withdrawn and arrested by adding 1 ml of 1 M sodium hydroxide solution. The organic layer was then analyzed by GLC and the relative rate constants calculated from the product ratios corrected by the mean concentrations of the aromatic hydrocarbons during the reactions

$$\frac{k_1}{k_2} = \frac{X_1}{C_1° - X_1/2} \bigg/ \frac{X_2}{C_2° - X_2/2}$$

where $C_1°$ and $C_2°$ are the initial concentrations of the hydrocarbons and $X_1$ and $X_2$ the concentrations of the corresponding hydroxyalkylation products.

*Apparatus.* The gas-chromatograms were run on a Perkin-Elmer Model 452 gas-chromatograph with a hot-wire detector or on a Perkin-Elmer Model F11 gas-chromatograph with a flame ionization detector. The PMR spectra were run on a Varian T-60 NMR spectrograph employing carbon tetrachloride as solvent and tetramethylsilane as internal standard. The mass spectra were recorded on a Hitachi Perkin-Elmer RMU-6E double focusing mass spectrometer.

## REFERENCES

1. Searles, S. In Weissberger, A., Ed., *The Chemistry of Heterocyclic Compounds, Heterocyclic Compounds with Three- and Four-Membered Rings*, Interscience, New York 1964, Part Two, Chapter IX.
2. Virtanen, P. O. I. *Suomen Kemistilehti* **B 39** (1966) 58, 64.
3. Schriesheim, A. In Olah, G. A., Ed., *Friedel-Crafts and Related Reactions*, Interscience, New York 1964, Vol. II, Part 1, Chapter XVIII.
4. Searles, S. *J. Am. Chem. Soc.* **76** (1954) 2313.
5. Nakamoto, Y., Nakajima, T. and Suga, S. *Kogyo Kagaku Zasshi* **72** (1969) 2594; *Chem. Abstr.* **72** (1970) 100192u.
6. Milstein, N. *J. Heterocyclic Chem.* **5** (1968) 337.
7. Somerville, W. T. and Spoerri, P. E. *J. Am. Chem. Soc.* **72** (1950) 2185.
8. Somerville, W. T. and Spoerri, P. E. *J. Am. Chem. Soc.* **73** (1951) 697.
9. Berti, G., Bottari, F., Ferrarini, P. L. and Macchia, B. *J. Org. Chem.* **30** (1965) 4091.
10. Biggs, J., Chapman, N. B. and Wray, V. *J. Chem. Soc.* **B 1971** 71.
11. Biggs, J., Chapman, N. B., Finch, A. F. and Wray, V. *J. Chem. Soc.* **B 1971** 55.
12. Virtanen, P. O. I. and Ruotsalainen, H. *Ann. Acad. Sci. Fennicae* **A II 143** (1968), and references therein.
13. Searles, Jr., S., Pollart, K. A. and Block, F. *J. Am. Chem. Soc.* **79** (1957) 952.
14. Virtanen, P. O. I. and Manninen, K. *Suomen Kemistilehti* **B 40** (1967) 341.
15. Searles, Jr., S., Pollart, K. A. and Lutz, E. F. *J. Am. Chem. Soc.* **79** (1957) 948.

16. Virtanen, P. O. I. *Suomen Kemistilehti* **B 40** (1967) 185.
17. Virtanen, P. O. I., Karjalainen, A. and Ruotsalainen, H. *Suomen Kemistilehti* **B 43** (1970) 219.
18. Ipatieff, V. N., Pines, H. and Olberg, R. C. *J. Am. Chem. Soc.* **70** (1948) 2123.
19. Stock, L. M. and Brown, H. C. *Advan. Phys. Org. Chem.* **1** (1963) 35.
20. Marino, G. and Brown, H. C. *J. Am. Chem. Soc.* **81** (1959) 5929.
21. Olah, G. A., Kuhn, S. J. and Flood, S. H. *J. Am. Chem. Soc.* **84** (1962) 1688.
22. Andrews, L. J. and Keefer, R. M. *J. Am. Chem. Soc.* **74** (1952) 4500.
23. Brown, H. C., Bolto, B. A. and Jensen, F. R. *J. Org. Chem.* **23** (1958) 417.
24. Jensen, F. R., *Ph. D. Thesis*, Purdue University 1955, quoted in Ref. 12.
25. Olah, G. A., Kuhn, S. J., Flood, S. H. and Hardie, B. A. *J. Am. Chem. Soc.* **86** (1964) 2203.
26. Lichtenberger, J. and Lichtenberger, R. *Bull. Soc. Chim. France* **15** (1948) 1002.
27. Eliel, E. L., Wilken, P. H. and Fang, F. T. *J. Org. Chem.* **22** (1957) 231.
28. Hauser, C. R., Tetenbaum, M. T. and Yost, R. S. *J. Org. Chem.* **23** (1958) 916.

# Mercury (II) Complexes of Methionine

BO BIRGERSSON, TORBJÖRN DRAKENBERG and
GEORGE A. NEVILLE*

*Organic Chemistry 2 and Physical Chemistry 2, Chemical Center, University of Lund,
Box 740, S-220 07 Lund, Sweden and The Institute of Hygiene, University of Lund,
Magle Stora Kyrkogata 12, S-223 50 Lund, Sweden*

Investigations of the complexation of methionine with mercury(II) chloride, acetate, and nitrate are described. With $HgCl_2$, the complex $(C_5H_{10}O_2NS)_3Hg_3(HCl)_3HgCl_4$ was obtained whereas the complex $(C_5H_{10}O_2NS)_2Hg$ was obtained from methionine directly with $Hg(OAc)_2$ and from lithium methioninate by reaction with either $Hg(OAc)_2$ or $HgCl_2$. $^1H$- and $^{13}C$-NMR spectral studies are reported, proton coupling for methionine is reported for the first time, and relative rotamer populations are compared to those of $S$-methylcysteine. In acidic aqueous solution, mercury bonding is localized to the sulphur of methionine which appears to adopt an extended chain configuration.

The nature of complexation of the amino acid, methionine, $CH_3SCH_2$-$CH_2CH(NH_2)COOH$ (Hmt), with a number of transition and non-transition metal ions has been studied in the solid state by infrared spectroscopy by McAuliffe, Quagliano and Vallarino.[1] Methionine appears to behave as an anionic ligand (mt) and generally forms neutral complexes. $M^{II}mt_2$ and $M^{III}mt_3$ in which the metal attains its usual higher coordination number by linking with the N atom of the $-NH_2$ group and with one or both of the O atoms of the $-COO^-$ group. In these complexes the S atom of the $-SCH_3$ group is still available for coordination, as shown by the formation of mixed-metal complexes with Ag(I).[1] From studies in solution by $^1H$-NMR spectroscopy, Li and Manning[2] concluded that the sulphur is not involved in coordination in methionine complexes of zinc, cadmium, and mercury. In a later study utilizing potentiometry, Lenz and Martell[3] concurred with the bidendate nature of methionine, $S$-methyl-L-cysteine, and ethionine, and they concluded that there is little or no involvement of substituted mercapto groups in chelation. More recently, Natusch and Porter[4,5] have provided evidence from $^1H$-NMR spectral studies that mercury(II) bonds to the sulphur of methionine in 1 M $HNO_3$.

---

As part of a study to investigate the nature of mercurial complexation with molecules of biochemical interest in order to obtain a better understanding of biotransformation and organomercurial toxicology,[6-8] we undertook a reinvestigation of mercurial complexation with methionine. In our studies, we have tried to prepare and isolate mercurial complexes for structural characterization using the mildest possible *in vitro* conditions in relation to the *in vivo* state. For this reason, mercurial complexation was restricted to acidic media in this investigation.

## DISCUSSION

*Complexation.* Preliminary experiments indicated that difficulties would be experienced in attempting to isolate mercurial complexes of methionine under acid conditions and that variable composition would be a feature of the products isolated. Systematic investigation was undertaken to determine the role of various solvents and acidic conditions in the complexation of methionine by mercury(II) chloride, nitrate, and acetate. Preparative work, summarized in Table 1, was first carried out, and then all products were analyzed at the same time as a group for mercury content by atomic absorption. The highly variable mercury content of the various products is evident from Table 1.

*Table 1.* Summary of reaction conditions and results for complexation of methionine with mercury(II) chloride.

| Methionine (mmol) | Solvent 95 % EtOH (ml) | Initial state[a] | HgCl$_2$ (mmol) | Solvent 95 % EtOH (ml) | State after addition[b] | Conditions for precipitation[c,d] | Yield (g) | Hg content (%) |
|---|---|---|---|---|---|---|---|---|
| 1 | 200 | S | 5 | 20 | N,C | R | 1.42 | [e] |
| 10 | 40 | H[f] | 5 | 20 | N | [g] | 0.84[h] | 0.9 |
| 5 | 20 | H[i] | 2.5 | 10 | N | R[j] Fr.A, | 0.12 | 4.1 |
|  |  |  |  |  |  | Fr.B, | 0.21 | 2.1 |
| 5 | 10 | H[k] | 2.5 | 10 | N,T | O | 0.42 | 52.1 |
| 5 | 20[l] | H[m] | 2.5 | 10 | N,T | R | 0.80 | 33.3 |
| 5 | 0[n] | H[o] | 2.5 | 10 | N,T | R | 0.65 | 46.1 |
| 10 | 0[p] | H | 5 | 20[q] | P[r] | Fr.A, O Fr.A, | 1.06 | 45.4 |
|  |  |  |  |  |  | Fr.B, R Fr.B, | 0.37 | 47.8 |

[a] S, suspension; H, hot solution. [b] N, no precipitation; C, clarified; T, tail-effect; P, precipitation. [c] R, refrigeration; O, standing overnight. [d] 95 % EtOH used for washing. [e] Gave excellent C, H, O, N, and S analysis for methionine. [f] Dissolution achieved by addition of just sufficient conc. HNO$_3$. [g] Hot syrup treated with acetonitrile until gum formed, then treated with acetone, heated to obtain solution followed by diethyl ether. Crystalline solid obtained at room temperature. [h] Shown by infrared spectra to be mainly methionine hydronitrate. [i] Dissolution achieved by minimal addition of trifluoroacetic acid (1.5 ml). [j] Treated with diethyl ether. [k] Dissolution effected by adding water (15 ml required) to nearly boiling suspension. [l] 1.5 ml HOAc added. [m] Dissolution achieved by adding water (2 ml) to hot suspension. [n] 10 ml HOAc. [o] Dissolution effected by adding water (1−2 ml) near boiling temperature of suspension. [p] 20 ml HOAc+ 3.0 ml H$_2$O. [q] Hot solution. [r] Initially, precipitate dissolved with stirring, later precipitate accumulated. At end, mixture treated with 10 ml EtOH and raised to b.p. to obtain solution.

The isolation of a mercury(II) chloride complex of methionine appears to require rather special conditions. When a large volume of 95 % ethanol is used to dissolve methionine (see example one of Table 1) before treatment with an ethanolic solution of $HgCl_2$, beautiful, long crystals were obtained which gave an excellent analysis for methionine. The superbly formed crystals of methionine obtained under these conditions contrast with the small and difficultly obtained plate and needle polymorphs of methionine.[9],[10] If a much smaller volume of ethanol is used to dissolve methionine aided by the addition of minimal water (see example four of Table 1), then a mercury(II) chloride complex of methionine is obtained having the composition $(C_5H_{10}O_2NS)_3Hg_3$-$(HCl)_3(HgCl_4)$. Examination of the complex by NMR is precluded by its insolubility in boiling water and by its degradation in dimethyl sulfoxide. X-Ray diffraction showed the product to be amorphous. By examining solutions of methionine in 1 M $HNO_3$ containing variable $Hg(NO_3)_2$ concentration, Natusch and Porter [4],[5] deduced evidence for mercurial bonding to sulphur and concluded that complexes of the type $M(LH_2)_2$ were formed. No complexes have been isolated from these systems. McAuliffe et al.[1] have reported the isolation of a yellow, polymeric mercury complex of methionine $(Hg\ mt_2)_n$ which was obtained from the lithium salt of methionine on treatment with mercury(II) perchlorate.

In contrast to the behaviour of methionine with $HgCl_2$, treatment with mercury(II) acetate readily gave a mercury complex having the composition, $(C_5H_{10}O_2NS)_2Hg$. X-Ray diffraction showed the substance to be crystalline and identical with the mercury complex obtained by reaction of lithium methioninate with either mercury(II) chloride or acetate. Infrared spectra showed the absence of the acetate moiety and this absence was confirmed by ^{13}C-NMR spectra.

Investigation of the formation and isolation of mercurial complexes of methionine in aqueous ethanol using mercury(II) nitrate was unrewarding and frustrated by the formation of glassy residues from intractable syrups.

*NMR spectral studies.* Natusch and Porter [4],[5] first reported ^{1}H-NMR evidence for the binding of $Hg^{2+}$ to the isolated sulphide group of methionine. The evidence was reported simply in the form of proton chemical shift differences ($\Delta v$ at 60 MHz) between the metal complexes and the corresponding free ligands but, as yet, no chemical shift or coupling data have been reported for methionine itself. In examining an aqueous solution * of the bis(methioninato)-mercury(II) complex by ^{1}H- and ^{13}C-NMR spectroscopy, we found it necessary to investigate similarly acidic aqueous solutions of methionine. As a result of this work the ^{13}C-NMR chemical shifts have been determined (Table 2) for both methionine and bis(methioninato) mercury(II), and the proton coupling parameters (Table 3) have been determined for the methionine system following iteration and computer simulation (Fig. 1).

A comparison of the ^{13}C-NMR chemical shifts (Table 2) for methionine and the mercury complex reveals deshielding of approximately 5 ppm for the *S*-methyl and -methylene carbons, respectively, of the complex relative to

---

* Dissolution of the complex was achieved on addition of a few drops of trifluoroacetic acid to a suspension of the solid in 5.0 ml $D_2O$ followed by gentle warming.

*Table 2.* ^{13}C NMR chemical shifts (ppm relative to TMS) for $D_2O$ solutions (pD 2.2) of methionine (Hmt) and bis(methioninato)mercury(II) [(mt)$_2$Hg].

$$\overset{5}{CH_3}S-\overset{4}{CH_2}-\overset{3}{CH_2}-\overset{2}{CH}(\overset{1}{ND_3}{}^+)COOD$$
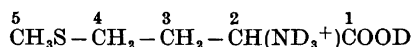
| Solute | Conc.(M) | 1 | 2 | 3 | 4 | 5 |
|--------|----------|-----|-----|------|------|------|
| Hmt | 0.2 | 173.4 | 53.4 | 30.1[a] | 29.5[a] | 14.8 |
| (mt)$_2$Hg | 0.2 | 172.9 | 53.4 | 29.7 | 34.6 | 19.7 |

[a] Tentative assignment.

*Table 3.* Proton chemical shift (ppm relative to external TMS) and coupling data (100 MHz) for methionine and bis(methioninato)mercury(II) in $D_2O$ (pD 2.2)

$$CH_3S-\overset{}{CH_2}-\overset{4,5}{CH_2}-\overset{}{CH}(\overset{}{ND_3})COOD$$
$$\quad\underset{2,3}{\quad}\qquad\qquad\underset{1}{\quad}$$

| Solute | Conc.(M) | CH$_3$ | SCH$_2$ | CH$_2$ | CH |
|--------|----------|--------|---------|------------|------|
| Hmt | 0.2 | 2.67 | 3.22 | 2.82, 2.72 | 4.66 |
| (mt)$_2$Hg | 0.2 | 3.24 | 3.85 | 2.9 | 4.67 |
| $J_{Hmt}$: | $J_{1,2}=J_{1,3}=0$ Hz | | | | |
| | $J_{2,4}=J_{2,5}=J_{3,4}=J_{3,5}=7.28$ Hz | | | | |
| | $J_{1,4}=6.03,\ J_{1,5}=7.10$ Hz | | | | |
| | $J_{2,3}=-11.00^{a},\ J_{4,5}=-14.88$ Hz | | | | |

[a] Assumed value.

those of methionine whereas there is no appreciable change in the values for the other carbon atoms. This evidence not only supports the conclusion of Natusch and Porter [5] that mercurial bonding is localized to the sulphide group, but it is also consistent with an extended chain configuration for the complex in solution in which the amino and carboxyl moieties are remote from the mercury atom.

An analysis of the relative rotamer populations for methionine was performed in the standard fashion [12-15] by assuming that the rotamer with the bulkiest substituents in the *trans* position (in this case $CH_3SCH_2$ or $NH_3$ and COOH) is sterically favoured. In this conformation, the sulphur atom is located proximate to the ammonium group which might afford a means for rotamer stabilization through dipolar attraction. Adopting values of 12.0 and 2.0 Hz for $J_t$ and $J_g$, respectively, which have been suggested by Martin and Mathur [16] for cysteine, one obtains the rotamer populations $P_t=(J_{1,5}-J_g)/(J_t-J_g)=0.51$, $P_g=(J_{1,4}-J_g)/(J_t-J_g)=0.403$ and $P_h=1-(P_t+P_g)=0.09$. These relative rotamer populations support the above conformational hypothesis and suggest that the alternate rotamer g (Fig. 2) with *trans* bulky substituents
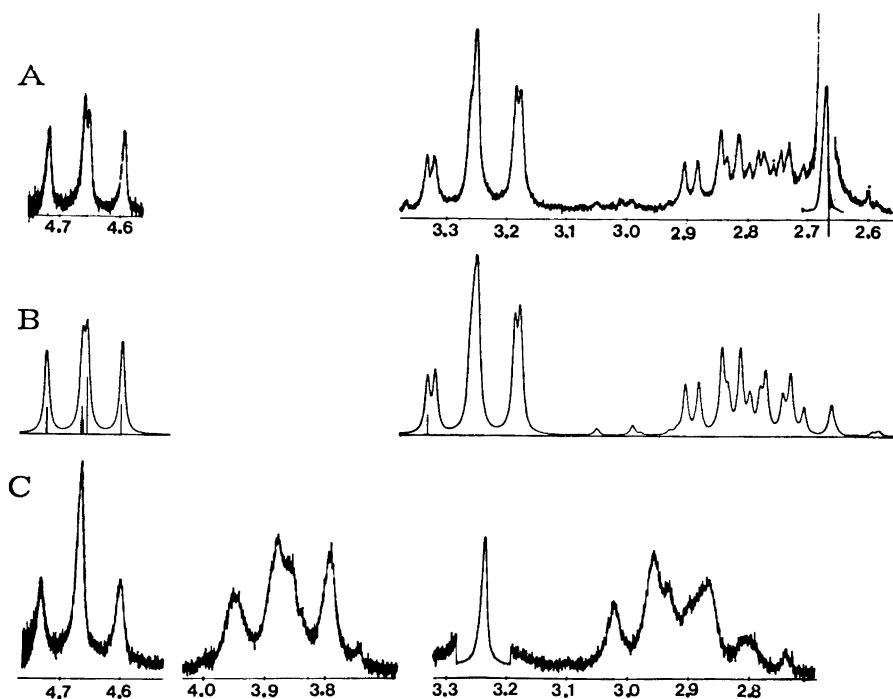
*Fig. 1.* ¹H-NMR spectra (100 HMz) in $D_2O$ at pD 2.2. A: Methionine. B: Simulated spectrum for methionine ($CH_3S-$ omitted). C: Bis-(methioninato)mercury(II).
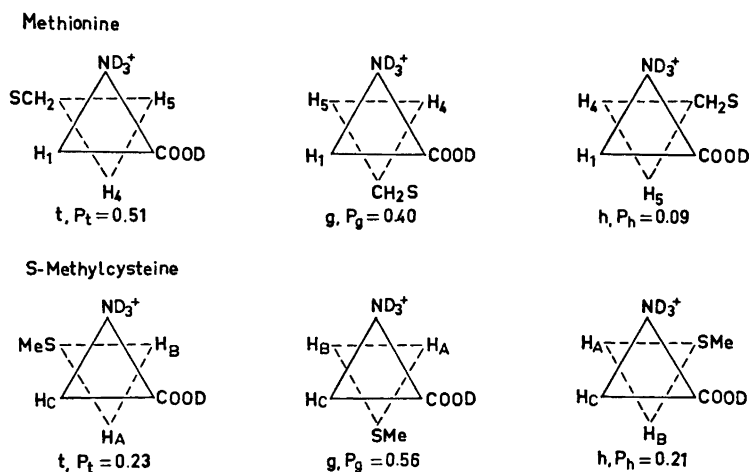


*Fig. 2.* Relative populations of the three staggered rotamers of methionine [$CH_3SCH_2CH_2CH(ND_3^+)CO_2D$] and of *S*-methylcysteine [$CH_3SCH_2CH(ND_3^+)CO_2D$] in $D_2O$ at pD 2.2.

may be stabilized by intramolecular hydrogen bonding ($COOH\cdots CH_3SCH_2$). In addition, the excellent spectral matching (Fig. 1) serves to confirm the assumed equivalence of the $S$-methylene protons and the identical vicinal coupling between pairs of methylene protons.

It is interesting to compare the relative rotamer populations of methionine with those of $S$-methyl cysteine obtained under similar conditions (pD 2.2). For methionine the two rotamers (t and g) with bulky *trans* substituents are nearly equally populated and there is a very small fraction of the sterically hindered rotamer (h). In the case of $S$-methylcysteine, for which we have determined $J_{AC} = 4.31$, $J_{BC} = 7.64$, and $J_{AB} = -15.02$, the most highly populated rotamer is assumed to be that (g) in which COOH and $SCH_3$ are adjacent when hydrogen bonding in a six-membered ring is expected to exert a stabilizing influence. The population of this rotamer is more than twice that of the rotamer (t) having adjacent $NH_3^+$ and $SCH_3$ which is assumed to be stabilized by a more weakly dipolar attraction. In contrast to methionine, the most sterically hindered rotamer of $S$-methylcysteine is essentially as highly populated as the least favoured rotamer with *trans* bulky substituents. It appears that the forces of repulsion in the sterically hindered rotamer of $S$-methylcysteine are compensated by a combination of attractive forces between $CH_3S$ and COOH (hydrogen bonding) and $NH_3^+$ (dipolar). It would appear that the reason that the sterically hindered rotamer of methionine is not as highly favoured as in $S$-methylcysteine is due to a combination of weaker hydrogen bonding in a seven-membered ring and the fact that a hydrogen-bonded $SCH_3$ group must be inclined away from the $NH_3^+$ group due to the presence of the extra methylene linkage resulting in reduced dipolar attraction. The sterically hindered rotamer of $S$-methylcysteine therefore appears to be unusually favoured by stabilizing forces.

The proton spectral features obtained for bis(methionineato)mercury(II) are shown in Fig. 1C. Unfortunately the broad nature of the bands makes it virtually impossible to find a unique set of coupling constants for the mercury complex because several combinations will give almost the same line shape. This situation arises because of the necessity in computer simulation of spectra to employ line widths related to experimental conditions, thus the derived line shapes do not allow one to discriminate between sets of possible parameters. It was possible, however, to conclude from these investigations of spectral matching that, unlike methionine, both methylene groups of the mercury complex possess non-equivalent protons.

## EXPERIMENTAL

*General methods.* $^{13}C$-NMR spectra were obtained at 27°C with a Varian XL-100 spectrometer following accumulation and Fourier transformation of signals in both proton decoupled and coupled modes. Frequencies were measured relative to dioxane and converted to the TMS scale ($\delta_{TMS} = \delta_{dioxane} + 67.4$ ppm).[17] Proton spectra were obtained at 35°C at 100 MHz. Solutions were prepared from $D_2O$ by acidification with trifluoroacetic acid, and pD values were obtained from the expression pD = scale reading $+ 0.4$.[18]

X-Ray diffraction patterns were obtained using Guinier-Hägg cameras.

Atomic absorption measurements were performed with a Perkin-Elmer Model 303

spectrometer. Samples (approx. 10 mg) were weighed accurately, digested with warming in a little water treated with concentrated hydrochloric acid, and then made up to volume in 50 ml volumetric flasks. Standard samples containing 200, 100, 50, 25, and 12.5 ppm of mercury were prepared from mercury(II) chloride (BDH Analar), and calibration analyses were performed both before and after analyzing the series of samples of unknown mercury content.

*Microanalyses.* Microanalyses were performed by Alfred Bernhardt, Mikroanalytisches Laboratorium, 5251 Elbach über Engelskirchen, Fritz-Pregl Strasse 14 – 16, W. Germany. Appropriate separatory processes were employed to eliminate the interference of mercury with the C, H, and Cl determinations. Sulphur was analyzed by a reductive process.

C, H, and N analyses of the lithium and hydronitrate salts of methionine were performed by Dr. Lars Haraldson, Analytical Chemistry, University of Lund, Sweden.

## Synthesis

*Mercury(II) chloride complex of methionine.* A suspension of D,L-methionine (0.745 g, 0.005 mol, Sigma 99.5 %) in nearly boiling ethanol (10 ml) was taken into solution by the addition of a minimum of water (~ 15 ml). To the magnetically stirred solution, a warm solution of mercury(II) chloride (0.681 g, 0.0025 mol, BDH Analar) in 95 % ethanol (5 ml) was slowly added. Although a "tail-effect" was seen during the addition, no precipitate formed immediately after the addition. On standing overnight at room temperature, the mixture produced a fine precipitate which had to be scraped from the flask. The solid (Fraction A, 0.416 g) was washed with 95 % ethanol and dried over NaOH *in vacuo.* X-Ray diffraction showed the product to be amorphous, and the solid was found to decompose above 115°. [Found: C 12.30; H 2.17; O 6.47; N 2.96; Hg 53.35; Cl 16.49; S 6.40. $(C_5H_{10}O_2NS)_3Hg_3(HCl)_3HgCl_4)$(M.W. 1488.3) requires C 12.10; H 2.23; O 6.45; N 2.82; Hg 53.91; Cl 16.68; S 6.46].

Following refrigeration, the mother liquor yielded second and third fractions (0.206 and 0.169 g, respectively) which were shown by X-ray diffraction to be methionine.

*Mercury(II) acetate complex with methionine.* A solution of D,L-methionine (0.745 g, 0.005 mol, Sigma 99.5 %) was obtained in 95 % ethanol (20 ml) with heating and magnetic stirring by addition of a minimum of water (4 – 5 ml). To this solution, a solution of mercury(II) acetate (0.798 g, 0.0025 mol, Merck 99 %) in methanol (10 ml) was slowly added. A gelatinous precipitate formed when nearly half the mercurial reagent had been added. After standing for 2 h, the mixture was filtered, and the product was washed with 95 % ethanol and dried over NaOH *in vacuo.* The yield was 1.065 g or 48 %, and the solid was found to decompose above 215°. X-Ray diffraction showed the solid to be crystalline. [Found: C 24.01; H 3.91; O 13.33 and 13.38; N 5.95; Hg 41.96; S 12.72 and 12.67. $(C_5H_{10}O_2NS)_2Hg$ (M.W. 497.01) requires C 24.16; H 4.06; O 12.88; N 5.64; Hg 40.36; S 12.90].

*Lithium methioninate.* The conditions reported by Halbert and Rogerson [11] for the preparation of a lithium salt of methionine (composition not reported) were used. A mixture of D,L-methionine (3.00 g, Sigma) and freshly opened lithium hydroxide mono-hydrate (0.800 g, BDH) in 95 % ethanol (40 ml) was heated (50 – 60°) with magnetic stirring. A solution was soon obtained. On cooling to room temperature, the solution deposited a small quantity of solid which did not increase with refrigeration. This solid (0.138 g) was shown by X-ray diffraction to be methionine.

The mother liquor was reduced to approximately 10 ml by rotary evaporation, then the concentrate was treated with diethyl ether (~ 15 ml) in small portions until turbidity was obtained. The mixture was refrigerated and treated periodically with more ether to obtain glistening, white flakes. The solid was collected, washed with ether-ethanol (1:1) and dried over NaOH *in vacuo.* The product (2.16 g) was found to be crystalline by X-ray diffraction and infrared spectra showed a marked change from the parent compound. [Found: C 38.40; H 7.08; N 9.00. $C_5H_{10}O_2NSLi$ ((M.W. 155.14) requires C 38.71; H 6.50; N 9.03].

*Bis(methioninato)mercury(II) from lithium methioninate and mercury(II) acetate or mercury(II) chloride.* To a magnetically stirred solution of lithium methioninate (0.500 g, 0.00323 mol), prepared at room temperature from water (2 ml) and 95 % ethanol (10 ml), was added dropwise a warm (40°C) solution of mercury(II) acetate

(1.015 g, 0.00323 mol, Merck, *p.a.*) in methanol (10 ml). Precipitation was immediate. The solid was too finely divided for suction filtration, thus the mixture was centrifuged (10 000 rpm) and washed three times with 95 % ethanol. The dry product (0.498 g, 62 % yield) was shown by X-ray diffraction to be crystalline and identical to the product obtained directly from methionine with mercury(II) acetate.

To an identical aqueous ethanolic solution of lithium methioninate (as above) was added dropwise a solution of mercury(II) chloride (0.875 g, 0.00323 mol, BDH Analar) in 95 % ethanol (10 ml). Precipitation was immediate and copious. After collection and washing with 95 % ethanol the dry solid (0.814 g, 100 % yield) was shown by X-ray diffraction to be crystalline and identical to the product obtained directly from methionine with mercury(II) acetate.

REFERENCES

1. McAuliffe, C. A., Quagliano, J. V. and Vallarino, L. M. *Inorg. Chem.* **5** (1966) 1996.
2. Li, N. C. and Manning, R. A. *J. Am. Chem. Soc.* **77** (1955) 5225.
3. Lenz, G. R. and Martell, A. E. *Biochemistry* **3** (1964) 745.
4. Natusch, D. F. S. and Porter, L. J. *J. Chem. Soc.* **D 1970** 596.
5. Natusch, D. F. S. and Porter, L. J. *J. Chem. Soc.* **A 1971** 2527.
6. Neville, G. A. and Berlin, M. *Environ. Res. In press.*
7. Neville, G. A. and Berlin, M. *Can. J. Chem.* **51** (1973) 3970.
8. Neville, G. A. and Drakenberg, T. *Can. J. Chem.* **52** (1974) 616.
9. Mathieson, A. McL., *Acta Cryst.* **5** (1952) 332.
10. Khawas, B. *Acta Cryst.* **B 26** (1970) 1919.
11. Halbert, E. J. and Rogerson, M. J. *Aust. J. Chem.* **25** (1972) 421.
12. Pachler, K. G. R. *Spectrochim. Acta* **19** (1963) 2085; **20** (1964) 581.
13. Pachler, K. G. R. *Z. anal. Chem.* **224** (1967) 211.
14. Cavanaugh, J. R. *J. Am. Chem. Soc.* **89** (1967) 1558; **90** (1968) 4533.
15. Neville, G. A., Deslauriers, R., Blackburn, B. J. and Smith, I. C. P. *J. Med. Chem.* **14** (1971) 717.
16. Martin, R. B. and Mathur, R. *J. Am. Chem. Soc.* **87** (1965) 1065.
17. Johnson, L. F. and Jankowski, W. C. In *Carbon-13 NMR Spectra*, Wiley, New York 1972.
18. Glasoe, P. K. and Long, F. A. *J. Phys. Chem.* **64** (1960) 188.

# The Crystal Structure of Squaric Acid

DAG SEMMINGSEN

*Department of Chemistry, University of Oslo, Oslo 3, Norway*

The crystal structure of squaric acid (3,4-dihydroxy-3-cyclobutene-1,2-dione) has been determined from three-dimensional X-ray diffraction data measured by counter methods. The compound crystallizes in the space group $P2_1/m$. The symmetry is pseudotetragonal with cell dimensions $a = 6.129(3)$, $b = 5.273(2)$, $c = 6.140(3)$ Å and $\beta = 90.00(1)°$. The data were corrected for extinction effects and refined by least-squares techniques to a conventional $R$ factor of 0.049. Hydrogen bonds of length 2.55 Å link the molecules into infinite sheets. The bond lengths indicate a high degree of conjugation in the molecule: $C=O$ 1.229(1) Å, $C-O$ 1.291(1) Å, $C=C$ 1.409(1) Å, $C-C$ 1.458(1) Å, $C-C$ 1.501(1) Å.

Squaric acid, $C_4H_2O_4$, (I), the smallest known member of the cyclic oxocarbon acids, was first synthesized by Cohen, Lacher and Park.[1]



I
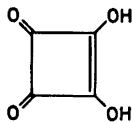
In view of the bond-angle strain associated with a four-membered ring, the squaric acid molecule is surprisingly stable: cyclobutene decomposes at room temperature, whereas squaric acid is stable up to 290°C. The molecule is unique among the oxocarbon acids in having an equal number of groups acting as donors and acceptors for hydrogen bonding. The compound is a strong acid ($pK_1 = 0.5$, $pK_2 = 3.5$), and the dianion $C_4O_4^{2-}$ has been shown to have a symmetrical structure,[2] indicating a substantial delocalization. The crystal structure analysis of squaric acid was carried out in order to obtain information about the influence of conjugation in the molecular system and to examine the hydrogen bonding properties of the compound. A brief description of the results of the X-ray crystal structure analysis has been published.[3]

## EXPERIMENTAL

Well developed bipyramidal crystals were obtained from an aqueous solution of commercially available squaric acid. Preliminary film investigations with CuKα radiation suggested the Laue symmetry to be 4/m. However, photographs from small crystals showed unexpected splitting of reflections with high θ values into triple spots instead of the normal $\alpha_1$, $\alpha_2$ pairs. Similar splittings were observed by scanning along 2θ with a manual Picker diffractometer, using both α and β components of the radiation. 2θ scans with the latter showed doublets instead of triplets. At high 2θ angles splitting was generally observed except for reflections corresponding to the unique axis and the diagonals in the plane normal to this axis. The observations were interpreted as due to twinning, thus implying a lower symmetry than tetragonal. After some effort a true single crystal was found, and this specimen was used in the following X-ray experiments.

The crystal was of rectangular shape with dimensions $0.59 \times 0.22 \times 0.60$ mm³. The Weissenberg and precession photographs showed systematic absences only for (0k0), $k = 2n + 1$. It was further evident from these photographs that only a pseudo fourfold axis was present. The space group is hence either $P2_1$ or $P2_1/m$. The latter was assumed and proved to be correct by the structure refinement. Cell dimensions were determined on a manual four-circle diffractometer using CuK radiation. Three-dimensional intensity data were recorded on an automatic Picker four-circle diffractometer using graphite crystal monochromated MoKα radiation, ($\lambda = 0.71069$). Integrated intensities were collected using the $\omega - 2\theta$ scan technique with a scan rate of 1°/min. The scan range was 0.7° below $2\theta(\alpha_1)$ and 0.7° above $2\theta(\alpha_2)$. Background counts were taken for 15 sec at each end of the scan range limits. The standard reflections measured after every 50 reflections declined in intensity by less than 4 % during the data collection and 2178 reflections within the sphere for 2θ less than 75° were measured. Two quadrants $(\pm h, k, \pm l)$ of the reciprocal space were examined and a total of 1849 reflections with intensities greater than $2\sigma(I)$ were obtained. The remaining 329 reflections were excluded from the structure refinement procedure. The intensities were corrected for Lorentz and polarization effects, assuming an ideal mosaic monochromator crystal. The standard reflections were used for scaling and a 2 % uncertainty in scaling and diffractometer stability was included in the standard deviations. Atomic scattering factors were those of Hanson et al.[4] except for hydrogen.[5] All programs applied are written or revised for CD-3300 by Dahl et al.[6]

## CRYSTAL DATA

Squaric acid, $C_4H_2O_4$, F.W. 114.1, monoclinic. $a = 6.129(3)$, $b = 5.273(2)$, $c = 6.140(3)$ Å, $\beta = 90.00(1)°$, $V = 198.4$ Å³, $F(000) = 116$, $Z = 2$, $\varrho_{obs} = 1.90$ g cm⁻³, $\varrho_{calc} = 1.908$ g cm⁻³. Space group $P2_1/m$.

## STRUCTURE DETERMINATION

There are two non-centrosymmetric molecules in the unit cell. Each molecule is thus constrained to lie on a mirror plane. From inspection of the intensity data it was evident that reflections with $h + k + l = 2n + 1$ were weak or absent, suggesting an approximately body-centered lattice. The orientation of the molecule was found from a three-dimensional Patterson synthesis. A trial parameter set in accordance with the above considerations was refined by the "minimum residual method".[7] The R value for 100 low order reflections dropped from 0.20 to 0.13 during refinement. Full matrix least-squares refinements of positional and anisotropic thermal parameters gave $R_w = 0.093$ and $R = 0.072$. At this stage the positions for the hydrogen atoms could be calculated and refinement including positional and isotropic thermal param-

*Table 1.* Observed and calculated structure factors. (The five columns list values of *h*, *k*, *l*, $10F_o$, and $10F_c$.)

*Table 2.* Positional and thermal parameters ($\times 10^5$) with estimated standard deviations. The temperature factor is given by $\exp-(B_{11}h^2+B_{22}k^2+B_{33}l^2+B_{12}hk+B_{13}hl+B_{23}kl)$.

| Atom | $x$ | $y$ | $z$ | $B_{11}(B)$ | $B_{22}$ | $B_{33}$ | $B_{12}$ | $B_{13}$ | $B_{23}$ |
|---|---|---|---|---|---|---|---|---|---|
| C1 | 19994 | 25000 | 9806 | 504 | 1555 | 513 | 0 | − 47 | 0 |
|    | 13    |       | 14   | 17  | 34   | 18  |   | 25    |   |
| C2 | 10677 | 25000 | 30788 | 511 | 1556 | 517 | 0 | − 54 | 0 |
|    | 13    |       | 13    | 18  | 34   | 18  |   | 25    |   |
| C3 | 32099 | 25000 | 41085 | 579 | 1488 | 484 | 0 | 7 | 0 |
|    | 13    |       | 14    | 18  | 34   | 18  |   | 25 |   |
| C4 | 42040 | 25000 | 18737 | 512 | 1509 | 521 | 0 | − 10 | 0 |
|    | 14    |       | 13    | 17  | 33   | 18  |   | 25    |   |
| O1 | 11415 | 25000 | − 9386 | 706 | 2433 | 445 | 0 | −213 | 0 |
|    | 11    |       | 10     | 17  | 35   | 16  |   | 23    |   |
| O2 | − 8699 | 25000 | 39065 | 459 | 2445 | 687 | 0 | 189 | 0 |
|    | 10     |       | 10    | 15  | 34   | 17  |   | 23  |   |
| O3 | 39265 | 25000 | 59777 | 767 | 2295 | 469 | 0 | −209 | 0 |
|    | 11    |       | 10    | 17  | 34   | 16  |   | 23    |   |
| O4 | 60567 | 25000 | 11132 | 461 | 2305 | 737 | 0 | 138 | 0 |
|    | 11    |       | 11    | 15  | 33   | 18  |   | 23  |   |
| H1 | 23029 | 25000 | − 21688 | 4.88 | | | | | |
|    | 212   |       | 260     | .53  | | | | | |
| H2 | − 21550 | 25000 | 26307 | 4.96 | | | | | |
|    | 228     |       | 229    | .54  | | | | | |

eters for all atoms gave $R_w = 0.086$ and $R = 0.072$. A comparison of observed and calculated structure factors revealed the presence of extinction effects. Isotropic secondary extinction corrections [6] were carried out giving $R_w = 0.076$ and $R = 0.064$.* However, it is evident that some structure factors had been undercorrected while others had been overcorrected, suggesting anisotropic extinction effects. Symmetry related reflections were then averaged. The total number of independent reflections observed twice became 898. The standard deviations for these reflections were taken as the average of the individual standard deviations. Another 52 reflections were also included in the data, increasing their standard deviations arbitrarily by 10 %. Further refinement decreased the residuals to $R_w = 0.062$ and $R = 0.049$.

The weight analysis showed negligible intensity dependence except for the smaller $F$-values. Observed and calculated structure factors are listed in Table 1 and atomic and thermal parameters in Table 2. Bond distances and angles are listed in Table 3, as well as in Fig. 1. The standard deviations in bond lengths and angles were calculated from the correlation matrix of the final least-squares cycle. Fig. 2 is a schematical drawing of the structure as viewed along the $b$ axis.

Successive least-squares refinements with increasing inner cut-off limits in $\sin \theta/\lambda$ were finally applied to the intensity data. A summary of these calculations is given in Table 4.

* The strong 020 reflections was omitted from refinement at this stage, being less than 2/3 of their calculated value after correction.

*Table 3.* Bond distances, bond angles, hydrogen bond lengths and angles (uncorrected values).

| Bond lengths (Å) | e.s.d. ($\times 10^4$) | Bond angles (°) | |
|---|---|---|---|
| C1 – C2 | 1.409 (11) | C1 – C2 – C3 | 91.8(.07) |
| C2 – C3 | 1.457 (11) | C2 – C3 – C4 | 88.2(.07) |
| C3 – C4 | 1.501 (11) | C3 – C4 – C1 | 88.2(.07) |
| C1 – C4 | 1.458 (11) | C4 – C1 – C2 | 91.8(.07) |
| C1 – O1 | 1.290 (10) | O1 – C1 – C2 | 132.0(.08) |
| C2 – O2 | 1.292 (10) | O1 – C1 – C4 | 136.1(.08) |
| C3 – O3 | 1.229 (10) | O2 – C2 – C3 | 131.1(.08) |
| C4 – O4 | 1.228 (10) | O2 – C2 – C1 | 137.1(.08) |
| O1 – H1 | 1.108(150) | O3 – C3 – C4 | 135.1(.08) |
| O2 – H2 | 1.040(140) | O3 – C3 – C2 | 136.7(.08) |
| | | O4 – C4 – C1 | 135.6(.08) |
| | | O4 – C4 – C3 | 136.3(.08) |

| Hydrogen bond lengths (Å) | | Hydrogen bond angles (°) | |
|---|---|---|---|
| O1···O3 | 2.549 (10) | O1 – H1···O3 | 177.9(1.2) |
| O2···O4 | 2.548 (10) | O2 – H2···O4 | 175.6(1.2) |
| O3···H1 | 1.510(160) | C1 – O1 – H1 | 112.7(0.7) |
| O4···H2 | 1.441(140) | C1 – O1···O3 | 113.9(0.06) |
| | | C2 – O2 – H2 | 112.0(0.7) |
| | | C2 – O2···O4 | 114.5(0.05) |
| | | C3 – O3···H1 | 117.9(0.5) |
| | | C3 – O3···O1 | 117.0(0.06) |
| | | C4 – O4···H2 | 117.2(0.5) |
| | | C4 – O4···O2 | 115.3(0.6) |
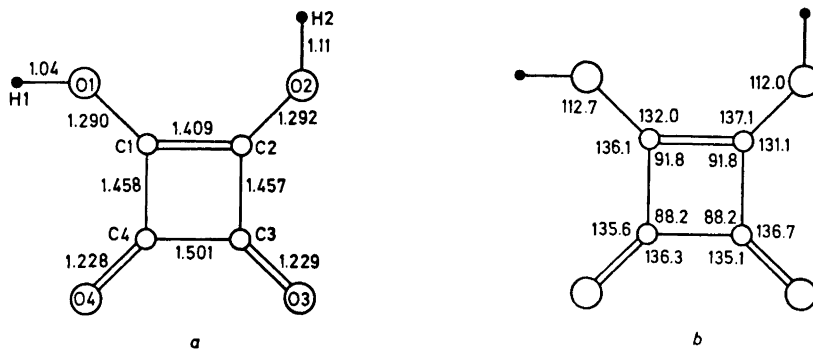


*Fig. 1.* Schematical drawings of the molecule showing (*a*) bond lengths (Å), (*b*) angles (°) (uncorrected values).

*Table 4.* Intramolecular distances (Å) as found with increasing inner cut-off in $\sin \theta/\lambda$ were employed in the least-squares refinements.

| $\sin \theta/\lambda$ lower limit | $R_1$ | $R_2$ | $R_w$ | $N$ | $k$ | $s$ | C1–O1 | C2–O2 | C3–O3 | C4–O4 | C1–C4 | C2–C3 | C1–C2 | C3–C4 | Average e.s.d. ($\times 10^4$) |
|---|---|---|---|---|---|---|---|---|---|---|---|---|---|---|---|
| 0.0 | .049 | .049 | .062 | 950 | .984 | 3.72 | 1.290 | 1.292 | 1.229 | 1.228 | 1.458 | 1.457 | 1.409 | 1.501 | 10 |
| 0.4 | .049 | .040 | .051 | 840 | .982 | 3.03 | 1.290 | 1.289 | 1.229 | 1.230 | 1.458 | 1.460 | 1.412 | 1.500 | 11 |
| 0.5 | .049 | .033 | .041 | 732 | .972 | 2.39 | 1.290 | 1.290 | 1.230 | 1.231 | 1.459 | 1.460 | 1.414 | 1.501 | 9 |
| 0.6 | .049 | .029 | .031 | 573 | .954 | 1.73 | 1.289 | 1.289 | 1.231 | 1.232 | 1.459 | 1.459 | 1.413 | 1.497 | 8 |

$R_1$ and $R_2$ include all data and data used in the refinement, respectively. $N$ denotes the number of data in the refinement procedure and $k$ is the scale factor from the refinement. The standard deviation of an observation of unit weight is $s = (\sum w \Delta F^2/N - m)^{\frac{1}{2}}$ where $m$ is the number of parameters.
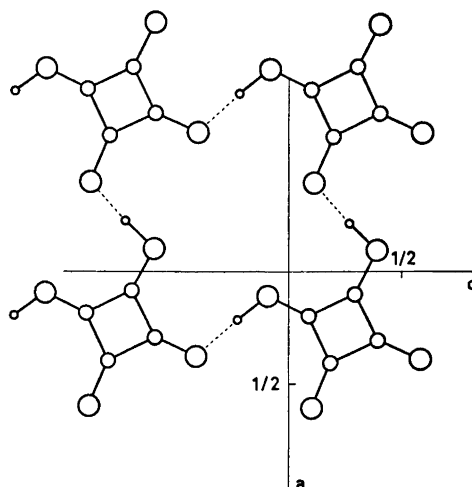
*Fig. 2.* Schematical drawing of molecules at $y = 1/4$ as viewed along the $b$ axis.

The thermal parameters of Table 1 were applied in the thermal analysis. Root-mean-square amplitudes and corresponding $B$-values for the atomic anisotropic thermal vibration along the principal axes together with the components of these axes along the crystal axes are given in Table 5. Largest component of the thermal motion is normal to the plane of the molecule. The carbon atoms in the ring have almost isotropic motion in this plane, whereas the oxygen atoms show small deviations from isotropic motion and have the larger component in the plane normal to the $C-O$ bonds.

*Table 5.* R.m.s. amplitudes of vibration $(\overline{u^2})^{\frac{1}{2}}$ (Å) and $B$-values (Å²) along the principal axes of vibration given by the components of a unit vector **e** in fractional coordinates ($\times 10^3$).

| Atom | $(\overline{u^2})^{\frac{1}{2}}$ | $B$ | $e_x$ | $e_y$ | $e_z$ | Atom | $(\overline{u^2})^{\frac{1}{2}}$ | $B$ | $e_x$ | $e_y$ | $e_z$ |
|------|------|------|------|------|------|------|------|------|------|------|------|
|     | .184 | 2.68 | 0 | 190 | 0 |     | .147 | 1.71 | 0 | 190 | 0 |
| O1  | .118 | 1.11 | −154 | 0 | 55 | C1  | .100 | .79 | −100 | 0 | 129 |
|     | .087 | .60 | 55 | 0 | 153 |     | .095 | .71 | 129 | 0 | 100 |
|     | .185 | 2.70 | 0 | 190 | 0 |     | .147 | 1.71 | 0 | 190 | 0 |
| O2  | .117 | 1.08 | 55 | 0 | 154 | C2  | .100 | .80 | −104 | 0 | 126 |
|     | .089 | .63 | −154 | 0 | 55 |     | .095 | .72 | 126 | 0 | 104 |
|     | .179 | 2.53 | 0 | 190 | 0 |     | .144 | 1.63 | 0 | 190 | 0 |
| O3  | .123 | 1.19 | −156 | 0 | 49 | C3  | .104 | .85 | 163 | 0 | 5 |
|     | .090 | .65 | 49 | 0 | 155 |     | .095 | .72 | − 51 | 0 | 163 |
|     | .179 | 2.54 | 0 | 190 | 0 |     | .145 | 1.65 | 0 | 190 | 0 |
| O4  | .119 | 1.12 | 37 | 0 | 159 | C4  | .099 | .77 | − 59 | 0 | 152 |
|     | .091 | .66 | −159 | 0 | 37 |     | .097 | .75 | 152 | 0 | 59 |

*Table 6.* Components of molecular translational $(T_{ij} \times 10^4 \text{ Å}^2)$ and librational $[L_{ij} (°)^2]$ tensors referred to the crystal axes, standard deviations in parentheses.

|   | 11 | 22 | 33 | 12 | 13 | 23 |
|---|----|----|----|----|----|----|
| **T** | 80 | 171 | 78 | 0 | − 3 | 0 |
|   | (2) | (3) | (2) | (2) | (3) | (3) |
| **L** | 8.5 | 3.5 | 9.9 | 0.0 | − 0.6 | 0.0 |
|   | (10.4) | (0.2) | (10.4) | (0.3) | (10.8) | (0.3) |

Principal axes of **T** (Å) and **L** (°) and their direction cosines

|   |   |   |   |   |
|---|---|---|---|---|
| **T** | 0.131 | 0.0 | 1.0 | 0.0 |
|   | 0.091 | 0.7993 | 0.0 | − 0.6010 |
|   | 0.087 | 0.6009 | 0.0 | 0.7993 |
| **L** | 3.18 | 0.3553 | 0.0 | − 0.9347 |
|   | 2.89 | 0.9347 | 0.0 | 0.3553 |
|   | 1.88 | 0.0 | 1.0 | 0.0 |

With the molecular center of mass as origin, the tensors of librational and vibrational motion with respect to the crystal axes were also derived in a rigid-body analysis [8] (Table 6). The root-mean-square deviation is 0.0004 Å². The atoms in the molecule lie, however, very close to the asymptotes of a hyperbola and thus approximately along a quadratic curve.[8] The two largest components in the libration tensor **L** occurring in the molecular plane have large standard deviations, probably indicating that the motion perpendicular to the molecular plane is poorly resolved. The two largest librational amplitudes occur around axes nearly parallel with the C − C bonds, while the two smaller amplitudes of the translational motion coincides nearly with the directions of the hydrogen bonds. As is expected for an approximately centrosymmetric molecule, the components of the correlation tensor **S** are very small. Similarly the **T** and **L** tensors are approximately diagonal. The "center of reaction" lies within 0.06 Å from the center of mass of the molecule.

Corrections in bond lengths for rigid-body motion are small and amount to 0.002 Å for the four terminal C − O bonds and about 0.004 Å for the C − C bonds. Owing to the large standard deviations in the **L** tensor these corrections may be rather uncertain. Corrections in bond lengths for "riding" motion [9] have been calculated for the terminal carbon oxygen bonds and amount to 0.007 Å.

## DISCUSSION

Refinement using different inner cut-off limits yielded only minor differences in the structural parameters. However, it will be seen from Table 4 that $R$, $R_w$, and $s$ continuously decrease with increasing inner cut-off. The

maximum difference of 0.004 Å in bond lengths is barely outside the experimental error. However, most of the variations in bond lengths (Table 4) are as expected, taking into consideration effects from lone pairs and bonding electrons.[10] In the following the values obtained from the refinement including all observed intensities will be discussed.

The molecular point group is $C_{2v}$, but only one mirror plane is retained in the crystal. The values found for chemically equivalent bonds agree very well, the largest deviation being only 0.0014 Å while standard deviations range from 0.0010 to 0.0012 Å.

*Table 7.* Bond distances in squaric acid and some related compounds.

|  | C1 − C2 | C1 − C4 | C3 − C4 | C1 − O1 | C3 − O3 | Ref. |
|---|---|---|---|---|---|---|
| 1-Cyclohexeneyl-1-cyclobutenedione | 1.395(18) | 1.483(18) | 1.547(18) | 1.198(18) | − | 11 |
| Phenylcyclobutenedione | 1.358(6) | 1.485(6) | 1.543(6) | 1.205(10) | − | 12 |
| Benzocyclobutenedione | 1.384(10) | 1.493(10) | 1.569(13) | 1.197(12) | − | 13 |
| 1,2-Dichloro-1-cyclobutenedione | 1.41(2) | 1.46(2) | 1.56(2) | 1.20(2) | − | 14 |
| 3,4-Dimethylenecyclobutene | 1.357(5) | 1.488(9) | 1.516(20) | − | − | 15 |
| This investigation | 1.409(1) | 1.458(1) | 1.501(1) | 1.229(1) | 1.291(1) | − |

The bond lengths in the cyclobutene ring show significant departures from those found in other investigations of the cyclobutenedione moiety. Table 7 contains a summary of relevant bond lengths in some similar molecules.[11-15] The single bonds C1 − C4 and C2 − C3 (1.458 Å) are appreciably shorter than corresponding bonds commonly found in cyclobutenediones. Similarly, the formal double bond C1 − C2 (1.409 Å) is longer than those listed in Table 7. Furthermore, the formal single bond distance in the diketonic group (1.501 Å) is shorter than the C − C distance in glyoxal [1.525(3) Å][16] and even shorter than similar bonds in pure hydrocarbons containing strained four-membered rings such as biphenylene [1.514(3) Å][17] and dimethylenecyclobutene [1.516(20) Å].[15] Thus it seems that the conjugation is higher in squaric acid than ordinarily found in cyclobutenediones and related conjugated systems. The conjugation in the molecule seems to extend to the C = O and C − O bonds, the two C = O bonds (1.229 Å) being longer than similar distances in other cyclobutenedione moieties. In investigations of acireductones ( − CO − COH = COH − ) the values of the C − O bonds range from 1.361(2) Å[18] in ascorbic acid to 1.308 Å[19] (1.297 Å neutron diffraction)[20] in dialuric acid. The C − O bond in squaric acid is probably somewhat shorter than that in dialuric acid. The values of the carbon-oxygen bonds in squaric acid are, however, comparable with those commonly found among the carboxylic acids: C = O 1.228(2) − 1.211(4) Å and C − O 1.278(2) − 1.322(4) Å.[21,22]

The high degree of conjugation revealed in the bond lengths is probably connected with the strong hydrogen bonding.

Striking examples of the influence of hydrogen bonding on electronic structure are found in recent investigations of the monomers and dimers of formic,[23] acetic,[24] and propionic acids [25] by electron diffraction in the vapour phase where the $C-O$ bond on average is 0.035 Å shorter in the dimer than in the monomer, whereas the $C=O$ bond on average is 0.014 Å longer in the dimer.

The bond angles within the ring closely conform to the $C_{2v}$ symmetry of the molecule and agree fairly well with corresponding angles in previous investigations of the cyclobutenedione moiety. The angles involving the hydroxylic oxygens and the carbon atoms in the ring depart, however, markedly from this symmetry, the angle on the same side as the hydrogen atom being expanded. Small distortions are also found in the external angles involving the carbonyl groups. Similar distortions have been found in several phenols [26] and may be explained by intramolecular non-bonded repulsions between the hydrogen bonded proton and the carbon atom carrying the hydroxyl group.[27] However, effects associated with the hydrogen bond formation may also be of importance.

The two short $O\cdots O$ distances of 2.549 Å indicate the presence of strong *inter*molecular hydrogen bonds. They are shorter than corresponding bonds found in the free carboxylic acids (2.63−2.67 Å).[28,29] As expected from the incomplete delocalization of the $\pi$ electrons between the heavy atoms, the hydrogen bonds are of the asymmetric type. The protons are located 1.04 Å and 1.11 Å from their respective hydroxyl oxygen atoms, the average bond length being slightly longer than the value (1.03 Å) predicted from the Naka-moto-Margoshes-Rundle curve of Hamilton and Ibers.[30] The hydrogen bonds are nearly linear, the $O-H\cdots O$ angles being 177.8° and 175.6°. The values are in good agreement with that of 176° calculated from the linear empirical relation between $O-H\cdots O$ angles and $O\cdots O$ distances of Hamilton.[31] The hydrogen atoms make angles with the carbonyl groups of 117.9° and 117.2°, respectively.

The four oxygen atoms in a molecule are linked to four other molecules by hydrogen bonds across pseudo fourfold inversion axes (see below). There are two crystallographically independent hydrogen bonds per molecule, and the molecules thus form infinite planar networks lying in the crystallographic mirror planes. Molecules in one layer are related to the layers above and below by screw axes. Thus they are fitted into the open regions in and be-tween the layers above and below, in such a way that each oxygen atom in a molecule is situated between two $O-C-C-O$ fragments from molecules in neighbouring sheets. This produces a very efficient stacking along the $b$ axis which partly explains the high density of the crystals.

As implied by the lattice constants and intensity symmetry the crystal structure is pseudo tetragonal. In addition to the space group symmetry operations there are approximate fourfold axes parallel to the $b$ axis through the molecules at $x=z=1/4$ and approximate fourfold inversion axes at $x=-z=1/4$, and the pseudo space group is therefore $I4/m$.

The most probable explanation of the reflection splitting observed in twinned crystals is an interchange of the $a$ axis with the slightly longer (0.01 Å) $c$ axis and *vice versa*, arising from a twin axis or twin plane along the diagonal

in the $a-c$ plane, or from a 90° rotation about the $b$ axis. The latter explanation is in accordance with the pseudosymmetry found in the single crystal investigation (while the former is not), and therefore seems to be the most probable one, although this kind of twin growth does not give a normal rotational twin.[32]

A final electron-density difference synthesis was calculated with the contributions from all atoms subtracted and with the scale factor and parameters given in Table 1. The resulting map is shown in Fig. 3. The highest peaks
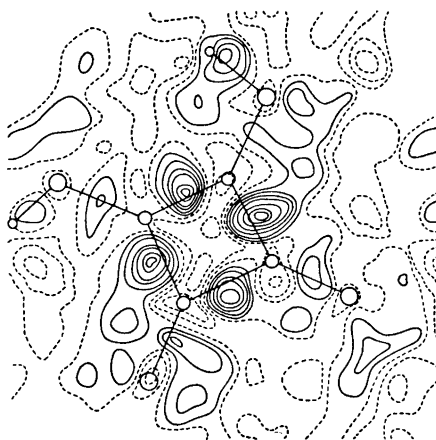


*Fig. 3.* Final electron density difference synthesis through the molecular plane. Contours at 0.05 eÅ⁻³. Zero and negative contours dotted.

are found in the regions between the C – C bonds, the terminal C – O bonds having smaller residuals. The positions of the maxima of the residual electron density in the C – C single bonds lie about 0.2 Å outside the lines joining the atomic centers, while that of the double bond lies less than 0.1 Å outside. The positions of these maxima seem to support the concept of bent bonds in strained rings, but the data in the present work are probably too inaccurate to warrant a detailed study of the residual electron density.

## REFERENCES

1. Cohen, S., Lacher, J. R. and Park, J. D. *J. Am. Chem. Soc.* **81** (1959) 3480.
2. Macintyre, W. M. and Werkema, M. S. *J. Chem. Phys.* **40** (1964) 3563.
3. Semmingsen, D. *Tetrahedron Letters* **1973** 807.
4. Hanson, H. P., Herman, F., Lea, J. D. and Skillman, S. *Acta Cryst.* **17** (1964) 1040.
5. Stewart, R. F., Davidson, E. R. and Simpson, W. T. *J. Chem. Phys.* **42** (1965) 3175.
6. Dahl, T., Gram, F., Groth, P., Kleve, B. and Rømming, Chr. *Acta Chem. Scand.* **24** (1970) 2232.
7. Stanley, E. *Acta Cryst.* **17** (1964) 1028.
8. Schomaker, V. and Trueblood, K. N. *Acta Cryst.* **B 24** (1968) 63.
9. Busing, W. R. and Levy, H. A. *Acta Cryst.* **17** (1964) 142.
10. Coppens, P. *Thermal Neutron Diffraction*, Oxford Univ. Press, London 1970.
11. Karle, I. L., Britts, K. and Brenner, S. *Acta Cryst.* **17** (1964) 1507.
12. Wong, C. H., Marsh, R. E. and Schomaker, V. *Acta Cryst.* **17** (1964) 131.

13. Trotter, J. and Allen, F. H. *J. Chem. Soc.* **B 1970** 916.
14. Mattes, R. and Schroebler, S. *Chem. Ber.* **105** (1972) 3761.
15. Skancke, A. *Acta Chem. Scand.* **22** (1968) 3239.
16. Kuchitsu, K., Fukuyama, T. and Morino, Y. *J. Mol. Struct.* **1** (1967 – 68) 463.
17. Fawcett, J. K. and Trotter, J. *Acta Cryst.* **20** (1966) 87.
18. Hvoslef, J. *Acta Cryst.* **B 24** (1968) 23.
19. Bolton, W. *Acta Cryst.* **19** (1965) 1051.
20. Craven, B. M. and Sabine, T. M. *Acta Cryst.* **B 25** (1969) 1970.
21. Benghiat, V. and Leizerowitz, L. *J. Chem. Soc. Perkin Trans. 2* **1972** 1778.
22. Filippakis, S. E., Leizerowitz, L., Rabinovich, D. and Schmidt, G. M. J. *J. Chem. Soc. Perkin Trans 2* **1972** 1750.
23. Almenningen, A., Bastiansen, O. and Motzfeldt, T. *Acta Chem. Scand.* **23** (1969) 2848.
24. Derissen, J. L. *J. Mol. Struct.* **7** (1971) 67.
25. Derissen, J. L. *J. Mol. Struct.* **7** (1971) 81.
26. Coppens, P. and Schmidt, G. M. J. *Acta Cryst.* **18** (1965) 654.
27. Hirshfeld, F. L. *Israel J. Chem.* **2** (1964) 87.
28. Jönsson, P.-G. *Acta Cryst.* **B 27** (1971) 893.
29. Jönsson, P.-G. and Hamilton, W. C. *J. Chem. Phys.* **56** (1972) 4433.
30. Hamilton, W. C. and Ibers, J. A. *Hydrogen Bonding in Solids*, Benjamin, N. Y. 1968.
31. Hamilton, W. C. *Ann. Rev. Phys. Chem.* **13** (1962) 19.
32. Hartshorne, N. H. and Stuart, A. *Practical Optical Crystallography*, Edward Arnold, 1964.

# Correlation of the Absolute Configurations of
# Tris-(*trans*-1,2-cyclohexanediamine) Complexes
# of Cr(III), Co(III), Rh(III), and Ir(III)
# by Means of X-Ray Powder Photographs of Active Racemates

P. ANDERSEN, F. GALSBØL, S. E. HARNUNG and T. LAIER

*Chemistry Department I (Inorganic Chemistry), H. C. Ørsted Institute,
Universitetsparken 5, DK 2100 Copenhagen Ø, Denmark*

Racemates and active compounds of [M chxn$_3$]Cl$_3$.aq and active racemates {[M'chxn$_3$][M''chxn$_3$]}Cl$_6$.aq have been prepared, where M is one of the metals Cr, Co, Rh, and Ir; M' and M'' denote two different metals, and chxn = *trans*-1,2-cyclohexanediamine. From X-ray powder photographs of these compounds it has been possible to conclude that the isomers of $(-)_{589}$[Co($+$)chxn$_3$]$^{3+}$, $(-)_{589}$[Cr($+$)-chxn$_3$]$^{3+}$, $(-)$[Rh($+$)chxn$_3$]$^{3+}$, and $(-)$[Ir($+$)chxn$_3$]$^{3+}$ which have a positive rotational strength for the spin-allowed ligand field band with lowest energy have the same absolute configuration. This absolute configuration is $\Lambda$ (from other considerations), and the ring conformation is $\delta$ (IUPAC 1968). A determination of the space groups by single crystal X-ray diffraction showed that the tetragonal cells of the racemates ($I\bar{4}2d$) differ only slightly from the orthorhombic cells of the active racemates ($I2_12_12_1$).

An earlier investigation[1] of the correlation of the absolute configurations of tris(diamine) complexes by means of X-ray powder photographs of active racemates included the tris(ethylenediamine) and tris(propylenediamine) complexes of chromium(III), cobalt(III), and rhodium(III). The tris-complexes were all of the lel$_3$ type[1] and the investigation led to a clear correlation of the absolute configurations within each of the two series. We concluded that the method is convenient for correlating the absolute configurations in such systems, and we present here a similar investigation of the lel$_3$ isomers of the tris(*trans*-1,2-cyclohexanediamine) complexes of chromium(III), cobalt(III), rhodium(III), and iridium(III).

We have prepared some of the active racemates, {$\Lambda$[M' chxn$_3$; lel$_3$] $\Lambda$[M'' chxn$_3$; lel$_3$]}Cl$_6$.aq, M' and M'' being two of the metals Cr, Co, Rh, and Ir, and compared their X-ray powder photographs with those of the ordinary racemates and active forms. In this way it has been possible to correlate the

P. ANDERSEN ET AL.

*Table 1.* X-Ray powder data of racemates and active racemates. Unit cell dimensions and densities for some of the table.

| h k l | [Cr chxn$_3$]Cl$_3$.aq rac, lel$_3$ | | | [Co chxn$_3$]Cl$_3$.aq rac, lel$_3$ | | | [Rh chxn$_3$]Cl$_3$.aq rac, lel$_3$ | | | [Ir chxn$_3$]Cl$_3$a.q rac, lel$_3$ | | |
|---|---|---|---|---|---|---|---|---|---|---|---|---|
| | $I_{obs}$ | $d_{obs}$(Å) | $d_{calc}$(Å) | $I_{obs}$ | $d_{obs}$(Å) | $d_{calc}$(Å) | $I_{obs}$ | $d_{obs}$(Å) | $d_{calc}$(Å) | $I_{obs}$ | $d_{obs}$(Å) | $d_{calc}$(Å) |
| 1 1 0 | | | | | | | | | | | | |
| 1 0 1 ⎫ 0 1 1 ⎬ | s | 11.27 | 11.26 | s | 11.00 | 11.01 | s | 11.26 | 11.27 | s | 11.31 | 11.31 |
| 2 0 0 ⎫ 0 2 0 ⎬ | s | 9.599 | 9.604 | s | 9.636 | 9.624 | s | 9.599 | 9.603 | ms | 9.577 | 9.582 |
| 2 1 1 ⎫ 1 2 1 ⎬ | vs | 7.310 | 7.307 | vs | 7.252 | 7.246 | vs | 7.307 | 7.307 | vs | 7.307 | 7.310 |
| 1 1 2 | m | 6.192 | 6.190 | ms | 6.024 | 6.014 | s | 6.184 | 6.192 | s | 6.216 | 6.222 |
| 3 1 0 ⎫ 1 3 0 ⎬ | ms | 6.076 | 6.074 | ms | 6.083 | 6.087 | s | 6.072 | 6.074 | ms | 6.059 | 6.061 |
| 3 0 1 ⎫ 0 3 1 ⎬ | vw | 5.825 | 5.816 | vvw | 5.788 | 5.788 | | | | | | |
| 2 0 2 ⎫ 0 2 2 ⎬ | vvw | 5.643 | 5.632 | | | | vw | 5.634 | 5.634 | w | 5.654 | 5.654 |
| 3 2 1 ⎫ 2 3 1 ⎬ | vw | 4.972 | 4.975 | vw | 4.960 | 4.961 | mw | 4.975 | 4.975 | ms | 4.970 | 4.970 |
| 3 1 2 ⎫ 1 3 2 ⎬ | w | 4.578 | 4.574 | w | 4.508 | 4.507 | w | 4.579 | 4.575 | w | 4.583 | 4.584 |
| 1 0 3 ⎫ 0 1 3 ⎬ | w | 4.508 | 4.507 | w | 4.354 | 4.354 | vw | 4.506 | 4.508 | | | |
| 4 1 1 ⎫ 1 4 1 ⎬ | mw | 4.419 | 4.417 | w | 4.411 | 4.409 | vw | 4.422 | 4.417 | vvw | 4.412 | 4.411 |
| 2 1 3 ⎫ 1 2 3 ⎬ | vvw | 4.081 | 4.080 | | | | vw | 4.082 | 4.081 | w | 4.101 | 4.101 |
| 4 0 2 ⎫ 0 4 2 ⎬ | vs | 3.951 | 3.951 | s | 3.910 | 3.910 | s | 3.953 | 3.951 | s | 3.954 | 3.955 |
| 3 3 2 | vw | 3.792 | 3.794 | vw | 3.758 | 3.757 | w | 3.795 | 3.794 | w | 3.797 | 3.796 |
| 5 1 0 ⎫ 1 5 0 ⎬ | | | | | | | w | 3.768 | 3.766 | w | 3.760 | 3.758 |
| 3 0 3 ⎫ 0 3 3 ⎬ | vvw | 3.757 | 3.755 | vvw | 3.667 | 3.668 | | | | | | |
| 4 3 1 ⎫ 3 4 1 ⎬ | w | 3.703 | 3.703 | vw | 3.701 | 3.700 | w | 3.700 | 3.702 | vw | 3.697 | 3.697 |
| 4 2 2 ⎫ 2 4 2 ⎬ | m | 3.653 | 3.654 | s | 3.622 | 3.622 | ms | 3.653 | 3.654 | m | 3.656 | 3.655 |
| 3 2 3 ⎫ 2 3 3 ⎬ | mw | 3.495 | 3.497 | mw | 3.428 | 3.427 | ms | 3.500 | 3.498 | ms | 3.509 | 3.508 |
| 0 0 4 | | | | vvw | 3.352 | 3.354 | w | 3.475 | 3.478 | | | |
| 5 2 1 ⎫ 2 5 1 ⎬ | w | 3.457 | 3.455 | w | 3.451 | 3.453 | m | 3.455 | 3.454 | mw | 3.449 | 3.449 |
| 4 4 0 | | | | | | | vvw | 3.397 | 3.395 | w | 3.387 | 3.388 |
| 5 3 0 ⎫ 3 5 0 ⎬ | | | | vvw | 3.299 | 3.301 | | | | | | |
| 4 1 3 ⎫ 1 4 3 ⎬ | mw | 3.287 | 3.286 | mw | 3.230 | 3.229 | w | 3.287 | 3.286 | mw | 3.293 | 3.294 |

$a=b=19.20_8$ Å $\quad\quad$ $a=b=19.24_8$ Å $\quad\quad$ $a=b=19.20_6$ Å $\quad\quad$ $a=b=19.16_4$ Å
$c=13.90_8$ Å $\quad\quad\quad$ $c=13.42_0$ Å $\quad\quad\quad$ $c=13.91_3$ Å $\quad\quad\quad$ $c=14.00_9$ Å
$\alpha=\beta=\gamma=90.0°$ $\quad$ $\alpha=\beta=\gamma=90.0°$ $\quad$ $\alpha=\beta=\gamma=90.0°$ $\quad$ $\alpha=\beta=\gamma=90.0°$

Density:
  exp.: 1.411 g/ml
  calc.: 1.405 g/ml$^d$

$a, b, c$ Refer to observed diffraction lines which are given twice in the table. $^d$ The densities are calculated on *per* metal atom (the average found for these compounds by thermogravimetric analysis).

the compounds (measured by flotation in carbon tetrachloride/toluene mixtures) are given at the bottom of

| CrCo chxn₆ Cl₆.aq act rac, lel₃ | | | CoRh chxn₆ Cl₆.aq act rac, lel₃ | | | CoIr chxn₆ Cl₆.aq act rac, lel₃ | | | | | |
|---|---|---|---|---|---|---|---|---|---|---|---|
| $I_{obs}$ | $d_{obs}$ (Å) | $d_{calc}$ (Å) | $I_{obs}$ | $d_{obs}$ (Å) | $d_{calc}$ (Å) | $I_{obs}$ | $d_{obs}$ (Å) | $d_{calc}$ (Å) | h | k | l |
| | | | | | | w | 13.61 | 13.59 | 1 | 1 | 0 |
| ms | 11.08 | 11.12 | vs | 11.17 | 11.16 | m (br.) | 11.19 | 11.21 | 1 | 0 | 1 |
| | | 11.06 | | | 11.12 | | | 11.14 | 0 | 1 | 1 |
| m | 9.697 | 9.695 | ms | 9.704 | 9.682 | mw | 9.704 | 9.704 | 2 | 0 | 0 |
| mw | 9.547 | 9.547 | ms | 9.577 | 9.547 | ms | 9.533 | 9.526 | 0 | 2 | 0 |
| ms | 7.278 | 7.291 | ms | 7.314 | 7.300 | s | 7.307 | 7.317 | 2 | 1 | 1 |
| m | 7.240 | 7.242 | ms | 7.268 | 7.255 | ms | 7.255 | 7.255 | 1 | 2 | 1 |
| m | 6.055$^a$ | 6.068 | s (br.) | 6.106 | 6.106 | s (br.) | 6.129 | 6.125 | 1 | 1 | 2 |
| mw | 6.116 | 6.122 | | | 6.114 | | | 6.127 | 3 | 1 | 0 |
| m | 6.055$^a$ | 6.047 | mw | 6.051 | 6.046 | mw | 6.036 | 6.034 | 1 | 3 | 0 |
| vvw | 5.841 | 5.834 | | | | | | | 3 | 0 | 1 |
| vvw | 5.778 | 5.762 | | | | | | | 0 | 3 | 1 |
| | | | | | | | | | 2 | 0 | 2 |
| | | | vvw | 5.556 | 5.557 | w | 5.564 | 5.566 | 0 | 2 | 2 |
| vvw (br.) | 4.969 | 4.978 | vw (br.) | 4.971 | 4.979 | w | 4.984 | 4.987 | 3 | 2 | 1 |
| | | 4.954 | | | 4.957 | w | 4.954 | 4.955 | 2 | 3 | 1 |
| vw | 4.544 | 4.544 | | | | | | | 3 | 1 | 2 |
| vvw | 4.510 | 4.513 | mw | 4.525 | 4.529 | w | 4.529 | 4.531 | 1 | 3 | 2 |
| w | 4.399$^b$ | 4.403 | vw (br.) | 4.432 | 4.435 | | | 4.452 | 1 | 0 | 3 |
| | | 4.400 | | | 4.432 | vw | 4.449 | 4.447 | 0 | 1 | 3 |
| vw | 4.438 | 4.439 | | | 4.438 | | | 4.449 | 4 | 1 | 1 |
| w | 4.399$^b$ | 4.386 | | | | | | | 1 | 4 | 1 |
| | | | | | | | | | 2 | 1 | 3 |
| | | | | | | | | | 1 | 2 | 3 |
| m | 3.943 | 3.943 | vs | 3.953 | 3.950 | m | 3.963 | 3.962 | 4 | 0 | 2 |
| m | 3.906 | 3.904 | vs | 3.912 | 3.914 | mw | 3.911 | 3.912 | 0 | 4 | 2 |
| vvw | 3.768 | 3.770 | mw | 3.778 | 3.777 | vw | 3.779 | 3.782 | 3 | 3 | 2 |
| | | | | | | | | | 5 | 1 | 0 |
| | | | | | | vw | 3.738 | 3.738 | 1 | 5 | 0 |
| | | | | | | | | | 3 | 0 | 3 |
| | | | | | | | | | 0 | 3 | 3 |
| vvw (br.) | 3.702 | 3.709 | | | | | | | 4 | 3 | 1 |
| | | 3.695 | | | | | | | 3 | 4 | 1 |
| mw | 3.646 | 3.645 | s | 3.650 | 3.650 | mw | 3.659 | 3.658 | 4 | 2 | 2 |
| mw | 3.620 | 3.622 | s | 3.629 | 3.628 | w | 3.628 | 3.628 | 2 | 4 | 2 |
| mw (br.) | 3.447$^c$ | 3.453 | w | 3.469$^a$ | 3.468 | mw | 3.476$^a$ | 3.477 | 3 | 2 | 3 |
| | | 3.446 | ms | 3.459 | 3.460 | mw | 3.465 | 3.466 | 2 | 3 | 3 |
| vvw | 3.385 | 3.390 | w | 3.408$^b$ | 3.418 | | | | 0 | 0 | 4 |
| vw | 3.473 | 3.473 | w | 3.469$^a$ | 3.471 | mw | 3.476$^a$ | 3.478 | 5 | 2 | 1 |
| mw (br.) | 3.447$^c$ | 3.437 | m | 3.441 | 3.438 | mw | 3.434 | 3.433 | 2 | 5 | 1 |
| | | | w | 3.408$^b$ | 3.399 | | | | 4 | 4 | 0 |
| vvw | 3.310 | 3.312 | | | | | | | 5 | 3 | 0 |
| | | | vw | 3.286 | 3.286 | | | | 3 | 5 | 0 |
| vw | 3.263 | 3.258 | mw | 3.270 | 3.269 | w | 3.281 | 3.279 | 4 | 1 | 3 |
| vw | 3.235 | 3.236 | mw | 3.252 | 3.249 | vw | 3.252 | 3.252 | 1 | 4 | 3 |

$a = 19.39_0$ Å          $a = 19.36_3$ Å          $a = 19.41_2$ Å
$b = 19.09_5$ Å          $b = 19.09_4$ Å          $b = 19.04_8$ Å
$c = 13.56_3$ Å          $c = 13.67_0$ Å          $c = 13.72_0$ Å
$\alpha = \beta = \gamma = 90.0°$          $\alpha = \beta = \gamma = 90.0°$          $\alpha = \beta = \gamma = 90.0°$

Density:
exp.: 1.456 g/ml
calc.: 1.440 g/ml$^d$

the basis of eight metal atoms *per* unit cell and on the assumption that there is one water of crystallization

absolute configurations of the ions act[M chxn$_3$; lel$_3$]$^{3+}$, M being Cr, Co, Rh, or Ir. The space groups have been determined for the racemates as well as for the active racemates from single crystal X-ray diffraction data.

## EXPERIMENTAL

*X-Ray powder photographs* were taken at 25°C with CuK$\alpha$ radiation using a focussing camera of the Guinier type, calibrated with silicon.

*Single crystal X-ray diffraction* has been carried out on rac[Co chxn$_3$; lel$_3$]Cl$_3$.aq and act rac{$\varDelta$[Co chxn$_3$; lel$_3$] $\varDelta$[Rh chxn$_3$; lel$_3$]}Cl$_6$.aq. Using CuK$\alpha$ radiation, equiinclination Weissenberg and precession photographs were obtained of crystals of dimensions 0.05, 0.05, and 0.3 mm in the *a*, *b*, and *c* direction, respectively, the *c*-axis being the axis of rotation.

*Optically active complexes* were prepared as described elsewhere: act[Cr chxn$_3$; lel$_3$]-Cl$_3$.aq,[2] act[Co chxn$_3$; lel$_3$]Cl$_3$.aq,[3] act[Rh chxn$_3$; lel$_3$]Cl$_3$.aq,[4] and act[Ir chxn$_3$; lel$_3$]Cl$_3$.aq.[5]

*Racemic complexes.* 0.25 g of rac[Cr chxn$_3$; lel$_3$]Cl$_3$.aq[2] was recrystallized from 7.0 ml of water at 47°C. After 1 h at 0°C 0.19 g was obtained. Recrystallization was repeated using 5.5 ml of water; yield 0.11 g.

rac[Co chxn$_3$; lel$_3$]Cl$_3$.aq was prepared from a solution of 1.0 g of $\varDelta$[Co chxn$_3$; lel$_3$]Cl$_3$. 4H$_2$O in 13 ml of water and a solution of 1.0 g of $\varDelta$[Co chxn$_3$; lel$_3$]Cl$_3$.4H$_2$O in 13 ml of water. The two solutions were heated to boiling and were rapidly mixed, and precipitation soon commenced. After cooling to room temperature the precipitate was filtered off, washed with 40 % ethanol, and dried in air; yield 0.95 g. Another crop was obtained by heating the mother liquor to boiling and adding 12 M hydrochloric acid to make the solution 0.5 M with respect to HCl. After cooling, the crystals were filtered off, washed with water, and dried in air; yield 0.49 g. The two fractions had identical X-ray powder photographs.

rac[Rh chxn$_3$; lel$_3$]Cl$_3$.aq (yield 0.79 + 0.78 g) was prepared in an analogous manner from 1.0 g of $\varDelta$[Rh chxn$_3$; lel$_3$]Cl$_3$.4H$_2$O in 16 ml of water and 1.0 g of $\varDelta$[Rh chxn$_3$; lel$_3$]Cl$_3$. 4H$_2$O in 22 ml of water.

Similarly rac[Ir chxn$_3$; lel$_3$]Cl$_3$.aq (yield 0.57 + 0.24 g) was prepared from 0.51 g of $\varDelta$[Ir chxn$_3$; lel$_3$]Cl$_3$ . 3.5H$_2$O in 7 ml of water and 0.51 g of $\varDelta$[Ir chxn$_3$; lel$_3$]Cl$_3$ . 3.5H$_2$O in 7 ml of water.

*Active racemates.* act rac{$\varDelta$[Cr chxn$_3$; lel$_3$]$\varDelta$[Co chxn$_3$; lel$_3$]}Cl$_6$.aq: 0.46 g of $\varDelta$[Cr chxn$_3$; lel$_3$]Cl$_3$.aq was dissolved in 6.4 ml of water at 65°C. This solution was rapidly mixed with a solution of 0.46 g of $\varDelta$[Co chxn$_3$; lel$_3$]Cl$_3$.aq in 3.2 ml of water at 65°C. The precipitate, 0.39 g, formed at 0°C, was recrystallized twice from water and the fractions had identical CD-spectra. In the last recrystallization 0.21 g of the active racemate was dissolved in 3.2 ml of water at 50°C. This solution was left for 1 h at 0°C to yield 0.12 g.

act rac{$\varDelta$[Co chxn$_3$; lel$_3$]$\varDelta$[Rh chxn$_3$; lel$_3$]}Cl$_6$.aq was prepared from a solution of 1.0 g of $\varDelta$[Rh chxn$_3$; lel$_3$]Cl$_3$.4H$_2$O in 16 ml of water and a solution of 1.0 g of $\varDelta$[Co chxn$_3$; lel$_3$]Cl$_3$.4H$_2$O in 13 ml of water. The two solutions were heated to boiling and rapidly mixed, and precipitation soon commenced. After cooling to room temperature the precipitate was filtered off, washed with 40 % ethanol and dried in air; yield 0.96 g. Another crop was obtained by heating the mother liquor to boiling and adding 12 M hydrochloric acid to make the solution 0.5 M with respect to HCl. After cooling the crystals were filtered off, washed with water, and dried in air; yield 0.60 g. The two fractions had identical X-ray powder photographs.

act rac{$\varDelta$[Co chxn$_3$; lel$_3$]$\varDelta$[Ir chxn$_3$; lel$_3$]}Cl$_6$.aq (yield 0.58 + 0.38 g) was prepared in an analogous way from 0.66 g of $\varDelta$[Ir chxn$_3$; lel$_3$]Cl$_3$.3.5H$_2$O in 9 ml of water and 0.59 g of $\varDelta$[Co chxn$_3$; lel$_3$]Cl$_3$.4H$_2$O in 8 ml of water.

## RESULTS AND CONCLUSION

The powder photographs of the racemates and active racemates have been indexed assuming tetragonal and orthorhombic unit cells, respectively. Observed and calculated *d*-spacings and relative intensities of the diffraction

lines are given in Table 1. The unit cell dimensions and densities are given at the bottom of the table.

Table 1 shows that all the powder photographs have similar patterns and correspondingly the indexing has a general resemblance for all the compounds. The powder diagrams of the racemates have been indexed on the basis of tetragonal unit cells, the active racemates on the basis of orthorhombic unit cells, and there are only small, variations in the unit cell dimensions from one compound to another. A comparison of the photographs of the racemates with those of the active racemates shows that many lines on the racemate diagrams appear to be split into two lines on the active racemate diagrams. In most cases two such lines have nearly equal intensities. As mentioned previously,[1] racemates and active racemates cannot be expected to belong to the same crystal system, because any symmetry element which might connect the catoptromers in the racemates must be absent in the active racemates. However, for the ethylenediamine and propylenediamine complexes it was found [1] that the racemates as well as the active racemates belong to the hexagonal system. In the present case of cyclohexanediamine complexes it is observed that the racemates belong to the tetragonal system, whereas the active racemates belong to the orthorhombic system. Here, the two tetragonal axes of equal length in the racemates correspond to two axes of slightly different lengths in the active racemates, giving rise to the observed splitting of diffraction lines with $h \neq k$.

The resemblance between all the powder photographs in Table 1, which is also reflected in the indexing, shows that the structures of the crystals involved are very much alike, from which we conclude that $(-)_{589}[Co(+)$-chxn$_3]^{3+}$, $(-)_{589}[Cr(+)$chxn$_3]^{3+}$, $(-)[Rh(+)$chxn$_3]^{3+}$, and $(-)[Ir(+)$chxn$_3]^{3+}$ (series I)* all have the same absolute configuration. From a single crystal structure analysis on $(-)_{589}[Co(+)$chxn$_3]Cl_3.5H_2O$ [6] it is known that the configuration of this complex is $\varLambda$,lel$_3$. This salt is one of the starting materials in our preparation of the active racemates. Thus all the tris(cyclohexanediamine) complexes in series I are of the $\varLambda$,lel$_3$ type, *i.e.* the configuration is $\varLambda\delta\delta\delta$ (IUPAC 1968).[7]

It is noted that all the complexes of series I have positive circular dichroism for the major component under the spin-allowed ligand field band with lowest energy.

X-Ray powder photographs have been taken of all act[M chxn$_3$; lel$_3$]-Cl$_3$.aq (M being Cr, Co, Rh, or Ir). These compounds show similar diffraction patterns (hexagonal [6]), which are different from those of the racemates. The absolute configuration of the lel$_3$ complexes follows as $\varLambda$ from the stereo-specific coordination of the active (+)cyclohexanediamine,[8,9] and it is seen that there is agreement between this assignment and the correlation found by the active racemate method.

The unit cell dimensions indicate similar metal-ligand distances for Cr(III),

---

* Attention is drawn to the fact that for Rh and Ir [4,5] there are two isomers with the formula $(-)[M(+)$chxn$_3]^{3+}$, namely the lel$_3$-isomer and the ob$_3$-isomer.[1] This investigation concerns only the lel$_3$-isomers as revealed in the arguments to follow.

Rh(III), and Ir(III), and somewhat shorter distances for Co(III). This is as found earlier [1,10] for complexes of other diamines.

The single crystal work on rac[Co chxn$_3$; lel$_3$]Cl$_3$.aq shows that the space group of this salt is $I\bar{4}2d$ (No. 122, *Intern. Tables*). This result is based on the systematic absence of reflexions ($h+k+l\neq2n$ for $hkl$, and $2h+l\neq4n$ for $hhl$), on diffraction symmetry, and on the condition that in the unit cell there are eight metal atoms (Table 1) which cannot be placed at mirror planes or at centers of inversion.

The space group of act rac$\{\varLambda$[Co chxn$_3$; lel$_3$]$\varDelta$[Rh chxn$_3$; lel$_3$]$\}$Cl$_6$.aq has in the same way (absent reflexions: $h+k+l\neq2n$ for $hkl$, and $2\times4$ metal atoms in the unit cell) been determined to be either $I222$ (No. 23, *Intern. Tables*) or $I2_12_12_1$ (No. 24, *Intern. Tables*). In the racemate the cobalt atoms must be placed at special positions, namely on 2-fold axes perpendicular to the 4-fold inversion axis. The 2-fold axes containing the one catoptromer are perpendicular to the 2-fold axes containing the other catoptromer. The choice of possible positions for the large complex molecules is thus highly restricted. When the metal of one of the catoptromers in the cobalt racemate is replaced by rhodium as in the active racemate, then the 4-fold inversion axes become 2-fold axes, the "diamond" glide planes vanish, and the $a$-axis need no longer be equal in length to the $b$-axis. If all other symmetry elements from $I\bar{4}2d$ are maintained and we still have $\alpha=\beta=\gamma=90°$, then just the orthorhombic subgroup of $I\bar{4}2d$, $I2_12_12_1$, is obtained. Thus $I222$ can be disregarded. This is supported by the fact that it seems impossible to place eight complex molecules in a unit cell of the dimensions found if the space group is $I222$.

## REFERENCES

1. Andersen, P., Galsbøl, F. and Harnung, S. E. *Acta Chem. Scand.* **23** (1969) 3027.
2. Harnung, S. E. and Laier, T. *Acta Chem. Scand. To be submitted.*
3. Harnung, S. E., Sørensen, B. S., Creaser (Olsen), I., Maegaard, H., Pfenninger, U. and Schäffer, C. E. *Acta Chem. Scand. To be submitted.*
4. Galsbøl, F., Steenbøl, P. and Sørensen, B. S. *Acta Chem. Scand.* **26** (1972) 3605.
5. Galsbøl, F. *Acta Chem. Scand. To be submitted.*
6. Marumo, F., Utsumi, Y. and Saito, Y. *Acta Cryst.* **B 26** (1970) 1492.
7. IUPAC, *Information Bulletin* No. 33 (1968) 68; *Inorg. Chem.* **9** (1970) 1; IUPAC, *Nomenclature of Inorganic Chemistry*, 2nd Ed., Definitive rules 1970, Butterworths, London 1971, p. 75.
8. Corey, E. J. and Bailar, J. C., Jr. *J. Am. Chem. Soc.* **81** (1959) 2620.
9. Sargeson, A. M. In Carlin, R. L., Ed., *Transition Metal Chemistry*, Marcel Dekker, New York 1966, Vol. 3, p. 303.
10. Andersen, P. and Josephsen, J. *Acta Chem. Scand.* **25** (1971) 3255.

# The Systems $K_3AlF_6$—$Li_3AlF_6$ and $Rb_3AlF_6$—$Li_3AlF_6$

## II. The Structure of the Melt

SHAHEER AZIZ MIKHAIEL*

*Institute of Inorganic Chemistry, The Technical University of Norway, Trondheim, Norway*

The phase diagrams of the binary systems $K_3AlF_6 - Li_3AlF_6$ and $Rb_3AlF_6 - Li_3AlF_6$ were used to find a structural model which can explain the equilibrium "solidus-liquidus" of the molten mixtures at either side of each system. From the course of the liquidus line of the $K_3AlF_6$- and the $Li_3AlF_6$-sides of the system $K_3AlF_6 - Li_3AlF_6$ it was found that the melt can be treated as a strictly regular ionic solution. The partial molar excess free energy of mixing can be written as:

$$\Delta \overline{G}_m^{\ E} = -5900(1 - X_{K_3AlF_6})^2 \qquad \text{at the } K_3AlF_6\text{-side}$$
$$\text{and} \quad \Delta \overline{G}_m^{\ E} = -6500(1 - X_{Li_3AlF_6})^2 \qquad \text{at the } Li_3AlF_6\text{-side}$$

where $X$ represents the mol fraction.

For the $Rb_3AlF_6$- and the $Li_3AlF_6$-sides of the system $Rb_3AlF_6 - Li_3AlF_6$ it was found that the melt can also be treated as a strictly regular ionic solution. The partial molar excess free energy of mixing can be written as:

$$\Delta \overline{G}_m^{\ E} = -5500(1 - X_{Rb_3AlF_6})^2 \qquad \text{at the } Rb_3AlF_6\text{-side}$$
$$\text{and} \quad \Delta \overline{G}_m^{\ E} = -6600(1 - X_{Li_3AlF_6})^2 \qquad \text{at the } Li_3AlF_6\text{-side}$$

In part I of this work [1] the two binary systems $K_3AlF_6 - Li_3AlF_6$ and $Rb_3AlF_6 - Li_3AlF_6$ were investigated using differential thermal analysis (DTA), low- and high-temperature X-ray diffraction, and density measurements. One intermediate incongruently melting compound was detected in each system; $K_2LiAlF_6$ at 780°C, and $Rb_2LiAlF_6$ at 700°C. In the first system, $K_3AlF_6 - Li_3AlF_6$, a peritectic point was found at 780°C and 41.5 mol % $Li_3AlF_6$ and a eutectic at 650°C and 75 mol % $Li_3AlF_6$. In the second system, $Rb_3AlF_6 - Li_3AlF_6$, a peritectic point was detected at 700°C and 44 mol % $Li_3AlF_6$ and a eutectic point at 605°C and 71 mol % $Li_3AlF_6$. The aim of this part of the work is to find a certain model which is able to explain the equilibrium "solidus-liquidus" of the molten mixtures of the investigated systems.

---

This model should give the best agreement between the calculated and the experimental results.

In case of a binary mixture of two components A and B, which are completely miscible in the liquid phase and have no solid solubility in each other, the general form of Le Chatelier[2] and Schröder[3] equations holds;

$$\ln a_{\mathrm{A}} = - \frac{\Delta H_{\mathrm{A}}^{\mathrm{f}}}{R} \left( \frac{1}{T_{\mathrm{A}}} - \frac{1}{T_{\mathrm{A}}^{\mathrm{f}}} \right) \tag{1}$$

where  $a_{\mathrm{A}}$  is the activity of A in the mixture,
$\Delta H_{\mathrm{A}}^{\mathrm{f}}$  is the enthalpy of fusion of component A, (taken to be independent of temperature within the interval $T_{\mathrm{A}} - T_{\mathrm{A}}^{\mathrm{f}}$),
$T_{\mathrm{A}}^{\mathrm{f}}$  is the melting point of component A,
$T_{\mathrm{A}}$  is the liquidus temperature, and
$R$  is the gas constant.

The terms $T_{\mathrm{A}}^{\mathrm{f}}$ and $T_{\mathrm{A}}$ are obtained experimentally, and therefore the activity $a_{\mathrm{A}}$ can be calculated, if $\Delta H_{\mathrm{A}}^{\mathrm{f}}$ is known. By knowing the activity, the activity coefficient $\gamma_{\mathrm{A}}$ can be obtained from the expression:

$$a_{\mathrm{A}} = X_{\mathrm{A}} \gamma_{\mathrm{A}} \tag{2}$$

where $X_{\mathrm{A}}$ is the mol fraction of component A.

## DETERMINATION OF AN UNKNOWN ENTHALPY OF FUSION

If data on the enthalpy of fusion, $\Delta H^{\mathrm{f}}$, are not available, an approximate value of it can be obtained from the experimental data of the liquidus line using any of the following methods. (a) The cryoscopic method, which was developed by Darmois[4] as well as by his co-workers Rolin[5] and Petit.[6] (b) The second method was developed and applied by Malinovský.[7] He made use of Schröder's equation in the following way:

In case of a dilute solution, the activity of the component A, $a_{\mathrm{A}}$, will be equal to its mol fraction, $X_{\mathrm{A}}$, which is approximately equal to unity. Schröder's equation can, therefore, be written in the following form:

$$T_{\mathrm{A}} = \mathrm{f}(X_{\mathrm{A}}) = \Delta H_{\mathrm{A}} / (\Delta H / T_{\mathrm{A}} - R \ln X_{\mathrm{A}}) \tag{3}$$

This expression represents the equation of the liquidus curve of the component A. The slope of the curve at any point can be determined by differentiating equation (3) with respect to $X_{\mathrm{A}}$;

$$\frac{\mathrm{d}T_{\mathrm{A}}}{\mathrm{d}X_{\mathrm{A}}} = \frac{\Delta T_{\mathrm{A}}}{\Delta X_{\mathrm{A}}} = \frac{R \Delta H_{\mathrm{A}}^{\mathrm{f}}}{X_{\mathrm{A}} (\Delta H_{\mathrm{A}}^{\mathrm{f}} / T_{\mathrm{A}}^{\mathrm{f}} - R \ln X_{\mathrm{A}})^2} \tag{4}$$

where $\Delta T = T_{\mathrm{A}}^{\mathrm{f}} - T_{\mathrm{A}}$, and $\Delta X_{\mathrm{A}} = 1 - X_{\mathrm{A}}$.

Therefore for the slope, $K_{\mathrm{A}}$, at the melting point of the component A, i.e. when $1 - X_{\mathrm{A}} = 0$, we have:

$$K_A = \lim (dT_A/dX_A)X_A \to 1$$
$$= \lim [\Delta T_A/(1 - X_A)]X_A \to 1$$
$$= (R/\Delta H_A^f)(T_A^f)^2 \tag{5}$$

If the term $\Delta T/(1 - X_A)$ is plotted as a function of $1 - X_A$, the value of $K_A$ is given by the intercept on the ordinate, *i.e.* $\Delta T/(1 - X_A) \to K_A$ when $1 - X_A \to 0$.

Just as for the cryoscopic method, eqn. (5) is valid when one molecule of the added salt B yields only one foreign particle in the melt of pure A. If the number of foreign particles is $r_B$, then;

$$K_A = \frac{R(T_A^f)^2}{\Delta H_A^f} r_B \tag{6}$$

$$\Delta H_A^f = \frac{R(T_A^f)^2}{K_A} r_B \tag{7}$$

## CALCULATION OF THE LIQUIDUS CURVE

*Ideal ionic solution.* In case of ionic melts, the concept "ideal ionic solution", given by Temkin,[8] is found to be very useful. It is successfully applied to different categories of molten systems. In the present investigation we deal with systems where the generally accepted dissociation scheme is as follows:

$$M_3AlF_6 \to 3 \ M^+ + AlF_6^{3-}$$

where $M = Li$, K, or Rb.

According to Temkin, the activity of the compound $M_3AlF_6$ can be written as follows:

$$a_{M_3AlF_6} = N_{M^+}^3 N_{AlF_6^{3-}}$$

where $N_{M^+}$ and $N_{AlF_6^{3-}}$ are the cation and anion fractions, respectively. And since

$$N_{M^+} = \frac{3X}{3X + 3Y} = X$$

and

$$N_{AlF_6^{3-}} = \frac{X + Y}{X + Y} = 1$$

we get for the activity

$$a_{M_3AlF_6} = X^3$$

and likewise

$$a_{R_3AlF_6} = Y^3$$

where $X$ and $Y$ are the mol fractions of $M_3AlF_6$ and $R_3AlF_6$, respectively, $(X + Y = 1)$.

*Regular ionic solution.* The regular ionic solution model assumes that the partial molar Gibbs free energy of mixing, $\Delta \bar{G}_{m,i}$, of component i in the mixture can be expressed as follows:[9]

$$\Delta\overline{G}_{m,i} = RT \ln \gamma_i = b(1 - X_{r,i})^2 \tag{8}$$

where $\gamma_i$ is the activity coefficient of component i in the binary mixture, and is equal to the ratio between the mol fraction of the component i, $X_{ideal} = $ activity $a_i$, which is obtained from the curve of the ideal ionic model at temperature $T$, and the mol fraction of i, $X_{r,i}$, from the experimental curve at the same temperature, $b$ is the interaction parameter.

## RESULTS AND DISCUSSION

### Enthalpies of fusion

The data given by Rolin, Latreille, and Pham [10] for the enthalpy of fusion of $Li_3AlF_6$, $\Delta H^f_{Li_3AlF_6} = 21.5$ kcal/mol, was used in the present calculations.

For $K_3AlF_6$, the only data on the enthalpy of fusion were published by Yoshioka and Kuroda [11] on the basis of the phase diagram of the system $Na_3AlF_6 - K_3AlF_6$. Their result for $\Delta H^f_{K_3AlF_6}$ (44.4 − 44.7 kcal/mol) seems to be unreasonably high, however. By use of the liquidus curve of the system $Li_3AlF_6 - K_3AlF_6$ obtained in the present work, Part 1, and by following the two previously reported procedures, $\Delta H^f_{K_3AlF_6}$ was found to be equal to 38.0 kcal/mol.

As no data on the enthalpy of fusion of $Rb_3AlF_6$ were found in the literature, calculations were made to evaluate it from the present experimental data of the liquidus curve of the system $Li_3AlF_6 - Rb_3AlF_6$.[1] The two previously reported procedures were used to determine $\Delta H^f_{Rb_3AlF_6}$. This was found to be equal to 37.0 kcal/mol.

### A model for the melt

By applying Temkin's model,[8] the calculated curves at both sides of each system were, in general, much higher than the experimental ones. However, the regular ionic solution model was successfully applied and the results can be summarized as follows:

*The system $K_3AlF_6 - Li_3AlF_6$.* (i) *The $Li_3AlF_6$-side.* The calculations, according to the regular ionic solution model, are summarized in Table 1, and

*Table 1.* Calculation of a regular ionic solution model for $Li_3AlF_6$ in the system $Li_3AlF_6 - K_3AlF_6$.

| $T$ K | $X_{id}$ | $X_r$ | $1 - X_r$ | $(1 - X_r)^2$ | $\gamma$ | $-RT \ln \gamma$ | $-b$ |
|---|---|---|---|---|---|---|---|
| 953 | 0.698 | 0.798 | 0.202 | 0.0408 | 0.875 | 252.4 | 6186 |
| 973 | 0.755 | 0.830 | 0.170 | 0.0289 | 0.910 | 182.9 | 6329 |
| 993 | 0.813 | 0.865 | 0.135 | 0.0182 | 0.940 | 122.2 | 6714 |
| 1013 | 0.873 | 0.902 | 0.098 | 0.0096 | 0.968 | 65.8 | 6854 |
| 1033 | 0.935 | 0.944 | 0.056 | 0.0031 | 0.991 | 19.9 | 6322 |
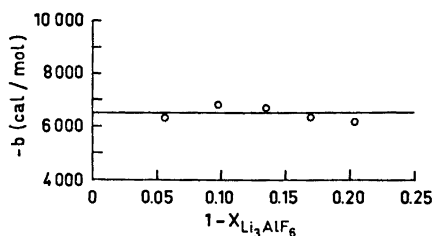
Fig. 1. The interaction parameter $b$ as a function of $1 - X_{Li_3AlF_6}$ on the basis of the phase diagram of the system $Li_3AlF_6 - K_3AlF_6$.
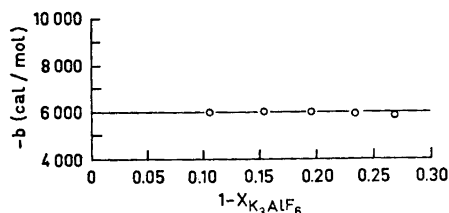
Fig. 2. The interaction parameter $b$ as a function of $1 - X_{K_3AlF_6}$ on the basis of the phase diagram of the system $Li_3AlF_6 - K_3AlF_6$.

the interaction parameter $b$ is presented as a function of $(1 - X_{Li_3AlF_6})$ in Fig. 1. From the figure it appears that $b$ has a constant value of $-6500 \pm 400$ cal/mol, and hence the mixture may be considered as a strictly regular ionic solution, i.e. the partial molar excess free energy of mixing, $\Delta\bar{G}_m^E$, is equal to the partial molar enthalpy of mixing, $\Delta\bar{H}_m$;

$$\Delta\bar{G}_m^E = \Delta\bar{H}_m = -6500(1 - X_{Li_3AlF_6})^2$$

while the partial molar excess entropy of mixing, expressed as:

$$\Delta\bar{S}_m^E = \partial\Delta\bar{G}_m^E/\partial T$$

will be equal to zero.

(ii) *The $K_3AlF_6$-side.* The calculations are summarized in Table 2, and the interaction parameter $b$ is presented as a function of $(1 - X_{K_3AlF_6})$ in Fig. 2. The interaction parameter $b$ was found to be constant and equal to $-5900 \pm 100$ cal/mol. Therefore the mixture may be considered as a strictly regular ionic solution. The partial molar excess free energy of mixing may be expressed as follows:

$$\Delta\bar{G}_m^E = \Delta\bar{H}_m = -5900 \ (1 - X_{K_3AlF_6})^2$$

and $\Delta S_m^E = 0$

Table 2. Calculation of a regular ionic solution model for $K_3AlF_6$ in the system $Li_3AlF_6 - K_3AlF_6$.

| $T$ K | $X_{id}$ | $X_r$ | $1 - X_r$ | $(1 - X_r)^2$ | $\gamma$ | $-RT \ln \gamma$ | $-b$ |
|---|---|---|---|---|---|---|---|
| 1153 | 0.608 | 0.731 | 0.267 | 0.0724 | 0.832 | 421.5 | 5822 |
| 1173 | 0.667 | 0.766 | 0.234 | 0.0548 | 0.871 | 322.0 | 5876 |
| 1193 | 0.730 | 0.804 | 0.196 | 0.0384 | 0.908 | 228.7 | 5956 |
| 1213 | 0.798 | 0.846 | 0.154 | 0.0237 | 0.943 | 141.6 | 5973 |
| 1233 | 0.870 | 0.891 | 0.106 | 0.0112 | 0.973 | 67.1 | 5991 |
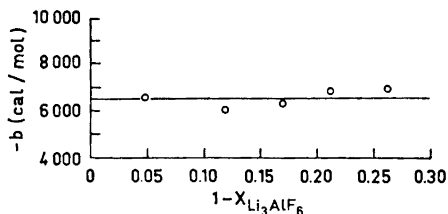
Fig. 3. The interaction parameter $b$ as a function of $1 - X_{Li_3AlF_6}$ on the basis of the phase diagram of the system $Li_3AlF_6 - Rb_3AlF_6$.
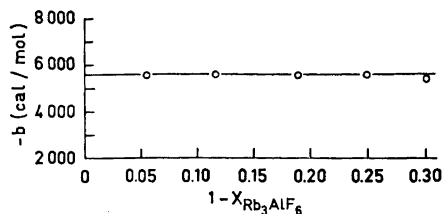
Fig. 4. The interaction parameter $b$ as a function of $1 - X_{Rb_3AlF_6}$ on the basis of the phase diagram of the system $Li_3AlF_6 - Rb_3AlF_6$.

*The system* $Rb_3AlF_6 - Li_3AlF_6$. (i) *The* $Li_3AlF_6$*-side:* Table 3 shows the calculations according to the regular ionic solution model, and Fig. 3 shows the interaction parameter $b$ as a function of $(1 - X_{Li_3AlF_6})$. The interaction parameter $b$ was found to be constant and equal to $-6600 \pm 400$ cal/mol. The mixture may, therefore, be treated as a strictly regular ionic solution. The partial molar excess free energy of mixing can be expressed as:

$$\Delta \overline{G}_m^{E} = \Delta \overline{H}_m = -6600(1 - X_{Li_3AlF_6})^2$$

and $\Delta \overline{S}_m^{E} = 0$

Table 3. Calculation of a regular ionic solution model for $Li_3AlF_6$ in the system $Li_3AlF_6 - Rb_3AlF_6$.

| $T$ K | $X_{id}$ | $X_r$ | $1 - X_r$ | $(1 - X_r)^2$ | $\gamma$ | $-RT \ln \gamma$ | $-b$ |
|---|---|---|---|---|---|---|---|
| 903 | 0.566 | 0.738 | 0.262 | 0.0686 | 0.767 | 475.9 | 6937 |
| 943 | 0.669 | 0.788 | 0.212 | 0.0449 | 0.849 | 306.8 | 6832 |
| 973 | 0.755 | 0.830 | 0.170 | 0.0289 | 0.910 | 182.9 | 6329 |
| 1003 | 0.844 | 0.881 | 0.119 | 0.0142 | 0.958 | 85.4 | 6028 |
| 1033 | 0.935 | 0.942 | 0.048 | 0.0023 | 0.993 | 15.1 | 6574 |

Table 4. Calculation of a regular ionic solution model for $Rb_3AlF_6$ in the system $Li_3AlF_6 - Rb_3AlF_6$.

| $T$ K | $X_{id}$ | $X_r$ | $1 - X_r$ | $(1 - X_r)^2$ | $\gamma$ | $-RT \ln \gamma$ | $-b$ |
|---|---|---|---|---|---|---|---|
| 1073 | 0.547 | 0.698 | 0.302 | 0.0966 | 0.784 | 518.9 | 5372 |
| 1103 | 0.641 | 0.751 | 0.249 | 0.0620 | 0.854 | 345.7 | 5577 |
| 1133 | 0.743 | 0.811 | 0.189 | 0.0357 | 0.918 | 197.5 | 5532 |
| 1163 | 0.856 | 0.884 | 0.116 | 0.0135 | 0.968 | 75.0 | 5573 |
| 1183 | 0.938 | 0.945 | 0.055 | 0.0030 | 0.993 | 16.3 | 5545 |

(ii) *The* $Rb_3AlF_6$-*side*. As in the previous cases, it seems that the mixture can be treated as a strictly regular ionic solution. The results of the calculations are presented in Table 4. Fig. 4 shows the interaction parameter as a function of $(1 - X_{Rb_3AlF_6})$. It is shown that $b$ has a constant value of $-5500 \pm 200$ cal/mol. The expression for the partial molar excess free energy of mixing may be written as:

$$\Delta \bar{G}_m{}^E = \Delta \bar{H}_m = -5500(1 - X_{Rb_3AlF_6})^2$$

and $\Delta \bar{S}_m{}^E = 0$

## REFERENCES

1. Grjotheim, K., Holm, J. L., Malinovský, M. and Mikhaiel, S. A. *Acta Chem. Scand.* **25** (1971) 1695.
2. Le Chatelier, H. *Compt. Rend.* **118** (1894) 638.
3. Schröder, J. *Z. physik. Chem. (Leipzig)* **11** (1893) 449.
4. Darmois, E. *Bull. Soc. Chim. France*, 5ᵉ Serie **17** (1950) 1.
5. Rolin, M. *Rev. Met. (Paris)* **48** (1951) 182.
6. Petit, G. *La cryométrie a haute temperature et ses applications*, Masson et Cie., Paris 1965.
7. Malinovský, M. *Private communication*.
8. Temkin, M *Acta Physicochim. URSS* **20** (1945) 411.
9. Lewis, G. N. and Randall, M. In *Thermodynamics*, McGraw, New York 1961 p. 284.
10. Rolin, M., Latreille, H. and Pham, H. *Bull. Soc. Chim. France* **1969** 2271.
11. Yoshioka, T. and Kuroda, T. *Denki Kagaku* **36** (1968) 797.

# The Primary Structure of Soybean Leghemoglobin

## IV. Fractionation and Sequence of Thermolytic Peptides of the Apoprotein of the Slow Component (Lba)

NILS ELLFOLK and GUNNEL SIEVERS

*Department of Biochemistry, University of Helsinki, SF-00170 Helsinki 17, Finland*

The peptides from the thermolytic digest of the apoprotein of soybean leghemoglobin were fractionated by high voltage paper electrophoresis. Partial sequences of some of these peptides were obtained. Most of the overlap peptides were isolated and it was thus possible to order the tryptic peptides and to propose a unique sequence of the Lba chain.

In the preceding paper[1] we reported that sixteen tryptic peptides[2,3] of the slow component of soybean leghemoglobin (Lba) could be combined into four fragments by studying the chymotryptic peptides. Two of these fragments could be assigned to the $NH_2$- and the COOH-terminal portions of the entire molecule of Lba. No direct evidence on the internal order of the other two fragments was obtained. Their order was decided by the distance between the two histidine residues, which was either 30 or 59 amino acid residues depending on the arrangement of the two fragments. A distance of 28 − 30 amino acid residues between the two hemin binding histidine residues is a general feature of hemoglobins and myoglobins.[4]

Because the specificity of thermolysin is known to differ from that of chymotrypsin, in the present experiments the thermolytic peptides of Lba were isolated in order to obtain direct evidence for the internal arrangement of the two middle fragments mentioned above. Further, it was hoped that the peptides resulting from the thermolytic digestion of Lba would enable us to derive the order of the tryptic peptides unequivocally and independently of the results of the chymotryptic digestion.

## MATERIALS AND METHODS

*Materials.* The apoprotein of the slow component of soybean leghemoglobin (Lba) was prepared as described previously.[5,6] Thermolysin was a crystalline preparation from Merck AG (West Germany). Trypsin was a crystalline chymotrypsin-free preparation

*Abbreviation.* 1-Dimethyl-amino-5-naphthalenesulfonyl-, dansyl-, DNS-.

obtained from Serva AG (Heidelberg, West Germany). Carboxypeptidase A was a crystallized, DFP-treated preparation from Sigma Chemical Company (St Louis, U.S.A.). All other materials were the same as described previously.[2,3]

*Thermolytic digestion.* Digestion of the heat denatured (95°C, 3 min) apoLba was carried out at 37°C in a pH-stat (Radiometer TT1) at pH 8.0. ApoLba was suspended in water at a concentration of 1 %, and dissolved by the addition of 1 N NaOH. Thermolysin (0.5 mg/ml in 0.001 M calcium acetate) was added to give a final concentration of 0.5 % (w/w) and digestion was allowed to proceed for 2 h. A second aliquot of enzyme was then added and digestion was continued for a further hour. The reaction was stopped by lowering the pH to 2.25 by addition of 6 N HCl. The digest was lyophilized.

*Isolation of thermolytic peptides.* The lyophilized digest was dissolved in 5 ml of water and the pH adjusted to 5 with 1 N NaOH. In contrast to the isolation of the tryptic and chymotryptic peptides, the thermolytic peptides were purified on high voltage paper electrophoresis at pH 6.5, 3.5, 1.9, and 8.9 as described previously.[2,3] A butanol – acetic acid – water (4:1:5) system was used for the paper chromatography.

*Amino acid analysis.* Quantitative and qualitative amino acid analyses were performed as described earlier.[2]

*Determination of $NH_2$-terminus and sequence.* The $NH_2$-terminal residues of the peptides were determined by the dansyl procedure and the derivatives identified by electrophoresis and chromatography, as described in the preceding paper.[1] Dansyl- and subtractive-Edman procedures, performed as described before,[3] were used to obtain the sequence. Some of the thermolytic peptides containing lysine were hydrolyzed with trypsin as described earlier.[1] Hydrolysis with carboxypeptidase A was performed as described previously.[3]

*Amide residues.* Amide residues were assigned according to Offord on the basis of electrophoretic mobilities of the peptides at pH 6.5.[7]

*Nomenclature of thermolytic peptides.* The principles employed for numbering the peptides were identical with those used previously.[2] The thermolytic peptides are represented by the letters Th followed by a number indicating their order from the anode on electrophoresis. *a* before Th indicates Lba.

## RESULTS AND DISCUSSION

The peptides from the thermolytic digestion of Lba were separated by repeated high voltage paper electrophoresis at different pH-values. Peptides found homogeneous on electrophoresis and chromatography in the butanol-acetic acid-water system were subjected to quantitative amino acid analysis with the results given in Table 1. Partial sequences were determined for some of these peptides by Edman degradation. These results are summarized in Table 2. For the sake of brevity, the data obtained after the application of only one or two steps of dansyl-Edman degradation have been omitted.

It was recently found[1] that the tryptic peptides could be arranged into four fragments by the overlap peptides from a chymotryptic digestion. The sequences of the thermolytic overlap peptides, combining these fragments in an unequivocal fashion, is given below.

*Peptide aTh21.* Dansylation showed phenylalanine to be the $NH_2$-terminal residue (Table 3). Two fragments, T1 and T2, were obtained on hydrolysis with trypsin. They were isolated by electrophoresis at pH 6.5 and their amino acid content is given in Table 3. Five steps of Edman degradation and digestion with carboxypeptidase A showed T1 to have the sequence *Ala-Asn-Ile-Pro-Gln-Tyr-Ser*, which is compatible with the $NH_2$-terminal sequence of the tryptic peptide *a*T18. $NH_2$-terminal analysis on T2 established the sequence *Phe-Lys*, representing the unique COOH-terminal sequence of the tryptic peptide *a*T13. *a*Th21, therefore provides, the overlap joining *a*T13 to *a*T18.

*Table 1.* Amino acid compositions of the thermolytic peptides of the slow component not corrected for losses of amino

| Amino acid | aTh1 | aTh2 | aTh3 | aTh4 | aTh5 | aTh6 | aTh7 |
|---|---|---|---|---|---|---|---|
| Aspartic acid | 1.05 | 1.10 | | 2.11 | 1.15 | 1.05 | 2.06 |
| Threonine | | | | | 0.80 | 0.94 | |
| Serine | | | | 0.90 | | | 1.81 |
| Glutamic acid | 1.07 | 1.17 | 1.08 | 1.09 | 2.03 | 2.23 | 1.41 |
| Proline | | | | | | | |
| Glycine | | | | 1.00 | | | 0.94 |
| Alanine | 1.01 | 1.90 | 1.00 | 0.92 | 1.08 | 1.00 | 1.81 |
| Valine | 1.00 | 0.96 | | 0.98 | | | 0.91 |
| Isoleucine | | | | | | | |
| Leucine | | 0.87 | | | | | 1.05 |
| Tyrosine | 0.87 | 0.32 | | | | | |
| Phenylalanine | | | 0.92 | | | 0.89 | |
| Tryptophan | | | | +[a] | | | +[a] |
| Lysine | | | | 1.01 | 0.94 | 0.89 | 1.17 |
| Histidine | | | | | | | |
| Arginine | | | | | | | 0.79 |
| No. of residues | 5 | 7 | 3 | 9 | 6 | 7 | 13 |
| $\dfrac{E_{Lys}}{E_{Asp}}$ | 0.63 | 0.57 | 0.50 | 0.42 | 0.28 | 0.28 | 0.28 |

[a] Positive Ehrlich reaction on paper.

| Amino acid | aTh14 | aTh15 | aTh16 | aTh17 | aTh18 | aTh19 |
|---|---|---|---|---|---|---|
| Aspartic acid | 1.15 | | | | | |
| Threonine | | 0.87 | | | | |
| Serine | 0.96 | 0.98 | | | | |
| Glutamic acid | 1.05 | 1.11 | | 0.93 | | |
| Proline | | 0.93 | | | | |
| Glycine | 1.03 | | | | | |
| Alanine | 1.03 | 1.16 | 2.96 | 0.85 | 1.07 | 1.03 |
| Valine | 0.97 | | | 1.44 | 0.93 | |
| Isoleucine | | 0.89 | | | | |
| Leucine | 0.88 | 0.99 | 1.01 | 1.03 | | 1.90 |
| Tyrosine | | | | | | |
| Phenylalanine | | | | | | 1.00 |
| Tryptophan | | | | | | |
| Lysine | | 1.05 | | 1.00 | | |
| Histidine | | | | | | |
| Arginine | 0.93 | | | | | |
| No. of residues | 8 | 8 | 4 | 6 | 2 | 4 |
| $\dfrac{E_{Lys}}{E_{Asp}}$ | neutr. | neutr. | neutr. | neutr. | neutr. | neutr. |

(Lba) of soybean leghemoglobin. The values given in the table are mol ratios and are
acids during hydrolysis.

| | aTh8 | aTh9 | aTh10 | aTh11 | aTh12 | aTh13 |
|---|---|---|---|---|---|---|
| | | | 3.39 | | | |
| | | | 1.06 | 1.09 | 1.08 | |
| | | 0.98 | | 1.05 | | 1.08 |
| | | | 1.82 | | | |
| | | | 1.10 | | 1.04 | 0.99 |
| | | | 1.07 | | | |
| | 1.21[b] | | 0.82 | | | |
| | | 1.00 | 0.76 | | 0.88 | 0.93 |
| | 0.88 | | | 0.86 | | |
| | 1.00 | 2.00 | | | | |
| | | | 0.98 | | | |
| | 4 | 4 | 11 | 3 | 3 | 3 |
| | neutr. | neutr. | neutr. | neutr. | neutr. | neutr. |

[b] 70 h hydrolysis gives two valines.

| aTh20 | aTh21 | aTh22 | aTh23 | aTh24 | aTh25 | aTh26 | aTh27 |
|---|---|---|---|---|---|---|---|
| 1.00 | 1.05 | | | | | | |
| | | 0.87 | 0.98 | | 1.00 | | |
| | 0.97 | | 1.06 | | | | |
| | 1.06 | 1.04 | | | | 1.16 | |
| | 0.84 | | | | | | |
| | | 1.09 | 1.04 | | | | |
| 2.00 | 1.14 | 1.12 | 1.03 | 2.10 | | 1.96 | 1.05 |
| | | | | | | 1.01 | |
| | 1.06 | | | 0.83 | | | 0.90 |
| | | 0.87 | 0.91 | | 2.00 | | |
| | 0.91 | | | | | | |
| | 0.96 | | | | | | |
| 1.08 | 1.03 | 1.02 | 0.98 | 1.08 | 1.25 | 1.30 | 2.05 |
| | | 0.64 | | | | 1.03 | |
| 4 | 9 | 7 | 6 | 4 | 4 | 6 | 4 |
| 0.04 | 0.28 | 0.28 | 0.44 | 0.44 | 0.44 | 0.68 | 0.90 |

*Table 2.* Deduced amino acid sequences of the thermolytic peptides from the slow component (Lb*a*) of soybean leghemoglobin.

| Peptide number | Amino acid sequence |
| --- | --- |
| *a*Th1 | Val-(Ala,Tyr,Asp,Glu) |
| *a*Th2 | Val-Ala-(Tyr,Asp,Glu,Leu,Ala) |
| *a*Th3 | Phe-(Glu,Ala) |
| *a*Th4 | Ala-Val-(Gly,Asp,Lys,Trp,Ser,Asp,Glu) |
| *a*Th5 | Thr-(Glu,Lys,Gln,Asp,Ala) |
| *a*Th6 | Phe-(Thr,Glu,Lys,Gln,Asp,Ala) |
| *a*Th7 | Ala-(Val,Gly,Asp,Lys,Trp,Ser,Asp,Glu,Leu,Ser,Arg,Ala) |
| *a*Th8 | Val-Val-Phe-Tyr |
| *a*Th9 | Leu-Phe-Ser-Phe |
| *a*Th10 | Leu-(Ala,Asn,Pro,Thr,Asp,Gly,Val,Asn,Pro,Lys) |
| *a*Th11 | Tyr-Thr-Ser |
| *a*Th12 | Leu-(Thr,Gly) |
| *a*Th13 | Leu-Gly-Ser |
| *a*Th14 | Leu-Val-(Arg,Asp,Ser,Ala,Gly,Gln) |
| *a*Th15 | Thr-(Ser,Ile,Leu,Glu,Lys,Ala,Pro) |
| *a*Th16 | Leu-Ala-Ala-Ala |
| *a*Th17 | Val-(Val,Lys,Glu,Ala,Leu) |
| *a*Th18 | Val-Ala |
| *a*Th19 | Leu-(Phe,Ala,Leu), |
| *a*Th20 | Ala-(Ala,Lys,Asp) |
| *a*Th21 | Phe-Lys-Ala-Asn-Ile-Pro-Gln-Tyr-Ser |
| *a*Th22 | Leu-(Thr,Gly,His,Ala,Glu,Lys) |
| *a*Th23 | Leu-Lys-Ala-(Ser,Gly,Thr) |
| *a*Th24 | Ile-(Lys-Ala-Ala) |
| *a*Th25 | Leu-Leu-Lys-Thr |
| *a*Th26 | Val-(His,Ala,Gln,Lys,Ala) |
| *a*Th27 | Ile-Lys-(Ala,Lys) |

*Table 3.* Amino acid sequence of peptide *a*Th21.

| Sequence *a*Th21 | Phe-Lys-Ala-Asn-Ile-Pro-Gln-Tyr-Ser |
| --- | --- |
| | \|—T2—\|——————————T1——————\| |
| Dansylation | DNS-Phe |
| Tryptic peptides | |
| T1 | Ala, 0.97; Asp, 1.00; Ile, 0.99; Pro, 1.03; Glu, 1.07; |
| (neutral) | Tyr, 0.60; Ser, 0.95 |
| Edman degradation | |
| Step 1 | *Ala, 0.00*  Asp, 1.03; Ile,0.98; Pro, 0.97; Glu, 1.10; Tyr, 0,97; Ser,0.95 |
| Step 2 | *Asp, 0.21*  Ile, 0.91;  Pro, 1.18; Glu; 1.04; Tyr, 0.89; Ser, 0.98 |
| Step 3 | *Ile, 0,32*  Pro, 1.03; Glu, 1.08; Tyr, 0.89; Ser, 1.01 |
| Step 4 | *Pro, 0.63*  Glu, 1.07; Tyr, 0.91; Ser, 1.02 |
| Step 5 | *Glu, 0.62*  Tyr, 0.83; Ser, 1.02 |
| Carboxypeptidase A 15 min | Ser, 1.00; Tyr,0.76 |
| T2 ($E_{Lys}$, 0.64) | Phe, 0.80; Lys, 1.14 |
| Dansylation | DNS-Phe |

*Peptide aTh23.* Leucine was found to be the $NH_2$-terminal amino acid residue. Digestion of aTh23 with trypsin yielded two fragments, T1 and T2, which were isolated by electrophoresis at pH 6.5. Their amino acid composition is given in Table 4. The sequence of T1, *Ala-(Ser,Gly,Thr)*, is compatible with the $NH_2$-terminal sequence of the tryptic peptide aT6. The sequence of T2 was found to be *Leu-Lys*, which represents the COOH-terminal sequence of peptide aT9 as well as that of aT10. Since aT10 is linked to aT5 (peptide aTh25), aTh23 provides the overlap linking aT9 to aT6.

Table 4. Amino acid sequences of peptides aTh23 and aTh25.

| Sequence aTh23 | Leu-Lys-Ala-[Ser,Gly,Thr] |
| | \|—T2—\|———T1———\| |
| Dansylation | DNS-Leu |
| Tryptic peptides | |
| T1 | Ala, 1.05; Ser, 1.00; Gly, 0.93; Thr, 1.02 |
| (neutral) | |
| Dansylation | DNS-Ala |
| T2 | Leu, 1.07; Lys, 0.93 |
| ($E_{Lys}$, 0.70) | |
| Dansylation | DNS-Leu |
| Sequence aTh25 | Leu-Leu-Lys-Thr |
| | \|———T2———\|—T1- |
| Dansylation | DNS-Leu |
| Tryptic peptides | |
| T1 | Thr, 1.00 |
| (neutral) | |
| T2 | Leu, 1.98; Lys, 1.02 |
| ($E_{Lys}$, 0.58) | |

*Peptide aTh25.* Leucine was established as the $NH_2$-terminal amino acid residue (Table 4). Tryptic digestion of aTh25 yielded two fragments, T1 and T2, which were electrophoretically separated at pH 6.5. T1 was found to be threonine, the $NH_2$-terminus of the tryptic peptide aT5. The sequence of T2 is concluded to be *Leu-Leu-Lys*, the unique $NH_2$-terminal sequence of the tryptic peptide aT10. aTh25, therefore, provides the overlap joining aT10 to aT5.

Because the sequences of the tryptic peptides of Lba have already been established the sequences of the thermolytic peptides could be evaluated from their amino acid composition and from their $NH_2$-terminal analyses. Consequently, we were able to decide in an unequivocal fashion which tryptic peptides were connected to each other in the original Lba chain (Fig. 1).

These results confirm the order of the tryptic peptides which was deduced from the chymotryptic peptides, and also show that no fragment was neglected during the isolation of tryptic peptides.

```
————————————T12————————|———————————————T13———————————————|————
NH₂-Val-Ala-Phe-Thr-Glu-Lys-Gln-Asp-Ala-Leu-Val-Ser-Ser-Ser-Phe-Glu-Ala-Phe-Lys-Ala-Asn
|————Th18—|———————————T6h———————————|          |————Th3————|————
              |—————————Th5—————————|
```

```
————————————————————T18————————————————————|————T2————|————
Ile-Pro-Gln-Tyr-Ser-Val-Val-Phe-Tyr-Thr-Ser-Ile-Leu-Glu-Lys-Ala-Pro-Ala-Ala-Lys-Asp-Leu-
—Th21————————————|————Th8———|——————————Th15—————————|————Th20—|———
                       |———Th11—|
```

```
————————————————T14————————————————————|————————T11—————————|——
Phe-Ser-Phe-Leu-Ala-Asn-Pro-Thr-Asp-Gly-Val-Asn-Pro-Lys-Leu-Thr-Gly-His-Ala-Glu-Lys-Leu·
————Th9———|———————————————Th10———————————————|————————Th22————————|———
                                             |————Th12————|
```

```
————————T3————————|————————T9—————————|———————————————————————T6-
Phe-Ala-Leu-Val-Arg-Asp-Ser-Ala-Gly-Gln-Leu-Lys-Ala-Ser-Gly-Thr-Val-Val-Ala-Asp-Ala-Ala-
        |——————————Th14——————————|——————Th23————|
——Th19—|
```

```
———————————————————————|————————————T7————————————|—————————T10-
Leu-Gly-Ser-Val-His-Ala-Gln-Lys-Ala-Val-Thr-Asn-Pro-Glu-Phe-Val-Val-Lys-Glu-Ala-Leu-Leu-
|— Th13—|——————————Th26——————|                    |————————Th17————|
                                                                   |———————
```

```
——|—— T5——|————————T8—————————|————————T16————————|———————————————
Lys-Thr-Ile-Lys-Ala-Ala-Val-Gly-Asp-Lys-Trp-Ser-Asp-Glu-Leu-Ser-Arg-Ala-Trp-Glu-Val-Ala-
—Th25—|        |——————————————————Th7——————————|            |——
       |       |——————————Th4——————|
       |———Th24——|
————T17—————————————————————|————T4——|
Tyr-Asp-Glu-Leu-Ala-Ala-Ala-Ile-Lys-Ala-Lys-COOH
——Th1——|————————Th16—|————Th27————|
————————Th2————|
```

*Fig. 1.* The amino acid sequence of soybean leghemoglobin *a*. The tryptic peptides (T) are shown above the sequence and the thermolytic peptides (Th) below it.

## REFERENCES

1. Ellfolk, N. and Sievers, G. *Acta Chem. Scand.* **27** (1973) 3817.
2. Ellfolk, N. and Sievers, G. *Acta Chem. Scand.* **26** (1972) 1155.
3. Ellfolk, N. and Sievers, G. *Acta Chem. Scand.* **27** (1973) 3371.
4. Dayhoff, M. O., Ed., *Atlas of Protein Sequence and Structure* **5** (1972).
5. Ellfolk, N. *Acta Chem. Scand.* **14** (1960) 609.
6. Ellfolk, N. *Acta Chem. Scand.* **16** (1962) 831.
7. Offord, R. E. *Nature* **211** (1966) 591.

Received June 28, 1973.

# The NMR Spectrum of a Conjugated Aldehyde:
# Sorbaldehyde

P. ALBRIKTSEN[a] and R. K. HARRIS[b]

[a] *Chemical Institute, University of Bergen, N-5000 Bergen, Norway and*
[b] *School of Chemical Sciences, University of East Anglia, Norwich NOR 88C, England*

The NMR spectrum of *trans*-sorbaldehyde has been fully analysed and is consistent with an all-*trans*-conformation. Coupling constants to the aldehyde proton are measurable for up to four bonds between the coupled nuclei, and there is some indication of more extensive coupling. The coupling constants to the methyl group are measurable for nuclei separated by up to six bonds. The values of the coupling constant are discussed in relation to those for acroleins and for *trans*-penta- and hexa-dienes.

Several NMR investigations of $\alpha$-$\beta$-unsaturated aldehydes have been reported.[1-4] Hoffman and Gronowitz[1] analysed the NMR spectrum of crotonaldehyde in order to explain the long-range coupling mechanism in unsaturated compounds. Moreover, the NMR analysis of acrolein has been published twice.[2,3] Klinck and Stothers[4] reported the chemical shift of the formyl proton in various aldehydes. Benzene-induced solvent shifts[5] have been used as an aid to the determination of stereochemistry for some $\alpha$,$\beta$-unsaturated compounds. Crotonic acid derivatives,[6] *trans*-2,4-pentadienoic acid,[7] and *trans*-2,4-hexadienoic esters[8] have been analysed in detail by NMR. No highly conjugated aldehydes have, however, been completely analysed by NMR. This is partly because the unsaturated aldehydes are reactive and hence it is difficult to obtain spectra of the monomers, and partly because of the number of coupled protons in the molecules. The *trans*-sorbaldehyde studied in this work has eight coupled nuclei, which is too large a spin system for many computers programs to handle. This investigation was undertaken to obtain information about configuration and long-range (H,H) coupling constants in highly unsaturated aldehydes. It is of special interest to compare the NMR parameters obtained with those found for buta- and penta-dienes.[9]

## EXPERIMENTAL

The 2,4-hexadienal, sorbaldehyde, was commercially available from Aldrich. The NMR spectrum of this compound showed two doublets in the aldehyde region with

intensities in the ratio *ca.* 1:20. The sorbaldehyde was purified by the following procedure: The crude mixture was cooled to *ca.* − 60°C, transferred to a pre-cooled filter funnel and allowed to warm up to *ca.* − 40°C. The mixture was then cooled to − 60°C again. The non-crystalline compounds or isomers were continuously sucked off. The cooling and heating cycle was repeated three times. The crystalline compound was allowed to melt and was collected. The NMR spectrum showed only one CHO doublet, which was taken as evidence of isomeric purity. The purified sorbaldehyde was assumed to be the all-*trans* isomer (see Fig. 1), as this isomer should show the higher melting point; this is confirmed by the NMR spectral analysis.

The sorbaldehyde (neat liquid) was introduced into a 5 mm O. D. sample tube, and a small quantity of TMS was added to serve as NMR locking and reference substance. The sample was degassed by the freeze, pump, thaw technique and sealed in the evacuated condition.

The spectra were recorded using a Varian Associates HA-100 spectrometer operating at 100 MHz. The spectra were recorded at ambient temperature (*ca.* 35°C) in the field-frequency lock mode with frequency sweep. The spectra for detailed measurement were recorded at 50 Hz sweep width and scan rate 0.02 Hz s$^{-1}$; they were calibrated every 5 Hz using a Hewlett-Packard 5212A frequency counter.

The computations were carried out using the IBM 360/50 computer at the University of Bergen and, in part, the Atlas Computer at the Science Research Council Atlas Laboratory, Chilton, Didcot, England. The results were plotted with a Calcomp Plotter.

## SPECTRAL ANALYSIS

The NMR spectrum of the all-*trans* sorbaldehyde gave well-separated bands for each of the nuclei involved except for protons A and B. The spectrum is therefore of the ABKMXY$_3$ type (see Fig. 1), with only one pair, AB, of
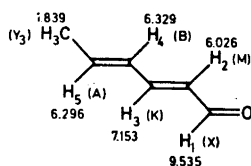


*Fig. 1. trans*-Sorbaldehyde: Notation, and chemical shifts in ppm from TMS.

tightly-coupled nuclei. Considerable second-order splittings were, however, observed. The high frequency doublet is easily assigned to the aldehyde proton, and the low-frequency band (Fig. 2) to the CH$_3$-group. The olefinic nuclei, with $\delta \sim 5.8$ to 7.5, can be assigned as follows: Assuming negligible or small coupling between the proton K and protons X or Y$_3$ and with the M nucleus in either the $\alpha$ or $\beta$ spin state, the spectrum of nucleus K should resemble the K part of an ABK spin system. In fact, the high frequency multiplet of the olefinic region looks like the K part of two ABK spin systems (Fig. 3). Therefore this multiplet is assigned to H$_K$, the separation of the two sub-spectra being $^3J_t$, *ca.* 15 Hz. The separation of certain strong pairs of lines in these abk-subspectra arising from H$_K$ gives an estimate of $|J_{AK} + J_{BK}| \simeq 10$ Hz. Moreover, each line in the K multiplet (Fig. 3) is further split due to the aldehyde proton and the methyl group. The low-frequency part of the olefinic signals (Fig. 4), a doublet of doublets with splittings of *ca.* 7.9 Hz and 15.3 Hz, is assigned to H$_M$ with coupling constants $J_{KM} \simeq 7.9$ Hz and $J_{KM} \simeq 15.3$ Hz. Each signal is further split into a complex pattern due to long-range coupling. The remaining signals are assigned to H$_A$ and H$_B$ (Fig. 5).
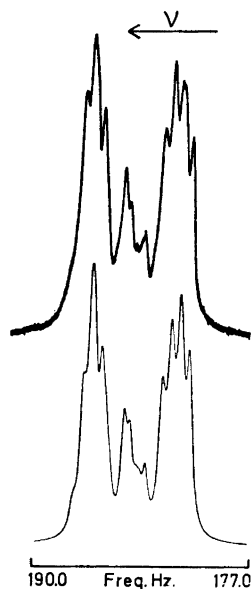
*Fig. 2.* Spectrum of the methyl protons: Upper, observed spectrum; lower, spectrum computed with the parameters of Table 1, with a linewidth of 0.2 Hz.
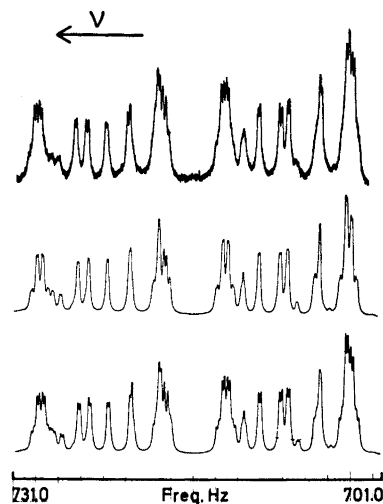
*Fig. 3.* Spectrum of $H_K$: Upper, observed spectrum; middle, spectrum computed with the parameters obtained from the iterative computations, *i.e.* $^4J_{KX} = -0.19$ Hz; lower, spectrum computed with the parameters of Table 1, *i.e.* with the parameters obtained from the iterative calculations apart from $^4J_{KX}$, which is changed to $-0.25$ Hz. The linewidth of the computed spectra is 0.2 Hz.

The coupling constants (Table 1) and chemical shifts (Fig. 1) were obtained using a modified version [10] of LAOCN3 [11] which accommodates eight spins. The final RMS error was 0.068 when 20 parameters were allowed to vary. The computed probable errors on the coupling constants are 0.01 to 0.02 Hz when 325 computed transitions were fitted to 125 observed lines. The figures show a good correlation between the theoretical spectrum, obtained for the parameters of Table 1, and the experimental spectrum. A better visual fit of

*Table 1.* Coupling constants for sorbaldehyde.[a,b,c,d]

| | | |
|---|---|---|
| $^3J_s(M,X) = 7.96$ Hz | $^4J_c(B,M) = -0.72$ Hz | $^3J(A,Y) = 6.89$ Hz |
| $^3J_s(B,K) = 10.96$ Hz | $^4J_c(A,K) = -9.92$ Hz | $^4J_c'(B,Y) = -1.55$ Hz |
| $^3J_t(K,M) = 15.34$ Hz | $^4J_c(K,X) = -0.25$ Hz[e] | $^5J_t'(K,Y) = 0.48$ Hz |
| $^3J_t(A,B) = 15.23$ Hz | $^5J_{cc}(A,M) = 0.66$ Hz | $^6J_{ct}'(M,Y) = -0.67$ Hz |

[a] Errors in the coupling constants are estimated to be $\pm 0.08$ Hz. [b] See Fig. 1. [c] $^5J(B,X)$, $^6J(A,X)$, and $^7J(X,Y)$ are all unobservable ($\leq 0.1$ Hz). [d] For the notation see Ref. 9. [e] The value obtained during the iterative calculation was $^4J_c = -0.19$ Hz (see the text and Fig. 3).
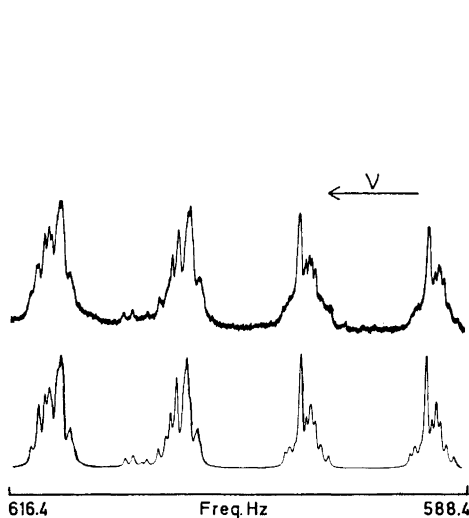
Fig. 4. Spectrum of $H_M$: Upper, experimental spectrum; lower, spectrum computed with the parameters if Table 1, with a linewidth of 0.2 Hz.
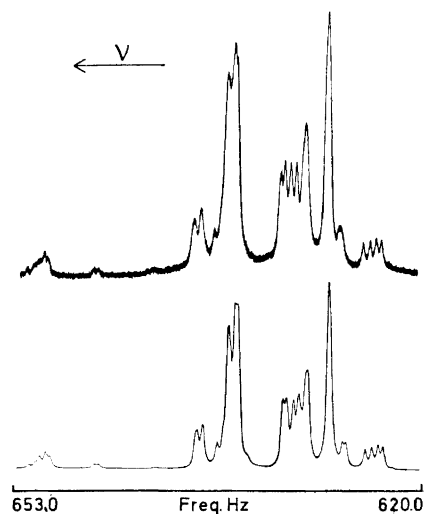
Fig. 5. Spectrum of $H_A$ and $H_B$: Upper, experimental spectrum; lower, spectrum computed with the parameters of Table 1, with a linewidth of 0.4 Hz.

observed and calculated spectra was obtained for $H_K$ (Fig. 3) with the value of $-0.25$ Hz for $^4J_{KX}$ instead of the value, $-0.19$ Hz, obtained during the iterative calculations.

## RESULTS AND DISCUSSION

The data for *trans*-sorbaldehyde (Table 1) are consistent with an all-*trans* configuration and an all-*trans* conformation of the molecule. It is unlikely that there is a significant population of other conformations. This statement is based on a comparison of the coupling constants with those for butadiene and acrolein derivatives. In making comparisons of coupling constants (see below) we have restricted our choice of model compounds to cases without steric hindrance, *i.e.* to molecules with all-*trans* configurations and with no side-chains. The chemical shifts for sorbaldehyde (Fig. 1) are unremarkable and in view of uncertainty due to solvent and concentration effects, we do not propose to make quantitative conclusions from the available data. Certain trends are, however, apparent. The chemical shift of the aldehyde proton, $\delta = 9.535$, lies within the range found for other conjugated aldehydes [2,3,12] (9.48 to 9.58 ppm). The *trans*-terminal methyl group is little affected ($< 0.2$ ppm) by the interposition of a $C = C$ double bond. The effect of a $C = O$ group on the olefinic protons shows the same trend as observed for acroleins, with the $\alpha$-proton shifted to low frequency and the *cis*-$\beta$-proton shifted to high frequency as compared to the remaining olefinic protons of the sorbaldehyde.

*Table 2.* Coupling constants for *trans*-substituted acroleins, $XCH=CH-CHO$.

| Molecule | X | $^3J_s$/Hz | $^4J_c$/Hz | Reference |
|---|---|---|---|---|
| Sorbaldehyde | a | 7.96 | −0.25 | this work |
| Acrolein | H | 7.49 to 8.11[b] | c | 3 |
| Crotonaldehyde | Me | 7.57<br>7.61 to 7.85[b] | −0.25<br>(−)0.32 | 2<br>12 |
| Cinnamaldehyde | Ph | 7.5<br>7.17 to 7.90[b] | −0.3<br>d | 13<br>12 |
| 2-Furylacrolein | e | 7.7 ± 0.1 | 0.0 ± 0.1 | 14 |
| 2-Thienylacrolein | f | 7.43 ± 0.1 | −0.11 ± 0.1 | 15 |
| 4-Ketohex-2-enal | COEt | 7.14 | 0.04 | 16 |
| N,N-Dimethylamino-<br>propenal | NMe₂ | 7.26 to 7.72[b] | c | 17 |
| Ethoxyacrolein | OEt | 8.12 | c | 18 |

*a* See Fig. 1. *b* Solvent and temperature dependent. *c* Not relevant to the present discussion. *d* Not obtained. *e* Structure I. *f* Structure II.



I                                        II
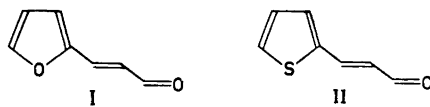
The value of $^3J_s$ to the aldehyde proton (7.96 Hz) lies within the rather narrow range (7.1 to 8.2 Hz) found for other *trans-β*-substituted acroleins, $X-CH=CH-CHO$, for which results are quoted in Table 2. There are several possible influences on $^3J_s$ in this series of compounds:

(i) Direct substituent effects; these appear to be small, presumably because the site of substitution is fairly remote from the coupled protons.

(ii) The effect of extended conjugation. This would be expected to influence principally the π-contributions to coupling (though the σ-contribution may be affected indirectly if the C−C formal single bond is changed in length). Cunliffe, Grinter and Harris[19] have presented theoretical results for $^3J_s$ in the butadiene-hexatriene-octatetraene series which suggest the effects of extended conjugation are small ( ≤ 0.2 Hz). In any case several of the values quoted above for acrolein derivatives are for compounds where extended conjugation is possible; there is no indication that this has a marked effect.

(iii) Rotational isomerism about the $C_1-C_2$ bond. It is possible that sorbaldehyde contains small amounts of *s-cis* or *s-gauche* forms. It has been estimated from a microwave study[20] that at 30°C acrolein may contain about 3 % of the *s-cis* form, and that there is an energy difference of about 10 kJ mol⁻¹ between the *s-cis* and *s-trans* isomers. The effect of isomerism on the NMR spectrum of acrolein has been investigated by Davies.[3] He tentatively attributed the small increase of $^3J_s$ as temperature decreased to the increased proportion of the predominant *s-trans* form. Similar comments have been made for cinnamaldehyde and crotonaldehyde.[12] The influence of isomerism has been

*Table 3.* Coupling constants for *trans,trans*-disubstituted butadienes, $XCH = CH - CH = CHY$.

| Molecule | X | Y | | $^3J_s$/Hz | $^4J_c$/Hz | $^5J_{cc}$/Hz | Reference |
|---|---|---|---|---|---|---|---|
| Sorbaldehyde | Me | CHO | | 10.96 | $-0.92^a$ | 0.66 | this work |
| | | | | | $-0.72^b$ | | |
| Methyl sorbate | Me | $CO_2Me$ | | 10.5 | $c$ | $c$ | 24 |
| Hexadiene | Me | Me | | 10.30 | $-0.84$ | 0.68 | 9 |
| Muconates | $CO_2R$ | $CO_2R$ | R = H | 11.7 | $-0.71$ | $\sim 0.5$ | 25 |
| | | | R = Me | 11.4 | $-0.7$ | 0.8 | 8 |
| | | | R = Et | 11.3 | $-0.8$ | 0.8 | 8 |
| | | | R = t-Bu | 11.5 | $-0.8$ | 0.7 | 8 |
| Diphenylbutadiene | Ph | Ph | | 10.80 | $-0.94$ | 0.90 | 26 |
| Dicyanobutadiene | CN | CN | | $10.3^d$ | $-1.0$ | 1.4 | 27 |
| | | | | $11.1^e$ | $-0.7$ | 0.9 | 8 |
| | | | | $11.11^f$ | $-0.64$ | 0.81 | 28 |
| Pentadiene | Me | H | | 10.30 | $-0.78^a$ | $g$ | 9 |
| | | | | 10.33 to $10.52^h$ | $-0.77$ to | | |
| | | | | | $-0.80^{a,h}$ | $g$ | 29 |
| t-Butylbutadiene | t-Bu | H | | 10.16 | $-0.78^a$ | $g$ | 29 |
| 2,4-Pentadienoic acid | $CO_2H$ | H | | 11.05 | $-0.71^a$ | $g$ | 7 |
| Butadiene | H | H | | 10.41 | $g$ | $g$ | 30 |
| | | | | 10.20 to $10.65^h$ | $g$ | $g$ | 29 |
| Methoxybutadiene | OMe | H | | 10.49 to $10.57^h$ | $g$ | $g$ | 31 |
| Dichlorobutadiene | Cl | Cl | | 11.24 | $g$ | $g$ | 32 |

$^a$ $^4J_c$ for the group $XCH = CH - CH$. $^b$ $^4J_c$ for the group $CH - CH = CHY$. $^c$ Not given. $^d$ $CDCl_3$ solution. $^e$ MeCN solution. $^f$ $Me_2SO$ solution. $^g$ Not relevant to the present discussion. $^h$ Solvent- and/or temperature-dependent.

*Table 4.* Coupling constants involving the methyl protons for sorbaldehyde and related compounds.

| Compound | $^3J'$/Hz | $^4J_c'$/Hz | $^5J_t'$/Hz | $^6J_{ct}'$/Hz | Reference |
|---|---|---|---|---|---|
| Sorbaldehyde | 6.89 | $-1.55$ | 0.48 | $-0.67$ | this work |
| Pentadiene | 6.69 | $-1.70$ | 0.45 | $-0.76$ | 9 |
| | 6.58 to $6.71^a$ | $-1.61$ to $-1.66^a$ | 0.37 to $0.46^a$ | $-0.69$ to $-0.70^a$ | 29 |
| Hexadiene | 6.84 | $-1.71$ | 0.42 | $-0.84$ | 9 |
| Methyl sorbate | 6.5 | $-1.6$ | $b$ | $b$ | 24 |

$^a$ Solvent-and/or temperature-dependent. $^b$ Not given.

discussed for the butadiene series by Bothner-By and Moser.[21] Kozerski and Dabrowski[22] have shown by direct NMR measurement of spectra showing separate bands for *s-cis* and *s-trans* isomers of protonated $N,N$-dimethyl-aminopropenal that this compound exists to 86 % in the *s-trans* form. In so far as our result for $^3J_s$ to the aldehyde proton of sorbaldehyde is on the high side for such compounds it may be assumed that the compound is predominantly *s-trans*. Rotational isomerism about the $C_3 - C_4$ bond will affect $^3J_s$ (M,X) much less than $^3J_s$(B,K); see below.

(iv) *Molecular deformations.* For the butadiene series these have been discussed theoretically by Bacon and Maciel [23] and from experimental results by Albriktsen, Cunliffe and Harris.[9] There is no suggestion of appreciable effects of this type for *trans*-substituted systems.

Reported values of $^3J_s$ across the central single bond of all-*trans* 1,3-dienes (see Table 3) also fall in a narrow range (10.1 to 11.7 Hz); our result for sorbaldehyde (10.96 Hz) is in the middle of this range. The influences of extended conjugation and substituent electronegativity are clearly not large and are difficult to analyse in any detail, particularly in view of the variable accuracy of the data quoted in Table 3 and of small variations with temperature and solvent. However it seems that both factors tend to increase $^3J_s$. It may be noted that when both substituents are alkyl groups or hydrogen, values of $^3J_s$ are in the lower part of the range. There is no evidence to suggest any appreciable population of conformations other than *s-trans* for sorbaldehyde.

The magnitude of $^3J_t$ for the MeCH = CH group of sorbaldehyde (15.23 Hz) is similar to the corresponding values for *trans*-pentadiene (15.00 to 15.06 Hz [9,29]), *trans,trans*-hexadiene (15.01 Hz[9]) and methyl sorbate (15.1 Hz [2]). The value of $^3J_t$ for the CH = CHCHO group of sorbaldehyde (15.34 Hz) should be compared to the data for methyl sorbate (15.8 Hz [24]), *trans,trans*-muconic acid and its esters (15.79 to 16.0 Hz [8,25]), *trans*-2,4-pentadienoic acid (15.41 Hz [7]) and cinnamaldehyde (15.71 to 15.93 Hz, [12] 15.9 Hz [13]). The fact that for sorbaldehyde $^3J_t$ is slightly larger for the CH = CHCHO group (*i.e.* for the "central" double bond) than for the MeCH = CH group is consistent with the results for methyl sorbate.[24]

Long-range coupling between the diene protons follows the pattern shown by *trans,trans*-hexadiene [9] and related compounds (see Table 3). However, the two values of $^4J_c$ differ by 0.2 Hz, the result for $J_{AK}$ being algebraically lower than for the other compounds of Table 3. Coupling constants to the methyl protons (Table 4) are measurable for up to six bonds between the nuclei concerned; the values are closely comparable with those for related molecules. In contrast long-range coupling to the aldehyde proton is small; in fact only for $^4J_c$ is it detectable ($-0.25$ Hz), as obtained by full analysis of the K region, though the linewidth of the aldehyde doublet, 0.7 Hz, gives some indication of more extensive coupling. The small magnitude of $^4J_c$ to aldehyde protons is well-known (see Table 2). The negative sign gave a better correlation of both line positions and intensities than a positive sign; this is consistent with signs for the diene series [9] and for acrolein.[3] We believe the magnitude of $^4J_c$ to the aldehyde proton to be accurate to 0.08 Hz. The lack of longer-range coupling to the aldehyde proton of sorbaldehyde is in contrast to the situation for hexatriene and its derivatives, for which both experimental [33,34] and theoretical [19] data have been reported.

## REFERENCES

1. Hoffman, R. A. and Gronowitz, S. *Acta Chem. Scand.* **13** (1959) 1377; *Arkiv Kemi* **16** (1961) 471.
2. Douglas, A. W. and Goldstein, J. H. *J. Mol. Spectry.* **16** (1965) 1.
3. Davies, J. E. D. *J. Mol. Spectry.* **29** (1969) 499.
4. Klinck, D. E. and Stothers, J. B. *Can. J. Chem.* **44** (1966) 45.

5. Ronayne, I. and Williams, D. H. *J. Chem. Soc.* **C 1967** 2642.
6. Collin, P. J. and Sternhell, S. *Aust. J. Chem.* **19** (1966) 317.
7. Kelly, D. P. *J. Mol. Spectry.* **28** (1968) 204.
8. Elvidge, J. A. and Ralph, P. D. *J. Chem. Soc.* **C 1966** 387.
9. Albriktsen, P., Cunliffe, A. V. and Harris, R. K. *J. Magn. Resonance* **2** (1970) 150, and references therein.
10. Albriktsen, P. *Unpublished work.*
11. Castellano, S. and Bothner-By, A. A. *J. Chem. Phys.* **41** (1964) 3863.
12. Scrimshaw, G. F. *M. Sc. Thesis*, University of East Anglia 1967.
13. Hoffman, R. A., Gestblom, B. and Rodmar, S. *J. Chem. Phys.* **42** (1965) 1695.
14. Schaefer, T. *Can. J. Chem.* **40** (1962) 1678.
15. Bothner-By, A. A. and Harris, R. K. *Unpublished work.*
16. Gilby, A. R. and Waterhouse, D. F. *Aust. J. Chem.* **17** (1964) 1311.
17. Dabrowski, J. and Kozerski, L. *Org. Magn. Resonance* **4** (1972) 137.
18. Bothner-By, A. A. and Harris, R. K. *J. Org. Chem.* **30** (1965) 254.
19. Cunliffe, A. V., Grinter, R. and Harris, R. K. *J. Magn. Resonance* **3** (1970) 299.
20. Wagner, R., Fine, J., Simmons, J. W. and Goldstein, J. H. *J. Chem. Phys.* **26** (1957) 634.
21. Bothner-By, A. A. and Moser, E. *J. Am. Chem. Soc.* **90** (1968) 2347.
22. Kozerski, L. and Dabrowski, J. *Org. Magn. Resonance* **4** (1972) 253.
23. Bacon, M. and Maciel, G. E. *Mol. Phys.* **21** (1971) 257.
24. Elvidge, J. A. and Ralph, P. D. *J. Chem. Soc.* **B 1966** 243.
25. Bishop, E. O. and Musher, J. I. *Mol. Phys.* **6** (1963) 621.
26. Bothner-By, A. A. and Harris, R. K. *J. Am. Chem. Soc.* **87** (1965) 3451.
27. Hall, J. H. and Patterson, E. *J. Am. Chem. Soc.* **89** (1967) 5856.
28. Wendisch, D. and Kurtz, P. *Z. Naturforsch.* **22b** (1967) 599.
29. Segre, A. I., Zetta, L. and DiCorato, A. *J. Mol. Spectry.* **32** (1969) 296.
30. Hobgood, R. T. and Goldstein, J. H. *J. Mol. Spectry.* **12** (1964) 76.
31. Diez, E. and Rico, M. *J. Mol. Spectry.* **37** (1971) 131.
32. Bothner-By, A. A. and Harris, R. K. *J. Am. Chem. Soc.* **87** (1965) 3445.
33. Albriktsen, P. and Harris, R. K. *Acta Chem. Scand.* **27** (1973) 1875.
34. Cunliffe, A. V., Grinter, R. and Harris, R. K. *J. Magn. Resonance* **2** (1970) 200.

# Nucleophilic Reactivity of Some Nitrogen Heterocycles

P. FRØYEN* and R. F. HUDSON

*University Chemical Laboratory, Canterbury, Kent, England*

The rates of reaction of 1,4-diazabicyclo[2.2.2]octane and quinuclidine with various substrates are explained by through bond coupling of the lone pairs in the diaza-compound. The relative reactivity of 1,2-oxazolidine and tetrahydro-1,2-oxazine towards p-nitrophenyl acetate indicates *weak* interaction between the lone pairs on adjacent nitrogen and oxygen atoms. The reactivities of piperidine and pyrrolidine are used as reference compounds to obtain a measure of steric hindrance. Comment is made on the high energy barrier to inversion of cyclic hydroxylamines.

Nucleophilic reactivity is usually discussed[1] in terms of polarisability and basicity (*i.e.* the $pK_a$ of the conjugate acid of the nucleophile), although solvation energies are particularly important in the reactions of anionic reagents.[2] In addition, steric hindrance frequently dominates a reaction sequence, as for example in the reactions of amines.[3]

It is now evident that reactions must be considered in orbital terms[4] rather than in terms of empirical parameters (*e.g.* free energy relationships), since orbital diagrams give a more detailed, albeit approximate, description of the reaction process. This approach has been developed recently[5] to explain
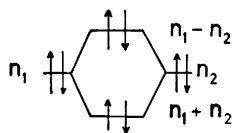


*Fig. 1.*
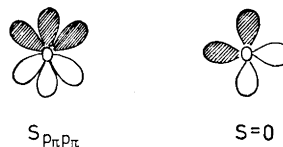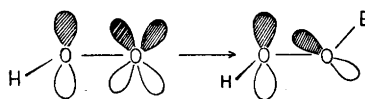


*Fig. 2.*

* Present address: Kjemisk Institutt, Universitetet i Bergen, Bergen, Norway.

the anomalously high reactivity of certain nucleophiles (*e.g.* $HO_2^-$, $ClO^-$) towards electrophilic centres. According to this explanation, lone pairs of the correct symmetry on adjacent atoms combine to give bonding and anti-bonding molecular orbitals as shown in Fig. 1.

For example, in the case of the hydroperoxide ion, $p\pi - p\pi$ overlap leads to electron repulsion * which is partially removed on formation of a $\sigma$-bond with an electrophile, E (Fig. 2).

This orbital splitting, and hence the repulsion energy is conformation dependent. We have demonstrated this by following the reactions of cyclic disulphides [6] with methyl fluorosulphonate in dimethyl sulphate solution,

$$(CH_2)_n \overset{\diagup S}{\underset{\diagdown S}{\Big|}} + MeOSO_2F \rightarrow (CH_2)_n \overset{\diagup \overset{+}{S}-Me}{\underset{\diagdown S}{\Big|}} + SO_3F^-$$
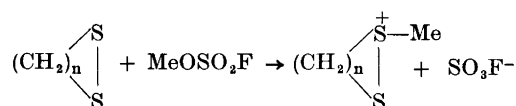
Sulphur compounds are particularly suitable for study because, unlike nitrogen, the lone pair electrons are in pure $p$ orbitals, orthogonal to the $C_{2v}$ $\sigma$-bond framework.[7] Accordingly, the reactivity, $k$, of the disulphide depends on the dihedral angle, $\theta$, between the $p_\pi$ orbitals, and on the extent of bond formation,** $\beta$, in the transition state as follows,

$$RT \ln k \simeq 2\beta E_\pi S \cos \theta$$

where $E_\pi$ is the orbital splitting energy (given directly by photoionisation spectra [7]), and $S_\pi$ the $p_\pi - p_\pi$ overlap integral for a disulphide bond.

In further work,[8] aromatic nitrogen heterocycles (*e.g.* pyrazine and iso-thiazole) were found to be considerably more reactive towards activated esters than predicted from their basicity. Here again lone-pair repulsions (in essentially $sp^2$ orbitals) lead to orbital splitting with consequent destabilisation of the molecule and increased nucleophilic reactivity. The situation with nitrogen compounds is by no means simple, owing to the combination of "lone-pair" orbitals with orbitals used in $\sigma$-bonding.[9] This modifies the behaviour of the nitrogen lone pair such that in certain molecules it may effectively "disappear" into the molecular structure.

In the present study we have measured the rate of reaction of some nitrogen heterocycles which may show through space or through bond coupling [10] of lone pair orbitals, with various electrophiles. In the present work we show that through space interaction of the lone pairs on adjacent oxygen and nitrogen atoms of cyclic hydroxylamines can lead to small increases in reactivity, when bond formation in the transition state is extensive. On the other hand, through bond coupling in 1,4-diazabicyclo[2.2.2]octane (DBCO) can lead to small rate enhancements when bonding in the transition state is very weak (low Brønsted $\beta$), but in most reactions the more basic homomorph [3] quinuclidine (Q) is more reactive than DBCO.

---

* Given by $4(\beta - \alpha S)/(1 - S^2)$ according to Hückel MO theory.

** This is given approximately by the Brønsted exponential coefficient, $\beta$.

## EXPERIMENTAL

*Materials.* Methyl tosylate was synthesized from tosyl chloride and methanol. Before use it was recrystallized several times from ether-petrol ether, m.p. 28°. *p*-Nitrophenyl acetate was prepared from acetic anhydride and *p*-nitrophenol, and was recrystallized from benzene-petrol ether, m.p. 78°. 4,4'-Tetramethyldiaminotriphenylmethane chloride (malachite green) a commercial product from B.D.H. Ltd. was used without further purification. The hydrochlorides of 1,2-oxazolidine and tetrahydro-1,2-oxazolidine and tetrahydro-1,2-oxazine were prepared according to King,[11] and were repeatedly recrystallized before use.

1,4-Diazabicyclo[2.2.2]octane and quinuclidine hydrochloride were obtained from R. H. Emanuel, Ltd. and were recrystallized from ethanol. Piperidine hydrochloride was prepared by treatment of piperidine with dry HCl. The product was crystallized twice from ethanol, m.p. 246°. Pyrrolidine (Fisons Chemicals) was dried over KOH pellets and distilled before use.

*Kinetic methods.* The rates of reaction were followed colourimetrically using a Unicam S.P. 800 spectrophotometer and a cell held at $25 \pm 0.1°$. The appearance of 4-nitrophenol and 4-nitrophenolate ion was followed at 330 and 400 nm, respectively, and the disappearance of malachite green was followed at 625 nm. The reactions of methyl tosylate were followed at 272 nm. Freshly prepared, aqueous, solutions were used in all cases, and a large excess of nucleophile ensured that the reactions proceeded under pseudo-unimolecular conditions. The bases thus served as buffer and nucleophile, and the concentration of free base was calculated from the $pK_a$ and pH of the solution used in each case. The rate constants, calculated by Guggenheim's method are given in Tables 1 and 2.

*Table 1.* Rates of reaction of several substrates with 1,4-diazabicyclo[2.2.2]octane and with quinuclidine in aqueous solution at 25°. (Second order rate constants are given as $1 \text{ mol}^{-1}\text{min}^{-1}$).

| Substrate | $\beta^a$ | 1,4-Diazabicyclo-[2.2.2]octane*[b] | Quinu-clidine | Relative reactivity |
|---|---|---|---|---|
| *p*-Nitrophenyl acetate | 0.83 | 1.1 | 148.3 | 135 |
| Malachite green | 0.41 | $5.6 \times 10^{-2}$ | 4.0 | 71 |
| Methyl tosylate | 0.10 | 4.3 | 10.7 | 2.5 |
| 2,4-Dinitrophenyl phosphate [12] | $\simeq 0$ | $5.11 \times 10^{-2}$ | $1.68 \times 10^{-2}$ | 0.3 |

[a] $\beta$ is the Brønsted coefficient for reactions with a series of amines. [b] Half of observed values.

*Table 2.* Reaction of *p*-nitrophenyl acetate and methyl phosphate with some cyclic amines and hydroxylamines. (Second order rate constants $1 \text{ mol}^{-1}\text{min}^{-1}$).

| Nucleophile | *p*-Nitrophenyl acetate | *p*-Nitrophenyl methylphosphonate [13] |
|---|---|---|
| Pyrrolidine | 9200 | 285 |
| Piperidine | 3180 | 48 |
| 1,2-Oxazolidine | 1.89 | 0.14 |
| Tetrahydro-1,2-oxazine | 0.21 | 0.075 |

## RESULTS AND DISCUSSION

The initial studies involved the reactions of 1,4-diazabicyclo [2.2.2]octane (DBCO) and quinuclidine (Q) with several electrophiles in aqueous solution (Table 1). Molecules of the same general structure, *e.g.* tertiary amines, normally show the same reactivity order to all substrates [†] as given quantitatively by the Brønsted equation, Hammett equation or similar linear free energy relationship.[4] The data of Table 1, however, show that DBCO is more reactive than Q towards 2,4-dinitrophenyl phosphate,[12] but less reactive towards the other reagents.

This change in reactivity order may be attributed to the unusual electronic structure of DBCO since the $pK_a$ is very low for a tertiary amine, but the ionisation potential is also low (7.52 eV; *cf.* 8.6 eV for quinuclidine).[10] Usually a low $pK_a$ is associated with a high ionisation potential for molecules of a given structure. In the case of DBCO, the combination of the lone pair orbitals with $\sigma$ and $\sigma^*$ orbitals of the $C-C$ bonds gives delocalised orbitals [9] as shown in Fig. 3.
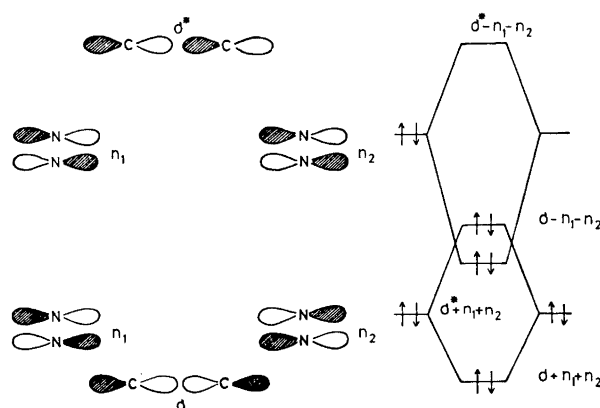


*Fig. 3.*

This orbital interaction has been confirmed elegantly by a study of the photoelectron spectrum by Heilbronner,[10] from which it may be concluded that in spite of the high energy occupied (symmetric) orbital (I.P. 7.52 eV), the molecule is more stable than quinuclidine (I.P. 8.6 eV).[††]

We can now explain the change in the reactivity order in the following way. For small interactions, as in the reaction of 2,4-dinitrophenyl phosphate ($\beta \simeq 0$), the electronic structure of the nucleophile is essentially unaltered, and the electrophilic L.U.M.O. ($\sigma^*$ orbital) interacts primarily with $n_1$ and $n_2$ of DBCO. (Fig. 4).

---

[†] Providing that differences in steric hindrance are negligible.

[††] Hence a greatly reduced $pK_a$ (8.8) compared to a tertiary amine, *e.g.* 11.2 for $Et_3N$ and 10.95 for quinuclidine.[14]
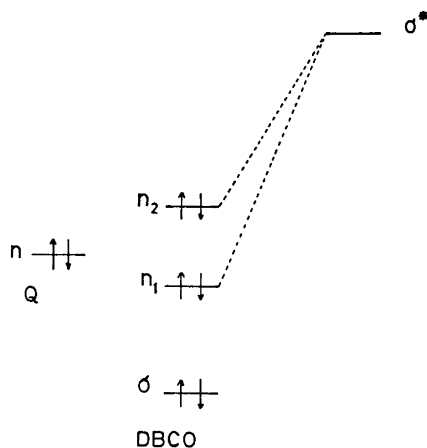
*Fig. 4.*

As predicted by Hoffmann,[9] and shown later by Heilbronner,[10] the average energy of $n_1$ and $n_2$ is less than the energy of n (for quinuclidine). Hence under these conditions the perturbation of DBCO is greater than that of Q, and the former is the more reactive. As the interaction in the transition state increases, the electrophile interacts more strongly with the available orbitals, $n_1$, $n_2$ and $\sigma$. In the limit, when the bond is (almost) fully formed in the transition state, e.g. as in acylation ($\beta = 0.83$), the reactivity is determined by the stability of the nucleophile (i.e. the total electronic energy), and quinuclidine is more reactive than DBCO (Table 1).

In further work we have compared the reactivity of cyclic hydroxylamines and cyclic amines. As shown by the data in Table 2 the relative reactivity of pyrrolidine and piperidine towards p-nitrophenyl methyl phosphonate (6.0) is greater than the relative reactivity towards p-nitrophenyl acetate (2.9). This is in line with greater steric hindrance towards phosphorylating agents than towards acylating agents.[15] Moreover, the relative reactivity of 1,2-oxazolidine and tetrahydro-1,2-oxazine towards p-nitrophenyl methyl phosphonate is appreciably less than the relative reactivity of the two cyclic amines. According to Edwards et al.[13] the rate differences are due to differences in steric hindrance produced mainly by the 3 and 5 axial H-atoms, and hence the cyclic hydroxylamines are expected, on this basis, to exert less steric hindrance than the corresponding cyclic amines.

On the other hand 1,2-oxazolidine is ca. 9 times more reactive than tetrahydro-1,2-oxazine towards p-nitrophenyl acetate, where steric hindrance differences are expected to be negligible (i.e. less than for the methylphosphonate). This rate increase is therefore probably due to the interaction of lone-pairs on adjacent nitrogen and oxygen atoms. The effect, however, is small compared with reactivity increases found for other α-nucleophiles, and this reduced effect may be due to the different symmetries of the lone pair orbitals on oxygen and nitrogen. Because of the (local) $C_3$ symmetry of the nitrogen atom, the lone pair orbital will combine with the σ-bond orbitals and the lone pair is effectively delocalised throughout the σ-bond framework.

This will reduce the repulsion exerted towards the lone pairs in the $p_\pi$ orbital of the oxygen atom.

In this connection it is found that isoxazolidines and tetrahydro-1,2-oxazines undergo nitrogen inversion slowly with barriers of the order of 14 − 17 kcal/mol.[16] The barriers for simple acyclic amines are of the order of 5 kcal/mol. The difference can be attributed to strong $p_\pi - p_\pi$ repulsions of the lone pairs in the transition state where the nitrogen atom adopts the trigonal configuration. An estimate of the repulsion energy, $\Delta E$, may be obtained from a simple Hückel treatment for the interaction of two $p$ orbitals,

$$\Delta E \simeq 4[(\beta - \alpha S)/(1 + S)][S/(1 - S)] \simeq 2E_\pi[S/(1 - S)]$$

where $E_\pi$ is the $\pi$-bond energy of a N − O single bond and S the corresponding overlap intergral. For $E_\pi \simeq 50$ kcal/mol* and $S_{N-O} \simeq 0.1$ we have a value of 11 kcal/mol for the inversion barrier. This is similar to the difference in energy barriers for cyclic N − O compounds and cyclic amines, and is in agreement with the assumption of a small lone-pair lone-pair repulsion energy in the ground state. Molecules of this kind therefore can exhibit only small rate enhancements ($\alpha$-effects) in nucleophilic substitutions.

## REFERENCES

1. Pearson, R. G. and Edwards, J. O. *J. Am. Chem. Soc.* **84** (1962) 16; Hudson, R. F. *Chimia* **16** (1962) 173.
2. Parker, A. J. *Quart. Rev.* **16** (1962) 163; *Advan. Phys. Org. Chem.* **5** (1967) 173.
3. Brown, H. C. *J. Am. Chem. Soc.* **67** (1945) 503.
4. Hudson, R. F. *Angew. Chem.* **85** (1973) 63; *Int. Ed.* **12** (1973) 36; Salem, L. *Chem. in Britain* **5** (1969) 449.
5. Aubort, J.-D. and Hudson, R. F. *Chem. Commun.* **1970** 937.
6. Filippini, F. and Hudson, R. F. *Chem. Commun.* **1972** 726.
7. Filippini, F. and Hudson, R. F. *Chem. Commun.* **1972** 522; Zoltewicz, J. A. and Jacobsen, H. L. *Tetrahedron Letters* **1972** 189; Zoltewicz, J. A. and Deady, L. W. *J. Am. Chem. Soc.* **94** (1972) 2765.
8. Hoffmann, R. *Accounts Chem. Res.* **4** (1971) 1.
9. Hoffmann, R., Inamura, A. and Hehre, J. W. *J. Am. Chem. Soc.* **90** (1968) 1499.
10. Heilbronner, E. and Muszkat, K. A. *J. Am. Chem. Soc.* **92** (1970) 3818.
11. King, H. *J. Chem. Soc.* **1943** 43.
12. Kirby, A. J. and Varvoglis, A. G. *J. Chem. Soc.* **A 1968** 135.
13. Brass, H. J., Edwards, J. O. and Fina, N. J. *J. Chem. Soc. Perkin Trans. 2* **1972** 726; Brass, H. J., Edwards, J. O. and Biallas, M. J. *J. Am. Chem. Soc.* **92** (1970) 4675.
14. Perrin, D. D. *Dissociation Constants of Organic Bases in Aqueous Solution*, 1965, p. 260.
15. Hudson, R. F. and Keay, L. *J. Chem. Soc.* **1956** 2463.
16. Griffith, D. L. and Olsen, B. L. *Chem. Commun.* **1968** 1682; Riddell, F. G., Lehn, J. M. and Wagner, J. *Ibid.* 1403.

Received June 29, 1973.

* Estimated from the value for a N − O double bond, and from double and single bond distances.

# The Ion Activity Function

## An Approach to the Study of Electrolyte Behavior in Concentrated Solutions III. Formal Species in the Systems LiCl-H₂O and LiBr-H₂O

### LESLIE LEIFER and ERIK HÖGFELDT

*Department of Chemistry, Michigan Institute of Technology, Houghton, Michigan, USA, and the Department of Inorganic Chemistry, Royal Institute of Technology, S-100 44 Stockholm 70, Sweden*

Employing a method developed by Högfeldt for the estimation of ionic hydration numbers from activity and $H_0$-data, the systems $LiCl - H_2O$ and $LiBr - H_2O$ from dilute up to saturated solution can be described by the following equilibria:

$$LiCl - H_2O$$

$$Li^+ + 5H_2O \rightleftharpoons Li(H_2O)_5^+$$
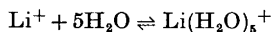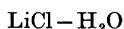
$$\log [Li(H_2O)_5^+] = -0.33 + \log \phi_0\{Li^+\} + 5 \log \{H_2O\}$$
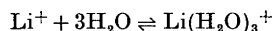
$$Li^+ + 3H_2O \rightleftharpoons Li(H_2O)_3^+$$

$$\log [Li(H_2O)_3^+] = -1.02 + \log \phi_0\{Li^+\} + 3 \log \{H_2O\}$$
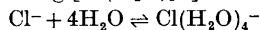
$$Cl^- + 4H_2O \rightleftharpoons Cl(H_2O)_4^-$$

$$\log [Cl(H_2O)_4^-] = 0.34 + \log \phi_0^{-1}\{Cl^-\} + 4 \log \{H_2O\}$$

$$\log [Cl^-]_{free} = -0.20 + \log \phi_0^{-1}\{Cl^-\}$$
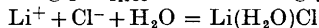
$$Li^+ + Cl^- + H_2O = Li(H_2O)Cl$$

$$\log [Li(H_2O)Cl] = -4.87 + \log \{Li^+\}\{Cl^-\} + \log \{H_2O\}$$

$$LiBr - H_2O$$

$$Li^+ + 5H_2O \rightleftharpoons Li(H_2O)_5^+$$
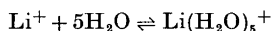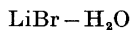
$$\log [Li(H_2O)_5^+] = -0.22 + \log \phi_0\{Li^+\} + 5 \log \{H_2O\}$$
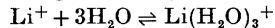
$$Li^+ + 3H_2O \rightleftharpoons Li(H_2O)_3^+$$

$$\log [Li(H_2O)_3^+] = -1.36 + \log \phi_0\{Li^+\} + 3 \log \{H_2O\}$$
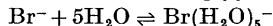
$$Br^- + 5H_2O \rightleftharpoons Br(H_2O)_5^-$$

$$\log [Br(H_2O)_5^-] = 0.31 + \log \phi_0^{-1}\{Br^-\} + 5 \log \{H_2O\}$$

$$\log [Br^-]_{free} = -0.53 + \log \phi_0^{-1}\{Br^-\}$$
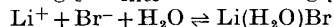
$$Li^+ + Br^- + H_2O \rightleftharpoons Li(H_2O)Br$$

$$\log [Li(H_2O)Br] = -6.22 + \log \{Li^+\}\{Br^-\} + \log \{H_2O\}$$

In the literature activities and activity coefficients of electrolytes in water are referred to the completely dissociated, unhydrated ions. For systems where the mean activity coefficient shows a large increase with a corresponding decrease in water activity when approaching saturation, it is obvious that ion-solvent interactions are responsible for a large part of the observed variation in excess free energy. Examples of such systems are mixtures of strong acids and water, where proton hydration is extensive, and the lithium salts, where the small $Li^+$ can be expected to interact strongly with water, e.g. for LiBr at 20 m (molal) $\gamma_\pm = 485$, which indicates that the choice of the species $Li^+$, $Br^-$ and $H_2O$ is a very poor one indeed.

Some time ago, the ion activity function concept, developed for mixtures of strong acids and water, was applied to the systems $LiCl - H_2O$ and $LiBr - H_2O$.[1] This application is based on the following assumption: the ion activity function of a given anion is the same in both acid and salt solutions, when compared at the same water activity. This assumption is made by analogy to the behavior of the proton activity function, which has been found to be the same at the same water activity for several strong acids.[2] Ojeda and Wyatt [3] found that the Hammett acidity function (or proton activity function) also is a unique function of water activity in salt-acid mixtures, at least in dilute solutions.

Both for LiCl and LiBr we have found [1] that the anion activity coefficient functions are the same at the same water activity in acid as well as salt solutions. Moreover, we found that the lithium ion seems to carry a substantial amount of water of hydration even at 20 m, while the anion seems to be practically unhydrated in 8 − 10 m solutions.

In this paper we describe the two systems in terms of differently hydrated species, as has been done for several strong acids.[4−6]

*The ion activity and activity coefficient functions.* In order to construct functions mainly dependent on the behavior of a single ion, the following approach has been adopted. First consider the Hammett acidity function, $H_0$. This function is determined by studying the protonation of a series of uncharged bases, mostly substituted nitroanilines. These indicators participate in the following reaction

$$BH^+ \rightleftharpoons B + H^+ \tag{1}$$

Application of the law of mass action to (1) gives

$$\{B\}\{H^+\}/\{BH^+\} = K_{BH^+} \tag{2}$$

By taking the logarithm of (2) and rearranging the terms we get

$$pK_{BH^+} + \log([B]/[BH^+]) = -\log \phi_0\{H^+\} = H_0 \tag{3}$$

where

$$pK_{BH^+} = -\log K_{BH^+}$$
$$\phi_0 = y_B/y_{BH^+} \tag{4a,b}$$

The left hand side of (3) shows how $H_0$ is obtained experimentally by determination of the ratio $[B]/[BH^+]$ spectrophotometrically, when $K_{BH^+}$ is known. In dilute solutions $K_{BH^+}$ is obtained by extrapolating the stoichio-

metric equilibrium constant to infinite dilution. At high concentrations of acid $K_{BH^+}$ is obtained in the range of overlap between two indicators. If $H_0$ is known (determined with another indicator) and the ratio [B]/[BH$^+$] determined spectrophotometrically $pK_{BH^+}$ can be computed from (3). The right hand side of eqn. (3) shows the physical meaning of $H_0$, being the product of the activity coefficient ratio $\phi_0$ and the proton activity {H$^+$}.

In reaction (1) hydration of the indicator base and acid forms should be taken into account and the reaction formulated

$$BH(H_2O)_m{}^+ \rightleftharpoons B(H_2O)_n + H^+ + (m-n)H_2O \tag{5}$$
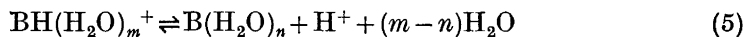
According to (5) only apparent hydration numbers can be obtained for the proton if the acid and base forms of the indicator are hydrated. The value $m-n$ should be added to the value estimated from the expression

$$\bar{n}_{H^+}{}' = -(\varDelta \log \phi_0 y_{H^+})/(\varDelta \log \{H_2O\}) \tag{6}$$

where $\phi_0 y_{H^+}$ is the proton activity coefficient function evaluated from

$$\log (\phi\{H^+\}/[H^+]_{tot}) = \log \phi_0 y_{H^+} \tag{7}$$

and [H$^+$]$_{tot}$ is the total molarity of all hydrated protons present in solution. Functions analogous to (6) can be written for anions as well as for cations other than H$^+$.

Since $m$ can be expected to be larger than $n$, $\bar{n}_{H^+}{}'$ represents a lower limit for the hydration of the proton. In order to obtain information on $m$ and $n$ Essig and Marinsky[7] determined the activity coefficient of unprotonated base form of Hammett indicators as well as the protonated form using a reasonable extra thermodynamic assumption. From these data Högfeldt et al.[8] estimated $m$ and $n$. It was found that $m-n$ is surprisingly small in concentrated solutions. This is the main reason why the method outlined above has so far given surprisingly reasonable numbers. For this reason we neglect $m-n$ in the following treatment.

Reaction (5) implies that $K_{BH^+}$ refers to the state of hydration that B and BH$^+$ have in the acidity range where B is transformed to BH$^+$ rather than to the state of infinite dilution in water as suggested by Hammett.[9]

In recent years various other acidity functions have appeared among them $H_R$ introduced by Deno et al.,[10,11] Boyds relative acidity function,[12] and the function $H_A$ of Yates et al.[13] etc. They have been discussed by Rochester,[14] and from this discussion it is evident that $H_0$ still is a most useful acidity function.

However, a comparison of various acidity functions with respect to the possibility of constructing a more useful set of ion activity functions certainly merits further consideration and we plan to do this in the near future. In the meantime a consistent formalism can be developed based on $H_0$. This function has some useful properties which may not be shared by all other acidity functions. Besides being a unique function of water activity for several strong acids as first shown by Wyatt[15] and later confirmed by Högfeldt for $H_0{}^2$ but not for $H_R$,[16] it has been found that the anion activity coefficient function sometimes stays constant over a considerable concentration range as found for NO$_3{}^-$ in HNO$_3$ – H$_2$O[5] and for Br$^-$ in LiBr – H$_2$O.[1] These observations are

interpreted in terms of formally unhydrated $NO_3^-$ and $Br^-$ in the concentration range under consideration.

According to (3) we can identify the proton activity function with $H_0$, i.e.

$$\log \phi_0\{H^+\} = -H_0$$

From the activity product $\{H^+\}\{A^-\}$, which can be obtained from the stoichiometric activity coefficient of HA, tabulated in the literature, and the proton activity function an anion activity function is obtained from

$$\log \phi_0^{-1}\{A^-\} = H_0 + \log \{H^+\}\{A^-\} \qquad (8)$$

For a two-proton acid like $H_2SO_4$, similar but slightly more complicated expressions are obtained.[2]

Similarly to (7) an anion activity coefficient function can be evaluated from

$$\log \phi_0^{-1}\{A^-\}/[A^-]_{tot} = \log \phi_0^{-1}y_{A^-} \qquad (9)$$

where $[A^-]_{tot}$ is the stoichiometric molarity of $A^-$ in the solution.

With the aid of the ion activity and ion activity coefficient functions we can estimate the minimum number of ion-water complexes necessary to fit the experimental data. We shall start with the anions, then consider the possibility of ion-pair formation and finally consider cation hydration.

*Anion hydration.* In Fig. 1 $\log \phi_0^{-1}y_{A^-}$ is plotted against $\log \{H_2O\}$ for $Cl^-$ and $Br^-$ in the two lithium salts employing the assumption that the anion activity functions are the same at the same water activity in both acid and salt. The rising part of the curves in Fig. 1 can be interpreted as due to formation of hydrates, the horizontal portion by unhydrated anion and the decreasing part by formation of ion-pairs.
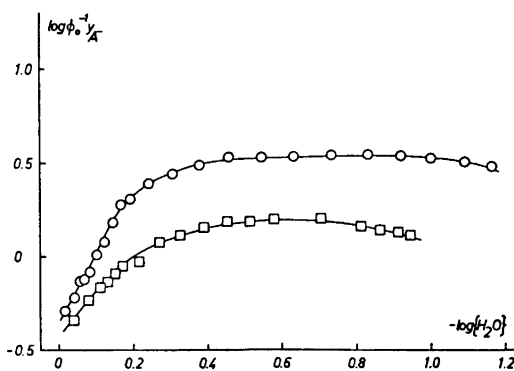


*Fig. 1.* The function $\log \phi_0^{-1}y_{A^-}$ plotted against $-\log \{H_2O\}$ for the systems (O) LiBr – $H_2O$ and (☐) LiCl – $H_2O$.

In order to find the minimum number of anionic species necessary to describe the experimental data we consider the following equilibrium

$$A^- + pH_2O \rightleftharpoons A(H_2O)_p^- \qquad (10)$$
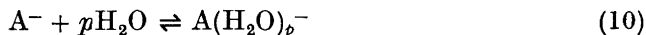
Application of the law of mass action to (10) gives

$$\{A(H_2O)_p^-\} = k\{A^-\}\{H_2O\}^p \tag{11}$$

We include the activity coefficient of $A(H_2O)_p^-$ in the equilibrium constant, use (8) for $\{A^-\}$ and get

$$[A(H_2O)_p^-] = k'10^{H_0} \{H^+\}\{A^-\}\{H_2O\}^p \tag{12}$$

where

$$k' = k\phi_0/y_{A(H_2O)_p^-} = k\frac{y_B}{y_{BH^+}\,y_{A(H_2O)_p^-}} \tag{13}$$

For the total concentration of $A^-$ the following expression is obtained

$$[A^-]_{tot} = 10^{H_0}\{H^+\}\{A^-\}\sum_0^p k_i'\{H_2O\}^i = \phi_0^{-1}\{A^-\}\sum k_i'\{H_2O\}^i \tag{14}$$

In the range where the unhydrated anion predominates eqn. (14) gives

$$[A^-]_{tot} = [A^-]_{free} = \phi_0^{-1}\{A^-\}k_0' \tag{15a}$$

or

$$\log [A^-]_{tot} = \log [A^-]_{free} = \log k_0' + \log \phi^{-1}\{A^-\} \tag{15b}$$

and

$$\log \phi_0^{-1}y_{A-} = -\log k_0' \tag{16}$$

According to (16) the horizontal asymptotes in Fig. 1 will give the values for $k_0'$ and we find

$$\log [Cl^-]_{free} = -0.20 + \log \phi_0^{-1}\{Cl^-\} = -0.20 + H_0 + \log \{H^+\}\{Cl^-\}$$
$$\log [Br^-]_{free} = -0.53 + \log \phi_0^{-1}\{Br^-\} = -0.53 + H_0 + \log \{H^+\}\{Br^-\} \tag{17a,b}$$

The concentration of unhydrated $Cl^-$ and $Br^-$ can be computed from eqns. (17a,b). By subtracting this amount from the total concentration the amount of hydrated anion is obtained.

In Fig. 2 $[\log ([A^-]_{tot} - [A^-]_{free})]/\phi_0^{-1}\{A^-\}$ is plotted against $-\log \{H_2O\}$. From Fig. 2 it is seen that two straight lines can be fitted to the data with slopes close to 4 for $Cl^-$ and 5 for $Br^-$. This indicates that one hydrate alone is sufficient to describe the data. If only one complex predominates over an extended concentration range we get from (14)

$$\log [A(H_2O)_p^-] = \log [A^-]_{tot} = \log k_p' + \log \phi_0^{-1}\{A^-\} + p \log \{H_2O\} \tag{18}$$

or

$$\log \frac{[A^-]_{tot}}{\phi_0^{-1}\{A^-\}} = -\log \phi_0^{-1}y_{A-} = \log k_p' + p \log \{H_2O\} \tag{19}$$

which is the equation of a straight line with a slope equal to $p$. According to (19) the data for dilute solutions are consistent with $Cl(H_2O)_4^-$ and $Br(H_2O)_5^-$.

The constants $k_4'$ and $k_5'$ were computed from (18) with $p = 4$ for $Cl^-$ and $p = 5$ for $Br^-$ and an acceptable fit was obtained with the following relations

$$\log [Cl(H_2O)_4^-] = 0.34 + \log \phi_0^{-1}\{Cl^-\} + 4 \log \{H_2O\}$$
$$\log [Br(H_2O)_5^-] = 0.31 + \log \phi_0^{-1}\{Br^-\} + 5 \log \{H_2O\} \tag{20a,b}$$

If the indicators are hydrated one must subtract the unknown quantity $(m-n)$ from the hydration numbers evaluated above. This indicates that in the range where formally unhydrated ions predominate either the indicators are practically unhydrated or the variation in hydration is cancelled by other effects, such as electrostatic interactions. In the latter case it would be surprising if these effects effectively cancel over a large range of water activity.
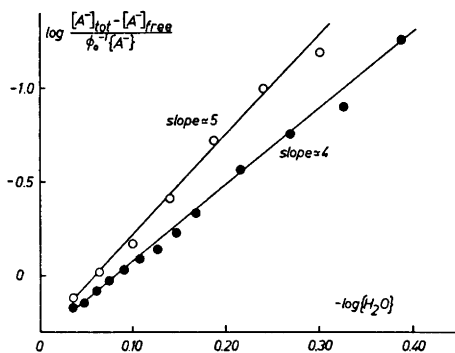


*Fig. 2.* $[\log([A^-]_{tot} - [A^-]_{free})]/(\phi^{-1}\{A^-\})$ plotted against $-\log\{H_2O\}$ for the systems (O) $Br^-$ in $LiBr - H_2O$ and ( ●) $Cl^-$ in $LiCl - H_2O$.
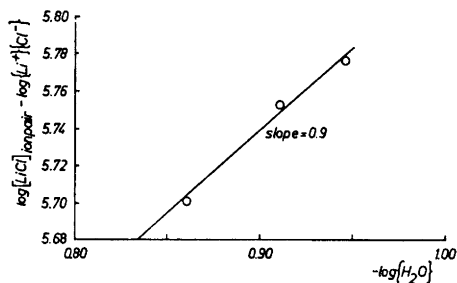
*Fig. 3.* $\log [LiCl(H_2O)_n] - \log \{Li^+\}\{Cl^-\}$ plotted against $-\log [H_2O]$ for the system: $LiCl - H_2O$. A straight line with a slope close to unity can be fitted to the data.

*Ion-pair formation.* The decreasing part of the curve in Fig. 1 was previously supposed to be due to formation of ion-pairs at high concentrations.[1] In the present paper the difference between the total concentration and the other two species is taken to be due to an ion-pair *i.e.*,

$$[LiA(H_2O)_q] = [A]_{tot} - [A]_{free} - [A(H_2O)_q^-] \tag{21}$$

This fits the data well for $Br^-$ and satisfactorily for $Cl^-$. The concentration of the ion-pair is obtained from the $\alpha$-values computed from the expressions

$$\log \alpha_{LiBr} = \log \phi_0^{-1} y_{Br^-} - 0.53$$

$$\log \alpha_{LiCl} = \log \phi_0^{-1} y_{Cl^-} - 0.20 \tag{22a,b}$$

derived previously,[1] which can be taken as a consistency test for the two methods of estimating the concentration of the ion-pair.

As indicated in (21) the ion-pair may be hydrated. In order to evaluate the hydration of the ion-pair, consider the following reaction
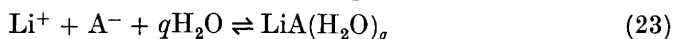
$$Li^+ + A^- + qH_2O \rightleftharpoons LiA(H_2O)_q \tag{23}$$

Assuming the activity coefficient of the hydrated ion-pair to be practically constant it is included in the equilibrium constant and the equilibrium law applied to (23) then gives

$$\log [LiA(H_2O)_q] = \log k_q + \log \{Li^+\}\{A^-\} + q \log \{H_2O\} \tag{24}$$

In Fig. 3 $\log [\text{LiA}(\text{H}_2\text{O})_n] - \log \{\text{Li}^+\}\{\text{Cl}^-\}$ with the first term computed from (21) is plotted against $\log \{\text{H}_2\text{O}\}$ for the system $\text{LiCl} - \text{H}_2\text{O}$. A straight line with a slope close to unity can be fitted to the data indicating that the predominant species might be $\text{LiCl.H}_2\text{O}$. Similarly for $\text{LiBr} - \text{H}_2\text{O}$ the ion-pair $\text{LiBr.H}_2\text{O}$ seemed to fit the data best. For reaction (24) with $n = 1$ the following constants are obtained

$$\log [\text{LiCl.H}_2\text{O}] = -4.87 + \log \{\text{Li}^+\}\{\text{Cl}^-\}\{\text{H}_2\text{O}\}$$

$$\log [\text{LiBr.H}_2\text{O}] = -6.22 + \log \{\text{Li}^+\}\{\text{Br}^-\}\{\text{H}_2\text{O}\}$$

(25a,b)

*Cation hydration.* From the activity product $\{\text{Li}^+\}\{\text{A}^-\}$ and $\phi_0^{-1}\{\text{A}^-\}$ we get the cation activity and activity coefficient functions according to the relations:

$$\log \phi_0\{\text{Li}^+\} = \log \{\text{Li}^+\}\{\text{A}^-\} - \log \phi_0^{-1}\{\text{A}^-\} \qquad (26)$$

$$\log \phi_0 y_{\text{Li}^+} = \log \phi_0\{\text{Li}^+\} - \log[\text{Li}^+]_{\text{tot}} \qquad (27)$$

Knowing the equilibrium constant for the formation of the ion-pair we can correct for the amount of lithium that participates in the ion-pair formation and evaluate the corrected ion activity coefficient function according to the relation

$$\log \phi_0 y_{\text{Li}^+\text{corr}} = \log \phi_0\{\text{Li}^+\}/\{\text{Li}^+\}_{\text{corr}} \qquad (28)$$

In Fig. 4 $\log \phi_0 y_{\text{Li}^+\text{corr}}$ is plotted against $-\log \{\text{H}_2\text{O}\}$ for the two systems. From Fig. 4 it is seen that to begin with the two curves coincide to about $\{\text{H}_2\text{O}\} = 10^{-0.5}$ where they start to deviate, although the limiting slopes of the curves in both cases approach a value of about 3 indicating a formal hydration number of 3 for $\text{Li}^+$, even close to saturation.
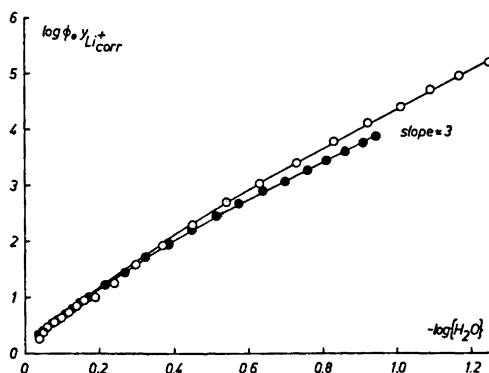


*Fig. 4.* $\log \phi_0 y_{\text{Li}}^+{}_{\text{corr}}$ plotted against $-\log \{\text{H}_2\text{O}\}$ for the systems (O) $\text{LiBr} - \text{H}_2\text{O}$ and ($\bullet$) $\text{LiCl} - \text{H}_2\text{O}$.

For the equilibrium
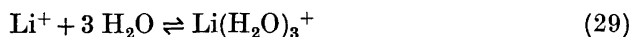
$$\text{Li}^+ + 3 \text{ H}_2\text{O} \rightleftharpoons \text{Li}(\text{H}_2\text{O})_3{}^+ \qquad (29)$$

we find

$$\text{LiCl} - \text{H}_2\text{O}: \ \log [\text{Li(H}_2\text{O)}_3{}^+] = -1.02 + \log \phi_0\{\text{Li}^+\} + 3 \log \{\text{H}_2\text{O}\}$$

$$\text{LiBr} - \text{H}_2\text{O}: \ \log [\text{Li(H}_2\text{O)}_3{}^+] = -1.36 + \log \phi_0\{\text{Li}^+\} + 3 \log \{\text{H}_2\text{O}\}$$

(30a,b)

Computing the amount of the trihydrato complex from (30) and subtracting it from the total lithium concentration we obtain

$$D = [\text{Li}^+]_{\text{tot}} - [\text{LiH}_2\text{OA}] - [\text{Li(H}_2\text{O)}_3{}^+] \tag{31}$$

In Fig. 5 $\log D - \log \phi_0\{\text{Li}^+\}$ is plotted against $-\log \{\text{H}_2\text{O}\}$ for the system $\text{LiBr} - \text{H}_2\text{O}$. A straight line with a slope of 5 can be fitted to the data indicating that we have a formal hydrate $\text{Li(H}_2\text{O)}_5{}^+$. Two lines with slopes of 4 and 6 are also indicated in Fig. 5, showing that 5 is the best choice. Similarly for $\text{LiCl} - \text{H}_2\text{O}$ the data can be fitted with a pentahydrate, although the spread is larger and the conclusion not so well-established as for the system $\text{LiBr} - \text{H}_2\text{O}$.
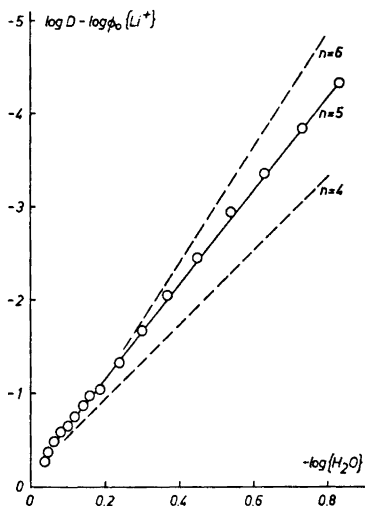


*Fig. 5.* $\log D - \log \phi_0\{\text{Li}^+\}$ plotted against $-\log \{\text{H}_2\text{O}\}$ for the system: $\text{LiBr} - \text{H}_2\text{O}$. A straight line with a slope of 5 has been fitted to the data. Two other straight lines with slopes 4 and 6 are also indicated.

For the equilibrium
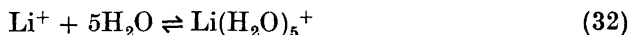
$$\text{Li}^+ + 5\text{H}_2\text{O} \rightleftharpoons \text{Li(H}_2\text{O)}_5{}^+ \tag{32}$$

we get

$$\text{LiCl} - \text{H}_2\text{O}: \ \log [\text{Li(H}_2\text{O)}_5{}^+] = -0.33 + \log \phi_0\{\text{Li}^+\} + 5 \log \{\text{H}_2\text{O}\}$$

$$\text{LiBr} - \text{H}_2\text{O}: \ \log [\text{Li(H}_2\text{O)}_5{}^+] = -0.20 + \log \phi_0\{\text{Li}^+\} + 5 \log \{\text{H}_2\text{O}\}$$

(33a,b)

The uncertainty in the various constants is about $\pm 0.03$. In Figs. $6-9$ the various anionic and cationic species present in the two systems are indicated and their sum compared with the total anion and cation concentration. As seen a reasonably good fit is obtained over the entire concentration range.
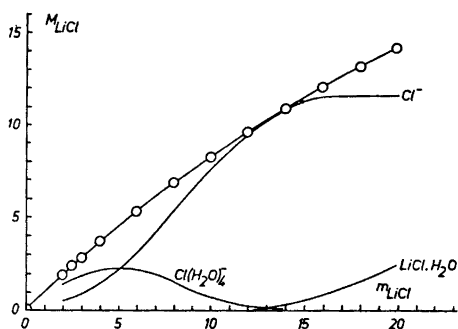
Fig 6. The stoichiometric molarity M plotted against the stoichiometric molality m for the system: LiCl − H₂O. The two anionic species and the ion-pair assumed to be present are indicated by the full-drawn curves and their sum compared with the stoichiometric molarity. (————) Stoic hiometric molarity and (O) computed sum for the three species present.
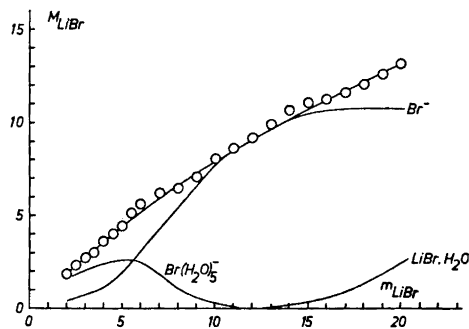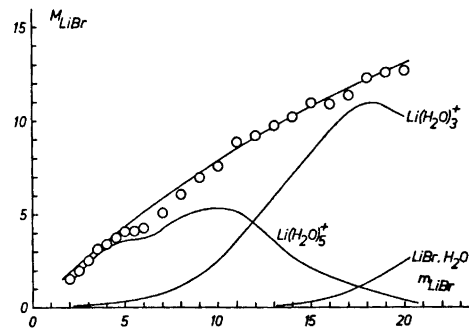
Fig. 7. The stoichiometric molarity M plotted against the stoichiometric molality m for the system: LiBr − H₂O. The two anionic species and the ion-pair assumed to be present are indicated by the full-drawn curves and their sum compared with the stoichiometric molarity. (————) Stoichiometric molarity and (O) computed sum for the three species present.
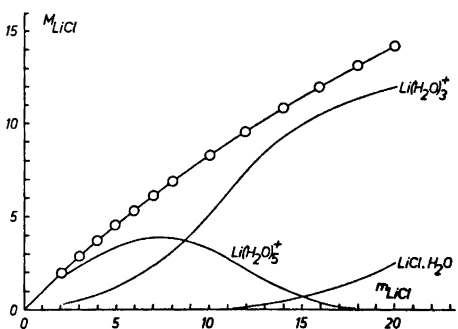


Fig. 8. The stoichiometric molarity M plotted against the stoichiometric molality m for the system: LiCl − H₂O. The two cationic species and the ion-pair assumed to be present are indicated by the full-drawn curves and their sum compared with the stoichiometric molarity. (————) Stoichiometric molarity and (O) computed sum for the three species present.

Fig. 9. The stoichiometric molarity M plotted against the stoichiometric molality m for the system. LiBr − H₂O. The two cationic species and the ion-pair assumed to be present are indicated by the full-drawn curves and their sum compared with the stoichiometric molarity. (————) Stoichiometric molarity and (O) computed sum for the three species present.

## DISCUSSION

The formal hydration numbers obtained in this approach differ from earlier estimates by being assigned to given complexes, and not being overall averages. Hitherto very few investigations have dealt with the variation of hydration

number with composition. As mentioned elsewhere,[1] the overall averages obtained from equations similar to (6) for cation and anion hydration compare favorably with other estimates of primary hydration. Further support can be adduced from the compilations of Bockris and his coworkers [17],[18] and of Desnoyers and Jolicoeur,[19] in which a coordination number close to $5 \pm 1$ is given for $Li^+$. An investigation covering the whole accessible concentration range has been made by Pottel.[20] From dielectric constant measurements he estimated the overall number of water molecules hindered from rotation. This overall value decreases from nine to two when going from dilute to concentrated LiCl solutions, which is surprisingly close to the overall hydration number obtained by us.[1] Although this coincidence might be fortuitous it is encouraging. Estimates from NMR measurements have been made by Crechmore and Reilly [21] from a study of the temperature dependent proton chemical shift. Although only $3-4$ m solutions were studied they obtained rather low values $\bar{n}(=3.4$ at 3.08 m and $\bar{n}=3.2$ at 4.62 m). They rationalized their results by assigning an hydration number of four to $Li^+$ and practically zero for $Cl^-$. Although not in exact agreement with our description their results give the same general picture with strong cation hydration and very little anion hydration.

That water is strongly attached to the lithium ion as illustrated by the results of Munson and Tyndall [22] who find about 6 $H_2O$ per $Li^+$ in noble gas atmosphere, which upon extrapolation of the ratio field strength/gas pressure seems to suggest $3-4$ $H_2O$ per $Li^+$. Although a gas phase is a considerably different environment from a concentrated aqueous solution, their results support ours in showing that water is strongly bound to the lithium ion.

For the anions our results are in qualitative agreement with those obtained by Robinson and Stokes [23] in their attempt to account for hydration in electrolyte solutions. On the other hand the very scanty information given by Bockris and Reddy [18] indicates roughly the same hydration by $Cl^-$ and $Br^-$ and *i.e.* $2 \pm 1$. If we compare the average hydration numbers for these anions as defined by the relation analogous to eqn. (6) we find that for $m_{LiCl} > 4$ they are practically the same. Only in more dilute solutions does the difference become appreciable, and at these low concentrations the assumption that most of the change in excess free energy is due to changes in energy of hydration becomes a poor one.

The formation of solvent-separated ion-pairs may be given as a simple explanation for the decreasing part of the curves in Fig. 1. As mentioned elsewhere,[1] through the formation of such ion-pairs enough water is released to provide three water molecules for the formation of $Li(H_2O)_3{}^+$ even above 18 m, where less water than $3H_2O/LiCl$ is present. However, these ion-pairs as well as the various hydrates suggested can at present only be regarded as formal entities permitting a very simple description of the two systems $LiCl-H_2O$ and $LiBr-H_2O$. It is most encouraging, however, that the present approach gives a rather simple description of the system, with only two cationic and two anionic species together with an hydrated ion-pair, all the way up to saturated solutions.

## REFERENCES

1. Högfeldt, E. and Leifer, L. *Acta Chem. Scand.* **17** (1963) 338.
2. Högfeldt, E. *Acta Chem. Scand.* **14** (1960) 1627.
3. Ojeda, M. and Wyatt, P. A. H. *J. Phys. Chem.* **68** (1964) 1857.
4. Leifer, L. and Högfeldt, E. In Friend, A. and Gutmann, F., Eds., *First Australian Conf. Electrochem.*, Pergamon, Oxford 1964, p. 107.
5. Högfeldt, E. *Svensk Kem. Tidskr.* **70** (1963) 63.
6. Högfeldt, E. *Acta Cient. Venez.* **17** (1966) 13.
7. Essig, T. R. and Marinsky, J. A. *Can. J. Chem.* **50** (1972) 2254.
8. Högfeldt, E., Marinsky, J. A. and Essig, T. R. *In preparation.*
9. Hammett, L. P. *Physical Organic Chemistry*, McGraw, New York 1940.
10. Deno, N. C., Jaruszelski, J. J. and Schriesheim, A. *J. Am. Chem. Soc.* **77** (1955) 3044.
11. Deno, N. C., Berkheimer, H. E., Evans, W. L. and Peterson, H. J. *J. Am. Chem. Soc.* **81** (1959) 2344, 6535.
12. Boyd, R. H. *J. Am. Chem. Soc.* **85** (1963) 1.
13. Yates, K., Stevens, J. B. and Katritzky, A. R. *Can. J. Chem.* **42** (1964) 1957.
14. Rochester, C. H. *Acidity functions*, Academic, London 1970.
15. Wyatt, P. A. H. *Discussions Faraday Soc.* **24** (1957) 162.
16. Högfeldt, E. *Acta Chem. Scand.* **16** (1962) 1054.
17. Bockris, J. O.' M. and Conway, B. E. *Modern Aspects of Electrochemistry*, London 1954, Vol. 1, p. 71.
18. Bockris, J. O. M. and Reddy, A. K. N. *Modern Electrochemistry*, Plenum Press, New York 1970, Vol. 1, p. 131.
19. Desnoyer, J. E. and Jolicoeur, C. In Bockris, J. O.' M. and Conway, B. E., Eds., *Modern Aspects of Electrochemistry*, Butterworths, London 1969, No. 5, p. 1.
20. Pottel, R. In Conway, B. E. and Barradas, R. G., Eds., *Chemical Physics of Ionic Solutions*, Wiley, New York 1966, p. 581.
21. Crechmore, R. W. and Reilly, C. N. *J. Phys. Chem.* **73** (1969) 1563.
22. Munson, R. J. and Tyndall, A. M. *Proc. Roy. Soc. (London)* **A 172** (1939) 28.
23. Robinson, R. A. and Stokes, R. H. *Electrolyte, Solutions*, 2nd Ed., Butterworths, London 1959, Chapter 9.

# Short Communications

## Kinetics of the Decomposition of Aqueous Chlorine Dioxide Solutions

GUNNAR von HEIJNE and ANTS TEDER

*Swedish Forest Products Research Laboratory (STFI), S-114 86 Stockholm, Sweden*

Chlorine dioxide is used extensively in the pulping industry as a bleaching agent. The industrially-prepared chlorine dioxide always contains some chlorine. During the bleaching almost half the chlorine dioxide is consumed by the unwanted side reaction [1]

$$2 \, ClO_2 + H_2O \rightarrow ClO_3^- + ClO_2^- + 2 \, H^+$$

It is known that the presence of chlorine and increased pH accelerates the decomposition,[2] but no kinetic studies on chlorine dioxide decomposition under the conditions prevailing during pulp bleaching could be found in the literature. Previous studies are limited to alkaline solutions, room temperature and/or very high chlorine dioxide concentrations.

In the present investigation, the kinetics of aqueous chlorine dioxide decompositions were studied under the conditions used in chlorine dioxide bleaching (temperature 40 – 80°C, pH 2 – 7, $ClO_2$ conc. = 0.001 – 0.01 mol/l, total chlorine conc. = 0 – 0.01 mol/l), but in the absence of pulp.

During each experiment the temperature and pH were kept constant, the latter by successive alkali additions controlled by a pH-stat. The reaction was monitored by removing samples after different reaction times. The chlorine dioxide concentration was determined spectrophotometrically using a Bausch and Lomb 600 instrument.[8] Mainly the initial rate, $r_0 = -(d[ClO_2]/dt)$ at $t = 0$, was studied. The reaction mixture was obtained by diluting chlorine dioxide

and "chlorine" stock solutions with distilled water.

The chlorine dioxide stock solution was prepared by absorbing chlorine dioxide gas in water. The chlorine dioxide gas was obtained as follows. Gaseous chlorine was absorbed in a solution of sodium chlorite. When the reaction was complete, as indicated by a change of colour from brown to yellow, the chlorine dioxide was driven off in a stream of nitrogen. The molar ratio chlorine dioxide/total chlorine (*i.e.* $\sum Cl_2 + HOCl + OCl^-$) was larger than 30 in the chlorine dioxide stock solution. The "chlorine" stock solution contained mainly HOCl and was prepared by absorbing chlorine in aqueous NaOH.

As a rule the chlorine dioxide concentration decreased according to a first order reaction. At pH values higher than 6, the "normal" decomposition was followed, after an induction period of up to 60 min, by a very rapid reaction, the rate of which, $d[ClO_2]/dt$, was denoted $r_r$. This rapid reaction had been previously observed by Rapson.[9] The nature of this autocatalytic reaction is obscure but it can be triggered by injecting minute amounts of 0.1 M HOCl into neutral or slightly alkaline chlorine dioxide solutions. Increased pH increased the rate of this rapid reaction in the absence of "chlorine" as well as that of the initial reaction in the presence of "chlorine". In the absence of chlorine, the pH seemed to have no significant effect on the initial rate of reaction (Fig. 1).

The initial rate of chlorine dioxide decomposition could be described by

$$r_0 = - \frac{d[ClO_2]}{dt} = k_1[ClO_2] + k_2[ClO_2][ClO^-]$$

At 78°C, the temperature at which most of the experiments were carried out, $k_1 = 3.0 \times 10^{-5} \, s^{-1}$ and $k_2 = 36 \, 1 \, mol^{-1}, \, s^{-1}$ were obtained using a value for the equilibrium constant
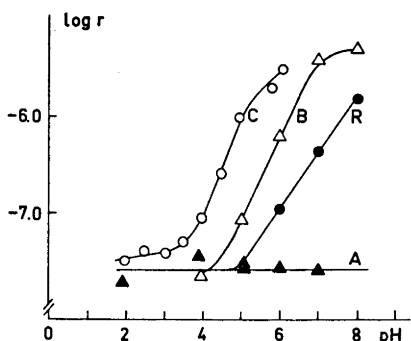
$$K_a = [ClO^-][H^+]/[HClO]$$

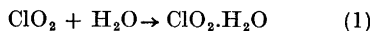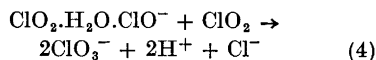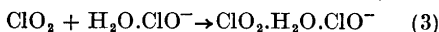*Fig. 1.* An example of the effect of pH and the presence of "chlorine" ($Cl_2 + HOCl + OCl^-$) on the rate of decomposition of aqueous chlorine dioxide solutions. The logarithm of the reaction rate in mol/s is plotted *versus* pH. Temp. 78°C. $[ClO_2] = 0.0028$ mol/l. The initial rate of decomposition $r_0$, at different "chlorine" concentrations: A (▲) $<1 \times 10^{-4}$, B(△) $2 \times 10^{-4}$, C (○) $1.5 \times 10^{-3}$ mol/l; as well as the rate $r_s$, of the rapid reaction R (●), that occurs after an induction period, are given.

of $1.59 \times 10^{-7}$ mol/l according to Flis.[10] Both rate constants have activation energies of about 45 kJ/mol. If the temperature dependence of the equilibrium $ClO^-/HClO$ is neglected, $k_2$ has an apparent activation energy of 70 kJ/mol. The rate equation proposed here, for conditions prevailing during chlorine dioxide bleaching, is different from those previously proposed for chlorine dioxide degradation under other conditions.[3-7]

The first term in the rate equation found can be described by the reactions

$$ClO_2 + H_2O \rightarrow ClO_2.H_2O \qquad (1)$$

$$ClO_2.H_2O + ClO_2 \rightarrow ClO_2^- + ClO_3^- + 2H^+ \qquad (2)$$

while the second term is described by

$$ClO_2 + H_2O.ClO^- \rightarrow ClO_2.H_2O.ClO^- \qquad (3)$$

$$ClO_2.H_2O.ClO^- + ClO_2 \rightarrow 2ClO_3^- + 2H^+ + Cl^- \qquad (4)$$

The reactions (1) and (3) are assumed to be slow and rate determining. This hypothesis is supported by the observation that the entropy of activation, $\Delta S^{\ddagger}$, for the chlorine dioxide decomposition is negative $-200$ J/K, mol in the absence and $-100$ J/K, mol in the presence of "chlorine". The entropy values observed

are typical for association reactions of the type (1) and (3).[11]

1. Rydholm, S. *Pulping Processes*, Interscience, London 1965.
2. Soila, R., Lehtikoski, O. and Virkola, N.-E. *Svensk Papperstid.* 65 (1962) 632.
3. Birgogne, M. *Compt. Rend.* 240 (1955) 311.
4. Bray, W. H. *Z. anorg. allgem. Chem.* 48 (1906) 217.
5. Brown, R. W. *Tappi* 35 (1952) 75.
6. Burghards, S. J. *Northwest Sci.* 25 (1951) 137.
7. Granstrom, M. and Lee, F. *Publ. Works* 88 (1957) 90.
8. Sjöström, L., Teder, A. and Tormund, D. *STFI Report Ser. B* (1973) No. 172.
9. Rapson, H. D. *Private communication.*
10. Flis, J. E. *J. Appl. Chem. USSR* 31 (1958) 1183.
11. Moore, W. J. *Physical Chemistry*, 4th Ed., Longmans, London 1963.

## Structural Studies of the *Klebsiella* O Group 8 Lipopolysaccharide

MARGARETA CURVALL,[a]
BENGT LINDBERG,[a]
JÖRGEN LÖNNGREN,[a] ULLA RUDÉN[a]
and WOLFGANG NIMMICH[b]

[a]*Department of Organic Chemistry, Arrhenius Laboratory, University of Stockholm, S-104 05 Stockholm, Sweden* and [b]*Institut für Medizinische Mikrobiologie und Epidemiologie der Universität Rostock, 25 Rostock 1, DDR*

Five of the twelve different *Klebsiella* O groups contain D-galactose as the only sugar in the O-specific side chains of their lipopolysaccharides (LPS).[1] We have reported structural studies of three of these, O groups 1 and 6 [2] (identical) and O group 9.[3] We now report similar studies of the O group 8 LPS.
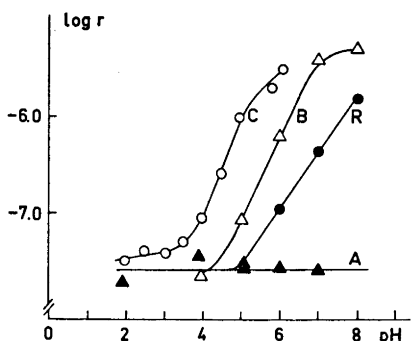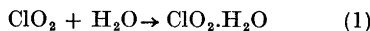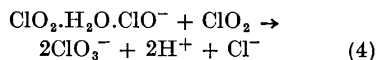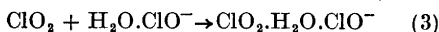
*Fig. 1.* An example of the effect of pH and the presence of "chlorine" ($Cl_2 + HOCl + OCl^-$) on the rate of decomposition of aqueous chlorine dioxide solutions. The logarithm of the reaction rate in mol/s is plotted *versus* pH. Temp. 78°C. $[ClO_2] = 0.0028$ mol/l. The initial rate of decomposition $r_0$, at different "chlorine" concentrations: A ($\blacktriangle$)$<1 \times 10^{-4}$, B($\triangle$)$2 \times 10^{-4}$, C (O) $1.5 \times 10^{-3}$ mol/l; as well as the rate $r_s$, of the rapid reaction R ($\bullet$), that occurs after an induction period, are given.

of $1.59 \times 10^{-7}$ mol/l according to Flis.[10] Both rate constants have activation energies of about 45 kJ/mol. If the temperature dependence of the equilibrium $ClO^-/HClO$ is neglected, $k_2$ has an apparent activation energy of 70 kJ/mol. The rate equation proposed here, for conditions prevailing during chlorine dioxide bleaching, is different from those previously proposed for chlorine dioxide degradation under other conditions.[3-7]

The first term in the rate equation found can be described by the reactions

$$ClO_2 + H_2O \rightarrow ClO_2.H_2O \tag{1}$$

$$ClO_2.H_2O + ClO_2 \rightarrow ClO_2^- + ClO_3^- + 2H^+ \tag{2}$$

while the second term is described by

$$ClO_2 + H_2O.ClO^- \rightarrow ClO_2.H_2O.ClO^- \tag{3}$$

$$ClO_2.H_2O.ClO^- + ClO_2 \rightarrow$$
$$2ClO_3^- + 2H^+ + Cl^- \tag{4}$$

The reactions (1) and (3) are assumed to be slow and rate determining. This hypothesis is supported by the observation that the entropy of activation, $\Delta S^{\ddagger}$, for the chlorine dioxide decomposition is negative $-200$ J/K, mol in the absence and $-100$ J/K, mol in the presence of "chlorine". The entropy values observed

are typical for association reactions of the type (1) and (3).[11]

1. Rydholm, S. *Pulping Processes*, Interscience, London 1965.
2. Soila, R., Lehtikoski, O. and Virkola, N.-E. *Svensk Papperstid.* **65** (1962) 632.
3. Birgogne, M. *Compt. Rend.* **240** (1955) 311.
4. Bray, W. H. *Z. anorg. allgem. Chem.* **48** (1906) 217.
5. Brown, R. W. *Tappi* **35** (1952) 75.
6. Burghards, S. J. *Northwest Sci.* **25** (1951) 137.
7. Granstrom, M. and Lee, F. *Publ. Works* **88** (1957) 90.
8. Sjöström, L., Teder, A. and Tormund, D. *STFI Report Ser. B* (1973) No. 172.
9. Rapson, H. D. *Private communication.*
10. Flis, J. E. *J. Appl. Chem. USSR* **31** (1958) 1183.
11. Moore, W. J. *Physical Chemistry*, 4th Ed., Longmans, London 1963.

# Structural Studies of the *Klebsiella* O Group 8 Lipopolysaccharide

MARGARETA CURVALL,[a]
BENGT LINDBERG,[a]
JÖRGEN LÖNNGREN,[a] ULLA RUDÉN[a]
and WOLFGANG NIMMICH[b]

[a]*Department of Organic Chemistry, Arrhenius Laboratory, University of Stockholm, S-104 05 Stockholm, Sweden and* [b]*Institut für Medizinische Mikrobiologie und Epidemiologie der Universität Rostock, 25 Rostock 1, DDR*

Five of the twelve different *Klebsiella* O groups contain D-galactose as the only sugar in the O-specific side chains of their lipopolysaccharides (LPS).[1] We have reported structural studies of three of these, O groups 1 and 6 [2] (identical) and O group 9.[3] We now report similar studies of the O group 8 LPS.

The LPS was isolated from *Klebsiella* O8:K69 as previously described[1] and showed $[\alpha]_{578} + 59°$. Analysis of a hydrolysate, using D-arabinose as an internal standard, showed that the LPS contained 36 % galactose, 2 % glucose, and 2 % heptose residues. The galactose has the D-configuration, as it reacts with galactose oxidase.[1] Assuming that the sugar residues account for the greater part of the optical rotation, most or all of the D-galactose residues should be α-linked. The LPS showed strong absorption in the IR at 1730 cm$^{-1}$, indicating the presence of O-acyl groups. These were transferred into benzyl esters and identified as acetyl groups by GLC−MS.[4]

A methylation analysis (Table 1, column A) showed that the O-specific side chains

Table 1. Methylation analyses of original and modified *Klebsiella* O group 8 LPS.

| Sugars[a] | $T^b$ | Mol %[c] | | |
|---|---|---|---|---|
| | | A | B | C |
| 1,2,4,5,6-Gal[d] | 0.46 | − | 20 | − |
| 2,3,4,6-G | 1.00 | 5 | 4 | 7 |
| 2,3,4,6-Gal | 1.17 | − | 28 | 5 |
| 2,5,6-Gal | 1.80 | 33 | 15 | 32[e] |
| 2,4,6-Gal | 1.99 | 63 | 34 | 56[f] |

[a] 1,2,4,5,6-Gal= 1,2,4,5,6-penta-O-methyl-D-galactitol; 2,3,4,6-G= 2,3,4,6-tetra-O-methyl-D-glucose, etc. [b] Retention time of the corresponding alditol acetate relative to 1,5-di-O-acetyl-2,3,4,6-tetra-O-methyl-D-glucitol on a SP-1000 glass capillary column at 220°. [c] A: original LPS; B: partially acid degraded LPS (see text); C: acetalated, trideuteriomethylated, hydrolysed and methylated LPS (see text). [d] Monodeuterated at C-1. [e] ≃18 % OCD$_3$-groups at position 2. [f] ≃12 % OCD$_3$-groups at position 2 and ≃12 % at position 6.

are linear and composed of (1→3)-linked furanosidic and pyranosidic D-galactose residues in the proportion 1:2. This proportion, for five different analyses, was 1:2±0.2. Arabinose and galactose (1:1.9) were identified after periodate oxidation, borohydride reduction and acid hydrolysis of the LPS.

A sample of the LPS was subjected to mild acid hydrolysis, whereby only the furanosidic linkages should be hydrolysed,
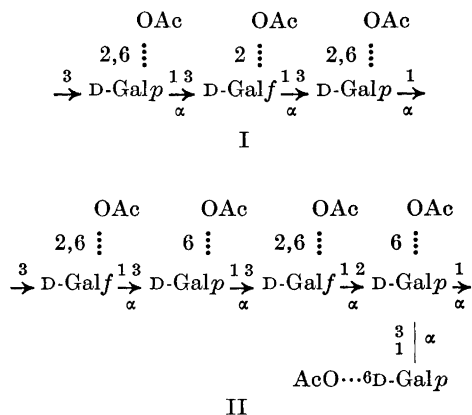
and the products were reduced (NaBD$_4$) and subjected to methylation analysis. The results (Table 1, column B) demonstrate that about half of the furanosidic linkages have been hydrolysed and, as 2,3,4,6- but no 2,3,5,6-tetra-O-methyl-D-galactose was found, that no galactofuranose residues are adjacent. The O-specific side chains in bacterial LPS are generally composed of oligosaccharide repeating units. The simplest unit for the present LPS should be a (1→3)-linked trisaccharide with one D-galactofuranose and two D-galactopyranose residues.

O-Acetyl groups were located by the method of de Belder and Norrman,[3,5] wherein hydroxyl groups are protected as acetals by treatment with methyl vinyl ether, and the product subjected to methylation analysis. The formation of 2-, 4-, and 6-O-methyl-D-galactose (15, 2, and 8 %, respectively) demonstrated the presence of O-acetyl groups in these positions in the original polysaccharide. The degree of substitution was 0.25.

Part of the acetalated polysaccharide was trideuteriomethylated, hydrolysed under mild conditions during which only the protecting acetal groups should be removed and remethylated (CH$_3$I). Analysis of this product (Table 1, column C) revealed that some furanosidic linkages had been cleaved, since a small portion of 2,3,4,6-tetra-O-methyl-D-galactose was obtained. MS of the derived alditol acetates showed the presence of trideuteriomethyl groups at C-2 in both furanosidic and pyranosidic residues and at C-6 in pyranosidic residues. The small percentage of O-acetyl groups in the 4-positions was not revealed by this procedure.

From the combined evidence presented above, structure I is proposed for the trisaccharide repeating unit in the O-specific side chains of the *Klebsiella* O group 8 LPS. A dotted line indicates a substituent that is not present in all repeating units. As no sugar deriving from the non-reducing terminal was observed in the methylation analysis it is inferred that the O-specific side chains are at least thirty repeating units long. The structure has structural features in common with the penta-saccharide repeating unit (II) proposed for the *Klebsiella* O group 9 LPS.[3] (Most sugar residues in I and II should be α-linked but not necessarily all, as indicated in the formulae.) Immunological cross-reactions between these two O groups may therefore be expected. The observation

by Kaluzewski[6] that they are serologically identical is, however, difficult to understand in the light of the present results.

$$
\begin{array}{ccc}
\text{OAc} & \text{OAc} & \text{OAc} \\
\text{2,6} \vdots & \text{2} \vdots & \text{2,6} \vdots \\
\overset{3}{\rightarrow} \text{D-Gal}p \overset{1\ 3}{\underset{\alpha}{\rightarrow}} \text{D-Gal}f \overset{1\ 3}{\underset{\alpha}{\rightarrow}} \text{D-Gal}p \overset{1}{\underset{\alpha}{\rightarrow}}
\end{array}
$$

I

$$
\begin{array}{cccc}
\text{OAc} & \text{OAc} & \text{OAc} & \text{OAc} \\
\text{2,6} \vdots & \text{6} \vdots & \text{2,6} \vdots & \text{6} \vdots \\
\overset{3}{\rightarrow} \text{D-Gal}f \overset{1\ 3}{\underset{\alpha}{\rightarrow}} \text{D-Gal}p \overset{1\ 3}{\underset{\alpha}{\rightarrow}} \text{D-Gal}f \overset{1\ 2}{\underset{\alpha}{\rightarrow}} \text{D-Gal}p \overset{1}{\underset{\alpha}{\rightarrow}}
\end{array}
$$

$$\begin{array}{c} 3 \\ 1 \end{array} \Big| \ \alpha$$

AcO···6D-Gal$p$

II

*Experimental.* General methods and methods for sugar analysis, methylation analysis, and location of O-acetyl groups were essentially the same as used in studies on the related *Klebsiella* O group 9 LPS.[3] GLC of the partially methylated alditol acetates was performed at 220° on a glass capillary column (0.25 mm × 25 m) containing SP-1000 as the stationary phase. For GLC−MS an OV-225 SCOT column was used. The LPS was isolated[1] from strain *Klebsiella* O8:K69 (889), and showed $[\alpha]_{578} + 59°$ (c 0.25, water). In the IR (KBr) a strong absorption at 1730 cm$^{-1}$ was observed. The LPS contained 1.8 % P.

*Analysis of partially hydrolysed LPS.* The LPS (5 mg) in 0.025 M sulphuric acid (5 ml) was kept at 100° for 2 h and neutralised (BaCO₃). Sodium borodeuteride (20 mg) was added and the solution kept for 3 h at room temperature. The solution was treated with Dowex 50 (H⁺), concentrated and boric acid removed by distillations with methanol. The product was dissolved in water, lyophilised and subjected to methylation analysis.

*Periodate oxidation of the LPS.* The LPS (5 mg) was dissolved in 0.1 M sodium acetate buffer of pH 3.9 (5 ml), 0.08 M sodium metaperiodate (2 ml) was added and the solution kept in the dark at 4° for 48 h. Excess periodate was reduced with ethylene glycol (0.5 ml) and the solution was dialysed against tapwater overnight. Sodium borohydride (60 mg) was added, the solution kept for 7 h at room temperature, excess borohydride decomposed by addition of 50 % acetic acid and the solution dialysed overnight. Sugar analysis of this

product showed arabinose and galactose in the molar proportion 1:1.9. D-Mannose (1 mg) was added as an internal standard, and the two sugars accounted for all the galactose in the original LPS.

1. Nimmich, W. and Korten, G. *Pathol. Microbiol.* 36 (1970) 179.
2. Björndal, H., Lindberg, B. and Nimmich, W. *Acta Chem. Scand.* 25 (1971) 750.
3. Lindberg, B., Lönngren, J. and Nimmich, W. *Carbohyd. Res.* 23 (1972) 47.
4. Bethge, P. O. and Lindström, K. *Svensk Papperstid.* 76 (1973) 645.
5. de Belder, A. N. and Norrman, B. *Carbohyd. Res.* 8 (1968) 1.
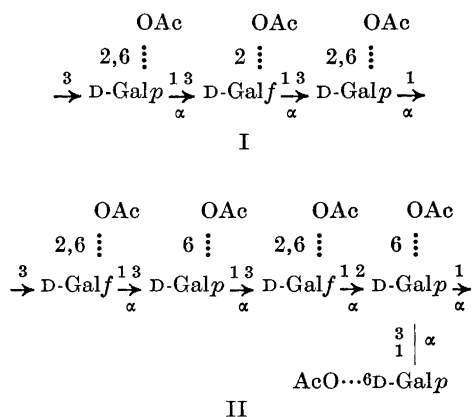6. Kaluzewski, S. *Med. dosw. Mikrobiol.* 17 (1965) 283.

# On the Calibration of Circular Dichroism Spectrometers

BENGT NORDÉN

*Inorganic Chemistry 1, Chemical Center, University of Lund, P.O.Box 740, S-220 07 Lund, Sweden*

Due to uncertainties about CD standards[1-3] we want to suggest two methods of calibrating a CD spectrometer. The first determines whether the instrument is actually measuring CD $= A_{1} - A_{r}$. It may also be used for the calibration over a wavelength range, in which the instrumental accuracy depends upon the wavelength program for the excitation voltage of the light modulation.[4] The second is appropriate for regular checking.

by Kaluzewski[6] that they are serologically identical is, however, difficult to understand in the light of the present results.

$$\underset{\alpha}{\overset{3}{\rightarrow}}\ \text{D-Gal}p\ \underset{\alpha}{\overset{1\ 3}{\rightarrow}}\ \text{D-Gal}f\ \underset{\alpha}{\overset{1\ 3}{\rightarrow}}\ \text{D-Gal}p\ \overset{1}{\underset{\alpha}{\rightarrow}}$$

OAc  OAc  OAc
2,6    2    2,6

I

$$\underset{\alpha}{\overset{3}{\rightarrow}}\ \text{D-Gal}f\ \underset{\alpha}{\overset{1\ 3}{\rightarrow}}\ \text{D-Gal}p\ \underset{\alpha}{\overset{1\ 3}{\rightarrow}}\ \text{D-Gal}f\ \underset{\alpha}{\overset{1\ 2}{\rightarrow}}\ \text{D-Gal}p\ \overset{1}{\underset{\alpha}{\rightarrow}}$$

OAc  OAc  OAc  OAc
2,6    6    2,6    6

$$\begin{array}{c}3\\1\end{array}\Big|\ \alpha$$

AcO$\cdots$6D-Gal$p$

II

*Experimental.* General methods and methods for sugar analysis, methylation analysis, and location of O-acetyl groups were essentially the same as used in studies on the related *Klebsiella* O group 9 LPS.[3] GLC of the partially methylated alditol acetates was performed at 220° on a glass capillary column (0.25 mm × 25 m) containing SP-1000 as the stationary phase. For GLC−MS an OV-225 SCOT column was used. The LPS was isolated[1] from strain *Klebsiella* O8:K69 (889), and showed $[\alpha]_{578} + 59°$ (c 0.25, water). In the IR (KBr) a strong absorption at 1730 cm$^{-1}$ was observed. The LPS contained 1.8 % P.

*Analysis of partially hydrolysed LPS.* The LPS (5 mg) in 0.025 M sulphuric acid (5 ml) was kept at 100° for 2 h and neutralised (BaCO$_3$). Sodium borodeuteride (20 mg) was added and the solution kept for 3 h at room temperature. The solution was treated with Dowex 50 (H$^+$), concentrated and boric acid removed by distillations with methanol. The product was dissolved in water, lyophilised and subjected to methylation analysis.

*Periodate oxidation of the LPS.* The LPS (5 mg) was dissolved in 0.1 M sodium acetate buffer of pH 3.9 (5 ml), 0.08 M sodium metaperiodate (2 ml) was added and the solution kept in the dark at 4° for 48 h. Excess periodate was reduced with ethylene glycol (0.5 ml) and the solution was dialysed against tap-water overnight. Sodium borohydride (60 mg) was added, the solution kept for 7 h at room temperature, excess borohydride decomposed by addition of 50 % acetic acid and the solution dialysed overnight. Sugar analysis of this

product showed arabinose and galactose in the molar proportion 1:1.9. D-Mannose (1 mg) was added as an internal standard, and the two sugars accounted for all the galactose in the original LPS.

1. Nimmich, W. and Korten, G. *Pathol. Microbiol.* **36** (1970) 179.
2. Björndal, H., Lindberg, B. and Nimmich, W. *Acta Chem. Scand.* **25** (1971) 750.
3. Lindberg, B., Lönngren, J. and Nimmich, W. *Carbohyd. Res.* **23** (1972) 47.
4. Bethge, P. O. and Lindström, K. *Svensk Papperstid.* **76** (1973) 645.
5. de Belder, A. N. and Norrman, B. *Carbohyd. Res.* **8** (1968) 1.
6. Kaluzewski, S. *Med. dosw. Mikrobiol.* **17** (1965) 283.

# On the Calibration of Circular Dichroism Spectrometers

BENGT NORDÉN

*Inorganic Chemistry 1, Chemical Center, University of Lund, P.O.Box 740, S-220 07 Lund, Sweden*

Due to uncertainties about CD standards[1-3] we want to suggest two methods of calibrating a CD spectrometer. The first determines whether the instrument is actually measuring $CD = A_l - A_r$. It may also be used for the calibration over a wavelength range, in which the instrumental accuracy depends upon the wavelength program for the excitation voltage of the light modulation.[4] The second is appropriate for regular checking.

The normal calibration methods are subject to the following uncertainties: 1. They require the use of a "standard" sample of previously established specific CD. This $\Delta\varepsilon$ may be inaccurate. 2. The standard may be of poor optical or chemical purity. 3. The chemical and instrumental conditions to which the $\Delta\varepsilon$ refers may be poorly defined. As none of the commercially available CD instruments yields an absolute CD, the first point is the most intractable.[4-6]

The first method does not require any optically active sample. Hence it does not rely upon a previously established specific CD. Instead it takes advantage of the fact that the accuracy of the optical decadic absorbance obtained from a spectrophotometer, $\log(I_0/I)$, can be determined easily.[7] A Glan polarizing prism was placed in a Zeiss PMQ − II spectrophotometer. The two orthogonal polarized absorptions, $A_{\parallel}$ and $A_{\perp}$,[8] of a stretched polyethylene film containing orientated 2,2'-bipyridyl were measured at 282 nm where the wavelength of the broad absorbance maximum coincides with a linear dichroism peak.[9] The film was of high homogeneity and was hermetically sealed with a water lock to ensure high reproducibility.[10] The concentration of 2,2'-bipyridyl could be decreased as desired by washing-out with chloroform.

An unstretched polyethylene film was inserted into the CD spectrometer (Jouan, Dichrographe Model B). In the light path behind this was placed the sample solution (0.01 cm d-fenchone). The film was stretched in steps until the apparent "CD" was zero. A quarter wave retardation had thus been obtained so that the instrument was now adapted to measure the linear dichroism, $A_{\parallel} - A_{\perp}$. The sample was replaced by a film containing 2,2'-bipyridyl orientated with its plane perpendicular to that of the incident light. Its stretch direction relative to the stretch direction of the "quarter wave film" was then adjusted until the deflection recorded on the instrument was a maximum.

Table 1 shows a satisfactory agreement between corresponding linear dichroism values obtained from the two instruments, particularly after one set was adjusted by 0.006 absorbance units. This correction was presumably due to a systematic error in the absorbance measurement, since a plot of the CD against concentration yielded a line passing through the origin. This conclusion was also supported by the results of an experiment in which samples of different concentrations were preceded in the light path by a *semi*-oriented "quarter-wave" film. The apparent CD recorded with the elliptically polarized light was about half the real CD (without film) and was also linear with respect to concentration, the line again passing through the origin. The systematic error was thus not due to some deficiency in the photo-elastic quarter-wave plate. Furthermore the error cannot be due to stray-light from the Zeiss monochromator since this would produce the opposite effect.

A second series of experiments was conducted to test the instrument at very high dichroisms. Fig. 1 shows absorbance differences obtained with the technique described above, but at 500 nm with samples of acridine orange orientated in stretched polyvinyl alcohol (PVA).[8] This

*Table 1.* Dichroisms, determined independently with two instruments, of a stretched polyethylene film containing various concentrations of orientated 2,2'-bipyridyl. For the absorption measurements, the estimated error in the last digit is given in parentheses. "Adjusted" refers to the correction necessary for the curve of $y=f(x)$ to pass through the origin.

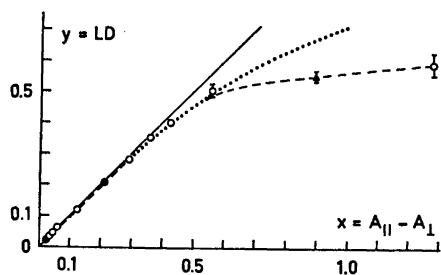| Dichroism (Jouan) | Absorbance (Zeiss) | | | |
|---|---|---|---|---|
| $y=A_{\parallel}-A_{\perp}=LD$ | $A_{\parallel}$ | $A_{\perp}$ | $x=A_{\parallel}-A_{\perp}$ | adjusted |
| 0.331 | 1.415 | 1.077 | 0.338(5) | 0.332 |
| 0.140 | 0.705 | 0.559 | 0.146(3) | 0.140 |
| 0.064 | 0.376 | 0.307 | 0.069(2) | 0.063 |
| 0.031 | 0.230 | 0.192 | 0.038(2) | 0.032 |
| 0.019 | 0.181 | 0.154 | 0.027(2) | 0.021 |
| 0.017 | 0.171 | 0.147 | 0.024(2) | 0.018 |

*Fig. 1.* Linear dichroism, $y$, obtained differentially (Jouan), plotted *versus* the difference, $x$, between separately determined $A_{||}$ and $A_\perp$ (Zeiss), from stretched PVA/acridine orange films measured at 500 nm. ● two selected high-quality films suitable as standards, ▲ $A_{||} = 1.45$, $A_\perp = 0.51$, ... $y = 2(\log \mathrm{e}) \tanh (x/2 \log \mathrm{e})$, —— $x = y$. Deviation of ... from —— at $x = 0.3$ is 4 %.

system is easier to handle than the first. In addition PVA retains its orientation and behaves as a clear, hard glass at room temperature, and much larger linear dichroisms can be produced. However, thickness and orientation cannot be reproduced as well as in the polyethylene/bipyridine system.

The CD spectrometer used here measures linear dichroisms lower than $0.3 - 0.4$ with satisfactory accuracy but for larger absorbance differences it gives too low a value. Such behaviour could actually be expected because the instrument is designed to register a deflection proportional to the hyperbolic tangent of the dichroism divided by $2^{10} \log \mathrm{e}$.[5]

For very high dichroisms the error exceeds even that expected on the above grounds. This is probably due to straylight, depolarization, *etc.*

PVA-acridine orange films of high quality can be combined with quarter wave plates to provide permanent standards. The CD values of two such were found to be stable ($\pm 3$ %) for at least 5 months.

To eliminate effects due to different photomultiplier sensitivity when measuring the absorbance for the two orthogonal polarizations, a depolarizer may be inserted after the sample film. For a rapid test the sample film can be rotated 90° and the measurements repeated.

It is of interest to observe that the conventional standard with which the

CD spectrometer employed here was calibrated was quite satisfactory ("Isoandrosterone", Jouan-Quétin Co.).

The polyethylene matrix used was stretched approximately 300 % and the PVA film $5 - 100$ %. The polyethylene quarter-wave films were more accurate at 280 nm than a tested commercial plate (Bernhard Halle Nachflgs., Berlin, 300 nm). The quarter-wave films mounted as permanent standards were made of PVA stretched at about 80°C a little more than that required to give quarter-wave effect. Relaxation to give exact zero-CD deflection was attained by adjusting the temperature to about 70° in an air thermostat for intervals of a few minutes.

The second method employs as a standard a solid-state solution of $d$-10-camphorsulphonic acid in PVA, which has been calibrated previously. It has proved to be very stable and is conveniently employed for regular checks of instrumental accuracy. Its use is certainly to be preferred to the "self-checking" systems of some instruments, *e.g.* the Jasco J-40 CD-spectrometer. Reproducibility of 0.5 % is easily attained, and even under unfavourable conditions differences are always less than a few percent.

The standard is prepared as follows: 20 ml of 10 % aqueous PVA solutions are mixed with 2 ml of 0.5 M aqueous $d$-10-camphorsulfonic acid. The resulting solution is centrifuged to remove bubbles and solid impurities from the PVA and then evaporated slowly (3 days) on a horizontal mirror glass, alternatively on a mercury surface. A piece is cut from the film for mounting either into a cell-holder or between quartz windows glued with a small amount of 10 % PVA. The presence of strains can be detected with a polarizing microscope, but this is not necessary if the film is carefully handled. Typically, a 0.011 cm thick film yielding a CD peak at 295 nm of 0.0131 absorbance units is obtained. The absorbance is 0.8. A 0.5 M aqueous $d$-10-camphorsulfonate solution of the same thickness, gives a peak at 290 nm with CD 0.0121.[1] The difference is presumably due to solvent effects, PVA being similar to ethanol. The temperature dependence is less than $\pm 2$ % for $\pm 5$°C at 24°C.

Certain CD instruments have recorders marked in ellipticity units, even though the instrument measures only the absorption difference $A_l - A_r$. It seems preferable, therefore, to recalibrate these in

terms of absorbance units using the relation $A_1 - A_r$ (CD in absorbance units) $= \theta$ (ellipticity in °)/33.0.

1. Cassim, J. Y. and Yang, J. T. *Biochemistry* 8 (1969) 1947.
2. Chau, K. H. and Yang, J. T. *Anal. Biochem.* 46 (1973) 616.
3. Håkansson, R. *Private communication.*
4. Velluz, L., Legrand, M. and Crosjean, M. *Optical Circular Dichroism*, Academic, London 1965.
5. Velluz, L. and Legrand, M. *Angew. Chem.* 73 (1961) 603.
6. Woldbye, F. In Jonassen, H. B. and Weissberger, A., Eds., *Technique of Inorganic Chemistry*, Interscience, London 1965, p. 249.
7. Hogness, A., Zscheile, B. and Sidwell, C. *J. Phys. Chem.* 41 (1937) 379.
8. Nordén, B. *Chemica Scripta* 1 (1971) 145.
9. Nordén, B., Håkansson, R. and Sundbom, M. *Acta Chem. Scand.* 26 (1972) 429.
10. Nordén, B. *Chem. Phys. Lett.* 23 (1973) 200.

# On the Structure of Gaseous Anisole

## H. M. SEIP and R. SEIP

*Department of Chemistry, University of Oslo, Oslo 3, Norway*

Anisole is usually assumed to have a planar heavy atom skeleton,[1] but some authors have suggested that the carbon in the methyl group does not lie in the ring plane.[2-5] Aroney *et al.*[2] measured the dipole moments and molar Kerr constants for anisole and some *para* substituted derivatives. They give an apparent torsional angle ($\phi$) around the $C_1 - O_7$ bond (see Fig. 1) of 18° for anisole. An extended Hückel calculation[4] gave minimum in energy for $\phi = 75°$, while $\phi = 0°$ was obtained by the CNDO/2 method if the methyl group was oriented to give minimum steric interaction between the methyl hydrogens and the *ortho* hydrogens in the ring.[5]

Electron diffraction data of anisole were recorded for two nozzle temperatures, the low temperature data (about 55°C) with Balzers Eldigraph KD-G2,[6,7] and the high temperature data (about 250°C) with the Oslo apparatus.[8] In both cases two nozzle-to-plate distances were used, and composite intensity curves covering the $s$-ranges $2.0 - 28.5$ Å$^{-1}$ and $2.0 - 40.0$ Å$^{-1}$ were calculated in the usual way.[9] The experimental radial distribution functions[9] calculated by Fourier inversion of the intensity curves, are shown in Fig. 1.

The mean amplitudes of vibration ($u$) for both temperatures computed as described by Stølevik *et al.*,[10] are included in Table 1. A simple force field, found to give $u$ values for benzene in good agreement with more refined calculations,[11] was used for the phenyl group. The other force constants were also estimated from force constants found in related molecules.

Least-squares refinements of the structural parameters were then carried out with a diagonal weight matrix. Except for the CO bond the phenyl group was assumed to have hexagonal symmetry, and the methyl group to have a threefold symmetry axis coinciding with the CO bond. For the low temperature data good agreement between experimental and theoretical intensity values was obtained for a model with planar skeleton and mean amplitudes computed as described above. The angle $\alpha$ (Fig. 1) was first assumed to be zero, but better agreement was obtained for $\alpha = 4°$. The most important $u$ values were then refined as shown in Table 1. A slightly better fit was obtained. The radial distribution curve calculated with these parameters is given in Fig. 1A. A very slight improvement was obtained if $\phi$ was increased to about 10°.

For the high temperature data the fit was not satisfactory if $\phi$ was assumed to be zero and the mean amplitudes kept at the computed values (Fig. 1). Much better agreement was obtained if the $u$ values were refined. However, the mean amplitudes for the distances from $C_8$ to the carbon atoms in the ring, became then considerably larger than the computed values.

Refinements were then carried out for various fixed values of $\phi$; the best agreement was obtained for $\phi = 40°$. It seemed likely that the torsional oscillations about $C_1 - O_7$ resulted in an apparent large devia-

terms of absorbance units using the relation $A_1 - A_r$ (CD in absorbance units) $= \theta$ (ellipticity in °)/33.0.

1. Cassim, J. Y. and Yang, J. T. *Biochemistry* **8** (1969) 1947.
2. Chau, K. H. and Yang, J. T. *Anal. Biochem.* **46** (1973) 616.
3. Håkansson, R. *Private communication.*
4. Velluz, L., Legrand, M. and Crosjean, M. *Optical Circular Dichroism*, Academic, London 1965.
5. Velluz, L. and Legrand, M. *Angew. Chem.* **73** (1961) 603.
6. Woldbye, F. In Jonassen, H. B. and Weissberger, A., Eds., *Technique of Inorganic Chemistry*, Interscience, London 1965, p. 249.
7. Hogness, A., Zscheile, B. and Sidwell, C. *J. Phys. Chem.* **41** (1937) 379.
8. Nordén, B. *Chemica Scripta* **1** (1971) 145.
9. Nordén, B., Håkansson, R. and Sundbom, M. *Acta Chem. Scand.* **26** (1972) 429.
10. Nordén, B. *Chem. Phys. Lett.* **23** (1973) 200.

# On the Structure of Gaseous Anisole

## H. M. SEIP and R. SEIP

*Department of Chemistry, University of Oslo, Oslo 3, Norway*

Anisole is usually assumed to have a planar heavy atom skeleton,[1] but some authors have suggested that the carbon in the methyl group does not lie in the ring plane.[2-5] Aroney *et al.*[2] measured the dipole moments and molar Kerr constants for anisole and some *para* substituted derivatives. They give an apparent torsional angle ($\phi$) around the $C_1 - O_7$ bond (see Fig. 1) of 18° for anisole. An extended Hückel calculation[4] gave minimum in energy for $\phi = 75°$, while $\phi = 0°$ was obtained by the CNDO/2 method if the methyl group was oriented to give minimum steric interac-

tion between the methyl hydrogens and the *ortho* hydrogens in the ring.[5]

Electron diffraction data of anisole were recorded for two nozzle temperatures, the low temperature data (about 55°C) with Balzers Eldigraph KD-G2,[6,7] and the high temperature data (about 250°C) with the Oslo apparatus.[8] In both cases two nozzle-to-plate distances were used, and composite intensity curves covering the $s$-ranges $2.0 - 28.5$ $Å^{-1}$ and $2.0 - 40.0$ $Å^{-1}$ were calculated in the usual way.[9] The experimental radial distribution functions[9] calculated by Fourier inversion of the intensity curves, are shown in Fig. 1.

The mean amplitudes of vibration ($u$) for both temperatures computed as described by Stølevik *et al.*,[10] are included in Table 1. A simple force field, found to give $u$ values for benzene in good agreement with more refined calculations,[11] was used for the phenyl group. The other force constants were also estimated from force constants found in related molecules.

Least-squares refinements of the structural parameters were then carried out with a diagonal weight matrix. Except for the CO bond the phenyl group was assumed to have hexagonal symmetry, and the methyl group to have a threefold symmetry axis coinciding with the CO bond. For the low temperature data good agreement between experimental and theoretical intensity values was obtained for a model with planar skeleton and mean amplitudes computed as described above. The angle $\alpha$ (Fig. 1) was first assumed to be zero, but better agreement was obtained for $\alpha = 4°$. The most important $u$ values were then refined as shown in Table 1. A slightly better fit was obtained. The radial distribution curve calculated with these parameters is given in Fig. 1A. A very slight improvement was obtained if $\phi$ was increased to about 10°.

For the high temperature data the fit was not satisfactory if $\phi$ was assumed to be zero and the mean amplitudes kept at the computed values (Fig. 1). Much better agreement was obtained if the $u$ values were refined. However, the mean amplitudes for the distances from $C_8$ to the carbon atoms in the ring, became then considerably larger than the computed values.

Refinements were then carried out for various fixed values of $\phi$; the best agreement was obtained for $\phi = 40°$. It seemed likely that the torsional oscillations about $C_1 - O_7$ resulted in an apparent large devia-
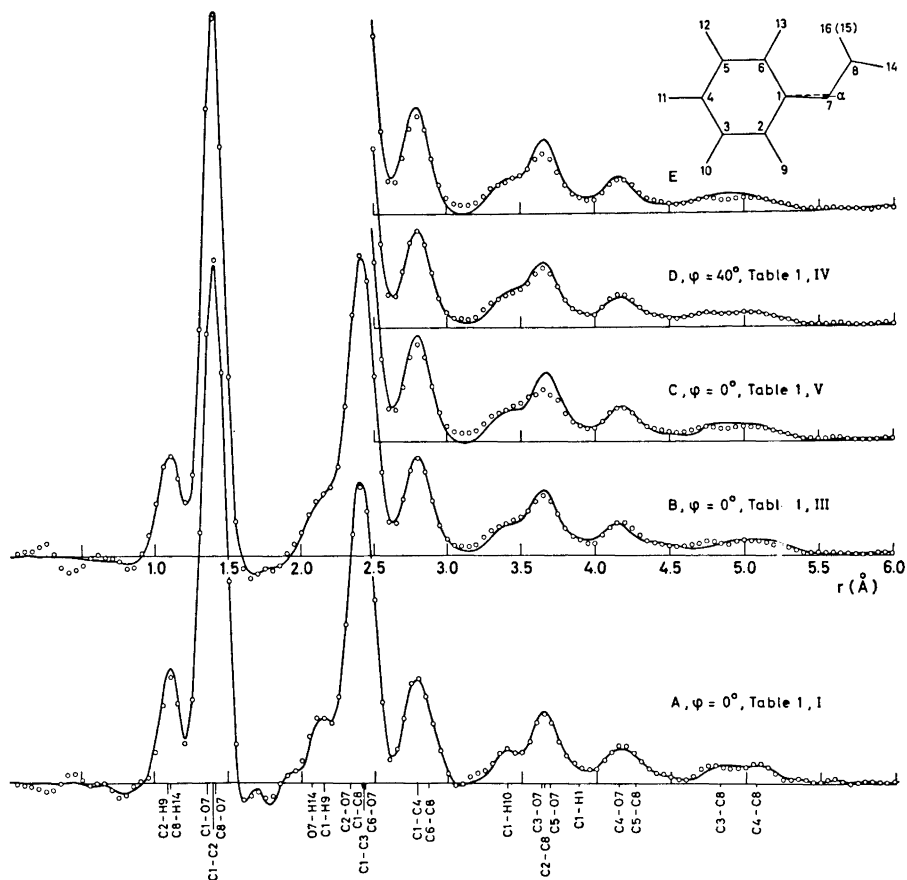
*Fig. 1.* Experimental (dotted) and theoretical radial distribution curves calculated with an artificial damping constant $k = 0.0015$ Å.[2] Curve A corresponds to the low temperature data, curves B − E to the high temperature. The parameters used to calculate the theoretical curves are given in Table 1. The theoretical curve in E was calculated by using eqn. (1) with
$$V_0 = 3 \text{ kcal/mol.}$$

tion from planarity. We therefore assumed a potential for internal rotation of the form

$$V(\phi) = (V_0/2)[1 - \cos(2\phi)] \qquad (1)$$

The corresponding probability distribution was calculated classically. Owen and Hester have reported a barrier of about 6 kcal/mol.[1] We found that if the computed mean amplitudes were used, satisfactory agreement was not obtained with this barrier. $V_0 = 3$ kcal/mol and $V_0 = 2$ kcal/mol gave only a slight improvement (Fig. 1E).

It is not possible from the electron-diffraction data to determine the potential for rotation about the $C_1 - O_7$ bond accurately. However, it seems very likely that $\phi = 0°$ corresponds to minimum in energy. This is in agreement with the result of a microwave investigation of *p*-fluoro-anisole.[12] The simple function (1) is probably not a good description of the potential. The large difference between the *u* values obtained for the two temperatures and the good agreement for the high temperature data for $\phi = 40°$ may be caused by

*Table 1.* Bond distances $(r_a)$, angles and mean amplitudes of vibration in anisole.[a] The standard deviations given in parentheses apply to the last decimal place.

| | Temperature 55°C | | Temperature 250°C | | |
| | I | II | III | IV | V |
| | exp. $u$ values | comp. $u$ values | exp. $u$ values | exp. $u$ values | comp. $u$ values |
|---|---|---|---|---|---|
| **Distances (Å)** | | | | | |
| $C_1-C_2$ | 1.397 | 1.398 | 1.398(8) | 1.398(11) | 1.398 |
| $C_8-O_7$ | 1.423(7) | 1.418(4) | 1.434(7) | 1.422(6) | 1.406 |
| $C_1-O_7$ | 1.357(6) | 1.359(3) | 1.351(5) | 1.365(6) | 1.379(3) |
| $C_2-H_9$ | 1.09 | 1.09 | 1.09 | 1.09 | 1.09 |
| $C_8-H_{14}$ | 1.11 | 1.11 | 1.11 | 1.11 | 1.11 |
| **Angles (degrees)** | | | | | |
| $\alpha$ | 4.0 | 4.0 | 4.0 | 4.0 | 4.0 |
| $\angle COC$ | 120.9(6) | 120.9(6) | 123.6(12) | 119.2(11) | 119.0 |
| $\angle CCH$ | 110.0 | 110.0 | 110.0 | 110.0 | 110.0 |
| $\phi$ | 0.0 | 0.0 | 0.0 | 40.0 | 40.0 |
| **Mean amplitudes [b] (Å)** | | | | | |
| $C_1-C_2$ | 0.045⎫ | 0.046 | 0.040⎫ | 0.043⎫ | 0.047 |
| $C_8-O_7$ | 0.048⎬(2) | 0.047 | 0.043⎬(2) | 0.046⎬(2) | 0.050 |
| $C_1-O_7$ | 0.046⎭ | 0.046 | 0.041⎭ | 0.044⎭ | 0.048 |
| $C_1\cdots C_4$ | 0.064⎫(2) | 0.059 | 0.062⎫(2) | 0.065⎫(2) | 0.064 |
| $C_1\cdots C_3$ | 0.058⎭ | 0.054 | 0.056⎭ | 0.059⎭ | 0.058 |
| $C_2\cdots O_7$ | 0.066⎫ | 0.060 | 0.061⎫ | 0.066⎫ | 0.068 |
| $C_3\cdots O_7$ | 0.068⎪ | 0.062 | 0.063⎪ | 0.068⎪ | 0.070 |
| $C_4\cdots O_7$ | 0.069⎬(6) | 0.063 | 0.064⎬(5) | 0.069⎬(5) | 0.071 |
| $C_5\cdots O_7$ | 0.064⎪ | 0.060 | 0.059⎪ | 0.064⎪ | 0.066 |
| $C_6\cdots O_7$ | 0.062⎭ | 0.057 | 0.057⎭ | 0.062⎭ | 0.064 |
| $C_1\cdots C_8$ | 0.056⎫ | 0.064 | 0.113⎫ | 0.098⎫ | 0.073 |
| $C_2\cdots C_8$ | 0.059⎪ | 0.067 | 0.116⎪ | 0.101⎪ | 0.076 |
| $C_3\cdots C_8$ | 0.066⎪(10) | 0.072 | 0.123⎪(18) | 0.108⎪(13) | 0.083 |
| $C_4\cdots C_8$ | 0.083⎪ | 0.085 | 0.140⎪ | 0.125⎪ | 0.100 |
| $C_5\cdots C_8$ | 0.098⎪ | 0.097 | 0.155⎪ | 0.140⎪ | 0.115 |
| $C_6\cdots C_8$ | 0.098⎭ | 0.094 | 0.155⎭ | 0.140⎭ | 0.115 |

[a] Parameters given without standard deviations were not refined with the other parameters.
[b] The mean amplitudes were refined in groups, the differences between the values in one group were assumed.

a secondary minimum in the potential function. The low resolution microwave spectra have given indications of the existence of conformers with non-planar skeletons for *p*-anisaldehyde[13] and *m*-bromoanisole.[14]

The bond distances and angles found by least-squares refinements are given in Table 1. The best values and error limits for the most important parameters seem to be: $r_a(C-C) = 1.398 \pm 0.003$ Å, $r_a(C_1-O_7) = 1.361 \pm 0.015$ Å, $r_a(C_8-O_7) = 1.423 \pm 0.015$ Å, $\angle COC = 120.0 \pm 2.0°$. The average

C−C bond distance is the same as in benzene[15] and the CO distances close to the values found in methyl-vinyl-ether, 1.358 Å and 1.424 Å.[16]

1. Owen, N. L. and Hester, R. E. *Spectrochim. Acta* **A 25** (1969) 343.
2. Aroney, M. J., Le Fevre, R. J. W., Pierens, R. K. and The, M. C. N. *J. Chem. Soc.* **B 1969** 666.
3. Horak, M., Lippincott, E. R. and Khanna, R. *Spectrochim. Acta* **A 23** (1967) 1111.
4. Tylli, H. *Finska Kemistsamfundets Medd.* **79** (1970) 22.
5. Tylli, H. *Finska Kemistsamfundets Medd.* **81** (1972) 19.
6. Bastiansen, O., Graber, R. and Wegmann, L. *Balzers High Vacuum Report* **25** (1969) p. 1.
7. Zeil, W., Haase, J. and Wegmann, L. *Z. Instrumentenk.* **74** (1966) 84.
8. Bastiansen, O., Hassel, O. and Risberg, F. *Acta Chem. Scand.* **9** (1955) 232.
9. Andersen, B., Seip, H. M., Strand, T. G. and Stølevik, R. *Acta Chem. Scand.* **23** (1969) 3224.
10. Stølevik, R., Seip, H. M. and Cyvin, S. J. *Chem. Phys. Lett.* **15** (1972) 263.
11. Cyvin, S. J. *Molecular Vibrations and Mean Square Amplitudes*, Universitetsforlaget, Oslo and Elsevier, Amsterdam 1968.
12. Lister, D. G. and Owen, N. L. *J. Chem. Soc. Faraday Trans. 2* **1973** 1304.
13. Steinmetz, W. E. *Private communication* 1973.
14. Bohn, R. *Private communication* 1973.
15. Seip, R. and Fernholt, L. *To be published*.
16. Owen, N. L. and Seip, H. M. *Chem. Phys. Lett.* **5** (1970) 162.
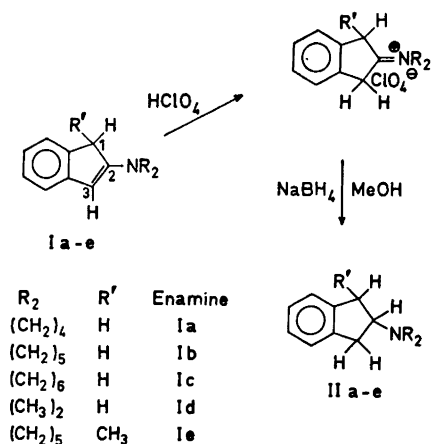
Received November 10, 1973.

# Preparation of Some N-Substituted 2-Aminoindanes

ULF EDLUND

*Department of Organic Chemistry,*
*University of Umeå, S-901 87 Umeå, Sweden*

In connection with the studies of enamines of 2-indanones [1,2] we want to report a versatile method for the preparation of some N-substituted 2-aminoindanes. Some of these compounds have been synthesized previously by catalytic reduction of the corresponding enamines at high pressure.[3] Structurally these indanamines form an interesting group of compounds since the presence of a phenethylamine skeleton relates them to the pharmacologically and physiologically well-known phenylisopropylamines. Thus these compounds are indane analogs corresponding to amphetamine. The pharmacological effect upon N-alkylation of 2-aminoindanes has earlier been reported.[4,5]

2-Indanone and 1-methyl-2-indanone are most conveniently prepared by oxidation of the corresponding indenes with performic acid.[1,6] The syntheses of the enamines are then easily achieved by mixing the ketone and the desired secondary amine in methanol at room temperature.[1,7] Since the reduction of enamines by hydride depends on the prior generation of an immonium salt,[8] we have prepared the stable perchlorate salts of our enamines.



| R₂ | R′ | Enamine |
|---|---|---|
| $(CH_2)_4$ | H | Ia |
| $(CH_2)_5$ | H | Ib |
| $(CH_2)_6$ | H | Ic |
| $(CH_3)_2$ | H | Id |
| $(CH_2)_5$ | CH₃ | Ie |

*Scheme 1.*

1. Owen, N. L. and Hester, R. E. *Spectrochim. Acta* **A 25** (1969) 343.
2. Aroney, M. J., Le Fevre, R. J. W., Pierens, R. K. and The, M. C. N. *J. Chem. Soc.* **B 1969** 666.
3. Horak, M., Lippincott, E. R. and Khanna, R. *Spectrochim. Acta* **A 23** (1967) 1111.
4. Tylli, H. *Finska Kemistsamfundets Medd.* **79** (1970) 22.
5. Tylli, H. *Finska Kemistsamfundets Medd.* **81** (1972) 19.
6. Bastiansen, O., Graber, R. and Wegmann, L. *Balzers High Vacuum Report* **25** (1969) p. 1.
7. Zeil, W., Haase, J. and Wegmann, L. *Z. Instrumentenk.* **74** (1966) 84.
8. Bastiansen, O., Hassel, O. and Risberg, F. *Acta Chem. Scand.* **9** (1955) 232.
9. Andersen, B., Seip, H. M., Strand, T. G. and Stølevik, R. *Acta Chem. Scand.* **23** (1969) 3224.
10. Stølevik, R., Seip, H. M. and Cyvin, S. J. *Chem. Phys. Lett.* **15** (1972) 263.
11. Cyvin, S. J. *Molecular Vibrations and Mean Square Amplitudes*, Universitetsforlaget, Oslo and Elsevier, Amsterdam 1968.
12. Lister, D. G. and Owen, N. L. *J. Chem. Soc. Faraday Trans. 2* **1973** 1304.
13. Steinmetz, W. E. *Private communication* 1973.
14. Bohn, R. *Private communication* 1973.
15. Seip, R. and Fernholt, L. *To be published*.
16. Owen, N. L. and Seip, H. M. *Chem. Phys. Lett.* **5** (1970) 162.
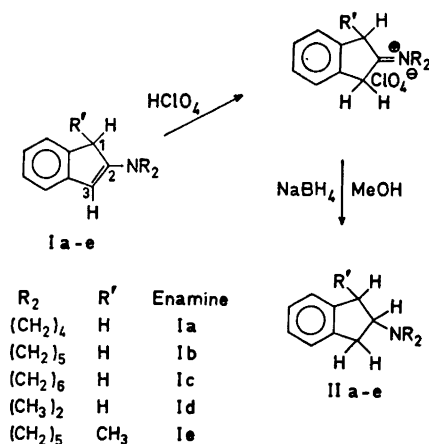
Received November 10, 1973.

# Preparation of Some N-Substituted 2-Aminoindanes

ULF EDLUND

*Department of Organic Chemistry, University of Umeå, S-901 87 Umeå, Sweden*

In connection with the studies of enamines of 2-indanones [1,2] we want to report a versatile method for the preparation of some N-substituted 2-aminoindanes. Some of these compounds have been synthesized previously by catalytic reduction of the corresponding enamines at high pressure.[3] Structurally these indanamines form an interesting group of compounds since the presence of a phenethylamine skeleton relates them to the pharmacologically and physiologically well-known phenylisopropylamines. Thus these compounds are indane analogs corresponding to amphetamine. The pharmacological effect upon N-alkylation of 2-aminoindanes has earlier been reported.[4,5]

2-Indanone and 1-methyl-2-indanone are most conveniently prepared by oxidation of the corresponding indenes with performic acid.[1,6] The syntheses of the enamines are then easily achieved by mixing the ketone and the desired secondary amine in methanol at room temperature.[1,7] Since the reduction of enamines by hydride depends on the prior generation of an immonium salt,[8] we have prepared the stable perchlorate salts of our enamines.



| $R_2$ | $R'$ | Enamine |
|-------|------|---------|
| $(CH_2)_4$ | H | I a |
| $(CH_2)_5$ | H | I b |
| $(CH_2)_6$ | H | I c |
| $(CH_3)_2$ | H | I d |
| $(CH_2)_5$ | $CH_3$ | I e |

*Scheme 1.*

Treatment of these salts with sodium borohydride in methanolic solution affords, after usual workup, the saturated tertiary amines in almost quantitative yields. A series of $N$-substituted 2-aminoindanes has been prepared in this way (Scheme 1).

Previous studies of the stereochemical course of lithium aluminium hydride reductions of an immonium salt [9] (Scheme 2) have shown that the two possible
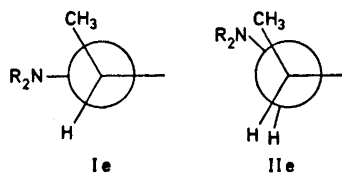


Scheme 2.
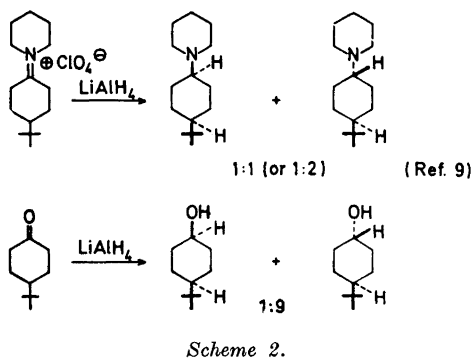
isomers are formed in almost equal proportions. This is in contrast to the reduction of the analogous ketone where the thermodynamically stable isomer predominates. In our 2-indanone system we have a more planar conformation and this framework is in good agreement with the open-chain model chosen to illustrate Cram's rule of steric control of asymmetric induction. In view of these considerations and the greater effective size of the borohydride we should therefore, in the case of reduction of the 1-methyl-2-($N$-piperidyl)indene (I e) salt, expect the *cis* isomer to be equally favoured or possibly more favoured compared with the product formed by "*product development control*". The isomer distribution we observed shows that one isomer predominates as determined by the ^{1}H NMR spectrum. A small doublet downfield the dominant methyl signal is ascribed to the other isomer. This contamination ( < 5 %) could not be eliminated by careful distillation. However, the recrystallization of the hydrochloride afforded pure product. In a ^{13}C NMR study where steric compression effects are more significant an upfield shift of about 3 ppm (Table 1) was observed compared with the methyl peak from (I e). Even if interpretations of small shielding

Table 1. Carbon-13 shieldings of some 2-($N$-piperidyl)indenes and their saturated analogs.[a,b]

| Compound | $C_1$ | $C_2$ | $C_3$ | R' |
|----------|------|-------|-------|------|
| I b | 37.4 | 157.9 | 98.9 | |
| II b | 37.3 | 67.6 | 37.3 | |
| I e | 42.1 | 163.1 | 99.3 | 18.0 |
| II e | 41.3 | 70.2 | 34.7 | 15.1 |

[a] $\delta$ ppm from TMS; 1 M solution in chloroform-D. [b] wide-band (noise) decoupled; pulse width 8 $\mu$s ($\pi/4$); repetition rate 1 sec.

changes must be approached with caution in ^{13}C NMR, it is invariably found that steric crowding produces an upfield shift of a carbon with a nucleus other than hydrogen in the $\gamma$ position.[10] Thus this shift difference implies increased steric



Scheme 3.

hindrance and confirms our proposal that the main isomer is the kinetically formed *cis* isomer (II e) (Scheme 3).

*Experimental.* All ^{1}H NMR- and ^{13}C NMR-work was performed on a JEOL JNM PFT-60 NMR spectrometer. The computer system (EC-100; 20 K core) allowed acquisition of 16 K spectral data points. The mass spectra were obtained with a LKB 9000 mass spectrometer.

*2-(N-Cycloamino)indenes (I a−c).* The enamines (I a−c) were prepared in good yields according to a method published by Schroth and Fischer[7] by simply mixing 2-indanone[6] and the cyclic secondary amine in methanol.

*2-(N-Dimethylamino)indene (I d).* To an ice-cooled solution of 2.64 g (0.020 mol) 2-indanone in 75 ml methanol p.a. were added 2.0 g (0.044 mol) dimethylamine (99 % GLC) in one portion. After a few minutes the crystalline product separated, m.p. 79.5− 80.0°C.

Yield; 2.50 g (79 %) $M^{+\cdot} = 159$. (Found: C 82.8; H 8.1; N 8.6. Calc. for $C_{11}H_{13}N$ (159): C 83.0; H 8.2; N 8.8). $^1$H NMR in chloroform-D (TMS) of (I d); 2.73 (6 H singlet), 3.23 (2 H singlet), 5.20 (1 H singlet), 6.50–7.17 (4 H complex) ($\delta$ ppm).

*1-Methyl-2-(N-piperidyl)indene (I e)*. The contaminated (I e) (4 % of the 3-isomer) was synthesized as we have earlier described from 4.38 g (0.030 mol) 1-methyl-2-indanone.[1] Yield: 62 %.

*The perchlorate salts of (I a−e)*. According to a method described by Blomquist and Moriconi[11] a solution of 25 ml 70 % perchloric acid and 25 ml abs. ethanol was added to a solution of (I a−e) in ether until pH<3 (Congo Red paper). Yields were almost quantitative.

*General procedure for the preparation of (II a−e)*. To an ice-cooled stirred slurry of 0.014 mol of the perchlorate salt in methanol p.a., 1.0 g (0.026 mol) sodium borohydride was added cautiously in small portions. The temperature was not allowed to exceed 5°C. After addition of the hydride the stirring was continued for another 15 min. The solution was then concentrated to a small volume. 50 ml 5 % sodium hydroxide was added and the mixture was extracted with ether. The combined ether layers were then dried over anhydrous sodium sulphate. Removal of solvent gave pure $N$-substituted 2-amino-indane (II a−e) in quantitative yield. Distillation under reduced pressure did not affect physical data or spectral characteristics.

*2-(N-Pyrrolidyl)indane (II a)*. Colourless crystals, m.p. 44.5−46.0°C. Hydrochloride (ethanol-ether); m.p. 234−236°C (lit.[3] 191−193°C). $M^{+\cdot} = 187$. (Found: C 83.3; H 9.2; N 7.3. Calc. for $C_{13}H_{17}N$ (187): C 83.4; H 9.2; N 7.5). $^1$H NMR in chloroform-D (TMS) of (II a); 1.50−1.90 (4 H complex), 2.25−2.65 (4 H complex), 2.86 (5 H complex), 6.93 (4 H singlet) ($\delta$ ppm).

*2-(N-Piperidyl)indane (II b)*. Colourless crystals, m.p. 59.0−60.0°C. Hydrochloride (ethanol−ether); m.p. 256−259°C (lit.[3] 252−253°C). $M^{+\cdot} = 201$. (Found: C 83.7; H 9.5; N 7.0). $^1$H NMR in chloroform-D (TMS) of (II b); 1.20−1.83 (6 H complex) 2.10−2.60 (4 H complex), 2.60−3.33 (5 H complex), 6.93 (4 H singlet) ($\delta$ ppm).

*2-(N-Hexamethyleneimino)indane (II c)*. Colourless oil, b.p. 164−166°C (10 mm). Hydrochloride (ethanol−ether); m.p. 194−196°C (lit.[3] 232°C). $M^{+\cdot} = 215$. (Found: C 83.6; H 9.8; N 6.5. Calc. for $C_{15}H_{21}N$ (215): C 83.7; H 9.8; N 6.5). $^1$H NMR in chloroform-D (TMS) of (II c); 1.30−1.83 (8 H complex)

2.30−3.70 (9 H complex) 6.93 (4 H complex) ($\delta$ ppm).

*2-(N-Dimethylamino)indane (II d)*. Fairly hygroscopic colourless oil, b.p. 99−101°C (10 mm). Hydrochloride (ethanol−ether); m.p. 205−207°C. $M^{+\cdot} = 161$. (Found: C 66.8; H 8.2; N 6.9; Cl 17.9. Calc. for $C_{11}H_{16}NCl$ (197.5); C 66.8; H 8.2; N 7.1; Cl 17.9). $^1$H NMR in chloroform-D (TMS) of (II d); 2.23 (6 H singlet), 2.90 (5 H complex), 7.00 (4 H singlet) ($\delta$ ppm).

*cis-1-Methyl-2-(N-piperidyl)indane (II e)*. The residue after evaporation consists mainly of (II e) as determined by $^1$H NMR and $^{13}$C NMR spectra. A small doublet in the $^1$H NMR spectrum at 1.27 ppm downfield TMS is ascribed to the other isomer. One recrystallization of the hydrochloride (ethanol−ether) followed by generation of the free amine affords pure (II e), b.p. 152−154°C (10 mm). Hydrochloride (ethanol−ether); m.p. 218−221°C. $M^{+\cdot} = 215$. (Found: C 83.3; H 9.9; N 6.5. Calc. for $C_{15}H_{21}N$ (215): C 83.7; H 9.8; N 6.5). $^1$H NMR in chloroform-D (TMS) of (II e): 1.05 (3 H doublet), 1.20−1.80 (6 H complex) 2.10−2.60 (4 H complex) 2.67−3.27 (4 H complex) 6.96 (4 H singlet) ($\delta$ ppm).

1. Edlund, U. and Bergson, G. *Acta Chem. Scand.* **25** (1971) 3625.
2. Edlund, U. *Acta Chem. Scand.* **26** (1972) 2972.
3. Brit. Patent 1.142.724; cf. *Chem. Abstr.* **71** (1969) 21937 s.
4. Levin, N., Graham, B. E. and Kolloff, H. G. *J. Org. Chem.* **9** (1944) 380.
5. Van der Schoot, J. B., Ariens, E. J., van Rossum, J. M. and Hurkmans, J. A. T. M. *Arzneimittel-Forsch.* **12** (1962) 902.
6. Horar, J. E. and Schliesser, R. W. *Org. Syn.* **41** (1961) 53.
7. Schroth, W. and Fischer, G. W. *Chem. Ber.* **102** (1969) 575.
8. Cook, A. G. *Enamines Synthesis, Structure and Reactions*, Dekker, New York 1969, pp. 185−192, 428−433.
9. Cabaret, D., Chauvière, G. and Welvart, Z. *Tetrahedron Letters* **1966** 4109.
10. a. Reich, H. J., Jautelat, M., Messe, M. T., Weigert, F. J. and Roberts, J. D. *J. Am. Chem. Soc.* **91** (1969) 7445; b. Balogh, B., Wilson, D. J. and Burlingame, A. L. *Nature* **233** (1971) 261; c. Gough, J. L., Guthrie, J. P. and Stothers, J. B. *J. Chem. Soc.* **D** 1972 979.
11. Blomquist, A. T. and Moriconi, E. J. *J. Org. Chem.* **26** (1961) 3761.

Received November 10, 1973.